Nuclear Structure and Nuclear Processes

Jan Kvasil

jan.kvasil@mff.cuni.cz

Institute of Particle and Nuclear Physics
Faculty of Mathematics and Physics
Charles University in Prague

July 7, 2023

Contents

Preface 1

1 Basic properties of nuclei, symmetry of nuclear Hamiltonian 3
1.1 Basic nuclear properties 3
1.1.1 Interactions of nucleons, many-body problem 3
1.1.2 Nuclear proportions and shapes, mass and charge distribution in nucleus 5
1.1.3 Mass of nucleus, nuclear binding energy 9
1.2 Isotopic symmetry of nuclear interaction 11
1.3 Space-time symmetries of nuclear Hamiltonian 18
1.3.1 Inversion of space axes - parity 18
1.3.2 Time reversal 18
1.4 Degrees of freedom of nuclear motion 24

2 Electromagnetic transition probabilities, static electromagnetic moments 32
2.1 Quantum description of a free electromagnetic field 32
2.1.1 Maxwell and wave equations, solutions of the wave equation 33
2.1.1.1 Derivation of the wave equation 33
2.1.1.2 Solution of wave equation - spherical waves . 36
2.1.1.3 Solution of wave equation - plane waves . . . 42
2.1.1.4 Relation between plane and spherical waves . 48
2.1.2 Lagrangian and Hamiltonian of a free electromagnetic field, quantization of el.mg. field 50
2.2 Interaction of electromagnetic field with the quantum bound object (nucleus) 60
2.2.1 Probability of electromagnetic transitions 60
2.2.2 Probability of the emission of the photon by the nucleus 62
2.2.2.1 Electric and magnetic multipole operators - transition probability 62

2.2.2.2 Longwave approximation 72
2.2.2.3 Reduced transition probabilities and the multipolarity mixing ratio 80
2.2.2.4 Reduced probability of el.mg. transitions in the framework of the simple model of independent particles - Weisskopf units 84
2.2.3 Absorption of photons by nuclei 88
2.3 Static electromagnetic moments of the nucleus 92
2.3.1 Electric dipole moment 99
2.3.2 Electric quadrupole moment 100
2.3.3 Magnetic dipole moment 102

3 Nucleon - nucleon interaction 104
3.1 Nucleon-nucleon interaction in the vacuum (bare nucleon-nucleon interaction) 105
3.1.1 Basic data on bare nucleon-nucleon interaction following from the deuteron properties 105
3.1.1.1 Central potential 106
3.1.1.2 Tensor forces 109
3.1.1.3 Electric quadrupole moment of the deuteron . 114
3.1.1.4 Magnetic dipole moment of the deuteron . . . 115
3.1.2 Information on the bare nucleon-nucleon interaction from the scattering of two nucleons 117
3.1.2.1 Scattering of neutron and proton by means of the central potential 118
3.1.2.2 Scattering of two protons by means of the central potential 120
3.1.2.3 Tensor forces 122
3.1.2.4 Phase shift analysis 131
3.1.3 Bare nucleon-nucleon potentials 133
3.1.3.1 Basic properties of the bare nucleon-nucleon forces and their physical premises 133
3.1.3.2 Exchange meson character of the bare nucleon-nucleon interaction 136
3.1.3.3 Phenomenological bare nucleon-nucleon potentials 143
3.2 Nucleon-nucleon effective interaction in the nuclear matter . . 150
3.2.1 Microscopic effective nucleon-nucleon interaction 151

3.2.2 Semi-phenomenological effective nucleon-nucleon interaction . . . 158
3.2.2.1 Skyrme effective nucleon-nucleon interaction . 160
3.2.2.2 Gogny effective nucleon-nucleon interaction . 161
3.2.3 Relativistic mean field approach . . . 162

4 Hartree-Fock method, particle-hole formalism, basic idea of shell model 168
4.1 Hartree-Fock method . . . 168
4.1.1 Hartree-Fock equation . . . 168
4.1.2 Ground state in the Hartree-Fock method . . . 177
4.1.3 Excited states in the HF approach (particle-hole formalism) . . . 181
4.1.4 Problems and questions in the HF method . . . 184
4.1.4.1 The question of taking into account of the short range residual interaction . . . 184
4.1.4.2 Questions of the stability of numerical calculations and of the absolute minimum . . . 185
4.1.4.3 Translation and rotation invariance of the nuclear hamiltonian, spurious modes . . . 186
4.1.4.4 The problem of the infinite potential (hard core) . . . 187
4.2 Shell model . . . 188

5 Model of independent particles in the nuclear physics 192
5.1 Phenomenological mean field . . . 194
5.1.1 Spherical mean field, magic numbers . . . 194
5.1.2 Phenomenological deformed mean field, Strutinski shell corrections, equilibrium deformation, fission barriers . . 206
5.1.2.1 Nilsson model of deformed mean field . . . 206
5.1.2.2 Strutinski shell model corrections . . . 216
5.1.2.3 Some application of the Strutinski shell model correction method . . . 221
5.1.2.3.1 Equilibrium deformations and nuclear masses . . . 221
5.1.2.3.2 Nuclear fission (fission barriers) . . . 223
5.2 Microscopical mean field . . . 237

6 Short range residual interaction, pairing correlations in nuclei 254
6.1 Experimental indications of nuclear pairing effects 256
6.2 Bardeen-Cooper-Schrieffer (BCS) theory, Bogoliubov transformation, Hartree-Fock-Bogoliubov (HFB) equation 260
6.2.1 Pairing interaction potential 260
6.2.2 Bardeen-Cooper-Schrieffer (BCS) theory 264
6.2.2.1 Bogoliubov transformation 264
6.2.2.2 BCS equations 268
6.2.2.3 Blocking effect 276
6.2.2.4 Standard deviation of the number of particles 278
6.2.2.5 Existence and nonexistence of nontrivial solution of the BCS equation 280
6.2.2.6 Neutron-proton pairing 281
6.2.2.7 Empirical (experimental) pairing gap Δ . . . 282
6.2.3 BCS with the general effective nucleon-nucleon interaction 284
6.2.4 Hartree-Fock-Bogoliubov approach 290
6.3 Simple algebraic model of the pairing, seniority scheme 306

7 Vibration of nuclei, long range residual interaction 316
7.1 Model Hamiltonian of vibrating and rotating deformed nucleus 317
7.2 Phenomenological models of intrinsic degrees of freedom of nuclear motion 331
7.2.1 Bohr geometrical model (nucleus as a drop of the nuclear matter) 332
7.2.1.1 Shape oscillation of the spherical nuclear droplet 334
7.2.1.2 Vibration and rotation of the deformed droplet 346
7.2.2 Algebraic description of nuclear collective motion (Interacting Boson Model) 357
7.2.2.1 Interacting Boson Model - 1 358
7.2.2.1.1 $U(5)$ limit (vibrator limit) 366
7.2.2.1.2 $SU(3)$ limit (axial rotor limit) 373
7.2.2.1.3 γ- unstable limit ($SO(6)$ limit) . . . 379
7.2.2.1.4 Casten symmetry triangle 383
7.2.2.2 Interacting Boson Model - 2 389
7.2.2.3 Interacting Boson-Fermion Model (IBFM) . . 400

7.3 Microscopical models of intrinsic degrees of freedom of nuclear motion (taking into account the long-range residual interaction) 404
7.3.1 Random-Phase-Approximation method 406
7.3.1.1 RPA for even-even nuclei 406
7.3.1.1.1 General RPA equation, phonons . . . 406
7.3.1.1.2 Fermion-boson mapping, RPA Hamiltonian, spurious modes. 418
7.3.1.1.3 Separable form of the RPA equation 433
7.3.1.2 RPA for odd-A and odd-odd nuclei 439
7.3.2 Application of the RPA approach for the interpretation of selected experimental data 446
7.3.2.1 RPA description of low- lying part of nuclear spectra 447
7.3.2.1.1 Low- lying states in spherical nuclei . 447
7.3.2.1.2 Intrinsic (non-rotational) low-lying states in deformed nuclei 457
7.3.2.2 RPA description of higher energy part of nuclear spectra 469
7.3.2.2.1 Isoscalar and isovector transitions, strength functions, sum rules 469
7.3.2.2.2 Giant resonances in spherical and deformed nuclei 476
7.3.3 Approaches going beyond the Random-Phase Approximation 513
7.3.3.1 Time-depending Hartree-Fock approach . . . 514
7.3.3.2 Generator coordinate method (Hill-Wheeler-Griffin theory) 515
7.3.3.2.1 Hill-Wheeler-Griffin theory (HWG theory) 515
7.3.3.2.2 Application of the GCM for nuclear structure 521
7.3.3.3 Large scale shell model 532
7.3.3.3.1 Quantum Monte Carlo Diagonalization (QMCD) - simplified Hamiltonian 536
7.3.3.3.2 Quantum Monte Carlo Diagonalization (QMCD) - general case 538
7.3.3.4 Equation of motion multi-phonon method . . 544

8 Rotation of nuclei **552**
8.1 Slow rotation . . . 552
8.1.1 Slow rotation of axially deformed $\mathscr{R}$-symmetric nuclei . 555
8.1.2 Slow rotation of axially deformed $\mathscr{S}$-symmetric (reflection asymmetric) nuclei . . . 559
8.1.3 Effect of the Coriolis interaction . . . 572
8.1.4 Moments of inertia . . . 580
8.2 Fast rotation . . . 584
8.2.1 Cranking model . . . 584
8.2.2 Cranking formula for moment of inertia . . . 595
8.2.3 Microscopic version of the cranking model (shape transitions induced by rotation) . . . 597
8.2.4 Giant resonances above the yrast band in fast rotating nuclei . . . 613

9 Alpha decay **621**
9.1 Basic data on alpha decay . . . 621
9.2 Theoretical determination of probability of the α- decay of even-even nuclei . . . 627
9.2.1 Alpha- transition from the ground state of even-even nucleus to the ground state of even-even nucleus . . . 631
9.2.1.1 Ground state to ground state alpha transitions in even-even nuclei within the model of independent particles (IP) . . . 631
9.2.1.2 Ground state to ground state alpha transitions in even-even nuclei within the model of independent quasiparticles (IP) . . . 632
9.2.2 Alpha- transition from the ground state of even-even nucleus to the excited state of even-even nucleus . . . 636
9.3 Probability of α- decay in odd-A nuclei . . . 639

10 Beta decay (beta transitions in nuclei) **649**
10.1 Kinematics of beta-decay . . . 651
10.2 Fermi theory of β- decay, allowed and forbidden β- transitions 654
10.3 Generalization of Fermi theory of β- transitions (parity violation) 658
10.4 Consequences for weak β-process amplitude coming from elementary processes experiments . . . 662
10.4.1 Electron spectrum from the β- decay of neutron . . . 663

10.4.2 Electron-antineutrino correlation in pure Fermi and Gamow-Teller β^- decays (V-A dominance) 670
10.4.3 Longitudinal polarization of electrons 672
10.4.4 V - A coupling constants C_A and C_V 676
10.4.5 Comments to the Standard Model of electro-weak interaction 679
10.5 β- processes in nuclei 685
10.5.1 Nuclear matrix element of β- interaction Hamiltonian . 685
10.5.2 Probability of β decay of nuclei 695
10.5.3 Higher energy Gamow-Teller and Fermi excitations (GM and F resonances) 705
10.5.3.1 Fermi and Gamow-Teller strength functions (Ikeda selection rules) 706

11 Basic theory of nuclear reactions 712
11.1 Mechanisms of nuclear reactions 712
11.1.1 Reaction going through compound nucleus 712
11.1.2 Direct nuclear reactions 714
11.2 Feshbach theory of nuclear reaction 718
11.2.1 Classification of channels and reactions 719
11.2.1.1 Open and closed channels 719
11.2.1.2 Prompt and time-delayed channels, "doorway" and "reminding" channels 720
11.2.2 P-space and Q-space formalism 723
11.2.2.1 P-space and Q-space of reaction channels . . 723
11.2.2.2 Resonance Breight-Wigner expression for reaction $\mathscr{T}$- matrix 729
11.2.2.3 Optical potential 741
11.2.2.4 Intermediate structures, doorway state resonances 750
11.2.3 Concluding remarks to the Feshbach formal theory . . 758
11.3 Many-channel description of reaction (reaction matrix, S-matrix, optical theorem) 761
11.3.1 General coupled channel equation system 761
11.3.2 S- matrix and reaction amplitudes for nuclear reactions, optical theorem 768
11.3.2.1 Reaction of spinless particles and nuclei . . . 769

11.3.2.2 Reaction of nuclei and particles with nonzero spin . . . 780
11.3.2.3 Properties of S- matrix . . . 782
11.3.2.3.1 Spherical ingoing and outgoing wave packets . . . 782
11.3.2.3.2 Unitarity of S- matrix . . . 784
11.3.2.3.3 Reciprocity theorem . . . 786
11.3.2.3.4 Principle of detailed balance . . . 787
11.4 Direct nuclear reactions . . . 789
11.4.1 Green function method for solving coupled channel equation system . . . 789
11.4.1.1 Plane wave Born approximation (PWBA) . . 793
11.4.1.2 Distorted wave Born approximation (DWBA) 793
11.4.1.3 Coupled channel method . . . 793
11.4.2 Elastic scattering from the point of view of the optical model . . . 794
11.4.3 Inelastic scattering from the point of view of the optical model . . . 797
11.4.3.1 Inelastic scattering excitation of spherical nucleus . . . 800
11.4.3.2 Inelastic scattering excitation of axially deformed nucleus . . . 802
11.4.4 One nucleon transfer reaction . . . 805
11.5 Compound nucleus reactions . . . 821
11.5.1 Statistical theory of compound nucleus reactions (Hauser-Feshbach approach) . . . 823
11.5.2 Application of Hauser-Feshbach theory of the CN reactions . . . 832
11.6 Concluding remarks to the Chapter 11 . . . 838

12 Statistical aspects of nuclear dynamics (energy density of nuclear states, fluctuation, radiative width, strength function 841
12.1 Introduction . . . 841
12.2 Energy density of nucleus states (density of levels) . . . 842
12.2.1 Density of quantum system states and its relation to canonical and grand-canonical partition function . . . 842

12.2.2 Energy density of grand-canonical systems of fermions in the model of independent particles (fermions of one type) . . . 846
12.2.3 Energy density of of states of Fermi systems with fermions of two types . . . 852
12.2.4 Energy density of of states of Fermi system with one type of fermions and with the given value of the angular momentum projection . . . 854
12.3 Fluctuation and their determination by means of the random matrices method . . . 859
12.3.1 Random distribution of two- dimensional matrix elements and their eigen values (Wigner and Poisson distributions) . . . 860
12.3.1.1 Random distribution of matrix elements of two- dimensional matrix . . . 860
12.3.1.2 Distribution of eigen-values and eigen-vectors of 2-dimensional matrices in Gaussian orthogonal ensemble . . . 864
12.3.2 Random distribution of matrix elements and eigen values of matrices with large dimensions . . . 872
12.3.2.1 Thomas-Porter distribution . . . 872
12.3.3 Some examples of distributions of levels and their widths in nuclear physics . . . 879
12.3.3.1 Energy distribution of levels observed in neutron capture and the energy distributions of neutron widths . . . 879
12.3.3.1.1 Energy distribution of levels in the compound nucleus formed during neutron capture . . . 883
12.3.3.1.2 Distribution of neutron widths . . . 885
12.3.3.2 Comparison of the level distribution of the Gauss Orthogonal Ensemble (GOE) and experimental level distribution of so called Nuclear Data Ensemble (NDE) . . . 887
12.3.4 Spectral characteristics of Two-body Random Ensembles (TBRE) and Realistic Two-body Random Ensembles (RTBRE) . . . 889
12.4 Strength function . . . 899

12.4.1 Strength functions of the square of the amplitude of one basis vector in the excitation states of the system Hamiltonian 900
12.4.1.1 Strength function $P_a(E)$ (see (12.153), (12.156)) in the case of the constant matrix elements $V_{a\alpha}$ 903
12.4.1.2 Strength function $P_a(E)$ (see (12.153), (12.156)) in the case when matrix elements $V_{a\alpha}$ are not constant 905
12.4.2 Photon strength function 909
12.4.2.1 Partial radiation widths and their connection with photo-absorption cross-section 910
12.4.2.2 Photon strength function and its connection with photoabsorption cross section 919
12.4.3 Photon radiation widths for finite temperature 925
12.4.4 Simulation of γ- cascades in complex nuclei 929

A Some expressions from the theory of angular moment 936
A.1 Coupling of two moments ($\vec{j} = \vec{j}_1 + \vec{j}_2$) 936
A.2 Coupling of three angular moments ($\vec{j} = \vec{j}_1 + \vec{j}_2 + \vec{j}_3$) 937
A.3 Coupling of four angular moments ($\vec{j} = \vec{j}_1 + \vec{j}_2 + \vec{j}_3 + \vec{j}_4$) 938
A.4 Tensor operators, reduced matrix elements 938
A.5 Rotation, Wigner D-functions 939
A.6 Spherical harmonics, vector spherical harmonics 945

B Creation and annihilation operators of fermions 950
B.1 Introduction of creation and annihilation operators 950
B.2 One-particle and two-particle operators expressed in terms of creation and annihilation operators 951
B.2.1 Single-particle operators 951
B.2.2 Two-particle operators 952
B.3 Normal product of creation and annihilation operators 955
B.3.1 Normal product with respect to particle vacuum $|-\rangle$. 955
B.3.2 Normal product with respect to Hartree-Fock ground state $|HF\rangle$ 955
B.4 Wick's theorem 957
B.5 Thouless theorem 960

C Approximative solution of the nonstationary problems 964
C.1 Schroedinger and Dirac description of the time evolution . . . 964

D Scattering of the spinless particle 968
D.1 Stationary states of the particle scattering on the spherically symmetric potential . . . 968
D.1.1 Scattering on a spherically symmetric finite-range potential ($\hat{V}(r) = 0$ for $r \geq a$) . . . 968
D.1.2 Scattering on the Coulomb potential $\hat{V}(r) = \frac{\gamma}{r}$ . . . 970
D.1.3 Scattering on a superposition of the finite-range central potential and the Coulomb potential . . . 970
D.2 Cross section of the spinless particle scattering . . . 971
D.2.1 Elastic scattering of the spinless particle . . . 971

E Lippman-Schwinger and Bethe-Goldstone equations, Born series for the scattering amplitude 978
E.1 Lippman-Schwinger equation . . . 978
E.2 Bethe-Goldstone equation . . . 981
E.3 Born series for the scattering amplitude . . . 982

F Strutinski shell-model corrections 986

G Penetration through the potential barrier 993

H Density of Fermi gas and Fermi sphere 997

I Collective Hamiltonian of the Liquid Drop Model (LDM) 999
I.1 Derivation of B_λ . . . 1001
I.2 Derivation of C_λ . . . 1002

J Some definitions and theorems from the group theory 1011
J.1 Definition of the group . . . 1011
J.2 Lie groups and Lie algebras . . . 1020
J.3 Examples of Lie groups and Lie algebras . . . 1024
J.3.1 Orthogonal group (algebra) $O(n)$ and special orthogonal group (algebra) $SO(n)$ . . . 1024
J.3.2 Unitary group (algebra) $U(n)$ and special unitary group (algebra) $SU(n)$ . . . 1027
J.4 Symmetry groups, dynamical groups, dynamical subgroup chain 1030

J.4.1 Symmetry groups (algebras) . . . 1030
J.4.2 Dynamical groups (algebras) . . . 1031
J.4.3 Dynamical subgroup chains [111] . . . 1032
J.4.4 Permutation symmetry, Young diagrams . . . 1033

K More details on the Interaction Boson Model 1040
K.1 IBM Hamiltonian . . . 1040
K.1.1 Anharmonic vibrator ($U(5)$) limit . . . 1050
K.1.2 Axial rotor ($SU(3)$) limit . . . 1060
K.1.3 γ- unstable ($SO(6)$) limit . . . 1064

L The quasiparticle representation of the general single-particle operator 1068

M Separable RPA 1073

N Projection method 1080
N.1 Projection operator . . . 1080
N.2 Particle number projection (PNP) . . . 1082
N.3 Angular momentum projection . . . 1085
N.4 Projection before and after the variation . . . 1088

O Sum rules of multipole strength functions 1090
O.1 EWSR for isoscalar multipole operators . . . 1090
O.2 EWSR for isovector multipole operators . . . 1098

P Selected expressions from quantum field theory 1104

Q Selected expressions from scattering theory 1108
Q.1 Lippman- Schwinger equation for the channel wave function, "in" and "out" waves . . . 1109
Q.2 S matrix . . . 1110
Q.3 Reaction matrix $\mathcal{T}$ and cross-section ($\hat{H}^+ = \hat{H}$) . . . 1111
Q.4 Scattering amplitude . . . 1113

R Detailed derivations and discussions of selected expressions of the Chapter 12 (Statistical aspects of nuclear dynamics)1115
R.1 Derivation of the expression for energy density of quantum canonical system states (expressions (12.17) and (12.18)) . . . 1115

R.2 Derivation of the expression (12.23) for the logarithm of the partition function $lnZ(\beta, \alpha)$ 1117
R.3 Classification of Gaussian ensembles of Hamiltonian matrices . 1119
R.4 Derivation of eigen values and eigen vectors of two- dimensional matrix H (derivation of exprs. (12.76)-(12.78)) 1121
R.5 Poisson Distribution 1122
R.6 Derivation of the expression for the distribution $P(C_1^{(\alpha)})$ (see (12.106)) of the amplitude $C_1^{(\alpha)}$ in the eigen vector of $N \times N$ matrices from GOE ensemble. 1126
R.7 Ergodicity of canonical systems - canonical ensemble as the mean value of all possible distributions 1127

S Importance sampling Monte Carlo integration 1132

Preface

This textbook was conceived as a collection of notes to my two-semester lecture on the theoretical nuclear physics for M.Sc. and Ph.D. students at the Faculty of Mathematics and Physics of the Charles University in Prague. The main attention is devoted to the theoretical description of nuclear structure using phenomenological as well as microscopical approaches. However it involves also the basic ideas of the description of processes in the nature involving atomic nuclei like α-, β-, γ- radioactivity and low-energy nuclear reations. The last chapter concerns statistical aspects of nuclear physics (density of nuclear levels, basic concepts of the chaos and regularity in the nuclear structure physics).

The preparing of lectures or writting a textbook in nuclear physics is always connected with a decision what aspect has priority, to give a maximum amount of information to the detriment of a profundity of discussed methods or reversely to go to the complete explanation of used approach with the restriction of the number of approaches. In this text I try to keep some balance between these two aspects. The whole content of the book is relevant to graduate students in theoretical nuclear physiscs. In order to use it for M.Sc. undergraduate students it is necessary to reduce some topics.

The book is essentially self-contained but requires an introductory course on quantum mechanics. The most important quantum mechanics topics needed for understanding of discussed nuclear models (like basic elements of the angular momentum theory, spherical and vector spherical harmonics, creation and annihilation operator formalism and others) are briefly described in appendixes. Most of the expressions and approaches, used in many of the existing textbooks with only refences to previous papers, are derived here in more details with the description of each step. I tried to minimize using the typical (and very unpleasant from the point of view of students) phrase "....after some simple and straightforward algebra one finds ....". Each approach discussed in the textbook is not only derived and described but in most casses the comparison of its result with corresponding experimental data is demonstrated.

The first introductory chapter is devoted to the basic nuclear properties (nuclear proportins and shapes, nuclear binding energies and masses, symmetries of nuclear Hamiltonian, division of degrees of freedom of nuclear motion). Then, in the second chapter, the nonrelativistic theory of electromagnetic transitions is discussed. The bare nucleon-nucleon interactions and

the effective nucleon-nucleon interactions in the nuclear medium are analyzed and sorted in the third chapter. The 4-th chapter is devoted to the theoretical determination of the nuclear single-particle mean field (Hartree-Fock method in nuclear physics) and particle-hole formalism. Some aspects of models of inedepent particles are discussed in the 5-th chapter (magic numbers, equilibrium deformation, fission barriers etc.). Approaches for taking into account of the short-range residual interactions are characterized in the 6-th chapter (BCS, HFB approaches). Vibrational degrees of freedom of nuclei generated by the long-range residual interaction are discussed in details in the 7-th chapter (phenomenological and microscopical description of nuclear vibrations, RPA method and beyond RPA description of nuclei). Some aspects of the slow and fast nuclear rotation are explained in the 8-th chapter. The 9-th and 10-th chapters are devoted to the α- and β- processes, respectively. Low-energy nuclear reactions, their sorting and model description, are discussed in the 11-th chapter, and as it was already mentioned, the last chapter is devoted to the selected statistical aspects of nuclear structure.

.....

1. Basic properties of nuclei, symmetry of nuclear Hamiltonian

In the first chapter the brief recapitulation of the basic nuclear properties is presented in the connection with two main problems of nuclear physics, namely the problem of the interaction of nucleons and the many body problem. In the second part of this chapter the symmetries of nuclear Hamiltonian are discussed.

1.1 Basic nuclear properties

1.1.1 Interactions of nucleons, many-body problem

Atomic nucleus is built from protons and neutrons. It is a finite system with number of nucleons going up to several hundreds. Opposite to atom or molecule where the interaction among constituents has electromagnetic character interactions among nucleons holding the nucleus together are not known precisely. Since the nucleus is usually many body system besides the problem of interaction any nuclear model should overcome also the many body problem. So, there are two main problems in nuclear physics:

- problem of nucleon interaction
- many body problem

Both these problems are briefly described below.

In nature four types of interactions are recognized, namely strong, weak, electromagnetic and gravitational. It is known that in dimensions characteristic for nucleus ($\approx 10^{-15}$ m) and nucleon masses (≈ 1 GeV) the gravitational interactions can be neglected with respect to remaining ones. So, the nucleus is a quantum system where strong, weak and electromagnetic interactions participate in the forming of nuclear structure and all nuclear processses. Moreover, after more than 70 year history of nuclear physics it is known that a dominant role in this forming is played by strong interaction.

However, in the theoretical description of the strong interaction systems one meets a fundamental problem - such a systems are always connected with variable number of particles and strong interaction generally need the quantum field techniques for the description. Theory of strong interactions has not been yet completed. The most promising theory of strong interaction is QCD (nucleon is considered as a system of three quarks exchanging gluons).

Fortunately for the nuclear structure the relativistic quantum field problem is simplified because the nucleus is relatively weakly bound system. Bound energy of one nucleon in the nucleus is averagely $\approx$ 8 MeV and the mean kinetic energy of the nucleon in the nucleus is $\approx$ 30 MeV. These energies are substantially less than a rest energy of nucleon ($\approx 10^3$ MeV) or a rest energy of pion ($m_\pi c^2 = 140$ MeV) or rest energies of heavier mesons (strong interacting mesons η, ρ, ω, ...). Therefore, in the description of a nucleus we can restrict ourseleves to nonrealtivistic approximation and take a nucleus as a system consisting from given fixed number of particles.

Strong interactions acting in the nucleus system are of very short-range. Therefore, these interactions act effectively only in the case when nucleons are very closed each other, practically only if they are in the same place of the space. From it the conclusion can be deduced that interactions among the nucleons in the nucleus have two-body character because there is a small probability that more than two nucleons meet in the same place and time.

Quantum field theory problems in the description of nucleon-nucleon interactions are bypassed by an introduction of so called effective nucleon-nucleon potentials describing interactions between nucleons inside nucleus matter. In the present time we have theories which are able to determine these effective nucleon-nucleon interactions in the presence of all other nucleons starting from "bare" nucleon-nucleon potentials describing the scattering of two nucleons in the vacuum and from the properties of the only bound state of two nucleons - deuteron.

In spite of the fact that Coulomb and weak interactions are not so crutial for the nucleus structure in the comparison with strong interaction they play an important role in many nuclear processes (e.g. nuclear fission is given by the competition of strong and Coulomb interaction or weak interaction is responsible for beta-decay). As a consequence of the weak interaction many nuclei are unstable and are changed over gradually by means of beta-decay to nuclei with smaller energy.

Nevertheless, the structure of the nucleus (its energy levels and corresponding wave functions) is formed dominantly by strong interaction in the combi-

nation with electromagnetic interaction. Therefore the nuclear Hamiltonian has symmetries which are typical for strong and electromagnetic interactions, namely it is invariant with respect to following transformations:

- inversion of the space-axes (parity)
- time reverse
- part of the Hamiltonian corresponding to strong interaction is isotopically invariant

These symmetries will be discussed in details in next subsections.

The forming of nuclear spectrum and corresponding wave functions is also substantially influenced by the Pauli principle (the total nucleus wave function should be antisymmetric with respect to an exchange of two arbitrary nucleons).

Besides the problem of relatively unknown effective interaction of nucleons in the nucleus the other problem, even more important from the point of view of the nuclear structure, is a many body problem. It is well known that we can solve precisely quantum-mechanic equations of motion only for a system of two bodies and three bodies (Fadeev equation). For the system with more particles than three we should use always some approximation in the solving of equations of motion. In the case of nuclear physics for a description of heavier nuclei the most important theoretical models are shell models and models based on so called mean field. Both these models together with some other phenomenological nuclear models will be discussed in next chapters.

1.1.2 Nuclear proportions and shapes, mass and charge distribution in nucleus

A big amount of experimental data confirms the fact that the nuclear mass density is approximately constant inside the nucleus and decreases quickly to zero on the nuclear surface (see e.g. famous Hofstadter experiments with electron scattering on nuclei in the fifties [1]). The radial dependence of the mass distribution (density) is described well by the Saxon-Woods expression (for spherical nuclei)

$$\rho(r) = \rho_0 \left(1 + e^{\alpha(r-R)}\right)^{-1}, \tag{1.1}$$

where $\alpha = 1/a$, a is so called diffuseness parameter. In (1.1) ρ_0 is the constant value of the mass density in the nucleus interior and R is the nuclear radius.

Nuclear radius is the distance from the nuclear center to the nuclear surface where the mass density decreases to half value of that in the interior and is given by

$$R = r_0 A^{1/3}, \tag{1.2}$$

where A is the number of nucleons in the given nucleus. Numerical values of parameters a and r_0 are: $r_0 = 1.2$ fm, $a = 0.5$ fm. The most precise value of nuclear radius is usually obtained from the scattering of high-energy electrons on nuclei and from the data on mesoatoms. Experimental values of nuclear radii are in agreement with the relation (1.2).

Besides spherical nuclei in the nature one meets also deformed nuclei. In fact, there are more deformed nuclei than spherical ones. The fact, if given nucleus is deformed or spherical, is given by the number of nucleons filling the last (valence) shell and this will be discussed later. Here only the way of the description of deformed shape of the nucleus is presented. General shape of any closed body (including a nucleus) is able to describe in mathematical way by Dirichlet decomposition in spherical functions $Y_{\lambda\,\mu}(\theta, \varphi)$:

$$R(\theta, \varphi) = R_0 \left\{ 1 + \sum_{\lambda,\mu} \alpha_{\lambda\,\mu}\, Y_{\lambda\,\mu}(\theta, \varphi) \right\}, \tag{1.3}$$

where generally $\lambda = 1,\ 2,\ 3, \ldots\ ;\ \mu \in \langle -\lambda, +\lambda \rangle$ and where R_0 is so called mean radius (the radius of the sphere with the same volume as the deformed body described by (1.3)). Coefficients $\alpha_{\lambda\,\mu}$ (so called deformation parameters) characterize given deformed shape: if $\forall\, \alpha_{\lambda\,\mu} = 0$ then sphere with the radius R_0, if $\alpha_{2\,0} \neq 0$ and all others $= 0$ then axially symmetric ellipsoid, if $\alpha_{2\,0} \neq 0$, $\alpha_{3\,0} \neq 0$ and all others $= 0$ then axially symmetric pear shape etc.

Deformation parameters $\alpha_{\lambda,\mu}$ are connected with static electric multipole moments (static multipole moments of any system with charge density $\rho_{ch}(\vec{r})$ and charge current $\vec{j}_{ch}(\vec{r})$ are discussed in details in the Section 2.3 and in the Appendix A). Because of nuclei in their ground states have not static electric dipole moments (see Subsection 2.3.1) the summation in (1.3) starts from $\lambda = 2$ ($\lambda \neq 1$). Experimental experience confirms that the most of so called "well" deformed nuclei in ground state have only $\alpha_{2\,0} \neq 0$ and $\alpha_{4\,0} \neq 0$ with $|\alpha_{2\,0}| >> |\alpha_{4\,0}|$ and all other $\alpha_{\lambda\,\mu} = 0$. This shape corresponds to axial symmetry.

If in (1.3) we restrict ourselves only to $\lambda = 2$ (that means only quadrupole

deformation is supposed) then

$$R(\theta,\varphi) = R_0 \left\{ 1 + \sum_{\mu} \alpha_{2\,\mu}\, Y_{2\,\mu}(\theta,\varphi) \right\} \tag{1.4}$$

and this is triaxial ellipsoid (if $|\alpha_{2\,\mu}| < 1$). Axes of the intrinsic coordinate system (fixed to the nucleus) are usually chosen in order to coincide with the principle axes of the quadrupole moment $Q_{ij} = \int (3x_i x_j - r^2\,\delta_{ij})\,\rho_{ch}(\vec{r})\,d^3r$ (see Subsection 2.3.2). In such a choice off-diagonal ($i \neq j$) components of the quadrupole moment tensor Q_{ij} are zero. Then, in the connection with it in (1.4) we also have $\alpha_{21} = \alpha_{2-1} = 0$ and $\alpha_{22} = \alpha_{2-2}$. So, from five components $\alpha_{2\,0}$, $\alpha_{2\,1}$, $\alpha_{2\,-1}$, $\alpha_{2\,2}$, $\alpha_{2\,2}$ only two remain independent: $\alpha_{2\,0}$, $\alpha_{2\,2}$. In the literature instead of deformation parameters $\alpha_{2\,0}$ and $\alpha_{2\,2}$ quadrupole deformation parameters β and γ are introduced:

$$\alpha_{2\,0} = \beta\, cos\gamma, \qquad \alpha_{2\,2} = \alpha_{2\,-2} = \frac{1}{\sqrt{2}}\beta\, sin\gamma, \tag{1.5}$$

In such a case the parameter β is a measure of the whole quadrupole deformation:

$$\sum_{\mu} |\alpha_{2\mu}|^2 = \beta^2 \tag{1.6}$$

and expr. (1.4) can be rewritten in the following form (shape in the fixed-body coordinate system)

$$\begin{aligned} R(\theta,\varphi) - R_0 \;\; = \;\; & R_0 \beta cos\gamma\, Y_{2\,0}(\theta,\varphi) + \\ & R_0 \frac{1}{\sqrt{2}} \beta sin\gamma\; (Y_{2\,2}(\theta,\varphi) + Y_{2\,-2}(\theta,\varphi)) \end{aligned} \tag{1.7}$$

Specially for the direction of the principal axes we have

$$\begin{aligned} \delta R_3 &= R(\theta = 0, \varphi) - R_0 = \sqrt{\frac{5}{4\pi}} R_0\, \beta\, cos\gamma \\ \delta R_2 &= R(\theta = \frac{\pi}{2}, \varphi = \frac{\pi}{2}) - R_0 = \sqrt{\frac{5}{4\pi}} R_0\, \beta\, cos(\gamma + \frac{2\pi}{3}) \\ \delta R_1 &= R(\theta = \frac{\pi}{2}, \varphi = 0) - R_0 = \sqrt{\frac{5}{4\pi}} R_0\, \beta\, cos(\gamma - \frac{2\pi}{3}) \end{aligned} \tag{1.8}$$

From (1.7) and (1.8) one can see that for the case $\gamma = 0$ we have an axial symmetry with respect to the 3^d axis (see the Fig. 1.1). If we restrict to this case of axial symmetry then

$$R(\theta,\varphi) = R_0 + R_0\, \beta\, Y_{2\,0}(\theta,\varphi). \tag{1.9}$$

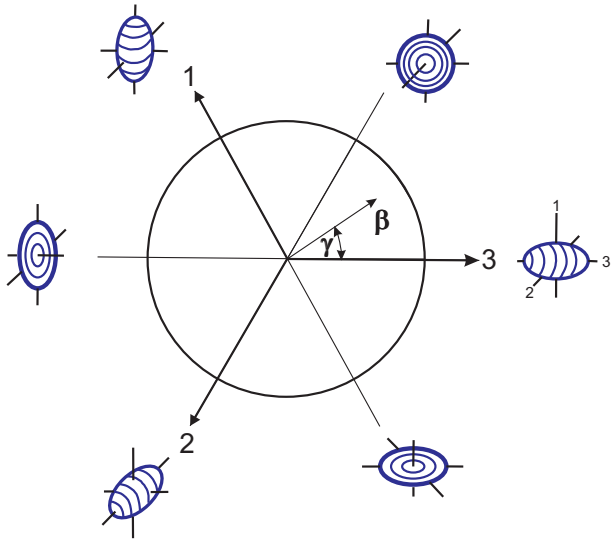


Figure 1.1: Various nuclear shapes in the (β, γ) plane. The axial symmetry occurs in the case when the values of γ corresponds to the principal axes $k = 1,\ 2,\ 3$ ($\gamma = 0, \frac{\pi}{3}, \frac{2\pi}{3}, \pi, , \frac{4\pi}{3}, \frac{5\pi}{3}$). If $\gamma > \frac{\pi}{3}$ then we can always rotate the nucleus in such a way that all possible quadrupole shapes are described by the γ from the interval $\frac{\pi}{3} > \gamma > 0$ and therefore only this interval of γ can be considered in practice. For $\gamma = 0$ the axially symmetric shape is elongated along the 3-d axis. For $\gamma = \frac{\pi}{6}$ the shape has axial symmetry but flattened like disc.

If we integrate in the expression for the static quadrupole moment (see exp. (2.189)) within the volume given by shape (1.9) assuming that the nuclear charge density is constant in the whole nuclear volume ($\rho_{ch}(\vec{r}) \approx \rho_{ch} = Ze\,(\frac{4}{3}\pi R_0^3)^{-1}$) then the static quadrupole moment of the nucleus is

$$
\begin{aligned}
Q_0 &= \int d^3r\,(3z^2 - r^2)\,\rho_{ch}(\vec{r}) = \rho_{ch}\sqrt{\frac{16\pi}{5}}\int d^3r\,r^2\,Y^*_{2\,0}(\hat{r}) = \\
&= \rho_{ch}\sqrt{\frac{16\pi}{5}}\int d\Omega\int dr\,r^4\,Y^*_{2\,0}(\hat{r}) = \\
&= \rho_{ch}\sqrt{\frac{16\pi}{5}}\int d\Omega\,Y^*_{2\,0}(\hat{r})\left[\frac{r^5}{5}\right]_0^{R(\theta,\varphi)} = \\
&= \rho_{ch}\sqrt{\frac{16\pi}{5}}\frac{R_0^5}{5}\int d\Omega\,Y_{2\,0}(\hat{r})(1+\beta\,Y_{2\,0}(\hat{r}))^5 = \\
&= \boxed{\begin{array}{c}\text{because}\\ (1+\beta\,Y_{2\,0})^5 \approx 1 + 5\,\beta\,Y_{2\,0} + 10\,\beta^2\,Y_{2\,0}\,Y_{2\,0} + \ldots\end{array}} =
\end{aligned}
$$

$$
\begin{aligned}
&= \sqrt{\frac{9}{5\pi}} Ze\, R_0^2\, \beta \\
&\quad \left\{ \int d\Omega\, Y^*_{2\,0}\, Y_{2\,0} + 2\beta \int d\Omega\, Y^*_{2\,0}\, Y_{2\,0}\, Y_{2\,0} + \ldots \right\} = \\
&= \boxed{\text{see e.g. exprs.(1) and (2) on the p. 148 in [2]}} = \\
&= \sqrt{\frac{9}{5\pi}} Ze\, R_0^2\, \left\{ \beta + 0.16\, \beta^2 + \ldots \right\}. \qquad (1.10)
\end{aligned}
$$

Since in the reality the charge density (similarly as mass density) is almost constant in the nucleus volume the expression (1.10) represents good approximation for the intrinsic static quadupole moment of the nucleus.

The mass density for deformed nuclei is also given by (1.1) but now the radius R is dependent on θ and φ and on deformation parameters:

$$
\rho(r,\theta,\varphi) = \rho_0 \left(1 + e^{\alpha(r - R(\theta,\varphi)}\right)^{-1} = \rho_0 \left[1 + e^{\alpha(r - R_0 - R_0 \sum_{\lambda\mu} \alpha_{\lambda\mu} Y_{\lambda\mu}(\theta,\varphi))}\right]^{-1} \qquad (1.11)
$$

1.1.3 Mass of nucleus, nuclear binding energy

Mass of the nucleus is always less than the sum of masses of individual nucleaon by the absolute value of nuclear binding energy:

$$
B(Z,N) = (M(A) - Z\, m_p - N\, m_n)\, c^2 \qquad (1.12)
$$

The total binding energy of the nucleus, $B(Z,N)$, is described by sufficiently precise Weizsacker semi-empirical formula [3] (1935 - liquid drop model of the nucleus)

$$
B(N,Z) = b_V A + b_S A^{2/3} + b_C \frac{Z^2}{A^{1/3}} + b_I \frac{(N-Z)^2}{A} - \delta(A), \qquad (1.13)
$$

where one obtains by a fit:

$$
\begin{aligned}
&b_V = -15.68\, MeV; \quad b_S = 18.56\, MeV; \quad b_C = 0.717\, MeV; \\
&b_I = 28.1\, MeV \quad \delta(A) = \left\{ \begin{array}{cc} 34\, A^{-3/4}\, MeV & \text{for even-even} \\ 0 & \text{for even-odd} \\ -34\, A^{-3/4}\, MeV & \text{for odd-odd} \end{array} \right\} \text{nuclei}
\end{aligned} \qquad (1.14)
$$

Formula (1.13) was deduced from the analogy of the nucleus and a liquid drop. The first term (involving b_V) is usually called volume term, because it

is proportional to A ($\approx R^3$ - see (1.2)). The second term (involving b_S) is proportional to $A^{2/3}$ ($\approx R^2$) and therefore it is called surface term. It results from the fact that the nucleons close to the surface contribute less to the total binding energy (parameter b_S determines the surface tension coefficient σ defined as the surface energy per unit area: $\sigma = b_S/4\pi r_0^2 = 1.03[MeV\ fm^{-2}]$ with $r_0 = 1.2fm$ - see (1.2)). The third term in (1.13) represents the Coulomb term and it reflects the static Coulomb energy, $\frac{3}{5}\frac{Z^2e^2}{4\pi\epsilon_0 R_C}$, of the homogeneously charged drop with the radius R_C. The fourth term in (1.13) reflects a tendency of nuclei towards a stability for $N = Z$ in the absence of the Coulomb interaction. This term cannot depend on the sign of $N - Z$ and in the framework of the Fermi gas model it can be shown (see e.g. p. 127 in [4]) that it is proportional to $(N - Z)^2/A$. The quadratic dependence of the binding energy on $(N - Z)$ is experimentally very well confirmed. Only the base of the experimental parabola is different according to whether we consider an even-even, even-odd or odd-odd nuclei. This is due to the so-called pairing effect which is discussed in the Chapter 6 and is taken care of by the last term in Eq.(1.13).

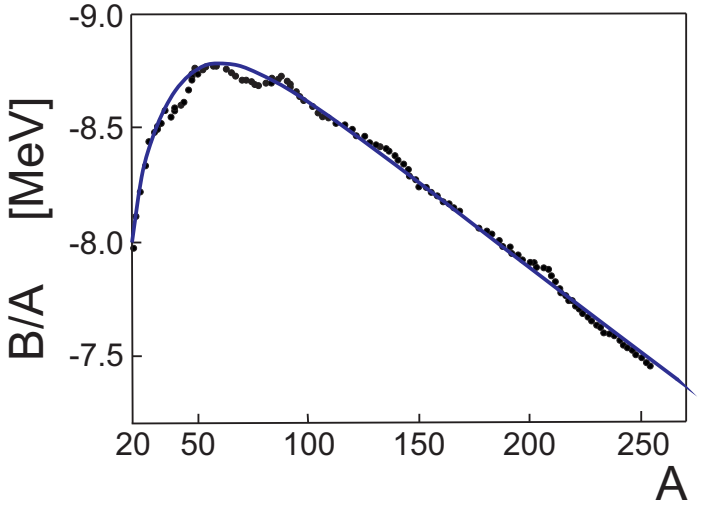


Figure 1.2: Experimental values of $B(Z,N)/A$ for β-stable odd-A nuclei and the calculated curve according to a mass formula (1.13) (from [5]).

The b- parameters (1.14) of the Weizsacker formula (1.13) were obtained by fitting to the experimental values of binding energy of nuclei from the broad region of isotopes. In Fig.1.2 the experimental vaues of binding energies per one nucleon, $B(Z,N)/A$, are compared with the curve obtaind by Eq.(1.13) with optimal values of parameters given in (1.14).

It should be noted that the formula (1.13) gives only an overall smooth fit

to the binding energy as a function of A, and that locally there are strong deviations from it as can be seen from Fig.1.2. This is due to shell effects, which will be discussed in the Section 5.1.2.

1.2 Isotopic symmetry of nuclear interaction

Since there is an assumption about the dominant role of the strong interaction of nucleons in nuclei which is charge independent one can expect that the interactions between two nucleons in a nucleus are the same (or alsmost the same because of a inconsiderable presence of the Coulomb interaction which is charge dependent) for all possible pairs: (n,p), (n,n) and (p,p). If it is so we can understand neutron and proton as a different states of the same particle. In the connection with it in the fifties the isotopic spin (isospin) as a new quantum nuber was introduced, projection of which distinquishes the neutron from proton. In such a way neutron and proton are different isotopic states of one particle - nucleon.

Not looking at the identity of neutron and and proton from the point of view of the strong interactions there are differences between them, namely:

- small difference in masses: $m_n \approx 940\ \mathrm{MeV}/c^2$, $m_p \approx 938\ \mathrm{MeV}/c^2 \Rightarrow \frac{m_n - m_p}{2(m_n+m_p)} \approx 1.4\,10^{-3}$;
- different magnetic dipole moments:
  $\mu_p = g_p^{(s)} \langle s_p \rangle \frac{e\hbar}{2mc} = \frac{1}{2} 5.586\ \frac{e\hbar}{2mc} = 2.79 \frac{e\hbar}{2mc}$
  $\mu_n = g_n^{(s)} \langle s_n \rangle \frac{e\hbar}{2mc} = -\frac{1}{2} 3.826\ \frac{e\hbar}{2mc} = -1.91 \frac{e\hbar}{2mc}$

These differences and a presence of the charge dependent Coulomb interaction cause that the isotopic symmetry of nuclear interaction is fulfilled only partly.

From the mathematical point of view proton and neutron are distinquished in terms of two different values of the projection of the isospin (in analogy with the spin 1/2):

$$\vec{t} = \frac{1}{2}\vec{\tau}; \qquad \text{proton } t_z = -\frac{1}{2}; \qquad \text{neutron } t_z = +\frac{1}{2}$$
$$\tau_x = \begin{pmatrix} 0 & 1 \\ 1 & 0 \end{pmatrix} \qquad \tau_y = \begin{pmatrix} 0 & -i \\ i & 0 \end{pmatrix} \qquad \tau_z = \begin{pmatrix} 1 & 0 \\ 0 & -1 \end{pmatrix} \tag{1.15}$$

where τ_x, τ_y, τ_z are isospin Pauli matrixes.
$\Rightarrow$ Corresponding s.p. wave functions of proton and neutron in the combined

configuration-spin-isospin Hilbert space are following:

$$\begin{aligned}
\langle\xi|n\rangle = \psi_n(\xi) = \psi(\xi)\begin{pmatrix}1\\0\end{pmatrix}; \qquad \tau_z\begin{pmatrix}1\\0\end{pmatrix} = \begin{pmatrix}1\\0\end{pmatrix}; \qquad |n\rangle = |\frac{1}{2}\frac{1}{2}\rangle \\
\langle\xi|p\rangle = \psi_p(\xi) = \psi(\xi)\begin{pmatrix}0\\1\end{pmatrix}; \;\; \tau_z\begin{pmatrix}0\\1\end{pmatrix} = -\begin{pmatrix}0\\1\end{pmatrix}; \;\; |p\rangle = |\frac{1}{2}-\frac{1}{2}\rangle
\end{aligned} \tag{1.16}$$

where $\xi \equiv (\vec{r},\ s)$ are configuration-spin variables (coordinates).

In the analogy with the angular momentum (spin) we can introduce step up and step down operators which, in the case of isospin, change neutron into proton and vice versa:

$$\begin{aligned}
&t_\pm = \frac{1}{2}(\tau_x \pm i\tau_y) \;\Rightarrow\; t_+ = \begin{pmatrix}0 & 1\\ 0 & 0\end{pmatrix};\; t_- = \begin{pmatrix}0 & 0\\ 1 & 0\end{pmatrix}; \\
&\Rightarrow t_+|p\rangle = \begin{pmatrix}0 & 1\\ 0 & 0\end{pmatrix}\begin{pmatrix}0\\1\end{pmatrix} = \begin{pmatrix}1\\0\end{pmatrix} = |n\rangle \\
&\quad t_-|n\rangle = \begin{pmatrix}0 & 0\\ 1 & 0\end{pmatrix}\begin{pmatrix}1\\0\end{pmatrix} = \begin{pmatrix}0\\1\end{pmatrix} = |p\rangle \\
&\quad t_+|n\rangle = \begin{pmatrix}0 & 1\\ 0 & 0\end{pmatrix}\begin{pmatrix}1\\0\end{pmatrix} = 0; \quad t_-|p\rangle = \begin{pmatrix}0 & 0\\ 1 & 0\end{pmatrix}\begin{pmatrix}0\\1\end{pmatrix} = 0,
\end{aligned} \tag{1.17}$$

and charge exchange operator $P^\tau_{ii'}$:

$$P^\tau_{ii'} \equiv \frac{1}{2}(1 + \vec{\tau}^{\,(i)} \cdot \vec{\tau}^{\,(i')}) = t^{(i)}_+ t^{(i')}_- + t^{(i)}_- t^{(i')}_+ + \frac{1}{2}(1 + \tau^{(i)}_z \tau^{(i')}_z). \tag{1.18}$$

Then

$$\begin{aligned}
P^\tau_{ii'}\,|n_i\rangle|p_{i'}\rangle = |p_i\rangle|n_{i'}\rangle; \qquad P^\tau_{ii'}\,|p_i\rangle|n_{i'}\rangle = |n_i\rangle|p_{i'}\rangle \\
P^\tau_{ii'}\,|p_i\rangle|p_{i'}\rangle = |p_i\rangle|p_{i'}\rangle; \qquad P^\tau_{ii'}\,|n_i\rangle|n_{i'}\rangle = |n_i\rangle|n_{i'}\rangle
\end{aligned} \tag{1.19}$$

Similarly as two or more angular momenta can be coupled to the total angular momenta (see Appendix A) two or more isospins can be coupled to the total one. For instance, for two nucleons we have a basis of kets in the isospin space:

$$|\frac{1}{2}\mu_1\rangle|\frac{1}{2}\mu_2\rangle \qquad |\frac{1}{2}\frac{1}{2}\rangle \to \text{neutron}, \qquad |\frac{1}{2}-\frac{1}{2}\rangle \to \text{proton},$$

However, we can construct another basis in the same isospin space:

$$|\frac{1}{2}\frac{1}{2}TM\rangle = \sum_{\substack{\mu_1\mu_2 \\ \mu_1+\mu_2=M}} C^{T\,M}_{1/2\,\mu_1\,1/2\,\mu_2} \;\; |\frac{1}{2}\,\mu_1\rangle\,|\frac{1}{2}\,\mu_1\rangle =$$

$$= C^{T\,M}_{1/2\,1/2\,1/2\,M-1/2}\,|\frac{1}{2}\,\frac{1}{2}\rangle|\frac{1}{2}\,M-\frac{1}{2}\rangle + C^{T\,M}_{1/2\,-1/2\,1/2\,M+1/2}\,|\frac{1}{2}\,-\frac{1}{2}\rangle|\frac{1}{2}\,M+\frac{1}{2}\rangle \qquad (1.20)$$

where T is the total isospin of the system of two nucleons ($T = 0,\, 1$) with the projection M and $C^{T\,M}_{1/2\,\mu_1\,1/2\,\mu_2}$ are Clebsch-Gordan coefficients for the coupling $\overrightarrow{1/2} + \overrightarrow{1/2} = \vec{T}$ - see Appendix A). In this case we have four possiblities of the coupling:

$$T=0 \quad M=0: \qquad |0\,0\rangle = \frac{1}{\sqrt{2}}\left(|\frac{1}{2}\,\frac{1}{2}\rangle|\frac{1}{2}\,-\frac{1}{2}\rangle - |\frac{1}{2}\,-\frac{1}{2}\rangle|\frac{1}{2}\,\frac{1}{2}\rangle\right)$$

$$T=1 \quad M=1: \qquad |1\,1\rangle = |\frac{1}{2}\,\frac{1}{2} > |\frac{1}{2}\,\frac{1}{2}\rangle$$

$$T=1 \quad M=0: \qquad |1\,0\rangle = \frac{1}{\sqrt{2}}\left(|\frac{1}{2}\,\frac{1}{2}\rangle|\frac{1}{2}\,-\frac{1}{2}\rangle + |\frac{1}{2}\,-\frac{1}{2}\rangle|\frac{1}{2}\,\frac{1}{2}\rangle\right)$$

$$T=1 \quad M=-1: \qquad |1\,-1\rangle = |\frac{1}{2}\,-\frac{1}{2}\rangle|\frac{1}{2}\,-\frac{1}{2}\rangle \qquad (1.21)$$

Since according to (1.20) $P^{\tau}_{ii'}\,|\frac{1}{2}\,\mu_1\rangle|\frac{1}{2}\,\mu_2\rangle = |\frac{1}{2}\,\mu_2\rangle|\frac{1}{2}\,\mu_1\rangle$ the expr. (1.21) gives the following symmetry

$$P^{\tau}_{ii'}\,|T=0\;M=0\rangle = -|T=0\;M=0\rangle$$
$$P^{\tau}_{ii'}\,|T=1\;M\rangle = |T=1\;M\rangle \text{ for } M=\pm 1,\,0$$
$$\Rightarrow \qquad < |P^{\tau}_{ii'}| >= \begin{cases} = +1 & \text{for } \; T=1 \;\; \text{(triplet state)} \\ = -1 & \text{for } \; T=0 \;\; \text{(singlet state)} \end{cases} \qquad (1.22)$$

For the nucleus, as the system of A nucleons, the total isospin is given by

$$\hat{\vec{T}} = \sum_{i=1}^{A} \hat{\vec{t}}^{(i)} \qquad (1.23)$$

with its z-component:

$$\hat{T}_z = \sum_{i=1}^{A} \hat{t}_z \tag{1.24}$$

Since, similarly as for angular momentum, $[\hat{T}^2,\ \hat{T}_z] = 0$ we can look for the common eigen-basis of the operators $\hat{T}^2$ and $\hat{T}_z$:

$$\begin{aligned} \hat{T}^2|TM\rangle &= T(T+1)\,|TM\rangle \\ \hat{T}_z|TM\rangle &= M\,|TM\rangle, \end{aligned} \tag{1.25}$$

with $T = 0,\ 1,\ 2, \ldots$ for even number of nucleons and $T = 1/2,\ 3/2,\ 5/2, \ldots$ for odd number of nucleos.

Because of $\hat{t}_z\,|p\rangle = -1/2|p\rangle$ and $\hat{t}_z\,|n\rangle = +1/2|n\rangle$ the expectation value of the operator $\hat{T}_z$ in any state of (Z, N) nucleus is:

$$\langle|\hat{T}_z|\rangle = \frac{N-Z}{2} \tag{1.26}$$

and corresponding expectation value of the operator $\hat{\vec{T}}^2$ has the following form

$$\begin{aligned} &\langle|\hat{\vec{T}}^2|\rangle = \\ = \ &\langle| \left(\sum_{i=1}^{A} \hat{\vec{t}}^{(i)} \right)^2 |\rangle = \langle| \sum_{i=1}^{A} (\hat{\vec{t}}^{(i)})^2 |\rangle + 2\,\langle| \sum_{i<i'} \hat{\vec{t}}^{(i)} \cdot \hat{\vec{t}}^{(i')} |\rangle = \\ = \ &\boxed{\text{see (1.18) and } \langle|(\hat{\vec{t}}^{(i)})^2|\rangle = 3/4} = \\ = \ &\sum_{i=1}^{A} \frac{3}{4} + \langle| \sum_{i<i'} (P^{\tau}_{ii'} - \frac{1}{2}) |\rangle = A - \frac{A^2}{4} + \langle| \sum_{i<i'} (P^{\tau}_{ii'} |\rangle \end{aligned} \tag{1.27}$$

Further we discuss exp. (1.27) from the point of view of two limiting cases:

1. If the isospin part of the wave function is totally symmetric, that means $\langle|P^{\tau}_{ii'}|\rangle = 1$ for all i, i', then

$$\langle| \sum_{i<i'} P^{\tau}_{ii'} |\rangle = \sum_{i<i'} 1 = \frac{A(A-1)}{2}$$

and exp. (1.27) gives:

$$\langle|\hat{\vec{T}}^2|\rangle = A - \frac{A^2}{4} + \frac{A(A-1)}{2} = \frac{A}{2}\,(\frac{A}{2} + 1) \tag{1.28}$$

So, in the case of the total symmetric isospin part of the A-particle wave function $|>$ it follows from the comparison of (1.28) and (1.25) that the total isospin is $T = \frac{A}{2}$.

2. For $A = 2$ the exp. (1.27) gives:

$$\langle|\hat{\vec{T}}^2|\rangle = \langle|(\hat{\vec{t}}^{(1)} + \hat{\vec{t}}^{(2)})^2|\rangle = 1 + \langle|P^{\tau}_{ii'}|\rangle$$
$$\Rightarrow \text{for } P^{\tau}_{12}|\rangle = |\rangle(\text{symmetric}) : \langle|\hat{\vec{T}}^2|\rangle = 2 \Rightarrow T = 1$$
$$\text{for } P^{\tau}_{12}|\rangle = -|\rangle(\text{antisymmetric}) : \langle|\hat{\vec{T}}^2|\rangle = 0 \Rightarrow T = 0$$

and it is consistent with (1.22).

We can introduce step up and step down operators of the total nucleus isospin:

$$\hat{T}_{\pm} = \sum_{i=1}^{A} \hat{t}^{(i)}_{\pm} = \hat{T}_x \pm \hat{T}_y \tag{1.29}$$

Then these operators fulfil the following commutator relations

$$[\hat{T}_x, \hat{T}_y] = i\hat{T}_z \quad \Rightarrow$$
$$\text{and cyclically}$$
$$\Rightarrow [\hat{T}_0, \hat{T}_+] = \hat{T}_+ \; ; \; [\hat{T}_0, \hat{T}_-] = -\hat{T}_- \; ; \; [\hat{T}_+, \hat{T}_-] = 2\hat{T}_0 \tag{1.30}$$

and the eigen-states of operators $\hat{T}^2$ and $\hat{T}_z$ fulfil:

$$\hat{T}_{\pm}\,|T\;M\rangle = \sqrt{(T \mp M)(T \pm M + 1)}\;\;|T\;M \pm 1\rangle$$
$$\Rightarrow \hat{T}_+\;\;|T\;T\rangle = 0\,; \qquad \hat{T}_-\;\;|T\;\;-T\rangle = 0 \tag{1.31}$$

The operator $\hat{T}_z$ of the z- component of the total nuclear isospin is connected with the operator of the charge by the simple relation, $\hat{Q} = \sum_{i=1}^{A} q^{(i)} = e\sum_{i=1}^{A}(1/2 - \hat{t}^{(i)}_z) = e\,(A/2 - \hat{T}_z)$. Since the operator of the nuclear charge always commute with the nuclear Hamiltonian to zero (a preservation of the nucleus charge) the operator $\hat{T}_z$ also fulfils the commutator $[\hat{H}, \hat{T}_z] = 0$ and therefore the operator $\hat{T}_z$ has the sharp eigen-value $(N - Z)/2$ for all nuclear states. However, this is not the case of the operator $\hat{\vec{T}}^2$ of the square of the total nuclear isospin. The operator $\hat{\vec{T}}^2$ commutes with the total nucleus Hamiltonian only in the case when the Coulomb (el.mg.) interaction can be neglected with the respect to the strong interaction in the Hamiltonian. It is fulfilled with a good approximation only for very light nuclei. For heavier

nuclei the Coulomb interaction plays an important role and cannot be neglected. For light nuclei, where the Coulomb interaction can be neglected in the comparison with the strong interactions, the total isospin quantum number T corresponding to the ground state of given nucleus is given only by the excess of protons or neutrons (because the isospin of each pair on neutron and proton occupying the same spatial states is zero in accordance with the demand that the wave function of such neutron-proton pair should be antisymmetric with respect to their mutual exchange (the antisymmetry of the wave function of this pair can be given only by its isospin part because the spatial-spin part of the wave function is symmetric - see (1.22)). Therefore

$$T = \frac{|N - Z|}{2} \tag{1.32}$$

for the ground state of light nucleus (when the Coulomb contribution to the nuclear Hamiltonian is neglected).

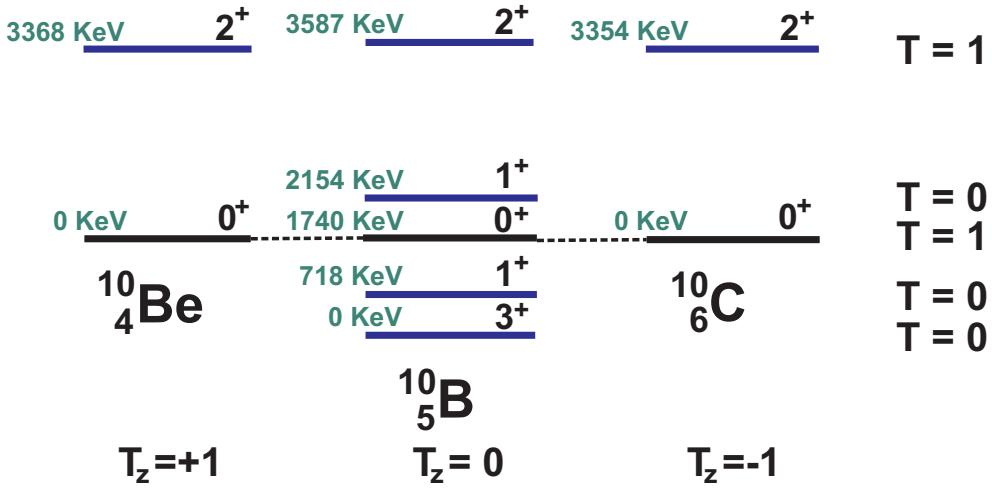


Figure 1.3: Isospin assign to the low-lying levels in the isobar nuclei: ^{10}Be, ^{10}B, ^{10}C.

As a simple example, we will show how to attribute total isospin to certain nuclear states. For three isobar nuclei: $^{10}_{4}$Be, $^{10}_{5}$B, $^{10}_{6}$C the z- component of the total isospin is $(T_z = (N - Z)/2)$

$$T_z^{(Be)} = +1\ , \qquad T_z^{(B)} = 0\ , \qquad T_z^{(C)} = -1$$

and according to (1.32) the total isospin of $^{10}_{4}$Be and $^{10}_{6}$C in their ground state is $T = 1$ (because $T \geq T_z$ but the ground state total isospin for ^{10}B should be zero.

In the case of $T = 1$ we speak about an isospin triplet, that means three $T = 1$ states which can be found in all three nuclei at the same total energy

(slight differences nevertheless occurs because of the Coulomb energy) and which are ground states only for ${}^{10}_{4}$Be and ${}^{10}_{6}$C. The case $T = 0$ is an isospin singlet, which can be observed as ground state only in ${}^{10}_{5}$B. In the Fig 1.3 the low-lying states of the three isobars and their identification with the isospin quantum numbers are shown.

In the Table 1.1 the experimental total binding energies of the isotopic triplet states (3-d column), the Coulomb contribution to the binding energies (4-th column) and strong interaction part of the total binding energies (binding energy without the Coulomb contribution) are mutually compared for two isotopic triplets. One can see that the strong interaction part of the total energy is almost the same for all states from one isotopic triplet.

nucleus	T_z	binding energy $B(N,Z$ [MeV]	Coulomb energy $\frac{3}{5}\frac{Z^2e^2}{4\pi\epsilon_0 R}$ [MeV]	strong interaction part energy $B(N,Z) - \frac{3}{5}\frac{Z^2e^2}{4\pi\epsilon_0 R}$ [MeV]
${}^{10}_{4}$Be$_6$	+1	-65.7	5.3	-71.0
${}^{10}_{5}$B$_5$	0	-63.0	8.3	-71.3
${}^{10}_{6}$C$_4$	-1	-60.0	11.9	-71.9
${}^{14}_{6}$C$_8$	+1	-105.7	10.7	-116.4
${}^{14}_{7}$N$_7$	0	-102.4	14.5	-116.9
${}^{14}_{8}$O$_6$	-1	-98.7	19.0	-117.7

Table 1.1: Binding energies, Coulomb energies, and strong interaction part energies for two isotopic triplets.

Coulomb field

$$\sum_{i<i'} \frac{e^2}{4\pi\epsilon_0} \frac{(\frac{1}{2} - \hat{t}_z^{(i)})(\frac{1}{2} - \hat{t}_z^{(i')})}{|\vec{r}_i - \vec{r}_{i'}|} =$$

$$= \sum_{i<i'} \frac{e^2}{4\pi\epsilon_0 \, |\vec{r}_i - \vec{r}_{i'}|} \left[\frac{1}{4} + \hat{t}_z^{(i)}\hat{t}_z^{(i')} - \frac{1}{2}\hat{t}_z^{(i)} - \frac{1}{2}\hat{t}_z^{(i')}\right]$$

commutes with the z-component, $\hat{T}_z = \sum_{i=1}^{A} \hat{t}_z^{(i)}$, of the total isospin but it does not commute with the square of the total isospin, $\hat{T}^2 = \left(\sum_{i=1}^{A} \hat{\vec{t}}^{(i)}\right)^2$. Therefore, after the switching on the Coulomb interaction the total isospin T is not a good quantum number (especially for heavy nuclei where the Coulomb energy is relatively big).

1.3 Space-time symmetries of nuclear Hamiltonian

1.3.1 Inversion of space axes - parity

As it was discussed in the previous section the nuclear Hamiltonian involves predominantly strong and electromagnetic interactions and both these interactions are invariant with respect to the inversion of the space axes. Weak interaction, which violates this symmetry, influences nuclear states very little. Therefore, we can assume with a good accuracy that the nuclear Hamiltonian commutes with the parity operator $\mathscr{P}$.

$$[\hat{H},\ \mathscr{P}] = 0 \tag{1.33}$$

As a result, nuclear states (eigen-states of the Hamiltonian) are simultaneously eigen states of the parity operator (and because of the square of the parity operator is the unity operator corresponding parity eigen values are ± 1):

$$\hat{H}|\psi_i\rangle = E_i|\psi_i\rangle; \quad \mathscr{P}|\psi_i\rangle = \pi_i|\psi_i\rangle; \quad \pi_i = \pm 1. \tag{1.34}$$

Non-preservation of the parity in the possible weak interaction leads to the presence of a very small components in the nuclear wave functions with the opposite parity than the parity of the dominant components in the given nuclear state. Because these componnets are very small they can be recognized only in experiments (processes) where effects of these components are strenghtened. Different experiments (e.g. a scattering of polarized particles on oriented targets) show that a probabilty of finding opposite parity components in the given nuclear state does not rise above 10^{-7}.

1.3.2 Time reversal

The acting of the time reversal operator $\mathscr{T}$ on coordinate operator $\hat{\vec{r}}$, linear momentum operator $\hat{\vec{p}}$, spin operator $\hat{\vec{\sigma}}$, and general linear momentum operator $\hat{\vec{I}}$ is obvious:

$$\begin{aligned} \mathscr{T}^{-1}\,\hat{\vec{r}}\,\mathscr{T} &= \hat{\vec{r}} & \mathscr{T}^{-1}\,\hat{\vec{p}}\,\mathscr{T} &= -\hat{\vec{p}} \\ \mathscr{T}^{-1}\,\hat{\vec{\sigma}}\,\mathscr{T} &= -\hat{\vec{\sigma}} & \mathscr{T}^{-1}\,\hat{\vec{I}}\,\mathscr{T} &= -\hat{\vec{I}}. \end{aligned} \tag{1.35}$$

This transformation cannot be described by an unitary operator because any unitary transformation preserves algebraic operations like commutators. If the time reversal transformation is unitary then the time reversal transformation of the commutator

$$[\hat{I}_x,\ \hat{I}_y] = i\,\hat{I}_z \tag{1.36}$$

is not consistent with the last equation in (1.35). It can be seen from the following consideration. The application of the time reversal to the l.h.s. of (1.36) gives:

$$\mathscr{T}^{-1}\,[\hat{I}_x,\,\hat{I}_y]\,\mathscr{T} = \mathscr{T}^{-1}\hat{I}_x\mathscr{T}\;\mathscr{T}^{-1}\hat{I}_y\mathscr{T} - \mathscr{T}^{-1}\hat{I}_y\mathscr{T}\;\mathscr{T}^{-1}\hat{I}_x\mathscr{T} =$$
$$= \boxed{\text{see (1.35)}} = \hat{I}_x\hat{I}_y - \hat{I}_y\hat{I}_x = [\hat{I}_x,\,\hat{I}_y] = \boxed{\text{see (1.36)}} = i\,\hat{I}_z \qquad (1.37)$$

However, provided the time reversal operator is an unitary operator the application of it to the r.h.s of (1.36) gives:

$$\mathscr{T}^{-1}\,i\,\hat{I}_z\,\mathscr{T} = i\,\mathscr{T}^{-1}\,\hat{I}_z\,\mathscr{T} = -i\,\hat{I}_z \qquad (1.38)$$

and it is in the contraversy with (1.37). Therefore the time reversal operator cannot be an unitary operator. In order the time reversal operation to be consistent with the expression (1.36) (that means in order this transformation gives the same result for l.h.s. and r.h.s.) the time reversal operator $\mathscr{T}$ should be expressed in the form of the product of the unitary operator $\hat{\mathscr{U}}$ and the complex conjugation operator $\hat{\mathscr{K}}$:

$$\mathscr{T} = \hat{\mathscr{U}}_\tau\,\hat{\mathscr{K}} \qquad (1.39)$$

Then really the time reversal transformation of the r.h.s. of (1.36) gives:

$$\mathscr{T}^{-1}\,i\,\hat{I}_z\,\mathscr{T} = (\hat{\mathscr{U}}_\tau\hat{\mathscr{K}})^{-1}\,i\,\hat{I}_z\,\hat{\mathscr{U}}_\tau\hat{\mathscr{K}} = i\,\hat{I}_z\,,$$

and this agrees to the transformation of the l.h.s. of (1.36) (see (1.37)).

Further the unitary part $\hat{\mathscr{U}}_\tau$ of the time reversal operator will be determined. In the coordinate representation any single-particle wave function involves space-configuration, spin and isospin parts and unitary part $\hat{\mathscr{U}}_\tau$ of the time reversal operator for all these parts is specified below [1] .

- **Space-configuration part**
  Since $\mathscr{T}\,|\vec{r}\rangle = |\vec{r}\rangle$ then the space-configuration part of the s.p. wave function, $\psi_\alpha(\vec{r}) \equiv \langle\vec{r}\,|\alpha\rangle$, is transformed by the time reversal operator into the time reversed s.p. wave function, $\psi_{\bar{\alpha}}(\vec{r})$, as it is given below:

$$\psi_{\bar{\alpha}}(\vec{r}) \equiv \langle\vec{r}\,|\bar{\alpha}\rangle = \langle\vec{r}\,|\mathscr{T}|\alpha\rangle = \langle\mathscr{T}^{-1}\,\vec{r}\,|\alpha\rangle^* = \langle\vec{r}\,|\,\alpha\rangle^* = \psi^*_\alpha(\vec{r})$$

[1] Difference of the action of the unitary ($\hat{\mathscr{U}}$) and anti-unitary ($\hat{\mathscr{T}}$) transformations on the scalar product of two kets (and consequently on matrix element of any operator $\hat{F}$) is shown below.

- unitary transformation ($|A'\rangle = \hat{\mathscr{U}}|A\rangle$, $|B'\rangle = \hat{\mathscr{U}}|B\rangle$):

$$\langle B'\mid A'\rangle = \langle\hat{\mathscr{U}}\,B\mid\hat{\mathscr{U}}\,A\rangle = \int d\xi\;\psi^+_B(\xi)\;\hat{\mathscr{U}}^+\hat{\mathscr{U}}\;\psi_A(\xi) = \int d\xi\;\psi^+_B(\xi)\;\psi_A(\xi) = \langle B\mid A\rangle$$
$$\Rightarrow \qquad \langle B'\mid\hat{F}'\mid A'\rangle = \langle B\mid\hat{F}\mid A\rangle$$

So, for the space-configuration part of the s.p. wave function the action of the time reversal operator reduces to the complex conjugation and therefore the space-configuration part of the unitary operator $\hat{\mathscr{U}_\tau}$ is

$$\hat{\mathscr{U}_\tau}^{(c)} = 1 \tag{1.40}$$

For instance, the eigen-vector $|lm\rangle$ of the square of angular momentum and of its z-component ($\hat{L}^2\,|lm\rangle = l(l+1)\,|lm\rangle$, $\hat{L}_z\,|lm\rangle = m\,|lm\rangle$, $\langle\vec{r}|lm\rangle = Y_{lm}(\vartheta,\varphi)$) is transformed under the action of the time reversal as

$$\mathscr{T}\,|lm\rangle = \boxed{\begin{array}{c}\text{because}\\ \mathscr{T}^{-1}\,Y_{lm}(\vartheta,\varphi)\,\mathscr{T} = Y^*_{lm}(\vartheta,\varphi) = (-1)^m\,Y_{l-m}(\vartheta,\varphi)\end{array}}$$
$$= (-1)^m\,|l-m\rangle$$

- **Spin part**

The operators of nucleon spin components, $\hat{s}_x = \frac{1}{2}\begin{pmatrix}0&1\\1&0\end{pmatrix}$, $\hat{s}_y = \frac{1}{2}\begin{pmatrix}0&-i\\i&0\end{pmatrix}$, $\hat{s}_z = \frac{1}{2}\begin{pmatrix}1&0\\0&-1\end{pmatrix}$ should fulfil following symmetries with respect to the time reversal (see (1.35))

$$\mathscr{T}^{-1}\,\hat{s}_x\,\mathscr{T} = -\hat{s}_x, \quad \mathscr{T}^{-1}\,\hat{s}_y\,\mathscr{T} = -\hat{s}_y, \quad \mathscr{T}^{-1}\,\hat{s}_z\,\mathscr{T} = -\hat{s}_z$$

Since in the spin space the time reversal operator is expected in the form: $\hat{\mathscr{U}_\tau}^{(s)}\,\hat{\mathscr{K}}$ and since the action of the complex conjugation on spin components is

$$\hat{\mathscr{K}}^{-1}\,\hat{s}_x\,\mathscr{K} = \hat{s}_x, \quad \mathscr{K}^{-1}\,\hat{s}_y\,\mathscr{K} = -\hat{s}_y, \quad \mathscr{K}^{-1}\,\hat{s}_z\,\mathscr{K} = \hat{s}_z$$

the action of the unitary part $\hat{\mathscr{U}_\tau}^{(s)}$ should be following

$$\hat{\mathscr{U}_\tau}^{(s)\,-1}\,\hat{s}_x\,\mathscr{K}_\tau^{(s)} = -\hat{s}_x,\ \hat{\mathscr{U}_\tau}^{(s)\,-1}\,\hat{s}_y\,\mathscr{K}_\tau^{(s)} = \hat{s}_y,\ \hat{\mathscr{U}_\tau}^{(s)\,-1}\,\hat{s}_z\,\mathscr{K}_\tau^{(s)} = -\hat{s}_z$$

- anti-unitary transformation ($|A'\rangle = \hat{\mathscr{T}}|A\rangle$, $|B'\rangle = \hat{\mathscr{T}}|B\rangle$) :

$$\langle B' \mid A'\rangle = \langle \hat{\mathscr{T}}B \mid \hat{\mathscr{T}}A\rangle = \int d\xi\,\left(\hat{\mathscr{U}}\hat{\mathscr{K}}\psi_B(\xi)\right)^+\left(\hat{\mathscr{U}}\hat{\mathscr{K}}\,\psi_A(\xi)\right) =$$
$$= \int d\xi\,\left(\hat{\mathscr{K}}\psi_B(\xi)\right)^+\hat{\mathscr{U}}^+\hat{\mathscr{U}}\,\left(\hat{\mathscr{K}}\psi_A(\xi)\right) = \int d\xi\,\left(\hat{\mathscr{K}}\psi_B(\xi)\right)^+\left(\hat{\mathscr{K}}\psi_A(\xi)\right) =$$
$$= \int d\xi\,\sum_i \psi_B^{(i)}(\xi)\ \psi_A^{(i)\,*}(\xi) = \langle A \mid B\rangle = \langle B \mid A\rangle^*$$
$$\Rightarrow \qquad \langle B' \mid \hat{F}' \mid A'\rangle = \langle B \mid \hat{F} \mid A\rangle^*$$

.

The properties of $\hat{\mathscr{U}_\tau^{(s)}}$ given in the expr. above are fulfilled e.g. by the operator of the inverse rotation by angle π round the y-axis (see exp.(1A-48) in [6])

$$\hat{\mathscr{U}_\tau^{(s)}} = \mathscr{R}_y^{-1}(\pi) = e^{i\pi\hat{s}_y} = e^{i\frac{\pi}{2}\hat{\sigma_y}} = cos\frac{\pi\,\hat{\sigma}_y}{2} + i\,sin\frac{\pi\,\hat{\sigma}_y}{2} =$$

$$= \boxed{\begin{array}{c}\text{Taylor expansion for } cos \text{ and } sin \\ \text{and } \hat{\sigma}_y^2 = 1\end{array}} =$$

$$= cos\frac{\pi}{2} + i\hat{\sigma}_y sin\frac{\pi}{2} = i\hat{\sigma}_y \tag{1.41}$$

Then the eigen-vector of the square of the spin and its z-projection is transformed under the action of the time reversal as

$$\mathscr{T}\,|s\mu\rangle \;=\; i\hat{\sigma}_y\,|\frac{1}{2}\mu\rangle = \boxed{\begin{array}{rl}\text{because} & |\frac{1}{2}\,\frac{1}{2}\rangle = \begin{pmatrix}1\\0\end{pmatrix} \\ & |\frac{1}{2}\,-\frac{1}{2}\rangle = \begin{pmatrix}0\\1\end{pmatrix}\end{array}} =$$

$$= \;(-1)^{\frac{1}{2}+\mu}|\frac{1}{2} - \mu\rangle = (-1)^{s+\mu}|s - \mu\rangle$$

- **Isospin part**
  By the same consideration as in the spin part of the time reversal operator (see above) we can obtain the isospin part, $\hat{\mathscr{U}_\tau^{(iso)}}$, of the unitary part of the time reversal operator (analogy with (1.41):

$$\hat{\mathscr{U}_\tau^{(iso)}} = e^{i\pi\hat{t}_y} = i\,\tau_y\ , \tag{1.42}$$

So, the total time reversal operator in the combined space-configuration, spin and isospin Hilbert space is

$$\mathscr{T} = \hat{\mathscr{U}_\tau^{(c)}}\,\hat{\mathscr{U}_\tau^{(s)}}\,\hat{\mathscr{U}_\tau^{(iso)}}\,\hat{\mathscr{K}} = e^{i\pi\hat{s}_y}\,e^{i\pi\hat{t}_y}\,\hat{\mathscr{K}} \tag{1.43}$$

example: Time-reversed single-particle wave function $\psi_{nljm}(\vec{r})$ in the con-

figuration - spin Hilbert space:

$$\mathscr{T}\psi_{nljm}(\vec{r}) = \mathscr{T}\langle\vec{r}\,|nljm\rangle = \mathscr{T}\sum_{m_l\,m_s} C^{jm}_{lm_lsm_s} R_{nl}(r) Y_{lm_l}(\vartheta,\varphi)\,\chi_{sm_s} =$$

$$= \boxed{\begin{array}{c}\mathscr{T}\,\chi_{sm_s} = (-1)^{s+m_s}\chi_{s-m_s} \\ \mathscr{T}\,Y_{lm_l} = Y^*_{lm_l}\end{array}} =$$

$$= \sum_{m_l\,m_s} C^{jm}_{lm_lsm_s}\, R_{nl}(r)\, Y^*_{lm_l}(\vartheta,\varphi)\,(-1)^{s+m_s}\,\chi_{s-m_s} =$$

$$= \sum_{m_l\,m_s} C^{jm}_{lm_lsm_s}(-1)^{\frac{1}{2}+m_l+m_s} R_{nl}(r)\, Y_{l-m_l}\,\chi_{s-m_s} = \boxed{\text{see (A3)}} =$$

$$= \sum_{m_l\,m_s} (-1)^{j-l-\frac{1}{2}}\, C^{j-m}_{l-m_ls-m_s}(-1)^{\frac{1}{2}+m} R_{nl}(r)\, Y_{l-m_l}\,\chi_{s-m_s} =$$

$$= (-1)^{l+j+m}\langle\vec{r}\,|nlj-m\rangle = (-1)^{l+j+m}\psi_{nlj-m}(\vec{r}) \tag{1.44}$$

The expr. (1.44) corresponds to so called Condon-Shortley phase convention (when all Clebsch-Gordan coefficients are real - see Appendix A). It is known from quantum mechanics that a wave function is determined up to the phase factor and that we have an arbitrariness in the choice of this phase factor. In order to simplify the notation of the action of the time reversal operator on the wave function in the space-configuration and spin parts of the Hilbert space the phase of the wave function is chosen frequently (see e.g. [6]) in such a way that instead of the spherical harmonics Y_{lm_l} in the function $\langle\vec{r}|nlm_l\rangle = R_{nl}Y_{lm_l}$ we take $i^l\,Y_{lm_l}$. That means the singleparticle wave function $\langle\vec{r}|nlm_l\rangle$ is written in the following form:

$$\langle\vec{r}\,|nlm_l\rangle = R_{nl}(r)\,i^l\,Y_{l_{m_l}}(\vartheta,\varphi) \tag{1.45}$$

Then the action of the time reversal operator is

$$\mathscr{T}\psi_{nlm_l}(\vec{r}) = \mathscr{T}\langle\vec{r}\,|nlm_l\rangle = (-1)^{l+m_l}\,\langle\vec{r}\,|nl-m_l\rangle \tag{1.46}$$

and the action of $\mathscr{T}$ on the whole s.p. wave function is:

$$\begin{aligned}&\mathscr{T}\psi_{nljm}(\vec{r}) = \mathscr{T}\langle\vec{r}\,|nljm\rangle = \\ &= \mathscr{T}\sum_{m_l\,m_s} C^{jm}_{lm_lsm_s} R_{nl}(r)\,i^l\,Y_{lm_l}(\vartheta,\varphi)\,\chi_{sm_s} = \\ &= (-1)^{j+m}\,\langle\vec{r}\,|nlj-m\rangle = (-1)^{j+m}\,\psi_{nlj-m}(\vec{r})\end{aligned} \tag{1.47}$$

So, generally the phase convention can be chosen so that time reversal oper-

ator and its action have the following form [6] (in the agreement with(1.47)):

$$\begin{aligned}
&\mathscr{T} = \mathscr{R}_y^{-1}(\pi)\,\mathscr{K} = e^{i\pi\hat{j}_y}\,\mathscr{K} \Rightarrow \mathscr{R}_y^{-1}(\pi)\,\mathscr{T} = \mathscr{K} \\
&\mathscr{K}\,|\alpha JM\rangle = |\alpha JM\rangle \\
&\overline{|\alpha JM\rangle} = \mathscr{T}\,|\alpha JM\rangle = \mathscr{R}_y^{-1}(\pi)\,|\alpha JM\rangle = (-1)^{J+M}\,|\alpha J-M\rangle
\end{aligned} \tag{1.48}$$

This phase convention is used often in nuclear physics and is known as Bohr-Mottelson phase convention (see [6]) [2] .

From (1.48) it follows

$$\begin{aligned}
&\mathscr{R}_y^2(\pi)\,\mathscr{T}^2\,|\alpha JM\rangle = \mathscr{K}^2\,|\alpha JM\rangle = |\alpha JM\rangle \\
&\text{or} \quad \mathscr{T}^2\,|\alpha JM\rangle = (\mathscr{R}_y^{-1}(\pi))^2\,|\alpha JM\rangle = e^{i\hat{J}_y 2\pi}\,|\alpha JM\rangle
\end{aligned} \tag{1.49}$$

The exp. (1.49) implies the conclusion that if we consider a nucleus with the half-integer spin (that means the odd number of nucleons) then (because matrix elements of $\hat{J}_y$ have a half-integer character):

$$\mathscr{T}^2\,|\alpha JM\rangle = -\,|\alpha JM\rangle\ , \tag{1.50}$$

and if a nucleus has the integer spin (that means even number of nucleons) then

$$\mathscr{T}^2\,|\alpha JM\rangle = |\alpha JM\rangle\ . \tag{1.51}$$

The expr. (1.50) excludes a possibility that states of the nucleus with odd number of nucleons are eigen states of the operator $\mathscr{T}$. It follows from the following consideration:

if $|A\rangle$ is an eigen state of the operator $\mathscr{T}$ then

$$\begin{aligned}
&\mathscr{T}\,|A\rangle = e^{i\varphi_A}|A\rangle \qquad \Rightarrow \\
&\mathscr{T}^2\,|A\rangle = \mathscr{T}\,e^{i\varphi_A}|A\rangle = e^{-i\varphi_A}\,\mathscr{T}|A\rangle = \\
&= e^{-i\varphi_A}\,e^{i\varphi_A}\,|A\rangle = |A\rangle \quad ,
\end{aligned}$$

but this is in conflict with (1.50).

In the case of the odd-number of particle system (e.g. in the case of single particle states) when corresponding Hamiltonian commutes with the time reversal operator, $[\hat{H},\ \mathscr{T}] = 0$, we cannot look for the common system of eigen states similtaneously for $\hat{H}$ and $\mathscr{T}$. We have just shown that for odd number of particles the eigenstates of the time reversal operator do not exist. However, if in this case (when $[\hat{H},\ \mathscr{T}] = 0$) the state $|A\rangle$ is the eigenstate of

[2] Using the Bohr-Mottelson phase convention for nucleus wave funtion ($\mathscr{T} = \mathscr{R}_y^{-1}(\pi)$) one should have in mind that in all single-particle wave functions the imaginary factor i^l is involved (see (1.45).

$\mathscr{T}$-symmetric Hamiltonian ($\hat{H}\,|A\rangle = E_A\,|A\rangle$) then the state $\mathscr{T}\,|A\rangle$ is also the eigenstate of the Hamiltonian $\hat{H}$ with the same eigen-energy E_A, because:

$$\hat{H}\;\mathscr{T}\,|A\rangle = \mathscr{T}\;\hat{H}\,|A\rangle = \mathscr{T}\;E_A\,|A\rangle = E_A\;\mathscr{T}\,|A\rangle$$

This fulfils also for single-paricle Hamiltonian. That means, if the single-particle Hamiltonian commutes with the time reversal operator then each single-particle level is at least twice degenerated.

1.4 Degrees of freedom of nuclear motion

As it was mentioned in the Section 1.1 the short range of the strong interaction causes predominantly two-body character of the nucleon-nucleon interaction. So, if we neglect three-body and higher interactions (and it is a good approximation for nuclear structure) then the nuclear Hamiltonians has the following form

$$\hat{H} = \sum_i \hat{t}_i + \sum_{i<j} \hat{V}_{i\,j} \quad , \tag{1.52}$$

where $\hat{t}_i = -\hbar^2\vec{\nabla}_i^2/2m$ is the kinetic energy of the i-th nucleon and $\hat{V}_{i\,j}$ is the effective interaction between i-th and j-th nucleon in the nucleus. For heavier nuclei usually so called nuclear mean (average) field $\hat{H}_{AV}$ is extracted from the Hamiltonian (1.52) which involves average singleparticle potential $\hat{U}_i$ acting on the i-th nucleon and caused by the presence of all other nucleons in the given nucleus. Then the nuclear Hamiltonian can be rewritten in the following form

$$\hat{H} = \underbrace{\sum_i \hat{h}_i}_{\hat{H}_{AV}=\sum_i(\hat{t}_i+\hat{U}_i)} + \sum_{i<j} \hat{V}_{i\,j}^{(res)} \tag{1.53}$$

The mean field $\hat{H}_{AV}$ is usually extracted from the starting Hamiltonian (1.52) in terms of the Hartree-Fock (HF) method which is discussed in the Chapter 4. The second term, $\sum_{i<j} \hat{V}_{i\,j}^{(res)}$, in (1.53) represents so called residual interactions and it will be discussed in Chapters 6 and 7.

Singleparticle degrees of freedom

The basic global properties of nuclei (e.g. binding energy, nuclear radius, shape of the nucleus, compressibility of nuclear matter etc) are given by the mean field $\hat{H}_{AV}$, that means by the singleparticle states of the mean field. In

accordance with the Pauli principle nucleons fill one by one individual s.p. states (eigen-states of $\hat{H}_{AV}$ from the bottom of the mean field potential up to the so called Fermi level - see Fig. 1.4.)

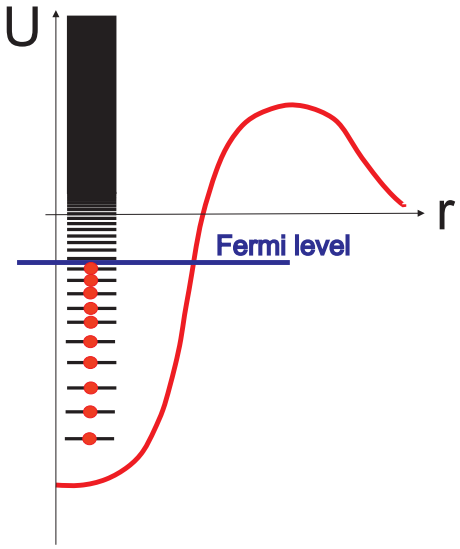


Figure 1.4: Schematic figure - nucleons fill eigen-states of the mean fild.

Mean field $\hat{H}_{AV}$ determines so called **singleparticle degrees** of freedom of the nuclear motion (individual nucleons move in the singleparticle states). If in the nuclear Hamiltonian only the mean field is included and the residual interactions are neglected then we speak about a **model of independent particles** (nucleons move in the average potential $\sum_i \hat{U}_i$ but do not interact mutually). The model of independent particles is discussed in details in the Chapter 5.

The shape of equipotential surfaces of the potential $\sum_i \hat{U}_i$ corresponds to the shape of the surfaces of the same value of the mass density. That means equipotential surfaces of the average potential $\sum_i \hat{U}_i$ of deformed nuclei (see Subsection 1.1.2) have the same shape as the shape of the whole deformed nucleus.

Collective vibrational degrees of freedom

Residual interactions, $\sum_{i<j} \hat{V}^{(res)}_{i\,j}$, represent the part of the nucleon-nucleon interactions not included in the mean field. Usually residual interactions are divided into two groups, short range residual interactions and long range residual interactions:

$$\hat{V}^{(res)} = \hat{V}^{(res)}_{short} + \hat{V}^{(res)}_{long} \tag{1.54}$$

Residual interactions of very short range, $\hat{V}^{(res)}_{short}$, are responsible for pairing

effects in the nucleus (a formation of the nucleon pairs) which are discussed in the Chapter 6. Long range residual interactions, $\hat{V}_{long}^{(res)}$, are responsible for collective vibrations of the whole nucleus (that means correlated motion of many nucleons).

The long range residual interactions, generating **collective vibrational degrees of freedom of a nuclear motion**, will be discussed in details in the Chapter 7. In many papers dealing with the structure of heavier nuclei the long range residual interactions are decomposed into multipole ($\hat{M}_{\lambda\mu}$) and spin-multipole ($\hat{S}_{\lambda\mu}$) operators (in the analogy with the electric and magnetic multipole operator decomposition of the interaction between a general microsystem with some charge density and current and an external electromagnetic field - see the Chapter 2 and the Appendix B). Schematically such decomposition is written as follows (see e.g. [7, 8, 9] and citations therein)

$$\begin{aligned}\hat{V}_{long}^{(res)} \;\approx\; & \sum_{\lambda=0}^{\infty}\sum_{\mu=-\lambda}^{\lambda}\sum_{\tau=n,p}\kappa_{\lambda}[\tau]\;\hat{M}^{+}_{\lambda\mu}\hat{M}_{\lambda\mu} + \\ & + \sum_{\lambda=0}^{\infty}\sum_{l=|\lambda-1|}^{\lambda+1}\sum_{\mu=-\lambda}^{\lambda}\sum_{\tau=n,p}\kappa_{l\lambda}[\tau]\;\hat{S}^{+}_{l\lambda\mu}\hat{S}_{l\lambda\mu}\,, \qquad (1.55)\end{aligned}$$

where $\hat{M}_{\lambda\mu}$ are multipole operators and $\hat{S}_{l\lambda\mu}$ are the spin-multipole operators with corresponding parity:

$$\begin{aligned}\hat{M}_{\lambda\mu} \;&\approx\; \sum_{i=1}^{A} f_{\lambda}(r_i)Y_{\lambda\mu}(\vartheta_i,\varphi_i) \quad || \quad \hat{\mathscr{P}}^{-1}\hat{M}_{\lambda\mu}\hat{\mathscr{P}} = (-1)^{\lambda}\hat{M}_{\lambda\mu} \\ \hat{S}_{l\lambda\mu} \;&\approx\; \sum_{i=1}^{A} f_{l\lambda}(r_i)[\vec{\sigma}\otimes Y_l(\vartheta_i,\varphi_i)]_{\lambda\mu} \quad || \quad \hat{\mathscr{P}}^{-1}\hat{S}_{l\lambda\mu}\hat{\mathscr{P}} = (-1)^{l}\hat{S}_{l\lambda\mu}\end{aligned} \qquad (1.56)$$

where $[\vec{\sigma}\otimes Y_l(\vartheta_i,\varphi_i)]_{\lambda\mu} = \sum_m C^{\lambda\mu}_{lm1\mu-m}Y_{lm}(\vartheta_i,\varphi_i)\,\sigma_{m-\mu}$. In (1.56) $f_{\lambda}(r_i)$ and $f_{l\lambda}(r_i)$ are corresponding radial dependences. The first term in (1.56) generates electric-like excitations (E0, E1, E2, ...) and the second term magnetic-type excitations (M1, M2, ...). Each term in (1.56) is responsible for vibrational excitations of the nucleus with given multipolarity and parity - see the classification of excitation modes corresponding to the decomposition (1.55) presented in the Table 1.2.

Each type (electric or magnetic), multipolarity and parity of given excitation mode correspond to the concrete vibration of the nuclear shape - see

$\hat{M}_{00}$	$\longrightarrow$	E0: 0^+	$\hat{S}_{01\mu}$	$\longrightarrow$	M1: 1^+
$\hat{M}_{1\mu}$	$\longrightarrow$	E1: 1^-	$\hat{S}_{12\mu},\ \hat{S}_{32\mu}$	$\longrightarrow$	M2: 2^-
$\hat{M}_{2\mu}$	$\longrightarrow$	E2: 2^+		$\vdots$	

Table 1.2: Classification of the collective vibration excitations

Fig.1.5. This classification of vibrational modes is not necessarily connected

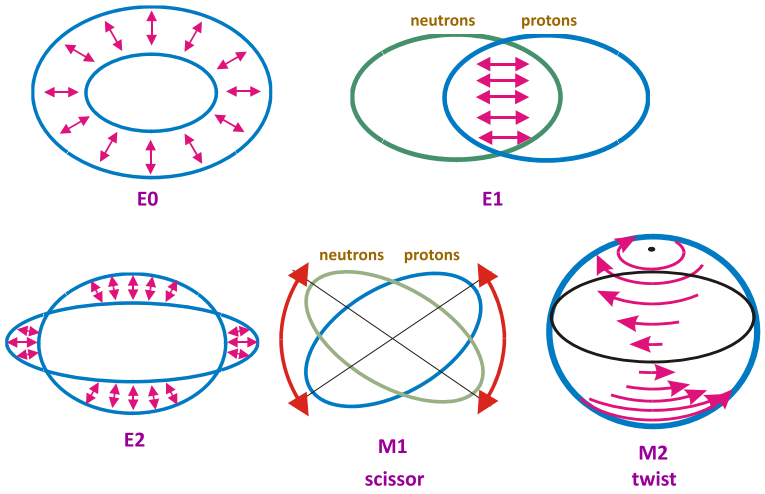


Figure 1.5: Schematic figure - different excitation modes of nuclear shape vibrations

only with the separable form of the long range residual interaction given by (1.55). The decomposition (1.55) only simplifies the solving of the equation of motion where long range residual interactions are taken into account (see the Chapter 7). Generally, the long range residual interactions have not the separable form of (1.55). The classification of excitation modes depends on the process by which the given nucleus is excited. From quantum mechanics it is known that if we excite the nucleus by some process from its ground state $|\rangle$ then the probability $P(|\rangle \to |\nu\rangle)$ of finding the nucleus in some concrete excited state $|\nu\rangle$ is proportional to the square of the matrix element of the transition operator $\hat{T}$ corresponding to the given process:

$$P(|\rangle \to |\nu\rangle) \approx |\langle\nu|\,\hat{T}\,|\rangle|^2 \quad . \tag{1.57}$$

For instance, if the excitation process is of the electromgnetic character (e.g. photoabsorption or electron scattering) then the transition operator $\hat{T}$ can be identified with the corresponding electric or magnetic transition operator with given multipolarity λ and its projection μ, $\hat{T} = \hat{\mathscr{M}}^{(X)}_{\lambda\mu}$, where X = electric or magnetic (for the derivation of electromagnetic transition operator $\hat{\mathscr{M}}^{(X)}_{\lambda\mu}$

see the Chapter 2 and Appendix B). Then the classification of excited states according to the Table 1.2 valids as well.

In the Fig.1.6 there is a schematic plot of the dependence of the probability of the electromagnetic E1 excitation $|\rangle \rightarrow |1^-_\nu\rangle$ on the excitation energy. A similar character of the excitation probability can be observed also for other electromagnetic transitions (E2, E3, ..., M1, M2, ...). From the Fig.1.6 one can see that low-energy part of the spectrum is discrete but the density of states increases rapidly with the excitation energy. Starting from some value of the excitation energy the spectrum becomes practically smooth, usually with huge broad peak called giant resonance of given type and multipolarity. So, the giant dipole resonance, quadrupole isovector and isoscalar resonances, magnetic dipole resonance etc. can be recognized among the nuclear excitations.

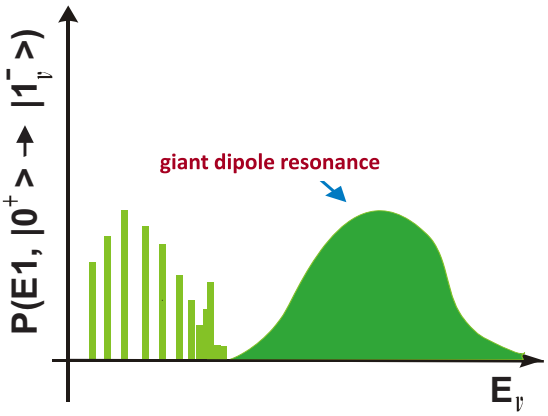


Figure 1.6: Schematic figure - probability of E1 excitations from the even-even nucleus ground state $|0^+\rangle$ to the excited states $|1^-_\nu\rangle$ in the dependence on the excitation energy. Index ν enumerates solutions of a nonspecified equation of motion (e.g. in the Chapter 7 the Random Phase Aproximation (RPA) equation of motion and their solving is discussed). The experimental spectrum of all 1^- states has also this character.

Collective rotational degrees of freedom

In the case of deformed nuclei (where equipotential surfaces of the mean field potential are deformed) the rotational degrees of freedom of the nuclear motion are observed in the laboratory frame. In the framework of the quantum mechanics spherically symmetric object (including spherical nucleus) cannot rotate. The reason is that quantum mechanics is not able to recognize a rotation of such objects. It can be seen from the following reflection.

In the spherical systems always Hamiltonian commutes with all

components of the total momentum, $[\hat{H}, \hat{J}_i] = 0 \quad \Rightarrow$ Hamiltonian is invariant with respect to a rotation by any angle $\vec{\theta}$: $e^{-i\hat{\vec{J}}\cdot\vec{\theta}}\hat{H}e^{i\hat{\vec{J}}\cdot\vec{\theta}} = \hat{H}$
After the rotation by angle $\vec{\theta}$ the new state $|\psi' >= e^{i\hat{\vec{J}}\cdot\vec{\theta}}|\psi >$ corresponds to the energy:
$E' = \langle\psi'|\hat{H}|\psi'\rangle = \langle\psi|e^{-i\hat{\vec{J}}\cdot\vec{\theta}}\hat{H}e^{i\hat{\vec{J}}\cdot\vec{\theta}}|\psi\rangle = \langle\psi|\hat{H}|\psi\rangle = E$
So, the total energy remains untouched by the rotation. The same can be said for the expectation value or matrix elements of any operator which is invariant with respect to rotation. So, the **quantum mechanics cannot recognize any rotation of the spherically symmetric system**.

Singleparticle and vibrational degrees of freedom of the nucleus motion are described in the intrisic frame connected with the nucleus (e.g. center of mass frame when axes of the coordinate system coincide with the principal axes of the nucleus quadrupole moment tensor). In such a frame, usually called intrinsic frame, some nuclei are deformed (that means the distribution of the matter in the nuclear volume is not spherically symmetric) and some other nuclei can have spherical shape in their ground states.

In the laboratory frame (rest frame of the detectors in terms of which given nucleus is observed) the deformed nucleus can rotate and quantum mechanics is able to recognize this rotation. The rotation degrees of freedom of nuclear motion show themselves as so called rotational bands in the spectrum of the nucleus which are discussed in the Chapter 8.

Precise separation of the rotational degrees of freedom in the heavier nuclei is quite complicated. It is connected with the complex tranformation of the Hamiltonian of the A nucleons nucleus with 3A degrees of freedom in the spatial space from the laboratory coordinate frame to the intrinsic frame rotating together with the nucleus. Therefore, quasi-phenomenological approaches are usually used for this purpose when an adiabatic separation of the rotational part of the nuclear Hamiltonian is usually supposed (see also Chapter 8):

$$\hat{H} = \hat{H}_{intr} + \hat{H}_{rot} \quad , \tag{1.58}$$

where the intrinsic part of the Hamiltonian $\hat{H}_{intr}$ given by the sum of the mean field $\hat{H}_{AV}$ and the residual interactions $\hat{V}^{(res)}$, $\hat{H}_{intr} = \hat{H}_{AV} + \hat{V}^{(res)}$, (the same as in (1.53) but now everything expressed in the intrinsic frame coordinates) is responsible for the intrinsic (single-particle and vibrational) degrees of freedom. In (1.58) $\hat{H}_{rot}$ is the part of the Hamiltonian connected with the

rotational motion, usually taken in the form of so called rotor Hamiltonian (in the analogy with the classical mechanics where the rotational energy of the rotating body is given by the square of the rotational angular momentum divided by two inertia moments):

$$\hat{H}_{rot} = \sum_{i=1}^{3} \frac{\hbar^2 \hat{R}_i^2}{2\mathscr{F}_i} \quad , \tag{1.59}$$

where $\hat{R}_i$ is the i-th component of the operator of rotational angular moment and $\mathscr{F}_i$ is the i-th principal value of the nucleus moment of inertia. Details of this Hamiltonian are discussed in the Chapter 8. It should be noted that the adiabatic division of the nuclear Hamiltonian (1.58) into the intrinsic and rotational parts valids with good precision only in the case of small rotational frequencies when rotational frequencies are much lower than the frequencies of the intrinsic single-particle and vibrational motions (so called adiabatic region). Good models for the description of the nuclear structure in this region are e.g. particle+rotor models discussed in the Chapters 7 and 8. For high rotational frequencies the intrinsic and rotational degrees of freedom are mixed by the Coriolis interaction and by other nonadiabatic couplings to large extend that it is hard to separate the intrinsic and rotational motion. If the rotational frequency is very high the nucleus behaves like gyroscop, that means rotates round the stable axis in the space. In such a case so called cranking models, described again in the Chapter 8, are usually used.

Summarizing the possible nuclear degrees of freedom there are three basic degrees of freedom of nuclear motion: i. single-particle, ii. vibrational, iii. rotational degrees of freedom. All these classes of nuclear degrees of freedom can be mixed in the real nuclear states and they are the subjects of the Chapters 5, 6, 7 and 8.

In order to give an outlook about character of nuclear states and nuclear models used for their description all possible bound nuclear states are illustrated in the schematic Fig. 1.7. The area of all possible states in the plane (excitation energy & total angular moment) is bordered from the bottom by so called yrast line [3]. From the side of the high energy the area of possible states is bordered by the fission line when the rotational frequencies and excitation energies are so high that the given nucleus cannot exist as a bound system. The whole area of possible states is divided into the sub-areas (indicated by different colors) according to the type of nuclear models used for

[3]The word yrast originates from Swedish and it means dizziest or the most bewildered.

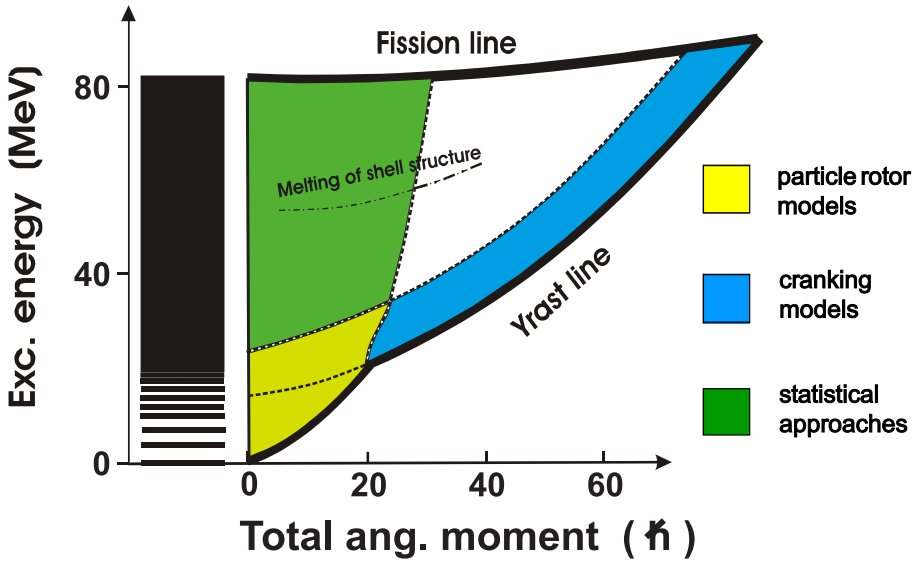


Figure 1.7: Schematic figure - Area of all possible nuclear states in the plane (excitation energy & total angular moment) is divided into sub-areas according to the type of the nuclear model for given sub-area.

the description of states belonging to the given sub-area (low excitation energy and low ang. moments - particle-rotor models; excitation energies close to the yrast line and with high ang. moments - collective cranking models; high excitation energies - statistical approaches should be applied). In the Fig.1.7 there is also demonstrated an increasing density of levels of excited states from the discrete spectrum for states with low energy up to the smooth spectrum for higher energy states.

2. Electromagnetic transition probabilities, static electromagnetic moments

Before nuclear structure models are discussed it is necessary to spend some time with the theoretical description of electromagnetic properties of nucleus (or generally of any quantum system). Besides the energy spectrum electromagnetic properties of any quantum system (electromagnetic transition probabilities or electromagnetic moments) are usually the most frequent measured properties in experiements. That is why this chapter is devoted to this problem. Throughout this chapter we speak about a nucleus but the theory of el.mg. transitions presented in this chapter is applicable to any bound quantum system (e.g. atoms, quantum dots, atomic clusters etc.).

The interaction of the nucleus with the external time-dependent electromagnetic field shows itself in the nucleus by two possible ways, namely:

- the nucleus absorbs photon from the external el.mg. field and this leads to the excitation of the nucleus;
- the external el.mg. field induces the deexcitation of the excited nucleus and during the deexcitation a photon is emitted.

Both these processes are discussed in this chapter. Throughout this chapter it is assumed that investigated system (nucleus) is composed from fermions.

In the first part of this chapter the quantum description of free electromagnetic field is discussed. The second part is devoted to the interaction of the nucleus with external (time dependent) electromagnetic field. In the end of the chapter the static electromagnetic moments of the nucleus are introduced as a result of the interaction of the nucleus with the static electromagnetic field.

2.1 Quantum description of a free electromagnetic field

The quantum description of free electromagnetic field starts with the classical solution of the wave equation which can be derived directly from Maxwell

equations. There are different solutions of wave equations. For the purpose of quantization of the electromagnetic field the most suitable is the solution of the wave equation in the form of plane waves. For the derivation of el.mg. transition probabilities a spherical wave solution is the most appropriate. Both these solutions of the wave equation and their connection are discussed in the first subsections of this section. Then the the quantization of the free el.mg. field can be obtained in terms of classical Lagrange approach.

2.1.1 Maxwell and wave equations, solutions of the wave equation

2.1.1.1 Derivation of the wave equation

Maxwell equations for general time-dependent el.mg. field are written as follows (assignment is obvious):

$$\begin{aligned} rot\vec{H} - \frac{\partial \vec{D}}{\partial t} &= \hat{j} \\ div\vec{D} &= \rho \\ rot\vec{E} + \frac{\partial \vec{B}}{\partial t} &= 0 \\ div\vec{B} &= 0 \end{aligned} \tag{2.1}$$

Sources of the el.mg. field, that means the charge density ρ and current density $\vec{j}$, are bound by the continuity equation:

$$div\vec{j} + \frac{\partial \rho}{\partial t} = 0 \tag{2.2}$$

Magnetic induction $\vec{B}$ and electric induction $\vec{D}$ are related with magnetic intensity $\vec{H}$ and electric intensity $\vec{E}$ by the well-known expressions involving electric permeability ϵ and magnetic permitivity μ (we suppose isotropic medium):

$$\begin{aligned} \vec{D} &= \epsilon_0 \vec{E} + \vec{P} = \epsilon \vec{E} \\ \vec{B} &= \mu_0(\vec{H} + \vec{M}) = \mu \vec{H} \end{aligned} \tag{2.3}$$

Scalar potential φ and vector potential $\vec{A}$ are usually introduced instead of $\vec{E}$ and $\vec{H}$:

$$\begin{aligned} \vec{B} &= rot\vec{A} \\ \vec{E} &= -\vec{\nabla}\varphi - \frac{\partial \vec{A}}{\partial t} \end{aligned} \tag{2.4}$$

Because of the identities:

$$\begin{aligned} div\, rot\vec{A} &= 0 \\ rot\, grad\varphi &= 0 \end{aligned} \tag{2.5}$$

the 3-d and 4-th equations from Maxwell equations (2.1) are automaticly fulfilled. The substitution of (2.4) into the 2-d equation of (2.1) gives:

$$\begin{aligned} & div\vec{D} = \epsilon\, div\vec{E} = -\epsilon\, div\, grad\varphi - \epsilon\, div\frac{\partial\vec{A}}{\partial t} = \rho \\ \Rightarrow \quad & \vec{\nabla}^2\varphi + \frac{\partial}{\partial t}(\vec{\nabla}\cdot\vec{A}) = -\frac{\rho}{\epsilon} \end{aligned} \tag{2.6}$$

and the substitution of (2.4) into the 1-st equation in (2.1) yields:

$$rot\vec{H} - \frac{\partial\vec{D}}{\partial t} = \frac{1}{\mu}\, rot\, rot\vec{A} + \epsilon\,\frac{\partial}{\partial t}(grad\varphi + \frac{\partial\vec{A}}{\partial t}) = \vec{j}$$

and using the identity $rot\, rot\vec{A} = -\,\vec{\nabla}^2\vec{A} + \vec{\nabla}\,(\vec{\nabla} div\vec{A})$ we obtain:

$$\begin{aligned} & \frac{1}{\mu}\,\vec{\nabla}^2\vec{A} - \epsilon\,\frac{\partial^2\vec{A}}{\partial t^2} = -\,\vec{j} + \frac{1}{\mu}\,\vec{\nabla}\,(\vec{\nabla}\cdot\vec{A}) + \epsilon\,\vec{\nabla}\frac{\partial\varphi}{\partial t} \\ \Rightarrow \quad & \vec{\nabla}^2\vec{A} - \epsilon\mu\,\frac{\partial^2\vec{A}}{\partial t^2} = \vec{\nabla}(div\vec{A} + \epsilon\mu\,\frac{\partial\varphi}{\partial t}) - \mu\,\vec{j} \end{aligned} \tag{2.7}$$

Equations (2.6) and (2.7) together with the definition (2.4) are fully equivalent to the Maxwell equations (2.1).

It is necessary to realize that the scalar potential φ and the vector potential $\vec{A}$ are not determined by their definition expressions (2.4) unambiguously. If instead of φ and $\vec{A}$ we take φ' and $\vec{A}'$ given by:

$$\begin{aligned} \vec{A}'(\vec{r},t) &= \vec{A}(\vec{r},t) + \vec{\nabla}\Lambda(\vec{r},t) \\ \varphi'(\vec{r},t) &= \varphi(\vec{r},t) - \frac{\partial}{\partial t}\Lambda(\vec{r},t) \quad , \end{aligned} \tag{2.8}$$

where $\Lambda(\vec{r},t)$ is arbitrary scalar function, then

$$\begin{aligned} rot\vec{A}' &= rot\vec{A} + rot\, grad\Lambda = \boxed{\begin{matrix}\text{see}\\(2.5)\end{matrix}} = \\ &= rot\vec{A} = \boxed{\begin{matrix}\text{see}\\(2.4)\end{matrix}} = \vec{B} \\ \vec{\nabla}\varphi' + \frac{\partial\vec{A}'}{\partial t} &= \vec{\nabla}\varphi - \vec{\nabla}\frac{\partial\Lambda}{\partial t} + \frac{\partial\vec{A}}{\partial t} + \vec{\nabla}\frac{\partial\Lambda}{\partial t} = \\ &= \vec{\nabla}\varphi + \frac{\partial\vec{A}}{\partial t} = \boxed{\begin{matrix}\text{see}\\(2.4)\end{matrix}} = -\vec{E} \end{aligned}$$

and one can see that φ' and $\vec{A}'$ give the same measurable intensities $\vec{B}$ and $\vec{E}$ as φ and $\vec{A}$. So, we have a freedom in the choosing of φ and $\vec{A}$ and therefore we may require an additional condition for φ and $\vec{A}$. In the literature so called Lorentz calibration condition is usually used:

$$\vec{\nabla}\cdot\vec{A} + \epsilon\mu\,\frac{\partial\varphi}{\partial t} = 0 \tag{2.9}$$

and we can always find φ and $\vec{A}$ in such a way that the condition (2.9) is fulfilled.

If the Lorentz calibration condition (2.9) is fulfilled by φ and $\vec{A}$ then equations (2.6) and (2.7) are simplified:

$$\begin{aligned} \vec{\nabla}^2\varphi + \frac{\partial}{\partial t}(\vec{\nabla}\cdot\vec{A}) &= \vec{\nabla}^2\varphi - \epsilon\mu\frac{\partial^2\varphi}{\partial t^2} = -\frac{\rho}{\epsilon} \\ \vec{\nabla}^2\vec{A} - \epsilon\mu\frac{\partial^2\vec{A}}{\partial t^2} &= -\mu\,\vec{j} \end{aligned} \tag{2.10}$$

where $\epsilon\mu = \frac{1}{c^2}$. Equations (2.10) are called wave equations with the sources. Wave equations (2.10) together with the definition (2.4) are fully equivalent to Maxwell equations (2.1).

In the stationary case $\frac{\partial\varphi}{\partial t} = \frac{\partial\vec{A}}{\partial t} = 0$ wave equations (2.10) give so called Poisson equations:

$$\begin{aligned} \vec{\nabla}^2\varphi &= -\frac{\rho}{\epsilon} \\ \vec{\nabla}^2\vec{A} &= -\mu\,\vec{j} \end{aligned} \tag{2.11}$$

with the explicit solution:

$$\begin{aligned} \varphi(\vec{r}) &= \frac{1}{4\pi\epsilon}\int \frac{\rho(\vec{r'})}{|\vec{r}-\vec{r'}|}\, d^3r' \\ \vec{A}(\vec{r}) &= \frac{\mu}{4\pi}\int \frac{\vec{j}(\vec{r'})}{|\vec{r}-\vec{r'}|}\, d^3r' \end{aligned} \tag{2.12}$$

2.1.1.2 Solution of wave equation - spherical waves

In next sections of this chapter the interaction of the electromagnetic field with the quantum micro-system will be discussed. This interaction shows itself as the absorption or emission of a photon by the micro-system. We assume that the source of the electromagnetic field is outside the micro-system. Therefore the form of the the wave equations (2.10) in the points inside the micro-system are following:

$$\begin{aligned} \vec{\nabla}^2\varphi - \epsilon\mu\frac{\partial^2\varphi}{\partial t^2} &= 0 \\ \vec{\nabla}^2\vec{A} - \epsilon\mu\frac{\partial^2\vec{A}}{\partial t^2} &= 0 \end{aligned} \tag{2.13}$$

Vector and scalar potentials $\vec{A}(\vec{r},t)$ and $\varphi(\vec{r},t)$ can be always chosen in such a way that they fulfil the Lorentz calibration condition (2.9). In the case of real nonvirtual photons the Lorentz calibration condition can be strengthened so that potentials $\vec{A}(\vec{r},t)$ and $\varphi(\vec{r},t)$ undergo following conditions:

$$\varphi(\vec{r},t) = 0 \qquad \vec{\nabla}\cdot\vec{A}(\vec{r},t) = 0 \tag{2.14}$$

So, in the case of real photons the electromagbetic field is described by one vector potential $\vec{A}$ which fulfils following wave equation ($\epsilon\mu = \frac{1}{c^2}$):

$$\vec{\nabla}^2\vec{A} - \frac{1}{c^2}\frac{\partial^2\vec{A}}{\partial t^2} = 0 \tag{2.15}$$

The time-dependence of the vector potential $\vec{A}(\vec{r},t)$ is usually looked for in the form:

$$\vec{A}(\vec{r},t) = \vec{A}(\vec{r})\, e^{-i\,\omega\, t} \tag{2.16}$$

Then, after the substitution of (2.16) into (2.15) the wave equation (2.15) can be rewritten as the equation for the unknown function $\vec{A}(\vec{r})$:

$$(\vec{\nabla}^2 + k^2)\,\vec{A}(\vec{r}) = 0 \tag{2.17}$$

where

$$k = \frac{\omega}{c} \tag{2.18}$$

The equation (2.17) can be transformed into spherical coordinates:

$$\left[\frac{1}{r^2}\,\frac{\partial}{\partial r}r^2\frac{\partial}{\partial r} + \underbrace{\frac{1}{r^2\,sin\vartheta}(\frac{\partial}{\partial\vartheta}sin\vartheta\frac{\partial}{\partial\vartheta}) + \frac{1}{r^2\,sin^2\vartheta}\frac{\partial^2}{\partial\varphi^2}}_{-\frac{\hat{\vec{L}}^2}{r^2}} + k^2\right]\vec{A}(r,\vartheta,\varphi) = 0 \tag{2.19}$$

where $\hat{\vec{L}}^2$ is the operator of the square of the orbital ang. moment. If we compare the equation (2.19) (for each component of the wave function $\vec{A}$) with the Schroedinger equation for free spinless particle (see any QM textbook, e.g. the appendix A in [12]) one can see that they are similar and therefore one could expect that the each component of $\vec{A}$ can be written as a product of the spherical harmomic $Y_{Lm}(\vartheta,\varphi)$ and radial function $R_L(r)$ which in the case of free particle is the combination of spherical Bessel and Neumann functions (see e.g. [12]). However, one should realize that the field $\vec{A}(\vec{r},t)$ describes the photon and a photon is not a spinless particle. Any photon has spin $S = 1$ and from the quantum mechanics it is known that any particle with spin $S = 1$ is described by a vector field which corresponds to the total moment $\vec{J}$ in the form of the vector sum of orbital moment $\vec{L}$ and spin $\vec{S}$

$$\vec{J} = \vec{L} + \vec{S}$$

where in the case of photons (electromagnetic field) $S = 1$. In this case the solution of the wave equation (2.17) can be searched for in the form of the linear combination of the following basis of functions:

$$\left\{f_L(kr)\,\vec{Y}_{LJM}(\vartheta,\varphi)\right\}, \qquad J = L \pm 1,\ L \tag{2.20}$$

where $\vec{Y}_{LJM}(\vartheta,\varphi) = \vec{Y}_{LJM}(\hat{r})$ are so called vector spherical harmonics defined as (see e.g. [2] and the Appendix A):

$$\vec{Y}_{LJM}(\hat{r}) = \sum_{m\mu} C^{J\,M}_{L\,m\,1\,\mu}\,Y_{Lm}(\hat{r})\,\vec{\xi}_\mu \tag{2.21}$$

with spherical harmonics $Y_{Lm}(\hat{r})$ and where $\vec{\xi}_\mu$ are spin functions - eigen functions of the square of spin and of the 3-d component of the spin operator [1] (see the Appendix A for more details):

$$\begin{aligned} \hat{S}^2\,\vec{\xi}_\mu &= 1\,(1+1)\,\vec{\xi}_\mu \\ \hat{S}_3\,\vec{\xi}_\mu &= \mu\,\vec{\xi}_\mu \quad , \qquad \mu = 0, \pm 1 \end{aligned} \tag{2.22}$$

The radial functions $f_L(kr)$ in (2.20) are given by spherical Bessel or Neumann functions. From (2.22) and (2.21) it follows that the vector spherical functions $\vec{Y}_{LJM}(\hat{r})$ fulfil following relations:

$$\begin{aligned} \hat{S}^2\,\vec{Y}_{LJM}(\hat{r}) &= 2\,\vec{Y}_{LJM}(\hat{r}) \\ \hat{L}^2\,\vec{Y}_{LJM}(\hat{r}) &= L(L+1)\,\vec{Y}_{LJM}(\hat{r}) \\ \hat{J}^{\,2}\,\vec{Y}_{LJM}(\hat{r}) &= J(J+1)\,\vec{Y}_{LJM}(\hat{r}) \\ \hat{J}_3\,\vec{Y}_{LJM}(\hat{r}) &= M\,\vec{Y}_{LJM}(\hat{r}) \end{aligned} \tag{2.23}$$

where $J = L,\ L \pm 1$ and $M = -J, -J+1, \ldots, J-1, J$.

Since vectors (2.20) are solutions of the equation (2.17) the general solution of the wave equation (2.15) can be written as the linear combination of the complete set of functions $f_L(kr)\vec{Y}_{LJM}(\hat{r})e^{-i\omega t}$ with $J = 1,\ 2,\ \ldots;\ L = J,\ J \pm 1;\ M = -J,\ \ldots,\ J$. However, one should have in mind that we search for the solution of the wave equation (2.15) which simultaneously fulfil the transverse calibration condition (2.14), that means $\vec{\nabla} \cdot \vec{A}(\vec{r}, t) = 0$, and this condition is not generally fulfilled by vectors $f_L(kr)\vec{Y}_{LJM}(\hat{r})e^{-i\omega t}$. Further we will construct such solutions from vectors $f_L(kr)\vec{Y}_{LJM}(\hat{r})e^{-i\omega t}$. Concretely, we take three vectors $f_L(kr)\vec{Y}_{LJM}(\hat{r})e^{-i\omega t}$ with $L = J,\ J \pm 1$ for fixed J and M and we will combine them in order to obtain new three solutions of the wave equation (2.15) which fulfil transverse calibration condition (2.14). We will see that in such a way we can obtain only two solutions of (2.15) which simultaneously fulfil the transverse calibration condition (2.14) (so called transverse solutions) and the third one, orthogonal to previous two, does not fulfil the condition (2.14) (longitudinal solution of (2.15)).

[1] The spin functions $\vec{\xi}_\mu$ are connected with the unit vectors $\vec{e}_1$, $\vec{e}_2$, and $\vec{e}_3$ along the coordinate axes by the well-known relation (see e.g. [2] and the Appendix A):

$$\begin{aligned} \vec{\xi}_0 &= \vec{e}_3 \\ \vec{\xi}_{+1} &= -\frac{1}{\sqrt{2}}\,(\vec{e}_1 + i\,\vec{e}_2) \\ \vec{\xi}_{-1} &= \frac{1}{\sqrt{2}}\,(\vec{e}_1 - i\,\vec{e}_2) \end{aligned}$$

1. Let us consider the vector (for fixed value J and M)

$$\hat{\vec{L}} f_J(kr) Y_{JM}(\hat{r}) = -i\,\vec{r}\times\vec{\nabla}\, f_J(kr) Y_{JM}(\hat{r}) = \boxed{\begin{array}{c}\text{see}\\(A.64)\end{array}} = \\ = \sqrt{J(J+1)}\,\vec{Y}_{JJM}(\hat{r})\, f_J(kr) \qquad (2.24)$$

Since $[\hat{\vec{L}}^2,\ \hat{\vec{L}}] = 0$ and $\vec{\nabla}^2 = \frac{1}{r^2}\frac{\partial}{\partial r} r^2 \frac{\partial}{\partial r} - \frac{1}{r^2}\hat{\vec{L}}^2$ we have $[\hat{\vec{L}}^2,\ \vec{\nabla}^2] = 0$. Therefore

$$(\vec{\nabla}^2 + k^2)\,\hat{\vec{L}}\, f_J(kr) Y_{JM}(\hat{r}) = \hat{\vec{L}}\,(\vec{\nabla}^2 + k^2) f_J(kr) Y_{JM}(\hat{r}) = \\ = \boxed{\begin{array}{c}\text{because the function } f_J(kr)Y_{JM}(\hat{r}),\text{ where}\\ f_J(kr) \text{ is sph. Bessel or Neumann function,}\\ \text{is a solution of (2.17)}\end{array}} = 0$$

Moreover, vector $\hat{\vec{L}} f_J(kr) Y_{JM}(\hat{r})$ fulfil the transverse calibration condition $\vec{\nabla}\cdot\vec{A}(\vec{r},t) = 0$ because:

$$\vec{\nabla}\cdot\hat{\vec{L}} f_J(kr) Y_{JM}(\hat{r}) = \vec{\nabla}\cdot(-i\,\vec{r}\times\vec{\nabla})\, f_J(kr) Y_{JM}(\hat{r}) = \\ = \boxed{\begin{array}{c}\text{because}\\ \Rightarrow\ \vec{\nabla}\cdot(-i\vec{r}\times\vec{\nabla})\vec{A} = 0\end{array}} = 0$$

So, we obtain the first transverse solution of the wave function (2.15) given by the vector $\hat{\vec{L}} f_J(kr) Y_{JM}(\hat{r}) e^{-i\omega t}$ which, after the suitable renormalization by a factor $\frac{1}{\sqrt{J(J+1)}}$, is:

$$\vec{A}^{(mag)}_{JM}(\vec{r},t) \equiv \frac{1}{\sqrt{J(J+1)}}\hat{\vec{L}}\, f_J(kr)\, Y_{JM}(\hat{r})\, e^{-i\omega t} = \\ = f_J(kr)\,\vec{Y}_{JJM}(\hat{r})\, e^{-i\omega t} \qquad (2.25)$$

2. For the searching of the second transverse solution of the wave equation we start with the vector:

$$(\vec{\nabla}\times\hat{\vec{L}})\, f_J(kr) Y_{JM}(\hat{r}) = \boxed{\begin{array}{c}\text{see}\\(A.64)\end{array}} = \qquad (2.26)$$
$$= \sqrt{J(J+1)}\,(\vec{\nabla}\times f_J(kr)\,\vec{Y}_{JJM}(\hat{r}))$$

Again it is possible to show that $[(\vec{\nabla} \times \hat{\vec{L}}),\ \vec{\nabla}^2] = 0$ and therefore that the vector (2.26) is the solution of the equation (2.17). The vector (2.26) also fulfils the transverse calibration condition (2.14) because:

$$\vec{\nabla} \cdot (\vec{\nabla} \times \hat{\vec{L}})\, f_J(kr)\, Y_{JM}(\hat{r}) = \boxed{\begin{array}{c}\text{because} \\ div\ rot\ \vec{a} = 0\end{array}} = 0$$

So, for given values of J and M we found the second transverse solution of the wave equation (2.15) (again suitable normalized):

$$\vec{A}^{(el)}_{JM}(\vec{r},t) \equiv \frac{1}{k\,\sqrt{J(J+1)}}\,(\vec{\nabla} \times \hat{\vec{L}})\, f_J(kr) Y_{JM}(\hat{r})\, e^{-i\omega t} =$$

$$\boxed{\begin{array}{c}\text{see} \\ (2.25)\end{array}} =$$

$$= \frac{1}{k}\,(\vec{\nabla} \times \vec{A}^{(mag)}_{JM}(\vec{r},t)) = \frac{1}{k}\,(\vec{\nabla} \times f_J(kr)\,\vec{Y}_{JJM}(\hat{r}))\, e^{-i\omega t} =$$

$$\boxed{\begin{array}{c}\text{see} \\ (A.63)\end{array}} =$$

$$= \frac{i}{k}\,[\quad (\frac{d}{dr} - \frac{J}{r})\, f_J(kr)\,\sqrt{\frac{J}{2J+1}}\,\vec{Y}_{J+1\,J\,M}(\hat{r}) +$$

$$(\frac{d}{dr} + \frac{J+1}{r})\, f_J(kr)\,\sqrt{\frac{J+1}{2J+1}}\,\vec{Y}_{J-1\,J\,M}(\hat{r})\quad]\, e^{-i\omega t} \tag{2.27}$$

Since $f_J(kr)$ represents spherical Bessel or Neumann function fulfilling the following identity

$$\begin{aligned}\frac{d}{dr}\, f_J(kr) &= \frac{J}{r}\, f_J(kr) - k\, f_{J+1}(kr) = \\ &= -\frac{J+1}{r}\, f_J(kr) + k\, f_{J-1}(kr)\end{aligned} \tag{2.28}$$

the solution $\vec{A}^{(el)}_{JM}(\vec{r},t)$ in (2.27) can be rewritten as follows

$$\begin{aligned}\vec{A}^{(el)}_{JM}(\vec{r},t) &= i\,\left\{\sqrt{\frac{J+1}{2J+1}}\, f_{J-1}(kr)\,\vec{Y}_{J-1\,J\,M}(\hat{r})\right. \\ &\quad \left. -\sqrt{\frac{J}{2J+1}}\, f_{J+1}(kr)\,\vec{Y}_{J+1\,J\,M}(\hat{r})\right\}\, e^{-i\omega t}\end{aligned} \tag{2.29}$$

It can be seen from the second row of (2.27) that the solutions $\vec{A}^{(el)}_{JM}(\vec{r},t)$ and $\vec{A}^{(mag)}_{JM}(\vec{r},t)$ are mutually orthogonal.

3. Now we will construct the third solution of the wave equation (2.15) which is orthogonal to both $\vec{A}^{(el)}_{JM}(\vec{r},t)$ and $\vec{A}^{(mag)}_{JM}(\vec{r},t)$. Let us take a vector $\vec{\nabla}\, f_J(kr)\, Y_{JM}(\hat{r})$. This vector is the solution of (2.17):

$$(\vec{\nabla}^2 + k^2)\, \vec{\nabla}\, f_J(kr)\, Y_{JM}(\hat{r}) = \vec{\nabla}\, (\vec{\nabla}^2 + k^2)\, f_J(kr)\, Y_{JM}(\hat{r}) =$$

$$= \boxed{\begin{array}{c}\text{because the function } f_J(kr)Y_{JM}(\hat{r}), \text{ where} \\ f_J(kr) \text{ is sph. Bessel or Neumann function,} \\ \text{is a solution of (2.17)}\end{array}} = 0$$

However, the vector $\vec{\nabla}\, f_J(kr)\, Y_{JM}(\hat{r})$ does not fulfil the transverse calibration condition $\vec{\nabla}\cdot\vec{A}(\vec{r},t) = 0$:

$$\begin{aligned}\vec{\nabla}\cdot\vec{\nabla}\, f_J(kr)\, Y_{JM}(\hat{r}) &= \boxed{\begin{array}{c}\text{because} \\ (\vec{\nabla}^2 + k^2)\, f_J(kr)\, Y_{JM}(\hat{r}) = 0\end{array}} = \\ &= -\,k^2\, f_J(kr)\, Y_{JM}(\hat{r}) \neq 0\end{aligned}$$

From the vector $\vec{\nabla}\, f_J(kr)\, Y_{JM}(\hat{r})$ we can construct the solution of the wave equation (2.15) (suitable normalized):

$$\begin{aligned}\vec{A}^{(long)}_{JM}(\vec{r},t) &= \frac{1}{k}\,\vec{\nabla}\, f_J(kr)\, Y_{JM}(\hat{r})\, e^{-i\omega t} = \boxed{\begin{array}{c}\text{see} \\ (A.62)\end{array}} = \\ &= \left\{ \sqrt{\frac{J}{2J+1}}\, f_{J-1}(kr)\, \vec{Y}_{J-1\,J\,M}(\hat{r}+ \right. \\ &\quad \left. \sqrt{\frac{J+1}{2J+1}}\, f_{J+1}(kr)\, \vec{Y}_{J+1\,J\,M}(\hat{r},t) \right\} e^{-i\omega t}\end{aligned} \tag{2.30}$$

Using (2.30), (2.29), (2.25) together with (A.65), (A.63) it is possible to show that the solution $\vec{A}^{(long)}_{JM}(\vec{r},t)$ is orthogonal to solutions $\vec{A}^{(el)}_{JM}(\vec{r},t)$ and $\vec{A}^{(mag)}_{JM}(\vec{r},t)$ (see also the discussion below).

So, we found a complete set of the solutions of the wave equation (2.15): $\vec{A}^{(mag)}_{JM}(\vec{r},t)$ (see(2.25)), $\vec{A}^{(el)}_{JM}(\vec{r},t)$ (see (2.29)), $\vec{A}^{(long)}_{JM}(\vec{r},t)$ (see (2.30), with $J = 1,\ldots,\infty$ and $M = -J,\ldots,J$. The first two, $\vec{A}^{(el)}_{JM}(\vec{r},t)$ and $\vec{A}^{(mag)}_{JM}(\vec{r},t)$,

fulfil the transverse calibration condition (2.14) ($\vec{\nabla} \cdot \vec{A}(\vec{r},t) = 0$) while the third one, does not fulfil. From (A.65) it follows that all these three vectors (for given J and M) are mutually orthogonal ($\vec{n} \equiv \frac{\vec{k}}{k}$):

$$\vec{n} \cdot \vec{A}^{(mag)}_{JM}(\vec{r},t) = \frac{1}{\sqrt{J(J+1)}} \frac{1}{k} \vec{k} \cdot \hat{\vec{L}} f_J(kr)\, Y_{JM}(\hat{r})\, e^{-i\omega t} =$$

$$= \boxed{\begin{array}{c}\text{because} \\ \vec{k} \cdot \hat{\vec{L}} = 0\end{array}} = 0$$

$$\vec{n} \cdot \vec{A}^{(el)}_{JM}(\vec{r},t) \;\; = \frac{1}{\sqrt{J(J+1)}} \frac{1}{k} \vec{k} \cdot (\vec{\nabla} \times \hat{\vec{L}}) f_J(kr)\, Y_{JM}(\hat{r})\, e^{-i\omega t} = 0$$

$$\vec{n} \cdot \vec{A}^{(long)}_{JM}(\vec{r},t) \neq 0 \tag{2.31}$$

So, the vector $\vec{A}^{(long)}_{JM}(\vec{r},t)$ is parallel to the vector $\vec{k}$ (the photon linear moment) and that is why this solution is called longitudinal while the transverse sulutions $\vec{A}^{(mag)}_{JM}(\vec{r},t)$ and $\vec{A}^{(el)}_{JM}(\vec{r},t)$ are perpendicular to $\vec{k}$.

Since vectors $\vec{A}^{(el)}_{JM}(\vec{r},t)$, $\vec{A}^{(mag)}_{JM}(\vec{r},t)$, and $\vec{A}^{(long)}_{JM}(\vec{r},t)$ are orthogonal each other and all of them (for all J and M) are solutions of the wave equation (2.15) and since they form the complete set every general solution of (2.15) can be expanded into these complete set of solutions. If we search for the solutions of (2.15) corresponding to the transverse calibration condition $\vec{\nabla} \cdot \vec{A}(\vec{r},t) = 0$ (real photons) then this expansion involves only transverse spherical waves $\vec{A}^{(el)}_{JM}(\vec{r},t)$ and $\vec{A}^{(mag)}_{JM}(\vec{r},t)$.

2.1.1.3 Solution of wave equation - plane waves

Spherical waves $\vec{A}^{(el)}_{JM}(\vec{r},t)$, $\vec{A}^{(mag)}_{JM}(\vec{r},t)$, $\vec{A}^{(long)}_{JM}(\vec{r},t)$ for $J = 1, \ldots, \infty$ and $M = -J, \ldots, +J$ are not the only complete orthogonal set of the solutions of the wave equation (2.15). The other set of solutions can be constructed from plane waves

$$\vec{A}_{\vec{k}}(\vec{r},t) = \vec{A}_0\, e^{\pm i\,(\vec{k}\vec{r} - \omega t)} \tag{2.32}$$

The substiution of (2.32) into the wave equation (2.15) gives:

$$k^2 = \frac{\omega^2}{c^2} \tag{2.33}$$

So, if $k = \omega/c$ then the plane waves (2.32) fulfil the wave equation (2.15).

Similarly as in the case of spherical waves we want to discuss real photons, that means the transverse calibration condition $\vec{\nabla} \cdot \vec{A}(\vec{r}, t) = 0$ is suposed. This gives the perpendicularity of $\vec{A}_{\vec{k}}(\vec{r}, t)$ and $\vec{k}$:

$$\vec{\nabla} \cdot \vec{A}_{\vec{k}}(\vec{r}, t) = \boxed{\begin{array}{c}\text{see}\\ (2.32)\end{array}} = \pm\, \vec{k} \cdot \vec{A}_{\vec{k}}(\vec{r}, t) = 0$$

$$\Longrightarrow \qquad k_1\, A_{\vec{k},\,1} + k_2\, A_{\vec{k},\,2} + k_3\, A_{\vec{k},\,3} = 0 \tag{2.34}$$

This means that for given direction of the linear momentum $\hbar\vec{k}$ of the photon only two components of the vector potential are independent (result of the tranverse calibration condition).

For further discussions two coordinate frames will be introduced:

- the coordinate frame $(x\,',\ y\,',\ z\,')$ when the $z\,'-$ axis is parallel to the vector $\vec{k}$:

$$\vec{e}_{x\,'} = \begin{pmatrix} 1 \\ 0 \\ 0 \end{pmatrix} \qquad \vec{e}_{y\,'} = \begin{pmatrix} 0 \\ 1 \\ 0 \end{pmatrix} \qquad \vec{e}_{z\,'} = \begin{pmatrix} 0 \\ 0 \\ 1 \end{pmatrix} \,||\, \vec{k}$$

- the general coordinate frame $(x,\ y,\ z)$ when $\vec{k}$ is not parallel to $z-$ axis

Linearly polarized plane waves

We suppose that we work in the coordinate frame $(x\,',\ y\,',\ z\,')$. Then from (2.34) it follows that $A_{\vec{k},\,z\,'} = 0$ and generally the vector $\vec{A}_{\vec{k}}$ should lie on the plane perpendicular to $\vec{e}_{z\,'}$. The general transverse solution $\vec{A}_{\vec{k}}(\vec{r}\,', t)$ of the wave equation expressed in the frame $(x\,',\ y\,',\ z\,')$ is a linear combination of the vectors:

$$\begin{aligned} \vec{A}_{\vec{k},\,x\,'}(\vec{r}\,', t) &= C_k\, \vec{e}_{x\,'}\, e^{i\,(\vec{k}\vec{r}\,' - \omega t)} \;\rightarrow\; \begin{array}{c}\text{linearly polarized wave}\\ \text{in the direction of } \vec{e}_{x\,'}\end{array} \\ \vec{A}_{\vec{k},\,y\,'}(\vec{r}\,', t) &= C_k\, \vec{e}_{y\,'}\, e^{i\,(\vec{k}\vec{r}\,' - \omega t)} \;\rightarrow\; \begin{array}{c}\text{linearly polarized wave}\\ \text{in the direction of } \vec{e}_{y\,'}\end{array} \end{aligned} \tag{2.35}$$

Since vectors $\vec{e}_{x\,'}$, $\vec{e}_{y\,'}$, $\vec{e}_{z\,'}$ form the orthonormal basis and since $\vec{k}$ is parallel to $\vec{e}_{z\,'}$ the following relation valids (see also (2.33)

$$\vec{k} = \frac{\omega}{c}\,(\vec{e}_{x\,'} \times \vec{e}_{y\,'}) \tag{2.36}$$

Coefficient C_k in (2.35) is a normalization factor which will be discussed later.

Circularly polarized plane wave

From the Appendix A (see (A.56) and (A.59)) we know that instead of vectors $\vec{e}_{x\,\prime}$, $\vec{e}_{y\,\prime}$ and $\vec{e}_{z\,\prime}$ (unit vectors in the directions of coordinate axes) we can take basis of vectors $\vec{\xi}_\mu$, $\mu = 0, \pm 1$:

$$\begin{aligned} \vec{\xi}_{+1} &= -\frac{1}{\sqrt{2}}\,(\vec{e}_{x\,\prime} + i\,\vec{e}_{y\,\prime}) \\ \vec{\xi}_0 &= \vec{e}_{z\,\prime} \\ \vec{\xi}_{-1} &= \frac{1}{\sqrt{2}}\,(\vec{e}_{x\,\prime} - i\,\vec{e}_{y\,\prime}) \end{aligned} \tag{2.37}$$

which are the eigenvectors of operators $\hat{\vec{S}}^{\,2}$ and $\hat{S}_{z\,\prime}$

$$\begin{aligned} \hat{\vec{S}}^{\,2}\,\vec{\xi}_\mu &= 2\,\vec{\xi}_\mu \\ \hat{S}_{z\,\prime}\,\vec{\xi}_\mu &= \mu\;\vec{\xi}_\mu \end{aligned} \tag{2.38}$$

We can perform the same transition like the one: $\vec{e}_{x\,\prime}$, $\vec{e}_{y\,\prime}$ and $\to \vec{\xi}_{+1}$, $\vec{\xi}_{-1}$ and instead of linearly polarized transverse plane waves $\vec{A}_{\vec{k},\,x\,\prime}(\vec{r}\,',t)$, $\vec{A}_{\vec{k},\,y\,\prime}(\vec{r}\,',t)$ (see (2.35) introduce so called circularly polarized plane waves $\vec{A}_{\vec{k},\,\tau=+1}(\vec{r}\,',t)$, $\vec{A}_{\vec{k},\tau=-1}(\vec{r}\,',t)$:

$$\begin{aligned} \vec{A}_{\vec{k},\,\tau=+1}(\vec{r}\,',t) &= C_k\,\vec{\xi}_{+1}e^{\,i\,(\vec{k}\vec{r}\,'-\omega t)} \;\to\; \text{right hand circularly polarized wave - spin of the photon is parallel to } \vec{e}_{z\,\prime} \\ \vec{A}_{\vec{k},\,\tau=-1}(\vec{r}\,',t) &= C_k\,\vec{\xi}_{-1}e^{\,i\,(\vec{k}\vec{r}\,'-\omega t)} \;\to\; \text{left hand circularly polarized wave - spin of the photon is antiparallel to } \vec{e}_{z\,\prime} \end{aligned} \tag{2.39}$$

It is necessary to realize that real photons correspond to the transverse calibrated vector potential ($\vec{k}\cdot\vec{A} = 0$ - see (2.34)). This means that from three basis vectors for given $\vec{k}$: $\vec{A}_{\vec{k},\,x\,\prime}$, $\vec{A}_{\vec{k},\,y\,\prime}$ $\vec{A}_{\vec{k},\,z\,\prime}$ or $\vec{A}_{\vec{k},\,\tau=+1}$, $\vec{A}_{\vec{k},\,\tau=-1}$ $\vec{A}_{\vec{k},\,\tau=0}$ always only two of them, $\vec{A}_{\vec{k},\,x\,\prime}$, $\vec{A}_{\vec{k},\,y\,\prime}$ for linearly polarized waves or $\vec{A}_{\vec{k},\,\tau=+1}$, $\vec{A}_{\vec{k},\,\tau=-1}$ for circularly polarized waves, have real physical sense (e.g. $\vec{A}_{\vec{k},\,\tau=0}$

is zero for real photon) [2].

The physical geometrical interpretation of the circularly polarized el.mg. waves follows e.g. from the time dependence of $x\,'$- and $y\,'$-components of the electric intensity $\vec{E}_{\vec{k},\,\tau}(\vec{r}\,',t)$. Let us take e.g. the right hand circularly polarized wave:

$$\vec{A}_{\vec{k},\,\tau=+1}(\vec{r}\,',t) = C_k\,\vec{\xi}_{+1}e^{i\,(\vec{k}\cdot\vec{r}\,'-\omega t)} = C_k\,e^{i\,(\vec{k}\cdot\vec{r}\,'-\omega t)}\,(-\frac{1}{\sqrt{2}})(\vec{e}_{x'}+i\,\vec{e}_{y\,'})$$

with the following $x\,'$- and $y\,'$- components:

$$(\vec{A}_{\vec{k},\,+1})_{x\,'} = -\tfrac{1}{\sqrt{2}}\,C_k e^{i\,(\vec{k}\cdot\vec{r}\,'-\omega t)} \quad , \qquad (\vec{A}_{\vec{k},\,+1})_{y\,'} = -\tfrac{i}{\sqrt{2}}\,C_k\,e^{i\,(\vec{k}\cdot\vec{r}\,'-\omega t)}$$

Corresponding intensity of the electric field $(\vec{E}_{\vec{k},\,+1}) =$ (see (2.4) with $\varphi = 0$) $= -\frac{\partial \vec{A}_{\vec{k},\,+1}}{\partial t}$ should be real and therefore usually the electric intensity is given by: $\vec{E}_{\vec{k},\,+1} = -\frac{\partial}{\partial t}(\vec{A}_{\vec{k},\,+1} + \vec{A}^{*}_{\vec{k},\,+1}) \Rightarrow$ corresponding components are:

$$\begin{aligned}
(\vec{E}_{\vec{k},\,+1})_{x\,'} &= -\frac{\partial}{\partial t}(\vec{A}_{\vec{k},\,+1} + \vec{A}^{*}_{\vec{k},\,+1})_{x\,'} = \sqrt{2}\,C_k\,\omega\,sin(\vec{k}\vec{r}\,' - \omega t) \\
(\vec{E}_{\vec{k},\,+1})_{y\,'} &= -\frac{\partial}{\partial t}(\vec{A}_{\vec{k},\,+1} + \vec{A}^{*}_{\vec{k},\,+1})_{y\,'} = \sqrt{2}\,C_k\,\omega\,cos(\vec{k}\vec{r}\,' - \omega t) \\
(\vec{E}_{\vec{k},\,+1})_{z\,'} &= -\frac{\partial}{\partial t}(\vec{A}_{\vec{k},\,+1} + \vec{A}^{*}_{\vec{k},\,+1})_{z\,'} = 0
\end{aligned} \tag{2.40}$$

From this expressions it follows that in the cut by the plane (x', y') the vector $\vec{E}_{\vec{k},\,+1}(\vec{r}\,',t)$ rotates in the anticlockwise direction - see the Fig. 2.1.

So, the right hand circularly polarized wave corresponds to the photon with spin oriented along its linear momentum (positive helicity) and left hand circular wave represents the photon with spin antiparallel with the linear momentum (negative helicity)- see (2.37), (2.38).

Further the normalization constant C_k will be determined (see (2.35), (2.39)). This constant is related to the normalization of the plane wave $\vec{A}_{\vec{k}}(\vec{r}\,',t)$. One can see from (2.35), (2.39) that general plane wave $\vec{A}_{\vec{k}}(\vec{r}\,',t)$ is a periodical function in coordinate components and time:

$$\vec{A}_{\vec{k}}(x\,'+L,\,y\,'+L,\,z\,'+L,t) = \vec{A}_{\vec{k}}(x\,',\,y\,',\,z\,',t)$$

[2] In the relativistic quantum field theories the space z'-component of the vector potential $\vec{A}_{\vec{k}}$ and its time-component do not contribute to the real energy of the electromagnetic field and therefore both these components are relevant only to virtual intermediate photons (Gupta-Bleuler theory) - see e.g. [13]

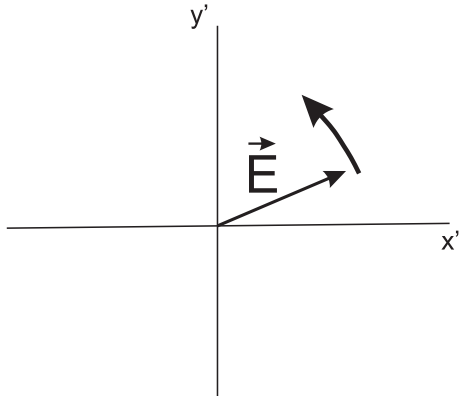


Figure 2.1: For given $z\,'$ the vector $\vec{E}_{\vec{k},\,\tau=+1}(\vec{r}\,',t)$ rotates in the $(x\,',y\,')$ plane in the anti-clockwise direction with time.

where L is the periodicity constant or the wave length. The substitution of (2.35) or (2.39) gives:

$$e^{i\,(\vec{k}\vec{r}\,'-\omega t)}\;e^{i\,L\,(k_{x\,'}+k_{y\,'}+k_{z\,'})}=e^{i\,(\vec{k}\vec{r}\,'-\omega t)}$$
$$\Rightarrow e^{i\,L\,(k_{x\,'}+k_{y\,'}+k_{z\,'})}=1=e^{i\,2\pi\,(n_x+n_y+n_z)}$$

where $n_x,\ n_y,\ n_z$ are any integer numbers. Therefore we have:

$$k_{x\,'}=\frac{2\pi}{L}\,n_x\qquad k_{y\,'}=\frac{2\pi}{L}\,n_y\qquad k_{z\,'}=\frac{2\pi}{L}\,n_z$$
$$\Rightarrow(n_x,\ n_y,\ n_z)\ =\ \frac{L}{2\pi}\,(k_{x\,'},\ k_{y\,'},\ k_{z\,'})$$
$$\Rightarrow k=|\vec{k}|=\frac{2\pi}{L}\,\sqrt{n_x^2+n_y^2+n_z^2}\qquad(2.41)$$

It seems from (2.41) that all results based on (2.41) depends on the choice of the box side L. However, as it will be seen farther, the final physical results do not depend on L

From (2.41) one can see that the photon linear momentum is discretized. Each three numbers $(n_x,\ n_y,\ n_z)$ determine one linear momentum state $\vec{k}=(k_{x\,'},\ k_{y\,'},\ k_{z\,'})$. The number of linear momentum states corresponding to the linear momentum space element $k^2\,dk\,d\Omega_k=k^2\,dk\,\hat{dk}$ is (according to (2.41) one linear momentum state occupies the volume $(2\pi)^3$ in the linear momentum space of the vector $\vec{k}$):

$$dn=\frac{L^3}{(2\pi)^3}\,d^3k=\frac{L^3}{(2\pi)^3}\,k^2\,\hat{dk}\,dk\qquad(2.42)$$

By other words dn represents the number of photons with the linear momentum in the interval $<k,\ k+dk>$ which fly to the space angle $\hat{dk}=d\Omega_k$.

Circularly polarized wave is usually normalized by the assumption that $\vec{A}_{\vec{k},\,\tau}(\vec{r}\,',t)+\vec{A}^{*}_{\vec{k},\,\tau}(\vec{r}\,',t)$ represents one photon in the box with the volume L^3 with its center in the point $\vec{r}\,'$. The energy of such a photon is (we assume that the side L of the box is so small that the $\vec{r}\,'$- dependence of electric and magnetic intensities is negligible inside the box) [3] :

$$\begin{aligned}
\hbar\,\omega &= \boxed{\begin{array}{c}\text{because the energy density}\\ \text{is } \frac{1}{2}\,(\vec{E}\cdot\vec{D}+\vec{H}\cdot\vec{B})\end{array}} = \\
&= \frac{1}{2}\int_{box}\left(\vec{E}\cdot\vec{D}+\vec{H}\cdot\vec{B}\right)\,d^3r = \\
&= \frac{1}{2}\int_{box}\left(\epsilon_0\,\vec{E}^2+\frac{\vec{B}^2}{\mu_0}\right)\,d^3r = \frac{1}{2\mu_0}\int_{box}\left(\frac{\vec{E}^2}{c^2}+\vec{B}^2\right)\,d^3r = \\
&= \boxed{\begin{array}{c}\text{because for plane wave (see footnote [3])}\\ \vec{B}^2=\vec{E}^2/c^2=2\,C_k^2\,\omega^2/c^2\end{array}} = \\
&= \frac{1}{\mu_0\,c^2}\,2\,C_k^2\,\omega^2\,L^3=\epsilon_0\,C_k^2\,2\,\omega^2\,L^3
\end{aligned} \tag{2.43}$$

So

$$C_k=\sqrt{\frac{\hbar}{2\,\epsilon_0\,L^3\,\omega}} \tag{2.44}$$

And the circularly plarized waves $\vec{A}_{\vec{k},\,\tau=0,\pm1}(\,\vec{r}\,',t)$ are written in the form:

$$\vec{A}_{\vec{k},\,\tau=0,\pm1}(\,\vec{r}\,',t)=\sqrt{\frac{\hbar}{2\epsilon_0 L^3\omega}}\,\vec{\xi}_\tau\,e^{i\,(\vec{k}\vec{r}\,'-\omega t)} \tag{2.45}$$

Vectors (2.45) for $\vec{k}\equiv(k_{x\,'},\,k_{y\,'},\,k_{z\,'})$, $k_{x\,',\,y\,',\,y\,'}\in(-\infty,\,\infty)$ and for $\tau=0,\pm1$ form the complete basis of the general solutions of the wave equation (2.15). If

[3] Similarly like in (2.40) for electric intensity of the plane wave the magnetic induction components are:

$$\begin{aligned}
(\vec{B}_{\vec{k},+1})_{x\,'} &= \left(\frac{\partial}{\partial y\,'}(\vec{A}_{\vec{k},+1}+\vec{A}^{*}_{\vec{k},+1})_{z\,'}-\frac{\partial}{\partial z\,'}(\vec{A}_{\vec{k},+1}+\vec{A}^{*}_{\vec{k},+1})_{y\,'}\right)=-\sqrt{2}\,C_k\,k\,cos(\vec{k}\vec{r}\,'-\omega t)\\
(\vec{B}_{\vec{k},+1})_{y\,'} &= \left(\frac{\partial}{\partial y\,'}(\vec{A}_{\vec{k},+1}+\vec{A}^{*}_{\vec{k},+1})_{x\,'}-\frac{\partial}{\partial x\,'}(\vec{A}_{\vec{k},+1}+\vec{A}^{*}_{\vec{k},+1})_{y\,'}\right)=\sqrt{2}\,C_k\,k\,sin(\vec{k}\vec{r}\,'-\omega t)\\
(\vec{B}_{\vec{k},+1})_{z\,'} &= \left(\frac{\partial}{\partial x\,'}(\vec{A}_{\vec{k},+1}+\vec{A}^{*}_{\vec{k},+1})_{y\,'}-\frac{\partial}{\partial y\,'}(\vec{A}_{\vec{k},+1}+\vec{A}^{*}_{\vec{k},+1})_{x\,'}\right)=0
\end{aligned}$$

Therefore (see (2.40))

$$\vec{B}^2=2\,C_k^2\,k^2=\frac{\vec{E}^2}{c^2}$$

we want to restrict ourselves only to the solutions with transverse calibration condition (2.14) then this basis is formed only by vectors (2.45) with $\tau = \pm 1$. So, each solution of (2.15) can be written as the linear combination of vectors $\vec{A}_{\vec{k},\,\tau}(\,\vec{r}\,',t)$:

$$\begin{aligned}\vec{A}(\vec{r}\,',t) &= \sum_{\vec{k},\,\tau}\left[\vec{A}_{\vec{k},\,\tau}(\,\vec{r}\,',t)\;a_{\vec{k},\,\tau} + \vec{A}^{*}_{\vec{k},\,\tau}(\,\vec{r}\,',t)\;a^{*}_{\vec{k},\,\tau}\right] = \\ &= \sum_{\vec{k},\,\tau} C_k\;\left[\vec{\xi}_\tau\, e^{\,i\,(\vec{k}\vec{r}\,'-\omega t)}\;a_{\vec{k},\,\tau} + \vec{\xi}^{*}_\tau\, e^{-\,i\,(\vec{k}\vec{r}\,'-\omega t)}\;a^{*}_{\vec{k},\,\tau}\right] = \\ &= \sum_{\vec{k},\,\tau}\sqrt{\frac{\hbar}{2\,\epsilon_0\,L^3\,\omega}}\;\left[\vec{\xi}_\tau\, e^{\,i\,(\vec{k}\vec{r}\,'-\omega t)}\;a_{\vec{k},\,\tau} + \vec{\xi}^{*}_\tau\, e^{-\,i\,(\vec{k}\vec{r}\,'-\omega t)}\;a^{*}_{\vec{k},\,\tau}\right]\end{aligned} \tag{2.46}$$

where $a_{\vec{k},\,\tau}$ are the decay amplitudes and generally $\tau = 0,\ \pm 1$. If $\vec{A}(\vec{r}\,',t)$ is transverse calibrated field then $\tau = \pm 1$ in the sum of (2.46).

2.1.1.4 Relation between plane and spherical waves

It is kmown from the previous subsections that we have two bases of vectors - solutions of the wave equation (2.15):

- spherical waves (see (2.25), (2.29), (2.30): $\vec{A}^{(mag)}_{JM}(\vec{r}\,',t)$, $\vec{A}^{(el)}_{JM}(\vec{r}\,',t)$, $\vec{A}^{(long)}_{JM}(\vec{r}\,',t)$, where $J = 1,2,\ldots,\infty$ and $M = -J,\ldots,+J$
- circularly polarized plane waves (see (2.45): $\vec{A}_{\vec{k},+1}(\vec{r}\,',t)$, $\vec{A}_{\vec{k},0}(\vec{r}\,',t)$, $\vec{A}_{\vec{k},-1}(\vec{r}\,',t)$, with $\vec{k} \equiv (k,\vartheta,\varphi)$, $k \in <0,\infty>$, $\vartheta \in <0,\pi>$, $\varphi \in <0,2\pi>$

If we restrict ourselves on real photons then we have only transverse waves and $\vec{A}^{(long)}_{JM}(\vec{r}\,',t)$ and $\vec{A}_{\vec{k},0}(\vec{r}\,',t)$ can be removed from our considerations (because they do not fulfil the transverse calibration condition $\vec{\nabla}\cdot\vec{A}(\vec{r},t) = 0$). Each of mentioned above basis is complete and therefore each one vector from one basis can be expressed as the linear combination of the second basis. Further we will determine this linear combination.

In the searching for this linear combination the following identity is used

(see e.g. [2]):

$$e^{i\,\vec{k}\cdot\vec{r}\,'} = 4\pi \sum_{L=0}^{\infty} \sum_{M=-L}^{L} i^L\, f_L(kr\,')\, Y^*_{LM}(\hat{k})\, Y_{LM}(\hat{r}\,') =$$

$$= \boxed{\begin{array}{c}\text{because}\\ P_L(cos\vartheta) = \frac{4\pi}{2L+1} \sum_{M=-L}^{L} Y^*_{LM}(\hat{k})\, Y_{LM}(\hat{r}\,')\end{array}} =$$

$$= \sum_{L=0}^{\infty} i^L\, (2L+1)\, f_L(k\,r\,')\, P_L(cos\vartheta) =$$

$$= \boxed{\begin{array}{c}\text{in the frame } (x\,', y\,', z\,') \text{ the vector } \vec{k}\;||\;\vec{e}_{z\,'}\\ \Rightarrow \text{ the angle } \vartheta \text{ is the angle between } \vec{r}\,' \text{ and } \vec{e}_{z\,'}\end{array}} =$$

$$= \sum_{L=0}^{\infty} i^L\, (2L+1)\, f_L(k\,r\,')\, P_L(\hat{r}\,') =$$

$$= \boxed{\begin{array}{c}\text{because}\\ Y_{L0}(\hat{r}\,') = \sqrt{\frac{2L+1}{4\pi}} P_L(cos\vartheta)\end{array}} =$$

$$= \sqrt{4\pi} \sum_{L=0}^{\infty} i^L\, (2L+1)^{1/2}\, f_L(k\,r\,')\, Y_{L0}(\hat{r}\,') \qquad (2.47)$$

where $f_L(k\,r\,')$ are spherical Bessel or Neumann functions. Using (2.47) the part containing the exponent and spin function in plane waves can be rewritten as follows

$$\vec{\xi}_\tau\, e^{i\,\vec{k}\vec{r}\,'} = \sqrt{4\pi} \sum_{L=0}^{\infty} i^L\, (2L+1)^{1/2}\, f_L(k\,r\,')\, \vec{\xi}_\tau\, Y_{L0}(\hat{r}\,') =$$

$$= \boxed{\begin{array}{c}\text{definition (A.53) of the vector spherical}\\ \text{harmonics can be inverted using (A.3)}\end{array}} =$$

$$= \sqrt{4\pi} \sum_{J=0}^{\infty} \sum_{L=|J-1|}^{J+1} i^L\, (2L+1)^{1/2}\, f_L(k\,r\,')\, C^{J\,\tau}_{L\,0\,1\,\tau}\, \vec{Y}_{LJM}(\hat{r}\,') \qquad (2.48)$$

Clebsch-Gordan coefficients involved in (2.48) are (see e.g. [2])

$$\begin{aligned} C^{J\,\tau}_{J\,0\,1\,\tau} &= -\frac{\tau}{\sqrt{2}} \\ C^{J\,\tau}_{J-1\,0\,1\,\tau} &= \frac{1}{\sqrt{2}}\sqrt{\frac{J+1}{2J-1}} \\ C^{J\,\tau}_{J+1\,0\,1\,\tau} &= \frac{1}{\sqrt{2}}\sqrt{\frac{J}{2J+3}} \end{aligned} \tag{2.49}$$

The substitution of (2.49) into (2.48) and then into (2.25) and (2.29) gives final expr. for transverse calibrated vector potential in the following form:

$$\begin{aligned} \vec{A}_{\vec{k},\tau=\pm1}(\vec{r}\,',t) = &- C_k\,\sqrt{2\pi}\sum_{J=1}^{\infty} i^J\,(2J+1)^{1/2} \\ &\left[\vec{A}^{(el)}_{J\,\tau}(\vec{r}\,',t) + \tau\,\vec{A}^{(mag)}_{J\,\tau}(\vec{r}\,',t)\right] \end{aligned} \tag{2.50}$$

Relation (2.50) valids only in the frame $(x\,',y\,',z\,')$ when $\vec{e}_{z\,'} \,||\, \vec{k}$. Since $\vec{A}^{(el)}_{JM}(\vec{r}\;',t)$ and $\vec{A}^{(mag)}_{JM}(\vec{r}\;',t)$ are tensor operators from the point of view of rotations and therefore in order to transform them to the general frame (x,y,z), when $\vec{e}_z$ is not parallel to $\vec{k}$, we can use the inverse transformation of (A.39). So, we have

$$\begin{aligned} \vec{A}_{\vec{k},\tau=\pm1}(\vec{r}\,',t) = &- C_k\,\sqrt{2\pi}\sum_{JM} i^J\,(2J+1)^{1/2} \\ &\left[\vec{A}^{(el)}_{JM}(\vec{r},t) + \tau\,\vec{A}^{(mag)}_{JM}(\vec{r},t)\right]\; D^{J\,*}_{M\,\tau}(\vec{e}_z\to\vec{k}) \end{aligned} \tag{2.51}$$

where $D^{J}_{\tau\,M}(\vec{e}_z\to\vec{k})$ are Wigner D-functions of the coordinate angles of the vector $\vec{e}_z$ in the frame $(x\,',y\,',z\,')$.

2.1.2 Lagrangian and Hamiltonian of a free electromagnetic field, quantization of el.mg. field

Up to now we have solved the classic wave equation (2.15) (derived from classic Maxwell equation) and solutions in the form of spherical waves (see (2.25),(2.29)) or of plane waves (see (2.39)) were obtained. These solutions represent bases for the classic vector potential (see (2.46)) of the free electromagnetic field. Up to now in (2.46) there are no any operators which would act on photons as on the quanta of electromagnetic field. At first we should

perform a quantization of electromagnetic field and introduce creation and annihilation operators of photons. This quantization can be obtained using the procedure which starts with the classic Lagrange formalizm of any field (not only electromagnetic one). Then we can derive a conjugated linear momentum field and postulate quantum mechanics commutator relations between given field and its conjugated linear momentum field in the analogy with the commutator relation between coordinate and linear momentum. Finally, this gives us creation and annihilation operators of the corresponding quanta of given field (in our case photons as quanta of electromagnetic field). It should be noted that this quantization procedure is general and it is applicable for any field not only electroamgnetic one (see any textbook of quantum field theory - eg. [13]).

Let us consider some field described by a potential $\psi(\vec{r}, t)$. For the simplicity only one-component potential $\psi(\vec{r}, t)$ is assumed. From the classic mechanics we know that a Lagrangian of some system is a function of generalized coordinates q_i and their time-derivatives $\dot{q}_i$, $L = L(q_i,\ \dot{q}_i)$ (assuming that the Lagrangian does not depend on time explicitely). In the analogy with the classic mechanics we suppose that a Lagrangian of the field depends on ψ, $\frac{\partial\,\psi}{\partial\,x_i}$, $\frac{\partial\,\psi}{\partial\,t}$ $(i = x, y, z)$. So,

$$L = \int d^3r\ \mathscr{L}(\psi,\ \vec{\nabla}\psi,\ \dot{\psi}) = \int d^3r\ \mathscr{L}(\psi, \frac{\partial\,\psi}{\partial\,x_i},\ \frac{\partial\,\psi}{\partial\,t}) \tag{2.52}$$

where $\mathscr{L}$ is the density of the Lagrangian. The action of the field ψ is defined by the following integral (again in the analogy with the classic mechanics)

$$\mathscr{S} = \int_{t_1}^{t_2} L\,dt = \int_{t_1}^{t_2} dt\ \int d^3r\ \ \mathscr{L}(\psi,\ \vec{\nabla}\psi,\ \dot{\psi}) \tag{2.53}$$

where t_1 and t_2 are the initial and final time of the time interval in which given field is developed.

Further the variation of the action of the field ψ will be investigated. The states of the field in the initial and final time are fixed. Therefore during the time evolution of the field only variation fulfilling the following conditions are allowed

$$\delta\psi(\vec{r}, t_1) = \delta\psi(\vec{r}, t_2) = 0 \tag{2.54}$$

for any $\vec{r}$.

The time evolution of the field (field trajectory) corresponds to the mini-

mal field action when the variation of the field action is zero:

$$\begin{aligned}&\delta\mathscr{S} = \\ &= \int_{t_1}^{t_2} dt \int d^3r \left[\frac{\partial\,\mathscr{L}}{\partial\,\psi}\,\delta\psi + \sum_i \frac{\partial\,\mathscr{L}}{\partial(\frac{\partial\psi}{\partial x_i})}\,\frac{\partial}{\partial x_i}\delta\psi + \frac{\partial\,\mathscr{L}}{\partial(\frac{\partial\psi}{\partial t})}\,\frac{\partial}{\partial t}\delta\psi\right] = 0\end{aligned} \tag{2.55}$$

where we used $\delta(\frac{\partial\psi}{\partial x_i}) = \frac{\partial}{\partial x_i}\delta\psi$ and $\delta(\frac{\partial\psi}{\partial t}) = \frac{\partial}{\partial t}\delta\psi$. Using the following identities

$$\begin{aligned}\frac{\partial}{\partial x_i}\left(\frac{\partial\,\mathscr{L}}{\partial(\frac{\partial\psi}{\partial x_i})}\,\delta\psi\right) &= \left[\frac{\partial}{\partial x_i}\left(\frac{\partial\,\mathscr{L}}{\partial(\frac{\partial\psi}{\partial x_i})}\right)\right]\delta\psi + \frac{\partial\,\mathscr{L}}{\partial(\frac{\partial\psi}{\partial x_i})}\,\frac{\partial(\delta\psi)}{\partial x_i} \\ \frac{\partial}{\partial t}\left(\frac{\partial\,\mathscr{L}}{\partial(\frac{\partial\psi}{\partial x_i})}\,\delta\psi\right) &= \left[\frac{\partial}{\partial t}\left(\frac{\partial\,\mathscr{L}}{\partial(\frac{\partial\psi}{\partial t})}\right)\right]\delta\psi + \frac{\partial\,\mathscr{L}}{\partial(\frac{\partial\psi}{\partial t})}\,\frac{\partial(\delta\psi)}{\partial t}\end{aligned} \tag{2.56}$$

the equation (2.55) can be rewritten as follows

$$\begin{aligned}\delta\mathscr{S} = &\int_{t_1}^{t_2} dt \int_{(V)} d^3r \frac{\partial\,\mathscr{L}}{\partial\,\psi}\,\delta\psi + \\ &+\sum_i \int_{t_1}^{t_2} dt \int_{(V)} d^3r \left(\left[\frac{\partial}{\partial x_i}\left(\frac{\partial\,\mathscr{L}}{\partial(\frac{\partial\psi}{\partial x_i})}\delta\psi\right)\right]\right. \\ &\qquad\left. - \left[\frac{\partial}{\partial x_i}\left(\frac{\partial\,\mathscr{L}}{\partial(\frac{\partial\psi}{\partial x_i})}\right)\right]\delta\psi\right) \\ &+\sum_i \int_{t_1}^{t_2} dt \int_{(V)} d^3r \left(\left[\frac{\partial}{\partial t}\left(\frac{\partial\,\mathscr{L}}{\partial(\frac{\partial\psi}{\partial t})}\delta\psi\right)\right]\right. \\ &\qquad\left. - \left[\frac{\partial}{\partial t}\left(\frac{\partial\,\mathscr{L}}{\partial(\frac{\partial\psi}{\partial t})}\right)\right]\delta\psi\right) = 0\end{aligned} \tag{2.57}$$

The volume (V), in which our electromagnetic field is stretched (possible values of $\vec{r}$), is so big that on the surface of this volume and outside of it the field function $\psi(\vec{r},t)$ is zero for all t, that means $\psi(\vec{r},t) = 0$ for $\vec{r} \in (\Sigma)$, where Σ is the surface of the volume V. So, we can use the Gauss formule from mathematics and write the following identity

$$\sum_i \int_{(V)} d^3r\ \frac{\partial}{\partial x_i}\left(\frac{\partial\,\mathscr{L}}{\partial(\frac{\partial\psi}{\partial x_i})}\delta\psi\right) = \sum_i \int_{(\Sigma)} d\Sigma_i\,\frac{\partial\,\mathscr{L}}{\partial(\frac{\partial\psi}{\partial x_i})} = 0 \tag{2.58}$$

The other identity can be obtained from (2.54):

$$\int_{t_1}^{t_2} dt\, \frac{\partial}{\partial t}\left(\frac{\partial\, \mathscr{L}}{\partial(\frac{\partial \psi}{\partial t})}\delta\psi\right) = \frac{\partial\, \mathscr{L}}{\partial(\frac{\partial \psi}{\partial t})}\, \delta\psi|_{t_1}^{t_2} = 0 \tag{2.59}$$

Using (2.58) and (2.59) the equation (2.57) can be modified as follows

$$\delta\mathscr{S} = \int_{t_1}^{t_2} dt \int_{(V)} d^3r \left[\frac{\partial\, \mathscr{L}}{\partial\, \psi} - \sum_i \frac{\partial}{\partial x_i}\left(\frac{\partial\, \mathscr{L}}{\partial(\frac{\partial \psi}{\partial x_i})}\right) - \frac{\partial}{\partial t}\left(\frac{\partial\, \mathscr{L}}{\partial(\frac{\partial \psi}{\partial t})}\right)\right]\delta\psi = 0 \tag{2.60}$$

Since $\delta\psi$ is arbitrary, finally we have

$$\frac{\partial\, \mathscr{L}}{\partial\, \psi} - \sum_i \frac{\partial}{\partial x_i}\left(\frac{\partial\, \mathscr{L}}{\partial(\frac{\partial \psi}{\partial x_i})}\right) - \frac{\partial}{\partial t}\left(\frac{\partial\, \mathscr{L}}{\partial(\frac{\partial \psi}{\partial t})}\right) = 0 \tag{2.61}$$

The equation (2.61) represents Lagrange equation of motion for the field $\psi(\vec{r}, t)$ (analogy with the classic mechanic where the Lagrange equation is: $\frac{\partial L}{\partial q_i} - \frac{1}{\partial t}(\frac{\partial L}{\partial \dot{q}}) = 0$).

In the analogy with the clasic meachanics (when the field ψ is treated as the generalized coordinate q_i) we can introduce linear momentum field $\pi(\vec{r}, t)$ (which is treated as linear momentum p_i conjugated to coordinate q, $p_i = \frac{\partial L}{\partial \dot{q}}$):

$$\pi(\vec{r}, t) = \frac{\partial \mathscr{L}}{\partial\, (\frac{\partial \psi(\vec{r},t)}{\partial t})} \tag{2.62}$$

The process of the quantization of the field $\psi(\vec{r}, t)$ consists in the following idea. After the quantization the field $\psi(\vec{r}, t)$ becames an operator $\hat{\psi}(\vec{r}, t)$ acting in the Fock space of the occupation number for the quanta of given field (photons in the case of el.mg. field) [4]. In the quantum mechanics it is known that the coordinate and the corresponding conjugated linear momentum commutes as:

$$[\, \hat{q}_i, \hat{p}_j\,] = i\hbar\, \delta_{ij}, \quad [\, \hat{q}_i, \hat{q}_j\,] = 0, \quad [\, \hat{p}_i, \hat{p}_j\,] = 0 \tag{2.63}$$

[4]The Fock space of the occupation numbers and corresponding creation and annihilation operators are introduced in many textbooks of the quantum mechanics (see e.g. [14]). Some basic information about the Fock space of the occupation numbers for fermions can be also find in the Appendix B - subsection B.1. Here we speak about Fock space for bosons (photons) but the idea is the same as for fermions.

The quantization of our field $\psi(\vec{r},t)$ can be simply performed by the postulate of the following commutation relation between the operator of the field $\hat{\psi}(\vec{r},t)$ and the operator of corresponding conjugated linear momentum field $\hat{\pi}(\vec{r},t)$ (analogy: $\hat{q}_i \to \hat{\psi}(\vec{r},t)$ and $\hat{p}_i \to \hat{\pi}(\vec{r},t)$)

$$[\,\hat{\psi}(\vec{r},t),\,\hat{\pi}(\vec{r}\,',t)\,] = i\hbar\,\delta(\vec{r}-\vec{r}\,')$$
$$[\,\hat{\psi}(\vec{r},t),\,\hat{\psi}(\vec{r}\,',t)\,] = [\,\hat{\pi}(\vec{r},t),\,\hat{\pi}(\vec{r}\,',t)\,] = 0 \qquad (2.64)$$

It is necessary to point out that all fields and conjugated fields involved in the commutation relations (2.64) are in the same time t. The other important fact is that the quantization conditions (2.64) valids for boson fileds when corresponding quanta are bosons (as it is for electromagnetic field where corresponding quanta are photons with the spin S=1).

So, after the quantization process the field $\hat{\psi}(\vec{r}.t)$ and its derivatives $\frac{\partial\hat{\psi}}{\partial t}$ and $\frac{\partial\hat{\psi}}{\partial x_i}$ are operators. Therefore the Lagrangian density $\mathscr{L}(\hat{\psi},\,\frac{\partial\hat{\psi}}{\partial x_i},\,\frac{\partial\hat{\psi}}{\partial t})$ is also an operator. In the analogy with the classic mechanics ($\psi(\vec{r},t) \leftrightarrow q_i,\ \pi(\vec{r},t) \leftrightarrow p_i,\ H = \sum_i p_i\,\dot{q}_i - L(q_i,\dot{q}_i)$) we can introduce the operator of the Hamiltonian density $\hat{\mathscr{H}}(\vec{r},t)$ corresponding to the field operator $\hat{\psi}(\vec{r},t)$:

$$\hat{\mathscr{H}}(\vec{r},t) = \hat{\pi}(\vec{r},t)\,\dot{\hat{\psi}}(\vec{r},t) - \hat{\mathscr{L}}(\vec{r},t) \qquad (2.65)$$

with its Hamiltonian:

$$\hat{H} = \int d^3r\,\hat{\mathscr{H}}(\vec{r},t) \qquad (2.66)$$

In many cases (like for el.mg. field) the field is not described by a one-dimensions function $\psi(\vec{r},t)$ but by many-component function (potential) $\psi_\alpha(\vec{r},t), \alpha = 1,\ldots,\,p$. In such a case the Lagrangian and Hamiltonian densities and corresponding Lagrange equation are (generalization of relations (2.61), (2.62), (2.64), (2.65)):

$$\mathscr{L} = \mathscr{L}(\psi_\alpha,\,\frac{\partial\psi_\alpha}{\partial\,x_i},\,\frac{\partial\psi_\alpha}{\partial\,t}), \qquad \pi_\alpha(\vec{r},t) = \frac{\partial\mathscr{L}}{\partial\,(\frac{\partial\,\psi_\alpha}{\partial\,t})}$$
$$\frac{\partial\mathscr{L}}{\partial\psi_\alpha} - \sum_i \frac{\partial}{\partial x_i}\left(\frac{\partial\,\mathscr{L}}{\partial(\frac{\partial\psi_\alpha}{\partial x_i})}\right) - \frac{\partial}{\partial t}\left(\frac{\partial\,\mathscr{L}}{\partial(\frac{\partial\psi_\alpha}{\partial t})}\right) = 0$$

$$\hat{\mathscr{H}}(\vec{r},t) = \sum_\alpha \hat{\pi}_\alpha(\vec{r},t)\,\dot{\hat{\psi}}_\alpha(\vec{r},t) - \hat{\mathscr{L}}(\vec{r},t)$$
$$\Big[\,\hat{\psi}_\alpha(\vec{r},t),\,\hat{\pi}_\beta(\vec{r}\,',t)\,\Big] = i\hbar\ \delta_{\alpha\,\beta}\ \delta(\vec{r}-\vec{r}\,') \qquad (2.67)$$

Now, we can go back to the electromagnetic field and derive the densities of Lagrangian and Hamiltonian for el.mg. field and show how the electromagnetic field can be quantized. Provided the transverse calibration condition ($\varphi = 0,\ \vec{\nabla} \cdot \vec{A}(\vec{r},t) = 0$) the electromagnetic field is described by three-component function (vector potential) $\vec{A}(\vec{r},t) \equiv (A_k(\vec{r},t),\ k = 1,2,3)$. The corresponding equation of motion is represented by the wave equation (2.15) (which was solved in previous subsections):

$$\vec{\nabla}^2 \vec{A} - \frac{1}{c^2}\frac{\partial^2 \vec{A}}{\partial t^2} = 0 \tag{2.68}$$

with corresponding measurable quantities, electric intensity $\vec{E}(\vec{r},t)$ and magnetic induction $\vec{B}(\vec{r},t)$:

$$\vec{E} = -\frac{\partial \vec{A}}{\partial t}, \qquad \vec{B} = \vec{\nabla} \times \vec{A}$$

Our task is to find the density Lagrangian of our electromagnetic field which gives the Lagrange equation precisely in the same form as the wave equation (2.15) is. If we take the density of Lagrangian in the following form

$$\begin{aligned} &\mathscr{L}_{elmg}(A_k,\ \frac{\partial A_k}{\partial x_i},\ \frac{\partial A_k}{\partial t}) = \frac{1}{2}\left[\vec{E}\cdot\vec{D} - \vec{H}\cdot\vec{B}\right] = \\ &= \frac{1}{2}\left[\epsilon_0\,\dot{\vec{A}}^2(\vec{r},t) - \frac{1}{2\,\mu_0}\sum_{k\,l}\left(\frac{\partial A_l}{\partial x_k} - \frac{\partial A_k}{\partial x_l}\right)^2\right] \end{aligned} \tag{2.69}$$

then, really, the Lagrange equation

$$\frac{\partial \mathscr{L}_{elmg}}{\partial A_k} - \sum_i \frac{\partial}{\partial x_i}\left(\frac{\partial\,\mathscr{L}_{elmg}}{\partial(\frac{\partial A_k}{\partial x_i})}\right) - \frac{\partial}{\partial t}\left(\frac{\partial\,\mathscr{L}_{elmg}}{\partial(\frac{\partial A_k}{\partial t})}\right) = 0 \tag{2.70}$$

gives the wave equation (2.68):

$$\frac{\partial \mathscr{L}_{elmg}}{\partial A_k} = 0 \qquad\qquad \frac{\partial \mathscr{L}_{elmg}}{\partial \dot{A}_k} = \epsilon_0 \, \dot{A}_k$$
$$\frac{\partial \mathscr{L}_{elmg}}{\partial(\frac{\partial A_k}{\partial x_i})} = -\frac{1}{\mu_0} \left(\frac{\partial A_k}{\partial x_i} - \frac{\partial A_i}{\partial x_k} \right)$$

$$\Longrightarrow$$

$$\frac{\partial \mathscr{L}_{elmg}}{\partial A_k} - \sum_i \frac{\partial}{\partial x_i} \left(\frac{\partial \mathscr{L}_{elmg}}{\partial(\frac{\partial A_k}{\partial x_i})} \right) - \frac{\partial}{\partial t} \left(\frac{\partial \mathscr{L}_{elmg}}{\partial(\frac{\partial A_k}{\partial t})} \right) =$$
$$= \frac{1}{\mu_0} \sum_i \frac{\partial}{\partial x_i} \left(\frac{\partial A_k}{\partial x_i} - \frac{\partial A_i}{\partial x_k} \right) - \epsilon_0 \, \ddot{A}_k =$$
$$= \frac{1}{\mu_0} \sum_i \frac{\partial^2 A_k}{\partial x_i^2} - \epsilon_0 \, \ddot{A}_k = 0$$

and it is (2.68). So, Lagrangian (2.69) is really Lagrangian of the free electromagnetic field because it gives the evolution equation which fully coincides with the standard wave equation of el.mg. field.

The linear momentum field $\vec{\Pi}(\vec{r},t)$ conjugated according to (2.62) to the vector potential $\vec{A}(\vec{r},t)$ is:

$$\begin{aligned} \vec{\Pi}(\vec{r},t) &= \frac{\partial \mathscr{L}_{elmg}}{\partial \dot{\vec{A}}(\vec{r},t)} = \epsilon_0 \, \dot{\vec{A}}(\vec{r},t) = \\ &= \boxed{\begin{array}{c}\text{because} \\ \vec{E} = -\frac{\partial \vec{A}}{\partial t}\end{array}} = -\epsilon_0 \, \vec{E}(\vec{r},t) \end{aligned} \tag{2.71}$$

Knowing the Lagrangian density (see (2.69) it is possible to determine the density of the Hamiltonian according to (2.67)

$$\begin{aligned} \mathscr{H}_{elmg} &= \vec{\Pi} \cdot \dot{\vec{A}} - \mathscr{L}_{elmg} = \epsilon_0 \, \vec{E} \cdot \vec{E} - \frac{1}{2} \, \epsilon_0 \, \vec{E} \cdot \vec{E} + \frac{1}{2} \, \vec{H} \cdot \vec{B} = \\ &= \frac{1}{2} \left(\vec{E} \cdot \vec{D} + \vec{H} \cdot \vec{B} \right) \end{aligned} \tag{2.72}$$

So, the Hamiltonian of the free electromagnetic field is

$$\begin{aligned} H_{elmg}(t) &= \int d^3r \;\; \mathscr{H}_{elmg}(\vec{r},t) \\ &= \frac{1}{2} \int d^3r \left(\vec{E}(\vec{r},t) \cdot \vec{D}(\vec{r},t) + \vec{H}(\vec{r},t) \cdot \vec{B}(\vec{r},t) \right) \end{aligned} \tag{2.73}$$

From (2.46) we know that any transverse calibrated solutions of the wave equation can be decomposed into the circularly polarized plane waves $\vec{A}_{\vec{k},\tau=\pm1}(\vec{r}',t)$:

$$\vec{A}(\vec{r}\,',t)=\sum_{\vec{k}}\sum_{\tau=\pm1}\left(\vec{A}_{\vec{k},\tau}(\vec{r}\,',t)\,a_{\vec{k},\tau}+\vec{A}^{*}_{\vec{k},\tau}(\vec{r}\,',t)\,a^{+}_{\vec{k},\tau}\right) \tag{2.74}$$

where (see (2.45)) $\vec{A}_{\vec{k},\tau}(\vec{r}',t)=C_k\,\vec{\xi}_\tau\,e^{i\,(\vec{k}\vec{r}\,'-\omega t)}$ with $C_k=\sqrt{\frac{\hbar}{2\,\epsilon_0\,L^3\,\omega}}$ and where opposite to (2.46) instead of $a^{*}_{\vec{k},\tau}$ in (2.74) we write $a^{+}_{\vec{k},\tau}$. The corresponding linear momentum field is (see (2.71))

$$\begin{aligned}\Pi(\vec{r}\,',t)&=\epsilon_0\,\dot{\vec{A}}(\vec{r}\,',t)=\\&=\sum_{\vec{k}}\sum_{\tau=\pm1}i\,\omega\,\epsilon_0\,\left(-\vec{A}_{\vec{k},\tau}(\vec{r}\,',t)\,a_{\vec{k},\tau}+\vec{A}^{*}_{\vec{k},\tau}(\vec{r}\,',t)\,a^{+}_{\vec{k},\tau}\right)\end{aligned} \tag{2.75}$$

Using the quantization postulation (2.64) applied to the case of electromagnetic field we can transform the classical quantities $\vec{A}(\vec{r}\,',t)$ (2.74), $\vec{\Pi}(\vec{r}\,',t)$ (2.75), $\mathscr{H}_{elmg}$ (2.72) etc. into quantum mechanical operators. According to (2.64) the quantization of el.mg. field means that the field $\vec{A}(\vec{r}\,',t)$ and corresponding conjugated linear momentum field $\vec{\Pi}(\vec{r}\,',t)$ are now operators and fulfil the following commutation relations

$$\begin{aligned}\left[\hat{\vec{A}}(\vec{r}_1\,',t),\;\hat{\vec{A}}(\vec{r}_2\,',t)\right]&=\left[\hat{\vec{\Pi}}(\vec{r}_1\,',t),\;\hat{\vec{\Pi}}(\vec{r}_2\,',t)\right]=0\\\left[\hat{A}_j(\vec{r}_1\,',t),\;\hat{\Pi}_l(\vec{r}_2\,',t)\right]&=i\,\hbar\,\delta_{l\,j}\,\delta(\vec{r}_1\,'-\vec{r}_2\,')\end{aligned} \tag{2.76}$$

After the quantization procedure amplitudes $a_{\vec{k},\tau}$ and $a^{+}_{\vec{k},\tau}$ in (2.74) and (2.75) become annihilation and creation operators, respectively. These operators fulfil the boson commutation relations

$$\begin{aligned}\left[a_{\vec{k},\tau},\;a_{\vec{k}\,',\tau'}\right]&=\left[a^{+}_{\vec{k},\tau},\;a^{+}_{\vec{k}\,',\tau'}\right]=0\\\left[a_{\vec{k},\tau},\;a^{+}_{\vec{k}\,',\tau'}\right]&=\delta_{\vec{k}\,\vec{k}\,'}\,\delta_{\tau\,\tau'}\end{aligned} \tag{2.77}$$

which is fully equivalent to (2.76). This equivalence can be easily shown by the substitution of eqs. (2.74) and (2.75) into the l.h.s. of (2.76). For instance if we take the commutator $\left[\hat{A}_j(\vec{r}_1\,',t),\;\hat{\Pi}_l(\vec{r}_2\,',t)\right]$ and if we substitute (2.74) and (2.75) into it and use the well-known eq. for Dirac δ- function:

$$\delta(\vec{r}-\vec{r}\,')=\frac{1}{(2\pi)^3}\int d^3k\,e^{i\,\vec{k}\cdot(\vec{r}-\vec{r}\,')}) \tag{2.78}$$

together with the postulation of (2.77) then we obtain r.h.s. of the second row expr. (2.76) [5]. The operator of the Lagrangian and Hamiltonian of el.mg. field can be obtained by the substitution of (2.74) and (2.75) into (2.69) and then into (2.72) and (2.73). The result is

$$\hat{H}_{elmg} = \sum_{\vec{k}} \sum_{\tau=\pm 1} \hbar\,\omega\,\left(a^{+}_{\vec{k}\,\tau} a_{\vec{k}\,\tau} + \frac{1}{2} \right) \tag{2.79}$$

From previous subsections it is known that $\hbar\,\omega = \hbar\,k\,c$ is the energy of the photon with the linear momentum $\hbar\,\vec{k}$. On the other hand if $a^{+}_{\vec{k},\tau}$ and $a_{\vec{k},\tau}$ are the creation and annihilation operators of particle with the quantum numbers $\vec{k}$, τ then the operator $a^{+}_{\vec{k},\tau} a_{\vec{k},\tau}$ is the operator of the number of particles with the quantum numbers $\vec{k}$, τ. From the point of view of these facts the expr. (2.79) can be interpreted as the operator of the total energy expressed as the sum over energies of all photons of investigated free electromagnetic field. [6] By other words the operators $a^{+}_{\vec{k},\tau}$ and $a_{\vec{k},\tau}$ are the creation and annihilation operators of the phonon with the linear momentum $\hbar\,\vec{k}$ and polarization τ with the corresponding photon vacuum

$$a_{\vec{k},\tau}\,|0\rangle = 0 \tag{2.80}$$

and one-photon, two-photon, etc. states

$$|\vec{k}\,\tau\rangle = a^{+}_{\vec{k}\,\tau}|0\rangle\,, \qquad |\vec{k}\,\tau,\,\vec{k}\,'\,\tau\rangle = a^{+}_{\vec{k}\,\tau}\,a^{+}_{\vec{k}\,',\tau}\,|0\rangle\,,\,\ldots \tag{2.81}$$

[5] In the showing of the equivalence of (2.76) and (2.77) we used also the following expressions,

$$\frac{1}{L^3}\sum_{\vec{k}} = \frac{1}{(2\pi)^3}\int d^3k \qquad , \qquad \frac{1}{(2\pi)^3}\int d^3r\,e^{i(\vec{k}-\vec{k}')\cdot\vec{r}} = \delta(\vec{k}-\vec{k}') \approx \delta_{\vec{k},\vec{k}'}$$

following from the exp. (2.41) which shows that each linear momentum state occupies the volume $(2\pi)^3$ in the linear momentum space of vectors $\vec{k}$, and also expressions below valid for the spin functions $\vec{\xi}_\tau$ for $\tau = \pm 1$,

$$\vec{\xi}^{\,*}_{\tau}\cdot\vec{\xi}_{\tau'} = \delta_{\tau,\tau'} \qquad , \qquad \vec{\xi}_{\tau}\cdot\vec{\xi}_{\tau'} = -\delta_{\tau,-\tau'}$$

[6] The fraction 1/2 in (2.79) gives the total energy of the photon vacuum added to all energies of possible photon states because the summation in (2.79) goes over infinite number of photon linear momenta. However we are not interested in the total energy of electromagnetic field including the energy of the photon vacuum. In order to get rid of this infinite vacuum energy the fraction 1/2 is usually omitted in (2.79) and the Hamiltonian of the electromagnetic field reads,

$$\hat{H}_{elmg} = \sum_{\vec{k}} \sum_{\tau=\pm 1} \hbar\,\omega\,a^{+}_{\vec{k}\,\tau} a_{\vec{k}\,\tau} \tag{2.79$'$}$$

One should also realize that because of the time periodical dependence of (2.74) and (2.75) on time the substitution of these expressions into (2.73) gives H_{elmg} not dependent on time (in the non-relativistic quantum mechanics when $\hat{H}_{elmg}$ does not change number of photons - see the chapter 1 in [13]).

Photons as quanta of electromagmetic field are described by a vector potential and from the quantum mechanics it means that they have spin $S = 1$ (in accordance with experiments). The transverse calibration condition ($\varphi = 0$, $\vec{\nabla} \cdot \vec{A} = 0$) ensures only two possible projections of the spin to the direction of the photon linear momentum $\hbar\vec{k}$. Concretely, the real photon can have only two values of circular polarizations, $\tau = \pm 1$. Virtual intermediate photons (interchanging of them mediates the electromagnetic interaction) may have all values of the polarizations, $\tau = 0, \pm 1$.

After the quantization the el.mg. vector potential (2.74) is the operator linearly dependent on the photon creation operator $a^+_{\vec{k}\,'\,\tau}$ and on the photon annihilation operator $a_{\vec{k}\,'\,\tau}$. Therefore the matrix element of this operator is nonzero only in the case when the bra state differs from the ket state by one photon. These matrix elements can be determined using the boson commutation relations (2.77) and rel. (2.80):

$$\begin{aligned}
\langle \vec{k}\,\tau|\hat{\vec{A}}(\vec{r}\,',t)|0\rangle = \langle 0|a_{\vec{k}\,\tau}\,\hat{\vec{A}}(\vec{r}\,',t)|0\rangle = \boxed{\begin{array}{c}\text{see}\\(2.72)\end{array}} = \\
= \sum_{\vec{k}\,'\,\tau'} \langle 0|\vec{A}_{\vec{k}\,'\,\tau'}(\vec{r}\,',t)\; a_{\vec{k}\,\tau} a_{\vec{k}\,'\,\tau'} + \vec{A}^*_{\vec{k}\,'\,\tau'}(\vec{r}\,',t)\; a_{\vec{k}\,\tau} a^+_{\vec{k}\,'\,\tau'}|0\rangle = \\
= \sum_{\vec{k}\,'\,\tau'} \langle 0|\vec{A}^*_{\vec{k}\,'\,\tau'}(\vec{r}\,',t)\;\; a_{\vec{k}\,\tau} a^+_{\vec{k}\,'\,\tau'}\,|0\rangle = \vec{A}^*_{\vec{k}\tau}(\vec{r}\,',t) = \\
= C_k\,\vec{\xi}^*_\tau e^{-i\,(\vec{k}\,\vec{r}\,'\,-\omega t)}
\end{aligned} \tag{2.82}$$

and similarly

$$\begin{aligned}
\langle 0|\hat{\vec{A}}(\vec{r}\,',t)|\vec{k}\tau\rangle = \langle 0|\hat{\vec{A}}(\vec{r}\,',t)\; a^+_{\vec{k}\tau}|0\rangle = \ldots = \\
= \vec{A}_{\vec{k}\tau}(\vec{r}\,'\,\tau) = C_k\,\vec{\xi}_\tau\; e^{i\,(\vec{k}\,\vec{r}\,'-\omega t)}
\end{aligned} \tag{2.83}$$

where $|\vec{k}\,\tau\rangle = a^+_{\vec{k},\tau}|0\rangle$ is the one-photons state. Generally:

$$\begin{aligned}
\langle n_{\vec{k}\,\tau} + 1|\hat{\vec{A}}(\vec{r}\,',t)|n_{\vec{k}\,\tau}\rangle &= \sqrt{n_{\vec{k}\,\tau}+1}\;\vec{A}^*_{\vec{k}\tau}(\vec{r}\,'\,\tau) \\
\langle n_{\vec{k}\,\tau} - 1|\hat{\vec{A}}(\vec{r}\,',t)|n_{\vec{k}\,\tau}\rangle &= \sqrt{n_{\vec{k}\,\tau}}\;\vec{A}_{\vec{k}\tau}(\vec{r}\,'\,\tau)
\end{aligned} \tag{2.84}$$

where $|n_{\vec{k}\,\tau}\rangle$ is the state involving $n_{\vec{k}\,\tau}$ photons with the linear momentum $\hbar\vec{k}$ and polarization τ.

2.2 Interaction of electromagnetic field with the quantum bound object (nucleus)

2.2.1 Probability of electromagnetic transitions

Let us consider the system consisting from electromagnetic field and a quantum bound object, e.g. a nucleus. The total Hamiltonian of such a system is

$$\hat{H} = \hat{H}_{elmg} + \hat{H}_{nuc} + \hat{H}_{int} \tag{2.85}$$

where $\hat{H}_{elmg}$ is the Hamiltonian of the electromagnetic field (see (2.79), $\hat{H}_{nuc}$ stands for the Hamiltonian of the nucleus (bound object) and $\hat{H}_{int}$ is the interaction between the nucleus and electromagnetic field. The nucleus Hamiltonian $\hat{H}_{nuc}$ will be specified later, for the moment it is not necessary to know its details.

From the classical physics (theory of the classical electromagnetic field) it is known that the interaction of the electromagnetic field with the operator of the scalar potential $\hat{\varphi}(\vec{r},t)$ and of the vector potential $\hat{\vec{A}}(\vec{r},t)$ with a system of charged particles (a nucleus) with the operator of the charge density $\hat{\rho}_{nuc}(\vec{r},t)$ and the operator of the current density $\hat{\vec{j}}_{nuc}(\vec{r},t)$ is given by the Hamiltonian

$$\hat{H}_{int} = \int d^3r \, \left[\hat{\rho}_{nuc}(\hat{r},t)\hat{\varphi}(\vec{r},t) - \hat{\vec{j}}_{nuc}(\vec{r},t)\cdot\hat{\vec{A}}(\vec{r},t)\right] \tag{2.86}$$

It should be pointed out that operators $\hat{\varphi}(\vec{r},t)$ and $\hat{\vec{A}}(\vec{r},t)$ act in the space of photons while operators $\hat{\rho}_{nuc}(\vec{r},t)$ and $\hat{\vec{j}}_{nuc}(\vec{r},t)$ act in the space of the nucleus wave funtions (e.g. eigen functions of the nucleus Hamiltonian $\hat{H}_{nuc}$).

If we suppose transverse calibration condition ($\hat{\varphi}(\vec{r},t) = 0$ and $\vec{\nabla}\hat{\vec{A}}(\vec{r},t) = 0$) then (2.86) can be rewritten as follows

$$\hat{H}_{int} = -\int d^3r \, \hat{\vec{j}}_{nuc}(\vec{r},t)\cdot\hat{\vec{A}}(\vec{r},t) \tag{2.87}$$

where the vector potential operator $\hat{\vec{A}}(\vec{r},t)$ is given by (2.74). The substitution of (2.74) into (2.87) gives the interaction Hamiltonian in the following form

$$\hat{H}_{int} = \hat{B}\, e^{-i\omega t} + \hat{B}^{+}\, e^{i\omega t} \tag{2.88}$$

where

$$\begin{aligned}
\hat{B} &= -\int d^3r\, \hat{\vec{j}}_{nuc}(\vec{r}) \cdot \sum_{\vec{k}\,\tau} C_k\, \vec{\xi}_\tau\, e^{i\vec{k}\vec{r}}\, a_{\vec{k},\tau} \\
\hat{B}^+ &= -\int d^3r\, \hat{\vec{j}}^+_{nuc}(\vec{r}) \cdot \sum_{\vec{k}\,\tau} C_k\, \vec{\xi}^+_\tau\, e^{-i\vec{k}\vec{r}}\, a^+_{\vec{k},\tau} = \\
&= -\int d^3r\, \hat{\vec{j}}_{nuc}(\vec{r}) \cdot \sum_{\vec{k}\,\tau} C_k\, \vec{\xi}^+_\tau\, e^{-i\vec{k}\vec{r}}\, a^+_{\vec{k},\tau}
\end{aligned} \tag{2.89}$$

where we supposed a stationary condition for the nucleus, that means the charge density and current density do not depend explicitly on time, and also the fact that the current density $\hat{\vec{j}}_{nuc}(\vec{r})$ is a hermitian operator.

The transition probability that our system "nucleus + external electromagnetic field" transfers from the initial state $|i\rangle$ to the final state $|f\rangle$ during the time interval $\langle t_0,\, t\rangle$ is given by the square of the matrix element of the evolution operator $\hat{S}(t, t_0)$ between the final and initial states (see Appendix C - exp. C.13)). In the first order of the nonstationary perturbation theory (see Appndix C) this transition probability is (see (C.17):

$$w_{i\to f}(t_0, t) = |\langle f|\hat{S}^{(1)}(t, t_0)|i\rangle|^2 \tag{2.90}$$

where

$$\langle f|\hat{S}^{(1)}(t, t_0)|i\rangle = \boxed{\begin{array}{c}\text{see}\\ (C.18)\end{array}} =$$

$$= \frac{e^{-i\,\omega_{fi}\,t_0}}{i\hbar} \int_{t_0}^{t} dt\,'\, e^{i\,\omega_{fi}\,t\,'} \langle f|\hat{H}_{int}(t\,')|i\rangle = \boxed{\begin{array}{c}\text{substitution}\\ \text{of (2.88)}\end{array}} =$$

$$\begin{aligned}
&= \frac{e^{-i\,\omega_{fi}\,t_0}}{i\hbar} \left(\langle f|\hat{B}|i\rangle \int_{t_0}^{t} dt\,' e^{i\,(\omega_{fi}-\omega)\,t\,'} + \right. \\
&\qquad \left. + \langle f|\hat{B}^+|i\rangle \int_{t_0}^{t} dt\,' e^{i\,(\omega_{fi}+\omega)\,t\,'} \right) = \\
&= -\frac{1}{\hbar} \left(\langle f|\hat{B}|i\rangle\, e^{-i\,\omega\,t}\, \frac{e^{i\,(\omega_{fi}-\omega)\,\Delta t}}{\omega_{fi}-\omega} + \right. \\
&\qquad \left. + \langle f|\hat{B}^+|i\rangle\, e^{i\,\omega\,t}\, \frac{e^{i\,(\omega_{fi}+\omega)\,\Delta t}}{\omega_{fi}+\omega} \right)
\end{aligned} \tag{2.91}$$

where $\omega_{fi} = \frac{E_f - E_i}{\hbar}$ (E_i is the energy of the unperturbed initial state $|i\rangle$, $(\hat{H}_{nuc} + \hat{H}_{elmg})|i\rangle = E_i\,|i\rangle$, and E_f is the energy of the unperturbed final state $|f\rangle$, $(\hat{H}_{nuc} + \hat{H}_{elmg})|f\rangle = E_f\,|f\rangle$) and $\Delta t = t - t_0$.

In principle, we have two possibilities of electromagnetic transitions in the nucleus (or generally in any bound quantum object):

- emission of the photon by the nucleus
- absorption of the photon by the nucleus.

Both these possibilities are discussed in details in next subsections.

2.2.2 Probability of the emission of the photon by the nucleus

2.2.2.1 Electric and magnetic multipole operators - transition probability

The probability of the transition $|i\rangle \to |f\rangle$ of the system nucleus + el.mg. field during the time interval $\langle t_0, t\rangle$ is given by (2.90). Futher we will specify the unperturbed states $|i\rangle$ and $|f\rangle$ of the system nucleus + external el.mg. field in the case when the photon with the linear momentum $\hbar\vec{k}$ and polarization $\tau = \pm 1$ is emitted during the transition:

$$\begin{array}{ccc} \text{initial state of the system:} \\ \text{nucleus + el.mg. field} \end{array} \quad \ldots . |i\rangle = |i,\,0\rangle \quad \begin{array}{c} \text{no photon, nucleus} \\ \text{in the state } |i\rangle \end{array}$$

$$\begin{array}{ccc} \text{final state of the system:} \\ \text{nucleus + el.mg. field} \end{array} \quad \begin{array}{c} \ldots . \\ \ldots . \end{array} \quad \begin{array}{c} |f\rangle = |f, \vec{k}\,\tau\rangle \\ = a^{+}_{\vec{k},\tau}|f,\,0\rangle \end{array} \quad \begin{array}{c} \text{one photon, nucleus} \\ \text{in the state } |f\rangle \end{array}$$

In this case the matrix elements $\langle f|\hat{B}|i\rangle$ and $\langle f|\hat{B}^{+}|i\rangle$ involved in (2.91) are following

$$\langle f|\hat{B}|i\rangle = \langle f, 0|a_{\vec{k},\tau}\,\hat{B}|i, 0\rangle = \boxed{\begin{array}{c}\text{see}\\(2.89)\end{array}} =$$

$$= -\sum_{\vec{k}\,'\,\tau\,'} \int d^3r \langle f|\,\hat{\vec{j}}_{nuc}(\vec{r})\,|i\rangle$$

$$C_{k\,'}\,\vec{\xi}_{\tau\,'}\,e^{i\vec{k}'\vec{r}}\langle 0|a_{\vec{k},\tau}\,a_{\vec{k}\,',\tau\,'}|0\rangle = 0 \qquad (2.92)$$

$$\langle f|\hat{B}^+|i\rangle = \langle f,0|a_{\vec{k},\tau}\ \hat{B}^+|i,0\rangle = \boxed{\begin{array}{c}\text{see}\\(2.89)\end{array}} =$$

$$= -\sum_{\vec{k}\,'\,\tau\,'}\int d^3r\langle f|\ \hat{\vec{j}}_{nuc}(\vec{r})\ |i\rangle$$

$$C_{k\,'}\ \vec{\xi}^{\,*}_{\tau\,'}\ e^{-i\vec{k}'\vec{r}}\langle 0|a_{\vec{k},\tau}\ a^{+}_{\vec{k}\,',\tau\,'}|0\rangle =$$

$$= -\int d^3r\ \langle f|\ \hat{\vec{j}}_{nuc}(\vec{r})\ |i\rangle C_k\ \vec{\xi}^{\,*}_{\tau}\ e^{-i\vec{k}\vec{r}} \qquad (2.93)$$

We substitute (2.93) into (2.91) and then into (2.90):

$$\begin{aligned}\omega_{i\to f}(t_0,t) &= \frac{1}{\hbar^2}\,|\langle f|\hat{B}^+|i\rangle|^2\ \left|\frac{e^{i\,(\omega_{fi}+\omega)\Delta t}-1}{\omega_{fi}+\omega}\right|^2 =\\ &= \frac{2\pi}{\hbar^2}\,|\langle f|\hat{B}^+|i\rangle|^2\,\delta_{\Delta t}(\omega_{fi}+\omega)\,\Delta t \qquad (2.94)\end{aligned}$$

where the function $\delta_{\Delta t}(\omega_{fi}+\omega)$ was introduced:

$$\delta_{\Delta t}(\omega_{fi}+\omega) = \frac{1}{2\pi\,\Delta t}\ \left|\frac{e^{i\,(\omega_{fi}+\omega)\,\Delta t}-1}{\omega_{fi}+\omega}\right|^2 \quad \xrightarrow[\Delta t\to\infty]{} \quad \delta(\omega_{fi}+\omega) \qquad (2.95)$$

So, the probability of the emission of the photon with the linear momentum $\hbar\vec{k}$ and energy $\hbar kc$ and with the polarization τ from the nucleus in the time unit is:

$$\begin{aligned}\omega_{i\to f} &= \frac{\omega_{i\to f}(t_0,t)}{\Delta t} = \frac{2\pi}{\hbar^2}\,|\langle f|\hat{B}^+|i\rangle|^2\ \delta_{\Delta t}(\omega_{fi}+\omega) =\\ &\xrightarrow[\Delta t\to\infty]{} \frac{2\pi}{\hbar^2}\ |\langle f|\hat{B}^+|i\rangle|^2\ \delta(\omega_{fi}+\omega) = \boxed{\begin{array}{c}\text{see}\\(2.93)\end{array}} =\\ &= \frac{2\pi}{\hbar}\,C_k^2\ \left|\int d^3r\langle f|\hat{\vec{j}}_{nuc}(\vec{r})|i\rangle\ \vec{\xi}^{\,*}_{\tau}\ e^{-i\vec{k}\vec{r}}\right|^2\delta(E_f-E_i+\hbar\omega)\end{aligned} \qquad (2.96)$$

Exp. (2.96) represents the probability that in the time unit the system of the nucleus and el.mg field makes transition from one concrete state $|i,0\rangle$ to one concrete final state $|f,\vec{k}\tau\rangle$. However, we should realize that the linear momentum $\hbar\vec{k}$ of the photon in the final state $|f,\vec{k}\tau\rangle$ has a continuous character and therefore we usually speak not about one concrete linear momentum but about an interval of the linear momentum. Therefore we modify the exp.

(2.96) in the following way:

$$T_{i\to f}(\vec{k},\tau)\,d\Omega_k = \frac{2\pi}{\hbar}\,C_k^2\,\left|\int d^3r\,\langle f|\hat{\vec{j}}_{nuc}(\vec{r})|i\rangle\,\vec{\xi}_\tau^{\,*}\,e^{-i\vec{k}\vec{r}}\right|^2\,\rho_{fin} \tag{2.97}$$

where $T_{i\to f}(\vec{k},\tau)$ is the probability that in the time unit the nucleus makes the transition $|i\rangle \to |f\rangle$ with the emission of one photon with the energy in the unit interval around the energy $\hbar kc = \hbar\omega$ and flying to the unit space angle around the direction of the linear momentum $\hbar\vec{k}$. The symbol $d\Omega_k$ represents the element of the space angle in the space of the vectors $\vec{k}$. The symbol ρ_{fin} is so called the density of final states of photons. Particularly, in the case of (2.97) it is the number of the photon states with the energy in the unit energy interval around the value $\hbar kc = \hbar\omega$ and with the linear momentum belonging to the linear momentum space element $d^3k = k^2\,dk\,d\Omega_k = \frac{1}{c^3}\,\omega^2\,d\omega\,d\Omega_k$. Taking into account the fact that one photon state $|\vec{k},\tau\rangle$ occupies in the linear momentum space (and in the phase space of vectors $(\vec{r},\vec{k})$ as well) the volume $(2\pi)^3$ (see (2.42)) the density of final state ρ_{fin} is given by

$$\rho_{fin} = \frac{L^3}{(2\pi)^3}\,\frac{d^3k}{d(\hbar\omega)} = \frac{L^3}{(2\pi)^3}\frac{\omega^2\,d\omega\,d\Omega_k}{c^3\,\hbar\,d\omega} = \frac{L^3\,\omega^2}{(2\pi)^3\,c^3\,\hbar}\,d\Omega_k \tag{2.98}$$

The substitution of (2.98) and (2.44) into (2.97) gives

$$T_{i\to f}(\vec{k},\tau)\,d\Omega_k = \frac{\omega}{8\pi^2\,\hbar\epsilon_0\,c^3}\,\left|\int d^3r\,\langle f|\hat{\vec{j}}_{nuc}(\vec{r})|i\rangle\,\vec{\xi}_\tau^{\,*}\,e^{-i\vec{k}\vec{r}}\right|^2\,d\Omega_k \tag{2.99}$$

In (2.99) the probability $T_{i\to f}(\vec{k},\tau)$ of electromagnetic transitions is expressed in terms of plane waves. For practical reasons, which will be seen later, it is more convenient to express this probability in terms of spherical waves. Leaving out the time dependence in the exprs. (2.25) and (2.29) electric and magnetic spherical waves are

$$\begin{aligned}\vec{A}_{JM}^{(el)}(\vec{r}) &= i\left\{\sqrt{\frac{J+1}{2J+1}}\,f_{J-1}(kr)\,\vec{Y}_{J-1\,J\,M}(\hat{r})\right.\\ &\qquad\left.-\sqrt{\frac{J}{2J+1}}\,f_{J+1}(kr)\,\vec{Y}_{J+1\,J\,M}(\hat{r})\right\}\\ \vec{A}_{JM}^{(mag)}(\vec{r}) &= f_J(kr)\,\vec{Y}_{JJM}(\hat{r})\end{aligned} \tag{2.100}$$

Similarly, if we omit the time dependence in the rel. (2.51) the plane waves for the polarizations $\tau = \pm 1$ are

$$C_k\,\vec{\xi}_\tau\,e^{i\vec{k}\vec{r}\,'} = -\,C_k\,\sqrt{2\pi}\sum_{JM} i^J\,(2J+1)^{1/2} \left[\vec{A}^{(el)}_{JM}(\vec{r}) + \tau\,\vec{A}^{(mag)}_{JM}(\vec{r})\right]\,D^{J\,*}_{M\,\tau}(\vec{e}_z \to \vec{k}) \tag{2.101}$$

So, we have

$$\begin{aligned}
\vec{\xi}_\tau\,e^{i\vec{k}\vec{r}\,'} &= -\sqrt{2\pi}\sum_{JM} i^J\,(2J+1)^{1/2} \left[\vec{A}^{(el)}_{JM}(\vec{r}) + \tau\,\vec{A}^{(mag)}_{JM}(\vec{r})\right]\,D^{J\,*}_{M\,\tau}(\vec{e}_z \to \vec{k}) \\
\vec{\xi}^{\,*}_\tau\,e^{-\,i\vec{k}\vec{r}\,'} &= -\sqrt{2\pi}\sum_{JM} i^{-J}\,(2J+1)^{1/2} \left[\vec{A}^{(el)\,*}_{JM}(\vec{r}) + \tau\,\vec{A}^{(mag)\,*}_{JM}(\vec{r})\right]\,D^{J}_{M\,\tau}(\vec{e}_z \to \vec{k}) = \\
&= \boxed{\begin{array}{c}\text{from (A.67) it follows: } \vec{A}^{(el)\,*}_{JM} = (-1)^{M+1}\vec{A}^{(el)}_{J\,-M} \\ \text{and similarly: } \vec{A}^{(mag)\,*}_{JM} = (-1)^{M+1}\vec{A}^{(mag)}_{J\,-M}\end{array}} = \\
&= -\sqrt{2\pi}\sum_{JM} i^{-J}\,(2J+1)^{1/2}\,(-1)^{M+1} \left[\vec{A}^{(el)}_{J\,-M}(\vec{r}) + \tau\,\vec{A}^{(mag)}_{J\,-M}(\vec{r})\right]\,D^{J}_{M\,\tau}(\vec{e}_z \to \vec{k})
\end{aligned} \tag{2.102}$$

In order to simplify next expressions it is very useful to introduce so called magnetic and electric multipole operators:

$$\begin{aligned}
\hat{\mathscr{M}}^{(mag)}_{JM}(k) &\equiv -i\,\frac{(2J+1)!!}{c\,k^J\,(J+1)}\,[J(J+1)]^{1/2}\int d^3r\,\hat{\vec{j}}_{nuc}(\vec{r})\,\vec{A}^{(mag)}_{JM}(\vec{r}) \\
\hat{\mathscr{M}}^{(el)}_{JM}(k) &\equiv \frac{(2J+1)!!}{c\,k^J\,(J+1)}\,[J(J+1)]^{1/2}\int d^3r\;\hat{\vec{j}}_{nuc}(\vec{r})\,\vec{A}^{(el)}_{JM}(\vec{r})
\end{aligned} \tag{2.103}$$

where $\hat{\vec{j}}_{nuc}(\vec{r})$ is the operator of the current density of the nucleus. In the (2.99) there are involved the matrix elements of the operator $\int d^3r\vec{\xi}^{\,*}_\tau\hat{\vec{j}}_{nuc}(\vec{r})e^{-i\vec{k}\vec{r}}$ between nuclear states $|f\rangle$ and $|i\rangle$. Using (2.102) and (2.103) this operator

can be rewritten as follows

$$\int d^3r\ \vec{\xi}^{*}_{\tau}\ \hat{\vec{j}}_{nuc}(\vec{r})\ e^{-i\vec{k}\vec{r}} = \int d^3r\,'\ \vec{\xi}^{*}_{\tau}\ \hat{\vec{j}}_{nuc}(\vec{r}\,')\ e^{-i\vec{k}\vec{r}\,'} =$$

$$= \boxed{\begin{array}{c}\text{substitution of}\\ (2.102)\end{array}} =$$

$$= -\sqrt{2\pi}\sum_{JM} i^{-J}(2J+1)^{1/2}(-1)^{M+1}D^{J}_{M\,\tau}(\vec{e}_z\to\vec{k})$$

$$\frac{k^J c}{(2J+1)!!}\left(\frac{J+1}{J}\right)^{1/2}\left[\hat{\mathscr{M}}^{(el)}_{J\,-M} + i\,\tau\hat{\mathscr{M}}^{(mag)}_{J\,-M}\right] =$$

$$= \boxed{\begin{array}{c}\text{because } \hat{\mathscr{M}}^{(mag)\,+}_{J\,M} = (-1)^M\hat{\mathscr{M}}^{(mag)}_{J\,-M}\\ \text{and } \hat{\mathscr{M}}^{(el)\,+}_{J\,M} = (-1)^{M+1}\hat{\mathscr{M}}^{(el)}_{J\,-M}\end{array}} =$$

$$= -\sqrt{2\pi}\sum_{JM} i^{-J}\,(2J+1)^{1/2}\,D^{J}_{M\,\tau}(\vec{e}_z\to\vec{k})$$

$$\frac{k^J c}{(2J+1)!!}\left(\frac{J+1}{J}\right)^{1/2}\left[\hat{\mathscr{M}}^{(el)\,+}_{J\,M}(k) - i\,\tau\hat{\mathscr{M}}^{(mag)\,+}_{J\,M}(k)\right] \tag{2.104}$$

the expression (2.104) represents the operator equation. In the exp. (2.99) for the transition probability there is the matrix element of this operator between the nuclear final state $|f\rangle$ and initial state $|i\rangle$.

$$\int d^3r\ \vec{\xi}^{*}_{\tau}\ \hat{\vec{j}}_{nuc;\,fi}(\vec{r})\ e^{-i\vec{k}\vec{r}} \equiv \int d^3r\ \vec{\xi}^{*}_{\tau}\,\langle f|\hat{\vec{j}}_{nuc;}(\vec{r})|i\rangle\,e^{-i\vec{k}\vec{r}} =$$

$$= -\sqrt{2\pi}\sum_{JM} i^{-J}\,(2J+1)^{1/2}\,D^{J}_{M\,\tau}(\vec{e}_z\to\vec{k})\,\frac{k^J c}{(2J+1)!!}\left(\frac{J+1}{J}\right)^{1/2}$$

$$\left[\langle f|\hat{\mathscr{M}}^{(el)\,+}_{J\,M}(k)|i\rangle - i\,\tau\langle f|\hat{\mathscr{M}}^{(mag)\,+}_{J\,M}(k)|i\rangle\right] \tag{2.105}$$

where

$$\left[\langle f|\hat{\mathscr{M}}^{(el)\,+}_{J\,M}(k)|i\rangle - i\,\tau\langle f|\hat{\mathscr{M}}^{(mag)\,+}_{J\,M}(k)|i\rangle\right] =$$

$$= (-1)^{M+1}\left[\langle f|\hat{\mathscr{M}}^{(el)}_{J\,-M}(k)|i\rangle + i\,\tau\langle f|\hat{\mathscr{M}}^{(mag)}_{J\,-M}(k)|i\rangle\right]$$

In the quantun systems (including nuclei) the Hamiltonian usually fulfils the following symmetries

$$[\hat{H}_{nuc},\hat{I}^2] = [\hat{H}_{nuc},\hat{I}_z] = 0 \tag{2.106}$$

Therefore, the eigen-states of the system Hamiltonian are simultaneously eigen-states of the square of the total angular momentum $\hat{I}^2$ and its z-component $\hat{I}_z$:

$$\begin{array}{ll} \text{initial state:} & |i\rangle = |\alpha_i\, j_i\, m_i\rangle \\ \text{final state:} & |f\rangle = |\alpha_f\, j_f\, m_f\rangle \end{array} \tag{2.107}$$

where index α represents all other quantum numbers (besides j and m) which chracterize the state of the nucleus.

Magnetic and electric multipole operators, $\hat{\mathscr{M}}^{(mag)}_{J\,M}$ and $\hat{\mathscr{M}}^{(el)}_{J\,M}$, are the tensor operators with respect to rotations (see subsection A.4 in the Appendix A). Therefore, we can use the Wigner-Eckart theorem (A.12) for the calculation of their matrix elements.

$$\begin{aligned} &\langle f|\hat{\mathscr{M}}^{(el,\,mag)}_{J\,-M}(k)|i\rangle = \langle \alpha_f\, j_f\, m_f|\hat{\mathscr{M}}^{(el,\,mag)}_{J\,-M}(k)|\alpha_i\, j_i\, m_i\rangle = \\ &= \boxed{\begin{array}{c}\text{see}\\ (A.12)\end{array}} = \\ &= \frac{1}{\sqrt{2j_f+1}}\, C^{j_f\, m_f}_{j_i\, m_i\, J\, -M} \langle \alpha_f\, j_f||\hat{\mathscr{M}}^{(el,\,mag)}_{J}(k)||\,\alpha_i\, j_i\rangle \end{aligned} \tag{2.108}$$

Then the expr. (2.105) can be rewritte as follows

$$\begin{aligned} &\langle \alpha_f\, j_f\, m_f| \int d^3r\ \vec{\xi}^*_\tau\ \hat{\vec{j}}_{nuc}(\vec{r})\ e^{-i\vec{k}\vec{r}}|\,\alpha_i\, j_i\, m_i\rangle = \\ &= -\sqrt{2\pi}\sum_{JM}(2J+1)^{1/2}\frac{(-ik)^J c}{(2J+1)!!}\left(\frac{J+1}{J}\right)^{1/2}\ D^J_{M\,\tau}(\vec{e}_z\to\vec{k}) \\ &\quad \frac{1}{\sqrt{2j_f+1}}\, C^{j_f\, m_f}_{j_i\, m_i\, J\, -M} \\ &\quad \Big[\langle \alpha_f\, j_f||\,\hat{\mathscr{M}}^{(el)}_J(k)\,||\,\alpha_i\, j_i\rangle + i\,\tau\langle \alpha_f\, j_f||\,\hat{\mathscr{M}}^{(mag)}_J(k)\,||\,\alpha_i\, j_i\rangle\Big] \end{aligned} \tag{2.109}$$

and the substitution of (2.109) into (2.99) gives for the transition probabilty

the following expression

$$
\begin{aligned}
T_{\alpha_i\, j_i\, m_i \to \alpha_f\, j_f\, m_f}(\vec{k},\tau) &= \frac{\omega}{8\pi^2\,\epsilon_0\,c^3\,\hbar} \\
&\langle \alpha_f\, j_f\, m_f| \int d^3r\ \vec{\xi}^{\,*}_{\tau}\ \hat{\vec{j}}_{nuc}(\vec{r})\ e^{-i\vec{k}\vec{r}}|\ \alpha_i\, j_i\, m_i\rangle^* \\
&\qquad \langle \alpha_f\, j_f\, m_f| \int d^3r\ \vec{\xi}^{\,*}_{\tau}\ \hat{\vec{j}}_{nuc}(\vec{r})\ e^{-i\vec{k}\vec{r}}|\ \alpha_i\, j_i\, m_i\rangle = \\
= \frac{\omega}{4\pi\,\epsilon_0\,c\,\hbar} &\sum_{JJ'} \frac{k^{J+J'}}{(2J+1)!!\,(2J'+1)!!}\ \frac{1}{2j_f+1} \\
&\left[\frac{(J+1)(J'+1)(2J+1)(2J'+1)}{J\ J'}\right]^{1/2} \\
&\left[\langle \alpha_f\, j_f||\hat{\mathscr{M}}^{(el)}_{J}(k)||\ \alpha_i\, j_i\rangle^* - i\,\tau\langle \alpha_f\, j_f||\hat{\mathscr{M}}^{(mag)}_{J}(k)||\ \alpha_i\, j_i\rangle^*\right] \\
&\left[\langle \alpha_f\, j_f||\hat{\mathscr{M}}^{(el)}_{J'}(k)||\ \alpha_i\, j_i\rangle + i\,\tau\langle \alpha_f\, j_f||\hat{\mathscr{M}}^{(mag)}_{J'}(k)||\ \alpha_i\, j_i\rangle\right] \\
&\sum_{M\,M'} D^{J\,*}_{M\tau}(\vec{e}_z\to\vec{k}) D^{J'}_{M'\tau}(\vec{e}_z\to\vec{k})\ C^{j_f\,m_f}_{j_i\,m_i\,J\,-M}\ C^{j_f\,m_f}_{j_i\,m_i\,J'\,-M'}
\end{aligned}
\tag{2.110}
$$

We should remind that $T_{\alpha_i\, j_i\, m_i \to \alpha_f\, j_f\, m_f}(\vec{k},\tau)$ is the probabilty in the time unit that the nucleus makes the transition from the initial state $|\ \alpha_i\, j_i\, m_i\rangle$ to the final state $|\ \alpha_f\, j_f\, m_f\rangle$ and simultaneously it emits the photon with the energy in the energy unit interval around the value $\hbar\omega = \hbar kc$ and with the linear momentum dirrected into the unit space angle around the dirrection of the vector $\vec{k}$.

If the nucleus is not spin oriented in the initial state $|\ \alpha_i\, j_i\, m_i\rangle$ (that means all projections m_i of its total momentum j_i are possible) and if in the final state the projection m_f is not also known then the corresponding transition probability is obtained from (2.110) by averaging over the initial projections m_i and sumation over final projections m_f. That means the last row of the

expr. (2.110) should be substituted by the following expression:

$$\frac{1}{2j_i+1}\sum_{M\,M'\,m_i\,m_f} D^{J\,*}_{M\tau}\;D^{J'}_{M'\tau}\,C^{j_f\,m_f}_{j_i\,m_i\,J\,-M}\,C^{j_f\,m_f}_{j_i\,m_i\,J'\,-M'} =$$

$$= \boxed{\begin{array}{c}\text{see (A.4):}\\ C^{j_f\,m_f}_{j_i\,m_i\,J\,-M} = (-1)^{j_i-m_i}\sqrt{\frac{2j_f+1}{2J+1}}\,C^{J\,M}_{j_i\,m_i\,j_f\,-m_f}\end{array}} =$$

$$= \frac{(2j_f+1)}{(2j_i+1)(2J+1)} \sum_{M\,M'\,m_i\,m_f} D^{J\,*}_{M\tau}\;D^{J'}_{M'\tau}\,C^{J\,M}_{j_i\,m_i\,j_f\,-m_f}\,C^{J'\,M'}_{j_i\,m_i\,j_f\,-m_f} =$$

$$= \boxed{\begin{array}{c}\text{see (A.3):}\\ \sum_{m_i\,m_f} C^{J\,M}_{j_i\,m_i\,j_f\,m_f}\,C^{J'\,M'}_{j_i\,m_i\,j_f\,m_f} = \delta_{J\,J'}\,\delta_{M\,M'}\end{array}} =$$

$$= \frac{\delta_{J\,J'}\,(2j_f+1)}{(2j_i+1)(2J+1)}\sum_{M} D^{J\,*}_{M\tau}\;D^{J'}_{M'\tau} =$$

$$= \boxed{\begin{array}{c}\text{because}\\ \sum_M D^{J\,*}_{M\tau}\;D^{J}_{M\tau} = 1\end{array}} =$$

$$= \frac{\delta_{J\,J'}\,(2j_f+1)}{(2j_i+1)(2J+1)} \tag{2.111}$$

So, after the averaging over m_i and sumation over m_f (that means the nucleus is not spin oriented before and as well as after the transition) the transition probabilty is

$$T_{\alpha_i\,j_i\to\alpha_f\,j_f}(\vec{k},\tau) = \frac{1}{2j_i+1}\sum_{m_i\,m_f} T_{\alpha_i\,j_i\,m_i\to\alpha_f\,j_f\,m_f}(\vec{k},\tau) =$$

$$= \frac{1}{4\pi\,\epsilon_0\,\hbar}\,\frac{1}{2j_i+1}\sum_J \frac{k^{2J+1}}{[(2J+1)!!]^2}\,\frac{J+1}{J}$$

$$\left|\langle\alpha_f\,j_f||\hat{\mathscr{M}}^{(el)}_J(k)||\,\alpha_i\,j_i\rangle + i\,\tau\,\langle\alpha_f\,j_f||\hat{\mathscr{M}}^{(mag)}_J(k)||\,\alpha_i\,j_i\rangle\right|^2 \tag{2.112}$$

If we do not know the polarization of the emitted photon (that means τ is not determined in (2.112) then the sumation over $\tau = \pm 1$ shoud be made in

(2.112).

$$T_{\alpha_i\, j_i \to \alpha_f\, j_f}(\vec{k}) = \sum_{\tau=\pm 1} T_{\alpha_i\, j_i \to \alpha_f\, j_f}(\vec{k},\tau) =$$
$$= \frac{1}{4\pi\,\epsilon_0\,\hbar}\,\frac{1}{2j_i+1}\sum_J \frac{k^{2J+1}}{[(2J+1)!!]^2}\,\frac{J+1}{J}$$
$$2\,\left[\left|\langle \alpha_f\, j_f||\hat{\mathscr{M}}_J^{(el)}(k)||\,\alpha_i\, j_i\rangle\right|^2 + \left|\langle \alpha_f\, j_f||\hat{\mathscr{M}}_J^{(mag)}(k)||\,\alpha_i\, j_i\rangle\right|^2\right] \tag{2.113}$$

From the (2.113) it follows that the expression $T_{\alpha_i\, j_i \to \alpha_f\, j_f}(\vec{k})\; d\Omega_k$ is the probability that during the time unit the nucleus makes the transition from the nonoriented initial state $|\alpha_i\, j_i\rangle$ to the nonoriented final state $|\alpha_f\, j_f\rangle$ with the simultanous emission of the unpolarized photon with the energy in the unit energy interval arround the value $\hbar\omega = \hbar kc$ and with the direction of the unit space angle vicinity of the space angle given by the dirrection of the vector $\vec{k}$.

If we want to determine the total probability that during the time unit the nucleus makes the transition $|\alpha_i\, j_i\rangle \to |\alpha_f\, j_f\rangle$ between two nonoriented states with the emission of the unpolarized photon with the energy in the unit interval arround the value $\hbar\, k\, c = \hbar\, \omega$ and flying to the arbitrary dirrection we should integrate the expr. (2.113) over the whole space angle (we also used the expression $\alpha = \frac{e^2}{4\pi\,\epsilon_0\,\hbar\,c} = \frac{1}{137}$ for the constant of the fine structure)

$$T_{\alpha_i\, j_i \to \alpha_f\, j_f}(k) = \int_{(4\pi)} T_{\alpha_i\, j_i \to \alpha_f\, j_f}(\vec{k})\; d\Omega_k =$$
$$= \frac{4\pi}{2\pi\,\epsilon_0\,\hbar}\,\frac{1}{2j_i+1}\sum_J \frac{k^{2J+1}}{[(2J+1)!!]^2}\,\frac{J+1}{J}$$
$$\left[\left|\langle \alpha_f\, j_f||\hat{\mathscr{M}}_J^{(el)}(k)||\,\alpha_i\, j_i\rangle\right|^2 + \left|\langle \alpha_f\, j_f||\hat{\mathscr{M}}_J^{(mag)}(k)||\,\alpha_i\, j_i\rangle\right|^2\right] =$$
$$= \frac{8\pi c\alpha}{e^2}\,\frac{1}{2j_i+1}\sum_J \frac{k^{2J+1}}{[(2J+1)!!]^2}\,\frac{J+1}{J}$$
$$\left[\left|\langle \alpha_f\, j_f||\hat{\mathscr{M}}_J^{(el)}(k)||\,\alpha_i\, j_i\rangle\right|^2 + \left|\langle \alpha_f\, j_f||\hat{\mathscr{M}}_J^{(mag)}(k)||\,\alpha_i\, j_i\rangle\right|^2\right] \tag{2.114}$$

We have to realize that the sum over J in (2.114) goes formally over all values $J = 1,\, 2, \ldots,\, \infty$ but in reality for given transition $|\alpha_i\, j_i\rangle \to |\alpha_f\, j_f\rangle$ only

values of J which fulfil the selection rules of the matrix elements of transition multipole operators $\langle \alpha_f\, j_f || \hat{\mathscr{M}}^{(el)}_{J\,M}(k) || \,\alpha_i\, j_i \rangle$ and $\langle \alpha_f\, j_f || \hat{\mathscr{M}}^{(mag)}_{J\,M}(k) || \,\alpha_i\, j_i \rangle$ (see also (2.109)) is allowed. These selection rules are given by triangle inequality.

$$|j_f - j_i| \;\leq\; J \;\leq\; j_f + j_i \tag{2.115}$$

Besides the selection rule (2.15) for angular momenta there are also selection rules for parity. We suppose that the nucleus Hamiltonian $\hat{H}_{nuc}$ commutes with the parity operator $\mathscr{P}$ (see(1.33))

$$[\hat{H}_{nuc}, \mathscr{P}] = 0 \tag{2.116}$$

From the subsection 1.3.1 we know that a small violation of the symmetry (2.116) exists through the presence of weak interaction but this is neglectible for electromagnetic transitions. So, if (2.116) valids then each eigenstate of the nuclear Hamiltonian $\hat{H}_{nuc}$ is simultaneously an eigenstate of the parity operator $\mathscr{P}$. Therefore

$$\begin{aligned} \mathscr{P}\,|i\rangle \;&=\; \mathscr{P}\,|\alpha_i\; j_i\; m_i\rangle \;=\; \Pi_i\,|i\rangle\,, \qquad \Pi_i = \pm 1 \\ \mathscr{P}\,|f\rangle \;&=\; \mathscr{P}\,|\alpha_f\; j_f\; m_f\rangle = \Pi_f\,|f\rangle\,, \qquad \Pi_f = \pm 1 \end{aligned} \tag{2.117}$$

Further we determine the transformation properties of the transition multipole operators $\hat{\mathscr{M}}^{(el)}_{J\,M}(k)$ and $\hat{\mathscr{M}}^{(mag)}_{J\,M}(k)$. Using the following symmetries with respect to the parity transformation

$$\begin{aligned} \mathscr{P}\, Y_{Lm}\, \mathscr{P}^{-1} \;&=\; (-1)^L\, Y_{lm} && \text{(see(A.48))} \\ \mathscr{P}\, \vec{\xi}_\mu\, \mathscr{P}^{-1} \;&=\; -\,\vec{\xi}_\mu && \text{(see(A.61))} \\ \mathscr{P}\, \vec{Y}_{LJM}\, \mathscr{P}^{-1} \;&=\; \sum_\mu C^{J\,M}_{l\;M-\mu\,1\,\mu}\, \mathscr{P}\, Y_{L\,m-\mu} \vec{\xi}_\mu\, \mathscr{P}^{-1} = (-1)^{L+1}\, \vec{Y}_{LJM} \end{aligned}$$

we obtain following symmetries for electric and magnetic transverse fields

$$\begin{aligned} \mathscr{P}\, \hat{\vec{j}}_{nuc}\, \mathscr{P}^{-1} \;&=\; -\hat{\vec{j}}_{nuc} \\ \mathscr{P}\, \vec{A}^{el}_{JM}\, \mathscr{P}^{-1} \;&=\; (-1)^{J+1}\, \vec{A}^{el}_{JM} && \text{(see (2.27))} \\ \mathscr{P}\, \vec{A}^{mag}_{JM}\, \mathscr{P}^{-1} \;&=\; (-1)^{J}\, \vec{A}^{mag}_{JM} && \text{(see (2.25))} \end{aligned}$$

and from the definition (2.103) it follows

$$\begin{aligned} \mathscr{P}\, \hat{\mathscr{M}}^{(el)}_{JM}(k)\, \mathscr{P}^{-1} \;&=\; (-1)^J\, \hat{\mathscr{M}}^{(el)}_{JM}(k) \\ \mathscr{P}\, \hat{\mathscr{M}}^{(mag)}_{JM}(k)\, \mathscr{P}^{-1} \;&=\; (-1)^{J+1}\, \hat{\mathscr{M}}^{(mag)}_{JM}(k) \end{aligned} \tag{2.118}$$

So, we have for the matrix elements of the electric and magnetic transition operators

$$\begin{aligned}
\langle f|\hat{\mathscr{M}}^{(el)}_{JM}(k)|i\rangle &= \langle f|\,\mathscr{P}^{-1}\,\mathscr{P}\hat{\mathscr{M}}^{(el)}_{JM}(k)\,\mathscr{P}^{-1}\,\mathscr{P}|i\rangle = \\
&= \Pi_i\,\Pi_f\,(-1)^J\,\langle f|\hat{\mathscr{M}}^{(el)}_{JM}(k)|i\rangle \\
\langle f|\hat{\mathscr{M}}^{(mag)}_{JM}(k)|i\rangle &= \langle f|\,\mathscr{P}^{-1}\,\mathscr{P}\hat{\mathscr{M}}^{(mag)}_{JM}(k)\,\mathscr{P}^{-1}\,\mathscr{P}|i\rangle = \\
&= \Pi_i\,\Pi_f\,(-1)^{J+1}\,\langle f|\hat{\mathscr{M}}^{(mag)}_{JM}(k)|i\rangle
\end{aligned} \tag{2.119}$$

We can summarize the main expressions for the el.mg. transition probability. The probability that during the time unit the nucleus makes the el.mg. transition $|\alpha_i\, j_i\rangle \to |\alpha_f\, j_f\rangle$ between two nonoriented states with the simultaneous emission of the unpolarized photon with the energy with values in the unit interval arround the value $\hbar\, k\, c = \hbar\,\omega$ and flying to any dirrection is given by (2.114). All possible total angular momenta J of emmited photon in this transition are determined by the triangle inequality (2.15)

$$|j_f - j_i| \;\leq\; J \;\leq\; j_f + j_i$$

and by the parity selection rules (2.16) which claim that the only values of J allowed in this transition have to fulfill the following conditions :

$$\begin{aligned}
&\text{for electric transitions:} && (-1)^J\,\Pi_i\Pi_f = 1 \\
&\text{for magnetic transitions:} && (-1)^{J+1}\,\Pi_i\Pi_f = 1
\end{aligned} \tag{2.120}$$

2.2.2.2 Longwave approximation

Electromagnetic transition probabilities (2.114) contains the squares of the matrix elements of the electric and magnetic multipole operators which, according to (2.103), involves spherical wave solutions $\vec{A}^{(el)}_{JM}(\vec{r})$ and $\vec{A}^{(mag)}_{JM}(\vec{r})$ (see (2.100) of the wave equation with the spherical Bessel function $f_J(kr)$. All these expressions are quite complicated but they can be substantionally simplified if we use so called longwave approximation. This approximation consists in the fact that the argument kr of the spherical Bessel function $f_J(kr)$ involved in (2.100) is sufficiently close to zero, that means

$$k\,r \;<<\; 1 \tag{2.121}$$

Then we can use approximative expression for the spherical Bessel function:

$$f_J(kr) = j_J(kr) \;\stackrel{kr\to 0}{\longrightarrow}\; \frac{(kr)^J}{(2J+1)!!} \tag{2.122}$$

This approximation simplifies all expressions for transition probabilities as it will be shown.

One can ask if the condition (2.121) is fulfilled for the el.mg. transition in nuclei (we remind that $\hbar kc = \hbar\omega$ is the energy of the emitted photon and simultaneously it is the transition energy). The answer is yes, the condition (2.121) is fulfilled for usual transitions in nuclei. For the nucleus the argument kr is always: $kr \leq kR$, where $R = 1.2A^{1/3}\ fm$ is the nucleus radius (see (1.2)). Therefore, the condition (2.121) means:

$$kR << 1 \quad \Rightarrow \quad k << \frac{1}{R}$$

$$\Rightarrow \hbar kc << \frac{\hbar c}{R} \approx \boxed{\begin{array}{c}\text{we suppose heavier nuclei}\\ \text{where} \quad R \approx 10\ fm\end{array}} \approx \frac{197 MeV.fm}{10\ fm}$$

$$\Rightarrow \text{transition energy:} \qquad \hbar\omega = \hbar kc << 20\ MeV \tag{2.123}$$

The energy 20 MeV is much higher than the standard el.mg. transition energies in nuclei which is usually less than 5 MeV (for heavier nuclei a typical transition energy between low-energy nuclear states does not exceed 1 MeV). So, the longwave approximation (2.121) can be considered as fulfilled for nuclei.

Further the electric and magnetic multipole operators in the longwave approximation are derived.

Electric multipole operator in the longwave approximation Electric multipole operator (see (2.103)) involves $\vec{A}^{(el)}_{JM}$ which, according to (2.100), has two terms, the first one involves $f_{J-1}(kr)$ and the second contains $f_{J+1}(kr)$. From the epr. (2.122) it follows that

$$\frac{f_{J+1}(kr)}{f_{J-1}(kr)} = \frac{(kr)^{J+1}}{(2J+3)!!}\,\frac{(2J-1)!!}{(kr)^{J-1}} = \frac{(kr)^2}{(2J+3)(2J+1)} \tag{2.124}$$

As we have just discussed the argument of these functions fulfills: $kr \leq kR << 1$ and therefore the ratio (2.124) is very small, $\frac{f_{J+1}(kr)}{f_{J-1}(kr)} \to 0$. This means that in the framework of the longwave approximation the second term in (2.100) is neglectible in the comparison with the first one and for $\vec{A}^{(el)}_{JM}$ we can write the following approximative expression

$$\vec{A}^{(el)}_{JM}(\vec{r}) \overset{kr<<1}{\longrightarrow} i\sqrt{\frac{J+1}{2J+1}}\ f_{J-1}(kr)\ \vec{Y}_{J-1\,J\,M}(\hat{r}) \tag{2.125}$$

Similarly, for the same reason in the framework of the longwave limit we can neglect the second term in the expression (2.30) for the longitudinal solution of the wave equation and we have (again we omit the time dependence)

$$\vec{A}^{(long)}_{JM}(\vec{r}) \overset{kr<<1}{\longrightarrow} \sqrt{\frac{J}{2J+1}}\, f_{J-1}(kr)\, \vec{Y}_{J-1\,J\,M}(\hat{r}) \tag{2.126}$$

So, in the framework of the longwave limit $\vec{A}^{(el)}_{JM}(\vec{r})$ and $\vec{A}^{(long)}_{JM}(\vec{r})$ are equal each other but for a factor:

$$\begin{aligned}
&\vec{A}^{(el)}_{JM}(\vec{r}) \overset{kr<<1}{\longrightarrow} i\sqrt{\frac{J+1}{J}}\, \vec{A}^{(long)}_{JM}(\vec{r}) \;= \\
&= \boxed{\begin{array}{c}\text{see}\\(2.30)\end{array}} = i\sqrt{\frac{J+1}{J}}\,\frac{1}{k}\,\vec{\nabla}\, f_J(kr)\, Y_{JM}(\hat{r}) = \\
&= \boxed{\begin{array}{c}\text{see}\\(2.122)\end{array}} = i\sqrt{\frac{J+1}{J}}\,\frac{1}{(2J+1)!!}\, k^{J-1}\,\vec{\nabla}\, r^J\, Y_{JM}(\hat{r})
\end{aligned} \tag{2.127}$$

The substitution of (2.127) into (2.103) gives the expression for the electric multipole operator $\hat{\mathscr{M}}^{(el)}_{J\,M}(k)$ in the longwave approximation:

$$\begin{aligned}
\hat{\mathscr{M}}^{(el)}_{J\,M}(k) &\overset{kr<<1}{\longrightarrow} \hat{\mathscr{M}}^{(el)}_{J\,M}(k=0) = i\,\frac{(2J+1)!!}{c\,k^J\,(J+1)}\,[J(J+1)]^{1/2}\,\frac{k^{J-1}}{(2J+1)!!}\sqrt{\frac{J+1}{J}} \\
&\qquad \cdot \int d^3r\, \hat{\vec{j}}_{nuc}(\vec{r})\,\vec{\nabla}\, r^J\, Y_{JM}(\hat{r}) = \\
&= \frac{i}{c\,k}\int d^3r\, \hat{\vec{j}}_{nuc}(\vec{r})\,\vec{\nabla}\, r^J\, Y_{JM}(\hat{r}) = \boxed{\begin{array}{c}\text{integration}\\\text{per partes}\end{array}} = \\
&= -\frac{i}{c\,k}\int d^3r\, r^J\, Y_{JM}(\hat{r})\,\vec{\nabla}\hat{\vec{j}}_{nuc}(\vec{r})
\end{aligned} \tag{2.128}$$

In order to determine the electromagnetic transition probabilities we have to

calculate matrix elements of the multipole operators (see (2.110)-(2.114)):

$$\langle f|\hat{\mathscr{M}}^{(el)}_{J\,M}(k=0)|i\rangle = -\frac{i}{ck}\int d^3r\, r^J\, Y_{JM}(\hat{r})\,\hat{\nabla}\cdot\langle f|\hat{\vec{j}}_{nuc}(\vec{r})|i\rangle =$$

$$= \left|\begin{array}{c}\text{for stationary states:}\\ \langle f|\hat{\vec{j}}_{nuc}(\vec{r},t)|i\rangle = \langle f|\hat{\vec{j}}_{nuc}(\vec{r})|i\rangle\, e^{\frac{i}{\hbar}(E_f-E_i)t}\\ \langle f|\hat{\rho}_{nuc}(\vec{r},t)|i\rangle = \langle f|\hat{\rho}_{nuc}(\vec{r})|i\rangle\, e^{\frac{i}{\hbar}(E_f-E_i)t}\\ \text{and using continuity equation (see the Chapter 5, expr.(5) in [332]) :}\\ \vec{\nabla}\cdot\langle f|\hat{\vec{j}}_{nuc}(\vec{r},t)|i\rangle = \vec{\nabla}\cdot\langle f|\hat{\vec{j}}_{nuc}(\vec{r})|i\rangle\, e^{\frac{i}{\hbar}(E_f-E_i)t} = -\frac{\partial}{\partial t}\langle f|\hat{\rho}_{nuc}(\vec{r},t)|i\rangle =\\ = -\frac{i(E_f-E_i)}{\hbar}\,\langle f|\hat{\rho}_{nuc}(\vec{r},t)|i\rangle = \frac{i(E_i-E_f)}{\hbar}\,\langle f|\hat{\rho}_{nuc}(\vec{r})|i\rangle\, e^{\frac{i}{\hbar}(E_f-E_i)t}\\ \Longrightarrow \langle f|\hat{\rho}_{nuc}(\vec{r})|i\rangle = -\frac{1}{i\omega_{fi}}\langle f|\vec{\nabla}\cdot\hat{\vec{j}}_{nuc}(\vec{r})|i\rangle \quad \text{where } \omega_{fi}\equiv\frac{E_f-E_i}{\hbar}\end{array}\right| =$$

$$= \frac{E_i-E_f}{\hbar kc}\int d^3r\, r^J\, Y_{JM}(\hat{r})\,\langle f|\hat{\rho}_{nuc}(\vec{r})|i\rangle = \tag{2.129}$$

So, the longwave limit electric multipole operator is given by ($E_i - E_f = \hbar kc$):

$$\hat{\mathscr{M}}^{(el)}_{J\,M}(k) \overset{kr<<1}{\longrightarrow} \hat{\mathscr{M}}^{(el)}_{J\,M}(k=0) = \int d^3r\, r^J\, Y_{JM}(\hat{r})\,\hat{\rho}_{nuc}(\vec{r}) \tag{2.130}$$

The operator of the charge density $\hat{\rho}_{nuc}(\vec{r})$ for the system (nucleus) consisted from A particles, each of them has the charge e_i and radius-vector $\vec{r}_i$, is given as follows

$$\hat{\rho}_{nuc}(\vec{r}) = \sum_{i=1}^{A} e_i\,\delta(\vec{r}-\vec{r}_i) \tag{2.131}$$

So, the electric multipole operator in the longwave approximation is

$$\hat{\mathscr{M}}^{(el)}_{J\,M}(k) \overset{kr<<1}{\longrightarrow} \hat{\mathscr{M}}^{(el)}_{J\,M} \equiv \hat{\mathscr{M}}^{(el)}_{J\,M}(k=0) = \sum_{i=1}^{A} e_i\, r_i^J\, Y_{JM}(\hat{r}_i) \tag{2.132}$$

Magnetic multipole operator in the longwave approximation Mag-

netic multipole operator was introduced in (2.103)

$$\begin{aligned}
&\hat{\mathscr{M}}_{JM}^{(mag)}(k) \equiv \\
&\quad \equiv -i\,\frac{(2J+1)!!}{c\,k^J\,(J+1)}\,[J(J+1)]^{1/2}\int d^3r\,\hat{\vec{j}}_{nuc}(\vec{r})\,\vec{A}_{JM}^{(mag)}(\vec{r}) = \\
&\quad = \boxed{\begin{array}{c}\text{see}\\(2.25)\end{array}} = \\
&\quad = -i\,\frac{(2J+1)!!}{c\,k^J\,(J+1)}\,[J(J+1)]^{1/2}\,\frac{1}{\sqrt{J(J+1)}} \\
&\qquad\qquad \int d^3r\,\hat{\vec{j}}_{nuc}(\vec{r})\cdot\hat{\vec{L}}\,f_J(kr)\,Y_{JM}(\hat{r}) \qquad (2.133)
\end{aligned}$$

In the longwave limit the spherical Bessel function $f_J(kr)$ is given by (2.122) and the substitution of (2.122) into (2.133) gives the longwave limit of the magnetic multipole operator in the following form

$$\begin{aligned}
&\hat{\mathscr{M}}_{JM}^{(mag)}(k) \overset{kr<<1}{\longrightarrow} \hat{\mathscr{M}}_{JM}^{(mag)}(k=0) = \frac{-\,i}{c\,(J+1)}\int d^3r\,\hat{\vec{j}}_{nuc}(\vec{r})\cdot\hat{\vec{L}}\,r^J\,Y_{JM}(\hat{r}) = \\
&\quad = \boxed{\begin{array}{c}\text{because}\\ \hat{\vec{L}} = -\,i\,\vec{r}\times\vec{\nabla}\end{array}} = \\
&\quad = \frac{-\,1}{c\,(J+1)}\int d^3r\,\hat{\vec{j}}_{nuc}(\vec{r})\cdot(\vec{r}\times\vec{\nabla})\,r^J\,Y_{JM}(\hat{r}) = \\
&\quad = \boxed{\begin{array}{c}\text{because}\\ \vec{a}\cdot(\vec{b}\times\vec{c}) = \vec{c}\cdot(\vec{a}\times\vec{b}) = -\vec{c}\cdot(\vec{b}\times\vec{a})\end{array}} = \\
&\quad = \frac{1}{c\,(J+1)}\int d^3r\,\left(\vec{r}\times\hat{\vec{j}}_{nuc}(\vec{r})\right)\cdot\vec{\nabla}\,r^J\,Y_{JM}(\hat{r}) \qquad (2.134)
\end{aligned}$$

The operator of the nucleus current density $\hat{\vec{j}}_{nuc}(\vec{r})$ consists from two parts

$$\hat{\vec{j}}_{nuc}(\vec{r}) = \hat{\vec{j}}_o(\vec{r}) + \hat{\vec{j}}_s(\vec{r}) \qquad (2.135)$$

where $\hat{\vec{j}}_o(\vec{r})$ is the operator of orbital part of the current density corresponding to the movement of the charged particles (protons in the case of the nucleus) and $\hat{\vec{j}}_s(\vec{r})$ is the operator or the current density part caused by the possible presence of the spin of particles (or more precisely by the magnetic dipole moments of particles). As a consequence of the nonzero magnetic moments

of the system particles (nucleons) the system has generally nonzero values of the magnetic dipole moment density $\hat{\vec{M}}_{spin}(\vec{r})$ (by other words $\hat{\vec{M}}_{spin}(\vec{r})$ is the operator of the magnetic dipole moment caused by the spin of the system particles corresponding to the unit volume of the system). From the classic theory of el.mg. field the spin (magnetization) current density is related to the magnetic dipole moment density $\hat{\vec{M}}_{spin}(\vec{r})$ by the following well-known formula

$$\hat{\vec{j}}_s(\vec{r}) = \vec{\nabla} \times \hat{\vec{M}}_{spin}(\vec{r}) \tag{2.136}$$

The substitution of (2.136) into (2.135) and then into (2.134) gives

$$\begin{aligned} \hat{\mathscr{M}}_{JM}^{(mag)}(k) \overset{kr<<1}{\longrightarrow} & \frac{1}{c\,(J+1)} \int d^3r\, (\vec{r} \times \hat{\vec{j}}_o(\vec{r})) \cdot \vec{\nabla}\, r^J\, Y_{JM}(\hat{r}) + \\ & + \frac{1}{c\,(J+1)} \int d^3r \left[\vec{r} \times \left(\vec{\nabla} \times \hat{\vec{M}}_{spin}(\vec{r})\right)\right] \cdot \vec{\nabla}\, r^J\, Y_{JM}(\hat{r}) \end{aligned} \tag{2.137}$$

Using the following identity

$$\int d^3r\, \vec{A}(\vec{r}) \cdot \left(\vec{\nabla} \times \vec{B}(\vec{r})\right) = \int d^3r\, \vec{B}(\vec{r}) \cdot \left(\vec{\nabla} \times \vec{A}(\vec{r})\right) \tag{2.138}$$

the second term in (2.137) can be rewritten

$$\frac{1}{c\,(J+1)}\int d^3r\left[\vec{r}\times\left(\vec{\nabla}\times\hat{\vec{M}}_{spin}(\vec{r})\right)\right]\cdot\vec{\nabla}\,r^J\,Y_{JM}(\hat{r})=$$

$$=\boxed{\begin{array}{c}\text{because}\\(\vec{a}\times\vec{b})\cdot\vec{c}=-\vec{b}\cdot(\vec{a}\times\vec{c})\end{array}}=$$

$$=-\frac{1}{c\,(J+1)}\int d^3r\,\left[\vec{\nabla}\times\hat{\vec{M}}_{spin}(\vec{r})\right]\cdot\left[\vec{r}\times\vec{\nabla}\right]\,r^J\,Y_{JM}(\hat{r})=$$

$$=\boxed{\begin{array}{c}\text{see (2.138) where}\\\vec{B}\leftrightarrow\hat{\vec{M}}_{spin}\quad\vec{A}\leftrightarrow[\vec{r}\times\vec{\nabla}r^J\,Y_{JM}(\hat{r})]\end{array}}=$$

$$=-\frac{1}{c\,(J+1)}\int d^3r\,\hat{\vec{M}}_{spin}(\vec{r})\cdot\left[\vec{\nabla}\times(\vec{r}\times\vec{\nabla})\right]\,r^J\,Y_{JM}(\hat{r})=$$

$$=\boxed{\begin{array}{c}\vec{\nabla}\times(\vec{r}\times\vec{\nabla})=-\vec{\nabla}\frac{\partial}{\partial r}r+\vec{r}\Delta\\\Delta\,r^JY_{JM}(\hat{r})=0\end{array}}=$$

$$=\frac{1}{c\,(J+1)}\int d^3r\,\hat{\vec{M}}_{spin}(\vec{r})\cdot\vec{\nabla}\frac{\partial}{\partial r}\,r^{J+1}\,Y_{JM}(\hat{r})=$$

$$=\frac{1}{c}\int d^3r\,\hat{\vec{M}}_{spin}(\vec{r})\cdot\vec{\nabla}\,r^J\,Y_{JM}(\hat{r}) \tag{2.139}$$

and the substitution of (2.139) into (2.137) gives the longwave limit of the magnetic multipole operator in the following form

$$\hat{\mathscr{M}}^{(mag)}_{JM}(k)\overset{kr<<1}{\longrightarrow}\hat{\mathscr{M}}^{(mag)}_{JM}\equiv\hat{\mathscr{M}}^{(mag)}_{JM}(k=0)=$$
$$=\frac{1}{c}\int d^3r\,\left[\hat{\vec{M}}_{spin}+\frac{1}{J+1}\left(\vec{r}\times\hat{\vec{j}}_o(\vec{r})\right)\right]\,\vec{\nabla}\,r^J\,Y_{JM}(\hat{r}) \tag{2.140}$$

The nucleus composed from A nucleons (each of them has the charge e_i, mass m_i, linear momentum $\hat{\vec{p}}_i$, radius vector $\vec{r}_i$, and magnetic dipole moment $\hat{\vec{\mu}}_i^{(s)}$) has following orbital part of the charge current density and magnetic moment density:

$$\hat{\vec{j}}_o(\vec{r})=\sum_{i=1}^{A}\frac{e_i}{m_i}\,\hat{\vec{p}}_i\,\delta(\vec{r}-\vec{r}_i)$$

$$\hat{\vec{M}}_{spin}(\vec{r})=\sum_{i=1}^{A}\hat{\vec{\mu}}_i^{(s)}\,\delta(\vec{r}-\vec{r}_i) \tag{2.141}$$

The substitution of (2.141) into (2.140) yields

$$\begin{aligned}
&\hat{\mathscr{M}}_{JM}^{(mag)}(k) \overset{kr<<1}{\longrightarrow} \hat{\mathscr{M}}_{JM}^{(mag)} = \\
&= \frac{1}{c} \sum_{i=1}^{A} \left[\hat{\vec{\mu}}_i^{(s)} + \frac{1}{J+1} \left(\vec{r}_i \times \hat{\vec{p}}_i \right) \frac{e_i}{m_i} \right] \vec{\nabla}_i \, r_i^J \, Y_{JM}(\hat{r}_i) = \\
&= \frac{1}{c} \sum_{i=1}^{A} \left[\hat{\vec{\mu}}_i^{(s)} + \frac{1}{J+1} \hbar \, \hat{\vec{l}}_i \, \frac{e_i}{m_i} \right] \vec{\nabla}_i \, r_i^J \, Y_{JM}(\hat{r}_i)
\end{aligned} \tag{2.142}$$

where $\hat{\vec{l}}_i$ is the operator of the orbital momentum of i-th particle. The particle magnetic dipole moment can be expressed in terms of its spin $\hat{\vec{s}}_i$ through gyromagnetic ratio $g_i^{(s)}$:

$$\hat{\vec{\mu}}_i^{(s)} = g_i^{(s)} \, \hat{\vec{s}}_i \, \frac{e \, \hbar}{2 \, m_i} = g_i^{(s)} \, \hat{\vec{s}}_i \, \mu_N^{(SI)} \tag{2.143}$$

where gyromagnetic ratios for nucleons are

$$g^{(s)} = 5.586 \text{ for protons}, \qquad g^{(s)} = -3.826 \text{ for neutrons} \tag{2.144}$$

and the nuclear magneton $\mu_N^{(SI)} = \frac{e\hbar}{2m_p}$ in the SI system of units was introduced, The substitution of (2.143) into (2.142) gives the final expression of the magnetic multipole operator in the framework of the longwave approximation

$$\begin{aligned}
&\hat{\mathscr{M}}_{JM}^{(mag)}(k) \overset{kr<<1}{\longrightarrow} \hat{\mathscr{M}}_{JM}^{(mag)} = \\
&= \sum_{i=1}^{A} \left[g_i^{(s)} \, \hat{\vec{s}}_i + + \frac{2}{J+1} \, g_i^{(l)} \, \hat{\vec{l}}_i \right] \mu_N \, \vec{\nabla}_i \, r_i^J \, Y_{JM}(\hat{r}_i)
\end{aligned} \tag{2.145}$$

where we introduced orbital gyromagnetic ratios $g_i^{(l)}$ and so called nuclear magneton μ_N [7] :

$$g^{(l)} = 1 \text{ for protons}, \quad g^{(l)} = 0 \text{ for neutrons}, \quad \mu_N = \mu_N^{(G)} = \frac{e\hbar}{2 \, m \, c} \tag{2.146}$$

and we supose that all particles forming the system (nucleons) have the same mass m and the charge of i-th particle is $e \, g_i^{(l)}$.

[7] In this textbook we use SI system of units but the nuclear magneton is defined as $\mu_N = \mu_N^{(G)} = \frac{e\hbar}{2 \, m_p \, c} = \frac{1}{c} \, \mu_N^{(SI)} = 0.105 \, fm$ which corresponds to the Gauss system of units. Such introducing is more convenient from the point of view of farther dimension analysis.

The expression (2.145) for $\hat{\mathscr{M}}^{(mag)}_{JM}$ can be rewritten into the equivalent and more used form applying following identities,

$$\vec{\nabla} r^J Y_{JM}(\hat{r}) = \boxed{\begin{array}{c}\text{see}\\ (A.62) \text{ and } (A.53)\end{array}} =$$

$$= \sqrt{J(2J+1)}\, r^{J-1} \sum_{m_l \mu} C^{JM}_{J-1\, m_j\, 1\, \mu} Y_{J-1,m_l}(\hat{r})\, \vec{\xi}_\mu$$

$$\Rightarrow \quad \vec{s}\cdot\vec{\nabla} r^J Y_{JM}(\hat{r}) = \sqrt{J(2J+1)} r^{J-1} \sum_{m_l \mu} C^{JM}_{J-1\, m_l\, 1\, \mu}\, s_\mu\, Y_{J-1,m_l}(\hat{r}) =$$

$$= \sqrt{J(2J+1)}\, r^{J-1} \left[\, s \otimes Y_{J-1}(\hat{r}) \,\right]_{JM}$$

$$\vec{l}\cdot\vec{\nabla} r^J Y_{JM}(\hat{r}) = \sqrt{J(2J+1)}\, r^{J-1} \left[\, l \otimes Y_{J-1}(\hat{r}) \,\right]_{JM}$$

and long-wave limit of $\hat{\mathscr{M}}^{(mag)}_{JM}$ reads

$$\hat{\mathscr{M}}^{(mag)}_{JM}(k) \overset{kr<<1}{\longrightarrow} \hat{\mathscr{M}}^{(mag)}_{JM} = \mu_N \sqrt{J(2J+1)}$$

$$\sum_{i=1}^{A} \left(\frac{2g_i^{(l)}}{J+1} \left[\hat{l}_i \otimes Y_{J-1}(\hat{r})\right]_{JM} + g_i^{(s)} \left[\hat{s}_i \otimes Y_{J-1}(\hat{r})\right]_{JM} \right) r^{J-1} \qquad (2.145')$$

Using of the longwave limits for the electric and magnetic multipole operators in the exprs. (2.110), (2.112), (2.113) and (2.114) simplifies substantionally the calculation of the transition probabilities. It is necessary to note that the condition $kR << 1$ for the longwave approximation (see(2.121)) is valid not only for nuclei as the systems of nucleons but also for other systems like electrons in the atomic or molecular shells or electrons in the quantum dots and others. In all these cases the usual transition energies $\hbar kc$ and the size (radius) R of the given system is so, that inequality $kR << 1$ is usually fulfilled.

2.2.2.3 Reduced transition probabilities and the multipolarity mixing ratio

From the expressions (2.110), (2.112), (2.113), (2.114) one can see that the electromagnetic transition probabilities depend explicitly on the transition energy $\hbar kc$. In order to have a quantity characterizing the transition probability without the dependence on the transition energy so called reduced transition probability $B(XJ,\, i \to f)$ of the given type $X = \mathit{electric}$ or $X = \mathit{magnetic}$ and of given multipolarity J for given nucleus transition

$|i\rangle \to |f\rangle$ is introduced:

$$B(XJ;\, i \to f) \equiv \frac{|\,\langle f||\,\hat{\mathscr{M}}_J^{(X)}(k)\,||i\rangle\,|^2}{2j_i+1} \approx \frac{|\,\langle f||\,\hat{\mathscr{M}}_J^{(X)}\,||i\rangle\,|^2}{2j_i+1} \qquad (2.147)$$

where $|\,i\rangle = |\,\alpha_i\; j_i\rangle$, $|\,f\rangle = |\,\alpha_f\; j_f\rangle$ are the initial and final states of the transition, respectively. Then the transition probability $T_{\alpha_i\, j_i \to \alpha_f\, j_f}(k)$ (see (2.114) can be rewritten as follows

$$\begin{aligned} T_{\alpha_i\, j_i \to \alpha_f\, j_f}(k) &= \frac{8\pi\, c\, \alpha}{e^2} \sum_J \frac{k^{2J+1}}{[(2J+1)!!]^2}\, \frac{J+1}{J} \\ &\qquad [B(el\; J,\; i \to f) + B(mag\; J,\; i \to f)] = \\ &= \frac{8\pi\, c\, \alpha}{e^2} \sum_J \frac{(\hbar\,\omega)^{2J+1}}{(\hbar\, c)^{2J+1}[(2J+1)!!]^2}\, \frac{J+1}{J} \\ &\qquad [B(el\; J,\; i \to f) + B(mag\; J,\; i \to f)] \end{aligned} \qquad (2.148)$$

It is necessary to realize that because of the parity selection rules (2.119) for given transition $|i\rangle \to |f\rangle$ and for given sumation index J in the r.h.s. of (2.148) alway only one term appears in the square bracket (that menas only electric or only magnetic reduced probability).

Further we will analyze the dimensions of all quantities involved in (2.148).

$$\begin{aligned} &8\pi\, c\, \alpha = 0.550352 * 10^8\, \frac{m}{s} \\ &\hbar\, c = 197\; MeV\; fm = 197 * 10^{-15}\; MeV\; m \\ &\mu_N \equiv \mu_N^{(G)} = \frac{e\hbar}{2mc} = \frac{1}{c}\, \mu_N^{(SI)} = 0.105\; fm \end{aligned}$$

$$[\; B(el\; J,\; i \to f)\;]_{dim} = \boxed{\begin{array}{c}\text{see (2.132)}\\ (2.147)\end{array}} = e^2\; fm^{2J} =$$

$$= e^2\; (10^{-15})^{2J}\; m^{2J}$$

$$[\; B(mag\; J,\; i \to f)\;]_{dim} = \boxed{\begin{array}{c}\text{see (2.142)}\\ (2.147)\end{array}} = \mu_N^2\; fm^{2J-2} =$$

$$= \left(\frac{e\,\hbar}{2m_p\, c}\right)^2\; fm^{2J-2} = e^2\; 1.105 * 10^{-2} * (10^{-15})^{2J}\; m^{2J}$$

where the nuclear magneton $\mu_N \equiv \mu_N^{(G)} = \frac{e\hbar}{2m_p\, c}$ was introduced.

So, the expression (2.148) for the transition probability $T_{\alpha_i\, j_i\to\alpha_f\, j_f}(k)$ can be rewritten in the more convenient form

$$T_{\alpha_i\, j_i\to\alpha_f\, j_f}(k)=\sum_J\Big(T^{(el)}_{\alpha_i\, j_i\to\alpha_f\, j_f}(J)+T^{(mag)}_{\alpha_i\, j_i\to\alpha_f\, j_f}(J)\Big) \tag{2.149}$$

where

$$\begin{aligned}
T^{(el)}_{\alpha_i\, j_i\to\alpha_f\, j_f}(J=1) &= 1.59059*10^{15}*(\hbar\,\omega)^3\,B(el\,1,\,i\to f)\\
T^{(mag)}_{\alpha_i\, j_i\to\alpha_f\, j_f}(J=1) &= 1.7598*10^{13}*(\hbar\,\omega)^3\,B(mag\,1,\,i\to f)\\
T^{(el)}_{\alpha_i\, j_i\to\alpha_f\, j_f}(J=2) &= 1.2254*10^{9}*(\hbar\,\omega)^5\,B(el\,2,\,i\to f)\\
T^{(mag)}_{\alpha_i\, j_i\to\alpha_f\, j_f}(J=2) &= 1.3558*10^{7}*(\hbar\,\omega)^5\,B(mag\,2,\,i\to f)\\
T^{(el)}_{\alpha_i\, j_i\to\alpha_f\, j_f}(J=3) &= 5.7112*10^{2}*(\hbar\,\omega)^7\,B(el\,3,\,i\to f)\\
T^{(mag)}_{\alpha_i\, j_i\to\alpha_f\, j_f}(J=3) &= 6.3113*10^{0}*(\hbar\,\omega)^7\,B(mag\,3,\,i\to f)
\end{aligned} \tag{2.150}$$

where the following dimensions in (2.150) should be used

$$\begin{aligned}
&[\,T^{(X)}_{i\to f}(J)\,]_{dim}=1/s && [\,B(el\,J,\,i\to f)\,]_{dim}=e^2\,fm^{2J}\\
&[\,\hbar\,\omega]_{dim}=MeV && [\,B(mag\,J,\,i\to f)\,]_{dim}=\mu_N^2\,fm^{2J-2}
\end{aligned}$$

In the nuclear physics literature it is possible to meet also so called absolute amplitudes $\gamma(X\,J,\,i\to f)$ of electric $(X=el)$ or magnetic $(X=el)$ type transition. These are defined as follows

$$\begin{aligned}
\gamma(el\,J,\,i\to f)\equiv i^J\,&\left[\frac{8\pi\,c\,\alpha}{e^2}\,\frac{k^{2J+1}(J+1)}{[(2J+1)!!]^2\,J\,(2j_i+1)}\right]^{1/2}\\
&\cdot\langle\alpha_f\,j_f||\hat{\mathscr{M}}^{(el)}_J||\,\alpha_i\,j_i\rangle\\
\gamma(mag\,J,\,i\to f)\equiv i^{J+1}\,&\left[\frac{8\pi\,c\,\alpha}{e^2}\,\frac{k^{2J+1}(J+1)}{[(2J+1)!!]^2\,J\,(2j_i+1)}\right]^{1/2}\\
&\cdot\langle\alpha_f\,j_f||\hat{\mathscr{M}}^{(mag)}_J||\,\alpha_i\,j_i\rangle
\end{aligned} \tag{2.151}$$

Then the transition probability $T_{\alpha_i\, j_i\to\alpha_f\, j_f}(k)$ (see (2.148)) is written as

$$T_{\alpha_i\, j_i\to\alpha_f\, j_f}(k)=\sum_J\left[|\gamma(el\,J,\,i\to f)|^2+|\gamma(mag\,J,\,i\to f)|^2\right] \tag{2.152}$$

Similarly as in (2.148) because of the parity selection rules (2.120) for electric and magnetic multipole operators in the square bracket on the r.h.s. of

(2.152) always only one term participates ($\gamma(el\ J,\ i \to f)|^2$ or $\gamma(mag\ J,\ i \to f)|^2$). In many real situations the selection rules (2.115) and (2.120) enable for given transition $|\alpha_i\ j_i\rangle \to |\alpha_f\ j_f\rangle$ the simultaneous presence in the expr. (2.152) of several terms with different multipolarities J and different types X (X =el or mag). For instance one meets very often the transitions between low-energy nuclear states with the mixture of $E2$ (el $J = 2$) and M1 (mag $J = 1$) transitions. For such cases it is convenient to introduce so called multipolarity mixing ratio (or factor)

$$\delta_{i\to f}\left(\frac{X\,J}{X'J'}\right) \equiv \frac{\gamma(X\ J, i \to f)}{\gamma(X'\ J', i \to f)} \tag{2.153}$$

e.g. for the mixing of E2 with M1

$$\begin{aligned}\delta_{i\to f}\left(\frac{E\,2}{M\,1}\right) &= \frac{\gamma(E2\ J, i \to f)}{\gamma(M1\ J, i \to f)} = \\ &= 0.835\,\hbar\omega\ [\mathrm{MeV}]\ \frac{\langle f||\ \hat{\mathscr{M}}_2^{(el)}||\ i\rangle\ [e\,b]}{\langle f||\ \hat{\mathscr{M}}_1^{(mag)}||\ i\rangle\ [\mu_n]}\end{aligned} \tag{2.154}$$

where $1\,b = 100\,fm^2$.

It is necessary to note that in the standard (unpolarized and nonoriented) spectroscopic experiments (e.g. from the measurement of the half-lives of excited levels or from the area of energy spectrum peaks) it is possible to obtain only an absolute value of the multipolarity mixing ratios $\delta_{i\to f}\left(\frac{XJ}{X'J'}\right)$. If we want to measure also the sign of $\delta_{i\to f}\left(\frac{XJ}{X'J'}\right)$ experiments with oriented nuclei and with polarized photons are necessary.

In the end of this subsection for the completeness the well-known expressions giving the connection betweeen the transition probability and the half-life of the excited level are shown. According to the decay law the number of nuclei in some sample sitting in the given excited initial state $|i>$ and decaying through electromagnetic transitions into final states $|f>$ with lower energies ($E_f < E_i$) depends on the time by the following formule

$$N^{(i)}(t) = N_0^{(i)}\ e^{-w_i\,t} \tag{2.155}$$

where $N_0^{(i)}$ is the initial number of nuclei excited to the initial state $|i>$ in the initial tine $t = 0$, $N^{(i)}(t)$ is the number of nuclei in this initial state in the time t. The factor w_i in the exponent of (2.155) is a total probability that the nucleus in the state $|i>$ makes electromagnetic transition to all possible (by selection rules) final states $|f>$ and it is given by the following sum

$$w_i = \sum_f T_{i\to f}(k) \qquad \text{with} \quad \hbar kc = E_i - E_f \tag{2.156}$$

where $T_{i\to f}(k)$ is given by (2.148) and where E_i and E_f are energies of states $|i>$ and $|f>$, respectively. Half-life $T^{(i)}_{1/2}$ of the state $|i>$ (or level E_i) is then defined as follows

$$N^{(i)}(T^{(i)}_{1/2}) = \frac{N^{(i)}_0}{2} = N^{(i)}_0\, e^{-w_i\ T^{(i)}_{1/2}} \ \Rightarrow\ T^{(i)}_{1/2} = \frac{ln\,2}{w_i} \tag{2.157}$$

Usual values of time-lives of the low-lying decaying nuclear levels are from picoseconds ($1ps\ =\ 10^{-12}s$) up to nanoseconds ($1ns\ =\ 10^{-9}s$).

2.2.2.4 Reduced probability of el.mg. transitions in the framework of the simple model of independent particles - Weisskopf units

Reduced el.mg. transition probabilty of given type $X = el$ or $X = mag$ with given multipolarity J is defined by (2.147), where then initial state $|i>$ and final state $|f\rangle$ is described in the case of a nucleus by some nuclear model which gives corresponding wave fnctions of the states $|i\rangle$ and $|f\rangle$.

In this subsection we assume very simple model when the nucleus is described by the Hamiltonian with some single-particle mean field potential [8] and residual two-particle interactions between nucleons placed in the mean field is neglected. As we will discuss in detail in the Chapter 5 in such a simple case the total nucleus wave function is represented by the antisymmetrized sum of products of single-particle wave functions of individual nucleons (Slater determinant - see (5.7)), where individual single-particle wave functions are obtained by the solving of the Schroedinger equation with the mentioned above single-paricle Hamiltonian. In the most simple idea the nucleus properties are given by so called valence particles, that means by nucleons occupying the last not fully occupied (with the highest energy) shell of the nuclear mean field (the simple shell model of the nucleus). For the total simplicity we assume that in the last shell there is only one nucleon (for instance the odd-A nucleus with one odd nucleon outside even-even core with closed shells). In such a simple case the properties of the whole nucleus are determined by this odd nucleon (more precisely by its single-particle wave function). Then the reduced matrix element in the expression (2.147) is calculated between the single-particle wave functions of the final and initial s.p.

[8] The microscopic and phenomenological nuclear models of independent particles will be discussed in more details in the Chapters 5 and 6, respectively. For the purpose of this chapter it is not necessary to specify the model of independent particles more presisely.

states of the odd nucleons:

$$|i\rangle = |n_i\, l_i\, j_i\, m_i\rangle = \sum_{\mu_i} C^{j_i\, m_i}_{l_i\, m_i-\mu_i\, \frac{1}{2}\, \mu_i} |n_i\, l_i\, m_i - \mu_i\rangle\, |\frac{1}{2}\, \mu_i\rangle$$
$$|f\rangle = |n_f\, l_f\, j_f\, m_f\rangle = \sum_{\mu_f} C^{j_f\, m_f}_{l_f\, m_f-\mu_f\, \frac{1}{2}\, \mu_f} |n_f\, l_f\, m_f - \mu_f\rangle\, |\frac{1}{2}\, \mu_f\rangle \tag{2.158}$$

which have the following form in the Schroedinger (coordinate) representation (we suppose the central character of the s.p. mean field potential and therefore the wave function has separated form of the radial, angular and spin parts)

$$\langle \vec{r}\,|\, i\rangle \;=\; R_{n_i l_i}(r) \sum_{\mu_i} C^{j_i\, m_i}_{l_i\, m_i-\mu_i\, \frac{1}{2}\, \mu_i}\, Y_{l_i\, m_i-\mu_i}(\hat{r})\, |\frac{1}{2}\, \mu_i\rangle$$
$$\langle \vec{r}\,|\, f\rangle \;=\; R_{n_f l_f}(r) \sum_{\mu_f} C^{j_f\, m_f}_{l_f\, m_f-\mu_f\, \frac{1}{2}\, \mu_f}\, Y_{l_f\, m_f-\mu_f}(\hat{r})\, |\frac{1}{2}\, \mu_f\rangle \tag{2.159}$$

Since the electromagnetic multipole operators (2.103) are tensor operators we can use the Wigner-Eckart theorem (see (A.12)) for the calculation of their matrix elements

$$\langle n_f l_f j_f m_f|\, \hat{\mathscr{M}}^{(el)}_{JM}\, |\, n_i l_i j_i m_i\rangle = \frac{C^{j_f\, m_f}_{j_i\, m_i\, J\, M}}{\sqrt{2j_f+1}}\, \langle n_f l_f j_f ||\, \hat{\mathscr{M}}^{(el)}_{J}\, ||\, n_i l_i j_i\rangle$$

This matrix element can be also determined using the longwave approximation (2.130) for the $\hat{\mathscr{M}}^{(el)}_{JM}$.

$$\langle n_f l_f j_f m_f|\, \hat{\mathscr{M}}^{(el)}_{JM}\, |\, n_i l_i j_i m_i\rangle = \boxed{\begin{matrix}\text{see (2.130)}\\ \text{(2.159)}\end{matrix}} =$$
$$= e \int_0^\infty dr\, R_{n_f l_f}(r)\, r^{J+2}\, R_{n_i l_i}(r)\, \langle l_f j_f m_f|\, Y_{JM}\, |\, l_i j_i m_i\rangle =$$
$$= \boxed{\begin{matrix}\text{Wigner-Eckart theorem for}\\ \langle l_f j_f m_f|\, Y_{JM}\, |\, l_i j_i m_i\rangle\end{matrix}} =$$
$$= e \int_0^\infty dr\, R_{n_f l_f}(r)\, r^{J+2}\, R_{n_i l_i}(r)\, \frac{C^{j_f\, m_f}_{j_i\, m_i\, J\, M}}{\sqrt{2j_f+1}}\, \langle l_f \frac{1}{2} j_f ||\, Y_J\, ||\, l_i \frac{1}{2} j_i\rangle$$

The comparison of two last expressions gives the reduced matrix element in the following form

$$\begin{aligned}&\langle n_f l_f j_f || \hat{\mathscr{M}}_J^{(el)} || n_i l_i j_i \rangle = \\ &= e \int_0^\infty dr\, R_{n_f l_f}(r)\, r^{J+2}\, R_{n_i l_i}(r)\ \langle l_f \frac{1}{2} j_f || Y_J || l_i \frac{1}{2} j_i \rangle \end{aligned} \tag{2.160}$$

and after the substitution of (2.160) into (2.147) the reduced transition probability $B(el\ J, n_i l_i j_i \to n_f l_f j_f)$ can be written as

$$\begin{aligned}&B(el\ J, n_i l_i j_i \to n_f l_f j_f) = \\ &= \frac{e^2}{2j_f+1} \left| \int_0^\infty dr R_{n_f l_f}(r)\, r^{J+2}\, R_{n_i l_i}(r) \right|^2 | \\ &\qquad\qquad \cdot \langle l_f \frac{1}{2} j_f || Y_J || l_i \frac{1}{2} j_i \rangle |^2 = \\ &= \frac{e^2}{4\pi} \left| \int_0^\infty dr\, R_{n_f l_f}(r)\, r^{J+2}\, R_{n_i l_i}(r) \right|^2 S^{(E)}(j_i, j_f, J) \end{aligned} \tag{2.161}$$

where we introduce a geometric factor

$$\begin{aligned}S^{(E)}(j_i, j_f, J) &= \frac{4\pi}{2j_f+1} |\langle l_f \frac{1}{2} j_f || Y_J || l_i \frac{1}{2} j_i \rangle|^2 = \\ &= \boxed{\begin{matrix}\text{see} \\ (A.15)\end{matrix}} = (2J+1) \left| C^{j_f\, \frac{1}{2}}_{j_i\, \frac{1}{2}\, J\, 0} \right|^2 \end{aligned} \tag{2.162}$$

The expression (2.161) for the reduced probabilty of electric transitions with the multipolarity J in the framework of the simple independent particle model was used by V.F. Weisskopf [15] for the introduction of so called single-particle units for the reduced probability of electric transitions. In (2.161) following approximations were applied.

- V.F. Weisskopf assumed the radial parts, $R_{n_i l_i}(r)$ and $R_{n_f l_f}(r)$, of the s.p. wave functions involved in (2.162) to be constant inside the nucleus and zero outside:

$$\begin{aligned}R_{nl}(r) &= C \qquad \text{for} \quad r \le R \\ R_{nl}(r) &= 0 \qquad \text{for} \quad r \ge R\end{aligned}$$

  where R is the nuclear radius and the constant C is given by the wave function normalization

$$\int_0^\infty dr\, |R_{nl}(r)|^2\ r^2 = C^2\, \frac{R^3}{3} = 1\ \Rightarrow\ C = \sqrt{\frac{3}{R^3}}$$

- Further V.F. Weisskopf assumed: $S^{(E)}(j_i, j_f, J) = 1$

Under such assumptions the reduced probabilty (2.161) becomes

$$B(el\ J)_W = \frac{e^2}{4\pi}\,\frac{9}{R^6}\,\left|\int_0^\infty r^{J+2} dr\right|^2 = \frac{9\,e^2\,R^{2J}}{4\pi\,(J+3)^2} =$$

$$= \boxed{\begin{array}{c}\text{see (1.2):}\\ R = r_0\,A^{1/3},\ r_0 = 1.2\ \text{fm}\end{array}} =$$

$$= \frac{(1.2)^{2J}}{4\pi}\,\left(\frac{3}{J+3}\right)^2\,A^{2J/3} \qquad [e^2\ fm^{2J}] \tag{2.163}$$

Similarly, with the use of the assumptions given above V.F. Weisskopf introduced the single-particle units for the reduced probability of magnetic transitions.

$$B(magJ)_W = \frac{10}{\pi}\,(1.2)^{2J-3}\,\left(\frac{3}{J+3}\right)^2\,A^{\frac{2J-2}{3}} \qquad [\mu_N^2\ fm^{2J-2}] \tag{2.164}$$

Weisskopf single-particle units (2.163) and (2.164) are often used for the experimental and theoretical values of reduced probabilities of electric and magnetic transitions.

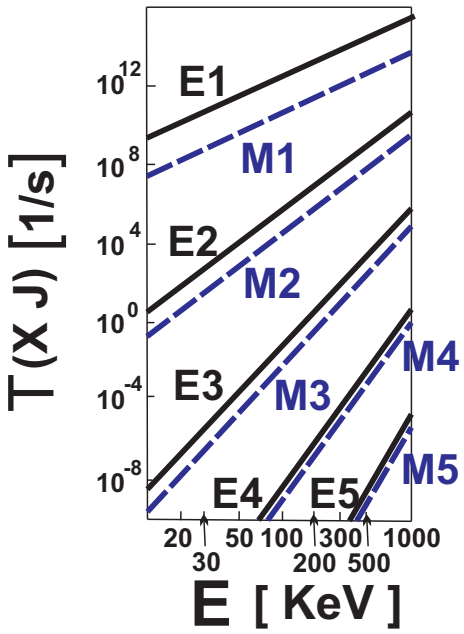


Figure 2.2: The Weisskopf values of the electric and magnetic probabilties $T^{(el)}(J)$ and $T^{(mag)}(J)$ as a function of the transition energy $E = \hbar\omega$ for several lowest values of $J = 1, 2, 3, 4, 5$. The rapid reduction of these probabilities with the increasing of J can be seen.

The probability that in one second the nucleus makes the electromagnetic transition from the state $|i\rangle$ to the state $|f\rangle$ with the simultaneous emission of the photon with the energy in the 1 MeV interval around the value $\hbar kc = \hbar\omega$ and with the arbitrary direction of the linear momentum $\hbar\vec{k}$ is given by (2.149) or (2.148). Experiments show (and theoretical calculations support it - see also (2.150)) that the contribution into the sum over J and $X = el, mag$ decreases very quickly with the increasing multipolarity J. This fact together with the selection rules (2.115) and (2.118) causes that in the sum over J in (2.149) only several J - terms participate (other are forbiden by selection rules or give the negligible contribution). The fact that the values $T^{(el)}_{i\to f}(J)$ and $T^{(mag)}_{i\to f}(J)$ in (2.149) decreases with the increasing J can be demonstrated when the Weisskopf single-particle units (2.163) and (2.164) are substituted into (2.149). Then we obtain Weisskopf single-particle values of probabilities $T^{(el)}(J)_W$ and $T^{(mag)}(J)_W$ and their ratio $\frac{T^{(el)}(J+1)_W}{T^{(el)}(J)_W}$ is following

$$\frac{T^{(el)}(J+1)_W}{T^{(el)}(J)_W} = \boxed{\begin{array}{c}\text{see}\\ (2.148)+(2.163)\end{array}} =$$

$$= \frac{J(J+2)}{(J+1)^2}\,\frac{1}{(2J+3)^2}\,\frac{(J+3)^2}{(J+4)^2}\,(kR)^2 << 1$$

because in accordance with the longwave approximation condition $kR << 1$. A similar result can be obtained for the ratio of magnetic probabilities. This rapid reduction of the values of the Weisskopf probabilities $T^{(el)}(J)_W$ and $T^{(mag)}(J)_W$ with the increasing J is demonstrated also in the Fig. 2.2.

2.2.3 Absorption of photons by nuclei

The probability $w_{i\to f}(t_0, t)$ of the transition in the time interval $\langle t_0, t\rangle$ of the system nucleus + outside electromagnetic field is given by (2.90) where the matrix elements of the evolution operator, $\langle f|\hat{S}^{(1)}(t, t_0)|i\rangle$, are specified in (2.91). For the case of the absorption of the photon by the nucleus we should at first determine the initial $|i\rangle$ and final $|f\rangle$ states of the system.

initial state of the system: nucleus + el.mg. field	$\cdots\cdots$ $\begin{array}{c}\|i\rangle = \|i, \vec{k}\,\tau\rangle\\ = a^+_{\vec{k},\tau}\|i,\ 0\rangle\end{array}$	one photon, nucleus in the state $\|i\rangle$
final state of the system: nucleus + el.mg. field	$\cdots\cdots$ $\|f,\ 0\rangle$	no photon, nucleus in the state $\|f\rangle$

In this case the matrix elements $\langle f|\hat{B}|i\rangle$ and $\langle f|\hat{B}^+|i\rangle$ involved in (2.91) are following

$$\langle f|\hat{B}|i\rangle \;=\; \langle f;0|\hat{B}|i;\vec{k}\tau\rangle = \boxed{\begin{array}{c}\text{see}\\(2.89)\end{array}} =$$

$$= -\int d^3r\langle f|\hat{\vec{j}}_{nuc}(\vec{r})|i\rangle\, C_k\, \vec{\xi}_\tau\, e^{i\,\vec{k}\vec{r}} \neq 0$$

$$\langle f|\hat{B}^+|i\rangle \;=\; \langle f;0|\hat{B}^+|i;\vec{k}\tau\rangle = \boxed{\begin{array}{c}\text{see}\\(2.89)\end{array}} =$$

$$= -\int d^3r\,\langle f|\hat{\vec{j}}^+_{nuc}(\vec{r})|i\rangle \sum_{\vec{k}\,'\,\tau\,'} C'_k\,\vec{\xi}^*_{\tau'}\, e^{-i\,\vec{k}\,'\vec{r}}\,\langle 0|\, a^+_{\vec{k}\,'\,\tau'}\, a^+_{\vec{k}\,\tau}|0\rangle =$$

$$= 0 \qquad (2.165)$$

Similarly as we obtained the probability (2.96) of the photon emission from (2.93) we can receive from the expr. (2.165) the probability that in one second the nucleus absorbs the photon with the linear momentum $\hbar\vec{k}$ and with the energy $\hbar kc$ and simultraneously it is excited from the state $|i\rangle$ to the state $|f\rangle$. This probability of the photon absorption is (the analog of emission probability in(2.96))

$$w_{i\to f} = \frac{2\pi}{\hbar}C_k^2\left|\int d^3r\,\langle f|\hat{\vec{j}}_{nuc}(\vec{r})|i\rangle\,\vec{\xi}_\tau\, e^{i\,\vec{k}\vec{r}}\right|^2 \delta(E_f - E_i - \hbar\omega) \qquad (2.166)$$

Since the normalization of the photon wave function corresponds to the one photon in the box with the volume L^3 (see exprs. (2.43) and (2.44)) the photon flow going to one nucleus with the light speed c is c/L^3. The photoabsorption cross section can be obtained by the ratio of the probability (2.166) and this flow. So, the photoabsorption cross section $\sigma(\vec{k}\tau,\, i\to f)$ for the absorption of the photon with the linear momentum $\hbar\vec{k}$ and the polarization τ is

$$\sigma(\vec{k}\tau,\, i\to f) = \frac{2\pi}{\hbar}C_k^2\,\frac{L^3}{c}\left|\int d^3r\,\langle f|\,\hat{\vec{j}}_{nuc}(\vec{r})\,|i\rangle\,\vec{\xi}_\tau\, e^{i\,\vec{k}\vec{r}}\right|^2 \delta(E_f - E_i - \hbar\omega) \qquad (2.167)$$

The integral $\int d^3r\;\langle f|\,\hat{\vec{j}}_{nuc}(\vec{r})\,|i\rangle\;\vec{\xi}_\tau\, e^{i\,\vec{k}\vec{r}}$ is given by the complex conjugation of the integral (2.105) or (2.109). So, after the substitution of the complex

conjugation of (2.109) into (2.167) the phoroabsorption cross section can be rewritten as follows

$$\begin{aligned}
&\sigma(\vec{k}\tau,\ \alpha_i j_i m_i \to \alpha_f j_f m_f) = \\
&= \frac{4\pi^2\, L^3\, C_k^2\, c}{\hbar} \sum_{J J'} \frac{k^{J+J'}}{(2J+1)!!\,(2J'+1)!!}\ \frac{1}{2j_f+1} \\
&\quad \left[\frac{(J+1)(J'+1)(2J+1)(2J'+1)}{J\ J'}\right]^{1/2} \\
&\quad \left[\langle \alpha_f\ j_f || \hat{\mathscr{M}}_J^{(el)}(k) ||\ \alpha_i\ j_i\rangle + i\,\tau\,\langle \alpha_f\ j_f || \hat{\mathscr{M}}_J^{(mag)}(k) ||\ \alpha_i\ j_i\rangle\right] \\
&\quad \left[\langle \alpha_f\ j_f || \hat{\mathscr{M}}_{J'}^{(el)}(k) ||\ \alpha_i\ j_i\rangle^* - i\,\tau\,\langle \alpha_f\ j_f || \hat{\mathscr{M}}_{J'}^{(mag)}(k) ||\ \alpha_i\ j_i\rangle^*\right] \\
&\quad \sum_{M\,M'} D^J_{M\tau}(\vec{e}_z \to \vec{k}) D^{J'*}_{M'\tau}(\vec{e}_z \to \vec{k})\ C^{j_f\ m_f}_{j_i\ m_i\ J\ -M}\ C^{j_f\ m_f}_{j_i\ m_i\ J'\ -M'}
\end{aligned} \tag{2.168}$$

If the nucleus in the initial and final state is not oriented then we should average over m_i and sum over m_f:

$$\begin{aligned}
&\sigma(\hbar k c = \hbar\omega\tau,\ \alpha_i j_i \to \alpha_f j_f) = \frac{1}{2j_i+1} \sum_{m_i m_f} \sigma(\vec{k}\tau,\ \alpha_i j_i m_i \to \alpha_f j_f m_f) = \\
&= \boxed{\begin{array}{c}\text{see}\\ (2.111)\end{array}} = \\
&= \frac{4\pi^2\, L^3\, C_k^2\, c}{\hbar}\ \frac{1}{2j_i+1} \sum_J \frac{k^{2J}}{[(2J+1)!!]^2} \frac{J+1}{J} \delta(\hbar\omega - E_f + E_i) \\
&\quad \left[\left|\langle \alpha_f j_f || \hat{\mathscr{M}}_J^{(el)}(k) ||\ \alpha_i j_i\rangle\right|^2 + \left|\langle \alpha_f j_f || \hat{\mathscr{M}}_J^{(mag)}(k) ||\ \alpha_i j_i\rangle\right|^2\right]
\end{aligned} \tag{2.169}$$

If the absorbed photon is not polarized then it is necessary to average in the exp. (2.169) over $\tau = \pm 1$:

$$\sigma(\hbar\omega,\ \alpha_i j_i \to \alpha_f j_f) = \frac{1}{2}\sum_{\tau=\pm 1} \sigma(\vec{k}\tau,\ \alpha_i j_i \to \alpha_f j_f) =$$
$$= \frac{4\pi^2\, L^3\, C_k^2\, c}{\hbar}\, \frac{1}{2j_i+1} \sum_J \frac{k^{2J}}{[(2J+1)!!]^2}\frac{J+1}{J}\delta(\hbar\omega - E_f + E_i)$$
$$\left[\left|\langle \alpha_f j_f || \hat{\mathscr{M}}_J^{(el)}(k) || \alpha_i j_i\rangle\right|^2 + \left|\langle \alpha_f j_f || \hat{\mathscr{M}}_J^{(mag)}(k) || \alpha_i j_i\rangle\right|^2\right] \tag{2.170}$$

Using the definition (2.147) of the reduced probability $B(XJ; i \to j)$ ($B(XJ; i \to j) = \frac{\left|\langle \alpha_f\, j_f || \hat{\mathscr{M}}_J^{(X)} || \alpha_i\, j_i\rangle\right|^2}{2j_i+1}$) and substituting the expression for C_k (see (2.44) the photoabsorption cross section (2.170) is given finally in the following form

$$\sigma(\hbar\omega,\ \alpha_i j_i \to \alpha_f j_f) =$$
$$= \frac{2\pi^2\, c}{\epsilon_0\, \omega} \sum_J \frac{k^{2J}}{[(2J+1)!!]^2}\frac{J+1}{J}\delta(\hbar\omega - E_f + E_i)$$
$$[B(el\ J; i \to j) + B(mag\ J; i \to j)] =$$
$$= \boxed{\begin{array}{c}\text{because fine structure constant is} \\ \alpha = \frac{e^2}{4\pi\,\epsilon_0\,\hbar c}\end{array}} =$$
$$= \frac{8\pi^3\,\hbar c^2\,\alpha}{\omega\, e^2} \sum_J \frac{k^{2J}}{[(2J+1)!!]^2}\frac{J+1}{J}$$
$$[B(el\ J; i \to j) + B(mag\ J; i \to j)]\ \delta(\hbar\omega - E_f + E_i) \tag{2.171}$$

2.3 Static electromagnetic moments of the nucleus

In the previous sections of this chapter the interaction of the nucleus (quantum system) with the external time-dependent electromagnetic field was discussed (the source of this el.mg. field was placed outside of the nucleus). This interaction induced the electromgnetic transitions in the nucleus which showed themselves as the absorption or emission of the photon by the nucleus. In this section we deal with the interaction of the nucleus as a system of charges and currents with the static (not dependent on time) electromagnetic field. This enables us to introduce static electric and magnetic moments of the nucleus.

The interaction of the nucleus (the system of charges with the static operator of the charge density $\hat{\rho}_{nuc}(\vec{r})$ and current density $\hat{\vec{j}}_{nuc}(\vec{r})$) with the static electromagnetic field with the scalar potential $\varphi(\vec{r})$ and the vector potential $\vec{A}(\vec{r})$ is again given by (2.86) but now all quantities are time-independent and the static electromagnetic field is not quantized:

$$\hat{H}_{int-stat} = \int d^3r \, \left[\hat{\rho}_{nuc}(\vec{r}) \;\; \varphi(\vec{r}) - \hat{\vec{j}}_{nuc}(\vec{r}) \cdot \vec{A}(\vec{r})\right] \tag{2.172}$$

Since the electromagnetic field is not quantized (it is not an operator) opposite to (2.86) the interaction Hamiltonian $\hat{H}_{int-stat}$ is the operator only in the space of the nuclear wave funtions (no any creation and annihilation operators of photons).

Further we will suppose that the sources of the static electromagnetic field are placed outside of the nucleus and therefore the scalar potential $\varphi(\vec{r})$ and the vector potential $\vec{A}(\vec{r})$ fulfil the wave equations (2.13) which are reduced, because $\varphi(\vec{r})$ and $\vec{A}(\vec{r})$ do not depend on t, to the Poisson equations (2.11) without r.h.s.:

$$\vec{\nabla}^2 \, \varphi(\vec{r}) = 0 \, , \qquad \vec{\nabla}^2 \, \vec{A}(\vec{r}) = 0 \tag{2.173}$$

Since the charge density $\hat{\rho}_{nuc}(\vec{r})$ and the current density $\hat{\vec{j}}_{nuc}(\vec{r})$ are nonzero only in the nucleus volume the integration in (2.172) goes only over the nucleus volume, that means over the small area close to the origin of the coordinate system. Therefore we are justified to decompose potentials $\varphi(\vec{r})$ and $\vec{A}(\vec{r})$ to Taylor series around the $\vec{r} = 0$ and to use in (2.172) only sveral

first terms of these series.

$$\varphi(\vec{r}) = \varphi_0 + \sum_{i=1}^{3} x_i \left(\frac{\partial\varphi}{\partial x_i}\right)_0 + \frac{1}{2!}\sum_{i,k=1}^{3} x_i\, x_k \left(\frac{\partial^2\varphi}{\partial x_i\,\partial x_j}\right)_0 + \dots$$
$$\vec{A}(\vec{r}) = \vec{A}_0 + \sum_{i=1}^{3} x_i \left(\frac{\partial\vec{A}}{\partial x_i}\right)_0 + \dots \tag{2.174}$$

At first we will analyze the 1-st term in the integral (2.172)

$$\begin{aligned}
&\int d^3r\ \hat{\rho}(\vec{r})\ \varphi(\vec{r}) = \\
&= \int d^3r\ \hat{\rho}_{nuc}(\vec{r})\ \varphi_0 + \sum_i \left(\frac{\partial\varphi}{\partial x_i}\right)_0 \int d^3r\ \hat{\rho}_{nuc}(\vec{r})\, x_i + \\
&\qquad + \sum_{ik} \frac{1}{2} \left(\frac{\partial^2\varphi}{\partial x_i\,\partial x_k}\right)_0 \int d^3r\ \hat{\rho}_{nuc}(\vec{r})\, x_i\, x_k = \\
&= \varphi_0\,\hat{q} + \hat{\vec{d}}\cdot(\vec{\nabla}\varphi)_0 + \frac{1}{6}\sum_{ik}\hat{Q}'_{ik}\left(\frac{\partial^2\varphi}{\partial x_i\,\partial x_k}\right)_0 + \dots
\end{aligned} \tag{2.175}$$

where

$$\begin{aligned}
&\hat{q} \equiv \int d^3r\ \hat{\rho}_{nuc}(\vec{r}) \ \rightarrow\ \text{the operator of the nucleus total charge} \\
&\hat{\vec{d}} \equiv \int d^3r\ \hat{\rho}_{nuc}(\vec{r})\,\vec{r} \ \rightarrow\ \begin{array}{c}\text{the operator of the electric}\\ \text{dipole nucleus moment}\end{array} \\
&\hat{Q}'_{ik} = 3\int d^3r\ \hat{\rho}_{nuc}(\vec{r})\, x_i\, x_k \ \rightarrow\ \begin{array}{c}\text{symmetric tensor of the 2-d}\\ \text{order which is connected with}\\ \text{the tensor of the quadrupole}\\ \text{moment } Q_{ik} \text{ (see further)}\end{array}
\end{aligned} \tag{2.176}$$

The operator of the quadrupole moment tensor $\hat{Q}_{ik}$ is defined as

$$\hat{Q}_{ik} = \hat{Q}'_{ik} - \hat{Q}\,\frac{1}{3}\,\delta_{ik} \tag{2.177}$$

where $\hat{Q} \equiv \sum_{i=1}^{3}\hat{Q}'_{ii}$. Tensor of the electric quadrupole tensor $\hat{Q}_{ik}$ is the symmetric tensor of the 2-d order with the zero trace ($Tr\,\{\hat{Q}_{ik}\} = \sum_i \hat{Q}_{ii} =$

0). Since (2.173) the last term in (2.175) does not change if the quadrupole moment tensor (2.177) is used instead of the tensor $\hat{Q}'_{ik}$ and we have

$$\begin{aligned}
&\sum_{i,k=1}^{3} \hat{Q}'_{ik} \left(\frac{\partial^2 \varphi}{\partial x_i \, \partial x_k} \right)_0 = \\
&= \sum_{i,k=1}^{3} \hat{Q}_{ik} \left(\frac{\partial^2 \varphi}{\partial x_i \, \partial x_k} \right)_0 + \frac{1}{3} \hat{Q} \sum_i \left(\frac{\partial^2 \varphi}{\partial x_i^2} \right)_0 = \\
&= \boxed{\begin{array}{c} \text{since (2.173)} \\ \sum_i \left(\frac{\partial^2 \varphi}{\partial x_i^2} \right)_0 = 0 \end{array}} = \sum_{i,k=1}^{3} \hat{Q}_{ik} \left(\frac{\partial^2 \varphi}{\partial x_i \, \partial x_k} \right)_0 = \\
&= \boxed{\begin{array}{c} \text{because of the stationarity} \\ \vec{E} = -\vec{\nabla}\varphi - \frac{\partial \vec{A}}{\partial t} = -\vec{\nabla}\varphi \end{array}} = - \sum_{ik} \hat{Q}_{ik} \left(\frac{\partial E_i}{\partial x_k} \right)_0
\end{aligned} \tag{2.178}$$

Since we suppose that the density $\hat{\rho}(\vec{r})$ and the field $\vec{A}(\vec{r})$ do not depend explicitly on the time we also have

$$\frac{\partial \hat{\vec{d}}}{\partial t} = 0 \,, \qquad\qquad \frac{\partial \hat{Q}_{ik}}{\partial t} = 0 \tag{2.179}$$

Further we analyze the second term in the integral in the relation (2.172)

$$\begin{aligned}
&\int d^3 r \, \hat{\vec{j}}_{nuc}(\vec{r}) \cdot \vec{A}(\vec{r}) = \boxed{\begin{array}{c} \text{see} \\ (2.174) \end{array}} = \\
&= \vec{A}_0 \int d^3 r \, \hat{\vec{j}}_{nuc}(\vec{r}) + \sum_i \left(\frac{\partial \vec{A}}{\partial x_i} \right)_0 \cdot \int d^3 r \, x_i \, \hat{\vec{j}}_{nuc}(\vec{r})
\end{aligned} \tag{2.180}$$

The first term in the r.h.s. of (2.180) is zero because

$$\frac{\partial \hat{\vec{d}}}{\partial t} = \boxed{\begin{array}{c}\text{see}\\(2.176)\end{array}} = \int d^3r\, \frac{\partial \hat{\rho}_{nuc}}{\partial t}\, \vec{r} = \boxed{\begin{array}{c}\text{see - continuity eq.}\\(2.2)\end{array}} =$$

$$= -\int d^3r\, \vec{r}\, (\vec{\nabla} \cdot \hat{\vec{j}}_{nuc}(\vec{r})) = -\sum_i \int d^3r\, \vec{r}\, \frac{\partial \hat{j}_i}{\partial x_i} =$$

$$= \sum_i \left[-\int d^3r\, \frac{\partial}{\partial x_i} \left((j_{nuc})_i\, \vec{r} \right) + \frac{1}{3} \int d^3r\, \vec{j}_{nuc}(\vec{r}) \right] =$$

$$= \sum_i \left[-\int_{(\Sigma)} \vec{r}\, \left(\hat{\vec{j}}_{nuc} \cdot \overrightarrow{d\Sigma} \right) + \frac{1}{3} \int d^3r\, \vec{j}_{nuc}(\vec{r}) \right] =$$

$$= \boxed{\begin{array}{c}\text{the first term is zero because}\\ \hat{\vec{j}}_{nuc} = 0 \text{ outside of the nucleus}\end{array}} = \sum_i \frac{1}{3} \int d^3r\, \vec{j}_{nuc}(\vec{r}) =$$

$$= \boxed{\begin{array}{c}\text{since we suppose (2.179)}\\ \frac{\partial \hat{\vec{d}}}{\partial t} = 0\end{array}} = 0 \qquad (2.181)$$

Therefore we can consider only the second term in (2.180)

$$\sum_i \left(\frac{\partial \vec{A}}{\partial x_i} \right)_0 \cdot \int d^3r\, x_i\ \hat{\vec{j}}_{nuc}(\vec{r}) = \sum_{ik} \left(\frac{\partial A_k}{\partial x_i} \right)_0 \int d^3r\, x_i\ (\hat{j}_k(\vec{r}))_{nuc} \qquad (2.182)$$

and it is the sum of the products of elements of two tensors, $\sum_{ik} T_{ik} U_{ik}$, where $T_{ik} = \left(\frac{\partial A_k}{\partial x_i} \right)_0$ and $U_{ik} = \int d^3r\, x_i\, \hat{j}_k(\vec{r})$. For both these tensors we construct corresponding symmetric and antisymmetric parts

$$\begin{aligned} T^{(S)}_{ik} &= \frac{1}{2}\, (T_{ik} + T_{ki})\ , \quad T^{(A)}_{ik} = \frac{1}{2}\, (T_{ik} - T_{ki})\ , \\ & \qquad\qquad T_{ik} = T^{(S)}_{ik} + T^{(A)}_{ik} \\ U^{(S)}_{ik} &= \frac{1}{2}\, (U_{ik} + U_{ki})\ , \quad U^{(A)}_{ik} = \frac{1}{2}\, (U_{ik} - U_{ki})\ , \\ & \qquad\qquad U_{ik} = U^{(S)}_{ik} + U^{A}_{ik} \end{aligned} \qquad (2.183)$$

and the sum of the products, $\sum_{ik} T_{ik}U_{ik}$, can be written as follows

$$\sum_{ik} T_{ik}U_{ik} = \sum_{ik} \left[T_{ik}^{(A)}U_{ik}^{(A)} + T_{ik}^{(S)}U_{ik}^{(A)} + T_{ik}^{(A)}U_{ik}^{S)} + T_{ik}^{(S)}U_{ik}^{(S)}\right] =$$
$$= \sum_{ik} \left[T_{ik}^{(A)}U_{ik}^{(A)} + T_{ik}^{(S)}U_{ik}^{(S)}\right] \tag{2.184}$$

In our case

$$T_{ik} \equiv \left(\frac{\partial A_k}{\partial x_i}\right)_0 \rightarrow$$
$$T_{ik}^{(A)} = \frac{1}{2}\left(\frac{\partial A_k}{\partial x_i} - \frac{\partial A_i}{\partial x_k}\right), \quad T_{ik}^{(S)} = \frac{1}{2}\left(\frac{\partial A_k}{\partial x_i} + \frac{\partial A_i}{\partial x_k}\right)$$
$$U_{ik} \equiv \int d^3r\, x_i\, (\hat{j}_{nuc})_k \rightarrow$$
$$U_{ik}^{(A)} = \frac{1}{2}\int d^3r \left(x_i\hat{j}_k - x_k\hat{j}_i\right)_{nuc}, U_{ik}^{(S)} = \frac{1}{2}\int d^3r \left(x_i\hat{j}_k + x_k\hat{j}_i\right)_{nuc} \tag{2.185}$$

For the second term in(2.184) we have

$$\sum_{ik} T_{ik}^{(S)}U_{ik}^{(S)} = \frac{1}{4}\sum_{ik}\left(\frac{\partial A_k}{\partial x_i} + \frac{\partial A_i}{\partial x_k}\right)\int d^3r\, (x_i\hat{j}_k + x_k\,\hat{j}_i)_{nuc} =$$
$$= \boxed{\begin{array}{c}\text{we suppose that } i,k,l \text{ form the complete} \\ \text{cyklical system of coordinates and, } l \neq i,k\end{array}} =$$
$$= \frac{1}{4}\sum_{ik}\left(\frac{\partial A_k}{\partial x_i} + \frac{\partial A_i}{\partial x_k}\right)$$
$$\int d^3r \left[\hat{j}_k\,\frac{\partial}{\partial x_k}(x_i\,x_k) + \hat{j}_i\,\frac{\partial}{\partial x_i}(x_i\,x_k) + \hat{j}_l\,\frac{\partial}{\partial x_l}(x_i\,x_k) + \right]_{nuc} =$$

$$= \boxed{\begin{array}{c}\text{because of (2.181) contributions from } i=k \text{ are zero}\\ \text{and the last term is zero because } l\neq i,k\\ \text{and subsequent integration per partes in each term}\end{array}} =$$

$$= -\frac{1}{4}\sum_{ik}\left[\frac{\partial A_k}{\partial x_i}+\frac{\partial A_i}{\partial x_k}\right]$$

$$\int d^3r\; x_i\; x_k\; \left(\frac{\partial \hat{j}_k}{\partial x_k}+\frac{\partial \hat{j}_i}{\partial x_i}+\frac{\partial \hat{j}_l}{\partial x_l}\right)_{nuc} =$$

$$= \boxed{\begin{array}{c}\text{nonzero contributions only for } i\neq k,\; i\neq l,\; k\neq l\\ \text{and for each } ikl \text{ the bracket () gives } \vec{\nabla}\hat{\vec{j}}_{nuc}=-\frac{\partial \hat{\rho}_{nuc}}{\partial t}\end{array}} =$$

$$= \frac{1}{4}\sum_{ik}\left[\frac{\partial A_k}{\partial x_i}+\frac{\partial A_i}{\partial x_k}\right]\int d^3r\; x_i\; x_k\; \frac{\partial \hat{\rho}_{nuc}}{\partial t} = \boxed{\begin{array}{c}\text{see}\\ (2.176)\end{array}} =$$

$$= \frac{1}{12}\sum_{ik}\left[\frac{\partial A_k}{\partial x_i}+\frac{\partial A_i}{\partial x_k}\right]\frac{\partial \hat{Q}'_{ik}}{\partial t} = \boxed{\begin{array}{c}\text{we suppose}\\ \frac{\partial \hat{Q}'_{ik}}{\partial t}=0\end{array}} = 0 \qquad (2.186)$$

So, in our case in the exp. (2.184) (which is equivqlent to (2.182)) only the first term remains and we have

$$\sum_i \left(\frac{\partial \vec{A}}{\partial x_i}\right)_0 \cdot \int d^3r\; x_i\; \hat{\vec{j}}_{nuc}(\vec{r}) = \sum_{ik} T^{(A)}_{ik}\; U^{(A)}_{ik} = \boxed{\begin{array}{c}\text{see}\\ (2.185)\end{array}} =$$

$$= 2\left(T^{(A)}_{12}\; U^{(A)}_{12} + T^{(A)}_{23}\; U^{(A)}_{23} + T^{(A)}_{31}\; U^{(A)}_{31}\right) = \boxed{\begin{array}{c}\text{see}\\ (2.185)\end{array}} =$$

$$= \frac{1}{2}\,[\;\left(\frac{\partial A_2}{\partial x_1}-\frac{\partial A_1}{\partial x_2}\right)_0 \int d^3r\; (x_1\,\hat{j}_2 - x_2\,\hat{j}_1)_{nuc} +$$

$$+\left(\frac{\partial A_3}{\partial x_2}-\frac{\partial A_2}{\partial x_3}\right)_0 \int d^3r\; (x_2\,\hat{j}_3 - x_3\,\hat{j}_2)_{nuc} +$$

$$\left(\frac{\partial A_1}{\partial x_3}-\frac{\partial A_3}{\partial x_1}\right)_0 \int d^3r\; (x_3\,\hat{j}_1 - x_1\,\hat{j}_3)_{nuc}\;\;] =$$

$$= rot\vec{A}_0 \cdot \frac{1}{2}\int d^3r\;[\,\vec{r}\times\hat{\vec{j}}_{nuc}(\vec{r}\,] = \vec{B}_0\cdot\hat{\vec{\mu}} \qquad (2.187)$$

where $\hat{\vec{\mu}} = \frac{1}{2} \int d^3r \, [\vec{r} \times \hat{\vec{j}}_{nuc}(\vec{r}) \,]$ is the operator of the magnetic dipole moment of the nucleus caused by the current density $\hat{\vec{j}}_{nuc}(\vec{r})$.

The expression (2.187) represents the final form of the expr. (2.182) and also, taking into account (2.181), of the second term in the expr. (2.180) for the interaction $\hat{H}_{int-stat}$ of the nucleus with the external static electromagnetic field. After the substitution of (2.187) and (2.175) into (2.172) this interaction can be rewritten in the following way

$$\hat{H}_{int-stat} = \hat{q} \, \varphi_0 - \hat{\vec{d}} \cdot \vec{E}_0 - \hat{\vec{\mu}} \cdot \vec{B}_0 - \frac{1}{6} \sum_{i,k=1}^{3} \hat{Q}_{ik} \, \left(\frac{\partial E_i}{\partial x_k} \right)_0 \tag{2.188}$$

where

$$\begin{aligned}
&\hat{q} = \int d^3r \, \hat{\rho}_{nuc}(\vec{r}) \\
&\hat{\vec{d}} = \int d^3r \, \hat{\rho}_{nuc}(\vec{r}) \, \vec{r} \\
&\hat{Q}_{ik} = \hat{Q}'_{ik} - \frac{1}{3} \hat{Q} \, \delta_{ik} = \int d^3r \, \left(3 \, x_i \, x_k - \delta_{ik} \, r^2 \right) \, \hat{\rho}_{nuc}(\vec{r}) \\
&\hat{\vec{\mu}} = \frac{1}{2} \int d^3r \, [\, \vec{r} \times \hat{\vec{j}}_{nuc}(\vec{r}) \,]
\end{aligned} \tag{2.189}$$

In (2.189) $\hat{q}$ is the operator of the nucleus charge, $\hat{\vec{d}}$ is the operator of the nucleus electric dipole moment, $\hat{Q}_{ik}$ is the operator of the ik-element of the quadrupole electric moment of the nucleus and $\hat{\vec{\mu}}$ stands for the operator of the nucleus magnetic dipole moment. These operators act in the space of the nucleus wave functions through the operators of the charge density $\hat{\rho}_{nuc}(\vec{r})$ and current density $\hat{\vec{j}}_{nuc}(\vec{r})$ of the nucleus:

$$\hat{\rho}_{nuc}(\vec{r}) = \boxed{\begin{array}{c}\text{see} \\ (2.131)\end{array}} = \sum_{i=1}^{A} e_i \, \delta(\vec{r} - \vec{r}_i) \tag{2.190}$$

$$\begin{aligned}
&\hat{\vec{j}}_{nuc}(\vec{r}) = \boxed{\begin{array}{c}\text{see} \\ (2.135)\end{array}} = \hat{\vec{j}}_o(\vec{r}) + \hat{\vec{j}}_s(\vec{r}) = \boxed{\begin{array}{c}\text{see} \\ (2.136), (2.141)\end{array}} = \\
&= \sum_{i=1}^{A} \frac{e_i}{m_i} \, \hat{\vec{p}}_i \, \delta(\vec{r} - \vec{r}_i) + \vec{\nabla} \times \sum_{i=1}^{A} \hat{\vec{\mu}}_i^{(s)} \, \delta(\vec{r} - \vec{r}_i)
\end{aligned} \tag{2.191}$$

2.3.1 Electric dipole moment

A classical electric dipole moment of the system with the charge density $\rho(\vec{r})$ is given by $\vec{d} = \int d^3r\ \rho(\vec{r})\ \vec{r}$. In the quantum mechanics it is represented by the operator (see (2.176))

$$\hat{\vec{d}} = \int d^3r\ \hat{\rho}_{nuc}(\vec{r})\ \vec{r} \tag{2.192}$$

where $\hat{\rho}_{nuc}(\vec{r})$ is the nucleus (system) charge density operator. The value of the electric dipole moment in the given state $|\alpha\rangle$ of the nucleus is determined by the expectation value (the diagonal matrix element) of the operator (2.192) in this state $|\alpha\rangle$

$$\vec{d}_\alpha = \langle\alpha|\ \hat{\vec{d}}\,|\alpha\rangle = \int d^3r\ \langle\alpha|\ \hat{\rho}_{nuc}(\vec{r})\ |\alpha\rangle\ \vec{r} \tag{2.193}$$

If the parity is a good quantum number for the state $|\alpha\rangle$, that means if the state $|\alpha\rangle$ is an eigen-state of the operator of the parity

$$\hat{\mathscr{P}}\ |\alpha\rangle = \Pi_\alpha\ |\alpha\rangle$$

then the expectation value (2.193) should be zero because

$$\langle\alpha|\hat{\vec{d}}|\alpha\rangle = \langle\alpha|\hat{\mathscr{P}}^{-1}\hat{\mathscr{P}}\ \hat{\vec{d}}\ \hat{\mathscr{P}}^{-1}\hat{\mathscr{P}}|\alpha\rangle = \Pi_\alpha^2\ \langle\alpha|\hat{\mathscr{P}}\ \hat{\vec{d}}\ \hat{\mathscr{P}}^{-1}|\alpha\rangle =$$

$$= \boxed{\begin{array}{c}\text{since from the definition of the electric}\\ \text{dipole moment it follows: } \hat{\mathscr{P}}\ \hat{\vec{d}}\hat{\mathscr{P}}^{-1} = -\ \hat{\vec{d}}\end{array}} = -\ \langle\alpha|\hat{\vec{d}}|\alpha\rangle$$

$$\Rightarrow \qquad \langle\alpha|\ \hat{\vec{d}}\,|\alpha\rangle = 0 \tag{2.194}$$

Since the nuclear states usually have good parities the dipole moments of them are zero.

The substitution of the expr. (2.190) for the charge density operator into (2.192) gives the alternative expr. for the electric dipole moment operator in the coordinate representation

$$\hat{\vec{d}} = \sum_{i=1}^{A} e_i \int d^3r\ \delta(\vec{r} - \vec{r}_i)\ \vec{r} = \sum_{i=1}^{A} e_i\ \vec{r}_i \tag{2.195}$$

This operator can be compared with the electric dipole operator $\hat{\mathscr{M}}^{(el)}_{1\,M}$ in the longwave limit (see (2.132))

$$\hat{\mathscr{M}}^{(el)}_{1\,M} = \sum_{i=1}^{A} e_i\ r_i\ Y_{1M}(\hat{r}_i) \tag{2.196}$$

Since the explicit exprs. for the spherical functions $Y_{1M}(\hat{r})$ are: $Y_{10}(\hat{r}) = \sqrt{\frac{3}{4\pi}}\frac{z}{r}$, $Y_{11}(\hat{r}) = -\sqrt{\frac{3}{8\pi}}\frac{1}{r}(x+iy)$, $Y_{1\,-1}(\hat{r}) = \sqrt{\frac{3}{8\pi}}\frac{1}{r}(x-iy)$ the relation between $\hat{\vec{d}}$ and $\hat{\mathscr{M}}^{(el)}_{1\,M}$ is

$$\hat{\mathscr{M}}^{(el)}_{10} = \sqrt{\frac{3}{4\pi}}\,\hat{\vec{d}}_z, \quad \hat{\mathscr{M}}^{(el)}_{11} = -\sqrt{\frac{3}{4\pi}}\,\frac{\hat{d}_x + i\,\hat{d}_y}{\sqrt{2}}, \qquad \hat{\mathscr{M}}^{(el)}_{1\,-1} = \sqrt{\frac{3}{4\pi}}\,\frac{\hat{d}_x - i\,\hat{d}_y}{\sqrt{2}} \tag{2.197}$$

2.3.2 Electric quadrupole moment

The operator of the electric quadrupole tensor operator $\hat{Q}_{ik}$ is given by (2.189). The substitution of the (2.190) for the charge density operator enables to rewrite (2.189) in the following way

$$\hat{Q}_{ik} = \sum_l e_l\,(\,3x^{(l)}_i x^{(l)}_k - \delta_{ik}\,r^2_l\,) \tag{2.198}$$

The value of the quadrupole electric moment of the given nucleus in the given state $|\,\alpha\,J_\alpha\rangle$ is in the nuclear physics defined as the expectation value of the $\hat{Q}_{33}$ component of the quadrupole tensor component

$$\begin{aligned} Q_\alpha \;\equiv\; Q_{33}(\alpha) \;=\; \frac{1}{e}\;\langle\,\alpha\,J_\alpha\,M_\alpha = J_\alpha|\,\hat{Q}_{33}\,|\,\alpha\,J_\alpha\,M_\alpha = J_\alpha\rangle \;= \\ = \frac{1}{e}\;\sum_{k=1}^{A} e_k \int d^3r_1 d^3r_2 \ldots d^3r_A \\ \Psi^*_{\alpha\,J_\alpha J_\alpha}(\vec{r}_1,\ldots,\vec{r}_A)\;\left[3\,(z^{(l)})^2 - (r^{(l)})^2\,\right]\;\Psi_{\alpha\,J_\alpha J_\alpha}(\vec{r}_1,\ldots,\vec{r}_A) \end{aligned} \tag{2.199}$$

where $\Psi_{\alpha\,J_\alpha M_\alpha}(\vec{r}_1,\ldots,\vec{r}_A)$ is the A-particle wave function of the nucleus in the state α in the coordinate representation.

The $\hat{Q}_{ij}$ is the symmetric second order tensor with the zero trace

$$\hat{Q}_{ij} = \hat{Q}_{ji}, \qquad Tr(\hat{Q}) = 0 \tag{2.200}$$

Therefore it has 5 independent components. The 5 independent components in the Kartezian coordinate system can be transormed into the spherical

coordinates and the quadrupole electric tensor in the spherical coordinate system can be expressed in terms of the spherical harmonics $Y_{2\mu}(\hat{r})$. For instance the component $\hat{Q}_{20}$ has the following form (because $r^2\, Y_{20}(\hat{r}) = \sqrt{\frac{5}{16\pi}}\,(3z^2 - r^2)$)

$$\hat{Q}_{20} = \sqrt{\frac{16\pi}{5}} \sum_{i=1}^{A} r_i^2\, Y_{20}(\hat{r}_i) = \sqrt{\frac{16\pi}{5}}\, \hat{\mathscr{M}}_{20}^{(el)} \tag{2.201}$$

and also other quadrupole moment components $\hat{Q}_{ij}$ can be expressed in terms of $\hat{\mathscr{M}}_{2\mu}^{(el)}$ for $\mu = 0,\ \pm 1, \pm 2$. The operator of the quadrupole moment $\hat{Q}_{ik} = \int d^3r (3x_i x_k - \delta_{ik} r^2)\, \hat{\rho}(\vec{r})$ can be also expressed in terms of the components of the angular momentum $\hat{J}_i$. As the symmetric tensor of the second order it can be written in terms of the component of the arbitrary vector operator (and therefore also in terms of the angular momentum components) exactly by one way

$$\begin{aligned} \hat{Q}_{ij} &= C\, \left[\frac{3}{2}\, (\hat{J}_i \hat{J}_j + \hat{J}_j\, \hat{J}_i) - \delta_{ij}\, \hat{J}^2 \right] \\ Q_{ij}(\alpha) &= C\, \langle \alpha\, J_\alpha\, M_\alpha\, | \frac{3}{2}\, (\hat{J}_i \hat{J}_j + \hat{J}_j\, \hat{J}_i) - \delta_{ij}\, \hat{J}^2 |\, \alpha\, J_\alpha\, M_\alpha \rangle \end{aligned} \tag{2.202}$$

where C is the normalization constant which can be related to the value of the quadrupole moment of the nucleus ground state $Q_0 \equiv Q_{33}(\alpha = ground) = \langle gr\ J_0 J_0 |\, \hat{Q}_{33}\, | gr\ J_0 J_0 \rangle$:

$$\begin{aligned} Q_0 &= \frac{C}{e}\, \langle gr\ J_0\ J_0 | 3\, \hat{J}_z^2 - \hat{J}^2 | gr\ J_0\ J_0 \rangle = \frac{C}{e}\, \left[3\, J_0^2 - J_0\, (J_0 + 1) \right] \\ &= \frac{C}{e}\, J_0\, (2\, J_0 - 1) \qquad \Rightarrow \qquad C = \frac{Q_0\, e}{J_0\, (2\, J_0 - 1)} \end{aligned} \tag{2.203}$$

So, the operator of the quadrupole moment expressed in terms of the components of the angular momentum is

$$\hat{Q}_{ij} = \frac{e\, Q_0}{J_0\, (2J_0 - 1)}\, \left[\frac{3}{2}\, \left(\hat{J}_i\, \hat{J}_j + \hat{J}_j\, \hat{J}_i \right) -\, \delta_{ij}\, \hat{J}^2 \right] \tag{2.204}$$

From the expr. (2.203) it can be seen that the nucleus quadrupole moment is zero, $Q_0 = 0$, if $J_0 = 0$ or $J_0 = 1/2$ and that the quadrupole moment can be nonzero only if the angular momentum of the given state is higher than $1/2$.

In the Chapter 1 (see (1.10)) it was shown that the quadrupole moment Q_0 is a measure of the quadrupole deformation of the nucleus. Spherical nuclei have zero quadrupole moments and with the increasing quadrupole deformation the nucleus has bigger value of the quadrupole moment.

2.3.3 Magnetic dipole moment

The operator of the magnetic dipole moment induced by the current density $\hat{\vec{j}}_{nuc}(\vec{r})$ is given by the expr. (2.189). So, the operator of the magnetic dipole moment of the nucleus is

$$\hat{\vec{\mu}} = \frac{1}{2} \int d^3r \, [\, \vec{r} \times \hat{\vec{j}}_{nuc}(\vec{r}) \,] \tag{2.205}$$

where $\hat{\vec{j}}_{nuc}(\vec{r})$ is the nuclear current density in the given point $\vec{r}$. This current density is given by the sum of the convectional (orbital) and magnetization (spin) parts - see (2.191):

$$\hat{\vec{j}}_{nuc}(\vec{r}) = \hat{\vec{j}}_o(\vec{r}) + \hat{\vec{j}}_s(\vec{r}) \tag{2.206}$$

with

$$\begin{aligned} \hat{\vec{j}}_o(\vec{r}) &= \sum_{i=1}^{A} \frac{e_i}{m_i} \, \hat{\vec{p}}_i \, \delta(\vec{r} - \vec{r}_i) \\ \hat{\vec{j}}_s(\vec{r}) &= \vec{\nabla} \times \sum_{i=1}^{A} \hat{\vec{\mu}}_s^{(i)} \, \delta(\vec{r} - \vec{r}_i) \end{aligned} \tag{2.207}$$

where $\hat{\vec{p}}_i$ is the operator of the linear momentum of $i-$the nucleon and $\hat{\vec{\mu}}_s^{(i)}$ is the magnetic dipole moment of the $i-$th nucleon which is connected with the spin of the ith nucleon through corresponding gyromagnetic ratio $g_s^{(i)}$ by

the expression (2.143). The substitution of (2.206) into (2.205) gives

$$\begin{aligned}
\hat{\vec{\mu}} &= \frac{1}{2}\int d^3r\,[\,\vec{r}\times(\hat{\vec{j}}_o(\vec{r})+\hat{\vec{j}}_s(\vec{r}))\,] = \\
&= \frac{1}{2}\sum_{i=1}^{A}\frac{e_i}{m_i}\,(\,\vec{r}_i\times\hat{\vec{p}}_i\,)+\frac{1}{2}\sum_{i=1}^{A}(\vec{r}_i\times(\vec{\nabla}_i\times\hat{\vec{\mu}}_s^{(i)})) = \\
&= \boxed{\begin{array}{c}\text{the second term can be}\\ \text{developed in the same way as in (2.139)}\end{array}} = \\
&= \frac{1}{2}\sum_{i=1}^{A}\frac{e_i}{m_i}\,(\,\vec{r}_i\times\hat{\vec{p}}_i\,)+\sum_{i=1}^{A}\hat{\vec{\mu}}_s^{(i)} = \sum_{i=1}^{A}(\,\hat{\vec{\mu}}_l^{(i)}+\hat{\vec{\mu}}_s^{(i)}\,)
\end{aligned} \tag{2.208}$$

where

$$\begin{aligned}
&\hat{\vec{\mu}}_s^{(i)} = g_s^{(i)}\,\mu_N\,\hat{\vec{s}}^{(i)} \qquad && g_s = \begin{cases}5.586 & \text{for protons}\\ -3.826 & \text{for neutrons}\end{cases}\\
&\hat{\vec{\mu}}_l^{(i)} = g_l^{(i)}\,\mu_N\,\hat{\vec{l}}^{(i)} \qquad && g_l = \begin{cases}1 & \text{for protons}\\ 0 & \text{for neutrons}\end{cases}
\end{aligned} \tag{2.209}$$

From the comparison of exprs.(2.208) and (2.145) it follows that the relation between the dipole moment $\hat{\vec{\mu}}$ of the nucleus and magnetic transition dipole operator $\hat{\mathscr{M}}_{1M}^{(mag)}$ is

$$\begin{aligned}
\hat{\mathscr{M}}_{10}^{(mag)} &= \sqrt{\frac{3}{4\pi}}\,\hat{\mu}_3\\
\hat{\mathscr{M}}_{1\pm1}^{(mag)} &= \mp\sqrt{\frac{3}{4\pi}}\,(\hat{\mu}_1\pm i\,\hat{\mu}_2)
\end{aligned} \tag{2.210}$$

The magnetic moment of the nucleus in the given state $\mid \alpha J_\alpha\rangle$ is defined as the following expectation value of the third component of the operator of the dipole magnetic moment

$$\mu_\alpha \;=\; \langle \alpha\; J_\alpha\; M_\alpha = J_\alpha \mid \hat{\mu}_3 \mid \alpha\; J_\alpha\; M_\alpha = J_\alpha\rangle \tag{2.211}$$

3. Nucleon - nucleon interaction

Energy region relevant for the nuclear structure covers values up to hundreds of MeV. Therefore in this chapter the properties of the nucleon-nucleon interaction as the strong and electromagnetic interactions among baryons with energies up to hundreds of MeV are discussed. At first we will deal with interactions between two nucleons without a presence of other nucleons (two nucleons in the vacuum) - so called bare nucleon-nucleon interaction. In the second half of this chapter the effective nucleon-nucleon interaction acting between nucleons in the nuclear medium (that means in the presence of all other nucleons in the nucleus) will be treated.

Basic information about the bare nucleon-nucleon interaction (that means interaction strength or depth and the interaction range) were roughly obtained from deuteron properties. However, the details of the bare nucleon-nucleon interactions with the energies up to several hundreds of MeV were exctracted from the nucleon-nucleon scattering experiments using so called phase analysis.

From the theoretical point of view the effective nucleon-nucleon interaction in the nuclear medium can be obtained from the bare nucleon-nucleon interaction by means of the microscopical approaches like Brueckner-Bethe method [18], [19]. The basic ideas of this method are presented in the end of this chapter. However, these microscopical approaches give only a general view of the effective nucleon-nucleon interaction and for a practical use of the concrete calculation of the structural properties of heavier nuclei the phenomenological or semi- phenomenological effective interactions (like Skyrme [20], Gogny [21] or relativistic mean field approach [22]) are applied. These effective interactions are also discussed in the end of this chapter.

3.1 Nucleon-nucleon interaction in the vacuum (bare nucleon-nucleon interaction)

3.1.1 Basic data on bare nucleon-nucleon interaction following from the deuteron properties

The deuteron, as the system consisting from neutron and proton, is the only bound system of two nucleons. It exists only in the ground state, it has no excited states. The basic experimental data on deuteron are following

- total angular momentum of the deuteron ground state is $J^{\pi} = 1^{+}$;
- ground state dipole magnetic moment is

$$\mu = (\ 0.857 \pm 0.000001\ )\ \mu_N = (\ \mu_p + \mu_n - 0.022209\ )\ \mu_N \tag{3.1}$$

  where $\mu_N = \frac{e\hbar}{2mc}$ is the nuclear magneton and $\mu_p = 2.793$, $\mu_n = -1.913$ (see (2.209));
- bound energy of the deuteron is $E = (-\ 2.22452 \pm 0.0001)\ MeV$;
- deuteron electric quadrupole moment: $Q = (0.282 \pm 0.001)\ fm^2$.

On basis of these experimental information we can do a rough estimation of basic characteristics of the deuteron ground state.

Since the deuteron magnetic dipole moment is almost equal to the sum of magnetic dipole moments of proton and neutron (see (3.1)) the orbital moment L of the deuteron should be closed to zero ($L \approx 0$). This conclusion follows from the expression (2.208) (in the combination with (2.111)) for the total magnetic dipole moment where this moment is given by the sum of the spin and orbital parts. Since (3.1) corresponds almost fully to the spin part the orbital part should be closed to zero. This implies the zero value of L. Therefore the total angular momentum of the deuteron, $\vec{J} = \vec{L} + \vec{S}$, is formed only by the total spin $\vec{S}$, which is $S = 1$, because it is the result of the coupling of two 1/2- spins of proton and neutron. Taking into account these facts one may conclude that the deuteron ground state is predominantly formed by the triplet spin component which is tagged in the spectroscopy as

$$^{3}S_{1} \tag{3.2}$$

where S means $L = 0$ ($L = 0 \rightarrow S$, $L = 1 \rightarrow P$, $L = 2 \rightarrow D$, ...) and 3 in the above left corner means $2S + 1 = 3$ and 1 in below right corner corresponds to $J = 1$.

On the other hand the nonzero value of the quadrupole moment ($Q = 0.282\ fm^2$) implies that the deuteron ground state cannot be a pure S-state. The space shape of the $L = 0$ wave function corresponds to a spherical symmetry and consequently to the zero value of Q. Therefore the nonzero value of Q means that the deuteron ground state should contain a small component of $L \neq 0$ state. Because the parity of the deuteron ground state is positive this small $L \neq 0$ component is expected to have $L = 2$, that means ${}^3D_1$ state.

In next subsections it will be shown that the existence of the deuteron ground state as a mixture of S- and D- states implies that the interaction between neutron and proton in the deuteron cannot have a simple central character, that it should contain a part which mixes different orbital momenta L. This conclusion lead to the introdusing of so called tensor term into the bare nucleon-nucleon interaction.

3.1.1.1 Central potential

In order to obtain the first insight into the neutron-proton interaction (what is the strength and range of the interaction) at first we will suppose a simple central potential for this interaction. In this case the deuteron wave function $\psi(\vec{r})$ is given by the simple Schroedinger equation:

$$\left[-\frac{\hbar^2}{2M_{red}}\vec{\nabla}^2 + V(r)\right]\ \psi(\vec{r}) = E\,\psi(\vec{r}) \tag{3.3}$$

where $\vec{r} = \vec{r}_n - \vec{r}_p$ and $M_{red} \approx M/2$ is the reduced mass of the system of proton and neutron (M- nucleon mass). If the potential has a central character we can look for the wave function $\psi(\vec{r})$ in the form of a product of the radial and angle parts (see any quantum mechanics textbook and the appendix D)

$$\psi(\vec{r}) = R_{nl}(r)\,Y_{lm}(\hat{r}) \tag{3.4}$$

where the angle part is well-known spherical function $Y_{lm}(\hat{r})$. The substitution of (3.4) into (3.3) gives the differential equation for the radial part $R_{nl}(r)$

$$\frac{d^2R_{nl}(r)}{dr^2} + \frac{2}{r}\frac{dR_{nl}(r)}{dr} + \frac{2M_{red}}{\hbar^2}\left[E - V(r) - \frac{\hbar^2 l(l+1)}{2M_{red}\,r^2}\right]R_{nl}(r) = 0 \tag{3.5}$$

or (after the substitution $u_{nl}(r) = r\,R_{nl}(r)$)

$$\frac{d^2u_{nl}(r)}{dr^2} + \frac{2M_{red}}{\hbar^2}\left[E - V(r) - \frac{\hbar^2 l(l+1)}{2M_{red}\,r^2}\right]u_{nl}(r) = 0 \tag{3.6}$$

On basis of the experimental data on deuteron (see (3.1) and (3.2)) we know that the dominant component of the deuteron ground state is the S-state ($l = m = 0$). Since $Y_{00}(\hat{r}) = 1/\sqrt{4\pi}$ the wave function $\psi(\vec{r})$ is (if we restrict oureselves on the central potential then there is no any l- mixing)

$$\psi(\vec{r}) = R(r)\frac{1}{\sqrt{4\pi}} = \frac{1}{\sqrt{4\pi}}\frac{u(r)}{r} \tag{3.7}$$

and the equation (3.6) can be rewritten as follows (for $l = 0$)

$$\left[\frac{d^2}{dr^2} + \frac{M}{\hbar^2}\left(E - V(r)\right)\right] u(r) = 0 \tag{3.8}$$

and the following boundary condition are required connected with the fact that $R(r \to 0)$ should be finite and for the bound system $R(r \to \infty) = 0$

$$u(0) = 0 \qquad u(\infty) = finite$$

For the simplicity the central potential $V(r)$ will be assumed in the form of the symmetric 3-dimensional well:

$$V(r) = \begin{cases} -V_0 \text{ for } r \leq r_0\,, \\ 0 \quad \text{for } r > r_0\,, \end{cases} \tag{3.9}$$

where r_0 is the potential range (please, do not confuse with the parameter $r_0 = 1.2\ fm$ in (1.2)). It is known from the basic quantum mechanics that in this case we can solve equation (3.8) very easily for both regions, $r \leq r_0$ and $r > r_0$, extra. From the condition of the smoothness of the logaritmic derivative of the function $u(r)$ in the point $r = r_0$ we obtain the equation for the energy E. Concretely, for the S-states ($L = 0$) this equation is (see e.g. [14])

$$cotg\left[\sqrt{M(V_0 + E)}\,\frac{r_0}{\hbar}\right] = -\frac{\sqrt{|E|}}{\sqrt{V_0 + E}}\,, \qquad E < 0 \tag{3.10}$$

Moreover, if we suppose $V_0 >> |E|$ (from the experimental deuteron data it is known that $|E| = 2.225$ MeV) then the condition (3.10) can be rewritten as

$$cotg\left[\sqrt{M(V_0 + E)}\,\frac{r_0}{\hbar}\right] \approx 0 \qquad \Rightarrow \qquad \sqrt{MV_0}\,\frac{r_0}{\hbar} \approx \frac{\pi}{2} \tag{3.11}$$

Another possibility could be $\sqrt{MV_0}\,\frac{r_0}{\hbar} \approx 3\,\frac{\pi}{2},\ 5\,\frac{\pi}{2},\ \ldots$ but this is excluded because in such cases the wave function have nodes and it is impossible for $L = 0$.

Various experimental data about nuclear forces give the range of nucleon-nucleon interaction: $r_0 \approx 1.7\ fm$. If this value is substituted to (3.11) we obtain

$$V_0 \approx 35.4\ MeV$$

and this is in agreement with the assumption $V_0 >> |E|$ for $|E| = 2.225 MeV$.

The solution of (3.8) for the region $r > r_0$ (that means $(d^2/dr^2 + ME/\hbar^2)u(r) = 0$) is the following function

$$u(r) = [2\alpha]^{1/2}\, e^{-\alpha\, r} \tag{3.12}$$

with

$$\alpha^2 = -\frac{ME}{\hbar^2} \tag{3.13}$$

The substitution of the experimental value, $E = -2.225$ MeV, into (3.13) gives

$$\alpha^{-1} = 4.3\ fm \tag{3.14}$$

If we substitute this value into (3.12) and subsequently we determine the expectation value $\langle r^2 \rangle = \int d^3r |\psi(\vec{r})|^2 r^2$ we figure that the proton and neutron in the deuteron are placed predominantly out of the interaction range (that means $\langle r^2 \rangle > r_0^2$). Therefore in the case of the potential well (3.9) the wave function in the region $r > r_0$ is decisive for the deuteron ground state.

The perpendicular potential well (3.9) with the depth $V_0 \approx 35\ MeV$ and the range $r_0 \approx 1.7\ fm$ has only one bound state ${}^3S_1$. The existence of a bound state with $L = 1$ (with the negative parity) is given by the condition (see quantum mechanics textbooks)

$$\sqrt{M\, V_0}\, \frac{r_0}{\hbar} \geq \pi$$

which is not possible for $V_0 \approx 35\ MeV$ and $r_0 \approx 1.7\ fm$.

In more realistic calculation of the deuteron the potential $V(r)$ is usually taken in the form of Hulten's potential

$$V(r) = -V_0\, \frac{e^{-\mu r}}{1 + e^{-\alpha r}} \tag{3.15}$$

and the differential equation (3.8) with this central potential gives following solution

$$u(r) = [2\alpha(\alpha + \mu)(2\alpha + \mu)]^{1/2}\, \mu^{-1}\, e^{-\alpha r}\, [1 + e^{-\mu r}] \tag{3.16}$$

The potential (3.15) has also only one bound state ${}^3S_1$.

The only one bound energy of the deuteron cannot give a sufficient amount of information for the determination of the nucleon-nucleon interaction. The nonzero value of the quadrupole electric moment and the experimental value of the magnetic dipole moment (see (3.1)) indicate that the ground state is a mixture of components with different L. In order to obtain such a mixing it is necessary to take into account also so called tensor interaction beside the central interaction.

3.1.1.2 Tensor forces

The Schroedinger equation for the deuteron wave function with the general noncentral potential is

$$\left[-\frac{\hbar^2}{M}\vec{\nabla}^2 + \hat{V}(\vec{r})\right]\psi(\vec{r}) = E\,\psi(\vec{r}) \tag{3.17}$$

where M is the nucleon mass (we suppose $M = M_p = M_n$; $M_{red} = M/2$). On basis of the experimental indications that the deuteron ground state is a mixture of S- and D- states the potential $V(\vec{r})$ in (3.17) should contain a term which mixes states with different orbital momenta L. The central potential, discussed in the previous subsections, does not cause any L- mixing and therefore so called tensor term is added into $\hat{V}(\vec{r})$ in order to obtain this mixing and the potential $\hat{V}(\vec{r})$ in (3.17) is taken in the following form

$$\hat{V}(\vec{r}) = \hat{V}_{centr}(r) + \hat{S}_{12}\,\hat{V}_T(r) \tag{3.18}$$

with

$$\hat{S}_{12} \equiv \frac{3}{r^2}\,(\vec{\sigma}_1\cdot\vec{r})\,(\vec{\sigma}_2\cdot\vec{r}) \;-\; \vec{\sigma}_1\cdot\vec{\sigma}_2 \tag{3.19}$$

where $\vec{\sigma}_1$ is the vector constructed from spin Pauli matrices of the 1-st nucleon and and $\vec{\sigma}_2$ from Pauli matrices of the 2-d nucleon. If we rewrite the operator $\hat{S}_{12}$ in the spherical coordinate we obtain

$$\hat{S}_{12} = \sqrt{24\pi}\;\left[(\sigma_1\,\sigma_2)_{\lambda=2}\,Y_{\lambda=2}\right]_{(22)\,00} \tag{3.20}$$

where $\vec{r} = \vec{r}_1 - \vec{r}_2$ is the mutual radius-vector between proton and neutron and

$$(\sigma_1\,\sigma_2)_{\lambda=2\,\mu} = \sum_{\Sigma} C^{2\,\mu}_{1\;\Sigma\,1\;\mu-\Sigma}\;(\sigma_1)_{1\Sigma}\,(\sigma_2)_{1\mu-\Sigma}$$

where

$$(\sigma)_{1\mu} = \begin{cases} -\frac{1}{\sqrt{2}}\,(\sigma_x + i\,\sigma_2) & \text{for } \mu = +1 \\ \sigma_z & \text{for } \mu = 0 \\ \frac{1}{\sqrt{2}}\,(\sigma_x - i\,\sigma_2) & \text{for } \mu = -1 \end{cases}$$

and

$$[(\sigma_1\,\sigma_2)_{\lambda=2}\,Y_{\lambda=2}]_{(22)\,00} = \sum_{m=-2}^{+2} C^{0\,0}_{2\,m\,2\,-m}\;(\sigma_1\,\sigma_2)_{2\,m}\,Y_{2-m}(\hat{r}) \tag{3.21}$$

The operator $\hat{S}_{12}$ itself is the scalar in the combined spatial-spin Hilbert space but in the spatial part of the space this operator is represented by the spherical function $Y_{2\mu}(\hat{r})$ which is a tensor of the second order. Similarly, in the spin part of the space the $\hat{S}_{12}$ is given by $(\sigma_1\,\sigma_2)_{2\mu}$ which is again the tensor of the second order. Therefore the operator $\hat{S}_{12}$ is often called as a tensor operator in the literature in spite of the fact that it is a scalar in the full Hilbert space.

The operator $\hat{S}_{12}$ was chosen in the form (3.18) because it is the only scalar with the second order power of $\vec{r}$ (which preserves the parity) and which is linear in $\vec{\sigma}_1$ and $\vec{\sigma}_2$. The second term with $\vec{\sigma}_1 \cdot \vec{\sigma}_2$ was added in order to obtain the zero value of the expectation value of the whole operator $\hat{S}_{12}$ (which is useful in the further considerations). In (3.19) it is sufficient to restrict to linear order terms in $\vec{\sigma}_1$ and $\vec{\sigma}_2$ because all terms with higher power of Pauli matrices can be reduced to the linear order in terms of the identities like this

$$(\vec{\sigma} \cdot \vec{A})\,(\vec{\sigma} \cdot \vec{B}) = \vec{A} \cdot \vec{B} + i\,\vec{\sigma} \cdot (\vec{A} \times \vec{B}) \tag{3.22}$$

The wave function $\psi(\vec{r})$ (the solution of the equation (3.17)) is usually searched for in the following form

$$\psi_{JM}(\vec{r}) = \sum_L \frac{u_L(r)}{r}\;\Phi_{LJM}(\hat{r}) \tag{3.23}$$

where

$$\Phi_{LJM}(\hat{r}) = \sum_{M_S=0,\pm1} C^{JM}_{L\,M-M_S\,1\,M_S}\,Y_{L\,M-M_S}(\hat{r})\,\chi_{M_S} \tag{3.24}$$

where $J = L,\ L \pm 1$. In (3.24) the fact was used that from the experimental deuteron data the total deuteron spin $S = 1$ was deduced (see the text below (3.1)). Functions $\Phi_{LJM}(\hat{r})$ form the complete system of orthonormal functions,

$$\int \hat{dr}\;\Phi^*_{L'J'M'}(\hat{r})\;\Phi_{LJM}(\hat{r}) = \delta_{LL'}\,\delta_{JJ'}\,\delta_{MM'} \tag{3.25}$$

and therefore we can look for the solution $\Phi_{JM}(\vec{r})$ in the form of the decomposition (3.23).

Since the parity of (3.23) should be a good quantum number and the parity of the function $\Phi_{JM}(\vec{r})$ is $(-1)^L$ ($\mathscr{P}\Phi_{JM}(\vec{r}) = (-1)^L\,\Phi_{JM}(\vec{r})$) the decomposition (3.23) for given J involves only $L = J$ or only $J = L \pm 1$. Because of the ground state of the deuteron has a positive parity and $J = 1$ the only possibility for L in (3.23) is $L = 0, 2$. We also know that $S = 1$ and therefore spin function χ_{M_S} in (3.23) corresponds to the triplet with $M_S = 0, \pm 1$:

$$
\begin{aligned}
&S = 1\ M_S = 0 \\
&\quad \chi_{M_S=0} = C^{1\,0}_{1/2\,1/2\,1/2\,-1/2}\ |1/2\ 1/2\rangle\,|1/2\ -1/2\rangle + \\
&\qquad\qquad + C^{1\,0}_{1/2\,-1/2\,1/2\,1/2}\ |1/2\ -1/2\rangle\,|1/2\ 1/2\rangle\ = \\
&\qquad = 1/\sqrt{2}\ \Big[\ |1/2\ 1/2\rangle\,|1/2\ -1/2\rangle + \\
&\qquad\qquad\qquad + |1/2\ -1/2\rangle\,|1/2\ 1/2\rangle\ \Big] \\
&S = 1\ M_S = 1 \\
&\quad \chi_{M_S=1}\ =\ C^{1\,1}_{1/2\,1/2\,1/2\,1/2}\ |1/2\ 1/2\rangle\,|1/2\ 1/2\rangle \\
&S = 1\ M_S = -1 \\
&\quad \chi_{M_S=-1}\ =\ C^{1\,-1}_{1/2\,-1/2\,1/2\,-1/2}\ |1/2\ -1/2\rangle\,|1/2\ -1/2\rangle
\end{aligned}
\tag{3.26}
$$

The searched for function $\psi_{JM}(\vec{r})$ fulfils the following normalization conditions

$$
\begin{aligned}
&\int d^3r\ \psi^*_{JM}(\vec{r})\ \psi_{JM}(\vec{r}) = \\
&= \sum_{LL'} \int_0^\infty dr\ u_{L'}(r)\ u_L(r)\ \int \hat{dr}\ \Phi^*_{L'JM}(\hat{r})\ \Phi_{LJM}(\hat{r}) = \\
&= \boxed{\begin{array}{c}\text{see}\\(3.25)\end{array}} = \sum_L \int_0^\infty dr\ u^2_L(r) = 1
\end{aligned}
\tag{3.27}
$$

We rewrite the equation (3.17) in the spherical coordinates

$$
\begin{aligned}
\Big\{\ \frac{d^2}{dr^2} + \frac{2}{r}\,\frac{d}{dr} + + \frac{M}{\hbar^2}\,\Big[E - \frac{\hbar^2}{M}\,\frac{(\hat{\vec{L}})^2}{r^2} - V_{centr}(r) - V_T(r)\,\hat{S}_{12}\Big]\ \Big\} \\
\cdot \sum_{L'} \frac{u_{L'}(r)}{r}\,\Phi_{L'JM}(\hat{r}) = 0
\end{aligned}
\tag{3.28}
$$

The multiplication of this equation by $\Phi^*_{LJM}(\hat{r})$ and the integration over $\hat{r}$ gives the system of differential equations for the radial parts $u_L(r)$ ($L = 0, 2$)

	$L' = J+1$	$L' = J$	$L' = J-1$
$L = J+1$	$-2\,(J+2)/(2J+1)$	0	$6\,\sqrt{J(J+1)}/(2J+1)$
$L = J$	0	2	0
$L = J-1$	$6\,\sqrt{J(J+1)}/(2J+1)$	0	$-2\,(J-1)/(2J+1)$

Table 3.1: The quantity $S_{JLL'}$ in the expr. (3.30)

of the wave function $\Psi_{JM}(\vec{r})$

$$\frac{d^2u_L(r)}{dr^2} + \frac{2M_{rel}}{\hbar^2}\left[E - \frac{\hbar^2}{2M_{rel}}\,\frac{L(L+1)}{r^2} - V_{centr}(r)\right] u_L(r) \\ - \frac{2M_{rel}}{\hbar^2}\,V_T(r) \sum_{L'=0,2} \int \hat{dr}\;\Phi^*_{LJM}(\hat{r})\;\hat{S}_{12}\;\Phi_{L'JM}(\hat{r})\;\; u_{L'}(r) \;=\; 0 \tag{3.29}$$

Further it is necessary to determine the matrix elements $\langle LJM|\hat{S}_{12}|L'J'M'\rangle = \int \hat{dr}\;\Phi^*_{LJM}(\hat{r})\;\hat{S}_{12}\;\Phi_{L'J'M'}(\hat{r})$:

$$\begin{aligned}
&\langle LJM|\hat{S}_{12}|L'J'M'\rangle = \\
&= \langle LJM|\;\sqrt{24\pi}\;\Big[(\sigma_1\sigma_2)_{\lambda=2}\;Y_{\lambda=2}\Big]_{(22)\,00}\;|L'J'M'\rangle = \\
&= \boxed{\begin{array}{c}\text{Wigner-Eckart}\\ \text{theorem } (A.12)\end{array}} = \\
&= C^{J\;M}_{J'\;M'\;0\;0}\;\frac{\sqrt{24\pi}}{\sqrt{2J+1}}\;\langle (L1)J||\;\Big[(\sigma_1\sigma_2)_{\lambda=2}\;Y_2\Big]_{(22)\,0}\;||(L'1)J'\rangle = \\
&= \delta_{JJ'}\;\delta_{MM'}\;(-1)^{J'+L'+1}\frac{\sqrt{24\pi(2J'+1)\;(2L+1)}}{\sqrt{15}}\;\begin{Bmatrix} L' & 1 & J\\ L & 1 & 2\end{Bmatrix} \\
&\qquad\qquad \cdot\langle L||Y_2||L'\rangle\;\langle 1||(\sigma_1\sigma_2)_2||1\rangle
\end{aligned}$$

The reduced matrix elements $\langle L||Y_2||L'\rangle$ and $\langle 1||(\sigma_1\sigma_2)||1\rangle$ can be found (e.g. in [2]) and finally we obtain

$$\langle LJM|\hat{S}_{12}|L'J'M'\rangle = \delta_{JJ'}\;\delta_{MM'}\;S_{JLL'} \tag{3.30}$$

where $S_{JLL'}$ are given in the table 3.1.

As it was mentioned several times above the main contribution to the wave function $\psi_{J=1\,M}(\vec{r})$ of the deuteron ground state is given by the configuration $^3S_1$. From the table 3.1 it can be seen that the tensor interaction can mix

this configuration with ${}^3D_1$. The state ${}^3D_1$ can be, in principle, mixed with some state with $L = 4$. However, because the deuteron ground state has $J = 1$ the component with $L = 4$ is excluded. So, the deuteron ground state can be written as the sum of $L = 0$ and $L = 2$ components.

$$\psi_{J=1\,M}(\vec{r}) = \frac{u_0(r)}{r}\,\Phi_{01M}(\hat{r}) + \frac{u_2(r)}{r}\,\Phi_{21M}(\hat{r}) \tag{3.31}$$

The explicit expression for $\Phi_{01M}(\hat{r})$ and $\Phi_{21M}(\hat{r})$ are

$$\begin{aligned}
&\Phi_{01M}(\hat{r}) = \frac{1}{\sqrt{4\pi}}\,\chi_M\,, \qquad\qquad M = -1,\,0,\,1\\
&\Phi_{211}(\hat{r}) = \sum_{M_s=-1}^{+1} C^{1\,1}_{2\,1-M_s\,1\,M_s}\,Y_{2\,1-M_s}(\hat{r})\,\chi_{M_s} =\\
&\quad = \sqrt{\frac{1}{10}}\,Y_{20}(\hat{r})\,\chi_1 - \sqrt{\frac{3}{10}}\,Y_{21}(\hat{r})\,\chi_0 + \sqrt{\frac{3}{5}}\,Y_{22}(\hat{r})\,\chi_{-1}\\
&\Phi_{210}(\hat{r}) = \sum_{M_s=-1}^{+1} C^{1\,0}_{2\,-M_s\,1\,M_s}\,Y_{2\,-M_s}(\hat{r})\,\chi_{M_s} =\\
&\quad = \sqrt{\frac{3}{10}}\,Y_{2\,-1}(\hat{r})\,\chi_1 - \sqrt{\frac{2}{5}}\,Y_{20}(\hat{r})\,\chi_0 + \sqrt{\frac{3}{10}}\,Y_{21}(\hat{r})\,\chi_{-1}\\
&\Phi_{21\,-1}(\hat{r}) = \sum_{M_s=-1}^{+1} C^{1\,-1}_{2\,-1-M_s\,1\,M_s}\,Y_{2\,-1-M_s}(\hat{r})\,\chi_{M_s} =\\
&\quad = \sqrt{\frac{3}{5}}\,Y_{2\,-2}(\hat{r})\,\chi_1 - \sqrt{\frac{3}{10}}\,Y_{2\,-1}(\hat{r})\,\chi_0 + \sqrt{\frac{1}{10}}\,Y_{20}(\hat{r})\,\chi_{-1}
\end{aligned} \tag{3.32}$$

and the normalization condition (3.27) is

$$\int_0^\infty dr\,\Big[u_0^2(r) + u_2^2(r)\Big] = 1 \tag{3.33}$$

The table 3.1 gives for $S_{1LL'}$ the following values

$$S_{120} = S_{102} = \sqrt{8}\,, \qquad\qquad S_{122} = 2$$

If these values are substituted into (3.30) and then into (3.29) the system of

eqs. (3.29) takes the following form

$$\begin{aligned}
&\frac{d^2u_0(r)}{dr^2} + \frac{M}{\hbar^2}\left[E - V_{centr}(r)\right] u_0(r) \\
&\qquad\qquad - \sqrt{8}\,\frac{M}{\hbar^2}\,V_T(r)\,u_2(r) = 0 \\
&\frac{d^2u_2(r)}{dr^2} + \frac{M}{\hbar^2}\left[E - \frac{6\hbar^2}{Mr^2} - V_{centr}(r) + 2\,V_T(r)\right] u_2(r) \\
&\qquad\qquad - \sqrt{8}\,\frac{M}{\hbar^2}\,V_T(r)\,u_0(r) = 0
\end{aligned} \tag{3.34}$$

Exprs. (3.34) represent the system of differential equations for $u_0(r)$ and $u_2(r)$. The concrete form of $V_{centr}(r)$ and $V_T(r)$ will be discussed later. Generally these radial functions are given by some empirical expressions containing free parameters which are fitted in order to obtain experimental value of the deuteron bind energy (besides other experimental data of the deuteron and data on the nucleon scattering - see further).

3.1.1.3 Electric quadrupole moment of the deuteron

The solution of the equation system (3.34) for $u_0(r)$ and $u_2(r)$ gives the wave function $\psi_{J=1\,M}(\vec{r})$ and the corresponding energy E of the deuteron ground state. Knowing the wave function we can determine the deuteron electric quadrupole moment using (2.199), (2.201)

$$Q_{deut} = \sqrt{\frac{16\pi}{5}} \int d^3r\; \psi^*_{1\,M=1}(\vec{r})\; \mathscr{M}^{(el)}_{20}\; \psi_{1\,M=1}(\vec{r}) \tag{3.35}$$

where the electric quadrupole transition operator $\mathscr{M}^{(el)}_{20}$ in the case of the deuteron is given by

$$\mathscr{M}^{(el)}_{20} = \sum_{i=p,n} e_i\, r_i^2\, Y_{20}(\hat{r}_i) \tag{3.36}$$

In the reality only proton contributes to (3.36). If we introduce relative radius-vector of the neutron with respect to the proton

$$\vec{r} = \vec{r}_p - \vec{r}_n\,, \qquad \vec{r}_p = \frac{1}{2}\,\vec{r}\,, \qquad \vec{r}_n = -\frac{1}{2}\,\vec{r} \tag{3.37}$$

the operator $\mathscr{M}^{(el)}_{20}$ can be rewritten as

$$\mathscr{M}^{(el)}_{20} = \frac{1}{4}\,r^2\,Y_{20}(\hat{r}) \tag{3.38}$$

and the deuteron quadrupole moment is

$$Q_{deut} = \sqrt{\frac{\pi}{5}} \int d^3r\, \psi^*_{1\,M=1}(\vec{r})\, r^2\, Y_{20}(\hat{r})\, \psi_{1\,M=1}(\vec{r}) = \boxed{\begin{array}{c}\text{see}\\ (3.31)\end{array}} =$$

$$= \sqrt{\frac{\pi}{5}} \int d^3r \left(\frac{u_0(r)}{r}\, \Phi^*_{011}(\hat{r}) + \frac{u_2(r)}{r}\, \phi^*_{211}(\hat{r})\right) r^2\, Y_{20}$$

$$\cdot\left(\frac{u_0(r)}{r}\, \Phi_{011}(\hat{r}) + \frac{u_2(r)}{r}\, \phi_{211}(\hat{r})\right) =$$

$$= \boxed{\begin{array}{c}\text{the substitution from (3.32) and the integration}\\ \text{over angles and using}\\ \int \hat{dr}\, Y^*_{l_3 m_3} Y_{l_2 m_2} Y_{l_1 m_1} = \sqrt{\frac{(2l_1+1)(2l_2+1)}{4\pi(2l_3+1)}} C^{l_3\,0}_{l_1\,0\,l_2\,0}\, C^{l_3\,m_3}_{l_1\,m_1\,l_2\,m_2}\end{array}} =$$

$$= \frac{\sqrt{2}}{10} \int_0^\infty dr\, r^2 \left(u_0(r)\, u_2(r) - \frac{\sqrt{2}}{4}\, u_2^2(r)\right) \tag{3.39}$$

From (3.39) one can see that, really, the electric quadrupole moment of the deuteron is nonzero only thanks to the $L = 2$ component with the nonzero $u_2(r)$.

3.1.1.4 Magnetic dipole moment of the deuteron

Deuteron magnetic moment is determined according to (2.211) as the expectation value of the operator $\hat{\mu}_3$ in the ground state $|J = 1\; M = 1\; gr\rangle$

$$\mu_{deut} \;=\; \langle J = 1\; M = 1\; gr|\; \hat{\mu}_3\; |J = 1\; M = 1\; gr\rangle \tag{3.40}$$

where $\hat{\mu}_3$ is the third component of the operator $\hat{\vec{\mu}}$ of the dipole magnetic moment (2.208) which can be written in terms of the isospin formalism as follows

$$\hat{\vec{\mu}} = \sum_{i=p,n} \left(\hat{\vec{\mu}}^{(i)}_l + \hat{\vec{\mu}}^{(i)}_s\right) =$$

$$= \Big\{ \sum_{i=p,n} \Big[\, \frac{1}{2}\,(1 - \tau_3)_i\, \frac{1}{\hbar}\, \vec{r}_i \times \hat{\vec{p}}_i \,\Big] + \; g^{(p)}_s\, \hat{\vec{s}}_p + \; g^{(n)}_s\, \hat{\vec{s}}_n \Big\}\, \mu_N$$

where $\hat{\vec{p}}_i$ is the operator of the linear momentum of the i-th nucleon, $(\tau_3)_i$ is the third isospin Pauli matrix for i-th nucleon. In the case of the deuteron we have (see (3.37))

$$\vec{r}_p = \frac{1}{2}\vec{r}\,, \qquad \vec{r}_n = -\frac{1}{2}\vec{r}\,, \qquad \hat{\vec{p}} = \hat{\vec{p}}_p = -\hat{\vec{p}}_n$$

and therefore

$$\hat{\vec{\mu}} = \left[\frac{1}{2\hbar}\,\vec{r}\times\hat{\vec{p}} + g_s^{(p)}\,\hat{\vec{s}}_p + g_s^{(n)}\,\hat{\vec{s}}_n\right]\frac{e\hbar}{2Mc} =$$
$$= \left[\frac{1}{2}\,\hat{\vec{L}} + \frac{1}{2}\left(g_s^{(p)} + g_s^{(n)}\right)\left(\hat{\vec{s}}_n + \hat{\vec{s}}_p\right) + \right.$$
$$\left. + \frac{1}{2}\left(g_s^{(p)} - g_s^{(n)}\right)\left(\hat{\vec{s}}_n - \hat{\vec{s}}_p\right)\right]\frac{e\hbar}{2Mc} \qquad (3.41)$$

Because the spin state of the deuteron is the triplet state ($S = 1$) the term with $(\hat{\vec{s}}_n - \hat{\vec{s}}_p)$ cannot give any contribution to the expectation value $\mu_{deut} = \langle J = 1\; M = 1|\,\hat{\mu}_3\,|J = 1 M = 1\rangle$ and the matrix elements of the dipole magnetic moment operator for the deuteron are

$$\langle J = 1\; M = 1|\,\hat{\mu}_3\,|J = 1\; M = 1\rangle =$$
$$= \langle J = 1\; M = 1|\,\frac{1}{2}\,\hat{L}_3 + \frac{1}{2}\left(g_s^{(p)} + g_s^{(n)}\right)\hat{s}_3\,|J = 1\; M = 1\rangle\;\mu_N =$$
$$= \langle J = 1\; M = 1|\,\frac{1}{2}\left(g_s^{(p)} + g_s^{(n)}\right)\hat{J}_3 -$$
$$\frac{1}{2}\left(g_s^{(p)} + g_s^{(n)}\right)\hat{L}_3 + \frac{1}{2}\,\hat{L}_3\,|J = 1\; M = 1\rangle\;\mu_N =$$
$$= \frac{1}{2}\left(g_s^{(p)} + g_s^{(n)}\right)\;\mu_N -$$
$$\frac{1}{2}\left(g_s^{(p)} + g_s^{(n)} - 1\right)\langle J = 1\; M = 1|\,\hat{L}_3\,|J = 1\; M = 1\rangle\;\mu_N =$$

$$= \boxed{\begin{array}{c}\text{see}\\(3.31)\end{array}} = \left[\frac{1}{2}\left(g_s^{(p)} + g_s^{(n)}\right) - \frac{1}{2}\left(g_s^{(p)} + g_s^{(n)} - 1\right)\right.$$
$$\left. \cdot \sum_{M_L=-2}^{+2}\left(C^{1\,1}_{2\,M_L\,1\,1-M_L}\right)^2 M_L\int_0^\infty dr\,u_2^2(r)\right]\mu_N =$$
$$= \left[\frac{1}{2}\left(g_s^{(p)} + g_s^{(n)}\right) - \frac{3}{4}\left(g_s^{(p)} + g_s^{(n)} - 1\right)\int_0^\infty dr\,u_2^2(r)\quad\right]\mu_N =$$
$$= \left[\frac{1}{2}\left(g_s^{(p)} + g_s^{(n)}\right) - \frac{3}{4}\left(g_s^{(p)} + g_s^{(n)} - 1\right)p_D\quad\right]\mu_N \qquad (3.42)$$

where $\mu_N = \frac{e\hbar}{2Mc}$ is the nuclear magneton and

$$p_D = \int_0^\infty dr\,u_2^2(r) \qquad (3.43)$$

is the probability for the finding the deuteron in the state D.

If the expression (3.44) is used for the evaluation of the p_D from the experimental value $\mu_{deut} = 0.875\,\mu_N$ (see (3.1)) then we obtain

$$p_D = \frac{4}{3}\,\frac{\mu_{deut} - \frac{1}{2}\left(g_s^{(p)} + g_s^{(n)}\right)}{g_s^{(p)} + g_s^{(n)} - 1} \approx 0.039 \tag{3.44}$$

Therefore the deuteron can be found in the D- state approximately in 4% of the whole time and this is in accordance with the assumption $|u_2(r)|^2 << |u_0(r)|^2$.

In this estimation of the p_D the following corrections are not involved

- the contribution of the magnetic dipole moments of mesons which are exchanged by the nucleons during their mutual interaction
- the relativistic corrections in the nucleons motion
- polarization effects in the pure proton and neutron magnetic moments caused by the presence of the second nucleon in the deuteron.

If these corrections are taken into account the probability p_D is

$$p_D \approx (3 \pm 1)\ \% \tag{3.45}$$

This value is also used for the testing of potentials $V_{centr}(r)$ and $V_T(r)$. If we solve the equation system (3.34) with the given $V_{centr}(r)$ and $V_T(r)$ and we obtain the function $u_2(r)$ we can determine $p_D = \int_0^\infty dr\, u_2^2(r)$ and in such a way obtained value can be compared with the value (3.45).

3.1.2 Information on the bare nucleon-nucleon interaction from the scattering of two nucleons

From the experimental data on the deuteron or from the information on nucleon-nucleon scattering in very low energies - less then 1 KeV (which was used in the forties but which is not discussed in this textbook) only very rough image about the nucleon-nucleon interaction can be deduced. As we saw in the previous subsection only the strength and range of the nucleon-nucleon interaction and the presence of the tensor force in this interaction was extracted from this data. For more details, which would enable to understand nucleon-nucleon interaction more deeply, it is necessary to have experimental data on other quantities directly connected with the bare nucleon-nucleon interactions.

Further information about the bare nucleon-nucleon interaction are obtained from the nucleon-nucleon scattering. As it was already mentioned in the introductory chapter the scattering energies relevant to the nuclear structure physics involve values from KeV up to hundreds MeV. This relatively low energy enables to describe scattering by means of the non-relativistic quantum mechanics and from the theoretical point of view the interaction between two nucleons during their scattering can be considered as the exchange of different mesons (quark and gluon degrees of freedom are applied in the higher energies). However, the meson exchange mechanism gives only functional dependencies of individual terms in the pure nucleon-nucleon interaction and these functions involve a lot of parameters. These parameters should be determined by a comparison of theoretical values of cross-sections of the nucleon-nucleon scattering with corresponding experimental values. The main ideas of this method, in the literature known as the phase analysis, are given in this subsection.

3.1.2.1 Scattering of neutron and proton by means of the central potential

In the case of the neutron - proton scattering the Coulomb interaction is not present. If only the central potential between the neutron and the proton is considered then there is no any orbital momentum L-mixing in the wave function of the neutron-proton system and as a consequence of it also spin of the system does not change during the scattering. So, the spin part of the wave function can be avoided from the consideration and we can use the expression for the scattering of the spinless particles (see the Appendix D). Further we suppose that the central scattering potential has a short range. Therefore the asymptotic form of the wave function of the neutron-proton system composes from the ingoing plane wave and outgoing spherical wave (see (D.16))

$$\Psi_{r\to\infty}(\vec{r}) = e^{ikz} + f(\theta)\frac{e^{ikr}}{r} \tag{3.46}$$

where $\vec{r} = \vec{r}_p - \vec{r}_n$ is the mutual radius-vector of the neutron and proton, θ is the scattering angle between vectors $\vec{r}$ and $\vec{k}$, $k^2 = \frac{ME}{\hbar^2}$ (E is the scattering energy) and $f(\theta)$ is the scattering amplitude (see the Appendix D). Differential cross-section of the n-p scattering is then given by (D.19))

$$\frac{d\sigma}{d\Omega} = |f(\theta)|^2 \tag{3.47}$$

The radial part $\frac{u_L(r)}{r}$ of the system wave function (see(D.20)), in the case of the central potential we have the axially symmetric scattering and therefore the second coordinate angle ϕ is irrelevant)

$$\Psi(\vec{r}) = \Psi(r,\theta) = \sum_{L=0}^{\infty} \frac{u_L(r)}{r} P_L(cos\theta)$$

is given by the solution of the Shroedinger equation (reduced mass is $M_{red} = M/2$) (see (D.21))

$$\Big[\frac{d^2}{dr^2} + k^2 - \frac{M}{\hbar^2} V(r) - \frac{L(L+1)}{r^2} \Big] u_L(r) = 0 \tag{3.48}$$

where $V(r)$ is the central scattering potential. In the asymptotic region ($\vec{r} \to \infty$) the radial function$u_L(r)$ has the following form (see (D.23))

$$u_L(r \to \infty) \;\approx\; (2L+1)\, i^L\, A_L\, \frac{1}{k}\, \sin(kr - \frac{\pi L}{2} + \delta_L) \tag{3.49}$$

where δ_L is the phase shift of the L-th partial wave. From the requirement that $\Psi(\vec{r}) - e^{ikz}$ should be outgoing spherical wave (see (3.46) and (D.24)) we obtain $A_L = e^{i\delta_L}$ and the scattering amplitude is (see (D.25)))

$$\begin{aligned} f(\theta) &= \frac{1}{2ik} \sum_{L=0}^{\infty} (2L+1) \Big[e^{2i\delta_L} - 1 \Big] P_L(\cos\theta) = \\ &= \frac{1}{k} \sum_{l=0}^{\infty} (2L+1)\, e^{i\delta_L}\, \sin\delta_L\, P_L(\cos\theta) \end{aligned} \tag{3.50}$$

where $P_L(x)$ is the Legendre polynomial of the L-th order. The substitution of (3.50) into (3.47) gives the differential cross section of the scattering in the following form (see (D.26))

$$\frac{d\sigma}{d\Omega}(\theta) = |f(\theta)|^2 = \frac{1}{k^2} \Big| \sum_{L=0}^{\infty} (2L+1)\, e^{i\delta_L}\, \sin\delta_L\, P_L(\cos\theta) \Big|^2 \tag{3.51}$$

and the total cross section of the neutron-proton scattering with the central potential is

$$\sigma = \int_0^{2\pi} d\phi \int_{-1}^{+1} \frac{d\sigma}{d\Omega}\, d(\cos\theta) = \frac{4\pi}{k^2} \sum_{L=0}^{\infty} (2L+1)\, \sin^2\delta_L \tag{3.52}$$

From the theory of the scattering in the quantum mechanics (see e.g. [14]) it is known that the phase shift is positive for the attractive potential ($V(r) < 0$)

and the phase shift is negative for the repulsive potential ($V(r) > 0$). We also know from the quantum mechanics that in the description of the scattering for given energy we can restrict ourselves to only several terms in the sum in (3.52). That means only several values of the phase shift δ_L are necessary and the contribution of terms with higher L is small. It should be pointed out that in the case of the only central scattering potential without any L-mixing each partial wave with the given L corresponds only to one phase shift δ_L.

3.1.2.2 Scattering of two protons by means of the central potential

In the case of the scattering of two protons it is necessary to involve the Coulomb interaction in the scattering potential. The Schroedinger equation for the function $u_L(r)$ from the radial part of the wave function $\Psi(\vec{r}) = \sum_L \frac{u_L(r)}{r} P_L(\cos\theta)$ of the system of two protons is (see (D.14) and compare with (3.48))

$$\left[\frac{d^2}{dr^2} + k^2 - \frac{M}{\hbar^2} V(r) - \frac{M}{\hbar^2} \frac{\gamma}{r} - \frac{L(L+1)}{r^2} \right] u_L(r) = 0 \tag{3.53}$$

where the factor γ in the Coulomb term is $\gamma = \frac{e^2}{4\pi\epsilon_0}$. The function $u_L(r)$ in this case fulfils the following boundary condition (see (D.15))

$$\begin{aligned} u_L(r) &\overset{r\to 0}{\to} 0 \\ u_L(r) &\overset{r\to\infty}{\to} (2l+1)\, i^l\, A_L \frac{1}{k} \sin\left(kr - \eta \cdot ln2kr - \frac{\pi L}{2} + \sigma_L + \delta_L\right) \end{aligned} \tag{3.54}$$

where $\eta = \frac{\gamma}{\hbar}\sqrt{\frac{M}{2E}}$ and σ_L is so called Coulomb shift which is defined (see Appendix A in [23] and (D12))

$$\Gamma(l+1+i\,\eta) = |\Gamma(l+1+i\,\eta)|\; e^{i\sigma_l} \tag{3.55}$$

where $\Gamma(z)$ is the Γ-function from mathematics. In (3.54) δ_L is again the phase shift for L-th partial wave caused by the short-range scattering potential.

Similarly as in (3.46) the asymptotic form of the wave function $\Psi(\vec{r})$ is

$$\Psi_{r\to\infty}(\vec{r}) = I(\vec{r}) + f(\theta)\frac{e^{ikr}}{r} \tag{3.56}$$

where the plane wave $I(\vec{r})$ in this case is not a simple power $e^{ikz} = e^{ikr\cos\theta}$ as in (3.46) but (ingoing plane wave is modified by the presence of the long-range

Coulomb interaction)

$$I(\vec{r}) = \left[1 - \eta \frac{ln2kr}{kr}\right] \; e^{i(kr - \eta\, ln2kr)\, \cos\theta} \tag{3.57}$$

The scattering amplitude $f(\theta)$ in the case of the presence of the Coulomb potential between the scattering protons is also changed in the comparison with (3.50) by the Coulomb shift

$$f(\theta) = -\frac{i}{2k} \sum_{L=0}^{\infty} (2L+1) \left[e^{2i\,(\delta_L + \sigma_L)} - 1\right] \; P_L(\cos\theta) \tag{3.58}$$

and corresponding cros section of the scattering is again given by $|f(\theta)|^2$, i.e.

$$\begin{aligned} \frac{d\sigma}{d\Omega} &= |f(\theta)|^2 = \\ &= \frac{1}{k^2} \left| \sum_{L=0}^{\infty} (2L+1) \left[e^{2i\,(\delta_L + \sigma_L)} - 1\right] \; P_L(\cos\theta) \right|^2 \end{aligned} \tag{3.59}$$

In the case of the mutual scattering of two protons the ingoing particle is the same as the target particle and as a consequence of it in accordance with the Pauli principle the wave function of the system of two protons (including the spin part which is not involved in (3.56)) should be antisymmetric with respect to the exchange of the ingoing and target protons (isospin part of the wave function is symmetric in this case). This fact gives the following relation of the total orbital moment L and the total spin S of two protons:

$$(-1)^{L+S} = 1 \tag{3.60}$$

This can be seen if the L-th component of the wave function of two protons in the coordinate-spin Hilbert space is analyzed

$$\begin{aligned} \text{wave function} \quad & R(r)\, Y_{LM}(\hat{r})\, |SM_s\rangle = \\ \text{of 2 protons:} \quad & = R(r)\, Y_{LM}(\hat{r}) \sum_{m_1\, m_2} C^{SM_s}_{\frac{1}{2}m_1\frac{1}{2}m_2} \, |\tfrac{1}{2}m_1\rangle |\tfrac{1}{2}m_2\rangle \end{aligned}$$

$$\begin{aligned} & R(r)\, Y_{LM}(-\hat{r}) \sum_{m_1\, m_2} C^{SM_s}_{\frac{1}{2}m_2\frac{1}{2}m_1} \, |\tfrac{1}{2}m_2\rangle |\tfrac{1}{2}m_1\rangle = \\ \text{exchange of} \quad & = (-1)^{L+1/2+1/2-S}\, R(r)\, Y_{LM}(\hat{r}) \\ \text{both protons:} \quad & \qquad \cdot \sum_{m_1\, m_2} C^{SM_s}_{\frac{1}{2}m_1\frac{1}{2}m_2} \, |\tfrac{1}{2}m_1\rangle |\tfrac{1}{2}m_2\rangle \end{aligned}$$

So, during the exchange of both protons the coordinate-spin wave function takes the factor $(-1)^{L+1-S}$ and, because the total wave function should be

antisymmetric with respect to the exchange, this factor is equal to -1 and we have (3.60).

We see that the factor $(-1)^L$ is a result of the action of the parity operator on the spherical function $Y_{LM}(\hat{r})$. The action of the operator parity comes out in the scattering amplitude $f(\theta)$ by the exchange: $f(\theta) \to f(\pi - \theta)$. So, if we want to involve the Pauli principle in the wave function (3.56) we can do it in the expr. (3.59) for the differential cross section by the exchange of $f(\theta)$ by

$$f(\theta) \pm f(\pi - \theta) \qquad\qquad \theta \in < 0, \pi/2 > \tag{3.61}$$

where the sign + is related to the singlet spin state ($S = 0$) (when L is even) and the sign $-$ corresponds to the triplet spin state ($S = 1$, where L should be odd). If the spin of the system of two protons is preserved during the scattering (no L- mixing) then in the expression, $\frac{d\sigma}{d\Omega} = |f(\theta)|^2$ for the differential cross section we should involve the spin singlet and the triplet states with corresponding weight factor (which are given by possibilities of the spin projections) as it is given in the following expression

$$\frac{d\sigma}{d\Omega} = \frac{1}{4}\ |f(\theta) + f(\pi - \theta)|^2 + \frac{3}{4}\ |f(\theta) - f(\pi - \theta)|^2 \tag{3.62}$$

3.1.2.3 Tensor forces

In the subsections 3.1.2.1 and 3.1.2.2 concerning the mutual scattering of two nucleons only central scattering potential not depended on spins was taken into account. Therefore the spin part of the wave function was not touched and did not changed during scattering and it could be cut out from the consideration. From the discussion on a deuteron (see subsection 3.1.1, particularly 3.1.1.2) it is known that the tensor interaction couples states with different orbital moments L (see the Tab. 3.1) but with the same value of the total angular momentum J. This means that the tensor interaction can come out only in the case of the scattering of two nucleons in the spin triplet state $S = 1$. Therefore in this subsection we restrict ourselves only for $S = 1$ (the spin singlet $S = 0$ case corresponds to the spinless situation discussed in the subsections 3.1.2.1 and 3.1.2.2).

The Schroedinger equation with the scattering potential involving the tensor interaction takes the following form (see (3.17) and (3.18))

$$\left[-\frac{\hbar^2}{M}\ \vec{\nabla}^2 + \hat{V}_{centr}(r) + \hat{V}_T(r)\ \hat{S}_{12}\right]\ \psi(\vec{r}\,) = E\ \psi(\vec{r}\,) \tag{3.63}$$

where $\hat{S}_{12}$ is called tensor operator (see(3.20)

$$\hat{S}_{12} = \sqrt{24\pi}\ [(\sigma_1\,\sigma_2)_{\lambda=2}\,Y_{\lambda=2}]_{(22)\,00} \tag{3.64}$$

Apart from the deuteron case, when $E < 0$, the scattering problem is connected with the continuous spectrum with $E > 0$. We can decompose the solution $\psi(\vec{r}\,)$ into the complete set of the functions $\Phi_{LJM}(\hat{r})$ (see (3.24))(we suppose $S = 1$)

$$\Phi_{LJM}(\hat{r}) = \sum_{M_S=0,\pm1} C^{JM}_{L\,M-M_s\,1\,M_s}\,Y_{L\,M-M_s}(\hat{r})\,\chi_{M_s} \tag{3.65}$$

and we can write

$$\psi_M(\vec{r}\,) = \sum_{J=0}^{\infty}\sum_{L=J-1}^{J+1}\frac{u_{JL}(r)}{r}\,\Phi_{LJM}(\hat{r}) \tag{3.66}$$

where the radial function $u_{JL}(r)$ fulfills the following system of differential equations (which can be derived from (3.63) using the orthonormality of the functions $\Phi_{LJM}(\hat{r})$)

$$\frac{d^2u_{JL}(r)}{dr^2} + \frac{M}{\hbar^2}\left[E - \frac{\hbar^2}{M\,r^2}L(L+1) - V_{centr}(r)\right]u_{JL}(r) - \frac{M}{\hbar^2}V_T(r)\sum_{L'}S_{JLL'}\,u_{JL'}(r) = 0 \tag{3.67}$$

where $S_{JLL'}$ are given in the Tab. 3.1 (see the text below (3.30)). The equation system (3.67) is relevant only for triplet spin state $S = 1$. In the singlet spin state $S = 0$ we have no system equations (3.67) because the term with the tensor interaction is not present. Therefore in the singlet spin $S = 0$ case the formalism given in the subsections 3.1.2.1 and 3.1.2.2 can be used and we can obtain the radial wave function $u_{JL=J}(r)$ by solving the equation (3.48) for neutrons and (3.53) for protons. In the case of $S = 1$ with given J the orbital momentum L can have three values, $L = J,\ J \pm 1$, and for the simplicity of the notation we introduce following assignment

$$u_J(r) \equiv u_{JL=J-1}(r)\,, \qquad v_J(r) \equiv u_{JL=J}(r) \qquad w_J(r) = u_{JL=J+1}(r) \tag{3.68}$$

The cross section of the nucleon scattering when the tensor term is involved in the scattering potential can be determined in the same way as in the case of the pure central scattering potential. That means the asymptotic limit of the

wave function (3.66) is compared with the relation (3.46) (for the scattering of two neutrons or neutron with proton) and with the relation (3.56) (for the scattering of two protons) where the spin part of the wave function is added. The plane wave involved in (3.46) and (3.56) is in the triplet case $S = 1$ multiplied by the spinor corresponding to $S = 1$ and the resulting function can be decomposed into spherical harmonics $Y_{LM}(\hat{r})$ using (D.22) (together with the relation $P_L(\cos\theta) = \sqrt{\frac{4\pi}{2L+1}}\, Y_{L0}(\hat{r})$)

$$
\begin{aligned}
e^{ikz}\,\chi_{S=1,M_s} &= \sum_{L=0}^{\infty} [4\pi(2L+1)]^{1/2}\; i^L\, j_L(kr)\, Y_{L0}(\hat{r})\, \chi_{M_s} = \\
&= \boxed{\begin{array}{c}\text{because (see (3.67))} \\ Y_{L0}(\hat{r})\,\chi_{M_s} = \sum_J\; C^{J\,M_s}_{L\,0\,1\,M_s}\,\Phi_{LJM_s}(\hat{r})\end{array}} = \\
&= \sum_{J=0}^{\infty}\sum_{L=J-1}^{J+1} [4\pi(2L+1)]^{1/2}\; i^L\, j_L(kr)\, C^{J\,M_s}_{L\,0\,1\,M_s}\,\Phi_{LJM_s}(\hat{r})
\end{aligned}
\tag{3.69}
$$

This expression gives for the asymptotic region $r \to \infty$ (see(D.6))

$$
\begin{aligned}
&e^{ikz}\,\chi_{M_s} \overset{r\to\infty}{\to} \\
&\quad \sum_J \sum_L [4\pi(2L+1)]^{1/2}\; i^L\; \sin(kr - \frac{\pi L}{2})\; C^{J\,M_s}_{L\,0\,1\,M_s}\,\Phi_{LJM_s}(\hat{r})
\end{aligned}
\tag{3.70}
$$

The case $L = J$

From the Tab. 3.1 it is known that the state with $L = J$ is always pure that means there is no mixing with any other $L \neq J$. In the asymptotic region the central potential $V_{centr}(r)$ and the central part $V_T(r)$ of the tensor term are equal to zero and therefore the radial part $v_J(r)$ of the wave function of the case $L = J$ has the same form as the radial wave function of free particles but with the phase shift $\delta_{JL=J}$ (see(D.23))

$$
\begin{aligned}
v_J(r) \overset{r\to\infty}{\to} C\, \sin(kr - \frac{\pi L}{2} + \delta_{JJ}) &= \\
&= C'\, \left(e^{-i\,(kr - \frac{\pi J}{2} + \delta_{JJ})} - e^{i\,(kr - \frac{\pi J}{2} + \delta_{JJ})}\right) = \\
&= e^{-i\,\delta_{JJ}} \left(A\, e^{-i\,(kr - \frac{\pi J}{2})} - B\, e^{i\,(kr - \frac{\pi J}{2})}\right) = \\
&= A\, e^{-i\,\delta_{JJ}} \left(e^{-i\,(kr - \frac{\pi J}{2})} - S\, e^{i\,(kr - \frac{\pi J}{2})}\right)
\end{aligned}
\tag{3.71}
$$

with $B = S\,A = e^{2i\,\delta_{JJ}}\,A$.

If we suppose the elastic scattering (and this is relevant to the nucleon scattering with energies up to several hundreds MeV) then the flux of ingoing and outgoing spherical waves involved in the wave function $\frac{v_J(r)}{r}\Phi_{JJM}(\hat{r})$ should be the same and we have

$$|S|^2 = 1 \tag{3.72}$$

with

$$S = e^{2i\delta_{JJ}} \tag{3.73}$$

This corresponds to (D.24) that $\psi_{M_s}(\vec{r}\,) - e^{ikz}\,\chi_{M_s}$ involves only outgoing spherical waves (see Appendix D for details). Therefore for the case of $L = J$ the expressions (3.52), (3.53) and (3.54) remain valid and one value of J corresponds to one phase shift δ_{JJ} (S-matrix is reduced to one element only).

The case $L = J \pm 1$

In this case the tensor interaction mixes the states with $L = J \pm 1$ (see the table 3.1) and the procedure of the introduction of the S-matrix is more complicated. For given J we have two radial functions $u_J(r)$ and $w_J(r)$ which are coupled in the equation system (3.69) by the tensor interaction. For each radial function, $u_J(r)$ and $w_J(r)$, asymptotic behavior (3.73) is expected

$$\begin{aligned} u_J(r) &\overset{r\to\infty}{\to} A_1\,e^{-i\,(kr-\frac{\pi\,(J-1)}{2})} - B_1\,e^{i\,(kr-\frac{\pi\,(J-1)}{2})} \\ w_J(r) &\overset{r\to\infty}{\to} A_2\,e^{-i\,(kr-\frac{\pi\,(J+1)}{2})} - B_2\,e^{i\,(kr-\frac{\pi\,(J+1)}{2})} \end{aligned} \tag{3.74}$$

and the generalisation of (3.73) for the case $L = J \pm 1$ is following

$$\begin{pmatrix} B_1 \\ B_2 \end{pmatrix} = \begin{pmatrix} S_{11} & S_{12} \\ S_{21} & S_{22} \end{pmatrix} \begin{pmatrix} A_1 \\ A_2 \end{pmatrix} \quad \Leftrightarrow \quad B = S\,A \tag{3.75}$$

That means the S-matrix is 2 dimensional. The condition of the preservation of the ingoing and outgoing probability flux

$$|A_1|^2 + |A_2|^2 = |B_1|^2 + |B_2|^2 \tag{3.76}$$

gives the unitarity of the S-matrix

$$S^+S = S\,S^+ = 1 \tag{3.77}$$

Morevoer, the S-matrix in our case should be symmetric. This follows from the following reason

- Coefficients in the system of equations (3.67) are real. Therefore functions $u_J(r)$ and $w_J(r)$ describe the same scattering as functions $u_J^*(r)$ and $w_J^*(r)$. We also know that the complex conjugation changes the outgoing wave into ingoing wave and vice versa. Therefore (3.75) can be also rewritten as follows

$$A^* = SB^* \tag{3.78}$$

- From the other hand we have

$$B = SA \qquad A = S^{-1}B = S^+B \qquad A^* = (S^+)^*B^* \tag{3.79}$$

and the comparison with (3.78) gives $(S^+)^* = S$, that means the matrix S is symmetric.

From the mathematics it is known that each unitary and symmetric matrix 2×2 has 3 independent real parameters and it can be written in the following form

$$S = Ue^{2i\Delta}\,U^{-1} \qquad\qquad e^{2i\Delta} = U^{-1}S\,U \tag{3.80}$$

where

$$U = \begin{pmatrix} \cos\epsilon_J & -\sin\epsilon_J \\ \sin\epsilon_J & \cos\epsilon_J \end{pmatrix} \qquad\qquad \Delta = \begin{pmatrix} \delta_{\alpha J} & 0 \\ 0 & \delta_{\gamma J} \end{pmatrix} \tag{3.81}$$

where ϵ_J is called mixing parameter and $\delta_{\alpha J}$ and $\delta_{\gamma J}$ are phase shifts of eigenvectors $A^{(\alpha,\,J)}$ and $A^{(\gamma,\,J)}$ of the S-matrix corresponding to the given value of total momentun J:

$$\begin{aligned} S\,A^{(\alpha,J)} &= \begin{pmatrix} S_{11} & S_{12} \\ S_{21} & S_{22} \end{pmatrix} \begin{pmatrix} A_1^{(\alpha,J)} \\ A_2^{(\alpha,J)} \end{pmatrix} = e^{2i\,\delta_J^{(\alpha)}} \begin{pmatrix} A_1^{(\alpha,J)} \\ A_2^{(\alpha,J)} \end{pmatrix} \\ S\,A^{(\gamma,J)} &= \begin{pmatrix} S_{11} & S_{12} \\ S_{21} & S_{22} \end{pmatrix} \begin{pmatrix} A_1^{(\gamma,J)} \\ A_2^{(\gamma,J)} \end{pmatrix} = e^{2i\,\delta_J^{(\gamma)}} \begin{pmatrix} A_1^{(\gamma,J)} \\ A_2^{(\gamma,J)} \end{pmatrix} \end{aligned} \tag{3.82}$$

If we know the eigen vectors $A^{(\alpha,J)}$ and $A^{(\gamma,J)}$ then the matrix U in (3.81) can be rewritten as follows

$$U = \begin{pmatrix} A_1^{(\alpha,J)} & A_1^{(\gamma,J)} \\ A_2^{(\alpha,J)} & A_2^{(\gamma,J)} \end{pmatrix} \tag{3.83}$$

This can be easily checked:

$$
\begin{aligned}
S\,U &= \begin{pmatrix} S_{11} & S_{12} \\ S_{21} & S_{22} \end{pmatrix} \begin{pmatrix} A_1^{(\alpha,J)} & A_1^{(\gamma,J)} \\ A_2^{(\alpha,J)} & A_2^{(\gamma,J)} \end{pmatrix} = \\
&= \begin{pmatrix} S_{11}A_1^{(\alpha,J)} + S_{12}A_2^{(\alpha,J)} & S_{11}A_1^{(\gamma,J)} + S_{12}A_2^{(\gamma,J)} \\ S_{21}A_1^{(\alpha,J)} + S_{22}A_2^{(\alpha,J)} & S_{21}A_1^{(\gamma,J)} + S_{22}A_2^{(\gamma,J)} \end{pmatrix} = \\
&= \boxed{\begin{matrix}\text{see} \\ (3.82)\end{matrix}} = \begin{pmatrix} e^{2i\,\delta_J^{(\alpha,J)}} A_1^{(\alpha,J)} & e^{2i\,\delta_J^{(\gamma,J)}} A_1^{(\gamma,J)} \\ e^{2i\,\delta_J^{(\alpha,J)}} A_2^{(\alpha,J)} & e^{2i\,\delta_J^{(\gamma,J)}} A_2^{(\gamma,J)} \end{pmatrix} = \\
&= \begin{pmatrix} A_1^{(\alpha,J)} & A_1^{(\gamma,J)} \\ A_2^{(\alpha,J)} & A_2^{(\gamma,J)} \end{pmatrix} \begin{pmatrix} e^{2i\,\delta_J^{(\alpha,J)}} & 0 \\ 0 & e^{2i\,\delta_J^{(\gamma,J)}} \end{pmatrix} = \\
&= U \begin{pmatrix} e^{2i\,\delta_J^{(\alpha,J)}} & 0 \\ 0 & e^{2i\,\delta_J^{(\gamma,J)}} \end{pmatrix} \\
\Rightarrow \qquad & U^{-1}\,S\,U = \begin{pmatrix} e^{2i\,\delta_J^{(\alpha,J)}} & 0 \\ 0 & e^{2i\,\delta_J^{(\gamma,J)}} \end{pmatrix} \equiv e^{2i\,\Delta_J} \qquad (3.84)
\end{aligned}
$$

From (3.84) one can see that the matrix U (with columns given by eigen vectors of the matrix S) diagonalizes the matrix S. The comparison of (3.83) with (3.81) gives

$$
\begin{aligned}
A_1^{(\alpha,J)} &= \cos\epsilon_j & A_1^{(\gamma,J)} &= -\sin\epsilon_j \\
A_2^{(\alpha,J)} &= \sin\epsilon_j & A_1^{(\gamma,J)} &= \cos\epsilon_j
\end{aligned} \qquad (3.85)
$$

The expression (3.75) can be then rewritten for each eigen vector separately

$$
\begin{aligned}
B^{(\alpha,J)} &= \begin{pmatrix} B_1^{(\alpha,J)} \\ B_2^{(\alpha,J)} \end{pmatrix} = e^{2i\,\delta_J^{(\alpha)}} \begin{pmatrix} A_1^{(\alpha,J)} \\ A_2^{(\alpha,J)} \end{pmatrix} = e^{2i\,\delta_J^{(\alpha)}}\; A^{(\alpha,J)} \\
B^{(\gamma,J)} &= \begin{pmatrix} B_1^{(\gamma,J)} \\ B_2^{(\gamma,J)} \end{pmatrix} = e^{2i\,\delta_J^{(\alpha)}} \begin{pmatrix} A_1^{(\gamma,J)} \\ A_2^{(\gamma,J)} \end{pmatrix} = e^{2i\,\delta_J^{(\gamma)}}\; A^{(\gamma,J)}
\end{aligned} \qquad (3.86)
$$

So, in the case of $L = J \pm 1$ we have two channels (2 values of L) which are mutually mixed if the tensor interaction is switched on. The asymptotic form of the radial functions $u_J(r)$ and $w_J(r)$ are given by (3.74) and (3.75). The expression (3.75) involves the S-matrix in the non-diagonal form. This expression can be transformed into the diagonal form and functions $u_J(r)$ and $w_J(r)$ can be expressed in terms of diagonal matrix elements of the S-matrix

and under appropriate normalization we have

$$u_J(r) = u_{J,\alpha}(r) + u_{J,\gamma}(r) \qquad , \qquad w_J(r) = w_{J,\alpha}(r) + w_{J,\gamma}(r) \tag{3.87}$$

where the asymptotic expressions for functions $u_{J,\alpha}$, $u_{J,\gamma}$, $w_{J,\alpha}$ and $w_{J,\gamma}$ are following

$$\begin{aligned} u_{J,\alpha}(r) \ &\overset{r\to\infty}{\to}\ A_1^{(\alpha,J)}\, e^{-i(kr-\frac{\pi(J-1)}{2})} - B_1^{(\alpha,J)}\, e^{i(kr-\frac{\pi(J-1)}{2})} = \\ &= \boxed{\begin{array}{c}\text{see}\\(3.86)\end{array}} = -2i\, A_1^{(\alpha,J)}\, e^{i\delta_J^{(\alpha)}}\, \sin\left(kr - \frac{\pi(J-1)}{2} + \delta_J^{(\alpha)}\right) \end{aligned} \tag{3.88}$$

$$\begin{aligned} w_{J,\alpha}(r) \ &\overset{r\to\infty}{\to}\ A_2^{(\alpha,J)}\, e^{-i(kr-\frac{\pi(J-1)}{2})} - B_2^{(\alpha,J)}\, e^{i(kr-\frac{\pi(J-1)}{2})} = \\ &= \boxed{\begin{array}{c}\text{see}\\(3.85)\end{array}} = -2i\, A_1^{(\alpha,J)}\, \tan\epsilon_J\ e^{i\delta_J^{(\alpha)}}\, \sin\left(kr - \frac{\pi(J-1)}{2} + \delta_J^{(\alpha)}\right) \end{aligned} \tag{3.89}$$

$$\begin{aligned} u_{J,\gamma}(r) \ &\overset{r\to\infty}{\to}\ A_1^{(\gamma,J)}\, e^{-i(kr-\frac{\pi(J+1)}{2})} - B_1^{(\gamma,J)}\, e^{i(kr-\frac{\pi(J+1)}{2})} = \\ &= \boxed{\begin{array}{c}\text{see}\\(3.85)\end{array}} = -2i\, A_1^{(\gamma,J)}\, e^{i\delta_J^{(\gamma)}}\, \sin\left(kr - \frac{\pi(J+1)}{2} + \delta_J^{(\gamma)}\right) \end{aligned} \tag{3.90}$$

$$\begin{aligned} w_{J,\gamma}(r) \ &\overset{r\to\infty}{\to}\ A_2^{(\gamma,J)}\, e^{-i(kr-\frac{\pi(J+1)}{2})} - B_2^{(\gamma,J)}\, e^{i(kr-\frac{\pi(J+1)}{2})} = \\ &= \boxed{\begin{array}{c}\text{see}\\(3.85)\end{array}} = 2i\, A_1^{(\alpha,J)}\, \cot\epsilon_J\, e^{i\delta_J^{(\gamma)}}\, \sin\left(kr - \frac{\pi(J+1)}{2} + \delta_J^{(\gamma)}\right) \end{aligned} \tag{3.91}$$

For the purpose of the consistent notation we ascribe the index β to the channel $L = J$ and for the radial function $u_{Jl+J}(r)$ and corresponding phase shift $\delta_{JL=J}$ the new assignment is introduced

$$v_{J,\beta}(r) \equiv v_J(r) = u_{JL=J}(r) \qquad , \qquad \delta_{JL=J} \equiv \delta_J^{\beta} \tag{3.92}$$

and the wave function (3.68) can be rewritten in the new form

$$\begin{aligned}\psi_{M_S}(\vec{r}\,) &= \sum_{J=0}^{\infty}\sum_{L=J-1}^{J+1}\frac{u_{JL}(r)}{r}\,\Phi_{LJM_s}(\hat{r}) = \\ &= \sum_{J=0}^{\infty}\frac{1}{r}\,\big[(u_{J,\alpha}(r)+u_{J,\gamma}(r))\;\Phi_{L=J-1,JM_S}(\hat{r})+ \\ &\qquad +v_{J,\beta}(r)\,\Phi_{L=J,JM_S}(\hat{r})+ \\ &\qquad +(w_{J,\alpha}(r)+w_{J,\gamma}(r))\;\Phi_{L=J+1,JM_S}(\hat{r})\big]\end{aligned}$$

$$\begin{aligned}&\overset{r\to\infty}{\to}\; -\frac{2i}{r}\sum_{J=0}^{\infty} \\ &\quad\big[A_1^{(\alpha,J)}\,e^{i\delta_J^{(\alpha)}}\;\sin\left(kr-\frac{\pi(J-1)}{2}+\delta_J^{(\alpha)}\right) \\ &\qquad\cdot\big(\Phi_{L=J-1,JM_S}(\hat{r})-\tan\epsilon_J\,\Phi_{L=J+1,JM_S}(\hat{r})\big)+ \\ &\quad+A_1^{(\beta,J)}\,e^{i\delta_J^{(\beta)}}\;\sin\left(kr-\frac{\pi(J-1)}{2}+\delta_J^{(\beta)}\right)\cdot\Phi_{L=J,JM_S}(\hat{r})+ \\ &\quad+A_1^{(\gamma,J)}\,e^{i\delta_J^{(\gamma)}}\;\sin\left(kr-\frac{\pi(J+1)}{2}+\delta_J^{(\gamma)}\right) \\ &\qquad\cdot\big(\tan\epsilon_J\,\Phi_{L=J+1,JM_S}(\hat{r})+\Phi_{L=J+1,JM_S}(\hat{r})\big)\big]\end{aligned} \tag{3.93}$$

The scattering amplitude in the $L = J \pm 1$ case can be again obtained by the comparison of (3.93) with usual asymptotic form (3.54) where the plane wave (the first term in (3.56)) is given by (3.70).

$$\begin{aligned}\psi_{M_S}(\vec{r}\,) &\overset{r\to\infty}{\to} e^{ikz}\,\chi_{M_S}+f_{M_S}(\theta,\varphi)\,\frac{e^{ikr}}{r} = \boxed{\begin{array}{c}\text{see}\\(3.70)\end{array}} = \\ &= \sum_{J=0}^{\infty}\sum_{L=J-1}^{J+1}\left\{[4\pi(2L+1)]^{1/2}\right. \\ &\quad\left.\cdot i^L\,\frac{1}{kr}\,\sin(kr-\frac{\pi l}{2})\,C^{J\,M_S}_{L\,0\,1\,M_S}\,\Phi_{LJM_S}(\hat{r})\right\}+f_{M_S}(\theta,\varphi)\,\frac{e^{(ikr)}}{r}\end{aligned} \tag{3.94}$$

And finally, the comparison of (3.94) and (3.93) gives the scattering amplitude

M_S	$A'_{JM_S\alpha}$	$A'_{JM_S\beta}$	$A'_{JM_S\gamma}$
1	$\sqrt{\frac{1}{2}(J+1)}\ \cos\epsilon_J$ $-\sqrt{\frac{1}{2}\,J}\ \sin\epsilon_J$	$-\sqrt{\frac{1}{2}(2J+1)}$	$\sqrt{\frac{1}{2}(J+1)}\ \sin\epsilon_J$ $+\sqrt{\frac{1}{2}\,J}\ \cos\epsilon_J$
0	$\sqrt{J}\ \cos\epsilon_J$ $+\sqrt{J+1}\ \sin\epsilon_J$	0	$\sqrt{J}\ \sin\epsilon_J$ $-\sqrt{J+1}\ \cos\epsilon_J$
-1	$\sqrt{\frac{1}{2}(J+1)}\ \cos\epsilon_J$ $-\sqrt{\frac{1}{2}\,J}\ \sin\epsilon_J$	$\sqrt{\frac{1}{2}(2J+1)}$	$\sqrt{\frac{1}{2}(J+1)}\ \sin\epsilon_J$ $+\sqrt{\frac{1}{2}\,J}\ \cos\epsilon_J$

Table 3.2: The coefficients $A'_{JM_S\lambda}$ ($\lambda=\alpha,\ \beta,\ \gamma$ involved in the expr. (3.95).

$f_{M_S}(\theta,\varphi)$ in the following form

$$
\begin{aligned}
f_{M_S}(\theta,\varphi) = \sqrt{4\pi}\frac{1}{k}\sum_{J=0}^{\infty}\Bigg\{ & \\
& A'_{JM_S\alpha}\, e^{i\,\delta_J^{(\alpha)}}\ \sin\delta_J^{(\alpha)} \\
& \qquad \cdot\big(\cos\epsilon_J\ \Phi_{L=J-1,J,M_S}(\hat{r}) - \sin\epsilon_J\ \Phi_{L=J+1,J,M_S}(\hat{r})\big) + \\
& + A'_{JM_S\beta}\, e^{i\delta_J^{(\beta)}}\ \sin\delta_J^{(\beta)}\ \Phi_{L=J,J,M_S}(\hat{r}) + \\
& + A'_{JM_S\gamma}\, e^{i\,\delta_J^{(\gamma)}}\ \sin\delta_J^{(\gamma)} \\
& \qquad \cdot\big(\sin\epsilon_J\ \Phi_{L=J-1,J,M_S}(\hat{r}) + \cos\epsilon_J\ \Phi_{L=J+1,J,M_S}(\hat{r})\big)\Bigg\}
\end{aligned}
\tag{3.95}
$$

where coefficients $A'_{JM_S\lambda}$ ($\lambda=\alpha,\beta,\gamma$) can be expressed in terms of the explicit expressions for Clebsch-Jordan coefficients $C^{J\,M_S}_{L\,0\,1\,M_S}$ and for $A_1^{(\alpha,J)}, A_1^{(\beta,J)}, A_1^{(\gamma,J)}$ (see (3.85). The result is given in the Tab. 3.2.

The differential cross section of the nucleon-nucleon scattering for the non-polarized incident beam and for the non-oriented target (in the case of the spin triplet $S=1$) is given by spin orientation averaging of the square of the scattering amplitude

$$
\frac{d\sigma_{S=1}}{d\Omega}(\theta,\varphi) = \frac{1}{3}\sum_{M_S=-1}^{1}|f_{M_S}(\theta,\varphi))|^2 \tag{3.96}
$$

where $f_{M_S}(\vartheta,\varphi))$ is given by (3.95). Using the orthonormality of the complete basis of functions $\phi_{LJM}(\hat{r})$ (see (3.63)) we can obtain the integral cross section

	$J=0$	$J=1$	$J=2$	$J=3$
T=0		${}^1P_1$ ${}^3S_1 + {}^3D_1$	 ${}^3D_2$	${}^1F_3$ ${}^3D_3 + {}^3G_3$
T=1	 ${}^1S_0$, ${}^3P_0$	 ${}^3P_1$	${}^1D_2$ ${}^3P_2 + {}^3F_2$	 ${}^3F_3$
	$J=4$	$J=5$	$J=6$	-
T=0	 ${}^3G_4$	${}^1H_5$ ${}^3G_5 + {}^3I_5$	 ${}^3I_6$	- -
T=1	${}^1G_4$ ${}^3F_4 + {}^3H_4$	 ${}^3H_5$	${}^1I_6$ ${}^3H_6 + {}^3J_6$	- -

Table 3.3: The states of the two-nucleon system which gives the substantial contribution to the nucleon scattering up to the energy 400 MeV (the state assignment is the same as in (3.2))

of the spin triplet state by the integration of (3.96) over the whole space angle

$$\sigma_{S=1} = \int \frac{d\sigma_{S=1}}{d\Omega}(\theta,\varphi))\, d\Omega = \\ = \frac{4\pi}{k^2} \sum_{J=0}^{\infty} \frac{1}{3}(2J+1) \left(\sin^2\delta_J^{(\alpha)} + \sin^2\delta_J^{(\beta)} + \sin^2\delta_J^{(\gamma)}\right) \qquad (3.97)$$

3.1.2.4 Phase shift analysis

The states of the two-nucleon system with the given isospin T, total ang. momentum J, orbital ang. momentum L and spin S, which can give a significant contribution to the total cross section, are given in the Table 3.3.

It is necessary to realize that not all states with the arbitrary combination of numbers T, J, L, S can give a contribution to the nucleon-nucleon scattering cross section because of the Pauli principle (the total wave function of two - nucleon system should be antisymmetric with respect to the exchange of nucleons). This reduces possibilities of combinations of numbers T, J, L, S. During the exchange of nucleons the two - nucleon wave function has the following symmetries (see (3.60) and the text below it)

$$\psi_{T,L,S,J,M}(2,1) = \hat{P}_{1\leftrightarrow 2}\, \psi_{T,L,S,J,M}(1,2) = \\ = (-1)^{T-\frac{1}{2}-\frac{1}{2}}\, (-1)^{S-\frac{1}{2}-\frac{1}{2}}\, (-1)^{L}\, \psi_{T,L,S,J,M}(1,2) = -\psi_{T,L,S,J,M}(1,2) \\ \Rightarrow \qquad (-1)^{T+L+S} = -1 \qquad (3.98)$$

From (3.98) it follows, for instance, that the state with $T = J = 0$ cannot

exist (because for this case we have two possibilities, $L = S = 0$ or $L = S = 1$, and both of them contradict (3.98).

From experimental values of $\frac{d\sigma}{d\Omega}(E)$ and $\sigma(E)$ (cross sections in the dependence on the scattering energy) it is possible to determine , using (3.95)-(3.97) and in terms of the χ^2-approach, values of all phase shifts δ_J for all possible values of T and J. These experimental values of phase shifts can be compared with theoretical values which can be obtained by the sewing of the logarithmic derivative of the radial function $u_{JL}(r)$ from the wave function $\psi_{M_s}(\vec{r}) = \sum_{J=0}^{\infty} \sum_{L=j-1}^{J+1} \frac{u_{JL}(r)}{r} \phi_{LJM}(\hat{r})$ in the point of the potential range. These radial functions $u_{JL}(r)$ in the region $r < a$ (for r less than the range a of the scattering potential) are solutions of the following differential equations (see (3.67))

$$
\begin{aligned}
&S = 1,\ L = J\ : \\
&\frac{d^2 u_{JJ}(r)}{dr^2} + \frac{M}{\hbar^2} \left[E - \frac{\hbar^2 J(J+1)}{M r^2} - V_{centr}(r) \right] u_{JJ}(r) \\
&\qquad\qquad - \frac{M}{\hbar^2} V_T(r)\, S_{JJJ}\, u_{JJ}(r) = 0
\end{aligned}
\tag{3.99}
$$

$$
\begin{aligned}
&S = 1,\ L = J \pm 1\ : \\
&\frac{d^2 u_{JJ-1}(r)}{dr^2} + \frac{M}{\hbar^2} \left[E - \frac{\hbar^2 (J-1) J}{M r^2} - V_{centr}(r) \right] u_{JJ-1}(r) \\
&\qquad\qquad - \frac{M}{\hbar^2} V_T(r) \sum_{L'=J\pm1} S_{JJ-1L'}\, u_{JL'}(r) = 0 \\
&\frac{d^2 u_{JJ+1}(r)}{dr^2} + \frac{M}{\hbar^2} \left[E - \frac{\hbar^2 (J+1)(J+2)}{M r^2} - V_{centr}(r) \right] u_{JJ+1}(r) \\
&\qquad\qquad - \frac{M}{\hbar^2} V_T(r) \sum_{L'=J\pm1} S_{JJ+1L'}\, u_{JL'}(r) = 0
\end{aligned}
$$

$$
\begin{aligned}
&S = 0,\ L = J\ : \\
&\frac{d^2 u_{JJ}(r)}{dr^2} + \frac{M}{\hbar^2} \left[E - \frac{\hbar^2 J(J+1)}{M r^2} - V_{centr}(r) \right] u_{JJ}(r) = 0
\end{aligned}
\tag{3.100}
$$

and the radial functions $u_{JL}(r)$ in the region out of the potential range ($r > a$) have the asymptotic form (see e.g (3.87)-(3.93)) for S=1 case). More details on this sewing can be found in the Appendix D (see (D.9). The comparison of experimental and theoretical phase shifts can serve as a test for

different potentials $V_{centr}(r)$ and $V_T(r)$ of bare nucleon-nucleon interaction. The determination of potentials $V_{centr}(r)$ and $V_T(r)$ using the comparison of experimental and theoretical phase shifts is known in the literature as the phase shift analysis. In the next subsection the forms of bare nucleon-nucleon interaction used in the nuclear structure calculations are discused in more details.

3.1.3 Bare nucleon-nucleon potentials

The phase shift analysis discussed in the end of the previous subsection provides a possibility to test different bare nucleon-nucleon potentials (potentials felt by two nucleons during their scattering in the vacuum) by the comparison of the experimental phase shifts with ones theoretically calculated. From the theoretical point of view the form of the bare nucleon-nucleon potential can be derived from the idea that the nucleon-nucleon interaction is mediated by the exchange of mesons of different types (this idea is discussed in the part 3.1.3.2). The functional dependencies of such potentials are quite complicated. Therefore historically the first approach to the determination of nucleon-nucleon potential was purely phenomenological when the rough form of the bare nucleon-nucleon potential was obtained from the symmetries of the nucleon-nucleon interaction. Both approaches, purely theoretical and phenomenological, give some functional dependencies containing free parameters which are usually determined by the phase shift analysis.

3.1.3.1 Basic properties of the bare nucleon-nucleon forces and their physical premises

Bare nucleon-nucleon forces (interaction) are of the short range

The deuteron properties show the short range character of the nucleon-nucleon interaction (see the text below expressions (3.9)-(3.11)). The short range of this interaction is also confirmed by the fact that the nuclear forces have so called saturation character. That means if one nucleon is added into the nucleus then the binding energy per nucleon does not change (see Fig. 1.2). This saturation assumes that the given nucleon interacts only with the small number of nucleons from the close vicinity (with the highest probability

only with the one nearest nucleon). In the opposite case, when the nucleon-nucleon interaction has a long range character, nuclear forces would involve higher number of nucleons simultaneously and as a result of this the binding energy per nucleon would increase with the increasing number of nucleons.

Bare nucleon-nucleon forces represent a mixture of attraction and repulsion

Experimental cross sections of the nucleon-nucleon scattering show values around 10 mb up to the scattering energies 400 MeV. However, tens of mb are values much lower in the comparison with the theoretical presumptions about nucleon-nucleon interactions. For instance, if we accept the Yukawa hypothesis about the meson exchange character of the nucleon-nucleon force then the cross section of the nucleon-nucleon scattering should have values near the range of the meson cloud surrounding each nucleon. According to the uncertainty principle the lightest meson, pion, can be departed mostly of the nucleon. This distance is equal roughly to the de Broglie wave length of pion, $\lambda = \frac{\hbar}{mc} \approx 1.41$ fm, and the corresponding value of the cross section is approximately given by $\sigma \approx \pi\,\lambda^2 \approx 600$ mb. This fact that the experimental nucleon-nucleon cross sections (10 mb) are much less than 600 mb lead in the past to the conclusion that the real nucleon-nucleon forces must be weaker than the pure attractive Yukawa potential. As a result of this conclusion the idea was risen that the nucleon-nucleon forces are the mixture of attractive and repulsive components and their partial cancellation leads to the reduction of the nucleon-nucleon cross section with respect to the pure Yukawa potential predictions.

The conclusion that the nucleon-nucleon forces are the mixture of the attraction and repulsion is supported by the phase shift analyzes of the nucleon-nucleon scattering. In the Fig. 3.1 the experimental phase shifts for the most important nucleon-nucleon states ($^1S_0$, $^3P_0$, $^3P_1$ for the isospin triple $T = 1$ channel) are demonstrated as a functions of transferred linear momentum k. It should be reminded that the most important state is $^1S_0$ with the zero orbital momentum $L = 0$ where the centrifugal barrier is missing. From the quantum mechanics it is known that the phase shift δ is positive for an attractive potential and negative for a repulsive potential. One can see from the Fig. 3.1 that the phase shift δ for the state $^1S_0$ changes the sign for $k \approx 1.4$ fm^{-1} going from the positive values for $k < 1.4$ fm^{-1} to negative values for $k > 1.4$ fm^{-1}. For $k > 1.4$ fm^{-1} both nucleons are very close each other: $r = 1/k < 0.7$ $fm = 1/1.41$ fm. In the region $r \in (0\,, 0.7\,fm)$ the phase

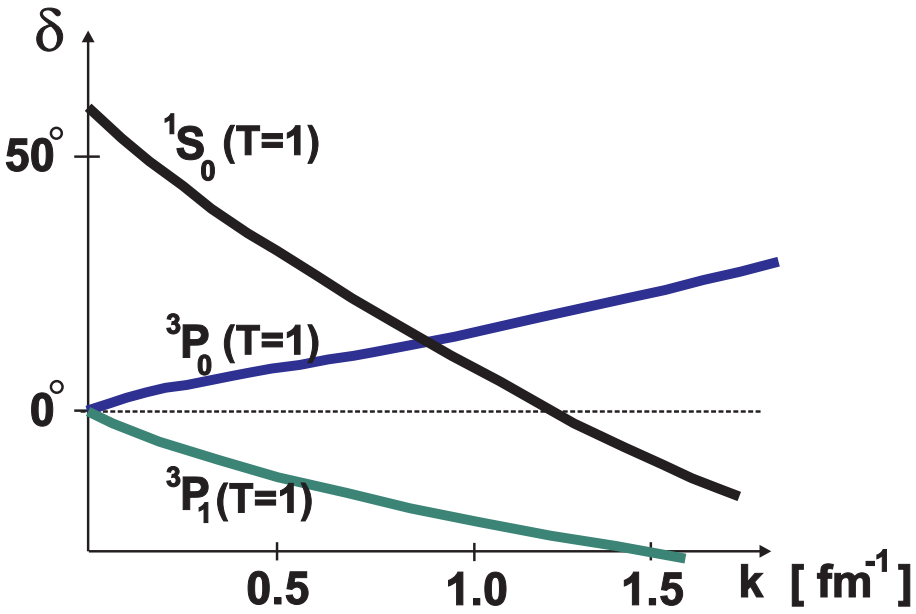


Figure 3.1: Nucleon-nucleon scattering experimental phase shifts for the states $^1S_0$, $^3P_0$, $^3P_1$ for isospin triple $T = 1$ channel

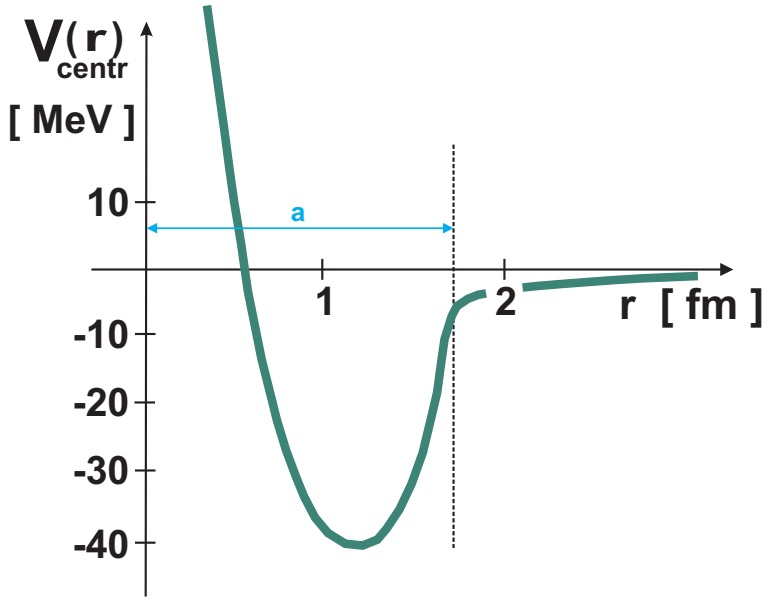


Figure 3.2: Radial dependence of the central nucleon-nucleon potential (schematic figure)

shift of ${}^1S_0$ is negative and this corresponds to the repulsive nucleon-nucleon potential. For higher distances, $r > 0.7\ fm$, the ${}^1S_0$ phase shift is positive and therefore the potential is attractive.

On the base of the phase shift analyzes and taking into account information about the nucleon-nucleon potential obtained from the deuteron (the strength and the range of the nucleon-nucleon interaction) the radial dependence of the nucleon-nucleon interaction given in the schematic figure Fig. 3.2 was deduced. In the interval $r \in \langle 0,\ 0.4\ fm\rangle$ the potential is strongly repulsive (so called repulsive core) while in the region $r > 0.4\ fm$ the potential is attractive with the range $\approx 1.4 - 2\,fm$. This potential is felt by two nucleons in the state ${}^1S_0$ (T=1) which is decisive for energies relevant for the nuclear structure (in the S-state the orbital ang. momentum is zero and therefore there is no centrifugal barrier and nucleons can get very close each other).

3.1.3.2 Exchange meson character of the bare nucleon-nucleon interaction

In 1937 Yukawa suggested the idea that the nucleon-nucleon force can be caused by the meson exchange. This suggestion was based in the analogy with the electrodynamics where the interaction was connected with the photon exchange. According to the Yukawa suggestion during the interaction of two nucleons an intermediate state with exchanged meson is created. This intermediate state can exist only within the time interval Δt which corresponds, according to the "energy uncertainty principle", to the energy uncertainty ΔE given by the following formula

$$\Delta t \cdot \Delta E \approx \hbar \quad \Rightarrow \quad \Delta t \approx \frac{\hbar}{mc^2} \quad \Rightarrow \quad \Delta t \cdot c \approx \frac{\hbar}{mc} \tag{3.101}$$

where m is the mass of the exchanged meson. The range of the force caused by the meson exchange is then characterized by the distance $\Delta t \cdot c \approx \hbar/mc$. The lightest meson is pion with the rest energy $m_\pi c^2 \approx 140$ MeV which corresponds to the range $\hbar/m_\pi c \approx 1.41$ fm. The exchange of heavier mesons is connected with the shorter ranges - see the Tab. 3.4.

If we accept the idea of the meson exchange mechanism of the bare nucleon-nucleon interaction then the scattering amplitude in the lowest order of the Dyson expansion of the S-matrix corresponds to the Feynman diagram given in the Fig. 3.3 (leading order of the process $N_1 + N_2 \to N_1' + N_2'$ - see any textbook of the quantum field theory). Corresponding expression for this scattering amplitude is [1].

[1] The derivation of the expression (3.103) is beyond the scope of this textbook.

particle (meson)	rest energy [MeV]	J^π	range $\frac{\hbar}{mc}$ [fm]
$\pi^\pm$	139.6	0^-	1.41
π^0	134.97	0^-	1.45
η	548.8	0^-	0.36
ρ	765.0	1^-	0.26
ω	783.4	1^-	0.25
$\eta\,'$	958.3	0^-	0.21
φ	1019.5	1^-	0.19
A_1	1070.0	1^+	0.18
$\vdots$	$\vdots$	$\vdots$	$\vdots$
fictive σ_0	≈ 550	0^+	0.36
fictive σ_1	≈ 600	1^+	0.33

Table 3.4: Properties of mesons echanged during the interaction of two nucleons

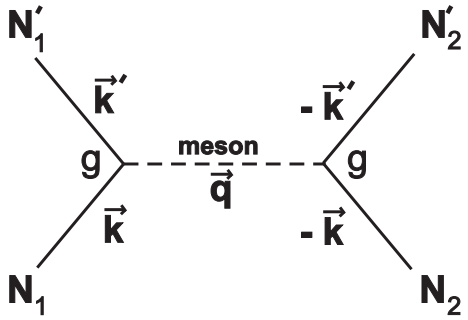


Figure 3.3: Leading order diagram of meson exchange proces $N_1 + N_2 \rightarrow N_1' + N_2'$

$$f(\vec{k}\,',\,\vec{k}) \approx \frac{g^2}{\mu^2 c^2 + q^2\hbar^2} \tag{3.102}$$

where the interaction is mediated by the intermedial meson with the mass μ and $\vec{q} = \vec{k} - \vec{k}\,'$ is the linear momentum transfer. From the other hand this scattering amplitude can be obtained also from the Born series (see (E.33)) using the Yukawa potential:

$$V(r) = -g^2 \frac{e^{-\frac{\mu r}{\hbar}\,r}}{r} \tag{3.103}$$

This can be demonstrated using the expression (E.33) in the Appendix E as it is shown below (in the nucleon-nucleon scattering the reduced mass is $M/2$

where M is the nucleon mass)

$$f^{(1)}(\vec{k}\,',\,\vec{k}) = \boxed{\begin{array}{c}\text{see}\\(E.33)\end{array}} = -\frac{M}{\hbar^2 q}\int_0^\infty dr\, r\, V(r)\, \sin qr =$$
$$= \frac{M}{\hbar^2 q}\, g^2 \int_0^\infty dr\, r\, \frac{e^{-\frac{\mu c}{\hbar}\, r}}{r}\, \sin qr = \frac{M g^2}{\hbar^2 q}\, \Im m \int_0^\infty dr\, e^{(iq-\frac{\mu c}{\hbar})\, r} =$$
$$= M g^2\, \frac{1}{\mu^2\, c^2 + q^2\, \hbar^2} \tag{3.104}$$

and this is equal to (3.102) up to the multiplicative factor. So, the exchange of the intermedial meson corresponds to the Yukawa potential (so called one-boson exchange potential - OBEP).

It is necessary to note that in the previous discussions concerning the exchange character of the nucleon-nucleon interaction (exprs. (3.102) - (3.104)) spin and isospin degrees of freedom were not considered. Their taking into account leads to new terms in the nucleon-nucleon bare potential (terms like $V_T(r)\, \hat{S}_{12}$, $V_{LS}(r)\, \vec{L}\cdot\vec{S}$ etc.). Just for the demonstration the potential terms corresponding to the exchange of the particular type mesons given in the Tab. 3.4 are discussed below.

i. **The exchange of the scalar mesons ($J^\pi = 0^+$)**

The density of the interaction Hamiltonian $\mathscr{H}_s(x)$ or the interaction Lagrangian $\mathscr{L}_s(x)$ corresponding to the interaction of the scalar meson field $\varphi^{(s)}(x)$ with the Dirac fields $\psi(x)$, $\bar{\psi}(x)$ is given by ($x \equiv (ct,\, \vec{r})$ is the point in the Minkowski space)

$$\mathscr{H}_s(x) = -\mathscr{L}_s(x) = \sqrt{4\pi}\, g_s\, \bar{\psi}(x)\, \psi(x)\, \varphi^{(s)}(x) \tag{3.105}$$

which is represented by the Feynman diagram given in the Fig. 3.4. In (3.105) $\psi(x)$ is the Dirac field describing the nucleon, $\bar{\psi}(x) = \psi^+(x)\, \gamma_0$, $\varphi^{(s)}(x)$ is the scalar meson field ($\mathscr{P}^{-1}\varphi^{(s)}(x)\mathscr{P} = \varphi^{(s)}(x)$) and g_s is the interaction strength constant. The corresponding potential term can be obtained by the comparison of the scattering amplitude expression of the process corresponding to the Fig. 3.3 (up to the 2-d order of the Dyson expansion for the S-matrix) with the scattering amplitude expression (E.33) obtained from the 1-st order

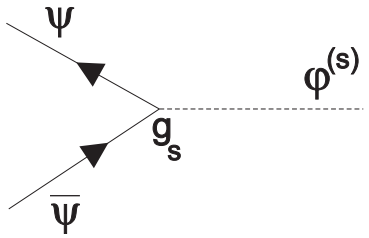


Figure 3.4: Feynman vertex digram for the interaction density Hamiltonian (3.106).

Born approximation. The result is

$$V_s(x_s) = g_s^2 m_s c^2 \left[-\left(1 - \frac{1}{4} m_s^2 M^{-2}\right) Y(x_s) + \right. \\ \left. + \frac{1}{2} m_s^2 M^{-2} \left(1 - \frac{1}{8} m_s^2 M^{-2}\right) J(x_s)\, \vec{L}\cdot\vec{S} \right] \qquad (3.106)$$

where m_s is the mass of the exchange scalar meson and

$$x_s = \frac{m_s c r}{\hbar} \quad , \quad Y(x_s) = -\frac{e^{-x_s}}{x_s} \, , \\ J(x) = \frac{1}{x}\frac{dY}{dx} \quad , \quad \vec{L}\cdot\vec{S} = \frac{1}{2}\vec{L}\,(\vec{\sigma}_1 + \vec{\sigma}_2) \qquad (3.107)$$

ii. **The exchange of the pseudoscalar mesons** ($J^\pi = 0^-$)
In this case the density of the interaction Hamiltonian is

$$\mathscr{H}_{PS}(x) = -\mathscr{L}_{PS}(x) = \sqrt{4\pi}\, g_s\, \bar{\psi}(x)\, \gamma_5\, \psi(x)\, \varphi^{(PS)}(x) \qquad (3.108)$$

where $\varphi^{(PS)}(x)$ is the pseudoscalar meson field ($\mathscr{P}^{-1}\varphi^{(PS)}(x)\mathscr{P} = -\varphi^{(PS)}(x)$). The corresponding potential $V_{PS}(r)$ obtained by the comparison of the 2-d order of the Dyson S-matrix expansion with the 1-st Born approximation is

$$V_{PS}(x_{PS}) = g_{PS}^2 m_{PS} c^2 \frac{1}{12} \left[m_{PS}^2 M^{-2} Y(x_{PS})\, \vec{\sigma}_1\cdot\vec{\sigma}_2 + \right. \\ \left. + m_{PS}^2 M^{-2}\, Z(x_{PS})\, S_{12} \right] \qquad (3.109)$$

where m_{PS} is the mass of the exchange pseudoscalar meson and

$$x_{PS} = \frac{m_{PS} c r}{\hbar} \, , \quad Z(x_{PS}) = \left(1 + 3x_{PS}^{-1} + 3x_{PS}^{-2}\right) Y(x_{PS}) \qquad (3.110)$$

iii. **The exchange of the vector mesons** ($J^\pi = 1^+$)

In the case of the exchange interaction mediated by vector mesons the density of the interaction Hamiltonian is

$$\mathscr{H}_V(x_V) = -\mathscr{L}_V(x_V) = \sqrt{4\pi}\, g_V\, \bar{\psi}(x_V)\, \gamma_\nu\, \psi(x_V)\, \varphi^{(V)\,\nu}(x_V) + \sqrt{4\pi}\, \frac{\hbar f_V}{2m_V c}\, \bar{\psi}(x_V)\sigma^{\mu\,\nu}\, \psi(x_V)\, \left[\partial_\nu \varphi_\mu^{(V)}(x_V) - \partial_\mu \varphi_\nu^{(V)}(x_V)\right] \tag{3.111}$$

and corresponding potential is given by:

$$V_V(x_V) = g_V^2 m_V c^2 \left\{ R_C\, \left(1 + \frac{1}{4}\lambda^2\right)\, Y(x_V) + \frac{3}{2}\lambda^2 R_{LS} J(x_V)\, \vec{L}\cdot\vec{S} + \frac{1}{12}\lambda^2\, R_{12}\, \left[2\, Y(x_V)\, \vec{\sigma}_1\cdot\vec{\sigma}_2 - Z(x_V)\, S_{12}\right] \right\} \tag{3.112}$$

where m_V is the mass of the vector meson and

$$x_V = \frac{m_V c r}{\hbar}\,, \quad R_C = 1 + \lambda\, \left(1 + \frac{1}{2}\lambda^2\right)^{-1}\, \frac{f_V}{g_V}$$
$$R_{12} = \left(1 + 2\,\lambda^{-1}\, \frac{f_V}{g_V}\right)^2\,, \quad R_{LS} = 1 + \frac{8}{3}\,\lambda^{-1}\, \frac{f_V}{g_V} \tag{3.113}$$

All formulas given above were obtained for isoscalar mesons (that means charge neutral mesons). For isovector mesons (like π^0, π^+, π^-) instead of $\varphi^{(S,\,PS\,V)}(x)$ the quantity $\vec{\tau}\cdot\vec{\varphi}^{S,\,PS,\,V}$ is involved in (3.105), (3.108), and (3.111) and corresponding terms in the potentials are multiplied by the scalar factor $\vec{\tau}_1\cdot\vec{\tau}_2$.

All expressions (3.106) - (3.113) for OBEP potentials corresponds to the exchange of one meson and all of them are known for 50 years. For instance, Bryan and Scott (1964-66) used these expressions for the first construction of the OBEP based on the exchange of π, η, ρ, ω, σ_0, σ_1 mesons. Strength constants g and f involved in this OBEP potential were fitted in order to reproduce the experimental phase shifts obtained in the nucleon-nucleon scattering (see e.g. [24]). The masses of the fictive mesons σ_0 and σ_1 were also fitted. These fictive mesons were introduced articially in order to obtain a good agreement of experimental and theoretical dependencies of phase shifts on the scattering energy for orbital momenta $L \geq 1$. The concrete values are given in the Tab 3.5.

particle	parameter g^2		particle	parameter g^2	
π	12.55		ω	17.26	$f/g = 0$
η	2.60		σ_0	8.19	$m = 550\ MeV$
ρ	1.81	$f/g = 1.33$	σ_1	1.65	$m = 600\ MeV$

Table 3.5: Parameters of the Bryan-Scott meson exchange interaction

However, the one boson exchange potentials, like Bryan-Scott one, are not able to explain sufficiently the effects connected with the hard repulsive nucleon-nucleon potential core ($V(r) \overset{r \to 0}{\to} \infty$ for $r < 0.7$ fm). As we saw in the subsection 3.1.3.1 this hard repulsive core is connected with the state ${}^1S_0$ (with the change of the sign of the phase shift of this state from the positive to negative values if the distance r increases through the point $r \approx 0.7$ fm - see the Fig. 3.1). That means OBEP potentials are not suitable for the description of the nucleon-nucleon interaction for the zero orbital momentum, $L = 0$.

The other problem with the OBEP potential is connected with the charge independence of the nucleon-nucleon interaction if it is described only with the leading order of the Dyson expansion of the S- matrix (which corresponds to the Fig. 3.3). From the Fig. 3.3 it is seen that the scattering $n_1 + n_2 \to n_1\,' + n_2\,'$ or $p_1 + p_2 \to p_1\,' + p_2\,'$ is mediated by the exchange of π^0 while the exchange of π^+ corresponds to the scattering $p_1 + n_2 \to p_1\,' + n_2\,'$.

In order to remove the problem of the hard repulsive core and the problem of the charge independence of the nucleon-nucleon interaction it is necessary to go beyond the leading order term and to take into account also the higher order terms corresponding to the exchange of more than one meson. In the case of the exchange of pions the next to leading order diagrams connected with the exchange of two pions are presented in the Fig. 3.5.

The next to leading order terms (2-nd order terms) represent the exchange of two mesons and they involves also the creation of new intermediate states - so called Δ resonances. The next to leading order terms are also charge dependent but the charge dependencies of the leading order terms and of the next to leading terms cancel each other. So, their sum is charge independent in accordance with the fact that the strong interaction part of the nucleon-nucleon interaction should be charge independent.

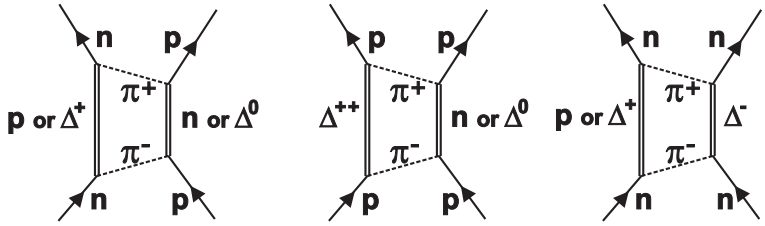


Figure 3.5: Feynman vertex diagrams of the next to leading order terms of the nucleon-nucleon interaction mediated by the π^- meson exchange.

The theory of potentials deduced from the idea of one- and two- meson exchange appeared in 70-ties and 80-ties under the name Refined Meson Theories, see e.g Paris potential [Lacombe et al., Phys. Rev. 21, 861 (1980)] or Bonn potential [Machleidt et al., Phys. Rep. 149, 1 (1987)]. These potentials were improved in 90-ties (e.g. CD-Bonn potential [Machleidt et al. 1996, 2001] or Argonne V18 potential [Wiringa et al. 1995]).

From the point of view of the present-day theory (from the standard Model of Particle Physics) the nucleon-nucleon interaction in the energies relevant to nuclear structure should be obtained from the low-energy limit of the Quantum Chromodynamics (QCD). The QCD describes the strong interaction as the interaction of quarks and gluons. While the QCD can be handled perturbatively at high energies, due to the so called asymptotic freedom the perturbative treatment breaks down in the low-energy regime relevant for nuclear structure. Moreover, it is an empirically established fact that the QCD is confining: while quarks an gluons carry individual color charges, only color-neutral bound states of quarks, the baryons and mesons, appear in the physical spectrum in the low-energy regime (see the Tab. 3.6). From the point of view of the low energy regime of the QCD the bare nucleon-nucleon interaction is connected with contact terms and one-, two-, and more- pion exchange terms (so called Chiral Perturbation Theory). It is possible (see e.g. [25]) to recognize the connection (equivalence) between Chiral Perturbation Theory and conventional meson exchange theory based on the exchange of different mesons (described above) - so called Resonance Saturation. This connection is shown in the Fig. 3.6. In this sense the older ideas of the different meson exchange character of the nucleon-nucleon interaction in the nucleus is confirmed by the QCD.

3 families of quarks			
$q = \frac{2}{3}\,\|e\|$	u	c	t
$q = \frac{1}{3}\,\|e\|$	d	s	b

quantum numbers of quarks								
	mass $[\frac{MeV}{c^2}]$	baryon number B	charge q $[\|e\|]$	isospin I_3	charm C	strangeness S	topness T	bottonness B'
u	1.5-3.3	+1/3	+2/3	+1/2	0	0	0	0
d	3.5-6.0	+1/3	-1/3	-1/2	0	0	0	0
c	1270^{+70}_{-110}	+1/3	+2/3	0	+1	0	0	0
s	104^{+26}_{-34}	+1/3	-1/3	0	0	-1	0	0
t	171200	+1/3	+2/3	0	0	0	+1	0
b	4200	+1/3	-1/3	0	0	0	0	-1

bound states of quarks	
$p = uud$	$\pi^+ = u\bar{d}$
$n = udd$	$\pi^0 = u\bar{u} + d\bar{d}$
	$\pi^- = \bar{u}d$

Table 3.6: Characteristics od quarks - each quark has its antiquark (e.g. antiquark of u is $\bar{u}$). Spin of all quarks is 1/2.

3.1.3.3 Phenomenological bare nucleon-nucleon potentials

As it was mentioned in the previous subsections the nucleon-nucleon (N-N) potentials derived from the one meson exchange mechanism is able to describe the interaction between two nucleons in the distances higher than 0.7 fm (corresponding to the higher orbital momenta L). Taking into account two and higher meson exchange helps only partly. The fully satisfactory description of the N-N potential hard core ($V(r) \approx \infty$ for $r \leq 0.7$ fm) is not available using only meson exchange mechanism. In the present time there are attempts (see e.g. [25]) to reproduce all N-N phase shifts (including $L = 0$ phase shift) in the framework of the Chiral Pertubation Theory using the inclusion of higher order Feynman diagrams of the pion exchange (next to next to leading order and higher). In the past, before Chiral Perturbation Theories, the

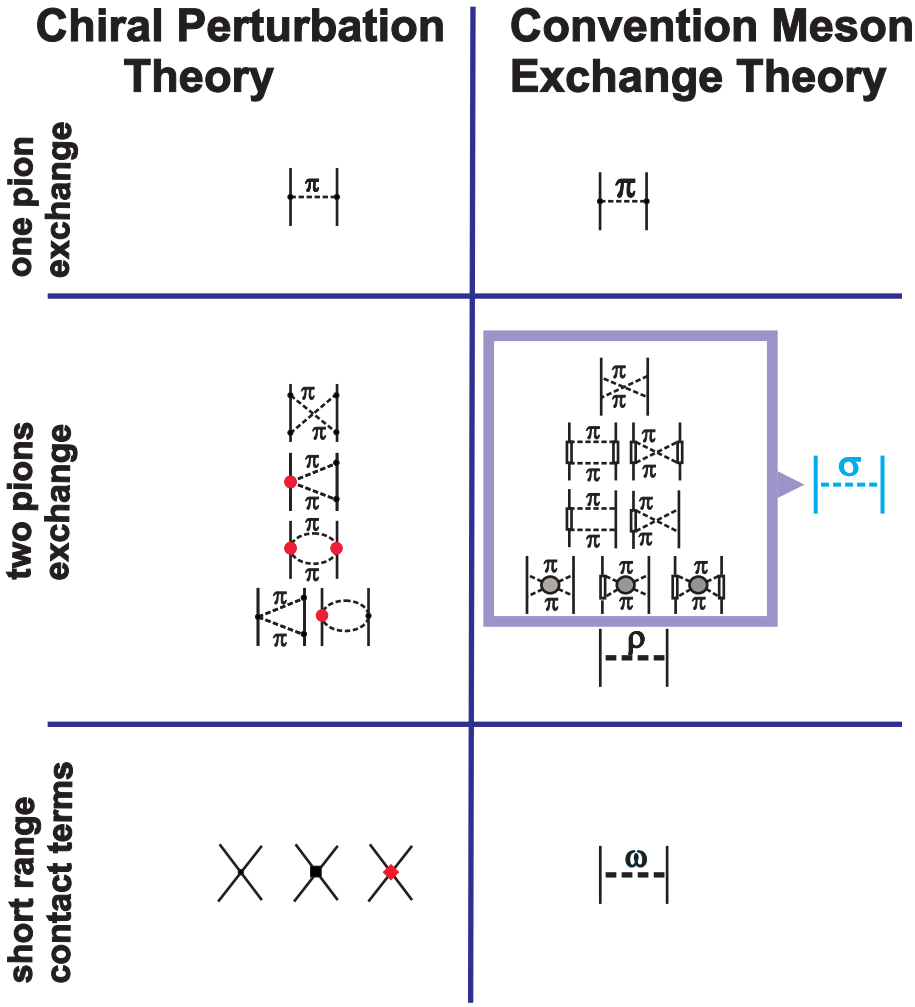


Figure 3.6: Equivalence of the Chiral Perturbation Theory with the Conventional Meson Exchange Theory (taken from the lecture of R.Machleidt in his web site: http://machleidt.weebly.com/lectures-on-nuclear-forces.html)

problem of the potential hard core (or $L = 0$ phase shifts) was overcome by the combination of meson exchange potentials (describing phase shifts for $L \geq 1$) and phenomenological potentials (describing $L = 0,\ 1$ phase shifts). The form of the phenomenological potentials was deduced from the general symmetries to be fulfilled by the N-N potential. Similarly as meson exchange potentials phenomenological potentials contain free parameters which should be determined by the fitting of theoretical phase shifts to experimental ones. Since the combination of meson exchange and phenomenological potentials are used in practical calculation of the nuclear structure characteristics up to now in this subsection the symmetries of the nucleon-nucleon potential and connected phenomenological forms of this potential are discussed in more details.

The symmetry requirement for the N-N potentials can be summarized in the following items.

1. From the Galilean invariance of the N-N potentials it follows that this potential can depend only on the distance r between two nucleons, on their relative linear momentum $\vec{p}$ and on spins $\vec{\sigma}_1$ and $\vec{\sigma}_2$ of these two nucleons.

2. The nucleon-nucleon potential should be Hermitian.

3. The N-N potential is invariant with respect to rotations.

4. The relative linear momentum $\vec{p}$ of two nucleons should be present in the expression for N-N potential in the lowest order as possible (preferably in the linear order).

Further we restrict ourselves on the terms in the N-N potential involving Pauli spin matrices $\vec{\sigma}_1$ and $\vec{\sigma}_2$ of two interacting nucleons in the linear order only. Higher order terms in $\vec{\sigma}_1$ and $\vec{\sigma}_2$ can be transformed into lower order terms using identities like (3.22) and finally we end with the linear order only.

Taking into account requirements 1. - 4. above the bare N-N potential involves terms with the following quantities.

$$r,\ \vec{p},\ \ \vec{\sigma}_1,\ \ \vec{\sigma}_2,\ \ \vec{\sigma}_1 \times \vec{\sigma}_2,\ \ \vec{\sigma}_1 \times \vec{r},\ \ \vec{\sigma}_2 \times \vec{r},\ \vec{r} \times \vec{p} \tag{3.114}$$

These quantities can participate in the N-N potential only in combinations which are scalars with respect to rotations. Using well-known identities:

$$\begin{aligned} &\vec{A} \times \vec{B} \times \vec{C} = \vec{B} \left(\vec{A} \cdot \vec{C} \right) - \vec{C} \left(\vec{A} \cdot \vec{B} \right) \\ &\left(\vec{A} \times \vec{B} \right) \cdot \left(\vec{C} \times \vec{D} \right) = \left(\vec{A} \cdot \vec{C} \right) \left(\vec{B} \cdot \vec{D} \right) - \left(\vec{A} \cdot \vec{D} \right) \left(\vec{B} \cdot \vec{C} \right) \end{aligned} \tag{3.115}$$

the following scalar combinations can be created

$$\begin{array}{llll} \vec{r} \cdot \vec{r} = r^2 & \vec{r} \cdot (\vec{\sigma}_1 \times \vec{\sigma}_2) & (\vec{\sigma}_1 \cdot \vec{\sigma}_2)\,(\vec{r} \cdot \vec{p}) & (\vec{\sigma}_1 \cdot \vec{r})\,(\vec{r} \cdot \vec{p}) \\ \vec{\sigma}_1 \cdot \vec{\sigma}_1 & \vec{p} \cdot (\vec{\sigma}_1 \times \vec{\sigma}_2) & (\vec{\sigma}_1 \cdot \vec{r})\,(\vec{\sigma}_2 \cdot \vec{r}) & (\vec{\sigma}_2 \cdot \vec{r})\,(\vec{r} \cdot \vec{p}) \\ \vec{\sigma}_1 \cdot \vec{r},\ \vec{\sigma}_2 \cdot \vec{r} & \vec{\sigma}_1 \cdot (\vec{r} \times \vec{p}) & (\vec{\sigma}_1 \cdot \vec{p})\,(\vec{\sigma}_2 \cdot \vec{p}) & (\vec{r} \cdot \vec{p})\,\vec{r} \cdot (\vec{\sigma}_1 \times \vec{\sigma}_2) \\ \vec{\sigma}_1 \cdot \vec{p},\ \vec{\sigma}_2 \cdot \vec{p} & \vec{\sigma}_2 \cdot (\vec{r} \times \vec{p}) & (\vec{\sigma}_2 \cdot \vec{r})\,(\vec{\sigma}_1 \cdot \vec{p}) & (\vec{r} \cdot \vec{p})\,(\vec{\sigma}_1 \cdot \vec{r})\,(\vec{\sigma}_2 \cdot \vec{r}) \\ \vec{r} \cdot \vec{p} & & & \end{array} \tag{3.116}$$

Except the requirements 1. - 4. above the following conditions are made for the N-N potential.

5. Because of the charge conservation the N-N potential operator should commute with the third component of the total isospin of two nucleons $\rightarrow \quad \left[\hat{V}, (\vec{\tau}_1 + \vec{\tau}_2)_3\right] = 0.$

6. The N-N potential should be symmetric with respect to the exchange of both nucleons (particle identity).

7. The N-N potential is invariant with respect to parity transformation ($\mathscr{P}^{-1}\hat{V}\mathscr{P} = \hat{V}$). However, the presence of small contributions violating parity preservation is not excluded (small contributions from weak interaction in the N-N potential).

8. The N-N potential should be invariant to the time reversal transformation. Again, there are possible small contributions which violate the time reversal symmetry of the N-N potential.

Scalar combinations (3.116) concerns only spatial-spin part of the Hilbert space of two nucleons. The combinations acting in the isospin space of the N-N interaction should be constructed from the isospin matrices $\vec{\tau}_1$ and $\vec{\tau}_2$ of both nucleons. The requirement 5. above allows only 5 combinations in the isospin part of the Hilbert space which can participate in the N-N potential $\hat{V}$, namely

$$1, \quad \vec{\tau}_1 \cdot \vec{\tau}_2, \quad (\vec{\tau}_1 + \vec{\tau}_2)_3\,, \quad (\vec{\tau}_1 - \vec{\tau}_2)_3\,, \quad (\vec{\tau}_1 \times \vec{\tau}_2)_3 \tag{3.117}$$

Under the time reversal transformation in the isospin part of the Hilbert space (see (1.42)) the combination $(\vec{\tau}_1 \times \vec{\tau}_2)_3$ changes the sign. Therefore the last combination, $(\vec{\tau}_1 \times \vec{\tau}_2)_3$, is excluded from our consideration. Further the requirement 5. above is strengthened and we require for the N-N potential $\hat{V}$ to be fully charge independent (in agreement with the empirical fact that the strong interaction is charge independent - see subsection 1.2). Therefore we exclude also combinations $(\vec{\tau}_1 \pm \vec{\tau}_2)_3$. So, only two combinations are possible in the isospin part of the Hilbert space,

$$1, \quad \vec{\tau}_1 \cdot \vec{\tau}_1 \tag{3.118}$$

The classification of combinations possible in the bare N-N interaction in the spatial-spin part of the Hilbert space (see (3.117) from the point of view of the parity $\mathscr{P}$ and time reversal $\mathscr{T}$ transformations is given in the Tab. 3.7.

time reversal sign	parity +	parity −
+	1	$\vec{r}\cdot(\vec{\sigma}_1-\vec{\sigma}_2)$
	$\vec{\sigma}_1\cdot\vec{\sigma}_1$	$(\vec{\sigma}_1+\vec{\sigma}_2)\cdot\vec{p}$
	$(\vec{\sigma}_1\cdot\vec{r})\,(\vec{\sigma}_2\cdot\vec{r})$	$((\vec{\sigma}_1+\vec{\sigma}_2)\cdot\vec{r})\,(\vec{r}\cdot\vec{p})$
	$(\vec{\sigma}_1+\vec{\sigma}_2)\cdot(\vec{r}\times\vec{p})$	$(\vec{\sigma}_1+\vec{\sigma}_2)\cdot\vec{p}$
	$(\vec{\sigma}_1-\vec{\sigma}_2)\cdot(\vec{r}\times\vec{p})$	$((\vec{\sigma}_1+\vec{\sigma}_2)\cdot\vec{r})\,(\vec{r}\cdot\vec{p})$
−	$\vec{r}\cdot\vec{p}$	$(\vec{\sigma}_1+\vec{\sigma}_2)\cdot\vec{r}$
	$(\vec{\sigma}_1\cdot\vec{\sigma}_2)\,(\vec{r}\cdot\vec{p})$	$(\vec{\sigma}_1\times\vec{\sigma}_2)\cdot\vec{p}$
	$(\vec{r}\cdot\vec{p})\,(\vec{\sigma}_1\vec{r})\,(\vec{\sigma}_2\vec{r})$	$(\vec{r}\cdot(\vec{\sigma}_1\times\vec{\sigma}_2))\,(\vec{r}\cdot\vec{p})$
	$(\vec{\sigma}_1\times\vec{\sigma}_2)\cdot(\vec{r}\times\vec{p})$	$(\vec{\sigma}_1+\vec{\sigma}_2)\cdot\vec{r}$

Table 3.7: Classification of combinations possible in the bare N-N interaction in the spatial-spin part of the Hilbert space (see (3.116) from the point of view of the sign of parity $\mathscr{P}$ and time reversal $\mathscr{T}$ transformations.

In the agreement with the requirements 7. and 8. above only spatial-spin terms which do not change sign under the parity and time reversal transformation (upper left corner in the Tab. 3.7) can be present in the N-N potential in the combination with isospin terms (3.119). It is necessary to realize that the term $(\vec{\sigma}_1-\vec{\sigma}_2)\cdot(\vec{r}\times\vec{p})$ (which changes the sign if we replace both nucleons mutually) should be combined with the operator from the isospin part of the Hilbert space which also changes the sign under the mutual replacing of both nucleons (because the whole combination should be invariant with respect to the replacing of both nucleons). However, as one can see in (3.119) such isospin operator does not exist. Therefore, the term with $(\vec{\sigma}_1-\vec{\sigma}_2)\cdot(\vec{r}\times\vec{p})$ cannot be present in the N-N potential.

So, if we require charge independence, invariance to the time reversal and

parity then the N-N potential can contain only following terms.

$$\left.\begin{array}{c} 1 \\ \vec{\sigma}_1 \cdot \vec{\sigma}_2 \\ (\vec{\sigma}_1 \cdot \vec{r})\,(\vec{\sigma}_2 \cdot \vec{r}) \\ (\vec{\sigma}_1 + \vec{\sigma}_2) \cdot (\vec{r} \times \vec{p}) \end{array}\right\} \text{in the combination with} \left\{\begin{array}{c} 1 \\ \vec{\tau}_1 \cdot \vec{\tau}_2 \end{array}\right. \tag{3.119}$$

and the general form of the N-N potential can be written as follows.

$$\begin{aligned} \hat{V}(\vec{r},\vec{p},\vec{\sigma}_1,\vec{\sigma}_2,\vec{\tau}_1,\vec{\tau}_2) = \\ & (V_c(r) + W_c(r)\,\vec{\tau}_1 \cdot \vec{\tau}_2) + \\ & + (V_{sc}(r) + W_{sc}(r)\,\vec{\tau}_1 \cdot \vec{\tau}_2)\;(\vec{\sigma}_1 \cdot \vec{\sigma}_2) + \\ & + (V_t(r) + W_t(r)\,\vec{\tau}_1 \cdot \vec{\tau}_2)\;[3\;(\vec{\sigma}_1 \cdot \vec{r})\,(\vec{\sigma}_2 \cdot \vec{r}) - \vec{\sigma}_1 \cdot \vec{\sigma}_2] + \\ & + (V_{ls}(r) + W_{ls}(r)\,\vec{\tau}_1 \cdot \vec{\tau}_2)\;(\vec{\sigma}_1 + \vec{\sigma}_2)\;(\vec{r} \times \vec{p}) + \\ & + (V_Q(r) + W_Q(r)\,\vec{\tau}_1 \cdot \vec{\tau}_2)\;[(\vec{\sigma}_1 + \vec{\sigma}_2)\;(\vec{r} \times \vec{p})]^2 \end{aligned} \tag{3.120}$$

The last term in (3.120), quadratic spin-orbital potential, violates the requirement 4. above, but even so it is sometimes taken into account.

All functions $V_i(r)$, $W_i(r)$ $(i = c, sc, t, ls, Q)$ are functions of the distance r between nucleons. In practice these radial functions are taken in the literature in different forms:

$$\begin{aligned} \text{finite well:} \quad & \left\{\begin{array}{l} V_i(r) = -V_0^{(i)}\;(\text{for } r < R_0) \\ V_i(r) = \;0 \qquad (\text{for } r > R_0) \end{array}\right. \\ \text{Gauss:} \quad & V_i(r) = -V_0^{(i)}\,e^{-\mu_i^2 r^2} \\ \text{exponential form:} \quad & V_i(r) = -V_0^{(i)}\,e^{-\mu_i r} \\ \text{Yukawa:} \quad & V_i(r) = -V_0^{(i)}\,r^{-1}\,e^{-\mu_i r} \\ \text{Hulten:} \quad & V_i(r) = -V_0^{(i)}\,e^{-\mu_i r}\,\left[1 - e^{-\mu_i r}\right]^{-1} \end{aligned} \tag{3.121}$$

where $V_0^{(i)}$ and μ_i are parameters for all i (usually fitted to experimental values of phase shifts).

Terms in (3.121) depending on $\vec{\sigma}_i$ and $\vec{\tau}_i$ $(i = 1, 2)$ are often written in terms of spin and isospin exchange operators $P_{12}^{(\sigma)}$ and $P_{12}^{(\tau)}$.

$$P_{12}^{(\sigma)} = \frac{1}{2}\;(1 + \vec{\sigma}_1 \cdot \vec{\sigma}_2) \qquad P_{12}^{(\tau)} = \frac{1}{2}\;(1 + \vec{\tau}_1 \cdot \vec{\tau}_2) \tag{3.122}$$

as is given below

$$\hat{V}(\vec{r},\vec{p},\vec{\sigma}_1,\vec{\sigma}_2,\vec{\tau}_1,\vec{\tau}_2) = V_W(r) + V_B(r)\, P_{12}^{(\tau)} + V_H(r)\, P_{12}^{(\tau)}\, P_{12}^{(\sigma)} + \\ + (V_t(r) + W_t(r)\, \vec{\tau}_1\cdot\vec{\tau}_2)\ [3\ (\vec{\sigma}_1\cdot\vec{r})\,(\vec{\sigma}_2\cdot\vec{r}) - \vec{\sigma}_1\cdot\vec{\sigma}_2] + \\ + (V_{ls}(r) + W_{ls}(r)\, \vec{\tau}_1\cdot\vec{\tau}_2)\ (\vec{\sigma}_1+\vec{\sigma}_2)\ (\vec{r}\times\vec{p}) + \\ + (V_Q(r) + W_Q(r)\, \vec{\tau}_1\cdot\vec{\tau}_2)\ [(\vec{\sigma}_1+\vec{\sigma}_2)\ (\vec{r}\times\vec{p})]^2 \qquad (3.123)$$

where functions $V_W(r)$, $V_M(r)$, $V_B(r)$ and $V_H(r)$ are connected with functions $V_c(r)$, $V_{sc}(r)$, $V_t(r)$, $V_{sc}(r)$ in (3.121) by following relations

$$\begin{aligned} V_W &= V_c - V_{sc} - W_c + W_{sc} \\ V_M &= -4\, W_{sc} \\ V_B &= 2\, V_{sc} - 2\, W_{sc} \\ V_H &= -2\ W_c + 2\, W_{sc} \end{aligned} \qquad (3.124)$$

The radial functions of the N-N potential should involve also the hard core for $r < 0.4$ fm. According to the hard core approach phenomenological potentials can be divided into two groups:

- hard core potentials with $V(r) = \infty$ for $r \leq 0.4$ fm,
- soft core potentials with $V(r) \to \infty$ for $r \to 0$.

So, the phenomenological parametrization of the bare N-N potential consists in the combination of the central, tenzor, spin-orbit and quadratic spin-orbital terms with, more or less, arbitrary radial dependencies (3.121) involving altogether many free parameters which should be consistent with the experimental phase shifts and deuteron data. These phenomenological N-N potentials are responsible for the nucleon-nucleon distances less than 0.7 fm. For the higher distances ($r > 0.7$ fm) these potentials transform to many meson exchange potentials (for orbital momenta $L \approx 1-4$). For more higher distances (corresponding to $L \geq 5$) the one meson exchange potentials are sufficient to describe the bare N-N interaction.

Some examples of the bare N-N potentials used in the literature are listed below.

i. Phenomenological potentials combined with meson exchange potentials:

- Hamada Johnston potential (T.Hamada, I.D.Johnston, Nucl. Phys. **34**, 382 (1962)

- Yale potential (F.Tabakin, et al., Phys. Rev. **126**, 881 (1962))
- Reid soft potential (P.V.Reid, Ann. Phys. (N.Y.) 50, 411 (1968))
- Paris potential (Lacombe et al., Phys. Rev. **21**, 861 (1980))
- Bonn potential (R.Machleidt et al., Phys. Rep. **149**, 1 (1987))

ii. Semiphenomenological + meson exchange (with some elements of the chiral theory)

- CD Bonn (Machleidt et al., 1996 + 2001)
- Argone V18 (Wiringa et al., 1995)

3.2 Nucleon-nucleon effective interaction in the nuclear matter

In the previous Section 3.1 the bare N-N interactions acting between two nucleons in the vacuum were discussed. These interactions are responsible for the nucleon-nucleon scattering in the vacuum and deuteron data. In fact, the nucleon-nucleon interaction in the nucleus is influenced by the presence of other nucleons. This influence can be realized as the manifold scattering of one nucleon on other nucleons in the nuclear medium.

For the description of many-body quantum systems (including nucleus) the Hartree-Fock (HF) (see the Chapter 4) or Hartree-Fock-Bogoliubov (HFB) (see the Chapter 6) in the combination with other methods (see the Chapter 7) are used. All these methods starts with the nucleon-nucleon interaction (N-N potential). In the past attempts was done to use the bare N-N potential as as input for HF or HFB calculations. However, the strongly repulsive infinite hard core of the bare N-N potential causes big numerical problems.

Both above problems (manifold scattering and infinite repulsive hard core) are removed by means of the introduction of so called effective nucleon-nucleon interaction (effective N-N potential) which acts effectively between two nucleons in the nuclear medium. This effective N-N potentials take into

account effectively manifold scattering as well as the infinite hard core of bare N-N interaction. From the point of view of the mathematical behaviour the effective N-N potentials are reasonable (finite near the coordinate origin - nucleus center of mass position) and their usage do not cause any numerical problems in the successive HF or HFB calculations.

The task to obtain effective N-N interaction from the bare N-N interaction by means of some pure microscopical way is not easy. The first attempts was done in 50-ties when effective N-N interaction was determined in terms of the Bethe-Goldstone equation (Brueckner-Bethe theory of effective interaction discussed in the Subsection 3.2.1). In last two decades (from 90-ties) another microscopic theories of the effective N-N interaction appeared (see e.g. [26]) which are also mentioned in the Subsection 3.2.1.

Fully microscopic approaches for the determination of the effective N-N interaction have minimum free parameters except those involved in the bare N-N interactions (which are fixed by the N-N scattering data). However, using of this fully microscopic effective interactions for the description of the concrete properties of heavier nuclei is not so good as concerned an agreement with experimental data. Therefore, up to now the phenomenological or semi-phenomenological effective interactions (e.g. Skyrme or Gogny effective interactions discussed in the Section 3.2.2) are used for this purpose. Phenomenological and semi-phenomenological effective N-N interactions contain always several free parameters which are usually fixed by the requirement that successive HF or HFB calculations give good agreement with some nuclear properties of heavier nuclei (usually bind energies, nuclear radii, compressibility of the nuclear matter of doubly-magic nuclei). Phenomenological effective N-N interactions are discussed in the Subsection 3.2.2.

3.2.1 Microscopic effective nucleon-nucleon interaction

Since the Brueckner-Bethe way (see [18], [19]) of the obtaining of the effective N-N interaction is used very often up to now and also because of its clear demonstration of the manifold scattering of one nucleon in the nuclear medium this method is discussed briefly in this subsection. The method is based on the Bethe-Goldstone equation derived and discussed in the Appendix E (see Subsections E.1 and E.2). The idea is following.

The system of nucleons mutually scattering in the nuclear medium have

the following Hamiltonian (see also (E.1))

$$\hat{H} = \hat{H}_0 + \hat{V} \tag{3.125}$$

where $\hat{H}_0$ is the single-particle (unperturbed) part of the Hamiltonian (e.g. total kinetic energy Hamiltonian of all nucleons). The symbol $\hat{V}$ stands for the residual interaction with respect to $\hat{H}_0$ (e.g. bare N-N interaction in the case when $\hat{H}_0$ is the total kinetic energy Hamiltonian of nucleons). We search for the eigen-system of the total Hamiltonian $\hat{H}$, that means for the eigen-vectors $|\psi\rangle$ and corresponding eigen-energies E:

$$\hat{H}\,|\psi\rangle = E\,|\psi\rangle \tag{3.126}$$

We suppose that we know the eigen-vectors $|\varphi\rangle$ of the unperturbed Hamiltonian $\hat{H}_0$ with the same energy E:

$$\hat{H}_0\,|\varphi >= E\,|\varphi\rangle \tag{3.127}$$

The goal of the Brueckner-Bethe method is to find the operator $\hat{G}$ which acting on the unperturbed vector $|\varphi\rangle$ gives the same result as the action of the potential $\hat{V}$ on the perturbed vector $|\psi\rangle$:

$$\hat{G}\,|\varphi\rangle = \hat{V}\,|\psi\rangle \tag{3.128}$$

In the Appendix E the derivation of the operator $\hat{G}$ is given and the result is so called Lippman-Schwinger equation (see (E.7)) for this operator $\hat{G}$,

$$\hat{G} = \hat{V} - \hat{V}\,\frac{1}{\hat{T} - E}\,\hat{G} \tag{3.129}$$

The meaning of the operator $\hat{G}$ introduced in (3.129) consists in the fact that matrix elements of the potential $\hat{V}$ constructed in the basis of the perturbed eigen-vectors $|\psi\rangle$ of the total Hamiltonian $\hat{H}$ can be replaced by matrix elements of the operator $\hat{G}$ formed in the basis of known unperturbed vectors $|\varphi\rangle$.

If we suppose infinite nuclear medium then the unperturbed Hamiltonian $\hat{H}_0$ can be chosen to be equal to the total kinetic energy operator, $H_0 = \hat{T}$, with the corresponding eigen-vectors in the form of plane waves $|\vec{k}_1\,\vec{k}_2\rangle$ ($\hat{H}_0|\vec{k}_1\,\vec{k}_2\rangle = \left(\frac{\hbar^2 k_1^2}{2m} + \frac{\hbar^2 k_2^2}{2m}\right)|\vec{k}_1\,\vec{k}_2\rangle$). Further we determine the matrix elements of the equation (3.129) between the eigen-vectors $|\vec{k}_1\,\vec{k}_2\rangle$ and $|\vec{k}\,'_1\,\vec{k}\,'_2\rangle$ of the unperturbed Hamiltonian $\hat{H}_0 = \hat{T}$ (we suppose the elastic scattering of each

two nucleons in the infinite nuclear medium when the energy before and after the scattering is the same - see (E.9)

$$\begin{aligned}\hat{H}_0\,|\vec{k}_1\,\vec{k}_2> &= \left(\frac{\hbar^2 k_1^2}{2m}+\frac{\hbar^2 k_2^2}{2m}\right)\,|\vec{k}_1\,\vec{k}_2\rangle = E\,|\vec{k}_1\,\vec{k}_2\rangle \\ \hat{H}_0\,|\vec{k}\,'_1\,\vec{k}\,'_2\rangle &= \left(\frac{\hbar^2 k\,'^2_1}{2m}+\frac{\hbar^2 k\,'^2_2}{2m}\right)\,|\vec{k}\,'_1\,\vec{k}\,'_2>= E\,|\vec{k}\,'_1\,\vec{k}\,'_2\rangle\end{aligned} \tag{3.130}$$

Using the completeness of the basis $|\vec{k}_1\,\vec{k}_2\rangle$ this matrix element is (see (E.10) (so called Lippman-Schwinger equation)

$$\begin{aligned}\langle\vec{k}_1\,\vec{k}_2\,|\hat{G}|\,\vec{k}\,'_1\,\vec{k}\,'_2\rangle = \langle\vec{k}_1\,\vec{k}_2\,|\hat{V}|\,\vec{k}\,'_1\,\vec{k}\,'_2\rangle + \\ \sum_{\vec{t}_1\,\vec{t}_2}\langle\vec{k}_1\,\vec{k}_2\,|\hat{V}|\,\vec{t}_1\,\vec{t}_2\rangle\,\frac{1}{E-\epsilon_{t_1}-\epsilon_{t_2}}\,\langle\vec{t}_1\,\vec{t}_2\,|\hat{G}|\,\vec{k}\,'_1\,\vec{k}\,'_2\rangle\end{aligned} \tag{3.131}$$

where $\epsilon_t = \frac{\hbar^2\,t^2}{2m}$ is the single-particle eigen-energy of the unperturbed Hamiltonian $\hat{H}_0$ (single-particle kinetic energy in the case of the infinite medium). The sequential substitution of the l.h.s. into the r.h.s. of (3.131) gives the Born series for the matrix element $\langle\vec{k}_1\,\vec{k}_2|\,\hat{G}\,|\vec{k}_1\,'\,\vec{k}_2\,'\rangle$ which can be grafically interpreted as the sum over ladder diagrams (see Fig. E.1 in the Appendix E). If we take into account the linear momentum conservation then the sum over linear momenta $\vec{t}_1$, $\vec{t}_2$ in (3.132) is reduced only to the sum over one linear momentum because the matrix element $\langle\vec{k}_1\,\vec{k}_2|\,\hat{G}\,|\vec{k}_1\,'\,\vec{k}_2\,'\rangle$ depends only on 3 linear momenta (see (E.11)- (E.13)):

$$\vec{k}\,'_1+\vec{k}\,'_2=\vec{k}_1+\vec{k}_2 \quad\Rightarrow\quad \vec{q}\equiv\vec{k}\,'_1-\vec{k}_1=\vec{k}_2-\vec{k}\,'_2 \tag{3.132}$$

and we have only 3 independent momenta, e.g. $\vec{k}_1$, $\vec{k}_2$, $\vec{q}$, because remain momenta $\vec{k}\,'_1$ and $\vec{k}\,'_2$ are given by

$$\vec{k}\,'_1=\vec{q}+\vec{k}_1 \qquad\qquad \vec{k}\,'_2=\vec{k}_2-\vec{q} \tag{3.133}$$

Then

$$\begin{aligned}\langle\vec{k}_1\,\vec{k}_2\,|\,\hat{G}\,|\,\vec{k}\,'_1\,\vec{k}\,'_2\rangle &= G(\vec{k}_1,\,\vec{k}_2,\,\vec{q}) \\ \langle\vec{k}_1\,\vec{k}_2\,|\,\hat{V}\,|\,\vec{k}\,'_1\,\vec{k}\,'_2\rangle &= \boxed{\begin{array}{c}\text{usually is}\\ \text{dependent only on } \vec{q}\end{array}} = V(\vec{q}\,)\end{aligned} \tag{3.134}$$

and the Lippman-Schwinger equation(3.131) can be rewritten as follows ($\sum_{\vec{t}_1\,\vec{t}_2} \to \sum_{\vec{k}} \to \int \frac{d^3k}{(2\pi)^3}$)

$$G(\vec{k}_1,\,\vec{k}_2,\,\vec{q}) = V(\vec{q}) + \\ + \int \frac{d^3k}{(2\pi)^3} V(\vec{q}-\vec{k}) \frac{1}{\frac{\hbar^2 k_1^2}{2m} + \frac{\hbar^2 k_2^2}{2m} - \frac{\hbar^2(\vec{k}_1+\vec{k})^2}{2m} - \frac{\hbar^2(\vec{k}_2-\vec{k})^2}{2m}} G(\vec{k}_1,\,\vec{k}_2,\,\vec{k}) \tag{3.135}$$

In the standard Lippman-Schwinger equation (3.131) there is no restriction on intermediate states (all states $\mid t_1\, t_2\rangle$ participate in the sum on the r.h.s. of (3.131)). For many-fermion systems (including the nucleus) the Pauli principle claims that all states $\mid t_1\, t_2\rangle$ with the momenta $\vec{t}_1$ and $\vec{t}_2$ inside the Fermi sphere (k_F is the modulus of the Fermi linear momentum)

$$\frac{\hbar^2 t_1^2}{2m} \le \frac{\hbar^2 k_F^2}{2m} \qquad\qquad \frac{\hbar^2 t_2^2}{2m} \le \frac{\hbar^2 k_F^2}{2m} \tag{3.136}$$

are occupied by one nucleon and that such states cannot be occupied once more. Therefore all intermediate states $\mid t_1\, t_2\rangle$ fulfilling (3.136) should be excluded from the sum $\sum_{\vec{t}_1\vec{t}_2}$ in (3.131). For equation (3.135) it means the following modification (see also (E.16), (E.17))

$$G(\vec{k}_1,\,\vec{k}_2,\,\vec{q}) = V(\vec{q}) + \\ + \int \frac{d^3k}{(2\pi)^3} V(\vec{q}-\vec{k}) \frac{(1-n_{\vec{k}_1+\vec{k}})\,(1-n_{\vec{k}_2-\vec{k}})}{\frac{\hbar^2 k_1^2}{2m} + \frac{\hbar^2 k_2^2}{2m} - \frac{\hbar^2(\vec{k}_1+\vec{k})^2}{2m} - \frac{\hbar^2(\vec{k}_2-\vec{k})^2}{2m}} G(\vec{k}_1,\,\vec{k}_2,\,\vec{k}) \tag{3.137}$$

where $n_{\vec{k}}$ is the usual Fermi distribution function (in the zero temperature)

$$n_{\vec{k}} = \begin{cases} 1 & \text{if } k \le k_F, \\ 0 & \text{if } k \ge k_F, \end{cases} \tag{3.138}$$

The equation (3.137) is called Bethe-Goldstone equation and the operator (or matrix) G is known in the literature as the G-matrix. Since the equation (3.137) depends on k_F it means that the G-matrix depends effectively on the medium (nuclear) density (the relation between the density ρ and Fermi linear momentum k_F for 3-dimensional Fermi gas of non-interacting particle is $\rho = \frac{k_F^3}{3\,\pi^2}$ (see e.g. (H.7)). One should also realize that the Bethe-Goldstone equation (3.138) is self-consistent and itis solved numerically for all possible values of $\vec{q}$ when $\vec{k}_1$ and $\vec{k}_2$ are fixed.

The single-particle unperturbed eigen-state $|\vec{k}\rangle$ of the unperturbed Hamiltonian $\hat{H}_0 = \hat{T}$ with the energy $\frac{\hbar^2 k^2}{2m}$ are represented in the coordinate representation by the plane waves $\langle\vec{r}|\vec{k}\rangle = \frac{1}{(2\pi)^3}\, e^{i\vec{k}\vec{r}}$. However, the usage of the plane waves as the intermediate single-particle states in the expr. (3.137) is relevant only in the case when the nuclear medium is infinite and homogeneous and the system of nucleons is taken as the Fermi gas of non-interacting particles with the Hamiltonian $\hat{H}_0$ given by the kinetic energy. Within such approximation the self-consistent solving of the Bethe-Goldsstone equation for infinite nuclear medium was made for the first time by K.A. Brueckner in the 50-ties (see [18]), and therefore this theory was called as Bethe-Brueckner theory. This theory is relatively simple in the non-relativistic case of the infinite nuclear medium. The problem of the effective interaction (G-matrix) is more complicated in the case of finite systems (realistic nucleus) when in each step of the itterative solving of the self-consistent equation (3.137) the intermediate states should be determined (e.g. by the Hartree-Fock method discussed in the following Chapter 4). The corresponding complex theory is known as the Brueckner-Hartree-Fock (BHF) method.

The complexity of the BHF method in the numerical solution of the finite system caused in the 70-ties and 80-ties its approximate simplification. The possible way was to use the G-matrix for the infinite homogeneous system in the successive HF self-consistent calculations where the G-interaction is taken as the effective N-N interaction for the corresponding finite system (see e.g. [27]). This approach was called as the Local Density Approximation (LDA).

In the exact approach of the determination of the effective N-N interaction in the presence of all other nucleons in the given nucleus the mentioned above BHF method should be used when the phenomenological or semi-phenomenological potentials discussed in the previous subsection 3.1.3 are taken as the initial bare N-N potentials (e.g. Reid's or Bonn potentials). As it was mentioned the form and all parameters of these bare potentials were set from the Feynman diagrams involving meson exchanges of different orders and from the fitting of all bare potential parameters in order to reproduce the N-N scattering phase shifts and deuteron data. Then, after the solving of the self-consistent Brueckner-Bethe BHF equations we obtain G-matrix which is used in subsequent calculations of the structure properties of heavier nuclei (HF, HFB, or RPA calculations discussed in next sections) as the effective N-N interaction.

Generally, the Brueckner-Bethe equation provides G-matrix in the non-

local form in the coordinate representation (for the non-local character of a two-particle operator see (B.17)). This causes some technical problems in calculations. Therefore in the subsequent HF and other calculations this non-local G-interaction is sometimes approximated by the sum of local functions depending on the Fermi linear momentum k_F. Effective N-N potential is often divided into the central part $V_C(r)$, spin-orbital part $V_{LS}(r)\,\vec{L}\cdot\vec{S} = V_{LS}(r)\,\vec{L}\cdot(\vec{\sigma}_1+\vec{\sigma}_2)$ and tensor part $V_T(r)\,\hat{S}_{12}$, $(\hat{S}_{12} = \frac{3}{r^2}\,(\vec{\sigma}_1\cdot\vec{r})\,(\vec{\sigma}_2\cdot\vec{r}) - \vec{\sigma}_1\cdot\vec{\sigma}_2)$. Then the radial function in each spin-isospin channel is approximated by the following sum.

$$V(r) = \sum_i C_i(k_F)\, e^{-\frac{r^2}{\lambda_i^2}} \tag{3.139}$$

where coefficients $C_i(k_F)$ and ranges λ_i for each value of the density of nuclear matter (which is unambiquously related to the Fermi momentum k_F) are fitted in order to obtain the good agreement of the local approximation of the effective interaction with the non-local G-matrix obtained from the exact solving of the Brueckner-Bethe equation. Such procedure was used in the paper [27] for the investigation of the different binding energy per nucleon (B/A) dependencies on k_F for different parametrizations (3.139) fitted to the exact G-matrix solution of the Brueckner-Bethe equation with the bare Reid's potential. This B/A binding energy is demonstrated in the Fig. 3.7.

The saturation point (i.e. minimum of the curves in the Fig. 3.7) is found to correspond to equilibrium density $\rho = \frac{k_F^3}{3\pi^2}$ (see (H.7)) with $k_F \cong 1.2 - 1.5\; fm^{-1}$. Experimental value of k_F (extracted from the extrapolation $A \to \infty$ of mass densities of heavy nuclei), $k_F = 1.37\, fm^{-1}$, is too low in the comparison with the value $k_F = 1.43\, fm^{-1}$ corresponding to the minimum of the curve with the mark Reid (exact solution of the Brueckner-Bethe equation with the bare Reid potential). Simultaneously infinite homogeneous nuclear matter minimal binding energy $B/A \approx -11$ MeV is too small with respect to the "experimental" value -15.68 MeV. [2] This is due to the fact that the G-matrix from the Brueckner-Bethe equation (3.138) takes into account only two-body contributions to the ladder diagrams. The three-body and four-body contributions to B/A are important, and when added to the previous

[2] From experimental values of the binding energy B/A for real finite nuclei (see e.g. Fig. 1.1 in the Section 1.1.3) we know that average value is ≈ -8 MeV. This value corresponds to the Weizsacker empirical formula (1.13) with parameters (1.14). For the infinite nuclear matter the relevant term in the Wiszacker formula (1.13) is only the first term, $b_V\, A$ $(b_V = -15.68\, MeV)$, all other terms concern only finite nuclei (we neglect here relatively small correction from the Coulomb term). So, for the infinite nuclear matter we take the value $B/A \approx b_V = -15.68$ MeV as the "experimental" value. The equilibrium density for finite nuclei is $\rho \approx 0.16\, fm^{-3}$ which corresponds to $k_F \approx 1.46\, fm^{-1}$.

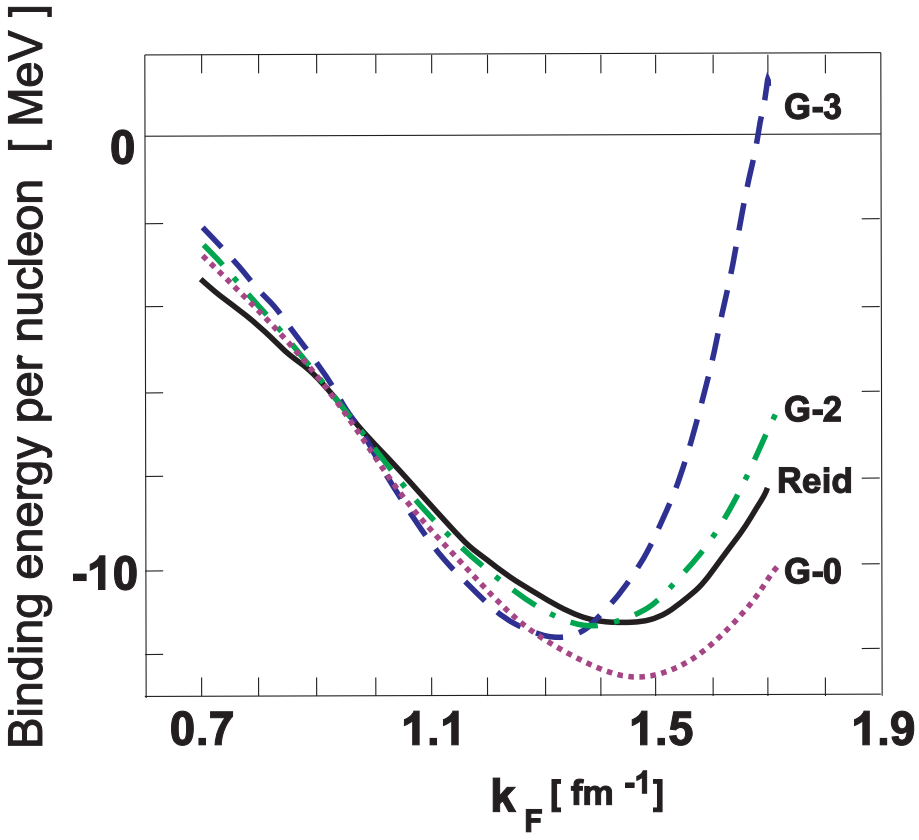


Figure 3.7: Binding energy per nucleon as a function of the Fermi momentum k_F obtained from Brueckner-Bethe equation for the infinite nuclear matter with the Reid's potential. The curve denoted by the mark Reid was obtained from the HF calculation with the exact solution of the Brueckner-Bethe eq. with Reid's potential. Curves with marks $G_0 - G_3$ corresponds to the binding energies B/A from the HF calculations with different parametrizations (3.40) fitted to the exact G-matrix with Reid's potebtial (see [27] for details).

ones make the calculated energy values B/A closer to the "experimental" value. Since it is very difficult to calculate accurately the three-body and four-body contributions to the effective interaction, what one does is simply to renormalize in an empirical way the effective interaction by slightly changing some of the Gaussian ranges in (3.139). In this way, by introducing two further parameters, it was possible to have saturation at $k_F = 1.35\, fm^{-1}$ and $B/A \approx -16.0$ MeV. Such effective renormalized interaction was then used for the HF calculation in finite nuclei using the lokal density approximation, in which k_F was replaced by it relation with density (see [28], [29], [30]). It should be noted that the Brueckner-Bethe equation method for the determination of effective interaction is used not only in nuclear physics but also in the case of other quantum systems - e.g. [31].

The Brueckner-Bethe theory is not the only microscopical theory for the

determination of the effective N-N interactions in nuclei from the bare N-N interaction in the vacuum. For instance in the paper [26] so called Unitary Correlation Operator Method (UCOM) was introduced. This method enables to transform the nucleus Hamiltonian involving kinetic energy, two-body, three-body and higher-body bare potentials into the correlated Hamiltonian with the effective interaction suitable for successive Hartree-Fock (HF) or Hartree-Fock-Bogoliubov (HFB) (or possible HFB+RPA) calculations. This unitary transformation does not contain any free parameters (all its parameters were determined from deuteron, triton, ^{3}He nuclei data and/or from ab initio calculations for very light nuclei (see e.g. [32]).

3.2.2 Semi-phenomenological effective nucleon-nucleon interaction

Microscopical theories of the effective nucleon-nucleon interactions in the finite nuclei (like Brueckner-Bethe theory described in the previous subsection or UCOM approach) are technically complicated and unambiguous. Therefore, for the practical numerical reason (especially for heavy nuclei) the semi-phenomenological effective N-N potentials are used. The form of these potentials has usually deeper theoretical background but they contain a lot of free parameters which should be determined by means of fitting to selected experimental data. Usually these parameters are specified by the requirement that Hartree-Fock or Hartree-Fock-Bogoliubov calculations with these effective potentials reproduce binding energy, radius and compressibility of selected double-magic nuclei.

The form of phenomenological potentials are often estimated from the expansion of the matrix elements of these potentials in the linear momentum space. Therefore, at first we will analyze the form of the effective potential in the spatial space corresponding to the lowest order terms of the expansion of this potential in the linear momentum space.

From the previous discussions we know that the bare N-N interaction is very short-range. This is true also for the range of the effective G-matrix discussed in the previous subsection 3.2.1. Therefore, the most simple ansatz is to suppose that the main contribution to the effective potential goes from the zero-range part described in the spatial space by the δ- function. The more realistic interaction has finite range but the finite range of the poten-

tial can be simulated by the linear momentum (or velocity) dependence in the coordinate representation. In order to show this we will transform the function $V(\vec{r}_1, \vec{r}_2) = V(\vec{r} = \vec{r}_1 - \vec{r}_2)$ (the effective potential) of the relative coordinate $\vec{r} = \vec{r}_1 - \vec{r}_2$ into the linear momentum space (further we use the symbol $\vec{p}$ for relative linear momentum of two interacting nucleons). At first we suppose the contact potential, $V(\vec{r}_1 - \vec{r}_2) = V_0\ \delta(\vec{r}_1 - \vec{r}_2)$. The linear momentum representation of the matrix element of the contact potential is [3]

$$\begin{aligned}
\langle \vec{p}\,|\,\hat{V}\,|\,\vec{p}\,'\rangle &= \int d^3r_1 \int d^3r_2\ \langle \vec{p}|\vec{r}_1\rangle\ \langle \vec{r}_1|\,\hat{V}\,|\vec{r}_2\rangle\ \langle \vec{r}_2|\vec{p}\,'\rangle = \\
&= \int d^3r_1 \int d^3r_2\ \langle \vec{p}\,|\,\vec{r}_1\rangle\ V(\vec{r}_1 - \vec{r}_2)\ \langle \vec{r}_2\,|\,\vec{p}\,'\rangle\ = \\
&= \boxed{\begin{array}{c}\text{because for local contact potential} \\ V(\vec{r}_1 - \vec{r}_2) = V_0\,\delta(\vec{r}_1 - \vec{r}_2)\end{array}} = \\
&= \int d^3r_1 \int d^3r_2\ \langle \vec{p}\,|\,\vec{r}_1\rangle\ \delta(\vec{r}_1 - \vec{r}_2)\ V_0\ \langle \vec{r}_2\,|\,\vec{p}\,'\rangle\ \equiv \\
&\equiv\ V_0\ \langle \vec{p}\,|\,\vec{p}\,'\rangle = V_0\,\delta(\vec{p} - \vec{p}\,')
\end{aligned} \tag{3.141}$$

So, the δ - interaction in the coordinate space is represented by the constant in the linear momentum space.

The general finite range potential in the coordinate representation is represented by the operator depending on the relative coordinate $\vec{r}$ and on the relative linear momentum operator $\hat{\vec{p}} = -i\,\hbar\,\vec{\nabla}$. The most simple rotationally invariant form of this contact potential is

$$\hat{V} = V_0\,\delta(\vec{r}) + V_1\ \left[\,\hat{\vec{p}}^{\,2}\,\delta(\vec{r}) + \delta(\vec{r})\,\hat{\vec{p}}^{\,2}\,\right] + V_2\,\hat{\vec{p}}\ \delta(\vec{r})\ \hat{\vec{p}} \tag{3.142}$$

[3] From the Appendix B (see (B.18) we know the general coordinate representation form of the two-body local potential is

$$V(\vec{r}_1, \vec{r}_2, \vec{r}_3, \vec{r}_4) = \delta(\vec{r}_1 - \vec{r}_3)\,\delta(\vec{r}_2 - \vec{r}_4)\,V(\vec{r}_1 - \vec{r}_2)$$

If moreover the local potential is contact then

$$V(\vec{r}_1, \vec{r}_2) = V(\vec{r}_1 - \vec{r}_2) = V_0\,\delta(\vec{r}_1 - \vec{r}_2) \tag{3.140}$$

with the following matrix elements

$$
\begin{aligned}
&\langle \vec{p} \,|\, \hat{V} \,|\, \vec{p}\,' \rangle = \\
&= \int d^3 r_1 \int d^3 r_2 \langle \vec{p} \,|\, \vec{r}_1 \rangle \, \langle \vec{r}_1 \,|\, \hat{V} \,|\, \vec{r}_2 \rangle \, \langle \vec{r}_2 \,|\, \vec{p}\,' \rangle = \\
&= \frac{1}{(2\pi\hbar)^3} \int d^3 r_1 \int d^3 r_2 \; e^{-\frac{i}{\hbar}\vec{p}\cdot\vec{r}_1} \\
&\quad \Big[V_0 \, \delta(\vec{r}_1 - \vec{r}_2) + V_1 \, \hat{\vec{p}}^{\,2} \, \delta(\vec{r}_1 - \vec{r}_2) + \\
&\qquad + \qquad V_1 \, \delta(\vec{r}_1 - \vec{r}_2) \, \hat{\vec{p}}^{\,2} + V_2 \, \hat{\vec{p}} \; \delta(\vec{r}_1 - \vec{r}_2) \; \hat{\vec{p}} \Big] \; e^{\frac{i}{\hbar}\vec{p}\,'\cdot\vec{r}_2} = \\
&= \boxed{\begin{array}{c} \text{because the operator } \hat{\vec{p}} \\ \text{is Hermitian} \end{array}} = \\
&= \frac{V_0}{(2\pi\hbar)^3} \int d^3 r e^{\frac{i}{\hbar}(\vec{p}\,' - \vec{p})\cdot\vec{r}} + \\
&\qquad + \frac{V_1}{(2\pi\hbar)^3} \int d^3 r e^{\frac{i}{\hbar}\vec{p}\,'\cdot\vec{r}} [i\hbar\vec{\nabla}]^2 \, e^{\frac{-i}{\hbar}\vec{p}\cdot\vec{r}} + \\
&\qquad\quad + \frac{V_1}{(2\pi\hbar)^3} \int d^3 r \, e^{\frac{-i}{\hbar}\vec{p}\cdot\vec{r}} [-i\hbar\vec{\nabla}]^2 \, e^{\frac{i}{\hbar}\vec{p}\,'\cdot\vec{r}} + \\
&\qquad\quad\quad + \frac{V_2}{(2\pi\hbar)^3} \int d^3 r \, [\, i\hbar\vec{\nabla} \, e^{\frac{-i}{\hbar}\vec{p}\cdot\vec{r}} \,] \, [\, -i\hbar\vec{\nabla} \, e^{\frac{i}{\hbar}\vec{p}\cdot\vec{r}} \,] = \\
&= \delta(\vec{p} - \vec{p}\,') \big(V_0 + V_1 \, \vec{p}^{\,2} + V_1 \, \vec{p}\,'^{\,2} + V_2 \, \vec{p} \cdot \vec{p}\,' \big)
\end{aligned}
\tag{3.143}
$$

One can see that this is the most simple expression in the linear momentum space, it contain the diagonal constant term and terms depending on squares of linear momenta $\vec{p}$ and $\vec{p}\,'$ and on the scalar product $\vec{p}\cdot\vec{p}\,'$. So, in the first approximation the basic form of the spatial part of the effective N-N potential in the coordinate representation is given by rel. (3.142). This spatial part should be combined with the spin and isospin parts and obtained terms of the effective N-N interaction in the whole spatial-spin-isospin Hilbert space form the basic terms of the so called Skyrme interaction discussed below (see also Section 5.2).

3.2.2.1 Skyrme effective nucleon-nucleon interaction

Above discussions around the expression (3.142) lead in fifties to the introduction of the effective phenomenological N-N interaction in the following

form (so called Skyrme effective interaction - see [20])

$$\hat{V} = \sum_{i<j} \hat{V}(i,j) + \sum_{i<j<k} \hat{V}(i,j,k) \tag{3.144}$$

where except terms involved in (3.142) the two-body part $V(i,j)$ contains also the spin-orbit term (last term in (3.145):

$$\begin{aligned} V(1,2) &= t_0\,(1+\kappa_0\,\hat{P}^{\,(\sigma)}_{12})\,\delta(\vec{r}_1-\vec{r}_2) + \\ &+\frac{1}{2}t_1\,[\,\delta(\vec{r}_1-\vec{r}_2)\overleftarrow{k}^{\,2} + \overrightarrow{k}^{\,2}\,\delta(\vec{r}_1-\vec{r}_2)\,] + \, t_2\,\overleftarrow{k}\,\delta(\vec{r}_1-\vec{r}_2)\,\overrightarrow{k}\, + \\ &+ i\,W_0\,(\vec{\sigma}_1+\vec{\sigma}_2)\cdot[\,\overleftarrow{k}\times\delta(\vec{r}_1-\vec{r}_2)\,\overrightarrow{k}\,] \end{aligned} \tag{3.145}$$

and Skyrme effective interaction involves also contact three-body term (last term in (3.144)):

$$V(1,2,3) = t_3\,\delta(\vec{r}_1-\vec{r}_2)\,\delta(\vec{r}_2-\vec{r}_3) \tag{3.146}$$

In (3.144)-(3.146) $\hat{P}^{\,(\sigma)}_{12}$ stands for the spin exchange operator (see (3.123)), $\overrightarrow{k} = \frac{1}{2i}(\overrightarrow{\nabla}_1 - \overrightarrow{\nabla}_2)$ acts to right, $\overleftarrow{k} = \frac{1}{2i}(\overleftarrow{\nabla}_1 - \overleftarrow{\nabla}_2)$ acts to left, and t_0, t_1, t_2, W_0, κ_0 are free parameters. These parameters (as it was already mentioned) are determined by the fitting the values of some nuclear properties of some double-magic nuclei (binding energy, nuclear radius, compressibility of the nuclear matter) calculated in terms of HF or HFB method to the corresponding experimental data. However, in such a way obtained parameters are not unambiguous and today a lot of Skyrme parametrizations exist which describe the properties above on the same level (each such parametrization describes some other, its own, properties better than other parametrizations). The Skyrme effective interaction parametrizations and some HF results obtained with them are discussed in more details in the Section 5.2.

3.2.2.2 Gogny effective nucleon-nucleon interaction

Another effective N-N interaction, which is often used up to now, is the finite-range Gogny interaction. Its phenomenological form is similar to that of phenomenological bare N-N interaction (3.124), only the Gaussian finite

range radial dependence is added (see e.g. [34])

$$\hat{V}(1,2) = \sum_{i=1}^{2} e^{-\frac{(\vec{r}_1-\vec{r}_2)^2}{\mu_i^2}} \left(W_i + B_i\, \hat{P}_{12}^{(\sigma)} + H_i\, \hat{P}_{12}^{(\tau)} + M_i\, \hat{P}_{12}^{(\sigma)}\, \hat{P}_{12}^{(\tau)} \right) +$$
$$+ i\, W_0\, (\vec{\sigma}_1 + \vec{\sigma}_2) \cdot [\overleftarrow{k} \times \delta(\vec{r}_1 - \vec{r}_2)\, \overrightarrow{k}] +$$
$$+ t_3\, (1 + \hat{P}_{12}^{(\sigma)})\, \delta(\vec{r}_1 - \vec{r}_2)\, \rho^{1/3}(\frac{\vec{r}_1 + \vec{r}_2}{2}) \qquad (3.147)$$

where $\hat{P}_{12}^{(\sigma)}$, $\hat{P}_{12}^{(\tau)}$ are spin and isospin exchange operators, respectively (see (3.122)), $\rho(\vec{r})$ is nuclear matter density [4] . Parameters μ_i, W_i, H_i, W_0 and t_3 are, similarly as for the Skyrme force, fitted to binding energies, nuclear radii and compressibility of selected double-magic nuclei.

3.2.3 Relativistic mean field approach

As it was mentioned several times the aim of the introducing the effective N-N interaction is to use it in successive Hartree-Fock (HF) and other calculations of the finite nucleus characteristics. The HF or HFB calculations give us the nuclear mean field with its single-particle basis (this will be discussed in details in Chapters 4, 5, 6). Relativistic Mean Field (RMF) approach does not provide the effective N-N potential explicitly but gives directly nuclear mean field single-particle states and energies (see e.g. [35] and citations therein) [5]. Since the theory of the RMF method is quite complicated and it is beyond the scope of this textbook here only very brief description of the basic idea is given.

The starting point of the relativistic mean field theory is the meson exchange picture of the strong-nucleon interaction (similar to that discussed in the Subsection 3.1.3.2 for meson exchange bare N-N interaction). In the RMF approach the nucleus is described as a system of nucleons, represented by the Dirac fields, interacting through the exchange of several intermediate-boson fields. Similarly as in the Subsection 3.1.3.2 for the bare N-N interaction the

[4] Density dependent term in the Gogny interaction was introduced in order to simulate a G-matrix through explicit dependence on the density $\rho(\vec{r})$

[5] In this textbook only Relativistic Mean Field (RMF) theory is discussed. The original RMF theory (see [36]) was later developed to so called Relativistic Hartree Bogoliubov (RHB) theory which includes also the pairing particle-particle interaction into account (see [35]).

isoscalar-scalar σ-meson field is responsible for the attraction between nucleons, whereas the isoscalar-vector ω-meson field is introduced to tune the isospin interaction. Finally, the photon field (A) accounts for the electromagnetic interaction. The π and η mesons with unnatural parity are not included in the original RMF approach because usually we work with nuclear states which have well-defined parity (in the RMF approach we restrict ourselves only to one-meson exchange diagrams - see e.g. [36]). RMF method uses the relativistic formalism of the quantum field theory. The model Lagrangian density reads (up to the end of this subsection we use $\hbar = c = 1$ convention)

$$\begin{aligned}
\mathscr{L}_{RMF}(x) &= \bar{\Psi}\left[\, i\not{D} - (m_N - g_{\sigma N}\sigma)\right]\Psi \; + \\
&+\frac{1}{2}\,\partial_\mu\sigma\,\partial^{\,\mu}\sigma - \frac{1}{2}m_\sigma^2\sigma^2 + \frac{1}{3}\,g_2\,\sigma^3 - \frac{1}{2}\,g_3\,\sigma^4 \\
&-\frac{1}{2}\,\left(\partial_\mu\omega_\nu - \partial_\nu\omega_\mu\right)\,\left(\partial^{\,\mu}\omega^\nu - \partial^{\,\nu}\omega^\mu\right) + \frac{1}{2}m_\omega^2\,\omega_\mu\,\omega^\mu + \frac{1}{4}d\,(\omega_\mu\,\omega^\mu)^2 \\
&-\frac{1}{4}\,\left(\partial_\mu\vec{\rho}_\nu - \partial_\nu\vec{\rho}_\mu\right)\,\left(\partial^{\,\mu}\vec{\rho}^{\,\nu} - \partial^{\,\nu}\vec{\rho}^{\,\mu}\right) + \frac{1}{2}m_\rho^2\,\vec{\rho}_\mu\cdot\vec{\rho}^{\,\mu} \\
&-\frac{1}{4}\,\left(\partial_\mu A_\mu - \partial_\nu A_\mu\right)\,\left(\partial^{\,\mu}A^\mu - \partial^{\,\nu}A^\mu\right)
\end{aligned} \tag{3.148}$$

where $\sigma = \sigma(x)$, $\omega_\mu = \omega_\mu(x)$, $\vec{\rho}_\mu = \vec{\rho}_\mu(x)$, $A^\mu = A^\mu(x)$ are corresponding meson and electromagnetic fields ($x = (ct,\ \vec{r}\ )$ is the coordinate in the Minkowski time-spatial space) and $\Psi = \Psi(x)$ is the nucleon- isospin doublet spinor

$$\Psi = \begin{pmatrix}\psi_p\\ \psi_n\end{pmatrix} \tag{3.149}$$

In (3.148) $\not{D} = \gamma^\mu\,D_\mu$ where D_μ is covariant derivative

$$D_\mu = \partial_\mu + i\,g_{\omega N}\,\omega + i\,\vec{\rho}_\mu\cdot\vec{\tau} + ie\frac{1}{2}\,(1+\tau_3)\,A_\mu \tag{3.150}$$

The arrow indicates the vector in the isospin space and $\vec{\tau}$ stands for the triplet of Pauli isospin matrices. The m_σ, m_ω and m_ρ are σ, ω, and ρ meson masses, respectively. The g_2, g_3 and d represent the strength of the scalar σ and vector ω field self-interaction. The meson coupling constants are specified by the RMF model parametrization. Similarly as in the case of the Skyrme effective interaction at the present time there are several RMF parametrizations (see e.g. [37]).

Using the standard Lagrange method for obtaining the motion equation known from any textbook of the quantum field theory (see also Subsection

2.1.2, but now we should use relativistic version) the Lagrangian density (3.148) yields the Dirac equation for nucleons

$$\left[i\,\partial\!\!\!/ - (m_N - g_{\sigma N}\,\sigma) - g_{\omega N}\,\gamma_\mu\,\omega^\mu \right. \\ \left. - g_{\rho N}\,\gamma_\mu\,\vec{\tau}\cdot\vec{\rho}^{\,\mu} - \gamma_\mu\,\frac{e}{2}\,(1+\tau_3)\,A^\mu\right]\,\Psi = 0 \tag{3.151}$$

and the Klein-Gordon, Proca, and Maxwell equations for the intermediate boson fields

$$\begin{aligned}
&\left(\partial_\nu\,\partial^{\,\nu} + m_\sigma^2\right)\,\sigma = g_{\sigma N}\bar{\Psi}\,\Psi + g_2\,\sigma^2 - g_3\,\sigma^3 \\
&\partial_\mu\,\left(\partial^{\,\mu}\,\omega^{\,\nu} - \partial^{\,\nu}\,\omega^{\,\mu}\right) + m_\omega^2\,\omega^{\,\nu} = g_{\omega N}\,\bar{\Psi}\,\gamma^\nu\,\Psi - d\,\omega^{\,\nu}\,\left(\omega_\mu\,\omega^{\,\mu}\right) \\
&\left(\partial_\mu - g_{\rho N}\,\vec{\rho}_\mu\times\right)\,\left(\partial^{\,\mu}\,\vec{\rho}^{\,\nu} - \partial^{\,\nu}\,\vec{\rho}^{\,\mu}\right) + m_\rho^2\,\vec{\rho}^{\,\nu} = g_{\rho N}\,\bar{\Psi}\,\gamma^\nu\,\vec{\tau}\,\Psi \\
&\partial_\mu\,\left(\partial^{\,\mu}\,A^\nu - \partial^{\,\nu}\,A^\mu\right) = e\,\bar{\Psi}\,\frac{1}{2}\,\left(1+\tau_3\right)\,\gamma^{\,\nu}\,\Psi
\end{aligned} \tag{3.152}$$

Equations (3.151), (3.152) are coupled non-linear quantum field equations and their exact solution is enormously complicated. Moreover, since we expect the coupling constants (except e) to be large, perturbative approaches are not useful. Fortunately, there exist an approximate solution, which becomes more and more valid as the nuclear density increases (see [36]). Namely, as the source terms on the r.h.s. of eq. (3.152) increase, the meson field operators can be replaced by their vacuum expectation values, which are classical fields.

Furthermore, symmetries simplify calculations considerably. For instance, if we look for the nuclear ground state of magic (spherical) nuclei, the rotational invariance implies that the angle part of the space-like components of the intermediate boson fields vanish. In this case the meson fields and also the source terms on the r.h.s. of equations of motion (3.152) depend only on the radial coordinate r. The electromagnetic charge conservation prohibits the charged component of the ρ-meson from appearing as classical fields. Finally, since we look for stationary states, the time derivatives of the boson fields vanish. Altogether, the meson fields are replaced by:

$$\begin{aligned}
\sigma(x) &\rightarrow \langle\sigma(x)\rangle = \sigma(r) \\
\omega_\mu(x) &\rightarrow \langle\omega_\mu(x)\rangle = \delta_{\mu\,0}\,\omega(r) \\
\rho_\mu^i(x) &\rightarrow \langle\rho_\mu^i(x)\rangle = \delta_{\mu\,0}\,\delta^{i\,3}\,\rho(r) \\
A_\mu(x) &\rightarrow \langle A_\mu(x)\rangle = \delta_{\mu\,0}\,A(r)
\end{aligned} \tag{3.153}$$

In the traditional RMF approach so called no-sea approximation of the nucleon field operator is used when the nucleon field operator is expanded as:

$$\Psi(x) = \sum_{i \leq A} \Psi_i(x)\, a_i \tag{3.154}$$

where a_i is the annihilation operator of the nucleon in the single-particle state i with the single-particle wave function $\Psi_i(x)$. In (3.155) the summation runs only over occupied positive-energy levels. With these assumptions we can write the field equation (3.152) - (3.153) in the following form.

$$\begin{aligned}
&\Big[-i\vec{\alpha}\cdot\vec{\nabla} + (m_N - g_{\sigma N}\,\sigma)\;\beta + \\
&\qquad\qquad + g_{\omega N}\,\omega + g_{\rho N}\,\tau_3\,\rho + \frac{e}{2}\;(1+\tau_3)\;A\Big]\;\Psi_i = E_i\,\Psi_i \\
&\left(-\nabla^2 + m_\sigma^2\right)\;\sigma = g_{\sigma N}\,\rho_s + g_2\,\sigma^2 - g_3\,\sigma^3 \\
&\left(-\nabla^2 + m_\omega^2\right)\;\omega = g_{\omega N}\,\rho_v - d\,\omega^4 \\
&\left(-\nabla^2 + m_\rho^2\right)\;\rho = g_{\rho n}\,\rho_3 \\
&\qquad -\nabla^2\,A_0 = e\,\rho_p
\end{aligned} \tag{3.155}$$

where matrices $\vec{\alpha}$ and β are connected with the standard γ-matrices from quantum field theory by well-known formulas, $\beta = \gamma^0$ and $\gamma^i = \beta\,\alpha_i$ ($i = 1,2,3$) and $E_i = i\partial_t\,\Psi_i$.

The densities on the r.h.s of (3.155) are defined as [6]

$$\begin{aligned}
\rho_s &= \langle 0| : \bar{\Psi}\,\Psi : |0\rangle = \sum_{i\leq A} \bar{\Psi}_i\,\Psi_i \\
\rho_v &= \langle 0| : \Psi^+\,\Psi : |0\rangle = \sum_{i\leq A} \Psi_i^+\,\Psi_i \\
\rho_3 &= \langle 0| : \Psi^+\,\tau_3\,\Psi : |0\rangle = \sum_{i\leq A} \Psi_i^+\,\tau_3\,\Psi_i \\
\rho_p &= \langle 0| : \Psi^+ \frac{1}{2}\,(1+\;\tau_3)\;\Psi : |0\rangle = \sum_{i\leq A} \Psi_i^+ \frac{1}{2}\,(1+\;\tau_3)\;\Psi_i
\end{aligned} \tag{3.156}$$

where no-sea approximation allows simple evaluation of the vacuum ($\equiv$ nuclear ground state) expectation values of normal ordered quantum field operator $\langle 0| : \ldots : |0\rangle$. The vector densities are normalized accordingly to the

[6] Here we do not take into account pairing correlations discussed in the Chapter 6. For the modification of exprs. (3.157) for the case when the pairing is taken into account - see [35]

number of protons and neutrons:

$$\begin{aligned} \int d^3x \rho_v(x) &= A \\ \int d^3x \rho_3(x) &= N - Z \\ \int d^3x \rho_p(x) &= Z \end{aligned} \tag{3.157}$$

with the nucleon number A, proton number Z, and neutron number N.

The total energy of the system E is a vacuum expectation value of the Hamiltonian via Legendre transform of the Lagrangian

$$\begin{aligned} E &= \langle 0| : p_i \dot{q}_i - L : |0\rangle = \\ &= \int d^3x \, \left(E_i \, \Psi_i^+ \, \Psi_i - \langle 0| : \mathscr{L}_{RMF}(x) : |0\rangle \right) = \\ &= \int d^3x \left\{ \langle 0| : \bar{\Psi} \, \left[-i \, \vec{\alpha} \cdot \vec{\nabla} + m_N - g_{\sigma N} \, \sigma \right. \right. \\ &\qquad \left. + g_{\omega N} \, \omega + g_{\rho N} \, \tau_3 \, \rho + \frac{e}{2} \, (1 + \tau_3) \right] \, \Psi : |0\rangle + \\ &\quad + \frac{1}{2} \, \left[(\nabla \sigma)^2 + m_\sigma^2 \, \sigma^2 \right] - \frac{1}{2} \, \left[(\nabla \omega)^2 + m_\omega^2 \, \omega^2 \right] \\ &\quad \left. - \frac{1}{2} \, \left[(\nabla \rho)^2 + m_\rho^2 \, \rho^2 \right] - \frac{1}{2} \, (\nabla \, A)^2 - \frac{1}{3} \, g_2 \, \sigma^3 + \frac{1}{4} \, d \, \omega^4 \right\} \end{aligned} \tag{3.158}$$

The vanishing of boson fields at large distances allows to perform the following partial integration

$$\begin{aligned} \frac{1}{2} \int d^3x \, \left[(\nabla \, \sigma)^2 + m_\sigma^2 \, \sigma^2 \right] &= \frac{1}{2} \int d^3x \, \sigma \, \left[-\nabla^2 + m_\sigma^2 \, \right] \, \sigma = \\ &= \frac{1}{2} \int d^3x \, \sigma \, \left(g_{\sigma N} \, \rho_s + g_2 \, \sigma^2 - g_3 \, \sigma^3 \right) \end{aligned} \tag{3.159}$$

Similar manipulation for remaining fields, using normalization conditions (3.158) and Euler-Lagrange equations (3.156), lead to the final expression

for the total energy: [7]

$$
\begin{aligned}
& E = \\
& = \sum_{i \leq A} E_i + \frac{1}{2} \int d^3x \ (g_{\sigma N}\, \sigma\, \rho_s - g_{\omega N}\, \omega\, \rho_v - g_{\rho N}\, \rho\, \rho_3 - e\, A\, \rho_p) + \\
& \quad + \frac{1}{2} \int d^3x \ \left(\frac{1}{3}\, g_2\, \sigma^3 - \frac{1}{3}\, g_3\, \sigma^4 - \frac{1}{2}\, d\, \omega^4 \right)
\end{aligned}
\tag{3.160}
$$

[7] Again it should be noted that if the pairing interaction is taken into account the expression for the total energy E involves not only terms from the r.h.s. of (3.160) but also other terms - see [35].

4. Hartree-Fock method, particle-hole formalism, basic idea of shell model

As it was mentioned in the Chapter 1 it is not possible to solve the nucleus many-body problem exactly for nuclei with the nucleon number higher than $A > 3$. For light nuclei ($A < 16$) so called ab initio calculations are possible (see e.g. [32] and citations therein) where the nuclear structure properties are calculated starting from the bare two- and three- particle nucleon-nucleon interactions using techniques with minimum approximations. However, because of technical numerical problems the ab initio calculations cannot be performed for heavier nuclei. In the present day there are two basic approaches for the theoretical determination of the structure of heavier nuclei, namely the shell model approach and mean field approach. Both these approaches are discussed in this and following chapters. Since the shell model approach for heavy nuclei (actinides and beyond) are also restricted by technical problems the main attention will be given to the mean field approach.

In this chapter the purely microscopical Hartree-Fock approach to obtain mean field is presented. This method is widely used not only in nuclear physics but also in atomic and molecular physics, in the physics of quantum dots and other nanoscale system. In the end of the chapter the basic ideas of the shell model approach is presented.

4.1 Hartree-Fock method

4.1.1 Hartree-Fock equation

We suppose the nucleus to be a quantum system described by the Hamiltonian

$$\hat{H} = \sum_i \hat{t}_i + \sum_{i<j} \hat{V}_{ij} \tag{4.1}$$

where $\hat{t}_i$ is the kinetic energy operator of i-th nucleon ($\hat{t}_i = -\frac{\hbar^2}{2M_i}\vec{\nabla}_i^2$) and $\hat{V}_{ij}$ is the effective interaction between i-th and j-th nucleons.

In the Hamiltonian (4.1) only effective two-particle interactions are involved. As it was already mentioned in the Chapter 1 it is believed that two-particle interactions play a dominant role in the determination of the nuclear characteristics. Nevertheless, in recent years there are a lot of papers where the importance of three-particle bare and effective- interactions $\sum_{i<j<k}\hat{V}_{ijk}$ have been shown (see e.g. [25, 32]). However, in many cases it is possible to transform three-particle interaction into two-particle density dependent terms. It will be discussed in the Chapter 5. Therefore here we suppose two-particle character of the potential in the Hamiltonian (4.1).

The Hartee-Fock method, discussed here, is fully microscopic approach for the determination of the nuclear mean field. Nuclear mean field is the single-particle operator involving mean potential which is felt by each nucleon as a result of averaging of all interactions of given nucleon with all other nucleons in the nucleus. The Hartree-Fock (HF) method is based on the variational principle.

In the framework of the HF approach we look for the A- fermion ground state wave function $\Psi(\xi_1, \xi_2, \ldots, \xi_A)$ of the nucleus with the Hamiltonian (4.1). Here by one symbol $\xi_i \equiv (\vec{r}_i, s_i, \tau_i)$ $(i = 1, \ldots, A)$ the particular point in the spatial-spin-isospin space is understood. Since we treat the system of fermions the ground state wave function $\Psi(\xi_1, \xi_2, \ldots, \xi_A)$ should be fully antisymmetrized according to Pauli principle. From this point of view the HF approach differs from the original Hartree method where the antisymmetrization was not required. The Pauli principle is described in more simple way if the formalism of single-particle creation and annihilation operators are used (see the Appendix B for brief introduction of these operators). In this formalism the Hamiltonian (4.1) reads (see the Subsection B.2.1 and B.2.2 in the Appendix B)

$$\hat{H} = \sum_{\alpha\beta}\langle\alpha|\hat{T}|\beta\rangle\, a_\alpha^+ a_\beta + \\ + \frac{1}{2}\sum_{\alpha\beta\gamma\delta}\langle\alpha\beta|\hat{V}|\gamma\delta\rangle\, a_\alpha^+ a_\beta^+ a_\delta\, a_\gamma \tag{4.2}$$

where

$$\langle\alpha|\vec{T}|\beta\rangle = \int d\xi\, \varphi_\alpha^*(\xi)\left(-\frac{\hbar^2}{2M}\vec{\nabla}^2\right)\varphi_\beta(\xi) \tag{4.3}$$

$$\langle\alpha\beta|\hat{V}|\gamma\delta\rangle = \boxed{\begin{array}{c}\text{for the simplicity the local two-particle}\\ \text{potential is supposed - see (B.18)}\end{array}} =$$

$$= \int d\xi_1 d\xi_2\, \varphi^*_\alpha(\xi_1)\, \varphi^*_\beta(\xi_2)\, V(\xi_1,\xi_2)\, \varphi_\gamma(\xi_1)\, \varphi_\delta(\xi_2) \tag{4.4}$$

In (4.2) a^+_α and a_α are the creation and annihilation operator of the nucleon in the single-particle state $\varphi_\alpha(\xi) = \langle\xi|\alpha\rangle$, respectively ($\{a_\alpha,\, a^+_\beta\} = \delta_{\alpha\,\beta}$).

The ground state wave function of the system of A nucleons can be expressed in terms of single-particle creation operators as follows (see also the Subsection B.3.2)

$$|HF\rangle = \prod_{\mu_<} a^+_{\mu_<}\,|0\rangle \tag{4.5}$$

where $|0\rangle$ is the state without any nucleon (vacuum for nucleons). Index $\mu_<$ is connected with the single-particle state μ with the energy below the Fermi level. In the next considerations the index $\sigma_>$ means the energy of the single-particle state σ is above the Fermi energy (see Fig. B.1). So, according to the Pauli principle the following relations valid (see also (B.25))

$$\begin{array}{lcl} a^+_{\lambda_<}\,|\,HF\rangle \;=\; 0 & \Leftrightarrow & \langle HF\,|\,a_{\lambda_<} = 0 \\ a_{\sigma_>}\,|\,HF\rangle \;=\; 0 & \Leftrightarrow & \langle HF\,|\,a^+_{\sigma_>} = 0 \end{array} \tag{4.6}$$

The ground state ket $|HF\rangle$ is expressed in the coordinate representation as the Slater determinant

$$\Psi_{\alpha_1,\alpha_2,\ldots,\alpha_A}(\xi_1,\xi_2,\ldots,\xi_A) \;=\; \langle\xi_1\xi_2\ldots\xi_A\,|\,\alpha_1\alpha_2\ldots\alpha_A\rangle \;= \\ = \frac{1}{\sqrt{A!}} \begin{vmatrix} \varphi_{\alpha_1}(\xi_1) & \varphi_{\alpha_2}(\xi_1) & \ldots & \varphi_{\alpha_A}(\xi_1) \\ \varphi_{\alpha_1}(\xi_2) & \varphi_{\alpha_2}(\xi_2) & \ldots & \varphi_{\alpha_A}(\xi_2) \\ \vdots & \vdots & \vdots & \\ \varphi_{\alpha_1}(\xi_A) & \varphi_{\alpha_2}(\xi_A) & \ldots & \varphi_{\alpha_A}(\xi_A) \end{vmatrix} \tag{4.7}$$

The single-particle wave functions $\varphi_\alpha(\xi)$ and corresponding single-particle energies ϵ_α (and therefore the corresponding nuclear mean field) are obtained in terms of the variational principle by variations of single-particle wave functions:

$$\begin{array}{lc} & \delta\langle HF\,|\hat{H}|\,HF\rangle \;=0 \\ \Rightarrow & \langle\delta\,HF\,|\hat{H}|\,HF\rangle + \langle HF\,|\hat{H}|\,\delta\,HF\rangle \;=0 \\ \Rightarrow & \langle\delta\,HF\,|\hat{H}|\,HF\rangle \;=\; \langle HF\,|\hat{H}|\,\delta\,HF\rangle \;=0 \end{array} \tag{4.8}$$

where $|\,\delta\, HF\rangle$ is the variation of the ket (4.5) or the variation of the Slater determinant (4.7) if we work in the coordinate representation. The variation of the determinant means that at least one of the single-particle functions involved in (4.7) is changed infinitesimally:

$$\varphi_{\lambda_<} \quad \longrightarrow \quad \varphi_{\lambda_<} + \eta\,\varphi_{\sigma_>} \qquad\qquad |\eta| << 1 \tag{4.9}$$

One should have in mind that in order to change the determinant in (4.7) as a result of the substitution (4.9) it is necessary the function $\varphi_{\sigma_>}$ to be orthogonal to all functions $\varphi_{\alpha_<}$ involved in (4.7) otherwise the row connected with $\varphi_{\lambda_<} + \eta\,\varphi_{\sigma_>}$ is nothing more than the linear combination of other determinant rows and the determinant remains unchanged. Therefore, the functions $\varphi_{\sigma_>}$ corresponds to some state $\sigma_>$ with the energy above the Fermi level. So, we can write

$$\varphi_{\lambda_<} \;\rightarrow\; \varphi_{\lambda_<} + \eta\,\varphi_{\sigma_>} \quad \Rightarrow \quad |\,\delta\, HF\rangle = \eta\, a^+_{\sigma_>}\, a_{\lambda_<}\,|\,HF\rangle \tag{4.10}$$

and the condition (4.8) can be rewritten as

$$\langle\, HF|\, a^+_{\lambda_<}\, a_{\sigma_>}\, \hat{H}\,|HF\rangle \;= 0 \tag{4.11}$$

The substitution of (4.2) into (4.11) gives

$$\begin{aligned}
&\sum_{\alpha\beta}\langle\alpha|\,\hat{T}\,|\beta\rangle\,\langle HF\,|a^+_{\lambda_<}a_{\sigma_>}a^+_\alpha\,a_\beta|\,HF\rangle\,+\\
&+\frac{1}{2}\sum_{\alpha\beta\gamma\delta}\langle\alpha\beta|\,\hat{V}\,|\gamma\delta\rangle\,\langle HF\,|a^+_{\lambda_<}a_{\sigma_>}a^+_\alpha\,a^+_\beta\,a_\delta\,a_\gamma|\,HF\rangle\;=\;0
\end{aligned} \tag{4.12}$$

and using the relation (4.6) with the anticommutator relation $\{a_\alpha,\, a^+_\beta\} = \delta_{\alpha\,\beta}$ we obtain for HF expectation values following expressions

$$\begin{aligned}
&\langle HF\,|a^+_{\lambda_<}a_{\sigma_>}a^+_\alpha\,a_\beta|\,HF\rangle\,=\\
&\qquad=\;\langle HF\,|a^+_{\lambda_<}\left(\delta_{\sigma_>\,\alpha}-a^+_\alpha\,a_{\sigma_>}\right)\,a_\beta|\,HF\rangle\;=\;\delta_{\sigma_>\,\alpha}\,\delta_{\lambda_<\,\beta}\\
&\langle HF\,|a^+_{\lambda_<}a_{\sigma_>}a^+_\alpha\,a^+_\beta\,a_\delta\,a_\gamma|\,HF\rangle\,=\\
&\qquad=\delta_{\alpha\,\gamma_<}\delta_{\beta\,\sigma_>}\,\delta_{\lambda_<\,\delta}-\delta_{\alpha\,\delta_<}\delta_{\beta\,\sigma_>}\,\delta_{\lambda_<\,\gamma}\,+\\
&\qquad\qquad+\,\delta_{\alpha\,\sigma_>}\delta_{\lambda_<\,\delta>}\,\delta_{\beta\,\gamma_<}-\delta_{\alpha\,\sigma_>}\delta_{\lambda_<\,\gamma}\,\delta_{\beta\,\delta_<}
\end{aligned} \tag{4.13}$$

and the substitution of (4.13) into (4.12) yields

$$\begin{aligned}
&\langle HF\,|a^+_{\lambda_<}\,a_{\sigma_>}\,\hat{H}|\,HF\rangle = \\
&= \langle\sigma_>|\,\hat{T}\,|\lambda_<\rangle + \\
&\quad +\frac{1}{2}\sum_{\mu_<=1}^{A}\Big[\,\langle\mu_<\,\sigma_>|\,\hat{V}\,|\mu_<\,\lambda_<\rangle - \langle\mu_<\,\sigma_>|\hat{V}|\lambda_<\,\mu_<\rangle \\
&\qquad\qquad -\langle\sigma_>\,\mu_<|\,\hat{V}\,|\mu_<\,\lambda_<\rangle + \langle\sigma_>\,\mu_<|\,\hat{V}\,|\lambda_<\,\mu_<\rangle\,\Big] = 0
\end{aligned} \tag{4.14}$$

Matrix elements (4.9) of two-particle potential fulfils following symmetry

$$\begin{aligned}
&\langle\alpha\beta|\,\hat{V}\,|\gamma\delta\rangle = \\
&\quad = \int d\xi_1\,d\xi_2\;\;\varphi^*_\alpha(\xi_1)\,\varphi^*_\beta(\xi_2)\;\;V(\xi_1,\xi_2)\;\;\varphi_\gamma(\xi_1)\,\varphi_\delta(\xi_2) = \\
&\quad = \boxed{\begin{array}{c}\text{we suppose}\\ V(\xi_1,\xi_2)=V(\xi_2,\xi_1)\end{array}} = \\
&\quad = \int d\xi_1\,d\xi_2\;\;\varphi^*_\alpha(\xi_2)\,\varphi^*_\beta(\xi_1)\;\;V(\xi_1,\xi_2)\;\;\varphi_\gamma(\xi_2)\,\varphi_\delta(\xi_1) = \\
&\quad = \quad\langle\beta\alpha|\,\hat{V}\,|\delta\gamma\rangle
\end{aligned} \tag{4.15}$$

and therefore the exp. (4.14) reads

$$\begin{aligned}
&\langle HF\,|a^+_{\lambda_<}\,a_{\sigma_>}\,\hat{H}|\,HF\rangle = \\
&= \langle\sigma_>|\,\hat{T}\,|\lambda_<\rangle + \\
&\quad + \sum_{\mu_<=1}^{A}\Big[\,\langle\mu_<\,\sigma_>|\,\hat{V}\,|\mu_<\,\lambda_<\rangle - \langle\mu_<\,\sigma_>|\hat{V}|\lambda_<\,\mu_<\rangle\Big] \\
&= \boxed{\begin{array}{c}\text{see}\\ (B.17)\end{array}} = \langle\sigma_>|\,\hat{T}\,|\lambda_<\rangle + \sum_{\mu_<=1}^{A}\langle\mu_<\,\sigma_>|\,\hat{V}\,|\widetilde{\mu_<\,\lambda_<}\rangle = \\
&\equiv \langle\sigma_>|\,\hat{T}\,|\lambda_<\rangle + \sum_{\mu_<=1}^{A} V_{\mu_<\,\sigma_>\,\mu_<\,\lambda_<} = 0
\end{aligned} \tag{4.16}$$

where we introduced two-particle antisymmetrized matrix elements $V_{\mu_<\,\sigma_>\,\mu_<\,\lambda_<}$ (see (B.17))

$$\begin{aligned}
V_{\mu_<\,\sigma_>\,\mu_<\,\lambda_<} &\equiv \langle\mu_<\,\sigma_>|\,\hat{V}\,|\mu_<\,\lambda_<\rangle - \langle\mu_<\,\sigma_>|\hat{V}|\lambda_<\,\mu_<\rangle \quad \equiv \\
&\equiv \langle\mu_<\,\sigma_>|\,\hat{V}\,|\widetilde{\mu_<\,\lambda_<}\rangle
\end{aligned} \tag{4.17}$$

Similarly, starting from the variational condition $\langle HF\,|\hat{H}|\,\delta\,HF\rangle\;=0$ (see (4.8)) the following equation can be obtained

$$\begin{aligned}\langle HF|\,\hat{H}\,a^{+}_{\sigma_>}\,a_{\lambda_<}\,|HF\rangle\;&=\\ &=\quad\langle\lambda_<|\,\hat{T}\,|\sigma_>\rangle+\sum_{\mu_<=1}^{A}\langle\lambda_<\,\mu_<|\,\hat{V}\,|\widetilde{\sigma_>\,\mu_<}\rangle\;=0\end{aligned}\tag{4.18}$$

Equations (4.16) and (4.18) should be fulfilled for all single-particle states $\lambda_<$ below Fermi level and $\sigma_>$ above Fermi level. These equations can be interpreted as the zero matrix elements of certain single-particle operator $\hat{H}_{AV}$ between single-particle states $\lambda_<$ (below Fermi level) and $\sigma_>$ (above Fermi level):

$$\begin{aligned}\langle\sigma_>|\,\hat{H}_{AV}\,|\lambda_<\rangle\;&\equiv\;\langle\sigma_>|\,\hat{T}\,|\lambda_<\rangle+\sum_{\mu_<=1}^{A}\langle\sigma_>\,\mu_<|\,\hat{V}\,|\widetilde{\lambda_<\,\mu_<}\rangle\;=0\\ \langle\lambda_<|\,\hat{H}_{AV}\,|\sigma_>\rangle\;&\equiv\;\langle\lambda_<|\,\hat{T}\,|\sigma_>\rangle+\sum_{\mu_<=1}^{A}\langle\lambda_<\,\mu_<|\,\hat{V}\,|\widetilde{\sigma_>\,\mu_<}\rangle\;=0\end{aligned}\tag{4.19}$$

It is evident that the operator $\hat{H}_{AV}$ is the single-particle operator (expr. (4.19) defines its nondiagonal matrix elements). So, one can conclude with the statement that the HF variational principle with the Slater determinant gives the zero matrix elements of the operator $\hat{H}_{AV}$ between single-particle states $\lambda_<$ (below Fermi level) and $\sigma_>$ (above Fermi level). This HF condition is usually strengthened and so called HF single-paticle basis is defined as the basis in which the matrix of the operator $\hat{H}_{AV}$ is diagonal:

$$\begin{aligned}\langle\alpha|\,\hat{H}_{AV}\,|\beta\rangle=\langle\alpha|\,\hat{T}\,|\beta\rangle+\sum_{\mu_<=1}^{A}\langle\alpha\,\mu_<|\,\hat{V}\,|\widetilde{\beta\,\mu_<}\rangle\;=\\ =\epsilon_\alpha\,\delta_{\alpha\,\beta}\end{aligned}\tag{4.20}$$

It is obvious that the Hartree-Fock basis fulfilling (4.20) fulfils also (4.19). The equation (4.20) is called in the literature as the Hartree-Fock equation. The single-particle operator $\hat{H}_{AV}$ represents the mean field which was extracted from the Hamiltonian (4.2) (or (4.1)) involving effective two-particle interaction $\hat{V}=\sum_{i<j}\hat{V}_{ij}$. This mean field has single-particle eigen-vectors

$|\alpha\rangle$ with eigen-energies ϵ_α. These single-particle states are filled by nucleons in the nuclear ground state from the lowest energy one to the single-particle state with the energy nearest below the Fermi level (see Fig. B.1).

The looking for the solution of the HF equation (4.20) means to solve the self-consistent problem. It can be seen more clearly if the HF equation (4.20) is rewritten in the coordinate representation

$$\begin{aligned}
\langle\alpha|\,\hat{H}_{AV}\,|\beta\rangle = & \boxed{\begin{array}{c}\text{see}\\ \text{(4.3) and (4.4)}\end{array}} = \\
= & \int d\xi\,\varphi^*_\alpha(\xi)\left(-\frac{\hbar^2}{2M}\,\vec{\nabla}^2\right)\varphi_\beta(\xi) + \\
& + \sum_{\mu_<=1}^{A}\int d\xi\,d\xi'\,\varphi^*_\alpha(\xi)\,\varphi^*_{\mu_<}(\xi')\,V(\xi,\xi')\,\varphi_\beta(\xi)\,\varphi_{\mu_<}(\xi') \\
& - \sum_{\mu_<=1}^{A}\int d\xi\,d\xi'\,\varphi^*_\alpha(\xi)\,\varphi^*_{\mu_<}(\xi')\,V(\xi,\xi')\,\varphi_{\mu_<}(\xi)\,\varphi_\beta(\xi') = \\
= & \,\epsilon_\alpha\int d\xi\,\varphi^*_\alpha(\xi)\,\varphi_\beta(\xi)
\end{aligned} \tag{4.21}$$

where the orthogonality, $\int d\xi\;\varphi^*_\alpha(\xi)\,\varphi_\beta(\xi) = \delta_{\alpha\,\beta}$, of the single-particle basis is assumed. The equation (4.21) can be rewritten (we omit the integration over ξ and the function $\varphi^*_\alpha(\xi)$ in the both sides of the equation (4.21)

$$\begin{aligned}
& -\frac{\hbar^2}{2M}\,\vec{\nabla}^2\,\varphi_\beta(\xi) + \sum_{\mu_<=1}^{A}\int d\xi'\,\varphi^*_{\mu_<}(\xi')\,V(\xi,\xi')\,\varphi_{\mu_<}(\xi')\,\varphi_\beta(\xi) \\
& -\sum_{\mu_<=1}^{A}\int d\xi'\,\varphi^*_{\mu_<}(\xi')\,V(\xi,\xi')\,\varphi_\beta(\xi')\,\varphi_{\mu_<}(\xi) \;=\; \epsilon_\beta\,\varphi_\beta(\xi)
\end{aligned} \tag{4.22}$$

Further we introduce following assignment

$$\begin{aligned}
U(\xi) \;&\equiv\; \sum_{\mu_<=1}^{A}\int d\xi'\,\varphi^*_{\mu_<}(\xi')\,V(\xi,\xi')\,\varphi_{\mu<}(\xi') \\
W(\xi,\xi') \;&\equiv\; \sum_{\mu_<=1}^{A}\varphi^*_{\mu_<}(\xi')\,V(\xi,\xi')\,\varphi_{\mu_<}(\xi)
\end{aligned} \tag{4.23}$$

and finally the HF equation takes the following form

$$-\frac{\hbar^2}{2M}\,\vec{\nabla}^2\,\varphi_\beta(\xi)+U(\xi)\,\varphi_\beta(\xi)-\int d\xi'\,W(\xi,\xi')\,\varphi_\beta(\xi')\;=\;\epsilon\,\varphi_\beta(\xi) \tag{4.24}$$

or, if we realize that $\xi\equiv(\vec{r},s,\tau)$

$$\begin{aligned}-\frac{\hbar^2}{2M}\,\vec{\nabla}^2\,\varphi_\beta(\vec{r},s,\tau)+U(\vec{r},s,\tau)\,\varphi_\beta(\vec{r},s,\tau)\\ -\sum_{s'\tau'}\int d^3r'\,W(\vec{r}s\tau,\;\vec{r}\,'s'\tau')\,\varphi_\beta(\vec{r}\,'s'\tau')\;=\;\epsilon_\beta\;\varphi_\beta(\vec{r},s,\tau)\end{aligned} \tag{4.25}$$

The equation system (4.25) for unknown functions $\varphi_\beta(\xi)$ and corresponding energies ϵ_β is self-consistent because "potentials" $U(\xi)$ and $W(\xi,\xi')$ depend on the result of the whole equation system (that means on all functions $\varphi_{\nu_<}(\xi)$). Such equation is usually solved by iterative way:

$$\left(\begin{array}{c}\text{We start with some}\\ \text{complete s.p. basis}\\ \varphi_\alpha^{(0)}(\xi)\text{ and corresponding}\\ \text{energies }\epsilon_\alpha^{(0)}\text{ , e.g. oscillator}\\ \text{function basis.}\end{array}\right)\;\rightarrow\;\left(\begin{array}{c}\text{With the basis}\\ \text{of functions}\varphi_\alpha^{(0)}(\xi)\\ \text{we determine}U^{(0)}(\xi)\\ \text{and }W^{(0)}(\xi,\xi')\\ \text{according to (4.23)}\end{array}\right)\;\rightarrow$$

$$\rightarrow\;\left(\begin{array}{c}\text{With }U^{(0)}(\xi)\text{ and}\\ W^{(0)}(\xi,\xi')\text{ the eq.}\\ \text{system(4.25)}\\ \text{is solved. As a result}\\ \text{we obtain new}\\ \text{basis }\varphi_\alpha^{(1)}(\xi)\text{ and }\epsilon_\alpha^{(1)}\end{array}\right)\;\rightarrow\;\left(\begin{array}{c}\text{With the new basis of}\\ \text{functions }\varphi_\alpha^{(1)}(\xi)\text{ we}\\ \text{determine }U^{(1)}(\xi)\text{ and}\\ W^{(1)}(\xi,\xi')\text{ according}\\ \text{to (4.23)}\end{array}\right)\;\rightarrow$$

$$\rightarrow\;\left(\begin{array}{c}\text{With }U^{(1)}(\xi)\text{ and}\\ W^{(1)}(\xi,\xi')\text{ the eq.}\\ \text{system(4.25)}\\ \text{is solved. As a result}\\ \text{we obtain new}\\ \text{basis }\varphi_\alpha^{(2)}(\xi)\text{ and }\epsilon_\alpha^{(2)}\end{array}\right)\;\rightarrow\;\ldots \tag{4.26}$$

We continue this chain of steps untill the n-th iteration when $|\epsilon_\alpha^{(n)} - \epsilon_\alpha^{(n-1)}| \leq \eta$ for all α, where η is arbitrary chosen small number. In such a way we obtain so called Hartree-Fock basis $\varphi_\alpha^{(HF)}(\xi) \equiv \varphi_\alpha^{(n)}(\xi)$, $\epsilon_\alpha^{(HF)} \equiv \epsilon_\alpha^{(n)}$. Knowing this HF basis the mean field Hamiltonian $\hat{H}_{AV}$ can be written as

$$\hat{H}_{AV} = \sum_\alpha \epsilon_\alpha^{(HF)} \, a_\alpha^+ a_\alpha \tag{4.27}$$

where a_α^+, a_α are nucleon creation and annihilation operators on nucleons in the HF s.p. basis.

It is necessary to realize that the HF mean field $\hat{H}_{AV}$ exhausts only part of the total Hamiltonian $\hat{H}$, that means $\hat{H}_{AV} \neq \hat{H}$. Always there is a part of the total Hamiltonian which is not involved in the HF mean field. This part is called in nuclear physics as residual interaction. So, after the solving the HF problem the total Hamiltonian can be expressed as follows.

$$\hat{H} = \hat{H}_{AV} + \hat{V}_{RES} \tag{4.28}$$

The size of the residual interaction, or by other words to what extend the mean field $\hat{H}_{AV}$ exhausts the whole Hamiltonian $\hat{H}$, depends on the character of interactions acting among A particles in the given system. For instance, in a system of electrons in an atom or in a system of particles forming nanostructures the HF mean field $\hat{H}_{AV}$ approximates the whole Hamiltonian $\hat{H}$ quite well and the residual interaction $\hat{V}_{RES}$ can be considered as only a small perturbation. However, in the atomic nucleus the residual interaction $\hat{V}_{RES}$ is usually big and it cannot be treated by perturbative way. In the nucleus case the HF mean field can describe only some global nucleus properties (like binding energy, magic numbers, shape of the nucleus, nuclear compressibility). If one wants to describe details of the spectrum of excited states in the nucleus or other more detailed characteristics it is necessary to take into account residual interactions.

Approaches based on the neglecting of the residual interactions, when the total Hamiltonian is approximated by the mean field only, is called in nuclear physics as a model of inedependent particles (nucleons move independently in the s.p. mean field potential). As it has been just mentioned such model is relevant only to global (bulk) nuclear properties. However, historically model of independent nucleons had important consequences and the Chapter 5 is devoted to it.

Residual interactions $\hat{V}_{RES}$ are usually divided into two parts, the short

range residual interactions $\hat{V}_{s.r.}^{(RES)}$ and long range ones $\hat{V}_{l.r.}^{(RES)}$

$$\hat{V}_{RES} = \hat{V}_{s.r.}^{(RES)} + \hat{V}_{l.r.}^{(RES)} \tag{4.29}$$

and their taking into account is discussed in the Chapters 6 and 7, respectively.

4.1.2 Ground state in the Hartree-Fock method

The ground state of the A fermion system is given by the Slater determinant (4.7) where the single-particle wave function $\varphi_\alpha(\xi) = \varphi_\alpha^{(HF)}(\xi)$ were obtained by the solving of the HF equation (4.22). In the Slater determinant (4.7) only single-particle wave functions of occupied states (below Fermi level) are involved. However, the total energy of the A fermion system is not given only by the sum of the single-particle energies of occupied states.

The total energy E_0 of the ground state $|HF\rangle$ is the corresponding expectation value of the total Hamiltonian $\hat{H}$

$$\begin{aligned} E_0 &= \langle HF\,|\hat{H}|\,HF\rangle = \boxed{\begin{array}{c}\text{see}\\(4.2)\end{array}} = \\ &= \sum_{\alpha\beta}\langle\alpha\,|\hat{T}|\,\alpha\rangle\,\langle HF\,|a_\alpha^+\alpha_\beta|\,HF\rangle + \\ &\quad +\frac{1}{2}\sum_{\alpha\beta\gamma\delta}\langle\alpha\beta\,|\hat{V}|\,\gamma\delta\rangle\,\langle HF\,|a_\alpha^+ a_\beta^+ a_\delta a_\gamma|\,HF\rangle \end{aligned} \tag{4.30}$$

where

$$\langle HF|a_\alpha^+ a_\beta|HF\rangle = \begin{cases} 0 & \text{if } \beta = \beta_> \\ \delta_{\alpha\beta_<} & \text{if } \beta = \beta_< \end{cases},$$

and similarly

$$\begin{aligned} \langle HF\,|a_\alpha^+ a_\beta^+ a_\delta a_\gamma|\,HF\rangle &= \langle HF\,|a_\alpha^+\,(\delta_{\beta\delta_<} - a_{\delta_<}\,a_\beta^+)\,a_\gamma|\,HF\rangle = \\ &= \delta_{\beta\delta_<}\,\delta_{\alpha\gamma_<} - \delta_{\alpha\delta_<}\,\delta_{\beta\gamma_<} \end{aligned}$$

The substitution into (4.30) gives the total energy in the HF ground state in

the following form

$$
\begin{aligned}
E_0 &= \sum_{\alpha\beta} \langle \alpha | \hat{T} | \beta \rangle \, \delta_{\alpha\beta_<} + \\
&\qquad + \frac{1}{2} \sum_{\alpha\beta\gamma\delta} \langle \alpha\beta | \hat{V} | \gamma\delta \rangle \, \left(\delta_{\beta\delta_<} \, \delta_{\alpha\gamma_<} - \delta_{\alpha\delta_<} \, \delta_{\beta\gamma_<} \right) = \\
&= \sum_{\alpha_<} \langle \alpha_< | \hat{T} | \alpha_< \rangle + \\
&\qquad + \frac{1}{2} \sum_{\alpha_<\beta_<} \Big(\langle \alpha_<\beta_< | \hat{V} | \alpha_<\beta_< \rangle - \langle \alpha_<\beta_< | \hat{V} | \beta_<\alpha_< \rangle \Big) = \\
&= \sum_{\alpha_<} \langle \alpha | \hat{T} | \alpha_< \rangle + \\
&\qquad + \sum_{\alpha_<\beta_<} \langle \alpha_<\beta_< | \hat{V} | \widetilde{\alpha_<\beta_<} \rangle - \frac{1}{2} \sum_{\alpha_<\beta_<} \langle \alpha_<\beta_< | \hat{V} | \widetilde{\alpha_<\beta_<} \rangle = \\
&= \boxed{\begin{array}{c}\text{see} \\ (4.20)\end{array}} = \sum_{\alpha_<} \epsilon_{\alpha_<} - \frac{1}{2} \sum_{\alpha_<\beta_<} \langle \alpha_<\beta_< | \hat{V} | \widetilde{\alpha_<\beta_<} \rangle
\end{aligned}
\tag{4.31}
$$

So, one can see that the total energy in the HF ground state is not given by the simple sum of the single-particle energies of occupied s.p. states.

In the connection with the expression (4.31) it is necessary to note that it is possible to derive the HF equation (4.22) directly from (4.31). One should realize that the expr. (4.31) valids not only for the HF basis (that means in the minimum of the total energy) but it is general expression for the expectation value of the Hamiltonian $\hat{H}$ in the general Slater determinant formed from any (trial) orthonormal basis of functions $\varphi_\alpha(\xi)$. In such a way the corresponding value of the total energy, $E[\varphi_\alpha(\xi)]$, can be consisered as

the functional of functions $\varphi_\alpha(\xi)$:

$$E[\varphi_\alpha(\xi)] = \sum_\alpha \langle\alpha|\hat{T}|\alpha\rangle + \\ + \frac{1}{2}\sum_{\alpha_<\beta_<}\Big(\langle\alpha_<\beta_<|\hat{V}|\alpha_<\beta_<\rangle - \langle\alpha_<\beta_<|\hat{V}|\beta_<\alpha_<\rangle\Big) = \\ = \sum_{\alpha_<}\int d\xi\,\varphi^*_{\alpha_<}(\xi)\,\left(-\frac{\hbar^2\vec{\nabla}^2}{2M}\right)\,\varphi_{\alpha_<}(\xi) + \\ + \frac{1}{2}\sum_{\alpha_<\beta_<}\int d\xi\,d\xi'\,\varphi^*_{\alpha_<}(\xi)\,\varphi^*_{\beta_<}(\xi')\,V(\xi,\xi')\,\varphi_{\alpha_<}(\xi)\,\varphi_{\beta_<}(\xi') \\ - \frac{1}{2}\sum_{\alpha_<\beta_<}\int d\xi\,d\xi'\,\varphi^*_{\alpha_<}(\xi)\,\varphi^*_{\beta_<}(\xi')\,V(\xi,\xi')\,\varphi_{\beta_<}(\xi)\,\varphi_{\alpha_<}(\xi')$$

Then the HF equation (4.22) is obtained as the condition of the extreme of the functional $E[\varphi_\alpha(\xi)]$ with the additional condition of the normalization of each single-particle function $\varphi_\alpha(\xi)$:

$$\frac{\partial}{\partial\varphi^*_\beta(\xi)}\left\{E[\varphi_\alpha(\xi)] - \sum_\alpha \epsilon_\alpha\,\left[\int d\xi'\,\varphi^*_\alpha(\xi')\,\varphi_\alpha(\xi') - 1\right]\right\} = \\ = -\frac{\hbar^2\vec{\nabla}^2}{2M}\,\varphi_\beta(\xi) + \sum_{\mu_<}\int d\xi'\,\varphi^*_{\mu_<}(\xi')\,V(\xi,\xi')\,\varphi_{\mu_<}(\xi')\,\varphi_\beta(\xi) \\ - \sum_{\mu_<}\int d\xi'\,\varphi^*_{\mu_<}(\xi')\,V(\xi,\xi')\,\varphi_{\mu_<}\xi)\,\varphi_\beta(\xi') - \epsilon_\beta\,\varphi_\beta(\xi) = 0 \tag{4.32}$$

The physical meaning of the single-particle energies ϵ_μ follows from the Koopmans theorem originally formulated for the molecular physics [38] [1]. This theorem claims:
Absolute value of the single-particle energy, $|\epsilon_\mu|$, is equal to the separation energy of the nucleon from the single-particle state μ.
The proof is following:

[1] It is interesting that Tjalling Koopmans, who formulated the theorem in 1934, became a Nobel lauerate in 1975, though neither in physics nor chemistry, but in economics.

Let us denote

$$|HF\rangle = \prod_{\nu_<=1}^{A} a^+_{\nu_<} |0\rangle \;\rightarrow\; \begin{array}{c}\text{HF ground state of the nucleus}\\ \text{with A nucleons (see (4.5))}\end{array}$$

$$|\Psi_{\mu_<}\rangle = \prod_{\substack{\nu_<=1\\ \nu_<\neq\mu_<}}^{A} a^+_{\nu_<} |0\rangle = a_{\mu_<} |HF\rangle \;\rightarrow\; \begin{array}{c}\text{state } \mu_< \text{ of the nucleus}\\ \text{with A-1 nucleons}\end{array}$$

The HF ground state energy of the nucleus with A nucleons is given by the energy E_0 given in (4.31)

$$E_0 = \sum_{\alpha_<} \langle \alpha_< | \hat{T} | \alpha_< \rangle + \frac{1}{2} \sum_{\alpha_< \beta_<} \langle \alpha_< \beta_< | \hat{V} | \widetilde{\alpha_< \beta_<} \rangle \tag{4.33}$$

The energy of the nucleus with A-1 nucleons in the state $|\Psi_{\mu_<}\rangle$ is given by the following expectation value

$$\begin{aligned} E_{\mu_<} \;&=\; \langle \Psi_{\mu_<} | \hat{H} | \Psi_{\mu_<} \rangle = \sum_{\alpha\beta} \langle \alpha | \hat{T} | \beta \rangle \, \langle HF | a^+_{\mu_<} a^+_\alpha a_\beta a_{\mu_<} | HF \rangle + \\ &+ \frac{1}{2} \sum_{\alpha\beta\gamma\delta} \langle \alpha\beta | \hat{V} | \gamma\delta \rangle \, \langle HF | a^+_{\mu_<} a^+_\alpha a^+_\beta a_\delta a_\gamma a_{\mu_<} | HF \rangle \end{aligned} \tag{4.34}$$

Using the anticommutator relations of the creation and annihilation particle operators, $\{a_\alpha, a^+_\beta\} = \delta_{\alpha\beta}$ and $\{a_\alpha, a_\beta\} = 0$, it is possible to show the following identities (one can obtain these identities also in terms of the Wick's theorem - see Subsection B.4 in the Appendix B)

$$\begin{aligned} &\langle HF | a^+_{\mu_<} a^+_\alpha a_\beta \, a_{\mu_<} | HF \rangle = \delta_{\alpha\beta} - \delta_{\mu_<\beta} \, \delta_{\mu_<\alpha} \\ &\langle HF | a^+_{\mu_<} a^+_\alpha a^+_\beta a_\delta \, a_\gamma \, a_{\mu_<} | HF \rangle = \delta_{\mu_<\beta} \, \delta_{\beta\gamma} \, \delta_{\alpha\mu_<} - \delta_{\mu_<\delta} \, \delta_{\beta\mu_<} \, \delta_{\alpha\gamma_<} \\ &\qquad + \delta_{\mu_<\gamma} \, \delta_{\beta\mu_<} \, \delta_{\alpha\delta_<} - \delta_{\mu_<\gamma} \, \delta_{\alpha\mu_<} \, \delta_{\alpha\delta_<} + \delta_{\beta\delta_<} \, \delta_{\alpha\gamma_<} - \delta_{\alpha\delta_<} \, \delta_{\beta\gamma_<} \end{aligned}$$

and the substitution of these identities into (4.34) gives

$$E_{\mu_<} = \sum_{\substack{\lambda_<=1\\ \lambda_<\neq\mu_<}} \langle \lambda_< | \hat{T} | \lambda_< \rangle + \frac{1}{2} \sum_{\substack{\lambda_<=1\\ \lambda_<\neq\mu_<}}^{A} \sum_{\substack{\nu_<=1\\ \nu_<\neq\mu_<}}^{A} \langle \lambda_< \nu_< | \hat{V} | \widetilde{\lambda_< \nu_<} \rangle \tag{4.35}$$

So, the difference $E_{\mu_<} - E_0$ is

$$
\begin{aligned}
& E_{\mu_<} - E_0 = \\
& = \sum_{\substack{\lambda_<=1 \\ \lambda_< \neq \mu_<}} \langle \lambda_< | \hat{T} | \lambda_< \rangle + \frac{1}{2} \sum_{\substack{\lambda_<=1 \\ \lambda_< \neq \mu_<}}^{A} \sum_{\substack{\nu_<=1 \\ \nu_< \neq \mu_<}}^{A} \langle \lambda_< \nu_< | \hat{V} | \widetilde{\lambda_< \nu_<} \rangle \\
& \quad - \left[\sum_{\alpha_<} \langle \alpha_< | \hat{T} | \alpha_< \rangle + \frac{1}{2} \sum_{\alpha_< \beta_<} \langle \alpha_< \beta_< | \hat{V} | \widetilde{\alpha_< \beta_<} \rangle \right] = \\
& = - \langle \mu_< | \hat{T} | \mu_< \rangle - \sum_{\lambda_<=1}^{A} \langle \mu_< \lambda_< | \hat{V} | \widetilde{\mu_< \lambda_<} \rangle \; = \; - \epsilon_{\mu_<}
\end{aligned}
\tag{4.36}
$$

So, really, the absolute value of the difference, $|E_{\mu_<} - E_0|$, of the total energies of the ground HF state of A nucleon nucleus and A-1 nucleon energy of the hole in the s.p. state $\mu_<$ (that means the separation energy of the nucleon from the s.p. state with the index $\mu_<$) is equal to the absolute value of the s.p. energy $|\epsilon_{\mu_<}|$. This is used for the testing of the reliability of used mean field. From some nuclear processes, like nuclear reactions (d,p) or (d,t), it is possible to extract the nucleon separation energies from particular s.p. states. According to Koopmans theorem these "experimental" separation energies should be equal to the single-particle energies. By such comparison we can check used mean field.

4.1.3 Excited states in the HF approach (particle-hole formalism)

The HF equation (4.22) or (4.25) determines single-particle wave functions $\varphi_\alpha(\xi)$ and in such a way also the HF ground state described by the corresponding Slater determinant $\langle \xi_1, \ldots, \xi_A | HF \rangle$ (see (4.7)). The HF s.p. wave functions were obtained by the variational principle searching for the minimum of the HF energy $\langle HF | \hat{H} | HF \rangle$ and therefore the HF method discussed in the previous subsection concerns only the HF ground state.

From the point of view of the exact theoretical approach excited states of the whole system of fermions can be also obtained by the variational principle searching for the minimum of the total energy but now with the additional condition of the orthogonality of the given excited states (it follows from the fact that all states describing ground state and all excited states in the framework of given Hamiltonian should form the complete orthogonal basis).

So for instance, the 1-st excited state $|\Phi_1\rangle$ can be obtained from the following variational principle

$$\delta\langle\Phi_1|\hat{H}|\phi_1\rangle = 0 \quad \text{with the condition } \langle\Phi_1|HF\rangle = 0 \tag{4.37}$$

and the 2-d excited state $|\Phi_2>$:

$$\delta\langle\Phi_2|\hat{H}|\phi_2\rangle = 0 \quad \text{with the condition } \langle\Phi_2|HF\rangle = \langle\Phi_2|\Phi_1\rangle = 0 \tag{4.38}$$

and so on. However, such procedure has two important problems:

- It is very complicated from the numerical point of view.
- Physical interpretation of such a way obtained excited states is not clear and the calculation of the matrix elements of transition operators with these states is also very complicated.

Therefore, in the practical approaches other methods are used for the description of excited states. These methods starts usually with the HF basis obtained from the variational principle for the HF ground state but the structure of excited states is not determined by the exact variational method described in (4.37) and (4.38). Some of such methods will be discussed in the Chapter 7.

The Slater determinant (4.7) or the HF ground state ket $|HF\rangle$ (see (4.5)) describes generally the even and odd number particle systems. However, in the calculation of the excited states of odd number particle system the starting step is usually the HF equation for the nearest even system (in the case of nucleus the even number of neutrons and protons, that means the even-even core of given odd-A or odd-odd-A nucleus).

At first we consider the even-even nucleus. Let us suppose that the solution of the HF equation (4.24) was found and we have Hartree-Fock single-particle basis $\varphi_\alpha(\xi)$. We also assume the total Hamiltonian is reduced only to the mean field $\hat{H}_{AV}$. The approach when the residual interaction $\hat{V}_{RES}$ in (4.28) is neglected and the total Hamiltonian $\hat{H}$ is approximated by the HF mean field $\hat{H}_{AV}$ is known in the literature as the model of independent particles. In this case the ground state of the even system is given by $|HF>$ and excited states are described by so called particle-hole configurations:

$$\begin{aligned} |\phi^{\sigma_>}_{\mu_<}\rangle &\equiv a^+_{\sigma_>} a_{\mu_<} |HF\rangle && \rightarrow \quad \text{1p-1h configurations} \\ |\phi^{\sigma_>\tau_>}_{\mu_<\nu_<}\rangle &\equiv a^+_{\sigma_>} a^+_{\tau_>} a_{\mu_<} a_{\nu_<} |HF\rangle && \rightarrow \quad \text{2p-2h configurations} \\ &\vdots \end{aligned} \tag{4.39}$$

These configurations are shown schematically in the Fig. 4.1. The energy

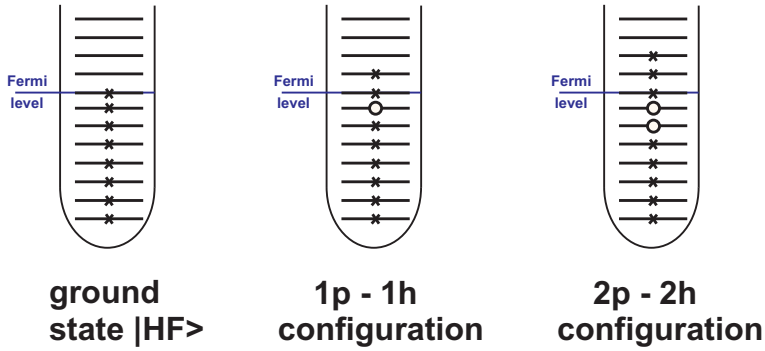


Figure 4.1: Schematic figure demonstrates the ground state, 1p-1h configurations, and 2p-2h configurations of the even neutron or proton system in the given nucleus.

of given particle-whole configuration is given by the expectation value of the mean field $\hat{H}_{AV}$ in this configuration. For instance, in the case of 1p-1h configuration $|\phi^{\sigma_>}_{\mu_<}>$ the corresponding energy in the model of independent particles reads as follows

$$E^{\sigma_>}_{\mu_<} = \langle\phi^{\sigma_>}_{\mu_<}|\hat{H}_{AV}|\phi^{\sigma_>}_{\mu_<}\rangle = \langle HF|\, a^+_{\mu_<}a_{\sigma_>}\, \hat{H}_{AV}\, a^+_{\sigma_>}a_{\mu_<}\,|HF\rangle =$$

$$= \boxed{\begin{array}{c}\text{see}\\(4.27)\end{array}} = \sum_\alpha \epsilon_\alpha \,\langle HF|\, a^+_{\mu_<}a_{\sigma_>}a^+_\alpha a_\alpha\, a^+_{\sigma_>}a_{\mu_<}\,|HF\rangle =$$

$$= \boxed{\begin{array}{c}\text{because}\\ \langle HF|\, a^+_{\mu_<}a_{\sigma_>}a^+_\alpha a_\alpha\, a^+_{\sigma_>}a_{\mu_<}\,|HF\rangle = \delta_{\sigma_>\alpha} - \delta_{\mu_<\alpha} + \begin{cases}1 \text{ for } \alpha = \alpha_<\\ 0 \text{ for } \alpha = \alpha_>\end{cases}\end{array}} =$$

$$= \epsilon_{\sigma_>} - \epsilon_{\mu_<} + \sum_{\alpha_<} \epsilon_{\alpha_<} \tag{4.40}$$

and the ground state energy in the framework of the model of independent particles (when $\hat{H} \approx \hat{H}_{AV}$) is given approximately by

$$\langle HF|\hat{H}_{AV}|HF\rangle = \sum_\alpha \epsilon_\alpha \,\langle HF|a^+_\alpha a_\alpha|HF\rangle = \sum_{\alpha_<} \epsilon_\alpha \tag{4.41}$$

That means in the framework of the approximation $\hat{H} \approx \hat{H}_{AV}$ the total ground state energy is estimated by the first term in (4.31) only. If the energy scale is chosen in accordance with $\sum_{\alpha_<} \epsilon_\alpha = 0$ then the energy of the 1p-1h configuration $|\Phi^{\sigma_>}_{\mu_<}\rangle$ is $\epsilon_{\sigma_>} - \epsilon_{\mu_>}$.

As it was mentioned above the odd number of particle system is usually treated as one particle above even particle core. That means, in the first step the HF problem for even core particle number is solved with corresponding $|HF\rangle$ state. Then the ground state of the odd system has one particle character, $a^+_{\lambda_>}|HF\rangle$, where the single-particle state $\lambda_>$ has the nearest s.p. energy above the Fermi level of the even particle number core. The corresponding excited states are (in the framework of the model of independent particles):

$$\begin{aligned} & a^+_{\lambda_>}|HF\rangle \quad \rightarrow \quad \text{particle states (including the ground state)} \\ & a^+_{\lambda_>}a^+_{\sigma_>}a_{\mu_<}|HF\rangle \quad \rightarrow \quad \text{particle + 1p-1h configurations} \\ & a^+_{\lambda_>}a^+_{\sigma_>}a^+_{\tau_>}a_{\mu_<}a_{\nu_<}|HF\rangle \quad \rightarrow \quad \text{particle + 2p-2h configurations} \\ & \quad \vdots \end{aligned} \tag{4.42}$$

One should point out that the description of excited states in terms of particle-hole configurations in the framework of the model of independent particles is far from the reality. The real excited states of the nucleus cannot be described by the approximation $\hat{H} \approx \hat{H}_{AV}$. In order to determine the structure and the spectrum of nuclear excited states it is always necessary to take into account residual interactions. This will be discussed in details in the Chapters 6 and 7.

4.1.4 Problems and questions in the HF method

As it can be seen from the previous subsection, from the purely theoretical point of view the Hartree-Fock method seems to be simple. However, the technical and numerical solution of the self-consistent HF equation represents a quite complex problem, especially for heavy nuclei where the big configuration space is necessary. In this subsection some of the most important questions connected with the HF method are discussed.

4.1.4.1 The question of taking into account of the short range residual interaction

The HF method enables to exctract from the total nuclear Hamiltonian the single-particle mean field $\hat{H}_{AV}$ and corresponding residual interaction $\hat{V}_{RES}$ (see (1.53) or (4.28)). As it was discussed (see (4.29)) the residual interaction involves short range part $\hat{V}^{(RES)}_{s.h.}$ and long range part $\hat{V}^{(RES)}_{l.h.}$. It turns out that

the short range residual interactions $\hat{V}_{s.h.}^{(RES)}$ lead to the formation of nuclear pairs. The creation of nucleon pairs has consequences even for global nucleus characteristics. Therefore in the case of deformed nuclei (where the pairing short-range residual interaction is especially strong) the only HF mean field is not able to describe nuclear global characteristics like binding energy, nuclear shape, radia etc. The approach which enables to take into account the pairing residual interaction is the Hartree-Fock-Bogoliubov and/or Bardeen-Cooper-Schriefer approaches. These approaches will be discussed in the Chapt. 6. The pairing of nucleons is important in the case of deformed nuclei where the number of nucleons corresponds to the partly occupation of the last mean field shell. For spherical nuclei where the number of nucleons filling the s.p. states is equal roughly to the full occupation of the closed shells the pairing does not contribute to the mean field characteristics and really, one can expect the bulk nuclear properties are well described by the Hartree-Fock mean field only.

4.1.4.2 Questions of the stability of numerical calculations and of the absolute minimum

The HF mean field was obtained by the finding of the functional extreme (minimum) of the total energy of given nucleus calculated in the state described by the Slater determinant. This means that the HF method involves all drawbacks of any variational method, concretely the variation of the s.p. energies does not give always stable minimum of the total energy functional. Further the simple condition is derived which gives some outlook if we have reached the minimum.

Let us suppose that $|HF\rangle$ is the HF ket giving the minimum E_0 of the total energy:

$$E_0 = \frac{\langle HF|\hat{H}|HF\rangle}{\langle HF|HF\rangle} \tag{4.43}$$

Now, we move the minimum ket $|HF\rangle$ to the new ket $|HF + \delta HF\rangle$ where $|\delta HF\rangle = \eta \; a^+_{\sigma_>} \, a_{\lambda_<} \, |HF\rangle$ is the variation (4.10). We obtain new energy

$$E'_0 = \frac{\langle HF + \delta HF|\hat{H}|HF + \delta HF\rangle}{\langle HF + \delta HF|HF + \delta HF\rangle} \tag{4.44}$$

If E_0 is the total energy minimum then for any variation $|\delta HF\rangle$ we should

have $E'_0 > E_0$. The eq. (4.44) can be rewitten as follows

$$\begin{aligned} E'_0 &= \boxed{\begin{array}{c}\text{because - see (4.8)}\\ \langle \delta HF|\hat{H}|HF\rangle = \langle HF|\hat{H}|\delta HF\rangle = 0\end{array}} = \\ &= E_0 + \eta^2 \langle HF|a^+_{\lambda_<} a_{\sigma_>}\ \hat{H}\ a^+_{\sigma_>} a_{\lambda_<}|HF\rangle = \\ &= \boxed{\begin{array}{c}\text{using anticommutator relations:}\\ \left\{a_\alpha,\ a^+_\beta\right\} = \delta_{\alpha\beta},\ \{a_\alpha,\ a_\beta\} = 0, \text{ and rel (4.6)}\end{array}} = \\ &= E_0 + |\eta|^2 \left\{E_0 + \epsilon_{\sigma_>} - \epsilon_{\lambda_<} - \langle \sigma_>\lambda_<|\hat{V}|\widetilde{\sigma_>\lambda_<}\rangle\right\} = \\ &= \boxed{\begin{array}{c}\text{within the independent particle model}\\ \text{see(4.40), (4.41)}\end{array}} = \\ &= E_0 + |\eta|^2 \left\{E^{\sigma_>}_{\lambda_<} - \langle \sigma_>\lambda_<|\hat{V}|\widetilde{\sigma_>\lambda_<}\rangle\right\} \end{aligned} \tag{4.45}$$

So, one can see that the minimum condition $E'_0 > E_0$ is fulfilled if

$$E^{\sigma_>}_{\lambda_<} \ > \ \langle \sigma_>\lambda_<|\hat{V}|\widetilde{\sigma_>\lambda_<}\rangle \tag{4.46}$$

Since absolute value of the matrix elements $\langle \sigma_>\lambda_<|\hat{V}|\widetilde{\sigma_>\lambda_<}\rangle$ is aboutA^{-1} in the most cases of heavier nuclei the inequality (4.46) is fufilled for all $\sigma_>$, $\lambda_<$. Nevertheless, the condition (4.46) would be taken as the additional condition for the HF variational principle to be sure that the energy functional extrem is related to the minimum.

4.1.4.3 Translation and rotation invariance of the nuclear hamiltonian, spurious modes

In the nuclear physics the Hamiltonian of the nucleus is translation and rotation invariant:

$$[\hat{H},\ \hat{\vec{P}}\,] = [\hat{H},\ \hat{\vec{J}}\,] = 0 \tag{4.47}$$

where $\hat{H}$ is the total nuclear Hamiltonian (4.2) in the laboratory frame, $\hat{\vec{P}}$ and $\hat{\vec{J}}$ are total linear and angular momentum operators in the laboratory frame, respectively. However, it does not mean that the mean field $\hat{H}_{AV}$ should have the same symmetries (4.47) as the total Hamiltonian. Generally

$$[\hat{H}_{AV},\ \hat{\vec{P}}\,] \neq 0 \qquad\qquad [\hat{H}_{AV},\ \hat{\vec{J}}\,] \neq 0 \tag{4.48}$$

This is caused by the fact that during the iterative solution of the HF equation (4.25) the HF ground state $|HF\rangle$ can loose the rotation and translation symmetry: $e^{i\vec{P}\cdot\vec{u}}|HF\rangle \neq |HF\rangle$, $e^{i\vec{J}\cdot\vec{n}\,\phi}|HF\rangle \neq |HF\rangle$ ($\vec{u}$ is the arbitrary space shift, ϕ is the arbitrary rotational angle around the axis directed along the unit vector $\vec{n}$). The general mean field $\hat{H}_{AV}$ is then deformed and translation noninvariant. This violation of the total Hamiltonian symmetries by the mean field is known in the literature as the spontaneous symmetry breaking.

If in the next step after the solving of the HF problem (that means after the obtaining the mean field $\hat{H}_{AV}$) some beyond HF method for the taking into account of the residual interaction $\hat{V}_{RES}$ is used then this method should restore the symmetry (4.47) of the total Hamiltonian $\hat{H} = \hat{H}_{AV} + \hat{V}_{RES}$. If it would not be so (that means if in the framework of used beyond mean field approach the residual interactions do not restore the total Hamiltonian symmetry violated by the mean field) then the rotational or translational nuclear states (which are spurious from the point of view of the intrinsic degrees of freedom of the nucleus motion) are mixed with the intrinsic (single-particle or vibrational) degrees of freedom. These spurious admixtures and states will be discussed in the Chapter 7 in the connection with the approaches taking into account residual interactions.

4.1.4.4 The problem of the infinite potential (hard core)

As it was mentioned in the Subsection 3.2 it is not possible (and it is also unphysical) to use bare two-particle nucleon-nucleon potential in the HF equation. The bare nucleon-nucleon potential involves strongly repulsive (infinite) interaction in very small distances which causes the infinite matrix elements $\langle\alpha\beta|\hat{V}_{bare}|\gamma\delta\rangle$ and as a consequence the HF equation is not solvable. Instead, the effective nucleon-nucleon interaction in the nuclear medium is necessary to use in the HF equation. This effective nucleon-nucleon interaction have a reasonable finite behaviour which does not cause any problem in the solution of the HF equation. By other words the input nucleon-nucleon potential in the HF equation should be reasonable from the point of view of the numerical solving of the HF equation.

4.2 Shell model

The model of independent particles, when the total Hamiltonian $\hat{H}$ is approximated by the single-particle mean field $\hat{H}$, is very rough approximation in the case of atomic nuclei. For realistic description of excited nuclear states it is necessary to go beyond the mean field and to take into account also the residual interaction. As it was already mentioned the residual interactions are quite strong in nuclei and it is not possible to use a perturbation theory for their taking into account. In the present days there are several approaches how to involve residual interactions in the theoretical unperturbative description of nuclear states. Some of the most popular are discussed in the Chapter 7. Here the basic ideas of the most simple one from the theoretical point of view (but not from the technical point of view), so called shell model [2], are presented.

Logically, the most simple way to take into account the whole nuclear Hamiltonian including residual interactions is to diagonalize the total Hamiltonian matrix in the infinite basis constructed from particle-hole configurations. In the case of the even-even nucleus this basis looks like (see also Fig. 4.1)

$$|HF\rangle;\ \underbrace{|\Phi^{\sigma_1>}_{\mu_1<}\rangle,\ |\Phi^{\sigma_2>}_{\mu_2<}\rangle,\ \ldots}_{1p-1h};\ \underbrace{|\Phi^{\sigma_1>\tau_1>}_{\mu_1<\nu_1<}\rangle,\ |\Phi^{\sigma_2>\tau_2>}_{\mu_2<\nu_2<}\rangle,\ \ldots}_{2p-2h};\ \underbrace{\ldots\ldots}_{3p-3h\text{ and more}} \tag{4.49}$$

and corresponding total Hamiltonian matrix has block structure as it is shown in the Table 4.1

In this matrix the ground state diagonal matrix element is given by the HF ground state energy

$$\langle HF|\hat{H}|HF\rangle = \boxed{\begin{matrix}\text{see}\\(4.31)\end{matrix}} = E_0 \tag{4.50}$$

The block between the HF ground state and 1p-1h configuration states contains zeros in accordance with the HF minimum condition (4.18) (if the basis

[2] In order to avoid misunderstanding concerning the terminology it is necessary to note that historically in the past the name "shell model" was used mainly for the simple model of independent nucleons in some phenomenological potential when individual nucleons occupied the s.p. states which were grouped to so called shells. In the present days the term "shell model" is used rather for approach when realistic nuclear states are obtained by the diagonalization of the matrix of he total Hamiltonian constructed in some complete basis of configurations. In such a sense this term is also used in this textbook.

	$\|HF\rangle$	$\ldots \|\Phi^{\sigma_>}_{\mu_<}\rangle \ldots$	$\ldots \|\Phi^{\sigma_>\tau_>}_{\mu_<\nu_<}\rangle \ldots$	$\ldots$
$\langle HF\|$	E_0	0	$\langle HF\|\hat{H}\|\Phi^{\sigma_>\tau_>}_{\mu_<\nu_<}\rangle$	$\ldots$
$\vdots$	$\vdots$	$\vdots$	$\vdots$	$\vdots$
$\langle\Phi^{\sigma'_<}_{\mu'_<}\|$	0	$\langle\Phi^{\sigma'_<}_{\mu'_<}\|\hat{H}\|\Phi^{\sigma_>}_{\mu_<}\rangle$	$\langle\Phi^{\sigma'_<}_{\mu'_<}\|\hat{H}\|\Phi^{\sigma_>\tau_>}_{\mu_<\nu_<}\rangle$	$\ldots$
$\vdots$	$\vdots$	$\vdots$	$\vdots$	$\vdots$
$\vdots$	$\vdots$	$\vdots$	$\vdots$	$\vdots$
$\langle\Phi^{\sigma'_>\tau'_>}_{\mu'_<\nu'_<}\|$	$\langle\Phi^{\sigma'_>\tau'_>}_{\mu'_<\nu'_<}\|\hat{H}\|HF\rangle$	$\langle\Phi^{\sigma'_>\tau'_>}_{\mu'_<\nu'_<}\|\hat{H}\|\Phi^{\sigma_>}_{\mu_<}\rangle$	$\langle\Phi^{\sigma'_>\tau'_>}_{\mu'_<\nu'_<}\|\hat{H}\|\Phi^{\sigma_>\tau_>}_{\mu_<\nu_<}\rangle$	$\ldots$
$\vdots$	$\vdots$	$\vdots$	$\vdots$	$\vdots$
$\vdots$	$\vdots$	$\vdots$	$\vdots$	$\vdots$

Table 4.1: Total Hamiltonian matrix in the particle-hole configuration space

of the particle-hole HF configurations are used for the construction of the Hamiltonian matrix),

$$\langle\Phi^{\sigma_>}_{\mu_<}|\hat{H}|HF\rangle = \langle HF|\hat{H}|\Phi^{\sigma_>}_{\mu_<}\rangle = \boxed{\begin{array}{c}\text{see}\\(4.18)\end{array}} = 0 \tag{4.51}$$

One should also realize that up to now only two-particle interactions are supposed to be involved in the Hamiltonian (4.1). This fact gives the zero values of elements of blocks in the Hamiltonian matrix where kets differs from bras by more than two particle-hole configurations. For instance, block containing bra $\langle HF|$ and kets formed by 3p-3h configurations $|\,\Phi^{a_> b_> c_>}_{\alpha_< \beta_< \gamma_<}\rangle = a^+_{a_>} a^+_{b_>} a^+_{c_>} a_{\gamma_<} a_{\beta_<} a_{\alpha_<}\,|\,HF\rangle$ involves only zeros because always $\langle HF|\, a^+_i a^+_j a_k a_l\; a^+_{a_>} a^+_{b_>} a^+_{c_>} a_{\gamma_<} a_{\beta_<} a_{\alpha_<}\,|\,HF\rangle = 0$. So generally, all blocks in the Hamiltonian matrix contain zero where kets differs from bras by more particle-hole configurations than the number of particle interaction involved in the Hamiltonian.

Generally matrix elements in all blocks can be obtain from (4.6) and anticommutator relations of single-particle creation and annihilation operators. For instance, the diagonal 1p-1h block involves following matrix elements

$$\begin{aligned}&\langle\Phi^{\sigma'_>}_{\mu'_<}|\hat{H}|\Phi^{\sigma'_>}_{\mu'_<}\rangle = \\ &= \begin{cases} -\langle\sigma'_>\mu'_<|\hat{V}|\widetilde{\sigma_>\mu_<}\rangle & \text{for } \sigma_> \neq \sigma'_>,\ \mu_< \neq \mu'_<, \\ E_0 + \epsilon_{\sigma_>} - \epsilon_{\mu_<} - \langle\sigma_>\mu_<|\hat{V}|\widetilde{\sigma_>\mu_<}\rangle & \text{for } \sigma_> = \sigma'_>,\ \mu_< = \mu'_< \end{cases}\end{aligned} \tag{4.52}$$

The diagonalization of the total Hamiltonian matrix given in the Table 4.1 gives the resultant nuclear energies and corresponding wave functions in the form of the linear combination of the basis vectors (4.49):

$$\tilde{E}_i \quad \rightarrow \quad |i\rangle = C_0^{(i)}\,|HF\rangle + \sum_{\mu_<\sigma_>} C^{(i)}_{\mu_<\sigma_>}\,|\Psi^{\sigma_>}_{\mu_<}\rangle + \\ + \sum_{\mu_<\sigma>\mu'_<\sigma'_>} C^{(i)}_{\mu_<\sigma>\mu'_<\sigma'_>}\,|\Psi^{\sigma_>\sigma'_>}_{\mu_<\mu'_<}\rangle + \ldots \qquad (4.53)$$

where index i enumerates all eigen-states of the total Hamiltonian matrix. It is necessary to point out that the lowest energy $\tilde{E}_{i=0}$ state $|i=0\rangle$ of the total Hamiltonian matrix corresponds to the new shell model ground state ($\tilde{E}_{i=0} \neq E_0$). This new ground state $|i=0\rangle$ is not equal to the HF ground state $|HF\rangle$ but generally it has also multiparticle-multiparticle components ($C^{(i=0)}_{\mu_<\sigma_>} \neq 0$, $C^{(i=0)}_{\mu_<\sigma>\mu'_<\sigma'_>} \neq 0, \ldots$) and in such a way it contains also so called particle-hole correlations. The importance of multiparticle-multiparticle components in the ground state and excited states was shown in the literature many times (see e.g. [39], [40], [41]).

The approach, when in the Hamiltonian matrix (see Table 4.1) we restrict only to the 1p-1h block (which is separated from the $|HF\rangle$ state due to (4.51), is called Tamm-Dancoff method (see e.g. [9]). The diagonalization of the 1p-1h block gives the excited states in the following form

$$|i^{(TD)}\rangle = \sum_{\mu_<\sigma_>} C^{(i)}_{\mu_<\sigma_>}\,a^+_{\sigma_>}a_\mu\,|HF\rangle \qquad (4.54)$$

In the Tamm-Dancoff approach the ground state is described by $|HF\rangle$ and it does not contain any particle-hole correlations.

The shell-model approach discussed above for even-even nuclei can be easily extended for odd-A nuclei. In this case the total Hamiltonian matrix is constructed within the basis (4.42) of particle+p-h configurations where particle states concerns neutron (for odd-neutron nucleus) or proton (for odd proton nucleus) single-particle states. After the diagonalization of the total Hamiltonian matrix the real odd-A nucleus states are obtained in the form of the linear combinations of basis states (4.42).

It is straightforward that to perform the diagonalization of the infinite matrix constructed within the infinite basis (4.49) or (4.42) is not possible in the reality. In the real situation we are always forced to cut off this infinite basis in order to have the finite dimension matrix. In this connection it is necessary to realize that present-day computers are able to diagonalize matrix

with the dimension $10^9 \times 10^9$. However, the heavy nuclei, like actinides, have cca 200-300 active single-particle states for proton and as well as for neutron system. If we want to involve all p-h configurations constructed from these s.p. states then we would have cca 100^2 p-h configurations and in this case only 1p-1h block in the Hamiltonian matrix has dimension $100^2 \times 100^2$ and 2p-2h block dimension is $100^4 \times 100^4$, ... So, one can see that such a full shell-model calculations are beyond the possibilities of present day computers. The other problem is the real computer time to construct such a huge matrices. On the other hand if we want to describe only some part of the nucleus spectrum, for instance the low-lying excitations, then we can restrict the Hamiltonian matrix only to p-h configurations constructed from single-particle states with energies not far from the ground state energy. The other possibility to reduce the configuration space is to use not the multiparticle-multihole HF basis but some other complete basis which has a priori some part of the p-h correlations built in. This can be achieved, for instance, by apropriate prediagonalization of blocks of the total Hamiltonian matrix (see e.g. [41]), or by choosing special basis with apropriate symmetry (see e.g.[42]).

Some concrete results of HF approach will be given in the Chapter 5 and some results of shell-model are also discussed in the Chapter 7.

5. Model of independent particles in the nuclear physics

As it was already shown in the Subsection 1.4, generally three types of degrees of freedom of nuclear motion are distinquished in the nucleus, namely, single-particle, vibrational, and rotational degrees of freedom. It was also shown there that the rotation of the nucleus in the laboratory frame can be recognized only in the case of deformed nuclei. If we use the adiabatic approximation for the extraction of the part of the Hamiltonian responsible for the nucleus rotation then the laboratory frame nucleus Hamiltonian is given by (1.58)

$$\hat{H} = \hat{H}_{intr} + \hat{H}_{rot} \tag{5.1}$$

where $\hat{H}_{intr}$ is the intrinsic part of the Hamiltonian corresponding to the intrinsic degrees of freedom (single-particle and vibrational) and $\hat{H}_{rot}$ is the rotor Hamiltonian (see (1.59) and the discussion above it). In the case of the spherically symmetric nucleus the rotational degrees of freedom do not exist and the total Hamiltonian $\hat{H}$ is identical with the intrinsic Hamiltonian $\hat{H}_{intr}$.

The intrinsic Hamiltonian $\hat{H}_{intr}$ of deformed nucleus or the total Hamiltonian $\hat{H} = \hat{H}_{intr}$ of spherical nucleus is usually written as the sum of the mean field $\hat{H}_{AV}$ and the residual interaction $\hat{V}_{RES}$ (see (4.28))

$$\hat{H}_{intr} = \hat{H}_{AV} + \hat{V}_{RES} \tag{5.2}$$

where in (5.2) the residual interactions $\hat{V}_{RES}$ are meant to be expressed in the intrinsic frame. The purely theoretical way of the determination of $\hat{H}_{AV}$ was discussed in the previous chapter. In this chapter we will deal in more details with the most simple approach when only the mean field $\hat{H}_{AV}$ is taken into account in the intrinsic Hamiltonian ($\hat{H}_{intr} \approx \hat{H}_{AV}$). It was already mentioned, this very rough approximation was called model independent particles. The model of independent particles in the nuclear physics was historically the first attempt in the 40-ties of 20-th century to determine semi-microscopically some nuclear properties. In that time they tried to describe the nucleus purely

in the framework of the quantum mechanics similarly as it had been done for atom [1]. In the 30-ties it was established that the electron clouds in the atom and molecules is possible to describe by means of the Hartree-Fock approach idea starting with the Hamiltonian involving the Coulomb interaction between electrons and the nuclei of atoms and the mutual Coulomb interaction between alectrons [43, 44, 45]. Using this purely quantum mechanical approach it was possible to understand the Mendeleev periodic table (see e.g. [46] and citation therein). In the second half of 40-ties nuclear physicists wanted to use the same approach for atomic nucleus and to describe in those days known nuclear experimental data using the concept of nucleon orbitals similarly as electron orbitals in the atomic physics. However, the problem was that in contrast to atomic electron clouds in the nucleus the interaction between nucleons was not known (and practically has not known precisely up to now). Moreover, in the nucleus for nucleons there is no any force center like the nucleus for electrons in the atom. This is the cause why the model of independent particle (mean field approach only) is able to describe , more or less qualitatively, only some bulk nuclear properties.

In the previous chapter the fully microscopical Hartre-Fock method for the extraction of the single-particle mean field $\hat{H}_{AV}$ from the total Hamiltonian $\hat{H}$ involving the kinetic energy and effective nucleon-nucleon interactions was discussed. Since this method is technically complicated and requiring complex numerical computer calculation not possible in the 40-ties they tried to "guess" the form of the mean field empirically and to obtain it phenomenologically. It was succeeded in 1948 to M. Goepert-Mayer and J.H.D. Jensen [2] for spherical nuclei and their mean field potential was extended in the 50-ties also for deformed nuclei.

In this chapter some basic results of phenomenological and microscopical model of independent particles are presented. The first part of the chapter is devoted to the phenomenological mean field, how they were introduced in the past, what nuclear properties are described by them, why they are applied in some cases up to now. In the connection with the phenomenological mean fields so called Strutinsky shell correction method is also discussed in this chapter which enables to determine the equillibrium deformation of used

[1] It should be noted that historically the first theoretical description of some nuclear properties was done in the 30-ties by means of the liquid drop model [3] mentioned in the Subsection 1.1.3. and discussed also in more details in the Chapter 7. The liquid drop model is semi-phenomenoligical model able to describe only smooth part of the nuclear binding energy and qualitatively some characteristics of collective vibrations of nucleus.

[2] M. Goepert-Mayer and J.H.D. Jensen obtained Nobel prize in 1963.

mean field and the surface maps of the mean field total energy of given nucleus which is necessary for the understanding of the nuclear fission process. In the second part of this chapter some results of the present-day microscopic Hartree-Fock calculations with modern effective nucleon-nucleon interaction are demonstrated.

5.1 Phenomenological mean field

5.1.1 Spherical mean field, magic numbers

In the first papers concerning the mean field potential (in the 40-ties) they tried to take the finite spherical potential well or 3-dimensional oscillator potential as the mean field potential. However, such a mean field potentials did not describe nuclear properties, especially magic numbers. Besides that later experimental data on the electron-nucleus scattering showed that the radial dependence of the mean field potential is something between the oscillator potential and the potential in the form of the spherical well and that this potential is finite.

Energy spectrum of the single-particle levels corresponds rougly to the spectrum of the harmonic oscillator with the angular frequency $\hbar\omega_0^{(0)} \approx 41\,A^{-1/3}$ MeV (in the case of spherical nuclei), that means the single-particle levels are:

$$\epsilon_N = \langle Nlm_lm_s|\hat{H}_0^{(0)}|Nlm_lm_s\rangle = \hbar\,\omega_0^{(0)}\,\left(N+\frac{3}{2}\right) \tag{5.3}$$

where $\hat{H}_0^{(0)} = \hat{T} + \frac{1}{2}\sum_{i=1}^{A} M(\omega_0^{(0)})^2 r_i^2$ is the spherically symmetric 3-dimensional harmonic oscillator Hamiltonian. The neutron or proton single-particle state of the harmonic oscillator Hamiltonan $\hat{H}_0^{(0)}$ is characterized by the quantum numbers N, l, m_l, m_s, m_t ($\hat{L}^2\ |Nlm_lm_sm_t\rangle = l\,(l+1)\ |Nlm_lm_sm_t\rangle$, $\hat{L}_3\ |Nlm_lm_sm_t\rangle = m_l\ |Nlm_lm_sm_t\rangle$, $\hat{s}_3\ |Nlm_lm_sm_t\rangle = m_s\,|Nlm_lm_sm_t\rangle$, $\hat{t}_3\,|Nlm_lm_s\rangle = m_t\,|Nlm_lm_s\rangle$) where for given N: $l = 0,\ 2,\ 4, \ldots,\ N$ for even N or $l = 1,\ 3,\ 5, \ldots,\ N$ for odd N; $m_l = -l, \ldots, l$; $m_s = \pm 1/2$; $m_t = 1/2$ for neutron and $m_t = -1/2$ for proton. For given type of nucleons (m_t is fixed) each level ϵ_N is degenerated with the degeneracy degree n_N given by:

$$n_N = \sum_{l=0(1)}^{N} 2\,(2l+1) = (N+1)\,(N+2) \tag{5.4}$$

The total number of nucleons of given type occupying levels from $N = 0$ up to given $N = N_0$ is following

$$\sum_{N=0}^{N_0} n_N = \sum_{N=0}^{N_0} (N+1)\,(N+2) = \frac{1}{3}(N_0+1)\,(N_0+2)\,(N_0+3) \qquad (5.5)$$

So, the individual nucleons of given type fill gradually the single-particle states given in the Table 5.1 One can see from the Table 5.1 that the har-

N	$\epsilon_N/\hbar\omega_0^{(0)}$	n, l	n_N	$\sum_N n_N$ —
0	3/2	1s	2	2
1	5/2	1p	6	8
2	7/2	2s, 1d	12	20
3	9/2	2p, 1f	20	40
4	11/2	3s, 2d, 1g	30	70
5	13/2	3p, 2f, 1h	42	112
6	15/2	4s, 3d, 2g, 1s	56	168

Table 5.1: Filling number for single-particle shells of the harmonic oscillator Hamiltonian

monic oscillator shells (that means levels ϵ_N) are filled when the number of protons and/or neutrons is equal to 2, 8, 20, 40, 70, 112, 168, ... In the analogy with the Mendeleev periodic table one would expect that there are the discontinuities in the dependence of various measurable quantities on N or Z for values of N and Z equal to the number given above (when oscillator shells are filled). However, these discontinuities were experimentally observed not for these numbers but for so called magic numbers $N(Z) = 2$, 8, 20, 28, 50, 82 and 126. As an example, in the Fig. 5.1 the dependence on Z and N of the difference of experimental masses of all stable nuclei from their average value is shown. From the Fig. 5.1 it is obvious that the nuclei with N and Z equal to some of magic numbers are much more stable than others (such nuclei have the mass minimum and therefore the biggest in absolute value binding energy - see (1.12)). Similar discontinuities are observed also in the dependence on Z and N of other quantities, e.g. separation energy of nucleons, energies of the first excited states 2^+ and others.

So, the filling numbers of oscillator shells do not correspond to experimental magic numbers. In order to remove this discrepancy M. Goepert-Mayer and J.H.D.Jensen (see e.g. [48, 49] and citations therein) added to the oscil-

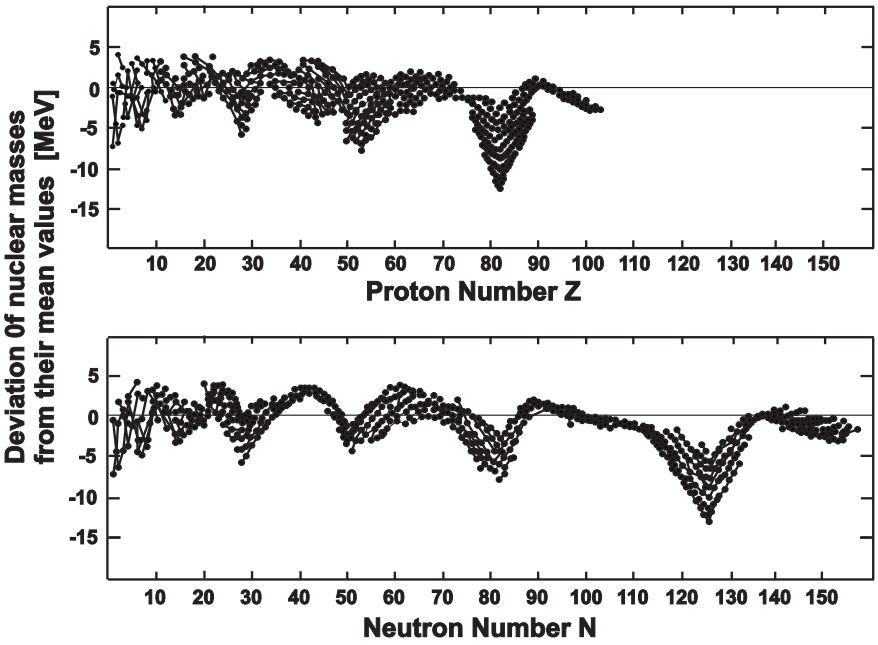


Figure 5.1: Deviation of nuclear masses from their mean values plotted as a function of neutron and proton number (data taken from [47])

lator mean field spin-orbital term:

$$\hat{V}_{LS} = -\sum_{i=1}^{A} V_{ls}(r_i)\,\hat{\vec{l}}_i \cdot \hat{\vec{s}}_i \tag{5.6}$$

where $\hat{\vec{l}}_i = \vec{r}_i \times \hat{\vec{p}}_i$ and $\hat{\vec{s}}_i$ is the orbital moment and the spin operator of the i-th nucleon. $V_{ls}(r)$ is the appropriately chosen radial dependence (see further). The spin-orbital term removes the degeneracy of the harmonic oscillator levels $\epsilon_N = \hbar\omega_0^{(0)}\,(N + 3/2)$ and taking account this term gives the new s.p. energy ϵ_{Nlj}:

$$\begin{aligned}
\epsilon_{Nlj} &= \langle Nljm|\,\hat{H}_0^{(0)} - \sum_i V_{ls}(r_i)\,\hat{\vec{l}}_i \cdot \hat{\vec{s}}_i\,|Nljm\rangle = \\
&= \boxed{\begin{array}{c}\text{because } \vec{j}^{\,2} = (\,\vec{l} + \vec{s}\,)^2 = \vec{l}^{\,2} + \vec{s}^{\,2} + 2\,\vec{l}\cdot\vec{s} \\ \Rightarrow \vec{l}\cdot\vec{s} = \frac{1}{2}\,(\,\vec{j}^{\,2} - \vec{l}^{\,2} - \vec{s}^{\,2}\,)\end{array}} = \\
&= (\,N + \frac{3}{2}\,)\,\hbar\omega_0^{(0)} - \langle V_{ls}\rangle_{Nl}\,\frac{1}{2}\left(j(j+1) - l(l+1) - \frac{3}{4}\right)
\end{aligned} \tag{5.7}$$

Since $\vec{j} = \vec{l} + \vec{s}$ we have two possibilities for j: $j = l \pm \frac{1}{2}$ and therefor the

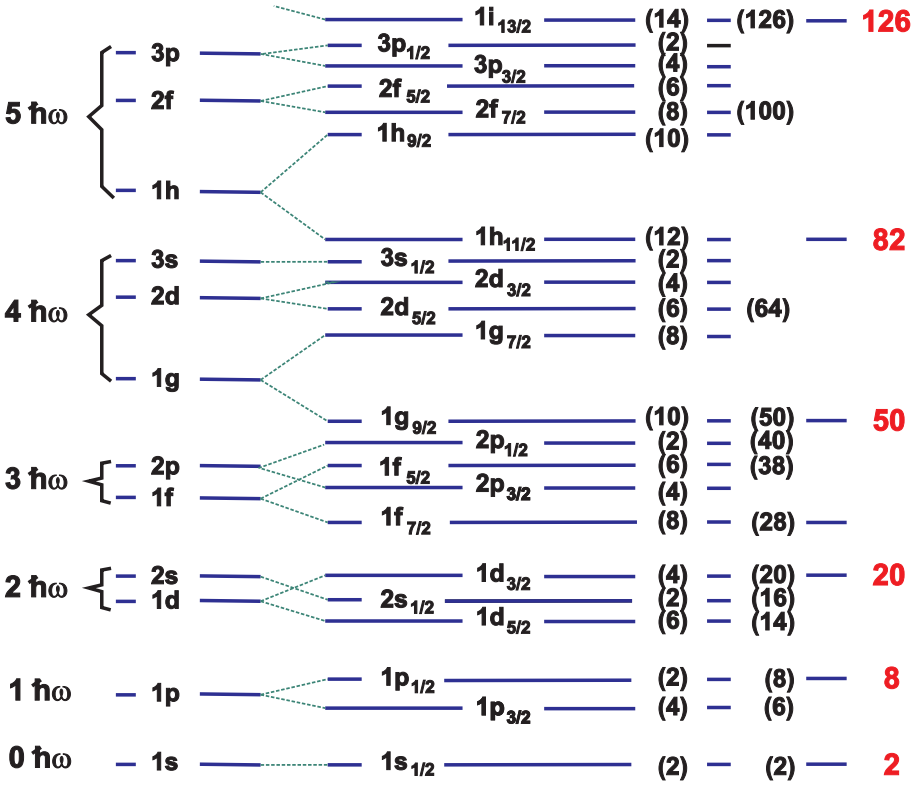


Figure 5.2: Schematic nuclear levels of the shell model with spin orbit term

relation (5.7) can be rewritten as follows:

$$\epsilon_{Nlj} = (N + \frac{3}{2}) \hbar\omega_0^{(0)} - \langle V_{ls} \rangle_{Nl} \begin{cases} \frac{1}{2}\, l & \text{for } j = l + 1/2 \\ -\frac{1}{2}\,(l+1) & \text{for } j = l - 1/2 \end{cases} \tag{5.8}$$

where $\langle V_{LS} \rangle_{Nl} = \int_0^\infty dr\, r^2\, R_{Nl}(r)\, V_{ls}(R)\, R_{Nl}(r)$ is the radial part of the diagonal matrix element $\langle Nljm|\hat{V}_{ls}|Nljm\rangle$ ($R_{Nl}(r)$ is the radial part of the corresponding single-particle wave function). This radial integral was not usually calculated and the quantity $\langle V_{LS} \rangle_{Nl}$ was taken as one of the free parameters for all quantum numbers Nl and it was adjusted according to the experimental data. Appropriate choice of this parameter enabled to achieve the single-particle spectrum corresponding to the filling number which reproduce the experimental magic numbers $N(Z) = 2,\ 8,\ 20,\ 28,\ 50,\ 82,\ 126$. This spin-orbit term gives the next 'magic' number 184 (corresponding to the valence shell N=6). The splitting of the oscillator shells by means of the spin-orbital term in the mean field Hamiltonian is shown schematically in the Fig. 5.2 (negative sign of the spin-orbital term means the l-s interaction is attractive).

The strength of the attractive spin-orbital coupling term needed for the sufficiently strong $j = l \pm 1$ splitting for obtaining good magic numbers according to the Fig. 5.2 was about an order higher in the comparison with the l-s coupling strength in the theory of electrons in an atom using a Lorentz invariant treatment (based on the Dirac equation). Later, in the 60-ties, when the nucleon-nucleon interaction including the l-s coupling was described by the meson exchange (as was discussed in the Chapter 3) it was shown that the meson exchange was able to give such a strong l-s coupling. However, in the 40-ties the idea to incorporate artificially strong l-s term into the single-particle oscillator Hamiltonian introduced in [49] and [48] was decisive for the understanding of the magic numbers.

In the 50-ties attempts were done to use as the single-particle potential not only pure harmonic oscillator but also other more realistic potentials, e.g.

- modified harmonic oscillator mean field [50]

$$\hat{H}_{AV} = \sum_{i=1}^{A} \left\{ \hat{t}_i + \frac{1}{2} M \, (\omega_0^{(0)})^2 \, r_i^2 + C \, \hat{\vec{l}}_i \cdot \hat{\vec{s}}_i + D \left(\hat{\vec{l}}_i^{\,2} - \langle l^2 \rangle \right) \right\} \tag{5.9}$$

  where C and D are parameters ($C < 0$, $D < 0$). The last term in (5.9) modifies the single-particle spectrum in order to obtain better agreement with the single-particle energies of odd-A spherical nuclei (see further).

- Wood-Saxon potential [51]

$$\hat{H}_{AV} = \sum_{i=1}^{A} \left\{ \hat{t}_i - \frac{V_0}{1 + e^{\frac{r - R_0}{a}}} + C \, \hat{\vec{l}}_i \cdot \hat{\vec{s}}_i \right\} + \hat{V}_{Coulomb} \tag{5.10}$$

  where $R_0 = 1.2 \, A^{1/3}$ fm is the nuclear radius. V_0 and a are parameters giving the width of the potential surface smearing - see Fig. 5.3 ($V_0 \approx 50$ MeV, $a \approx 0.5$ fm)

The success of the simple shell model of the phenomenological mean field did not consist only in the explanation of magic numbers but also in the description of other nuclear properties, e.g. of the total angular moments of the odd-A spherical nuclei. The main assumption in this case was based on the experimental fact that all spherical even-even nuclei have ground states 0^+ ($J = 0$, positive parity). This means that the spherical odd-A nucleus properties are given by the single-particle characteristics of the state occupied by the odd nucleon above the even-even core. Under such assumption the

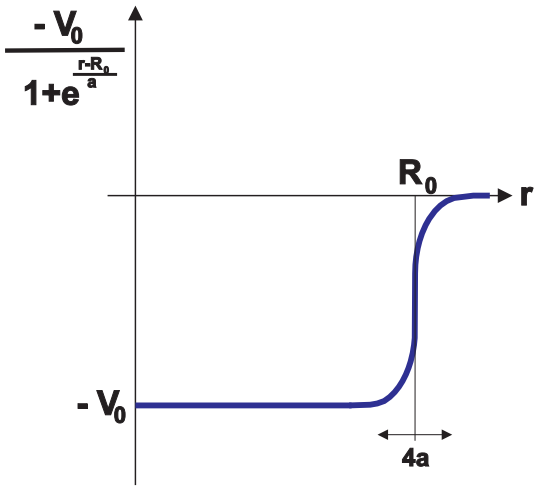


Figure 5.3: Shape of the Woods-Saxon potential

total angular moment of the odd nucleon state gives the total angular moment of the whole odd-A nucleus. In the Table 5.2 the comparison of the simple shell model angular moments of the odd-Z nuclear single-particle ground states and experimental angular moments of ground state spherical odd-A nuclei are shown.

The simple shell model with the phenomenological mean potential was also successful in the description of the electromagnetic transitions and of the static electromagnetic moments of odd-A spherical nuclei. From (2.148) we know that the probability of the electromagnetic transition from the state $|i\rangle$ to the state $|f\rangle$ in one second is given by

$$T_{i\to f} = \sum_{\lambda=1}^{\infty} \left(T_{i\to f}(el,\ \lambda) + T_{i\to f}(mag,\ \lambda) \right) \tag{5.11}$$

with (see (2.148)) ($X = el,\ mag$)

$$T_{i\to f}(X,\ \lambda) = \frac{8\pi c\alpha}{e^2} \frac{(\hbar\omega)^{2\lambda+1}(J+1)}{(\hbar c)^{2\lambda+1}\left[(2\lambda+1)!!\right]^2}\ B(X\lambda;\ i\to f) \tag{5.12}$$

where the energy of the transition is $\hbar\omega = E_i - E_f$ (we suppose deexcitation, $E_i > E_f$). In the case of electromagnetic transitions in the odd-A nuclei (when in the model of independent particles the nucleus wave function can be approximated by the single-particle wave function of the odd nucleon) the electromagnetic reduced probabilities are given by (2.147) where initial $|i\rangle$ and final $|f\rangle$ states are corresponding single-particle kets $|N_i l_i j_i m_i\rangle$ and

elem.	Z	$1s_{1/2}$	$1p_{3/2}$	$1p_{1/2}$	$1d_{5/2}$	$2s_{1/2}$	$1d_{3/2}$	$1f_{7/2}$	config.	theor. J	exp. J
^{1}H	1	1							$s_{1/2}$	1/2	1/2
^{7}Li	3	2	1						$p_{3/2}$	3/2	3/2
^{11}B	5	2	3						$(p_{3/2})^{-1}$	3/2	3/2
^{15}N	7	2	4	1					$p_{1/2}$	1/2	1/2
^{17}F	9	2	4	2	1				$d_{5/2}$	5/2	5/2
^{19}F	9	2	4	2	1				$(d_{5/2})^{-1}$	5/2	1/2
^{23}Na	13	2	4	2	3				$(d_{5/2})^{3}$	5/2	3/2
^{31}P	15	2	4	2	6	1			$s_{1/2}$	1/2	1/2
^{35}Cl	17	2	4	2	6	2	1		$d_{3/2}$	3/2	3/2
^{37}Cl	17	2	4	2	6	2	1		$d_{3/2}$	3/2	3/2
^{39}K	19	2	4	2	6	2	3		$(d_{3/2})^{-1}$	3/2	3/2
^{41}K	19	2	4	2	6	2	3		$(d_{3/2})^{-1}$	3/2	3/2
^{45}Sc	21	2	4	2	6	2	4	1	$f_{7/2}$	7/2	7/2
^{51}V	23	2	4	2	6	2	4	3	$(f_{7/2})^{3}$	7/2	7/2
^{55}Mn	25	2	4	2	6	2	4	5	$(f_{7/2})^{5}$	7/2	7/2
^{59}Mn	27	2	4	2	6	2	4	7	$(f_{7/2})^{7}$	7/2	7/2

Table 5.2: Simple shell model subshell occupation for light odd-Z nuclei - Note that the angular moments given in the column "theor.", which result from the simple spherical shell model (see Fig. 5.2), are in agreement with observed ground state angular moments given in the column "exp.". The only exception is found in the case of ^{19}F and ^{23}Na. However these two nuclei can be described as deformed and the simple shell model for spherical nucleus is not relevant for them.

$|N_f l_f j_f m_f\rangle$, respectively

$$B(el\ \lambda;\ N_i l_i\ j_i \to N_f l_f\ j_f) = \boxed{\begin{array}{c}\text{see}\\(2.147)\end{array}} =$$

$$= \frac{|\ \langle N_f l_f\ j_f||\hat{\mathscr{M}}^{(el)}_{\lambda}||N_i l_i\ j_i\rangle\ |^2}{2j_i+1} = \boxed{\begin{array}{c}\text{see (2.130)}\\(A.12),(A.3)\end{array}} =$$

$$= \sum_{m_f \mu} |\ \langle N_f l_f\ j_f\ m_f| \int d^3r\ \hat{\rho}(\vec{r})\ r^{\lambda} Y_{\lambda\mu}(\hat{r})\ \ |N_i l_i\ j_i\ m_i\rangle\ |^2 \tag{5.13}$$

where the operator of the charge density $\hat{\rho}(\vec{r})$ is introduced (see (2.131))

$$\hat{\rho}(\vec{r}\,) = \sum_{i=1}^{A} e_i\ \delta(\vec{r} - \vec{r}_i) \tag{5.14}$$

Similarly for the reduced probability of the magnetic transition we have

$$B(mag\ \lambda;\ N_i l_i\ j_i \to N_f l_f\ j_j) = \boxed{\begin{array}{c}\text{see}\\(2.147)\end{array}} =$$

$$= \frac{|\ \langle N_f l_f\ j_f||\hat{\mathscr{M}}_\lambda^{(mag)}||N_i l_i\ j_i\rangle\ |^2}{2j_i+1} = \boxed{\begin{array}{c}\text{see (2.145)}\\(A.12),(A.3)\end{array}} =$$

$$= \sum_{m_f \mu} \Bigg| \langle N_f l_f\ j_f\ m_f|\ \sum_{i=1}^{A} \left\{ g_s^{(i)}\ \hat{\vec{s}}_i + \frac{2}{2\lambda+1}\ g_l^{(i)}\ \hat{\vec{l}}_i \right\}\ \frac{e\hbar}{2Mc}$$

$$\cdot \vec{\nabla}_i\ r_i^\lambda\ Y_{\lambda\mu}(\hat{r}_i)\ \ |N_i l_i\ j_i\ m_i\rangle \Bigg|^2 \tag{5.15}$$

where (see (2.144), (2.146))

$$\begin{aligned} &e^{(i)} = e \text{ for protons}, \quad g_s^{(i)} = 5.586 \text{ for protons}, \quad g_l^{(i)} = 1 \text{ for protons},\\ &e^{(i)} = 0 \text{ for neutrons}, \ g_s^{(i)} = 5.586 \text{ for neutrons}, \ g_l^{(i)} = 0 \text{ for neutrons} \end{aligned} \tag{5.16}$$

The values of charges e_i and gyromagnetic ratios $g_s^{(i)}$ are values for free nucleons. In the case of the nucleons in the nucleus instead of the values for free particles so called effective charges and gyromagnetic ratios are used in the concrete calculations

$$e^{(i)} \to e_{eff}^{(i)}\, e \qquad g_s^{(i)} \to g_{eff}^{(i)}\, g_s^{(i)} \tag{5.17}$$

The introduction of the effective gyromagnetic ratios $g_{eff}^{(i)}$ is explained by many-particle effects and effects connected with the meson exchange between nucleons in the nucleus (see e.g. [52]). From the analyses of experimental data on M1 transitions it appeared that its value is $g_{eff}^{(i)} \approx 0.7$ [52]. In the case of odd-A nucleus the effective charge $e_{eff}^{(i)}$ involves effects connected with the relative motion of the odd nucleon with the mass M, charge $(1-\tau_z)\, e/2$ ($\tau_z = -1$ for protons and $\tau_z = +1$ for neutrons), coordinate $\vec{r}_1$ with respect to the even-even core (with the mass $M\,(A-1)$ and charge $[Z-(1-\tau_z)/2]\, e$ and the core center of mass coordinate $\vec{r}_0$). Then the center of mass of the whole odd-A nucleus is $\vec{R}_0 = [\vec{r}_1 + \vec{r}_0(A-1)]/A$. The effective charge of the odd nucleon is then defined for the electric transition with the multipolarity

λ by the following expression ($\vec{r} = \vec{r}_1 - \vec{r}_0$ is the relative coordinate of the odd nucleon with respect to the even-even core)

$$e^{(i)}_{eff}(\lambda)\,\vec{r}^{\,\lambda} \equiv \frac{1-\tau_z}{2}\,\left(\vec{r}_1 - \vec{R}_0\right)^{\lambda} + \left(Z - \frac{1-\tau_z}{2}\right)\,\left(\vec{r}_0 - \vec{R}_0\right)^{\lambda} =$$

$$= \frac{1-\tau_z}{2}\left[\vec{r}_1 - \frac{1}{A}\vec{r}_1 - \frac{A-1}{A}\vec{r}_0\right]^{\lambda} +$$

$$+ \left(Z - \frac{1-\tau_z}{2}\right)\,\left[\vec{r}_0 - \frac{1}{a}\vec{r}_1 - \frac{A-1}{A}\vec{r}_0\right]^{\lambda} =$$

$$= \left\{\frac{1-\tau_z}{2}\left(\frac{A-1}{A}\right)^{\lambda} + \left(Z - \frac{1-\tau_z}{2}\right)\left(-\frac{1}{A}\right)^{\lambda}\right\}\,\vec{r}^{\,\lambda}$$

and therefore

$$e^{(i)}_{eff}(\lambda) \;\equiv\; \frac{1-\tau_z}{2}\,\left(\frac{A-1}{A}\right)^{\lambda} + \left(Z - \frac{1-\tau_z}{2}\right)\left(-\frac{1}{A}\right)^{\lambda} \tag{5.18}$$

For instance, for $\lambda = 1$ we have: $e^{(i)}_{eff} = (A-1)/A - (Z-1)/A \approx 1 - Z/A = N/A$ for protons and $e^{(i)}_{eff}$ = -Z/A for neutrons. It should be noted that there are other, more sofisticated, ways for obtaining the effective nucleon charges (see e.g. [9], [53]).

Since in the coordinate representation the simple shell model single-particle wave function is

$$\langle\vec{r}|Nljm\rangle = \sum_{m_l\,m_s} C^{jm}_{lm_l\,\frac{1}{2}m_s}\,R_{Nlj}(r)\,Y_{lm_l}(\hat{r})\,|\frac{1}{2}m_s\rangle \tag{5.19}$$

the expression (5.13) for the electric reduced probability $B(el\;\lambda;\;N_i l_i\;j_i \rightarrow$

$N_f l_f\, j_f$) (see (2.147), (2.161)) can be rewritten as follows

$$
\begin{aligned}
&B(el\,\lambda;\; N_i l_i\, j_i \to N_f l_f\, j_f) = \\
&\quad = (e_{eff}(\lambda)\, e)^2 \left| \int_0^\infty dr\; R_{N_f l_f\, j_f}(r)\, r^{\lambda+2}\, R_{N_i l_i\, j_i}(r) \right|^2 \\
&\qquad \sum_{\mu m_f} \sum_{m_{l_i}} \sum_{m_{s_i}} \sum_{m_{l_f}\, m_{s_f}} \left(C^{j_i m_i}_{l_i m_{l_i}\, \frac{1}{2} m_{s_i}} \right)^2 \left(C^{j_f m_f}_{l_f m_{l_f}\, \frac{1}{2} m_{s_f}} \right)^2 \\
&\qquad\qquad \left| \int d\hat{r}\; Y^*_{l_f m_{l_f}}(\hat{r})\; Y_{\lambda\mu}(\hat{r}) Y_{l_i m_{l_i}}(\hat{r}) \right|^2 \delta_{m_{s_i}\, m_{s_f}} = \\
&\quad = \boxed{\begin{array}{c}\text{see also} \\ (2.162)\end{array}} = \\
&\quad = (e_{eff}(\lambda)\, e)^2\, \frac{2\lambda+1}{4\pi}\, C^{j_f \frac{1}{2}}_{j_i \frac{1}{2} \lambda 0} \left| \int_0^\infty dr\; R_{N_f l_f\, j_f}(r)\, r^{\lambda+2}\, R_{N_i l_i\, j_i}(r) \right|^2
\end{aligned}
\tag{5.20}
$$

and the similar expression for the reduced single-particle probability $B(mag\lambda; N_i l_i j_i \to N_f l_f\, j_f)$ of magnetic transitions can be obtained.

The application of the expression (5.20) for the spherical odd-A nuclei (where there are no rotational degrees of freedom) gave the qualitative agreement with the experimental probabilities of electromagnetic transitions between low-lying single-particle states in these spherical near closed shell nuclei. Simple expresions (5.20) lead on the 50-ties to the introduction of so called Wisskopf units for electric (and similar expression for magnetic) reduced probabilities (see Subsection 2.2.2.4 for more details). However, it is necessary to point out that expression (5.20) is suitable only for odd-A nuclei close to magic closed shell nuclei. In the nuclei more far from closed shell ones the mixing of configurations occurs and as a result we cannot use simple spherically symmetric shell model of independent particles.

Next measurable quantity, which was qualitatively explained by the simple shell model of independent particles, was magnetic dipole moment of odd-A nuclei. The magnetic dipole moment of the nucleus is defined by the epression (2.211). In the framework of the model of independent particles for the odd-A

nuclei the expression (2.211) reads as follows

$$\mu = \langle Nljm = j|\, \hat{\mu}_3\, |Nljm = j\rangle = \boxed{\begin{array}{c}\text{see}\\ \text{(2.208), (2.209)}\end{array}} =$$
$$= \langle Nljm = j|\, (g_l\, \hat{l}_3 + g_s\, \hat{s}_3)\, \mu_N\, |Nljm = j\rangle \tag{5.21}$$

where $\mu_N = e\hbar/2Mc$ is the nucleon magneton. The relation (5.21) can be rewritten using so called projection theorem for any vector operator $\hat{\vec{A}}$ (see e.g. [9]):

$$\langle jm|\, \hat{\vec{A}}\, |jm\rangle = \langle jm\, |\hat{\vec{j}}|\, jm\rangle\, \frac{\langle jm = j|\, \hat{\vec{A}} \cdot \hat{\vec{j}}\, |jm = j\rangle}{j(j+1)} \tag{5.22}$$

as follows

$$\mu = \frac{j}{j(j+1)}\, \langle Nljm = j|\ \ \hat{\vec{j}} \cdot (g_s\, \hat{\vec{s}} + g_l\, \hat{\vec{l}})\, \mu_N\, |Nljm = j\rangle =$$
$$= \boxed{\begin{array}{r}\text{because}\ \ 2\,\vec{j}\cdot\vec{s} = \vec{j}^{\,2} + \vec{s}^{\,2} - \vec{l}^{\,2}\\ 2\,\vec{j}\cdot\vec{l} = \vec{j}^{\,2} + \vec{l}^{\,2} - \vec{s}^{\,2}\end{array}} =$$
$$= \frac{1}{j+1}\, \frac{1}{2}\, \Big\{ g_l\, [j(j+1) + l(l+1) - \frac{3}{4}]$$
$$+ g_s\, [j(j+1) + \frac{3}{4} - l(l+1)] \Big\}\, \mu_N =$$
$$= \frac{1}{j+1}\, \frac{1}{2}\, \Big\{ (g_l + g_s)\, j(j+1) + (g_l - g_s)\, [l(l+1) - \frac{3}{4}] \Big\}\, \mu_N \tag{5.23}$$

Since $j = l \pm \frac{1}{2}$ we have two possibilities:

$$\mu = \begin{cases} [\,(j - \frac{1}{2})\, g_l + \frac{1}{2}\, g_s\,]\, \mu_N & \text{for}\ \ j = l + \frac{1}{2} \\ \frac{j}{j+1}\, [\,(j + \frac{3}{2})\, g_l - \frac{1}{2}\, g_s\,]\, \mu_N & \text{for}\ \ j = l - \frac{1}{2} \end{cases} \tag{5.24}$$

The curves $\mu = \mu(j)$ given by (5.24) are called Schmidt lines. They are plotted in the Fig. 5.4 together with experimental values of the magnetic dipole moment μ for odd-A nuclei in the ground state. One can see that all experimental values lay between two Schmidt lines but the best agreement of experimental values of μ with Schmidt lines are found for odd-A nuclei ^{15}N, ^{17}O, ^{39}K and ^{207}Pb and other odd-A nuclei just next to closed shell even-even nuclei.

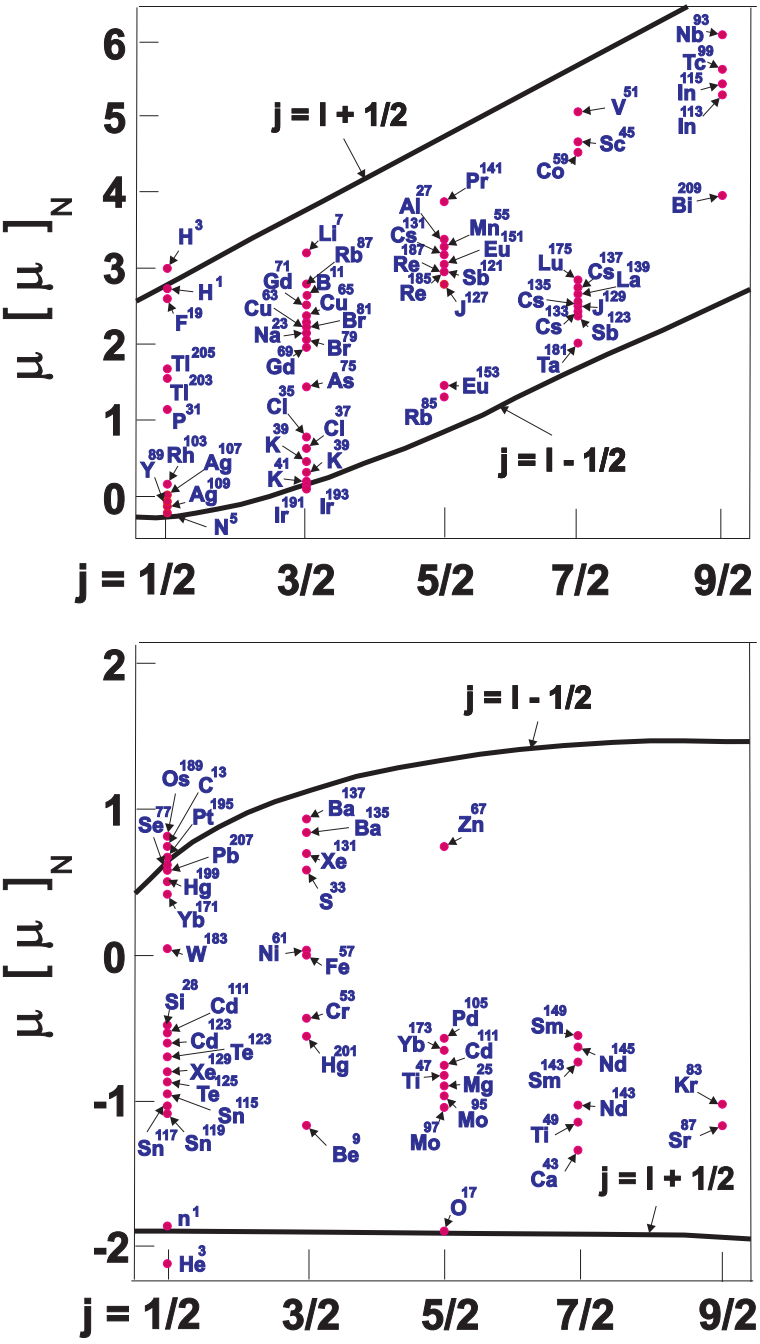


Figure 5.4: Magnetic moments for Z-odd (upper panel) and N-odd (bottom panel) as a function of angular momentum (data taken from [54])

The fact that dipole moments calculated in the framework of the spherically symmetric simple shell model of independent particles for nuclei more far from closed shell ones do not agree with the Schmidt lines is related with the deformation of the mean field of these nuclei. In the nuclei with the number of nucleons corresponding to the filling of around half of the valence shell the mean field potential has deformed equipotential surfaces and the usage of the simple spherically symmetric shell model of independent particles is not relevant.

5.1.2 Phenomenological deformed mean field, Strutinski shell corrections, equilibrium deformation, fission barriers

5.1.2.1 Nilsson model of deformed mean field

Experimental data on nucleon spectra in the beginning of the 50-ties showed the existence of the rotational bands in the nuclei with the number of nucleons corresponding to the partly filling of the valence shell [3]. Rotational degrees of freedom of nuclear motion will be discussed in details in the Chapter 8. Here it is necessary only to remind that the rotation of the quantum objects is possible to recognize in the quantum mechanics only in deformed systems (see the text under the Fig.1.5 and above the expr. (1.58)). So, if the rotational bands were observed in the specta of some nuclei it meant that these nuclei were deformed. To be more precise, the equipotential surfaces of the mean field potential were deformed. The deformation of the mean field of the nuclei with partly filled valence shell was confirmed later also by the fully self-consistent Hartree-Fock calculations (we will discuss this point in the end of this chapter). In the connection with the expectation of the deformation of some nuclei in the beginning of the 50-ties the simple spherically symmetric shell model of independent particles discussed in the previous subsection was modified and so called Nilsson model of deformed mean field was introduced [50].

As it was discussed in the subsection 1.1.2 the surface of any deformed object can be described by the decomposition (1.3) (we suppose the coordinate

[3]The rotational bands in the quantum systems were known from the 30-ties and 40-ties from spectra of deformed molecules.

frame fixed to the rotating nucleus - so called fixed body frame)

$$R(\theta,\varphi) = R_0 \left(1 + \sum_{\lambda\mu} \alpha_{\lambda\mu}\, Y_{\lambda\mu}(\theta,\varphi)\right) \tag{5.25}$$

The analysis of nuclear spectra and probabilities of electromagnetic transitions showed that the static electric dipole moments of nuclei in their ground state are zero and as a result the sum in (5.25) starts from $\lambda = 2$. Based on the more detailed inspection of nuclear data and on the analogy with the molecule physics it was found that the most important contribution in the sum (5.25) comes from the quadrupole term $\lambda = 2$ with the axial symmetry $\mu = 0$. Then the nucleus shape can be approximated by the axially symmetric ellipsoid (see also (1.4) and text below it):

$$R(\theta,\varphi) = R_0\ (1 + \alpha_{20}\, Y_{20}(\theta,\varphi)) \tag{5.26}$$

where R_0 in (5.26), (5.25) is the radius of the sphere with the same volume as the one of the ellipsoid (5.26). In the nucleus case R_0 is given by (1.2), $R_0 = 1.2\, A^{1/3}$ fm.

Usually it is assumed that the equipotential surfaces have the same shape as the mass distribution (the surfaces with the same density), that means these surfaces are described by the following equation (r_0 different but fixed)

$$r(\theta,\varphi) = r_0\ (1 + \alpha_{20}\, Y_{20}(\theta,\varphi)) \equiv r_0\, f(\alpha_{20},\theta,\varphi) \tag{5.27}$$

with the same quadrupole deformation α_{20} as in (5.26). The starting point of the derivation of the phenomenological deformed mean field of the Nilson model is the modified harmonic oscillator mean field for spherical case - see (5.9), where the requirement of equilibrium surfaces in the form (5.27) is added:

$$\hat{H}_{AV} = \sum_i \Big\{ -\frac{\hbar^2}{2M_i}\vec{\nabla}_i^2 + \frac{1}{2}M_i\omega_0^2 \left(\frac{r_i}{f(\alpha_{20},\theta,\varphi)}\right)^2 + \\ + C\,\vec{l_i}\cdot\vec{s}_i + D\,(\vec{l}_i^{\,2} - \langle l^2\rangle)\Big\} \tag{5.28}$$

Then, really, the second term in (5.28) gives equipotential surfaces $r/f(\alpha_{20},\theta,\varphi) = const = r_0$. In the next step the Taylor expansion according to the deformation parameter α_{20} is applied and up to the linear terms in α_{20} we obtain:

$$\hat{H}_{AV} = \hat{H}_0^{(0)} - \sum_i \Big\{ M\,\omega_0^2\, r_i^2\, \alpha_{20}\, Y_{20}(\theta_i,\varphi_i) + \\ - C\,\vec{l_i}\cdot\vec{s}_i - D\,(\vec{l}_i^{\,2} - \langle l^2\rangle)\Big\} \tag{5.29}$$

with the spherical harmonic oscillator Hamiltonian $\hat{H}_0^{(0)}$

$$\hat{H}_0^{(0)} = -\frac{\hbar^2}{2M}\sum_i \vec{\nabla}_i^2 + \sum_i \frac{1}{2}\, M\, \omega_0^2\, r_i^2 \tag{5.30}$$

Parametrization of the quadrupole deformation according to α_{20} is not the only possibility. There is an alternative introduction of the quadrupole deformation:

$$\hat{H}_{AV} = \sum_i \left\{ -\frac{\hbar^2}{2M}\vec{\nabla}^2 + \frac{1}{2}\, M\, \left(\omega_x^2\, x^2 + \omega_y^2\, y^2 + \omega_z^2\, z^2\right) + \right.$$
$$\left. + C\, \hat{\vec{l}}\cdot\hat{\vec{s}} + D\, \left(\hat{\vec{l}}^{\,2} - \langle l^2\rangle_N\right)\right\}_i \tag{5.31}$$

where the alternative quadrupole deformation parameter ϵ is installed by means of the following definition (for axially symmetric case)

$$\omega_{perp} \equiv \omega_x = \omega_y = \omega_0(\epsilon)\, \left(1 + \frac{1}{3}\,\epsilon\right)$$
$$\omega_z = \omega_0(\epsilon)\, \left(1 - \frac{2}{3}\,\epsilon\right) \tag{5.32}$$

The substitution of (5.32) into (5.31) gives (up to the linear terms in ϵ)

$$\hat{H}_{AV} = \sum_i \left\{ -\frac{\hbar^2}{2M}\vec{\nabla}^2 + \frac{1}{2}M\, \omega_0^2\, r^2 + m\, \omega_0^2\, \epsilon\, \left(\frac{x^2}{3} + \frac{y^2}{3} - \frac{2z^2}{3}\right) + \right.$$
$$\left. + C\, \hat{\vec{l}}\cdot\hat{\vec{s}} + D\, \left(\hat{\vec{l}}^{\,2} - \langle l^2\rangle_N\right)\right\}_i \tag{5.33}$$

Using the expression for the spherical harmonics $Y_{20}(\theta,\varphi)$:

$$2\sqrt{\frac{\pi}{5}}\, r^2\, Y_{20}(\theta,\varphi) = -\frac{1}{2}\, (x^2 + y^2 - 2z^2) \tag{5.34}$$

the expression (5.33) can be rewritten as follows

$$\hat{H}_{AV} = \sum_i \left\{ -\frac{\hbar^2}{2M}\vec{\nabla}^2 + \frac{1}{2}M\, \omega_0^2\, r^2 - \frac{4}{3}\sqrt{\frac{\pi}{5}}\, \epsilon\, r^2\, Y_{20}(\theta,\varphi) + \right.$$
$$\left. + C\, \hat{\vec{l}}\cdot\hat{\vec{s}} + D\, \left(\hat{\vec{l}}^{\,2} - \langle l^2\rangle_N\right)\right\}_i \tag{5.35}$$

The comparison of (5.35) with (5.29) gives the relation between quadrupole deformation parameters α_{20} and ϵ (sometimes this parameter is denoted as $\epsilon_2 = \epsilon$):

$$\alpha_{20} = \frac{4\sqrt{\pi}}{3\sqrt{5}}\, \epsilon \tag{5.36}$$

If the last two terms in (5.31) are neglected then the shape of the equipotential surfaces is rotationally symmetric ellipsoid

$$\omega_x^2\, x^2 + \omega_y^2\, y^2 + \omega_z^2\, z^2 = const$$

$$\Rightarrow \boxed{\begin{array}{c}\text{see}\\ (5.32)\end{array}} \Rightarrow$$

$$\frac{x^2+y^2}{1/\omega_{perp}^2} + \frac{z^2}{1/\omega_z^2} = const' \tag{5.37}$$

what represents the equation of the ellipsoid with semi-axes: $a = b = 1/\omega_{perp}$ and $c = 1/\omega_z$ with the volume $\frac{4}{3}\pi a^2 c = \frac{4}{3}\pi \frac{1}{\omega_{perp}^2 \omega_z}$. We suppose that this volume is equal to the volume of the sphere with the radius $1/\omega_0^{(0)}$ (where $\hbar\omega_0^{(0)} = 41\, A^{-1/3}$ MeV) and this gives

$$\omega_0^3(\epsilon)\, \left(1+\frac{1}{3}\epsilon\right)^2 \left(1-\frac{2}{3}\epsilon\right) = (\omega_0^{(0)})^3$$

$$\Rightarrow \qquad \omega_0(\epsilon) = \omega_0^{(0)} \left(1 - \frac{1}{3}\epsilon^2 - \frac{2}{27}\epsilon^3\right)^{-1/3} \tag{5.38}$$

which is known in the literature as the volume conservarion condition.

The single-particle states and corresponding single-particle energies of the mean field are eigen-states and eigen-values of the Hamiltonian (5.29)

$$\hat{H}_{AV} = \sum_i \left\{ -\frac{\hbar^2}{2M}\vec{\nabla}^2 + \frac{1}{2}M\,\omega_0^2\, r^2 - M\,\omega_0^2\, r^2\, Y_{20}(\theta,\varphi)\,\beta + \right.$$

$$\left. + C\,\hat{\vec{l}}\cdot\hat{\vec{s}} + D\,\left(\hat{\vec{l}}^{\,2} - \langle l^2\rangle_N\right)\right\}_i =$$

$$= \boxed{\begin{array}{c}\text{substitution}\ \ \rho = r\,\sqrt{\frac{M\omega_0^{(0)}}{\hbar}}\\ \text{introduction of new parameters}\ \ \kappa \equiv -\frac{1}{2}\frac{C}{\hbar\omega_0^{(0)}},\ \ \mu \equiv \frac{2D}{C}\end{array}} =$$

$$= \hat{H}_0^{(0)} -$$

$$\hbar\omega_0^{(0)} \sum_i \left\{ \beta\,\frac{\omega_0(\epsilon)}{\omega_0^{(0)}}\,\rho^2\, Y_{20}(\theta,\varphi) + 2\kappa\,\hat{\vec{l}}\cdot\hat{\vec{s}} + \kappa\mu\left(\hat{\vec{l}}^{\,2} - \langle l^2\rangle_N\right)\right\}_i \tag{5.39}$$

where we introduced familiar notation of quadrupole deformation $\beta = \alpha_{20}$.

Since in the case of the axial symmetry the mean field Hamiltonian fulfills the following commutator relations

$$\left[\hat{H}_{AV}, \hat{\vec{J}}^2\right] \neq 0\,, \qquad \left[\hat{H}_{AV}, \hat{J}_z\right] = 0 \tag{5.40}$$

there is the common system of the eigen-kets, $|K_\nu \nu\rangle$, of operators $\hat{H}_{AV}$ and $\hat{J}_z$:

$$\hat{H}_{AV}\,|K_\nu\nu\rangle = e_\nu\,|K_\nu\nu\rangle, \qquad \hat{J}_z\,|K_\nu\nu\rangle = K_\nu\,|K_\nu\nu\rangle \tag{5.41}$$

These eigen-kets $|K_\nu\nu\rangle$ and eigen-energies e_ν can be obtained by the diagonalization of the mean field Hamiltonian $\hat{H}_{AV}$ in some complete basis of kets, e.g. $|Nl\Lambda\Sigma\rangle$:

$$\begin{aligned}
\hat{H}_0^{(0)}\,|Nl\Lambda\Sigma\rangle &= \hbar\,\omega_0\,(N+3/2)\,|Nl\Lambda\Sigma\rangle \\
\hat{\vec{l}}^{\,2}\,|Nl\Lambda\Sigma\rangle &= l(l+1)\,|Nl\Lambda\Sigma\rangle \\
\hat{l}_z\,|Nl\Lambda\Sigma\rangle &= \Lambda\,|Nl\Lambda\Sigma\rangle \\
\hat{s}_z\,|Nl\Lambda\Sigma\rangle &= \Sigma\,|Nl\Lambda\Sigma\rangle
\end{aligned} \tag{5.42}$$

The matrix elements $\langle N'l'\Lambda'\Sigma'|\hat{H}_{AV}|Nl\Lambda\Sigma\rangle$ are nonzero only when the following selection rules are fulfilled ($K = \Lambda + \Sigma$, $K' = \Lambda' + \Sigma'$) [50]

$$\begin{aligned}
K = K'\,, \qquad & l = l'\,, \qquad & N = N'\,, \\
& l = l' \pm 2\,, \quad & N = N' \pm 2
\end{aligned}$$

After the diagonalization of the matrix $\left\{\langle N'l'\Lambda'\Sigma'|\hat{H}_{AV}|Nl\Lambda\Sigma\rangle\right\}$ we obtain single-particle energies e_ν and corresponding eigen-kets $|K_\nu\nu\rangle$ in the form of the linear combination of the basis vectors $|Nl\Lambda\Sigma\rangle$ ($K_\nu = \Lambda + \Sigma$):

$$e_\nu \quad \longrightarrow \quad |K_\nu\nu\rangle = \sum_{Nl\Lambda\Sigma} a_{Nl\Lambda\Sigma}^{(K_\nu\nu)}\;|Nl\Lambda\Sigma\rangle \tag{5.43}$$

The mean field Hamiltonian matrix can be also constructed in the alternative basis of states $|Nljk\rangle$:

$$|Nljk\rangle = \sum_{\Lambda\Sigma} C_{l\Lambda\frac{1}{2}\Sigma}^{jk}\,|Nl\Lambda\Sigma\rangle \tag{5.44}$$

when

$$\begin{aligned}
\hat{H}_0^{(0)}\,|Nljk\rangle &= \hbar\,\omega_0\,(N+3/2)\,|Nljk\rangle \\
\hat{\vec{l}}^{\,2}\,|Nljk\rangle &= l(l+1)\,|Nljk\rangle \\
\hat{\vec{j}}^{\,2}\,|Nljk\rangle &= j(j+1)\,|Nljk\rangle \\
\hat{j}_z\,|Nljk\rangle &= k\,|Nljk\rangle
\end{aligned} \tag{5.45}$$

Then after the diagonalization of the matrix $\left\{\langle N'l'j'K'|\hat{H}_{AV}|Nljk\rangle\right\}$ we obtain the eigen-vectors $|K_\nu\nu\rangle$ in the form of the linear combination of the basis vectors $|Nljk\rangle$:

$$e_\nu \quad \longrightarrow \quad |K_\nu\nu\rangle = \sum_{Nlj} c_{Nlj}^{(K_\nu\nu)} \; |NljK\rangle \tag{5.46}$$

when the relation between amplitudes $c_{Nlj}^{(K_\nu\nu)}$ and $a_{Nl\Lambda\Sigma}^{(K_\nu\nu)}$ is

$$c_{Nlj}^{(K_\nu\nu)} = \sum_{l\Lambda} a_{Nl\Lambda\Sigma}^{(K_\nu\nu)} \, C_{l\Lambda\frac{1}{2}\Sigma}^{jK} \tag{5.47}$$

It is necessary to realize that because of $[\hat{H}_{AV}, \hat{J}_z] = 0$ and $[\hat{H}_{AV}, \mathscr{P}] = 0$ the angular momentum projection K_ν and parity π_ν are good quantum numbers of the eigen-vectors of the mean field Hamiltonian $\hat{H}_{AV}$. Therefore the diagonalization of the matrix $\left\{\langle N'l'\Lambda'\Sigma'|\hat{H}_{AV}|Nl\Lambda\Sigma\rangle\right\}$ and/or $\left\{\langle N'l'j'K'|\hat{H}_{AV}|NljK\rangle\right\}$ can be performed separately for each value of $K = \Lambda + \Sigma = \Lambda' + \Sigma'$ and parity $\pi = \pm 1$. However, since the mean field Hamiltonian is time invariant ($[\hat{H}_{AV}, \mathscr{T}] = 0$) each single-particle energy e_ν is twice degenerated (eigenstate $|K_\nu\nu\rangle$ and $\mathscr{T}\,|K_\nu\nu\rangle \approx |-K_\nu\nu\rangle$ [4] have the same eigen-energy e_ν). That means, the diagonalization can be done only for positive projections $K = 1/2,\, 3/2, \ldots$ because the eigen-vectors $|-K_\nu\nu\rangle$ can be obtained by the time-reversal transformation of the states $|K_\nu\nu\rangle$ with positive projection.

Index ν for the resultant single-particle state $|K_\nu\nu\rangle$ (see (5.44) and (5.46)) enumerates the single-eigen states of the mean field Hamiltonian $\hat{H}_{AV}$. Historically (see [50]) instead of the simple numerization of the solutions of the diagonalization by one number ν so called Nilsson asymptotic numbers $[Nn_3\Lambda]K^\pi$ were introduced (one value of the index ν corresponds to one ensemble of Nilsson numbers). The physical meaning of the Nilsson asymptotic numbers is following.

---

[4]

$$\begin{aligned}
&\mathscr{T}\,|K\rho\rangle = \sum_{Nlj} c_{Nlj}^{K\rho}\, \mathscr{T}\,|NljK\rangle = \boxed{\begin{array}{c}\text{see}\\(1.44)\end{array}} = \\
&= \sum_{Nlj} c_{Nlj}^{(K\rho)}\,(-1)^{l+j+K}\,|Nlj-K\rangle = (-1)^{K+\frac{1}{2}} \sum_{Nlj} c_{Nlj}^{(K\rho)}\,(-1)^{l+j-\frac{1}{2}}\,|Nlj-K\rangle = \\
&= \sum_{\Lambda\Sigma}\sum_{Nlj}(-1)^{K+\frac{1}{2}}\, c_{Nlj}^{(K\rho)}\,(-1)^{l+j-\frac{1}{2}}\, C_{l-\Lambda\frac{1}{2}-\Sigma}^{j-K}\,|Nl-\Lambda-\Sigma\rangle = \\
&= (-1)^{K+\frac{1}{2}} \sum_{N\Lambda\Sigma} a_{Nl-\Lambda-\Sigma}^{K\rho}\,|Nl\Lambda\Sigma\rangle = (-1)^{K+\frac{1}{2}}\,|-K\rho\rangle
\end{aligned}$$

If the deformation ϵ (or β) in (5.39) is sufficiently big one particular component $|Nl\Lambda\Sigma\rangle$ in the decomposition (5.43) for $|K_\nu\nu\rangle$ prevails and in the limit $\beta \to \infty$ its amplitude is closed to one. The numbers N, Λ in the Nilsson asymptotic numbers $[Nn_3\Lambda]K^\pi$ corresponds to the number N, Λ of this particular prevailing component $|Nl\Lambda\Sigma\rangle$ of given single-particle state $|K_\nu\nu\rangle$. The number n_3 is the quantum number characterizing the oscillation of the nucleon in the given state $|K_\nu\nu\rangle$ with respect to the symmetry axis of the nucleus (the principal harmonic oscillator quantum number $N = n_1 + n_2 + n_3$). It can be shown that the number n_3 can be unambiguously determined from given N, Λ and given angular momentum projection K_ν. The number π in the Nilsson asymptotic numbers $[Nn_3\Lambda]K^\pi$ is the parity ± 1 of the given state ($\pi = (-1)^N$). It can be shown that each eigen-vector $|K_\nu\nu\rangle$ corresponds to one ensemble of Nilsoon numbers $[Nn_3\Lambda]K^\pi$.

In the Fig. 5.5 the example of the single-particle spectrum energies e_ν in the dependence on the quadrupole deformation parameter ϵ (introduced in (5.32) and (5.36)) is shown (concretely in the Fig.5.5 there is the single-particle spectrum for protons in the heavy nuclei with $A \approx 165$, the other parts of s.p. spectra of protons and neutrons have similar character).

From the Fig. 5.5 the degeneracy of the single-particle energies according to the angular momentum projection can be seen for the zero quadrupole deformation $\epsilon = 0$. This degeneracy is removed for $\epsilon \neq 0$ and each shell single-particle level e_{Nlj} for $\epsilon = 0$ is splitted into the multiplet of levels e_ν according to the projection $K = 1/2,\ 3/2,\ 5/2, \ldots,\ j$ for $\epsilon \neq 0$. The numbers in small circles are the number of nucleons of given type occupying single-particle levels below the given circle (since the mean field Hamiltonian is time reverse invariant each level denoted by corresponding Nilsson asymptotic numbers is twice degenerated with possible two nucleon occupying it - see the end of the Subsection 1.3). Therefore the numbers in circles for zero deformation $\epsilon = 0$ are equal to magic numbers.

If there is an energy gap between single-particle levels for given deformation ϵ it means that it is necessary more energy for the excitation of the nucleus from the single-particle level below the gap to the single-particle level above the gap. If this situation occurs for the valence nucleon the corresponding nucleus is more stable from the point of view single-particle degrees of freedom. The biggest gaps are seen for magic numbers for $\epsilon = 0$ and this is in accordance with the fact that nuclei with the number of protons or neutrons equal to the magic number are more stable than other ones. The smaller energy gaps with corresponding small circles can be observed also for deformed

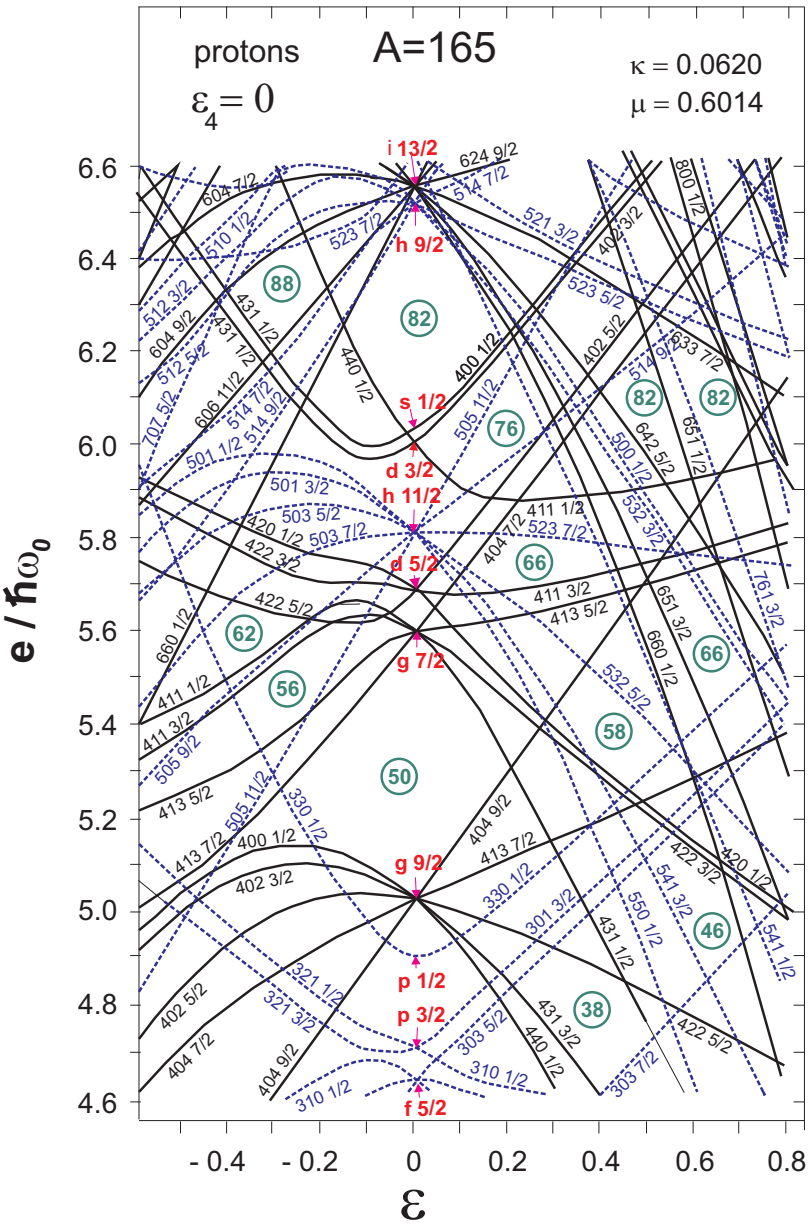


Figure 5.5: The example of the single-particle spectrum of deformed Nilsson mean field Hamiltonian as a function of the quadrupole deformation ϵ (the example concerns the proton system for a nucleus with $A \approx 165$; data taken from [55]). the solid lines corresponds positive parity levels, the dashed lines to those with negative parity.

nuclei with $\epsilon \neq 0$. One can expect that the deformed nuclei with number of nucleons corresponding to numbers in these $\epsilon \neq 0$ circles are also more stable.

	protons		neutrons	
	κ	μ	κ	μ
rare earths	0.0620	0.614	0.0636	0.393
actinides	0.0577	0.650	0.0635	0.325

Table 5.3: Nilsson mean field potential parameters κ and μ (see (5.39)) for rare earth and actinide nuclei (data taken from [55].

Parameters κ and μ of the Nilsson mean field Hamiltonian (5.39) were specified during past decades from the systematic comparison of the experimentally observed and calculated single-particle energies e_ν (see e.g. [55]). The experimental values of e_ν were obtained mostly from nuclear reactions with one-nucleon transfer. Since in the Nilsson mean field potential the Coulomb interactions is not taken into accound explicitely this interaction is in numerical calculations simulated by different parameters κ and μ for proton and neutron systems. Moreover, in order to get the best agreement of calculated e_ν with experimental ones parameters κ and μ were allowed to be different for different groups of nuclei. In the table there are fitted values of parameters κ and μ for deformed nuclei from rare earth and actinide regions.

In the past (in the 50-ties and the 60-ties) there was a problem with the equilibrium deformation for given nucleus with N neutrons and Z protons (A=Z+N) in its ground state. Natural way for the determination of the equilibrium deformation was to calculate the total energy E_0 of given nucleus as a function of the deformation β in the framework of the model of independent particles (when the total ground state energy E_0 is given by the sum of s.p. energies of occupied states - see (4.41)). The next step was to find the value of β corresponding to the absolute minimum of the function $E_0(\beta)$ [5]. However , it was found that the experimental nucleus total energy was not described by the values calculated in such a way when the simple model of independent particles with phenomenological mean field was applied. The problem was that the simple phenomenological mean field describes only single-particle states not far from the Fermi level. Deeply bound levels, for instance, cannot

[5]In the case when more than only one quadrupole deformation parameter β is taken into account in the Nilsson mean field potential we search for the minimum of the total energy E_0 as a function of all these deformation parameters.

be described by the simple oscillator-type or other phenomenological potentials. On the other hand in the beginning 60-ties it was already known that other phenomenological model, the liquid drop model with appropriate fitted parameters, was able to specify the gross character of the binding energy of nuclei from a broad region of the mass number A (see the smooth curve in the Fig. 1.1 in the Subsection 1.1.3) but not small fluctuations observed in the experimental binding energiy B/A - see the Fig. 1.1. Therefore in the second half of the 60-ties the method combining the liquid drop model and simple shell model of independent particles was introduced. This method is known in the literature under the name Strutinski Shell Model Correction Method according to its author V.M.Strutinski [56]. This method is discussed in the next subsection together with its most successful results including the equilibrium deformation. It should be pointed out that in spite of the fact that in the present days the Hartree-Fock and Hartree-Fock-Bogoliubov calculations with the microscopic effective nucleon-nucleon interaction are provided by modern computers the importance of the single mean field approach with the Strutinski shell model corrections remains valid up to the present time. This relatively simple method is still important, especially in the connection with the interpretation experimental data and further predictions for future experiments. This point will be discussed in the end of this chapter.

In the later calculations with the simple phenomenological mean field potentials not only quadrupole deformation parameter $\beta = \alpha_{20}$ was taken into account but also other deformation parameters: quadrupole triaxial deformation parameter γ (see (1.5)), hexadecapole deformation parameter $\epsilon_4 \approx \alpha_{40}$ and other ones with higher multipolarities $\lambda > 2$ were involved in he consideration. In such cases to find the equilibrium deformation means to find the minimum of the function $E_0(\beta_2,\ \gamma,\ \beta_4,\ \ldots)$ in the multi-dimesional parameter space of all deformation parameters taken into accounts. In the later calculations not only oscillator-type Nilsson potential was used but also other coordinate dependent mean potentials, like deformed Saxon-Wood potential:

$$\hat{H}_{AV} = \sum_i \left\{ -\frac{\hbar^2}{2M}\vec{\nabla}^2 - \frac{V_0}{1+e^{\frac{r-R(\theta,\,\varphi)}{a}}} + + C\,\hat{\vec{l}}\cdot\hat{\vec{s}} \right\}_i + \hat{V}_{coul} \tag{5.48}$$

where $R(\theta,\varphi)$ is generally given by (5.25) and $\hat{V}_{coul}$ is the Coulomb potential acting between protons. Similarly as in the Nilsson harmonic oscillator case the parameters of the Wood-Saxon potential (V_0, a, C) for neutron and proton systems were determined by the fitting procedure in order to reproduce the experimental spectrum of the low-lying single-particle states (see e.g. [57]).

For other type of phenomenological mean field models in nuclear physics see e.g. [9] and citation therein.

5.1.2.2 Strutinski shell model corrections

In the framework of the phenomenological methods of the theoretical description of the nuclear structure in the past there were two basic approaches:

1. Liquid Drop Model (LDNM
   The LDM is based on the idea that the nucleus can be understood as the drop of the charged nuclear liquid (liquid without vortexes, with the surface tension, described by the hydrodynamics equations e.t.c.). The starting basic expression of the LDM is the semi-empirical formula (1.13) for the total binding energy of the nuclear drop:

$$B(N,Z) = b_V A + b_S A^{2/3} + b_C \frac{Z^2}{A^{1/3}} + b_I \frac{(N-Z)^2}{A} - \delta(A), \quad (5.49)$$

   with the parameters given in (1.14).

2. Simple Shell Model (SSM)
   The SSM (e.g. Nilsson model described in the part 5.1.2.1), starting with the idea that nucleus moves independently in the spherical or deformed phenomenological mean field, is able to reproduce some properties of nuclear states near the Fermi level or ground state properties of odd-A nuclei (s.p. spectrum or magnetic dipole moments). However, the SSM misfires totally if we want to describe the global nuclear characteristics like binding energy or nuclear inertia momentum and others.

Since no one from above mentioned approaches was able to provide a good simultaneous description of single-particle degrees of freedom and the global nuclear characteristics the method combining both above approaches (LDM and SSM) was introduced in the 60-ties. The method was named Strutinski Shell Correction Method (SSCM) according to its author V.M. Strutinski [56]. This method keeps some importance up to now (as it will be discussed in the end of this section) therefore the basic idea of it is given below [6].

[6] Today there are attempts to reproduce the total binding energy including its fluctuation in the framework of microscopical methods like Hartree-Fock or Hartree-Fock-Bogoliubov approaches with realistic effective nucleon-nucleon interaction (see the Section 5.2). However, since the solving of the HF or HFB equations with realistic effective nucleon-nucleon interaction is relatively complex problem the Strutinski shell correction method is often used in the present time. Mainly in cases when the values of binding energy is necessary in many points like in the case of drawing the landscape energy surfaces in the space of deformation parameters which is necessary in the determination of the equilibrium deformation of the mean field and in the evaluation of the nuclear fission probabilities (see the end of this subsection).

From the Fig. 1.1 it is clear that the binding energy of the nucleus (which can be idetified with the total nucleus energy in the ground state) can be written as the sum of two terms: smooth part described by the liquid drop model and small fluctuation

$$E = E_{LDM} + E_{OSC} \tag{5.50}$$

where E_{LDM} is the LDM binding energy and E_{OSC} are small fluctuations (oscillations). Altogether these terms give experimental values of the binding energy represented by points in the Fig. 1.2. The basic idea of the Strutinski was (Strutinski assumptions):

- *The smooth part of the total nuclear energy in the dependence on A is given by the smooth part of the energy density of nuclear states and this part corresponds to the liquid drop model values of the nuclear energy which is equal to values given by the Weiczacker expression (5.49). The fluctuation (or oscillation) part of the total energy should be connected with the oscillation part of the energy density of states which should be given by the shell structure of the nuclear spectrum.*

Similarly as for the total energy E in the (5.50) the total shell model energy E_{SM} can be divided into the smooth part $\tilde{E}_{SM}$ and small oscillation corrections $E_{OSC}^{(SM)}$

$$E_{SM} = E_{OSC}^{(SM)} + \tilde{E}_{SM} = \boxed{\begin{array}{c}\text{in the model of}\\ \text{independent particles}\end{array}} \approx \sum_{i=1}^{A} e_i \tag{5.51}$$

where the oscillation part $E_{OSC}^{(SM)}$ of the total shell model energy is the same, according to the Strutinski assumption, as the E_{OSC} involved in the (5.50), $E_{OSC}^{(SM)} = E_{OSC}$. So, the eq. (5.50) can be rewritten as follows

$$E = E_{LDM} + E_{OSC} = E_{LDM} + E_{SM} - \tilde{E}_{SM} \tag{5.52}$$

where the extraction of the $\tilde{E}_{SM}$ should be done entirely in the framework of the shell model. By other words, according to the Strutinski assumption the smooth part $\tilde{E}_{SM}$ of the shell model total energy E_{SM} does not describe the smooth part of the total energy E properly while the oscillation part E_{OSC} of the total energy is fully determined by the shell model. The opposite is true for the liquid drop model which is able to describe well only the smooth part of the total energy E.

The spectrum of any mean field shell model (phenomenological as well as microscopical) for spherical and closed to the spherical nuclei is characterized by the shells when the single-particle levels are concentrated to groups (shells). The energy distances between single-particle levels belonging to one group (shell) are much less than the energy distance between any levels from different shells (see schematic Fig. 5.2). The average energy distamce between two neighbour shells is $\hbar\omega_0^{(0)} \approx 41\, A^{-1/3}$ (see (5.3). In the reality it is also known that the energy density of states of any bound system including nucleus increases with the energy. So, one can expect that the real energy density $g(e)$ of single-particle nucleon states fluctuates around the average smooth increasing curve with the energy distance $\approx \hbar\omega_0^{(0)}$ between two neighbour maxima of the fluctuations (see Fig.5.6).

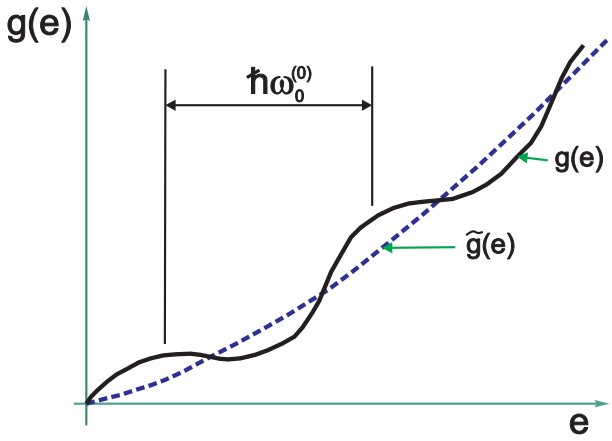


Figure 5.6: Schematic figure of the dependence of the energy density of nucleons on the single-particle energy. Solid curve corresponds to the full single-particle nucleon density, dashed curve represents the smooth part $\tilde{g}(e)$ of the nucleon density.

The energy density $g(e)$ of nucleons as a function of the single-particle energy e is given by the following sum over the occupied single-particle states

$$g(e) = \sum_{i_<=1}^{A} \delta(e - e_{i_<}) = \sum_i n_i\, \delta(e - e_i) \tag{5.53}$$

where e_i is the single-particle energy of the single-particle state with the index i ($\hat{H}_{AV}|i\rangle = e_i\,|i\rangle$) and $n_i = 1$ for occupied state i and $n_i = 0$ for unoccupied state i. The Fermi energy λ is then defined by the following expression.

$$A = \int_{-\infty}^{\lambda} g(e)\, de = \sum_i n_i \tag{5.54}$$

It can be noted that the value λ for given type of nucleons can be usually found between the single-particle energy of the highest occupied level and the lowest unoccupied level.

The total SM energy of the nucleus with the energy density $g(e)$ of nucleons is then given by the following expression (in the framework of the model of independent particles)

$$E_{SM} = \int_{-\infty}^{\lambda} e\, g(e)\, de = \sum_i n_i\, e_i \tag{5.55}$$

For the reason of the determination of the smooth part $\tilde{E}_{SM}$ of the total nuclear energy it is suitable to introduce the smooth part $\tilde{g}(e)$ of the energy density of nucleons ($\tilde{g}(e)$ has no any fluctuation - see the Appendix F for more details). The integration of the density $\tilde{g}(e)$ over occupied single-particle spectrum of single-particle energies e defines the corresponding "smooth" Fermi level $\tilde{\lambda}$ (in the analogy with (5.54)

$$A = \int_{-\infty}^{\tilde{\lambda}} \tilde{g}(e)\, de = \sum_i \tilde{n}_i \tag{5.56}$$

where $\tilde{n}_i$ can be considered as the generalized ("smooth") occupation numbers. The corresponding smooth part $\tilde{E}_{SM}$ of the total nuclear energy is defined as

$$\tilde{E}_{SM} = \int_{-\infty}^{\tilde{\lambda}} e\, \tilde{g}(e)\, de = \sum_i \tilde{n}_i\, e_i \tag{5.57}$$

The main task of the Strutinski shell model corrections is to determine the smooth part of the energy density $\tilde{g}(e)$. In order to remove fluctuations from the function $g(e)$ and to obtain the smooth part $\tilde{g}(e)$ of the energy density it is necessary to use some averaging function f and to average the density $g(e)$ in some energy interval γ which should be sufficiently wide, that means

$$\tilde{g}(e) = \frac{1}{\gamma} \int_{-\infty}^{\infty} g(e')\, f\left(\frac{e'-e}{\gamma}\right)\, de' \tag{5.58}$$

Usually $\gamma \approx \hbar\omega_0^{(0)}$. So, we take energies e from $-\infty$ up to ∞ and we average locally $g(e)$ with the averaging function f in the interval γ. The averaging function $f\left(\frac{e'-e}{\gamma}\right)$ is given by the requirement that the averaging procedure (5.58) when applied to $\tilde{g}(e)$ provides again the same fuction $\tilde{g}(e)$ (see also Appendix F):

$$\tilde{g}(e) = \frac{1}{\gamma} \int_{-\infty}^{\infty} \tilde{g}(e')\, f\left(\frac{e'-e}{\gamma}\right)\, de' \tag{5.59}$$

The determination of the averaging function $f\left(\frac{e'-e}{\gamma}\right)$ and of the smooth part $\tilde{g}(e)$ of the energy density is described in details in the Appendix F. When the smooth part $\tilde{g}(e)$ of the energy density is obtained then the smooth part $\tilde{E}_{SM}$ of the simple shell model energy is determined from (5.57) and the oscillation shell correction part E_{OSC} is given by:

$$\begin{aligned} E_{OSC} &= E_{SM} - \tilde{E}_{SM} = \boxed{\begin{array}{c}\text{see}\\ \text{(5.55) and (5.57)}\end{array}} = \\ &= \int_{-\infty}^{\lambda} e\, g(e)\, de - \int_{-\infty}^{\tilde{\lambda}} e\, \tilde{g}(e)\, de = \sum_i e_i\, (n_i - \tilde{n}_i) \\ &\equiv \sum_i e_i\, \delta n_i \end{aligned} \tag{5.60}$$

where $\sum_i e_i\, \tilde{n}_i = \int_{-\infty}^{\tilde{\lambda}} e\, \tilde{g}(e)\, de$, $\delta n_i \equiv n_i - \tilde{n}_i$.

If we know δn_i we can determine also the shell corrections to the local $\rho(\vec{r})$ and nonlocal $\rho(\vec{r}, \vec{r}\,')$ densities in the spatial space:

$$\begin{aligned} \rho(\vec{r}) &= \sum_{i=1}^{A} \varphi_i(\vec{r})\, \varphi_i^*(\vec{r}) \quad \rightarrow \quad \rho_{OSC}(\vec{r}) = \sum_{i=1}^{A} \varphi_i(\vec{r})\, \varphi_i^*(\vec{r})\, \delta n_i \\ \rho(\vec{r}, \vec{r}\,') &= \sum_{i=1}^{A} \varphi_i(\vec{r})\, \varphi_i^*(\vec{r}\,') \quad \rightarrow \quad \rho_{OSC}(\vec{r}, \vec{r}\,') = \sum_{i=1}^{A} \varphi_i(\vec{r})\, \varphi_i^*(\vec{r}\,')\, \delta n_i \end{aligned} \tag{5.61}$$

and the ground state expectation value $\langle \hat{F} \rangle$ of any operator $\hat{F}$ is then obtained as

$$\langle\, \hat{F}\, \rangle = \int d^3r F(\vec{r})\, \rho(\vec{r}) = \int d^3r F(\vec{r})\, \left[\rho_{LDM}(\vec{r}) + \rho_{OSC}(\vec{r})\right] \tag{5.62}$$

when again the smooth part $\tilde{\rho}_{SM}(\vec{r}) = \sum_{i=1}^{A} \varphi_i(\vec{r})\, \varphi_i^*(\vec{r})\, \tilde{n}_i$ of the shell model spatial density is substituted by the liquid drop model density $\rho_{LDM}(\vec{r})$. The total energy E_{LDM} given by (5.49) or (1.13) involves also the pairing energy [7]. Therefore, the shell correction term E_{OSC} should contain also the pairing part and the final expression for the total energy becomes

$$E = E_{LDM} + E_{SM} - \tilde{E}_{SM} + P_{BCS} - \tilde{P}_{BCS} \tag{5.63}$$

[7] From the microscopical point of view the pairing effects in the nucleus is connected with the short-rangle residual interactions and they are discussed in details in the Chapter 6. In the liquid drop model total energy (see (5.49) and (1.13)) the contribution from the pairing is represented by the last term.

where P_{BCS} is the pairing energy (which will be discussed in the Chapter 6) and $\tilde{P}_{BCS}$ is the smooth part of this pairing energy.

5.1.2.3 Some application of the Strutinski shell model correction method

In this subsection some most important results of Strutinski shell correction calculations are discussed. As it was mentioned several times in spite of the fact that Strutinsky method is known for 50 years this type of the calculations has its value up to now. Present computational facilities give possibility to calculate the total energy of the nucleus using the Hartree-Fock method (even beyond the HF or HFB method) starting with the realistic effective nucleon-nucleon interactions but the comparison with experimental values of the total nuclear energies (nucleas masses) (which is necessary for the interpretation of experimental data or predictions for new experiments) was not so good. It was not the case for Strutinski shell correction calculations and therefore it is applied up to now.

5.1.2.3.1 Equilibrium deformations and nuclear masses Experimental values of nuclear deformations (deformation parameters $\alpha_{\lambda\mu}(\lambda > 2)$ or $\beta, \gamma, \epsilon_2, \epsilon_4, \ldots$ - see subsection 1.1.2) can be obtained from different nuclear measurable properties. For instance, using expression (1.10) the quadrupole deformation parameter $\beta = \alpha_{20} = \frac{4\sqrt{\pi}}{3\sqrt{5}}\epsilon_2$ can be determined from the experimental value of the nucleus quadrupole moment Q_0. Deformation parameters are possible to obtain also from electric transition probabilities or photoabsorption cross sections as it will be discussed later in the Chapter 7. The nuclear deformation is implicitly hidden in the total nuclear energy E and therefore also in the nuclear mass (see (1.12)):

$$\begin{aligned} M(Z,N)\,c^2 &= Z\,m_p\,c^2 + N\,m_p\,c^2 + B(Z,N) = \\ &= Z\,m_p\,c^2 + N\,m_p\,c^2 + E \end{aligned} \tag{5.64}$$

where the total energy $E = E(\epsilon_2,\ \epsilon_4,\ \gamma, \cdots)$ is the function of deformation parameters. The expression (5.64) is used for the determination of the experimental values of the total energy E and this experimental value E can be compared with the corresponding theoretical values obtained from different nuclear models.

In the time before the Strutinski shell correction method was invented (before 1967) the total nuclear energy as a function of deformation parameters was determined in terms of the model of independent particles as sum of the

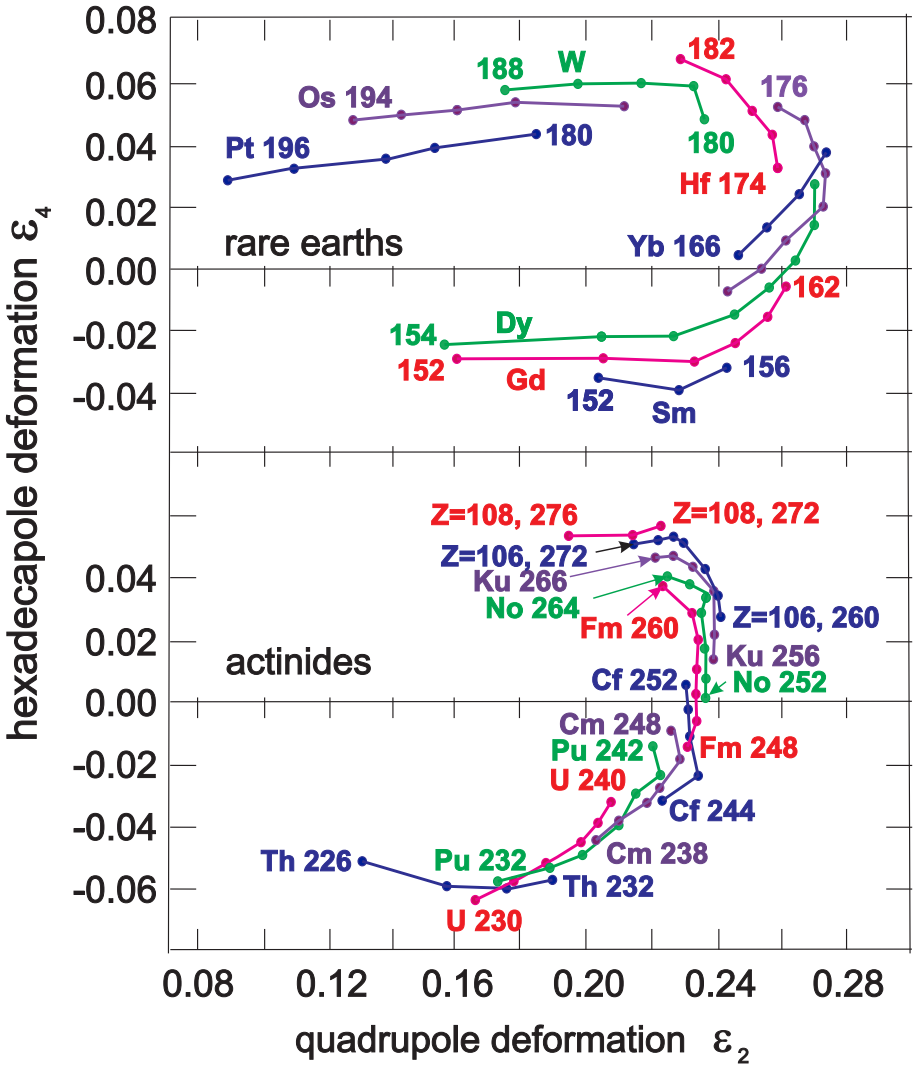


Figure 5.7: Equilibrium quadrupole ϵ_2 and hexadecapole ϵ_4 deformation parameters for rare earth and actinide isotopes calculated by the Strutinski shell correction method with the Nilsson mean field Hamiltonian (taken from [60])

single-particle energies of all nucleons - see (5.55)

$$E(\epsilon_2,\ \epsilon_4, \gamma, \ldots) = E_{SM}(\epsilon_2, \epsilon_4, \gamma, \ldots) = \sum_{i=1}^{A} n_i\, e_i(\epsilon_2, \epsilon_4, \gamma, \ldots) \qquad (5.65)$$

However, as it was already mentioned, such way of the determination of the total nuclear energy failed from the point of view of the comparison with the experimental values. Only after the introduction of Strutinski shell correction method it was possible to obtain the agreement with the total energy calculated from (5.63)

$$\begin{aligned} E(\epsilon_2, \epsilon_4, \gamma, \ldots) &= E_{LDM} + E_{SM}(\epsilon_2, \epsilon_4, \gamma, \ldots) - \tilde{E}_{SM}(\epsilon_2, \epsilon_4, \gamma, \ldots) \\ &+ P_{BCS}(\epsilon_2, \epsilon_4, \gamma, \ldots) - \tilde{P}_{BCS}(\epsilon_2, \epsilon_4, \gamma, \ldots) \end{aligned} \qquad (5.66)$$

with corresponding experimental values if in (5.66) the equilibrium deformation parameters are used. Equilibrium deformation parameters are obtained as values corresponding to the minimum of the function $E(\epsilon_2, \epsilon_4.\gamma, \ldots)$ in the space $(\epsilon_2, \epsilon_4, \gamma, \ldots)$ of deformation parameters. As an example, in the Fig. 5.7 the equilibrium deformation parameters ϵ_2, ϵ_4 for different isotope chains from the rare earth and actinide regions are demonstrated for the case of the Strutinski shell correction method applied for the simple Nilsson model with two deformation parameters, quadrupole ϵ_2 and hexadecapole ϵ_4 [60].

The nuclear masses obtained by (5.64) with the total energy from (5.66) calculated with equilibrium deformation parameters are compared with experimental values in the Fig. 5.8. One can see very good agreement with experimental values (within the accuracy ± 1 MeV). It should be noted that the fully microscopic HF calculations with realistic effective nucleon-nucleon interactions give the total energy with much less accuracy (more than one order worse than Strutinski shell correction method with simple phenomenological mean fields).

5.1.2.3.2 Nuclear fission (fission barriers) In the beginning of this subsection a few information from the history are given. In 1927-38 O. Hahn and L. Meitner discovered nuclear fission [62], more precisely the induced fission by thermal neutrons:

$$n\ +\ ^{235}U \quad \rightarrow \quad X_1 + X_2 + (2-3)n + \ energy\ (\approx\ 200\, MeV)$$

Shortly after the discovery of neutron fission attempts were made to understand this phenomenon using the concept of the nuclear drop model

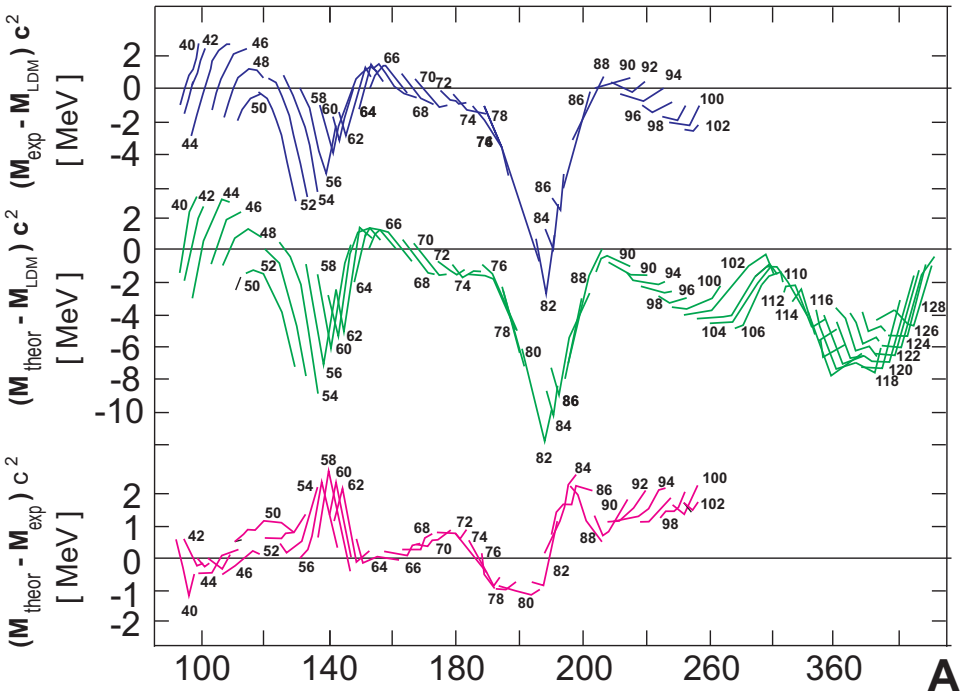


Figure 5.8: Experimental masses(upper graph) and theoretical masses obtained from (5.64) with the total energy E given by Strutinski shell correction expression (5.66) (central graph) relative to the spherical liquid drop value M_{LDM}. The bottom graph shows the difference between theoretical and experimental masses. Each curve corresponds to one isotopic chain characterized by proton number Z. As seen in the lower part of the figure, the shell correction method masses are obtained with a typical accuracy ± 1 MeV (taken from [61]).

[63, 64, 65]. In 1940 Russian physisists Petrzhak and Flerow discovered spontaneous fission (not induced by neutrons) of heavy element nucleus (actinides). The spontaneous fission half-life is one of the most directly measured quantity associated with the fission. The longest half-life for actinides was determined to be 10^{17} years for ^{235}U and the shortest is of the order of 0.1 ms (see Fig. 5.14).

Shell effects are clearly observed in another quantity connected with the fission, mass distribution of the fission fragments. In the Fig. 5.9 mass distribution of the fission fragments for the spontaneous fission of $^{252}_{98}$Cf, $^{256}_{100}$Fm and $^{257}_{100}$Fm and for neutron induced fission of $^{257}_{100}$Fm are shown. The asymmetry in the distribution of fragment masses is given by the fact that the nuclei with the number of nucleons equals to magic numbers are more stable and also more probable if they are formed as fragments in the dividing nucleus. One can see in the Fig. 5.9 the trend toward symmetric fission with the increasing mass and also for neutron-induced fission in the comparison with the spontaneous fission.

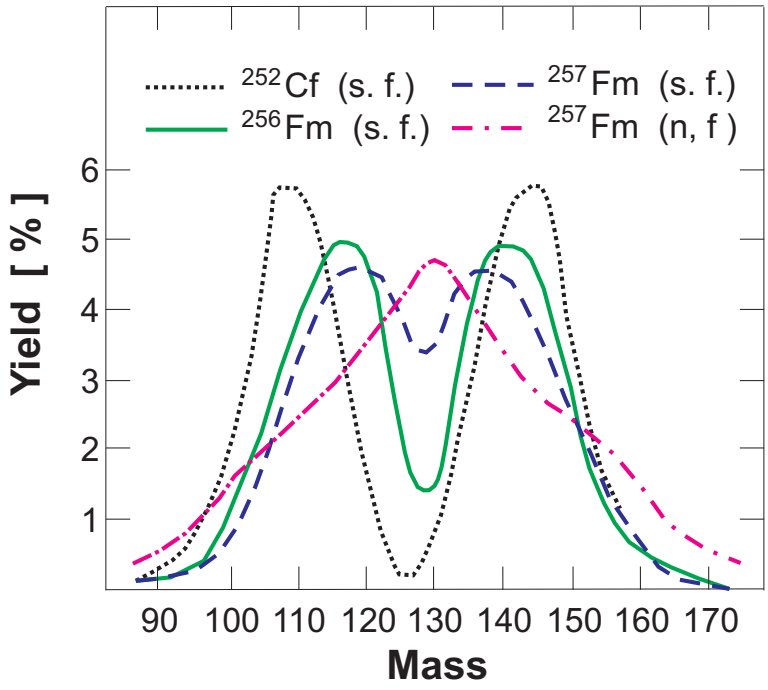


Figure 5.9: Mass distribution of the fission fragments for spontaneous fission of $^{252}_{98}$Cf, $^{256}_{100}$Fm and $^{257}_{100}$Fm and for neutron induced fission of $^{257}_{100}$Fm. (taken from [66])

Another quantity which can be extracted from experimental data is the fission barrier height. This barrier is seen in the dependence of the nucleus total energy on the prolongation (deformation) of the nuclear shape during the process of the fission. Since the first model which was used for the explanation of this dependence was the liquid drop model (LDM) we start with the simple version of the LDM.

The liquid drop model of Bohr and Wheeler starts with the expression (5.49) for the total nucleus energy E_{LDM} where parameters b_V, b_s, b_c, b_I where fitted to experimental values extracted from the measured masses of selected nuclei. Since the prolongation of the nucleus during its fission does not change its volume the decisive role is played by the surface term (2-d term in (5.49)) and Coulomb term (3-d term in (5.49):

$$E_s^{(0)} = b_s\, A^{2/3} \qquad\qquad E_C^{(0)} = b_c\, \frac{Z^2}{A^{1/3}} \tag{5.67}$$

where the parameter b_s is related to the surface tension parameter σ, $b_s = 4\pi r_0^2\, \sigma$, where $r_0 \approx 1.2$ fm (see (1.2)) and $\sigma = 1.03\ MeV/fm^2$. It should be pointed out that the LDM expressions (5.49), (5.67) valid only for spherically symmetric nuclei.

During the fission the nucleus is prolonged before its splitting to frag-

ments and its shape is described by the decomposition (1.3) into spherical harmonics:

$$R(\theta,\varphi) = R_\alpha \left(1 + \sum_{\lambda\mu} \alpha_{\lambda\mu} Y_{\lambda\mu}(\theta,\varphi)\right) \tag{5.68}$$

where the mean radius R_α is fixed by the volume conservation condition ($\hat{r} \equiv (\theta,\varphi)$):

$$\begin{aligned} \frac{4\pi}{3} R_0^3 &= \int dV = \int \hat{dr} \int_0^{R(\theta,\varphi)} dr\, r^2 = \boxed{\begin{array}{c}\text{see}\\ \text{(A.43) and (A.45)}\end{array}} = \\ &= \frac{4\pi}{3} R_\alpha^3 \left(1 + \frac{3}{4\pi}\, 2 \sum_{\lambda\mu} \mid \alpha_{\lambda\mu} \mid^2 + O(\alpha^3)\right) \end{aligned} \tag{5.69}$$

As it was already mentioned above the relevant part of the total LDM energy (5.49) is given by the sum of the surface $E_s(\alpha_{\lambda\mu})$ and Coulomb $E_C(\alpha_{\lambda\mu})$ terms which are now dependent on the deformation parameters $\alpha_{\lambda\mu}$:

$$E_{fish.}(\alpha_{\lambda\mu}) = E_s(\alpha_{\lambda\mu}) + E_C(\alpha_{\lambda\mu}) \tag{5.70}$$

where $E_s(\alpha_{\lambda\mu})$ is determined by the surface tension of the nuclear drop, $\sigma = \frac{b_s}{4\pi r_0^2}$ (Σ is the surface of the area given by (5.68))

$$\begin{aligned} E_s(\alpha_{\lambda\mu}) &= \sigma \int_{(\Sigma)} dS = \\ &= \boxed{\begin{array}{c}\text{see expr. (I.23) in the Appendix I where}\\ E_s(\alpha_{\lambda\mu}) = V_{surf} + \sigma\, 4\pi R_0^2 = V_{surf} + E_s^{(0)}\end{array}} = \\ &= E_s^{(0)} \left(1 + \frac{1}{8\pi} \sum_{\lambda\mu} (\lambda-1)\,(\lambda+1) \mid \alpha_{\lambda\mu} \mid^2 + O(\alpha^3)\right) \end{aligned} \tag{5.71}$$

and the Coulomb term is

$$E_C(\alpha_{\lambda\mu}) = \frac{1}{2}\,\frac{1}{4\pi\epsilon_0}\int \frac{\rho^{(el)}(\vec{r}_1)\,\rho^{(el)}(\vec{r}_1)}{|\vec{r}_1-\vec{r}_2|} d^3r_1\,d^3r_2 =$$

$$= \boxed{\begin{array}{c}\text{we supose } \rho^{(el)}(\vec{r}) = \rho_0 = Ze/\frac{4\pi}{3}\,R_0^3 \text{ for } r \le R(\Theta,\varphi)\\ \text{and } \rho^{(el)}(\vec{r}) = 0 \text{ for } r \ge R(\Theta,\varphi),\\ \text{see also analogy with exprs. (I.27)}\\ \text{and (I.32) in the Appendix I, where}\\ E_C(\alpha_{\lambda\mu}) = V_{coul} + \frac{1}{2}\int d^3r\;\rho_0\,\varphi_0^{(el)}(\vec{r}) = V_{coul} + E_C^{(0)}\end{array}} =$$

$$= E_C^{(0)}\left(1 - \frac{5}{4\pi}\sum_{\lambda\mu}\frac{\lambda-1}{2\lambda+1}\,|\,\alpha_{\lambda\mu}\,|^{\,2} + O(\alpha^3)\right) \qquad (5.72)$$

It can be shown (see e.g. [67]) that for good description of the nuclear fission we should determine $E_s(\alpha_{\lambda\mu})$ and $E_C(\alpha_{\lambda\mu})$ at least up to terms with $\alpha^3_{\lambda\mu}$. For the simplicity further the axially symmetric quadrupole deformation of the splitting nucleus is assumed only, $\alpha_{\lambda\mu} = 0$ for $\mu \neq 0$ and $\alpha_{\lambda\mu} = 0$ for $\lambda > 2$. Then the shape (5.68) is determined only by one quadrupole deformation parameter $\beta = \alpha_{20}$:

$$\begin{aligned} R(\theta) &= R_\beta\;(1+\beta\,Y_{20}(\theta,\varphi)) = R_\beta\left(1+\beta\sqrt{\frac{5}{4\pi}}\,P_2(\cos\theta)\right) = \\ &= R_\beta\;(1+a_2\,P_2(\cos\theta)) \end{aligned}$$

where $a_2 = \beta\sqrt{\frac{5}{4\pi}}$ and the expressions for $E_s(\alpha_{\lambda\mu})$ and $E_C(\alpha_{\lambda\mu})$ is simplified for the case $\lambda = 2$ as follows (see [67]) (up to the terms with a_2^2)

$$\begin{aligned} E_s(\alpha_{\lambda\mu}) &= E_s(a_2) = E_s^{(0)}\left(1 + \frac{3}{2}\,\frac{1}{5}\,a_2^2 + O(a_2^3)\right) \\ E_C(\alpha_{\lambda\mu}) &= E_C(a_2) = E_C^{(0)}\left(1 - \frac{1}{5}\,a_2^2 + O(a_2^3)\right) \end{aligned} \qquad (5.73)$$

In the literature so called fissility parameter x is introduced (see e.g. [9, 67])

$$x \equiv \frac{E_C^{(0)}}{2E_s^{(0)}} = \boxed{\begin{array}{c}\text{see}\\ (5.67)\end{array}} = \frac{b_C}{2b_s}\,\frac{Z^2}{A} \approx 0.01965\,\frac{Z^2}{A} \qquad (5.74)$$

Then the deformation contribution (5.70) to the energy $E_{fish.}(\alpha_{\lambda\mu}) \cong E_{fish.}(a_2)$ is

$$\Delta E_{fish.}(a_2) = E_s(a_2) + E_C(a_2) - E_s^{(0)} - E_C^{(0)} = \\ = E_s^{(0)} \left(\frac{2}{5} \left(\frac{3}{4} - x \right) a_2^2 + O(a_2^3) \right) \tag{5.75}$$

If the asymmetry term in the LDM semi-empirical expr. (5.49) (the term

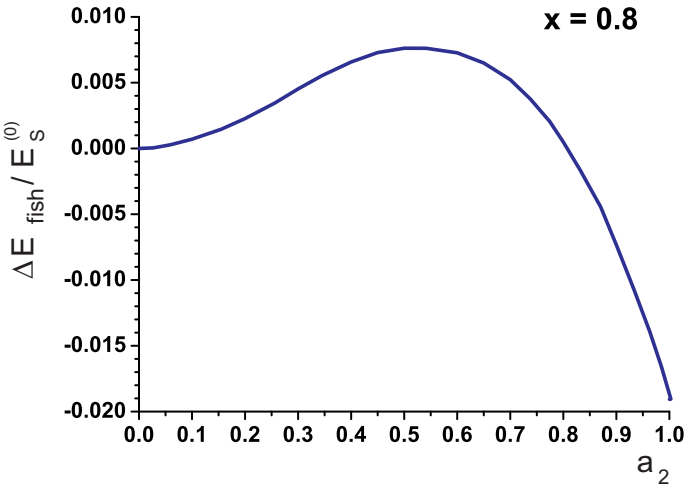


Figure 5.10: Dependence of $\Delta E_{fish.}$ (see (5.76)) on the quadrupole deformation parameter a_2 for the fissility $x = 0.8$. From the figure it is seen that the simple LDM model gives the spherical minimum of the total energy ($a_2 = 0$) and one barrier maximum ($a_2 = 0.55$).

with b_I in r.h.s of (5.49)) is taken into account in the fission process and if the terms with a_2^3 is also involved in (5.73) then the expression (5.75) is slightly modified (see [67]):

$$\Delta E_{fish.}(a_2) = E_s(a_2) + E_C(a_2) - E_s^{(0)} - E_C^{(0)} = \\ = E_s^{(0)} \left(\frac{2}{5} (1 - x) a_2^2 - \frac{4}{105} (1 + 2x) a_2^3 + \ldots \right) \tag{5.76}$$

The stability of given nucleus (with given fisility parameter $x = 0.01965 \frac{Z^2}{A}$ - see (5.74)) for given deformation a_2 is determined by the derivative

$$\frac{\partial \Delta E_{fish.}(a_2)}{\partial a_2} = E_s^{(0)} \left\{ \frac{4}{5} (1 - x) a_2 - \frac{4}{35} (1 + 2x) a_2^2 + \ldots \right\} \tag{5.77}$$

One can see that for $x < 1$ the deformation contribution derivative (slope) is positive for small deformations a_2 (the first term in the r.h.s. of (5.77) is positive and higher then the negative second term) while for $x > 1$ the slope

of $\Delta E_{fish.}(a_2)$ is always negative. Negative slope means that the nucleus tends to increase the deformation and to go to the fission. So, according to this simple consideration, nuclei with the fissility $x > 1$ cannot be stable because immediately they undergo the fission process. If we plot the fission energy $\Delta E_{fish.}(a_2)$ as a function of the deformation parameter a_2 then the maximum can be seen for nuclei with the fissility $x < 1$ (see Fig. 5.10). That means the nuclei with $x < 1$ feels the energy barrier with respect to the direct fission. The fission for such nuclei is possible only thanks to the tunneling process through the barrier. The nuclei with $x > 1$ ($\frac{Z^2}{A} > 50$) have no any barrier and are fully unstable with respect to the spontaneus fisssion in the framework of this simple LDM model.

The extreme condition for the function $\Delta E_{fish.}(a_2)$ (see (5.76)) is

$$\frac{\partial \Delta E_{fish.}(a_2)}{\partial a_2} = 0 = E_s^{(0)} \left\{ \frac{4}{5}(1-x)\, a_2 - \frac{4}{35}(1+2x)\, a_2^2 + \ldots \right\}$$

	Z^2/A	x	E_{barr} [MeV]	$a_2^{(barr)}$	$\beta^{(barr)}$
$^{209}_{83}$Bi	32.96	0.700	17.9	0.88	1.40
$^{232}_{90}$Th	34.91	0.753	9.7	0.69	1.09
$^{238}_{92}$U	35.56	0.769	7.8	0.64	1.01
$^{242}_{94}$Pu	36.51	0.787	6.0	0.58	0.92
$^{254}_{100}$Fm	39.37	0.841	2.4	0.41	0.65
$^{294}_{110}$Ds	41.16	0.912	0.4	0.22	0.35

Table 5.4: Fissility parameters, energy barriers and maximum barrier deformations determined in the framework of the simple liquid drop model (see exprs. (5.74), (5.78)).

This equation has two roots: 1) $a_2 = 0$ and 2) $a_2 = 7\,\frac{1-x}{1+2x}$. The first corresponds to the spherical minimum, the second to the barrier maximum with the value:

$$E_{barr} = \frac{98}{15}\,\frac{(1-x)^3}{(1+2x)^2}\,E_s^{(0} \tag{5.78}$$

It is useful to point out that all these expressions are valid only for small values of $(1-x)$. One may also ask if the expansion (5.76) with respect to a_2 is convergent. In fact it is not so beyond $a_2 \approx 0.7$.

In the Table 5.4 there are values of Z^2/A, x, E_{barr}, $a_2^{(barr)}$ and $\beta^{(barr)}$ for a few heavy nuclei along the β- stability line. One can see from the Tab.

5.4 that actinide nuclei have $x < 1$ although empirically they are observed to be unstable with respect to spontaneous fission. However, fissilities x are close to 1 and therefore the barriers are rather low and the tunneling process is probable. The maximum barrier energies (5.78) are given in the fourth column. The nuclear shape corresponding to the barrier maximum is indicated in the last column.

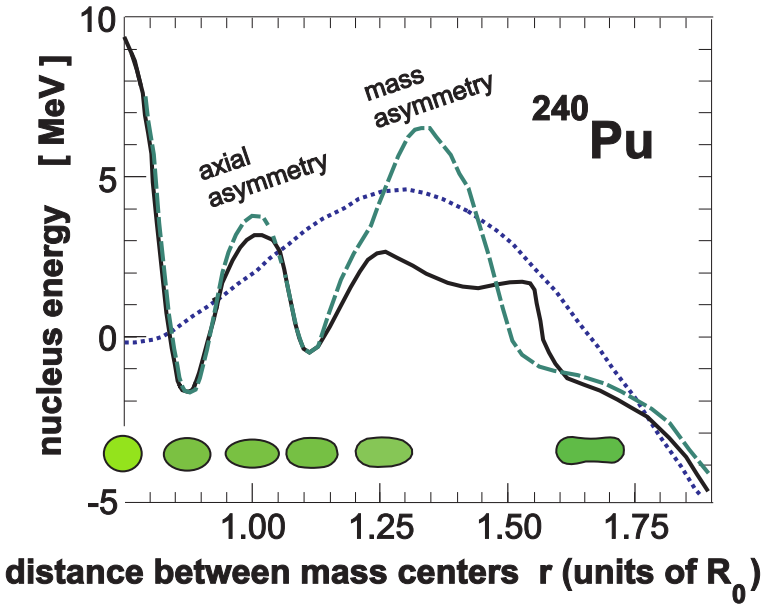


Figure 5.11: The total nucleus (^{240}Pu) energy as a function of the distance r between mass center of two fission fragments. The dotted line corresponds to the calculation within the simple liquid drop model ($E = E_{LDM}(\alpha_{\lambda\mu})$). The dashed line was obtained by the Strutinski shell correction approach ($E = E_{LDM} + E_{OSC}$) when the simple Nilsson model was used with only axial quadrupole α_{20} and hexadecapole α_{40} deformation parameters were taken into account. The solid line is connected again with the Strutinski-Nilsson approach but with $\alpha_{20} \neq 0$, $\alpha_{40} \neq 0$, $\alpha_{22} \neq 0$, $\alpha_{30} \neq 0$ (from [68]).

The energy barrier for the fission can be determined not only by the simple liquid drop model with one deformation β as it has just been discussed. It is evident that the considerations above can be extended also for the case of more deformation parameters and also for cases when total nucleus energy is calculated by other models. In the Fig. 5.11 there is the total nucleus energy E as a function of the distance r between mass centers of two fragments from the fission of ^{240}Pu (taken from [68]). In the fission stage before two fragments are separated this distance is directly connected with the deformation of the dividing nucleus (in the case of the simple liquid drop model discussed above this distance is proportional to the deformation parameter a_2). The dotted line in the Fig.5.11 corresponds to the calculation when the total en-

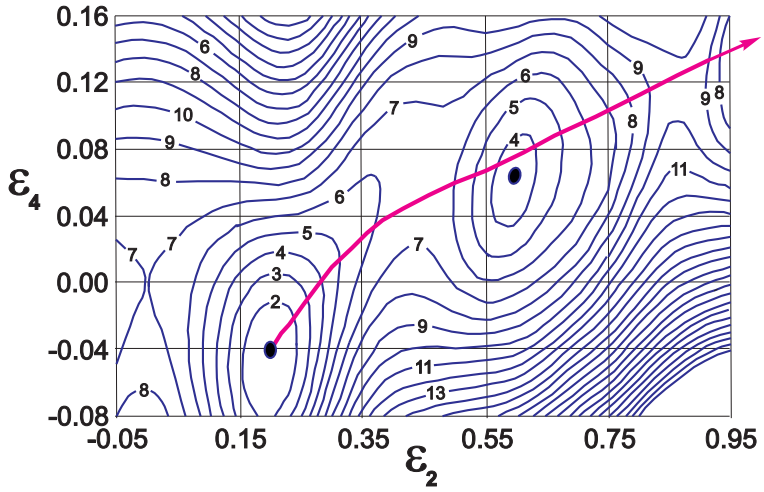


Figure 5.12: Surface map of the total energy of ^{236}U in the plane (ϵ_2, ϵ_4) of the quadrupole ϵ_2 and hexadecapole ϵ_4 deformation parameters. Thick solid line with the arrow shows the way along with the fission of ^{236}U proceeds (from [69]).

ergy E is calculated in the framework of the simple liquid drop model (that means $E = E_{LDM}(a_2)$, where $E_{LDM}(a_2)$ is determined by (5.49) and where the surface and Coulomb parts are substituted by $E_{fish.}(\alpha_{\lambda\mu})$ - see (5.70)). The dashed line was obtained by the Strutinski shell correction approach, $E = E_{LDM} + E_{OSC}$ (see (5.50), where the simple Nilsson shell model was used with only axial symmetric quadrupole and hexadecapole deformation parameters were involved ($\alpha_{20} \neq 0$, $\alpha_{40} \neq 0$, all other $\alpha_{\lambda\mu} = 0$). The solid line is connected with the Strutinski-Nilsson model when besides the axial quadrupole and hexadecapole deformations also the triaxial quadrupole α_{22} and axial octupole α_{30} deformation parameters are involved ($\alpha_{20} \neq 0$, $\alpha_{40} \neq 0$, $\alpha_{22} \neq 0$, $\alpha_{30} \neq 0$, and all other $\alpha_{\lambda\mu} = 0$). From the Fig. 5.11 it is seen that during the fission process the nucleus ^{240}Pu should goes through at least two barriers. One can also recognize that the simple liquid drop model gives only one broad barrier with one maximum and one minimum for zero deformation. The inclusion of the Strutinski shell corrections provides at least two barriers with two maxima and the first minimum at nonzero deformation. The nonzero deformation minimum corresponds to the reality because the nucleus ^{240}Pu is deformed in its ground state with the deformation corresponding to the position of the total energy minimum.

The Fig. 5.12 shows the surface map of the total energy of ^{236}U in the plane (ϵ_2, ϵ_4) of the quadrupole deformation ϵ_2 (see (5.36) and hexadecapole ϵ_4 ($\epsilon_4 \approx \alpha_{40}$) deformations. The total energy $E(\epsilon_2, \epsilon_4)$ was calculated using the LDM+Strutinski shell correction method based on the Nilsson mean field

involving deformation parameters ϵ_2 and ϵ_4. One can see two minima of the total energy separated by the barrier. The position of the deepest minimum ($\epsilon_2 \approx 0.19$, $\epsilon_4 \approx -0.04$) correspomds to the ground state deformation of ^{236}U. During the fission process the deformation of the ^{236}U nucleus changes as is indicated by the thick solid line with the arrow. The nucleus ^{236}U goes through the first barrier to the second minimum ($\epsilon_2 \approx 0.6$, $\epsilon_4 \approx 0.065$), then through the second barrier and during this way the deformations ϵ_2 and ϵ_4 are increasing (the nucleus is more and more prolonged). Finally the nucleus reaches the point where it is splitted into two fragments. The shapes characterized by the parameters (ϵ_2, ϵ_4) during this process are given in the Fig. 5.13. It should be noted that the parametrization of the deformed shapes in terms of ϵ_2 and ϵ_4 (so called Nilsson parametrization) is not the only one. In the literature also different parametrizations are used (e.g. Lawrence or Cassinian ovaloids - see e.g. [72]).

The path in the space od deformation parameters along which the shape of the nucleus is evolved during the fission (solid line in the Fig. 5.12) is determined by the WKB method (see e.g. [70, 14]) in the combination with the semi-microscopic cluster-decay theory (e.g. [71]). More detailed explanation can be found in [72]. Here only the basic ides is given.

From the WKB theory it is known that the probability of the penetration of the particle with the mass M through potential barrier $V(q)$ (we cosider here one-dimensional case when the potential is dependent only on one variable q) is given by (see Fig. 5.14 and Appendix G)

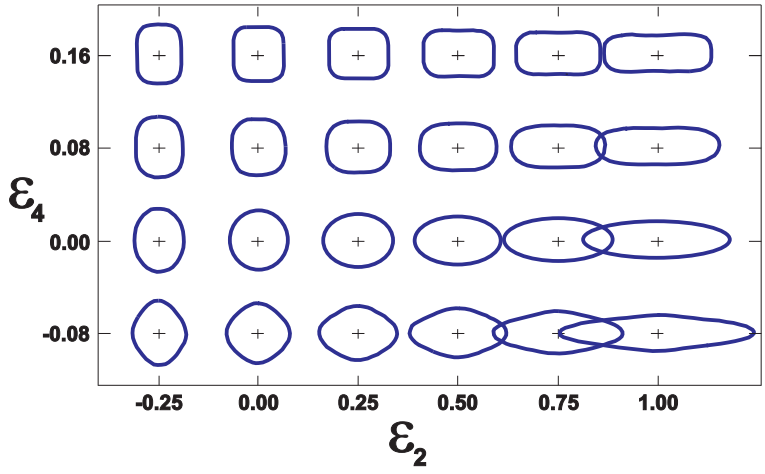


Figure 5.13: Shapes characterized by different quadrupole ϵ_2 and hexadecapole ϵ_4 deformation parameters.

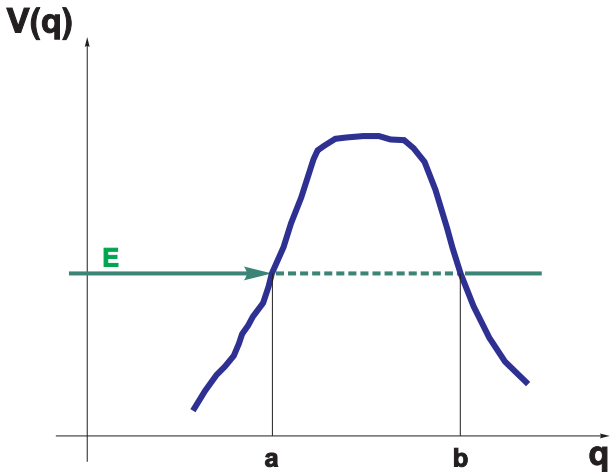


Figure 5.14: Schematic figure - tunneling effect of the particle with the energy through the barrier $V(q)$.

$$w \approx \boxed{\begin{array}{c}\text{see Appendix G}\\ (G.20)\end{array}} = e^{-\frac{2}{\hbar}\int_a^b dq\,\sqrt{2M\,[V(q)-E]}} \tag{5.79}$$

This simple one-dimesional expression is in the general WKB method generalized into the multi-dimensional case:

$$w_{WKB} \approx e^{-\frac{2}{\hbar}\int_{\vec{a}}^{\vec{b}} ds'\,\sqrt{2B(s')\,|V(\vec{q}_s(s'))-E|}} = e^{-\frac{2}{\hbar}S_s(\vec{a},\vec{b},E)} \tag{5.80}$$

where the integral in the exponent is the path integral from the point $\vec{a}$ into the point $\vec{b}$ in the multi-dimensional space of generalized coordinates $\vec{q}$ along the path $\vec{q}_s(s')$ (index s characterizes the path and the variable s' corresponds to the given point on the path s). In our case the $\vec{q}$- space is the space of deformation parameters, $\vec{q} = (\epsilon_2, \epsilon_4)$, and the pont $\vec{a}$ is the position $\vec{a} = (\epsilon_2 = 0.19, \epsilon_4 = -0.04)$ of the ground state minimum in the Fig. 5.12 and $\vec{b}$ is the point in the (ϵ_2, ϵ_4)- plane where the splitting of the nucleus is expected. The symbol $S_s(\vec{a},\ \vec{b},\ E)$ is so called action corresponding to the trajectory s between two points $\vec{a}$ and $\vec{b}$ in the q- space:

$$S_s(\vec{a},\ \vec{b},\ E) = \int_{\vec{a}}^{\vec{b}} ds'\,\sqrt{2B(s')\,|V(\vec{q}_s(s')) - E|} \tag{5.81}$$

The symbol $B(s')$ in (5.80) and (5.81) stands for mass factor which can be determined from single-particle wave functions of the used mean field corresponding to the deformation $\vec{q}(s') = (\epsilon_2, \epsilon_4)_{s'}$ (see [72] for more information).

In order to get right fission path $\vec{q}_s(s')$ from the point $\vec{a}$ to the point $(\vec{b})$ along which we should integrate in (5.80) it is necessary to find the minimum

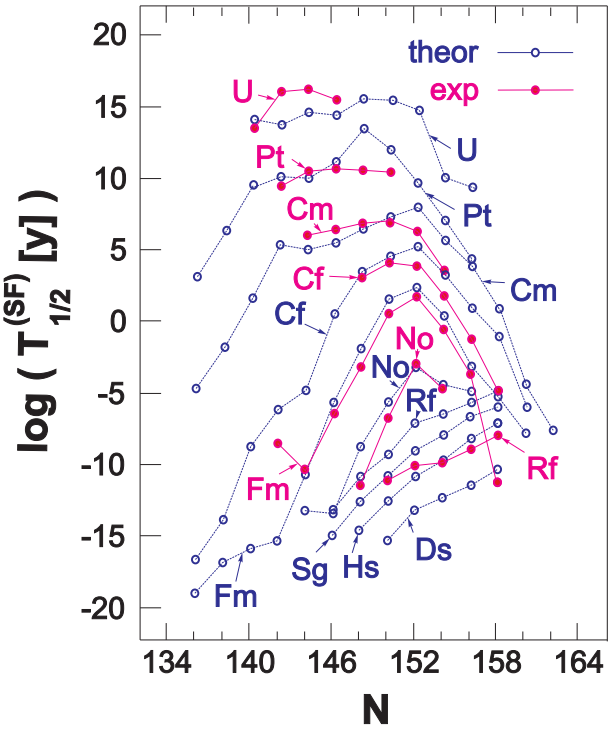


Figure 5.15: Experimental and calculated half-lives of some superheavy actinides. Theoretical values were obtained using (5.82) and (5.80) - see [73].

of the action $S_s(\vec{a}, \vec{b}, E)$ from the point of view of all possible paths for given points $\vec{a}$ and $\vec{b}$ and given energy E.

In the Fig. 5.15 there are spontaneous fission half-lives

$$T_{1/2}^{(SF)} = \frac{ln\, 2}{w_{WKB}} \tag{5.82}$$

where w_{WKB} was obtained using the minimal-action paths in the Strutinski-Nilsson energy surface in the space of deformation parameters ϵ_2, ϵ_3, ϵ_4 and ϵ_5 (see [73]). One can see the huge range of half-lives covering almost 40 orders and qualitative agreement between calculated and experimental values.

The determination of the spontaneous fission half-lives is very important in the present time when many experimental attempts are done to find more stable superheavy elements. The spontaneous fission, besides the alpha decay, is the main decay-channel for superheavy actinide nuclei. It is the cause why all heavier actinides than $Z > 92$ are not stable. In the Table 5.5 experimental half-lives of some superheavy elements with $Z > 100$ are presented.

From the Subsection 5.1.1 we know that the nuclei with the number of protons and/or neutrons equal to magic numbers 2, 8, 20, 28, 50, 126 are more stable and spherical. The number of protons and/or neutrons corre-

Z	name	longest-lived isotope	experimental half-life
100	Fermium	^{257}Fm	100.5 days
101	Mendelevium	^{258}Md	51.5 days
102	Nobelium	^{259}No	58 minutes
103	Lawrencium	^{262}Lr	10 hours
104	Ruthefordium	^{267}Rf	$\approx$ 1.3 hours
105	Dubnium	^{268}Db	30 hours
106	Seaborgium	^{271}Sg	$\approx$ 3 minutes
107	Bohrium	^{274}Bh	60 seconds
108	Hassium	^{270}Hs	$\approx$ 30 seconds
109	Meitnerium	^{278}Mt	4 seconds
110	Darmstadtium	^{281}Ds	$\approx$ 14 seconds
111	Roentgenium	^{281}Rg	$\approx$ 2 minutes
112	Copernicium	^{285m}Cn	$\approx$ 30 seconds
113	Nihonium	^{286}Nh	$\approx$ 8 seconds
114	Flerovium	^{289}Fl	$\approx$ 2 seconds
115	Moscovium	^{290}Mc	$\approx$ 0.8 seconds
116	Livermorium	^{293}Lv	$\approx$ 60 milliseconds
117	Tennesine	^{294}Ts	$\approx$ 50 milliseconds
118	Oganesson	^{294}Og	$\approx$ 0.7 milliseconds

Table 5.5: Table of superheavy elements with $Z \geq 100$ (from [75, 76]).

sponding to the filling of the shell with the principal quantum number $N = 6$ (see the text under the expression (5.8)) is 184. Therefore one can expect that the nuclei with $Z \approx 126$ and/or $N \approx 184$ can be more stable and can form so called "stability island" (see Fig. 5.16). However, the most of these superheavy nuclei are deformed with magic numbers a little bit shifted from 126 and 184 (see Fig. 5.5). Fo instance, there are theoretical predictions (see e.g. [74]) that some heavier isotopes of Hs can be candidates for more stability. However, theoretical predictions in this direction are not so precise up to now. The problem also is how to reach experimentally (through what nuclear reactions) this "stability island". The searching for it is today one of the most challenging topic in the nuclear physics.

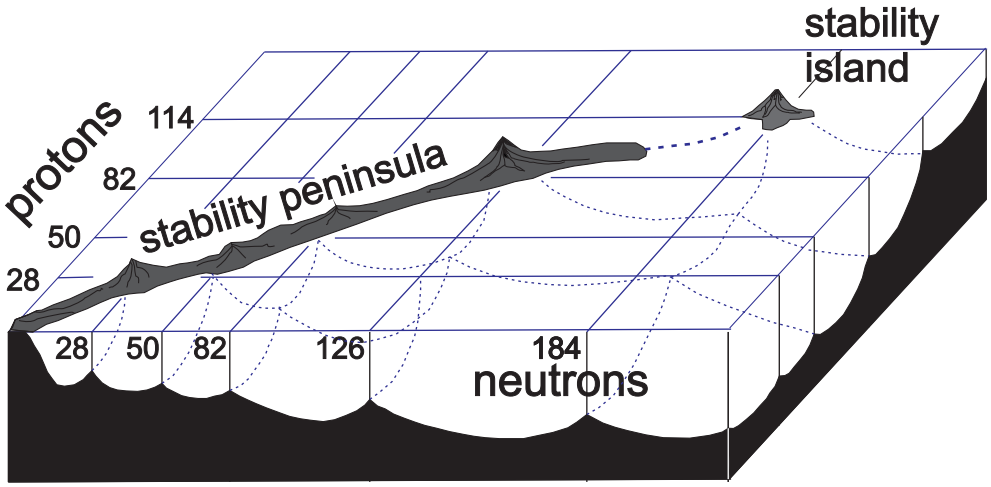


Figure 5.16: Schematic figure - surface map of the absolute value of the total nucleus energy in the plane of (N,Z) (chart of nuclides). More stable isotopes form so called "stability peninsula" and expected more stable superheavy nuclei can create so called "stability island".

In the end of this subsection it is necessary to note that in the present time (2019) there are more microscopic theoretical models for the determination of the total energy surface maps and subsequently the spontaneous fission half-lives. These approaches are mostly based on the microscopical HFB calculations (no phenomenological mean fields but HF and HFB calculations with more realistic microscopical effective nucleon-nucleon interactions as it will be discussed in next chapters) - see e.g. [77, 78] and citations therein. Some of these models goes beyond the mean field approach and take into account also residual interactions in the nucleus Hamiltonian and the contributions to the fission barriers coming from the rotational degrees of freedom of nuclear motion. However, it is necessary to point out that up to now the predictive power of these microscopical calculations does not reach the accuracy of the Strutnski shell correction approach with phenomenological mean fields discussed above.

5.2 Microscopical mean field

By the microscopical mean field we mean the single-particle mean field which is obtained in terms of the Hartree-Fock method from the realistic effective nucleon-nucleon interactios (involving possible three- and more- particle terms). As it was discussed in the Subsection 3.2.2 the present theory is not able to provide us precisely and unambiguously the effective nucleon-nucleon interaction starting with the bare nucleon-nucleon interaction (the bare nucleon-nucleon interaction is defined as the interaction of nucleons in the vacuum and it was discussed in the Subsection 3.1). Microscopical theories like Brueckner-Bethe one (see the Subsection 3.2.1) or UCOM (see e.g. [26]) give only some function dependences of effective interactions on nucleon coordinates in the spatial-spin-isospin Hilbert space. However, the real effective interactions contain in these functions always free parameters which should be determined by the fitting calculated values of selected nucleus properties on corresponding experimental data. Most frequently the bulk nuclear properties (e.g. bind energy, nuclear radius, compressibility of nuclear matter) of selected double magic nuclei are used for this purpose (see e.g. [79] and citations therein). Up to now there is no microscopical fully self-consistent theory which would give the nuclear spectra and wave functions of excited states of heavier nuclei with the sufficient accuracy (comparable with experimental data) without any additional adjustment of the effective n-n interaction. Certainly, the challenge for theoretical nuclear physics is to create such microscopical theory which minimizes number of free parameters as much as possible. However, as it was mentioned in the introductory Chapter 1 the many-body problem and the problem of the strong interaction between elementary particles (including nucleons) are not solvable precisely and one can only try to be precise and accurate as much as possible in the theoretical description of given particular quantum many-body system (nucleus in our case) in the framework of the present knowledge and present computional possibilities.

In this subsection we discuss one example of the Hartree-Fock treatment and results with the Skyrme effective interaction (see (3.144) in the Subsection 3.2.2.1). The Hartree-Fock approach with the Skyrme effective nucleon-nucleon interaction is one of the three most used microscopical methods for the determination of the nuclear mean field in the present time. The other two are mean fields obtained with the Gogny effective interaction (see the Subsection 3.2.2.2) and the relativistic mean field approach (see the Subsec-

tion 3.2.3). On the base of the example of the Skyrme effective interaction we demonstrate below so called energy functional approach to the mean field.

The form of the Skyrme interaction was discussed in the part 3.2.2.1 (expr. (3.144))

$$\hat{V}_{Skyrme} = \sum_{i<j} \hat{V}^{(2)}_{Skyrme}(i,j) + \sum_{i<j<k} \hat{V}^{(3)}_{Skyrme}(i,j,k) \tag{5.83}$$

where two-body and three-body components in (5.83) have a contact character depending on the linear momentum (that means non-local interaction) (see (3.145), (3.146))

$$\begin{aligned}\hat{V}^{(2)}_{Skyrme}(i,j) &= t_0\,(1+\kappa_0\,\hat{P}^{\,(\sigma)}_{ij})\,\delta(\vec{r}_i-\vec{r}_j) + \\ &+\frac{1}{2}t_1\,[\,\delta(\vec{r}_i-\vec{r}_j)\overleftarrow{k}^{\,2} + \overrightarrow{k}^{\,2}\,\delta(\vec{r}_i-\vec{r}_j)\,] + \, t_2\,\overleftarrow{k}\,\delta(\vec{r}_i-\vec{r}_j)\,\overrightarrow{k}\, + \\ &+ i\,W_0\,(\vec{\sigma}_i+\vec{\sigma}_j)\cdot[\,\overleftarrow{k}\,\times\delta(\vec{r}_i-\vec{r}_j)\,\overrightarrow{k}\,]\end{aligned} \tag{5.84}$$

$$\hat{V}^{(3)}_{Skyrme}(i,j,k) = t_3\,\delta(\vec{r}_i-\vec{r}_j)\,\delta(\vec{r}_j-\vec{r}_k) \tag{5.85}$$

where t_0, t_1, t_2, W_0, t_3 are strength constants (free parameters) and $\hat{P}^{(\sigma)}_{ij} = \frac{1}{2}(1+\vec{\sigma}_i\cdot\vec{\sigma}_j)$ is the spin exchange operator between the i-th and j-th nucleons. The symbol $\overrightarrow{k}$ and $\overleftarrow{k}$ are relative linear momentum operators acting to right and to left, respectively:

$$\overrightarrow{k} = \frac{\overrightarrow{\nabla}_i - \overrightarrow{\nabla}_j}{2i}\,, \qquad\qquad \overleftarrow{k} = \frac{\overleftarrow{\nabla}_i - \overleftarrow{\nabla}_j}{2i} \tag{5.86}$$

The first and the second terms in (5.84) represents so called s-wave interaction because their matrix elements are nonzero only when orbital moments of the relative motion of the bra- and ket- states in the matrix element are both equal to zero as it is seen below (s.p. state: $\varphi_i(\vec{r}) = \langle\vec{r}\,|\,i\rangle = R_{n_il_i}(r)\,Y_{l_im_i}(\hat{r})$,

where for the simplicity the spin and isospin variables are omitted)

$$\langle 1\,'\,2\,'|\hat{V}^{(2)}|1\,2\rangle =$$
$$= \int d^3r_1 \int d^3r_2 \;\varphi^*_{1\,'}(\vec{r}_1)\,\varphi^*_{2\,'}(\vec{r}_2)\;V^{(2)}(\vec{r}_1,\vec{r}_2)\;\varphi_1(\vec{r}_1)\,\varphi_2(\vec{r}_2) =$$

Moshinsky transformation:
$(\vec{r}_1,\vec{r}_2) \to \vec{r} = \vec{r}_1 - \vec{r}_2, \quad \vec{r}_t = \frac{1}{2}(\vec{r}_1 + \vec{r}_2)$,
where $\vec{r}$ is relative coordinate, $\vec{r}_t$ is the center of mass coordinate of two nucleons. Then:

$$= \varphi_1(\vec{r}_1)\varphi_2(\vec{r}_2) = \sum_{nln_tl_t}(nl,\; n_tl_t|n_1l_1,\; n_2l_2)\; R_{nl}(r)Y_{lm}(\hat{r})\; R_{n_tl_t}(r_t)Y_{l_tm_t}(\hat{r}_t)$$

where $(nl,\; n_tl_t|n_1l_1,\; n_2l_2)$ are so called Moshinsky brackets - see [80, 81, 82]. We also suppose

$$V^{(2)}(\vec{r}_1,\vec{r}_2) = V(\vec{r} = \vec{r}_1 - \vec{r}_2)$$

$$= \sum\sum(\;|\;)\;(\;|\;) \int d^3r\; R_{n\,'l\,'}(r)Y^*_{l\,'m\,'}(\hat{r})\; V(\vec{r}\,)\; R_{nl}(r)Y_{lm}(\hat{r})$$
$$\int d^3r_t\; R_{n\,'_tl\,'_t}(r_t)Y^*_{l\,'_tm\,'_t}(\hat{r}_t)\; R_{n_tl_t}(r_t)Y_{l_tm_t}(\hat{r}_t) =$$
$$= \sum\sum(\;|\;)\;(\;|\;) \int d^3r\; R_{n\,'l\,'}(r)Y^*_{l\,'m\,'}(\hat{r})\; V(\vec{r}\,)\; R_{nl}(r)Y_{lm}(\hat{r})$$
$$\cdot\,\delta_{n\,'_t\,l\,'_t\,m\,'_t,\,n_t\,l_t\,m_t} \tag{5.87}$$

So, the contribution to the matrix element from the 1-st term in (5.84) is proportional to:

$$\int d^3r\; R_{n\,'l\,'}(r)\; Y^*_{l\,'m\,'}(\hat{r})\;\delta(\vec{r})\; R_{nl}(r)\; Y_{lm}(\hat{r}) =$$
$$= R_{n\,'l\,'}(0)\; Y_{l\,'m\,'}(\hat{0})\; R_{nl}(0)\; Y_{lm}(\hat{0}) \tag{5.88}$$

However, for the oscillator case [14]: $R_{nl}(r) = N_{nl}\; e^{-\frac{\nu r^2}{2}}\; r^l\; L^{l+\frac{1}{2}}_{n+l+\frac{1}{2}}(\nu r^2)$ and therefore (5.88) can be nonzero only for $l = l' = 0$, that means only for s-waves. Similarly for the contribution of the 2-d term in (5.84) we obtain

$$\int d^3r\; R_{n\,'l\,'}(r)\; Y^*_{l\,'m\,'}(\hat{r})\;\overleftarrow{\nabla}^2\;\delta(\vec{r})\; R_{nl}(r)\; Y_{lm}(\hat{r}) =$$
$$= R_{n\,'l\,'}(0)\; Y_{l\,'m\,'}(\hat{0})\;\overleftarrow{\nabla}^2\; R_{nl}(0)\; Y_{lm}(\hat{0}) \tag{5.89}$$

and again it is nonzero only for $l = l' = 0$.

The third term in (5.84) is so called p-wave interaction because this term gives the contribution to the matrix element $\langle 1\,'\,2\,'|\hat{V}^{(2)}|1\,2\rangle$ which is proportional to (analogy with (5.88))

$$\int d^3r\, R_{n\,'l\,'}(r)\, Y^*_{l\,'m\,'}(\hat{r})\, \overleftarrow{\nabla}\, \delta(\vec{r})\, \overrightarrow{\nabla}\, R_{nl}(r)\, Y_{lm}(\hat{r}) = \\ = \left(\vec{\nabla} R_{n\,'l\,'}(0)\, Y^*_{l\,'m\,'}(\hat{0})\right) \cdot \left(\vec{\nabla} R_{n\,l}(0)\, Y^*_{l\,m}(\hat{0})\right) \tag{5.90}$$

However, because of $R_{nl}(r) = N_{nl}\, e^{-\frac{\nu r^2}{2}}\, r^l\, L^{l+\frac{1}{2}}_{n+l+\frac{1}{2}}(\nu r^2)$ the expr. (5.90) is nonzero only for $l = l' = 0$ or $l = l' = 1$ or $l = 0$, $l' = 1$ or $l = 1$, $l' = 0$, that means for s- or p- waves.

The nucleus Hamiltonian with the Skyrme effective interaction (5.83) can be rewritten in terms of single-particle creation and annihilation operators as follows

$$\begin{aligned} \hat{H} &= \sum_{ij} \langle i|\, \hat{T}\, |j\rangle\, a_i^+ a_j + \frac{1}{2} \sum_{ijkl} \langle ij|\, \hat{V}^{(2)}\, |kl\rangle\, a_i^+ a_j^+ a_l\, a_k + \\ &\quad + \frac{1}{6} \sum_{ijklmn} \langle ijk|\, \hat{V}^{(3)}\, |\, lmn\rangle\, a_i^+ a_j^+ a_k^+ a_n\, a_m\, a_l \end{aligned} \tag{5.91}$$

where $\hat{V}^{(2)} = \hat{V}^{(2)}_{Skyrme} + \hat{V}^{(2)}_{Coulomb}$ is two-body part of the effective interaction and $\hat{V}^{(3)} = \hat{V}^{(3)}_{Skyrme}$ is the three-body part of the interaction. The first term in (5.91) is standard one-body kinetic energy operator and a_i^+, a_i are single-particle creation and annihilation operators, respectively (see Appendix B).

Further the usual Hartree-Fock (HF) approach is used for the determination of the HF mean field (see Subsection 4.1). That means the minimum of the total energy is search for where the total energy E is calculated as the expectation value of the Hamiltonian (5.91) in the Slater determinant $|HF\rangle$ (see (4.5), (4.7)).

$$\begin{aligned} E &= \langle HF|\, \hat{H}\, |HF\rangle = \\ &= \sum_{ij} \langle i|\, \hat{T}\, |j\rangle \langle HF|\, a_i^+ a_j\, |HF\rangle + \\ &\quad + \frac{1}{2} \sum_{ijkl} \langle ij|\, \hat{V}^{(2)}\, |kl\rangle\ < HF|\, a_i^+ a_j^+ a_l\, a_k\, |HF\rangle + \\ &\quad + \frac{1}{6} \sum_{ijklmn} \langle ijk|\, \hat{V}^{(3)}\, |\, lmn\rangle\ < HF|\, a_i^+ a_j^+ a_k^+ a_n\, a_m\, a_l\, |HF\rangle \end{aligned} \tag{5.92}$$

Using the well-known properties of the HF ground state $|HF\rangle$ ($a^+_{i_<}|HF\rangle = 0$, $a_{l_>}|HF\rangle = 0$ - see (4.6)) the expectation values in the r.h.s. of (5.92) are

$$\langle HF|\, a^+_i a_j\, |HF\rangle = \begin{cases} 0 & \text{for } j = j_> \\ \delta_{j\,l_<} & \text{for } j = j_< \end{cases}$$

$$\langle HF|\, a^+_i a^+_j a_l\, a_k\, |HF\rangle = \begin{cases} 0 \text{ for } l = l_>,\ k = k_> \\ \delta_{j\,l_<}\delta_{i\,k_<} - \delta_{j\,k_<}\delta_{i\,l_<} \text{ for other cases} \end{cases}$$

$$\langle HF|\, a^+_i a^+_j a^+_k a_n\, a_m a_l\, |HF\rangle = \\ \begin{cases} 0 \text{ for } n = n_>, \text{ or } m = m_>, \text{ or } l = l_> \\ \begin{pmatrix} +\delta_{k\,n_<}\delta_{j\,m_<}\delta_{i\,l_<} - \delta_{k\,m_<}\delta_{j\,l_<}\delta_{i\,m_<} \\ -\delta_{j\,n_<}\delta_{k\,m_<}\delta_{i\,l_<} + \delta_{k\,m_<}\delta_{i\,n_<}\delta_{j\,l_<} \\ +\delta_{j\,n_<}\delta_{i\,m_<}\delta_{k\,l_<} - \delta_{i\,n_<}\delta_{j\,m_<}\delta_{k\,l_<} \end{pmatrix} \text{ for other cases} \end{cases}$$

where single-particle state with the index $i_<$ means the state below Fermi level and single-particle state with the index $i_>$ is state above Fermi level. So, the total energy expression (5.92) can be rewritten as follows

$$\begin{aligned} E &= \sum_{i_<=1}^{A} \langle\, i_<|\, \hat{T}\, |i_<\rangle + \frac{1}{2}\sum_{i_<j_<}^{A} \langle\, i_<j_<|\, \hat{V}^{(2)}\, |\, i_<j_< - j_<i_<\,\rangle + \\ &\quad + \frac{1}{6}\sum_{i_<j_<k_<}^{A} \langle\, i_<j_<k_<\,|\, \hat{V}^{(3)}\, |\, i_<j_<k_< - j_<i_<k_< + j_<k_<i_< \\ &\qquad\qquad -i_<k_<j_< + k_<i_<j_< - k_<j_<i_<\,\rangle = \\ &= \int \mathscr{H}(\vec{r})\, d^3r \end{aligned} \tag{5.93}$$

where $\mathscr{H}(\vec{r})$ is the density of the Hamiltonian (density of the energy). After the relatively simple but tedious calculations the explicite expression for the

energy density $\mathscr{H}(\vec{r})$ for the Skyrme Hamiltonian is following (e.g. [83])

$$\begin{aligned}
\mathscr{H}(\vec{r}) &= \frac{\hbar^2}{2M}\,\tau(\vec{r}) + \\
&+\frac{t_0}{2}\,\Big[\,(1+\frac{\kappa_0}{2})\,\rho^2(\vec{r}) \\
&-(\kappa_0+\frac{1}{2})\left(\rho_p^2(\vec{r})+\rho_n^2(\vec{r})+\frac{\kappa_0}{2}\,\vec{s}^{\,2}(\vec{r})-\frac{1}{2}\,\left(\vec{s}^{\,2}_p(\vec{r})+\vec{s}^{\,2}_n(\vec{r})\right)\right)\Big] \\
&+\frac{1}{4}\,(t_1+t_2)\,\Big[\rho(\vec{r})\,\tau(\vec{r})-\vec{j}^{\,2}(\vec{r})\Big]+\frac{1}{16}\,(t_2-3t_1)\,\rho(\vec{r})\,(\Delta\rho(\vec{r}))+ \\
&+\frac{1}{32}(t_2+3t_1)\sum_{q=n,p}\,[\,\rho_q(\vec{r})\,(\Delta\rho(\vec{r}))+\vec{s}_q(\vec{r})\cdot(\Delta\vec{s}_q(\vec{r}))\,]+ \\
&+\frac{t_3}{4}\,\Big[\rho_p(\vec{r})\,(\rho_n^2(\vec{r})-\vec{s}^{\,2}_n(\vec{r}))+\rho_n(\vec{r})\,(\rho_p^2(\vec{r})-\vec{s}^{\,2}_p(\vec{r}))\Big]+ \\
&+\frac{1}{8}\,(t_2-t_1)\,\sum_q\Big[\,\rho_q(\vec{r})\,\tau_q(\vec{r})-\vec{j}_q^{\,2}(\vec{r})+\vec{s}_q(\vec{r})\cdot\vec{T}_q(\vec{r})-\vec{J}_q^{\,2}\,\Big] \\
&-\frac{1}{2}W_0\,\sum_{qq'}(1+\delta_{qq'})\,\Big[\vec{s}_q\cdot(\vec{\nabla}\times\vec{j}_{q'}(\vec{r}))+\rho_q(\vec{r})\,(\vec{\nabla}\cdot\vec{J}_q(\vec{r}))\,\Big]+ \\
&+\mathscr{H}_C(\vec{r})
\end{aligned} \tag{5.94}$$

where

$$\mathscr{H}_C(\vec{r}) = \frac{e^2}{4\pi\epsilon_0}\,\frac{1}{2}\int d^3r'\,\frac{\rho_p(\vec{r})\,\rho_p(\vec{r}\,')}{|\vec{r}-\vec{r}\,'|}-\frac{3}{4}\,\left(\frac{3}{\pi}\right)^{1/3}\,\rho_p^{4/3}(\vec{r}) \tag{5.95}$$

is the part of the energy density originating from the Coulomb interaction between protons. In (5.94) and (5.95) the following densities and currents are introduced

$$\begin{aligned}
\rho(\vec{r}) &= \rho_p(\vec{r}\,)+\rho_n(\vec{r}\,) \quad\rightarrow\quad \text{density} \\
\rho_{q=n,p}(\vec{r}) &= \langle HF|\,\hat{\rho}_q(\vec{r}\,)\,|HF\rangle = \\
&= \sum_{ij\in q}\sum_{\sigma=\pm1/2}\varphi_i^*(\vec{r}\,\sigma)\,\varphi_j(\vec{r}\,\sigma)\,\langle HF|\,a_i^+\,a_j\,|HF\rangle = \\
&= \sum_{i_<\in q}\sum_{\sigma=\pm1/2}\varphi_{i_<}^*(\vec{r}\,\sigma)\,\varphi_{i_<}(\vec{r}\,\sigma)=\sum_{i_<\in\,q}\Phi_{i_<}^+(\vec{r}\,)\,\Phi_{i_<}(\vec{r}\,)
\end{aligned} \tag{5.96}$$

$$
\begin{aligned}
\tau(\vec{r}) &= \tau_p(\vec{r}\,) + \tau_n(\vec{r}\,) \quad \rightarrow \quad \text{kinetic energy density} \\
\tau_{q=n,p}(\vec{r}) &= \langle HF|\, \hat{\tau}_q(\vec{r}\,)\, |HF\rangle = \\
&= \sum_{ij\in q} \sum_{\sigma=\pm 1/2} (\vec{\nabla}\varphi_i^*(\vec{r}\,\sigma)) \cdot (\vec{\nabla}\varphi_j(\vec{r}\,\sigma))\, \langle HF|\, a_i^+\, a_j\, |HF\rangle = \\
&= \sum_{i_<\in q} \sum_{\sigma=\pm 1/2} (\vec{\nabla}\varphi_{i_<}^*(\vec{r}\,\sigma)) \cdot (\vec{\nabla}\varphi_{i_<}(\vec{r}\,\sigma)) = \\
&= \sum_{i_<\in\, q} \Big(\vec{\nabla}\Phi_{i_<}^+(\vec{r}\,)\Big) \cdot \Big(\vec{\nabla}\Phi_{i_<}(\vec{r}\,)\Big)
\end{aligned}
\tag{5.97}
$$

$$
\begin{aligned}
\vec{J}(\vec{r}) &= \vec{J}_p(\vec{r}\,) + \vec{J}_n(\vec{r}\,) \quad \rightarrow \quad \text{spin-orbital current} \\
\vec{J}_{q=n,p}(\vec{r}) &= \langle HF|\, \hat{\vec{J}}_q(\vec{r}\,)\, |HF\rangle = \\
&= \sum_{ij\in q} (-\frac{i}{2}) \, \Big\{\Phi_i^+(\vec{r}\,)\, [(\vec{\nabla}\times\vec{\sigma})\, \Phi_j(\vec{r}\,)] \\
&\qquad\qquad -[(\vec{\nabla}\times\vec{\sigma})\, \Phi_j(\vec{r}\,)]^+\, \Phi_i(\vec{r}\,)\Big\}\, \langle HF|\, a_i^+\, a_j\, |HF\rangle = \\
&= \sum_{i_<\in\, q} (-\frac{i}{2}) \, \Big\{\Phi_i^+(\vec{r}\,)\, [(\vec{\nabla}\times\vec{\sigma})\, \Phi_i(\vec{r}\,)] \\
&\qquad\qquad - [(\vec{\nabla}\times\vec{\sigma})\, \Phi_{i_<}(\vec{r}\,)]^+\, \Phi_{i_<}(\vec{r}\,)\Big\}
\end{aligned}
\tag{5.98}
$$

$$
\begin{aligned}
\vec{s}(\vec{r}) &= \vec{s}_p(\vec{r}\,) + \vec{s}_n(\vec{r}\,) \quad \rightarrow \quad \text{spin current} \\
\vec{s}_{q=n,p}(\vec{r}) &= \langle HF|\, \hat{\vec{s}}_q(\vec{r}\,)\, |HF\rangle = \\
&= \sum_{ij\in\, q} \Phi_i^+(\vec{r}\,)\, \vec{\sigma}\; \Phi_j(\vec{r}\,)\, \langle HF|\, a_i^+\, a_j\, |HF\rangle = \\
&= \sum_{i_<\in\, q} \Phi_{i_<}^+(\vec{r}\,)\, \vec{\sigma}\; \Phi_{i_<(}\vec{r}\,)
\end{aligned}
\tag{5.99}
$$

$$
\begin{aligned}
\vec{j}(\vec{r}) &= \vec{j}_p(\vec{r}) + \vec{j}_n(\vec{r}) \quad \rightarrow \quad \text{current} \\
\vec{j}_{q=n,p}(\vec{r}) &= \langle HF| \hat{\vec{j}}_q(\vec{r}) \, |HF\rangle = \\
&= \sum_{ij\in q} \frac{i}{2} \left\{ \left(\vec{\nabla} \Phi_i^+(\vec{r}) \right) \, \Phi_j(\vec{r}) \right. \\
&\quad \left. - \; \Phi_i^+(\vec{r}) \, \left(\vec{\nabla} \Phi_j(\vec{r}) \right) \right\} \, \langle HF| \, a_i^+ \, a_j \, |HF\rangle = \\
&= \sum_{i_< \in \, q} \frac{i}{2} \left\{ \left(\vec{\nabla} \Phi_{i_<}^+(\vec{r}) \right) \, \Phi_{i_<}(\vec{r}) - \; \Phi_{i_<}^+(\vec{r}) \, \left(\vec{\nabla} \Phi_{i_<}(\vec{r}) \right) \right\}
\end{aligned}
\tag{5.100}
$$

$$
\begin{aligned}
\vec{T}(\vec{r}) &= \vec{j}_p(\vec{r}) + \vec{j}_n(\vec{r}) \quad \rightarrow \quad \text{kinetic energy spin current} \\
\vec{T}_{q=n,p}(\vec{r}) &= \langle HF| \, \hat{\vec{T}}_q(\vec{r}) \, |HF\rangle = \\
&= \sum_{ij\in q} \left(\vec{\nabla} \Phi_i^+(\vec{r}) \right) \, \vec{\sigma} \cdot \left(\vec{\nabla} \Phi_j(\vec{r}) \right) \, \langle HF| \, a_i^+ \, a_j \, |HF\rangle = \\
&= \sum_{i_< \in \, q} \left(\vec{\nabla} \Phi_{i_<}^+(\vec{r}) \right) \, \vec{\sigma} \cdot \left(\vec{\nabla} \Phi_{i_<}(\vec{r}) \right)
\end{aligned}
\tag{5.101}
$$

where in (5.96)-(5.101) the spinor single-particle wave functions

$$
\Phi_{i_<}(\vec{r}) = \begin{pmatrix} \varphi_i(\vec{r}, \sigma = +1/2) \\ \varphi_i(\vec{r}, \sigma = -1/2) \end{pmatrix}
\tag{5.102}
$$

were introduced.

From the expressions (5.94) and (5.95) we can see that the energy density $\mathscr{H}(\vec{r})$ depends on the coordinate vector $\vec{r}$ through the densities and currents $\mathscr{J}_\alpha(\vec{r})$:

$$
\mathscr{H}(\vec{r}) = \mathscr{H}(\mathscr{J}_\alpha(\vec{r}))
\tag{5.103}
$$

where

$$
\begin{aligned}
\mathscr{J}_{\alpha=\rho}(\vec{r}) &= \rho(\vec{r}) \, , \quad \mathscr{J}_{\alpha=\tau}(\vec{r}) = \tau(\vec{r}) \, , \quad \mathscr{J}_{\alpha=\vec{J}}(\vec{r}) = \vec{J}(\vec{r}) \, , \\
\mathscr{J}_{\alpha=\vec{s}}(\vec{r}) &= \vec{s}(\vec{r}) \, , \quad \mathscr{J}_{\alpha=\vec{j}}(\vec{r}) = \vec{j}(\vec{r}) \, , \quad \mathscr{J}_{\alpha=\vec{T}}(\vec{r}) = \vec{T}(\vec{r}) \, ,
\end{aligned}
\tag{5.104}
$$

and the energy functional E depends on the single-particle wave functions $\varphi_i(\vec{r}\sigma)$ again through these densities and currents, $E[\varphi_i(\vec{r}\sigma)] = E[\mathscr{J}_\alpha(\varphi_i(\vec{r}\sigma))]$. Then the Hartree-Fock equation can be obtained as the condition of the min-

imum of the functional $E[\varphi_i(\vec{r}\sigma)]$ (see (4.32)).

$$\frac{\partial}{\partial\varphi_i^*(\vec{r}\sigma)}\left\{E[\varphi_i(\vec{r}\sigma)]-\sum_k\epsilon_k\left[\sum_{\sigma'}\int d^3x\,\varphi_k^*(\vec{x}\sigma')\,\varphi_k(\vec{x}\sigma')-1\right]\right\}=0$$
$$\Rightarrow\frac{\partial E}{\partial\varphi_i^*(\vec{r}\sigma)}=\sum_\alpha\frac{\partial E}{\partial\mathscr{J}_\alpha(\vec{r}\,)}\frac{\partial\mathscr{J}_\alpha(\vec{r}\,)}{\partial\varphi_i^*(\vec{r}\sigma)}\equiv H_{AV}(\vec{r})\,\varphi_i(\vec{r}\sigma)=\epsilon_i\,\varphi_i(\vec{r}\sigma) \tag{5.105}$$

In such a way we obtained the mean field single-particle field $\hat{H}_{AV}$ in the following form

$$\hat{H}_{AV}=\int d^3r\sum_\alpha\frac{\partial E}{\partial\mathscr{J}_\alpha(\vec{r}\,)}\hat{\mathscr{J}}_\alpha(\vec{r})=\int d^3r\sum_\alpha\frac{\partial\int d^3x\,\mathscr{H}(\vec{x})}{\partial\mathscr{J}_\alpha(\vec{r}\,)}\hat{\mathscr{J}}_\alpha(\vec{r}) \tag{5.106}$$

because

$$\langle i|\hat{H}_{AV}|j\rangle=$$
$$=\boxed{\begin{array}{c}\text{from the point}\\ \text{of view of (5.106)}\end{array}}=\int d^3r\sum_\alpha\frac{\partial\int d^3x\,\mathscr{H}(\vec{x})}{\partial\mathscr{J}_\alpha(\vec{r}\,)}\langle i|\,\hat{\mathscr{J}}_\alpha(\vec{r}\,)\,|j\rangle$$
$$=\boxed{\begin{array}{c}\text{from the point}\\ \text{of view of (5.105)}\end{array}}=\int d^3r\,\varphi_i^*(\vec{r}\sigma)\sum_\alpha\frac{\partial\int d^3x\,\mathscr{H}(\vec{x})}{\partial\mathscr{J}_\alpha(\vec{r}\,)}\frac{\partial\mathscr{J}_\alpha(\vec{r}\,)}{\partial\varphi_j^*(\vec{r}\sigma)}$$

and the expressions (5.105) and (5.106) are mutually consistent.

Densities and currents (5.96)-(5.101) involved in the energy functional (5.94) have the following symmetries with respect to the time-reverse transformation

$$\begin{array}{lll}\mathscr{T}\,\hat{\rho}(\vec{r}\,)\,\mathscr{T}^{-1} &=& \hat{\rho}(\vec{r}\,) \qquad\qquad \mathscr{T}\,\hat{\vec{s}}(\vec{r}\,)\,\mathscr{T}^{-1}=-\hat{\vec{s}}(\vec{r}\,)\\ \mathscr{T}\,\hat{\tau}(\vec{r}\,)\,\mathscr{T}^{-1} &=& \hat{\tau}(\vec{r}\,) \qquad\qquad \mathscr{T}\,\hat{\vec{j}}(\vec{r}\,)\,\mathscr{T}^{-1}=-\hat{\vec{j}}(\vec{r}\,)\\ \mathscr{T}\,\hat{\vec{J}}(\vec{r}\,)\,\mathscr{T}^{-1} &=& \hat{\vec{J}}(\vec{r}\,) \qquad\qquad \mathscr{T}\,\hat{\vec{T}}(\vec{r}\,)\,\mathscr{T}^{-1}=-\hat{\vec{T}}(\vec{r}\,)\end{array} \tag{5.107}$$

The Skyrme mean field Hamiltonian $\hat{H}_{AV}$ is time-reversal invariant

$$\mathscr{T}\,\hat{H}_{AV}\,\mathscr{T}^{-1}=\hat{H}_{AV} \tag{5.108}$$

and corresponding ground state $|HF\rangle$ is also invariant with respect to time-reversal transformation

$$\mathscr{T}\,|HF\rangle=|HF\rangle \tag{5.109}$$

From (5.108) it follows that the $\hat{H}_{AV}$ given by (5.106) should contain only time-even densities and currents, that means only $\hat{\rho}(\vec{r}\,)$, $\hat{\tau}(\vec{r}\,)$ and $\hat{\vec{J}}(\vec{r}\,)$ (see (5.107). So not all terms of the energy density $\mathscr{H}(\vec{r}\,)$ (see (5.94) give a contribution to $\hat{H}_{AV}$. However, one should realize that this is true only for the mean field $\hat{H}_{AV}$. If we go beyond the mean field and if we want to take into account also residual interactions all terms in (5.94) play role.

In the first pioneering paper with the Skyrme functional (see [84]) the functional (5.94) was used in the simplified version for the case of $N = Z$ nucleus ($\rho_n(\vec{r}\,) = \rho_p(\vec{r}\,) = \rho(\vec{r}\,)/2$ and the parameter $\kappa_0 = 1$. In [84] only relevant terms involving only time-even densities and currents were taken into account. The Coulomb term was neglected as well. So, the energy density $\mathscr{H}$ was reduced to the simple form:

$$\begin{aligned}\mathscr{H} = & \frac{\hbar^2}{2M}\,\tau(\vec{r}) + \frac{3}{2}\,t_0\,\rho^2(\vec{r}\,) + \frac{1}{16}\,t_3\,\rho^3(\vec{r}\,) + \\ & + \frac{1}{16}\,(3t_1 + 5t_2)\,\rho(\vec{r}\,)\,\tau(\vec{r}\,) + \frac{1}{64}\,(9t_1 - 5t_2)\,(\vec{\nabla}\rho(\vec{r}\,))^2 \\ & - \frac{3}{4}\,W_0\,\vec{\nabla}\vec{J}(\vec{r}\,) + \frac{1}{32}\,(t_1 - t_2)\,\vec{J}^{\,2}(\vec{r}\,) \end{aligned} \tag{5.110}$$

With such simplified functional it is possible to determine explicitely binding energy per nucleon and the incompressibility of the infinite nuclear matter. In the case of the infinite nuclear matter the Hamiltonian $\hat{H}$ (as well as the functional $\mathscr{H}(\mathscr{J}_\alpha(\vec{r}\,))$ is translational invariant and the single-particle wave function (eigenstates of the corresponding infinite mean field) are given by the plane waves in the spatial part of the Hilbert space (now we consider wave functions in the whole spatial-spin-isospin Hilbert space)

$$\begin{aligned} \varphi_{\vec{k}\sigma t}(\vec{r}\,) &= \frac{1}{(2\pi)^{3/2}}\,e^{i\,\vec{k}\cdot\vec{r}}\,\chi_\sigma\,\chi_t \\ \int d^3r\,\varphi^*_{\vec{k}\sigma t}(\vec{r}\,)\,\varphi_{\vec{k}\,'\sigma' t'}(\vec{r}\,) &= \delta(\vec{k} - \vec{k}\,')\,\delta_{\sigma\sigma'}\,\delta_{tt'} \end{aligned} \tag{5.111}$$

In this case the density $\rho(\vec{r}\,)$ (see (5.96)) and kinetic energy density $\tau(\vec{r}\,)$ (see

(5.97)) can be expressed explicitely as follows

$$\begin{aligned}
\rho(\vec{r}\,) &= \langle HF|\,\hat{\rho}(\vec{r}\,)\,|HF\rangle = \boxed{\begin{array}{c}\text{see}\\(5.96)\end{array}} = \sum_{i\sigma_i t_i} |\,\varphi_i(\vec{r}\,\sigma_i\,t_i)\,|^2 = \\
&= \boxed{\begin{array}{c}\text{see}\\(5.111)\end{array}} = \frac{1}{(2\pi)^3}\sum_{\sigma=\pm1}\sum_{t=\pm1}\int d^3k\,|\,e^{i\,\vec{k}\cdot\vec{r}}\,\chi_\sigma\,\chi_t\,|^2 = \\
&= \frac{4\pi}{(2\pi)^3}\sum_{\sigma t}\int_0^{k_F} dk\,k^2\,|\,\chi_\sigma\,\chi_t\,|^2 = \frac{4\pi}{(2\pi)^3}\,\frac{k_F^3}{3}\sum_{\sigma t}|\,\chi_\sigma\,\chi_t\,|^2 = \\
&= \boxed{\begin{array}{c}\text{because}\\ \chi_{\sigma=1} = \begin{pmatrix}1\\0\end{pmatrix} \quad \chi_{\sigma=-1} = \begin{pmatrix}0\\1\end{pmatrix} \\ \chi_{t=1} = \begin{pmatrix}1\\0\end{pmatrix} \quad \chi_{t=-1} = \begin{pmatrix}0\\1\end{pmatrix}\end{array}} = \frac{4\pi}{(2\pi)^3}\,\frac{k_F^3}{3}\,4 = \\
&= \frac{2}{3\pi^2}\,k_F^3 \qquad (5.112)
\end{aligned}$$

and

$$\begin{aligned}
\tau(\vec{r}\,) &= \langle HF|\,\hat{\tau}(\vec{r}\,)\,|HF\rangle = \boxed{\begin{array}{c}\text{see}\\(5.97)\end{array}} = \sum_{i\sigma_i t_i}|\,\vec{\nabla}\,\varphi_i(\vec{r}\,\sigma_i\,t_i)\,|^2 = \\
&= \frac{1}{(2\pi)^3}\sum_{\sigma=\pm1}\sum_{t=\pm1}\int_{|\vec{k}|\le k_F} d^3k\,|\vec{\nabla}e^{i\,\vec{k}\cdot\vec{r}}\,\chi_\sigma\,\chi_t\,|^2 = \\
&= \frac{1}{(2\pi)^3}\sum_{\sigma=\pm1}\sum_{t=\pm1}\int_{|\vec{k}|\le k_F} d^3k\,|\,\vec{k}\,e^{i\,\vec{k}\cdot\vec{r}}\,\chi_\sigma\,\chi_t\,|^2 = \\
&= \frac{4\pi}{(2\pi)^3}\int_0^{k_F} dk\,k^4\,4 = \frac{2}{5\pi^2}\,k_F^5 = \boxed{\begin{array}{c}\text{see}\\(5.112)\end{array}} = \\
&= \frac{3}{5}\left(\frac{3\pi^2}{2}\right)^{2/3}\rho^{5/3} \qquad (5.113)
\end{aligned}$$

From(5.112) and (5.113) we can see that in the case of the infinite matter densities $\rho(\vec{r}\,)$ and $\tau(\vec{r}\,)$ are constant (independent on $\vec{r}$). This is in accordance with the fact that in the translation invariant system the condition $\vec{\nabla}\rho = \vec{\nabla}\tau = 0$ should be fulfilled. It is possible to show (and intuitively it is clear)

that the translational invariance gives also $\vec{\nabla} \cdot \vec{J}(\vec{r}\,) = 0$. So, the terms in (5.110) with $(\vec{\nabla}\rho(\vec{r}))^2$ (5-th term) and $(\vec{\nabla} \cdot \vec{J}(\vec{r}))$ (6-th term) vanish. Besides that in the paper [84] it was shown that the last term in (5.110) is possible to neglect. So, the total energy of the fictive infinite nucleus with $N = Z$ is

$$\begin{aligned} E_0 &= \int d^3r\, \mathscr{H}(\vec{r}\,) = \\ &= \left[\frac{\hbar^2}{2M}\,\tau + \frac{3}{8}\,t_0\,\rho^2 + \frac{1}{16}\,t_3\,\rho^3 + \frac{1}{16}\,(3t_1 + 5t_2)\,\rho\,\tau\right] V \end{aligned} \tag{5.114}$$

where ρ and τ are given by (5.112) and (5.113), respectively, and V is the "volume" of the infinite nucleus. Then the binding energy per nucleon, E_0/A, is

$$\frac{E_0}{A} = \frac{\mathscr{H}}{\rho} = \frac{3}{5}\,\frac{\hbar^2}{2M}\,k_F^2 + \frac{3}{8}\,t_0\,\rho + \frac{1}{16}\,t_3\,\rho^2 + \frac{3}{80}\,(3t_1 + 5t_2)\,\rho\,k_F^2 \tag{5.115}$$

where $k_F = (3\,\pi^2\rho/2)^{1/3}$ (see (5.112)).

The nuclear matter occurs in so called saturated state when the density ρ has equilibrium value given by the condition of the minimum of the total energy per nucleon, E/A or, more precisely, by the condition of the zero preassure, $P = \rho^2\,\frac{\partial(E/A)}{\partial\rho} = 0$ [8] . In the case of the infinity nuclear matter, when the total energy per nucleon is given by (5.115), this condition reads

$$\begin{aligned} &\frac{\partial}{\partial\rho}\left(\frac{E_0}{A}\right)_{\rho=\rho_0} = 0 = \\ &= \left(\frac{2}{5}\frac{\hbar^2}{2M}\,k_F^2\,\rho^{-1} + \frac{3}{8}t_0 + \frac{1}{8}t_3\,\rho + \frac{1}{16}\,(3t_1 + 5t_2)\,k_F^2\right)_{\rho=\rho_0} \end{aligned} \tag{5.116}$$

This equation gives the equilibrium density ρ_0 as a function of the Skyrme interaction paremeters t_0, t_1, t_2, t_3. If we know the equilibrium density ρ_0 it

[8] From classical thermodynamics the preasure $P = -\frac{\partial E}{\partial V}$, where $V = \frac{N}{\rho}$ is the volume of the system with N particleas. Therefore $dV = -\frac{N}{\rho^2}\,d\rho$ and the preassure is

$$P = -\frac{\partial E}{\partial V} = -\frac{\partial E}{\frac{N}{\rho^2}\partial\rho} = \rho^2\,\frac{\partial(E/N)}{\partial\rho}$$

is possible to determine so called incompressibility K_∞ of the infinite nuclear matter [9]

$$\frac{K_\infty}{\rho} = \frac{\partial}{\partial\rho}\left(\rho^2\,\frac{\partial(E_0/A)}{\partial\rho}\right)_{\rho=\rho_0} = \\ = \left(\frac{2}{5}\,\frac{\hbar^2}{2M}\,k_F^2 + \frac{3}{4}\,t_0\,\rho + \frac{3}{8}\,t_3\,\rho^2 + \frac{1}{6}\,(3t_1+5t_2)\,\rho\,k_F^2\right)_{\rho=\rho_0} \tag{5.117}$$

In the otiginal paper of D. Vautherin and D.M. Bring [84] the incompressibility K_∞ was not determined by (5.117) but it was introduced as the curvature of the binding energy E_0/A with respect to the Fermi momentum k_F for the equilibrium density ρ_0

$$K_\infty^{(VB)} = k_F^2\,\frac{\partial}{\partial\rho}\left(\rho^2\,\frac{\partial(E_0/A)}{\partial k_F^2}\right)_{\rho=\rho_0} = \\ = \left(\frac{6}{5}\,\frac{\hbar^2}{2M}\,k_F^2 + \frac{9}{4}\,t_0\,\rho + \frac{15}{8}\,t_3\,\rho^2 + \frac{3}{4}\,(3t_1+5t_2)\,\rho\,k_F^2\right)_{\rho=\rho_0} \tag{5.118}$$

Equations (5.115), (5.116) and (5.117) or (5.118) enable to express Skyrme interaction parameters t_0, t_3 and the combination $(3t_1+5t_2)$ in terms of values E_0/A, ρ_0 and K_∞ and these values can be extracted from experimental data. However, one should be careful because expressions (5.115), (5.116), (5.117) and (5.118) were obtained for the infinite nuclear matter in the saturation equilibrium ($P = 0$) but not for a real finite nuclei. Therefore, for instance,

[9] In the thermodynamics investigation of the state equation $V = V(T,P)$ in the solid state or liquid system so called linear approximation is often used:

$$V(T,P) = V_0\,[\,1 + \alpha\,(T-T_0) - \mu\,(P-P_0)\,]$$

where $V(T_0,P_0)$ is arbitrary initial volume of the system and α and μ are expansion and compressibility coefficients, respectively

$$\alpha = \frac{1}{V}\frac{\partial V}{\partial T}\Big|_{P=P_0} \qquad \mu = -\frac{1}{V}\frac{\partial V}{\partial P}\Big|_{T=T_0}$$

The incompressibility (incompressibility coefficient) is defined as the inverse value of the compressibility coefficient

$$K = \frac{1}{\mu} = -V\frac{\partial P}{\partial V} = \boxed{\begin{array}{c}\text{because } V = \frac{N}{\rho} \Rightarrow\ P = -\frac{\partial E}{\partial V} = \rho^2\frac{\partial(E/N)}{\partial\rho} \\ \Rightarrow\ dV = -\frac{N}{\rho^2}d\rho\end{array}} = \\ = V\,\frac{\rho^2}{N}\frac{\partial}{\partial\rho}\left(\rho^2\,\frac{\partial(E/N)}{\partial\rho}\right) = \rho\,\frac{\partial}{\partial\rho}\left(\rho^2\,\frac{\partial(E/N)}{\partial\rho}\right)$$

the calculated value E_0/A given by (5.115) should be compared with the value ≈ -16 MeV corresponding to the first (volume) term in the Weiszacker semi-empirical expression (1.13) (other terms in (1.13) corresponds to the finitness of real nuclei and to the Coulomb term which is not also taken into account in (5.115)). The value $k_F = (3\pi^2\rho/2)^{1/3}$ with the ρ obtained from the Brueckner-Bethe calculations (see Fig. 3.7) is $k_F \approx 1.43\ fm^{-1}$. This value as a little bit higher than the experimental value $k_F \approx 1.37\ fm^{-1}$ obtained from the experimental masses and radia of $N = Z$ nuclei. The Brueckner-Bethe calculations (see the Subsection 3.2.1) gives for the incompressibility K_∞/ρ values $\approx$ 150-200 MeV and the corresponding experimental values for heavy nucleus ^{208}Pb obtained from the position of E0 resonance (it will be discussed in the Chapter 7) are $\approx$ 200 MeV [10] On the base of these values the first Skyrme interaction parameters were determined in the 70-ties (e.g. parametrizations SkI, SKII - see [79] and citation therein). In that time experimental values of binding energies and nucleus radia and incompressibilies for ^{16}O and ^{40}Ca were used for the determination of these parameters. Later on other spherical nuclei were added and other parametrizations were obtained by means of the analyses of the quantities E/A, ρ_0, K/ρ_0 (^{16}O, ^{40}Ca, ^{90}Zr, ^{208}Pb - see parametrizations SKIII, SkIV - see [79]). For instance, the parametrization SkIII is

$$\begin{aligned} t_0 &= -1128.75\ MeV\ fm^3 & t_1 &= 395.0\ MeV\ fm^5 \\ t_2 &= -95.0\ MeV\ fm^5 & t_3 &= 14000.0\ MeV\ fm^6 \\ W_0 &= 120\ MeV\ fm^5 & \kappa_0 &= 0.45 \end{aligned}$$

During the analyses of experimental data of spherical and deformed nuclei in last decades the original form of the Skyrme energy density functionals $\mathscr{H}(\vec{r}\,)$ (5.110) was extended by additional terms up to (5.94) in order to fulfil Galilean invariance of the whole functional. The other reason for this extension was to describe other experimental data. However, in all these extensions always the requirement of good description of the bulk properties of double magic nuclei ^{16}O, ^{40}Ca, ^{90}Zr, and ^{208}Pb was kept [85].

Today there are several tenths of Skyrme parametrizations which describe not only E/A, ρ_0, K/ρ_0 but also other quantities of selected nuclei [11].

[10] For finite nuclei with A nucleons the incompressibility K_A can be again defined according to (5.118) but instead of the infinite matter energy E_0 we should put the total energy E of given finite nucleus [79],

$$K_A = \left(k^2\,\frac{\partial^2(E/A)}{\partial k^2}\right)_{k=k_F} = 9\left(\rho^2\frac{\partial^2(E/A)}{\partial\rho^2}\right)_{\rho=\rho_0} \tag{5.119}$$

[11] Different Skyrme interaction parametrizations are named by abbreviations according to the authors or

Knowing the Skyrme interaction (or Skyrme energy functional) parameters we can determine the deformation of mean fields of deformed nuclei. If we restrict to the quadrupole axial deformation of the mean field, $\beta = \alpha_{20}$ (see (1.5), (1.10) the procedure of the determination of the deformation parameter β is following.

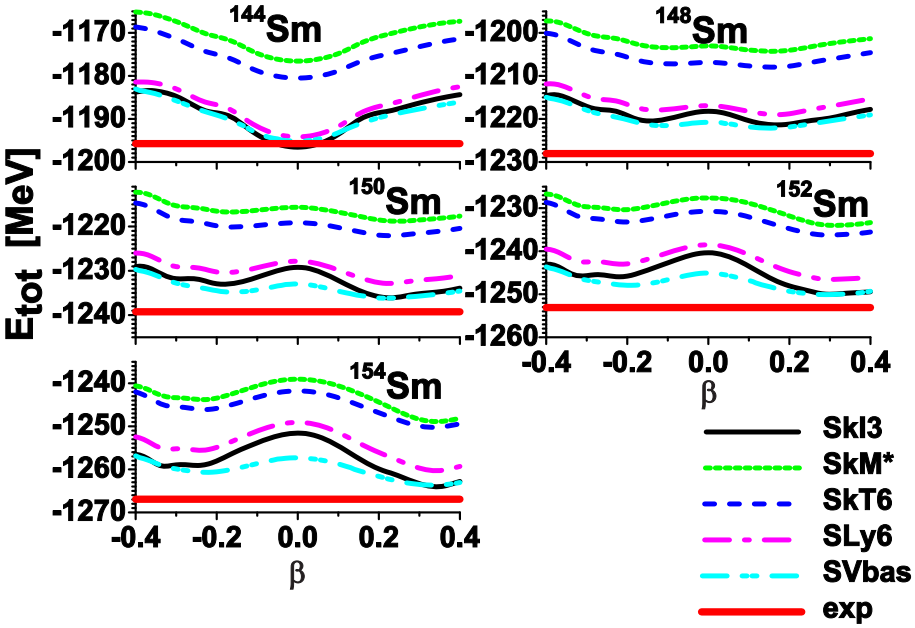


Figure 5.17: The total HFB energy $E(\beta) = \langle HFB| \hat{H} |HFB\rangle$ in the dependence on quadrupole deformation β for $^{144-154}$Sm and for different Skyrme interaction parametrizations SkM*, SkT6, SLy6, SkI3 and SVbas (taken from Kv13). Experimental values of the binding energy (thick horizontal line) were obtained using (1.12) from known experimental masses [93].

We solve the Hartree-Fock equation (5.105) with the additional condition when we require the resultant quadrupole moment $\langle HF| \hat{Q}_{33} |HF\rangle$ (see (2.201)) in the HF ground state is equal to the value $Q_0 = \sqrt{\frac{9}{5\pi}}\, ZeR_0^2\, (\beta + 0.16\,\beta^2)$ (see (1.10)) which corresponds to the reserved value of the deforma-

institutions where given parametrization was developed. Each such parametrization should describle bulk properties (binding energy, radius, approximatively incompressibility of nuclear matter) of double magic nuclei given above but also some other property for which it was modified from previous parametrizations. Some examples: SGII [86] - bulk properties + spin-isospin Landau parameters, SkI3 [87] - bulk properties + spin-orbit splitting, SkM* [88] - bulk properies + fission barriers, SkO [89] - bulk properties + shape coexistence, SkT6 [90] - bulk properties + fission barriers + selected spectroscopic properties, SLy6 [91] - bulk properties + isospin properties of nuclei far from the stability line, SVbas [79] - bulk properties + giant resonances.

tion parameter β

$$\frac{\partial}{\partial\varphi_i^*(\vec{r}\sigma)}\left\{E-\sum_k\epsilon_k\left[\sum_{\sigma'}\int d^3x\,\varphi_i^*(\vec{x}\sigma')\,\varphi_i(\vec{x}\sigma')-1\right]+\right.$$
$$\left.+C\left[\sum_k\sum_{\sigma'}\int d^3x\,\varphi_i^*(\vec{x}\sigma')\,\sqrt{\frac{16\pi}{5}}\,x^2\,Y_{20}(\hat{x})\,\varphi_k(\vec{x}\sigma')-Q_0\right]^2\right\}$$
$$=0 \qquad (5.120)$$

where C determines the priority which we want to have the value of the quadrupole moment equal to $Q_0=\sqrt{\frac{9}{5\pi}}\,ZeR_0^2\,(\beta+0.16\,\beta^2)$. The HF equation (5.120) with the additional condition for the quadrupole moment is solved for the mesh of different values of quadrupole deformations β and for each value of β we have corresponding total energy $E(\beta)=\langle HF(\beta)|\,\hat{H}_{AV}\,|HF(\beta)\rangle$. The resultant equilibrium deformation β_0 corresponds to the minimum of the function $E(\beta)$. As an example of such calculation in the Fig. 5.17 the total energy $E(\beta)$ as a function of the quadrupole deformation β is compared with the experimental binding energy for the chain of Sm isotopes going from the spherical ^{144}Sm to the well-deformed ^{154}Sm for 5 Skyrme interaction parametrizations (SkM*, SkT6, SLy6, SkI3, SVbas).

From the Fig. 5.17 one can see that in spite of the fact that all Skyrme parametrizations were obtained by the fitting to experimental binding energies and other bulk properties of the double magic nuclei the agreement between calculated and experimental values of binding energies is not good. Even for the spherical case ^{144}Sm (which is not double-magic) there is the agreement for only some parametrizations (only for SLy6, SkI3 and SVbas). Nevertheless, the equilibrium deformation β is practically the same for all Skyrme interaction parametrizations for all Sm isotopes.

Besides the Skyrme energy functional other functionals (effective nucleon-nucleon interactions) are used for the determination of the nuclear mean field. The most important are Gogny functional (see Subsection 3.2.2.2) and Relativistic mean field approach (see Subsection 3.2.3). The predictable power of both these methods are more or less the same as in the case of the Skyrme interaction. From theoretical point of view the Relativistic Mean Field approach is more fundamental (more microscopical) then the Skyrme and Gogny cases. At the present time there are attempts to develop more types of energy functionals (see e.g. [94]).

Today aim of the theoretical nuclear physics is to construct the nuclear

energy functional which is based on some fundamental microscopic theory (like Brueckner-Bethe or UCOM) and which at the same time is able with the minimum of free parameters to describe properties of nuclei from (if possible) the whole periodic table. Simultaneously this energy functional should describe not only nuclear bulk properties (in the mean field level) but also the spectroscopic properties (spectra of excited states) connected with the residual interactions (beyond mean field).

In next chapters we will go beyond mean field (beyond the model of independent particles) and we will take into account also residual interactions responsible for the pairing effects and the collective degrees of freeedom of the nuclear motion.

6. Short range residual interaction, pairing correlations in nuclei

In the previous chapter the nuclear mean field $\hat{H}_{AV}$ was discussed in details. From the theoretical point of view the mean field $\hat{H}_{AV}$ was obtained from the total nuclear Hamiltonian $\hat{H}$ (for simplicity the nucleon interactions in the nucleus is suposed to be of two-body character - see (4.1). (4.2))

$$\begin{aligned} \hat{H} &= \sum_i \hat{t}_i + \sum_{i \leq j} \hat{V}_{ij} = \\ &= \sum_{\alpha\beta} \langle \alpha | \, \hat{T} \, | \beta \rangle \, a_\alpha^+ \, a_\beta + \frac{1}{2} \sum_{\alpha\beta\gamma\delta} \langle \alpha\beta | \, \hat{V} \, | \, \gamma\delta \rangle \, a_\alpha^+ \, a_\beta^+ \, a_\delta \, a_\gamma \end{aligned} \tag{6.1}$$

by means of the Hartree-Fock method described in details in the Subsection 4.1.1. As a result (see (4.28)) the total Hamiltonian (5.1) can be rewritten as the sum of the one-body mean field $\hat{H}_{AV}$ and two-body residual interactions

$$\hat{H} = \hat{H}_{AV} + \hat{V}_{RES} \tag{6.2}$$

with $\hat{H}_{AV}$ (see (4.27))

$$\hat{H}_{AV} = \sum_\alpha \epsilon_\alpha^{(HF)} \, a_\alpha^+ \, a_\alpha \tag{6.3}$$

where $\epsilon_\alpha^{(HF)}$ are Hartree-Fock single-particle energies with corresponding single-particle creation (annihilation) operators $a_\alpha^+(a_\alpha)$. If we know Hartree-Fock single-particle basis of states with corresponding Hartree-Fock ground state $|HF\rangle$ ($|\alpha\rangle = a_\alpha^+ \, |-\rangle$, where $|-\rangle$ is the vacuum for nucleons) then the Wick's theorem (with respect to the ground state $|HF\rangle$ - see (B.35)) applied to the second (interaction) term in (6.1) gives the residual interaction $\hat{V}_{RES}$ in the

following form (see (B.35)) [1]

$$\hat{V}_{RES} = \frac{1}{4} \sum_{\alpha\beta\gamma\delta} V_{\alpha\beta\gamma\delta} \ : a_\alpha^+ \, a_\beta^+ \, a_\delta \, a_\gamma : \tag{6.4}$$

where (see (B.17))

$$V_{\alpha\beta\gamma\delta} = \langle \alpha\beta | \, \hat{V} \, | \gamma\delta \rangle - \langle \alpha\beta | \, \hat{V} \, | \delta\gamma \rangle \tag{6.5}$$

is antisymmetrized matrix element of the two-body effective interaction (the second term in (6.1)) and the symbol $: a_\alpha^+ \, a_\beta^+ \, a_\delta \, a_\gamma :$ is the normal product of operators taken with respect to the Hartree-Fock ground state $|HF\rangle$ (see the Appendix B, subsection B.3).

The expression (6.4) for the residual interaction is rather formal. In the reality the residual interaction is divided into the short-range and long-range parts (see (4.29))

$$\hat{V}_{RES} = \hat{V}_{s.r.}^{(RES)} + \hat{V}_{l.r.}^{(RES)} \tag{6.6}$$

This division of the residual interaction corresponds to the character of the bare nucleon-nucleon interaction (very short-range repulsive hard core and relatively longer range attractive potential - see Fig. 3.2) and it reflects also the experimental indications that there are short-range attractive forces between nucleons which are responsible for so called pairing effects. This pairing interaction is quite strong. It modifies the mean field in the open-shell nuclei and as a result of it instead of the single-particle mean field we have so called quasiparticle mean field. The long-range residual interactions $\hat{V}_{l.r.}^{(RES)}$ generate collective vibrational states in nuclei and will be discussed in the Chapter 7.

In this chapter the pairing short-range residual interaction $\hat{V}_{s.r.}^{(RES)}$ is discussed. At first, some experimental indications of the existence of such a type residual interaction are presented. Then the microscopical model of J.Bardeen, L.N.Cooper and J.R.Schiefer (BCS) and the Hartree-Fock-Bogoliubov (HFB) approach describing the pairing interaction are discussed in details. In the end of this chapter the simple algebraic model of the pairing scheme in a nucleus (seniority scheme) is demonstrated as an example that the pairing effects can be understood also by means of algebraic approaches.

[1] The Wick's theorem applied to the product $a_\alpha^+ \, a_\beta^+ \, a_\delta \, a_\gamma$ gives generally the expression (B.34). However, if we apply it with respect to the Hartree-Fock ground state $|HF\rangle$ fulfilling (4.6) or (B.26) then the expression (B.34) becomes (B.35) and the residual interaction is given only by the first term in (B.35) (other terms contribute to the Hartree-Fock mean field $\hat{H}_{AV}$).

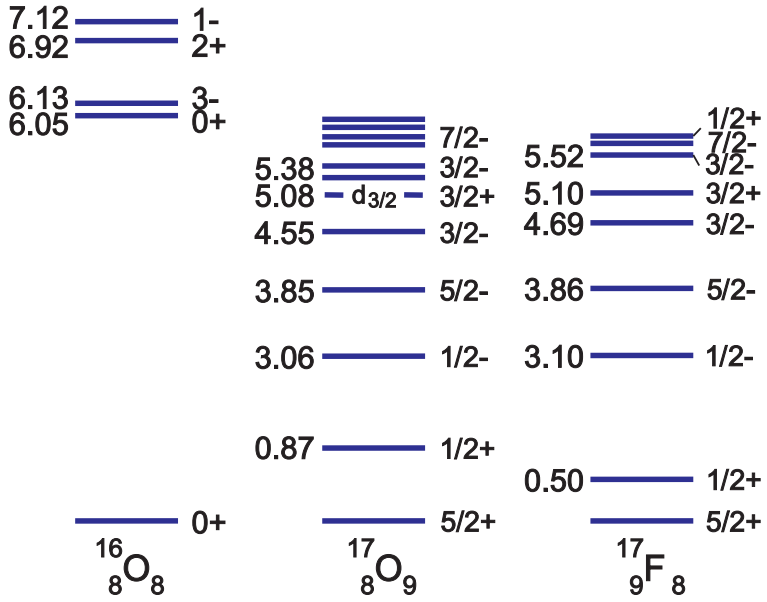


Figure 6.1: Low-lying part of experimental spectra of ^{16}O, ^{17}O and ^{17}F nuclei. Energy (in MeV) is indicated on the right and total s.p. momentum on the left side of each level.

6.1 Experimental indications of nuclear pairing effects

A. Energy gap in the specta of even-even nuclei

In the Fig. 6.1 experimental spectra of low-lying states in even-even spherical ${}^{16}_{8}O_8$, odd-N spherical ${}^{17}_{8}O_9$ and odd-Z spherical ${}^{17}_{9}F_8$ nuclei are compared mutually. The low energy part of the spectrum of even-even spherical nuclei involves very few levels and excited states are separated from the ground state by energy gap. In the case of odd-A nuclei such energy gap is not seen and the energy density of states is higher starting from the ground state. Similar situation is observed for odd-odd spherical nuclei where again there is no energy gap.

B. Masses of odd-A nuclei are always bigger than masses of neighbouring even-even nuclei

The systematic comparison of experimental binding energies in the dependence on A shows that the absolute values of binding energy of odd-A nuclei is always less than the average value of absolute values of binding energies of two neighbouring even-even nuclei (with the same Z or N) - see the Fig. 6.2. That means

$$\frac{|E_{A-1}| + |E_{A+1}|}{2} - |E_{A(odd)}| > 0 \;\Rightarrow\; M_{A\,(odd)} > \frac{M_{A-1} + M_{A+1}}{2} \qquad (6.7)$$

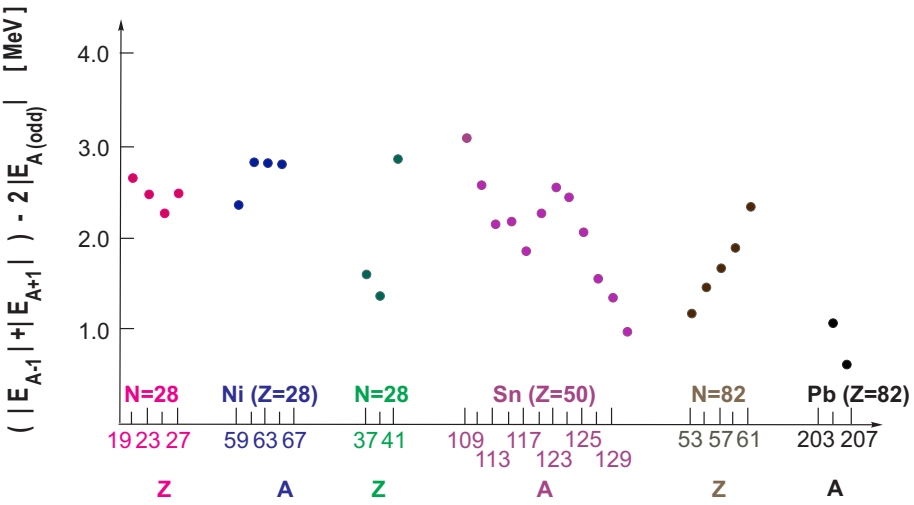


Figure 6.2: Even-odd A mass differences. The dots are the experimental binding energy differences $|E_{A-1}| + |E_{A+1}| - 2\,|E_{A\,(odd)}|$.

C. Ground states of all even-even nuclei are always 0^+

Already in 50-ties experiments confirmed that

- total angular momenta of ground states of even-even nuclei are always 0 with the positive parity
- total angular momenta and parities of ground states of odd-A nuclei are almost always given by the angular momentum and parity of the state occupied by the odd nucleon.

All these (and also other - see e.g. [9]) experimental information lead in the second half of the 50-ties to the conclusion that all nucleons in the even-even nuclei are groupped into pairs of nucleons of the same type (neutron or proton) and that the angular momentum of each such pair is 0 with the positive parity.

If such grouping is realized then there should be an interaction which creates such pairs. This pairing interaction should be a part of residual interactions and be attractive. It should couple angular momenta of both nucleons in the pair into the zero total momentum. Below it is shown that this pairing interaction has very short range.

Let us consider two nucleons of the same type occupying the same shell nlj of the spherically symmetric mean field. Their wave function is

$$|\, nl(j)^2;\, JM\rangle = \sum_{m_1 m_2} C^{JM}_{jm_1jm_2}\, |nljm_1\rangle\, |nljm_2\rangle \qquad (6.8)$$

Further we suppose that these two nucleons interact through the attractive δ-interaction, $V(\vec{r}_1, \vec{r}_2) = -\delta(\vec{r}_1 - \vec{r}_2)$. Following the paper [95] (see also [11]) the energy spectrum of this interaction is given by

$$E_J = \langle nl(j)^2;\ J \mid \hat{V} \mid nl(j)^2;\ J\rangle = -\frac{R}{4\pi}\,(j+1/2)\,\left(\,C^{j1/2}_{J0j1/2}\,\right)^2 \qquad (6.9)$$

where R is the radial integral

$$R = \int dr\, r^2\ (R_{nl}(r))^4$$

with $R_{nl}(r)$ being the radial part of the single-particle wave function $\langle\vec{r}|nljm\rangle$. The spectrum is shown in the Fig. 6.3 for the case $j = 15/2$.

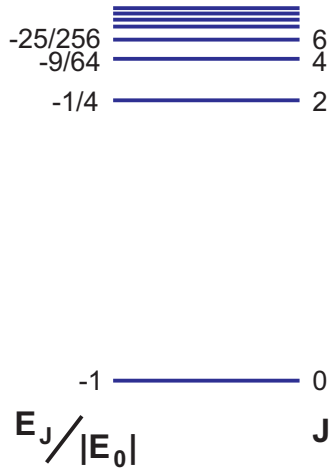


Figure 6.3: Spectrum for two nucleons in a $(j = 15/2)^2$ configuration with δ-interaction $V(\vec{r}_1, \vec{r}_2) = -\delta(\vec{r}_1 - \vec{r}_2)$ (taken from [95]).

It is seen that the $J = 0$ state

$$\mid nl(j)^2;\ J = 0\ M = 0\rangle = \sum_m C^{00}_{jmj-m}\,|nljm\rangle\,|nlj-m\rangle =$$

$$= \frac{1}{\sqrt{2j+1}}\,\sum_m |nljm\rangle\,|nlj-m\rangle \qquad (6.10)$$

corresponds to the lowest energy and therefore is much more strongly bound than others. This is because in a $J = 0$ state the nucleons come particularly close each other.

The Pauli principle prevents for two nucleons of the same type to be in the same single-particle state and therefore the most energy favourite state

where two nucleons are most close each other is just the state (6.10). If we have more than two nucleons in the shell and if it is known that there is very short-range two-body interaction (of δ-force type) betweeen them then the best many particle configuration from the energy point of view corresponds to the coupling of all nucleons pairwise to $J = 0$. Thus for an even number n of particles in a $(j)^n$ configuration, the pair-coupled wave function is

$$\Psi = \mathscr{A}\,\{\psi_0(1\,2)\ \psi_0(3\,4)\ \ldots\} \tag{6.11}$$

where $\psi_0(1\,2) = \psi_0(\vec{r}_1, \vec{r}_2) \equiv \langle \vec{r}_1 \vec{r}_2 \mid nl(j)^2,\ J = 0\ M = 0\rangle$ and the symbol $\mathscr{A}\,\{\ldots\}$ stands for the antisymmetrization of the product of single-particle wave functions inside the bracket.

So, in the even even nuclei we expect that all nucleons are paired as it is indicated in (6.11) if there is the very short-range interaction present. This pairing is in the agreement with the experimental indications presented above. For instance, if we want to excite even-even nucleus with such pairs we should either shift the whole one nucleon pair into pair state with higher energy or to break the pair and to move one nucleon from this broken pair to energy higher single-particle state. Both these ways are energy more demanding than just shifting of one nucleon to higher single-particle state as it occurs in the case of the exciting the odd-A nucleus. This is qualitative explanation of the energy gap observed in the low-lying spectra of even even nuclei and it explains also the higher odd-A nucleus mass with respect to neighbouring even-even nuclei.

6.2 Bardeen-Cooper-Schrieffer (BCS) theory, Bogoliubov transformation, Hartree-Fock-Bogoliubov (HFB) equation

6.2.1 Pairing interaction potential

Pairing interaction is a two-body interaction and therefore formally it can be written as follows (see(B.21))

$$\begin{aligned}\hat{V}_{pair} &= \hat{V}_{s.r}^{(RES)} = \frac{1}{2}\sum_{ijkl} \langle ij|\, \hat{V}_{pair}\, |kl\rangle\, a_i^+ a_j^+\, a_l\, a_k = \\ &= \frac{1}{4}\sum_{ijkl} V_{ijkl}^{(pair)}\, a_i^+ a_j^+\, a_l\, a_k \end{aligned} \tag{6.12}$$

where $V_{ijkl}^{(pair)} = \langle ij|\, \hat{V}_{pair}\, |kl - lk\rangle$. In (6.12) a_i^+ (a_i) is the single-particle creation (annihilation) operator of the nucleon in the single-particle state characterized by the index i. Usually single-particle states are eigen-states of the nuclear spherical or deformed mean field. In the case of the spherical mean field the single-particle index i means the quantum numbers $Nljm$ and the corresponding single-particle energy ϵ_{Nlj} is degenerated with respect to the projection m of the s.p. angular momentum $\vec{j}$ (see (5.8)). If also isospin part of the Hilbert space is involved in the wave function then we should add also the quantum number $t_3 = \pm 1/2$ of the projection of the s.p. isospin. If we use the Condon-Shortley phase convention for wave functions (see (1.44)) the action of the time-reversal transformation on the single-particle ket $|Nljm\rangle$ is following

$$\overline{|Nljm\rangle} \equiv \mathscr{T}\, |Nljm\rangle = \boxed{\begin{array}{c}\text{see}\\(1.44)\end{array}} = (-1)^{l+j+m}\, |Nlj\, -m\rangle \tag{6.13}$$

In the case of axially deformed mean field the single-particle index i represents the angular momentum projection K on the symmetry axis and some other quantum numbers ν which specify unambiguously given single-particle state (e.g. Nilsson asymptotic quantum numbers described in the text below the expression (5.47)). The action of the time-reversal operator on the ket

$|K\nu\rangle$ is

$$\overline{|K\nu\rangle} \equiv \mathscr{T}\,|K\nu\rangle = \boxed{\begin{array}{c}\text{see}\\(5.43)\end{array}} = \sum_{Nl\Lambda\Sigma} a^{(K\nu)}_{NL\Lambda\Sigma}\,\mathscr{T}\,|Nl\Lambda\Sigma\rangle =$$

$$= \boxed{\begin{array}{c}\text{because - see Subsection 1.3.2}\\ \mathscr{T}\,|\,l\Lambda\rangle = (-1)^{\Lambda}\,|\,l\,-\Lambda\rangle\\ \mathscr{T}\,|\,\frac{1}{2}\Sigma\rangle = (-1)^{\frac{1}{2}+\Sigma}\,|\,\frac{1}{2}\,-\Sigma\,\rangle\end{array}} =$$

$$= \sum_{Nl\Lambda\Sigma} a^{(K\nu)}_{Nl\Lambda\Sigma}\,(-1)^{\Lambda+\Sigma+\frac{1}{2}}\;|Nl\,-\Lambda\,-\Sigma\rangle =$$

$$= (-1)^{K+\frac{1}{2}} \sum_{Nl\Lambda\Sigma} a^{(K\nu)}_{NL\lambda\Sigma}\,|Nl\,-\Lambda\,-\Sigma\rangle = (-1)^{K+\frac{1}{2}}\,|\,-K\nu\rangle \tag{6.14}$$

So, in both cases (spherical as well as deformed) the single-particle wave function changes the sign of the angular momentum projection under the action of the time reverse transformation. For the simplicity of the notation further we will extract from the single-particle quantum numbers one index $\sigma = \pm 1$ which is the sign of the angular momentum projection and simultaneously the conjugation with respect to time reversal transformation (for both spherical and deformed cases we assume $m_i > 0,\ K_i > 0$)

$$\begin{aligned}
\varphi_i(\vec{r}\,) &= \langle\vec{r}\,|\,i\rangle = \langle\vec{r}\,|\,N_i l_i j_i m_i\rangle \equiv \langle\vec{r}\,|\,i\,\sigma_i = +1\rangle\\
\mathscr{T}\,\varphi_i(\vec{r}) &= \langle\vec{r}\,|\,\bar{i}\rangle = \langle\vec{r}\,|\,\overline{N_i l_i j_i m_i}\rangle = (-1)^{l_i+j_i+m_i}\,\varphi_{N_i l_i j_i - m_i}(\vec{r}) =\\
&= (-1)^{l_i+j_i+m_i}\;\langle\vec{r}\,|\,N_i l_i j_i\;-m_i\rangle \equiv \langle\vec{r}\,|\,i\,\sigma_i = -1\rangle
\end{aligned} \tag{6.15}$$

for spherical case and

$$\begin{aligned}
\varphi_i(\vec{r}\,) &= \langle\vec{r}\,|\,i\rangle = \langle\vec{r}\,|\,K_i\,i\rangle \equiv \langle\vec{r}\,|\,i\,\sigma_i = +1\rangle\\
\mathscr{T}\,\varphi_i(\vec{r}) &= \varphi_{\bar{i}}(\vec{r}) = \langle\vec{r}\,|\,\bar{i}\rangle = (-1)^{K_i+\frac{1}{2}}\,\langle\vec{r}\,|\;-K_i\,i\rangle =\\
&\equiv \langle\vec{r}\,|\,i\,\sigma_i = -1\rangle
\end{aligned} \tag{6.16}$$

for deformed case. So, within this new notation we can write generally for both cases (see also (1.50), (1.51))

$$\begin{aligned}
\mathscr{T}\,|\,\bar{i}\,\rangle &= \mathscr{T}\,|\,i\,\sigma = -1\,\rangle = -|\,i\,\rangle = -|\,i\sigma = +1\,\rangle\\
\mathscr{T}\,|\,i\,\rangle &= \mathscr{T}\,|\,i\,\sigma = +1\,\rangle = +|\,\bar{i}\;\rangle = +|\,i\sigma = -1\,\rangle\\
&\Rightarrow \mathscr{T}\,|\,i\,\sigma\,\rangle = \sigma\,|\,i\;-\sigma\,\rangle
\end{aligned} \tag{6.17}$$

and the pairing interaction (6.12) has following form

$$\hat{V}_{pair} = \frac{1}{2} \sum_{ijkl} \sum_{\sigma_i\sigma_j\sigma_k\sigma_l=\pm 1} \langle i\sigma_i,\ j\sigma_j \mid \hat{V}_{pair} \mid k\sigma_k,\ l\sigma_l\rangle\ a^+_{i\sigma_i} a^+_{j\sigma_j}\ a_{l\sigma_l} a_{k\sigma_k} \qquad (6.18)$$

From discussions in the Subsection 6.1 it is known that the pairing interaction is of very short range and it acts only between nucleons occupying the single-particle states with the same quantum numbers except the sign of the angular momentum projection. According to (6.13)-(6.17) such single-particle states are mutually time reversed. So, it is possible to expect that the short-range pairing interaction acts between nucleons sitting in the mutually time-reversed states and the matrix elements $\langle i\sigma_i,\ j\sigma_j \mid \hat{V}_{pair} \mid k\sigma_k,\ l\sigma_l\rangle$ are nonzero only if $i = j$, $\sigma_i = -\sigma_j$ and $k = l$, $\sigma_k = -\sigma_l$ (other matrix elements can be neglected). Therefore the sums in the r.h.s. of (6.18) is reduced as follows

$$\hat{V}_{pair} = \sum_{ij>0} \langle i+,\ i-\ \mid \hat{V}_{pair} \mid j+,\ j-\rangle\ a^+_{i+} a^+_{i-}\ a_{j-}\ a_{j+} \qquad (6.19)$$

where the summation index $ij > 0$ means that the sum goes only over the single-particle states with positive angular momentum projections. Since the pairing interaction is of very short range it is possible to suppose in the first approximation that it has the form of a δ-force

$$\begin{aligned} V_{pair}(\vec{r}, \vec{r}\,') &= -G'\,\delta(\vec{r} - \vec{r}\,') = \\ &= -G'\,\frac{\delta(r - r')}{r^2} \sum_{l=0}^{\infty} \sum_{m=-l}^{+l} Y^*_{lm}(\hat{r})\, Y_{lm}(\hat{r}\,') \end{aligned} \qquad (6.20)$$

and within this approximation the matrix element $\langle i+,\ i-\ \mid \hat{V}_{pair} \mid j+,\ j-\rangle$ is

$$\begin{aligned} &\langle i+,\ i-\ \mid \hat{V}_{pair} \mid j+,\ j-\rangle = \\ &= -G' \int d^3r \int d^3r'\, \varphi^*_{i+}(\vec{r}\,)\, \varphi^*_{i-}(\vec{r}\,')\, \frac{\delta(r - r')}{r^2} \\ &\qquad \sum_{lm} Y^*_{lm}(\hat{r})\, Y_{lm}(\hat{r}\,')\, \varphi_{j+}(\vec{r}\,)\, \varphi_{j-}(\vec{r}\,') \end{aligned} \qquad (6.21)$$

Further the spherical mean field case is considered only (the deformed case

gives the same result)

$$\langle i+,\, i-\, |\, \hat{V}_{pair}\, |\, j+,\, j-\rangle = \boxed{\begin{array}{c}\text{see}\\ (6.15)\end{array}} =$$

$$= -G^{'} \int d^3r \int d^3r' \varphi^*_{N_i l_i j_i m_i}(\vec{r})\, \varphi^*_{N_i l_i j_i -m_i}(\vec{r}\,')$$

$$\frac{\delta(r-r\,')}{r^2} \sum_{lm} Y^*_{lm}(\hat{r})\, Y_{lm}(\hat{r}\,')$$

$$\varphi_{N_j l_j j_j m_j}(\vec{r})\, \varphi_{N_j l_j j_j -m_j}(\vec{r}\,')\, (-1)^{l_i+j_i+m_i}\, (-1)^{l_j+j_j+m_j} =$$

$$= \boxed{\begin{array}{c}\text{because}\\ \varphi_{Nljm}(\vec{r}) = \sum_{\Lambda\Sigma} C^{jm}_{l\Lambda\frac{1}{2}\Sigma} R_{Nlj}(r)\, Y_{l\Lambda}(\hat{r})\, |\tfrac{1}{2}\Sigma\rangle\end{array}} =$$

$$= -G^{'} \sum_{lm} \sum_{\Lambda_i\Sigma_i} \sum_{\Lambda'_i\Sigma'_i} \sum_{\Lambda_j\Sigma_j} \sum_{\Lambda'_j\Sigma'_j} C^{j_i m_i}_{l_i\Lambda_i\frac{1}{2}\Sigma_i}\, C^{j_i -m_i}_{l_i\Lambda'_i\frac{1}{2}\Sigma'_i}\, C^{j_j m_j}_{l_j\Lambda_j\frac{1}{2}\Sigma_j}\, C^{j_j -m_j}_{l_j\Lambda'_j\frac{1}{2}\Sigma'_j}$$

$$(-1)^{l_i+l_j+j_i+j_j+m_i+m_j} \int dr\, r^2 \int dr'\, r'^{\,2}$$

$$R_{N_i l_i j_i}(r)\, R_{N_i l_i j_i}(r')\, \frac{\delta(r-r')}{r^2}\, R_{N_j l_j j_j}(r)\, R_{N_j l_j j_j}(r')$$

$$\int d\hat{r}\, Y^*_{l_i\Lambda_i}(\hat{r})\, Y^*_{lm}(\hat{r})\, Y_{l_j\Lambda_j}(\hat{r}) \int d\hat{r}'\, Y^*_{l_i-\Lambda_i}(\hat{r}')\, Y_{lm}(\hat{r}')\, Y_{l_j-\Lambda_j}(\hat{r}')$$

$$\langle\, \frac{1}{2}\, \Sigma_i \,|\, \frac{1}{2}\, \Sigma_j \,\rangle\, \langle\, \frac{1}{2} - \Sigma_i \,|\, \frac{1}{2} - \Sigma_j \,\rangle \qquad (6.22)$$

Further we restrict ourselves only to the monopole term $l = m = 0$ in the decomposition of the δ-function in (6.20)-(6.22). The experience shows that the monopole term gives the decisive contribution to the above matrix element. Then, using the orthogonality of spherical functions (see (A.45), (A.53)) and the orthogonality of spin kets, $\langle\, \frac{1}{2}\, \Sigma_i \,|\, \frac{1}{2}\, \Sigma_j \,\rangle = \delta_{\Sigma_i\Sigma_j}$, and the well-known expression, $Y_{00}(\hat{r}) = 1/\sqrt{4\pi}$, we obtains

$$\langle i+,\, i-\, |\, \hat{V}_{pair}\, |\, j+, j-\rangle \approx -G' \frac{1}{4\pi} \int dr\, r^2\, \left(R_{N_i l_i j_i}(r)\right)^4\, \delta_{ij} =$$

$$= \boxed{\begin{array}{c}\text{it can be shown that the radial integral above}\\ \text{is almost independent on } N_i l_i j_i\end{array}} =$$

$$\equiv -G \qquad (6.23)$$

where G is a constant for each type of nucleons (for all neutrons and/or for all protons). So in this monopole approximation the pairing potential $\hat{V}_{prot}$ (see(6.19)) is

$$\begin{aligned} \hat{V}_{pair} &= \sum_{ij>0} \langle i+,\, i-\, |\, \hat{V}_{pair}\, |\, j+,\, j-\rangle\; a^+_{i+} a^+_{i-}\, a_{j-}\, a_{j+} = \\ &= -G \sum_{ij>0} a^+_{i+} a^+_{i-}\, a_{j-}\, a_{j+} \end{aligned} \tag{6.24}$$

Further we denote the part of the nucleus Hamiltonian involving the mean field and the pairing residual interaction as $\hat{H}_P$ and it is given by

$$\hat{H}_P = \hat{H}_{AV} + \hat{V}_{pair} = \langle HF|\, \hat{H}_P\, |HF\rangle + \hat{H}_P(prot) + \hat{H}_P(neut) \tag{6.25}$$

where (see (6.3) and (6.24)

$$\begin{aligned} \hat{H}_P(prot) &= \sum_{\substack{i>0 \\ i\in prot}} \sum_{\sigma=\pm} \epsilon_i\, a^+_{i\sigma}\, a_{i\sigma} - G_P \sum_{\substack{ij>0 \\ ij\in prot}} a^+_{i+} a^+_{i-}\, a_{j-}\, a_{j+} \\ \hat{H}_P(neut) &= \sum_{\substack{i>0 \\ i\in neut}} \sum_{\sigma=\pm} \epsilon_i\, a^+_{i\sigma}\, a_{i\sigma} - G_N \sum_{\substack{ij>0 \\ ij\in neut}} a^+_{i+} a^+_{i-}\, a_{j-}\, a_{j+} \end{aligned} \tag{6.26}$$

6.2.2 Bardeen-Cooper-Schrieffer (BCS) theory

6.2.2.1 Bogoliubov transformation

J. Bardeen, L.N. Cooper, J.R. Schrieffer formulated their theory in 1957 [96] in order to explain the superconductive effect that means exactly zero resistance in certain materials when cooled below a characteristic critical temperature [2]. The basic idea of the BCS theory was that the conductivity of such materials is not mediated by individual electrons as it is in standard conductors but instead the pairs of electrons (so called Cooper pairs) are created which represent the charge particles for electric current. Since the electron pairs are bosons these pairs are not tied by the Pauli princilple for

[2] J. Bardeen, L.N. Cooper and J.R. Schrieffer were awarded the Nobel Prize in 1972 for the BCS theory.

fermions and they can form Bose-Einstein condensate in very low temperatures (when all boson pairs occupy one state and there is not any restriction for the number of bosons in this state). The BCS theory starts from the assumption that there is some attraction between electrons, which can overcome the Coulomb repulsion and in some particular materials it can create the electron pairs (in very low temperatures below the critical value). So, the BCS theory explains the superconductivity current as a superfluid of Cooper pairs, pairs of electrons interacting through the exchange of phonons (vibrational collective quanta of the whole system of electrons and crystal lattice of ions in the given solid state material). The origin of the Cooper pairing in superconductors is the electromagnetic interaction between electrons mutually and between electrons and vibrating crystal lattice of ions. The BCS theory in 1957 was based on the Bogoliubov transformation from the system of particle (electron) creation and annihilation operators to the quasiparticle ones (see [97]).

One year after the introduction of the BCS theory for superconductors, in 1958, this theory was adapted by A. Bohr, B.R. Mottelson and D. Pines [98] for the nuclear physics where experimental indications for the pairing interaction between nucleons discussed in the Subsection 6.1 was already known in that time. Opposite to electronic superconductor case the pairing interaction of nucleons (see the Subsection 6.2.1) is of very short range and it has orgin in the strong interaction. However, the idea of the BCS theory together with the Bogoliubov transformation is again apllicable and it is presented in this Subsection.

We start with the assumption that the basis of the single-particle eigen states of the mean field $\hat{H}_{AV}$ is known

$$\begin{aligned} \varphi_{i\sigma}(\vec{r}) &\equiv \langle \vec{r} \,|\, i\sigma \rangle = \langle \vec{r} \,|\, a^{+}_{i\sigma}|- \rangle \\ \hat{H}_{AV} \,|\, i\sigma \rangle &= \epsilon_i^{(\,0\,)} \,|\, i\sigma \rangle \end{aligned} \tag{6.27}$$

where $|-\rangle$ is the particle vacuum ($a_{i\sigma}\,|-\rangle = 0$ for all i and σ). The starting point of the BCS approach is the prerequisite that the ground state of the system of fermions (neutron or proton system in the nucleus) with the even number of particles is given by the ket $|BCS\rangle$

$$|BCS\rangle = \prod_{\substack{i>0 \\ i\,\in\, p,\,n}} \left(\mathscr{U}_i + \mathscr{V}_i \, a^{+}_{i+} \, a^{+}_{i-} \right) \, |-\rangle \tag{6.28}$$

The square of the amplitude $\mathscr{V}_i^2$ is the probability that in the ground state

$|BCS\rangle$ of the whole system of particles given pair of the single-particle states $|i+\rangle$ and $|i-\rangle$ is filled by two particles and $\mathscr{U}_i{}^2$ is the probability that this pair of the single-particle states is empty. The normalization of these amplitudes is obvious (amplitudes $\mathscr{V}_i$ and $\mathscr{U}_i$ are real)

$$\mathscr{U}_i{}^2 + \mathscr{V}_i{}^2 = 1 \tag{6.29}$$

for all i. The form (6.28) of the ground state $|BCS\rangle$ reflects the supposition that there is the attractive interaction between particles of the system which causes the formation of the pair of particles sitting in the states $|\,i+\rangle$ and $|\,i-\rangle$. The great advantage of the form (6.28) for the ground state $|\,BCS\rangle$ is the fact that this state is a vacuum for the new ensemble of the single-particle creation and annihilation operators, $\alpha^+_{i\sigma}$ and $\alpha_{i\sigma}$, which are called as quasiparticle operators and which are related to the original creation and annihilatiom operators $a^+_{i\sigma}$ and $a_{i\sigma}$ by the Bogoliubov transformation

$$\begin{array}{l} \alpha^+_{i+} = \mathscr{U}_i\, a^+_{i+} - \mathscr{V}_i\, a_{i-} \\ \alpha^+_{i-} = \mathscr{U}_i\, a^+_{i-} + \mathscr{V}_i\, a_{i+} \end{array} \quad \Leftrightarrow \quad \begin{array}{l} \alpha^+_{i\sigma} = \mathscr{U}_i\, a^+_{i\sigma} - \sigma\, \mathscr{V}_i\, a_{i-\sigma} \\ \alpha_{i\sigma} = \mathscr{U}_i\, a_{i\sigma} - \sigma\, \mathscr{V}_i\, a^+_{i-\sigma} \end{array} \tag{6.30}$$

Really, the $|BCS\rangle$ state is the vacuum for quasiparticle operator:

$$\alpha_{i+}\,|BCS\rangle = \boxed{\begin{array}{c}\text{see}\\ \text{(6.30), (6.28)}\end{array}} =$$

$$= \big(\mathscr{U}_i\, a_{i+} - \mathscr{V}_i\, a^+_{i-}\big) \prod_{j\,>\,0} \big(\mathscr{U}_j + \mathscr{V}_j\, a^+_{j+}\, a^+_{j-}\big)\ |-\rangle =$$

$$= \big(\mathscr{U}_i\, a_{i+} - \mathscr{V}_i\, a^+_{i-}\big)\, \big(\mathscr{U}_i + \mathscr{V}_i\, a^+_{i+}\, a^+_{i-}\big) \prod_{\substack{j\,>\,0,\, j\neq i \\ j\,\in\, p,\, n}} \big(\mathscr{U}_j + \mathscr{V}_j\, a^+_{j+}\, a^+_{j-}\big)\,|-\rangle =$$

$$= \big[\mathscr{U}_i{}^2\, a_{i+} - \mathscr{V}_i\mathscr{U}_i\, a^+_{i-} + \mathscr{U}_i\mathscr{V}_i\, a_{i+}\, a^+_{i+}\, a^+_{i-} - \mathscr{V}_i{}^2\, a^+_{i-}\, a^+_{i+}\, a^+_{i-}\big] \prod_{\substack{j\,>\,0,\, j\neq i \\ j\,\in\, p,\, n}} \big(\mathscr{U}_j + \mathscr{V}_j\, a^+_{j+}\, a^+_{j-}\big)\,|-\rangle =$$

$$= \boxed{\begin{array}{c}\text{the 1-st and 4-th terms give zero, because of}\\ \text{the Pauli principle for fermions}\end{array}} =$$

$$= \left[-\mathscr{V}_i\mathscr{U}_i\, a^+_{i-} + \mathscr{U}_i\mathscr{V}_i\,(1 - a^+_{i+}\, a_{i+})\, a^+_{i-}\right] \prod_{\substack{j>0,\, j\neq i \\ j\in p,\, n}} \left(\mathscr{U}_j + \mathscr{V}_j\, a^+_{j+}\, a^+_{j-}\right)|-\rangle =$$

$$= -\mathscr{U}_i\mathscr{V}_i\, a^+_{i+}\, a_{i+}\, a^+_{i-} \prod_{\substack{j>0,\, j\neq i \\ j\in p,\, n}} \left(\mathscr{U}_j + \mathscr{V}_j\, a^+_{j+}\, a^+_{j-}\right)|-\rangle =$$

$$= \boxed{\begin{array}{c}\text{because} \\ a_{i+}\,|-\rangle = 0\end{array}} = 0 \tag{6.31}$$

Since the original operators $a^+_{i\sigma}$, $a_{i\sigma}$ fulfil the Pauli anticommutator conditions for fermions, $\{a_{i\sigma},\ a^+_{i'\sigma'}\} = \delta_{ii'}\delta_{\sigma\sigma'}$, $\{a_{i\sigma},\ a_{i'\sigma'}\} = 0$, the new quasiparticle creation and annihilation operators also suit these conditions

$$\left\{\alpha_{i\sigma},\ \alpha^+_{i'\sigma'}\right\} = \boxed{\begin{array}{c}\text{substitution} \\ \text{from (6.30)}\end{array}} =$$

$$= \mathscr{U}_i\mathscr{U}_{i'}\left\{a_{i\sigma},\ a^+_{i'\sigma'}\right\} - \sigma\,\mathscr{V}_i\mathscr{V}_i\left\{a^+_{i-\sigma},\ a^+_{i'\sigma'}\right\} - \sigma'\,\mathscr{U}_i\mathscr{U}_{i'}\left\{a_{i\sigma},\ a_{i'-\sigma'}\right\} + \sigma\sigma'\,\mathscr{V}_i\mathscr{V}_{i'}\left\{a^+_{i-\sigma},\ a_{i'-\sigma'}\right\} =$$

$$= \left(\mathscr{U}_i^2 + \mathscr{V}_i^2\right)\,\delta_{ii'}\,\delta_{\sigma\sigma'} = \boxed{\begin{array}{c}\text{substitution} \\ \text{from (6.29)}\end{array}} = \delta_{ii'}\,\delta_{\sigma\sigma'}$$

and similarly

$$\{\alpha_{i\sigma},\ \alpha_{i'\sigma'}\} = \boxed{\begin{array}{c}\text{substitution} \\ \text{from (6.30)}\end{array}} = 0$$

So the quasiparticles are also fermions:

$$\begin{aligned}\left\{\alpha_{i\sigma},\ \alpha^+_{i'\sigma'}\right\} &= \delta_{ii'}\,\delta_{\sigma\sigma'} \\ \{\alpha_{i\sigma},\ \alpha_{i'\sigma'}\} &= \left\{\alpha^+_{i\sigma},\ \alpha^+_{i'\sigma'}\right\} = 0\end{aligned} \tag{6.32}$$

The Bogoliubov transformation from $a^+_{i\sigma}$, $a_{i\sigma}$ to $\alpha^+_{i\sigma}$, $\alpha_{i\sigma}$ can be inverted:

$$\begin{aligned}&\left.\begin{aligned}\alpha^+_{i+} &= \mathscr{U}_i\, a^+_{i+} - \mathscr{V}_i\, a_{i-} \\ \alpha_{i-} &= \mathscr{U}_i\, a_{i-} + \mathscr{V}_i\, a^+_{i+}\end{aligned}\right\} \Rightarrow \begin{aligned}\mathscr{U}_i\,\alpha^+_{i+} &= \mathscr{U}_i^2\, a^+_{i+} - \mathscr{U}_i\mathscr{V}_i\, a_{i-} \\ \mathscr{V}_i\,\alpha_{i-} &= \mathscr{U}_i\mathscr{V}_i\, a_{i-} + \mathscr{V}_i^2\, a^+_{i+}\end{aligned} \\ \Rightarrow\ &\begin{aligned}a^+_{i+} &= \mathscr{U}_i\,\alpha^+_{i+} + \mathscr{V}_i\,\alpha_{i-} \\ a^+_{i-} &= \mathscr{T}^{-1} a^+_{i+}\mathscr{T} = \mathscr{U}_i\,\alpha^+_{i-} - \mathscr{V}_i\, a_{i+}\end{aligned} \\ \Rightarrow\ &\begin{aligned}a^+_{i\sigma} &= \mathscr{U}_i\,\alpha^+_{i\sigma} + \sigma\mathscr{V}_i\,\alpha_{i-\sigma} \\ a_{i\sigma} &= \mathscr{U}_i\,\alpha_{i\sigma} + \sigma\mathscr{V}_i\, a^+_{i-\sigma}\end{aligned}\end{aligned} \tag{6.33}$$

In the derivation of (6.33) we used $\mathscr{T}^{-1}\alpha_{i-}\mathscr{T} = -\alpha_{i+}$ (see (1.50).

So the attractive pairing interaction can be taken into account by the Bogoliubov transformation (6.30) or (6.31) from the particle system to quasiparticle system of creation and annihilation operators. Corresponding ground state $|BCS\rangle$ is not eigen state of the operator of the number of particles.

$$\begin{aligned} |BCS\rangle &= \prod_{\substack{i>0 \\ i\in p,\,n}} \left(\mathscr{U}_i + \mathscr{V}_i\, a^+_{i+} a^+_{i-}\right) |-\rangle = \\ &= a_0\,|N=0\rangle + a_2\,|N=2\rangle + a_4\,|N=4\rangle + \ldots \end{aligned} \tag{6.34}$$

The BCS vacuum $|BCS\rangle$ is a sum of the components without particle ($N = 0$) with two particles ($N = 2$), with four particles ($N = 4$), ... In the case of the superconductivity of solid systems where the superconductivity is caused by the pairing of the practically infinite number of electrons contained in the bulk material the nonconserving of the number of particles does not mean any problem. However in the case of the nucleus with the finite number of nucleons it is the problem and it will be discussed later.

6.2.2.2 BCS equations

It remains to determine amplitudes $\mathscr{U}_i$, $\mathscr{V}_i$ in the BCS vacuum (6.28) and in the Bogoliubov transformation (6.30) or (6.33). This is usually done by the variational method seaching for the minimum of the total energy, $\langle BCS|\,\hat{H}_P(\tau = neut, prot)\,|BCS\rangle$, of the neutron or proton system with additional condition of the number of particles in the state $|BCS\rangle$, $\langle BCS|\,\hat{n}_{\tau=neut,\,prot}\,|BCS\rangle$, is equal to $N_\tau = A - Z$ for neutrons or $N_\tau = Z$ for protons, where

$$\hat{n}_\tau = \sum_{\substack{i>0 \\ i\in\tau}} \sum_{\sigma=\pm} a^+_{i\sigma}\, a_{i\sigma} \tag{6.35}$$

is the operator of the number of nucleons of given type (τ = neut or prot). The other additional condition is the normalization (6.29) of amplitudes $\mathscr{U}_i$ and $\mathscr{V}_i$ for all i. So the variation principle gives the following equation

$$\begin{aligned} \delta\Big\{ &\langle BCS|\,\hat{H}_P(\tau) - \lambda_\tau\,(\hat{n}_\tau - N_\tau)\,|BCS\rangle \\ &- \sum_{\substack{i>0 \\ i\in\tau}} E_i{}'\,\left(\mathscr{U}_i^2 + \mathscr{V}_i^2 - 1\right)\Big\} = 0 \end{aligned} \tag{6.36}$$

where variations are performed with respect to all amplitudes $\mathscr{U}_i$ and $\mathscr{V}_i$. In (6.36) $\hat{H}_P(\tau = neut, prot)$ is the Hamiltonian (6.26). The λ_τ ($\tau = neut, prot$) and $E_i\,'$ are Lagrange multipliers the physical meaning of which will come out later.

Furher we introduce new notation $\hat{H}'_P(\tau = neut,\ prot)$:

$$\hat{H}'_P(\tau) \equiv \hat{H}_P(\tau) - \lambda_\tau \hat{n}_\tau = \boxed{\begin{array}{c}\text{see}\\ (6.26)\end{array}} =$$

$$= \sum_{\substack{i>0\\ i\in\tau}} (\epsilon_i^{(0)} - \lambda_\tau)\,(a^+_{i+}a_{i+} + a^+_{i-}a_{i-}) - G_\tau \sum_{\substack{i,i'>0\\ i,i'\in\tau}} a^+_{i+}a^+_{i-}a_{i'-}a_{i'+} \tag{6.37}$$

The expectation value of the number of particle operator $\hat{n}_\tau$ in the BCS state is

$$\langle BCS|\,\hat{n}_\tau\,|BCS\rangle = \sum_{\substack{i>0\\ i\in\tau}} \sum_{\sigma=\pm} \langle BCS|\,a^+_{i\sigma}a_{i\sigma}\,|BCS\rangle =$$

$$= \boxed{\begin{array}{c}\text{substitution}\\ \text{from (6.30)}\end{array}} =$$

$$= \sum_{\substack{i>0\\ i\in\tau}} \sum_{\sigma=\pm} \langle BCS|\,\left(\mathscr{U}_i\,\alpha^+_{i\sigma} + \sigma\mathscr{V}_i\,\alpha_{i-\sigma}\right)$$

$$\left(\mathscr{U}_i\,\alpha_{i\sigma} + \sigma\mathscr{V}_i\,\alpha^+_{i-\sigma}\right)\,|BCS\rangle =$$

$$= \boxed{\begin{array}{c}\text{because}\\ \alpha_{i\sigma}\,|BCS\rangle\end{array}} = 2\sum_{\substack{i>0\\ i\in\tau}} \mathscr{V}_i^2 = N_\tau \tag{6.38}$$

where $N_{\tau=neut} = N = A - Z$ and $N_{\tau=prot} = Z$.

Further the variation of the functional in the brackets in the l.h.s. of (6.36) will be calculated. At first we determine the first term, $\langle BCS|\hat{H}'_P(\tau)|BCS\rangle = \langle BCS|\,\hat{H}_P(\tau) - \lambda_\tau\,\hat{n}_\tau\,|BCS\rangle$. We express $\hat{H}'_P(\tau)$ in terms of the quasiparticle

creation and annihilation operators

$$\hat{H}'_P(\tau) \equiv \hat{H}_P(\tau) - \lambda_\tau \hat{n}_\tau = \boxed{\begin{array}{c}\text{see}\\(6.26)\end{array}} =$$

$$= \sum_{\substack{i>0\\ i\in\tau}} (\epsilon_i^{(0)} - \lambda_\tau)\,(a_{i+}^+ a_{i+} + a_{i-}^+ a_{i-}) - G_\tau \sum_{\substack{i,i'>0\\ i,i'\in\tau}} a_{i+}^+ a_{i-}^+ a_{i'-} a_{i'+} =$$

$$= \sum_{\substack{i>0\\ i\in\tau}} (\epsilon_i^{(0)} - \lambda_\tau)\,\Big[(\mathscr{U}_i\alpha_{i+}^+ + \mathscr{V}_i\alpha_{i-})(\mathscr{U}_i\alpha_{i+} + \mathscr{V}_i\alpha_{i-}^+) + (\mathscr{U}_i\alpha_{i-}^+ + \mathscr{V}_i\alpha_{i+})(\mathscr{U}_i\alpha_{i-} + \mathscr{V}_i\alpha_{i+}^+)\Big]$$

$$-G_\tau \sum_{\substack{i,i'>0\\ i,i'\in\tau}} (\mathscr{U}_i\alpha_{i+}^+ + \mathscr{V}_i\alpha_{i-})(\mathscr{U}_i\alpha_{i-}^+ - \mathscr{V}_i\alpha_{i+}^+)\,(\mathscr{U}_{i'}\alpha_{i'-} - \mathscr{V}_{i'}\alpha_{i'+})(\mathscr{U}_{i'}\alpha_{i'+} + \mathscr{V}_{i'}\alpha_{i-}^+) =$$

$$\equiv U^{(\tau)} + \hat{H}^{(\tau)}_{P(1,1)} + \hat{H}^{(\tau)}_{P(2,0)} + \hat{H}^{(\tau)}_{res} \tag{6.39}$$

where

$$U^{(\tau)} = \sum_{\substack{i>0\\ i\in\tau}} \Big[2\,(\epsilon_i^{(0)} - \lambda_\tau) - G_\tau\,\mathscr{V}_i^2\Big]\,\mathscr{V}_i^2 - G_\tau\Big(\sum_{\substack{i>0\\ i\in\tau}} \mathscr{U}_i\,\mathscr{V}_i\Big)^2$$

$$\hat{H}^{(\tau)}_{P(1,1)} = \sum_{\substack{i>0\\ i\in\tau}} \Big\{\Big[\epsilon_i^{(0)} - \lambda_\tau - G_\tau\,\mathscr{V}_i^2\Big]\,(\mathscr{U}_i^2 - \mathscr{V}_i^2) + 2\,G_\tau\Big(\sum_{\substack{j>0\\ j\in\tau}} \mathscr{U}_j\,\mathscr{V}_j\Big)\mathscr{U}_i\mathscr{V}_i\Big\}\,(\alpha_{i+}^+\alpha_{i+} + \alpha_{i-}^+\alpha_{i-})$$

$$H^{(\tau)}_{P(2,0)} = \sum_{\substack{i>0\\ i\in\tau}} \Big\{\Big[2\,(\epsilon_i^{(0)} - \lambda_\tau) - G_\tau\,\mathscr{V}_i^2\Big]\,\mathscr{U}_i\mathscr{V}_i - G_\tau\Big(\sum_{\substack{j>0\\ j\in\tau}} \mathscr{U}_j\,\mathscr{V}_j\Big)\,(\mathscr{U}_i^2 - \mathscr{V}_i^2)\Big\}\,(\alpha_{i+}^+\alpha_{i-}^+ + \alpha_{i-}\alpha_{i+})$$

(6.40)

and the pairing residual interaction is

$$\hat{H}_{P.res} = -G_\tau \sum_{\substack{ij>0\\ij\in\tau}}$$

$$\Big\{ \mathscr{U}_i^2\,\mathscr{U}_j^2\,\alpha_i^+\,\alpha_{\bar{i}}^+\,\alpha_{\bar{j}}\,\alpha_j - \mathscr{V}_i\,\mathscr{U}_i\,\mathscr{U}_j^2\,\alpha_{\bar{i}}^+\,\alpha_{\bar{i}}\,\alpha_{\bar{j}}\,\alpha_j$$
$$- \mathscr{U}_i\,\mathscr{V}_i\,\mathscr{U}_j^2\,\alpha_i^+\,\alpha_i\,\alpha_{\bar{j}}\,\alpha_j - \mathscr{V}_i^2\,\mathscr{U}_j^2\,\alpha_{\bar{i}}\,\alpha_i\,\alpha_{\bar{j}}\,\alpha_j$$
$$- \mathscr{U}_i^2\,\mathscr{V}_j\,\mathscr{U}_j\,\alpha_i^+\,\alpha_{\bar{i}}^+\,\alpha_{\bar{j}}^+\,\alpha_j - \mathscr{V}_i\,\mathscr{U}_i\,\mathscr{V}_j\,\mathscr{U}_j\,\alpha_{\bar{i}}^+\,\alpha_j\,\alpha_{\bar{i}}\,\alpha_j$$
$$- \mathscr{U}_i\,\mathscr{V}_i\,\mathscr{V}_j\,\mathscr{U}_j\,\alpha_i^+\,\alpha_j^+\,\alpha_i\,\alpha_j + \mathscr{V}_i^2\,\mathscr{V}_j\,\mathscr{U}_j\,\alpha_j^+\,\alpha_{\bar{j}}\,\alpha_i\,\alpha_j$$
$$-\mathscr{U}_i^2\,\mathscr{U}_j\,\mathscr{V}_j\,\alpha_i^+\,\alpha_{\bar{i}}^+\,\alpha_{\bar{j}}^+\,\alpha_{\bar{j}} - \mathscr{V}_i\,\mathscr{U}_i\,\mathscr{U}_j\,\mathscr{V}_j\,\alpha_{\bar{i}}^+\,\alpha_{\bar{j}}^+\,\alpha_{\bar{i}}\,\alpha_{\bar{j}}$$
$$- \mathscr{U}_i\,\mathscr{V}_i\,\mathscr{U}_j\,\mathscr{V}_j\,\alpha_i^+\,\alpha_{\bar{j}}^+\,\alpha_i\,\alpha_{\bar{j}} + \mathscr{V}_i^2\,\mathscr{V}_j\,\mathscr{U}_j\,\alpha_{\bar{j}}^+\,\alpha_{\bar{i}}\,\alpha_i\,\alpha_{\bar{j}}$$
$$- \mathscr{U}_i^2\,\mathscr{V}_j^2\,\alpha_i^+\,\alpha_{\bar{i}}^+\,\alpha_j^+\,\alpha_{\bar{j}}^+ + \mathscr{V}_i\,\mathscr{U}_i\,\mathscr{V}_j^2\,\alpha_{\bar{i}}^+\,\alpha_j^+\,\alpha_{\bar{j}}^+\,\alpha_{\bar{j}}$$
$$+ \mathscr{U}_i\,\mathscr{V}_i\,\mathscr{V}_j^2\,\alpha_i^+\,\alpha_j^+\,\alpha_{\bar{j}}\,\alpha_i + \mathscr{V}_i^2\,\mathscr{V}_j^2\,\alpha_j^+\,\alpha_{\bar{j}}^+\,\alpha_{\bar{i}}\,\alpha_i \Big\} \tag{6.41}$$

Since $\alpha_{i\sigma}\,|BCS\rangle = 0$ we obtain

$$\langle BCS|\,\hat{H}'_P(\tau)\,|BCS\rangle = U^{(\tau)} \tag{6.42}$$

Then the expr. (6.36) (variation condition) can be rewritten as

$$\delta\Big\{U^{(\tau)} - \sum_{\substack{i>0\\i\in\tau}} E_i^{'}\,\left(\mathscr{U}_i^2 + \mathscr{V}_i^2 - 1\right)\Big\} = 0 \tag{6.43}$$

That means the amplitudes $\mathscr{U}_i$ and $\mathscr{V}_i$ should correspond to the extrem (minimum) of the expression in the bractets of (6.43) taken as the function of $\mathscr{U}_i$ and $\mathscr{V}_i$ and this gives following equations

$$\frac{\partial\{\quad\}}{\partial\mathscr{V}_i} = 4\,(\epsilon_i^{(0)} - \lambda_\tau)\,\mathscr{V}_i - 4\,G_\tau\,\mathscr{V}_i^3$$
$$-2\;G_\tau\Big(\sum_{\substack{j>0\\j\in\tau}}\mathscr{U}_j\,\mathscr{V}_j\Big)\,\mathscr{U}_i - 2\,E_i^{'}\,\mathscr{V}_i = 0 \tag{6.44}$$

$$\frac{\partial\{\quad\}}{\partial\mathscr{U}_i} = -2\;G_\tau\Big(\sum_{\substack{j>0\\j\in\tau}}\mathscr{U}_j\mathscr{V}_j\Big)\,\mathscr{V}_i - 2\,E_i^{'}\,\mathscr{U}_i = 0 \tag{6.45}$$

From (6.45)

$$E_i^{'} = -\frac{G_\tau \left(\sum_{\substack{j>0 \\ j\in\tau}} \mathscr{U}_j \mathscr{V}_j \right) \mathscr{V}_i}{\mathscr{U}_i}$$

and the substitution to (6.44) gives

$$2\,\mathscr{V}_i\,(\epsilon_i^{(0)} - \lambda_\tau - G_\tau\,\mathscr{V}_i^2) - G_\tau \Big(\sum_{\substack{j>0 \\ j\in\tau}} \mathscr{U}_j\,\mathscr{V}_j \Big)\,\mathscr{U}_i + \\ + \frac{1}{\mathscr{U}_i}\,G_\tau \Big(\sum_{\substack{j>0 \\ j\in\tau}} \mathscr{U}_j\,\mathscr{V}_j \Big)\,\mathscr{V}_i^2 = 0 \qquad (6.46)$$

Further we define

$$\Delta_\tau \equiv G_\tau \sum_{\substack{j>0 \\ j\in\tau}} \mathscr{U}_j\,\mathscr{V}_j \qquad (6.47)$$

$$\epsilon_i \equiv \epsilon_i^{(0)} - G_\tau\,\mathscr{V}_i^2 \text{ for all i} \qquad (6.48)$$

It should be pointed out that the second term in the r.h.s. of (6.48), $-G_\tau\,\mathscr{V}_i^2$, is very small in the comparison with $\epsilon_i^{(0)}$ and therefore the difference between ϵ_i and $\epsilon_i^{(0)}$ is often neglected (see e.g. [7, 8]). In the new notation (6.47), (6.48) the equation (6.46) has following form

$$2\,(\epsilon_i - \lambda_\tau)\,\mathscr{U}_i\mathscr{V}_i - \Delta_\tau\,(\mathscr{U}_i^2 - \mathscr{V}_i^2) = 0 \qquad (6.49)$$

This equation in the combination with definitions (6.47), (6.48) and together with the normalization conditions (6.29) and (6.38) can be understood as the equation system for amplitudes $\mathscr{U}_i$ and $\mathscr{V}_i$.

In fact, we have two type of solutions of (6.49)

i. trivial: $\mathscr{U}_i\mathscr{V}_i = 0$ for all i, that means $\Delta_\tau = 0$. This solution corresponds to the model of independent particles with the mean field $\hat{H}_{AV}$ because this model has

$$\begin{aligned} &\mathscr{V}_i = 1,\ \mathscr{U}_i = 0 \quad \text{for } \epsilon_i < \lambda_\tau \\ &\mathscr{V}_i = 0,\ \mathscr{U}_i = 1 \quad \text{for } \epsilon_i > \lambda_\tau \end{aligned} \qquad (6.50)$$

which really gives $\mathscr{U}_i\mathscr{V}_i = 0$ for all i. The Bogoliubov transformation (6.30) for this case is

$$\begin{aligned} \alpha^+_{i\sigma} &= -\sigma\, a_{i-\sigma} \quad \text{for } \epsilon_i < \lambda_\tau \\ \alpha^+_{i\sigma} &= a^+_{i\sigma} \qquad\quad \text{for } \epsilon_i > \lambda_\tau \end{aligned} \tag{6.51}$$

That means the quasiparticle creation operator $\alpha^+_{i\sigma}$ creates the particle in the single-particle state i if its energy is above the Fermi level and $\alpha^+_{i\sigma}$ creates the hole (annihilates particle) if the single-particle state i has energy ϵ_i below the Fermi level.

nontrivial:, which is usually written in the following form

$$\begin{aligned} \mathscr{U}_i^2 &= \frac{1}{2}\left\{1 + \frac{\epsilon_i - \lambda_\tau}{\sqrt{(\epsilon_i - \lambda_\tau)^2 + \Delta_\tau^2}}\right\} \\ \mathscr{V}_i^2 &= \frac{1}{2}\left\{1 - \frac{\epsilon_i - \lambda_\tau}{\sqrt{(\epsilon_i - \lambda_\tau)^2 + \Delta_\tau^2}}\right\} \end{aligned} \tag{6.52}$$

If we substitute this into the equation (6.49) we obtain

$$\begin{aligned} &2\,(\epsilon_i - \lambda_\tau)\,\mathscr{U}_i\mathscr{V}_i = \Delta_\tau\,(\mathscr{U}_i^2 - \mathscr{V}_i^2) = \\ &= \frac{(\epsilon_i - \lambda_\tau)\,\Delta_\tau}{\sqrt{(\epsilon_i - \lambda_\tau)^2 + \Delta_\tau^2}} \quad \Rightarrow \quad \mathscr{U}_i\mathscr{V}_i = \frac{\Delta_\tau}{2\sqrt{(\epsilon_i - \lambda_\tau)^2 + \Delta_\tau^2}} \end{aligned} \tag{6.53}$$

The substitution of (6.53) into the definition (6.47) gives

$$\Delta_\tau = \frac{G_\tau\,\Delta_\tau}{2} \sum_{\substack{i>0 \\ i\in\tau}} \frac{1}{\sqrt{(\epsilon_i - \lambda_\tau)^2 + \Delta_\tau^2}}$$

$$\Rightarrow \qquad 1 = \frac{1}{2}\,G_\tau \sum_{\substack{i>0 \\ i\in\tau}} \frac{1}{\sqrt{(\epsilon_i - \lambda_\tau)^2 + \Delta_\tau^2}} \tag{6.54}$$

This is the first equation for unknowns λ_τ and Δ_τ. The second one is obtained by the substitution of (6.52) into (6.38):

$$N_\tau = 2 \sum_{\substack{i>0 \\ i\in\tau}} \mathscr{V}_i^2 = \sum_{\substack{i>0 \\ i\in\tau}} \left\{1 - \frac{\epsilon_i - \lambda_\tau}{\sqrt{(\epsilon_i - \lambda_\tau)^2 + \Delta_\tau^2}}\right\} \tag{6.55}$$

So the variational principle (6.43) provides the system of two equations (6.54) and (6.55) for unknowns λ_τ and Δ_τ. After the solving it the substitution of λ_τ and Δ_τ into (6.52) gives the amplitudes $\mathscr{U}_i$ and $\mathscr{V}_i$ for all i (we suppose that we know the single-particle energies ϵ_i, for instance, from the previous solving the Hartree-Fock problem).

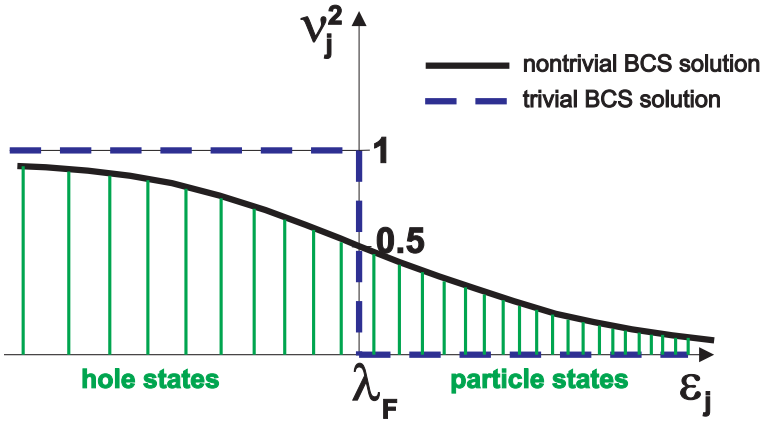


Figure 6.4: Occupation probability $\mathscr{V}_i^2$ of the single-particle (single-quasiparticle) states as a function of the single-particle energy ϵ_i for the case of the nontrivial solution (solid line) and trivial solution (dashed line) of the BCS equation (6.49) (schematic figure).

In the Fig. 6.4 the occupation probability $\mathscr{V}_i^2$ of the single-particle (or single-quasiparticle) states as the function of the single-particle energy ϵ_i is demonstrated for the cases of the trivial solution of the BCS equation (see (6.51)) (dashed line) and the nontrivial solution of the BCS function (see (6.52)) (solid line). One can see that for the nontrivial solution (6.52) the occupation probability of single-particle or single-quasiparticle states are smared in the comparison with the case of the trivial solution when all single-particle states up to the Fermi level are occupied and those above the Fermi level are empty.

Knowing the amplitudes $\mathscr{U}_i$ and $\mathscr{V}_i$ of quasiparticle states we can rewrite the one-body part of the Hamiltonian $\hat{H}_P^{'}(\tau)$ (see (6.39),(6.40) as follows (supposing of the existence of the nontrivial solution of the BCS equation (6.49))

$$\hat{H}_P^{(\tau)}(1,1) = \sum_{\substack{i>0 \\ i\in\tau}} \left[(\epsilon_i - \lambda_\tau)\,(\mathscr{U}_i^2 - \mathscr{V}_i^2) + 2\,\Delta_\tau\,\mathscr{U}_i\mathscr{V}_i\right] \left(\alpha_{i+}^+\alpha_{i+} + \alpha_{i-}^+\alpha_{i-}\right) =$$

$$= \boxed{\begin{array}{c}\text{see} \\ (6.49),(6.53)\end{array}} =$$

$$= \sum_{\substack{i>0\\ i\in\tau}} \left[(\epsilon_i - \lambda_\tau) \frac{\epsilon_i - \lambda_\tau}{\sqrt{(\epsilon_i - \lambda_\tau)^2 + \Delta_\tau^2}} + \frac{\Delta_\tau^2}{\sqrt{(\epsilon_i - \lambda_\tau)^2 + \Delta_\tau^2}} \right] \left(\alpha_{i+}^+ \alpha_{i+} + \alpha_{i-}^+ \alpha_{i-}\right) =$$

$$= \sum_{\substack{i>0\\ i\in\tau}} \sqrt{(\epsilon_i - \lambda_\tau)^2 + \Delta_\tau^2} \left(\alpha_{i+}^+ \alpha_{i+} + \alpha_{i-}^+ \alpha_{i-}\right) =$$

$$\equiv \sum_{\substack{i>0\\ i\in\tau}} E_i \left(\alpha_{i+}^+ \alpha_{i+} + \alpha_{i-}^+ \alpha_{i-}\right) \tag{6.56}$$

and

$$\hat{H}_P^{(\tau)}(2,0) = \sum_{\substack{i>0\\ i\in\tau}} \left[2\left(\epsilon_i - \lambda_\tau\right) \mathscr{U}_i \mathscr{V}_i - \Delta_\tau \left(\mathscr{U}_i{}^2 - \mathscr{V}_i{}^2\right)\right] \left(\alpha_{i+}^+ \alpha_{i-}^+ + \alpha_{i-}\alpha_{i+}\right) =$$

$$= \boxed{\begin{array}{c}\text{see}\\ (6.49), (6.53)\end{array}} = 0 \tag{6.57}$$

where so called quasiparticle energy $E_i = \sqrt{(\epsilon_i - \lambda_\tau)^2 + \Delta_\tau^2}$ was introduced. So, after the solving of the HFB equations the Hamiltonian $\hat{H}_P(\tau)$ (see (6.37) and (6.40)) can be rewritten as follows

$$\hat{H}_P(\tau) = \langle BCS|\, \hat{H}_P(\tau)\, |BCS\rangle + \hat{H}_{P(1,\,1)}^{(\tau)} + \hat{H}_{P(2,\,0)}^{(\tau)} + \hat{H}_{P,\,res}^{(\tau)} =$$

$$= \langle BCS|\, \hat{H}_P(\tau)\, |BCS\rangle + \sum_{\substack{i>0\\ i\in\tau}} E_i \left(\alpha_{i+}^+ \alpha_{i+} + \alpha_{i-}^+ \alpha_{i-}\right) + \hat{H}_{P,\,res}^{(\tau)} \tag{6.58}$$

where (see (6.36))

$$\begin{aligned} \langle BCS|\, \hat{H}_P^{(\tau)}\, |BCS\rangle &= \langle BCS|\, \hat{H}_P{}'^{(\tau)}\, |BCS\rangle + \lambda_\tau\, N_\tau = \\ &= U^{(\tau)} + \lambda_\tau\, N_\tau \end{aligned} \tag{6.59}$$

We can see that similarly as in the Subsection 4.1.1 we extracted one-body mean field Hamiltonian (4.27), $\hat{H}_{AV} = \sum_{i\sigma} \epsilon_i^{(HF)} a_{i\sigma}^+ a_{i\sigma}$, from the total Hamiltonian (4.28) now we can extract the quasiparticle mean field $\hat{H}_{BCS} = \hat{H}_{P(1,1)} = \sum_{i>0,\,\in\tau} E_i \left(\alpha_{i+}^+ \alpha_{i+} + \alpha_{i-}^+ \alpha_{i-}\right)$ from the Hamiltonian $\sum_\tau \hat{H}_P^{(\tau)}$. If in the Hamiltonian $\hat{H}_P^{(\tau)}$ the pairing residual interaction $\hat{H}_{P,\,res}$ is neglected then we speak

about the model of independent quasiparticles. The quasiparticle mean field $\hat{H}_{BCS} = \hat{H}_{P(1,1)}$ represents the one-quasiparticle operator and the pairing residual interaction term $\hat{H}_{P,\,res}$ is two-quasiparticle operator (from the point of view of quasiparticle creation and annihilation operators).

In the case of the model of independent quasiparticles when the whole nucleus Hamiltonian is approximated only by $\hat{H}_{BCS} = \hat{H}_{P,(1,1)}$ the excitation states are given by one-, two-, three-, and so on, quasiparticle states (we ommit in (6.60) s.p. indexes):

$$\begin{aligned} \alpha^+ \left|BCS\right\rangle,\ \alpha^+\alpha^+\alpha^+ \left|BCS\right\rangle, \ldots \quad &\rightarrow \quad \begin{array}{c}\text{for the system}\\ \text{with odd number}\\ \text{of particles}\end{array} \\ \alpha^+\alpha^+ \left|BCS\right\rangle,\ \alpha^+\alpha^+\alpha^+\alpha^+ \left|BCS\right\rangle, \ldots \quad &\rightarrow \quad \begin{array}{c}\text{for the system}\\ \text{with even number}\\ \text{of particles}\end{array} \end{aligned} \tag{6.60}$$

The ground state of the system with the even number of particles is given by the ket $\left|BCS\right\rangle$ (6.28). In the case of the odd number of particle system the ground state is one of the one-quasiparticle states $\alpha_i^+ \left|BCS\right\rangle$ with the lowest quasiparticle energy E_i of this system. For the odd number of particle systems (odd-A nuclei with the odd Z or odd N) it is usually assumed that the BCS equations are solved for the corresponding even number core (the system with the even number of particles with one particle removed from the state closest to the Fermi level of the investigated odd number of particle system) and in such a way obtained amplitudes $\mathscr{U}_i$ and $\mathscr{V}_i$ are used for all excitation states of the odd number of particle system. If we want to be more precise in the determination of the ground state of the odd number of particle system we whould take into account so called blocking effect (see the next subsection).

Further some comments on the BCS method are given

6.2.2.3 Blocking effect

The blocking effect is connected with the fact that in the ground state of the odd number of particle system there is one particle sitting in the single-particle state with the highest s.p. energy (with the index i_0) which is odd and therefore it cannot be paired by the pairing interaction and therefore the single-particle state with this index i_0 is blocked in the forming of the BCS

state. Corresponding ground state of this odd system is

$$|BCS\rangle_{i_0} = a^+_{i_0} \prod_{\substack{i>0 \\ i\neq i_0}} \left(\mathscr{U}_i^{(i_0)} + \mathscr{V}_i^{(i_0)}\, a^+_{i+} a^+_{i-} \right) |-\rangle \tag{6.61}$$

and amplitudes $\mathscr{U}_i^{(i_0)}$ and $\mathscr{V}_i^{(i_0)}$ are obtained by modified variational principle (a modification of (6.36))

$$\delta \Big\{ {}_{i_0}\langle BCS|\, \hat{H}_P(\tau) - \lambda_\tau \left(\hat{n}_\tau - N_\tau\right) |BCS\rangle_{i_0} - \sum_{\substack{i>0 \\ i\in\tau}} E_i{}' \left(\mathscr{U}_i^{(i_0)\,2} + \mathscr{V}_i^{(i_0)\,2} - 1 \right) \Big\} = 0 \tag{6.62}$$

where $\tau = neut$ or $\tau = prot$ according to the type of the odd-A nucleus. The anologous solving of this variational principle problem as it was performed in the derivation of (6.54) and (6.55) provides the following equations for unknowns $\lambda_\tau^{(i_0)}$ and $\Delta_\tau^{(i_0)}$

$$\begin{aligned} 1 &= \frac{1}{2} G_\tau \sum_{\substack{i>0 \\ i\neq i_0}} \frac{1}{\sqrt{(\epsilon_i - \lambda_\tau^{(i_0)})^2 + \Delta_\tau^{(i_0)\,2}}} \\ N_\tau &= 1 + \sum_{\substack{i>0 \\ i\neq i_0}} \left\{ 1 - \frac{\epsilon_i - \lambda_\tau^{(i_0)}}{\sqrt{(\epsilon_i - \lambda_\tau^{(i_0)})^2 + \Delta_\tau^{(i_0)\,2}}} \right\} \end{aligned} \tag{6.63}$$

The Fermi energy $\lambda_\tau^{(i_0)}$ and pairing gap $\Delta_\tau^{(i_0)}$ are now dependent on the blocked s.p. state i_0. The corresponding amplitudes $\mathscr{U}_i^{(i_0)}$ and $\mathscr{V}_i^{(i_0)}$ are also dependent on the blocked s.p. state i_0:

$$\begin{aligned} \mathscr{U}_i^{(i_0)\,2} &= \frac{1}{2} \left\{ 1 + \frac{\epsilon_i - \lambda_\tau^{(i_0)}}{\sqrt{(\epsilon_i - \lambda_\tau^{(i_0)})^2 + \Delta_\tau^{(i_0)\,2}}} \right\} \\ \mathscr{V}_i^{(i_0)\,2} &= \frac{1}{2} \left\{ 1 - \frac{\epsilon_i - \lambda_\tau^{(i_0)}}{\sqrt{(\epsilon_i - \lambda_\tau^{(i_0)})^2 + \Delta_\tau^{(i_0)\,2}}} \right\} \end{aligned} \tag{6.64}$$

In principle, we should involve this blocking effect in the calculation of amplitudes $\mathscr{U}_i$ and $\mathscr{V}_i$ for all quasiparticle excitation states where we have some unpaired nucleons but in this case these excitations determined with different blocking states are not orthogonal each other and we have problems with the calculation of matrix elements of different transition operators with such nonorthogonal states. This blocking effect is often neglected and BCS variation principle problem is solved only one time for the ground state of the even number of particle core.

If the blocking effect is neglected in the calculation of the excitations of the even number of particle system then the lowest excitations have two-quasiparticle character (in the model of independent quasiparticles):

$$\begin{aligned} \hat{H}_{BCS}\, \alpha^+_{i_1}\alpha^+_{i_2}\, |BCS\rangle \;&\approx\; \left(\hat{H}_{P(1,1)} + \hat{H}_{P(2,0)}\right)\, \alpha^+_{i_1}\alpha^+_{i_2}\, |BCS\rangle = \\ &=\; (E_{i_1} + E_{i_2})\; \alpha^+_{i_1}\alpha^+_{i_2}\, |BCS\rangle \end{aligned} \tag{6.65}$$

where

$$E_{i_1} + E_{i_2} = \sqrt{(\epsilon_{i_1} - \lambda_\tau)^2 + \Delta^2_\tau} + \sqrt{(\epsilon_{i_2} - \lambda_\tau)^2 + \Delta^2_\tau} \tag{6.66}$$

From (6.66) it follows that the minimal energy of the two-quasiparticle state is $2\Delta_\tau$ and this is the explanation of the energy gap between the ground state and the first excitation state observed in the even-even nuclei. In the odd-A nuclei the lowest excitations have one-quasiparticle character (we neglect the blocking effect):

$$\hat{H}_{BCS}\, \alpha^+_{i\sigma}|BCS\rangle \approx \sum_{\substack{j>0 \\ j\in\tau}} \sum_{\sigma=\pm} E_j\, \alpha^+_{j\sigma_j}\alpha_{j\sigma_j}\, \alpha^+_i\, |BCS\rangle = E_i\, \alpha^+_i\, |BCS\rangle \tag{6.67}$$

with the energy equal to the corresponding one-quasiparticle energy E_i and the excitation energy $E_i - E_{i_0}$, where the state $|\, i_0\rangle = \alpha^+_{i_0}|BCS\rangle$ is the ground state of the odd number of particle system. The difference $E_i - E_{i_0}$ is not separated from the zero by any energy gap and therefore in the spectra of the odd-A or odd-odd nuclei any energy gap is not observed.

6.2.2.4 Standard deviation of the number of particles

It was already mentioned that the BCS ket $|BCS\rangle$, introduced as the vacuum for the quasiparticle creation and annihilation operators, is not an eigenstate of the number of particle operator (see (6.34). In order to be accurate

we should project the parts of the $|BCS\rangle$ and of all quasiparticle states correspondingly into the good number N_τ of the particles subspace using so called good number of particle projection operator $\hat{P}_{N_\tau}$, and to construct all the theory with these projected states (see Appendix N and [9] for details). However, the projecting of all states is technically complex and therefore the projection is not usually done and the number of particle preservation is included only in average in terms of taking into account of the term $-\lambda_\tau(\hat{n}_\tau - N_\tau)$ in the variation of the functional (6.36). Therefore, before the using of this approximation, it is necessary to check if the approximative replacement $\hat{P}_{N_\tau}|BCS\rangle \to |BCS\rangle$ (that means involving only the term $-\lambda_\tau(\hat{n}_\tau - N_\tau)$ in the functional) does not cause too big error. The measure of the accuracy or inaccuracy of this approximative approach from the point of view of the number of particle conservation is the fluctuation or deviation of the number of particle $\Delta N_\tau = \sqrt{(\Delta N_\tau)^2}$, where

$$\begin{aligned}(\Delta N_\tau)^2 &\equiv \langle BCS|\,(\hat{n}_\tau - N_\tau)^2\,|BCS\rangle = \\ &= \langle BCS|\,\hat{n}_\tau^2\,|BCS\rangle - N_\tau^2 \end{aligned} \tag{6.68}$$

with

$$\langle BCS|\,\hat{n}_\tau^2\,|BCS\rangle = \boxed{\begin{array}{c}\text{see}\\(6.35)\end{array}} =$$

$$= \sum_{\substack{ij>0\\ij\in\tau}} \langle BCS|\,(a_{i+}^+ a_{i+} + a_{i-}^+ a_{i-})\,(a_{j+}^+ a_{j+} + a_{j-}^+ a_{j-})\,|BCS\rangle =$$

$$= \boxed{\begin{array}{c}\text{substitution from Boliubov transformation (6.30)}\\ \text{and using } \alpha_i\,|BCS\rangle = 0,\ \langle BCS|\,\alpha_i^+ = 0\end{array}} =$$

$$= \sum_{\substack{ij>0\\ij\in\tau}} \langle BCS|\,(2\mathscr{V}_i^2 + 2\mathscr{V}_i\mathscr{U}_i\,\alpha_{i-}\alpha_{i+})(2\mathscr{V}_j^2 + 2\mathscr{V}_j\mathscr{U}_j\,\alpha_{j+}^+\alpha_{j-}^+)\,|BCS\rangle =$$

$$= 4\sum_{\substack{ij>0\\ij\in\tau}} \mathscr{V}_i^2\mathscr{V}_j^2 + 4\sum_{\substack{ij>0\\ij\in\tau}} \mathscr{U}_i\mathscr{V}_i\mathscr{U}_j\mathscr{V}_j\ \langle BCS|\,\alpha_{i-}\alpha_{i+}\alpha_{j+}^+\alpha_{j-}^+\,|BCS\rangle =$$

$$= N_\tau^2 + 4\sum_{\substack{i>0\\i\in\tau}} \mathscr{U}_i^2\mathscr{V}_i^2 \qquad \Rightarrow \qquad (\Delta N_\tau)^2 = 4\sum_{\substack{i>0\\i\in\tau}} \mathscr{U}_i^2\mathscr{V}_i^2 \tag{6.69}$$

From this expression one can see that for the trivial solution of the BCS equation (6.49), when $\mathscr{U}_i\mathscr{V}_i = 0$ for all i, the fluctuation ΔN_τ is always zero. In this case $|BCS\rangle = |HF\rangle$ and the ground state $|HF\rangle$ is the eigen-state of the number of particle operator. In any case the value $(\Delta N_\tau)^2$ given by (6.69) should be small if we want to use the BCS method without any particle number projection.

6.2.2.5 Existence and nonexistence of nontrivial solution of the BCS equation

As it was already noted the BCS equation (6.49) has generally two types of solutions: trivial ($\mathscr{V}_i\mathscr{U}_i = 0$ for all i) and nontrivial ($\mathscr{V}_i\mathscr{U}_i \neq 0$). The nontrivial solution exists not in all cases and, if it exists, then its energy in the BCS ground state is always less then that for trivial solution.

In the framework of the simple schematic model it will be shown that if the pairing strength constant G is too small then the nontrivial solution of the BCS equation does not exist.

Let us consider the simple model of two degenerated levels ϵ_1 and ϵ_2, $\epsilon_1 < \epsilon_2$. Let us assume further that the number of particles in the system is so that the level ϵ_1 is fully occupied and the level ϵ_2 is empty. In such a case the Fermi level for the trivial solution is identical with ϵ_1 ($\lambda_{trivial} = \epsilon_1$). It is evident that if the nontrivial solution exists then at least one $\mathscr{V}_i\mathscr{U}_i \neq 0$ and corresponding Fermi level $\lambda_{nontrivial} \neq \epsilon_1$ and it lies higher somewhere between ϵ_1 and ϵ_2. It corresponds to the situation that not all particles in the ground state of the system sit permanently in the level ϵ_1. Let us assume further that the pairing strength constant for such a λ is so low that

$$\frac{G}{2}\sum_{i>0}\frac{1}{\epsilon_i - \lambda} < 1$$

Then the equation (6.54) for the energy gap Δ

$$\frac{G}{2}\sum_{i>0}\frac{1}{(\epsilon_i - \lambda)\sqrt{1 + \frac{\Delta^2}{(\epsilon_i - \lambda)^2}}} = 1$$

cannot have any solution. This simple model corresponds to the nuclei with the closed shells when the pairing interaction is not sufficiently strong enough to lift at least sometimes the pair of particles to the next empty shell (the principal shells are separated each other by quite big energy gap - see magic numbers discussed in the subsection 5.1). For the nuclei with partly filled valence shell the single-particle energies close to the Fermi level are in energy

much closer each other and therefore the nontrivial solution always exists even with the low pairing strength constant G.

However, one should realize that the nonexistence of the nontrivial solution of the BCS equation does not mean that the pairing interaction has not any effect. It only means that the pairing interaction does not cause the transformation from the particle to the quasiparticle phase of the nuclear matter and the quaiparticle mean field $\hat{H}_{BCS}$ coincides with the particle mean field $\hat{H}_{AV}$. However, even in this case the pairing interaction contributes to the residual interactions ($\hat{H}_{P,\,res} \neq 0$). For instance it causes so called pairing vibrations - see the Chapter 7.

6.2.2.6 Neutron-proton pairing

There is a question why we can do the BCS calculation of the amplitudes $\mathscr{U}_i$ and $\mathscr{V}_i$ and the Fermi level λ_τ independently for given type of nucleus, $\tau = \mathit{prot}$ and $\tau = \mathit{neut}$, that means why it is possible to take the pairing interaction in the form (see (6.24), (6.25))

$$\begin{aligned} \hat{V}_{pair} \;=\; -\,G_P \sum_{\substack{ij>0\\ ij\in\, prot}} a^+_{i+}a^+_{i-}a_{j-}a_{j+} \\ -\,G_N \sum_{\substack{ij>0\\ ij\in\, neut}} a^+_{i+}a^+_{i-}a_{j-}a_{j+} \end{aligned} \tag{6.70}$$

and why there is not also the contribution from the term

$$-\,G_{NP}\sum_{ij>O} a^+_{i_n+}a^+_{i_p-}a_{j_p-}a_{j_n+}$$

in the pairing interaction which would create the neutron-proton pairs where in such pair neutron and proton occupy the same single-particle states except the sign of the projection of the angular momentum and the sign of the isospin projection. The answer to this question is connected with the short range of the paring interaction. In the overwhelming majority of nuclei the number of the protons is different from the number of neutrons and therefore the Fermi level of protons differs from the Fermi level of neutrons. As a result of this difference the valence shells of protons and of neutrons (and these valence shells are most relevant) are also different (quantum numbers of valence proton states are different from valence neutron state quantum numbers). Therefore the valence neutrons are found in another places in the

space than the valence protons and therefore they cannot interact through very short range pairing interaction.

Only in the nuclei with $N \approx Z$ it would be possible to observe proton-neutron pairing. However nuclei with $N = Z$ and with not closed valence shells (because only in the open shell nuclei the quasiparticle mean field is created) can be experimentally observed. Such nuclei can be found only far from the stability line and therefor they are are very unstable and not sufficient amount of experimental data is available.

6.2.2.7 Empirical (experimental) pairing gap Δ

The experimental fact that the masses of odd-A nuclei are always bigger than masses of neighboring even-even nuclei is used for the experimental estimation of the pairing energy gap. The idea is based on the mass formula for even number A and $A+2$ nuclei and for odd $A+1$ nucleus (A - even) (see (1.12)):

$$\begin{aligned} M(A)\,c^2 &= \sum_{i=1}^{A} m\,c^2 + E_A^{(GS)} \\ M(A+2)\,c^2 &= \sum_{i=1}^{A} m\,c^2 + 2\,m\,c^2 + E_{A+2}^{(GS)} \\ M(A+1)\,c^2 &= \sum_{i=1}^{A} m\,c^2 + m\,c^2 + E_{A+1}^{(GS)} \end{aligned} \tag{6.71}$$

where m is the nucleon mass; $E_A^{(GS)}$, $E_{A+2}^{(GS)}$ and $E_{A+1}^{(GS)}$ are ground state (binding) energies of the even nuclei with A, $A+2$ nucleons and odd-(A+1) nucleus, respectively (one should have in mind that all these binding energies are negative). Since the $A+2$ nucleus is imposed to be obtained from the A- nucleus by the adding of one pair of nucleons of the same type into the two-quasiparticle state with the index i the relation between $E_A^{(GS)}$ and $E_{A+2}^{(GS)}$ is following

$$E_{A+2}^{(GS)} = E_A^{(GS)} - 2\,E_i \tag{6.72}$$

where E_i is the corresponding quasiparticle energy ($E_i = \sqrt{(\epsilon_i - \lambda)^2 + \Delta^2}$ is always positive). Similarly the odd-(A+1) nucleus was formed from the A-nucleus by adding of one nucleon into the single-particle state i (the same i as in (6.72)) and therefore we have

$$E_{A+1}^{(GS)} = E_A^{(GS)} - \epsilon_i \tag{6.73}$$

So we can write

$$\frac{1}{2}\left\{M(A+2)\,c^2 + M(A)\,c^2 - 2\,M(A+1)\,c^2\right\} =$$
$$= \frac{1}{2}\left(E^{(GS)}_{A+2} + E^{(GS)}_{A}\right) - E^{(GS)}_{A+1} = -E_i + \epsilon_i =$$
$$= \boxed{\begin{array}{c}\text{because}\\ E_i = \sqrt{(\epsilon_i - \lambda)^2 + \Delta^2}\end{array}} \approx -\Delta < 0 \qquad (6.74)$$

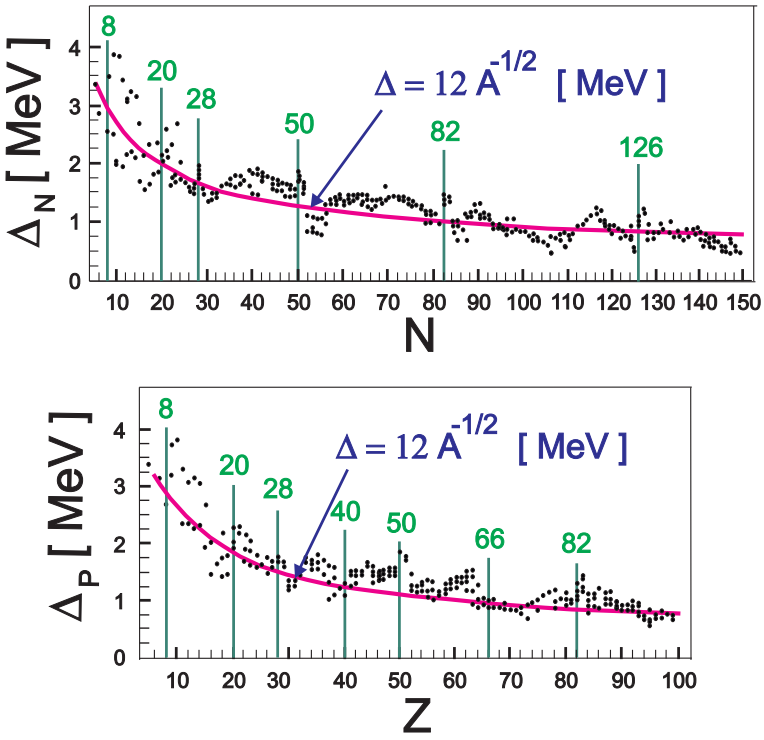


Figure 6.5: Dependence of the experimental neutron Δ_n and proton Δ_p gaps on the neutron and proton number (taken from [99]).

The l.h.s of the expression (6.74) [3] is used for the determination of the pairing gaps. Such "experimental" values of neutron and proton pairing energy gaps Δ_n and Δ_p for different nuclei as the function of neutron and proton numbers are given in the Fig.6.5. One can see that the empirical formula for Δ can be extracted from the Fig.6.5

$$\Delta_{n,\,p} \approx 12\,A^{-1/2}\,[MeV] \qquad (6.75)$$

Values of the empirical energy pairing gaps in the Fig. 6.5 were used for the obtaining the empirical values of the pairing strength constants G_N and G_P.

[3] Similar expression to (6.75) but involving masses not only of three neighbouring nuclei but five are also used for the determination of the pairing gap.

For instance in [7] the phenomenological Saxon-Woods mean field with the BCS approach with the pairing interaction in the form (6.70) was used for the comparison of the calculated gaps Δ_n and Δ_p with the empirical ones given in the Fig. 6.5. The extracted from this comparison values of G_N and G_P are following

$$G_P = \frac{17}{A}\,[MeV] \qquad\qquad G_N = \frac{23}{A}\,[MeV] \tag{6.76}$$

The lower value of G_P in the comparison with G_N is caused by the presence of the Coulomb repulsion in the proton system.

6.2.3 BCS with the general effective nucleon-nucleon interaction

In the section 6.1 it was shown that the experimental data support the very short range (almost contact) character of the pairing interaction and that this interaction acts most strongly in the case when two nucleons of the same type and from the same shell occupy the two-particle state $|nl(j)^2; J=0\ M=0\rangle$ (see (6.10) and discussion there). This lead to the conclusion that the most important part of the pairing interaction is given by the potential (6.24) and the original BCS theory discussed in the previous subsections started with the pairing interaction in this form (so callled monopole pairing when $\langle (j)^2; J|\, V_{pair}\, |(j^{'})^2; J\rangle = 0$ for all $J > 0$ and for all shells with j, $j^{'}$ including only the case $j = j^{'}$, that means when only $\langle (j)^2; J=0|\, V_{pair}\, |(j)^2; J=0\rangle \neq 0$). However, the BCS theory can be formulated for general two-particle interaction as the version of more general Hartree-Fock-Bogoliubov (HFB) theory which is discussed in details in the next subsection. Further this generalization of the BCS theory for the general effective nucleon-nucleon interaction is hinted.

Instead of the special Hamiltonian $\hat{H}_P$ (see (6.26)) now we start with the general Hamiltonian

$$\begin{aligned}\hat{H} &= \sum_{ij\,(all)} \langle i|\,\hat{t}\,|j\rangle\, a_i^+ a_j + \frac{1}{2}\sum_{ijmn\,(all)} \langle ij|\,\hat{V}\,|mn\rangle\, a_i^+ a_j^+ a_n a_m = \\ &= \sum_{ij\,(all)} t_{ij}\, a_i^+ a_j + \frac{1}{4}\sum_{ijmn\,(all)} V_{ijmn}\, a_i^+ a_j^+ a_n a_m \end{aligned} \tag{6.77}$$

where $V_{ijmn} = \langle ij|\,\hat{V}\,|mn\rangle - \langle ij|\,\hat{V}\,|nm\rangle$ are antisymmetrized matrix element of the effective nucleon-nucleon interaction (we restric ourselves only to the two-body interaction - see (B.17)) and a_i, a_i^+ are single-particle annihilation

and creation operators of nucleons in the mean field single-particle state i. Summation in the expr. (6.77) goes over all single-particle states with both $\pm$ signs of ang. momentum projections (time reversed as well as non-reversed s.p. states) which is indicated by the symbol (all) and this will be used in further expressions as well. We supose that the nucleon-nucleon interaction $\hat{V}$ does not contain any term which changes neutron to proton and vice versa. Therefore the nucleus represents two systems of particles, neutron system and proton system, each with the fixed number of particles. Similarly as in the case of the standard BCS we create quasiparticle system of operators α_i, α_i^+ by means of Bogoliubov tranformation (6.30) or (6.33) with the corresponding quasiparticle vacuum $|BCS\rangle$ in the form (6.28). And similarly as in the Subsection 6.2.2.2 the Bogoliubov amplitudes $\mathscr{U}_i$ and $\mathscr{V}_i$ are obtained from the variational principle by the searching for the minimum of $\langle BCS|\hat{H}'|BCS\rangle$ for the Hamiltonian

$$\hat{H}' = \sum_{ij\,(all)} (t_{ij} - \lambda\,\delta_{ij})\, a_i^+ a_j + \frac{1}{4} \sum_{ijmn\,(all)} V_{ijmn}\, a_i^+ a_j^+ a_n a_m \tag{6.78}$$

where λ is a Lagrange multiplier (chemical potential) given by

$$\frac{\partial}{\partial N} \langle BCS|\, \hat{H}'\, |BCS\rangle = 0 \qquad \text{or} \qquad \lambda = \frac{\partial}{\partial N} \langle BCS|\, \hat{H}\, |BCS\rangle \tag{6.79}$$

Further we suppose the time-reversal invariance of the potential $\hat{V}$, $\mathscr{T}^{-1}\hat{V}\mathscr{T} = \hat{V}$. Then

$$\begin{aligned} &\langle \bar{i}'\,\bar{j}'|\,\hat{V}\,|\,\bar{i}\,\bar{j}\,\rangle = \langle \mathscr{T} i'\,j'|\,\hat{V}\,|\mathscr{T} ij\,\rangle = \langle i'\,j'|\,\mathscr{T}^{-1}\hat{V}\mathscr{T}\,|ij\,\rangle^* = \\ &= \langle i'\,j'|\,\hat{V}\,|ij\,\rangle^* = \boxed{\begin{array}{c}\text{because we suppose}\\ \hat{V}^+ = \hat{V}\end{array}} = \langle ij\,|\,\hat{V}\,|\,i'\,j'\,\rangle \end{aligned} \tag{6.80}$$

$$\begin{aligned} &\langle \bar{i}\,i'|\,\hat{V}\,|\,\bar{j}\,j'\,\rangle = \langle \mathscr{T} i\,\bar{i}'|\,\hat{V}\,|\mathscr{T} j\,\bar{j}'\,\rangle = \langle i\,\bar{i}'|\,\mathscr{T}^{-1}\hat{V}\mathscr{T}\,|j\,\bar{j}'\,\rangle^* = \\ &= \langle i\,\bar{i}'|\,\hat{V}\,|j\,\bar{j}'\,\rangle^* = \langle j\,\bar{j}'\,|\,\hat{V}\,|\,i\,\bar{i}'\,\rangle \end{aligned} \tag{6.81}$$

and the same symmetries hold for the antisymmetrized matrix elements $V_{ijmn} = \langle i\,j\,|\,\hat{V}\,|m\,n\rangle - \langle i\,j\,|\,\hat{V}\,|n\,m\rangle$.

Using the Wick's theorem (see (B.34)) taken with respect to the BCS vacuum $|BCS\rangle$ the expression (6.78) for the Hamiltonian $\hat{H}'$ can be rewritten as follows

$$\hat{H}' = H'^{\,0} + \hat{H}'^{\,1,1} + \hat{H}'^{\,2,0} + \hat{V}_{res} \tag{6.82}$$

where

$$H'^{\,0} \equiv \sum_{ii'\,(all)} \left[(t_{ii'} - \lambda\,\delta_{ii'}) + \frac{1}{2} \sum_{jj'\,(all)} V_{j\,ij\,'i'}\,\langle a_j^+ a_{j'}\rangle \right] \langle a_i^+ a_{i'}\rangle + \\ + \frac{1}{4} \sum_{iji'j'\,(all)} V_{ij\,i'j'}\,\langle a_i^+ a_j^+\rangle\,\langle a_{j'} a_{i'}\rangle \qquad (6.83)$$

$$\hat{H}'^{\,1,1} = \sum_{i\,i'\,(all)} \left[(t_{ii'} - \lambda\,\delta_{ii'}) + \sum_{jj'\,(all)} V_{ij\,i'j'}\,\langle a_j^+ a_{j'}\rangle \right] :\, a_i^+ a_{i'} : \qquad (6.84)$$

$$\hat{H}'^{\,2.0} = \frac{1}{4} \sum_{ij\,i'j'\,(all)} V_{ij\,i'j'} \left[\langle a_i^+ a_j^+\rangle \,:\, a_{j'} a_{i'} : + \langle a_{j'}^+ a_{i'}^+\rangle \,:\, a_i^+ a_j^+ :\, \right] \qquad (6.85)$$

$$\hat{V}_{res} = \frac{1}{4} \sum_{ij\,i'j'\,(all)} V_{ij\,i'j'} \,:\, a_i^+ a_j^+ a_{j'} a_{i'} : \qquad (6.86)$$

where in (6.86) and further in this subsection $\langle \hat{A}\,\rangle \equiv \langle BCS|\,\hat{A}\,|BCS\rangle$. In (6.82)-(6.85) the expectation values $\langle ab\rangle$ are (after the substitution of the Bogoliubov transformation (6.33) and using of $\alpha_i|BCS\rangle = 0$, $\langle HFB|\alpha_i^+ = 0$)

$$\begin{aligned}
\langle a_i^+ a_{i'}\rangle &= \langle HFB|\,a_i^+ a_{i'}\,|HFB\rangle = \boxed{\text{see (6.33)}} = \mathscr{V}_i^2\,\delta_{\bar{i}\,\bar{i}'} \\
\langle a_{\bar{i}}^+ a_{\bar{i}'}\rangle &= \langle HFB|\,a_{\bar{i}}^+ a_{\bar{i}'}\,|HFB\rangle = \mathscr{V}_i^2\,\delta_{i\,i'} \\
\langle a_i^+ a_{\bar{i}'}\rangle &= \langle HFB|\,a_i^+ a_{\bar{i}'}\,|HFB\rangle = 0 \\
\langle a_{\bar{i}}^+ a_{i'}\rangle &= \langle HFB|\,a_{\bar{i}}^+ a_{i'}\,|HFB\rangle = 0 \\
\langle a_{i'}^+ a_{\bar{i}}^+\rangle &= \langle HFB|\,a_{i'}^+ a_{\bar{i}}^+\,|HFB\rangle = \mathscr{U}_i \mathscr{V}_i\,\delta_{\bar{i}'\bar{i}} \\
\langle a_i a_{\bar{i}'}\rangle &= -\langle a_{\bar{i}'} a_i\rangle = \langle HFB|\,a_i a_{\bar{i}'}\,|HFB\rangle = -\mathscr{U}_i \mathscr{V}_i\,\delta_{i\,i'} \\
\langle a_i a_{i'}\rangle &= \langle HFB|\,a_i a_{i'}\,|HFB\rangle = 0 \\
\langle a_{i'}^+ a_i^+\rangle &= \langle HFB|\,a_{i'}^+ a_i^+\,|HFB\rangle = 0
\end{aligned} \qquad (6.87)$$

Further expressions can be simplified by introducing the following notation

$$h_{i\,i'} \equiv t_{i\,i'} + \sum_{j\,j'\,(all)} V_{ij\,i'j'}\,\langle a_j^+ a_{j'}\rangle = \\ = t_{i\,i'} + \sum_{j\,(all)} V_{ij\,i'j}\,\mathscr{V}_j^2 \qquad (6.88)$$

$$\Delta_{i\,i'} \equiv -\frac{1}{2}\sum_{j\,j'\,(all)} V_{\bar{j}j'\bar{i}\,i'}\langle a_j^+ a_{\bar{j}'}^+\rangle = \boxed{\text{see (6.81), (6.87)}} =$$

$$= \frac{1}{2}\sum_{j\,j'\,(all)} V_{i\,\bar{i}'\,j\;\bar{j}'}\langle a_j a_{\bar{j}'}\rangle = -\frac{1}{2}\sum_{j\,(all)} V_{i\,\bar{i}'\,j\,\bar{j}}\mathscr{U}_j\mathscr{V}_j \tag{6.89}$$

Then using (6.87)

$$H'^{\,0} = \sum_{i\,(all)}\left[(t_{ii} - \lambda\,\delta_{ii'}) + \frac{1}{2}\sum_{j\,(all)} V_{ij\,ij}\,\mathscr{V}_j^2\right]\mathscr{V}_i^2 +$$

$$-\frac{1}{4}\sum_{ij\,(all)} V_{i\bar{i}j\bar{j}}\,\mathscr{U}_i\mathscr{V}_i\mathscr{U}_j\mathscr{V}_j \tag{6.90}$$

The condition for the minimum of $H'^{\,0}$ with the simultaneous additional normalization condition gives (the analog of (6.43)-(6.45)):

$$\frac{\partial}{\partial\mathscr{U}_k}\left\{H'^{\,0} - \sum_j \mu_j\,(\mathscr{U}_j^2 + \mathscr{V}_j^2 - 1)\right\} = 0 \tag{6.91}$$

$$\frac{\partial}{\partial\mathscr{V}_k}\left\{H'^{\,0} - \sum_j \mu_j\,(\mathscr{U}_j^2 + \mathscr{V}_j^2 - 1)\right\} = 0 \tag{6.92}$$

where μ_j are Lagrange multipliers. After the substitution of (6.90) into (6.91) we obtain

$$\sum_{j\,(all)}(t_{jj} - \lambda)\,2\,\mathscr{V}_j\,\delta_{kj} + \frac{1}{2}\sum_{ij\,(all)} V_{ijij}\Big[2\,\mathscr{V}_i\,\delta_{ik}\,\mathscr{V}_j^2 + \mathscr{V}_i^2\,2\,\mathscr{V}_j\,\delta_{jk}\Big] +$$

$$-\frac{1}{4}\sum_{ij\,(all)} V_{i\bar{i}\,j\bar{j}}\,\mathscr{U}_i\mathscr{V}_i\,(\mathscr{V}_i\,\delta_{jk} + \mathscr{V}_j\,\delta_{ik}) + 2\,\mu_k\,\mathscr{V}_k =$$

$$= 2\,(t_{kk} - \lambda)\,\mathscr{V}_k + 2\sum_{i\,(all)} V_{ikik}\,\mathscr{V}_k\,\mathscr{V}_i^2 -$$

$$\frac{1}{2}\sum_{i\,(all)} V_{i\bar{i}\,k\bar{k}}\,\mathscr{U}_i\mathscr{V}_i\mathscr{U}_k + 2\,\mu_k\,\mathscr{V}_k =$$

$$= \boxed{\begin{array}{c}\text{see}\\ (6.88), (6.89)\end{array}} = 2\,(h_{kk} - \lambda)\,\mathscr{V}_k + \Delta_{kk}\,\mathscr{U}_k + 2\,\mu_k\,\mathscr{V}_k = 0 \tag{6.93}$$

and the equation (6.92) gives

$$-\frac{1}{4}\sum_{ij\,(all)} V_{i\bar{i}\,j\bar{j}}\,\mathscr{U}_i\mathscr{V}_j\,(\mathscr{U}_i\,\delta_{jk}+\mathscr{U}_j\,\delta_{ik})+2\,\mu_k\,\mathscr{U}_k=$$

$$=-\frac{1}{2}\sum_{i\,(all)} V_{i\bar{i}\,k\bar{k}}\,\mathscr{U}_i\mathscr{V}_i\mathscr{V}_k+2\,\mu_k\,\mathscr{U}_k=\boxed{\begin{array}{c}\text{see}\\(6.89)\end{array}}=$$

$$=\Delta_{kk}\,\mathscr{V}_k+2\,\mu_k\,\mathscr{U}_k=0 \tag{6.94}$$

From (6.94):

$$2\,\mu_k=-\frac{\Delta_{kk}\,\mathscr{V}_k}{\mathscr{U}_k} \tag{6.95}$$

and after the substitution (6.95) into (6.93) we obtain the generalized BCS equation:

$$2\,(h_{kk}-\lambda)\,\mathscr{V}_k\mathscr{U}_k+\Delta_{kk}\left(\mathscr{U}_k^2-\mathscr{V}_k^2\right)=0 \tag{6.96}$$

which is the analog of the standard monopole BCS equation (6.49) (only the sign of the energy gap is opposite) and similarly we have the nontrivial solution of it in the form similar to (6.52)

$$\begin{aligned}\mathscr{U}_k^2 &= \frac{1}{2}\left\{1+\frac{h_{kk}-\lambda}{\sqrt{(h_{kk}-\lambda)^2+\Delta_{kk}^2}}\right\}\\ \mathscr{V}_k^2 &= \frac{1}{2}\left\{1-\frac{h_{kk}-\lambda}{\sqrt{(h_{kk}-\lambda)^2+\Delta_{kk}^2}}\right\}\end{aligned} \tag{6.97}$$

which fulfils the following equation

$$\Delta_{ii}=\frac{1}{2}\sum_{k>0} V_{i\bar{i}'k\bar{k}}\frac{\Delta_{kk}}{\sqrt{(h_{kk}-\lambda)^2+\Delta_{kk}^2}}$$

with the number of particle N given by

$$N=\sum_{i\,(all)}\mathscr{V}_i^2=2\sum_{i>0}\mathscr{V}_i^2=\sum_{k>0}\left\{1-\frac{h_{kk}-\lambda}{\sqrt{(h_{kk}-\lambda)^2+\Delta_{kk}^2}}\right\} \tag{6.98}$$

where the symbol $k>0$ in the sums means that given summation index k goes over single- particle states with the positive ang. momentum projection (we suppose the time-reverse symmetry of the nucleus Hamiltonian). Usually the single-particle basis is chosen as the Hartree-Fock basis which diagonalizes

the mean field Hamiltonian (see (4.20)). In our notation (6.88) it corresponds to the basis in which the matrix $h_{kk'}$ is diagonal

$$h_{kk'} = t_{kk'} + \sum_j V_{kj\,k'j}\,\mathcal{V}_j^2 = \epsilon_k\,\delta_{kk'} \tag{6.99}$$

It can be easily shown that in such a basis the expressions for $H'^{\,0}$, $\hat{H}'^{\,1,1}$, and $\hat{H}'^{\,2,0} = \hat{H}^{\,2,0}$ (see (6.82)-(6.85)) become (using (6.99), (6.98))

$$H'^{\,0} = \sum_{i\,(all)} \Big[(\epsilon_i - \lambda) - \frac{1}{2}\sum_{j\,(all)} V_{ijij}\,\mathcal{V}_j^2\Big]\,\mathcal{V}_i^2 - \frac{1}{2}\sum_{i\,(all)} \Delta_{ii}\,\mathcal{U}_i\mathcal{V}_i$$

$$\hat{H}'^{\,1,1} = \sum_{i\,(all)} \Big[(\epsilon_i - \lambda)^2 + \Delta_{ii}^2\Big]\,\alpha_i^+\alpha_i \equiv \sum_{i>0} E_i\,(\alpha_i^+\alpha_i + \alpha_{\bar{i}}^+\,\alpha_{\bar{i}})$$

$$\hat{H}'^{\,2,0} = 0 \tag{6.100}$$

with $E_i = \sqrt{(\epsilon_i - \lambda)^2 + \Delta_{ii}^2}$, $\quad \Delta_{ii} = -\frac{1}{2}\sum_j V_{i\bar{i}\,j\bar{j}}\,\mathcal{V}_j\mathcal{U}_j = -\sum_{j>0} V_{i\bar{i}\,j\bar{j}}\,\mathcal{V}_j\mathcal{U}_j$. These expressions are the same as in (6.56), (6.57) except the fact that the gap Δ_{ii} is not the same for all single-particle states i (as it is in the standard monopole BCS theory described in the Subsection 6.2.2.2) but it is different for different single-particle states i.

6.2.4 Hartree-Fock-Bogoliubov approach

In the previous subsection 6.2.2.8 we presented the generalized BCS theory which started with the general Hamiltonian in the form (6.78) or (6.82). Implicitly (and in (6.99), (6.100) explicitly) we supposed that the starting single-particle basis (with the corresponding creation and annihilation operators $(a_i^+,\ a_i)$) is the basis of eigen-vectors of the nuclear Hartree-Fock mean field with the corresponding diagonal matrix $h_{kk'}$ - see (6.99). In this subsection we discuss even more general case when the starting basis is the arbitrary complete basis of single-particle states with corresponding creation and annihilation operators c_i^+ and c_i, respectively. Further we suppose that operators $(c_i,\ c_i^+)$ correspond to the arbitrary starting basis and operators $(a_i,\ a_i^+)$ are connected with the Hartree-Fock basis (sometimes called canonical basis). This general Hartree-Fock-Bogoliubov (HFB) approach combines the Hartree-Fock and BCS approaches. In the interpretation of the HFB method we follow the way given in [9].

So our starting nucleus Hamiltonian expressed in terms of the creation and annihilation operators c_i^+ and c_i of the arbitrary single-particle basis (analog of (6.77) but now expressed in the arbitrary starting basis)

$$\begin{aligned}\hat{H} &= \sum_{ij} \langle i|\ \hat{t}\ |j\rangle\ c_i^+ c_j + \frac{1}{2}\ \sum_{\substack{ij\\mn}} \langle ij|\ \hat{V}\ |mn\rangle\ c_i^+ c_j^+ c_n c_m = \\ &= \sum_{ij} t_{ij}\ c_i^+ c_j + \frac{1}{4}\ \sum_{\substack{ij\\mn}} V_{ijmn}\ c_i^+ c_j^+ c_n c_m \end{aligned} \tag{6.101}$$

and we suppose that the configuration space of the single-particle states i involves M states $(i = 1, \ldots,\ M)$.

Further we introduce quasiparticle system of operators $(\beta_i,\ \beta_i^+)$ by means of the generalized Bogoliubov transformation (generalization of (6.36))

$$\begin{aligned}\beta_i &= \sum_{k=1}^{M} \left(u_{ki}^*\ c_k + v_{ki}^*\ c_k^+\right) = \sum_{k=1}^{M} \left(u_{ik}^+\ c_k + v_{ik}^+\ c_k^+\right) \\ \beta_i^+ &= \sum_{k=1}^{M} \left(u_{ki}\ c_k^+ + v_{ki}\ c_k\right) = \sum_{k=1}^{M} \left(u_{ik}^T\ c_k + v_{ik}^T\ c_k^+\right) \end{aligned} \tag{6.102}$$

This unitary transformation is a transformation from the system of single-particle operators $(c_1, \ldots,\ c_M;\ c_1^+, \ldots,\ c_k^+)$ to the system of quasiparticle op-

erators $(\beta_1, \ldots, \beta_M; \beta_1^+, \ldots, \beta_k^+)$. It can be written in the matrix form:

$$\begin{pmatrix} \beta \\ \beta^+ \end{pmatrix} = \begin{pmatrix} \mathscr{U}^+ & \mathscr{V}^+ \\ \mathscr{V}^T & \mathscr{U}^T \end{pmatrix} \begin{pmatrix} c \\ c^+ \end{pmatrix} \equiv \mathscr{W}^+ \begin{pmatrix} c \\ c^+ \end{pmatrix} \tag{6.103}$$

where the new matrix $\mathscr{U} \equiv \{u_{ik}\}$ and $\mathscr{V} \equiv \{v_{ik}\}$ (each with the dimension $(M \times M)$ were introduced together with $(2M \times 2M)$ supermatrix

$$\mathscr{W} \equiv \begin{pmatrix} \mathscr{U} & \mathscr{V}^* \\ \mathscr{V} & \mathscr{U}^* \end{pmatrix} \qquad \Leftrightarrow \qquad \mathscr{W}^+ \equiv \begin{pmatrix} \mathscr{U}^+ & \mathscr{V}^+ \\ \mathscr{V}^T & \mathscr{U}^T \end{pmatrix} \tag{6.104}$$

Similarly as in the BCS case we suppose that both the systems of operators, $(c_i,\, c_i^+)$ and $(\beta_i,\, \beta_i^+)$, fulfil the fermion anticommutator relations. This gives the following conditions for matrixes $\mathscr{U}$ and $\mathscr{V}$:

$$\begin{aligned} \mathscr{U}^+\,\mathscr{U} + \mathscr{V}^+\,\mathscr{V} &= 1 \qquad & \mathscr{U}\,\mathscr{U}^+ + \mathscr{V}^*\,\mathscr{V}^T &= 1 \\ \mathscr{U}^T\,\mathscr{V} + \mathscr{V}^T\,\mathscr{U} &= 0 \qquad & \mathscr{U}\,\mathscr{V}^+ + \mathscr{V}^*\,\mathscr{U}^T &= 0 \end{aligned} \tag{6.105}$$

or

$$\mathscr{W}^+\,\mathscr{W} = \mathscr{W}\,\mathscr{W}^+ = 1 \tag{6.106}$$

which means that the Bogoliubov transormation (6.103) is unitary and it can be easily inverted

$$\begin{pmatrix} c \\ c^+ \end{pmatrix} = \mathscr{W} \begin{pmatrix} \beta \\ \beta^+ \end{pmatrix} = \begin{pmatrix} \mathscr{U} & \mathscr{V}^* \\ \mathscr{V} & \mathscr{U}^* \end{pmatrix} \begin{pmatrix} \beta \\ \beta^+ \end{pmatrix} \tag{6.107}$$

or

$$\begin{aligned} c_l &= \sum_{i=1}^{M} \Big(u_{li}\,\beta_i + v_{li}^*\,\beta_i^+ \Big) \\ c_l^+ &= \sum_{i=1}^{M} \Big(u_{li}^*\,\beta_i^+ + v_{li}\,\beta_i \Big) \end{aligned} \tag{6.108}$$

The vacuum state $|HFB\rangle$ for the system of quasiparticle operators ($\beta_i|HFB\rangle = 0$) is the ground state in the model of independent quasipaticles and similarly as the state $|BCS\rangle$ in the BCS approach the vacuum $|HFB\rangle$ does not preserve the number of particles (nucleons).

The basic blocks of the HFB theory are the density matrixes ($(M \times M)$ matrices)

$$\rho_{ij} \equiv \langle HFB|\, c_j^+\, c_i\, |HFB\rangle \qquad \kappa_{ij} \equiv \langle HFB|\, c_j\, c_i\, |HFB\rangle \tag{6.109}$$

Using (6.108) these densities can be expressed in terms of matrixes $\mathscr{U}$ and $\mathscr{V}$:

$$\rho_{ij} = \sum_{kk'} \langle HFB| \left(u^*_{jk}\, \beta^+_k + v_{jk}\, \beta_k\right) \left(u_{ik'}\, \beta_{k'} + v^*_{ik'}\, \beta^+_{k'}\right) |HFB\rangle =$$

$$= \boxed{\begin{array}{c}\text{because}\\ \beta_k\, |HFB\rangle = 0\end{array}} = \sum_{kk'} v_{jk} v^*_{ik'}\, \langle HFB|\, \beta_k \beta^+_{k'}\, |HFB\rangle =$$

$$= \sum_k v_{jk} v^*_{ik} = \sum_k v^*_{ik} v^T_{kj} = \left(\mathscr{V}^* \mathscr{V}^T\right)_{ij} \tag{6.110}$$

$$\kappa_{ij} = \sum_{kk'} \langle HFB| \left(u_{jk}\, \beta_k + v^*_{jk}\, \beta^+_k\right) \left(u_{ik'}\, \beta_{k'} + v^*_{ik'}\, \beta^+_{k'}\right) |HFB\rangle =$$

$$= \sum_{kk'} u_{jk} v^*_{ik'}\, \langle HFB|\, \beta_k \beta^+_{k'}\, |HFB\rangle = \sum_k u_{jk} v^*_{ik} =$$

$$= \sum_k v^*_{ik} u^T_{kj} \tag{6.111}$$

The density ρ_{ij} is Hermitian

$$\rho^+_{ij} = \rho^*_{ji} = \boxed{\begin{array}{c}\text{see}\\ (6.110)\end{array}} = \left(\mathscr{V}^* \mathscr{V}^T\right)^*_{ji} = \sum_k v_{jk} v^{T\,*}_{ki} = \sum_k v^*_{ik} v^T_{kj} =$$

$$= \left(\mathscr{V}^* \mathscr{V}^T\right)_{ij} = \rho_{ij} \tag{6.112}$$

$$\kappa^T_{ij} = \kappa_{ji} = \left(\mathscr{V}^* \mathscr{U}^T\right)^*_{ji} = \boxed{\begin{array}{c}\text{see}\\ (6.105)\end{array}} = -\left(\mathscr{U} \mathscr{V}^+\right)_{ji} =$$

$$= -\sum_k u_{jk}\, v^+_{ki} = -\sum_k u^T_{kj}\, v^*_{ik} = -\left(\mathscr{V}^*\, \mathscr{U}^T\right)_{ij} = -\kappa_{ij} \tag{6.113}$$

Using the inverse Bogoliubov transformation (6.108) the Hamiltonian $\hat{H}$ (see (6.101)) can be expressed in terms of the generalized quasiparticle operators (the substitution of (6.108) into (6.101)):

$$\hat{H} = H^0 + \sum_{k_1 k_2} H^{1\,1}_{k_1 k_2}\, \beta^+_{k_1} \beta_{k_2} + \frac{1}{2} \sum_{k_1 < k_2} \left(H^{2\,0}_{k_1 k_2}\, \beta^+_{k_1} \beta^+_{k_2} + h.c.\right) +$$

$$
\begin{aligned}
&+ \sum_{k_1k_2k_3k_4} \Big(H^{4\,0}_{k_1k_2k_3k_4}\, \beta^+_{k_1}\beta^+_{k_2}\beta^+_{k_3}\beta^+_{k_4} + h.c. \Big) + \\
&+ \sum_{k_1k_2k_3k_4} \Big(H^{3\,1}_{k_1k_2k_3k_4}\, \beta^+_{k_1}\beta^+_{k_2}\beta^+_{k_3}\beta_{k_4} + h.c. \Big) + \\
&+ \frac{1}{4} \sum_{k_1k_2k_3k_4} H^{2\,2}_{k_1k_2k_3k_4}\, \beta^+_{k_1}\beta^+_{k_2}\beta_{k_3}\beta_{k_4}
\end{aligned} \tag{6.114}
$$

With the following definition

$$
\begin{aligned}
h_{lm} &= t_{lm} + \Gamma_{lm}\,, \qquad\qquad \Gamma_{lm} = \sum_{pq} V_{lqmp}\,\rho_{pq} \\
\Delta_{lm} &= \frac{1}{2}\sum_{pq} V_{lmpq}\,\kappa_{pq}
\end{aligned} \tag{6.115}
$$

the expressions for H^0 and matrixes $H^{1\,1}$, $H^{2\,0}$, $H^{4\,0}$, $H^{3\,1}$ and $H^{2\,2}$ are following

$$
\begin{aligned}
H^{\,0} &= \sum_k \Big(t\rho + \frac{1}{2}\Gamma\rho + \frac{1}{2}\Delta\kappa^* \Big)_{kk} \\
H^{1\,1} &= \mathscr{U}^+ h\,\mathscr{U} - \mathscr{V}^+ h^T\,\mathscr{V} + \mathscr{U}^+\Delta\,\mathscr{V} - \mathscr{V}^+\Delta^*\,\mathscr{U} \\
H^{2\,0} &= \mathscr{U}^+ h\,\mathscr{V}^* - \mathscr{V}^+ h^T\,\mathscr{U}^* + \mathscr{U}^+\Delta\,\mathscr{U}^* - \mathscr{V}^+\Delta^*\,\mathscr{V}^*
\end{aligned} \tag{6.116}
$$

$$
H^{4\,0}_{k_1k_2k_3k_4} = \frac{1}{4}\sum_{l_1l_2l_3l_4} V_{l_1l_2l_3l_4}\, u^*_{l_1k_1}\, u^*_{l_2k_2}\, v^*_{l_4k_3}\, v^*_{l_3k_4} \tag{6.117}
$$

$$
\begin{aligned}
H^{3\,1}_{k_1k_2k_3k_4} = \frac{1}{2}\sum_{l_1l_2l_3l_4} V_{l_1l_2l_3l_4} \Big(& u^*_{l_1k_1}\, u^*_{l_4k_2}\, v^*_{l_3k_3}\, v_{l_2k_4} + \\
& + v^*_{l_3k_1}\, u^*_{l_2k_2}\, u^*_{l_1k_3}\, u_{l_4k_4} \Big)
\end{aligned} \tag{6.118}
$$

$$
\begin{aligned}
&H^{2\,2}_{k_1k_2k_3k_4} = \\
&= \sum_{l_1l_2l_3l_4} V_{l_1l_2l_3l_4} \Big[\Big(u^*_{l_1k_1} v^*_{l_4k_2} v_{l_2k_3} u_{l_3k_4} - (k_1 \leftrightarrow k_2) \Big) - (k_3 \leftrightarrow k_4) + \\
&\qquad u^*_{l_1k_1} u^*_{l_2k_2} u_{l_3k_3} u_{l_4k_4} + v^*_{l_3k_1} v^*_{l_4k_2} v_{l_1k_3} v_{l_2k_4} \Big]
\end{aligned} \tag{6.119}
$$

The last three terms in (6.114) are usually involved in so called residual interaction term $\hat{H}_{int}$. So, the exp. (6.114) is written as

$$
\hat{H} = H^{\,0} + \sum_{k_1k_2} H^{1\,1}_{k_1k_2}\, \beta^+_{k_1}\beta_{k_2} + \sum_{k_1k_2} \Big(H^{2\,0}_{k_1k_2}\, \beta^+_{k_1}\beta^+_{k_2} + h.c. \Big) + \hat{H}_{int} \tag{6.120}
$$

Similarly as in the case of the BCS approach (see previous subsection) the quasiparticle vacuum $|HFB\rangle$ is searched for by the variational principle (minimum of the total energy $\langle HFB|\,\hat{H}\,|HFB\rangle$). As in the BCS model the state $|HFB\rangle$ violates the symmetry connected with the particle number. Again we have to use in the variation of the expectation value $\langle HFB|\,\hat{H}\,|HFB\rangle$ a constraint on the particle number N and to vary the Hamiltonian $\hat{H}^{'} = \hat{H}_P = \hat{H} - \lambda\,\hat{n}$ where the particle number operator is (see (6.35))

$$\hat{n} = \sum_{l_1 l_2} n_{l_1 l_2}\, c^{+}_{l_1} c_{l_2}\,, \qquad\qquad n_{l_1 l_2} = \delta_{l_1 l_2} \tag{6.121}$$

expressed in terms of the quasiparticle operators is (the substitution of (6.108) into (6.121))

$$\hat{n} = N^{\,0} + \sum_{k_1 k_2} N^{1\,1}_{k_1 k_2}\,\beta^{+}_{k_1}\beta_{k_2} + \frac{1}{2}\sum_{k_1 k_2}\Big(N^{2\,0}_{k_1 k_2}\,\beta^{+}_{k_1}\beta^{+}_{k_2} + h.c.\Big) \tag{6.122}$$

with

$$\begin{aligned} N^{\,0} &= \sum_{k}(n\rho)_{kk} = \sum_{k}\rho_{kk}\,, \quad N^{1\,1}_{k_1 k_2} = \Big(\mathscr{U}^{+}\,n\,\mathscr{U} - \mathscr{V}^{+}\,n\,\mathscr{V}\Big)_{k_1 k_2} \\ N^{2\,0}_{k_1 k_2} &= \Big(\mathscr{U}^{+}\,n\,\mathscr{V}^{*} - \mathscr{V}^{+}\,n\,\mathscr{U}^{*}\Big)_{k_1 k_2} \end{aligned} \tag{6.123}$$

Starting from the variation principle

$$\delta\langle\Phi|\,\hat{H}^{'}\,|\Phi\rangle = 0 \tag{6.124}$$

we have to investigate small variation of the trial function $|\Phi\rangle$ in the vicinity of the HFB function $|HFB\rangle$. Since we consider only wave function $|\Phi\rangle$ of the HFB type the connection between $|\Phi\rangle$ and the equilibrium solution $|HFB\rangle$ of the equation (6.124) is given by the Thouless theorem (B.38) (see the Subsecrion B.5 in the Appendix B)

$$\begin{aligned} |\Phi\rangle = e^{\sum_{k<k'} Z_{kk'}\,\beta^{+}_{k}\beta^{+}_{k'}}\,|HFB\rangle \approx \boxed{\begin{array}{c}\text{up to the second}\\ \text{order in } Z\end{array}} \approx \\ \approx \Big(1 + \sum_{k<k'} Z_{kk'}\,\beta^{+}_{k}\beta^{+}_{k'} + \frac{1}{2}\sum_{\substack{k<k'\\ l<l'}} Z_{kk'}\,Z_{kk'}\,\beta^{+}_{k}\beta^{+}_{k'}\beta^{+}_{l}\beta^{+}_{l'}\Big)\,|HFB\rangle \end{aligned} \tag{6.125}$$

So the variation (6.124) can be written as follows

$$\begin{aligned}
&\langle \Phi \mid \hat{H}^{'} \mid \Phi \rangle = \\
&= \langle HFB| \Big\{ 1 + \sum_{k_f < k_f^{'}} Z^{*}_{k_f k_f^{'}} \, \beta_{k_f^{'}} \beta_{k_f} + \\
&\qquad + \frac{1}{2} \sum_{\substack{m_f < m_f^{'} \\ l_f < l_f^{'}}} Z^{*}_{m_f m_f^{'}} \, Z^{*}_{l_f l_f^{'}} \, \beta_{l_f^{'}} \beta_{l_f} \beta_{m_f^{'}} \beta_{m_f} \Big\} \mid \hat{H}^{'} \mid \\
&\quad \Big\{ 1 + \sum_{k_i < k_i^{'}} Z^{*}_{k_i k_i^{'}} \, \beta^{+}_{k_i} \beta^{+}_{k_i^{'}} + \\
&\qquad + \frac{1}{2} \sum_{\substack{m_i < m_i^{'} \\ l_i < l_i^{'}}} Z_{m_i m_i^{'}} \, Z_{l_i l_i^{'}} \, \beta^{+}_{m_i} \beta^{+}_{m_i^{'}} \beta^{+}_{l_i} \beta^{+}_{l_i^{'}} \Big\} \mid HFB \rangle = \\
&= \boxed{\begin{array}{c} \text{up to the second} \\ \text{order in } Z \end{array}} = \\
&= \langle HFB| \, \hat{H}^{'} \, |HFB\rangle + \sum_{k_f < k_f^{'}} Z^{*}_{k_f k_f^{'}} \, \langle HFB| \, \beta_{k^{'}} \beta_{k_f} \, \hat{H}^{'} \, |HFB\rangle + \\
&+ \sum_{k_i < k_i^{'}} Z_{k_i k_i^{'}} \, \langle HFB| \, \hat{H}^{'} \, \beta^{+}_{k_i} \beta^{+}_{k_i^{'}} \, |HFB\rangle + \\
&+ \frac{1}{2} \sum_{\substack{m_f < m_f^{'} \\ l_f < l_f^{'}}} Z^{*}_{m_f m_f^{'}} \, Z^{*}_{l_f l_f^{'}} \, \langle HFB| \, \beta_{l_f^{'}} \beta_{l_f} \beta_{m_f^{'}} \beta_{m_f} \, \hat{H}^{'} \, |HFB\rangle + \\
&+ \frac{1}{2} \sum_{\substack{m_i < m_i^{'} \\ l_i < l_i^{'}}} Z_{m_i m_i^{'}} \, Z_{l_i l_i^{'}} \, \langle HFB| \, \hat{H}^{'} \, \beta^{+}_{m_i} \beta^{+}_{m_i^{'}} \beta^{+}_{l_i} \beta^{+}_{l_i^{'}} \, |HFB\rangle + \\
&+ \sum_{\substack{m_i < m_i^{'} \\ l_i < l_i^{'}}} Z^{*}_{k_f k_f^{'}} \, Z_{k_i l_k^{'}} \, \langle HFB| \, \beta_{k_f^{'}} \beta_{k_f} \, \hat{H}^{'} \, \beta^{+}_{k_i} \beta^{+}_{k_i^{'}} \, |HFB\rangle
\end{aligned} \tag{6.126}$$

It is evident that

$$
\begin{aligned}
H^{'0} &= \langle HFB|\, \hat{H}^{'} \,|HFB\rangle = h^0 - \lambda\, N^0 \\
H^{'11}_{kk'} &= \left(H^{11} - \lambda\, N^{11}\right)_{kk'} = \boxed{\begin{array}{c}\text{see}\\ (6.120)\end{array}} = \\
&= \langle HFB|\, \beta_k\, \hat{H}^{'}\, \beta^{+}_{k'} \,|HFB\rangle \\
H^{'20}_{kk'} &= \left(H^{20} - \lambda\, N^{20}\right)_{kk'} = \boxed{\begin{array}{c}\text{see}\\ (6.120) \text{ and } H^{'20}_{kk'} = -H^{'20}_{k'k}\end{array}} = \\
&= \langle HFB|\beta_{k'}\beta_k\, \hat{H}^{'} \,|HFB\rangle = \langle HFB|\, \hat{H}^{'}\, \beta^{+}_{k}\beta^{+}_{k'} \,|HFB\rangle^*
\end{aligned}
\tag{6.127}
$$

Further we introduce new notation

$$
\begin{aligned}
A_{kk'll'} &= \langle HFB|\, \Big[\beta_{k'}\beta_k\,,\, [\hat{H}^{'},\, \beta^{+}_{l}\beta^{+}_{l'}]\Big] \,|HFB\rangle = \\
&= \langle HFB|\, \beta_{k'}\beta_k\,,\, [\hat{H}^{'},\, \beta^{+}_{l}\beta^{+}_{l'}] \,|HFB\rangle = \\
&= \langle HFB|\, \beta_{k'}\beta_k\, \hat{H}^{'}\, \beta^{+}_{l}\beta^{+}_{l'} - \beta_{k'}\beta_k\, \beta^{+}_{l}\beta^{+}_{l'}\, \hat{H}^{'} \,|HFB\rangle = \\
&= \langle HFB|\, \beta_{k'}\beta_k\, \hat{H}^{'}\, \beta^{+}_{l}\beta^{+}_{l'} \,|HFB\rangle \\
&\qquad\qquad - (\delta_{kl}\delta_{k'l'} - \delta_{kl'}\delta_{k'l})\, \langle HFB|\, \hat{H}^{'} \,|HFB\rangle = \\
&= \boxed{\begin{array}{c}\text{we can choose the energy scale}\\ \text{so that } \langle HFB|\, \hat{H}^{'} \,|HFB\rangle = 0\end{array}} = \\
&= \langle HFB|\, \beta_{k'}\beta_k\, \hat{H}^{'}\, \beta^{+}_{l}\beta^{+}_{l'} \,|HFB\rangle
\end{aligned}
\tag{6.128}
$$

and

$$
\begin{aligned}
B_{kk'll'} &= -\langle HFB|\, \Big[\beta_{k'}\beta_k\,,\, [\hat{H}^{'},\, \beta_{l'}\beta_l]\Big] \,|HFB\rangle = \\
&= -\langle HFB|\, \beta_{k'}\beta_k\,,\, [\hat{H}^{'},\, \beta_{l'}\beta_l] \,|HFB\rangle = \\
&= \langle HFB|\, -\beta_{k'}\beta_k\, \hat{H}^{'}\, \beta_{l'}\beta_l + \beta_{k'}\beta_k\, \beta_{l'}\beta_l\, \hat{H}^{'} \,|HFB\rangle = \\
&= \boxed{\begin{array}{c}\text{because}\\ \beta_l\,|HFB\rangle\end{array}} = \\
&= \langle HFB|\, \beta_{k'}\beta_k\, \beta_{l'}\beta_l\, \hat{H}^{'} \,|HFB\rangle
\end{aligned}
\tag{6.129}
$$

So the expectation value $\langle\Phi|\, \hat{H}^{'}|\, \Phi\rangle$ (see (6.126) - (6.129)) can be rewritten

as

$$\langle\Phi|\,\hat{H}^{'}\,|\,\Phi\rangle = H^{'0} + \left(H^{'20\,*}\;\; H^{'20}\right)\begin{pmatrix} Z \\ Z^{*}\end{pmatrix} + \\ +\frac{1}{2}\left(Z^{*}\;Z\right)\begin{pmatrix} A & B \\ B^{*} & A^{*}\end{pmatrix}\begin{pmatrix} Z \\ Z^{*}\end{pmatrix} \tag{6.130}$$

Equation (6.130) gives a quadratic approximation of the multidimensional energy surface $\langle\Phi|\,\hat{H}^{'}\,|\Phi\rangle$ as a function of the variables $Z_{kk'}$. In the BCS case (see previous section) this energy surface $\langle BCS|\,\hat{H}^{'}\,|BCS\rangle$ was investigated as a function of variables $\mathscr{U}_i$ and $\mathscr{V}_i$ which satisfied the normalization condition (6.29). Now we have total energy $\langle\Phi|\,\hat{H}^{'}\,|\Phi\rangle$ as a function of variables $Z_{kk'}$ $(k < k^{'})$ and these variables are independent without any additional condition. From(6.125) we know also that the solution $|HFB\rangle$ of variational principle (6.124) corresponds ro $Z_{kk'} = 0$. The variation of (6.130) with respect to $Z_{kk'}$ and $Z^{*}_{kk'}$ gives at the stationary point $Z_{kk'} = 0$ following conditions

$$\begin{aligned} \frac{\partial}{\partial Z^{*}_{kk'}}\langle\Phi|\,\hat{H}^{'}\,|\Phi\rangle\Big|_{Z=0} &= \boxed{\begin{matrix}\text{see}\\(6.129)\end{matrix}} = H^{'20}_{kk'} = 0 \\ \frac{\partial}{\partial Z_{kk'}}\langle\Phi|\,\hat{H}^{'}\,|\Phi\rangle\Big|_{Z=0} &= H^{'20\,*}_{kk'} = 0 \end{aligned} \tag{6.131}$$

This means that the linear terms (in Z) in the eq. (6.130) vanish at the stationary point $Z = 0$. The matrix

$$\mathcal{D} \equiv \begin{pmatrix} A & B \\ B^{*} & A^{*}\end{pmatrix} \tag{6.132}$$

is called the stability matrix (or curvature tensor). If the stationary point $Z = 0$ corresponds to the minimum of (6.132) in the space of variables $Z_{kk'}$ then this stability matrix should be positively definite.

In order to see the physical meaning of eqs. (6.130), (6.131) and the connection of these equations to the BCS approach discussed in the previous subsection it is necessary to go back to the transformation (6.107) from the system of particle operators (c, c^{+}) to the quasiparticle operators (β, β^{+}). This unitary transformation is mediated by the matrix $\mathscr{W}$. There is a famous theorem of Bloch and Messiah [100] which states that a unitary matrix $\mathscr{W}$ of the form of (6.104) can always be decomposed into three matrices of very

special form

$$\mathscr{W} = \begin{pmatrix} D & 0 \\ 0 & D^* \end{pmatrix} \begin{pmatrix} \bar{\mathscr{U}} & \bar{\mathscr{V}} \\ \bar{\mathscr{V}}^* & \bar{\mathscr{U}}^* \end{pmatrix} \begin{pmatrix} C & 0 \\ 0 & C^* \end{pmatrix} = \\ = \begin{pmatrix} D\bar{\mathscr{U}}C & D\bar{\mathscr{V}}C^* \\ D^*\bar{\mathscr{V}}C & D^*\bar{\mathscr{U}}C^* \end{pmatrix}$$

$$\Leftrightarrow \boxed{\begin{matrix}\text{see} \\ (6.104)\end{matrix}} \qquad \mathscr{U} = D\bar{\mathscr{U}}C \qquad\qquad \mathscr{V} = D^*\bar{\mathscr{V}}C \tag{6.133}$$

where D and C are unitary $(M \times M)$ matrixes and $\bar{\mathscr{U}}$, $\bar{\mathscr{V}}$ are real $(M \times M)$ matrixes of the following form

$$\bar{\mathscr{U}} = \begin{pmatrix} 0 & & & & & & & & & & \\ & \ddots & & & & & & & & & \\ & & 0 & & & & & & & & \\ & & & U_1 & 0 & & & & & 0 & \\ & & & 0 & U_1 & & & & & & \\ & & & & & \ddots & & & & & \\ & & & & & & U_n & 0 & & & \\ & 0 & & & & & 0 & U_n & & & \\ & & & & & & & & 1 & & \\ & & & & & & & & & \ddots & \\ & & & & & & & & & & 1 \end{pmatrix}$$

$$\bar{\mathscr{V}} = \begin{pmatrix} 1 & & & & & & & & & & \\ & \ddots & & & & & & & & & \\ & & 1 & & & & & & & & \\ & & & 0 & V_1 & & & & & 0 & \\ & & & -V_1 & 0 & & & & & & \\ & & & & & \ddots & & & & & \\ & & & & & & 0 & V_n & & & \\ & 0 & & & & & -V_n & 0 & & & \\ & & & & & & & & 0 & & \\ & & & & & & & & & \ddots & \\ & & & & & & & & & & 0 \end{pmatrix}$$

(6.134)

The proof of this theorem can be found in the Appendix E of the book

[9]. The meaning of the Bloch-Messiah theorem is that the transformation (6.107), $(c,\ c^+) \to (\beta,\ \beta^+)$, can be decomposed into three steps:

$$\left.\begin{array}{ccc} c & \to & a \\ c^+ & \to & a^+ \end{array}\right\} \quad \to \quad \left\{\begin{array}{ccc} \alpha & \to & \beta \\ \alpha^+ & \to & \beta^+ \end{array}\right. \\ C \qquad\qquad \bar{\mathscr{U}},\ \bar{\mathscr{V}} \qquad\qquad D \tag{6.135}$$

1. an unitary transformation of operators c^+ among themselves

$$a_k^+ = \sum_l C_{lk}\, c_l^+ \qquad\qquad a_k = \sum_l C_{lk}^*\, c_l \tag{6.136}$$

This corresponds to the Hartree-Fock case when the selfconsistent HF equation system (4.25) is solved. In the case of HF we can also search for the single-particle wave functions $\varphi_k(\vec{r}s\tau) = \langle \vec{r}s\tau|k\rangle = \langle \vec{r}s\tau|a_k^+|HFB\rangle$ in the form of the decomposition into the orthonormal set of basis functions $\langle \vec{r}s\tau|\ l\rangle = \langle \vec{r}s\tau|c_l^+|HFB\rangle$ (e.g. products of the 3-dimensional oscillator eigen function and spin and isospin s.p. wave functions) where a_i^+ and c_l^+ are related by (6.136).

2. a special Bogoliubov transformation which distinguishes between "paired" levels ($U_p > 0$, $V_p > 0$)

$$\begin{aligned} \alpha_p^+ &= U_p\, a_p^+ - V_p\, a_{\bar{p}} \\ \alpha_{\bar{p}}^+ &= U_p\, a_{\bar{p}}^+ + V_p\, a_p \end{aligned} \tag{6.137}$$

where $(p,\ \bar{p})$ are defined by the (2×2) boxes in the equation (6.134) and blocked (nonpaired) levels, which are either occupied ($V_i = 1$, $U_i = 0$) or empty ($V_i = 0$, $U_i = 1$):

$$\begin{aligned} \alpha_i^+ &= a_i \qquad \alpha_i = a_i^+ \qquad \text{for } (U_i = 1,\ V_i = 0) \\ \alpha_m^+ &= a_m^+ \qquad \alpha_m = a_m \qquad \text{for } (U_m = 0,\ V_m = 1) \end{aligned} \tag{6.138}$$

It is obvious that (6.137) corresponds to the nontrivial solution of the BCS equation (see (6.30) with (6.52) while (6.138) corresponds to the trivial solution of the BCS equation (see (6.50), (6.51)).

3. an unitary transformation of the quasiparticle operators α_k^+ among themselves

$$\beta_k^+ = \sum_{k'} D_{k'\,k}\, \alpha_{k'}^+ \tag{6.139}$$

We can summarize. The first part of the transformation (see (6.135) is equivalent to the solving of the HF equation and the second transformation (6.136) solves the BCS problem. It should be noted that the variation condition (6.131) giving equation $H^{'}_{k\,k'} = 0$ for all k, $k^{'}$ is not affected by the third transformation (6.139) because

$$H^{'\,2\,0}_{k\,k'} = \boxed{\begin{array}{c}\text{see}\\(6.127)\end{array}} = \langle HFB|\, \beta_{k'}\beta_k\, \hat{H}^{'}\, |HFB\rangle =$$

$$= \boxed{\begin{array}{c}\text{see}\\(6.139)\end{array}} = \sum_{l\,l'} D^{*}_{l'k'}\, D^{*}_{lk}\, \langle HFB|\, \alpha_{l'}\alpha_l\, |HFB\rangle = 0$$

$$\Rightarrow \quad H^{'\,2\,0}_{l\,l'}(\alpha) \equiv \langle HFB|\, \alpha_{l'}\alpha_l\, \hat{H}^{'}\, |HFB\rangle = 0 \quad \text{for all}\, l\, l^{'}$$

So, really, the condition $H^{'\,2\,0}_{k\,k'} = 0$ for all $(k\,k^{'})$ valids in the both representations (with α operators and β operators) and the variation (6.131) is not influenced by the transformation (6.139). The requirement $H^{'\,2\,0}_{k\,k'} = 0$ determines, therefore, only the first two of Bloch-Messiah transformations. The third transformation can be used for any additional requirement. This additional requirement usually is the diagonalization of the $H^{'\,1\,1}$ part in (6.120). Together with (6.131) this corresponds to the fact that the supermatrix

$$\mathscr{K} \equiv \begin{pmatrix} H^{'\,1\,1} & H^{'\,2\,0} \\ -H^{'\,2\,0\,*} & -H^{'\,1\,1\,*} \end{pmatrix} \tag{6.140}$$

is diagonal.

The elements of the supermatrix $\mathscr{K}$ can be expressed also in the following form:

$$\langle HFB|\, \left\{[\beta_k,\, \hat{H}^{'}],\, \beta^{+}_{k'}\right\} |HFB\rangle = \langle HFB|\, [\beta_k,\, \hat{H}^{'}]\, \beta^{+}_{k'}\, |HFB\rangle =$$
$$= \langle HFB|\beta_k\, \hat{H}^{'}\, \beta^{+}_{k'} - \hat{H}^{'}\, \beta_k\, \beta^{+}_{k'}\, |HFB\rangle =$$
$$= \langle HFB|\beta_k\, \hat{H}^{'}\, \beta^{+}_{k'}\, |HFB\rangle - \delta_{k\,k'}\, \langle HFB|\, \hat{H}^{'}\, |HFB\rangle =$$
$$= \boxed{\begin{array}{c}\text{see}\\(6.127)\end{array}} = H^{'\,1\,1}_{k\,k'} - \delta_{k\,k'}\, H^{'\,0} = \boxed{\begin{array}{c}\text{we choose energy}\\\text{scale: } H^{'\,0} = 0\end{array}} =$$
$$= H^{'\,1\,1}_{k\,k'} \tag{6.141}$$

$$\langle HFB|\, \left\{[\beta^{+}_k,\, \hat{H}^{'}],\, \beta^{+}_{k'}\right\} |HFB\rangle = \langle HFB|\, [\beta^{+}_k,\, \hat{H}^{'}]\, \beta^{+}_{k'}\, |HFB\rangle =$$

$$= -\langle HFB|\, \hat{H}^{'}\, \beta^{+}_k\, \beta^{+}_{k'}\, |HFB\rangle = \boxed{\begin{array}{c}\text{see}\\(6.127)\end{array}} = -H^{'\,*\,2\,0}_{k\,k'} \tag{6.142}$$

$$\langle HFB|\left\{[\beta_k,\,\hat{H}'],\,\beta_{k'}\right\}|HFB\rangle = \langle HFB|\,\beta_{k'}\,[\beta_k^+,\,\hat{H}']\,|HFB\rangle =$$

$$= \langle HFB|\,\beta_{k'}\beta_k\,\hat{H}'\,|HFB\rangle = \boxed{\begin{array}{c}\text{see}\\(6.127)\end{array}} = H'^{20}_{k\,k'} \tag{6.143}$$

$$\langle HFB|\left\{[\beta_k^+,\,\hat{H}'],\,\beta_{k'}\right\}|HFB\rangle = \langle HFB|\,\beta_{k'}\,[\beta_k^+,\,\hat{H}']\,|HFB\rangle =$$
$$= \langle HFB|\beta_{k'}\beta_k^+\,\hat{H}' - \beta_{k'}\hat{H}'\,\beta_k^+\,|HFB\rangle =$$
$$= \delta_{k\,k'}\,\langle HFB|\,\hat{H}'\,|HFB\rangle - \langle HFB|\beta_k\,\hat{H}'\,\beta_{k'}^+\,|HFB\rangle =$$
$$= \boxed{\begin{array}{c}\text{see}\\(6.127)\end{array}} = \delta_{k\,k'}\,H'^0 - H'^{11}_{k'k} =$$
$$= \boxed{\begin{array}{c}\text{we choose energy scale: } H'^0 = 0\\ \text{because matrix } H'^{11} \text{ is Hermitian}\end{array}} = -H'^{11*}_{k\,k'} \tag{6.144}$$

So the supermatrix $\mathscr{K}$ is given by (for the purpose of the short notation in (6.145) $|\,\rangle \equiv |HFB\rangle$)

$$\mathscr{K} = \begin{pmatrix} H'^{11} & H'^{20} \\ -H'^{20*} & -H'^{11*} \end{pmatrix} =$$
$$= \begin{pmatrix} \langle\,|\left\{[\beta_k,\,\hat{H}'],\,\beta_{k'}^+\right\}|\,\rangle & \langle\,|\left\{[\beta_k,\,\hat{H}'],\,\beta_{k'}\right\}|\,\rangle \\ \langle\,|\left\{[\beta_k^+,\,\hat{H}'],\,\beta_{k'}^+\right\}|\,\rangle & \langle\,|\left\{[\beta_k^+,\,\hat{H}'],\,\beta_{k'}\right\}|\,\rangle \end{pmatrix} \tag{6.145}$$

and this supermatrix is diagonal.

In (6.145) the quasiparticle operators $(\beta_k,\,\beta_k^+)$ are involved. Using (6.102) or (6.103) we can transform the supermatrix (6.145) so that it involves operators $(c_k,\,c_k^+)$:

$$\mathscr{K} = \begin{pmatrix} H'^{11} & H'^{20} \\ -H'^{20*} & -H'^{11*} \end{pmatrix} = \mathscr{W}^+ \begin{pmatrix} h & \Delta \\ -\Delta^* & -h^* \end{pmatrix} \mathscr{W} = E \tag{6.146}$$

where E is the diagonal matrix with elements E_k and (in the analogy with

(6.141) and (6.143))

$$h_{k\,k'} \equiv \langle HFB| \left\{ [c_k,\, \hat{H}'],\, c^+_{k'} \right\} |HFB\rangle = \boxed{\begin{array}{c}\text{in analogy with}\\ (6.88)\end{array}} =$$
$$= t_{k\,k'} - \lambda\, \delta_{k\,k'} + \sum_{l\,l'} V_{kl\,k'l'}\, \rho_{l\,l'}$$

$$\Delta_{k\,k'} \equiv \langle HFB| \left\{ [c_k,\, \hat{H}'],\, c_{k'} \right\} |HFB\rangle = \boxed{\begin{array}{c}\text{in analogy with}\\ (6.89)\end{array}} =$$
$$= \frac{1}{2} \sum_{l\,l'} V_{k\,k'l\,l'}\, \kappa_{l\,l'} \tag{6.147}$$

with $\rho_{l\,l'}$ and $\kappa_{l\,l'}$ defined in (6.110) and (6.111), respectively.

Equation (6.146) can be also rewritten in the following form (using unitarity, $\mathscr{W}\,\mathscr{W}^+ = 1$):

$$\begin{pmatrix} h & \Delta \\ -\Delta^* & -h^* \end{pmatrix} \mathscr{W} = E\,\mathscr{W}$$
$$\Rightarrow \begin{pmatrix} h & \Delta \\ -\Delta^* & -h^* \end{pmatrix} \begin{pmatrix} \mathscr{U} & \mathscr{V}^* \\ \mathscr{V} & \mathscr{U}^* \end{pmatrix} = E \begin{pmatrix} \mathscr{U} & \mathscr{V}^* \\ \mathscr{V} & \mathscr{U}^* \end{pmatrix}$$

or

$$\mathscr{H} \begin{pmatrix} U^{(i)} \\ V^{(i)} \end{pmatrix} \equiv \begin{pmatrix} h & \Delta \\ -\Delta^* & -h^* \end{pmatrix} \begin{pmatrix} U^{(i)} \\ V^{(i)} \end{pmatrix} = E_i \begin{pmatrix} U^{(i)} \\ V^{(i)} \end{pmatrix} \tag{6.148}$$

where $U^{(i)}$ and $V^{(i)}$ are one column matrixes defined as (see (6.102), (6.103))

$$U^{(i)} \equiv \begin{pmatrix} u_{1i} \\ u_{2i} \\ \vdots \\ u_{Mi} \end{pmatrix} \qquad V^{(i)} \equiv \begin{pmatrix} v_{1i} \\ v_{2i} \\ \vdots \\ v_{Mi} \end{pmatrix} \tag{6.149}$$

which determine the quasiparticle creation operator $\beta^+_i = \sum_k (u_{ki}\, c^+_k + v_{ki}\, c_k)$ (see (6.102)).

Similarly as the Hartree-Fock equation (see (4.25) and (4.26)) the HFB equation (6.148) is also selfconsistent. That means the $2M$- dimensional matrix $\mathscr{H}$ depends on resultant matrix $\mathscr{U}$ and $\mathscr{V}$. Such equation should be solved iteratively: we start with some basis corresponding to (c_k, c^+_k) in which we have matrix $V_{k\,k'l\,l'}$ of used effective nucleon-nucleon interaction. Within this basis we determine $\rho^{[1]}_{k\,k'}$ and $\kappa^{[1]}_{k\,k'}$ (using (6.110), (6.111)), then $h^{[1]}_{k\,k'}$ and $\Delta^{[1]}_{k\,k'}$ (using (6.147)) and we have matrix $\mathscr{H}^{[1]}$ which can be diagonalized.

After that we obtain the first iteration matrixes $U^{(i)}_{[1]}$ and $V^{(i)}_{[1]}$ and we can go on with the second iteration: determination of $\rho^{[2]}_{k\,k'}$ and $\kappa^{[2]}_{k\,k'}$, then $h^{[2]}_{k\,k'}$ and $\Delta^{[2]}_{k\,k'}$, then matrix $\mathscr{H}^{[2]}$. After the diagonalization of $\mathscr{H}^{[2]}$ we obtain matrixes $U^{(i)}_{[2]}$ and $V^{(i)}_{[2]}$ and the third iteration can be started. The iteration process is stopped when the changes of the eigen values $E_i^{[n-1]}$ of $(n-1)$-th iteration and $E_i^{[n]}$ of n-th iteration are smaller than given small number.

One should realize that the matrix $\mathscr{H}$ in the HFB equation (6.148) is $2M$- dimensional and we have $2M$ eigenvalues and eigenvectors. In order to construct a set of quasiparticle operators $(\beta_1^+, \ldots, \beta_M^+)$, and for the calculation of matrix $\rho_{k\,k'}$ and $\kappa_{k\,k'}$ $(k,\ k^{'} = 1, \ldots,\ M)$ we have to choose only M of them (physical solutions). The extraction of this physical solutions is simple. As is easily recognized and we demonstrate it below, to each eigenvector $(U^{(i)},\ V^{(i)})$ with the eigenvalue E_i there exists one eigenvector $(V^{(i)\,*},\ U^{(i)\,*})$ with the eigenvalue $-E_i$. This is shown below.

From (6.148) we have

$$\begin{array}{c} h\,U^{(i)} + \Delta\,V^{(i)} = E_i\,U^{(i)} \\ -\Delta^*\,U^{(i)} - h^*\,V^{(i)} = E_i\,V^{(i)} \end{array} \Rightarrow \begin{array}{c} \Delta^*\,U^{(i)} + h^*\,V^{(i)\,*} = -E_i\,V^{(i)\,*} \\ -h\,U^{(i)} - \Delta\,V^{(i)\}} = -E_i\,U^{(i)} \end{array}$$

$$\Rightarrow \begin{array}{c} \Delta\,U^{(i)\,*} + h\,V^{(i)\,*} = -E_i\,V^{(i)\,*} \\ -h^*\,U^{(i)\,*} - \Delta^*\,V^{(i)\,*} = -E_i\,U^{(i)\,*} \end{array}$$

$$\Rightarrow \begin{array}{c} h\,V^{(i)\,*} + \Delta\,U^{(i)\,*} = -E_i\,V^{(i)\,*} \\ \Delta^*\,V^{(i)\,*} - -h^*\,U^{(i)\,*} = -E_i\,U^{(i)\,*} \end{array}$$

$$\Rightarrow \quad \begin{pmatrix} h & \Delta \\ -\Delta^* & -h^* \end{pmatrix} \begin{pmatrix} V^{(i)\,*} \\ U^{(i)\,*} \end{pmatrix} = -E_i \begin{pmatrix} V^{(i)\,*} \\ U^{(i)\,*} \end{pmatrix}$$

So in the case of the even number of particles in the system (nucleus), when even number of particles occupy the s.p. levels up to the Fermi level in the system ground state, all solutions of (6.148) with the positive energies $E_i > 0$ can be interpreted as single-quasiparticle states $(U^{(i)},\ V^{(i)})$ with the single-quasiparticle energies $E_i > 0$.

After the solving of the equation (6.148) and after the obtaining the quasiparticle system $(U^{(i)},\ V^{(i)})$ with corresponding energies $E_i > 0$ the nucleus Hamiltonian (6.120) can be rewritten as follows

$$\hat{H}^{'} = H^{'\,0} + \sum_{\substack{i \\ (E_i > 0)}} E_i\,\beta_i^+\beta_i + \hat{H}_{int} \tag{6.150}$$

where $\hat{H}_{int}$ involves last three terms of (6.114) (terms with $\hat{H}^{4\,0}$, $\hat{H}^{3\,1}$, $\hat{H}^{2\,2}$). If we restrict ourselves into the quasiparticle mean field only and we neglect the term $\hat{H}_{int}$ in (6.150) then we speak about the model of independent quasiparticles with the diagonal Hamiltonian

$$\hat{H}^{'} = H^{'\,0} + \sum_{\substack{i \\ (E_i > 0)}} E_i\, \beta_i^{+} \beta_i \tag{6.151}$$

with the eigenstate:

- quasiparticle vacuum $|HFB\rangle$ with the energy $H^{'\,0}$;
- one-quasiparticle states $\beta_i^{+}\,|HFB\rangle$ with correspondimng energies $E_i + H^{'\,0}$;
- two-quasiparticle states $\beta_i^{+}\beta_{i'}^{+}\,|HFB\rangle$ with energies $E_i + E_{i'} + H^{'\,0}$;

$\vdots$

Using the variation principle (6.124) or (6.131), which gave us the HFB equation (6.148), we search for the absolute minimum of the total energy (in the space of variables $Z_{k\,k'}$). If we use as the starting basis (in which matrix elements V_{ijkl} of the nucleon-nucleon effective interaction are determined) the basis which has another symmetry than the resultant mean field , we can never get an eventual absolute minimum which breaks the symmetry of starting basis. Unrestricted HF and HFB calculations give only one point on the energy surface, namely local minimum. We are often interested in other points on the energy surface, too: we can impose certain auxiliary conditions defined by them. Sometimes we want to calculate the energy surface as a function of one (or several) collective parameter q, such as the quadrupole deformation. In all these cases we are interested in a wave function $|\Phi(q)\rangle$, which minimizes the total energy under the constraint that a certain single-particle operator $\hat{Q}$ has a fixed expectation value (this is exactly the same situation as we discussed the HF variation principle with the additional constraints - see (5.120))

$$q = \langle\Phi(q)|\,\hat{Q}\,|\Phi(q)\rangle \tag{6.152}$$

The simpliest method for the solving this problem is the adding the condition with the Lagrange multiplier Λ to the Hamiltonian and minimizing the following expectation value (so called linear constraint)

$$\langle\Phi|\,\hat{H}^{''}\,|\Phi\rangle \equiv \langle\Phi|\,\hat{H}^{'}\,|\Phi\rangle - \Lambda\,\Big(\langle\Phi|\,\hat{Q}\,|\Phi\rangle - q\Big) \tag{6.153}$$

This can be involved by several methods, e.g. using this linear constraint and changing the value Λ in each step of the iteration in such a way that the condition (6.152) is fulfilled. This can be done for a mesh of points in the space of parameter or parameters q in order to find the absolute minimum of (6.153). This was done, for instance, with the solving of the HFB equations with the Skyrme effective interaction in order to find the absolute minimum of the total HFB energy of the isotopes Sm - see Fig.5.17.

In the end of this subsection concerning the HFB approach let us give a different derivation of the HFB equation which is much simpler than that given above (but not explaining all important aspects of the HFB method). Starting with the Hamiltonian (6.101) we can rewrite it using the theorem of Wick applied with respect to the quasiparticle vacuum $|HFB\rangle$ (see subsection B.4 in the Appendix B)

$$c_k^+ \, c_{k'} \; = \; \langle HFB| \, c_k^+ \, c_{k'} \, |HFB\rangle + : c_k^+ \, c_{k'} : = \; \rho_{k'k} + : c_k^+ \, c_{k'} :$$

$$\begin{aligned} c_{k_1}^+ \, c_{k_2}^+ \, c_{k_4} \, c_{k_3} = \rho_{k_3 k_1} \, \rho_{k_4 k_2} - \; \rho_{k_3 k_2} \, \rho_{k_4 k_1} + \; \kappa^*_{k_1 k_2} \, \kappa_{k_3 k_4} \\ + \rho_{k_3 k_1} \; : c_{k_2}^+ \, c_{k_4} : + \rho_{k_4 k_2} \; : c_{k_1}^+ \, c_{k_3} : - \, (l_3 \leftrightarrow l_4) + \\ + \kappa^*_{k_1 k_2} \; : c_{k_4} c_{k_3} : + \kappa_{k_3 k_4} \; : c_{k_1}^+ \, c_{k_2}^+ : + \; : c_{k_1}^+ \, c_{k_2}^+ \, c_{k_4} \, c_{k_3} : \end{aligned} \tag{6.154}$$

This can be substituted into the Hamiltonian (6.101) and using the definition (6.147) the Hamiltonian can be rewritten as follows

$$\begin{aligned} \hat{H} = H^0 + \frac{1}{2} \; : (c^+ \, c) \begin{pmatrix} h & \Delta \\ -\Delta^* & -h^* \end{pmatrix} \begin{pmatrix} c \\ c^+ \end{pmatrix} : \; + \\ + \; \frac{1}{4} \sum_{k_1 k_2 k_3 k_4} V_{k_1 k_2 k_3 k_4} \; : c_{k_1}^+ \, c_{k_2}^+ \, c_{k_4} \, c_{k_3} : \end{aligned} \tag{6.155}$$

The last term corresponds to the last three terms in (6.114) containing $\hat{H}^{4\,0}$, $\hat{H}^{3\,1}$ and $\hat{H}^{2\,2}$ and it involves only product of four-quasiparticle operators. It represents the residual interactions above the quasiparticle mean field. In the model of independent quasiparticles the last term in (6.155) is neglected. The rest is a quadratic form in the operators $(c, \, c^+)$, which can be diagonalized exactly by the general Bogoliubov transformation (6.102). Again we find the HFB equation (6.148) with the solution (6.150) or (6.151).

6.3 Simple algebraic model of the pairing, seniority scheme

In this section we demonstrate the simple model of the description of the pairing effects in nuclei. In the section 6.1 it was shown that there are many experimental indications supporting the existence of very short range pairing interaction which creates the pairs of nucleons of one type occupying the single-particle states with the same quantum numbers except the sign of the angular momentum projection. In the framework of the simple model of nucleons of one type filling one j-shell with momentum projections $m = -j, \ldots, +j$ it will be shown that the pairs of nucleons, $(m, -m)$, sitting in the states $|jm\rangle$ and $|j-m\rangle$ behave like bosons. This model is based on so called quasi-spin formalism demonstrating in the 60-ties for the first time a boson character of the low-lying excitations in the even-even nuclei (see e.g. [101]).

Let us consider N fermions (nucleons of one type) accupying $(2j+1)$-fold degenerate j-shell (that means all states $|jm\rangle$ have the same energy). Let us suppose further that we switch on the pairing interaction of (6.24) type acting among these particles:

$$\hat{V}_{pair} = -G \sum_{m,\, m'>0} a_m^+ a_{-m}^+ a_{-m'} a_{m'} \equiv -G\, \hat{S}_+ \hat{S}_- \tag{6.156}$$

where

$$\hat{S}_+ = \sum_{m>0} a_m^+ a_{-m}^+ \tag{6.157}$$

is the quasi-spin step up operator and

$$\hat{S}_- = \sum_{m>0} a_{-m} a_m \tag{6.158}$$

is the quasi-spin step down operator. The reason why these operators are called step up and step down will be given later. Further we introduce following operators

$$\begin{aligned}
\hat{s}_+^{(m)} &\equiv a_m^+ a_{-m}^+ \rightarrow \begin{array}{c}\text{creates the pair of particles in the states} \\ |jm\rangle \text{ and } |j-m\rangle \text{ (so called } (m,\,-m) \text{ pair)}\end{array} \\
\hat{s}_-^{(m)} &\equiv a_{-m} a_m \rightarrow \text{ annihilates the pair } (m,\,-m) \text{ of particles} \\
\hat{s}_0^{(m)} &\equiv \frac{1}{2}\left(a_m^+ a_m + a_{-m}^+ a_{-m} - 1\right)
\end{aligned} \tag{6.159}$$

We denote by Ω the maximum number of $(m, -m)$ pairs which can be created within the given j-shell:

$$\begin{aligned}
&j = \frac{1}{2} \quad \rightarrow \quad \text{maximum 1 pair: } (\frac{1}{2},\, -\frac{1}{2}) \\
&j = \frac{3}{2} \quad \rightarrow \quad \text{maximum 2 pairs: } (\frac{1}{2},\, -\frac{1}{2}),\, (\frac{3}{2},\, -\frac{3}{2}) \\
&j = \frac{5}{2} \quad \rightarrow \quad \text{maximum 3 pairs: } (\frac{1}{2},\, -\frac{1}{2}),\, (\frac{3}{2},\, -\frac{3}{2}),\, (\frac{5}{2},\, -\frac{5}{2}) \\
&\vdots \\
&j \qquad \rightarrow \quad \text{maximum } j + \frac{1}{2} \text{ pairs} \\
&\qquad\qquad \Rightarrow \qquad \Omega = j + \frac{1}{2}
\end{aligned} \tag{6.160}$$

where Ω is the integer number.

Operators (6.159), $s_+^{(m)}$, $s_-^{(m)}$, $s_0^{(m)}$, fulfil the following commutation relations

$$\begin{aligned}
&\left[\hat{s}_+^{(m)},\, \hat{s}_-^{(m')}\right] = a_m^+\, a_{-m}^+\, a_{-m'}\, a_{m'} - a_{-m'}\, a_{m'}\, a_m^+\, a_{-m}^+ = \\
&= \boxed{\begin{array}{c}\text{because} \\ \{a_m,\, a_{m'}^+\} = \delta_{m\,m'},\ \{a_m,\, a_{m'}\} = 0\end{array}} = \\
&= \delta_{m\,m'}\,(\, a_m^+\, a_m + a_{-m}^+ a_{-m} - 1\,) = \boxed{\begin{array}{c}\text{see} \\ (6.159)\end{array}} = 2\,\hat{s}_0^{(m)}\,\delta_{m\,m'}
\end{aligned} \tag{6.161}$$

and similarly

$$\left[\hat{s}_0^{(m)},\, \hat{s}_+^{(m')}\right] = \hat{s}_+^{(m)}\,\delta_{m\,m'} \quad , \quad \left[\hat{s}_0^{(m)},\, \hat{s}_-^{(m')}\right] = -\hat{s}_-^{(m)}\,\delta_{m\,m'} \tag{6.162}$$

From (6.161), (6.162) one can see that these operators $\hat{s}_+^{(m)}$, $\hat{s}_-^{(m)}$, $\hat{s}_0^{(m)}$ fulfil the same commutation relations as the angular momentum operators $\hat{j}_+ = \hat{j}_1 + i\hat{j}_2$, $\hat{j}_- = \hat{j}_1 - i\hat{j}_2$, $\hat{j}_0 = \hat{j}_3$. Therefore the oparators $\hat{s}_+^{(m)}$, $\hat{s}_-^{(m)}$ are called quasi-spin step up and step down operators (in the analogy with $\hat{j}_+$ and $\hat{j}_-$)

and the following components of the quasi-spin operator can be introduced

$$\begin{aligned} \hat{s}_1^{(m)} &= \frac{1}{2}\left(\hat{s}_+^{(m)} + \hat{s}_-^{(m)}\right) \\ \hat{s}_2^{(m)} &= \frac{1}{2}\left(\hat{s}_+^{(m)} - \hat{s}_-^{(m)}\right) \\ \hat{s}_3^{(m)} &= \hat{s}_0^{(m)} \end{aligned} \tag{6.163}$$

with the corresponding commutation relations

$$\left[\hat{s}_i^{(m)},\ \hat{s}_j^{(m)}\right] = i\,\epsilon_{ij\,k}\,\hat{s}_k^{(m)} \tag{6.164}$$

One can realize that the eigen-values of the operator $\hat{s}_3^{(m)} = \hat{s}_0^{(m)} = 1/2(a_m^+ a_m + a_{-m}^+\,a_{-m} - 1)$ are following (because $a_m^+\,a_m$ $(a_{-m}^+\,a_{-m})$ is the operator of the number of particles in the state $|jm\rangle$ $(|j\ -m\rangle)$):

$$\begin{array}{cl} -1/2 & \text{if the pair of states } (m,\,-m) \text{ is empty} \\ +1/2 & \text{if the pair of states } (m,\,-m) \text{ is occupied by 2 particles} \\ 0 & \text{if the pair of states } (m,\,-m) \text{ is occupied by 1 particle} \end{array} \tag{6.165}$$

The scalar product of two quasi-spin opertors $\vec{\hat{s}}^{(m)}$ and $\vec{\hat{s}}^{(m')}$ is

$$\begin{aligned} \vec{\hat{s}}^{(m)} \cdot \vec{\hat{s}}^{(m')} &= \hat{s}_1^{(m)}\,\hat{s}_1^{(m')} + \hat{s}_2^{(m)}\,\hat{s}_2^{(m')} + \hat{s}_3^{(m)}\,\hat{s}_3^{(m')} = \\ &= \boxed{\begin{array}{c}\text{substitution}\\ \text{from (6.163)}\end{array}} = \\ &= \frac{1}{2}\left(\,\hat{s}_+^{(m)}\,\hat{s}_-^{(m')} + \hat{s}_+^{(m')}\,\hat{s}_-^{(m)}\,\right) - \hat{s}_0^{(m)}\,\delta_{m\,m'} + \hat{s}_0^{(m)}\,\hat{s}_0^{(m')} \\ \Rightarrow \qquad \hat{s}_+^{(m)}\,\hat{s}_-^{(m)} &= \vec{\hat{s}}^{(m)} \cdot \vec{\hat{s}}^{(m)} + \hat{s}_0^{(m)} - \hat{s}_0^{(m)}\,\hat{s}_0^{(m)} \end{aligned} \tag{6.166}$$

Further so called total quasi-spin operator is introduced

$$\begin{array}{lll} \hat{S}_+ = \sum_{m>0} a_m^+ a_{-m}^+ = \sum_{m>O}\hat{s}_+^{(m)} & & \hat{S}_1 = \sum_{m>0}\hat{s}_1^{(m)} \\ \hat{S}_- = \sum_{m>0} a_{-m} a_m = \sum_{m>O}\hat{s}_-^{(m)} & \Rightarrow & \hat{S}_2 = \sum_{m>0}\hat{s}_2^{(m)} \\ \hat{S}_0 = \sum_{m>0}\hat{s}_0^{(m)} & & \hat{S}_3 = \sum_{m>0}\hat{s}_3^{(m)} \end{array} \tag{6.167}$$

Because of (6.164) the total quasi-spin component operators fulfil the standard commutation relations typical for angular momentum

$$\begin{array}{l} [\hat{S}_0,\ \hat{S}_+] = \hat{S}_+ \\ [\hat{S}_0,\ \hat{S}_-] = -\hat{S}_- \\ [\hat{S}_+,\ \hat{S}_-] = 2\,\hat{S}_0 \end{array} \qquad \Rightarrow \qquad [\hat{S}_i,\ \hat{S}_j] = i\,\epsilon_{ijk}\,\hat{S}_k \tag{6.168}$$

and similarly as in (6.166) we have

$$\hat{S}_+ \, \hat{S}_- = \vec{\hat{S}} \cdot \vec{\hat{S}} + \hat{S}_0 - \hat{S}_0^2 \tag{6.169}$$

The substitution for $\hat{s}_0^{(m)}$ from (6.159) into (6.167) gives

$$\hat{S}_0 = \sum_{m>0} \hat{s}_0^{(m)} = \frac{1}{2} \sum_{m>0} (\, a_m^+ \, a_m + a_{-m}^+ \, a_{-m} - 1 \,) =$$

$$= \boxed{\begin{array}{c}\text{because the number of particle operator:} \\ \hat{N} = \sum_{m>0} (\, a_m^+ \, a_m + a_{-m}^+ \, a_{-m} \,)\end{array}} =$$

$$= \frac{1}{2} \, \hat{N} - \frac{1}{2} \sum_{m>0} 1 = \boxed{\begin{array}{c}\text{see} \\ (6.160)\end{array}} = \frac{1}{2} \, \hat{N} - \frac{1}{2} \, \Omega \tag{6.170}$$

where Ω is the maximum number of pairs $(m, \, -m)$ formed in the framework of the given j-shell, $\Omega = j + 1/2$ (see (6.160)). Since N and Ω are always integer the eigenvalues of $\hat{S}_0$ is an integer or half integer.

The components $\hat{S}_i$ of the total quasi-spin fulfil the commutation relations (6.168) typical for the components of the ang. momentum (including the relation $[\hat{S}_i, \, \hat{S}^2] = 0$ where $\hat{S}^2 = \hat{S}_1^2 \, + \hat{S}_1^2 \, + \hat{S}_3^2$). Therefor we can find the common system of eigen-vectors $|S \, S_0 >$ for operators $\hat{S}^2$ and $\hat{S}_3$:

$$\begin{aligned} &\hat{S}^2 \mid S \, S_0 \rangle = S \, (S+1) \mid S \, S_0 \rangle \\ &\hat{S}_0 \mid S \, S_0 \rangle = \hat{S}_3 \mid S \, S_0 \rangle = S_0 \mid S \, S_0 \rangle \\ &\hat{S}_\pm \mid S \, S_0 \rangle \equiv \mid S \, S_0 \pm 1 \rangle \end{aligned} \tag{6.171}$$

where $S_0 = (\,\text{see}\,(6.170)\,) = (N - \Omega)/2$. Since the value of S should be always higher or equal to its projection S_0 we have for given number of nucleons N:

$$S \geq \mid S_0 \mid = \frac{1}{2} \mid N - \Omega \mid \tag{6.172}$$

The value of S is given by the maximal value of the projection $|S_0|$ and this occurs for $N = 0$ if S_0 is half-integer - see (6.160), or for $N = 1$ if S_0 is integer - se (6.160). So, the spectrum of values of S for given N is (both S and S_0 should be simultaneously odd or even)

$$\begin{aligned} S &= \left| \frac{\Omega}{2} - \frac{N}{2} \right|, \left| \frac{\Omega}{2} - \frac{N}{2} + 1 \right|, \, \ldots, \, \frac{\Omega}{2} - 1, \, \frac{\Omega}{2} && \text{for } N \text{ even} \\ S &= \left| \frac{\Omega}{2} - \frac{N}{2} \right|, \left| \frac{\Omega}{2} - \frac{N}{2} + 1 \right|, \, \ldots, \, \frac{\Omega}{2} - \frac{3}{2}, \, \frac{\Omega}{2} - \frac{1}{2} && \text{for } N \text{ odd} \end{aligned} \tag{6.173}$$

The pairing interaction (6.156) can be also expressed in the folllowing form (using (6.169))

$$\begin{aligned}
\hat{V}_{pair} \mid S\, S_0\rangle &= \boxed{\begin{array}{c}\text{see}\\ (6.156),\ (6.169)\end{array}} = \\
&= -G\, \left[S\,(S+1) - S_0^2 + S_0\right] \mid S\, S_0\rangle = \boxed{\begin{array}{c}\text{because}\\ S_0 = (N-\Omega)/2\end{array}} = \\
&= -G\, \left[S\,(S+1) - \frac{(N-\Omega)^2}{2} + \frac{N-\Omega}{2}\right] \mid S\, S_0\rangle = \\
&\equiv E(S\, S_0 = (N-\Omega)/2) \mid S\, S_0\rangle
\end{aligned} \tag{6.174}$$

for given number N of particles in the given j-shell and for given $\Omega = j+1/2$.

Instead of the quantum number S the new state index, seniority s, is usually introduced by the following definition

$$S = \frac{1}{2}\,(\Omega - s) \qquad \Leftrightarrow \qquad s = \Omega - 2\,S \tag{6.175}$$

Since the spectrum of possible S is given by (6.173) the definition (6.175) give the following possible values of the seniority

$$\begin{aligned}
s &= 0,\ 2,\ 4,\ \ldots,\ N \qquad \text{for } N \text{ even} \\
s &= 1,\ 3,\ 5,\ \ldots,\ N \qquad \text{for } N \text{ odd}
\end{aligned} \tag{6.176}$$

So, we have two basis of kets for the quasi-spin Hilbert space:

$$\begin{aligned}
&\mid S\, S_0\rangle \qquad S_0 = \frac{N}{2} - \frac{\Omega}{2} \\
&\qquad S = |S_0|,\ |S_0|+1,\ \ldots,\ \frac{\Omega}{2} \qquad \text{for } N \text{ even} \\
&\qquad S = |S_0|,\ |S_0|+1,\ \ldots,\ \frac{\Omega}{2} - \frac{1}{2} \quad \text{for } N \text{ odd}
\end{aligned}$$

or

$$\begin{aligned}
&|N\, s\rangle \qquad s = 0,\ 2,\ 4,\ \ldots,\ N \quad \text{for } N \text{ even} \\
&\qquad\qquad\ \ s = 1,\ 3,\ 5,\ \ldots,\ N \quad \text{for } N \text{ odd}
\end{aligned} \tag{6.177}$$

and the correspondence of these two basis is following

$$\begin{aligned}
\mid N\ s=0\rangle \quad &\leftrightarrow \quad \Big| S=\frac{\Omega}{2} \qquad S_0=\frac{N-\Omega}{2}\Big\rangle \\
\mid N\ s=2\rangle \quad &\leftrightarrow \quad \Big| S=\frac{\Omega}{2}-1 \quad S_0=\frac{N-\Omega}{2}\Big\rangle \\
\mid N\ s=4\rangle \quad &\leftrightarrow \quad \Big| S=\frac{\Omega}{2}-2 \quad S_0=\frac{N-\Omega}{2}\Big\rangle \\
&\vdots \\
\mid N\ s=N\rangle \quad &\leftrightarrow \quad \Big| S=\frac{\Omega}{2}-\frac{N}{2} \quad S_0=\frac{N-\Omega}{2}\Big\rangle
\end{aligned} \tag{6.178}$$

for N even and

$$\begin{aligned}
\mid N\ s=1\rangle \quad &\leftrightarrow \quad \Big| S=\frac{\Omega}{2}-\frac{1}{2} \quad S_0=\frac{N-\Omega}{2}\Big\rangle \\
\mid N\ s=3\rangle \quad &\leftrightarrow \quad \Big| S=\frac{\Omega}{2}-\frac{3}{2} \quad S_0=\frac{N-\Omega}{2}\Big\rangle \\
\mid N\ s=3\rangle \quad &\leftrightarrow \quad \Big| S=\frac{\Omega}{2}-\frac{5}{2} \quad S_0=\frac{N-\Omega}{2}\Big\rangle \\
&\vdots \\
\mid N\ s=N\rangle \quad &\leftrightarrow \quad \Big| S=\frac{\Omega}{2}-\frac{N}{2} \quad S_0=\frac{N-\Omega}{2}\Big\rangle
\end{aligned} \tag{6.179}$$

for N odd. Simultaneously we should have in mind the following possibilties for the number of particles

$$\begin{aligned}
N &= 2\,\Omega,\ 2\,\Omega-2,\ 2\,\Omega-4,\ \ldots,\ 0 \qquad \text{for } N \text{ even} \\
N &= 2\,\Omega-1,\ 2\,\Omega-3,\ 2\,\Omega-5,\ \ldots,\ 1 \qquad \text{for } N \text{ odd}
\end{aligned}$$

After the substitution of (6.175) the spectrum of the pairing interaction (6.174) becomes

$$\begin{aligned}
&E(N,s) \equiv E(S, S_0=(N-\Omega)/2) = \\
&= -G\left[\, S\,(S+1) - \frac{(N-\Omega)^2}{4} + \frac{N-\Omega}{2}\,\right] = \boxed{\begin{array}{c}\text{substitution}\\ \text{from (6.175)}\end{array}} = \\
&= -\frac{G}{4}\left[s^2 - 2\,s\,(\Omega+1) + 2\,N\,(\Omega+1) - N^2\,\right]
\end{aligned} \tag{6.180}$$

The following conclusions can be extracted from (6.180)

1. For given N the lowest energy occurs for $s=0$ in the case of N even

and for $s = 1$ in the case of N odd:

$$E_{min}(N\ even) = E(N\ s = 0) = \frac{G}{4}\, N \left[N - 2\,(\Omega + 1)\right]$$
$$E_{min}(N\ odd) = E(N\ s = 1) = \frac{G}{4}\,(N-1) \left[N + 1 - 2\,(\Omega + 1)\right] \tag{6.181}$$

2. For given N the highest energy occurs for $s = N$ for both cases, N even and N odd:

$$E_{max}(N) = E(N\ s = N) =$$
$$= -\frac{G}{4} \left[N^2 - 2\,N\,(\Omega + 1) + 2\,N\,(\Omega + 1) - N^2\right] = 0 \tag{6.182}$$

Further we show that the quantum number seniority represents the number of unpaired nucleons in the given state $|N\,s\rangle$. Let us consider for the simplicity two nucleons in the j-shell. Two identical particles in one j-shell can have their angular momenta coupled in such a way that their total momentum is only: $J = 0,\ 2,\ 4,\ \ldots,\ 2j - 1$ because other values are excluded by Pauli principle. It can be seen from the following.

$$|j_1 j_2;\ JM\rangle = \sum_{\substack{m_1\, m_2 \\ m_1 + m_2 = M}} C^{JM}_{j_1 m_1\, j_2 m_2}\, |j_1 m_1\rangle\, |j_2\, m_2\rangle$$

$$|j_2 j_1;\ JM\rangle = \sum_{\substack{m_1\, m_2 \\ m_1 + m_2 = M}} C^{JM}_{j_2 m_2\, j_1 m_1}\, |j_2 m_2\rangle\, |j_1\, m_1\rangle = \boxed{\begin{array}{c}\text{see} \\ (A.4)\end{array}} =$$

$$= \sum_{\substack{m_1\, m_2 \\ m_1 + m_2 = M}} C^{JM}_{j_1 m_1\, j_2 m_2}\, (-1)^{J - j_1 - j_2}\, |j_1 m_1\rangle\, |j_2\, m_2\rangle =$$

$$= (-1)^{J - j_1 - j_2}\, |j_1 j_2;\ JM\rangle = \boxed{\begin{array}{c}\text{according to} \\ \text{Pauli principle}\end{array}} =$$

$$= -\,|j_1 j_2;\ JM\rangle$$

$$\Rightarrow \qquad (-1)^{J - j_1 - j_2} = -1 \tag{6.183}$$

If both the particles sit in the same j-shell ($j_1 = j_2 = j$) then

$$(-1)^{J-2\,j} = -1 \quad \Rightarrow \boxed{\begin{array}{c}\text{because}\\ 2j \text{ is odd}\end{array}} \Rightarrow \quad J \text{ is even}$$

So all states of two nucleons in one j-shell should have only even values of the total ang. momentum: $J = 0,\ 2,\ 4,\ \ldots,\ 2j-1$. Both particles belong to the one j-shell with the quantum numbers $(N\,l\,j)$ (see e.g. (5.8)). If the pairing interaction is swithched off both particles have the same energy in all $|jj;\ JM\rangle$ states. When the pairing interaction (6.156) is swithched on the original degeneracy is removed and because of the contact character of this pairing interaction the lowest energy belongs to the state $|jj;\ J = M = 0\rangle$. It can be shown e.g. for the pairing interaction of the δ-form - see (6.9) and Fig. 6.3. The nature of the contact interaction (6.156) is even so that it acts only on the state $|jj;\ J = M = 0\rangle$ lowering its energy and all other states $|jj;\ JM\rangle$ with $J \neq 0$ have the original degenerated energy before the switching on the pairing interaction. In the language of the quasi-spin formalism with the states $|N\ s\rangle$ we have two states $|N = 2\ s = 0\rangle$ and $|N = 2\ s = 2\rangle$ for two particles in one j-shell (see (6.177), (6.178)). The energy of the state $|N = 2\ s = 2\rangle$ is higher than that of the state $|N = 2\ s = 0\rangle$. According to (6.181), (6.182) these energies are following

$$\begin{aligned} E(N = 2\ s = 0) &= \frac{G}{2}\Big[2 - 2\,(\Omega + 1)\Big] = -G\,\Omega \\ E(N = 2\ s = 2) &= 0 \end{aligned}$$

So the state $|N = 2\ s = 2\rangle$ is excited and the state $|N = 2\ s = 0\rangle$ is the ground state which can be identified with the state $|jj\ ;\ J = 0\ M = 0\rangle$ (with the lowest energy from the states $|jj\ ;\ J\ M\rangle$). The excitation energy of the excited state $|N = 2\ s = 2\rangle$ is

$$E(N = 2\ s = 2) - E(N = 2\ s = 0) = G\,\Omega \tag{6.184}$$

So we can conclude:
in the ground state $|N = 2\ s = 0\rangle = |jj\ ;\ J = 0 M = 0\rangle$ of the two nucleos in one j-shell both nucleons are paired to the one pair with the total ang. momentum $J = 0$ while in the excited state $|N = 2\ s = 2\rangle$ these nucleons can have the total ang. momenta $J = 2,\ 4,\ \ldots,\ 2j-1$.

The energy spectrum (6.184) of the pairing interaction (6.156) is in the Fig. 6.6 compared schematically with the experimental spectrum of the lowest

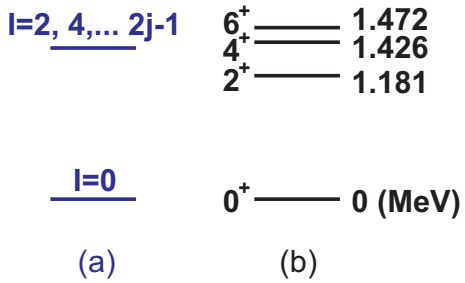


Figure 6.6: (a) Two-particle spectrum of the pure pairing interaction (6.156). (b) The low-lying spectrum of $^{210}_{84}$Po (2 protons in the $1h9/2$ shell).

states of ^{210}Po which has two protons in the $1h_{9/2}$ ($j = 9/2$) shell outside the "double magic" even-even core ^{208}Pb and therefore it can be approximated by two protons in one j-shell. One can see a rough qualitative agreement of the simple quasi-spin paring model with the experimental spectrum of the lowest states of ^{210}Po.

The wave function $|S\ S_0\rangle$ for N even can be constructed from the state $|-\rangle \equiv |N = 0\ s = 0\rangle$ = (see (6.178)) = $|S = \Omega/2\ S_0 = -\Omega/2\rangle$ (the state without particles, $\hat{S}_-\ |-\rangle = 0$) in terms of the step up operators $\hat{S}_+$. For instance the ground state $|N\ s = 0\rangle$ is:

$$|N\ s = 0\rangle = \boxed{\begin{array}{c}\text{see}\\(6.178)\end{array}} = |S = \frac{\Omega}{2}\ S_0 = \frac{(N-\Omega)}{2}\rangle =$$

$$= \boxed{\begin{array}{c}\text{see}\\(6.171)\end{array}} \approx \hat{S}_+^{\frac{N}{2}}\ |S = \frac{\Omega}{2}\ S_0 = -\frac{\Omega}{2}\rangle = \hat{S}_+^{\frac{N}{2}}\ |-\rangle \qquad (6.185)$$

The state $|N\ s = 0\rangle$ with the lowest energy for N (N even) nucleons in one j-shell given in (6.185) contains $N/2$ pairs of nucleons paired to $J = 0$ (that means $N/2$ bosons with $J = 0$) and therefore it can be understood as the boson condensate.

The discussed quasi-spin Hilbert space of states $|S\ S_0\rangle$ for two fermions in one shell is intirely different from the Hilbert space of states $|jj;\ JM\rangle$. The latter one is the standard Hilbert space of two fermion states $|jj';\ JM\rangle$ while the quasi-spin space is connected with the artifical quasi-spin states $|S\ S_0\rangle$ which are the eigen-states of the special Hamiltonian (6.156). For the nuclear physics the expression (6.156) is only an approximative expression for the short-range residual interaction reflecting only roughly some experimental indications that such a type of interaction among nucleons is present. All other nuclear properties (or degrees of freedom of nuclear motion) are ignored

by this interaction. Therefore one cannot expect that the approximative interaction (6.156) is able to descibe the experimental spectrum precisely. One can only obtain some rough qualitative agreement with experimental data similar to one given in the Fig.6.6. The simple quasi-spin model discussed in this section belongs to so called algebraic models which are able to describe usually only some selected degrees of freedom of nuclear motion. Models aspiring to more general and more quantitative description of possibly all nucleus degrees of freedom should be based on realistic interactions among nucleons and not only on some intuitive Hamiltonian acting in the very restricted Hilbert space involving only selected nuclear variables.

7. Vibration of nuclei, long range residual interaction

In this chapter the taking into account of the long range residual interactiom is discussed. The long range residual interactions are responsible for the vibration of the nuclear shape. Historically the first description of the nuclear vibration was given by the phenomenological droplet model of the nucleus (see section 7.2). However, phenomenological models like the model of the spherical or deformed droplet (so called Bohr's geometrical model [102]) or Interacting Boson Model (IBM) (see e.g. [103] and citations therein) are able to describe only purely vibrational degrees of freedom of the lowest multipolarity, that means very restricted space of the nucleus degrees of freedom. Phenomenological models cannot give an answer to the question of the connection of the nucleus vibrational degrees of freedom with the degrees of freedom of the individual nucleons. Nevertheless phenomenological models gave very good physical interpretation of the lowest part of experimental nuclear spectra, particularly the connection of different types of the spectrum with the symmetry of the nuclear Hamiltonian. Therefore these relatively simple models are discussed in section 7.2. From theoretical point of view the most interesting are so called microscopical models which aspire to connect all nuclear degrees of freedom with the nucleon-nucleon effective interaction. Microscopical models are discussed in the section 7.3.

The vibrational degrees of freedom of the nucleus motion are coupled with other degrees of freedom (single-particle and rotational motions). In fact, only in some cases it is possible to distinquish the intrinsic (single-particle and vibrational) degrees of freedom of the nuclear motion. The calssification of degrees of freedom of the nucleus motion is connected with the form of the nuclear Hamiltonian which is discussed in the section 7.1.

7.1 Model Hamiltonian of vibrating and rotating deformed nucleus

In the Section 1.4 all types of nuclear motion were briefly introduced, namely single-particle motion of individual nucleons (each nucleon moves in the mean field potential created by other nucleons), as well as the correlated motion of many nucleons which can be interpreted as the vibration of the nuclear shape, and, in the case of the deformed mean field, we can recognize a rotation of the nucleus in the lab system. All degrees of freedome connected with these types of nuclear motion should be described by means of the Shroedinger equation with the nuclear Hamiltonian $\hat{H}$ written in the laboratory frame.

It was shown in the Chapter 4 that the single-particle nuclear mean field Hamiltonian $\hat{H}_{AV}$ can be extracted from the total Hamiltonian by means of the Hartree-Fock method. The rest of the total Hamiltonian - residual interactions (see (4.28))

$$\hat{V}_{RES} = \hat{H} - \hat{H}_{AV} = \hat{V}_{s.r.}^{(RES)} + \hat{V}_{l.r.}^{(RES)\,\prime} \tag{7.1}$$

are divided according to their range into the short range part $\hat{V}_{s.r.}^{(RES)}$ and the long range part $\hat{V}_{l.r.}^{(RES)\,\prime}$. The short range residual interaction part $\hat{V}_{s.r.}^{(RES)}$ was discussed in details in the Chapter 6 and it was shown that this part of the residual interactions is quite strong, especially in deformed nuclei (nuclei with the valence shell of the mean field filled only partly), and it leads to the pairing effects. It was demonstrated there also that the pairing short range residual interactions are taken into account in terms of the BCS (subsection 6.2.2) or HFB (see Subsection 6.2.3) using the Bogoliubov transformation from the system od single-particle creation and annihilation operators to the system of quasiparticle operators. In such cases after the solving of the BCS or HFB equations we speak about single-quasiparticle rather than single-particle degrees of freedom.

The subject of this chapter is the inclusion of the long range residual interaction $\hat{V}_{l.r.}^{(RES)\,\prime}$. It was already mentioned in the Chapter 1 that the long-range residual interactions are responsible for the collective vibrational motion of the whole nucleus. In the case of nuclei with the deformed mean field, when $\hat{H}_{AV}$ violates the rotational invariance of the total Hamiltonian, the deformed mean field $\hat{H}_{AV}$ does not commute with components $\hat{I}_i$ of the total ang. momentum ($\hat{I}_i$ is the operator of the i-th projection of the total

angular momentum onto the intrinsic frame axes [1]

$$\left[\hat{H}_{AV}, \hat{I}_i\right] \neq 0 \qquad (i = 1, 2, 3) \tag{7.2}$$

That means the long range residual interaction $\hat{V}_{l.s_{\hat{s}}}^{(RES)\,\prime}$ should restore the rotational invariance of the whole Hamiltonan ($[\hat{H}, \hat{I}_i] = 0$). By other words it means that in this case the long range residual interactions $\hat{V}_{l.r.}^{(RES)\,\prime}$ involves also the rotational degrees of freedom and they are responsible for both the vibrational and rotational motion of the nucleus in the lab frame.

The partition of the nucleus degrees of freedom into single-particle, vibrational and rotational parts is purely model image. From the theoretical point of view in order to find the A-particle wave functions and energy spectrum of the nuclear states we should solve the Schroedinger equation with the nuclear Hamiltonian containing the kinetic energy and general effective two-body, three-body and more-body interactions. Generally it is a problem of A- particle system with $2 \times 3A$ degrees of freedom ($3A$- degrees of freedom are connected with the spatial space and the factor of 2 corresponds to two spin projections of each nucleon). These $2 \times 3A$ degrees of freedom should involve all types of the nuclear motion, single-particle, vibrational and possible rotational. Generally the partition of all degrees of freedom into single-particle, vibrational and rotational ones is a hard problem because all these types of the motion are mutually tied. However in some cases the coupling between these types of degrees of freedom is not so big and a mutual extraction of them is possible. For instance this extraction can be done easily if the angular frequency ω_{rot} of the nuclear rotation is much lower than the angular frequencies $\omega_{s.p.}$ and ω_{vib} typical for the single-particle and vibrational motions:

$$\omega_{rot} << \omega_{s.p.} \qquad \omega_{rot} << \omega_{vib} \tag{7.3}$$

Then the nuclear Hamiltonian can be rewritten in the following form

$$\hat{H} = \hat{H}_{intr} + \hat{H}_{rot} \tag{7.4}$$

where

$$\hat{H}_{intr} = \hat{H}_{AV} + \hat{V}_{s.r.}^{(RES)} + \hat{V}_{l.r.}^{(RES)} \tag{7.5}$$

is the intrinsic Hamiltonian acting in the Hilbert space in the intrinsic frame rotating with the rotating nucleus (so called fixed-body frame). $\hat{H}_{rot}$ is the

[1] By indexes $i = 1, 2, 3$ we denote axes of the intrinsic frame rotating with the nucleus and indexes x, y, z concern the axes of the lab system.

Hamiltonian part responsible for rotational degrees of freedom and $\hat{V}_{l.r.}^{(RES)} = \hat{V}_{l.r.}^{(RES)\,\prime} - \hat{H}_{rot}$ is the part of the long range residual interaction describing nuclear vibrations in the fixed-body frame. The rotational part $\hat{H}_{rot}$ is determined from the analogy with the solid-body rotation in the classical physics where the rotational energy E_{rot} and rotational momentum M of the body rotating around the axis with respect to which the moment of inertia is $\mathscr{F}$, are given by

$$E_{rot} = \frac{1}{2}\,\mathscr{F}\,\Omega^2 \qquad\qquad M = \mathscr{F}\,\Omega$$
$$\Rightarrow E_{rot} = \frac{M^2}{2\mathscr{F}} \tag{7.6}$$

It is clear that this analogy gives the rotational Hamiltonian $\hat{H}_{rot}$ in the form

$$\hat{H}_{rot} = \sum_{i=1}^{3} \frac{\hbar^2\,\hat{R}_i^2}{2\mathscr{F}_i} \tag{7.7}$$

where $\hat{R}_i$ $(i = 1, 2, 3)$ are rotational angular momentum components and $\mathscr{F}_i \equiv \mathscr{F}_{ii}$ are principal components of the tensor of inertia moment (we suppose that the axes of the rotating fixed-body frame coincide with the principal axes of the inertia moment).

It should be pointed out that the adiabatic condition (7.3) is usually valid in the low-lying part of the nuclear spectrum (the rotational energies $\hbar\omega_{rot} \approx$ tens up to hundreds KeV while $\hbar\omega_{s.p.}$ and $\hbar\omega_{vib}$ are units of MeV and more). Therefore the partition (7.4) is usually used for the description of the low-lying part of the nucleus spectrum (in the Fig.1.7 this part of the spectrum is denoted as the part where so called particle-rotor models are used).

In the case of the adiabatic rotation the total angular moment $\vec{I}$ of the rotating nucleus is given as the sum of the rotational ang. moment $\vec{R}$ and the intrinsic ang. moment $\vec{j}$

$$\vec{I} = \vec{R} + \vec{j} \qquad \Rightarrow \qquad \vec{R} = \vec{I} - \vec{j} \tag{7.8}$$

which reflects the similar partition of the Hamiltonian $\hat{H}$ given in (7.4). The substitution of (7.8) into (7.7) gives

$$\hat{H}_{rot} = \sum_{i=1}^{3} \frac{(\hat{I}_i - \hat{j}_i)^2\hbar^2}{2\mathscr{F}_i} \tag{7.9}$$

As it was mentioned several times the most of deformed nuclei is axially symmetric in their ground state. In such a case we can always choose the 3-d

intrinsic frame axis to be the symmetry axis (the symmetry axis concerns the symmetry of the shape of the mass distribution of given nucleus). We know also from the Chapter 1 that it is not possible to identify the rotation of any quantum object around the symmetry axis. That means for axially symmetric nucleus with respect to the 3-d intrinsic frame axis the 3-d component of the rotational momentum is always zero

$$\hat{R}_3 = \hat{I}_3 - \hat{j}_3 = 0 \tag{7.10}$$

and the moment of inertia components $\mathscr{F}_1$ and $\mathscr{F}_2$ are equal

$$\mathscr{F}_1 = \mathscr{F}_2 \equiv \mathscr{F} \tag{7.11}$$

In the Fig. 7.1 the coupling of the total nucleus angular momentum $\vec{I}$ and

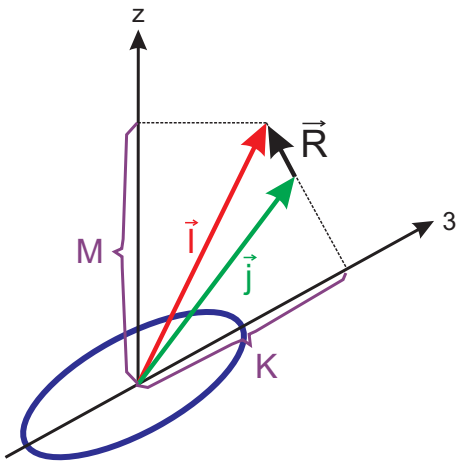


Figure 7.1: Schematic figure of the coupling of the intrinsic and total lab. ang. momenta in the axially symmetric deformed nucleus.

intrinsic angular momentum $\vec{j}$ for the axially symmetric deformed nucleus is schematically demonstrated.

In the case of the axially symmetry the rotational part $\hat{H}_{rot}$ of the nucleus Hamiltonian can be rewritten as follows

$$\hat{H}_{rot} = \frac{\hbar^2}{2\mathscr{F}}\left[(\hat{I}_1 - \hat{j}_1)^2 + (\hat{I}_2 - \hat{j}_2)^2\right] = \boxed{\begin{array}{c}\hat{I}_\pm = \hat{I}_1 \pm i\,\hat{I}_2 \\ \hat{j}_\pm = \hat{j}_1 \pm i\,\hat{j}_2\end{array}} =$$

$$= \frac{\hbar^2}{2\mathscr{F}}\left[\hat{I}^2 - \hat{I}_3^2\right] - \frac{\hbar^2}{2\mathscr{F}}\left[\hat{I}_+\hat{j}_- + \hat{I}_-\hat{j}_+\right] + \frac{\hbar^2}{2\mathscr{F}}\left[\hat{j}_1^2 + \hat{j}_2^2\right] \equiv$$

$$\equiv \frac{\hbar^2}{2\mathscr{F}}\left[\hat{I}^2 - \hat{I}_3^2\right] + \hat{H}_{Cor} + \hat{H}_{centrif} \tag{7.12}$$

where

$$\hat{H}_{cor} = -\frac{\hbar^2}{2\mathscr{F}} [\hat{I}_+ \hat{j}_- + \hat{I}_- \hat{j}_+] \tag{7.13}$$

is so called Coriolis interaction and

$$\hat{H}_{centrif} = \frac{\hbar^2}{2\mathscr{F}} [\hat{j}_1^2 + \hat{j}_2^2] \tag{7.14}$$

is the centrifugal interaction (centrifugal from the point of view of the fixed body frame).

So in the case when the adiabatic condition (7.3) is fulfilled the deformed nucleus total Hamiltonian is (see (7.1)

$$\begin{aligned} \hat{H} &= \hat{H}_{AV} + \hat{V}_{s.r.}^{(RES)} + \hat{V}_{l.r.}^{(RES)\,\prime} = \\ &= \hat{H}_{AV} + \hat{V}_{s.r.}^{(RES)} + \hat{V}_{l.r.}^{(RES)} + \hat{H}_{rot} \equiv \hat{H}_{intr} + \hat{H}_{rot} \end{aligned} \tag{7.15}$$

where

$$\hat{H}_{intr} = \hat{H}_{AV} + \hat{V}_{s.r.}^{(RES)} + \hat{V}_{l.r.}^{(RES)} \tag{7.16}$$

is the intrinsic Hamiltonian expressed in terms of the variables concerning the fixed body frame and $\hat{H}_{rot}$ is the rotating part of the nucleus Hamiltonian responsible for the rotational degrees of freedom of nuclear motion given by (7.12).

The Coriolis interaction term $\hat{H}_{cor}$ involved in (7.12) represents the coupling between the intrinsic and rotational degrees of freedom (one should realize that the operators $\hat{j}_\pm$ act on the intrinsic part of the wave function and operators $\hat{I}_\pm$ act on the rotational external (laboratory) part of the wave function). For the low-lying part of the nuclear spectrum (low rotational frequencies) the Coriolis term is small and it can be treated as a perturbation. However, as it will be discussed in the Chapter 8 the Coriolis term increases with the increasing rotational frequency and therefore for higher rotational frequency the coupling between the intrinsic and rotational degrees of freedom becomes strong and the separation of the intrinsic and rotational degrees of freedom is more difficult and problematic. However, for very high rotational frequency the nucleus starts to behave like flywheel. That means it rotates steadily in the laboratory space with the stable rotational axis. In this case the situation with the coupling of the intrinsic moment $\hat{\vec{j}}$ and the rotational one $\hat{\vec{R}}$ becomes again more simple and the extraction of the intrinsic and rotational degrees of freedom can be done easily (this situation will be discussed in the Subsection 8.2).

In the simple case when the Coriolis and centrifugal terms in the Hamiltonian (7.15) are neglected and the whole Hamiltonian is approximated by

$$\hat{H} \approx \hat{H}_{intr} + \frac{\hbar^2}{2\mathscr{F}} (\hat{I}^2 - \hat{I}_3^2) \tag{7.17}$$

the corresponding eigen-states can be written as the product of the eigen-function $\psi_{K\rho}(\xi)$ of the intrinsic part $\hat{H}_{intr}$:

$$\hat{H}_{intr}\psi_{K\rho}(\xi) = E_{K\rho}\,\psi_{K\rho}(\xi) \tag{7.18}$$

and the eigen-function of the pure rotational part $\frac{\hbar^2}{2\mathscr{F}} (\hat{I}^2 - \hat{I}_3^2)$:

$$\frac{\hbar^2}{2\mathscr{F}} (\hat{I}^2 - \hat{I}_3^2)\, D^I_{MK}(\theta) = \frac{\hbar^2}{2\mathscr{F}} [I(I+1) - K^2]\, D^I_{MK}(\theta) \tag{7.19}$$

In (7.18) $\psi_{K\rho}(\xi)$ is the intrinsic wave function of the intrinsic variables ξ. Since in the case af the axially symmetry $[\hat{H}_{intr}, \hat{J}_3] = 0$ this wave function is simultaneously the eigen function of the 3-d component $\hat{j}_3$ of the intrinsic angular moment, $\hat{j}_3\,\psi_{K\rho}(\xi) = K\,\psi_{K\rho}(\xi)$. In (7.19) $D^I_{MK}(\theta)$ stands for the Wigner D- function (see Appendix A, part A.5) of the Euler angles which are characterized here by one symbol θ. These Wigner D- functions are eigen-functions of the operators $\hat{I}^2$, $\hat{I}_3$ and $\hat{I}_z$:

$$\begin{aligned} \hat{I}^2\, D^I_{MK}(\theta) &= I(I+1)\, D^I_{MK}(\theta) \\ \hat{I}_3\, D^I_{MK}(\theta) &= K\, D^I_{MK}(\theta) \\ \hat{I}_z\, D^I_{MK}(\theta) &= M\, D^I_{MK}(\theta) \end{aligned} \tag{7.20}$$

where $\hat{I}_3$ is the total moment projection onto the 3-d axis of the intrinsic frame and $\hat{I}_z$ is the total moment projection onto the z- axis of the laboratory frame. Then the energy spectrum of the Hamiltonian (7.17) is

$$\langle IMK\rho|\hat{H}|IMK\rho\rangle \approx E_{K\rho} + \frac{\hbar^2}{2\mathscr{F}} [I(I+1) - K^2] \tag{7.21}$$

where the corresponding eigen wave functions have the form of the product of the intrinsic wave functions a Wigner D-functions:

$$\Psi_{IMK\rho}(\xi,\theta) = \langle\theta,\xi|IMK\rho\rangle \approx D^I_{MK}(\theta)\,\psi_{K\rho}(\xi) \tag{7.22}$$

and these lab. frame wave functions fulfill the following relations

$$\begin{aligned} \hat{H}_{int}\,|IMK\rho\rangle &= E_{K\rho}\,|IMK\rho\rangle & \hat{I}^2\,|IMK\rho\rangle &= I(I+1)\,|IMK\rho\rangle \\ \hat{j}_3\,|IMK\rho\rangle &= K\,|IMK\rho\rangle & \hat{I}_z\,|IMK\rho\rangle &= M\,|IMK\rho\rangle \\ & & \hat{I}_3\,|IMK\rho\rangle &= K\,|IMK\rho\rangle \end{aligned} \tag{7.23}$$

Further we suppose that the intrinsic Hamiltonian $\hat{H}_{intr}$ corresponds to the axially symmetric deformed nuclei and it is invariant with respect to the time reversal transformation

$$\left[\hat{H}_{intr}, \hat{\mathscr{T}}\right] = 0 \quad \Rightarrow \boxed{\begin{array}{c}\text{see also the end of}\\ \text{the section 1.4}\end{array}}$$

$$\Rightarrow \quad \hat{H}_{intr}\,\hat{\mathscr{T}}\,|K\rho\rangle = \hat{\mathscr{T}}\,\hat{H}_{intr}\,|K\rho\rangle \tag{7.24}$$

and we see that the state $|K\rho\rangle$ has the same energy $E_{K\rho}$ as the state $\mathscr{T}|K\rho\rangle$. We know from (1.44) that $\mathscr{T}\,|K\rho\rangle \approx |-K\,\rho\rangle$ (the action of the time reversal operator $\mathscr{T}$ on the eigen state of the projection $\hat{j}_3$ changes the sign of the projection: $K \to -K$). As a result of this we can restrict ourselves only to non negative K, $K \geq 0$.

In the case of the nucleus axial spheroidal symmetry the intrinsic Hamiltonian $\hat{H}_{AV}$ is also invariant with respect to the turn of the nucleus round the arbitrary intrinsic body-fixed frame axis by angle π. That means

$$\left[\hat{H}_{intr}\,, \hat{\mathscr{R}}_i\right] = 0 \tag{7.25}$$

where

$$\hat{\mathscr{R}}_i \equiv \hat{\mathscr{R}}_i(\pi) \equiv e^{\,-i\,\pi\,\hat{j}_i} \tag{7.26}$$

Since $\hat{\mathscr{T}} = \hat{\mathscr{R}}_2^{-1}\,K$ (see (1.48)) the symmetry $[\hat{H}_{\,intr}, \hat{\mathscr{T}}] = 0$ is equivalent to the symmetry $[\hat{H}_{intr}, \hat{\mathscr{R}}_2] = 0$. Because of the identity, $\hat{\mathscr{R}}_1\hat{\mathscr{R}}_2\hat{\mathscr{R}}_3 = \mathbb{I}$, and because of the axial symmetry, $[\hat{H}_{\,int}, \hat{j}_3] = 0$, the commutator $[\hat{H}_{\,intr}, \hat{\mathscr{R}}_3]$ is equal to zero automatically. So the condition (7.25) gives the only new information that the intrinsic state with the wave function $\hat{\mathscr{R}}_1\,|K\rho\rangle$ should have the same intrinsic energy $E_{K\rho}$ as the intrinsic state $|K\rho\rangle$. In the agreement with it we should symmetrize the laboratory wave function $\Psi_{IMK\rho}(\xi,\theta)$ (see (7.22)) as follows (see e.g. [99])

$$\Psi_{IMK\rho}(\xi,\theta) = \langle\xi,\theta|IMK\rho\rangle = \\ = \sqrt{\frac{2I+1}{16\pi^2(1+\delta_{K0})}}\,\left(1 + \hat{\mathscr{R}}_e^{-1}(1)\,\hat{\mathscr{R}}_1(\pi)\right)\,D^I_{MK}(\theta)\,\psi_{K\rho}(\xi) \tag{7.27}$$

where $\hat{\mathscr{R}}_1(\pi) \equiv \hat{\mathscr{R}}_1$ is the operator of the turn round the 1-st intrinsic frame axis by angle π. The symbol $\hat{R}_e(1)$ stands for the operator of the same turn round the 1-st intrinsic axis but performed in the laboratory frame and therefore generally $\hat{\mathscr{R}}_e^{-1}(1)\,\hat{\mathscr{R}}_1(\pi) = \mathbb{I}$. The differences between $\hat{\mathscr{R}}_1(\pi)$ and

$\hat{\mathscr{R}}_e(1)$ is that the turn round the 1-st intrinsic axis by angle π is accomplished through the variables ξ in the case of the operator $\hat{\mathscr{R}}_1$ while through the Euler angles θ in the case of the operator $\hat{\mathscr{R}}_e(1)$. So the operator $\hat{\mathscr{R}}_1(\pi)$ acts on the intrinsic wave function $\psi_{K\rho}(\xi)$ and the operator $\hat{\mathscr{R}}_e(1)$ acts only on the Wigner D- functions $D^I_{MK}(\theta)$ (because $\hat{\mathscr{R}}_e(1) = e^{-i\,\hat{I}_3\,\pi}$). From mathematics it is known that (see e.g. [2])

$$\hat{\mathscr{R}}_e(1)\; D^I_{MK}(\theta) = (-1)^I\; D^I_{M\,-K}(\theta) \tag{7.28}$$

and so we have

$$\Psi_{IMK\rho}(\xi,\theta) = \sqrt{\frac{2I+1}{16\pi^2(1+\delta_{K0})}}\;\Big[D^I_{MK}(\theta)\;\psi_{K\rho}(\xi) + \\ + (-1)^I\; D^I_{M\,-K}(\theta)\;\hat{\mathscr{R}}_1(\pi)\;\psi_{K\rho}(\xi)\Big] \tag{7.29}$$

The factor $\sqrt{\frac{2I+1}{16\pi^2(1+\delta_{K0})}}$ in (7.28) and (7.29) is introduced from the normalization reason:

$$\int d\theta\; D^{I\,*}_{MK}(\theta)\; D^{I'}_{M'K'}(\theta) = \frac{8\pi^2}{2I+1}\;\delta_{II'}\;\delta_{MM'}\;\delta_{KK'} \quad \Rightarrow$$
$$\langle IMK\rho\,|I'M'K'\rho'\rangle = \int d\theta \int d\xi\;\; \Psi^*_{IMK\rho}(\theta,\xi)\;\; \Psi_{I'M'K'\rho'}(\theta,\xi) = \\ = \delta_{II'}\;\delta_{MM'}\;\delta_{KK'}\;\delta_{\rho\rho'} \tag{7.30}$$

So, if the Coriolis and the centrifugal terms are neglected in (7.15) and the total Hamiltonian of the nucleus is approximated by the Hamiltonian (7.17) then the normalized eigen states of the Hamiltonian (7.17) are given by (7.29) with the corresponding energy spectrum (7.21). This spectrum demonstrates the forming of so called rotational bands: above each intrinsic state with the energy $E_{K\rho}$ and with the wave function $\psi_{K\rho}(\xi)$ the sequence (band) of levels is formed where level energies

$$E_{IK\rho} = \langle IMK\rho\,|\hat{H}_{intr} + \frac{\hbar^2}{2\mathscr{F}}\;\left(\hat{I}^2 - \hat{I}_3^2\right)\;|IMK\rho\rangle = \\ = E_{K\rho} + \frac{\hbar^2}{2\mathscr{F}}\;\left[I(I+1) - K^2\right] \tag{7.31}$$

are determined by the total angular momentum I (one should realize that each level energy is degenerate with respect to the projection M of the total

ang. momentum $\vec{I}$ on the z- axis of the laboratory frame). From the point of view of the value K two types of rotational bands can be distinguished in even-even nuclei

1. $K = 0$ **bands**
   It is clear that $\hat{\mathscr{R}}_1\,\psi_{K\rho}(\xi) \approx \psi_{-K\,\rho}(\xi)$. It means the following symmetry for the case of $K = 0$ (we suppose even-even nucleus)

$$\begin{aligned} \hat{\mathscr{R}}_1\,\psi_{K=0\,\rho}(\xi) = r_1\,\psi_{K=0\,\rho}(\xi) \qquad & \hat{\mathscr{R}}_1^{\,2} = e^{-i\,j_1\,2\pi} = \mathbb{I} \\ \Rightarrow \qquad r_1^2 = 1 \qquad & \Rightarrow \quad r_1 = \pm 1 \end{aligned} \tag{7.32}$$

   So in the case of $K = 0$ the intrinsic state $\psi_{K=0\,\rho}(\xi)$ is simultaneously the eigen state of the operator $\hat{\mathscr{R}}_1$ with the corresponding eigen value $r = \pm 1$. The substitution of (7.32) into (7.29) gives for $K = 0$

$$\begin{aligned} &\Psi_{IM\,K=0\,\rho}(\xi,\theta) = \\ &\quad = \sqrt{\frac{2I+1}{32\pi^2}}\,\left(1 + (-1)^I\,r_1\right)\,D^I_{M\,K=0}(\theta)\;\psi_{K=0\,\rho}(\xi) \end{aligned} \tag{7.33}$$

   and this lab. wave function is not equal to zero only if

$$(-1)^I\,r_1 = 1$$

   So, in the $K = 0$ case, for the intrinsic wave function $\psi_{K=0\,\rho}(\xi)$ with $r_1 = +1$ the corresponding rotational band involves only levels with the even value of I while in the case of $\psi_{K=0\,\rho}(\xi)$ with $r_1 = -1$ the corresponding rotational band can have only levels with odd values of I:

$$\begin{aligned} &\text{for } r_1 = +1: \qquad I = 0,\,2,\,4,\,6,\ldots \qquad \text{only even } I \\ &\text{for } r_1 = -1: \qquad I = 1,\,3,\,5,\ldots \qquad \text{only odd } I \end{aligned} \tag{7.34}$$

2. $K \neq 0$ **bands**
   In this case there is no any restriction of I and I can have all values $I \geq |K|$:

$$I = |K|,\,|K|+1,\,|K|+2,\ldots \qquad \begin{array}{c}\text{both even and odd values} \\ \text{of } I \text{ are possible}\end{array} \tag{7.35}$$

As an example, in the Fig. 7.2 there is the low-lying part of the experimental energy spectrum of well deformed nucleus ^{154}Sm. The well developed

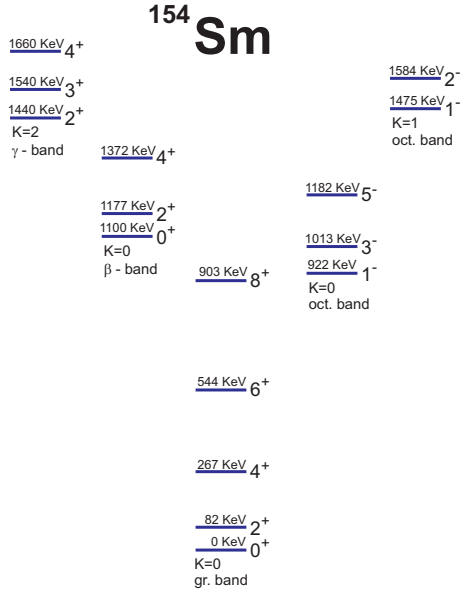


Figure 7.2: Experimental level scheme of well deformed nucleus ^{154}Sm. The ground state rotational band (gr, $K = 0$, $r_1 = 1$), quadrupole β - vibration band (β - vibr, $K = 0$, $r_1 = 1$), quadrupole γ - vibration band (γ - vibr, $K = 2$), octupole $oct.$ - vibration band (oct - vibr, $K = 0$, $r_1 = -1$), oct - vibr, $K = 1$) can be recognized.

rotational bands built on the intrinsic quadrupole and octupole vibration states can be recognized.

Knowing the wave function $\Psi_{IMK\rho}(\xi, \theta) = \langle \xi\theta \, | IMK\rho \rangle$ (see (7.29)) the probabilities of electromagnetic transitions can be determined. The reduced probability of the electromagnetic transition of the type X ($X = el$ or $X = mag$) with the multipolarity λ is defined by the expression (2.147)

$$B(X\lambda;\ I_iK_i\rho_i \to I_fK_f\rho_f) = \frac{1}{2I_i + 1} \left| \langle I_fK_f\rho_f || \mathscr{M}_\lambda^{(X)} || I_iK_i\rho_i \rangle \right|^2 \tag{7.36}$$

where the initial state $|I_iM_iK_i\rho_i\rangle$ and final state $|I_fM_fK_f\rho_f\rangle$ are given by (7.29) (in the framework of the approximation (7.17)). In (7.36) $\mathscr{M}_{\lambda\mu}^{(X)}$ is the transition oprerator of the given transition (in the long- wave approximation these transition operators are given by (2.128) for electric transitions, and (2.140) for magnetic transitions). Further the reduced matrix elements $\langle I_fK_f\rho_f \, || \hat{\mathscr{M}}_\lambda^{(X)} || I_iK_i\rho_i \rangle$ are determined. It is necessary to realize that the operators $\hat{\mathscr{M}}_{\lambda\mu}^{(X)}$ given in (2.128) or (2.140) are expressed in terms of laboratory variables. Because of the expression (7.29), where laboratory frame wave functions are expressed in terms of the intrinsic variables ξ (in the body-fixed frame) and by means of the Euler angles θ giving the orientation of the body-

fixed frame with respect to the external laboratory frame, it is convenient to transform the lab. frame transition operator $\hat{\mathscr{M}}^{(X)}_{\lambda\mu}$ into the body-fixed frame form $\hat{\mathscr{M}}^{(X)\,(\theta)}$. This can be done using the rel. (A.39):

$$\hat{\mathscr{M}}^{(X)}_{\lambda\mu} = \sum_{\nu} D^{\lambda}_{\mu\nu}(\theta)\, \hat{\mathscr{M}}^{(X)\,(\theta)}_{\lambda\nu} \tag{7.37}$$

Then the matrix elements $\langle I_f M_f K_f \rho_f \,|\hat{\mathscr{M}}^{(X)}_{\lambda\mu}|I_i M_i K_i \rho_i\rangle$ can be easily determined as follows

$$\begin{aligned}
&\langle I_f M_f K_f \rho_f \,|\hat{\mathscr{M}}^{(X)}_{\lambda\mu}|I_i M_i K_i \rho_i\rangle = \\
&= \sqrt{\frac{(2I_i+1)(2I_f+1)}{16^2\pi^4(1+\delta_{K_i 0})(1+\delta_{K_f 0})}} \int d\xi \int d\theta \\
&\quad \Big[D^{I_f\,*}_{M_f K_f}(\theta)\, \psi^{*}_{K_f\rho_f}(\xi) + (-1)^{I_f}\, D^{I_f\,*}_{M_f\,-K_f}(\theta)\, \hat{\mathscr{R}}_1\, \psi^{*}_{K_f\rho_f}(\xi)\Big] \\
&\quad \sum_{\nu} D^{\lambda}_{\mu\nu}(\theta)\, \hat{\mathscr{M}}^{(X)\,(\theta)} \\
&\quad \Big[D^{I_i}_{M_i K_i}(\theta)\, \psi_{K_i\rho_i}(\xi) + (-1)^{I_i}\, D^{I_i\,*}_{M_i\,-K_i}(\theta)\, \hat{\mathscr{R}}_1\, \psi^{*}_{K_i\rho_i}(\xi)\Big] = \\
&= \boxed{\begin{array}{c}
\int d\theta\, D^{J_3\,*}_{M_3 M_3'}(\theta)\, D^{J_2}_{M_2 M_2'}(\theta)\, D^{J_1}_{M_1 M_1'}(\theta) = \\
= \frac{8\pi^2}{2J_3+1}\, C^{J_3 M_3}_{J_1 M_1 J_2 M_2}\, C^{J_3 M_3'}_{J_1 M_1' J_2 M_2'}\,; \\
\hat{\mathscr{R}}_1^{-1}\, \hat{\mathscr{M}}^{(X)\,(\theta)}_{\lambda\,-\nu}\, \hat{\mathscr{R}}_1 = (-1)^{\lambda}\, \hat{\mathscr{M}}^{(X)\,(\theta)}_{\lambda\mu}\,; \\
\hat{\mathscr{R}}_1 = e^{-i\pi\hat{j}_1} \;\Rightarrow\; \hat{\mathscr{R}}_1^{\,2} = (-1)^{2I} \;\Rightarrow \\
\hat{\mathscr{R}}_1^{-1}\, \hat{\mathscr{M}}^{(X)\,(\theta)}_{\lambda\,-\nu} = \hat{\mathscr{R}}_1^{-1}\, \hat{\mathscr{M}}^{(X)\,(\theta)}_{\lambda\,-\nu}\, \hat{\mathscr{R}}_1^{\,2}\, (-1)^{2I} = \\
= (-1)^{\lambda-2I}\, \hat{\mathscr{M}}^{(X)\,(\theta)}_{\lambda-\nu}\, \hat{\mathscr{R}}_1
\end{array}} = \\
&= \sqrt{\frac{2I_i+1}{2I_f+1}}\, \frac{C^{I_f M_f}_{I_i M_i \lambda\mu}}{\sqrt{(1+\delta_{K0})(1+\delta_{K_f 0})}} \\
&\quad \Big[C^{I_f K_f}_{I_i K_i \lambda\; K_f - K_i}\, \langle K_f\rho_f \,|\hat{\mathscr{M}}^{(X)\,(\theta)}_{\lambda\;\nu=K_f-K_i}|K_i\rho_i\rangle \\
&\qquad + (-1)^{I_i}\, C^{I_f K_f}_{I_i - K_i \lambda\; K_f + K_i}\, \langle K_f\rho_f \,|\hat{\mathscr{M}}^{(X)\,(\theta)}_{\lambda\;\nu=K_f+K_i}\, \hat{R}_1|K_i\rho_i\rangle\Big]
\end{aligned} \tag{7.38}$$

This matrix element can be also expressed by means of the Wigner-Eckart

theorem (see (A.12))

$$\langle I_f M_f K_f \rho_f \,|\hat{\mathscr{M}}^{(X)}_{\lambda\mu}|I_i M_i K_i \rho_i\rangle = \\ = \frac{1}{\sqrt{2I_f+1}}\, C^{I_f M_f}_{I_i M_i \lambda\mu}\, \langle I_f K_f \rho_f \,||\hat{\mathscr{M}}^{(X)}_{\lambda}||I_i K_i \rho_i\rangle \tag{7.39}$$

The comparison of (7.39) and (7.38) gives

$$\langle I_f K_f \rho_f \,||\hat{\mathscr{M}}^{(X)}_{\lambda}||I_i K_i \rho_i\rangle = \\ = \sqrt{\frac{(2I_i+1)}{(1+\delta_{K_i 0})(1+\delta_{K_f 0})}}\, \Big[C^{I_f K_f}_{I_i K_i \lambda\, K_f - K_i}\, \langle K_f \rho_f \,|\hat{\mathscr{M}}^{(X)\,(\theta)}_{\lambda\,\nu=K_f-K_i}|K_i\rho_i\rangle \\ + (-1)^{I_i}\, C^{I_f K_f}_{I_i - K_i \lambda\, K_f + K_i}\, \langle K_f \rho_f \,|\hat{\mathscr{M}}^{(X)\,(\theta)}_{\lambda\,\nu=K_f+K_i}\, \hat{R}_1 |K_i\rho_i\rangle\Big] = \tag{7.40}$$

where the laboratory frame transition operators in the long wave approximation are following (see (2.128) and (2.140))

$$\hat{\mathscr{M}}^{(el)}_{\lambda\,\mu} = \sum_{\nu=-\lambda}^{+\lambda} D^{\lambda}_{\mu\,\nu}(\theta)\, \sum_{i=1}^{A} e_i\, r_i^{\lambda}\, Y_{\lambda\mu}(\hat{r}_i) \\ \hat{\mathscr{M}}^{(mag)}_{\lambda=1\,\mu} = \sqrt{\frac{3}{4\pi}}\, \sum_{\nu=-1}^{+1} D^{1}_{\mu\,\nu}(\theta) \Big\{ \sum_{i=1}^{A} \Big[g_l^{(i)} \hat{l}_\nu^{(i)} + g_s^{(i)} \hat{s}_\nu^{(i)}\Big]\, \mu_N \Big\} + \\ + \sqrt{\frac{3}{4\pi}}\, \mu_N\, g_R\, \hat{R}_\mu \tag{7.41}$$

where $\vec{r}_i$ is the coordinate vector of the i-th nucleon in the intrinsic frame, $\hat{l}_\nu^{(i)}$ and $\hat{s}_\nu^{(i)}$ are orbital and spin intrinsic momentum spherical $\nu-$ component ($\nu = 0, \pm 1$), respectively, and $g_R \approx \frac{Z}{A}$ is so called rotor gyromagnetic ratio (see further discussion in this chapter).

The substitution of (7.40) into (7.36) gives the reduced probability $B(X\lambda; I_i K_i \rho_i \to I_f K_f \rho_f)$ in the following form

$$B(X\lambda;\, I_i K_i \rho_i \to I_f K_f \rho_f) = \\ = \Big| C^{I_f K_f}_{I_i K_i \lambda\, K_f - K_i}\, \langle K_f \rho_f \,|\hat{\mathscr{M}}^{(X)\,(\theta)}_{\lambda\,\nu=K_f-K_i}|K_i\rho_i\rangle \\ + (-1)^{I_i}\, C^{I_f K_f}_{I_i - K_i \lambda\, K_f + K_i}\, \langle K_f \rho_f \,|\hat{\mathscr{M}}^{(X)\,(\theta)}_{\lambda\,\nu=K_f+K_i} \hat{\mathscr{R}}_1 |K_i\rho_i\rangle \Big|^2 \tag{7.42}$$

Keeping the assumption of the neglecting of the Coriolis and centrifugal interactions in (7.15) the reduced probability for so called intraband transitions ($K_i\rho_i = K_f\rho_f \equiv K\rho$) are given by (because the second term in (7.42) is zero for $K \neq 0$ [2] and for the case $K = 0$ the second term is equal to the first term if the condition $(-1)^I r_1^{(i)} = 1$ is fulfilled)

$$B(X\lambda;\ I_iK\rho \to I_fK\rho) \approx \left(C^{I_fK}_{I_iK\lambda 0}\right)^2 \left|\langle K\rho\,|\hat{\mathscr{M}}^{(X)\,(\theta)}_{\lambda\,0}|K\rho\rangle\right|^2 \tag{7.43}$$

where $\langle K\rho\,|\hat{\mathscr{M}}^{(X)\,(\theta)}_{\lambda\,0}|K\rho\rangle$ is the intrinsic diagonal matrix element of the corresponding multipole transition operator. Usually it can be shown that the diagonal matrix elements of multipole transition operators are much bigger in the comparison with the nondiagonal matrix elements. This is connected with the symmetry of the mean field. For instance, in the case of the quadrupole deformed nucleus we have

$$\begin{aligned}
\left|\langle K\rho|\hat{\mathscr{M}}^{(el)\,(\theta)}_{2\,0}|K\rho\rangle\right|^2 &= \boxed{\begin{array}{c}\text{see}\\(2.201)\end{array}} = \\
&= \frac{5}{16\pi}\left|\langle K\rho|\hat{Q}_{33}|K\rho\rangle\right|^2 \approx \boxed{\begin{array}{c}\text{approximatelly we can write:}\\ Q_0 \approx \langle K\rho|\hat{Q}_{33}|K\rho\rangle \text{ for all } K\rho\end{array}} \approx \\
&\approx \frac{5}{16\pi}|Q_0|^2 \quad >> \left|\langle K\rho|\hat{\mathscr{M}}^{(el)\,(\theta)}_{2\,0}|K'\rho'\rangle\right|^2 \quad \text{for all } \rho\,K \neq \rho'\,K'
\end{aligned} \tag{7.44}$$

where Q_0 is the intrinsic quadrupole moment of the nucleus (see (2.202)).

So, in the case of the nuclei with the quadrupole deformation the reduced probability of E2 intraband transitions are substatially bigger than the reduced probabilities of any extraband transitions.

This conclusion is demonstrated in the Fig. 7.3 with the experimental values of the reduced probabilities $B(E2)$ of E2 transitions going from the ground state 0^+ to the first 2^+_1 excited state in even-even nuclei from a broad interval of the mass number A.

One can see from the Fig.7.3 an increase in the reduced probability $B(E2; O^+ \to 2^+_1)$ in the regions of well deformed nuclei with the stable quadrupole $a_{20} = \beta$ deformation. For these well deformed nuclei the first 2^+_1 state corresponds to the second level of the ground state rotational band (that means the transition $0^+ \to 2^+_1$ is the intraband transition). In the spherical nuclei the first

[2] For intraband transitions the multipole transition operator should have the zero projection of its multipolarity and therefore in the case of $K_i = K_f \neq 0$ the projection selection rules for the second term cannot be fulfilled.

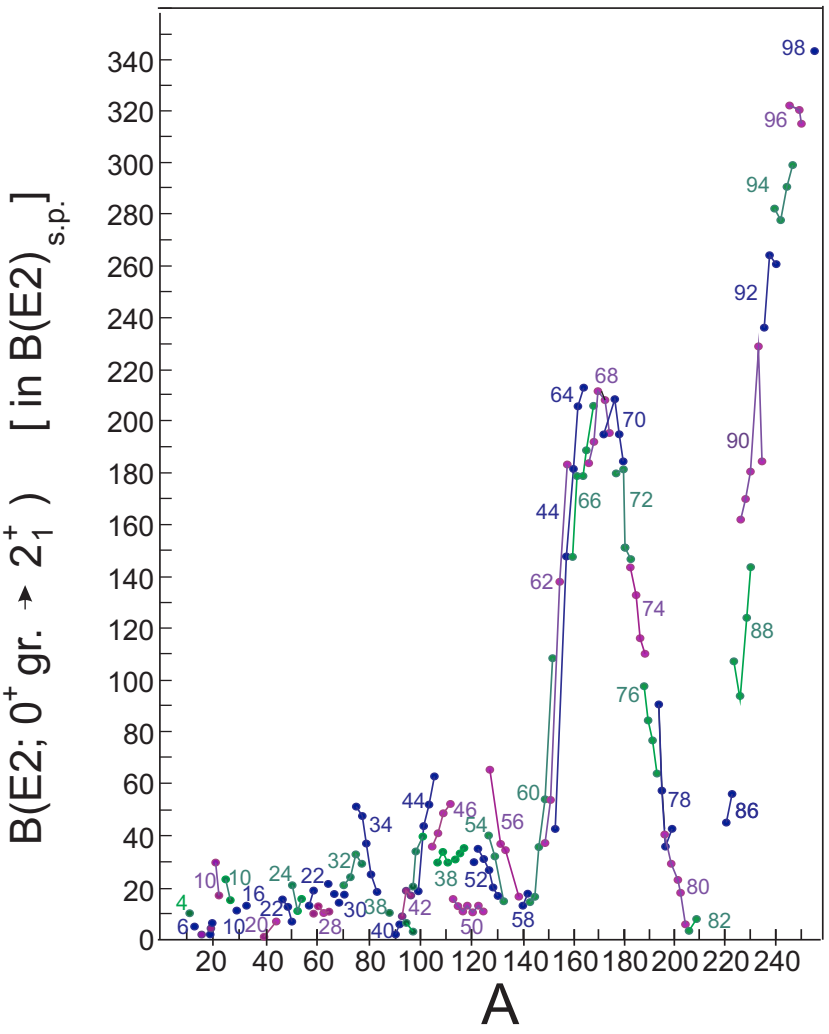


Figure 7.3: Experimental values of reduced probabilities of E2 transitions of the excitation of first 2_1^+ state from the ground state in the dependence on the mass number A. The reduced probabilities $B(E2;\ 0^+gr. \to 2_1^+)$ are given in so called s.p. units $B(E2)_{s.p.}$ which are connected with the Weisskopf units $B(E2)_{Weiss}$ defined by (2.163) as, $B(E2)_{s.p.} = 5\,B(E2)_{Weiss}$. The numbers close to the expreimental values for given chain of isotopes give the number of protons Z characterizing given isotope chain (exp. values taken from [105]).

2_1^+ state is the intrinsic vibrational state (as it will be seen in the subsection 7.2.1) and the transition $0^+ \to 2_1^+$ is not an intraband and therefore is weak. It should be noted that the square of the nondiagonal matrix elements $\left|\langle K\rho|\hat{\mathscr{M}}_{2\,0}^{(el)\,(\theta)}|K^{'}\rho^{'}\rangle\right|^2$ $(K \neq K^{'})$ or $(\rho \neq \rho^{'})$ have values equal to $\approx 1\, B(E2)_{Weiss}$.

The spectra of rotating nuclei including the taking into account of the Coriolis term in the Hamiltonian will be discused in details in the Chapter 8. Here, in the following section of the Chapter 7, the detailed discussion of the finding of the intrinsic wave function $\psi_{K\rho}(\xi)$ with the corresponding energy $E_{K\rho}$ in the framework of different approaches is given.

As it was mentioned in the previous section (see also the Chapter 1) the intrinsic degrees of freedom are represented by the single-particle motion (single nucleons move in the nuclear single-particle mean field) and by the oscillations of the nuclear shape (vibrational degrees of freedom). In the case of the spherical nuclei, where the rotational motion is not recognized, the intrinsic Hamiltonian is identical with the total Hamiltonian and single-particle and vibrational degrees of freedom form all possible degrees of freedom of the nuclear motion.

Single-particle and vibrational motions are generally strongly coupled and it is difficult from the microscopical point of view to separate them. In addition, both these types of the motion manifest themselves differently in even-even, odd-A and odd-odd nuclei. In the even-even nuclei the lowest intrinsic excitations have vibrational character while in the odd-A or in the odd-odd A nucleus the lowest states are formed mostly by single-particle (in odd-A case) or neutron s.p. - proton s.p. configurations (in odd-odd case). The even-even core of odd-A or of odd-odd A nuclei is in its ground state and the character of the lowest excitations in these nuclei are given by single-particle configurations of odd nucleons. All these aspects of the intrinsic degrees of freedom of nuclear motion are discussed in next sections of this chapter and some details also in the Chapter 8.

7.2 Phenomenological models of intrinsic degrees of freedom of nuclear motion

The problem of the extraction of the intrinsic variables ξ describing the intrinsic degrees of freedom of deformed nucleus in the case of phenomenological models is usually solved intuitively. For instance, when we want to describe

vibrations of the nuclear shape of the quadrupole character we start with the assumption that the nucleus shape in the laboratory frame in each time t is described by the Dirichlet formula (see (1.3))

$$R(\vartheta, \phi, t) = R_0 \left[\sum_{\mu=-2}^{+2} \alpha_{2\mu}(t)\, Y_{2\mu}(\vartheta, \phi) + 1 \right] \tag{7.45}$$

where parameters of the quadrupole deformation, $\alpha_{2\mu}(t)$, describe in the given time t the quadrupole form of the nucleus in the laboratoty frame. That means the quadrupole shape of the nucleus in the lab. frame is described by 5 variables $\alpha_{2\mu}(t)$ ($\mu = 0, \pm 1, \pm 2$). If we suppose that vibrating quadrupole deformed nucleus rotates in the laboratory frame and the intrinsic vibration is connected with the intrinsic parameters $a_{2\mu}(t)$ characterizing the shape of the nucleus in the time t in the intrinsic frame then the connection of the lab deformation parameters $\alpha_{2\mu}$ with the fixed body rotating frame is given by the Wigner functions:

$$\alpha_{2\mu}(t) = \sum_{\nu} a_{2\nu}(t)\, D^2_{\mu\nu}(\theta(t)) \tag{7.46}$$

Without the lack of the generality we can choose the axes of the intrinsic frame to coincide with the principal axes of the moment of inerta of the rotating nucleus. In such a case we have

$$a_{21} = a_{2-1} = 0 \qquad\qquad a_{22} = a_{2-2} \tag{7.47}$$

So instead of 5 functions $\alpha_{2\mu}(t)$ characterizing the time- dependence of the nucleus quadrupole shape in the laboratory frame we have 3 Euler angles $\theta(t)$ giving the orientation of the rotating nucleus in the given time in the lab system and 2 intrinsic variables $\xi \equiv a_{20}(t)$, $a_{22}(t)$ determining the shape of the vibrating nucleus in the intrinsic frame. Further the phenomenological approaches to the theoretical description of the intrinsic nuclear motion is discussed in more details.

7.2.1 Bohr geometrical model (nucleus as a drop of the nuclear matter)

The basic idea of the Bohr geometrical model (BGM) is based on the analogy between the nucleus and the drop of the classical liquid. The liquid drop

model (LDM) of the nucleus was already mentioned in the subsection 1.1.3 in the connection with the Weizsacker semi-empirical formula (1.13) for the nuclear binding energy. Some aspects of the LDM was also discussed in the subsection 5.1.2.3.2 in the relation to the shape of the nucleus during the fission process. In the BGM theory the liquid drop model is used for the determination of the collective Hamiltonian as a function of the collective coordinates describing the shape of the vibrating nucleus.

The shape of the nucleus in given time t is described by the Dirichlet formula (1.3) which is now written in the following form

$$R(\vartheta,\phi) = R_0 \left(1 + \sum_{\lambda=1}^{\infty} \sum_{\mu=-\lambda}^{\lambda} \alpha^*_{\lambda\mu}(t)\, Y_{\lambda\mu}(\vartheta,\phi) \right) \tag{7.48}$$

where $R(\vartheta,\phi)$ is the distance from the center of mass of the nucleus (the origin of the center of mass coordinate frame) to the nucleus surface in the direction given by angles ϑ and ϕ. In the case of the shape oscillation of the nucleus the deformation parameters $\alpha_\lambda(t)$ are functions of the time t. Since the distance $R(\vartheta,\phi)$ is real and because of the identity $Y^*_{\lambda\mu}(\vartheta,\phi) = (-1)^\mu\, Y_{\lambda\,-\mu}(\vartheta,\phi)$ the deformation parameters $\alpha_{\lambda\mu}(t)$ fulfill also this condition

$$\alpha^*_{\lambda\mu}(t) = (-1)^\mu\, \alpha_{\lambda\,-\mu}(t) \tag{7.49}$$

The deformation parameters $\alpha_{\lambda\mu}(t)$ are tensors of the rang λ from the point of view of the rotations of the coordinate frame. Therefore we have (see (A.39))

$$\alpha_{\lambda\mu}(t) = \sum_{\mu'} D^\lambda_{\mu\mu'}(\theta(t))\, a_{\lambda\mu'}(t) \tag{7.50}$$

where $a_{\lambda\mu'}(t)$ are deformation parameters in the coordinate frame (fixed-body frame) turned by Euler angles $\theta(t)$ with respect to the original coordinate frame (lab. frame) in which the deformation parameters are $\alpha_{\lambda\mu}$. Shape oscillation means the periodical dependence of $a_{\lambda\mu}$ on the time t. In the case of the spherical nucleus the equilibrium shape is the sphere:

$$\bar{a}_{\lambda\mu} = 0 \tag{7.51}$$

while the equilibrium shape of the deformed nucleus is deformed and characterized by the nonzero equilibrium deformation parameters:

$$\bar{a}_{\lambda\mu} \neq 0 \tag{7.52}$$

At first we will discuss shape vibrations of spherical nuclei. Then we will go over the vibrations of deformed nuclei where the situation is more complicated because the shape vibrations are coupled with the rotations of the nucleus.

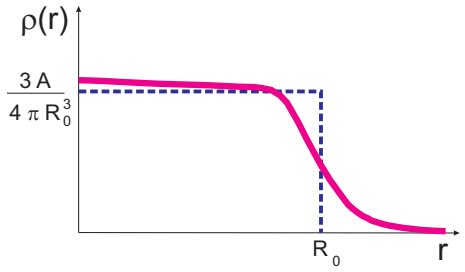


Figure 7.4: Comparison of the mass density as a function of the distance r from the center of the spherical nucleus (solid line) and the classical drop (dashed line).

7.2.1.1 Shape oscillation of the spherical nuclear droplet

In the case of the shape vibration of the spherical nucleus (the shape of the nucleus in its ground state is the sphere) the equilibrium deformation parameters for all λ and μ are zero, $\bar{\alpha}_{\lambda\mu} = \bar{a}_{\lambda\mu} = 0$. If we compare the spherical nucleus with the classical spherical drop of a liquid we can see a difference in the mass density (see Fig. 7.4). The mass density in the classical drop is supposed to be constant and the same in the whole volume of the drop from its center up to its surface. The density in the nucleus is not the same, it changes with the distance r from the nuclear center up to the nucleus surface as can be seen from the Fig.7.4. However, in each time t we suppose that the surfaces of the same density are described by the same deformation parameters $\alpha_{\lambda\mu}(t)$ as the nucleus surface (7.25). That means the surfaces of the same density are described by:

$$r(\vartheta,\phi) = r_0 \left(1 + \sum_{\lambda=1}^{\infty} \sum_{\mu=-\lambda}^{\lambda} \alpha^*_{\lambda\mu}(t)\, Y_{\lambda\mu}(\vartheta,\phi)\right) \tag{7.53}$$

where $0 < r_0 \leq R_0$. This assumption corresponds to the **irrotational fluid** for the nuclear matter in each time. The second assumption which is usually used in the LDM is the **incompressibility** of the nuclear matter. In the Appendix I it is shown that these two assumptions enable to determine all collective LDM Hamiltonian parameters.

As it was mentioned above we expect that the nuclear shape vibrations are small amplitude harmonic oscillations around the equilibrium spherical shape given by the ensamble of functions - variables $\alpha_{\lambda\mu}(t)$. By other words we expect that from the classical physics point of view the functions $\alpha_{\lambda\mu}(t)$ should be harmonic periodical functions which are solutions of the equation of motion with the harmonic oscillator Hamiltonian. That means the total

collective classical Hamiltonian H_c or Lagrangtian L_c reads

$$\begin{aligned} H_c &= \frac{1}{2}\sum_{\lambda\mu}\left(B_\lambda\,|\dot{\alpha}_{\lambda\mu}|^2 + C_\lambda\,|\alpha_{\lambda\mu}|^2\right) \\ \text{or}\quad L_c &= \frac{1}{2}\sum_{\lambda\mu}\left(B_\lambda\,|\dot{\alpha}_{\lambda\mu}|^2 - C_\lambda\,|\alpha_{\lambda\mu}|^2\right) \end{aligned} \tag{7.54}$$

Classical solutions of the equation of motion with the Lagrangian L_c is well known:

$$\alpha_{\lambda\mu}(t) = A_{\lambda\mu}\,cos\omega_\lambda t \qquad\qquad \omega = \sqrt{\frac{C_\lambda}{B_\lambda}} \tag{7.55}$$

with the total energy in the form:

$$E = \frac{1}{2}\sum_{\lambda\mu}|A_{\lambda\mu}|^2\omega_\lambda^2 B_\lambda \tag{7.56}$$

where $A_{\lambda\mu}$ are the corresponding oscillation amplitudes.

In the case with the spherical symmetry the mass parameters B_λ and potential parameteres C_λ do not depend on the multipolarity projections μ. From the point of view of the quantum mechanics the Hamiltonian (7.31) should be quantized. It can be done by the introduction of the linear moments $\pi_{\lambda\mu}$ conjugated to the collective coordinates $\alpha_{\lambda\mu}$:

$$\pi_{\lambda\mu} = \frac{\partial L_c}{\partial\dot{\alpha}_{\lambda\mu}} = B_\lambda\,\dot{\alpha}^*_{\lambda\mu} \tag{7.57}$$

by the following postulation of the commutator relations for coordinate $\hat{\alpha}_{\lambda\mu}$ and linear moment $\hat{\pi}_{\lambda\mu}$ operators

$$[\hat{\alpha}_{\lambda\mu},\hat{\pi}_{\lambda'\mu'}] = i\hbar\,\delta_{\lambda\lambda'}\delta_{\mu\mu'} \quad\Leftrightarrow\quad \hat{\pi}_{\lambda\mu} = -i\hbar\,\frac{\partial}{\partial\alpha_{\lambda\mu}} \tag{7.58}$$

From the quantum mechanics of the harmonic oscillator it is known that for each λ and μ we can introduce so called oscillator quanta (see e.g. [104, 14]) which are known in the nuclear physics as phonons. The corresponding

creation ($Q^+_{\lambda\mu}$) and annihilation ($Q_{\lambda\mu}$) operators are:

$$Q^+_{\lambda\mu} = \left(\frac{\omega_\lambda\, B_\lambda}{2\hbar}\right)^{1/2}\left(\hat\alpha_{\lambda\mu} - \frac{i(-1)^\mu}{\omega_\lambda B_\lambda}\,\hat\pi_{\lambda-\mu}\right)$$
$$Q_{\lambda\mu} = \left(\frac{\omega_\lambda\, B_\lambda}{2\hbar}\right)^{1/2}\left((-1)^\mu\,\hat\alpha_{\lambda-\mu} + \frac{i}{\omega_\lambda B_\lambda}\,\hat\pi_{\lambda\mu}\right)$$

or inversely

$$\hat\alpha_{\lambda\mu} = \left(\frac{\hbar}{2B_\lambda\omega_\lambda}\right)^{1/2}\left(Q^+_{\lambda\mu} + (-1)^\mu\, Q_{\lambda-\mu}\right)$$
$$\hat\pi_{\lambda\mu} = \left(\frac{\hbar B_\lambda\omega_\lambda}{2}\right)^{1/2}\left((-1)^\mu\, Q^+_{\lambda-\mu} - Q_{\lambda\mu}\right) \tag{7.59}$$

Then the commutator relations (7.58) are equivalent to the following boson commutator relations

$$\left[Q_{\lambda\mu}\,, Q^+_{\lambda'\mu'}\right] = \delta_{\lambda\lambda'}\,\delta_{\mu\mu'} \tag{7.60}$$

That means phonons (7.59) have boson character. The energy $\hbar\omega_\lambda$ of each boson can be then obtained from the following quantum oscillator equations

$$\left[\hat H_c\,, Q^+_{\lambda\mu}\right] = \hbar\omega_\lambda\, Q^+_{\lambda\mu} \qquad\qquad \left[\hat H_c\,, Q_{\lambda\mu}\right] = -\hbar\omega_\lambda\, Q_{\lambda\mu} \tag{7.61}$$

with the corresponding phonon vacuum $|0\rangle$

$$Q_{\lambda\mu}|0\rangle = 0 \tag{7.62}$$

for all λ and μ.

From (7.55) it follows that if the mass and potential parameters B_λ and C_λ are known then the energies of collective vibrational states, $Q^+_{\lambda\mu}|0\rangle$, $Q^+_{\lambda_1\mu_1}Q^+_{\lambda_2\mu_2}|0\rangle, \ldots$ are given by $\hbar\omega_\lambda$, $\hbar\omega_{\lambda_1} + \hbar\omega_{\lambda_2}$, ...

The value of B_λ and C_λ for all λ are usually determined from the LDM (see e.g. [9, 99]) using the irrotational and incompressibility assumptions. The derivation of them is shown in the Appendix I and result is (see (I.13) and(I.34))

$$B_\lambda = \frac{M\rho_0 R_0^5}{\lambda} = \boxed{\begin{array}{c}\text{in the 1-st approximation}\\ \rho_0 = A/\frac{4}{3}\pi R_0^3\end{array}} = \frac{3}{4\pi\lambda}AMR_0^2$$
$$C_\lambda = \sigma\, R_0^2(\lambda-1)(\lambda+2) - \frac{3}{2\pi}\frac{Z^2\, e\,\tilde e}{R_0}\frac{\lambda-1}{2\lambda+1} \tag{7.63}$$

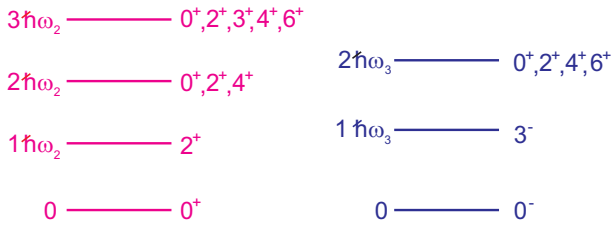


Figure 7.5: Qudrupole and octupole vibrational spectra, respectively. In the l.h.s. of each spectrum there are energies and in the r.h.s. the possible total ang. momenta are given (schematic figure).

where $\tilde{e} = e/4\pi\epsilon_0$ and σ is the nucleus surface tension parameter (see the text under the expression (1.14)). So for each λ we obtain the sequence of excited states generated from the ground state $|0\rangle$ by sequential application of the creation operator $Q^+_{\lambda\mu}$ (one- phonon states $Q^+_{\lambda\mu}$. two- phonon states $Q^+_{\lambda_1\mu_1}Q^+_{\lambda_2\mu_2}|0\rangle$, ...) with the corresponding spectrum given in the schematic figure Fig.7.5 for $\lambda = 2, 3$. It is necessary to realize that for given number of phonons in the given excited state not all total angular moments allowed by the coupling of ang. moments are possible. This is connected with the fact that the possible total moments are also restricted by the requirement of the complete symmmetry of the N- boson wave function. We will demonstrate it on the case of two- quadrupole phonon states constructed from two-quadrupole phonons:

$$|2\,\mu\rangle \equiv Q^+_{2\mu}\,|0\rangle \qquad\qquad |2'\,\mu'\rangle \equiv Q^+_{2\mu'}\,|0\rangle$$

The corresponding wave function coupled to the total angular moment I with its projection M to the 3-d axis is following

$$|2\,2';\,IM\rangle = \sum_{\substack{\mu\,\mu' \\ \mu+\mu'=M}} C^{IM}_{2\,\mu\,2'\mu'}\,|2\mu\rangle\,|2'\mu'\rangle \tag{7.64}$$

and if the sequence of the coupling is reversed then

$$|2'\,2;\,IM\rangle = \sum_{\substack{\mu\,\mu' \\ \mu+\mu'=M}} C^{IM}_{2'\mu'\,2\,\mu}\,|2'\mu'\rangle\,|2\,\mu\rangle = \boxed{\begin{matrix}\text{see} \\ (A.4)\end{matrix}} =$$

$$= (-1)^{I-4} \sum_{\substack{\mu\,\mu' \\ \mu+\mu'=M}} C^{IM}_{2\,\mu\,2'\mu'}\,|2\mu\rangle\,|2'\mu'\rangle \tag{7.65}$$

Since phonons are bosons the two- boson wave function $|2\,2^{'};\,IM\rangle$ should be symmetric with respect to the exchange $|2\mu\rangle \leftrightarrow |2^{'}\mu^{'}\rangle$ and the comparison of (7.64) and (7.65) gives

$$(-1)^{I-4} = 1 \qquad \Rightarrow \qquad I \ \text{ is even} \tag{7.66}$$

Therefore two- quadrupole phonon states can have only moments with $I =$

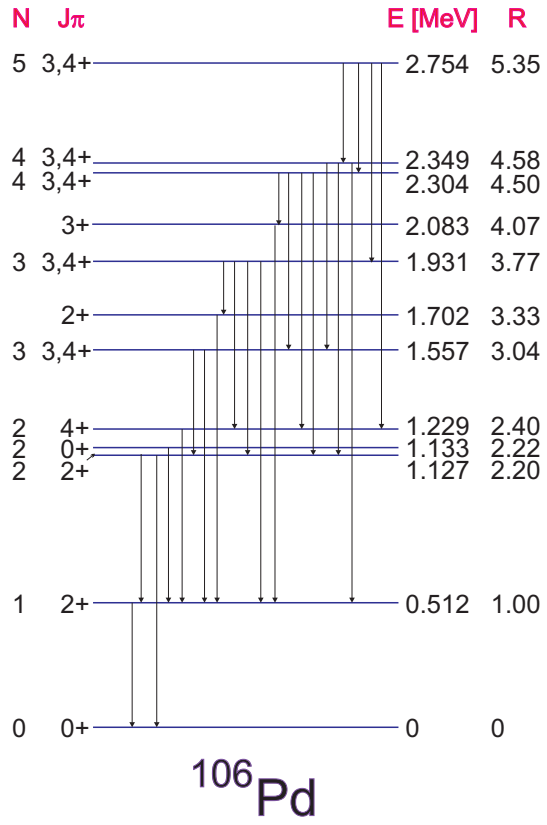


Figure 7.6: Positive parity vibrational spectrum of ^{106}Pd (N is the number of quadrupole phonons in given state, $J\pi$ is the ang. moment and parity of given state, R is the excitation energy of given state in the units of the excitation energy of the first excited state = one-quadrupole phonon state)

0, 2, 4 as it is seen in the Fig. 7.5. Since in the case of the spherical symmetry of the nucleus all phonon energies $\hbar\omega_\lambda$ does not depend on the multipolarity projection all states $|2\,2^{'};\,IM\rangle$ (for all $I = 0,\ 2,\ 4$ and all M) have the same energy $2\,\omega_{\lambda=2}$ as it can be also seen in the Fig. 7.5. The symmetry of the coupled wave functions for the general multi- phonon states give the similar restriction for values of the total angular moment. For instance, 3 quadrupole phonon states with the energy $3\,\hbar\omega_{\lambda=2}$ can have only angular moment $I = 0,\ 2,\ 3,\ 4,\ 6$ or the total angular moment of the 2- octupole phonon states can be equal to $I = 0,\ 2,\ 4,\ 6$.

If the harmonic spectrum given in the Fig. 7.5 is compared with the experimental spectrum of the realistic spherical nucleus then the degeneracy of the multi- phonon states with respect to their angular moment is not observed exactly. However, as it can be seen from the Fig. 7.6 with the experimental spectrum of ^{106}Pd, some traces of this degeneracy can be seen (e.g. the triplet 2^+, 0^+, 4^+ observed around the energy 1.1 - 1.2 MeV corresponds to the two-quadrupole phonon states).

Knowing the phonon operators $Q^+_{\lambda\mu}$, $Q_{\lambda\mu}$ (see (7.59)) with their energies $\hbar\omega_\lambda$ we can determine not only spectra but also other nuclear properties in the framework of discussed LDM, e.g. the probabilities of electromagnetic transitions. From the Chapter 2 (see (2.147), (2.148)) it is known that these electromagnetic transition probabilities are given by the square of the electric and magnetic transition multipole operator matrix elements. For instance the electric multipole operator in the long wave approximation (see (2.130)) is given by:

$$\hat{\mathscr{M}}^{(el)}_{\lambda\mu} = e \int d^3r \; \hat{\rho}_p(\vec{r}) \; r^\lambda Y_{\lambda\mu}(\hat{r}) \tag{7.67}$$

where $\hat{\rho}_p(\vec{r})$ is the operator of the proton density. In the simple version of the LDM discussed here the proton density is constant in the nucleus volume: $\rho_p(\vec{r}) \approx Z \;/\; \frac{4}{3}\pi R_0^3 = \frac{3Z}{4\pi R_0^3}$ for $\vec{r}$ inside the nucleus. In order to calculate the matrix elements of the operator $\hat{\mathscr{M}}^{(el)}_{\lambda\mu}$ we should express it in terms of the collective coordinator operators $\hat{\alpha}_{\lambda\mu}$ or phonon operators $Q^+_{\lambda\mu}$, $Q_{\lambda\mu}$. Since the proton density is nonzero only in the volume of the nucleus the expression (7.67) can be rewritten as follows

$$\begin{aligned}
\hat{\mathscr{M}}^{(el)}_{\lambda\mu} &= \frac{3Ze}{4\pi R_0^3} \int d\Omega \int_0^{R(\vartheta,\phi)} dr \; r^{\lambda+2} Y_{\lambda\mu}(\hat{r}) = \frac{3Ze}{4\pi R_0^3} \int d\Omega \left[\frac{r^{\lambda+3}}{\lambda+3} \right]_0^{R(\vartheta,\phi)} Y_{\lambda\mu}(\hat{r}) = \\
&= \frac{3Ze}{4\pi R_0^3(\lambda+3)} \int d\Omega \; Y_{\lambda\mu}(\vartheta,\phi) \; (R(\vartheta,\phi))^{\lambda+3} = \boxed{\begin{array}{c}\text{see}\\(7.48)\end{array}} = \\
&= \frac{3Ze}{4\pi R_0^3(\lambda+3)} \int d\Omega \; Y_{\lambda\mu}(\vartheta,\phi) \; R_0^{\lambda+3} \left(1 + \sum_{\lambda\mu} \hat{\alpha}_{\lambda\mu} Y^*_{\lambda\mu}(\hat{r}) \right)^{\lambda+3}
\end{aligned} \tag{7.68}$$

Further we use the identity, $(1+x)^n = \sum_k \binom{n}{k} 1^k \, x^{n-k}$, and for the simplicity

we restrict ourselves to $\lambda = 2$

$$\hat{\mathscr{M}}^{(el)}_{2\mu} = \frac{3ZeR_0^5}{20\,\pi R_0^3}\int d\Omega\ Y_{2\mu}(\vartheta,\phi)\,\big(\,1+\sum_{\lambda'\mu'}\hat{\alpha}_{\lambda'\mu'}Y^*_{\lambda'\mu'}(\hat{r})\,\big)^5 \approx$$

$$\approx \frac{3ZeR_0^5}{20\,\pi R_0^3}\int d\Omega\ Y_{2\mu}(\vartheta,\phi)\,\Big(\,1+5\sum_{\lambda'\mu'}\hat{\alpha}_{\lambda'\mu'}Y^*_{\lambda'\mu'}(\hat{r}) +$$

$$+\,10\sum_{\substack{\lambda'\mu'\\ \lambda''\mu''}}\hat{\alpha}^+_{\lambda''\mu''}\hat{\alpha}_{\lambda'\mu'}\,Y^*_{\lambda''\mu''}(\hat{r})Y_{\lambda'\mu'}(\hat{r})\ +\ \ldots\Big) =$$

$$= \boxed{\begin{array}{c}\text{because } \int d\Omega\, Y_{20}=0,\ \int d\Omega\, Y_{2\mu}Y^*_{\lambda'\mu'} = \delta_{\lambda'2}\,\delta_{\mu'\mu}\\ \text{and we restrict ourselves up to the linear terms in } \hat{\alpha}_{\lambda\mu}\end{array}} =$$

$$= \frac{3ZeR_0^2}{4\pi}\,\hat{\alpha}_{2\mu} \tag{7.69}$$

Generally up to the quadratic order in $\hat{\alpha}_{\lambda\mu}$ and for general λ it is possible to show the following expression for $\hat{\mathscr{M}}^{(el)}_{\lambda\mu}$

$$\hat{\mathscr{M}}^{(el)}_{\lambda\mu} = \frac{3Ze^2}{4\pi}R_0^\lambda\left[\hat{\alpha}_{\lambda\mu} + \right.$$

$$+\frac{\lambda+2}{2}\sum_{\substack{\lambda_1\mu_1\\ \lambda_2\mu_2}}\hat{\alpha}_{\lambda_1\mu_1}\hat{\alpha}_{\lambda_2\mu_2}\,(-1)^\mu\sqrt{\frac{(2\lambda+1)(2\lambda_1+1)(2\lambda_2+1)}{4\pi}}$$

$$\left.\begin{pmatrix}\lambda_1 & \lambda_2 & \lambda\\ 0 & 0 & 0\end{pmatrix}\begin{pmatrix}\lambda_1 & \lambda_2 & \lambda\\ -\mu_1 & -\mu_2 & \mu\end{pmatrix}\right] \tag{7.70}$$

Matrix elements of the electric multipole operator (7.70) between multiphonon states can be then calculated if this operator is expressed in terms of the phonon operator (using(7.59)) and the boson commutator relations (7.60) together with (7.63) are applied.

Similarly as for electric multipole operator it is necessary to express also magnetic multipole operator in terms of operators $\hat{\alpha}_{\lambda\mu}$. Magnetic multipole operator in the long wave approximation is given by (2.134):

$$\hat{\mathscr{M}}^{(mag)}_{\lambda\mu} = \frac{1}{c(\lambda+1)}\int d^3r\ \left(\vec{r}\times\hat{\vec{j}}_p(\vec{r})\right)\cdot\left(\vec{\nabla}r^\lambda Y_{\lambda\mu}(\hat{r})\right) \tag{7.71}$$

Similarly as the expressions (7.63) for the mass B_λ and potential C_λ parameters were derived using the assumption of the incompressibility and irrotationality of the nuclear matter - see the Appendix I, it is possible to use these assumptions to express the charge current density $\hat{\vec{j}}_p(\vec{r})$ (and therefore also the whole operator (7.71)) in terms of the operators $\hat{\alpha}_{\lambda\mu}$ and $\hat{\pi}_{\lambda\mu}$. Then, applying (7.59), (7.60) with (7.62) the matrix elements of the magnetic multipole operator $\hat{\mathscr{M}}_{\lambda\mu}$ between multi- phonon states can be determined (see [9]). Since this procedure is quite involved we do not give it here. We will only show the determination of the multi-phonon matrix elements of the operator $\hat{\mathscr{M}}_{1\mu}$ (dipole case) where the derivation is simple if the spin part of the nuclear charge current is neglected.

In the case of $\lambda = 1$ the magnetic dipole transition operator $\hat{\mathscr{M}}_{1\mu}$ is related to the operator of the static magnetic dipole moment $\hat{\vec{\mu}}$ by the expression (2.210)

$$\hat{\mathscr{M}}_{1\mu} = \sqrt{\frac{3}{4\pi}}\,\hat{\mu}_\mu\ , \qquad \mu = 0, \pm 1 \tag{7.72}$$

where (see (2.205))

$$\hat{\vec{\mu}} = \frac{1}{2c}\int_{(V)} d^3r\,\left(\vec{r}\times\vec{j}_p(\vec{r})\right) = \boxed{\begin{array}{c}\text{if the spin part of the current}\\ \text{density is neglected: } \vec{j}_p(\vec{r}) = \frac{Ze}{A}\vec{v}\end{array}} =$$

$$= \frac{Ze}{2AMc}\int_{(V)} d^3r\,(\vec{r}\times M\vec{v}) = \boxed{\begin{array}{c}\text{because}\\ \vec{I} \approx \frac{1}{\hbar}\int_{(V)} d^3r\,(\vec{r}\times M\vec{v})\end{array}} =$$

$$\approx \frac{Z}{A}\,\frac{e\hbar}{2Mc}\,\hat{\vec{I}} \equiv g_R\,\hat{\vec{I}}\,\mu_N \tag{7.73}$$

where $\mu_N = \frac{e\hbar}{2Mc}$ is so called nucleon magneton, $\hat{\vec{I}}$ is the operator of the total ang. moment and

$$g_R \equiv \frac{Z}{A} \tag{7.74}$$

is the rotor gyromagnetic ratio. The calculation of the absolute transition probabilities of transitions from excited states (the half lifes of the excited states) requires the knowledge of the corresponding reduced probabilities $B(X\lambda;\ I_i \to I_f)$ (see (2.148), (2.147))

$$B(X\lambda;\ I_i \to I_f) = \frac{1}{2I_i+1}\,|\,\langle I_f\nu_f||\hat{\mathscr{M}}^{(X)}{}_\lambda||\ I_i\nu_i\rangle|^2 =$$

$$= \sum_{\mu M_f} |\,\langle I_f M_f\nu_f|\hat{\mathscr{M}}^{(X)}{}_{\lambda\mu}|\ I_i M_i\nu_i\rangle|^2 \tag{7.75}$$

with $X = el,\ mag$. If we substitute (7.72) together with the approximation (7.73) into (7.75) we see that we need the matrix elements $\langle I_f \nu_f || \hat{I}_\mu || I_i \nu_i \rangle$ which are given by (see the page 489 in [2])

$$\langle I_f \nu_f || \hat{I}_\mu || I_i \nu_i \rangle = \delta_{I_i I_f}\, \delta_{\nu_i \nu_f}\, \sqrt{I(I+1)(2I+1)} \tag{7.76}$$

So within the approximation (7.73) the reduced matrix element of the operator $\hat{\mathscr{M}}^{(mag)}_{1\mu}$ is nonzero only in the case of the diagonal matrix element, that means for the unphysical transition $|I\nu\rangle \to |I\nu\rangle$. Therefore the realistic M1 transitions are forbidden in the framework of the approximation (7.73). Even in the case, when we go beyond this approximation and we take into account the spin part of the nuclear charge current, the LDM or BGM gives the M1 transitions very weak (underestimation with respect to the experimental values).

Next example of the application of the LDM or BGM is the reduced probability $B(E2)$ for E2 transitions from the ground state $|0\rangle$ to the one- phonon states $Q^+_{2\mu}|0\rangle$. According to (7.69) and (7.75) these reduced probabilities read

$$B(E2;\ 0^+ \to 2^+_1) = \sum_{\mu'=-2}^{2} \left| \frac{3ZeR_0^2}{4\pi} \right|^2 \left| \langle 0 | Q_{2\mu}\, \hat{\alpha}_{2\mu'} | 0 \rangle \right|^2 = \boxed{\begin{array}{c}\text{see}\\(7.59)\end{array}} =$$

$$= \left| \frac{3ZeR_0^2}{4\pi} \right|^2 \frac{\hbar}{2B_2\omega_2} \sum_{\mu'=-2}^{2} \left| \langle 0 | Q_{2\mu}\, Q^+_{2\mu'} | 0 \rangle \right|^2 = \left| \frac{3ZeR_0^2}{4\pi} \right|^2 \frac{5\,\hbar}{2B_2\omega_2} \tag{7.77}$$

where (see (7.63), (7.55))

$$B_2 = \frac{3}{8\pi}\, AMR_0^2\,, \quad C_2 = 3\sigma R_0^2 - \frac{3}{10\pi}\frac{Ze\tilde{e}}{R_0}\,, \quad \omega_2 = \sqrt{\frac{C_2}{B_2}} \tag{7.78}$$

In order to compare the result of the LDM for $B(E2;\ 2_1\mu \to 0^+)$ with the experimental results it is necessary to clarify what experimental data we can describe in terms of the LDM. In the schematic figure Fig. 7.7 the typical spectrum of the 2^+ states in the nucleus are sketched. The spectrum of 2^+ states consists from discrete levels in the low- energy part and the continuous part in the higher energies. Among the discrete levels there is usually one with quite high value $B(E2;\ 2^+\mu \to 0^+)$ in the comparison with other discrete levels and usually this level is the lowest in the energy. The

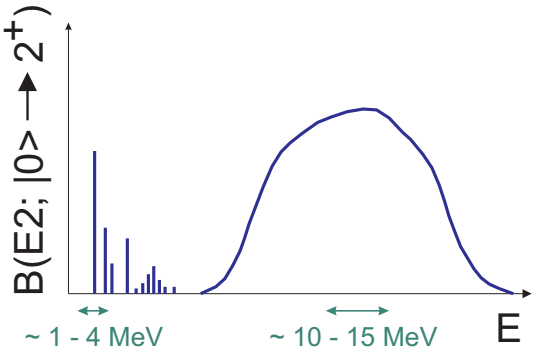


Figure 7.7: Schematic figure of the 2^+ spectra in nuclei. The ordinate gives the $B(E2)$ values for the discrete levels and the distribution of the $B(E2)$ strength in the resonance region. The energy of the isoscalar E2 resonance maximum depends on the A and it is about 15-20 MeV and the energy of the first 2^+ level is about 1-5 MeV (for rare-earths and actinides) also depending on A.

value $B(E2;\, 2^+\mu \to 0^+)$ of this level for spherical nuclei is about 10-20 times higher than the single-particle Weisskopf units (see (2.163)),

$$B(E2)_{Weis} = \frac{(1.2)^4}{4\pi} \left(\frac{3}{5}\right)^2 A^{4/3}\,.$$

So the state corresponding to this level has usually collective character (that means many nucleons contribute to this value of $B(E2;\, 2^+\mu \to 0^+)$ and therefore this state is interpreted as the surface quadrupole vibration (e.g. the first excited state 2^+ in the Fig. 7.6 of the vibrational ^{106}Pd spectrum). Therefore in the framework of the LDM one- phonon state $Q_{2\mu}|0\rangle$ can be identify with this experimental first excited $|2_1^+\rangle$ state. In the Fig. 7.8 the experimental energies of the first 2_1^+ levels are compared for a broad region of isotopes with the calculated one- quadrupole LDM phonon energies (7.78), $E_2^{(LDM)} = \hbar\omega_2 = \hbar\sqrt{\frac{C_2}{B_2}}$ (solid line in the Fig. 7.8 corresponds to the energy 0.2 $E_2^{(LDM)}$). From the Fig. 7.8 one observes large shell effects. Only the average trend is given by the LDM expr. (7.77), the Fig. 7.8 shows a general overestimation of the energies E_{2_1} by the LDM - the absolute value is off by a factor of five for spherical nuclei. For deformed nuclei the experimental values of E_{2_1} are even smaller (see interval $150 \leq A \leq 185$ for rare earths and $A > 200$ for actinides). This is because the character of the $|2_1^+\rangle$ state in deformed nuclei is not of vibrational type but the first $|2_1^+\rangle$ states in deformed nuclei belong to the ground rotational band where the first excitation energy is much lower than for vibrational states (rotational bands will be discussed in details in the Chapter 8).

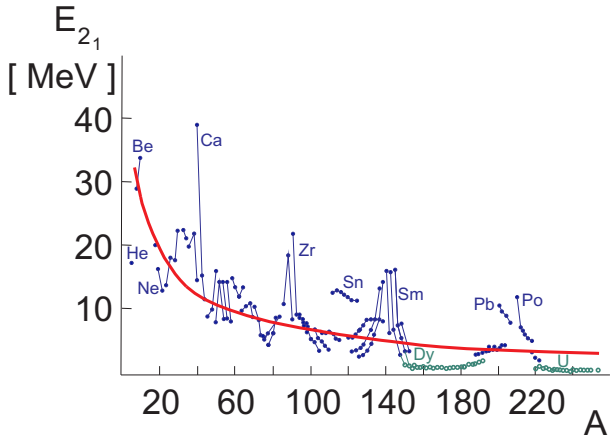


Figure 7.8: The energy of the first 2^+ state in even-even nuclei. Well-deformed nuclei are marked by green open circles. Solid red line corresponds to energies calculated as $0.2\,\hbar\,\omega_2$ where ω_2 is given by (7.77). Exp. data taken from [105].

From the point of view of the comparison of the LDM phonon energy $\hbar\omega_2 = \sqrt{\frac{C_2}{B_2}}$ with experimental data it is probably better to compare them not with the energy $E^+_{2_1}$ of the first excited 2^+ level but with the energy E_{GQR} of the centroid of the isoscalar quadrupole giant resonance (e.g. the energy of the centroid of the isoscalar E2 resonance for nuclei with $A \approx 200$ is $\approx$ 10-15 MeV while the energy $E^+_{2_1} \approx 4$ MeV). Then, if we suppose that one LDM level with $\lambda = 2$ describes the whole isoscalar E2 resonance, the agreement of the LDM energy $\hbar\omega_2$ with E_{GQR} is much better than if we compare it with $E^+_{2_1}$ (without any factor of 5 mentioned above). The assumption that all isoscalar E2 strength is concentrated in a small energy interval (even in one level) is in the agreement with other models from the past (see e.g. [99, 106]).

Concerning the comparison of experimental values of $B(E2;\ 0^+ \rightarrow 2^+_1)$ with corresponding LDM values (7.77) it is better to compare the ratio $B(E2;\ 2^+_1 \rightarrow 2^+_2)\ /B(E2;\ 0^+ \rightarrow 2^+_1)$ (direct comparison of the exp. values of $B(E2;\ 0^+ \rightarrow 2^+_1)$ with calculated ones in the framework of different models will be discussed in the Chapter 8). In the framework of the LDM the second 2^+ state $|2^+_2\mu\rangle$ is the two- quadrupole phonon state $|2^+_2\mu\rangle \approx \sum_{\mu_1\mu_2} C^{2\mu}_{2\mu_1 2\mu_2} Q^+_{2\mu_1} Q^+_{2\mu_2}\ |0\rangle$. That means in the framework of the LDM the

reduced probability $B(E2;\ 2_1^+ \to 2_2^+)$ reads

$$\begin{aligned} & B(E2;\ 2_1^+\mu \to 2_2^+\mu') = \\ & = \left|\frac{3ZeR_0^2}{4\pi}\right|^2 \frac{5\,\hbar}{2B_2\omega_2} \sum_{\nu'=-2}^{2} |\sum_{\mu_1\mu_2} C^{2\mu'}_{2\mu_1 2\mu_2} \langle 0|\ Q_{2\mu_2} Q_{2\mu_1} Q^+_{2\nu} Q^+_{2\mu}\ |0\rangle|^2 = \\ & = 2\ \left|\frac{3ZeR_0^2}{4\pi}\right|^2 \frac{5\,\hbar\,\delta_{\mu\mu'}}{2B_2\omega_2} = \boxed{\begin{array}{c}\text{see}\\(7.77)\end{array}} = 2\ B(E2;\ 0^+ \to 2_1^+) \end{aligned} \tag{7.79}$$

That means the LDM gives the following ratio

$$\frac{B(E2;\ 2_1^+\mu \to 2_2^+\mu_1+\mu_2)}{B(E2;\ 0^+ \to 2_1^+\mu)} = 2 \tag{7.80}$$

The corresponding experimental values for a broad region of even-even spherical nuclei are

$$\frac{B(E2;\ 2_1^+ \to 2_2^+)}{B(E2;\ 0^+ \to 2_1^+)} = 0.5\ -\ 1.6 \tag{7.81}$$

From the comparison of experimental data about energies and electromagnetic transition probabilities discussed above it follows that the LDM gives only a very qualitative agreement. It is clear that the shell effects seen in the Fig. 7.8 as a fluctuation of the $E_{2_1^+}$ in the dependence on A cannot be explained by the LDM. Similar fluctuations are observed not only for $\lambda^\pi = 2^+$ but also for other multipolarities and parities.

From the schematic Fig. 7.7 of the spectrum of 2^+ states it is obvious for the given $\lambda = 2$ that we have not only one degenerate level $E_{2_1^+}$ corresponding to 5 states with the ang. moment projections $\mu = -2,\ -1,\ 0,\ 1,\ 2$ but there are a lot of states 2^+ which in the higher energy create a quadrupole giant resonance (a broad continuous higher energy peak in the Fig. 7.7). This discrepancy between the LDM or BGM predictions and the reality is caused by the fact that the collective vibrational degrees of freedom are in the LDM one-phonon level with given λ restricted only to $2\lambda+1$ phonon states $Q^+_{\lambda\mu}|0\rangle$ with $\mu = -\lambda, \ldots, +\lambda$. The LDM does not take into account the single-particle degrees of freedom. In the reality each state with given λ (e.g. quadrupole excited states $\lambda^\pi = 2^+$) is a certain mixture of the single-particle and vibrational degrees of freedom with different degree of a collectivity. In order to explain this mixture it is necessary to go beyond phenomenological models of the LDM or BGM type and to use some more microscopical approach. This is discussed in the section 7.3.

This subsection has involved only the LDM of the harmonic shape vibrations of the spherical nuclei around their spherical equilibrium shape. In the next subsection the version of the LDM for deformed nuclei will be discussed.

7.2.1.2 Vibration and rotation of the deformed droplet

In the original version of the LDM discussed in the previous subsection the small vibrations of the quantum droplett were assumed around the spherical equilibrium shape. In this subsection the small shape vibrations are treated in the framework of the LDM with the deformed equilibrium shape.

As it was already mentioned in the beginning of this chapter the shape of the vibrating deformed nucleus is described by the Dirichlet formula (7.48) (in the laboratory frame) but now the equilibrium deformation parameters are nonzero ($\bar{\alpha}_{\lambda\mu} \neq 0$ - see (7.52)). It should be realized that in the case of the nonzero equilibrium deformation the dynamical deformation parameters $\alpha_{\lambda\mu}(t)$ in the formula (7.48) describe not only the vibrations of the deformed droplet in the laboratory frame but also its rotation.

If the deformed nuclear droplet is axially symmetric and the symmetry axis coincides with the 3-d axis of the intrinsic coordinate frame, rotating together with the nucleus, then the eigen-function of the intrinsic part of the nucleus Hamiltonian is simultaneously the eigen-function of the 3-d component of the intrinsic angular momentum ($\hat{j}_3\ \phi_{K\rho}(\xi) = K\ \phi_{K\rho}(\xi)$ - see (7.18)). An arbitrary turn round the 3-d intrinsic axis generates only the phase factor in the wave function ($e^{ij_3\phi}\phi_{K\rho}(\xi) = e^{iK\rho}\psi_{k\rho}(\xi)$ which does not change the values of measurable quantities. Therefore the rotations round the 3-d intrinsic axis are not distinguishable (see also the text below expression (7.9)).

Since the quadrupole ($\lambda = 2$) deformation component in the sum (7.48) is the most dominate component in all well-deformed nuclei in their ground state further we restrict ourselves only to $\lambda = 2$. We also suppose that the coordinate axis of the intrinsic frame coincides with the principal axes of the nucleus moment of inertia (which are usually also the principal axes of the nucleus electric quadrupole moment tensor).

If we restrict ourselves only to $\lambda = 2$ then in the framework of the LDM we have 5 variables, $\alpha_{2\mu}(t)$ with $\mu = 0,\ \pm 1,\ \pm 2$, which determine in each time t the shape of the vibrating nucleus in the laboratory system (see (7.45)). These 5 variables can be transformed from the laboratory frame to the in-

trinsic one, $a_{2\nu}(t)$, according to (7.46)

$$\alpha_{2\mu}(t) = \sum_{\nu} D^{2}_{\mu\nu}(\theta(t))\, a_{2\nu}(t) \quad \leftrightarrow \quad a_{2\nu}(t) = \sum_{\mu} D^{2\,*}_{\mu\nu}(\theta(t))\, \alpha_{2\mu}(t) \qquad (7.82)$$

If the intrinsic frame axes coincide with the principal axes of the nucleus quadrupole moment tensor then 5 laboratory collective variables $\alpha_{2\mu}(t)$ can be transformed into 3 Euler angles $\theta(t)$ and two intrinsic quadrupole variables $a_{20}(t)$ and $a_{22}(t)$ (see (7.47)) [3]. So the space of the quadrupole variables in the intrinsic frame are reduced to 2 dimensions (2 independent variables, $a_{20}(t)$ and $a_{22}(t)$, determines in each time the quadrupole shape of the vibrating nucleus in the intrinsic frame). Instead of these two variables, $a_{20}(t)$ and $a_{22}(t)$, another two deformation variables, $\beta(t)$ and $\gamma(t)$ (see (1.5)), are usually introduced

$$a_{20}(t) = \beta(t)\, cos\, \gamma(t) \qquad a_{22}(t) = a_{2-2}(t) = \frac{1}{\sqrt{2}}\, \beta(t)\, sin\, \gamma(t) \qquad (7.83)$$

Using the transformation (7.82) and definition (7.83) we can rewrite the laboratory frame quadrupole vibrating deformed nucleus Hamiltonian (see (7.54))

$$H_c = \frac{1}{2} \sum_{\mu=\pm 2,\pm 1,0} B_2 \left|\dot{\alpha}_{2\mu}\right|^2 + \frac{1}{2} \sum_{\mu=\pm 2,\pm 1,0} C_{2\mu} \left|\alpha_{2\mu}\right|^2, \qquad (7.84)$$

expressed in terms of the laboratory frame variables $\alpha_{2\mu}(t)$, and transform it into the intrinsic frame quadrupole variables $\beta(t)$ and $\gamma(t)$ and angular velocities $\dot{\varphi}_k$ with respect to the intrinsic frame axes $k = 1, 2, 3$. After the relatively simple but tedious procedure (see [107]) we obtain classical quadrupole collective Hamiltonian in the following form ($C_{2-2} = C_{22}$)

$$H_c = T_{rot} + \frac{1}{2}\, B_2\, (\dot{\beta}^2 + \beta^2\, \dot{\gamma}^2) + U(\beta, \gamma) \qquad (7.85)$$

where the potential energy $U(\beta, \gamma)$ of quadrupole vibrations is

$$U(\beta, \gamma) = \frac{1}{2}\, C_{20} \left[a_{20}(\beta(t), \gamma(t)) - \bar{a}_{20}\right]^2 + \\ + C_{22} \left[a_{22}(\beta(t), \gamma(t)) - \bar{a}_{22}\right]^2 \qquad (7.86)$$

[3] We have only two intrinsic quadrupole shape variables because in the reality the intrinsic variables $a_{2\nu=\pm 1}(t)$ do not represent the intrinsic vibrational degrees of freedom. They are connected with the nucleus rotation (see e.g. [99]). Therefore from the point of view of the intrinsic nonrotating degrees of freedom variables $a_{2\nu=\pm 1}(t)$ are spurious.

and T_{rot} is the kinetic energy of the rotational motion

$$T_{rot} = \frac{1}{2} \sum_{k=1}^{3} \mathscr{F}_k \, \dot{\varphi}_k^2 \tag{7.87}$$

For fixed value of β and γ, T_{rot} is the collective rotational kinetic energy with moments of inertia $\mathscr{F}_k$. With β and γ changing with the time, the collective rotational and β, γ vibrational energies become coupled in a complicated way. Using the irrotational value for B_2 (see (7.63)) these moments of inertia become (so called irrotational fluid values)

$$\mathscr{F}_k^{(irr)} = \frac{3}{2\pi} \, M \, A \, R_0^2 \, \beta^2 \, sin^2(\gamma - \frac{2\pi}{3} \, k) \tag{7.88}$$

This gives for the axially symmetric case ($\gamma = 0$) (the symmetry axis corresponds to $k = 3$)

$$\mathscr{F}_1^{(irr)} = \mathscr{F}_2^{(irr)} = \frac{9}{8\pi} \, M \, A \, R_0^2 \, \beta^2 \tag{7.89}$$

Irrotational moment of inertia differs from so called rigid body value which is determined from the assumption that the nucleus is a rigid body with the constant density $\rho = MA/\frac{4}{3}\pi R_0^3$

$$\mathscr{F}_1^{(rig)} = \rho \int d\Omega \int_0^{R(\vartheta,\varphi)} dr \, r^2 \, (x_2^2 + x_3^2) \tag{7.90}$$

and similarly for $k = 2, 3$. This gives

$$\mathscr{F}_k^{(rig)} = \frac{2}{5} \, A \, M \, R_0^2 \left(1 - \sqrt{\frac{5}{4\pi}} \beta \cos(\gamma - \frac{2\pi}{3} k)\right) \tag{7.91}$$

which for $\gamma = 0$ provides

$$\mathscr{F}_1^{(rig)} = \frac{2}{5} \, A \, M \, R_0^2 \, (1 + 0.31 \, \beta) \tag{7.92}$$

Irrotational and rigid-body moments of inertia can be compared with the experimental values. The way how experimental values of the inertia moment are extracted from the rotational spectra of nuclei will be discussed in details in the Chapter 8 (subsection 8.1.4). Generally the following inequality valids

$$\mathscr{F}_1^{(rig)} > \mathscr{F}_1^{(exp)} > \mathscr{F}_1^{(irr)} \tag{7.93}$$

but the detail discussion of nuclear moments of inertia is given in the Chapter 8 in the connection with the theoretical interpretation of experimental low-lying spectra of different type nuclei.

The next step is the quantization of the classical Hamiltonian (7.85). There is no unique prescription in order to quantize the motion relating to the β and γ variables. Usually one adopts the Pauli prescription giving rise to the Bohr Hamiltonian (see [107])

$$\hat{H}_{coll} = -\frac{\hbar^2}{2B_2}\left[\beta^{-4}\frac{\partial}{\partial\beta}\Big(\beta^4\frac{\partial}{\partial\beta}\Big) + \frac{1}{\beta^2\sin 3\gamma}\,\frac{\partial}{\partial\gamma}\Big(sin3\gamma\,\frac{\partial}{\partial\gamma}\Big)\right] + \\ + \;\hat{T}_{rot} \;+\; \hat{U}(\beta,\gamma) \tag{7.94}$$

with

$$\hat{T}_{rot} = \frac{\hat{I}_1^2}{2\mathscr{F}_1} + \frac{\hat{I}_2^2}{2\mathscr{F}_2} + \frac{\hat{I}_3^2}{2\mathscr{F}_3} \tag{7.95}$$

and $\hat{U}(\beta,\gamma)$ is given by (7.86) where a_{20} and a_{22} are taken as operators 7.59 acting in the intrinsic fixed to body frame. In (7.95) the operators $\hat{I}_k$ represent the total angular momentum projections onto body-fixed axes. The orientation and the projection quantum numbers are indicated in Fig.7.9.

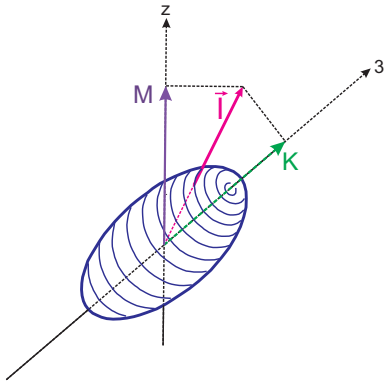


Figure 7.9: Schematic figure of the total angular momentum $\vec{I}$ projection M and K on the laboratory frame z- axis and the intrinsic body-fixed frame 3-d axis, respectively.

A general expression for the eigen- functions of the Hamiltonian (7.94) is derived as

$$\Psi_{IM}(\beta,\gamma,\theta) = \sum_K \psi_{K\rho}(\beta,\gamma)\,\sqrt{\frac{2I+1}{8\pi^2}}\,D^I_{MK}(\theta) \tag{7.96}$$

where $\psi_{K\rho}(\beta,\gamma)$ is the intrinsic part of the wave function and $D^I_{MK}(\theta)$ are Wigner functions of the Euler angles specifying by one symbol θ (see the analogy with the text under the expression (7.21)). The index ρ stands for the other quantum numbers (apart from K) characterizing the intrinsic state (in the case of the quadrupole collective Hamiltonian (7.96) it is the number of $\beta-$ and $\gamma-$ phonons - see below). The form of the wave functions

(7.96) depends also on symmetries of the intrinsic Hamiltonian. A number of these symmetry operations are related to the axially symmetric rotor and these symmetries put constraints on the collective wave functions (7.96): $\Psi_{IMK}(\beta,\gamma,\theta) = \psi_{K\rho}(\beta,\gamma)\sqrt{\frac{2I+1}{8\pi^2}}\,D^I_{Mk}(\theta)$. Some other symmetries are discussed in more details in the Chapter 8. At present we go through the most simple modes of motion related to the collective Bohr Hamiltonian of an axially symmetric case in the equilibrium position $\bar{\gamma} = 0$

Supposing a deep minimum in $U(\beta,\gamma)$ at the equilibrium deformation $\beta = \bar{\beta}$ and $\gamma = 0$ we expect nucleus rotation superimposing a small amplitude vibrations. Without a loss of generality we can suppose the rotational axes perpendicular to the nucleus symmetry axis (the 3-d axis of the body-fixed frame). Then the rotational kinetic energy operator (7.95) is

$$\hat{T}_{rot} = \frac{\hat{I}_1^2 + \hat{I}_2^2}{2\mathscr{F}_0} = \frac{\hat{I}^2 - \hat{I}_3^2}{2\mathscr{F}_0} \tag{7.97}$$

with $\mathscr{F}_0 = \mathscr{F}_1(\beta = \bar{\beta},\ \gamma = 0) = \mathscr{F}_2(\beta = \bar{\beta},\ \gamma = 0)$, and the intrinsic part of the collective Hamiltonian can be approximated by harmonic oscillators with respect to $\beta-$ and $\gamma-$ variables. Superimposed on each intrinsic vibrational state (characterized by the numbers n_β and n_γ of $\beta-$ phonons and $\gamma-$ phonons, respectively) a rotational band is constructed with the level sequence given by the sequence of the total angular momentum values I. In accordance with the text under te expression (7.31) (see (7.32) - (7.35)) we here distinguish two possibilities for even-even nuclei:

- $K = 0$ bands ($I_3 = 0$)
  Since the rotational and axial vibrational motions decouple the laboratory frame wave function becomes

$$\Psi_{IMK=0\,\rho=(n_\beta,n_\gamma)}(\beta,\gamma,\theta) = \psi_{K=0\,\rho}(\beta,\gamma)\sqrt{\frac{2I+1}{8\pi^2}}\,D^I_{MK=0}(\theta) \tag{7.98}$$

  In the case of the quadrupole vibrations with $K = 0$ the intrinsic wave function $\psi_{K=0\,\rho}(\beta,\gamma)$ is symmetric with respect to the turn $\hat{R}_1$ by angle π round the the 1-st intrinsic frame axis with $r_1 = +1$ (see (7.32)) and therefore the spin sequence $I = 0,\ 2,\ 4,\ \ldots$ of levels appears in the rotational band above this intrinsic state. The total eigen energy of the Hamiltonian (7.94) is

$$E_{n_\beta,n_\gamma,K=0}(I) = \hbar\omega_\beta\,(n_\beta + \frac{1}{2}) + \hbar\omega_\gamma\,(2\,n_\gamma + 1) + \frac{\hbar^2}{2\mathscr{F}_0} I\,(I+1) \tag{7.99}$$

with $n_\beta = 0,\ 1,\ 2,\ \ldots$; $n_\gamma = 0,\ 1,\ 2,\ \ldots$ and with ω_β and ω_γ the $\beta-$ and $\gamma-$ vibrational frequencies ($\hbar\omega_\beta = \sqrt{C_{20}/B_2}$, $\hbar\omega_{22} = \sqrt{C_{22}/B_2}$) .

- $K \neq 0$ bands
  Here, symmetrized laboratory frame rotational wave functions are needed, to give good parity, with the following form

$$\Psi_{IMK\rho=(n_\beta,n_\gamma)}(\beta,\gamma,\theta) = \\ = \psi_{K\rho=(n_\beta,n_\gamma)}(\beta,\gamma)\,\frac{1}{\sqrt{2}}\sqrt{\frac{2I+1}{8\pi^2}}\left[D^I_{MK}(\theta) + (-1)^I\,D^I_{M-K}(\theta)\right] \tag{7.100}$$

  and with even K values. For such $K \neq 0$ bands the angular momentum sequence results with $I = |K|,\ |K|+1,\ |K|+2,\ \ldots$ (in accordance with (7.35)). Here now, the $\gamma-$ vibration couples to the rotational motion with the following energy spectrum

$$E_{n_\beta,n_\gamma,K}(I) = \hbar\omega_\beta\,(n_\beta + \frac{1}{2}) + \hbar\omega_\gamma\,(2\,n_\gamma + 1 + \frac{|K|}{2}) + \\ + \frac{\hbar^2}{2\mathscr{F}_0}\left[I\,(I+1) - K^2\right] \tag{7.101}$$

These rotational bands, in particular $n_\beta = 1$, $n_\gamma = 0$ and $n_\beta = 0$, $n_\gamma = 1$, have been observed in many nuclei. A schematic figure of various combined modes are given in the Fig. 7.10.

It should be noted that the Hamiltonian (7.94) containing the intrinsic and rotational parts corresponds to the model Hamiltonian (7.17) where the Coriolis coupling term was neglected. Wave functions (7.98) and (7.100) have also the form of the product of the intrinsic wave function and the Wigner function of Euler angles similarly as in the case of the Hamiltonian (7.17). The energy spectrum (7.21) is practicallly the same as the spectrum (7.101) (sum of the intrinsic and rotational energies) but in (7.101) the intrinsic modes are restrict only to the quadrupole harmonic $\beta-$ and $\gamma-$ vibrations while in (7.17) - (7.21) the intrinsic motion is not specified, it depends on the model used for the description of the intrinsic nonrotating degrees of freedom. In this sense the Hamiltonian (7.15) - (7.17)) is more general and its eigen modes will be disussed in details in the Chapter 8 for particular cases of even-even, odd A, and odd-odd nuclei [4]

[4]The Liquid Drop Model (LDM) theory with the collective vibration degrees of freedom in spherical and

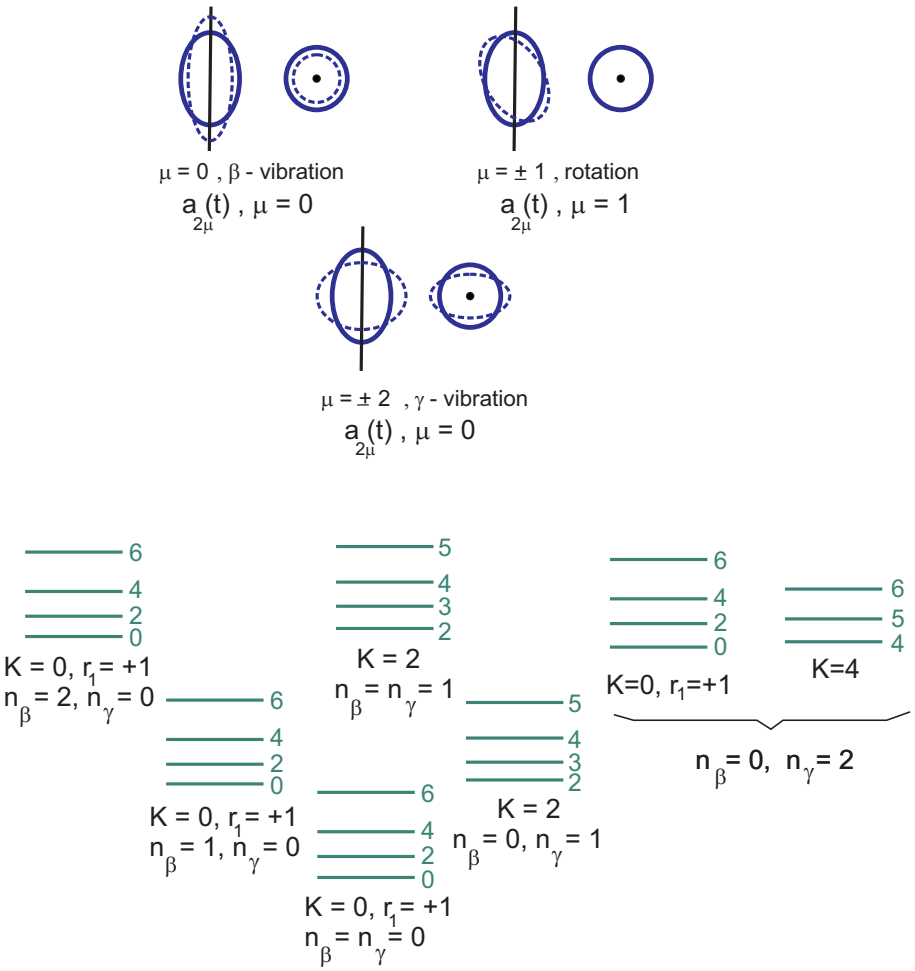


Figure 7.10: Various quadrupole shape oscillations in the axially deformed nucleus. The upper part shows projections of the nuclear shape in directions perpendicular and parallel to the symmetry axis. The lower panel shows the spectrum associated with excitations of one or two vibrational quanta (phonons), including the specific values of the various oscillation energies $\hbar\omega_\beta$, $\hbar\omega_\gamma$. The rotational energy is assumed to be given by $I(I+1) - K^2$ and harmonic oscillator spectra for the intrinsic energy are supposed.

Above discussion of a standard Bohr Hamiltonian giving the regular rotational bands following a $I(I+1)$ momentum law above each intrinsic state, described as the $\beta-$ and /or $\gamma-$ vibrational states, is an idealized situation. In real nuclei there is always coupling between vibrational and rotational degrees of freedom. In the spherical nuclei (as it was discussed in the previous 7.2.1.1 subsection) there is no rotational degrees of freedom and the lowest part of the energy spectrum has pure oscillator character (see the discussion of the Fig. 7.3). On the other side the lowest parts of the energy spectra of well axially deformed nuclei are close to the situation given in the lower panel of the schematic Fig. 7.10 with well developed rotational bands. There are many, so called transitional, nuclei with the spectra lying between the purely harmonic quadrupole vibrational pattern and the rotational limit. A good indicator to specify the type of the spectrum of the given nucleus is the energy ratio of the first 4_1^+ level and the first 2_1^+ level. As it can be seen from the Figs. 7.2 and 7.5, in the spherical nuclei the state 4_1^+ has two-phonon character with the energy $2\,\hbar\omega_{\lambda=2}$, and the energy of the state 2_1^+ is $\hbar\omega_{\lambda=2}$. In well-deformed nuclei with the axial symmetry both 2_1^+ and 4_1^+ levels are members of the ground rotational band above the intrinsic ground state $n_\beta = n_\gamma = 0$ (see Fig. 7.10 and (7.101)). Therefore the ration $E_{4_1^+}/E_{2_1^+}$ for the axially deformed limit is

$$\frac{E_{4_1^+}}{E_{2_1^+}} = \frac{4 \times 5}{2 \times 3} = 3.333 \tag{7.102}$$

The lowest 2^+ and 4^+ states in the even-even nuclei with number of nucleons closed to magic numbers (closed shell nuclei) have 2p-2h character and the ratio $E_{4_1^+}/E_{2_1^+}$ is closed to 1 (it can be seen from experiments as well as from the shell-model calculations). In the Fig. 7.11 the experimental values of the ratio $E_{4_1^+}/E_{2_1^+}$ are demonstrated for a broad interval of the mass number A. One can recognize spherical nucleus and deformed nucleus regions.

The Bohr generalized LDM model was able to describe for the first time in the beginning of the 50-ties observed two type of low-lying spectra of atomic nuclei: vibrational type of spherical nuclei and rotational type of deformed nuclei. The transition from the rotational model, on one side, and the vibrational one (with $\beta-$ and $\gamma-$ vibrations included), on the other side,

deformed nuclei was created by A. Bohr and B.R. Mottelson in the beginning of the 50-ties (see [102, 108]) based on the original version of the LDM from the 30-ies (see [109, 65]). Then the idea of the LDM collective motion was generalized and the connection between the collective motion and particle motion was found (see [99] and citation therein). For this achievement A. Bohr and B.R. Mottelson were awarded by the Nobel prize in 1975.

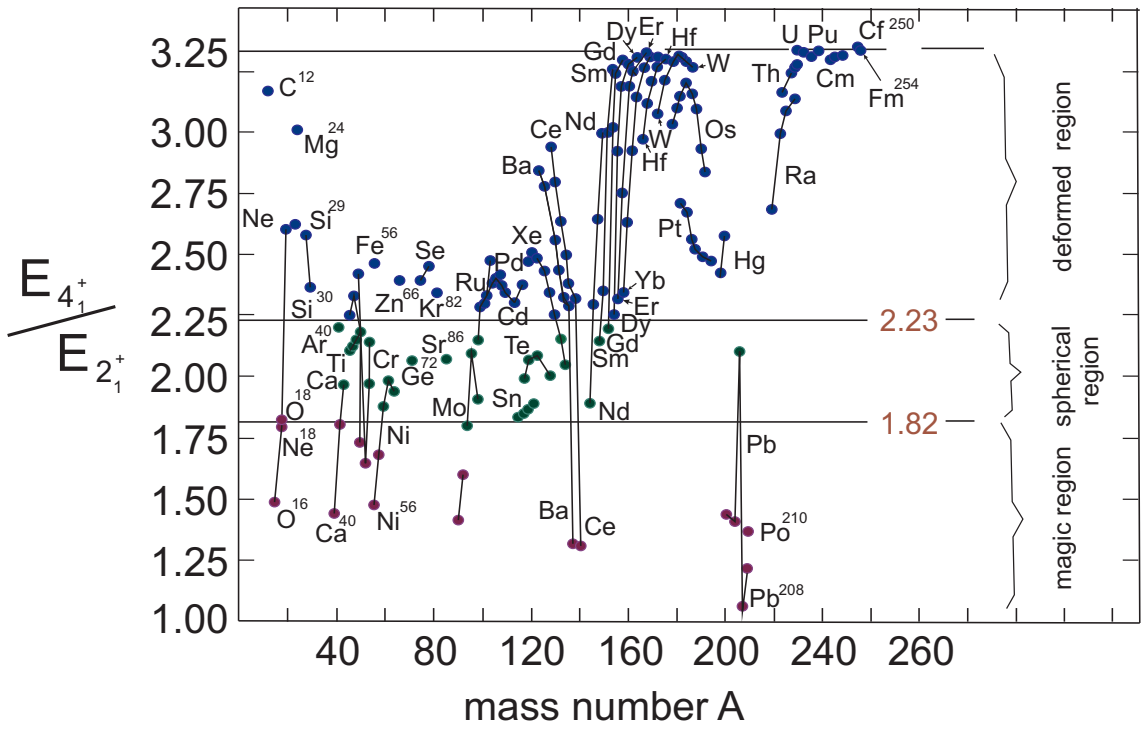


Figure 7.11: Experimental values of the $R = E_{4_1^+}/E_{2_1^+}$ ratio in even-even nuclei. The top horizontal line corresponds to the ideal rotor ratio $R = 3.33$. The interval $2.67 \leq R \leq 3.33$ fit most nuclei in the well deformed region. Values $2.23 \leq R \leq 2.67$ corresponds rather to the transitional nuclei. For values $R \leq 2.23$ the rotational motion goes away and the moment of inertia vanishes (spherical nucleus region). The nuclei with an even smaller ratio of R ($R < 1.82$) correspond to nuclei having just a few nucleons (two) outside a closed shell configuration (data taken from [110]).

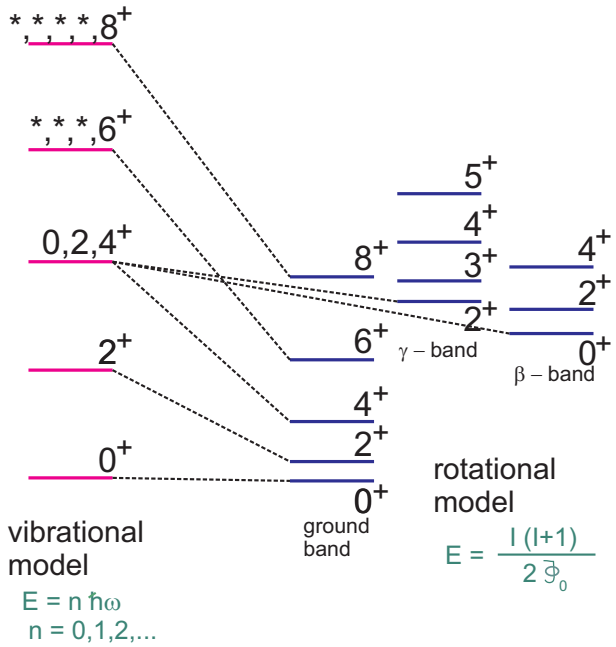


Figure 7.12: Schematic figure giving the connection between the vibrational spectrum of the spherival nucleus with the rotational spectrum of the axially deformed nucleus.

is schematically illustrated in the Fig. 7.12.

Besides the energy spectrum, other obervables indicate also the presence of coherent collective vibrational and rotational motion in nuclei such as electric E2 transition probabilities (see Fig. 7.3) and quadrupole moments of nuclei. We will discuss these quantities in the framework of the Bohr geometrical model with the quadrupole degrees of freedom.

From the section 7.1 we know that in the deformed nuclei the electromagnetic transitions can be divided into two groups: intraband and extraband transitions. In the low-lying part of the spectrum of the axialy symmetric deformed nucleus (if the Coriolis and centrifugal terms in the Hamiltonian (7.12) are neglected) the general reduced probability of the electromagnetic transition of the type X (X = el., mag.) from the state $|I_i K_i \rho_i\rangle$ to the state $|I_f K_f \rho_f\rangle$ is given by (7.42). For the intraband electric $E2$ transitions $|I_i K \rho\rangle \to |I_f K \rho\rangle$ the expression (7.42) reduces to the exp. (7.43) (see also (2.201)):

$$B(E2;\ I_i K \rho \to I_f K \rho) = \left(C^{I_f K}_{I_i K 20}\right)^2 \frac{5}{16\pi} \left|\langle K\rho \mid \hat{Q}_{33} \mid K\rho\rangle\right|^2 \qquad (7.103)$$

where $\langle K\rho|\hat{Q}_{33}|K\rho\rangle$ is the diagonal intrinsic matrix element of the quadrupole

moment operator

$$\hat{Q}_{33} = \boxed{\begin{array}{c}\text{see}\\(2.201)\end{array}} = \sqrt{\frac{16\pi}{5}}\,\hat{\mathscr{M}}^{(el)}_{20} \tag{7.104}$$

where $\hat{\mathscr{M}}_{20}$ is given by (7.70). The transformation into the intrinsic body-fixed system results in the intrinsic quadrupole moment in the following form (up to the linear order in β)

$$Q_0 = \langle K\rho \,|\, \hat{Q}_{33} \,|\, K\rho\rangle \approx \sqrt{\frac{16\pi}{5}}\,\frac{3}{4\pi}\,ZeR_0^2\,\beta \tag{7.105}$$

This relation valids approximately for all low-lying intrinsic states (for the grouns state, for one $\beta-$ phonon state, for one $\gamma-$ phonon state, ...). So, for the low- lying intraband transition the reduced E2 probabilities are

$$B(E2;\; I_iK\rho \to I_fK\rho) \approx \frac{5}{16\pi}\,Q_0^2\,\left(C^{I_fK}_{I_iK20}\right)^2 \tag{7.106}$$

For $K = 0$ (for intraband ground state band or $\beta-$ band transitions) using the explicit form of the Clebsch-Gordan coefficient, one obtains

$$\begin{aligned} B(E2;\; I_i + 2\;K = 0 \to I_i\;K = 0) = \\ = \frac{5}{16\pi}\,Q_0^2\,\frac{3}{2}\,\frac{(I_i+2)(I_i+1)}{(2I_i+3)(2I_i+5)} \end{aligned} \tag{7.107}$$

Besides the intrinsic quadrupole moment Q_0 (see (7.105)) so called spectroscopic quadrupole moment is introduced in accordance with the definition (2.199):

$$\begin{aligned} Q &= \langle I\;M = I\;K\rho \,|\, \hat{Q}_{33} \,|\, I\;M = I\;K\rho\rangle = \\ &= \boxed{\begin{array}{c}\text{substitution from (7.29) and using of}\\ Q_0 = \langle K\rho|\hat{Q}_{33}|K\rho\rangle \text{ and (7.82)}\end{array}} = \frac{3K^2 - I(I+1)}{2I(I+1)}\,Q_0 \end{aligned} \tag{7.108}$$

So, in general, the band-heads with $I = K$ has a non-vanishing spectroscopic quadrupole moment Q, except the $K = 0$ ($I = 0$) band. For these $K = 0$ bands the information on Q_0 can be obtained by studying excited higher energy states (using (7.107)). By this way it was shown in the past that the Q_0 value and thus deformation β remains a constant to relatively quite high I, even in those cases where the energy spacings deviate from the $I(I+1)$

law. The collectivity (which manifests itself by high values of Q_0) is easily observed by plotting the $B(E2)$ values of ground-state rotational band for various mass regions (see e.g. Fig. 7.3). Values up to 200 Weisskopf units in the rare earth region $A \approx 160 - 180$ and even extending 350 Weisskopf units in the actinide region $A > 220$, observed in the Fig. 7.3, indicate the enhanced and coherent rotational modes of the deformed nucleus motion.

7.2.2 Algebraic description of nuclear collective motion (Interacting Boson Model)

In the previous subsection the simple phenomenological Bohr-Mottelson model was discussed. This model gave the first explanation of collective vibrational and rotational degrees of freedom of spherical and deformed nuclei. As we saw the lowest collective vibrational states in the even-even nuclei was described by the oscillator quanta - phonons with boson character (in the simplest version of the Bohr-Mottelson geometrical model these phonons were obtained by the quantization of the 5- dimensional Hamiltonian written in terms of the classical quadrupole variables $\alpha_{2\mu}$ and subsequent finding of the corresponding solutions of the eigen problem). Another type of boson model, in the literature known as the Interacting Boson Model (IBM), describes the well-ordered coherent motion of nucleons, by the concept of symmetries related to algebraic description of the nuclear many-body system. In this subsection the basic elements of this model are presented.

Since the IBM is based on the algebraic approach the reader of this textbook not acquainted with the basic elements of the group theory is asked to read at first the Appendix J. In this subsection only a brief description of the IBM is presented. More details of the simplest version of this model, the IBM-1, can be found in the Appendix K.

In the first part 7.2.2.1 of this subsection the simplest version of the IBM model (IBM-1) is briefly presented. The IBM-1 was introduced in 1975 [124] as modified approach of [117] (more detailed presentation of the IBM-1 model can be found in [113]). The modification of Jolos-Janssen approach [117] consists in the fact that in the IBM the monopole or scalar s- bosons appear in addition to the usually used quadrupole d- bosons. In the simplest version IBM-1 the neutrons and protons are not distinct. The introduction of s- and d- bosons can be regarded as the Schwinger [125] type representation of $U(6)$

algebra. The IBM-1 was the first model which was able to describe transition from the spherical vibrational nuclei to deformed vibrational-rotational nuclei within one consistent approach.

The second part 7.2.2.2. of this subsection is devoted to the modified version of the Interacting Boson Model, so called IBM-2. In the IBM-2 the neutron and proton degrees of freedom are distinct (s- and d- bosons for neutrons and protons are introduced). Opposite to the IBM-1 the version IBM-2 takes into account also neutron-proton interactions. More details concerning the IBM-2 model can be found e.g. in [114, 118].

The extension of the IBM, formulated originally for even-even nuclei, to the odd-A nuclei (so called interacting boson-fermion model - IBFM) is discussed briefly in the third part of this subsection. In the framework of the IBFM aproach the nucleus is considered as the even-even core described by the IBM-1 or IBM-2 and by the extra odd nucleon occupying single- particle states of some s.p. configuration space (see [126]). This odd nucleon can interact with s- and d- bosons of the core.

7.2.2.1 Interacting Boson Model - 1

In the 70-ties (when IBM-1 model was introduced) it had been known for decades that the lowest positive parity states of the even-even spherical nuclei and the lowest intrinsic (nonrotational) states in the even-even deformed nuclei had quadrupole collective character. The other well-known fact was the existence of the magic numbers in the atomic nuclei connected with the relative inertness of the nuclei with the number of protons and/or neutrons equal to magic numbers given by the closed shells. This led to the conclusions (as it was discussed in previous chapters) that the main properties of nuclei were given by the valence nucleons above closed shells. The pairing correlations between one-type nucleons (see the chapter 6) were also known in the 70-ties.

All these facts led A. Arima and F. Iachello in [124] to the introduction of simple IBM model with the following assumption and ideas:

- Closed shells of either protons or neutrons, and excitations out of these shells, are neglected.
- The low-lying excitations of even-even nuclei depend only on the valence space.
- The valence nucleons are treated in pairs, as s- and d- bosons, with

angular momenta 0 and 2. In the IBM-1 no distinction is made between proton and neutron bosons. The number of bosons is equal to the half the number of valence protons and neutrons, both of which are always counted to the nearest proton and neutron closed shells. This finite number of bosons causes often effects that are different from those of the Bohr-Mottelson geometric model.

- The states of this boson system depend only on the s- and d- boson energies and on interactions between bosons. These interactions are assumed to be simple (at most two-body).

So the assumed configuration space of the IBM-1 can be reduced to the N- boson space formed by quadrupole ($l = 2$) and monopole ($l = 0$) bosons with corresponding creation operators $d^+_\mu \equiv b^+_{l=2\,\mu}$ ($\mu = 0, \pm 1, \pm 2$) and $s^+ \equiv b^+_{l=0\,\mu=0}$, respectively. Further assumption is that these $l = 2$ and $l = 0$ bosons can fill only two levels: s- level with the energy ϵ_s and d- level with the energy ϵ_d (which is degenerated with respect to the angular momentum projection). These quadrupole and monopole bosons interact mutually by the two-boson interaction $\hat{V}$ and the general Hamiltonian consists from the one- boson and two- boson parts as follows (see also (K.1))

$$\hat{H} = \sum_{\substack{l=0,2 \\ m}} \epsilon_l \, b^+_{lm} \, b_{lm} + \\ + \frac{1}{2} \sum_{\substack{l_1,\, l_2=0,2 \\ m_1, m_2}} \sum_{\substack{l_1^{'},\, l_2^{'}=0,2 \\ m_1^{'}, m_2^{'}}} \langle \, l_1 m_1 l_2 m_2 | \hat{V} | \, l_1^{'} m_1^{'} l_2^{'} m_2^{'} \rangle \;\; b^+_{l_1 m_1} b^+_{l_2 m_2} b_{l_2^{'} m_2^{'}} b_{l_1^{'} m_1^{'}} \tag{7.109}$$

Using the coupling scheme (see (K.4), (K.5))

$$\begin{aligned} \left(b^+_{l_1} \, b^+_{l_2}\right)_{(l_1 l_2;\, LM)} &= \sum_{m_1} C^{LM}_{l_1 m_1 l_2 M - m_1} \;\; b^+_{l_1 m_1} \, b^+_{l_2 m_2} \\ \left(\tilde{b}_{l_1^{'}} \, \tilde{b}_{l_2^{'}}\right)_{(\, l_1^{'} l_2^{'};\, L\, -M)} &= \sum_{m_1} C^{LM}_{l_1 m_1 l_2 M - m_1} \, (-1)^{L+M} \, b_{l_2 m_2} \, b_{l_1 m_1} \end{aligned} \tag{7.110}$$

where

$$\tilde{b}_{\, l_1 m_1} \equiv (-1)^{l_1 + m_1} \, b_{\, l_1 \, -m_1} \tag{7.111}$$

the Hamiltonian (7.109) can be rewritten as follows (see (K.3)-(K.6))

$$\hat{H} = \sum_{\substack{l=0,2 \\ m}} \epsilon_l \, b^+_{lm} \, b_{lm} +$$

$$+ \sum_{L=0,2,4} \frac{1}{2} \, (2L+1)^{1/2} \sum_{\substack{l_1=0,2 \\ l_1'=0,2}} \sum_{\substack{l_2=0,2 \\ l_2'=0,2}} \langle \, l_1 l_2 L \mid \hat{V} \mid l_1' l_2' L \rangle$$

$$\left[\left(b^+_{l_1} \, b^+_{l_2} \right)_{(\, l_1 \, l_2; \, L)} \left(\tilde{b}_{l_1'} \, \tilde{b}_{l_2'} \right)_{(\, l_1' l_2'; \, L)} \right]_{(LL; \, 00)} \tag{7.112}$$

and if the sums in (7.112) are written explicitly (see (K.7))

$$\hat{H} = \epsilon_0 \, s^+ s + \epsilon_2 \sum_{m \, = -2}^{2} d^+_m d_m +$$

$$+ \sum_{L=0, \, 2, \, 4} \frac{\sqrt{2L+1}}{2} \, \langle \, d^{\, 2} L \mid \hat{V} \mid d^2 L \rangle \, \left[(d^+ d^+)_{(22; \, L)} \, (\tilde{d} \, \tilde{d})_{(22; \, L)} \right]_{(LL; \, 0)}$$

$$+ \frac{\sqrt{5}}{2} \, \langle \, d^{\, 2} L = 2 \mid \hat{V} \mid ds L = 2 \rangle$$

$$\left[(d^+ d^+)_{(22; \, 2)} \, (\tilde{d} \, \tilde{s})_{(20; \, 2)} + (d^+ s^+)_{(20; \, 2)} \, (\tilde{d} \, \tilde{d})_{(22; \, 2)} \right]_{(22; \, 0)}$$

$$+ \frac{1}{2} \, \langle \, d^{\, 2} L = 0 \mid \hat{V} \mid ss L = 0 \rangle$$

$$\left[(d^+ d^+)_{(22; \, 0)} \, (\tilde{s} \, \tilde{s})_{(00; \, 0)} + (s^+ s^+)_{(00; \, 0)} \, (\tilde{d} \, \tilde{d})_{(22; \, 0)} \right]_{(00; \, 0)}$$

$$+ \sqrt{5} \, \langle \, ds L = 2 \mid \hat{V} \mid ds L = 2 \rangle \, \left[(d^+ s^+)_{(20; \, 0)} \, (\tilde{d} \, \tilde{s})_{(20; \, 2)} \right]_{(22; \, 0)}$$

$$+ \frac{1}{2} \, \langle \, ss L = 0 \mid \hat{V} \mid ss L = 0 \rangle \, \left[(s^+ s^+)_{(00; \, 0)} \, (\tilde{s} \, \tilde{s})_{(00; \, 00} \right]_{(00; \, 0)} =$$

$$
\begin{aligned}
&= \epsilon_0\, s^+ s + \epsilon_2 \sum_{m=-2}^{2} d_m^+ d_m + \\
&\quad + \sum_{L=0,\,2,\,4} \frac{\sqrt{2L+1}}{2}\, c_L \, \Big[(d^+ d^+)_{(22;\,L)}\, (\tilde{d}\,\tilde{d})_{(22;\,L)} \Big]_{(LL;\,0)} \\
&\quad + \tilde{v}_2 \, \Big[(d^+ d^+)_{(22;\,2)}\, (\tilde{d}\,\tilde{s})_{(20;\,2)} + (d^+ s^+)_{(20;\,2)}\, (\tilde{d}\,\tilde{d})_{(22;\,2)} \Big]_{(22;\,0)} \\
&\quad + \tilde{v}_0 \, \Big[(d^+ d^+)_{(22;\,0)}\, (\tilde{s}\,\tilde{s})_{(00;\,0)} + (s^+ s^+)_{(00;\,0)}\, (\tilde{d}\,\tilde{d})_{(22;\,0)} \Big]_{(00;\,0)} \\
&\quad + \tilde{u}_2 \, \Big[(d^+ s^+)_{(20;\,2)}\, (\tilde{d}\,\tilde{s})_{(20;\,2)} \Big]_{(22;\,0)} \\
&\quad + \tilde{u}_0 \, \Big[(s^+ s^+)_{(00;\,0)}\, (\tilde{s}\,\tilde{s})_{(00;\,00} \Big]_{(00;\,0)}
\end{aligned}
\tag{7.113}
$$

where the following matrix elements are taken further as parameters (see (K.8))

$$
\begin{aligned}
& c_L \equiv \langle\, d^{\,2} L |\, \hat{V} \,|\, d^{\,2} L \rangle \quad , \quad \tilde{v}_2 \equiv \frac{\sqrt{5}}{2} \langle\, d^{\,2} L = 2 |\, \hat{V} \,|\, ds L = 2 \rangle \\
& \tilde{v}_0 \equiv \frac{1}{2} \langle\, d^{\,2} L = 0 |\, \hat{V} \,|\, s^{\,2} L = 0 \rangle \quad , \quad \tilde{u}_2 \equiv \sqrt{5}\, \langle ds L = 2 |\, \hat{V} \,|\, ds L = 2 \rangle \\
& \tilde{u}_0 \equiv \frac{1}{2}\, \langle\, s^{\,2} L = 0 |\, \hat{V} \,|\, s^{\,2} L = 0 \rangle
\end{aligned}
\tag{7.114}
$$

One can see from (7.113) that the IBM-1 Hamiltonian involves generally 9 parameters ϵ_0, ϵ_2, c_L $(L = 0, 2, 4)$, $\tilde{v}_2$, $\tilde{v}_0$,$\tilde{u}_2$, $\tilde{u}_0$. It is necessary to realize that the operators $\hat{n}_s = s^+ s$ and $\hat{n}_d = \sum_m d_m^+ d_m$ are the operators of the number of monopole and quadrupole bosons, respectively (we should have in mind that the number $N = n_d + n_s$ is finite and fixed and it is determined as the half of the number of valence nucleons for the given nucleus).

In [124] it was shown that the column vector

$$
B^+ \equiv \begin{pmatrix} B_1^+ \\ B_2^+ \\ \vdots \\ B_6^+ \end{pmatrix} \equiv \begin{pmatrix} s^+ \\ d_2^+ \\ \vdots \\ d_{-2}^+ \end{pmatrix}
\tag{7.115}
$$

constructed from the six boson creation operators s^+, d_2^+, d_1^+, d_0^+, d_{-1}^+, d_{-2}^+ transforms according to the group $U(6)$ and the s- and d- multi-boson states

$$
B_\mu^+ B_\nu^+ \cdots \,|\, 0 \rangle
\tag{7.116}
$$

represent vectors in the Hilbert space for the totally symmetric representation of the group $U(6)$, which is characterized by the number of bosons N and which is further labeled by a single label $[N]$ (see [124]). The 36 bilinear combinations

$$\hat{G}_{\mu\nu} \equiv B^{+}_{\mu} B_{\nu} \qquad \mu,\, \nu = 1, \cdots,\, 6 \tag{7.117}$$

form the corresponding $U(6)$ algebra and are generators of this algebra that are closed under the commutation (J.77). The explicit form of these generators are given below

$$\begin{aligned} G_{U(6)} \equiv \Big\{ & (s^{+}\tilde{s})_{(00;\,0)},\ (d^{+}\tilde{s})_{(20;\,2m)},\ (s^{+}\tilde{d})_{(02;\,2m)},\ (d^{+}\tilde{d})_{(22;\,0)}, \\ & (d^{+}\tilde{d})_{(22;\,1m)},\ (d^{+}\tilde{d})_{(22;\,2m)},\ (d^{+}\tilde{d})_{(22;\,3m)},\ (d^{+}\tilde{d})_{(22;\,4m)} \Big\} \end{aligned} \tag{7.118}$$

From the point of view of the $U(6)$ generators (7.118) the Hamiltonian (7.113) can be understood written as follows

$$\hat{H} = \sum_{\mu} \epsilon_{\mu} \hat{G}_{\mu\mu} + \underbrace{\frac{1}{2} \sum_{\mu\nu\kappa\sigma} U_{\mu\nu,\,\kappa\sigma} \hat{G}_{\mu\nu} \hat{G}_{\kappa\sigma}}_{\hat{H}'} \tag{7.119}$$

The first term in (7.119) should be identified with two first terms in (7.113) (one- boson part of the Hamiltonian of the boson system) and the rest of (7.119), denoted by $\hat{H}'$, represents the interaction between bosons. This means that in the absence of the interaction $\hat{H}'$ we have a system of non-interacting bosons when all possible states (7.116) for a given n_s, n_d are degenerated in energy. The interaction $\hat{H}'$ splits the different possible states for a given n_s, n_d and one needs to solve the eigenvalue problem in the most general situation (for given $N = n_s + n_d$).

In order to determine the electromagnetic transition probabilities in the framework of the IBM it is necessary to specify electromagnetic transition operators $\hat{\mathscr{M}}^{(el)}_{JM}$ and $\hat{\mathscr{M}}^{(mg)}_{JM}$ and to express them in terms of the monopole and quadrupole boson creation and annihilation operators. The el.mg. transition operators $\hat{\mathscr{M}}^{(X=el,mg)}_{JM}$ are tensor operators from the point of view of the $SO(3)$ group of rotations and they are one-boson operators. Therefore they can be

expressed as follows (see the appendix K - expr. (K.13))

$$\hat{\mathscr{M}}^{(X)}_{JM} = \sum_{\substack{l_1=0,2 \\ m_1}} \sum_{\substack{l_2=0,2 \\ m_2}} \langle l_1 m_1 |\, \hat{\mathscr{M}}^{(X)}_{JM} \,|\, l_2 m_2 \rangle \; b^{+}_{l_1\, m_1} b_{l_2\, m_2} =$$

$$= \tilde{\alpha}_J \; \delta_{J2} \; \Big\{ (d^{+} \tilde{s})_{(20;\, 2M)} + (s^{+} \tilde{d})_{(02;\, 2M)} \Big\} + \\ + \beta_J \; (d^{+} \tilde{d})_{(22;\, JM)} + \gamma_0 \; \delta_{J0} \delta_{M0} \; (s^{+} \tilde{s})_{(00;\, 0)} \qquad (7.120)$$

where $J = 0, 1, 2, 3, 4$ and the following parameters $\tilde{\alpha}_J$, γ_0, β_J were introduced

$$\tilde{\alpha}_2 = \langle d ||\, \hat{\mathscr{M}}^{(X)}_{J=2} \,||\, s \rangle \; \frac{1}{\sqrt{5}} \; , \qquad \beta_J = \langle d ||\, \hat{\mathscr{M}}^{(X)}_{J} \,||\, d \rangle \; \frac{1}{\sqrt{2J+1}}$$
$$\gamma_0 = \langle s ||\, \hat{\mathscr{M}}^{(X)}_{J} \,||\, s \rangle \qquad (7.121)$$

That means, for instance, the electric quadrupole transition operator is given by two parameters, $\tilde{\alpha}_2$ and β_2:

$$\hat{\mathscr{M}}^{(el)}_{2M} = \tilde{\alpha}_2 \; \Big\{ (d^{+} \tilde{s})_{(20;\, 2M)} + (s^{+} \tilde{d})_{(20;\, 2M)} \Big\} + \; \beta_2 \; (d^{+} \tilde{d})_{(22;\, 2M)} \qquad (7.122)$$

and magnetic dipole transition operator by one parameter β_1:

$$\hat{\mathscr{M}}^{(mg)}_{1M} = \beta_1 \; (d^{+} \tilde{d})_{(22;\, 1M)} \qquad (7.123)$$

Natural basis for the construction of the matrix of the Hamiltonian (7.112) is $|[N]; s^{N-n_d}\, d^{\,n_d}; \Gamma L M\rangle$. Here N is the total number of s- and d- bosons, n_d is the number of quadrupole bosons, $n_s = N - n_d$ is the number of monopole s-bosons, L is the angular momentum quantum number with the projection M of the whole system of N bosons and the symbol Γ represents all other possible quantum numbers. The action of the Hamiltonian $\hat{H}$ on this ket

$|[N]; s^{N-n_d}\, d^{\,n_d}; \Gamma LM\rangle$ is following (see (K.17) - (K.25))

$$
\begin{aligned}
&\hat{H}\,|[N]; s^{N-n_d}\, d^{\,n_d}; \Gamma LM\rangle = \\
&= \Big\{\epsilon_s(N-n_d) + \epsilon_d n_d + \sum_{L=0,2,4} \frac{\sqrt{2L+1}}{2}\, c_L\, \left[(d^+d^+)_{(22;\,L)}\, (\tilde{d}\tilde{d})_{(22;\,L)}\right]_{(LL;\,0)} \\
&\quad +\tilde{u}_2(N-n_d)\, n_d + \tilde{u}_0(N-n_d)(N-n_d-1)\Big\}\, |[N]; s^{N-n_d}\, d^{\,n_d}; \Gamma LM\rangle \\
&\quad +\tilde{v}_2\, \Big\{ \left[(d^+d^+)_{(22;\,2)}\, \tilde{d}_2\right]_{(22;\,0)} \sqrt{N-n_d}\ \, |[N-1]; s^{N-n_d-1}\, d^{\,n_d}; \Gamma LM\rangle \\
&\qquad + \left[d_2^+\, (\tilde{d}\tilde{d})_{(22;\,2)}\right]_{(22;\,0)} \sqrt{N-n_d+1}\ \, |[N+1]; s^{N-n_d+1}\, d^{\,n_d}; \Gamma LM\rangle \Big\} \\
&\quad +\tilde{v}_0\, \Big\{ (d^+d^+)_{(22;\,0)}\, \sqrt{(N-n_d)(N-n_d-1)}\ \, |[N-2]; s^{N-n_d-2}\, d^{\,n_d}; \Gamma LM\rangle \\
&\qquad + (\tilde{d}\tilde{d})_{(22;\,0)} \sqrt{(N-n_d+1)(N-n_d+2)}\, |[N+2]; s^{N-n_d+2}\, d^{\,n_d}; \Gamma LM\rangle \Big\}
\end{aligned}
\tag{7.124}
$$

Using(7.124) the Hamiltonian matrix within the basis of states $|[N]; s^{N-n_d} d^{\,n_d}; \Gamma LM\rangle$ can be constructed. The eigen energies and corresponding eigen vectors can be obtained by the diagonalization of this matrix. This will be discussed later.

The s- bosons, in principle, have no physical meaning. Therefore degrees of freedom connected with s- bosons are usually omitted in (7.124) and the action of the Hamiltonian can be rewritten as follows (see (K.26) in the appendix K for details)

$$
\begin{aligned}
&\hat{H}\,|N; d^{\,n_d}; \Gamma LM\rangle = \\
&= \Big\{h_0 + \epsilon\, \hat{n}_d + \sum_{L=0,2,4} \frac{\sqrt{2L+1}}{2}\ c_L^{'}\ \left[(d^+d^+]_{(22;\,L)}\, (\tilde{d}\tilde{d})_{(22;\,L)}\right]_{(LL;\,0)} + \\
&\quad + \tilde{v}_2 \Big(\left[(d^+d^+)_{(22;\,2)}\, \tilde{d}\right]_{(22;\,0)} \sqrt{N-n_d}\ \, + \\
&\qquad\qquad + \ \left[d^+\, (\tilde{d}\tilde{d})_{(22;\,2)}\right]_{(22;\,0)} \sqrt{N-n_d+1}\, \Big)\ + \\
&\quad + \tilde{v}_0 \Big((d^+d^+)_{(22;\,0)}\, \sqrt{(N-n_d)(N-n_d-1)}\ \, + \\
&\qquad\qquad + \ (\tilde{d}\tilde{d})_{(22;\,0)}\, \sqrt{(N-n_d+1)(N-n_d+2)}\Big)\ \Big\} \\
&\quad |N; d^{\,n_d}; \Gamma LM\rangle
\end{aligned}
\tag{7.125}
$$

where

$$
\begin{aligned}
&h_0 = \epsilon_s\, N \qquad , \qquad \epsilon = \epsilon_d + (\tilde{u}_2 - \tilde{u}_0)(N-n_d) \\
&c_L^{'} = c_L + \tilde{u}_0\, \delta_{L0}
\end{aligned}
\tag{7.126}
$$

Similarly the action of the quadrupole electric transition operator $\hat{\mathscr{M}}^{(el)}_{2M}$ (7.122) is (see (K.18) - (K.31) in the appendix K)

$$\begin{aligned}\hat{\mathscr{M}}^{el}_{2M'}\,|N;d^{n_d};\,\Gamma LM\rangle = \\ = \Big\{\tilde{\alpha}_2\left[\sqrt{N-n_d}\,d^{+}_{M'} \;+\; \sqrt{N-n_d+1}\,(-1)^{M'}\,d_{-M'}\right] \;+ \\ +\;\beta_2\,(d^{+}\tilde{d})_{(22;\,2M')}\Big\}\,|N;d^{n_d};\,\Gamma LM\rangle\end{aligned} \tag{7.127}$$

So, if in our configuration space only d- bosons are involved (basis vectors $|N;d^{n_d};\,\Gamma LM\rangle$ then from the expression (7.125) one can see that the IBM-1 Hamiltonian involves 7 parameters. The parameter h_0 determines only the absolute scale of the energy and therefore we can put e.g. $h_0 = 0$. Therefore in reality the IBM-1 Hamiltonian is determined by 6 parameters ϵ, $c^{'}_{L}$ $(L = 0, 2, 4)$, $\tilde{v}_2$ and $\tilde{v}_0$. From (7.127) it follows that the electric quadrupole transition operator $\hat{\mathscr{M}}^{(el)}_{2M'}$ is given by two parameters $\tilde{\alpha}$ and β_2.

Eigen-spectrum and eigen-vectors of the IBM-1 Hamiltonian $\hat{H}$ can be obtained by the diagonalization of the Hamiltonian matrix within the space of basis vectors $|N;d^{n_d};\Gamma LM\rangle$ (after the specification of the additional quantum numbers Γ). However, for the special values of the parameters the IBM-1 Hamiltonian can be written as the combination of Casimir operators of chains of subgroups of the $U(6)$ algebra (it is necessary to remaind here that the IBM-1 Hamiltonian is constructed from generators of the $U(6)$ algebra - see (K.12)). In such cases the eigen-vectors of the IBM-1 Hamiltonian are characterized by the quantum numbers which label irreps of subgroups in the given chain and no diagonalization is needed. From the point of view of the IBM-1 Hamiltonian there are 3 possible subgroup chains of the group $U(6)$ (see subsection J.4.3 for more details of subgroup chain) (e.g. [118])

$$\begin{aligned}&U(6)\supset U(5)\supset SO(5)\supset SO(3)\supset SO(2) \;-\; \text{vibrator limit}\\ &U(6)\supset SU(3)\supset SO(3)\supset SO(2) \qquad -\quad \text{axial rotor limit}\\ &U(6)\supset SO(6)\supset SO(5)\supset SO(3)\supset SO(2) \;-\; \gamma\text{- unstable limit}\end{aligned} \tag{7.128}$$

which correspond to so called anharmonic vibrator limit, axial rotor limit and γ- unstable limit, respectively. As it will be shown in next subsections the anharmonic vibrator limit subgroup chain gives the low-lying spectrum which is similar to the spectrum of low-lying (vibrational) states in spherical nuclei

while the axial-rotor limit subgroup chain corresponds to the low-lying rotational bands observed in well- deformed nuclei. If the dynamical symmetry of the IBM-1 Hamiltonian is given by the 3-d subgroup chain in (K.32) (the γ- unstable limit chain) then the corresponding low-lying spectrum resembles the low-lying spectrum of so called γ- unstable nuclei (the nuclei where the total energy as a function of the quadrupole deformation parameter γ (see (1.5)) does not provide any distinct minimum). In the next subsections all these limits are discussed in more details.

7.2.2.1.1 $U(5)$ **limit (vibrator limit)** The $U(5)$ limit corresponds to the first $U(6)$ subgroup chain in (7.128) when parameters of the general IBM Hamiltonian (7.124), (7.125) or (7.113) are chosen in such a way that the resulting reduced Hamiltonian has the form of the combination of the Casimir operators of the corresponding $U(6)$ subgroups in the chain $U(6) \supset U(5) \supset SO(5) \supset SO(3) \supset SO(2)$.

The set of 25 generator operators of the subgroup $U(5)$ is [118] (see also subsection K.1.1 in the appendix K):

$$G_{U(5)} \equiv \Big\{(d^+\tilde{d})_{(22;\,00)},\ (d^+\tilde{d})_{(22;\,1m)},\ (d^+\tilde{d})_{(22;\,2m)},\ (d^+\tilde{d})_{(22;\,3m)},\ (d^+\tilde{d})_{(22;\,4m)}\Big\} \tag{7.129}$$

and the set $G_{SO(5)}$ of 10 generators of the subgroup $SO(5)$ is close under the commutations (J.77) (see also (K.74)):

$$G_{SO(5)} \equiv \Big\{(d^+\tilde{d})_{(22;\,1m)},\ (d^+\tilde{d})_{(22;\,3m)}\Big\} \tag{7.130}$$

The group $SO(5)$ involves the subgroup $SO(3)$ (angular momentum group) with 3 generators

$$G_{SO(3)} \equiv \Big\{(d^+\tilde{d})_{(22;\,1m)}\Big\} \tag{7.131}$$

If the structure of the general IBM Hamiltonian (7.124) is compared with the set of generators $G_{U(5)}$ (see (7.129)) of the subgroup $U(5)$ we can see that the choice of the parameters $\epsilon_0 = \tilde{v}_2 = \tilde{v}_0 = \tilde{u}_2 = \tilde{u}_0 = 0$ corresponds to the situation when the Hamiltonian is given by the combination of generators (7.129) of the subgroup $U(5)$ (generators $(d^+\tilde{d})_{(22;\,1m)}$, $(d^+\tilde{d})_{(22;\,3m)}$ cannot participate in the quadrupole 2- boson Hamiltonian because two quadrupole boson wave functions cannot have angular momentum $L = 1, 3$). So the $U(5)$

limit Hamiltonian is

$$\hat{H}_{vib} = \epsilon \sum_{m=-2}^{2} d_m^+ d_m \; + \\ + \sum_{L=0,2,4} \frac{\sqrt{2L+1}}{2} \, c_L^{'} \left[(d^+ d^+)_{(22;\, L)} \, (\tilde{d}\tilde{d})_{(22;\, L)} \right]_{(LL;\, 0)} \qquad (7.132)$$

The quantum number characterizing the totally symmetric representation of the group $U(5)$ is n_d (the number of d- bosons). The representations of the group $SO(5)$ are labeled by the index ν and the eigen values of the quadratic Casimir operator of $SO(5)$ [5] (see also (K.75))

$$\hat{C}_2[SO(5)] = \frac{1}{3} \, (d^+ \tilde{d})_{(22,\, 1)} \cdot (d^+ \tilde{d})_{(22,\, 1)} + \frac{1}{3} \, (d^+ \tilde{d})_{(22,\, 3)} \cdot (d^+ \tilde{d})_{(22,\, 3)} \qquad (7.133)$$

are given by $\frac{1}{6} \, \nu(\nu + 3)$. The Casimir operator of the group $SO(3)$ is given by well-known operator of the square of the angular momentum

$$\hat{C}_2[SO(3)] \equiv \hat{L}^2 = 10 \, (d^+ \tilde{d})_{(22;\, 1)} \cdot (d^+ \tilde{d})_{(22;\, 1)} \qquad (7.134)$$

with the eigen value $L(L+1)$.

The Hamiltonian (7.132) can be rewritten also in terms of the Casimir operators (7.133) and (7.134) as follows (see [118, 113])

$$\hat{H}_{vib} = \epsilon^{''} \, \hat{n}_d + \kappa_1 \, \hat{n}_d(\hat{n}_d - 1) + \kappa_2 \, \hat{C}_2[SO(5)] + \kappa_3 \, \hat{L}^2 \qquad (7.135)$$

where parameters $\epsilon^{''}$, κ_1, κ_2, κ_3 are connected with the parameters ϵ, c_0, c_2, c_4 involved in (7.132) by [118]

$$\begin{aligned} \epsilon &= \epsilon^{''} + \frac{2}{3}\kappa_2 + 6\kappa_3 \\ c_0^{'} &= 2\kappa_1 - \frac{4}{3}\kappa_2 - 12\kappa_3 \\ c_2^{'} &= 2\kappa_1 + \frac{1}{3}\kappa_2 - 6\kappa_3 \\ c_4^{'} &= 2\kappa_1 + \frac{1}{3}\kappa_2 + 8\kappa_3 \end{aligned} \qquad (7.136)$$

The eigen vectors $|[N]; n_d \nu n_\Delta; LM\rangle$ of the Hamiltonian $\hat{H}_{vib}$ are characterized by the quantum numbers labeling the irreps of the corresponding subggroup

[5] The Casimir operator is called quadratic if it is given by the quadratic form of the two- boson combinations $(d^+ \tilde{d})_{(22;\, Lm)}$. This is always indicated by the index 2.

chain (see also (K.72))

$$\begin{array}{ccccccccc} U(6) & \supset & U(5) & \supset & SO(5) & \supset & SO(3) & \supset & SO(2) \\ \vdots & & \vdots & & \vdots & & \vdots & & \vdots \\ N & & n_d & & \nu & ..n_\Delta.. & L & & M \end{array} \tag{7.137}$$

The physical meaning of these quantum numbers is discussed in details in the appendix K (see (K.35) - (K.37)): N is the number of s- and d- bosons, n_d is the number of d- bosons, ν is so called seniority - the number of unpaired bosons when by the boson pair are understood two d- bosons with the total angular momentum 0, the quantum number n_Δ determines the number of boson triplets with the zero angular momentum. The quantum numbers L and M are the total angular momentum and its projection. The allowed values for these quantum numbers are given by (see (K.35)-(K.36) in the appendix K)

$$\begin{aligned} & N \geq n_d \geq \nu \\ & \lambda = (\nu - 3\, n_\Delta) \geq 0 \\ & 2\,\lambda \geq L \geq \lambda \end{aligned} \tag{7.138}$$

where $L = 2\,\lambda - 1$ is excluded.
The corresponding eigen-energies of the Hamiltonian (7.135)
($\hat{H}_{vib}\ |[N];\, n_d \nu n_\Delta;\, LM\rangle = E_{n_d \nu L}\ |[N];\, n_d \nu n_\Delta;\, LM\rangle$) are (see e.g. [118, 113]):

$$E_{n_d \nu L} = \epsilon^{''} n_d + \kappa_1\, n_d(n_d - 1) + \kappa_2\, \frac{1}{6}\, \nu(\nu + 3) + \kappa_3\, L(L + 1) \tag{7.139}$$

The other possibility for the Hamiltonian $\hat{H}_{vib}$ is to express it in terms of so called boson pairing operator $\hat{\mathscr{P}}$ (see (K.39), (K.40)) [113]

$$\hat{H}_{vib} = \epsilon^{'} \hat{n}_d + \sum_{i<j} \left(\alpha\, 1_{ij} + \beta\, \hat{\mathscr{P}}_{ij} + \gamma\, \hat{\mathscr{L}}_{ij} \right) \tag{7.140}$$

where 1_{ij} are matrix elements of the unity operator between i-th and j-th bosons ($1 = \sum_{i<j} 1_{ij}$) and (see (K.40), (K.41))

$$\begin{aligned} & \hat{\mathscr{P}} \equiv 4\, \hat{S}_+\, \hat{S}_- \quad , \quad \hat{S}_+ \equiv \frac{1}{2} \sum_{m=-2}^{2} (-1)^m d_m^+ d_{-m}^+ \qquad \hat{S}_- = \hat{S}_+^+ \\ & \mathscr{L}_{ij} = 2\, \hat{\vec{l}}_i \cdot \hat{\vec{l}}_j \end{aligned} \tag{7.141}$$

with $\hat{\vec{l}}_i$ and $\hat{\vec{l}}_j$ angular momenta of i-th and j-th quadrupole bosons, respectively. In the Appendix K there is a detailed derivation of the expression for the eigen energies $E_{n_d \nu L}$ in terms of the parameters α, β, γ (see (K.65))

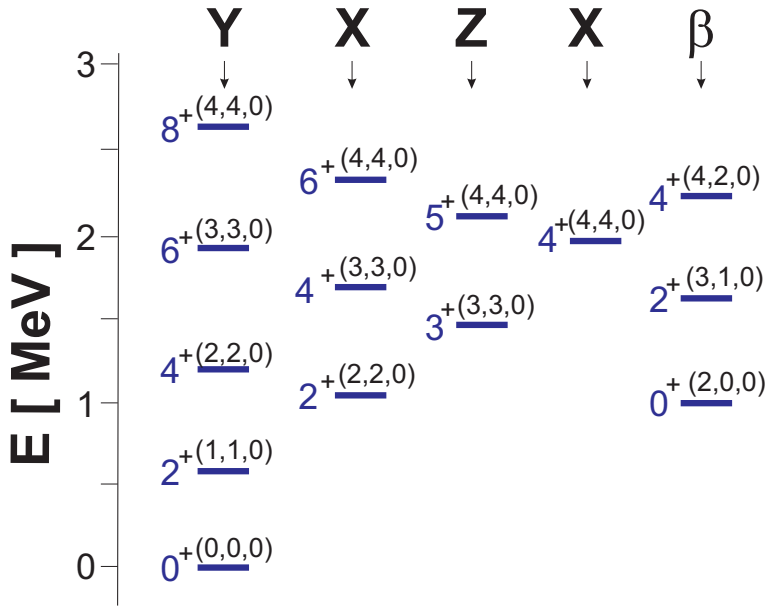


Figure 7.13: Typical spectrum of positive parity levels $E_{n_d\nu L}$ given by (K.65) or (7.142) and (K.66) or (7.143) with the parameters: $\epsilon = 579$ KeV, $c_4^{'} = 39.4$ KeV, $c_2^{'} = -95.3$ KeV, $c_0^{'} = -27.4$ KeV (see [113]). In the parentheses shown above each level there are quantum numbers (n_d, ν, n_Δ) and on the left there are angular momenta L.

$$E_{n_d\nu l} = \langle [N]; n_d\nu n_\Delta; LM|\hat{H}_{vib}|[N];\ n_d\nu n_\Delta LM\rangle =$$
$$= \epsilon^{'}\, n_d + \alpha\,\frac{1}{2}\,n_d\,(n_d-1) + \beta\,(n_d-\nu)(n_d+\nu+3) +$$
$$+\gamma\,\left[L(L+1) - 6\,n_d\right] \qquad (7.142)$$

with the following relation of the parameter set ϵ, c_0, c_2, c_4 and the set $\epsilon^{'}$, α, β, γ (see (K.66))

$$\epsilon = \epsilon^{'} + \frac{10}{3}\,\beta \qquad c_0 = \alpha + \frac{10}{3}\,\beta - 12\,\gamma$$
$$c_2 = \alpha + \frac{5}{3}\,\beta - 6\,\gamma \qquad c_4 = \alpha + \frac{5}{3}\,\beta + 8\,\gamma \qquad (7.143)$$

In order to compare the eigen energies $E_{n_d\nu L}$ with the experimental low-lying levels A.Arima and F.Iachello in [113] divided the states $|[N]; n_d\nu n_\Delta LM\rangle$

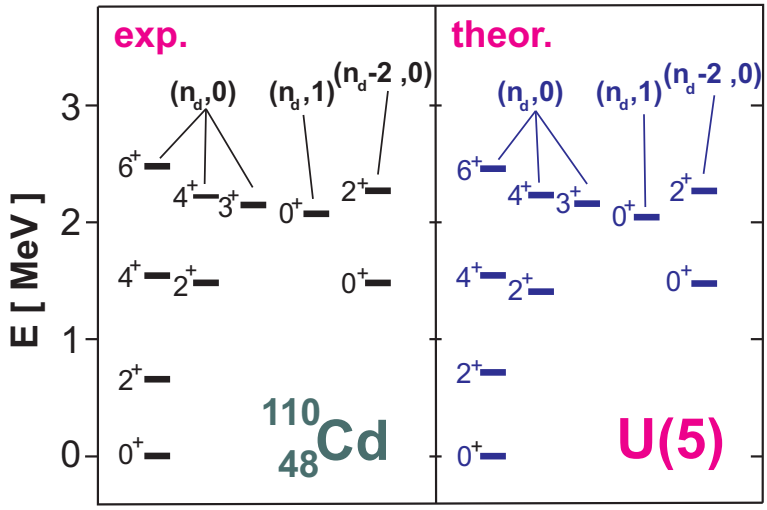


Figure 7.14: An example of a spectrum with $U(5)$ symmetry: $^{110}_{48}$Cd, $(N = 7)$. The theoretical energies are calculated using (7.142) with $\epsilon^{'} = 722$ KeV, $\alpha = 16$ KeV, $\beta = 10.3$ KeV, $\gamma = 10$ KeV.

into "bands" Y, X, Z, $X^{'}$, β, ... as is given below (see eq. (4.31) in [113])

$$\begin{aligned}
\text{Y band} &: |\, n_d\,,\ \nu = n_d\,,\ n_\Delta = 0\,,\ L = 2\,n_d\,;\ M\rangle \qquad n_d = 0, 1, 2, \ldots \\
\text{X band} &: |\, n_d\,,\ \nu = n_d\,,\ n_\Delta = 0\,,\ L = 2\,n_d - 2\,;\ M\rangle \qquad n_d = 2, 3, 4 \ldots \\
\text{Z band} &: |\, n_d\,,\ \nu = n_d\,,\ n_\Delta = 0\,,\ L = 2\,n_d - 3\,;\ M\rangle \qquad n_d = 3, 4, 5 \ldots \\
\text{X' band} &: |\, n_d\,,\ \nu = n_d\,,\ n_\Delta = 0\,,\ L = 2\,n_d - 4\,;\ M\rangle \qquad n_d = 4, 5, 6 \ldots \\
\beta \text{ band} &: |\, n_d\,,\ \nu = n_d - 2\,,\ n_\Delta = 0\,,\ L = 2\,n_d - 4\,;\ M\rangle \qquad n_d = 2, 3, 4 \ldots \\
&\vdots
\end{aligned}$$

Corresponding level scheme is shown in the Fig. 7.13. If we compare the spectrum of levels $E_{n_d\nu L}$ given on the Fig. 7.13 with the experimental spectrum of the lowest states in the spherical nuclei (see e.g. the spectrum of ^{106}Pd in the Fig.7.6) one can see that the lowest levels of the spectrum of $E_{n_d\nu L}$ resembles the experimental spectrum, particularly the first 0^+_1, 2^+_1, 2^+_2, 0^+_2, 4^+_1 levels (see also fig. 7.12). It was the success of the simple IBM-1 model that the explicit expressions for $E_{n_d\nu L}$ describe the low-lying parts of the spectra of vibrational nuclei. The example of the comparison of the $U(5)$ limit spectrum (7.142) with experimental energies is shown in the Fig. 7.14 with the lowest spectrum of $^{110}_{48}$Cd nucleus. One can see very good agreement of the energies calculated from (7.142) with the corresponding experimental values. A similar agreement was obtained also for other vibrational nuclei (see e.g. [118, 113, 123]).

The electric quadrupole transition operator is given by (7.127). For higher

values of N it is usually rewritten as follows (see (K.34))

$$\hat{\mathscr{M}}^{(el)}_{2M} = \boxed{\begin{array}{c}\text{see}\\(7.122)\end{array}} =$$

$$= e_2\left[(s^+\tilde{d})_{(02;\,2M)} + (d^+\tilde{s})_{(20;\,2M)}\right] + \chi\,(d^+\tilde{d})_{(22;\,2M)} = \boxed{\begin{array}{c}\text{see}\\(K.34)\end{array}} =$$

$$= q_2\left(d^+_M + (-1)^M\,d_{-M}\right) + q_2^{'}\,(d^+\tilde{d})_{(22;\,2M)} \tag{7.144}$$

with two parameters q_2, $q_2^{'}$ or e_2, χ. The corresponding reduced probability $B(E2;\,([N];\,n_d\nu n_\Delta;\,L)_i \to ([N];\,n_d\nu n_\Delta;\,L)_f)$ of the transition going from the state of the spherical nucleus with the angular momentum L_i to the state with L_f is determined by (see (2.147), (K.67))

$$\begin{aligned} &B(E2;\,([N];\,n_d\nu n_\Delta;\,L)_i \to ([N];\,n_d\nu n_\Delta;\,L)_f) = \\ &= \frac{\left|\langle([N];\,n_d\nu n_\Delta;\,L)_f\,||\hat{\mathscr{M}}^{(el)}_2||\,([N];\,n_d\nu n_\Delta;\,L)_i\rangle\right|^2}{2L_i+1} \end{aligned} \tag{7.145}$$

So it is given by the square of the reduced matrix elements of the operator $\hat{\mathscr{M}}^{(el)}_2$, which can be finally expressed by the reduced matrix elements $\langle([N];\,n_d\nu n_\Delta;\,L)_f\,||d^+||\,([N];\,n_d\nu n_\Delta;\,L)_i\rangle$ which are determined by so called parentage (genealogic) coefficients [99]. For instance, for $n_d = 2$ we have (see [99], p.690)

$$\langle n_d = 2\;L_f||\;d^+\;||\;n_d = 1\;L_i = 2\rangle = \left[2\,(2L_f+1)\right]^2 \tag{7.146}$$

Generally E2 transition operator (7.144) can change the number of d- bosons at most by one, which gives the selection rule for E2 transitions: $\Delta n_d = 0, \pm 1$. For instance, the $B(E2)$ strength for transition in the g.s. band (it means Y band in the Fig. 7.13) is given by

$$\begin{aligned} &B(E2;\,L^{'} = 2n_d + 2 \to L = 2n_d) = \\ &= \frac{\left|\langle[N], n_d^{\prime} L\,||\hat{\mathscr{M}}^{(el)}_2||[N], n_d+1, L^{'}\rangle\right|^2}{2L+1} = \\ &= \boxed{\begin{array}{c}\text{see}\\[118]\end{array}} = e_2^2\,(N-n_d)(n_d+1) \end{aligned} \tag{7.147}$$

which gives for the lowest level transition:

$$\begin{aligned} B(E2;\,2_1^+ \to 0_1^+) &= e_2^2\,N \\ B(E2;\,2_2^+ \to 2_1^+) &= 2\,e_2^2\,(N-1) \end{aligned} \tag{7.148}$$

and

$$R = \Big[\frac{B(E2;\, 2_2^+ \to 2_1^+)}{B(E2;\, 2_1^+ \to 0_1^+)}\Big]_{U(5)} = 2\,\frac{N-1}{N} \tag{7.149}$$

This ratio, given by the IBM $U(5)$ limit, is different in the comparison with this ratio determined by the Bohr-Mottelson geometrical model (7.80). For example, eq. (7.144) gives $R = 1.71$ for the typical value $N = 7$ (the value $N = 7$ was used in the Fig.7.14) while Bohr-Mottelson geometrical model gives $R = 2$ (see (7.80)). In this sence the value given by the $U(5)$ limit of the IBM is a little bit closer to experimental values then the Bohr-Mottelson model - see (7.81). However, for the limit $N \to \infty$ both these models give the same value $R = 2$.

For the case of the $M1$ transitions we start with the expression (7.120) (see also (K.13)) for the general transition operator $\hat{\mathscr{M}}^{(X)}_{JM}$. For $M1$ only term $\beta_1\,(d^+\tilde{d})_{22;\,1M}$ can work in (7.120). So we have

$$\begin{aligned}\hat{\mathscr{M}}^{(mag)}_{1M} &= m_1\,(d^+\tilde{d})_{22;\,1M} = \\ &= m_1 \sum_{m=-2}^{+2} C^{1M}_{2m\,2\,M-m}\, d^+_m\, \tilde{d}_{M-m}\end{aligned} \tag{7.150}$$

and it can be easily shown that the reduced matrix of (7.150) is diagonal

$$\begin{aligned}\langle n_d \nu n_\Delta L||\hat{\mathscr{M}}^{(mag)}_1||\; n_d^{'}\nu^{'} n_\Delta^{'} L^{'}\rangle &= \\ = m_1 \sqrt{\frac{L(L+1)(2L+1)}{10}}\,\delta_{n_d n_d^{'}}\,\delta_{\nu\nu^{'}}\,\delta_{n_\Delta n_\Delta^{i}}\,\delta_{LL^{'}}\end{aligned} \tag{7.151}$$

However it means that all $M1$ transitions with $L_i \to L_f$, $L_i \neq L_f$ are not possible if the corresponding $M1$ transition operator is given only by (7.150). Therefore in order to describe nonzero $M1$ transitions observed in experiments the additional second order term was introduced into $\hat{\mathscr{M}}^{(mag)}_{1M}$ (see [113, 114]):

$$\begin{aligned}\hat{\mathscr{M}}^{(mag)}_{1M} &= m1\,(d^+\tilde{d})_{(22;\,1M)} + \\ &+ m_1^{'}\Big\{\big[d^+\,(d^+\tilde{d})_{(22,\,1)}\big]_{(21;\,1M)} + \big[(d^+\tilde{d})_{(22;\,1)}\tilde{d}\big]_{(12,1M)}\Big\}\end{aligned} \tag{7.152}$$

where m_1 and $m_1^{'}$ are free parameters. In the analogy with (7.144)-(7.146) the $M1$ reduced probabilities can be also expressed in terms of the parentage genealogic coefficients (see [99]). By the appropriate choice of the parameters m_1, $m_1^{'}$ it is possible to obtain relatively good agreement with the corresponding experimental value. More discussions about the comparison of the $U(5)$ IBM limit el.mg. probabilities with experimental values can be found in e.g. [118, 113].

7.2.2.1.2 $SU(3)$ **limit (axial rotor limit)** In the previous subsection the vibrator limit of the IBM Hamiltonian was discussed when the general IBM-1 Hamiltonian (7.113) was reduced to the $\hat{H}_{vib}$ given in (7.132) or (7.135). Another simplification of the IBM-1 Hamiltonian occurs when the general IBM-1 Hamiltonian (7.113) is reduced to the combination of Casimir operators of the subgroups from the group chain $U(6) \supset SU(3) \supset SO(3) \supset SO(2)$ (the second subgroup chain in (7.128)). This reduction corresponds to so called axial rotor limit because, as it will be seen further, the obtained spectrum in this limit resembles the low- lying spectrum of the axially deformed nuclei (see also appendix K, subsection K.1.2).

The procedure to obtain $SU(3)$ limit is essentially the same as for the $U(5)$ limit dicussed in the precious subsection. In the following the derivation is only sketched (see also the subsection K.1.2). The details can be found e.g. in [114].

The set of eight $SU(3)$ generators is

$$G_{SU(3)} \equiv \left\{ \hat{Q}^{(2)}_m,\ \hat{L}^{(1)}_m \right\} \tag{7.153}$$

where

$$\begin{aligned} \hat{Q}^{(2)}_m &= \boxed{\begin{array}{c}\text{see}\\ (K.89)\end{array}} = \\ &= \left[(d^+ \tilde{s})_{(\,20;\,2m)} + (s^+ \tilde{d})_{(\,02;\,2m)} \right] - \frac{7^{1/2}}{2} \, (d^+ \tilde{d})_{(\,22;\,2m)} \end{aligned} \tag{7.154}$$

with $m = \pm 2, \pm 1, 0$ and

$$\hat{L}^{(1)}_m = \boxed{\begin{array}{c}\text{see}\\ (K.90)\end{array}} = \sqrt{10} \, (d^+ \tilde{d})_{(\,22;\,1m)} \tag{7.155}$$

with $m = \pm 1, 0$.

It should be noted that in the IBM literature the modification of the operator $\hat{Q}^{(2)}_m$ is often used in the sense that instead of (7.154) the quadrupole operator $\hat{Q}^{(2)}_m(\chi)$, dependent in the parameter χ, is introduced:

$$\hat{Q}^{(2)}_m(\chi) = \left[(d^+ \tilde{s})_{(\,20;\,2m)} + (s^+ \tilde{d})_{(\,02;\,2m)} \right] + \chi \, (d^+ \tilde{d})_{(\,22;\,2m)} \tag{7.156}$$

However, it should be pointed out that the $SU(3)$ generator corresponds only to $\chi = -\sqrt{7}/2$.

The corresponding quadratic Casimir operator is [114]

$$\hat{C}_2(SU(3)) = 2 \sum_{m=-2}^{+2} (-1)^m \hat{Q}_m^{(2)} \hat{Q}_{-m}^{(2)} + \frac{3}{4} \sum_{m=-1}^{+1} (-1)^m \hat{L}_m^{(1)} \hat{L}_{-m}^{(1)} \qquad (7.157)$$

In the $SU(3)$ scheme the basis states are labeled as

$$| \, [N]; \, (\lambda\mu) \, KLM \rangle \qquad (7.158)$$

where $[N]$ charcterizes the totally symmetric irreducible representation of the group $U(6)$ (N is the number of s- and d- bosons), $(\lambda\mu)$ corresponds to the irrep of the group $SU(3)$; L and M label the angular momentum and its projection onto z- axis (the labels of the irrep of the $SO(3)$ group), and K is the additional quantum number which distinguishes the states with the same (λ, μ) and L:

$$\begin{array}{ccccccc} U(6) & \supset & SU(3) & \supset & SO(3) & \supset & SO(2) \\ \vdots & & \vdots & & \vdots & & \vdots \\ N & & (\lambda\mu) & ..K.. & L & & M \end{array} \qquad (7.159)$$

Again without any details the quantum numbers λ, N, μ and M are tied by following conditions [114]

$$\begin{aligned} & 0 \leq \lambda \leq 2N - 2\mu - 6M \\ & M \geq 0 \quad \text{integer} \\ & \mu \geq 0 \quad \text{integer, even} \end{aligned} \qquad (7.160)$$

and we accept the interpretation of the Elliott's paper [119] (see also appendix K) that the additional quantum number K represents the projection of the angular momentum onto the nucleus symmetry axis. Then the connection of K and L is following

$$\begin{aligned} & L = K, \; K+1, \; K+2, \cdots, \; (K + max(\lambda, \mu)) \quad \text{for } K \neq 0 \\ & L = max(\lambda, \mu), \; max(\lambda, \mu) - 2, \cdots, \; 1 \text{ or } 0 \quad \text{for } K = 0 \end{aligned} \qquad (7.161)$$

where

$$K = \text{ integer } = min(\lambda, \mu), \; \min(\lambda, \mu) - 2, \cdots, \; 1 \text{ or } 0 \qquad (7.162)$$

As was the case for the $U(5)$ limit, the Hamiltonian is diagonal in the base (7.158) if it can be written in terms of the generators (7.154) of the subgroup $SU(3)$, concretely in the case of the $SU(3)$ limit the Hamiltonian is following

$$\hat{H}_{rot} = -\kappa \sum_{m=-2}^{+2} (-1)^m \hat{\vec{Q}}_m^{(2)} \, \hat{\vec{Q}}_{-m}^{(2)} - \kappa' \sum_{m=-1}^{+2} (-1)^m \hat{\vec{L}}_m^{(1)} \, \hat{\vec{L}}_{-m}^{(1)} \qquad (7.163)$$

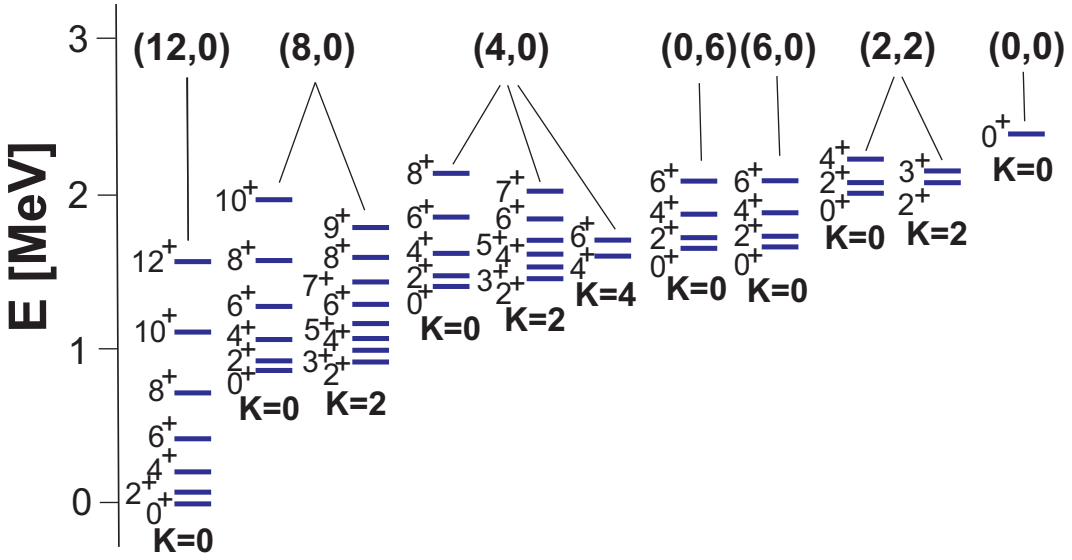


Figure 7.15: Typical spectrum of positive parity levels $E([N](\lambda\mu)KL)$ given by (7.164) calculated with $N = 6$ and $\kappa \approx 7.2$, $\kappa' = 0$ KeV. Individual levels with given L are sorted to the bands characterized by the quantum numbers $(\lambda\mu)$ and K. All quantum numbers λ, μ, M, L, K are tied by the conditions (7.160), (7.161) and (7.162).

with the eigen energy

$$E([N],\,(\lambda\mu),\,KL) = \left(\frac{3}{4}\,\kappa - \kappa'\right)\,L(L+1) - \kappa\,C(\lambda\mu) \tag{7.164}$$

where $C(\lambda\mu)$ are eigen values of the quadratic Casimir operator (7.157) of the subgroup $SU(3)$ [114]

$$C(\lambda\mu) = \lambda^2 + \mu^2 + \lambda\mu + 3\,(\lambda + \mu) \tag{7.165}$$

The substitution of (7.154) and (7.155) into (7.163) enables to compare the Hamiltonian $\hat{H}_{rot}$ in (7.163) with the general IBM-1 Hamiltonian (7.113). The comparison shows that the $SU(3)$ limit Hamiltonian (7.163) can be obtain from the general Hamiltonian (7.133) if its parameters are following

$$\begin{aligned}
\epsilon_s &= -10\,\kappa & c_0 &= -7\,\kappa + 12\,\kappa' \\
\epsilon_d &= -\frac{11}{2}\,\kappa - 6\,\kappa' & c_2 &= \frac{3}{2}\,\kappa + 6\,\kappa' \\
\tilde{v}_2 &= \sqrt{140}\,\kappa & c_4 &= -2\,\kappa - 8\,\kappa' \\
\tilde{v}_0 &= -2\,\sqrt{5}\,\kappa \\
\tilde{u}_2 &= -4\,\sqrt{5}\,\kappa \\
\tilde{u}_0 &= -2\,\sqrt{5}\,\kappa
\end{aligned} \tag{7.166}$$

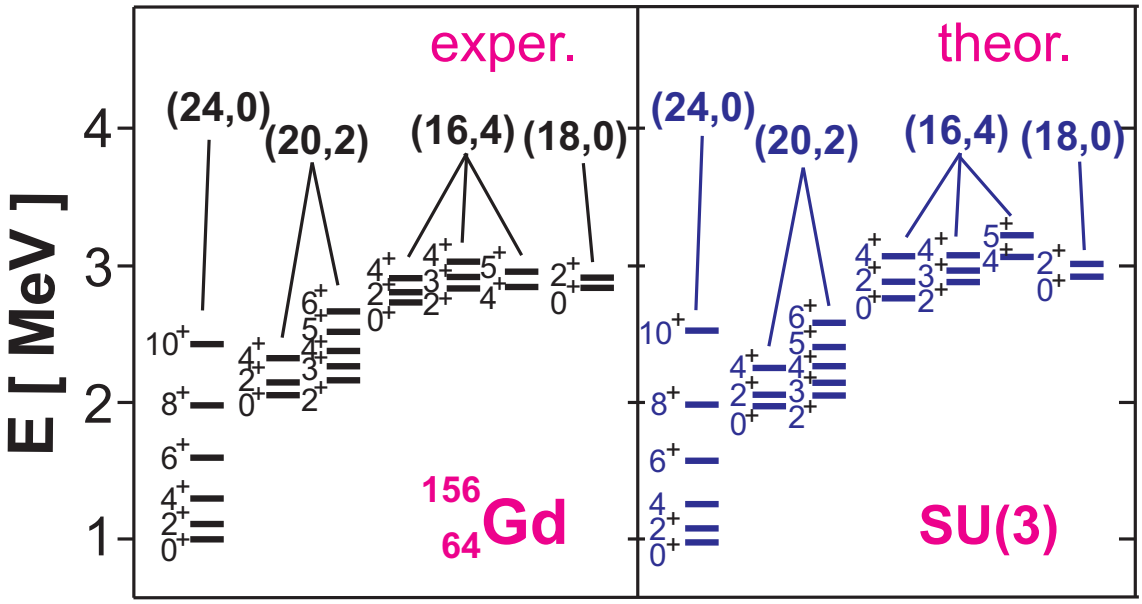


Figure 7.16: An example of a spectrum with $SU(3)$ symmetry: $^{156}_{64}$Gd, (N=12). The theoretical spectrum is calculated using eq. (7.164) with $\kappa = 7.25$ KeV and $\kappa^{'} = 8.56$ KeV.

A typical $SU(3)$ spectrum (7.164) is shown in the Fig. 7.15. The spectrum is equivalent to that of a rigid axially symmetric rotor in the sense that the energies in each band go as $L(L+1)$. Really, if we compare the spectrum in the Fig.7.15 with the spectrum of the lowest positive parity rotational band spectrum of well deformed axially symmetric nuclei (see e.g. Fig.7.2 where the low-lying spectrum of well deformed nucleus ^{154}Sm is shown) one can see that they are similar (the ground state band $K = 0$, β- and γ- rotational bands can be recognized in the Fig. 7.15). The main difference between the $SU(3)$ limit spectrum (7.164) and axially symmetric rotor spectrum is that in the case of $SU(3)$ the bands are terminated at a certain angular momentum while in the axially symmetric rotor they continue up to infinity. The other difference is that in the case of axially symmetric rotor the rotational bands based on the β- and γ- vibrational states are not degenerate while in the $SU(3)$ scheme the levels with the same spin L and the same $(\lambda\mu)$ but with different K are degenerated in the energy. The comparison of the $SU(3)$ spectrum (7.164) with the experimental low- lying spectrum of ^{156}Gd is also shown in the Fig. 7.16. The qualitative agreement between calculated and experimental spectra is very good. However one should have in mind that the IBM is phenomenological (without any connection to the realistic nucleon-nucleon interaction) and that the physical meaning of parameters (7.166) is under the question.

Up to now two limiting cases of the IBM were discussed: vibrator ($U(5)$) limit, suitable for spherical nuclei, and rotor ($SU(3)$) limit, describing well deformed nuclei with rotational bands in their spectra. The merit of the IBM is the fact that these limits (together with their γ- unstable ($SO(6)$) limit which will be discussed in the next subsection 7.2.2.2.3) are only special cases of the more general Hamiltonian (7.125) with $U(6)$ symmetry, which acts on a finite dimensional space with low dimension and which can be therefore easily diagonalized e.g. within the basis of $U(5)$ limit states $\mid [N];\ n_d \nu n_\Delta;\ LM\rangle$ or $SU(3)$ limit states $\mid [N];\ (\lambda\mu);\ KLM\rangle$. This allows to give a unified and simple description of not only limits mentioned above but also all case in between. This was, for instance, done in the paper [127] using a very simple Hamiltonian and other transition operators for the chain of Sm isotopes going from the spherical ^{146}Sm up to well deformed ^{156}Sm. Parameters of this simple Hamiltonian were taken constant or varied at most linearly with the neutron number. In this way it was demonstrated that in the framework of the simple IBM-1 model it is possible to describe the transition from the spherical to deformed nuclei (changing of energy spectra and of other properties if one goes in one isotopic chain from spherical nuclei to deformed ones).

The simplest Hamiltonian that can describe within one approach both vibrational and rotational spectra is following (compare with (7.163) and (7.135))

$$\hat{H}_{U(5)-SU(3)} = \epsilon\, \hat{n}_d - \kappa \sum_{m=-2}^{+2} (-1)^m\, \hat{Q}^{(2)}_m \hat{Q}^{(2)}_{-m} - \kappa' \sum_{m=-1}^{+1} (-1)^m\, \hat{L}^{(1)}_m \hat{L}^{(1)}_{-m} \quad (7.167)$$

Here ϵ, κ and κ' are free parameters that in general depend on N_ν and N_π, the neutron and proton boson number, respectively. In the description of the Samarium isotopes parameters κ and κ' were kept constant and ϵ varied according to

$$\epsilon = \epsilon_c - \theta\, N_\nu \quad (7.168)$$

With this simple parametrization for $\hat{H}_{U(5)-SU(3)}$ they could recover the $U(5)$ limit if ϵ was large compared to N, κ and κ' where $N = N_\nu + N_\pi$ (see [127, 118]) while the $SU(3)$ limit was obtained if ϵ was small. Therefore the Hamiltonian $\hat{H}_{U(5)-SU(3)}$ in (7.167) describes the transition from the vibrational to rotational limit. In the both limits, $U(5)$ and $SU(3)$, there exist analytical formulas (see (7.139) for $U(5)$ symmetry and (7.164) for $SU(3)$ limit). In the transitional region between these limits they had to obtain eigen energies of the Hamiltonian $\hat{H}_{U(5)-SU(3)}$ numerically by the diagonalization of its matrix.

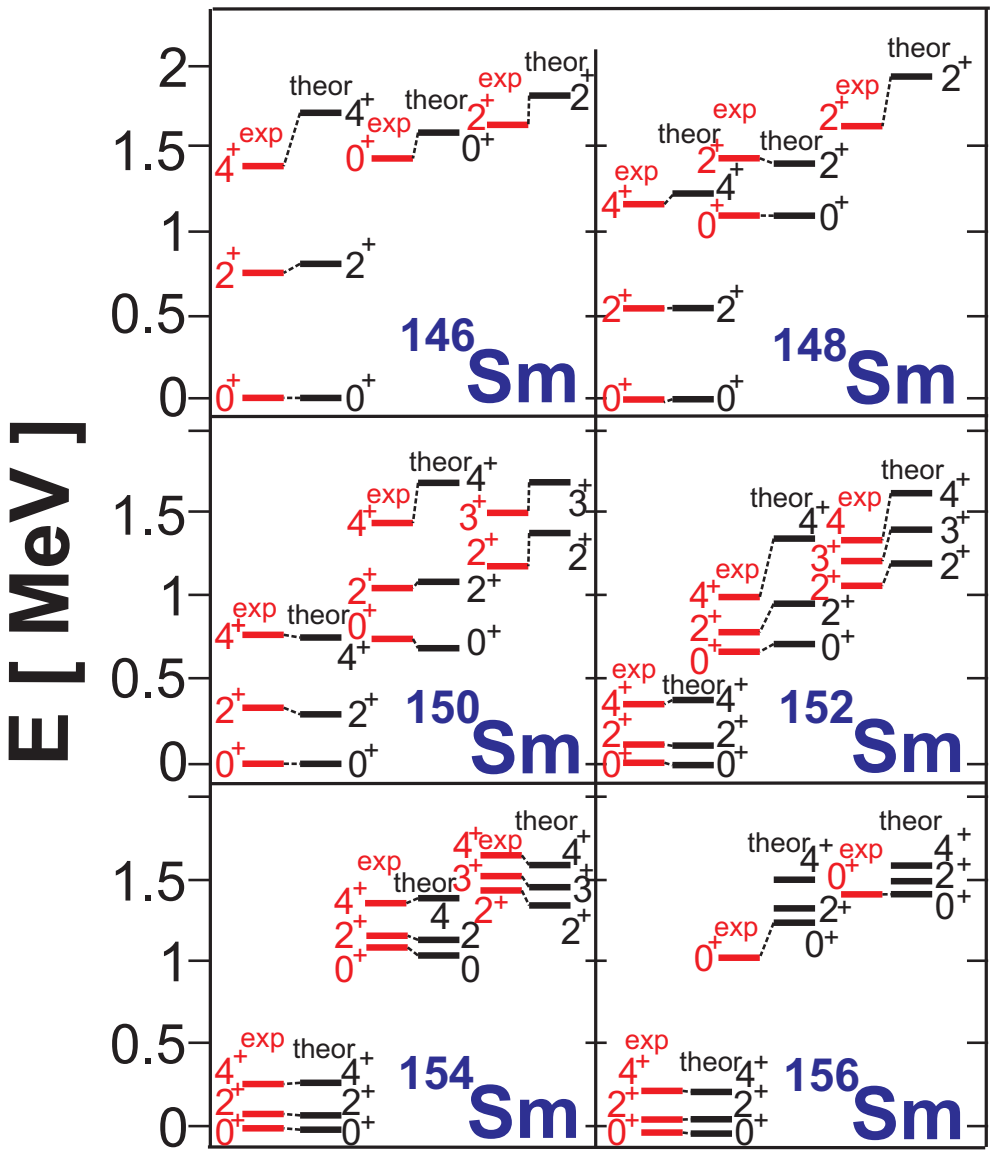


Figure 7.17: Comparison between calculated (theor) and experimental (exp) energy levels in the Sm isotopes. Only levels O_1^+, O_2^+, 2_1^+, 2_2^+, 2_3^+, 3_1^+, 4_1^+, 4_2^+, 4_3^+ below 2 MeV are shown (taken from [118]).

The boson number was determined in the following way. The Samarium has 62 protons and the number of neutrons for Sm isotopes ranges from 84 (^{146}Sm) to 94 (^{156}Sm). Counting from the proton closed shell at $Z = 50$ and the neutron closed shell at $N = 82$ the number of proton and neutron valence pairs (bosons) are $N_\pi = 6$ and $N_\nu = 1$ to 6 (according to the receipt given in the text above the exp. (7.104)). Therefore the total number of bosons, $N = N_\pi + N_\nu$, ranges from 7 for ^{146}Sm to 12 for ^{156}Sm.

The values of the parameters of the Hamiltonian $\hat{H}_{U(5)-SU(3)}$ (see (7.167), (7.168)), used in the calculations, was following

$$\begin{aligned} \epsilon_c &= 1260\text{keV} \quad , \qquad \theta = 170 \text{ keV} \quad , \\ \kappa &= 9.75 \text{ keV} \quad , \qquad \kappa^{'} = -6 \text{ keV} \end{aligned} \tag{7.169}$$

The result of the diagonalization of the Hamiltonian (7.167) is compared with the measured excitation energies of the Sm isotopes in Fig. 7.17. The spectrum of ^{146}Sm has clear vibrational structure with a triplet of states at about twice the energy of the 2_1^+ state. ^{156}Sm is a good example of a $SU(3)$ spectrum with a well developed rotational bands. Furthermore the $K = 0$ and $K = 2$ bands ($\lambda = 2N - 4$, $\mu = 2$) multiplet lie relatively high and close together in the spectrum.

The simple model with the Hamiltonian (7.167) was used also for the calculation of other properties of Sm isotopes (two neutron separation energy, reduced probabilities of E2 and E4 transitions, quadrupole moments, cross sections of (p,t) reactions etc. - see [118]) and similarly as in the energy spectrum case this simple model with small number of parameters describes the corresponding experimental data very well.

7.2.2.1.3 γ- unstable limit ($SO(6)$ limit) Besides two limits of the IBM-1 discussed in the previous subsections there is the third limit called as γ-unstable or γ- soft limit. This limit corresponds to the third subgroup chain decomposition of the $U(6)$ totally symmetric representation given in (7.128) and therefore it is sometimes called as $SO(6)$ limit. The name "γ unstable or γ-soft limit" is connected with the fact that the energy spectrum and el.mg. reduced transition probabilities given by this $SO(6)$ limit corresponds to the experimental data of nuclei from the region of isotope table where the mean field total energy calculations give the broad plateau minimum in the dependence on the quadrupole γ- deformation of the mean field (see the discussion further). Therefore these nuclei are γ- unstable or γ- soft.

According to the scheme used in the previous subsections if the Hamiltonian can be written in terms of the generators (or more precisely in terms of the combination of Casimir operators) of the subgroups in the subgroup chain decomposition of the $U(6)$ irrep then the eigen vectors of the Hamiltonian involves quantum numbers which label the irreps of the subgroups in the chain and the eigen energies can be expressed explicitly by means of these quantum numbers. This scheme is used also now for the subgroup chain $U(6) \supset SO(6) \supset SO(5) \supset SO(3) \supset SO(2)$ (see also the Appendix K, subsection K.1.3). The fifteen $SO(6)$ generators are

$$G_{SO(6)} \equiv \left\{ \left((s^+ \tilde{d})_{(02;\,2m)} + (d^+ \tilde{s})_{(20;\,2m)} \right),\ (d^+ \tilde{d})_{(22;\,3m)},\ (d^+ \tilde{d})_{(22;\,1m)} \right\} \quad (7.170)$$

and ten operators

$$G_{SO(5)} \equiv \left\{ (d^+ \tilde{d})_{(22;\,1m)},\ (d^+ \tilde{d})_{(22;\,3m)} \right\} \quad (7.171)$$

form the set of generators of the group $SO(5)$ and three operators

$$G_{SO(3)} \equiv \left\{ (d^+ \tilde{d})_{(22;\,1m)} \right\} \quad (7.172)$$

are generators of the group $SO(3)$. From (7.170) we see immediately that the generators of $SO(5)$ and $SO(3)$ are contained in the set of generators of $SO(6)$ and this gives rise to the group reduction $U(6) \supset SO(6) \supset SO(5) \supset SO(3) \supset SO(2)$. The quadratic Casimir operator of $SO(6)$ is given by [115, 118]

$$\begin{aligned} \hat{C}_2[SO(6)] = \hat{N}(\hat{N}+4) \\ -8 \Big\{ \frac{5}{4} \big[(d^+ d^+)_{(22;\,0)}\ (\tilde{d}\tilde{d})_{(22;\,0)} \big]_{(00;\,0)} \\ -\frac{\sqrt{5}}{4} \left[(d^+ d^+)_{(22;\,0)}\ (\tilde{s}\tilde{s})_{(00;\,0)} + h.c. \right]_{(00;\,0)} \\ +\frac{1}{4} \left[(s^+ s^+)_{(00;\,0)}\ (\tilde{s}\tilde{s})_{(00;\,0)} \right]_{(00;\,0)} \Big\} \end{aligned} \quad (7.173)$$

This operator has eigen values $2\sigma(\sigma+4)$ where σ label the different $SO(6)$ multiplets [115, 118].

In accordance with the group reduction $U(6) \supset SO(6) \supset SO(5) \supset SO(3) \supset SO(2)$ the $SO(6)$ limit basis states are labeled as $|\,[N];\ \sigma\nu n_\Delta :\ LM\rangle$:

$$\begin{array}{ccccccccc} U(6) & \supset & SO(6)) & \supset & SO(5) & \supset & SO(3) & \supset & SO(2) \\ \vdots & & \vdots & & \vdots & & \vdots & & \\ N & & \sigma & & \nu & ..n_\Delta.. & L & & M \end{array} \quad (7.174)$$

This resembles the labeling of irreps in the vibrator limit group chain (see (7.137)) but instead of the quantum number n_d now we have the quantum number σ. The meaning of the numbers ν and n_d are the same as in (7.137). The allowed values for the quantum numbers are [115, 118] are

$$\begin{aligned}
&\sigma = N,\ N-2,\ N-4, \cdots, 0 \text{ or } 1 \\
&0 \leq \nu \leq \sigma \\
&\lambda = \nu - 3n_\Delta \geq 0 \\
&L = \lambda,\ \lambda+1,\ \lambda+2, \cdots, 2\lambda-2,\ 2\lambda
\end{aligned} \tag{7.175}$$

where the last two equalities are the same as in (7.138). The most general Hamiltonian with the $SO(6)$ symmetry can be then written as

$$\begin{aligned}
\hat{H}_{\gamma- \, soft} = A\,\frac{1}{8}\left\{2\hat{N}(\hat{N}+4) - \hat{C}_2[SO(6)]\right\} + \\
+B\,\hat{C}_2[SO(5)] + C\,\hat{L}^2
\end{aligned} \tag{7.176}$$

where $\hat{C}_2[SO(6)]$ is given by (7.173), $\hat{C}_2[SO(5)]$ by (7.133) and $\hat{L}^2$ by (7.134). The eigen values of (7.176) in the basis of states $|\,[N];\,\sigma\,\nu\,n_\Delta;\,L\,M\rangle$ are [118]

$$\begin{aligned}
E(N,\sigma,\nu,n_\Delta,L) = A\,\frac{1}{4}(N-\sigma)(N+\sigma+4) + \\
+B\,\frac{1}{6}\nu(\nu+3) + C\,L(L+1)
\end{aligned} \tag{7.177}$$

The $SO(6)$ limit Hamiltonian $\hat{H}_{\gamma- \, soft}$ (see (7.176)) corresponds to a particular choice of the coefficients of the general IBM-1 $U(6)$ Hamiltonian (7.124):

$$\begin{aligned}
&\epsilon_0 = 0 \quad , \qquad\qquad \epsilon_d = \frac{5}{2}\,A + \frac{2}{3}\,B + 6\,C\,, \\
&c_0 = -\frac{1}{3}\,B - 12\,C\,, \quad c_2 = \frac{1}{3} - 6\,C\,, \quad c_4 = \frac{1}{3}\,B + 8\,C \\
&\tilde{v}_2 = 0\,, \qquad \tilde{v}_0 = \frac{\sqrt{5}}{4}\,A\,, \qquad \tilde{u}_2 = 0\,, \qquad \tilde{u}_0 = \frac{1}{4}\,A
\end{aligned} \tag{7.178}$$

A typical spectrum is shown in the fig. 7.18. A characteristic property of this $SO(6)$ limit is the repeated occurrence of a sequence of states 0^+, 2^+ and a doublet $(4^+, 2^+)$, where the energy difference between the doublet and the ground 0^+ in each multiplet is about 2.5 times as large as the energy difference between the first 2^+ and ground 0^+ level of each (σ, n_Δ) multiplet. Although at the first glance the spectrum resembles that of the $U(5)$ limit (see Fig 7.13), there are an important difference. In the $U(5)$ limit there is a

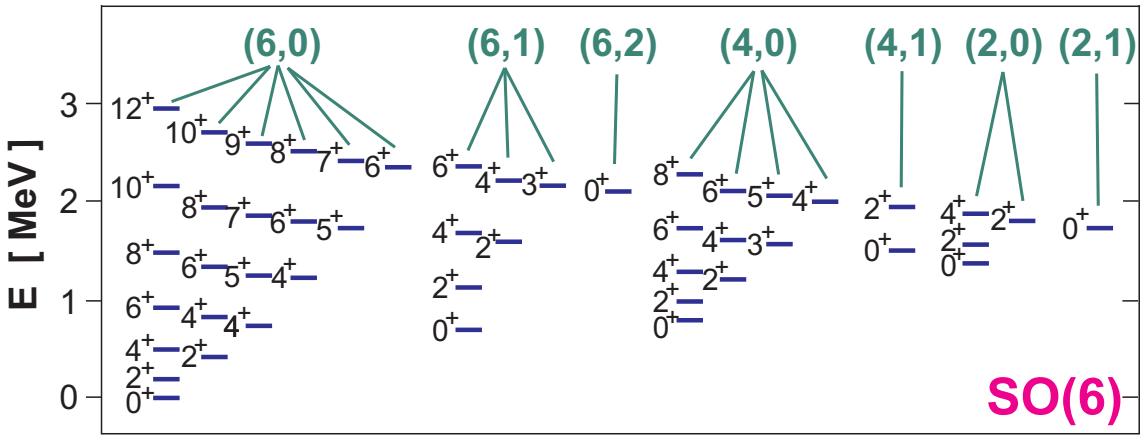


Figure 7.18: Typical spectrum of positive parity levels with $SO(6)$ symmetry and $N = 6$. In parenthesis are the value of σ and n_Δ.

triplet of states $(0^+, 2^+, 4^+)$ at $E_x \approx 2\epsilon$ (see Fig. 7.13) while in $SO(6)$ there is only a doublet. Also marked differences occur in the $B(E2)$ transition probabilities as it will be discussed further.

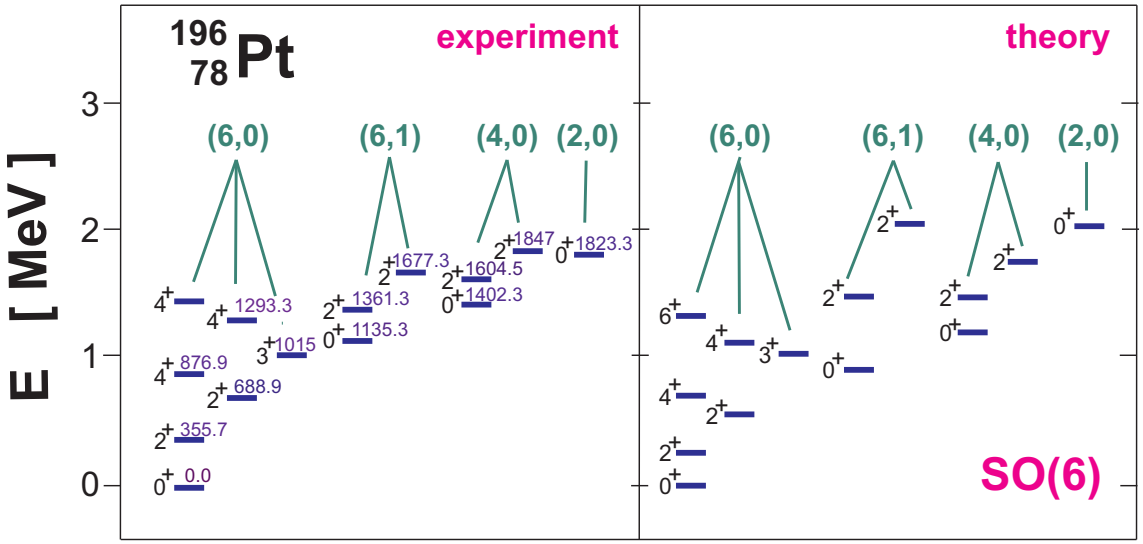


Figure 7.19: Example of a spectrum of the nucleus with $SO(6)$ dynamical symmetry: ^{196}Pt. The theoretical spectrum was calculated using (K.102) with $A = 43$ keV, $B = 33.2$ keV, $C = 10$ keV and N=6. The value of the energy in keV is shown above each experimental level. Experimental energies were taken from [122].

The name "γ- soft" came from the paper of Meyer-ter-Vehn [120] where it was shown that the most resembles with $SO(6)$ limit is the γ- unstable model of Wilets and Jean [121]. This model corresponds to considering only $\sigma = N$ multiplets of $SO(6)$ in the limit of $N \to \infty$. As an example of the $SO(6)$ limit in the fig. 7.19 the spectrum of ^{196}Pt is shown. One can see very

good agreement of the calculated energies with experimental ones in spite of the fact that we used a little number of parameters (A, B, C, N).

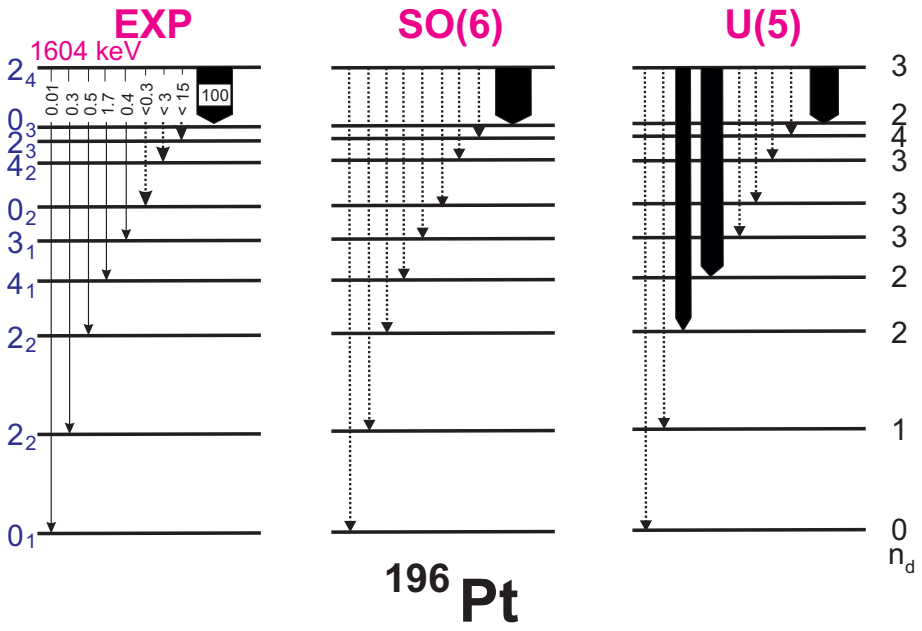


Figure 7.20: Comparison of the decay of the 1604 keV level in ^{196}Pt with $SO(6)$ and $U(5)$ limit predictions (taken from [122]).

The $SO(6)$ nuclei are now well known in two regions: the Pt isotopes, especially ^{196}Pt and Xe-Ba nuclei near $A \approx 130$. A comparison of the ^{196}Pt level scheme with the $SO(6)$ limit is shown in the fig. 7.19. Similar comparisons for other nuclei from regions mentioned above can be found e.g. in [118, 123]. Although the energy spectra obtained in the framework of the $U(5)$ and $SO(6)$ limits are quite similar the selection rule $\Delta\nu = \pm 1$ for E2 transitions in the $SO(6)$ limit gives much better results in the comparison with the experimental values of reduced probabilities than the $U(5)$ limit. This can be seen from the Fig.7.20 where the experimental decay of the 1604.5 keV level in ^{196}Pt is compared with with the theoretical $SO(6)$ and $U(5)$ limit predictions.

7.2.2.1.4 Casten symmetry triangle In order to analyze simultaneously 3 limit cases discussed in previous subsections using one Hamiltonian even 3 parameter Hamiltonian (7.167) is too complex. For the transparent demonstration of these three limits usually two- parameter Hamiltonian is extracted from the six- parameter general IBM-1 Hamiltonian (7.125) or from the 3-parameter Hamiltonian (7.167) and the $U(5)$, $SU(3)$, and $SO(6)$ limits are then reached for some particular point in the 2- dimensional parameter space.

In such a way this two- dimensional parameter manifold can be mapped onto so called Casten symmetry triangle, whose vertices correspond to these limits. This triangle enables also the transparent demonstration of the shape transition from the spherical symmetry to the deformation of nuclei and simultaneously to classify these transitions as phase transitions.

The suitable 2- parameter Hamiltonian for the simultaneous analysis of $U(5)$, $SU(3)$, and $SO(6)$ limits is following (see e.g. [128, 129] and compare with (7.167)) [6]

$$\hat{H}_{Casten} = \epsilon\, \hat{n}_d - \kappa \sum_{m=-2}^{+2} (-1)^m\, \hat{Q}^{(2)}_m(\chi)\, \hat{Q}^{(2)}_{-m}(\chi) \tag{7.179}$$

where $\hat{Q}^{(2)}_m(\chi)$ is given by (7.156). One can see that if $\chi = -\frac{\sqrt{7}}{2}$ Hamiltonian (7.179) is the combination of Casimir operators: $\hat{C}_1[U(5)] = \hat{n}_d$ and $\frac{1}{2}\hat{C}_2[SU(3)] - \frac{3}{8}\hat{C}_2[SO(3)]$ (see (7.157), (7.134)). For $\kappa \to 0$ (or $\kappa << \epsilon$) the Hamiltonian (7.179) has $U(5)$ symmetry while for $\epsilon \to 0$ (or $\epsilon << \kappa$) the symmetry of the Hamiltonian $\hat{H}_{Casten}$ corresponds to the $SU(3)$ or $SO(6)$ limits [128]. The $SU(3)$ and $SO(6)$ limits with $\epsilon \to 0$ are distinguished by the parameter χ: if $\chi = -\frac{\sqrt{7}}{2}$ then we have $SU(3)$ limit (compare with (7.163)) and for $\chi = 0$ we treat the $SO(6)$ limit (compare with (7.176)). In order to describe the transitions $U(5)$ - $SU(3)$ ($\chi = 0$) and $U(5)$ - $SO(6)$ ($\chi = -\frac{\sqrt{7}}{2}$) it is convenient to reparametrize the ratio ϵ/κ as

$$\frac{\epsilon}{\kappa} = \frac{1-\xi}{\xi} \tag{7.180}$$

Then the symmetry transitions $U(5) - SU(3)$ and $U(5) - SO(6)$ are labeled by one control parameter ξ ($0 \le \xi \le 1$): $\xi = 0$ for $U(5)$ limit and $\xi = 1$ for $SU(3)$ and $SO(6)$ limits). The changing the parameter χ (for $\xi = +1$ fixed) from $\chi = -\sqrt{7}/2$ to $\chi = 0$ we go from $SU(3)$ limit to $SO(6)$ limit. Both transitions, $U(5) - SU(3)$ and $SU(3) - SO(6)$, can be then represented grafically by the triangle (so called Casten symmetry triangle [128]) given in the Fig.7.21.

Vertexes of the symmetry triangle corresponds to 3 limits $U(5)$, $SU(3)$ and $SO(6)$. Changing χ from $-\sqrt{7}/2$ to 0, one moves along the side $SU(3) - SO(6)$ of the triangle. The value of χ for a point inside the triangle is given

[6] In fact, the Hamiltonian (7.179) has 3 parameters ϵ, κ and χ. However from the point of view of the transitions $U(5)$ - $SU(3)$ and $U(5)$ - $SO(6)$ only the ratio ϵ/κ of two parameters is relevant as is discussed further.

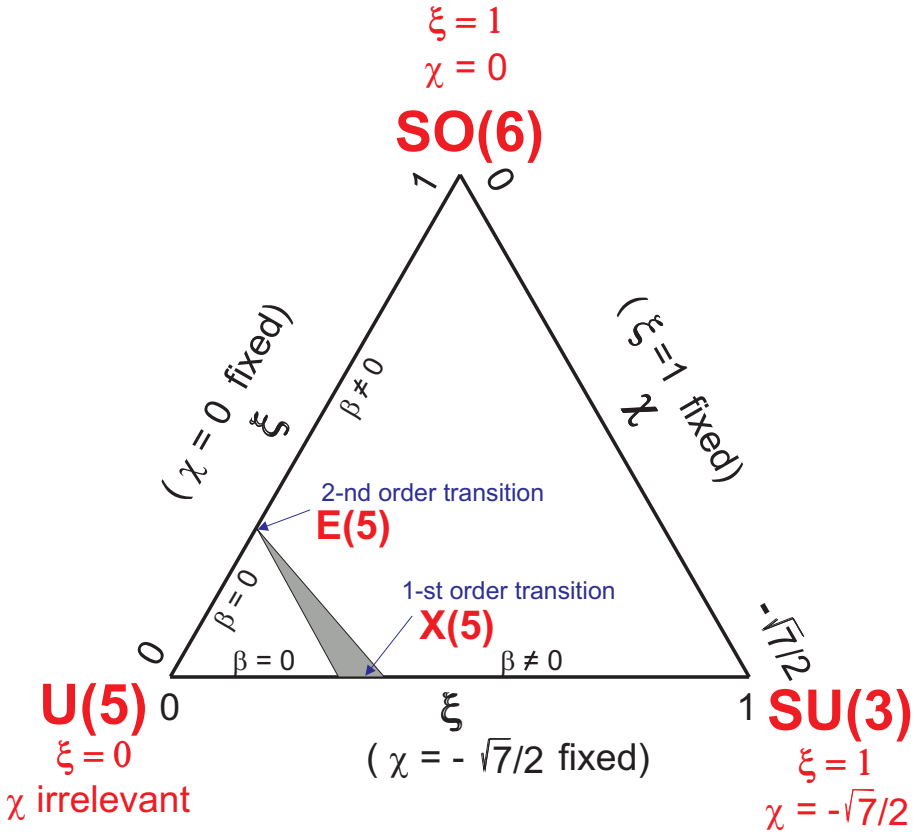


Figure 7.21: The symmetry triangle for the IBM-1 showing schematically the region of parameter space corresponding to $U(5)$,SU(3) and $SO(6)$ limits. Shaded area corresponds to parameters ξ and χ of the Hamiltonian (7.179) when the total energy (7.183) has two minima corresponding to two different values of the deformation β. This corresponds to the phase coexistence discussed in the text.

by the intersection of the line, originating from the $U(5)$ vertex and passing through the given point, with the $SU(3) - SO(6)$ side of the triangle. Going from the $U(5)$ vertex with $\xi = 0$, where the equilibrium quadrupole deformation is zero, $\beta = 0$, in the direction to the $SU(3) - SO(6)$ side of the triangle at some values of the control parameter ξ the shape transition from the spherical $\beta = 0$ shape to the deformed one with $\beta \neq 0$ occurs. This transition region corresponds to the shaded area in the Fig.7.21. In the determination of this area we follow the approach introduced in [130] as it is further briefly discussed (see also [128]).

In order to investigate deformation effects in the IBM in the paper [130] instead of the uncorrelated multiboson states (7.117) with the pure monopole s^+ and quadrupole d^+_m $(m = \pm 2, \pm 1, 0)$ creation operators the basis of the

correlated multiphonon states:

$$|N;\ \alpha\rangle \equiv \left(s^{+} + \sum_{\mu=-2}^{+2} \alpha_{2\mu}\, d_{\mu}^{+}\right)^{N} |\ 0\rangle \tag{7.181}$$

was suggested. In (7.181) $\alpha_{2\mu}$ are quadrupole deformation parameters (see (7.48)-(7.53)) and the symbol α involves 5 quadrupole deformation parameters $\alpha_{2\mu}$ ($\mu = \pm 2, \pm 1, 0$). In the case of the nonzero equilibrium deformation we can transform 5 variable $\alpha_{2\mu}$ in the lab. frame into 2 intrinsic coordinates $a_{20} = \beta\, cos\gamma$, $a_{22} = a_{2-2} = \frac{1}{\sqrt{2}}\, \beta\, sin\gamma$ (see (7.82), (7.83)) and 3 Euler angles θ (see (7.82)). In such a way we obtain the intrinsic frame multiboson state $|N;\ \beta\gamma\rangle$. Then we can determine the total energy of the Hamiltomian (7.179) in the intrinsic multiboson state $|N;\ \beta\gamma\rangle$:

$$E(N;\ \beta, \gamma) \equiv \frac{\langle N; \beta\gamma |\ \hat{H}_{Ca}\ |\ N;\ \beta\gamma\rangle}{\langle N; \beta\gamma |\ N;\ \beta\gamma\rangle} \tag{7.182}$$

and minimize it with respect to β and γ ($\frac{\partial E(N;\beta,\gamma)}{\partial \beta} = \frac{\partial E(N;\beta,\gamma)}{\partial \gamma} = 0$). This algorithm provides a rigorous definition of the equilibrium "shape" associated with the given boson Hamiltonian ($\hat{H}_{Ca}$ in our case) and the boson number N, which has the property of converging to the classical equilibrium shape when $N \to \infty$. In the case of the Hamiltonian (7.179) the procedure (7.182) gives (see [128])

$$\begin{aligned} E(N;\beta,\gamma) = {} & \frac{N\,\beta^2}{1+\beta^2}\left[1 - \xi\,(\chi^2 - 3)\right] \\ & - \frac{N\,(N-1)}{(1+\beta^2)^2}\,\xi\left[4\xi^2 - 4\sqrt{\frac{2}{7}}\,\chi\,\beta^3\, cos3\gamma + \frac{2}{7}\,\chi^2\,\beta^4\right] \end{aligned} \tag{7.183}$$

By means of the minimizing of the (7.183) in the each point of the symmetry triangle we can determine the equilibrium deformation β, γ.

Further we concentrate on the values of the control parameters ξ and χ near the shaded area in the triangle Fig.7.21 where the transition between two "phases" , spherical one with $\beta = 0$ and deformed one $\beta \neq 0$, occurs. In [128] it was shown that for values of ξ in the narrow interval around the value 0.026 and for $\chi > 0$ the energy (7.182) has two minima ($\beta_1 = 0$, $\gamma = 0$) and ($\beta_2 \neq 0$, $\gamma = 0$). The values of β_2 depends on χ: $\beta_2 = 0$ for $\chi = 0$ (that means only one minimum) up to $\beta_2 \approx 0.5$ for $\chi = -\frac{\sqrt{7}}{2}$. This situation is depicted in the Fig.7.22.

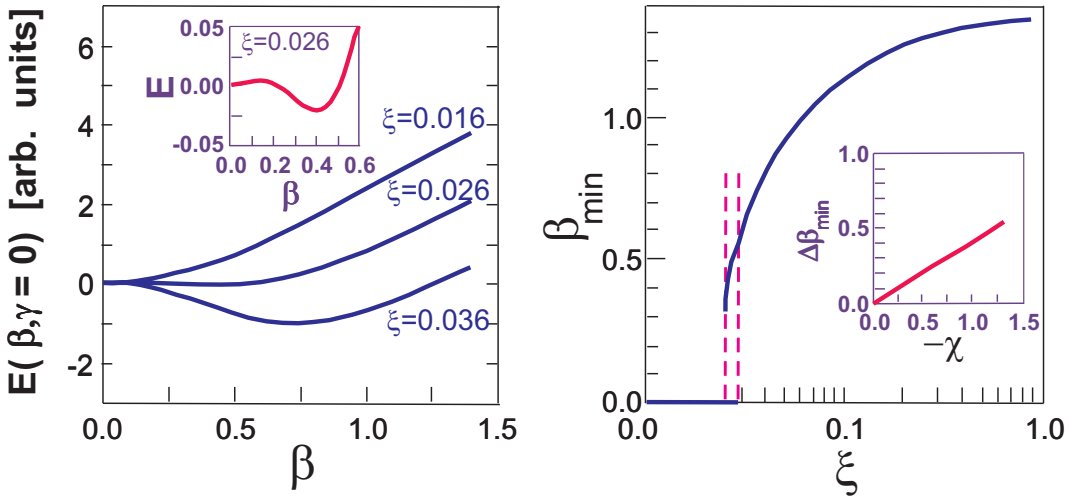


Figure 7.22: **Left panel**: Energy surfaces as a function of the deformation (order) parameter β (see (7.183). The inset shows, on an expanded scale, the two shallow coexisting minima that arise for a narrow range of values of the parameter ξ near 0.026. The upper and lower curves have one minima only, either for a spherical or a deformed shape. **Right panel**: Value(s) of the location of the minima of the energy surfaces. Note the two minima for a small range of ξ values around the value 0.026. The calculation was done for $N = 10$ and $\chi = -\frac{\sqrt{7}}{2}$. The inset shows the difference in β_{min}values, $\Delta\beta_{min} = \beta_2 - \beta_1$, as a function of the parameter χ when $\xi = 0.026$ (taken from [128]).

In the left panel of the Fig. 7.22 there is the dependence of the energy $E(N = 10;\ \beta,\ \gamma = 0)$ on the deformation β for 3 values of the control parameter ξ: $\xi = 0.036,\ 0.026,\ 0.016$. In the left panel the value(s) of the location β_{min} of the minima of the energy $E(N = 10;\ \beta,\ \gamma = 0)$ as a function of the parameter ξ is shown for $N = 10$ and $\chi = -\sqrt{7}/2$. The inset in the right panel shows the difference $\Delta\beta_{min} = \beta_2 - \beta_1$ in the dependence on the parameter χ for $\xi = 0.026$ fixed. The inset in the left panel demonstrates positions of two minima, $\beta_1 = 0$ and $\beta_2 \neq 0$, of the energy surface $E(N = 10;\ \beta,\ \gamma = 0)$ depicted as a function of the deformation parameter β which occur for fixed value $\xi = 0.026$. From the right panel one can see the narrow interval of ξ around $\xi = 0.026$ where the energy $E(N = 10;\ \beta,\ \gamma = 0)$ has two different minima β_1 and β_2. These values of the parameter ξ are also depicted in the schematic figure Fig.7.21 as the shaded area. It should be pointed out that the values of parameters $\xi = \epsilon/\kappa = 0.032$, $\chi = -\sqrt{7}/2$ of the Hamiltonian (7.179) and $N = 10$ give the low- lying spectrum of excited states which agrees with experimental spectrum of ^{152}Sm (for ^{152}Sm $N = N_\pi + N_\nu = 6 + 4 = 10$). This means that the ^{152}Sm is very close to the critical point ($\xi = 0.026$, $\chi = \sqrt{7}/2$) where the shape transition from the

spherical shape to deformed one occurs (see [128]).

From the point of view of the classical physics the equilibrium deformation β_{min} plays a role of the order parameter in the phase transition (it determines the phase: spherical one for $\beta = 0$ and deformed one for $\beta \neq 0$) [7] . Further we know from the statistical physics (see e.g. [131]) that the phase transition of the 1-st type is connected with the phase coexistence. That means in the phase transition point with the critical control parameters $\xi_0 = 0.026$, $\chi_0 = -\sqrt{7}/2$ two phases (two equilibrium deformations β_1 and β_2, $\beta_1 \neq \beta_2$) exist simultaneously. From the Fig. 7.22 and Fig. 7.21 one can see that this is just the case of the $U(5)-SU(3)$ transition for the control parameter ξ in the vicinity of the value 0.026 (generally the whole shaded area in the Fig. 7.21 is connected with the two minima of the energy and therefore with the phase coexistence). The $U(5)-SO(6)$ transition with $\chi = 0$ is connected with only one minimum of the energy (7.182) (one phase) that is characteristic for the phase transition of the 2-nd order. It should be noted that for the first time the transition $U(5)-SU(3)$ was identified with the 1-st order phase transition and the transition $U(5) - SO(6)$ with the 2-d order phase transition in the paper [130].

In the paper of F. Iachello [140] the phase transition of the second order on the Casten triangle side $U(5)-SO(6)$ was analyzed by means of the Bohr Hamiltonian (see the Subsection 7.2.1.2). It was found that this shape phase transition is connected with the Eucklidean dynamical symmetry $E(5)$. Later on in papers [141, 142] F. Iachello found that the first order transition on the Casten triangle side $U(5)-SU(3)$ had a link to the $X(5)$ dynamical symmetry of the reduced form of the Bohr Hamiltonian. So the dynamical symmetries of the simplified IBM-1 Hamiltonian $\hat{H}_{Casten}$ of the Bohr Hamiltonian $\hat{H}_c$ (see (7.66) play a role not only the Casten triangle vertexes but also in the triangle points connected with the shape-phase transitions (see the $E(5)$ and $X(5)$ points in the Casten triangle on the Fig.7.21). It should be realized that in reality the nuclear Hamiltonian is only close to the Hamiltonian with the symmetry corresponding to given dynamical symmetry and eigen-functions of the real nuclear Hamiltonian are not characterized by the quantum numbers of given dynamical symmetry precisely. It means only that the realistic nuclear Hamiltonian for given system parameters (e.g. number of nucleons of given type) is not far from the given dynamical symmetry and therefor

[7] One should have in mind, however, that about a phase transition we can speak only in the case $N \to \infty$ (that means for the infinite degrees of freedom system). Real nucleus is the finite number of particle system and therefore it would be better to speak only about an indication of the phase transition.

it is useful to use the basis corresponding to this particular symmetry for the construction and subsequent diagonalization of the nuclear Hamiltonian matrix. One can then expect that the dimension of such matrix, necessary for good description of experimental reality, is less in the comparison with the situation when the Hamiltonian matrix is constructed within any other basis. More details on the dynamical algebras and corresponding symmetries can be found in the Appendix J (subsections J.4.1 and J.4.2) .

7.2.2.2 Interacting Boson Model - 2

In the previous subsection the simplest version IBM-1 of the Interacting Boson Model was discussed, which has a strong root in group-theoretical methods, and which was highly successful in describing many facets of nuclear collective quadrupole motion, especially the evolution of the low-lying parts of the positive parity nuclear spectrum if one goes from the spherical nuclei to well-deformed ones. In the framework of the IBM-1 neutrons and protons were not distinguished and s- and d- bosons were connected with the pair of nucleons as one type particles (see (7.109)-(7.119)). Using this approximation the many- boson states are realized as fully symmetric representation of the $U(6)$ group structure (see (7.116), (7.115)) and these many boson states (for given N) exhaust the full model space.

If the neutrons and protons are distinguished, as is treated in the Interacting Boson Model - 2 (IBM-2), then the bosons are connected with the pairs of neutrons and protons separately and the many- boson basis of states is now spanned by the irrep of the product group $U_\pi(6) \otimes U_\nu(6)$ "[8]. This enlarges the boson space in the comparison with the IBM-1 and simultaneously enables to interpret the neutron and proton bosons in terms of the shell model neutron and proton single-particle states.

In the IBM-1 we restrict ourselves only to s- and d- bosons for the description of the low-lying part of the spectrum and this approximation was used more or less intuitively. Similarly in the IBM-2 the simple idea that only proton and neutron s- and d- bosons are taken into account, is also used. Further the justification for this approximation based on the shell model results is briefly described.

J.P. Schiffer and W.W. True in [132] determined from the shell model calculations the diagonal two body matrix element of the shell model Hamiltonian for the one type nucleon pair with angular momentum L from $1g_{9/2}$ shell

[8]Further the index π is connected with the proton system and the index ν with the neutron system

(concretely the contribution to the total nucleus energy, $\langle(\pi g_{9/2})^2 L|\hat{H}_{shell\ model}|(\pi g_{9/2})^2$ of the proton pair originating from the $1\,\pi g_{9/2}$ shell and with the pair ang. momentum L.

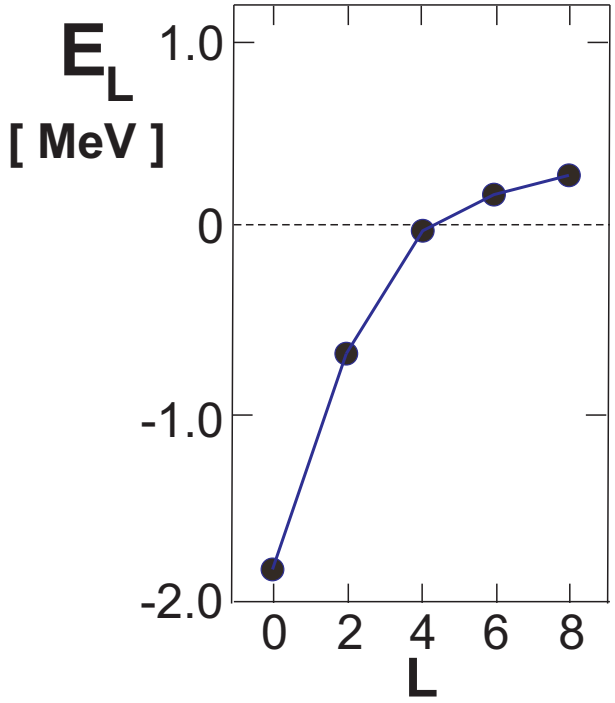


Figure 7.23: Diagonal matrix element $\langle(\pi g_{9/2})^2\ L\ |\hat{H}_{shell\ model}|\ \ (\pi g_{9/2})^2\ L\rangle$, of the proton pair originating from the $1\,\pi g_{9/2}$ for different values $J = 0, 2, 4, 6, 8$ which represents the contribution to the nucleus energy from pairs (bosons) with given ang. momentum L (taken from [132].

The Fig.7.23 shows the contribution $\langle(\pi g_{9/2})^2\ L\ |\hat{H}_{shell\ model}|\ \ (\pi g_{9/2})^2\ L\rangle$ to the nucleus energy is strongly attractive (negative) when the two nucleons are in $L = 0$ S-state. This is well known as the pairing property of the nucleon-nucleon interaction (see the Fig. 6.3, exprs. (6.9), (6.10)). As it can be seen from the Fig.7.23, the interaction remains attractive for two nucleons in a $L = 2$ D-state. For $L \geq 4$ it becomes repulsive. Consequently the nucleus tends to form pairs with relative angular momentum $L = 0$ or $L = 2$ (see [118]). This is the typical feature of the two-particle matrix elements $\langle(\pi g_{9/2})^2\ L\ |\hat{H}_{shell\ model}|\ \ (\pi g_{9/2})^2\ L\rangle$ for all used shell model Hamiltonians.

As an example let us consider a nucleus with only two nucleons outside a closed shell core, e.g. the $N = 50$ closed shell. The two extra nucleons can occupy the valence orbits $2d_{5/2}$, $1g_{7/2}$, $1h_{11/2}$, $2d_{3/2}$ or $3s_{1/2}$ (see Figs.5.2, 5.5), that form the major shell $N = 50 - 82$. If we restrict ourselves only to this configuration space of two particle states $|(nlj)^2\ L\rangle$ there are five possible

two-particle states $|(nlj)^2\ L = 0\rangle$ with the angular momentum $L = 0$ for given type of nucleons.

The residual interaction causes that of these five states only one, the collective state, comes much lower in energy than the other four. This collective $L = 0$ state will be denoted in the following as the $|\ S\rangle$ state and can be written schematically as the following linear combination

$$|\ S\rangle = \sum_{\substack{nlj \\ \in \text{ shell 50-82}}} a_{nlj}\ |(nlj)^2\ L = 0\rangle \tag{7.184}$$

where the sumation runs over the orbitals in the valence shell 50-82 (explicit contributions from possible orbitals outside the valence shell can be neglected in the collective state (7.184) because they lie at a too high energy).

A similar argument also holds for the $L = 2$ states. Of all possible $L = 2$ states originating from the major shell 50-82, only one state will come much lower in energy. This collective $L = 2$ state will be denoted as $|\ D\rangle$

$$|\ D\rangle = \sum_{\substack{nlj \\ \in \text{ shell 50-82}}} b_{nlj}\ |(nlj)^2\ L = 2\rangle \tag{7.185}$$

where again the sumation runs over the valence orbits.

Further we may view a nucleus with $2N$ nucleons of one type (e.g. neutrons) outside a closed shell 50 (for simplicity the number Z of protons of the nucleus corresponds to the closed major shell). Since there is a strong attractive nucleon-nucleon interaction which bounds valence $2N$ neutrons into the $L = 0$ and $L = 2$ pairs (see the Fig.7.23) we can expect that collective low-lying states of this nucleus can be described within the configuration space formed by the multiphonon states constructed from pairs of $|S\rangle$ and $|D\rangle$ states. To calculate properties of the nucleus in the low-lying state (here we consider only even-even nucleus) it is therefore sufficient to give a description in terms of these S and D degrees of freedom. What we have gained by this procedure is that instead of having to use the full shell model space it is sufficient to consider the much smaller (S, D) subspace [133, 134] to approximate collective states of the nucleus. For instance, for a typical nucleus from the rare earth region, ^{156}Sm, this results in a reduction from a 10^{14} to a 10^3 dimensional space. Athough we can no longer describe all the states of the even-even nucleus, this approximation works well for the low-lying collective states of the nucleus.

In describing a general nucleus ${}^{A}_{Z}X_{N}$ containing a large number of valence nucleons outside a closed major shell, the pairing properties discussed above give rise to strongly bound $L = 0^+$ and 2^+ pairs. It is evident that there is the possibility to relate 0^+ and 2^+ coupled pairs to s- and d- boson configurations introduced in the IBM-1 (see previous subsection).

The 0^+, 2^+ pair truncation of the shell model configuration space discussed above (called S, D pair truncation) allows to use a restricted model space in order to describe the main, low-lying collective excitations of the even-even nucleus ${}^{A}_{Z}X_{N}$. The corresponding fermion basis states can be written as

$$\left\{ [(S^+_\pi)^{n_{s_\pi}} (D^+_\pi)^{n_{d_\pi}}] \otimes [(S^+_\nu)^{n_{s_\nu}} (D^+_\nu)^{n}_{d_\nu}] \right\}_{(LM)} | \, 0\rangle_F \tag{7.186}$$

with

$$\begin{aligned} & n_{s_\pi} + n_{d_\pi} = N_\pi \quad , \qquad n_{s_\nu} + n_{d_\nu} = N_\nu \\ & S_\rho \, | \, 0\rangle_F = D_\rho \, | \, 0\rangle_F = 0 \qquad , \qquad \rho = \pi, \, \nu \end{aligned} \tag{7.187}$$

where N_π (N_ν) denotes the number of valence proton (neutron) pairs.

Using the Otsuka-Arima-Iachello (OAI) mapping procedure [134] outlined in the text above, the fermion many pair configurations (7.186) are mapped onto real phenomenological boson states using the correspondence $S_\rho \rightarrow s_\rho$, $D_\rho \rightarrow d_\rho$ ($\rho = \pi, \nu$). Generally the mapping procedure starts with some effective nucleon-nucleon interaction involved in the standard shell model Hamiltonian $\hat{H}_F$ for nucleons as fermions and acting in the space of multi-fermion collective states $|\Psi_F\rangle$ of the type (7.186) then the mapping $S_\rho \rightarrow s_\rho, D_\rho \rightarrow d_\rho$ is done in such a way that the matrix elements $\langle \Psi_F | \hat{H}_F | \Psi^{'}_F \rangle$ should be the same as the matrix elements $\langle \Psi_B | \hat{H}_B | \Psi^{'}_B \rangle$ where $|\Psi_B\rangle$ are the multi-boson states

$$\begin{aligned} & \left\{ [(s^+_\pi)^{n_{s_\pi}} (d^+_\pi)^{n_{d_\pi}}] \otimes [(s^+_\nu)^{n_{s_\nu}} (d^+_\nu)^{n}_{d_\nu}] \right\}_{(LM)} | \, 0\rangle_B \\ & s_\rho \, | \, 0\rangle_B = d_\rho \, | \, 0\rangle_B = 0 \qquad , \qquad \rho = \pi, \, \nu \end{aligned} \tag{7.188}$$

where $\hat{H}_B$ is the boson image of the fermion Hamiltonian $\hat{H}_F$, that means the requirement for the mapping is

$$\langle \Psi_F | \hat{H}_F | \Psi^{'}_F \rangle = \langle \Psi_B | \hat{H}_B | \Psi^{'}_B \rangle \tag{7.189}$$

A schematic mapping scheme is shown in the Table 7.1. The symbol ν in the table means the seniority, the number of nucleons not involved in the pairs with $L = 0$. The index μ determining the projection of the momentum $L = 2$ for the creation operator D^+ and d^+ is missing in the Table 7.1.

fermion space			boson space		
$N=0$	$\nu=0$	$\|0\rangle_F$	$N=0$	$n_d=0$	$\|0\rangle_B$
$N=2$	$\nu=0$	$S^+\|0\rangle_F$	$N=2$	$n_d=0$	$s^+\|0\rangle_B$
	$\nu=2$	$D^+\|0\rangle_F$		$n_d=1$	$d^+\|0\rangle_B$
$N=4$	$\nu=0$	$(S^+)^2\|0\rangle_F$	$N=4$	$n_d=0$	$(s^+)^2\|0\rangle_B$
	$\nu=2$	$S^+D^+\|0\rangle_F$		$n_d=1$	$s^+d^+\|0\rangle_B$
	$\nu=4$	$(D^+)^2\|0\rangle_F$		$n_d=2$	$(d^+)^2\|0\rangle_B$

Table 7.1: Schematic table of the fermion-boson mapping in the IBM-2.

The whole mapping process is schematically shown in the Fig.24 where we start from the full fermion space and finish with the boson $(s-d)$ model space.

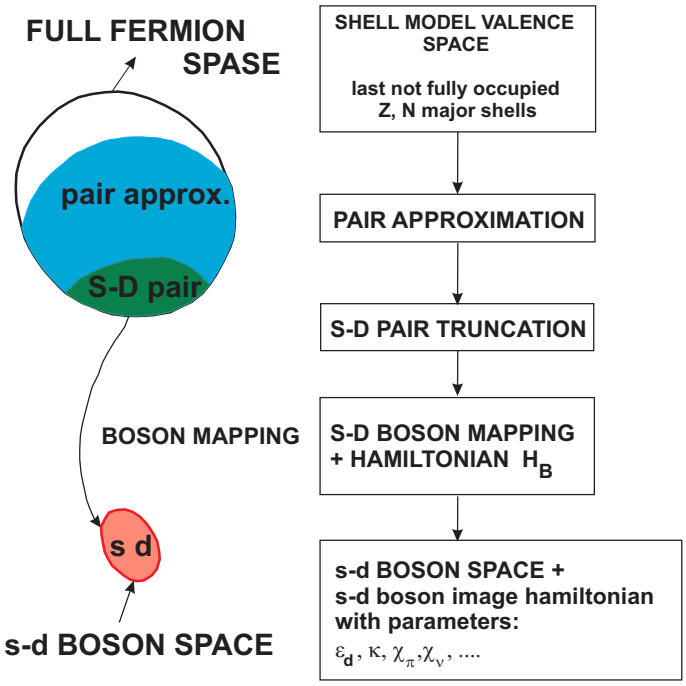


Figure 7.24: Schematic figure of the fermion-boson mapping in the IBM.

Starting from a general large-scale shell model space using the S- and D- pairing approximation (7.184), (7.185) and corresponding pair truncation with the fermion-boson mapping from the Table 7.1 the boson s, d space can be obtained with the corresponding boson Hamiltonian $\hat{H}_B$.

For a simple fermion Hamiltonian containing pairing and quadrupole-quadrupole interaction (see the first term in (1.55) for fixed $\lambda = 2$) the general form of the boson Hamiltonian, using OAI mapping (see Table 7.1)

and equation (7.189), is following [118]

$$\hat{H}_B = E_0 + \epsilon_{d_\pi}\hat{n}_{d_\pi} + \epsilon_{d_\nu}\hat{n}_{d_\nu} + \kappa \sum_{m=-2}^{+2}(-1)^m \hat{Q}^{(2)}_{m;\,\nu}(\chi)\,\hat{Q}^{(2)}_{-m;\,\pi}(\chi) + \\ + \hat{V}_{\pi\pi} + \hat{V}_{\nu\nu} + \hat{M}_{\pi\nu} \tag{7.190}$$

where

$$\hat{V}_{\rho\rho} = \sum_{L=0,2,4} c_L^{(\rho)}\,\sqrt{2L+1}\,\left[(d^+_\rho d^+_\rho)_{(22;\,L)}(\tilde{d}_\rho\tilde{d}_\rho)_{22;\,L)}\right]_{(LL;\,0)}\,, \quad \rho = \nu,\pi \tag{7.191}$$

$$\hat{M}_{\pi\nu} \;=\; \xi_2 \sum_{m=-2}^{+2}(-1)^m\left(s^+_\nu d^+_\pi - d^+_\nu s^+_\pi\right)_{(02;\,2-m)}\left(\tilde{s}_\nu\tilde{d}_\pi - \tilde{d}_\nu\tilde{s}_\pi\right)_{(02;\,2-m)} \\ + \sum_{k=1,3}\xi_k \sum_{m=-k}^{+k}(-1)^m(d^+_\nu d^+_\pi)_{(22;\,km)}(\tilde{d}_\nu\tilde{d}_\pi)_{(22;\,k-m)} \tag{7.192}$$

Here (see (7.156)

$$\hat{Q}^{(2)}_{m;\,\rho}(\chi_\rho) = (d^+_\rho\tilde{s}_\rho)_{(20;\,2m)} + (s^+_\rho\tilde{d}_\rho)_{(02;\,2m)} + \chi_\rho\,(d^+_\rho\tilde{d}_\rho)_{(22;\,2m)} \tag{7.193}$$

with $\rho = \pi, \nu$.

The structure of the boson Hamiltonian (7.190) with its parameters E_0, ϵ_{d_π}, ϵ_{d_ν}, κ, $c_L^{(\rho)}$ $(L = 0, 2, 4)$, ξ_k $(k = 1, 2, 3)$, χ_ρ $(\rho = \pi, \nu)$ can be understood qualitatively if we compare it with the general forces of the shell model Hamiltonian. In the standard shell model approach we start with the Hamiltonian containing the total nucleus kinetic energy term and some effective nucleon-nucleon interaction term (see e.g. (6.1). Using the Hartree-Fock (HF) approach (see Chapter 4) and subsequent BCS methos (see Chapter 6) [9] we can rewrite the nucleus Hamiltonian as a sum of the quasiparticle mean field and corresponding residual interaction (see (6.82) with (6.100) or (6.155)):

$$\hat{H} = \hat{h}_{HFB} + \hat{V}_{res} \tag{7.194}$$

In the standard shell model approach the matrix of the Hamiltonian (7.194) is then constructed in the basis of many quasiparticle states (in the case of even-even nucleus the basis consists from quasiparticle vacuum, 2-quasiparticle

[9] Instead of the HF+BCS approach we can apply simultaneously Hartree-Fock-Bogoliubov (HFB) methos - see Subsection 6.2.3.

configurations, 4-quasiparticle configurations, ...) and then this Hamiltonian matrix is diagonalized. In such a way we obtain eigen vectors and eigen spectrum of the nucleus Hamiltonian. The construction of the Hamiltonian matrix is much easier if we decompose the residual interaction into the series of multipole-multipole and spinmultipole-spinmultipole terms - see (1.55). From the point of view of the low-lying states the most important is the quadrupole-quadrupole term (monopole-monopole terms are already involved in the quasiparticle mean field $\hat{h}_{HFB}$. The quasiparticle mean field involves also substantial parts of the proton-proton and neutron-neutron quadrupole-quadrupole terms. So for the even-even nuclei the most important for the description of low-lying states is the quadrupole-quadrupole neutron-proton term in residual interactions which is in the boson Hamiltonian (7.190) represented by the 4-th term ($\kappa\, \hat{Q}_{\pi}^{(2)} \cdot \hat{Q}_{\nu}^{(2)}$ term). From the point of view of the boson picture the terms $E_0 + \epsilon_{d_\pi} \hat{n}_{d_\pi} + \epsilon_{d_\nu} \hat{n}_{d_\nu}$ in (7.194) corresponds to the mean field part of the fermion Hamiltonian (7.194). The last 3 terms in (7.190) are connected with all left parts in $\hat{V}_{res}$ not involved in the neutron-proton quadrupole-quadrupole term.

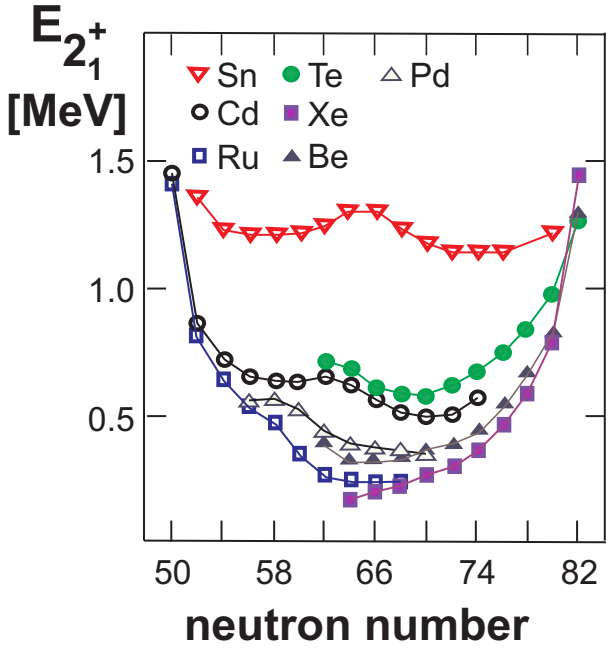


Figure 7.25: The energy of the 2_1^+ state of the Ru, Pd, Cd, Sn Te, Xe and Ba isotopes in the 50-84 neutron shell in the dependence on the neutron number (taken from [118]).

The fact that there is no strong atractive quadrupole-quadrupole interaction between like nucleons (proton-proton or neutron-neutron) in the the residual interaction of $\hat{H}_B$ (see (7.190)) and that the most important from

the quadrupole-quadrupole interaction is the neutron-proton part can be also seen from the experimental data, particularly from the plot of the experimental energy of the 2_1^+ state for even-even nuclei Ru, Pd, Cd, Sn, Te, Xe and Ba in the dependence on the neutron number between 50 and 82 - see Fig. 7.25.

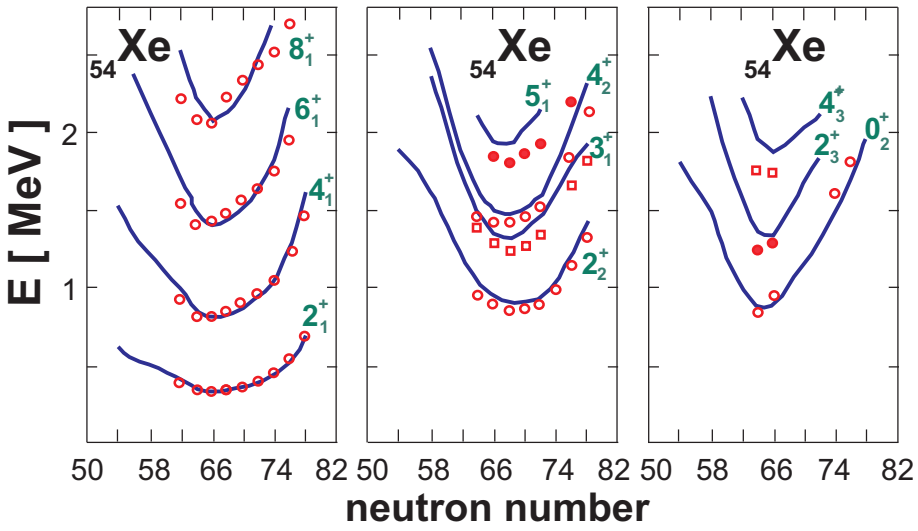


Figure 7.26: Comparison between calculated and experimental energy levels in Xe (taken from [118]).

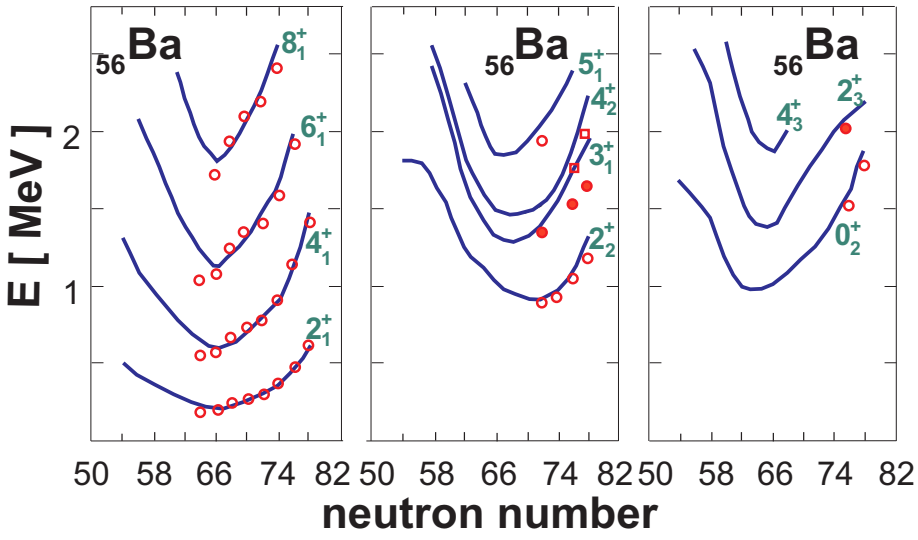


Figure 7.27: The same as in the Fig.7.26 but for Ba isotopes.

In the Sn isotopes, which have a $Z = 50$ closed proton core, the energy of the 2_1^+ state is essentially constant, i.e. independent on the number of neutrons in the 50-82 major shell. This is in the contradiction with the expecta-

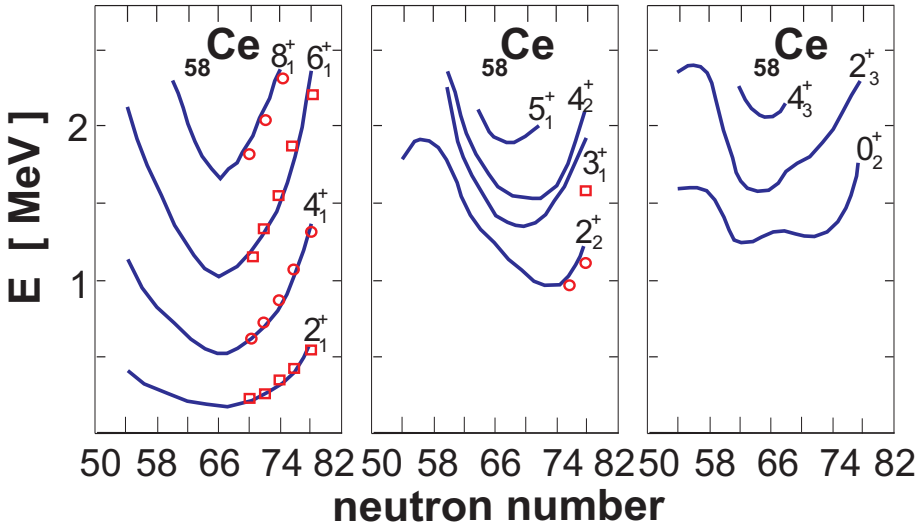


Figure 7.28: The same as in the Fig.7.26 but for Ce isotopes.

tion that neutron-neutron quadrupole-quadrupole force lower the excitation energy of the 2_1^+ state (because the quadrupole-quadrupole force is attractive - see Fig.7.24) once there are several neutrons added to the $N = 50$ core. If there is only one proton pair with respect to the $Z = 50$ core (particle-like for $_{52}$Te or hole-like for $_{48}$Cd isotopes) the situation is completely different. When neutron pair is added to the closed shells (particle/like for $N = 50$ and hole-like for $N = 82$) the energy of the 2_1^+ state is lowered considerably. This effect is even more pronounced when there are more (two for Pd and Xe or three for Ru and Ra) proton pairs outside the closed shell. This shows clearly that the neutron-proton quadrupole-quadrupole interaction term in (7.190) plays a dominant role in the low-lying part of the spectra of even-even nuclei.

If the form of the IBM-2 Hamiltonian $\hat{H}_B$ given in (7.190) is compared with the IBM-1 Hamiltonians (see (7.113) or (7.135), (7.163), (7.176)) one can see that all terms in the IBM-2 Hamiltonian (7.190) are already involved in the IBM-1 Hamiltonian (7.113) for separate neutron and proton sectors except the neutron-proton quadrupole-quadrupole (the 4-th term in (7.190)) and so called Majorana term (the last term $\hat{M}_{\pi\nu}$ in (7.190)).

Incorporating the proton and neutron degrees of freedom into the IBM-2 the group structure becomes (compare with the group structure of the IBM-1 given in (7.128))

$$U_\pi(6) \otimes U_\nu(6) \supset U_{\pi+\nu}(6) \supset \dots$$

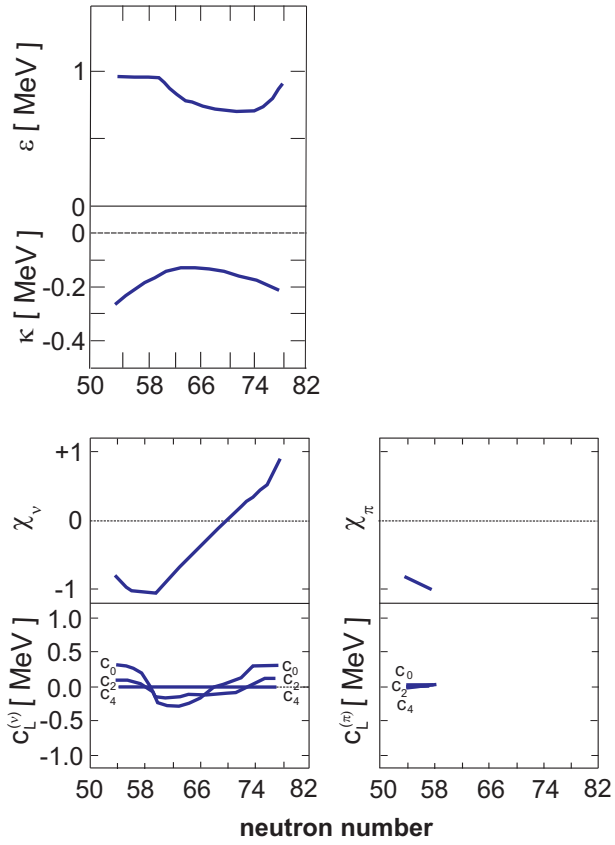


Figure 7.29: The parameters ϵ_{n_d}, κ, $c_L^{(\rho)}$ ($L = 0, 2, 4$; $\rho = \pi, \nu$) of the IBM-2 Hamiltonian used in the calculations fo Xe, Ba and Ce isotopes with results presented in Figs. 7.26, 7.27 and 7.28 (taken from [118]).

where the irrep are formed from the product irrep as follows

$$[N_\pi] \oplus [N_\pi + N_\nu, 0, \ldots] \oplus [N_\pi + N_\nu - 1, 1, 0, \ldots] \oplus [N_\pi + N_\nu - 2, 2, 0, \ldots] \tag{7.195}$$

Now, the one-row irrep (the 1-st term in (7.195) corresponding to one-row Young diagram - see the section J.4.4 in the Appendix J), two-row (the second term in (7.195)) and even more complicated and less symmetric irrep can be constructed. These states are called in the literature as mixed-symmetry states, which correspond to non-symmetric couplings of the basic proton and neutron bosons. It can be shown from the spectra of even-even nuclei that these mixed-symmetry states do not occur below an excitation energy of about 2 MeV. To obtain this in the calculation one needs, besides the quadrupole-quadrupole force represented in (7.190) by the 4-th, 5-th and 6-th terms, so called Majorana force given by the last term in (7.190) [118].

From the theoretical point of view the parameters ϵ_{d_π}, ϵ_{d_ν}, κ, $c^{(\rho)}{}_L$, ξ_k, χ_ρ involved in the boson Hamiltonian (7.190) can be determined from the shell

model Hamiltonian [118] but connected calculations are very complicated and approximate. In practice these parameters are obtained phenomenologically by fitting them in order to obtain the agreement with experimental values of energies of selected low-lying states in the given nucleus. Obtained by this way parameters should behave reasonably and smoothly in the dependence on the number of protons and neutrons.

As an example of the IBM-2 calculation in the Figs. 7.26, 7.27 and 7.28 there is the comparison between calculated and experimental energies of low-lying states in Xe, Ba and Ce isotopes, respectively. Corresponding parameters ϵ_{d_ρ}, κ, $c_L^{(\rho)}$ $(L = 0, 2, 4;\ \rho = \pi, \nu)$, $\chi^{(\rho)}$ $(\rho = \pi, \nu)$ are shown in the Fig. 7.29. Since there is no information on the location of the states with mixed neutron-proton symmetry the parameters ξ_k $(k = 1, 2, 3)$ were kept constant for all investigated nuclei with the following values: $\xi_1 \approx \xi_2 = 0.12$ MeV; $\xi_3 = -0.9$ MeV. One can see that we can obtain very good agreement of theoretical energies with the experimental ones with the reasonable behavior of parameters of the Hamiltonian (7.190).

We can analyze and compare IBM-2 theoretical and experimental values of not only energies but also other properties of nuclei (e.g. E2 transition rates, quadrupole moments, ...) - see e.g. [118, 114, 123]. However, these aspects of the IBM-2 are beyond the scope of this textbook.

The IBM-1 and IBM-2 can be used not only for the description of the positive parity low-lying states but also for negative parity states. This can be done by the introduction of octupole $L = 3$, so called f- bosons [113, 114, 127]. However, by adding the f- bosons the boson Hamiltonian becomes complex with many parameters and the beauty of the simple description is lost. Nevertheless, by appropriate fitting of parameters it is possible to obtain a good agreement of calculated and experimental energies of the low-lying negative parity states.

In order to extend the region of applicability of the IBM to light nuclei it is necessary to treat not only proton-proton and neutron-neutron bosons and their interaction but also to add to the consideration proton-neutron pairs. This is because the building blocks of the IBM-2 (proton-proton and neutron-neutron bosons) do not form an isospin invariant model. Therefore the extension by including so called δ- boson with the isospin $T = 1$ and projection $M_T = 0$, and even further, by also taking anto account both the $T = 1$ and $T = 0$ (with projection $M_T = 0$) proton-neutron bosons have been done and the IBM-3 and IBM-4 versions of the interacting boson model was introduced (see e.g. [135]) for more details about various extensions of the

IBM).

It should be noted that the IBM is not the first boson model. At level of phenomenology there were several attempts to describe the low-lying state in the even-even nucleus (with the integer angular momentum) by means of the introduction of boson quanta and corresponding boson Hamiltonian. These models usually started with the Bohr Hamiltonian in which the collective motion is described in terms of five quadrupole degrees of freedom $\alpha_{2\mu}$ (see the subsection 7.2.1). Common problem connected with these models is that the boson-boson Hamiltomian cannot be restricted to two-body boson-boson interaction. The importance of higher order terms in the interaction was, for instance, confirmed by Kishimoto and Tamura [136]. In order to solve the problem of infinite boson expansions Janssen, Jolos and Doenau [117] introduced a cut-off factor. This was an application of the Holstein-Primacoff way of the fermion-boson mapping [137]. In the IBM the problem of higher order boson terms in the Hamiltonian is simulated by the introduction of s-bosons. As we saw this allowed to understand the phenomenological s- and d- bosons as the collective pairs of nucleons. However, the IBM way of such interpretation of bosons is too trivial if we want to describe not only collective states in even-even nuclei. The problem of the fermion-boson mapping in this sence is not finished. More about this mapping can be found in the Chapter 9 of the Ring-Shuck book [9] (see also.....).

7.2.2.3 Interacting Boson-Fermion Model (IBFM)

Up to now we were concerned with the even-even nuclei. The IBM is possible to extend also for odd-A nuclei by so called Interacting Boson-Fermion Model (IBFM) (see e.g. [118, 135, 138]). Here we will not go into details, only basic idea is indicated.

The IBFM is a straghtforward extension of the IBM in which additional single-particle degrees of freedom are introduced and coupled to the system of s- and d- bosons. The IBFM Hamiltonian is supposed to be in the following form

$$\hat{H}_{IBFM} = \hat{H}_B + \hat{H}_F + \hat{V}_{BF} \tag{7.196}$$

with $\hat{H}_B$ the Hamiltonian for the even-even core, $\hat{H}_F$ the single-particle Hamiltonian for the odd nucleon, and $\hat{V}_{BF}$ the coupling between the s- and d-bosons of the core and odd nucleon. For $\hat{H}_B$ the usual IBM-1 Hamiltonian is used. The using of the IBM-2 Hamiltonian would involve too many degrees of freedom and too many parameters and corresponding Hamiltonian matrix

would be too large. The single-paricle Hamiltonian $\hat{H}_F$ of the odd nucleon is taken as

$$\hat{H}_F = \sum_j \sum_{m=-j}^{j} \epsilon_j \, a^+_{jm} \, \tilde{a}_{jm} \tag{7.197}$$

where a^+_{jm} (a_{jm}) are the creation (annihilation) operators for a nucleon in one of the valence single-particle spherically symmetric orbitals with energy ϵ_j.

The most general two-body boson-fermion interaction $\hat{V}_{BF}$ can be written as [118, 113]

$$\begin{aligned}\hat{V}_{BF} = &\sum_j u_j \left[(s^+\tilde{s})_{(00;\,2)} \, (a^+_j \tilde{a}_j)_{(jj;\,0)}\right]_{(00;\,0)} + \\ &+ \sum_{jj'} v_{jj'} \left\{\left[(d^+\tilde{s})_{(20;\,2)} \, (a^+_j \tilde{a}_{j'})_{(jj;\,2)}\right]_{(22;\,0)} + h.c.\right\} + \\ &+ \sum_{jj'k} w^{(k)}_{jj'} \left[(d^+\tilde{d})_{(22;\,k)} \, (a^+_j \tilde{a}_{j'})_{(jj';\,k)}\right]_{(kk;\,0)}\end{aligned} \tag{7.198}$$

where $\tilde{a}_{jm} = (-1)^{j-m} a_{j-m}$. In (7.198) u_j, $v_{jj'}$, $w^{(k)}_{jj'}$ are parameters. The number of parameters in (7.198) can be large, i.e. for an odd nucleon restricted to the modest space of single-particle orbitals, $2d_{5/2}$, and $1g_{7/2}$, there are 18 linearly independent parameters.

Then the matrix pf the Hamiltonian $\hat{H}_{IBFM}$ is costructed within the basis [118]

$$\left[a^+_j \left(s^{N-n_d} d^{\,n_d};\, \alpha L\right)\right]_{(jL;\,JM)} \mid 0\rangle \tag{7.199}$$

where the symbol α stands for all quantum numbers except L characterizing the s- and d- multi-boson states of the nucleus core, and $|0\rangle$ is a product of the vacua for bosons and odd nucleon ($a_j \mid 0\rangle = 0,\ s \mid 0\rangle = d \mid 0\rangle = 0$). It should be noted that the states (7.199) are not generally orthonormal each other but one can apply orthonormalization procedure (see e.g. [118]) in order to obtain orthonormal basis. In practice usually the basis involves states with only $n_d = 0, 1$. After the diagonalization of this matrix we obtain eigen-states of the Hamiltonian $\hat{H}_{IBFM}$ with corresponding energy spectrum.

The concrete results of the IBFM calculations are not presented here. They can be found e.g. in [118]. Similarly as in the case of even-even nuclei we can obtain $U(5)$, $SU(3)$ and $SO(6)$ limits according to the symmetry of the boson part $\hat{H}_B$ of the IBFM Hamiltonian of investigated odd-A nucleus. Using the appropriate ensemble of parameters we can obtain good agreement with the experimental energie of low-lying states in spherical (vibrational),

deformed (rotational) or γ- softh odd-A nuclei ([118, 135, 138] [10]. One can also construct the IBFM transition operators combining the corresponding expressions for these operators in s-d boson and single-particle valence nucleon spaces.

In the end of this section 7.2 we summarize some advantages an drawbacks of the phenomenological (algebraic) models of nuclear motion.

- The big advantage of phenomenological approaches to the description of the degrees of freedome of nuclear motion is the relative simplicity. Using a small number of model parameters it is possible to describe the basic features of the low-lying states of nuclei. Particularly the IBM was successful in describing the shape transition if we go in the isotope table from spherical magic number nuclei (with the closed major shells) to deformed ones (with only partly occupied major valence shell).

- The beauty of phenomenological models consists also in their clear physical interpretation. For instance, the Bohr geometrical model based on the concept of the nucleus as a droplet of the nuclear fluid enabled to interprete low-lying states of even-even nuclei as nuclear shape vibrations and rotations (for deformed nuclei).

- The main drawback of the phenomenological models is the fact that they cannot aspire to describe all degrees of freedom of nuclear motion. Because of the restricted configuration space for bosons (only s- and d-bosons with maximally f- boson) the IBM-1 or IBM-2 can treat only collective modes in even-even nuclei up to the multipolarity $\lambda = 3$ (if f-bosons are taken into account). This restriction of the space is more or less O.K. for low-lying collective states but not for higher excitations or for intruder states. This is connected with the very primitive fermion-boson mapping used in the IBM and with the fact that it is not possible to restrict boson Hamiltonian only to two-body s- and d- boson interactions (for instance it is not possible to describe particle-hole excitations in even-even nuclei).

- The other problem of phenomenological models is connected with the impossibility to obtain an internal structure of collective states in even-even nuclei. Obtained eigenstates of the boson Hamiltonian given as combinations of multi-boson base vectors do not give any connection of the

[10]The spectra and other properties of odd-A and odd-odd nuclei are discussed in more details in the Chapter 8.

collective excitation states with single-particle configurations of nucleons (opposite to the shell model or to the Random-Phase-Approximation (RPA) approach or Generalized-Coordinate Method (GCM) discussed in the next sections of this chapter).

- Next problem of phenomenological models is the physical meaning of parameters involved in the model Hamiltonian. For instance the explanation of the boson $|S\rangle$ and $|D\rangle$ states in the IBM-2 as the combination of two-nucleon single-particle states (see (7.185), (7.184), (7.186)) of nucleon pairs from the valence shell is too simple and vague. Therefore to connect the IBM-2 Hamiltonian parameters with some multipole-multipole decompositions of the realistic effective nucleon-nucleon interactions, as was suggested e.g. in [118], is very approximative (qualitative) and impossible in the quantitative level.

7.3 Microscopical models of intrinsic degrees of freedom of nuclear motion (taking into account the long-range residual interaction)

In this section microscopical approaches to the description of nucleus degrees of freedom are discussed. These approaches usually start with the nucleus Hamiltonian in the general form (4.2) of the sum of the kinetic energy part and the effective nucleon-nucleon interaction part. Using the Hartree-Fock method (see the Chapter 4) or relativistic mean field approach (see the Subsection 3.2.3) the nucleus single-particle mean field H_{AV} is extracted and the nucleus Hamiltonian reads (see (7.1))

$$\hat{H} = \hat{H}_{AV} + \hat{V}_{(RES)} = \hat{H}_{AV} + \hat{V}_{s.r.}^{(RES)} + \hat{V}_{l.r.}^{(RES)\,\prime} \tag{7.200}$$

as a sum of the mean field and residual interactions which has a short range ($\hat{V}_{s.r}^{(RES)}$) and long range ($\hat{V}_{s.r}^{(RES)}$) parts. As it was already discussed (see (7.3), (7.4) and (7.5)) short range residual interactions are responsible for nucleon pairing effects discussed in the Chapter 6. Long range residual interactions give rise to the correlated collective motion, nucleus shape vibrations, and in the case of deformed mean field also rotations. It was already mentioned (see the text between exprs. (7.1) and (7.5)) that in the low-lying part of the deformed nucleus spectrum we can use the adiabatic condition (7.3) and extract the rotational degrees of freedom from single-particle and vibrational ones. In such a case the nucleus Hamiltonian (in the lab. frame) can be written in the following form (see (7.4), (7.5) and (7.7))

$$\hat{H} = \hat{H}_{intr} + \hat{H}_{rot} = \hat{H}_{AV} + \hat{V}_{s.r.}^{(RES)} + \hat{V}_{l.r.}^{(RES)} + \hat{H}_{rot} \tag{7.201}$$

where $\hat{V}_{l.r.}^{(RES)}$ are parts of the long-residual interactions responsible only for vibrational degrees of freedom (the part of $\hat{V}_{l.r.}^{(RES)\,\prime}$ connected with rotations is removed, $V_{l.r.}^{(RES)} = V_{l.r.}^{(RES)\,\prime} - \hat{H}_{rot}$). In the case of nuclei with the spherical mean field the rotational degrees of freedom are not recognized and $\hat{V}^{(RES)\,\prime} = \hat{V}^{(RES)}$. In this case the intrinsic frame (with the Hamiltonian $\hat{H}_{intr}$) coincides with the the center of mass laboratory frame.

In this section we will search for the eigen-states and eigen-energies of the intrinsic Hamiltian $\hat{H}_{intr}$

$$\hat{H}_{intr} = \hat{H}_{AV} + \hat{V}_{s.r.}^{(RES)} + \hat{V}_{l.r.}^{(RES)} \tag{7.202}$$

which is the whole nucleus Hamiltonian for spherical nuclei (in the center of mass frame) or the nucleus Hamiltonian in the intrinsic center of mass frame rotating with the deformed nucleus.

In the Chapter 6 the taking into account of the short-range residual interaction $\hat{V}_{s.r.}^{(RES)}$ was discussed in details. Particularly it was shown there that starting with the intrinsic Hamiltonian in the general form (6.78) [11] using the BCS approach (Subsection 6.2.2.1) or the HFB (Subsection 6.2.3) one can rewrite the intrinsic Hamiltonian in the form of the sum of the quasiparticle mean field and corresponding residual interaction (see (6.82)-(6.86)) and (6.100):

$$\hat{H}_{intr} = \langle BCS|\, \hat{H}_{intr}|BCS\rangle + \hat{H}_{BCS} + \hat{V}_{res} \tag{7.203}$$

with

$$\hat{H}_{BCS} = \sum_{\substack{i \\ (all)}} E_i\, \alpha_i^+ \alpha_i$$

$$\hat{V}_{res} = \boxed{\begin{array}{c}\text{see} \\ (6.86)\end{array}} = \frac{1}{4} \sum_{\substack{ij\, i'\, j' \\ (all)}} V_{ij\, i'j'} \; : a_i^+ a_j^+ a_{j'} a_{i'} : \tag{7.204}$$

where E_i are single-quasiparticle energies, $E_i = \sqrt{(\varepsilon_i - \lambda)^2 + \Delta_{ii}^2}$, ($\varepsilon_i$ - mean field s.p. energies for given type of nucleons, λ - Fermi level for given type of nucleons), and the symbol $: a_i^+ a_j^+ a_{j'} a_{i'} :$ is the normal product of the single-particle creation and annihilation operators $a_i^+ a_j^+ a_{j'} a_{i'}$ with respect to the quasiparticle vacuum $|BCS\rangle$. Generally the antisymmetrized matrix elements $\hat{V}_{ij\, i'j'}$ are two-nucleon matrix elements of the starting effective nucleon-nucleon interaction. If the normal ordering of the s.p. operators in $\hat{V}_{res}$ is taken with respect to the BCS vacuum then the residual interaction $\hat{V}_{res}$ involves automatically the long-range residual interaction $\hat{V}_{l.r.}^{(RES)}$ from (7.202) and the part of $\hat{V}_{s.r.}^{(RES)}$ not involved in the quasiparticle mean field $\hat{H}_{BCS}$.

In the further consideration in this chapter we suppose that we solved the BCS problem and the Hamiltonian (7.203) is known (quasiparticle energy E_i and corresponding $\mathscr{U}_i$, $\mathscr{V}_i$ coefficient from the Bogoliubov transformation

[11] The Hamiltonian $\hat{H}'$ (see (6.78) involves the term $-\sum_{ij} \lambda\, \delta_{ij}\, a_i^+ a_j$ which is not important for the fixed number of nucleons if we investigate individual eigen-states and eigen-energies of the intrinsic Hamiltonian. The inclusion of this term for fixed number of nucleos only shifts the scale of the total energy and does not change relative energies of the states and corresponding wave functions.

(6.33) or (B.36)). We will search for the eigen states and eigen energies of the intrinsic Hamiltonian (7.103).

7.3.1 Random-Phase-Approximation method

The original version of the Random-Phase-Approximation (RPA) method for nuclear structure calculation was designed for even-even nuclei (see e.g. [139]). From the point of view of the mean field (or model of independent particles) the basic building blocks for the forming of low-lying excitations in the even-even nucleus are particle-hole configurations $a^+_{\sigma_>} a_{\mu_<} \, |HF\rangle$ (see (4.39)). In the case when the pairing residual interaction contributes to the forming of the quasiparticle mean field the basic building blocks for excitations in the even-even nucleus are two-quasiparticle configurations $\alpha^+_i \alpha^+_j \, |BCS\rangle$ (see (6.60), (6.65)). Therefore the particle-hole configurations or two-quasiparticle configurations form the configuration space for the RPA approach where the low-lying excitations are supposed to be created by so called phonon creation operators with boson character. Each phonon creation operator represents a linear combination of particle-hole or two-quasiparticle configuration vectors. In the first subsection of this section the determination of these linear combinations and corresponding phonon energies are discussed in details. The extension of the RPA for the case of odd-A and odd-odd nuclei is discussed in subsequent subsections.

7.3.1.1 RPA for even-even nuclei

7.3.1.1.1 General RPA equation, phonons Before the discussion of the RPA method for taking into account the residual interaction (7.204) we should remind more simple and more approximative Tamm-Dancoff-Approximation (TDA) method already mentioned in the Chapter 4 (see the text around exp. (4.54)). In the TDA approach the matrix of the Hamiltonian (7.203) was constructed within the space of the particle-hole configuration (in the case when the pairing effects can be neglected in the mean field) or within the space of two-quasiparticle states (in the case with the pairing involved on the mean field level) and then this matrix is diagonalized. The eigen-states of the Hamiltonian (7.203) for even-even nuclei are obtained in the form of the

linear combinations of the particle-hole configurations (see (4.54))

$$|\nu^{(TDA)}\rangle = \sum_{\mu_< \ \sigma_>} C^{(\nu)}_{\mu_< \ \sigma_>} \ a^+_{\sigma_>} \ a_{\mu_<} \ |HF\rangle \tag{7.205}$$

or two-quasiparticle configurations (see (6.60))

$$|\nu^{(TDA)}\rangle = \sum_{\substack{ij \\ (all)}} C^{(\nu)}_{ij} \ \alpha^+_i \ \alpha^+_j \ |BCS\rangle \tag{7.206}$$

with corresponding eigen-energies. It should be pointed out that in the framework of the TDA the ground state is given by $|HF\rangle$ or $|BCS\rangle$ and it is not mixed with the excited states given by $|\nu^{(TDA)}\rangle$. In the literature this fact is known as that the TDA does not provide any ground state correlation. This drawback of the TDA is up to certain extend removed in the Random-Phase-Approximation (RPA) [12]

In the RPA approach the eigenvectors of the Hamiltonian (7.203) are built by means of the generally collective excitations in the form of the combination of two-quasiparticle creation and annihilation operators [13]

$$Q^+_\nu = \sum_{ij} \left(X^{(\nu)}_{ij} \ \alpha^+_i \alpha^+_j - Y^{(\nu)}_{ij} \ \alpha_j \alpha_i \right) \tag{7.207}$$

where the summation indexes ij go over all single-quasiparticle states (that means over all states $|i\rangle = |i\sigma_i\rangle$ with all i and $\sigma_i = \pm 1$ - see the s.p. notation (6.17)). This operator is called in the nuclear physics literature as the phonon creation operator. The minus sign in (7.207) has been chosen for convenience. The RPA ground state $|RPA\rangle$ is defined as the vacuum for phonons

$$\begin{aligned} Q_\nu \ |RPA\rangle = \sum_{ij} \left(X^{(\nu)\,*}_{ij} \ \alpha_j \alpha_i - Y^{(\nu)\,*}_{ij} \ \alpha^+_i \alpha^+_j \right) |RPA\rangle = 0 \\ \Rightarrow \langle RPA| \ Q^+_\nu = 0 \end{aligned} \tag{7.208}$$

[12] The RPA was introduced by Bohm and Pines in 1953 [143] in the theory of plasma oscillations. The derivation of the original version of the RPA involves so called random phase of wave function and therefore the method was called Random-Phase-Approximation (RPA). Different RPA derivations were given also by other authors, see e.g. [144, 145]. Further we follow the derivation of the RPA given in [9].

[13] In (7.207) we suppose that the pairing correlations are taken into account by the BCS or HFB approach and therefore the phonon creation operators (7.207) are built from quasiparticle operators. If the pairing effects on the level of the mean field can be neglected then instead of (7.207) the phonon creation operator is formed from the combinations of particle-hole configurations

$$Q^+_\nu = \sum_{\mu_< \ \sigma_>} \left(X^{(\nu)}_{\sigma_> \mu_<} \ a^+_{\sigma_>} \ a_{\mu_<} - Y^{(\nu)}_{\sigma_> \mu_<} \ a^+_{\mu_<} \ a_{\sigma_>} \right)$$

Further we will always suppose that the pairing effects are taken into account and therefore we will always work with quasiparticle creation and annihilation operators

for all ν. Because of the anticommutator relations for quasiparticle operators ($\{\alpha_i,\ \alpha_j^+\} = \delta_{ij},\ \{\alpha_i^+,\ \alpha_j^+\} = 0$) the amplitudes $X_{ij}^{(\nu)}$ and $Y_{ij}^{(\nu)}$ fulfill the following symmetries

$$X_{ij}^{(\nu)} = -X_{ji}^{(\nu)} \quad , \qquad Y_{ij}^{(\nu)} = -Y_{ji}^{(\nu)} \tag{7.209}$$

Without loosing the generality the RPA ground state energy can be chosen to be equal zero

$$\hat{H}_{intr}|RPA\rangle = 0\,|RPA\rangle = 0 \tag{7.210}$$

The aim is to find the eigen system of the Hamiltonian $\hat{H}_{intr}$

$$\hat{H}_{intr}|\nu\rangle = \hbar\omega_\nu\,|\nu\rangle \tag{7.211}$$

where $|\nu\rangle = Q_\nu^+\,|RPA\rangle$ with $\hbar\omega_\nu$ as the phonon energy. In (7.207)-(7.211) the index ν enumerates the individual RPA eigen-vectors. The equation (7.211) can be rewritten as follows

$$\begin{aligned}\left[\hat{H}_{intr},\ Q_\nu^+\right]|RPA\rangle &= (\hat{H}_{intr}\,Q_\nu^+ - Q_\nu^+\,\hat{H}_{intr})\,|RPA\rangle = \\ &= \hbar\omega_\nu\,Q_\nu^+\,|RPA\rangle\end{aligned} \tag{7.212}$$

The eigen system of the $\hat{H}_{intr}$ (amplitudes $X_{ij}^{(\nu)}$ and $Y_{ij}^{(\nu)}$ with the corresponding energies $\hbar\omega_\nu$) is usually searched for in terms of the variation principle. The simpliest variaion $\delta Q|RPA\rangle$ of the one- phonon state has two possibilities

$$\delta Q\,|RPA\rangle = \begin{cases} \alpha_i^+\alpha_j^+\,|RPA\rangle\,\delta X_{ij} \\ \alpha_j\alpha_i\,|RPA\rangle\,\delta Y_{ij} \end{cases} \tag{7.213}$$

and variation principle gives for (7.212) [14]

$$\langle RPA|\,\delta Q\,[\hat{H}_{intr},\ Q_\nu^+]\,|RPA\rangle = \hbar\omega_\nu\,\langle RPA|\,\delta Q\,Q_\nu^+\,|RPA\rangle \tag{7.215}$$

Because of, $\langle RPA|\,Q_\nu^+ = 0$, $\hat{H}_{intr}\,|RPA\rangle = 0$, $\langle RPA|\,\hat{H}_{intr} = 0$ the l.h.s. of the equation (7.215) can be rewritten:

$$\begin{aligned}\langle RPA|\,\delta Q\,\hat{H}_{intr}\,Q_\nu^+ - \delta Q\,Q_\nu^+\,\hat{H}_{intr}|\,RPA\rangle &= \\ = \langle RPA|\,\left[\delta Q,\ [\hat{H}_{intr},\ Q_\nu^+]\right]\,|RPA\rangle\end{aligned}$$

[14] The variation principle can be also formulated as

$$\delta\Big\{\langle RPA|Q_\nu\,\hat{H}_{intr}Q_\nu^+|RPA\rangle - \hbar\omega_\nu\,\big(\langle RPA|Q_\nu Q_\nu^+|RPA\rangle - 1\big)\Big\} = 0 \tag{7.214}$$

where the variation of the functional in the bracket is performed with respect to amplitudes X_{ij} and Y_{ij}. The second term in the bracket represents the additional normalization condition with corresponding Lagrange multipliers $\hbar\omega_\nu$.

and equation (7.115) reads

$$\langle RPA|\left[\delta Q,\,[\hat{H}_{intr},\,Q_\nu^+]\right]|RPA = \\ = \hbar\omega_\nu\,\langle RPA|\,[\delta Q,\,Q_\nu^+]\,|RPA\rangle \qquad (7.216)$$

Since there are two possibilities for $\delta Q\,|RPA\rangle$ (see(7.213)) the equation (7.216) represents two equations

$$\langle RPA|\left[\alpha_j\alpha_i,\,[\hat{H}_{intr},\,Q_\nu^+]\,\right]|RPA\rangle = \\ = \hbar\omega_\nu\,\langle RPA|\,[\alpha_j\alpha_i,\,Q_\nu^+]\,|RPA\rangle \qquad (7.217)$$

$$\langle RPA|\left[\alpha_i^+\alpha_j^+,\,[\hat{H}_{intr},\,Q_\nu^+]\,\right]|RPA\rangle = \\ = \hbar\omega_\nu\,\langle RPA|\,[\alpha_i^+\alpha_j^+,\,Q_\nu^+]\,|RPA\rangle \qquad (7.218)$$

Further we introduce two-quasiparticle creation (annihilation) operators b_{ij}^+, b_{ij}

$$b_{ij}^+ \equiv \alpha_i^+\alpha_j^+ \quad , \qquad b_{ij} \equiv \alpha_j\alpha_i \qquad (7.219)$$

and so called quasi-boson approximation is used. This approximation is based on the assumption that the correlated RPA ground state $|RPA\rangle$ of phonons does not differ very much from the BCS quasiparticle vacuum $|BCS\rangle$ and the expectation value of the commutator, $\langle RPA|\,[b_{ij},\,b_{i'j'}^+]\,|RPA\rangle$ in the phonon vacuum $|RPA\rangle$ can be substituted by the expectation of this commutator calculated in the quasiparticle vacuum $|BCS\rangle$. So

$$\langle RPA|\,[b_{ij},\,b_{i'j'}^+]\,|RPA\rangle \approx \langle BCS|\,[b_{ij},\,b_{i'j'}^+]\,|BCS\rangle = \\ = \langle BCS|\,\alpha_j\alpha_i\,\alpha_{i'}^+\alpha_{j'}^+ - \alpha_{i'}^+\alpha_{j'}^+\,\alpha_j\alpha_i\,|BCS\rangle = \boxed{\begin{array}{c}\text{see}\\(6.32),(6.31)\end{array}} = \\ = \langle BCS|\,\delta_{ii'}\,\alpha_j\alpha_{j'}^+ - \delta_{ji'}\alpha_i\alpha_{j'}^+ + \delta_{ij'}\,\alpha_{i'}^+\alpha_j - \delta_{jj'}\,\alpha_{i'}^+\alpha_i\,|BCS\rangle = \\ = \delta_{ii'}\delta_{jj'} - \delta_{ij'}\delta_{ji'} \qquad (7.220)$$

and similarly

$$\langle RPA|\,[b_{ij},\,b_{i'j'}]\,|RPA\rangle = \langle BCS|\,[b_{ij}^+,\,b_{i'j'}^+]\,|BCS\rangle = 0 \qquad (7.221)$$

We can choose the 2-quasiparticle basis (ij) in such a way that only one of two possibilities (ij) or (ji) are involved in the basis ensemble for given i and j $(i \neq j)$ (e.g. for the axial deformation case only $K_i \geq K_j$ is always fulfilled). If we expept this assumption the expression (7.220) is reduced to the following form (because the second term in (7.220) is irrelevant),

$$\langle RPA|[b_{ij},b_{i'j'}^+]|RPA\rangle = \delta_{ii'}\delta_{jj'} \qquad (7.220')$$

From (7.221) and (7.220') the operators follows that b_{ij} (b_{ij}^+) behave as the boson annihilation (creation) operators in the quasi-boson approximation. In the framework of this approximation we have

$$\langle RPA|\,[\alpha_j\alpha_i,\,Q_\nu^+]\,|RPA\rangle \approx \boxed{\begin{array}{c}\text{see}\\(7.207)\end{array}} \approx$$

$$\approx \sum_{i'j'} X^{(\nu)}_{i'j'}\,\langle BCS|\,[\alpha_j\alpha_i,\,\alpha_{i'}^+\alpha_{j'}^+]\,|BCS\rangle - \sum_{i'j'} Y^{(\nu)}_{i'j'}\,\langle BCS|\,[\alpha_j\alpha_i,\,\alpha_{j'}\alpha_{i'}]\,|BCS\rangle =$$

$$= \sum_{i'j'} \left(X^{(\nu)}_{i'j'}\,\delta_{ii'}\,\delta_{jj'} - X^{(\nu)}_{i'j'}\,\delta_{ij'}\,\delta_{ii'}\right) = X^{(\nu)}_{ij} \tag{7.222}$$

and similarly

$$\langle RPA|\,[\alpha_i^+\alpha_j^+,\,Q_\nu^+]\,|RPA\rangle \approx$$

$$\approx \sum_{i'j'} X^{(\nu)}_{i'j'}\,\langle BCS|\,[\alpha_i^+\alpha_j^+,\,\alpha_{i'}^+\alpha_{j'}^+]\,|BCS\rangle - \sum_{i'j'} Y^{(\nu)}_{i'j'}\,\langle BCS|\,[\alpha_i^+\alpha_j^+,\,\alpha_{j'}\alpha_{i'}]\,|BCS\rangle =$$

$$= \sum_{i'j'} \left(Y^{(\nu)}_{i'j'}\,\delta_{ii'}\,\delta_{jj'} - Y^{(\nu)}_{i'j'}\,\delta_{ij'}\,\delta_{ii'}\right) = Y^{(\nu)}_{ij} \tag{7.223}$$

So, if we accept the quasi-boson approximation the RPA equations (7.217) and (7.218) read

$$\langle BCS|\,\left[\alpha_j\alpha_i,\,[\hat{H}_{BCS}+\hat{V}_{res},\,Q_\nu^+]\,\right]\,|BCS\rangle = \hbar\omega_\nu\,X^{(\nu)}_{ij} \tag{7.224}$$

$$\langle BCS|\,\left[\alpha_i^+\alpha_j^+,\,[\hat{H}_{BCS}+\hat{V}_{res},\,Q_\nu^+]\,\right]\,|BCS\rangle = \hbar\omega_\nu\,Y^{(\nu)}_{ij} \tag{7.225}$$

and these equations can be further rewritten as follows. For (7.224) we have

$$\langle BCS|\,\left[\alpha_j\alpha_i,\,[\hat{H}_{BCS}+\hat{V}_{res},\,Q_\nu^+]\,\right]\,|BCS\rangle =$$

$$\sum_{i'j'}\langle BCS|\,\left[\alpha_j\alpha_i,\,[\hat{H}_{BCS}+\hat{V}_{res},\alpha_{i'}^+\alpha_{j'}^+]\right]\,|BCS\rangle\,X^{(\nu)}_{i'j'} - \sum_{i'j'}\langle BCS|\,\left[\alpha_j\alpha_i,\,[\hat{H}_{BCS}+\hat{V}_{res},\alpha_{j'}\alpha_{i'}]\right]\,|BCS\rangle\,Y^{(\nu)}_{i'j'} \equiv$$

$$\equiv \sum_{i'j'}\left(\,A_{ij\,i'j'}\,X^{(\nu)}_{i'j'} + B_{ij\,i'j'}\,Y^{(\nu)}_{i'j'}\,\right) = \hbar\,\omega_\nu\,X^{(\nu)}_{ij} \tag{7.226}$$

where

$$A_{ij\,i'j'} \equiv \langle BCS|\,\left[\alpha_j\alpha_i,\,[\hat{H}_{BCS}+\hat{V}_{res},\,\alpha^+_{i'}\alpha^+_{j'}]\right]|BCS\rangle$$
$$B_{ij\,i'j'} \equiv -\langle BCS|\,\left[\alpha_j\alpha_i,\,[\hat{H}_{BCS}+\hat{V}_{res},\,\alpha_{j'}\alpha_{i'}]\right]|BCS\rangle \qquad (7.227)$$

One can see that the matrix A is Hermitian and the matrix B is symmetric. Similarly the eq. (7.225) has the following form

$$\langle BCS|\,\left[\alpha^+_i\alpha^+_j,\,[\hat{H}_{BCS}+\hat{V}_{res},\,\hat{Q}^+_\nu]\,\right]|BCS\rangle =$$
$$= \sum_{i'j'}\langle BCS|\,\left[\alpha^+_i\alpha^+_j,\,[\hat{H}_{BCS}+\hat{V}_{res},\alpha^+_{i'}\alpha^+_{j'}]\right]|BCS\rangle\,X^{(\nu)}_{i'j'}$$
$$-\sum_{i'j'}\langle BCS|\,\left[\alpha^+_i\alpha^+_j,\,[\hat{H}_{BCS}+\hat{V}_{res},\alpha_{j'}\alpha_{i'}]\right]|BCS\rangle\,Y^{(\nu)}_{i'j'} \equiv$$
$$\equiv -\sum_{i'j'}\left(\,B^*_{ij\,i'j'}\,X^{(\nu)}_{i'j'} + A^*_{ij\,i'j'}\,Y^{(\nu)}_{i'j'}\,\right) = \hbar\,\omega_\nu\,Y^{(\nu)}_{ij} \qquad (7.228)$$

So instead of (7.224) and (7.225) we have the following system of eqs. for unknowns $X^{(\nu)}_{ij}$ and $Y^{(\nu)}_{ij}$

$$\sum_{i'j'}\left(\,A_{ij\,i'j'}\,X^{(\nu)}_{i'j'} + B_{ij\,i'j'}\,Y^{(\nu)}_{i'j'}\,\right) = \hbar\,\omega_\nu\,X^{(\nu)}_{ij}$$
$$\sum_{i'j'}\left(\,B^*_{ij\,i'j'}\,X^{(\nu)}_{i'j'} + A^*_{ij\,i'j'}\,Y^{(\nu)}_{i'j'}\,\right) = -\hbar\,\omega_\nu\,Y^{(\nu)}_{ij} \qquad (7.229)$$

or (in the matrix representation)

$$\begin{pmatrix} A & B \\ B^* & A^* \end{pmatrix}\begin{pmatrix} X^{(\nu)} \\ Y^{(\nu)} \end{pmatrix} = \hbar\omega_\nu\begin{pmatrix} 1 & 0 \\ 0 & -1 \end{pmatrix}\begin{pmatrix} X^{(\nu)} \\ Y^{(\nu)} \end{pmatrix} \qquad (7.230)$$

Since

$$\langle BCS|\,\alpha_j\alpha_i\,\hat{H}_{BCS}\,\alpha^+_{i'}\alpha^+_{j'}\,|BCS\rangle = \boxed{\begin{matrix}\text{see}\\(7.204)\end{matrix}} =$$
$$= \sum_k E_k\,\langle BCS|\,\alpha_j\alpha_i\;\alpha^+_k\alpha_k\;\alpha^+_{i'}\alpha^+_{j'}|BCS\rangle =$$
$$= 2\,E_i\,\delta_{ii'}\delta_{jj'} - 2\,E_j\,\delta_{ij'}\delta_{ji'} \qquad (7.231)$$

we can write

$$\langle BCS|\,\Big[\,\alpha_j\alpha_i,\,[\hat{H}_{BCS},\,\alpha^+_{i'}\alpha^+_{j'}]\,\Big]\,|BCS\rangle =$$
$$= 2\,E_i\,\delta_{ii'}\delta_{jj'} - 2\,E_j\,\delta_{ij'}\delta_{ji'} \qquad (7.232)$$

and we also have

$$\langle BCS| \Big[\alpha_j \alpha_i,\, [\hat{H}_{BCS},\, \alpha_{j'} \alpha_{i'}] \Big] |BCS\rangle = 0 \tag{7.233}$$

The substitution of (7.232) and (7.233) into (7.226) and (7.227) allows to rewrite the definition (7.227) as follows

$$A_{ij\,i'j'} = (E_i + E_j)\, \delta_{ii'}\, \delta_{jj'} + \langle BCS| \left[\alpha_j \alpha_i,\, [\hat{V}_{res},\, \alpha^+_{i'} \alpha^+_{j'}]\right] |BCS\rangle \tag{7.234}$$

$$B_{ij\,i'j'} = -\langle BCS| \left[\alpha_j \alpha_i,\, [\hat{V}_{res},\, \alpha_{j'} \alpha_{i'}]\right] |BCS\rangle \tag{7.235}$$

where $\hat{V}_{res}$ is given in (7.204):

$$\begin{aligned}
\hat{V}_{res} &= \frac{1}{4} \sum_{ijkl} V_{ijkl}\ :a^+_i a^+_j a_l\, a_k: = \boxed{\begin{array}{c}\text{see}\\ (6.33)\end{array}} = \\
&= \frac{1}{4} \sum_{i\sigma_i j\sigma_j} \sum_{k\sigma_k l\sigma_l} V_{i\sigma_i j\sigma_j k\sigma_k l\sigma_l} \\
&\qquad :\big(\mathscr{U}_i \alpha^+_{i\sigma_i} + \sigma_i \mathscr{V}_i \alpha_{i-\sigma_i}\big)\big(\mathscr{U}_j \alpha^+_{j\sigma_j} + \sigma_j \mathscr{V}_j \alpha_{j-\sigma_i}\big) \\
&\qquad\qquad \big(\mathscr{U}_l\, \alpha_{l\sigma_l} + \sigma_l \mathscr{V}_l\, \alpha^+_{l-\sigma_l}\big)\big(\mathscr{U}_k\, \alpha_{k\sigma_k} + \sigma_k \mathscr{V}_k\, \alpha^+_{k-\sigma_k}\big) : = \\
&= \boxed{\begin{array}{c}\text{in analogy}\\ \text{with (6.114)}\end{array}} = \\
&= \sum_{ijkl} H^{40}_{ijkl}\ :\big(\alpha^+_i \alpha^+_j \alpha^+_k \alpha^+_l + h.c.\big): + \\
&\qquad + \sum_{ijkl} H^{31}_{ijkl}\ :\big(\alpha^+_i \alpha^+_j \alpha^+_k \alpha_l + h.c.\big): + \\
&\qquad\qquad + \sum_{ijkl} H^{22}_{ijkl}\ :\big(\alpha^+_i \alpha^+_j \alpha_k\, \alpha_l\big):
\end{aligned} \tag{7.236}$$

where in H^{40}_{ijkl} all terms with 4 quasiparticle creation or annihilation operators are collected, the H^{31}_{ijkl} contains all terms with 3 creation quasiparticle operators and 1 annihilation operator (and their Hermitian conjugated partners), and the H^{22}_{ijkl} collects all terms with 2 creation and 2 annihilation quasiparticle operators. Since the explicit expressions for H^{40}_{ijkl}, H^{31}_{ijkl} and H^{22}_{ijkl} are very lengthy we do not present them here. The substitution of (7.236) into

(7.235) gives [15]

$$A_{ij\ i'j'} = (E_i + E_j)\,\delta_{ii'}\delta_{jj'} + 4\,H^{22}_{ij\ i'j'}$$
$$B_{ij\ i'j'} = 24\,H^{40}_{ij\ i'j'} \qquad (7.237)$$

The diagonalization of the RPA matrix $\begin{pmatrix} A & B \\ B^* & A^* \end{pmatrix}$ (see (7.230)) gives the structure of phonons (amplitudes X^ν_{ij} and Y^ν_{ij}) and corresponding energies $\hbar\omega_\nu$. In many cases it is then necessary to determine the matrix element of the concrete one-body operator $\hat{F}$ between the RPA vacuum $|RPA\rangle$ and one-phonon state $|\nu\rangle = Q^+_\nu\,|RPA\rangle$. For instance it is the case of electromagnetic transition probabilities which are given by the square of the matrix element of electric and magnetic transition multipole operators (see e.g. (2.113)). Further we will suppose that this operator $\hat{F}$ is Hermitian and is invariant or antiinvariant with respect to the time-reversal operator (see Appendix L for details)

$$\mathscr{T}\,\hat{F}\,\mathscr{T}^{-1} = \gamma^{(F)}_T\,\hat{F} \qquad\qquad \gamma_T = \pm 1 \qquad (7.238)$$

Then the single-particle matrix elements of this operator fulfill the following symmetries (we use the notation (6.17) of the single-particle states: $|i\rangle = |i\sigma_i\rangle$, $\sigma_i = \pm 1$, $\mathscr{T}\,|i\sigma_i\rangle = \sigma_i\,|i\ -\sigma_i\rangle$) (see Appendix L)

$$F_{j-\sigma_j i\sigma_i} = \langle j\ -\sigma_j|\,\hat{F}\,|i\ \sigma_i\rangle = \langle i\ \sigma_i|\hat{F}^+|j\ -\sigma_j\rangle^* = \langle i\ \sigma_i|\hat{F}|j\ -\sigma_j\rangle^* =$$
$$= \langle i\sigma_i|\,\mathscr{T}^{-1}\mathscr{T}\,\hat{F}\,\mathscr{T}^{-1}\mathscr{T}\,|j\ -\sigma_j\rangle^* = -\sigma_i\sigma_j\,\langle i\ -\sigma_i|\,\mathscr{T}\hat{F}\mathscr{T}^{-1}\,|j\ \sigma_j\rangle =$$
$$= -\sigma_i\sigma_j\,\gamma^{(F)}_T\,\langle i\ -\sigma_i|\,\hat{F}\,|j\sigma_j\rangle = -\sigma_i\sigma_j\,\gamma^{(F)}_T\,F_{i-\sigma_i j\sigma_j} \qquad (7.239)$$

Then the matrix element $\langle RPA|\hat{F}|\nu\rangle$ of the operator $\hat{F}$ between the RPA vacuum $|RPA\rangle$ and one-phonon state $|\nu\rangle$ is following

$$\langle RPA|\hat{F}|\nu\rangle = \langle RPA|\hat{F}\,Q^+_\nu|RPA\rangle \approx \langle BCS|\left[\hat{F},\,Q^+_\nu\right]|RPA\rangle =$$
$$= \boxed{\begin{array}{c}\hat{F} = \sum_{k\sigma_k l\sigma_l} F_{k\sigma_k l\sigma_l} a^+_{k\sigma_k} a_{l\sigma_l} \\ \text{and see (7.207)}\end{array}} =$$
$$= \sum_{k\sigma_k l\sigma_l}\ \sum_{i\sigma_i j\sigma_j} F_{k\sigma_k l\sigma_l}\Big\{X^{(\nu)}_{i\sigma_i j\sigma_j}\,\langle BCS|\,\left[a^+_{k\sigma_k}a_{l\sigma_l},\,\alpha^+_{i\sigma_i}\alpha^+_{j\sigma_j}\right]\,|\,BCS\rangle$$
$$- Y^{(\nu)}_{i\sigma_i j\sigma_j}\,\langle BCS|\,\left[a^+_{k\sigma_k}a_{l\sigma_l},\,\alpha_{j\,\sigma_j}\alpha_{i\sigma_i}\right]\,|\,BCS\rangle\Big\} =$$

[15] It should be pointed out that the RPA equations (7.230) concerns the even-even nucleus. As it is discussed further in this subsection the term in (7.236) with $H^{31}_{ij\,kl}$ does not contribute to the RPA equations for even-even nucleus. Generally it contributes to the equation of motion for odd-A and odd-odd nuclei.

$$
\begin{aligned}
&= \boxed{\begin{array}{c}\text{substitution}\\ \text{from (6.30)}\end{array}} = \\
&= \sum_{k\sigma_k l\sigma_l} \sum_{i\sigma_i j\sigma_j} F_{k\sigma_k l\sigma_l} \\
&\qquad \Big\{ X^{(\nu)}_{i\sigma_i j\sigma_j}\, \sigma_k\, \mathscr{V}_k \mathscr{U}_l\ \langle BCS|\, \alpha_{k-\sigma_k}\alpha_{l\sigma_l}\, \alpha^+_{i\sigma_i}\alpha^+_{j\sigma_j}\,|\, BCS\rangle \\
&\qquad + Y^{(\nu)}_{i\sigma_i j\sigma_j}\, \sigma_l\, \mathscr{U}_k \mathscr{V}_l\ \langle BCS|\, \alpha_{j\sigma_j}\alpha_{i\sigma_i}\, \alpha^+_{k\,\sigma_k}\alpha^+_{l-\sigma_l}\,|\, BCS\rangle \Big\} = \\
&= \sum_{k\sigma_k l\sigma_l} \sum_{i\sigma_i j\sigma_j} F_{k\sigma_k l\sigma_l} \\
&\qquad \Big\{ X^{(\nu)}_{i\sigma_i j\sigma_j}\, \sigma_k\, \mathscr{V}_k \mathscr{U}_l\ \left(\delta_{l\sigma_l,\, i\sigma_i}\, \delta_{k-\sigma_k,\, j\sigma_j} - \delta_{l\sigma_l,\, j\sigma_j}\, \delta_{k-\sigma_k,\, i\sigma_i}\right) \\
&\qquad + Y^{(\nu)}_{i\sigma_i j\sigma_j}\, \sigma_l\, \mathscr{U}_k \mathscr{V}_l\ \left(\delta_{i\sigma_i,\, k\sigma_k}\, \delta_{j\sigma_j,\, l-\sigma_l} - \delta_{i\sigma_i,\, l-\sigma_l}\, \delta_{j\sigma_j,\, k\sigma_k}\right) \Big\} = \\
&= \sum_{i\sigma_i j\sigma_j} \Big\{ X^{(\nu)}_{i\sigma_i j\sigma_j} \left(\sigma_j\, \mathscr{V}_j \mathscr{U}_i\, F_{j-\sigma_j i\sigma_i} - \sigma_i\, \mathscr{V}_i \mathscr{U}_j\, F_{i-\sigma_i j\sigma_j}\right) \\
&\qquad\qquad + Y^{(\nu)}_{i\sigma_i j\sigma_j} \left(\sigma_j\, \mathscr{U}_i \mathscr{V}_j\, F_{i\sigma_i j-\sigma_j} - \sigma_i\, \mathscr{U}_j \mathscr{V}_i\, F_{j\sigma_j i-\sigma_i}\right) \Big\} = \\
&= \boxed{\begin{array}{c}\text{see}\\ (7.239)\end{array}} = \\
&= \sum_{i\sigma_i j\sigma_j} \left(\mathscr{U}_i \mathscr{V}_j + \gamma_T^{(F)}\, \mathscr{V}_i \mathscr{U}_j\right) F_{i\sigma_i\, j-\sigma_j}\, \sigma_j \left(X^{(\nu)}_{i\sigma_i j\sigma_j} + Y^{(\nu)}_{i\sigma_i j\sigma_j}\right)
\end{aligned}
\tag{7.240}
$$

The expression (7.240) enables to calculate matrix elements of any single-particle operator $\hat{F}$ with symmetries (7.238) between the RPA ground state and general one-phonon state $|\nu\rangle = Q^+_\nu|RPA\rangle$ (if the single-particle matrix elements $F_{i\sigma_i j\sigma_j}$ are known). It should be noted that it can be used also for matrix elements of electric (see (2.132)) and magnetic (see (2.134)) transition operators if these operators are symmetrized in order to be Hermitian. One should realize that $\gamma_T^{(F)} = +1$ for electric type transition operators and $\gamma_T^{(F)} = -1$ for magnetic type operators - see Appendix L.

For further consideration it is convenient to introduce matrix $\mathscr{S}$

$$
\mathscr{S} = \begin{pmatrix} A & B \\ B^* & A^* \end{pmatrix} \tag{7.241}
$$

This matrix is known in the literature as the stability matrix (see e.g. exprs. (8.73) in [9]). The reason for this name consists in the fact that it is possible

to show (see e.g. [9]) that this matrix is positive definite when the used quasiparticle system of states corresponds to the minimum of the total BCS energy $\langle BCS|\,\hat{H}\,|BCS\rangle$ of the nucleus Hamiltonian. Then from mathematics we know that if the matrix $\mathscr{S}$ is positive definite then there exists the matrix $\mathscr{S}^{1/2}$ such as $\mathscr{S}^{1/2}\mathscr{S}^{1/2} = \mathscr{S}$. So the RPA equation (7.230) can be rewritten as follows

$$\mathscr{S}\begin{pmatrix} X \\ Y \end{pmatrix} = \hbar\omega \begin{pmatrix} 1 & 0 \\ 0 & -1 \end{pmatrix}\begin{pmatrix} X \\ Y \end{pmatrix} \tag{7.242}$$

$$\begin{aligned}
\Rightarrow \qquad & \begin{pmatrix} 1 & 0 \\ 0 & -1 \end{pmatrix}\mathscr{S}^{1/2}\,\mathscr{S}^{1/2}\begin{pmatrix} X \\ Y \end{pmatrix} = \hbar\omega\begin{pmatrix} X \\ Y \end{pmatrix} \\
\Rightarrow \qquad & \mathscr{S}^{1/2}\begin{pmatrix} 1 & 0 \\ 0 & -1 \end{pmatrix}\mathscr{S}^{1/2}\,\mathscr{S}^{1/2}\begin{pmatrix} X \\ Y \end{pmatrix} = \hbar\omega\,\mathscr{S}^{1/2}\begin{pmatrix} X \\ Y \end{pmatrix} \\
\Rightarrow \qquad & \mathscr{S}^{1/2}\begin{pmatrix} 1 & 0 \\ 0 & -1 \end{pmatrix}\mathscr{S}^{1/2}\begin{pmatrix} \tilde{X} \\ \tilde{Y} \end{pmatrix} = \hbar\omega\begin{pmatrix} \tilde{X} \\ \tilde{Y} \end{pmatrix}
\end{aligned} \tag{7.243}$$

where

$$\begin{pmatrix} \tilde{X} \\ \tilde{Y} \end{pmatrix} \equiv \mathscr{S}^{1/2}\begin{pmatrix} X \\ Y \end{pmatrix} \tag{7.244}$$

So the solving of the RPA equation (7.230) is equivalent to the eigenvalue problem of the matrix $\mathscr{S}^{1/2}\begin{pmatrix} 1 & 0 \\ 0 & -1 \end{pmatrix}\mathscr{S}^{1/2}$. Since the matrix $\mathscr{S}$ is Hermitian the matrix $\mathscr{S}^{1/2}\begin{pmatrix} 1 & 0 \\ 0 & -1 \end{pmatrix}\mathscr{S}^{1/2}$ is also Hermitian and the corresponding eigenvalues $\hbar\omega_\nu$ are real. However, it holds only in the case when the BCS energy $\langle BCS|\,\hat{H}\,|BCS\rangle$ is in the minimum (that means pairing amplitudes $\mathscr{U}_i$, $\mathscr{V}_i$ were obtained by the solving of the BCS equations (6.96)-(6.99)) because only in this case the matrix $\mathscr{S}$ is positive definite and we can introduce the matrix $\mathscr{S}^{1/2}$. If we are not in the BCS minimum the eigenvalues $\hbar\omega_\nu$ are not necessarily real.

Further the orthonormality of solutions of the RPA equation is investigated. Using the quasi-boson approximation (7.220), (7.221) the normaliza-

tion condition of the one-phonon states should be expected as

$$\langle \nu \,|\, \nu^{'} \rangle = \langle RPA|\, Q_\nu \, Q^+_{\nu'} \,|RPA\rangle = \langle RPA|\, \left[Q_\nu,\ Q^+_{\nu'}\right] |RPA\rangle \approx$$

$$\approx \frac{1}{4} \sum_{ij} \sum_{i'j'} \Big\{ X^{(\nu)\,*}_{ij} \, X^{(\nu^{'})}_{i'j'} \, \langle BCS|\, \left[\alpha_j \alpha_i,\ \alpha^+_{i'} \alpha^+_{j'}\right] |BCS\rangle$$

$$- Y^{(\nu)\,*}_{ij} \, Y^{(\nu^{'})}_{i'j'} \, \langle BCS|\, \left[\alpha_{j'} \alpha_{i'},\ \alpha^+_i \alpha^+_j\right] |BCS\rangle \Big\} =$$

$$= \boxed{\begin{array}{c}\text{see}\\ (7.220)\end{array}} =$$

$$= \sum_{ij} \sum_{i'j'} \Big(X^{(\nu)\,*}_{ij} \, X^{(\nu^{'})}_{i'j'} - Y^{(\nu)\,*}_{ij} \, Y^{(\nu^{'})}_{i'j'} \Big) \big(\delta_{i'i} \, \delta_{j'j} - \delta_{j'i} \, \delta_{i'j} \big) =$$

$$= \sum_{ij} \Big(X^{(\nu)\,*}_{ij} \, X^{(\nu^{'})}_{ij} - Y^{(\nu)\,*}_{ij} \, Y^{(\nu^{'})}_{ij} \Big) = \delta_{\nu\nu'} \qquad (7.245)$$

To show the orthogonality of the RPA solutions in the sence of (7.245) it should be realized that for each eigenvector $\begin{pmatrix} X^{(\nu)} \\ Y^{(\nu)} \end{pmatrix}$ with the energy $\hbar\omega_\nu$ we have another eigenvector $\begin{pmatrix} Y^{(\nu)\,*} \\ X^{(\nu)\,*} \end{pmatrix}$ with the energy $-\hbar\omega_\nu$. This can be seen directly from (7.230)

$$\begin{pmatrix} A & B \\ B^* & A^* \end{pmatrix} \begin{pmatrix} X^{(\nu)} \\ Y^{(\nu)} \end{pmatrix} = \hbar\omega_\nu \begin{pmatrix} 1 & 0 \\ 0 & -1 \end{pmatrix} \begin{pmatrix} X^{(\nu)} \\ Y^{(\nu)} \end{pmatrix}$$

$$\begin{aligned} \Rightarrow \qquad & A\ X^{(\nu)} + B\ Y^{(\nu)} = \hbar\omega_\nu \, X^{(\nu)} \\ & B^* \, X^{(\nu)} + A^* \, Y^{(\nu)} = -\hbar\omega_\nu \, Y^{(\nu)} \\ \Rightarrow \qquad & A\ Y^{(\nu)\,*} + B\ X^{(\nu)\,*} = -\hbar\omega_\nu \, Y^{(\nu)\,*} \\ & B^* \, Y^{(\nu)\,*} + A^* \, X^{(\nu)\,*} = \hbar\omega_\nu \, X^{(\nu)\,*} \\ \Rightarrow \qquad & \begin{pmatrix} A & B \\ B^* & A^* \end{pmatrix} \begin{pmatrix} Y^{(\nu)\,*} \\ X^{(\nu)\,*} \end{pmatrix} = -\hbar\omega_\nu \begin{pmatrix} 1 & 0 \\ 0 & -1 \end{pmatrix} \begin{pmatrix} Y^{(\nu)\,*} \\ X^{(\nu)\,*} \end{pmatrix} \end{aligned} \qquad (7.246)$$

Further we show that both these two solutions have the same absolute norm in the sense of (7.245) but with the opposite sign and that they are orthogonal each other. The completeness of all solutions of the RPA is also demonstrated.

We introduce the matrices Ξ and Π

$$\Xi = \begin{pmatrix} X & Y^* \\ Y & X^* \end{pmatrix} \equiv \begin{pmatrix} X^{(\nu)}_{ij} & Y^{(\nu)\,*}_{ij} \\ Y^{(\nu)}_{ij} & X^{(\nu)\,*}_{ij} \end{pmatrix} \quad , \qquad \Pi \equiv \begin{pmatrix} 1 & 0 \\ 0 & -1 \end{pmatrix} \qquad (7.247)$$

where indexes ij (labeling rows) go over the configuration 2- quasiparticle basis and index ν (labeling columns) runs over all solutions of the RPA equation (7.230) (the number of the RPA solutions is the same as the dimension of 2- quasiparticle configuration space, that means the dimension of the matrix Π is the same as that of matrix Ξ and $\mathscr{S}$. Then the RPA equation (7.230) can be written also as follows

$$\mathscr{S}\,\Xi = \Pi\,\Xi\,\Omega \tag{7.248}$$

where the matrix Ω

$$\Omega = \begin{pmatrix} \hbar\omega & 0 \\ 0 & -\hbar\omega \end{pmatrix} \tag{7.249}$$

is the diagonal real matrix. With using of (7.248) the following identity can be written

$$\begin{aligned} \left[\Omega,\, \Xi^{+}\,\Pi\,\Xi\right] &= \Omega\,\Xi^{+}\,\Pi\,\Xi - \Xi^{+}\,\Pi\,\Xi\,\Omega = \left(\Pi\,\Xi\,\Omega\right)^{+}\Xi - \Xi^{+}\left(\Pi\,\Xi\,\Omega\right) = \\ &= \boxed{\begin{array}{c}\text{see}\\(7.248)\end{array}} = \left(\mathscr{S}\,\Xi\right)^{+}\Xi - \Xi^{+}\,\mathscr{S}\,\Xi \;=\; \Xi^{+}\,\mathscr{S}^{+}\,\Xi - \Xi^{+}\,\mathscr{S}\,\Xi \;= \\ &= \boxed{\begin{array}{c}\text{because}\\ \mathscr{S}\text{ is Hermitian}\end{array}} = 0 \end{aligned} \tag{7.250}$$

Since the norm of the vector $\begin{pmatrix} X \\ Y \end{pmatrix}$ is open for the moment we can determine the normalization of it according to the additional condition which can be chosen as follows

$$\Xi^{+}\,\Pi\,\Xi = \Pi \tag{7.251}$$

Concretely this means

$$\begin{aligned} \Xi^{+}\,\Pi\,\Xi &= \begin{pmatrix} X^{+} & Y^{+} \\ (Y^{*})^{+} & (X^{*})^{+} \end{pmatrix}\begin{pmatrix} 1 & 0 \\ 0 & -1 \end{pmatrix}\begin{pmatrix} X & Y^{*} \\ Y & X^{*} \end{pmatrix} = \\ &= \begin{pmatrix} X^{+}X - Y^{+}Y & X^{+}Y^{*} - Y^{+}X^{*} \\ (Y^{*})^{+}X - (X^{*})^{+}Y & (Y^{*})^{+}Y^{*} - (X^{*})^{+}X^{*} \end{pmatrix} = \\ &= \begin{pmatrix} \sum_{ij}\left(X_{ij}^{(\nu)\,*}X_{ij}^{(\nu')} - Y_{ij}^{(\nu)\,*}Y_{ij}^{(\nu')}\right) & \sum_{ij}\left(X_{ij}^{(\nu)}Y_{ij}^{(\nu')\,*} - Y_{ij}^{(\nu)}X_{ij}^{(\nu')\,*}\right) \\ \sum_{ij}\left(Y_{ij}^{(\nu)}X_{ij}^{(\nu')} - X_{ij}^{(\nu)}Y_{ij}^{(\nu')}\right) & \sum_{ij}\left(Y_{ij}^{(\nu)}Y_{ij}^{(\nu')\,*} - X_{ij}^{(\nu)}X_{ij}^{(\nu')\,*}\right) \end{pmatrix} = \\ &= \Pi = \boxed{\begin{array}{c}\text{see}\\(7.247)\end{array}} = \begin{pmatrix} \delta_{\nu\nu'} & 0 \\ 0 & -\delta_{\nu\nu'} \end{pmatrix} \end{aligned} \tag{7.252}$$

The relation (7.252) is in accordance with the expectation (7.245) and also with the orthonormality of all solutions of the RPA equation (with positive as well as negative eigen energies, $\pm\hbar\omega$). The condition of the completeness (or closure condition) of the ensemble of all RPA solutions can be obtained by multiplying the equation (7.251) by the matrix Π:

$$\Pi\,\Xi^{+}\,\Pi\,\Xi = \Pi^{2} = 1 \tag{7.253}$$

From (7.253) it follows that the matrix $\frac{1}{2}\Pi\Xi^{+}\Pi$ is the inverse matrix to Ξ:

$$\begin{aligned} \Xi^{-1} &= \Pi\,\Xi^{+}\,\Pi \qquad \Rightarrow \qquad (\Xi^{+})^{-1} = \Pi\,\Xi\,\Pi \\ \Rightarrow \qquad & (\Xi^{+})^{\,-1}\,\Xi^{+} = \Pi\,\Xi\,\Pi\,\Xi^{+} = 1 \\ \Rightarrow \qquad & \boxed{\begin{array}{c}\text{because}\\ \Pi^{2}=1\end{array}} \quad \Rightarrow \quad \Xi\,\Pi\,\Xi^{+} = \Pi \end{aligned} \tag{7.254}$$

and this gives explicitly

$$\begin{pmatrix} X & Y^{*} \\ Y & X^{*} \end{pmatrix} \begin{pmatrix} 1 & 0 \\ 0 & 1 \end{pmatrix} \begin{pmatrix} X^{+} & Y^{+} \\ (Y^{*})^{+} & (X^{*})^{+} \end{pmatrix} =$$

$$= \begin{pmatrix} \sum_{\nu}\left(X_{ij}^{(\nu)}X_{i'j'}^{(\nu)\,*} - Y_{ij}^{(\nu)\,*}Y_{i'j'}^{(\nu)}\right) & \sum_{\nu}\left(X_{ij}^{(\nu)}Y_{i'j'}^{(\nu)\,*} - Y_{ij}^{(\nu)\,*}X_{i'j'}^{(\nu)}\right) \\ \sum_{\nu}\left(Y_{ij}^{(\nu)}X_{i'j;}^{(\nu)\,*} - X_{ij}^{(\nu)\,*}Y_{i'j'}^{(\nu)}\right) & \sum_{\nu}\left(Y_{ij}^{(\nu)}Y_{i'j'}^{(\nu)\,*} - X_{ij}^{(\nu)\,*}X_{i'j'}^{(\nu)}\right) \end{pmatrix} =$$

$$= \begin{pmatrix} \delta_{ij,\,i'j'} & 0 \\ 0 & -\delta_{ij,\,i'j'} \end{pmatrix} \tag{7.255}$$

One can see that the equation (7.255) corresponds to (7.245) and represents the closure conditions for sectors of the RPA solutions with positive and negative energies and equation (7.252) shows the orthonormality of these two sectors. The physical meaning has only the sector of the RPA solutions with positive energy.

7.3.1.1.2 Fermion-boson mapping, RPA Hamiltonian, spurious modes. In the derivation of the RPA equations (7.230), (7.234), (7.235) we used the quasi-boson approximation (7.220) when the two-quasiparticle creation and annihilation operators b_{ij}^{+} and b_{ij} (see (7.219)) were supposed to behave like boson

creation and annihilation operators (see (7.220) and (7.221), $b^+_{ij} \equiv \alpha^+_i\, \alpha^+_j$)

$$\begin{aligned}\left[b_{ij},\, b^+_{i'j'}\right] &= \delta_{ii'}\,\delta_{jj'} - \delta_{ij'}\,\delta_{ji'} \\ &+ \delta_{ij'}\,\alpha^+_j\alpha_{i'} + \delta_{ji'}\,\alpha^+_i\alpha_{j'} - \delta_{jj'}\,\alpha^+_i\alpha_{i'} - \delta_{ii'}\,\alpha^+_j\alpha_{j'} \;\approx \\ &\approx\; \delta_{ii'}\,\delta_{jj'} - \delta_{ij'}\,\delta_{j\,i'} = \boxed{\begin{array}{c}\text{see the text above}\\ \text{the expr. (7.220')}\end{array}} = \delta_{ii'}\,\delta_{jj'}\end{aligned}$$

$$\left[b_{ij},\, b_{i'j'}\right] = 0 \tag{7.256}$$

This assumption (known as quasi-boson approximation) is a non-controlled approximation. Generally it can be shown (see e.g. the Chapter 9 in [9]) that we should use a boson mapping from the space of fermion operators α^+_i, α_i to the space of pure boson operators B^+_μ, B_μ which fulfill precisely the boson commutator relations

$$\left[B_\mu,\, B^+_{\mu'}\right] = \delta_{\mu\mu'} \quad , \qquad \left[B_\mu,\, B_{\mu'}\right] = 0 \tag{7.257}$$

This mapping allows to rewrite for even-even nucleus (generally for the quantum system formed by the even number of fermions) all quantum mechanics operators including corresponding equation of motion, originally formulated for fermion system, by means of the boson operators. We discussed already a simple version of such mapping in the connection with the Interacting Boson Model (see the Subsection 7.2.2.2, the Table 7.1 and the Fig. 7.2.4) where the collective fermion $L = 0$ and $L = 2$ low-lying states in the even-even nuclei were mapped into the boson s- and d- states. In the general case (not only for $L = 0,\ 2$ states) the mapping procedure is complicated from the mathematical point of view (see the Chapter 9 in [9]) and it has not been completed entirely up to now. This procedure is beyond the scope of this textbook. We can only say that the boson image of two- fermion operators $\alpha^+_i\alpha^+_j$ and $\alpha^+_i\alpha_j$ can be written in the form of the generally infinite series in terms of the pure boson operators B^+_μ, B_μ (see (9.40) in [9] and also [146])

$$(b^+_{ij})_B \equiv (\alpha^+_i\alpha^+_j)_B = \sum_\mu x^{(1)}_{ij,\,\mu}\, B^+_\mu + \sum_{\rho\nu\lambda} x^{(3)}_{ij,\,\rho\nu\lambda}\, B^+_\nu B^+_\rho B_\lambda + \ldots \tag{7.258}$$

$$(\alpha^+_i\alpha_j)_B = y^{(0)}_{ij} + \sum_{\rho\lambda} y^{(2)}_{ij,\,\rho\lambda}\, B^+_\rho B_\lambda + \ldots \tag{7.259}$$

where the coefficients $x^{(i)}$ and $y^{(i)}$ can be determined by the condition that the anticommutation relations $\{\alpha_i, \alpha^+_j\} = \delta_{ij}$, $\{\alpha_i, \alpha_j\} = 0$ are satisfied for all

i and j. There are basically 3 methods suggested for the determination of the boson mapping (7.258) which are used in the literature, namely perturbative boson expansion (e.g. [147, 146]), the Boson Expansion of Marumori [148, 149], and Boson Expansion of Dyson [150]. More detailed description of these methods can be found in the chapter 9 of [9].

From the discussion above it is clear that in the quasi-boson approximation (7.220) or (7.256) all higher order terms with B_μ or B_μ^+ in (7.258) are neglected and

$$(b_{ij}^+)_B = (\alpha_i^+ \alpha_j^+)_B \approx B_{\mu=ij}^+ \tag{7.260}$$

Usually it is very convenient to express all operators, such as Hamiltonian $\hat{H}$ or transition operators, in terms of the boson operators. Generally it is shown in the chapter 9 of [9]. Here we shall do it only in the framework of the RPA (quasiboson approximation) or, by other words, harmonic order only. Further we determine the boson (or RPA) Hamiltonian $\hat{H}_{RPA}$ as the Hamiltonian containing only terms quadratic in the quasi-boson operators b, b^+, that means only terms with b^+b, bb and b^+b^+, which simultaneously give the same RPA equations as the total Hamiltonian $\hat{H}$ (in the framework of the quasi-boson approximation). By other words the matrices A and B (see (7.227)) participating in the RPA equation (7.230) are given now by

$$\begin{aligned} A_{ij\,i'j'} &= \langle BCS| \left[b_{ij},\, [\hat{H},\, b_{i'j'}^+] \right] |BCS\rangle = \\ &\equiv_B \langle BCS| \left[B_{ij},\, [\hat{H}_{RPA} + \hat{V}_{res},\, B_{i'j'}^+] \right] |BCS\rangle_B \\ B_{ij\,i'j'} &= -\langle BCS| \left[b_{ij},\, [\hat{H},\, b_{i'j'}] \right] |BCS\rangle = \\ &\equiv -{}_B\langle BCS| \left[B_{ij},\, [\hat{V}_{res},\, B_{i'j'}] \right] |BCS\rangle_B \end{aligned} \tag{7.261}$$

where $|BCS\rangle_B$ is the boson image of the quasiparticle vacuum $|BCS\rangle$:

$$B_{ij}\,|BCS\rangle_B = 0 \qquad , \qquad {}_B\langle BCS|\, B_{ij}^+ = 0 \tag{7.262}$$

and B_{ij} and B_{ij}^+ are boson images of the two-quasiparticle creation and annihilation operators $b_{ij} = \alpha_j \alpha_i$ and $b_{ij}^+ = \alpha_i^+ \alpha_j^+$, respectively. The pure boson operators B_{ij} and B_{ij}^+ are supposed to fulfill boson commutation relation (7.257) precisely. In the literature with the RPA (see e.g. [57]) usually boson images are not mentioned and in the corresponding expressions quasi-boson two-quasiparticle operators b_{ij} and b_{ij}^+ are used directly with the statement that in all commutators of any two one-boson operators quasi-boson approximation (7.220) is used (corresponding commutator is substituted by the BCS

expectation value of this commutator). By other words it means that in these commutator we use the approximation (7.256) and two-quasiparticle operaors behave like boson operators. Using this formulation of the quasi-boson approximation it is not necessary to introduce any boson images B_{ij}, B^+_{ij} and $|BCS\rangle_B$ and we can work with operators b_{ij}, b^+_{ij} and with the BCS quasiparticle vacuum $|BCS\rangle$ directly assuming that operators b_{ij} and b^+_{ij} are boson operators and $|BCS\rangle$ is the vacuum for two-quasiparticle quasi-bosons:

$$b_{ij}\,|BCS\rangle = 0 \qquad , \qquad \langle BCS|\,b^+_{ij} = 0 \tag{7.263}$$

This formulation of the quasi-boson approximation is used further and then the equations (7.261) can be rewritten as follows

$$\begin{aligned} A_{ij\,i'j'} &= \langle BCS|\,\big[b_{ij},\,[\hat{H},\,b^+_{i'j'}]\,\big]|BCS\rangle = \\ &\equiv_B \langle BCS|\,\big[b_{ij},\,[\hat{H}_{RPA},\,b^+_{i'j'}]\,\big]|BCS\rangle_B \\ B_{ij\,i'j'} &= -\langle BCS|\,\big[b_{ij},\,[\hat{H},\,b_{i'j'}]\,\big]|BCS\rangle = \\ &\equiv -{}_B\langle BCS|\,\big[b_{ij},\,[\hat{H}_{RPA},\,b_{i'j'}]\,\big]|BCS\rangle_B \end{aligned} \tag{7.264}$$

Further we show that the definition expression (7.264) for the RPA Hamiltonian $\hat{H}_{RPA}$ corresponds to the $\hat{H}_{RPA}$ in the following form

$$\begin{aligned} \hat{H}_{RPA} = E_{BCS} &+ \sum_{ij\,i'j'} A_{ij\,i'j'}\,b^+_{ij}\;b_{i'j'} + \\ &+\frac{1}{2}\sum_{ij\,i'j'}\big(\,B_{ij\,i'j'}\,b^+_{ij}\,b^+_{i'j'} + B^*_{ij\,i'j'}\,b_{i'j'}b_{ij}\,\big) \end{aligned} \tag{7.265}$$

We can easily prove that, really, if the RPA Hamiltonian (7.265) is substituted into the r.h.s. of the (7.264) then we obtain back $A_{ij\,i'j'}$ and $B_{ij\,i'j'}$:

$$\begin{aligned} &\big[b_{ij},\,[\hat{H}_{RPA},\,b^+_{i'j'}]\,\big] = \sum_{kl\,k'l'} A_{kl\,k'l'}\,\big[b_{ij},\,[b^+_{kl}\,b_{k'l'},\,b^+_{i'j'}]\,\big] = \\ &= \boxed{\begin{array}{c}\text{because } [AB,C] = A\,[B,C] + [A,C]\,B \\ \text{and } [b_{ij},\,b^+_{i'j'}] = \delta_{ii'}\delta_{jj'}\end{array}} = \\ &= \sum_{kl\,k'l'} A_{kl\,k'l'}\;[b_{ij},\,b^+_{kl}]\,(\delta_{k'i'}\,\delta_{l'j'}\,\delta_{l'i'}) = \\ &= \sum_{kl\,k'l'} A_{kl\,k'l'}\,(\delta_{ik}\delta_{j\,l})\,(\delta_{k'i'}\,\delta_{l'j'}) = A_{ij\,i'j'} \end{aligned}$$

and similarly

$$\left[b_{ij},\,[\hat{H}_{RPA},\,b_{i'j'}]\,\right] = \frac{1}{2}\sum_{kl\,k'l'} B_{kl\,k'l'}\,\left[b_{ij},\,[b^+_{kl}\,b^+_{k'l'},\,b_{i'j'}]\,\right] =$$

$$= -\frac{1}{2}\sum_{kl\,k'l'} B_{kl\,k'l'}\,\left\{\,[b_{ij},\,b^+_{kl}]\,\delta_{k'i'}\,\delta_{l'j'} + [b_{ij},\,b^+_{k'l'}]\,\delta_{ki'}\,\delta_{lj'}\,\right\} =$$

$$= -\frac{1}{2}\sum_{kl\,k'l'} B_{kl\,k'l'}\,\left(\delta_{ik}\delta_{jk}\delta_{k'i'}\delta_{l'j'} + \delta_{ik'}\delta_{jl'}\delta_{ki'}\delta_{lj'}\right) =$$

$$-\frac{1}{2}\left(B_{iji'j'} + B_{i'j'ij}\right) = \boxed{\begin{array}{c}\text{because}\\ B_{iji'j'} = B_{i'j'ij}\end{array}} = -B_{iji'j'}$$

So the Hamiltonian H_{RPA} in (7.265) fulfills the definition (7.261) and therefore gives the same RPA equations as the total Hamiltonian $\hat{H}$ (if quasi-boson approximation is assumed).

The total BCS energy E_{BCS} involved in (7.265) is given by (see (6.100))

$$E_{BCS} = \langle BCS|\,\hat{H}\,|BCS\rangle = \langle BCS|\,\hat{H}_{RPA}\,|BCS\rangle =$$
$$= \sum_i \epsilon_i\,\mathcal{V}_i^2 - \frac{1}{2}\sum_{ij} V_{ij\,ij}\;\mathcal{V}_i^2\,\mathcal{V}_j^2 - \frac{1}{2}\sum_i \Delta_{ii}\,\mathcal{U}_j\,\mathcal{V}_j \qquad (7.266)$$

with (see (6.89))

$$\Delta_{ii} = -\frac{1}{2}\sum_j V_{i\tilde{i}j\tilde{j}}\,\mathcal{U}_j\,\mathcal{V}_j \qquad (7.267)$$

The definition of the fonon, (7.207)

$$Q^+_\nu = \sum_{ij}\left(X^{(\nu)}_{ij}\,b^+_{ij} - Y^{(\nu)}_{ij}\,b_{ij}\right) \qquad (7.268)$$

can be understood as the unitary transformation from the space of the quasi-boson creation and annihilation operators b_{ij}, b^+_{ij} into the space of the phonon cration and annihilation operators Q^+_ν, Q_ν. This transformation can be inverted as it follows

$$Q^+_\nu = \sum_{ij}\left(X^{(\nu)}_{ij}\,b^+_{ij} - Y^{(\nu)}_{ij}\,b_{ij}\right) \qquad |\cdot X^{(\nu)\,*}_{i'j'}$$

$$Q_\nu = \sum_{ij}\left(X^{(\nu)\,*}_{ij}\,b_{ij} - Y^{(\nu)\,*}_{ij}\,b^+_{ij}\right) \qquad |\cdot Y^{(\nu)}_{i'j'}$$

Both these equations can be summed over phonon index ν and we have

$$\begin{aligned}
&\sum_{\nu} X^{(\nu)\,*}_{i'j'}\, Q^{+}_{\nu} + \sum_{\nu} Y^{(\nu)\,*}_{i'j'}\, Q_{\nu} = \\
&= \sum_{\nu\, ij} \big\{ X^{(\nu)\,*}_{i'j'}\, X^{(\nu)}_{ij}\, b^{+}_{ij} - X^{(\nu)\,*}_{i'j'}\, Y^{(\nu)}_{ij}\, b_{ij} \\
&\qquad\qquad + Y^{(\nu)}_{i'j'}\, X^{(\nu)\,*}_{ij}\, b^{+}_{ij} - Y^{(\nu)}_{i'j'}\, Y^{(\nu)\,*}_{ij}\, b^{+}_{ij} \big\} = \\
&= \sum_{ij} \Big\{ \sum_{\nu} \big(X^{(\nu)\,*}_{i'j'}\, X^{(\nu)}_{ij} - Y^{(\nu)}_{i'j'}\, X^{(\nu)\,*}_{ij} \big)\, b^{+}_{ij} \\
&\qquad\qquad + \sum_{\nu} \big(Y^{(\nu)}_{i'j'}\, X^{(\nu)\,*}_{ij} - X^{(\nu)\,*}_{i'j'}\, Y^{(\nu)}_{ij} \big)\, b_{ij} \Big\} = \\
&= \boxed{\begin{array}{c}\text{see}\\ (7.255)\end{array}} = \sum_{ij} \big\{ \delta_{ii'}\delta_{jj'}\, b^{+}_{ij} + 0 \big\} = b^{+}_{i'j'}
\end{aligned}$$

So the inverse transformation for (7.268) is following

$$\begin{aligned}
b^{+}_{ij} &= \sum_{\nu} \big(X^{(\nu)\,*}_{ij}\, Q^{+}_{\nu} + Y^{(\nu)}_{ij}\, Q_{\nu} \big) \\
b_{ij} &= \sum_{\nu} \big(X^{(\nu)}_{ij}\, Q_{\nu} + Y^{(\nu)\,*}_{ij}\, Q^{+}_{\nu} \big)
\end{aligned} \tag{7.269}$$

The substitution of (7.269) into the expression (7.265) gives the RPA Hamil-

tonian expressed in terms of the phonon creation and annihilation operators.

$$
\begin{aligned}
&\hat{H}_{RPA} = E_{BCS} + \\
&+\sum_{ijj'i'} A_{iji'j'} \sum_{\nu\nu'} \left(X^{(\nu)\,*}_{ij} Q^{+}_{\nu} + Y^{(\nu)}_{ij}\, Q_{\nu}\right) \left(X^{(\nu')}_{i'j'}\, Q_{\nu'} + Y^{(\nu')\,*}_{i'j'} Q^{+}_{\nu'}\right) \\
&+\frac{1}{2} \sum_{ijj'i'} \sum_{\nu\nu'} \Big\{ B_{iji'j'} \left(X^{(\nu)*}_{ij} Q_{\nu} + Y^{(\nu)}_{ij}\, Q^{+}_{\nu}\right) \left(X^{(\nu'^{*})}_{i'j'}\, Q^{+}_{\nu'} + Y^{(\nu')*}_{i'j'} Q_{\nu'}\right) \\
&\qquad +B^{*}_{iji'j'} \left(X^{(\nu)}_{ij} Q_{\nu} + Y^{(\nu)\,*}_{ij}\, Q^{+}_{\nu}\right) \left(X^{(\nu')}_{i'j'}\, Q_{\nu'} + Y^{(\nu')\,*}_{i'j'} Q^{+}_{\nu'}\right) \Big\} = \\
&= E_{BCS} + \\
&+\sum_{\nu\nu'} Q^{+}_{\nu} \sum_{ijj'i'} \Big[X^{(\nu)\,*}_{ij} A_{iji'j'} X^{(\nu')}_{i'j'} + \frac{1}{2}\, X^{(\nu)\,*}_{ij} B_{iji'j'} Y^{(\nu')}_{i'j'} + \\
&\qquad\qquad + \frac{1}{2}\, Y^{(\nu)\,*}_{ij} B^{*}_{iji'j'} X^{(\nu')}_{i'j'} \Big]\, Q_{\nu'} + \\
&+\sum_{\nu\nu'} Q_{\nu} \sum_{ijj'i'} \Big[Y^{(\nu)}_{ij} A_{iji'j'} Y^{(\nu')\,*}_{i'j'} + \frac{1}{2}\, Y^{(\nu)}_{ij} B_{iji'j'} X^{(\nu')\,*}_{i'j'} + \\
&\qquad\qquad + \frac{1}{2}\, X^{(\nu)}_{ij} B^{*}_{iji'j'} Y^{(\nu')\,*}_{i'j'} \Big]\, Q^{+}_{\nu'} + \\
&+\sum_{\nu\nu'} Q_{\nu} \sum_{ijj'i'} \Big[Y^{(\nu)}_{ij} A_{iji'j'} X^{(\nu')}_{i'j'} + \frac{1}{2}\, Y^{(\nu)}_{ij} B_{iji'j'} Y^{(\nu')}_{i'j'} + \\
&\qquad\qquad + \frac{1}{2}\, X^{(\nu)}_{ij} B^{*}_{iji'j'} X^{(\nu')}_{i'j'} \Big]\, Q_{\nu'} + \\
&+\sum_{\nu\nu'} Q^{+}_{\nu} \sum_{ijj'i'} \Big[X^{(\nu)\,*}_{ij} A_{iji'j'} Y^{(\nu')\,*}_{i'j'} + \frac{1}{2}\, X^{(\nu)\,*}_{ij} B_{iji'j'} X^{(\nu')\,*}_{i'j'} + \\
&\qquad\qquad + \frac{1}{2}\, Y^{(\nu)\,*}_{ij} B^{*}_{iji'j'} Y^{(\nu')\,*}_{i'j'} \Big]\, Q_{\nu'} = \\
&= \boxed{\begin{array}{c} \text{because} \\ A_{iji'j'} = A^{+}_{iji'j'} = A^{*}_{i'j'ij} \end{array}} = \\
&= E_{BCS} + \\
&+\frac{1}{2} \sum_{\nu\nu'} Q^{+}_{\nu} \sum_{ijj'i'} \Big[X^{(\nu)\,*}_{ij} A_{iji'j'} X^{(\nu')}_{i'j'} + X^{(\nu)\,*}_{ij} B_{iji'j'} Y^{(\nu')}_{i'j'} + \\
&\qquad + \quad X^{(\nu)\,*}_{ij} A_{i'j'ij} X^{(\nu')}_{i'j'} + Y^{(\nu)\,*}_{ij} B^{*}_{iji'j'} X^{(\nu')}_{i'j'} \Big]\, Q_{\nu'} +
\end{aligned}
$$

$$+\frac{1}{2}\sum_{\nu\nu'}Q_\nu\sum_{iji'j'}\big[Y^{(\nu)}_{ij}A_{iji'j'}Y^{(\nu')*}_{i'j'}+Y^{(\nu)}_{ij}B_{iji'j'}X^{(\nu')*}_{i'j'}+$$
$$+\;Y^{(\nu)}_{ij}A_{i'j'ij}Y^{(\nu')*}_{i'j'}+X^{(\nu)}_{ij}B^{*}_{iji'j'}Y^{(\nu')*}_{i'j'}\big]\,Q^{+}_{\nu'}\;+$$
$$+\frac{1}{2}\sum_{\nu\nu'}Q_\nu\sum_{iji'j'}\big[Y^{(\nu)}_{ij}A_{iji'j'}X^{(\nu')}_{i'j'}+Y^{(\nu)}_{ij}B_{iji'j'}Y^{(\nu')}_{i'j'}+$$
$$+\quad Y^{(\nu)}_{ij}A_{i'j'ij}X^{(\nu')}_{i'j'}+X^{(\nu)}_{ij}B^{*}_{iji'j'}X^{(\nu')}_{i'j'}\big]\,Q_{\nu'}\;+$$
$$+\frac{1}{2}\sum_{\nu\nu'}Q^{+}_\nu\sum_{iji'j'}\big[X^{(\nu)*}_{ij}A_{iji'j'}Y^{(\nu')*}_{i'j'}+X^{(\nu)*}_{ij}B_{iji'j'}X^{(\nu')*}_{i'j'}+$$
$$+\;X^{(\nu)*}_{ij}A_{i'j'ij}Y^{(\nu')*}_{i'j'}+Y^{(\nu)*}_{ij}B^{*}_{iji'j'}Y^{(\nu')*}_{i'j'}\big]\,Q^{+}_{\nu'}\;=$$

$$=\boxed{\begin{array}{c}\text{using (7.229) and complex conjugated (7.229) :}\\ \sum_{i'j'}\left(A^{*}_{iji'j'}X^{(\nu)*}_{i'j'}+B^{*}_{iji'j'}Y^{(\nu)*}_{i'j'}=\hbar\omega_\nu\,X^{(\nu)*}_{i'j'}\right.\\ \sum_{i'j'}\left(B_{iji'j'}X^{(\nu)*}_{i'j'}+A^{*}_{iji'j'}Y^{(\nu)*}_{i'j'}=-\hbar\omega_\nu\,X^{(\nu)*}_{i'j'}\right.\end{array}}=$$

$$=E_{BCS}+$$
$$+\frac{1}{2}\sum_{\nu\nu'}Q^{+}_\nu\sum_{ij}\left\{X^{(\nu)*}_{ij}\hbar\omega_{\nu'}X^{(\nu')}_{ij}+X^{(\nu)*}_{ij}\hbar\omega_{\nu'}X^{(\nu')}_{ij}\right\}Q_{\nu'}+$$
$$+\frac{1}{2}\sum_{\nu\nu'}Q_\nu\sum_{ij}\left\{-Y^{(\nu)}_{ij}\hbar\omega_{\nu'}Y^{(\nu')*}_{ij}-Y^{(\nu)}_{ij}\hbar\omega_{\nu'}Y^{(\nu')*}_{ij}\right\}Q^{+}_{\nu'}+$$
$$+\frac{1}{2}\sum_{\nu\nu'}Q_\nu\sum_{ij}\left\{Y^{(\nu)}_{ij}\hbar\omega_{\nu'}X^{(\nu')}_{ij}-Y^{(\nu)}_{ij}\hbar\omega_{\nu'}X^{(\nu')}_{ij}\right\}Q_{\nu'}+$$
$$+\frac{1}{2}\sum_{\nu\nu'}Q^{+}_\nu\sum_{ij}\left\{-X^{(\nu)}_{ij}\hbar\omega_{\nu'}Y^{(\nu')*}_{ij}-X^{(\nu)}_{ij}\hbar\omega_{\nu'}Y^{(\nu')*}_{ij}\right\}Q_{\nu'}=$$

$$=\boxed{\begin{array}{c}\text{because } Q_\nu Q^{+}_{\nu'}=\delta_{\nu\nu'}+Q^{+}_{\nu'}Q_\nu\\ \text{and (7.252)}\end{array}}=$$
$$=E_{BCS}-\sum_\nu\hbar\omega_\nu\sum_{ij}|Y^{(\nu)}_{ij}|^2+\sum_\nu\hbar\omega_\nu\,Q^{+}_\nu Q_\nu\equiv$$
$$\equiv E_{RPA}+\sum_\nu\hbar\omega_\nu\,Q^{+}_\nu Q_\nu \qquad (7.270)$$

where we introduced energy E_{RPA} of the vacuum of the RPA phonons

$$E_{RPA} = \langle RPA|\hat{H}_{RPA}|RPA\rangle = \\ = E_{BCS} - \sum_{\nu} \hbar\omega_{\nu} \sum_{ij} |Y_{ij}^{(\nu)}|^2 \qquad (7.271)$$

and E_{BCS} is given by (7.264).

From (7.270) it can be easily seen that the RPA Hamiltonian $\hat{H}_{RPA}$ has the form of the sum of harmonic oscillators. Therefore the RPA is often knows as the harmonic oscillator approximation with phonons as the oscillator quanta. Using the standard quantum mechanics formalism for harmonic oscillator instead of the phonon operators Q_{ν}^{+}, Q_{ν} (oscillator quanta) we can introduce the generalized coordinate operators $\mathscr{X}_{\nu}$ and conjugated linear momenta $\mathscr{P}_{\nu}$ ($\mathscr{X}_{\nu}^{+} = \mathscr{X}_{\nu}$, $\mathscr{P}_{\nu}^{+} = \mathscr{P}_{\nu}$)

$$\mathscr{P}_{\nu} \equiv \frac{\hbar}{i}\sqrt{\frac{M_{\nu}\,\omega_{\nu}}{2\hbar}}\left(Q_{\nu} - Q_{\nu}^{+}\right) \quad , \quad \mathscr{X}_{\nu} \equiv \sqrt{\frac{\hbar}{2\,M_{\nu}\,\omega_{\nu}}}\left(Q_{\nu} + Q_{\nu}^{+}\right) \qquad (7.272)$$

or inversely

$$Q_{\nu} = \sqrt{\frac{M_{\nu}\,\omega_{\nu}}{2\hbar}}\,\mathscr{X}_{\nu} + \frac{i}{\sqrt{2\,\hbar\,M_{\nu}\,\omega_{\nu}}}\,\mathscr{P}_{\nu} \quad , \\ Q_{\nu}^{+} = \sqrt{\frac{M_{\nu}\,\omega_{\nu}}{2\hbar}}\,\mathscr{X}_{\nu} - \frac{i}{\sqrt{2\,\hbar\,M_{\nu}\,\omega_{\nu}}}\,\mathscr{P}_{\nu} \qquad (7.273)$$

Then the quasi-boson commutation relations, $[Q_{\nu},\, Q_{\nu'}^{+}] = \delta_{\nu\nu'}$, $[Q_{\nu},\, Q_{\nu'}] = 0$, are equivalent to the standard "coordinate - momentum" commutation relations:

$$\left[\mathscr{X}_{\nu},\, \mathscr{P}_{\nu'}\right] = i\hbar\,\delta_{\nu\nu'} \;, \quad \left[\mathscr{X}_{\nu},\, \mathscr{X}_{\nu'}\right] = 0 \;, \quad \left[\mathscr{P}_{\nu},\, \mathscr{P}_{\nu'}\right] = 0 \qquad (7.274)$$

and the expression (7.270) for the RPA Hamiltonian $\hat{H}_{RPA}$ can be rewritten as follows

$$\hat{H}_{RPA} = E_{RPA} - \frac{1}{2}\sum_{\nu}\hbar\omega_{\nu} + \sum_{\nu}\left(\frac{\mathscr{P}_{\nu}^{2}}{2\,M_{\nu}} + \frac{1}{2}\,M_{\nu}\,\omega_{\nu}^{2}\,\mathscr{X}_{\nu}^{2}\right) \qquad (7.275)$$

In (7.272) - (7.275) the mass parameter M_{ν} for each RPA solution ν is arbitrary in this moment. The RPA equations (7.230) can be now written as the oscillator equations:

$$\begin{array}{lcl} \left[\hat{H}_{RPA},\, Q_{\nu}^{+}\right] = \hbar\,\omega_{\nu}Q_{\nu}^{+} & & \left[\hat{H}_{RPA},\, \mathscr{P}_{\nu}\right] = i\,\hbar\,M_{\nu}\,\omega_{\nu}^{2}\,\mathscr{X}_{\nu} \\ \left[\hat{H}_{RPA},\, Q_{\nu}\right] = -\,\hbar\,\omega_{\nu}Q_{\nu} & \Leftrightarrow & \left[\hat{H}_{RPA},\, \mathscr{X}_{\nu}\right] = -\dfrac{i\,\hbar}{M_{\nu}}\,\mathscr{P}_{\nu} \\ \left[Q_{\nu},\, Q_{\nu'}^{+}\right] = \delta_{\nu\nu'} & & \left[\mathscr{X}_{\nu},\, \mathscr{P}_{\nu'}\right] = i\hbar\,\delta_{\nu\nu'} \end{array} \qquad (7.276)$$

In the framework of the quasi-boson approximation the generalized coordinates and linear momenta are expressed in terms of the quasi-boson operators b_{ij}^{+} and b_{ij} as follows

$$\mathscr{P}_{\nu} = \sum_{ij} \left(\mathscr{P}_{ij}^{(\nu)} \, b_{ij}^{+} + \mathscr{P}_{ij}^{(\nu)\,*} \, b_{ij} \right) \quad , \qquad \mathscr{P}_{ij}^{(\nu)} = -\mathscr{P}_{ji}^{(\nu)}$$
$$\mathscr{X}_{\nu} = \sum_{ij} \left(\mathscr{X}_{ij}^{(\nu)} \, b_{ij}^{+} + \mathscr{X}_{ij}^{(\nu)\,*} \, b_{ij} \right) \quad , \qquad \mathscr{X}_{ij}^{(\nu)} = -\mathscr{X}_{ji}^{(\nu)} \tag{7.277}$$

The substitution of (7.277) into (7.273) and subsequent comparison with (7.268) gives the relation between amplitudes $\mathscr{X}_{ij}^{(\nu)}$, $\mathscr{P}_{ij}^{(\nu)}$ and $X_{ij}^{(\nu)}$, $Y_{ij}^{(\nu)}$

$$\mathscr{P}_{ij}^{(\nu)} = i \sqrt{\frac{\hbar \, M_{\nu} \, \omega_{\nu}}{2}} \left(X_{ij}^{(\nu)} + Y_{ij}^{(\nu)\,*} \right)$$
$$\mathscr{X}_{ij}^{(\nu)} = \sqrt{\frac{\hbar}{2 \, M_{\nu} \, \omega_{\nu}}} \left(X_{ij}^{(\nu)} - Y_{ij}^{(\nu)\,*} \right)$$

or inversely

$$X_{ij}^{(\nu)} = \sqrt{\frac{M_{\nu} \, \omega_{\nu}}{2\hbar}} \, \mathscr{X}_{ij}^{(\nu)} - \frac{i}{\sqrt{2\hbar \, M_{\nu} \, \omega_{\nu}}} \, \mathscr{P}_{ij}^{(\nu)}$$
$$Y_{ij}^{(\nu)} = -\sqrt{\frac{M_{\nu} \, \omega_{\nu}}{2\hbar}} \, \mathscr{X}_{ij}^{(\nu)\,*} + \frac{i}{\sqrt{2\hbar \, M_{\nu} \, \omega_{\nu}}} \, \mathscr{P}_{ij}^{(\nu)\,*} \tag{7.278}$$

Then the RPA equations (7.276) can be expressed (analogy with (7.230))

$$\begin{pmatrix} A & B \\ B^{*} & A^{*} \end{pmatrix} \begin{pmatrix} \mathscr{P}^{(\nu)} \\ -\mathscr{P}^{(\nu)\,*} \end{pmatrix} = i \, \hbar \, \omega_{\nu}^{2} \, M_{\nu} \begin{pmatrix} \mathscr{X}^{(\nu)} \\ \mathscr{X}^{(\nu)\,*} \end{pmatrix}$$
$$\begin{pmatrix} A & B \\ B^{*} & A^{*} \end{pmatrix} \begin{pmatrix} \mathscr{X}^{(\nu)} \\ -\mathscr{X}^{(\nu)\,*} \end{pmatrix} = \frac{\hbar}{i} \, \frac{1}{M_{\nu}} \begin{pmatrix} \mathscr{P}^{(\nu)} \\ \mathscr{P}^{(\nu)\,*} \end{pmatrix} \tag{7.279}$$

The normalization of one-column vectors $\mathscr{X}^{(\nu)}$ and $\mathscr{P}^{(\nu)}$ is given by (7.276), $[\mathscr{X}_{\nu}, \, \mathscr{P}_{\nu'}] = i\hbar \, \delta_{\nu\nu'}$, which explicitly gives

$$\left[\mathscr{X}_{\nu}, \, \mathscr{P}_{\nu'} \right] =$$
$$= \frac{1}{2} \sum_{ij \, i'j'} \left[\mathscr{X}_{ij}^{(\nu)} \, b_{ij}^{+} \, + \, \mathscr{X}_{ij}^{(\nu)\,*} \, b_{ij} \, , \, \mathscr{P}_{i'j'}^{(\nu')} \, b_{i'j'}^{+} \, + \, \mathscr{P}_{i'j'}^{(\nu')\,*} \, b_{i'j'} \right] =$$
$$= \frac{1}{2} \sum_{ij \, i'j'} \left\{ \mathscr{X}_{ij}^{(\nu)\,*} \, \mathscr{P}_{i'j'}^{(\nu')} \left[b_{ij} \, , \, b_{i'j'}^{+} \right] \, + \, \mathscr{X}_{ij}^{(\nu)} \, \mathscr{P}_{i'j'}^{(\nu')\,*} \left[b_{ij}^{+} \, , \, b_{i'j'} \right] \right\} =$$

$$= \frac{1}{2} \sum_{ij\, i'j'} \left(\mathscr{X}^{(\nu)\,*}_{ij}\, \mathscr{P}^{(\nu')}_{i'j'} \; - \; \mathscr{X}^{(\nu)}_{ij}\, \mathscr{P}^{(\nu')\,*}_{i'j'} \right) \left(\delta_{ii'}\delta_{jj'} - \delta_{ij'}\delta_{ji'} \right) =$$

$$= \sum_{ij} \left(\mathscr{X}^{(\nu)\,*}_{ij}\, \mathscr{P}^{(\nu')}_{ij} \; - \; \mathscr{X}^{(\nu)}_{ij}\, \mathscr{P}^{(\nu')\,*}_{ij} \right) =$$

$$= \left(\mathscr{X}^{(\nu)\,+}\, \mathscr{P}^{(\nu')} \; - \; \mathscr{X}^{(\nu)\,T}\, \mathscr{P}^{(\nu')\,*} = i\,\hbar\; \delta_{\nu\nu'} \right. \tag{7.280}$$

where $\mathscr{X}^{(\nu)}$ and $\mathscr{P}^{(\nu)}$ (with only upper indexes and without lower indexes) are one-column matrices constructed from the amlitudes $\mathscr{X}^{(\nu)}_{ij}$ and $\mathscr{P}^{(\nu)}_{ij}$ as their elements, respectively.

The RPA ground state $|RPA\rangle$ is defined as the vacuum for phonons (see (7.208))

$$Q_\nu \, |RPA\rangle = 0 \qquad\qquad \text{for all } \nu \tag{7.281}$$

We can construct it from the BCS ground state $|BCS\rangle$ using Thouless theorem (see Subsection B.5 where the Thouless theorem is proved for two different vacua of the fermion system; it can be proved also for the case of the phonon $|RPA\rangle$ and the quasiparticle $|BCS\rangle$ vacua - see [9] for details):

$$|RPA\rangle = N_0 \, e^{\hat{Z}} \, |BCS\rangle \tag{7.282}$$

where

$$\hat{Z} = \frac{1}{2} \sum_{ijkl} Z_{ijkl}\, b^{+}_{ij} b_{kl}$$

and N_0 is the normalization factor. It can be shown (see [9]) that

$$Z_{ijkl} = \left(Y^{*}\, X^{-1\,*} \right)_{ijkl} = \sum_{(\nu)} Y^{(\nu)\,*}_{ij}\, X^{(\nu)\,*\,-1}_{kl} \tag{7.283}$$

The RPA ground state energy E_{RPA},

$$\hat{H} \, |RPA\rangle = E_{RPA} \, |RPA\rangle \quad , \tag{7.284}$$

is given by (7.271), where it can be seen that E_{RPA} is always lower than E_{BCS}. The reason for it is that the RPA takes into account higher correlation than the BCS.

Further we consider a possible spontaneous symmetry breaking of the total Hamiltonian $\hat{H}$ by the BCS mean field Hamiltonian $\hat{H}_{BCS}$ ($\hat{H}$ =

$\langle BCS|\ \hat{H}\ |BCS\rangle + \hat{H}_{BCS} + \hat{V}_{res}$ - see (7.203)) and the corresponding occurrence of the spurious modes among the solutions of the RPA equations. Let us suppose that the nucleus Hamiltonian $\hat{H}$ fulfills the symmetry generated by means of some one-body operator $\hat{P}_0$. By other words it means that [16]

$$\left[\hat{H},\ \hat{P}_0\right] = 0 \tag{7.285}$$

We should expect that this symmetry is fulfilled also in the framework of the RPA (that means in the framework of the quasi-boson approximation):

$$\left[\hat{H}_{RPA},\ \hat{P}_0\right] = 0 \tag{7.286}$$

If we compare equation (7.286) with the RPA equations (7.276), namely with: $[\hat{H}_{RPA},\ \hat{P}_0] = i\hbar\ M_\nu\ \omega^2\ \mathscr{X}_\nu$, we can identify the operator $\hat{P}_0$ with the operator $\hat{\mathscr{P}}_0$ of the generalized linear momentum with the zero energy $\hbar\omega_0 \equiv \hbar\omega_{\nu=0} = 0$. Then the equations (7.279) for this particular RPA solution $(\mathscr{X}_0,\ \mathscr{P}_0 = P_0)$ reads

$$\begin{pmatrix} A & B \\ B^* & A^* \end{pmatrix} \begin{pmatrix} \mathscr{P}^{(0)} \\ -\mathscr{P}^{(0)\,*} \end{pmatrix} = 0$$
$$\begin{pmatrix} A & B \\ B^* & A^* \end{pmatrix} \begin{pmatrix} \mathscr{X}^{(0)} \\ -\mathscr{X}^{(0)\,*} \end{pmatrix} = \frac{\hbar}{i}\,\frac{1}{M_0} \begin{pmatrix} \mathscr{P}^{(0)} \\ \mathscr{P}^{(0)\,*} \end{pmatrix} \tag{7.287}$$

From (7.287) the expression for $1/M_0$ can be obtained:

$$\left(\mathscr{X}^{(0)\,+} - \mathscr{X}^{(0)\,T}\right) \begin{pmatrix} A & B \\ B^* & A^* \end{pmatrix} \begin{pmatrix} \mathscr{X}^{(0)} \\ -\mathscr{X}^{(0)\,*} \end{pmatrix} =$$
$$= \frac{\hbar}{i}\,\frac{1}{M_0} \left(\mathscr{X}^{(0)\,+} - \mathscr{X}^{(0)\,T}\right) \begin{pmatrix} \mathscr{P}^{(0)} \\ \mathscr{P}^{(0)\,*} \end{pmatrix} =$$
$$= \boxed{\begin{array}{c} \text{because - see (7.280)}\ :\ \left(\mathscr{X}^{(0)\,+} - \mathscr{X}^{(0)\,T}\right) \begin{pmatrix} \mathscr{P}^{(0)} \\ \mathscr{P}^{(0)\,*} \end{pmatrix} = \\ = \mathscr{X}^{(0)\,+}\,\mathscr{P}^{(0)} - \mathscr{X}^{(0)\,T}\,\mathscr{P}^{(0)\,*} = i\hbar \end{array}} =$$
$$= \frac{\hbar^2}{M_0}$$

So we have

$$\frac{\hbar^2}{M_0} = \left(\mathscr{X}^{(0)\,+} - \mathscr{X}^{(0)\,T}\right) \begin{pmatrix} A & B \\ B^* & A^* \end{pmatrix} \begin{pmatrix} \mathscr{X}^{(0)} \\ -\mathscr{X}^{(0)\,*} \end{pmatrix} \tag{7.288}$$

[16] In the real situations the operator $\hat{P}_0$ can be identified with the total linear momentum of the nucleus in the case of the translation invariance or with the components of the total angular momentum in the case of the rotational invariance of the total Hamiltonian.

Without loosing a generality we can suppose that $\mathscr{X}^{(0)}_{ij}$ is real. Then, because of (7.280), the corresponding $\mathscr{P}^{(0)}_{ij}$ should be purely imaginary. Then the expression (7.288) can be rewritten as follows

$$M_0 = 2\,\mathscr{P}^{(0)\,+}\,\frac{1}{A-B}\,\mathscr{P}^{(0)} \tag{7.289}$$

where A, B are matrices involved in the RPA equation (see (7.234), (7.234)). This can be easily proved:

$$\begin{aligned}
&\frac{\hbar^2}{M_0} = \boxed{\begin{array}{c}\text{see}\\(7.288)\end{array}} = \\
&= \mathscr{X}^{(0)\,+} A \mathscr{X}^{(0)} - \mathscr{X}^{(0)\,+} B \mathscr{X}^{(0)\,*} \\
&\qquad\qquad - \mathscr{X}^{(0)\,T} B^* \mathscr{X}^{(0)} + \mathscr{X}^{(0)\,T} A^* \mathscr{X}^{(0)\,*} = \\
&= \boxed{\begin{array}{c}\mathscr{X}_0 \text{ is supposed to be real and the phases of the wave}\\ \text{function are chosen in order the matrices } A \text{ and } B \text{ are real}\end{array}} = \\
&= 2\left(\mathscr{X}^{(0)\,T} A \mathscr{X}^{(0)} - \mathscr{X}^{(0)\,T} B \mathscr{X}^{(0)}\right) = 2\,\mathscr{X}^{(0)\,T}\big(A-B\big)\,\mathscr{X}^{(0)}
\end{aligned}$$

So

$$\begin{aligned}
M_0 &= \frac{\hbar^2}{2}\,\frac{1}{\mathscr{X}^{(0)}\,(A-B)\,\mathscr{X}^{(0)\,T}} = \\
&= \frac{\hbar^2}{2}\,\frac{\left(\mathscr{P}^{(0)\,+} - \mathscr{P}^{(0)\,T}\right)\,\left(\mathscr{P}^{(0)} - \mathscr{P}^{(0)\,*}\right)}{\left(\mathscr{P}^{(0)\,+} - \mathscr{P}^{(0)\,T}\right)\,\mathscr{X}^{(0)}\,(A-B)\mathscr{X}^{(0)\,T}\,\left(\mathscr{P}^{(0)} - \mathscr{P}^{(0)\,*}\right)} = \\
&= \boxed{\begin{array}{c}\text{because - see (7.280) and } \mathscr{X}^{(0)} \text{ are real :}\\ \mathscr{X}^{(0)\,T}\left(\mathscr{P}^{(0)} - \mathscr{P}^{(0)\,*}\right) = -\left(\mathscr{P}^{(0)\,+} - \mathscr{P}^{(0)\,T}\right)\mathscr{X}^{(0)} = i\hbar\end{array}} = \\
&= \frac{1}{2}\big(\mathscr{P}^{(0)\,+} - \mathscr{P}^{(0)\,T}\big)\,\frac{1}{A-B}\,\left(\mathscr{P}^{(0)} - \mathscr{P}^{(0)\,*}\right) = \\
&= \boxed{\begin{array}{c}\text{because } \mathscr{P}^{(0)}\\ \text{is purely imaginary}\end{array}} = 2\,\mathscr{P}^{(0)\,+}\,\frac{1}{A-B}\,\mathscr{P}^{(0)}
\end{aligned} \tag{7.290}$$

and the expression (7.289) is proved.

So, if among the RPA solutions ν of the Hamiltonian $\hat{H}$ there is one, $\nu = 0$, with the zero energy then the RPA Hamiltonian (7.275) can be rewritten

as follows

$$\hat{H}_{RPA} = E_{RPA} - \frac{1}{2}\sum_{\nu>0}\hbar\omega_\nu + \sum_{\nu>0}\left(\frac{\mathscr{P}_\nu^2}{2M_\nu} + \frac{1}{2}\,M_\nu\,\omega_\nu^2\,\mathscr{X}_\nu^2\right) + \frac{P_0^2}{2M_0} =$$

$$= E_{RPA} + \sum_{\nu>0}\hbar\omega_\nu\,Q_\nu^+ Q_\nu + \frac{P_0^2}{2M_0} \tag{7.291}$$

In practice usually the symmetry operator $\hat{\vec{P}}_0$ is represented by the total linear momentum of the nucleus (translation symmetry of the total Hamiltonian) or by the total angular momentum $\hat{\vec{I}}$ of the nucleus (rotational symmetry of the total Hamiltonian). Both these cases are discussed further.

Translation symmetry ($\hat{P}_0$ is the operator of the total linear momentum component)

The total linear momentum $\hat{P}_0$ (here we assume that $\hat{P}_0$ is one of the component of the linear momentum) is conjugated to the corresponding center of mass coordinate $\hat{X}_0$:

$$\left[\hat{X}_0,\,\hat{P}_0\right] = i\hbar \tag{7.292}$$

The definition of the center of mass coordinate $\hat{X}_0$ corresponds to (m is the nucleon mass)

$$\left[\hat{H},\,\hat{X}_0\right] = \frac{-i\hbar}{Am}\,\hat{P}_0 \tag{7.293}$$

So we have

$$\left[\hat{X}_0,\,\left[\hat{H},\,\hat{X}_0\right]\right] = -\frac{i\hbar}{Am}\left[\hat{X}_0,\,\hat{P}_0\right] = \frac{\hbar^2}{Am} \tag{7.294}$$

From the other side the expression (7.291) gives for the quasi-boson approximation (RPA)

$$\left[\hat{X}_0,\,\left[\hat{H}_{RPA},\,\hat{X}_0\right]\right] = \boxed{\begin{array}{c}\text{because}\\ \left[\hat{X}_0,\,Q_\nu\right] = \left[\hat{P}_0,\,Q_\nu\right] = 0 \text{ for all } \nu \neq 0\end{array}} =$$

$$= \left[\hat{X}_0,\,\left[\frac{\hat{P}_0^2}{2M_0},\,\hat{X}_0\right]\right] = \frac{\hbar^2}{M_0} \tag{7.295}$$

and the comparison of (7.294) with (7.295) gives the mass parameter M_0 (in the framework of the RPA)

$$M_0 \approx Am \tag{7.296}$$

Rotation symmetry ($\hat{P}_0$ is the operator of the total angular momentum component)

Let us suppose that $\hat{P}_0$ is the 1-st component of the total angular momentum, $\hat{P}_0 = \hat{I}_1$. Then the conjugated coordinate tp $\hat{P}_0 = \hat{I}_1$ is the angle θ_1 of the rotation round the 1-st axis:

$$\left[\hat{\theta}_1,\ \hat{I}_1\right] = i \tag{7.297}$$

The corresponding mass parameter M_0 is now represented by the 1-st principal component $\mathscr{F}_1$ of the moment of inertia tensor (we suppose the intrinsic frame axes coincide with the principal axes of the tensor of the moment of inertia). So according to (7.290) we have

$$\begin{aligned}
\mathscr{F}_1 &= 2\sum_{ij\,i'j'}(I_1^*)_{ij}\,\frac{1}{(A-B)_{ij\,i'j'}}\,(I_1)_{i'j'} = \\
&= 2\sum_{ij\,i'j'}(I_1^*)_{ij}\,\frac{1}{\left(E_i+E_j\right)\delta_{ii'}\delta_{jj'} + 4\,H^{22}_{ij\,i'j'} - 24\,H^{40}_{ij\,i'j'}}\,(I_1)_{i'j'} = \\
&= \boxed{\begin{array}{c}\text{if we neglect terms}\\ \text{with } H^{22}_{ij\,i'j'} \text{ and } H^{40}_{ij\,i'j'}\end{array}} = 2\sum_{ij}(I_1^*)_{ij}\,\frac{1}{E_i+E_j}\,(I_1)_{ij}
\end{aligned} \tag{7.298}$$

where $(I_1)_{ij} = \langle BCS|\ \alpha_j\alpha_i\hat{I}_1\ |BCS\rangle = \langle BCS|\ \hat{I}_1\alpha_i^+\alpha_j^+\ |BCS\rangle$ is the two-quasiparticle matrix element of the operator $\hat{I}_1$ which can be expressed in terms of the single-particle matrix element and pairing amplitudes $\mathscr{U}_i$, $\mathscr{V}_i$ (see Appendix L). If we do it we obtain the 1-st principal component of the moment of inertia in the following form

$$\mathscr{F}_1 = 2\hbar^2\sum_{ij>0}\frac{|(\mathscr{U}_i\mathscr{V}_j - \mathscr{U}_j\mathscr{V}_i)|^2\ |\langle i|\ \hat{I}_1\ |j\rangle|^2}{E_i+E_j} \tag{7.299}$$

The expression (7.299) is well-known Belyaev formula for the moment of inertia (see [151, 152]).The rotation of nuclei will be discussed in details in the Chapter 8, including the moment of inertia.

Expressions (7.298) can be also expressed not in terms of the 2-qp matrix elements but in terms of the one- phonon matrix elements, as is described

below,

$$\mathscr{F} = 2 \sum_{ij\, i'j'} (\hat{I}_1^*)_{ij} \frac{1}{(A-B)_{ij\, i'j'}} (I_1)_{i'j'} =$$

$$= 2 \sum_{ij\, i'j'} \langle BCS| \hat{I}_1 |ij\rangle \frac{1}{(A-B)_{ij\, i'j'}} \langle i'j'| \hat{I}_1 |BCS\rangle =$$

$$= \boxed{\begin{array}{l} \text{we use the approximations } E_{RPA} = 0 \text{ and } |BCS\rangle \approx |BCS\rangle_B \text{ in (7.264)} \\ A_{ij\, i'j'} = \langle BCS| \, [b_{ij} \, , \, [\hat{H}_{RPA}, b^+_{i'j'}]] \, |BCS\rangle = \langle BCS| \, b_{ij} \, \hat{H}_{RPA} \, b^+_{i'j'} \, |BCS\rangle \\ B_{ij\, i'j'} = - \langle BCS| \, [b_{ij} \, , \, [\hat{H}_{RPA}, b_{i'j'}]] \, |BCS\rangle \approx 0 \end{array}} =$$

$$= 2 \sum_{ij\, i'j'} \sum_{\nu\nu'} \langle BCS| \hat{I}_1 |\nu\rangle\langle\nu|ij\rangle \frac{1}{\langle ij| \hat{H}_{RPA} |i'j'\rangle} \langle i'j'|\nu'\rangle\langle\nu'| \hat{I}_1 |BCS\rangle =$$

$$= 2 \sum_{\nu\nu'} \langle BCS| \hat{I}_1 |\nu\rangle \frac{1}{\langle\nu| \sum_{\nu''} \hbar\omega_{\nu''} Q^+_{\nu''} Q_{\nu''} |\nu'\rangle} \langle\nu'| \hat{I}_1 |BCS\rangle =$$

$$= 2 \sum_{\nu} \langle BCS| \hat{I}_1 |\nu\rangle \frac{1}{\hbar\omega_\nu} \langle\nu| \hat{I}_1 |BCS\rangle = 2 \sum_{\nu} (I_1^*)_\nu \frac{1}{\hbar\omega_\nu} (I_1)_\nu \qquad (7.298')$$

where $(I_1)_\nu = \langle RPA| \, Q_\nu \hat{I}_1 \, |RPA\rangle$. The expression (7.298') is known as the Thoulless-Valatin moment of inertia (see e.g the expr. (8.142) in [9]).

The other symmetry operator, often met in parctice, is the number of particle operator. Every such symmetry operator commuting with the RPA Hamiltonian to zero, represents a zero energy RPA solution which is, from the point of view of the intrinsic degrees of freedom, spurious (unphysical).

7.3.1.1.3 Separable form of the RPA equation RPA equations have very simple form in the case when the effective nucleon-nucleon interactions are in the separable form of the product of two single-particle operators. For instance this is the case when the nucleon-nucleon interaction in the nuclear Hamiltonian is assumed to be decomposed into the multipole-multipole and spin-multipole - spin-multipole terms (see (1.55)). Such decompositions were used often in the past and the importance of this approach has persisted up to now. The separable form of the effective nucleon-nucleon interaction enables to show also in the clear way the connection between used effective nucleon-nucleon interaction and the mean field with corresponding residual interactions.

In order to show the simplicity of the RPA approach with the separable nucleon-nucleon interaction we start with the nuclear Hamiltonian in the following form

$$\hat{H}_{intr} = \hat{T} - \frac{1}{2}\sum_{\tau\tau'}\sum_{kk'} \kappa_{k\tau\, k'\tau'}\, \hat{Z}_{k\tau}\, \hat{Z}_{k'\tau'} \tag{7.300}$$

where $\hat{Z}_{k\tau}$ $(k = 1, \cdots, N_{op})$ is the ensemble of the Hermitian single-particle operators with their proton and neutron parts ($\tau = prot,\ neut$) and $\kappa_{k\tau\, k'\tau'}$ are corresponding strength constants forming the symmetric matrix κ. In the past (in the 60-80 ties) operators $\hat{Z}_{k\tau}$ were represented by symmetrized Hermitian multipoles or spin-multipoles and constants $\kappa_{k\tau\, k'\tau'}$ were obtained by the fitting procedure in order to describe selected properties of selected nuclei (see e.g. [7, 8] and the citation therein). In the present time the separable form (7.300) can be obtained by microscopic linear response theory approach (see e.g. [154, 153]) starting from the known effective nucleon-nucleon interaction. The separable form of the residual interaction is obtained in the microscopic approaches [154, 153] directly from the effective nucleon-nucleon interaction (e.g. Skyrme- type effective interaction) without any introduction of new free parameters. That means these approaches do not bring new parameters and the nuclear Hamiltonian is determined only by used effective nucleon-nucleon interaction.

Further we assume the single-particle operators $\hat{Z}_k$ in (7.300) are hermitian operators with the following symmetries

$$\begin{aligned}
&\mathscr{T}^{-1}\hat{Z}_k\mathscr{T} = \gamma_T^{(Z_k)}\, \hat{Z}_k && \gamma_T^{(X_k)} = \pm 1 \\
&\langle i|\hat{Z}_k|j\rangle^* = \gamma_c^{(Z_k)}\, \langle i|\hat{Z}_k|j\rangle && \gamma_c^{(X_k)} = \pm 1 \\
&\hat{Z}_k^+ = \hat{Z}_k &&
\end{aligned} \tag{7.301}$$

In the Appendix L it is shown that such operators can be expressed in terms of the creation and annihilation quasiparticle operators α_i^+, α_i as follows (see (L.5))

$$\hat{Z} = \langle BCS|\hat{Z}|BCS\rangle + \hat{Z}^{(1)} + \hat{Z}^{(2)} \tag{7.302}$$

where $\hat{Z}^{(1)}$ are terms involving two creation or two annihilation quasiparticle operators ($\alpha^+\alpha^+$- or $\alpha\alpha$- type terms) and $\hat{Z}^{(2)}$ involves terms with one creation and one annihilation quasiparticle operators ($\alpha^+\alpha$- type terms) - see (L.6) for detailed expressions.

The substitution of (7.302) into (7.300) gives the Hamiltonian in the fol-

lowing form

$$\hat{H}_{intr} = \hat{T} - \frac{1}{2}\sum_{\tau\tau'}\sum_{kk'}\kappa_{k\tau\,k'\tau'}\left(\langle BCS|\hat{Z}_{k\tau}|BCS\rangle + \hat{Z}^{(1)}_{k\tau} + \hat{Z}^{(2)}_{k\tau}\right)\cdot$$
$$\left(\langle BCS|\hat{Z}_{k'\tau'}|BCS\rangle + \hat{Z}^{(1)}_{k'\tau'} + \hat{Z}^{(2)}_{k'\tau'}\right) =$$
$$= \hat{H}_{BCS} + \hat{V}_{RES} \tag{7.303}$$

where

$$\hat{H}_{BCS} = \hat{T} - \frac{1}{2}\sum_{\tau\tau'}\sum_{kk'}\kappa_{k\tau\,k'\tau'}\Big(- \langle BCS|\hat{Z}_{k\tau}|BCS\rangle\,\langle BCS|\hat{Z}_{k'\tau'}|BCS\rangle + $$
$$+\ \langle BCS|\hat{Z}_{k\tau}|BCS\rangle\,\hat{Z}_{k'\tau'} + \ \hat{Z}_{k\tau}\,\langle BCS|\hat{Z}_{k'\tau'}|BCS\rangle\Big) \tag{7.304}$$

is the quasiparticle BCS mean field (the single-quasiparticle operator involving only terms of the $\alpha^+\alpha$ type and/or c- numbers) and

$$\hat{V}_{RES} = -\frac{1}{2}\sum_{kk'}\kappa_{k\tau\,k'\tau'}\Big(\hat{Z}^{(1)}_{k\tau}\hat{Z}^{(1)}_{k'\tau'} + \hat{Z}^{(2)}_{k\tau}\hat{Z}^{(1)}_{k'\tau'} +$$
$$+\ \hat{Z}^{(1)}_{k\tau}\hat{Z}^{(2)}_{k'\tau'} + \hat{Z}^{(2)}_{k\tau}\hat{Z}^{(2)}_{k'\tau'}\Big) \tag{7.305}$$

represents the quasiparticle residual interaction with respect to the quasiparticle mean field $\hat{H}_{BCS}$.

For the description of the excited states in the even-even nuclei we start again with the RPA idea that the lowest excited states are generated by the phonon creation operator (7.207)

$$Q^+_\nu = \frac{1}{2}\sum_{\tau=n,p}\sum_{\substack{\varpi=ij,\,i\bar{j},\,\bar{i}\bar{j}\\ \varpi\in\tau}}\left(X^{(\nu)}_\varpi\, b^+_\varpi - Y^{(\nu)}_\varpi\, b_{\bar{\varpi}}\right), \qquad b^+_\varpi = \begin{cases} \alpha^+_i\alpha^+_j, \\ \alpha^+_i\alpha^+_{\bar{j}}, \\ \alpha^+_{\bar{i}}\alpha^+_{\bar{j}}. \end{cases} \tag{7.306}$$

The corresponding eigen problem for an even-even nucleus with the whole

intrinsic Hamiltonian,

$$\hat{H}_{even-even} = \hat{H}_{intr} = \hat{H}_{BCS} + \hat{V}_{RES} = \\ = \hat{H}_{BCS} - \frac{1}{2}\sum_{\tau\tau'}\sum_{kk'}\kappa_{k\tau\,k'\tau'}\hat{Z}^{(1)}_{k\tau}\hat{Z}^{(1)}_{k'\tau'} - \frac{1}{2}\sum_{\tau\tau'}\sum_{kk'}\kappa_{k\tau\,k'\tau'}\hat{Z}^{(2)}_{k\tau}\hat{Z}^{(2)}_{k'\tau'} \\ -\frac{1}{2}\sum_{\tau\tau'}\sum_{kk'}\kappa_{k\tau\,k'\tau'}\big(\hat{Z}^{(1)}_{k\tau}\hat{Z}^{(2)}_{k'\tau'} + \hat{Z}^{(2)}_{k\tau}\hat{Z}^{(1)}_{k'\tau'}\big) \qquad (7.307)$$

Usually the searching of the eigenvectors of the Hamiltonian $\hat{H}_{even-even}$ is performed in two steps.

In the first step the RPA equations (see (7.212))

$$\big[\hat{H}'_{even-even}\,,\, Q^+_\nu\big] = \hbar\omega_\nu\, Q^+_\nu \qquad \big[\hat{H}'_{even-even}\,,\, Q_\nu\big] = -\hbar\omega_\nu\, Q_\nu \\ \big[Q_\nu,\, Q^+_{\nu'}\big] = \delta_{\nu\nu'} \qquad (7.308)$$

are solved with the simplified Hamiltonian

$$\hat{H}'_{even-even} = \hat{H}_{BCS} - \frac{1}{2}\sum_{\tau\tau'}\sum_{kk'}\kappa_{k\tau\,k'\tau'}\hat{Z}^{(1)}_{k\tau}\hat{Z}^{(1)}_{k'\tau'} \qquad (7.309)$$

As a result we obtain the structure of individual phonons (two-quasiparticle amplitudes $X^{(\nu)}_\varpi$ and $Y^{(\nu)}_\varpi$ for all RPA solutions ν with correspondig energies $\hbar\omega_\nu$).

In the second step the last 2 terms in (7.307) is taken into account in terms of the second step variational principle

$$\delta\Big\{\langle\rho\,|\hat{H}_{even-even}|\,\rho\rangle - E_\rho\,\big(\langle\rho\,|\,\rho\rangle - 1\big)\Big\} = 0 \qquad (7.310)$$

where the minimum of the total enrgy $\langle\rho\,|\hat{H}_{even-even}|\,\rho\rangle$ is searched for in the framework of the trial wave function $|\,\rho\rangle$ involving one- and two- phonon components [17]

$$|\,\rho\rangle = \Big\{\sum_\nu C^{(\rho)}_\nu Q^+_\nu + \sum_{\nu_1\nu_2} D^{(\rho)}_{\nu_1\nu_2} Q^+_{\nu_1} Q^+_{\nu_2}\Big\}\,|\,RPA\rangle \qquad (7.311)$$

and variation of the functional in the parenthesis in (7.310) is performed in terms of the variation of amplitudes $C^{(\rho)}_\nu$ and $D^{(\rho)}_{\nu_1\nu_2}$. Finally we obtained these amplitudes and corresponding eigen energies E_ρ for all eigen-vectors $|\,\rho\rangle$ of the Hamiltonian (7.307) (see [7, 8]).

[17] In principle it is possible to add to (7.311) three- phonon and even higher phonon components.

Further the solving of the RPA equations (7.308)

$$\left[\hat{H}^{'}_{even-even}, Q^{+}_{\nu}\right] = \hbar\omega_{\nu} Q^{+}_{\nu} \qquad\qquad \left[\hat{H}^{'}_{even-even}, Q_{\nu}\right] = -\hbar\omega_{\nu} Q_{\nu} \tag{7.312}$$

is briefly discussed. In the Appendix M it is shown in details that the simple form (7.309) of the RPA Hamiltoian enables to rewrite the RPA equations (7.312) for unknown amplitudes $X^{(\nu)}_{\varpi}$ and $Y^{(\nu)}_{\varpi}$ and corresponding phonon energy $\hbar\omega_{\nu}$ (see (7.306)) as follows (see also (M.19) and (M.20)))

$$\begin{aligned} X^{(\nu)}_{\substack{\varpi=ij,\, i\bar{j},\, \bar{i}\bar{j} \\ \varpi\in\tau}} &= 4\,\xi_{\varpi}\,\frac{\sum_{\tau'}\sum_{kk'}\kappa_{k\tau\,k'\tau'}\,R^{(\nu)}_{k\tau}\,\langle\varpi\,|\hat{Z}^{(1)}_{k'\tau'}|\,BCS\rangle}{\epsilon_{\varpi}-\hbar\omega_{\nu}} \\ Y^{(\nu)}_{\substack{\varpi=ij,\, i\bar{j},\, \bar{i}\bar{j} \\ \varpi\in\tau}} &= 4\,\xi_{\varpi}\,\frac{\sum_{\tau'}\sum_{kk'}\kappa_{k\tau\,k'\tau'}\,R^{(\nu)}_{k\tau}\,\langle\varpi\,|\hat{Z}^{(1)}_{k'\tau'}|\,BCS\rangle}{\epsilon_{\varpi}+\hbar\omega_{\nu}} \end{aligned} \tag{7.313}$$

where $\tau = prot,\ neut$ and $\xi_{\varpi} = 1/4$ for $\varpi = ij,\ \bar{i}\bar{j}$ or $1/2$ for $\varpi = i\bar{j}$. The unknown quantities $R^{(\nu)}_{k\tau}$ are solutions of the homogeneous algebraic equation system (see (M.23) in the Appendix M)

$$\sum_{\tilde{\tau}\tau'}\sum_{k'\tilde{k}}\left\{\kappa_{k\tau\,k'\tau'}\,F^{(\nu)}_{k'\tau'\,\tilde{k}\tilde{\tau}} - \delta_{k\tilde{k}}\,\delta_{\tau\tilde{\tau}}\,\delta_{kk'}\delta_{\tau\tau'}\right\}R^{(\nu)}_{\tilde{k}\tilde{\tau}} = 0 \tag{7.314}$$

for $k = 1, \cdots, N_{op}$ and $\tau = prot,\ neut$. In (7.314) the matrix elements $F^{(\nu)}_{k\tau\,k'\tau'}$ are given by the two-quasiparticle matrix elements, $\langle\varpi\,|\hat{Z}^{(1)}_{k\tau}|\,BCS\rangle$ of the operators $\hat{Z}^{(1)}_{k\tau}$ $(k = 1, \cdots, N_{op})$ (see (M.22)):

$$F^{(\nu)}_{k\tau\,k'\tau'} = 2\,\delta_{\tau\tau'}\sum_{\substack{\varpi=ij,\, i\bar{j}, \\ \varpi\in\tau}}\frac{\epsilon_{\varpi}\langle\varpi\,|\hat{Z}^{(1)}_{k'\tau'}|\,BCS\rangle\,\langle\varpi\,|\hat{Z}^{(1)}_{k\tau}|\,BCS\rangle^{*}}{\epsilon^{2}_{\varpi}-(\hbar\omega_{\nu})^{2}}$$

for the case when $\gamma^{(Z_l)}_{c} = \gamma^{(Z_{l'})}_{c}$, and

$$F^{(\nu)}_{l\tau\,l'\tau'} = 2\,\delta_{\tau\tau'}\sum_{\substack{\varpi=ij,\, i\bar{j} \\ \varpi\in\tau}}\frac{\hbar\omega_{\nu}\langle\varpi\,|\hat{Z}^{(1)}_{l'\tau'}|\,BCS\rangle\,\langle\varpi\,|\hat{Z}^{(1)}_{l\tau}|\,BCS\rangle^{*}}{\epsilon^{2}_{\varpi}-(\hbar\omega_{\nu})^{2}} \tag{7.315}$$

for $\gamma^{(Z_l)}_{c} = -\gamma^{(Z_{l'})}_{c}$. The phonon energies $\hbar\omega_{\nu}$ are determined by the condition of the solvability of the equation system (7.314):

$$det\{\kappa\,F - 1\} = 0 \tag{7.316}$$

Index ν enumerates all solutions of the equation system (7.314). The number of the RPA solutions (number of the RPA phonons) is given by the number of two quasiparticle configurations $\varpi = ij,\ i\bar{j}\ (\ \varpi > 0)$ involved in the configuration basis states used in (7.306).

Opposite to the general RPA equations with the non-separable interaction (see (7.230)) the dimension of the equation system (7.314) is very low. The dimension of matrices in (7.230) is given by the number of two-quasiparticle states $\varpi = ij,\ i\bar{j},\ \bar{i}\bar{j}$ and it can reach several thousands (up to 30 thousands for actinide region). The dimension of the equation system (7.314) is equal to $2N_{op}$ where N_{op} is the number of the separable terms in the interaction involved in the Hamiltonian (7.300). Since the number of the separable terms usually does not exceed 5 (see [154]) the dimension of the equation system (7.314) is below 10. This small dimension is a big advantage of the separable interaction approaches and it allows to obtain numerical results for very heavy nuclei where a big configuration space needed in standard RPA approaches makes the standard RPA calculations practically impossible or at least very difficult because of huge matrices.

The phonon creation operators (7.306) (or (7.207) determine excitation states in the given nucleus. The intrinsic low-lying excitation states in the even-even nuclei have usually one-phonon character:

$$|\nu\rangle = Q_\nu^+ \,|RPA\rangle \tag{7.317}$$

with the one-phonon excitation energy $\hbar\omega$.

The structure of one-phonon states $|\nu\rangle = Q_\nu^+ \,|RPA\rangle$ is often characterized by contributions of individual components $\varpi = ij,\ \bar{i}\bar{j},\ i\bar{j}$ with which these components enter the normalization condition:

$$\begin{aligned}\langle \nu \,|\, \nu\rangle = \langle RPA|\, Q_\nu Q_\nu^+ \,|RPA\rangle = \langle RPA|\, \left[Q_\nu \,,\, Q_\nu^+\right] \,|RPA\rangle = \\ = \sum_{\tau=n,p} \sum_{\substack{\varpi=ij,\,\bar{i}\bar{j},\,i\bar{j},\\ \varpi\in\tau}} p_\varpi = 1\end{aligned} \tag{7.318}$$

with

$$p_\varpi = \begin{cases} 1/2\ (|X_{ij}^{\nu)}|^2 - |Y_{ij}^{\nu)}|^2) & \text{for } \varpi = ij \\ 1/2\ (|X_{\bar{i}\bar{j}}^{\nu)}|^2 - |Y_{\bar{i}\bar{j}}^{\nu)}|^2) & \text{for } \varpi = \bar{i}\bar{j} \\ 1/4\ (|X_{i\bar{j}}^{\nu)}|^2 - |Y_{i\bar{j}}^{\nu)}|^2) & \text{for } \varpi = i\bar{j} \end{cases} \tag{7.319}$$

In (7.318) p_ϖ is the probability of the finding given component ϖ in the one phonon state $Q_\nu^+ \,|RPA\rangle$. From the point of view of the umber of such components one can recognize collective or noncollective states:

1. If in the sum (7.318) many components effectively participate then the given one phonon state $|\nu\rangle = Q_\nu^+ |RPA\rangle$ is considered as collective (that means in the sum (7.318) we have many terms).

2. If in the sum (7.318) one terms ϖ_0 dominates and all others are negligible the then the one phonon state $|\nu\rangle = Q_\nu^+ |RPA\rangle$ is noncollective with the two-quasiparticle character:

$$Q_\nu^+ \approx X_{\varpi_0}^{(\nu)} b_{\varpi_0}^+ - Y_{\varpi_0}^{(\nu)} b_{\varpi_0} \tag{7.320}$$

Examples of some numerical results of separable RPA approaches and corresponding comparison with experimental data of selected even-even nuclei are discussed in the Subsection 7.3.1.4. The detailed derivation of the separable RPA equation system (7.314) can be found in the Appendix M.

7.3.1.2 RPA for odd-A and odd-odd nuclei

The odd-A nuclei are characterized by the odd nucleon outside the vibrating even-even core. The long-range residual interaction produces a coupling of the odd nucleon states with the phonon states of the vibrating even-even core. If the long-range residual interactions are not taken into account (that means the even-even core does not vibrate and stays in its ground state) then the lowest excited states of odd-A nucleus have one-quasiparticle character, $\alpha_{\rho\sigma}^+ |BCS\rangle$ ($\sigma = \pm$), (if the pairing interaction is present - see (6.60), (6.67), or one- particle character (if the pairing interaction is not present in the mean field). If the long-range residual interactions are present in the nucleus Hamiltonian and the vibration of the even-even core are taken into account then the low-lying states of a spherical odd-A nucleus are characterized by the angular momentum j and can be searched for in the following form (see e.g. [7, 99])

$$\begin{aligned} &|jm;\, \nu\rangle = \\ &= \left\{ \sum_\rho \delta_{jj_\rho}\, c_\rho^{(j,\,\nu)}\, a_{j_\rho m}^+ + \sum_{j_\rho \lambda_i} d_{\rho\lambda_i}^{(j,\,\nu)} \sum_{m_\rho \mu_i} C_{j_\rho m_\rho \lambda_i \mu_i}^{jm}\, a_{j_\rho m_\rho}^+\, Q_{\lambda_i \mu_i,\, i}^+ \right\} | \, 0\rangle \end{aligned} \tag{7.321}$$

where the first term represents the sum over one- particle components of the odd- A state $|jm;\, \nu\rangle$ and the second term is the sum over all particle-phonon

components (index ρ enumerates all single-particle states with given j_ρ and index i enumerates all core phonon states with given angular momentum λ). When the studied odd-A nucleus is axially deformed then the intrinsic low-lying states are characterized by the projection K onto the symmetry axis and the (7.317) should be modified into the following form (angular momentum projections K, $K_\rho, \mu_i \geq 0$ and $\sigma_\rho, \sigma_i = \pm 1$, and in the axially deformed nuclei the projection K of the angular momentum is a good quantum number)

$$|K;\ \nu\rangle_{odd} = \\ = \Big\{ \sum_{\rho} c_{\rho}^{(K,\,\nu)}\ \alpha_{\rho +}^{+} + \sum_{\substack{\rho\, K_\rho\, \sigma_\rho \\ i\, \mu_i\, \sigma_i}} d_{\rho i}^{(K;\,\nu)}\ \alpha_{\rho K_\rho}^{+}\ Q_{i\mu_i}^{+}\ \delta_{K_\rho \sigma_\rho + \mu_i \sigma_i,\, K} \Big\} \mid 0\rangle \tag{7.322}$$

where $Q_{i\mu_i}^{+}$ are phonon creation operator with given angular momentum projection μ_i corresponding to the axially deformed vibrating even-even core.

In (7.321) $c_{\rho}^{(j,\,\nu)}$ and $d_{\rho\lambda_i}^{(j,\,\nu)}$ represent one-particle and one-particle + phonon components, respectively, in the spherically symmetric case, while in (7.322) $c_{\rho K}^{K,\,\nu)}$ and $d_{\rho K_\rho i}^{(K,\,\nu)}$ are the corresponding components of the intrinsic state in axially deformed nuclei. The symbol $|0\rangle$ stands for the combined phonon-quasiparticle (or phonon particle) vacuum, $|0\rangle = |RPA\rangle|BCS\rangle_{val}$ or $|0\rangle = |RPA\rangle|HF\rangle_{val}$), where $|RPA\rangle$ is the vacuum for RPA phonons of the even-even core and $|BCS\rangle_{val}$ (or $|HF\rangle_{val}$) is the vacuum for valence quasiparticles (or HF gr. state) of odd nucleon. The total Hilbert space of the odd-A nucleus states is divided into the space of even-even core phonons and the space of valence quasiparticles (for deformed nuclei, where pairing interactions participate in the mean field) or space of valence particle states (for spherical nuclei where pairing interactions does not participate in the forming of mean fields).

In order not to violate the Pauli principle it is necessary the valence quasiparticles (or valence particle states) of odd nucleon not to enter the structure of the phonons of the even-even core. That means the Pauli principle requires the following conditions:

$$\left[\alpha_{\rho\sigma},\ Q_{i\mu_i}^{+}\right] = \left[\alpha_{\rho\sigma}^{+},\ Q_{i\mu_i}^{+}\right] = 0$$

or

$$\left[a_{j_\rho m_\rho},\ Q_{i\lambda_i\mu_i}^{+}\right] = \left[a_{j_\rho m_\rho}^{+},\ Q_{i\lambda_i\mu_i}^{+}\right] = 0 \tag{7.323}$$

Using the condition (7.323) the boson commutation relations for phonon creation and annihilation operators and fermion anti-commutation relations for quasiparticles the normalization condition for wave function (7.322) can be written as follows

$$ {}_{odd}\langle K;\ \nu | K;\ \nu \rangle_{odd} = \sum_{\rho} |\ c_{\rho}^{(K,\,\nu)}|^{\,2} + 2\ \sum_{\rho i} |\ d_{\rho i}^{(K,\,\nu)}|^{\,2} = 1 \qquad (7.324) $$

for axially deformed case, and similarly for wave function (7.317) in the spherically symmetric case.

Amplitudes $c_{\rho}^{(K,\,\nu)}$, $d_{\rho i}^{(K,\,\nu)}$ together with the corresponding energies η_{ν} can be obtained using the variation principle by searching for the minimum of the total energy ${}_{odd}\langle K;\ \nu |\ \hat{H}\ | K;\ \nu \rangle_{odd}$ calculated within the trial wave functions (7.322) in the case of deformed mean field or within the wave functions (7.321) for the spherical mean field. Further we suppose the deformed mean field and therefore we work with (7.322). The corresponding vibrational principle condition can be expressed as follows

$$ \delta \left\{ {}_{odd}\langle K;\ \nu \mid \hat{H}_{intr} \mid K;\ \nu \rangle_{odd} \ -\ \eta_{\nu}\ [\ {}_{odd}\langle K;\ \nu \mid K;\ \nu \rangle_{odd} - 1] \right\} = 0 \quad (7.325) $$

where the second term represents the condition of the normalization (see (7.324)). The variation of the functional in parenthesis in (7.325) is performed with respect of amplitudes $c_{\rho}^{(k,\,\nu)}$ and $d_{\rho i}^{(K,\,\nu)}$. The Lagrange multiplier η_{ν} has the sense of the energy of the state $|K;\ \nu\rangle_{odd}$. The system of equations for these amplitudes obtained from the variation principle (7.325) is quite complex and is not given here. It can be found e.g. in [7, 156]. here we demonstrate only the scheme of the looking for the eigenstates $|K;\ \nu\rangle_{odd}$ the intrinsic odd-A nucleus Hamiltonian in the case when the effective nucleon-nucleon interaction is in the separable form (see (7.300)).

As it was discussed in the subsection 7.3.1.1.3 in the case of the separable effective nucleon-nucleon interaction (7.300) the residual interaction corresponding to the quasiparticle mean field can be written in the form (see (7.305))

$$ \hat{V}_{RES} = -\frac{1}{2} \sum_{\tau,\tau'=n,p} \sum_{\substack{k\in\tau \\ k'\in\tau'}} \kappa_{k\tau\,k'\tau'} \Big(\hat{Z}_{k\tau}^{(1)} \hat{Z}_{k'\tau'}^{(1)} + \hat{Z}_{k\tau}^{(2)} \hat{Z}_{k'\tau'}^{(1)} $$

$$ + \hat{Z}_{k\tau}^{(1)} \hat{Z}_{k'\tau'}^{(2)} + \hat{Z}_{k\tau}^{(2)} \hat{Z}_{k'\tau'}^{(2)} \Big) \qquad (7.326) $$

This type of the residual interaction is used by e.g. Dubna group (see e.g. [156] and citations therein). Using this residual interaction the searching for the odd-A eigenstates $|K;\,\nu\rangle$ of the intrinsic Hamiltonian $\hat{H}_{intr} = \hat{H}_{BCS} + \hat{V}_{RES}$ (see (7.303)) [18] goes on in the following steps:

1. At first, the one-phonon states of the vibrating even-even core are found, that means, one-phonon states $|i\rangle = Q_i^+ \,|RPA\rangle$ of the simplified Hamiltonian $\hat{H}'_{even-even}$ with its energy $\hbar\omega_i$ (see (7.309))

$$\hat{H}'_{even-even} = \hat{H}^{(core)}_{BCS} - \frac{1}{2} \sum_{\substack{k\in\tau \\ k'\in\tau'}} \kappa_{k\tau\,k'\tau'}\, \hat{Z}^{(1)}_{k\tau}\, \hat{Z}^{(1)}_{k'\tau'} = \sum_i \hbar\omega_i\, Q_i^+ Q_i \quad (7.327)$$

2. In the second step, the part of the Hilbert space corresponding to the valence quasiparticles, possibly occupied by odd nucleon, is added to the Hilbert space of phonons of even-even core. That means we add to the even-even core Hamiltonian (7.327) the valence part to the BCS Hamiltonian, $\hat{H}^{(val)}_{BCS} = \sum_{k\in val} E_k\,(\alpha_k^+\alpha_k + \alpha_{\bar{k}}^+\alpha_{\bar{k}})$ and as well as the coupling between the valence single-quasiparticle states and phonons of the even-even core represented by the part $-1/2\,\sum_{kk'\tau\tau'} \kappa_{k\tau\,k'\tau'}\,(\hat{Z}^{(2)}_{k\tau}\hat{Z}^{(1)}_{k'\tau'} + \hat{Z}^{(1)}_{k\tau}\hat{Z}^{(2)}_{k'\tau'})$ of the residual interaction (7.305) or (7.309) (see also the text below (7.306) where the explanation, why this term represents phonon-quasiparticle coupling, can be found). In such a way we obtain the Hamiltonian of the odd-A nuclei in the following form [19]

$$\begin{aligned}\hat{H}_{odd} = &\sum_i \hbar\omega_i\, Q_i^+ Q_i + \sum_{k\in val} E_k\,(\alpha_k^+\alpha_k + \alpha_{\bar{k}}^+\alpha_{\bar{k}}) \\ &-\frac{1}{2} \sum_{\substack{k\in\tau \\ k'\in\tau'}} \kappa_{k\tau\,k'\tau'} \left(\hat{Z}^{(1)}_{k\tau}\hat{Z}^{(2)}_{k'\tau'} + \hat{Z}^{(2)}_{k\tau}\hat{Z}^{(1)}_{k'\tau'}\right) \end{aligned} \quad (7.328)$$

and this Hamiltonian enters the variational principle problem (7.325) for the states of odd-A nucleus. The solving of the corresponding equation (see [156]) gives the amlitudes $c_\rho^{(K,\,\nu)}$ and $d_{\rho i}^{(K,\,\nu)}$ and corresponding intrinsic energies η_ν of the state $|K;\,\nu\rangle$ of given odd-A nucleus.

[18] We speak about the intrinsic Hamiltonian but this is the intrinsic Hamiltonian only in the case of deformed nuclei. When the investigated nucleus is spherical then $\hat{H}$ represents the total nucleus Hamiltonian.

[19] The part $-1/2\,\sum_{kk'\tau\tau'} \kappa_{k\tau\,k'\tau'}\,\hat{Z}^{(2)}_{k\tau}\hat{Z}^{(2)}_{k'\tau'}$ is usually neglected in the case of odd-A nuclei.

In the subsection 7.3.1.3 some concrete results of the solving of the variational problem (7.325) for low-lying states in odd-A nuclei are compared with corresponding experimental data.

In the end of this subsection the intrinsic (for deformed case) or laboratory (for spherical case) wave function of odd-odd nuclei are briefly discussed. The ideas presented above for odd-A nuclei can be extended for the case of odd-odd nuclei. From this point of view the odd-odd nucleus can be considered as the odd proton and odd neutron outside the vibrating even-even core. Similarly as in odd-A nucleus discussed above we assume that the nucleus is axially deformed (modification for spherically symmetric nucleus is obvious). Then, in the analogue with (7.322), the intrinsic state of the odd-odd nucleus involves neutron-proton two-quasiparticles, coupled to the even-even core, components:

$$|K;\ \nu\rangle_{odd-odd} = \Big\{ \sum_{\substack{\rho_n\rho_p \\ \sigma_n,\sigma_p=\pm}} c^{(K,\,\nu)}_{\rho_n\rho_p}\ \alpha^{+}_{\rho_n\sigma_n}\ \alpha^{+}_{\rho_p\sigma_p}\ \delta_{K_{\rho_p\sigma_p}+K_{\rho_n\sigma_n},\,K}\ + $$

$$+ \sum_{\substack{\rho_n\rho_p \\ \sigma_n,\sigma_p=\pm}} \sum_{i\sigma_i} d^{(K;\,\nu)}_{\rho_n\rho_p\,i}\ \alpha^{+}_{\rho_n\sigma_n}\ \alpha^{+}_{\rho_p\sigma_p}\ Q^{+}_{i}\ \delta_{K_{\rho_p\sigma_p}+K_{\rho_n\sigma_n}+\sigma_i\mu_i,\,K} \Big\} |0\rangle \tag{7.329}$$

where again $|0\rangle = |RPA\rangle|BCS\rangle$ represents the combined phonon and valence proton quasiparticle vacuum. Using the anti-commutation relations for valence proton and valence neutron quasiparticles the normalization condition for wave function (7.329) is (analogue of (7.324)

$$_{odd-odd}\langle K;\ \nu\ |\ K;\ \nu\rangle_{odd-odd} = \sum_{\substack{\rho_n\rho_p \\ \sigma_n,\sigma_p=\pm}} |\ c^{(K,\,\nu)}_{\rho_n\rho_p}|^{\,2}\ \delta_{K_{\rho_p\sigma_p}+K_{\rho_n\sigma_n},\,K}\ +$$

$$+\,2 \sum_{\substack{\rho_n\rho_p \\ \sigma_n,\sigma_p=\pm}} \sum_{i\sigma_i} |\ d^{(K,\,\nu)}_{\rho_n\rho_p\,i}|^{\,2}\ \delta_{K_{\rho_p\sigma_p}+K_{\rho_n\sigma_n}+\sigma_i\mu_i,\,K}\ =\ 1 \tag{7.330}$$

Amplitudes $c^{(K,\,\nu)}_{\rho_n\rho_p}$ and $d^{(K,\,\nu)}_{\rho_n\rho_p\,i}$ can be obtained from the variational principle equation similar to (7.325)

$$\delta\{\ _{odd-odd}\langle K;\ \nu\ |\ \hat{H}_{intr}\ |\ K;\ \nu\rangle_{odd-odd} - \eta_\nu\ [\ _{odd-odd}\langle K;\ \nu\ |\ K;\ \nu\rangle_{odd-odd} - 1\ ]\ \} = 0 \tag{7.331}$$

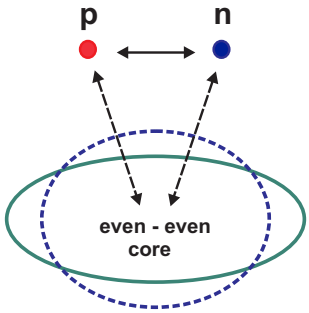


Figure 7.30: Schematic figure of an odd-odd nucleus

Similarly as was discussed for odd-A nuclei we can demonstrate for odd-odd nucleus on the case of the separable residual interaction (7.326) what parts of the residual interaction give an contribution to the expectation value ${}_{odd-odd}\langle K;\ \nu \mid \hat{H}_{intr} \mid K;\ \nu\rangle_{odd-odd}$ in (7.331). On the base of the discussions concerning odd-A nuclei given above we know that the part of the residual interaction (7.326), $-1/2\ \sum_{k\tau}\sum_{k'\tau'}\kappa_{k\tau\,k'\tau'}(\hat{Z}^{(1)}_{k\tau}\hat{Z}^{(2)}_{k'\tau'}+\hat{Z}^{(2)}_{k\tau}\hat{Z}^{(1)}_{k'\tau'})$, represents the interaction between odd particles (odd proton and/or odd neutron) with the vibrating even-even core and this interaction is depicted on the simple schematic figure Fig.7.30 by the dashed arrows. From this figure and from the expr. (7.326) it is clear that the last term in (7.326), $-1/2\ \sum_{k\tau}\sum_{k'\tau'}\kappa_{k\tau\,k'\tau'}\,\hat{Z}^{(2)}_{k\tau}\hat{Z}^{(2)}_{k'\tau'}$, should involve the interaction between odd proton and odd neutron (solid arrow in the Fig.7.30). All these terms should be take into account in the Hamiltonian of odd-odd nucleus [20]

$$\hat{H}_{odd-odd}=\hat{H}'_{even-even}+\sum_{\substack{k\in val\\ k\in p,n}}E_k\,(\alpha^+_k\alpha_k+\alpha^+_{\bar{k}}\alpha_{\bar{k}})$$

$$-\frac{1}{2}\sum_{\substack{k\tau\\ k'\tau'}}\kappa_{k\tau\,k'\tau'}\,(\hat{Z}^{(1)}_{k\tau}\hat{Z}^{(2)}_{k'\tau'}+\hat{Z}^{(2)}_{k\tau}\hat{Z}^{(1)}_{k'\tau'})$$

$$-\frac{1}{2}\sum_{\substack{k\tau\\ k'\tau'}}\kappa_{k\tau\,k'\tau'}\hat{Z}^{(2)}_{k\tau}\hat{Z}^{(2)}_{k'\tau'}=$$

[20] The interaction between odd proton and odd neutron is connected with so called Gallagher-Moszkowski splitting which will be discussed in more details in the subsection 7.3.1.3.1.1.

$$= \hat{H}_{odd} - \frac{1}{2} \sum_{\substack{k\tau \\ k'\tau'}} \kappa_{k\tau\, k'\tau'} \hat{Z}^{(2)}_{k\tau} \hat{Z}^{(2)}_{k'\tau'} \tag{7.332}$$

The analysis of the structure of the odd-odd nucleus using the trial functions (7.329) with the variational principle problem (7.331) is not the only one used in the literature. The other approach is so-called neutron-proton RPA (npRPA). It starts with the ansatz of the odd-odd nucleus states in the form (here we suppose the spherical nucleus where the total angular momentum is good quantum number - see e.g. [158, 157, 153])

$$\begin{aligned} |K^{\pi}_{\nu};\nu\rangle &= Q^{(np)\,+}_{K^{\pi}_{\nu}} |RPA\rangle = \\ &= \sum_{pn} \delta_{K_\nu,\,|K_n - K_p|} \left(X^{(K^\pi \nu)}_{pn}\, \alpha^{+}_{p} \alpha^{+}_{n} - Y^{(K^\pi \nu)}_{pn}\, \alpha_n \alpha_p \right) |RPA\rangle \end{aligned} \tag{7.333}$$

That means the low-lying odd-odd nucleus states are considered as neutron-proton one- phonon states where p-n phonon creation operator $Q^{(np)\,+}_{K^{\pi}_{\nu}}$ can be searched for in the form of the linear combination of neutron-proton two-quasiparticle states with corresponding amplitudes $X^{(K^\pi \nu)}_{pn}$ and $Y^{(K^\pi \nu)}_{pn}$ which can be obtained from the variation principle condition together with its energy η_ν:

$$\delta \left\{ \langle K^{\pi}_{\nu};\nu|\, \hat{H}_{intr}\, |K^{\pi}_{\nu};\nu\rangle - \eta_{K^{\pi}_{\nu}} \left(\langle K^{\pi}_{\nu}, \nu \mid K^{\pi}_{\nu};\nu\rangle - 1 \right) \right\} = 0 \tag{7.334}$$

Opposite to the standard RPA approach for even-even nuclei discussed in the subsection 7.3.1.1, where the phonons were built from neutron two-quasiparticle states or proton two-quasiparticle states, in the case of odd-odd nucleus we have neutron-proton two-quasiparticle states. The symbol $|RPA\rangle$ in (7.333) stands for the ground state of even-even core (neutron-proton phonon vacuum). This fact requires the terms in the Hamiltonian involving the step-up and step-down isospin operators which change the neutron into proton and vice versa (see the section 1.2). For instance, such approach was used in [157] where the states of odd-odd nucleus appears as the intermediate states in the double-beta decay of even-even nucleus [21].

[21] The double-beta decay is discussed in the section 10.....

7.3.2 Application of the RPA approach for the interpretation of selected experimental data

In this subsection selected RPA results are compared with corresponding experimental values. As it was already mentioned (see (7.200)) the RPA approach starts with the Hamiltonian in the form of the sum of the mean field and residual interactions

$$\hat{H}_{intr} = \hat{H}_{AV} + \hat{V}_{res} \tag{7.335}$$

where the mean field part $\hat{H}_{AV}$ can be obtained by the HF method or, in the case when pairing interaction contributes to the mean field, by the HFB method. Here it is necessary to point out again that in the case of **deformed nuclei** [22] the Hamiltonian (7.335) is the Hamiltonian in the **intrinsic non-rotating frame**. In principle, the HF or HFB method gives the possibility to obtain the intrinsic Hamiltonian $\hat{H}_{intr}$ from the total Hamiltonian $\hat{H}$ in the laboratory frame by the the space frame transformation (rotation) of coordinate frame but in this case we should be careful and we have to get rid of the spurious (unphysical from the point of view of the intrinsic degrees of freedom) solutions of the subsequent RPA equations (connected with the nucleus rotation in the lab. frame) - see the discussion of the possible spontaneous symmetry breaking of the total Hamiltonian by the mean field discussed in the subsection 7.3.1.1.2 (see (7.283)-(7.299)) [23]. In the case of **spherical nuclei**, where we have no rotational degrees of freedom, the Hamiltonian (7.335) represents the **total Hamiltonian in laboratory frame**.

Historically, the first calculations with the RPA were phenomenological where the mean field $\hat{H}_{AV}$ was taken in the simple form with the oscillator or Wood-Saxon potential with the l-s coupling (see (5.9) and (5.10)) [7, 99, 159]. Since this approach was used in the beginning of 70-ties also for odd-A nuclei with quasiparticle - phonon wave functions (7.322) all models of this type are known in literature as **Quasiparticle- Phonon Model (QPM)**. Calculations based on theoretically more erudite RPA approaches with the HF and/or HFB methods starting with realistic effective nucleon-nucleon interactions appeared a decade later in 70-ties and 80-ties (see e.g. [160, 161] and citations therein).

From the point of view of the comparison of the RPA calculation results with corresponding experimental values it is better to discuss separately the

[22] The deformed nucleus is understand here as the nucleus which has deformed surfaces with the same fixed density of nucleons in its ground state.

[23] The rotational degrees of freedom of nucleus motion is discussed in details in the Chapter 8

discrete low-lying part of the nucleus energy spectrum and the very dense energetically higher-lying excitation states (giant resonances, already mentioned - see the schematic figure Fig.1.6). The reason for it is the different accuracy of the reproduction of experimental values for these two energy regions of the nuclear spectra obtained by the simple phenomenological and more complex microscopical approaches. While the parameters of the phenomenological mean field Nilsson or Wood-Saxon potentials, usually used in phenomenological models, are fitted in order to describe experimental single-particle low-lying energies (see e.g. [7]), the parameters of the effective nucleon-nucleon interaction, used in microscopical models (e.g. Skyrme, Gogny or relatiovistic mean field interaction), are obtained from the comparison of calculated and experimental values of nuclear bulk properties (bind energies, nuclear radia, compressibility) of selected nuclei (see e.g. [79]). As a result of it the prediction power of phenomenological approaches for the lowest parts of the nuclear spectra is higher than that of microscopical models. However, it is not the case of higher lying collective states - giant resonances. Although the recent progress in the computer possibilities gives the hope that the microscopical models will be able to describe the low-lying states relatively better (see e.g. [162]). One should have always in mind that from the theoretical point of view the microscopical models are more fundamental because their residual interactions are consistent with their mean fields and this residual interaction does not bring any new parameters which is the case of phenomenological approaches.

7.3.2.1 RPA description of low- lying part of nuclear spectra

In this subsection the energetically low-lying states in spherical and deformed nuclei are discussed from the point of view of the RPA approach. At first, some RPA results for spherical nuclei are demonstrated and then some comments to deformed nuclei are given. From reasons given above we demonstrate RPA results, concerning low-lying states, mainly using the separable version of the RPA described in the subsection 7.3.1.1.3.

7.3.2.1.1 Low- lying states in spherical nuclei In spherical nuclei the total nucleus Hamiltonian $\hat{H} = \hat{H}_{intr}$ (see (7.334)) is invariant with respect to rotations and as a result of it the total angular momentum J (together with the parity π) is a good quantum number for states in the spherical even-even nucleus as well as in the spherical odd-A and odd-odd nuclei.

i. Even-even spherical nuclei

In the framework of the RPA the low-lying states in the spherical even-even nuclei can be searched for in the form (7.311) where $\rho \to J^\pi_\rho$, $\nu \to \lambda i$, $\nu_1 \to \lambda_1 i_1$, $\nu_2 \to \lambda_2 i_2$ (index λ characterizes the multipolarity or angular momentum of the given phonon $Q^+_{\lambda i}$ and the index i enumerates phonons with the same multipolarity λ). Then the expression (7.311) can be written as follows

$$|J^\pi_\rho M_\rho\rangle = \Big\{ \sum_i C^{(J^\pi_\rho)}_{J_\rho i}\, Q^+_{J_\rho M_\rho i} + \\ + \sum_{\substack{\lambda_1 i_1 \\ \lambda_2 i_2}} D^{(J^\pi_\rho)}_{\lambda_1 i_1 \lambda_2 i_2} \sum_{\mu_1 \mu_2} C^{J_\rho M_\rho}_{\lambda_1 \mu_1 \lambda_2 \mu_2}\, Q^+_{\lambda_1 \mu_1 i_1}\, Q^+_{\lambda_2 \mu_2 i_2} \Big\}\, |RPA\rangle \qquad (7.336)$$

where the spherical nucleus phonon operators are:

$$Q^+_{\lambda\mu;i} = \frac{1}{2} \sum_{j_1 j_2} \left(X^{(\lambda i)}_{j_1 j_2}\ [\alpha^+_{j_1} \alpha^+_{j_2}]_{(j_1 j_2;\, \lambda\mu)} - Y^{(\lambda i)}_{j_1 j_2}\ [\alpha_{j_1} \alpha_{j_2}]_{(j_1 j_2;\, \lambda\mu)} \right) \qquad (7.337)$$

with

$$[\alpha^+_{j_1} \alpha^+_{j_2}]_{(j_1 j_2; \lambda\mu)} = \sum_{m_1 m_2} C^{\lambda\mu}_{j_1 m_1 j_2 m_2}\, \alpha^+_{j_1 m_1} \alpha^+_{j_2 m_2} \qquad (7.338)$$

In the case of spherical nuclei we should have in mind that the eigen-energies $E_{J^\pi_\rho}$ of the Hamiltonian $\hat{H} = \hat{H}_{intr}$ ($\hat{H}|J^\pi_\rho M_\rho\rangle = E_{J^\pi_\rho}|J^\pi_\rho M_\rho\rangle$) are degenerated with respect to the projection M_ρ. The amplitudes $X^{(\lambda i)}_{j_1 j_2}$, $Y^{(\lambda i)}_{j_1 j_2}$ in (7.337) and $C^{(J^\pi_\rho)}_{J_\rho M_\rho}$, $D^{(J^\pi_\rho)}_{\lambda_1 i_1\, \lambda_2 i_2}$ in (7.336) together with corresponding energies are found by the solving of corresponding variational principle equations (7.308) and (7.310).

As an example of results obtained by this method we show in the Tab. 7.2 the comparison of calculated energies of the lowest quadrupole ($J^\pi_\rho = 2^+_1, 2^+_2$), octupole ($J^\pi_\rho = 3^-_1$) and hexadecapole ($J^\pi_\rho = 4^+_1$) states with corresponding experimental energies for selected spherical nuclei. In the table contributions of the highest one- phonon components, $|\, C^{(J^\pi_\rho)}_{\lambda\, i}|^2$, and two-phonon components, $|\, D^{(j^\pi_\rho)}_{\lambda_1 i_1\, \lambda_2 i_2}|^2$, in (7.336), with which given component enters the normalization condition:

$$\langle J^\pi_\rho M_\rho \mid J^\pi_\rho M_\rho \rangle = \sum_i |\, C^{(J^\pi_\rho)}_{J_\rho\, i}|^{\,2} + 2 \sum_{\substack{\lambda_1 i_1 \\ \lambda_2 i_2}} |\, D^{(J^\pi_\rho)}_{\lambda_1 i_1\, \lambda_2 i_2}|^{\,2} = 1\ , \qquad (7.339)$$

Nucleus	J^π_ρ	$E_{J^\pi_\rho}$ exp. [MeV]	$E_{J^\pi_\rho}$ theor. [MeV]	highest components				
				λi	$\lvert C^{(J^\pi_\rho)}_{\lambda i}\rvert^2$	$\lambda_1 i_1$	$\lambda_2 i_2$	$2\lvert D^{(J^\pi_\rho)}_{\lambda_1 i_1\,\lambda_2 i_2}\rvert^2$
^{114}Sn	2^+_1	1.30	1.29	21	0.90	21	21	0.01
	2^+_2	2.17	2.53	22	0.21	21	21	0.58
	3^-_1	2.28	2.22	31	0.91	31	21	0.09
	4^+_1	2.19	2.60	41	0.22	21	21	0.57
^{142}Sm	2^+_1	0.77	0.64	21	0.79	21	21	0.05
	2^+_2	1.66	1.52	22	0.39	21	21	0.34
	3^-_1	1.78	1.76	31	0.91	31	21	0.08
	4^+_1	1.79	1.60	41	0.26	21	21	0.23
^{146}Gd	2^+_1	1.97	2.00	21	0.94	31	31	0.05
	2^+_2	3.37	3.43	21	0.05	31	31	0.94
	3^-_1	1.57	1.54	31	0.96	21	31	0.03
^{208}Pb	2^+_1	4.08	4.43	21	0.97	31	31	0.03
	3^-_1	2.61	2.60	31	0.99	-	-	-

Table 7.2: Energies $E_{J^\pi_\rho}$ and the structure (highest 1-phonon and 2-phonon components) of the low-lying states (7.336) calculated with the Hamitonian involving the separable interaction (1.55) and the mean field potential in the Saxon-Wood form (5.10) (exp. data taken from [163], theoretical data taken from [164])

are shown as well.

The Hamiltonian, used in the calculation, was taken in the phenomenological form with the separable multipole-multipole and spin multipole- spin-multipole nucleon-nucleon interactions (1.55) [164]. In [164] it is shown that only isoscalar multipole-multipole interaction can be taken into account for the description of low-lying states, that means the multipole-multipole strength constants in (1.55) are following [164]

$$\kappa_\lambda[n] = \kappa_\lambda[p] = \kappa_\lambda[np] \equiv \kappa_\lambda \tag{7.340}$$

where the value for dipole part ($\lambda = 1$), κ_1, was determined from the requirement of the zero energy of isoscalar electric dipole $\lambda = 1^-$ one- phonon state which represents the spurious unphysical mode connected with the nucleus center of mass motion (see the text below (7.286)). The electric quadrupole

($\lambda = 2$), octupole ($\lambda = 3$) and hexadecapole ($\lambda = 4$) strength constants κ_2, κ_3 and κ_4 were determined from the fitting of the calculated quadrupole, octupole and hexadecapole energies ($E_{J^\pi_\rho} = E_{2^+_1}$, $E_{3^-_1}$, $E_{4^+_1}$) of the lowest levels to the corresponding experimental values for a broad regions of nuclei. For instance, for quadrupole and octupole strength constants κ_2 and κ_3 this systematic analyses, performed for spherical and deformed nuclei, gave the following empirical values (see [164])

$$\kappa_2 \approx \frac{400}{A^{7/3}} \frac{MeV}{fm^4} \qquad \kappa_3 \approx \frac{200}{A^3} \frac{MeV}{fm^6} \tag{7.341}$$

for nuclei rare-earth region, and

$$\kappa_2 \approx \frac{310}{A^{7/3}} \frac{MeV}{fm^4} \qquad \kappa_3 \approx \frac{180}{A^3} \frac{MeV}{fm^6} \tag{7.342}$$

for actinide region. Similar systematic analyses for spin multipole - spin multipole constants $\kappa_{l\lambda}[\tau]$ gave (see [164, 7])

$$\kappa_{l\lambda}[n] = \kappa_{l\lambda}[p] = \kappa_{l\lambda}[np] \equiv \kappa_{l\lambda} \approx -4\pi \frac{25}{A} \langle r^{2\lambda} \rangle \frac{MeV}{fm^{2\lambda}} \tag{7.343}$$

where the values of strength constants given in (7.341) - (7.343) were obtained with the interaction (1.55) using the radial dependencies in the simple form $f_\lambda(r) = f_{l\lambda}(r) = r^\lambda$. The parameters of the Wood-Saxon mean field potential used in the calculations for Table 7.3 and 7.4 are given in [7].

It can be seen from the Table 7.2 that the lowest J^π_ρ ($\rho = 1$) states have one- phonon character ($|C^{(J^\pi_1)}_{J_1\,1}|^2 \geq 0.8$). The substantial higher two- phonon components are found for some second and higher $|J^\pi_\rho\rangle$ ($\rho \geq 2$) states. This is a general feature of spherical nuclei (not only for isotopes discussed in the Table 7.2). All nuclei, given in the Table 7.2, are spherical and magic or very closed to magic. A typical feature for these nuclei is the fact that the structure of the lowest phonons $Q^+_{\lambda\mu;\,i=1}$ is almost pure two- quasiparticle (that means $X^{(\lambda 1)}_{jj} \approx 1$ for the last valence occupied shell j and almost zero for all other $X^{(\lambda 1)}_{j_1\,j_2}$ and all $Y^{(\lambda i)}_{j_1\,j_2}$ [7]). As it will be seen further this is not the case of deformed nuclei.

Knowing the structure of the wave function (7.336) of the lowest states one can determine electromagnetic probabilities of the excitation of low-lying states $|J^\pi_\rho\rangle$ from the ground state $|0^+_{g.s.}\rangle = |RPA\rangle$. For instance, the reduced probability $B(E\lambda; 0^+_{g.s.} \rightarrow J^\pi_\rho = \lambda)$ of the electric $E\lambda$ transition from the

ground state $|0^+_{g.s.}\rangle$ to the state $|J^\pi_\rho = \lambda^\pi_\rho\rangle$ is given by (see [164])

$$B(E\lambda;\, 0^+_{g.s.} \to J^\pi_\rho) = \frac{1}{2\lambda+1} \Big| \sum_{\tau=n,p} e^{(\lambda=J_\rho)}_{eff}[\tau] \sum_{j,j'\in\tau} \langle j||\hat{\mathscr{M}}^{el}_{J_\rho}||j'\rangle \cdot$$
$$\Big\{ \sum_i C^{(J^\pi_\rho)}_{J_\rho i} \left(X^{(J_\rho i)}_{jj'} + Y^{(J_\rho i)}_{jj'} \right) u^{(+)}_{jj'} +$$
$$+ \sum_{\substack{\lambda_1 i_1 \\ \lambda_2 i_2}} \sum_{j''} D^{(J^\pi_\rho)}_{\lambda_1 i_1\, \lambda_2 i_2} \langle j||\hat{\mathscr{M}}_{J_\rho}||j'\rangle\, v^{(-)}_{jj'}\, (2\lambda_1+1)(2\lambda_2+1) \cdot$$
$$\begin{Bmatrix} \lambda_1 & \lambda_2 & \lambda \\ j & j' & j'' \end{Bmatrix} \left(X^{(\lambda_1 i_1)}_{j'j''}\, Y^{(\lambda_2 i_2)}_{j''j} + Y^{(\lambda_1 i_1)}_{j'j''}\, X^{(\lambda_2 i_2)}_{j''j} \right) \Big\}\Big|^2 \qquad (7.344)$$

where $u^{(\pm)}_{jj'} = \mathscr{U}_j \mathscr{V}_{j'} \pm \mathscr{V}_j \mathscr{U}_{j'}$, $v^{(\pm)}_{jj'} = \mathscr{U}_j \mathscr{U}_{j'} \pm \mathscr{V}_j \mathscr{V}_{j'}$ are pairing factors ($\mathscr{U}_j$, $\mathscr{V}_j$ are amplitudes from the Bogoliubov transformation for given one- quasiparticle state $\alpha^+_{j\sigma}\,|BCS\rangle$ - see (6.30)); $\langle j||\hat{\mathscr{M}}^{(el)}_\lambda||j'\rangle$ are reduced s.p. matrix elements of the electric transition operator $\hat{\mathscr{M}}^{(el)}_{\lambda\mu}$ (see (2.103) or (2.132) for its long-wave limit); $\langle j||\hat{M}_\lambda||j'\rangle$ are reduced matrix elements of the multipole operator $\hat{M}_{\lambda\mu}$ involved in the separable interaction (1.55); and $e^{(\lambda)}_{eff}[\tau]$ are effective nucleon ($\tau = n$ - neutron, $\tau = p$ - proton) charges depending on the transition process (e.g. for standard electric transitions for $\lambda > 1$: $e^{(\lambda)}_{eff}[p] = 1, e^{(\lambda)}_{eff}[n] = 0$). The expression (7.344) can be obtained from the definition (2.147) by the substitution $|i\rangle = |0^+_{g.s.}\rangle = |RPA\rangle$ and $|f\rangle = |J^\pi_\rho\rangle$ from (7.336) after the expressing the single-particle transition operator $\hat{\mathscr{M}}^{(el)}_{\lambda\mu}$ in terms of quasiparticle creation and annihilation operators (see (L.5)) and subsequently in terms of the phonon creation and annihilation operators (7.337) (for details see [164, 7]).

In the table 7.3 the excitation reduced probabilities for the lowest states in selected spherical nuclei calculated by (7.344) are compared with the corresponding experimental values. The Table 7.3 contains also excitation energies. From the Table 7.3 one can see that the agreement of calculated and experimental values of $B(E\lambda;\, 0^+_1 \to J^\pi_\rho)$ is only approximate, only in some cases the agreement can be considered as good. However, here it is necessary to note that the more theoretically erudite approaches, like Skyrme RPA approach - see e.g. [165, 162], do not give better results for reduced el.mg. probabilities of transitions in the lowest part of the excitation state spectra of spherical or deformed nuclei.

Nucleus	final state		transition	$B(E\lambda;\ 0_1^+ \to J_\rho^\pi)$	
	J_ρ^π	Energy [MeV]	type	exp. [W.u.]	theor. [W.u.]
^{114}Sn	2_1^+	1.299	E2	16	19
	3_1^-	2.275	E3	11	28
^{116}Sn	2_1^+	1.294	E2	12.9	22
	2_2^+	2.114	E2	0.05	0.05
	3_1^-	2.266	E3	39	37
^{144}Sm	2_1^+	1.660	E2	17	20
^{146}Gd	2_1^+	1.970	E2	>0.4	15
	3_1^-	1.580	E3	37	36
^{208}Gd	2_1^+	4.086	E2	8.0	7.8
	3_1^-	2.614	E3	38	35

Table 7.3: Reduced probabilities of $E\lambda$ transitions from the ground state to low-lying excited states (exp. data taken from [163], theoretical data taken from [164]). Reduced probabilities are presented in the Weisskopf units (2.163).

ii. Odd-A spherical nuclei

In the framework of the QPM model with the separable interaction (1.55) and using the double variational principle (7.310) and (7.325)) the odd-A nucleus low-lying eigen states of the Hamiltonian are searched for in the following form (the spherical analogue of the axially deformed nucleus wave function (7.311))

$$|JM;\nu\rangle_{odd} = C^{(J;\nu)} \left\{ \alpha^+_{JM} + \sum_{\lambda ij} D^{(J;\nu)}_{j\lambda i} \sum_{m\mu} C^{JM}_{jm\lambda\mu}\, \alpha^+_{jm} Q^+_{\lambda\mu i} \right\} |0\rangle \qquad (7.345)$$

with the normalization

$$\langle JM;\ \nu\,|JM;\ \nu\rangle = \left|\, C^{(J;\,\nu)}\right|^2 \left\{ 1 + \sum_{\lambda ij} \left| D^{(J,\,\nu)}_{j\lambda i}\right|^2 \right\} \qquad (7.346)$$

Amplitudes $C^{(J;\,\nu)}$ and $D^{(J;\,\nu)}_{j\lambda i}$ and structure of even-even core phonons $Q^+_{\lambda\mu i}$, together with the eigen energies $E_{J,\,\nu}$ of the states $|JM;\nu\rangle_{odd}$, can be obtained by the two- step method described in the text around expressions (7.327)-(7.328).

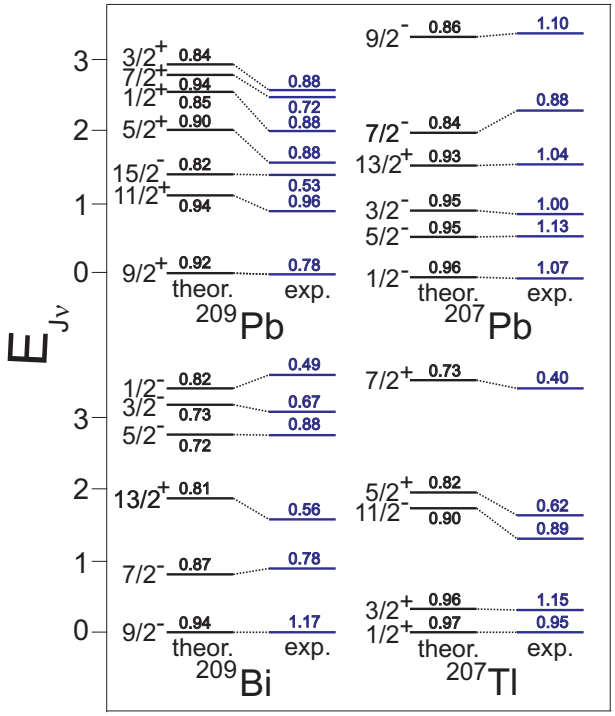


Figure 7.31: Comparison of low-lying excitation energies $E_{J\nu}$ and spectroscopic factors $S_J^{(\nu)}$, calculated by QPM approach, with corresponding experimental values (data taken from [164])

As an example of the comparison of calculated and experimental low-lying spectrum in the Fig. 7.31 the spectra of odd-A spherical nuclei ^{209}Bi, ^{207}Tl and ^{207,209}Pb (nuclei differing by one nucleon from the double magic ^{208}Pb) are shown. In the Fig. 7.31, the number above each calculated (theor.) level $E_{J\nu}$ is the value $|C^{(J,\,\nu)}|^2$ (the probability of finding the single-quasiparticle component $\alpha^+_{JM}|0\rangle$ in the given state $|JM;\,\nu\rangle_{odd}$). This number can be directly compared with the experimental value of the spectroscopic factor, which is defined as

$$S_J^{(\nu)} \equiv |\langle 0|\,\alpha_{JM}\,|JM;\,\nu\rangle|^2 = |C^{(J;\,\nu)}|^2 \qquad (7.347)$$

and which enters the expressions for cross sections of nuclear reactions with one nucleon transfer (so called stripping or pick up reactions discussed in the Chapter 11). The experimental values of $S_J^{(\nu)}$ were extracted from the experimental one- nucleon transfer reaction cross sections and their corresponding values are given above each experimental energy in the spectra shown in the Fig. 7.31. From the Fig. 7.31 relatively good agreement of calculated and experimental values for both energies and spectroscopic factors can be seen.

The results concerning the low-lying states in spherical nuclei presented above were obtained by the Quasiparticle+Phonon Model (QPM) (see [164]

and citations there in). The original version of this model started with the separable nucleon-nucleon interaction (1.55) and the RPA equations (7.308) and variational principle equations (7.310) (for even-even nuclei) or (7.325) (for odd-A nuclei) were solved using the quasi-boson approximation (7.256) and using the assumption (for add-A and odd-odd nuclei) that the valence quasiparticles of odd nucleons do not enter the structure of the even-even core phonons, which is expressed by (7.323). In later versions of the QPM (see e.g. [164, 166, 167, 168]) effects connected with more precise involving the Pauli principle (beyond the quasi-boson approximations) were discussed as well. However, these aspects go beyond the scope of this textbook. Some other methods going beyond the RPA are discussed also in the Section 7.3.2.

iii. Odd-odd spherical nuclei

As it was already mentioned the odd-odd nucleus is usually treated as the odd proton and odd neutron outside the vibrating even-even core with the Hamiltonian (7.332) which can be rewritten as follows

$$\hat{H} = \hat{H}_n + \hat{H}_p + \hat{H}_{core} + \hat{H}_{pcore} + \hat{H}_{ncore} + \hat{V}_{pn} \tag{7.348}$$

where $\hat{H}_n$ ($\hat{H}_p$) is the single-particle Hamiltonian of valence neutron (proton) (the second term in the first equation in (7.332), $\hat{H}_{pcore}$ ($\hat{H}_{ncore}$) is the interaction term between odd proton (odd neutron) and vibrating even-even core (the third term in the first equation in (7.332), and $\hat{V}_{np}$ is the interaction between odd proton and neutron (this interaction is involved in the last term in the first equation in (7.332).

In the case of spherical odd-odd nucleus the neutron and proton mean field are spherically symmetric with eigen vectors $|\nu_n j_n m_n\rangle$ ($\hat{H}_n|\nu_n j_n m_n\rangle = \epsilon_{\nu_n j_n}|\nu_n j_n m_n\rangle$) and $|\nu_p j_p m_p\rangle$ ($\hat{H}_p|\nu_p j_p m_p\rangle = \epsilon_{\nu_p j_p}|\nu_p j_p m_p\rangle$), where j_n (j_p) is the angular momentum of the odd neutron (proton) with the projection m_n (m_p) and ν_n (ν_p) are other quantum numbers (besides j and m) which characterize given single particle states. Then the eigen-vectors of the Hamiltonian $\hat{H}_n + \hat{H}_p$ is

$$|\nu_n\nu_p;\, j_n j_p;\, jm\rangle = \sum_{m_p m_n} C^{jm}_{j_n m_n\, j_p m_p}\, |\nu_n j_n m_n\rangle\, |\nu_p j_p m_p\rangle \tag{7.349}$$

$$\left(\hat{H}_n + \hat{H}_p\right) |\nu_n\nu_p;\, j_n j_p;\, jm\rangle = \mathscr{E}_{\nu_n j_n\, \nu_p j_p}\, |\nu_n\nu_p;\, j_n j_p;\, jm\rangle \tag{7.350}$$

with the corresponding energy

$$\mathscr{E}_{\nu_n j_n\, \nu_p j_p} = \epsilon_{\nu_n j_n} + \epsilon_{\nu_p j_p} \tag{7.351}$$

and with the possible values of the odd np pair angular momentum

$$j = |j_n - j_p|,\ |j_n - j_p| + 1,\ \ldots,\ j_n + j_p \tag{7.352}$$

That means, if the even-even core is fixed in its ground state and we can neglect term $\hat{H}_{pcore} + \hat{H}_{ncore} + \hat{V}_{np}$ in (7.348) then the energies of odd-odd nucleus states are $\mathscr{E}_{\nu_n j_n\, \nu_p j_p} + E^{(core)}_{g.s.}$, where $E^{(core)}_{g.s.}$ is the even-even core ground state energy ($\hat{H}_{core}|0\rangle_{core} = E^{(core)}_{g.s.}|0\rangle_{core}$). In such a case the energy of levels of odd-odd nucleus would be degenerated with respect to the values (7.352) of the the angular momentum j of the odd np- pair and with respect to all projections m (or m_n and m_p).

Experiments in the 60-ties showed that the lowest levels in the spectra of the spherical odd-odd nuclei are not degenerated with respect to the values of j. In order to get the splitting of energies according to j it is necessary to take into account the residual interaction $\hat{H}_{pcore} + \hat{H}_{ncore} + \hat{V}_{np}$. In the first papers with this problem the even-even core was suggested to be fixed in its ground state and from the residual interaction $\hat{H}_{pcore} + \hat{H}_{ncore} + \hat{V}_{np}$ only the neutron-proton interaction $\hat{V}_{np}$ was taken into account (residual interaction part corresponding to the interaction of odd-particles with the vibrations of the even-even core was neglected). The $\hat{V}_{np}$ interaction was supposed to be of a short range, e.g. δ- interaction or Yukawa type interaction with the tensor S_{12} term - see [173]

$$V_{np}(\vec{r} = \vec{r}_n - \vec{r}_p) \approx V_0\, \delta(\vec{r}) \qquad \text{or} \qquad V_{np}(\vec{r}) \approx V_0\, \frac{e^{-\mu r}}{r} + \tilde{V}_0\, \frac{e^{-\tilde{\mu} r}}{r}\, S_{12} \tag{7.353}$$

The taking into account of the residual interaction $\hat{V}_{np}$ was carried out by the construction and subsequent diagonalization of the matrix of the Hamiltonian $\hat{H} \approx \hat{H}_n + \hat{H}_p + \hat{V}_{np}$ within the basis of states $|\nu_n \nu_p;\ j_n j_p;\ jm\rangle$ for each fixed values ν_n, ν_p, j_n, j_p and with $j = |j_n - j_p|,\ \ldots,\ j_n + j_p$ (for spherical nuclei these matrix elements do not depend on m). After such diagonalization we obtain odd-odd nucleus wave functions in the form of linear combination of basis states $|\nu_n \nu_p; j_n j_p; jm\rangle$ and corresponding energies $E_{\nu_n \nu_p j_n j_p j}$. These eigen energies $E_{\nu_n \nu_p j_n j_p j}$ are not degenerated according to j. That means that from each originally degenerated level $\mathscr{E}_{\nu_n j_n\, \nu_p j_p}$ (for given $\nu_n \nu_p j_n j_p$) the multiplet of levels $E_{\nu_n \nu_p j_n j_p j}$ for $j = |j_n - j_p|,\ \ldots,\ j_n + j_p$ are created (see e.g. [174] where such approach was used for the first time).

The questions arised, which of multiplet levels $E_{\nu_n \nu_p j_n j_p j}$ ($j = |j_n - j_p|, \ldots, j_n + j_p$) corresponds to the minimal energy (for given $\nu_n \nu_p j_n j_p$). From theoretical point of view the answer is not unambiquous because different forms of the

$\hat{V}_{np}$ gives different results. The systematic analyses of experimental spectra of odd-odd nuclei, made in the end of the 40-ties allowed to formulate so called Nordheim's rules [175], which give the answer, at least partly:

- Weak Nordeim's rule: if, for given single particle states of odd neutron and proton, $|n_n l_n j_n m_n\rangle$ and $|n_p l_p j_p m_p\rangle$, spins of odd nucleons couple with orbital momenta parallelly (that means $j_p = l_p + 1/2$ and $j_n = l_n + 1/2$) or antiparallelly ($j_p = l_p - 1/2$ and $j_n = l_n - 1/2$), then the lowest level of the given multiplet $\nu_n j_n \nu_p j_p$ is not unambiguously determined and it can be arbitrary level $E_{\nu_n \nu_p j_n j_p j}$ with $j = |j_n - j_p|, \ldots, j_n + j_p$.
- Strong Nordheim's rule: if $j_p = l_p + 1/2$ and $j_n = l_n - 1/2$ or $j_p = l_p - 1/2$ and $j_n = l_n + 1/2$ then the lowest level $E_{\nu_n \nu_p j_n j_p j}$ from the multiplet $\nu_n j_n \nu_p j_p$ is one with $j = |j_n - j_p|$.

However, it must be remembered that there are many observed violations of Nordheim's rules.

Later, in the 70-ties and 80-ties, besides the interaction $\hat{V}_{np}$ also the coupling between odd nucleons and vibrating even-even core was taken into account (e.g. [176, 177] and citations therein). Methods involving all residual interactions $\hat{H}_{ncore} + \hat{H}_{pcore} + \hat{V}_{np}$ usually used the Bohr geometrical model, described in the Subsection 7.2.1, for the description of the vibrating even-even core (that means for the part $\hat{H}_{core}$ of the Hamiltonian (7.348)), and the Nilsson or Wood-Saxon spherical mean field for $\hat{H}_n + \hat{H}_p$. Used particle-core vibration, $\hat{H}_{pcore} + \hat{H}_{ncore}$, part of the Hamiltonian (7.348) is described in details in [6, 99] (see also [178] and citations therein).

As an example of the comparison of such calculations with experimental data in the Fig.7.32 the theoretical energies $E_{\nu_n \nu_p j_n j_p j}$ $j = |j_n - j_p|, \ldots, j_n + j_p$ of individual multiplets, created by the splitting of originally degenerated level $\mathscr{E}_{\nu_n j_n \nu_p j_p}$, with the corresponding experimental data are shown for ^{48}Sc and ^{122}Sb (exp. as well as theor. data taken from [176]). Each multiplet in this figure shows the parabolic character of the energy level splitting in the dependence on $j(j+1)$. In the paper [176], so called parabolic rule is formulated for this dependence. In [176] the residual interactions involves only part $\hat{H}_{pcore} + \hat{H}_{ncore}$, which was interpreted as the exchange of the quadrupole 2^+ and magnetic dipole 1^+ phonons between odd neutron and proton. The multiplets shown in panels a) and b) fulfill to the strong Nordheim rule, when the lowest level $E_{\nu_n \nu_p j_n j_p j}$ corresponds to $j = |j_n - j_p|$, while the multiples in panels c) and d) agree with the weak Nordheim rules.

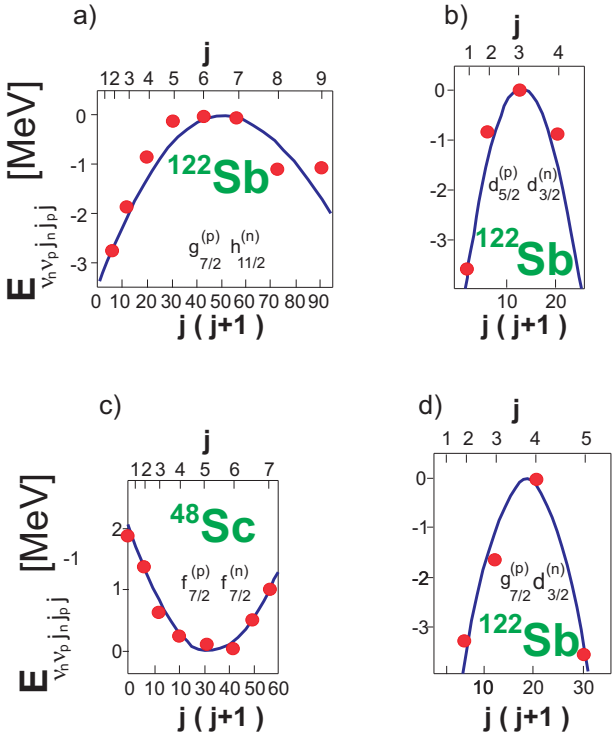


Figure 7.32: Demonstration of parabolic splitting of originally degenerated levels $\mathscr{E}_{\nu_n j_n \nu_p j_p}$ into multiplets $E_{\nu_n \nu_p j_n j_p j}$ ($j = |j_n - j_p|, \ldots, j_n + j_p$) in spherical odd-odd nuclei ^{48}Sc and ^{122}Sb. Circles corresponds to experimental energies and solid lines to the calculation performed in [176] with the exchange of 2^+ and 1^+ even-even core phonons between odd neutron and proton of the given odd-odd nucleus. The energies in each multiplet are read with respect to the parabola extreme. Each panel corresponds to one multiplet characterized by the spectroscopic assignment of the original neutron-proton configuration with the energy $\mathscr{E}_{\nu_n j_n \nu_p j_p}$ (data taken from [176]).

7.3.2.1.2 Intrinsic (non-rotational) low-lying states in deformed nuclei In this subsection some examples of the RPA results for low-lying states in axially deformed nuclei are discussed. We start again with the QPM Hamiltonian with the separable residual interaction (1.55) and the mean field in the form of deformed Wood-Saxon field with the l-s coupling [7, 166, 167]. Since the deformed nuclei are nuclei with only partly occupied valence proton and neutron shells and fully non-occupied shells are characteristic by strong pairing interaction (see the end of the Subsection 6.2.2.5), it is necessary to involve into the Hamiltonian the pairing interaction term. In the case of the simple version of the QPM this term is represented by the monopole pairing (see (6.24), (6.26)) which is taken into account by the simple BCS method discussed in the Subsections 6.2.2.1 and 6.2.2.2. Parameters of the used Wood-Saxon mean field potential and monopole pairing strength constants G_P and G_N for both

K^{π}_{ρ}	$E_{K\rho}$ MeV		$B(E\lambda)$ W.u.		$p^{(\rho)}_{\varpi} = \frac{1}{2}\left(\lvert X^{(\rho)}_{\varpi}\rvert^2 - \lvert Y^{(\rho)}_{\varpi}\rvert^2\right)$	
	exp	theor	exp	theor	in percentage	
0^-	0.922	0.9	8.1	8.3	$nn[651]\uparrow[521]\uparrow$ 30.2	$pp[532]\uparrow[413]\downarrow$ 29.6
oct					$nn[642]\uparrow[523]\downarrow$ 3.9	$pp[541]\uparrow[411]\uparrow$ 3.1
					$pp[550]\uparrow[400]\uparrow$ 2.4	$nn[615]\uparrow[505]\uparrow$ 2.4
0^+	1.100	1.0	1.0	2.0	$pp[413]\downarrow[413]\downarrow$ 40.4	$pp[532]\uparrow[532]\uparrow$ 38.8
β					$nn[505]\uparrow[505]\uparrow$ 6.6	$nn[651]\uparrow[651]\uparrow$ 3.5
					$nn[402]\downarrow[402]\downarrow$ 2.6	$nn[642]\uparrow[642]\uparrow$ 2.3
2^+	1.440	1.3	2.8	4.5	$nn[642]\uparrow[660]\uparrow$ 28.6	$nn[651]\uparrow[660]\uparrow$ 15.0
γ					$nn[402]\downarrow[400]\uparrow$ 10.8	$nn[521]\uparrow[521]\downarrow$ 10.7
					$nn[523]\downarrow[521]\downarrow$ 4.4	$pp[413]\downarrow[411]\downarrow$ 3.0
1^-	1.475	1.5	6.0	5.5	$pp[532]\uparrow[411]\downarrow$ 47.4	$nn[642]\uparrow[521]\uparrow$ 20.6
oct					$nn[523]\downarrow[651]\uparrow$ 5.8	$nn[521]\uparrow[400]\uparrow$ 2.4
					$nn[523]\downarrow[402]\downarrow$ 2.0	$nn[521]\downarrow[660]\uparrow$ 1.8
0^-		1.6		0.6	$pp[532]\uparrow[413]\downarrow$ 67.8	$nn[651]\uparrow[521]\uparrow$ 26.4
					$nn[642]\uparrow[523]\downarrow$ 1.2	
0^+		1.8		0.3	$pp[532]\uparrow[532]\uparrow$ 31.5	$pp[413]\downarrow[413]\downarrow$ 29.6
					$nn[505]\uparrow[505]\uparrow$ 13.5	$nn[651]\uparrow[651]\uparrow$ 8.2
					$nn[642]\uparrow[642]\uparrow$ 5.9	$nn[402]\downarrow[402]\downarrow$ 4.8
2^-		2.0		3.4	$nn[660]\uparrow[521]\uparrow$ 21.2	$nn[633]\uparrow[521]\uparrow$ 12.7
					$pp[532]\uparrow[420]\uparrow$ 11.7	$nn[642]\uparrow[530]\uparrow$ 10.6
					$nn[523]\downarrow[660]\uparrow$ 7.4	$pp[523]\uparrow[411]\uparrow$ 5.8
1^-		2.1		0.2	$pp[532]\uparrow[411]\uparrow$ 46.7	$nn[642]\uparrow[521]\uparrow$ 41.7
					$nn[523]\downarrow[651]\uparrow$ 6.1	
2^-		2.5		0.4	$nn[660]\uparrow[521]\uparrow$ 77.0	$nn[523]\downarrow[660]\uparrow$ 7.2
					$pp[532]\uparrow[420]\uparrow$ 4.0	$nn[633]\uparrow[521]\uparrow$ 2.8
					$nn[642]\uparrow[530]\uparrow$ 2.4	$pp[523]\uparrow[411]\uparrow$ 1.4

Table 7.4: One- phonon low-lying states in ^{154}Sm (data taken from [169]).

rare-earth and actinide regions of deformed nuclei are specified in [7, 169]. Strength constants of the multipole-multipole and spin multipole - spin multipole terms in the separable residual interaction (1.55) were determined by (7.341)-(7.343). The intrinsic non-rotational states $|K\rho\rangle$ of axially deformed nuclei are simultaneously eigen vectors of the intrinsic QPM Hamiltonian and the operator of the projection K of the angular momentum on the 3-d axis of the intrinsic fixed-body frame ($\hat{H}_{intr}\,|K\rho\rangle = E_{K\rho}\,|K\rho\rangle$, $\hat{I}_3\,|K\rho\rangle = K\,|K\rho\rangle$) - see (7.15), (7.18). It is necessary to remind that in the case of deformed nuclei the intrinsic Hamiltonian (in our case the intrinsic QPM Hamiltonian) gives only the intrinsic non-rotating states $|K\rho\rangle$ with their intrinsic energies $E_{K\rho}$. The real measurable spectrum corresponds to the spectrum in the laboratory frame which involves also rotational degrees of freedom. In this measurable spectrum of deformed nucleus we can always recognize rotational bands where each rotational band is built on the corresponding intrinsic state - see the discussion in the Subsection 7.1 and the example of the spectrum of ^{154}Sm given in the Fig.7.2. Further in this subsection only the intrinsic states and their energies are discussed for even-even, odd-A and odd-odd axially deformed nuclei.

i. Even-even axially deformed nuclei

In the Tab. 7.4 calculated QPM intrinsic energies $E_{K\rho}$ of the lowest intrinsic states $|K\rho\rangle$, taken as one- phonon states:

$$|K\rho\rangle = Q^{+}_{K^{\pi}_{\rho},\rho}|RPA\rangle = \boxed{\begin{array}{c}\text{see}\\(7.306)\end{array}} = \\ = \frac{1}{2}\sum_{\tau=n,p}\sum_{\varpi=ij,i\bar{j},\bar{i}\bar{j}}\left(X^{(\rho)}_{\varpi}\,b^{+}_{\varpi} - Y^{(\rho)}_{\varpi}\,b_{\varpi}\right)|RPA\rangle \qquad (7.354)$$

are compared with corresponding experimental energies [24] for ^{154}Sm. Besides intrinsic energies the Tab. 7.4 involves also the percentage $p^{(\rho)}_{\varpi}$ with which the highest neutron and proton two- quasiparticle components, created by the

[24] As the experimental energies the energies of the lowest level in the rotatinal bands built on the corresponding intrinsic states are taken in the Tab. 7.4 (compare energies of the lowest level in rotational bands given in the Fig. 7.2 with the "experimental" energies presented in the Tab. 7.4). This is only an approximation because we neglect here the difference between the energy of the lowest level in the given rotational band and corresponding intrinsic energy $E_{K\rho}$. For instance, if we neglect the Coriolis and centrifugal terms in the laboratory Hamiltonian (7.15), and the laboratory Hamiltonian is approximated by (7.17), then the energy of the lowest level of the rotational band built on the intrinsic state $|K\rho\rangle$ is given by (7.21) with $I = K$, which is different from $E_{K\rho}$ ($\langle I = KMK\rho|\hat{H}|I = KMK\rho\rangle \neq E_{K\rho}$). This difference is usually small and it is neglected in the Tab. 7.4

two- quasiparticle operator b^+_ϖ, enter the normalization condition of given intrinsic state (see (7.318) and (7.319)). Here every quasiparticle state is characterized by the corresponding Nilsson assignment $[Nn_3\Lambda]\ K^\pi$ (see the text above the Fig.5.5 in the Subsection 5.1.2.1), e.g. $[651]\uparrow \equiv [651]K^\pi = 3/2^+$, or $[521]\uparrow \equiv [521]K^\pi = 3/2^-$.

The Tab. 7.4 shows also the QPM reduced excitation probabilities $B(E\lambda; |0^+\rangle \to |K\rho\rangle)$ for the given intrinsic state $|K\rho\rangle$ in the comparison with corresponding experimental values (reduced probabilities are given in the Weisskopf single-particle units (2.163)).

From the Tab. 7.4 one can see that the most of the intrinsic low-lying states are collective, that means there are several two- quasiparticle components (not only one or two) giving a quite big contribution to the normalization (7.318) of the given intrinsic states. It is a general feature that the low lying intrinsic states in well-deformed nuclei, like β- and γ- quadrupole vibrations (see the Fig. 7.2), are collective in this sence.

ii. Odd-A axially deformed nuclei

As an example of the QPM results for odd-A nuclei in the Fig.7.33 the comparison of the calculated and experimental low-lying spectrum of ^{229}Ra. Since the nucleus ^{229}Ra is supposed to be axially deformed nucleus (quadrupole and hexadecapole deformation parameters are $\beta_2 \approx 0.15$, $\beta_4 \approx 0.065$) all levels of this nucleus are grouped to rotational bands. Each rotational band is built on corresponding intrinsic state $|K;\rho\rangle_{odd}$ (see (7.322)) ($K_\rho, K_i > 0$, $\mu_\nu \geq 0$; $\sigma_i, \sigma_\nu = \pm$):

$$|K_\rho;\ \rho\rangle_{odd} = \\ = \Big\{ \sum_i c_i^{(K_\rho,\,\rho)}\ \alpha^+_{i+} + \sum_{\substack{i\ K_i\ \sigma_i \\ \nu\ \mu_\nu\ \sigma_\nu}} d_{i\nu}^{(K_\rho;\,\rho)}\ \alpha^+_{i\sigma_i}\ Q^+_{\nu\mu_\nu}\ \delta_{K_i\sigma_i+\mu_\nu\sigma_\nu,\,K_\rho} \Big\} \mid 0\rangle \tag{7.355}$$

The structure of the intrinsic states (amplitudes $c_i^{(K_\rho,\,\rho)}$ and $d_{i\nu}^{(K_\rho;\,\rho)}$) and corresponding intrinsic energies $E_{K_\rho\rho}$ were obtained by the method given in the Subsection 7.3.1.2 applied for the QPM Hamiltonian with the separable residual interaction (1.55) with parameters (7.341)-(7.343). Theoretical energies of all levels in rotational bands demonstrated in the Fig.7.33 were determined by the diagonalization of the total Hamiltonian (7.15) matrix constructed within the basis of functions $|IMK\rho\rangle$ (see (7.27)) for each value of the total

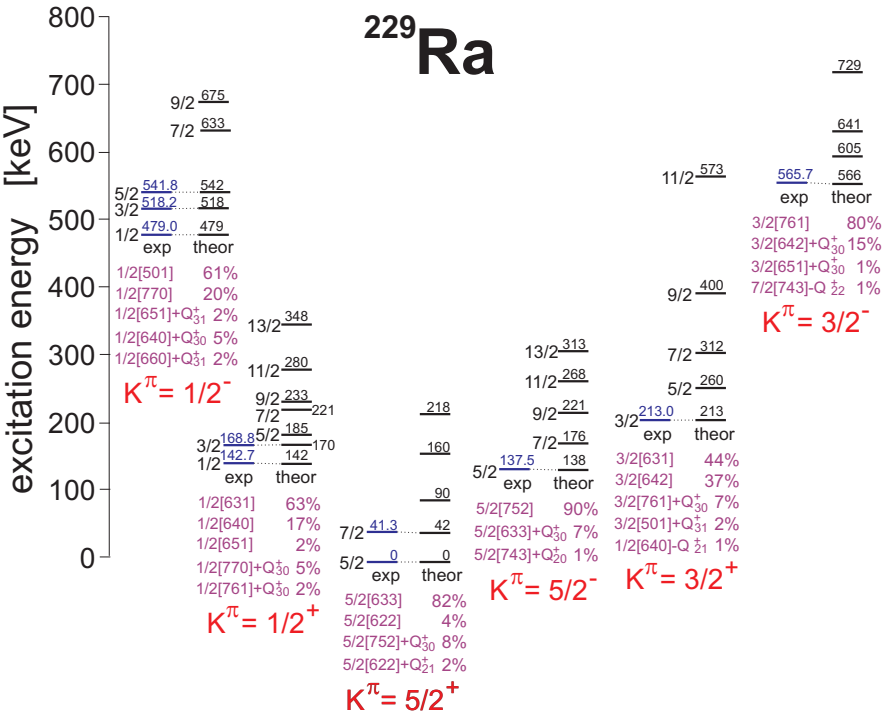


Figure 7.33: Energy levels of ^{229}Ra calculated using the QPM including Coriolis coupling are compared with those found experimentally (data taken from [170])

angular momentum I. The total Hamiltonian (7.15) involving intrinsic QPM Hamiltonian, pure rotational term $\frac{\hbar^2}{2\mathscr{F}}(\hat{I}^2 - \hat{I}_3^2)$ (see (7.17), (7.19)), Coriolis term (7.13), and centrifugal term (7.14) was used. The derivation of its matrix elements $\langle IMK\rho|\ \hat{H}\ |I'M'K'\rho'\rangle$ for odd-A nuclei is discussed in details in the Chapter 8 and here we do not discuss it. It is necessary only to note that during the diagonalization process the inertia parameters $\frac{\hbar^2}{2\mathscr{F}(+)}$ and $\frac{\hbar^2}{2\mathscr{F}(-)}$ for positive parity and negative parity bands were optimized in order to obtain good agreement of calculated energies with experimental ones. Optimal values of these parameters were $\frac{\hbar^2}{2\mathscr{F}(+)} = 7.92\ keV$ and $\frac{\hbar^2}{2\mathscr{F}(-)} = 7.79\, keV$.

In the Fig.7.33, under each rotational band (characterized by the angular momentum projection K and parity π) the highest one- quasiparticle and quasiparicle+phonon components of the corresponding intrinsic state (7.349) are listed together with their contribution $|c_i^{(K_\rho,\rho)}|^2$ and $|d_{i\nu}^{(K_\rho,\rho)}|^2$ into the normalization (7.324) (in percentage) of the given intrinsic state $|K_\rho;\rho\rangle_{odd}$. One can see that the most intrinsic low-lying states in deformed odd-A nucleus have one-quasiparticle character. This is a general feature of the well deformed odd-A nuclei (see [7, 164, 170, 171]).

Nuclei from the low-A edge of the deformed actinide region (Ra-Th re-

gion) are characteristic by so called octupole correlations (see e.g. [172]). In some nuclei from this region the octupole correlations are so strong that their mean field can have nonzero octupole deformation. In the presence of the nonzero octupole deformation a character of the nucleus spectrum changes in the comparison with the spectrum of the nucleus with only even multipolarity deformed mean field (see [6]). This situation is discussed in the Chapter 8. High octupole correlations in ^{229}Ra is also confirmed in the QPM calculation with even- λ deformations β_λ, concretely by large octupole phonon ($\lambda = 3$) components in the structure of the low-lying intrinsic states as it can be seen in the Fig.7.33 (see e.g. [171, 170]). The usual well deformed nuclei in the ground states and in the low-lying excitaion states have deformations with even λ. However, the odd λ deformations of the mean field can appear in the nucleus excited states with high values of angular momentum I if we take into account a dynamical changes of mean field deformations with the increase of I (fast rotations of nuclei) [25] .

iii. Odd-odd axially deformed nuclei

Similarly as in the case of deformed odd-A nuclei we will demonstrate the comparison of the theoretical and experimental low-lying spectra of odd-odd deformed nuclei starting with the Hamiltonian (7.15) ($\hat{H} = \hat{H}_{intr} + \hat{H}_{rot}$) with the intrinsic Hamiltonian in the QPM form (7.348)

$$\hat{H}_{intr} = \hat{H}_n + \hat{H}_p + \hat{H}_{ncore} + \hat{H}_{pcore} + \hat{V}_{pn} \tag{7.356}$$

and with the rotational part $\hat{H}_{rot}$ with the general form (7.12):

$$\hat{H}_{rot} = \frac{\hbar^2}{2\mathscr{F}} \left[\hat{I}^2 - \hat{I}_3^2\right] + \hat{H}_{cor} + \hat{H}_{centrifug} \tag{7.357}$$

For the purpose of simplicity, in this subsection we neglect the Coriolis term $\hat{H}_{cor}$ and centrifugal term $\hat{H}_{centrifug}$, so the rotational Hamiltonian is given only by the pure rotational term $\frac{\hbar^2}{2\mathscr{F}}\left[\hat{H}^2 - \hat{I}_3^2\right]$ (the Coriolis and centrifugal terms will be discussed in the Chapter 8). In such approximation the eigen vectors of the total Hamiltonian $\hat{H}$ in the lab. frame are described by kets $|IMK\rho\rangle$ (see (7.27)) with the corresponding eigen-energies (7.21):

$$E_{K_\rho,\,\rho}(I) = \langle IMK\rho|\hat{H}_{intr} + \frac{\hbar^2}{2\mathscr{F}}\left[\hat{I}^2 - \hat{I}_3^2\right]|IMK\rho\rangle \approx$$
$$\approx E_{K_\rho,\,\rho} + \frac{\hbar^2}{2\mathscr{F}}\left[I(I+1) - K^2\right] \tag{7.358}$$

[25] Dynamical changes of mean field deformations are discussed in the connection with so called cranking models discussed in the Subsection 8....

where $E_{K_\rho,\,\rho}$ is the intrinsic energy corresponding to the intrinsic state $|K_\rho\rho\rangle_{odd-odd}$ which is the eigen ket of the intrinsic QPM Hamiltonian $\hat{H}_{intr}$ ($\hat{H}_{intr}|K_\rho\rho\rangle_{odd-odd} = E_{K_\rho,\,\rho}\,|K_\rho\,\rho\rangle_{odd-odd}$). From the Subsection 7.3.1.2 we know that in the framework of the QPM with the odd-odd axially deformed nucleus the intrinsic wave function can be searched in the form (7.329) applied for the axially deformed nucleus where the angular momentum projection K_ρ on the 3-d intrinsic frame axis is the good quantum number (we suppose $K_{\nu_n}, K_{\nu_p} > 0;\ \sigma_n, \sigma_p, \sigma_i = \pm;\ K_\rho \geq 0;\ \mu_i \geq 0$) [26]:

$$|K_\rho\,\rho\,+\rangle_{odd-odd} = \Big\{ \sum_{\substack{\nu_n\nu_p \\ \sigma_n,\sigma_p=\pm}} c^{(K_\rho\,\rho)}_{\nu_n\nu_p}\ \alpha^+_{\nu_n\sigma_n}\alpha^+_{\nu_p\sigma_p}\ \delta_{K_{\nu_p}.\,\sigma_p+K_{\nu_n}.\,\sigma_n,\,K_\rho}$$

$$+ \sum_{\substack{\nu_n\nu_p \\ \sigma_n,\sigma_p=\pm}} \sum_{\substack{i\lambda_i\mu_i \\ \sigma_i=\pm}} d^{(K_\rho\,\rho)}_{\nu_n\nu_p\,i\lambda_i\mu_i}\ \alpha^+_{\nu_n\sigma_n}\alpha^+_{\nu_p\sigma_p}\ Q^+_{i\lambda_i\mu_i}\ \delta_{K_{\nu_p}.\,\sigma_p+K_{\nu_n}.\,\sigma_n+\mu_i.\,\sigma_i,\,K_\rho}\Big\}\ |0\rangle \tag{7.359}$$

where the action of the time reversal transformation on $|K_\rho\ \rho\,+\rangle_{odd-odd}$ is $|K_\rho\rho-\rangle_{odd-odd} \equiv \mathscr{T}\,|K_\rho\rho+\rangle_{odd-odd}$, which is the intrinsic state with the ket by a factor different from that with the opposite projection sign, $|-K_\rho\,\rho\rangle_{odd-odd}$ (see (1.48)).

It should be noted that usually in the low-lying intrinsics states $|K_\rho\rho+\rangle_{odd-odd}$ one two-quasiparticle component, say $\alpha^+_{\rho_n\sigma_n}\alpha^+_{\rho_p\sigma_p}\,|0\rangle$ predominates with the corresponding angular momentum projection $K = K_{\rho_n} + K_{\rho_p}$ (if $\sigma_n = \sigma_p$) or $K = |K_{\rho_n} - K_{\rho_p}|$ (if $\sigma_n = -\sigma_p$). Two intrinsic states $|K_\rho\,\rho = \rho_n\rho_p\rangle$ with $K_\rho = K_{\rho_n} + K_{\rho_p}$ and $K_\rho = |K_{\rho_n} - K_{\rho_p}|$ have a similar structure (that means amplitudes $c^{(K_\rho\,\rho)}_{\nu_n\nu_p}$ and $d^{(K_\rho\,\rho)}_{\nu_n\nu_p\,i\lambda_i\mu_i}$) and they form the well known Gallagher-Mozskowski (GM) doublet with the corresponding GM splittining energy

$$\Delta E^{(GM)}_{\rho=\rho_n\rho_p} = E_{K_\rho=|K_{\rho n}-K_{\rho p}|,\ \rho} - E_{K_\rho=K_{\rho n}+K_{\rho p},\ \rho} \tag{7.360}$$

One should realize that the nonzero value of this GM splitting energy is caused by the residual interaction $\hat{H}_{ncore}+\hat{H}_{pcore}+\hat{V}_{np}$ in the intrinsic Hamilto-

[26] Indexes σ_n, σ_p, σ_i mean the sign of the angular momentum projections K_{ν_n}, K_{ν_p}, μ_i of the odd neutron, odd proton and core phonon, respectively ($\sigma_n, \sigma_p, \sigma_i = \pm 1$). In the case of the axial deformation only angular momentum projections are good quantum numbers. That means angular momentum (or multipolarity) λ_i of the phonon $Q^+_{i\lambda_i\mu_i}$ is not generally good quantum number (only the projection μ_i and the parity π_i is good quantum numbers) but in the case of the QPM the coupling between core phonons of different multipolarities (e.g. quadrupole $\lambda = 2$ with hexadecapole $\lambda = 4$ or with higher multipolarity $\lambda > 4$) can be neglected (see e.g. [7]) and therefore we use the phonon mutipolarity λ_i as one of the identification indexes for phonons $Q^+_{i\lambda_i\mu_i}$ as well. We remind that the index i enumerates phonons with the same λ and μ.

nian (7.356). If this residual interaction is neglected and the intrinsic Hamiltonian is formed only by neutron and proton mean field ($\hat{H}_{intr} \approx \hat{H}_n + \hat{H}_p$) then the GM splittiong energy is zero and we have degenerated GM doublet. So, the value of the $\Delta E^{(GM)}_{\rho=\rho_n\rho_p}$,which is directly connected with the difference, $E_{K_\rho=|K_{\rho_n}-K_{\rho_p}|,\,\rho=\rho_n\rho_p}(I=|K_{\rho_n}-K_{\rho_p}|)-E_{K_\rho=K_{\rho_n}+K_{\rho_p},\,\rho=\rho_n\rho_p}(I=K_{\rho_n}+K_{\rho_n})$, between the lowest levels of two bands built on the same intrinsic configuration $\rho=\rho_n\rho_p$ but with different projections $K_\rho=|K_{\rho_n}-K_{\rho_p}|$ and $K_\rho=K_{\rho_n}+K_{\rho_p}$, can give some information about the residual interaction $\hat{H}_{ncore}+\hat{H}_{pcore}+\hat{V}_{np}$.

From (7.358) one can see that above each intrinsic state with the energy $E_{K_\rho,\,\rho}$ the rotational band with levels $E_{K_\rho,\,\rho}(I)$ is created. From the Section 7.1 it is known (see (7.32) - (7.35)) that in the case of even-even or odd-odd axially deformed nuclei (where total angular momenta I are integer) two type of rotational bands can be recognized: band with $K_\rho=0$ and band with $K_\rho\neq 0$. In the case of $K_\rho\neq 0$ the corresponding rotational band involves levels $E_{K_\rho,\,\rho}(I)$ with the standard sequence of total angular momenta: $I=K_\rho,\ K_\rho+1,\ K_\rho+2,\ \ldots$ (see (7.35)). However the intrinsic state $|K_\rho=0,\ \rho+\rangle_{odd-odd}$ with the zero projection has additional symmetry (7.32), $\hat{R}_1\,|K_\rho=0,\ \rho+\rangle = r_1\,|K_\rho=0,\ \rho+\rangle$ with the signature r_1 ($r_1=\pm 1$) being a good quantum number. As a result, in fact, we have two rotational bands for $K_\rho=0$ for two values of the signature $r_1=\pm 1$ with two different sequences of total angular momenta (see (7.34):

$$\begin{aligned} &\text{for } r_1=+1: \qquad I=0,\ 2,\ 4,\ 6,\ldots \qquad \text{only even } I \\ &\text{for } r_1=-1: \qquad I=0,\ 1,\ 3,\ 5,\ldots \qquad \text{only odd } I \end{aligned} \tag{7.361}$$

and for the case $K_\rho=0$ so called Newby shift can be defined (see e.g. [179])

$$\Delta E^{(N)}_{\rho\,K_\rho=0} \equiv E_{K_\rho=0\,\rho\,r_1=-1} - E_{K_\rho=0\,\rho\,r_1=+1} \tag{7.362}$$

which determines the energy shift between two $K_\rho=0$ rotational bands with the same internal structure differing only by the signature quantum number $r_1=\pm 1$.

As an example, in the Fig.7.34 the experimental low-lying rotational bands in axially deformed ^{166}Ho is shown. Below each rotational band the angular momentum projection K and parity π are given. Two rotational bands, marked with the same capital letter, are built on the intrinsic states where the same proton-neutron two-quasiparticle component $\rho_1\rho_2$ plays a dominant role. That means, if the residual interaction in the intrinsic Hamiltonian is neglected then the corresponding intrinsic states of these two bands form the

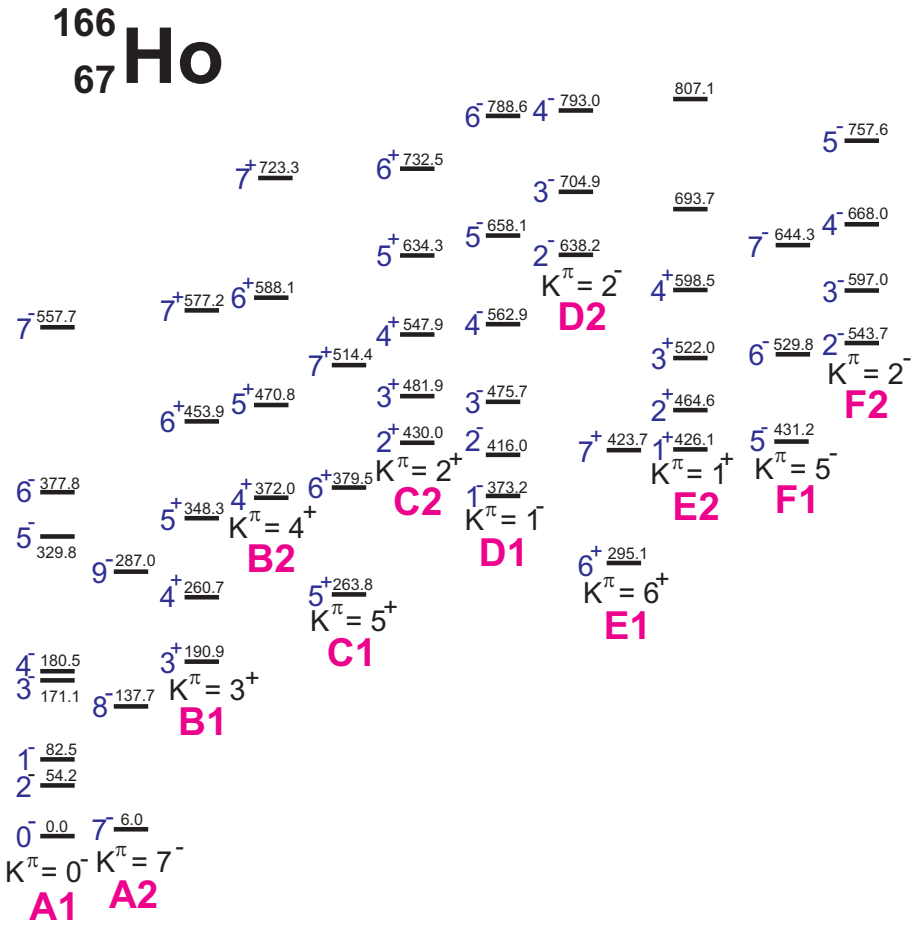


Figure 7.34: Experimental low-lying levels of rotational bands observed in the axially deformed odd-odd nucleus ^{166}Ho (data taken from [179]).

GM doublet. For instance, two bands, denoted in the Fig.7.34 as A1 and A2, have the same dominant proton-neutron two-quasiparticle component, $(p\,\frac{7}{2}[523] \pm n\,\frac{7}{2}[633])$ (see the Tab.7.5), with angular momentum projections $K = |K_n \pm K_p| = |7/2 \pm 7/2|$, which gives $K = 0$ for the band A1 and $K = 7$ for the band A2. Both the bands, A1 and A2, have the negative parity $\pi = -1$. A similar situation accurs for bands B1 and B2 or C1 and C2 etc. Each level, presented in the spectrum in the Fig.7.34, is characterized by its experimental energy in keV (the number above each level) and by the angular momentum I and parity π (the number on the left). The Fig.7.34 involves only rotational bands with bandheads (the lowest level in the given rotational band) up to the energy 500 keV.

The structure of the intrinsic states, above which rotational bands shown in the Fig.7.34 are built, is given in the Table 7.5. The corresponding band assignment is given in the first column of this table. The second column

Table 7.5: Structure and energies of the intrinsic states in ^{166}Ho (data taken from [179]).

band	structure of the intrinsic state $\lvert K_\rho, \rho+\rangle_{odd-odd}$	first level of rotational band (theory) [keV]	first level of rotational band (exper.) [keV]
A1	$\left(p\frac{7}{2}[523] - n\frac{7}{2}[633]\right)$ 95%	0.0	0.0
$K^\pi = 0^-$	$\left(p\frac{7}{2}[523] - n\frac{3}{2}[651]\right) - Q^+_{22}$ 5%	$\Delta E^{(N)} = 32.6$ keV	
A2	$\left(p\frac{7}{2}[523] + n\frac{7}{2}[633]\right)$ 83%		
$K^\pi = 7^-$	$\left(p\frac{7}{2}[523] - n\frac{3}{2}[521]\right) + Q^+_{32}$ 4%		
	$\left(p\frac{3}{2}[411] + n\frac{7}{2}[633]\right) + Q^+_{32}$ 4%		
	$\left(p\frac{7}{2}[523] + n\frac{3}{2}[651]\right) + Q^+_{22}$ 3%		
	$\left(p\frac{3}{2}[541] + n\frac{7}{2}[633]\right) + Q^+_{22}$ 2%		
	$\left(p\frac{3}{2}[521] + n\frac{7}{2}[633]\right) + Q^+_{32}$ 1%	13.2	5.9
B1	$\left(p\frac{7}{2}[523] - n\frac{1}{2}[521]\right)$ 60%		
$K^\pi = 3^+$	$\left(p\frac{1}{2}[411] - n\frac{7}{2}[633]\right)$ 31%		
	$\left(p\frac{3}{2}[411] + n\frac{7}{2}[633]\right) - Q^+_{22}$ 2%		
	$\left(p\frac{3}{2}[541] + n\frac{7}{2}[633]\right) - Q^+_{32}$ 1%	142.2	190.9
B2	$\left(p\frac{7}{2}[523] + n\frac{1}{2}[521]\right)$ 70%		
$K^\pi = 4^+$	$\left(p\frac{1}{2}[411] + n\frac{7}{2}[633]\right)$ 10%		
	$\left(p\frac{7}{2}[523] - n\frac{7}{2}[633]\right) + Q^+_{22}$ 8%		
	$\left(p\frac{7}{2}[523] + n\frac{5}{2}[512]\right) - Q^+_{22}$ 6%	305.2	371.9
C1	$\left(p\frac{7}{2}[523] + n\frac{3}{2}[521]\right)$ 30%		
$K^\pi = 5^+$	$\left(p\frac{3}{2}[411] + n\frac{7}{2}[633]\right)$ 60%		
	$\left(p\frac{7}{2}[523] + n\frac{7}{2}[633]\right) - Q^+_{32}$ 5%		
	$\left(p\frac{7}{2}[541] - n\frac{1}{2}[521]\right) + Q^+_{22}$ 2%	292.1	263.8
C2	$\left(p\frac{7}{2}[523] - n\frac{3}{2}[521]\right)$ 39%		
$K^\pi = 2^+$	$\left(p\frac{3}{2}[411] - n\frac{7}{2}[633]\right)$ 50%		
	$\left(p\frac{7}{2}[523] - n\frac{7}{2}[633]\right) + Q^+_{32}$ 4%		
	$\left(p\frac{7}{2}[523] + n\frac{1}{2}[521]\right) - Q^+_{22}$ 3%	592.1	430.0

band	structure of the intrinsic state $\lvert K_\rho, \rho+\rangle_{odd-odd}$	first level of rotational band (theory) [keV]	first level of rotational band (exper.) [keV]
D1	$\left(p\frac{3}{2}[411] - n\frac{1}{2}[521]\right)$ 94%		
$K^\pi = 5^-$	$\left(p\frac{3}{2}[411] + n\frac{1}{2}[521]\right) - Q^+_{22}$ 1%		
	$\left(p\frac{3}{2}[411] + n\frac{3}{2}[651]\right) - Q^+_{32}$ 1%		
	$\left(p\frac{3}{2}[411] - n\frac{5}{2}[642]\right) + Q^+_{32}$ 1%	369.0	373.1
D2	$\left(p\frac{3}{2}[411] + n\frac{1}{2}[521]\right)$ 95%		
$K^\pi = 2^-$	$\left(p\frac{7}{2}[523] + n\frac{1}{2}[521]\right) - Q^+_{32}$ 1%		
	$\left(p\frac{3}{2}[541] + n\frac{1}{2}[521]\right) + Q^+_{30}$ 1%	531.2	638.2
E1	$\left(p\frac{7}{2}[523] + n\frac{5}{2}[512]\right)$ 80%		
$K^\pi = 6^+$	$\left(p\frac{7}{2}[523] + n\frac{5}{2}[523]\right)$ 10%		
	$\left(p\frac{7}{2}[523] + n\frac{1}{2}[510]\right) + Q^+_{22}$ 5%		
	$\left(p\frac{7}{2}[523] - n\frac{9}{2}[514]\right) - Q^+_{22}$ 4%	362.3	295.1
E1	$\left(p\frac{7}{2}[523] - n\frac{5}{2}[512]\right)$ 76%		
$K^\pi = 1^+$	$\left(p\frac{7}{2}[513] - n\frac{5}{2}[523]\right)$ 10%		
	$\left(p\frac{7}{2}[523] + n\frac{9}{2}[514]\right) + Q^+_{22}$ 4%		
	$\left(p\frac{7}{2}[523] - n\frac{1}{2}[400]\right) - Q^+_{32}$ 4%	407.9	426.1
F1	$\left(p\frac{7}{2}[523] + n\frac{3}{2}[651]\right)$ 81%		
$K^\pi = 5^-$	$\left(p\frac{3}{2}[541] + n\frac{7}{2}[633]\right)$ 12%		
	$\left(p\frac{7}{2}[523] - n\frac{7}{2}[633]\right) - Q^+_{22}$ 6%	452.5	531.2
F2	$\left(p\frac{7}{2}[523] - n\frac{3}{2}[651]\right)$ 62%		
$K^\pi = 2^-$	$\left(p\frac{3}{2}[541] - n\frac{7}{2}[633]\right)$ 5%		
	$\left(p\frac{7}{2}[523] - n\frac{7}{2}[633]\right) + Q^+_{22}$ 26%		
	$\left(p\frac{7}{2}[523] + n\frac{1}{2}[660]\right) - Q^+_{22}$ 7%	527.1	543.7

contains the components and percentages with which they enter the structure of the corresponding intrinsic state $|K^{\pi}_{\rho}\ \rho+\rangle$ ($|c^{(K_\rho,\rho)}_{\nu_n\nu_p}|^2$ for two-quasiparticle components and $|d^{(K_\rho,\rho)}_{\nu_n\nu_p i\ \lambda_i\mu_i}|^2$ for two-quasiparticle plus phonon components). The third column contains the energy of the first member of the rotational band built on the corresponding intrinsic state. These values were obtained by means of the standard $I(I+1)$ formula (7.358) without an inclusion of Coriolis coupling (i.e. $\big[E_{K_\rho,\rho}(I) - E_{K_0,\rho_0} + \frac{\hbar^2}{2\mathscr{F}}[I(I+1) - K^2_\rho]_{I=K_\rho} - \frac{\hbar^2}{2\mathscr{F}}[I(I+1) - K^2_0]_{I=K_\rho}\big]$. The inertial parameters were assumed to be $\frac{\hbar^2}{2\mathscr{F}} \approx 9$ keV for all bands.The individual GM doublets are separated by the double-line. The GM splitting energy (7.360) can be deduced from the third column for each GM doublet. When $K = 0$. the third column also contains the Newby shift (7.362).

It can be observed from the Tab.7.5 that the low-lying intrinsic states in the odd-odd ^{166}Ho have predominantly proton-neutron two-quasiparticle character with a small vibrating even-even core components (see [179] for more details).

7.3.2.2 RPA description of higher energy part of nuclear spectra

7.3.2.2.1 Isoscalar and isovector transitions, strength functions, sum rules Nuclei, similarly as all bound quantum systems, are characterized by the increasing density of levels with the increasing excitation energy. It was already mentioned in the beginning of the Subsection 7.3.1.3.1 (see also schematic Fig. 1.6) that, starting with some relatively high excitation energy, the density of individual levels is so high that it is not possible to distinguish experimentally each individual level and in some concrete experiments (e.g. in the photoabsorption cross section measurements or in the cross-section experiments of other nuclear reactions) only the envelope curve involving many individual levels can be observed. Very often we meet the situation when this envelope curve for a particular quantity, e.g. probability of the excitation of the nucleus in the concrete process or the cross-section of the concrete nuclear reaction, shows the broad peak. In the case when this broad peak concerns the excitation probability we speak about giant resonances of nuclei.

The excitation probability of given nuclear process is determined by the square of the matrix element of the corresponding transition operator of the given process, calculated between the final (excited) and initial (usually ground state) states. In this subsection we restrict ourselves to the discussion of the electromagnetic excitations in the framework of the RPA. From the Subsection 2.2.2.2 we know that in the framework of the long-wave approximation the electric and magnetic transition operators, $\hat{\mathscr{M}}^{(el)}_{\lambda\mu}$ and $\hat{\mathscr{M}}^{(mag)}_{\lambda\mu}$, with the multipolarity λ and its projection μ are given by (2.132) and (2.145), respectively. Further these operators will be rewritten in order to specify the isospin character of the corresponding transition. For electric type transition operators we have

$$\hat{\mathscr{M}}^{(el)}_{\lambda\mu} = \boxed{\begin{array}{c}\text{see}\\(2.132)\end{array}} = \sum_{k=1}^{A} e_k\, r_k^{\lambda}\, Y_{\lambda\mu}(\hat{r}_k) = \boxed{\begin{array}{c}\text{because of (1.15):}\\ e_k = e\,(\frac{1}{2} - (\hat{t}_z)_k)\end{array}} =$$

$$= \frac{e}{2}\sum_{k=1}^{A} r_k^{\lambda}\, Y_{\lambda\mu}(\hat{r}_k) - e\sum_{k=1}^{A}(\hat{t}_z)_k\, r_k^{\lambda}\, Y_{\lambda\mu}(\hat{r}_k) =$$

$$= \frac{e}{2}\,\hat{\mathscr{M}}^{(el)}_{\lambda\mu}(\Delta T = 0, \Delta T_z = 0) - \frac{e}{2}\,\hat{\mathscr{M}}^{(el)}_{\lambda\mu}(\Delta T = 1, \Delta T_z = 0) \qquad (7.363)$$

where we defined isoscalar electric, $\hat{\mathscr{M}}^{(el)}_{\lambda\mu}(\Delta T = 0, \Delta T_z = 0)$, and isovector

electric, $\hat{\mathscr{M}}^{(el)}_{\lambda\mu}(\Delta T=1,\Delta T_z=0)$, transition operators [27]:

$$\hat{\mathscr{M}}^{(el)}_{\lambda\mu}(\Delta T=0,\Delta T_z=0)\equiv\sum_{k=1}^{A} r_k^{\lambda}\,Y_{\lambda\mu}(\hat{r}_k)$$
$$\hat{\mathscr{M}}^{(el)}_{\lambda\mu}(\Delta T=1,\Delta T_z=0)\equiv\sum_{k=1}^{A} 2(\hat{t}_z)_k\,r_k^{\lambda}\,Y_{\lambda\mu}(\hat{r}_k) \qquad (7.364)$$

Processes, connected with the isoscalar electric transition operators $\hat{\mathscr{M}}^{(el)}_{\lambda\mu}(\Delta T=0,\Delta T_z=0)$, do not change the isospin during the transition ($\Delta T=\Delta T_z=0$). The isovector transition operators, $\hat{\mathscr{M}}^{(el)}_{\lambda\mu}(\Delta T=1,\Delta T_z=0)$, correspond to the electromagnetic transitions with the change $\Delta T=1$ of the nucleus isospin. Since during electromagnetic transitions in nuclei the charge of the nucleus (which is directly connected with the z- component of the isospin - see the text below (1.31): $\hat{Q}=e\,(A/2-\hat{T}_z)$) the z- component of the nucleus isospin is not changed during the electromagnetic transition for both $\Delta T=0$ and $\Delta T=1$ cases we have $\Delta T_z=0$.

Similarly for magnetic type transitions we have (using long-wave approximation):

$$\hat{\mathscr{M}}^{(mag)}_{\lambda\mu}=\boxed{\begin{array}{c}\text{see}\\(2.145)\end{array}}=\sum_{k=1}^{A}\left[g_k^{(s)}\hat{\vec{s}}_k+\frac{2}{\lambda+1}g_k^{(l)}\hat{\vec{l}}_k\right]\mu_N\,\vec{\nabla}_k\,r_k^{\lambda}Y_{\lambda\mu}(\hat{r})=$$
$$=\boxed{\begin{array}{c}\text{because of (2.144), (2.146):}\\ g_k^{(l)}=\frac{1}{2}-(t_z)_k;\ g_k^{(s)}=\frac{1}{2}\,(g_p^{(s)}+g_n^{(s)})-(t_z)_k\,(g_p-g_n)\end{array}}=$$
$$=\mu_N\sum_{k=1}^{A}\Big[\,\frac{g_n+g_p}{2}\,\hat{\vec{s}}_k+\frac{1}{\lambda+1}\,\hat{\vec{l}}_k\,\Big]\,\vec{\nabla}_k\,r_k^{\lambda}Y_{\lambda\mu}(\hat{r}_k)$$
$$+\mu_N\sum_{k=1}^{A}\Big[\,(g_n-g_p)\,\hat{\vec{s}}_k-\frac{2}{\lambda+1}\,\hat{\vec{l}}_k\,\Big]\,(\hat{t}_z)_k\,\vec{\nabla}_k\,r_k^{\lambda}Y_{\lambda\mu}(\hat{r}_k)\equiv$$
$$=\hat{\mathscr{M}}^{(mag)}_{\lambda\mu}(\Delta T=0,\ \Delta T_z=0)-\ \hat{\mathscr{M}}^{(mag)}_{\lambda\mu}(\Delta T=1,\ \Delta T_z=0) \qquad (7.365)$$

[27] The isovector electric transition operator is defined sometimes (see e.g. [181]) without a factor 2, that means

$$\hat{\mathscr{M}}^{(el)}_{\lambda\mu}(\Delta T=1,\Delta T_z=0)\equiv\sum_{k=1}^{A}(\hat{t}_z)_k\,r_k^{\lambda}\,Y_{\lambda\mu}(\hat{r}_k)$$

where isoscalar magnetic, $\hat{\mathscr{M}}^{(mag)}_{\lambda\mu}(\Delta T=0,\Delta T_z=0)$, and isovector magnetic, $\hat{\mathscr{M}}^{(mag)}_{\lambda\mu}(\Delta T=1,\ \Delta T_z=0)$, transition operators are introduced:

$$\begin{aligned}
&\hat{\mathscr{M}}^{(mag)}_{\lambda\mu}(\Delta T=0,\Delta T_z=0)\equiv\\
&\quad\equiv\mu_N\sum_{k=1}^{A}\Big[\,\frac{g_n+g_p}{2}\,\hat{\vec{s}}_k+\frac{1}{\lambda+1}\,\hat{\vec{l}}_k\,\Big]\,\vec{\nabla}_k\,r_k^{\lambda}Y_{\lambda\mu}(\hat{r}_k)\\
&\hat{\mathscr{M}}^{(mag)}_{\lambda\mu}(\Delta T=1,\Delta T_z=0)\equiv\\
&\quad\equiv-\mu_N\sum_{k=1}^{A}\Big[\,(g_n-g_p)\,\hat{\vec{s}}_k-\frac{2}{\lambda+1}\,\hat{\vec{l}}_k\,\Big]\,(\hat{t}_z)_k\,\vec{\nabla}_k\,r_k^{\lambda}Y_{\lambda\mu}(\hat{r}_k)
\end{aligned}\tag{7.366}$$

All these electromagnetic transition operators can be rewritten in more compact form:

$$\begin{aligned}
\hat{\mathscr{M}}^{(el)}_{\lambda\mu}(\Delta T)&=e\,\sum_{k=1}^{A}e_k^{(eff)}(\Delta T)\,r_k^{\lambda}\,Y_{\lambda\mu}(\hat{r}_k)\\
\hat{\mathscr{M}}^{(mag)}_{\lambda\mu}(\Delta T)&=-\mu_N\sum_{k=1}^{A}\Big[\,g_k^{(s;\,eff)}(\Delta T)\,\hat{\vec{s}}_k+\frac{1}{\lambda+1}g_k^{(l;\,eff)}(\Delta T)\,\hat{\vec{l}}_k\,\Big]\\
&\qquad\cdot\vec{\nabla}_k\,r_k^{\lambda}\,Y_{\lambda\mu}(\hat{r}_k)
\end{aligned}\tag{7.367}$$

where μ_N is so called nuclear magneton $\mu_N=\frac{e\hbar}{2mc}$ (see the text between (2.148) and (2.149)) and

$$\begin{aligned}
e_k^{(eff)}(\Delta T=0)&=\begin{cases}+1 & \text{for protons}\\ +1 & \text{for neutrons}\end{cases}\\
e_k^{(eff)}(\Delta T=1)&=\begin{cases}-1 & \text{for protons}\\ +1 & \text{for neutrons}\end{cases}\\
e_k^{(eff)}(\Delta T=p)&=\begin{cases}+1 & \text{for protons}\\ 0 & \text{for neutrons}\end{cases}
\end{aligned}\tag{7.368}$$

for electric transitions and

$$\begin{aligned}
g_k^{(s,\,eff)}(\Delta T=0)&=\begin{cases}\big(g_p^{(s)}+g_n^{(s)}\big)/2 & \text{for protons}\\ \big(g_p^{(s)}+g_n^{(s)}\big)/2 & \text{for neutrons}\end{cases}\\
g_k^{(s,\,eff)}(\Delta T=1)&=\begin{cases}-(g_n^{(s)}-g_p^{(s)})/2 & \text{for protons}\\ +(g_n^{(s)}-g_p^{(s)})/2 & \text{for neutrons}\end{cases}
\end{aligned}$$

$$
\begin{aligned}
g_k^{(s,\,eff)}(\Delta T = p) &= \begin{cases} g_p^{(s)} & \text{for protons} \\ g_n^{(s)} & \text{for neutrons} \end{cases} \\
g_k^{(l,\,eff)}(\Delta T = 0) &= \begin{cases} +1 & \text{for protons} \\ +1 & \text{for neutrons} \end{cases} \\
g_k^{(l,\,eff)}(\Delta T = 1) &= \begin{cases} +1 & \text{for protons} \\ -1 & \text{for neutrons} \end{cases} \\
g_k^{(l,\,eff)}(\Delta T = p) &= \begin{cases} +1 & \text{for protons} \\ 0 & \text{for neutrons} \end{cases}
\end{aligned}
\tag{7.369}
$$

for magnetic transitions. In (7.368) - (7.369), $\Delta T = 0$ concerns isoscalar transitions, $\Delta T = 1$ is connected with isovector transitions, and $\Delta T = p$ is a label for the full (standard) electric or magnetic transition operators (7.363) or (7.365) (that means only proton contribution for electric transitions; and $g_k^{(l)} = 1$ for protons, $g_k^{(l)} = 0$ f or neutrons, $g_k^{(s)} = g_p^{(s)}$ for protons and $g_k^{(s)} = g_n^{(s)}$ for neutrons in the case of magnetic transitions). In all expressions (7.365) - (7.369):

$$
g_p^{(s)} = \boxed{\begin{array}{c}\text{see} \\ (2.144)\end{array}} = 5.586\,\zeta \qquad g_n^{(s)} = \boxed{\begin{array}{c}\text{see} \\ (2.144)\end{array}} = -3.826\,\zeta \tag{7.370}
$$

where $\zeta \approx 0.7$ is a reducing or quenching factor connected with the meson exchange currents in nuclei (see [52] and citations therein).

Standard electromagnetic excitation process of nuclei (like photoabsorption) is connected with transition operator (7.367) where effective charges (7.368) and effective gyromagnetic ratios (7.369) correspond to $\Delta T = p$. Other processes can be connected with isoscalar or isovector transition operators. For instance, inelastic scattering of alpha particles, which is often used for obtaining experimental information on giant resonances, is associated with isoscalar transition operators (because the isospin of the alpha particle is zero).

For the description of the envelope curve mentioned above, describing excitation probability of the nucleus as a function of the excitation energy in the given process, it is useful to introduce so called strength function. Usually the strength function for given type of the excitation is defined as the energy

distribution of the excitation probability ($X = el.$ or $mag.$; $\Delta T = 0,\ 1,\ p$) [28]

$$S_0(X\lambda\mu;\ \Delta T;\ E) \equiv \sum_{\nu\neq 0} \left|\langle\nu|\ \mathscr{M}^{(X)}_{\lambda\mu}(\Delta T)\ |0\rangle\right|^2 \delta(E - E_\nu) \qquad (7.371)$$

where the summation $\sum_{\nu\neq 0}$ goes through all excited states $|\nu\rangle$ with nonzero excitation energy E_ν calculated in the framework of the used model (it means all RPA one-phonon states in this subsection), and $|0\rangle$ is the model ground state ($|0\rangle = |RPA\rangle$ in this subsection). Very often this definition of the strength function is extended and so called energy weighted strength function of the k-th order,

$$S_k(X\lambda\mu;\ \Delta T;\ E) \equiv \sum_{\nu\neq 0} E^k_\nu\ \left|\langle\nu|\ \mathscr{M}^{(X)}_{\lambda\mu}(\Delta T)\ |0\rangle\right|^2 \delta(E - E_\nu), \qquad (7.372)$$

is introduced.

In order to simulate so called escape width (coupling of each bound state $|\nu\rangle$ with states of the continuum spectrum) and also the coupling to complex configurations (coupling of one-phonon states with more-phonon components of the excited state wave function) the delta- function $\delta(E - E_\nu)$ in the definition (7.372) or (7.371) is usually substituted by Lorentz weight function (see [53]):

$$\xi_\Delta(E - E_\nu) = \frac{1}{2\pi}\frac{\Delta}{(E - E_\nu)^2 + \frac{\Delta^2}{4}}, \qquad \lim_{\Delta\to 0}\xi_\Delta(E - E_\nu) = \delta(E - E_\nu) \quad (7.373)$$

and the energy weighted strength function (7.372) can be rewritten as follows

$$S^{(\Delta)}_k(X\lambda\mu;\ \Delta T;\ E) = \sum_{\nu\neq 0} E^k_\nu\ \left|\langle\nu|\ \mathscr{M}^{(X)}_{\lambda\mu}(\Delta T)\ |0\rangle\right|^2 \xi(E - E_\nu), \qquad (7.374)$$

The value of the local averaging energy interval Δ for particular giant resonances will be determined in next subsections.

Useful quantity is introduced for the given strength function, namely the moment $m_k(X\lambda\mu;\ \Delta T)$ of the k-th order ($X = el.,\ mag.$):

$$m_k(X\lambda\mu;\ \Delta T) \equiv \int_0^\infty S_k(X\lambda\mu;\ \Delta T;\ E)\, dE = \\ = \sum_\nu E^k_\nu\ |\ \langle\nu|\ \hat{\mathscr{M}}^{(X)}_{\lambda\mu}(\Delta T)\ |\ 0\rangle\ |^2 \qquad (7.375)$$

[28] In this subsection we assume the excitation probability from the ground state $|0\rangle$ of even-even nuclei

These moments can be calculated also using ground state expectation values of commutators or anti-commutators involving given transition operator $\hat{\mathscr{M}}^{(X)}_{\lambda\mu}$ (further the hermicity of the transition operator is assumed)

$$\begin{aligned} m_0(\hat{\mathscr{M}}) &= \frac{1}{2}\,\langle 0|\,\{\hat{\mathscr{M}},\hat{\mathscr{M}}\}\,|\,0\rangle - \big|\,\langle 0|\,\hat{\mathscr{M}}\,|\,0\rangle\,\big|^2 = \\ &= \langle 0|\,\hat{\mathscr{M}}^{\,2}\,|\,0\rangle - \big|\,\langle 0|\,\hat{\mathscr{M}}\,|\,0\rangle\,\big|^2 = \\ &= \sum_{\nu}\langle 0|\,\hat{\mathscr{M}}\;|\nu\rangle\langle\nu|\,\hat{\mathscr{M}}\,|\,0\rangle - \big|\,\langle 0|\,\hat{\mathscr{M}}\,|\,0\rangle\,\big|^2 = \\ &= \sum_{\nu\neq 0}\big|\,\langle\nu|\,\hat{\mathscr{M}}\,|\,0\rangle\,\big|^2 \end{aligned} \tag{7.376}$$

$$\begin{aligned} m_1(\hat{\mathscr{M}}) &= \frac{1}{2}\,\langle 0|\,\big[\hat{\mathscr{M}}^{+},\,[\hat{H},\hat{\mathscr{M}}]\big]\,|\,0\rangle = \\ &= \frac{1}{2}\,\langle 0|\,2\hat{\mathscr{M}}\,\hat{H}\,\hat{\mathscr{M}} - \hat{\mathscr{M}}\,\hat{\mathscr{M}}\,\hat{H} - \hat{H}\,\hat{\mathscr{M}}\,\hat{\mathscr{M}}\,|\,0\rangle = \\ &= \langle 0|\,\hat{\mathscr{M}}\,\hat{H}\,\hat{\mathscr{M}} - E_0\,\hat{\mathscr{M}}\,\hat{\mathscr{M}}\,|0\rangle = \\ &= \sum_{\nu_1\nu_2}\langle 0|\,\hat{\mathscr{M}}\,|\nu_1\rangle\langle\nu_1|\,\hat{H}\,|\nu_2\rangle\langle\nu_2|\,\hat{\mathscr{M}}\,|\,0\rangle \\ &\qquad\qquad -E_0\;\sum_{\nu}\langle 0|\,\hat{\mathscr{M}}\,|\nu\rangle\langle\nu|\,\hat{\mathscr{M}}\,|\,0\rangle = \\ &= \sum_{\nu}\big(E_\nu - E_0\big)\,\big|\langle\nu|\,\hat{\mathscr{M}}\,|\,0\rangle\,\big|^2 = \sum_{\nu\neq 0}E_\nu\,\big|\langle\nu|\,\hat{\mathscr{M}}\,|\,0\rangle\big|^2 \end{aligned} \tag{7.377}$$

and similarly

$$\begin{aligned} m_2(\hat{\mathscr{M}}) &= \frac{1}{2}\,\langle 0|\,\big\{\,\big[\hat{\mathscr{M}},\,\hat{H}\big],\,\big[\hat{H},\,\hat{\mathscr{M}}\big]\,\big\}\,|\,0\rangle = \\ &\qquad\qquad = \cdots\cdots = \sum_{\nu\neq 0}E_\nu^2\,\big|\langle\nu|\,\hat{\mathscr{M}}\,|\,0\rangle\big|^2 \\ m_3(\hat{\mathscr{M}}) &= \frac{1}{2}\,\langle 0|\,\Big[\,\big[\hat{\mathscr{M}},\,\hat{H}\big],\,\big[\hat{H},\,\big[\hat{H},\,\hat{\mathscr{M}}\big]\,\big]\,\Big]\,|\,0\rangle = \\ &\qquad\qquad = \cdots\cdots = \sum_{\nu\neq 0}E_\nu^3\,\big|\langle\nu|\,\hat{\mathscr{M}}\,|\,0\rangle\big|^2 \end{aligned} \tag{7.378}$$

and so on. It should be noted that moments $m_k(\hat{\mathscr{M}})$ with odd k involve only commutators of $\hat{\mathscr{M}}$ with the Hamiltonian $\hat{H}$ while k- even moments $m_k(\hat{\mathscr{M}})$ contain anti-commutators (see [53, 180] for more details).

From the point of view of the statistical analyses of the shape of the strength function $S_0(\hat{\mathscr{M}};\ E)$ (see (7.371)) the above introduced moments $m_k(\hat{\mathscr{M}})$ are very useful [53, 180]. We can define set of energies

$$\omega_{k,\,k-2} = \sqrt{\frac{m_k(\hat{\mathscr{M}})}{m_{k-2}(\hat{\mathscr{M}})}} \quad , \quad \omega_{k,\,k-1} = \frac{m_k(\hat{\mathscr{M}})}{m_{k-1}(\hat{\mathscr{M}})} \tag{7.379}$$

which characterize the strength distribution of $S_0(\hat{\mathscr{M}};\ E)$. If this distribution is sharply peaked at a certain energy then all $\omega_{k,k-2}$ coincide. The degree to which they are different reflects the width of the distribution (see below for square fluctuation). Using the Schwartz inequality for moments:

$$\sqrt{m_k \cdot m_{k-2}} \ > \ m_{k-1} \tag{7.380}$$

we deduce

$$\cdots > \ \omega_{k,\,k-1} \ > \ \omega_{k,\,k-2} \ > \ \omega_{k-1,\,k-2} \ > \ \omega_{k-1,\,k-3} \ > \cdots \tag{7.381}$$

In the case when the distribution (strength function) has a form of modified Lorentzian, $\sigma(E) = (\sigma_0 E^2\Gamma^2)/[\,(E^2 - \bar{E}^2)^2 + E^2\Gamma^2\,]$, then it can be deduced (see e.g. [53]) that the centroid $\bar{E}$ and the width at half maximum, $\Gamma_{1/2}$, are

$$\bar{E} = \omega_{1,-1} \qquad\qquad \Gamma_{1/2} \ \propto \ \sqrt{\frac{m_1}{m_{-1}} - (\frac{m_0}{m_{-1}})^2} \tag{7.382}$$

The knowledge of an infinite set of such moments determines, in principle, the strength function $S_0(\hat{\mathscr{M}};\ E)$. However, the possibility is limited by the convergence of the moment expansion (see [180]). In practice it is possible to calculate only a few moments and therefore a method for the determination of $S_0(\hat{\mathscr{M}};\ E)$ based on moments $m_k(\hat{\mathscr{M}})$ is practically useful only when a few moments are able to characterize the whole strength function (e.g. if the given strength function represents a resonance with a form close to the modified Lorentzian mentioned above).

The RPA is based on the quasi-boson approximation (7.220), which, by other words, says that the expectation ground state value of the commutator of two single-particle operators does not depend on the fact if the ground state is described by the quasiparticle vacuum $|BCS\rangle$, or by phonon vacuum $|RPA\rangle$ (see (7.220), (7.221)) (see e.g. [9]). So, if the residual interaction involved in the commutator (7.377) with the Hamiltonian $\hat{H}$ commutes with the given transition operator $\hat{\mathscr{M}}$ (and therefore only kinetic energy operator in $\hat{H}$ acts effectively in the commutator) then the value of the moment

$m_1(\hat{\mathscr{M}})$ does not depend on the fact if it is calculated with $|\,0\rangle = |BCS\rangle$ or $|\,0\rangle = |RPA\rangle$. In such case the moment $m_1(\hat{\mathscr{M}})$ can be understood as model independent and the value of $m_1(\hat{\mathscr{M}})$ calculated in the framework of the RPA is equal to the value of this moment determined in the framework of the model of independent quasiparticles. This is used very often in the literature and the value of the $m_1(\hat{\mathscr{M}})$ calculated by (7.377), where the Hamiltonian $\hat{H}$ is approximated only by the kinetic energy part of the quasiparticle mean field, is used as the comparative unit for the more precise RPA values (e.g. so called Thomas-Reiche-Kuhn (TRK) sum rule values for electric dipole transitions). The moments $m_1(\hat{\mathscr{M}})$ are known as Energy Weighted Sum Rules (EWSR) and their comparative unit values for particular multipole operators are discussed in the Appendix O (see also [99, 181] and citations therein).

In the next subsections the concrete giant resonances in spherical and deformed nuclei are briefly discussed.

7.3.2.2.2 Giant resonances in spherical and deformed nuclei Further giant resonances of different types and multipolarities are subsequently discussed.

Electric giant monopole E0 resonance

In the connection with the electric giant monopole resonance we will discuss primarily the isoscalar giant monopole resonance. From theoretical point of view the electric isoscalar giant monopole resonance (ISGMR) in nuclei (the broad peak of the energy distribution of the isoscalar excitations of 0^+ states in even-even nuclei with the transition operator $\hat{\mathscr{M}}^{(el)}_{00}(\Delta T = 0) = \sum_{k=1}^{A} r_k^2 Y_{00}(\hat{r}_k)$ was predicted in the 60- ties (see e.g. [182, 9, 181] and citations therein). Experimentally it was observed for the first time in the 70-ties [183, 184] using $(\alpha, \alpha^{'})$ reaction at very forward angles. Energies of centroids of the observed isoscalar giant monopole resonance was found in the energy region 13-22 MeV depending on the mas number A as is demonstrated in the lower panel of the Fig.7.35.

In the upper panel of the Fig.7.35 there is the fraction of the ISGMR

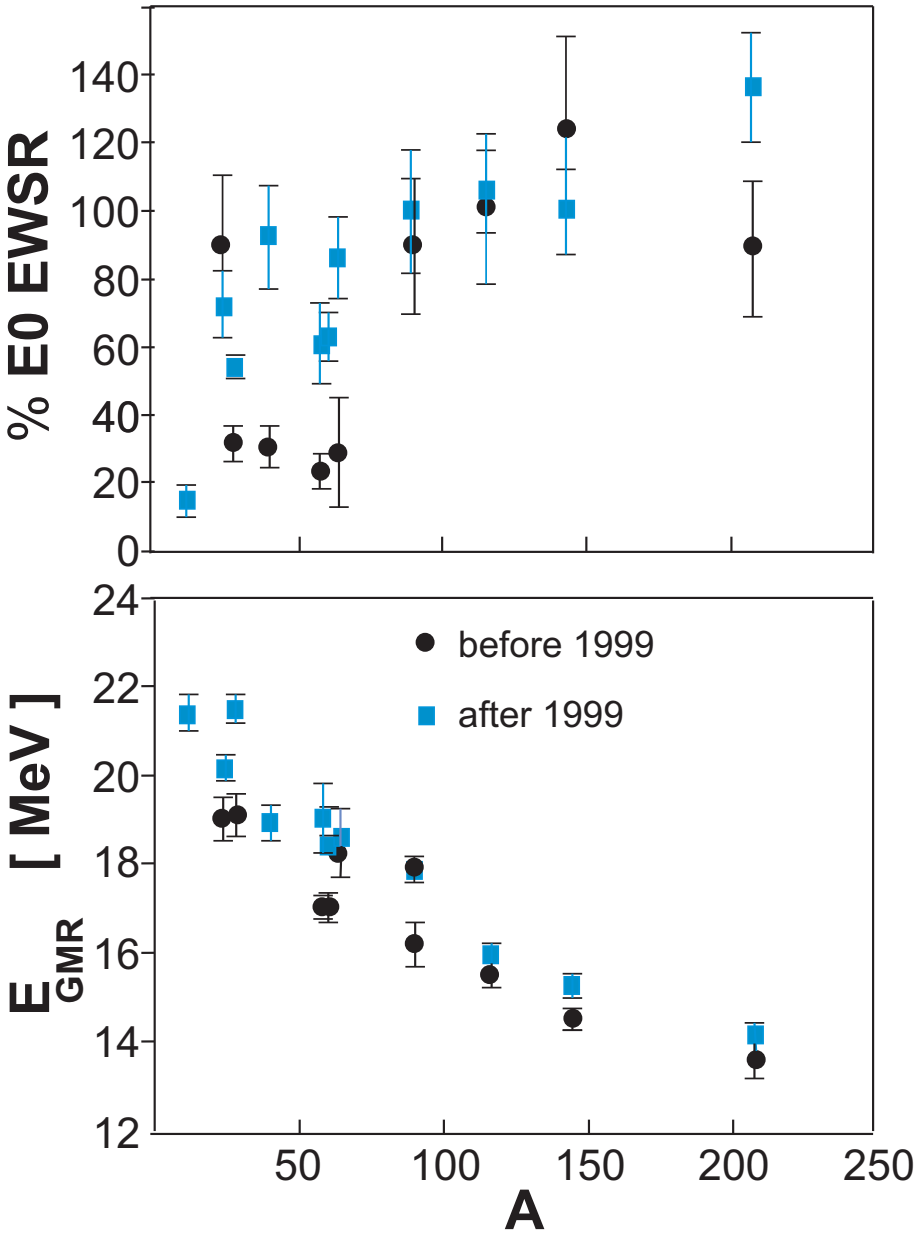


Figure 7.35: Overview of ISGMR data on GMR centroid energies and fractions of EWSR versus A. Data indicated by squares are from summary [185] and the circles from [186]. Adapted from [181].

EWSR value, $m_1^{(kin)}(\hat{\mathscr{M}}_{00}^{(el)}(\Delta T=0))$ (see Appendix 0):

$$EWSR_{ISGMR} = m_1^{(kin)}(\hat{\mathscr{M}}_{00}^{(el)}(\Delta T=0) = \sum_{k=1}^{A} r_k^2 Y_{00}(\hat{r}_k)) =$$

$$= \boxed{\begin{matrix}\text{see} \\ (O.12)\end{matrix}} =$$

$$= \frac{\hbar^2}{8\pi m}\{ \int d^3r \left|\vec{\nabla}\, r^2\right|^2 \rho(\vec{r}) - \frac{1}{A}\left| \int d^3r \left(\vec{\nabla}\, r^2\right) \rho(\vec{r})\right|^2 \} =$$

$$= \boxed{\begin{array}{c}\text{because } \vec{\nabla}\, r^2 = 2\vec{r} \text{ and } \rho(\vec{r}) \text{ is parity even: } \rho(\vec{r}) = \rho(-\vec{r}) \\ \Rightarrow \int d^3r\, (\vec{\nabla}\, r^2)\, \rho(\vec{r}) = 2 \int d^3r\, \vec{r}\, \rho(\vec{r}) = 0\end{array}} =$$

$$= \frac{\hbar^2}{8\pi m}\, 4 \int d^3r\, \vec{r}^{\,2}\, \rho(\vec{r}) = \frac{\hbar^2}{2\pi m}\, A\, \langle r^2 \rangle_A \qquad (7.383)$$

exhausted in the experimental determination of the ISGMR centroid (in percentage).

Simple hydrodynamical type oscillator model (see e.g. [182]) showed that the ISGMR can be interpreted geometrically as the breathing mode (breathing oscillation of the nuclear surface) - see schematic figure Fig.7.36.

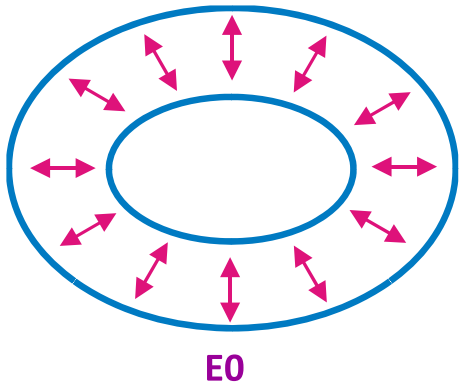


Figure 7.36: ISGMR has a character of the breathing oscillation of nuclear surface (schematic figure).

From this simple geometrical interpretation of the ISGMR one can expect that the GMR is directly connected with the incompressibility modulus K_A [29] of the finite nucleus. This connection is characterized by the following relation of K_A to the GMR centroid E_{GMR} (for the derivation of this relation see e.g. [182, 187])

$$E_{GMR} = \sqrt{\frac{\hbar^2\, K_A}{m\, \langle r^2 \rangle_A}} \qquad (7.384)$$

The finite nucleus incompressibility modulus K_A is unambigously related to the infinite nuclear matter incompressibility modulus K_∞ defined in the text below expr. (5.118). We do not present this relation between K_A and K_∞

[29] General incompressibility modulus is defined in the footnote under the expression (5.117); the incompressibility K_∞ of the infinite nuclear matter for the case of the Skyrme effective nucleon-nucleon interaction is discussed in (5.117); the finite nucleus incompressibility modulus K_A is connected with the infinite nuclear matter modulus K_∞ through the expression similar to the Weitzacker formula for the nucleus bind energy where only volume term is involved (for details see e.g. [188] and citations therein, see also (5.119)).

here. The readers are only asked to realize that using (7.384) it is possible to obtain "experimental" value of K_A from the experimental value of the GMR centroid E_{GMR}. Such an "experimental" value of K_A is then used for the determination of the infinite matter incompressibility modulus K_∞ which belongs to the one of main bulk properties (in addition to the nuclear radius and nuclear bind energy) of nuclei used for the determination of the effective nucleon-nucleon interaction parameters (see e.g. [79]). The important role of the incompressibility in the fitting of the effective nucleon-nucleon interaction parameters caused that the ISGMR is a subject of an intensive investigation from the 60-ties up to now.

In last two decades the experimental data have concerned not only the ISGMR centroids but also the shape of the GMR (see e.g. [189, 190, 191, 192, 193, 194]). These experimental data showed the dependence of the shape of the GMR on the nucleus deformation. In the case of spherical nuclei the GMR has one- peak character while the axially deformed nuclei show two-peak shape. Theoretical explanation of this deformation effect is based on the coupling of the monopole electric E0 and quadrupole electric E2 (with the ang. momentum projection $K = 0$) modes (see [195, 196]). The idea is following. In the spherical nuclei the total angular momentum is a good quantum number for the nucleus states (with corresponding energies degenerated with respect to the projection K). As a result there is not any coupling between modes with different I (particularly between monopole $I^\pi = 0^+$ and quadrupole $I^\pi = 2^+$ modes for the ang. projection $K = 0$). In the case of axially deformed nuclei the angular momentum projection onto the intrinsic 3-d axis is good quantum number for nucleus intrinsic states (total ang. momentum I is not good quantum number in the deformed case). Therefore the coupling between monopole and quadrupole modes (with the same projection $K = 0$) is allowed now. Since the unperturbed (uncoupled) monopole and quadrupole resonances are located in different energies the resultant (perturbed) monopole resonance has two- peak structure. As an example in the Fig.7.37 the calculated E0 strength function $S_0(E00,\ \Delta T = 0,\ E)$ (see (7.372)) is compared with corresponding experimental values, extracted from the $(\alpha,\ \alpha^{'})$ reactions, for the chain of Sm isotopes, going from the spherical ^{144}Sm to the well-deformed axial ^{154}Sm.

From the Fig.7.37 the evolution of the ISGMR shape with the increasing quadrupole deformation β can be observed. The GMR in the spherical nucleus ^{144}Sm has clearly one- peak character in both experiments (Texas TAMU data [189] and Japan RCNP data [191]), which is confirmed by cal-

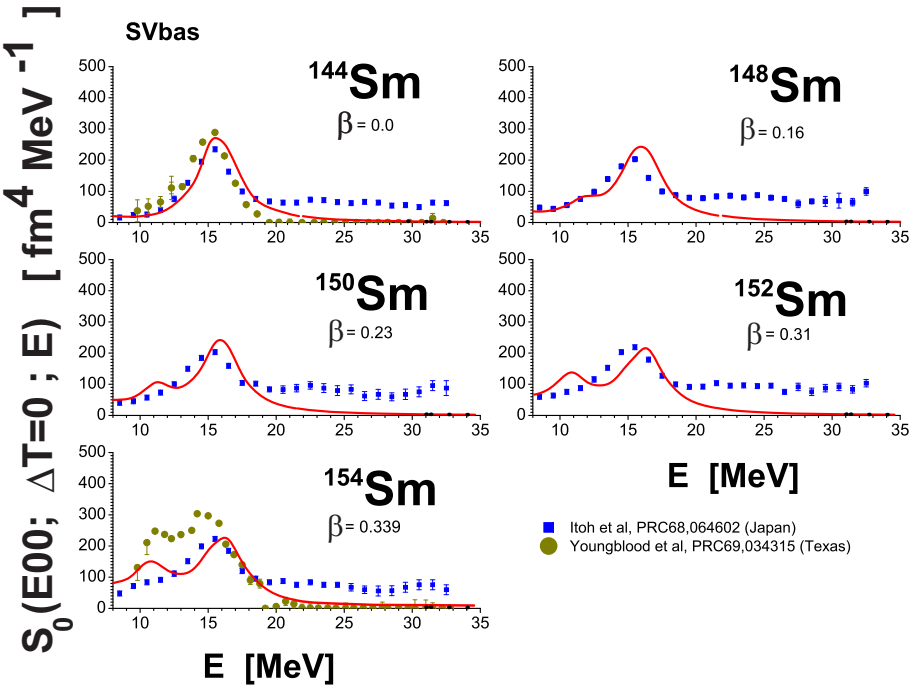


Figure 7.37: Comparison of the strength function of the electric isoscalar monopole excitations for the chain of Sm isotopes calculated in the framework of the Skyrme effective n-n interaction HFB+RPA approach [196] (solid curve) with corresponding experimental ISGMR data (Texas TAMU data [189] - denoted by circles, and Japan RCNP data [191] denoted by squares). Skyrme effective n-n interaction with its SV-bas parametrization [79] was used in the calculation [196]. The E0 strength fumction was calculated using (7.372) and (7.373) with the Lorentz energy averaging interval $\Delta = 2\ MeV$.

culation [196]. The shape of the calculated ISGMR in the well-deformed nucleus ^{154}Sm is two-humped which is also observed in the Texas experiment [189]. Experimental data of Japan group [191] did not show two-humped character directly nevertheless the broadening of the GMR in the direction of lower energies can be seen. Here it should be noted that the absolute value normalization of experimental values of $S_0(E00;\ \Delta T = 0;\ E)$ of both experimental groups was based on the approximative comparison of the total experimental strength with the kinetic energy EWSR estimations (7.383) and therefore is only indicative.

It can be noticed in the Fig.7.37 that the energy scale starts from 8 MeV. The reason is the presence of so called spurious peak near the zero energy which is connected with the non-physical solutions of the RPA equations from the point of the intrinsic degrees of freedom of the nuclear motion. In the case of the ISGMR these non-physical RPA solutions are related to the number of proton and neutron conservation in the RPA calculation, where

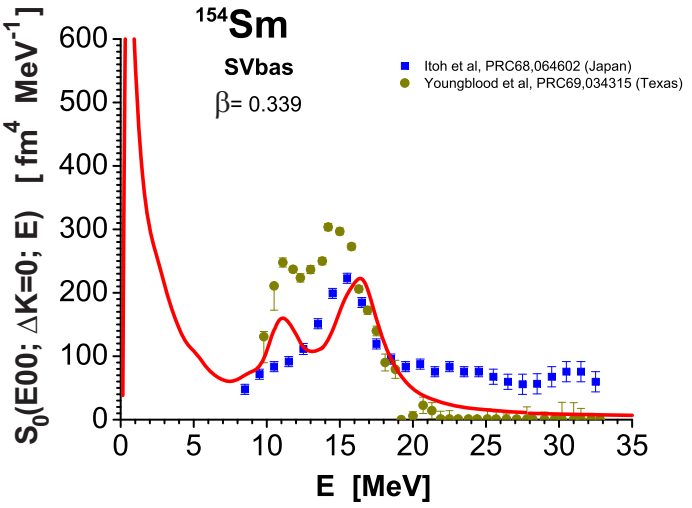


Figure 7.38: The same as in the last panel of the Fig.7.37 but with the excitation energies starting from zero.

we require the nuclear Hamiltonian to commute to zero with the operator of the number of protons ($\hat{N}_Z$) and number of neutron ($\hat{N}_N$) (compare with (7.286) if $\hat{P}_0 = \hat{N}_Z$ *or* $\hat{N}_N$)

$$\left[\hat{H}_{RPA},\ \hat{N}_Z\right] = \left[\hat{H}_{RPA},\ \hat{N}_N\right] = 0 \tag{7.385}$$

According to the discussion under the eq. (7.286) we know, from the comparison of (7.385) with the RPA equations (7.276) (particularly with $[\hat{H}_{RPA}, \hat{\mathscr{P}}_\nu] = i\hbar M_\nu \omega_\nu^2\ \hat{\mathscr{X}}_\nu$), that operators $\hat{N}_Z$ and $\hat{N}_N$ can be identified with generalized linear momenta $\hat{\mathscr{P}}_0$ of the zero energy RPA solutions ($\hbar\omega_0 = 0$). That means, if our RPA theory fulfill precisely to (7.385) we would have zero energy RPA solutions which are non-physical from the point of the intrinsic states of the nucleus. However, since our nuclear Hamiltonian and the full RPA approach itself is not precise (at least due to the fact that used configuration space is finite and not complete in any case) the relations (7.385) are fulfilled only approximately. That means, in reality we have no zero energy RPA solutions and the strength of these spurious modes is now spread out in the lowest nonzero energy RPA solutions. As a result in the strength function $S_0(E00;\ \Delta K = 0;\ E)$ instead of zero width peak at zero energy we have a finite width peak at low nonzero energy. Just for a demonstration we show in the Fig.7.38 the strength function $S_0(E00;\ \Delta K = 0;\ E)$ for ^{154}Sm (see last panel in the Fig.7.37) with the full energy interval starting with the zero energy.

The Fig.7.38 shows that the part of the energy spectrum up to energies ≈ 6 MeV is soiled by these spurious non-physical RPA solutions (the spurious

peak at energies 0-5 Mev is clearly recognized). Spectrum with energies higher than 8 MeV is sufficiently far from the spusious solutions and it can be supposed to be free from the spuriosity.

In order to get rid of this spuriosity it is necessary to use very big configuration space (the increasing configuration space causes the spurious peak more narrow and shifted closer to the zero energy) and simultaneously to apply some special procedure. For instance in [197] the special orthogonalization procedure for all nonzero energy RPA solutions to be orthogonal to the zero energy solutions connected with $\hat{N}_Z$ and $\hat{N}_N$ was used. Another method is to work with the intrinsic RPA solutions projected to the Hilbert space with sharp value of the number of protons and neutrons (for projection methods see the Appendix N). As it was mentioned above for the energy region typical for the ISGMR we can suppose that the spuriosity connected with the number of particle conservation is irrelevant. However, if we are interested in the low-lying part of the spectrum, the additional procedures should be used to get rid of this spuriosity.

In the connection with the monopole E0 resonance we have discussed up to now the isoscalar $\Delta T = 0$ monopole resonance where the experimental information is usally obtained from $(\alpha, \alpha^{'})$ reaction. The obtaining of an information about isovector E0 resonance is much more difficult and it is not so direct. In the cross section of $(\alpha, \alpha^{'})$ reaction the dominant role is played by the isoscalar transition operator $\hat{\mathscr{M}}_{00}(\Delta T = 0, \Delta T_3 = 0)$ and the contribution of $\Delta T = 1$ transitions, connected with $\hat{\mathscr{M}}_{00}(\Delta T = 1, \Delta T_3 = 0)$, is very small, experimentally practically not accessible. Another story is the isovector monopole modes connected with the transition operator $\hat{\mathscr{M}}_{00}(\Delta T = 1, \Delta T_3 = \pm 1) = \sum_{k=1}^{A} r_k^2 \, Y_{00}(\hat{r}_k) \, (\hat{t}_{\pm})_k$ (so called non-spin-flip isovector monopole transitions [30]). Experimental information about resonance corresponding to such mode can be obtained by charge-exchange reactions ($\Delta T = 1$, $\Delta T_3 = \pm 1$) at small momentum transfer (see [181] and citations therein). We will not discuss isovector monopole excitations in this textbook, readers are referred to the monography [181].

Electric giant dipole E1 resonance

In the Appendix O the zero value of the EWSR for the isoscalar electric dipole strength function connected with the transition operator $\sum_{\mu=-1}^{+1} \hat{\mathscr{M}}_{1\mu}^{(el)}(\Delta T =$

[30] The non-spin-flip transitions are connected with the transition operators not involving spin operators of nucleons. For onstance, electric type transitions belong to non-spin-flip transitions. The spin-flip transitions correspond to the transition operators involving spins of nucleon. As an example of spin-flip transition the magnetic type transitions can be taken.

$0) = \sum_{\mu=1}^{+1} \sum_{k=1}^{A} r_k Y_{1\mu}(\hat{r}_k)$ was shown (see (O.16). It is in accordance with the fact that, except spurious zero energy E1 excitation (connected with the nucleus center of mass motion - see the Appendix O), there are no any isoscalar excitations. Therefore we will concentrate our discussion of the electric dipole resonance only to the isovector electric giant dipole resonance (IVGDR) connected with the transition operators $\hat{\mathscr{M}}_{1\mu}^{(el)}(\Delta T = 1,\ \Delta T_z = 0) = \sum_{k=1}^{A} r_k Y_{1\mu}(\hat{r}_k)\, 2(\hat{t}_z)$ with $(\mu = 0, \pm 1)$ or, more precisely, with the transition operators $\hat{\mathscr{M}}_{1\mu}^{(el)}(eff) = \sum_{k=1}^{A} e_k^{(eff)} r_k Y_{1\mu}(\hat{r}_k)$ with the effective charges $e_p^{(eff)} = N/A$ and $e_n^{(eff)} = -Z/A$ (see (O.38) and (O.39)), which are equivalent to the operators $\hat{\mathscr{M}}_{1\mu}^{(el)}(\Delta T = 1, \Delta T_z = 0)$ if we work in the center of mass frame (see (O.37), (O.39), (O.40)). In the Appendix O it is also shown that the EWSR estimation for the isovector electric dipole resonance is (see (O.37) or (O.40))

$$EWSR_{IVGDR} = m_1^{(kin)}(\sum_{\mu-1}^{+1} \hat{\mathscr{M}}_{1\mu}^{(el)}(eff)) = \frac{9\hbar^2}{8\pi m}\frac{NZ}{A} \tag{7.386}$$

Isovector giant dipole resonance (IVGDR) is the oldest and best known giant resonance. It was observed in the early 50s in photo-absorption experiments (e.g. [198]) where the connection between photo-absorption cross section $\sigma_\gamma(E)$ (see (2.171)) and the strength function $\sum_{\mu=-1}^{+1} S_1(E1\mu;\ \Delta T = 1;\ E)$ is simple. If we realize that the dominant contribution to the sum over J in the photo-absorption cross section (2.171) comes from the component with $J = 1$ and all components with $J > 1$ are negligible then the comparison of (2.171) with (7.372) gives the following relation

$$\begin{aligned}
\sigma_\gamma(E,\ 0^+ \to \sum_\nu |\nu\rangle) &= \boxed{\begin{array}{c}\text{see}\\(2.171)\end{array}} = \\
&= \frac{16\pi^3\alpha_F}{9} \sum_\nu E_\nu\, B(E1;\ 0^+ \to \nu\rangle)\, \delta(E - E_\nu) = \\
&= \frac{16\pi^3\alpha_F}{9} \sum_{\mu=-1}^{+1} S_1(E1\mu;\ \Delta T = 1;\ E)
\end{aligned} \tag{7.387}$$

with

$$\sigma_{\gamma}^{(theor)} = \int_0^{\infty} dE\, \sigma_{\gamma}(E;\, 0^+ \to \sum_{\nu} |\nu\rangle) = \boxed{\begin{array}{c}\text{see}\\ (7.375)\end{array}} =$$

$$= \frac{16\pi\alpha_F}{9} \sum_{\mu=-1}^{+1} m_1(E1\mu;\, \Delta T = 1) \tag{7.388}$$

where in (7.386) and (7.387) α_F is the fine structure constant. If the EWSR estimation (7.386) is used as $\sum_{\mu} m_1(E1\mu;\, \Delta T = 1)$ in (7.388) we obtain EWSR estimation of the photo-absorption cross section

$$\sigma_{\gamma}^{(EWSR)} = \frac{2\pi^3\alpha_F\hbar^2c^2}{\pi mc^2}\,\frac{NZ}{A} = 6\,\frac{NZ}{A}\,MeV\;fm^2 \tag{7.389}$$

From experimental point of view the photo-absorption cross section in medium-heavy and heavy nuclei is given by $(\gamma,\, xn)$ reactions:

$$\sigma_{\gamma}^{(exp)} = \int dE\, \sigma_{\gamma}^{(exp)}(E) = \sum_{x} \sigma(\gamma, xn) \tag{7.390}$$

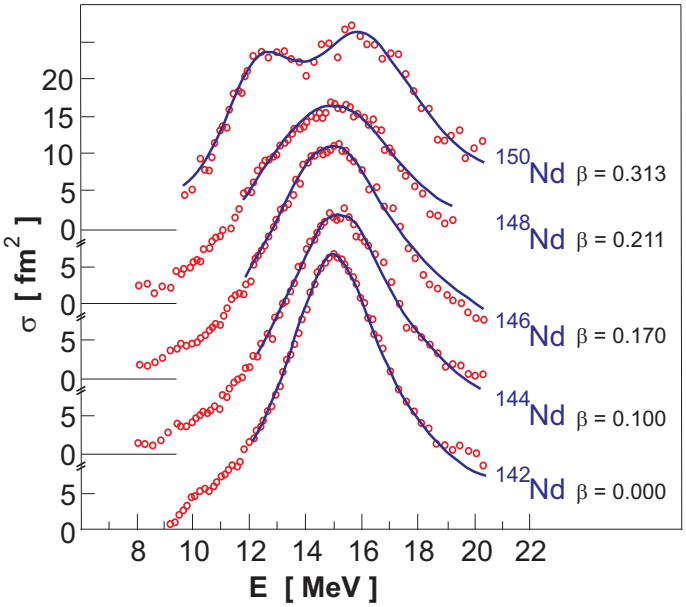
because the (γ, p) and $(\gamma, \gamma^{'})$ cross sections are negligible small. For actinide nuclei also fission induced by photon (γ, f) cross sections have to be added.

In the Fig.7.39 the experimental photo-absorption cross sections $\sigma_{\gamma}^{(exp)}(E)$ in the dependence on the excitation energy (absorbed photon energy) for the chain of Nd isotopes going from the spherical ^{142}Nd ($\beta = 0$) to the well-deformed ^{150}Nd ($\beta = 0.352$) are shown. One can see that in IVGDR in the spherical ^{142}Nd has one- peak character while two- humped character can be seen in the case of deformed nuclei.

Experimental groups usually fit the experimental values of the photo-absorption cross section with the modified Lorentzians: for spherical nuclei with one modified Lorentzian and for deformed nuclei by two modified Lorentzians:

$$\sigma_{\gamma}^{(exp)}(E) = \sum_{i=1}^{2} \frac{\sigma_{0i} E^2 \Gamma_{0i}^2}{\left(E^2 - E_{0i}^2\right)^2 + E^2\,\Gamma_{0i}^2} \tag{7.391}$$

where σ_0, E_0 and Γ are fitting parameters. For the case of the chain of Nd isotopes with experimental photo- absorption cross sections shown in upper part of the Fig.7.39 the optimal values of these parameters are involved in the table given in the lower part of this figure (see [199]).



	^{142}Nd	^{144}Nd	^{146}Nd	^{148}Nd	^{150}Nd	
E_0 [MeV]	14.9	15.0	14.8	14.7	12.3	16.0
σ_0 [fm^2]	36.0	32.0	31.0	26.0	17.0	22.0
Γ [MeV]	4.4	5.3	6.0	7.2	3.3	5.2

Figure 7.39: Experimental photo-absorption cross section for Nd isotopes (upper part). The curves are fits with one Lorentzian (for $^{142,-,148}$Nd) or with two Lorentzians (for well-deformed ^{150}Nd) - see (7.40). Table given in the lower part contains parameters of Lorentzians for all Nd isotopes. Data taken from [199].

Single- peak structure of the IVGDR for spherical nuclei and double- peak structure for axially deformed nuclei can be understood from the simple schematic interpretation of the IVGDR shown in the Fig.7.40.

Simple geometrical oscillator model of the IVGDR (see e.g. [99]) gave a simple interpretation of the IVGDR as the vibration of the neutron system with respect to the proton system. In the case of spherical nucleus this vibration means the oscillation of proton sphere versus neutron sphere as is depicted in the upper panel of the Fig.7.40. In the axially deformed nucleus both proton and neutron systems are ellipsoidally deformed and there are two main directions for such vibrations: along the long (symmetry) axis or perpendicularly to the symmetry axis, as is demonstrated in the lower panel of the Fig.7.40. As it will be shown later, these two possibilities of E1 vibrations of proton with respect to neutrons are related to two possible projections μ of the angular momentum $\lambda = 1$ of dipole E1 vibrations in axially deformed

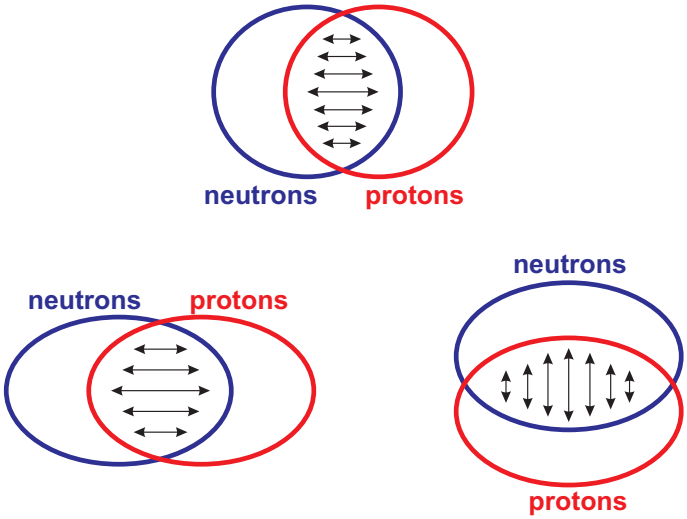


Figure 7.40: Schematic figure of the interpretation of the IVGDR as the vibration of the neutron system with respect to the proton system. The uper part corresponds to the spherical nucleus and the lower panel to the deformed nucleus. In the case of axially deformed nucleus (lower panel) there are two possible oscillations of neutrons versus protons: i. along the long axis of ellipsoid or ii. along the short axis of rotationally symmetric prolonged ellipsoid and these two possibilities correspond to two peaks observed in the $\sigma_{\gamma}^{(exp)}(E)$ for axially deformed nuclei.

nucleus: $\mu = 0$ and $\mu = \pm 1$.

Maxima of the photo-absorption cross section $\sigma_{\gamma}^{(exp)}(E)$ (see the Fig.7.39) in spherical nuclei, that means E_{01} energy in the fitted Lorentzian (7.391) (only one Lorentzian for spherical nucleus) can be well reproduced by a two-term functions [165, 181]:

$$E_{01} = 31.2\, A^{-1/3} + 20.6\, A^{-1/6}\ MeV \tag{7.392}$$

which has a simple hydrodynamical model interpretation - see [181].

As an example of microscopical description of the $\sigma_{\gamma}(E)$ in the Fig.7.41 the comparison of the calculated $\sigma_{\gamma}^{(theor)}(E)$ in the framework of the Skyrme BCS+RPA model with the corresponding experimental $\sigma_{\gamma}^{(exp)}(E)$ values is demonstrated for the chain of Nd isotopes, going from the spherical ^{142}Nd to the well- deformed ^{152}Nd. The Skyrme BCS+RPA calculation was done with the SLy6 Skyrme effective n-n interaction parametrization [91]. Fig.7.41 shows a good agreement of experimental data with calculated values for all Nd isotopes using this parametrization. In the Fig.7.41 microscopic Skyrme BCS+RPA approach demonstrates the evolution of the double-peak structure of the IVGDR with the increasing quadrupole deformation β. One can also see that in the case of nonzero deformation with two peaks in the IVGDR the

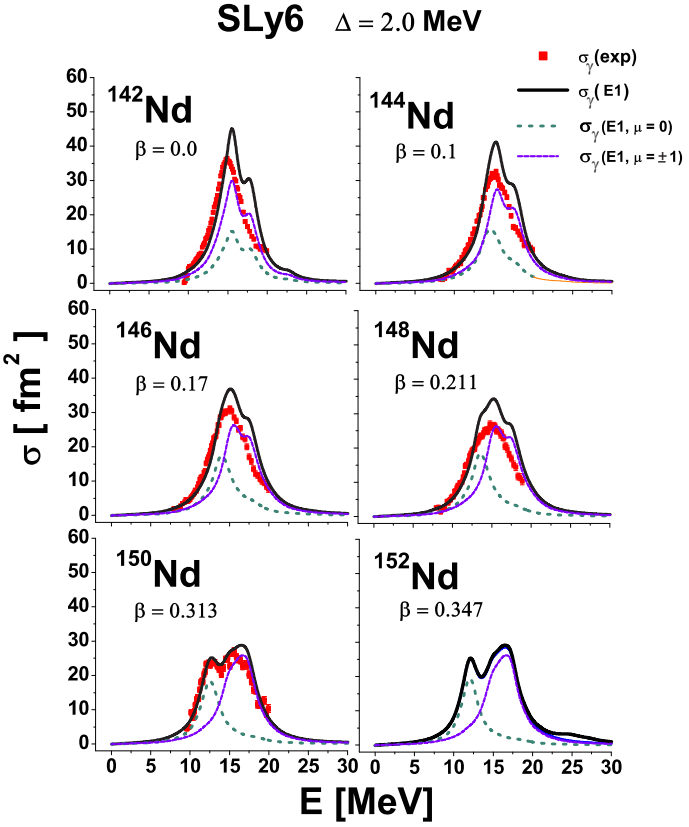


Figure 7.41: The comparison of the calculated photo-absorption cross section $\sigma_\gamma^{(theor)}(E)$ (solid curve) with experimental $\sigma_\gamma^{(exp)}(E)$ (squares) for the chain of Nd isotopes. Calculation was pergormed using exp. (7.387) and (7.374) with the Lorentz averaging interval $\Delta = 2MeV$ in the framework of the Skyrme BCS-RPA method with the Skyrme effective parametrization SLy6. The dotted and dashed curves correspond to calculated $\mu = 0$ and $\mu = \pm 1$ components of the IVGDR photo-absorption cross section. The equilibrium quadrupole deformation β, obtained from the position of the ground state total energy minimum -see the text below (5.120), is also given for each Nd isotope. Experimental data taken from [199].

energetically lower peak is formed by the $\mu = 0$ component of the IVGDR and higher peak is connected with $\mu = \pm 1$ component.

Up to now in the Subsection 7.3.1.3.2 (see eq. (7.363)-(7.367) and (7.383)-(7.392)) we worked in the framework of so called long-wave approximation (see the Subsection 2.2.2.2) where the transition electric multipole operators were approximated by (2.130), $\hat{\mathscr{M}}^{(el)}_{\lambda\mu}(k) \stackrel{kr<<1}{\to} \hat{\mathscr{M}}^{(el)}_{\lambda\mu} = \int d^3r\, r^\lambda\, Y_{\lambda\mu}(\hat{r})\, \hat{\rho}_{nuc}(\vec{r})$, that means for the dipole ($\lambda = 1$) transition operator $\hat{\mathscr{M}}^{(el)}_{1\mu} = \int d^3r r Y_{1\mu}(\hat{r})\hat{\rho}(\vec{r}) = \sum_{k=1}^{A} r_k\, Y_{1\mu}(\hat{r}_k)$. The recent experimental facilities are able to obtain information about strength functions of transition operators which represent the second order terms in the long-wave decompositions of electric multipole op-

erators (2.130). Concretely, for electric dipole transitions these second order transition operators are toroidal electric dipole operator $\hat{\mathscr{M}}^{(tor)}_{1\mu}$ and electric compression dipole operator $\hat{\mathscr{M}}^{(com)}_{1\mu}$. Before the discussion of the theoretical interpretation of experimental data on dipole compression and toroidal modes the theoretical connection of the toroidal and compression transition operators with the electric transition operators (2.130) should be given.

We start with the general expression (2.103) for electric multipole transition operator $\hat{\mathscr{M}}^{(el)}_{\lambda\mu}(k)$ (no long-wave approximation) together with the expr. (2.27) for the electric vector potential $\vec{A}^{(el)}_{\lambda\mu}(\hat{r})$ and then the following expansion of the spherical Bessel function into powers in the transferred linear momentum k is incorporated into (2.27) and then into (2.103) (see e.g. (B.68) in [9])

$$j_\lambda(kr) = \frac{(kr)^\lambda}{(2\lambda+1)!!}\left[1 - \frac{k^2r^2}{2(2\lambda+3)} + \cdots\right] \tag{7.393}$$

So, the (2.103) can be rewritten as follows

$$\hat{\mathscr{M}}^{(el)}_{\lambda\mu}(k) = \boxed{\begin{array}{c}\text{see}\\(2.103)\end{array}} =$$

$$= \frac{(2\lambda+1)!!}{ck^\lambda(\lambda+1)}\left[\lambda(\lambda+1)\right]^{1/2}\int d^3r\,\hat{\vec{j}}_{nuc}(\vec{r})\cdot\hat{\vec{A}}^{(el)}_{\lambda\mu}(\vec{r}) = \boxed{\begin{array}{c}\text{see}\\(2.27)\end{array}} =$$

$$= \frac{(2\lambda+1)!!}{ck^{\lambda+1}(\lambda+1)}\int d^3r\,\hat{\vec{j}}_{nuc}(\vec{r})\cdot\left(\vec{\nabla}\times\hat{\vec{L}}\right) f_\lambda(kr)\,Y_{\lambda\mu}(\hat{r}) =$$

$$= \boxed{\begin{array}{c}\text{because - see (A.64)}\\ \hat{\vec{L}}\,f_\lambda(r)\,Y_{\lambda\mu}(\hat{r}) = \sqrt{\lambda(\lambda+1)}\,f_\lambda(kr)\,\vec{Y}_{\lambda\lambda\mu}(\hat{r})\end{array}} =$$

$$= \frac{(2\lambda+1)!!\,\sqrt{\lambda(\lambda+1)}}{k^{\lambda+1}\,c\,(\lambda+1)} \int d^3r\,\hat{\vec{j}}_{nuc}(\vec{r}) \cdot \left[\vec{\nabla} \times f_\lambda(kr)\,\vec{Y}_{\lambda\lambda\mu}(\hat{r})\right] =$$

$$= \boxed{\begin{array}{c}\text{see}\\(A.63)\end{array}} =$$

$$= \frac{(2\lambda+1)!!\,\sqrt{\lambda(\lambda+1)}}{k^{\lambda+1}\,c\,(\lambda+1)} \int d^3r\,\hat{\vec{j}}_{nuc}(\vec{r}) \cdot$$

$$\cdot\Big[\, i\,\sqrt{\frac{\lambda}{2\lambda+1}}\,\Big(\frac{d}{dr} - \frac{\lambda}{r}\Big)\,f_\lambda(kr)\,\vec{Y}_{\lambda+1\,\lambda\mu}(\hat{r}) +$$

$$+ i\sqrt{\frac{\lambda+1}{2\lambda+1}}\,\Big(\frac{d}{dr} + \frac{\lambda+1}{r}\Big)\,f_\lambda(kr)\,\vec{Y}_{\lambda-1\,\lambda\mu}(\hat{r})\,\Big] =$$

$$= \boxed{\begin{array}{c}\text{using expansion (7.393) of spherical Bessel function}\\ f_\lambda(kr) = j_\lambda(kr) = \frac{(kr)^\lambda}{(2\lambda+1)!!}\left[1 - \frac{k^2r^2}{2(2\lambda+3)} + \cdots\right]\\ \text{and carrying out all derivatives}\end{array}} =$$

$$= \frac{i\sqrt{\lambda(2\lambda+1)}}{kc} \int d^3r\,\hat{\vec{j}}_{nuc}(\vec{r})\,r^{\lambda-1}\,\cdot\vec{Y}_{\lambda-1\,\lambda\mu}(\hat{r})$$

$$-\frac{ik}{c}\sqrt{\frac{\lambda}{(\lambda+1)(2\lambda+1)}} \int d^3r\,\hat{\vec{j}}_{nuc}(\vec{r}) \cdot$$

$$\cdot\Big[\frac{\sqrt{\lambda}}{2\lambda+3}\,r^{\lambda+1}\,\vec{Y}_{\lambda+1\,\lambda\mu}(\hat{r}) + \frac{\sqrt{\lambda+1}}{2}\,r^{\lambda+1}\,\vec{Y}_{\lambda-1\,\lambda\mu}(\hat{r})\Big] + \cdots$$

$$= \boxed{\begin{array}{c}\text{because - see (A.62)}\\ \vec{\nabla}\,r^\lambda\,Y_{\lambda\mu}(\hat{r}) = \sqrt{\lambda(2\lambda+1)}\,r^{\lambda-1}\,\vec{Y}_{\lambda-1\,\lambda\mu}(\hat{r})\end{array}} =$$

$$= \frac{i}{kc} \int d^3r\,\hat{\vec{j}}_{nuc}(\vec{r})\,\big(\nabla r^\lambda\,Y_{\lambda\mu}(\hat{r})\big)$$

$$-\frac{ik}{c}\sqrt{\frac{\lambda}{(\lambda+1)(2\lambda+1)}} \int d^3r\,\hat{\vec{j}}_{nuc}(\vec{r}) \cdot$$

$$\cdot\Big[\frac{\sqrt{\lambda}}{2\lambda+3}\,r^{\lambda+1}\,\vec{Y}_{\lambda+1\,\lambda\mu}(\hat{r}) + \frac{\sqrt{\lambda+1}}{2}\,r^{\lambda+1}\,\vec{Y}_{\lambda-1\,\lambda\mu}(\hat{r})\Big] + \cdots$$

$$\equiv \hat{\mathscr{M}}^{(el)}_{\lambda\mu}(k=0) + k\,\hat{\mathscr{M}}^{(tor)}_{\lambda\mu}(k=0) + \cdots \qquad (7.394)$$

where

$$\hat{\mathscr{M}}^{(el)}_{\lambda\mu}(k=0) \equiv \frac{i}{kc}\int d^3r\,\hat{\vec{j}}_{nuc}(\vec{r})\cdot\left(\vec{\nabla}\,r^{\lambda}\,Y_{\lambda\mu}(\hat{r})\right) = \boxed{\begin{array}{c}\text{integration}\\ \text{per partes}\end{array}} =$$

$$= -\frac{i}{kc}\int d^3r\,r^{\lambda}\,Y_{\lambda\mu}(\hat{r})\,\left(\vec{\nabla}\,\hat{\vec{j}}_{nuc}(\hat{r})\right) =$$

$$= \boxed{\begin{array}{c}\text{because - see (2.128)}\\ \vec{\nabla}\hat{\vec{j}}_{nuc}(\vec{r}) = \frac{i}{\hbar}[\hat{H},\,\hat{\rho}(\vec{r})] = ikc\,\hat{\rho}_{nuc}(\vec{r})\end{array}} =$$

$$= \int d^3r\,r^{\lambda}\,Y_{\lambda\mu}(\hat{r})\,\hat{\rho}_{nuc}(\vec{r}) \tag{7.395}$$

is the long-wave limit of the electric multipole operator (see (2.130)) and

$$\hat{\mathscr{M}}^{(tor)}_{\lambda\mu}(k=0) \equiv \frac{-i}{c}\sqrt{\frac{\lambda}{2\lambda+1}}\,\frac{1}{2}\int d^3r\,\hat{\vec{j}}_{nuc}(\vec{r})\cdot$$

$$\cdot\,r^{\lambda+1}\left[\vec{Y}_{\lambda-1\,\lambda\mu}(\hat{r}) + \sqrt{\frac{\lambda}{\lambda+1}}\,\frac{2}{2\lambda+3}\,\vec{Y}_{\lambda+1\,\lambda\mu}(\hat{r})\right] =$$

$$= \boxed{\begin{array}{c}\text{because } \int d^3r\,\vec{a}(\vec{r})\cdot\left(\vec{\nabla}\times\vec{b}(\vec{r})\right) = \int d^3r\,\vec{b}(\vec{r})\cdot\left(\vec{\nabla}\times\vec{a}(\vec{r})\right)\\ \text{and } (A.63)\end{array}} =$$

$$= -\frac{1}{2c}\sqrt{\frac{\lambda}{\lambda+1}}\,\frac{1}{2\lambda+3}\int d^3r\,r^{\lambda+2}\,\vec{Y}_{\lambda\lambda\mu}(\hat{r})\cdot\left[\vec{\nabla}\times\hat{\vec{j}}_{nuc}(\vec{r})\right] \tag{7.396}$$

is the long-wave limit of the dipole toroidal transition operator.

Similarly as the decomposition (7.394) was derived another decomposition of $\hat{\mathscr{M}}^{(el)}_{\lambda\mu}$ can be obtained (see [200]):

$$\hat{\mathscr{M}}^{(el)}_{\lambda\mu}(k) \equiv \hat{\mathscr{M}}^{(el)}_{\lambda\mu}(k=0) + k\left(\hat{\mathscr{M}}^{(V)}_{\lambda\mu}(k=0) - \hat{\mathscr{M}}^{(com)}_{\lambda\mu}(k=0)\right) + \cdots \tag{7.397}$$

where

$$\hat{\mathscr{M}}^{(V)}_{\lambda\mu}(k=0) = -\frac{i\sqrt{2\lambda+1}}{c(2\lambda+3)\sqrt{\lambda+1}}\int d^3r\,r^{\lambda+1}\,\hat{\vec{j}}_{nuc}(\vec{r})\cdot\vec{Y}_{\lambda+1\,\lambda\mu}(\hat{r}) \tag{7.398}$$

and the compression multipole transition operator is introduced:

$$\hat{\mathscr{M}}^{(com)}_{\lambda\mu}(k=0) = -\frac{i}{2c(2\lambda+3)} \int d^3r\, r^{\lambda+2}\, Y_{\lambda\mu}(\hat{r}) \left[\vec{\nabla}\cdot\hat{\vec{j}}_{nuc}(\vec{r})\right] =$$

$$= \boxed{\begin{array}{c}\text{because - see (2.128)}\\ \vec{\nabla}\hat{\vec{j}}_{nuc}(\vec{r}) = \frac{i}{\hbar}[\hat{H},\ \hat{\rho}(\vec{r})] = ikc\,\hat{\rho}_{nuc}(\vec{r})\end{array}} =$$

$$= \frac{k}{2(2\lambda+3)} \int d^3r\, r^{\lambda+2}\, \hat{\rho}(\vec{r})\, Y_{\lambda\mu}(\hat{r}) \equiv k\,\hat{\mathscr{M}}'^{(com)}(k=0) \tag{7.399}$$

where $\hat{\mathscr{M}}'^{(com)}(k=0)$ is the familiar density-dependent form of the compression electric multipole operator (see [181, 202]). The comparison of (7.397) with (7.394) gives the relation between long-wave limits of operators $\hat{\mathscr{M}}^{(tor)}_{\lambda\mu}(k=0)$, $\hat{\mathscr{M}}^{(V)}_{\lambda\mu}(k=0)$ and $\hat{\mathscr{M}}^{(com)}_{\lambda\mu}(k=0)$:

$$\hat{\mathscr{M}}^{(tor)}_{\lambda\mu}(k=0) = \hat{\mathscr{M}}^{(V)}_{\lambda\mu}(k=0) - \hat{\mathscr{M}}^{(com)}_{\lambda\mu}(k=0) \tag{7.400}$$

Further we apply expressions (7.396) and (7.399) for the interpretation of the compression dipole $\lambda=1$ and toroidal dipole data on the isoscalar strength function. In the case of $\lambda=1$ it is necessary to involve in the expressions for $\hat{\mathscr{M}}'^{(com)}_{1\mu}(k=0)$ and $\hat{\mathscr{M}}^{(tor)}_{1\mu}(k=0)$ the correction to the center of mass motion (see e.g. [200, 201]):

$$\hat{\mathscr{M}}^{(tor)}_{1\mu}(k=0) = -\frac{i}{2c\sqrt{3}} \int d^3r \left[\frac{\sqrt{2}}{5}\, r^2\, \vec{Y}_{12\mu}(\hat{r}) + \left(r^2 - \langle r^2\rangle_A\right) \hat{Y}_{10\mu}(\hat{r})\right] \cdot \hat{\vec{j}}_{nuc}(\vec{r}) \tag{7.401}$$

$$\hat{\mathscr{M}}'^{(com)}_{1\mu}(k=0) = \frac{1}{10} \int d^3r\, \hat{\rho}_{nuc}(\vec{r}) \left[r^3 - \frac{5}{3}\,\langle r^2\rangle_A\, r\right] Y_{1\mu}(\hat{r}) \tag{7.402}$$

Here $\langle r^2\rangle_A = \frac{1}{A}\int d^3r\, \hat{\rho}_{nuc}(\vec{r})\, r^2$ is the ground state squared radius (see also (O.18)). The center of mass corrections are connected with the terms in (7.401) and (7.402) involving $\langle r^2\rangle_A$.

Once the theoretical connection of the toroidal and compression multipole operators with the general electric multipole operator is settled we can return to the interpretation of corresponding experimental data. In the Fig.7.42 the experimental isovector E1 strength energy distribution (extracted mainly from the photo-absorption cross section [203, 204, 205]) is shown in the energy interval 5-17 MeV for ^{208}Pb. One can recognize a broad peak of the IVGDR in the interval 9-16 MeV and a bunch of 1^- states with energies 7-9 MeV.

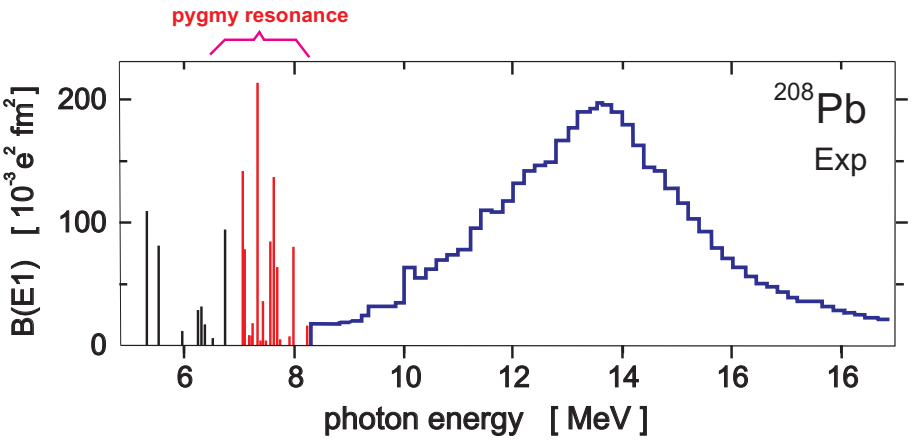


Figure 7.42: Isovector E1 strength function in ^{208}Pb in the dependence on the excitation (photon in the case of the photo-absorption) enrgy. So called pygmy resonance region is marked. Experimental data taken from [203, 204, 205].

This bunch is known in the literature as so called pygmy resonance, though it is not a resonance in the right sense.

The geometrical interpretation of the pygmy resonance is connected with the transition densities of protons and neutrons in the given nucleus, which are defined as

$$\delta\rho_\nu^{(\tau)} \equiv \langle\nu|\ \hat{\rho}_\tau(\vec{r})\ |\,0\rangle \qquad\qquad \tau \in n,p \tag{7.403}$$

where $|\,0\rangle$ is the ground state (in the RPA case it is the phonon vacuum), $|\nu\rangle$ are the excited states (in the framework of the RPA we restricted ourselves to one- phonon states) and $\hat{\rho}_{\tau=n}(\vec{r}) = \sum_{i=1}^{N} \delta(\vec{r}-\vec{r}_i)$, $\hat{\rho}_{\tau=p}(\vec{r}) = \sum_{i=1}^{Z} \delta(\vec{r}-\vec{r}_i)$ are neutron and proton density operators. Since in the pygmy energy region (6-8.8 MeV in ^{208}Pb) there is a high density of states, which can vary from state to state and so hide common feature of the density. Thus it is necessary to consider transition densities averaged over given energy intervals. Incoherent (that means not dependent on numerical phases of individual solutions of the RPA equations) averaging requires expressions which are bilinear in the excited states $|\nu\rangle$. This is achieved by summing transition densities weighted by the matrix elements of transition operator (not necessarily the same transition operator as that corresponding to investigated strength function but the transition operator $\hat{D}$ with the same momentum and parity selection

rules). So instead of (7.403) the following averaged density will be analyzed

$$\delta\rho_{\tau}^{(\hat{D})}(\vec{r}) = \sum_{\nu\in[\omega_1,\omega_2]} \langle\nu|\ \hat{D}\ |0\rangle\ \delta\rho_{\nu}^{(\tau)}(\vec{r}) = \\ = \sum_{\nu\in[\omega_1,\omega_2]} \langle\nu|\ \hat{D}\ |0\rangle\ \langle\nu|\ \hat{\rho}_{\tau}(\vec{r})\ |\ 0\rangle \qquad (7.404)$$

The sum in (7.404) involve all the excited states $|\nu\rangle$ with energies in the interval $\langle\omega_1,\ \omega_2\rangle$. For the investigation of the pygmy resonance in ^{208}Pb we will use the interval 6.0-8.8 MeV.

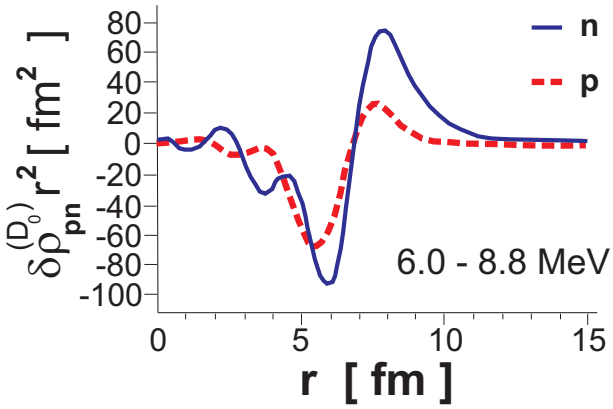


Figure 7.43: Summed r^2- weighted proton and neutron transition densities $\delta\rho_{p,n}^{(\hat{D}_0)}(r)$ at energy interval 6.0-8.8 MeV in ^{208}Pb (taken from [206]).

In the Fig.7.43 the r^2- weighted proton and neutron transition densities $\delta\rho_{\tau=p,n}^{(\hat{D}_0)}(\vec{r})$ averaged in the energy interval 6.0-8.8 MeV by the matrix elements of the operator $\hat{D} = \sum_{i=1}^{A} r_i^3\, Y_{10}(\hat{r}_i)$ [31] (compression dipole operator (7.402) - see [206]) for details).

From the Fig.7.43 it is clearly seen that near the nucleus surface ($r \approx 7-8$ fm for ^{208}Pb) the neutron density dominates over proton density as it can be expected for $N >> Z$ nucleus ^{208}Pb. This fact lead to the simple interpretation of the pygmy resonance as the oscillation of the neutron skin (the $N-Z$ excess of neutrons with respect to protons) versus the $N=Z$ core [207, 208, 209], which is demonstrated in the schematic Fig.7.44.

However in the paper [206] it is shown that the interpretation of the pygmy resonance as the oscillation of the neutron skin versus the $N=Z$ core is not the only one and that it can be connected also with the dipole toroidal

[31] Very similar averaged density is obtained if the transition density is weghted by the matrix elements of the standard E1 transition operator $\hat{D} = \sum_{i=1}^{A} r_i\, Y_{10}(\hat{r}_i)$.

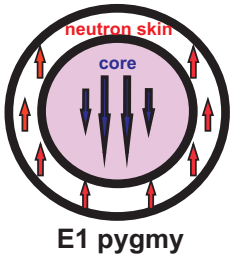


Figure 7.44: Schematic figure of the geometrical interpretation of the pygmy resonance.

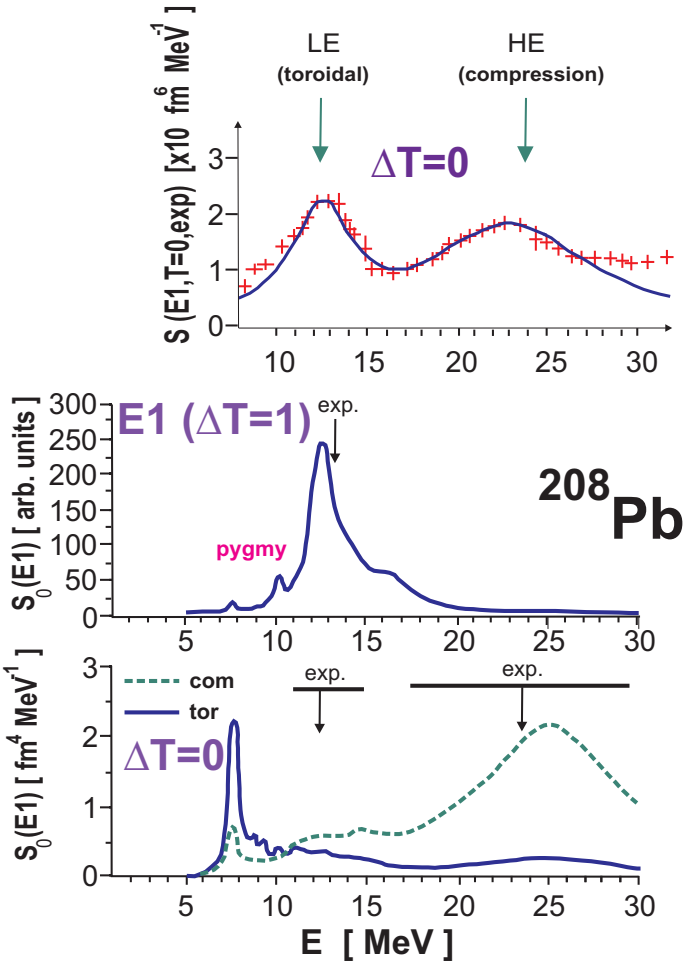


Figure 7.45: Isovector ($\Delta T = 1$) and isoscalar ($\Delta T = 0$) E1 strength functions in ^{208}Pb. Upper panel shows the experimental isoscalar E1 strength function (toroidal dipole and/or compression dipole strength) - experimental data taken from [190]. The middle panel demonstrates calculated isovector ($\Delta T = 1$) E1 strength function using the Skyrme BCS+RPA approach with the SLy6 Skyrme parametrization [206]. The lowest panel involves the calculated isoscalar ($\Delta T = 0$) toroidal dipole (solid curve) and isoscalar ($\Delta T = 0$) compression dipole (dashed curve) strength functions.

strength which has a peak in the pygmy energy region. This connection can

be seen in the Fig.7.45.

The upper panel of the Fig.7.45 shows the experimental isoscalar ($\Delta T = 0$) E1 strength function. Here it should be noted that the term "isoscalar E1" is used in the literature incorrectly. As it was already mentioned in the beginning of the current paragraph concerning the electric giant dipole resonance and as it was also discussed in the Appendix O, the isoscalar E1 excitations connected with the transition operator $\hat{\mathscr{M}}^{(el)}_{1\mu}(\Delta T = 0) = \sum_{k=1}^{A} e_k^{(eff)}(\Delta T = 0)\, r_k\, Y_{1\mu}(\hat{r}_k)$ do not exist (except the non-physical spurious mode connected with the center of mass translation motion). That means to speak about the realistic isoscalar E1 strength function is a nonsense. Nevertheless in the literature became to be used the term "isoscalar E1 strength function" for the isoscalar ($\Delta T = 0$) strength function connected with the second order terms in the long-wave decomposition of the standard E1 transition operator (2.103), that means with the isoscalar compression dipole isoscalar operator $\hat{\mathscr{M}}^{'(com)}_{1\mu}(k = 0, \Delta T = 0)$ (see (7.402) which is directly connected with the isoscalar dipole toroidal operator $\hat{\mathscr{M}}^{(tor)}_{1\mu}(k = 0, \Delta T = 0)$ (see (7.400), (7.396). So the experimental strength function $S(E1, T = 0, exp)$ (extracted from the $(\alpha, \alpha^{'})$ reaction cross section in [190]) should be compared with the bottom panel of the Fig.7.45. Concretly, in the bottom panel the isoscalar toroidal dipole (solid curve) and isoscalar compression dipole (dashed curve) strength functions calculated with the Skyrme BCS+RPA approach with the SLy6 Skyrme force parametrization [206] are demonstrated. The arrows, depicted in the bottom panel, mark the position of the experimental peaks demonstrated in the upper panel. From the comparison of the upper and bottom panels in the fig.7.45 it follows that the experimental lower energy peak (denoted as LE in the upper panel) is connected with the toroidal dipole strength and the higher energy peak (denoted as HE) is associated with the compression dipole character. Just for a comparison in the middle panel there is the calculated isovector E1 strength function (again with the SLy6 Skyrme BCS+RPA approach [206]). The comparison of the middle panel with the bottom panel demonstrates the toroidal character of 1^- excitations with energies in the pygmy resonance region (the toroidal dipole peak in the bottom panel corresponds very well in energy with the pygmy resonance region in the middle panel). In the middle panel the arrow shows the position of the experimental centroid of the IVGDR which is in accordance with the position of the maximum of the calculated IVGDR.

The toroidal character of the states with the excitation energies in the

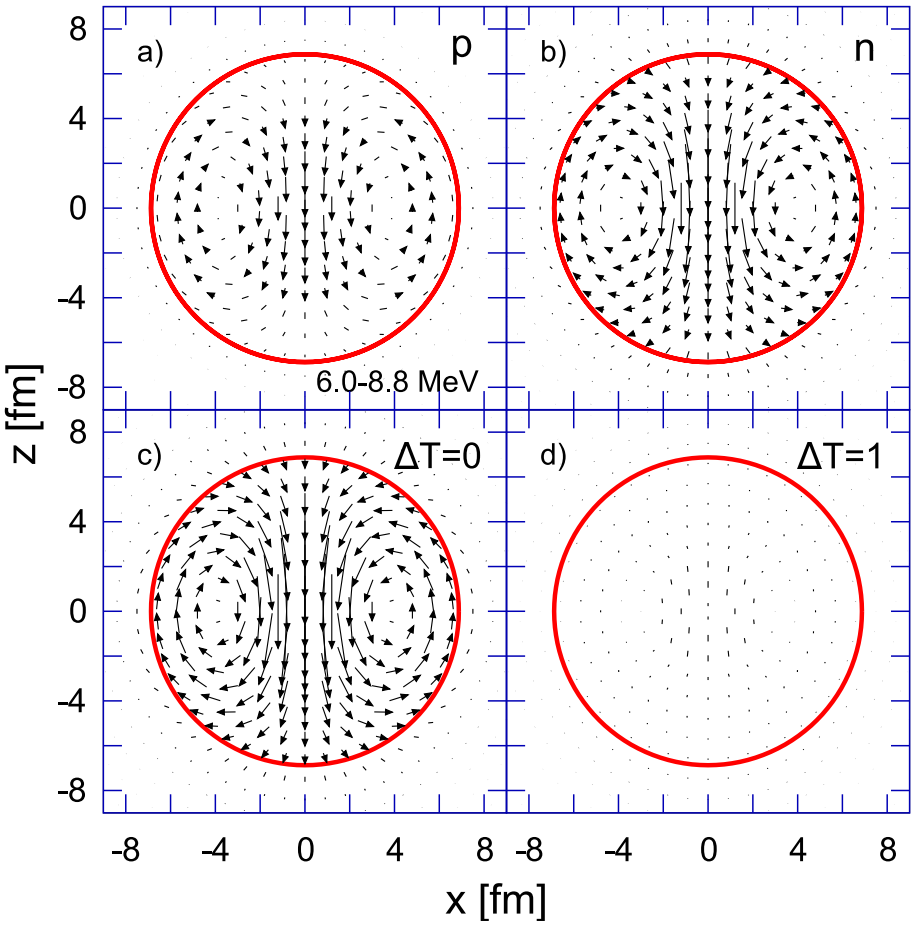


Figure 7.46: Proton (a), neutron (b), isoscalar $\Delta T = 0$ (c), and isovector $\Delta T = 1$ (d) transition current density $\delta\vec{j}_\tau^{(\hat{D}_1)}$ (see (7.406) in ^{208}Pb, averaged and weighted in the energy interval 6.0-8.8 MeV (taken from [206]).

pygmy resonance region can be clearly seen if the shape of the nucleon transition current is depicted. Similarly as the transition density (7.403) is averaged in (7.404) inside the energy interval $\langle\omega_1, \omega_2\rangle$ we can average the nucleon transition current

$$\delta\vec{j}_\nu^{(\tau)}(\vec{r}) \equiv \langle\nu|\,\hat{\vec{j}}_\tau(\vec{r})\,|\,0\rangle \qquad\qquad \tau = n, p \tag{7.405}$$

where $\hat{\vec{j}}_\tau(\vec{r}) = \hat{\vec{j}}_{nuc,\,\tau}(\vec{r})$ is the proton ($\tau = p$) or neutron ($\tau = n$) nucleon current density operator (see (2.135), (2.136), (2.141)). So the averaged in the energy interval $\langle\omega_1, \omega_2\rangle$ transition current, weighted by the matrix elements

of the operator $\hat{D}$, is (the analogy with(7.404))

$$\delta\vec{j}_{\tau}^{(\hat{D})}(\vec{r}) = \sum_{\nu\in[\omega_1,\,\omega_2]} \langle\nu|\,\hat{D}\,|\,0\rangle\;\delta\vec{j}_{\nu}^{(\tau)}(\vec{r}) = \\ = \sum_{\nu\in[\omega_1,\,\omega_2]} \langle\nu|\,\hat{D}\,|\,0\rangle\;\langle\nu|\,\hat{\vec{j}}_{\tau}(\vec{r})\,|\,0\rangle \qquad (7.406)$$

Again for the investigation of the pygmy resonance in ^{208}Pb we use the energy interval 6.0-8.8 MeV.

In the Fig.7.46 the cut of the current field $\vec{j}_{\tau}^{(\hat{D}_1)}(\vec{r})$ on the (x,z) plane of the center of mass frame of the ^{208}Pb calculated in the framework of the Skyrme BCS+RPA approach with the SLy6 Skyrme interaction parametrization. The calculation was done with effective gyromagnetic ratios (7.369) for $\tau = \Delta T = p$ (only proton part of the nucleon corrent - left upper panel), $\tau = \Delta T = n$ (only neutron part of the nucleon current - right upper panel), $\tau = \Delta T = 0$ (isoscalar nucleon current - left bottom panel) and $\tau = \Delta T = 1$ (isovector nucleon current - right bottom panel) (see [206] for details). Matrix elements of the operator $\hat{D} = \hat{D}_1 = \sum_{k=1}^{A} r_k Y_{10}(\hat{r}_k)$ were used in the averaging of the density current (7.406) in the interval $\langle\omega_1,\omega_2\rangle = \langle 6.0\;MeV,\;8.8\;MeV\rangle$. From the Fig.7.46 the toroidal character of the E1 oscillation of the nucleon flow in the excitation states with energies in the pygmy resonance region for neutrons ($\Delta T = n$) and isoscalar case ($\Delta T = 0$) is clearly seen. The figure demonstrates also the isoscalar character of the pygmy resonance (practically no E1 isovector $\Delta T = 1$ flow is observed). Similar situation was obtained also for other spherical and deformed nuclei (see e.g. [210, 211]).

Shapes of the nucleon flow in the excited states with energies in the pygmy resonance region obtained for ^{208}Pb and other nuclei indicate a new (alternative) interpretaion of the pygmy resonance, or more precise a modificaltion of the interpretation given in the Fig.7.44. Figures Fig.7.45 (high toroidal dipole strength in the pygmy resonance energy region) and Fig.7.46 (toroidal shape of the neutron and/or isoscalar flow of nucleons) illustrate that to interpret the pygmy resonance only as the vibration of the neutron skin versus the $N = Z$ core is not precise and that, more likely, the better interpretation is the toroidal oscillation of the neutron flow - see the right panel of the Fig.7.47.

From the schematic figures Fig.7.47 one can see that the older interpretation of the pygmy resonance as the vibration of the neutron skin versus $N = Z$ core presented in the left part of the Fig.7.47 does not contradict entirely to the new interpretation of the toroidal oscillation of the neutron or

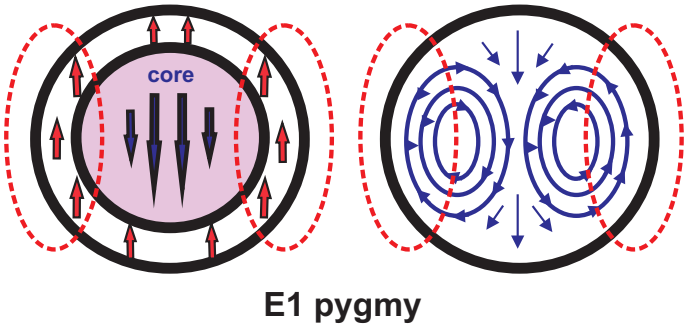


Figure 7.47: Schematic figure of the modified geometrical interpretation of the pygmy resonance. The left figure is the same as in the Fig7.44 and it shows the original interpretation of the pygmy resonance as the vibration of the neutron skin against the $N = Z$ core. The right figure demonstrate the new modified interpretation of the pygmy resonance where this resonance is formed predominantly by toroidal oscillations of the neutron flow. From the point of view of the periferal parts of the nucleus, denoted by the dashed ovals, both interpretations do not contradict each other.

isoscalar flow. If we inspect the peripheral parts of the nucleus denoted by the dashed ovals the same shape of the flow near the nucleus surface can be observed in the right and left part of the Fig.7.47.

Electric giant quadrupole E2 resonance

Giant quadrupole E2 resonance (GQR) is connected with the transition operators $\hat{\mathscr{M}}^{(el)}_{2\mu}(\Delta T = 0) = \sum_{k=1}^{A} r_k^2\, Y_{2\mu}(\hat{r})$, $(\mu = 0, \pm 1, \pm 2)$ (for isoscalar E2 transitions - isoscalar quadrupole resonance (ISGQR)) and $\hat{\mathscr{M}}^{(el)}_{2\mu}(\Delta T = 1,\ \Delta T_z = 0) = \sum_{k=1}^{A} r_k^2\, Y_{2\mu}(\hat{r})\, 2(\hat{t}_z)_k$, $(\mu = 0, \pm 1, \pm 2)$ (for isovector E2 transitions - isovector quadrupole resonance (IVGQR)) (see (7.364)). Unlike the electric dipole resonance, where only isovector dipole resonance connected with the electric transition operators $\hat{\mathscr{M}}^{(el)}_{1\mu}(\Delta T = 1,\ \Delta T_z = 0)$ can be experimentally observed, in the case of the electric giant quadrupole resonance both isoscalar (ISGQR) and isovector (IVGQR) E2 resonances are possible to see in experiments. The experimental data on the ISGQR are mainly obtained from the analysis of the inelastic α and ^{3}He scattering at very forward angles [32] and experimental information on the IVGQR can be extracted using (γ, n), (n, γ) reactions or by the inelastic scattering of electrons (see [181] and citations therein). The experimental energies of the ISGQR centroids

[32] In the (α, α') and $(^3He, ^3He')$ scattering the analysis of the theoretical cross sections using the distorted wave Born approximation (DWBA) discussed in the Chapter ... show the rapid decreasing cross section contribution of the ISGMR as a function of angle with its minimum at $\approx 3^\circ$ and a quick change of the IVGDR in the angle interval $\langle 0^\circ, 5^\circ \rangle$. However the monopole and quadrupole resonances are relatively smooth in this angle interval. This fact allows to separate ISGQR from the ISGMR and IVGDR (see [181]).

can be approximated by the following expression, obtained by the fitting to the experimental values of many spherical nuclei [181],

$$E^{(exp)}_{ISGQR}(A) \approx (61 \pm 1.7)\, A^{-1/3}\ MeV \tag{7.407}$$

and experimental energies of the IVGQR centroids are estimated by [181]:

$$E^{(exp)}_{IVGQR}(A) \approx (59.2 \pm 2.6)\, A^{-1/6}\ MeV \tag{7.408}$$

In the Fig.7.48 the proton part ($\Delta T = p$ - see (7.368)) of the GQR, calculated in the framework of the BCS+RPA method with the Skyrme effective interaction using different Skyrme parametrizations (listed in the figure), is shown. The left panels concern spherical nucleus ^{142}Nd and in the right panels the results for axially deformed ^{150}Nd nucleus are demonstrated. Equilibrium quadrupole deformation β for individual Skyrme parametrizations was obtained by the minimizing of the total BCS energy as a function of β. One can see that this equlibrium deformations do not differ so much for given nucleus. In the case of the spherical nucleus ^{142}Nd all projections $\mu = 0,\ \pm 1,\ \pm 2$ of the transition operator $\hat{\mathscr{M}}^{(el)}_{2\mu}(\Delta T = p) = \sum_{k=1}^{Z} r_k^2\, Y_{2\mu}(\hat{r}_k)$ give the same strength function $S_0(E2\mu;\ \Delta T = p;\ E)$ (μ- degeneracy) [33] . For the deformed nucleus ^{152}Nd we observe the μ- splitting and each μ-component gives the different E2 strength function $S_0(E2\mu;\ \Delta T = p\ ;\ E)$. This lead to the substantial broadening of peak structure for the deformed nucleus. For the spherical ^{142}Nd (left panels) two peaks can be clearly recognized for all Skyrme parametrizations. Energetically lower peak corresponds to the ISGQR ($\Delta T = 0$) and higher peak to the IVGQR ($\Delta T = 1$). So the proton E2 strength function represents the mixture of the isoscalar ISGQR and isovector IVGQR as it was expected. The deformation effect of the μ-splitting for deformed nuclei causes a partly stretching out the ISGQR and IVGQR peaks. The red arrows in all panels show the position of the ISGQR experimental centroid (lower panel) and of the IVGQR experimental centroid (higher energy) estimated by (7.407) and (7.408), respectively. From the figure only a qualitative agreement of calculated peaks with experimental centroids can be observed (the best agreement was obtained for the Skyrme interaction parametrization SKM* and SkT6). One should realize in this comparison that all E2 excitations obtained by the RPA approach are supposed to have one- phonon character and all two- phonon and more- phonon

[33] Since for $\mu \neq 0$ the strength function presented in the Fig.7.48 is the sum of $\mu = |\mu|$ and $\mu = -|\mu|$ components the contribution of $\mu \neq 0$ to the total strength function is 2- times higher than the contribution of the $\mu = 0$ projection.

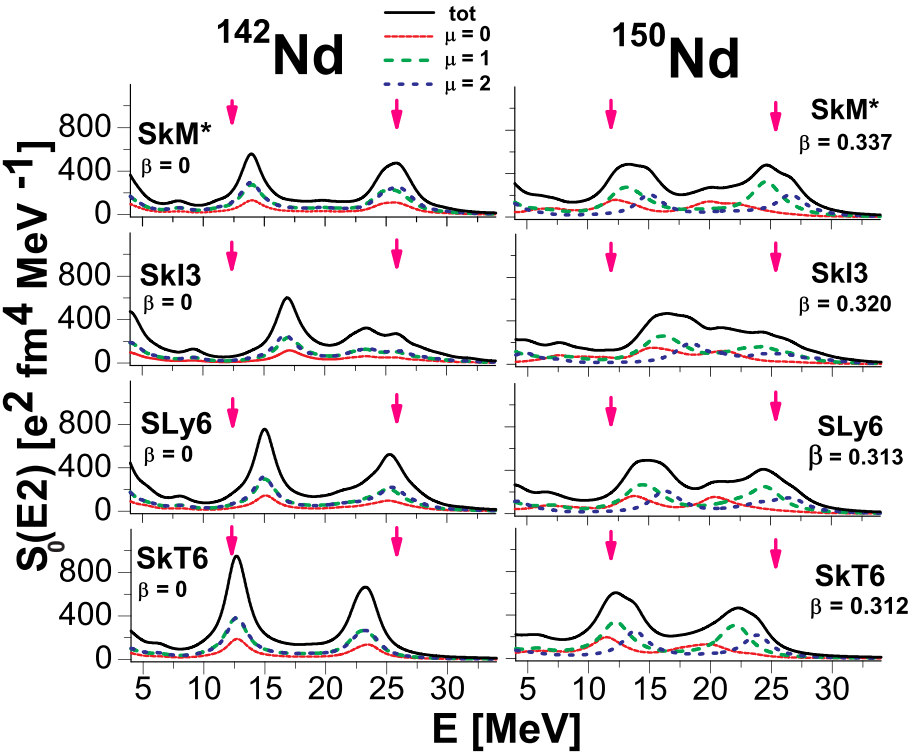


Figure 7.48: Proton (with pure electromagnetic effective charges $\Delta T = p$ - see (7.368)) E2 strength function in the spherical ^{142}Nd and axially deformed ^{150}Nd isotopes calculated in the framework of the Skyrme BCS+RPA approach with different Skyrme interaction parametrizations (SkM^*, $SkI3$, $SLy6$ and $SkT6$ parametrizations). The estimation of the position of the experimental isocalar (lower energy) and isovector (higher energy) giant quadrupole resonance centroids (see (7.407) and (7.408)) are denoted by red arrows. The red short dashed curve corresponds to the $\mu = 0$ component of the E2 excitations, the green dashed curve to the $\mu = \pm 1$ components of the E2 and the blue dotted curve to $\mu = \pm 2$ component of E2 resonance. The solid black line is the total E2 strength function. Equilibrium deformation given for each Skyrme parametrization for deformed ^{152}Nd was obtained from the minimum of the total BCS bind energy as a function of the deformation β for each Skyrme parametrization.

components in excitation states are neglected. Taking into account of these complex configurations could give the ISGQR and IVGQR more fragmented and as a result corresponding peaks can be shifted and their widths changed.

As another example of the E2 strength function the energy weighted ISGQR strength function $S_1(E2;\ \Delta T = 0;\ E)$ is compared in the upper part of the Fig7.49 with the experimental values for deformed nucleus ^{154}Sm ($\beta = 0.339$). The calculation was done with the Skyrme SkT6 BCS+RPA approach with the Lorentz averaging function with $\Delta = 1$ MeV (see (7.372) and (7.373)) (the details of corresponding codes can be found in [212]). We can see again the μ- splitting according to the angular momentum projection

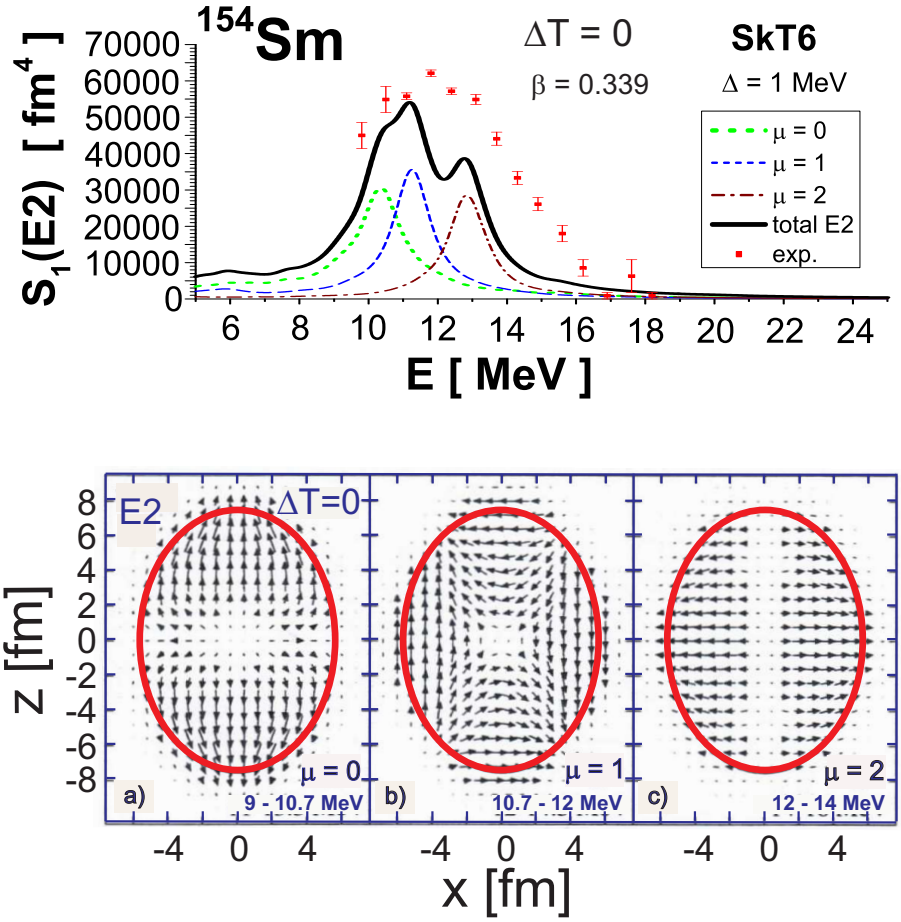


Figure 7.49: Energy weighted ISGQR strength function $S_1(E2;\Delta T=0;E)$, calculated in the framework of the Skyrme SkT6 BCS + RPA approach [212], is compared with corresponding experimental values in the upper panel. In lower panels the cuts on the (x,z) plane of the intrinsic coordinate frame of the isoscalar nucleon transition current (7.409) calculated for different E2 RPA excitations with different angular momentum projections $\mu=0,\pm1,\pm2$ and averaged by the quadrupole transition operators in the energy intervals given in each panel.

$\mu = 0,\ \pm1,\ \pm2$. In the lower panel of the Fig7.49 the figures of the transition isoscalar ($\Delta T = 0$) nucleon current (see the analogy with the transition density in (7.404))

$$\delta\vec{j}_\tau^{\hat{D}_2}(\vec{r}) = \sum_{\nu\in\langle\omega_1,\omega_2\rangle} \langle 0|\ \hat{D}_2\ |\nu\rangle\ \delta\vec{j}_\nu^{(\tau=\Delta T=0)}(\vec{r}) =$$

$$= \sum_{\nu\in[\omega_1,\omega_2]} \langle 0|\ \hat{D}_2\ |\nu\rangle\ \langle\nu|\ \hat{\vec{j}}_\tau(\vec{r})\ |\ 0\rangle \qquad (7.409)$$

where the isoscalar nucleon current operator $\hat{\vec{j}}_\tau(\vec{r})$ is [34]

$$\hat{\vec{j}}_{\tau=0} = -i \sum_{i=1}^{A} e_i^{(eff)}(\Delta T = 0) \left(\delta(\vec{r} - \vec{r}_i)\, \vec{\nabla}_i - \vec{\nabla}_i\, \delta(\vec{r} - \vec{r}_i)\right) \qquad (7.410)$$

with corresponding effective charges $e_i^{(eff)}(\Delta T = 0)$ given in (7.368), and the matrix elements of the standard long wave electric quadrupole operator $\hat{D}_2 = \sum_{i=1}^{A} r_i^2\, Y_{2\mu}(\hat{r}_i)$ are used in the corresponding energy interval $\langle \omega_1, \omega_2 \rangle$. More precisely, in the lower part of the Fig.7.49 the cuts of the isoscalar transition nucleon current (7.409) field on the (x, z) plane of the frame fixed to the nucleus are presented for different ang. momentum projections. In the panel a) the RPA states $|\nu\rangle = |\mu = 0, \nu\rangle$ with the ang. momentum projection $\mu = 0$ are used in (7.409). The pane b) corresponds to the projection $\mu = 1$ and the panel c) to the projection $\mu = 2$. The corresponding averaging energy intervals (9-10.7 MeV for the panel a), 10.7 - 12 MeV for the panel b), 12 - 14 MeV for the panel c)) are intervals where the corresponding μ- component strength function peak in the upper panel gives the biggest contribution to the total $S_1(E2)$ strength function. The panel a) and panel c) correspond to the standard geometric interpretation of quadrupole beta and quadrupole gamma shape vibrations, respectively, which are demonstrated in the upper part of the schematic figure Fig.7.10.

From the upper part pf the Fig.7.49 a good agreement of the calculated ISGQR with the experimental values can be seen if the Skyrme SkT6 effective interaction parametrization is used in the calculations. However it is necessary to note that this parametrization is not so good in the comparison of experimental and calculated IVGDR (see e.g. [92]). This is a general feature of the Skyrme effective nucleon-nucleon interaction that there is no Skyrme interaction parametrization which gives the good agreement with experimental values simultaneously for all giant resonances.

M1 giant resonance (scissor and spin-flip resonances)

M1 giant resonance is connected with the transition operator (see (7.367) or (2.145) for $\lambda = 1$)

$$\hat{\mathscr{M}}_{1\mu}^{(mag)} = \mu_n \sqrt{\frac{3}{4\pi}} \sum_{i=1}^{A} \left(g_i^{(l;\, eff)}\, \hat{l}_\mu^{(i)} + g_i^{(s;\, eff)}\, \hat{s}_\mu^{(i)}\right) \qquad \mu = \pm 1, 0 \qquad (7.411)$$

[34] In the [212] it is shown that the magnetization part of the nucleon current gives very small contribution to (7.409).

where $\hat{l}_{\mu}^{(i)}$, $\hat{s}_{\mu}^{(i)}$ are single-particle operators of the orbital momentum and spin momentum components $\mu = \pm 1, 0$, respectively. Symbols $g_i^{(l,\,eff)}$ and $g_i^{(s,\,eff)}$ stand for the orbital and spin effective gyromagnetic ratios, respectively (see (7.369)), and μ_N is the nuclear magneton (see (2.146)). Similarly as in the case of electric monopole, dipole and quadrupole resonances discussed in previous part of this subsection the M1 resonances in even-even nuclei will be discussed only. From the experimental point of view the orbital part of the M1 transition operator (7.411) participates mainly in the $(e, e^{'})$ and γ-absorption experiments while the spin part of the (7.411) is important in the excitations by $(e, e^{'})$ and $(p, p^{'})$ reactions [181].

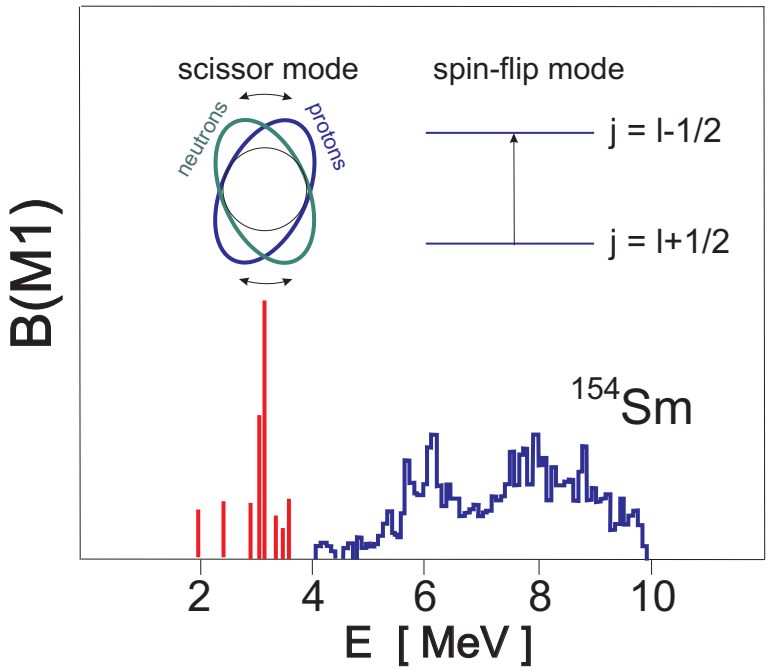


Figure 7.50: Illustrative figure of the orbital (scissor) and spin-flip parts of the magnetic dipole resonance (from [181], see also [214]).

In the Fig.7.50 the typical spectrum of 1^+ state excited in terms of the M1 transition operator (7.411) is illustrated for deformed nucleus ^{154}Sm. In the case of deformed nucleus the spectrum of 1^+ states can be divided into the low- energy part (a cluster of individual excited states known as scissor resonance) and high- energy part (spin-flip resonance) generated by the spin part of the M1 transition operator (7.411). The spin part of the operator (7.411) is the $\Delta T_z = 0$ component of the Gamow-Teller transition operator

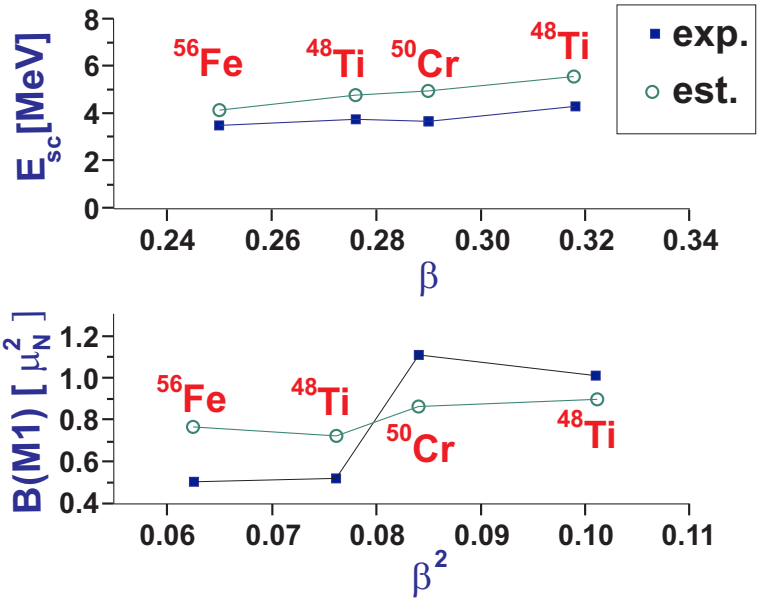


Figure 7.51: Comparison of the simple two- rotor model [213] estimations (7.415) and (7.416) of the scissor mode excitation energies and excitation reduced probabilities to the scissor $\mu^{\pi} = 1^{+}$ states with the corresponding experimental energies taken from [215, 216, 217].

$\hat{\mathcal{M}}^{(\beta\ allowed\ GT)}_{1M}$ (see (10.136)):

$$\hat{\mathcal{M}}^{(\beta\ allowed\ GT)}_{1M}(\Delta T_z) = \hat{\mathcal{M}}^{(\beta)}_{01M;\,\sigma;\,\tau\mu=\Delta T_z} \approx \sum_{i=1}^{A} (\hat{s}_M)_i\ (\hat{t}_{\mu=\Delta T_z})_i \quad , \quad M = 0,\ \pm 1 \tag{7.412}$$

where $\hat{t}_{\mu=\Delta T_z} = \frac{1}{2}\hat{\tau}_{\mu=\Delta T_z}$ with $\Delta T_z = 0, \pm 1$ are operators of components of the single-nucleon isospin and $\hat{s}_M = \frac{1}{2}\hat{\sigma}_M$ with $M = 0,\ \pm 1$ are the single-particle spin component operators ($\hat{\vec{\sigma}}_\mu$ and $\hat{\vec{\tau}}_\mu$ (with $\mu = 0, \pm 1$) are components of the vector formed by the spin or isospin Pauli matrices, respectively), and

$$\hat{\mathcal{M}}^{(\beta)}_{LJM;\,\sigma;\,\tau\mu} = \sum_{j=1}^{A} r_j^L\ \left[Y_L(\hat{r}_j) \otimes \vec{\sigma}^{(j)}\right]_{JM} (\hat{t}_\mu)_j \tag{7.413}$$

with $M = -J, \cdots, +J$ and $\mu = 0, \pm 1$ are general spin-flip β- multipole transition operators which, together with the non-spin-flip Fermi β- transition operators (see (10.136) for $J = 0$ Fermi allowed transition case)

$$\hat{\mathcal{M}}^{(\beta)}_{JM;\,\tau\mu} = \sum_{j=1}^{A} r_j^J\ Y_{JM}(\hat{r}_j)\ (\hat{t}_\mu)_j \quad , \tag{7.414}$$

generate the β- transitions in nuclei discussed in the Chapter 10.

The qualitative explanation of both parts of the spectrum of 1^+ states can be done by the following consideration. The simple two-rotor model (see [213, 214]) showed that the orbital part of the M1 transition operator (7.411) generates in the deformed nuclei an angular oscillation of the axially deformed proton system versus neutron system around an axis perpendicular to the symmetry axis of the nucleus (so called scissor modes - see the left upper corner in the Fig.7.50). The spin part of the M1 transition operator (7.411) is responsible for so called M1 spin-flip transitions with corresponding M1 spin-flip resonance. As it was mentioned above, this spin-flip part of (7.411) can be identified with the operator $\hat{\mathscr{M}}^{(\beta)}_{L=0\ J=1\ M;\ \sigma;\ \tau\mu=0}$ and therefore acting on the ground state of even-even nuclei this operator excites states with $J^\pi = 1^+$ and these $\Delta L = 0$, $\Delta S = 1$ transitions can occur between the single-particle partners $j = l \pm 1/2$: $j = l + 1/2 \to j = l - 1/2$ (see the right upper corner of the Fig.7.50) [35] . The energy splitting of the orbital scissor resonance and spin-flip resonance can be understood if we look what happens if the residual interaction is taken into account by the RPA calculation. The unperturbed mean field particle-hole states are scattered over an energy interval of about 8-10 MeV (from about 2 MeV to about 10 MeV in rare-earth nuclei) and orbital and spin-flip states are mingled. The residual particle-hole interaction is known to be strong and repulsive in the $\sigma\tau$ channel and turns out to be weak in the orbital part. Hence, by switching the residual interaction on, the collective spin-flip strength having about 90% of the total M1 strength will move to higher energies while the weakly collective orbital strength practically does not move. As a result, the two components will split in energy: the lower part is due to orbital and the higher part to spin-flip excitations. As a consequence, in deformed nucleus the scissor and spin-flip modes are located at low and high energy, respectively, as is illustrated in the Fig.7.50.

From the schematic figure of the scissor M1 excitation (see the left upper corner of the Fig.7.50) one can expect that this type of excitation can be observed only in deformed nuclei. Really, the two-rotor model of Lo Iudice and Richter [213] gave the following estimation for the energy of the scissor resonance

$$E_{scissor} \approx 66\,(0.95\,\beta)\,A^{-1/3} \qquad MeV \tag{7.415}$$

[35] However one should realize that the excitation by the operator $\hat{\mathscr{M}}^{(\beta)}_{L=0\ J=1\ M;\ \sigma;\ \tau\mu=0}$ of only single-particle partners $j = l \pm 1/2$ from the even-even nucleus ground state valids only in the case when the ground state is described as the Hartee-Fock ground state $|HF\rangle$ (or BCS ground state $|BCS\rangle$) where correlations with particle-hole or two-quasiparticle configurations are not taken into account. If these correlations in the ground state are taken into account and cannot be neglected then not only single-particle $j = l \pm 1/2$ partners can be excited by the transition operator $\hat{\mathscr{M}}^{(\beta)}_{L=0\ J=1\ M;\ \sigma;\ \tau\mu=0}$ (with the selection rules $\Delta L = 0$, $\Delta S = 1$).

with the excitation M1 reduced probability from the even-even nuclei ground state to the states $\mu^\pi = 1^+$ in the axially deformed nuclei:

$$B_{scissor}(M1;\, 0^+ \to \mu^\pi = 1^+) \approx 0.004\, E_{scissor}\, A^{5/3}\, (0.95\,\beta)^2 \left(2\frac{Z}{A}\right)^2 \mu_N^2 \quad (7.416)$$

In the Fig. 7.51 these estimations for light nuclei ^{56}Fe, ^{48}Ti, ^{50}Cr and ^{48}Ti are compared with the corresponding experimental values taken from [215, 216, 217].

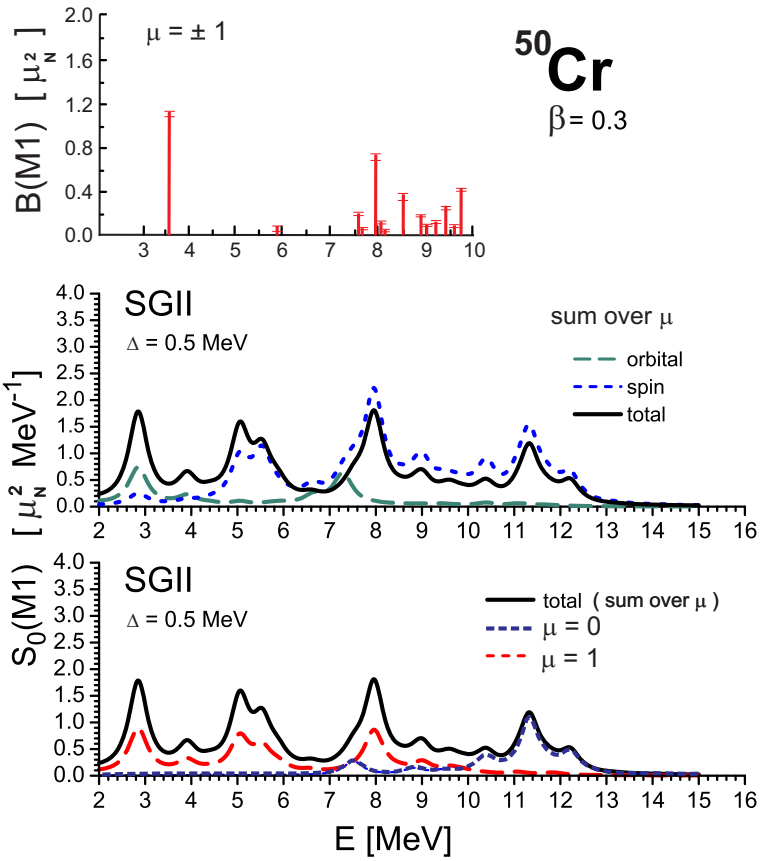


Figure 7.52: The experimental $B(M1)$ distribution (the upper panel) are compared with the calculated M1 strength function (the middle and the bottom panels). The middle panel demonstrates the contributions to the $S_0(M1;\, total)$ going from the spin and orbital parts of the M1 transition operator (7.411) while the bottom panel shows the contribution to the $S_0(M1;\, total)$ from individual M1 multipolarity projections $\mu = 0,\, +1$. Calculations were performed using the Skyrme BCS+RPA approach with the SGII Skyrme n-n interaction parametrization and using the averaging interval $\Delta = 0.5$ MeV in the expression (7.374) for the strength function $S_0^{(\Delta)}(M1\mu;\, \Delta T = p\,;\, E)$ with the effective gyromagnetic ratios given in (7.369) for $\Delta T = p$ (taken from [218]).

From the scissor energy estimation (7.415) it can be seen the almost horizontal linear dependence on the quadrupole deformation β. The weak dependence of the scissor excitation energy on A according to (7.415) is also

confirmed by experiment (scissor mode energies can be found in the energy interval 2.5 - 4.5 for a broad region of A, from ≈ 4 MeV in light nuclei to $\approx$ 2.5 MeV for actinides.).

More detailed comparison of the Skyrme BCS+RPA M1 strength function with the experimental excitation B(M1) values is shown in the Fig.7.52 for the case of ^{50}Cr isotope. In the top panel of this figure there is the experimental spectrum of the B(M1) excitation strength of the $\mu^{\pi} = 1^{+}$ states [218]. The first peak at 3.6 MeV is suggested in [218] to be interpreted as the scissor M1 state. This was confirmed by the results of the Skyrme BCS+RPA calculations with the SkII Skyrme parametrization which gave the M1 strength function $S_0(M1)$ presented in the middle and bottom panels. In the middle panel of the Fig.7.52 the black solid curve corresponds to the total $S_0(M1,\ total)$ strength function (that means the M1 strength function is summed over all projections $\mu = 0,\ \pm 1$), the blue short dashed curve corresponds to the M1 strength function where only spin part of the M1 transition operator (7.411) (that means $\hat{\mathscr{M}}^{(mag)}_{1\mu}(spin) = \mu_N \sqrt{\frac{3}{4\pi}} \sum_{i=1}^{A} g_i^{(s;\,eff)}\, \hat{s}^{(i)}_{\mu}$) was used in the RPA calculations. The green long dashed line was obtained with only the orbital part, $\hat{\mathscr{M}}^{(mag)}_{1\mu}(orbit) = \mu_N \sqrt{\frac{3}{4\pi}} \sum_{i=1}^{A} g_i^{(l;\,eff)}\, \hat{l}^{(i)}_{\mu}$, of the M1 transition operator (7.411). Comparing the top and middle panels one can conclude that the first experimental peak in the top panel correponds to the first peak of the calculated strength function $S_0(M1)$, in which the dominant contribution comes from the orbital part of the M1 transition (it is necessary to realize that the total strength function $S_0(M1;\ total)$ is not a simple sum of the spin $S_0(M1;\ spin)$ and orbital $S_0(M1,\ orbit)$ parts but that both these parts interfere, that means $S_0(M1;\ total) = (\sqrt{S_0(M1;\ spin)} + \sqrt{S_0(M1;\ orbit)})^2$). In the bottom panel of the Fig.7.52 the contributions of different multipolarity $\lambda = 1$ projections, $\mu = 0, \pm 1$, to the total M1 strength are demonstrated. Opposite to the spin and orbital contributions the contributions of multipolarity projections are additive, that means $S_0(M1;\ total) = \sum_{\mu=0,\pm 1} S_0(M1\mu)$. The red long dashed line in the bottom panel corresponds to $\mu = +1$ and the blue short dashed line to the projection $\mu = 0$ (the $\mu = -1$ contribution is not shown in the bottom panel because it is the same as the $\mu = 1$ contribution). From the bottom panel it is clear that the projection $\mu = 0$ manifests itself only in the higher energies (above 10 MeV) while the projections $\mu = \pm 1$ form practically all M1 strength function up to the energies 10 MeV.

In the Fig.7.53 strength function $S_0(M1\mu = 1;\ \Delta T = p;\ E)$ (see the upper panel) calculated in the framework of the Skyrme BCS+RPA method (that

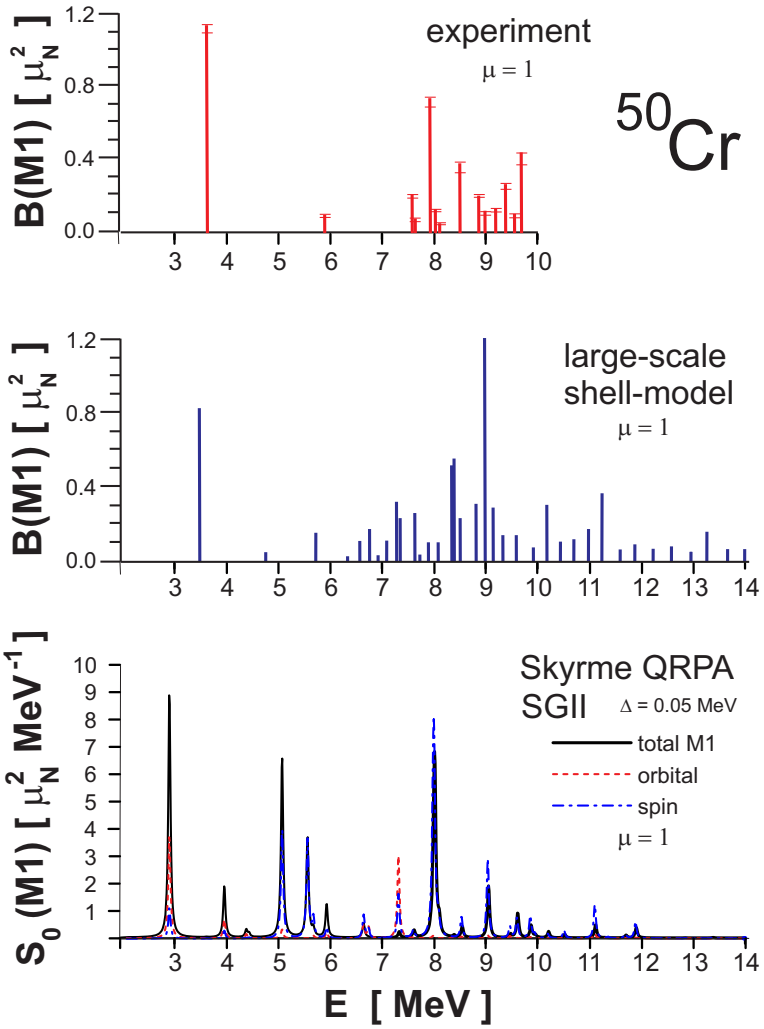


Figure 7.53: Excitation M1 reduced probability for 1^+ states in the dependence on the excitation energy in ^{50}Cr. The upper panel demonstrates experimental values extracted from the photon scattering (see [218]). Corresponding theoretical values calculated within a large-scale shell-model with the KB3G interaction [217] are shown in the middle panel. The M1 strength function $S_0(M1\mu = 1;\ \Delta T = p\ ;\ E)$ calculated in the framework of the SGII Skyrme QRPA approach [212, 218] according to (7.372) with the Lorentz averaging interval $\Delta = 0.05$ MeV is depicted in the bottom panel.

means the solving of the RPA equation (7.230) with the BCS quasiparticle basis obtained from the BCS equations (6.96)-(6.98) with the Skyrme effective interaction (5.83) and subsequent determination of the strength function (7.373) with (7.369) for $\Delta T = p$ - see [212, 218] for details) is compared with the results of the large-scale shell-model (LSSM) calculations [39] (see the middle panel) and with the experimental values (see the upper panel). In the bottom panel, with the SGII Skyrme QRPA results, the black solid curve corresponds to the total $S_0(M1)$ strength, the red dashed curve to the M1

orbital transitions and the blue dot-dashed curve to the M1 spin-flip transitions. Opposite to the Fig.7.52 in the bottom panel of the Fig.7.53 the SGII Skyrme QRPA strength function $S_0(M1)$ was determined with the very small Lorentz averaging interval $\Delta = 0.05$ MeV. This enables to observe individual RPA solutions in the plot and to compare them with the individual solutions of the large-scale shell-model and with the experimental excited states in ^{50}Cr.

Comparing the middle and bottom panels more $\mu^\pi = 1^+$ states can be observed in the energy interval 2-14 MeV for the LSSM than for the SGII Skyrme QRPA approach . This is because the LSSM (using a diagonalization of large Hamiltonian matrix) involves automatically complex many-particle - many-hole configurations (not only RPA one-phonon states). On the other hand side both these approaches interpret the first solution (with the energy $\approx$ 3.5 MeV for the LSSM and 2.92 MeV for the Skyrme QRPA) as the scissor state excited predominantly by the orbital part of the M1 transition operators as it can be seen from the bottom panel if the red dashed and blue dot-dashed curves are compared with the black solid curve (see [218] for more details). States with energies in the interval 5-14 MeV are predominantly of the spin-flip character excited by the spin part of the M1 operator as it can be indicated again in the bottom panel and as it is confirmed by the middle panel in the Fig.7.52 with the orbital and spin contributions to the M1 strength function (calculated with the Lorentz averaging interval $\Delta = 0.5$ MeV) where $S_0(M1)$ in the energy interval 5-14 MeV is formed mainly by the spin part of the M1 transition operator. These results of the theoretical analyses in [217, 218] lead to the interpretation of the lowest energy 1^+ state with the energy 3.628 MeV in ^{50}Cr observed in the experiment [218] to be the scissor state. This result, that the M1 excitations in the energy region around 3 MeV have a scissor character, is in the agreement with similar analyses performed for other nuclei (as it was already mentioned in the text below the Fig.7.51).

In order to show the character of the nucleon flow in the RPA excitation $|\nu\rangle$ with the energy 2.92 MeV, which was interpreted as the scissor state, in the Fig.7.54 the cuts on the (x, z) plane of the intrinsic coordinate frame of the proton (left panel) and neutron (right panel) transition current field calculated according to (7.406) is shown. Since we analyze the transition current corresponding to the excitation of one RPA state $|\nu\rangle$ (with the energy 2.92 MeV) there is not any sum in the expression (7.406) and it is not necessary to do any additional averaging of the current by matrix elements

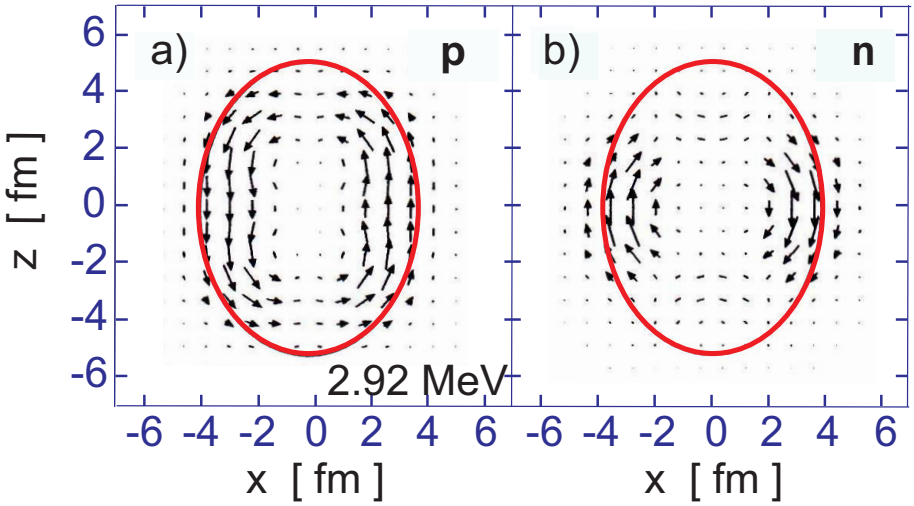


Figure 7.54: The cuts on the (x, z) plane of the intrinsic coordinate frame of the nucleon transition current field (7.406) calculated for M1 RPA excitation $|\nu\rangle$ with the energy 2.92 MeV and weighted by the corresponding matrix element of the quadrupole transition operator $\hat{D} = \sum_i r_i^2 Y_{21}(\hat{r}_i)$. The calculation was done within the Skyrme SGII RPA approach [212].

of any transition operator (in the case of one RPA state there is no conflict of phases of several RPA vawe functions) and we can use directly the expr. (7.405). The figure demonstrates clearly the scissor character of the nucleon flow, as it can be seen from the comparison of the Fig.7.54 with the schematic picture in the left corner of the Fig.7.50.

The situation with the spin-flip part of the M1 resonance is more complicated than with the scissor (orbital) part. Opposite to the orbital part of the M1 resonance (where the most of the effective nucleon-nucleon interactions give the scissor excitation in the energy around 3 MeV for all isotopes) in the case of the spin-flip part the different nucleon-nucleon interactions give different shapes and positions of the M1 spin-flip resonance. In the Fig.7.55 the M1 resonance in the spin-flip energy region in ^{238}U (4-10 MeV) calculated with 8 different Skyrme parametrization using the Skyrme QRPA method are compared with the corresponding experimental data taken from [220]. One can see that none of used parametrizations agrees with experimental values. From this point of view relatively the best one is the SGII parametrization.

It was already mentioned (see the text bellow the expr. (7.414)) that the spin-orbit energy splitting of the dominant single-particle partners $j = l \pm 1/2$ represents a crucial ingredient in the description of the spin-flip M1 mode (see e.g. [181, 219]). Usually the centroid of the proton peak E^p_{so} (calculated from the unperturbed M1 strength function where the residual

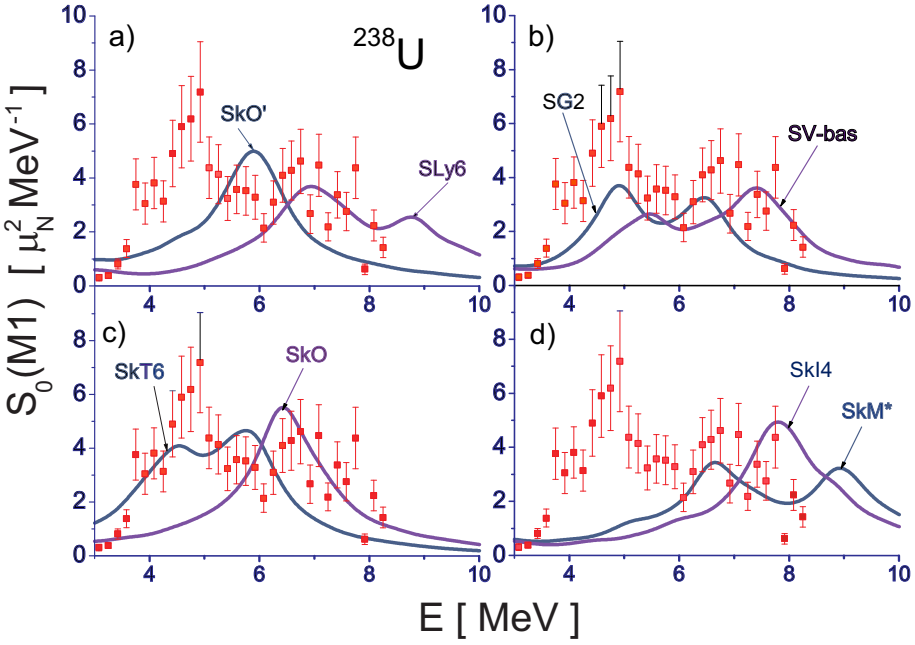


Figure 7.55: Spin-flip resonance in deformed ^{238}U ($\beta = 0.275$) described with eight Skyrme parametrizations as indicated. The experimental data are from [220].

interaction is switched off) is less than the centroid of the neutron peak centroid E^n_{so}, $E^p_{so} < E^n_{so}$, which leads in rare-earth and actinide nuclei to a two-peak structure of the spin-flip resonance with dominant proton (neutron) origin of the lower (upper) peak. This is demonstrated for ^{238}U in the Fig.7.56 (a) where the proton and neutron components of the M1 strength function, obtained with the QRPA approach are shown. The lower panel of the Fig.7.56 exhibits proton and neutron splittings $E_{so} \equiv |E^p_{so} - E^p_{so}|$ for different Skyrme parametrizations. The results strongly depend on the parametrization. In the most cases we have $E^p_{so} < E^n_{so}$ with $E_{so} = |E^p_{so} - E^n_{so}| \approx 1 - 2MeV$, but SkI4, SkO and SkO$'$ give very close splittings with even $E^p_{so} > E^n_{so}$ for SkI4 and SkO. It is necessary to note that the experimental proton-neutron splitting in the M1 strength function is $\approx$ 2 MeV in ^{238}U and zero in the spherical ^{208}Pb (see [221, 222]) and therefore one spin-flip M1 peak for ^{208}Pb. Generally one can say (see [219]) that different Skyrme parametrizations give the double-peak structure of the spin-flip resonance for deformed rare-earth and actinide nuclei but without a precise agreement with experimental data. However only some of the Skyrme parametrizations (SkO, SkO$'$ (see [219])) provide one-peak structure seen in the double-magic ^{208}Pb and ^{48}Ca nuclei and again there is no any agreement with the experimental data on the shape

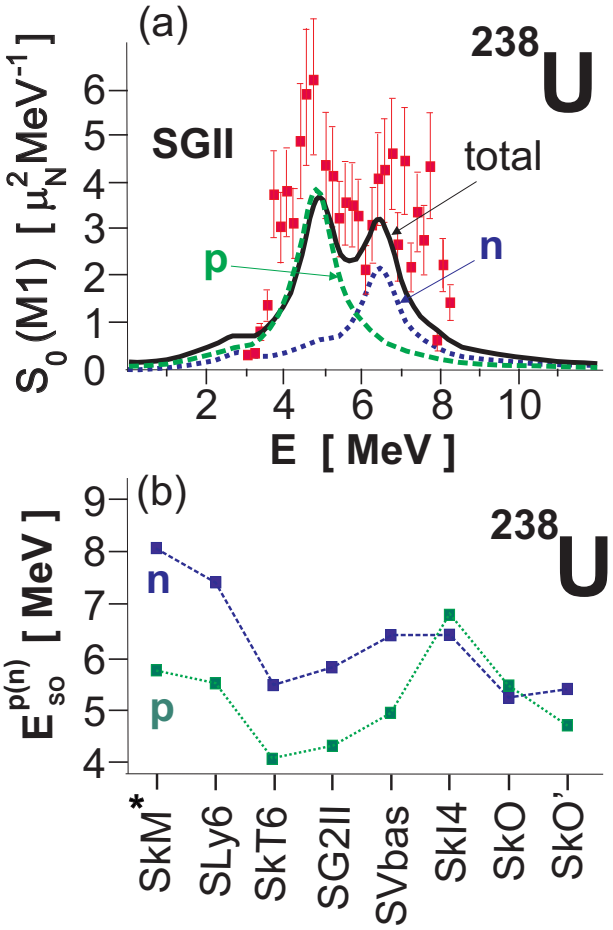


Figure 7.56: (a) Spin-flip resonance in ^{238}U calculated with the SGII Skyrme interaction: total (black solid line), proton (blue dotted line), neutron (green dashed line) strength function. The experimental data taken from [220]; (b) proton and neutron unperturbed spin-orbit splitting energies $E_{so}^{p(n)}$ for different Skyrme interactions in ^{238}U.

of the spin-flip resonance [219]. The reason, why the Skyrme QRPA does not give a better agreement with the experimental data on the spin-flip M1 mode, is probably connected with neglecting of the complex configurations (more-phonon configurations) in the QRPA method.

7.3.3 Approaches going beyond the Random-Phase Approximation

The RPA, discussed in the previous subsection 7.3.1, was based on the harmonic approximation when the even-even nucleus excitations states were approximated by one-, two-, or more- phonon states generated by the phonon creation operator Q_ν^+ (see (7.207)). The structure of the phonon creation operators Q_ν^+, that means amplitudes $X_{ij}^{(\nu)}$ and $Y_{ij}^{(\nu)}$ in (7.207), was obtained from the simple harmonic oscillator equations (see (7.276)). The RPA ground state energy E_{RPA} (energy of the RPA phonon vacuum) is always lower then the BCS (or HF) ground state energy (see (7.271)) but the particle-hole or many- quasiparticle correlations in the RPA ground state are taken into account only very roughly and partly. As a result the RPA can aspire for the description of the basic characters of the small- amplitude vibration motion of nuclei (like giant resonances). If we want to analyze anharmonic effects of the nuclear motion or large- amplitude motion we should go beyond the RPA. It should be mentioned that the RPA fails also in the critical situations when the HF or HFB (or BCS) total energy has only very shallow minimum (which occur in the cases where a HF or HFB mean field changes its symmetry, e.g. if it goes from spherical to deformed symmetry). In such cases the energy of the first solution of the RPA equation goes to zero or even is not real (see the discussion under the expr. (7.244) and [9] for details). In all these cases the methods going beyond the RPA should be applied.

Some of the approaches going beyond the RPA were already mentioned. Namely, the shell model (see the Section 4.2) and the inclusion of two- phonon components in the wave function (7.311) of the even-even nuclei. [36]

In this section the approaches going beyond the RPA are discussed in some details. As it was mentioned in the Chapter 1 this textbook concerns mainly middle-heavy and heavy nuclei. Therefore we will not speak about ab-initio approaches noticed in the beginning of the Chapter 4 which try to describe nuclear properties starting from the bare nucleon-nucleon interaction and which are, because of their complexity, suitable only for light nuclei ($Z < 20$). From the point of view of the heavier nuclei the most important microscopic approaches are Generator Coordinate Method (GCM) and Large-Scale-Shell Model (LSSM). Both these methods are discussed in this section.

[36] The RPA for odd-A and odd-odd nuclei discussed in the Subsection 7.3.1.2 goes also beyond the RPA

7.3.3.1 Time-depending Hartree-Fock approach

The time dependent Hartree-Fock (TDHF) belongs to the one of the most general method for the solving of the many-body fermionic system. It starts with the time-dependent variation equation

$$\frac{\delta \int_{t_1}^{t_2} dt \, \langle \Psi(t)| \, \hat{H} - i\hbar \frac{\partial}{\partial t} \, |\Psi(t)\rangle}{\delta \, \Psi} = 0 \tag{7.417}$$

restricting the variation to the set of HF or HFB states (we speak about the time-dependent Hartree-Fock (TDHF) or time-dependent Hartree-Fock-Bogoliubov (TDHFB) approaches). Generally we can connect the wave function $|\Psi(t)\rangle$ of the general nuclear state of even-even nucleus in the time t with the wave function $|\,0\rangle \equiv |\Psi(t=0)\rangle$ in the time $t=0$ by the Thouless theorem (see the Subsection B.5 - expr. (B.38) or (B.44))

$$|\Psi(t)\rangle \approx e^{\frac{1}{2}\sum_{ij} Z_{ij}(t)\, \alpha_i^+ \alpha_j^+} |\,0\rangle \tag{7.418}$$

where we suppose that $|0\rangle$ is the ground state given by the quasiparticle HFB vacuum and α_i^+ is the quasiparticle creation operator [37] .

If we substitute (7.418) into (7.417) and performing the variation in (7.417) with respect to $Z_{ij}(t)$ we obtain a complex integral-differential system of equations for amplitudes $Z_{ij}(t)$. Knowing the nuclear Hamiltonian $\hat{H}$ we can describe (using found amplitudes $Z_{ij}(t)$) any large amplitude motion of the system generated by the given Hamiltonian. However technical complexity is enormous (even with nowadays computational facilities). In the case when we want to analyze only a small amplitude motion it is sufficient to decompose (7.418) into the Taylor series in $Z_{ij}(t)$ and to substitute to (7.417) only terms up to the linear order in $Z_{ij}(t)$ (linear TDHFB). It can be shown (see e.g. [9]) that the linear TDHFB approximation is equivalent to the RPA approach discussed in the previous section 7.3.1. The technical complexity of the TDHFB approach causes that the most used beyond the RPA methods (for heavier nuclei) are numerically simpler Generator Coordinate Method (GCM) and Large-Scale-Shell Model (LSSM) discussed in the next subsections.

[37] The TDHF or TDHFB method provides an unified description of all types of collective motions in the nucleus, starting with the static solution for the ground state to large amplitude collective motion, such as fission, fusion, compound nucleus formation etc. Using (7.417), (7.418) the system (nucleus) determines self-consistently the path on the multidimensional energy surface (given by the amplitude $Z_{ij}(t)$), which includes all configurations representable by product stets $\Psi(t)\rangle$ and which determines the time evolution of the system from its ground state. In particular, we are not forced to choose a priory some collective coordinates (like in the GCM discussed in the next subsection), nor to force the system to a motion within some external fields (like in the case of the linear response approaches).

7.3.3.2 Generator coordinate method (Hill-Wheeler-Griffin theory)

The Generator Coordinate Method (GCM) is based on the assumption that particular collective motion of the nucleus, which we are interested in, is connected with a set of collective variables $\vec{q} \equiv (q_1, \cdots, q_n)$, so called generator coordinates, and the dependence on time of the nuclear wave function $|\Psi(t)\rangle$ can be written as the continuous decomposition into the basis of generating functions $|\Phi(\vec{q}\,)\rangle$ (see also (N.1), (N.3) in the Appendix N)

$$|\Psi(t)\rangle = \int d\vec{q}\, f(\vec{q}, t)\, |\Phi(\vec{q}\,)\rangle \tag{7.419}$$

The set of generation functions $|\Phi(\vec{q}\,)\rangle$ and generator coordinates $\vec{q}$, as well as the limits of the integration in the eq. (7.419) are chosen according to the actual physical problem. Usually the generating functions $|\Phi(\vec{q}\,)\rangle$ are wave functions of HF or HFB states for given type of the nucleus (e.g. for even-even nucleus) depending on deformation variables $\vec{q}$ (see e.g. [223] for the using of the GCM in the nuclear structure calculation or [224] and [225] for the using of the GCM in the fission theory). The weight function $f(\vec{q}, t)$ in (7.419) can be determined using the variational principle (7.417) applied on the wave function (7.419). Some recent applications of the GCM for the nuclear structure calculation is demonstrated in the Subsection 7.3.2.2.2. Since these results were obtained on the time-independent version of the GCM the basic ideas of the GCM, know as the Hill-Wheeler-Griffin (HWG) theory (see [226, 227]), are discussed in the Subsection 7.3.2.2.1 for the time-independent case.

7.3.3.2.1 Hill-Wheeler-Griffin theory (HWG theory) We search for the nucleus wave function $|\Psi\rangle$ (HWG wave function) in the form of the decomposition into a set of the generating functions $|\Phi(\vec{q}\,)\rangle$

$$|\Psi\rangle = \int d\vec{q}\, f(\vec{q}\,)\, |\Phi(\vec{q}\,)\rangle \tag{7.420}$$

The weight function $f(\vec{q})$ is assumed to be a well behaved function of variables $\vec{q}$ (for mathematical rigor see e.g. [228]) and it can be obtained from the variational principle:

$$\delta\, \frac{\langle\Psi|\, \hat{H}\, |\Psi\rangle}{\langle\Psi \mid \Psi\rangle} = 0$$

or

$$\delta \left\{ \langle\Psi|\, \hat{H}\, |\Psi\rangle - E\, \langle\Psi \mid \Psi\rangle \right\} = 0 \tag{7.421}$$

where the variation is performed according to $f(\vec{q}\,)$ and $f^*(\vec{q}\,)$ [38] . More specifically

$$\langle\Psi|\,\hat{H}\,|\Psi\rangle = \int d\vec{q}_1 \int d\vec{q}_2\, f^*(\vec{q}_1\,)\, f(\vec{q}_2\,)\,\langle\Phi(\vec{q}_1\,)|\,\hat{H}\mid\Phi(\vec{q}_2\,)\rangle$$

$$\frac{\delta}{\delta f^*(\vec{q}\,)}\Big\{\int d\vec{q}_1 \int d\vec{q}_2\, f^*(\vec{q}_1\,)\, f(\vec{q}_2\,)\,\langle\Phi(\vec{q}_1\,)|\,\hat{H}\mid\Phi(\vec{q}_2\,)\rangle$$

$$-E\int d\vec{q}_1 \int d\vec{q}_2\, f^*(\vec{q}_1\,)\, f(\vec{q}_2\,)\,\langle\Phi(\vec{q}_1\,)|\,\Phi(\vec{q}_2\,)\rangle\Big\} = 0$$

Hence we obtain equation for $f(\vec{q}\,)$:

$$\int d\vec{q}_2\, f(\vec{q}_2)\,\langle\Phi(\vec{q}\,)|\,\hat{H}\mid\Phi(\vec{q}_2\,)\rangle = E\int d\vec{q}_2\, f(\vec{q}_2)\,\langle\Phi(\vec{q}\,)|\,\Phi(\vec{q}_2\,)\rangle \qquad (7.422)$$

A similar equation can be obtained for $f^*(\vec{q}\,)$ if the variation of the functional (7.421) is done according to $f(\vec{q}\,)$. Further the following assignment is used

$$\begin{aligned}\mathscr{H}(\vec{q}_1,\vec{q}_2) &\equiv \langle\Phi(\vec{q}_1\,)|\,\hat{H}\mid\Phi(\vec{q}_2\,)\rangle\\ \mathscr{N}(\vec{q}_1,\vec{q}_2) &\equiv \langle\Phi(\vec{q}_1\,)|\,\Phi(\vec{q}_2\,)\rangle\end{aligned} \qquad (7.423)$$

Then the equation (7.422) can be rewritten in a matrix form

$$\mathscr{H}\,f = E\,\mathscr{N}\,f \quad\Leftrightarrow\quad (\mathscr{H} - E\,\mathscr{N})\,f = 0 \qquad (7.424)$$

where matrices $\mathscr{H}$, $\mathscr{N}$ and f are infinite (continuous) matrices constructed within the generator coordinates $\vec{q}_1$ and $\vec{q}_2$. In practice the variables $\vec{q}_1$, $\vec{q}_2$ are not continues but they are discretized and we work within the mesh of M vectors in the n- dimensional space: $\vec{q}_1, \cdots, \vec{q}_M$. Formally the equation (7.424) looks like the diagonalization of the Hamiltonian M- dimensional matrix with elements $\mathscr{H}_{ij} \equiv \langle\Phi(\vec{q}_i\,)|\,\hat{H}\,|\Phi(\vec{q}_j\,)\rangle$ in the nonorthogonal basis of generator states $|\Phi(\vec{q}_i\,)\rangle$ $(i = 1, \cdots, M)$.

The formal solution of the equation (7.424) is easy. If we can invert the overlap matrix $\mathscr{N}$ we can rewrite (7.424) as follows

$$\mathscr{N}^{-1}\,\mathscr{H}\,f = E\,f \qquad (7.425)$$

which means the diagonalization of generally non- Hermitian matrix $\mathscr{N}^{-1}\mathscr{H}$ because the set of $|\Phi(\vec{q}_i\,)\rangle$ is, in general, linearly dependent. The problem of the diagonalization of non- Hermitian matrices is usually solved by an orthogonalization of the set $|\Phi(\vec{q}_i\,)\rangle$. There are several methods for this

[38] Since the weight function $f(\vec{q}\,)$ is generally complex we should treat $f(\vec{q}\,)$ and $f^*(\vec{q}\,)$ as independent.

purpose. The most used is so called symmetric orthogonalization which is applicable also in the continuous non-discretized case. This approach starts with the diagonalization of the overlap matrix $\mathscr{N}$:

$$\int d\vec{q}_1 \, \mathscr{N}(\vec{q}, \vec{q}_1\,) \, u_k(\vec{q}_1\,) = n_k \, u_k(\vec{q}\,) \tag{7.426}$$

Further we assume that the spectrum n_k ($k = 1, 2, \cdots$) is discrete (the theory can be slightly modified if it is necessary to take into account also a continuous part of the spectrum of eigen- values n_k). Since the spectrum of functions $u_k(\vec{q})$ is a result of the diagonalization (7.426) the functions $u_k(\vec{q}\,)$ form a complete orthonormal set of functions in the space of weight functions $f(\vec{q}\,)$:

$$\sum_k u_k(\vec{q}\,) \, u_k^*(\vec{q}\,') = \delta(\vec{q} - \vec{q}\,') \,, \qquad \int d\vec{q} \;\, u_k^*(\vec{q}\,) \, u_k(\vec{q}\,) = \delta_{k\,k'} \tag{7.427}$$

Knowing all eigen-values n_k and eigen-vectors $u_k(\vec{q}\,)$ we can express the operator (or matrix) $\mathscr{N}$ in the following form [39]

$$\mathscr{N}(\vec{q}, \vec{q}\,') = \sum_k u_k(\vec{q}\,) \, n_k \, u_k^*(\vec{q}\,') \tag{7.428}$$

This overlap matrix can be also written as ($\mathscr{N} = \mathscr{N}^{1/2} \, \mathscr{N}^{1/2}$):

$$\mathscr{N}(\vec{q}_1, \vec{q}_2) = \int d\vec{q} \, \mathscr{N}^{1/2}(\vec{q}_1, \vec{q}\,) \, \mathscr{N}^{1/2}(\vec{q}, \vec{q}_2\,) \tag{7.429}$$

with

$$\mathscr{N}^{1/2}(\vec{q}, \vec{q}\,') = \sum_k u_k(\vec{q}\,) \, \sqrt{n_k} \;\, u_k(\vec{q}\,') \tag{7.430}$$

Then the equation (7.425) for the weight function $f(\vec{q}\,)$ reads

$$\begin{aligned} & \mathscr{N}^{-1/2} \, \mathscr{N}^{-1/2} \, \mathscr{H} \, \mathscr{N}^{-1/2} \, \mathscr{N}^{1/2} \, f = \mathscr{N}^{-1/2} \, E \, \mathscr{N}^{1/2} \, f \\ \Rightarrow \quad & \mathscr{N}^{-1/2} \, \mathscr{N}^{-1/2} \, \mathscr{H} \, \mathscr{N}^{-1/2} \, g = \mathscr{N}^{-1/2} \, E \, g \\ \Rightarrow \quad & \mathscr{N}^{-1/2} \, \mathscr{H} \, \mathscr{N}^{-1/2} \, g = E \, g \end{aligned} \tag{7.431}$$

[39] The expression (7.428) can be easily checked:

$$\int d\vec{q}\,' \, \mathscr{N}(\vec{q}, \vec{q}\,') \, u_k(\vec{q}\,') = \int d\vec{q}\,' \sum_{k'} u_{k'}(\vec{q}) n_{k'} \, u_{k'}^*(\vec{q}\,') \, u_k(\vec{q}\,') =$$

$$= \boxed{\begin{array}{c}\text{because see}\\ (7.427)\end{array}} = \sum_{k'} u_{k'}(\vec{q}\,) \, n_{k'} \, \delta_{k\,k'} = n_k \, u_k(\vec{q}\,)$$

and we can see that the expression (7.428) reproduces (7.426).

with

$$g = \mathscr{N}^{1/2}\, f \qquad \text{or} \qquad f = \mathscr{N}^{-1/2}\, g \tag{7.432}$$

From mathematics it is known that the matrix $\mathscr{N}^{1/2}$ (see (7.430)) cannot be inverted if the matrix $\mathscr{N}$ has zero eigen-values ($n_{k\in\{0\}} = 0$, where $\{0\}$ is the subspace of indexes k with the zero values of eigen-values, $n_k = 0$). The norm of all states $|\Psi_{k\in\{0\}}\rangle \approx f^{(k\in\{0\})}(\vec{q})\,|\Psi(\vec{q})\rangle$ (where index k corresponds to some zero value eigen-value $n_k = 0$ of the matrix $\mathscr{N}(\vec{q}_1, \vec{q}_2)$) is zero:

$$\begin{aligned}
&\langle \Psi_{k\in\{0\}}|\ \Psi_{k'\in\{0\}}\rangle \approx \\
&= \int d\vec{q}_1 \int d\vec{q}_2\ f^{(k\in\{0\})\,*}(\vec{q}_1)\ \ f^{(k'\in\{0\})}(\vec{q}_2)\ \ \langle\Phi(\vec{q}_1)|\Phi(\vec{q}_2)\rangle = \\
&= \boxed{\begin{array}{c}\text{see}\\ (7.423)\end{array}} = \\
&= \int d\vec{q}_1 \int d\vec{q}_2\ \ f^{(k\in\{0\})\,*}(\vec{q}_1)\ \ \mathscr{N}(\vec{q}_1, \vec{q}_2)\ \ f^{(k'\in\{0\})}(\vec{q}_2) = \\
&= \boxed{\begin{array}{c}\text{because}\\ \int d\vec{q}\,'\mathscr{N}(\vec{q}, \vec{q}\,')\ f^{(k'\in\{0\})}(\vec{q}\,') = 0 \text{ for } k' \in \{0\}\end{array}} = \\
&= 0
\end{aligned} \tag{7.433}$$

If there exists a zero eigen-values of the operator $\mathscr{N}$ ($n_k = 0$ for $k \in \{0\}$) then the weight function $f(\vec{q})$, corresponding to the HWG state $\Psi\rangle$, is not determined uniquely by the equation (7.431). We can always add a function $f^{(k\in\{0\})}$) to any solution g of (7.431) and we obtain the same solution (because $f = \mathscr{N}(g + f^{(k\in\{0\})}) = \mathscr{N} g$) and therefore the same $|\Psi\rangle$. To find a unique correspondence between $|\Psi\rangle$ and the weight function $f(\vec{q})$ we should restrict $f(\vec{q})$ to weight functions that are linear combinations of functions $u_k(\vec{q})$ with k corresponding to non-zero $n_k \neq 0$. For each of these functions $u_k(\vec{q})$ ($k \neq 0$) there exists a normalized vector in the Hilbert space of the many-body wave function $|\Psi\rangle$:

$$|k\rangle = \frac{1}{\sqrt{n_k}} \int d\vec{q}\ u_k(\vec{q}\,)\,|\,\Phi(\vec{q})\rangle \quad , \qquad n_k \neq 0 \tag{7.434}$$

These vectors are called natural states and they form orthonormal basis

$$\langle k|k^{'}\rangle = \frac{1}{\sqrt{n_k n_{k^{'}}}} \int d\vec{q}_1 \int d\vec{q}_2 \; u_k^*(\vec{q}_1) \; u_{k^{'}}(\vec{q}_2) \; \langle \Phi(\vec{q}_1)| \, \Phi(\vec{q}_2)\rangle =$$

$$= \frac{1}{\sqrt{n_k n_{k'}}} \int d\vec{q}_1 \int d\vec{q}_2 \; u_k^*(\vec{q}_1) \, \mathscr{N}(\vec{q}_1, \vec{q}_2) \, u_{k^{'}}(\vec{q}_2) =$$

$$= \boxed{\begin{array}{c}\text{see}\\(7.426)\end{array}} = \frac{1}{\sqrt{n_k n_{k^{'}}}} \int d\vec{q}_1 \int d\vec{q}_2 \; u_k^*(\vec{q}_1) \, n_{k^{'}} \, u_k(\vec{q}_2) =$$

$$= \boxed{\begin{array}{c}\text{see}\\(7.427)\end{array}} = \frac{n_{k'}}{\sqrt{n_k n_{k^{'}}}} \, \delta_{kk^{'}} = \delta_{kk^{'}} \tag{7.435}$$

Vectors (7.344) span a sub-Hilbert space, so called "collective" subspace. It is the smallest Hilbert space which contains all generating states $|\Phi(\vec{q})\rangle$.

From (7.426) and (7.427) we know that the eigen-functions $u_k(\vec{q}\,)$ of the overlap matrix $\mathscr{N}(\vec{q}, \vec{q}^{\,'})$ form the complete set of functions in the space of possible weight functions $f(\vec{q}\,)$ (or functions $g(\vec{q}\,)$) - see (7.432). From discussions above it is also known that in order to have a unique correspondence between the many-body wave function $|\Psi\rangle$ and $f(\vec{q}\,)$ it is necessary to work only within the subspace of the eigen-vectors $u_k(\vec{q}\,)$ with k corresponding to $n_k \neq 0$. Therefor the weight functions $f(\vec{q}\,)$ or $g(\vec{q}\,)$ can be searched for in the following form

$$f^{(\nu)}(\vec{q}\,) = \sum_{k \; (n_k \neq 0)} \tilde{f}_k^{(\nu)} \, u_k(\vec{q}\,) \, , \quad g^{(\nu)}(\vec{q}\,) = \sum_{k \; (n_k \neq 0)} \tilde{g}_k^{(\nu)} \, u_k(\vec{q}\,) \, , \quad \tilde{f}_k^{(\nu)} = \frac{\tilde{g}_k^{(\nu)}}{\sqrt{n_k}}$$

$$\Rightarrow \qquad \tilde{g}_k^{(\nu)} = \int d\vec{q} \; u_k^*(\vec{q}\,) \, g^{\nu)}(\vec{q}\,) \tag{7.436}$$

where we introduced the index ν which enumerates the solutions of the equation (7.431). The equation (7.431) can be rewritten in more details as

$$\int d\vec{q}_1 d\vec{q}_2 d\vec{q}_3 \mathscr{N}^{-1/2}(\vec{q}, \vec{q}_1) \mathscr{H}(\vec{q}_1, \vec{q}_2) \mathscr{N}^{-1/2}(\vec{q}_2, \vec{q}_3) g^{(\nu)}(\vec{q}_3) = E_\nu g^{(\nu)}(\vec{q}) \tag{7.437}$$

Multiplying this equation by $u_k^*(\vec{q})$, then integrating over $\vec{q}$, and finally using the orthogonality (7.427) of the eigen-functions $u_k(\vec{q}\,)$ and applying (7.428) we obtain (k corresponds to $n_k \neq 0$)

$$\sum_{k^{'}(n_{k^{'}} \neq 0)} \int d\vec{q}_1 d\vec{q}_2 \; u_k^*(\vec{q}_1) \frac{1}{\sqrt{n_k}} \, \mathscr{H}(\vec{q}_1, \vec{q}_2) \, \frac{1}{\sqrt{n_{k^{'}}}} u_{k^{'}}(\vec{q}_2) \, \tilde{g}_{k^{'}}^{(\nu)} = E_\nu \, \tilde{g}_k^{(\nu)} \tag{7.438}$$

or

$$\sum_{k^{'}(n_{k^{'}}\neq 0)} \langle k|\ \hat{H}\ |k^{'}\rangle\ \tilde{g}^{(\nu)}_{k^{'}} = E_{\nu}\ \tilde{g}^{(\nu)}_{k} \tag{7.439}$$

with ($n_k \neq 0$, $n_{k^{'}} \neq 0$)

$$\langle k|\ \hat{H}\ |k^{'}\rangle \equiv \int d\vec{q}_1 d\vec{q}_2\ \frac{u^{*}_{k}(\vec{q}_1)}{\sqrt{n_k}}\ \mathscr{H}(\vec{q}_1,\vec{q}_2)\ \frac{u_{k^{'}}(\vec{q}_2)}{\sqrt{n_{k^{'}}}} \tag{7.440}$$

The index ν in (7.437)-(7.439) enumerates all solutions of the equation system (7.437) or (7.438) or (7.439).

The elements $\langle k|\ \hat{H}\ |k^{'}\rangle$, with $n_k \neq 0$, $n_{k^{'}} \neq 0$, can be understood as the matrix elements of the Hamiltonian $\hat{H}$ projected to the "collective" subspace spanned by the set of the vectors $|k\rangle$ (see (7.434)) corresponding to $n_k \neq 0$, that means

$$\langle k|\ \hat{H}\ |k^{'}\rangle = \left(\hat{P}_c \hat{H} \hat{P}_c\right)_{kk^{'}} \tag{7.441}$$

with the projection operator

$$\hat{P}_c = \sum_{k\ (n_k\neq 0)} |k\rangle\langle k| \tag{7.442}$$

The diagonalization (7.439) provides all unknown coefficients $\tilde{g}^{(\nu)}_{k}$ and in such a way weight funcions $f^{(\nu)}(\vec{q})$ or $f^{(\nu)}(\vec{q})$ (see (7.436)) are determined together with the corresponding many-body HWG wave functions $|\Psi_\nu\rangle$:

$$\begin{aligned} |\Psi_\nu\rangle &= \sum_{k(n_k\neq 0)} \tilde{g}^{(\nu)}_{k}\ |k\rangle = \sum_{k(n_k\neq 0)} \frac{\tilde{g}^{(\nu)}_{k}}{\sqrt{n_k}} \int d\vec{q}\, u_k(\vec{q})\ |\Phi(\vec{q})\rangle = \\ &= \sum_{k(n_k\neq 0)} f^{(\nu)}(\vec{q})\ |\Phi(\vec{q})\rangle \end{aligned} \tag{7.443}$$

From (7.443) we see that $|f^{(\nu)}(\vec{q})|^2$ represents the probability of the finding of the state $|\Psi_\nu\rangle$ with the given value of the collective coordinate (defomation) $\vec{q}$.

Based on the scheme described above we can roughly say that GCM ansatz (7.420) (or more precisely (7.443)) represents an expansion of the many-body wave function $|\Psi_\nu\rangle$ in terms of the nonorthogonal generating functions $|\Phi(\vec{q})\rangle$ with the weight functions $f^{(\nu)}(\vec{q}\,)$. However, one should have in mind that the exact wave function of the system (nucleus) can be approximated by (7.443) only in the case when the system Hamiltonian $\hat{H}$ commutes with the projection operator $\hat{P}_c$ (see (7.442))

$$\left[\hat{H},\ \hat{P}_c\right] = 0 \tag{7.444}$$

with a good approximation. If there is only a finite number of eigen-values $n_k \neq 0$ of the overlap matrix $\mathcal{N}(\vec{q}_1, \vec{q}_2)$ then the weight functions $f^{(\nu)}(\vec{q})$ are always well defined by (7.436). In the continuous case, however, there are usually several values $n_k = 0$ in the limiting case on the border of the region of the integration over collective coordinates $\vec{q}$ and the functions $f^{(\nu)}(\vec{q})$ diverge there. Then we should modify the theory a little bit (see [9]).

One should also realize that obtained many-body wave functions $|\Psi^{(\nu)}\rangle$ describe the nucleus states only in the case when these states are connected with the collective coordinates $\vec{q}$ relevant to the nucleus degrees of freedom which are investigated. The good description is dependent on the proper choice of coordinates $\vec{q}$.

Above discussed GCM scheme seems to be relatively easy. However, the practical realization of it for the realistic nuclei represents a complex problem as it is demonstrated in the next subsection.

7.3.3.2.2 Application of the GCM for nuclear structure General scheme of the GCM, based on the HWG theory and discussed in the previous subsection, is demonstrated on the example of the calculation of the energy spectrum of the lowest positive parity states in the light deformed nucleus ^{24}Mg [223]. It was several times pointed out that in the case of deformed nucleus the HF and HFB mean field is deformed and violates the rotational symmetry of the total Hamiltonian in the laboratory frame. Moreover, the HFB or BCS mean field violates the number of particle (neutron and proton) conservation which is connected with the breaking the total Hamiltonian symmetry with respect to rotation in the gauge space (generated by the angle φ_g - see the part N.2 in the Appendix N). As it was mentioned in the text above the expression (7.419) the generating functions $|\Phi(\vec{q})\rangle$ in the HWB theory (see (7.420)) are supposed to be the HF Slater determinants or HFB (BCS) quasiparticle vacuum for different sets of deformation parameters $\vec{q}$. That means the generating functions $|\Phi(\vec{q})\rangle$ violates the rotational symmetry and, in the HFB or BCS case, also the number of particle conservation is generally broken. On the other hand side, the searched for many-body functions $|\Psi^{(\nu)}\rangle$ (see (7.420), (7.443)) are the wave functions of the nucleus in the laboratory frame (eigen-functions of the total Hamiltonian in the laboratory system) and therefore these functions $|\Psi^{(\nu)}\rangle$ should be rotationally invariant and with the good (sharp) number of nucleons. By other words, the GCM approach (HWG theory) should restore the rotational and particle-number symmetry of the many body wave functions $|\Psi^{(\nu)}\rangle$ violated by the generat-

ing HFB (BCS) functions $|\phi(\vec{q}\,)\rangle$ (here the set of deformation parameters is denoted by one symbol $\vec{q}\,$).

The restoration of the symmetry of the nucleus wave function in the lab. system violated by the intrinsic deformed functions $|\phi(\vec{q})\rangle$ is usually done by the projection method described in the Appendix N (for particle number projection - see the Subsection N.2, for angular momentum projection - see the Subsection N.3). This projection can be performed before or after the variation (7.421). Both these possibilities (variation before projection (VBP) and variation after projection (VAP)) are described in the Subsection N.4 of the Appendix N). Since the VAP approach uses the projected (to good number N and Z of particles and sharp value I of the angular momentum) wave functions in the each iteration step during the solving of the variation equation the VAP approach is considered to be more precise than the VBP approach where the projection is performed only once, after the minimum of the energy functional was found (see e.g. [111, 9]). In such a way the VAP approach takes into account the dynamical changing of the deformation in the calculation of the excited states of the nucleus. Recent papers based on the GCM use always the VAP method (see e.g. [229, 230, 231, 232, 238, 234, 235, 236, 237, 233] for axially symmetric mean fields and [239] for the triaxial case (but without a particle projection).

The application of the GCM for the description of the structure of low-lying states of deformed nuclei is further demonstrated for ^{24}Mg (see [223]). In [223] the triaxial version of the GCM with the particle number and angular momentum projection (GCM-PNAMP approach) was introduced where the generating coordinates were quadrupole $\beta-$ and $\gamma-$ deformations, $\vec{q} \equiv (\beta, \gamma)$. The starting step is the finding of the set of the HFB functions $|\phi(\beta, \gamma)\rangle$ (quasiparticle vacuum for given (β, γ)) by the minimizing the particle number projected energy functional $E^{N,\,Z}[\phi(\beta, \gamma)]$

$$\delta E^{N,\,Z}[\phi(\beta, \gamma)] = 0 \tag{7.445}$$

The variation is performed with respect to the trial functions $\phi(\beta, \gamma)$ for given β, γ. The functional $E^{N,\,Z}[\beta, \gamma]$ is determined with the Gogny effective interaction (3.147) using the HFB method (see the Subsection 6.2.3) with the

deformation constrant of given values of (β, γ) [240]

$$E^{N,Z}[\phi] = \frac{\langle\phi|\ \hat{H}_{Gogny}\hat{P}^{(N)}\hat{P}^{(Z)}\ |\ \phi\rangle}{\langle\phi|\ \hat{P}^{(N)}\hat{P}^{(Z)}\ |\ \phi\rangle} - \lambda_{q_{20}}\ \big(\ \langle\phi\ \hat{Q}_{20}^{(mass)}\ |\phi\rangle - q_{20}(\beta,\gamma)\big) - \lambda_{q_{22}}\ \big(\ \langle\phi\ \hat{Q}_{22}^{(mass)}\ |\phi\rangle - q_{22}(\beta,\gamma)\big) \tag{7.446}$$

where $\hat{P}^{(N)}$ and $\hat{P}^{(Z)}$ are neutron and proton number projection operators (see (N.19))

$$\hat{P}^{(N_\tau)} = \frac{1}{2\pi}\int_0^{2\pi} d\varphi_g\ \ e^{i\,\varphi_g\,(\hat{N}_\tau - N_\tau)} \tag{7.447}$$

with $N_\tau = N$ or $N_\tau = Z$ for neutrons and protons. In (7.446) $\hat{H}_{Gogny}$ is the nucleus Hamiltonian with the Gogny effective interaction (3.147). The last two terms in (7.446), with corresponding Lagrange multipliers $\lambda_{q_{20}}$ and $\lambda_{q_{22}}$, ensure that the expectation values of the mass quadrupole momentum operators $\hat{Q}_{20}^{(mass)}$ and $\hat{Q}_{22}^{(mass)}$, defined as (see(2.201) for $\lambda\mu = 20$ with $e_i = 1$)

$$\hat{Q}_{20}^{(mass)} = \sqrt{\frac{16\pi}{5}}\sum_{i=1}^{A} r_i^2\ Y_{20}(\hat{r}_i) \quad , \quad \hat{Q}_{22}^{(mass)} = \sqrt{\frac{32\pi}{15}}\sum_{i=1}^{A} r_i^2\ Y_{22}(\hat{r}_i), \tag{7.448}$$

are equal to the values q_{20} and q_{22}, respectively, which are determined by the deformation parameter β and γ by (see [9] and also (1.10) with $Z = A$ and $e = 1$ for $\gamma = 0$)

$$q_{20} = \frac{1}{\sqrt{5\pi}}\ 3\,r_0^2\ A^{5/3}\ \beta\ \cos\gamma \qquad (\text{in } fm^2)$$
$$q_{22} = \frac{1}{\sqrt{10\pi}}\ 3\,r_0^2\ A^{5/3}\ \beta\ \sin\gamma \qquad (\text{in } fm^2) \tag{7.449}$$

After the variation procedure (7.445) we have HFB functions $|\phi(\beta,\gamma)\rangle$ which minimize functionals $E^N[\phi(\beta,\gamma)]$ and $E^Z[\phi(\beta,\gamma)]$ for all values of β and γ [40]. In order to determine the GCM generating functions $|\Phi(\vec{q}\,)\rangle$ (see (7.419)) the obtained HFB functions $|\phi(\beta,\gamma)\rangle$ are projected for good sharp value of the total angular momentum I, its projection M onto the laboratory z- axis, its projection K onto the 3-d intrinsic axis, the sharp value of the number N of neutrons and the number Z of protons (see (N.19), (N.28))

$$|IMK;\ NZ;\ \beta\gamma\rangle = \frac{2I+1}{8\pi^2}\int d\Omega\ D^I_{MK}(\Omega)\ \hat{R}(\Omega)\ \hat{P}^{(N)}\ \hat{P}^{(Z)}\ |\phi(\beta,\gamma)\rangle \tag{7.450}$$

[40] In the papers [241, 242] the extension of the triaxial GCM-PNAMP approach with the Gogny effective interaction was introduced where besides the deformation constraints also the cranking constraint to the sharp value of the angular momentum is made. Then the variation (7.445) is performed with the energy

Then these functions fulfill

$$\begin{aligned}
\hat{N}\,|IMK;\ NZ;\ \beta\gamma\rangle &= N\,|IMK;\ NZ;\ \beta\gamma\rangle \\
\hat{Z}\,|IMK;\ NZ;\ \beta\gamma\rangle &= Z\,|IMK;\ NZ;\ \beta\gamma\rangle \\
\hat{I}^2\,|IMK;\ NZ;\ \beta\gamma\rangle &= I(I+1)\,|IMK;\ NZ;\ \beta\gamma\rangle \\
\hat{I}_z\,|IMK;\ NZ;\ \beta\gamma\rangle &= M\,|IMK;\ NZ;\ \beta\gamma\rangle \\
\hat{I}_3\,|IMK;\ NZ;\ \beta\gamma\rangle &= K\,|IMK;\ NZ;\ \beta\gamma\rangle
\end{aligned} \tag{7.451}$$

and they represent GCM generating functions (realization of functions $|\Phi(\vec{q})\rangle$ in the Subsection 7.3.2.2.1). Then the general GCM many-body wave functions (see (7.420)) reads

$$|IM;\ NZ;\ \nu\rangle = \sum_{K\beta\gamma} f^{I;\,NZ;\,\nu}_{K\beta\gamma}\,|IMK;\ NZ;\ \beta\gamma\rangle \tag{7.452}$$

It should be pointed out that the generating functions $|IMK;\ NZ;\ \beta\gamma\rangle$ are not mutually orthogonal (similarly as functions $|\Phi(\vec{q})\rangle$ in the previous subsection). The deformations β and γ in (7.452) are supposed to be discretized and therefore in the expr (7.452) the sum over β and γ is present instead of the integration. The final spectrum (energies $E^{I;\,NZ;\,\nu}$) together with the corresponding GCM many-body wave functions (7.452) (given by the weight functions $f^{I;\,NZ;\,\nu}_{K\beta\gamma}$) are then obtained by the minimizing of the total energy with respect to the trial weight functions $f^{I;\,NZ;\,\nu}_{K\beta\gamma}$ (see (7.422), (7.423), (7.424))

$$\sum_{K'\beta'\gamma'} \Big(\mathscr{H}^{I;\,NZ}_{K\beta\gamma\ K'\beta'\gamma'} - E^{I;\,NZ;\,\nu}\,\mathscr{N}^{I;\,NZ}_{K\beta\gamma\ K'\beta'\gamma'} \Big)\, f^{I;\,NZ;\,\nu}_{K'\beta'\gamma'} = 0 \tag{7.453}$$

where index ν labels individual solutions of the equations and (analogy with (7.423))

$$\begin{aligned}
\mathscr{N}^{I;\,NZ}_{K\beta\gamma\ K'\beta'\gamma'} &= \langle IMK:\ NZ;\ \beta\gamma\,|\,IMK';\ NZ;\ \beta'\gamma'\rangle \\
\mathscr{H}^{I;\,NZ}_{K\beta\gamma\ K'\beta'\gamma'} &= \langle IMK:\ NZ;\ \beta\gamma|\,\hat{H}_{Gogny}\,|IMK';\ NZ;\ \beta'\gamma'\rangle
\end{aligned} \tag{7.454}$$

---

functional

$$\begin{aligned}
E^{N,Z}[\phi] = \frac{\langle\phi|\,\hat{H}_{Gogny}\hat{P}^{(N)}\hat{P}^{(Z)}\,|\,\phi\rangle}{\langle\phi|\,\hat{P}^{(N)}\hat{P}^{(Z)}\,|\,\phi\rangle} \\
-\lambda_{q_{20}}\left(\,\langle\phi|\,\hat{Q}_{20}\,|\phi\rangle - q_{20}(\beta,\gamma)\right) \\
-\lambda_{q_{22}}\left(\,\langle\phi|\ \hat{Q}_{22}\,|\phi\rangle - q_{22}(\beta,\gamma)\right) \\
-\omega_{rot}\left(\langle\phi|\,\hat{I}_x\,|\phi\rangle - \sqrt{I(I+1)}\right)
\end{aligned}$$

where $\omega_{rot} = \hbar\,\langle\phi|\,\hat{I}_1\,|\phi\rangle/\mathscr{F}_1$ is the rotational angular frequency of the cranking rotation round the intrinsic first axis. The cranking models of rotations are discussed in the Chapter 8.

Since the basis of states $|IMK;\ NZ;\ \beta\gamma\rangle$ are not orthogonal the orthonormalization procedure described in the previous subsection is used (see (7.434)-(7.440)). At first, the orthonormal set of eigen-functions of the overlap matrix $\mathcal{N}^{I;\,NZ}_{K\beta\gamma\ K'\beta'\gamma'}$ is found (analogy with $u_k(\vec{q})$ - see (7.426))

$$\sum_{K'\beta'\gamma'} \mathcal{N}^{I;\,NZ}_{K\beta\gamma\ K'\beta'\gamma'}\ u^{I;\,NZ}_{K'\beta'\gamma';\ k} = n^{I;\,NZ}_k\ u^{I;\,NZ}_{K\beta\gamma;\ k} \tag{7.455}$$

where index k enumerates the eigen-states of the overlap matrix. Using the overlap matrix eigen-functions $u^{I;\,NZ}_{K\beta\gamma;\ k}$ the mutually orthonormal vectors of so called natural basis (see (7.434)) are constructed [41]

$$|k^{IM;\,NZ}\rangle \equiv \sum_{K\beta\gamma} \frac{u^{I;\,NZ}_{K\beta\gamma;\ k}}{\sqrt{n^{I;\,NZ}_k}}\,|IMK;\ NZ;\ \beta\gamma\rangle \tag{7.456}$$

Then, using this natural basis vectors, the HWG equation system (7.453) for unknown weight functions $f^{I;\,NZ;\,\nu}_{K\beta\gamma}$ (functions of β and γ) can be rewritten as the equation system for unknown amplitudes $\tilde{g}^{I;\,NZ;\,\nu}_k$ (see (7.439))

$$\sum_{k'}\langle k^{I;\,NZ;\,\nu}|\ \hat{H}\ |\ k'^{\,I;\,NZ;\,\nu}\rangle\ \tilde{g}^{I;\,NZ;\,\nu}_{k'} = E^{I;\,NZ;\,\nu}\ \tilde{g}^{I;\,NZ;\,\nu}_k \tag{7.457}$$

which determine the weight function $f^{I;\,NZ;\,\nu}_{K\beta\gamma}$ (see (7.436))

$$f^{I;\,NZ;\,\nu}_{K\beta\gamma} = \sum_k \frac{1}{\sqrt{n^{I;\,NZ}_k}}\ \tilde{g}^{I;\,NZ;\,\nu}_k\ u^{I;\,NZ}_{K\beta\gamma;\,k} = \equiv \sum_k \tilde{f}^{I;\,NZ;\,\nu}_k\ u^{I;\,NZ}_{K\beta\gamma;\,k} \tag{7.458}$$

Knowing the weight functions $f^{I;\,NZ;\,\nu}_{K\beta\gamma}$ for all solutions ν the many-body wave functions $|IM;\ NZ;\ \nu\rangle$ (see (7.452)) are determined for given angular momentum I, given number N of neutrons, and given number Z of protons:

$$|IM;\ NZ;\ \nu\rangle = \sum_{K\beta\gamma}\sum_k \frac{1}{\sqrt{n^{I;\,NZ}_k}}\ \tilde{g}^{I;\,NZ;\,\nu}_k\ u^{I;\,NZ}_{K\beta\gamma;\,k}\,|IMK;\ NZ;\ \beta\gamma\rangle =$$

$$= \boxed{\begin{array}{c}\text{see}\\(7.456)\end{array}} = \sum_k \tilde{g}^{I;\,NZ;\,\nu}_k\ \ |\ k^{IM;NZ}\rangle \tag{7.459}$$

[41] In the natural basis only components k participate for which $n^{I;\,NZ}_k/n^{I;\,NZ}_{nmax} > \xi$, where ξ is the fixed small number. This cutoff ensures the linear independency of the natural basis.

with corresponding final energies $E^{I;\,NZ;\,\nu}$ ($\tilde{g}_k^{I;\,NZ;\,\nu}$ for all k and $E^{I;\,NZ;\,\nu}$ are solutions of (7.457), and the index ν enumerates all solutions of (7.457)).

It is necessary to realize that the many-body wave functions $|IM;\,NZ;\,\nu\rangle$ (see (7.459)) do not correspond to the sharp value of deformations β and γ. Each function $|IM;\,NZ;\,\nu\rangle$ represents the mixture of components with different (β,γ). Therefore, in [223] so called collective wave functions $F^{I;\,NZ;\,\nu}(\beta,\gamma)$, normalized by $\int (F^{I;\,NZ;\,\nu}(\beta,\gamma))^*\, F^{I;\,NZ;\,\nu}(\beta,\gamma))\, d\beta\, d\gamma = 1$, are introduced:

$$F^{I;\,NZ;\,\nu}(\beta,\gamma) \approx \sum_{kK} \tilde{g}_k^{I;\,NZ;\,\nu}\; u_{K\beta\gamma;\,k}^{I;\,NZ} \equiv \sum_K F_K^{I;\,NZ;\,\nu}(\beta,\gamma) \qquad (7.460)$$

Then $|F^{I;\,NZ;\,\nu}(\beta,\gamma)|^2$ means the probability density of finding the state $|IM;\;NZ;\;\nu\rangle$ with the given deformation (β,γ) and $|F_K^{I;\,NZ;\,\nu}(\beta,\gamma)|^2$ is the probability of finding the state $|IM;\,NZ;\,\nu\rangle$ with the given deformation (β,γ) and with the given projection K of the angular momentum onto the 3-d intrinsic axis. The average deformation $(\bar{\beta}^{I\nu},\bar{\gamma}^{I\nu})$ corresponding to the given excitation with the wave function $|IM;\,NZ;\,\nu\rangle$ is $\bar{\beta}^{I\nu} = \sum_{\beta,\gamma} \beta |F^{I;NZ;\nu}(\beta,\gamma)|^2$ and $\bar{\gamma}^{I\nu} = \sum_{\beta,\gamma} \beta\, |F^{I;NZ;\nu}(\beta,\gamma)|^2$.

The procedure described above is repeated for all angular momenta I and as a result for given nucleus (given N and Z) we obtain the whole spectrum of levels $E^{I;\,NZ;\,\nu}$ with corresponding eigen-states $|IM;\;NZ;\;\nu\rangle$. Then the reduced matrix elements of any transitional operator (e.g. electromagnetic $\mathscr{M}_{\lambda\mu}^{(X)}$ - see (2.145) for $X = mag$, or (2.130) for $X = el$) can be determined:

$$\begin{aligned}
&\langle I_1;\; NZ;\; \nu_1 || \,\hat{\mathscr{M}}_\lambda^{(X)} \,||\, I_2;\; NZ;\; \nu_2\rangle = \\
&= \sum_{kk'} \sum_{\substack{K\beta\gamma \\ K'\beta'\gamma'}} \tilde{g}^{I;\,NZ;\,\nu_1\,*} \frac{u_{K\beta\gamma;\,k}^{I_1;\,NZ;\,\nu_1\,*}}{\sqrt{n_k^{I_1;\,NZ}}} \\
&\qquad \cdot \langle I_1 K;\; NZ;\; \beta\gamma || \,\hat{\mathscr{M}}_\lambda^{(X)} \,||\, I_2 K';\; NZ;\; \beta'\gamma' \rangle \\
&\qquad\qquad \cdot \frac{u_{K'\beta'\gamma';\,k'}^{I_2;\,NZ;\,\nu_2}}{\sqrt{n_{k'}^{I_2;\,NZ}}}\; \tilde{g}_{k'}^{I_2;\,NZ;\,\nu_2}
\end{aligned} \qquad (7.461)$$

where the explicit expressions for reduced matrix elements $\langle I_1 K;\; NZ;\; \beta\gamma || \,\hat{\mathscr{M}}_\lambda^{(X)} \,||\, I_2 K';\; NZ;\; \beta'\gamma' \rangle$ within the states (7.450) is straightforward (see e.g. [9, 239, 223]).

In the paper [223] the triaxial (β,γ) GCM-PNAMP approach discussed above was used for the analysis of the lowest level spectrum of the positive

parity states in ^{24}Mg. The parametrization (β, γ) for the quadrupole deformation (see (1.5)) gives a triple degeneracy in the range $0 \leq \gamma \leq 360^\circ$ if we consider time-reversal conserving wave functions $|\phi(\beta, \gamma)\rangle$. This degeneracy corresponds to the three possible orientations of the principal quadrupole moment axes with respect to the intrinsic 3-d axis (see the Fig.1.1) (e.g. that means $\gamma = 0^\circ$, 120°, 240° give the same prolate shape of the nucleus). In such a way the interval $0^\circ \leq \gamma \leq 60^\circ$ covers all possible quadrupole deformations. This enables to reduce intervals of the integration over Euler angles (a, b, c) to $0 \leq a \leq \pi/2$, $0 \leq b \leq \pi/2$, $0 \leq c \leq \pi$. Authors of [223] used the mesh of 18 points for the integration over a, 16 points for the integration over b and 16 points for the integration over c. For the integration over deformation (β, γ) 90 points triangular mesh with the $0 \leq \beta \leq 1.6$ and $0^\circ \leq \gamma \leq 60^\circ$ was used, and 9 points were used for the integration over gauge angle φ_g. The convergence of results for these number of points for integrations was checked in [223]. The variation equation (7.446) was solved using the Gogny effective interaction (3.146) with the D1S parametrization (see [243]) with the monopole pairing and proton Coulomb interaction.

Authors of [223] made two calculations for ^{24}Mg. The first one concerned the axially symmetric case when the GCM equations discussed above were solved with the fixed $\gamma = 0$. That means in (7.453), (7.455), (7.456), (7.459), (7.461) there is no summation over γ and only the sum over β (or integration over β) remained. In the axially symmetric case the resultant wave functions (7.459) are linear combinations of the functions $|IMK;\ NZ;\ \beta\rangle$ (no dependence on γ)

$$|IMK;\ NZ;\ \nu\rangle = \sum_{K\beta} \sum_{k} \frac{1}{\sqrt{n_k^{I;NZ}}}\, u_{K\beta;\,k}^{I;\,NZ}\, |IMK;\ NZ;\ \beta\rangle \qquad (7.462)$$

and the collective wave functions $F^{I;\,NZ}(\beta)$ or $F_K^{I;\,NZ}(\beta)$ (see (7.460) do not depend on γ now. In the upper panel of the Fig.7.57 the potential energy surface are shown as a function of the deformation β for $I = 0, 2, 4, 6, 8$. They were obtained for each value of the angular momentum $I = 0$, 2, 4, 6, 8 as the energies $E_{PNAMP}^{I;\,NZ;\,\sigma=1,2}(\beta)$ of the lowest solutions, $\sigma = 1, 2$, of so called PNAMP equations for the functions $|IM;\ NZ;\ \beta;\ \sigma\rangle_{PNAMP}$:

$$|IM;\ NZ;\ \beta;\ \sigma\rangle_{PNAMP} = \sum_{K} h_K^{I;\,NZ;\,\sigma}(\beta)\, |IMK;\ NZ,\ \beta\rangle \qquad (7.463)$$

with amplitudes $h_K^{I;\,NZ;\,\sigma}(\beta)$ determined from a simplified (PNAMP) version

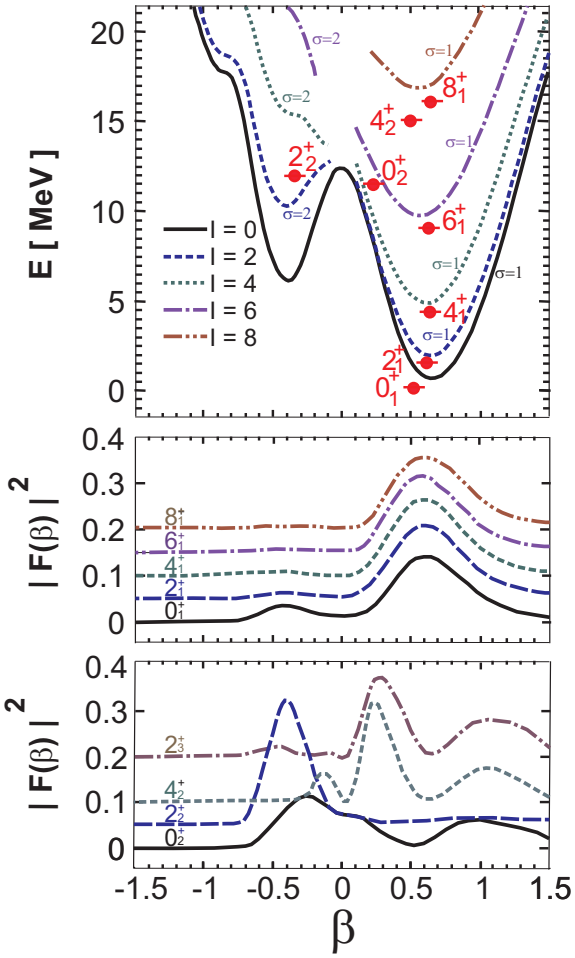


Figure 7.57: The upper panel show potential energy surfaces $E^{I;\,NZ;\,\sigma=1,2}_{PNAMP}(\beta)$ (see (7.463) for particle number and angular momentum projection (PNAMP) for different values of the ang. momentum I (^{24}Mg). The bullets corresponds to the excitation full GCM energies $E^{I;\,NZ;\,\nu}$ (see the eqs. (7.457)) with their positions at the equilibrium deformations $\bar{\beta}^{I\nu} = \sum_\beta \beta\, |F^{I;\,NZ;\,\nu}(\beta)|^2$. The energy is normalized to the full GCM ground state (0^+_1). The central panel demonstrates collective wave functions $|F^{I;\,NZ;\,\nu=1}(\beta)|^2$ for the first $\nu = 1$ full GCM levels. The values of the ordinate axis are displayed by 0.05 with increasing angular momentum. The bottom panel shows the same as the central panel but for $\nu = 2$ full GCM levels and 2^+_3 state (taken from [223]).

of the full HWG equations (see (7.454) for fixed γ)

$$\sum_{K'} \left(\mathscr{H}^{I;\,NZ}_{K\beta\,K'\beta} - E^{I;\,NZ;\,\sigma}_{PNAMP}(\beta)\, \mathscr{N}^{I;\,NZ}_{K\beta\,K'\beta} \right) h^{I;\,NZ;\,\sigma}_{K'}(\beta) = 0 \qquad (7.464)$$

The index σ enumerates the solutions of (7.464) [42]. The bullets in the upper panel of the Fig.7.57 correspond to the excitation energies $E^{I;\,NZ;\,\nu}$ ($\nu = 1, 2$)

[42]PNAMP version of the GCM equations (7.464) differs from the full GCM equations (7.453) by the fact that in the full GCM equation (7.453) the mixing of different deformation configurations are taken into account by the summation over deformations, while in the PNAMP version of the GCM equations (7.464) the summation over deformations is missing. The PNAMP GCM equations (7.464) were part of so called

(see (7.457) of the full GCM states $|IM;\, NZ;\, \nu\rangle$ (see (7.459) with their positions at $\bar{\beta}^{I,\nu} \equiv \sum_\beta \beta |F^{I;\,NZ;\,\nu}(\beta)|^2$. The energy is normalized to the full GCM ground state energy $E^{I=0;\,NZ;\,\nu=1}$. Differences between the minima of the potential energy surfaces $E^{I;\,NZ;\,\sigma}_{PNAMP}(\beta_0)$ and the full GCM energies $E^{I;\,NZ;\,\nu=\sigma}$ (bullets) demonstrate difference between simplified PNAMP (VAMPIR) version of the GCM and the full GCM approaches.

The corresponding collective wave functions $|F^{I;\,NZ;\,\nu}(\beta)|^2$ are plotted in the middle panel ($\nu = 1$) and the bottom panel ($\nu = 2$) and 2^+_3 ($\nu = 3$). In these panels we can see that the $\nu = 1$ states are members of ground rotational band, with most of the intensity of the collective wave functions concentrates around $\beta = 0.6$. This deformation corresponds to the location of the prolate minima of the potential energy surfaces corresponing to the different angular momenta $I = 0,\ 2;\ 4,\ 6,\ 8$ (see the upper panel of the Fig.7.57). The situation is rather different for the $\nu = 2$ states. The second 0^+_2 state is a mixing of oblate and prolate configurations whereas the wave function of the 2^+_2 state peaks in the oblate minimum of the corresponding potential energy surface and the 4^+_2 state could be considered as a vibration built on the $I = 4$ prolate well with a small contribution of slightly oblate states. In the 2^+_3 state the prolate deformations are again favored. The final spectrum of this axially symmetric calculation are demonstrated in the left side of the Fig.7.58 and it can be compared with the experimental spectrum in the right side of the Fig.7.58.

The second physical result of the [223] concerns the triaxial full GCM approach when the GCM equations (7.457), (7.456) besides the summation over β involve also the summation over γ. The final wave functions (7.459) involves the summation over both β and γ deformations, and the collective wave functions (7.460) are dependent also on both β and γ. In the cen-

---

VAMPIR approches, which had been used in the past before the full GCM equations were able to be solved numerically (see [244, 245]). The VAMPIR approaches generally consist from following steps:

1. In the framework of the given set of deformation points $\vec{q}_i \equiv (\beta_i, \gamma_i)$, or $\vec{q}_i \equiv (\beta_i)$ in the axially symmetric case, the equations (7.445), (7.446) are solved and as a result we obtain wave functions $|\phi(\vec{q}_i)\rangle$;
2. For given values of N, Z, I and K the PNAMP projected wave functions $|IMK;\, NZ;\, \vec{q}_i\rangle$ are found;
3. For each deformation point $\vec{q}_i \equiv (\beta_i, \gamma_i)$ or $\vec{q}_i \equiv \beta_i$ the PNAMP HWG equations (7.464), (7.463) are solved and wave functions $|IM;\, NZ;\, \vec{q}_i,\, \sigma\rangle_{PNAMP}$ with their energies $E^{I;\,NZ;\,\sigma}_{PNAMP}(\vec{q}_i)$ are found;
4. For each value of the angular momentum I and the index σ the minimum of energies $E^{I;\,NZ;\,\sigma}_{PNAMP}(\vec{q}_i)$ are found in the space of deformations $\vec{q}_i$ and we obtain the position $\vec{q}_0^{\,(I\sigma)}$ of this minimum. Corresponding to this minima wave functions $|IM;\, NZ;\, \vec{q}_0^{\,(I\sigma)};\, \sigma\rangle$ and energies $E^{I;\,NZ;\,\sigma}_{PNAMP}(\vec{q}_0)$ determine the final spectrum of the nucleus for all values of I and σ.

tral panel of the Fig.7.58 the spectrum of ^{24}Mg extracted from the triaxial full GCM calculations is demonstrated. The levels in the three bands were classified according to the corresponding $B(E2)$ values (strong inter-band E2 transitions). The ground state band is formed by a sequence of even angular momentum states with a level spacing very similar to that of a general rotational band. The first excited band consists of states with $I = 2, 3, 5, 6, 7$, as specified for a γ- band. The third band is built of even- I states on top of the second 0_2^+ state.

Concerning transition probabilities, the strong E2 intraband transitions are observed in the Fig.7.58 whereas the interband transitions are much weaker. This fact indicates the different intrinsic structure of the bands and the absence of mixing between them. The internal nature of these bands can be seen from the Table 7.6 where, besides the energy of each state, the K-components of the collective wave functions $|F^{I;NZ;\nu}(\beta,\gamma)|^2$, summed over all deformations (β,γ) for each K, are shown for all values I and ν. One can clearly see that the first and third bands are rather pure $K = 0$ whereas the second band corresponds to $|K| = 2$. Furthermore, for each level the $K = \pm 2$ components have the same values and it is a direct consequence of the time-reversal conservation of the intrinsic wave function.

If we compare the axial symmetry results with the triaxial case it is clearly observed that the triaxial case spectrum is much closer to the experimental situation.

From the above given discussion of the full GCM approach and its simpli-

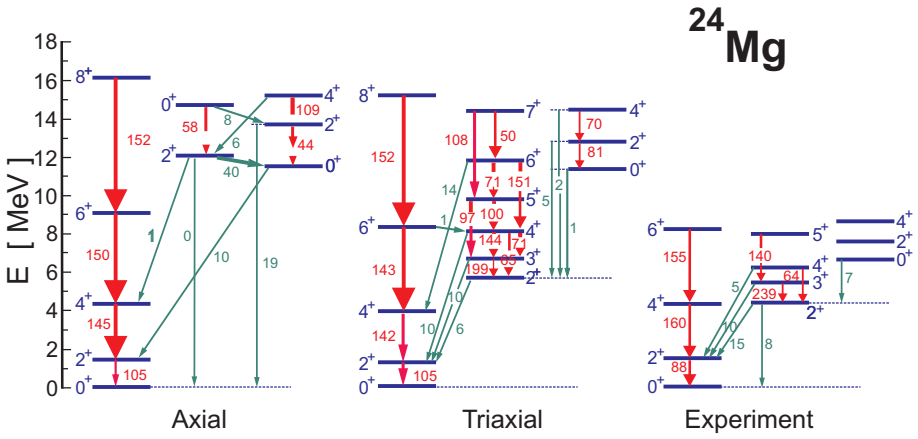


Figure 7.58: Calculated excitation energies and reduced transition probabilities B(E2) (in $e^2\ fm^4$) in ^{24}Mg obtained using axially symmetric full GCM (left) and triaxial full GCN (middle) approaches compared to the experimental values (right). The calculation results taken from [223] and experimental values are taken from [246].

I^+_ν	E [MeV]	$K=0$	$K=\pm2$	$K=\pm4$	$K=\pm6$	$K=\pm8$
0^+_1	0.000	**1.000**	-	-	-	-
2^+_1	1.202	**0.922**	0.039	-	-	-
4^+_1	3.875	**0.904**	0.016	0.032	-	-
6^+_1	8.256	**0.882**	0.011	0.015	0.033	-
8^+_1	15.198	**0.834**	0.040	0.017	0.016	0.010
2^+_2	5.616	0.188	**0.406**	-	-	-
3^+_1	6.564	0.000	**0.500**	-	-	-
4^+_2	7.990	0.081	**0.413**	0.046	-	-
5^+_1	9.718	0.000	**0.407**	0.093	-	-
6^+_2	11.688	0.078	**0.398**	0.007	0.056	-
7^+_1	14.349	0.000	**0.379**	0.036	0.085	-
0^+_2	11.265	**1.000**	-	-	-	-
2^+_3	12.686	**0.958**	0.021	-	-	-
4^+_3	14.363	**0.795**	0.048	0.055	-	-

Table 7.6: Decomposition of the norm of GCM-PNAMP collective functions into K components, $\sum_{\beta,\gamma} |F^{I;\,NZ;\,\nu}(\beta,\gamma)|^2$, for the first ($\nu=1$), second ($\nu=2$), and third ($\nu=3$) bands. The highest components are printed boldface. The excitation energies of the corresponding states are also provided (taken from [223]).

fied PNAMP (VAMPIR) version one can see that both these methods enable to investigate the dynamical changing (evolution) of the nuclear deformations with the increasing excitation energy. This is big advantage of these methods compared to the standard RPA approaches discussed in the Subsection 7.3.1 (or compared to the phenomenological approaches in the Section 7.2), where the deformations of the nucleus mean field were determined only one time from the minimum of the HF or HF+BCS total energy as a function of deformation for ground state (or using the Strutinski shell corrections discussed in the Subsection 5.1.2).

The application of the GCM was demontrated here on the results presented in the paper [223] published by the Madrid group. The GCM is used also by other groups (see e.g. [239] for angular projection VAMPIR version of the GCM without any particle number projection and using the relativistic mean field approach). However, the full GCM approach has been used only by Madrid group (at least up to year 2016).

7.3.3.3 Large scale shell model

The other approach going beyond the RPA is the large scale shell model (LSSM) approach (see e.g. [247, 248] and citations therein). The basic idea of the shell models was already discussed schematically in the Section 4.2. - the construction of the Hamiltonian matrix within the complete set of the configuration space basis functions, preferably within the set of HF many particle - many hole configuration states (for even-even nuclei - see (4.49)) or within the set of HFB or BCS many quasiparticle states (see (6.60)). However, using only these type of bases, without any other detail specification concerning a possible violation of the nucleus of the nucleus Hamiltonian symmetries by the HF or HFB (BCS) mean field, would lead to a problem of the physical interpretation of obtained results. For instance, if the total nucleus Hamiltonian concerns the laboratory frame then it should be rotationally invariant and the angular momentum I should be a good quantum number. In this case used shell model should ensure that the resultant eigen-functions obtained by the diagonalization of the total nuclear Hamiltonian matrix have sharp value of I. A similar problem concerns the sharp value of the number of protons and neutrons in the case when the pairing interaction contribute to the BCS mean field. Therefore, similarly as in the case of the GCM approach, discussed in the previous subsection, the starting LSSM configuration basis for heavier nuclei does not involve many p-h HF or many quasiparticle HFB configurations directly but rather their projections for a good (sharp) value of angular momentum I and number of protons and neutrons. Then the Hamiltonian matrix is constructed and diagonalized separately for each value of angular momentum I within the basis of projected HF or HFB many-particle or many-quasiparticle states. A similar problem, which should be solved in shell model approaches, is the removing of the center of mass (CoM) motion from the physical internal nucleus degrees of freedom.

General problem of shell model calculations is a size of used configuration space. As it was already mentioned in the end of the Section 4.2 the size of the configuration space (or dimension of the Hamiltonian shell model matrix) is restricted by the memory and the computing speed of nowadays computers. Here it is necessary to note that in modern codes for diagonalization of big matrices it is not necessary to keep all their matrix elements in the memory, it is sufficient to remember only nonzero matrix elements. Nevertheless the number of nonzero matrix elements is enormous, even for configuration

spaces relevant for light nuclei. From the point of view of the size of used configuration space we recognize two types of shell model approaches, no core shell model and core shell model approaches.

In the no core shell model calculations the NCSM configuration space is used for the description of the whole nucleus with all its neutrons and protons (without an introduction of any even-even core with the magic number of nucleons as it is done in the core shell model). Because of problems with the memory and computing speed, mentioned above, no core shell model calculations are possible only for very light nuclei (see e.g. [249]). For instance, in [249] it is shown for the heaviest nucleus calculated within the no core shell approach in 2013, oxygen ^{28}O, that the dimension of the Hamiltonian matrix was $\approx 10^{11}$ and needed memory was 56×10^{15} bytes (if two-body NN and three-body NNN nucleon interaction was taken into account). No core shell model calculations usually start with the "bare" NN and NNN nucleon interactions (for "bare" nucleon interactions see the Section 3.1) using some renormalization method, like Suzuki-Lee scheme [250]. In the last decade a new class of NN potentials was developed, mostly by means of unitary transformations of the standard bare NN potentials (e.g. CD-Bonn potential [251] or Argonne V18 potential [252]). These include Low-K [253], the UCOM [111], or SRGNN [254]. The NCSN calculations with this type of NN and NNN nucleon interactions (based on bare potentials), called also *ab initio* no core shell calculations, usually use the harmonic oscillator (HO) basis for the construction and diagonalization of Hamiltonian matrices. In such calculations the HO frequency and the basis truncation parameter are used as variation parameters in order to obtain convergence to the exact results (see e.g. [249]). The *ab initio* NCSM treats all A nucleons using the modern NN and NNN interactions and successfully describes properties of lightest nuclei. A detail expanation and discussion of the *ab initio* no core shell model is beyond the scope of this textbook. The readers, more interested in this topic, are referred to the review [249].

In the case of the core shell model (CSM) approach the configuration space is restricted only to valence nucleons outside the usually double magic even-even core. The even-even core is considered as inert. Then the properties of given nucleus is supposed to be formed by these valence nucleons. This enables to reduce the size of the configuration space basis and to use the CSM for heavier nuclei in the comparison with no core shell model approaches [248, 247].

The CSM approaches start also with effective interactions based on the

bare NN interactions. However the using of the bare NN interaction as in the NCSM (where interaction was directly connected with the bare NN interaction through the G- matrix calculations or unitary transformation of the UCOM type) leads to results not sufficiently precise for a comparison with experimental data on heavier nuclei. Therefore effective nucleon-nucleon interaction used in the CSM is usually slightly modified and adjusted in order to reproduce selected experimental data. For instance, in the paper [255], starting with the effective interaction [257], derived from the Bonn-C potential, the iteration fitting method was used for the new effective interaction GXPF1 (G-matrix interaction based on the Bonn-C bare interaction). The iterative fitting procedure involved 700 experimental energy data of 87 nuclei (mainly the energies of the first 2_1^+ states in even-even nuclei). This effective interaction was then specified several times (e.g. interaction GXPF2, A3DA ...) [258].

As an example of the CSM calculations we present here results of the Tokyo group [248] with the demonstration of the shape evolution of exotic Ni isotopes. Autors of [248] used so called Monte Carlo shell model (MCSH) version of the LSSM [259]. This method starts with the valence nucleus Hamiltonian

$$\hat{H}_{val} = \sum_{i,j=1}^{N_{sp}} \epsilon_{ij}\ c_i^+ c_j + \frac{1}{4} \sum_{i,j,k,l=1}^{N_{sp}} V_{ijkl}\ c_i^+ c_j^+\ c_l\ c_k \tag{7.465}$$

where the number of the valence spherical single-particle states is denoted as N_{sp} (e.g. $N_{sp} = 24$ for sd shell and $N_{sp} = 40$ for pf shell). In (7.465) c_i^+ stands for the single-particle creatioon operator for given spherical single-particle state of appropriately chosen starting spherical basis - e.g. harmonic oscillator basis.

At first, the separabilization of the two-body interaction involved in (7.465) is done (similar to multipole-multipole and spinmultipole-spinmultipole one in (1.55) and (1.56)):

$$\hat{H}_{val} = \sum_{i,j=1}^{N_{sp}} \epsilon_{ij}\ c_i^+ c_j + \hat{V} \tag{7.466}$$

where

$$\hat{V} = \frac{1}{4} \sum_{abcd} \sum_{JT} \sqrt{(1+\delta_{ab})(1+\delta_{cd})}\ V_{JT}^A(ab,cd)\ A_{JT;MT_z}^+(ab)\ A_{JT;MT_z}(cd) \tag{7.467}$$

with

$$A^{+}_{JT;MT_z}(ab) = \sum_{m_a m_b} \sum_{t_a t_b} C^{JM}_{j_a m_a j_b m_b} \, C^{TT_z}_{\frac{1}{2} t_a \frac{1}{2} t_b} c^{+}_{j_b m_b t_b} c^{+}_{j_a m_a t_a} \tag{7.468}$$

It can be rewritten further into a separable form (see [259])

$$\hat{V} = \frac{1}{2} \sum_{JT} \sum_{\alpha} \lambda_{JT}(\alpha) \sum_{M \geq 0} \big[: \hat{Q}^2_{JMT}(\alpha) : + : \hat{P}^2_{JMT}(\alpha) : \big] \tag{7.469}$$

where amplitudes $\lambda_{JT}(\alpha)$ and operators $\hat{Q}_{JMT}(\alpha)$ and $\hat{P}_{JMT}(\alpha)$ are given vy two-body matrix elements $V^{A}_{JT}(ab, cd)$ of the starting two-body interaction $\hat{V}$ in (7.466) (see the expr. (65) in [259]). Then the whole Hamiltonian $\hat{H}_{val}$ can be schematically rewritten as (see (22) in [259]),

$$\hat{H}_{val} \approx \sum_{\alpha=1}^{N_f} \big(E_\alpha \hat{Q}_\alpha + \frac{1}{2} V_\alpha \hat{Q}^2_\alpha \big) \tag{7.470}$$

where N_f is the number of separable terms and the N_f can be at most N^2_{sp} but usually is maller (see the subsection 4.6.5 in [259]).

Let us suppose that E_i is the i-th eigen-value of $\hat{H}_{val}$ and $|\Phi_i\rangle$ is its eigen-function, and let us introduce the general wave packet,

$$|\Psi\rangle = \sum_i c_i \, |\Phi_i\rangle \tag{7.471}$$

where c_i stands for an amplitude. Further we introduce imaginary-time evolution operator $e^{-\beta \hat{H}_{val}}$ ($\hat{H}_{val}$ is supposed to be time-independent). Here, β is a real number and it represents a parameter. If this evolution operator acts on the wave packet (7.471) then,

$$e^{-\beta \hat{H}_{val}} \, |\Psi\rangle = \sum_i e^{-\beta E_i} \, c_i \, |\Phi_i\rangle \stackrel{\beta \to \infty}{\longrightarrow} |\Phi_g\rangle \tag{7.472}$$

For β large enough the amplitudes of the eigen-states $|\phi_i\rangle$ with small energies E_i become relatively large in the expansion (7.472) and at $\beta \to \infty$ only the ground state $|\Phi_g\rangle$ survives. Therefore the operator $e^{-\beta \hat{H}_{val}}$ can be understood as the projection operator for the lowest eigen-states in the spectrum of the Hamiltonian $\hat{H}_{val}$. This enables to formulate variation principle (searching for a minimum of the ground state energy $\langle \Psi_{gr} | \hat{H}_{val} | \Psi_{gr} \rangle / \langle \Psi_{gr} | \Psi_{gr} \rangle$) as the searching of the minimum of

$$\frac{\langle \Psi | \hat{H}_{val} \, e^{-\beta \hat{H}_{val}} | \Psi \rangle}{\langle \Psi | e^{-\beta \hat{H}_{val}} | \Psi \rangle} \stackrel{\beta \to \infty}{\longrightarrow} \frac{\langle \Phi_g | \hat{H}_{val} | \Phi_g \rangle}{\langle \Phi_g | \Phi_g \rangle} \tag{7.473}$$

starting with any wave packet (7.471). However, to use this feature of the evolution opoerator $e^{-\beta \hat{H}_{val}}$ is technically complex. In order to avoid these technical problems the Metropolis Monte Carlo diagonalization method can be used (see [259]). We shall explain this method in a simple example.

7.3.3.3.1 Quantum Monte Carlo Diagonalization (QMCD) - simplified Hamiltonian We shall start with the simplified Hamiltonian (instead of (7.470)),

$$\hat{H} = \frac{1}{2}\, V\, \hat{Q}^2 \tag{7.474}$$

where for simplicity we assume $V < 0$. Then the imaginary-time evolution operator is,

$$e^{-\beta \hat{H}} = e^{-\frac{1}{2}\,\beta\, V\, \hat{Q}^2} \tag{7.475}$$

Further we use following expressions from mathematics

$$\begin{aligned} \int_{-\infty}^{\infty} d\sigma\, e^{-a(\sigma+c)^2} &= \sqrt{\frac{\pi}{a}} \qquad\qquad (a>0) \\ \text{or} \qquad e^{ac^2} &= \sqrt{\frac{a}{\pi}} \int_{-\infty}^{\infty} d\sigma\, e^{-a\sigma^2-2a\sigma c} \end{aligned} \tag{7.476}$$

where σ means the integration variable, and c and a are parameters. By substitution $a \to -\frac{1}{2}\beta V$ and $c \to \hat{Q}$ the equation (7.476) can be rewritten as,

$$e^{-\beta \hat{H}} = e^{-\frac{1}{2}\beta V \hat{Q}^2} = \int_{-\infty}^{\infty} d\sigma \sqrt{\frac{\beta|V|}{2\pi}}\, e^{-\beta|V|\sigma^2} \cdot e^{-\beta|V|\sigma\hat{Q}} \tag{7.477}$$

This equation is exact, but not practical at all. The idea of the quantum Monte Carlo calculation comes now, the integration (7.477) is approximated, apart from the normalization, by a Monte Carlo (MC) sampling as (see the Appendix S for details),

$$e^{-\frac{1}{2}\beta V \hat{Q}^2} \approx \sum_{MC:\sigma} \sqrt{\frac{\beta|V|}{2\pi}}\, e^{-\beta\,|V|\,\sigma\,\hat{Q}} \tag{7.478}$$

where the integration over variable σ in (7.477) is sampled by Monte Carlo method with the Gaussian sampling probability weight (see (S...)),

$$G(\sigma) \approx e^{-\frac{\beta}{2}|V|\sigma^2} \tag{7.479}$$

Equation (7.478) becomes exact if the MC sampling is complete.

By combining equations (7.472),(7.474) and (7.478) one can see that, apart from the normalization, the ground state can be obtained for $\beta \to \infty$ by,

$$|\Phi_g\rangle \approx \sum_{MC:\sigma} \sqrt{\frac{\beta|V|}{2\pi}}\, e^{-\beta\,\hat{h}(\sigma)}\, |\Phi^{(0)}\rangle \tag{7.480}$$

where $\hat{h}(\sigma)$ is called the one-body Hamiltonian and is defined as,

$$\hat{h}(\sigma) = |V|\sigma\hat{Q} \tag{7.481}$$

So far, we assume $V < 0$. In the case of $V > 0$ the above arguments should be modified, and the general definition of $\hat{h}(\sigma)$ is given by,

$$\hat{h}(\sigma) = s\,V\,\sigma\,\hat{Q}\;, \qquad \text{with } s = \pm 1 \text{ for } V < 0,\; s = \pm i \text{ for } V > 0, \tag{7.482}$$

Then the ground state energy is given by (7.473) for the Hamiltonian $\hat{H}$:

$$E_g = \frac{\langle\Phi_g|\hat{H}|\Phi_g\rangle}{\langle\Phi_g|\Phi_g\rangle} \approx \frac{\langle\Psi^{(0)}|\hat{H}\,\sum_{MC;\sigma} e^{-\beta\,\hat{h}(\sigma)}|\Psi^{(0)}\rangle}{\langle\Psi^{(0)}|\sum_{MC;\sigma} e^{-\beta\,\hat{h}(\sigma)}|\Psi^{(0)}\rangle} \tag{7.483}$$

starting with some wave packet $|\Psi^{(0)}\rangle$ (usually taken as HF or HFB Slater determinants obtained independently from constraint variational principle).

So, basic concept of the QMCD method starts with $|\Psi^{(0)}\rangle$ and we create a basis vectors $|\Phi(\sigma)\rangle$,

$$\sum_{MC;\sigma} e^{-\beta\,\hat{h}(\sigma)}|\Psi^{(0)}\rangle \equiv \sum_{MC;\sigma} |\Phi(\sigma)\rangle \tag{7.484}$$

introduced by,

$$|\Phi(\sigma)\rangle \approx e^{-\beta\,\hat{h}(\sigma)}|\Psi^{(0)}\rangle \tag{7.485}$$

By having different values of the random variable σ we can generate different basis vectors $|\Phi(\sigma)\rangle$. Then we can diagonalize Hamiltonian matrix in a subspace spanned by these basis vectors. To be more precise, let us suppose that some basis vectors are already obtained. We then create a state $|\Phi(\sigma = \sigma_1)\rangle$ according to (7.485) using a value σ_1 of this random variable. Then we diagonalize the Hamiltonian in a subspace spanned by the previously obtained basis vectors and this new vector $|\Phi(\sigma = \sigma_1)\rangle$. One can then check the contribution of the state $|\Phi(\sigma = \sigma_1)\rangle$ for the change of the eigenvalues being calculated in the previous step (mainly lowering the lowest eigenvalue). If the contribution is large enough, one can add the state $|\Phi(\sigma = \sigma_1)\rangle$ to the set of basis vectors to be kept and used in the next step. If the contribution from

$|\Phi(\sigma = \sigma_1)\rangle$ is not sufficient, we forget this state, and should look for another basis vector generated from another value of the random number, say σ_2. We repeat this iterative process and obtain more basis vectors, until we come to a reasonable convergence of the energy eigenvalues as a function of the number of basis vectors. One can thus select only important basis vectors (their number is usually much less than the number of any complete initial basis for the Hamiltonian $\hat{H}$). By having such selected basis vectors, the ground state state wave function corresponding to the lowest eigenvalue is obtained as a result of the diagonalization of the Hamiltonian in a subspace spanned by the basis vectors from the last iteration. However, we should realize that the procedure described above was applied for lowering the lowest eigenvalue starting with the original $|\Psi^{(0)}\rangle$ (see (7.484)). The other thing which should be realized is the fact that the basis vectors $|\Phi(\sigma)\rangle$ obtained in each iteration are not mutually orthogonal and we should use some orthonormalization procedure before each diagonalization (e.g. Gram-Schmidt method).

If we want to have more than one eigenstate of the Hamiltonian (not only the ground state) then one first determines the basis vectors for the lowest eigenstate (the ground state). After a reasonable convergence is attained, one can switch to the second lowest eigenstate. Keeping the basis vectors for the lowest eigenstate, one generates basis vectors by the equation (7.485), and check them according to their contribution to the change of the second eigenvalue. In diagonalizing the Hamiltonian matrix, one merges the basis vectors for the lowest eigenvalue and those for the second eigenstate, but uses the second the second eigenvalue for selecting the basis vectors for the second eigenstate. This is repeated until a reasonable convergence is reached for the second eigenstate. By repeating this procedure we can obtain higher eigenstates as well.

7.3.3.3.2 Quantum Monte Carlo Diagonalization (QMCD) - general case Going back to the general separable Hamiltonian (7.470), the one-body Hamiltonian $\hat{h}(\sigma)$ (see (7.481) or (7.482)) can be generalized as,

$$\hat{h}(\sigma) = \sum_{\alpha=1}^{N_f} (E_\alpha + s_\alpha V_\alpha \sigma_\alpha)\, \hat{Q}_\alpha \tag{7.486}$$

and the imaginary-time evolution operator $e^{-\beta\,\hat{H}_{val}}$ obtain following form (see (7.477)),

$$e^{-\beta\,\hat{H}_{val}} \approx \int_{-\infty}^{\infty} \prod_{\alpha} d\sigma_{\alpha} \Big(\frac{\beta |V_{\alpha}|^2}{2\pi} \Big) \cdot G(\vec{\sigma}) \cdot e^{-\beta\,\hat{h}(\vec{\sigma})} \tag{7.487}$$

where $\vec{\sigma} \equiv \{\sigma_{\alpha}\}$, $\alpha = 1, \cdots, N_f$ means a set of random numbers (auxiliary fields). For $\hat{H}_{val}$ (see (7.470)) containing many terms, this is an approximate relation and becomes exact only in the limit of small β, because the $\hat{Q}_{\alpha}$-s do not commute with each other in general. The Gaussian weight factor $G(\sigma)$ in general case is defined by (see (7.479)),

$$G(\vec{\sigma}) = e^{-\sum_{\alpha} \frac{\beta}{2} |V_{\alpha}| \sigma_{\alpha}^2} \tag{7.488}$$

where one should realize that in order to express the (7.488) as the probability weight function for the multi-dimensional case $\alpha = 1, \cdots, N_f$ and simultaneously we want (7.484) and (7.485) to be valid it is necessary to work with the decompossition of $e^{-\beta \hat{H}_{val}}$ up to the linear order in β if generally $[\hat{Q}_{\alpha}, \hat{Q}_{\alpha'}] \neq 0$ (which is general case). So in (7.487), we need small β but this is in contradiction with (7.473). However, the equation (7.485) can be applied to smaller imaginary time intervals by dividing β into N_t time slices,

$$e^{-\beta \hat{H}_{val}} = \prod_{n=1}^{N_t} e^{-\Delta\beta\,\hat{H}_{val}} \tag{7.489}$$

where $\Delta\beta = \frac{\beta}{N_t}$. Then the eq. (7.487) can be rewritten as,

$$e^{-\beta \hat{H}_{val}} \approx \prod_{n=1}^{N_t} \int_{-\infty}^{\infty} \prod_{\alpha=1}^{N_f} d\sigma_{\alpha,n} \Big(\frac{\Delta\beta\,|V_{\alpha}|}{2\pi} \Big)^{1/2} \cdot G(\vec{\sigma_n}) \cdot e^{-\Delta\beta\,\hat{h}(\vec{\sigma}_n)} \tag{7.490}$$

where $\vec{\sigma}_n$ stands for the n-th time slice. The nonzero commutation relations between different $\hat{Q}_{\alpha}$-s can be neglected in usual quantum Monte Carlo calculations for small $\Delta\beta$ (that means in the usual QMCD method).

So, the basis generation process for the general case consists from following steps.

1. In the first step, we take an initial state $|\Psi^{(0)}\rangle$ (see (7.471)) which can be determined e.g. by a HF or HFB mean field method. The initial energy is calculated as $E^{(1)} = \langle \Psi^{(0)} | \hat{H}_{val} | \Psi^{(0)} \rangle$.

   If the present step is not the initial step, there should be k basis vectors already selected, and the lowest energy eigenvalue obtained by the diagonalization with these basis vectors is called $E^{(k)}$.

2. A set of random numbers (auxiliary fields) is given:

$$\sigma \equiv \{\vec{\sigma}_1, \vec{\sigma}_2, \cdots, \vec{\sigma}_{N_t}\} \tag{7.491}$$

for time slices $n = 1, 2, \cdots, N_t$ with $\vec{\sigma}_n = \{\sigma_{\alpha=1,n}, \sigma_{\alpha=2,n}, \cdots, \sigma_{\alpha=N_t,n}\}$.

3. The wave function $|\phi(\sigma)\rangle$ is calculated for the present set σ (see (7.485) and (7.490)) after the Monte Carlo diagonalization),

$$|\Phi(\sigma)\rangle \approx \prod_{n=1}^{N_t} e^{-\Delta\beta\,\hat{h}(\sigma_n)}\,|\Psi^{(0)}\rangle \tag{7.492}$$

which is obtained by applying the idea of eq. (7.485) to eq. (7.490).

4. The state $|\Phi(\sigma)\rangle$ is a candidate for the $(k+1)$-th basis vector. It is orthonormalized by means of the Gram-Schmidt method against the first k-th basis states already fixed.

5. By including the state $|\Phi(\sigma)\rangle$, we diagonalize the Hamiltonian $\hat{H}_{val}$ matrix, and obtain an improved (perturbed) lowest eigen-energy E.

6. The perturbed lowest energy eigenvalue E is compared to E^k (see the step 1.), i.e. to the lowest eigen- energy obtained by the diagonalization within the k basis vectors already fixed. If the lowest eigen-energy E (after the diagonalization with the state $|\Phi(\sigma)\rangle$ added) is lowered significantly compared to E^k then the $|\Phi(\sigma)\rangle$ is adopted as the new, i.e. $(k+1)$-th basis vector. In this case, we increase k by one, and move to the step 1. Otherwise, $|\Phi(\sigma)\rangle$ is discarded and steps 2 to 5 are repeated.

The iterations are continued and k is increased, until the lowest energy eigenvalue converges reasonably well.

The adopted basis vectors are called Quantum Monte Carlo Diagonalization (QMCD) basis. The number of QMCD basis vectors is referred to as the QMCD dimension. The Hilbert subspace spanned by this QMCD basis is called QMCD space. We emphasize that energies and wave functions are determined by the diagonalization.

Up to now we determined only the QMCD basis for the lowest energy eigenstate. If one needs to calculate more than one lowest eigenstate, one starts with the lowest eigenstate, and select the QMCD basis for it. One then looks for the basis for the second eigenstate similarly, but diagonalization should be done in the combained space where QMCD (that means the steps 2-6 are performed for the second eigenvalue with the combined (merged) space

of the first (lowest) and the second eigenstates). Thus, the orthogonality between eigenstates is guaranteed. By doing this way, one can calculate many eigenstates successively. Note that the relevant basis vectors can be quite different for different eigenvalues.

As it was already mentioned, the initial state $|\Psi^{(0)}\rangle$ is usually taken in the form of the HF (or HFB) mean field ground state (Slater determinant or BCS function). In such a case the one-body Hamiltonian $\hat{h}(\vec{\sigma})$ used in (7.482) has the following form (see [259]),

$$\hat{h}(\sigma_n) = \hat{h}_{MF} + \sum_{\alpha} V_\alpha s_\alpha \hat{Q}_\alpha \tag{7.493}$$

The nucleus is an isolated system and conserves several symmetries (e.g. parity symmetry, rotational symmetry, number of neutrons and protons). That means the Hamiltonian $\hat{H}_{val}$ should have these symmetries. However, the states $|\Phi(\sigma)\rangle$ in (7.488) are not an eigenstates of the total angular momentum in general because the initial state $|\Psi^{(0)}\rangle$ breaks the rotational symmetry in general. We therefore restore the rotational symmetry by means of the angular momentum projection operator $\hat{P}^I_{MK}$ (see the expr. (7.450)) and the Appendix N (exprs (N.25), (N.26)),

$$\hat{P}^I_{MK} = \frac{2I+1}{8\pi^2} \int d\Omega D^I_{MK}(\Omega)\, e^{-i\alpha\hat{J}_z} e^{-i\beta\hat{J}_y} e^{-i\gamma\hat{J}_z} \tag{7.494}$$

acting on the states $|\Phi(\sigma)\rangle$ (see (7.492)). Usually, we do not need directly wave functions $|\Phi(\sigma)\rangle$ but their matrix elements (which are involved in the steps 1 - 6 above). That means we need projected matrix elements in the following form (e.g. for scalar single-particle operator $\hat{Q}$),

$$\langle\Phi(\sigma')|\,\hat{Q}\,\hat{P}^I_{MK}\,|\Phi(\sigma)\rangle = \boxed{\begin{array}{c}\text{see}\\ (7.494)\,,\ (A.21)\end{array}} =$$

$$= \frac{2J+1}{8\pi^2} \int_0^{2\pi} d\gamma \int_0^{\pi} sin\beta\, d\beta \int_0^{2\pi} d\alpha\, e^{-iM\gamma} d^I_M K(\beta)\, e^{-iK\alpha}$$

$$\langle\Phi(\sigma')|\,\hat{Q}\, e^{i\hat{J}_z\gamma} e^{i\hat{J}_y\beta}\, e^{i\hat{J}_z\alpha}\,|\Phi(\sigma)\rangle \tag{7.495}$$

Here it is necessary to note that the z-axis does not coincide generally with the intrinsic 3-d axis of a deformed nucleus (defined as the 3-d principal axis of the intrinsic quadrupole moment or moment of inertia -see the Fig.7.1).

So, after the applying QMCD procedure for finding the eigen-vectors and eigenvalues of the Hamiltonian $\hat{H}_{cal}$ (see steps 1 - 6 above) the resultant

eigen-functions has following form

$$|\Psi_{I^\pi M;\,\nu}\rangle = \sum_{i=1}^{N} \sum_{K=-I}^{I} f_{i,K}^{(\nu,N)}\, \hat{P}_{MK}^{I}\, |\Phi_i\rangle \tag{7.496}$$

where N is the QMCD dimension and $|\Phi_i\rangle$ are QMCD basis vectors constructed from the Slater determinants using the Monte Carlo importance sampling method described by the points 1 - 6 above and $f_{i,K}^{(N)}$ are corresponding amplitudes obtained by the digonalization of the Hamiltonian $\hat{H}_{val}$ within the projected QMCD basis. Index ν enumerates solutions of the eigen problem.

In order to investigate the evolution of deformation with the excitation energy in the excited states $|\Psi_{I^\pi M;\,\nu}\rangle$ for $\nu = 1, 2, \cdots$ it is necessary to set a deformation structure of these states. It requires, at first, to determine

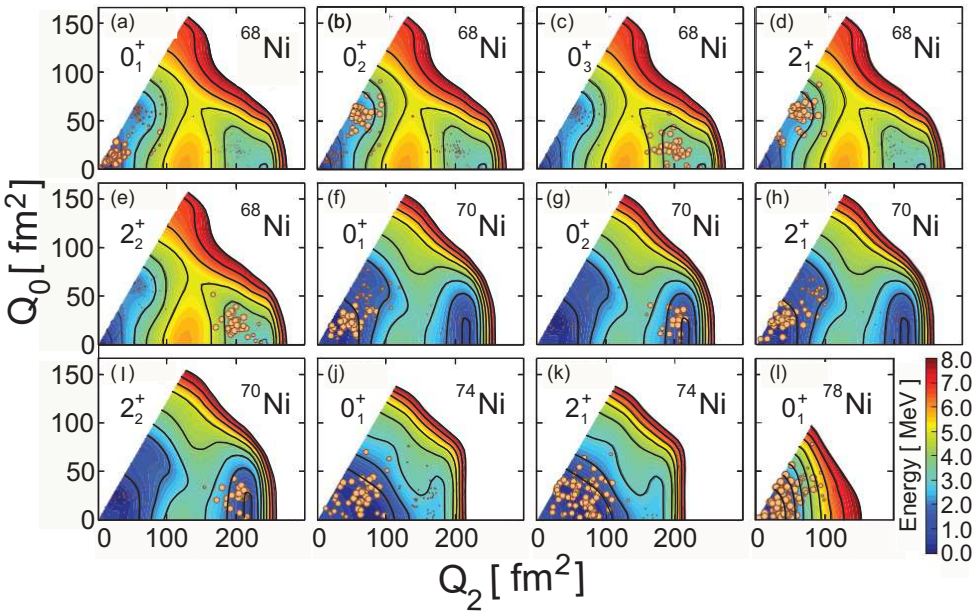


Figure 7.59: Potential energy surfaces (PESs) of Ni isotopes, coordinated by the quadrupole moments Q_0 and Q_2. Circles on the each PES represent (β, γ) shapes of components of the corresponding excitation state (see the text for more details) - taken from [248].

the intrinsic coordinate frame for each Slater determinant $|\Phi_i\rangle$ entering the structure of excited states $|\Psi_{I^\pi M;\,\nu}\rangle$ (see (7.496)). It is done by the calculation of all components of the quadrupole moment tenzor in the given Slater determinant $|\Phi_i\rangle$ (see [248])

$$Q_{2\mu}^{(i)} = \langle \Phi_i |\, \hat{Q}_{2\mu}\, |\, \Phi_i \rangle \tag{7.497}$$

The intrinsic coordinate frame is defined as the frame where the quadrupole moment component $Q^{(i)}_{2\mu=\pm1}$ are zero ($Q^{(i)}_{2\mu=\pm1}=0$). So we diagonalize matric $Q^{(i)}_{2\mu}$ (for $\mu=0,\pm1,\pm2$) and obtained diagonal values

$$Q^{(i)}_0 \equiv Q^{(i)}_{20} \quad , \quad Q^{(i)}_2 \equiv Q^{(i)}_{22} = Q^{(i)}_{2-2} \tag{7.498}$$

define the intrinsic values of the quadrupole moment for given $|\Phi_i\rangle$. These values, $Q^{(i)}_0$ and $Q^{(i)}_2$, can be then recalculated to the internal quadrupole deformation parameters $\beta^{i)}$ and $\gamma^{(i)}$ according to (7.449). In such a way for each Slater determinant $|\Phi_i\rangle$ (and this is also for its projection $P^I_{MK}\,|\Phi_i\rangle$) we obtain corresponding deformation parameters $\beta^{(i)}, \gamma^i$. Then we can determine the overlap probability

$$p^{(I^\pi\ \nu)}_i \equiv \sum_K |\ \langle\Phi_i|\ P^I_{MK}\ |\Psi_{I^\pi M;\,\nu}\rangle\ |^2 \tag{7.499}$$

of finding the resultant state $|\Psi_{I^\pi M;\,\nu}\rangle$ with the internal deformation $\beta^{(i)}$, $\gamma^{(i)}$.

For the comparison of deformations of different components $P^{I\pi}_{MK}\,|\Phi_i\rangle$ of given resultant excitation MCSM states $|\Psi_{I^\pi M;\,\nu}\rangle$ the potential energy surface (PES) is determined for given nucleus. This is done in [248] by standard way using the solving of the deformation constrained HF equation (7.446) with the valence nuclear Hamiltonian (7.465) for a mesh of deformation points $(Q_0(\beta,\gamma), Q_2(\beta,\gamma))$ [43]. As a result we obtain HF Slater determinant $|\Phi(\beta,\gamma)\rangle$ at each point of the mesh of deformations and the PES can be depicted as the dependence of the total HF energy $E_{HF}(\beta,\gamma)=\langle\Phi(\beta,\gamma)|\ \hat{H}_{val}\ |\ \phi(\beta,\gamma)\rangle$ on deformations β and γ (or on $Q_0(\beta,\gamma)$ and $Q_2(\beta,\gamma)$). In the Fig.7.59 the potential energy surfaces (PESs) of Ni isotopes, obtained by the step described above, coordinated by the $Q_0(\beta,\gamma)$ and $Q_2(\beta,\gamma)$, are demonstrated for selected Ni isotopes (^{68,70,74,78}Ni). Circles are placed on PES at each point corresponding to the point $Q_0(\beta^{(i)},\gamma^{(i)})$ and $Q_2(\beta^{(i)},\gamma^{(i)})$ obtained by the (7.499). The size (i.e. area) of each circle is set to be proportional to the overlap probability $p^{(I^\pi\ \nu)}_i$ (see (7.499)) for given i and the excitation state $|\Psi_{I^\pi M;\,\nu}\rangle$ (each panel in the Fig.59 corresponds to one excitation state $|\Psi_{I^\pi M;\,\nu}\rangle \equiv |\ I^\pi_\nu\rangle$ of given nucleus).

[43] Potential energy surfaces (PESs) in [248] is determined in the simpliest way by the calculation of $\langle\Phi(\beta,\gamma)|\ \hat{H}\ |\Phi(\beta,\gamma)\rangle$ in the mesh of deformation points with the deformation constrained HF Slater determinants $|\Phi(\beta,\gamma)\rangle$. Therefore we obtain one PES for one nucleus. It cannot be directly compared with the more sophisticated determination of PES discussed in the upper panel of the Fig.7.57 where te VAMPIR method (see the footnote under the eq. (7.464)) was used. The Vampir method is connected with the solving of the eq. (7.464) and this gives us the PES for each state I^π_ν (for different solutions $\nu=1,2,\cdots$ of the eq.(7.464)).

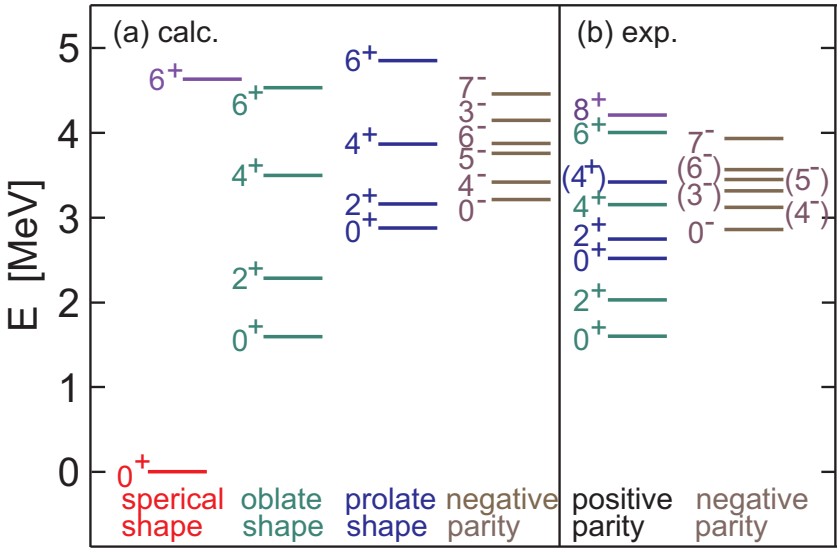


Figure 7.60: The lowest spectrum of ^{68}Ni, calculated by the MCSM approach with the valence Hamiltonian (7.465) with the A3DA interaction [258], are compared with the experimental spectrum (right part of the figure - taken from [248].

Fig.7.59(a) shows the potential energy surface and circles described above for the ground state $|\,0_1^+\rangle$ ($\nu = 1$ for I^π) of ^{68}Ni. one can see that there are many circles around the spherical $Q_0 = Q_2 = 0$ point. That means the ground state is formed predominantly with the spherical components. The 0_2^+ state in the Fig.7.59(b) shows a situation for 0_2^+ state in ^{68}Ni. In this case the oblate shape components play a dominant role in the state $|\Psi_{0^+0;\,\nu}\rangle = |\,0_2^+\rangle$ with Q_0 and Q_2 corresponding to $\beta \approx 0.2$ and $\gamma \approx 60^o$. In the state $|\,0_3^+\rangle$ in ^{68}Ni (the panel (c) in the Fig.7.59) the dominant role is played by components with the prolate shape. A similar shape evolution for excited states with $I_\nu^+ = 0_1^+,\ 0_2^+,\ 2_1^+,\ 2_2^+$ can be seen also for other isotopes $^{70,\,74}$Ni.

In the Fig.7.60 the comparison of calculated MCSM energies $E_{I^\pi\,\nu}$ with the corresponding experimental spectrum for the lowest excited states in ^{68}Ni are shown. The shape of the dominant components of the given I_ν^π states is mentioned in the bottom of the figure. The excited states are sorted to the bands according the similarity of shapes of dominant components. One can see relatively good agreement of the MCSM spectrum with experimental one.

7.3.3.4 Equation of motion multi-phonon method

The last example of beyond RPA approach is so called equation-of-motion phonon method (EMPM) [41, 261]. The EMPM derives and solves iteratively a set of equations of motion to generate an orthonormal basis of multi-phonon

states built on phonons obtained in the Tamm-Dancoff approximation. The basic stones of the EMPM are Tamm-Dancoff phonons built as linear combinations of 1p-1h configurations (see (4.54) and the text around) with the following creation operator

$$Q^+_\lambda = \sum_{ph} c^\lambda_{p\,h}\, a^+_p a_h \tag{7.500}$$

where a^+_p (a_h) creates a particle (hole) out of the unperturbed ground state (the mean field ground state, e.g. Hartree-Fock mean field ground state). The TDA phonon amplitudes $c^\lambda_{p\,h}$ are obtained from the general Hamiltonian

$$\hat{H} = \sum_i \epsilon_i\, a^+_i\, a_i + \frac{1}{4}\sum_{ij\,kl} V_{ij\,kl}\;\; a^+_i a^+_j\, a_l\, a_k \tag{7.501}$$

by the solving of the TDA eigen-value problem (diagonalization of the Hamiltonian 1p-1h block - see the Fig.4.1),

$$\sum_{p'h'} A_{p\,h\,p'h'}\, c^\lambda_{p'h'} = E_\lambda\, c^\lambda_{p\,h} \tag{7.502}$$

where

$$A_{p\,h\,p'h'} = \delta_{hh'}\delta_{pp'}\,(\epsilon_p - \epsilon_h) + V_{p\tilde{h}'\,\tilde{h}p} \tag{7.503}$$

In (7.503) $\tilde{h}$ denotes time reversal of h. The goal of the EMPM is to construct n-phonon basis states $\mid n;\, \beta\rangle$ obtained by the acting of the TDA phonons (7.500) on all $n-1$ phonon basis states

$$\mid n;\, \beta\rangle = \sum_{\lambda\alpha} C^{(\beta)}_{\lambda\alpha}\, Q^+_\lambda \mid n-1;\, \alpha\rangle \tag{7.504}$$

Amplitudes $C^{(\beta)}_{\lambda\alpha}$ are then obtained by the diagonalization of the Hamiltonian matrix constructed in the space of states $Q^+_\lambda \mid n-1;\, \alpha\rangle$. The basis of this states is non-orthogonal and redundant. The redundancy is removed by the special approach based on the Cholesky decomposition method (see [41] and citation therein). In such a way we obtain for each n-phonon subspace an orthogonal set of n-phonon states $\mid n;\, \beta\rangle$ starting from $n = 1$ (for $n = 1$ we have the TDA one-phonon space) up to the desired value of n (technical limits of the memory and computing speed of computers in 2015 allowed to do this calculation up to 2-phonons for heavy nuclei and up to 3-phonons for $A \approx 20$ nuclei with the effective n-n interaction based on the chiral $V_{chi} = NNLO_{opt}$ potential [262] as it is discussed in [261]). As a result

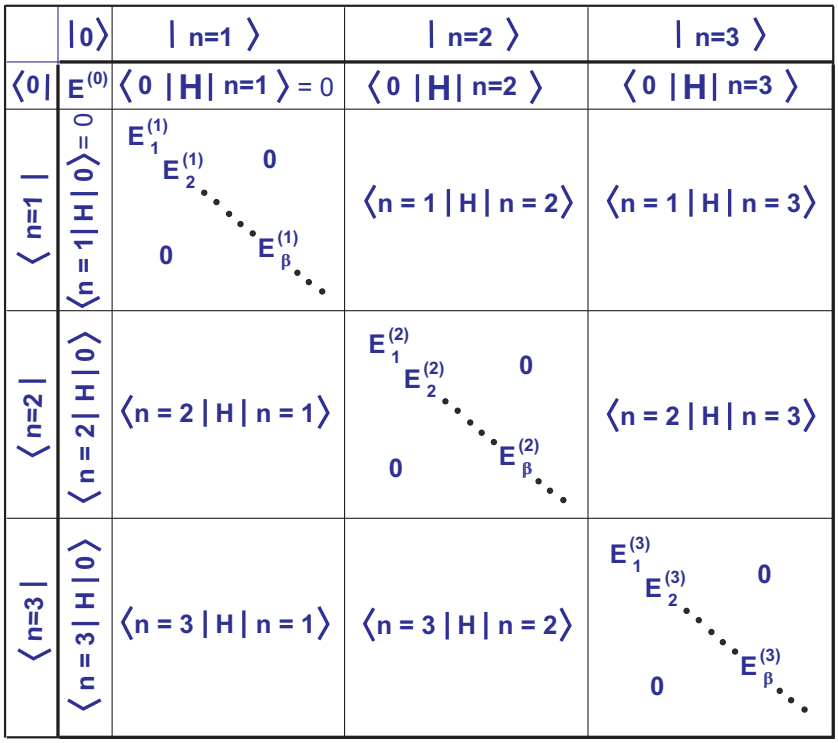


Figure 7.61: Schematic figure of the Hamiltonian matrix decomposed in the EMPM into blocks according to n-phonon subspaces ($n = 0,\ 1,\ 2,\ 3$).

the total Hamiltonian matrix is decomposed into blocks as it is schematically shown in the Fig.7.61. The diagonal blocks belonging to the given number n of TDA phonons are diagonal in the EMPM orthogonal basis of $\mid n;\ \beta\rangle$ states with energies $E^{(n)}_{\beta} = \langle\, n,\ \beta \mid \hat{H} \mid n;\ \beta\rangle$ where the index β enumerates the energies for given n-phonon block.

In the next step the total Hamiltonian matrix shown in the Fig.7.61 is diagonalized in the whole basis of states $\mid n;\ \beta\rangle$ ($n = 0,\ 1,\ 2;\ 3$, where $\mid n = 0\rangle \equiv \mid 0\rangle$ is the unperturbed mean field ground state - e.g. Hartree-Fock ground state for given nucleus). This diagonalization provides us perturbed ground state $|\Psi_{\nu=0}\rangle$ and all excited eigen-states $|\Psi_{\nu}\rangle$ in the form of the linear combination of the basis of states $\mid n;\ \beta\rangle$,

$$|\Psi_{\nu}\rangle = \sum_{n=0}^{3} \sum_{\alpha} d^{(\nu)}_{n\alpha} \mid n;\ \alpha\rangle \tag{7.505}$$

together with their corresponding eigen-energies E_{ν} of the whole Hamiltonian matrix shown in the Fig.7.61.

Originally EMPM was formulated in the particle-hole scheme and applied to ^{16}O for the calculation of the low-lying spectrum and isovector and isoscalar

E1 and isoscalar E2 strength functions [263, 264]. Later the E1 responce in heavier nuclei was analyzed using the EMPM [265]. In the first original version of the EMPM the Hamiltonian was taken in the form of the sum of the Nilsson mean field and the residual interaction taken from the chiral $V_\chi = NNLO_{opt}$ potential. More recent calculations [266, 267] were fully selfconsistent with the HF mean field and residual interaction obtained from the chiral V_χ potential. In the latest version of the EMPM the quasiparticle BCS formalism was added with the aim of the description of open shell nuclei [268]. The spurious CoM mode is separated by the special method discussed in [269].

As a demonstration of the influence of multiphonon components in the low-lyiong states and E1 resonances the spectrum of ^{16}O is discussed further.

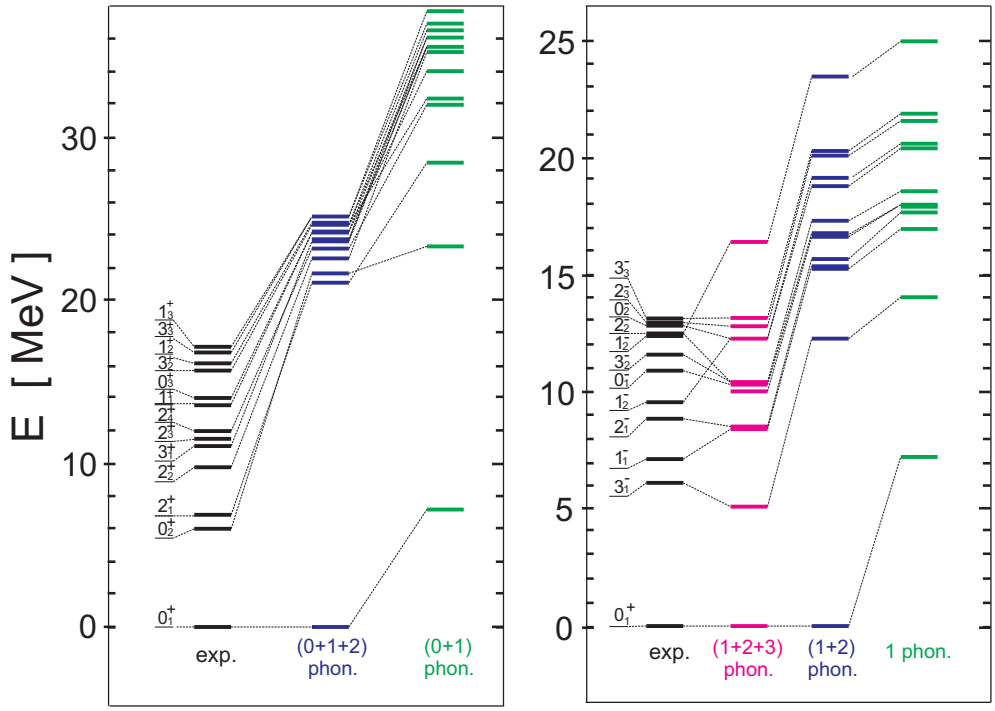


Figure 7.62: Experimental and calculated (within the EMPM) spectrum of low-lying states in ^{16}O. The EMPM calculations with the 1- phonon, (1+2)- phonon, and (1+2+3)-phonon subspaces in the configuration space are mutually compared. In the case of the positive parity state the mean field ground state is added to 1-phonon or (1+2)- phonon or (1+2+3)-phonon configuration spaces - taken from [264].

In the Fig.7.62 the low-lying spectrum in ^{16}O, calculated within the EMPM, is compared with the corresponding experimental values [263, 264]. In the left panel the positive parity levels are shown and the right panel involves the negative parity part of the spectrum. In the case of the positive parity

spectrum the calculation was performed only with the configuration space involving the number of TDA phonons up to 2 phonons while negative parity calculations involve the configuration space up to 3 phonons. The reason was the computer memory which did not allowed to increase configuration space for more than 2 phonon subspaces. Selected low-lying states and structure of wave functions are listed in the Table 7.7.

Authors of [263, 264] did not pretend to reproduce the experimental binding energy and therefore they set the energy of the lowest perturbed or correlated 0^+ state (the lowest 0^+ state obtained by the diagonalization of the whole Hamiltonian matrix in the Fig.7.61) as the reference level. Energies of all positive parity excited states (obtained by calculations involving unperturbed mean field states with 1- TDA phonons ((0+1)- configuration space), or with 1- and 2- TDA phonons ((0+1+2)- configuration space) are taken with respect to the energy of the perturbed ground state obtained with (0+1+2) configuration space. It should be realized that the lowest 0^+ state in the case of (0+1) configuration space calculation corresponds to the unperturbed particle-whole TDA ground state (it is a result of the fact that the HF (mean field) ground state does not mix with the 1p-1h block (or 1 TDA phonon block) states in the Hamiltonian matrix (see the Table 4.1 in the Section 4.2)). In the case of negative parity states, energies were related to the energy of the lowest 0^+ state obtained with the (0+1+2) configuration space (the same as for positive parity states) and, opposite to the positive parity case, the negative parity state calculations involved also the calculation with (1+2+3) configuration space.

From the left side of the Fig.7.62 one can see that the ground state correlations, obtained by the mixing of the unperturbed mean field ground state with the unperturbed 2- phonon states and represented in the Table 7.7 by the 19.86 % component in the perturbed ground state 0_1^+, lower the energy of the perturbed (correlated) (0+1+2) ground state by about 7 MeV. nevertheless, the calculated positive parity spectrum is in complete disagreement with the experimental one. The calculated 0_2^+ state in the (0+1+2)- calculation lies 22 MeV above the ground state 0_1^+, while the experimental 0_2^+ level is only at about 6 MeV. It is even worse situation than in the case of (0+1)-configuration space calculation where the 0_2^+ state lies only about 16.5 MeV above the corresponding (0+1) ground state. However, this is in accordance with the shell model calculation of Haxton et al. [40] which shows the essential role of the 4p-4h configurations. In the language of the EMPM this is equivalent to the inclusion of 4- TDA phonon subspace into the configuration

J^π	E	phonon content (%)			J^π	E	phonon content (%)		
	(MeV)	n=1	n=2	n=3		(MeV)	n=0	n=1	n=2
0_1^-	10.44	80.91	6.14	12.95	$0_{g.s.}^+$	0.00	79.58	0.56	19.86
0_2^-	12.27	80.43	6.77	12.80	0_2^+	21.70	0.86	67.30	31.84
0_3^-	20.70	77.28	7.00	15.72	0_3^+	23.21	5.07	13.40	81.53
1_1^-	8.47	78.36	8.11	13.53	1_1^+	24.19	0.00	0.25	99.75
1_2^-	12.33	80.11	6.91	12.98	1_2^+	24.73	0.00	0.17	99.83
1_3^-	16.38	78.56	8.15	13.29	1_3^+	24.87	0.00	0.48	99.52
2_1^-	8.51	79.27	8.31	12.42	2_1^+	21.13	0.00	10.57	89.43
2_2^-	10.09	81.74	6.40	11.86	2_2^+	22.65	0.00	2.02	97.98
2_3^-	13.18	77.06	8.45	14.49	2_2^+	23.85	0.00	2.53	97.47
3_1^-	5.10	80.37	5.95	13.68	3_1^+	23.62	0.00	2.65	97.35
3_2^-	10.35	81.79	6.12	12.09	3_2^+	24.86	0.00	4.03	95.97
3_3^-	12.87	78.82	7.85	13.33	3_3^+	25.22	0.00	0.81	99.19

Table 7.7: Energies and phonon structure of low-lying states in ^{16}O obtained by the EMPM calculations with (1+2+3) configuration space for negative parity states and with (0+1+2) configuration space for positive parity states - taken from [264]

space. That means one can believe that the inclusion of 4-phonon subspace would improve the situation and brings the calculated spectrum closer to the experimental one. The Table 7.7 shows that the (0+1+2) calculation gives for the ground state 0_1^+ the contribution of about 80 % of the unperturbed mean field ground state (TDA phonon vacuum) and about 20 % of the 2-TDA phonon admixtures. Results of no core shell model calculation in [42] performed in a complete configuration space up to 6 $\hbar\omega$ showed that the unperturbed particle-hole vacuum plus 2p-2h configuration account for 80 % of the perturbed ground state and the rest 20 % is connected with more complex configurations (4p-4h and higher). This support again the idea that the indirect coupling of the TDA phonon vacuum with 4 phonon configurations play an important role in the description of low-lying spectrum and it would be taken into account. However, because of computer memory space limitation, authors of [263, 264] were not able to do it.

In the case of negative parity states, a complete set of states up to three TDA phonons was included in [263, 264]. The dimension of the basis in M-scheme reached 25800. As it is apparent from the right panel of the Fig.62, the 2- and 3- phonon configurations push the energy of all states down about 2 MeV and 7 MeV, respectively. After inclusion of the 3- phonon states, a reasonable description of the experimental spectrum was achieved.

The effect of the inclusion of the multiphonon components in the E1

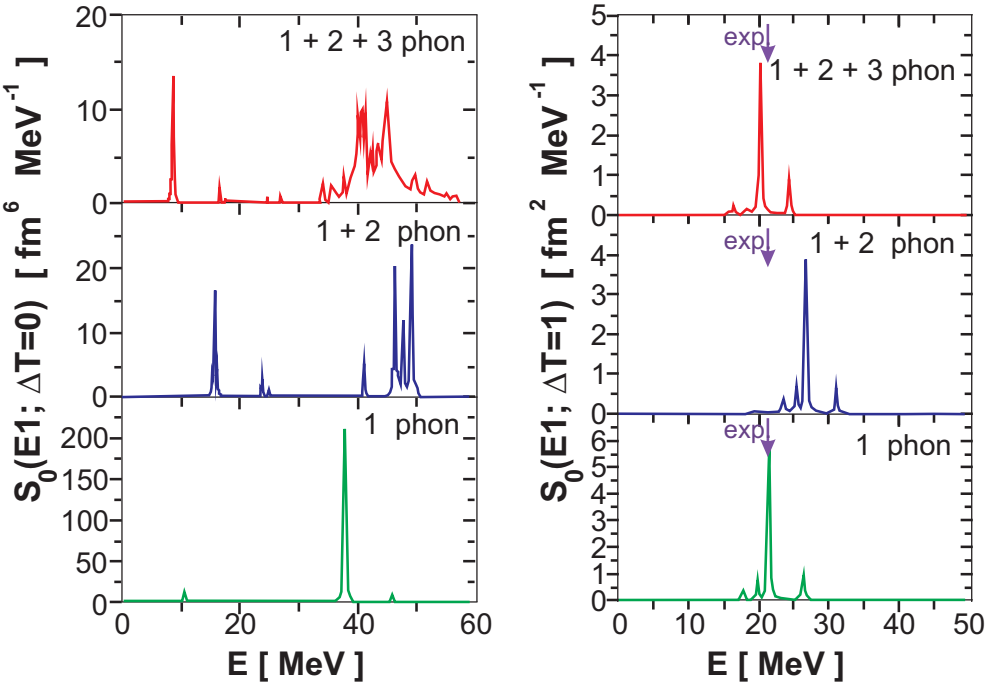


Figure 7.63: Isoscalar (left panel) and isovector (right panel) E1 strength function in ^{16}O calculated in the framework of the EMPM with 1- , (1+2)- and (1+2+3)- TDA phonon subspaces in the configuration space. Width of the averaging Lorentzian $\Delta = 0.5$ MeV - taken from [264].

isoscalar and isovector E1 resonance is shown in the Fig.7.63. In the left part of the Fig.7.63 the isoscalar E1 strength function (so called compression E1 strength function), generated by the transition operator $\hat{\mathscr{M}}'^{(com)}_{1\mu}(k=0)$ (see (7.402)) and summed over $\mu = 0, \pm 1$, is demonstrated. In the right part of the Fig.7.63 the isovector E1 strength function, generated by the transition operator $\hat{\mathscr{M}}^{(el)}_{1\mu}(eff)$ (see (O.38)), is shown. Arrows in the right panel denotes the position of the centroid of the experimental isovector GDR ($\approx$ 21 MeV). Similarly as in the case of the low-lying part of the ^{16}O spectrum in the Fig.7.62, the (1+2)- configuration space calculation provides the shift of the isovector E1 strength funcion to higher energies and the (1+2+3)- configuration space calculation bring it back to the position of 1- phonon configuration space calculation and closer to the experimental GMR centroid. The other effect of multi-phonon calculations is the higher fragmentation, as it can be seen especially in the isoscalar E1 strength function calculated with (1+2)- and (1+2+3)- phonon configuration space calculations.

Above discussed approaches (GCM, LSSM, EMPM) are not the only one methods going beyond the RPA. In last decade several other approaches appeared, some of them are more fundamental from the theoretical point of view. For instance, the relativistic quasiparticle time blocking approximation (RTBA), framed within a covariant energy density functional theory, couples two-quasiparticle states to collective vibrations [197, 270]. Two- particle-hole configurations are explicitly included in the self-consistent second RPA calculations, employing realistic interactions derived by means of the unitary correlation operator method (UCOM) [271] or Skyrme forces [272].

Though some of these methods are theoretically more fundamental than methods discussed above (e.g. no core approaches based on the gauge bare nucleon-nucleon interaction [249], or the meson-exchange nucleon-nucleon interaction covariant density-functional theory as [270]) above discussed beyond RPA methods are more physical transparent from the pedagogical reason. They provide also more direct comparison with experimental data because they are easier tractable numerically. However, we can believe that the rapid progress in the computer facilities enables to use in practice approaches emploing bare nucleon-nucleon interactions and simultaneously sophisticated many-body methods without any new adjusting parameters except those involved in the bare n-n interaction.

8. Rotation of nuclei

From discussions in previous chapters we know that in the case when nuclear mean field is deformed the rotational bands are recognized in the measurable spectrum of given nucleus. It was already mentioned also that the separation of degrees of freedom of nuclear motion to the intrinsic ones (single-particle and vibrational) and rotational ones is generally a complex problem because all these degrees of freedom are generally mixed in the nucleus laboratory frame wave functions. The problem is to define precisely the intrinsic (rotating with the nucleus) frame. Usually the coordinate axes of the intrinsic frame are identified with the principal axes of the tenzor of the quadrupole moment determined in the mean field ground state. However, as it was already pointed out in the Subsection 7.3.2.3 concerning the large scale shell model, the principal values of the quadrupole moment (and therefore an orientation of the intrinsic frame axes) depend on the excitation energy of excited states (sometimes this dependence is quite drastical even for low-lying excited states - see e.g. Fig.7.59). So to extract or to separate rotational degrees of freedom from the internal ones cannot be done generally exactly (especially for the nuclei which are soft with respect to deformation).

This problem of the extraction of nucleus rotation from other degrees of freedom can be done for well-deformed nuclei, with some degree of approximation, only in special cases: (i) when expected rotational frequency is much less than the frequency of other types of motion - so called slow rotation (see (7.3)) or (ii) on the contrary in the case when the rotational frequency is very high - so called fast rotation. Both these limits are discussed in following sections in more details.

8.1 Slow rotation

Many aspects of slow rotation were already discussed in the previous chapter. In the Section 7.1 it was shown that in the case of low rotational frequency rotational degrees of freedom are represented in the Hamiltonian by the rotor

term $\hat{H}_{rot}$ (7.7) and that the axially deformed nuclei Hamiltonian can be written as the sum of the intrinsic part $\hat{H}_{intr}$ and rotational part $\hat{H}_{rot}$ (see (7.4))

$$\hat{H} = \hat{H}_{intr} + \hat{H}_{rot} \tag{8.1}$$

where $\hat{H}_{rot}$ is given by (7.12). In the slow rotation limit and for low- energy states we can neglect the Coriolis term involved in the rotational Hamiltonian $\hat{H}_{rot}$ (see (7.12)) which mixes the internal degrees of freedom ξ with the rotational degrees of freedom represented by the Euler angles θ between external (laboratory) and internal (rotating with the nucleus) frame. So, in the slow rotations case the total Hamiltonian in the laboratory frame can be approximated by (7.17)

$$\hat{H} \approx \hat{H}_{intr} + \hat{H}_{pure\,rot} \quad , \quad \hat{H}_{pure\,rot} = \frac{\hbar^2}{2\mathscr{F}} \left[\hat{I}^2 - \hat{I}_3^2\right] \tag{8.2}$$

and the corresponding laboratory eigen-functions can be written as

$$\Psi_{IMK\rho}(\xi,\theta) = \langle \xi\theta \mid IMK\rho\rangle \approx D^I_{MK}(\theta)\, \psi_{K\rho}(\xi) \tag{8.3}$$

with (see (7.18) and (7.20))

$$\begin{aligned} &\hat{H}_{intr}\, \psi_{K\rho}(\xi) = E_{k\rho}\, \psi_{K\rho}(\xi) \\ &\hat{H}_{pure\,rot}\, D^I_{MK}(\theta) = \frac{\hbar^2}{2\mathscr{F}} \left[\, I(I+1) - K^2 \,\right] D^I_{MK}(\theta) \end{aligned} \tag{8.4}$$

In (8.1)-(8.4) $\hat{H}_{intr}$ stands for the intrinsic Hamiltonian expressed in the intrinsic variables ξ and consisting from the mean field and residual interactions (see(7.5)). It was shown (see (7.5)) that this division of the Hamiltonian into the intrinsic and rotational parts enabled to recognize the nucleus rotational motion in the nucleus spectrum (in the laboratory frame) in the form of rotational bands built on the intrinsic states (that means on the eigen-states of the intrinsic Hamiltonian $\hat{H}_{intr}$). The character of rotational bands (that means the type of the sequence of angular momenta of levels in the given rotational band) depends on the symmetry of the intrinsic Hamiltonian. For instance, the symmetrization of the laboratory wave function (7.27), which gave two type of rotational bands ($K = 0$ bands and $K \neq 0$ bands - see (7.34) and (7.35)), was determined by the $\mathscr{R}_i$- symmetry of the intrinsic Hamiltonian (invariance of $\hat{H}_{intr}$ with regard to rotations $\hat{\mathscr{R}}_i \equiv \hat{\mathscr{R}}_i(\pi)$ $(i = 1, 2, 3)$ by angle π round the i-th intrinsic frame axis - see (7.25)). This $\mathscr{R}_i$ - invariance of the intrinsic Hamiltonian occurs in the case of quadrupole deformation of

the nucleus (generally in the case when the nuclear shape is described by the Dirichlet expansion (7.48) in the intrinsic frame with the even multipolarities λ)). The big majority of deformed nuclei has in their ground states shapes corresponding to the quadrupole axial deformation ($\lambda\mu = 20$) with a small contribution of a hexadecapolar ($\lambda\mu = 40$) deformations (see the Fig.5.7) and therefore the sequence of levels in their rotational bands in the low- energy spectrum corresponds to the rule given by (7.34) and (7.35) (see the Fig.7.2 for a typical low-energy spectrum of R_i - symmetric deformed nucleus).There are strong experimental indications for an existence of small groups of nuclei with a stable octupole ($\lambda = 3$) deformation (see e.g. [273, 172]). Namely, the nuclei from the beginning of the actinide region (Th-Ra region) and some nuclei, in the less extend, from Ba-Nd region are candidates to be nuclei with stable octupole deformation [273]. The rotational bands of nuclei with the stable octupole deformation ($a_{30} \neq 0$) are characterized by the parity double structure (or close to parity doublet) structure as it will be discussed further.

In the next subsection the properties of the rotational bands in the $\mathscr{R}$-symmetric nuclei are summarized again and then the following subsection is devoted to the nuclei with stable octupole deformation.

8.1.1 Slow rotation of axially deformed $\mathscr{R}$-symmetric nuclei

In this subsection we suppose axial symmetric $\mathscr{R}_i(\pi)$- deformed nuclei. This case was already discussed in the Section 7.1 However, in order to understand the differences between the character of rotational spectrum of $\mathscr{R}_i(\pi)$- symmetric nucleus with the good parity (reflection symmetric nucleus) and of the reflection asymmetric nucleus, where $\mathscr{R}_i(\pi)$ and parity invariances of the intrinsic Hamiltonian are violated and which are discussed in the next subsection, we give below again the basic idea leading to the typical rotational band structure of the reflection symmetric nuclei.

In the case of $\mathscr{R}_i-$ and parity $\mathscr{P}$- symmetric nuclei the intrinsic Hamiltonian involves the mean field with the deformation of its equipotential surfaces corresponding to the Dirichlet decomposition (7.48) in the intrinsic frame with only even multipolarities λ. Then the intrinsic Hamiltonian is invariant with respect to the rotations by angle π round the intrinsic coordinate axes (principal axes of the intrinsic quadrupole tenzor) (see (7.25), (7.26))

$$\left[\hat{H}_{intr},\, \hat{\mathscr{R}}_i(\pi)\right] = 0 \quad , \quad i = 1,2,3 \tag{8.5}$$

We suppose also the invariance of the intrinsic Hamiltonian with respect to the time reversal transformation, $[\hat{H}_{intr},\, \hat{\mathscr{T}}] = 0$ where the phase convention corresponds to the time reversal operator in the form $\hat{\mathscr{T}} = \hat{\mathscr{R}}_2^{-1}(\pi)\mathscr{K}$ (see the Subsection 1.3.2). Since the nuclear shape is characterized by even multipolarities λ the parity is good quantum number for the eigen-states of the intrinsic Hamiltonian ($[\hat{H}_{intr}, \hat{\mathscr{P}}] = 0$ where $\hat{\mathscr{P}}$ is the parity operator in the intrinsic frame).

The next assumption is the axial symmetry of the intrinsic Hamiltonian, which ensures the zero value of the commutator $[\hat{H}_{inntr}, \hat{j}_3] = [\hat{H}_{inntr}, \hat{I}_3] = 0$. Therefore the angular momemtum projection K is good quantum number for the intrinsic wave function $\psi_{K\rho}(\xi)$ ($\hat{H}_{intr}\, \psi_{K\rho}(\xi) = E_{K\rho}\, \psi_{K\rho}(\xi)$, $\hat{j}_3\, \psi_{K\rho}(\xi) = K\, \psi_{K\rho}(\xi)$ - see (7.18)). This gives $[\hat{H}_{intr}, \hat{R}_3(\pi)] = 0$ and the only new information contained in (8.5) is the invariance of the intrinsic Hamiltonian $\hat{H}_{intr}$ with respect to $\hat{R}_1(\pi)$, $[\hat{H}_{intr}, \hat{\mathscr{R}}_1(\pi)] = 0$. This implicates the same intrinsic energy $E_{k\rho}$ for the states $\psi_{K\rho}(\xi)$ and $\hat{\mathscr{R}}_1(\pi)\psi_{K\rho}(\xi)$.

The $\mathscr{R}_1(\pi)$- symmetry of the intrinsic Hamiltonian should be taken into account also in the laboratory frame wave function $\Psi_{IMK\rho}(\xi, \theta)$ (see (8.3)).This leads to the properly normalized and symmetrized laboratory wave function

$\Psi_{IMK\rho}(\xi,\theta)$ in the following form (see (7.29)) $(K \geq 0)$ [1]

$$\Psi_{IMK\rho}(\xi,\theta) = \sqrt{\frac{2I+1}{16\pi}} \Big[D^I_{M\,K}(\theta)\, \psi_{K\rho}(\xi) + \\ + (-1)^I D^I_{M-K}(\theta)\, \hat{\mathscr{R}}_1(\pi)\, \psi_{K\rho}(\xi) \Big] \tag{8.6}$$

with the energies (7.31)

$$E_{IK\rho} = E_{K\rho} + \frac{\hbar^2}{2\mathscr{F}} \left[I(I+1) - K^2 \right] \tag{8.7}$$

demonstrating the rotational bands with $I(I+1)$- dependence built on each intrinsic state $\psi_{k\rho}(\xi)$ with the intrinsic energy $E_{K\rho}$. For the case $K=0$ the intrinsic states $\psi_{K=0\rho}(\xi)$ of even-even or odd-odd nucleus are simultaneously eigen- states of the operator $\hat{\mathscr{R}}_1(\pi)$ [2]

$$\hat{\mathscr{R}}_1(\pi)\, \psi_{K=0\,\rho}(\xi) = r_1^{(\rho)}\, \psi_{K=0\,\rho}(\xi) \quad , \quad r_1^{(\rho)} = \pm 1 \tag{8.8}$$

while this is not the case for $K \neq 0$ (for $K \neq 0$ the symmetry $[\hat{H}_{intr}, \hat{\mathscr{R}}_1(\pi)] = 0$ ensures only the same energy $E_{K\rho}$ for states $\psi_{K\rho}(\xi)$ and $\hat{\mathscr{R}}_1(\pi)\, \psi_{K\rho}(\xi)$).

[1] We can restrict ourselves to $K \geq 0$ because the wave function $\Psi_{IM-K\rho}(\xi,\theta)$ can be obtained from $\Psi_{IMK\rho}(\xi,\theta)$ by the action of the operator $\hat{\mathscr{R}}_1(\pi) = \hat{\mathscr{R}}_e(1)$, where the operator $\hat{\mathscr{R}}_e(1)$ is also the operator of the rotation round the 1-st intrinsic axis by angle π but performed in the external laboratory frame, that means acting on the Wigner D-functions,

$$\hat{\mathscr{R}}_e(1)\, \Psi_{IMK\rho}(\xi,\theta) = \sqrt{\frac{2I+1}{16\pi}} \Big[(-1)^I\, D^I_{M\,-K}(\theta)\, \psi_{K\rho}(\xi) + D^I_{M\,K}(\theta)\, \hat{\mathscr{R}}_1(\pi)\, \psi_{K\rho}(\xi) \Big] = \\ = (-1))^I \sqrt{\frac{2I+1}{16\pi}} \Big[D^I_{M\,-K}(\theta)\, \psi_{K\rho}(\xi) + (-1)^I D^I_{M\,K}(\theta)\, \hat{\mathscr{R}}_1(\pi)\, \psi_{K\rho}(\xi) \Big] = \\ \equiv (-1)^I \Psi_{IM-K\rho}(\xi,\theta)$$

[2] In the case of the $\mathscr{R}_i(\pi)$- symmetry of the intrinsic Hamiltonian it is convenient to choose the phase convention for wave functions so that the time reversal operator is $\hat{\mathscr{T}} = \hat{R}_2^{-1}(\pi)\mathscr{K}$ (see (1.48)). Since $\hat{\mathscr{R}}_1(\pi)\hat{\mathscr{R}}_2(\pi)\hat{\mathscr{R}}_3(\pi) = 1$ the action of the operator $\hat{\mathscr{R}}_1(\pi)$ on the intrinsic wave function with the zero projection can be written as follows

$$\hat{\mathscr{R}}_1(\pi)\, \psi_{K=0\,\rho}(\xi) = \hat{\mathscr{R}}_3^{-1}(\pi)\hat{\mathscr{R}}_2^{-1}(\pi)\, \psi_{K=0\,\rho}(\xi) = \hat{\mathscr{R}}_3^{-1}(\pi)\, \hat{\mathscr{T}}\mathscr{K}\, \psi_{K=0\,\rho}(\xi) = \\ = \hat{\mathscr{R}}_3^{-1}(\pi)\, \hat{\mathscr{T}}\, \psi^*_{K=0\,\rho}(\xi) = e^{-i\pi\hat{j}_3} \hat{\mathscr{T}}\, \psi^*_{K=0\,\rho}(\xi) = \boxed{\begin{array}{c}\text{because} \\ \hat{j}_3\, \psi_{K=0\,\rho}(\xi) = 0\end{array}} = \\ = \hat{\mathscr{T}}\, \psi^*_{K=0\,\rho}(\xi)$$

So in the case of the zero ang. momentum projection intrinsic wave function, $\psi_{K=0\,\rho}(\xi)$, the action of the operator $\hat{\mathscr{R}}_1(\pi)$ on $\psi_{K=0\,\rho}(\xi)$ is the same as the action of the time-reversal operator $\hat{\mathscr{T}}$ on $\psi^*_{K=0\,\rho}(\xi)$. It is known (see e.g. [99] for details) that the phase of wave functions corresponding to $\hat{\mathscr{T}} = \hat{\mathscr{R}}_2^{-1}(\pi)\mathscr{K}$ ensures the wave functions $\psi_{K=0\,\rho}(\xi)$ to be simultaneously eigen-functions of the time-reversal operator $\hat{\mathscr{T}}$ with the eigen values ± 1. Therefore the intrinsic wave functions $\psi_{K=0\,\rho}(\xi)$ are simultaneously eigen-functions of the operator $\hat{\mathscr{R}}_1(\pi)$ with the same eigen-values $r_1^{(\rho)} = \pm 1$.

This different behaviour of the intrinsic wave function $\psi_{K\rho}(\xi)$ with respect to $\hat{\mathscr{R}}_1(\pi)$ transformation for $K=0$ and $K\neq 0$ causes the different sequences of angular momenta of rotational band levels for rotational bands built on the intrinsic states with $K=0$ and $K\neq 0$.

For $K=0$ band the substitution of (8.8) into (8.6) gives

$$\Psi_{IMK=0\rho}(\xi,\theta)\,\sqrt{\frac{2I+1}{16\pi^2(1+\delta_{k0})}}\,D^I_{MK=0}(\theta)\left(1+(-1)^I\,r_1^{(\rho)}\right)\psi_{K=0\rho}(\xi) \quad (8.9)$$

which is nonzero only in the following cases

$$\begin{aligned} &\text{for } r_1^{(\rho)}=+1 \qquad \text{if } I=0,\,2,\,4,\,6,\,8,\cdots \\ &\text{for } r_1^{(\rho)}=-1 \qquad \text{if } I=1,\,3,\,5,\,7,\,9,\cdots \end{aligned} \quad (8.10)$$

So, for $K=0$ and given ρ we have generally two different rotational bands (one with even values of I and the other with odd values of I).

For $K\neq 0$ there is no any restriction for I and the corresponding rotational band built on intrinsic state $\psi_{K\rho}(\xi)$ $(K\neq 0)$, has standard sequence of levels with all angular momenta $I\geq |K|$ (see (7.35).

The other typical property of the rotational bands in the slow- rotation limit is a strong E2- intraband transitions, much stroger than extra-band transitions. As it was shown in the Section 7.1 (see the text between expressions (7.42) and the end of the Section 7.1), the reduced probabilities of $E\lambda$ intra-band transitions are given by (7.43)

$$B(E\lambda;\,I_iK\rho\to I_fK\rho)\approx\left(C^{I_fK}_{I_iK\lambda 0}\right)^2\left|\langle K\rho|\,\hat{\mathscr{M}}^{(E)\,(\theta)}_{\lambda 0}\,|K\rho\rangle\right|^2 \quad (8.11)$$

for even values of λ (for λ odd the intrinsic diagonal matrix elements $\langle K\rho|\hat{\mathscr{M}}^{(E)\,(\theta)}_{\lambda\mu}|K\rho\rangle=0$ because $\hat{\mathscr{P}}\hat{\mathscr{M}}^{(E)\,(\theta)}_{\lambda\mu}\hat{\mathscr{P}}^{-1}=(-1)^\lambda\hat{\mathscr{M}}^{(E)\,(\theta)}_{\lambda\mu}$ and $\hat{\mathscr{P}}\psi_{K\rho}(\xi)=\pm\,\psi_{K\rho}(\xi)$). The intra-band E2 transition probabilities are therefore much bigger in the comparison with the extra- band transition probabilities $B(E\lambda;I_iK_i\rho_i\to I_fK_f\rho_f)$ $(I_iK_i\rho_i\neq I_fK_f\rho_f)$ which depends on the square of the nondiagonal intrinsic matrix elements $\langle K_f\rho_f|\,\hat{\mathscr{M}}^{(E)\,(\theta)}_{\lambda\mu}\,|K_i\rho_i\rangle$ which are much less than the diagonal ones. One should have in mind that in the case of the slow- rotation regime the intrinsic matrix elements $\langle K\rho|\,\hat{\mathscr{M}}^{(E)\,(\theta)}_{\lambda 0}\,|K\rho\rangle$ do not depend on I and therefore are the same for all levels of the given roational band built on the intrinsic state $\psi_{K\rho}(\xi)$.

The most of deformed nuclei have axial $\mathscr{R}$-symmetry with rotational bands characterized by the sequence of levels given by (7.34) (or (8.10) and (7.35)

which corresponds to the stable quadrupole deformation a_{20} in their ground states (with small contribution of a_{40}). However, there are some indication of an existence of a small group of nuclei with the stable octupole deformation a_{30} in their ground state. The nonzero value of a_{30} changes the character of the nucleus spectrum and this is a subject of our discussion in the next subsection.

8.1.2 Slow rotation of axially deformed $\mathscr{S}$-symmetric (reflection asymmetric) nuclei

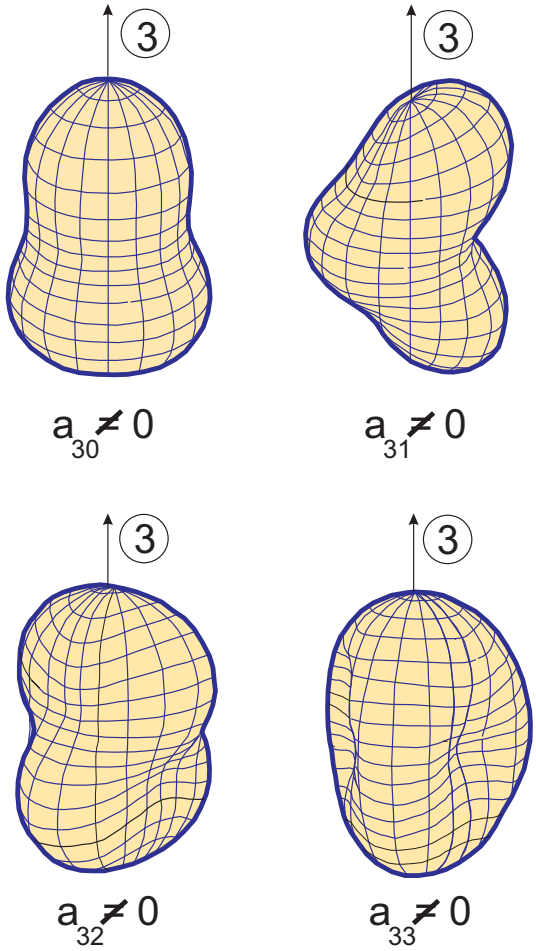


Figure 8.1: Quadrupole-octupole shapes represented by Dirichlet multipole expansion, $R(\vartheta,\phi) = R_0\left[1+\sum_{\lambda=2,3}\sum_{\mu=-\lambda}^{+\lambda} a_{\lambda\mu}\, Y_{\lambda\mu}(\vartheta,\phi)\right]$ with only $\mu = 0$ qudrupole term involved ($a_{20} = 0.6$), and all other $a_{2\mu} = 0$. Each shape, shown in the figure, corresponds to octupole $\lambda = 3$ term with one projection $\mu \geq 0$ ($a_{3-\mu} = (-1)^\mu a_{3\mu} = 0.175$). Arrows denote the orientation of the 3-d intrinsic frame axis (taken from [273]).

The shape of the intrinsic mean field equipotential surfaces of reflection asymmetric nuclei is characterized by the Dirichlet decomposition (1.3) in the intrisic frame, rotating with the nucleus, involving at least one odd-multipolarity (λ odd) deformation parameter. For the simplicity we consider here only one quadrupole and one octupole axially symmetric terms,

$$R(\vartheta,\phi) = R_0\left[1+\sum_{\lambda=2,3} a_{\lambda 0}\, Y_{\lambda\mu=0}(\vartheta,\phi)\right] \tag{8.12}$$

Because of the presence of the $\lambda = 3$ term the expr. (8.12) represents

the pear shape with the 3-d intrinsic frame axis being the symmetric axis (see the Fig.8.1). Here it is necessary to note that the nonzero values of different octupole deformation parameters (not only a_{30}) means the reflection asymmetric shapes with regard to different intrinsic planes as it can be seen from the Fig.8.1. However, further we restrict ourselves to only axially symmetric shapes with only $a_{20} \neq 0$ and $a_{30} \neq 0$. So the $\mathscr{R}$- and $\mathscr{P}$-symmetry is violated but the symmetry with regard to the combine transormations $\hat{\mathscr{S}}_i \equiv \hat{\mathscr{P}}\,\hat{\mathscr{R}}_i^{-1}(\pi)$ $(i = 1, 2)$ remains (axially symmetric pear shape - the left upper corner of the Fig.8.1). This shape corresponds to the following symmetries of the intrinsic Hamiltonian

$$\left[\hat{H}_{intr},\, \hat{\mathscr{R}}_i(\pi)\right] \neq 0 \quad (i = 1, 2) \quad , \qquad \left[\hat{H}_{intr},\, \hat{\mathscr{P}}\right] \neq 0$$
$$\left[\hat{H}_{intr},\, \hat{\mathscr{S}}_i(\pi)\right] = 0 \quad (i = 1, 2) \tag{8.13}$$

and the nucleus with this shape is reflection asymmetric with regards to the plane in the intrinsic frame determined by the 1-st and 2-d axes, $[\hat{H}_{intr}, \hat{\mathscr{S}}_3] \neq 0$. Our further assumption is the time-reversal invariance of the intrinsic Hamiltonian, $[\hat{H}_{intr}, \hat{\mathscr{T}}] = 0$. In the case of the $\mathscr{S}$- symmetric shape (8.12) it is more convenient to choose wave function phase convention not according (1.48) but as

$$\hat{\mathscr{T}} = \hat{\mathscr{S}}_2^{-1}\hat{\mathscr{K}} \tag{8.14}$$

That means the only relevant new information going from the last symmetry condition in (8.13) is

$$\left[\hat{H}_{intr},\, \hat{\mathscr{S}}_1(\pi)\right] = 0 \quad , \quad \hat{\mathscr{S}}_1 = \hat{\mathscr{P}}\,\hat{R}_1^{-1}(\pi) \tag{8.15}$$

because the symmetry of $\hat{H}_{intr}$ with regard to $\mathscr{S}_2$ is, within the phase convention (8.14), equivalent to the time reversal invariance of the intrinsic Hamiltonian, $[\hat{H}_{intr}, \hat{\mathscr{T}}] = 0$. Using (8.15) the parity operator $\hat{\mathscr{P}}$ can be expressed as

$$\hat{\mathscr{P}} = \hat{\mathscr{S}}_1\,\hat{\mathscr{R}}_1(\pi) = \hat{\mathscr{S}}_1\,\hat{\mathscr{R}}_e(1) \tag{8.16}$$

where $\hat{\mathscr{R}}_1(\pi) = e^{-i\pi\hat{j}_1}$ is the operator of the rotation by an angle π round the first intrinsic axis acting in the intrinsic rotating frame system. The $\hat{\mathscr{R}}_e(1)$ is the same turn operator but acting in the external laboratory frame. So in the action of the parity operator $\hat{\mathscr{P}}$ on the laboratory frame wave function the operator $\hat{\mathscr{S}}_1$ acts on the intrinsic wave function $\psi_{K\rho}(\xi)$ while the operator $\hat{\mathscr{R}}_e(1)$ acts on the rotational part of the wave function (that

means on the Wigner D- function (see (7.28))). So the properly symmetrized and normalized laboratory wave functions $\Psi_{\pi IMK\rho}(\xi,\theta)$ is $(K \geq 0)$ [3]

$$\Psi_{\pi IMK\rho}(\xi,\theta) = \sqrt{\frac{2I+1}{16\pi}}\,\Big[D^I_{M\,K}(\theta)\,\psi_{K\rho}(\xi) + \\ + \pi\,(-1)^I D^I_{M-K}(\theta)\,\hat{\mathscr{S}}_1\,\psi_{K\rho}(\xi)\Big] \tag{8.17}$$

with

$$\begin{aligned}
&\hat{\mathscr{P}}\,\Psi_{\pi IMK\rho}(\xi,\theta) = \pi\,\Psi_{\pi IMK\rho}(\xi,\theta)\\
&\hat{I}^2\,\Psi_{\pi IMK\rho}(\xi,\theta) = I(I+1)\,\Psi_{\pi IMK\rho}(\xi,\theta)\\
&\hat{I}_z\,\Psi_{\pi IMK\rho}(\xi,\theta) = M\,\Psi_{\pi IMK\rho}(\xi,\theta)\\
&\hat{I}_3\,\Psi_{\pi IMK\rho}(\xi,\theta) = K\,\Psi_{\pi IMK\rho}(\xi,\theta)
\end{aligned} \tag{8.18}$$

where $\pi = \pm 1$ is the parity of given state in the laboratory frame (because of (8.13) parity of intrinsic sates is violated and we can speak about the sharp parity only in the laboratory Hilbert space). We can check back if the first equation in (8.18) is fulfilled:

$$\begin{aligned}
\hat{\mathscr{P}}\,\Psi_{\pi IMK\rho}(\xi,\theta) &= \hat{\mathscr{S}}_1\,\hat{\mathscr{R}}_e(1)\,\sqrt{\frac{2I+1}{16\pi}}\,\Big[D^I_{M\,K}(\theta)\,\psi_{K\rho}(\xi) + \\
&\qquad + \pi\,(-1)^I D^I_{M-K}(\theta)\,\hat{\mathscr{S}}_1\,\psi_{K\rho}(\xi)\Big] = \\
&= \hat{\mathscr{S}}_1\,\sqrt{\frac{2I+1}{16\pi}}\,\Big[(-1)^I\,D^I_{M\,-K}(\theta)\,\psi_{K\rho}(\xi) + \\
&\qquad + \pi\,D^I_{MK}(\theta)\,\hat{\mathscr{S}}_1\,\psi_{K\rho}(\xi)\Big] = \\
&= \pi\,\Psi_{\pi IMK\rho}(\xi,\theta)
\end{aligned} \tag{8.19}$$

If we neglect Coriolis and centrifugal parts of the rotor Hamiltonian and the rotor Hamiltonian is approximated by the pure-rotor term then the laboratory frame energy corresponding to the wave function (8.17) is again given

[3] We can restrict ourselves only to $K \geq 0$ because the states with the negative $-K$ can be obtained from $\Psi_{\pi IMK\rho}(\xi,\theta)$ by the rotation $\hat{R}_e(1)$:

$$\begin{aligned}
\hat{\mathscr{R}}_e(1)\,\Psi_{\pi IMK\rho}(\xi,\theta) &= \sqrt{\frac{2I+1}{16\pi}}\,\Big[(-1)^I\,D^I_{M\,-K}(\theta)\,\psi_{K\rho}(\xi) + \pi D^I_{M\,K}(\theta)\,\hat{\mathscr{S}}_1\,\psi_{K\rho}(\xi)\Big] = \\
&= (-1)^I\,\sqrt{\frac{2I+1}{16\pi}}\,\Big[D^I_{M\,-K}(\theta)\,\psi_{K\rho}(\xi) + \pi\,(-1)^I D^I_{M\,K}(\theta)\,\hat{\mathscr{S}}_1\,\psi_{K\rho}(\xi)\Big] = \\
&\equiv (-1)^I \Psi_{\pi IM-K\rho}(\xi,\theta)
\end{aligned}$$

and has the same energy as the state $\Psi_{\pi IMK\rho}(\xi,\theta)$.

by (8.7)

$$E_{IK\rho} = E_{K\rho} + \frac{\hbar^2}{2\mathscr{F}}\left[I(I+1) - K^2\right] \tag{8.20}$$

and is degenerated with regards to $\pi = \pm 1$ for each level with given I and K and ρ if $K \neq 0$. So for reflection asymmetric (or $\mathscr{S}$-symmetric) axial nuclei we obtain two bands, same in the energy levels, with the standard $I(I+1)$-dependence on I ($I \geq K$), one for positive parity $\pi = +1$ described by wave functions $\Psi_{\pi=+1\, IMK\rho}(\xi,\theta)$ and other for negative parity $\pi = -1$ described by the wave functions $\Psi_{\pi=-1\, IMK\rho}(\xi,\theta)$.

Similarly as in the case of $\mathscr{R}_i(\pi)$- axial symmetric nuclei also for $\mathscr{S}_{i=1,2}$-axial symmetric nuclei the character of rotational bands built on the intrinsic states with the zero angular momentum projection, $\psi_{K=0\,\rho}(\xi)$, are different than rotational bands built on the intrinsic states $\psi_{K\neq 0\,\rho}(\xi)$. In the case of $\mathscr{S}_{i=1,2}$ symmetry of the $\mathscr{T}$-symmetric intrinsic Hamiltonian we can choose the phase convention of wave functions so that the time reversal operator is (8.14) ($\hat{\mathscr{T}}\hat{H}_{intr}\hat{\mathscr{T}}^{-1} = \hat{H}_{intr}$). Then the intrinsic eigen-states $\psi_{K=0\,\rho}(\xi)$ with the zero projection K are simultaneously eigen-states of the operator $\hat{\mathscr{S}}_1$ [4]

$$\hat{\mathscr{S}}_1\, \psi_{K=0\,\rho}(\xi) = s_1^{(\rho)}\, \psi_{K=0\,\rho}(\xi) \quad , \quad s_1^{(\rho)} = \pm 1 \tag{8.21}$$

The substitution of (8.21) into (8.17) gives

$$\Psi_{\pi\, IM\, K=0\,\rho}(\xi,\theta) = \sqrt{\frac{2I+1}{16\pi}}\; D^I_{M\,K=0}(\theta)\left[1 + \pi(-1)^I\, s_1^{(\rho)}\right]\psi_{K=0\,\rho}(\xi) \tag{8.22}$$

So the laboratory wave function $\Psi_{\pi\, IM\, K=0\,\rho}(\xi,\theta)$ is nonzero only when

$$\pi\,(-1)^I\, s_1^{(\rho)} = 1 \tag{8.23}$$

[4] In the case of the $\mathscr{S}_i$ ($i = 1, 2$) symmetry of the intrinsic Hamiltonian we always can choose the time-reversal operator in the form of (8.14). This, together with the identity $\hat{\mathscr{S}}_1\hat{\mathscr{S}}_2\hat{\mathscr{S}}_3 = \hat{\mathscr{P}}$, causes that the action of the operator $\hat{\mathscr{S}}_1$ on the $\psi_{K=0\,\rho}(\xi)$ is following

$$\hat{\mathscr{S}}_1\, \psi_{K=0\,\rho}(\xi) = \hat{\mathscr{P}}\hat{\mathscr{S}}_3^{-1}\hat{\mathscr{S}}_2^{-1}\, \psi_{K=0\,\rho}(\xi) = \hat{\mathscr{P}}\hat{\mathscr{S}}_3^{-1}\hat{\mathscr{T}}\mathscr{K}\, \psi_{K=0\,\rho}(\xi) = \hat{\mathscr{P}}\hat{\mathscr{S}}_3^{-1}\hat{\mathscr{T}}\, \psi^*_{K=0\,\rho}(\xi) =$$

$$= \boxed{\begin{array}{c}\text{because}\\ \hat{\mathscr{S}}_3 = \hat{\mathscr{P}}\hat{\mathscr{R}}_3^{-1}(\pi)\end{array}} = \hat{\mathscr{P}}^{\,2}\,\hat{\mathscr{R}}_3^{-1}(\pi)\hat{\mathscr{T}}\, \psi^*_{K=0\,\rho}(\xi) = \boxed{\begin{array}{c}\text{because}\\ \hat{j}_3\, \psi^*_{K=0\,\rho}(\xi) = 0\end{array}} = \hat{\mathscr{T}}\, \psi^*_{K=0\,\rho}(\xi)$$

So the action of the operator $\hat{\mathscr{S}}_1$ on $\psi_{K=0\,\rho}(\xi)$ is the same as the action of the time reversal operator $\hat{\mathscr{T}}$ on $\psi^*_{K=0\,\rho}(\xi)$. It is known that in the case of $\hat{\mathscr{T}}$- symmetric Hamiltonian the eigen-states $\psi_{K=0\,\rho}(\xi)$ with the zero ang. momentum projection $K = 0$ are simultaneously eigen-states of the time reversal operator with the eigen-values ± 1 (see [99]). Therefore from the expression above it follows that the phase convention (8.14) ensures that the intrinsic Hamiltonian eigen-states $\psi_{K=0\,\rho}(\xi)$ are simultaneously eigen-states of $\hat{\mathscr{S}}_1$ with the eigen-values $s_1^{(\rho)} = \pm 1$.

which gives for $K = 0$ and for given ρ two rotational bands (one for $s_1^{(\rho)} = +1$ and the other for $s_1^{(\rho)} = -1$):

$$
\begin{aligned}
& s_1^{(\rho)} = +1 \quad \begin{cases} \pi = +1 \text{ with } \; I = 0^+,\, 2^+,\, 4^+, \cdots & , \\ \pi = -1 \text{ with } \; I = 1^-,\, 3^-,\, 5^-, \cdots & . \end{cases} \\
& \text{and} \\
& s_1^{(\rho)} = -1 \quad \begin{cases} \pi = +1 \text{ with } \; I = 1^+,\, 3^+,\, 5^+, \cdots & , \\ \pi = -1 \text{ with } \; I = 0^-,\, 2^-,\, 4^-, \cdots & . \end{cases}
\end{aligned}
\tag{8.24}
$$

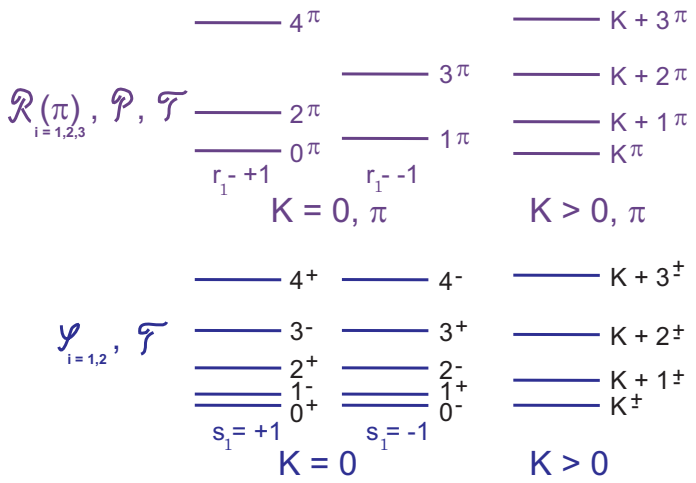


Figure 8.2: Schematic figure of rotational bands of axially deformed nuclei with the $\mathscr{R}_i(\pi)$-, $\mathscr{P}$-, $\mathscr{T}$- symmetric intrinsic Hamiltonian (upper panel) and with the $\mathscr{S}_{I=1,2}$ -, $\mathscr{T}$ - symmetric intrinsic Hamiltonian (lower panel). The intrinsic states in the case $\mathscr{R}_i(\pi)$ -, $\mathscr{T}$ - symmetry have sharp values of parity and therefore all levels in the band built on the given intrinsic states have the same parity (upper panel). The spectrum of $\mathscr{S}_i(\pi)$-, $\mathscr{T}$- symmetric nuclei has a parity doublet character (lower panel).

That means the energy spectrum of the axially deformed nucleus with the intrinsic $\mathscr{T}$- symmetric Hamiltonian violating the $\mathscr{P}$- and $\mathscr{R}_i(\pi)$- symmetry, but keeping the invariance with regard to $\hat{\mathscr{S}}_{i=1,2} = \hat{\mathscr{P}}\hat{\mathscr{R}}^{-1}_{i=1,2}(\pi)$ transformations, has totally doublet character for both $K = 0$ and $K \neq 0$ cases, as it is seen also in the lower panel of the Fig.8.2.

The schematic comparison of the spectrum of the axially deformed nucleus with the $\mathscr{T}$-, $\mathscr{R}_{i=1,2,3}(\pi)$-, and $\mathscr{P}$- symmetric intrinsic Hamiltonian (upper panel) with the spectrum of the axially deformed nucleus with $\mathscr{T}$- symmetric intrinsic Hamiltonian violating $\mathscr{P}$- and $\mathscr{R}_i(\pi)$- symmetries but keeping the invariance with regards to $\hat{\mathscr{S}}_i = \hat{\mathscr{P}}\hat{\mathscr{R}}^{-1}_i(\pi)$ $(i = 1, 2)$ reflection transformations (lower panel) is shown in the Fig.8.2. The lower panel with the doublet character spectrum takes place precisely when the deformation of the nucleus

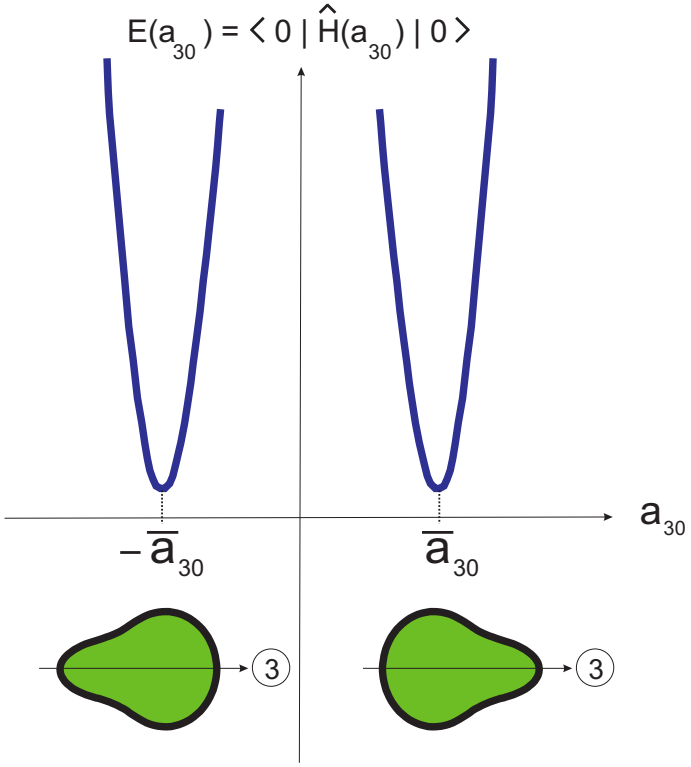


Figure 8.3: Schematic figure of the dependence of the total energy in the ground state of the axial reflection asymmetric nucleus ($a_{30} \neq 0$) on the octupole deformation a_{30}. Equilibrium deformations ($a_{30} = \bar{a}_{30}$ and $a_{30} = -\bar{a}_{30}$) corresponds to two energy minima separated by the infinite barrier which are connected with two reflection positions of the pear-shaped nucleus in the intrinsic frame.

is characterized by an odd- values of λ with $\mu = 0$ in the Dirichlet decomposition, e.g. if deformation with $\lambda = 3$ and $\mu = 0$ is involved in (8.12), and when the energy surface dependence on a_{30} (that means $E(a_{30}) = \langle 0|\hat{H}_{intr}(a_{30})|0\rangle$) has a form of two infinite wells separated by the infinite barrier as is depicted in the Fig.8.3 (one well corresponds to $a_{30} > 0$ and the second one to $a_{30} < 0$) . Then there is no any energy shift between doublet partners caused by the tunnel transition through the barrier.

However one should realize that the dependence of the total energy $E(a_{30})$, as it is shown in the Fig.8.3, is a very special case. Usually the presence in the nucleus Hamiltonian of other degrees of freedom than that connected with a_{30} leads to the decreasing the barrier between two minima at $a_{30} = \pm\bar{a}_{30}$ from the infinite value to the finite one. As a result the tunneling effect occurs and the intrinsic state with $a_{30} = \bar{a}_{30}$ can pass to the intrinsic state with $a_{30} = -\bar{a}_{30}$ and vice versa. This leads to the violation of the mentioned above degeneracy of the laboratory spectrum and the states with negative

parity are shifted in energy with respect to the laboratory states with the positive parity. The violation of the parity degeneracy occurs also in the case when the minima $E(\bar{a}_{30})$ and $E(-\bar{a}_{30})$ have different values as it will be discussed later.

When the intrinsic states $\psi_\rho(\xi) = \langle \xi|\rho\rangle$ are not eigen-states of the parity operator (that means $[\hat{H}_{intr},\ \hat{\mathscr{P}}] \neq 0$) then we cannot use (2.194) and we have nonzero values of the intrinsic electric dipole moments (see (2.194))

$$\langle \rho|\ \hat{\vec{d}}\ |\ \rho\rangle \neq 0 \quad \text{or (see (2.197))} \quad \langle \rho|\ \hat{\mathscr{M}}^{(el)\,(\theta)}_{1\mu}\ |\ \rho\rangle \neq 0 \tag{8.25}$$

If moreover we have axial symmetry with respect to the 3-d intrinsic axis and the angular momentum projection K is a good quantum number then

$$\langle K\rho|\ \hat{\mathscr{M}}^{(el)\,(\theta)}_{10}\ |K\rho\rangle \neq 0 \quad \text{and} \quad \langle K\rho|\ \hat{M}^{(el)\,(\theta)}_{1\,\mu=\pm1}\ |\ K\rho\rangle = 0 \tag{8.26}$$

Then the reduced electric transition probabilities, defined by (7.36) for $X = el$, between the laboratory frame wave functions $\Psi_{\pi IMK\rho}(\xi,\theta) = \langle \xi\theta|\pi IMK\rho\rangle$ (see (8.16)) are (analogy with (7.42))

$$\begin{aligned} &B(E\lambda;\ \pi_i I_i K_i \rho_i \to \pi_f I_f K_f \rho_f) = \\ &= \Big|\ C^{I_f K_f}_{I_i K_i \lambda\ K_f - K_i}\ \langle K_f\rho_f|\ \hat{\mathscr{M}}^{(el)\,(\theta)}_{\lambda\nu=K_f-K_i}\ |\ K_i\rho_i\rangle + \\ &\qquad +(-1)^{I_i}\ \pi_i\ C^{I_f K_f}_{I_i K_i \lambda\ K_f + K_i}\ \langle K_f\rho_f|\hat{\mathscr{M}}^{(el)\,(\theta)}_{\lambda\nu=K_f+K_i}\ \hat{\mathscr{S}}_1\ |\ K_i\rho_i\rangle\ \Big|^2 \end{aligned} \tag{8.27}$$

For intraband transitions ($\rho K \equiv \rho_i K_i = \rho_f K_f$ ($K_i > 0$) or $s_1\rho K \equiv s_1^{(\rho_i)}\rho_i K_i = s_1^{(\rho_f)}\rho_f K_f$ ($K_i = 0$)) the expression (8.27) gives

$$B(E\lambda;\ \pi_i I_i K\rho \to \pi_f I_f K\rho) = \Big(\ C^{I_f K}_{I_i K \lambda 0}\Big)^2\ \Big|\langle K\rho|\ \hat{\mathscr{M}}^{(el)\,(\theta)}_{\lambda 0}\ |\ K\rho\rangle\ \Big|^2 \tag{8.28}$$

where opposite to (8.11) for $\mathscr{R}$-symmetric axial nuclei, where only even values of λ were possible, now for $\mathscr{S}$-symmetric nuclei both even and odd values of λ are allowed (there is no any parity selection rule which gives some restriction for $\langle K\rho|\ \hat{\mathscr{M}}^{(el)\,(\theta)}_{\lambda 0}\ |\ K\rho\rangle$ as was the case for R- symmetric axial nuclei). For instance, if the nucleus has a_{30} deformation there are strong intraband E1 transitions which are excluded for $\mathscr{R}$-symmetric nuclei.

The mechanism responsible for the appearance of the static deformation is connected with the Jahn-Teller effect [274] when the stable deformation of given multipolarity appears as a result of strong instability with respect to

the shape vibration of the same multipolarity. Particularly a stable reflection-asymmetric deformation of the nucleus mean field in the intrinsic body-fixed frame can be attributed to a parity breaking odd-multipolarity interaction. For instance, in the deformed even-even nuclei from the beginning of the actinide region (Th-Pa region) the lowest states are collective octupole vibration states which is a result of the strong octupole character interaction between s.p. states near the Fermi level. In some nuclei from this region this octupole interaction can be so strong that corresponding mean field can obtain a nonzero $\lambda\mu = 30$ deformation (besides the standard quadrupole $\lambda\mu = 20$ deformation) [273, 172]. Then the structure of rotational bands should have a character close to parity-doublet character described in (8.20) and (8.24) (see also the Fig.8.2).

We will demonstrate the mechanism of the formation of the stable octupole deformation in the simple model with the Hamiltonian involving the separable multipole-multipole residual interaction and monopole pairing (see e.g. [273])

$$\hat{H} = \sum_{j} e_j \, c_j^+ \, c_j - \frac{1}{2} \sum_{\lambda=2,3} \kappa_\lambda \sum_{\mu=-\lambda}^{\lambda} \hat{Z}_{\lambda\mu}^+ \, \hat{Z}_{\lambda\mu} + \hat{H}_{pair} \tag{8.29}$$

with

$$\hat{Z}_{\lambda\mu}^+ = \sum_{jj'} \langle j | \, f_\lambda(r) \, Y_{\lambda\mu}(\hat{r}) \, | \, j' \rangle \, c_j^+ \, c_{j'} \tag{8.30}$$

where $f_\lambda(r)$ is the radial form factor (given e.g. by the derivative of the average potential [99]). A coupling between single-particle states of opposite parity is produced by the octupole-octupole ($\lambda = 3$) residual interaction in (8.29). The excitation energies E_{oct} of octupole vibration states generating by the octupole-octupole interaction in (8.29) can be computed by means of the RPA. They are solutions of the dispersion equation (see e.g. [9, 11, 7]) [5]

$$\sum_{jj'} \frac{\left| \langle j || \hat{Z}_3 || j' \rangle \right|^2 (\mathscr{U}_j \mathscr{V}_{j'} + \mathscr{U}_{j'} \mathscr{V}_j)^2 \, (E_j + E_{j'})}{(E_j + E_{j'})^2 - E_{oct}^2} = \frac{7}{\kappa_3} \tag{8.31}$$

where $E_j = \sqrt{(e_j - \lambda)^2 + \Delta^2}$ are quasiparticle BCS energies and $\mathscr{U}_j$ and $\mathscr{V}_j$ are usual BCS occupation amplitudes (see 6.64).

[5] For general separable residual interaction involved in the Hamiltonian (M.1) the RPA approach is formulated in the Appendix M. Corresponding dispersion equation determining the excitation energies $\hbar\omega_\nu$ is (M.24) for the case of many separable terms in the Hamiltonian (M.1). The Hamiltonian (8.29) for negative parity excitation involves only octupole-octupole $\lambda = 3$ term and this corresponds to the Hamiltonian (M.1) with only one term. Then the dispersion equation (M.24) reduces to (8.31).

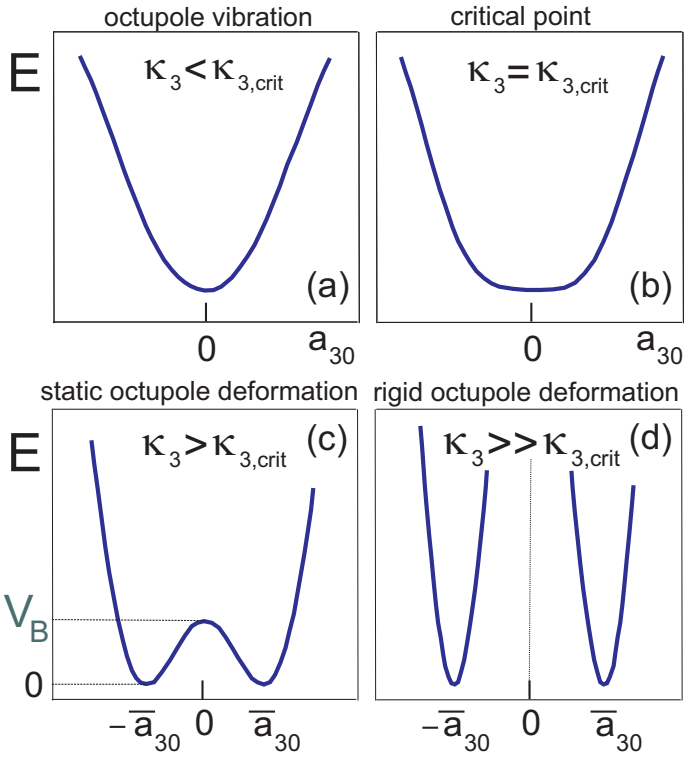


Figure 8.4: The total nucleus energy as a function of the octupole deformation a_{30} for different values of the octupole coupling constant κ_3 in the Hamiltonian (8.29). Small values of κ_3 corresponds to the octupole vibrational limit when the nucleus performs octupole vibrations round the nucleus shape without a stable octupole deformation (panel (a)). At the critical point, $\kappa_3 = \kappa_{3,crit}$, the energy of the lowest negative parity (octupole) RPA solution goes to zero and this corresponds to the nucleus instability to octupole vibrations (panel (b)). For $\kappa > \kappa_{3,crit}$ the system is permanently a_{30}-deformed (panel (c)) but the parity doublets are splitted because of a tunneling between two degenerate minima at $a_{30} = \pm\bar{a}_{30}$, separated by a finite barrier V_B. In the limit of the rigid octupole deformation (panel (d)) the barrier V_B becomes infinite and the spectrum has parity doublet character without any splitting - taken from [273].

The lowest root of the equation (8.31) represents the energy of the low-frequency collective octupole vibration. In the Fig.8.4 the total BCS energy, calculated within the model with the Hamiltonian (8.29), in the dependence on the octupole deformation parameter a_{30} (with the quadrupole coupling constant κ_2 fixed) is shown. This dependence for given value κ_3 can be obtained e.g. by means of the Hartree-Fock + BCS method with the constraint to given value of octupole deformation a_{30} or by the calculation of the total energy using the Strutinski shell correction method for each value of mean field deformation a_{30}. In such a way we can obtain the total energy in the mean field ground state as a function of a_{30}, $E(a_{30}) = \langle 0 | \hat{H} | 0 \rangle$, (in analogy with the total energy dependence on quadrupole deformation discussed in

the Fig.5.17). From the Fig.8.4 we can see that for small octupole coupling constant κ_3 we have the total energy minimum at $a_{30} = 0$. Then the lowest negative parity RPA solution with the Hamiltonian (8.29) represents the nucleus vibration round the stable equilibrium shape with $\bar{a}_{30} = 0$. If the value of κ_3 is increased, vibration in the lowest RPA state becomes more and more collective and the vibrational energy E_{oct} of this lowest octupole state decreases. At the critical point of the coupling constant κ_3,

$$\kappa_{3,\,crit} \equiv 7 \Big[\sum_{jj'} \frac{\left|\langle j||\hat{Z}_3||j'\rangle\right|^2 (\mathscr{U}_j\mathscr{V}_{j'} + \mathscr{U}_{j'}\mathscr{V}_j)^2}{E_j + E_{j'}} \Big]^{-1} \tag{8.32}$$

the lowest solution of the equation (8.31) has zero energy, i.e. the lowest octupole collective vibrational state becomes degenerate with the ground state (Fig.8.4(b)). At this point the RPA breaks down (the RPA stability matrix $\mathscr{S}$ (see (7.241)) becomes no positive definite and the lowest RPA solution of (8.31) becomes complex - see the text below (7.241)). At the critical point $\kappa_3 = \kappa_{3,\,crit}$ the system becomes unstable against vibration induced by the octupole-octupole force (see [275]).

Further increase of the coupling constant κ_3 leads to a stable octupole deformation $\bar{a}_{30}$ (more precisely to two minima of the total energy - see Fig.8.4(c) and Fig.8.4(d)). Then we should involve the stable octupole deformation in the mean field (e.g. by the HF or HFB method). If the coupling constant κ_3 is above the critical point (but not in the infinity) then there is the finite barrier with the finite height V_B between these two minima. Then in the spectrum the splitting of parity doublets can be observed which is a result from tunneling between two degenerate minima at $a_{30} = \pm\bar{a}_{30}$. In the limit of the rigid octupole deformation, $\kappa_3 >> \kappa_{3,\,crit}$ (see Fig.8.4(d)) the barrier V_B increases to infinity and the corresponding spectrum obtains a parity doublet character [273]. The inclusion of the pairing interaction manifests itself through the reductive $\mathscr{U} - \mathscr{V}$ factor in the numerator and the change in the denominator in the Eq. (8.31). So the pairing has a tendency to increase the critical value $\kappa_{3,\,crit}$ and to make the nucleus less octupole deformed.

It is important to point out that in the reality the rigid static octupole deformation corresponding to two total energy minima separated by an infinite barrier (the Fig.8.4(d)) is never approached. It is because that the actual nuclei are relatively small systems and the finite-size effects (fluctuations) wash out transitions from "spherical" to "deformed" phase. As a result of these finite-size fluctuation we have a smooth and continuous pattern of E_{oct}

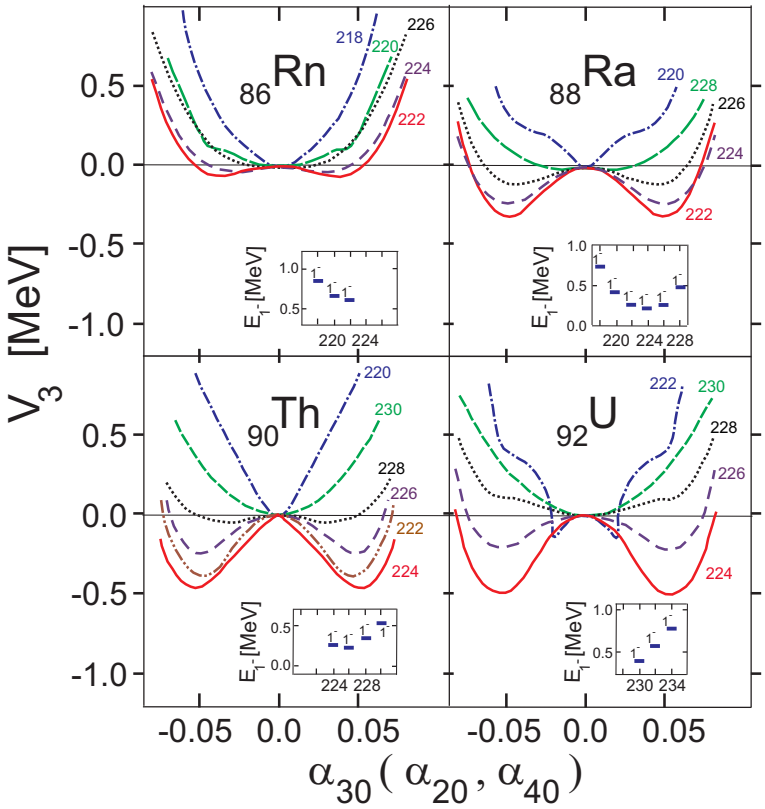


Figure 8.5: Octupole- deformation energy curves for even-even isotopes Rn, Ra, Th, and U obtained by the Strutinski shell correction method using the Saxon-Woods + BCS mean field. Insets show experimental energies of the lowest negative-parity 1^- states in these isotopes (taken from [286]).

and octupole deformation (which is proportional to $\langle 0_1^+ || \hat{\mathscr{M}}_3^{(\theta)} || \, 3_1^+ \rangle$). Nevertheless, there are strong experimental indications that some nuclei in the Th-Pa region have a nonzero octupole deformation in their ground state (see e.g. [172, 276, 277, 278]) with close to the parity doublet character of the their spectra and with alternating parity rotatinal bands. This is also confirmed by theoretical calculations (see e.g. Strutinski shell-corrected liquid drop models - [279], mean field approaches [280, 281, 282], α-clustering models [283, 284], or algebraic models [285]). For instance the experimental data on ^{220}Rn and ^{224}Ra obtained in [172] demonstrate strong octupole correlation in the ground state in both nuclei. However in ^{220}Rn only octupole vibrations were recognized (which corresponds to the Fig.8.4(a)) while in ^{224}Ra the stable octupole deformation, corresponding to the Fig.8.4(c), was obtained from the E1 intraband transitions [172].

In the Fig.8.5 the octupole-deformation total energies V_3 as a function of a_{30} calculated in the framework of the Strutinski shell correction method

with the Saxon-Woods + BCS mean field are shown for Rn, Ra, Th, and U isotope chains (octupole-deformation energy was in [286] defined as the shell-correction total energy where the liquid drop part energy involved only surface and Coulomb terms - see [286] for details). In the calculation there quadrupole a_{20} and hexadecapole a_{40} deformation parameters were fixed in their equilibrium values. Insets in the Fig.8.5 show experimental energies of the lowest negative-parity states in these isotopes. One can see that the even-even nuclei ^{222,224,226}Ra and ^{224,226}Th are the most promising candidates for a stable octupole deformation (because the minima of V_3 are deepest and their values of E_{1^-} are close to the minimum in the dependence on A).

The strong octupole correlations in the ground states are observed also in the odd-A nuclei from the Th-Ra region (see the Fig.7.33 and the text around). As it can be seen from the Fig.7.33, where the lowest rotational bands were calculated in the framework of the Nilsson+BCS+RPA+particle-rotor approach without any stable octupole deformation, the strong octupole correlations in the odd-A nuclei from this region manifest themselves as relatively high quasiparticle-phonon components in the lowest intrinsic states (see also [287] and citations therein).

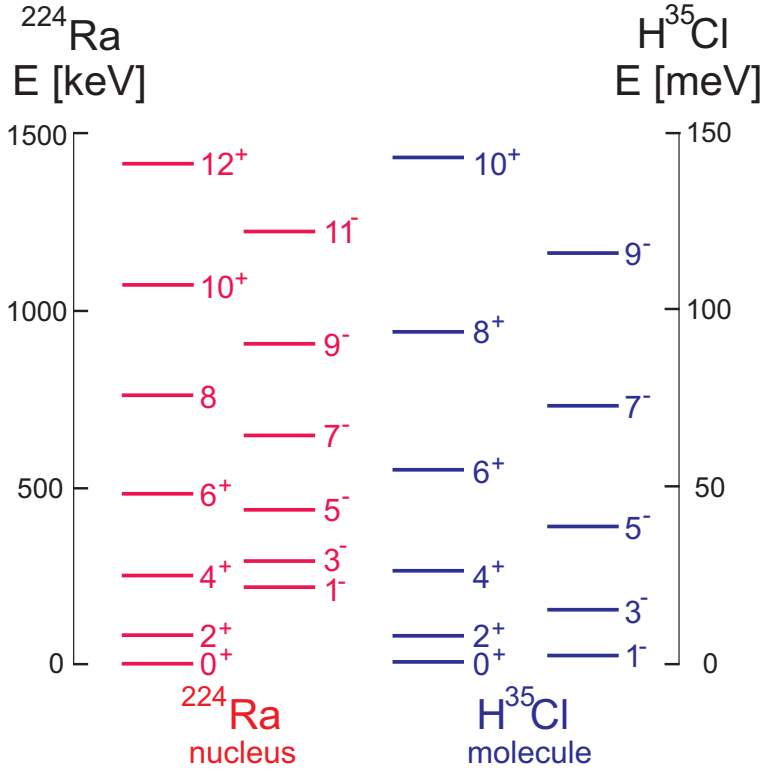


Figure 8.6: The low-lying rotational spectra of ^{224}Ra, compared with that of the H^{35}Cl molecule (taken from [273]).

In the end of this subsection regarding to the reflection asymmetric shapes of nuclei a historical remark is done. The existence of nuclei with stable deformed shapes was realized already in the beginning of the fifties in the connection with large quadrupole moments observed in some nuclei. The nonzero quadrupole moments led to the suggestion that the given nuclei have spheroidal shapes. For most deformed nuclei the shape described as axial and reflection symmetric spheroid is adequate to reproduce the observed rotational band character of the low-lying spectrum. We saw in the Subsection 8.1.1 that because the axial spheroidal shape is symmetric under space inversion (parity) all members of any rotational band built on the given intrinsic state have the same parity. However, with the first observation of negative-parity states near the ground state by the Berkeley group in the fifties [288, 289] the possibility arose that some nuclei might have a shape asymmetric under a reflection, such as pear shape [290]. We saw in (8.24) and (8.20) that in the case of the axial reflection- asymmetric shape the rotational bands involved levels with alternaring parities. Such rotational bands were known in the fifties from the spectra of reflection asymmetric molecules (see [291]). However, extensive investigation into the structure of nuclei with low-lying intrinsic negative parity states lead to the conclusion that the nucleus reflection-asymmetric shapes are not so stable as the familiar quadrupole deformations. The situation is illustrated by the low-lying spectrum of ^{224}Ra in the comparison with the spectrum of the linear molecule H^{35}Cl in the Fig.8.6. From the HCl spectrum we can see that the lowest positive parity and negative parity levels form one rotational band with typical $I(I+1)$-dependence (8.20). In the ^{224}Ra spectrum we recognize also low-lying states of both parities but rather then to involve them into one rotational band it is better to group them into two bands, one with the positive parity levels only and the other one with only negative parity levels. By other words the lowest band in HCl molecule corresponds precisely to the $K = 0$ with $s_1^{(\rho)} = +1$ (see (8.24)) while the lowest levels in ^{224}Ra resembles the ground rotational band built on intrinsic $K = 0$ state of the reflection symmetric nucleus (positive parity levels) and negative-parity rotational band built on the octupole vibration intrinsic state. Nevertheless the character of the ^{224}Rn- spectrum is very similar to one of the HCl spectrum. The strong octupole correlations in ^{224}Ra are pointed out also by strong extra-band E1- transitions between positive parity band and negative parity band levels. From theoretical point view it is hard to decide if the nucleus^{224}Ra has a stable octupole deformation in the ground state or it is a nucleus which is only very soft towards

the octupole vibrations. This question is discused in the literature up to now (e.g. [172, 287]).

8.1.3 Effect of the Coriolis interaction

In previous sections 8.1.1 and 8.1.2 the Coriolis term $\hat{H}_{cor}$ (see (7.13))

$$\hat{H}_{cor} = -\frac{\hbar^2}{2\mathscr{F}} [\hat{I}_+ \hat{j}_- + \hat{I}_- \hat{j}_+] \tag{8.33}$$

was neglected and the rotational part of the nucleus total laboratory Hamiltonian of the axially symmetric nucleus (see (7.12))

$$\hat{H}_{rot} = \hat{H}_{pure\,rot} + \hat{H}_{cor} + \hat{H}_{centrifug} \tag{8.34}$$

was approximated only by $\hat{H}_{pure\,rot} = \frac{\hbar^2}{2\mathscr{F}} [\hat{I}^2 - \hat{I}_3^2]$ (see (8.2)). As it was already mentioned (see the text below (7.16)) the Coriolis term represents the coupling between the intrinsic (single-particle and vibration) and rotational degrees of freedom and its neglecting can be used only at very low rotational frequences or rotational energies. In the approximation when the Coriolis term is neglected the intrinsic and rotational degrees of freedom are separated in the total laboratory Hamiltonian without any coupling and the corresponding laboratory frame wave function $\Psi_{IMK\rho}(\xi, \theta)$ can be written as a product of the intrinsic wave function $\psi_{K\rho}(\xi)$ and the Wigner $D^I_{MK}(\theta)$ function (see (8.3)). Further in this subsection we restrict orselves only to the axial $\hat{\mathscr{R}}_{i=1,2}(\pi)$-symmetric nuclei because almost all well-deformed nuclei have $\mathscr{R}_i$-symmetry in their ground state. Then, when the Coriolis interaction is neglected, the laboratory wave function can be symmetrized as follows (see (7.29) or (8.6))

$$\Psi_{IMK\rho}(\xi, \theta) = \sqrt{\frac{2I+1}{16\pi(1+\delta_{K0})}} \Big[D^I_{M\,K}(\theta)\, \psi_{K\rho}(\xi) + \\ + (-1)^I D^I_{M-K}(\theta)\, \hat{\mathscr{R}}_1(\pi)\, \psi_{K\rho}(\xi) \Big] \tag{8.35}$$

which gives for $K = 0$ wave function (8.9).

In the slow rotaion limit the taking into account the Coriolis and centrifugal intercation is usually done by the construction and diagonaliation of the

matrix of the total Hamiltonian (see (7.4), (7.12))

$$\hat{H} = \hat{H}_{intr} + \\ + \frac{\hbar^2}{2\mathscr{F}}\,[\hat{I}^2 - \hat{I}_3^2] - \frac{\hbar^2}{2\mathscr{F}}\,[\hat{I}_+\hat{j}_- + \hat{I}_-\hat{j}_+] + \frac{\hbar^2}{2\mathscr{F}}\,[\hat{j}_1^2 + \hat{j}_2^2] \tag{8.36}$$

within the basis of wave functions (8.35). Further we determine the single parts of the matrix elements $\langle I^{'} M^{'} K^{'} \rho^{'} |\, \hat{H} \,|\, IMK\rho \rangle$.

i) Matrix elements of the part $\hat{H}_{intr} + \frac{\hbar^2}{2\mathscr{G}}[\hat{I}^2 - \hat{I}_3^2]$ are diagonal and they were already determined - see e.g. (8.7)

$$\langle I^{'} M^{'} K^{'} \rho^{'} |\, \hat{H}_{intr} + \frac{\hbar^2}{2\mathscr{G}}[\hat{I}^2 - \hat{I}_3^2] \,|\, IMK\rho \rangle = \\ = \left[\, E_{K\rho} + \frac{\hbar^2}{2\mathscr{F}}[\, I(I+1) - K^2\,]\,\right] \delta_{I\,I^{'}}\, \delta_{M\,M^{'}}\, \delta_{K\,K^{'}}\, \delta_{\rho\,\rho^{'}} \tag{8.37}$$

ii) Matrix elements of the Coriolis term,

$$\langle I^{'} M^{'} K^{'} \rho^{'} | \hat{H}_{cor} | IMK\rho \rangle = \langle I^{'} M^{'} K^{'} \rho^{'} | - \frac{\hbar^2}{2\mathscr{F}}[\hat{I}_+\hat{j}_- + \hat{I}_-\hat{j}_+] | IMK\rho \rangle \tag{8.38}$$

involve the intrinsic matrix elements $\langle K^{'} \rho^{'} | \hat{j}_\pm | K\rho \rangle$ with $\hat{j}_\pm = \hat{j}_1 \pm i\hat{j}_2$ and the matrix elements of the operators $\hat{I}_\pm$ which act on the Wigner D- functions (see the Subsection (A.5)). The operators $\hat{j}_\pm$ are the standard angular momentum step-up and step-down operators acting in the intrinsic frame,

$$\hat{j}_\pm \,|\, jK\rangle = \sqrt{(j \mp K)(j \pm K + 1)}\ \,|\, j\ K \pm 1\rangle \tag{8.39}$$

However the action of $\hat{I}_\pm = \hat{I}_1 \pm i\hat{I}_2$ (when $\hat{I}_1$ and $\hat{I}_2$ are total angular projections on the 1-st and the 2-nd intrinsic axes, respectively) is opposite (see (A.38))

$$\hat{I}_\pm\, D^I_{MK}(\theta) = \sqrt{(I \pm K)(I \mp K + 1)}\ \ D^I_{MK\mp 1}(\theta) \tag{8.40}$$

Since the rotation $\hat{\mathscr{R}}_1(\pi)$ acts on the components $\hat{j}_i$ $(i = 1, 2, 3)$ of the intrinsic angular momentum by standard way ($\hat{\mathscr{R}}_1^{-1}(\pi)\hat{j}_1\hat{\mathscr{R}}_1(\pi) = \hat{j}_1$, $\hat{\mathscr{R}}_1^{-1}(\pi)\hat{j}_2\hat{\mathscr{R}}_1(\pi) = -\hat{j}_2$, $\hat{\mathscr{R}}_1^{-1}(\pi)\hat{j}_3\hat{\mathscr{R}}_1(\pi) = -\hat{j}_3$) the operators $j_\pm$ fulfill following conditions under the action of the transformation by the operator $\hat{\mathscr{R}}_1(\pi)$ (we should realize that $\hat{\mathscr{R}}_1^{\,2}(\pi) = e^{i\hat{j}_1 2\pi} = 1$ in the action on a wave function of a nucleus with even number of nucleons and $\hat{\mathscr{R}}_1^{\,2}(\pi) = e^{i\hat{j}_1 2\pi} = -1$ in the action on a wave function of an odd nucleon number nucleus)

$$\hat{\mathscr{R}}_1^{-1}(\pi)\, \hat{j}_\pm\, \hat{\mathscr{R}}_1(\pi) = \hat{j}_\mp \quad , \quad \hat{\mathscr{R}}_1^{-1}(\pi)\, \hat{j}_\pm = \pm\hat{j}_\mp\, \hat{\mathscr{R}}_1(\pi) \tag{8.41}$$

where the the upper sign is for even number of nucleons and the lower sign for odd-A nuclei. Taking into account (8.35), (8.38), (8.39), (8.40), and (A.27) the Coriolis term matrix elements for even-even and odd-odd nucleus are following

$$\begin{aligned}
&\langle I^{'} M^{'} K^{'} \rho^{'} \mid \hat{H}_{cor} \mid IMK\rho\rangle = \langle IMK\rho \mid \hat{H}_{cor} \mid I^{'} M^{'} K^{'} \rho^{'}\rangle = \\
&= -\frac{\hbar^2}{2\mathscr{F}} \Big\{ \sqrt{(I+K)(I-K+1)}\ \langle K^{'} \rho^{'} \mid \hat{j}_{-} \mid K\rho\rangle\ \delta_{K^{'},K-1}\,(1-\delta_{K0}) \\
&+\sqrt{(I-K)(I+K+1)}\ \langle K^{'} \rho^{'} \mid \hat{j}_{+} \mid K\rho\rangle\ \ \delta_{K^{'},K+1}\ (1-\delta_{K0}) \\
&+\frac{1}{\sqrt{2}} \left(1+(-1)^I\, r_1^{(\rho)}\right) \sqrt{I(I+1)}\, \langle K^{'}\ \rho^{'} \mid \hat{j}_{+} \mid K\ \rho\rangle\, \delta_{K0}\, \delta_{K^{'}1} \Big\}\, \delta_{II^{'}}\, \delta_{MM^{'}}
\end{aligned} \tag{8.42}$$

and for odd-A nuclei we have

$$\begin{aligned}
&\langle I^{'} M^{'} K^{'} \rho^{'} \mid \hat{H}_{cor} \mid IMK\rho\rangle = \langle IMK\rho \mid \hat{H}_{cor} \mid I^{'} M^{'} K^{'} \rho^{'}\rangle = \\
&= -\frac{\hbar^2}{2\mathscr{F}} \sqrt{(I+K)(I-K+1)}\, \langle K^{'} \rho^{'} \mid \hat{j}_{-} \mid K\rho\rangle\, \delta_{II^{'}}\, \delta_{MM^{'}}\, \delta_{K^{'},K-1} \\
&\quad -\frac{\hbar^2}{2\mathscr{F}} \sqrt{(I-K)(I+K+1)}\, \langle K^{'} \rho^{'} \mid \hat{j}_{+} \mid K\rho\rangle\, \delta_{II^{'}}\, \delta_{MM^{'}}\, \delta_{K^{'},K+1} \\
&\quad -\frac{\hbar^2}{2\mathscr{F}} (-1)^I\, (I+\frac{1}{2})\, \langle K^{'} = 1/2\, \rho^{'} \mid \hat{j}_{+}\, \hat{\mathscr{R}}_1(\pi) \mid K = 1/2\, \rho\rangle
\end{aligned} \tag{8.43}$$

iii) Matrix elements of the centrifugal term $\hat{H}_{centrifug} = \frac{\hbar^2}{2\mathscr{F}}\,[\hat{j}_1^2 + \hat{j}_2^2]$ are following

$$\begin{aligned}
&\langle I^{'} M^{'} K^{'} \rho^{'} \mid \hat{H}_{centrifug} \mid IMK\rho\rangle = \\
&= \frac{\hbar^2}{2\mathscr{F}}\, \langle K^{'} \rho^{'} \mid \hat{j}_1^2 + \hat{j}_2^2 \mid K\rho\rangle\ \left(1+(-1)^I r_1^{(\rho)}\, \delta_{K0}\right) \delta_{II^{'}}\ \ \delta_{MM^{'}}\, \delta_{K^{'}K}
\end{aligned} \tag{8.44}$$

Substitutions of (8.37), (8.42), or (8.43), and (8.44) into the matrix elements

$\langle I^{'}M^{'}K^{'}\rho^{'}\mid \hat{H}\mid IMK\rho\rangle$ of the total nucleus Hamilonian gives

$$\begin{aligned}
&\langle I^{'}M^{'}K^{'}\rho^{'}\mid \hat{H}\mid IMK\rho\rangle = \\
&= \Big[\, E_{K\rho} + \frac{\hbar^2}{2\mathscr{F}}[\, I(I+1) - K^2\,]\,\Big]\,\delta_{I\,I^{'}}\,\delta_{M\,M^{'}}\,\delta_{K\,K^{'}}\,\delta_{\rho\,\rho^{'}} \\
&-\frac{\hbar^2}{2\mathscr{F}}\Big\{\sqrt{(I+K)(I-K+1)}\;\langle K^{'}\rho^{'}\mid \hat{j}_-\mid K\rho\rangle\;\delta_{K^{'},K-1}\,(1-\delta_{K0}) \\
&+\sqrt{(I-K)(I+K+1)}\;\langle K^{'}\rho^{'}\mid \hat{j}_+\mid K\rho\rangle\;\;\delta_{K^{'},K+1}\;\,(1-\delta_{K0}) \\
&+\frac{1}{\sqrt{2}}\left(1+(-1)^I\,r_1^{(\rho)}\right)\sqrt{I(I+1)}\,\langle K^{'}\,\rho^{'}\mid \hat{j}_+\mid K\,\rho\rangle\,\delta_{K0}\,\delta_{K^{'}1}\Big\}\,\delta_{II^{'}}\,\delta_{MM^{'}} \\
&+\frac{\hbar^2}{2\mathscr{F}}\,\langle K^{'}\rho^{'}\mid \hat{j}_1^2+\hat{j}_2^2\mid K\rho\rangle\;\left(1+(-1)^I r_1^{(\rho)}\,\delta_{K0}\right)\,\delta_{II^{'}}\;\,\delta_{MM^{'}}\,\delta_{K^{'}K}
\end{aligned} \tag{8.45}$$

for even-even and odd-odd nuclei and

$$\begin{aligned}
&\langle I^{'}M^{'}K^{'}\rho^{'}\mid \hat{H}\mid IMK\rho\rangle = \\
&= \Big[\, E_{K\rho} + \frac{\hbar^2}{2\mathscr{F}}[\, I(I+1) - K^2\,]\,\Big]\,\delta_{I\,I^{'}}\,\delta_{M\,M^{'}}\,\delta_{K\,K^{'}}\,\delta_{\rho\,\rho^{'}} \\
&-\frac{\hbar^2}{2\mathscr{F}}\,\sqrt{(I+K)(I-K+1)}\,\langle K^{'}\rho^{'}\mid \hat{j}_-\mid K\rho\rangle\,\delta_{II^{'}}\,\delta_{MM^{'}}\,\delta_{K^{'},K-1} \\
&-\frac{\hbar^2}{2\mathscr{F}}\,\sqrt{(I-K)(I+K+1)}\,\langle K^{'}\rho^{'}\mid \hat{j}_+\mid K\rho\rangle\,\delta_{II^{'}}\,\delta_{MM^{'}}\,\delta_{K^{'},K+1} \\
&+\frac{\hbar^2}{2\mathscr{F}}\,(-1)^{I+\frac{1}{2}}\,(I+\frac{1}{2})\;\,a_{\rho^{'}\rho}\;\,\delta_{II^{'}}\;\,\delta_{MM^{'}}\,\delta_{K^{'}K}\,\delta_{K\,1/2} \\
&+\frac{\hbar^2}{2\mathscr{F}}\,\langle K^{'}\rho^{'}\mid \hat{j}_1^2+\hat{j}_2^2\mid K\rho\rangle\;\,\delta_{II^{'}}\;\,\delta_{MM^{'}}\,\delta_{K^{'}K}
\end{aligned} \tag{8.46}$$

for odd-A nuclei. In (8.46) the symbol $a_{\rho^{'}\rho}$ stands for so called decoupling parameter [6]

$$\begin{aligned}
&a_{\rho^{'}\rho} = -(-1)^{-1/2}\,\langle K^{'}=\frac{1}{2}\,\rho^{'}\mid \hat{j}_+\,\hat{\mathscr{R}}_1(\pi)\mid K=1/2\,\rho\rangle = \\
&= -(-1)^{-1/2}\,\pi_\rho\,(-1)^{1/2}\,\langle K^{'}=\frac{1}{2}\,\rho^{'}\mid \hat{j}_+\mid \overline{K=1/2\,\rho}\rangle = \\
&= -\pi_\rho\,\langle K^{'}=\frac{1}{2}\,\rho^{'}\mid \hat{j}_+\mid \overline{K=1/2\,\rho}\rangle
\end{aligned} \tag{8.47}$$

where $\pi_{\rho^{'}} = \pi_\rho$.

So, in the case when the Coriolis and centrifugal interactions are taken into account the eigen-functions and eigen-energies of the total Hamiltonian

[6]The connection between $\hat{\mathscr{R}}_1(\pi)\,|K\rho\rangle$ and $\hat{\mathscr{T}}\,|K\rho\rangle$, where $|K\rho\rangle$ is the single-particle state (5.46), is

of the axially deformed $\mathscr{R}$-symmetric nucleus can be found following the steps below.

1. The appropriate ensemble of basis functions $|IMK\rho\rangle$ (see (8.35)) is chosen for given value of the total ang. momentum I. Generally this basis is infinite but in reality it is sufficient to reduce it only into vectors $|IMK\rho\rangle$ with intrinsic states $|K\rho\rangle$ near the Fermi level of the intrinsic Hamiltonian.

2. In the framework of chosen basis of laboratory states $|IMK\rho\rangle$ the total Hamiltonian matrix is constructed with matrix elements (8.45) for even-A nuclei or (8.46) for odd-A nuclei. After the diagonalization of this matrix we obtain eigen-states $|IM\nu\rangle$ and egen-energies $E_{I\nu}$ of the total Hamiltonian (8.46),

$$\hat{H}\,|IM\nu\rangle = E_{I\nu}\,|IM\nu\rangle \quad , \quad |IM\nu\rangle = \sum_{K\rho} b_{K\rho}^{(I\nu)}\,|IMK\rho\rangle \tag{8.48}$$

One should realize that, since the total Hamiltonian $\hat{H}$ in the laboratory frame is rotationally invariant and all its matrix elements (8.45) or (8.46) are diagonal with respect to I, the diagonalization can be done separately for given I. It can be done also for given value of the parity because the

---

following,

$$\begin{aligned}
&\hat{\mathscr{R}}_1(\pi)\,|\,K\rho\rangle = \hat{\mathscr{R}}_1(\pi)\,\sum_{Nlj} c_{Nlj}^{(\rho K)}\,\sum_{\Lambda\Sigma} C^{jK}_{l\Lambda\frac{1}{2}\Sigma}\,|\,Nl\Lambda\Sigma\rangle = \\
&= \sum_{Nlj} c_{Nlj}^{(\rho K)}\,\sum_{\Lambda\Sigma} C^{jK}_{l\Lambda\frac{1}{2}\Sigma}\,(-1)^l\,|\,Nl-\Lambda\rangle\,\hat{\mathscr{R}}_1(\pi)\,|\frac{1}{2}\,\Sigma\rangle = \\
&= \sum_{Nlj} c_{Nlj}^{(\rho K)}\,\sum_{\Lambda\Sigma} C^{jK}_{l\Lambda\frac{1}{2}\Sigma}\,(-1)^l\,|\,Nl-\Lambda\rangle\,\hat{\mathscr{R}}_3^{-1}(\pi)\;\hat{\mathscr{R}}_2^{-1}(\pi)\,|\frac{1}{2}\,\Sigma\rangle = \\
&= \sum_{Nlj} c_{Nlj}^{(\rho K)}\,(-1)^{l+\frac{1}{2}+1}\,\sum_{\Lambda\Sigma} C^{jK}_{l\Lambda\frac{1}{2}\Sigma}\,|\,Nl-\Lambda-\Sigma\rangle = \\
&= -\sum_{Nlj} c_{Nlj}^{(\rho K)}\,(-1)^j\,|\,Nlj-K\rangle
\end{aligned}$$

and

$$\begin{aligned}
&\hat{\mathscr{T}}\,|\,K\rho\rangle = \sum_{Nlj} c^{(\rho K)}\,|Nlj K\rangle = \boxed{\begin{array}{c}\text{see}\\(1.44)\end{array}} = \sum_{Nlj} c^{(\rho K)}\,(-1)^{l+j+K}\,|Nlj-K\rangle = \\
&= \pi_\rho\,(-1)^K\,\sum_{Nlj} c_{Nlj}^{(\rho K)}\,(-1)^j\,|\,Nlj-K\rangle
\end{aligned}$$

So

$$\hat{\mathscr{R}}_1(\pi)\,|\,K\rho\rangle = \pi_\rho\,(-1)^K\,\hat{\mathscr{T}}\,|\,K\rho\rangle = \pi_\rho\,(-1)^K\,|\overline{K\rho}\rangle$$

Hamiltonian $\hat{H}$ is invariant also regarding parity (the Hamiltonian matrix has a block-diagonal character where each block is characterized by the total angular momentum I and the parity $\pi = \pm 1$).

As it was already mentioned in several places the effect of the Coriolis interaction encreases with the higher rotational frequency (energy). In the low rotational frequency the Coriolis interaction is weak and it can be neglected. As it can be seen from (8.45) and (8.46) nondiagonall matrix elements of the Coriolis interaction fulfill the selection rule $\Delta K = \pm 1$. These nondiagonal matrix elements represents the coupling between different rotational bands (that means the coupling between different angular momentum projections K in the wave functions (8.48).

For the case of the even-even axially deformed nuclei the selection rules of the Coriolis coupling ($\Delta K = \pm 1$) does not find their use in the lowest part of the spectrum of positive parity rotational bands. As it is shown in the Table 7.4 for ^{154}Sm (see the Subsection 7.3.1.3.1.2) the lowest positive parity rotational bands are built on the intrinsic ground state $K^\pi = 0_1^+$, the beta- vibration state $K^\pi = 0_2^+$, and gamma- vibration state $K^\pi = 2_1^+$ (see also the Fig.7.2 for ^{154}Sm - see the p. 326). Therefore there is no direct Coriolis coupling between these positive parity bands. The other situation is with the negative parity rotational bands in even-even nuclei where the lowest negative parity bands are built on the octupole vibration states with $K^\pi = 0^-, 1^-, 2^-, 3^-$ and the direct Coriolis coupling is possible. The Coriolis coupling between octupole vibration rotational bands is discussed in details e.g. in [292, 293].

One can see from the Fig.7.33 (see the p. 460) of the low-lying part of the spectrum of ^{229}Ra that the lowest intrinsic states in axially deformed odd-A nuclei have predominantly one quasiparticle character with smaller collective phonon-quasiparticle components. In the vicinity of the intrinsic ground state of the deformed odd-A nucleus there are always several intrinsic states with angular momentum projections K differing mutually and with the intrinsic ground state by 1 and in such a way fulfilling the Coriolis interaction selection rules $\Delta K = \pm 1$. Therefore it is always possible to construct a matrix of the total Hamiltonian within the ensemble of wave functions $\Psi_{IMK\rho}(\xi, \theta)$ with nonzero nondiagonal matrix elements caused by the Coriolis interaction. In the Fig.7.33 (see the Subsection 7.3.1.3.1.2) the comparison of energies of the lowest rotational bands, obtained by the diagonalization of such matrix for ^{229}Ra for gradually increasing angular momentum I and for both parity $\pi = \pm 1$, with corresponding experimental values is presented. In the Table 8.1

there is the list of the intrinsic states of both parities used in the construction of mentioned above Hamiltonan matrixes for the obtaining the spectrum demonstrated in the Fig.7.33. The number of intrinsic states with given parity involved in the Table 8.1 is simultaneously the dimension of the total Hamiltonian matrix for given π and for angular momenta $I \geq K_{max}$, where K_{max} is the maximum angular momentum projection of intrinsic states with the given parity π listed in the Table 8.1. For lower values of I, $I < K_{max}$, only intrinsic states from the Table 8.1 for which $K \leq I$ participate in the construction of the total Hamiltonian matrix for given I and π.

The first and the second columns of this table provide the highest one quasiparticle or quasiparticle+phonon component (using the Nilsson assignment) and its percentage with which this component enters the norm (7.324) of the given intrinsic state (the list of more components of intrinsic states of experimentally observed rotational bands is presented directly in the Fig.7.33; for the structure of intrinsic states not observed experimentally see [170]). The third column presents the experimental bandhead energies of corresponding rotational bands. The fourth column shows the calculated intrinsic energies (using the quasiparticle-phonon model described in the text around the Fig.7.33) related to the intrinsic ground state energy. The last fifth column involves the intrinsic energies obtained by the fitting of these intrinsic energies in order to obtain an agreement of calculated and experimental energies of all observed levels in all rotational bands depicted in the Fig.7.33. The bandheads of rotational bands not observed experimentally were obtained from (8.7) for $I = K$ using calculated intrinsic energies given in the fourt column. Besides the bandhead energies of observed rotational bands inertial factors $\frac{\hbar^2}{2\mathscr{F}^\pi}$ ($\pi = \pm 1$) were fitted separately for both parities (but were kept the same for all rotational bands with given parity), particularly for ^{229}Ra these inertial factors were $\frac{\hbar^2}{2\mathscr{F}^+} = 7.92$ keV and $\frac{\hbar^2}{2\mathscr{F}^-} = 7.79$ keV (for details see [170]).

The effect of the decoupling parameter $a_{\rho\rho}$ in the matrix elements of the total Hamiltonian matrix for axially deformed nucleus (see (8.46)) can be clearly seen in the Fig.7.33 as irregularities in the sequence of levels in the rotational bands built on the intrinsic $K^\pi = \frac{1}{2}^\pm$ states in the comparison with the standard level sequence observed in other $K \neq \frac{1}{2}^\pm$ rotational bands.

Very similar method for taking into account the Coriolis and centrifugal terms in the total laboratory frame Hamiltonian to what described above can be applied also for odd-odd nuclei - see [294] and the citation therein.

Knowing the eigen-vectors (8.48) of the total Hamiltonian the reduced elec-

$\psi_{K\rho}(\xi)$	[%]	bandhead energy exp. [KeV]	QPM intrinsic energy [keV] $E_{K\rho} - E_{K_0\rho_0}$	fitted intrinsic energy [keV] $E^{fit}_{K\rho} - E^{fit}_{K_0\rho_0}$
$5/2^+$ [633]	82	0.0	0.0	0.0
$5/2^-$ [752]	90	137.5	147.3	-18.5
$3/2^+$ [631]	44	213.0	250.1	193.4
$3/2^-$ [761]	80	565.7	431.7	631.5
$1/2^-$ [501]	61	479.0	367.5	450.3
$1/2^+$ [631]	63	142.7	102.8	213.0
$5/2^+$ [622]	90	107.1	129.9	19.6
$1/2^+$ [640]	68	(501)	511.2	456.9
$3/2^+$ [631]	48	(563)	542.1	193.4
$7/2^-$ [743]	84	-	577.0	-
$7/2^+$ [624]	51	-	773.3	-
$1/2^+$ [651]	46	-	620.7	-
$5/2^-$ ([633] + Q^+_{30})	83	-	891.3	-
$1/2^-$ [501]	51	-	921.8	-
$3/2^-$ ([631] + Q^+_{30})	83	-	1055.2	-

Table 8.1: The list of intrinsics states of both parities involved in the doagonalization of the total Hamiltonian matrixes (8.46) for the calculation of the low-lying energy spectrum of ^{229}Ra presented in the Fig.7.33. The first column provides the highest one quasiparticle or quasiparticle-phonon components (using the Nilsson assignment), the second column involves the corresponding percentage with which the highest component enters the norm (7.324). The third column shows the experimental bandhead energies of the corresponding rotational band. The fourth column presents the corresponding calculated intrinsic energy $E_{K\rho}$ (related to the intrinsic ground state energy $E_{K_0\rho_0}$) using the quasiparticle-phonon model (see the text below the expr. (7.355) and [170]). The last column involves the intrinsic energy related to the intrinsic ground state energy obtained by the fitting procedure (see the text for details).

tromagnetic transition probabilities $B(X\lambda;\, I_iM_i\nu_i \to I_fM_f\nu_f)$ of the transition $|I_iM_i\nu_i\rangle \to I_fM_f\nu_f\rangle$ of the type $X = el.\, or\, mag.$ and multipolariy λ can

be obtained by the generalization of the expression (7.36),

$$
\begin{aligned}
&B(X\lambda;\; I_iM_i\nu_i \to I_fM_f\nu_f) = \\
&\quad = \frac{1}{2I_i+1}\Big|\sum_{K_i\rho_i}\sum_{K_f\rho_f} b^{(I_i\nu_i)}_{K_i\rho_i}\, b^{(I_f\nu_f)}_{K_f\rho_f}\, \langle I_fK_f\rho_f||\, \hat{\mathscr{M}}^{(X)}_{\lambda}\, ||\, I_iK_i\rho_i\rangle\Big|^2 = \\
&\quad = \boxed{\begin{array}{c}\text{see}\\(7.40)\end{array}} = \\
&\quad = \Big|\sum_{K_i\rho_i}\sum_{K_f\rho_f} b^{(I_i\nu_i)}_{K_i\rho_i}\, b^{(I_f\nu_f)}_{K_f\rho_f}\, \Big[\, C^{I_fK_f}_{I_iK_i\lambda K_f-K_i}\, \langle K_f\rho_f|\, \hat{\mathscr{M}}^{(X)\,(\theta)}_{\lambda\mu=K_f-K_i}\, |\, K_i\rho_i\rangle \\
&\qquad + \quad (-1)^{I_i}\, C^{I_fK_f}_{I_i-K_i\lambda K_f+K_i}\, \langle K_f\rho_f|\, \hat{\mathscr{M}}^{(X)\,(\theta)}_{\lambda\mu=K_f-K_i}\, \hat{\mathscr{R}}_i(\pi)\, |\, K_i\rho_i\rangle\Big]\Big|^2
\end{aligned}
\tag{8.49}
$$

Comparisons of the reduced transition probabilities calculted using (8.48) in the framework of the quasiparticle+phonon model (QPM) with experimental values for selected actinides can be found e.g. in [171, 170, 295, 296, 297, 298, 299, 300]. One should realize in the comparison of the calculated results with experimental data on the intrinsic state energies that the predictive power of the microscopic and semi-microscopic approaches like the QPM is not more precise than 100 keV. Therefore in all papers cited above the intrinsic energies of experimentally observed rotational bands were fitted in the diagonalization of the laboratory total Hamiltonian and obtained optimal values of intrinsic energies were then compared with the QPM values. The Coriolis mixing of rotational bands is very sensitive to the relative positions of rotational bands and therefore one cannot expect that microscopic models of the intrinsic degrees of freedom give a sufficiently precise intrinsic energies for the determination of positions of rotational bands relevant to the correct Coriolis mixing. As one can see from papers [171, 170, 295, 296, 297, 298, 299, 300], approaches for taking into account the Coriolis mixing using the optimal (fitted) intrinsic energies gave qualitatively good agreement of calculated and experimental reduced transition probabilities.

8.1.4 Moments of inertia

In this subsection we continue with the assumption of the slow rotating axially deformed and $\mathscr{R}_{i=1,2}(\pi)$- symmetric nucleus round the 1-st intrinsic axis when

the total Hamiltonian is given by (8.36). In all expressions concerned such rotation (see (8.33)-(8.46)) the moment of inertia $\mathscr{F}$ was supposed to be taken with regard to the 1-st intrinsic axis which is perpendicular to the symmetry axis of the rotating nucleus. If the nucleus is assumed to be a rigid body then the corresponding expression for $\mathscr{F}$ is (7.91) for $k = 1$ and $\gamma = 0$

$$\mathscr{F} = \mathscr{F}^{(rig)} = \frac{2}{5} AM\ R_0^2\,(1 + 0,31\beta) \tag{8.50}$$

If the rotating nucleus is described as the rotating drop of the irrotational and incompressible liquid then (see (7.88) for $\gamma = 0$),

$$\mathscr{F} = \mathscr{F}^{(irr)} = \frac{3}{2\pi}\ AM\ R_0^2\,\beta^2\ sin^2\frac{2\pi}{3} \tag{8.51}$$

From experimental point of view the moment of inertial is calculated from the simple $I(I+1)$- formula (8.7) applied for the even-even nucleus ground state rotational band (with energy levels $E_{IK_0\rho_0}$)

$$\frac{\hbar^2}{2\mathscr{F}_I^{(exp)}} = \frac{\partial E_{IK_0\rho_0}}{\partial[I(I+1)]} \approx \frac{E_{IK_0\rho_0} - E_{I-2K_0\rho_0}}{(2I-1)}$$

$$\Rightarrow \quad \mathscr{F}_I^{(exp)} \approx \frac{\hbar^2\,(2I-1)}{E_{IK_0\rho_0} - E_{I-2K_0\rho_0}} \tag{8.52}$$

The experimental moment of inertia depends generally on the angular momentum I. For low lying levels in rotational bands moments of inertia are treated as constant and they are usually extracted from the lowest experimental levels in the given rotational band. For instance for the even-even nucleus ground rotational band we have

$$\mathscr{F}^{(exp)} \equiv \mathscr{F}_{I=2}^{(exp)} \approx \frac{3\,\hbar^2}{E_{I=2\,K_0\rho_0} - E_{I=0\,K_0\rho_0}} \tag{8.53}$$

One should realize that the ground state rotational band in the even-even nucleus does not mix with other rotational bands by means of the Coriolis interaction because the even-even nucleus ground state corresponds to $K^\pi = 0_1^+$ and the nearest $K^\pi = 1^+$ states are placed very high in the spectrum to be directly mixed with $K^\pi = 0_1^+$ states in terms of the Coriolis interaction.

The moment of inertia determined by (8.52) corresponds to the finite dif-

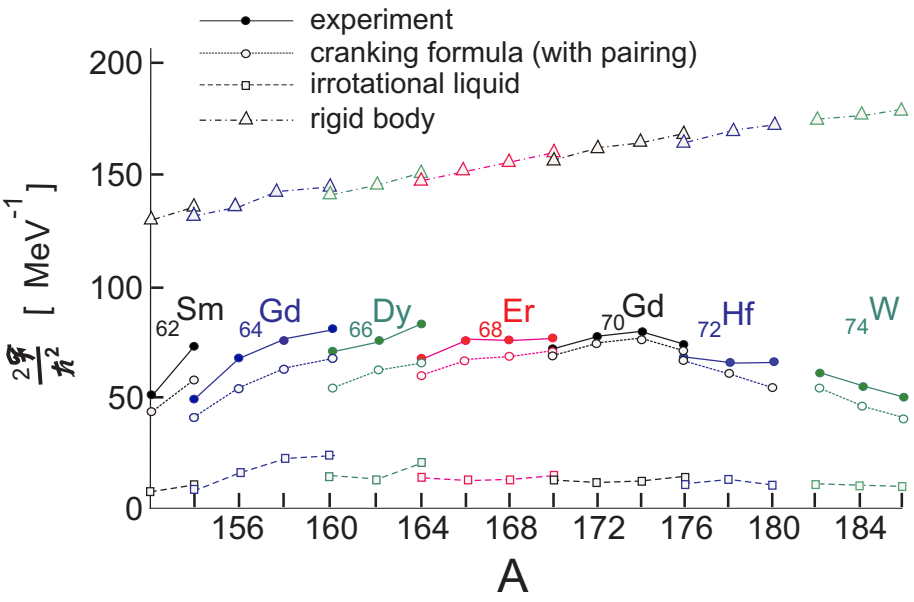


Figure 8.7: Moments of inertia calculated for selected rare-earth even-even nuclei in the framework of different models (irrotational liquid drop model - see (8.51), rigid body approach - see (8.50), and cranking formula - see (7.299) and the Subsection 8.2.2) are compared with experimental values obtained by (8.53) (adapted from [7]).

ference approximation of so called kinematic moment of inertia [7] ,

$$\mathscr{F}^{(1)} \equiv \hbar \frac{\sqrt{I(I+1)}}{\Omega} = \frac{\hbar^2 \tilde{I}}{[\frac{\partial E_{IK\rho}}{\partial \tilde{I}}]} \tag{8.54}$$

where $\tilde{I} \equiv \sqrt{I(I+1)}$ and Ω is the rotational frequency.

As it was alerady mentioned (see (7.93)) the experimental values $\mathscr{F}^{(exp)}$ lie between $\mathscr{F}^{(irr)}$ and $\mathscr{F}^{(rig)}$,

$$\mathscr{F}^{(irr)} < \mathscr{F}^{(exp)} < \mathscr{F}^{(rig)} \tag{8.55}$$

[7] The classic physics formula for the rotational energy $E(\Omega)$ corresponds to $E(I)$ as follows

$$E(\Omega) = E(0) + \frac{1}{2}\mathscr{F}^{(1)}\,\Omega^2 = E(I) = E(0) + \frac{\hbar^2\, I(I+1)}{2\,\mathscr{F}^{(1)}}$$

with kinematic moment of inertia defined as

$$\mathscr{F}^{(1)} = \hbar \frac{\sqrt{I(I+1)}}{\Omega} = \hbar \frac{\tilde{I}}{\Omega}$$

Then

$$\frac{\partial E}{\partial \tilde{I}} = \frac{\partial}{\partial \tilde{I}} \frac{\hbar^2\, \tilde{I}^2}{2\,\mathscr{F}^{(1)}} = \hbar^2 \frac{\tilde{I}}{\mathscr{F}^{(1)}}$$

So

$$\mathscr{F}^{(1)} = \frac{\hbar^2\, \tilde{I}}{(\frac{\partial E}{\partial \tilde{I}})}$$

In the Fig.8.7 the experimental values $\mathscr{F}^{(exp)}$ of moments of inertia are compared with irrotational liquid drop and rigid body values for several rare earth nuclei. One can see that rigid body values $\mathscr{F}^{(rig)}$ are about twice as big as the experimental ones and the irrotational liquid drop values are very small in the comparison with experimental values. In the Fig.8.7 the cranking formula values of inertia moments are given as well (see (7.299) and the Subsection 8.2.2).

8.2 Fast rotation

8.2.1 Cranking model

In the previous section the slow rotation of axially deformed nuclei was discussed where the moment of inertia was constant and independent on rotational frequency. As it was already mentioned (see the text below the exp. (7.16)) the role of the Coriolis interaction, which mixes the intrinsic and rotational degrees of freedom, increases very rapidly with rotational frequency and therefore for higher rotational frequency the separation of the intrinsic and rotational degrees of freedom becomes problematic. However, for very high rotational frequency the nucleus starts to behave like flywheel, that means it rotates steadily in the laboratory frame round the stable axis. Then without loosing a generality, we can choose the x-th laboratory frame axis as the rotation axis and simultaneously this rotation axis can be identified with the 1-st axis of the intrinsic frame (fixed body frame).

We start with the assumption that in the time $t = 0$ the nucleus begins to rotate with the constant frequency Ω. Then the laboratory wave function $\Psi_{\Omega}^{(lab)}(t)$ is given by the time evolution (analogy with (A.16) where $\vec{n}$ is the unit vector along the 1-st intrinsic axis)

$$\Psi_{\Omega}^{(lab)}(t) = e^{-i\Omega t\,\hat{I}_1}\,\Psi_{\Omega}^{(lab)}(t=0) = e^{-i\Omega t\,\hat{I}_1}\;\psi_{\Omega}^{(intr)}(t=0) \tag{8.56}$$

where in the time $t = 0$ laboratory and intrinsic frames are merged, $\Psi_{\Omega}^{(lab)}(t = 0) = \psi_{\Omega}^{(intr)}(t = 0)$. The laboratory frame wave function $\Psi_{\Omega}^{(lab)}(t)$ fulfills the standard Schroedinger equation

$$i\hbar\,\frac{\partial\Psi_{\Omega}^{(lab)}(t)}{\partial t} = \hat{H}\;\Psi_{\Omega}^{(lab)}(t) \tag{8.57}$$

where $\hat{H}$ is the total nucleus Hamiltonian in the laboratory frame. The corresponding Schroedinger equation for the intrinsic wave function $\Psi_{\Omega}^{(intr)}(t)$ is

$$\begin{aligned} i\hbar\,\frac{\partial\Psi_{\Omega}^{(intr)}(t)}{\partial t} &= i\hbar\;\frac{\partial e^{i\Omega t\hat{I}_1}\;\psi_{\Omega}^{(lab)}(t)}{\partial t} = \\ &= -\hbar\Omega\;\hat{I}_1\,e^{i\Omega t\,\hat{I}_1}\,\Psi_{\Omega}^{(lab)}(t) + e^{i\Omega t\,\hat{I}_1}\;\hat{H}\;\Psi_{\Omega}^{(lab)}(t) = \\ &= \boxed{\begin{array}{c}\text{because}\\ \left[\hat{H}\;,\;\hat{I}_1\right] = 0\end{array}} = \left(-\hbar\Omega\;\hat{I}_1 + \hat{H}\right)\psi_{\Omega}^{(intr)}(t) \equiv \\ &= \hat{H}_{\Omega}\;\psi_{\Omega}^{(intr)}(t) \end{aligned} \tag{8.58}$$

So the intrinsic wave function $\psi_{\Omega}^{(intr)}(t)$ fulfills the Schroedinger equation with the effective Hamiltonian $\hat{H}_{\Omega}$

$$\hat{H}_{\Omega} \equiv \hat{H} - \hbar\Omega\, \hat{I}_1 \tag{8.59}$$

In the stationary case, when the total Hamiltonian and rotational frequency Ω does not depend on time, the intrinsic wave function of the nucleus, $\psi_{\Omega}^{(intr)}$, is the eigen function of the effective Hamiltonian $\hat{H}_{\Omega}$

$$\hat{H}_{\Omega}\, \psi_{\Omega,\,\nu}^{(intr)} = R_{\Omega,\,\nu}^{(intr)}\, \psi_{\Omega,\,\nu}^{(intr)} \tag{8.60}$$

with the energy $R_{\Omega,\,\nu}^{(intr)}$ in the intrinsic frame (index ν enumerates solution of the equation (8.60)). This equation can be solved similarly as the standard time-nonindependent Schroedinger equation $\hat{H}\,\Psi = E\,\Psi$ with the laboratory frame Hamiltonian (8.1), that means for given rotational frequency Ω we can find single-particle mean field $\hat{H}_{AV}^{(\Omega)}$ (e.g. using Hartree-Fock method with the intrinsic effective Hamiltonian $\hat{H}_{\Omega}$) and corresponding two-body (generally many body) residual interaction $\hat{V}_{res}^{(\Omega)}$,

$$\hat{H}_{\Omega} = \hat{H}_{AV}^{(\Omega)} + \hat{V}_{res}^{(\Omega)} \tag{8.61}$$

In the next steps the short-range part of the residual interaction $\hat{V}_{res}^{(\Omega)}$ can be taken into account by means of the BCS or HFB method (for given value of Ω) and the long-range part of $\hat{V}_{res}^{(\Omega)}$ can be included by the RPA and other beyond RPA methods. From the theoretical point of view the main difference between the solving of the Schroedinger equation (8.60) with the intrinsic Hamiltonian (8.59) and the standard Schroedinger equation $\hat{H}\,\Psi = E\,\Psi$ with the laboratory frame Hamiltonian (8.1) corresponding to the slow rotation regime is the fact that opposite to the slow rotation case (where the total Hamiltonian (8.1) together with its mean field was invariant with respect to the time reversal transformation) the effective intrinsic Hamiltonian $\hat{H}_{\Omega}$ is not invariant under the time reversal,

$$\hat{\mathscr{T}}\, \hat{H}_{\Omega}\, \hat{\mathscr{T}} \neq \hat{H}_{\Omega} \tag{8.62}$$

because the second term in (8.59) (so called cranking term) involves $\hat{I}_1$ with $\hat{\mathscr{T}}^{-1}\, \hat{I}_1\, \hat{\mathscr{T}} = -\hat{I}_1$.

On the other hand side the intrinsic Hamiltonian $\hat{H}_{\Omega}$ is invariant as regards the rotation by angle π round the intrinsic 1-st axis with the rotation operator $\hat{\mathscr{R}}_1(\pi)$,

$$\left[\hat{H}_{\Omega}\,,\, \hat{\mathscr{R}}_1(\pi)\right] = \left[\hat{H}_{\Omega}\,,\, e^{-i\,\pi\,\hat{I}_1}\right] = 0 \tag{8.63}$$

Then

$$\hat{\mathscr{R}}_1(\pi)\,\psi^{(intr)}_{\Omega,\,\nu,\,r_\nu} = r_\nu\,\psi^{(intr)}_{\Omega,\,\nu,\,r_\nu}$$
$$\hat{\mathscr{R}}_1{}^2(\pi)\,\psi^{(intr)}_{\Omega,\,\nu,\,r_\nu} = \begin{cases} \psi^{(intr)}_{\Omega,\,\nu,\,r_\nu} & \text{for even number of nucleons} \\ -\psi^{(intr)}_{\Omega,\,\nu,\,r_\nu} & \text{for odd number of nucleons} \end{cases} \tag{8.64}$$

and we see that the intrinsic wave function $\psi^{(intr)}_{\Omega,\,\nu,\,r_\nu}$ (solution of the eq. (8.60)) is also the eigen-function of the operator $\hat{\mathscr{R}}_1(\pi)$. The corresponding eigen value $r_\nu = \pm 1$ (for even number of nucleons) and $r_\nu = \pm i$ (for odd number of nucleons) is called as signature and can be added to the quantum numbers characterizing the intrinsic state [8] .

Examples of the solving of the equation (8.60) and the comparison of results with experimental data will be discussed later.

In the fast rotation regime the scheme of the coupling of the intrinsic angular momentum $\vec{j}$ and the rotational angular momentum $\hat{R}$ into the total angular momentum $\hat{I}$ is different than in the case of the slow rotation limit. The coupling $\vec{I} = \vec{j} + \vec{R}$ for slow rotation was demonstrated in the Fig.7.1 (see the p. 320). Fast rotation with the high rotational frequency Ω is connected with the high value of the rotational angular momentum $\vec{R}$ which is oriented along the x-axis of the laboratory frame (because of the stable rotation in the laboratory frame we can always choose the axes of laboratory and intrinsic frames so that laboratory x-axis and intrinsic 1-st axis coincide). The absolute value of $\vec{R}$ is so big in the comparison with the value of $\vec{j}$ that the total angular momentum $\vec{I} = \vec{j} + \vec{R}$ is almost oriented along laboratory x- and simultaneously along intrinsic 1-st axes as it is shown in the schematic Fig.8.8.

If the total angular momentum $\vec{I}$ is almost parallel with the laboratory frame x-axis (and simultaneously with the intrinsic 1-st axis) the following expresion is valid with good approximation

$$\langle \psi^{(intr}_{\Omega,\,\nu,\,r}|\ \hat{I}_1\ |\ \psi^{(intr}_{\Omega,\,\nu,\,r}\rangle \approx \sqrt{I(I+1)} \equiv \tilde{I} \tag{8.65}$$

From other side using the definition of the kinematic moment of inertia (see

[8] In the case of odd-A nuclei wave functions (including the single-particle or single-quasiparticle states) instead of the signature eigen-value $r = \pm i$ another signature quantum quantum number $\alpha = \pm\frac{1}{2}$ is sometimes introduced. The connection between the quantum numbers r and α is following

$$r = e^{-i\pi\,\alpha}$$

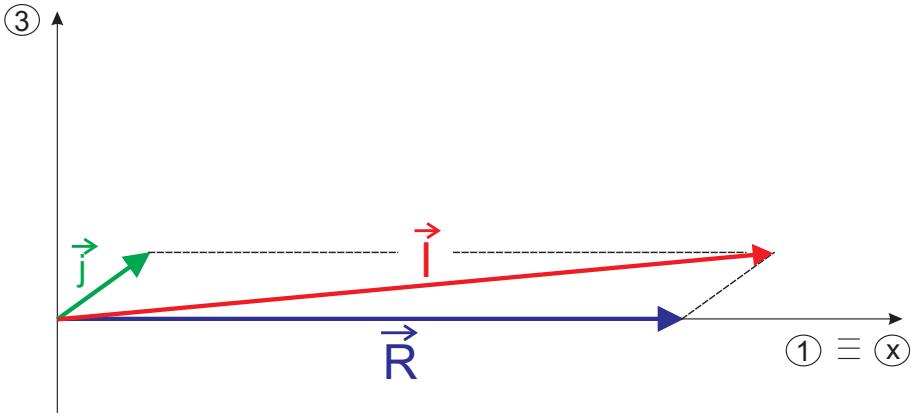


Figure 8.8: Schematic figure of the coupling of the intrinsic angular momentum $\vec{j}$ with the rotational ang. momentum $\vec{R}$ into the total ang. momentum $\vec{I} = \vec{j} + \vec{R}$ in the fast rotation regime.

(8.54)) gives

$$\mathscr{F}^{(1)}_{I,\,\nu,\,r}\,\Omega = \hbar\,\tilde{I} \approx \hbar\,\langle\psi^{(intr)}_{\Omega,\,\nu,\,r}|\;\hat{I}_1\;|\psi^{(intr)}_{\Omega,\nu,r}\rangle \tag{8.66}$$

The expressions (8.65),(8.66) provide us the connection between the value of I and rotational frequency Ω. In order to obtain the total angular momentum I we should at first solve the equation (8.60) in the framework of given model for a mesh of point Ω and using (8.65) determine the dependence $I(\Omega)$. From this dependence we can deduce the precise value of $\Omega_{I,\,\nu}$ corresponding to given value of I and for given rotational band ν (rotational band ν connects solutions of (8.60) with similar internal structure which are usually solutions of (8.60) for given signature r with the same index ν for different values of Ω). The solutions $\psi^{(intr)}_{\Omega_I,\,\nu_1,\,r=+}$ of (8.60) with the lowest energy $R^{(intr)}_{\Omega_{I,\,\nu_1,\,r=+}}$ (even nucleus ground state of the intrinsic Hamiltonian $\hat{H}_\Omega$ for given I) corresponds to the states with the lowest energy for given I. Laboratory energies of such states , $E^{(lab)}_{\nu_1,\,I,\,r=+} \equiv R^{(intr)}_{\Omega_I,\,\nu_1,r=+} + \hbar\Omega_{I,\,\nu_1}\langle\psi^{(intr)}_{\Omega_I,\,\nu_1,\,r=+}|\hat{I}_1|\psi^{(intr)}_{\Omega_I,\,\nu_1,\,r=+}\rangle$, for different I form the yrast line (see the Fig.1.7). Energies $E^{(lab)}_{\nu_i,\,I,\,r}$ $(i > 1)$ of intrinsic states $\psi^{(intr)}_{\Omega_I,\,\nu_i,\,r=+}$ form the excited bands which are "parallel" with the yrast line as it is shown in the schematic Fig.8.9 for a nucleus with even number of nucleons.

Theoretical interpretation of the solutions of the equation (8.60) demonstrated in the Fig.8.9 corresponds to the experimental spectrum as it is explained below. The fast rotation is experimentally connected with long rotational bands extended to high excitations (high frequencies or high ang. momenta). Such excitations are achieved in terms of heavy ion reactions (see

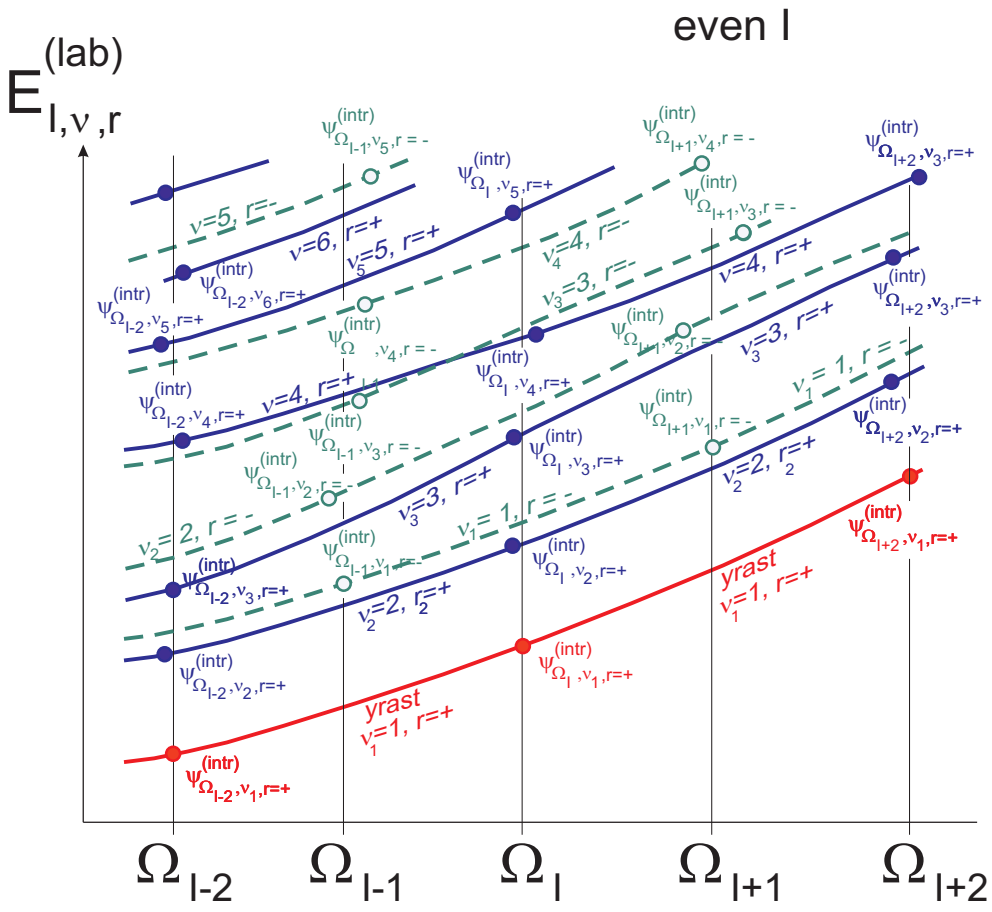


Figure 8.9: Schematic figure of excitations of fast rotating nucleus - yrast line with the indexes $\nu_1 \equiv 1$, $r = +1$ (red curve), excited band states with positive signature $r = +1$ (blue solid curves) and excited states with negative signature (green dashed curves). The value of the I in the figure is supposed to be even. From the $\mathscr{R}_1(\pi)$- symmetry of the intrinsic Hamiltonian $\hat{H}_\Omega$ (see (8.63)) and from the form of the operator $\hat{\mathscr{R}}_1(\pi) = e^{i\pi \hat{I}_1}$ ($I_1 \approx I$ for a fast rotation) it follows that the even values of the angular momentum ($\cdots$, $I-4$, $I-2$, I, $I+2, \cdots$) corresponds to bands with $r = +1$ while the odd values of angular momentum ($\cdots$, $I-3$, $I-1$, $I+1, \cdots$ where here I is supposed to be even) corresponds to r=-1. The yrast line of even-even nucleus is connected always with $r = +1$ and therefore to even values of angular momentum. Since moments of inertia of different rotational bands (different ν and r) differ mutually a little bit for given I states with the same I are not placed in the figure on the same vertical.

e.g. [301, 302]). The target nucleus is bombarded by α-particles or heavy ions having energy much above the Coulomb barrier so that a compound nucleus [9] with a large angular momentum and excitation energy is formed. Subsequently the compound system de-excites by evaporating a few neutrons, each carying 1 or 2 units ($\hbar$) of angular momentum. With the emission of neutrons, the residual compound nucleus gradually approaches the yrast line

[9] Nuclear reactions going through so called compound nucleus are discussed in details in the Chapter 11.

until it comes close in energy to it that the emission of any more neutrons is not energetically possible. The nucleus then emits several γ- quanta and de-excites to the yrast states at angular momentum concerned. Then a chain of γ-rays is emitted due to the transitions to the successively lower members of the yrast line until the nucleus ends up through the rotational ground band in its ground state. Ideally, each of these γ- transitions is expected to be of the E2-type and strongly enhanced due to collective effects. The procedure described above is schematically shown in the Fig.8.10 (see also the Fig1.7)

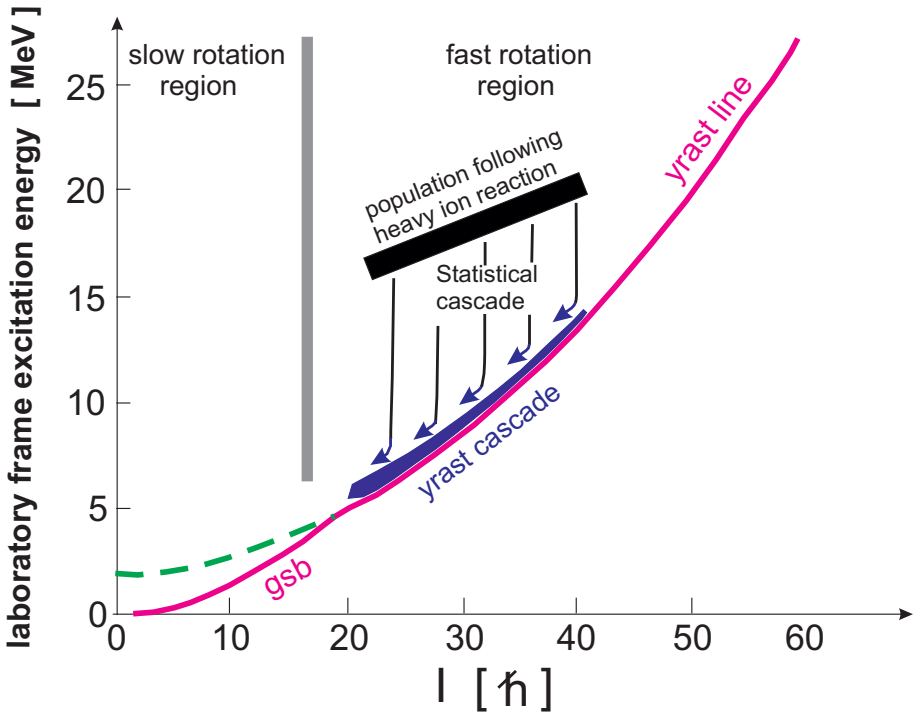


Figure 8.10: Diagram showing de-excitation of product of the heavy ion reaction (following [301]).

The long rotational bands observed in the final nucleus from heavy ion reaction cannot be described by the simple $I(I+1)$- formula of (8.7)- type with a constant moment of inertia. This can be done using the angular momentum dependent moment of inertia when the energy levels of the given rotational band νr are given by the modified expression,

$$E^{(lab)}_{I,\nu,r} = E_{bandhead,\nu,r} + \frac{\hbar^2}{2\mathscr{F}^{(1)}_{I,\nu,r}} I(I+1) = \\ = E_{bandhead,\nu} + \frac{\hbar^2}{2\mathscr{F}^{(1)}_{I,\nu,r}} \tilde{I}^2 \qquad (8.67)$$

where $\mathscr{F}^{(1)}_{I,\nu,r}$ is the kinematic moment of inertia (8.66) and $E_{bandhead,\nu,r}$ is the lowest energy level given by constant for each rotational band with indexes νr. Then

$$\frac{dE^{(lab)}_{I,\nu,r}}{d\tilde{I}} \approx \frac{\hbar^2\,\tilde{I}}{\mathscr{F}^{(1)}_{I,\nu,r}} = \boxed{\begin{array}{c}\text{see}\\(8.66)\end{array}} = \hbar\,\Omega_{I,\nu,r} \tag{8.68}$$

$$\frac{dE^{(lab)}_{I,\nu,r}}{d(\tilde{I}^{\,2})} \approx \frac{\hbar^2}{2\,\mathscr{F}^{(1)}_{I,\nu,r}} \tag{8.69}$$

Besides the kinematic moment of inertia, defined as $\mathscr{F}^{(1)}_{I,\nu,r} = \hbar\,\frac{\tilde{I}}{\Omega_{I,\nu,r}}$ (see (8.54)), so called dynamical moment of inertia $\mathscr{F}^{(2)}_{I,\nu,r}$ is introduced in literature,

$$\mathscr{F}^{(2)}_{I,\nu,r} \equiv \hbar\,\frac{d\tilde{I}}{d\Omega_{I,\nu,r}} \tag{8.70}$$

Both the kinematic and dynamical moments of inertia can be obtained directly from the intrinsic energy $R^{(intr)}_{\Omega,\nu,r}$ (eigen-energy of the intrinsic Hamiltonian $\hat{H}_\Omega$ corresponding to $\psi_{\Omega,\nu,r}$) as it can be seen from following expressions.

The laboratory energy $E^{(lab)}_{\Omega,\nu,r}$ is connected with the intrinsic energy $R^{(intr)}_{\Omega,\nu,r}$ by (8.59),

$$E^{(lab)}_{\Omega,\nu,r} = \boxed{\begin{array}{c}\text{see}\\(8.59)\end{array}} = R^{(intr)}_{\Omega,\nu,r} + \hbar\,\Omega_{\nu,r}\ \langle\psi_{\Omega,\nu,r}|\,\hat{I}_1\,|\psi_{\Omega,\nu,r}\rangle \approx$$

$$= \boxed{\begin{array}{c}\text{see}\\(8.66)\end{array}} \approx R^{(intr)}_{\Omega,\nu,r} + \hbar\,\Omega_{\nu,r}\,\tilde{I} \tag{8.71}$$

From (8.71) it follows for kinematic moment of inertia,

$$\frac{dE^{(lab)}_{\Omega,\nu,r}}{d\Omega_{\nu,r}} = \frac{dR^{(intr)}_{\Omega,\nu,r}}{d\Omega_{\nu,r}} + \hbar\,\tilde{I} + \hbar\,\Omega_{\nu,r}\,\frac{d\tilde{I}}{d\Omega_{\nu,r}} =$$

$$= \boxed{\begin{array}{c}\text{see}\\(8.68)\end{array}} = \frac{dR^{(intr)}_{\Omega,\nu,r}}{d\Omega_{\nu,r}} + \hbar\,\tilde{I} + \frac{dE^{(lab)}_{\Omega,\nu,r}}{d\tilde{I}}\,\frac{d\tilde{I}}{d\Omega_{\nu,r}} =$$

$$= \frac{dR^{(intr)}_{\Omega,\nu,r}}{d\Omega_{\nu,r}} + \hbar\,\tilde{I} + \frac{dE^{(lab)}_{\Omega,\nu,r}}{d\Omega_{\nu,r}} \quad \Rightarrow \quad \frac{dR^{(intr)}_{\Omega,\nu,r}}{d\Omega_{\nu,r}} = -\hbar\,\tilde{I}$$

$$\Rightarrow \quad \mathscr{F}^{(1)}_{\Omega,\nu,r} = \frac{\hbar\,\tilde{I}}{\Omega_{\nu,r}} = -\frac{1}{\Omega_{\nu,r}}\,\frac{dR^{(intr)}_{\Omega,\nu,r}}{d\Omega_{\nu,r}} \tag{8.72}$$

and for dynamical moment of inertia we obtain

$$\frac{d^2 E^{(lab)}_{\Omega,\,\nu,\,r}}{d\Omega^2_{\nu,\,r}} = \frac{d^2 R^{(intr)}_{\Omega,\,\nu,\,r}}{d\Omega^2_{\nu,\,r}} + 2\,\hbar\,\frac{d\tilde{I}}{d\Omega_{\nu,\,r}} + \hbar\,\Omega_{\nu,\,r}\,\frac{d^2\tilde{I}}{d\Omega^2_{\nu,\,r}}$$

$$\Rightarrow \quad \frac{d^2 R^{(intr)}_{\Omega,\,\nu,\,r}}{d\Omega^2_{\nu,\,r}} = \frac{d^2 E^{(lab)}_{\Omega,\,\nu,\,r}}{d\Omega^2_{\nu,\,r}} - 2\,\hbar\,\frac{d\tilde{I}}{d\Omega_{\nu,\,r}} - \hbar\,\Omega_{\nu,\,r}\,\frac{d^2\tilde{I}}{d\Omega^2_{\nu,\,r}} =$$

$$= \frac{d}{d\Omega_{\nu,\,r}}\Big(\frac{dE^{(lab)}_{\Omega,\,\nu,\,r}}{d\tilde{I}}\frac{d\tilde{I}}{d\Omega_{\nu,\,r}}\Big) - 2\,\hbar\,\frac{d\tilde{I}}{d\Omega_{\nu,\,r}} - \hbar\,\Omega_{\nu,\,r}\,\frac{d^2\tilde{I}}{d\Omega^2_{\nu,\,r}} =$$

$$= \boxed{\begin{array}{c}\text{see}\\(8.68)\end{array}} =$$

$$= \frac{d}{d\Omega_{\nu,\,r}}\Big(\hbar\,\Omega_{\nu,\,r}\,\frac{d\tilde{I}}{d\Omega_{\nu,\,r}}\Big) - 2\,\hbar\,\frac{d\tilde{I}}{d\Omega_{\nu,\,r}} - \hbar\,\Omega_{\nu,\,r}\,\frac{d^2\tilde{I}}{d\Omega^2_{\nu,\,r}} =$$

$$= -\hbar\,\frac{d\tilde{I}}{d\Omega_{\nu,\,r}} = -\mathscr{F}^{(2)}_{\Omega,\,\nu,\,r}$$

$$\Rightarrow \qquad \mathscr{F}^{(2)}_{\Omega,\,\nu,\,r} = \hbar\,\frac{d\tilde{I}}{d\Omega_{\nu,\,r}} = -\frac{d^2 R^{(intr)}_{\Omega,\,\nu,\,r}}{d\Omega^2_{\nu,\,r}} \tag{8.73}$$

Expressions (8.68), (8.69) and (8.73) allow to extract the experimental values of the rotational frequency $\hbar\Omega_{I,\,\nu,\,r}$, kinematic moment of inertia $\mathscr{F}^{(1)}_{I,\,\nu,\,r}$ and dynamical moment of inertia $\mathscr{F}^{(2)}_{I,\,\nu,\,r}$, respectively, if the derivatives are evaluated by corresponding differences:

$$\hbar\Omega_{I,\,\nu,\,r} = \frac{E^{(lab)}_{I,\,\nu,\,r} - E^{(lab)}_{I-2,\,\nu,\,r}}{\sqrt{I(I+1)} - \sqrt{(I-2)(I-1)}} \approx \frac{E^{(lab)}_{I,\,\nu,\,r} - E^{(lab)}_{I-2,\,\nu,\,r}}{2} \tag{8.74}$$

$$\frac{\hbar^2}{2\mathscr{F}^{(1)\,(exp)}_{I,\,\nu,\,r}} = \frac{E^{(lab)}_{I,\,\nu,\,r} - E^{(lab)}_{I-2,\,\nu,\,r}}{I(I+1) - (I-2)(I-1)} = \frac{E^{(lab)}_{I,\,\nu,\,r} - E^{(lab)}_{I-2,\,\nu,\,r}}{2(2I-1)} \tag{8.75}$$

$$\mathscr{F}^{(2)\,(exp)}_{I,\,\nu,\,r} = \hbar\,\frac{d\tilde{I}}{d\Omega_{I,\,\nu,\,r}} = \frac{2\hbar}{\Omega_{I+2,\,\nu,\,r} - \Omega_{I,\,\nu,\,r}} = \boxed{\begin{array}{c}\text{see}\\(8.74)\end{array}} =$$

$$= \frac{4\,\hbar}{E^{(lab)}_{I+4,\,\nu,\,r} - 2\,E^{(lab)}_{I+2,\,\nu,\,r} - E^{(lab)}_{I,\,\nu,\,r}} \tag{8.76}$$

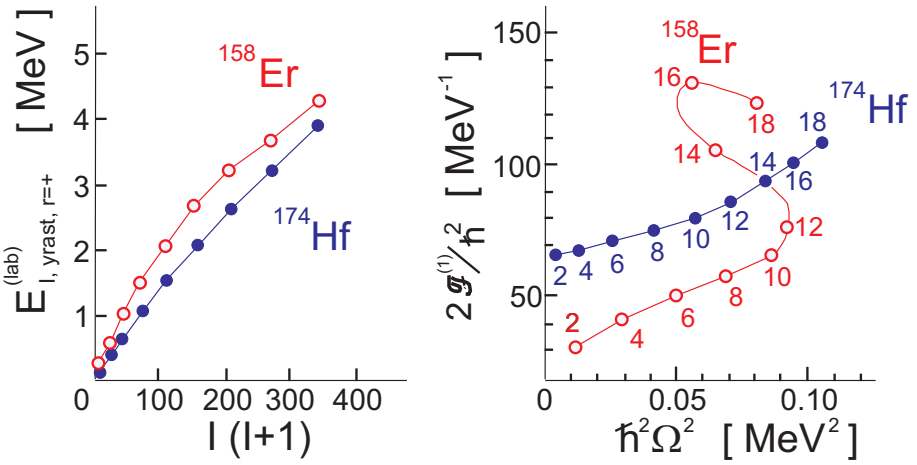


Figure 8.11: Dependence of the experimental yrast line laboratory energies $E^{(lab)}_{I,\,\nu=1,\,r=+}$ on $I(I+1)$ (left figure) and the yrast line kinetic moment of inertia $\mathscr{F}^{(1)}_{I,\,\nu=1,\,r=+}$ in the dependence on $\hbar^2\Omega^2_{I,\,\nu=1,\,r=+}$ (right figure). Kinetic moment of inertia was determined by (8.75) from the experimental yrast line energies (adapted from [304, 303]).

As an example of experimental data in the Fig.8.11 the experimental yrast line energies for ^{158}Er and ^{174}Hf in the dependence on $I(I+1)$ and kinetic moment of inertial $\mathscr{F}^{(1)}_{I,\,\nu=1,\,r=+1}$ in the dependence on $\hbar^2\Omega^2_{I,\,\nu=1,\,r=+1}$ are demonstrated. One can see that the dependence of $\mathscr{F}^{(1)}_{I,\,\nu=1,\,r=+1}$ on $\hbar^2\Omega^2_{I,\,\nu=1,\,r=+1}$ (right figure of the Fig.8.11) show the backbending behaviour in ^{158}Er (so called backbending effect).

The comparison of experimental values of the yrast line kinetic moment of inertia $\mathscr{F}^{(1),\,exp}_{I,\,yrast,\,r=i}$ for odd-A ^{159}Er and $\mathscr{F}^{(1),\,exp}_{I,\,yrast,\,r=+1}$ for even-even ^{158,160}Er in the dependence on $(\hbar\Omega_{I,\,yrast,\,r})^2$ are shown in the Fig.8.12.

It is a general feature that the backbending effect is observed in even-even nuclei more frequently and at lower angular momenta than in odd-A nuclei (as it can be seen from the example shown in the Fig.8.12). It is connected with so called Coriolis anti-pairing effect. The Coriolis interaction tends to align angular momenta of all nucleons in single-particle states near the Fermi level to be oriented along the rotational axis of the whole nucleus. In such a way its effect goes against the pairing residual interaction which tends to create pairs of nucleons with the zero angular momentum in each of these pairs (see the Chapter 6). Since the influence of the Coriolis interaction increases rapidly with the rotation frequency Ω the intrinsic excitation energy above the yrast line of the lowest 2-quasiparticle state in the even-even nucleus with aligned angular momenta of each quasiparticle in the pair (so called 2-qp unpaired band) goes down with the increasing Ω. Finally, at some criti-

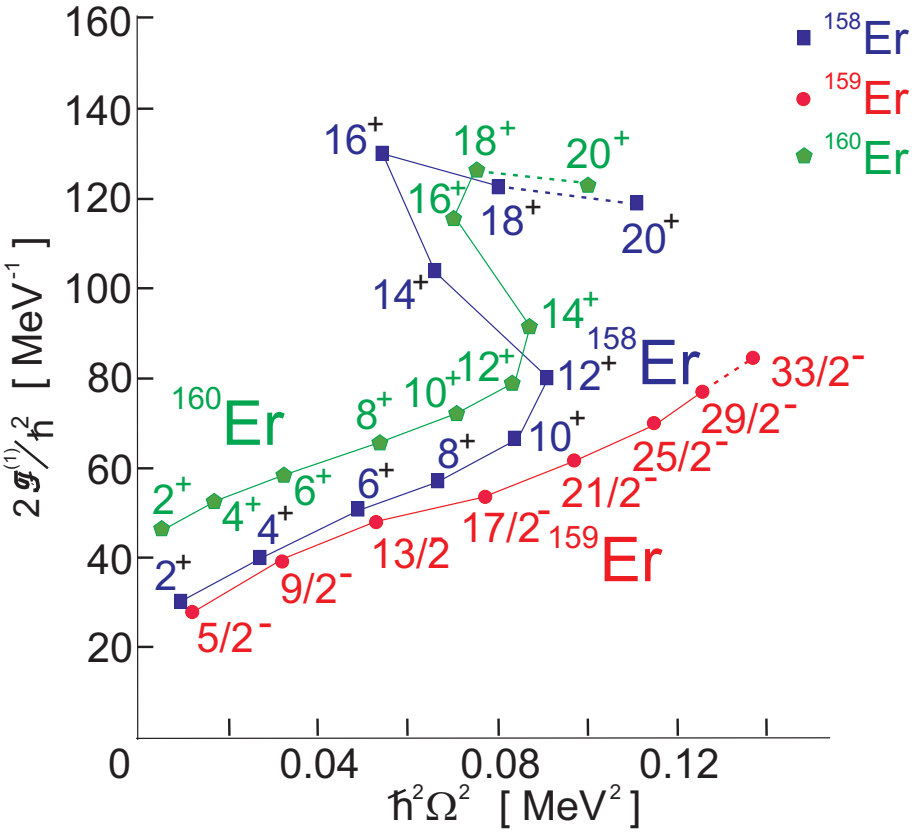


Figure 8.12: The comparison of the experimental yrast band kinetic moment of inertia as the function of the square of the rotational frequency for even-even ^{158,160}Er with kinetic inertia moment of odd-A ^{159}Er. One should realize that for given rotational band ν the signature r_ν is connected with the total angular momentum I_ν by $r_\nu = (-1)^{-i\pi I_\nu}$. So, for even nucleus yrast band (the lowest band with $r = +1$) we always have even values of I while for the yrast band in odd-A nuclei (the lowest band with $r = -i$) we have $I = 1/2,\ 5/2,\ 9/2,\ 13/2, \cdots$ (adapted from [301]).

cal rotational frequency Ω_c (or corresponding critical angular momentum I_c) intrinsic excitation energy of this unpaired two-quasiparticle state becomes zero and it merges with the ground rotational band states (vacuum for the quasiparticles for given value of rotational frequency). This situation is depicted in the schematic Fig.8.10 as the merging of the green dashed curve (the lowest 2-quasiparticle energies) with the ground state rotational band denoted as gsb. As a result the yrast line, which begins as ground rotational band at very low rotational frequencies, changes rapidly its its structure at this critical rotational frequency Ω_c which leads also to the quick changes in the dependence of the moment of inertia on the Ω in the vicinity of the critical value Ω_c (backbending effect). In odd-A nuclei there is always one nucleon unpaired and it sits in the single-particle state which is blocked with respect

to pairing. As a result the lowest excitation of the odd-A nucleus containing the unpaired aligned 2-quasiparticle state (that means the lowest particle + 2-quasiparticle configuration in the odd-A nucleus) is always higher in energy than the intrinsic energy of the lowest unpaired aligned 2-quasiparticle state in the neighbouring even-even nuclei. Therefore the first changes of the structure of the yrast band (the first backbending) occurs in odd-A nucleus at higher rotational frequency than in the neighbourning even-even nucleus. The Coriolis anti-pairing effect is discussed in more details in the Subsection 8.2.3.

8.2.2 Cranking formula for moment of inertia

The cranking formula for the 1-st principal component of the moment of inertia tenzor was already derived, see (7.298) or (7.299), as a mass parameter (7.289) for the spurious RPA solution connected with the invariance of the Hamiltonian with respect to the rotation by angle π round the first axis (which coincides with the 1-st principal axis of the inertia moment tenzor). However, historically the first derivation of the cranking formula (7.299) for the moment of inertia was performed in [151, 152] on the base of the low-roational frequency limit of the cranking model discussed in the previous subsection. Below the basic idea of this derivation is given.

Starting point of this derivation is the expression (8.59) which gives for the total laboratory frame Hamiltonian

$$\hat{H} = \hat{H}_{\Omega} + \hbar\Omega\, \hat{I}_1 \tag{8.77}$$

and corresponding yrast band stationary solution $\Psi^{(lab)}_{yrast,\,\Omega}$ of the total laboratory Hamiltonian can be ontained from the following equation

$$i\hbar\, \frac{\partial \Psi^{(lab)}_{yrast,\,\Omega}}{\partial t} = \hat{H}\, \Psi^{(lab)}_{yrast,\,\Omega} = E^{(lab)}_{yrast,\,\Omega}\, \Psi^{(lab)}_{yrast,\,\Omega} \tag{8.78}$$

If the rotational frequency Ω is small the total laboratory frame energy $E^{(lab)}_{yrast,\,\Omega}$ can be determined by the perturbation theory where the perturbation is given by $\hbar\Omega\, \hat{I}_1$ and for the yrast band states (which for the low Ω can be identified with the ground state rotational band) the unperturbed Hamiltonian is $\hat{H}_{intr} \equiv \hat{H}_{\Omega=0}$ with its eigen-vectors $|k\rangle$,

$$\hat{H}_{intr}\, |k\rangle = E^{(intr)}_{k}\, |k\rangle \tag{8.79}$$

where the state $|\, 0\rangle \equiv |\, k = 0\rangle$ corresponds to the unperturbed intrinsic ground state for $\Omega = 0$. Then

$$E^{(lab)}_{yrast,\,\Omega} \equiv \langle \Psi^{(lab)}_{yrast,\,\Omega}|\, \hat{H}\, |\, \Psi^{(lab)}_{yrast,\,\Omega}\rangle = \langle \Psi^{(lab)}_{yrast,\,\Omega}|\, \hat{H}_{intr} + \hbar\Omega\, \hat{I}_1\, |\, \Psi^{(lab)}_{yrast,\,\Omega}\rangle =$$

$$= \boxed{\begin{array}{c}\text{using perturbation theory}\\ \text{up to the second order in } \Omega\end{array}} =$$

$$= E^{(intr)}_{0} + \hbar\Omega\, \langle 0|\, \hat{I}_1\, |\, 0\rangle + \hbar^2\Omega^2 \sum_{k\neq 0} \frac{|\, \langle\, k\, |\, \hat{I}_1\, |\, 0\rangle\, |^2}{E^{(intr)}_{k} - E^{(intr)}_{0}} =$$

$$= \boxed{\begin{array}{c} \text{since } [\hat{H}_{intr}\ ,\ \hat{\mathscr{T}}\ ] = 0 \text{ then } \hat{\mathscr{T}}\ |\ 0\ \rangle = |\ 0\ \rangle \\ \text{and since } \hat{\mathscr{T}}\ \hat{I}_1\ \hat{\mathscr{T}}^{-1} = -\hat{I}_1 \quad \Longrightarrow \quad \langle\ 0\ |\ \hat{I}_1\ |\ 0\ \rangle = 0 \end{array}} =$$

$$= E_0^{(intr)} + \hbar^2\Omega^2 \sum_{k\neq 0} \frac{|\ \langle\ k\ |\ \hat{I}_1\ |\ 0\rangle\ |^2}{E_k^{(intr)} - E_0^{(intr)}} \tag{8.80}$$

This equation can be compared with the classical one,

$$E^{(lab)}_{yrast,\,\Omega} \approx\ E_0^{(intr)} + \frac{1}{2}\,\mathscr{F}_1\,\Omega^2 \tag{8.81}$$

and the resulting moment of inertia $\mathscr{F}$ can be idetified with

$$\mathscr{F}_1 = 2\hbar^2 \sum_{k\neq 0} \frac{|\ \langle\ k\ |\ \hat{I}_1\ |\ 0\rangle\ |^2}{E_k^{(intr)} - E_0^{(intr)}} \tag{8.82}$$

If the intrinsic Hamiltonian $\hat{H}_{intr}$ is treated in the framework of the model of independent quasiparticles then the expression (8.82) can be written as (7.299) (for even-even nucleus):

$$\mathscr{F}_1 = 2\hbar^2 \sum_{ij>0} \frac{|\ (\mathscr{U}_i\mathscr{V}_j - \mathscr{V}_i\mathscr{U}_j)\ \langle\ i\ |\ \hat{I}_1\ |\ j\rangle\ |^2}{E_i + E_j} \tag{8.83}$$

which is known as Belyaev formula (see [151, 152]). In (8.83) $\mathscr{U}_i$ and $\mathscr{V}_i$ stand for the pairing occupation amplitudes for the given quasiparticle state with the index i, E_i is the corresponding quasiparticle energy, and $\langle\ i\ |\ \hat{I}_1\ |\ j\rangle$ is the single-particle matrix element of the operator $\hat{I}_1$ (see the Chapter 6 for details and (7.299)).

The formula (8.83) was used for the determination of the moment of inertia depicted as "cranking formula" values in the Fig.8.7. These values were obtained in [305] using the Nilsson model with the pairing residual interaction in the simple monopole form - see (6.26). As it can be seen from the Fig.8.7 calculated moments of inertia according to (8.83) agree qualitatively with experimental values.

8.2.3 Microscopic version of the cranking model (shape transitions induced by rotation)

In this subsection selected results of the microscopic versions of the cranking model and their comparison with experimental data are discussed. As it was already mentioned in the Subsection 8.2.1 any microscopic or semimicroscopic treatment of the cranking model, that means the solving the equation (8.60), consists from two steps.

i. In the first step the single-particle mean field $\hat{H}^{(\Omega)}_{AV}$ should be obtained for all values of rotational frequencies Ω_I corresponding to all angular momenta I of levels investigated in the spectrum of given nucleus. From the strict theoretical point of view this single-particle mean field can be obtained by the HF method applied for given intrinsic Haliltonian $\hat{H}_\Omega$. In the more sophisticated approaches the HFB method for $\hat{H}_\Omega$ can be used for obtaining quasiparticle mean field directly which enables to take into account also the pairing residual interaction involved in the $\hat{H}_\Omega$. In order to obtain rotational frequency Ω_I corresponding to given I it is necessary to solve this HFB equation (see (6.148)) with the Hamiltonian $\hat{H}_\Omega$ for a mesh of values Ω. In such a way for each value Ω of this mesh we obtain the system of quasiparticle creation operators $\beta^+_i(\Omega)$ (see (6.102)) with corresponding vacuum $|HFB\rangle$ ($\beta_i(\Omega)|HFB\rangle_\Omega = 0$) which represents the ground state of the nucleus for given value of Ω (yrast state for given Ω). Then we calculate ${}_\Omega\langle HFB|\,\hat{I}_1\,|\,HFB\rangle_\Omega$ which, according to (8.65), corresponds to $\tilde{I} = \sqrt{I(I+1)}$. If it is done for all values of Ω from the mesh we obtain the dependence $I(\Omega)$ from which the values of the frequency Ω_I corresponding to the particular angular momentum I can be determined. Then for each investigated I we solve again the HFB equation (6.148) and obtain quasiparticle creation (annihilation) operators $\beta^+_i(I)$ ($\beta_i(I)$) with the corresponding vacuum $|HFB\rangle_I$. That means the quasiparticle mean field $\hat{H}^{(I)}_{qp}$ (see (6.151))

$$\hat{H}^{(I)}_{qp} = {}_I\langle HFB|\,\hat{H}_\Omega\,|\,HFB\rangle_I + \sum_i E^{(I)}_i\;\beta^+_i(I)\,\beta_i(I) \tag{8.84}$$

with corresponding residual interaction $\hat{V}^{(I)}_{res}$ ($\hat{H}_{\Omega_I} = \hat{H}^{(I)}_{qp} + \hat{V}^{(I)}_{res}$) are determined. In (8.84) E^I_i is the quasiparticle energy corresponding to the given one-quasiparticle state $|i\rangle_I = \beta^+_i(I)\,|\,HFB\rangle_I$ (with its $\mathscr{U}^{(i)}_{(I)}$ and $\mathscr{V}^{(i)}_{(I)}$ amplitudes for the given I - see (6.149)).

Since in this subsection we suppose that the intrinsic Hamiltonian quasi-

particle mean field $\hat{H}^{(\Omega)}_{qp}$ is invariant with respect to the rotation by angle π round the 1-st intrinsic axis ($[\hat{H}^{(\Omega)}_{qp}, \hat{\mathscr{R}}_1(\pi)] = 0$) for each value of Ω (or I) and also is invariant with respect to parity ($[\hat{H}^{(\Omega)}_{qp}, \hat{\mathscr{P}}] = 0$) the signature $r_j = \pm i$ and parity $\pi_j = \pm 1$ are good quantum numbers for all single-quasiparticle states $|j\rangle_I \equiv |\, \pi_j,\, r_j,\, j\,\rangle_I = \beta^+(I)_j \,|\, HFB\rangle_I$,

$$\begin{aligned}
&\hat{H}^{(I)}_{qp} \,|\, \pi_j,\, r_j,\, j\rangle = E^{(I)}_j \,|\, \pi_j,\, r_j,\, j\,\rangle_I \\
&\hat{\mathscr{R}}_1(\pi) \,|\, \pi_j,\, r_j,\, j\,\rangle = r_j \,|\, \pi_j,\, r_j,\, j\,\rangle_I \qquad\qquad (r_j = \pm i) \\
&\hat{\mathscr{P}} \,|\, \pi_j,\, r_j,\, j\,\rangle = \pi_j \,|\, \pi_j,\, r_j,\, j\,\rangle_I \qquad\qquad (\pi_j = \pm 1)
\end{aligned} \tag{8.85}$$

It can be shown (see e.g. [302]) that it is enough to solve the HFB equation for one signature only (e.g. $r_j = -i$ which corresponds to the positive $\alpha = +1/2$ - see the footnote below the expression (8.64)) but for both positive and negative energies since the negative signature quasiparticle eigen states (with $r_j = +i$) are obtained from the positive ones according to the relation

$$(\, -E^{(I)}_j,\, \mathscr{U}^{(j)}_{(I)},\, \mathscr{V}^{(j)}_{(I)}\,) \quad \rightarrow \quad (\, E^{(I)}_{\tilde{j}},\, \mathscr{V}^{(\tilde{j})}_{(I)},\, \mathscr{U}^{(\tilde{j})}_{(I)}\,) \tag{8.86}$$

where the quasiparticle $\tilde{j}$ denotes the signature partner of the quasiparticle j ($\beta^+_{\tilde{j}} \equiv \mathscr{R}_1(\pi)\, \beta^+_j\, \mathscr{R}^{-1}_1(\pi)$). One should also realize that the HFB equation (6.148) with the cranking Hamiltonian $\hat{H}_\Omega$ provides half of the HFB solutions $|\, \pi_j,\, r_j,\, j\,\rangle_\Omega$ with positive energies $E^{(\Omega)}_j$ and half with negative energies $E^{(\Omega)}_j$. Only solutions with positive quasiparticle energies have physical meaning (see [302]) [10].

ii In the second step residual interactions $\hat{V}^{(I)}_{res} = \hat{V}^{(\Omega_I)}_{res}$ are taken into account by means of the RPA or some beyond RPA methods for each value of the rotational frequency Ω_I. In the case of the RPA we should solve the following equation (see (7.230)) for each value if I corresponding to Ω_I,

$$\begin{pmatrix} A(\Omega) & B(\Omega) \\ B^*(\Omega) & A^*(\Omega) \end{pmatrix} \begin{pmatrix} X^{(\nu)}(\Omega) \\ Y^{(\nu)}(\Omega) \end{pmatrix} = \hbar\omega^{(\Omega)}_\nu \begin{pmatrix} 1 & 0 \\ 0 & -1 \end{pmatrix} \begin{pmatrix} X^{(\nu)}(\Omega) \\ Y^{(\nu)}(\Omega) \end{pmatrix} \tag{8.87}$$

[10] Generally the HFB equation (6.148) with the cranking intrinsic Hamiltonian $\hat{H}_I = \hat{H}_{\Omega_I}$ (which is not time-reversal invatiant) gives half solutions (quasiparticles) with the positive energies, $E^{(I)}_j = E^{(I)}_{\pi_j,\, r_j,\, j} > 0$, and half with the negative energy solutions $\tilde{E}^{(I)}_j = \tilde{E}^{(I)}_{\pi_j,\, r_j,\, j} < 0$. Such energy spectrum is symmetric with respect to the zero energy value, that means we have negative energy spectrum reflection image, $\tilde{E}^{(I)}_{\pi_j,\, r_j,\, j}$, of the positive energy part of the spectrum, $E^{(I)}_{\pi_j,\, r_j,\, j}$, with the following condition corresponding to (8.86),

$$\tilde{E}^{(I)}_{\pi_j,\, r_j,\, j} = -E^{(I)}_{\pi_j,\, -r_j,\, j}$$

and only positive energy part of the spectrum has a physical meaning.

where (see (7.34), (7.35))

$$A_{ij,\,i'j'}(\Omega) = \left(E_i^{(\Omega)} + E_j^{(\Omega)}\right)\delta_{ii'}\,\delta_{jj'} + \\ +\frac{1}{2}\;{}_\Omega\langle HFB|\,\left[\,\beta_j(\Omega)\beta_i(\Omega),\,\left[\,\hat{V}_{res}^{(\Omega)},\,\beta_{i'}^{(\Omega)\,+}\beta_{j'}^{(\Omega)\,+}\,\right]\,\right]\,|\,HFB\rangle_\Omega$$

$$B_{ij,\,i'j'}(\Omega) = -\frac{1}{2}\;{}_\Omega\langle HFB|\,\left[\,\beta_j(\Omega)\beta_i(\Omega),\,\left[\hat{V}_{res}^{(\Omega)},\,\beta_{j'}\beta_{i'}\,\right]\,\right]\,|\,HFB\rangle_\Omega \tag{8.88}$$

The solving gives the phonon energies $\hbar\omega_\nu^{(\Omega)}$ with corresponding amplitudes $X_{ij}^{(\nu)}(\Omega)$ and $Y_{ij}^{(\nu)}(\Omega)$ of all RPA phonons $Q_\nu^+(\Omega)$ (see (7.207)) [11] ,

$$Q_\nu^+(\Omega) = \frac{1}{2}\sum_{ij}\left(X_{ij}^{(\nu)}\,(\Omega)\,\beta_i^+(\Omega)\,\beta_j^+(\Omega) - Y_{ij}^{(\nu)}\,(\Omega)\,\beta_j(\Omega)\,\beta_i(\Omega)\right) \tag{8.89}$$

For low excitation intrinsic even-even nucleus states above the yrast line states $|\psi_{\Omega,\,yrast}^{(intr)}\rangle \equiv |\,HFB\rangle_\Omega$ a one-phonon character can be assumed. Since $[\,\hat{H}_\Omega,\,\hat{\mathscr{R}}_1(\pi)\,] = [\,\hat{H}_\Omega,\,\hat{\mathscr{P}}\,] = 0$ the phonons $Q_\nu^+ \equiv Q_{\nu,\,\pi_\nu,\,r_\nu}^+$ are characterized by the sharp value of the parity $\pi_\nu = \pm 1$ and signature $r_\nu = \pm 1$,

$$\left[\,\hat{H}_\Omega,\,Q_{\nu,\,\pi_\nu,\,r_\nu}^+(\Omega)\,\right] = \hbar\omega_\nu^{(\Omega)}\,Q_{\nu,\,\pi_\nu,\,r_\nu}^+(\Omega)$$
$$\left[\,\hat{H}_\Omega,\,Q_{\nu,\,\pi_\nu,\,r_\nu}(\Omega)\,\right] = -\hbar\omega_\nu^{(\Omega)}\,Q_{\nu,\,\pi_\nu,\,r_\nu}(\Omega)$$
$$\hat{\mathscr{P}}\,Q_{\nu,\,\pi_\nu,\,r_\nu}^+(\Omega)\,\hat{\mathscr{P}}^{-1} = \pi_\nu\,Q_{\nu,\,\pi_\nu,\,r_\nu}^+(\Omega) \qquad (\pi_\nu = \pm 1)$$
$$\hat{\mathscr{R}}_1(\pi)\,Q_{\nu,\,\pi_\nu,\,r_\nu}^+(\Omega)\,\hat{\mathscr{R}}_1^{-1}(\pi) = r_\nu\,Q_{\nu,\,\pi_\nu,\,r_\nu}^+(\Omega) \qquad (r_\nu = \pm 1) \tag{8.90}$$

It is clear that the positive signature phonon $Q_{\nu,\,\pi_\nu,\,r_\nu=+1}^+$ defined by (8.89) involves two-quasiparticle components $\beta_i^+(\Omega)\,\beta_j^+(\Omega)$ where the single-particles i and j are of the opposite signature ($r_\nu = r_i r_j = -i\;i = +1$) while the negative signature phonon $Q_{\nu,\,\pi_\nu,\,r_\nu=-1}^+$ involves two-quasiparticle components $\beta_i^+(\Omega)\,\beta_j^+(\Omega)$ with the signature r_i equal to the signature r_j (because $r_\nu = r_i r_j = i\;i = -1$). If the lowest excited rotational bands, schematically shown in the Fig.8.9, have one-phonon character the states $|\psi_{\Omega_I,\,\nu,\,r_\nu=+1}^{(intr)}\rangle$, $|\psi_{\Omega_{I\pm2},\,\nu,\,r_\nu=+1}^{(intr)}\rangle$, $|\psi_{\Omega_{I\pm4},\,\nu,\,r_\nu=+1}^{(intr)}\rangle$, $\cdots$ are created by $Q_{\nu,\,\pi_\nu,\,r_\nu=+1}^+(\Omega_I)$, $Q_{\nu,\,\pi_\nu,\,r_\nu=+1}^+(\Omega_{I\pm2})$, $Q_{\nu,\,\pi_\nu,\,r_\nu=+1}^+(\Omega_{I\pm4})$, $\cdots$ acting on $\psi_{\Omega_I,\,yrast,\,r=+1}^{(intr)} = |HFB\rangle_I$, $\psi_{\Omega_{I\pm2},\,yrast,\,r=+1}^{(intr)} = |HFB\rangle_{I\pm2}$, $\psi_{\Omega_{I\pm4},\,yrast,\,r=+1}^{(intr)} = |HFB\rangle_{I\pm4}$, $\cdots$, respectively (here we suppose

[11] In the case when residual interactions $\hat{V}_{res}^{(\Omega)}$ have a separable form the amplitudes $X_{ij}^{(\nu)}(\Omega)$ and $Y_{ij}^{(\nu)}(\Omega)$ together with phonon energies $\hbar\omega_\nu^{(\Omega)}$ can be obtained by the simplified version of the RPA descibed in the Subsection 7.3.1.1.3 (see (7.313), (7.314), (7.315), (7.316)).

even I). The states with odd values of ang. momentum, $|\psi^{(intr)}_{\Omega_{I\pm1},\,\nu,\,r_\nu=-1}\rangle$, $|\psi^{(intr)}_{\Omega_{I\pm3},\,\nu,\,r_\nu=-1}\rangle$, $\cdots$ are created by $Q^+_{\nu,\,\pi_\nu,\,r_\nu=-1}(\Omega_I)$, $Q^+_{\nu,\,\pi_\nu,\,r_\nu=-1}(\Omega_{I\pm2})$, $\cdots$ acting on $|HFB\rangle_I$, $|HFB\rangle_{I\pm2}$, $\cdots$, respectively (as it can be seen in the Fig.8.9).

As an example of a semi-microscopic cranking model calculations some results for ^{156}Dy and ^{162}Yb taken from [306] are demonstrated. The calculations were based on the phenomenological cranked Nilsson single-particle mean field $\hat{H}_{Nilss}-\hbar\Omega\hat{I}_1$ (where $\hat{H}_{Nilss}=\hat{H}_{AV}$ - see (5.35)) with the monopole pairing residual interaction $\hat{V}_{pair}$ and long-range residual interaction $\hat{V}_{l.res}$ in the form of the quadrupole-quadrupole and spin-spin separable form (see [306] for details). The cranking intrinsic Hamiltonian was

$$\hat{H}_\Omega=\hat{H}_{Nilss}-\hbar\Omega\hat{I}_1+\hat{V}_{pair}+\hat{V}_{l.res} \tag{8.91}$$

The quasiparticle mean field $\hat{H}^{(\Omega)}_{qp}$ for each value of Ω with corresponding quasiparticle creation operators (see (6.102)),

$$\begin{aligned}
&\beta^+_i(\Omega)=\sum_k\left(\,\mathscr{U}^{(i)}_k(\Omega)\,c^+_k+\mathscr{V}^{(i)}_{\bar{k}}(\Omega)\,c_{\bar{k}}\,\right)\\
&\beta^+_{\bar{i}}(\Omega)=\sum_k\left(\,\mathscr{U}^{(i)}_k(\Omega)\,c^+_{\bar{k}}-\mathscr{V}^{(i)}_{\bar{k}}(\Omega)\,c_k\,\right)\equiv\\
&\equiv\sum_k\left(\,\mathscr{U}^{(\bar{i})}_{\bar{k}}(\Omega)\,c^+_{\bar{k}}+\mathscr{V}^{(\bar{i})}_k(\Omega)\,c_k\,\right),\quad\left(\,\mathscr{U}^{(\bar{i})}_{\bar{k}}\equiv\mathscr{U}^{(i)}_k\,,\;\mathscr{V}^{(\bar{i})}_k\equiv-\mathscr{V}^{(i)}_{\bar{k}}\,\right)
\end{aligned} \tag{8.92}$$

were obtained by the solving of the HFB equations (6.148) which had the following form in the case of the Hamiltonian (8.91)

$$\begin{aligned}
&\begin{pmatrix}h^{(\Omega)}(1)&\Delta^{(\Omega)}\\ \Delta^{(\Omega)}&h^{(\Omega)}(2)\end{pmatrix}\begin{pmatrix}\mathscr{U}^{(i)}(\Omega)\\ \mathscr{V}^{(i)}(\Omega)\end{pmatrix}=E^{(\Omega)}_i\begin{pmatrix}\mathscr{U}^{(i)}(\Omega)\\ \mathscr{V}^{(i)}(\Omega)\end{pmatrix}\\
&\begin{pmatrix}h^{(\Omega)}(1)&\Delta^{(\Omega)}\\ \Delta^{(\Omega)}&h^{(\Omega)}(2)\end{pmatrix}\begin{pmatrix}\mathscr{V}^{(\bar{i})}(\Omega)\\ \mathscr{U}^{(\bar{i})}(\Omega)\end{pmatrix}=-E^{(\Omega)}_{\bar{i}}\begin{pmatrix}\mathscr{V}^{(\bar{i})}(\Omega)\\ \mathscr{U}^{(\bar{i})}(\Omega)\end{pmatrix}
\end{aligned} \tag{8.93}$$

where

$$\begin{aligned}
\big(h^{(\Omega)}(1)\big)_{kl}&=\langle k|\,\hat{H}_{Nilss}\,|\,l\rangle-\hbar\Omega\langle k|\,\hat{I}_1\,|\,l\rangle\\
\big(h^{(\Omega)}(2)\big)_{kl}&=-\langle k|\,\hat{H}_{Nilss}\,|\,l\rangle-\hbar\Omega\langle k|\,\hat{I}_1\,|\,l\rangle\\
\big(\Delta^{(\Omega)}\big)_{kl}&=-\delta_{kl}\,G_{\tau\,\Omega}\langle HFB|\sum_{l'}c_{\bar{l}'}\,c_{l'}\,|\,HFB\rangle_\Omega=\\
&=\delta_{kl}\,G_\tau\sum_{il'}\mathscr{U}^{(i)}_{l'}\,\mathscr{V}^{(i)}_{\bar{l}'}
\end{aligned} \tag{8.94}$$

with

$$\left(\begin{array}{c} \mathscr{U}^{(i)}(\Omega) \\ \mathscr{V}^{(i)}(\Omega) \end{array} \right) \equiv \left[\begin{array}{c} \mathscr{U}_1^{(i)}(\Omega) \\ \mathscr{U}_2^{(i)}(\Omega) \\ \vdots \\ \mathscr{V}_{\bar{1}}^{(i)}(\Omega) \\ \mathscr{V}_{\bar{2}}^{(i)}(\Omega) \\ \vdots \end{array} \right] \qquad \left(\begin{array}{c} \mathscr{V}^{(\bar{i})}(\Omega) \\ \mathscr{U}^{(\bar{i})}(\Omega) \end{array} \right) \equiv \left[\begin{array}{c} \mathscr{V}_1^{(\bar{i})}(\Omega) \\ \mathscr{V}_2^{(\bar{i})}(\Omega) \\ \vdots \\ \mathscr{U}_{\bar{1}}^{(\bar{i})}(\Omega) \\ \mathscr{U}_{\bar{2}}^{(\bar{i})}(\Omega) \\ \vdots \end{array} \right] \tag{8.95}$$

The solving of (8.93) can be performed independently for protons ($\tau = prot$) and neutrons ($\tau = neut$) and for given parity gradually for all needed values Ω. In (8.92)-(8.94) indexes $k, \bar{k}, l, \bar{l}$ denotes so called Goodman oscillator basis vectors $|k\rangle \equiv c_k^+ \, |-\rangle \equiv |N_k l_k j_k K_k\rangle_G$ which is connected with the standard oscillator vectors $|N_k l_k j_k K_k\rangle$ by the following definition ($K > 0$)

$$|Nljk\rangle_G \equiv \frac{1}{\sqrt{2}} \left(\, |NLJK\rangle + i \, \mathscr{R}_1(\pi) \, |NLJK\rangle \, \right) =$$

$$= \boxed{\begin{array}{c} \text{because - see (1.48)} \\ \mathscr{R}_1(\pi) \, |NLJK\rangle = \mathscr{R}_3^{-1}(\pi) \mathscr{R}_2^{-1}(\pi) \, |Nljk\rangle = \\ = \mathscr{R}_3^{-1}(\pi) \, |\overline{NLJK}\rangle = e^{i\pi K} \, |\overline{Nljk}\rangle = i \, (-1)^{K-\frac{1}{2}} |\overline{Nljk}\rangle \end{array}} =$$

$$= \frac{1}{\sqrt{2}} \left(\, |NLjK\rangle - (-1)^{K-\frac{1}{2}} \, |\overline{Nljk}\rangle \, \right) \tag{8.96}$$

$$|\overline{NLjk}\rangle_G = \hat{\mathscr{T}} |NLjk\rangle_G = \frac{1}{\sqrt{2}} \left(\, |\overline{NLjk}\rangle + (-1)^{K-\frac{1}{2}} |NLjk\rangle \, \right) =$$

$$= \frac{(-1)^{K-\frac{1}{2}}}{\sqrt{2}} \left(\, |NLjk\rangle - i \, \mathscr{R}_1(\pi) \, |NLjk\rangle \, \right) \tag{8.97}$$

The Goodman oscillator basis $|Nljk\rangle_G$ is very convenient for the cranking model because the signature of the state $|k\rangle_i = |N_k l_k j_k K_k\rangle_G$ is $r_k = -i$ and $r_{\bar{k}} = -i$ for $|\bar{k}\rangle = |\overline{N_k l_k j_k K_k}\rangle_G$,

$$\begin{aligned} \hat{\mathscr{R}}_1(\pi) \, |k\rangle &= \hat{\mathscr{R}}_1(\pi) \, |N_k l_k j_k K_k\rangle_G = -i \, |N_k l_k j_k K_k\rangle_G \\ \hat{\mathscr{R}}_1(\pi) \, |\bar{k}\rangle &= \hat{\mathscr{R}}_1(\pi) \, |\overline{N_k l_k j_k K_k}\rangle_G = i \, |\overline{N_k l_k j_k K_k}\rangle_G \end{aligned} \tag{8.98}$$

From the generalized Bogoliubov transformation (8.92) it is clearly seen that the one-quasiparticle states $\beta_i^+(\Omega) \, |HFB\rangle_\Omega$ and $\beta_{\bar{i}}^+(\Omega) \, |HFB\rangle_\Omega$ have also signatures $r_i = -i$ and $r_{\bar{i}} = -i$, respectively,

$$\begin{aligned} \hat{\mathscr{R}}_1(\pi) \, \beta_i^+(\Omega) \, |HFB\rangle_\Omega &= -i \, \beta_i^+(\Omega) \, |HFB\rangle_\Omega \\ \hat{\mathscr{R}}_1(\pi) \, \beta_{\bar{i}}^+(\Omega) \, |HFB\rangle_\Omega &= i \, \beta_{\bar{i}}^+(\Omega) \, |HFB\rangle_\Omega \end{aligned} \tag{8.99}$$

So, we solve HFB equations (8.93) and we take solutions with the positive quasiparticle energies ($E_i^{(\Omega)} > 0$, $E_{\bar{i}}^{(\Omega)}) > 0$) (but with the both signatures) which have only the physical meaning.

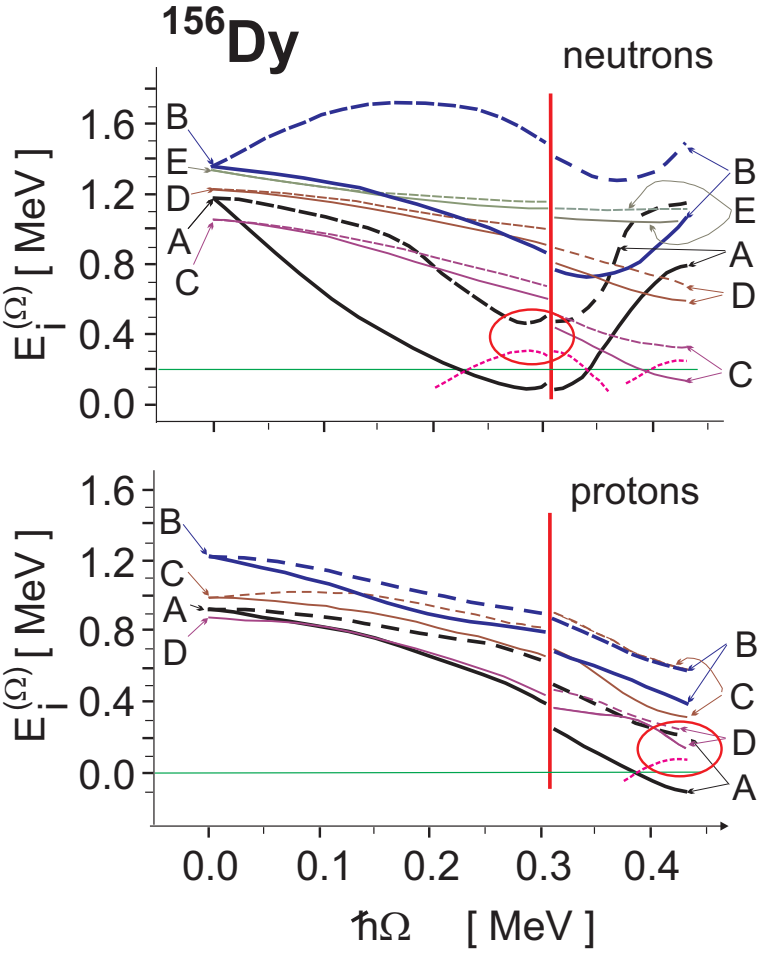


Figure 8.13: Lowest quasineutron energies (upper panel) and quasiproton energies (lower panel) for ^{156}Dy in the dependence on the rotational frequency $\hbar\Omega$. Thick (thin) lines are used for positive (negative) parity quasiparticles. The positive (negative) signature quasiparticle levels are connected by solid (dashed) lines. At $\Omega = 0$, quasineutron levels (upper panel) denoted by A, B, C, D, and E corresponds to the Nilsson quantum numbers 3/2[651], 1/2[660], 3/2[521], 5/2[521], and 11/2[505], respectively. Quasiproton levels (lower panel) for $\Omega = 0$ denoted by A, B, C, and D are connected with Nilsson quantum numbers 3/2[523], 5/2[532], 3/2[411], and 5/2[411], respectively. For $\Omega > 0$ each originally Nilsson quasiparticle level i splits into two levels, E_i and $E_{\bar{i}}$, according to the signature $r_i = -i$ and $r_{\bar{i}} = +i$. The shape transition point (discussed further in the text) is denoted by the vertical red line. The lowest quasicrossings are surrounded by circles (taken from [306]).

In the Fig.8.13 the dependence of the lowest quasineutron (top panel) and quasiproton (bottom panel) energies $E_i^{(\Omega)}$ and $E_{\bar{i}}^{(\Omega)}$ on the rotational frequency Ω is demonstrated for ^{156}Dy. One can see that quasiparticle levels

with different parities or with different signatures can cross each other as a function of Ω but levels with the same parity and the same signature cannot cross because they repulse each other in the Fig.8.13. The places in the figure where two levels with the same parity and signature are closest each other are called as quasicrossings. At $\Omega = 0$, each quasiparticle can be characterized by the Nilsson quantum numbers (see the text below the expr. (5.47)) and the angular momentum projection K is good quantum number if there is only axial deformation of the intrinsic mean field at $\Omega = 0$. For $\Omega = 0$ the quasiparticle i (with given parity π_i and signature $r_i = -i$) has the same energy as the quasiparticle $\bar{i}$ (that means the same quasiparticle energy for two quasiparticles with given parity $\pi_{\bar{i}} = \pi_i$ and with the opposite signature $r_{\bar{i}} = -r_i = i$). In the rotating case, $\Omega \neq 0$, the energies of these two quasiparticles i and $\bar{i}$ split due to the nonzero cranking term in the Hamiltonian $\hat{H}_\Omega$ as can be seen in the Fig.8.13. The Nilsson asymptotic quantum numbers lose also their validity in the rotating case because of the strong mixing caused by the cranking term. The analysis of the quasiparticle proton and neutron spectra in the dependence on Ω indicates that the lowest quasicrossing occur at $\hbar\Omega \approx 0.275$ (0.42) MeV for neutron (proton) system in ^{156}Dy and it is surrounded by red circle in the Fig.8.13. Similar quasicrossings was observed in [306] for ^{162}Yb and this effect is known for all rotating deformed nuclei (see e.g. [302]).

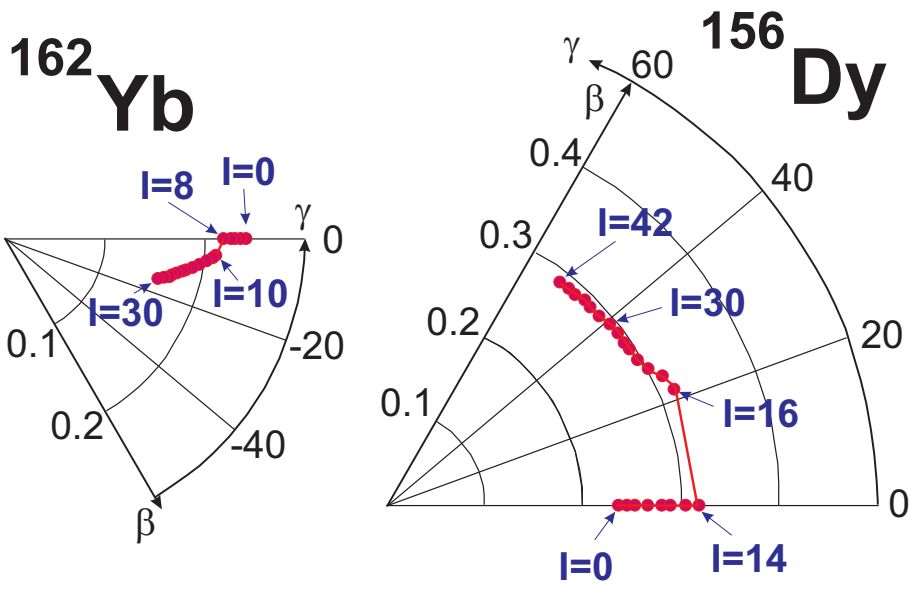


Figure 8.14: Equilibrium deformations in $\beta-\gamma$ plane as a function of the angular momentum $I \approx {}_\Omega\langle HFB|\,\hat{I}_1\,|\,HFB\rangle_\Omega$ in units of $\hbar$ (taken from [310]).

Knowing the neutron and proton quasiparticle systems with correspond-

ing vacua $\mid HFB\rangle_{\Omega}^{(neut)}$, $\mid HFB\rangle_{\Omega}^{(prot)}$ in the dependence on Ω we can calculate quadrupole mass moments $q_{20}^{(\Omega)}$ and $q_{22}^{(\Omega)}$, which are connected with the quadrupole deformation parameters β_{Ω} and γ_{Ω} by (see (7.449))

$$
\begin{aligned}
q_{20} =_{\Omega} \langle HFB| \hat{Q}_{00}^{(mass)} \mid HFB\rangle_{\Omega} = \\
= \frac{1}{\sqrt{20\pi}} 3\, r_0^2\, A^{5/3}\, \beta_{\Omega}\, \cos\gamma_{\Omega} \qquad (\text{in } fm^2) \\
q_{22} =_{\Omega} \langle HFB| \hat{Q}_{22}^{(mass)} \mid HFB\rangle_{\Omega} = \\
= \frac{1}{\sqrt{40\pi}} 3\, r_0^2\, A^{5/3}\, \beta_{\Omega}\, \sin\gamma_{\Omega} \qquad (\text{in } fm^2) \qquad (8.100)
\end{aligned}
$$

In the Fig.8.14 the dependence of the equilibrium deformations β_{Ω} and γ_{Ω} obtained from (8.100) for values of Ω_I which gives the angular momentum I according to (8.66), ${}_{\Omega}\langle HFB|\hat{I}_1|HFB\rangle_{\Omega} = \sqrt{I(I+1)}$, for ^{156}Dy and ^{162}Yb. One can see that both nuclei, ^{156}Dy and ^{162}Yb, are non-axially deformed ($\gamma_{\Omega_I} \neq .0$) starting from some values of I (so called critical point), for $I_c \approx 14-16$ in ^{156}Dy and $I_c \approx 8-10$ which corresponds to $\hbar\Omega_c \approx 0.3$ MeV for ^{156}Dy and $\hbar\Omega_c \approx 0.25$ MeV for ^{162}Yb. At the critical rotational frequency Ω_c the shape of the both nuclei in the yrast line is quickly (by jump) changed from the axial deformation $\gamma = 0$ into the non-axial one $\gamma \neq 0$ (shape transition). It corresponds to the jump change of the structure of the quasiparticle vacuum $|HFB\rangle_{\Omega}$ for $\Omega = \Omega_c$. In the literature this shape transition is considered as the phase transition from he axial deformation phase into the non-axial deformation shape. For instance, based on the energy surface (β, γ) minima analysis in the [306] it is shown that the axial-nonaxial deformation shape transition in ^{156}Dy possesses typical features of the first-order phase transition while this shape transition in ^{162}Yb can be probably classified as the phase transition of the second order. In [306] it is also discussed the connection of the shape transition and the lowest quasi-crossing of the quasiparticle levels (compare the critical value $\Omega_c = 0.3$ MeV with the lowest quasi-crossing of quasi- neutron levels at $\hbar\Omega \approx 0.275$ MeV in the ^{156}Dy observed in the Fig.8.13).

In the Fig.8.15 the kinematic moments of inertia $\mathscr{F}^{(1)}$ calculated in [306] by means of (8.66) are compared with experimental values obtained by (8.75) for ^{156}Dy and ^{162}Yb. One can see the quantitative agreement. The backbending effect is seen in the both investigated nuclei ^{156}Dy and ^{162}Yb.

Using calculated quasiparticle systems for all needed rotational frequencies Ω obtained by the solving of the HFB equation (8.93) the RPA equations (8.87) can be solved for both signatures $r = \pm 1$ and both parities $\pi = \pm 1$

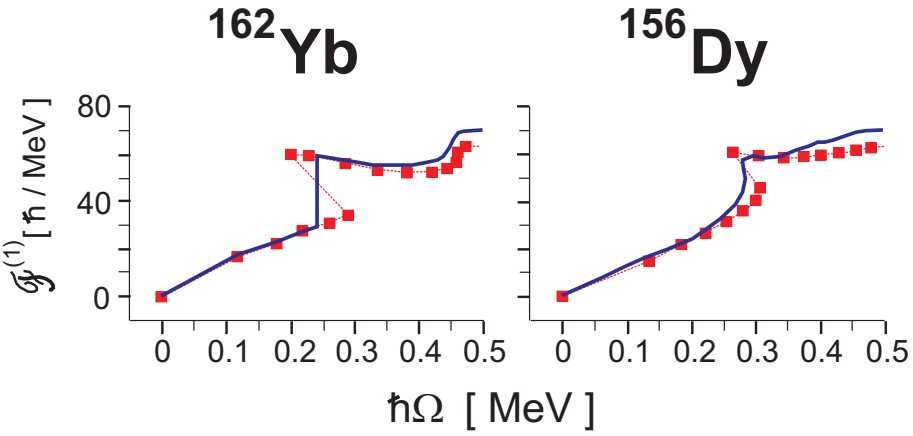


Figure 8.15: Calculated kinematical moment of inertia for ^{156}Dy and ^{162}Yb (blue solid line) are compared with corresponding experimental values. Experimetal values (red squares) are connected with the dashed lines (taken from [306]).

(see [306]). Calculated excitation energies $\hbar\omega_\nu$ (see [306]) for two lowest RPA solutions, $\nu = 1$ and $\nu = 2$, and for positive signature $r_\nu = +1$, and positive parity $\pi_\nu = +1$, are compared with corresponding experimental values in the Fig.8.16. It is clearly seen that the first positive signature and parity excitation energy $\hbar\omega_{\nu=1}$ goes to zero in both nuclei ^{162}Yb and ^{156}Dy for rotational frequency close to critical rotational frequency $\hbar\Omega_c$ of the first quasicrossing or shape transition rotational frequency discussed above. By other words it means that the first positive parity and positive signature rotational band, connecting the lowest RPA solutions with the excitation energy $\hbar\omega_\nu$ above the yrast line energies, merges with the ground (yrast) band at rotational frequencies near the critical first quasicrossing frequency $\hbar\Omega_c$. Historically this first excited band with $\nu = 1$ was called as "Stockholm" band (s-band) because its merging with the ground band for rotational frequency around $\hbar\Omega_\nu$ was discussed for the first time in papers of Stockholm group in the beginning of the 70-ties (see [307, 308, 302]).

In order to see in more details what happens with the quasiparticle mean field (with its quasiparticle vacua $|HFB\rangle_\Omega$) in the shape phase transition region with the rotational frequencies near the critical $\hbar\Omega_c$ the Fig.8.17 is presented with dependence of the neutron pairing gaps Δ_n on the square of the rotational frequency $(\hbar\Omega)^2$ for ^{166,168,170}Yb where backbending effect was observed (see [309]). The calculation in [309] was performed in the framework of the phenomenological independent quasiparticle model with the HFB approach without the long range residual interaction (without the RPA). In the upper panels of the fig.8.17 the neutron pairing gaps $\Delta_n =$

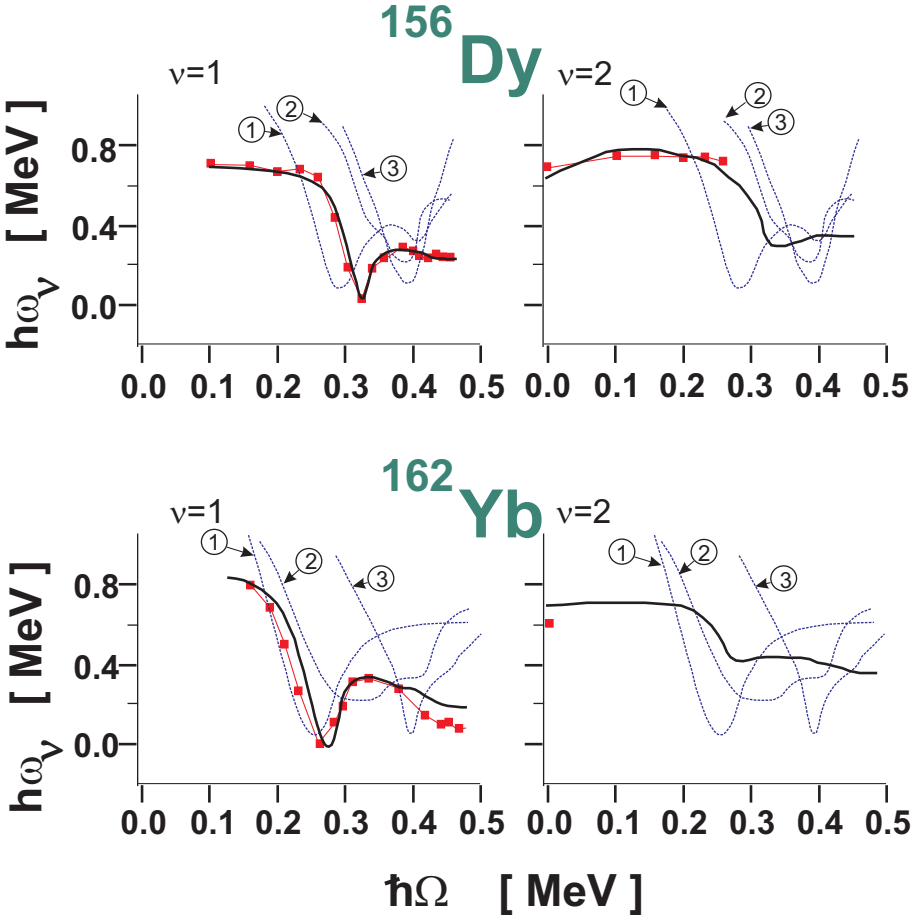


Figure 8.16: Experimental (red squares) and calculated RPA (black solid line) excitation energies $\hbar\omega_\nu$ for two lowest RPA solutions ($\nu = 1, 2$) as a function of the rotational frequency $\hbar\Omega$ (or of the angular momentum I). For the comparison the first three two-quasiparticle energies, indicated by arrows, are shown as well. Two-quasiparticle energies, indicated by arrows with numbers 1, 2, and 3 in circles, originate from Nilsson states ($n\bar{n}\frac{3}{2}[651]$, $\frac{3}{2}[651]$), ($p\bar{p}\frac{7}{2}[523]$, $\frac{7}{2}[523]$), and ($n\bar{n}\frac{1}{2}[651]$, $\frac{5}{2}[651]$), respectively (taken from [310]).

$G_{N\ \Omega}\langle HFB|\ \sum_l c_{\bar{l}}c_l\ |HFB\rangle_\Omega$ are demonstrated as a function of $(\hbar\Omega)^2$. In the bottom panels the calculated kinematic moment of inertia (solid curves) are compared with the corresponding experimental values. One can see backbending effect in ^{166}Yb and ^{170}Yb. In the ^{168}Yb this effect manifests itself only as "upbending" of the dependence $\mathscr{F}^{(1)}(\Omega)$ (upbending effect). The upper panels demonstrate the Coriolis antipairing effect when the pairing gap Δ_n decreases rapidly with the increasing Ω in the backbending region (braking of the pairing by increasing Coriolis interaction). In [309] the alignment of the single-quasiparticle angular moments with the rotational axis (with the vector of the rotational frequency $\vec{\Omega}$) in the backbending region is also demonstrated (in agreement with other papers - see [302] and citations

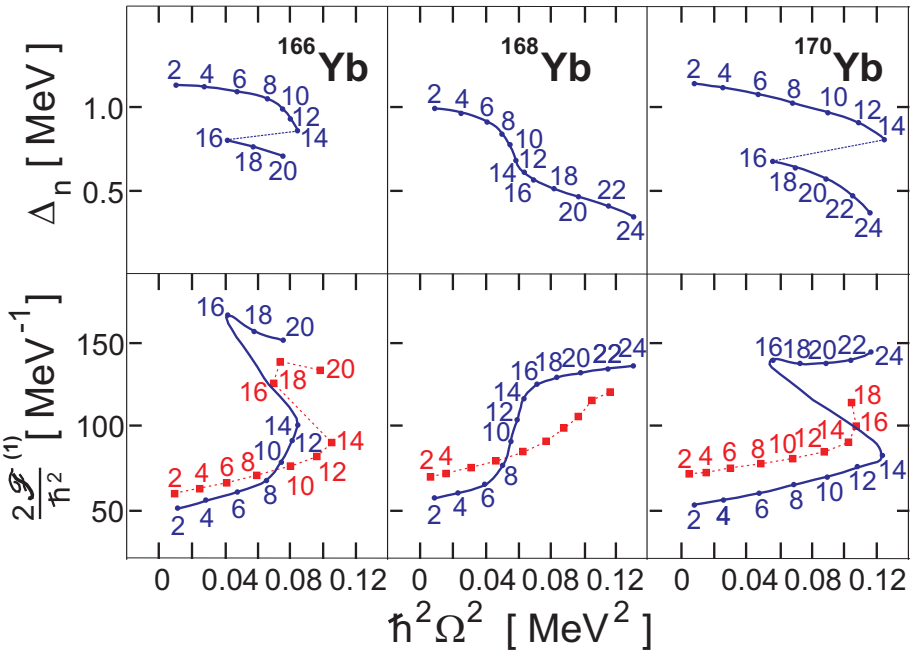


Figure 8.17: Twice the kinematical moment of inertia versus Ω^2 for the $^{166,\,168,\,170}$Yb nuclei (bottom panel). Upper panel demonstrates the dependence of the neutron pairing gap on the square of the rotational frequency. The blue solid lines corresponds to the HFB calculations with the Wood-Saxon mean field with the pairing monopole residual interaction. The deformations of the Wood-Saxon potential for neutron and proton systems were obtained by the Strutinski shell-correction method and were kept independent on Ω with the values $\beta_2 = 0.28$, $\beta_4 = -0.035$ for ^{166}Yb; $\beta_2 = 0.30$, $\beta_4 = -0.014$ for ^{168}Yb, $\beta_2 = 0.30$, $\beta_4 = -0.025$ for ^{170}Yb. The monopole pairing strength constants G_N and G_P (see (6.37)) were $G_N \approx 18.95$ MeV, $G_N \approx 17.9$ MeV (see [309] for details). Experimental values of the kinematical moment of iertia are indicated by red squares (adapted from [309]).

therein).

In experiments multiple backbending or multiple shape transition effect can be observed when it is possible to obtain the nucleus in very high spin states. It is connected with the possibility that the yrast states change their structure several times with the increasing rotational frequency. Each such abrupt change of the structure of yrast states means usually also the change of symmetry (or shape) of the mean field. As an example further this multiple backbending is shown in ^{152}Dy where the second backbending is connected with the shape transition from the normal to so called superdeformation (see [311, 310]). In the [312] 6 superdeformed rotational bands with very high quadrupole deformation ($\beta \approx 0.6$) were recognize in the experimental spectrum of ^{152}Dy (see also [313]) which were denoted as SD1, SD2, SD3, SD4, SD5 SD6. Energetically the lowest one, SD1, at angular momenta $I \approx 40$ merges with the yrast line and as a result of it at angular momenta

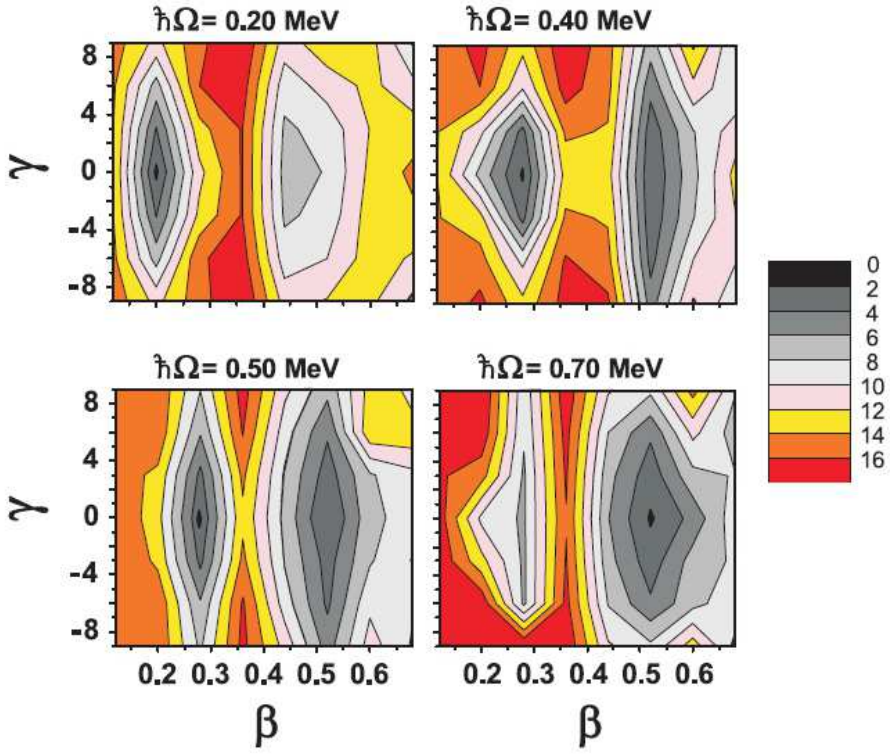


Figure 8.18: The β and γ contour plots of the cranked Nilsson plus pairing HFB surfaces at different rotational frequencies Ω in ^{152}Dy. The surfaces give the relative energies $E(\beta,\gamma) - E_{min}$ (taken from [310]).

higher than 40 the yrast line states are represented by the ground states of the intrinsic Hamiltonian $\hat{H}_\Omega$ with the deformed mean field with very high quadrupole deformation β ($\beta \approx 0.6$). In the paper [310] it is shown that this shape transition to the superdeformed mean field is connected with the second backbending of the kinematic moment of inertia (or of the angular momentum ${}_\Omega\langle HFB|\hat{H}_1|HFB\rangle_\Omega$) as a function of Ω. The calculations in [310] was again based on the cranked Nilsson HFB+RPA approach. In the Fig.8.18 the shape evolution of the HFB mean field energy surfaces (the plots of the total HFB ground state energies as a function of quadrupole deformation parameters β and γ) are shown in the dependence on $\hbar\Omega$ for four values $\hbar\Omega = 0.2,\ 0.4,\ 0.5$ and 0.6 MeV. The plots demonstrate two minima with $\gamma = 0$ for all values of Ω. In the rotational frequency interval $0 \leq \hbar\Omega \leq 0.3$ MeV we have the deepest minimum at $\beta \approx 0.2$ and the second minimum at $\beta \approx 0.45$ (superdeformed minimum). At $\hbar\Omega \approx 0.3 - 0.35$ MeV these minima are slightly shifted to $\beta \approx 0.28$ (the deepest one) and $\beta \approx 0.5 - 0.6$ (superdeformed one) and these deformations are kept for $\hbar\Omega$ in the interval $0.35 \leq \hbar\Omega \leq 0.67$. In the frequency $\hbar\Omega \geq 0.67$ MeV the superdeformed

minimum becames the deepest (taken from [310]).

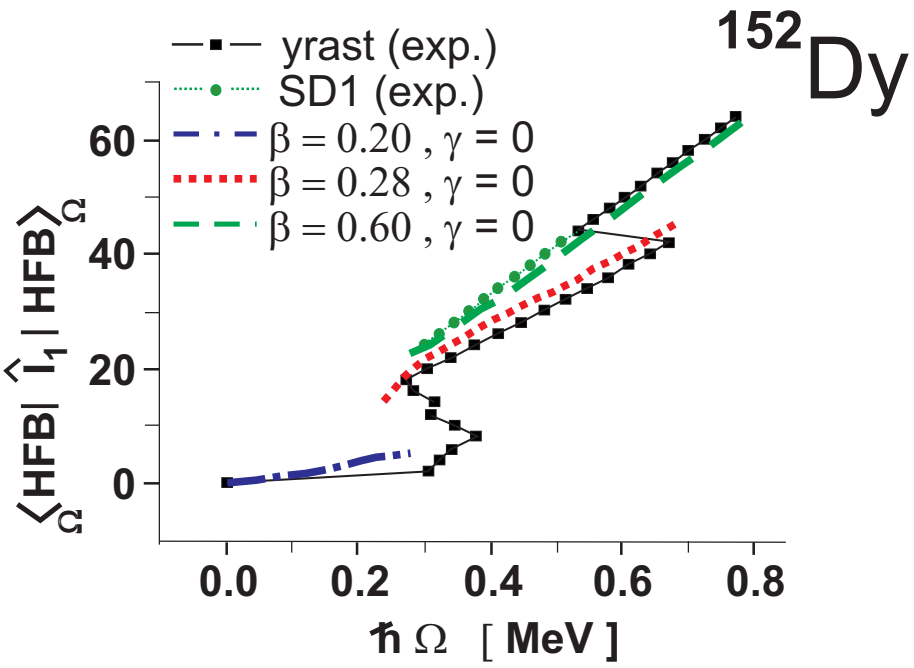


Figure 8.19: Yrast line angular momenta versus rotational frequency. For an appropriate comparison with experiments, the angular momentum over the whole SD yrast band (SD1 band) is plotted. The SD1 band coincides with the yrast band only for $\hbar\Omega \geq 0.67$ MeV (taken from [310]).

In the Fig.8.19 two backbendings in the dependence of the angular momentum $I \approx {}_\Omega\langle HFB|\, \hat{I}_1 \,|\, HFB\rangle_\Omega$ on the rotational frequency $\hbar\Omega$ are shown for ^{152}Dy. The first backbending occurs for $\hbar\Omega \approx 0.28 - 0.3$ MeV where the yrast states changes their mean field deformation from ($\beta = 0.2$, $\gamma = 0$) (blue dashed-dotted curve) to ($\beta = 0.28$, $\gamma = 0$) (red dotted curve). The second backbending at $\hbar\Omega \approx 0.6$ MeV is connected with the yrast band transition from ($\beta = 0.28$, $\gamma = 0$) (red dotted curve) to superdeformed ($\beta \approx 0.6$, $\gamma = 0$) (green dashed curve). The experimental values of the angular momentum I in the dependence on $\hbar\Omega_I$ (obtained by (8.74)) for the yrast band are indicated in the Fig.8.19 by black squares and the experimental points $I(\Omega_I)$ obtained by (8.74) for the superdeformed band SD1 are given by green circles. The merging of the SD1 band with the yrast band at $\hbar\Omega \approx 0.6$ MeV is clearly seen.

Fig 8.20 shows how the lowest RPA energies, built on the superdeformed yrast (SD1) band states as phonon vacua, evolve with the rotational ferqency (calculations made in [310]). We should point out that in accordance with the Fig.9.19 the SD1 band becomes the nucleus yrast band for $\hbar\Omega \geq 0.67$ MeV.

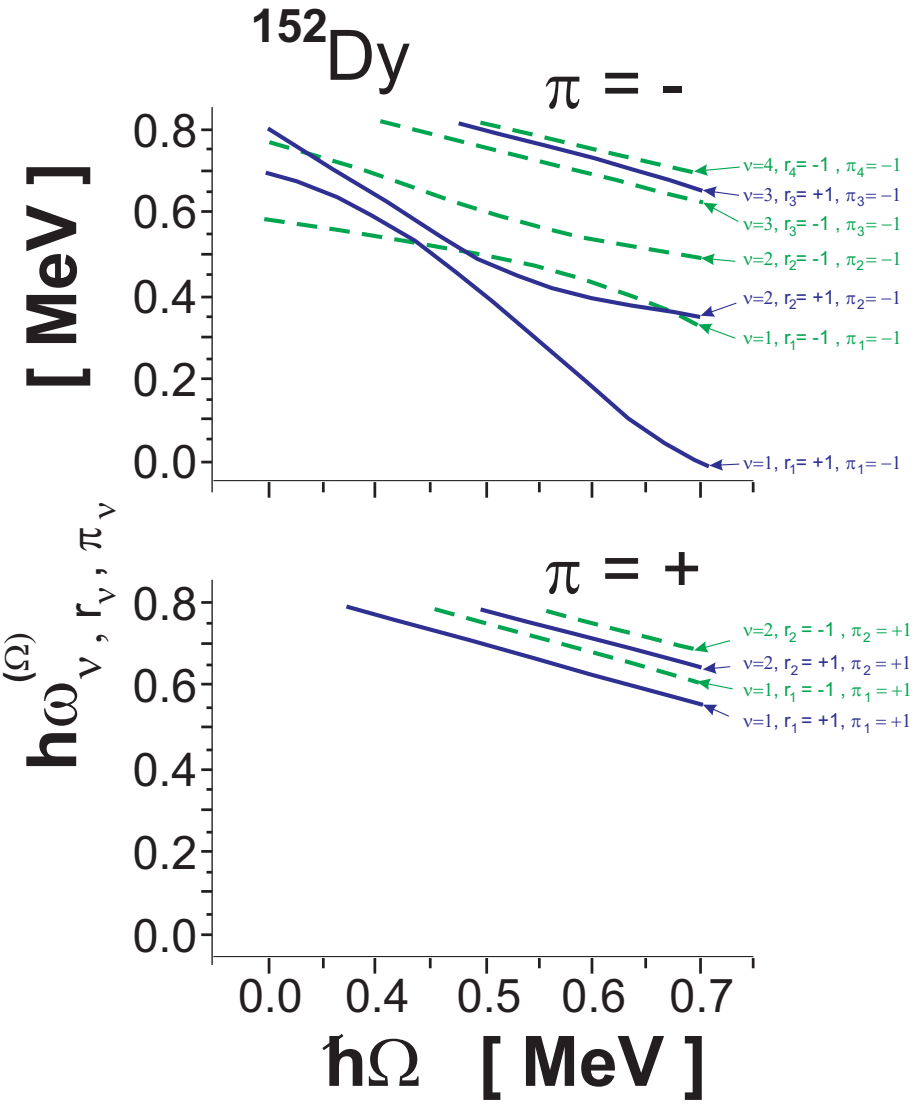


Figure 8.20: Negative parity (upper panel) and positive parity (lower panel) lowest RPA intrinsic energies $\hbar\omega_\nu^{(\Omega)}$ versus rotational frequency $\hbar\Omega$. Solid and dashed lines correspond to positive and negative signatures, respectively. Quasi-crossings of the lowest $\nu = 1$ and $\nu = 2$ bands for $\pi = -1$ and $r = \pm 1$ can be seen in the upper panel.

In accordance with other calculations (see e.g. [312]), the negative parity RPA phonons are lowest in energy for higher rotational frequencies, because of the strong octupole correlations present in the SD states. One may note the quasi-crossings of two lowest negative parity bands with either positive ($(\nu = 1,\ r_1 = +,\ \pi_1 = -)$ with $(\nu = 2,\ r_2 = +,\ \pi_2 = -)$) or negative ($(\nu = 1,\ r_1 = -,\ \pi_1 = -)$ with $(\nu = 2,\ r_2 = -,\ \pi_2 = -)$) signature. These quasi-crossings have effects on the dynamical moment of inertia.

Dynamical moment of inertia is given by (8.73) where $R^{(intr)}_{\Omega,\nu}$ is the intrinsic energy (eigenvalue of the intrinsic Hamiltonian $\hat{H}_\Omega$. In the framework of the

RPA the intrinsic energy $R^{(intr)}_{\Omega,\,\nu,\,r,\,\pi}$ can be approximated by

$$R^{(intr)}_{\Omega,\,\nu,\,r,\,\pi} \approx R^{(intr)}_{\Omega,\,yrast} + \hbar\omega^{(\Omega)}_{\nu,\,r,\,\pi} \tag{8.101}$$

The substitution of (8.101) into (8.73) gives

$$\begin{aligned}\mathscr{F}^{(2)}_{\Omega,\,\nu,\,r,\,\pi} &= -\frac{d^{\,2}}{d\Omega^2}\big(R^{(intr)}_{\Omega,\,yrast} + \hbar\omega^{(\Omega)}_{\nu,\,r,\,\pi}\big) = \\ &= \mathscr{F}^{(2)}_{\Omega,\,yrast} - \frac{d^{\,2}\hbar\omega^{(\Omega)}_{\nu,\,r,\,\pi}}{d\Omega^2}\end{aligned} \tag{8.102}$$

where $\mathscr{F}^{(2)}_{\Omega,\,yrast}$ is the dynamical moment of inertia of the yrast band which can be described approximately by the Harris formula

$$\mathscr{F}^{(2)}_{\Omega,\,yrast} = a + b\,\Omega^2 \tag{8.103}$$

The fit of the yrast band of ^{152}Dy yields for the parameters $a = 88.5\hbar^2\,MeV^{-1}$ and $a = -11.9\,\hbar^4\,MeV^{-3}$ (see [310]). The fluctuation part originates from the second derivative of the phonon energy $\hbar\omega^{(\Omega)}_{\nu,\,r,\,\pi}$ which is computed in the RPA for a given band at different rotational frequencies Ω.

Experimental dynamical moment of inertia was extracted from the experimental spectrum of SD bands, $E^{(lab)}_{I,\,\nu}$, according to (8.76). These energies for ^{152}Dy were taken from [314] for all observed excited SD bands (ν = SD2, SD3, SD4, SD5, SD6) above the SD yrast band SD1. According to (8.102), only moments of inertia of the negative-parity quasi-crossing bands, which yield nonzero second derivatives for the energy $\hbar\omega^{(\Omega)}_{\nu,\,r,\,\pi=-}$, should be appreciably affected by the rotation. This is confirmed empirically. As shown in the Fig.8.21, the dynamical moment of inertia, $\mathscr{F}^{(2)}_{\nu}$, undergoes strong variation with Ω only for negative-parity and positive signature bands SD2, SD3 as well as for negative-parity and negative-signature band SD6. The computed quantities are in fair agreement with empirical moments of inertia of these three bands.

The fluctuation induced by the RPA phonons (by long-range residual interaction) on the dynamical moment of inertia $\mathscr{F}^{(2)}_{\nu}(\Omega)$ of the SD4 and SD5 are negligible, in qualitative agreement with experiments. The experimental quantities, in fact, undergo small oscillations and do not get far from the SD yrast values determined by the Harris formula (dashed curves in the Fig.8.21). The RPA, however, is unable to reproduce the observed modes fluctuation, suggesting that they may be related to anharmonic effects caused by neglected in [310] multi-phonon components in the lowest SD bands (that means neglecting the compex cofiguration cantribution).

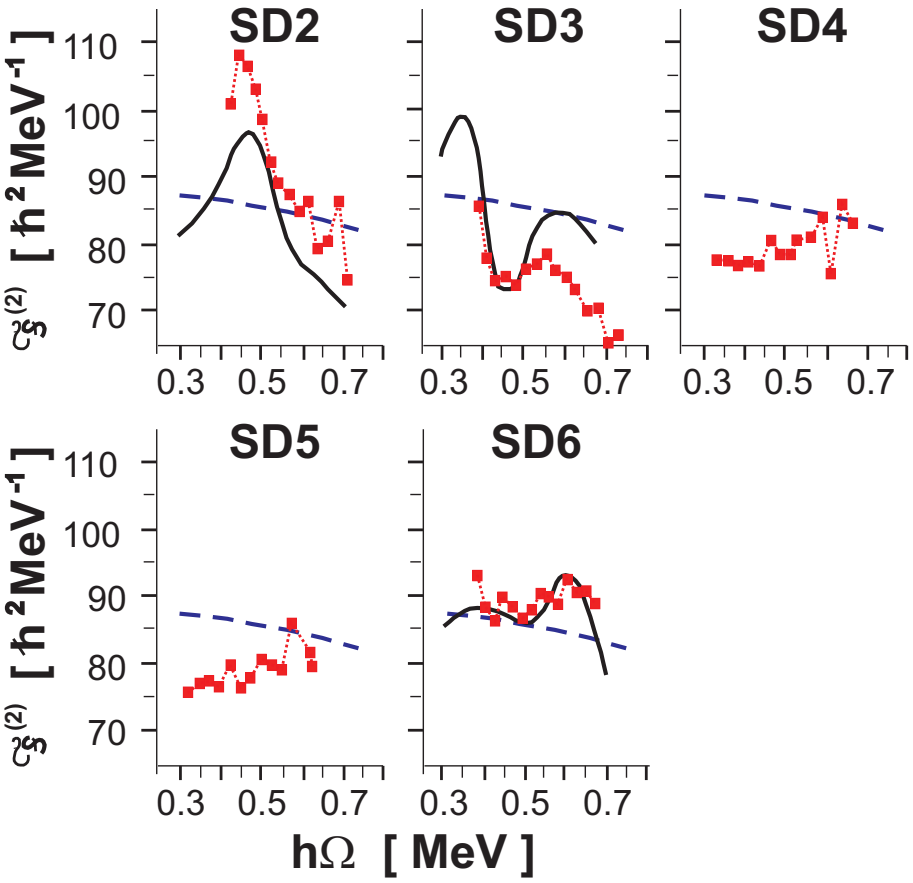


Figure 8.21: Theoretical dynamical moments of inertia of excited SD bands in ^{152}Dy determined by (8.102) (black solid curves) are compared with the corresponding experimental values obtained by (8.76). The blue dashed curves correspond to the Harris fit (8.103) for the yrast SD1 band.

Results published in [310] and discussed here are consistent with calculations and conclusions drawn in other papers (see e.g. [312]) where it was pointed out the importance of the octupole correlations in shaping the dependence of the dynamical moment of inertia with rotational frequency in SD nuclei like ^{152}Dy. From this point of view the octupole deformation, apart from quadrupole superdeformation, can be present in the yrast band states with $\Omega \geq 0.67$ MeV. So the second backbending observed in ^{152}Dy can serve as an example of the shape transition from the normal quadrupole deformation to the quadrupole superdeformation and , prbably, simultaneously the octupole deformation.

8.2.4 Giant resonances above the yrast band in fast rotating nuclei

In this subsection the evolution of the shape of giant resonances E0, E1, E2, and M1 in the dependence on the rotation ferquency Ω is discussed. Results published in [310], using the cranked Nilsson mean field with the monopole pairing and long-range residual interaction in the separable multipole-multipole form taken into account in the framework of the RPA, are used again for the demonstration of the approach.

As it was discussed in the subsection 7.3.1.3.2 giant resonances are observed as the broad peaks of the envelope curve (strength function) of the probabilities of transitions induced by some nuclear reaction from the given initial state (most often from ground state) to individual excited states. In the Subsection 7.3.1.3.2 the electromagnetic giant resonances of different types ($X = el.$ or $X = mag.$) and multipolarities λ was analysed in the case when the initial state for the electromagnetic excitation was the ground state. For even-even nuclei discussed here the ground state has always zero angular momentum and positive parity; $|gr.st.\rangle \equiv |0^+\rangle$. Therefore in the even-even nucleus only states with low values of the angular momentum I can be excited from the ground state by electromagnetic transitions with low values of the multipolarity λ, $I = \lambda = 0,\ 1,\ 2$, discussed in the Subsection 7.3.1.3.2. In the case of axially deformed even-even nuclei (when the low-lying intrinsic states $|\nu\rangle$ are characterized by the sharp value of the angular momentum projection K_ν on the 3-d intrinsic axis) it means that only lowest levels of rotational bands built on the intrinsic state $|\nu\rangle$ allowed by the selection rule of the given electromagnetic transition operator ($K_\nu \leq \lambda$) can be excited for given λ. Then we can use the scheme of the excitation typical for low rotation when the laboratory wave functions are given by (8.6) and corresponding excitation reduced probabilities by (8.11). Concretely, for ecitations going from the ground state of the even-even nucleus and when the intrinsic states are approximated as the RPA one-phonon states $|\nu\ K_\nu\rangle = Q^+_{\nu\,K}\,|\,RPA\rangle$ the corresponding reduced probability is

$$B(X\lambda;\ 0^+_{gr} \rightarrow K\nu) = \left|C^{IK}_{00\,\lambda K}\right|^2 \left|\ \langle RPA|\ Q_{\nu K}\ \hat{\mathscr{M}}^{(X)}_{\lambda\mu_3=K}\ |\ RPA\rangle\ \right|^2 =$$
$$= \delta_{I\,\lambda}\ \langle RPA|\ \left[\ Q_{\nu K},\ \hat{\mathscr{M}}^{(X)}_{\lambda\,\mu_3=K}(\Delta T)\ \right]\ |\ RPA\rangle\ |^2 \qquad (8.104)$$

with corresponding strength function (see (7.371))

$$S_0(X\lambda;\ \Delta T;\ E) = \sum_{K=-\lambda}^{+\lambda} \sum_{\nu} B(X\lambda;\ \Delta T;\ 0^+_{gr} \to K\nu)\ \delta(E - \hbar\omega_\nu) =$$

$$= \sum_{K=-\lambda}^{+\lambda} \sum_{\nu} \left|\ \langle RPA|\ Q_{\nu K}\ \hat{\mathscr{M}}^{(X)}_{\lambda\mu_3=K}(\Delta T)\ |\ RPA\rangle\ \right|^2 \qquad (8.105)$$

This slow rotation scheme of excitation for the quadrupole case $\lambda = 2$ is

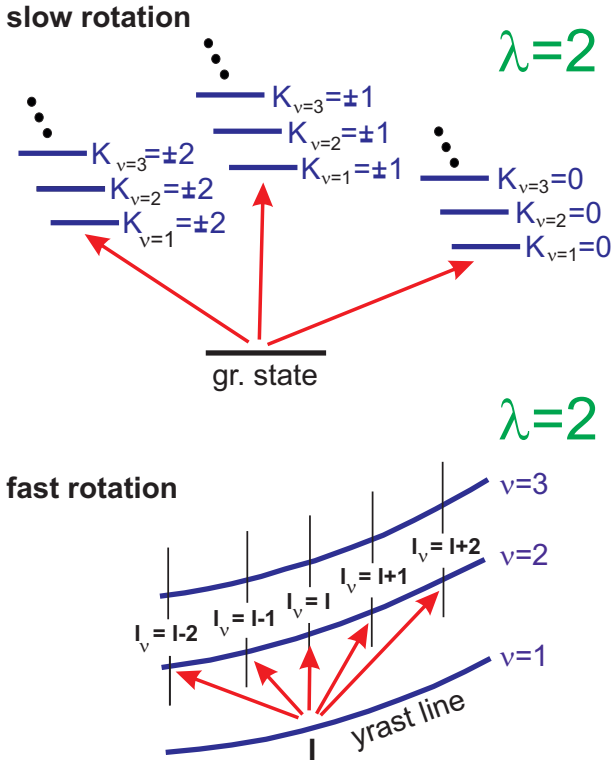


Figure 8.22: Schematic figure of the quadrupole excitations for the determination of the strength function $S_0(X\lambda;\ \Delta T;\ E)$ for the slow rotation limit (upper panel) and for the fast rotation limit (lower panel).

schematically shown in the upper panel of the Fig.8.22.

In the case of the fast rotation (cranking model) the nuclear angular momentum is aligned in the direction of the rotation axis (the 1-st intrinsic axis) and the excitation scheme is shown in the Fig.8.9. Then, instead of the ground state, the concrete yrast band state $|\psi^{(intr)}_{\Omega,yrast}\rangle$ should be taken as the initial state. In the framework of the cranked RPA the yrast line state is approximated by the phonon vacuum for given rotational frequency Ω_I, $|\psi^{(intr)}_{\Omega,yrast}\rangle \equiv |\ RPA;\ \Omega_I\rangle$. Corresponding excitation probabilty of the electromagnetic transition of given type X and multipolarity λ going from

the yrast state $|RPA,\ \Omega_I\rangle$ to the excited one-phonon state $|\psi^{(intr)}_{\Omega_{I_\nu},\,\nu,\,r_\nu,\,\pi_\nu}\rangle = Q^{+}_{\nu,\,r_\nu,\,\pi_\nu}(\Omega_{I_\nu})\mid RPA;\ \Omega_I\rangle$ ($I_\nu = I \pm \lambda,\ I \pm (\lambda-1),\ \ldots,\ I$) reads ($\Delta I = \pm\lambda,\ \pm(\lambda-1),\ \ldots,\ 0$)

$$B^{(\Omega_I)}(X\lambda;\Delta T;\ I\ yrast \to I+\Delta I,\ \nu) = \Big|\ C^{I+\Delta I\ I+\Delta I}_{I\,I\ 2\Delta I}\ \Big|^2 \cdot\Big|\ \langle RPA;\ \Omega_I|\ \big[Q_{\mu,\,r_\nu,\,\pi_\nu}(\Omega_{I_\nu}),\ \hat{\mathscr{M}}^{(X)}_{\lambda\,\mu_1=\Delta I}(\Delta T)\big]\mid RPA;\ \Omega_I\rangle\ \Big|^2 \tag{8.106}$$

with corresponding strength function

$$S^{(\Omega_I)}_0(X\lambda;\ \Delta T;\ E) = = \sum_{\Delta I=-\lambda}^{+\lambda}\ \sum_{\nu} B(X\lambda;\Delta T;\ I\ yrast \to I+\Delta I;\ \nu)\ \delta(E-\hbar\omega^{(\Omega_I)}_{\nu}) \tag{8.107}$$

The fast rotation scheme of the excitations from given yrast state $|RPA;\ \Omega_I\rangle$ for $\lambda = 2$ is demonstrated in the lower panel of the Fig.8.22.

In the following figures, Figs.8.23-8.26, the reduced probabilities of E0, E1, E2, and M1 transitions, going from the paricular yrast band state $|\,RPA,\ \Omega_I\rangle$ to all possible excited states allowed by the selection rules of given transition operator, are demonstrated for several values of Ω_I in ^{152}Dy.

Electric monopole E0 reduced probabilities in the Fig.8.23 (giant monopole resonance GMR) illustrate a broadening of the GMR with the increasing rotational frequency and a slight shift to higher energy connected with the shape transition from the normal deformation to the superdeformation seen in ^{152}Dy at $\hbar\Omega \approx 0.67$ MeV (see the Fig.8.19).

The dependence of the shape of the electric giant dipole resonance (GDR), generated by the transition operator $\hat{\mathscr{M}}^{(el)}_{1\mu}(\Delta T=1) = \sum_{k=1}^{A} e\ e^{(eff)}_{k\,,\,\Delta T=1}\ r_k Y_{1\mu}(\hat{r}_k)$, $\mu = 0, \pm 1$, $e^{(eff)}_{k,\,\Delta T=1} = N/A$ for $k \in protons$ and $e^{(eff)}_{k,\,\Delta T=1} = -Z/A$ for $k \in neutrons$ (see (O.38), (O.39)), is demonstrated in the Fig.8.24. Again the broadening of the GDR can be recognized during the shape transition from the normal deformation to the superdeformation (for $\hbar\Omega \geq 0.67$ MeV in ^{152}Dy).

Giant quadrupole resonance (GQR) (that means the dependence of the excitation reduced probabilities $B(E2) \equiv \sum_{\mu=0,\pm1,\pm2} B(E2;\Delta T=p;yrast\Omega_I \to 2^+\mu)$, generated by the quadrupole electric transition operators $\hat{\mathscr{M}}^{(el)}_{2\mu}(\Delta T = 1) = \sum_{k=1}^{Z} e\, r_k\, Y_{2\mu}(\hat{r}_k)$, $\mu = 0,\ \pm1,\ \pm2$, on the excitation energy E) is shown

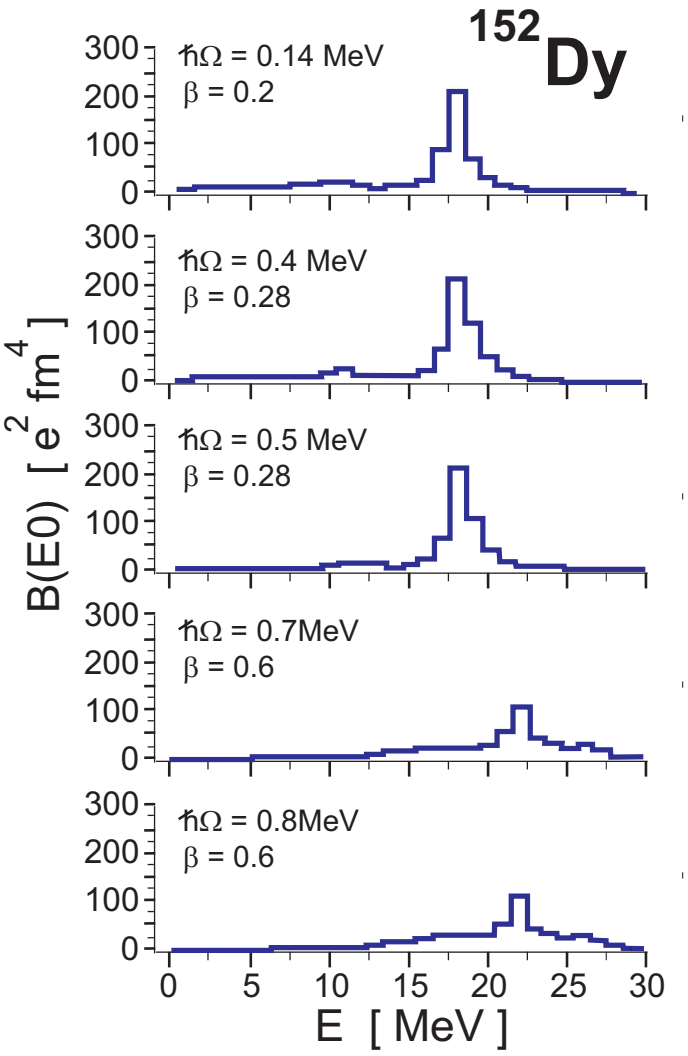


Figure 8.23: Reduced probabilities of electric monopole transitions E0 in ^{152}Dy, going from the yrast band state $\mid RPA,\ \Omega_I\rangle$ to all possible excited states allowed by the selection rules for the electric E0 transiton operator $\hat{\mathscr{M}}^{(el)}_{00}(\Delta T = p) = \sum_{k=1}^{Z} e\, r_k^2\, Y_{00}(\hat{r}_k)$ (see (7.367), (7.368)) are demonstrated as a function of the excitation energy for five values of the rotational frequency ($\hbar\Omega_I = 0.14$ MeV, 0.4 MeV, 0.5 MeV, 0.7 MeV, and 0.8 MeV). Equlibrium deformation β for all rotational frequenies is given in all panels. The reduced strengths are summed in bins of 1 MeV around the energy E (adopted from [310]).

in the Fig.8.25 for five values of the rotational frequency. The broadening of the GQR and the shift to the higher energies can be recognized in the superdeformation transition rotational frequency region $\hbar\Omega \approx 0.67$ MeV.

The behaviour of the M1 strength appears to be more interesting. In the Fig8.26 the giant M1 resonance is demonstrated in the dependence on rotational frequency$\hbar\Omega$. From the Subsection 7.3.1.3.2.2 we know that the

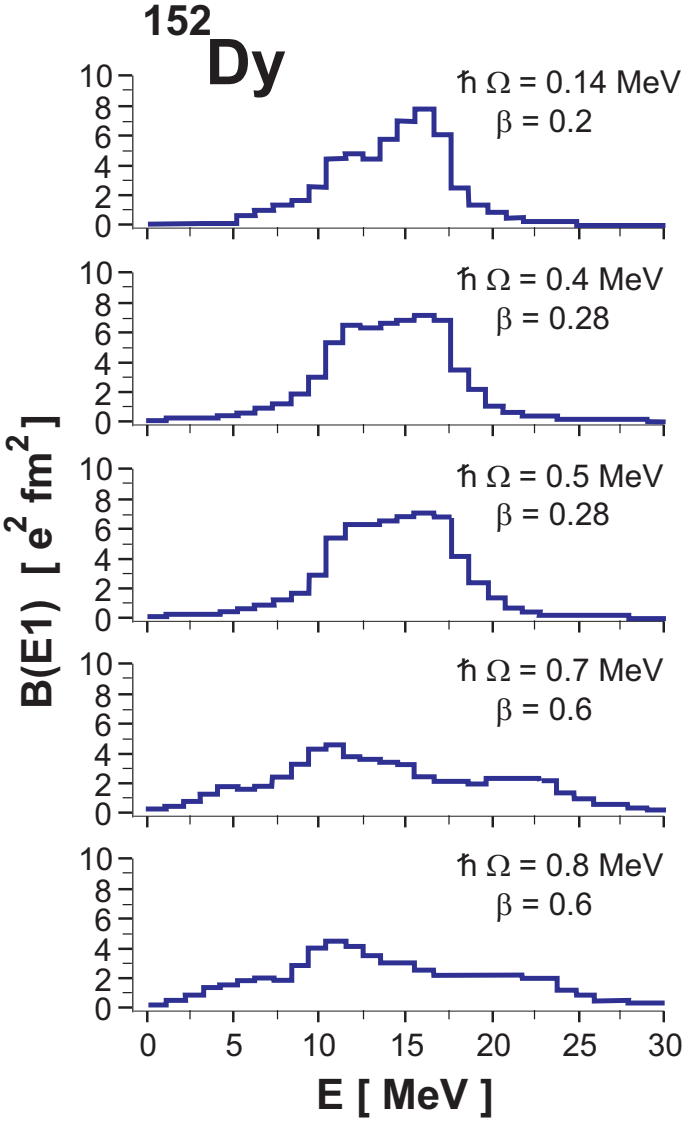


Figure 8.24: The same as for the Fig.8.23 but for the reduced isovector E1 probabilities (giant dipole resonance GDR), $\sum_{\mu=0,\pm1} B(E1,\ \Delta T=1, yrast\, \Omega_I \rightarrow 1\mu)$, generated by the electric dipole transition operators $\hat{\mathscr{M}}^{(el)}_{1\mu}(\Delta T=1) = \sum_{k=1}^{A} e e^{(eff)}_{k,\,\Delta T=1}\, r_k Y_{1\mu}(\hat{r}_k)$, in the dependence on the excitation energies for five values of the rotational frequency. The reduced probabilities are again summed in bins of 1 MeV around the energy E (adopted from [310]).

standard M1 giant resonance is generated by the transition operators (7.411),

$$\hat{\mathscr{M}}^{(mag)}_{1\mu} = \mu_N \sqrt{\frac{3}{4\pi}} \sum_{i=1}^{A} \left(g_i^{(l,\,eff)}\, \hat{l}^{(i)}_{\mu} + g_i^{(s,\,eff)}\, \hat{s}^{(i)}_{\mu} \right) \qquad \mu = 0, \pm 1 \qquad (8.108)$$

with effective orbital and spin gyromagnetic ratios $g_i^{(l,\,eff)}$ and $g_i^{(s,\,eff)}$ given by, $g_i^{(l,\,eff)} = 1$ for protons, $g_i^{(l,\,eff)} = 0$ for neutrons, $g_i^{(s,\,eff)} = 5.586\,\xi$ for protons, $g_i^{(s,\,eff)} = -3.826\,\xi$ for neutrons, with $\xi \approx 0.7$ (see (7.370)). The

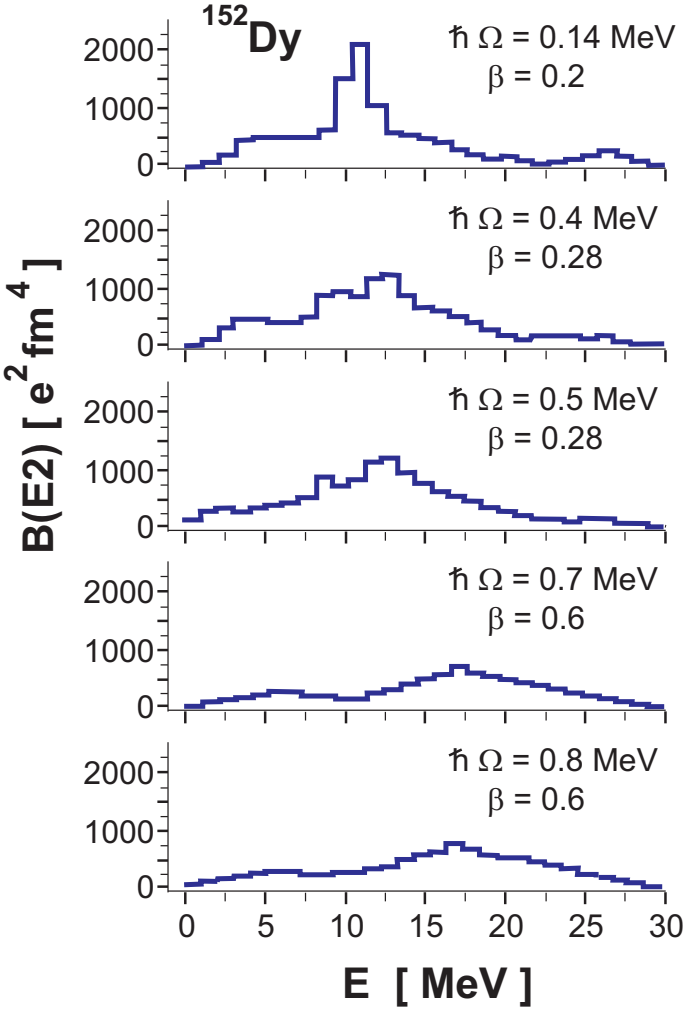


Figure 8.25: The same as for the Fig.8.23 but for the reduced quadrupole E2 probabilities $B(E2) = \sum_{\mu=0,\pm1,\pm2} B(E2;\, \Delta T = p\,;\, yrast\, \Omega_I \rightarrow 2+\mu)$ in the dependence on the excitation energy Ω for five values of the rotational frequency $\hbar\Omega$ (giant quadrupole resonance GQR). The reduced probability $B(E2)$ is again summed in bins of 1 MeV (adopted from [310]).

Fig.8.26 shows the most of the M1 strength is concentrated in the energy range 2-10 MeV at all rotational frequencies and deformations. At low rotational frequency and normal deformation ($\beta \approx 0.2$), most of the M1 strength is due to spin excitations. It is only in the low-energy tail (2-4 MeV) that the orbital contribution is comparable with the one that is due to spin.

The first shape transition ($\beta = 0.2 \rightarrow \beta = 0.28$) induces an overall enhancement of the orbital transition, especially at low energy, with a consequent downward shift of the total M1 strength. For fixed deformation, rotation has a damping effect on spin and affects marginally the orbital strength.

The onset of superdeformation induces more dramatic changes. It inhances strongly the orbital strength, which becomes strongly peaked around 6 MeV

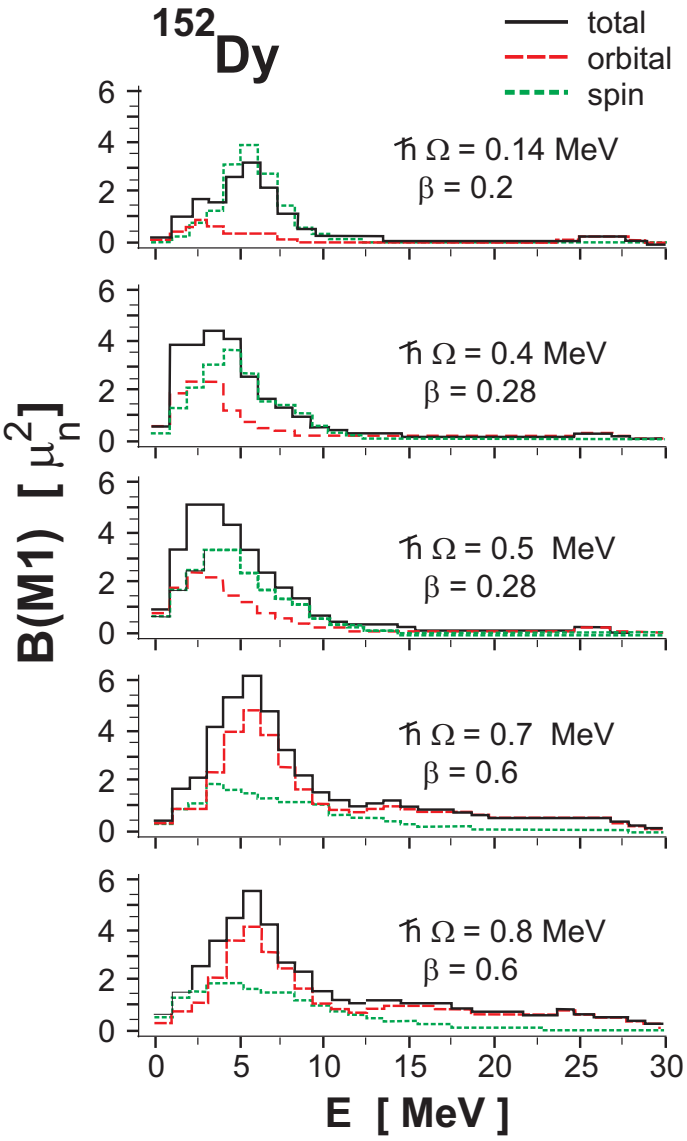


Figure 8.26: Orbital part (red dashed lines), spin part (dotted green lines) and the total (black solid lines) M1 strength functions for different angular frequencies and deformations. The reduced strengths are summed in bins as in the Figs.8.22-8.25 (taken from [310]).

and has a damping and spreading effect on spin transormations, which get scattered all along the 2-10 MeV interval. Further increase of the rotational frequency above the superdeformed critical value $\hbar\Omega_c \approx 0.67$ MeV no longer affects appreciably either orbital or the spin contribution once the nucleus is settled down in the SD phase.

The ehancement of the low-lying orbital M1 trnsition over the spin with the increasing nucleus deformation (or with the increasing rotational frequency if this causes the increase of the deformation) is in the agreement with the expr. (7.415) discussed in the Subsection 7.3.1.3.2.2 and also with

calculations performed in [315]. This effect was obtained not only in ^{152}Dy but also in others nuclei (see eg. [316] for ^{190,192,194}Hg).

The topic of the fast rotating nuclei with high angular momenta is actual from the experimental (see e.g. [317, 318]) as well as theoretical (see e.g. [320, 319]).

9. Alpha decay

9.1 Basic data on alpha decay

During alpha decay alpha particle is emitted from the nucleus. Opposite to beta decay the emission of alpha particle is two-body process,

$$Z^A \rightarrow (Z-2)^{A-4} + {}^4_2He \tag{9.1}$$

when given nucleus with Z protons and A nucleons emits alpha particle ${}^4_2He$ and the final nucleus has $Z-2$ protons and $A-4$ nucleons. Energy Q released in this process is given by the difference of masses of the initial nucleus and final products [1]

$$Q = (M_A - M_{A-4} - M_\alpha)\, c^2 \tag{9.2}$$

This energy is divided into the kinetic energy, and potentially excitation energy, of the daughter nucleus and kinetic energy of the alpha particle. Usually the mass of the daughter nucleus is much higher than the mass of the alpha particle, $M_{A-4} >> M_\alpha$. Therefore the velocity (kinetic energy) of the daughter nucleus in the CoM frame is negligible in the comparison with the velocity (kinetic energy) of the alpha particle.

Spin of the alpha particle is zero. Therefore the angular momentum released in the alpha decay, which is given by the difference $\vec{I_i} - \vec{I_f}$ of the angular momentum $\vec{I_i}$ of the initial nucleus and angular momentum $\vec{I_f}$ of the daughter nucleus , is equal to the orbital momentum $\vec{L}$ of the relative motion of the alpha particle and daughter nucleus,

$$\vec{L} = \vec{I_i} - \vec{I_f} \quad \Rightarrow \quad |I_i - I_f| \leq L \leq I_i + I_f \tag{9.3}$$

Internal parity of the alpha particle is +1 and parity of the relative motion of the alpha particle and daughter nucleus is $(-1)^L$. So the parity π_i of the initial state of the initial nucleus and the parity π_f of the final state of the daughter nucleus fulfill following condition

$$\pi_i\, \pi_f = (-1)^L \tag{9.4}$$

[1] The mass of the daughter nucleus $M_{A-4}\, c^2$ involves also possible excitation energy of the daughter nucleus.

Total probability of the alpha decay of given nucleus in the initial state $|i\rangle$ in one second is connected with the half-life $t_{1/2}^{(i)}$ by the well-known relation [2],

$$\omega_i = \frac{ln\, 2}{t_{1/2}^{(i)}} \tag{9.5}$$

Given initial nucleus in its state $|i\rangle$ can decay to different final states $|f\rangle$ of the final daughter nucleus, so the probability $\omega_{i\to f}$ of the alpha decay $|i\rangle \to |f\rangle$ can be introduced. Then the total probability ω_i of the alpha decay from the state $|i\rangle$ of the initial nucleus Z^A going to all possible, by selection rules (9.3) and (9.4), states $|f\rangle$ of the daughter nucleus $(Z-2)^{(A-4)}$ is

$$\omega_i = \sum_f \omega_{i\to f} \tag{9.6}$$

Experimental measurement of nuclear masses show that practically all neutron-deficit nuclei are α- radioactive. However, the number of nuclei where alpha decay can be used for the investigation of the structure of excited states is very reduced and the data are restricted only to low-energy excitations. The reason for it is the empirical Geiger-Nuttall rule, empirically introduced in [321]. According to this rule the probability $\omega_0(E_\alpha,\, Z)$ of the alpha decay from the ground state of the initial (mother) nucleus going to the ground state of the final (daughter) nucleus $(Z-2)^{(A-4)}$ depends on the total kinetic energy E_{kin} of the alpha particle and daughter nucleus by the following expression,

$$ln\, \omega_0(E_{kin},\, Z) = -\frac{K_1(Z)}{\sqrt{E_{kin}}} + K_2(Z) \tag{9.7}$$

where the probability $\omega_0(E_{kin},\, Z)$ is expressed in $1/s$ and $K_1(Z)$ with $K_2(Z)$ are functions of Z obtained by fitting to selected alpha decays as

$$\begin{aligned} K_1(Z) &= 139.8 + 1.83\,(Z-90) \;+\; 0.012\,(Z-90)^2 \\ K_2(Z) &= \;\; 52.1 + 0.30\,(Z-90) \;+\; 0.001\,(Z-90)^2 \end{aligned} \tag{9.8}$$

In the most cases the kinetic energy of the daughter nucleus is negigible in the comparison with the kinetic energy E_α of the alpha particle and therefor

[2] Expression (9.5) can be easily derived from the standard decay rule

$$N_i(t) = N_0\, e^{-\omega_i\, t} \;\Rightarrow\; \frac{N_0}{2} = N_0\, e^{-\omega_i\, t_{1/2}^{(i)}}$$

$$\Rightarrow \quad ln\, N_0 - ln\, 2 = ln\, N_0 - \omega_i\, t_{1/2}^{(i)} \;\Rightarrow\; \omega_i = \frac{ln\, 2}{t_{1/2}^{(i)}}$$

$E_{kin} \approx E_\alpha$. From theoretical point of view the Geiger-Nuttall rule (9.7) can be qualitatively derived considering an alpha particle in the nucleus as a particle in the box. The alpha particle is in a bound state because of the presence of the attractive strong interaction potential. It will constantly bounce from one side to the other side of the box, and due to the possibility of quantum tunneling by the wave through the potential barrier, each time it bounces, then will be a small likelihood for it to escape (see [322], see also Appendix G).

From the energy conservation rule it is evident that

$$Q = E_\alpha + E_{A-4} \tag{9.9}$$

where E_α stands for the kinetic energy of the α- particle and E_{A-4} is the kinetic energy of the daughter nucleus (a possible excitation energy of the daughter nucleus is involved in Q). The expression (9.9) valids for the α-decay between the ground states of the initial and daughter nucleus ($Q = (E_\alpha)_0 + (E_{A-4})_0$) as well as for α- decay between excited states ($Q = (E_\alpha)_{exc} + (E_\alpha)_{exc}$),

$$\begin{aligned} & Q = (E_\alpha)_0 + (E_{A-4})_0 = (E_\alpha)_{exc} + (E_{A-4})_{exc} \\ \Rightarrow \qquad & (E_{A-4})_{exc} - (E_{A-4})_0 = (E_\alpha)_0 - (E_\alpha)_{exc} > 0 \end{aligned} \tag{9.10}$$

therefore always $(E_\alpha)_0 > (E_\alpha)_{exc}$. So,

$$\Big(\frac{1}{\sqrt{E_\alpha}}\Big)_0 < \Big(\frac{1}{\sqrt{E_\alpha}}\Big)_{exc} \tag{9.11}$$

In the first approximation an assumption is done that the Geiger-Nuttall expression (9.7) valids also for α- decays going between excited states of the initial and daughter nucleus. Then from (9.11) it follows the following relation (we also use the approximation $E_{kin} \approx E_\alpha$, and one should realize that the funcion $ln\,\omega_0$ in (9.7) is the decreasing function of E_α),

$$ln\,\omega_0 > ln\,\omega_{exc} \tag{9.12}$$

and it is necessary to have in mind that the dependence of the probability ω on the energy E_α is drastic as it is shown below:

Let us suppose, for instance, that $(E_\alpha)_0 = 2$ MeV and $(E_\alpha)_{exc} = 1$ MeV with $Z = 90$, then from (9.7) we obtain for $ln\,\omega_0$ and $ln\,\omega_{exc}$ following values,

$$ln\,\omega_0 \approx -\frac{139.8}{\sqrt{2}} + 52 \approx -46.85 \quad \Rightarrow \quad \omega_0 \approx 4.5\,10^{-21}\,\frac{1}{s}$$

$$ln\,\omega_{exc} \approx -\frac{139.8}{\sqrt{1}} + 52 \approx -87.8 \quad \Rightarrow \quad \omega_{exc} \approx 7.3\,10^{-39}\,\frac{1}{s}$$

and we see that the α- decay from the ground state to the ground state is by many orders stronger than the α- decay to the excited states of the daughter nucleus even in the case when the excitation energy of the final excited state is small ($1MeV$). So the probability of the α- decay going to excited states decreases very quickly with the excitation energy. That is why the α- decay can provide an information only about states with very low excitation energy.

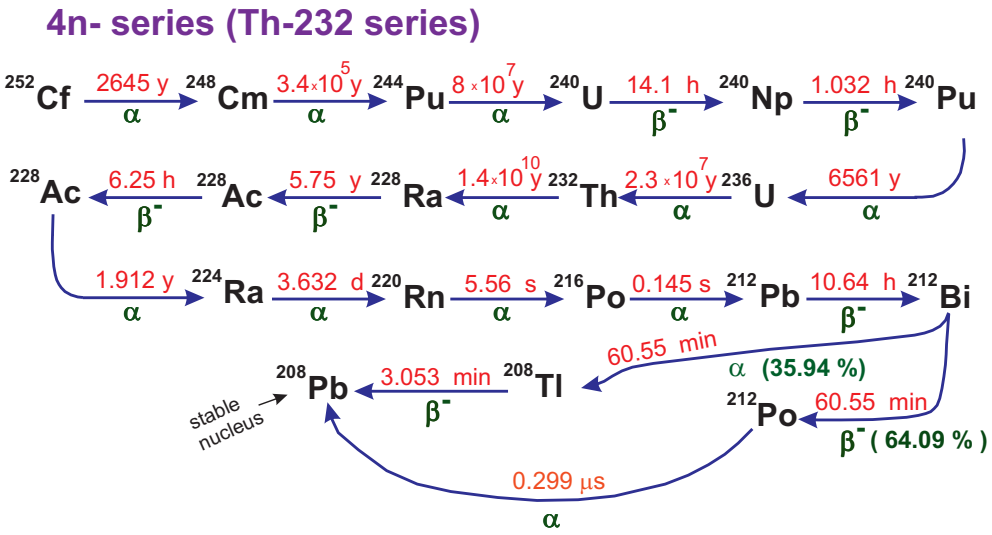


Figure 9.1: The 4n series (chain) is historically called the "thoriun series". The series terminates with the stable nucleus ^{208}Pb.

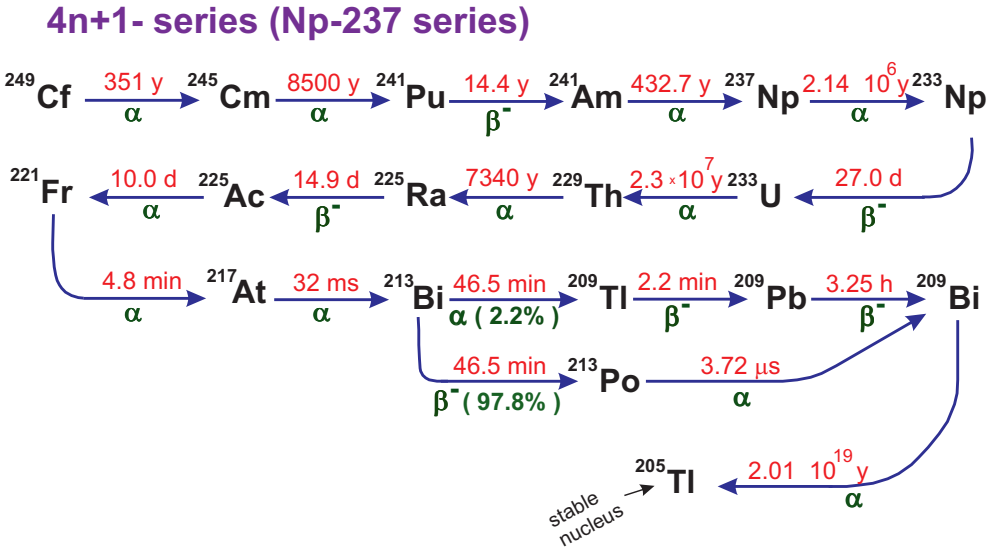


Figure 9.2: The 4n+1 series is historically called the "Np-237 series". The series terminates with the stable nucleus ^{205}Tl.

As it was already mentioned the kinetic energy of the daughter nucleus

is negligible in the comparison with the kinetic energy E_α of the emitted α- particle. Therefore from (9.9) follows that the kinetic energy of α- particle E_α is equal, with good approximation, to the energy Q of the given α- decay (one should realize that α- particle, ^{4}He, has no excited states). The α- decay energy Q is always discrete (because possible low- excitation energies of the daughter nucleus, involved in the mass M_{A-4} in (9.2), are always discrete) and therefore (9.9) gives the energy spectrum of emitted α- particles also discrete with peaks corresponding to possilble discrete excitation energies of the daughter nucleus.

Experimental measurements of half lifes of α- decays provide values in a broad interval from a small fraction of second up to thousands of years. The most of neutron- deficite nuclei with $A > 150$ are unstable with respect to α- decay. For heavy unstable nuclei (actinides) the α- decay, together with spontaneous fission and sometimes β- decay, is the main decay channel (see e.g. http://www-nds.iaea.org).

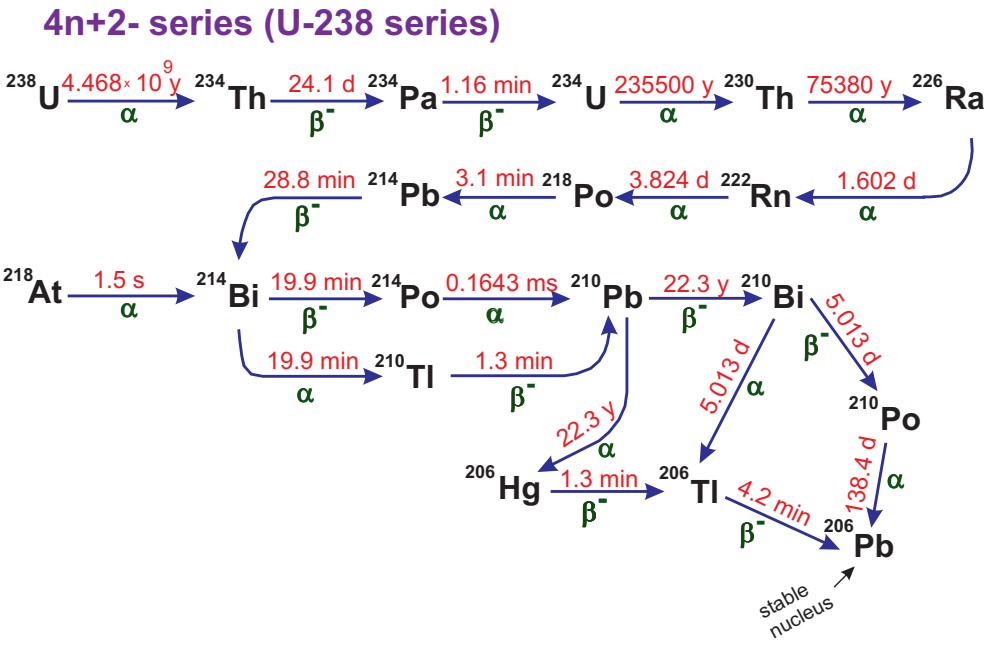


Figure 9.3: The 4n+2 series (chain) is historically called the "U-238". The series terminates with the stable nucleus ^{206}Pb.

From the point of view of the α- decay of heavy isotopes historically four decay series (chains) are recognized which are results of the balance between α- and β- deay rates (so called 4n-, (4n+1)-, (4n+2)-, and (4n+3)- series) (see e.g. [323]). These series are demonstrates in Figs. 9.1, 9.2, 9.3, and 9.4. Each series starts with unstable actinide nucleus with A equal to the multiple of the number 4: $A = 4n$ (for $4n$- series, $A = 4n + 1$ for (4n+1)-

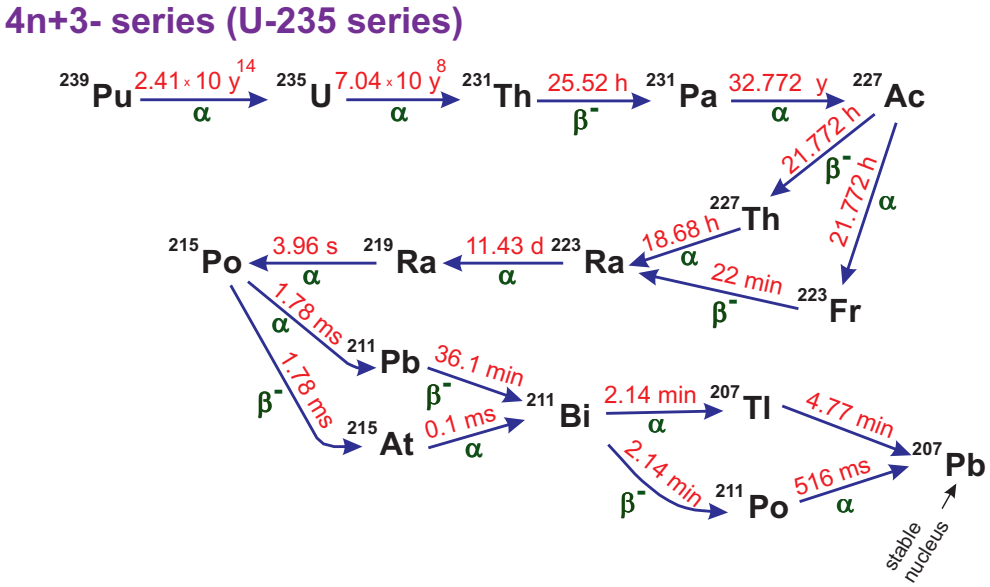


Figure 9.4: The 4n+1 series is historically called the "U-235 series". The series terminates with the stable nucleus ^{207}Pb.

series, $A = 4n + 2$ for (4n+2)- series, and $A = 4n + 3$ for (4n+3)- series). Each of these series ends with a stable nucleus.

Fig. 9.5 demonstrates a dependence of the energy E_α of emitted α- particle for α- decays going from ground states of initial nuclei to ground states of daughter nuclei in the dependence on the mass number A of initial nuclei. One can see that for heavy nuclei ($A > 212$) the energy E_α of the α- particle decreases with the increasing A. According to the Geiger-Nuttall rule (9.7) it means that with increasing A also the α- decay probability ω_α becomes lower. That means for given chain of isotopes (for given Z) the life-time of the initial nucleus increases, for instance, for the U- isotope chain we have: ${}^{227}_{92}\mathrm{U} \rightarrow t_{1/2} = 0.51\ s$, ... , ${}^{238}_{92}\mathrm{U} \rightarrow t_{1/2} = 10^{32}\ s$ (see e.g. http://www-nds.iaea.org).

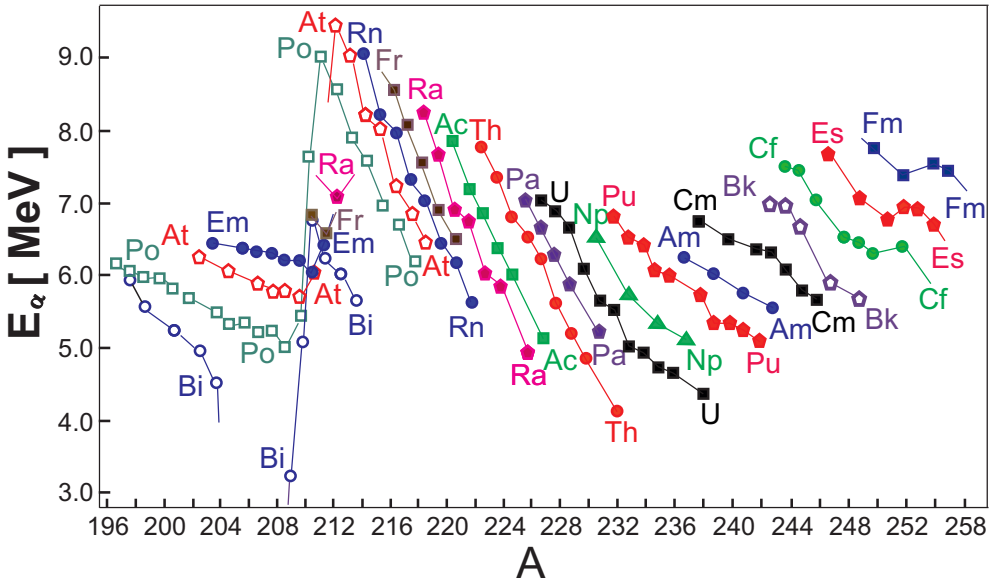


Figure 9.5: The dependence of energy of α- particle emitted by the ground state to ground state α- decay of heavy nuclei on the mass number A for selected isotope chains (taken from [323]).

9.2 Theoretical determination of probability of the α-decay of even-even nuclei

From theoretical point of view the process of the α- decay can be divided into two steps:

1. the forming of the α- particle in the initial nucleus,

2. the penetration of the α- particle through the Coulomb and centrifugal barriers [3] which separate α- particle formed in the initial nucleus from the infinity.

So, the α- particle probability can be written as,

$$\omega_{i\to f}(E_\alpha, Z, A) = \left|\mathscr{K}_{fi}^{(\alpha)}\right|^2 P_\alpha(E_\alpha) \tag{9.13}$$

where $\left|\mathscr{K}_{fi}^{(\alpha)}\right|^2$ is the probability of the forming (creation) of the α- particle inside initial nucleus and $P_\alpha(E_\alpha)$ is the coefficient of the penetration of the α- particle through the potential barrier given by well-known formula (see (G.20) in the appendix G)

$$P_\alpha(E_\alpha) \approx e^{-\frac{2}{\hbar}\int_0^\infty dr\,\sqrt{2M_\alpha(V(r)-E_\alpha)+\frac{\hbar^2 l\,(l+1)}{r^2}}} \tag{9.14}$$

with the α- particle mass M_α.

One should realize that in the case of the α- transition from ground state of even-even nucleus to the ground state of the daughter nucleus the orbital angular momentum l is always zero, $l = 0$ (α- transition $\mid 0^+\rangle \to \mid 0^+\rangle$).

Process of the forming of the α- particle inside the initial nucleus Z^A in the given point $\vec{r}$ is described by the creation operator

$$\hat{A}_\alpha^+ = \frac{1}{4} \sum_{\substack{i_n\sigma_{i_n} i_p\sigma_{i_p} \\ j_n\sigma_{j_n} j_p\sigma_{j_p}}}\sum A^{(\alpha)}_{i_n\sigma_{i_n}\, j_n\sigma_{j_n};\, i_p\,\sigma_{i_p}\, j_p\,\sigma_{j_p}}(\vec{r}\,)\;\; a^+_{i_n\sigma_{i_n}} a^+_{j_n\sigma_{j_n}} a^+_{i_p\sigma_{i_p}} a^+_{j_p\sigma_{j_p}} \tag{9.15}$$

where

$$A^{(\alpha)}_{i_n\sigma_{i_n}\, j_n\sigma_{j_n};\, i_p\,\sigma_{i_p}\, j_p\,\sigma_{j_p}}(\vec{r}\,) \;\equiv\; \langle i_n\sigma_{i_n},\; j_n\sigma_{j_n}; i_p\,\sigma_{i_p},\; j_p\,\sigma_{j_p} \mid \alpha;\; \vec{r}\,\rangle \tag{9.16}$$

In (9.15) $a^+_{i_n\sigma_{i_n}}$ ($a^+_{i_p\sigma_{i_p}}$) is the creation operator of the neutron (proton) in the single particle state $|i_n\sigma_{i_n}\rangle$ ($|i_p\sigma_{i_p}\rangle$), where $\sigma_{i_n} = \pm 1$ represents the sign

[3] The concept of a centrifugal barrier is connected with the particular term in the Schroedinger equation. For instance, the zero spin particle placed in the central potential $V(\vec{r})$ is described by the wave function $\psi(\vec{r}) = R(r)\,Y_{lm}(\hat{r})$ which can be factorized into a radial function $R(r)$ and the spherical function $Y_{lm}(\hat{r})$ of the angles $\hat{r} = \theta,\, \phi$ of the coordinate $\vec{r} = (r,\, \theta,\, \phi)$. Then the stationary Schr. equation for the radial part$R(r)$ reads

$$-\frac{\hbar^2}{2M}\left\{\frac{\partial^2}{\partial r^2} + \frac{2}{r}\frac{\partial}{\partial r}\right\} R(r) + \left\{\frac{\hbar^2}{2M}\frac{l\,(\,l+1\,)}{r^2} + V(r) - E\right\} R(r) = 0$$

and the first term in the second bracket, $\frac{\hbar^2}{2M}\frac{l\,(\,l+1\,)}{r^2}$, represents so called centrifugal barrier.

of the projection of the single neutron (proton) angular momentum $\vec{j}_n$ ($\vec{j}_p$) in the given s.p. state (from the Chapter 6, see (6.15)-(6.18), we know that the s.p. state with $\sigma_{i_n} = -1$ is connected with the s.p. state with $\sigma_{i_n} = +1$ by the time reversal, $\hat{\mathscr{T}}\, a^+_{i_n\sigma_{i_n}=+1}\hat{\mathscr{T}}^{-1} = a^+_{i_n\sigma_{i_n}=-1}$). The symbol $\langle i_n\sigma_{i_n},\ j_n\sigma_{j_n};\ i_p\sigma_{i_p}, j_p\sigma_{j_p}|\ \alpha;\ \vec{r}\,\rangle$ stands for the overlap scalar product of the wave function $|\alpha; \vec{r}\rangle$ of the α- particle in the given point $\vec{r}$ with the product of four s.p. wave functions, $|i_n\sigma_{i_n},\ j_n\sigma_{j_n};\ i_n\sigma_{i_p},\ j_n\sigma_{j_p}\rangle = a^+_{i_n\sigma_{i_n}} a^+_{j_n\sigma_{j_n}} a^+_{i_p\sigma_{i_p}} a^+_{j_p\sigma_{j_p}}\,|\,\rangle$, which is antisymmetrized with respect to the exchange of two neutrons or two protons,

$$A^{(\alpha)}_{i_n\sigma_{in}\ j_n\sigma_{jn};\, i_p\,\sigma_{ip}\ j_p\,\sigma_{jp}}(\vec{r}\,) = -A^{(\alpha)}_{j_n\sigma_{jn}\ i_n\sigma_{in};\, i_p\,\sigma_{ip}\ j_p\,\sigma_{jp}}(\vec{r}\,) = \\ = -A^{(\alpha)}_{i_n\sigma_{in}\ j_n\sigma_{jn};\, j_p\,\sigma_{jp}\ i_p\,\sigma_{ip}}(\vec{r}\,) \tag{9.17}$$

The amplitude of the forming of the α- particle, $\mathscr{K}^{(\alpha)}_{fi}$, is then determined by the matrix element of the operator $\hat{A}_\alpha(\vec{r})$ between the final state $|f\rangle$ of the daughter nucleus $(Z-2)^{A-4}$ and the initial state $|i\rangle$ of the initial nucleus, calculated in the nucleus surface (because the forming of the α- particle is supposed to occur usually on the surface of the nucleus), that means (here we assume the spherical nucleus)

$$\mathscr{K}^{(\alpha)}_{fi} \approx \langle f|\ \hat{A}_\alpha(r = R_0)\ |\ i\rangle \tag{9.18}$$

where $|i\rangle$ is the initial state of the initial nucleus and $|f\rangle$ the final state of the final nucleus.

Theoretical absolute values of transition probabilities $\omega_{i\to f}(E_\alpha, Z, A)$ of the α- decay contains uncertainties connected with the way how to treat the surface region of the nucleus (where α- particle is usually formed) and also with many-body aspects of the clasterization (see [324, 325]). Therefore instead of the probability $\omega_{i\to f}(E_\alpha, Z, A)$ so called hindrance factor is used which is defined as the ratio of the probability $\omega_{gr,Z,A}(E_{\alpha 0}, Z, A)$ of the α-decay from the ground state of the initial nucleus to the ground state of the daughter nucleus and the probability $\omega_{i\to f}(E_\alpha, Z, A)$ of the investigated α-transition $|i\rangle \to |f\rangle$ (here we suppose even A, Z),

$$F^{(\alpha)}_{i\to f;\, l} \equiv \frac{\omega_{gr,\,Z,\,A}(E_{\alpha 0}, Z, A)}{\omega_{i\to f}(E_\alpha, Z, A)} = \boxed{\begin{array}{c}see\\(9.13)\end{array}} = \\ = \frac{|\ \langle gr;\ Z-2, A-4|\ \hat{A}_\alpha(r \approx R_0)\ |\ gr;\ Z,\ A\rangle\ |^2}{|\ \langle f|\ \hat{A}_\alpha(r \approx R_0)\ |\ i\rangle\ |^2}\ \frac{P_0(E_{\alpha 0})}{P_f(E_\alpha)} \tag{9.19}$$

where according to (9.14)

$$P_0 \approx e^{-2\int_{(R_0)} d^3r \sqrt{\frac{2M_\alpha}{\hbar^2}\left(\frac{Z_\alpha Z_A \tilde{e}}{r} - E_{\alpha 0}\right)}}$$
$$P_f \approx e^{-2\int_{(R_0)} d^3r \sqrt{\frac{2M_\alpha}{\hbar^2}\left(\frac{Z_\alpha Z_A \tilde{e}}{r} - E_{\alpha 0}\right) + \frac{l(l+1)}{r^2}}} \tag{9.20}$$

with $\tilde{e} = e/4\pi\epsilon_0$ and where $\int_{(R_0($ d^3r means the integration over the surface region where α- particle is found. So we have following ratio

$$\frac{P_0(E_{\alpha 0})}{P_f(E_\alpha)} \approx e^{-2\int_{(R_0)} d^3r \left\{\sqrt{\frac{2M_\alpha}{\hbar^2}\left(\frac{Z_\alpha Z_A \tilde{e}^2}{r} - E_{\alpha 0}\right)} - \sqrt{\frac{2M_\alpha}{\hbar^2}\left(\frac{Z_\alpha Z_A \tilde{e}^2}{r} - E_{\alpha 0}\right) + \frac{l(l+1)}{r^2}}\right\}} \approx$$
$$\approx e^{-2\,\frac{l(l+1)}{\kappa R_0}} \tag{9.21}$$

where

$$\kappa \approx \sqrt{\frac{2M_\alpha}{\hbar^2}\frac{Z_\alpha Z_A\, \tilde{e}^2}{R_0}} \tag{9.22}$$

In such a way it is usually assumed that in the hindrance factor (9.19) the most of uncertainties are canceled by the approximation (9.21) and the hindrance factor can be written as

$$F^{(\alpha)}_{i\to f;\, l} \approx \frac{|\,\langle gr;\ Z-2, A-4|\,\hat{A}_\alpha(r \approx R_0)\,|\,gr;\ Z,\ A\rangle\,|^2}{|\,\langle f|\,\hat{A}_\alpha(r \approx R_0)\,|\,i\rangle\,|^2}\, e^{-2\,\frac{l(l+1)}{\kappa R_0}} \tag{9.23}$$

The approximation (9.21) was deduced for spherical nuclei. However most of neutron deficit nuclei with $A > 150$ (where α- decay is observed) are deformed. That means the ration P_0/P_f in (9.19) should be determined for deformed nuclei with the shape described by (1.3). Then the integrals (9.20) should be calculated effectively only inside deformed surface region and it brings some accuracy improvement. However our aim now is not to present here the precise expressions for α- decay rates but rather to sort α- decays according to their magnitude. From this point od view we can accept more approximations. In most cases we found that the ratio (9.21) is close to 1 and then the hindrance factor is determined only by the matrix elements of the operator $\hat{A}_\alpha(\vec{r})$ (here we again assume even A and Z),

$$F^{(\alpha)}_{i\to f} \approx \frac{|\,\langle gr;\ Z-2, A-4|\,\hat{A}_\alpha(r \approx R_0)\,|\,gr;\ Z,\ A\rangle\,|^2}{|\,\langle f|\,\hat{A}_\alpha(r \approx R_0)\,|\,i\rangle\,|^2} \tag{9.24}$$

9.2.1 Alpha- transition from the ground state of even-even nucleus to the ground state of even-even nucleus

Expressions (9.19) - (9.23) for hindrance factor are valid for all α- transitions. In hindrance factors investigated α- decay rate (denominator in (9.19)) is always compared with the rate of the α- transition between ground states of the nearest even-even mother and daughter nuclei. In this subsection the α- decays between ground states are discussed. Concretely we will compare the ground state - ground state α- transition probabilities from the point of view of two models of nuclear structure,

1. model of independent particles, when the mother and daughter nuclei Hamiltonians are approximated by corresponding mean fields ($\hat{H}_{intr} \approx \hat{H}_{AV}$ - see (5.2));

2. model of independent quasiparticles, when Hamiltonians of the mother and daughter nuclei involve only quasiparticle mean fields ($\hat{H}_{intr} \approx \hat{H}'_P$ - see (6.2)).

It will be shown that the taking into account of the pairing interaction is very important for the theoretical description of α- decay.

9.2.1.1 Ground state to ground state alpha transitions in even-even nuclei within the model of independent particles (IP)

In this case Z and A are even numbers and in the ground state all single-paricle states are occupied up to the Fermi level in pairs. The ground state of the mother even-even nucleus can be expressed as

$$|gr;\ Z,A\rangle_{HF} = \prod_{\nu_p<} \prod_{\nu_n<} a^+_{\nu_p+}\ a^+_{\nu_p-}\ a^+_{\nu_n+}\ a^+_{\nu_n-}\ |-\rangle = \\ = a^+_{\nu_p(F)+}\ a^+_{\nu_p(F)-}\ a^+_{\nu_n(F)+}\ a^+_{\nu_n(F)-}\ |gr;\ Z-2,A-4\rangle \qquad (9.25)$$

where $|-\rangle$ is the particle vacuum, $\nu_p(F)+$, $\nu_p(F)-$ are indices of single-particle states of two protons sitting on the proton Fermi level and similarly $\nu_n(F)+$, $\nu_n(F)-$ are indices of two neutrons from the neutron Fermi level. Index $\nu<$ means that the given single-particle state is occupied. We suppose that in the HF ground state of the even-even nucleus each single-particle level $e_{\nu<}$ below the Fermi level is occupied by two protons or neutrons in the single-particle states $\nu+$ and $\nu-$ differing only by the sign of the single-particle angular momentum. When two prorons and two neutrons sitting on

the proton and neutron Fermi levels ($\nu_p(F)+$, $\nu_p(F)-$ and $\nu_n(F)+$, $\nu_n(F)-$) are removed from the mother nucleus in the form of the α- particle we obtain the ground state $|gr;\ Z-2, A-4\rangle$ of the daughter nucleus. In such an approximation we have for the matrix element $\langle gr;\ Z-2, A-4|\,\hat{A}_\alpha(\vec{r})\,|\,gr;\ Z, A\rangle$ in (9.18) the following expression

$$\mathscr{K}^{(\alpha)}_{gr\,gr}(IP) \approx {}_{HF}\langle gr;\ Z-2, A-4|\,\hat{A}_\alpha(\vec{r}\,|\,gr;\ Z, A\rangle_{HF} =$$

$$= \boxed{\begin{array}{c} see \\ (9.25), (9.15) \end{array}} =$$

$$= \frac{1}{4} \sum_{\substack{i_p j_p \in prot \\ \sigma_{i_p}\sigma_{j_p}}} \sum_{\substack{i_n j_n \in neut \\ \sigma_{i_n}\sigma_{j_n}}} A^{(\alpha)}_{i_n\sigma_{i_n}\ j_n\sigma_{i_n}\ ;\ i_p\sigma_{i_p}\ j_p\sigma_{i_p}}$$

$$\langle -|\ a_{j_p\sigma_{j_p}}\ a_{i_p\sigma_{i_p}}\ a^+_{\nu_p(F)+}\ a^+_{\nu_p(F)-}\ |\ -\rangle$$

$$\langle -|\ a_{j_n\sigma_{j_n}}\ a_{i_n\sigma_{i_n}}\ a^+_{\nu_n(F)+}\ a^+_{\nu_n(F)-}\ |\ -\rangle =$$

$$= \boxed{\begin{array}{c} using \\ (9.17) \end{array}} = A^{(\alpha)}_{\nu_n(F)+\ \nu_n(F)-\ ;\ \nu_p(F)+\ \nu_p(F)-} \tag{9.26}$$

So, in the framework of the model of independent particles the probability of the α- decay from the ground state to the ground state of even-even nuclei (see (9.13)) depends only on the proton and neutron Fermi states $\nu_p(F)\pm$ and $\nu_n(F)\pm$ of the mother nucleus.

9.2.1.2 Ground state to ground state alpha transitions in even-even nuclei within the model of independent quasiparticles (IP)

In the framework of the model of independent quasiparticles usually the BCS approach described in the Section 6.2.2 is used. Within the BCS approximation the ground state of the even number of particle system is given by the quasiparticle vacuum $|BCS\rangle$ (see (6.28)). So, the ground state of the mother

and daughter nucleus can be written as follows

$$|gr;\ Z,A\rangle_{BCS} = |BCS,N\rangle\,|BCS,Z\rangle = \boxed{\begin{array}{c}see\\(6.28)\end{array}} =$$

$$= \prod_{\substack{\nu_p>0\\ \nu_p\in prot}}\ \prod_{\substack{\nu_n>0\\ \nu_n\in neut}} \left(\mathscr{U}_{\nu_p}^{(Z)} + \mathscr{V}_{\nu_p}^{(Z)}\, a^+_{\nu_p+}\, a^+_{\nu_p-}\right)\left(\mathscr{U}_{\nu_n}^{(N)} + \mathscr{V}_{\nu_n}^{(N)}\, a^+_{\nu_n+}\, a^+_{\nu_n-}\right)|-\rangle$$

$$|gr;\ Z-2,A-4\rangle_{BCS} = |BCS,N-2\rangle\,|BCS,Z-2\rangle = \boxed{\begin{array}{c}see\\(6.28)\end{array}} =$$

$$= \prod_{\substack{\nu_p>0\\ \nu_p\in prot}}\ \prod_{\substack{\nu_n>0\\ \nu_n\in neut}} \left(\mathscr{U}_{\nu_p}^{(Z-2)} + \mathscr{V}_{\nu_p}^{(Z-2)}\, a^+_{\nu_p+}\, a^+_{\nu_p-}\right)$$
$$\left(\mathscr{U}_{\nu_n}^{(N-2)} + \mathscr{V}_{\nu_n}^{(N-2)}\, a^+_{\nu_n+}\, a^+_{\nu_n-}\right)|-\rangle \qquad (9.27)$$

where $\mathscr{U}_\nu^{(Z)}$, $\mathscr{V}_\nu^{(Z)}$ are pairing BCS amplitudes (6.28), (6.52) for the system of Z protons and $\mathscr{U}_\nu^{(N)}$, $\mathscr{V}_\nu^{(N)}$ for the system of N neutrons. Similarly $\mathscr{U}_\nu^{(Z-2)}$, $\mathscr{V}_\nu^{(Z-2)}$,$\mathscr{U}_\nu^{(N-2)}$, $\mathscr{V}_\nu^{(N-2)}$ are pairning amplitudes for the system of $Z-2$ protons and $N-2$ neutrons. The substitution of (9.27) into (9.18) gives

$$\mathscr{K}^{(\alpha)}_{gr\to gr}(IQP) = {}_{BCS}\langle gr;\ Z-2,A-4|\ \hat{A}_\alpha(\vec{r})\,|gr;\ Z,A\rangle_{BCS} =$$

$$= \frac{1}{4}\sum_{\substack{i_p,j_p>0\\ \sigma_{ip}\sigma_{jp}}}\ \sum_{\substack{i_n,j_n>0\\ \sigma_{in}\sigma_{jn}}} A^{(\alpha)}_{i_n\sigma_{in}\ j_n\sigma_{jn};\ i_p\sigma_{ip}\ j_p\sigma_{jp}} \prod_{\nu_p>0}\prod_{\nu_n>0}\prod_{\nu_p'>0}\prod_{\nu_n'>0}$$

$$\langle -|\left(\mathscr{U}_{\nu_p'}^{(Z-2)} + \mathscr{V}_{\nu_p'}^{(Z-2)} a_{\nu_p'-}\, a_{\nu_p'+}\right)$$
$$a_{i_p\sigma_{ip}}\, a_{j_p\sigma_{jp}}\left(\mathscr{U}_{\nu_p}^{(Z)} + \mathscr{V}_{\nu_p}^{(Z)} a^+_{\nu_p+}\, a^+_{\nu_p-}\right)|-\rangle$$

$$\langle -|\left(\mathscr{U}_{\nu_n'}^{(N-2)} + \mathscr{V}_{\nu_n'}^{(N-2)} a_{\nu_n'-}\, a_{\nu_n'+}\right)$$
$$a_{i_n\sigma_{in}}\, a_{j_n\sigma_{jn}}\left(\mathscr{U}_{\nu_n}^{(N)} + \mathscr{V}_{\nu_n}^{(N)} a^+_{\nu_n+}\, a^+_{\nu_n-}\right)|-\rangle =$$

$$= \sum_{i_n,\,j_p>0} A^{(\alpha)}_{i_n+\ i_n-;\ j_p+\ j_p-}\ \ \xi_{i_n}(N)\,\xi_{j_p}(Z) \qquad (9.28)$$

where

$$\xi_i(N) \equiv \mathscr{U}_i^{(N-2)}\mathscr{V}_i^{(N)} \prod_{\nu\neq i}\left(\mathscr{U}_\nu^{(N-2)}\mathscr{U}_\nu^{(N)} + \mathscr{V}_\nu^{(N-2)}\mathscr{V}_\nu^{(N)}\right)$$
$$\xi_i(Z) \equiv \mathscr{U}_i^{(Z-2)}\mathscr{V}_i^{(Z)} \prod_{\nu\neq i}\left(\mathscr{U}_\nu^{(Z-2)}\mathscr{U}_\nu^{(Z)} + \mathscr{V}_\nu^{(Z-2)}\mathscr{V}_\nu^{(Z)}\right) \qquad (9.29)$$

Further we can use the following appproximation which fulfils especially for heavier nuclei where difference between $\mathscr{U}_\nu^{(Z)}$, $\mathscr{V}_\nu^{(Z)}$ from $\mathscr{U}_\nu^{(Z-2)}$, $\mathscr{V}_\nu^{(Z-2)}$ is small

$$\prod_{\nu\neq i}\left(\mathscr{U}_\nu^{(N-2)}\mathscr{U}_\nu^{(N)}+\mathscr{V}_\nu^{(N-2)}\mathscr{V}_\nu^{(N)}\right)\approx\prod_{\nu\neq i}\left(\mathscr{U}_\nu^{(N)}\mathscr{U}_\nu^{(N)}+\mathscr{V}_\nu^{(N)}\mathscr{V}_\nu^{(N)}\right)=$$

$$=\boxed{\begin{array}{c}see\\(6.29)\end{array}}=1 \tag{9.30}$$

Then

$$\xi_i(N)\approx\mathscr{U}_i^{(N-2)}\mathscr{V}_i^{(N)}\qquad\qquad\xi_i(Z)\approx\mathscr{U}_i^{(Z-2)}\mathscr{V}_i^{(Z)} \tag{9.31}$$

and (9.28) can be rewritten into the following form

$$\begin{aligned}\mathscr{K}_{gr\to gr}^{(\alpha)}(IQP)=&{}_{BCS}\langle gr\ ;\ Z-2,A-4|\ \hat{A}_\alpha(\vec{r})\ |gr\ ;\ Z,A\rangle\approx\\&\approx\sum_{i_nj_p>0}A_{i_n+\,i_n-;\ j_p+\,j_p-}\ \mathscr{U}_{i_n}^{(N-2)}\ \mathscr{V}_{i_n}^{(N)}\ \mathscr{U}_{j_p}^{(Z-2)}\ \mathscr{V}_{j_p}^{(Z)}\end{aligned} \tag{9.32}$$

So, opposite to the case of the model of independent particles (see (9.29), the model of independent quasiparticle gives the amplitude $\mathscr{K}_{fi}^{(\alpha)}$ and consequently α- decay probability dependent on all single-particle states (not only on the Fermi states).

Now we can compare the probabilities of ground state - ground state α-decay of even-even nuclei determined in the framework of the model of independent particles with that of the model of independent quasiparticles. Because of (9.26) the α- decay probability for the model of independent particles depends only on the neutron and proton Fermi states. Since the Fermi states change drastically with Z and A of the mother nucleus the α- decay probabilities must also change with Z and A discontinuously for the model of independent particles. In the case of the model of independent quasiparticles with the α- decay amplitude (9.28) or (9.32) the ground state α- decay probability depends on Z and A through the square of (9.32) which is the continuous dependence. The continuous character of the even-even nucleus ground state - ground state α- decay probability dependence on Z and A was confirmed experimentally. In such a way the inclusion of the pairing correlation in the model description leads to the improvement of the agreement with the experimental data (see e.g. [7] and citation therein).

Taking into account the pairing interaction leads also to the increasing of the α- decay probability between ground states of even-even nuclei. In order to estimate this α- decay probability strengthening further we use following simplification - we will suppose that the matrix elements $A^{(\alpha)}_{i_n+\, i_n-;\, j_p+\, j_p-}$ are constant and not dependent on states i_n and j_p ,

$$A^{(\alpha)}_{i_n+\, i_n-;\, j_p+\, j_p-} \equiv \; W = const \tag{9.33}$$

This approximation is quite rough. As it was shown in the paper [326] different elements $A^{(\alpha)}_{i_n+\, i_n-;\, j_p+\, j_p-}$ can vary by a factor 20-50. Nevertheless the approximation (9.33) is useful for rough estimation of the role of pairing interaction. Using the approximation (9.33) in the model of independent particle (see (9.26)) we obtain

$$\mathscr{K}^{(\alpha)}_{gr\to gr}(IPM) = {}_{HF}\langle gr;\; Z-2, A-4|\; \hat{A}_\alpha(\vec{r})\; |gr;\; Z, A\rangle_{HF} \approx W \tag{9.34}$$

while this approximation for the model of independent quasiparticles gives (see (9.28))

$$\begin{aligned}\mathscr{K}^{(\alpha)}_{gr\to gr}(IQM) = \; {}_{BCS}\langle gr;\; Z-2, A-4|\; \hat{A}_\alpha(\vec{r})\; |gr;\; Z, A\rangle_{BCS} \approx \\ \approx \; W \sum_{i_n\; i_p>0} \xi_{i_n}(N)\, \xi_{i_p}(Z)\end{aligned} \tag{9.35}$$

where

$$\sum_{i_n>0} \xi_{i_n}(N) = \sum_{i_n>0} \mathscr{U}^{(N-2)}_{i_n}\, \mathscr{V}^{(N)}_{i_n} \approx \sum_{i_n>0} \mathscr{U}^{(N)}_{i_n}\, \mathscr{V}^{(N)}_{i_n} =$$

$$= \boxed{\begin{array}{c}\text{because (6.47)} \\ \Delta_{neut} = G_N \sum_{i_n>0} \mathscr{U}^{(N)}_{i_n}\, \mathscr{V}^{(N)}_{i_n}\end{array}} \approx \frac{\Delta_{neut}}{G_N}$$

$$\sum_{j_p>0} \xi_{j_p}(Z) \approx \frac{\Delta_{prot}}{G_p} \tag{9.36}$$

So within the approximation (9.33)

$$\mathscr{K}^{(\alpha)}_{gr\to gr}(IQM) \approx W\, \frac{\Delta_{prot}}{G_P}\, \frac{\Delta_{neut}}{G_N} \tag{9.37}$$

and for the ratio of $gr \to gr$ α- decay probabilities for even-even nuclei determined by the model of independent quasiparticles and model of independent

particles we have,

$$\frac{\omega_{gr\to gr}(E_\alpha,Z,A)_{BCS}}{\omega_{gr\to gr}(E_\alpha,Z,A)_{HF}} \approx \boxed{\begin{array}{c}\text{see}\\(9.13)\end{array}} \approx \frac{\left|\mathcal{K}^{(\alpha)}_{gr\to gr}(IQM)\right|^2}{\left|\mathcal{K}^{(\alpha)}_{gr\to gr}(IPM)\right|^2} \approx$$
$$\approx \frac{\left|\,{}_{BCS}\langle\, gr;Z-2,A-4|\,\hat{A}_\alpha\,|\,gr;Z,A\rangle_{BCS}\,\right|^2}{\left|\,{}_{HF}\langle\, gr;Z-2,A-4|\,\hat{A}_\alpha\,|\,gr;Z,A\rangle_{HF}\,\right|^2} \approx$$
$$\approx \frac{W^2\left(\sum_{i_n>0}\xi_{i_n}(N)\right)^2\left(\sum_{i_p>0}\xi_{i_p}(Z)\right)^2}{W^2} = \frac{\Delta^2_{neut}\,\Delta^2_{prot}}{G^2_N\,G^2_P} \tag{9.38}$$

For instance, if the product $\left(\sum_{i_n>0}\xi_{i_n}(N)\right)^2\left(\sum_{i_p>0}\xi_{i_p}(Z)\right)^2$ was calculated in the framework of the BCS theory with the phenomenological mean field of the Saxon-Woods type (see (5.46)) and the pairing interaction was taken in the monopole form (6.24), when sums over i_n and i_p involved all Saxon-Woods single-particle states from the bottom of the potential well up to single-particle states with zero energy, then the product $\left(\sum_{i_n>0}\xi_{i_n}(N)\right)^2\left(\sum_{i_p>0}\xi_{i_p}(Z)\right)^2$ reaches value s of 2000 - 3000 for deformed nuclei (see [7]). That means the pairing correlations increase the value of the $gr\to gr$ α- decay probabilities by a factor of 3 orders in the comparison with the model of independent particles with only the mean field in the Hamiltonian. These increased $gr\to gr$ α- decay rate values for the model of independent quasiparticles are in the agreement with the experimental data for deformed nuclei. In the case of spherical nuclei this strengthening of α- decay rates is not so big and it gives only 1 order factor [7].

9.2.2 Alpha- transition from the ground state of even-even nucleus to the excited state of even-even nucleus

In this subsection hindrance factors for α- transitions from the ground state of the even-even mother nuclei to excited states of doughter nuclei are evaluated from the point of view of the model of independent partilcles and the model of independent quasiparticles. That means we analyze the influence of the taking into account of the pairing correlation on these α- transitions.

In the framework of the model of independent quasiparticle the initial state (ground state) of the mother nucleus (Z,A) and the final excited state

of the daughter nucleus [4] are

$$|i\rangle = |gr;\ Z, A\rangle_{BCS} = |BCS;\ N\rangle\,|BCS;\ Z\rangle = \\ = \prod_{\substack{\nu_n>0 \\ \nu_n\in neut}} \prod_{\substack{\nu_p>0 \\ \nu_p\in prot}} \Big(\mathscr{U}^{(N)}_{\nu_n} + \mathscr{U}^{(N)}_{\nu_n} a^+_{\nu_n+} a^+_{\nu_n-}\Big)\Big(\mathscr{U}^{(Z)}_{\nu_p} + \mathscr{U}^{(Z)}_{\nu_p} a^+_{\nu_p+} a^+_{\nu_p-}\Big)\,|-\rangle$$

$$|f\rangle = |\rho_1\sigma_1, \rho_2\sigma_2;\ Z-2, A-4\rangle = \\ = \alpha^+_{\rho_1\sigma_1}\alpha^+_{\rho_2\sigma_2}\,|BCS;\ N-2\rangle\,|BCS;\ Z-2\rangle \tag{9.39}$$

where we suppose that the final states of the daughter nucleus is neutron two-quasiparticle states created by two- quasiparticle creation operators $\alpha^+_{\rho_1\sigma_1}\alpha^+_{\rho_2\sigma_2}$ acting on the ground state $|BCS;\ N-2\rangle\,|BCS;\ Z-2\rangle$ ($\sigma_1,\ \sigma_2 = \pm$). Further the approximation is used that the quasiparticle vacuum for the mother nucleus is simultaneously quasiparticle vacuum for the daughter nucleus. So the matrix element $\langle f|\,\hat{A}_\alpha\,|i\rangle$ of the oparator (9.15) is

$$\langle f|\,\hat{A}_\alpha\,|i\rangle = \frac{1}{4}\sum_{\substack{i_n\ j_p \\ \sigma_{i_n}\ \sigma_{j_p}}}\ \sum_{\substack{j_n\ i_p \\ \sigma_{j_n}\ \sigma_{i_p}}} A^{(\alpha)}_{i_n\sigma_{i_n}\ j_n\sigma_{j_n},\, i_p\sigma_{i_p}\ j_p\sigma_{j_p}}$$

$$\langle BCS;\ Z-2|\,a_{j_p\sigma_{j_p}} a_{i_p\sigma_{i_p}}\,|BCS;\ Z\rangle$$

$$\langle BCS;\ N-2|\,\alpha_{\rho_2\sigma_2}\alpha_{\rho_1\sigma_1}\ a_{j_n\sigma_{j_n}} a_{i_n\sigma_{i_n}}\,|BCS;\ N\rangle =$$

$$= \boxed{\begin{array}{c}\text{particle operators } a_{i\sigma_i} \text{ are expressed in terms of} \\ \text{quasiparticle operators } \alpha_{i\sigma_i} \text{ using Bogoliubov} \\ \text{transformation and then anticommutator} \\ \text{relations for } \alpha^+_{i\sigma_i},\ \alpha_{i\sigma_i} \text{ are used}\end{array}} =$$

$$= \sum_{i_p>0} \xi_{i_p}(Z)\ \mathscr{V}^{(N)}_{\rho_1}\mathscr{V}^{(N)}_{\rho_2}\ \sigma_{\rho_1}\sigma_{\rho_2}\ A^{(\alpha)}_{\rho_2\sigma_2\ \rho_1\sigma_1,\, i_p+\ j_p-} \tag{9.40}$$

Now the matrix element (9.40) can be substituted into the denominator of the expr. (9.24) for the hindrance factor. The subsequent substitution of the ground state - ground state α- decay probability (9.28) into the (9.24) gives the hindrance factor in the form

$$F^{(\alpha)}_{gr\to\rho_1\sigma_1,\,\rho_2\sigma_1} = \frac{\Big|\ \sum_{i_n,\,j_p>0} A^{(\alpha)}_{i_n+\ i_n-;\ j_p+\ j_p-}\ \ \xi_{i_n}(N)\,\xi_{j_p}(Z)\ \Big|^2}{\Big|\ \sum_{i_p>0}\xi_{i_p}(Z)\ \mathscr{V}^{(N)}_{\rho_1}\mathscr{V}^{(N)}_{\rho_2}\ \sigma_{\rho_1}\sigma_{\rho_2}\ A^{(\alpha)}_{\rho_2\sigma_2\ \rho_1\sigma_1,\, i_p+\ j_p-}\ \Big|^2} \tag{9.41}$$

[4] The low- lying excited state of even-even nuclei in the model of independent quasiparticles have two-quasiparticle character.

It turns out that the nondiagonal matrix elements $A^{(\alpha)}_{\rho_2\sigma_2\,\rho_1\sigma_1;\,i_p+\,i_p-}$ ($\rho_1 \neq \rho_2$, $\sigma_1 \neq -\sigma_2$) are very small with respect to the diagonal ones with ($\rho_1 = \rho_2$, $\sigma_1 = -\sigma_2$). So we can accept the approximation $A_{\rho_2-\sigma_2\,\rho_1-\sigma_1;\,i_p+\,i_p-} \approx 0$ for $\rho_1 \neq \rho_2$; $\sigma_1 \neq -\sigma_2$. If further the approximation (9.33) is used the expression (9.41) for the hindrance factor of ground state to excited states α- transition in even-even nuclei can be rewritten in the following simplified form (in the framework of the model of independent quasiparticles)

$$F^{(\alpha)}_{gr\to\rho_1\sigma_1,\,\rho_2\sigma_1} \approx \delta_{\rho_1\rho_2}\,\delta_{\sigma_1,\,-\sigma_2}\,\frac{\left(\sum_{i_n>0}\xi_{i_n}(N)\right)^2\left(\sum_{j_p>o}\xi_{i_n}(Z)\right)^2}{\mathscr{V}^{(N)\,2}_{\rho_1}\,\mathscr{V}^{(N)\,2}_{\rho_2}\left(\sum_{i_p>0}\xi_{i_p}(Z)\right)} \approx$$

$$\approx \delta_{\rho_1\rho_2}\,\delta_{\sigma_1,\,-\sigma_2}\,\frac{\left(\sum_{i_n>0}\xi_{i_n}(N)\right)^2}{\mathscr{V}^{(N)\,2}_{\rho_1}\mathscr{V}^{(N)\,2}_{\rho_2}} \tag{9.42}$$

In the framework of the independent particle model the initial state (ground state of the even-even nucleus is described by the HF Slater determinants $|HF;\,N\rangle|HF;\,Z\rangle$ and final state are low-lying particle-hole excitations (we suppoese neutron p-h state $a^+_{\rho_1>\sigma_1}a_{\rho_2<\sigma_1}\,|gr;Z-2,A-4\rangle$)

$$|i\rangle = |gr;\,Z,A\rangle_{HF} = |HF;\,N\rangle\,|HF;\,Z\rangle = \boxed{\begin{array}{c}\text{see}\\(4.5)\end{array}} =$$

$$= \prod_{\nu_p<}\prod_{\nu_n<} a^+_{\nu_p<}\,a^+_{\nu_n<}\,|-\rangle$$

$$|f\rangle = |\rho_{1>\,\sigma_1}\,\rho_{2<\,\sigma_2};\,Z-2,A-4\rangle =$$

$$= a^+_{\rho_1>\,\sigma_1}\,a_{\rho_2<\,\sigma_2}\,|HF;\,N-2\rangle\,|HF;\,Z-2\rangle \tag{9.43}$$

Then

$$\langle f|\,\hat{A}_\alpha\,|i\rangle = \frac{1}{4}\sum_{\substack{i_n\,j_p\\ \sigma_{i_n}\,\sigma_{j_p}}}\sum_{\substack{i_p\,j_n\\ \sigma_{i_p}\,\sigma_{j_n}}} A^{(\alpha)}_{i_n\sigma_{i_n}\,j_n\sigma_{j_n};\,i_p\sigma_{i_p}\,j_p\sigma_{j_p}}$$

$$\langle HF;\,Z-2|\,a_{j_p\sigma_{j_p}}a_{i_p\sigma_{i_p}}|\,HF;\,N\rangle$$

$$\langle HF;\,N-2|\,a^+_{\rho_2<\,\sigma_2}\,a_{\rho_1>\,\sigma_1}\,a_{j_n\sigma_{j_n}}a_{i_n\sigma_{i_n}}|\,HF;\,N\rangle =$$

$$= \boxed{\begin{array}{c}\text{again we use the diagonal approximation for the matrix}\\ \text{elements of } \hat{A}_\alpha \text{ and (9.33)}\end{array}} \approx$$

$$\approx W \tag{9.44}$$

The substitution of the square of (9.44) into the denominator of (9.24) and square of (9.26) ($\mathscr{K}^{(\alpha)}_{gr\to gr}(IP) \approx W$) into the nominator of (9.24) gives the hindrance factor in the following form

$$F^{(\alpha)}_{gr\to\rho_1>\,\sigma_1\ \ \rho_2>\,\sigma_2}(IPM) \ \approx \ 1\,\delta_{\rho_1,\,\rho_2}\,\delta_{\sigma_1,-\sigma_2} \tag{9.45}$$

So the model of independent particles gives hindrance factors for ground state - excited states α- transitions in even-even nuclei with values about unity.

The estimation of the hindrance factor (9.42) calculated in the framework of the model of independent quasiparticles using phenomenological Saxon-Woods mean field with the monopole pairing for deformed rare-earth nuclei made in the sixties (see e.g. [7]) gives values about two orders higher,

$$F^{(\alpha)}_{gr\to\rho_1>\,\sigma_1\ \ \rho_2>\,\sigma_2}(IQM) \ \approx (200-500)\,\delta_{\rho_1,\,\rho_2}\,\delta_{\sigma_1,-\sigma_2} \tag{9.46}$$

That means the taking into account the pairing correlation leads to substantial increase of the gr. state -excited state α- decay hindrance factor for even-even nuclei in the comparison with the pure model of independent particles. By other words the inclusion of the pairing interaction in the nucleus Hamiltonian means the reduction of the calculated gr. state - excited state α- decay probability by two orders and it is in agreement with the experimental observations [7]. High values of the hindrance factor in even-even nuclei for transitions to excited states is also in agreement with the experimental experience that the probability of the α- decay going to the excited states of the daughter nucleus is much smaller then the α- decay to its ground state.

In this section we analyzed α- decay rates in even-even nuclei within the model of independent quasiparticles when the nucleus Hamiltonian involved mean field and pairing interaction (the nucleus Hamiltonian was approximated by the quasiparticle mean field). It was shown that taking into account pairing interaction changed drastically calculated α-decay probabilities and lead to the better agreement with experimental values. Further inclusion of the residual interaction (that means going beyond the model of independent quasiparticles) has no big influence on the α- particle probabilities (see e.g. [7] and citations therein).

9.3 Probability of α- decay in odd-A nuclei

Similarly as in the previous section concerning α- decay in even-even nuclei in this section we analyze α- decay probability in odd-A nuclei in the framework

of the model of independent particles and the model of independent quasiparticles. If the residual interaction is neglected in the nucleus Hamiltonian then

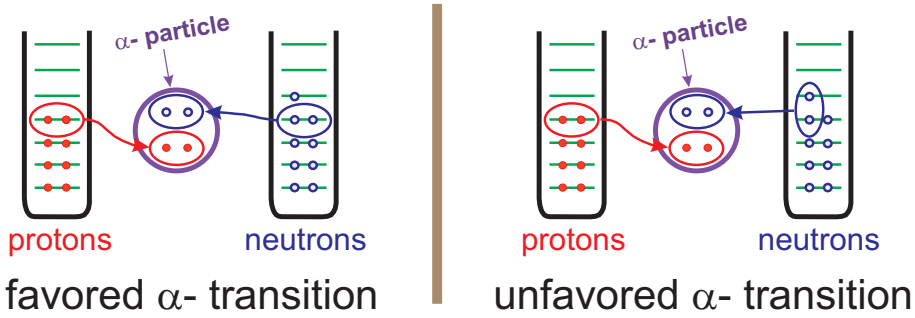


Figure 9.6: Schematic figure of the creation of the α- particle during favored and unfavored α- decay of odd neutron nucleus.

the ground state and the lowest excited states in odd-A nucleus have one-particle character (in the model of independent particles when $\hat{H} \approx \hat{H}_{AV}$) or one- quasiparticle character (in the model of independent quasiparticles when $\hat{H} \approx \hat{H}_{AV} + \hat{V}_{pair}$ - see (6.26).

From the point of view of the origin of neutrons and protons forming the α- particle emitted in the α- decay of the odd A nucleus we recognize two types of the α- transitions, (i) favored α- transitions and (ii) unfavored α- transitions (see the Fig. 9.6).

Favored α- transitions are transitions when the emitted α- particle is formed only by correlated proton and neutron pairs which were created in the mother nucleus by the pairing interaction.

Unfavored α- transitions are transitions when in the emitted α- particle the odd unpaired nucleon (odd proton or odd neutron) is present (see the right part of the Fig. 9.6). Intuitively one can expect that in this case the probability of the α- decay is reduced in the comparison with favored α- transitions (because in this case it is necessary to break one pair of nucleons during the formation of the α- particle).

In the Fig.9.7 the α- decay from the ground state of the isotope $^{249}_{98}\mathrm{Cf}_{151}$, with the angular momentum $I^{\pi} = 9/2^{-}$ with the projection $K = 7/2$ and with the main single-particle component characterized by the Nilsson labeling $K[Nn_z\Lambda] = 7/2[734]$ (see the text below expression (5.47)), going to low-lying states of the axially deformed $^{245}_{96}\mathrm{Cm}_{149}$ is demonstrated. One can see that this α- decay populates levels belonging to 3 rotational bands (ground rotational band built on the intrinsic state with the dominant single-particle component 7/2 [624], rotational band built on the single-particle state 5/2 [622]

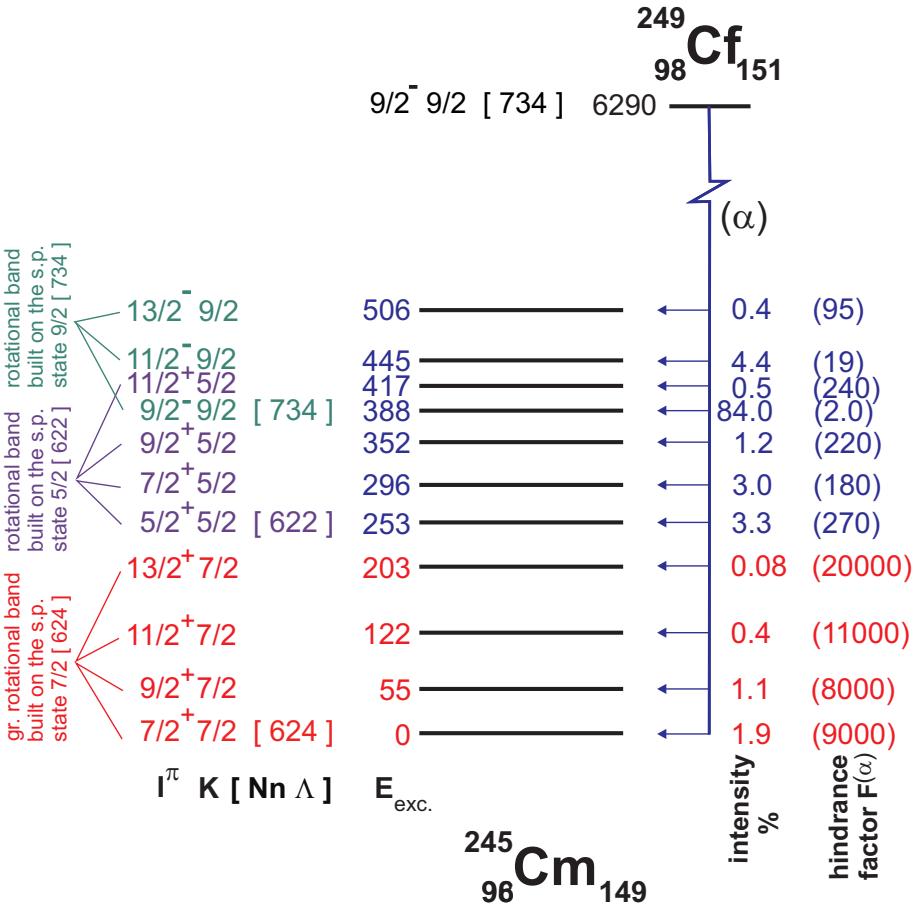


Figure 9.7: The experimental low- lying spectrum of ^{245}Cm populated by the α- decay from the ground state of ^{249}Cf (with the dominant single-paricle component $I^\pi\ K\,[Nn_z\Lambda] = 9/2\ 9/2[734]$). On the left side the total angular momentum I^π, its projection K and the Nilsson labeling $[Nn_z\Lambda]$ of the main single-particle component forming given excited state together with corresponding excitation energy is given. On the right side there is the relative intensity of the population of given excited state together with the experimental value of the corresponding hindrance factor.

and rotational band built on the single-particle state 7/2 [734]). From all α-transitions going to different states in ^{245}Cm only transitions 9/2 9/2 [734] (in ^{249}Cf) $\rightarrow$ 9/2 9/2 [734] (in ^{245}Cm) can be considered as favored α- transition. In this α- transition odd neutron occupies the same intrinsic state in the odd-A daughter and mother nuclei (with dominant single-particle state $K\,[Nn_z\Lambda] = 7/2\,[734]$) and therefore the emitted α- particle should be formed from two paired protons and two paired neutrons. All other α- transitions going to another intrinsic states of the daughter nucleus are unfavored transitions where the odd neutron from the ground state of the daughter nucleus $^{249}_{98}$Cf$_{151}$ is involved in the emitted α- particle and as a result of it the odd neutron of the daughter nucleus $^{245}_{96}$Cm$_{149}$ occupies another intrinsic states

then the ground state of the mother nucleus. As it is seen from the Fig. 7.6 the favored transition 9/2 9/2[734] $\rightarrow$ 9/2 9/2[734] has the lowest hindrance factor from all α- transitions ^{249}Cf $\rightarrow$ ^{244}Cm going from the ground state of ^{249}Cf. Consequently the favored α- transition 9/2 9/2[734] $\rightarrow$ 9/2 9/2[734] is the most intensive (84%) of all observed α- transitions - see Fig. 9.7. The hindrance factor of the favored α- transition going to the state 9/2 9/2[734] with the excitation energy 388 KeV is $F^{(\alpha)} \approx 2$ while for instance the ground state $\rightarrow$ ground state unfavored α- transition has the hindrance factor $F^{(\alpha)} \approx 9000$. That means the ground state $\rightarrow$ ground state α- transition is strongly suppressed.

The explanation why the hindrance factor for favored α- transitions in odd-A nuclei is substantially less in the comparison with the unfavored transitions is again given by the pairing of nucleons. Hindrance factor for transitions in odd-A nuclei is described by the expression (9.24) where in the nominator there is the square of the matrix element of the operator $\hat{A}_\alpha$ between ground states of neighbouring even-even nuclei and in the denominator the square of the matrix element of $\hat{A}_\alpha$ for investigated α- transition of odd-A nuclei (mother nucleus $(Z, A+1)$ and daughter nucleus $(Z-2, A-3)$) (A- even)

$$F^{(\alpha)}_{i\rightarrow f} = \boxed{\begin{array}{c}\text{see}\\(9.24)\end{array}} = \\ = \frac{\left|\, \langle gr;\ Z-2, A-4|\ \hat{A}_\alpha\ |gr;\ Z, A\rangle \,\right|^2}{\left|\, \langle f \equiv \rho_f\sigma_f;\ Z-2, A-3|\ \hat{A}_\alpha\ |i \equiv \rho_i\sigma_i;\ Z, A+1\rangle \,\right|^2} \qquad (9.47)$$

where we suppose that the neutron odd-A daughter nucleus $(Z-2, A-3)$ is investigated. That means

$$|\, gr;\ Z, A = Z+N\rangle \rightarrow \boxed{\begin{array}{c}\text{ground state of the even-even nucleus with}\\ Z \text{ protons and } N \text{ neutrons (the core of}\\ \text{the mother nucleus } (N \text{ and } Z \text{ are even}))\end{array}}$$

$$| \, i = gr \equiv \rho_i \sigma_i; \; Z, A+1\rangle \rightarrow$$

initial state = ground state of the mother nucleus $(Z, A+1)$ = single-particle ground state $|\rho_i \sigma_i\rangle = a_i^+ |HF\rangle$ in the model of independent particles or neutron one-quasiparticle ground state $|\rho_i \sigma_i\rangle = \alpha_i^+ |BCS\rangle$ in the model of independent quasiparticles

$$|f \equiv \rho_f \sigma_f; \; Z-2, A-3\rangle \rightarrow$$

final state of the daughter nucleus $(Z-2, A-3)$ = single-particle state $|\rho_f \sigma_f\rangle = a_f^+ |HF\rangle$ in the model of independent particles or neutron one-quasiparticle state $|\rho_f \sigma_f\rangle = \alpha_f^+ |BCS\rangle$ in the model of independent quasiparticles

If we use the diagonal approximation for the matrix element of the operator $\hat{A}_\alpha$ together with (9.33) the model of independent particles gives values of hindrance factors of favored as well as unfavored α- decays of odd-A nuclei about unity which is far from the experimental data.

Further we estimate the influence of the pairing on the hindrance factor of α- transitions in odd-A nuclei. That means the determination of the matrix elements of the operator $\hat{A}_\alpha$ in the framework of the model of independent quasiparticles. At first we should specify the initial and final states of odd-A mother and daughter nuclei in more details. The initial state is given by the neutron one-quasiparticle state (we suppose mother and daughter nuclei to

be neutron odd-A).

$$
\begin{aligned}
&|\, i = \rho_i\sigma_i;\ Z, A+1\rangle = \alpha^+_{\rho_i\sigma_i}\ |BCS;\ N\rangle\, |BCS;\ Z\rangle = \\
&= \boxed{\begin{array}{c} \text{because} \quad \alpha^+_{\rho_i\sigma_i}|BCS;\ N\rangle = \\ = (\mathscr{U}_{\rho_i} a^+_{\rho_i\sigma_i} - \sigma_i \mathscr{V}_{\rho_i} a_{\rho_i-\sigma_i}) \prod_{\nu_n} (\mathscr{U}_{\nu_n} + \mathscr{V}_{\nu_n} a^+_{\nu_n+} a^+_{\nu_n-})\, |-\rangle = \\ = \text{(using Pauli principle)} = \\ = a^+_{\rho_i\sigma_i} \prod_{\nu_n \neq \rho_i} (\mathscr{U}_{\nu_n} + \mathscr{V}_{\nu_n}\, a^+_{\nu_n+} a^+_{\nu_n-})\, |-\rangle \end{array}} = \\
&= a^+_{\rho_i\sigma_i} \prod_{\substack{\nu_n \neq \rho_i \\ \nu_n \geq 0}} \left(\mathscr{U}^{(N)}_{\nu_n} + \mathscr{V}^{(N)}_{\nu_n} a^+_{\nu_n+} a^+_{\nu_n-}\right) \prod_{\nu_p \geq 0} \left(\mathscr{U}^{(N)}_{\nu_p} + \mathscr{V}^{(N)}_{\nu_p} a^+_{\nu_p+} a^+_{\nu_p-}\right) |-\rangle
\end{aligned}
\tag{9.48}
$$

and similarly for the final state of the daughter nucleus

$$
\begin{aligned}
|\, f = \rho_f\sigma_f;\ Z-2, A-3\rangle = \\
= a^+_{\rho_f\sigma_f} \prod_{\substack{\nu_n \neq \rho_f \\ \nu_n \geq 0}} \left(\mathscr{U}^{(N-2)}_{\nu_n} + \mathscr{V}^{(N-2)}_{\nu_n} a^+_{\nu_n+} a^+_{\nu_n-}\right) \\
\prod_{\nu_p \geq 0} \left(\mathscr{U}^{(Z-2)}_{\nu_p} + \mathscr{V}^{(Z-2)}_{\nu_p} a^+_{\nu_p+} a^+_{\nu_p-}\right) |-\rangle
\end{aligned}
\tag{9.49}
$$

In the case of favored α- transitions the final state $|\rho_f\sigma_f\rangle$ of the odd-A daughter nucleus (odd- neutron in our case) is the same as the initial state $|\rho_i\sigma_i\rangle$ of the mother nucleus ($|\rho_i\sigma_i\rangle = |\rho_f\sigma_f\rangle$). If further we suppose that the quasiparticle neutron and proton vacua for the daughter nucleus are not so different from the corresponding quasiparticle vacua of the mother nucleus ($|BCS;\ N\rangle \approx |BCS;\ N-2\rangle$, $|BCS;\ Z\rangle \approx |BCS;\ Z-2\rangle$) then the matrix

element $\langle f|\,\hat{A}_\alpha|\,i\rangle$ for favored α- transitions reads

$$\langle f=\rho_i\sigma_i;\ Z-2, A+3|\,\hat{A}_\alpha\,|i=\rho_i\sigma_i;\ Z, A+1\rangle =$$

$$=\frac{1}{4}\sum_{\substack{i_n j_p\\ \sigma_{i_n}\sigma_{j_p}}}\ \sum_{\substack{i_p j_n\\ \sigma_{i_p}\sigma_{j_n}}} A^{(\alpha)}_{i_n\sigma_{i_n}\,j_n\sigma_{j_n},\,i_p\sigma_{i_p}\,j_p\sigma_{j_p}}$$

$$\langle BCS;\ Z-2|\,a_{j_p\sigma_{j_p}}a_{i_p\sigma_{i_p}}\,|\,BCS;\ Z\rangle$$

$$\langle BCS;\ N-2|\,\alpha_{\rho_i\sigma_i}a_{j_n\sigma_{j_n}}a_{i_n\sigma_{i_n}}\alpha^+_{\rho_i\sigma_i}\,|\,BCS;\ N\rangle =$$

$$=\boxed{\begin{array}{c}\text{using Bogoliubov transformation s.p operators } a_{i\sigma_i} \text{ are}\\ \text{expressed in terms of quasiparticle operators } \alpha_{i\sigma_i}\\ \text{and then anticommutator relations for } \alpha^+_{i\sigma_i},\ \alpha_{i\sigma_i}\\ \text{are used together with } \alpha_{i\sigma_i}|BCS\rangle=0\end{array}} =$$

$$=\sum_{i_p\geq 0}\ \sum_{\substack{i_n\neq\rho_i\\ i_n\geq 0}} A^{(\alpha)}_{i_n+\,i_n-,\,i_p+\,i_p-}\ \ \xi_{i_p}(Z)\ \mathscr{U}^{(N-2)}_{i_n}\,\mathscr{V}^{(N)}_{i_n} =$$

$$=\boxed{\begin{array}{c}\text{approximation } \mathscr{U}^{(N-2)}_{i_n}\approx\mathscr{U}^{(N)}_{i_n}\\ \text{and (9.33)}\end{array}}\approx$$

$$\approx W\sum_{i_p\geq 0}\ \sum_{\substack{i_n\neq\rho_i\\ i_n\geq 0}}\xi_{i_p}(Z)\,\mathscr{U}^{(N)}_{i_n}\,\mathscr{V}^{(N)}_{i_n} \tag{9.50}$$

The square of this matrix element participates in the denominator of the expression (9.47) for corresponding hindrance factor of favored α- transition in odd-A nuclei. The nominator of (9.47) is determined by the square of the matrix element $\langle gr;\ Z-2, A-4|\,\hat{A}_\alpha\,|\,gr;\ Z, A\rangle$ (α- transitions between ground states of the neighbouring even-even nuclei) and this matrix element in the model of independent quasiparticles is approximated by (9.23). The substitution of (9.35) and (9.50) into (9.47) gives the estimation for hindrance factor of favored α- transition in odd-A nuclei in the following form

$$F^{(\alpha)}_{(\rho_i\to\rho_i)}\approx\frac{(\sum_{i_n\geq 0}\ \xi_{i_n}(N))^2}{(\sum\limits_{\substack{i_n\neq\rho_i\\ i_n\geq 0}}\ \mathscr{U}^{(N)}_{\rho_i}\mathscr{V}^{(N)}_{\rho_i})^2} \tag{9.51}$$

This expression was used in the second half of the sixties for the first numerical estimation of favored α- transition hindrance factors in odd-A nuclei

state	favored	hindrance factor $F^{(\alpha)}_{\rho_i\to\rho_i}$	
ρ_i	α- transition	experiment	theory
$7/2^+$ [613]	^{255}Fm $\to$ ^{251}Cf	1.2	1.5
$1/2^+$ [620]	^{253}Fm $\to$ ^{249}Cf	3.3	1.8
$1/2^+$ [620]	^{251}Cf $\to$ ^{247}Cm	1.8	1.7
$9/2^-$ [734]	^{249}Cf $\to$ ^{245}Cm	2.0	2.0
$7/2^+$ [624]	^{245}Cm $\to$ ^{241}Pu	1.3	1.7
$5/2^+$ [622]	^{243}Cm $\to$ ^{239}Pu	1.6	1.7
$5/2^+$ [622]	^{241}Pu $\to$ ^{237}U	1.3	1.7
$1/2^+$ [631]	^{241}Cm $\to$ ^{237}Pu	2.7	2.0
$1/2^+$ [613]	^{239}Pu $\to$ ^{235}U	3.0	2.0
$7/2^+$ [633]	^{253}Es $\to$ ^{249}Bk	1.8	1.7
$7/2^+$ [633]	^{249}Bk $\to$ ^{245}Am	1.3	1.7
$3/2^-$ [521]	^{245}Bk $\to$ ^{241}Am	2.4	1.7
$5/2^-$ [523]	^{243}Am $\to$ ^{239}Np	1.3	1.5
$5/2^+$ [523]	^{241}Am $\to$ ^{237}Np	1.3	1.5

Table 9.1: Comparison of calculated and experimental hindrance factors of favored *alpha*-transitions in selected actinides (taken from [7])

[7]. The mother and daughter nuclei were described by the independent quasiparticle model Hamiltonian with the phenomenological mean field of the Saxon-Woods type and with the monopole pairing interaction. This approach gave for favored α- transition hindrance factors of nuclei from the actinide region values in the following interval [7],

$$1.2 < F^{(\alpha)}_{(\rho_i\to\rho_i)} < 3.0 \tag{9.52}$$

and these theoretical estimations are in good agreement with experimental values as it can be seen from the Table 9.1.

In the case of unfavored α- transitions the initial state $|\rho_i\sigma_i\rangle$ of the odd nucleon (here we suppose odd neutron) in the mother nucleus is different from the final state $|\rho_f\sigma_f\rangle$ of the odd nucleon in the daughter nucleus ($\rho_i \neq \rho_f$).

Then the analogous procedure as in (9.50) but for $\rho_i \neq \rho_f$ gives

$$\begin{aligned}
&\langle f = \rho_f \sigma_f;\ Z-2, A-3|\ \hat{A}_\alpha\ |i = \rho_i \sigma_i;\ Z, A+1\rangle = \\
&= \frac{1}{4} \sum_{\substack{i_n j_p \\ \sigma_{i_n} \sigma_{j_p}}} \sum_{\substack{i_p j_n \\ \sigma_{i_p} \sigma_{j_n}}} A^{(\alpha)}_{i_n \sigma_{i_n}\, j_n \sigma_{j_n},\, i_p \sigma_{i_p}\, j_p \sigma_{j_p}} \\
&\qquad \langle BCS;\ Z-2|\ a_{j_p \sigma_{j_p}} a_{i_p \sigma_{i_p}}\ |\ BCS;\ Z\rangle \\
&\qquad\qquad \langle BCS;\ N-2|\ \alpha_{\rho_f \sigma_f} a_{j_n \sigma_{j_n}} a_{i_n \sigma_{i_n}} \alpha^{+}_{\rho_i \sigma_i}\ |\ BCS;\ N\rangle \approx \\
&\approx W\ \mathscr{U}^{(N-2)}_{\rho_i} \mathscr{V}^{(N)}_{\rho_f} \sum_{i_p \geq 0} \xi_{i_p}(Z) \approx W\ \mathscr{U}^{(N)}_{\rho_i} \mathscr{V}^{(N)}_{\rho_f} \sum_{i_p \geq 0} \xi_{i_p}(Z)
\end{aligned} \tag{9.53}$$

Then the substitution of (9.53) and (9.35) into (9.47) gives the hindrance factor for unfavored α- transitions in the odd-N nuclei in the following form

$$F^{(\alpha)}_{(\rho_i \to \rho_f)} \approx \frac{(\sum_{i_n \geq 0}\ \xi_{i_n}(N))^2}{(\mathscr{U}^{(N)}_{\rho_i} \mathscr{V}^{(N)}_{\rho_f})^2} \tag{9.54}$$

If again the simple model of independent quasiparticles from the sixties involving phenomenological Saxon-Woods mean field and monopole pairing interaction is used then the hindrance factor estimation (9.54) for unfavored odd-A nuclei have following values:

- $F^{(\alpha)}_{(\rho_i \to \rho_f)} \approx 50 - 100$ for unfavored α- decays of odd-A nuclei going to the ground state of the daughter nucleus;
- $F^{(\alpha)}_{(\rho_i \to \rho_f)} \approx 200 - 800$ for unfavored α- decays going to so called $F+2$ state (that means 2-d state above the Fermi level of the daughter nucleus);
- $F^{(\alpha)}_{(\rho_i \to \rho_f)} \approx 10^3$ for unfavored α- decays going to $F+3$ and higher states of the daughter nucleus.

As concerned α- transitions in odd-odd nuclei the corresponding expressions for hindrance factors can be easily obtained by the extension and slight modification of the method discussed above for odd-A nuclei. According to the origin of protons and neutrons in the emitted α- particle from the odd-odd nucleus we can recognize following types of α- transitions:

- Favored-favored α- transitions $\to$ α- particle consists from originally paired neutrons and paired protons;
- favored-unfavored α- transitions $\to$ emitted α- particle contains originally paired neutrons and originally unpaired protons;

- unfavored - favored α- transitions $\rightarrow$ emitted α- particle is formed from originally unpaired neutrons and originally paired protons;
- unfavored - unfavored α- transitions $\rightarrow$ emitted α- particle contains originally unpaired nucleons (both protons and neutrons).

In the end of this chapter it is necessary to note that the inclusion of the residual interaction and going beyond the model of independent quasiparticles has no big influence on the α- decay rates (hindrance factors) in the comparison with the model of independent quasiparticles where the long-range residual interaction is neglected (similarly as for α- transitions in even-even nuclei discussed in the previous subsection).

10. Beta decay (beta transitions in nuclei)

As it was already pointed out in the first chapter the role of the weak interaction in the forming of nuclear states is negligible and the structure of nuclear states is determines by the strong and electromagnetic interactions between nucleons. The only process in nuclear physics which is fully connected with the weak interaction is beta decay of nuclei.

Beta transitions in nuclear physics involve three processes, β^-- decay (emission of electron and its antineutrino), β^+- decay (emission of positron and its neutrino) and the electron capture (the capture of the electron from the electron cloud of given atom),

$$\begin{aligned} &\beta^-\text{- decay:} && Z^{(A)} \to (Z+1)^{(A)} + e^- + \tilde{\nu}_e \\ &\beta^+ \text{ decay:} && Z^{(A)} \to (Z-1)^{(A)} + e^+ + \nu_e \\ &\text{electron capture:} && Z^{(A)} + e^- \to (Z-1)^{(A)} + \nu_e \end{aligned} \tag{10.1}$$

Energy Q released during β- decay or during electron capture is given by the difference of masses of parent and daughter nuclei, e.g. in the case of the β^--decay:

$$Q = \left(M_Z^A - M_{Z+1}^A\right) c^2 \tag{10.2}$$

where M_Z^A and M_{Z+1}^A are rest masses of the parent (mother) and daughter nuclei. This energy is divided among decay products (in the case of β^- decay among electron, antineutrino and daughter nucleus, or among positron, neutrino and daughter nucleus for β^+ decay). Special case is the electron capture. It is a process in which the proton-rich nucleus Z^A of an electrically neutral atom absorbs an inner atomic electron, usually from K or L electron shell. As a result a nuclear proton changes to a neutron and simultaneously an electron antineutrino is emitted. The daughter nucleus, if it is in excited states, then undergoes the transitions to its ground state. Usually a gamma ray photons are emitted during this transition, but the nuclear de-excitation may also take place by internal conversion. [1] Following capture of an inner electron from the atom, an outer electron replaces the electron that was

[1] Internal conversion is a radioactive process where an excited nucleus interacts electromagnetically with

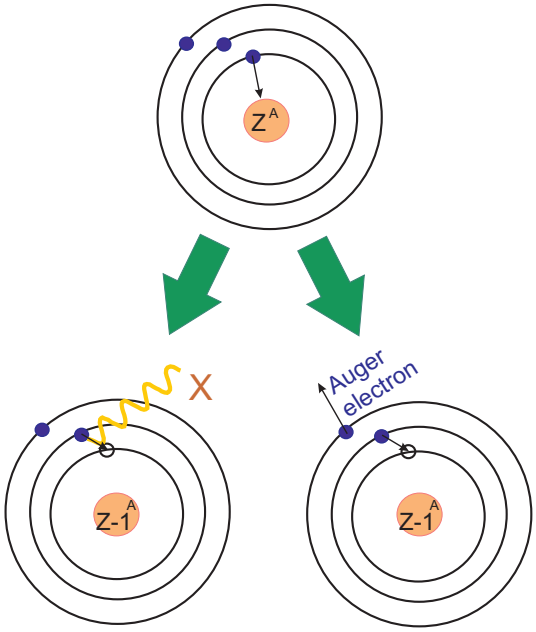


Figure 10.1: Schematic figure of the electron capture. Top: The nucleus absorbs an electron from its atom. Lower left: An outer electron fills the hole left by captured inner electron and during this process the X-ray photon is emitted. Lower left: The energy released during the filling the hole by outer electron is transferred to an outer Auger electron which is then ejected, leaving a positive ion (adapted from wikipedia).

captured and one or more characteristic X-ray photons is emitted in this process. Electron capture sometimes also results in the Auger effect, where an electron is ejected from the atom's electron shell due to interactions between the atom's electrons in the process of seeking a lower energy state. This two types of the filling of the hole, left by the captured electron, with outer electron (with characteristic X-ray photons or with Auger electron(s)) are schematically demonstrated in the Fig. 10.1.

The theory of the electron conversion is in large extend more connected with the theory of electron shells in atom than with the nuclear physics and it is beyond the scope of this textbook. Therefore further only β^- and β^+ decays are discussed.

The kinetic energy of electrons from β^- decay (or positrons from β^+ de-

one of the orbital electrons. This causes the electron to be ejected from the atom, but not from the nucleus. For this reason, the high-speed electrons resulting from internal conversion are not called beta particles, since the latter come from beta decay, where they are newly created in the nuclear decay process. Internal conversion is possible whenever gamma decay is possible, except in the case where the atom is fully ionized. During internal conversion the atomic number does not change, and thus (similarly as in the case of gamma decay) no transmutation of one element to another takes place. Since an electron is lost from the atom, a hole appears in an electron shell which is subsequently filled by other electrons from higher in energy electron levels. This filling is accompanied by the emission of characteristic X-ray(s) or Auger electron(s), or both. The atom thus emits high-energy electrons and X-ray photons, none of which originate in the nucleus.

cay) can attain big values in the comparison with the rest energy of electron (positron). That means emitted electrons or positrons (generally leptons) should be treated in terms of relativistic approaches. Therefore in the description of the lepton sector of beta decay the relativistic formalism should be used.

10.1 Kinematics of beta-decay

Beta decay (spontaneous emission of electrons) is known from the end of the 19-th century. All beta decay experiments provided a continue spectrum of emitted electrons or positrons with energy up to the maximum value E_0 close to the total β- decay energy (10.2)

$$E_0 \approx Q = (M_Z^A - M_{Z\pm1}^A)\, c^2 \approx$$

$$\approx \boxed{\begin{array}{c}\text{further in this section the relativistic system of units,}\\ \text{so called natural system of units, } \hbar = c = 1 \text{ , is used}\end{array}} \approx$$

$$\approx M_Z^A - M_{Z\pm1}^A \tag{10.3}$$

where M_{Z-1}^A (M_{Z+1}^A) concerns β^- (β^+) decay. This fact lead W. Pauli in the thirties to the introduction of the new neutral particle (known later as neutrino) which is simultaneously emitted together electron or positron during the beta decay. The reason was that in the case of the 3 - particle decay each produced particle has always continuous spectrum (opposite to the 2 - particle decay, as e.g. α- decay $M_Z^A \to M_{Z-2}^{A-4} + {}_2^4He$, where final particles have discrete spectra). Later on it was found that during β^+ decay the positron together with corresponding neutrino is formed. Today it is known that each known lepton (e^-, μ^-, τ^-) has corresponding neutrino (ν_e, ν_μ, ν_τ) and each known antilepton (e^+, μ^+, τ^+) has its antineutrino ($\tilde{\nu}_e$, $\tilde{\nu}_\mu$, $\tilde{\nu}_\tau$)

$$\begin{array}{ccc} e^- & \leftrightarrow & \nu_e \\ \mu^- & \leftrightarrow & \nu_\mu \\ \tau^- & \leftrightarrow & \nu_\tau \end{array} \qquad \begin{array}{ccc} e^+ & \leftrightarrow & \tilde{\nu}_e \\ \mu^+ & \leftrightarrow & \tilde{\nu}_\mu \\ \tau^+ & \leftrightarrow & \tilde{\nu}_\tau \end{array} \tag{10.4}$$

Because of the fact that the energy spectrum of emitted electrons (positrons) in β^- (β^+) decay ends with the energy E_0 which is almost equal to the total energy Q of the β^- (β^+) decay, $E_0 \approx Q$, the rest mass of the neutrino (antineutrino) should be close to zero. The recent experiments with neutrinos indicates very small (but nonzero) rest energies of neutrinos and antineutrinos.

At first the kinematics of the elementary β^- decay of the neutron,

$$n \rightarrow p + e^- + \tilde{\nu}_e \qquad \Leftrightarrow \qquad e^+ + n \rightarrow p + \tilde{\nu}_e \tag{10.5}$$

is discussed. During this process the total four- momentum before the β^- decay (that means the four- momentum $P \equiv (E_\mu\,,\,\vec{P})$ of the neutron is equal to the total four- momentum [2] of all products of the β^- decay (that means the sum of the four momentum $k \equiv (E_e\,,\,\vec{k})$ of emitted electron, four- momentum $k^{'} \equiv (E_{\tilde{\nu}}\,,\,\vec{k})$ of emitted antineutrino, and four- momentum of the proton, $p \equiv (E_p\,,\vec{p})$,

$$P = p + k + k^{'} \qquad \Leftrightarrow \qquad P - k = p + k^{'} \tag{10.6}$$

It is known that the square of the total linear four- momentum is the Lorentz invariant. Therefore the right equation in (10.6) gives

$$(P - k)^2 = (p + k^{'})^2 \tag{10.7}$$

where the l.h.s. of (10.7) can be determined in the laboratory frame (more precisely in the neutron rest frame) and the r.h.s. of (10.7) in the center of mass system of proton + antineutrino (where $\vec{p} = -\vec{k}^{\,'}$). Then the equation (10.7) can be rewritten as,

$$\begin{aligned} \text{r.h.s. of (10.7)} = (p + k^{'})^2 = E_p^{(c.m.)\,2} + 2E_p^{(c.m.)}E_{\tilde{\nu}}^{(c.m.)} + E_{\tilde{\nu}}^{(c.m.)\,2} = \\ = (\,E_p^{(c.m.)} + E_{\tilde{\nu}}^{(c.m.)}\,)^2 \geq (m_p + m_{\tilde{\nu}})^2 \end{aligned}$$

$$\begin{aligned} \text{l.h.s. of (10.7)} = (P - k)^2 = P^2 + k^2 - 2Pk = \\ = m_n^2 + E_e^2 - 2m_nE_e - |\vec{k}|^2 \end{aligned}$$

So,

$$\begin{aligned} m_n^2 + E_e^2 - 2m_nE_e - |\vec{k}|^2 \;&\geq\; (m_p + m_{\tilde{\nu}})^2 \\ 2m_nE_e \;&\leq\; m_n^2 + m_e^2 - (m_p + m_{\tilde{\nu}})^2 \end{aligned} \tag{10.8}$$

and we see that the upper bound for the electron energy is

$$E_e^{max} = \frac{m_n^2 + m_e^2 - (m_p + m_{\tilde{\nu}})^2}{2m_n} \approx \frac{m_n^2 - m_p^2 + m_e^2}{2m_n} \tag{10.9}$$

where in (10.9) the terms involving possible small rest mass of antineutrino are neglected in the comparison with m_n^2 and m_p^2.

[2] The zero- component of any linear four- momentum is given by the energy $P_0 = E$ and the remaining three components are formed by the components of the linear momentum vector $\vec{P}$.

Similarly as the first equality in (10.9) we can obtain the upper bound for proton and antineutrino

$$E_p^{max} = \frac{m_n^2 + m_p^2 - (m_e + m_{\tilde{\nu}})^2}{2m_n}$$
$$E_{\tilde{\nu}}^{max} = \frac{m_n^2 + m_p^2 - (m_p + m_e)^2}{2m_n} \tag{10.10}$$

The substitution of experimental values of rest masses of neutron ($m_n = 929.59$ MeV), proton ($m_p = 928.27$ MeV), and electron ($m_e = 0.511$ MeV) into (10.9) gives the maximum energy of emitted electron,

$$E_e^{max} \approx \frac{m_n^2 + m_e^2 - m_p^2}{2m_n} \approx \frac{m_n^2 - m_p^2}{2m_n} \approx$$
$$\approx m_n - m_p = \Delta m = 1.29\, MeV \tag{10.11}$$

From the expr. (10.11) follows that the velocity of emitted electrons is relativistic (at least near the E_e^{max}) as it is demonstrated below,

$$E_e^{max} = \frac{m_e}{\sqrt{1 - (\beta_e^{max})^2}} \quad \Rightarrow \quad \beta_e^{max} = v_e^{max} = \sqrt{1 - \frac{m_e^2}{(E_e^{max})^2}} \approx$$
$$\approx 1 - \frac{1}{2}\frac{m_e^2}{(\Delta m)^2} \approx 0.92 \tag{10.12}$$

That means the velocity of emitted electrons is not far from the light velocity and therefore we should use the relativistic formalism for the description of their kinematics. Using (10.10) the similar estimation can be done for protons and we obtain

$$\beta_p^{max} \approx \sqrt{1 - \frac{m_p^2}{(E_p^{max})^2}} \approx \frac{\Delta m}{m_p} \approx 1.37 \times 10^{-3} \tag{10.13}$$

So, opposite to emitted electrons, proton can be treated in the framework of a non-relativistic approach (with the non-relativistic reduction of the relativistic quantum field theory). Here we obtained this conclusion for the elementary β^- decay of neutron but it holds for any nucleus β^- and β^+ decay, always leptons emitted from β- decays of nucleons should be described relativistically opposite to the non-relativistic kinematics of nuclei.

10.2 Fermi theory of β- decay, allowed and forbidden β- transitions

The first theory of β- decay was formulated by E. Fermi in 1934 [327]. Fermi suggested contact interaction of 4 Dirac fields (each with the spin 1/2) corresponding to neutron, proton, electron and electron antineutrino in the elementary process (10.5). This interaction is represented by the interaction Hamiltonian density in the following form

$$\hat{\mathcal{H}}_{int}^{(Fermi)} = G \left(\hat{\bar{\psi}}_p(x)\, \gamma^\mu\, \hat{\psi}_n(x)\right) \left(\hat{\bar{\psi}}_e(x)\, \gamma_\mu\, \hat{\psi}_{\tilde{\nu}}(x)\right) \,+\, h.c. \tag{10.14}$$

where G is the coupling constant, $\psi(x)$ are bispinor fields of investigated Dirac fields (neutron, proton, electron and antineutrino in the process (10.5)) and $\bar{\psi}(x) = \psi^+(x)\, \gamma_0$ (see the Appendix P). The corresponding interaction Lagrangian density is (expression (10.15) involves the summation over $\mu = 0, 1, 2, 3$)

$$\hat{\mathcal{L}}_{int}^{(Fermi)} = -\, G \left(\hat{\bar{\psi}}_p(x)\, \gamma^\mu\, \hat{\psi}_n(x)\right) \left(\hat{\bar{\psi}}_e(x)\, \gamma_\mu\, \hat{\psi}_{\tilde{\nu}}(x)\right) \,+\, h.c. \tag{10.15}$$

This suggestion of the contact interaction was based on the analogy with the electromagnetic interaction, where the density of the interaction Lagrangian between Dirac particles (with the spin 1/2 and the charge q) and the external electromagnetic field characterized by the four- potential $A_\mu(x)$ ($\mu = 0, 1, 2, 3$) is given by well-known expression (see e.g. [13])

$$\hat{\mathcal{L}}_{int}^{(elmg)}(x) \;=\; \hat{s}^\mu(x)\, \hat{A}_\mu(x) \;\equiv\; -q\, \hat{\bar{\psi}}(x)\, \gamma^\mu\, \hat{\psi}(x)\, \hat{A}_\mu(x) \,+\, h.c. \tag{10.16}$$

where the assumption of E. Fermi was the analogy between the electromagnetic four- current $\hat{s}^\mu(x)$ in (10.16) and the current of lepton fields, $\hat{\bar{\psi}}_e(x)\, \gamma^\mu\, \hat{\psi}_{\tilde{\nu}}(x)$, in (10.15). As we will see later, the analogy between (10.15) and (10.16) can be seen more clearly if we compare both the electromagnetic and the beta- process amplitudes determined by the first order of the Born perturbation theory using the Hamiltonian density (8.14) with the amplitudes calculated in the framework of the lowest order of the Dyson quantum field decomposition with the interaction Lagrangian (10.15).

However, one should realize also differences of electromagnetic (10.16) and weak beta- (10.14) interactions. Expressions (10.14) or (10.15) represent the contact interaction with the zero range. The zero range is opposite to the long range of the electromagnetic interaction (10.16). This is a result of the fact that the electromagnetic interaction is mediated by the exchange of

the massless photons while the weak interaction, responsible for beta- decay, is mediated by the exchange of very heavy intermedial W- bosons which leads to a very short range interaction. The genius of E. Fermi in the thirties consists in the fact that without any knowledge about some heavy intermedial exchanged mesons he was able to guess the main zero range (contact) part of the whole weak interaction.

According to the quantum field theory the lowest leading order of the Dyson perturbation theory (see Appendix P) gives for the amplitude of the beta- process (10.5) the following expression (see (P.4) and [13])

$$\mathcal{M}_{fi}^{(1)(Fermi)} = G\,\left[\bar{u}_{p;\,r'}(\vec{p})\,\gamma^{\mu}\,u_{n;\,r}(\vec{P})\right]\,\left[\bar{u}_{e;\,s}(\vec{k})\,\gamma_{\mu}\,v_{\tilde{\nu};\,s'}(\vec{k}\,')\right] \tag{10.17}$$

which corresponds to the Fig.10.2 and where $u_{n;\,r}(\vec{P})$, $u_{p;\,r'}(\vec{p})$, $u_{e;\,s}(\vec{k})$ and $v_{\tilde{\nu};\,s'}(\vec{k}\,')$ are bispinor functions in the momentum representation for neutron, proton, electron and electron antineutrino, respectively (see the Appendix P, expression (P.8)). Further we suppose to work in the neutron rest frame ($E_n = m_n$).

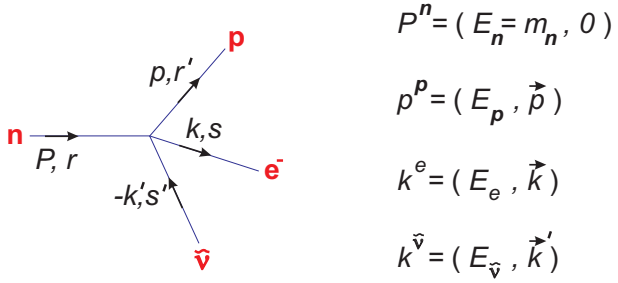


Figure 10.2: β- decay of neutron

As it was mentioned above in the neutron rest frame the proton from the neutron β^{-}- decay has not relativistic energy and therefore for neutron and proton bispinor functions $u_{n;\,r}(\vec{P})$ and $u_{p;\,r}(\vec{p})$ it is possible to use non relativistic reduction (see (P.10))

$$u_{n\,;\,r}(\vec{P}) \to u_{n\,;\,r}(0) = \begin{pmatrix} U_{n\,;\,r} \\ 0 \end{pmatrix} \qquad u_{p\,;\,r'}(\vec{p}) \to u_{p\,;\,r'}(0) = \begin{pmatrix} U_{p\,;\,r'} \\ 0 \end{pmatrix} \tag{10.18}$$

and the hadron current in (10.17) reads ($\mu = 0, 1, 2, 3$ and $j = 1, 2, 3$)

$$\bar{u}_{p\,;\,r'}(\vec{p})\,\gamma^{\mu}\,u_{n\,;\,r}(\vec{P}) \quad \rightarrow \quad \bar{u}_{p\,;\,r'}(0)\,\gamma^{\mu}\,u_{n\,;\,r}(0)$$

$$\bar{u}_{p\,;\,r'}(0)\,\gamma^{0}\,u_{n\,;\,r}(0) = \left(U^{+}_{p\,;\,r'}\;\;0\right)\gamma^{0}\gamma^{0}\begin{pmatrix} U_{n\,;\,r} \\ 0 \end{pmatrix} = U^{+}_{p\,;\,r'}\,U_{n\,;\,r} =$$

$$\boxed{\begin{array}{c}\text{see (P.8)} \\ \text{and } \chi^{+}_{r'}\,\chi_{r} = \delta_{rr'}\end{array}} = \delta_{r\,r'}\,\sqrt{2m_p}\sqrt{2m_n}$$

$$\bar{u}_{p\,;\,r'}(0)\,\gamma^{j}\,u_{n\,;\,r}(0) = \left(U^{+}_{p\,;\,r'}\;\;0\right)\gamma^{0}\gamma^{j}\begin{pmatrix} U_{n\,;\,r} \\ 0 \end{pmatrix} =$$

$$= \left(U^{+}_{p\,;\,r'}\;\;0\right)\begin{pmatrix} 1 & 0 \\ 0 & -1 \end{pmatrix}\begin{pmatrix} 0 & \sigma_j \\ -\sigma_j & 0 \end{pmatrix}\begin{pmatrix} U_{n\,;\,r} \\ 0 \end{pmatrix} =$$

$$= \left(U^{+}_{p\,,\,r^{''}}\;\;0\right)\begin{pmatrix} 0 & \sigma_j \\ \sigma_j & 0 \end{pmatrix}\begin{pmatrix} U_{n\,;\,r} \\ 0 \end{pmatrix} = 0 \qquad (10.19)$$

The substitution of (10.19) into (10.17) gives

$$\mathcal{M}^{(1)}_{fi} \approx G\,\sqrt{4m_p m_n}\,\left[\,\bar{u}_{e;\,s}(\vec{k})\,\gamma_{\mu}\,v_{\tilde{\nu};\,s'}(\vec{k}^{\,\prime})\,\right]\,\delta_{rr'} \qquad (10.20)$$

Expression (10.20) leads to the conclusion that Fermi beta interaction (10.15) or (10.14) for the β^- - decay of neutron does not involve any change of the spin states of the nucleus during the beta- decay (because $r = r^{'}$). So, according to the Fermi theory of β- decay the spin states of nucleons during the process $n \rightarrow p + e^{-} + \tilde{\nu}_e$ (generally spin states of mother and daughter nuclei in all beta- decays) remain unchanged. However rapid progress in the nuclear spectroscopy in the fifties showed experimentally that there are β- transitions (in the elementary process $n \rightarrow p + e^{-} + \tilde{\nu}_e$ as well as in the general β- decays of nuclei) in which the spin states of nucleons in the mother and daughter nuclei are different (spin projections are changed). Spin-flip changes in β- decays are not possible to explain by the Fermi theory based on the simple contact interaction (10.14). More sophisticated theory of beta- processes developed in the sixties and which explains also spin-flip effects in β- decays are discussed in next sections 10.3 and 10.4.

From historical reason β- transitions are divided into two groups, allowed and forbidden transitions, according to the change of the mother and daughter nucleus angular momenta and parities. If the initial mother nucleus (neutron in the elementary process (10.5)) has angular momentum $\vec{J}_i$ and the momentum of the daughter nucleus (proton in the elementary process (10.5))

is $\vec{J}_f$ then the change of the nuclear (hadron) ang. momentum during the β-process, $\Delta\vec{J} \equiv \vec{J}_i - \vec{J}_f$, is equal to the sum of the orbital momentum $\vec{L}$ of the final decay products and the total spin $\vec{S}$ of leptons created during the β-decay (this is the result of the conservation of the total angular momentum),

$$\vec{J}_i = \vec{J}_f + \vec{L} + \vec{S} \qquad \Rightarrow \qquad \Delta\vec{J} = \vec{J}_i - \vec{J}_f = \vec{L} + \vec{S} \tag{10.21}$$

Corresponding change of nuclear parities during the β- decay is

$$\Delta\pi = \pi_i \, \pi_f \quad , \tag{10.22}$$

where π_i is the parity of the mother initial nucleus and π_f is the parity of the daughter nucleus.

Allowed β- transitions are defined as the transition where the relative orbital momentum of lepton products with respect to the nucleus is zero and the nuclear parity does not change during the β- process ($\Delta\pi = +1$). Since in the β- decay always two leptons with half- spins are formed (electron and electron antineutrino or positron and positron neutrino) then for $L = 0$,

$$\Delta\vec{J} = \vec{S} = 1\vec{/}2 + 1\vec{/}2 \qquad \Rightarrow \qquad \Delta J = 0, \pm 1 \tag{10.23}$$

The case $S = 0$ ($\Delta J = 0$, $L = 0$) is called Fermi allowed transitions and the case $S = 1$, $L = 0$ ($\Delta J = \pm 1$ for $J_i > 0$, $J_f > 0$ or $|\Delta J| = 1$ for $J_i = 0$ *or* $J_f = 0$) is known as Gamow-Teller allowed transitions [3] (in all allowed β-decays $\Delta\pi = +1$).

As an example of the pure allowed Fermi transition the β^- decay of ^{14}O from its ground state 0^+ can be taken,

$$^{14}O_{(0^+)} \quad \rightarrow \quad ^{14}N_{(0^+)} \, + \, e^- \, + \, \tilde{\nu}_e \tag{10.24}$$

and examples of pure allowed Gamow-Teller transitions are

$$\begin{aligned} ^{6}He_{(0^+)} \quad &\rightarrow \quad ^{6}Li_{(1^+)} \, + \, e^- \, + \, \tilde{\nu}_e \\ ^{12}B_{(1^+)} \quad &\rightarrow \quad ^{12}C_{(0^+)} \, + \, e^- \, + \, \tilde{\nu}_e \end{aligned} \tag{10.25}$$

It is clear that in the case $J_i - J_f = 0$ (J_i,$J_f > 0$ we can have so called "mixed" allowed transitions (Fermi type simultaneously with Gamow-Teller

[3] In the case of Gamow-Teller transitions only the angular momentum of leptons with respect to final nucleus are supposed to be zero. Mutual relative ang. momentum of electron and electron antineutrino can be nonzero and it is equal to 1 in the case of allowed Gamow-Teller β^- transition, and it corresponds to $L = 1$.

type).

Forbidden β- transitions are connected with the nonzero orbital momentum ($L \neq 0$), that means $\Delta J > 1$ and/or with the change of nuclear parity during β- process, that means $\Delta\pi = -1$.

10.3 Generalization of Fermi theory of β- transitions (parity violation)

Fermi theory of β- processes described in the previous section was not able to explain experimental data on β- decays obtained experimentally in the fifties. Therefore in the beginning of fifties a big effort was devoted to the generalization of Fermi theory in order to obtain theory relevant to the new experimental data on β- decays. Since this generalization is described in many textbooks concerning electro-weak interactions (standard model), see e.g. [13, 256], here only a brief recapitulation is given.

From the quantum field theory (formulated in the end of the forties) it was known that the Lagrangian density should be invariant with respect to Lorentz transformation. Fermi interaction with the Lagrangian density (10.15) has a form of the scalar product of two four- currents which is a scalar with respect to Lorentz transformation. However, this is not the only scalar formed from four bispinor functions $\psi_n(x)$, $\psi_p(x)$, $\psi_e(x)$ and $\psi_{\tilde{\nu}}(x)$ of particles participating in the elementary process $n \to p + e^- + \tilde{\nu}_e$. From the quantum theory of Dirac fields it is also known that it is possible to create following objects from two Dirac fields $\psi_1(x)$ and $\psi_2(x)$ which has following properties with respect to Lorentz transformation and with respect to the reverse of the coordinate frame axes (parity transformation: $x \equiv (x^0,\ \vec{x}) \to x^{'} \equiv (x^0,\ -\vec{x})$,

when bispinor function transforms as $\psi(x) \to \psi^{'}(x^{'}) = \gamma_0\,\psi(x)$ [256, 13]) [4]

$$\bar{\psi}_1(x)\,\psi_2(x) \quad \to \quad Lorentz\ scalar,$$
$$\hat{\mathcal{P}}^{-1}\bar{\psi}_1(x)\psi_2(x)\,\hat{\mathcal{P}} = \bar{\psi}_1(x)\psi_2(x)$$

$$\bar{\psi}_1(x)\,\gamma^\mu\,\psi_2(x) \quad \to \quad Lorentz\ four-\ vector,$$
$$\hat{\mathcal{P}}^{-1}\bar{\psi}_1(x)\,\gamma^\mu\,\psi_2(x)\,\hat{\mathcal{P}} = \bar{\psi}_1(x)\,\gamma^\mu\,\psi_2(x)$$

$$\bar{\psi}_1(x)\,\gamma^\mu\gamma^5\,\psi_2(x) \quad \to \quad Lorentz\ axial\ four-\ vector,$$
$$\hat{\mathcal{P}}^{-1}\bar{\psi}_1(x)\,\gamma^\mu\gamma^5\,\psi_2(x)\,\hat{\mathcal{P}} = -\,\bar{\psi}_1(x)\,\gamma^\mu\gamma^5\,\psi_2(x)$$

$$\bar{\psi}_1(x)\,\sigma^{\mu\nu}\,\psi_2(x) \quad \to \quad Lorentz\ tenzor,$$
$$\hat{\mathcal{P}}^{-1}\bar{\psi}_1(x)\,\sigma^{\mu\nu}\,\psi_2(x)\,\hat{\mathcal{P}} = \bar{\psi}_1(x)\,\sigma^{\mu\nu}\,\psi_2(x)$$

$$\bar{\psi}_1(x)\,\gamma^5\,\psi_2(x) \quad \to \quad Lorentz\ pseudo\ scalar,$$
$$\hat{\mathcal{P}}^{-1}\bar{\psi}_1(x)\,\gamma^5\,\psi_2(x)\,\hat{\mathcal{P}} = -\,\bar{\psi}_1(x)\,\gamma^5\,\psi_2(x) \qquad (10.26)$$

where $\gamma^5 = \gamma_5 = i\,\gamma^0\gamma^1\gamma^2\gamma^3$ and $\sigma^{\mu\nu} = \frac{i}{2}[\gamma^\mu,\,\gamma^\nu]$.

These objects can be constructed from hadron bispinor functions $\psi_n(x)$ and $\psi_p(x)$ and independently from lepton bispinor functions $\psi_e(x)$ and $\psi_{\tilde{\nu}}(x)$. Hadron and lepton objects are then combined to Lorents scalar and the final

[4] Lorentz transformation of four- coordinate, $x^{\mu^{'}} = \Lambda^\mu{}_\nu x^\nu$, implies the transformation of bispinor function $\psi^{'}(x^{'}) = \hat{S}(\Lambda)\,\psi(x)$ or $\psi^{'}_\alpha(x) = \sum_\beta S_{\alpha\beta}(\Lambda)\,\psi_\beta(x)$. In the case of infinitesimal Lorentz transformation, $\Lambda_{\mu\nu} = g_{\mu\nu} + \epsilon_{\mu\nu}$ (where $g_{\mu\nu}$ is the metric tensor and $\epsilon_{\mu\nu}$ are infinitesimal corrections above the metric tenzor), corresponding transformation operator $\hat{S}(\Lambda)$ for bispinor field $\psi(x)$ is $\hat{S}(\Lambda) = 1 + \frac{1}{2}\epsilon_{\mu\nu}C^{\mu\nu}$ with $C^{\mu\nu} = \frac{1}{2}\gamma^\mu\gamma^\nu$.

For instance for the rotation by angle ϕ round the axis directed by the unit vector $\vec{n}$ the transformation of bispinor functions reads

$$\psi^{'}(x) = e^{i\vec{L}\cdot\vec{n}\,\phi}\hat{S}(\phi,\vec{n})\,\psi(x) = e^{i(\vec{L}+\frac{1}{2}\Sigma)\cdot\vec{n}\,\phi}\psi(x)$$

where $\vec{\Sigma} = \begin{pmatrix} \vec{\sigma} & 0 \\ 0 & \vec{\sigma} \end{pmatrix}$.

For the parity transformation we have,

$$x^{'} \equiv (x^0, -\vec{x}) \qquad \psi^{'}(x^{'}) = \hat{\mathcal{P}}\psi(x) = \gamma_0\,\psi(x)$$

Possible parity violation, described by the Lagrangian density (10.27), is provided by the identity

$$\hat{S}^{-1}(\Lambda)\,\gamma_5\,\hat{S}(\Lambda) = det\Lambda\ \gamma_5$$

where $det\Lambda = +1$ for special Lorentz transformations along coordinate axes (so called Lorentz boosts) and rotations and $det\Lambda = -1$ for the parity transformation.

Lagrangian density of β- process can be expected in the following form (see e.g. [13, 256])

$$\hat{\mathcal{L}}_{int}^{(\beta)} = \sum_{j=S,V,A,T,P} C_j \left[\hat{\bar{\psi}}_p(x)\, \Gamma_j\, \hat{\psi}_n(x)\right] \left[\hat{\bar{\psi}}_e(x)\, (1+\alpha_j\, \gamma^5)\, \Gamma^j\, \hat{\psi}_{\tilde{\nu}}(x)\right] \tag{10.27}$$

where terms with $\alpha_j\, \gamma_5$ were introduced because the violation of the parity conservation was expected in β- processes (which was confirmed later in 1957 by the famous experiment of Mrs. Wu [328]). The symbols Γ_j and Γ^j stands for the scalar, vector, axial vector, tensor, and pseudoscalar combinations,

$$\begin{aligned} &\Gamma_j = 1\ (j=1),\ \gamma_\mu\ (j=V),\ \gamma_5\gamma_\mu\ (j=A),\ \sigma_{\mu\nu}\ (j=T),\ \gamma_5\ (j=P) \\ &\Gamma^j = 1\ (j=1),\ \gamma^\mu\ (j=V),\ \gamma^5\gamma^\mu\ (j=A),\ \sigma^{\mu\nu}\ (j=T),\ \gamma^5\ (j=P) \end{aligned} \tag{10.28}$$

Real parameters C_j and α_j $(j = S, V, A, T, P)$ were obtained from experimental data on elementary processes like $n \to p + e^- + \tilde{\nu}_e$ and this procedure is discussed in the next section.

Lagrangian density (10.27) is the minimal realization of the Lorentz invariant Lagrangian constructed from two hadron bispinor functions $\psi_p(x)$, $\psi_n(x)$ and two lepton bispinor functions $\psi_e(x)$, $\psi_{\tilde{\nu}}(x)$. We could construct also other Lorentz invariant terms, involving derivatives of these bispinor functions, which could contribute to the Lagrangian density (higher order terms). However these complex terms would bring new parameters above ten parameters C_j and α_j $(j = S, V, A, T, P)$. Even 10 parameters involved in (10.27) is quite big number and the theory based on (10.27) is not so elegant as the former Fermi theory with the Lagrangian density (10.15) involving only one parameter G.

Using standard quantum field theory techniques the lowest order amplitude of the process $n \to p + e^- + \tilde{\nu}_e$ corresponding to the interaction Lagrangian density (10.27) can be written as follows [13, 256],

$$\mathcal{M}_{fi}^{(1)(\beta)} = \sum_{j=S,V,A,T,P} C_j \left[\bar{u}_{p;\,r'}(\vec{p})\, \Gamma_j\, u_{n;\,r}(\vec{P})\right] \left[\bar{u}_{e;\,s}(\vec{k})\, (1+\alpha_j\, \gamma^5)\, \Gamma^j\, v_{\tilde{\nu};\,s'}(\vec{k}')\right] \tag{10.29}$$

Further, similarly as in (10.20) for the Fermi amplitude (10.17), we perform the non-relativistic reduction in the nucleon current $\bar{u}_{p;\,r'}(\vec{p})\, \Gamma_j\, u_{n;\,r}(\vec{P})$ for all $j = S, V, A, T, P$ (because we know that neutron and proton in the process

$n \to p + e^- + \tilde{\nu}_e$ have non-relativistic velocities). Using the explicit expressions for 4×4 Dirac matrices γ^μ ($\mu = 0, 1, 2, 3, 5$),

$$\gamma^0 = \begin{pmatrix} 1 & 0 \\ 0 & -1 \end{pmatrix} \quad \gamma^j = -\gamma_j = \begin{pmatrix} 0 & \sigma_j \\ \sigma_j & 0 \end{pmatrix}, \; j = 1, 2, 3$$

$$\gamma^5 = \gamma_5 = i\,\gamma^0\gamma^1\gamma^2\gamma^3 = \begin{pmatrix} 0 & 1 \\ 1 & 0 \end{pmatrix} \tag{10.30}$$

and using the non-relativistic reduction (10.18) of the bispinor functions $u_{p;\,r'}(\vec{p})$ and $u_{n;\,r}(\vec{P})$ we obtain the following expressions for reduced $\bar{u}_{p;\,r'}(\vec{p})\Gamma_j u_{n;\,r}(\vec{P})$ for all $j = S, V, A, T, P$,

$$\begin{aligned}
j = S \qquad & \bar{u}_{p;\,r'}(\vec{p})\; u_{n;\,r}(\vec{P}) \qquad \to \quad \bar{u}_{p;\,r'}(0)\; u_{n;\,r}(0) = U^+_{p;\,r'}\, U_{n;\,r} \\
j = V \qquad & \bar{u}_{p;\,r'}(\vec{p})\; \gamma_\mu\, u_{n;\,r}(\vec{P}) \qquad \to \quad \bar{u}_{p;\,r'}(0)\; \gamma_\mu\, u_{n;\,r}(0) = U^+_{p;\,r'}\, U_{n;\,r} \\
j = A \qquad & \bar{u}_{p;\,r'}(\vec{p})\; \gamma_5\gamma_\mu\, u_{n;\,r}(\vec{P}) \quad \to \; \bar{u}_{p;\,r'}(0)\; \gamma_5\gamma_\mu\, u_{n;\,r}(0) = U^+_{p;\,r'}\vec{\sigma}\; U_{n;\,r} \\
j = T \qquad & \bar{u}_{p;\,r'}(\vec{p})\; \sigma_{\mu\nu}\, u_{n;\,r}(\vec{P}) \qquad \to \quad \bar{u}_{p;\,r'}(0)\; \sigma_{\mu\nu}\, u_{n;\,r}(0) = U^+_{p;\,r'}\vec{\sigma}\, U_{n;\,r} \\
j = P \qquad & \bar{u}_{p;\,r'}(\vec{p})\; \gamma_5\, u_{n;\,r}(\vec{P}) \qquad \to \quad \bar{u}_{p;\,r'}(0)\; \gamma_5\, u_{n;\,r}(0) = 0
\end{aligned} \tag{10.31}$$

which gives the Feynman amplitude (10.29) in the following form (we should realize that $U^+_{p;\,r'}\, U_{n;\,r} = \delta_{rr'}\, \sqrt{4m_n m_p}$)

$$\mathcal{M}^{(1)(\beta)}_{fi} \equiv \mathcal{M}^{(1)(\beta)}_{Pr\to pr';\,ks;\,k's'} = \mathcal{M}_S + \mathcal{M}_V + \mathcal{M}_A + \mathcal{M}_T + \mathcal{M}_P \tag{10.32}$$

where

$$\begin{aligned}
\mathcal{M}_S &= C_S\, \left(U^+_{p;\,r'} U_{n;\,r}\right)\, \left[\; \bar{u}_{e;\,s}\, (1 + \alpha_j\, \gamma^5)\, v_{\tilde{\nu};\,s'}\; \right]\, \delta_{rr'} \\
\mathcal{M}_V &= C_V\, \left(U^+_{p;\,r'} U_{n;\,r}\right)\, \left[\; \bar{u}_{e;\,s}\, (1 + \alpha_j\, \gamma^5)\, \gamma^0\, v_{\tilde{\nu};\,s'}\; \right]\, \delta_{rr'} \\
\mathcal{M}_A &= C_A\, \left(U^+_{p;\,r'}\, \sigma_j\, U_{n;\,r}\right)\, \left[\; \bar{u}_{e;\,s}\, (1 + \alpha_j\, \gamma^5)\, \gamma^5\gamma^j\, v_{\tilde{\nu};\,s'}\; \right] \\
\mathcal{M}_T &= C_T\, \left(U^+_{p;\,r'}\, \sigma_{\mu\nu}\, U_{n;\,r}\right)\, \left[\; \bar{u}_{e;\,s}\, (1 + \alpha_j\, \gamma^5)\, \Sigma^j\, v_{\tilde{\nu};\,s'}\; \right] \\
\mathcal{M}_P &= 0
\end{aligned} \tag{10.33}$$

where

$$\Sigma^j = \frac{1}{2}\, \epsilon^{jkl}\sigma^{kl} = \frac{1}{2} \begin{pmatrix} \sigma_j & 0 \\ 0 & \sigma_j \end{pmatrix} \tag{10.34}$$

So, on the base of (10.33) we can conclude,

- pseudoscalar term $j = P$ in the Lagrange density (10.27) does not contribute to the transition Feynman amplitude;

- scalar $j = S$ and vector $j = V$ terms in (10.27) give in the amplitude $\mathcal{M}_{fi}^{(1)(\beta)}$ terms $\mathcal{M}_S$ and $\mathcal{M}_V$ involving $\delta_{rr'}$ (that means $r = r^{'}$). That means the spin state of the neutron is the same as the spin state of proton. Therefore in the case of allowed β- transitions ($L = 0$) these terms $\mathcal{M}_S$ and $\mathcal{M}_V$ can contribute only to Fermi β- transitions ($\Delta J = 0$);

- axial vector and tensor terms, $\mathcal{M}_A$ and $\mathcal{M}_T$, involve Pauli matrices σ_j ($j = 1, 2, 3$) and therefore they contribute only in the allowed β-transitions with the change of the angular momentum, that means only in the case when $\Delta\vec{J} = \vec{1}$ corresponding to Gamow-Teller β- transitions.

The amplitude (10.32) is used to be written in the literature also in the following form (see [13, 256]),

$$\mathcal{M}_{fi}^{(1)(\beta)} = \mathcal{M}_{fi}^{(F)} + \mathcal{M}_{fi}^{(GT)} \tag{10.35}$$

with the Fermi amplitude,

$$\mathcal{M}_{fi}^{(F)} = \mathcal{M}_S + \mathcal{M}_V \tag{10.36}$$

and Gamow-Teller amplitude

$$\mathcal{M}_{fi}^{(GT)} = \mathcal{M}_A + \mathcal{M}_T \tag{10.37}$$

10.4 Consequences for weak β-process amplitude coming from elementary processes experiments

The β-decay Feynman amplitude $\mathcal{M}_{fi}^{(1)(\beta)}$ derived in the previous section for the elementary process $n \to p + e^- + \tilde{\nu}_e$ (see (10.32) with(10.33)) involves 8 parameters, C_S, C_V, C_A, C_T and α_S, α_V, α_A, α_T. These parameters should be determined from the experimental data on this elementary process. In this section the concrete experimental data used for the setting of these parameters are briefly discussed (more details can be found e.g. in [256]). In the connection with the amplitude (10.32) of the elementary process $n \to p + e^- + \tilde{\nu}_e$ one should realize that this process is fundamental from the point of view nuclear physics. If all parameters of the interaction Lagrangian (10.27) are known then the β- transition mechanism in all nuclei is set and in the framework of the given model of nuclear structure all properties of β- transition can be calculated as it is discussed in the next section 10.5.

10.4.1 Electron spectrum from the β- decay of neutron

In order to determine the energy spectrum of electrons produced in the process $n \to p + e^- + \tilde{\nu}_e$ it is necessary to calculate corresponding probability of the emission of electron with the given energy E_e. From the quantum field theory (see (P.12)) it is known that the probability of the neutron β^-- decay ($n \to p + e^- + \tilde{\nu}_e$), with the four- linear momentum $P \equiv (E_n;\, \vec{P})$ and spin index r, per 1 second, when emitted electron (with the linear four- momentum $k \equiv (E_e = E_{\vec{k}}\,;\, \vec{k})$) with spin index s and the linear momentum $\vec{k}$ is directed to the d^3k vicinity of the vector $\vec{k}$, and with the proton (with the linear four-momentum $p \equiv (E_{\vec{p}}\,;\, \vec{p})$) having the spin index $r^{'}$ and linear momentum directed to the d^3p vicinity of the vector $\vec{p}$, and with the antineutrino $\tilde{\nu}_e$, with the linear four- momentum $k^{'} \equiv (E_{\vec{k}'}\,;\, \vec{k}^{\,'})$ having the spin index $s^{'}$ and linear momentum directed to the $d^3k^{'}$ vicinity of the vector $\vec{k}^{\,'}$, is given by (P.12) (see e.g. [13])

$$d\Gamma_{Pr \to pr',\, ks,\, k's'} \;=\; (2\pi)^4 \;\delta^{(4)}(P - k - k^{'} - p) \\ \frac{1}{2m_n}\,\frac{d^3k}{(2\pi)^3\,2E_{\vec{k}}}\,\frac{d^3k^{'}_f}{(2\pi)^3\,2E_{\vec{k}'}}\,\frac{d^3p}{(2\pi)^3\,2E_{\vec{p}}}\,\left|\mathcal{M}^{(1)(\beta)}_{fi}\right|^2 \qquad (10.38)$$

where we suppose that we work in the neutron rest frame (when the neutron energy is equal to its rest energy, $E_n = m_n$).

Further the case is discussed where all particles in the elementary process $n \to p + e^- + \tilde{\nu}_e$ are not polarized. That means in the expression (10.38) we should sum over spin index of all final particles and average over spin index of neutron, that means instead of $|\mathcal{M}^{(1)(\beta)}_{i\to f}|^{\,2} = |\mathcal{M}^{(1)(\beta)}_{Pr\to pr',\, ks,\, k's'}|^{\,2}$ in (10.38) the following sum should be used,

$$\left|\,\mathcal{M}^{(1)(\beta)}_{fi}\,\right|^{\,2} \longrightarrow \left|\,\bar{\mathcal{M}}_{fi}\,\right|^{\,2} = \frac{1}{2}\sum_{rr'}\sum_{ss'}\left|\,\mathcal{M}^{(1)(\beta)}_{Pr\to pr',\, ks,\, k's'}\right|^{\,2} \qquad (10.39)$$

In the case of the Feynman amplitude (10.32), (10.33) it means to calculate $\frac{1}{2}\sum_{rr'}\sum_{ss'}|\mathcal{M}_S + \mathcal{M}_V + \mathcal{M}_A + \mathcal{M}_T|^{\,2}$. From quantum field theory it is known that such a sum is usually determined by means of the traces of corresponding products of 4×4 matrices (10.33) involved in (10.32), in our case traces of nucleon matrices and lepton matrices involved in (10.33). From the product of nucleon matrices follows that there is no interference terms between the Fermi (S, V) and Gamow-Teller (A,T) parts of matrices (10.33), (10.35), (10.36) and (10.37). It is evident that such interference term in

$\sum |\mathcal{M}|^2 = \sum \mathcal{M}^*\mathcal{M}$ (see (10.39)) would involve the nucleon factor,

$$(U^+_{n;\,r}U_{p\,;\,r'})\,(U^+_{p\,;\,r'}\,\sigma_j\,U_{n;\,r}) \tag{10.40}$$

and according to the quantum theory it means to determine the trace (see e.g. [13]),

$$\begin{aligned}
&\sum_{rr'} Tr\big((U^+_{n;\,r}U_{p\,;\,r'})\,(U^+_{p\,;\,r'}\,\sigma_j\,U_{n;\,r})\big) = \\
&\quad = \sum_{rr'}\sum_{ikl}(U^+_{n;\,r})_i\,(U_{p\,;\,r'})_i\,(U^+_{p\,;\,r'})_k\,(\sigma_j)_{kl}\,(U^+_{n;\,r})_l = \\
&\quad = \sum_{ikl}\Big[\,\Big(\sum_{r'}(U_{p\,,\,r'})_i\,(U_{p\,,\,r'})_k\Big)\,\Big(\sum_{r}(U_{n\,;\,r})_l\,(U^+_{n\,;\,r})_i\,(\sigma_j)_{kl}\Big)\,\Big]
\end{aligned} \tag{10.41}$$

and we have (with the assignment $M = \frac{1}{2}(m_n + m_p)$),

$$\begin{aligned}
\sum_{r'} U_{p\,;\,r'}U^+_{p\,;\,r'} &= \boxed{\begin{array}{c}\text{see}\\(P.10)\end{array}} = \\
&= \big(\sqrt{2M}\big)^2\,\Big[\begin{pmatrix}1\\0\end{pmatrix}(1\,0) + \begin{pmatrix}0\\1\end{pmatrix}(0\,1)\Big] = \\
&= 2M\,\Big[\begin{pmatrix}1&0\\0&0\end{pmatrix} + \begin{pmatrix}0&0\\0&1\end{pmatrix}\Big] = 2M\begin{pmatrix}1&0\\0&1\end{pmatrix}
\end{aligned} \tag{10.42}$$

and similarly

$$\sum_{r'} U_{n\,;\,r'}U^+_{n\,;\,r'} = 2M\begin{pmatrix}1&0\\0&1\end{pmatrix} \tag{10.43}$$

Hence,

$$\sum_{r'}(U_{p\,;\,r'})_i\,(U_{p\,;\,r'})_k = 2M\,\delta_{ik} \quad \sum_{r}(U_{p\,;\,r})_i\,(U_{p\,;\,r})_k = 2M\,\delta_{ik} \tag{10.44}$$

and (10.41) can be rewritten,

$$\begin{aligned}
&\sum_{rr'} Tr\big((U^+_{n;\,r}U_{p\,;\,r'})\,(U^+_{p\,;\,r'}\,\sigma_j\,U_{n;\,r})\big) = \sum_{ikl} 4M^2\,\delta_{ik}\,\delta_{li}\,(\sigma_j)_{kl} = \\
&\quad = 4M^2\,\sum_k(\sigma_j)_{kk} = \boxed{\begin{array}{c}\text{because the trace}\\\text{of Pauli matrix is}\\\text{zero for all } j=1,2,3\end{array}} = 0
\end{aligned} \tag{10.45}$$

So we can really conclude that there is no interference term between $\mathcal{M}_F$ and $\mathcal{M}_{GT}$ in (10.39) (or in (10.35)) and $|\bar{\mathcal{M}}_{fi}|^2$ in (10.39) has the following form,

$$\begin{aligned} \left|\bar{\mathcal{M}}_{fi}\right|^2 &= \left|\bar{\mathcal{M}}_{fi}^{(S)} + \bar{\mathcal{M}}_{fi}^{(V)}\right|^2 + \left|\bar{\mathcal{M}}_{fi}^{(A)} + \bar{\mathcal{M}}_{fi}^{(T)}\right|^2 = \\ &= \left|\bar{\mathcal{M}}_{fi}^{(F)}\right|^2 + \left|\bar{\mathcal{M}}_{fi}^{(GT)}\right|^2 \end{aligned} \tag{10.46}$$

At first we determine the Fermi part $|\bar{\mathcal{M}}_{fi}^{(F)}|^2$,

$$\left|\bar{\mathcal{M}}_{fi}^{(F)}\right|^2 = \left|\bar{\mathcal{M}}_{fi}^{(S)}\right|^2 + \left|\bar{\mathcal{M}}_{fi}^{(V)}\right|^2 + \bar{\mathcal{M}}_{fi}^{(S)}\bar{\mathcal{M}}_{fi}^{(V)\,*} = \boxed{\begin{array}{c}\text{see}\\ (10.33)\end{array}} =$$

$$\begin{aligned} &= \; C_S^2\, Tr\left[U_p U_p^+ U_n U_n^+\right]\, Tr\left[u_e\bar{u}_e\,(1+\alpha_S\gamma_5)\,v_{\tilde{\nu}}\bar{v}_{\tilde{\nu}}\,(1-\alpha_s\gamma_5)\right] \\ &\quad + C_V^2\, Tr\left[U_p U_p^+ U_n U_n^+\right]\, Tr\left[u_e\bar{u}_e\,(1+\alpha_S\gamma_5)\,\gamma_0\,v_{\tilde{\nu}}\bar{v}_{\tilde{\nu}}\,(1-\alpha_s\gamma_5)\,\gamma_0\right] \\ &\quad + C_S^2 C_V^2\, Tr\left[U_p U_p^+ U_n U_n^+\right]\, Tr\left[u_e\bar{u}_e\,(1+\alpha_S\gamma_5)\,v_{\tilde{\nu}}\bar{v}_{\tilde{\nu}}\,(1-\alpha_s\gamma_5)\,\gamma_0\right] \\ &\quad + c.c. \;\; = \end{aligned}$$

$$= \boxed{\begin{array}{c}\text{using identities}\\ \sum_r u_r(\vec{p})\,\bar{u}_r(\vec{p}) = \not{p} + m \quad , \quad \sum_r v_r(\vec{p})\,\bar{v}_r(\vec{p}) = \not{p} - m\\ \text{and using (10.45)}\end{array}} =$$

$$\begin{aligned} &= \; 4\,C_S^2\,M^2\;Tr\left[(\not{k}+m_e)\,(1+\alpha_S\gamma_5)\,\not{k}'(1-\alpha_S\gamma_5)\right] \\ &\quad + 4\,C_V^2\,M^2\;Tr\left[(\not{k}+m_e)\,(1+\alpha_S\gamma_5)\,\gamma_0\,\not{k}'(1+\alpha_S\gamma_5)\,\gamma_0\right] \\ &\quad + 4\,C_V C_S\,M^2\;Tr\left[(\not{k}+m_e)\,(1+\alpha_S\gamma_5)\,\not{k}'(1+\alpha_S\gamma_5)\,\gamma_0\right] \;+\; c.c. \;\; = \end{aligned}$$

$$= \boxed{\begin{array}{c}\text{using expressions for calculation of traces of products of}\\ \gamma\text{- matrices - see e.g. corresponding appendixes in [13, 256]}\end{array}} =$$

$$\begin{aligned} &= \; 4\,C_S^2\,(1+\alpha_S^2)\,M^2\,Tr(\not{k}\not{k}') \\ &\quad + 4\,C_S^2\,(1+\alpha_S^2)\,M^2\,Tr(\not{k}\,\gamma_0\,\not{k}'\gamma_0) \\ &\quad + 4\,C_S C_V\,(1-\alpha_S\,\alpha_V)\,m_e\,M^2\,Tr(\not{k}'\gamma_0) \;+\; c.c. \;\; = \end{aligned}$$

$$= \boxed{\begin{array}{c}\text{because e.g.}\\ Tr(\not{k}\not{k}') = 4\,k\,k' \text{ e.t.c. - see [13]}\end{array}} =$$

$$\begin{aligned} &= \; 16\,C_S^2\;(1+\alpha_S^2)M^2\,(k\cdot k') \;+\; 16\,C_V^2\,(1+\alpha_S^2)M^2\,(2\,E_e\,E_{\tilde{\nu}} - k\cdot k') \\ &\quad + 32\,C_S\,C_V\,(1-\alpha_S\,\alpha_V)\,m_e\,M^2\,E_{\tilde{\nu}} \;\; = \end{aligned}$$

$$= \boxed{\begin{array}{c}\text{because } k\cdot k^{'} = E_e E_{\tilde{\nu}}\, cos\vartheta = E_e E_{\tilde{\nu}}(1-\beta_e\, cos\vartheta) \\ \text{with the assumption of zero neutrino mass,}\quad E_{\tilde{\mu}} = |\vec{k}^{\,'}|\end{array}} =$$

$$= 16\, M^2\, E_e\, E_{\tilde{\nu}}\, \big[C_S^2\,(1+\alpha_S^2)\,(1-\beta_e\, cos\vartheta) + C_V^2\,(1+\alpha_V^2)\,(1+\beta_e\, cos\vartheta)\; +\; 2C_S\, C_V\,(1-\alpha_S\,\alpha_V)\,\frac{m_e}{E_e}\big] \tag{10.47}$$

Similarly we can obtain for GT part $|\bar{\mathcal{M}}|^2$ of (10.46),

$$\big|\bar{\mathcal{M}}_{fi}^{(GT)}\big|^2 = \big|\bar{\mathcal{M}}_{fi}^{(A)} + \bar{\mathcal{M}}_{fi}^{(T)}\big|^2 = = 16\, M^2\, E_e\, E_{\tilde{\nu}}\, \big[3\, C_A\,(1+\alpha_A^2)\,(1-\frac{1}{3}\,\beta_e\, cos\vartheta) +12\, C_T^2\,(1+\alpha_T^2)\,(1+\frac{1}{3}\,\beta_e\, cos\vartheta)\; -\; 12\, C_A\, C_T\,(1-\alpha_A\,\alpha_T)\,\frac{m_e}{E_e}\big] \tag{10.48}$$

So, the interference between $\bar{\mathcal{M}}^{(F)}$ and $\bar{\mathcal{M}}^{(A)}$ does not exist but we have an interference $\bar{\mathcal{M}}^{(S)}$ - $\bar{\mathcal{M}}^{(V)}$ and $\bar{\mathcal{M}}^{(A)}$ - $\bar{\mathcal{M}}^{(T)}$ (terms with $C_S C_V$ and $C_A C_T$).

Let us go back to the expression (10.38) for the probability of the β- decay of neutron per 1 second where all participated particles were polarized (that means with spin indexes). For non-polarized particles we should apply the substitution (10.39) and the probability (10.38) for non-polarized particles (spin indexes are not determined) reads,

$$d\Gamma_{P\to p,\,k,\,k^{'}} = (2\pi)^4\,\delta^{(4)}(P-k-k^{'}-p)\; \frac{1}{2m_n}\,\frac{d^3k}{(2\pi)^3\,2E_{\vec{k}}}\,\frac{d^3k^{'}}{(2\pi)^3\,2E_{\vec{k}^{'}}}\,\frac{d^3p}{(2\pi)^3\,2E_{\vec{p}}}\,\big|\bar{\mathcal{M}}_{fi}\big|^2 \tag{10.49}$$

where $|\bar{\mathcal{M}}_{fi}|^2$ is given by (10.46). This is the probability of the β- decay $n\to p+e^-+\tilde{\nu}_e$ with the final proton flying to the d^3p vicinity of the direction $\vec{p}$ (out of other characteristics of this β- decay).

If we are not interested in the direction of the linear momentum of the final proton $\vec{p}$ then the integration over d^3p should be performed. Because of the assumption that we work in the neutron rest frame ($P^\mu \equiv (m_n,\,\vec{0})$) and because of the presence of the four dimensional Dirac δ- function in (10.49) ($E_e \equiv E_{\vec{k}}$, $E_{\tilde{\nu}} \equiv E_{\vec{k}^{\,\prime}}$, $E_p \equiv E_{\vec{p}}$),

$$\delta^{(4)}(P-k-k^{'}-p) = \delta^{(3)}(\vec{0}-\vec{k}-\vec{k}^{\,'}-\vec{p})\;\delta(m_n-E_e-E_{\tilde{\nu}}-E_p)$$

the integration over d^3p is simple (simply we substitute $\vec{p} = \vec{k} + \vec{k}^{\,\prime}$). Because of the relatively high proton mass we can use also the approximation $\frac{1}{E_p} \approx \frac{1}{m_p}$ and finally we obtain,

$$d\Gamma_{P\to k,\,k^{\prime}} = \\ = \frac{2\pi}{2m_n} \left|\bar{\mathcal{M}}_{fi}\right|^2 \frac{d^3k}{(2\pi)^3\, 2E_{\vec{k}}} \frac{d^3k^{\,\prime}}{(2\pi)^3\, 2E_{\vec{k}^{\,\prime}}} \frac{1}{2m_p}\, \delta(m_n - E_e - E_{\tilde{\nu}} - E_p) \tag{10.50}$$

where $\delta\Gamma_{P\to\vec{k},\,\vec{k}^{\,\prime}}$ is the probability per second that during the elementary process $n \to p + e^- + \tilde{\nu}_e$ the electron e^- flyies into the d^3k vicinity of the direction of the vector $\vec{k}$ and the antineutrino goes to the $d^3k^{\,\prime}$ vicinity of the direction of the vector $\vec{k}^{\,\prime}$. If we are not interested in the linear momentum and the energy of the antineutrino then we integrate (10.50) over $d^3k^{\,\prime} = |\vec{k}^{\,\prime}|^2\, d|\vec{k}^{\,\prime}|\, d\Omega_{\tilde{\nu}}$. At first we integrate over $d|\vec{k}^{\,\prime}|$. If the antineutrino mass in neglected then $|\vec{k}^{\,\prime}| = E_{\tilde{\nu}}$. Further we denote as $x \equiv |\vec{k}^{\,\prime}| = E_{\tilde{\nu}}$. Then the δ-function in (8.50), representing the preservation of the total energy, can be written as $\delta(f(x))$ where

$$f(x) = m_n - E_e - x - \sqrt{m_p^2 + |\vec{k} + \vec{k}^{\,\prime}|^2} = \\ = m_n - E_e - x - \sqrt{m_p^2 + |\vec{k}|^2 + x^2 + 2x|\vec{k}|\, cos\, \vartheta} \tag{10.51}$$

where ϑ is the angle between $\vec{k}$ and $\vec{k}^{\,\prime}$. The preservation of the total energy means the condition $f(x_0) = 0$, then

$$x_0 = E_{\tilde{\nu}} = \frac{m_n^2 - m_p^2 + m_e^2 - 2m_nE_e}{2m_p - 2E_e + 2|\vec{k}|cos\, \vartheta} \tag{10.52}$$

In the integration of (10.50) over $d|\vec{k}^{\,\prime}|$ we use well-known identity,

$$\delta(f(x)) = \frac{1}{|f^{\,\prime}(x_0)|}\, \delta(x - x_0) \tag{10.53}$$

where

$$f^{\,\prime}(x_0) = \frac{df}{dx}(x = x_0) = -1 - \frac{2\, x_0 + 2\, |\vec{k}|\, cos\, \vartheta}{2\, \sqrt{m_p^2 + |\vec{k}|^2 + x_0^2 + 2\, x_0\, |\vec{k}|\, cos\, \vartheta}} = \\ = \boxed{\begin{array}{c}\text{because}\\ f(x_0) = 0\end{array}} = \frac{-m_n + E_e - |\vec{k}|\, cos\, \vartheta}{m_n - E_e - x_0} \tag{10.54}$$

Since $m_n > E_e - |\vec{k}|\, cos\, \vartheta$,

$$|f(x_0)| = \frac{m_n - E_e + |\vec{k}|\, cos\, \vartheta}{m_n - E_e - x_0} =$$

$$= \boxed{\begin{array}{c}\text{if the proton kinetic energy is neglected} \\ x_0 = E_{\tilde{\nu}} = m_n - m_p - E_e = \Delta m - E_e\end{array}} =$$

$$= \frac{m_n - E_e + |\vec{k}|\, cos\, \vartheta}{m_n - E_e - \Delta m + E_e} \approx \boxed{\begin{array}{c}\text{because} \\ m_n >> E_e - |\vec{k}|\, cos\, \vartheta\end{array}} \approx 1 \qquad (10.55)$$

Now we can perform the integration over $d|\vec{k}^{\,\prime}|$ with the fixed $d\Omega_{\tilde{\nu}}$ (where $d\Omega_{\tilde{\nu}} = sin\, \vartheta\, d\vartheta\, d\phi$ is the element of the space angle of the antineutrino linear momentum - ϑ is the angle between fixed $\vec{k}$ and $\vec{k}^{\,\prime}$),

$$d\Gamma_{P\to k,\,\vartheta,\,\phi} = \frac{1}{2m_n}\, |\bar{\mathcal{M}}_{fi}|^{\,2} \frac{1}{2m_p}\, \frac{d^3k}{(2\pi)^3 2E_e}\, \frac{d\Omega_{\tilde{\nu}}}{4\pi^2} \int dx\, \frac{x}{2}\, \delta(x - x_0) =$$

$$= \boxed{\begin{array}{c}\text{we use} \\ m_p \approx m_n \approx M = \frac{m_p + m_n}{2}\end{array}} = \frac{1}{8M^2}\, |\bar{\mathcal{M}}_{fi}|^{\,2}\, E_{\tilde{\nu}}\, \frac{d^3k}{(2\pi)^3 2E_e}\, \frac{d\Omega_{\tilde{\nu}}}{4\pi} \qquad (10.56)$$

If we are not interested in the direction of resulting antineutrino we integrate over $d\Omega_{\tilde{\nu}}$ and after the substitution of (10.46) into (10.56) we obtain the probability of the beta- decay of the neutron per second with the electron with the energy E_e and linear momentum in the vicinity of d^3k in the following form,

$$d\Gamma_{P\to k} = \frac{1}{8M^2}\, E_{\tilde{\nu}}\, \frac{d^3k}{(2\pi)^3 2E_e}\, \frac{1}{4\pi^2} \int_0^{\pi} d\vartheta \int_0^{2\pi} d\phi\, sin\vartheta\, \left\{|\bar{\mathcal{M}}_F|^2 + |\bar{\mathcal{M}}_{GT}|^2\right\} =$$

$$= \boxed{\begin{array}{c}\text{we substitute from (10.47) and (10.48) but the terms} \\ \text{with } cos\vartheta \text{ go away because} \\ \int_0^{\pi} d\vartheta sin\vartheta\ cos\vartheta = -\int_{-1}^{1} d(cos\vartheta)\, cos\vartheta = \int_{-1}^{1} x\, dx = 0\end{array}} =$$

$$= 2\, E_{\tilde{\nu}}\, \frac{d^3k}{(2\pi)^3 2E_e}\, \frac{1}{\pi}$$

$$\left\{E_e E_{\tilde{\nu}} \left[C_S^2\, (1 + \alpha_S^2) + C_V^2\, (1 + \alpha_V^2) + 2C_S C_V\, (1 - \alpha_S \alpha_V) \frac{m_e}{E_e}\right]\right.$$

$$\left. + E_e E_{\tilde{\nu}} \left[3C_A^2\, (1 + \alpha_A^2) + 12C_T^2\, (1 + \alpha_T^2) - 12C_A C_T\, (1 - \alpha_A \alpha_T) \frac{m_e}{E_e}\right]\right\} \qquad (10.57)$$

In order to obtain the energy spectrum of resulting electron from the decay $n \to p + e^- + \tilde{\nu}_e$ it is necessary to integrate (10.57) over all directions of outgoing electrons, that means the integration over $d\Omega_e$ ($d^3k = |\vec{k}|^2\, d|\vec{k}|\, d\Omega_e$)

$$
\begin{aligned}
d\Gamma_{i\to f}(E_e) &= \int d\Omega_e\, d\Gamma_{P\to k} = \\
&= \frac{1}{8\pi^4}\int d\Omega_e\, |\vec{k}|^2\, d|\vec{k}|\, E_{\tilde{\nu}}^2 \\
&\quad \Big\{ C_S^2\,(1+\alpha_S^2) + C_V^2\,(1+\alpha_V^2) + 2C_SC_V\,(1-\alpha_S\alpha_V)\frac{m_e}{E_e} \\
&\quad + 3C_A^2\,(1+\alpha_A^2) + 12C_T^2\,(1+\alpha_T^2) - 12C_AC_T\,(1-\alpha_A\alpha_T)\frac{m_e}{E_e}\Big\} = \\
&= \boxed{\begin{array}{c}\text{because} \\ E_e = \sqrt{m_e^2+|\vec{k}|^2} \quad \Rightarrow \quad dE_e = \frac{2\,|\vec{k}|\,d|\vec{k}|}{2\sqrt{m_e^2+|\vec{k}|^2}} = \frac{|\vec{k}|\,d|\vec{k}|}{E_e}\end{array}} = \\
&= \frac{1}{8\pi^4}\int d\Omega_e\, |\vec{k}|\, E_e\, dE_e\, E_{\tilde{\nu}}^2 \\
&\quad \Big\{ C_S^2\,(1+\alpha_S^2) + C_V^2\,(1+\alpha_V^2) + 2C_SC_V\,(1-\alpha_S\alpha_V)\frac{m_e}{E_e} \\
&\quad + 3C_A^2\,(1+\alpha_A^2) + 12C_T^2\,(1+\alpha_T^2) - 12C_AC_T\,(1-\alpha_A\alpha_T)\frac{m_e}{E_e}\Big\}
\end{aligned}
\tag{10.58}
$$

The function under the integral in (10.58) does not depend on angles of the vector $\vec{k}$. Therefore the integration over $d\Omega_e$ in (10.58) gives only a factor 4π. Then using energy preservation law, $E_{\tilde{\nu}} = m_n - m_p - E_e = \Delta m - E_e$, and (10.11), $E_e^{max} \approx \Delta m$, the expr. (10.58) can be rewritten as,

$$
\begin{aligned}
&d\Gamma_{i\to f}(E_e) = \\
&\quad = \frac{1}{2\pi^3}\Big\{ C_S^2\,(1+\alpha_S^2) + C_V^2\,(1+\alpha_V^2) + 2C_SC_V\,(1-\alpha_S\alpha_V)\frac{m_e}{E_e} \\
&\qquad + 3C_A^2\,(1+\alpha_A^2) + 12C_T^2\,(1+\alpha_T^2) - 12C_AC_T\,(1-\alpha_A\alpha_T)\frac{m_e}{E_e}\Big\} \\
&\qquad |\vec{k}|\, E_e\, (E_e^{max} - E_e)^2\, dE_e
\end{aligned}
\tag{10.59}
$$

Terms involving $\frac{m_e}{E_e}$ are known as Friez interference terms. As we will see farther all up to date experimental data (from all possible known β- processes) confirm the fact that

$$
C_SC_V\,(1-\alpha_S\alpha_V) = C_AC_T\,(1-\alpha_A\alpha_T) = 0 \tag{10.60}
$$

and therefore the energy spectrum of electrons from the process $n \to p + e^- + \tilde{\nu}_e$ is (using $|\vec{k}| = \sqrt{E_e^2 - m_e^2}$),

$$d\Gamma_{i\to f}(E_e) =$$
$$= \frac{1}{2\pi^3}\left\{C_S^2\,(1+\alpha_S^2) + C_V^2\,(1+\alpha_V^2) + 3C_A^2\,(1+\alpha_A^2) + 12C_T^2\,(1+\alpha_T^2)\right\}$$
$$|\vec{k}|\,E_e\,(E_e^{max} - E_e)^2\,dE_e \approx\ const\,\sqrt{E_e^2 - m_e^2}\ \ E_e\ \ (E_e^{max} - E_e)^2\,dE_e \tag{10.61}$$

The condition (10.60) is discussed in details in the next section.

From (10.61) it is clear that the electron spectrum from the elementary process $n \to p + e^- + \tilde{\nu}_e$ does not provide any suitable information for parameters $C_S,\ C_V,\ C_A,\ C_T,\quad \alpha_S,\ \alpha_A,\quad \alpha_A,\quad \alpha_T$ involved in the β- decay Feynman amplitude (10.35) (except its normalization). Therefore it is necessary to analyze not only the shape of the electron spectrum of $n \to p + e^- + \tilde{\nu}_e$ but also other data from β- decays in order to determine parameters of the Lagrangian density (10.27) of β- process.

The spectrum (10.59) or (10.61) for the electron spectrum was derived for the elementary process of the neutron β- decay. One can expect that the energy dependence (10.61) is valid not only in the case of the elementary process $n \to p + e^- + \tilde{\nu}_e$ but also for all allowed β- decays of atomic nuclei (allowed and forbidden β- decays of nuclei are discussed in the section 10.5).

10.4.2 Electron-antineutrino correlation in pure Fermi and Gamow-Teller β^- decays (V-A dominance)

Relevant information for the determination of the parameters of the β- process amplitude was extracted from the experimental angle correlations between electron and neutrino from the pure Fermi and Gamow-Teller β^- decays. In order to analyze this correlation from theoretical point of view it is necessary to go back to the expression (10.50). We discussed it in the previous subsection in the connection with the elementary process $n \to p + e^- + \tilde{\nu}_e$ but one should realize that it valids also for any β- decay $|i\rangle \to |f\rangle$. The square $|\bar{\mathcal{M}}_{fi}|^2$ in (10.50) is given by (10.46) where $|\bar{\mathcal{M}}_{fi}^{(F)}|^2$ is given by (10.47) and $|\bar{\mathcal{M}}_{fi}^{(GT)}|^2$ by (10.48). As it can be seen from(10.47) and (10.48) the angle ϑ between vectors $\vec{k}$ and $\vec{k}'$ (that means between electron and antineutrino) are present there only through $cos\,\vartheta$. Experimentally it is possible to determine the electron-antineutrino angle correlation independently for pure Fermi and pure Gamow-Teller transitions. From (10.47) and (10.48) it is evident that

for the case of the pure Fermi β- transition the probability is (see (10.50) with (10.47) where again the Fierz ineterference terms are neglected),

$$\frac{d\Gamma_F}{d\Omega_{\tilde{\nu}}} \approx const' \left[C_S^2(1+\alpha_S^2)(1-\beta_e cos\,\vartheta) + C_V^2(1+\alpha_V^2)(1+\beta_e cos\,\vartheta)\right] =$$
$$= const' \left[C_S^2(1+\alpha_S^2) + C_V^2(1+\alpha_V^2) + \left(C_V^2(1+\alpha_V^2) - C_S^2(1+\alpha_S^2)\right)\beta_e cos\,\vartheta\right] \approx$$
$$= const\left[1 + a_F\,\beta_e\,cos\,\vartheta\right] \tag{10.62}$$

where

$$a_F = \frac{C_V^2\,(1+\alpha_V^2)\;-\;C_S^2\,(1+\alpha_S^2)}{C_S^2\,(1+\alpha_S^2)\;+\;C_V^2\,(1+\alpha_V^2)} \tag{10.63}$$

Similarly for the pure GT transition the electron-antineutrino angle distribution is given by,

$$\frac{d\Gamma_{GT}}{d\Omega_{\tilde{\nu}}} \approx const\left[1 + a_{GT}\,\beta_e\,cos\,\vartheta\right] \tag{10.64}$$

with

$$a_{GT} = -\frac{1}{3}\,\frac{C_A^2\,(1+\alpha_A^2)\;-\;4\,C_T^2\,(1+\alpha_T^2)}{C_A^2\,(1+\alpha_A^2)\;+\;4\,C_T^2\,(1+\alpha_T^2)} \tag{10.65}$$

It is necessary to note that the angle ϑ between vectors $\vec{k}$ and $\vec{k}'$ does not depend on the non-preservation of the parity in β- processes, because this angle is invariant with respect to the frame axis inversion (both the vectors $\vec{k}$ and $\vec{k}'$ are linear momenta and therefore the angle between them does not change if the frame axes are inverted).

Further we will analyze expressions (10.62)-(10.65),

$$\text{if } C_V = 0 \text{ for the pure Fermi transition } \Rightarrow \boxed{\begin{matrix}\text{see}\\(10.63)\end{matrix}} \Rightarrow a_F = -1$$

$$\text{if } C_S = 0 \text{ for the pure Fermi transition } \Rightarrow \boxed{\begin{matrix}\text{see}\\(10.63)\end{matrix}} \Rightarrow a_F = +1$$

$$\text{if } C_A = 0 \text{ for the pure GT transition } \Rightarrow \boxed{\begin{matrix}\text{see}\\(10.65)\end{matrix}} \Rightarrow a_{GT} = +1/3$$

$$\text{if } C_T = 0 \text{ for the pure GT transition } \Rightarrow \boxed{\begin{matrix}\text{see}\\(10.65)\end{matrix}} \Rightarrow a_{GT} = -1/3 \tag{10.66}$$

All up to date data on pure Fermi and Gamow-Teller transitions have shown that for these transitions we always have

$$a_F = 1 \qquad\qquad a_{GT} = -1/3 \tag{10.67}$$

That means the experimental data on the pure Fermi β- transitions gave $C_S = 0$ (only the contribution of the vector part gave nonzero value of the corrsponding transition amplitude) and experimental data on the pure Gamow-Teller β- transitions have confirmed $C_T = 0$ (only the nonzero contribution of the axial vector components was confirmed). So the experimental data on the electron-antineutrino angle correlation provide:

$$C_S = C_T = 0 \tag{10.68}$$

and therefore the nonzero contribution to the transition amplitude came from only the vector and axial vector terms in the β- process interaction Lagrangian. From (10.68) also the condition (10.60) follows.

The zero values of parameters C_S and C_T (see (10.68) together with the zero contribution of the pseudoscalar term in the β- process Feynman amplitude (see (10.32) and (10.33)) mean that the β- process Lagrangian density (10.27) effectively involves only vector and axial vector terms,

$$\hat{\mathcal{L}}_{int}^{(\beta^-)}(x) = \\ = \sum_{j=V,\,A} C_j \left[\hat{\bar{\psi}}_p(x)\,\Gamma_j\,\hat{\psi}_n(x)\right]\left[\hat{\bar{\psi}}_e(x)\,(1+\alpha_j\gamma^5)\,\Gamma^j\,\hat{\psi}_{\tilde{\nu}}(x)\right] \tag{10.69}$$

and the corresponding lowest order Feynman amplitude (10.29) is reduced to

$$\mathcal{M}_{fi}^{(1)(\beta)} = \sum_{j=V,A} C_j \left[\bar{u}_{p;\,r'}(\vec{p})\,\Gamma_j\,u_{n;\,r}(\vec{P})\right] \\ \left[\bar{u}_{e;\,s}(\vec{k})\,(1+\alpha_j\,\gamma^5)\,\Gamma^j\,v_{\tilde{\nu};\,s'}(\vec{k}')\right] \tag{10.70}$$

This conclusion is known in literature as the vector-axial vector coupling dominance (V-A dominance). In the comparison with the original form of the operator of the interaction Lagrangian density for the process $n \to p + e^- + \tilde{\nu}_e$ (see (10.27)) the number of parameters in (10.69) is reduced from 8 to 4 (parameters C_s, C_A, α_s, α_A). In next subsections it will be shown how these parameters can be determined from further data on the decay $n \to p + e^- + \tilde{\nu}_e$.

10.4.3 Longitudinal polarization of electrons

So far we have not analyze the non-preservation of the parity in β- processes. Historically the first experimental confirmation of the violation of parity in β-

processes was made in the experiment of Mrs. Wu [328]. In this experiment the angle distribution between the linear momentum $\vec{k}$ of electron and the nucleus total angular momentum in the β- decay of ^{60}Co was analyzed. A change of this angle distribution was detected if the orientation of the nucleus angular momentum was reversed. It means that the scalar product of the total nucleus angular momentum and the electron linear momentum is not preserved during the inversion of the frame axes (parity transformation). By other words it means that there should be terms in the β- interaction Hamiltonian which changes the sign during the parity transformation. Such parity violating terms are expressed in the interaction Lagrangian (10.69) by terms involving $\alpha_j \, \gamma^5$ $(j = V, A)$.

In this subsection we will concentrate to other quantity providing information on the violation of the parity in β- process, namely the helicity of electrons in the case when the mother nucleus is not oriented. The degree of the longitudinal polarization (helicity) of electrons in β^-- decay is,

$$P_e = \frac{N_r - N_L}{N_R + N_L} \tag{10.71}$$

where N_R and N_L denotes the number of electrons with positive (right handed electrons) and negative (left handed electrons) helicity.

From theoretical point of view the longitudinal polarization P_e for given energy E_e of emitted electrons can be determined as,

$$P_e = \frac{d\Gamma_R(E_e) - \Gamma_L(E_e)}{d\Gamma_R(E_e) + \Gamma_L(E_e)} \tag{10.72}$$

where $d\Gamma_R(E_e)$ and $d\Gamma_L(E_e)$ is the β^-- decay probability per sec. when the electron with the energy in the dE_e vicinity of E_e is emitted with positive helicity (right handed electrons) and negative helicity (left handed electrons), respectively. The helicity of electron is defined as the projection of the electron spin onto the direction of the electron linear momentum,

$$\hat{h} \equiv \frac{\hat{\vec{\Sigma}} \cdot \hat{\vec{k}}}{|\vec{k}|} \tag{10.73}$$

where the spin of the electron is given by the spin operator acting in the space of bispinors (see (10.34)),

$$\hat{\vec{s}} = \frac{1}{2}\hat{\vec{\Sigma}} = \frac{1}{2}\begin{pmatrix} \vec{\sigma} & 0 \\ 0 & \vec{\sigma} \end{pmatrix} \tag{10.74}$$

Derivation of the P_e defined by (10.72) is beyond the scope of this textbook (for detailed derivation see e.g. [256, 147]). Here we present only resultant expressions. In the case of the pure Fermi β- decay of neutron, when only vector coupling is acting the polarization P_e is,

$$P_e^{(V)} = -\frac{2\,\alpha_V}{1+\alpha_V^2}\,\beta_e \tag{10.75}$$

and in the case of the pure GM transition the polarization P_e is given only by the axial vector term in the β^- Lagrangian,

$$P_e^{(A)} = -\frac{2\,\alpha_A}{1+\alpha_A^2}\,\beta_e \tag{10.76}$$

If the both types of β^-- decay (Fermi as well as Gammow-Teller) are present (as in the case of the neutron decay) then the polarization $P_e^{(V,A)}$ is (see [256])

$$P_e^{(V,A)} = -\,\beta_e\,\frac{2\,\alpha_V\,C_V^2 + 2\,\alpha_A\,3\,C_A^2}{(1+\alpha_V^2)\,C_V^2 + (1+\alpha_A^2)\,3\,C_A^2} \tag{10.77}$$

It should be noted that expressions (10.75), (10.76) and (10.77) derived in [256] for free neutron decay valid in principle also for β^- decay of any nucleus. Various experiments with different types of β^-- decay where the helicity of emitted electrons were measured, showed that always electron longitudinal polarization is ($\beta_e = v_e$ in the $\hbar = c = 1$ convention used in this chapter)

$$P_e^{(exp)} = -\beta_e \tag{10.78}$$

If we want to obtain this value from theoretical expressions (10.75), (10.76) and (10.77) we should take

$$\alpha_V = \alpha_A = 1 \tag{10.79}$$

The substitution of (10.79) into (10.69) gives the interaction Lagrangian density of the β^- decay of neutron in the following form

$$\begin{aligned}
\hat{\mathcal{L}}_{int}^{(\beta^-)}(x) = & \\
&= C_V\,\left[\hat{\bar{\psi}}_p(x)\,\gamma_\mu\,\hat{\psi}_n(x)\right]\,\left[\hat{\bar{\psi}}_e(x)\,(1+\gamma^5)\,\gamma^\mu\,\hat{\psi}_{\tilde{\nu}}(x)\right] + \\
&\quad + C_A\,\left[\hat{\bar{\psi}}_p(x)\,\gamma_5\gamma_\mu\,\hat{\psi}_n(x)\right]\,\left[\hat{\bar{\psi}}_e(x)\,(1+\gamma^5)\,\gamma_5\,\gamma^\mu\,\hat{\psi}_{\tilde{\nu}}(x)\right] = \\
&= \boxed{\begin{array}{c}\text{because}\\ \gamma_5^2 = 1\end{array}} = \\
&= C_V\,\left[\hat{\bar{\psi}}_p(x)\,\gamma_\mu\,\hat{\psi}_n(x)\right]\,\left[\hat{\bar{\psi}}_e(x)\,(1+\gamma^5)\,\gamma^\mu\,\hat{\psi}_{\tilde{\nu}}(x)\right] + \\
&\quad + C_A\,\left[\hat{\bar{\psi}}_p(x)\,\gamma_5\gamma_\mu\,\hat{\psi}_n(x)\right]\,\left[\hat{\bar{\psi}}_e(x)\,(1+\gamma^5)\,\gamma^\mu\,\hat{\psi}_{\tilde{\nu}}(x)\right]
\end{aligned} \tag{10.80}$$

Similarly we can obtain the Lagrangian density for β^+ process $p \to n + e^+ + \nu_e$ (which has not yet been observed)

$$\begin{aligned}\hat{\mathcal{L}}_{int}^{(\beta^+)}(x) = \\ = C_V \left[\hat{\bar{\psi}}_n(x)\, \gamma_\mu\, \hat{\psi}_p(x)\right] \left[\hat{\bar{\psi}}_\nu(x)\, (1+\gamma^5)\, \gamma^\mu\, \hat{\psi}_e(x)\right] + \\ + C_A \left[\hat{\bar{\psi}}_n(x)\, \gamma_5 \gamma_\mu\, \hat{\psi}_p(x)\right] \left[\hat{\bar{\psi}}_\nu(x)\, (1+\gamma^5)\, \gamma^\mu\, \hat{\psi}_e(x)\right]\end{aligned} \tag{10.81}$$

Corresponding Feynman amplitudes are (here there is not present the non-relativistic approximation for nucleus - see (10.70))

$$\begin{aligned}\mathcal{M}_{fi}^{(1)(\beta^-)} = \\ = C_V \left[\bar{u}_{p;\,r'}(\vec{p})\, \gamma_\mu\ u_{n;\,r}(\vec{P})\right] \left[\bar{u}_{e;\,s}(\vec{k})\, \gamma^\mu\, (1-\gamma^5)\, v_{\tilde{\nu};\,s'}(\vec{k}')\right] + \\ + C_A \left[\bar{u}_{p;\,r'}(\vec{p})\, \gamma_5\, \gamma_\mu\, u_{n;\,r}(\vec{P})\right] \left[\bar{u}_{e;\,s}(\vec{k})\, \gamma^\mu\, (1-\gamma^5)\, v_{\tilde{\nu};\,s'}(\vec{k}')\right]\end{aligned} \tag{10.82}$$

for the process $n \to p + e^- + \tilde{\nu}_e$, and

$$\begin{aligned}\mathcal{M}_{fi}^{(1)(\beta^+)} = \\ = C_V \left[\bar{u}_{n;\,r}(\vec{P})\, \gamma_\mu\, u_{p;\,r'}(\vec{p})\right] \left[\bar{u}_{\nu;\,s'}(\vec{k}')\, (1+\gamma^5)\, \gamma^\mu\ v_{e;\,s'}(\vec{k}')\right] + \\ + C_A \left[\bar{u}_{n;\,r}(\vec{P})\, \gamma_5\, \gamma_\mu\, u_{p;\,r'}(\vec{p})\right] \left[\bar{u}_{\nu;\,s'}(\vec{k}')\, (1+\gamma^5)\, \gamma^\mu\ v_{e;\,s}(\vec{k}')\right]\end{aligned} \tag{10.83}$$

for the process $p \to n + e^+ + \nu_e$.

From (10.82) and (10.83) the well known fact follows that in β^- decay only right handed antineutrina with positive helicity can be produced and in the β^+ decay only left handed neutrina with negative helicity are created. This is because the quantum field theory gives the projection operator onto the positive helicity (right handed) as $\frac{1}{2}(1+\gamma_5)$ and onto negative helicity (left handed) in the form $\frac{1}{2}(1-\gamma_5)$ for particles without mass (with bispinors

$u(\vec{k})$) and opposite for massless antiparicles $v(\vec{k})$ - see [13] [5],

$$\begin{aligned} u_L \equiv \frac{1-\gamma_5}{2}\, u \quad &\Rightarrow \quad \bar{u}_L = \bar{u}\, \frac{1+\gamma_5}{2} \quad \Rightarrow \quad \bar{u}_L\,(1+\gamma_5) \neq 0 \\ u_R \equiv \frac{1+\gamma_5}{2}\, u \quad &\Rightarrow \quad \bar{u}_R = \bar{u}\, \frac{1-\gamma_5}{2} \quad \Rightarrow \quad \bar{u}_L\,(1+\gamma_5) = 0 \end{aligned} \tag{10.84}$$

$$\begin{aligned} v_L \equiv \frac{1+\gamma_5}{2}\, v \quad &\Rightarrow \quad (1-\gamma_5)\, v_L = 0 \\ v_R \equiv \frac{1-\gamma_5}{2}\, v \quad &\Rightarrow \quad (1-\gamma_5)\, v_R \neq 0 \end{aligned} \tag{10.85}$$

and really from (10.84) and (10.82) follows that in the β^- decay only right handed antineutrina survives ($v_{\tilde{\nu},s'}(\vec{k}') = v_R(\vec{k}')$) and in the β^+ decay (see (10.85), (10.83)) only left handed neutrina are produced ($v_{\nu,s'}(\vec{k}') = v_L(\vec{k}')$) [256, 13].

10.4.4 V - A coupling constants C_A and C_V

Using facts about parameters of β process Lagrangian discussed in previous subsections, namely $C_S = C_T = 0$ (see (10.68)) and $\alpha_V = \alpha_A = 1$ (see (10.79)) the total amplitude (10.46) of β^- decay of neutron (with nucleon non-relativistic approximation) is given by

$$\begin{aligned} &\left|\bar{\mathcal{M}}_{fi}\right|^2 = \left|\bar{\mathcal{M}}^{(V)}_{fi}\right|^2 + \left|\bar{\mathcal{M}}^{(A)}_{fi}\right|^2 = \\ &= 32\, M^2\, E_e\, E_{\tilde{\nu}}\, C_V^2\, (1+\beta_e\, cos\vartheta) + 32\, M^2\, E_e\, E_{\tilde{\nu}}\, 3\, C_A^2\, (1-\frac{1}{3}\beta_e\, cos\vartheta) = \\ &= 32\, M^2\, E_e\, E_{\tilde{\nu}}\, \left(C_V^2 + 3\, C_A^2 + (C_V^2 - C_A^2)\, \beta_e\, cos\vartheta\right) \end{aligned} \tag{10.86}$$

So in order to fix amplitude $\bar{\mathcal{M}}_{fi}$ it remains to determine coupling constants C_V and C_A. The relation between C_V and C_A can be obtained from data on the electron-antineutrino angular correlations for mixed F-GT decay. Similarly as we obtained angular distribution probability $\frac{d\Gamma_F}{d\Omega_{\tilde{\nu}}}$ for pure Fermi β-transition (see (10.62)) from the square of the Fermi transition amplitude (10.47) (or (10.64) from (10.48) for pure GT transition) we can determine

[5] In all SM theory discussed in this chapter we suppose that the mass of neutrino and antineutrino is zero. In reality there are strong indications that the mass of neutrinos is nonzero but small. The nowadays upper limit mass for $\tilde{\nu}_e$ was obtained from the Troitzk experiment [329], $m_{\tilde{\nu}_e} < 2.05$ eV. Several new experiments with the intention to obtain lower limit of neutrino mass are in the preparation (e.g. Katrin experiment [330]). The nonzero neutrino mass means a slight modification of the original SM.

angular distribution from the square of the mixed F-GT transition amplitude (10.86),

$$\frac{d\Gamma_F}{d\Omega_{\tilde{\nu}}} \approx const^{'} \left[C_V^2 + 3\,C_A^2 + (C_v^2 - C_A^2)\,\beta_e\,cos\vartheta\right] =$$
$$= const^{'}\,(C_v^2 + 3\,C_A^2)\left[1 + \frac{C_V^2 - C_A^2}{C_V^2 + 3\,C_A^2}\,\beta_e\,cos\vartheta\right] =$$
$$= const\left(1 + a_n\,\beta_e\,cos\vartheta\right) \tag{10.87}$$

with

$$a_n = \frac{1-\lambda^2}{1+3\lambda^2} \quad , \qquad \lambda = \frac{C_A}{C_V} \tag{10.88}$$

where ϑ is the angle between electron linear momentum $\vec{k}$ and antineutrino linear momentum $\vec{k}^{'}$. Experimental value obtained from different β- decays of nuclei gave $|\lambda| = 1.26$. This value was also confirmed by the calculation of the angular distribution between neutron spin (total ang. momentum of the mother nucleus) and the linear momentum $\vec{k}$ of produced electron (for detailed derivation see [256]),

$$\frac{d\Gamma_F^{(theor)}}{d\Omega_{\tilde{\nu}}} \approx const\left(1 + A_n\,\beta_e\,cos\vartheta\right) \tag{10.89}$$

with

$$A_n = 2\,\frac{\lambda - \lambda^2}{1 + 3\,\lambda^2} \tag{10.90}$$

where the experimental neutron spin - electron linear moment angular distribution for the process $n \to p + e^- + \tilde{\nu}_e$ gave again

$$\lambda = \frac{C_A}{C_V} = 1.26 \tag{10.91}$$

Further it was necessary to determine the last remaining undetermined parameter C_V in the β- transition amplitudes (10.82), (10.83) or in corresponding interaction Lagrangians (10.80), (10.81). The value of C_V can be deduced from the experimental value of half-life $T_{1/2}(n) = 613.9\,s$ or life time $\tau_n = 885.7\,s$ of the neutron,

$$T_{1/2}(n) = \frac{ln2}{\Gamma} \quad , \qquad \tau_n = \frac{1}{\Gamma} \tag{10.92}$$

where Γ is total decay probability of the process $n \to p\ + e^- + \tilde{\nu}_e$ with all possible energies, linear momenta and spin indexes of all produced particles.

This total probability can be obtained by the integration of the (10.61) (where $\alpha_V = \alpha_A = 1$ and $C_A = \lambda\, C_V$) over $E_e \in \langle m_e,\, E_e^{max}\rangle$ of all possible energies of produced electron,

$$\begin{aligned}\Gamma &= \int_{m_e}^{E_e^{max}} \frac{d\Gamma(E_e)}{dE_e}\, dE_e = \\ &= \int_{m_e}^{E_e^{max}} \frac{1}{\pi^3}\big[C_V^2 + 3\, C_A^2\big]\, \sqrt{E_e^2 - m_e^2}\, E_e\, \big(E_e^{max} - E_e\big)^2\, dE_e = \\ &= \frac{1}{\pi^3}\, \big(C_V^2 + 3\, C_A^2\big)\, I_f = \frac{C_V^2}{\pi^3}\big(1 + 3\, \lambda^2\big)\, I_f \end{aligned} \tag{10.93}$$

where

$$I_f = \int_{m_e}^{E_e^{max}} \big(E_e^{max} - E_e\big)^2\, \sqrt{E_e^2 - m_e^2}\;\, E_e\; dE_e = \frac{1}{30}\, (E_e^{max})^5\, K \tag{10.94}$$

where $K \approx 0.46$ and $E_e^{max} \approx \Delta m = 1.29\, MeV$ (see (10.11)). Putting these numbers to (10.93) we obtain for the neutron β^- decay the value $\Gamma \approx 6.77 \times 10^{-25}\, MeV$ and according to (10.92) corresponding neutron life-time τ_n is $\tau_n = \Gamma^{-1} \approx 1.48 \times 10^{24}\, MeV^{-1}$. Converting this value to ordinary units (that means multiplying it by $\hbar = 6.58 \times 10^{-22}\, MeV\, s$) one gets finally $\tau_n \approx 974\, s$ which differs a little bit from experimental value 885.7 s.

In more precise calculation of the probability Γ it is necessary to take into account Coulomb interaction of emitted electron and resultant proton. This correction is discussed briefly in the next section and it lead to the additional correction factor function $F(E_e, Z = 1)$ in the (10.93). Resultant corrected expression for Γ is [6] ,

$$\Gamma = \frac{C_V^2}{\pi^3}\big(1 + 3\, \lambda^2\big)\, F(E_e, Z = 1)\, I_f \tag{10.95}$$

The substitution of (10.93), (10.95) to (10.92) for the elementary process $n \to p\, + e^- + \tilde{\nu}_e$ with the neutron experimental time-life $\tau_n = 885.7\, s$ gives for C_V following value [256],

$$C_V \equiv \frac{-G_\beta}{\sqrt{2}} \quad , \qquad G_\beta = 1.136 \times 10^{-5}\, GeV^{-2} \tag{10.96}$$

where G_β are given in the natural system of units. So, now we have all parameters of the β interaction Lagrangian (10.80) responsible for the elementary

[6] Correction factor $F(E_e, Z)$ for Coulomb interaction between daughter nucleus $(Z+1)^{(A)}$ and produced electron e^- in the β^- decay $Z^{(A)} \to (Z+1)^{(A)} + e^- + \tilde{\nu}_e$ is determined from the wave functions of emitted electron ($s-$, $p-$, ... electron wave functions).

neutron β^- decay fixed and final expression is

$$\begin{aligned}
\hat{\mathcal{L}}_{int}^{(\beta^-)}(x) &= C_V \left[\hat{\bar{\psi}}_p(x)\,\gamma_\mu\,\hat{\psi}_n(x)\right]\left[\hat{\bar{\psi}}_e(x)\,(1+\gamma^5)\,\gamma^\mu\,\hat{\psi}_{\tilde{\nu}}(x)\right] + \\
&\quad + C_A \left[\hat{\bar{\psi}}_p(x)\,\gamma_5\gamma_\mu\,\hat{\psi}_n(x)\right]\left[\hat{\bar{\psi}}_e(x)\,(1+\gamma^5)\,\gamma^\mu\,\hat{\psi}_{\tilde{\nu}}(x)\right] = \\
&= \boxed{\begin{array}{c}\text{see}\\(10.88)\end{array}} = \\
&= C_V \left[\hat{\bar{\psi}}_p(x)\,(1+\lambda\,\gamma_5)\,\gamma_\mu\,\hat{\psi}_n(x)\right]\left[\hat{\bar{\psi}}_e(x)\,(1+\gamma^5)\,\gamma^\mu\,\hat{\psi}_{\tilde{\nu}}(x)\right] = \\
&= \boxed{\begin{array}{c}\text{because}\\\{\gamma^\mu\,,\,\gamma_5\} = 0 \text{ and } (10.96)\end{array}} = \\
&= -\frac{G_\beta}{\sqrt{2}}\left[\hat{\bar{\psi}}_p(x)\,\gamma_\mu\,(1-\lambda\,\gamma_5)\,\hat{\psi}_n(x)\right]\left[\hat{\bar{\psi}}_e(x)\,\gamma^\mu\,(1-\gamma^5)\,\hat{\psi}_{\tilde{\nu}}(x)\right]
\end{aligned} \tag{10.97}$$

and corresponding Feynman amplitude (10.82) obtains following form,

$$\begin{aligned}
\mathcal{M}_{fi}^{(1)(\beta^-)} &= \boxed{\begin{array}{c}\text{see}\\(10.82)\end{array}} = \\
&= -\frac{G_\beta}{\sqrt{2}}\left[\bar{u}_{p;\,r'}(\vec{p})\,\gamma_\mu\,(1-\lambda\,\gamma_5)\,u_{n;\,r}(\vec{P})\right]\left[\bar{u}_{e;\,s}(\vec{k})\,\gamma^\mu\,(1-\gamma_5)\,v_{\tilde{\nu}_e;\,s'}(\vec{k'})\right]
\end{aligned} \tag{10.98}$$

and the same coupling constants C_V and C_A should be used for β^+ interaction Lagrangian (10.81) and β^+ Feynman amplitude (10.83) for the process $p \to n + e^+ + \nu_e$.

10.4.5 Comments to the Standard Model of electro-weak interaction

The nowadays Standard Model of electro-weak interaction (SM) operates not only with neutrons and protons (in the hadron sector) and with electrons (positrons) and corresponding electron neutrinos (antineutrinos) (in the lepton sector) but with all possible hadrons and the whole family of leptons (electrons, mions, taons with their antiparticles and corresponding neutrinos). The detailed discussion and derivation of the SM is beyond the scope of this book and it can be found in many textbooks (see e.g. [256, 13]). However in order to give a link between the theory of β processes in nuclei and

the SM some basic features of the SM are breafly listed in this subsection without and derivations.

The coupling constant G_β (or C_V - see (10.95)) determined from the nuclear $\beta^\pm$ decays is a little bit different from the universal constant G_F of weak interaction introduced by R. Feynman and M. Gell-Mann in [331] where they posited the density of the weak interaction Lagrangian in the form of the product of two currents,

$$\hat{\mathcal{L}}^{(w)}_{int}(x) = -\frac{G_F}{\sqrt{2}}\, \hat{J}^\rho(x)\hat{J}^+_\rho(x) \tag{10.99}$$

where so called weak current $\hat{J}^\rho(x)$ consists from the lepton and hadron parts,

$$\begin{aligned}\hat{J}^\rho(x) \;&=\; \hat{J}^\rho_{lepton}(x) + \hat{J}^\rho_{hadron}(x) = \\ &= \hat{\bar{\psi}}_{\nu_e}(x)\,\gamma^\rho\,(1-\gamma_5)\,\hat{\psi}_e(x) \;+\; \hat{\bar{\psi}}_{\nu_\mu}(x)\,\gamma^\rho\,(1-\gamma_5)\,\hat{\psi}_\mu(x) + \\ &\quad +\; \hat{\bar{\psi}}_{\nu_\tau}(x)\,\gamma^\rho\,(1-\gamma_5)\,\hat{\psi}_\tau(x) +\; \hat{J}^\rho_{hadron}(x)\end{aligned} \tag{10.100}$$

where lepton part is formed by electron, mion and taon contributions. It is assumed that the hadron part of the current $\hat{J}^\rho_{hadron}(x)$ has also V-A structure from the point of view of the Lorentz transformation but it is not necessary to express it by means of the field operators of physical hadrons (because of the complex structure of hadrons). It is only supposed that $\hat{J}^\rho_{hadron}(x)$ is an operator which has non-trivial matrix elements between the physical hadron states. In fact the $\hat{J}^\rho_{hadron}(x)$ represents a phenomenological tool which enables to avoid complex theories of hadron sector of the SM (e.g. QCD). It is evident that using different combinations of lepton and hadron parts in both currents in (10.99) we can describe different weak processes - see two examples below,

- neutron β^- decay is described by the interaction Lagrangian (10.99) with the hadron part $\approx \hat{\bar{\psi}}_p(x)\,\gamma^\mu\,(1-\lambda\,\gamma_5)\,\hat{\psi}_\mu(x)$ and it does not involve any terms $\hat{J}^\rho_{hadron}(x)\;\hat{J}^+_{\rho\,hadron}(x)$ and $\hat{J}^\rho_{lepton}(x)\;\hat{J}^+_{\rho\,lepton}(x)$;
- other example is the pure weak decay of mion, $\mu^- \to e^- + \tilde{\nu}_e + \nu_\mu$, where in the interaction Lagrangian the hadron part is missing entirely.

One can expect that the most clear way how to determine the coupling constant G_F is to use the pure weak process where the hadron current is not present at all, e.g. from the mion decay $\mu \to e^- + \tilde{\nu}_e + \nu_\mu$. From the measured life-time of mion ($\tau_\mu = 2.2 \times 10^{-6}$s) the following value of G_F was

deduced,

$$\begin{aligned} G_F &= 1.166 \times 10^{-5} \quad GeV^{-2} \qquad \text{(in natural system of units)} \\ G_F &= 8.685 \times 10^{-5}\, MeV\, fm^3 \qquad \text{(in standard system of units)} \end{aligned} \tag{10.101}$$

The relation between G_F (see (10.101)) and G_β (see (10.96)) is characterized by the Cabbibo angle Θ_C,

$$\frac{G_\beta}{G_F} = cos\Theta_C \quad \Rightarrow \qquad \Theta_C = 13^o \tag{10.102}$$

The Cabbibo angle is related to the decomposition of the hadron current to part preserving the strangeness ($\Delta S = 0$) and part non-preserving the strangeness ($\Delta S \neq 0$) (see e.g. [13, 256]),

$$J_{\rho\, hadron}(x) = J_\rho^{(\Delta S=0)}\, cos\Theta_C + J_\rho^{(\Delta S\neq 0)} sin\Theta_C \tag{10.103}$$

If the quark structure of nucleons is taken into account (see Table 3.6 in the Subsection 3.1.3.2),

$$p = uud \qquad , \qquad n = udd \tag{10.104}$$

then

$$p = \hat{t}_-\, n \qquad \Leftrightarrow \qquad u = \hat{t}_-\, d \tag{10.105}$$

The introduction of the Cabbibo angle Θ_C is connected with the fact that in the SM instead of the quark d we have a mixture of quark d and the strange quark s,

$$d \qquad \rightarrow \qquad d\, cos\Theta_C + s\, sin\Theta_C \tag{10.106}$$

where s is the strange quark with the strangeness 1 (see the Table 3.6 and [256, 13]). In the case of the β^- decay of neutrons (where interaction Lagrangian is given by (10.97)) the hadron current is represented by,

$$\hat{J}^\rho_{hadron}(x) \;\approx\; \bar{\psi}_p(x)\, \gamma^\rho \left(1 - \lambda\, \gamma_5\right) \hat{\psi}_n(x) \tag{10.107}$$

This hadron current can be rewritten within the isospin formalism as follows

$$\hat{J}^\rho_{hadron}(x) \;\approx\; \bar{\psi}_f(x)\, \gamma^\rho \left(1 - \lambda\, \gamma_5\right) \hat{t}_-\, \hat{\psi}_i(x) \tag{10.108}$$

where $\hat{t}_-$ is the step-down single-particle operator acting in the isospin part of the configuration space ($\psi_p(x) = \hat{t}_-\, \psi_n(x)$, $\hat{t}_-\, \psi_p(x) = 0$ - see (1.17) [7]) and $\psi_i(x)$ and $\psi_f(x)$ are general single-particle nucleon bispinor functions (or operators after the quantization procedure).

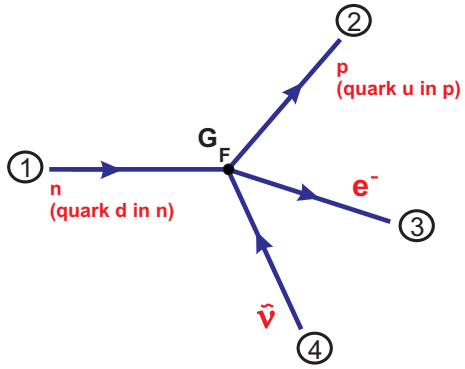


Figure 10.3: β- decay of neutron with the contact interaction (10.97).

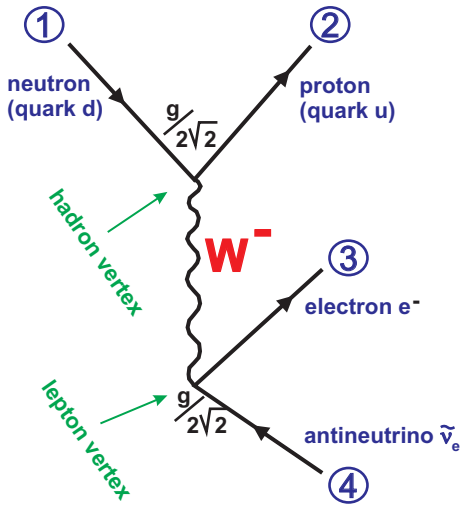


Figure 10.4: β- decay of neutron with the exchange of W^-,

In the SM the lowest order transition β^- amplitudes with the contact V-A interaction with the Lagrangian density (10.97), demonstrated by the schematic figure Fig. 10.4, can be explained as the exchange of vector bosons $W^{\pm}$. Corresponding lowest order Feynman diagram is shown in the Fig. 10.4. Each lepton vertex in all such Feynman diagrams with 3 lines going to or from given vertex reprents part of the transition amplitude corresponding to the general elementary β interaction Lagrangian,

$$\hat{\mathcal{L}}_{int}^{(gen,\beta)}(x) = -\frac{g}{2\sqrt{2}}\,\hat{\bar{\psi}}_l(x)\,\gamma^\mu\,\left(1-\gamma_5\right)\,\hat{\psi}_{\nu_l}(x)\,\hat{W}_\mu^+(x)\;+\;h.c. \qquad (10.109)$$

where $l = electron,\ mion,\ taon.$ In (10.109) g is the universal weak interaction coupling constant. This weak interaction Lagrangian is analo-

[7]One should have in mind that in the nuclear physics the isospin of nucleons introduced by (1.17) is opposite to one used in the particle physics, where $|p\rangle = \hat{t}_+\,|n\rangle$. That means if we use particle physics convention then we should substitute $\hat{t}_-$ operator by $\hat{t}_+$ operator in all expressions in this textbook.

gous to the elementary electromagnetic interaction Lagrangian $\hat{\mathcal{L}}_{int}^{(el.mag.)}(x) = -e\,\hat{\bar{\psi}}_1(x)\,\gamma^\mu\,\hat{\psi}_2(x)\,A_\mu(x)$ where $\psi_1(x)$ and $\psi_2(x)$ are bispinor functions (or field operators after the quantization) of 2 Dirac particles interacting through the exchange of photon with electromagnetic four- potential $A_\mu(x)$ $(\mu = 0, 1, 2, 3)$.

In the original theory of weak interaction based on the exchange of vector bosons $W^\pm$ (so called intermediate vector boson theory) only charged vector bosons participated (see also the SU(2) gauge invariant theory of weak interaction). Later, in the connection with the extension of the weak interaction theory to be invariant with respect to the combined SU(2) × U(1) gauge transformation, it was shown that besides charged vector bosons $W^\pm$ connected with the charged weak currents $\bar{\psi}_l\,\gamma^\mu(1-\gamma_5)\,\psi_{\tilde{\nu}_l}$ also neutral vector bosons Z^0 exist which are connected with the neutral currents in the Lagrangian density [256, 13],

$$\hat{\bar{\psi}}_{\nu_e}(x)\,\gamma^\mu\left(1-\gamma_5\right)\hat{\psi}_{\nu_e}(x)$$
$$\text{or generally}\quad \hat{\bar{\psi}}_l(x)\,\gamma^\mu\left(1-4\,sin^2\Theta_W-\gamma_5\right)\hat{\psi}_{l'}(x) \tag{10.110}$$

where $\hat{\psi}_l(x)$ and $\hat{\psi}_{l'}(x)$ are general bispinor functions (field operators) with $l, l^{'} = e, \mu, \tau, \nu_e, \nu_\mu, \nu_\tau$. In (10.110) Θ_W represents so called Weinberg angle. The value of this angle obtained from different experiments is $\Theta_W \approx 28.4^o$. The non-zero value of Θ_W lead to the unification of the weak and electromagnetic interaction (e.g. [256, 13]) provided,

$$g\,sin\Theta_W = e \tag{10.111}$$

where g is the strength constant in the universal weak interaction Lagrangian (10.109). Taking into account (10.111), (10.110) and arguments discussed above the elementary universal weak interaction Lagrangian corresponding to one lepton vertex in Feynman diagrams in electro-weak SM theory is

$$\hat{\mathcal{L}}_{int}^{(weak)}(x) = -\frac{e}{2\sqrt{2}\,sin\theta_W}\sum_{l=e,\,\mu,\,\tau}\hat{\bar{\psi}}_l(x)\,\gamma^\mu\,(1-\gamma_5)\,\hat{\psi}_{\tilde{\nu}_l}(x)\,\hat{W}_\mu^+(x) +$$
$$+\,h.c.\,+\,\text{terms with the the neutral vector meson } Z^0 \text{ exchange} \tag{10.112}$$

where $\hat{W}_\mu^\pm(x)$ $(\mu = 0, 1, 2, 3)$ is the fields operator of the charged vector meson $W^\pm$.

As it was already mentioned the β decay strength constant $G_\beta = G_F cos\Theta_C$ (see (10.102)) was obtained from measuring of the life-time of mion $(\mu^- \rightarrow$

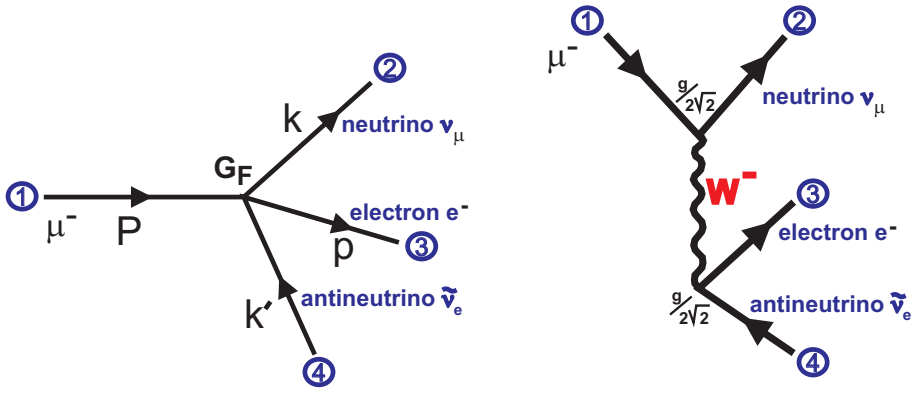


Figure 10.5: The lowest order of the transition amplitude β decay of mion with the exchange of intermediate vector boson W^- (right diagram) and the lowest order amplitude of the β decay of mion ($\mu^- \to e^- + \nu_\mu + \tilde{\nu}_e$) described by the contact interaction Lagrangian $\hat{\mathcal{L}}^{(\beta^-)}_{int}(x) = G_F \left[\hat{\bar{\psi}}_{\nu_\mu}(x)\,\gamma_\mu\,(1-\lambda\,\gamma_5)\,\hat{\psi}_\mu(x)\right]\left[\hat{\bar{\psi}}_e(x)\,\gamma^\mu\,(1-\gamma^5)\,\hat{\psi}_{\tilde{\nu}}(x)\right]$ (left diagram).

$e^- + \nu_\mu + \tilde{\nu}_e$) with the transition amplitude corresponding to the Feynman diagrams demonstrated in the Fig.10.5, right diagram corresponds to the lowest order (2-d order) transition amplitude with the interaction Lagrangian (10.112) and the left diagram shows the the first order transition amplitude of the same process with the contact interaction Lagrangian $\hat{\mathcal{L}}^{(\beta^-)}_{int}(x) = G_F \left[\hat{\bar{\psi}}_{\nu_\mu}(x)\,\gamma_\mu\,(1-\lambda\,\gamma_5)\,\hat{\psi}_\mu(x)\right]\left[\hat{\bar{\psi}}_e(x)\,\gamma^\mu\,(1-\gamma^5)\,\hat{\psi}_{\tilde{\nu}}(x)\right]$. Since both diagrams in the Fig.10.5 concern the same process (β^- decay of mion) we can compare corresponding transition amplitudes and this comparison gives for coupling constants G_F and g,

$$\frac{G_F}{\sqrt{2}} = \left(\frac{g}{m_W\,2\,\sqrt{2}}\right)^2 = \boxed{\begin{array}{c}\text{see}\\(10.111)\end{array}} = \frac{e^2}{8\,m_W^2\,sin^2\Theta_W}$$

$$\Rightarrow \boxed{\begin{array}{c}\text{see}\\(10.102)\end{array}} \Rightarrow \qquad G_\beta = \sqrt{2}\,\frac{e^2\,cos\Theta_C}{8\,m_W^2\,sin^2\Theta_W} \qquad (10.113)$$

where the mass of exchanged intermediate boson W appears in (10.113) because of the meson propagator in the right diagram in the Fig.10.5. From experimental values of coupling constants G_F and G_β (see (10.101) and (10.96)) and from (10.113) the mass m_W of intermediate vector boson W was estimated,

$$m_W \approx 90\,GeV \qquad (10.114)$$

More precise values for intermediate boson masses obtained from different

experiments are

$$m_{Z^0} = 91.2\, GeV \qquad m_W = 80.4\, GeV \tag{10.115}$$

As it was mentioned in the beginning of this subsection only brief outlook of the SM was presented. Detailed explanation can be found in many textbooks (see e.g. [256, 13]).

10.5 β- processes in nuclei

Amplitude (10.98) is concerned with the elementary β^- decay of the free neutron. In the case of the β^- decay of a nucleus an arbitrary neutron in the nucleus can undergo such elementary β^- decay. The answer to the question which of neutrons participates in the nucleus β^- decay and what is the probability of this nuclear β^- decay depends on the wave function of the initial state of the mother nucleus. In this section the incorporation of nuclear degrees of freedom into the elementary β decay probability is discussed in details.

10.5.1 Nuclear matrix element of β- interaction Hamiltonian

In order to take into account nuclear wave functions in the β - decay of the nucleus we again start with the density (10.97) of the β^- decay interaction Hamiltonian of the elementary process $n \to p + e^- + \tilde{\nu}_e$,

$$\begin{aligned} &\hat{\mathcal{H}}^{\beta^-}_{int}(x) = -\hat{\mathcal{L}}^{\beta^-}_{int}(x) = \\ &= \frac{G_\beta}{\sqrt{2}} \left[\hat{\bar{\psi}}_p(x)\, \gamma_\mu\, (1 - \lambda\, \gamma_5)\, \hat{\psi}_n(x)\right] \left[\hat{\bar{\psi}}_e(x)\, \gamma^\mu\, (1 - \gamma^5)\, \hat{\psi}_{\tilde{\nu}}(x)\right] \end{aligned} \tag{10.116}$$

where Dirac field operators $\hat{\bar{\psi}}_p(x)$, $\hat{\psi}_n(x)$, $\hat{\bar{\psi}}_e(x)$ and $\hat{\psi}_{\tilde{\nu}}(x)$ are given by corresponding plane wave decompositions (P.6) (see also [13])

$$\hat{\bar{\psi}}_p(x) = \sum_{r_p} \int \frac{d^3 k_p}{(2\pi)^{3/2}\, \sqrt{2E_p}}\; a^+_p(r_p\,, \vec{k}_p)\; e^{i\, k_p\, x}\; \bar{u}_p(r_p\,, \vec{k}_p) \tag{10.117a}$$

$$\hat{\psi}_n(x) = \sum_{r_n} \int \frac{d^3k_n}{(2\pi)^{3/2}\,\sqrt{2E_n}}\; a_n(r_n\,,\vec{k}_n)\; e^{-\,i\,k_n\,x}\; u_n(r_n\,,\vec{k}_n) \qquad (10.117b)$$

$$\hat{\bar{\psi}}_e(x) = \sum_{s_e} \int \frac{d^3k_e}{(2\pi)^{3/2}\,\sqrt{2E_e}}\; b_e^+(s_e,\vec{k}_e)\; e^{i\,k_e\,x}\; \bar{u}_e(s_e,\vec{k}_e) \qquad (10.117c)$$

$$\hat{\psi}_{\tilde{\nu}}(x) = \sum_{s_{\tilde{\nu}}} \int \frac{d^3k_{\tilde{\nu}}}{(2\pi)^{3/2}\,\sqrt{2E_{\tilde{\nu}}}}\; d_{\tilde{\nu}}^+(s_{\tilde{\nu}},\vec{k}_{\tilde{\nu}})\; e^{i\,k_{\tilde{\nu}}\,x}\; \bar{v}_{\tilde{\nu}}(s_{\tilde{\nu}},\vec{k}_{\tilde{\nu}}) \qquad (10.117d)$$

where $a_p^+(r_p,\vec{k}_p)$ is the creation operator of the final proton with the spin state r_p and linear momentum $\vec{k}_p$, and similarly for annihilation operator $a_n(r_n,\vec{k}_n)$ of the initial neutron, creation operator $b_e^+(s_e,\vec{k}_e)$ of the final electron, and creation operator $d_{\tilde{\nu}}^+(s_{\tilde{\nu}},\vec{k}_{\tilde{\nu}})$ of the final electron-antineutrino. The initial state is given by the neutron state with spin state r_n and linear momentum $\vec{k}_n$

$$|\,i\rangle = |n(\vec{k}_n,r_n)\rangle = a_n^+(r_n,\vec{k}_n)\,|-\rangle \qquad (10.118)$$

and in the final state there are proton, electron and electron antineutrino,

$$\begin{aligned} |\,f\rangle &= |\,p(\vec{k}_p,\;r_p),\;e(\vec{k}_e,\;s_e),\;\tilde{\nu}(\vec{k}_{\tilde{\nu}},\;s_{\tilde{\nu}})\rangle = \\ &= a_p^+(r_p,\vec{k}_p)\,b_e^+(s_e,\vec{k}_e)\,d_{\tilde{\nu}}^+(s_{\tilde{\nu}},\vec{k}_{\tilde{\nu}})\,|-\rangle \end{aligned} \qquad (10.119)$$

The Hamiltonian density (10.116) corresponds to the contact interaction with the following transition matrix element of the transition Hamiltonian

$$\langle f|\,\hat{H}_{int}^{\beta^-}(t)\,|i\rangle = \int d^3x\,\langle -|\,d_{\tilde{\nu}}(s_{\tilde{\nu}},\vec{k}_{\tilde{\nu}})\,b_e(s_e,\vec{k}_e)\,a_p(r_p,\vec{k}_p)\,\times$$
$$\frac{G_\beta}{\sqrt{2}}\left[\hat{\bar{\psi}}_p(x)\,\gamma_\mu\,(1-\lambda\,\gamma_5)\,\hat{\psi}_n(x)\right]\left[\hat{\bar{\psi}}_e(x)\,\gamma^\mu\,(1-\gamma^5)\,\hat{\psi}_{\tilde{\nu}}(x)\right]a_n^+(r_n,\vec{k}_n)\,|-\rangle =$$

$$= \boxed{\begin{array}{c}\text{see}\\(10.117)\end{array}} =$$

$$= \frac{1}{(2\pi)^6}\frac{1}{(2E_n\,2E_p\,2E_e\,2E_{\tilde{\nu}})^{1/2}}\,\frac{G_\beta}{\sqrt{2}}\,e^{i\,(E_p+E_e+E_{\tilde{\nu}}-E_n)\,t}\;\times$$
$$\times\int d^3x\,e^{i\,(\vec{k}_n-\vec{k}_p-\vec{k}_e-\vec{k}_{\tilde{\nu}})\,\vec{x}}\left[\bar{u}_p(r_p,\vec{k}_p)\,\gamma_\mu(1-\lambda\gamma_5)\,u_n(r_n,\vec{k}_n)\right]\;\times$$
$$\times\left[\bar{u}_e(s_e,\vec{k}_e)\gamma^\mu(1-\gamma_5)\,v_{\tilde{\nu}}(s_{\tilde{\nu}},\vec{k}_{\tilde{\nu}})\right]\;=$$

$$= \boxed{\begin{array}{c}\text{we suppose neutron rest frame } \vec{k}_n = 0, \\ \text{the recoil of the final proton is neglibible in} \\ \text{the neutron frame and } \vec{q} \equiv \vec{k}_e + \vec{k}_{\tilde{\nu}} = \vec{k}_n - \vec{k}_p\end{array}} =$$

$$= \frac{1}{(2\pi)^6} \frac{1}{2M\ (2E_e\ 2E_{\tilde{\nu}})^{1/2}} \frac{G_\beta}{\sqrt{2}}\, e^{i\,(E_e+E_{\tilde{\nu}})\,t}\ \times$$
$$\times \int d^3x\, e^{i\,(\vec{k}_n-\vec{k}_p)\cdot\vec{x}} \left[\bar{u}_p(r_p,\vec{k}_p)\ \gamma_\mu(1-\lambda\gamma_5)\ u_n(r_n,\vec{k}_n)\right]\ \times$$
$$\times\left[\bar{u}_e(s_e,\vec{k}_e)\gamma^\mu(1-\gamma_5)\ v_{\tilde{\nu}}(s_{\tilde{\nu}},\vec{k}_{\tilde{\nu}})\right] e^{-i\,\vec{q}\cdot\vec{x}} =$$

$$= \boxed{\begin{array}{c}\text{see} \\ (P.8)\end{array}} =$$

$$= \frac{G_\beta}{\sqrt{2}}\, e^{i\,(E_e+E_{\tilde{\nu}})\,t} \int d^3x$$
$$\frac{\chi^+_{p;\,r_p}\, e^{-i\vec{k}_p\cdot\vec{x}}}{(2\pi)^{3/2}} \begin{pmatrix} 1 & \frac{\vec{\sigma}\cdot\vec{k}_p}{2M}\end{pmatrix} \begin{pmatrix} 1 & 0 \\ 0 & -1\end{pmatrix} \gamma_\mu\ (1-\lambda\gamma_5) \begin{pmatrix} 1 \\ \frac{\vec{\sigma}\cdot\vec{k}_n}{2M}\end{pmatrix} \frac{\chi_{n;\,r_n}\, e^{i\,\vec{k}_n\cdot\vec{x}}}{(2\pi)^{3/2}}$$
$$\frac{1}{(2\pi)^3} \frac{1}{\sqrt{2E_e 2E_{\tilde{\nu}}}} \left[\bar{u}_e(s_e,\vec{k}_e)\ \gamma^\mu\ (1-\gamma_5)\ v_{\tilde{\nu}}(s_{\tilde{\nu}},\vec{k}_{\tilde{\nu}})\right] e^{-i\,\vec{q}\cdot\vec{x}} \tag{10.120}$$

The expression in the last but one row in (10.120) can be considered as the matrix element of the nuclear four- current, $\hat{J}^{(nuc)}_\mu = \hat{J}^{(V)}_\mu + \hat{J}^{(A)}_\mu$ ($\mu = 0, 1, 2, 3$), between proton and neutron plane waves,

$$\hat{J}^{(V)}_\mu = \begin{pmatrix} 1 & \frac{\vec{\sigma}\cdot\overleftarrow{k}_p}{2M}\end{pmatrix} \begin{pmatrix} 1 & 0 \\ 0 & -1\end{pmatrix} \gamma_\mu \begin{pmatrix} 1 \\ \frac{\vec{\sigma}\cdot\hat{\vec{k}}_n}{2M}\end{pmatrix} \tag{10.121a}$$

$$\hat{J}^{(A)}_\mu = -\lambda \begin{pmatrix} 1 & \frac{\vec{\sigma}\cdot\overleftarrow{k}_p}{2M}\end{pmatrix} \begin{pmatrix} 1 & 0 \\ 0 & -1\end{pmatrix} \gamma_\mu\,\gamma_5 \begin{pmatrix} 1 \\ \frac{\vec{\sigma}\cdot\hat{\vec{k}}_n}{2M}\end{pmatrix} \tag{10.121b}$$

where $\hat{J}^{(V)}_\mu$ is the operator of the μ-th component of the vector nucleon current and $\hat{J}^{(A)}_\mu$ represents the operator of the μ-th component of the axial vector current (the operator $\hat{\vec{k}}_n = -i\hbar\vec{\nabla}_n$ acts on the right direction on the neutron

wave function and the operator $\overleftarrow{k}_p = -i\hbar\overleftarrow{\nabla}_p$ acts on the left direction on the proton wave function. So the expr. (10.120) reads [8]

$$\begin{aligned}\langle f|\,\hat{H}^{(\beta)}_{int}(t)\,|i\rangle &= \\ &= \frac{G_\beta}{\sqrt{2}} e^{i\,(E_e+E_{\tilde\nu})\,t}\int d^3x\;\varphi^*_p(\vec{x},r_p)\,\left(\hat{J}^{(V)}_\mu+\hat{J}^{(A)}_\mu\right)\varphi_n(\vec{x},r_n)\,\times \\ &\quad\times\frac{1}{(2\pi)^3}\frac{1}{\sqrt{2E_e\;2E_{\tilde\nu}}}\left[\;\bar{u}_e(s_e,\vec{k}_e)\,\gamma^\mu\,(1-\gamma_5)\;\;v_{\tilde\nu}(s_{\tilde\nu},\vec{k}_{\tilde\nu})\;\right]e^{-i\,\vec{q}\cdot\,\vec{x}}\end{aligned} \tag{10.122}$$

where

$$\varphi_p(\vec{x},r_p)=\frac{1}{(2\pi)^{3/2}}\,e^{i\,\vec{k}_p\cdot\,\vec{x}}\,\chi_{r_p}\quad,\quad\varphi_n(\vec{x},r_n)=\frac{1}{(2\pi)^{3/2}}\,e^{i\,\vec{k}_n\cdot\,\vec{x}}\,\chi_{r_n} \tag{10.123}$$

are wave functions of proton and neutron, respectively (here in the form of plane wave functions). The last row in (10.122) represents the lepton flow in the elementary process $n\to p+e^-+\tilde\nu_e$ caused by the final electron and final electron neutrino.

Further we express vector and axial-vector currents (10.121) in components,

$$\begin{aligned}\hat{J}^{(V)\,0} &= \begin{pmatrix}1 & \frac{\vec\sigma\cdot\overleftarrow{k}_p}{2M}\end{pmatrix}\begin{pmatrix}1&0\\0&-1\end{pmatrix}\begin{pmatrix}1&0\\0&-1\end{pmatrix}\begin{pmatrix}1\\ \frac{\vec\sigma\cdot\hat{\vec k}_n}{2M}\end{pmatrix}= \\ &= 1+\frac{\vec\sigma\cdot\overleftarrow{k}_p}{2M}\,\frac{\vec\sigma\cdot\hat{\vec k}_n}{2M}\end{aligned} \tag{10.124a}$$

$$\begin{aligned}\hat{\vec J}^{(V)} &= \begin{pmatrix}1 & \frac{\vec\sigma\cdot\overleftarrow{k}_p}{2M}\end{pmatrix}\begin{pmatrix}1&0\\0&-1\end{pmatrix}\begin{pmatrix}0&\sigma\\-\sigma&0\end{pmatrix}\begin{pmatrix}1\\ \frac{\vec\sigma\cdot\hat{\vec k}_n}{2M}\end{pmatrix}= \\ &= \vec\sigma\,\frac{\vec\sigma\cdot\hat{\vec k}_n}{2M}+\frac{\vec\sigma\cdot\overleftarrow{k}_n}{2M}\,\vec\sigma=\frac{\hat{\vec k}_n+\overleftarrow{k}_p}{2M}+i\,\frac{\vec\sigma\times(\overleftarrow{k}_p-\hat{\vec k}_n)}{2M}\end{aligned} \tag{10.124b}$$

$$\begin{aligned}\hat{J}^{(A)\,0} &= -\lambda\,\begin{pmatrix}1 & \frac{\vec\sigma\cdot\overleftarrow{k}_p}{2M}\end{pmatrix}\begin{pmatrix}1&0\\0&-1\end{pmatrix}\begin{pmatrix}0&1\\1&0\end{pmatrix}\begin{pmatrix}1\\ \frac{\vec\sigma\cdot\hat{\vec k}_n}{2M}\end{pmatrix}= \\ &= -\lambda\,\frac{\vec\sigma\cdot(\overleftarrow{k}_p+\hat{\vec k}_p)}{2M}\end{aligned} \tag{10.124c}$$

[8] One should realize that $\hat{H}^{(beta)}_{int}(t)$, $\hat{J}^{(V)}_\mu$, and $\hat{J}^{(A)}_\mu$ in (10.122) are operators acting in the space of spatial wave functions of nucleons.

$$\hat{\vec{J}}^{(A)} = -\lambda \begin{pmatrix} 1 & \frac{\vec{\sigma}\cdot\overleftarrow{k}_p}{2M} \end{pmatrix} \begin{pmatrix} 1 & 0 \\ 0 & -1 \end{pmatrix} \begin{pmatrix} 0 & \sigma \\ -\sigma & 0 \end{pmatrix} \begin{pmatrix} 0 & 1 \\ 1 & 0 \end{pmatrix} \begin{pmatrix} 1 \\ \frac{\vec{\sigma}\cdot\hat{\vec{k}}_n}{2M} \end{pmatrix} =$$

$$= -\lambda\,\vec{\sigma} - \lambda\,\frac{(\vec{\sigma}\cdot\overleftarrow{k}_p)\,\vec{\sigma}\,(\vec{\sigma}\cdot\hat{\vec{k}}_n)}{4M^2} \tag{10.124d}$$

The last terms in (10.124b) and (10.124d) are small in the comparison with other terms for usual β transitions in nuclei. Therefore they are usually neglected and then

$$\hat{J}^{(V)\,0} = 1 \tag{10.125a}$$

$$\hat{\vec{J}}^{(V)} = \frac{\hat{\vec{k}}_n + \overleftarrow{k}_p}{2M} \tag{10.125b}$$

$$\hat{J}^{(A)\,0} = -\lambda\,\frac{\vec{\sigma}\cdot(\hat{\vec{k}}_n + \overleftarrow{k}_p)}{2M} \tag{10.125c}$$

$$\hat{\vec{J}}^{(A)} = -\lambda\,\vec{\sigma} \tag{10.125d}$$

Experience shows that in usual β transitions nucleus matrix elements of $\hat{\vec{J}}^{(V)}$ and $\hat{J}^{(A)\,0}$ are more then order smaller than the matrix elements of $\hat{J}^{(V)\,0}$ and $\hat{\vec{J}}^{(A)}$ (absolute values of matrix elements of $\hat{J}^{(V)\,0}$ and $\hat{\vec{J}}^{(A)}$ are about 20-times less than absolute values of matrix elements of $\hat{\vec{J}}^{(V)}$ or $\hat{J}^{(A)\,0}$). So we neglect matrix elements of $\hat{J}^{(A)\,0}$ and $\hat{\vec{J}}^{(V)}$,

$$\hat{J}^{\,(V)\,0} = 1 \quad , \quad \hat{\vec{J}}^{(V)} \approx 0 \quad , \quad \hat{J}^{\,(A)\,0} \approx 0 \quad , \quad \hat{\vec{J}}^{(A)} = -\lambda\,\vec{\sigma} \tag{10.126}$$

and corresponding matrix element (10.122) reads (we used also $\gamma^i = -\,\gamma_i$ for $i = 1, 2, 3$),

$$\langle f|\,\hat{H}^{(\beta^-)}_{int}(t)\,|\,i\rangle = \frac{G_\beta}{\sqrt{2}}\; e^{i\,(E_e+E_{\tilde{\nu}})\,t}\;\times$$

$$\times \int d^3x \Big\{\; \varphi^*_p(\vec{x}, r_p)\,\varphi_n(\vec{x}, r_n)\,e^{-i\,\vec{q}\cdot\,\vec{x}}\;\frac{1}{(2\pi)^3}\;\frac{1}{\sqrt{2E_e\;2E_{\tilde{\nu}}}}$$

$$\Big[\bar{u}_e(s_e, \vec{k}_e)\,\gamma_0\,(1-\gamma_5)\,v_{\tilde{\nu}}(s_{\tilde{\nu}}, \vec{k}_{\tilde{\nu}})\Big]$$

$$+\lambda\;\varphi^*_p(\vec{x}, r_p)\,\vec{\sigma}\,\varphi_n(\vec{x}, r_n)\,e^{-i\,\vec{q}\cdot\,\vec{x}}\;\frac{1}{(2\pi)^3}\;\frac{1}{\sqrt{2E_e\;2E_{\tilde{\nu}}}}$$

$$\cdot\Big[\bar{u}_e(s_e, \vec{k}_e)\,\vec{\gamma}\,(1-\gamma_5)\,v_{\tilde{\nu}}(s_{\tilde{\nu}}, \vec{k}_{\tilde{\nu}})\Big]\;\Big\} \tag{10.127}$$

If neutron and proton are taken into account as one type particles differing only by the isospin projection (see (1.17)) ($\varphi_p(\vec{x}, r_p) = \hat{t}_- \, \varphi_n(\vec{x}, r_n)$) then the β^- interaction matrix element (10.127) can be rewritten as follows,

$$\begin{aligned}
\langle f| \, \hat{H}^{(\beta^-)}_{int}(t) \, | \, i\rangle = \frac{G_\beta}{\sqrt{2}} \; e^{i\,(E_e + E_{\tilde{\nu}})\,t} \; \times \\
\times \int d^3x \Big\{ \; \varphi^*_f(\vec{x}, r_p) \, \hat{t}_- \, \varphi_i(\vec{x}, r_n) \, e^{-i\,\vec{q}\cdot\,\vec{x}} \; \frac{1}{(2\pi)^3} \; \frac{1}{\sqrt{2E_e \; 2E_{\tilde{\nu}}}} \\
\Big[\bar{u}_e(s_e, \vec{k}_e) \; \gamma_0 \; (1 - \gamma_5) \; v_{\tilde{\nu}}(s_{\tilde{\nu}}, \vec{k}_{\tilde{\nu}}) \Big] \\
+ \lambda \; \varphi^*_f(\vec{x}, r_p) \; \vec{\sigma} \; \hat{t}_- \; \varphi_i(\vec{x}, r_n) \; e^{-i\,\vec{q}\cdot\,\vec{x}} \; \frac{1}{(2\pi)^3} \; \frac{1}{\sqrt{2E_e \; 2E_{\tilde{\nu}}}} \\
\cdot \Big[\bar{u}_e(s_e, \vec{k}_e) \; \vec{\gamma} \; (1 - \gamma_5) \; v_{\tilde{\nu}}(s_{\tilde{\nu}}, \vec{k}_{\tilde{\nu}}) \Big] \; \Big\}
\end{aligned} \tag{10.128}$$

where $\varphi_f(\vec{x}, r_f)$ and $\varphi_i(\vec{(r)}, r_i)$ are wave functions of free nucleons.

In the expression (10.128) $\varphi_i(\vec{x}, r_i)$ and $\varphi_f(\vec{x}, r_f)$ are wave functions of free nucleons in the elementary process $n \to p + e^- + \tilde{\nu}_e$. If the nuclear β^- decay is considered (that means $Z^A \to (Z+1)^A + e^- + \tilde{\nu}_e$) then the functions $\varphi_i(\vec{x}, r_i)$ and $\varphi_f(\vec{x}, r_f)$ are single-particle wave functions of nucleons bound in the mother and daughter nuclei in the investigated β^- decay. These single-particle wave functions are built in the corresponding many nucleons wave functions of the initial (mother) and final (daughter) nucleus,

$$\begin{aligned}
\Phi_i(\vec{x}_1 r_1, \vec{x}_2 r_2, \cdots, \vec{x}_A r_A) \quad &\to \quad \text{mother nucleus initial state} \\
\Phi_f(\vec{x}_1 r_1, \vec{x}_2 r_2, \cdots, \vec{x}_A r_A) \quad &\to \quad \text{daughter nucleus final state}
\end{aligned} \tag{10.129}$$

In the usual β^- decay the initial mother nucleus is in its ground state with the wave function $\Phi_i(\xi_1, \xi_2, \cdots, \xi_A)$ ($\xi_k \equiv \vec{x}_k r_k$) given, for instance, by the Slater determinant (4.7) (in the mean field approximation), or by $|BCS\rangle$ quasiparticle vacuum (6.18) (in the quasiparticle mean field approximation), or by RPA phonon vacuum $|RPA\rangle$ (in the framework of the random-phase-approximation), etc. The final daughter nucleus is mostly in some excited state and corresponding final wave function $\Phi_f(\xi_1, \xi_2, \cdots, \xi_A)$ should be determined within appropriate nuclear model, the same one as used for the mother nucleus initial state. Therefore in the nuclear β^- decay the interac-

tion matrix element (10.128) should be modified as

$$\langle f|\,\hat{H}_{int}^{(\beta^-)}(t)\,|\,i\rangle = \frac{G_\beta}{\sqrt{2}}\; e^{i\,(E_e+E_{\tilde{\nu}})\,t}$$
$$\Big\{\;\langle\Phi_f\mid \sum_{j=1}^{A}\hat{t}_-^{(j)}\,e^{-i\vec{q}\cdot\,\vec{x}_j}\mid\Phi_i\rangle$$
$$\frac{1}{(2\pi)^3}\,\frac{1}{\sqrt{2E_e\;2E_{\tilde{\nu}}}}\Big[\bar{u}_e(s_e,\vec{k}_e)\,\gamma_0\,(1-\gamma_5)\,v_{\tilde{\nu}}(s_{\tilde{\nu}},\vec{k}_{\tilde{\nu}})\Big]$$
$$+\,\lambda\,\langle\Phi_f|\sum_{j=1}^{A}\big(\vec{\sigma}\,\hat{t}_-\big)_j\,e^{-i\vec{q}\cdot\,\vec{x}_j}|\;\Phi_i\rangle$$
$$\frac{1}{(2\pi)^3}\,\frac{1}{\sqrt{2E_e\;2E_{\tilde{\nu}}}}\cdot\Big[\bar{u}_e(s_e,\vec{k}_e)\,\vec{\gamma}\,(1-\gamma_5)\,v_{\tilde{\nu}}(s_{\tilde{\nu}},\vec{k}_{\tilde{\nu}})\Big]\;\Big\} \tag{10.130}$$

It is necessary to remind that the expr. (10.130) valids for the case of nucleon non-relativistic approximation (10.126) while the lepton degrees of freedom are treated fully relativistically. If we want to be more precise and to use the approximation (10.125) instead of (10.126) then

$$\langle f|\,\hat{H}_{int}^{(\beta^-)}\,|i\rangle = \frac{G_\beta}{\sqrt{2}}\,e^{i(E_e+E_{\tilde{\nu}})\,t}$$
$$\Big\{\langle\Phi_f\mid\sum_{j=1}^{A}\hat{t}_-^{(j)}e^{-i\vec{q}\cdot\vec{x}_j}\mid\Phi_i\rangle$$
$$\frac{1}{(2\pi)^3}\,\frac{1}{\sqrt{2E_e\;2E_{\tilde{\nu}}}}\Big[\bar{u}_e(s_e,\vec{k}_e)\,\gamma_0\,(1-\gamma_5)\,v_{\tilde{\nu}}(s_{\tilde{\nu}},\vec{k}_{\tilde{\nu}})\Big] \tag{10.131a}$$

$$-\,\langle\Phi_f\mid\sum_{j=1}^{A}\frac{\overleftarrow{k}_f+\hat{\vec{k}}_i}{2M}\;\hat{t}_-^{(j)}\;e^{-i\vec{q}\cdot\vec{x}_j}\mid\Phi_i\rangle$$
$$\frac{1}{(2\pi)^3}\,\frac{1}{\sqrt{2E_e\;2E_{\tilde{\nu}}}}\cdot\Big[\bar{u}_e(s_e,\vec{k}_e)\,\vec{\gamma}\,(1-\gamma_5)\,v_{\tilde{\nu}}(s_{\tilde{\nu}},\vec{k}_{\tilde{\nu}})\Big] \tag{10.131b}$$

$$-\,\lambda\,\langle\Phi_f\mid\sum_{j=1}^{A}\frac{\vec{\sigma}_j\cdot(\overleftarrow{k}_f+\hat{\vec{k}}_i)}{2M}\;\hat{t}_-^{(j)}\;e^{-i\vec{q}\cdot\vec{x}_j}\mid\Phi_i\rangle$$
$$\frac{1}{(2\pi)^3}\,\frac{1}{\sqrt{2E_e\;2E_{\tilde{\nu}}}}\Big[\bar{u}_e(s_e,\vec{k}_e)\,\gamma_0\,(1-\gamma_5)\,v_{\tilde{\nu}}(s_{\tilde{\nu}},\vec{k}_{\tilde{\nu}})\Big] \tag{10.131c}$$

$$+ \lambda \, \langle \Phi_f \mid \sum_{j=1}^{A} \; \vec{\sigma}_j \, \hat{t}_-^{(j)} \; e^{-i\vec{q}\cdot\vec{x}_j} \mid \Phi_i \rangle$$

$$\frac{1}{(2\pi)^3} \frac{1}{\sqrt{2E_e \, 2E_{\tilde{\nu}}}} \cdot \left[\bar{u}_e(s_e, \vec{k}_e) \, \vec{\gamma} \, (1 - \gamma_5) \, v_{\tilde{\nu}}(s_{\tilde{\nu}}, \vec{k}_{\tilde{\nu}}) \right] \Big\} \qquad (10.131d)$$

The first term (10.131a) originates from $\hat{J}^{(V)\,0}$, the second term (10.131) from $\hat{\vec{J}}^{(V)}$, the third from $\hat{J}^{(A)\,0}$ and the fourth from $\hat{\vec{J}}^{(A)}$. The expression (10.131) can be easily extended into the non- approximate case of all terms in (10.124) involved in the vector and axial-vector currents.

Nuclear matrix elements (10.130) or (10.131) involves power function $e^{-i\vec{q}\cdot\vec{x}}$, where $\vec{q} = \vec{k}_e + \vec{k}_{\tilde{\nu}} = \vec{k}_i - \vec{k}_f$ (see (10.120). In analogy with electromagnetic transitions (see (2.47)) this function can be decomposed into spherical harmonics in all terms in (10.130) or (10.131). In the combination of this decomposition with spin (Pauli matrices $\vec{\sigma}$) and linear momenta $\vec{k}_i, \vec{k}_f$ (or transef momentum $\vec{q}$) involved in (10.130) or (10.131) this spherical harmonics decomposition gives the decomposition into multipoles and spin-multipoles of different types (see e.g. [332, 99]). However further we will discuss only allowed β transitions which corresponds to the first term (unity) in the Taylor decomposition of $e^{-i\vec{q}\cdot\vec{x}}$ with respect to $\vec{q}$,

$$e^{-i\vec{q}\cdot\vec{x}} = 1 - i\vec{q}\cdot\vec{x} + \cdots \qquad (10.132)$$

We can restrict ourself only by the first term in (10.132) because the power function (10.132) participates in (10.130) or (10.131) only in the framework of the nuclear matrix element, that means effectively only in the integrals over the nuclear volume where the nucleon desities and currents are nonzero. Effectively this integration is performed over d^3x in the interval $0 \leq q|\vec{x}| \leq q|R_0|$ where $R_0 \approx 1.2 \times A^{1/3}$ fm. Because of the usual β transition transfer moment $\vec{q}$ does not exceed 20-30 MeV the product $\vec{q}\cdot\vec{x}$ is sufficiently small to restrict overself only to the first term in (10.132) (arguments analogic to ones for the long-wave approximation in the case of elelectromagnetic transitions - see (2.123) in the Subsection 2.2.2.2). Further we show that the restriction $e^{-i\vec{q}\cdot\vec{x}} \approx 1$ corresponds to the Fermi allowed and Gamow-Teller allowed transitions discussed in the Section 10.2.

In the lowest order of the Taylor expansion (10.132) ($e^{-i\vec{q}\cdot\vec{x}} \approx 1$) the nuclear matrix parts in (10.130) reduce to $\langle \Phi_f | \sum_{j=1}^{A} \hat{t}_-^{(j)} | \Phi_i \rangle$ for the first term (originating from $\hat{J}^{(V)\,0}$) and to $\langle \Phi_f | \sum_{j=1}^{A} \vec{\sigma}_j \, \hat{t}_-^{(j)} | \Phi_i \rangle$ for the second term (origination from $\hat{\vec{J}}^{(A)}$). Angular momentum and parity selection rules for

these matrix elements are

$$\pi_i\pi_f = 1\ ,\ |\Delta J| = |J_f - J_i| = 0 \qquad \text{for } \langle\Phi|\sum_j \hat{t}^j_-\,|\Phi_i\rangle$$

$$\pi_i\pi_f = 1\ ,\ |\Delta J| = |J_f - J_i| = \begin{cases} 0,1\ \ (J_i, J_f > 0) \\ 1\ \begin{pmatrix} J_i = 0 \\ \text{or } J_f = 0 \end{pmatrix} \end{cases} \text{for } \langle\Phi|\sum_j \vec{\sigma}_j\,\hat{t}^j_-\,|\Phi_i\rangle \tag{10.133}$$

The selection rules from the first row of (10.133) (of the matrix element $\langle\Phi|\ \sum_j \hat{t}^j_-\ |\Phi_i\rangle$) is in accordanec with the selection rule for allowed Fermi β transitions and selection rules in the second row of (10.133) corresponds to the selection rules of allowed Gamow-Teller β transitions (selection rule for allowed β transitions were introduced in the text below expr. (10.23).

Involving the next to the lowest order term in the expansion (10.132) (the term with $\vec{q}\cdot\vec{x}$) in the both terms (10.131a) and (10.131d) or involving terms (10.131b) and (10.131c) (with simultaneously $e^{-i\vec{q}\cdot\vec{x}} \approx 1$) give so called first forbidden transitions with the following selection rules,

$$\begin{aligned}
&\text{term with } \langle\Phi_f\,|\sum_{j=1}^{A} \vec{x}_j\,\hat{t}^{(j)}_-\,|\Phi_i\rangle \to \quad \pi_i\pi_f = -1\ ,\ \Delta J = 0,\pm 1 \\
&\text{term with } \langle\Phi_f\,|\sum_{j=1}^{A} \frac{\overleftarrow{k}_f + \hat{\vec{k}}_i}{2M}\ \hat{t}^{(j)}_-\,|\Phi_i\rangle \to \\
&\qquad\qquad \to \quad \pi_i\pi_f = -1\ ,\ \Delta J = 0,\pm 1 \\
&\text{term with } \langle\Phi_f\,|\sum_{j=1}^{A} \frac{\vec{\sigma}_j\cdot(\overleftarrow{k}_f + \hat{\vec{k}}_i)}{2M}\ \hat{t}^{(j)}_-\,|\Phi_i\rangle \\
&\qquad\qquad \to \quad \pi_i\pi_f = -1\ ,\ \Delta J = 0,\pm 1,\pm 2 \\
&\text{term with } \langle\Phi_f\,|\sum_{j=1}^{A} \vec{\sigma}_j\cdot\vec{x}_j\,\hat{t}^{(j)}_-\,|\Phi_i\rangle \to \\
&\qquad\qquad \to \quad \pi_i\pi_f = -1\ ,\ \Delta J = 0,\pm 1,\pm 2
\end{aligned} \tag{10.134}$$

In average the square of the first forbidden transition matrix elements $\langle f|\hat{H}^{(\beta^-)}_{int}|i\rangle$ (with nucleus terms (10.134) involved) represent not more than 10% of the square of allowed β transition element (10.128) with $e^{-i\vec{q}\cdot\vec{x}} \approx 1$.

We can continue and take into account terms originating from hiher order terms of the decomposition (10.132) (which are linked with the higer multipolarity terms in multipole decompositions mentioned above) and analyze

the corresponding angular momentum and parity selection rules. Since these terms contain effectively higher order powers of small factors $\approx qR_0$ and $\frac{k}{M}$ one can expect that the corresponding transition matrix element decreases with the rang of the transition prohibition.

In next subsections we will discuss only Fermi and Gamow-Teller allowed transitions. Fermi allowed transitions are connected with the first term (10.131a) in the nuclear β^- decay matrix element (10.131) with the approximation $e^{-i\vec{q}\cdot\vec{x}} \approx 1$ used and Gamow-Teller allowed transition with the last term (10.131d) of (10.131) where again the approximation $e^{-i\vec{q}\cdot\vec{x}} \approx 1$ is used. So the allowed β^- decay matrix element of the β interaction Hamiltonian is

$$\begin{aligned}\langle f|\, \hat{H}_{int}^{(\beta\, allowed)}(t)\, |i\rangle = \mathcal{M}_{fi}^{(\beta^-\, allowed\, F)}\, \frac{1}{(2\pi)^3}\, \frac{G_\beta}{\sqrt{2}}\, e^{i(E_e+E_{\tilde{\nu}})\, t} \frac{1}{\sqrt{2E_e\, 2E_{\tilde{\nu}}}}\, \times \\ \times \Big[\, \bar{u}_e(s_e, \vec{k}_e)\, \gamma_0\, (1-\gamma_5)\, v_{\tilde{\nu}}(s_{\tilde{\nu}}, \vec{k}_{\tilde{\nu}})\, \Big] \\ +\, \lambda\, \vec{\mathcal{M}}_{fi}^{(\beta^-\, allowed\, GT)}\, \frac{G_\beta}{\sqrt{2}}\, e^{i(E_e+E_{\tilde{\nu}})\, t} \frac{1}{(2\pi)^3}\, \frac{1}{\sqrt{2E_e\, 2E_{\tilde{\nu}}}}\, \times \\ \cdot \Big[\, \bar{u}_e(s_e, \vec{k}_e)\, \vec{\gamma}\, (1-\gamma_5)\, v_{\tilde{\nu}}(s_{\tilde{\nu}}, \vec{k}_{\tilde{\nu}})\, \Big]\end{aligned} \tag{10.135}$$

where

$$\begin{aligned}\mathcal{M}_{fi}^{(\beta^-\, allowed\, F)} &= \langle \Phi_f|\, \hat{\mathcal{M}}^{(\beta^-\, allowed\, F)}\, |\, \Phi_i\rangle = \langle \Phi_f|\, \sum_{j=1}^{A} \hat{t}_-^{(j)}\, |\Phi_i\rangle \\ \hat{\vec{\mathcal{M}}}_{fi}^{(\beta^-\, allowed\, GT)} &= \langle \Phi_f|\, \hat{\vec{\mathcal{M}}}^{(\beta^-\, allowed\, GT)}\, |\, \Phi_i\rangle = \langle \Phi_f|\, \sum_{j=1}^{A} \vec{\sigma}_j\, \hat{t}_-^{(j)}\, |\Phi_i\rangle\end{aligned} \tag{10.136}$$

Fermi allowed transition operator $\hat{\mathcal{M}}^{(\beta^-\, allowed\, F)} = \sum_{j=1}^{A} \hat{t}_+^{(j)}$ is directly connected with the isovector electric monopole E0 transition operator $\hat{\mathscr{M}}_{00}^{(el)}(\Delta T = 1, \Delta T_z = -1)$ given in (7.364),

$$\begin{aligned}\hat{\mathcal{M}}^{(\beta^-\, allowed\, F)} &= \sum_{j=1}^{A} \hat{t}_-^{(j)} = \frac{\sqrt{4\pi}}{2}\, \hat{\mathscr{M}}_{00}^{(el)}(\Delta T = 1, \Delta T_z = -1) \\ \hat{\mathcal{M}}^{(\beta^+\, allowed\, F)} &= \sum_{j=1}^{A} \hat{t}_+^{(j)} = \frac{\sqrt{4\pi}}{2}\, \hat{\mathscr{M}}_{00}^{(el)}(\Delta T = 1, \Delta T_z = +1)\end{aligned} \tag{10.137}$$

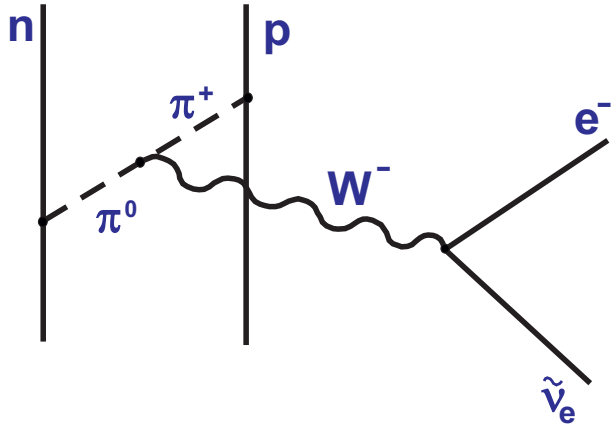


Figure 10.6: Feynman diagram corresponding to the decay $\pi^0 \to \pi^+ + W^- \to \pi^+ + e^- + \tilde{\nu}_e$ of the intermediate π^0 exchanged by the neutron and proton in the nuclear medium.

and similarly the components of the Gamow-Teller allowed transition operator $\hat{\vec{\mathcal{M}}}^{(\beta^- \, allowed \, GT)} = \sum_{j=1}^{A} \vec{\sigma} \, \hat{t}_-^{(j)} \, |\Phi_i\rangle$ can be directly linked with the components $\mu = 0, \pm 1$ of the dipole isovector magnetic $M1\mu$ transition operator $\hat{\mathscr{M}}^{(mag)}_{1\mu=0,\pm1}(\Delta T = 1, \Delta T_z = \pm 1)$ (see (7.366) with corresponding gyromagnetic ratios.

Up to now we discussed only expressions for β interaction matrix elements based on the lowest order Feynman diagram shown in the Fig.10.5. In principle we can construct higher order Feynman diagrams for the same transition as, for instant, diagram with the non-nucleon degrees of freedom shown in the Fig.10.6. This diagram corresponds to the β^- decay of the intermediate pions exchanged by nucleons in the nuclear medium. In the case of allowed β^- transitions the contribution of such diagrams is negligible but for the first forbidden β^- transitions the diagrams like one in the Fig.10.6 can give a contribution about 10%.

10.5.2 Probability of β decay of nuclei

In this subsection the probability of nuclear allowed β transition is derived at first. We start with the transition matrix element (10.135),

$$\begin{aligned}\langle f| \, \hat{H}_{int}^{(\beta \, allowed)}(t) \, |i\rangle = \frac{1}{(2\pi)^3} \, \frac{G_\beta}{\sqrt{2}} \, e^{i(E_e + E_{\tilde{\nu}}) \, t} \frac{1}{\sqrt{2E_e \, 2E_{\tilde{\nu}}}} \, \times \\ \times \Big\{ \, \mathcal{M}_{fi}^{(\beta^- \, allowed \, F)} \, \Big[\, \bar{u}_e(s_e, \vec{k}_e) \, \gamma_0 \, (1 - \gamma_5) \, v_{\tilde{\nu}}(s_{\tilde{\nu}}, \vec{k}_{\tilde{\nu}}) \, \Big] \, + \\ + \lambda \, \vec{\mathcal{M}}_{fi}^{(\beta^- \, allowed \, GT)} \cdot \Big[\, \bar{u}_e(s_e, \vec{k}_e) \, \vec{\gamma} \, (1 - \gamma_5) \, v_{\tilde{\nu}}(s_{\tilde{\nu}}, \vec{k}_{\tilde{\nu}}) \, \Big] \, \Big\}\end{aligned} \tag{10.138}$$

where the nuclear matrix elements $\mathcal{M}_{fi}^{(\beta^- \, allowed \, F)} = \langle \Phi_f | \sum_j \hat{t}_-^{(j)} | \Phi_i \rangle$ and $\vec{\mathcal{M}}_{fi}^{(\beta^- \, allowed \, GT)} = \langle \Phi_f | \sum_j \vec{\sigma}_j \hat{t}_-^{(j)} | \Phi_i \rangle$ are supposed to be known in the framework of used nuclear model. From (10.138) one can see that the nuclear part of the β interaction Hamiltonian is periodical function of the time similarly as the electromagnetic interaction Hamiltonian of the nucleus and external electromagnetic field. Therefore we can used for the derivation of the β decay probability per 1 sec. the same procedure as for the probability of electromagnetic emission of photon (see the text between (2.90) and (2.96)). Specifically, for the β^- decay we obtain (opposite to the Chapter 2 now we suppose to work in the natural unit system where $\hbar = c = 1$) [9]

$$\omega_{i \to f} = 2\pi \left| \langle f | \hat{H}^{(\beta^- \, allowed)} | i \rangle \right|^2 \delta(E_i - E_f - E_e - E_{\tilde{\nu}}) \tag{10.139}$$

Particularly $\omega_{i \to f}$ is the probability per second of the β^- decay of the parent nucleus being in the initial state $|\Phi_i\rangle$ with the daughter nucleus being in the final state $|\Phi_f\rangle$ and during the β^- decay the electron with the linear momentum $\vec{k}_i$ and spin (helicity) state s_e (and energy $E_e = \sqrt{m_e^2 + \vec{k}_e^2}$) and the electron antineutrino with the linear momentum $\vec{k}_{\tilde{\nu}}$ and helicity state $S_{\tilde{\nu}}$ (and the energy $E_{\tilde{\nu}} \approx |\vec{k}_{\tilde{\nu}}|$) are emitted.

If we analyze the probability of a β^- decay, where in the final state we have electron not in one state $(\vec{k}_e; s_e)$ but in the ensemble of states with linear momenta in the interval $\langle \vec{k}_e, \vec{k}_e + d^3 k_e \rangle$ and in the final state there is antineutrino not in one state $(\vec{k}_{\tilde{\nu}}; s_{\tilde{\nu}})$ but in the ensemble of states with the linear momenta in the interval $\langle \vec{k}_{\tilde{\nu}}, \vec{k}_{\tilde{\nu}} + d^3 k_{\tilde{\nu}} \rangle$ then the β^- decay probability per one second is (in the analogy with (2.92), (2.93))

$$\begin{aligned} d\omega_{i \to f}^{(6)} &= 2\pi \left| \langle f | \hat{H}^{(\beta^- \, allowed)} | i \rangle \right|^2 \times \\ &\times \frac{|\vec{k}_e|^2 \, d|\vec{k}_e| \, d\Omega_e}{(2\pi)^3} \, \frac{|\vec{k}_{\tilde{\nu}}|^2 \, d|\vec{k}_{\tilde{\nu}}| \, d\Omega_{\tilde{\nu}}}{(2\pi)^3} \, \delta(Q - E_e - E_{\tilde{\nu}}) \end{aligned} \tag{10.140}$$

where $Q = E_i - E_f$ is the energy released for electron and antineutrino. Differentials $|d\vec{k}_e|$ and $|d\vec{k}_{\tilde{\nu}}|$ can be transformed to energy differentials dE_e and $dE_{\tilde{\nu}}$, respectively,

$$\begin{aligned} E_e = \sqrt{m_e^2 + |\vec{k}_e|^2} \quad &\Rightarrow \quad |\vec{k}_e| \, d|\vec{k}_e| = E_e \, dE_e \\ E_{\tilde{\nu}} = |\vec{k}_{\tilde{\nu}}| \quad &\Rightarrow \quad |\vec{k}_{\tilde{\nu}}| \, d|\vec{k}_{\tilde{\nu}}| = E_{\tilde{\nu}} \, dE_{\tilde{\nu}} \end{aligned} \tag{10.141}$$

[9] The expression (10.139) is in the literature often called as the application of "Fermi golder rule" for β^- decay.

The presence of δ- function in (10.140) represents the energy conservation law, $E_{\tilde{\nu}} + E_e = Q = E_i - E_f$ and thank to this δ-function in (10.140) we can easily integrate (10.140) over energies of antineutrino

$$d\omega^{(5)}_{i\to f} \equiv \int dE_{\tilde{\nu}}\, d\omega^{(6)}_{i\to f} = \\ = \frac{1}{(2\pi)^5} \left|\langle f|\hat{H}^{(\beta^- \, allowed)}|i\rangle\right|^2 \, |\vec{k}_e|\, E_e \left(Q - E_e\right)^2 dE_e\, d\Omega_e\, d\Omega_{\tilde{\nu}} \tag{10.142}$$

If we are not interested on the direction of emitted electron and antineutrino we should integrate (10.142) over $d\Omega_e$ and $d\Omega_{\tilde{\nu}}$. Since in the case of allowed β^- transitions the square $\left|\langle f|\hat{H}^{(\beta^- \, allowed)}|i\rangle\right|^2$ does not depend on the angles of electron and antineutrino emission the integrations oved $d\Omega_e$ and $d\Omega_{\tilde{\nu}}$ give only a factor $(4\pi)^2$ and we obtain

$$d\omega_{i\to f} = \frac{1}{(2\pi)^3} \, \left|\langle f|\hat{H}^{(\beta^- \, allowed)}|i\rangle\right|^2 \, \sqrt{E_e^2 - m_e^2}\; E_e \; \left(Q - E_e\right)^2 dE_e \tag{10.143}$$

where the square of the matrix element of allowed β^- transition interaction Hamiltonian, $\left|\langle f|\hat{H}^{(\beta^- \, allowed)}|i\rangle\right|^2$, is given by (10.138) without the power $e^{i(E_e+E_{\tilde{\nu}})t}$. Nuclear states in the laboratory frame are usually characterized by eigen-vectors of operators $\hat{H}_{nucleus}$, $\hat{\vec{J}}^2$, $\hat{J}_z$, that means

$$|\Phi_i\rangle = |\nu_i\,;\; J_i M_i\rangle \qquad , \qquad |\Phi_f\rangle = |\nu_f\,;\; J_f M_f\rangle \tag{10.144}$$

Then the matrix elements (10.136) can be rewritten using Wigner-Eckart theorem (see (A.12))

$$\mathcal{M}^{(\beta^- allowed\, F)}_{fi} = \langle \nu_f\,;\; J_f M_f| \sum_{j=1}^{A} t^{(j)}_-| \,\nu_i\,;\; J_i M_i\rangle = \\ = \frac{\delta_{J_i J_f}}{\sqrt{2J_I+1}} \, \langle \nu_f\,;\; J_f|| \sum_{j=1}^{A} t^{(j)}_-|| \,\nu_i\,;\; J_i\rangle \tag{10.145}$$

$$\vec{\mathcal{M}}^{(\beta^- allowed\, GT)}_{fi} = \langle \nu_f\,;\; J_f M_f| \sum_{j=1}^{A} \vec{\sigma}_j \, t^{(j)}_-| \,\nu_i\,;\; J_i M_i\rangle = \\ = \frac{C^{J_f M_f}_{J_i M_i 1\,\mu}}{\sqrt{2J_I+1}} \, \langle \nu_f\,;\; J_f|| \sum_{j=1}^{A} (\vec{\sigma}_j)_1 \; t^{(j)}_-|| \,\nu_i\,;\; J_i\rangle \tag{10.146}$$

where $(\vec{\sigma})_{1\,u}$ is the μ-th component of the tensor of rang 1 constructed from the componnets of the vector of Pauli matrices $\vec{\sigma} \equiv (\sigma_x,\ \sigma_y,\ \sigma_z)$ by the standard way, $(\vec{\sigma})_{1\pm1} = \mp\frac{1}{\sqrt{2}}(\sigma_x \pm i\sigma_y)$, $(\vec{\sigma})_{10} = \sigma_z$.

In usual case we do not know polarisation of parent and daughter nuclei (that means angular momentum projections M_i and M_f). Then, after the substitution of (10.145) and (10.146) into (10.135), we should sum over M_f and average over M_i. If further we are not interested in helicite states of emitted electron and antineutrino then in (10.135) the additional summation over the spin indeces s_e and $s_{\tilde{\nu}}$ should be done. Then, using the techniques of the calculation of traces of products of γ- matrices (in the analogy with obtaining (10.39) from (10.32) and subsequently (10.59) and (10.61); see also [332]) we obtain finally,

$$\frac{d\omega_{i\to f}}{dE_e} = \frac{G_\beta^2}{2\pi^3}\,\xi_{fi}^{-}\,\sqrt{E_e^2 - m_e^2}\,E_e\,(Q - E_e)^2 \tag{10.147}$$

with

$$\xi_{fi}^{-} = \frac{1}{2J_i+1}\Big(\ \big|\langle \nu_f J_f||\,\hat{\mathcal{M}}^{(\beta^- allowedF)}||\nu_i J_i\rangle\big|^2 + \\ +\ \lambda^2\,\big|\langle \nu_f J_f||\hat{\vec{\mathcal{M}}}^{(\beta^- allowed\,GT)}||\,\nu_i J_i\rangle\big|^2\ \Big) \tag{10.148}$$

where $\hat{\mathcal{M}}^{(\beta^- allowed\,F)}$ and $\hat{\vec{\mathcal{M}}}^{(\beta^- allowed\,GT)}$ are defined by (10.146).

In the past it was also shown that in the expression (10.147) it is necessary to involve corrections caused by the Coulomb interaction between charged protons in the daughter nucleus and emitted electron. In the derivation of (10.147) and in all expressions involving the nuclear matrix element $\langle f|\,\hat{H}_{int}^{(\beta^-)}\,|\,i\rangle$ we always supposed that the spatial wave function of emitted electron was in the form of the plane wave $\approx e^{-i\,\vec{k}_e\cdot\vec{x}}$ (see (10.117), which lead to the power $\approx e^{-i\,\vec{q}\cdot\vec{x}}$ in expressions (10.120), (10.122), (10.127), (10.128), (10.130), (10.131) and which was approximated by the long-wave approximation $e^{-i\,\vec{q}\cdot\vec{x}} \approx 1$ for allowed β transitions. In the nuclear β^- decay the Coulomb interaction between protons in the daughter nucleus and emitted electron lead to the modification of the spatial electron wave function. Other modification comes from the relativistic higher order diagrams and from the three-body effects in the final state of the whole system. All these modifications are simulated by the additional factor function $F(\pm Z_f, E_e)$ (so called Fermi function) in the probability (10.147) and the final expression for the

spectrum of emitted electrons or protons from the $\beta^{\pm}$ decay reads,

$$\frac{d\omega_{i\to f}^{(\beta^{\mp})}}{dE_e} = \frac{G_\beta^2}{2\pi^3}\ \xi_{fi}^{\mp}\ F(\pm Z_f, E_e)\ \sqrt{E_e^2 - m_e^2}\ E_e\ (Q - E_e)^2 \tag{10.149}$$

with

$$\xi_{fi}^{\mp} \equiv \frac{1}{2J_i+1}\ \Big(\ \big|\langle \nu_f J_f||\ \hat{\mathcal{M}}^{(\beta^{\mp}\ allowed\ F)}||\nu_i J_i\rangle\big|^2 + \\ +\ \lambda^2\ \big|\langle \nu_f J_f||\hat{\vec{\mathcal{M}}}^{(\beta^{\mp}\ allowed\ GT)}||\ \nu_i J_i\rangle\big|^2\ \Big) \tag{10.150}$$

where (see (10.136) and (10.137) extended also for β^+ decay)

$$\hat{\mathcal{M}}^{(\beta^{\pm}\ allowed\ F)} = \sum_{j=1}^{A} \hat{t}_{\pm}^{(j)}$$

$$\hat{\vec{\mathcal{M}}}_{1\mu}^{(\beta^{\pm}\ allowed\ GT)} = \sum_{j=1}^{A} (\vec{\sigma})_{1\mu}\ \hat{t}_{\pm}^{(j)} \tag{10.151}$$

The Fermi function $F(\pm Z_f, E_e)$, discussed in detail e.g. in the subsection 7.2.3 of [158], can be written analytically in a nonrelativistic approximation known as the Primacoff-Rosen approximation [333] [10]

$$F(\pm Z_f, E_e) \approx \frac{E_e}{|\vec{k}_e|}\ \frac{\pm 2\pi\ \alpha\ Z_f}{1 - e^{\mp 2\pi\ \alpha\ Z_f}} = \frac{E_e}{\sqrt{E_e^2 - m_e^2}}\ \frac{\pm 2\pi\ \alpha\ Z_f}{1 - e^{\mp 2\pi\ \alpha\ Z_f}} \tag{10.152}$$

with $\alpha = 1/137$ and upper (lower) sign is used for β^- (β^+) decay. For large $|\vec{k}_e|$ and small Z_f the Fermi function $F(\pm Z_f, E_e)$ is closed to unity. This factor is bigger for β^- decay than for β^+ decay for the same Z_f which is in accordance with the attractive (repulsive) interaction between electron (positron) and protons of the daughter nucleus.

Integration of (10.149) over the whole spectrum of emitted electrons or

[10] The distortion of the electron (positron) wave function caused by the Coulomb interaction with protons in the daughter nucleus consists in the lowest order in the renormalization of the electron (positron) plane wave by the electron (positron) wave function in the origin,

$$F(\pm Z_f, E_e) \approx |\phi_e(r=0;\ Z_f)|^2 \approx \frac{2\pi\ \eta}{1 - e^{-2\pi\ \eta}} \approx \frac{E_e}{|\vec{k}_e|}\ \frac{\pm 2\pi\ \alpha\ Z_f}{1 - e^{\mp 2\pi\ \alpha\ Z_f}}$$

where $\eta = \frac{\pm Z_f\ e^2}{4\pi\epsilon_0 \hbar v_e}$ with the final velocity v_e of the electron or positron. The upper (lower) sign is used for β^- (β^+) decay.

positrons gives us the total probability $\omega_{i\to f}^{(\beta^{\mp})}$ of the investigated $\beta^{\mp}$ decay,

$$\begin{aligned}\omega_{i\to f}^{(\beta^{\mp})} &= \int_{m_e}^{Q} \frac{d\omega_{i\to f}^{(\beta^{\mp})}}{dE_e}\, dE_e = \\ &= \int_{m_e}^{Q} dE_e\ \frac{G_\beta^2}{2\pi^3}\ \xi_{fi}^{\mp}\ F(\pm Z_f, E_e)\ \sqrt{E_e^2 - m_e^2}\, E_e\, (Q - E_e)^2 = \\ &= \frac{G_\beta^2}{2\pi^3}\, \xi_{fi}^{\mp} \int_{m_e}^{Q} dE_e\, F(\pm Z_f, E_e)\, \sqrt{E_e^2 - m_e^2}\, E_e\, (Q - E_e)^2 = \\ &\equiv \frac{G_\beta^2}{2\pi^3}\, \xi_{fi}^{\mp}\, m_e^5\, f^{(\mp)}(Z_f, \epsilon_0) \end{aligned} \tag{10.153}$$

where the phase-space factor $f^{(\mp)}(Z_f, \epsilon_0)$ is introduced,

$$f^{(\mp)}(Z_f, \epsilon_0) \equiv \int_1^{\epsilon_0} d\epsilon\ \ F(\pm Z_f, m\epsilon)\, \sqrt{\epsilon^2 - 1}\, \epsilon\, (\epsilon_0 - \epsilon)^2 \tag{10.154}$$

with $Q = m_e\epsilon_0$, $E_e = m_e\epsilon$. One should realize that the phase-space factor $f^{(\mp)}(Z_f, \epsilon_0)$ contains all lepton kinematics. The integral (10.154) can be calculated and the resultant phase-space factor used in the practical calculation is (see [158])

$$f^{(\mp)}(Z_f, \epsilon_0) \approx \frac{1}{30}\left(\epsilon_0^5 - 10\epsilon_0^2 + 15\epsilon_0 - 6\right) F_0^{(PR)}(\pm Z_f) \tag{10.155}$$

with

$$F_0^{(PR)}(\pm Z_f) \equiv \frac{\pm 2\pi\, \alpha\, Z_f}{1 - e^{\mp 2\pi\, \alpha\, Z_f}} \tag{10.156}$$

where upper (lower) sign correspond to β^- (β^+) decay.

The half-life of the parent nucleus corresponding to the $\beta_{i\to f}^{\mp}$ decay is given by well-known expression (see (2.157))

$$T_{1/2}^{(i\to f)} = \frac{ln2}{\omega_{i\to f}^{(\beta^{\mp})}} = \frac{2\pi^3\, ln2}{G_\beta^2\, m_e^5\, f^{(\mp)}(Z_f, \epsilon_0)}\, \frac{1}{\xi_{fi}^{\mp}} \tag{10.157}$$

or

$$\begin{aligned} f^{(\mp)}(Z_f, \epsilon_0)\, T_{1/2}^{(i\to f)} &= \kappa\, \frac{1}{\xi_{fi}^{\mp}} = \\ &= \kappa\, \frac{2J_i + 1}{\left|\langle \nu_f J_f || \hat{\mathcal{M}}^{(\beta^{\mp}\ allowedF)}\ ||\nu_i J_i\rangle\right|^2 + \lambda^2\, \left|\langle \nu_f J_f ||\ \hat{\mathcal{M}}_1^{(\beta^{\mp}\ allowedGT)}\ ||\nu_i J_i\rangle\right|^2} \end{aligned} \tag{10.158}$$

where the value of κ is

$$\kappa \equiv \frac{2\pi^3\, ln2}{G_\beta^2\, m_e^5} = \boxed{\begin{array}{c}\text{in the standard}\\ \text{unit frame}\end{array}} = \frac{2\pi^3\, \hbar^7 ln2}{G_\beta^2\, m_e^5\, c^4} =$$

$$= \boxed{\begin{array}{c}\text{substitution}\\ \text{form (10.101) and (10.102)}\end{array}} = 6549\ s \qquad (10.159)$$

In practical calculations (see e.g. [158]) the value for κ , slightly different is used, $\kappa = 6147$ s.

The quantity $fT_{1/2}$ given in (10.158) depends only on dynamical variables, that means on the reduced matrix elements of allowed β- transition operators (10.150) (as it was mentioned only allowed β- transitions are discussed in this textbook). However similar expressions for $fT_{1/2}$ values can be derived also for forbidden β transitions (see e.g. [110]).

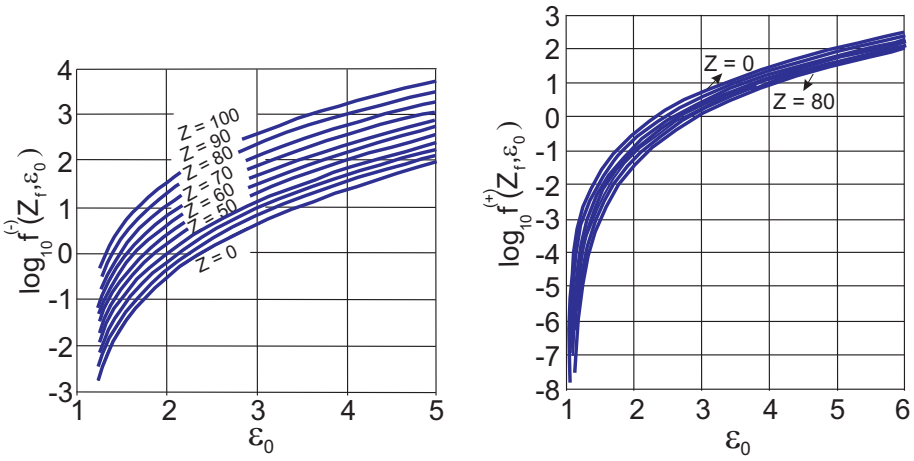


Figure 10.7: The quantity $log_{10}f^{(\mp)}(Z_f,\, \epsilon_0)$ as a function of the total β- decay energy ϵ_0 for different values of atomic number Z_f of the daughter nucleus for electrons (left panel) and positrons (right panel). Data taken from [336].

Because of the numerical and experimental values of the quantity $fT_{1/2}$ for usual $\beta^\mp$ decays this quantity is usually presented in literature in the logarithmic form, $log_{10}f^{(\mp)}(Z_f,\epsilon_0)\, T_{1/2}^{(i\to f)} = log_{10}f^{(\mp)}(Z_f,\epsilon_0) + log_{10}T_{1/2}^{(i\to f)}$. In the Fig.10.7 values $log_{10}f^{(\mp)}(Z_f,\epsilon_0)$ are shown in the dependence on ϵ_0 for several values of Z_f. The experimental values of $f^{(-)}(Z_f,\epsilon_0)\, T_{1/2}^{(0^+\to 0^+)}$ for so called superallowed β^- decays (that means for pure Fermi allowed $0^+ \to 0^+$ transitions) are given in the Fig.10.8. One can see that for the pure Fermi allowed β transitions the value $log_{10}f^{(-)}(Z_f,\epsilon_0)T_{1/2}^{(0^+\to 0^+)}$ varies closely around 3.5,

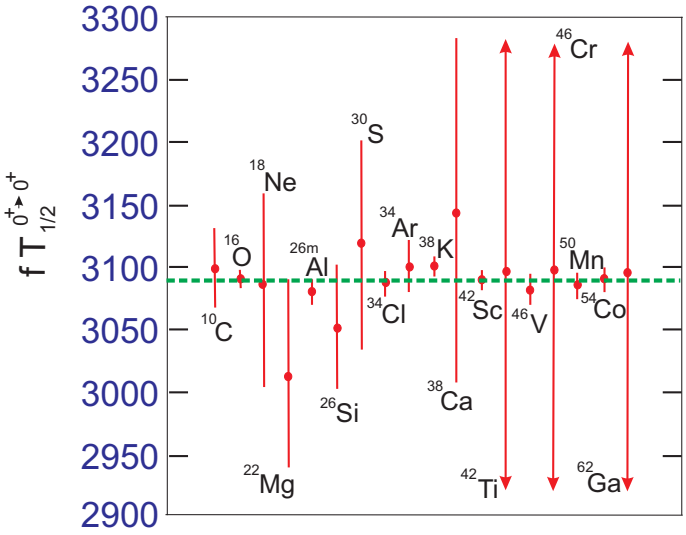


Figure 10.8: The quantity $f^{(-)}\, T_{1/2}^{(0^+\to 0^+)}(exp)$ for various superallowed pure Fermi $0^+ \to 0^+$ β^- decays. The fT average of $\approx$ 3089 s is indicated by horizontal green line (data taken from [337]).

$$log_{10}\, f^{(-)}(Z_f, \epsilon_0)\; T_{1/2}^{(0^+\to 0^+)} \approx 3.5 \tag{10.160}$$

Values of $log_{10} f\, T_{1/2}^{i\to f}$ increases by about 4 units if we compare $log_{10} fT$ values for $(L+1)$-th and L-th forbidden β transitions (estimation was done for $E_e \approx 1\; MeV$ and nuclei with radius $R \approx 5\; fm$). Typical experimental $log_{10} fT$ values for allowed, 1-st firbidden, ..., 4-th forbidden β- decays are shown in the Fig.10.9.

In the end of this subsection we will discuss the spectrum of emitted electrons (positrons) from β^- (β^+) decay. This spectrum is given by the differential probability (10.149),

$$N_{e;\, i\to f}^{(\beta^\mp)}(E_e) \approx N_0\, \frac{d\omega_{i\to f}^{(\beta^\mp)}}{dE_e} \tag{10.161}$$

where N_0 is the number of parent nuclei in the radioactive source. From the shape of the function $\frac{d\omega_{i\to f}^{(\beta^\mp)}}{dE_e}(E_e)$ in (10.149) one can see that the quantity $K_{i\to f}(E_e)$, defined as

$$K_{i\to f}^{(\beta^\mp)}(E_e) \equiv \sqrt{\frac{N_e^{(\beta^\mp)}(E_e)}{E_e\, \sqrt{E_e^2 - m_e^2}\, F(\pm Z_f,\; E_e)}} \approx (Q - E_e)\, \sqrt{\xi_{fi}^\mp} \tag{10.162}$$

should be linearly decreasing function of the electron (positron) energy E_e. This dependence is known in the literature as Fermi-Kurie plot. In the

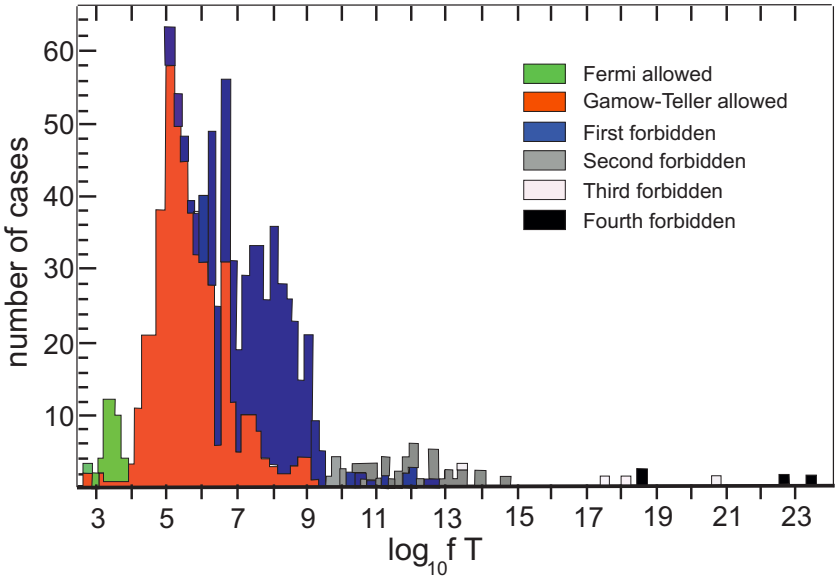


Figure 10.9: Systematics of experimental $log_{10}fT$ values for β^- allowed and forbidden decays (data taken from [338]).

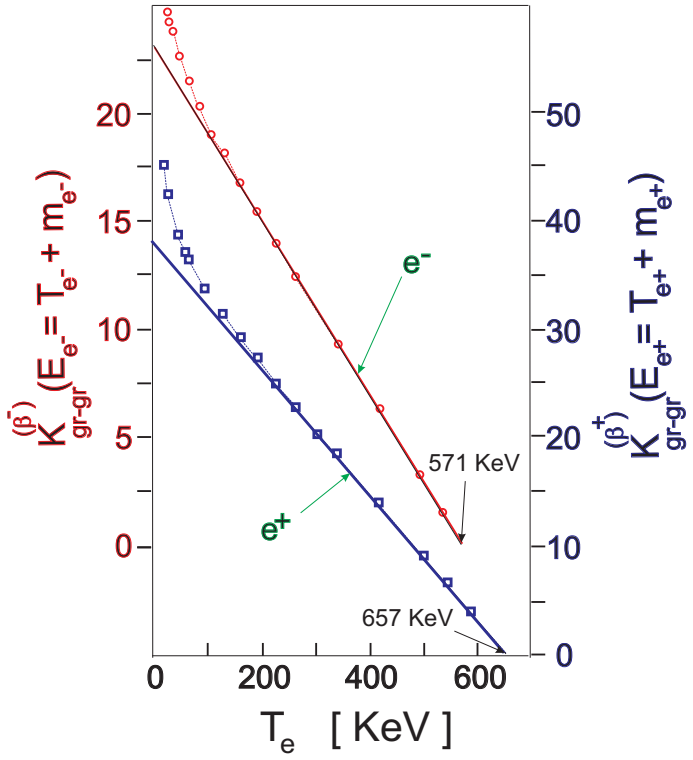


Figure 10.10: Kurie plot for electron and positron spectra of ^{64}Cu (data taken from [334]).

Fig.10.10 Kurie plots for electron (positron) emitted during β^- and β^+ decays of ^{64}Cu are demonstrated as a function of the kinetic energy T_e of electron or positron ($E_e \approx T_e + m_e$, $T_e^{(max)} = Q - m_e$). The linearly decreasing character

of the Kurie plots (see (10.162)) was obtained from (10.149) where the zero rest mass of the antineutrino or neutrino was supposed (see (10.141)). In the case when nonzero neutrino (antineutrino) mass is admitted the probability $\frac{d\omega_{i\to f}^{(\beta^{\mp})}}{dE_e}(E_e)$ (see (10.149)) should be modified as follows (see [110]) (instead $E_{\tilde{\nu}} = |\vec{k}_{\tilde{\nu}}|$ we should take $E_{\tilde{\nu}} = \sqrt{m_{\tilde{\nu}}^2 + |\vec{k}_{\tilde{\nu}}|^2}$ in (10.140))

$$\frac{d\omega_{i\to f}^{(\beta^{\mp})}}{dE_e} = \\ = \frac{G_\beta^2}{2\pi^3}\ \xi_{fi}^{\mp}\ F(\pm Z_f, E_e)\ \sqrt{E_e^2 - m_e^2}\ E_e\ (Q - E_e)\ \sqrt{(Q - E_e)^2 - m_{\tilde{\nu}}^2} \tag{10.163}$$

which corresponds to the modification of the Fermi-Kurie plot (see (10.162)) to the new expression,

$$K_{i\to f}^{(\beta^{\mp})}(E_e) \equiv \sqrt{\frac{N_e^{(\beta^{\mp})}(E_e)}{E_e\ \sqrt{E_e^2 - m_e^2}\ F(\pm Z_f,\ E_e)}} \approx \\ \approx \sqrt{\xi_{fi}^{\mp}}\ (Q - E_e)^{1/2}\ [(Q - E_e)^2 - m_{\tilde{\nu}}^2]^{1/4} \tag{10.164}$$

where $m_{\tilde{\nu}}$ is the rest mass of the antineutrino (neutrino). In the Fig 10.11

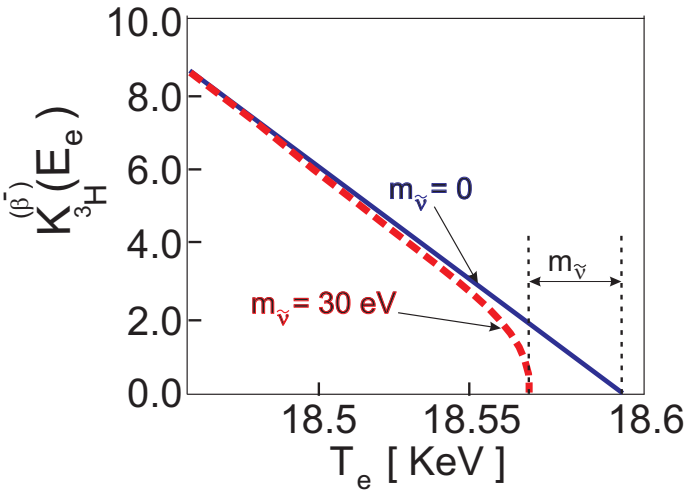


Figure 10.11: Illustration of the Fermi-Kurie plot for ^{3}H β^- decay to ^{3}He in the hypothetical case of decay with a non-vanishing neutrino mass of $m_{\tilde{\nu}} = 30$ eV and the zero mass situation $m_{\tilde{\nu}} = 0$ eV.

there is the comparison of the fictive Fermi-Kurie plot for the ^{3}H β decay with

a non-vanishing antineutrino mass $m_{\tilde{\nu}} = 30$ eV with the Fermi-Kurie plot obtained by (10.162) with the zero mass of antineutrino. One can see that in principle it is possible to estimate antineutrino (neutrino) mass through the analysis of the end-point part of the Kurie plot. Nowadays (2018) experiments, where electron antineutrino mass is exctracted from the Kurie plot, give the upper limit for antineutrino mass, $m_{\tilde{\nu}} < 1.5$ eV. In order to obtain more precise value several new big collaboration experiments are in the preparation (see e.g. KATRIN experiment [335] with the tritium β^- decay).

10.5.3 Higher energy Gamow-Teller and Fermi excitations (GM and F resonances)

In the previous subsection β-transitions from the mother nucleus initial state $|i\rangle$ into the final state $|f\rangle$ of the daughter nucleus were discussed. Probabilities of these β-transitions are given by the square of the matrix element, $|\langle f|\,\hat{H}^{(\beta)}_{int}\,|i\rangle|^2$, of the β-interaction Hamiltonian (see (10.131)). Our discussion there was restricted mainly to allowed Fermi and Gamow-Teller transitions where the transition matrix elements $|\langle f|\,\hat{H}^{(\beta)}_{int}\,|i\rangle|^2$ is given by the matrix elements of the allowed F and GM transition operators $\hat{\mathcal{M}}^{(\beta^{\pm}allowed\,F)} = \sum_{j=1}^{A} \hat{t}^{(j)}_{\pm}$ and $\hat{\vec{\mathcal{M}}}^{(\beta^{\pm}allowed\,GT)} = \sum_{j=1}^{A} \vec{\sigma}_j \hat{t}^{(j)}_{\pm}$, respectively (see (10.138) and (10.151)). It was also shown that allowed Fermi transition operator $\hat{\mathcal{M}}^{(\beta^{\pm}allowed\,F)}$ is linked directly with the isovector monopole E0 transition operator $\hat{\mathcal{M}}^{(el)}_{00}(\Delta T = 1, \Delta T_z = \pm 1)$ (see (10.137)) and allowed GT transition operator $\hat{\mathcal{M}}^{(\beta^{\pm}allowed\,GT)}$ is connected with the spin part of the magnetic dipole isovector transition operator $\hat{\mathcal{M}}^{(mag)}_{1\mu}(\Delta T = 1,\, \Delta T_z = \pm 1)$ (see (7.412),(7.413),(10.137) and the text below). From the theory of electromagnetic transitions (see the Chapter 2) we know that it is possible to excite nucleus through processes where the excitation probability or corresponding cross-sections depend also on the square of the matrix elements of isovector or isoscalar electromagnetic multipole transition operators (e.g. photo-absorption cross section - see the subsection 2.2.3, Coulomb excitation or (e,e') reaction [332], or (α, α') reaction). Such processes allow to study excitations with higher excitation energies (strength functions or giant resonances of different types and multipolarities - see the subsection 7.3.1.3.2). In this subsection strength functions of β-transition operators, particularly of allowed Fermi and Gamow-Teller transition operators, are discussed. Both these transition operators are connected with β-decay discussed in the previous subsection and with the charge-exchange reactions involving the isovector projection change (e.g. (p,n), (^{3}He,t) reactions for

$\hat{\mathcal{M}}^{(\beta^- allowed\, F)}$ and $\hat{\vec{\mathcal{M}}}^{(\beta^- allowed\, GT)}$ or (n,p), (t,^{3}He) reactions for $\hat{\mathcal{M}}^{(\beta^+ allowed\, F)}$ and $\hat{\vec{\mathcal{M}}}^{(\beta^+ allowed\, GT)}$ - see e.g. [181]). Opposite to β-decay rates the cross section of reactions mentioned above allow to obtain information about nucleus excitations with higher excitation energies, particularly about strength functions of Fermi and Gamow-Teller transition operators [181], as will be shown later.

10.5.3.1 Fermi and Gamow-Teller strength functions (Ikeda selection rules)

Further the strength functions of the Fermi and Gamow-Teller transition operators (see (10.137),

$$\hat{\mathcal{M}}^{(\beta^\pm allowed\, F)} = \sum_{j=1}^{A} \hat{t}_\pm^{(j)} \quad , \quad \hat{\vec{\mathcal{M}}}^{(\beta^\pm allowed\, GT)} = \sum_{j=1}^{A} \vec{\sigma}_j\, \hat{t}_\pm^{(j)} \tag{10.165}$$

are determined. According to (7.372) and (7.374) corresponding energy weighted strength functions of the k-th order are

$$\begin{aligned} S^\pm(F;E) &\equiv S_k^\pm(F;\ \Delta T = 1, \Delta T_z = \pm 1;\ E) = \\ &= \sum_{\nu \neq 0} E_\nu^k\ \left| \langle \nu |\, \mathcal{M}^{(\beta^\pm allowed\, F)}\, |0\rangle \right|^2 \xi_\Delta(E - E_\nu) \\ S^\pm(GT;E) &\equiv S_k^\pm(GT;\ \Delta T = 1, \Delta T_z = \pm 1;\ E) = \\ &= \sum_{\nu \neq 0} E_\nu^k\ \left| \langle \nu |\, \hat{\vec{\mathcal{M}}}^{(\beta^\pm allowed\, GT)}\, |0\rangle \right|^2 \xi_\Delta(E - E_\nu) \end{aligned} \tag{10.166}$$

with corresponding moments (see (7.375))

$$\begin{aligned} m_k^\pm(F) &= \sum_\nu E_\nu^k\ \left| \langle \nu |\, \hat{\mathcal{M}}^{(\beta^\pm allowed\, F}\, |0\rangle \right|^2 = \int_0^\infty dE\, E^k\, S_0^\pm(F;E) \\ m_k^\pm(GT) &= \sum_\nu E_\nu^k\ \left| \langle \nu |\, \hat{\vec{\mathcal{M}}}^{(\beta^\pm allowed\, GT}\, |0\rangle \right|^2 = \int_0^\infty dE\, E^k\, S_0^\pm(GT;E) \end{aligned} \tag{10.167}$$

where $|0\rangle$ is the ground state of the target nucleus, $|\nu\rangle$ are individual excitation states of the final nucleus with the excitation energies E_ν of the final nucleus (e.g. for (p,n) reaction $Q_{gs} = E_\nu + E_n - E_p$ where Q_{gs} is the ground state Q value of the given reaction (p,n)) [11] and $\xi_\Delta(E - E_\nu)$ is the

[11] In exprs. (10.166) and (10.167) we supposed implicitly that we discuss β-transitions from the ground state $|0\rangle$ of initial (target) nucleus to the excitation states $|\nu\rangle$ of the final nucleus.

Lorentz energy averaging function (7.373) in the energy smearing interval Δ (see (7.373)).

Further the zero order moments for allowed Fermi ($m_0^{\pm}(F)$), and allowed Gamow-Teller ($m_0^{\pm}(GT)$) transitions are discussed. These moments cannot be generally determined model-independently. They can be calculated numerically according to (10.166) and (10.167) for $k = 0$ in the framework of used shell-model space in which ground state correlations and Pauli principle are taken properly into account (e.g. as in the proton-neutron RPA approach mentioned in (7.333) and (7.334) [12]. However the difference of GT and F moments, $m_0^-(GT) - m_0^+(GT)$ or $m_0^-(F) - m_0^+(F)$, can be obtained model-independently and are only functions of the neutron or proton excess:

$$
\begin{aligned}
m_0^{\pm}(GT) = & \boxed{\begin{array}{c}\text{see}\\ (10.167)\end{array}} = \\
& = \sum_{\mu=0,\pm1} \sum_{\nu} \langle\nu|\, \hat{\mathcal{M}}_{\mu}^{(\beta^{\pm} allowed\, GT)}\, |0\rangle^{*}\, \langle\nu|\, \hat{\mathcal{M}}_{\mu}^{(\beta^{\pm} allowed\, GT)}\, |0\rangle = \\
& = \sum_{\mu=0,\pm1} \sum_{\nu} \langle 0|\, \hat{\mathcal{M}}_{\mu}^{(\beta^{\pm} allowed\, GT+)}\, |\nu\rangle\, \langle\nu|\, \hat{\mathcal{M}}_{\mu}^{(\beta^{\pm} allowed\, GT)}\, |0\rangle = \\
& = \sum_{\mu=0,\pm1} \langle 0|\, \hat{\mathcal{M}}_{\mu}^{(\beta^{\pm} allowed\, GT+)}\, \hat{\mathcal{M}}_{\mu}^{(\beta^{\pm} allowed\, GT)}\, |0\rangle \qquad (10.168)
\end{aligned}
$$

and similarly

$$
m_0^{\pm}(F) = \langle 0|\, \hat{\mathcal{M}}^{(\beta^{\pm} allowed\, F+)}\, \hat{\mathcal{M}}^{(\beta^{\pm} allowed\, F)}\, |0\rangle \qquad (10.169)
$$

[12] If the target nucleus is even-even nucleus with the ground state $|RPA\rangle$ then the states of the final nucleus in e.g. (p,n) reaction is odd-odd nucleus with states created by the proton-neutron RPA phonon operator given by (7.333) in the framework of the standard RPA.

Then we obtain for the difference $m_0^-(GT) - m_0^+(GT)$ following expression

$$
\begin{aligned}
& m_0^-(GT) - m_0^+(GT) = \\
& \quad = \sum_{\mu=0,\pm1} \langle 0| \, \hat{\mathcal{M}}_\mu^{(\beta^- allowed\, GT+)} \, \hat{\mathcal{M}}_\mu^{(\beta^- allowed\, GT)} \\
& \qquad\qquad - \hat{\mathcal{M}}_\mu^{(\beta^+ allowed\, GT+)} \, \hat{\mathcal{M}}_\mu^{(\beta^+ allowed\, GT)} \, |0\rangle = \\
& \quad = \boxed{\begin{array}{c} \text{see (10.165)} \\ \text{with } \hat{t}_\pm^{(j)} = \frac{1}{2}\tau_\pm^{(j)} \end{array}} = \\
& \quad = \frac{1}{4} \sum_{\mu=0,\pm1} \sum_{j,j'=1}^{A} \langle 0| \, \sigma_\mu^{(j)+} \tau_-^{(j)+} \, \sigma_\mu^{(j')} \tau_-^{(j')} - \sigma_\mu^{(j)+} \tau_+^{(j)+} \, \sigma_\mu^{(j')} \tau_+^{(j')} \, |0\rangle = \\
& \quad = \boxed{\begin{array}{c} \text{because } \sum_\mu \sigma_\mu^+ \sigma_\mu = \sigma^2 \text{ and } \sigma^2 = \sigma_1^2 + \sigma_2^2 + \sigma_3^2 = 3) \\ \text{and } (\tau_\pm)^+ = \tau_\mp \, , \; \langle 0| \, \tau_+^{(j)} \tau_-^{j'} \, |0\rangle = 0 \text{ for } j \neq j' \end{array}} = \\
& \qquad = \frac{3}{4} \, \langle 0| \, \sum_{j=1}^{A} [\, \tau_+^{(j)} \tau_-^{(j)} - \tau_-^{(j)} \tau_+^{(j)} \,] \, |0\rangle = \\
& \qquad = \boxed{\begin{array}{c} \text{because } \tau_+\tau_- \, |n\rangle = 4 \, |n\rangle) \quad \tau_-\tau_+ \, |p\rangle = 4 \, |p\rangle) \\ \tau_+\tau_- \, |p\rangle = \tau_-\tau_+ \, |n\rangle = 0 \end{array}} = \\
& \qquad = \frac{3}{4} \, (4N - 4Z) = 3 \, (N - Z)
\end{aligned}
\tag{10.170}
$$

and similarly for the difference $m_0^-(F) - m_0^+(F)$,

$$
\begin{aligned}
& m_0^-(F) - m_0^+(F) = \\
& \qquad = \frac{1}{4} \sum_\nu \left| \langle \nu| \, \sum_{j=1}^{A} \tau_-^{(j)} \, |0\rangle \right|^2 - \frac{1}{4} \sum_\nu \left| \langle \nu| \, \sum_{j=1}^{A} \tau_+^{(j)} \, |0\rangle \right|^2 = \\
& \qquad = N - Z
\end{aligned}
\tag{10.171}
$$

Expressions (10.170) and (10.171) are known as Ikeda sum rule and they are fully model-independent.

As an example of the theoretical determination of the GT strength function $S_0^-(GT, E)$ in the Fig.10.12 the GT strength distribution for ^{120}Sn, calculated in the framework of the quasiparticle + random phase approximation (QRPA) and or of the quasiparticle-vibration coupling (QPVC) (see [339]), are compared with the experimental GT strength extracted from (^{3}He,t) and (p,n)

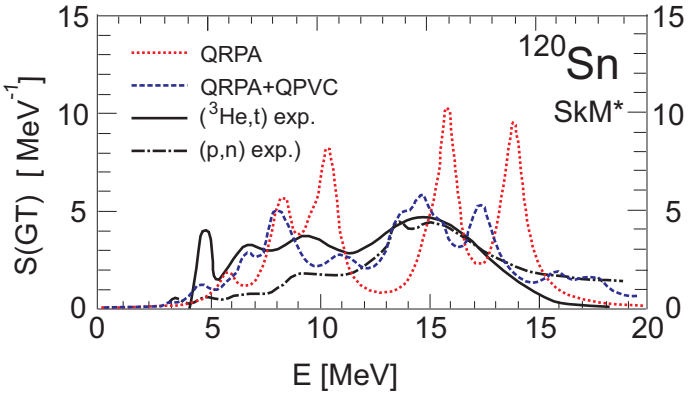


Figure 10.12: Gamow-Teller strength function for ^{120}Sn calculated by QRPA (red dotted curve) and QRPA+QPVC (blue dashed curve) approaches using the SkM* Skyrme interaction. The smearing file energy interval Δ=0.5 MeV is used. Experimental results from (^{3}He,t) and (p,n) reactions are shown for comparison. The cross section from (^{3}He,t) experiment is scaled by a factor of 1.6 so that the main GT strength exhausts 65% of Ikeda sum rule [341]. The cross section from (p,n) reaction is normalized by the unit cross section [342] (see also [181]) (taken from [339]).

reaction cross-section (see discussions further). The RPA results shown in the Fig.10.12 were obtained using the neutron-proton RPA approach where nucleon excitations are described as neutron-proton states $Q^+_\nu|RPA\rangle$ (see (7.333),(7.334)). The RPA results show in the fig.10.12 were obtained using the neutron-proton RPA approach where nucleon excitations are described as neutron-proton states $Q^+_\nu|RPA\rangle$ (see (7.333), (7.334)). The QPVC values are results of the calculation of $S^-_0(GT;E) = \sum_{\mu=0,\pm1}\sum_A |\langle a|\hat{\vec{\mathcal{M}}}^{(\beta^-\ allowed\ GT)}|0\rangle|^2$ where the excitation states $|a\rangle$ involve the coupling of the proton-neutron phonons with the nuclear states in the continues part of the spectrum (see [339] for details) [13].

The GT sum rule (10.170) has been checked many times using (p,n) and (n,p) reaction cross section (the way how to extract GT strength function $S^\pm_0(GT;\ E)$ from (p,n) and (n,p) reaction differential cross section at 0^o is discussed further). In the case of the (p,n) reaction on heavy and medium heavy nuclei due to Pauli principle blocking $S^+_0(GT,\ E) = 0$. According to the GT sum rule (10.170) it means that for (p,n) reaction on heavier nuclei $m^-_0(GT) \approx 3\times(N-Z)$. However obtained RPA values of $(m^-_0(GT))_{RPA}$ are about $\approx 0.5\, m^-_0(GT) = 0.5\times 3\times(N-Z)$ and therefore we have a "missing" strength problem if the RPA is used. It is expected that this RPA

[13]The coupling of RPA n-p phonons with nuclear states in the continues part of the spectrum is obtained by the finding of the eigen states of the effective complex Hamiltonian with the imaginary part simulating the escape strength function into the continues spectrum (see [339],[340]).

quenching of the GT strength function can be explained by the coupling of the 1p-1h (or 2- quasiparticle) RPA states either to 2p-2h (or 4- quasiparticle) states (as they are involved in (10.172) or to the Δ_{33}- particle nucleon hole $(\Delta - h)$ state at 300 MeV excitation (see e.g. [181]). However, the value of $(m_0^-(GT))_{RPA+QPVC}$ calculated from the QVPC exp. data in the Fig.10.12 is only by 10% higher than the value $(m_0^-(GT))_{RPA}$ and therefore it seems that the taking into account the coupling between 1p-1h and 2p-2h (or 2-qp and 4-qp) configurations does not explain fully the "missing" problem of the GT strength (see [339] for details).

In the end of this subsection the connection between moments $m_0^{\pm}(GT)$ and $m_0^{\pm}(F)$ with the $f^{\pm}T_{1/2}$ quantity of $\beta^{\pm}$-decay ($f^{\pm}T_{1/2} = \sum_f f^{\pm}T_{1/2}^{(i\to f)}$ - see (10.158)) and with the cross sections of reactions (p,n) (for $m_0^-(GT)$) and (n,p) (for $m_0^+(GT)$) are discussed. These connections allow one to extract values of $m_0^{\pm}(GT)$ and $m_0^{\pm}(F)$ from experimental values of $\beta^{\pm}$-decay half lives and from experimental values of differential cross sections of (p,n) and (n,p) reactions.

The half lives $T_{1/2}^{(i)}$ of the $\beta^{\pm}$- decay from the initial state $|i\rangle$ of the mother nucleus to all possible final states $|\nu\rangle$ of the daughter nucleus is given by (see (10.157))

$$T_{1/2}^{(i)} = \frac{ln2}{\sum_\nu w_{i\to\nu}^{(\beta^{\pm})}} = \boxed{\begin{array}{c}\text{see}\\(10.158)\end{array}} = \frac{1}{\sum_\nu \xi_{\nu i}^{\pm}} \frac{\kappa}{f^{(\pm)}(Z_f,\,\epsilon_0)} = \boxed{\begin{array}{c}\text{see}\\(10.150)\end{array}} =$$

$$= \frac{\kappa}{f^{(\pm)}(Z_f,\,\epsilon_0)} \frac{2J_i+1}{\sum_\nu \left[\, |\langle\nu||\,\hat{\mathcal{M}}^{(\beta^{\pm}\,allowed\,F)}\,||i\rangle|^2 + \lambda^2\,\langle\nu||\,\hat{\mathcal{M}}_1^{(\beta^{\pm}\,allowed\,GT)}\,||i\rangle|^2\right]} \tag{10.172}$$

Usually the mother nucleus is in its ground state ($|i\rangle = |0\rangle$. Then, using (10.168), (10.169) and Wigner-Eckard theorem, we obtain the following expression for the quantity $f\,T_{1/2}$,

$$f^{(\pm)}(Z_f,\,\epsilon_0)\,T_{1/2}^{(0)} = \frac{\kappa}{m^{\pm}(F) + \lambda^2\,m^{\pm}(GT)} \tag{10.173}$$

where $\kappa = 6549$s (or more precisely 6.147 ± 7s - see (10.159)). Therefore measuring of $\beta^{\pm}$- decay half-lives for pure Fermi or Gamov-teller β- transitions provide experimental values of $m_0^{(\pm)}(F)$ or $m_0^{(\pm)}(GT)$. However, usually we have problem because not all $\beta^{\pm}$- transitions $|0\rangle \to |f\rangle$ are pure Fermi or

pure GT transitions for the $\beta^{\pm}$- decay of given mother nucleus. Therefore more suitable way is to use charge-exchange reactions like (p,n) or (n,p) for the determination of $m_0^{(\pm)}(F)$ or $m_0^{(\pm)}(GT)$.

The reaction (p,n) is connected with the β^- transition operator $\hat{\mathcal{M}}^{(\beta^- \, allowed \, F)}$ and $\hat{\mathcal{M}}^{(\beta^- \, allowed \, GT)}$ and therefore for (p,n) reaction $m_0^-(F) \neq 0$, $m_0^-(GT) \neq 0$, $m_0^+(F) = 0$, $m_0^+(GT) = 0$ (because of the isovector selection rule). The opposite is true for the (n,p) reaction. In usual energies of the initial particles (tens or hundreds MeV) these reactions can be understood as direct reactions (see [181] and the Chapter 11). The distorted wave Born approximation for the description of the direct reactions (see the Subsection 11....) allows to parametrize the cross section of the (p,n) reaction for $L = 0$ transitions (that means allowed F and allowed GT transitions) as (see [343])

$$\frac{d\sigma}{d\Omega} \approx \sigma_\alpha(E_p, A) \, F_\alpha(q, \omega) \, m_0^-(\alpha) \tag{10.174}$$

where $\alpha = GT$ or F (according to the spin and isospin selection rules for the particular nuclear transition $|i\rangle \rightarrow |f\rangle$). In (10.174) E_p is the energy of the initial proton, q is the linear momentum transfer, and $\omega = E - Q_{gs}$ is the energy loss (E is the energy of the final nucleus and Q_{gs} is the ground state Q- value of the (p,n) reaction). The factor $\sigma_\alpha(E_p, A)$ is so called "unit cross section" which via its atomic mass A and bombarding energy E_p dependence connects measurement for different A and E_p . The factor F_α describes the shape of differential cross section where for $q \rightarrow 0$, $\omega \rightarrow 0$ (that means the zero angle between linear momenta of outgoing neutron and the final nucleus) the function $F_\alpha(q, \omega) \rightarrow 1$. So for the zero angle the differential cross section $d\sigma/d\omega(0^o)$ is proportional to $m_0^-(\alpha)$ and this proportionality can be used for the determination of $m_0^-(\alpha)$ ($\alpha = GT, F$) from the experimental values of $d\sigma/d\omega(0^o)$. Similar expression as (10.174) can be also obtained for (n,p) reactions for the determination of $m_0^+(\alpha)$. These expressions were used for the obtaining experimental values presented in the Fig.10.12.

11. Basic theory of nuclear reactions

11.1 Mechanisms of nuclear reactions

Up to now theoretical description of nuclear states has been discussed. Nuclear reactions were mentioned only in cases when it was necessary to demonstrate a quality of given nuclear model on the description of data from nuclear reactions, mainly data on cross sections (see e.g. photo-absorption reaction in the subsection 2.2.3, or nuclear fission in the subsection 5.1.2.3.2). Unlike the previous chapters in this chapter the main topic is the theoretical description of nuclear reactions with impacting particles having energy up to several hundreds of MeV. There are two main mechanisms of nuclear reactions with these energies, particularly

- reactions going through so called compound nucleus
- direct nuclear reactions

Which mechanism is applicable for given reaction depends on the kinetic energy of impacting particle and on the width Γ and mutual energy distances D of excitation states of the system impacting particle+target nucleus. Further the short and only qualitative descriptions of both mechanisms are given.

11.1.1 Reaction going through compound nucleus

Let us investigate the nucleus reaction where impacting particle a is absorbed by the target nucleus A and the whole energy of the particle is exhausted for the forming the final compound nucleus (CN) consisting from the impacting particle and target nucleus. The final compound nucleus is generally excited by the energy brought by the absorbed particle a. One can expect that the cross section of this absorption process increases when the energy of absorbed particle a is equal to the energy of some excitation state of the compound nucleus. By other words one can expect a resonance character of the cross section in dependence on the energy of the impacting particle

a. Each resonance corresponds to some excitation energy of the compound nucleus. However in real experiments we have no one impacting particle but mono-energetic beam of particles a with average energy E_a and the ability to recognize individual resonances in the cross section depends on the energy dispersion ΔE_a around average energy E_a of this beam. If the energy dispersion ΔE_a is sufficiently less than the width Γ_{CN} of individual excited CN state and both the ΔE_a and Γ_{CN} are sufficiently less than the average distance D_{CN} between two neighboring CN excitations, that means

$$\Delta E_a << \Gamma_{CN} << D_{CN} \tag{11.1}$$

then individual resonances in the absorption cross section can be observed. If the inequality (11.1) is not fulfilled then individual narrow resonances in the energy dependence of the cross section cannot be detected. Example of such absorption reaction is the neutron capture of low-energy neutrons. In this case the compound nucleus formed after the neutron capture is in relatively high excitation states where the density of excitation levels is big (with relatively small average distances D between neighboring excitation CN levels, $\Gamma_{CN} \approx D_{CN} \approx 1$ eV). So the cross section of the neutron capture in the dependence on the neutron energy has narrow resonances with widths given by narrow widths of the CN excitation states but only in the case when the inequality (11.1) is fulfilled.

The absorption reaction described above forms the first step of so called "nuclear reactions going through the compound nucleus" or shortly "compound nucleus reactions". So the result of this first step is the compound nucleus. The energy brought by the incoming particle to the compound nucleus provides the CN excited state where the kinetic energy of incoming particle is statistically spread out among all nucleons of the compound nucleus but the energy of each individual nucleon is not so big to leave the compound nucleus. As a result the life time of the compound nucleus is relatively big, much bigger than the time characteristic for typical electromagnetic transitions in nuclei. Nevertheless after relatively long CN life time some of nucleons during many-fold scattering with other nucleons obtains sufficient energy to fly out from the compound nucleus. This leaving of one or several nucleons from the compound nucleus is the second step of the compound nucleus reaction.

The idea of the compound nucleus reaction originates from the thirties of the 20-th century (see [344]) when N. Bohr introduced CN mechanism in the connection with the description of the resonance structure of cross sections of the neutron capture. In the connection with the two-step character of the

CN reactions mentioned above the cross section $\sigma_{\alpha\beta}$ of the CN reaction going from the channel α (consisting from the incoming particle a and the target nucleus A) to the channel B (with out-going particle b and the resulting nucleus B) through the compound nucleus (CN),

$$a + A \to CN \to b + B \tag{11.2}$$

was supposed to have the form of the product of two terms

$$\sigma_{\alpha\beta} = \sigma_{\alpha(CN)} \cdot P_{(CN)\beta} \tag{11.3}$$

where $\sigma_{\alpha(CN)}$ is the cross section of the creation of the CN from the initial channel α and $P_{(CN)\beta}$ is the probability of the decay of the CN into the channel β consisting from the resultant particle b and the final nucleus B. Since the life time of the compound nucleus is relatively big the final channel $\beta \equiv b + B$ "does not feel" all characteristics of the initial channel $\alpha \equiv a + A$ (that means spin and other internal characteristics of the initial particle a and the target nucleus A together with the relative linear momentum of the particle a with respect to the target nucleus A). This idea was introduced by the N. Bohr and it is known in the literature as the Bohr's hypothesis of the statistical independence of the decay and forming of the CN. The derivation and the discussion of both factors in (11.2) is presented in the next sections of this chapter.

11.1.2 Direct nuclear reactions

In the case of the CN reactions all wave functions of possible formation and decay channels of the given CN (in the form of the product of the internal wave functions of all particles (nuclei) in each channel and wave function of their relative motion) are spread out in all volume of the compound nucleus among all its nucleons. As a result the cross section of the CN reaction (11.2) is not dependent on the individual discrete eigenstates of the CN. Usual excitation energies of the CN in reactions (11.2) is high where the distances between neighboring CN levels are very small and corresponding eigen state wave functions overlap each other. Therefore the CN reaction cross section has no visible narrow resonances (the inequality (11.3) does not valid) and is smooth in the dependence on the energy of the incoming particle a or on the energy of the outgoing resultant particle b.

However in the second half of the forties and in the fifties of the 20-th century new cyclotrons enabled to measure nuclear reaction cross sections with

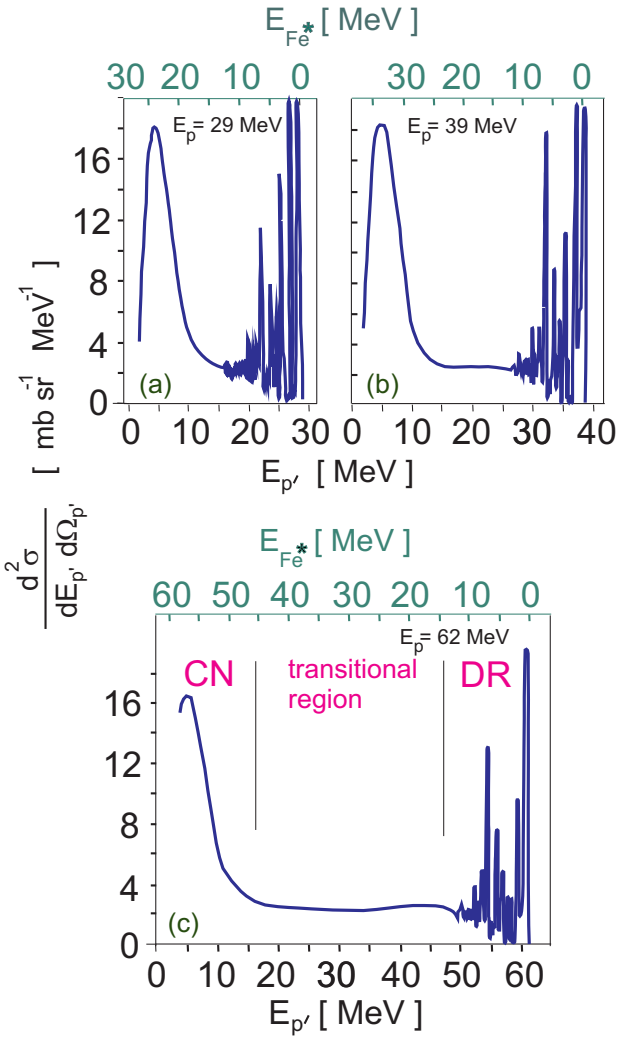


Figure 11.1: Differential cross section $d^2\sigma/dE_{p'}d\Omega_{p'}$ of the reaction $^{54}Fe(p,p')^{54}Fe^*$ for fixed scattering angle $\theta = 40$ degrees as a function of the energy of the scattered proton (lower horizontal axis in each panel) or as a function of the excitation energy of the final nucleus $^{54}Fe^*$ (top horizontal axis in each panel). Panels (a), (b), and (c) correspond to energies of incoming proton $E_p = 29$, 39, and 62 MeV, respectively. The CN reaction, direct reaction, and transitional regions are indicated in the panel (c) (adapted from [345] where exp. data from [346] were used)

higher energies (tens of MeV) of incoming particles (nucleons, deuterons and α- particles). It was found that if the incoming particle energy is sufficiently high (more than 20 MeV) then in the differential cross section $d^2\sigma/dE_b\, d\Omega_b$ in the dependence on the energy E_b of the outgoing particle b from the reaction $a + A \rightarrow b + B$ broad (1-2 MeV) maxima (resonances) appeared with mutual average distance about 1-2 MeV (see the Fig.11.1 where the differential cross section $d^2\sigma/dE_{p'}\, d\Omega_{p'}$ for the reaction $^{54}Fe(p,p')^{54}Fe^*$ is demonstrated in the dependence on the scattered proton energy $E_{p'}$ for fixed

scattering angle $\theta = 40^o$ and for three energies of incoming proton energies, E_p = 29, 39, 62 MeV - see [345]). One should realize that the sum of the excitation energy of the nucleus $^{54}Fe^*$ and the energy of the scattered proton in the inelastic proton scattering is equal to the energy E_p of the incoming proton, $E_p = E_{p'} + E_{Fe^*}$, in each panel of the figure. The smooth broad maximum (of the Maxwell form) in the beginning of all plots in the Fig.11.1 can be explained by the CN mechanism (when inequality (11.1) is not fulfilled and narrow and dense CN resonances are washed out). However resonances observed in higher energy part of observed cross section spectra ($E_{p'} > 20$ MeV in the panel (a), $E_{p'} > 30$ MeV in the panel (b) and $E_{p'} > 50$ MeV in the panel (c) of the Fig.11.1) cannot be explained by the compound nucleus mechanism (CN resonances have widths and mutual average energy distance about $1 - 2$ eV and it is six order less than observed widths and mutual distances of resonances observed in the higher energy parts of plots in the Fig.11.1). These relatively broad maxima in the higher energy part of the cross section spectrum were explained in [347] by so called optical potential model when the wave function of the relative motion of particle and nucleus in the initial ($\alpha \equiv a + A$) and the final ($\beta \equiv b + B$) channels of the reaction $\alpha \to \beta$ were obtained by the solving of the Shroedinger equation with the complex optical potential. Feshbach and collaborators supposed that only one or very restricted number of solutions of the Schroedinger equation with the complex optical potential contribute effectively to given relatively broad resonance in the Fig.11.1. As we will see later each such solution is connected with the excitation state of the final resultant nucleus B and therefore one can say that the relatively broad higher energy resonances (broad from the point of view of the particle b- energy - e.g. scattered proton energy $E_{p'}$ in the case of the inelastic scattering of protons on ^{54}Fe depicted on the Fig.11.1) are given by the widths of the low-energy excitation levels in the final resultant nucleus B (excited final nucleus $^{54}Fe^*$ in the case of the $^{54}Fe(p,p')^{54}Fe^*$ reaction denonstrated in the Fig.11.1). By other words it means that the solution of the Schroedinger equation for relative motion of particle and nuclei in channels α and β are not spread out inside the CN. As we will see later the optical potential for given channel α or β can be obtained by the averaging of nuucleon-nucleon interaction over several states of the CN in a small energy interval of the CN excitation energies around energy corresponding to the relative motion in the given channel (usually from elastic scattering $\alpha \to \alpha$ or $\beta \to \beta$). One can imagine that the incoming particle a interacts only with one, two or very restricted number of nucleons in the target nucleus (no with

all nucleons as it is in the CN reactions). During this interaction in a small part of the nucleus the output final channel β is formed (final particle b and final nucleus B). Reaction time is much smaller in the comparison with the CN reaction when all target nucleons interact with the incoming particle a. A small energy interval for the averaging over CN eigen-states needed for the creation of the optical potential is connected with relatively long free path of the incoming particle (more CN eigen-states used in the averaging in the creation of the complex optical means bigger its imaginary part and as a result of it also higher probability of the absorption of the incoming particle by the target nucleus and the forming of the compound nucleus). The shorter interaction time and the longer free path of the incoming particle means also higher probability of only one interaction with one nucleon of the target nucleus and that the incoming particle can escape without change (elastic or inelastic scattering, no the case where the target nucleus A are different from the final nucleus B, that means $A = B$).

In the reality both mechanisms described above assert themselves simultaneously in the given nuclear reaction. Which of these mechanisms prevails depends on the energy of the incoming particle. Each mechanism of reaction has its own models for the determination of differential or integral cross sections of the given reaction. Models of the direct reactions are usually used for the description of the higher energies of incoming particle (lower exc. energies of the final nucleus) where the resonance character of cross sections is connected with isolated excitations of the final nucleus (broad resonances in the higher energy part of the cross section spectrum - see the Fig.11.1). The models of CN reactions, with the averaging over a big energy interval of higher excitation CN states corresponding to the dispersion ΔE of the band of incoming particles, are convenient for the description of the cross sections in the lower part of the spectrum. Indeed in the spectra of outgoing final particles from nuclear reactions accomplished in the sixties both mechanisms were complementary: the lower energy smooth part of the cross section spectrum described by the CN reaction model was immediately followed by the broad resonances part corresponding to the direct reaction mechanism (see the panel(a) in the Fig.11.1). Developments in the accelerator techniques reached in the seventies allowed to investigate cross sections of nuclear reactions with the higher energy initial particle beams (nucleon or light nucleus beams). In the cross section spectra of nuclear reactions with higher energy of incoming particle the energy distance between the low-energy smooth Maxwell type peak (described by the CN mechanism) and the high energy

broad resonances part of the spectrum (described by the direct reaction mechanism) increased and so called transitional region was observed - see panels (b) and (c) in the Fig.11.1. This transitional region was possible to describe neither by the CN reaction mechanism nor by the direct reaction mechanism.

In next sections of this chapter both mechanisms described above qualitatively are discussed in details. At first the theory of Feshbach and Weiscopf is introduced where both mechanisms are formally taken into account in one approach [23].

11.2 Feshbach theory of nuclear reaction

In this section the formal general theory of reactions of two quantum micro-systems based on so called multi-channel formalism is discussed. This theory was introduced by H. Feshbach and collaborators in early fifties (see e.g. [23, 347] and citation therein). The theory is general in the sense that it is applicable not only for nuclear physics but for any reaction of two bound quantum systems with many possible output channels. The initial channel is formed by the incoming particle a (incoming micro-system) and target nucleus A (target micro-system). As a consequence of the interaction between particle a and target nucleus A in the initial channel generally a lot of output channels can be created (among them there is the elastic scattering and inelastic scattering channel $a + A$ and possible channels $b_i + B_i$ with final particle b_i and final nucleus B_i in each such output channel characterized by the index i (see the Fig.11.2). The concrete reaction $a + A \rightarrow b_i + B_i$

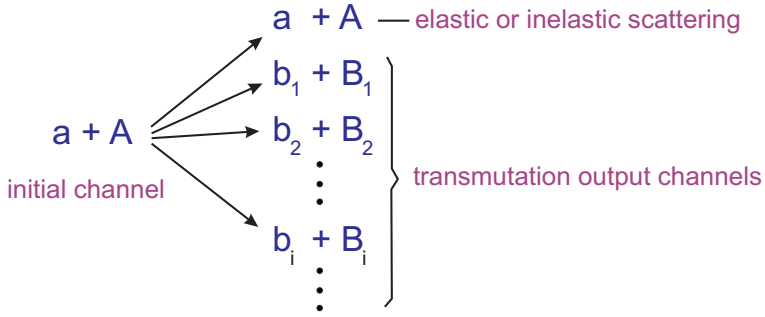


Figure 11.2: Schematic figure of output channels created by the interaction of initical particle a and target nucleus A in the initial channel $a + A$.

can proceed in terms of different mechanisms. Not in all cases all output

channels are known or some of them are too complicated for the theoretical description. The theory of Feshbach enables effectively to take into account channels which are not known or which we want to neglect for the different reasons. In this sense the theory is also general.

11.2.1 Classification of channels and reactions

11.2.1.1 Open and closed channels

The wave function of any channel (e.g. $b+B$) can be written as the product of the intrinsic wave function of the channel (product of the intrinsic wave functions of the particle b and the nucleus B) and the wave function of the relative motion of the particle b with respect to the nucleus B. Relative motion wave function is a solution of the stationary Schroedinger equation with the interaction between the particle b and the nucleus B in the channel $b+B$. It is known (see e.g. (D.32) for elastic scattering channel) that this relative motion function in the asymptotic region ($r \to \infty$) can be generally written in the form of the sum of outgoing spherical waves (terms with e^{ikr}/r in (D.32) with $k > 0$) and ingoing spherical waves (terms with e^{-ikr}/r in (D.32) with $k > 0$). If the relative motion wave function wave function in the given channel contains both spherical ingoing and outgoing terms or only outgoing terms then we speak about **open channels**. If the channel relative motion wave function in the asymptotic region ($r \to \infty$) is formed only by ingoing spherical waves then this channel is refereed to as **closed channel**. By other words it means that open channel involves in asymptotic region two separated bound objects - the particle b and the nucleus B.

One should realize that for the given particle b and the nucleus B the fact, if the given channel is open and closed, depends on the energy E of the relative motion of the particle b with respect to nucleus B. We can demonstrate it on the case of the elastic and inelastic scattering of the pion on the nucleus (we choose a pion and not e.g. nucleon because we want to avoid the problem with the Pauli principle). The initial channel of this scattering is always open and it has wave function in the form $u_0(\vec{k}_0, \vec{r})\psi_0(\xi)$ where $\psi_0(\xi)$ is the ground state wave function of the target nucleus (with the zero ground state energy) and $u_0(\vec{k}_0, \vec{r})$ is the corresponding wave function of the relative motion of the pion (with the kinetic energy $E \equiv \hbar^2 k_0^2/2m > 0$ where m is the relative motion reduced mass of the pion and ground state nucleus in the given pion-nucleus channel) and $\vec{r}$ is the relative coordinate of the pion with respect to the center of mass of the system pion+nucleus. In the inelastic scattering pion+nucleus

channel only part of the pion energy is passed to the target nucleus to excite it to the excitation state $\psi_n(\xi)$ with the energy $\varepsilon_n > 0$ ($\hat{H}_{nucleus}|\psi_n\rangle = \varepsilon_n\,|\psi_n\rangle$). Therefore the kinetic energy of the scattered pion is $\hbar^2 k_n^2/2m$ with the relative motion wave function $u_n(\vec{k}_n, \vec{r}) \overset{r\to\infty}{\longrightarrow}\approx e^{ik_n r}/r$ where $k_n = \sqrt{2m(E-\varepsilon_n)/\hbar^2}$. If $E - \varepsilon_n > 0$ then the k_n is real and the wave function $u_n(k_n r)$ represents really outgoing spherical wave and the inelastic channel is open by definition. If $E - \varepsilon_n < 0$ then the k_n is purely imaginary with the relative motion wave function $u_n(\vec{k}_n, \vec{r}) \overset{r\to\infty}{\longrightarrow}\approx e^{-|k_n|r}/r$. Then the pion is absorbed by the nucleus and corresponding inelastic scattering channel becomes closed channel. That means in the open channel the function $u_n(k_n r)$ is generally complex and in the closed channel the function $u_n(k_n r)$ is real and goes to zero for $r \to \infty$.

The creation of the open or closed (absorption) channel during the inelastic scattering in the dependence on the energy of the incoming particle a can be also seen in the Fig.11.3. Let us suppose that we analyze the inelastic scattering of some particle a (e.g. nucleon) whith the incoming energy E on the target nucleus A in the ground state and during this scattering the target nucleus is excited to the state with the excitation energy ϵ_n. In the upper part of the Fig.11.3 the situation is demonstrated when $E - \epsilon_n > 0$. In this case after the scattering the energy $E - \epsilon_n$ of the scattered particle is positive and the final channel is open with real scattered particle a. In the lower part of the Fig.11.3 the opposite situation is shown, $E - \epsilon_n < 0$. "Scattered particle a" has negative energy and the final channel (with not real scattered particle) cannot be open channel. In this case the incoming particle a is absorbed (captured) by the target nucleus and the final channel is closed (e.g. nucleon capture reaction). The Fig 11.3 is schematic, e.g. the only single-particle excitation of the target nucleus A is demonstrated in the figure. In reality not only single-particle excitations are present but also collective rotational and vibrational excitations of the target nucleus can be evoked during the interaction with the incoming particle a.

11.2.1.2 Prompt and time-delayed channels, "doorway" and "reminding" channels

The other classification of reaction channels corresponds to mechanism which prevails in the creation of given final channel $\beta_i \to b_i + B_i$ where the index i characterizes the given final channel in the ensemble of all possible final channels originating from the initial channel $\alpha \equiv a + A$ (see the Fig.11.2). In the Section 11.1 it was mentioned that generally there are two types of nuclear reaction mechanism, reactions going through the compound nucleus and di-

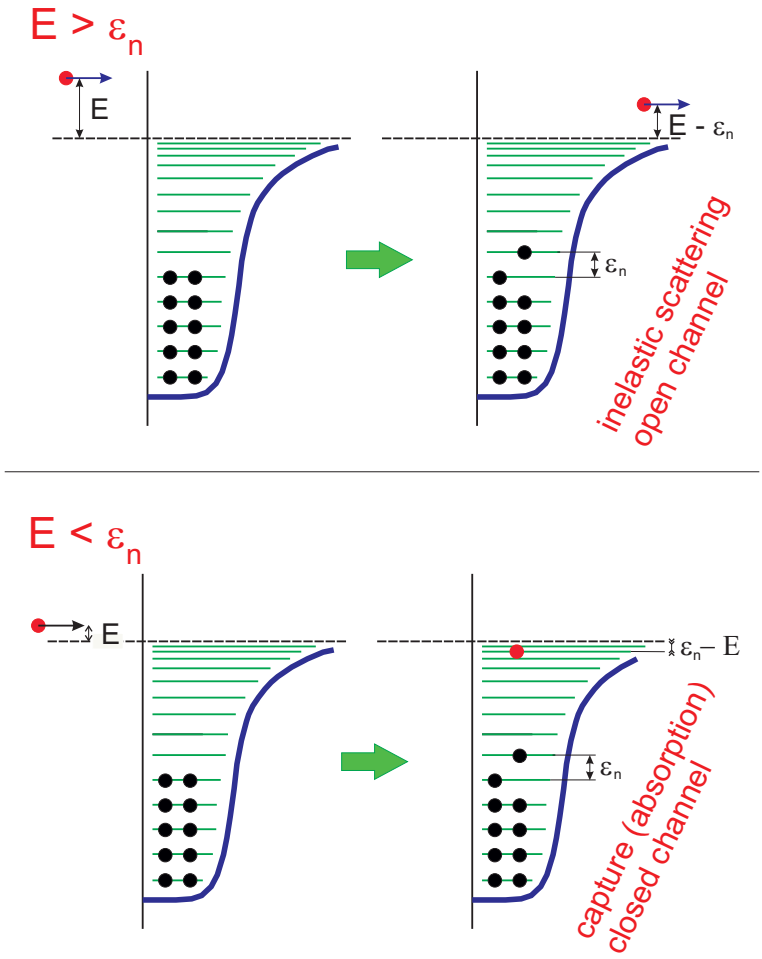


Figure 11.3: Schematic figure of the inelastic scattering of particle a (e.g. nucleon) on the target nucleus A in the ground state when in the final channel the nucleus is excited with the excitation energy ϵ_n. The upper part of the figure demonstrates the situation when the energy E of the incoming particle is bigger than the excitation energy ϵ_n of the final nucleus which corresponds to the standard inelasic scattering. The lower part of the figure shows the case when $E < \epsilon_n$ which means the absorption of the incoming particle and the creation of the closed final channel (e.g. nucleon capture reaction).

rect nuclear reactions, and that nuclear reactions going through a compound nucleus are much slower than the direct nuclear reactions. From this point of view H. Feshbach (see [23]) suggested to classify nuclear reactions according to the reaction time as prompt reactions (fast) and time-delayed reactions (slow). The direct nuclear reactions discussed in the Subsection 11.1.2 produce the final prompt channels (but not only) and the compound nucleus (CN) reactions are examples of reactions producing final time-delayed channels. However, as it was already mentioned, starting with the initial channel $a + A$ the given reaction $a + A \to b_i + B_i$ can go simultaneously directly (as prompt) and as well as through CN mechanism (as time-delayed). This situa-

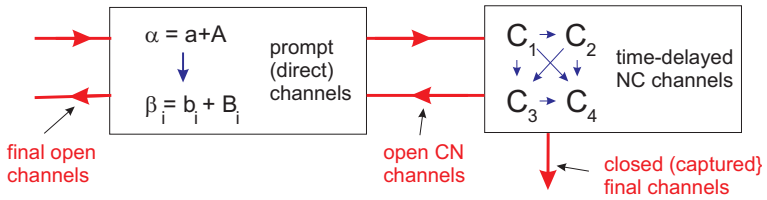


Figure 11.4: Schematic figure of the prompt and time-delayed channels. Final open channels $\beta_i \equiv b_i + B_i$ can be created from the initial channel $\alpha \equiv a + A$ either by prompt direct processes or through time-delayed processes. The total Hamiltonian of the system $a + A$ (and or any system $b_i + B_i$) couples directly all prompt channels mutually and with the initial channel while the final output open channels $b_i + B_i$ obtained through the compound nucleus is not coupled to the initial channel $a + A$ directly by the total Hamiltonian. As a result the probability of the transition leading to the final channel $b_i + B_i$ through the compound nucleus is much less than if the final channel $b_i + B_i$ is prompt channel obtained directly by the Hamiltonian interaction with the initial channel. Therefore the final channels obtained through the compound nucleus channels are time-delayed.

tion is schematically shown in the Fig.11.4. One can see that if the compound nucleus is formed it can decay back to open channels or it remains with the given number of nucleons in the different final closed capture channels.

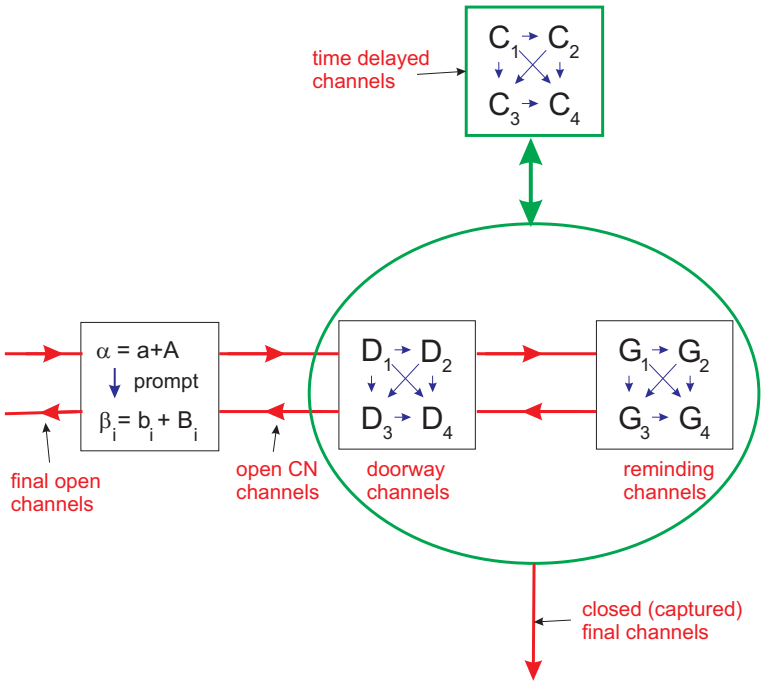


Figure 11.5: Schematic figure of the prompt, time-delayed, doorway- and reminding channels.

The channels $b_i + B_i$ formed through the compound nucleus states were divided by H. Feshbach into two groups according to the transition probability from the initial channel into the final channel, $a + A \to C \to b_i + B_i$:

- doorway channels D_1, D_2, ...
- reminding channels G_1, G_2, ...

Doorway channels D_i are channels which are created through the CN states but the interaction in the CN Hamiltonian provides relatively strong coupling between the given final channel $b_i + B_i$ and all prompt channels originating from given initial channel $a + A$ (involving the initial channel itself).

Reminding channels G_i involve CN channels which are weekly coupled to the prompt channels with the given initial channell. That means there is no direct transition between remainding CN channels and the initial channel $a + A$. This classification of CN channels as doorway D_i and reminding G_i is schematically figured in the Fig. 11.5.

If the given CN reaction proceeds through the doorway channels and not through reminding channels G_i then the relatively strong coupling of the doorway channel with fast prompt channels causes the high probability (faster going) of this reaction in the comparison with CN reactions going through reminding channels G_i. By other words the reaction

$$a + A \to D \to G \to D \to b_i + B_i \tag{11.4}$$

is slower than the reaction

$$a + A \to D \to b_i + B_i \tag{11.5}$$

because in the process (11.4) the compound nucleus remains for a long time in the reminding states G_1, $G_2, \cdots$ which are not coupled directly with the prompt channes.

Qualitative considerations above are formulated in more details in next subsections.

11.2.2 P-space and Q-space formalism

11.2.2.1 P-space and Q-space of reaction channels

According to the previous subsections all channels, which arise in the given reaction from one initial channel $a + A$, are divided into two groups, prompt and time-delayed channels (see the Fig. 11.4). In this subsection we do not take into account the possible existence of the doorway channels which will be discussed later (see subsection ....). So in the space of all channels connected with the system $a + A$ we can recognize two subspaces,

- P-space = space of prompt (usually open) channels which are connected mutually and with the initial channel $a + A$ by relatively strong interaction. The reaction from the initial channel $a + A$ to the prompt final channels is always very fast.

- Q-space = space of time-delayed (usually closed) channels which are weakly coupled with the initial channel. Reaction time of processes going through the Q-space channels is much higher than in the case of reactions going to the channels from P-space.

The choice of P- and Q- subspaces of channels, originating from the given initial channel $a + A$, depends on investigated process (reaction) and is directly connected with the edge (asymptotic) conditions for the relative wave function in each possible channel. For instance the initial prompt channel $a + A$ (with the target nucleus in the ground state) has relative wave function $u_0(\vec{k}_0.\vec{r})$ of the incoming particle a with respect to the target nucleus A which in the asymptotic region $r \to \infty$ is the sum of the incoming wave (usually plane wave describing incoming particle a) and spherical outgoing wave (describing the scattered particle a in the elastic channel $a + A \to a + A$). Next inelastic prompt channels in the space P corresponds in the asymptotic region $r \to \infty$ to the outgoing spherical wave describing inelastic scattering $a + A \to a + A^*$ or outgoing spherical waves describing scattered particle b in the transmutation reaction $a + A \to b + B$. Channel $a + A$ is fully involved in the Q- space when the particle a is captured and bound by the nucleus A and there is no any elastic or inelastic $a + A$ scattering. In such a case the relative motion wave function of the particle a with respect to the nucleus A (after the subtraction of incoming plane wave) should exponentially decreases to zero for $r \to \infty$ and particle a and target nucleus form the bound system. The non-initial channel $b + B$ is closed and usually involved in the Q-space when the mutual realtive wave function of particle b with respect to the nucleus B exponentially degreases with $r \to \infty$.

Furher we introduce projection operators $\hat{P}$ and $\hat{Q}$ which project out from the general ket $|\Psi\rangle$ of the system $a + A$ the part (component) belonging to the P-space and Q-space, respectively,

$$|\Psi\rangle = \hat{P}\,|\Psi\rangle + \hat{Q}\,|\Psi\rangle \tag{11.6}$$

with

$$\hat{Q}\hat{P}\,|\Psi\rangle = 0 \quad , \quad \hat{P}\hat{Q}\,|\Psi\rangle = 0 \tag{11.7}$$

and with usual properties of projection operators,

$$\begin{aligned} &\hat{P}^+ = \hat{P} \qquad \hat{Q}^+ = \hat{Q} \qquad \hat{P} + \hat{Q} = 1 \\ &\hat{P}^2 = \hat{P} \qquad \hat{Q}^2 = \hat{Q} \end{aligned} \tag{11.8}$$

In (11.6) we suppose that the general ket (state) $|\Psi\rangle$ fulfils following stationary condition

$$(\hat{H} - E)\,|\Psi\rangle = 0 \tag{11.9}$$

where $\hat{H}$ is the Hamiltonian of the system $a + A$ formed in the initial channel $a + A$. It should be noted that the general ket $|\Psi\rangle$ represents a linear combination of components belonging to all channels which can reachable from the given initial channel $a + A$ (see the Fig. 11.2). All these channel kets are now divided into two groups corresponding to P- and Q- spaces.

The equation (11.9) can be rewritten into two separate equations in the P- and Q- spaces (using (11.6), (11.7))

$$\begin{aligned} &(E - \hat{H})\,(\hat{P}\,|\Psi\rangle + \hat{Q}\,|\Psi\rangle) = 0 \\ &\quad \Rightarrow \qquad (E - \hat{H}_{PP})\,\hat{P}\,|\Psi\rangle = \hat{H}_{PQ}\,\hat{Q}\,|\psi\rangle \\ &\qquad\qquad (E - \hat{H}_{QQ})\,\hat{Q}\,|\Psi\rangle = \hat{H}_{QP}\,\hat{P}\,|\psi\rangle \end{aligned} \tag{11.10}$$

where

$$\begin{aligned} &\hat{H}_{PP} \equiv \hat{P}\hat{H}\hat{P} \qquad\qquad \hat{H}_{PQ} \equiv \hat{P}\hat{H}\hat{Q} \\ &\hat{H}_{QQ} \equiv \hat{Q}\hat{H}\hat{Q} \qquad\qquad \hat{H}_{QP} \equiv \hat{Q}\hat{H}\hat{P} \end{aligned} \tag{11.11}$$

Total Hamiltonian $\hat{H}$ corresponds to the Hilbert space of the system $a + A$ and therefore generally can be written as the sum of two terms (see also the Appendix Q) ,

$$\hat{H} = \hat{H}_0 + \hat{V} \tag{11.12}$$

where $\hat{H}_0$ represents the sum of Hamiltonans relevant to the internal degrees of freedom of the particle a and the target nucleus A and of the kinetic energy Hamiltonian of the poarticle a with respect to the nucleus A. The symbol $\hat{V}$ in (11.12) stands for the interaction between the projectile a and the targer A which generally involve also the interaction leading to the process going to the channels other than is the initial one.

The Hamiltonian $\hat{H}_0$ in (11.12) is supposed to be expressed in the internal coordinates of particle a and the nucleus A and their mutual relative coordinate. However it is necessary to realize that for the purpose of the determination of the cross-section (and other characteristics) of the reaction

$a + A \to b_i + B_i$ (where index i enumerates all open channels reachable from the initial channel $a + A$) we should re-transform the whole Hamiltonian $\hat{H}$ in 11.12) into the internal and relative coordinates corresponding to particles (nuclei) in the channel $b_i + B_i$. In the case of the reaction going through the compound nucleus $a + A \to C \to b_i + B_i$ we have to express also this Hamiltonian in terms of the internal coordiates of the compound nucleus.

The other condition which is usually fulfilled is that

$$\hat{H}_{PQ} = \hat{V}_{PQ} \qquad\qquad \hat{H}_{QP} = \hat{V}_{QP} \tag{11.13}$$

That means the interaction which bound the prompt channels from P-space with the time-delayed channels from Q-space is involved only in the interaction $\hat{V}$ ($\hat{V}_{PQ} = \hat{P}\hat{V}\hat{Q}$, $\hat{V}_{QP} = \hat{Q}\hat{V}\hat{P}$).

Equation (11.10) can be formally solved,

$$\begin{aligned}
&\hat{Q}|\Psi\rangle = \frac{1}{E^{(+)} - \hat{H}_{QQ}}\hat{H}_{QP}|\Psi\rangle \\
&\Rightarrow \quad (E - \hat{H}_{PP})\hat{P}|\Psi\rangle = \hat{H}_{PQ}\frac{1}{E^{(+)} - \hat{H}_{QQ}}\hat{H}_{QP}\hat{P}|\Psi\rangle \\
&\Rightarrow \quad (E - \hat{H}_{eff})\hat{P}|\Psi\rangle = 0
\end{aligned} \tag{11.14}$$

where

$$\hat{H}_{eff} = \hat{H}_{PP} + \hat{H}_{PQ}\frac{1}{E^{(+)} - \hat{H}_{QQ}}\hat{H}_{QP} \tag{11.15}$$

The index (+) in $E^{(+)}$ is connected with the possibility that the incoming particle a can be caught in some state of the compound nucleus with the excitation energy equal to the energy E. In such a case the fraction in (11.15) is singular. The index (+) corresponds the bypassing of this singularity when $E^{(+)} = E + i\eta$ with $\eta \to 0+$ (η goes to zero from the right side). This is also connected with the fact that all channels in the Q-space are closed, that means corresponding wave function of the relative motion of any particle and nuclei in any closed Q-space channel should go to zero if the relative distance r between particle and nucleus goes to ifinity - see the Appendix Q for details.

The effective Hamiltonian $\hat{H}_{eff}$ in (11.15) can be interpreted as follows,

1. the first term in (11.15) describes the pure prompt processes within the P-space;

2. the second term describes the time-delayed processes when the channel (state) $\hat{P}|\Psi\rangle$ from the P-space is at first coupled with the Q-space

in terms of the interaction $\hat{H}_{QP}$ then is propagated (developed) in the Q-space in terms of the propagator $1/(E^{(+)} - \hat{H}_{QQ})$ and then, finally re-transformed to the P-space by means of the interaction $\hat{H}_{PQ}$. The Schroedinger equation (11.14) iterates this process.

The effective Hamiltonian $\hat{H}_{eff}$ is generally energy dependent (because of the presence of $1/(E^{(+)} - \hat{H}_{QQ})$) and generally non-local. Moreover the Hamiltonian $\hat{H}_{eff}$ is complex. Further we show that exists the disperse relation between the real and imaginary parts of $\hat{H}_{eff}$.

At first $\hat{H}_{eff} - \hat{H}_{PP}$ in (11.15) are expressed in terms of the eigen-states of the Hamiltonian $\hat{H}_{QQ}$. Generally the Q-space Hamiltonian $\hat{H}_{QQ}$ has simultaneously discrete and continuous spectrum of eigen-states,

$$\hat{H}_{QQ}|\phi_s\rangle = \epsilon_s \, |\phi_s\rangle \qquad\qquad \hat{H}_{QQ}|\phi(\epsilon,\alpha)\rangle = \epsilon \, |\phi(\epsilon,\alpha)\rangle \tag{11.16}$$

where the index s characterizes the eigen-state of the Hamiltonian $\hat{H}_{QQ}$ with the energy ϵ_s in the discrete part of the spectrum and the continuous index α together with the energy ϵ characterize the state $|\phi(\epsilon,\alpha)\rangle$ from the continuous part of the eigen-states of the Hamiltonian $\hat{H}_{QQ}$. We suppose that the eigen-states $|\phi_s\rangle$ and $|\phi(\epsilon,\alpha)\rangle$ form the complete and ortonormalized basis.

$$\begin{aligned}
&\langle\phi_s|\phi_{s'}\rangle = \delta_{ss'} \qquad \langle\phi(\epsilon,\alpha)|\phi(\epsilon',\alpha') = \delta(\epsilon-\epsilon')\,\delta(\alpha-\alpha') \\
&\langle\phi_s|\phi(\epsilon,\alpha)\rangle = 0 \\
&\sum_s |\phi_s\rangle\langle\phi_s| + \int d\alpha \int d\epsilon \, |\phi(\epsilon,\alpha)\rangle \, \langle\phi(\epsilon,\alpha)| = 1
\end{aligned} \tag{11.17}$$

Since the continuous part of the energy spectrum is taken into account in (11.17) (that means energies ϵ in the basis $\{|\phi_s\rangle, |\phi(\epsilon,\alpha)\rangle\}$ are from the interval $\epsilon \in \langle 0, \infty)$) these energies cover all, open and closed, channels from the Q-space. It is necessary also to realize that for any energy E of impacting particle a in the initial channel $a + A$ we are able to find energy ϵ from the spectrum of the operator $\hat{H}_{QQ}$ such as E is close to ϵ ($E \approx \epsilon$). Using the completeness (11.17) of the basis $\{|\phi_s\rangle, |\phi(\epsilon,\alpha)\rangle\}$ the expression (11.15) can be rewritten as,

$$\begin{aligned}
&\hat{H}_{eff} - \hat{H}_{PP} = \\
&= \sum_s \frac{\hat{H}_{PQ} \, |\phi_s\rangle\langle\phi_s| \, \hat{H}_{QP}}{E - \epsilon_s} + \int d\alpha \int d\epsilon \frac{\hat{H}_{PQ} \, |\phi(\epsilon,\alpha)\rangle\langle\phi(\epsilon,\alpha)| \, \hat{H}_{QP}}{E^{(+)} - \epsilon}
\end{aligned} \tag{11.18}$$

If the impacting particle energy E is higher than any eigen-energy ϵ_s from the discrete part of the spectra of the Hamiltonian $\hat{H}_{QQ}$ then the function of ϵ under the integral of the second term in (11.18) has a pole for $\epsilon = E$. Therefore we add to the energy E in the denominator of the fraction in the second term of (11.18) the index $(+)$ in the agreement with the comment in the text under the expression (11.15). Further we modify the second term in (11.18) using the following expression known from mathematics.

$$\frac{f(\epsilon)}{E^{(+)} - \epsilon} = \mathcal{P}\left\{\frac{f(\epsilon)}{E - \epsilon}\right\} - i\,\pi\, f(\epsilon)\,\delta(E - \epsilon)$$

$$\text{where}\quad \mathcal{P}\left\{\frac{f(\epsilon)}{E - \epsilon}\right\} = \int_{-\infty}^{E-\delta} d\epsilon\, \frac{f(\epsilon)}{E - \epsilon} + \int_{E+\delta}^{\infty} d\epsilon\, \frac{f(\epsilon)}{E - \epsilon} \tag{11.19}$$

where the symbol $\mathcal{P}$ indicates so called principal value of the possible integral $\int \frac{d\epsilon\, f(\epsilon)}{E-\epsilon}$ (see the footnote [1] with the Fig. 11.6) So the expression (11.18) can be rewritten as

$$\hat{H}_{eff} - \hat{H}_{PP} = Re(\hat{H}_{eff} - \hat{H}_{PP}) + i\, Im(\hat{H}_{eff} - \hat{H}_{PP}) \tag{11.20}$$

with

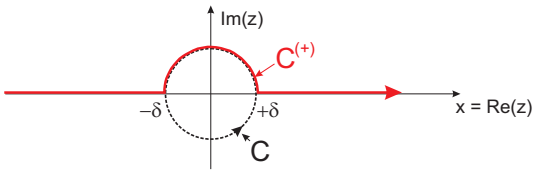


Figure 11.6: Scheme of the integration along the curve C and $C^{(+)}$.

[1]

$$\int_{-\infty}^{\infty} \frac{f(x)}{x} = \boxed{\begin{array}{c}\text{see}\\ \text{Fig. 11.6}\end{array}} = \int_{-\infty}^{-\delta} dx \frac{f(x)}{x} + \int_{+\delta}^{\infty} dx \frac{f(x)}{x} + \int_{(C)} dz \frac{f(z)}{z} = \boxed{\begin{array}{c}\text{because}\\ z = \delta\, e^{i\varphi}\end{array}} =$$

$$= \int_{-\infty}^{-\delta} dx \frac{f(x)}{x} + \int_{+\delta}^{\infty} dx \frac{f(x)}{x} + \frac{1}{2} \oint_{C^{(+)}} \frac{f(z)}{z} = \boxed{\begin{array}{c}\text{Cauchy residuum}\\ \text{theorem}\end{array}} =$$

$$= \int_{-\infty}^{-\delta} dx \frac{f(x)}{x} + \int_{+\delta}^{\infty} dx \frac{f(x)}{x} - \frac{1}{2}\, 2\pi i \int_{-\infty}^{+\infty} dx f(x)\, \delta(x) =$$

$$= \int_{-\infty}^{-\delta} dx \frac{f(x)}{x} + \int_{+\delta}^{\infty} dx \frac{f(x)}{x} - i\pi\, f(0) \equiv \mathcal{P}\{\frac{f(x)}{x}\} - i\pi\, f(0)$$

where

$$\mathcal{P}\{\frac{f(x)}{x}\} \equiv \int_{-\infty}^{-\delta} dx \frac{f(x)}{x} + \int_{+\delta}^{\infty} dx \frac{f(x)}{x}$$

is known as the principal value of the integral $\int dx \frac{f(x)}{x}$.

$$Re(\hat{H}_{eff} - \hat{H}_{PP}) =$$
$$= \sum_s \frac{\hat{H}_{QP} \, |\phi_s\rangle\langle\phi_s| \, \hat{H}_{QP}}{E - \epsilon_s} + \mathcal{P}\Big\{ \frac{1}{E-\epsilon} \int d\alpha \hat{H}_{PQ} \, |\phi(\epsilon,\alpha)\rangle\langle\phi(\epsilon,\alpha) \, \hat{H}_{QP} \Big\}$$
$$Im(\hat{H}_{eff} - \hat{H}_{PP}) = -\pi \int d\alpha \, \hat{H}_{PQ} \, |\phi(E,\alpha)\rangle\langle\phi(E,\alpha) \, \hat{H}_{QP} \tag{11.21}$$

We can substitute from the second equation of (11.21) into the first one and we obtain,

$$Re(\hat{H}_{eff} - \hat{H}_{PP}) =$$
$$= \sum_s \frac{\hat{H}_{QP} \, |\phi_s\rangle\langle\phi_s| \, \hat{H}_{QP}}{E - \epsilon_s} - \frac{1}{\pi} \mathcal{P}\Big\{ \frac{1}{E-\epsilon} \, Im(\hat{H}_{eff}(\epsilon) - \hat{H}_{PP}(\epsilon)) \Big\} \tag{11.22}$$

The Hamiltonian $\hat{H}_{PP}$ is usually real so we have,

$$Re(\hat{H}_{eff}) =$$
$$= \hat{H}_{PP} + \sum_s \frac{\hat{H}_{QP} \, |\phi_s\rangle\langle\phi_s| \, \hat{H}_{QP}}{E - \epsilon_s} - \frac{1}{\pi} \, \mathcal{P}\Big\{ \frac{1}{E-\epsilon} \, Im(\hat{H}_{eff}(\epsilon)) \Big\}$$
$$Im(\hat{H}_{eff}) = -\pi \int d\alpha \, \hat{H}_{PQ} \, |\phi(E,\alpha)\rangle\langle\phi(E,\alpha)| \, \hat{H}_{QP} \tag{11.23}$$

and this gives the disperse relation between the real and imaginary parts of the effective Hamiltonian $\hat{H}_{eff}$ acting in the P-space. One can see that even in the case when the Hamiltonian $\hat{H}_{PP}$ is real the presence of the Q-space and the interaction between P- and Q- spaces lead to the complexity of the effective Hamiltonian $\hat{H}_{eff}$ in the P-space.

11.2.2.2 Resonance Breight-Wigner expression for reaction $\mathscr{T}$- matrix

Further we will go back to the expr. (11.18) for the effective Hamiltonian in the P-space. We will suppose that the energy of the impacting particle is low and corresponds to the discrete energies of the Hamiltonian $\hat{H}_{QQ}$ and the value E is close to some particular eigen-energy ϵ_s of the bound eigen-state of $\hat{H}_{QQ}$ (Hamiltonian of the compound nucleus) [2], $(E \to \epsilon_s)$. Then the expression (11.18) is rewritten in the following form,

$$\hat{H}_{eff} = \hat{\tilde{H}}_{PP} + \frac{\hat{H}_{PQ} \, |\phi_s\rangle\langle\phi_s| \, \hat{H}_{QP}}{E - \epsilon_s} \tag{11.24}$$

[2] One should realize that the low energy of the impacting particle is usually connected with the reaction going through the compound nucleus - see the example of the reaction (p, p') demonstrated in the Fig.11.1.

where the small second term in (11.18) (because E lies in the energy interval of discrete eigen-energies, $E < \epsilon$) and all other eigen-state terms in the sum in the first term in (11.18) with different indexes from the particular s are supposed to be involved in $\hat{\bar{H}}_{PP}$ (together with $\hat{H}_{PP}$ itself). One should realize that the Hamiltonian $\hat{\bar{H}}_{PP}$ is generally complex and energy dependent. Then the stationary Schroedinger equation (11.14) for the wave function $\hat{P}|\Psi\rangle$ in the P-space can be rewritten as,

$$(E - \hat{\bar{H}}_{PP})\, \hat{P}|\Psi\rangle = \frac{\hat{H}_{PQ}|\phi_s\rangle\langle\phi_s|\ \hat{H}_{QP}\, \hat{P}|\Psi\rangle}{E - \epsilon_s} \tag{11.25}$$

In the coordinate representation this equation represents differential equation with right-hand-side term. From mathematical point of view it is known that general solution of such equation can be always written as the sum of one particular solution $\{\bar{\chi}^{(\pm)}\rangle$ of corresponding equation without right-hand-side term [3],

$$(E - \hat{\bar{H}}_{PP})\, |\bar{\chi}^{(\pm)}\rangle = 0 \tag{11.26}$$

and a formal solution of (11.25),

$$\hat{P}|\Psi\rangle_{form} = \frac{1}{E^{(+)} - \hat{\bar{H}}_{PP}}\, \frac{\hat{H}_{PQ}\, |\phi_s\rangle\langle\phi_s|\hat{H}_{QP}\, \hat{P}|\Psi\rangle}{E - \epsilon_s} \tag{11.27}$$

Indexes $(\pm)$ for the solution $|\bar{\chi}^{(\pm)}\rangle$ of the equation (11.26) (without right-hand-side term) is connected with the asymptotic ($r \to \infty$) behaviour of the wave function $\hat{P}|\Psi\rangle$ in the particular channel (see the Appendix Q for details). One should realize that in the asymptotic region $r \to \infty$ particles and nuclei in the given channel are infinitely far each other where both $\hat{H}_{PQ}$ and $\hat{H}_{QP}$ go to zero. So really, solution $|\bar{\chi}^{(\pm)}\rangle$ of the equation (11.26) represents the channel wave function in the asymptotic region and indexes $(\pm)$ characterizes the asymptotic behaviour:

- $$(E - \hat{\bar{H}}_{PP})\, |\bar{\chi}_i^{(+)}\rangle = 0 \tag{11.28}$$

  and $|\bar{\chi}_i^{(+)}\rangle$ is the solution of equation (11.26) (or (11.25) without right-hand-side term) when the initial channel wave function $|\bar{\chi}_i\rangle$ for the initial channel i in the P-space (expressed in the coordinate representation)

[3] One should realize that the Hamiltonian $\hat{\bar{H}}_{PP}$ involves a part of the interaction $\hat{H}_{QP}$ because it is supposed that the sum $\sum_{s' \neq s} \frac{\hat{H}_{QP}\, |\phi'_s\rangle\langle\phi'_s|\, \hat{H}_{QP}}{E - \epsilon'_s}$ is taken into account in $\hat{\bar{H}}_{PP}$. Therefore the solutions $|\bar{\chi}^{(\pm)}\rangle$ represent ingoing or outgoing distorted waves rather than ingoing and outgoing plane or spherical waves.

involves impacting wave (incoming plane or distorted wave) describing impacting particle and target nucleus and their relative motion in the initial channel i.

- $$(E - \hat{\bar{H}}_{PP})\,|\bar{\chi}_f^{(-)}\rangle = 0 \tag{11.29}$$

  and $|\bar{\chi}_f^{(-)}\rangle$ is the solution of equation (11.26) (or (11.25) without right-hand-side term) when the final channel wave function $|\bar{\chi}_f\rangle$ for the channel f in the P-space (expressed in the coordinate representation) involves outgoing wave (outgoing spherical or outgoing distorted wave) describing final particle and final nucleus in the final channel f.

So the general solution of the equation (11.25) for all P- channels reachable from the initial channel with the index i (e.g. $a + A$ channel) is

$$\begin{aligned}\hat{P}\,|\Psi\rangle &= |\bar{\chi}_i^{(+)}\rangle + \hat{P}\,|\Psi_{form}\rangle = \\ &= |\bar{\chi}_i\rangle + \frac{1}{E^{(+)} - \hat{\bar{H}}_{PP}}\,\frac{\hat{H}_{PQ}|\phi_s\rangle\langle\phi_s|\;\hat{H}_{QP}\,\hat{P}|\Psi\rangle}{E - \epsilon_s}\end{aligned} \tag{11.30}$$

or

$$(E^{(+)} - \hat{\bar{H}}_{PP})\,|\hat{P}\Psi\rangle = (E^{(+)} - \hat{\bar{H}}_{PP})|\bar{\chi}_i^{(+)}\rangle + \frac{\hat{H}_{PQ}|\phi_s\rangle\langle\phi_s|\hat{H}_{QP}|\hat{P}\Psi\rangle}{E - \epsilon_s} \tag{11.31}$$

On the base of the expression (11.13) and taking into account evident formula, $\hat{H} = \hat{P}\hat{H}\hat{P} + \hat{P}\hat{H}\hat{Q} + \hat{Q}\hat{H}\hat{P} + \hat{Q}\hat{H}\hat{Q}$, we will denote formally $\hat{V}_{int} \approx E^{(+)} - \hat{\bar{H}}_{PP}$ (as we will see the sign is not important), where $\hat{V}_{int}$ represents an interaction between P-space channels and Q-space channels. So eq. (11.31) can be rewritten as,

$$\hat{V}_{int}\,|\hat{P}\Psi_i\rangle = \hat{V}_{int}\,|\bar{\chi}_i^{(+)}\rangle + \frac{\hat{H}_{PQ}|\phi_s\rangle\langle\phi_s|\hat{H}_{QP}|\hat{P}\Psi_i\rangle}{E - \epsilon_s} \quad \text{with } \hat{V}_{int} = E^{(+)} - \hat{\bar{H}}_{PP} \tag{11.32}$$

where we added the index i to $|\Psi_i\rangle$ in order to point out that the channel state $|\Psi_i\rangle$ corresponds to the initial asymptotic state $|\bar{\chi}_i^{(+)}\rangle$. This equation is further multiplied by the bra $\langle\bar{\chi}_f^{(-)}|$ and we obtain,

$$\langle\bar{\chi}_f^{(-)}|\hat{V}_{int}\,|\hat{P}\Psi_i\rangle = \langle\bar{\chi}_f^{(-)}|\hat{V}_{int}\,|\bar{\chi}_i^{(+)}\rangle + \frac{\langle\bar{\chi}_f^{(-)}|\hat{H}_{PQ}|\phi_s\rangle\langle\phi_s|\hat{H}_{QP}|\hat{P}\Psi_i\rangle}{E - \epsilon_s} \tag{11.33}$$

However, if we compare $\langle\bar{\chi}_f^{(-)}|\hat{V}_{int}\,|\hat{P}\Psi_i\rangle$ with the expr. (Q.14) for the reaction matrix element $\mathcal{T}_{fi}$ in the Appendix Q then we can interpret $\mathcal{T}_{fi} = \langle\bar{\chi}_f^{(-)}|\hat{V}_{int}\,|\hat{P}\Psi_i\rangle$ as the total reaction matrix element $\mathcal{T}_{fi}$ of the process $i \to f$ between two channels i and f from the P-space where the reaction can go promptly and directly within the P-space (represented by the first term in the r.h.s. of (11.33), $\langle\bar{\chi}_f^{(-)}|\hat{V}_{int}\,|\bar{\chi}_i^{(+)}\rangle$) and /or through the Q-space as the time-delayed process (the second term in the r.h.s. of (11.33)). From this point of view the equation (11.33) can be rewritten as follows

$$\mathcal{T}_{fi} = \mathcal{T}_{fi}^{(P)} + \frac{\langle\bar{\chi}_f^{(-)}|\hat{H}_{PQ}|\phi_s\rangle\langle\phi_s|\hat{H}_{QP}|\hat{P}\Psi_i\rangle}{E-\epsilon_s} \tag{11.34}$$

where (see (Q.14))

$$\mathcal{T}_{fi} = \langle\bar{\chi}_f^{(-)}|\hat{V}_{int}\,|\hat{P}\Psi_i\rangle \tag{11.35}$$

is the total reaction $\mathcal{T}$- matrix element of the process $i \to f$ and

$$\mathcal{T}_{fi}^{(P)} = \langle\bar{\chi}_f^{(-)}|\hat{V}_{int}\,|\bar{\chi}_i^{(+)}\rangle \tag{11.36}$$

is the prompt fast amplitude associated with the first term in the r.h.s of (11.30).

Returning to the expr. (11.30) the multiplying both sides of it by $\langle\phi_s|\hat{H}_{QP}$ yields

$$\begin{aligned}
&\langle\phi_s|\hat{H}_{QP}|\hat{P}\Psi_i\rangle = \\
&= \langle\phi_s|\hat{H}_{QP}|\bar{\chi}_i^{(+)}\rangle + \frac{\langle\phi_s|\hat{H}_{QP}\,\frac{1}{E^{(+)}-\hat{\bar{H}}_{PP}}\hat{H}_{PQ}\,|\phi_s\rangle\,\langle\phi_s|\hat{H}_{QP}|\hat{P}\Psi_i\rangle}{E-\epsilon_s} = \\
&= \langle\phi_s|\hat{H}_{QP}|\bar{\chi}_i^{(+)}\rangle + \frac{\langle\phi_s|\,\hat{W}_{QQ}\,|\phi_s\rangle\,\langle\phi_s|\hat{H}_{QP}|\hat{P}\Psi_i\rangle}{E-\epsilon_s}
\end{aligned} \tag{11.37}$$

where the operator $\hat{W}_{QQ}$,

$$\hat{W}_{QQ}(E) \equiv \hat{H}_{QP}\frac{1}{E^{(+)}-\hat{\bar{H}}_{PP}}\hat{H}_{PQ} \tag{11.38}$$

was introduced and this operator is complex (at least because $E^{(+)} = E+i\eta$). We can express explicitely $\langle\phi_s|\hat{H}_{QP}|\hat{P}\Psi_i\rangle$ from the equation (11.37) as

$$\langle\phi_s|\hat{H}_{QP}|\hat{P}\Psi_i\rangle = \frac{(E-\epsilon_s)\,\langle\phi_s|\hat{H}_{QP}|\bar{\chi}_i^{(+)}\rangle}{E-\epsilon_s-\langle\phi_s|\hat{W}_{QQ}(E)|\phi_s\rangle} \tag{11.39}$$

and this can be substituted back to (11.34) and the total reaction $\mathcal{T}$- matrix element $\mathcal{T}_{fi}$ obtains following form

$$\mathcal{T}_{fi} = \mathcal{T}_{fi}^{(P)} + \frac{\langle \bar{\chi}_f^{(-)} | \hat{H}_{PQ} | \phi_s \rangle \, \langle \phi_s | \hat{H}_{QP} | \bar{\chi}_i^{(+)} \rangle}{E - \epsilon_s - \langle \phi_s | \hat{W}_{QQ}(E) | \phi_s \rangle} \tag{11.40}$$

Since the energy dependent operator $\hat{W}$ is complex its expectation value $\langle \phi_s | \hat{W}_{QQ}(E) | \phi_s \rangle$ is also complex and it can be always expressed as follows,

$$\langle \phi_s | \hat{W}_{QQ}(E) | \phi_s \rangle \equiv \Delta_s(E) - \frac{i}{2} \Gamma_s(E) \tag{11.41}$$

with its real and imaginary energy dependent parts. The substitution of (11.41) into (11.40) demonstrates a resonance character of the $\mathcal{T}$- matrix element,

$$\begin{aligned}
\mathcal{T}_{fi}(E) &= \mathcal{T}_{fi}^{(P)} + \frac{\langle \bar{\chi}_f^{(-)} | \hat{H}_{PQ} | \phi_s \rangle \, \langle \phi_s | \hat{H}_{QP} | \bar{\chi}_i^{(+)} \rangle}{E - \epsilon_s - \Delta_s(E) + \frac{i}{2} \Gamma_s(E)} = \\
&= \mathcal{T}_{fi}^{(P)} + \frac{\langle \bar{\chi}_f^{(-)} | \hat{H}_{PQ} | \phi_s \rangle \, \langle \phi_s | \hat{H}_{QP} | \bar{\chi}_i^{(+)} \rangle}{E - E_s(E) + \frac{i}{2} \Gamma_s(E)} = \\
&= \mathcal{T}_{fi}^{(P)} + \frac{[E - E_s(E) - \frac{i}{2} \Gamma_s(E)] \, \langle \bar{\chi}_f^{(-)} | \hat{H}_{PQ} | \phi_s \rangle \, \langle \phi_s | \hat{H}_{QP} | \bar{\chi}_i^{(+)} \rangle}{(E - E_s(E))^2 + \frac{1}{4} \Gamma_s^2(E)}
\end{aligned} \tag{11.42}$$

where we introduced

$$E_s(E) \equiv \epsilon_s + \Delta_s(E) \tag{11.43}$$

and it represents the position of the resonance of the amplitude $\mathcal{T}_{fi}(E)$ of the process $i \to f$ going through the eigenstate $|\phi_s\rangle$ of the Hamiltonian $\hat{H}_{QQ}$ with the eigen-energy ϵ_s close to the energy E. The real part $\Delta_s(E)$ of the expectation value (11.41) shifts the maximum of the resonance from the eigen-energy ϵ_s and this shift is induced by the interaction of the P-space channels with the channels from the Q-space. It is possible to see from the expression (11.42) that the imaginary part $\Gamma_s(E)/2$ of the expectation value $\langle \phi_s | \hat{W}_{QQ} | \phi_s \rangle$ determines the width of the resonance. However one should realize that both $\Delta_s(E)$ and $\Gamma_s(E)$ generally depend on the energy E and if we want to understand expression (11.42) as the resonance in the dependence on the energy E then the energy dependence $E_s(E)$ and $\Gamma_s(E)$ should be very weak, almost negligible.

Further we derive more concrete expressions for the width $\Gamma_s(E)$ and the energy shift $\Delta_s(E)$. We start with the definition (11.38) for the operator $\hat{W}_{QQ}$ and then using the identity (11.19) the expression for $\langle\phi_s|\hat{W}_{QQ}|\phi_s\rangle$ can be rewritten as follows

$$\langle\phi_s|\hat{W}_{QQ}(E)|\phi_s\rangle = \langle\phi_s|\hat{H}_{QP}\frac{1}{E^{(+)}-\hat{\bar{H}}_{PP}}\hat{H}_{PQ}|\phi_s\rangle = \boxed{\begin{array}{c}\text{see}\\(11.19)\end{array}} =$$

$$= \langle\phi_s|\hat{H}_{QP}\mathscr{P}\{\frac{1}{E-\hat{\bar{H}}_{PP}}\}\hat{\bar{H}}_{QP}\,|\phi_s\rangle - i\pi\langle\phi_s\,|\hat{H}_{QP}\,\delta(E-\hat{\bar{H}}_{PP})\,\hat{H}_{PQ}|\phi_s\rangle \tag{11.44}$$

and the comparison of (11.44) with (11.41) gives

$$\Gamma_s(E) = 2\pi\langle\phi_s\,|\hat{H}_{QP}\,\delta(E-\hat{\bar{H}}_{PP})\,\hat{H}_{PQ}|\phi_s\rangle \tag{11.45}$$

$$\Delta_s(E) = \langle\phi_s|\hat{H}_{QP}\mathscr{P}\{\frac{1}{E-\hat{\bar{H}}_{PP}}\}\hat{\bar{H}}_{QP}\,|\phi_s\rangle \tag{11.46}$$

The expression (11.45) for the width can be further modified using the complete set of eigen-states $|\bar{\chi}_r^{(+)}\rangle$ of the Hamiltonian $\hat{\bar{H}}_{PP}$ with the eigen-energy E_r ($\hat{\bar{H}}_{PP}|\bar{\chi}_r\rangle = E_r\,|\bar{\chi}_r\rangle$)

$$\Gamma_s(E) = 2\pi\sum_r\langle\phi_s|\hat{H}_{QP}|\bar{\chi}_r\rangle\,\delta(E-E_r)\,\langle\bar{\chi}_r|\hat{H}_{QP}|\phi_s\rangle$$

$$= \boxed{\begin{array}{c}\text{because}\\\hat{H}^{+}_{PQ}=\hat{H}_{QP}\end{array}} = 2\pi\sum_r|\langle\phi_s|\hat{H}_{QP}|\bar{\chi}_r\rangle|^2\,\delta(E-E_r) =$$

$$= \sum_r\Gamma_{sr}(E) \tag{11.47}$$

where

$$\Gamma_{sr}(E) \equiv 2\pi\,|\langle\phi_s|\hat{H}_{QP}|\bar{\chi}_r\rangle|^2\,\delta(E-E_r) \tag{11.48}$$

is so called partial width corresponding to the decay of the boud channel state $|\phi_s\rangle$ of the Hamiltonian $\hat{H}_{QQ}$ back to various possible P-space channels $|\bar{\chi}_r\rangle$ with the energy E (it is necessary to realize that ensemble of states $\{|\bar{\chi}_r\rangle\}$ form the basis of open channel states in the P-space).

Similarly for $\Delta_s(E)$ (see (11.46)) we obtain

$$\Delta_s(E) = \sum_r \langle\phi_s|\hat{H}_{QP}|\bar{\chi}_r\rangle\, \mathcal{P}\{\frac{1}{E-E_r}\}\, \langle\bar{\chi}_r|\hat{H}_{PQ}|\phi_s\rangle =$$
$$= \sum_r |\langle\phi_s|\hat{H}_{QP}|\bar{\chi}_r\rangle|^2\, \langle\bar{\chi}_r|\mathcal{P}\{\frac{1}{E-E_r}\}|\bar{\chi}_r\rangle =$$
$$= \sum_r \int dE'\, \delta(E_r - E')\, |\langle\phi_s|\hat{H}_{QP}|\bar{\chi}_r\rangle|^2\, \langle\bar{\chi}_r|\mathcal{P}\{\frac{1}{E-E'}\}|\bar{\chi}_r\rangle ==$$
$$= \boxed{\begin{array}{c}\text{see}\\ \text{(11.47) and (11.48)}\end{array}} = \frac{1}{2\pi}\,\mathcal{P}\{\frac{\Gamma_s(E')}{E-E'}\} \qquad (11.49)$$

The last equation in (11.49) represents the dispersion relation between the width $\Gamma_s(E)$ and the shift $\Delta_s(E)$.

The numerator of the resonance term in (11.42), particularly $\langle\bar{\chi}_f^{(-)}|\hat{H}_{PQ}|\phi_s\rangle$ and $\langle\phi_s|\hat{H}_{PQ}|\bar{\chi}_i^{(+)}\rangle$, is related to corresponding partial widths Γ_{si} and Γ_{sf},

$$\langle\phi_s|\hat{H}_{QP}|\bar{\chi}_i^{(+)}\rangle = e^{i\delta_i}\sqrt{\frac{\Gamma_{si}}{2\pi}} \equiv e^{i\delta_i}\,\frac{g_{si}}{\sqrt{2\pi}}$$
$$\langle\bar{\chi}_f^{(-)}|\hat{H}_{PQ}|\phi_s\rangle = e^{i\delta_f}\sqrt{\frac{\Gamma_{sf}}{2\pi}} \equiv e^{i\delta_f}\,\frac{g_{sf}}{\sqrt{2\pi}} \qquad (11.50)$$

where δ_f and δ_i stands for the phases of $|\bar{\chi}_f^{(+)}\rangle$ and $|\bar{\chi}_i^{(+)}\rangle$, respectively (in coordinate representation),

$$|\bar{\chi}_i\rangle = e^{i\delta_i}|F_i\rangle \qquad\qquad |\bar{\chi}_f\rangle = e^{i\delta_f}|F_f\rangle \qquad (11.51)$$

where $|F_i\rangle$ and $|F_f\rangle$ are real (see e.g. (D.7),(D.8),(D.24) or (D.31) with (D.28) for elastic scattering $i \equiv a + A \to a + A \equiv f$ where we had only one channel with $\delta = \delta_i = \delta_f$. The equation (11.51) assumes that $|\bar{\chi}_i\rangle$ and $|\bar{\chi}_f\rangle$ are eigenstates of the evolution operator $\hat{S}^{(PP)}$ connected with the Hamiltonian $\hat{H}_{PP}$, $\hat{S}^{(PP)}|\bar{\chi}_i^{(+)}\rangle \approx e^{2i\delta_i}|\bar{\chi}_i^{(+)}\rangle$ and $\hat{S}^{(PP)}|\bar{\chi}_f^{(+)}\rangle \approx e^{2i\delta_f}|\bar{\chi}^{(+)}\rangle$ (see (D.31)) for pure elastic scattering where for particular partial wave $\langle\vec{r}|\chi_{l,i}\rangle \approx P_l(cos\theta)\frac{e^{-ik_i r}}{r}$ and $\langle\vec{r}|\chi_{l,f}\rangle \approx P_l(cos\theta)\frac{e^{ik_f r}}{r}$ and $S_{el}^{(l)} = e^{2i\delta_l}$. The phases of the matrix elements (11.50) are given only by wave functions $\bar{\chi}_i\rangle$ and $\bar{\chi}_f\rangle$ because bound wave functions $|\phi_s\rangle$ are always real (since in the coordinate representation bound wave functions $\langle\vec{r}|\phi_s\rangle$ always go to zero for $\to\infty$ as $e^{-|k_s|r}$ - see the Subsection 11.2.1.1, and they are real). Then the substitution of (11.50) into (11.42) gives

$$\mathcal{T}_{fi}(E) = \mathcal{T}_{fi}^{(P)}(E) + \frac{1}{2\pi}\, e^{i(\delta_i+\delta_f)}\frac{g_{si}(E)\, g_{sf}(E)}{E - E_s(E) + \frac{i}{2}\Gamma_s(E)} \qquad (11.52)$$

The expression (11.52) is known in literature as one-channel Breight-Wigner resonance formula for $\mathcal{T}$- matrix element between one initial channel i and one final channel f from P-space where the reaction $i \to f$ can go promptly within the P-space (which corresponds to $\mathcal{T}_{fi}^{(P)}$ in (11.52) or through **one** channel state s from the Q-space (one particular eigen-state of the Hamiltonian $\hat{H}_{QQ}$ with the eigen-energy ϵ_s) - see the text above (11.24)).

If incoming initial asymptotic wave $\bar{\chi}_i^{(+)}\rangle$ and outgoing final wave $\bar{\chi}_f^{(-)}\rangle$ are solutions of (11.28) and (11.29) then the expression for the reaction matrix element $\mathcal{T}_{fi}$ in (11.52) can be rewritten as (here we assume that the P-space involves only two channels with indexes i and f),

$$\mathcal{T}_{fi} = \frac{1}{2\pi i}(1 - e^{2i\delta_i})\,\delta_{if} + \frac{e^{i(\delta_i+\delta_f)}}{2\pi}\frac{g_{si}g_{sf}}{E - E_s + \frac{i}{2}\Gamma_s} \tag{11.53}$$

where the first term, $\mathcal{T}_{fi}^{(P)} \equiv \frac{1}{2\pi i}(1 - e^{2i\delta_i})\,\delta_{if}$ represents the elastic scattering matrix element (see (Q.25) with (D.28)).

The index s in (11.16) represent all quantum numbers unambiguously characterizing the bound channel state $|\phi_s\rangle$ (closed channel in the Q-space) with the energy ϵ_s (usually index s involves the total angular momentum and total parity of the gives state $|\phi_s\rangle$). The expressions (11.42) or (11.52) valid in the case when the energy E is closed the some eigen-energy ϵ_s of the Hamiltonian $\hat{H}_{QQ}$. However this energy closeness is not the only condition of the validity of resonance expressions (11.42) or (11.52). The resonance character of these expressions can be seen only when the energy distances between the eigen-energy ϵ_s and the neighboring eigen-energies of $\hat{H}_{QQ}$ (further denoted as D) is sufficiently high. By other words resonances in $\mathcal{T}_{fi}$ caused by the neighboring eigen-states $|\phi_s\rangle$ should be separated. In the case when the energy distance D between neighboring eigen-energies ϵ_s is comparable or less then the width Γ_s of the resonance ($D \leq \Gamma_s$) then the exprs. (11.42) or (11.52) should be modified because resonance overlap. The modification consists in the fact that we do not start with the expression (11.24) but directly from the general equations (11.10).

At first the first equation in (11.10) is solved,

$$|\hat{P}\Psi_i\rangle = |\bar{\chi}_i^{(+)}\rangle + \frac{1}{E^{(+)} - \hat{H}_{PP}}\,\hat{H}_{PQ}\,|\hat{Q}\Psi_i\rangle \tag{11.54}$$

where the index i is again added in $|\Psi_i\rangle$ in order to point out that the general channel state is supposed to be created from the initial asymptotic wave $|\bar{\chi}_i^{(+)}\rangle$. The expression (11.54) reflects the fact that the general solution of the

first equation in (11.10) can be obtained as a sum of one particular solution $|\bar{\chi}_i^{(+)}\rangle$ of the corresponding equation without right-hand-side and the formal solution (the second term in (11.54)) of the first equation in (11.10). Similarly as we obtained expression (11.34) from (11.30) for the reaction matrix element in the case of the derivation of the one-channel Breight-Wigner formula the expression (11.54) gives the reaction $\mathcal{T}$- matrix element in the following form,

$$\begin{aligned}
\mathcal{T}_{fi} &= \langle \bar{\chi}_f^{(-)} | \hat{V}_{int} | \hat{P}\Psi_i \rangle = \\
&= \boxed{\begin{array}{c}\text{we suppose } \hat{V}_{int} \approx E^{(+)} - \hat{H}_{PP}, \text{ in the analogy} \\ \text{with the text below the expr. (11.31)}\end{array}} = \\
&= \langle \bar{\chi}_f^{(-)} | \hat{V}_{int} | \bar{\chi}_i^{(+)} \rangle + \langle \chi_f^{(-)} | \hat{H}_{PQ} | \hat{Q}\Psi_i \rangle = \\
&= \mathcal{T}_{fi}^{(P)} + \langle \bar{\chi}_f^{(-)} | \hat{H}_{PQ} | \hat{Q}\Psi_i \rangle
\end{aligned} \tag{11.55}$$

The substitution of (11.54) into the second equation in (11.10) yields,

$$\begin{aligned}
& (E - \hat{H}_{QQ}) \, |\hat{Q}\Psi_i\rangle = \hat{H}_{QP} \left[\, |\chi_i^{(+)}\rangle + \frac{1}{E^{(+)} - \hat{H}_{PP}} \, \hat{H}_{PQ} \, |\hat{Q}\Psi_i\rangle \, \right] \\
\Rightarrow \quad & \left(\, E - \hat{H}_{QQ} - \hat{H}_{QP} \frac{1}{E^{(+)} - \hat{H}_{PP}} \hat{H}_{PQ} \, \right) |\hat{Q}\Psi_i\rangle = \hat{H}_{QP} \, |\bar{\chi}_i^{(+)}\rangle
\end{aligned} \tag{11.56}$$

and using the definition (11.38) the expression (11.56) can be rewritten as,

$$\left(\, E - \hat{H}_{QQ} - \hat{W}_{QQ} \, \right) |\hat{Q}\Psi_i\rangle = \hat{H}_{QP} \, |\bar{\chi}_i^{(+)}\rangle \tag{11.57}$$

and we obtain

$$|\hat{Q}\Psi_i\rangle = \frac{1}{E^{(+)} - \hat{H}_{QQ} - \hat{W}_{QQ}} \, \hat{H}_{QP} \, |\bar{\chi}_i^{(+)}\rangle \tag{11.58}$$

Then the substitution of (11.58) into (11.55) gives for the $\mathcal{T}$- matrix element the following form,

$$\mathcal{T}_{fi} = \mathcal{T}_{fi}^{(P)} + \langle \bar{\chi}_f^{(-)} | \, \hat{H}_{PQ} \frac{1}{E^{(+)} - \hat{H}_{QQ} - \hat{W}_{QQ}} \hat{H}_{QP} \, |\bar{\chi}_i^{(+)}\rangle \tag{11.59}$$

Then we use the completeness of the discrete part of the system of eigen-states of the Hamiltonian $\hat{H}_{QQ}$ (see (11.17) where the second term can be neglected because the energy E in the denominator in (11.59) is supposed to be far from the continuous eigen-energies of the Hamiltonian $\hat{H}_{QQ}$. So for the

purpose of the modification of (11.59) only approximate completeness of the discrete part of eigen-states $|\phi_s\rangle$ of the operator $\hat{H}_{QQ}$ is further taken into account (only the first term in (11.17) can be used),

$$\hat{H}_{QQ}\,|\phi_s\rangle = \epsilon_s\,|\phi_s\rangle \qquad , \qquad \sum_s |\phi_s\rangle\langle\phi_s| \approx 1 \tag{11.60}$$

and it gives

$$\begin{aligned}
\mathcal{T}_{fi} &= \mathcal{T}_{fi}^{(P)} + \\
&\quad + \sum_{ss'} \langle\bar{\chi}_f^{(-)}|\,\hat{H}_{PQ}|\phi_s\rangle\langle\phi_s|\frac{1}{E^{(+)} - \hat{H}_{QQ} - \hat{W}_{QQ}}|\phi_{s'}\rangle\langle\phi_{s'}|\hat{H}_{QP}\,|\bar{\chi}_i^{(+)}\rangle = \\
&= \mathcal{T}_{fi}^{(P)} + \\
&\quad + \sum_{ss'} \langle\bar{\chi}_f^{(-)}|\,\hat{H}_{PQ}|\phi_s\rangle\frac{1}{E^{(+)} - \epsilon_{s'}\delta_{ss'} - \langle\phi_s|\hat{W}_{QQ}|\phi_{s'}\rangle}\langle\phi_{s'}|\hat{H}_{QP}\,|\bar{\chi}_i^{(+)}\rangle = \\
&\quad = \boxed{\begin{array}{c}\text{using the approximation} \\ \langle\phi_s|\hat{W}_{QQ}|\phi_{s'}\rangle \approx \langle\phi_s|\hat{W}_{QQ}|\phi_{s'}\rangle\,\delta_{ss'}\end{array}} \approx \\
&\approx \mathcal{T}_{fi}^{(P)} + \\
&\quad + \sum_{s} \langle\bar{\chi}_f^{(-)}|\,\hat{H}_{PQ}|\phi_s\rangle\frac{1}{E^{(+)} - \epsilon_s - \langle\phi_s|\hat{W}_{QQ}|\phi_s\rangle}\langle\phi_s|\hat{H}_{QP}\,|\bar{\chi}_i^{(+)}\rangle
\end{aligned} \tag{11.61}$$

where it is necessary to realize that $\langle\phi_s|\hat{W}_{QQ}|\phi_s\rangle = \Delta_s - \frac{i}{2}\Gamma_s$ (see (11.41))are generally complex and therefore the expression (11.61) represents again resonance formula but opposite to (11.40) or (11.42) with many resonances under the sum over s. Expression (11.61) is the Breight-Wigner resonance expression for $\mathcal{T}$- matrix element $\mathcal{T}_{fi}$ for the reaction $i \to f$ between one initial channel i from the P-space and one final channel f from P-space. The first term corresponds to the prompt transition $i \to f$ and the second term describes the time-delayed transition $i \to f$ going generally through all possible discrete states $|\phi_s\rangle$ of the compound nucleus states (discrete eigen-states of the Hamiltonian $\hat{H}_{QQ}$).

It is clear that the one-channel Breight-Wigner formula (11.52) can be obtained from (11.61) if only one term in the sum $\sum_s$ is taken into account (only term s with ϵ_s close to energy E).

In the end of this subsection we will go back to the one-channel Breight-Wigner formula (11.52) or (11.53). This formula was derived on the base

of (11.51) for the plane asymptotic wave $|\bar{\chi}_i^{(+)}\rangle$ and the outgoing spherical wave $|\bar{\chi}_f^{(-)}\rangle$ (see e.g. (D.24) for elastic scattering) or, equvalently, on the base of (D.31) where the asymptotic initial wave has radial spherical ingoing character and asymptotic final wave is represented again by radial spherical but outgoing wave. One should realize that if the scattering goes through bound states of $\hat{H}_{QQ}$ the linear momentum then $\vec{k}$ is purely imaginary and as a result the only complexity in (D.24) originates from $e^{2i\delta_l}$. Such an asymptotic waves are simultaneously eigen-states of the evolution operator $\hat{S}_P$ (connected with the Hamiltonian $\hat{\bar{H}}_{PP}$) with the eigen-values $e^{2i\delta_i}$ and $e^{2i\delta_f}$ ($\hat{S}_P|\bar{\chi}_i^{(+)}\rangle = e^{2i\delta_i}|\bar{\chi}_i^{(+)}\rangle$, $\hat{S}_P|\bar{\chi}_f^{(-)}\rangle = e^{2i\delta_f}|\bar{\chi}_f^{(-)}\rangle$). The other assumption for (11.53) was that the prompt P-space involves only two channels i and f.

When there are more prompt channels in the P-space then at first we approximate the solution of equation

$$(E - \hat{\bar{H}}_{PP})\,|\bar{\chi}_\alpha\rangle = 0$$

by spherical type asymptotic waves for all prompt channels in the P-space with their "pure" phase shifts Δ_α for all channels α in the P-space. Then, according to (11.53), we can introduce "unperturbed" $\mathcal{T}$- matrix within the P-space,

$$\mathcal{T}_{\alpha\beta}^{(unpert)} = \frac{1}{2\pi i}(1 - e^{2i\Delta_\alpha})\,\delta_{\alpha\beta} + \frac{e^{i(\Delta_\alpha+\Delta_\beta)}}{2\pi}\,\frac{g_{s\alpha}g_{s\beta}}{E - E_s + \frac{i}{2}\Gamma_s} \tag{11.62}$$

where $g_{s\alpha}$ gives the magnitude of $\langle\phi_s|\hat{H}|\bar{\chi}_\alpha\rangle$. From other side the perturbed $\mathcal{T}$- matrix in the given channel P-space can be obtained also by other more sophisticated approaches then that given by (11.61) based on the spherical asymptotic waves. Some of these more sophisticated methods (e.g. distorted wave approximation (DWA) method or coupled channel approximation (CCA) approach will be discussed in the Section 11.4.1.2 or 11.4.1.3. In any case it is always possible to find the transformation real orthogonal unitary matrix M which transform the unperturbed $\mathcal{T}$- matrix into the perturbed $\mathcal{T}$- matrix with matrix element,

$$\begin{aligned}\mathcal{T}_{fi} &= \sum_{\alpha\beta} M_{f\alpha}^{-1}\,\mathcal{T}_{\alpha\beta}\,M_{\beta i} = \sum_{\alpha\beta} M_{f\alpha}^{+}\,\mathcal{T}_{\alpha\beta}\,M_{\beta i} = \\ &= \sum_{\alpha\beta} M_{\alpha f}\Big[\,\frac{1}{2\pi i}(1 - e^{2i\Delta_\alpha})\,\delta_{\alpha\beta} + \frac{e^{i(\Delta_\alpha+\Delta_\beta)}}{2\pi}\,\frac{g_{s\alpha}g_{s\beta}}{E - E_s + \frac{i}{2}\Gamma_s}\,\Big]\,M_{\beta i}\end{aligned} \tag{11.63}$$

where channels i and f belong to the open prompt channels described by the DWA or CCA aproach. The first term in the r.h.s. of (11.63) represents prompt $i \to f$ process while the second term is relevant for the time-delayed process $i \to CN \to f$ going through the compound nucleus state $|\phi_s\rangle$.

Knowing matrix element $\mathcal{T}_{fi}$ (see e.g. (11.52), (11.53) or (11.60), (11.62)) of the process $i \to f$ it is possible to determine the corresponding differential cross section using the expression (Q.21) in the Appendix Q

$$\frac{d\sigma_{fi}}{d\Omega_f} = \frac{1}{(2\pi)^2} \frac{\mu_i \mu_f \, k_f}{\hbar^4 \, k_i} \, |\mathcal{T}_{fi}|^2 \tag{11.64}$$

where μ_i and μ_f are reduced masses of particle and nucleus in the initial and final channel, respectively, and $\hbar k_i$ is the absolute value of the relative linear momentum of the particle with respect to the nucleus in the initial channel i. Similarly the $\hbar k_f$ is the absolute value of the linear momentum of the relative motion of the particle and the nucleus in the final channel. In the connection with the expr. (11.64) it is necessary to point out again that the factor of the proportionality between differential cross-section and $|\mathcal{T}_{fi}|^2$ depends on the normalization of the asymptotic waves $|\chi_i^{(+)}\rangle$ and $|\chi_f^{(-)}\rangle$. The expr. (11.64) corresponds to the normalization of asymptotic waves as is given in (Q.28) where the intrinsic degrees of freedom of particle and nucleus in the given channel are involved in the energy density of the channel states (see the text below the expr. (Q.27) (see also [23]).

Other important fact should be mentioned again that all resonance expressions (11.42), (11.52), (11.53) or (11.61) derived in this subsection were based on the assumption that the energy E brought to the reaction by the incoming particle in the initial channel belongs to the energy interval of the discrete eigen-energies of the Hamiltonian $\hat{H}_{QQ}$ (discrete excitation energies of the compound nucleus). In the reality these resonances could be seen only in the case when the distance D between neghboring eigen-energies of $\hat{H}_{QQ}$ is much bigger then the widths Γ_s of individual eigen-states and also much bigger than the experimental energy blurring of the bunch of the impacting initial particles. Otherwise individual resonances are smudged and observed dependence of the reaction cross-section on the energy of the impacting particles or on the excitation energy of the final nucleus is continous without any resonances (as it is demonstrated in the Fig. 11.1 where dependence of the cross-section of the reaction (p,p') on $E_{p'}$ is continuous in the compound nucleus region of energies).

11.2.2.3 Optical potential

Optical potential is the effective potential used in the Schroedinger equation for the relative particle-nucleus motion wave function in the given open prompt channel. Model of the optical potential was formulated in the first half of the fifties (see [347]), originally for the case when only elastic open channel was involved in the P-space. Optical potential is complex and its imaginary part is induced by the existence of the channels not taken into account explicitly. In the language of the P- and Q- channels it means that for the description of the elastic process $a + A \to a + A$ in the P-space we have one channel $a + A$. Then we should solve the Schroedinger equation for this elastic prompt channel wave function $|\hat{P}\Psi\rangle$

$$(E - \hat{H}_{opt})\,|\hat{P}\Psi\rangle = 0 \tag{11.65}$$

with the complex optical Hamiltonian $\hat{H}_{opt}$ involving complex optical potential. Its form should be obtained from "known" Hamiltonians $\hat{H}_{PP}$, $\hat{H}_{PQ}$, $\hat{H}_{QP}$ and $\hat{H}_{QQ}$ (see (11.11)) by some averaging approach which is described further in this subsection. After that the solution of (11.65) is sewn logarithmically in some region of relative coordinates in the given P-channel, where the short-range interaction between a and A is zero, with the known free particle-nucleus $a - A$ wave function. As a result of this sewing we obtain partial wave phase shifts $\delta_l \equiv \delta_{i,l} = \delta_{f,l}$ and subsequently corresponding elastic matrix element of the S-matrix which finally determines elastic cross-section as is described in the Appendix D (see (D.26), (D.27)).

If there are more than one channel in the P-space then we should determine at first the optical potential for each channel in the P-space (usually using phase shift analysis for elastic scattering in each channel) and then the $\mathcal{T}$- matrix element $\mathcal{T}_{fi}$ can be obtained within the P-space (for instance so called destroyed wave Born approximation (DWBA) or coupled channel approximation (CCA) which will be discussed in Sections 11.4.1.3 and 11.4.1.3).

Further the averaging procedure of obtaining the optical Hamiltonian (potential) from $\hat{H}_{PP}$, $\hat{H}_{PQ}$, $\hat{H}_{QP}$ and $\hat{H}_{QQ}$ is shortly described. As it was mentioned above in order to determine the optical potential for given prompt channel $a + A$ the elastic scattering process $a + A \to a + A$ is analyzed. The interaction potential between the particle a and the nucleus A should be constructed by the averaging of all individual narrow resonances caused by the existence of bound states of the system $a + A$ (bound states of the corresponding compound nucleus) over the energy interval ΔE around the energy

E brought to the system $a + A$ by the impacting particle a. This averaging energy interval ΔE should be wider then the widths and mutual distances of individual compound nucleus resonances. However on the other side the averaging interval should be narrower than the energy interval where the important changes in the cross-section of the investigated process are expected or experimentally observed. The fluctuations in cross-section usually measured have widths of the order of hundreds of KeV to the units of MeV (see e.g. energy fluctuations of the cross-section of the reaction ^{26}Mg(p,p')^{26}Mg shown in the Fig.11.1). Usual magnitude of the width Γ of the CN resonances and their mutual distance D is of the order of eV. So the averaging interval ΔE should be somewhere between these values (between tents eV and hundreds of keV).

The starting point of averaging process mentioned above is the first equation in (11.10) (or equation (11.54)),

$$|\hat{P}\Psi_i\rangle = |\bar{\chi}_i^{(+)}\rangle + \frac{1}{E^{(+)} - \hat{H}_{PP}} \hat{H}_{PQ} \, |\hat{Q}\Psi_i\rangle \tag{11.66}$$

Further both sides of this equations are averaged over the interval ΔE also mentioned above. At the same time we suppose that the prompt part $|\bar{\chi}_i^{(+)}\rangle$ of (11.66) does not change much with the energy E (in the framework of the energy interval ΔE around the value E) and therefore the averaging concerns only the second term in (11.66) connected with the Q-space (with the state $|\hat{Q}\Psi_i\rangle$). Therefore after the averaging the expression (11.66) can be formally rewritten as,

$$|\left\langle \hat{P}\Psi_i \right\rangle\rangle = |\bar{\chi}_i^{(+)}\rangle + \frac{1}{E^{(+)} - \hat{H}_{PP}} \hat{H}_{PQ} \, |\left\langle \hat{Q}\Psi_i \right\rangle\rangle \tag{11.67}$$

where the symbol $|\left\langle \hat{P}\Psi_i \right\rangle$ or $|\left\langle \hat{Q}\Psi_i \right\rangle\rangle$ means the averaging.

Further the transition $\mathcal{T}$- matrix element $\mathcal{T}_{fi}$ for two prompt channels, the initial i and the final f, are averaged in the sense of the discussion above (for the elastic scattering $i = f$). Similarly as we obtained expression (11.55) from the expression (11.54) the expression (11.67) gives the following expression for the averaged transition $\mathcal{T}$- matrix element,

$$\left\langle \mathcal{T}_{fi} \right\rangle = \mathcal{T}_{fi}^{P} + \langle \bar{\chi}_f^{(-)}| \, \hat{H}_{PQ} \, |\left\langle \hat{Q}\Psi_i \right\rangle\rangle \tag{11.68}$$

The averaged wave function $|\left\langle \hat{Q}\Psi_i \right\rangle\rangle$ involved in (11.67) can be obtained by

the averaging of the equation (11.58)

$$|\left\langle \hat{Q}\Psi_i \right\rangle\rangle = \left\langle \frac{1}{E^{(+)} - \hat{H}_{QQ} - \hat{W}_{QQ}} \right\rangle \hat{H}_{QP} \, |\chi_i^{(+)}\rangle \tag{11.69}$$

Further the way af the averaging of the fraction $1/(E^{(+)} - \hat{H}_{QQ} - \hat{W}_{QQ})$ will be discussed. The substitution of (11.69) into (11.67) gives,

$$|\left\langle \hat{P}\Psi_i \right\rangle\rangle = |\bar{\chi}^{(+)}\rangle + \frac{1}{E^{(+)} - \hat{H}_{PP}} \hat{H}_{PQ} \left\langle \frac{1}{\hat{e}_{QQ}} \right\rangle \hat{H}_{QP} \, |\chi_i^{(+)}\rangle \tag{11.70}$$

where the operator $\hat{e}_{QQ}$ was defined as

$$\hat{e}_{QQ} = E^{(+)} - \hat{H}_{QQ} - \hat{W}_{QQ} \tag{11.71}$$

The action of the operator $(E^{(+)} - \hat{H}_{PP})$ on (11.70) yields (because in the P-space $(E^{(+)} - \hat{H}_{PP})|\left\langle \hat{P}\Psi_i \right\rangle\rangle = (E - \hat{H}_{PP})|\left\langle \hat{P}\Psi_i \right\rangle\rangle$)

$$(E - \hat{H}_{PP})|\left\langle \hat{P}\Psi_i \right\rangle\rangle = (E - \hat{H}_{PP}) \, |\bar{\chi}_i^{(+)}\rangle + \hat{H}_{PQ} \left\langle \frac{1}{\hat{e}_{QQ}} \right\rangle \hat{H}_{QP} \, |\bar{\chi}_i^{(+)}\rangle =$$

$$= \boxed{\begin{array}{c}\text{because } |\bar{\chi}_i^{(+)}\rangle \text{ is the solution of} \\ \text{the equation } (E - \hat{H}_{PP}) \, |\bar{\chi}_i^{(+)}\rangle = 0\end{array}} =$$

$$= \hat{H}_{PQ} \left\langle \frac{1}{\hat{e}_{QQ}} \right\rangle \hat{H}_{QP} \, |\bar{\chi}_i^{(+)}\rangle \tag{11.72}$$

The $|\bar{\chi}_i^{(+)}\rangle$ involved in (11.72) can be substituted by the formal solution of (11.70)

$$|\bar{\chi}_i^{(+)}\rangle = \frac{1}{1 + \frac{1}{E^{(+)} - \hat{H}_{PP}} \hat{H}_{PQ} \left\langle \frac{1}{\hat{e}_{QQ}} \right\rangle \hat{H}_{QP}} \, |\left\langle \hat{P}\Psi_i \right\rangle\rangle \tag{11.73}$$

and therefore (11.72) can be rewritten as

$$(E - \hat{H}_{PP})|\left\langle \hat{P}\Psi_i \right\rangle\rangle =$$

$$= \hat{H}_{PQ} \left\langle \frac{1}{\hat{e}_{QQ}} \right\rangle \hat{H}_{QP} \, \frac{1}{1 + \frac{1}{E^{(+)} - \hat{H}_{PP}} \hat{H}_{PQ} \left\langle \frac{1}{\hat{e}_{QQ}} \right\rangle \hat{H}_{QP}} \, |\left\langle \hat{P}\Psi_i \right\rangle\rangle \tag{11.74}$$

Further we apply following identity [4]

$$\hat{B} \frac{1}{1 + \hat{C}\hat{A}\hat{B}} = \frac{1}{1 + \hat{B}\hat{C}\hat{A}} \hat{B} \tag{11.75}$$

[4] Identity (11.75) follows evidently from:

$$(1 + \hat{B}\hat{C}\hat{A})\hat{B} = \hat{B}(1 + \hat{C}\hat{A}\hat{B}) \;\Rightarrow\; \hat{B} \frac{1}{1 + \hat{C}\hat{A}\hat{B}} = \frac{1}{1 + \hat{B}\hat{C}\hat{A}} \hat{B}$$

with

$$\hat{A} \equiv \left\langle \frac{1}{\hat{e}_{QQ}} \right\rangle \quad , \quad \hat{B} \equiv \hat{H}_{QP} \quad , \quad \hat{C} \equiv \frac{1}{E^{(+)} - \hat{H}_{PP}} \hat{H}_{PQ}$$

and (11.74) reads,

$$\begin{aligned}
&(E - \hat{H}_{PP}) | \left\langle \hat{P}\Psi_i \right\rangle\rangle = \hat{H}_{PQ} \left\langle \frac{1}{\hat{e}_{QQ}} \right\rangle \hat{B} \, \frac{1}{1 + \hat{C}\hat{A}\hat{B}} \, | \left\langle \hat{P}\Psi_i \right\rangle\rangle = \\
&= \hat{H}_{PQ} \left\langle \frac{1}{\hat{e}_{QQ}} \right\rangle \frac{1}{1 + \hat{B}\hat{C}\hat{A}} \hat{B} \, | \left\langle \hat{P}\Psi_i \right\rangle\rangle = \\
&= \hat{H}_{PQ} \left\langle \frac{1}{\hat{e}_{QQ}} \right\rangle \frac{1}{1 + \hat{H}_{QP} \frac{1}{E^{(+)} - \hat{H}_{PP}} \hat{H}_{PQ} \left\langle \frac{1}{\hat{e}_{QQ}} \right\rangle} \hat{H}_{QP} \, | \left\langle \hat{P}\Psi_i \right\rangle\rangle = \\
&= \boxed{\begin{array}{c}\text{see} \\ (11.57)\end{array}} = \hat{H}_{PQ} \left\langle \frac{1}{\hat{e}_{QQ}} \right\rangle \frac{1}{1 + \hat{W}_{QQ} \left\langle \frac{1}{\hat{e}_{QQ}} \right\rangle} \hat{H}_{QP} \, | \left\langle \hat{P}\Psi_i \right\rangle\rangle
\end{aligned} \tag{11.76}$$

So we obtain following equation for $| \left\langle \hat{P}\Psi_i \right\rangle\rangle$,

$$\left\{ E - \hat{H}_{PP} - \hat{H}_{PQ} \frac{1}{\left\langle \frac{1}{\hat{e}_{QQ}} \right\rangle^{-1} + \hat{W}_{QQ}} \hat{H}_{QP} \right\} | \left\langle \hat{P}\Psi_i \right\rangle\rangle = 0 \tag{11.77}$$

or

$$\left\{ E - \hat{H}_{opt} \right\} | \left\langle \hat{P}\Psi_i \right\rangle\rangle = 0 \tag{11.78}$$

where the optical Hamiltonian (with the complex optical potential) was introduced,

$$\hat{H}_{opt} \equiv \hat{H}_{PP} + \hat{H}_{PQ} \frac{1}{\left\langle \frac{1}{\hat{e}_{QQ}} \right\rangle^{-1} + \hat{W}_{QQ}} \hat{H}_{QP} \tag{11.79}$$

where the Hamiltonian $\hat{H}_{PP}$ involves the sum of the kinetic energy operator and the interaction potential for the relative motion of the particle a and the nucleus A and the internal Hamiltonians of the particle a and the nucleus A in the initial elastic channel. The second term represents the interaction active in the case when the elastic scattering goes through bound states of the corresponding compound nucleus. That means the optical potential is given by $\hat{H}_{opt}$ where the kinetic energy of the relative motion in the elastic channel together with the internal Hamiltonian of the particle a and the nucleus A are subtracted. Since the second term in (11.79) is always complex the optical potential is also always complex if in the given elastic process the branch

going through the compound nucleus bound states is possible (energetically with given energy of the impacting particle a or by other selection rules for the excitation of the compound nucleus bound states).

One can see from (11.78) that the optical Hamiltonian $\hat{H}_{opt}$ represents the Hamiltonian for the stationary Schroedinger equation for averaged channel state $|\left\langle \hat{P}\Psi_i \right\rangle\rangle$ from the P-space. It is evident that if the averaging is not performed then,

$$\left\langle \frac{1}{\hat{e}_{QQ}} \right\rangle \to \frac{1}{\hat{e}_{QQ}} \qquad \Rightarrow \qquad \left\langle \frac{1}{\hat{e}_{QQ}} \right\rangle^{-1} \to \hat{e}_{QQ} = E^{(+)} - \hat{H}_{QQ} - \hat{W}_{QQ} \quad (11.80)$$

and taking into account (11.57) we obtain,

$$\hat{H}_{opt} \to \hat{H}_{PP} + \hat{H}_{PQ} \frac{1}{E^{(+)} - \hat{H}_{QQ} - \hat{W}_{QQ} + \hat{W}_{QQ}} \hat{H}_{QP} =$$

$$= \boxed{\begin{array}{c}\text{see}\\(11.15)\end{array}} = \hat{H}_{eff} \qquad (11.81)$$

So without averaging equation (11.78) becomes the same as the equation (11.14).

The term $\left\langle \frac{1}{\hat{e}_{QQ}} \right\rangle$ represents the averaged influence of channels not taken in the P-space. Therefore the averaged quantity $\left\langle \frac{1}{\hat{e}_{QQ}} \right\rangle$ depends on the choice of P- and Q- spaces. In practice it is usually supposed that in the first step the channels in the P-space don't interact mutually. That means in the $\hat{H}_{opt}$ only "diagonal" part of the relative motion potential responsible for the elastic scattering in individual open channels in the P- space is taken into account in (11.79) (without any mutual interaction of channels in the P- space). By other words it corresponds to the situation when only elastic process in all P- channels are analyzed independently ignoring their mutual interaction.

If we want to take into account also the interaction between different P-space channels then in the second step nondiagonal interaction terms in the $\hat{H}_{PP}$ should be involved in the system of equations for P- space channels. In such a case instead of the individual equations (11.78) without right-hand-side we have the system of coupled integral-differential equations for all prompt open channels (that means for $|\left\langle \hat{P}\Psi_i \right\rangle\rangle_\nu$ with $\nu = 1, 2, \cdots$, all prompt channels) with corresponding non-diagonal matrix elements of the $\hat{H}_{PP}$ in the right-hand-side of (11.78). This coupled channel approach will be discussed in the Sections 11.4.1.2 and 11.4.1.3 in the connection with the coupled channel approximation and distorted wave Born approximation).

Generally one can say that the optical potential (Hamiltonian) is an absorptive type of potential for the description of prompt channel processes where the imaginary part is responsible for the absorption of the probability flow escaping to Q- channels involving bound states of the compound nucleus.

Further the procedure of the averaging of $\left\langle \frac{1}{\hat{e}_{QQ}} \right\rangle$ is shown in more details. Let the $F(E)$ is arbitrary function (or operator) depending on the energy E. Its locally averaged value for the certain normalized density (or folding function) $\rho(E, E')$ is

$$\left\langle F(E) \right\rangle = \int \rho(E, E')\, F(E')\, dE' \tag{11.82}$$

where

$$\int \rho(E, E')\, dE' = 1 \tag{11.83}$$

So the averaged quantity $\left\langle \frac{1}{\hat{e}_{QQ}} \right\rangle$ is

$$\begin{aligned} \left\langle \frac{1}{\hat{e}_{QQ}} \right\rangle &= \int \rho(E, E')\, \frac{1}{\hat{e}_{QQ}(E')}\, dE' = \boxed{\begin{array}{c}\text{see}\\(11.71)\end{array}} = \\ &= \int \rho(E, E')\, \frac{1}{E' - \hat{H}_{QQ} - \hat{W}_{QQ}}\, dE' \end{aligned} \tag{11.84}$$

It is necessary to realize that $\frac{1}{\hat{e}_{QQ}(E)}$ has poles in the dependence on E and in the vicinity of these poles its value changes very quickly. For the averaging density $\rho(E, E')$ different functions can be used. The most usual are following two, Lorentzian form

$$\rho(E, E') = \frac{\Delta}{2\pi}\, \frac{1}{(E - E')^2 + \frac{\Delta^2}{4}} \tag{11.85}$$

and "box" averaging form

$$\rho(E, E') = \begin{cases} \frac{1}{\Delta E} & \text{for } |E - E'| < \frac{E}{2} \\ 0 & \text{for } |E - E'| > \frac{E}{2} \end{cases} \tag{11.86}$$

Both these types of averaging take differently into account the compound nucleus resonances which are energetically far from the energy E. In the case of the "box" averaging more distant resonances are not included at all (as it follows from (11.86)). Further both way of averaging are discussed in details.

Lorentzian averaging ($\frac{1}{\hat{e}_{QQ}} \to \left\langle \frac{1}{\hat{e}_{QQ}} \right\rangle_{Lorentz}$)

$$\left\langle F(E) \right\rangle = \frac{\Delta}{2\pi} \int_{-\infty}^{\infty} \frac{F(E')}{(E-E')^2 + \frac{\Delta^2}{4}}\, dE' = \tag{11.87}$$

If it is possible to suppose that the function (operator) $F(z)$, taken as dependent on the complex variable z, has no any singularity and behaves well in the upper half of the complex z- plane, it is convenient to evaluate the integral (11.87) using the calculus of residues (that means $\int_{-\infty}^{\infty} f(E')dE' = \oint_C f(z)dz$ where C is the "infinite" semicircle in the upper half of the complex z- plane)

$$\left\langle F(E) \right\rangle = \frac{\Delta}{2\pi} \oint_C \frac{F(z)}{(E-z)^2 + \frac{\Delta^2}{4}}\, dz =$$

$$= \boxed{\begin{array}{c}\text{residue theorem: } \oint \frac{f(z)}{g(z)}dz = 2\pi i \sum_i res(\frac{f}{g})_i \\ \text{where } g(z_i) = 0 \text{ and } res(\frac{f}{g})_i = \frac{f(z_i)}{g'(z_i)}\end{array}} =$$

$$= \frac{\Delta}{2\pi}\, 2\pi i\, res\Big(\frac{F(z)}{(E-z)^2 + \frac{\Delta^2}{4}}\Big)_{z=E+\frac{i\Delta}{2}} =$$

$$= \frac{\Delta}{2\pi}\, 2\pi i\, \frac{F(z = E + i\frac{\Delta}{2})}{i\Delta} = F(z = E + \frac{i\Delta}{2}) \tag{11.88}$$

In our case $F(z) = \frac{1}{z - \hat{H}_{QQ} - \hat{W}_{QQ}}$ and (11.88) gives

$$\left\langle \frac{1}{\hat{e}_{QQ}} \right\rangle = \frac{1}{E + \frac{i\Delta}{2} - \hat{H}_{QQ} - \hat{W}_{QQ}} \tag{11.89}$$

Before we started averaging the width of each reaction amplitude resonance had been given by Γ_s (see (11.40), (11.41) and (11.42) - for one-channel Breight-Wigner resonance) involved in (11.41)

$$\langle \psi_s | \hat{W}_{QQ}(E) | \phi_s \rangle = \Delta_s - \frac{i}{2}\Gamma_s(E) \tag{11.90}$$

From the expression (11.89) one can see that thanks to the averaging the width of each resonance increases by the Δ. Since the Δ is substantially higher than the original width $\Gamma_s(E)$ the fluctuations caused by the individual compound nucleus resonance are washed out and the contribution of $\hat{W}_{QQ}$ into (11.89) can be neglected. The expression (11.89) is further substituted into (11.80) and the optical Hamiltonian obtain following form (the contribution from $\hat{W}_{QQ}$ is neglected)

$$\left(\hat{H}_{opt}\right)_{Lorentz} = \hat{H}_{PP} + \hat{H}_{PQ}\, \frac{1}{E - \hat{H}_{QQ} + \frac{i\Delta}{2}}\, \hat{H}_{QP} \tag{11.91}$$

where Δ is the width of the local averaging by the Lorentz- type function (11.85).

"Box" averaging

Further we suppose that we analyze optical potential in energies E which are very close to one concrete eigen-energy ϵ_s of te Hamiltonian $\hat{H_{QQ}}$ and that the difference $E - E_s = E - \epsilon_s - \Delta_s$ (see (11.43) is very low, much lower that the energy interval ΔE of the averaging,

$$\Gamma_s << E - E_s << \frac{\Delta E}{2} \tag{11.92}$$

The substitution of (11.86) into (11.84) gives,

$$\begin{aligned}
\left\langle \frac{1}{\hat{e}_{QQ}} \right\rangle &= \frac{1}{\Delta E} \int_{E-\frac{\Delta E}{2}}^{E+\frac{\Delta E}{2}} \frac{dE'}{E' - \hat{H}_{QQ} - \hat{W}_{QQ}} \approx \\
&\approx \frac{1}{\Delta E} \int_{E-\frac{\Delta E}{2}}^{E+\frac{\Delta E}{2}} \frac{dE'}{E' - \langle \phi_s | \hat{H}_{QQ} | \phi_s \rangle - \langle \phi_s | \hat{W}_{QQ} | \psi_s \rangle} = \boxed{\begin{array}{c}\text{see} \\ (11.41)\end{array}} = \\
&= \frac{1}{\Delta E} \int_{E-\frac{\Delta E}{2}}^{E+\frac{\Delta E}{2}} \frac{dE'}{E' - \epsilon_s - \Delta_s(E) + \frac{i}{2}\Gamma_s(E)} = \boxed{\begin{array}{c}\text{see} \\ (11.43)\end{array}} = \\
&= \frac{1}{\Delta E} \int_{E-\frac{\Delta E}{2}}^{E+\frac{\Delta E}{2}} \frac{dE'}{E' - E_s(E) + \frac{i}{2}\Gamma_s(E)} =
\end{aligned}$$

$$
\begin{aligned}
&= \frac{1}{\Delta E}\int_{E-\frac{\Delta E}{2}}^{E+\frac{\Delta E}{2}} dE' \frac{E'-E_s-\frac{i}{2}\Gamma_s}{(E'-E_s)^2+\frac{\Gamma_s^2}{4}} = \\
&= \frac{1}{\Delta E}\,\frac{\frac{\Gamma_s}{2}}{\frac{\Gamma_s^2}{4}}\int_{E-\frac{\Delta E}{2}}^{E+\frac{\Delta E}{2}} dE' \frac{\frac{2(E'-E_s)}{\Gamma_s}-i}{\left(\frac{2(E'-E_s)}{\Gamma_s}\right)^2+1} = \boxed{\begin{array}{c}\text{substitution}\\ x=\frac{2(E'-E_s)}{\Gamma_s}\end{array}} = \\
&= \frac{1}{\Delta E}\int_{\frac{2}{\Gamma_s}(E-E_s-\frac{\Delta E}{2}}^{\frac{2}{\Gamma_s}(E-E_s+\frac{\Delta E}{2}} \frac{x-i}{x^2+1}\,dx = \boxed{\begin{array}{c}\text{see}\\ (11.92)\end{array}} \approx \\
&\approx \frac{1}{\Delta E}\int_{-\frac{\Delta E}{\Gamma_s}}^{+\frac{\Delta E}{\Gamma_s}} \frac{dx}{x+i} = \boxed{\begin{array}{c}\text{substitution}\\ y=x+i;\ dy=dx\end{array}} = \\
&= \frac{1}{\Delta E}\int_{-\frac{\Delta E}{\Gamma_s}+i}^{+\frac{\Delta E}{\Gamma_s}+i} \frac{dy}{y} = \frac{1}{\Delta E}\Big(\ln\big(\frac{\Delta E}{\Gamma_s}+i\big)-\ln\big(-\frac{\Delta E}{\Gamma_s}+i\big)\Big) = \\
&= \boxed{\begin{array}{c}\text{because } \ln z=\ln(x+iy)=\ln r\,e^{i\phi}=\ln r+i\phi\\ \text{and because (11.92) } (\frac{\Delta E}{\Gamma_s}\to\infty)\\ \Rightarrow \phi(\frac{\Delta E}{\Gamma_s}+i)\to 0\ ,\ \phi(\frac{\Delta E}{\Gamma_s}-i)\to\pi\end{array}} = \\
&= \frac{1}{\Delta E}\Big(\ln r+0i-\ln r-\pi i\Big) = -\frac{i\pi}{\Delta E} \qquad (11.93)
\end{aligned}
$$

The expression (11.93) is then substituted into (11.79) and we obtain the optical Hamiltonian in the following form,

$$\Big(\hat{H}_{opt}\Big)_{"Box"} = \hat{H}_{PP} - \frac{i\pi}{\Delta}\,\hat{H}_{PQ}\,\frac{1}{1-\frac{i\pi}{\Delta E}\,\hat{W}_{QQ}}\,\hat{H}_{QP} \qquad (11.94)$$

In the both averaging (Lorentzian as well as "Box" type) the optical Hamiltonian (potential) is complex. In the limit of big Δ (or ΔE) its imaginary part is negatively definite and this is in accordance with the fact that the optical potential is always absorptive (because imaginary part of the optical potential is responsible effectively for the escaping of the probability flow from the given prompt P-channel to all time-delayed Q- channels).

In subsections 11.2.2.2 and 11.2.2.3 the space of channels was divided into two subspaces, P-subspace involving prompt open channels and Q-subspace of closed (mainly compound nucleus) channels. This enabled us to express the reaction $\mathcal{T}$- matrix element $\mathcal{T}_{fi}$ of the given reaction $i \to f$ between initial and final open channels (from the P-subspace) as a sum of two terms (see e.g. (11.61). The first term (see $\mathcal{T}_{fi}^{(P)}$ in (11.61) is relevant to the reaction $i \to f$ when the channels i and f are strongly directly coupled and this leads to the

prompt and fast process $i \to f$ (direct reaction). The second term in (11.61) corresponds to the time-delayed reaction $i \to f$ going through the compound nucleus. Depending on the mutual relation between the widths Γ_{CN} of the compound nucleus levels, their mutual distances D_{CN} in the spectrum and the experimental energy fuzziness ΔE_i of the impacting particle beam in the initial channel this second term in (11.61) leads to the resonance character of the matrix element $\mathcal{T}_{fi}$ (and consequently to the resonance character of the reaction cross section in the dependence on the energy E) in the case when $\Delta E_i < \Gamma_{CN} < D_{CN}$ or we should average $\mathcal{T}_{fi}$ over several overlaping compound nucleus states. This averaging then provides the smooth behaviour of the cross section in the dependence on the energy E without any narrow compound nucleus resonances. In the case of the elastic scattering this averaging leads to the complex optical potential as has been discussed in this subsection.

However the direct reaction mechanism and the compound nucleus mechanism describe the high- energy and low- energy parts of the dependence of the cross section on the final particle energy of the reaction $i \to f$, respectively (see the example of the reaction (p, p') in the Fig.11.1). In practice there is the region of intermediate energies where neither the direct mechanism nor the compound nucleus mechanism is able to describe the observed structures in the cross section of the $i \to f$ process. Typical examples of such structures are giant resonances of different types and multipolarities which are observed in some reactions (e.g. giant dipole resonance in the photo-absorption cross section). The states responsible for these intermediate energy structures in the cross section are known in the literature as doorway state resonances (see [349]). These doorway states and corresponding intermediate structures in the cross section are discussed in the next subsection.

11.2.2.4 Intermediate structures, doorway state resonances

This subsection is devoted to the description of the intermediate structures observed in the energy dependence of the cross section of given reaction between energy region where the cross section is described dominantly by fast prompt reaction mechanism (higher energies of the final particle) and the lower energy region where the reaction goes through the compound nucleus. The fact if these intermediate structures can be observed or not depends on the scale (more precisely on the doorway state width) of Γ_d in the comparison

with the low compound nucleus state widths Γ_{CN} and with the width Γ_{SP} of the gross structure that would appear in the cross section for single-channel elastic scattering produced by a real local potential, and also with the energy interval ΔE of the local averaging of the cross section. Usually Γ_d lies somewhere between Γ_{CN} and Γ_{SP},

$$\Gamma_{SP} >> \Gamma_d >> \Gamma_{CN} \tag{11.95}$$

To observe intermediate structure it is necessary to average the cross section

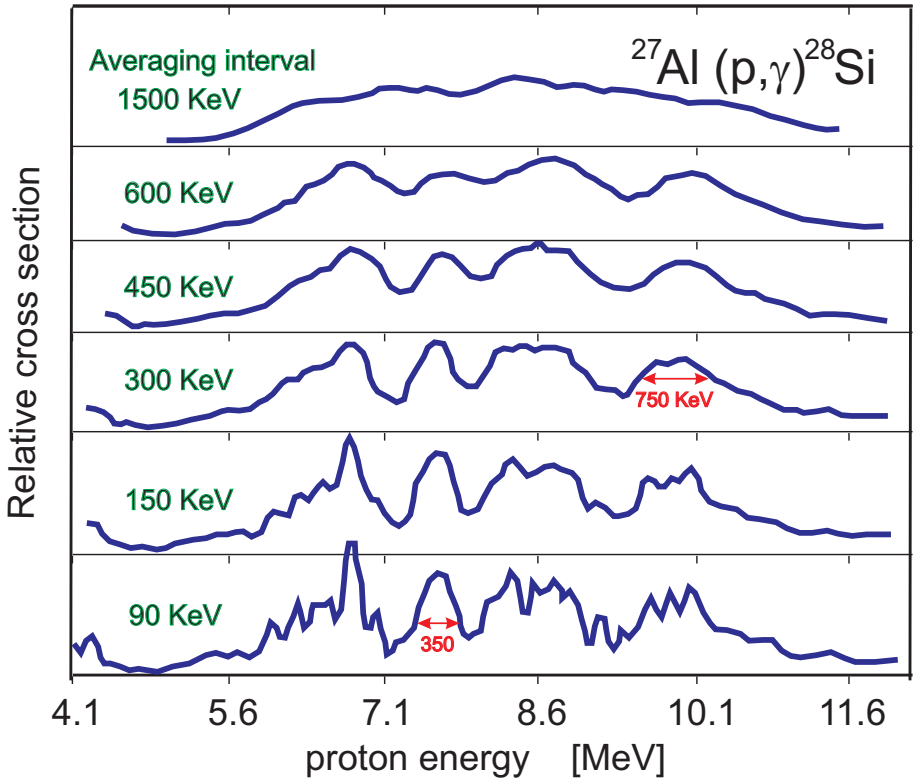


Figure 11.7: Relative cross section of the reaction ^{27}Al (p,p')^{28}Si (photocapture of protons by ^{27}Al going to the ground state of ^{28}Si). The data is presented for various energy resolutions (adapted from [350], see also p.101 in [4] and p.180 in [23]).

(either by numerical averaging of good resolution data or by using poorer, but not too poor, experimental energy resolution). In this way the fine fluctuations in the cross section are washed out and larger widths become visible. The energy interval ΔE over which the averaging is performed should be less then Γ_d but much greater than Γ_{CN} and D (the spacing of compound nucleus levels), This process is demonstrated in the Fig.11.7 where the cross section of the reaction ^{27}Al (p,p')^{28}Si is demonstrated for different values of the averaging interval ΔE. One can see that the appropriate averaging interval ΔE makes more visible particular structures with different withs Γ_d.

Many examples of different intermediate structures can be quoted (e.g. giant resonances of different types and multipolarities). States corresponding to these intermediate structures are referred as doorway states and the corresponding resonances as doorway state resonances (see e.g. [349]) to point out that they serve as the first stage beyond the entrance channel in the development of the complex compound nucleus states. That means the system should pass through doorway state before the full complexity of compound nucleus states could be generated. This is illustrated in the Fig 11.8.

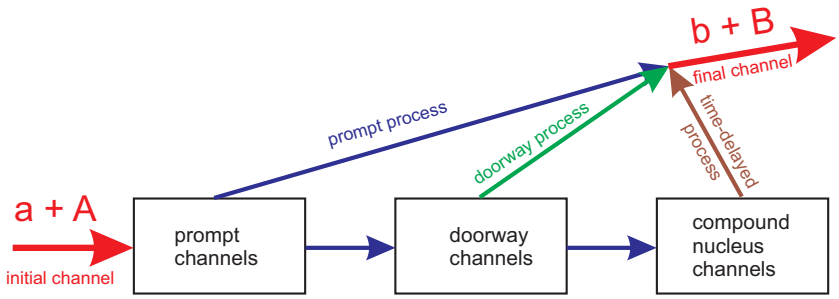


Figure 11.8: Schematic figure demonstrates the three possible ways of the forming the reaction $i \equiv a + A \to f \equiv b + B$: (i) as direct prompt process (responsible for gross structures in cross section for the higher final particle energies and connected with the lower excitations in the final nucleus), (ii) as doorway process going through the doorway quasi-bound states of the $a + A$ system and responsible for the intermediate structures in the cross section for the intermediate final particle energies, and (iii) as time-delayed orocess going through the fine (narrow) compound nucleus states and responsible for possible very narrow resonances in the cross section for lower final particle energies. These three ways of the forming the reaction $i \to f$ contribute simultaneously to the reactio matrix $\mathcal{T}_{fi}$ and interfere in the corresponding cross section $\sigma_{i\to f} \approx |\mathcal{T}_{fi}|^2$ differently in different energy regions. It should be also realized that the fine- and intermediate structures in the cross section of the reaction can be observed only if we do not perform any numerical averaging and the experimental energy resolution is ideal (see the text).

The doorway state is relatively simple state, not as complex as the compound nucleus states, but on the other side not as simple as the entrance channel state. The hypothesis that such simple doorway states exist and that they are the only states that couple strongly with the entrance channel is referred in the literature to as the doorway state hypothesis.

In order to understand the doorway state hypothesis in more concrete way let us consider following somewhat idealized example. Suppose that the incident projectile is a nucleon. Let us suppose further that its energy is such that no interaction is possible and therefore only elastic scattering is available. Then the entrance asymptotic wave function, $|\bar{\chi}_i^{(+)}\rangle$, describes the relative motion of the incident nucleon in the field of the target nu-

cleus and corresponding nucleon-nuclear interaction is specified by a model Hamiltonian relevant to the energy of relative projectile-target nucleus motion. Let us further suppose that the target nucleus has a closed shell so the model intrinsic Hamiltoia of the target nucleus is the single-particle mean field Hamiltonian. From the point of view of the intrinsic degrees of freedom the entrance channel intrinsic wave function is one-particle state in the shell model terminology. The residual nucleon-target nucleus interaction acting on the entrance channel wave function $|\bar{\chi}_i^{(+)}\rangle$ can excite a particle-hole pair and the incident nucleon changing its 1 particle state for two-particle-one hole (2p-1h) state or linear combination of such (2p-1h) states. The states produced in this fashion are doorway states since they are only ones that are coupled by the residual interaction to the entrance channel. All these created (2p-1h) states (or their combinations forming possible collective states of (2p-1h) character) are doorway states. A resonance in the elastic scattering cross section dependence on the energy occurs whenever there is an appropriate state of the system nucleon+target nucleus which is bound and its energy is equal to the total energy of the system (that means the total energy of the doorway state equals to the incident kinetic energy). In such a case the doorway state resonance occurs and it leads to the forming of the intermediate structures (peaks) in the cross section.

The resonant doorway state is not an exact stationary eigenstate of the nuclear Hamiltonian. It will decay with time and therefore has a width. In addition to the escape width $\Gamma_d^{\uparrow}$ caused by transitions to various exit channels and common to all types of resonances, there is the width, which is a consequence of the possible transition to states of higher complexity (where the energy is spread to other compound nucleus states than the doorway states, roughly speaking to the compound nucleus fine structure states (see the Fig.11.8). This width, $\Gamma_d^{\downarrow}$, is referred to as the spreading width. The total doorway width, Γ_d, is the sum of these two,

$$\Gamma_d = \Gamma_d^{\uparrow} + \Gamma_d^{\downarrow} \tag{11.96}$$

The visibility of the doorway state resonance depends critically on Γ_d. If Γ_d is too large, intermediate structure is not seen. To see this let us turn to the

expression for the $l = 0$ elastic scattering cross section (see (11.53) for $l = 0$),

$$\begin{aligned}\sigma_{el}(l=0) &\approx \frac{\pi}{k^2}\left|\frac{1-e^{2i\delta}}{i} + e^{i\delta}\,\frac{\Gamma_d^{\uparrow}}{(E-E_d)+\frac{i}{2}(\Gamma_d^{\uparrow}+\Gamma_d^{\downarrow})}\right|^2 = \\ &= \frac{4\pi}{k^2}\left|sin\,\delta + e^{i\delta}\,\frac{\frac{\Gamma_d^{\uparrow}}{2}}{(E-E_d)+\frac{i}{2}(\Gamma_d^{\uparrow}+\Gamma_d^{\downarrow})}\right|^2 \end{aligned} \tag{11.97}$$

where δ is the $l = 0$ elastic scattering phase shift. We can see that $\Gamma_d^{\downarrow}$ acts as an additional absorption. The maximum magnitude of the resonant doorway term (the second term in (11.98)) occurs at $E = E_d$ and is equal to $\Gamma_d^{\uparrow}/\Gamma_d$. That means if Γ_d is large with respect to $\Gamma_d^{\uparrow}$ then the structure given by the doorway resonance (the second term in (11.97)) cannot be observed.

Above discussion leads to the conclusion that it is not sufficient generally to divide the space of channels only to the P-space of prompt channels and Q-space of time-delayed channel. Simplified example of elastic scattering of nucleon on target nucleus presented above demonstrated possible (in reality quite often) existence of doorway channels which do not belong to the P-space but simultaneously cannot be involved in the Q-space of time delayed channels because they are coupled quite strongly with P- channels. Therefore in further consideration in order to take into account the general existence of doorway channels it is necessary to divide Q-space into two parts, the subspace Q' of genuin time-delayed channels and the subspace D of doorway channels with corresponding projection operators $\hat{Q}'$ and $\hat{D}$ (compare with (11.8)),

$$\begin{aligned} &\hat{P}^+ = \hat{P} \qquad &&\hat{P}^2 = \hat{P} \\ &\hat{D}^+ = \hat{D} \qquad &&\hat{D}^2 = \hat{D} \qquad &&\hat{P} + \hat{D} + \hat{Q}' = 1 \\ &\hat{Q}'^{+} = \hat{Q}' \qquad &&\hat{Q}'^{2} = \hat{Q}' \end{aligned} \tag{11.98}$$

We introduce also the projection operator $\hat{P}'$ which project out simultaneously the P-channels and D-channels,

$$\hat{P}' = \hat{P} + \hat{D} \qquad\qquad \hat{P}' + \hat{Q}' = 1 \tag{11.99}$$

Introduction of this projection operator $\hat{P}'$ enables us to rewrite all expressions derived in the subsection 11.2.2 (where we had $\hat{P} + \hat{Q} = 1$) for the case when the doorway channels exist (that means where we have $\hat{P} + \hat{D} + \hat{Q}' = \hat{P}' + \hat{Q}' = 1$). For instance, the expression (11.59) can be immediately

rewritten as,

$$\mathcal{T}_{fi} = \mathcal{T}_{fi}^{(P')} + \langle \bar{\phi}_f^{(-)} | \hat{H}_{P'Q'} \frac{1}{E^{(+)} - \hat{H}_{Q'Q'} - \hat{W}_{Q'Q'}} \hat{H}_{Q'P'} | \bar{\phi}_i^{(+)} \rangle \qquad (11.100)$$

where $\hat{W}_{Q'Q'} \equiv \hat{H}_{Q'P'} \frac{1}{E^{(+)} - \hat{H}_{P'P'}} \hat{H}_{P'Q'}$ and where $|\bar{\phi}_i\rangle$ and $|\bar{\phi}_f\rangle$ are asymptotic initial and final channel wave functions fulfilling

$$(E - \hat{H}_{P'P'})\, |\bar{\phi}_f^{(-)}\rangle = 0 \qquad (E - \hat{H}_{P'P'})\, |\bar{\phi}_i^{(-)}\rangle = 0 \qquad (11.101)$$

with the corresponding asymptotic behaviour for initial and final channels (the analogy of (11.28) and (11.29) but for $\hat{H}_{P'P'}$). These asymptotic functions can be resolved into prompt and doorway components $|\hat{P}\bar{\phi}\rangle$ and $|\hat{D}\bar{\phi}\rangle$ satisfying the following equations

$$\begin{aligned} (E - \hat{H}_{PP})\, |\hat{P}\bar{\phi}\rangle &= \hat{H}_{PD} |\hat{D}\bar{\phi}\rangle \\ (E - \hat{H}_{DD})\, |\hat{D}\bar{\phi}\rangle &= \hat{H}_{DP} |\hat{P}\bar{\phi}\rangle \end{aligned} \qquad (11.102)$$

in analogy with (11.10). The $\mathcal{T}_{fi}^{(P')}$ is the transition amplitude corresponding

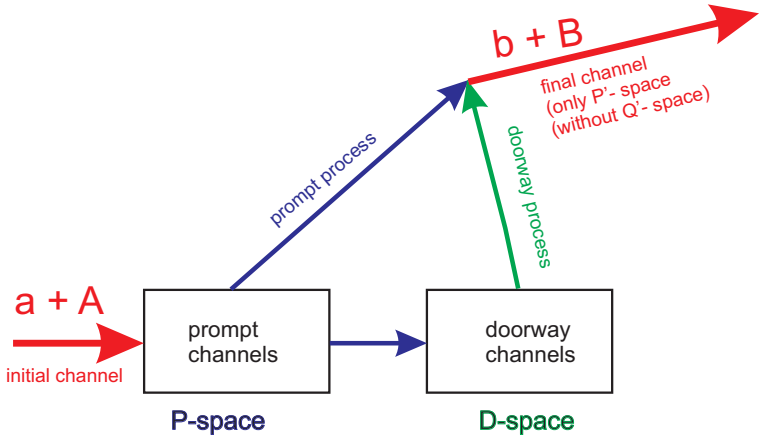


Figure 11.9: Schematic figure demonstrating reaction $a + A \to b + B$ where Q'- space of channels is neglected and the reaction can only run as prompt direct reaction or through doorway D- channels.

to the P'- space. Since the equations (11.102) are identical in the form with (11.10) (simply replace $\hat{Q}$ by $\hat{D}$) it is entirely possible to exhibit resonances which are presented in $\mathcal{T}_{fi}^{(P')}$ in the analogy with (11.52) or (11.59) (see also the Fig.11.9). Only instead of $|\bar{\chi}_i^{(+)}\rangle$, $|\bar{\chi}_f^{(+)}\rangle$ we should use $|\bar{\phi}_i^{(+)}\rangle$, $|\bar{\phi}_f^{(+)}\rangle$ and the $\hat{H}_{QQ}$, $\hat{W}_{QQ}$ should be replaced by $\hat{H}_{DD}$, $\hat{W}_{DD}$ and $\hat{H}_{PQ}$, $\hat{H}_{QP}$ by $\hat{H}_{PD}$, $\hat{H}_{DP}$. These resonances are generated by the presence of doorway states (the

Q'-space is not taken into account) and they have a width that is roughly the escape width $\Gamma_d^{\uparrow}$. In order to obtain the full width it is necessary to average over the fine (compound nucleus) structure connected with the Q'- space channels (compound nucleus states), that is , we should obtain the optical potential for this case. Instead of (11.78) now the optical Hamiltonian gives the following equation for the wave function describing the elastic process $a + A \to a + A$,

$$(E - \hat{H}_{opt}) \left\langle \hat{P}' \Psi_i \right\rangle = 0 \tag{11.103}$$

with the optical Hamiltonian in the following form (in analogy with (11.79)),

$$\hat{H}_{opt} \equiv \hat{H}_{P'P'} + \hat{H}_{P'Q'} \frac{1}{\left\langle \frac{1}{\hat{e}_{Q'Q'}} \right\rangle^{-1} + \hat{W}_{Q'Q'}} \hat{H}_{Q'P'} \tag{11.104}$$

where

$$\hat{e}_{Q'Q'} \equiv E^{(+)} - \hat{H}_{Q'Q'} - \hat{W}_{Q'Q'} \tag{11.105}$$

Now we introduce the important assumption, which we shall refer to as the strong doorway assumption, namely that the P- space channels couple only to the doorway D- space . In other words, Q'- space does not couple directly to the P- space channels. This assumption leads to the equations,

$$\hat{H}_{PQ'} = 0 \qquad\qquad \hat{H}_{P'Q'} = \hat{H}_{DQ'} \tag{11.106}$$

and (11.104) can be rewritten as,

$$\hat{H}_{opt} \equiv \hat{H}_{P'P'} + \hat{H}_{DQ'} \frac{1}{\left\langle \frac{1}{\hat{e}_{Q'Q'}} \right\rangle^{-1} + \hat{W}_{Q'Q'}} \hat{H}_{Q'D} \tag{11.107}$$

The other possibility to obtain expressions for $\mathcal{T}_{fi}$ and $\hat{H}_{opt}$ in the case of the presence of doorway states is to use directly the decomposition (11.99) of the total channel space into P-, D-, and Q'-subspaces. Using the properties of projection operators (see (11.106) the general channel stationary Schroedinger equation $(E - \hat{H}) |\Psi\rangle = 0$ can be rewritten in terms of three equations,

$$\begin{aligned} (E - \hat{H}_{PP}) |\hat{P}\Psi\rangle &= \hat{H}_{PD} |\hat{D}\Psi\rangle \\ (E - \hat{H}_{DD}) |\hat{P}\Psi\rangle &= \hat{H}_{DP} |\hat{P}\Psi\rangle + \hat{H}_{DQ'} |\hat{Q}'\Psi\rangle \\ (E - \hat{H}_{Q'Q'}) |\hat{Q}'\Psi\rangle &= \hat{H}_{Q'D} |\hat{D}\Psi\rangle \end{aligned} \tag{11.108}$$

where $\hat{H}_{PD} = \hat{P}\hat{H}\hat{D}$, $\hat{H}_{PP} = \hat{P}\hat{H}\hat{P}$, $\hat{H}_{DD} = \hat{D}\hat{H}\hat{D}$, $\hat{H}_{DP} = \hat{D}\hat{H}\hat{P}$, $\hat{H}_{DQ'} = \hat{D}\hat{H}\hat{Q}'$, $\hat{H}_{Q'Q'} = Q'\hat{H}\hat{Q}'$, $\hat{H}_{Q'D} = Q'\hat{H}D$. The substitution from the third equation in (11.108) reduces the 3 equations (11.108) into only two,

$$\begin{aligned}
&(E - \hat{H}_{PP})\,|\hat{P}\Psi\rangle = \hat{H}_{PD}\,|\hat{D}\Psi\rangle \\
&(E - \hat{H}_{DD} - \hat{H}_{DP'}\frac{1}{E - \hat{H}_{Q'Q'}}\hat{H}_{Q'D}\,|\hat{D}\Psi\rangle = \hat{H}_{DP})\,|\hat{P}\Psi\rangle
\end{aligned} \tag{11.109}$$

The first equation in (11.109) can be formally solved and $|\hat{P}\Psi\rangle$ can be written as the sum of one particular solution of this equation without the r.h.s., $(E - \hat{H}_{PP})\,|\bar{\chi}\rangle = 0$ (which is e.g. asymptotic channel wave function $|\bar{\chi}_i\rangle$ - see (11.28)), and the general solution of this equation (exactly in the some way as in (11.54)),

$$|\hat{P}\Psi_i\rangle = |\bar{\chi}_i\rangle + \frac{1}{E^{(+)} - \hat{H}_{PP}}\,\hat{H}_{PD}|\hat{D}\Psi_i\rangle \tag{11.110}$$

where the index i is again added in $|\hat{P}\Psi_i\rangle$ in order to point out that the general channel state is assumed to be created from the initial asymptotic wave $|\bar{\chi}_i^{(+)}\rangle$. Then the reaction amplitude $\mathcal{T}_{fi}$ is (see (11.55)),

$$\begin{aligned}
\mathcal{T}_{fi} &= \langle\bar{\chi}_f^{(-)}|\hat{V}_{int}|\hat{P}\Psi_i\rangle \approx \\
&\approx \boxed{\begin{array}{c}\text{see} \\ (11.55), (11.110)\end{array}} \approx \mathcal{T}_{fi}^{(P)} + \langle\bar{\chi}_f^{(-)}|\hat{H}_{PD}|\hat{D}\Psi_i\rangle
\end{aligned} \tag{11.111}$$

The substitution of (11.110) into the second equation in (11.109) gives

$$\begin{aligned}
&(E - \hat{H}_{DD} - \hat{H}_{PQ'}\frac{1}{E - \hat{H}_{Q'Q'}}\hat{H}_{Q'D})\,|\hat{D}\Psi_i\rangle = \\
&\qquad = \hat{H}_{DP}\,[\,|\bar{\chi}_i^{(+)}\rangle + \frac{1}{E - \hat{H}_{PP}}\hat{H}_{PD}|\hat{D}\Psi_i\rangle\,] \\
&\Rightarrow \\
&\left\{E - \hat{H}_{DD} - \hat{H}_{DQ'}\frac{1}{E - \hat{H}_{Q'Q'}}\hat{H}_{Q'D} - \hat{H}_{DP}\frac{1}{E - \hat{H}_{PP}}\hat{H}_{PD}\right\}\,|\hat{D}\Psi_i\rangle = \\
&\qquad = \hat{H}_{DP}\,|\bar{\chi}_i^{(+)}\rangle \\
&\Rightarrow \\
&\qquad |\hat{D}\Psi_i\rangle = \frac{1}{E - \hat{H}_{DD} - \hat{W}_{DD} - \hat{W}_{Q'Q'}}\hat{H}_{DP}\,|\bar{\chi}_i^{(+)}\rangle
\end{aligned} \tag{11.112}$$

where $\hat{W}_{DD}$ and $\hat{W}_{Q'Q'}$ were introduced as,

$$\hat{W}_{DD} \equiv \hat{H}_{DP}\frac{1}{E - \hat{H}_{PP}}\hat{H}_{PD} \quad , \quad \hat{W}_{Q'Q'} \equiv \hat{H}_{DQ'}\frac{1}{E - \hat{H}_{Q'Q'}}\hat{H}_{Q'D} \tag{11.113}$$

The substitution of (11.113) into (11.111) provides the amplitude $\mathcal{T}_{fi}$ in the following form,

$$\mathcal{T}_{fi} = \mathcal{T}_{fi}^{(P)} + \langle \bar{\chi}_f^{(-)} | \hat{H}_{PD} \frac{1}{E - \hat{H}_{DD} - \hat{W}_{DD} - \hat{W}_{Q'Q'}} \hat{H}_{DP} \, | \bar{\chi}_i^{(+)} \rangle \tag{11.114}$$

One can see that the coupling of doorway D- space channels with the time-delayed Q'- channels leads to the last term $\hat{W}_{Q'Q'}$ in the denominator. This term (this coupling) provides (after averaging) additional energy shift to the doorway resonances and additional broadening of the doorway resonance widths (if the D-Q'coupling is swithched on) in the comparison with the case when this term is not present in the denominaor of (11.114) and we have the doorway width generated only through the P-D coupling in terms of the $\hat{W}_{DD}$ (compare figures Fig.11.9 and Fig.11.8). Since $\hat{W}_{DD}$ involves $\hat{H}_{DP}$ and $\hat{H}_{PD}$ this term is connected with the escape width $\Gamma_d^{\uparrow}$ while the term $\hat{W}_{Q'Q'}$ involves $\hat{H}_{DQ'}$ and $\hat{H}_{Q'D}$ and therefore is connected with the spreding width $\Gamma_d^{\downarrow}$. One should only realize that energy averaging interval (for the taking into account of $\hat{W}_{Q'Q'}$) should be chosen appropriately in order to observe the intermediate structures in the cross section generated by the existence of doorway states (see the text under the expr. (11.96)).

11.2.3 Concluding remarks to the Feshbach formal theory

Feshbach theory is the nuclear reaction theory which is able qualitatively to describe both the direct promp reactions and the reactions going through compound nucleus within one formalism. This formalism is based on the assumption that all possible channels which can be formed from the initial channel of impacting particle (with given kinetic energy) and target nucleus can be divided into P- space and Q- space of channels. Among the P- channels there are all final open channels which are mutually strongly coupled and also directly coupled with the initial channel. The Q-space involves all other channels reachable from the initial channel (by energy conservation law and by other selection rules) but not coupled directly to the initial channel and to P- channels. The given reaction $i \to f$ between initial (i) and final (f) open channels from the P-space can be realized either in the framework of the P- space as the fast direct reaction or through the Q- space channels as the time-delayed reaction (see the Fig.11.4). From this point of view the

cross section of the given reaction $i \to f$ is determined by the square of the reaction amplitude $\mathcal{T}_{fi}$ (see e.g. (11.64)) where the $\mathcal{T}_{fi}$ is the sum of the direct $\mathcal{T}_{fi}^{(P)}$ term (giving the fast direct component of the reaction $i \to f$) and the term describing the slow (time-delayed) run of the reaction $i \to f$ (going through Q- space - see the 2-d term in exprs. (11.34), (11.40), (11.42), (11.52), (11.53), (11.59), (11.61).

The division of the full space of channels, reachable from the given initial channel into the P- space of prompt channels and Q- space of time-delayed channels, enables to introduce the projection operators $\hat{P}$ and $\hat{Q}$ (see (11.6)-(11.8)) which project out the Hamiltonan $\hat{H}_{PP}$ acting in the P- space and the Hamiltonian $\hat{H}_{QQ}$ relevant to the Q-space and simultaneously to obtain interactions $\hat{H}_{PQ}$ and $\hat{H}_{QP}$ between P- and Q- channel spaces (see (11.11), (11.13)).

Which of two parts of the reaction matrix element $\mathcal{T}_{fi}$ mentioned above (that means the first prompt term $\mathcal{T}_{fi}^{(P)}$ in exprs. (11.52) or (11.53) or the second time-delayed term in these exprs.) predominates depends on the distribution of the energy brought by the initial channel $i \equiv a + A$ into the system $a + A$ among the kinetic energy of the final particle b and the excitation energy of the final nucleus B in the final channel $f \equiv b + B$ (see the fig 11.1). Usually in the case when the excitation energy of the final nucleus is high (close to the total initial energy) and the kinetic energy of the final particle is consequently small then the full reaction matrix element $\mathcal{T}_{fi}$ is mainly formed by the second term in (11.52) or (11.61) (reaction goes mainly through Q-space) and the first term $\mathcal{T}_{fi}^{(P)}$ represents only a background. In this case, depending on the energy distance and width of the eigen-states of the Hamiltonian $\hat{H}_{QQ}$, the reaction matrix element $\mathcal{T}_{fi}$ can have a resonance character. If the widths of the individual eigen states of $\hat{H}_{QQ}$ are small (narrow eigen-states of the compound nucleus) with respect to their mutual distances then the reaction matrix element $\mathcal{T}_{fi}$ is described by the one-channel Breight-Wigner resonance formule (see the second term in (11.52)). If the distances between eigen-states of the Hamiltonian $\hat{H}_{QQ}$ are not so big and they are comparable with their widths then we should use the many-channel Breight-Wigner formule (the second term in (11.61). One should however realize that in both these case (one-channel or many-channel Breight-Wigner formule) this resonance character of the transition matrix element $\mathcal{T}_{fi}$ can be observed in the cross section only provided that the energy blurring of the impacting particles is much smaller than the widths and mutual distances of

the eigen-states of the Hamiltonian $\hat{H}_{QQ}$ (eigenstates of the compound nucleus). Otherwise all Breight-Wigner resonances discussed above are washed out and we do not see any fine individual resonances caused by the compud nucleus eigen-states (eigen-states of $\hat{H}_{QQ}$).

If the kinetic energy of final particle is high (close to the total initial energy) and consequently the excitation energy of the final nucleus is small (close to zero) then the second term in the expression for the reaction matrix element $\mathcal{T}_{fi}$ (see e.g. (11.53) or (11.61)) is small and the first term is dominant. In such a cases the reaction $i \to f$ goes mainly as the direct prompt process. However even in this case the presence of the Q-space and its interaction with P- channel wave functions $|\hat{P}\Psi\rangle$ manifest themselves in the imaginary part of the optical potential participating in the Schroedinger equations for P- channel wave function $|\hat{P}\Psi\rangle$ (see (11.79)), which determines corresponding prompt part $\mathcal{T}_{fi}^{(P)}$ of the reaction matrix element $\mathcal{T}_{fi}$ - see (11.35). This imaginary part of the optical potential (Hamiltonian) is obtained by the averaging procedure described in the subsection 11.2.2.3.

In the case when in some of the final channels $b_f + B_f$ of the reaction $a+A \to b_f+B_f$ (index f enumerates all open final channels) the quasi-bound system $b_f + B_f$ can be formed then this quasi-bound system represents the doorway channel responsible for the possible intermediate structure in the cross section of the corresponding reaction $i \to f$. In this case we should divide the Q- space into the doorway subspace D and the subspace Q' of channels which are not coupled with the P- space channels. The coupling of doorway D- channels with P- channels leads to the resonance in the cross section with the escape width $\Gamma_d^{\uparrow}$ and the averaged coupling between D- channels and Q'- channels (fine structure compound nucleus channels) provide additional, so called spreading, width $\Gamma_d^{\downarrow}$ of the doorway resonance as is described in the Subsection 11.2.2.4 (see also the section 3.4 in [23]).

Feshbach theory presented in this section is a formal theory. Mentioned above division of the configuration channel space into P- and Q- subspaces depends on the concrete situation (reaction energy, selection rules, impacting particle and target nucleus etc.) and the Hamiltonian parts $\hat{H}_{PP}$, $\hat{H}_{QQ}$, $\hat{H}_{PQ}$ and $\hat{H}_{QP}$ are not known generally. So in order to use this theory in practice we should apply some phenomenology to it. For instance, in real calculations of the prompt $i \to f$ reaction cross section with heavier target nuclei usually at first diagonal matrix element of the optical potential in channels i and f are phenomenologically parametrized (their real as well as imaginary parts) and parameters are obtained by the fitting procedure on experimental

cross sections of elastic scatterings in the each prompt channels i and f independently (fitting of optical potential parameters on experimental elastic scattering phase shifts through the solving of the equation (11.78) and subsequent determination of the theoretical elastic scattering phase shifts). In the next step the nondiagonal matrix elements of the optical potential between $|\hat{P}\Psi_i\rangle$ and $|\hat{P}\Psi_f\rangle$ (that means between so called distorted waves in channels i and f), is then taken (again more or less in phenomenologic form) and the corresponding reaction matrix element $\mathcal{T}_{fi}^{(P)}$ can be determined (in the framework of the Distorted Wave Aprroximation (DWA) or by the solving of the Coupled Channel (CCH) problem in the P- space). Both these steps are discussed in more details in the next section concerning the prompt direct nuclear reactions.

11.3 Many-channel description of reaction (reaction matrix, S-matrix, optical theorem)

11.3.1 General coupled channel equation system

In the previous section general formal Feshbach theory of nuclear reaction was presented. It was shown there that we can always express the total reaction matrix element $\mathcal{T}_{fi}$ for given nuclear reaction $\alpha_i \equiv a + A \to b_f + B_f \equiv \beta_f$ as the sum of so called prompt (direct) part $\mathcal{T}_{fi}^{(P)}$ and the time-delayed $\mathcal{T}_{fi}^{(Q)}$ part (the second term in the expressions (11.59), (11.61)). This partition of the $\mathcal{T}_{fi}$ was a result of the division of the total space of reaction channels into the P- subspace of prompt (mutually coupled) channels and the space of time-delayed (or compound nucleus) channels. As a result given reaction $i \to f$ between two open channels can run generally by two mechanisms, either as prompt direct process or as time-delayed process through the compound nucleus states. Since the cross section of the reaction $i \to f$ is given by the square $| \approx \mathcal{T}_{fi}|^2$ both these mechanism ways "interfere" and, depending on the kinetic energy E of the incident particle a, in the given region of the energy E, one mechanism can be dominated. It was already mentioned several times (see e.g. the last subsection in the previous section) that in the situation when the kinetic energy of the final particle b_f is relatively high and the excitation energy of the final nucleus B_f is small then the $\mathcal{T}_{fi}^{(P)}$ prevails and the reaction $i \to f$ goes predominantly as the fast prompt process while when the opposite is true then the reaction goes through the compound nucleus states. In this section the many-channel formalism for the description of

the reaction $\alpha_i \to \beta_f$ between two prompt channels α_i and β_f is introduced which is more practical than the Feshbach formal theory. In the framework of this formalism the existence of the Q-channels and the interaction between P-channels and Q-channels are taken into account through the imaginary part of the optical Hamiltonian (potential) for each prompt channel and the complex optical potential in each prompt channel is divided into so called diagonal part describing the elastic scattering in each prompt channel (e.g. $\alpha_i \to \alpha_i$ or $\beta_f \to \beta_f$) and the nondiagonal part characterizing the mutual interactions between each channel pair (α_i, β_f), where $\alpha_i \neq \beta_f$) which is responsible for mutual coupling of prompt channels and subsequent reaction $\alpha_i \to \beta_f$.

As it was shortly mentioned in the end of the subsection 11.2.3 the Feshbach theory of nuclear reactions is the formal and abstract theory and real calculation of cross sections of direct reactions need some phenomenological approximations consisting in the appropriate parametrization of the complex diagonal part of the optical potential for each channel involved in the P-space. Corresponding optical potential parameters are determined through the fitting procedure of calculated elastic scattering cross section to the experimental elastic scattering data. Then the cross section of given nonelastic reaction $i \to f$ ($f \neq i$) is obtained by the solving of the distorted wave approximation (DWA) or Coupled Channel (CCh) equations (in the framework of the P- space channel space) which involve non-diagonal complex part of the optical potential. This approach is discussed in details in next parts of this section.

The cross section of any reaction $i \to f$ between two channels i and f is determined by the corresponding reaction matrix element $\mathcal{T}_{fi}$ (see (Q.14), (11.55) and (Q.21)),

$$\mathcal{T}_{fi} = \langle \phi_f^{(-)} | \, \hat{V} \, | \hat{P}\Psi_i \rangle = \langle \phi_f^{(-)} | \, \hat{\mathcal{T}}(E) \, | \phi_i^{(+)} \rangle \qquad (11.115)$$

where $|\hat{P}\Psi_i\rangle$ is the initial channel wave function ($|\phi_f^{(-)}\rangle$ is the asymptotic outgoing final channel wave function and $\hat{V}$ is the reaction interaction. The wave function $|\phi_i^{(+)}\rangle$ describes the asymptotic ingoing initial wave function and $\hat{\mathcal{T}}$ is the reaction "evolution" operator given by (Q.15). Repeating substitution of $\hat{T}(E)$ in (Q.15) gives the reaction operator $\hat{T}(E)$ in the form of the series with respect to the interaction $\hat{V}$. For instance up to the 3-d order the expression (Q.15) yields the reaction matrix element $\mathcal{T}_{fi}$ in the following

form,

$$\mathcal{T}_{fi} = \langle \phi_f^{(-)} | \, \hat{V} \, | \phi_i^{(+)} \rangle + \langle \phi_f^{(-)} | \, \hat{V} \frac{1}{E - \hat{H}_0} \hat{V} \, | \phi_i^{(+)} \rangle + \\ + \langle \phi_f^{(-)} | \, \hat{V} \frac{1}{E - \hat{H}_0} \hat{V} \frac{1}{E - \hat{H}_0} \hat{V} \, | \phi_i^{(+)} \rangle + \cdots \qquad (11.116)$$

where $\hat{H}_0$ is the intermediate state Hamiltonian. This expression is suitable for the case when the interaction $\hat{V}$ is relatively weak and we can restrict ourselves only to a few terms in the series (11.116). The series (11.116) can be also understood as describing the many-step process. The first term in (11.116) describes the one-step process when the impacting particle interacts with one nucleon in the target through the interaction $\hat{V}$ and as a result the final particle and final nucleus is formed. The second term in (11.116) corresponds to the two-step process when the impacting initial particle interacts with one nucleon and after a propagation in the intermediate state (through the propagator $\frac{1}{E-\hat{H}_0}$) the second scattering occurs (through the interaction $\hat{V}$) and the final particle and final nucleus is formed. The third term in (11.116) describes the 3-step process (3 scatterings before the forming of the final particle and final nucleus) and in this way we can continue to higher order processes.

However the interaction $\hat{V}$ in (11.116) is generally quite strong and we should take into account many terms in (11.116) in order to obtain a convergence. Therefore the formalism based on (11.116) is not convenient for the most of nuclear reactions. So instead of (11.116) usually so called multichannel optical model is used where the P-channel wave functions (or more precise wave function packet) $|\hat{P}\Psi_i\rangle$ involved in (11.115) are obtained by the solving of the equations,

$$(E - \hat{H}_{opt}) \, |\hat{P}\Psi_\beta\rangle = 0 \qquad (11.117)$$

where optical Hamiltonian $\hat{H}_{opt}$ involves (opposite to the $\hat{H}_{opt}$ discussed in the Subsection 11.2.2.3) not only the interaction of individual P-space channel wave function $|\Psi_\beta\rangle$ with the Q- space but also the mutual self-consistent interactions between different channels in the P- space. From this point of view the equation (11.117) represents the system of equations for all prompt P- channels involved in the P- space as will be discussed further. That means the optical Hamiltonians in (11.117) for different β involves imaginary parts depending on the choice of prompt channels in the P- space (in addition to imaginary part coming from the interaction of P- space channels with the Q-

space channels discussed in subsections 11.2.2). That means in this section we will consider only P- space channels and the presence of Q- space channels and possible multi-step processes are felt only through the imaginarity of the optical potential (in agreement with the Feshbach theory discussed in the previous section).

So in the beginning we have initial particle a impacting on the target nucleus A which create the unbound system $a + A$ immediately decaying into different final channels $b_f + B_f$ including the elastic one $a + A$ (see the Fig. 11.2). The wave function of the system $a + A$ created by the initial channel will be further denoted as $\Psi_{(\vec{k}_{\alpha i})}$ which generally depends on the linear momentum of the relative motion in the initial channel (see also the Subsection Q.1 in the Appendix Q). This wave function can be expressed as a linear combination of wave functions of all channels taken into account in the P- space of prompt open channels (see e.g. [23], p.509, expr. (2.1)) [5]

$$\Psi_{(\vec{k}_{\alpha i})}(\vec{r}, \xi) = \sum_{\beta j} u^{(\alpha i)}_{\beta j}(\vec{k}_{\beta j}, \vec{r}_{\beta})\, \psi_{\beta j}(\xi_{\beta}) \tag{11.118}$$

where $u^{(\alpha i)}_{\beta j}(\vec{k}_{\beta j}, \vec{r}_{\beta})$ is the wave function of the relative motion of the particle and the nucleus in the channel βj (the index β characterizes the types of particle and the nucleus in the channel β and the index j specifies their internal states). The upper index α characterizes type of the particle a and the target nucleus A in the initial channel and the index i specifies the internal states of the particle a and the target nucleus A - usually ground states. The symbol $\psi_{\beta j}(\xi_{\beta}) = \langle \xi_{\beta} | \beta j \rangle$ represents the product of internal wave functions of particles (nuclei) in the output channel βj which are functions of the internal variables (coordinates) ξ_{β} of particles (nuclei) in the channel βj. The relative motion wave function $u^{(\alpha i)}_{\beta j}(\vec{k}_{\beta j}, \vec{r}_{\beta})$ represents the wave packet in the sense of the expr. (Q.7) (see the Appendix Q) when the relative linear momentum $\vec{k}_{\beta j}$ of particles (nuclei) in the channel βj and corresponding relative coordinate $\vec{r}_{\beta}$ can be used as simultaneous characteristics of the relative motion state. The sum over βj in (11.117) means the sum over all open P- channels which mutually interact and this sum involves also initial channel itself (elastic process). One should also realize that the index (αi) is present in the (11.118) in order to specify the initial channel for all processes involved in the general wave function packet (11.118). The other remark should be done in the

[5] In (11.118) the anti-symmetrization between nucleons of the same type in the particle (consisting from nucleons) and the nucleus (target or final) in each channel βj is not taken into account. The example of such function can be found e.g. in the exprs. (2.1) on the p. 464 and p. 509 in [23] or the expr. (4.6) on the p. 73 of [351].

connection with the wave function packet (11.118). The divisions of the coordinates $(\vec{r}_\beta, \xi_\beta)$ in all channels βj are not independent. They are dependent on the interaction responsible for particular transmutation reaction $\alpha i \to \beta j$. This point will be discussed in more details in the section 11.4.

In the asymptotic region ($r_\beta \to \infty$) the stationary relative wave functions in all channels involved in the wave function packet (11.118) have the form of outgoing spherical waves describing the scattered particles in all final channels. In the case of the elastic scattering (initial channel $\alpha_i \equiv a + A$) we should add also the plane wave describing the ingoing particles a impacting on the target nucleus A (see the Fig. D.1 in the Appendix D). So in the asymptotic region wave function packet (11.118) has the following form (see e.g. expr. (4.1) on the p. 72 in [351])

$$\Psi_{(\vec{k}_{\alpha i})} \quad \stackrel{r\to\infty}{\longrightarrow} \quad \psi_{\alpha i}(\xi_\alpha)\, e^{i\vec{k}_{\alpha i}\cdot\vec{r}_\alpha} + \sum_{\beta j} f(\vec{k}_{\alpha i} \to \vec{k}_{\beta j})\, \psi_{\beta j}(\xi_\beta)\, \frac{e^{ik_{\beta j} r_\beta}}{r_\beta} \qquad (11.119)$$

Functions $f(\vec{k}_{\alpha i} \to \vec{k}_{\beta j}) \equiv f(\vec{k}_{\beta j}, \vec{k}_{\alpha i})$ in (11.119) are scattering (or reaction) amplitudes in the channel βj and they are functions of the scattering angle between vectors $\vec{k}_{\alpha i}$ and $\vec{k}_{\beta j}$ (we will always supposed that the differential cross-section of the reactions $(\alpha i) \to (\beta j)$ is analyzed always with the same direction given by the linear momentum $\vec{k}_{\beta j}$ for all internal states $\psi_{\beta j}(\xi)$ given by the index j for given $\beta \equiv b + B$, that means the direction of all vectors $\vec{k}_{\beta j}$ is the same for all j and only the absolute value of the vectors $\vec{k}_{\beta j}$ can depends on j). In all further consideration the axis z of the CoM coordinate frame is supposed to be in the direction of the relative motion linear momentum $\vec{k}_{\alpha i}$ in the initial channel (that means $e^{i\vec{k}_{\alpha i}\cdot\vec{r}_\alpha} = e^{ik_{\alpha i} z}$). These scattering amplitudes determine the cross sections $\sigma_{\alpha i\, \beta j}$ as it will be described in next subsections.

General P-channel wave function packet (11.118) can be obtained by the solving of the stationary Schroedinger equation,

$$\hat{H}\, \Psi_{(\vec{k}_{\alpha i})} = E\, \Psi_{(\vec{k}_{\alpha i})} \qquad (11.120)$$

where $\hat{H}$ is the total Hamiltonian of the system created by the initial channel (αi). This Hamiltonian can be expressed in terms of variables relevant to each channel (βj) involved in the P- space (involving the elastic channel) (αi) - see e.g. exprs. (4.3), (4.4) in [351],

$$\hat{H} = \hat{H}_\alpha + \hat{T}_\alpha + \hat{V}_\alpha = \hat{H}_\beta + \hat{T}_\beta + \hat{V}_\beta \qquad (11.121)$$

where $\hat{H}_\alpha$ (or $\hat{H}_\beta$) represents the internal Hamiltonian of the particle and nucleus in the channel α (or β), $\hat{T}_\alpha$ (or $\hat{T}_\beta$) is the operator of the kinetic

energy of the relative motion of particles (nuclei) in the given channel α (or β), and $\hat{V}_\alpha$ or $\hat{V}_\beta$ stands for the interaction between the particle and the nucleus in the given channel α (or β) together with the interaction between given channel α (or β) with other channels involved in the P-space. This interaction $\hat{V}$ drives the relative particle-nucleus motion in the given channel α (or β) and is responsible also for transformation processes from the given channel α (or β) into other P-channels. It is clear that the internal channel wave function $\psi_{\beta j}(\xi_\beta) = \langle \xi_\beta | \beta j \rangle$ fulfills the Schroedinger equation with the internal Hamiltonian $\hat{H}_\beta \equiv \hat{H}_b + \hat{H}_B$,

$$\hat{H}_\beta \, \psi_{\beta j}(\xi_\beta) = E_{\beta j} \, \psi_{\beta j}(\xi_\beta) \tag{11.122}$$

where index j characterizes the internal (excitation) states of the particle b and the nucleus B in the channel β. So the equation (11.120) can be rewritten as follows,

$$\hat{H} \, \Psi_{(\vec{k}_{\alpha i})} = \boxed{\begin{array}{c}\text{see}\\(11.118)\end{array}} =$$

$$= \hat{H} \sum_{\beta j} u^{(\alpha i)}_{\beta j}(\vec{k}_{\beta j}, \vec{r}_\beta) \, \psi_{\beta j}(\xi_\beta) = E \sum_{\beta j} u^{(\alpha i)}_{\beta j}(\vec{k}_{\beta j}, \vec{r}_\beta) \, \psi_{\beta j}(\xi_\beta)$$

$$\Rightarrow \boxed{\begin{array}{c}\text{see}\\(11.122)\end{array}} \Rightarrow$$

$$\sum_{\beta' j'} \left(E_{\beta' j'} + \hat{T}_{\beta'} + \hat{V}_{\beta'} \right) u^{(\alpha i)}_{\beta' j'}(\vec{k}_{\beta' j'}, r_{\beta'}) \, \psi_{\beta' j'}(\xi_{\beta'}) =$$

$$= E \sum_{\beta' j'} u^{(\alpha i)}_{\beta' j'}(\vec{k}_{\beta' j'} r_{\beta'}) \, \psi_{\beta' j'}(\xi_{\beta'}) \tag{11.123}$$

The equation (11.123) is further multiplied by $\psi^*_{\beta j}(\xi) \equiv \langle \beta j | \xi \rangle$ and integrated over the internal variables ξ,

$$\sum_{\beta' j'} \left(E_{\beta' j'} + \hat{T}_{\beta'} \right) u^{(\alpha i)}_{\beta' j'}(\vec{k}_{\beta' j'}, r_{\beta'}) \langle \beta j | \beta' j' \rangle + \sum_{\beta' j'} \langle \beta j | \hat{V}_{\beta'} | \beta' j' \rangle \, u^{(\alpha i)}_{\beta' j'}(\vec{k}_{\beta' j'}, r_{\beta'}) =$$

$$= E \sum_{\beta' j'} \langle \beta j | \beta' j' \rangle \, u^{(\alpha i)}_{\beta' j'}(\vec{k}_{\beta' j'}, r_{\beta'})$$

which can be rewritten as,

$$\sum_{\beta' j'} \left(E_{\beta' j'} + \hat{T}_{\beta'} - E \right) \langle \beta j | \beta' j' \rangle \, u^{(\alpha i)}_{\beta' j'}(\vec{k}_{\beta' j'}, r_{\beta'}) + \langle \beta j | \hat{V}_\beta | \beta j \rangle \, u^{(\alpha i)}_{\beta j}(\vec{k}_{\beta j}, r_\beta) =$$

$$= \sum_{\beta' j'} \left[\langle \beta j | \hat{V}_\beta | \beta j \rangle \, \delta_{\beta j, \beta' j'} - \langle \beta j | \hat{V}_{\beta'}(\vec{r} | \beta' j' \rangle \right] u^{(\alpha i)}_{\beta' j'}(\vec{k}_{\beta' j'}, r_{\beta'}) \tag{11.124}$$

Equations (11.124) represent the system of equations for unknown relative motion wave functions $u^{(\alpha i)}_{\beta j}(\vec{k}_{\beta j}, \vec{r}_\beta)$ for coupled channels βj (inedexes βj enumerate all channels in the P-space including the elastic one).

Generally the internal wave functions $\psi_{\beta j}(\xi) = \langle \xi | \beta j \rangle$ are not orthogonal each other for different β, $\langle \beta j | \beta' j' \rangle \neq \delta_{\beta\beta'}\delta_{jj'}$. For particular $\beta = b + B$ and different j they are orthogonal, $\langle \beta j | \beta j' \rangle = \delta_{jj'}$ (because excitation states of the particle b and the nucleus B form the orthogonal bases) but for different β generally, $\langle \beta j | \beta' j' \rangle \neq \delta_{\beta\beta'}\delta_{jj'}$ (for $\beta \neq \beta'$). However usually in the framework of the distorted wave approximation (DWA) calculations of coupled channel (CCh) calculations the approximation

$$\langle \beta j | \beta' j' \rangle = \int d\xi \; \psi^*_{\beta j}(\xi) \; \psi_{\beta' j'}(\xi) \approx \delta_{\beta\beta'}\delta_{jj'} \tag{11.125}$$

is used (see e.g. p.148 in [352]). Under such approximation the equations (11.124) can be further rewritten as follows,

$$\begin{aligned} \left(\hat{T}_\beta - \epsilon_{\beta j} + \hat{U}^{(opt)}_{\beta j}(\vec{r})\right) u^{(\alpha i)}_{\beta j}(\vec{k}_{\beta j}, \vec{r}) \approx \\ \approx \sum_{\beta' j'} \left[\hat{U}^{opt}_{\beta j}(\vec{r}) \; \delta_{\beta j, \beta' j'} - \langle \beta j | \hat{V}_{\beta'}(\vec{r}_{\beta'}) | \beta' j' \rangle\right] u^{(\alpha i)}_{\beta' j'}(\vec{k}_{\beta' j'}, \vec{r}) = \\ = -\sum_{\beta' j'} \langle \beta j | \; \hat{W}^{(opt)}(\vec{r}) \; | \beta' j' \rangle \; u^{(\alpha i)}_{\beta' j'}(\vec{k}_{\beta' j'}, \vec{r}) \end{aligned} \tag{11.126}$$

where

$$\epsilon_{\beta j} \equiv E - E_{\beta j} \tag{11.127}$$

is the energy of the relative motion in the channel, and

$$\hat{U}^{(opt)}_{\beta j}(\vec{r}) = \langle \beta j | \hat{V}_\beta(\vec{r}, \xi) | \beta j \rangle = \int d\xi \psi^*_{\beta j}(\xi) \hat{V}_\beta(\vec{r}, \xi) \psi_{\beta j}(\xi) \tag{11.128}$$

is the effective "diagonal" optical potential in the channel βj (in realistic calculations usually approximated for all j by the elastic scattering $b + B \to b + B$ where b and B are in the ground states). In (11.126) we introduced also the residual "nondiagonal" interaction $\hat{W}^{(opt)}_{\beta j,\, \beta' j'}(\vec{r})$ between channels βj and $\beta' j'$,

$$\langle \beta j | \; \hat{W}^{(opt)}(\vec{r}) \; | \beta' j' \rangle \equiv \langle \beta j | \; \hat{V}_\beta(\vec{r}) \; | \beta' j' \rangle - \hat{U}^{(opt)}_{\beta j}(\vec{r}) \tag{11.129}$$

and this expression is only schematic because possible and necessary anti-symmetrization of intrinsic wave functions $\psi_{\beta j}(\xi)$ and $\psi_{\beta' j'}(\xi)$ is not specified here (for more information about anti-symmetrization see [23]).

There are also more fine approximations going beyond (11.125) allowing to solve the equation system (11.124) more presisely (see e.g. [352]) but their explanation goes beyond the scope of this textbook. Equation system (11.124), or more approximative (11.126), for unknown relative motion wave functions $u^{(\alpha i)}_{\beta j}(\hat{k}_{\beta j}, \vec{r}_\beta)$ for all channels βj involved in the P-space are known as coupled channel equation system. If the coupling of channels is switched off, that mans all $\langle \beta j | \hat{W}^{(opt)}(\vec{r}) | \beta' j' \rangle = 0$, then we have independent (without coupling) equations,

$$\left(\hat{T}_\beta - \epsilon_{\beta j} + \hat{U}^{(opt)}_{\beta j}(\vec{r}_\beta)\right) u^{(\alpha i}_{\beta j}(\vec{k}_{\beta j}, \vec{r}_\beta) = 0 \tag{11.130}$$

for relative motion wave functions in all channels βj and we speak about so called distorted wave approximation (DWA). In all these CCh or DWA approaches the "diagonal" optical potential $\hat{U}^{(opt)}_{\beta j}$ and "non-diagonal" channel iteractions $\hat{W}^{(opt)}_{\beta j\,,\,\beta' j'}$ are generally complex operators where imaginary parts should be obtained through the Feshbach averaging procedure described in the Section 11.2. In realistic calculations all optical potentials $\hat{U}^{(opt)}_{\beta j}$ (and possible interaction $\hat{W}^{(opt)}_{\beta j\,,\,\beta' j'}$) are parametrized using phenomenological expressions for concrete reactions. Some results and comparison with experimental data are discussed in the next section 11.4.

Knowing DWA or CCh sulutions $u^{(\alpha i)}_{\beta j}(\hat{k}_{\beta j}, \vec{r}_\beta)$ we can calculate reaction amplitude $f_{\vec{k}_{\alpha i} \to \vec{k}_{\beta j}} \equiv f_{\vec{k}_{\beta j}\,,\,\vec{k}_{\alpha i}}$ or corresponding S- matrix element $S_{\alpha i \to \beta j}$ and then subsequently the cross section of the particular reaction $\alpha i \to \beta j$ (see (11.64), (Q.21)). In next subsections the S- matrix of given reaction and its connection with the reaction amplitude is discussed in details.

11.3.2 S- matrix and reaction amplitudes for nuclear reactions, optical theorem

Reaction (scattering) amplitude $f_{(\vec{k}_{\alpha i} \to \vec{k}_{\beta j})}$ of the reaction $\alpha i \to \beta j$ is connected with the asymptotic behavior of the general channel wave function $\Psi_{(\vec{k}_{\alpha i})}$ of the system formed by the initial channel αi and decaying into several final open channels βj (see (11.119)). In order to specify asymptotic behavior of the wave function $\Psi_{(\vec{k}_{\alpha i})}$ (see (11.118) in more details we will suppose that all interactions $\hat{V}_\beta$ in (11.121) have short range (that means it goes to zero with $r \to \infty$ more quickly than $\frac{1}{r}$). Then in the asymptotic region all relative motion wave functions $u^{(\alpha i)}_{\beta j}(\vec{k}_{\beta j}, \vec{r}_\beta)$ behave as the wave functions (more

precisely as the wave packets) of free particles with the following asymptotic conditions,

1. relative motion wave function $u_{\beta j}^{(\alpha i)}(\vec{k}_{\beta j}, \vec{r}_{\beta})$ should involve the plane wave $e^{i\vec{k}_{\alpha i}\cdot\vec{r}_{\alpha}} = e^{ik_{\alpha}z_{\alpha}}$ describing the incoming beam of initial particle a and the target nucleus A in the CoM frame and outgoing spherical wave $\frac{1}{r_{\alpha}}e^{ik_{\alpha i}r_{\alpha}}$ describing ealastic scattering of particle a on the target nucleus A;
2. relative motion wave function $u_{\beta j}^{(\alpha i)}(\vec{k}_{\beta j}, \vec{r}_{\beta})$ for $\beta j \neq \alpha i$ should involve only spherical wave $\frac{1}{r_{\beta}}e^{ik_{\beta j}r_{\beta}}$ describing the relative motion of the outgoing final particle and final nucleus B after the reaction (or inelastic scattering) $\alpha i \to \beta j$.

11.3.2.1 Reaction of spinless particles and nuclei

In order to simplify the explanation at first we will suppose that all particles and nuclei participated in all considered channels have zero internal spins (zero intrinsic angular momenta). We will see later that the generalization of this rough assumption into the realistic case with nonzero spins of the particles (nuclei) in all considered channels can be done quite easily.

So we start with the general P-space channel wave function (11.118) with its asymptotic form (11.119). Our aim is the derivation of the expression for the reaction amplitude $f(\vec{k}_{\beta j}, \vec{k}_{\alpha i})$. Besides the assumption of the short range of interaction between particle and the nucleus in each of the considered channel it is usually supposed that this interaction depends only on the relative distance between particle and nucleus in all channels (that means only central character of these interaction is supposed). From the quantum mechanics it is known that under such assumption the orbital angular momentum L is good quantum number for the relative motion wave function (there is no any mixing between different L). We also know (see the expression (D.1) in the Appendix D) that in such a case the relative motion wave function for each value L can be written as the product of the radial part (depending on r_{β}) and the part depending on coordinate angles (φ_{β}, θ_{β}). That means in the case when the interaction between particle and the nucleus in each channel βj depends only on r_{β} the partial relative motion wave functions for different L do not mix. In general case (when the interaction in the channel βj is also dependent on $(\varphi_{\beta}, \theta_{\beta})$ the relative motion channel wave functions $u_{\beta j}^{(\alpha i)}(\vec{k}_{\beta j}, \vec{r}_{\beta})$

is a linear combination of partial channel wave functions with different L [6],

$$u_{\beta j}^{(\alpha i)}(\vec{k}_{\beta j}, \vec{r}_{\beta}) = \sum_{L} \frac{u_{L}^{(\alpha i, \beta j)}(r_{\beta})}{r_{\beta}} P_{L}(cos\theta_{\beta j}) \tag{11.131}$$

where $\frac{u^{(\alpha i, \beta j)}}{r_{\beta}}$ is the radial wave function and $P_L(cos\theta_{\beta j})$ is the Legendre polynomials depending on the angle $\theta_{\beta j}$ between vectors $\vec{k}_{\alpha i}$ and $\vec{k}_{\beta j}$ (we remind that the initial linear momentum vector $\vec{k}_{\alpha i}$ is directed to the z- axis of the CoM frame of the initial channel and the Legendre polynonials are present in the spherical functions $Y_{LM}(\vartheta, \varphi)$ - see any quantum mechanics textbook). Since we assumed that the interaction between particle and the nucleus in each channel in the asymptotic region $r \to \infty$ is zero then the particle and the nucleus behave like free particles for $r \to \infty$. From quantum mechanics it is also known that the radial part of the relative motion wave function of two particles (nuclei) in the region where there is no interaction between them can be written as the linear combination of the spherical Besel and spherical Neumann functions (see the expression (D.5) and the text above

[6] However in this general case the spin degrees of freedom should be taken into account and depending on the rotation symmetry of the interaction of particle and the nucleus in each channel the total angular momentum J is usually a good quantum number for the channel relative motion wave function. This aspect is not discussed in the subsection and partly will be mentioned in the next subsection 11.3.1.2.

it). Therefore the radial L-partial wave function is [7],

$$\frac{u_L^{(\alpha i,\beta j)}(r)}{r} = A_L^{\prime(\alpha i)} j_L(k_{\beta j}\, r) + B_L^{\prime(\alpha i)} n_L(k_{\beta j}\, r) =$$

$$= \boxed{\begin{array}{c}\text{in the asymptotic region}\\ (r \to \infty) \text{ - see (D.6)}\end{array}} =$$

$$\stackrel{r\to\infty}{\longrightarrow} \quad \frac{A_L^{\prime(\alpha i)}}{k_{\beta j}\, r}\, \sin\,(k_{\beta j}\, r - \frac{\pi L}{2}) - \frac{B_L^{\prime(\alpha i)}}{k_{\beta j}\, r}\, \cos\,(k_{\beta j}\, r - \frac{\pi L}{2}) =$$

$$= \boxed{\begin{array}{c}\text{because we can always write}\\ A_L^{\prime(\alpha i)} = C_L^{(\alpha i)} \cos\delta_L\ ,\ B_L^{\prime(\alpha i)} = C_L^{(\alpha i)} \sin\delta_L\end{array}} =$$

$$= \frac{C_L^{(\alpha i)}}{k_{\beta j}\, r} \sin\,(k_{\beta j}\, r - \frac{\pi L}{2} + \delta_L) =$$

$$= \frac{C_L^{(\alpha i)}}{2i\, k_{\beta j}\, r} \left[e^{i(k_{\beta j}\, r - \frac{\pi L}{2} + \delta_L)} - e^{-i(k_{\beta j}\, r - \frac{\pi L}{2} + \delta_L)}\right] =$$

$$= \frac{C_L^{(\alpha i)}}{2i\, k_{\beta j}\, r}\, e^{-i\delta_L} \left[\, e^{2i\delta_L}\, e^{i(k_{\beta j}\, r - \frac{\pi L}{2})} - e^{-i(k_{\beta j}\, r - \frac{\pi L}{2})}\, \right] \qquad (11.132)$$

In the case of elastic scattering $\alpha i \to \alpha i$ (that means $\beta j = \alpha i$ in (11.132)), discussed in the Subsection D.2.1 in the Appendix D, we introduced elastic S- matrix element (see (D.28)),

$$S^{(L)}_{\alpha i \to \alpha i} = e^{2i\delta_L} \qquad (11.133)$$

So the radial function $u_L^{(\alpha i,\alpha i)}(r)$ for elastic scattering can be rewritten as follows (in the asymptotic region)

$$u_L^{(\alpha i,\alpha i)}(r) \quad \stackrel{r\to\infty}{\longrightarrow} \quad \boxed{\begin{array}{c}\text{see}\\ \text{(11.132 and (11.133))}\end{array}} \quad \stackrel{r\to\infty}{\longrightarrow}$$

$$\stackrel{r\to\infty}{\longrightarrow} \quad A_L^{(\alpha i)} \left[\, S^{(L)}_{\alpha i \to \alpha i}\ e^{i(k_{\alpha i}\, r - \frac{\pi l}{2})} - e^{-i(k_{\alpha i}\, r - \frac{\pi l}{2})}\, \right] \qquad (11.134)$$

[7] If the different partial wave functions (different L) are mixed by the interaction then orbital angular momentum L of relative motion in the channel βj is not good quantum number but the rotation symmetry of the interaction is usually preserved which corresponds to the conserving of the total angular momentum J ($\vec{J} = \vec{L} + \vec{S}$), In such a case we should take into account also spin configuration space of the particle and the nucleus in all channels and the treating of the asymptotic relative motion in each channel should be modified in the sence of the subsection 3.1.2.3 where the elastic scattering of two nucleons via the tensor interaction was discussed. However this modification goes beyond the scope of this textbook. Some aspects of it will be also mentioned in the next discussions concerning the taking into account spin degrees of freedom in each channel (see Subsection 11.3.1.2).

while for the reaction $\alpha i \to \beta j$ ($\alpha i \neq \beta j$ we have the asymptotic radial L-partial wave function involving only outgoing spherical radial wave [8],

$$u_L^{(\alpha i,\beta j)}(r) \quad \stackrel{r\to\infty}{\longrightarrow} \quad B_L^{(\beta j)}\, S^{(L)}_{\alpha i\to\beta j}\; e^{i(k_{\beta j}\, r - \frac{\pi l}{2})} \tag{11.135}$$

The normalization constants $A_L^{(\alpha i)}$ and $B_L^{(\beta j)}$ are to be determined from the condition (1) and (2) given in the beginning of this section, that means:

1. the constant $A_L^{(\alpha i)}$ for given L is given by the condition that in the asymptotic region we require the function $\Psi_{(\vec{k}_{\alpha i})} - \psi_{\alpha i}(\xi)\, e^{ik_{\alpha i}z}$ to involve only outgoing spherical radial waves (for all L separately);

2. the constant $B_L^{(\beta j)}$ is determined by the requirement that the total spherical ingoing flux of probability for each L is equal to the total spherical outgoing flux of probability (in the sence of the integral of the flux over the whole space angle 4π).

Further the determination of $A_L^{(\alpha i)}$ and $B_L^{(\beta j)}$ is discussed in more details.

At first in agreement with the requirement (1) we should determine the following difference,

$$\Psi_{(\vec{k}_{\alpha i})} - \psi_{\alpha i}(\xi)\, e^{i\vec{k}_{\alpha i}\cdot\vec{r}_\alpha} = \boxed{\begin{array}{c}\text{see}\\ (11.118)\end{array}} =$$

$$= \psi_{\alpha i}(\xi)\, u^{(\alpha i)}_{\alpha i}(\vec{k}_{\alpha i},\vec{r}_\alpha) - \psi_{\alpha i}(\xi)\; e^{i\vec{k}_{\alpha i}\cdot\vec{r}_\alpha} + \sum_{\beta j\neq\alpha i} \psi_{\beta j}(\xi)\; u^{(\alpha i)}_{\beta j}(\vec{k}_{\beta j},\vec{r}_\beta) =$$

$$= \boxed{\begin{array}{c}\text{see}\\ (11.131),(D.22)\end{array}} =$$

$$= \psi_{\alpha i}(\xi) \sum_L \frac{u_L^{(\alpha i,\alpha i)}(r_\alpha)}{r_\alpha}\, P_L(\cos\theta_{\alpha i})$$

$$- \psi_{\alpha i}(\xi) \sum_L (2L+1)\, P_L(\cos\theta_{\alpha i})\, \frac{i^L}{2ik_{\alpha i}r_\alpha}\left[e^{i(k_{\alpha i}r_\alpha - \frac{\pi L}{2})} - e^{-i(k_{\alpha i}r_\alpha - \frac{\pi L}{2})}\right]$$

$$+ \sum_{\beta j\neq\alpha i} \psi_{\beta j}(\xi) \sum_L \frac{u_L^{(\alpha i,\beta j)}(r_\beta)}{r_\beta}\, P_L(\cos\theta_{\beta j}) \tag{11.136}$$

[8] In this textbook the S-matrix element of the reaction $\alpha \to \beta$ is denoted as $S_{\alpha\to\beta}$ or $S_{\beta,\alpha}$ ($S_{\alpha\to\beta} = S_{\beta,\alpha}$)

In the asymptotic region this expression has the following form,

$$\Psi_{(\vec{k}_{\alpha i})} - \psi_{\alpha i}(\xi)\, e^{i\vec{k}_{\alpha i}\cdot\vec{r}_\alpha} \quad \overset{r_\alpha, r_\beta \to \infty}{\longrightarrow} \quad \boxed{\begin{array}{c}\text{see}\\ (11.134), (11.135)\end{array}} =$$

$$= \psi_{\alpha i}(\xi) \sum_L \frac{A^{(\alpha i)} \left[S_{\alpha i,\alpha i}(L)\, e^{i(k_{\alpha i} r_\alpha - \frac{\pi L}{2})} - e^{-i(k_{\alpha i} r_\alpha - \frac{\pi L}{2})} \right]}{r_\alpha} P_L(\cos\theta_{\alpha i})$$

$$+ \psi_{\alpha i}(\xi) \sum_L \frac{i^L (2L+1) \left[e^{-i(k_{\alpha i} r_\alpha - \frac{\pi L}{2})} - e^{i(k_{\alpha i} r_\alpha - \frac{\pi L}{2})} \right]}{2ik_{\alpha i} r_\alpha} P_L(\cos\theta_{\alpha i})$$

$$+ \sum_{\beta j \neq \alpha i} \psi_{\beta j}(\xi) \sum_L \frac{B_L^{(\beta j)}}{r_\beta} S_{\alpha i \to \beta j}(L)\, e^{i(k_{\beta j} r_{\beta j} - \frac{\pi L}{2})} P_L(\cos\theta_{\beta j}) \qquad (11.137)$$

So the requirement that (11.137) cannot involve the ingoing spherical wave functions for all L gives the following value for $A_L^{(\alpha i)}$,

$$A_L^{(\alpha i)} = (2L+1) \frac{i^L}{2ik_{\alpha i}} \qquad (11.138)$$

and the substitution of (11.138) back to (11.137) yields,

$$\Psi_{(\vec{k}_{\alpha i})} \quad \overset{r_\alpha, r_\beta \to \infty}{\longrightarrow} \quad \psi_{\alpha i}(\xi)\, e^{i\vec{k}_{\alpha i}\cdot\vec{r}_\alpha} +$$

$$+ \ \psi_{\alpha i}(\xi) \sum_L \frac{i^L (2L+1)}{2ik_{\alpha i} r_\alpha} \left(S^{(L)}_{\alpha i \to \alpha i} - 1 \right) e^{i(k_{\alpha i}\cdot r_\alpha - \frac{\pi L}{2})} P_L(\cos\theta_{\alpha i})$$

$$+ \sum_{\beta j \neq \alpha i} \psi_{\beta j}(\xi) \sum_L \frac{B_L^{(\beta j)}}{r_\beta} S^{(L)}_{\alpha i \to \beta j} \ e^{i(k_{\beta j} r_{\beta j} - \frac{\pi L}{2})} \ P_L(\cos\theta_{\beta j}) = \qquad (11.139)$$

$$= \boxed{\begin{array}{c}\text{see}\\(D.22)\end{array}} =$$

$$= \psi_{\alpha i}(\xi) \sum_L \frac{i^L (2L+1) P_L(\cos\theta_{\alpha i})}{2ik_{\alpha i} r_\alpha} \Big[\, e^{i(k_{\alpha i} r_\alpha - \frac{\pi L}{2})} - e^{-i(k_{\alpha i} r_\alpha - \frac{\pi L}{2})} \,\Big]$$

$$+ \ \psi_{\alpha i}(\xi) \sum_L \frac{i^L (2L+1) P_L(\cos\theta_{\alpha i})}{2ik_{\alpha i} r_\alpha} \Big[\, S^{(L)}_{\alpha i \to \alpha i} - 1 \Big]\, e^{i(k_{\alpha i} r_\alpha - \frac{\pi L}{2})}$$

$$+ \sum_{\beta j \neq \alpha i} \psi_{\beta j}(\xi) \sum_L \frac{B^{(\beta j)}_L}{r_\beta}\, S^{(L)}_{\alpha i \to \beta j}\ e^{i(k_{\beta j} r_{\beta j} - \frac{\pi L}{2})}\ P_L(\cos\theta_{\beta j}) =$$

$$= \ \psi_{\alpha i}(\xi) \sum_L \frac{i^L (2L+1) P_L(\cos\theta_{\alpha i})}{2ik_{\alpha i} r_\alpha} \Big[\, S^{(L)}_{\alpha i \to \alpha i}\, e^{i(k_{\alpha i} r_\alpha - \frac{\pi L}{2})} - e^{-i(k_{\alpha i} r_\alpha - \frac{\pi L}{2})} \,\Big]$$

$$+ \sum_{\beta j \neq \alpha i} \psi_{\beta j}(\xi) \sum_L \frac{B^{(\beta j)}_L}{r_\beta}\, S^{(L)}_{\alpha i \to \beta j}\ e^{i(k_{\beta j} r_{\beta j} - \frac{\pi L}{2})}\ P_L(\cos\theta_{\beta j}) \qquad (11.140)$$

Further the amplitude $B^{(\beta j)}_L$ is determined from the requirement (2) above that the total spherical ingoing probability flux for each L should be equal to the total spherical outgoing probability flux,

$$\text{(probability "flux in" for given } L) =$$

$$= \int_0^\pi d\theta_{\alpha i} \int_0^{2\pi} d\phi_{\alpha i}\ r^2\ \sin\theta_{\alpha i}\ j^{(in)}_{r,\,\alpha i}(r_{\alpha i}, \phi_{\alpha i}, \theta_{\alpha i}) =$$

$$= \boxed{\begin{array}{c}\text{see (D.18) for the ingoing part}\\ \text{of the 1-st term in (11.140)}\end{array}} =$$

$$= \int_0^\pi d\theta_{\alpha i} \int_0^{2\pi} d\phi_{\alpha i}\ r^2\ \sin\theta_{\alpha i}\ (2L+1)^2\ \frac{\hbar k_{\alpha i}}{4k^2_{\alpha i} r^2 M_{\alpha i}}\ \Big|P_L(\cos\theta_{\alpha i})\Big|^2 =$$

$$= (2L+1)^2\ \frac{2\pi\hbar k_{\alpha i}}{4k^2_{\alpha i} M_\alpha} \int_0^\pi \Big|P_L(\cos\theta_{\alpha i})\Big|^2\ \sin\theta i\ d\theta_{\alpha i} \qquad (11.141)$$

and

$$\text{(probability "flux out" for given } L) =$$

$$= \int_0^\pi d\theta_{\alpha i} \int_0^{2\pi} d\phi_{\alpha i}\ r^2\ \sin\theta_{\alpha i}\ j^{(out)}_{r,\,\alpha i}(r_{\alpha i}, \phi_{\alpha i}, \theta_{\alpha i})$$

$$+ \sum_{\beta j \neq \alpha i} \int_0^\pi d\theta_{\beta j} \int_0^{2\pi} d\phi_{\beta j}\ r^2\ \sin\theta_{\beta j}\ j^{(out)}_{r,\,\beta j}(r_{\beta i}, \phi_{\beta i}, \theta_{\beta i}) =$$

$$= \boxed{\begin{array}{c}\text{see (D.18) for the outgoing part of the first}\\ \text{term in (11.140) and for the 2-d term in (11.140}\end{array}} =$$

$$= (2L+1)^2\,\frac{2\pi\hbar k_{\alpha i}}{4k_{\alpha i}^2 M_\alpha}\,\left|S^{(L)}_{\alpha i\to\alpha i}\right|^2\int_0^\pi \left|P_L(\cos\theta_{\alpha i})\right|^2\,\sin\theta_{\alpha i}\,d\theta_{\alpha i}$$
$$+\sum_{\beta j\neq\alpha i}\frac{2\pi B_L^{(\beta j)\,2}\,\hbar k_{\beta j}}{M_{\beta j}}\,\left|S^{(L)}_{\alpha i\to\beta j}\right|^2\int_0^\pi d\theta_{\beta j}\;\; r^2\,\left|P_L(\cos\theta_{\beta j})\right|^2\,\sin\theta_{\beta j} \tag{11.142}$$

Expression (11.141) should be equal to (11.142) $\Rightarrow$

$$\frac{(2L+1)^2\hbar k_{\alpha i}}{4k_{\alpha i}^2 M_{\alpha i}} = \frac{(2L+1)^2\hbar k_{\alpha i}}{4k_{\alpha i}^2 M_{\alpha i}}\,\left|S^{(L)}_{\alpha i\to\alpha i}\right|^2 + \sum_{\beta j\neq\alpha i} B_L^{(\beta j)\,2}\,\frac{\hbar k_{\beta j}}{M_{\beta j}}\left|S^{(L)}_{\alpha i\to\beta j}\right|^2 \tag{11.143}$$

This equation is valid if we choose,

$$B_L^{(\beta j)\,2} = \frac{(2L+1)^2 M_{\beta j}k_{\alpha i}}{4k_{\alpha i}^2 M_{\alpha i}k_{\beta j}} \quad\Rightarrow\quad B_L^{(\beta j)} = (2L+1)\frac{i^L}{2ik_{\alpha i}}\sqrt{\frac{M_{\beta j}k_{\alpha i}}{M_{\alpha i}k_{\beta j}}} \tag{11.144}$$

and simultaneously,

$$\sum_{\beta j(all)}\left|S^{(L)}_{\alpha i\to\beta j}\right|^2 = 1 \tag{11.145}$$

where the sum over βj in (11.145) involves both $\beta j\neq\alpha i$ and $\beta j=\alpha i$.

If the expression (11.144) is substituted into (11.139) then the asymptotic expression for $\Psi_{(\vec{k}_{\alpha i})}$ becomes,

$$\Psi_{(\vec{k}_{\alpha i})} \overset{r_\alpha, r_\beta\to\infty}{\longrightarrow} \psi_{\alpha i}(\xi_\alpha)\,e^{i\vec{k}_{\alpha i}\cdot\vec{r}_\alpha}$$
$$+\frac{1}{2ik_{\alpha i}}\sum_{\beta j\,(all)}\psi_{\beta j}(\xi_\beta)\sqrt{\frac{M_{\beta j}k_{\alpha i}}{M_{\alpha i}k_{\beta j}}}\;\sum_L(2L+1)\cdot$$
$$\cdot\left[S^{(L)}_{\alpha i\to\beta j}-\delta_{ij}\delta_{\alpha\beta}\right]\,P_L(\cos\theta_{\beta j})\,\frac{e^{ik_{\beta j}r_\beta}}{r_\beta} =$$

$$= \boxed{\begin{array}{c}\text{see}\\ (D.22)\end{array}} =$$

$$= -\frac{1}{2ik_{\alpha i}}\psi_{\alpha i}(\xi_\alpha)\sum_L (2L+1)\frac{e^{-ik_{\alpha i}r_\alpha}}{r_\alpha}(-1)^L P_L(\cos\theta_{\alpha i})$$

$$+\frac{1}{2ik_{\alpha i}}\sum_{\beta j\ (all)}\psi_{\beta j}(\xi_\beta)\sqrt{\frac{M_{\beta j}k_{\alpha i}}{M_{\alpha i}k_{\beta j}}}\sum_L (2L+1)S^{(L)}_{\alpha i\to\beta j}\,P_L(\cos\theta_{\beta j})\,\frac{e^{ik_{\beta j}r_\beta}}{r_\beta} = \tag{11.146}$$

Then the expression (11.146) is compared with the original expression (11.119) and as a result we obtain the expression for the reaction amplitude $f(\vec{k}_{\alpha i}\to\vec{k}_{\beta j})\equiv f(\vec{k}_{\beta j},\vec{k}_{\alpha i})$,

$$f(\vec{k}_{\beta j},\vec{k}_{\alpha i}) = \frac{1}{2ik_{\alpha i}}\sqrt{\frac{M_{\beta j}k_{\alpha i}}{M_{\alpha i}k_{\beta j}}}\sum_L (2L+1)\left[S^{(L)}_{\alpha i\to\beta j}-\delta_{ij}\delta_{\alpha\beta}\right]P_L(\cos\theta_{\beta j}) \tag{11.147}$$

where angle $\theta_{\beta j}$ is the angle between vectors $\vec{k}_{\beta j}$ and $\vec{k}_{\alpha i}$. In the analogy with the derivation of the differential cross section of the elastic process (see the Appendix D, expr. (D.16)-(D.19)) the differential cross section of the general reaction $\alpha i\to\beta j$ has the following form,

$$\frac{d\sigma_{\alpha i\to\beta j}}{d\Omega_\beta} = \frac{\left(\begin{array}{c}\text{flux of outgoing wave to the channel } \beta j \text{ and}\\ \text{to the unit space angle in the dirrection } \theta_{\beta j},\phi_{\beta j}\end{array}\right)}{\text{flux of the incident plane wave in the channel } \alpha i} =$$

$$= \boxed{\begin{array}{c}\text{see}\\ (D.17),(D.18)\end{array}} = \frac{\left|f(\vec{k}_{\alpha i}\to\vec{k}_{\beta j})\right|^2\frac{\hbar k_{\beta j}}{M_{\beta j}}}{\frac{\hbar k_{\alpha i}}{M_{\alpha i}}} = \frac{M_{\alpha i}k_{\beta j}}{M_{\beta j}k_{\alpha i}}\left|f(\vec{k}_{\alpha i}\to\vec{k}_{\beta j})\right|^2 \tag{11.148}$$

where angles $\theta_{\beta j},\phi_{\beta j}$ characterize the dirrection of the vector $\vec{k}_{\beta j}$ with respect to the vector $\vec{k}_{\alpha i}$ in the frame where the z- axis is parallel to the vector $\vec{k}_{\alpha i}$. The expression (11.148) is valid for inelastic processes $\alpha i\neq\beta j$ as well as for elastic one $\alpha i=\beta j$. Corresponding integral cross sections are derived further.

Integral cross section of the elastic scattering $\alpha i = \beta j$ is,

$$\sigma_{el} = \sigma_{\alpha i \to \alpha i} = \int d\Omega_{\alpha i} \big| f(\vec{k}_{\alpha i}, \vec{k}_{\alpha i}) \big|^2 = \boxed{\begin{array}{c}\text{see}\\ (11.147)\end{array}} =$$

$$= \frac{1}{4k_{\alpha i}^2} \sum_{L,L'} (2L+1)(2L'+1) \big(S_{\alpha i,\alpha i}^{(L')\,*} - 1\big) \big(S_{\alpha i,\alpha i}^{(L)} - 1\big) \cdot$$

$$\cdot \int d\Omega_{\alpha i} \; P_{L'}(\cos\theta_{\alpha i}) \, P_L(\cos\theta_{\alpha i}) =$$

$$= \boxed{\begin{array}{c}\text{using following math. identity}\\ \int d\Omega \, P_{L'}(\cos\theta) \, P_L(\cos\theta) = \frac{4\pi\delta_{L,L'}}{2L+1}\end{array}} =$$

$$= \frac{\pi}{k_{\alpha i}^2} \sum_{L} (2L+1) \big(S_{\alpha i,\alpha i}^{(L)\,*} - 1\big) \big(S_{\alpha i,\alpha i}^{(L)} - 1\big) =$$

$$= \frac{\pi}{k_{\alpha i}^2} \sum_{L} (2L+1) \big|1 - S_{\alpha i,\alpha i}^{(L)}\big|^2 \tag{11.149}$$

Integral cross section of the reaction $\alpha i \to \beta j$ ($\beta j \neq \alpha i$) has following form,

$$\sigma_{\alpha i \to \beta j} = \int d\Omega_{\beta j} \frac{M_{\alpha i} k_{\beta j}}{M_{\beta j} k_{\alpha i}} \big| f(\vec{k}_{\beta j}, \vec{k}_{\alpha i}) \big|^2 = \boxed{\begin{array}{c}\text{see}\\ (11.147) \text{ for } \beta j \neq \alpha i\end{array}} =$$

$$= \frac{1}{4k_{\alpha i}^2} \sum_{L,L'} (2L+1)(2L'+1) S_{\alpha i \to \beta j}^{(L')\,*} \, S_{\alpha i \to \beta j}^{(L)} \cdot$$

$$\cdot \int d\Omega_{\beta j} \; P_{L'}(\cos\theta_{\beta j}) \, P_L(\cos\theta_{\beta j}) =$$

$$= \frac{\pi}{k_{\alpha i}^2} \sum_{L} (2L+1) \big|S_{\alpha i \to \beta j}^{(L)}\big|^2 \tag{11.150}$$

Integral cross section for all inelastic process is,

$$\sigma_{inel} = \sum_{\beta j \neq \alpha i} \sigma_{\alpha i \to \beta j} = \frac{\pi}{k_{\alpha i}^2} \sum_{L} (2L+1) \sum_{\beta j \neq \alpha i} \big|S_{\alpha i \to \beta j}^{(L)}\big|^2 =$$

$$= \boxed{\begin{array}{c}\text{see}\\ (11.145)\end{array}} = \frac{\pi}{k_{\alpha i}^2} \sum_{L} (2L+1) \left(1 - \big|S_{\alpha i,\alpha i}^{(L)}\big|^2\right) \tag{11.151}$$

and finally the total integral cross section for all elastic and inelastic process

is given by the sum of σ_{el} and σ_{inel},

$$\begin{aligned}
\sigma_{total} &= \sigma_{el} + \sigma_{inel} = \\
&= \frac{\pi}{k_{\alpha i}^2} \sum_L (2L+1) \\
&\qquad \cdot \Big[\big| S_{\alpha i,\alpha i}(L) \big|^2 - S^{(L)}_{\alpha i,\alpha i} - S^{(L)\,*}_{\alpha i,\alpha i} + 1 + 1 - \big| S^{(L)}_{\alpha i,\alpha i} \big|^2 \Big] = \\
&= \frac{\pi}{k_{\alpha i}^2} \sum_L (2L+1) \big(2 - S^{(L)}_{\alpha i,\alpha i} - S^{(L)\,*}_{\alpha i,\alpha i} \big) = \\
&= \frac{\pi}{k_{\alpha i}^2} \sum_L (2L+1) \left(2 - 2\, Re S^{(L)}_{\alpha i,\alpha i} \right)
\end{aligned} \tag{11.152}$$

The expression (11.152) demonstrates that the knowledge of the elastic S-matrix elements $S^{(L)}_{\alpha i,\alpha i}$ is sufficient for the determination of the total integral cross section σ_{total} (which involves information about inelastic or reaction scattering). The fact that the elastic scattering amplitude $f(\vec{k}_{\alpha i} \to \vec{k}_{\beta j})$ for zero angle between $\vec{k}_{\alpha i}$ and $\vec{k}_{\beta j}$ fully determines the total integral cross section follows from so called optical theorem which is discussed below.

Let us determine the reaction amplitude (11.147) for the zero angle between $\vec{k}_{\alpha i}$ and $\vec{k}_{\beta j}$,

$$\begin{aligned}
& f_{\theta=0}(\vec{k}_{\alpha i} \to \vec{k}_{\beta j}) \equiv f_{\beta j,\,\alpha i}(\theta = 0) = \\
&\quad = \frac{1}{2ik_{\alpha i}} \sqrt{\frac{M_{\beta j} k_{\alpha i}}{M_{\alpha i} k_{\beta j}}} \sum_L (2L+1) \left(S^{(L)}_{\alpha i \to\, \beta j} - \delta_{ij}\delta_{\alpha\beta} \right) P_L(1) = \\
&= \boxed{\begin{array}{c} \text{because} \\ P_L(1) = 1 \text{ for all } L \end{array}} = \\
&= \frac{1}{2ik_{\alpha i}} \sqrt{\frac{M_{\beta j} k_{\alpha i}}{M_{\alpha i} k_{\beta j}}} \sum_L (2L+1) \left(S^{(L)}_{\alpha i \to\, \beta j} - \delta_{ij}\delta_{\alpha\beta} \right) = \\
&= \frac{1}{2ik_{\alpha i}} \sqrt{\frac{M_{\beta j} k_{\alpha i}}{M_{\alpha i} k_{\beta j}}} \sum_L (2L+1) \left[Re S^{(L)}_{\alpha i \to\, \beta j} + i\, Im S^{(L)}_{\alpha i \to \beta j} - \delta_{ij}\delta_{\alpha\beta} \right] = \\
&= \frac{1}{2k_{\alpha i}} \sqrt{\frac{M_{\beta j} k_{\alpha i}}{M_{\alpha i} k_{\beta j}}} \sum_L (2L+1) \left[Im S^{(L)}_{\alpha i \to\, \beta j} + i \big(\delta_{\alpha i,\,\beta j} - Re S^{(L)}_{\alpha i \to\, \beta j} \big) \right]
\end{aligned} \tag{11.153}$$

So we obtained

$$Imf_{\alpha i\to\beta j}(\theta=0)=\frac{1}{2k_{\alpha i}}\sqrt{\frac{M_{\beta j}k_{\alpha i}}{M_{\alpha i}k_{\beta j}}}\sum_{L}(2L+1)\big(\delta_{\alpha i,\beta j}-ReS^{(L)}_{\alpha i,\alpha i}\big)$$

$$\Rightarrow\quad Imf_{\alpha i,\alpha i}(\theta=0)=\frac{1}{2k_{\alpha i}}\sum_{L}(2L+1)\big(1-ReS^{(L)}_{\alpha i,\alpha i}\big) \tag{11.154}$$

and the comparison of (11.154) with (11.152) gives

$$\sigma_{total}=\frac{4\pi}{k_{\alpha i}}\,Imf_{\alpha i,\,\alpha i}(\theta=0) \tag{11.155}$$

This expression is known in literature as the optical theorem. One can see that the elastic scattering amplitude for the forward direction ($\theta=0$) fully determines the total integral cross section including inelastic processes.

It is necessary to realize that all information about interactions among particles and nuclei in all channels involved in our configuration space enter the expressions (11.149)-(11.152) through the complex S-matrix elements. These S- matrix elements are directly connected with phase shifts of relative motion wave functions in all investigated channels. For instance the case of pure elastic scattering of two particles interacting mutually by central potential was discussed in the Subsection D.2.1 and it was shown there that each partial wave with orbital angular momentum L is connected with one phase shift δ_L and that in this case for given L we have only one diagonal S- matrix element $S^{(L)}_{\alpha i,\alpha i}=e^{2i\delta_L}$ (see (D.28)). In the case when not only elastic channel is taken into account and/or the interaction between particles is not central (depending only on their relative distance) then the situation is more complicated and each partial wave is not characterized only by the orbital angular momentum L and for each partial wave we have not only one phase shift (see the Subsection 3.1.2.3 where the elastic scattering of two nucleons interacting by the tensor force is discussed). However in any case the phase shifts of relative motion wave functions in individual channels (and consequently the S-matrix elements, defined by (11.134) and (11.135)) can be obtained from potentials $\hat{V}_\beta$ participating in the equation system of coupled channels (see (11.126)) in terms of the phase shift analysis method discussed in the Subsection 3.1.2.4 (for the case of two nucleon scattering). The other possibility is to express the reaction amplitude $f(\hat{k}_{\alpha i},\hat{k}_{\beta j})$ in terms of the optical potential matrix elements using the perturbation Born series as will be discussed in the Section 11.4.

The other thing which should be pointed out is that in realistic calculations we always restrict ourselves into the finite number of P- channels (some prompt channels are always neglected) and always the Q- space channels are present. According to the averaging procedure involved an the formal Feshbach theory it means that all matrix elements of interaction potentials have non-zero imaginary parts and therefore are complex.

11.3.2.2 Reaction of nuclei and particles with nonzero spin

In the case when nonzero spin of nuclei and particles participating in the reaction are take into account the expressions (11.118) and (11.131) for the general P-channel wave function $\Psi_{(\vec{k}_{\alpha i})}$ connected with the initial channel αi takes more complicated form [9]

$$\Psi_{\alpha i \equiv (J_{Ai}, m_{Ai}, s_{ai}, \mu_{ai}, \vec{k}_{\alpha i})} = \\ = \sum_{\beta j(all)} \sum_{LJS} \sum_{\mu_{bj} m_{Bj} m} C^{S\,\mu_{bj}+m_{Bj}}_{s_{bj}\,\mu_{bj} J_{Bj} m_{Bj}}\; C^{J\,\mu_{bj}+m_{Bj}+m}_{S\,\mu_{bj}+m_{Bj}\;L\,m}\; \psi_{J_{Bj} m_{Bj}}(\xi_{Bj})\; \psi_{s_{bj}\mu_{bj}}(\xi_{bj}) \cdot \\ \cdot \frac{u^{(\alpha i,\beta j)}_{LJ}(r_{\beta j})}{r_{\beta j}}\; Y_{Lm}(\theta_{\beta j}, \phi_{\beta j}) \qquad (11.156)$$

where in each channel βj (including the initial one) the total angular momentum $\vec{J} = \vec{S} + \vec{L}$ with $\vec{S} = \vec{J}_B + \vec{s}_b$ been the total spin (intrinsic angular momentum) of the nucleus B and the particle b in the given channel βj and $\vec{L}$ is the orbital momentum of the relative motion in the given partial wave characterized by the quantum numbers SLJ. Functions $\psi_{J_{Bj} m_{Bj}}(\xi_{Bj})$ and $\psi_{s_{bj}\mu_{bj}}(\xi_{bj})$ are the internal wave functions of the nucleus B and the particle b corresponding to the internal state j of the channel. The function $\frac{u^{(\alpha i,\beta j)}_{LJ}(\xi_{\beta j})}{r_{\beta j}}$ stands for the radial part of the relative motion wave function where angle part is given by the spherical function $Y_{Lm}(\theta_{\beta j}, \phi_{\beta j})$.

Presumed asymptotic form of the general wave function $\Psi_{\alpha i}$ can be expressed as follows (we use the expression (D.22), the math. identity $Y_{L0}(\theta, \phi) = \sqrt{\frac{2L+1}{4\pi}}\, P_L(\cos\theta)$ and the assumption that in each final channel the relative motion part of the wave function has a form of the spherical outgoing wave

[9] Opposite to the Subsection 11.3.1.1. now we suppose possible interaction dependence on spins and rotation invariance of the relative motion interaction of particles and nuclei in each channel and therefor the partial wave functions are characterized not only by L (orbital momentum) but quantum numbers SLJ (orbital and total ang. momenta)

- see (11.119)),

$$\Psi_{\alpha i} =$$
$$= \sum_{LJS} C^{S\,\mu_{ai}+m_{Ai}}_{s_{ai}\,\mu_{ai}\,J_{Ai}\,m_{Ai}} C^{J\,\mu_{ai}+m_{Ai}}_{S\,\mu_{ai}+m_{Ai}\,L\,0} \sqrt{\frac{4\pi}{2L+1}} Y_{L0}(\theta_{\alpha i}, \phi_{\alpha i})$$
$$\psi_{J_{Ai}m_{Ai}}(\xi_{Ai})\, \psi_{(s_{ai}m_{ai})}(\xi_{ai})\, \frac{i^L}{2ik_{\alpha i}r_{\alpha i}} \left[e^{i(k_{\alpha i}r_\alpha - \frac{\pi L}{2})} - e^{-i(k_{\alpha i}r_\alpha - \frac{\pi L}{2})} \right] +$$
$$+ \sum_j f_{\alpha i \to \alpha j}\, \frac{e^{ik_{\alpha j}r_{\alpha j}}}{r_{\alpha j}}\, \psi_{AJ_{Ai}\mu_{Ai}}(\xi_{Aj})\, \psi_{as_{Ai}\mu_{ai}}(\xi_{aj})$$
$$+ \sum_{\beta j \neq \alpha i} f_{\alpha i \to \beta j}\, \frac{e^{ik_{\beta j}r_\beta}}{r_{\beta j}}\, \psi_{BJ_{Bj}\mu_{Bj}}(\xi_{Bj})\, \psi_{bs_{bj}\mu_{bj}}(\xi_{bj}) \tag{11.157}$$

where $\alpha i \equiv (J_{Ai},\, m_{Ai},\, s_{ai},\, \mu_{ai},\, \vec{k}_{\alpha i})$ and $\beta j \equiv (J_{Bj},\, m_{Bj},\, s_{bj},\, \mu_{aj},\, \vec{k}_{\beta j})$ characterize corresponding channels. The first term (plane wave in the form of the decomposition into the partial waves) corresponds to the initial channel αi, the second term describes all scattering $\alpha i \to \alpha j$ of the particle a and the target nucleus A (elastic scattering for $j = i$ as well as inelastic scattering for $i \neq j$), and the third term is connected with the transmutation reaction $\alpha i \to \beta j$ $(a + A \to b + B,\ \alpha \neq \beta$, where the indexes i or j characterize the intrinsic state of the particle and the nucleus in the given channel αi or βj). One should realize that if in the given channels αi and βj the orientations of spins of particle and nucleus are detected (that means the nucleus is spin-oriented and the particle is spin-polarized) then the corresponding ensembles of indexes characterizing given channel involve ang. momentum projections m_{Ai}, μ_{ai} and m_{Bj}, μ_{bj}.

The reaction amplitudes $f_{\alpha i \to \alpha j}$ and $f_{\alpha i \to \beta j}$ can be generally obtained by the comparison of presumed form of the asymptotic wave function (11.157) with the asymptotic form of the wave function (11.156) given by the asymptotic behavior of the radial wave functions $u^{(\alpha i, \beta j)}_{LJ}(r_{\beta j})$ (all βj) (analogy with (11.134) and (11.135) but with the inclusion of the spin degrees of freedom),

$$u^{(\alpha i, \alpha j)}_{SLJ}(r_{\alpha i}) = A^{(\alpha i)}_{SLJ} \left[S^{(SLJ)}_{\alpha i,\, \alpha i}\, e^{i(\vec{k}_{\alpha i}\vec{r}_{\alpha i} - \frac{\pi l}{2})} - e^{-i(\vec{k}_{\alpha i}\vec{r}_{\alpha i} - \frac{\pi l}{2})} \right]$$
$$u^{(\alpha i, \beta j)}_{SLJ}(r_{\beta j}) = B^{(\beta j)}_{SLJ}\, S^{(SLJ)}_{\alpha i,\, \beta j}\, e^{i(\vec{k}_{\alpha i}\vec{r}_{\beta j} - \frac{\pi l}{2})} \tag{11.158}$$

where the normalization constants $A^{(\alpha i)}_{SLJ}$ can be determined by the requirement that for each partial wave given by SLJ the asymptotic form of the

wave function (see (11.157)),

$$\Psi_{(\vec{k}_{\alpha i})} - \sum_{SLJ} C^{S\,\mu_{ai}+m_{Ai}}_{s_{ai}\,\mu_{ai}\,J_{Ai}\,m_{Ai}} C^{J\,\mu_{ai}+m_{Ai}}_{S\,\mu_{ai}+m_{Ai}\,L\,0} \sqrt{\frac{4\pi}{2L+1}} Y_{L0}(\theta_{\alpha i}, \phi_{\alpha i}) \cdot$$

$$\cdot\, \psi_{J_{Ai}m_{Ai}}(\xi_{Ai})\, \psi_{(s_{ai}m_{ai})}(\xi_{ai})\, \frac{i^L}{2ik_{\alpha i}r_{\alpha i}} \left[e^{i(k_{\alpha i}r_\alpha - \frac{\pi L}{2})} - e^{-i(k_{\alpha i}r_\alpha - \frac{\pi L}{2})}\right]$$

becomes only outgoing spherical wave. The constants $B^{(\beta j)}_{SLJ}$ are given by the requirement that for fixed SLJ the whole ingoing spherical probability flux (integrated over the whole 4π space) in the function $\Psi_{\alpha i}$ should be equal to the whole outgoing spherical probability flux with the simultaneous condition $\sum_{\beta j\,(all)} |S^{(SLJ)}_{\alpha i,\,\beta j}|^2 = 1$. This is the analogy with (11.145) for spinless case discussed in the previous subsection. In such a case we can express the reaction amplitudes $f_{\alpha i\to\beta j}$ for all reactions $\alpha i \to \beta j$ (for given initial channel αi) in terms of the corresponding S- matrix which can be determined e.g. by the phase analysis method with given channel interaction. In the subsequent step the differential cross section of all reactions $\alpha i \to \beta j$ are determined by the square power of the reaction amplitudes.

The scheme discussed above is more or less formal because all channel interactions are not known generally and we should determine it phenomenologically for each particular physical situation. For instance in the next section the inelastic scattering and reactions with one nucleon transfer with the incoming particles (nucleons, light nuclei) will be discussed in details.

In the expression (11.157) we supposed that the channel intrinsic spin projections $m_{Aj} + \mu_{aj}$ or $m_{Bj} + \mu_{bj}$ are known. In reality they are not known generally (that means spin orientation of nucleus and polarization of particle in all channels are not known). In such a case in the determination of the cross sections we should average over projections $\mu_{\alpha j}$ and sum over internal ang. momenta $\mu_{\beta j}$ for all final channels.

Detailed expressions for cross sections in general case (with nonzero spins of reaction participants) are not given here. We will discuss cross sections (particularly their comparison with experimental values) for some concrete reactions in the next section.

11.3.2.3 Properties of S- matrix

11.3.2.3.1 Spherical ingoing and outgoing wave packets Up to now reactions were described in a stationary way. That means incoming particles were supplied continually from the source independently on time and corresponding

beam of incoming particles was also time-independent. As a result the outgoing waves corresponding to all final channels were also stationary without any dependence on time. From now on we will consider the idealized case when the source of the incoming particles is switched on for the time interval T and then it is switched off. Then in the initial channel we have spherical wave packet with the length $L_\alpha = v_\alpha\, T$, where $v_\alpha = \frac{k_\alpha}{M_\alpha}$ is the velocity of the incoming particle in the CoM frame (M_α is the channel effective mass). That means before the reaction the wave function $\Psi_\alpha \equiv \Psi_{k_\alpha}$ is characterized by the ingoing spherical wave (see the first term in (11.146) and after the reaction all final channels β contain the outgoing spherical wave (see the second term in (11.146)) [10].

In next consideration we restrict ourselves in (11.146) only on the partial waves with $L = 0$. The partial waves for $L > 0$ can be treated similarly, only corresponding expressions are a little bit more complicated. Then the incoming spherical $L = 0$ packet can be written as (see the first term in (11.146) for $L = 0$ and one should realize that for $L = 0$ the Legendre polynomials are $P_{L=0}(\cos\theta) = 1$ for all θ),

$$\Psi^{(L=0)}_{\alpha;\, in} = -\, C\, \frac{1}{\sqrt{4\pi v_\alpha}}\, \psi_\alpha(\xi)\, \frac{e^{-ik_{\alpha r_\alpha}}}{r_\alpha} \tag{11.159}$$

where the constant C is obtained from the normalization condition,

$$\int \Psi^{(L=0)\,*}_{\alpha;\, in}\, \Psi^{(L=0)}_{\alpha;\, in}\, d\tau =$$

$$= \boxed{\begin{array}{c}\text{integration over } d\tau \text{ means the integration over} \\ \text{intrinsic and relative motion variables , } d\tau = d^3 r_\alpha\, d\xi_\alpha\end{array}} =$$

$$= |C|^2\, \frac{1}{4\pi v_\alpha} \int d^3 r_\alpha\, e^{ik_\alpha r_\alpha}\, e^{-ik_\alpha r_\alpha} \frac{4\pi r_\alpha^2}{r_\alpha^2} \int d\xi_\alpha\, \psi^*_\alpha(\xi_\alpha)\, \psi_\alpha(\xi_\alpha) =$$

$$= \boxed{\begin{array}{c}\text{because} \\ \int d\xi\, \psi^*_\alpha(\xi)\, \psi_\alpha(\xi) = 1\end{array}} =$$

$$= |C|^2\, \frac{1}{v_\alpha} \int dr_\alpha = |C|^2\, \frac{L_\alpha}{v_\alpha} = |C|^2\, T = 1$$

$$\Rightarrow \qquad C = \sqrt{T^{-1}} \tag{11.160}$$

[10] For a simplicity in this subsection we return back to the assumption of the spinless particles and nuclei when partial waves are characterized only by the orbital angular momentum L. We also omit the indexes i and/or j characterizing the internal states of the particle and the nucleus in the given channel, see (11.146), in order to have expressions simpler.

As was mentioned above after the reaction all final channels β contain the outgoing spherical wave packets with the length $L_\beta = v_\beta T$ (we suppose that the time, during of which the detector in the channel β registered particle b and the nucleus B, is the same as the time interval T of the switching on the producing of impacting particles a in the initial channel α - that means we neglect effects connected with the quantum mechanics mechanism expansion of the packet [11]. So after the reaction the wave function $\Psi_{\alpha,\,out}(L=0)$ of the whole system $a+A$ is following (see the second term in (11.146) for $L=0$),

$$\Psi^{(L=0)}_{\alpha,\,out} = \sum_\beta \Psi^{(L=0)}_{\substack{\alpha,\beta \\ out}} = \sum_\beta C\, S^{(L=0)}_{\beta,\,\alpha}\, \frac{1}{4\pi v_\beta}\, \frac{e^{ik_\beta r_\beta}}{r_\beta}\, \psi_\beta(\xi_\beta) \qquad (11.161)$$

where $S^{(L=0)}_{\alpha,\,\beta}$ is the element of the S- matrix for the partial wave $L=0$ (see the second term in the expr. (11.146)). The probability of finding the reaction product in the channel β is (for the partial wave $L=0$)

$$\int \left|\Psi^{(L=0)}_{\substack{\alpha,\beta \\ out}}\right|^2 d^3r_\beta\, d\xi_\beta = |C|^2 \left|S^{(L=0)}_{\alpha\to\beta}\right|^2 \frac{L_\beta}{v_\beta} = \boxed{\begin{array}{c}\text{see} \\ (11.160)\end{array}} = \left|S^{(L=0)}_{\alpha\to\beta}\right|^2 \quad (11.162)$$

and similar expressions can be derived for another partial waves with $L>0$.

11.3.2.3.2 Unitarity of S- matrix Let $\hat{H}$ is the hermitian Hamiltonian driving the general wave function Ψ_α (this Hamiltonian can be identified with the effective Hamiltonian $\hat{H}_{eff}$ in (11.15) for P- channels). Then,

$$\begin{aligned} & \hat{H}|\Psi_\alpha\rangle = i\hbar \frac{\partial|\Psi_\alpha\rangle}{\partial t} \\ \Rightarrow \quad & \frac{\partial}{\partial t}\langle\Psi_\alpha|\Psi_\alpha\rangle = \langle\frac{\partial\Psi_\alpha}{\partial t}|\Psi_\alpha\rangle + \langle\Psi_\alpha|\frac{\partial\Psi_\alpha}{\partial t}\rangle = \\ & = \frac{i}{\hbar}\langle\hat{H}\Psi_\alpha|\Psi_\alpha\rangle - \frac{i}{\hbar}\langle\Psi_\alpha|\hat{H}\Psi_\alpha\rangle = \boxed{\begin{array}{c}\text{because } \hat{H} \\ \text{is hermitian}\end{array}} = 0 \end{aligned} \qquad (11.163)$$

That means the norm of the function $\Psi_\alpha(\vec{r},\xi)$ is not dependent on time (for any partial wave L - see (11.162) [12],

$$\sum_\beta \Psi^{(L)\,*}_{\alpha,\beta}\, \Psi^{(L)}_{\alpha,\beta}\, d^3r\, d\xi = \boxed{\begin{array}{c}\text{see (11.162)} \\ \text{for any } L\end{array}} = \sum_\beta \left|S^{(L)}_{\alpha\to\beta}\right|^2 = 1 \qquad (11.164)$$

[11] In the quantum mechanics it is known that each wave packet expands with time but we suppose that this expansion is much slower in the comparison with the velocity v_α or v_β.

[12] In this paragraph we again suppose the spinless case when the partial wave is characterized by the orbital momentum quantum number L. In order to simplify expressions we omit the internal state index for each channle α or β.

This expression is the same as (11.145) and it ensures the total probability conservation for partial wave with given L (total probability "flux in" is equal to the total probability "flux out" for given L). It is necessary to emphasize here that we assume that all interactions do not mix different L.

The expression (11.164) can be generalized for the case of the general scalar product of any channel waves with given Hamiltonian,

$$\frac{\partial}{\partial t}\langle\Psi|\Phi\rangle = \langle\frac{\partial\Psi}{\partial t}|\Phi\rangle + \langle\Psi|\frac{\partial\Phi}{\partial t}\rangle =$$

$$= \frac{i}{\hbar}\langle\hat{H}\Psi|\Phi\rangle - \frac{i}{\hbar}\langle\Psi|\hat{H}\Phi\rangle = \boxed{\begin{array}{c}\text{because } \hat{H}\\ \text{is hermitian}\end{array}} = 0 \qquad (11.165)$$

Let us suppose now that Ψ_α and Ψ_β ($\alpha \neq \beta$) are total general channel wave functions corresponding to the same system (consisting from the same nucleons) but in the case of Ψ_α the system was created through the initial channel α while Ψ_β corresponds to the initial channel β. Before the reaction (before the creation of our system) both functions Ψ_α and Ψ_β are mutually ortogonal because Ψ_α is localized (nonzero) only in the channel α while Ψ_β is nonzero in the channel β and $\alpha \neq \beta$. However according to (11.165) the scalar product $\langle\Psi_\alpha|\Psi_\beta\rangle = 0$ is preserves in all times so we can write $\langle\Psi_\alpha|\Psi_\beta\rangle = 0$ for any time and it valids for any partial wave (and we suppose also that all interactions do not mix different L),

$$\langle\Psi_\alpha^{(L)}|\Psi_\beta^{(L')}\rangle = \delta_{\alpha\beta}\,\delta_{LL'} \qquad (11.166)$$

For instance for $L = 0$ and $\alpha \neq \beta$ this expression gives,

$$0 = \langle\Psi_\alpha^{(L=0)}|\Psi_\beta^{(L=0)}\rangle = \boxed{\begin{array}{c}\text{see}\\ (11.161)\end{array}} = \sum_{\gamma,\delta}\langle\Psi_{\alpha,\gamma}^{(L=0)}|\Psi_{\beta,\delta}^{(L=0)}\rangle =$$

$$= \sum_{\gamma,\delta} S_{\gamma,\alpha}^{(L=0)\,*}\, S_{\delta,\beta}^{(L=0)}\, \frac{C_\gamma C_\delta}{\sqrt{4\pi v_\gamma\, 4\pi v_\delta}} \int d^3r \frac{e^{i(k_\delta - k_\gamma)r}}{r^2} \int d\xi\, \psi_\gamma^*(\xi)\, \psi_\delta(\xi) =$$

$$= \boxed{\begin{array}{c}\text{because of } \int d\xi\, \psi_\gamma^*(\xi)\, \psi_\delta(\xi) \approx \delta_{\gamma,\delta} \text{ and we suppose the time}\\ \text{interval } T \text{ is the same for channels } \delta \text{ and } \gamma\text{; see also (11.160)}\end{array}} =$$

$$= \sum_\gamma S_{\gamma,\alpha}^{(L=0)*}\, S_{\gamma,\beta}^{(L=0)} = \sum_\gamma S_{\alpha,\gamma}^{(L=0)+}\, S_{\gamma,\beta}^{(L=0)} = 0 \qquad \text{for } \alpha \neq \beta \qquad (11.167)$$

and the combination of expressions (11.167) and (11.164) gives,

$$\sum_\gamma S_{\alpha,\gamma}^{(L=0)+}\, S_{\gamma,\beta}^{(L=0)} = \delta_{\alpha,\beta} \quad \Rightarrow \quad S^{(L=0)+}\, S^{(L=0)} = S^{(L=0)}\, S^{(L=0)+} = 1$$

and it can be shown that this expression valids also for any L. So we have,

$$S^{(L)+}\, S^{(L)} = S^{(L)}\, S^{(L)+} = 1 \tag{11.168}$$

That means the S- matrix is unitary and this fact degreases the number of independent matrix elements. Since generally S- matrix elements are complex the N- channel process is characterized by N^2 complex matrix elements ($2N^2$ real parameters) and the unitarity conditions (11.168) represents $\frac{1}{2}N(N+1)$ conditions for these parameters. So it remains $2N^2 - \frac{1}{2}(N^2+N) = \frac{1}{2}N(3N-1)$ independent parameters.

11.3.2.3.3 Reciprocity theorem Reciprocity theorem relates the probability of the process $\alpha \to \beta$ with the probability of the time- reversed process $\bar{\beta} \to \bar{\alpha}$ where $\bar{\alpha}$ and $\bar{\beta}$ are connected with α and β by the time- reverse transformation. The operator corresponding to the time- reverse transformation is the anti-unitary operator (see (1.39)),

$$\mathscr{T} = \hat{\mathscr{U}}_T \hat{K} \tag{11.169}$$

where $\hat{\mathscr{U}}_T$ is unitary operator and $\hat{K}$ is the complex conjugation operator. From the Subsection 1.3.2 we know that usual choice of the wave function phase corresponds to $\hat{\mathscr{U}}_T = \mathscr{R}_y^{-1}(\pi)$, that means to the rotation by angle π around the y- axis of the current frame (see (11.48). It is also known that under the action of the time-reverse operator on the wave function with the sharp value of the angular momentum projection changes the sign of this projection (see e.g. (1.48)). In the next consideration the following marking is used for the time-reverse general channel wave function $\Psi_\alpha^{(L)}(\xi, \vec{r})$,

$$\mathscr{T}\Psi_\alpha^{(L)}(\xi, \vec{r}) = \Psi_{\bar{\alpha}}^{(L)}(\xi, \vec{r}) \tag{11.170}$$

It is clear that the time- reverse transormation of the incoming spherical wave packet (11.159) is following (again we restrict ourselves into $L = 0$, the general case $L \neq 0$ is a little bit more complicated but the idea is the same),

$$\begin{aligned} &\Psi_{\alpha,\, in}^{(L=0)}(\xi, \vec{r}) = -C\, \frac{1}{\sqrt{4\pi v_\alpha}}\, \psi_\alpha(\xi)\, \frac{e^{-ik_\alpha r}}{r} \\ &\overset{\text{time revesed}}{\longrightarrow} \qquad \mathscr{T}\Psi_{\alpha,\, in}^{(L=0)}(\xi, \vec{r}) = -C\, \frac{1}{\sqrt{4\pi v_\alpha}}\, \psi_{\bar{\alpha}}(\xi)\, \frac{e^{ik_\alpha r}}{r} \end{aligned} \tag{11.171}$$

and the time-reverse transformation of the wave packet after the reaction (see (11.161) is following ($S_{\alpha\to\beta} \equiv S_{\beta,\alpha}$),

$$\Psi_{\alpha}^{(L=0)}(\xi,\vec{r}) = \sum_{\beta} C\, S_{\alpha\to\beta}^{(L=0)}\, \frac{1}{\sqrt{4\pi v_\beta}}\, \psi_\beta(\xi)\, \frac{e^{ik_\beta r}}{r}$$

$$\overset{\text{time revesed}}{\longrightarrow} \qquad \mathscr{T}\Psi_{\alpha}^{(L=0)}(\xi,\vec{r}) = \sum_{\beta} C\, S_{\alpha\to\beta}^{(L=0)*}\, \frac{1}{\sqrt{4\pi v_\beta}}\, \psi_{\bar\beta}(\xi)\, \frac{e^{-ik_\beta r}}{r} \tag{11.172}$$

Further we will define time-reverse matrix elements of the S- matrix,

$$\Psi_{\bar\alpha}^{(L=0)}(\xi,\vec{r}) = \sum_{\beta} C\, S_{\bar\alpha\to\bar\beta}^{(L=0)*}\, \frac{1}{\sqrt{4\pi v_\beta}}\, \psi_{\bar\beta}(\xi)\, \frac{e^{-ik_\beta r}}{r} \tag{11.173}$$

and the comparison of (11.173) and (11.172) gives (see e.g. p.285, expr.(11.3) in [351])

$$S_{\bar\beta,\bar\alpha}^{(L)} \equiv S_{\bar\alpha\to\bar\beta}^{(L)} = S_{\beta,\alpha}^{(L)} \equiv S_{\alpha\to\beta}^{(L)}$$

$$\Longrightarrow \boxed{\begin{array}{c}\text{because S- matrix}\\ \text{is unitary}\end{array}} \Longrightarrow S_{\bar\beta,\bar\alpha}^{(L)} = S_{\beta,\alpha}^{(L)} = \left(S_{\alpha,\beta}^{(L)\,-1}\right)^* \tag{11.174}$$

where we generalized the comparison of (11.173) and (11.172) for general case of any L (not only $L = 0$)(It can be shown that it is possible to do.). The expression (11.174) represents the reciprocity theorem.

The expression (11.174) also gives,

$$\left|S_{\bar\beta,\bar\alpha}\right|^2 = \left|S_{\alpha,\beta}^{-1}\right|^2 \tag{11.175}$$

From (11.162) we know that $|S_{\beta,\alpha}^{(L)}|^2$ represents the probability of finding the reaction products $b+B$ of the channel β in the general channel wave function Ψ_α. Therefore the reciprocity theorem can be also expressed by the following sentence.

The probability of the process $\alpha \to \beta$ going in the direction of the increasing time is identical with the probability of the inverse transition $\bar\beta \to \bar\alpha$ when time goes inversly.

11.3.2.3.4 Principle of detailed balance Principle of detailed balance relates the unpolarized differential cross section of the reaction $\alpha \to \beta$ and thime reversed reaction $\bar\beta \to \bar\alpha$. Polarized differential cross section of the reaction

$\alpha \equiv (\alpha;\ J_A m_A s_a \mu_a;\ \vec{k}_\alpha) \to \beta \equiv (\beta;\ J_B m_B s_b \mu_b;\ \vec{k}_\beta)$ is given by (Q.21) (see also (11.148) with (Q.27)),

$$\frac{d\sigma^{(a+A\to b+B)}_{J_A m_A s_a \mu_a \to J_B m_B s_b \mu_b}(pol)}{d\Omega_b} = \frac{M_\alpha k_\beta}{M_\beta k_\alpha} \left| f^{(\vec{k}_\alpha \to \vec{k}_\beta)}_{\alpha: J_A m_A s_a \mu_a \to \beta; J_B m_B s_b \mu_b} \right|^2 =$$

$$= \boxed{\begin{array}{c}\text{see}\\ (Q.27)\end{array}} = \frac{M_\alpha M_\beta k_\beta}{4\pi^2 \hbar^4\ k_\alpha} \left| \mathcal{T}^{(\vec{k}_\alpha \to \vec{k}_\beta)}_{\alpha: J_A m_A s_a \mu_a \to \beta; J_B m_B s_b \mu_b} \right|^2 \qquad (11.176)$$

and corresponding polarized differential cross section of the time-reversed reaction $\bar{\beta} \equiv (\bar{\beta};\ J_B - m_B s_b\ - \mu_b; -\vec{k}_\beta) \to \bar{\alpha} \equiv (\bar{\alpha};\ J_A - m_A s_a - \mu_a; -\vec{k}_\alpha)$ is

$$\frac{d\sigma^{(\bar{b}+\bar{B}\to\bar{a}+\bar{A})}_{J_B - m_B s_b - \mu_b \to J_A - m_A s_a - \mu_a}(pol)}{d\Omega_{\bar{a}}} =$$

$$= \frac{M_\alpha M_\beta k_\alpha}{4\pi^2 \hbar^4\ k_\beta} \left| \mathcal{T}^{(-\vec{k}_\beta \to -\vec{k}_\alpha)}_{\bar{\beta}: J_B - m_B s_b - \mu_b \to \bar{\alpha}; J_A - m_A s_a - \mu_a} \right|^2 \qquad (11.177)$$

Unpolarized differential cross section is obtained from polarized one by the averaging over initial channel angular momentum projections and by the summation over the final channel angular momentum projections,

$$\frac{d\sigma^{(a+A\to b+B)}_{J_A s_a \to J_B s_b}(unpol)}{d\Omega_b} =$$

$$= \frac{1}{(2J_A+1)(2s_a+1)} \sum_{m_A \mu_a} \sum_{m_B \mu_b} \frac{d\sigma^{(a+A\to b+B)}_{J_A m_A s_a \mu_a \to J_B m_B s_b \mu_b}(pol)}{d\Omega_b} =$$

$$= \frac{1}{(2J_A+1)(2s_a+1)} \frac{M_\alpha M_\beta}{4\pi^2\hbar^2} \frac{k_\beta}{k_\alpha} \sum_{m_A \mu_a} \sum_{m_B \mu_b} \left| \mathcal{T}^{(\vec{k}_\alpha \to \vec{k}_\beta)}_{\alpha: J_A m_A s_a \mu_a \to \beta; J_B m_B s_b \mu_b} \right|^2 \qquad (11.178)$$

and

$$\frac{d\sigma^{(\bar{b}+\bar{B}\to\bar{a}+\bar{A})}_{J_B s_b \to J_A s_a}(unpol)}{d\Omega_{\bar{a}}} =$$

$$= \frac{1}{(2J_B+1)(2s_b+1)} \sum_{m_B \mu_b} \sum_{m_A \mu_a} \frac{d\sigma^{(\bar{b}+\bar{B}\to\bar{a}+\bar{A})}_{J_B - m_B s_b - \mu_b \to J_A - m_A s_a - \mu_a}(pol)}{d\Omega_{\bar{a}}} =$$

$$= \frac{1}{(2J_A+1)(2s_a+1)} \frac{M_\alpha M_\beta}{4\pi^2\hbar^2} \frac{k_\alpha}{k_\beta}$$

$$\sum_{m_A \mu_a} \sum_{m_B \mu_b} \left| \mathcal{T}^{(-\vec{k}_\beta \to -\vec{k}_\alpha)}_{\bar{\beta}: J_B - m_B s_b - \mu_b \to \bar{\alpha}; J_A - m_A s_a - \mu_a} \right|^2 \qquad (11.179)$$

Because of the reciprocity theorem (11.175) and using (Q.25) we have following identity,

$$\sum_{m_A\mu_a}\sum_{m_B\mu_b}\left|\mathcal{T}^{(\vec{k}_\alpha\to\vec{k}_\beta)}_{\alpha:J_Am_As_a\mu_a\to\beta;J_Bm_Bs_b\mu_b}\right|^2 = \\ = \sum_{m_A\mu_a}\sum_{m_B\mu_b}\left|\mathcal{T}^{(-\vec{k}_\beta\to-\vec{k}_\alpha)}_{\bar{\beta}:J_B-m_Bs_b-\mu_b\to\bar{\alpha};J_A-m_As_a-\mu_a}\right|^2 \qquad (11.180)$$

So the sums in the r.h.s. of (11.178) and (11.179) are the same and we obtain following equation,

$$k_\alpha^2(2J_A+1)(2s_a+1)\frac{d\sigma^{(a+A\to b+B)}_{J_As_a\to J_Bs_b}(unpol)}{d\Omega_b} = \\ = k_\beta^2(2J_B+1)(2s_b+1)\frac{d\sigma^{(\bar{b}+\bar{B}\to\bar{a}+\bar{A})}_{J_Bs_b\to J_As_a}(unpol)}{d\Omega_{\bar{a}}} \qquad (11.181)$$

This relation is known in the literature as the "principle of detailed balance" and it gives relation between unpolarized cross section for a transition $\alpha\to\beta$ and its "time reverse" $\bar{\beta}\to\bar{\alpha}$.

11.4 Direct nuclear reactions

In this section the concrete results of numerical calculations and their comparison with experimental data on cross sections for selected nuclear reactions are presented. Particularly the question how the information about the structure of target and final nuclei enters the expressions for the cross section is discussed. We restrict ourselves on the direct nuclear reactions between prompt channels but the existence of time-delayed Q- channels is also taken into account through the imaginary part of the optical potentials in each P-channel.

11.4.1 Green function method for solving coupled channel equation system

From the Section 11.3.1 we know that the relative motion wave functions $u^{(\alpha i)}_{\beta j}(\vec{k}_{\beta j},\vec{r}_\beta)$ in the outgoing channel βj with the given initial channel αi can be obtained by the solving of the general coupled channel equation system (11.126). This equation system can be solved using the Green function method (see e.g [351] - expr. (4.26)) which is shortly explained further.

Let us suppose we are interested for the calculation of cross section of given reaction $\alpha i \to \beta j$. At first we solve the equations (11.126) without the right-hand-side,

$$\left(\hat{T}_\beta - \epsilon_{\beta j} - \hat{U}^{(opt)}_{\beta j}(\vec{r}_\beta)\right) u^{(\alpha i)}_{\beta j}(\vec{k}_{\beta j}, \vec{r}_\beta) = 0 \tag{11.182}$$

According to Green function approach the solution of the equation system (11.126) with the nonzero right-hand-side can be expressed in terms of the so called Green function $G(\vec{r}, \vec{r}\,')$ which is the solution of the following equation,

$$\left(\hat{T} - \epsilon_{\beta j} + \hat{U}^{(opt)}_{\beta j}(\vec{r})\right) G(\vec{r}, \vec{r}\,') = \delta(\vec{r} - \vec{r}\,') \tag{11.183}$$

where $\hat{U}^{(opt)}_{\beta j}(\vec{r})$ is the optical potential in the channel βj (see (11.128)). Then the general solution of the equation system (11.126) can be written as follows,

$$\begin{aligned} u^{(\alpha i)}_{\beta j}(\vec{k}_{\beta j}, \vec{r}_\beta) &= \delta_{\alpha i, \beta j}\ u^{(\alpha i)}_{\alpha i}(\vec{k}_{\alpha i}, \vec{r}_\beta) \\ &- \int d^3 r'\, G(\vec{r}_\beta, \vec{r}\,') \sum_{\beta' j'} \langle \beta j \mid \hat{W}^{(opt)}(\vec{r}\,') \mid \beta' j' \rangle\, u^{(\alpha i)}_{\beta' j'}(\vec{k}_{\beta' j'}, \vec{r}\,') \end{aligned} \tag{11.184}$$

where $\langle \beta j \mid \hat{W}^{(opt)}(\vec{r}\,') \mid \beta' j' \rangle$ are given by (11.129). One can easily check that the substitution of (11.184) back into the left-hand-side of (11.126) and the use of the (11.183) automatically gives the right-hand-side of (11.126).

Further the Green function approach procedure similar to one used for the scattering of two particles where the scattering amplitude (E.27) is derived. For the nuclear reaction case this procedure is described in the book [351] (see the section 4.2 with the derivation of the reaction amplitude expression (4.26), see also [353]). Using the decomposition of the Green function $G(\vec{r}, \vec{r}\,')$ and δ- function $\delta(\vec{r} - \vec{r}\,')$ in (11.183) into spherical harmonics, we can rewrite the equation (11.183) into the equations for Green function partial waves. The resultant Green function partial wave decomposition is then substituted back into the expression (11.184) and the expression (11.184) obtains following form (here the asymptotic form of the $u_\beta(\vec{k}_{\beta j}, \vec{r})$ is supposed to have outgoing diverging spherical wave character - see analogy with (E.25),(E.26), (E.27)),

$$\begin{aligned} \langle \beta j \mid \Psi_{(\vec{k}_\alpha)}(\vec{r}_\beta) \rangle &= u^{(\alpha i)}_{\beta j}(\vec{k}_{\beta j}, \vec{r}_\beta) = \delta_{\alpha i, \beta j}\, u^{(\alpha i)}_{\alpha i}(\vec{k}_{\alpha i}, \vec{r}_\beta) \\ &- \frac{M_\beta}{2\pi\hbar^2} \int d^3 r'\, u^{(\alpha i)}_{\beta j}(-\vec{k}_{\beta j}, \vec{r}\,')\, \langle \beta j \mid \hat{W}^{(opt)}(\vec{r}\,') \mid \Psi_{(\vec{k}_\alpha)}(\vec{r}\,') \rangle \end{aligned} \tag{11.185}$$

with $\mid \Psi_{(\vec{k}_{\alpha i})}(\vec{r})\rangle = \sum_{\beta j} u^{(\alpha i)}_{\beta j}(\vec{k}_{\beta j}, \vec{r}) \mid \beta j\rangle$ (see (11.118)) and

$$\langle \beta j \mid \hat{W}^{(opt)}(\vec{r}\,') \mid \Psi_{(\vec{k}_{\alpha})}(\vec{r}\,')\rangle = \boxed{\begin{array}{c}\text{see}\\ (11.118), (11.129)\end{array}} =$$

$$= \sum_{\beta' j'} \langle \beta j \mid (\hat{V}_{\beta}(\vec{r}\,') - \hat{U}^{(opt)}_{\beta j}(\vec{r}\,') \mid \beta' j'\rangle \; u^{(\alpha i)}_{\beta' j'}(\vec{k}_{\beta' j'}, \vec{r}\,') \tag{11.186}$$

where

$$\begin{aligned} u^{(\alpha i)}_{\alpha i}(\vec{k}_{\beta j}, \vec{r}_{\alpha}) &\overset{r_{\alpha}\to\infty}{\longrightarrow} e^{i\vec{k}_{\alpha i}\cdot\vec{r}_{\alpha}} \quad \text{for ingoing elas. scattering channel } \alpha i \\ u^{(\alpha i)}_{\beta j}(\vec{k}_{\beta j}, \vec{r}_{\beta}) &\overset{r_{\beta}\to\infty}{\longrightarrow} \frac{e^{ik_{\beta j} r_{\beta}}}{r_{\beta}} \quad \text{for all outgoing channels } \beta j \neq \alpha i \end{aligned} \tag{11.187}$$

The expression (11.185) can be substituted into (11.118) and obtained expression for $|\Psi_{(\vec{k})_{\alpha}}\rangle$ can be compared with the asymptotic expression following directly from (11.119) and this gives us the final expression for the reaction amplitude ($\beta j \neq \alpha i$) (see (E.27)),

$$f_{(\vec{k}_{\alpha i}\to\vec{k}_{\beta j})} = -\frac{M_{\beta}}{2\pi\hbar^2}\int d^3r \;\; u^{(\alpha i)}_{\beta j}(-\vec{k}_{\beta j}, \vec{r}) \; \langle \beta j \mid \hat{W}^{(opt)}(\vec{r}) \mid \Psi_{(\vec{k}_{\alpha i})}(\vec{r})\rangle \tag{11.188}$$

In the first order of the Born perturbation series we can substitute $|\Psi_{\vec{k}_{\alpha i}}(\vec{r})\rangle \to u_{\alpha i}(\vec{k}_{\alpha i}, \vec{r}) \;\; |\alpha i\rangle$ and this approximation gives for (11.188) [13],

$$f^{(1)}_{(\vec{k}_{\alpha i}\to\vec{k}_{\beta j})} \approx -\frac{M_{\beta}}{2\pi\hbar^2}\int d^3r \;\; u^{(\alpha i)}_{\beta j}(-\vec{k}_{\beta j}, \vec{r}) \; \langle \beta j \mid \hat{W}^{(opt)}(\vec{r}) \mid \alpha i\rangle \; u^{(\alpha i)}_{\alpha i}(\vec{k}_{\alpha i}, \vec{r}) \tag{11.189}$$

where $\langle \beta j \mid \hat{W}^{(opt)}(\vec{r}) \mid \alpha i\rangle = \int d\xi \; \psi_{\beta j}(\xi)\big(V_{\beta}(\vec{r}, \xi) - U^{(opt)}_{\beta j}(\vec{r})\big) \; \psi_{\alpha i}(\xi)$ represents the pure effective non-diagonal interaction between relative motion wave functions in the channels αi and βj. One should realize that the general interaction $V(\vec{r}, \xi)$ in (11.189) involves the interaction between particle and nucleus within given channel together with interaction between channels. The optical potential $U^{(opt)}_{\beta j}(\vec{r})$ represents the interaction between the particle and nucleus in the given channel βj (it does not involve the interaction between

[13] If the asymptotic behavior of $u^{(\alpha i)}_{\beta j}(\vec{k}_{\beta j}, \vec{r})$ for all βj is $u^{(\alpha i)}_{\beta j}(\vec{k}_{\beta j}, \vec{r}) \overset{r\to\infty}{\to} e^{i\vec{k}_{\beta j}\cdot\vec{r}}$ then,

$$f^{(1)}_{(\vec{k}_{\alpha i}\to\vec{k}_{\beta j})} \approx -\frac{M_{\beta}}{2\pi\hbar}\int d^3r' \langle \beta j \mid \hat{W}(\vec{r}\,') \mid \alpha i\rangle \; e^{i(\vec{k}_{\alpha i} - \vec{k}_{\beta j})}$$

which is similar to the expression (E.32) for the elastic scattering amplitude.

different channels). That means the difference $V_\beta(\vec{r},\xi) - U^{(opt)}_{\beta j}(\vec{r})$ involves the interaction of the channel βj with other channels.

In the connection with derived expressions (11.188) and (11.189) it is necessary to be realized that this derivation is only formal and not fully precise from the point of view of mathematics. The problem is that the whole system of nucleons formed by the initial channel αi is the same also for the forming of the final channel βj but the internal variables ξ_α in the initial channel and ξ_β in the final channel and subsequently relative motion coordinates $\vec{r}_\alpha$ and $\vec{r}_\beta$ are different if $a \neq b$ and $A \neq B$. The number of degrees of freedom of the system $a + A$ formed by the initial channel generally is given by $N_\alpha \equiv 2 \times (3 \times A_a + 3 \times A_A) + 1$, where A_a and A_A are number of nucleons in the particle a and in the target nucleus A, respectively. So there is a question how to understand the integration over d^3r and $d\xi$ in expressions (11.188) and (11.189). In order to answer this question one should realize that the division of degrees of freedom $(\vec{r}_\alpha, \xi_\alpha)$ to the relative motion $\vec{r}_\alpha$ and internal ξ_α ones in the channel α is different from the similar division $(\vec{r}_\beta, \xi_\beta)$ for the channel β and their connection depends on the interaction $\hat{W}^{(opt)}$ responsible for the transmutation $\alpha \to \beta$. Their mutual dependence is given by the mechanism of the transfer (or transmutation) $a \to b$, $A \to B$. Generally the interaction $\hat{W}^{(opt)}(\vec{r})$ in (11.188) and (11.189) depends on all nucleon N_α coordinates (degrees of freedom) involved in the system of nucleons formed by the initial channel but the given transition separates these nucleon coordinates into a set containing the two relative motion variables $\vec{r}_\alpha$ and $\vec{r}_\beta$ and the remainder which is further denoted as ξ. From this point of view it is more precise to rewrite e.g. the expression for the DWBA transition amplitude (11.189) as follows,

$$f_{(\vec{k}_{\alpha i} \to \vec{k}_{\beta j})} \approx$$
$$\approx -\frac{M_\beta}{2\pi\hbar^2} \int d^3r_\alpha d^3r_\beta \; u^*_{\beta j}(\vec{k}_{\beta j}, \vec{r}_\beta) \, \langle \beta j \mid \hat{W}^{(opt)}(\vec{r}_\alpha, \vec{r}_\beta) \mid \alpha i \rangle \, u_{\alpha i}(\vec{k}_{\alpha i}, \vec{r}_\alpha) \tag{11.190}$$

with $\langle \beta j | \, \hat{W}^{(opt)}(\vec{r}_\alpha, \vec{r}_\beta) \, | \alpha i \rangle = \mathcal{J} \int d\xi \, \psi^*_{\beta j}(\xi) \, W^{(opt)}(\vec{r}_\alpha, \vec{r}_\beta, \xi) \, \psi_{\alpha i}(\xi)$, where $\mathcal{J}$ is the Jacobian of the transformation (schematically)

$$\big(\text{all } N_\alpha = 2 \times (3 \times A_a + 3 \times A_A) + 1 \text{ coordinates}\big) \longrightarrow (\vec{r}_\alpha, \vec{r}_\beta, \xi) \tag{11.191}$$

This will be discussed in more details for nucleon transfer reaction in the Subsection 11.4.4.

Since all interactions involved in $V(\vec{r},\xi)$ and $U_{\beta j}^{(opt)}(\vec{r})$ are not generally known in practical calculations these potentials are parametrized using some phenomenological function dependencies and these parameters are then determined from experimental data on concrete reaction. For instance the parameters of the optical potential $U_{\beta j}^{(opt)}(\vec{r})$ are usually obtained from the fitting procedure to experimental values of elastic scattering cross sections in the given channel β where differences between different excitation indexes j in given channel $\beta \equiv b + B$ are usually ignored. This is discussed in next subsections in more details.

11.4.1.1 Plane wave Born approximation (PWBA)

The PWBA consists in the using of the first order Born perturbation approximation (11.190) for the reaction amplitude $f_{(\vec{k}_{\alpha i}\to\vec{k}_{\beta j})}$ where additional rough simplification is done, namely the substitution of wave functions $u_{\alpha i}(\vec{k}_{\alpha i},\vec{r})$ and $u_{\beta j}(\vec{k}_{\beta j},\vec{r})$ by plane waves,

$$u_{\alpha i}(\vec{k}_{\alpha i},\vec{r}_{\alpha}) \approx e^{i\vec{k}_{\alpha i}\cdot\vec{r}_{\alpha}} \qquad\qquad u_{\beta j}(\vec{k}_{\beta j},\vec{r}_{\beta}) \approx e^{i\vec{k}_{\beta j}\cdot\vec{r}_{\beta}} \tag{11.192}$$

Then we speak about the plane wave Born approximation. That means the differential equations (11.182) are not solved within the PWBA. This approximation is very rough and it was used in the early papers in the fifties when big computer numerical calculations were not possible.

11.4.1.2 Distorted wave Born approximation (DWBA)

The approximation, where the first order Born perturbation expression (11.190) is used for the calculation of the reaction amplitude, is known in literature as the distorted wave Born approximation (DWBA). This approximation uses the solutions of equations (11.182) for $u_{\alpha i}(\vec{k}_{\alpha i},\vec{r}_{\alpha})$ and $u_{\beta j}(\vec{k}_{\beta j},\vec{r}_{\beta})$ in (11.190) with the asymptotic forms as the outgoing spherical waves which were called as distorted waves in the past (plane waves were distorted). In the framework of the DWBA the coupled channel equation system (11.126) is not solved and the corresponding second term in (11.184) is ignored. The DWBA approach is often applied up to now (see e.g. ....).

11.4.1.3 Coupled channel method

If the reaction amplitude $f_{(\vec{k}_{\alpha i}\to\vec{k}_{\beta j})}$ is calculated according to (11.188) with the whole wave function $\Psi_{\vec{k}_{\alpha}}$ given by (11.118) where generally all βj participate

in the sum over βj and all relative motion wave functions $u^{(\alpha i)}_{\beta j}(\vec{k}_{\beta j}, \vec{r}_{\beta})$ in $\Psi_{\vec{k}_{\alpha}}$ are determined by the solving of the coupled channel equation system (11.126) then we speak about the coupled channel approach (CCA) of the determination of the reaction amplitude (see e.g. ...). However even in the present time the general coupled channel approach is quite complicated for nowadays computers and is not often used for usual calculations of reaction amplitudes and corresponding cross sections, especially in the heaver nuclei cases.

11.4.2 Elastic scattering from the point of view of the optical model

In the previous section we discussed the determination of the reaction amplitude $f_{\vec{k}_{\alpha i} \to \vec{k}_{\beta j}}$ (see (11.190)) in the framework of the optical DWBA or CA methods. For the elastic scattering the key role in this determination is played by the complex optical potential $\hat{U}^{(opt)}_{\beta}(\vec{r})$ in each channel βj with the index j corresponding to the ground states of the particle b and the nucleus B. Corresponding elastic scattering amplitude is given by ($k_{\beta j} = k'_{\beta j}$)

$$f^{(elas)}_{\vec{k}_{\beta j} \to \vec{k}'_{\beta j}} \approx \int d^3 r \; u_{\beta j}(-\vec{k}'_{\beta j}, \vec{r}) \; \hat{U}^{opt)}_{\beta j}(\vec{r}) \; u_{\beta j}(\vec{k}'_{\beta j}, \vec{r}) \tag{11.193}$$

for $j = gr$, and the square of $f^{(el)}_{\vec{k}_{\beta j} \to \vec{k}'_{\beta j}}$ determines the elastic scattering differential cross-section (see e.g. [356, 351]). Since the interactions between the particle b and the nucleus B in the each channel are not usually sufficiently known from microscopical theories the optical potential in the each channel $\beta j \equiv \beta gr$ involved in the P- space is approximated by some reasonable function dependencies and involved corresponding parameters are obtained by the fitting procedure in order to obtain an agreement with the experimental differential cross-section of the elastic scattering of the particle b on the target nucleus B. The most frequent form of the complex optical potential is the radial Wood-Saxon and Gaussian dependence of the optical potential involving the $\vec{L} \cdot \vec{S}$ coupling ($\vec{L}$ is the total channel angular momentum and $\vec{S}$ is the total channel spin),

$$\begin{aligned} \hat{U}^{(opt)}_{\beta j}(\vec{r}) = \hat{U}^{(opt)}_{\beta j}(r) = \\ = \hat{V}_{Coulomb}(r) + U \; f_1(r) + iW \left[\, \alpha \; f_2(r) + (1-\alpha) \; g(r) \, \right] + \\ + \left(\frac{\hbar}{m_{\pi} c}\right) \left[\, U_s \frac{df_1(r)}{dr} + iW_s \, \frac{df_2(r)}{dr} \, \right] \frac{1}{r} \, \vec{L} \cdot \vec{S} \end{aligned} \tag{11.194}$$

where U, W, U_s and W_s are real parameters for given β, and $f_1(r)$, $f_2(r)$, $g(r)$ are so called form-factors that means functional Wood-Saxon or Gaussian dependencies on the relative distance r between particle b and the nucleus B (see e.g. [354]),

$$f_1(r, r_1, a_1) \equiv \frac{1}{1 + e^{\frac{r-r_1}{a_1}}} \qquad , \qquad f_2(r, r_2, a_2) \equiv \frac{1}{1 + e^{\frac{r-r_2}{a_2}}}$$
$$g(r, b) = e^{-\frac{(r-R_0)^2}{b^2}} \qquad \text{with } R_0 = r_0\, A^{1/3} \tag{11.195}$$

where r_1, r_2, r_0, a, b are also real parameters. All these parameters U, W, U_s, W_s, r_1, r_2, r_0, a, b are determined by the optimizing to the experimental differential cross-section of the elastic scattering in the channel $\beta \equiv b + B$ in the dependence on the CoM energy E and the mass number A of the nucleus B.

For instance the systematic analyses of experimental differential cross-sections of proton and neutron elastic scattering on nuclei with $A > 40$ using the optical model performed in [355] gave the following values of these parameters for energies $E < 50\, MeV$ (so called optical potential with volume interaction - see also [351], epr. (8.12), (8.13)),

protons:

$$U = \left(54 - 0.32E + 24\frac{N-Z}{A} + 0.4\frac{Z}{A^2}\right) MeV$$
$$r_1 = 1.17fm \qquad a_1 = 0.75fm$$
$$W = 0.22E - 2.7 \text{ or zero, whichever is greater}$$
$$r_2 = 1.32fm \qquad a_2 = \left(0.51 + 0.7\frac{N-Z}{A}\right) fm \qquad b \approx 1fm$$

neutrons:

$$U = \left(56.3 - 0.32E - 24\frac{N-Z}{A} + 0.4\frac{Z}{A^2}\right) MeV$$
$$r_1 = 1.17fm \qquad a_1 = 0.75fm$$
$$W = 0.22E - 1.56 \text{ or zero, whichever is greater}$$
$$r_2 = 1.26fm \qquad a_2 = 0.58fm \qquad b \approx 1fm$$

As an example of such analysis in the Fig. 11.10 the effect of different radii for real and imaginary parts of the optical potential is demonstrated for the case of the elastic proton scattering on the ^{26}Al isotope. One can see that the oscillations in the differential CoM cross-section is very dependent on the radii r_1 and r_2 in optical potential radial dependencies (11.194) [354].

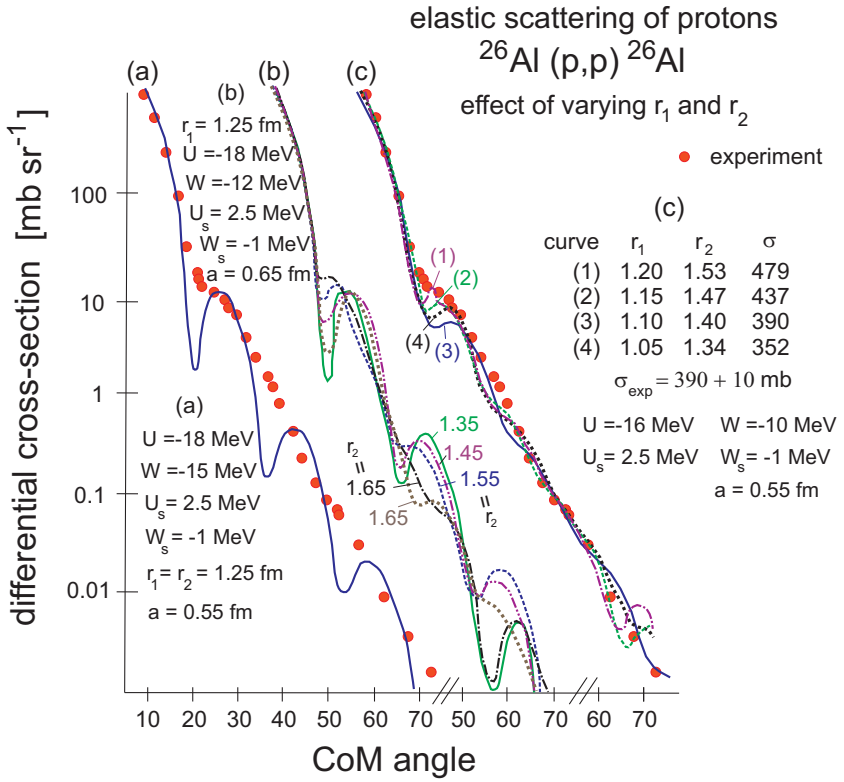


Figure 11.10: (a) Experimental differential cross-section for the elastic scattering of 183-MeV protons by ^{26}Al calculated in the framework of the DWBA using the optical potential (11.191) and (11.192) with $\alpha = 0.5$, $r_0 = 1.25$fm, $b = 1$fm (other parameters are given directly in the figure); (b) Calculated differential cross-section for the same reaction with increasing values of the radius of the absorbing (imaginary) potential; (c) The same for a series of radii with $r_2 = 1.27\, r_1$ (adapted from [354]).

Above described way of the determination of parameters of the optical potential in each channel βj using the elastic scattering experimental data on the cross-section was applied in the sixties and the seventies. The effect of the anti-symmetrization of the whole channel wave function was not taken into account (that means the anti-symmetrization of the wave function of the system "particle b plus nucleon B" with respect to any exchange of two nucleons of the same type). Later attempts of involving this anti-symmetrization of the optical potential were done (see e.g. [352]) but the most of the DWBA calculations works with the optical potential determined without proper anti-symmetrization.

Optical potential parametrizations are not determined only for channels where impacting particle is nucleon but also for channels with more complex impacting particle (e.g. light nucleus as deuteron, α-particle or other light nuclei). This point will be discussed also in next subsections.

11.4.3 Inelastic scattering from the point of view of the optical model

In the previous subsection the case of the elastic scattering of the particle a on the nucleus A ($a + A \to a + A$) was discussed in the framework of the DWBA. According to the DWBA at first the equation (11.182) was solved for given channel $\alpha \equiv a + A$ (where the nucleus A and the particle a were in their ground states) and the distorted wave $u_{\alpha i}(\vec{k}_{\alpha i}, \vec{r}_\alpha)$ was found for given optical potential $\hat{U}^{(opt)}(\vec{r})$. This distorted wave was then substituted to the scattering amplitude $f_{(\vec{k}_{\alpha i} \to \vec{k}_{\alpha i})}$ and corresponding differential cross-section of the elastic scattering $\frac{d\sigma_{\alpha i \Rightarrow \alpha i}}{d\Omega} = |f_{(\vec{k}_{\alpha i} \to \vec{k}_{\alpha i})}|^2$ (see (11.148)) could be determined.

In this subsection the inelastic scattering of the particle a on the nucleus A is studied, that means during the scattering besides the elastic channel also the inelastic channels $a + A \to a + A^*$ are analyzed when the target nucleus is excited after the scattering (see the Fig.11.11) and all transmutation reactions are not explicitly taken into account (they are involved only implicitly through the imaginary part of the optical potential). Wave function of the

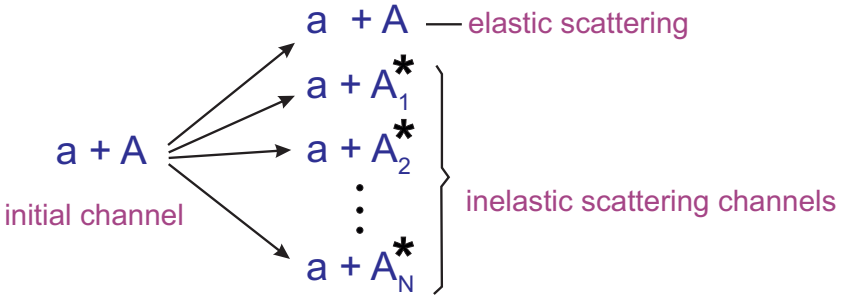


Figure 11.11: Schematic figure of elastic and inelastic channels. In the elastic scattering the initial particle a and the target nucleus A stay in their ground states during the scattering while in the inelastic scattering the target nucleus is excited during the scattering. Transmutation processes $a + A \to b + B$ is not taken into account explicitly but they are involved implicitly by the imaginary part of the optical potential in each elastic and inelastic channels.

relative motion in each inelastic channel, $u_\alpha^{(\alpha i)}(\vec{k}_{\alpha j}, \vec{r}_\alpha)$, can be determined by the solving of the system of equations (11.126) for $j = 0(gr), 1, 2, \cdots, N$ (that means for $N + 1$ unknown functions $u_{\alpha j}^{(\alpha i)}(\vec{k}_{\alpha j}, \vec{r}_\alpha)$ - see also (11.128),

(11.129)),

$$\left(\hat{T}_\alpha + U_{\alpha j}^{(opt)}(r) - \epsilon_{\alpha j}\right) v_{\alpha j}^{(\alpha i)}(\vec{k}_{\alpha j}, \vec{r}) =$$
$$= -\sum_{j'} \int d\xi\, \psi_{\alpha j}^*(\xi) \left(\hat{V}_\alpha(\vec{r}, \xi) - U_{\alpha j}^{(opt)}(r)\right) \psi_{\alpha j'}(\xi)\, u_{\alpha j'}^{(\alpha i)}(\vec{k}_{\alpha j'}, \vec{r}) \tag{11.196}$$

where $\hat{V}_\alpha(\vec{r}, \xi)$ represents the interaction between the particle a and the nucleus A and simultaneously the interaction between different channel (αj). In (11.194) the optical potential $U_{\alpha j}^{(opt)}(r) = \int d\xi\, \psi_{\alpha j}^*(\xi)\, \hat{V}_\alpha(\vec{r}, \xi)\, \psi_{\alpha j}^*(\xi)$ is supposed to be dependent only on the $r \equiv |\vec{r}|$ (radial dependency). For the simplicity of expressions further the spins of the particle a and the nucleus A are not considered (spinless particle a and the nucleus A). Further we use the decomposition of the relative motion wave functions $u_{\alpha j}^{(\alpha i)}(\vec{k}_{\alpha j}, \vec{r})$ for all $j,\ j' = 0, 1, \cdots, N$ into partial waves (see (11.131)) [14]

$$u_{\alpha j}^{(\alpha i)}(\vec{k}_{\alpha j}, \vec{r}) = \sum_L \frac{u_L^{(\alpha_i, \alpha j)}(r)}{r} P_L(\cos\Theta_{\alpha j}) \tag{11.197}$$

where $\Theta_{\alpha j}$ is the angle between $\vec{k}_{\alpha j}$ and $\vec{r}$. Then we substitute (11.197) into (11.196) for all j and j' and multiply each equation by $P_L(\cos\Theta_{\alpha j})$ and integrate over $\Theta_{\alpha j}$. Then using the ortogonality of Legendre polynomials (see the footnote [15] in the bottom of this page) and the transformation of the kinetic energy operator $\hat{T}_\alpha = -\frac{\hbar^2}{2M_\alpha}\vec{\nabla}^2$ to the spherical coordinates the system of equations (11.196) can be rewritten to the system of equations for radial functions $u_L^{\alpha i, \alpha j)}(r)$ for given $i \equiv gr$ and $j = 0(gr), 1, 2, \cdots, N$ and all

[14] The consideration of nonzero spins of the particle a and the nucleus A only makes the decomposition (11.195) more complex - each partial wave is characterized not only by the orbital momentum L but also by the total channel spin S and the total angular momentum J (see (11.158)).

[15] Legendre polynomials fulfill following orthogonality conditions,

$$\int P_L(\vec{n}\cdot\vec{n}_1)\, P_{L'}(\vec{n}\cdot\vec{n}_2)\, d\hat{r} = \frac{4\pi}{2L+1} P_L(\vec{n}_1\cdot\vec{n}_2)\, \delta_{LL'}$$

where $\vec{n} = \frac{\vec{r}}{r}$ ($d\hat{r} \equiv d\Omega$ is the space angle element of the vector $\vec{r}$) and $\vec{n}_1$, $\vec{n}_2$ are unit vectors ($\vec{n}_1\cdot\vec{n}_2 = \cos\Theta$, where Θ is the angle between $\vec{n}_1$ and $\vec{n}_1$).

L involved in the decomposition (11.197) (see (11.128), (11.129)),

$$\Big\{\frac{d^2}{dr^2}-\frac{L(L+1)}{r^2}+\frac{2M_\alpha}{\hbar^2}\epsilon_{\alpha j}-\frac{2M_\alpha}{\hbar^2}U_{\alpha j}^{(opt)}(r)\Big\}\,u_L^{(\alpha i,\alpha j)}(r)=$$
$$=\sum_{j'\neq j}\int d\Omega\,P_L(\cos\Theta_{\alpha j})$$
$$\int d\xi\,\psi_{\alpha j}^*(\xi)\big(V_\alpha(\vec r,\xi)-U_{\alpha j}^{(opt)}(r)\big)\psi_{\alpha j'}(\xi)\,P_{L'}(\cos\Theta_{\alpha j'})\,u_{L'}^{(\alpha i,\alpha j')}(r) \tag{11.198}$$

where $\Theta_{\alpha j}=\Theta_{\alpha j'}=\Theta$ is the angle between $\vec r$ and $\vec k_{\alpha j}$ (we suppose that all channels αj have linear momenta in the same direction for all $j=0(elastic),1,2,\cdots,N$ - see the text under the exp. (11.119).

The solving of the equation system (11.198) gives the radial wave function $u_L^{(\alpha i,\alpha j)}(r)$ for all excitations $j=0,1,\cdots,N$ in the inelastic scattering channels and for all L and in such a way we obtain all excitation wave functions $u_{\alpha j}^{(\alpha i,\alpha j)}(\vec k_{\alpha j},\vec r)$ of the relative motion in the inelastic process $\alpha i\to\alpha j$ (see (11.197)). The substitution of these $u_{\alpha j}^{(\alpha i,\alpha j)}(\vec k_{\alpha j},\vec r)$ into (11.193) gives the first order Born approximation inelastic scattering amplitude

$$f^{(inelas)}_{(\vec k_{\alpha i}\to\vec k_{\alpha j})}\approx$$
$$\approx\frac{M_\alpha}{2\pi\hbar^2}\int d^3r\,u_{\alpha j}^{(\alpha i)^*}(\vec k_{\alpha j},\vec r)\,\langle\alpha j|\hat W_\alpha(\vec r)|\alpha i\rangle\,u_{\alpha i}^{(\alpha i)}(\vec k_{\alpha i},\vec r) \tag{11.199}$$

where $W_{\alpha j\,,\,\alpha i}(\vec r)\equiv\langle\alpha j\,|\hat W_\alpha(\vec r)|\,\alpha i\rangle=\langle\alpha j\,|\hat V_\alpha|\,\alpha i\rangle-U_{\alpha i}^{(opt)}(r)=$ $\int d\xi\,\psi_{\alpha j}^*(\xi)\,V_\alpha(\vec r,\xi)\,\psi_{\alpha i}(\xi)-U_{\alpha i}^{(opt)}(r)$ is the interaction between the particle a and the nucleus A leading to the excitation of the nucleus A and therefore it represents the "non-diagonal" interaction between elastic and non-elastic channels (see also (11.129) and the text below it). Then the square of this amplitude determines the differential cross-section of the inelastic scattering $\alpha i\to\alpha j$. One should realize that if in (11.199) the relative motion wave functions $u_{\alpha j}^{(\alpha i)}(\vec k_{\alpha j},\vec r)$ are determined by the solving of the equation system (11.196) (that means with the nonzero r.h.s. in (11.196) we speak about coupled channel Born approximation (CCBA) determination of the scattering cross-section. If the coupling between channels (r.h.s. of (11.196) is neglected and $u_{\alpha j}^{(\alpha i)}(\vec k_{\alpha j},\vec r)$ and $u_{\alpha i}^{(\alpha i)}(\vec k_{\alpha i},\vec r)$ involved in (11.196) where obtained independently by solving (11.196) without r.h.s. then the method is called as distorted wave Born approximation (DWBA).

From the expression (11.199) it can be seen that the structure of the internal excitation states $|\alpha j\rangle$ influences the cross-section of the inelastic scattering $\alpha i \to \alpha j$ $(i \equiv gr)$ through the internal matrix element $\langle \alpha j|\hat{W}_\alpha(\vec{r})|\alpha i\rangle$. Further we will discuss how this matrix element can be determined in the framework of nuclear models, particularly in terms of the Bohr-Mottelson liquid drop model.

From the point of view of the nuclear structure it is necessary to distinguish spherical nuclei from deformed ones. As we know from the Chapter 7 in the case of the spherical nucleus we have only single-particle and collective vibrational degrees of freedom of the nuclear motion while in deformed nuclei besides the single-particle and vibrational motion also rotational degrees of freedom are observed. Both these cases have different character of the lowest excitations. The lowest states in spherical nuclei can be described mostly as vibrational states (see the Subsection 7.2.1.1) while the lowest states in deformed nuclei belong usually to the ground state rotational band (see the Subsection 7.2.1.2). Therefore the effect of the internal structure of the target nucleus on the cross-section of inelastic scattering leading to the lowest excitations of the target nucleus is a little bit different for spherical and deformed nucleus.

11.4.3.1 Inelastic scattering excitation of spherical nucleus

The lowest excitations of spherical even-even nuclei have vibrational character and in the simplified picture these states can be described as vibrations of the nucleus around the spherical equilibrium "shape". in this subsection we restrict ourselves on the liquid drop model (LDM) description of these states where the nuclear shape is described by the Dirichlet decomposition into spherical harmonics (see (7.53)),

$$R(\theta,\phi) = R_0\left(1 + \sum_{\lambda\mu} \alpha^*_{\lambda\mu}(t)\, Y_{\lambda\mu}(\theta,\phi)\right) \approx$$

$$\approx \boxed{\begin{array}{c}\text{the lowest excitations of spherical even-even nuclei}\\ \text{have quadrupole axial character - see the subsection 7.2.1.1}\end{array}} \approx$$

$$\approx R_0\left(1 + \sum_{\mu} \alpha^*_{2\mu}(t)\, Y_{2\mu}(\theta,\phi)\right) \qquad (11.200)$$

From the Subsection 7.2.1.1 we know that in the framework of the LDM quadrupole excitations are driven by the collective Hamiltonian (see (7.54)-

(7.57)) (after the quantizing procedure),

$$\hat{H}_c = \sum_{\mu} \big(\frac{\hat{\pi}^+_{2\mu} \hat{\pi}_{2\mu}}{2B_2} + \frac{1}{2}\, C_2\, \hat{\alpha}^+_{2\mu} \hat{\alpha}_{2\mu} \big) \tag{11.201}$$

and vibration excitations are described in terms of the creation ($Q^+_{2\mu}$) and annihilation ($Q_{2\mu}$) operators of phonons (vibrational quanta) (see (7.59) with excitation energies $\hbar\omega_2 = \hbar\frac{C_2}{B_2}$ (see (7.55)),

$$Q^+_{2\mu} = \big(\frac{\omega_2\, B_2}{2\hbar} \big) \, \big((-1)^{\mu}\, \hat{\alpha}_{2-\mu} + \frac{i}{\omega_2\, B_2}\, \hat{\pi}_{2\mu} \big) \tag{11.202}$$

and the lowest excitations have one- or two- phonon character (we suppose that the scattering particle a stays in its ground state during inelastic scattering and therefor the whole intrinsic wave function in the channel $\alpha \equiv a + A$ is given by the intrinsic wave function of the target nucleus A),

$$\psi_{2\mu}(\xi) = \psi_{2\mu}(\xi \equiv \alpha_{2\mu}) \qquad or \qquad |\psi_{2\mu}\rangle = Q^+_{2\mu}\, |0\rangle \tag{11.203}$$

(see the text below expression (7.62) and the Fig. 7.5). In the framework of the LDM the potential $V_\alpha(\vec{r}, \xi \equiv \alpha_{2\mu})$ involved in the interaction $\hat{W}_\alpha(\vec{r})$ in (11.199) is supposed to be dependent on the distance from the surface of the vibrating nucleus,

$$\begin{aligned} V_\alpha(\vec{r}, \xi \equiv \alpha_{2\mu}) = V_\alpha(r - R(\theta,\phi)) \approx \boxed{\begin{array}{c}\text{see}\\ (11.200)\end{array}} \approx \\ \approx V_\alpha(r - R_0) - \sum_{\mu} \alpha^*_{2\mu}\, Y_{2\mu}(\theta,\phi) R_0\, \frac{dV_\alpha(r)}{dr} \\ + \frac{1}{2}\, \big(\sum_{\mu} \alpha^*_{2\mu}\, Y_{2\mu}(\theta,\phi) \big)^2\, R_0^2\, \frac{d^2 V_\alpha(r)}{dr^2} \end{aligned} \tag{11.204}$$

Then the simplification is usually used that the first term $V_\alpha(r - R_0)$ in (11.204) can be approximated by the optical potential $U^{(opt)}_{\alpha i}$ (see (11.194)) where parameters of which were determined by the analysis of the elastic scattering as was discussed in the Subsection 11.4.2 and therefore it is known. So we have for $W_\alpha(\vec{r})$ in (11.199) following approximation (after the quantizing procedure),

$$\hat{W}_\alpha(\vec{r}) \approx - \sum_{\mu} \hat{\alpha}_{2\mu}\, Y_{2\mu}(\theta,\phi) R_0\, \frac{dV_\alpha(r)}{dr} + \frac{1}{2}\, \big(\sum_{\mu} \hat{\alpha}_{2\mu}\, Y_{2\mu}(\theta,\phi) \big)^2\, R_0^2\, \frac{d^2 V_\alpha(r)}{dr^2} \tag{11.205}$$

where the operator $\hat{\alpha}_{2\mu}$ of the generalized coordinate can be expressed in terms of the creation and annihilation operators of phonons (see (7.59) and subsequently the matrix elements $W_{\alpha j,\,\alpha 0}$, involved in (11.199), between the ground state and excited vibrational one- and/or two- phonon states of the target nucleus can be determined.

11.4.3.2 Inelastic scattering excitation of axially deformed nucleus

In the case of deformed nuclei the rotational band is formed above each intrinsic state and the lowest excited states belong to the rotational band based on the intrinsic ground state (see the Section 7.1 - Fig 7.2, or the Subsection 8.1.1). In the laboratory external frame the wave function of the states from the ground rotational band is following (see (8.9) for $K = 0$ and $r_1 = +1$),

$$\Psi_{IMK\rho}(\xi, \theta_{Eu}) \equiv \langle \theta_{Eu}, \xi \mid IMK = 0\rho \equiv gr \rangle \approx$$
$$\approx \sqrt{\frac{2I+1}{8\pi^2}}\, D^I_{MK=0}(\theta_{Eu})\, \langle \xi | gr \rangle \tag{11.206}$$

where $I = 0, 2, 4, \cdots$ for individual levels of the ground rotational band, θ_{Eu} are Euler angles transforming the laboratory external frame into the intrinsic frame rotating with the nucleus, $\psi_{K=0,\rho=gr}(\xi) = \langle \xi | gr \rangle$ is the intrinsic ground state wave function (phonon vacuum for even-even nuclei) of the intrinsic variables ξ (see (7.33) for $K = 0$, $r_1 = +1$), and $D^I_{MK}(\theta_{Eu})$ are Wigner functions (see the Appendix A). From the Subsection 8.1.1 it is known that the laboratory frame even-even nucleus wave function for rotational bands built on the intrinsic multi-phonon states $\psi_{K\rho}(\xi)$ is generally given by (8.6) (if Coriolis mixing is neglected), where $\psi_{K\rho}(\xi) = \langle \xi | K\rho \rangle$ have multi-phonon vibration character (one- phonon $|K\rho\rangle = Q^+_{K\rho}|gr\rangle$, two- phonon $|K\rho\rangle = |K = K_1 + K_2\ \rho = \rho_1\rho_2\rangle = Q^+_{K_1\rho_1} Q^+_{K_2\rho_2}|gr\rangle$, etc.). In any case the low energy excited intrinsic states of axially deformed nuclei are connected with the stable equilibrium quadrupole deformation β and the shape of such nuclei is given by the following expression with good approximation (compare with (11.200))

$$R(\theta, \phi) \approx R_0 \left(1 + \beta\, Y_{20}(\theta, \phi)\right) \tag{11.207}$$

with fixed deformation parameter β. Now the deformation β is not linked directly with any quantizing of the collective quadrupole Hamiltonian and the deformation β in (11.207) is just real parameter and phonons $Q^+_{K\rho}$ are determined using e.g. Bohr-Mottelsaon deformed LDM approach (see the

Subsection 7.2.1.2) or by the microscopic RPA approach (see the Subsection 7.3.1.1) or by other models for the intrinsic degrees of freedom of deformed nuclei. However, similarly as in the spherical case, the interaction $V_\alpha(\vec{r},\xi)$ involved in (11.199) is dependent only on the distance from the surface of the deformed nucleus given by (11.207). So

$$V_\alpha(\vec{r}\,',\xi) = V_\alpha(r\,' - R(\theta',\phi')) \approx \boxed{\begin{array}{c}\text{see}\\(11.207)\end{array}} \approx$$

$$\approx V_\alpha(r\,' - R_0) - \beta\, R_0\, Y_{20}(\theta',\phi')\, \frac{dV_\alpha(r\,')}{dr\,'} \tag{11.208}$$

where $\vec{r}\,' \equiv (r\,',\theta',\phi')$ is the radius-vector in the intrinsic frame rotating with the nucleus and again the approximation is used that the first term in (11.208) is approximated by the optical potential $U^{(opt)}_{\alpha i}(r\,')$ which gives for $W_\alpha(\vec{r}\,')$ in (11.199),

$$W_\alpha(\vec{r}\,') \approx -\beta\, R_0\, Y_{20}(\theta',\phi')\, \frac{dV_\alpha(r\,')}{dr\,'} \tag{11.209}$$

In order to calculate the matrix elements $W_{\alpha j,\,\alpha 0}(\vec{r})$ between different nuclear wave functions expressed in the external laboratory frame (for excitations in the ground rotational band) or generally between different wave functions (8.9) it is necessary to transform the operator (11.209), expressed in the intrinsic fix-body rotating frame into the external laboratory frame (similarly as was done for matrix elements (7.37) of electromagnetic transition operators). However it can be easily done and the integral over Euler angles can be calculated (as in (7.38)) and searched for the matrix elements $W_{\alpha j,\,\alpha 0}(\vec{r})$ for (11.199) can be obtained.

So, if we accept the hypothesis that the interaction $V_\alpha(\vec{r},\xi)$ responsible for elastic scattering going to the lowest excited states of the nucleus A in the given channel $\alpha \equiv a + A$ is determined by (11.204) (for spherical nuclei) or by (11.208) (for axially deformed nuclei) with $V_\alpha(r - R_0)$ been represented by the elastic optical potential then the inelastic DWBA scattering amplitude is given by(11.199) where $W_{\alpha j,\,\alpha i}(\vec{r})$ are determined by (11.205) for spherical nuclei or by (11.209) for axially deformed nuclei. Since parameters of elastic scattering optical potential $U^{(opt)}_{\alpha i}(r)$ involved in (11.205) or (11.209) were obtained by the fitting procedure (usually the least square method) to the experimental elastic scattering cross-section is without free parameters (we suppose that the intrinsic Hamiltonian giving the excitation state wave

functions of the target nucleus and the equilibrium deformation β in the case of deformed nucleus are known from other data, independent on investigated scattering.

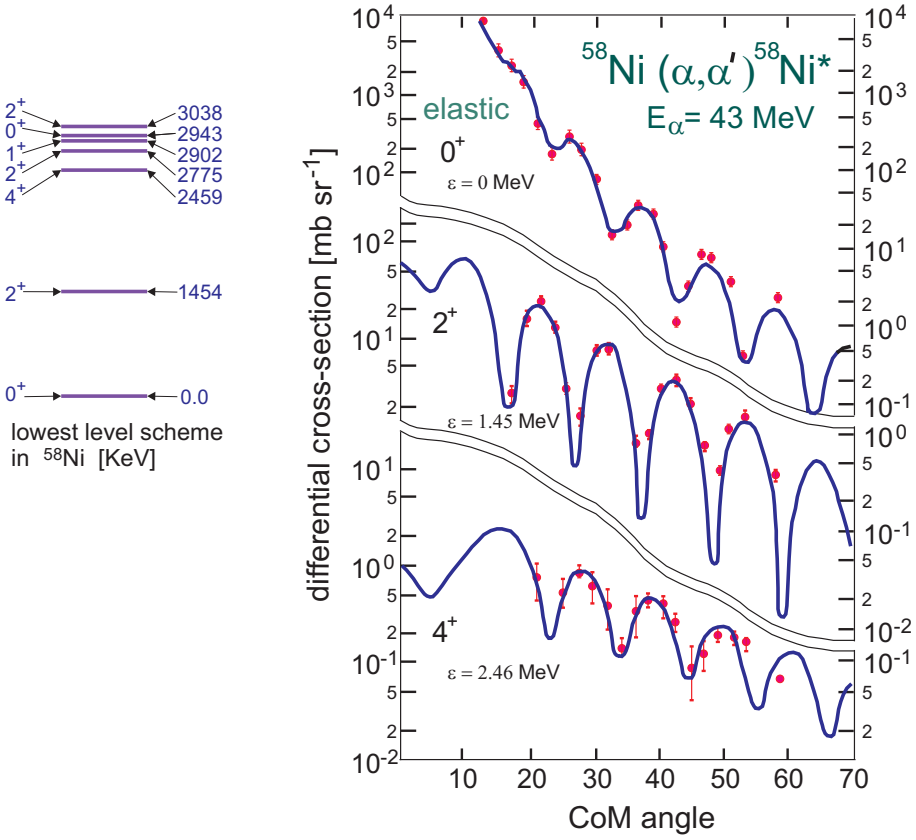


Figure 11.12: Elastic and inelastic scattering differential cross-sections of $E_\alpha = 43$ MeV α- particles leading to the lowest excited states of ^{58}Ni are compared with the DWBA curves calculated with the interaction W_α given by (11.203). The 2- phonon 4^+ curve is the prediction of the LDM vibrational model where the calculated 2- phonon amplitude was artificially increased by a factor 1.5. For the comparison there is the level scheme of the lowest excitations of ^{58}Ni shown on the l.h.s. of the figure (adapted from [357]).

As an example of the comparison of the calculated DWBA differential cross-sections with corresponding experimental results in the right part of the Fig. 11.12 the differential cross-section of the α- particle scattering $^{58}Ni(\alpha,\alpha')^{58}Ni^*$ leading to the ground state 0^+, the first 2^+ state and the first 4^+ state in the ^{58}Ni isotopes are shown (see [357]). The elastic scattering differential cross-section (upper plot in the right part of the figure) for the ground state of ^{58}Ni with the zero excitation energy $\epsilon = 0$ MeV served as the data for obtaining parameters of the optical potential $U^{(opt)}_{\alpha\,^{58}Ni}$ (see [358]). The nucleus ^{58}Ni was supposed to be spherical and the first quadrupole state 2^+ with the energy $\epsilon \approx 1.45 MeV$ was considered as one- quadrupole phonon

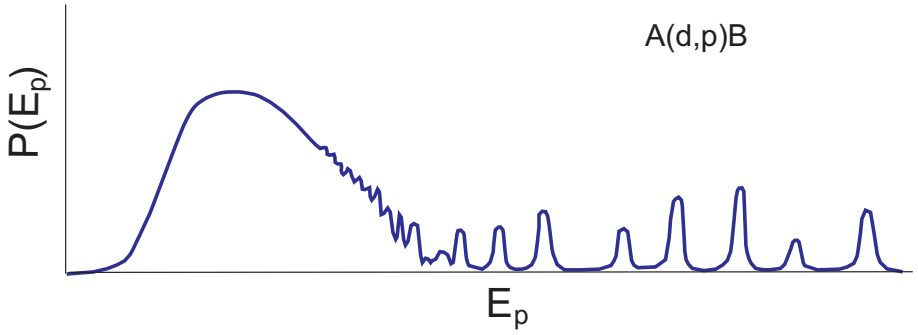


Figure 11.13: Energy distribution of protons from (d,p) reaction with the fixed ingoing deuteron energy.

LDM state generated in the inelastic scattering by the first term in (11.205). The first hexadecapole state 4^+at the energy $\epsilon \approx 2.46$ MeV was interpreted as two- quadrupole phonon LDM state generated by the second term in (11.205). The calculated differential cross-section for the first excited 2^+ state (the middle plot in the right part of the Fig. 11.12) is in very good agreement with the experimental values. In order to obtain at least qualitative agreement of calculated curve for two- phonon state 4^+ at the energy ≈ 2.46 MeV with the experimental values the author of [358] had to increase the two- phonon amplitude by 50 percents. This discrepancy can be explained by the very simple pure LDM vibrational approach used in the calculation or it may be an effect of the neglect of the antisymmetrization in the DWBA theory. The other cause for this discrepancy can be the neglect of the coupling of the 4_1^+ excitation channel with other hexadecapole excitations channels. It is the general drawback of the DWBA and CCBA calculations performed in the sixties and seventies that they used relatively simple nuclear structure models for the determination of the interaction $W_\alpha(\vec{r})$ in expressions (11.198) and (11.199).

11.4.4 One nucleon transfer reaction

The application of the optical model is further demonstrated on the example of the reaction with one nucleon transfer. The most often observed one nucleon transfer reaction is so called stripping (d,p) reaction and therefore we will concentrate primarily on this reaction.

The typical energy distribution of protons from the reaction (d,p) with the fixed energy of ingoing deuterons (several tens up to hundreds MeV) is demonstrated on the schematic figure Fig.11.13. In higher energies of

outgoing protons (that means the lower excitation of the final nucleus B) the discrete peaks are observed which are connected with the discrete spectrum of the final nucleus B. In the low energies of protons (up to 10-20 MeV), what corresponds to higher excitation energies of final nucleus, the excitation curve in the Fig.11.13 is continuous (we can see a similarity with the Fig.11.1 for inelastic scattering (p, p')).

If further the angle distribution of final protons at different but fixed proton energies (that means the differential cross-section of the reaction (d,p)) is analyzed then there is a big difference for protons originated from discrete higher energy peaks in the Fig.11.13 and for protons from a lower energy continuous part of the spectrum in the Fig.11.13, namely (it should be remanded that the deuteron energy is fixed),

- protons with fixed energy from the lower continuous part of their spectrum have the angle distribution (differential cross-section of (d,p) reaction) symmetric with respect to 90^o and usually almost isotropic;
- protons with fixed higher energy (that means originating from the higher energy discrete peaks of their spectrum in the Fig.11.13) demonstrate the non-symmetric angular distribution and in many cases a lot of protons flies to the opposite direction than incoming deuterons ($\theta \approx 180^o$).

From the section 11.1 we know that the symmetric almost isotropic angular distribution is typical for the reactions going through the compound nucleus when the final channel "forgets about" the initial channel (particularly about the direction of the incoming deuterons). On the contrary the non-symmetric and unisotropic angular distribution with some structure is characteristic for the direct nuclear reactions when the incoming particle (deuteron) reacts with one or with very small number of nucleons from the target nucleus and the final particle is formed practically immediately (so the final channel "resembles" the initial channel). These two reaction mechanisms can participate in the (d,p) reaction as well as is schematically depicted on the Fig11.14.

Possible other mechanisms of the reaction A(d,p)B are of higher order of the Born formalism and are usually neglected.

Further we will describe the (d,p) reaction in the framework of the optical model when the reaction $d + A \to p + B$ ongoes as the direct reaction (DR). Within the DWBA approach the DR reaction amplitude is given by (11.190),

$$f_{(\vec{k}_{dA\,i} \to \vec{k}_{pBj})} \approx -\frac{M_\beta}{2\pi\hbar^2} \int d^3r_\alpha \int d^3r_\beta \;\; u^*_{pBj}(\vec{k}_{pBj}, \vec{r}_\beta) \\ \langle\, pB\; j|\; \hat{V}_{pB} - \hat{U}^{(opt)}_{pB} \;|dA\; i\rangle \; u_{dA\,i}(\vec{k}_{dA\,i}, \vec{r}) \qquad (11.210)$$

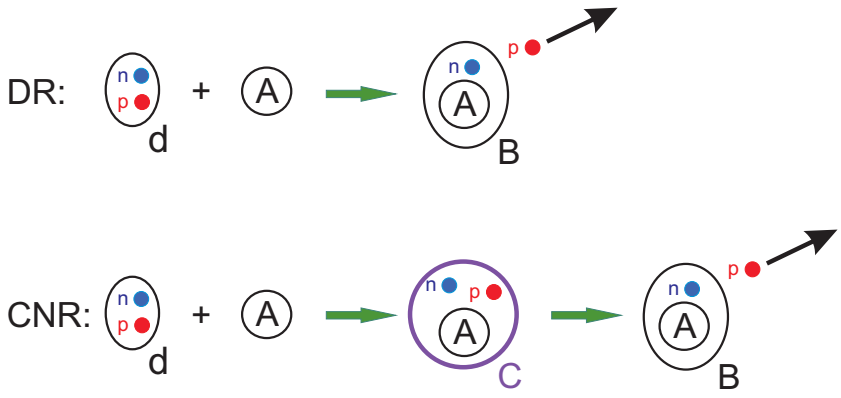


Figure 11.14: Direct reaction (DR) mechanism (upper fihure) and compound nucleus reaction (CNR) mechanism (lower figure) of the stripping reaction A(d,p)B.

where $\langle\, pB\; j|\; \hat{V}_{pB} - \hat{U}_{pB}^{(opt)}\; |dA\; i\rangle$ is the intrinsic matrix element, which can be expressed as the integral over the internal coordinates as will be shown further. The symbol $u_{pBj}(\vec{k}_{pbj}, \vec{r})$ stands for the relative motion wave function (distorted wave) in the channel $\beta \equiv p{+}B$ which is the solution of the equation (see(11.182)),

$$\left(\hat{T}_\beta - \epsilon_{pBj} - \hat{U}_{pB}^{(opt)}(\vec{r}_\beta)\right) u_{pBj}(\vec{k}_{pBj}, \vec{r}_\beta) = 0 \qquad (11.211)$$

with the optical potential $U_{pb}^{(opt)}(\vec{r})$ in the channel $\beta \equiv p + B$, parameters of which were obtained by the analysis of the elastic scattering $p + B \to p + B$. Similarly the relative motion wave function (distorted wave) in the channel $\alpha \equiv d + A$, $v_{dA\,i}(\vec{k}_{dA\,i}, \vec{r})$, is the solution of the DWBA equation

$$\left(\hat{T}_\alpha - \epsilon_{dA\,i} - \hat{U}_{dA}^{(opt)}(\vec{r}_\alpha)\right) u_{dA\,i}(\vec{k}_{dA\,i}, \vec{r}_\alpha) = 0 \qquad (11.212)$$

with the optical potential $U_{dA}^{(opt)}(\vec{r})$ determined from the elastic scattering $d + A \to d + A$ (as it was mentioned in the Subsection 11.4.2).

In order to calculate the intrinsic matrix element $\langle\, pB\; j|\; \hat{V}_{pB} - \hat{U}_{pB}^{(opt)}\; |dA\; i\rangle$ in (11.210) we should concretize interaction $\hat{V}_{pB} - \hat{U}_{pB}^{(opt)}$ and the kets $|dA\; i\rangle$ and $|pB\; j\rangle$.

The direct reaction part of the stripping reaction (d,p) is schematically shown in the figure Fig.11.15. The Hamiltonian $\hat{H}$ of the whole system formated by the initial channel $\alpha \equiv a + A = d + A$ can be expressed in terms

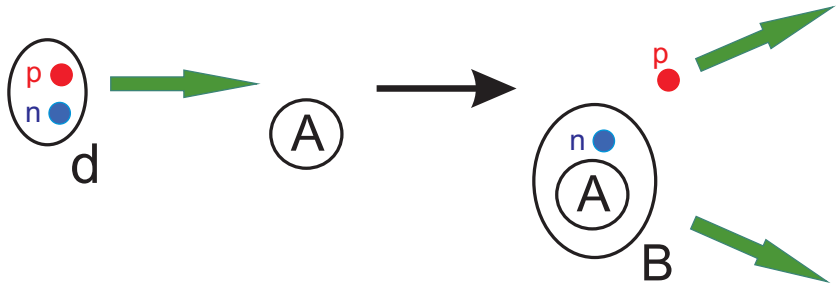


Figure 11.15: Schematic figure of the stripping (d,p) reaction. The deuteron d impacts on the target nucleus A with the linear momentum $\hbar\vec{k}_{dA\,i}$ (in the CoM frame). Then the neutron n is stripped from the deuteron and the final nucleus B and the proton p are formed with the relative linear momentum $\hbar\vec{k}_{pBj}$ (again in the CoM frame).

of variables corresponding to the channel $\alpha = d + A$,

$$\hat{H} = \boxed{\begin{array}{c}\text{see}\\(11.121)\end{array}} = \hat{T}_{dA} + \hat{H}_{dA} + \hat{V}_{dA} =$$

$$= \boxed{\begin{array}{c}\text{because}\\ \hat{H}_{dA} = \hat{H}_d + \hat{H}_A\ ,\ \hat{V}_{dA} = \hat{V}_{pA} + \hat{V}_{nA}\end{array}} =$$

$$= \hat{T}_{dA} + \hat{H}_d + \hat{H}_A + \hat{V}_{pA} + \hat{V}_{nA} = \boxed{\begin{array}{c}\text{because}\\ \hat{H}_d = \hat{T}_{pn} + \hat{V}_{pn}\end{array}} =$$

$$= \hat{T}_{dA} + \hat{T}_{pn} + \hat{V}_{pn} + \hat{H}_A + \hat{V}_{pA} + \hat{V}_{nA} \qquad (11.213)$$

or in terms of variables corresponding to the channel $\beta \equiv p + B$,

$$\hat{H} = \hat{T}_{pB} + \hat{H}_{pB} + \hat{V}_{pB} = \boxed{\begin{array}{c}\text{because}\\ \hat{H}_{pB} = \hat{H}_B = \hat{H}_A + \hat{T}_{nA} + \hat{V}_{nA}\\ \hat{V}_{pB} = \hat{V}_{pn} + \hat{V}_{pA}\end{array}} =$$

$$= \hat{T}_{pB} + \hat{T}_{nA} + \hat{V}_{pn} + \hat{V}_{nA} + \hat{V}_{pA} + \hat{H}_A \qquad (11.214)$$

where $\hat{H}_{dA} \equiv \hat{H}_A + \hat{H}_d = \hat{H}_A + \hat{T}_{pn} + \hat{V}_{pn}$ is the intrinsic Hamiltonian in the initial channel $\alpha \equiv d + A$, and $\hat{H}_{pB} = \hat{H}_B = \hat{H}_A + \hat{T}_{nA} + \hat{V}_{nA}$ is the intrinsic Hamiltonian in the final channel $\beta \equiv p + B$ which is simultaneously the intrinsic Hamiltonian of the final nucleus B because the proton has no any intrinsic structure. Other notations in (11.213) and (11.214) are straightforward. The interaction between the incoming deuteron and the target nucleus A is,

$$\hat{V}_\alpha = \hat{V}_{dA} = \hat{V}_{pA} + \hat{V}_{nA} \qquad (11.215)$$

and similarly the interaction between the final proton and final nucleus B is,

$$\hat{V}_\beta \equiv \hat{V}_{pB} = \hat{V}_{pA} + \hat{V}_{pn} \tag{11.216}$$

That means the interaction $\hat{V}_\beta - \hat{U}_{pB}^{(opt)} = \hat{V}_{pB} - \hat{U}_{pB}^{(opt)}$ involved in (11.210) reads as,

$$\hat{V}_{pB} - \hat{U}_{pB}^{(opt)} = \hat{V}_{pA} + \hat{V}_{pn} - \hat{U}_{pB}^{(opt)} \tag{11.217}$$

The main assumption used in the most of the DWBA calculations for the reaction (d,p) is following:
In the final channel $\beta \equiv p + B$ only stripped neutron in the final nucleus interacts effectively with the final proton and that

$$\hat{V}_{pA} \approx \hat{U}_{pB}^{(opt)} \tag{11.218}$$

Using this assumption the interaction (11.217) can be rewritten as follows,

$$\hat{V}_{pB} - \hat{U}_{pB}^{(opt)} \approx \hat{V}_{pn} \tag{11.219}$$

This approximation was verified in many calculations and corresponding comparisons of calculated and experimental cross-sections (see e.g. [359], [351]-p.443, [360], or [352]-p.215). The approximation (11.219) is also supported by the detailed balance principle (see the Subsection 11.3.2.3.4) when the calculated pick up reaction (p,d) DWBA cross-section with the similar approximation, which agreed with the (p,d) experimental data, was transformed using the detailed balance principle expression (11.177) into the stripping (d,p) cross-section and the agreement with experimental (d,p) cross-section was also achieved.

The substitution of (11.219) into (11.190) or (11.210) gives the following amplitude of the (d,p) reaction ($\vec{k}_{\alpha i} \equiv \vec{k}_{dAi}$, $\vec{k}_{\beta j} \equiv \vec{k}_{pBj}$),

$$\begin{aligned} & f_{(\vec{k}_{\alpha i} \to \vec{k}_{\beta j})} \approx \\ & \approx -\frac{M_\beta}{2\pi\hbar^2} \int d^3 r_\alpha d^3 r_\beta \; u^*_{pBj}(\vec{k}_{pBj}, \vec{r}_\beta) \, \langle pBj \mid \hat{V}_{pn} \mid dAi \rangle \, u_{dAi}(\vec{k}_{dAi}, \vec{r}_\alpha) \end{aligned} \tag{11.220}$$

Further the intrinsic matrix element $\langle pBj | \, \hat{V}_{pn} \, | dAi \rangle$ is specified, particularly we should extract dependence of this intrinsic matrix element on variables $\vec{r}_\alpha \equiv \vec{r}_{dA}$ and $\vec{r}_\beta \equiv \vec{r}_{pB}$ and to perform the integration over the reminder variables ξ as is indicated in the expression (11.190). At first the connection between the relative motion coordinates $\vec{r}_{np} = \vec{r}_n - \vec{r}_p$ (between stripped

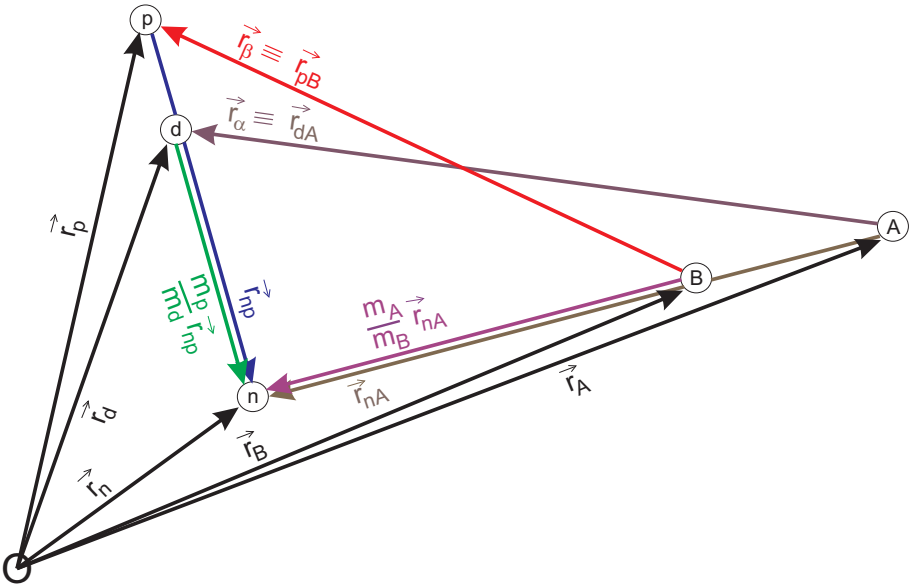


Figure 11.16: The scheme of coordinates of participants of the $A(d,p)B$ reaction. The point O represents the origin of the external frame (usually CoM frame of the system $d+A$ and/or $p+B$.

neutron and final proton) and $\vec{r}_{nA} = \vec{r}_A - \vec{r}_d$ (between stripped neutron and the centre of mass of the target nucleus A) should be clarify. This connection, following from the Fig.11.16, gives the transformation $(\vec{r}_{np}, \vec{r}_{nA}) \to (\vec{r}_\alpha, \vec{r}_\beta)$,

$$\begin{aligned} \vec{r}_\alpha &= \vec{r}_{nA} - \frac{m_p}{m_d}\,\vec{r}_{np} \\ \vec{r}_\beta &= \frac{m_A}{m_B}\,\vec{r}_{nA} - \vec{r}_{np} \end{aligned} \qquad (11.221)$$

which transforms the internal variables $\vec{r}_{np}$ (in the deuteron) and $\vec{r}_{nA}$ (in the final nucleus B) into the external variables $\vec{r}_\alpha = \vec{r}_{dA}$ and $\vec{r}_\beta = \vec{r}_{pB}$ giving the mutual position deuteron-target nucleus A and proton-final nucleus B, respectively. In (11.221) m_A, m_d, m_B and m_p are masses of the target nucleus, impacting deuteron, final nucleus and final proton, respectively.

Further we should specify the intrinsic wave functions $|dAi\rangle$ and $\langle pBj|$ together with the interaction $\hat{V}_{np}$, all in the coordinate representation (see

Fig.11.15),

$$\langle \vec{r}_{np}\,, s_n, s_p; \xi_A \,|dAi\rangle = \psi_d(\vec{r}_{np})\; \chi^{(d)}_{1\mu_d}(s_n, s_p)\; \psi^{(A)}_{I_a M_a i}(\xi_A)$$
$$\langle pBj \,|\xi_A, \vec{r}_{nA}; s_n, s_p\rangle = \chi^{(p)\,*}_{\frac{1}{2}\mu_p}(s_p)\; \psi^{(B)\,*}_{I_B M_B j}(\xi_A, \vec{r}_{nA}, s_n)$$
$$\langle \xi_A, \vec{r}_{nA}; s_n, s_p \mid \hat{V}_{np} \,|\vec{r}_{np}\,, s_n, s_p; \xi_A\rangle \approx \boxed{\begin{array}{c}\text{see}\\ (11.219)\end{array}} \approx V_{pn}(\vec{r}_{np}) \tag{11.222}$$

where $\psi_d(\vec{r}_{np})$ and $\chi^{(d)}_{1\mu_d}(s_n, s_p)$ are configuration and spin part of the deuteron wave function, respectively (we suppose the deuteron bound state is approximated only by pure S-state - see the Subsection 3.1.1, s_n and s_p are formal spin variables of neutron and proton). The symbol $\psi^{(A)}_{I_A m_A i}(\xi_A)$ stands for the wave function of the target nucleus A (I_A and M_A are total angular momentum and its projection and ξ_A represents all internal variables of the target nucleus A), $\chi^{(p)}_{\frac{1}{2}\mu_p}(s_p)$ is the spin wave function of the final proton and $\psi^{(B)}_{I_b M_b j}(\xi_A, \vec{r}_{nA}, s_n)$ is the wave function of the final nucleus B in the final state $I_B M_B j$ which is the function of the internal variables ξ_A of the nucleus A and mutual coordinate $\vec{r}_{nA}$ of the stripped neutron and the CoM of the nucleus A (inside the nucleus B - see the Fig.11.15). The relative coordinate $\vec{r}_{nA}$ can be expressed in terms of $\vec{r}_\alpha \equiv \vec{r}_{dA}$ and $\vec{r}_\beta \equiv \vec{r}_{pB}$ with the use of (11.221) (we eliminate the variable $\vec{r}_{np}$ from equations (11.221)),

$$\vec{r}_{nA} = \vec{r}_{nA}(\vec{r}_\alpha, \vec{r}_\beta) = \frac{m_d\, m_B}{m_d\, m_B - m_p\, m_A}\left(\vec{r}_\alpha - \frac{m_p}{m_d}\,\vec{r}_\beta\right) \tag{11.223}$$

So the integration $\int d^3r_\alpha \int d^3r_\beta$ involved in (11.220) is connected with the integration $\int d^3r_{nA} \int d^3r_\beta$ by the Jacobi transformation,

$$\int d^3r_\beta \int d^3r_{nA} = \mathcal{J} \int d^3r_\beta \int d^3r_\alpha \tag{11.224}$$

with the Jacobian (see (11.223)),

$$\mathcal{J} \equiv \left|\frac{\partial \vec{r}_{nA}}{\partial \vec{r}_\alpha}\right| = \left(\frac{m_d\, m_B}{m_d\, m_B - m_p\, m_A}\right)^3 \tag{11.225}$$

Then the expression for the reaction amplitude (11.220) can be rewritten as

follows,

$$f^{(I_A M_A i,\, \mu_d \to I_b M_b j,\, \mu_p)}_{(\vec{k}_{\alpha i} \to \vec{k}_{\beta j})} = -\frac{M_\beta}{2\pi\hbar^2}\, \mathcal{J} \int d^3r_\alpha \int d^3r_\beta \int d\xi_A \int d^3r_{np} \int ds_n \int ds_p$$
$$u^*_{\beta j}(\vec{k}_{\beta j}, \vec{r}_\beta)\ \chi^{(p)\,*}_{\frac{1}{2}\mu_p}(s_p)\ \psi^{(B)\,*}_{I_b M_B j}(\xi_A, \vec{r}_{nA}(\vec{r}_\alpha, \vec{r}_\beta), s_n)\ V_{np}(\vec{r}_{np})$$
$$\psi_d(\vec{r}_{np})\ \chi^{(d)}_{1\mu_d}(s_n, s_p)\ \psi^{(A)}_{I_A M_A i}(\xi_A)\ u_{\alpha i}(\vec{k}_{\alpha i}, \vec{r}_\alpha) \tag{11.226}$$

The action of the interaction $V_{np}(\vec{r}_{np})$ on the deuteron wave function $\psi_d(\vec{r}_{np})$ can be determined easily if this wave function is approximated only by simple S-state component (see (3.7) with (3.8)),

$$\psi_d(\vec{r}_{np}) = \psi_d(r_{np}) = D_0\, \frac{e^{-k_d\, r_{np}}}{r_{np}} \tag{11.227}$$

which is the solution of the Schroedinger equation

$$\Big(-\frac{\hbar^2}{2\mu_{np}}\, \nabla^2_{np} + V_{np}(r_{np}) - \epsilon_d \Big)\, \psi_d(r_{np}) = 0 \tag{11.228}$$

So the action $V_{np}(r_{np})\, \psi_d(r_{np})$ is

$$V_{np}(r_{np})\, \psi_d(r_{np}) = \Big(\frac{\hbar^2}{2\mu_{np}}\, \nabla^2_{np} + \epsilon_d\Big)\, \psi_d(r_{np}) =$$
$$= \frac{\hbar^2\, D_o}{2\mu_{np}} \left(\nabla^2_{np} - k_d^2\right) \frac{e^{-k_d r_{np}}}{r_{np}} = \boxed{\begin{array}{c}\text{because} \\ \nabla^2 \frac{1}{r} = -4\pi\, \delta(\vec{r})\end{array}} =$$
$$= -\frac{2\pi D_0 \hbar^2}{\mu_{np}}\, \delta(\vec{r}_{np})\, e^{-k_d r_{np}} \tag{11.229}$$

where ϵ_d is the deuteron bound energy and $k_d^2 = -\frac{2\mu_{np}}{\hbar^2}\, \epsilon_d$. So the integration

over d^3r_{np} in (11.226) gives the reaction amplitude in the following form,

$$f^{(I_AM_Ai,\,\mu_d\to I_bM_bj,\,\mu_p)}_{(\vec{k}_{\alpha i}\to\vec{k}_{\beta j})} = -\frac{M_\beta D_0}{\mu_{np}}\,\mathcal{J}\int d^3r_\alpha\int d^3r_\beta\int d\xi_A\int d^3r_{np}\int ds_n\int ds_p$$
$$u^*_{\beta j}(\vec{k}_{\beta j},\vec{r}_\beta)\;\chi^{(p)\,*}_{\frac{1}{2}\mu_p}(s_p)\;\psi^{(B)\,*}_{I_bM_Bj}(\xi_A,\vec{r}_{nA}(\vec{r}_\alpha,\vec{r}_\beta),s_n)$$
$$\delta(\vec{r}_{np}=\vec{r}_\beta-\frac{m_A}{m_\beta})\;\chi^{(d)}_{1\mu_d}(s_n,s_p)\;\psi^{(A)}_{I_AM_Ai}(\xi_A)\;u_{\alpha i}(\vec{k}_{\alpha i},\vec{r}_\alpha)=$$

$$=\boxed{\begin{array}{c}\text{because (see (11.223))}\\ \int d^3r_\beta\int d^3r_\alpha=\mathcal{J}^{-1}\int d^3r_\beta\int d^3r_{nA}\text{ and }\vec{r_\beta}=\frac{m_A}{m_B}\,\vec{r}_{nA}\end{array}}=$$

$$=\frac{M_\beta D_0}{\mu_{np}}\int d^3r_{nA}\int d\xi_A\int ds_n\int ds_p$$
$$u^*_{\beta j}(\vec{k}_{\beta j},\frac{m_A}{m_B}\vec{r}_{nA})\;\chi^{(p)\,*}_{\frac{1}{2}\mu_p}(s_p)\;\psi^{(B)\,*}_{I_bM_Bj}(\xi_A,\vec{r}_{nA},s_n)$$
$$\chi^{(d)}_{1\mu_d}(s_n,s_p)\,\psi^{(A)}_{I_AM_Ai}(\xi_A)\;u_{\alpha i}(\vec{k}_{\alpha i},\vec{r}_{nA})\qquad(11.230)$$

The S-state approximation for the deuteron wave function (11.227) and following approximation (11.229) for the action of the potential $V_{np}(\vec{r}_{np})$ on the wave function $\psi_d(\vec{r}_{np})$ is called in the literature as the zero-range approximation for (d,p) reactions.

Further the wave function $\psi^{(B)}_{I_BM_Bj}(\xi_A,\vec{r}_{nA},s_n)$ and $\chi^{(d)}_{1\mu_d}(s_n,s_p)$ are decomposed as follows,

$$\psi^{(B)}_{I_BM_Bj}(\xi_A,\vec{r}_{nA},s_n)=$$
$$=\sum_{JLM'_Ai}\Theta^{(ji)}_{nLJ}\;\psi^{(A)}_{I_AM'_Ai}(\xi_A)\;\phi^{(n)}_{nLJM_B-M'_A}(\vec{r}_{nA},s_n)\;C^{I_BM_B}_{I_AM'_AJM_B-M'_A}=$$

$$=\boxed{\begin{array}{c}\text{single-neutron wave function }\phi^{(n)}_{nLJM_B-M'_A}\text{ is}\\ \text{decomposed into radial, angle and spin components}\end{array}}=$$

$$=\sum_{JLM'_AM_Li}\Theta^{(ji)}_{nLJ}\,\psi^{(A)}_{I_AM'_Ai}(\xi_A)\,R_{nLJ}(r_{nA})\,Y_{LM_L}(\hat{r}_{nA})\,\chi^{(n)}_{\frac{1}{2}M_B-M'_A-M_L}$$
$$C^{I_BM_B}_{I_AM'_AJM_B-M'_A}\;C^{JM_B-M'_A}_{LM_L\frac{1}{2}M_B-M'_A-M_L}\qquad(11.231)$$

and

$$\chi^{(d)}_{1\mu_d}(s_n,s_p)=\sum_{\mu_n=\pm\frac{1}{2}}C^{1\mu_d}_{\frac{1}{2}\mu_n\frac{1}{2}\mu_d-\mu_n}\,\chi^{(n)}_{\frac{1}{2}\mu_n}(s_n)\,\chi^{(p)}_{\frac{1}{2}\mu_p}(s_p)\qquad(11.232)$$

where $\Theta^{(ji)}_{nLJ}$ is so called spectroscopic amplitude and its square is known in

the literature as the spectroscopic factor,

$$S^{(ji)}_{nLJ} = \Theta^{(ji)\,2}_{nLJ} \tag{11.233}$$

Since the spectroscopic amplitude $\Theta^{(ji)}_{nLJ}$ is a coefficient in an expansion (11.231) in complete sets of the target states $\psi_{I_A M_A i}(\xi_A)$ and single-particle states $\phi^{n)}_{nLJM_j}$ which are orthonormal,

$$\begin{aligned} \int d\xi_A \, \psi^{(A)}_{I'_A M'_A i'}(\xi_A) \, \psi^{(A)}_{I_A M_A i}(\xi_A) &= \delta_{I'_A I_A} \, \delta_{M'_A M_A} \, \delta_{i'i} \\ \int ds \int d^3r \, \phi^{(n)\,*}_{n'L'J'M'_J}(\vec{r}, s) \;\; \phi^{(n)\,*}_{nLJM_J}(\vec{r}, s) &= \delta_{n'n} \, \delta_{L'L} \, \delta_{J'J} \, \delta_{M'_J M_J} \end{aligned} \tag{11.234}$$

the spectroscopic factor represents the probability for the nucleus B with the angular momentum (I_B, M_B) in the state j to be describable as the nucleus A in the state i with the angular momentum (I_A, M_A) plus a neutron in the single-particle orbit (nLJ) in the field of the nucleus A. Its determination and extraction from the experimental data will be discussed later.

The substitution of (11.231) and (11.232) into (11.230) gives the amplitude (11.230) in the following form,

$$\begin{aligned} & f^{(I_A M_A i,\, \mu_d \to I_b M_b j,\, \mu_p)}_{(\vec{k}_{\alpha i} \to \vec{k}_{\beta j})} = \\ & = \frac{M_\beta D_0}{\mu_{np}} \int d^3 r_{nA} \int d\xi_A \int ds_n \int ds_p \sum_{JLM'_A i' \mu_n} \Theta^{(ji')}_{nLJ} \\ & u^*_{\beta j}(\vec{k}_{\beta j}, \frac{m_A}{m_B} \vec{r}_{nA}) \;\; \chi^{(p)\,*}_{\frac{1}{2}\mu_p}(s_p) \;\; \psi^{(A)\,*}_{I_A M'_A i'}(\xi_A) \, R_{nLJ}(r_{nA}) \, Y^*_{LM_L}(\hat{r}_{nA}) \\ & \chi^{(n)\,*}_{\frac{1}{2} M_B - M'_A - M_L}(s_n) \, \chi^{(n)}_{\frac{1}{2}\mu_n}(s_n) \, \chi^{(p)}_{\frac{1}{2}\mu_d - \mu_n}(s_p) \;\; \psi^{(A)}_{I_A M_A i}(\xi_A) \;\; v_{\alpha i}(\vec{k}_{\alpha i}, \vec{r}_{nA}) \\ & \qquad\qquad C^{I_B M_B}_{I_A M'_A J M_B - M'_A} \, C^{J M_B - M'_A}_{L M_L \frac{1}{2}\, M_B - M'_A - M_L} \, C^{1\mu_d}_{\frac{1}{2}\mu_n \frac{1}{2}\, \mu_d - \mu_n} = \\ & = \boxed{\begin{array}{c} \text{see (11.234) and} \\ \int ds_n \, \chi^{(n)\,*}_{\frac{1}{2} M_B - M'_A - M_L}(s_n) \, \chi^{(n)}_{\frac{1}{2}\mu_n}(s_n) = \delta_{M_B - M'_A - M_L \,,\, \mu_n} \\ \int ds_p \, \chi^{(p)\,*}_{\frac{1}{2}\mu_p}(s_p) \, \chi^{(p)}_{\frac{1}{2}\mu_d - \mu_n}(s_p) = \delta_{\mu_p \,,\, \mu_d - \mu_n} \end{array}} = \\ & = \frac{M_\beta D_0}{\mu_{np}} \sum_{LJ} \Theta^{(ji)}_{nLJ} \int d^3 r \, v^*_{\beta j}(\vec{k}_{\beta j}, \frac{m_A}{m_B} \vec{r}) \, R_{nLJ}(r) \, Y^*_{LM_L}(\hat{r}) \, v_{\alpha i}(\vec{k}_{\alpha i}, \vec{r}) \\ & C^{I_B M_B}_{I_A M_A J M_B - M_A} \, C^{J M_B - M_A}_{L M_L \frac{1}{2}\, M_B - M_A - M_L} \, C^{1\mu_d}_{\frac{1}{2} M_B - M_A - M_L \frac{1}{2}\, \mu_d - M_B + M_A + M_L} \end{aligned} \tag{11.235}$$

where $M_L = \mu_p + M_B - \mu_d - M_A$ and $|I_A - I_B| \leq J \leq I_A + I_B$ and $|J - 1/2| \leq L \leq J + 1/2$. The intrinsic parity change in the $d + A \to p + B$ reaction is

$$\Delta\pi = \pi_d \cdot \pi_A \cdot \pi_p \cdot \pi_B = \boxed{\begin{array}{c}\text{because}\\ \pi_d = +1,\ \pi_p = +1\end{array}} = \pi_A\, \pi_B \tag{11.236}$$

and owing to the law of parity conservation this change of intrinsic parity must be compensated by an equal change of parity of the relative motion.

The square of the reaction amplitude (11.235) determines the polarized differential cross-section of the reaction $A(d,p)B$ (see (11.148)),

$$\frac{d\sigma^{[pol]}_{I_A M_A i:1\mu_d \to I_B M_B j;\frac{1}{2}\mu_p}(\vec{k}_{\alpha i} \to \vec{k}_{\beta j})}{d\Omega_\beta} = \frac{M_\alpha\, k_{\beta j}}{M_\beta\, k_{\alpha i}} \left| f^{(I_A M_A i;\mu_d \to I_B M_B j;\mu_p)}_{(\vec{k}_{\alpha i} \to \vec{k}_{\beta j})} \right|^2 \tag{11.237}$$

where polarization is given by angular momentum projections μ_d, M_A, and μ_p, M_B. In order to obtain unpolarized cross-section we should average over projections μ_d, M_A and sum over final channel projections μ_p, M_B,

$$\begin{aligned}&\frac{d\sigma^{[unpol]}_{I_A M_A i:1\mu_d \to I_B M_B j;\frac{1}{2}\mu_p}(\vec{k}_{\alpha i} \to \vec{k}_{\beta j})}{d\Omega_\beta} =\\ &= \frac{1}{(2s_d+1)(2I_A+1)} \sum_{M_A \mu_d M_B \mu_p} \frac{d\sigma^{[pol]}_{I_A M_A i:1\mu_d \to I_B M_B j;\frac{1}{2}\mu_p}(\vec{k}_{\alpha i} \to \vec{k}_{\beta j})}{d\Omega_\beta}\end{aligned} \tag{11.238}$$

One should realize that the unpolarized differential cross-section of the stripping reaction $A(d,p)B$ is connected with the unpolarized differential cross-section of the time-reversed pick up reaction $\bar{B}(\bar{p},\bar{d})\bar{A}$ by the detailed balance principle relation (11.181). This connection allows to combine knowledges of both (p,d) and (d,p) reaction cross-sections in the interpretation of corresponding experimental data of both these reactions.

If the target nucleus is even-even one and if it is in its 0^+ ground state then the expression (11.235) simplifies as ($I_A = M_A = 0,\ J = I_B$),

$$\begin{aligned}f^{(00gr,\mu_d \to I_B M_B j,\mu_p)}_{(\vec{k}_{\alpha i \equiv gr} \to \vec{k}_{\beta j})} &= \frac{M_\beta D_0}{\mu_{np}} \sum_{L = I_B \pm \frac{1}{2}} \Theta^{(ji=gr)}_{nLJ=I_B} \int d^3r\, v^*_{\beta j}(\vec{k}_{\beta j}, \frac{m_A}{m_B}\vec{r})\\ &R_{nLJ=I_B}(r)\, Y_{LM_L}(\hat{r})\, v_{\alpha gr}(\vec{k}_{\alpha i}, \vec{r})\, C^{I_B M_B}_{LM_L \frac{1}{2} M_B - M_L}\, C^{1\mu_d}_{\frac{1}{2}\, M_B - M_L \frac{1}{2}\, \mu_d - M_B + M_L}\end{aligned} \tag{11.239}$$

where $M_L = \mu_p + M_B - \mu_d$. Then the substitution of (11.239) into (11.237) gives the following differential polaried cross-section of the (d,p) reaction,

$$\frac{d\sigma^{[pol]}_{I_A=M_A=0,\,gr;\,\mu_d\to I_B M_B j;\,\mu_p}(\vec{k}_{\alpha i}\to\vec{k}_{\beta j})}{d\Omega_\beta} = \\ = \sum_{L=I_B\pm\frac{1}{2}} S^{(ji=gr)}_{nLI_B}\, F_{LI_BM_Bj\,\mu_p;\,\mu_d}(E_\alpha,\theta_\beta) \qquad (11.240)$$

where θ_β is the angle between $\vec{k}_{\alpha i}$ and $\vec{k}_{\beta j}$, $E_\alpha \approx \frac{\hbar^2 k^2_{\alpha i}}{2\mu_\alpha}$ is the CoM kinetic energy in the initial channel with μ_α been the relative mass in the initial channel $a + A$, and

$$F_{LI_BM_Bj\,\mu_p;\,\mu_d}(E_\alpha,\theta_\beta) = \Big|\big(\frac{M_\alpha k_{\beta j}}{M_\beta k_{\alpha i}}\big)^{1/2}\frac{M_\beta D_0}{\mu_{np}}\int d^3r\, v^*_{\beta j}(\vec{k}_{\beta j},\frac{m_A}{m_B}\vec{r}) \\ R_{nLJ=I_B}(r)\, Y_{LM_L}(\hat{r})\, v_{\alpha gr}(\vec{k}_{\alpha i},\vec{r})\, C^{I_BM_B}_{LM_L\frac{1}{2}M_B-M_L}\, C^{1\mu_d}_{\frac{1}{2}\,M_B-M_L\,\frac{1}{2}\,\mu_d-M_B+M_L}\Big|^2 \qquad (11.241)$$

(with $M_L = \mu_p + M_B - \mu_d$) is so called dynamical factor which is determined fully by the optical model (we should have in mind that $v_{\alpha i=gr}(\vec{k}_{\alpha i},\vec{r})$ and $v_{\beta j}(\vec{k}_{\beta j},\vec{r}) \approx v_{\beta j=gr}(\vec{k}_{\beta j},\vec{r})$ are destroyed waves of the initial and final channels which are usually determined by the fitting procedure to corresponding elastic scattering in channels $\alpha \equiv d + A$ and $\beta \equiv p + B$). In the expression (11.240) there is the sum over $L = I_B \pm \frac{1}{2}$ but in the reality only one value of L works for given I_B and j which is given by the parity of the final nucleus state I_BM_Bj. It is also necessary to realize that the wave function $\phi^{(n)}_{nLJM_B-M'_A}(\vec{r}_{nA},s_n)$ in (11.231) are for (d,p) reaction the single-neutron wave function of the neutron mean field in the nucleus B and they are usually taken from some phenomenological mean field model (e.g. with simple Wood-Saxon potential or with Nilsson potential with the L-S coupling). In such a case the dynamical factor (11.241) is not directly connected with the model used for the description of the final nucleus B states. So from this point of view the dynamical factor $F_{LI_BM_Bj\,\mu_p;\,\mu_d}(E_\alpha,\theta_\beta)$ is independent on nuclear structure models and the whole information about the structure of the nucleus A and/or B is involved in the spectroscopic factors $S^{(ji\equiv gr)}_{nLI_B} = |\Theta^{(ji=gr)}_{nLJ=I_B}|^2$ (see (11.231)). Spectroscopic amplitudes $\Theta^{(ji=gr)}_{nLJ=I_B}$ were defined in (11.231) through the formal decomposition of the final nucleus wave function $\psi^{(B)}_{I_BM_Bj}(\xi_A,\vec{r}_{nA},s_n)$ into the set of internal states $\psi^{(A)}_{I_AM_Ai}(\xi_A)$ of the target nucleus (for given I_A) and into the phenomenological neutron

single-particle wave functions $\phi^{(n)}_{nLJM_B-M'_A}(\vec{r}_{nA}, s_n)$. In the case when target nucleus is even-even and stays in its ground state then

$$\psi^{(B)}_{I_B M_B j}(\xi_A, \vec{r}_{nA}, s_n) = \\ = \sum_{L=I_B\pm\frac{1}{2}} \Theta^{(ji=gr)}_{nLJ=I_B} \psi^{(A)}_{I_A=M_A=0,\,gr}(\xi_A)\, \phi^{(n)}_{nLI_BM_B}(\vec{r}_{nA}, s_n)$$

and therefor

$$\Theta^{(ji=gr)}_{nLJ=I_B} = \int ds_n\, d^3r_{nA}\, d\xi_A \\ \phi^{(n)\,*}_{nLI_BM_B}(\vec{r}_{nA}, s_n)\, \psi^{(A)\,*}_{I_A=M_A=0,\,gr}(\xi_A)\, \psi^{(B)}_{I_BM_Bj}(\xi_A, \vec{r}_{nA}, s_n) \tag{11.242}$$

which is independent on M_B (consequence of the rotational symmetry in the CoM frame of the system $n + A$ forming the final nucleus B).

The expression (11.240) for the (d,p) differential polarized cross-section (or for unpolarized differential cross-section if the expression (11.240) is averaged over μ_d and summed over μ_p and M_B) can be used for the testing of different models of the structure of the final nucleus B. However in such tests one should realize that the expression (11.240) was derived in the framework of the approximative DWBA approach. These tests are done often inversely, that means at first the expression (11.240) for differential cross-section is used for the fitting spectroscopic factors $S^{(ji\equiv gr)}_{nLI_B} = |\Theta^{(ji=gr)}_{nLJ=I_B}|^2$ in order to obtain an agreement of calculated cross-section with corresponding experimental values . This procedure provides us optimal, so called experimental, spectroscopic factors which can be further compared with theoretical values obtained by (11.242) for different models of the wave function $\psi^{(B)}_{I_BM_Bj}(\xi_A, \vec{r}_{nA}, s_n)$ of the final nucleus B.

As an example of the DWBA calculations for (d,p) reaction going to low-energy excitations of the final nucleus B the unpolarized differential DWBA cross-section of ^{40}Ca(d,p)^{41}Ca reaction with the deuteron energy $E_d = 12$ MeV are compared with corresponding experimental values. The comparison is shown for ^{41}Ca ground state $f_{7/2}$ ($\epsilon = 0$ MeV), $p_{3/2}$ state ($\epsilon = 3.195$ MeV), $p_{3/2}$ state ($\epsilon = 2.47$ MeV) and $p_{1/2}$ state ($\epsilon = 3.95$ MeV). Calculations were done in [361] with two different optical potential parametrizations for proton elastic scattering ^{41}Ca(p,p)^{41}Ca denoted in the Fig.11.17 as L (see [362]) and BG (see [363]). Absolute values of differential cross-section for each final nucleus excitation level was fitted to the experimental points in

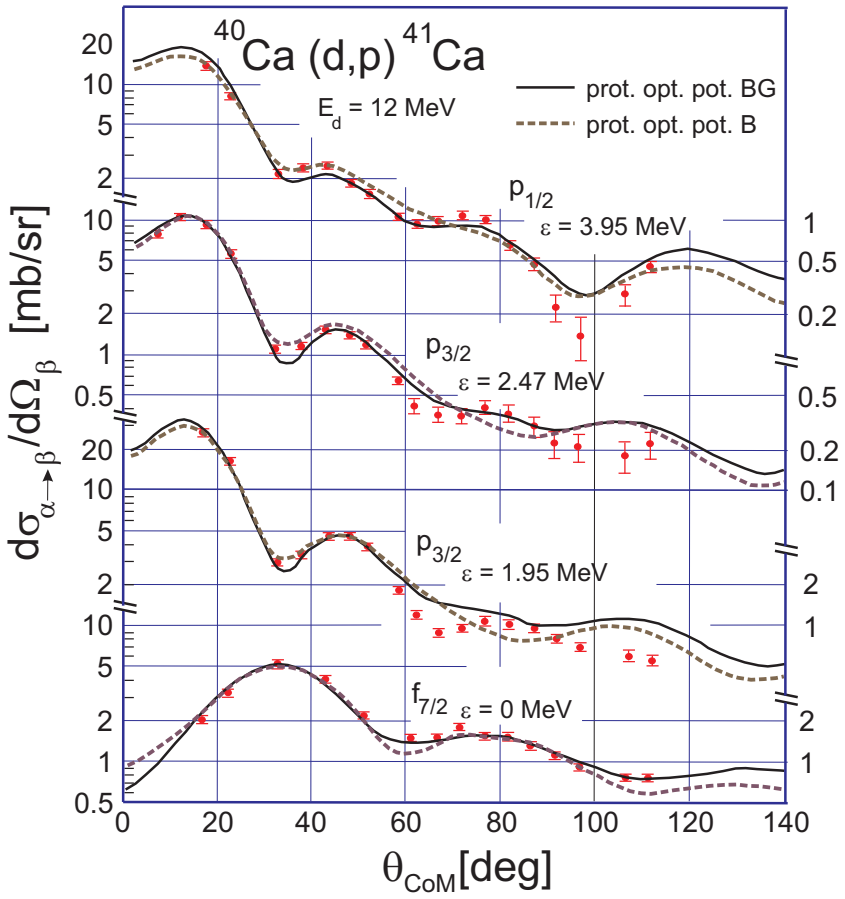


Figure 11.17: Experimental cross-sections for the ^{40}Ca(d,p)^{41}Ca reaction going to several states of ^{41}Ca, compared with the DWBA calculations using two different proton optical potentials [361].

order to obtain corresponding spectroscopic factor. In such a way obtained spectroscopic factors are collected in the Table 11.1. The table shows very

state	$f_{7/2}$	$p_{3/2}$	$p_{3/2}$	$p_{1/2}$
ϵ [MeV]	0	1.949	2.471	3.954
proton L	0.72	0.58	0.19	0.53
proton BG	0.76	0.67	0.21	0.64

Table 11.1: Spectroscopic factors corresponding to low-energy excitations in ^{41}Ca excited by the reaction ^{31}Ca(d,p)^{40}Ca for two proton optical potential parametrizations (taken from [361])

small optimal (experimental) spectroscopic factor ≈ 0.2 for the excitation level in ^{41}Ca with the exc. energy $\epsilon = 2.471$ MeV. That means the experiment indicates small spectroscopic amplitude (overlap integral) (11.242) for this

level. Such a small value means that corresponding wave function $\psi^{(B)}_{I_B M_B j}$ for this level is probably collective with a small component of the single-neutron state $p_{3/2}$ and this gives a small overlap.

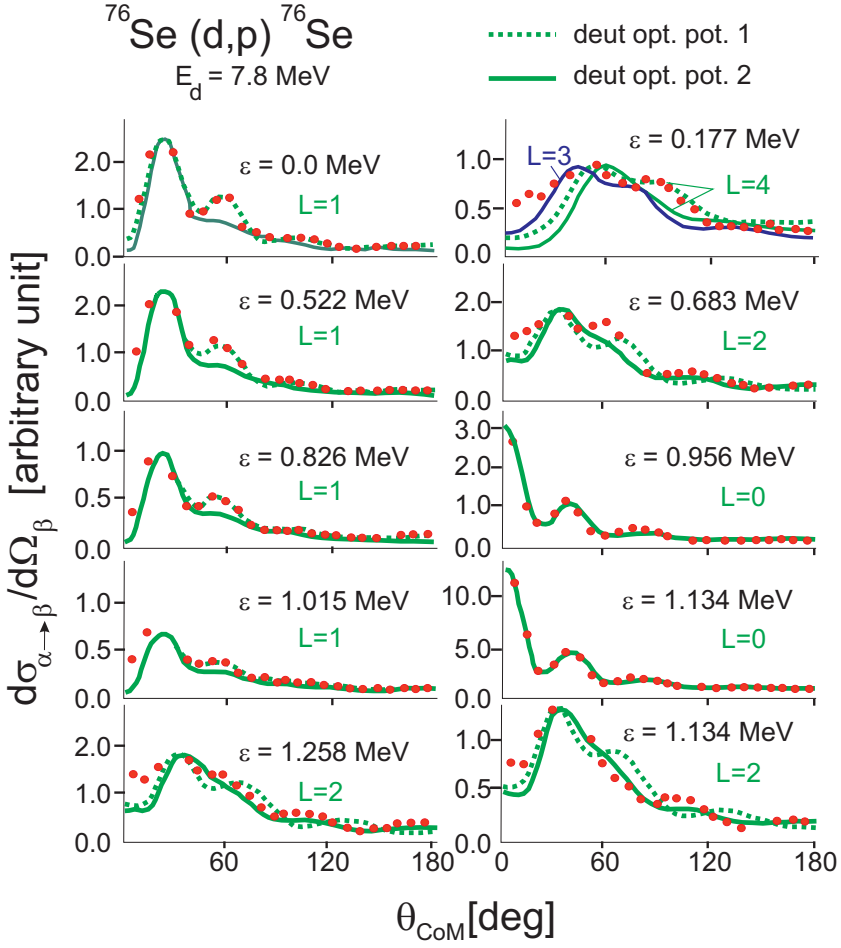


Figure 11.18: Experimental data for ^{76}Se(d,p^{77}Se reaction to several states of the final nucleus, compared with the DWBA calculations using optical potentials derived from the appropriate elastic scattering data. The full and dotted curves correspond to calculations using two different deuteron optical potentials that give equally good fits to the deuteron elastic scattering data [364].

Next figure Fig.11.18 shows unpolarized differential cross-sections of the reaction ^{76}Se(d,p)^{77}Se going to different low-lying excitation states in ^{77}Se (ground state $1/2^-$ ($L = 1$), $\epsilon = 0$ MeV; $9/2^+$ or $7/2^+$ ($L = 4$), $\epsilon = 0.177$ MeV; $1/2^-$ or $3/2^-$ ($L = 1$), $\epsilon = 0.522$ MeV; $3/2^+$ or $5/2^+$ ($L = 4$), $\epsilon = 0.682$ MeV; $1/2^-$ or $3/2^-$ ($L = 1$), $\epsilon = 0.826$ MeV; $1/2^+$ ($L = 0$) $\epsilon = 0.956$ MeV; $1/2^-$ or $3/2^-$ ($L = 1$), $\epsilon = 1.01$ MeV; $1/2^+$ ($L = 0$) $\epsilon = 1.134$ MeV; $3/2^+$ or $5/2^+$ ($L = 2$), $\epsilon = 1.258$ MeV; $3/2^+$ or $5/2^+$ ($L = 2$), $\epsilon = 1.424$ MeV (see [364]). Calculations of differential cross-sections in [364] was done for

two sets of deuteron optical potential parameters denoted in the Fig.11.18 as deut. opt. pot. 1 and deut. opt. pot. 2 and these parameters are given in the Table 2 of [364].

It is clearly seen from the Fig.11.18 that the shape of the differential cross-section for each neutron level of the final nucleus depends strongly on the orbital momentum L of the neutron single-particle state of the final nucleus. That means we can determine orbital momentum L from the shape of the (d,p) differential cross-section corresponding to each excitation state of the final nucleus and in such a way to obtain quantum characteristics of low-lying states in the final nucleus. This procedure was successfully used in the past for many nuclei (see e.g. [352, 351]).

The DWBA calculations for (d,p) reaction discussed above were used as a simple examples of the theoretical determination of cross-sections of direct reactions with one nucleon transfer. The DWBA and coupled channel Born approximations (CCA) can be used also for reaction with more nucleons transfer (see e.g. [352, 351]). The method is more complicated but the ideas are similar however detail discussion of multi-nucleon transfer reactions is beyond the scope of this textbook.

Although the DWBA method is known for more 5 decades the approach has been used intensively up to now, e.g. for the determination of cross-sections of reactions important for astrophysics (see e.g. [365]). As it was mentioned in the introductory section 11.1 in the case of the compound nucleus reaction $a + A \to C \to b + B$, the impacting particle a is cached by the target nucleus A and the compound nucleus C is formed in its excitation state. The energy brought by the impacting particle is fully absorbed by the compound nucleus and spread among all its nucleus. After some time, which is several orders of magnitude longer in the comparison with the time of the corresponding direct reactions, the compound nucleus decays to several final channels with the particular channel $b + B$ among them. We also know from the previous sections of the Chapter 11 that both mechanisms can occur simultaneously and that the given reaction $a + A \to b + B$ goes on partly as the direct reaction and partly through the CN. Which mechanism prevails it depends om the energy of the final particle b and on the excitation energy of the final nucleus.

11.5 Compound nucleus reactions

Reactions going through compound nucleus (CN) represent the second, complementary to the direct nuclear reactions, mechanism of the nuclear reactions with heavier nuclei. As it was mentioned in the introductory section 11.1 in the case of the compound nucleus reaction $a+A \to C \to b+B$, the impacting particle a is cached by the target nucleus A and the compound nucleus C is formed in its excitation state. The energy brought by the impacting particle is fully absorbed by the compound nucleus and spread among all its nucleus. After some time, which is several orders of magnitude longer in the comparison with the time of the corresponding direct reactions, the compound nucleus decays to several final channels with the particular channel $b + B$ among them. We also know from the previous sections of the Chapter 11 that both mechanisms can occur simultaneously and that the given reaction $a + A \to b + B$ goes on partly as the direct reaction and partly through the CN. Which mechanism prevails it depends on the energy of the final particle b and on the excitation energy of the final nucleus B.

In the introductory section 11.1 (see the discussion connected with the Fig.11.1) it was shown that in the lowest energies of the final particle b (which, as a consequence of the conserving energy law, corresponds to the highest excitation energies of the final nucleus B) the compound nucleus mechanism is dominant while opposite is true if the final particle energy is close to the energy brought to the system $a + A$ by the impacting particle a (and consequently the excitation energy of the final nucleus B is amall, close to zero). The Fig.11.1 shows also usual situation when for low energies of final particles, where the CN mechanism is dominant, the cross-section is usually smooth in the dependence on E_b. It was already demonstrated in the previous subsections that the CN is usually excited in high energies where the energy density of the CN eigen-states is very high (and consequently the energy distance D between CN excitation levels is low) and corresponding peaks in the differential cross-section as a function of E_b are very narrow (the average width Γ of the CN state peaks is very small). The fact, if the narrow and dense peaks connected with the individual CN excitation states can be or not be observed in the dependence of cross-section on E_b, is given by the relation between D_{CN}, Γ_{CN}, and energy smearing ΔE_a of the impacting band of initial particles a. Further possibilities of the dependency of the CN cross-section on the energy E_b of the final particles b for different relations of ΔE_a, Γ_{CN} and D_{CN} are summarized.

1. If $\Delta E_a < \Gamma_{CN} < D_{CN}$ (see (11.1) then excitation states of the CN (that means the eigen-states of the H_{QQ} Hamiltonian (see (11.16) and the Paragraph 11.2.2.2) are well separated and the cross-section has significant resonance character where each narrow resonance is connected with one NC excitation state. The energy smearing ΔE_a is so small that maximally one CN state falls into the each interval ΔE_a of energy. However, because usual values of Γ_{CN} and D_{CN} are units of eV and usual values of ΔE_a are bigger than units and tents of KeV the inequality (11.1) is not usually fulfilled (the exception is the neutron capture reactions which will be discussed in the Chapter 12). Nevertheless if we admit the validity of (11.1) then, as is described in details in the Paragraph 11.2.2.2, the reaction matrix $\mathcal{T}_{\beta\alpha}$ ($\alpha = a + A$, $\beta = b + B$) is given by the second term in (11.52) which gives the resonance character of the CN reaction cross-section (so called one-channel Breight-Wigner resonance formula (11.52) for $\mathcal{T}_{\beta\alpha}$).

2. If $\Delta E_a < \Gamma_{CN} \approx D_{CN}$ then two neighbouring levels of the CN overlap each other. In this case we can use also Breight-Wigner resonance expression for the reaction matrix element $\mathcal{T}_{\beta\alpha}$ but in the multi-channel version - see the second CN term in (11.61).

3. If $\Delta E_a < \Gamma_{CN}$ but $\Gamma_{CN} > D_{CN}$ then many CN levels mutually overlap and fluctuations are observed in the $\alpha \to \beta$ reaction cross-section dependencies on the energy E_b. However, these fluctuations have complicated character and it is not possible to connect them with contributions from individual CN excitations.

4. If $\Delta E_a > \Gamma_{CN} \approx D_{CN}$ (usual situation) then many CN states can be excited by the impacting band of particles a and the $\alpha \to \beta$ reaction cross-section is smooth without any peaks and fluctuations in the dependence on E_b. Then the cross-section should be analyzed in the framework of some statistical approach using some averaging techniques,

The CN mechanism is applicable mainly for low energies of the final particles b (less than 10 MeV) where its contribution to the total cross-section of the reaction $\alpha \to \beta$ is dominant. For higher energy E_b of particle b (starting from $\approx$ 15 MeV) the contribution of the CN mechanism to $\sigma_{\alpha\to\beta}$ is small and the direct reaction mechanism is the main mechanism for the reaction (see the Fig.11.1). However there is no any sharp border from which we can say that the only direct reaction mechanism is relevant for the description of

the reaction $\alpha \to \beta$ and that the CN mechanism is fully negligible. Even for higher energies E_b there is always nonzero part of the reaction $\alpha \to \beta$ going through compound nucleus.

11.5.1 Statistical theory of compound nucleus reactions (Hauser-Feshbach approach)

In this subsection we suppose that the given reaction $a + A \to b + B = B$ goes on according to the CN mechanism. That means the energy brought to the system $a + A = b + B$ by the incoming particle is divided between the final particle b and the target nucleus B so that the CN mechanism is dominant and the direct reaction can be neglected. If we accept this assumption we can say that the initial channel $\alpha \equiv a + A$ can initiate elastic scattering $a + A \to a + A$ and all inelastic final channels are formed through the compound nucleus. From (11.151) we know that the integral cross-section for inelastic processes is given by (in the contrast to the expression (11.151) here we do not consider spins and orbital moments of a, A, b, B),

$$\sigma_\alpha^{(CN)} \approx \frac{\pi}{k_\alpha^2}\left(1 - |S_{\alpha\alpha}|^2\right) \equiv \frac{\pi}{k_\alpha^2}\, T_\alpha \tag{11.243}$$

where we introduced so called transmission coefficient $T_\alpha \equiv (1-|S_{\alpha\alpha}|^2)$. From discussions above it is also known that the CN excitation states, excited after the absorption of the particle a, cause the narrow resonances in the cross-section $\sigma_\alpha^{(CN)}$, usually much narrower than the energy smearing of the incoming band of particles a - see the case 4. above, $\Delta E_a > \Gamma_{CN} \approx D_{CN}$. So in order to obtain more realistic cross-section $\sigma_\alpha^{(CN)}$ of the forming of the CN eigen states (according to our assumption during the formation of the CN the only open channel is the elastic channel $a + A \to a + A$ and all other inelastic channels are connected with the CN, therefor the CN Hamiltonian can be identified with the Q- space Hamiltonian $\hat{H}_{QQ}$ - see (11.16)) with energies falling to the energy interval ΔE_a around the energy $E_\alpha \equiv E_a$. So it is more consistent to rewrite (11.243) in the following averaged form,

$$\sigma_\alpha^{(CN)} \approx \frac{\pi}{k_\alpha^2}\left(1 - |\langle S_{\alpha\alpha}\rangle|^2\right) \equiv \frac{\pi}{k_\alpha^2}\, T_\alpha \tag{11.244}$$

The transmission coefficient T_α in (11.244) can be determined from the deff-inition,

$$T_\alpha = 1 - |\langle S_{\alpha\alpha}\rangle|^2 \tag{11.245}$$

where $\langle S_\alpha \rangle$ is the averaged elastic scattering S- matrix element which can be obtained from the optical model for elastic scattering using some averaging techniques described in the Subsection 11.2.2.3 (see also the width-fluctuation correction described in [351], pages 199-292, and it will be discussed also in the end of this subsection). So summarizing, the cross-section (11.244) can be understood as the cross-section of the formation of the CN through the initial channel $\alpha \equiv a + A$ because this is the cross-section of all inelastic processes initialized by the channel α and according to our assumption all inelastic process goes on through the CN.

In order to determine the cross-section of the concrete reaction $\alpha = a + A \to b + B = \beta$ it is necessary to have not only the elastic scattering S- matrix element $S_{\alpha\alpha}$ but also the non-diagonal averaged matrix element $\langle S_{\beta\alpha} \rangle \equiv \langle S_{\alpha\to\beta} \rangle$. Then the cross-section $\sigma^{(CN)}_{\alpha\to\beta}$ is given by (11.150),

$$\sigma^{(CN)}_{\alpha\to\beta} \approx \frac{\pi}{k^2_\alpha} \left| \langle S_{\beta\alpha} \rangle \right|^2 \tag{11.246}$$

where, similarly as in (11.243), we simplify the expression (11.150) into the spinless form. Purely theoretically the non-diagonal matrix elemen $\langle S_{\beta\alpha} \rangle$ can be determined by the abstract Feshbach theory described in the Section 11.3 but, as was mentioned several times, the Feshbach theory is too formal for practical application. Therefor in the paper [366] H. Feshbach and W. Hauser formulated their method for practical calculations. This method is based on the assumption of the hypothesis of the independence of the CN decay and formation (see the expr. (11.3) and on the reciprocity theorem giving the the relation between the S- matrix elements $S_{\alpha\to\beta}$ of the process $\alpha \to \beta$ and $S_{\bar\beta\to\bar\alpha}$ of the time-reversed process (see (11.175)).

According to the reciprocity theorem (see (11.175)),

$$\langle S_{\alpha\to\beta} \rangle = \langle S_{\bar\beta\to\bar\alpha} \rangle \tag{11.247}$$

and from (11.246),

$$\begin{aligned} \sigma^{(CN)}_{\alpha\to\beta} \approx \frac{\pi}{k^2_\alpha} \left| \langle S_{\alpha\to\beta} \rangle \right|^2 \quad , \quad \sigma^{(CN)}_{\bar\beta\to\bar\alpha} \approx \frac{\pi}{k^2_\beta} \left| \langle S_{\bar\beta\to\bar\alpha} \rangle \right|^2 \\ \Rightarrow \ \left| \langle S_{\alpha\to\beta} \rangle \right|^2 = \frac{k^2_\alpha \, \sigma^{(CN)}_{\alpha\to\beta}}{\pi} \quad , \quad \left| \langle S_{\bar\beta\to\bar\alpha} \rangle \right|^2 = \frac{k^2_\beta \, \sigma^{(CN)}_{\bar\beta\to\bar\alpha}}{\pi} \end{aligned} \tag{11.248}$$

and the substitution of (11.248) into (11.247) gives,

$$\frac{k^2_\alpha \, \sigma^{(CN)}_{\alpha\to\beta}}{\pi} = \frac{k^2_\beta \, \sigma^{(CN)}_{\bar\beta\to\bar\alpha}}{\pi} \quad \Rightarrow \quad k^2_\alpha \, \sigma^{(CN)}_{\alpha\to\beta} = k^2_\beta \, \sigma^{(CN)}_{\bar\beta\to\bar\alpha} \tag{11.249}$$

The hypothesis of the independence of the CN formation and decay can be mathematically expressed by the expression (11.3) giving the cross-section of the reaction $a + A \to C \to b + B$ as the product of the cross-section $\sigma_{\alpha}^{(CN)}$ of the CN creation and the probability of its decay into the channel β,

$$\sigma_{\alpha\to\beta}^{(CN)} = \sigma_{\alpha}^{(CN)}\, P_{\beta} \approx \boxed{\begin{array}{c}\text{see}\\(11.244)\end{array}} \approx \frac{\pi\, T_{\alpha} P_{\beta}}{k_{\alpha}^{2}}$$

$$\sigma_{\bar{\beta}\to\bar{\alpha}}^{(CN)} \approx \frac{\pi\, T_{\bar{\beta}} P_{\bar{\alpha}}}{k_{\beta}^{2}} \tag{11.250}$$

and the substitution of (11.250) into (11.249) yields,

$$\lambda \equiv \frac{P_{\bar{\alpha}}}{T_{\alpha}} = \frac{P_{\beta}}{T_{\bar{\beta}}} \tag{11.251}$$

where λ is the constant which can be determined from the normalization of the CN decay,

$$\sum_{\alpha} P_{\bar{\alpha}} = \sum_{\beta} P_{\beta} = 1 \quad \Rightarrow \quad \lambda \sum_{\alpha} T_{\alpha} = 1 \quad \Rightarrow \quad \lambda = \frac{1}{\sum_{\alpha} T_{\alpha}} \tag{11.252}$$

so we have,

$$P_{\beta} = \boxed{\begin{array}{c}\text{see}\\(11.251)\end{array}} = \lambda\, T_{\bar{\beta}} = \boxed{\begin{array}{c}\text{see}\\(11.252)\end{array}} = \frac{T_{\bar{\beta}}}{\sum_{\gamma} T_{\gamma}} \tag{11.253}$$

and we should realize that in the denominator of (11.253) the sum over all open channels participates, that means the sum over elastic scattering channel and all open final channels related to the initial channel through the CN. The substitution of (11.253) into (11.250) gives the cross-section $\sigma_{\alpha\to\beta}^{(CN)}$ in the following form,

$$\sigma_{\alpha\to\beta}^{(CN)} = \frac{\pi\, T_{\alpha} T_{\bar{\beta}}}{k_{\alpha}^{2} \sum_{\gamma} T_{\gamma}} \tag{11.254}$$

This expression is known in the literature as the spinless version of the Hauser-Feshbach expression for the integral cross-section of the process $\alpha \to \beta$ going fully through the CN.

In the most cases the CN reaction $a + A \to C \to b + B$ involves particles and nuclei with nonzero spins and with nonzero mutual $a - A$ and $b - B$ orbital moments. If we want to take into account these spins and moments

we should perform corresponding averaging and summing for analyses of unpolarized and polarized cross-sections.

Let us investigate cross-section of the reaction $a + A \to C \to b + B$ going on through the compound nucleus C. Further we will introduce following notation: $\vec{I}_A$ is the internal angular momentum of the nucleus A, $\vec{i}_a$ stands for the spin of the particle a, $\vec{L}_\alpha$ represents the orbital momentum of the relative motion of the particle a and the nucleus A. Then the total angular momentum $\vec{J}$ of the system $a+A$ (that means simultanously the total angular momentum of the compound nucleus) reads,

$$\vec{J} = \vec{i}_a + \vec{I}_A + \vec{L}_\alpha \equiv \vec{j}_\alpha + \vec{L}_\alpha \tag{11.255}$$

where the symbol $\vec{j}_\alpha \equiv \vec{i}_a + \vec{I}_A$ is the internal angular momentum of the channel α. Similarly we will introduce equivalent symbols for the channel β,

$$\vec{J} = \vec{i}_b + \vec{I}_B + \vec{L}_\beta \equiv \vec{j}_\beta + \vec{L}_\beta \tag{11.256}$$

where, according to the conservation law for the total angular momentum the momentum, $\vec{J}$ is the same for the channel α and β (and for the compound nucleus states with the given angular moments $\vec{J}$).

Further we suppose that in the energy interval ΔE_α around the energy E_α of the relative motion in the initial channel α we always have some states of the compound nucleus (or of the system $a + A = C$ with the angular momentum J). The correspondingg cross-section of the forming the compound nucleus C in the state with the given J of the total angular momentum and its projection M is (see (11.244) which is modify now involving the spins and relative motion angular momentum in the initial channel α),

$$\sigma^{(CN)\,JM}_{\alpha L_\alpha j_\alpha} = \frac{\pi}{k_\alpha^2}\,(2L_\alpha + 1)\;\, T^{(CN)\,(J)}_{\alpha L_\alpha j_\alpha}\;\, \left|\, C^{JM}_{L_\alpha 0\, j_\alpha M}\,\right|^2 \tag{11.257}$$

where $|JM\rangle = C^{JM}_{L_\alpha 0\, j_\alpha M}\, |L_\alpha 0\rangle\, |j_\alpha M\rangle$ is the wave function (ket) of the compound nucleus in the state with the angular momentum J and its projection M (where we suppose that the coordinate frame axis z is penpendicular to the orbital momentum $\vec{L}_\alpha$ or that this axis z is oriented paralelly with the linear momentum $\vec{k}_\alpha$ of the relative motion in the channel α). Now the transmission coefficient $T^{(CN)\,(J)}_{\alpha L_\alpha j_\alpha}$ depends on L_α, j_α, and J (we suppose that the interaction between a and A is rotational invariant and therefor the transmission coefficient is not dependent on M).

The wave function (ket) $|JM\rangle$ of the compound nucleus can be decomposed into the orbital ket $|L_\beta M_\beta\rangle$ and the intrinsic ket $|j_\beta M - M_\beta\rangle$ in the

final channel β,

$$|JM\rangle = \sum_{M_\beta} C^{JM}_{L_\beta M_\beta j_\beta M-M_\beta} \, |L_\beta M_\beta\rangle \, |j_\beta M - M_\beta\rangle$$

or

$$\langle\theta_\beta\phi_\beta|JM\rangle = \sum_{\beta} C^{JM}_{L_\beta M_\beta j_\beta M-M_\beta} \, Y_{L_\beta M_\beta}(\theta_\beta\phi_\beta) \, |j_\beta M - M_\beta\rangle \tag{11.258}$$

where $(\theta_\beta, \phi_\beta)$ are coordinate angles of the relative $b - B$ vector in the CoM frame. Therefor the probability of the decay of the compound nucleus with the total angular momentum J with its projection M into the channel β with the quantum numbers $\beta L_\beta M_\beta j_\beta M - M_\beta$ is not given only by P_β (see (11.250)) but by,

$$P_\beta \, \Big| \, C^{JM}_{L_\beta M_\beta \, j_\beta M-M_\beta} \, \Big|^2 \, \Big| Y_{L_\beta M_\beta}(\theta_\beta, \phi_\beta) \Big|^2 \tag{11.259}$$

and the corresponding expression for the polarized differential cross-section of the process $\alpha L_\alpha j_\alpha M \to JM \to \beta L_\beta j_\beta M$ is,

$$\frac{d\sigma^{(CN)\,(JM)}_{\alpha L_\alpha j_\alpha \to \beta L_\beta j_\beta}}{d\Omega_\beta}(\theta, \phi) = \sum_{M_\beta} \sigma^{(CN)}_{\alpha L_\alpha j_\alpha} P_\beta \Big| \, C^{JM}_{L_\beta M_\beta \, j_\beta M-M_\beta} \, \Big|^2 \, \Big| Y_{L_\beta M_\beta}(\theta, \phi) \Big|^2 =$$

$$= \boxed{\begin{array}{c}\text{see} \\ (11.257)\end{array}} =$$

$$= \frac{\pi}{k_\alpha^2}(2L_\alpha + 1) \, T^{(CN)\,(J)}_{\alpha L_\alpha j_\alpha} \, \Big| \, C^{JM}_{L_\alpha 0 \, j_\alpha M} \, \Big|^2$$

$$\sum_{M_\beta} P_\beta \Big| \, C^{JM}_{L_\beta M_\beta \, j_\beta M-M_\beta} \, \Big|^2 \, \Big| Y_{L_\beta M_\beta}(\theta, \phi) \Big|^2 \tag{11.260}$$

where

$$P_\beta = \boxed{\begin{array}{c}\text{see (11.253)} \\ \text{modified for given J}\end{array}} = \frac{T^{(CN)\,(J)}_{\bar\beta L_\beta j_\beta}}{\sum_{\gamma L_\gamma j_\gamma} T^{(CN)\,(J)}_{\gamma L_\gamma j_\gamma}} \tag{11.261}$$

Finally we rewrite the expression (11.260) into the following form,

$$\frac{d\sigma^{(CN)\,(JM)}_{\alpha L_\alpha j_\alpha \to \beta L_\beta j_\beta}}{d\Omega_\beta}(\theta, \phi) = \frac{\pi}{k_\alpha^2} \, A^{(JM)}_{j_\alpha L_\alpha ; j_\beta L_\beta}(\theta, \phi) \;\; \frac{T^{(CN)\,(J)}_{\alpha L_\alpha j_\alpha} \; T^{(CN)\,(J)}_{\bar\beta L_\beta j_\beta}}{\sum_{\gamma L_\gamma j_\gamma} T^{(CN)\,(J)}_{\gamma L_\gamma j_\gamma}} \tag{11.262}$$

where

$$A^{(JM)}_{j_\alpha L_\alpha; j_\beta L_\beta}(\theta,\phi) = \sum_{M_\beta} \mid C^{JM}_{L_\beta M_\beta\, j_\beta M - M_\beta} \mid^2 \mid C^{JM}_{L_\alpha 0\, j_\alpha M} \mid^2 |Y_{L_\beta M_\beta}(\theta,\phi)|^2 \quad (11.263)$$

The expression (11.262) represents the polarized differential cross-section of the reaction $a + A \to C \to b + B$ because it depends on projections m_a, m_A, m_b, m_B of angular momenta $\vec{i}_a$, $\vec{I}_A$, $\vec{i}_b$, $\vec{I}_B$ of particle a, nucleus A, particle b, nucleus B, respectively (we should realize that we work in the CoM coordinate frame where the projection M_α of the orbital momentum $\vec{L}_\alpha$ in the channel α is zero and therefor the projection M of the total angular momentum $\vec{J}$ of the compound nucleus is $M = m_a + m_A = m_b + m_B + M_\beta$. As a result in reality the projection M_β in (11.263) is fixed with the value $M_\beta = m_a + m_A - m_b - m_B$ and effectively there is no sum over M_β in (11.263)).

In order to obtain unpolarized differential cross-section comparable with experimetal values we should average over m_a and m_A (or over M) and sum over L_α, j_α, L_β, j_β and $J = |j_\alpha - L_\alpha|, \cdots, j_\alpha + L_\alpha$,

$$\frac{d\sigma^{(CN)}_{\alpha\, i_a I_A \to \beta\, i_b I_B}}{d\Omega_\beta}(\theta,\phi) = \frac{\pi}{k^2_\alpha} \sum_{j_\alpha L_\alpha j_\beta L_\beta JM} \frac{(2L_\alpha+1)}{(2i_a+1)(2I_A+1)} A^{(JM)}_{j_\alpha L_\alpha; j_\beta L_\beta}(\theta,\phi)\, \frac{T^{(CN)\,(J)}_{\alpha L_\alpha j_\alpha}\; T^{(CN)\,(J)}_{\bar{\beta} L_\beta j_\beta}}{\sum_{\gamma L_\gamma j_\gamma} T^{(CN)\,(J)}_{\gamma L_\gamma j_\gamma}} \quad (11.264)$$

where the following triangle inequalities should be fulfilled (see (11.205) and (11.256),

$$\begin{aligned} |I_A - i_a| \le j_\alpha \le I_A + i_a \qquad & |j_\alpha - L_\alpha| \le J \le j_\alpha + L_\alpha \\ |I_B - i_b| \le j_\beta \le I_B + i_b \qquad & |j_\beta - L_\beta| \le J \le j_\beta + L_\beta \end{aligned} \quad (11.265)$$

together with the parity conservation law,

$$\pi_a \pi_A (-1)^{L_\alpha} = \pi_b \pi_B (-1)^{L_\beta} \quad (11.266)$$

where π_a, π_A, π_b, and π_B are internal parities of the particle a, the nucleus A, the particle b and the nucleus B, respectively. The expression (11.264) can be further modified using the alsgebra of angular momentum coupling (see [351] p.288 or [367]) into the following expression without the dependence on

ϕ,

$$\frac{d\sigma^{(CN)}_{\alpha\, i_a\, I_A\to\beta\, i_b I_B}}{d\Omega_\beta}(\theta) = \frac{\pi}{k_\alpha^2}\sum_{j_\alpha L_\alpha j_\beta L_\beta JM}\frac{(2L_\alpha+1)}{(2i_a+1)(2I_A+1)} \tilde{A}^{(JM)}_{j_\alpha L_\alpha; j_\beta L_\beta}(\theta)\,\frac{T^{(CN)\,(J)}_{\alpha L_\alpha j_\alpha}\; T^{(CN)\,(J)}_{\bar{\beta} L_\beta j_\beta}}{\sum_{\gamma L_\gamma j_\gamma} T^{(CN)\,(J)}_{\gamma L_\gamma j_\gamma}} \tag{11.267}$$

where

$$\tilde{A}^{(JM)}_{j_\alpha L_\alpha; j_\beta L_\beta}(\theta) = \frac{(2L_\beta+1)(2J+1)}{4\pi} \Big|\sum_L \begin{pmatrix} L & L_\alpha & L_\alpha \\ 0 & 0 & 0 \end{pmatrix}\begin{pmatrix} L & L_\beta & L_\beta \\ 0 & 0 & 0 \end{pmatrix} W(JJL_\alpha L_\alpha;\, Lj_\alpha)\, W(JJL_\beta L_\beta;\, Lj_\beta)\, P_L(\cos\theta)\Big|^2 \tag{11.268}$$

where the summation over L goes over values from the interval $0 \le L \le min(2L_\alpha, 2L_\beta, 2J)$ and L is even, and $\begin{pmatrix} a & b & c \\ d & e & f \end{pmatrix}$ are 3-j symbols (see (A.5)), and $W(a,b,c,d;ef)$ are so called Racah coefficients related to the 6-j symbols $\begin{Bmatrix} a & b & c \\ d & e & f \end{Bmatrix}$ (see (A.8)) by,

$$\begin{Bmatrix} a & b & c \\ d & e & f \end{Bmatrix} = (-1)^{a+b+d+e}\, W(abcd;\, ef)$$

Three conclusions follow from the final expressions (11.267) and (11.268)

- the expression for $\tilde{A}^{(JM)}_{j_\alpha L_\alpha; j_\beta L_\beta}(\theta)$ is symmetric with respect to $\theta = 90^o$ (this is a consequence of the fact that L are even and for even L $P_L(\cos\theta)$ is symmetric according to $\theta = 90^o$);
- if $L_\alpha = L_\beta = 0$ and $J = 0$ or $1/2$, then $L = 0$ and $\tilde{A}^{(JM)}_{j_\alpha L_\alpha; j_\beta L_\beta}(\theta)$ is not dependent on $\theta \Rightarrow$ for low energies where s- waves are dominant the angular distribution of particles b is almost isotropic;
- the anisotropy grows up with the increasing of L, that means if big values L dominate in (11.268) then we can expect higher anisotropy in the differential cross-section.

Transmission coefficients $T^{(CN\,(J)}_{\alpha\, L_\alpha\, j_\alpha}$, $T^{(CN\,(J)}_{\beta\, L_\beta\, j_\beta}$ are determined from the definition expression (11.245). The diagonal S- matrix elements $\langle S_{\alpha\alpha}\rangle$ or $\langle S_{\beta\beta}\rangle$

in (11.245) are connected through (Q.25) and (Q.27) with the elastic scattering amplitud which is directly related to the optical potential $\hat{U}_{\alpha}^{(opt)}(\vec{r})$ or $\hat{U}_{\beta}^{(opt)}(\vec{r})$ (see (11.193)). That means the transmission coefficients $T_{\alpha L_\alpha j_\alpha}^{(CN)\,(J)}$ or $T_{\beta L_\beta j_\beta}^{(CN)\,(J)}$ can be determined by the analysis of the elastic scattering in the channel $\alpha = a + A$ or $\beta = b + B$. For the determination of transmission coefficients generally we should known the elastic scattering experimental data on excited nuclei but they are not available. Therefor it is usually assumed that the optical potential is more or less independent on the excitation of the nucleus during elastic scattering and therefor transmission coefficients corresponding to channels with nucleus excited states are approximated by transmission coefficients for nucleus ground state. This way of the determination of the transmission coefficients is also used for all coefficients involved in the sum in the determination of (11.267).

The CN cross-section (11.207) requires knowledge of spins of all states involved in the denominator sum in this expression. In general case there are thousands and even millions of such states in the denominator of (11.267). Therefor for this sum the following approximation is often used,

$$\sum_{\gamma L_\gamma j_\gamma} T_{\gamma L_\gamma j_\gamma}^{(CN)\,(J)} \approx {\sum_{\gamma L_\gamma j_\gamma}}' T_{\gamma L_\gamma j_\gamma}^{(CN)\,(J)} + \sum_{\gamma Lj} \int dE\, w_j(E)\; T_{\gamma Lj}^{(CN)\,(J)}(E) \qquad (11.269)$$

where $w_J(E)$ is the energy density of CN states with the angular momentum J (which will be discussed in the next chapter). The symbol $\sum'_{\gamma LJ}$ means the sum over channels leading to the several lowest discrete levels in the final nucleus. All other channels are involved in the second term in (11.269). The division of all channels between two terms in (11.269) is more or less arbitrary. For instance this division is determined by the excitation energy above which the spins of excited states are not known (corresponding levels are so much dense that characteristics of individual levels cannot be determined) but we can obtain some phenomenological dependence of the energy density $w_J(E)$ (see [351], section 11.3 for details).

Hauser-Feshbach theory of the CN reactions is based on the assumption of the independence of the formation and the decay of the CN. This assumption is quite strong and it is the reason why the cross-section expression (11.154) (for spinless case) or (11.262) (if spins of reaction participants are taken into account) is not sufficiently accurate for the comparison with experimental cross-section. In the reality the process of formation and decay of the CN are not completely independent. On the other hand the Feshbach theory of

nuclear reactions, discussed in the Section 11.2, which is formally precise, is not applicable for practical calculations as well. For instance the second term in (11.52) for the CN part of the $\mathcal{T}$- matrix element,

$$\mathcal{T}_{\beta\alpha}^{(CN)} \approx \frac{g_\alpha\, g_\beta}{(E - E_s) + \frac{i}{2}\Gamma_s} \tag{11.270}$$

giving the CN cross-section $\sigma_{\alpha\to\beta}^{(CN)} \approx |\mathcal{T}_{\beta\alpha}^{(CN)}|^{\,2}$ in the form of the one-channel Breight-Wigner expression for the CN reaction cross-section ($\Gamma_\alpha = g_\alpha^2$, $\Gamma_\beta = g_\beta^2$)

$$\sigma_{\alpha\to\beta}^{(CN)} = \frac{\pi}{k_\alpha^2}\, \frac{\Gamma_\alpha\, \Gamma_\beta}{(E - E_s)^2 + \frac{1}{4}\Gamma_s^{\,2}} \tag{11.271}$$

with g_α and g_β defined by (11.45) and (11.46) is formally precise but it is valid only in the narrow surroundings of the eigen- energy of the CN (or $\hat{H}_{QQ}$) Hamiltonian which is not usually known. It is also known that there are usually thousands (and even more) of such eigen-energies in the experimental smearing energy interval ΔE_α around the average a- particle beam energy E_α and it is not possible to involve all of them in the numerical calculations for usual values of ΔE_α. These facts make impossible numerical calculations using only pure Feshbach formal theory. That is why in the sixties the correction method, so called the width-fluctuation correction method, was developed (see e.g. [351] or [368] and citations therein) using averaging techniques applied for Hauser-Feshbach approach in the connection with the Breight-Wigner formula (11.271) in order to modify the expression (11.254) into the following one [16]

$$\langle \sigma_{\alpha\to\beta}^{(CN)} \rangle = \frac{\pi}{k_\alpha^2}\, \frac{T_\alpha\, T_\beta}{\sum_\gamma T_\gamma}\, W_{\alpha\beta} \tag{11.272}$$

where the factor $W_{\alpha\beta}$ is derived e.g. in [351] or [369]. In order to calculate $W_{\alpha\beta}$ it is necessary to know the distribution of levels in the CN formed in the initial channel. This distribution may be calculated from the statistical model of nuclear excitations (it will be discussed in the next chapter 12), and a useful form is the Poter-Thomas distribution [370],

$$P(x)\, dx = \frac{1}{\sqrt{2\pi x}}\, e^{-x/2}\, dx \tag{11.273}$$

[16] Here we present only spinless expression for the cross-section. The expressions involving spins of participants in the reaction $\alpha \to \beta$ are not given here but the idea is same

where $x = \Gamma/\langle\Gamma\rangle$. In this form the distribution is normalized and has mean unity. This statistical approach finally gives following expression for $W_{\alpha\beta}$ [371]

$$W_{\alpha\beta} = (1 + 2\delta_{\alpha\beta}) \left(\sum_{\gamma} T_{\gamma} \right) \int_0^{\infty} dx \, (1 + 2xT_{\alpha})^{-1} \, (1 + 2xT_{\beta})^{-1} \, \prod_{\gamma} (1 + 2xT_{\gamma})^{-1/2} \tag{11.274}$$

and simultaneously if this CN resonance interference effect is taken into account the transmission coefficients T_α and T_β in (11.172) becomes (see [371]),

$$\begin{aligned} T_{\alpha} \to T_{\alpha}^{R} &= \frac{2}{Q_{\alpha}} \left[1 - \sqrt{1 - Q_{\alpha} T_{\alpha}} \right] \\ T_{\beta} \to T_{\beta}^{R} &= \frac{2}{Q_{\beta}} \left[1 - \sqrt{1 - Q_{\beta} T_{\beta}} \right] \end{aligned} \tag{11.275}$$

where Q_α and Q_β depends on the amplitudes of the nuclear states i the channel α and β. Since it is difficult to estimate Q_α and Q_β, calculations are usually made with some fixed value Q (usually $Q \approx 0$ or $Q \approx 1$).

So in real calculations the Hauser-Feshbach approach in the modified version with (11.272) and (11.275) is usually used. Some examples of the comparison of results of such calculations with corresponding experimental cross-sections are discussed in the next subsection.

11.5.2 Application of Hauser-Feshbach theory of the CN reactions

From the previous subsection we know that given reaction $\alpha \equiv a + A \to b + B \equiv \beta$ can pass of simultaneously as the direct reaction and the reaction going through the compound nucleus. It was also shown that which of these two mechanisms prevails it depends on the distribution of energy, brought by the initial channel α into the whole system $CN = a + A$, among all nucleons of this system and finally on the energy distribution between the final particle b and the final nucleus B. If some reaction $\alpha \to \beta$ is analyzed in the low-energy region of the relative $b - B$ motion of the final particle b with respect to the final nucleus B (that means, according to the energy conservation law, high excitation energy of the final nucleus) then one can expect that this reaction goes predominantly through the formation of the compound nucleus (see the Fig.11.1 and the text below it). In such a case the cross-section of the reaction $\alpha \to \beta$ is usually determined by means of the Hauser-Feshbach

formalism discussed in the previous subsection - see (11.254) for spinless case or (11.264) if spins of a, A, b, B are taken into account, eventually using (11.272) if the width-fluctuation correction is applied. In all these expressions the transmission coefficients T_α, T_β are determined in terms of the optical model with the optical potential fixed by the experimental elastic scattering cross-section in channels α, β.

Denominator, $\sum_\gamma T_\gamma$, in (11.254) and similar denominator in (11.264) or (11.272) is calculated using (11.269) where transission coefficients in the first term are again determined in terms of the optical model for all channels involved in the sum $\sum'_{\gamma L_\gamma j_\gamma}$. The rest of channels, involved in the second term in (11.269), is taken into account by means of phenomenological dependences of the energy level density $w_j(E)$ and of the transmission coefficient function $T^{(CN)\,(J)}_{\gamma Lj}(E)$ on the energy E.

However the Hauser-Feshbach formalism described above can be used only when the whole reaction $\alpha \to \beta$ goes only through the compound nucleus that means all probability flux from the initial channel α is exhausted for the formation of the CN and after it continues to the final channels β (no direct reaction mechanism). In the reality, even in the case when the CN reaction mechanism is dominant, some part of this probability flux from the channel α escapes into the final channel β directly as the prompt process without forming the CN. This is the reason why the CN cross-sections $\sigma^{(CN)}_{\alpha\to\beta}$ determined only by means of Hauser-Feshbach formalism are overestimated and should be reduced. Therefor the reduce factor is introduced as follows,

$$\sigma^{(CN)}_{\alpha\to\beta} - \sigma^{(direct)}_{\alpha\to\beta} = R\,\sigma^{(CN)}_{\alpha\to\beta} \quad \Leftrightarrow \quad R = 1 - \frac{\sigma^{(direct)}_{\alpha\to\beta}}{\sigma^{(CN)}_{\alpha\to\beta}} \tag{11.276}$$

This reduce factor R can be different for different final channels β and therefor the reduce factor $R_{\alpha\to\beta}$ is defined for each reaction $\alpha \to \beta$ and e.g. differential cross-section $d\sigma_{\alpha\to\beta}/d\Omega_\beta$ comparble with experimental values is,

$$\frac{d\sigma_{\alpha\to\beta}}{d\Omega_\beta} = R_{\alpha\to\beta}\,\Big(\,\frac{d\sigma^{Hauser-Feshbach)}_{\alpha\to\beta}}{d\Omega_\beta}\,\Big) \tag{11.277}$$

where $R_{\alpha\to\beta}$ is used as adjustable parametr by means of which the calculated Hauser-Feshbach angle distribution is normalized in the absolute values according to the experimental distribution (it is evident that $0 < R_{\alpha\to\beta} < 1$).

As an example of such calculations in the Fig.11.19 the differential cross-section of the reaction ^{31}P(p,α)^{28}Si is shown for two cases. The upper panel

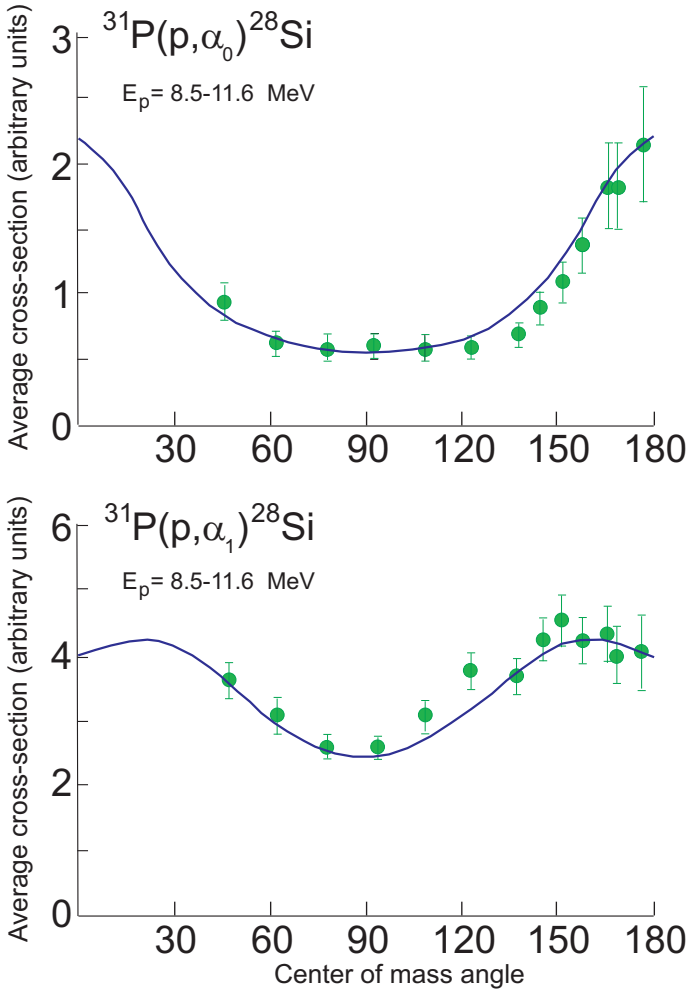


Figure 11.19: Averaged angular distribution of α-particles from the reaction ^{31}P(p,α)^{28}Si for two cases, the first one ^{31}P(p,α_0)^{28}Si corresponds to the ground state of the final nucleus ^{28}Si and the second one, ^{31}P(p,α_2)^{28}Si, to the first excited state of ^{28}Si (both averaged over proton energies $E_p = 8.5 - 11.6$ MeV). The solid curves represent the Hauser-Feshbach calculations. Both theoretical and experimental values are normalized at 177^o (taken from [372]).

involves the angular distribution of α- particles in the α-^{28}Si CoM frame when the final nucleus ^{28}Si stays in its ground state. In the lower panel the angular distribution is demonstrated when the final nucleus ^{28}Si is in its first excited state. In both panels the differential cross-section is averaged over the proton in-beam energy interval $E_p \in \langle 8.5 \text{ MeV}, 11.6 MeV \rangle$ and the theoretical and experimental values are normalized at 177^o (see [372]). One can see that both angular distributions of α- particles in the Fig.11.19 are symmetric with respect to the angle 90^o and that the differential cross-section with the first excited state in ^{28}Si (lower panel) is closer to the isotropic distribution in the comparison with the differential cross-section corresponding to the ground

state of ^{28}Si (upper panel). Both these features are in accordance with the CN reaction characteristics discussed above.

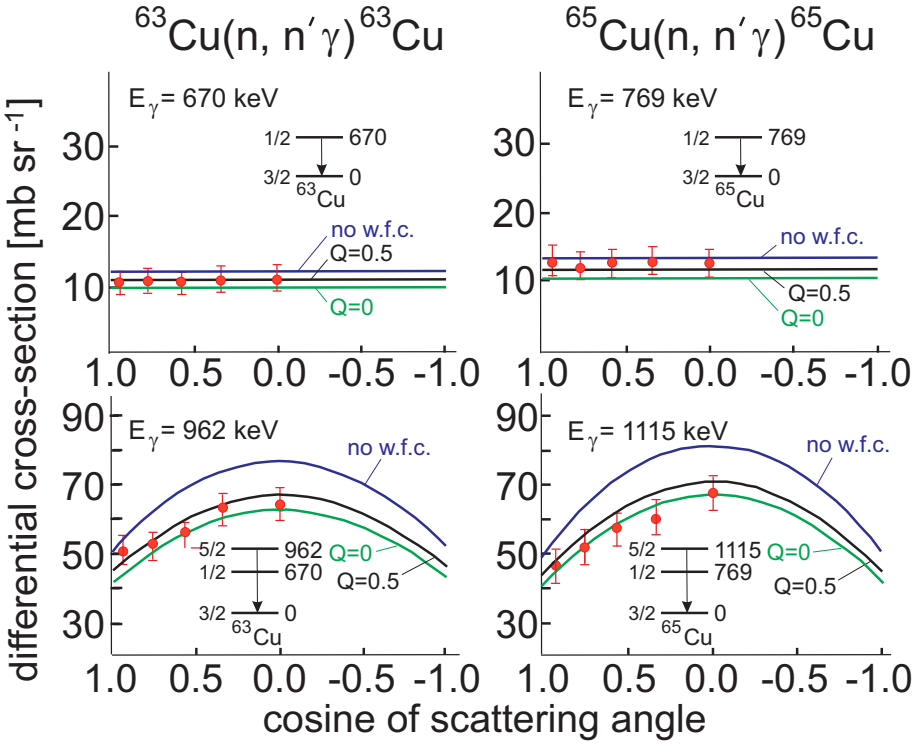


Figure 11.20: Experimental and theoretical angular distributions of photons from the reactions ^{63}Cu(n,n'γ)^{63}Cu (left panels) and ^{65}Cu(n,n'γ)^{65}Cu (right panels). The Hauser-Feshbach calculations for the cross-section of the inelastic scattering of neutrons leading to two excited states in ^{63}Cu and ^{63}Cu were made with and without the width-fluctuation correction, and those including it are labeled with the corresponding value of $Q_\alpha = 0$ and $Q_\beta = Q = 0,\ 0.5$ (see (11.275) used in calculations. The final nucleus state populations for individual excitations determined using the Hauser-Feshbach cross-section were then used for the calculation of theoretical photon angular distributions (taken from [373]).

The fact, that if in the given CN reaction the target and the final nucleus states have angular momenta very low (0, 1/2 or 3/2), with corresponding orbital momenta L_α ad L_β of partial waves in the cross-section (11.267) closed to zero, then the angular distributions of final particles are almost isotropic, is demonstrated in the Fig.11.20. This figure shows the angular distributions of photons produced in reactions ^{63}Cu(n,n'γ)^{63}Cu (left panels) and ^{65}Cu(n,n'γ)^{65}Cu (right panels) when the final nuclei are excited from the ground state $3/2^-$ to the first excited states $1/2^-$ for both ^{63,65}Cu (see upper panels) and to the second excited states $5/2^-$ for both ^{63,65}Cu (see lower panels). The experimental values of photon angular distributions are compared with theoretical ones calculated with the final nucleus populations

for individual excitations determined using the Hauser-Feshbach cross-section with and without the width-fluctuation corrections (see (11.272), (11.274), (11.275) with $Q = 0$ and $Q = 0.5$). One can see that upper panels (with partial s-waves in (11.267) demonstrate isotropic photon angular distributions while the lower panels (where not only partial s-waves participate in (11.267)) show anisotropic photon angular distributions. However in all cases the symmetry of angular distributions with respect to the angle 90^o remains.

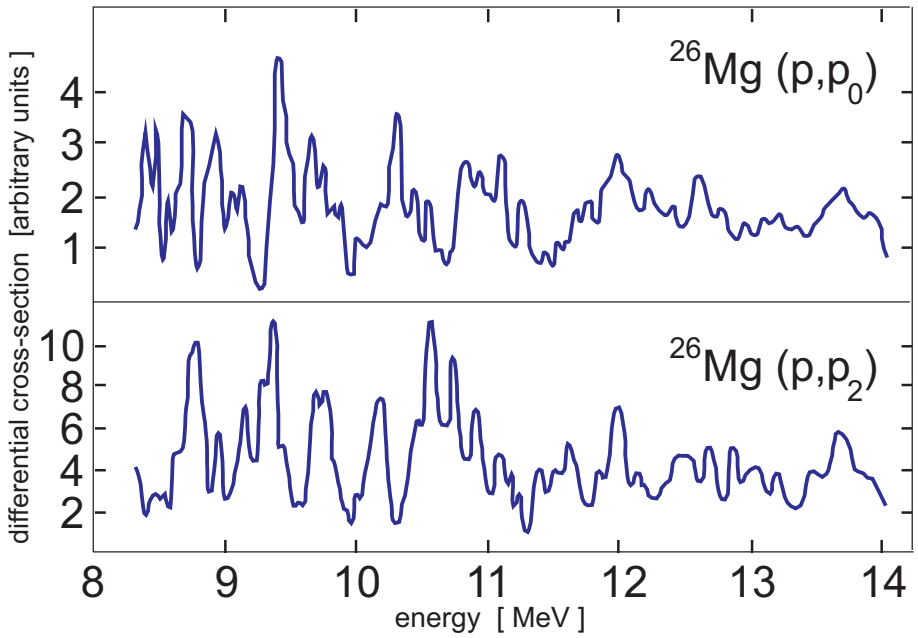


Figure 11.21: Excitation function for the reaction $^{26}\mathrm{Mg}(p, p_0)^{26}\mathrm{Mg}$ (going to the ground state of ^{26}Mg) and $^{26}\mathrm{Mg}(p, p_2)^{26}\mathrm{Mg}$ (going to the second excites state in ^{26}Mg), showing the degrease in the amplitude of fluctuations as the energy of protons increases. This is due to the increasing the contribution of direct process to the reaction (taken from [374]).

As it was already mentioned the Hauser-Feshbach formalism can be used only in the case when the given reaction goes on predominantly through the formation of the compound nucleus. So if we want to describe theoretically given reaction (using the Hauser-Feshbach approach or standard optical model method) we should know what reaction mechanism is dominant for given energy of impacting particles (compound nucleus or direct reaction mechanism). The simplest way for the determination what mechanism is dominant is to measure so called excitation function, that means the dependence of the differential cross-section $d\sigma_{\alpha\to\beta}/d\Omega_\beta$ on the energy E_α of the incoming particle a for the fixed scattering angle. If this excitation func-

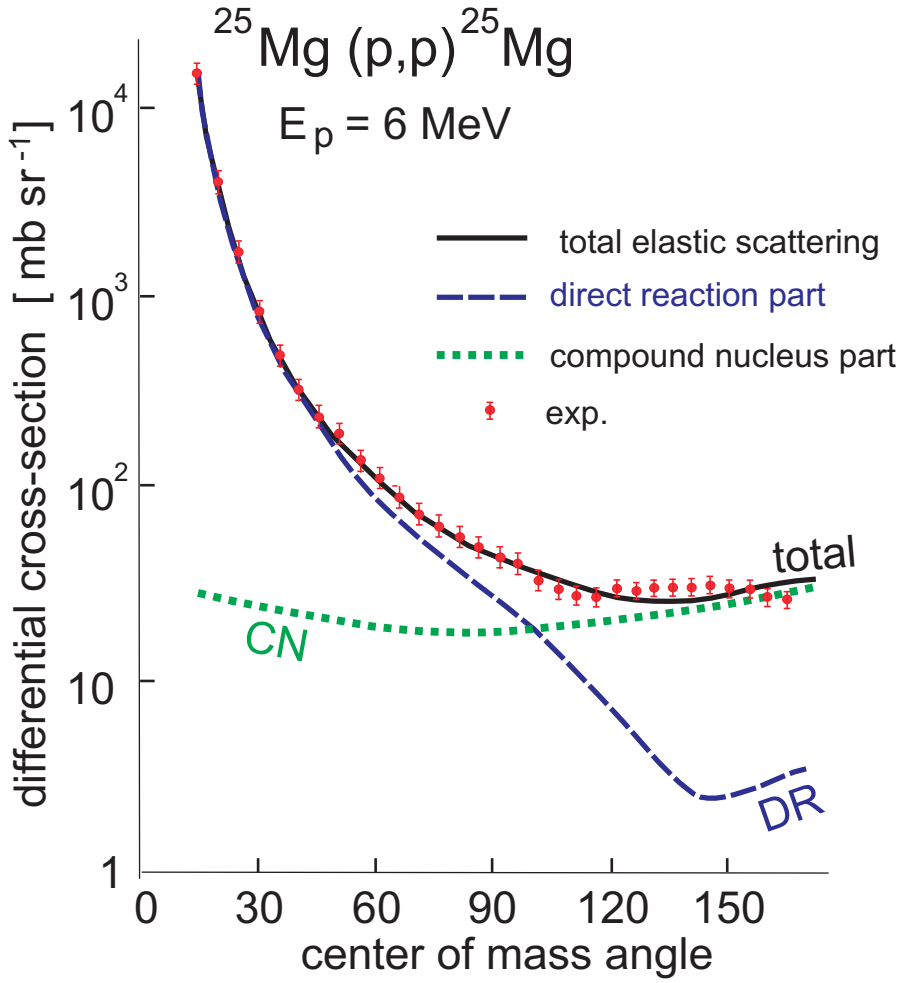


Figure 11.22: Differential cross-section for the elastic scattering of 6 MeV prons by ^{25}Mg. Experimental values are compared with theoretical values calculated by (11.279) (the curve denoted as total). The direct reaction part (the first term in (11.279)) and the compound nucleus part (the second term in)11.279) are shown as well (taken from [375]).

tion fluctuates between zero and values several times higher than its mean value then the transition $\alpha \to \beta$ goes almost predominantly through the compound nucleus. If opposite situation occurs and the strength function is a smooth function without significant fluctuations then the direct reaction mechanism is dominant. As an example the excitation function for the reactions $^{26}\mathrm{Mg}(p,p_0)^{26}\mathrm{Mg}$ (elastic scattering) and $^{26}\mathrm{Mg}(p,p_2)^{26}$ (the final nucleus ^{26}Mg is excited in the second excitation state) are demonstrated in the Fig.11.21. The figure shows that the fluctuations in the differential cross-section decrease with increasing proton energy E_p. Therefor for sufficiently high energies E_α of initial particles the CN effect can be neglected and given

reaction can be considered as the direct process. On the contrary the low energy E_α is characteristic for the compound nucleus mechanism where the Hauser-Feshbach approach can be used.

Starting from (11.276) the total cross-section of the process $\alpha \to \beta$ consists from the compound nucleus part and the direct reaction part,

$$\sigma_{\alpha\to\beta} = \sigma_{\alpha\to\beta}^{(direct)} + R_{\alpha\to\beta}\, \sigma_{\alpha\to\beta}^{(CN)} \tag{11.278}$$

where $\sigma_{\alpha\to\beta}^{(CN)}$ is calculated using Hauser-Feshbach formalism (see the Subsection 11.5.1) and $\sigma_{\alpha\to\beta}^{(direct)}$ is determined in the framework of the direct reaction mechanism (see the Section 11.4). The expression (11.278) valids not only for transmutation reactions ($\alpha \neq \beta$) but also for elastic and inelastic scattering. It is applicable for any energies of the impacting particles a and also for differential cross-sections,

$$\frac{d\sigma_{\alpha\to\beta}(\theta)}{d\Omega_\beta} = \frac{d\sigma_{\alpha\to\beta}^{(direct)}(\theta)}{d\Omega_\beta} + R_{\alpha\to\beta}\, \frac{d\sigma_{\alpha\to\beta}^{(CN)}(\theta)}{d\Omega_\beta} \tag{11.279}$$

where the factor $R_{\alpha\to\beta}$ is not dependent on the scattering angle θ. For instance in the Fig.11.22 the experimental cross-section of the elastic scattering ^{25}Mg(p,p)^{25}Mg is compared with the calculated one according to (11.279) (the curve denoted as total). The Fig.11.22 involves also the angle dependence of the first term in (11.279) (denoted as DR) and of the second term in (11.279) (denoted as CN). For angles $\theta < 90^o$ the contribution of the direct reaction part is dominant while for angles $\theta > 90^o$ the CN mechanism prevails (for the energy $E_p = 6$ MeV of protons).

11.6 Concluding remarks to the Chapter 11

In this chapter only basic methods, the direct nuclear reaction approach and the compound nucleus reaction model, were discussed. Both these approaches were introduced more than 60 years ago but they are used intensively up to now, especially for middle heavy and heavy target nuclei where other more microscopic models of nuclear reactions cannot be applied (because of huge configuration spaces). Both these models are more suitable for reactions where impacting particles (nucleons, mesons or light nuclei) are much lighter than target nuclei.

Reactions with heavy ions, where masses and proportions of impacting nuclei are comparable with the mass and proportion of target nucleus, are

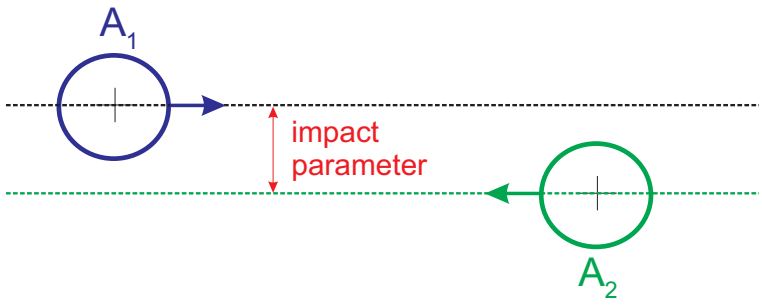


Figure 11.23: Schematic figure of the initial channel $\alpha \equiv A_1 + A_2$ of the heavy-ion reaction.

considered as dissipative or deep-inelastic collisions (DIC). In the case of the DIC impacting and target nuclei come close with the intermediate impact parameter [17] (see the Fig.11.23), that means impact parameter is less then the sum of radii of nuclei A_1 and A_2 and on the other side is higher than zero. As a result of it many degrees of freedom in both collision partners are excited. These excitations absorb a large amount of the initial energy and both nuclei are highly heated similarly as in the case of the compound nucleus reaction. However the DIC are not compound nucleus reactions because the collision partners do not overlap completely. They do not stay together for a long time as it is so for a compound nucleus. They retain their identity except for the exchange of a few nucleons. The cross-sections of the DIC reaction are usually derived semi-classically (e.g. Langevin equations, Fokker-Planck equation -see the part E in [352]) but these derivations are beyond the scope of this textbook. The DIC reactions are described in details e.g. in the book [352]) where the derivation of corresponding cross-sections can be found (see the part E therein).

On the other side the recent progress in computational techniques allowed to use fully microscopic theories for the description of the nuclear reaction with light nuclei. For instance ab initio approach starting with the bare nucleon-nucleon interactions was used for the determination of the cross-section of light-nuclei reactions without any other parameters except those involved in the bare nucleon-nucleon interaction (see e.g. [376, 377, 378]). There are also attempts to use these ab initio calculations also for the evaluation of optical potentials , that means optical potential parameters for given channel are not determined from by means of the fitting procedure to the elastic scattering as usually but they are obtained using ab initio ap-

[17] Impact parameter of the given reaction initialized by the channel $\alpha \equiv A_1 + A_2$ is the perpendicular distance of the CoM of the target nucleus A_2 from the trajectory of the CoM of the impacting nucleus A_1 - see the Fig.11.23

proach from given bare nucleon-nucleon interaction without any fitting (see e.g. [380, 379]). We can hope that further development of computer facilities enables to extend such ab initio calculations for reactions with heavier nuclei.

12. Statistical aspects of nuclear dynamics (energy density of nuclear states, fluctuation, radiative width, strength function

12.1 Introduction

The energy density of states increases with the excitation energy in all bound systems including atomic nuclei. In the case of middle heavy and heavy nuclei the energy density of states with energies above 5 MeV is so high that there is a problem of determination of characteristics of all individual states in terms of the solving of corresponding equations of motion (see the Fig.12.1). Therefore statistical approaches should be used in the description of higher

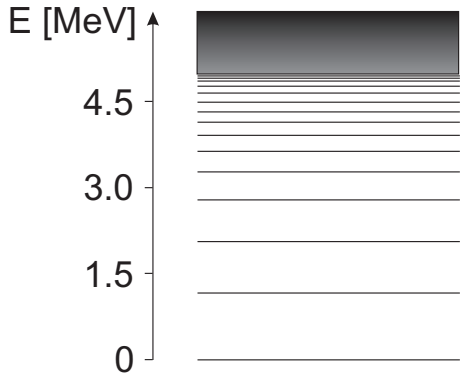


Figure 12.1: Typical spectrum of bound system (heavier nuclei): lower discrete spectrum changes to the continuous one with the increasing excitation energy

energy states. In this chapter statistical methods of the description of nuclear dynamics are discussed. In the first part of this chapter the Bethe formula for the density of nuclear levels is derived. Then the discussion involves statistical fluctuations of different physical quantities together with their determination by means of the theory of random matrices. In the second part of this chapter we discuss electromagnetic (photon) strength functions and their relation to the partial radiative width of electromagnetic de-excitation and photo-absorption cross-section (at zero as well as finite nuclear temperatures).

12.2 Energy density of nucleus states (density of levels)

12.2.1 Density of quantum system states and its relation to canonical and grand-canonical partition function

At first some terms from statistical physics are reminded (see e.g.[381]):

Canonical ensemble = ensemble of identical systems in the same heat bath (reservoir) and every these systems can exchange with its heat bath only energy but no particles (the number of particle in the system is constant).
The probability that each system from canonical ensemble is in the state n with the energy E_n for given temperature T is,

$$\omega_n = e^{\frac{F-E_n}{kT}} \tag{12.1}$$

with the Botzmann constant k and where F is the free energy of the system which is connected with the system internal energy U and the system entropy S by,

$$F = U - TS \tag{12.2}$$

The canonical partition function of the canonical ensemble is defined as,

$$Z = \sum_n e^{\frac{E_n}{kT}} \tag{12.3}$$

In the classical physics it is shown following relation for free energy ($\beta = \frac{1}{kT}$),

$$F = -kT\, lnZ = -\frac{1}{\beta}\, lnZ \tag{12.4}$$

Grand-canonical ensemble= ensemble of canonical systems with different number of particles, $N_1, N_2, \cdots, N_k, \cdots$.
The probability that randomly chosen system from grand canonical ensemble have the number N of particles and is in the state n with the energy E_{nN} is given by,

$$\omega_{nN} = e^{\frac{\Omega - E_{nN} - \mu N}{kT}} \tag{12.5}$$

with the chemical potential μ and where Ω is so called grand-canonical potential which is defined as,

$$\Omega = F - G = (U - TS) - (U - TS + PV) = -PV \tag{12.6}$$

where G is so called Gibbs potential (T - temperature, S - entropy, P - preasure, V - volume of the system). In the statistical physics so called grand-canonical partition function is introduced,

$$\Xi = \sum_{N,n} e^{\mu N - \beta E_{nN}} \tag{12.7}$$

Now we can go back to nuclei. Let us suppose that $\hat{H}$ is the nucleus Hamiltonian (quantum system Hamiltonian) with its energies $E_1,\ E_2, \cdots,\ E_k, \cdots$. Corresponding canonical partition function is (see (12.3)),

$$Z(\beta \approx \frac{1}{T}) = \sum_k e^{-\beta E_k} = \int dE\ \rho(E)\ e^{-\beta E} \tag{12.8}$$

where $1/\beta$ is called as the nucleus "temperature" which will be discussed later. The symbol $\rho(E)$ represents the energy density of nucleus states,

$$\rho(E) = \sum_k \delta(E - E_k) \tag{12.9}$$

The relation (12.8) can be interpreted as the Laplace transformation from the function $\rho(E)$ (E is real) to the function $Z(\beta)$ where the number β is a complex number from the mathematics point of view (in our case we can restrict ourselves only to pure imaginary number β). The inverse transormation to (12.8) is (see e.g. [58] - see also the footnote below), [1]

$$\rho(E) = \frac{1}{2\pi i} \int_{-i\infty}^{i\infty} d\beta\ Z(\beta)\ e^{\beta E} = \frac{1}{2\pi} \int_{-\infty}^{\infty} d\tilde{\beta}\ \ Z(i\tilde{\beta})\ e^{i\tilde{\beta}E} \tag{12.10}$$

The function inside the integral (12.10) represents quickly oscillating function of the real variable $\tilde{\beta} = -i\beta$. It is evident that the main contribution to the integral (12.10) comes from not big region around the value β_0 where the expression inside the integral (12.10) is stationary (not so oscillating). This

[1] Proof of (12.10):

$$\frac{1}{2\pi i} \int_{-i\infty}^{i\infty} Z(\beta)\, d\beta = \frac{1}{2\pi} \int_{-\infty}^{\infty} d\tilde{\beta} \int_0^{\infty} dE' \rho(E') e^{-i\tilde{\beta}E' + i\tilde{\beta}E} =$$
$$= \frac{1}{2\pi} \int_{-\infty}^{\infty} d\tilde{\beta} \int_0^{\infty} dE' \sum_k \delta(E' - E_k)\, e^{-i\tilde{\beta}E' + i\tilde{\beta}E} = \sum_k \frac{1}{2\pi} \int_{-\infty}^{\infty} d\tilde{\beta}\, e^{i\tilde{\beta}(E - E_k)}$$
$$= \sum_k \delta(E - E_k) = \rho(E)$$

value β_0 is given by the following condition,

$$\frac{\partial}{\partial\beta}\big(Z(\beta)e^{\beta E}\big)_{\beta=\beta_0} = \frac{\partial}{\partial\beta}\big(e^{lnZ(\beta)+\beta E}\big)_{\beta=\beta_0} =$$
$$= \big[\frac{d}{d\beta}lnZ(\beta)+E\big]_{\beta=\beta_0} e^{lnZ(\beta)+\beta E}|_{\beta=\beta_0} = 0$$
$$\Rightarrow \quad E = -\frac{d}{d\beta}lnZ(\beta=\beta_0) \tag{12.11}$$

So in the calculation of the integral in (12.10) the Taylor expansion of the function in the integral can be used in the vicinity of the value β_0,

$$\rho(E) = \frac{1}{2\pi i}\int_{-i\infty}^{i\infty} d\beta\, e^{lnZ(\beta)+\beta E} =$$
$$= \boxed{\begin{array}{c}\text{because (up to the terms with } (\beta-\beta_0)^2)\\ lnZ(\beta)+\beta E = ln(\beta_0)+\beta_0 E + (\beta-\beta_0)\big(\frac{d}{d\beta}lnZ(\beta)+E\big)_{\beta_0}\\ +(\beta-\beta_0)^2\,\frac{1}{2}\big(\frac{d^2}{d\beta^2}lnZ(\beta)\big)_{\beta_0}+\cdots\\ \text{and because of (12.11)}\end{array}} =$$
$$= \frac{1}{2\pi i}\; e^{lnZ(\beta_0)+\beta_0 E}\int_{-i\infty}^{i\infty} d\beta\, e^{\frac{1}{2}\left(\frac{d^2}{d\beta^2}lnZ(\beta_0)\right)(\beta-\beta_0)^2} =$$
$$= \boxed{\begin{array}{c}\text{substitution}\\ i\gamma = \beta-\beta_0\end{array}} =$$

$$= e^{lnZ(\beta_0)+\beta_0 E}\frac{i}{2\pi i}\int_{-\infty}^{\infty} d\gamma\, e^{-\frac{1}{2}\left(\frac{d^2}{d\beta^2}lnZ(\beta)\right)_{\beta=\beta_0}\gamma^2} =$$
$$= \boxed{\begin{array}{c}\text{because}\\ \int_{-\infty}^{\infty} e^{-c\,x^2}dx = \frac{\sqrt{\pi}}{\sqrt{c}}\end{array}} = e^{lnZ(\beta_0)+\beta_0 E}\frac{1}{2\pi}\,\frac{\sqrt{\pi}}{\sqrt{\frac{1}{2}\big(\frac{d^2}{d\beta^2}lnZ(\beta)\big)_{\beta=\beta_0}}} =$$
$$= \frac{e^{lnZ(\beta_0)+\beta_0 E}}{\sqrt{2\pi}\,\big(\frac{d^2}{d\beta^2}lnZ(\beta)\big)_{\beta=\beta_0}} \tag{12.12}$$

Generally in the quantum mechanics theories the eigen vectors of the Hamiltonian depends on quantum numbers q characterizing the eigen values of operators commuting mutually and commuting to zero with the Hamiltonian (that means operators belonging to the one complete set of commuting operators involving the Hamiltonian). Then corresponding density of levels with

the given energy E and given quantum numbers q is,

$$\rho(E,q) = \sum_i \delta(q-q_i)\ \ \delta(E-E_i) \tag{12.13}$$

In this case the corresponding canonical partition function is (see (12.8) [2],

$$Z(\beta,\alpha) = \sum_i e^{\alpha q_i - \beta E_i} = \int dE\, dq\, \rho(E,q)\, e^{\alpha q - \beta E} \tag{12.14}$$

Similarly as we obtained the expression (12.10) for $\rho(E)$ by the inversion of the Laplace transformation (12.8) the expression (12.14) can be understood as the Laplace transformation from $\rho(E,q)$ into $Z(\beta,\alpha)$ which can be inverted as follows,

$$\rho(E,q) = \frac{1}{(2\pi i)^2} \int_{-i\infty}^{i\infty} d\beta \int_{-i\infty}^{i\infty} d\alpha\ \ Z(\beta,\alpha)\ \ e^{\beta E - \alpha q} \tag{12.15}$$

Again the function inside the integrals (12.15) is oscillating besides the stationary region around the point (β_0,α_0) given by the following stationary conditions (analogy with (12.11),

$$E + \frac{\partial}{\partial\beta} lnZ(\beta_0,\alpha_0) = 0 \quad , \quad q - \frac{\partial}{\partial\alpha} lnZ(\beta_0,\alpha_0) = 0 \tag{12.16}$$

and again the main contribution into the integrals (12.15) comes from the relatively narrow region around the point (β_0,α_0). Therefore the Taylor expansion around the point (β_0,α_0) can be used in the exponent under the integral (12.15) and only the terms up to the $(\beta-\beta_0)^2$, $(\alpha-\alpha_0)^2$ and $(\beta-\beta_0)(\alpha-\alpha_0)$ are kept (together with the using of (12.16)). Then the integrals (12.15) can be calculated (see the Appendix R, the section R.1) and the result is following,

$$\rho(E,q) = \frac{1}{2\pi\ \ (det\ R)^{1/2}}\ \ e^{\Big(lnZ(\beta,\alpha)+\beta E-\alpha q\Big)_{\alpha,\beta=\alpha_0,\beta_0}} \tag{12.17}$$

where

$$det\ R = \left| \begin{array}{cc} \frac{\partial^2\, lnZ(\beta,\alpha)}{\partial\beta^2} & \frac{\partial^2\, lnZ(\beta,\alpha)}{\partial\beta\partial\alpha} \\ \frac{\partial^2\, lnZ(\beta,\alpha)}{\partial\alpha\partial\beta} & \frac{\partial^2\, lnZ(\beta,\alpha)}{\partial\alpha^2} \end{array} \right|_{\alpha,\beta=\alpha_0,\beta_0} \tag{12.18}$$

[2] In the case when among quantum numbers q_i there is also number of particle number N of the system (that means $[\hat{H},\hat{N}] = 0$) then we should speak about grand-canonical ensemble instead of the canonical ensemble.

12.2.2 Energy density of grand-canonical systems of fermions in the model of independent particles (fermions of one type)

In this subsection we will consider the quantum systems formed by mutually non-interacting fermions of one type. Each state of the system is characterized by the occupation numbers $(n_s)_i$ for all possible single-particle states s which can be filled by individual fermions and for all possible whole system states characterized by the index i. According to the Pauli principle these occupation numbers can be only $(n_s)_i = 0, 1$. It is evident that the total number of particles in the system and the total system energy are given by,

$$N = \sum_s (n_s)_i \qquad , \qquad E_i = \sum_s (n_s)_i \, e_s \tag{12.19}$$

where e_s are single-particle energies and the index i enumerates the eigenstates of the whole N- fermion system. One should also realize that because we analyse canonical systems the number of fermions in each system is fixed and therefore the number of particles N in the system is independent on the index i.

Further we will fix the number of fermions in each canonical quantum system by A. Then the density of system levels as a function of the system energy E and particle number N is given by,

$$\rho(E, A) = \sum_{N,i} \delta(A - N) \, \delta(E - E_i(N)) \tag{12.20}$$

where N and E_i are given by (12.19). The corresponding partition function is (see (12.14)),

$$\begin{aligned} Z(\beta, \alpha) &= \int_0^\infty dA \int_0^\infty dE \, \rho(E, A) \, e^{\alpha A - \beta E} = \\ &= \sum_{N,i} e^{\alpha N - \beta E_i(N)} = \sum_{n_s=0,1} e^{\alpha \sum_s (n_s)_i - \beta \sum_s e_s (n_s)_i} = \\ &= \sum_{n_1=0,1} e^{(\alpha - \beta e_1) n_1} \sum_{n_2=0,1} e^{(\alpha - \beta e_2) n_2} \ldots = \\ &= \prod_s \left(1 + e^{\alpha - \beta e_s}\right) \end{aligned} \tag{12.21}$$

In each factor the term with 1 comes from $n_s = 0$ and the exponential term comes from $n_s = 1$.

Further we determine the equilibrium stationary total energy E and the number A of particles according to (12.16) where $q = A$. So we need to

find the stationary point α_0, β_0 and to determine $lnZ(\beta, \alpha)$. This logarithm is derived in the Appendix R (see the Section R.2). In this derivation the approximation was used that the energy density of single-particle states,

$$g(e) = \sum_s \delta(e - e_s) \tag{12.22}$$

has no any discontinuities around the single-particle energy $e \approx \alpha/\beta$. Further we will see that the physical meaning of the ratio α/β in the stationary point $\alpha/\beta = \alpha_0/\beta_0$ (see (12.16)) is the Fermi energy for fermions forming the investigated quantum system. We can expect that the single-particle energy density has a minimum around the Fermi energy and therefore its reasonable behavior giving the possibility of the using the Taylor expansion for $g(e)$ in the region of e around the fermi energy. This is the crucial point in the derivation of the following expression for $lnZ(\beta, \alpha)$ (see the expression (R.11) in the Appendix R),

$$lnZ(\beta, \alpha) \approx \beta \int_0^{\mu} dx\, g(x)(\mu - x) + \frac{\pi^2}{6\beta} g(\mu) + \frac{7\pi^4}{360\beta^3} g''(\mu) + \cdots \tag{12.23}$$

where $\mu = \alpha/\beta$, $x = e - \alpha/\beta$, $g'(x) = \frac{dg(x)}{dx}$, $g''(x) = \frac{d^2 g(x)}{dx}$.

In the ground state of the fermion system all single-particle levels are filled up to the Fermi level e_F which is given by the energy density normalization for given number of particles,

$$\int_0^{e_F} g(e)\, de = A \tag{12.24}$$

with the following total energy in the ground state,

$$E_0 = \int_0^{e_F} g(e)\, e\, de \tag{12.25}$$

From statistical physics side the ground state corresponds to the thermodynamical stationary point given by the condition (12.16) [3],

$$\begin{aligned} A = N(\beta_0, \alpha_0) &= \frac{\partial}{\partial \alpha} lnZ(\beta, \alpha)_{\alpha, \beta = \alpha_0, \beta_0} \\ E_0 = E(\beta_0, \alpha_0) &= -\frac{\partial}{\partial \beta} lnZ(\beta, \alpha)_{\alpha, \beta = \alpha_0, \beta_0} \end{aligned} \tag{12.26}$$

[3]Further we suppose that β and α are real (because if they are purely imaginary then $lnZ(\beta, \alpha)$ is also purely imaginary and $E_0(\beta_0, \alpha_0)$ and $N(\beta_0, \alpha_0)$ are remained real)

We substitute (12.23) into the equation for A in (12.26) (simultaneously we neglect terms in (12.23) with derivatives of $g(\mu)$ - see the page 284 in [6]),

$$\begin{aligned}
A &= \frac{\partial}{\partial\alpha} lnZ(\beta,\alpha)_{\alpha,\beta=\alpha_0,\beta_0} \approx \\
&\approx \frac{\partial}{\partial\alpha}\Big(\int_0^{\frac{\alpha}{\beta}} de\, g(e)\,(\alpha-\beta e) + \frac{\pi^2}{6\beta}\, g(\frac{\alpha}{\beta})\,\Big)_{\alpha,\beta=\alpha_0,\beta_0} = \\
&= \boxed{\begin{array}{c}\text{in the case of the ground state}\\ \text{the "temperature" } 1/\beta_0 \text{ is zero}\end{array}} = \\
&= \frac{\partial}{\partial\alpha}\Big(\int_0^{\alpha/\beta} de\, g(e)\,(\alpha-\beta e)\Big)_{\alpha,\beta=\alpha_0,\beta_0} = \\
&= \frac{\partial}{\partial\alpha}\Big(\int_0^{\alpha/\beta} de\, \alpha\, g(e)\Big)_{\alpha,\beta=\alpha_0,\beta_0} = \int_0^{\alpha_0/\beta_0} de\, g(e) \qquad (12.27)
\end{aligned}$$

And the comparison of (12.27) with (12.24) gives,

$$e_F = \alpha_o/\beta_0 \qquad (12.28)$$

Further we substitute (12.23) into the expression for E_0 in (12.26) (see the page 284 in [6]),

$$\begin{aligned}
&E(\beta_0,\alpha_0) = \\
&= -\frac{\partial}{\partial\beta} lnZ(\beta,\alpha)_{\alpha,\beta=\alpha_0,\beta_0} = \boxed{\begin{array}{c}\text{substitution from (12.23)}\\ \text{and neglecting terms with}\\ g''(\mu)\end{array}} = \\
&= -\frac{\partial}{\partial\beta}\Big(\int_0^{\alpha/\beta} de\, g(e)\,(\alpha-\beta e) + \frac{\pi^2}{6\beta}\, g(\frac{\alpha}{\beta})\,\Big)_{\alpha,\beta=\alpha_0,\beta_0} = \\
&= \boxed{\begin{array}{c}\text{we neglect derivative}\\ \text{over } \beta \text{ of the upper}\\ \text{limit of the integral}\end{array}} \approx \\
&\approx \int_0^{e_F} de\, g(e)\, e + \frac{\pi^2}{6\beta_0^2}\, g(e_F) = \boxed{\begin{array}{c}\text{see}\\ (12.25)\end{array}} \\
&= E_0 + \frac{\pi^2}{6\beta_0^2}\, g(e_F) \qquad (12.29)
\end{aligned}$$

where e_F is the Fermi energy. The expressions (12.29) and (12.25) imply the

conclusion that

$$E_{ex}(\beta_0) \approx E(\beta_0, \alpha_0) - E_0 \approx \frac{\pi^2}{6\beta_0^2}\, g(e_F) \tag{12.30}$$

represents the excitation energy of the system corresponding to the system "temperature" $\frac{1}{\beta_0}$.

Further we determine the energy density of states using expressions (12.17) and (12.18) ($E = E(\beta, \alpha)\,;\; q = N(\beta, \alpha)$),

$$\frac{\partial^2 lnZ(\beta,\alpha)}{\partial\alpha^2} = \boxed{\begin{array}{c}\text{see}\\ (12.27)\end{array}} = \frac{\partial}{\partial\alpha}\int_0^{\alpha/\beta} de\, g(e) = \frac{1}{\beta}\, g(\frac{\alpha}{\beta})$$

$$\frac{\partial^2 lnZ(\beta,\alpha)}{\partial\beta\partial\alpha} = \frac{\partial}{\partial\beta}\int_0^{\alpha/\beta} de\, g(e) = -\frac{\alpha}{\beta^2}\, g(\frac{\alpha}{\beta})$$

$$\frac{\partial^2 lnZ(\beta,\alpha)}{\partial\beta^2} = \boxed{\begin{array}{c}\text{see}\\ (12.29)\end{array}} = -\frac{\partial}{\partial\beta}\Big(\int_o^{\alpha/\beta} g(e)\, e\, de + \frac{\pi^2}{6\beta^2}\, g(\frac{\alpha}{\beta})\Big) =$$

$$= \boxed{\begin{array}{c}\text{because}\\ e \approx \frac{\alpha}{\beta}\end{array}} = \frac{\alpha}{\beta^2}\, g(\frac{\alpha}{\beta})\, \frac{\alpha}{\beta} + \frac{\pi^2}{6}\, \frac{2\beta}{\beta^4}\, g(\frac{\alpha}{\beta}) + \frac{\pi^2}{6\beta^2}\, g'(\frac{\alpha}{\beta})\, \frac{\alpha}{\beta^2} =$$

$$= \boxed{\begin{array}{c}g' \text{ is}\\ \text{neglected}\end{array}} = \frac{\alpha^2}{\beta^3}\, g(\frac{\alpha}{\beta}) + \frac{\pi^2}{3}\, \frac{1}{\beta^3}\, g(\frac{\alpha}{\beta})$$

$$\frac{\partial^2 lnZ(\beta,\alpha)}{\partial\alpha\partial\beta} \approx -\frac{\partial}{\partial\alpha}\Big(\int_0^{\alpha/\beta} g(e)\, e\, de + \frac{\pi^2}{6\beta^2} g(\frac{\alpha}{\beta})\Big) \approx$$

$$\approx -\frac{1}{\beta}\, g(\frac{\alpha}{\beta})\, \frac{\alpha}{\beta} = -\frac{\alpha}{\beta^2}\, g(\frac{\alpha}{\beta}) \tag{12.31}$$

The the determinant $det\ R$ (see (12.18)) is,

$$det\ R = \Big(\frac{\partial^2 lnZ(\beta,\alpha)}{\partial\beta^2}\Big)\Big(\frac{\partial^2 lnZ(\beta,\alpha)}{\partial\alpha^2}\Big) - \Big(\frac{\partial^2 lnZ(\beta,\alpha)}{\partial\alpha\partial\beta}\Big) =$$

$$= \frac{1}{\beta}\, g(\frac{\alpha}{\beta})\, \Big[\, \frac{\alpha^2}{\beta^3}\, g(\frac{\alpha}{\beta}) + \frac{\pi^2}{3}\frac{1}{\beta^3}\, g(\frac{\alpha}{\beta})\, \Big] - \frac{\alpha^2}{\beta^4}\, g^2(\frac{\alpha}{\beta}) =$$

$$= \frac{\pi^2}{3}\frac{1}{\beta^4}\, g^2(\frac{\alpha}{\beta}) \tag{12.32}$$

and the nominator of (12.17) is,

$$
\begin{aligned}
ln Z(\beta,\alpha) &= \boxed{\begin{array}{c}\text{see (12.23)}\\ \text{where } g' \text{ is neglected}\end{array}} = \\
&\approx \beta \int_0^{\alpha/\beta} de\, g(e)\,(\frac{\alpha}{\beta} - e) + \frac{\pi^2}{6\beta}\, g(\frac{\alpha}{\beta}) = \\
&= \alpha \int_0^{\alpha/\beta} de\, g(e) - \beta \int_0^{\alpha/\beta} de\, g(e)\, e + \frac{\pi^2}{6\beta}\, g(\frac{\alpha}{\beta}) = \boxed{\begin{array}{c}\text{see (12.27)}\\ \text{and (12.29)}\end{array}} = \\
&= \alpha\, N(\beta,\alpha) - \beta\, E(\beta,\alpha) + \beta\, E_{ex}(\beta) \\
\Longrightarrow \quad ln Z(\beta,\alpha) &+ \beta\, E(\beta,\alpha) - \alpha\, N(\beta,\alpha) = \boxed{\begin{array}{c}\text{see}\\ \text{(12.30)}\end{array}} = \frac{\pi^2}{6\beta}\, g(\frac{\alpha}{\beta})
\end{aligned}
\tag{12.33}
$$

The substitution of (12.32) and (12.33) into (12.17) and (12.18) (where $E = E(\beta_0,\alpha_0)$, $q = N(\beta_0,\alpha_0)$) gives the expression for the level density of the system of A non-interacting fermions of one type with the given excitation energy E_{ex} (under the assumption that each of single-particle level is not degenerated and $A = N(\beta_0,\alpha_0)$),

$$
\begin{aligned}
\rho(E_{ex},\, A) &= \frac{1}{2\pi\,\sqrt{det\, R}}\, e^{ln Z(\beta_0,\alpha_0) + \beta_0\, E(\beta_0,\alpha_0) - \alpha_0\, N(\beta_0,\alpha_0)} = \\
&= \frac{1}{2\pi}\, \frac{1}{\frac{\pi}{\sqrt{3}}\frac{1}{\beta^2}\, g(\frac{\alpha_0}{\beta_0})} e^{\frac{\pi^2}{6\beta_0}\, g(\frac{\alpha_0}{\beta_0})} = \boxed{\begin{array}{c}\text{because - see (12.30)}\\ \beta_0 = \sqrt{\frac{\pi^2\, g(\frac{\alpha_0}{\beta_0})}{6E_{ex}}}\end{array}} = \\
&= \frac{1}{E_{ex}\,\sqrt{48}}\; e^{\sqrt{\frac{\pi^2}{6}\, g(e_F)\, E_{ex}}}
\end{aligned}
\tag{12.34}
$$

where $e_F = \frac{\alpha_0}{\beta_0}$, $A = \int_0^{e_F} g(e)\, de$.

However in many cases in the reality the Hamiltonian of the system is invariant with respect to the time-reverse transformation (e.g. intrinsic Hamiltonian of well-deformed nuclei with the even-multipolarity deformation parameters - see the Subsection 8.1.1). In such cases each single-particle level is at least twice degenerated (eigen-states with the opposite sign of the s.p. angular momentum projection onto the 3-d intrinsic axis have the same s.p. energy). If each single-particle energy is twice degenerated then the density

of s.p. eigen-states is twice higher than the density of eigen-levels,

$$A = 2 \int_0^{e_F} de\, g(e) \qquad , \qquad E_{ex} = 2\, \frac{\pi^2}{6\beta_0^2}\, g(e_F) \tag{12.35}$$

and in this case the density of states of the whole system of A fermions of one type (when the single-particle level density is $g(e)$ and all single-particle levels with energies $e < e_F$ are occupied by 2 particles and the whole system is excited to the energy E_{ex}) should be modified as follows,

$$\rho(E_{ex}, A) = \frac{1}{E_{ex}\,\sqrt{48}}\; e^{2\,\sqrt{\frac{\pi^2}{6}\, g(e_F)\, E_{ex}}} \tag{12.36}$$

In the derivation of this expression several relatively rough approximations were used which are listed below,

- **The replacement of the single-particle density by a smooth function in the calculation of $lnZ(\beta, \alpha)$ in (12.23) (particularly in the evaluation of the integral (R.7) - see the Section R.2 in the Appendix R)**
  This approximation is valid provided (see the text below (R.7)),

  $$\beta_0^{-1}\, g(e_F) >> 1 \tag{12.37}$$

  which is equivalent to (see (12.30)

  $$E_{ex} >> \frac{1}{g(e_F)} \tag{12.38}$$

  This condition reflects the fact that average level density $\rho(E, A)$ is not defined until we come to excitation energies E_{ex} large compared with the energy $g^{-1}(e_F)$ of the first excited state.

- **The neglect of terms depending on the derivatives of $g(e)$ (e.g. the last term in (12.23))**
  In [6] it was shown that this neglect can be done if the following condition is fulfilled,

  $$\frac{(g''(e_F))^2\, E_{ex}}{(g(e_F))^3} << 1 \tag{12.39}$$

  According to [6] this condition is usually fulfilled for a Fermi gas. For a system with the shell structure (like a nucleus), the one-particle level density may vary more rapidly and irregularly than for a Fermi gas and the condition (12.39) should be checked individually.

In the end of this subsection it is necessary to point out that the system "temperature", β_0^{-1}, has nothing to do with the standard temperature in the thermodynamics. In the quantum mechanics the "temperature" β_0^{-1} is only a parameter characterizing the density of levels in the given excitation energy E_{ex} of the given quantum system with$A$ particles. From the expression (12.30) or (12.35) one can see that the system "temperature" is related to the excitation energy E_{ex} as $\beta_0^{-1} \approx \sqrt{E_{ex}}$.

12.2.3 Energy density of of states of Fermi systems with fermions of two types

Atomic nucleus consists from neutrons and protons, that means from fermions of two types. Therefore its partition function Z (see (12.21) depends on three variables (parameters) α_n, α_p, β (nucleus is characterized by 3 quantities: energy E, number N of neutrons, number Z of protons),

$$
\begin{aligned}
Z(\beta,\alpha_n,\alpha_p) = & \boxed{\begin{array}{c}\text{see}\\ (12.21)\end{array}} = \\
= & \sum_{n_1^{(n)}=0,1} e^{(\alpha_n-\beta e^{(n)}{}_1)} \sum_{n_2^{(n)}=0,1} e^{(\alpha_n-\beta e^{(n)}{}_2)} \cdots \\
& \sum_{n_1^{(p)}=0,1} e^{(\alpha_p-\beta e^{(p)}{}_1)} \sum_{n_2^{(p)}=0,1} e^{(\alpha_p-\beta e^{(p)}{}_2)} \cdots = \\
= & \prod_{s_n} \left(1+e^{\alpha_n-\beta e_{s_n}}\right) \prod_{s_p} \left(1+e^{\alpha_p-\beta e_{s_p}}\right) \qquad (12.40)
\end{aligned}
$$

where e_{s_n} (e_{s_p}) are single-particle energies of neutron (proton) system.

Further, in the analogy with expressions (12.22)-(12.36)) for one type fermion systems, the energy level density (or energy state density) are determined for two type fermion systems. For this aim we need the logarithm of the partition function (12.40) (analogy with one type fermion expression

(R.7) in the Appendix R or (12.23)),

$$lnZ(\beta,\alpha_n,\alpha_p)=\sum_{s_n} ln(1+e^{\alpha_n-\beta e_{s_n}})+\sum_{s_p} ln(1+e^{\alpha_p-\beta e_{s_p}})=$$

$$=\boxed{\begin{array}{c}\text{because}\\ g_n(e)=\sum_{s_n}\delta(e-e_{s_n})\ ,\ \ g_p(e)=\sum_{s_p}\delta(e-e_{s_p})\end{array}}=$$

$$=\int_0^\infty g_n(e)\ ln(1+e^{\beta\,(\frac{\alpha_n}{\beta}-e)})\,de+\int_0^\infty g_p(e)\ ln(1+e^{\beta\,(\frac{\alpha_p}{\beta}-e)})\,de \tag{12.41}$$

Both these integrals can be determined using the same approximations as in the case of the derivation of the density $\rho(E,\alpha)$ (see (12.35)) for the system with fermions of one type - see the Subsection 12.3.2). For instance, in the analogy with (12.23) we obtain for $lnZ(\beta,\alpha_n,\alpha_p)$ (again the derivatives g'' are neglected),

$$lnZ(\beta,\alpha_n,\alpha_p)\approx\int_0^{\frac{\alpha_n}{\beta}} g_n(e)\ (\alpha_n-\beta e)\,de+\int_0^{\frac{\alpha_p}{\beta}} g_p(e)\ (\alpha_p-\beta e)\,de\ \ +$$
$$+\ \frac{\pi^2}{6\beta}\ (\ g_n(\frac{\alpha_n}{\beta})+g_p(\frac{\alpha_p}{\beta})\ ) \tag{12.42}$$

and in the stationary point $(\beta_0,(\alpha_n)_0,(\alpha_p)_0)$ (equilibrium condition) is given by,

$$N(\beta,(\alpha_n)_0,(\alpha_p)_0)=\frac{\partial}{\partial\alpha_n}lnZ(\beta,\alpha_n,\alpha_p)|_{\beta,\alpha_n,\alpha_p=\beta_0,(\alpha_n)_0,(\alpha_p)_0}$$
$$Z(\beta,(\alpha_n)_0,(\alpha_p)_0)=\frac{\partial}{\partial\alpha_p}lnZ(\beta,\alpha_n,\alpha_p)|_{\beta,\alpha_n,\alpha_p=\beta_0,(\alpha_n)_0,(\alpha_p)_0}$$
$$E(\beta,(\alpha_n)_0,(\alpha_p)_0)=-\frac{\partial}{\partial\beta}lnZ(\beta,\alpha_n,\alpha_p)|_{\beta,\alpha_n,\alpha_p=\beta_0,(\alpha_n)_0,(\alpha_p)_0} \tag{12.43}$$

The generalization of the expression (12.30) for neutron-proton type fermion system (nucleus) gives following expression for the excitation energy of the nucleus,

$$E_{ex}=E(\beta_0,(\alpha_n)_0,(\alpha_p)_0)-E_0=\frac{\pi^2}{6\beta_0^2}\ (\ g_n(e_F^{(n)})+g_p(e_F^{(p)})\ ) \tag{12.44}$$

where $E_0=\int_0^{e_F} de\ g(e)\ e$, $(\alpha_n)_0=e_F^{(n)}\beta_0$, $(\alpha_p)_0=e_F^{(p)}\beta_0$. Similarly generalization of the expressions (12.17) and (12.18) for one-type systems gives the

expression for the density of states of nuclei (systems with two-type fermions),

$$\rho(E,N,Z) = \frac{1}{2\pi\ (detR)^{1/2}}\ e^{lnZ(\beta_0,(\alpha_n)_0,(\alpha_p)_0)\ +\ \beta_0 E\ -\ (\alpha_n)_0 N\ -\ (\alpha_n)_0 Z} \tag{12.45}$$

where

$$det\ R = \left| \begin{array}{ccc} \frac{\partial^2\ lnZ(\beta,\alpha_n,\alpha_p)}{\partial\beta^2} & \frac{\partial^2\ lnZ(\beta,\alpha_n,\alpha_p)}{\partial\beta\ \partial\alpha_n} & \frac{\partial^2\ lnZ(\beta,\alpha_n,\alpha_p)}{\partial\beta\ \partial\alpha_p} \\ \frac{\partial^2\ lnZ(\beta,\alpha_n,\alpha_p)}{\partial\alpha_n\ \partial\beta} & \frac{\partial^2\ lnZ(\beta,\alpha_n,\alpha_p)}{\partial\alpha_n^2} & \frac{\partial^2\ lnZ(\beta,\alpha_n,\alpha_p)}{\partial\alpha_n\ \partial\alpha_p} \\ \frac{\partial^2\ lnZ(\beta,\alpha_n,\alpha_p)}{\partial\alpha_p\ \partial\beta} & \frac{\partial^2\ lnZ(\beta,\alpha_n,\alpha_p)}{\partial\alpha_p\ \partial\alpha_n} & \frac{\partial^2\ lnZ(\beta,\alpha_n,\alpha_p)}{\partial\alpha_p^2} \end{array} \right|_{\alpha_n,\alpha_p,\beta=(\alpha_n)_0,(\alpha_p)_0,\beta_0} \tag{12.46}$$

The substitution of (12.41 into (12.45) and (12.46) gives the following energy density of nucleus states with the excitation energy E_{ex} (see (12.44), given number N of neutrons and given number Z of protons,

$$\rho(E_{ex},N,Z) = \frac{6^{\frac{1}{4}}}{12}\ g_0\ \Big(\frac{g_0^2}{4\ g_n(e_F^{(n)})\ \ g_p(e_F^{(p)})}\Big)^{\frac{1}{2}}\ (g_0 E_{ex})^{-\frac{5}{4}}\ \ e^{2\sqrt{\frac{\pi^2}{6}g_0 E_{ex}}} \tag{12.47}$$

where $g_0 \equiv g_n(e_F^{(n)}) + g_n(e_F^{(p)})$ ($g_n(e_F^{(n)})$ and $g_p(e_F^{(p)})$) are neutron and proton single-particle energy densities around corresponding Fermi energies, respectively). The expression (12.47) has the same exponential dependence on E_{ex} as does (12.36) with $g(e_F)$ replased by g_0, but the coefficient in front of the exponential is somewhat modified by the presence of two different kinds of particles.

12.2.4 Energy density of of states of Fermi system with one type of fermions and with the given value of the angular momentum projection

The calculation of the energy density of states of canonical quantum systems can be extended in order to treat not only energy and number of particle but also other quantum numbers. As an example we will consider the projection M of the angular momentum on the third axis of the laboratory frame. For the simplicity we are assuming only one kind of particles in the canonical quantum systems. Then, the partition function depends on three parameters

(generalization of the expression (12.14)),

$$Z(\beta,\alpha,\gamma) = \int dE \int dN \int dM \;\; \rho(E,N,M) \;\; e^{\alpha N - \beta E - \gamma M} = \boxed{\begin{array}{c}\text{see}\\ (12.20)\end{array}} =$$

$$= \sum_{i,N,M_i} e^{\alpha N - \beta E_i - \gamma M_i} = \boxed{\begin{array}{c}\text{because } N = \sum_s (n_s)_i \;, \\ E_i = \sum_s (n_s)_i \, e_s \;,\; M_i = \sum_s (n_s)_i \, m_s\end{array}} =$$

$$= \boxed{\begin{array}{c}\text{analogy with}\\ (12.40)\end{array}} = \sum_{n_1=0,1} e^{\alpha - \beta e_1 - \gamma m_1} \sum_{n_2=0,1} e^{\alpha - \beta e_2 - \gamma m_2} \ldots =$$

$$= \prod_s \left(1 + e^{\alpha - \beta e_s - \gamma m_s} \right) \tag{12.48}$$

The expression for $lnZ(\beta,\alpha,\gamma)$ can be obtained in the analogical way as in the case of the expression (12.41) (using the same approximations),

$$lnZ(\beta,\alpha,\gamma) =$$

$$= \sum_s ln(1 + e^{\alpha - \beta e_s - \gamma m_s}) = \boxed{\begin{array}{c}\text{because energy s.p. density:}\\ g(e,m) = \sum_s \delta(e - e_s)\delta(m - m_s)\end{array}} =$$

$$= \int_0^\infty de \int_0^\infty dm \;\; g(e,m) \, ln(1 + e^{\alpha - \beta e - \gamma m}) \tag{12.49}$$

Similarly as we got (12.42) from (12.41) (or (R.11)) from (12.21) the expression (12.49) can be rewritten as follows (again the second derivatives g'' are neglected),

$$lnZ(\beta,\alpha,\gamma) = \int_0^{\frac{\alpha}{\beta}} de \, g(e) \, (\alpha - \beta e) + \frac{\pi^2}{6\beta} \, g(\frac{\alpha}{\beta}) + \frac{\gamma^2}{2\beta} \, g(\frac{\alpha}{\beta}) \, \langle m^2 \rangle \tag{12.50}$$

where $g(e) = \int_{-\infty}^{\infty} dm \; g(e,m)$, $g(e = \frac{\alpha}{\beta}) \, \langle m^2 \rangle \equiv \int_{-\infty}^{\infty} dm \; g(e,m) \, m^2$. From the expression (12.50) follows that the quantity $\langle m^2 \rangle$ represents the average value of the square of the s.p. angular momentum projection m^2 for the Fermi surface.

The expresion (12.49) for the partition function $Z(\beta,\alpha,\gamma)$ can be understood as the Laplace transformation $\rho(E,N,M) \;\; \rightarrow \;\; Z(\beta,\alpha,\gamma)$. Similarly as in the case of expressions (12.14) and (12.15) this transformation can be inverted:

$$\rho(E,N,M) = \frac{1}{(2\pi i)^3} \int_{-i\infty}^{i\infty} d\gamma \int_{-i\infty}^{i\infty} d\beta \int_{-i\infty}^{i\infty} d\alpha \, e^{lnZ(\beta,\alpha,\gamma) + \beta E + \gamma M - \alpha N} \tag{12.51}$$

The stationary point of the integrand of the inverse Laplace transformation (12.51) is given by the following condition (see (12.50)),

$$
\begin{aligned}
N &= \frac{\partial\, lnZ(\beta,\alpha,\gamma)}{\partial\alpha}|_{\alpha,\beta,\gamma=\alpha_0,\beta_0,\gamma_0} = \int_0^{\alpha_0/\beta_0} g(e)\, de \\
E &= -\frac{\partial\, lnZ(\beta,\alpha,\gamma)}{\partial\beta}|_{\alpha,\beta,\gamma=\alpha_0,\beta_0,\gamma_0} = \\
&= \int_0^{\alpha_0/\beta_0} g(e)\, e\, de + \frac{\pi^2}{6\beta_0^2} g(e_F) + \frac{1}{2}\big(\frac{\gamma_0}{\beta_0}\big)^2 g(e_F) \\
M &= -\frac{\partial\, lnZ(\beta,\alpha,\gamma)}{\partial\gamma}|_{\alpha,\beta,\gamma=\alpha_0,\beta_0,\gamma_0} = -\frac{\gamma_0}{\beta_0}\, g(e_F)\, \langle m^2\rangle
\end{aligned}
\tag{12.52}
$$

where $e_F = \frac{\alpha_0}{\beta_0}$, $\frac{\pi^2}{6\beta_0^2}\, g(e_F) = E - E_0 - \frac{1}{2}\frac{\gamma_0^2}{\beta_0^2}\, g(e_F) = E - E_0 - \frac{M^2}{2g(e_F)\langle m^2\rangle} = E_{ex} - \frac{M^2}{2g(e_F)\langle m^2\rangle}$.

Similarly as in (12.12) we can expand the exponent in the integrand of the integral in (12.52) using the Taylor expansion around the stationary point $(\alpha_0, \beta_0, \gamma_0)$ and we obtain the expression for the state density $\rho(E, N, M)$ in the form analogical to the expression (12.17) or (12.45),

$$
\rho(E,N,M) = \frac{1}{2\pi\, (detR)^{1/2}}\, e^{lnZ(\beta_0,\alpha_0,\gamma_0)\, +\, \beta_0 E\, +\gamma_0 M\, -\, \alpha_0 N}
\tag{12.53}
$$

where

$$
det\ R = \left|
\begin{array}{ccc}
\frac{\partial^2\, lnZ(\beta,\alpha,\gamma)}{\partial\beta^2} & \frac{\partial^2\, lnZ(\beta,\alpha,\gamma)}{\partial\beta\,\partial\alpha} & \frac{\partial^2\, lnZ(\beta,\alpha,\gamma)}{\partial\beta\,\partial\gamma} \\
\frac{\partial^2\, lnZ(\beta,\alpha,\gamma)}{\partial\alpha\,\partial\beta} & \frac{\partial^2\, lnZ(\beta,\alpha,\gamma)}{\partial\alpha^2} & \frac{\partial^2\, lnZ(\beta,\alpha,\gamma)}{\partial\alpha\,\partial\gamma} \\
\frac{\partial^2\, lnZ(\beta,\alpha,\gamma)}{\partial\gamma\,\partial\beta} & \frac{\partial^2\, lnZ(\beta,\alpha,\gamma)}{\partial\gamma\,\partial\alpha} & \frac{\partial^2\, lnZ(\beta,\alpha,\gamma)}{\partial\gamma^2}
\end{array}
\right|_{\alpha,\beta,\gamma=\alpha_0,\beta_0,\gamma_0}
\tag{12.54}
$$

Then the substitution of (12.52) into (12.53) and (12.54) gives the energy density of the system states in the following form,

$$
\rho(E_{ex},N,M) = \frac{6^{\frac{1}{4}}}{24}\Big(\frac{g_0}{\langle m^2\rangle}\Big)^{\frac{1}{2}}\Big[g_0 E_{ex} - \frac{M^2}{2\langle m^2\rangle}\Big]^{-5/4} e^{2\Big[\frac{\pi^2}{6}\Big(g_0 E_{ex} - \frac{M^2}{2\langle m^2\rangle}\Big)\Big]^{1/2}}
\tag{12.55}
$$

where the fact that 2 fermions differing by the sign of the angular momentum projection can sit in one single-particle level (which is a result of the invariance of the system Hamiltonian with respect to the time-reverse and taking into account of the nucleus spin degrees of freedom).

Further we should determine $\langle m^2\rangle$ defined by the expression under the (12.50). We will do it in the framework of the Fermi gas model (Fermi gas

model is described in the Appendix H) [4]. Then we can introduce the density $g(\vec{p},\vec{r})$ of the single-particle states in the phase space,

$$g(\vec{p},\vec{r}) = 2\big(\frac{1}{2\pi\hbar}\big)^3 \tag{12.56}$$

where the factor 2 corresponds to the taking into account the spin degrees of freedom. The expectation value $\langle m^2\rangle$, defined by expressions below the (12.50), means the averaging over single-particle states with single-particle energies equal approximately to the Fermi energy $\frac{p_F^2}{2M_n} = \frac{\hbar^2 k_F^2}{2M_n}$ where M_n is the nucleon mass. Therefore (we should realize that m is the 3-d projection of the angular momentum),

$$g_0\,\langle m^2\rangle = \int d^3p \int d^3r\; g(\vec{p},\vec{r})\;\delta\big(\frac{p^2}{2M_n} - \frac{(p_F(\vec{r})^2)}{2M_n}\big)\;\frac{1}{\hbar^2}\;(xp_y - yp_x)^2 \tag{12.57}$$

where $g(\vec{p},\vec{r})$ is given by (12.56) and $p_F(\vec{r})$ is average linear momentum of the Fermi gas per volume unit given by (H.7) (see the Appendic H),

$$p_F(\vec{r}) = \hbar k_F = \hbar\big(3\pi^2\rho(\vec{r})\big)^{\frac{1}{3}} \tag{12.58}$$

Since the linear momenta are in the Fermi gas distributed isotropically at each point, the cross term involving $p_x p_y$ does not contribute, and the integrals in (12.57) become (using (12.56) and following expressions from mathematics:

[4]The model of the Fermi gas is discussed shortly in the Appendix H. It corresponds to the infinite system of non-interacting fermions where the whole Hamiltonian $\hat{H}$ is given only by the kinetic energy term. In this case the single-particle states are represented by the plane waves $\langle\vec{r}|\vec{p}_\nu\rangle = \frac{1}{(2\pi\hbar)^3}e^{i\vec{p}_\nu\cdot\vec{r}}$ (see the unperturbed Hamiltonian $\hat{H}_0$ in (3.130)). Then the individual fermions fill the single-particle states $|\vec{p}_\nu\rangle$ up to the Fermi linear momentum ($|\vec{p}_\nu| \leq p_F = \hbar k_F$ - see the Appendix H). If the spin degrees of freedom are accounted then each linear momentum single-particle level $\frac{\hbar^2 k_\nu^2}{2M_n}$ (M_n - mass of nucleon) is filled by 2 particles with different sign of the spin projection.

$\delta(\alpha x) = \frac{1}{|\alpha|}\,\delta(x)\,, \delta(f(x)) = \sum_j \frac{1}{|f'(x_j)|}\,\delta(x - x_j)$ where $f(x_j) = 0$),

$$
\begin{aligned}
& g_0\,\langle m^2\rangle = \\
& = \int d^3p \int d^3r\, \frac{2}{(2\pi\hbar)^3}\,\delta\big(\frac{p^2}{2M_n} - \frac{(p_F(\vec{r})^2)}{2M_n}\big)\,\frac{1}{\hbar^2}\,(x^2p_y^2 + y^2p_x^2) = \\
& = \boxed{\begin{array}{c}\text{because of isotropic distribution} \\ p_y^2 = p_x^2 = \frac{1}{3}\,p^2\end{array}} = \\
& = \int d^3p \int d^3r\, \frac{2}{(2\pi\hbar)^3}\frac{1}{3\,\hbar^2}\,\delta\big(\frac{p^2}{2M_n} - \frac{(p_F(\vec{r})^2)}{2M_n}\big)\;(x^2 + y^2)\,p^2 = \\
& = \boxed{\begin{array}{c}\text{because} \\ \delta\big(\frac{p^2}{2M_n} - \frac{(p_F(\vec{(}r))^2}{2M_n}\big) = \frac{M_n}{p_F(\vec{r})}\,\delta(p - p_F(\vec{r}))\end{array}} = \\
& = M_n \int d^3r\,(x^2 + y^2)\,\frac{8\pi}{(2\pi\hbar)^3\,\hbar^2\,3}\frac{1}{p_F(\vec{r})}\int_0^\infty dp\,p^4\,\delta(p - p_F(\vec{r})) = \\
& = M_n \int d^3r\,(x^2 + y^2)\,\frac{8\pi}{(2\pi\hbar)^3\,\hbar^2\,3}\,p_F^3(\vec{r}) = \boxed{\begin{array}{c}\text{see} \\ (12.58)\end{array}} = \\
& = M_n \int d^3r\,(x^2 + y^2)\,\frac{8\pi}{(2\pi\hbar)^3\,\hbar^2\,3}3\pi^2\,\hbar^3\,\rho(\vec{r}) = \\
& = \frac{M_n}{\hbar^2}\int d^3r\,\rho(\vec{r})\,(x^2 + y^2) = \frac{\mathcal{F}_{rig}}{\hbar^2}
\end{aligned}
\tag{12.59}
$$

where $\mathcal{F}_{rig} = \int d^3r\,\rho(\vec{r})\,(x^2 + y^2)$ is the moment of inertia with respect to the 3-d axis of the intrinsic frame of a rigid body with the same density distribution as the Fermi gas.

The expression (12.55) represents the energy density of Fermi gas with the excitation energy E_{ex}, with the given number N of fermions and with the given angular momentum projection M onto the 3-d frame axis. It is necessary to realize that into the given angular momentum projection all angular momenta $I = M,\ M + 1,\ M + 2, \cdots$ contributes. Therefore the density of states with the given total angular momentum I can be obtained

from the differentiation of $\rho(E_{ex}, N, M)$ (see (12.55)) with respect to M,

$$\begin{aligned}
&\rho(E_{ex}, N, I) = \rho(E_{ex}, N, M = I) - \rho(E_{ex}, N, M = I + 1) = \\
&\approx -\Big(\frac{\partial \rho(E_{ex}, N, M)}{\partial M}\Big)\Big|_{M=I+1/2} = \\
&\approx \frac{\pi}{48} 6^{-1/4} \, (2I + 1) \, g_0 \, \big(\frac{g_0 \hbar^2}{\mathcal{F}_{rig}}\big)^{\frac{3}{2}} \, \big[g_0 \, \big(E_{ex} - \frac{I(I+1)\,\hbar^2}{2\mathcal{F}_{rig}}\big)\big]^{-\frac{7}{4}} \\
&\qquad\qquad e^{2\left[\frac{\pi^2}{6} g_0 \left(E_{ex} - \frac{I(I+1)\,\hbar^2}{2\mathcal{F}_{rig}}\right)\right]^{\frac{1}{2}}}
\end{aligned} \tag{12.60}$$

In the calculation of the derivative we have neglected relatively weak dependence of the coefficient in front of the exponential.

Expressions above for energy density of states of the Fermi gas system were derived for the systems with one type fermions. If the Fermi gas system formed by two-type fermions (e.g. protons and neutrons) is considered then the derivation of the energy density $\rho(E_{ex}, N, Z, I)$ should be extended adequately. For instance, for the special case of the nucleus with $N = Z = A/2$ the density of states characterized by a value of the total angular momentum I, and parity π this derivation gives following expression (see the page 155 in [6]),

$$\begin{aligned}
&\rho(A, E_{ex}, I\pi) = \\
&\approx \frac{2I + 1}{24} \big(\frac{\pi^2}{6} g_0\big)^{1/2} \, \big(\frac{\hbar^2}{2\,\mathcal{F}_{rig}}\big)^{\frac{3}{2}} \, \big[E_{ex} - \frac{I(I+1)\,\hbar^2}{2\mathcal{F}_{rig}}\big]^{-2} \\
&\qquad\qquad e^{2\left[\frac{\pi^2}{6} g_0 \left(E_{ex} - \frac{I(I+1)\,\hbar^2}{2\mathcal{F}_{rig}}\right)\right]^{\frac{1}{2}}}
\end{aligned} \tag{12.61}$$

12.3 Fluctuation and their determination by means of the random matrices method

In this section statistical features of the spectra of Hamiltonian matrices are discussed. These features are results of the random probability distribution of individual matrix elements of Hamiltonian (see [6, 402]).

12.3.1 Random distribution of two- dimensional matrix elements and their eigen values (Wigner and Poisson distributions)

12.3.1.1 Random distribution of matrix elements of two- dimensional matrix

Let us suppose that some quantum system is described by the Hamiltonian in the two- dimensional configuration space with the following Hamiltonian matrix,

$$H = \begin{pmatrix} H_{11} & H_{12} \\ H_{21} & H_{22} \end{pmatrix} \tag{12.62}$$

Further we assume that the matrix is Hermitian, invariant with respect to orthogonal transformation (rotation) and with the Hamiltonian time-reverse invariant. The rotation invariance ensures that the matrix H connects only states with the same value of the angular momentum I and its projection M. Other conserved quantum numbers can be e.g. parity, isospin, etc.

From the rotation and time-reverse invariance of the Hamiltonian $\hat{H}$ follows that the Hamiltonian matrix has real matrix elements and its eigen-vectors are real vectors in the basis $|IM\rangle$ of eigen-states of the square of the angular momentum operator $\hat{I}^2$ and its projection $\hat{I}_3$,

$$\langle I_2 M_2|\hat{H}|I_1 M_1\rangle = \boxed{\begin{array}{c}\text{time-reverse invariance - see (1.48)} \\ \hat{\mathscr{T}}^{-1}\hat{H}\hat{\mathscr{T}} = \hat{H}\ ,\ \text{with}\ \hat{\mathscr{T}} = \hat{R}_y(\pi)\,\hat{\mathscr{K}}\end{array}} =$$

$$= \langle I_2 M_2|\hat{\mathscr{T}}^{-1}\hat{H}\hat{\mathscr{T}}|I_1 M_1\rangle = \langle\overline{I_2 M_2}|\hat{H}|\overline{I_1 M_1}\rangle^* =$$

$$= \boxed{\begin{array}{c}\text{see)} \\ (1.48)\end{array}} = (-1)^{I_1+M_1+I_2+M_2}\,\langle I_2 - M_2|\hat{H}|I_1 - M_1\rangle^* =$$

$$= \boxed{\begin{array}{c}\text{because rotation invariance of } \hat{H} \text{ and} \\ \hat{R}_y(\pi)|IM\rangle = (-1)^{I+M}|I - M\rangle\end{array}} =$$

$$= \langle I_2 M_2|\hat{R}_y^{-1}(\pi)\,\hat{H}\,\hat{R}_y(\pi)|I_1 M_1\rangle^* = \langle I_2 M_2|\hat{H}|I_1 M_1\rangle^*$$

From mathematics it is known that real Hermitian matrix is symmetric (further the kets $|IM\rangle$ are denoted by one index $|i\rangle \equiv |IM\rangle$),

$$\langle j|\hat{H}|i\rangle = \langle i|\hat{H}^+|j\rangle^* = \langle i|\hat{H}|j\rangle^* = \langle i|\hat{H}|j\rangle$$

So our matrix (12.61) is determined by 3 independent matrix elements H_{11}, H_{12} and H_{22},

$$H = \begin{pmatrix} H_{11} & H_{12} \\ H_{12} & H_{22} \end{pmatrix} \tag{12.63}$$

Further we consider the ensemble of matrices (12.63). Let us denote as $P(H)$ the probability that given matrix H is raised from the ensemble during random picking out from the ensemble. The probability distribution $P(H)$ is characterized by the following two properties,

1. If the matrix elements H_{11}, H_{12} and H_{22} are statistically independent (uncorrelated) then,

$$\begin{aligned} & P(H) = \\ & = P_{11}(H_{11}, H_{12}, H_{22}) \cdot P_{12}(H_{11}, H_{12}, H_{22}) \cdot P_{22}(H_{11}, H_{12}, H_{22}) = \\ & = \boxed{\begin{array}{c} \text{if matrix elements are statistically independent} \\ P_{ij}(H_{12}, H_{12}, H_{22}) = P_{ij}(H_{ij}) \end{array}} = \\ & = P_{11}(H_{11}) \cdot P_{12}(H_{12}) \cdot P_{22}(H_{22}) \end{aligned} \tag{12.64}$$

   where $P_{ij}(H_{ij})$ is the probability that pulled out matrix has matrix element H_{ij}.

2. Since the original basis states $|1\rangle$ and $|2\rangle$ ($H_{11} = \langle 1|\hat{H}|1\rangle$ etc.) were chosen arbitrary and because the matrix (12.63) is supposed to be invariant with respect to any orthogonal transformation (including rotations) from vectors $|1\rangle$, $|2\rangle$ into the vectors $|1'\rangle$, $|2'\rangle$ the probability $P(H)$ does not change in any orthogonal transormation:

$$\begin{aligned} & P(H) = P(H') \quad , \quad H_{ij} = \langle i|\hat{H}|j\rangle \quad , \quad H_{i'j'} = \langle i'|\hat{H}|j'\rangle \\ & H = \begin{pmatrix} H_{11} & H_{12} \\ H_{12} & H_{22} \end{pmatrix} \quad , \quad H' = \begin{pmatrix} H_{1'1'} & H_{1'2'} \\ H_{1'2'} & H_{2'2'} \end{pmatrix} \end{aligned} \tag{12.65}$$

Since we restrict ourselves only to the transformations keeping the matrix elements real the unitary transformations are orthogonal in 2- dimensional space (real 2- dimensional space). Further the only infinitesimal transformations can be considered because any finite rotation can be always composed of a sum of infinitesimal transformations,

$$\begin{aligned} & |1'\rangle = |1\rangle + \epsilon\,|2\rangle \quad , \quad \langle i'|j'\rangle = \delta_{i'j'} \\ & |2'\rangle = -\epsilon\,|1\rangle + |2\rangle \quad , \quad \langle i|j\rangle = \delta_{ij} \end{aligned} \tag{12.66}$$

Within the new basis the Hamilton matrix elements can be expressed as

follows (up to the linear terms in ϵ),

$$\begin{aligned} H_{1'1'} &= \big(\langle 1| + \epsilon \langle 2|\big)\, \hat{H}\, (|1\rangle + \epsilon\, |2\,\rangle) \approx H_{11} + 2\,\epsilon\, H_{12} \\ H_{1'2'} &= \big(\langle 1| + \epsilon \langle 2|\big)\, \hat{H}\, \big(-\epsilon\, |1\rangle + |\epsilon\, |2\rangle\big) \approx H_{12} + \epsilon\, \big(H_{22} - H_{11}\big) \\ H_{2'2'} &= \big(-\epsilon \langle 1| + \epsilon \langle 2|\big)\, \hat{H}\, \big(-\epsilon\, |1\rangle + |2\rangle\big) \approx H_{12} - 2\,\epsilon\, H_{12} \end{aligned} \tag{12.67}$$

For corresponding probability $P_{ij}(H_{i'j'})$ the Taylor expansion up to linear terms in ϵ is used,

$$\begin{aligned} P_{11}(H_{1'1'}) &= P_{11}(H_{11} + 2\,\epsilon\, H_{12}) \approx P_{11}(H_{11}) + 2\,\epsilon\, H_{12}\, \frac{dP_{11}}{dH_{11}} \\ P_{12}(H_{1'2'}) &= P_{12}(H_{12} + \epsilon\, (H_{22} - H_{11})) \approx \\ &\qquad \approx P_{11}(H_{12} + \epsilon\, (H_{22} - H_{11}))\, \frac{dP_{12}}{dH_{12}} \\ P_{22}(H_{2'2'}) &= P_{22}(H_{22} - 2\,\epsilon\, H_{12}) \approx P_{22}(H_{22}) - 2\,\epsilon\, H_{12}\, \frac{dP_{22}}{dH_{22}} \end{aligned} \tag{12.68}$$

The substitution of (12.67) into (12.64) gives,

$$P(H) = P(H') = P_{11}(H') \cdot P_{12}(H') \cdot P_{22}(H') = \boxed{\begin{array}{c}\text{up to linear} \\ \text{terms in } \epsilon\end{array}} =$$

$$\begin{aligned} &= P_{11}(H_{11})\, P_{12}(H_{12})\, P_{22}(H_{22}) + P_{11}(H_{11})\, P_{22}(H_{22})\, \epsilon\, (H_{22} - H_{11})\, \frac{dP_{12}}{dH_{12}} \\ &\quad +2\,\epsilon\, H_{12}\, \frac{dP_{11}}{dH_{11}}\, P_{12}(H_{12})\, P_{22}(H_{22}) - 2\,\epsilon\, H_{12}\, \frac{dP_{22}}{dH_{22}}\, P_{11}(H_{12})\, P_{11}(H_{11}) = \\ &= P_{11}(H_{11})\, P_{12}(H_{12})\, P_{22}(H_{22}) \\ &\qquad \big\{1 + \epsilon\, \big[\frac{2H_{12}}{P_{11}(H_{11})} \frac{dP_{11}}{dH_{11}} + \frac{H_{22} - H_{11}}{P_{12}(H_{12})} \frac{dP_{12}}{dH_{12}} - \frac{2H_{12}}{P_{22}(H_{22})} \frac{dP_{22}}{dH_{22}}\big]\big\} = \\ &= P(H)\, \big\{1 + \epsilon\, \big[\frac{2H_{12}}{P_{11}(H_{11})} \frac{dP_{11}}{dH_{11}} + \frac{H_{22} - H_{11}}{P_{12}(H_{12})} \frac{dP_{12}}{dH_{12}} - \frac{2H_{12}}{P_{22}(H_{22})} \frac{dP_{22}}{dH_{22}}\big]\big\} \end{aligned} \tag{12.69}$$

If we suppose the invariance of $P(H)$ with respect to the orthogonal transformation (that means $P(H) = P(H')$) than the rectangular parenthesis (terms with ϵ) should be zero. That means,

$$\begin{aligned} &\frac{1}{H_{12}\, P_{12}(H_{12})}\, \frac{dP_{12}}{dH_{12}} = \\ &= -\frac{2}{H_{22} - H_{11}} \Big(\frac{1}{P_{11}(H_{11})} \frac{dP_{11}}{dH_{11}} - \frac{1}{P_{22}(H_{22})} \frac{dP_{22}}{dH_{22}} \Big) = -C \end{aligned} \tag{12.70}$$

where C is a constant. Since the function on the left hand side of (12.70) is a function of H_{12} while the right hand side depends only on H_{11} and H_{22} the equalities in (12.70) represent two differential equations. The first one is following,

$$\frac{dP_{12}}{dH_{12}} = -C\, H_{12}\, P_{12} \quad \Rightarrow \quad \frac{dP_{12}}{P_{12}} = -C\, H_{12}\, dH_{12}$$
$$\Rightarrow \quad lnP_{12} = -C\, \frac{H_{12}^2}{2} \quad \Rightarrow \quad P_{12} = \big(\frac{C}{2\pi}\big)^{1/2}\, e^{-\frac{C}{2}\, H_{12}^2} \tag{12.71}$$

The expression (12.71) represents the normalized probability because,

$$\int_{-\infty}^{\infty} P_{12}(H_{12})\, dH_{12} = \big(\frac{C}{2\pi}\big)^{1/2} \int_{-\infty}^{\infty} e^{-\frac{C}{2}\, H_{12}^2}\, dH_{12} =$$
$$= \boxed{\begin{array}{c}\text{substitution } x^2 = \frac{C}{2} H_{12}^2 \\ \Rightarrow x = \sqrt{\frac{C}{2}} H_{12}\end{array}} = \frac{1}{\sqrt{\pi}} \int_{-\infty}^{\infty} e^{-x^2}\, dx = \frac{\sqrt{\pi}}{\sqrt{\pi}} = 1$$

The second equation following from (12.70) is:

$$\frac{2}{P_{11}} \frac{dP_{11}}{dH_{11}} - \frac{2}{P_{22}} \frac{dP_{22}}{dH_{22}} = C\, H_{22} - C\, H_{11} \tag{12.72}$$

Again we can separate parts dependent on H_{11} and H_{22},

$$\frac{2}{P_{11}}\, \frac{dP_{11}}{dH_{11}} + C\, H_{11} = \frac{2}{P_{22}}\, \frac{dP_{22}}{dH_{22}} + C\, H_{22} = A \tag{12.73}$$

where A is a constant. The change of the constant A shifts merely the zero point of the energy scale and therefore we can set $A = 0$ and obtain (similarly as we obtained (12.71)),

$$\frac{dP_{11}}{P_{11}} = -\frac{C}{2}\, H_{11}\, dH_{11} \quad \Rightarrow \quad P_{11} = \big(\frac{C}{4\pi}\big)^{1/2}\, e^{-\frac{C}{4}\, H_{11}^2}$$
$$\frac{dP_{22}}{P_{22}} = -\frac{C}{2}\, H_{22}\, dH_{22} \quad \Rightarrow \quad P_{22} = \big(\frac{C}{4\pi}\big)^{1/2}\, e^{-\frac{C}{4}\, H_{22}^2} \tag{12.74}$$

The constant C in (12.71) and (12.74) is in fact determined by the average magnitude of the matrix elements (that means we want $\int P_{ij}(H)\, H\, dH$ to be equal to given values) and in the consequence of it the constant C is related to the average value of the level spacing (as we will be seen in the next subsection 12.3.1.2 the diagonalization of the matrix with the matrix elements distributed by $P_{ij}(H_{ij})$ gives the level spectrum with the distribution $P(s)$ of the level spacing s between 2 neighboring eigen values of this matrix).

According to the expression (12.64) the distribution P(H) corresponding to (12.71) and (12.74) is

$$P(H) = P_{11}(H_{11}) \cdot P_{12}(H_{12}) \cdot P_{22}(H_{22}) = \\ = \frac{C^{3/2}}{2(2\pi)^{3/2}} \, e^{-\frac{C}{4}\,(H_{11}^2+H_{22}^2+2H_{12}^2)} = K_2 \, e^{-\frac{C}{4}\,Tr(H^2)} \tag{12.75}$$

where $K_2 = \frac{C}{2(2\pi)^{3/2}}$ and $Tr(H^2) = H_{11}^2 + H_{22}^2 + 2H_{12}^2$ is the trace of the matrix H^2.

The expression (12.75) for the probability distribution $P(H)$ represents the product of Gaussian distributions $P_{ij}(H_{ij})$ [5] with the zero mean value ($\langle H_{ij} \rangle = 0$ for $i \leq j$) and with the standard quadratic deviation $\langle |(H_{ij} - \langle H_{ij} \rangle)^2| \rangle = \langle H_{ij}^2 \rangle = (1 + \delta_{ij})\, \sigma^2$. therefore the ensemble of matrix (12.63) is called as Gauss orthogonal ensemble (GOE) of two-dimensional real matrix of the Hermitian time-reverse invariant Hamiltonians (see the classification of ensembles of orthogonal and/or unitary Hermitian matrices discussed in the Section R.3 of the Appendix R).

It is necessary to point out that from the point of view of quantum mechanics we should involve into the GOE only part of the Hamiltonian matrix (or the part of the configuration space) which corresponds to given quantum numbers I^π (in the case of $I^\pi = 1/2^\pi$ two-dimensional configuration space). If we involve into the GOE also states with other quantum numbers then we cannot require invariance $P(H') = P_{11}(H'_{11}) \cdot P_{12}(H'_{12}) \cdots P_{NN}(H'_{NN}) = P_{11}(H_{11}) \cdot P_{12}(H_{12}) \cdots P_{NN}(H_{NN}) = P(H)$. So we should always construct ensemble matrices only in the framework of the Hilbert configuration subspace corresponding to given chosen quantum numbers. This determines also the number of statistically independent matrix elements of each matrix of the ensemble (which is directly related to the dimension of matrices in the ensemble - see the Section R.3).

12.3.1.2 Distribution of eigen-values and eigen-vectors of 2-dimensional matrices in Gaussian orthogonal ensemble

In this subsection the probability distribution $P(s)$ of level spacing s between two neighboring levels of the Hamiltonian matrix of the quantum system randomly chosen from the Gauss orthogonal ensemble (GOE) is derived. The eigen values and eigen vectors of the matrix H (Hamiltonian $\hat{H}$) are given

[5] Gaussian distribution is defined as $P_{\mu,\sigma}(x) = \frac{1}{\sigma\sqrt{4\pi}} e^{-\frac{(x-\mu)^2}{2\sigma^2}}$ where μ is the mean or expectation value of the distribution (and also its median) and σ is its standard deviation.

by,

$$\hat{H}|\alpha\rangle = E_\alpha|\alpha\rangle \quad , \quad \langle\alpha|\alpha\rangle = 1$$
$$\hat{H}|\beta\rangle = E_\beta|\beta\rangle \quad , \quad \langle\beta|\beta\rangle = 1 \quad , \quad \langle\alpha|\beta\rangle = 0 \tag{12.76}$$

We suppose that the eigen vectors $|\alpha\rangle$ and $|\beta\rangle$ are search for in the form of the linear combination of basis vectors $|1\rangle$ and $|2\rangle$ ($\langle 1|1\rangle = 1$, $\langle 2|2\rangle = 1$, $\langle 1|2\rangle = 0$, $H_{11} = \langle 1|\hat{H}|1\rangle$, $H_{22} = \langle 2|\hat{H}|2\rangle$, $H_{21} = H_{12} = \langle 1|\hat{H}|2\rangle$. Diagonalization of the matrix H gives the following eigen values (see the Appendix R for details),

$$E_\alpha = \frac{1}{2}\,(H_{11} + H_{22}) + \frac{1}{2}\,\sqrt{(H_{11} - H_{22})^2 + 4\,H_{12}^2}$$
$$E_\beta = \frac{1}{2}\,(H_{11} + H_{22}) - \frac{1}{2}\,\sqrt{(H_{11} - H_{22})^2 + 4\,H_{12}^2} \tag{12.77}$$

with corresponding eigen vectors,

$$|\alpha\rangle = \cos\theta\,|1\rangle + \sin\theta\,|2\rangle$$
$$|\beta\rangle = -\sin\theta\,|1\rangle + \cos\theta\,|2\rangle \quad , \quad -\frac{\pi}{2} \le \theta \le \frac{\pi}{2} \tag{12.78}$$

where (see (R.18) and (R.16))

$$cotg\,\theta = -\frac{1}{2H_{12}}\,\left[\,H_{22} - H_{11} - \sqrt{(H_{11} - H_{22})^2 + 4\,H_{12}^2}\,\right] \tag{12.79}$$

Expressions (12.77)-(12.79) are derived in the Section R.4 of the Appendix R.

Further the distribution $P(H)$ in (12.64),

$$P(H) = P(H_{11}, H_{12}, H_{22}) =$$
$$= P_{11}(H_{11}, H_{12}, H_{22}) \cdot P_{12}(H_{11}, H_{12}, H_{22}) \cdot P_{22}(H_{11}, H_{12}, H_{22}) \tag{12.80}$$

is transformed from variables H_{11}, H_{12}, H_{22} into the variables E_α, E_β, θ. The new and old variables are related by the expressions (12.77) and (12.79). The transformation of the distribution $P(H_{11}, H_{12}, H_{22})$ to the distribution $P(E_\alpha, E_\beta, \theta)$ is given by,

$$P(H_{11}, H_{12}, H_{22})\,dH_{11}\,dH_{12}\,dH_{22} =$$
$$= P(H_{11}(E_\alpha, E_\beta, \theta),\ H_{12}(E_\alpha, E_\beta, \theta),\ H_{22}(E_\alpha, E_\beta, \theta))$$
$$\frac{\partial(H_{11}, H_{12}, H_{22})}{\partial(E_\alpha, E_\beta, \theta)}\,dE_\alpha\,dE_\beta\,d\theta =$$
$$= P(E_\alpha, E_\beta, \theta)\,\frac{\partial(H_{11}, H_{12}, H_{22})}{\partial(E_\alpha, E_\beta, \theta)}\,dE_\alpha\,dE_\beta\,d\theta \tag{12.81}$$

Further the Jacobian $\frac{\partial(H_{11},H_{12},H_{22})}{\partial(E_\alpha,E_\beta,\theta)}$ is determined. From expressions (12.77) and (12.79) we obtain,

$$\begin{aligned} H_{11} &= E_\alpha \cos^2\theta + E_\beta \sin^2\theta \quad , \quad H_{12} = (E_\alpha - E_\beta) \sin\theta \cos\theta \\ H_{22} &= E_\alpha \sin^2\theta + E_\beta \cos^2\theta \end{aligned} \tag{12.82}$$

Hence,

$$\begin{aligned} &\frac{\partial H_{11}}{\partial E_\alpha} = \cos^2\theta \qquad \frac{\partial H_{12}}{\partial E_\alpha} = \sin\theta \cos\theta \qquad \frac{\partial H_{22}}{\partial E_\alpha} = \sin^2\theta \\ &\frac{\partial H_{11}}{\partial E_\beta} = \sin^2\theta \qquad \frac{\partial H_{12}}{\partial E_\beta} = -\sin\theta \cos\theta \qquad \frac{\partial H_{22}}{\partial E_\beta} = \cos^2\theta \\ &\frac{\partial H_{11}}{\partial \theta} = -2(E_\alpha - E_\beta) \sin\theta \cos\theta \\ &\frac{\partial H_{12}}{\partial \theta} = (E_\alpha - E_\beta)(-\cos^2\theta + \sin^2\theta) \\ &\frac{\partial H_{22}}{\partial \theta} = 2(E_\alpha - E_\beta) \sin\theta \cos\theta \end{aligned}$$

So the Jacobian is

$$\begin{aligned} &\frac{\partial(H_{11},H_{12},H_{22})}{\partial(E_\alpha,E_\beta,\theta)} = \begin{vmatrix} \frac{\partial H_{11}}{\partial E_\alpha} & \frac{\partial H_{22}}{\partial E_\alpha} & \frac{\partial H_{12}}{\partial E_\alpha} \\ \frac{\partial H_{11}}{\partial E_\beta} & \frac{\partial H_{22}}{\partial E_\beta} & \frac{\partial H_{12}}{\partial E_\beta} \\ \frac{\partial H_{11}}{\partial \theta} & \frac{\partial H_{22}}{\partial \theta} & \frac{\partial H_{12}}{\partial \theta} \end{vmatrix} = \\ &= \cdots = (E_\alpha - E_\beta)\,[1 - 8 \sin^2\theta \cos^2\theta] \approx E_\alpha - E_\beta \end{aligned} \tag{12.83}$$

The substitution of (12.83), (12.75) into (12.81) gives (see also [6], p.297):

$$\begin{aligned} &P(E_\alpha,E_\beta,\theta) = \\ &= P_{11}(H_{11}(E_\alpha,E_\beta,\theta) \cdot P_{22}(H_{22}(E_\alpha,E_\beta,\theta) \cdot P_{12}(H_{12}(E_\alpha,E_\beta,\theta) \\ &\qquad\qquad \frac{\partial(H_{11},H_{22},H_{12})}{\partial(E_\alpha,E_\beta,\theta)} = \\ &\approx \frac{C^{3/2}}{2(2\pi)^{3/2}} (E_\alpha - E_\beta)\, e^{-\frac{C}{4}(H_{11}^2+H_{22}^2+2H_{12}^2)} = \\ &= \frac{C^{3/2}}{2(2\pi)^{3/2}} (E_\alpha - E_\beta)\, e^{-\frac{C}{4}(E_\alpha^2+E_\beta^2)} \end{aligned} \tag{12.84}$$

In this expression the probability distribution $P(H)$ is expressed in terms of the eigen energies E_α, E_β and the mixing angle θ. The dependence on θ is supposed to be weak and is neglected in (12.83) and (12.84) (see [6] for details).

The probability $P(s)$ that in random picking out from 2-dimensional GOE ensemble we obtain the matrix H with the level spacing s ($s = E_\alpha - E_\beta$, $E_\alpha > E_\beta$) is given by following integral over variables $E_\alpha, E_\beta, \theta$ (more precisely, $P(s)$ is the probability that in the random picking out from the GOE we have matrix H with the eigen-level spacing in the unit energy interval around the value s),

$$P'(s) = \int dE_\alpha \int dE_\beta \int d\theta \; P(E_\alpha, E_\beta, \theta)\, \delta(s - (E_\alpha - E_\beta)) =$$

$$= \boxed{\begin{array}{c}\text{see} \\ (12.84)\end{array}} =$$

$$= \frac{C^{3/2}}{2(2\pi)^{3/2}} \int dE_\alpha \int dE_\beta \int d\theta \; \delta(s - (E_\alpha - E_\beta))\, e^{-\frac{C}{4}\,(E_\alpha^2 + E_\beta^2)}\, (E_\alpha - E_\beta) =$$

$$= \frac{C^{3/2}}{2(2\pi)^{3/3}}\, \pi \int_0^\infty dE_\beta \; s\, e^{-\frac{C}{4}\,[s^2 + 2sE_\beta + E_\beta^2]} =$$

$$= \frac{C^{3/2}}{2(2\pi)^{3/2}}\, \pi\, e^{-\frac{Cs^2}{8}} \int dE_\beta \; e^{-\frac{C}{2}\,(\frac{s}{2} + E_\beta)^2} = \boxed{\begin{array}{c}\text{substitution} \\ y = E_\beta + \frac{s}{2}\,,\; dy = dE_\beta\end{array}} =$$

$$= \frac{C^{3/2}}{2(2\pi)^{3/2}}\, \pi\, e^{-\frac{Cs^2}{8}} \int dy \; e^{-\frac{C}{2}\,y^2} = \boxed{\begin{array}{c}\text{because} \\ \int_0^\infty dy \; e^{-a^2\,y^2} = \frac{\sqrt{\pi}}{2a}\,,\; a = \sqrt{\frac{C}{2}}\end{array}} =$$

$$= \frac{C}{8}\, s\, e^{-\frac{Cs^2}{8}} \tag{12.85}$$

where $s = E_\alpha - E_\beta \in < 0, \infty)$ is the level spacing between eigen energies of the two- dimensional matrix H. The normalization condition, $\int_0^\infty ds\, P(s) = 1$, gives

$$\int_0^\infty ds\; P'(s) = \frac{C}{8} \int_0^\infty ds\; s\, e^{-\frac{Cs^2}{8}} = \boxed{\begin{array}{c}\text{substitution} \\ y = \frac{Cs^2}{8}\,,\; s\, ds = \frac{4}{C} dy\end{array}} =$$

$$= \frac{C}{8}\frac{4}{C} \int_0^\infty dy\; e^{-y} = \frac{1}{2} \int_{-\infty}^0 dx\; e^x = \frac{1}{2} \tag{12.86}$$

Therefore in order to obtain correctly normalized level spacing distribution we should multiply $P'(s)$ by 2, $P(s) = 2\, P'(s)$,

$$P(s) = \frac{C}{4}\, s\, e^{-\frac{Cs^2}{8}} \qquad \text{with} \quad \int_0^\infty ds\; P(s) = 1 \tag{12.87}$$

The constant C can be related to the mean spacing D,

$$\int_0^\infty s\,P(s)\,ds = D = \frac{C}{4}\int_0^\infty s^2\,e^{-\frac{Cs^2}{8}}\,ds = \boxed{\begin{array}{c}\text{the new notation:}\\ a=\frac{C}{8}\end{array}} =$$

$$= \frac{C}{4}\int_0^\infty s^2\,e^{-a\,s^2} = \boxed{\begin{array}{c}\text{because}\\ \int_0^\infty ds\,e^{-a\,s^2}\,s^2 = \frac{\sqrt{\pi}}{4a^{3/2}}\end{array}} = \sqrt{\frac{2\pi}{C}}$$

$$\Rightarrow \quad C = \frac{2\pi}{D^2}$$

and we obtain so called **Wigner distribution** of level spacing (with the average spacing D):

$$P_{Wigner}(s) = \frac{\pi}{2D^2}\,s\,e^{-\frac{\pi\,s^2}{4\,D^2}} \tag{12.88}$$

From (12.88) it is possible to see that the Wigner distribution gives zero for $s \to 0$. This is understandable because for $s \to 0$ the eigen values are degenerated ($E_\alpha = E_\beta$). In order to be degenerated it is necessary (see (12.77) to fulfill simultaneously the conditions $H_{12} = 0$ and $H_{11} = H_{22}$. The probability of both these special values simultaneous is vanishingly small. The exception is if we have 2-dimensional configuration space of two non-interacting particles (that means $H_{12} = H_{21} = 0$) sitting in 2 states with the same energy (e.g. 2 single-particle states $I^\pi = \frac{1}{2}^\pi$ differing only by the sign of angular momentum projection for the rotationally invariant single-particle Hamiltonian).

The Wigner distribution (12.88) was derived on the base of the expansion (12.64) for the probability distribution $P(H)$ of the random picking out the matrix H from the ensemble of matrices with given symmetries (in our case Hermitian rotationally and time-reverse invariant 2- dimensional matrices - see the Appendix R for details). As it was discussed above the Wigner level spacing distribution fulfills, $\lim_{s\to 0} P_{Wigner}(s) = 0$. For non-interacting particles ($H_{12} = H_{21} = 0$) the derivation of the Wigner level spacing distribution requires alway degenerated spectrum ($E_\alpha = H_{11} = E_\beta = H_{22}$). However there is the question if really we should require both these conditions valid simultaneously for the derivation of $P(s)$.

There is an alternative level spacing distribution with the different ansatz from the one used for the Wigner distribution. Specifically so called Poisson distribution is derived starting with the assumption that the eigen values E_α and E_β are randomly distributed in Hamiltonian matrix (the derivation is

given in the Appendix R in the Section R.5 - expr. (R.35)),

$$P_{Poisson}(s) = \frac{1}{D}\, e^{-\frac{s}{D}} \tag{12.89}$$

where D is the mean spacing between E_α end E_β ($s = E_\alpha - E_\beta$), $\int_0^\infty ds\, P(s) = 1$, $\int_0^\infty ds\, s\, P(s) = D$. Randomly distributed eigen values E_α are characteristics (with good approximation) for the Fermi gas model systems with no configuration mixing (no-interacting particles). Opposite to the Wigner distribution (12.88) the Poisson distribution fulfills: $\lim_{s\to 0} P_{Poisson}(s) = \frac{1}{D} \neq 0$. The greatly reduced fluctuations for $s \to 0$ in the spacing implied by the Wigner distribution (12.88) as compared with the Poisson distribution (12.89) imply a tendency for neighboring levels to repel each other (Wigner probability $P_{Wigner}(s)$ goes quickly to zero for $s \to 0$ and therefore if the eigen value distribution is described by the Wigner distribution the spectrum of levels prefers to have spacing with $s \neq 0$). So if the spectrum spacing distribution $P(s)$ for given ensemble of two- dimensional Hermitian rotationally invariant matrices is closed to the Wigner distribution (12.88) one can expect that the corresponding quantum system have eigen vectors $|\alpha\rangle$ and $|\beta\rangle$ which involve mixing of original basis vectors $|1\rangle$ and $|2\rangle$ (the angle $\theta \neq 0$ in (12.78) while if the $P(s)$ is close to the Poisson distribution (12.89) the the original configurations $|1\rangle$ and $|2\rangle$ are not mixed (θ in (12.78) is close to 0).

Randomly distributed eigen values E_α and E_β used in the derivation of the Poisson distribution $P_{Poisson}(s)$ for quantum systems (see the Section R.5) corresponds to the chaotic behavior of solutions of the classic equation of motion (if these systems are described as classic, no quantum, objects). The Wigner spacing distribution $P_{Wigner}(s)$ with a configuration mixing corresponds to the regular behavior in classical physics. Chaotic system in classical physics are connected with more or less homogeneous distribution of classic trajectory traces in so called Poincare cuts of the phase space of the system [6] . On the contrary the regular classical system has these traces (points) in the cut concentrated to regular patterns corresponding to regular closed trajectories in the phase space.

Further we will investigate the question what is the probability distri-

[6]The classical equation of motion equations provides the trajectory of the investigated classical system in the phase space of coordinates and linear momenta $(\vec{r}_i, \vec{p}_i)$ as a function of time (index i enumerates particles forming investigated system, $i = 1, \cdots, n$). The analyzes of traces of trajectories of the system in different cuts of the phase space (so called Poincare cuts) can give information about chaotic or regular behavior of the system. Roughly speaking, if these traces (points) are spread more or less randomly and homogeneously over Poincare cuts the system behaves chaotically. If these traces (points) form regular patterns in the cut the system is regular.

bution of the concrete basis state component in the given eigen state. For instance, we are interested in the probability distribution of the amplitude of the basis state $|1\rangle$ in the eigen state $|\alpha\rangle$ (see (12.78), that means the probability distribution of the amplitude $C_1 = \cos\theta$. We start with the probability distribution $P(E_\alpha, E_\beta, \theta)$ involving the approximation (12.83). The expression (12.84) for $P(E_\alpha, E_\beta, \theta)$ gives the probability that in the random pulling out the matrix H from the GOE ensemble of t- dimensional Hermitian matrices we obtain the matrix H with eigen values E_α, E_β and corresponding eigen vectors $|\alpha\rangle$ and $|\beta\rangle$ characterized by the mixing angle θ. If the approximation (12.83) is valid then the distribution (12.84) is not correlated with the eigen-vectors directly and the probability $P(\theta)$ of the random pulling out the matrix H with the mixing angle θ can be obtained by the integration of $P(E_\alpha, E_\beta, \theta)$ over θ,

$$P'(\theta) = \int_0^\infty dE_\alpha \int_0^\infty dE_\beta \, P(E_\alpha, E_\beta, \theta) = \boxed{\begin{array}{c}\text{see (12.84)}\\ \text{and } E_\alpha \geq E_\beta\end{array}} =$$

$$= \frac{C^{3/2}}{2(2\pi)^{3/2}} \int_0^\infty dE_\alpha \int_0^\infty dE_\beta \, (E_\alpha - E_\beta) \, e^{-\frac{C}{4}(E_\alpha^2 + E_\beta^2)} =$$

$$= \boxed{\begin{array}{c}\text{substitution: } x = E_\alpha - E_\beta \, , \; y = E_\alpha + E_\beta \\ \Rightarrow \; E_\alpha = \frac{1}{2}(x+y) \, , \; E_\beta = \frac{1}{2}(y-x) \quad \Rightarrow \; \frac{\partial(E_\alpha, E_\beta)}{\partial(x,y)} = \frac{1}{2}\end{array}} =$$

$$= \frac{C^{3/2}}{4(2\pi)^{3/2}} \int_0^\infty dx \, x \int_0^\infty dy \, y \, e^{-\frac{C}{8}(x^2+y^2)} = \frac{C^{3/2}}{4(2\pi)^{3/2}} \frac{\Gamma(1)}{2(\frac{C}{8})} \frac{\sqrt{\pi}}{2\frac{\sqrt{C}}{\sqrt{8}}} =$$

$$= \frac{1}{2\pi} \quad \Rightarrow \quad \text{properly normalized distribution: } P(\theta) \approx \frac{1}{\pi} \qquad (12.90)$$

with the normalization $\int_{-\frac{\pi}{2}}^{\frac{\pi}{2}} P(\theta) \, d\theta = 1$. And corresponding probability $P(C_1)$ is

$$P(C_1) \, dC_1 = P(\theta) \, d\theta \quad \Rightarrow$$

$$\Rightarrow P(C_1) = P(\theta) \, \big(\frac{dC_1}{d\theta}\big)^{-1} = \boxed{\begin{array}{c}\text{because}\\ C_1 = \cos\theta\end{array}} \approx P(\theta) \, \frac{1}{\sin\theta} =$$

$$= \frac{P(\theta)}{\sqrt{1 - C_1^2}} = \frac{1}{\pi \sqrt{1 - C_1^{\,2}}} \qquad (12.91)$$

The result (12.91) can be obtained by alternative way. The original GOE ensemble involve the rotationally invariant two dimensional Hamiltonian matrices. It means that matrix elements $\langle i|\hat{H}|j\rangle$ $(i = 1, 2)$ are invariant with

respect to rotations of the basis vectors $|1\rangle$ and $|2\rangle$. As a consequence the normalization $C_1^2 + C_2^2 = 1$ of components in eigen vectors $|1\rangle$ and $|2\rangle$ (see (12.77)) is also invariant with respect to rotations. Therefore the distribution function $P(C_1, C_2)$ for amplitudes in random matrix eigen vectors has following form (because of rotational invariance the distribution $P(C_1, C_2)$ does not depend on θ),

$$P(C_1, C_2) = \frac{1}{\pi}\,\delta(1 - C_1^2 - C_2^2)) \tag{12.92}$$

and the integration of (12.91) over C_2 gives,

$$P(C_1) = \int_0^1 dC_2\, P(C_1, C_2) = \frac{1}{\pi}\int_0^1 dC_2\, \delta(1 - C_1^2 - C_2^2) =$$

$$= \boxed{\begin{array}{c}\text{because}\\ \delta(f(x)) = \sum_{j-1}^{n} \frac{\delta(x-x_j)}{|f\,'(x_j)|}\ ,\ f(x_j) = 0\ ,\ C_2 = \pm\sqrt{1 - C_1^2}\end{array}} =$$

$$= \frac{1}{\pi}\int_0^1 dC_2 \left(\frac{\delta(C_2 - \sqrt{1 - C_1^2})}{2\sqrt{1 - C_1^2}} + \frac{\delta(C_2 + \sqrt{1 - C_1^2})}{2\sqrt{1 - C_1^2}}\right) =$$

$$= \frac{1}{\pi}\frac{1}{2\sqrt{1 - C_1^2}}\int_0^1 dC_2 \left(\delta(C_2 - \sqrt{1 - C_1^2}) + C_2 + \sqrt{1 - C_1^2})\right) =$$

$$= \frac{1}{\pi}\frac{1}{\sqrt{1 - C_1^2}} = (12.91)$$

The linear dependence of the Wigner level spacing distribution $P(s)$ (see (12.88) is a consequence of symmetries assumed for the Hamiltonian matrix (12.62) that means Hermicity, time-reverse invariance, rotational invariance). If these symmetries are reduced we obtain different level spacing from the Wigner one and different number of statistically independent real parameters characterizing each matrix H from the investigated ensemble of matrices with given symmetry (not 3 real parameters H_{11}, H_{12} and H_{22} as in the case of the GOE with2- dimensional matrices). The classification of Gaussian ensembles according to symmetries are discussed in the Section R.3 of the Appendix R (see also the text on the page 298 of [6]).

12.3.2 Random distribution of matrix elements and eigen values of matrices with large dimensions

12.3.2.1 Thomas-Porter distribution

In the case of the analysis of level distributions of energy distances which are not low in the comparison with the mean level distance it is necessary to consider matrices with large dimension N. In the case of large N we start again with the GOE assumptions that the Hamiltonian matrices are Hermitian, time-reverse invariant and invariant with respect to rotations. In the analogy with (12.64) and (12.65) for 2- dimensional matrices we will suppose that also in the case of N-dimensional matrices following assumptions are fulfilled.

1. Hamiltonian matrices with the general dimension N are real, time-reverse invariant (and therefore symmetric) and that the probability $P(H)$ of the picking out the given matrix from the matrix ensemble is (see (12.64)),

$$P(H) = \prod_{i \leq j=1}^{N} P_{ij}(H_{ij}) \tag{12.93}$$

   where $P_{ij}(H_{ij})$ is the probability that picked out matrix has matrix element H_{ij}

2. Since vectors $|1\rangle, |2\rangle, \cdots, |N\rangle$ of the basis, in which the matrices $N \times N$ are constructed, are chosen randomly and all these matrices are invariant with respect to any orthogonal transformations we can simultaneously assume that distribution (12.93) is also invariant with respect to any transformation of the basis $|1\rangle$, $|2\rangle, \cdots, |N\rangle$. Any such transformation can be divided into a product of infinitesimal transformations of the type (12.66). Therefore for the obtaining of the distributions $P_{ii}(H_{ii})$, $P_{ij}(H_{ij})$ $(i, j = 1, \cdots, N)$ the same derivation as in (12.66)-(12.74) can be used with the final same expressions (see (12.71),(12.74)) ,

$$\begin{aligned} P_{ii}(H_{ii}) &= \Big(\frac{C}{4\pi}\Big)^{1/2} e^{-\frac{C}{4} H_{ii}^2} \\ P_{ii}(H_{ij}) &= \Big(\frac{C}{2\pi}\Big)^{1/2} e^{-\frac{C}{2} H_{ij}^2} \quad \text{for } i \neq j \end{aligned} \tag{12.94}$$

The substitution of (12.94) into (12.93) gives,

$$P(H) = \frac{1}{2^{N/2}}\left(\frac{C}{2\pi}\right)^{\frac{N(N+1)}{4}} e^{-\frac{C}{4}(H_{11}^2+H_{22}^2+\cdots H_{NN}^2+2H_{12}+2H_{13}^2+\cdots)} =$$
$$= \frac{1}{2^{N/2}}\left(\frac{C}{2\pi}\right)^{\frac{N(N+1)}{4}} e^{-\frac{C}{4}TrH^2} \tag{12.95}$$

Diagonalization of the $N \times N$ matrix H means, in fact, to find the unitary transformation from the original basis vectors $|1\rangle, |2\rangle, \cdots, |N\rangle$ to the new one in which the matrix H is diagonal with the eigen values E_α ($\alpha = 1, \cdots, N$) on the diagonal. Corresponding eigen vectors are given by linear combinations of the original basis vectors,

$$|\alpha_i\rangle = \sum_{j=1}^{N} C_j^{(\alpha_i)} |j\rangle \qquad , \qquad i = 1, \cdots, N \tag{12.96}$$

However, it is necessary to realize that as a consequence of assumed symmetries of the matrix H (symmetric and real) not all amplitudes $C_j^{(\alpha_i)}$ ($j = 1, \cdots, N$) are independent. The total number of matrix elements of real $N \times N$ matrix is $N(N+1)/2$ and if the matrix H is also symmetric then we have only $N(N-1)/2$ independent matrix elements. Therefore after the diagonalization we have N independent eigen vectors with only $N(N-1)/2$ independent amplitudes $C_j^{(\alpha_i)}$ for all α_i and all j.

The other thing which should be realized is the fact that the TrH^2 in the exponent of (12.95) is invariant with respect to unitary transformations and therefore it can be determined after the diagonalization,

$$TrH^2 = \sum_{\alpha+1}^{N} E_\alpha^2 \tag{12.97}$$

So, similarly as in the case of 2-dimensional matrices (see (12.77) amplitudes $C_j^{(\alpha}$ can be characterized by $N(N-1)/2$ independent angles $\theta_1, \cdots, \theta_\nu$ ($\nu = \frac{N(N_1)}{2}$) and we can search for the distributions $P(E_1, \cdots, E_N, \theta_1, \cdots, \theta_\nu)$ (the probability that picked out the matrix has eigen energies $E_1, \cdots, E_N$ and "angles" θ_i ($i = 1, \cdots, \nu = \frac{N(N-1)}{2}$) in the analogy with (12.82). In the case of the degeneration of eigen energies the corresponding eigen vectors are not determined unambiguously and the Jacobian is equal to zero. Further we know that the functions $H_{ij}(E_\alpha, \theta)$ are linear combinations of E_α (see the expression (12.82) for $N = 2$) and therefore the Jacobian must be a symmetric polynomial of the order $\frac{N(N-1)}{2}$ in E_α. From these considerations the joint

distribution function $P(E_1, \cdots, E_N, \theta_1, \cdots, \theta_\nu)$ can be deduced (analogy with (12.84) - see also the expression (2C-23) in [6]),

$$P(E_1, \cdots, E_N, \theta_1, \cdots, \theta_\nu) = \\ = \mu(\theta_1, \cdots, \theta_\nu) \prod_{\alpha<\beta} |E_\alpha - E_\beta| \, e^{-\frac{C}{4}\sum_\alpha E_\alpha^2} \tag{12.98}$$

where $\theta_1, \cdots, \theta_\nu$ are $N(N-1)/2$ parameters characterizing the structure of N eigen-functions of the matrix H and the function $\mu(\theta_1, \cdots, \theta_\nu)$ is given by the Jacobian of the transformation,

$$H_{ij} \text{ with } i \leq j \\ \rightarrow \quad E_\alpha \, (\alpha = 1, \cdots, N) \;\; ; \;\; \theta_i \, (i = 1, \cdots, \nu = \frac{N(N-1)}{2})$$

When we integrate (12.98) over all angles θ_i $(i = 1, \cdots, \nu)$ we obtain the probability $P_N(E_1, \cdots, E_N)$ (the analog of (12.75) for the case $N = 2$ where $P(E_\alpha, E_\beta, \theta)$ does not depend on θ),

$$P_N(E1, \cdots, E_N) = C_N \, e^{-\frac{1}{4\sigma^2}\sum_i E_i^2} \prod_{j>i} |E_i - E_j| \tag{12.99}$$

where σ is the standard quadratic deviation (see the text under the expression (12.75)). This distribution contains all information about the eigen energies E_i and the statistical correlations among them. The last factor in (12.99) demonstrates the repulsion of levels when the low energy distance between levels are always reduced (not probable).

Integration of (12.99) over all variables E_i except one,

$$\bar{\rho}(E_1) = \int P_N(E_1, E_2, \cdots, E_N) \, dE_2 \cdots dE_N \tag{12.100}$$

gives the following expression (in the limit of large N),

$$\bar{\rho}(E) = \begin{cases} \frac{1}{2\pi\sigma^2} \sqrt{4N\sigma^2 - E^2} & \text{for } E < 2\sqrt{\sigma^2 N} \\ 0 & \text{for } E > 2\sqrt{\sigma^2 N} \end{cases} \tag{12.101}$$

where $\bar{\rho}(E)$ is normalized to N,

$$\int_0^\infty \bar{\rho}(E) \, dE = N \tag{12.102}$$

This normalization enables to interpret $\bar{\rho}(E)$ as the mean energy density of levels (that means the number of levels in the unit energy interval around the

energy E - because N levels are distributed into the whole energy interval $\langle 0, \infty)$ with the energy density $\bar{\rho}(E)$). The mean energy distance between two neighboring levels is then given by,

$$\bar{D} = \frac{1}{\bar{\rho}(E)} \tag{12.103}$$

The expression (12.101) can be rewritten as,

$$\bar{\rho}^2(E) + \frac{E^2}{4\pi^2\sigma^4} = \frac{N^2}{\pi^2\sigma^2} \tag{12.104}$$

and this represents the equation for the ellipse in the plane $(E, \bar{\rho})$. In the literature the equation (12.104) is known as "Wigner semicircle law".

Further the distribution of amplitudes $C_j^{(\alpha)}$ $(j = 1, \cdots .N)$ in the eigenstate (α) of randomly picked out matrix from the GOE ensemble of matrices with $N > 2$ (for $N = 2$ this distribution is given by (12.91)). This distribution can be obtained from the assumption that each matrix from the GOE ensemble is invariant with respect to orthogonal transformation of the basis, that means for all bases (within which given matrix is constructed) we have normalization $\sum_j C_j^{(\alpha)\,2} = 1$ for all α. In the space of amplitudes $(C_1^{(\alpha)}, C_2^{(\alpha)}, \cdots, C_N^{(\alpha)})$ we are located on the surface of the sphere with unit radius in the N- dimensional space. Therefore the general distribution function for N amplitudes is given by,

$$P(C_1^{(\alpha)}, \cdots, C_N^{(\alpha)}) = \frac{2}{\Omega_N}\, \delta\big(1 - \sum_{j=1}^{N} C_j^{(\alpha)\,2}\big) \qquad \text{for all } \alpha \tag{12.105}$$

where Ω_N is the surface of the sphere with the unit radius in the N- dimensional space (or by other words N- dimension space angle) - see p.300 in [6],

$$\Omega_N = \frac{N\,\pi^{N/2}}{\Gamma(\frac{N}{2}+1)} \tag{12.106}$$

where γ is the Gamma function [7] . The factor 2 in (12.105) is connected with the fact that only half of the unit radius sphere has a sense in fact because the other half corresponds to the exchange $C_i = -C_i$.

Distribution of one amplitude, e.g. $P(C_1^{(\alpha)})$, can be obtained by the integration over $C_2^{(\alpha)}, \cdots, C_N^{(\alpha)}$. This can be done by the introduction of polar

[7] Values $\Gamma(\frac{1}{2}) = \sqrt{\pi}$, $\Gamma(1) = O! = 1$, $\Gamma(\frac{3}{2}) = \frac{\sqrt{\pi}}{2}$, $\Gamma(2) = 1$, $\Gamma(\frac{5}{2}) = \frac{3}{4}\sqrt{\pi}$, gives following surfaces of unit radius sphere in 3D and 2D spaces, $\Omega_3 = \frac{3\pi^{3/2}}{\Gamma(\frac{5}{2})} = 4\pi$ and $\Omega_2 = \frac{2\pi}{\Gamma(2)} = 2\pi$

coordinates in the $N-1$ dimensional subspace of amplitudes $C_2^{(\alpha)}, \cdots, C_N^{(\alpha)}$ (see the Appendix R - Section R.6 for details). The result is,

$$P(C_1) = \frac{\Omega_{N-1}}{\Omega_N} \, (1 - C_1^2)^{\frac{N-3}{2}} \tag{12.107}$$

For the determination of Ω_N and Ω_{N-1} (see (12.107) in the limit of big N the Stirling formule,

$$\Gamma(n) \approx (n-1)! \approx (n-1)^{n-1} \, e^{-n+1} \, \sqrt{2\pi(n-1)} \tag{12.108}$$

can be used and we obtain,

$$\begin{aligned}
\Omega_N &= \frac{N \, \pi^{N/2}}{\Gamma(\frac{N}{2}+1)} \approx \frac{N \, \pi^{N/2}}{(\frac{N}{2})^{\frac{N}{2}} \, e^{-\frac{N}{2}} \, N^{\frac{1}{2}} \sqrt{\pi}} \\
\Omega_{N-1} &\approx \frac{(N-1) \, \pi^{\frac{N-1}{2}}}{(\frac{N-1}{2})^{\frac{N-1}{2}} \, e^{-\frac{N-1}{2}} \, (N-1) \, \sqrt{\pi}} \\
\Rightarrow \quad \frac{\Omega_{N-1}}{\Omega_N} &\approx \frac{1}{\sqrt{2\pi}} \, e^{-\frac{1}{2}} \, \sqrt{\frac{N^{N-1}}{(N-1)^{N-2}}} \quad \overset{N\to\infty}{\to} \quad \sqrt{\frac{N}{2\pi}}
\end{aligned} \tag{12.109}$$

The substitution of (12.109) into (12.107) gives the distribution $P(C_1)$ in the following form [8],

$$P(C_1^{(\alpha)}) \approx \sqrt{\frac{N}{2\pi}} \, e^{-\frac{N}{2} \, C_1^{(\alpha)\,2}} \tag{12.110}$$

This result is important for analysis of distributions of all physical quantities which are determined by one amplitude (e.g. C_1) of the wave function of

[8]

$$P(C_1^{(\alpha)}) = \boxed{\begin{array}{c}\text{see (12.107)} \\ \text{(12.109)}\end{array}} = \sqrt{\frac{N}{2\pi}} \, (1 - C_1^{(\alpha)}) = \boxed{\begin{array}{c}\text{Taylor expansion} \\ \text{in } C_1^{(\alpha)\,2}\end{array}} =$$

$$= \sqrt{\frac{N}{2\pi}} \, [1 - \frac{N-1}{2} \, C_1^{(\alpha)\,2} + \cdots]$$

From other side,

$$\sqrt{\frac{N}{2\pi}} \, e^{-\frac{N}{2} \, C_1^{(\alpha)\,2}} \approx \boxed{\begin{array}{c}\text{Taylor expansion} \\ \text{in } C_1^{(\alpha)\,2}\end{array}} = \sqrt{\frac{N}{2\pi}} \, [1 - \frac{N}{2} \, C_1^{(\alpha)\,2} + \cdots]$$

Therefore for $N \to \infty$ we have,

$$P(C_1^{(\alpha)}) \approx \sqrt{\frac{N}{2\pi}} \, e^{-\frac{N}{2} \, C_1^{(\alpha)\,2}} = (12.110)$$

the given eigen state of the system. For instance, in the case of neutron capture such quantity is so called neutron strength function which is related to the reduced neutron width $\Gamma_n^{(0)}$ of the distribution of the component of the captured state connected with the neutron single-particle state in which the neutron is captured. This neutron single-particle state belongs to components of the collective resonance states of the compound nucleus which is formed during the neutron capture - see the discussion in the next Subsection 12.3.3. The partial width distribution $P(\Gamma_n^{(0)})$ is then unambiguously determined by the distribution $P(C_1)$,

$$\Gamma^{(0)} = k\, C_1^2 \quad \Rightarrow \quad P(\Gamma^{(0)})\, |d\Gamma^{(0)}| = P(C_1)\, |dC_1|\, 2\, k \tag{12.111}$$

where k is some proportionality coefficient which is related to the given process (e.g. neutron capture). From (12.111),

$$P(\Gamma^{(0)}) = P(C_1)\, \Big|\frac{2\, dC_1}{d\Gamma^{(0)}}\Big| = \boxed{\begin{array}{c}\text{see}\\ (12.110)\end{array}} =$$

$$= \sqrt{\frac{N}{2\pi}}\, e^{-\frac{N}{2}C_1^2} \frac{2}{2kC_1} = \sqrt{\frac{N}{2\pi k\, \Gamma^{(0)}}}\, e^{-\frac{N}{2k}\Gamma^{(0)}} \tag{12.112}$$

Corresponding mean value of the reduced width is,

$$\langle \Gamma^{(0)} \rangle = \int_0^\infty \Gamma^{(0)}\, P(\Gamma^{(0)})\, d\Gamma^{(0)} = \sqrt{\frac{N}{2k\pi}} \int_0^\infty d\Gamma^{(0)}\, \sqrt{\Gamma^{(0)}}\, e^{-\frac{N}{2k}\,\Gamma^{(0}} =$$

$$= \boxed{\begin{array}{c}\text{substitution}\\ x = \frac{N}{2k}\Gamma^{(0)} \;\Rightarrow\; dx = \frac{N}{2k} d\Gamma^{(0)}\end{array}} = \sqrt{\frac{N}{2k\pi}} \int_0^\infty dx\, \big(\frac{2k}{N}\big)^{3/2} \sqrt{x}\, e^{-x} =$$

$$= \boxed{\begin{array}{c}\text{because}\\ \int_0^\infty dx\, x^r\, e^{-x} = \Gamma(r+1)\end{array}} = \frac{2k}{N\sqrt{\pi}}\, \Gamma(\frac{3}{2}) = \boxed{\begin{array}{c}\text{because}\\ \Gamma(\frac{3}{2}) = \frac{\sqrt{\pi}}{2}\end{array}} =$$

$$= \frac{k}{N} \tag{12.113}$$

Then the expression (12.112) can be rewritten as follows,

$$P(\Gamma^{(0)}) = \frac{1}{\sqrt{2\pi\, \langle \Gamma^{(0)} \rangle\, \Gamma^{(0)}}}\, e^{-\frac{\Gamma^{(0)}}{2\langle \Gamma^{(0)} \rangle}} \tag{12.114}$$

The distribution (12.114) is known in the literature as the Thomas-Porter distribution. The mean square deviation of this distribution is [9],

$$\langle\, (\; \Gamma^{(0)} - \langle \Gamma^{(0)} \rangle)^2 \,\rangle = 2\, \langle \Gamma^{(0)} \rangle^2 \tag{12.115}$$

[9]

$$\langle\, (\; \Gamma^{(0)} - \langle \Gamma^{(0)} \rangle)^2 \,\rangle = 2\, \langle \Gamma^{(0)} \rangle^2 = \langle \Gamma^{(0)\,2} \rangle - \langle \Gamma^{(0)} \rangle^2$$

We can see that the mean square deviation of the Thomas-Porter distribution is relatively big in the comparison with the mean value $\langle\Gamma^{(0)}\rangle$. So big fluctuation is related to our assumption that only one channel, connected with the amplitude $C_1^{(\alpha)}$ through its square ($\Gamma^{(0)} \approx C_1^2$), is open.

In the case when given excites state α, formed in some process, decays not only through one channel (one transition) into the ground state (e.g. through the emission of one photon connected with the partial width $\Gamma^{(0)} \approx C_1^{(\alpha)\,2}$), but it is possible to de-excite given state by transitions into other lower energy states (that means through several decay channels), then we have ν partial widths, $\Gamma^{(1)} \propto C_1^{(\alpha)\,2}$, $\Gamma^{(2)} \propto C_2^{(\alpha)\,2}$, $\cdots$, $\Gamma^{(\nu)} \propto C_\nu^{(\alpha)\,2}$. Then we can introduce a total width as a sum $\Gamma \equiv \sum_{i=1}^{\nu} \Gamma^{(i)}$. If further we suppose the statistical independence of each decay channel and that the mean partial widhs of all channels are the same,

$$\langle\Gamma^{(j)}\rangle = \frac{1}{\nu}\,\langle\Gamma\rangle \tag{12.116}$$

then the corresponding probabilty distribution $P_\nu(\Gamma)$ is given by the "folding"of Thomas-Porter distributions of individual partial decay channels,

$$\begin{aligned} &P_\nu(\Gamma) = \\ &= \int P(\Gamma^{(1)}) \cdot P(\Gamma^{(2)}) \cdots P(\Gamma^{(\nu)}) \;\; \delta(\Gamma - \sum_{i=1}^{\nu} \Gamma^{(i)}) \;\; d\Gamma^{(1)}\, d\Gamma^{(2)} \cdots d\Gamma^{(\nu)} \end{aligned} \tag{12.117}$$

The δ- function in this expression can be expressed as,

$$\delta(\Gamma - \sum_{i=1}^{\nu} \Gamma^{(i)}) = \frac{1}{2\pi} \int dk\, e^{ik(\Gamma - \sum_i \Gamma^{(i)})} \tag{12.118}$$

---

where

$$\langle\, \Gamma^{(0)\,2}\,\rangle = \int_0^\infty d\Gamma^{(0)}\, \Gamma^{(0)\,2}\, P(\Gamma^{(0)}) = \frac{1}{\sqrt{2\pi\,\langle\Gamma^{(0)}\rangle}} \int_0^\infty \frac{\Gamma^{(0)\,2}}{\sqrt{\Gamma^{(0)}}}\, e^{-\frac{\Gamma^{(0)}}{2\langle\Gamma^{(0)}\rangle}}\, d\Gamma^{(0)} =$$

$$= \boxed{\begin{array}{c}\text{substitution} \\ x = \frac{\Gamma^{(0)}}{2\langle\Gamma^{(0)}\rangle} \;\;\Rightarrow\;\; d\Gamma^{(0)} = 2\langle\Gamma^{(0)}\rangle\, dx\end{array}} = \frac{2\langle\Gamma^{(0)}}{\sqrt{2\pi\,\langle\Gamma^{(0)}\rangle}} \left(2\langle\Gamma^{(0)}\rangle\right)^{3/2} \int_0^\infty dx\, x^{\frac{3}{2}}\, e^{-x} =$$

$$= \boxed{\begin{array}{c}\text{because} \\ \int_0^\infty dx\, x^r\, e^{-x} = \Gamma(r+1)\end{array}} = \frac{4\,\langle\Gamma^{(0)}\rangle^2}{\sqrt{\pi}}\, \Gamma(\frac{5}{2}) = \boxed{\begin{array}{c}\text{because} \\ \Gamma(\frac{5}{2}) = \frac{3}{4}\sqrt{\pi}\end{array}} = 3\langle\Gamma^{(0)}\rangle^2$$

So we have

$$\langle\,(\;\Gamma^{(0)} - \langle\Gamma^{(0)}\rangle)^2\,\rangle = 3\langle\Gamma^{(0)}\rangle^2 - \langle\Gamma^{(0)}\rangle^2 = 2\langle\Gamma^{(0)}\rangle^2$$

and the substitution of (12.118) into (12.117) gives,

$$P_\nu(\Gamma) = \frac{1}{2\pi} \int dk\, e^{i\Gamma k} \left[\prod_{i=1}^{\nu} P(\Gamma^{(i)})\, e^{-ik\Gamma^{(i)}}\, d\Gamma^{(i)} \right]$$

which, using (12.116) and (12.114) for each i, finally gives (see [6] expr. (2C-29)),

$$P_\nu(\Gamma) = \Big(\frac{\nu\,\Gamma}{2\langle\Gamma\rangle}\Big)^{\nu/2} \big[(\frac{\nu}{2}-1)!\big]^{-1}\, e^{-\frac{\nu\Gamma}{2\langle\Gamma\rangle}}\, \frac{1}{\Gamma} \tag{12.119}$$

The distribution (12.119) is so called χ^2 distribution with ν degrees of freedom. Mean square deviation of χ^2 distribution is,

$$\langle|(\Gamma - \langle\Gamma\rangle)^2|\rangle = \frac{2}{\nu}\,\langle\Gamma\rangle^2 \tag{12.120}$$

and we see that it decreases with increasing ν.

For $\nu = 2$ the expression (12.119) gives the Poisson distribution (see (12.90).

$$P_2(\Gamma) = P_{Poisson}(\Gamma) = \frac{1}{\langle\Gamma\rangle}\, e^{-\frac{\Gamma}{\langle\Gamma\rangle}} \tag{12.121}$$

12.3.3 Some examples of distributions of levels and their widths in nuclear physics

12.3.3.1 Energy distribution of levels observed in neutron capture and the energy distributions of neutron widths

In the history of nuclear physics one of the main sources of information about structure of nuclear states with high excitation was the investigation of resonances observed in the capture reaction of low-energy (thermal) neutrons (with the energy E_n up to hundreds of eV) - see the Fig.12.2. The Fig.12.2 shows the dependence of the cross-section of the neutron capture by the nucleus ^{232}Th with the neutron energies $20\,eV < E_n < 210\,eV$.

As a consequence of the presence of so called centrifugal barrier in the effective interaction involved in the nuclear Hamiltonian (centrigugal barrier is given by the term $\frac{l(l+1)}{r^2}$ in (D.2)) the capture eigen states of the resultant compound nucleus [10] (^{233}Th in the Fig12.2) which are observed as the narrow

[10] It is necessary to realize that, because of the fact that the absolute value of the binding energy of ^{233}Th is less than the binding energy of ^{232}Th (in the ground state), the capture states in ^{233}Th have excitation energies E_{ex} not far from the absolute value of one neutron separation energy ($E_{ex} \approx |E_{bind}^{(A+1)}| - |E_{bind}^{(A)}| + E_n$). That means, during neutron capture in the even-even nucleus the resulting odd-A nucleus is a compound nucleus in the states with high excitation energies where the level density is big. In the next step this compound nucleus decays through different channels ($\gamma-$ de-excitation, emission of nucleons etc.).

resonances in the neutron capture cross-section, correspond to the orbital momentum $l = 0$ with much higher probability than to higher orbital momenta $l > 0$. For instance in the book [6] it is demonstrated that the widths of resonance with the orbital momentum $l = 1$ for neutron energies $E_n \approx 100$ eV is $\approx 10^4$-times less than the width of $l = 0$ resonance (it is necessary to remind that the width of the resonance is proportional to the intensity with which the resonance is observed in the neutron capture experiments). Therefore the probability that observed resonances correspond to $l > 0$ is negligible with respect to the probability that these resonances have $l = 0$. Nevertheless, the increase of the energy resolution of nowadays experimental equipments enabled to observe also $l = 1$ resonances and one should always check if the experimental data involve only $l = 0$ resonances.

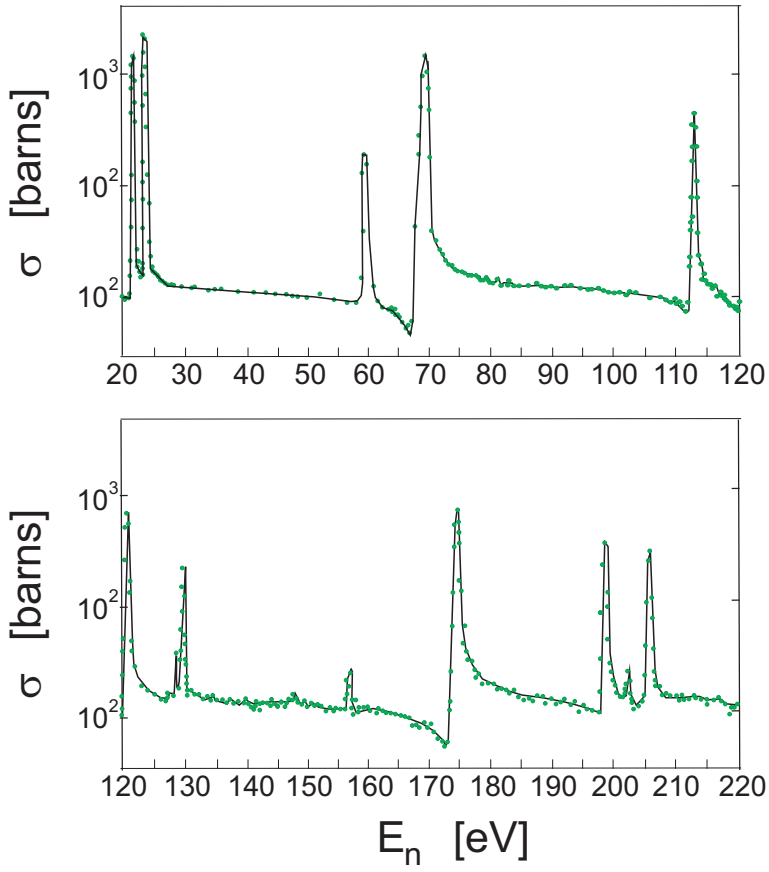


Figure 12.2: Total cross-section of the reaction n+^{232}Th as a function of the neutron energy E_n (figure taken from [6] (see the fig. 2-8) therein).

If the assumption that the experimental data concern only $l = 0$ resonances is accepted then the angular momentum I_r and parity π_r of the resonance

state in the final nucleus are following,

$$I_r = I_0 \pm \frac{1}{2} \qquad , \qquad \pi_r = \pi_0 \tag{12.122}$$

where I_0 and π_0 are the angular momentum and parity of the target nucleus ground state (^{232}Th with $I_0 = 0$ and $\pi_0 = +1$ in the Fig.12.2). For even-even nuclei the ground state values are always $I_0 = 0$ and $\pi_0 = +1$ and therefore in the neutron capture experiments with the even-even target nuclei we observe in the final nucleus predominantly resonances with $I_r = 1/2$ and $\pi_r = +1$, that means compound nucleus states with $I_r^{\pi_r} = \frac{1}{2}^+$.

From the neutron capture experiments it is known that the mean level spacing for resultant nucleus states is $\langle s \rangle \approx 16$ eV (see [6] and citation therein). This value is $\approx 10^6$ times less than the energy spacing between two neighboring levels of the single-particle states of the nuclear mean field. This corresponds to the big density of single-particle states (because the level spacing is inversely proportional to the level density). This indicates that the spectrum of excited states of resultant compound nuclei after the neutron capture cannot be formed by single-particle states and that these states should have an collective character. This fact can be demonstrated on the next rough estimation.

Our estimation starts with the Fermi gas expression (12.61) for the energy density of states in the nucleus with $N = Z = A/2$ when the rotation of the nucleus is taken into account,

$$\begin{aligned} &\rho(A, E_{ex}, I\pi) = \\ &\approx \frac{2I+1}{24}\Big(\frac{\pi^2}{6}g_0\Big)^{1/2}\,\Big(\frac{\hbar^2}{2\,\mathcal{F}_{rig}}\Big)^{\frac{3}{2}}\,\Big[E_{ex} - \frac{I(I+1)\,\hbar^2}{2\mathcal{F}_{rig}}\Big]^{-2} \\ &\qquad\qquad e^{2\left[\frac{\pi^2}{6}g_0\left(E_{ex}-\frac{I(I+1)\,\hbar^2}{2\mathcal{F}_{rig}}\right)\right]^{\frac{1}{2}}} \end{aligned} \tag{12.123}$$

where $\mathcal{F}_{rig} = M_n \int d^3r\rho(\vec{r})\,(x^2+y^2) \approx \frac{2}{3}\int d^3r\rho(\vec{r})\,r^2$ (where $r^2 = x^2+y^2+z^2$ and the surfaces of the same density are supposed to be spheres) is the inertial moment of the nucleus determined as the inertial moment of the rigid body with respect to the rotation axis perpendicular to the 3-d axis of the nucleus intrinsic frame. The symbol g_0 in (12.123) is the total density of the single-particle states on the Fermi level [11]

$$g_0 = \frac{3}{2}\frac{A}{\epsilon_F} \tag{12.125}$$

[11] We suppose that nucleons in the nucleus are described as the Fermi gas where the relation between number of nucleon states and the single-particle linear momentum k is given by the expression (H.4) in the

where A is the number of nucleons and ϵ_F is the Fermi energy ($\epsilon_F = \frac{\hbar^2 k_F^2}{2M}$, $k_F = (see\,(12.7) = \left(3\pi^2 A/V\right)^{1/3}$, $V = \frac{4}{3}\pi r_0^3 A$ is the nucleus volume $\approx$ volume of the sphere with the radius $R = r_0 A^{1/3}$ fm (see (1.2)). The estimation of ϵ_F gives,

$$\epsilon_F = \frac{\hbar^2 k_F^2}{2M} = \frac{\hbar^2}{2M}\left(3\pi^2 A/V\right)^{2/3} \approx 50 \ \text{MeV}$$

$$\Rightarrow \quad g_0 \approx \frac{3}{2}\frac{A}{50\ MeV} \approx \boxed{\begin{array}{c}\text{for estimation}\\ A = 232\end{array}} \approx 7\ MeV^{-1} \qquad (12.126)$$

This estimation can be compared with the corresponding experimental value which can be obtained from known experimental level spacing $\langle s \rangle_{exp} \approx 16$ eV which is connected with the single-particle energy density (12.123) as,

$$\langle s \rangle \approx [\,\rho(E, E_{ex}, I\pi)]^{-1} = \langle s \rangle_{exp} \approx 16 \text{ eV} \qquad (12.127)$$

If this expression (using (12.123) with $E_{ex} \approx 5\ MeV$, $I^\pi \approx \frac{1}{2}^+$) is undersood as the equation for g_0 we obtain solution $g_0^{(exp)} \approx 10\ MeV^{-1}$ which is in accordance with our Fermi gas estimation (12.126). From this very rough comparison of the Fermi gas approximation for g_0 with the experimental value one can conclude that the rotational degrees of freedom involved in the expression (12.123) for the energy density of states , lead to the improvement of the comparison with experimental data.

As it can be observed from the Fig.12.2 (and even better from the Fig. 12.4) The neutron width of resonances changes their values in the dependence

---

Appendix H (nucleus is the 3- dimensional object $\Rightarrow$ $D = 3$ in (H.4)),

$$2\,d^3k = \left(\frac{2\pi}{L}\right)^3 d^3n \qquad \Leftrightarrow \qquad d^3n = \frac{2V}{(2\pi)^3}\,d^3k \qquad (12.124)$$

where the factor 2 is connected with the 2 possibilities of the spin projection for each nucleon. The integration of (12.124) over the sphere in the linear momentum space with the radius k gives,

$$n = \frac{2V}{(2\pi)^3}\frac{4}{3}\pi k^3 = \boxed{\begin{array}{c}\text{because}\\ \epsilon = \frac{\hbar^2 k^2}{2M}\end{array}} = \frac{2V}{(2\pi)^3}\frac{4}{3}\pi\left(\frac{2M}{\hbar^2}\right)^{3/2}\epsilon^{3/2}$$

$$\Rightarrow \qquad \frac{dn}{d\epsilon} = \frac{3}{2}\frac{n}{\epsilon}$$

In our case $n = A$ and therefore,

$$g_0 \equiv \frac{dn}{d\epsilon}(\epsilon = \epsilon_F) = \frac{3}{2}\frac{A}{\epsilon_F} = (12.125)$$

on the excitation energy but their mean value is about (see [6]) [12],

$$\bar{\Gamma}_n \approx 1.2\,10^{-3}\,(E_n)^{1/2} \tag{12.128}$$

where both width $\bar{\Gamma}_n$ and energies E_n are in eV. This value is about 10^6 times less than single-particle estimation based on the Fermi gas model (see the expression (3F-51) in [6]). This is again a confirmation of the fact that the real excited states in the final nucleus (after the neutron capture) have a collective character.

The final compound nucleus (after the neutron capture) decays through several channels (e.g. reverse reaction ^{233}Th $\rightarrow$ n + ^{232}Th, or emissions of photon, or fission reaction (n,f)). It was shown that the total width with respect to the emission of γ-quantum, Γ_γ, is approximately the same for all resonances (e.g. for ^{233}Th $\Gamma_\gamma \approx 2.5\,10^{-2}$ eV). Since the E1 γ- transition dominates usually in the γ- de-excitation of the final compound nucleus the E1 character of γ- cascade de-excitation is preferred in the statistical modeling of the whole neutron capture process (including the decay of the compound nucleus formed during neutron capture). However, in the connection with the improvement of the resolution ability of modern experimental equipments it is possible to observed the influence of higher multipolarities γ- transitions (and not only electric one) following the neutron capture (see [382] and citations therein, see also the subsection 12.4.4).

12.3.3.1.1 Energy distribution of levels in the compound nucleus formed during neutron capture Statistical distribution of level spacing and widths of neutron resonances provide information about the structure of resonance states. As an example the level spacing between resonances in the system n+^{232}Th (that means in the final compound nucleus ^{233}Th) is demonstrated in the Fig.12.3. Particularly in the Fig.12.3 the experimental neutron resonance level spacing in ^{233}Th is compared with calculated Wigner and Poisson distributions of the ratio $x = s/D$ where D is the mean level spacing.

$$P_W(x) = P_W(s)\,\frac{ds}{dx} = \boxed{\begin{array}{c}\text{see}\\(12.88)\end{array}} = \frac{\pi}{2\langle x^2\rangle}\,x\,e^{-\frac{\pi}{4}\frac{x^2}{\langle x^2\rangle}}$$

$$P_P(x) = P_P(s)\,\frac{ds}{dx} = \boxed{\begin{array}{c}\text{see}\\(12.89)\end{array}} = \frac{1}{\langle x\rangle}\,e^{-\frac{x}{\langle x\rangle}} \tag{12.129}$$

[12] Mean value $\bar{\Gamma}_n$ divided by the mean value of the level spacing s defines so called neutron strength function which is discussed in the Subsection 12.4.4.

As we know the derivation of the Wigner distribution (see (12.88) and the text below the expr. (12.89) this distribution valids in the case when the basis vectors (in which Hamiltonian matrices were constructed) are mixed. In the case of resonance states of ^{233}Th the basis vectors are represented by single-particle neutron and proton states of the mean field of ^{232}Th. From

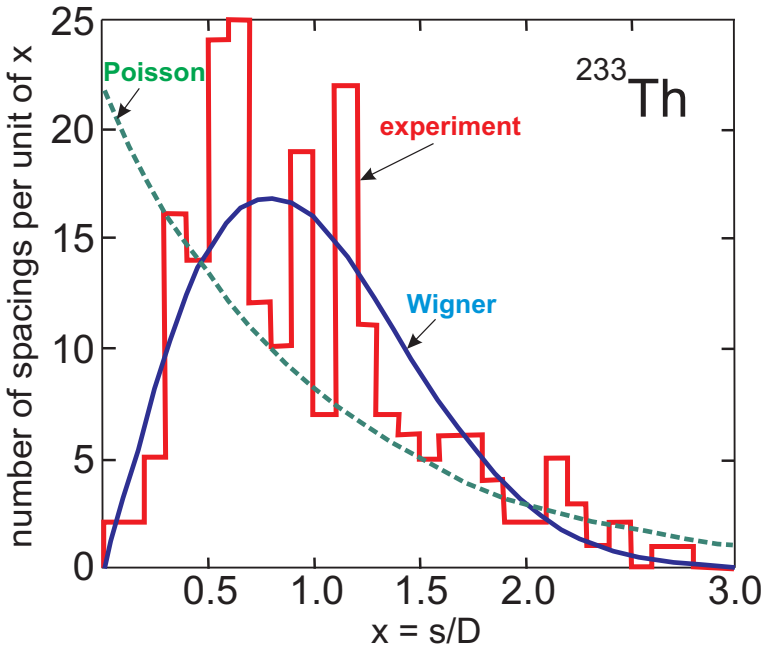


Figure 12.3: Probability distribution of spacings, $x = s/D$, between adjacent resonance levels in the reaction n+^{232}Th up to an energy $E_n = 3.9$ keV (223 resonances were involved in statistical ensemble). The average level spacing is denoted by D. The data taken from [383] (see also the Fig.2-9 in [6])

the Fig.12.3 it is evident that the experimental distribution corresponds to the Wigner distribution and therefore the resonance neutron states in ^{233}Th involve mixing of the basis single-particle states. By other words these resonance have a collective character.

However, in the connection with the Fig.12.3 (and similar figures) it is necessary to note that the experimental data from which experimental points in the Fig.12.3 were taken, involved also weak resonances where angular momenta and parities were not determined. It was supposed in the construction of the experimental statistical ensemble of spacings that these weak resonances did not belong to the group of resonances corresponding to $I^\pi = \frac{1}{2}^+$ (with the orbital momentum $l = 0$) but they correspond to higher orbital momenta $l > 0$. Therefore these weak resonances were not involved in the Fig.12.3. However it is a question of this assumption.

Analyzes of the configuration mixing, performed in the framework of the

random matrices approach, should involve also a long-order in sequence of resonance energies (not only spacing of neighboring levels). For this aim F.J. Dyson and M.Mehta (see [384]) introduced the quantity Δ_3 that measures the mean square deviation of the number $N(E)$ of levels up to the energy from the best straight line fit on the energy interval $\langle -L, +L \rangle$,

$$\Delta_3(L) = \min_{A,B} \Big[\frac{1}{2L} \int_{-L}^{+L} [N(E) - AE - B]^2 dE \Big] \tag{12.130}$$

where A, B are optimal parameters of the optimal straight line. The random matrix model (see [384]) gave for limit case when the number of resonances in the ensemble is very large the following expression (see also [6]),

$$\Delta_3 \approx \frac{1}{\pi^2} \big[\, ln \, n - 0.0687 \, \big] \tag{12.131}$$

where n is the number of resonances included in the ensemble. The value of Δ obtained from the experimental energies of the first 154 resonances in the ^{233}Th was $\Delta_{exp} = 3.12$. From other side the expression (12.131) corresponding to the Wigner distribution of spacings gave $\Delta_3 \approx 0.5$ [6]. The big difference between these values indicates the problem of the prediction of configuration mixing followed from the random matrices model. However one should be careful because the experimental value $\Delta_{exp} = 3.12$ was determined on the base of the assumption that the sample of the first 154 resonances is complete ensemble of the first $I^\pi = \frac{1}{2}^+$ resonances (that means we should exclude cases when resonances do not have $I^\pi = \frac{1}{2}^+$ or some of $I^\pi = \frac{1}{2}^+$ resonances were omitted). This fact was not fully checked [6].

The analysis of the ^{233}Th resonances is very simple because the target nucleus ^{232}Th has $I_0 = 0$ which corresponds to $l = 0$ and therefore all resonances have $I_r = \frac{1}{2}^+$. However, the random matrices model conclusion that the experimental level spacing distribution corresponds to the Wigner distribution was confirmed later by other neutron capture measurements with the both even-even and odd-A target nuclei (some of these results are discussed in the Subsection 12.3.3.2.

12.3.3.1.2 Distribution of neutron widths Further information about the structure of neutron resonances can be obtained by the analysis of widths. It will be again demonstrated on the case of the nucleus ^{233}Th (neutron capture n+ ^{232}Th $\rightarrow$ ^{233}Th - see [6]). As it was discussed in the connection with the expression (12.128) the average value of the neutron width $\bar{\Gamma}_n$ is proportional

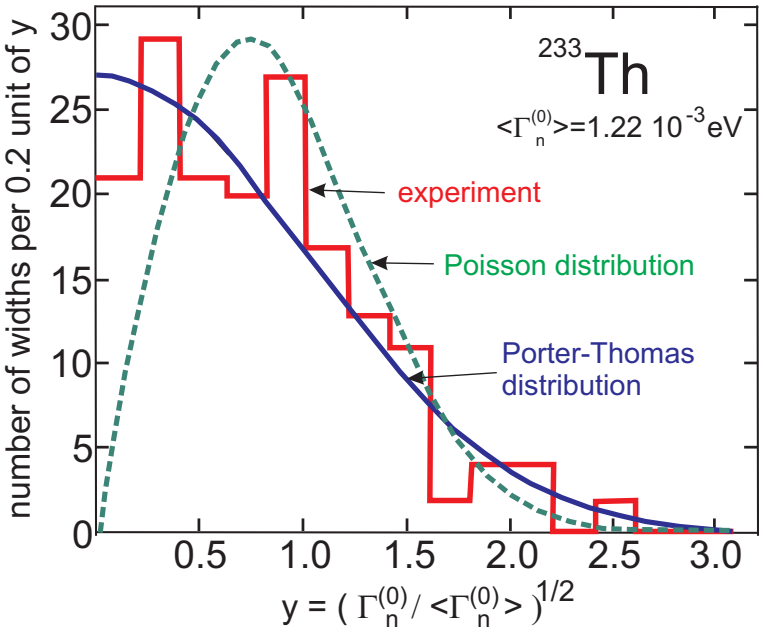


Figure 12.4: Probability distribution of the reduced neutron widths $\Gamma_n^{(0)}[r]$ (see (12.132)) (converted to the distribution of the quantity $y \equiv \sqrt{\Gamma_n^{(0)}(E_n)/\langle\Gamma_n^{(0)}\rangle}$) observed in the reaction n+^{232}Th. The same experimental ensemble of neutron resonance is used as in the Fig.12.3. The data taken from [383] (see also the Fig.2-9 in [6])

to $E_n^{1/2}$. In order to get rid of the dependence on $E_n[r]$ (index r enumerates resonances with $l = 0$) a distribution of so called reduced neutron widths defined as,

$$\Gamma_n^{(0)}[r] \equiv E_n^{-1/2}[r]\ \Gamma_n(E_n[r]) \tag{12.132}$$

were introduced. These reduced neutron widths are independent on resonance energies and they are connected with the intrinsic properties of the resonance with the given index r

As an example the probability distribution of the reduced neutron widths $\Gamma_n^{(0)}[r]$ observed in the neutron capture n+^{232}Th = ^{233}Th (normalized to the total number of 171 $l = 0$ resonances, $\sum_{r=1}^{171} P(\Gamma_n^{(0)}(E_r) = 1$, with resonance energies $E_r \in \langle\ 0\ , E_{max} = 3\ keV\ \rangle$) is shown in the Fig.12.4. Particularly, experimental distribution of the quantity $y \equiv \sqrt{\Gamma_n^{(0)}(E_n)/\langle\Gamma_n^{(0)}\rangle}$ is demonstrated there. The experimental distribution of the quantity y is compared with the theoretical distributions $P(y)$ of the quantity y corresponding to the

Thomas-Porter distribution (12.114),

$$P_{T.P.}(\Gamma_n^{(0)}) = \frac{1}{\sqrt{2\pi\langle\Gamma_n^{(0)}\rangle\Gamma_n^{(0)}}}\, e^{-\frac{\Gamma_n^{(0)}}{2\langle\Gamma_n^{(0)}\rangle}} \quad \Leftrightarrow \quad P_{T.P.}(y) = \sqrt{\frac{2}{\pi}}\, e^{-\frac{y^2}{2}}$$

$$\text{because :} \quad P_{T.P.}(y)\, dy = P_{T.P.}(\Gamma_n^{(0)})\, d\Gamma_n^{(0)}$$

$$\Rightarrow \quad P_{T.P.}(y) = P_{T.P.}(\Gamma_n^{(0)})\, \frac{d\Gamma_n^{(0)}}{dy} = \boxed{\begin{array}{c}\text{since}\\ \Gamma_n^{(0)} = \langle\Gamma_n^{(0)}\rangle y^2\end{array}} = \sqrt{\frac{2}{\pi}}\, e^{-\frac{y^2}{2}} \tag{12.133}$$

and to the Poisson distribution (12.121),

$$P_{Poiss.}(\Gamma_n^{(0)}) = \frac{1}{\langle\Gamma_n^{(0)}\rangle}\, e^{-\frac{\Gamma_n^{(0)}}{\langle\Gamma_n^{(0)}\rangle}} \quad \Leftrightarrow \quad P_{Poiss.}(y) = 2y\, e^{-y^2}$$

$$\text{because : } P_{Poiss.}(y) = P_{Poiss.}(\Gamma_n^{(0)})\, \frac{d\Gamma_n^{(0)}}{dy} = 2y\, e^{-y^2} \tag{12.134}$$

From the Fig.12.4 it follows that the experimental distribution of the quantity y corresponds to the Porter-Thomas distribution of the reduced neutron widths while the Poisson distribution of the reduced neutron widths does not agree with the experiment.

12.3.3.2 Comparison of the level distribution of the Gauss Orthogonal Ensemble (GOE) and experimental level distribution of so called Nuclear Data Ensemble (NDE)

In the previous subsection 12.3.3.1 results of calculations for Gauss orthogonal ensemble of random matrices (level spacing distributions and neutron width distributions) were compared with experimental data of the compound nucleus formed during the neutron capture. We investigated always one type compound nucleus , particularly ^{233}Th. However the data from one nucleus do not provide sufficient statistics for the comparison with random matrices calculations (the neutron capture on one nucleus can give only about 100 neutron resonances). On the other side it is known that reasonable energies of all compound nuclei formed by the neutron capture and other reactions have the same fluctuation properties. Therefore in the paper [385] the ensemble of experimental data of different nuclei obtained from different reactions,

1. Slow neutron resonance reaction data on $^{110,-,114}$Cd, ^{152,154}Sm, $^{154,-,160}$Gd, $^{160,-,164}$Dy, $^{166,-,170}$Er, $^{172,-,176}$Yb,$^{182,-,186}$W, ^{232}Th, ^{236}U;

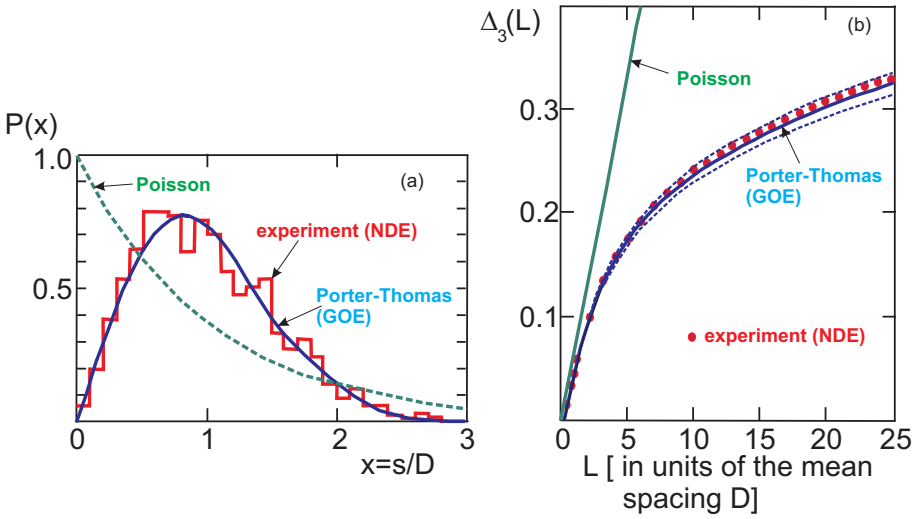


Figure 12.5: Left panel: nearest neighbor experimental spacing distribution $P(x = s/D)$ is compared with the Thomas-Porter (GOE) (full blue line) and Poisson (full green line) spacing distribution predictions (dashed lines correspond, for GOE, to one standard deviation from the average value). Right panel: Dyson-Mehta statistic $\Delta_3 L$ distributions (experimental (NDE), Thomas-Porter (GOE), Poisson) are plotted for the comparison (the figure is taken from [387])

2. Proton resonance data on ^{44}Ca ($J^\pi = \frac{1}{2}^-$), ^{44}Ca ($J^\pi = \frac{1}{2}^+$), ^{48}Ti ($J^\pi = \frac{1}{2}^+$);

3. (n,γ) reaction data on ^{177}Hf ($J = 3$), ^{177}Hf ($J = 4$), ^{179}Hf ($J = 5$);

was collected. This ensemble contains altogether 1407 resonances from 27 nuclei. It is necessary to realize that on the given energy interval we should have the complete ensemble of resonances with the given value J^π in order all prerequisites for the GOE are fulfilled.

Above mentioned ensemble of experimental data is called as "Nuclear Data Ensemble" (NDE). These data were used for the test of GOE ensembles - see e.g. [386]. As an example of such comparison the Fig.12.5 shows the level spacing distribution $P(s)$ and the distribution of the quantity $\Delta_3(L)$ (least square deviation - see (12.130)) in the comparison with corresponding experimental data taken from the NDE (see [385, 387]).

Again it can be seen that experimental NDE distributions are in agreement with the Thomas-Porter GOE distribution and the Poisson distribution does not corresponds to experimental values.

12.3.4 Spectral characteristics of Two-body Random Ensembles (TBRE) and Realistic Two-body Random Ensembles (RTBRE)

In the previous subsections of this chapter the Gauss orthogonal ensemble of Hamiltonians was discussed. This ensemble involves Hamiltonian matrices with randomly generated matrix elements within the n-particle Hilbert space corresponding to given J^π (that means all matrices were invariant with respect to rotations and parity). Random generation of matrix elements means that using the generator of random numbers we generate the numbers P_{ii} and P_{ij} in the interval $\langle 0, 1\rangle$ and then in terms of expressions (see (12.94) and the text under the expr. (12.74)),

$$P_{ii}(H_{ii}) = \big(\frac{C}{4\pi}\big)^{1/2} e^{-\frac{C}{4} H_{ii}^2} \quad , \quad P_{ii}(H_{ij}) = \big(\frac{C}{2\pi}\big)^{1/2} e^{-\frac{C}{2} H_{ij}^2}$$
$$\langle H_{ij}\rangle = 0 \quad \text{for } i \neq j \ , \ \langle |\, (H_{ij} - \langle H_{ij}\rangle)^2 \,|\rangle = (1 + \delta_{ij})\, \sigma^2 \quad , \quad C = \frac{1}{\sigma^2} \tag{12.135}$$

the matrix elements H_{ii} and H_{ij} are obtained. In such a way obtained each matrix is diagonalized and eigen-vectors and eigen-energies are determined. this procedure is performed many times in order to obtain good statistics. Resultant eigen-energy spectra form the Gauss orthogonal ensemble (GOE) of spectra and we can investigate corresponding distributions of level spacings s or distributions of widths $\Gamma^{(0)}$ or distributions of other quantities. The main results of analyses of statistics of the GOE spectra discussed in the previous subsection can be summarized in two following points,

- Statistics of the level spacing s between two nighboring levels is controlled by the Wigner distribution (12.87) (corresponding mean vales of level density $\bar{\rho}(E)$ is controllled by the Wigner semicircle law (12.104);
- Statistics of the neutron resonance widths is controlled by the Thomas-Porter distribution (12.114).

Discussed above way of generating of GOE matrix assumes that all Hamiltonian is taken into account (the mean field part together with all residual interactions), that means all parts of the interaction among particles forming the quantum system. However in the nucleus (and also in many other quantum systems) the two-particle nucleon-nucleon interaction prevails and three-particle and more particle interactions are usually neglected. By other

words in the usual models of nuclei the Hamiltonian of the A-nucleon system is transformed into the one-particle mean field and so called residual interactions which have dominantly two-particle character (see (4.28)),

$$\hat{H} = \hat{H}_{AV} + \hat{V}_{res} \quad \text{with } \hat{V}_{res} = \frac{1}{2}\sum_{abcd}\langle ab|\hat{V}|cd\rangle \ :a_a^+ a_b^+ a_c a_d: \qquad (12.136)$$

where $\hat{H}_{AV}$ is the one- particle mean field and $\hat{V}_{res}$ represents the residual two-particle interaction acting within the space of the n valence nucleons above the core (for no core nucleus shell models $n = A$). So in the nucleus case we can suppose that only two-particle interactions participate. Therefore in the beginning of the seventies so called "Two-Body Random Ensemble" (TBRE) (see [388] or [389]) method was developed. The TBRE specifies the GOE approach for systems with two- particle residual interaction. Approaches working with the TBRE are also called as "embedded ensemble"methods. Historically analyses based on the embedded ensemble approaches can be divided into two phases,

1. Two-body random ensemble (TBRE)
   In the first papers with embedded ensemble in the 70-ties and 80-ties the rough assumption was done that the one-particle nuclear mean field $\hat{H}_{AV}$ gives the degenerated spectrum, that means the same energy for all particle-hole mean field configurations (the even-even nucleus is supposed to be analyzed) for given angular momentum J and the parity π. Because of the Hamiltonian matrices are then randomly generated for given J^π we can always choose energies of all these p-h configurations as zero. Gaussian TBRE generating of the Hamiltonian matrices proceeds in following steps,
   - for n- particle system (even-even nucleus) the basis of particle-hole eigen states of the mean field $\hat{H}_{AV}$ is introduced for given J^π (with degenerated eigen-energies settled as zero);
   - in the framework of this basis (for fixed value of J^π) matrix elements are generated. That means at first the random numbers $P_{ii} \in \langle 0, 1\rangle$ and $P_{ij} \in \langle 0, 1\rangle$ are generated (indexes i and j enumerates the particle-hole eigen states of $\hat{H}_{AV}$). Then using expressions (12.135),

   $$P_{ii}(H_{ii}) = \Big(\frac{C}{4\pi}\Big)^{1/2} e^{-\frac{C}{4}H_{ii}^2} \quad , \quad P_{ii}(H_{ij}) = \Big(\frac{C}{2\pi}\Big)^{1/2} e^{-\frac{C}{2}H_{ij}^2} \qquad (12.137)$$

   the matrix elements H_{ii} and H_{ij} are determined;
   - in such a way randomly created matrix is diagonalized and the spec-

trum of eigen-energies with corresponding eigen-vectors of the Hamiltonian matrix are obtained.
This procedure is repeated many times and the ensemble of the TBRE spectra is obtained. Resultant ensemble is then statistically worked out similarly as was done before for the GOE spectra.

2. Realistic two-body random ensemble (RTBRE)
In the 90-ties the mentioned above TBRE method was modified in the sense that the degeneration of the mean field spectrum was not expected and instead realistic mean field non-degenerated particle-hole eigen-states were taken as the starting point (see e.g. [390] and citations therein). The particular steps of the RTBRE procedure were following,
- for investigated even-even nucleus the basis of particle-hole eigen configurations of the mean field Hamiltonian H_{AV} for given J^{π} is determined together with corresponding p-h eigen-energies e_i;
- then, in the framework of this p-h basis, matrix elements H_{ii} and H_{ij} of the matrix of the whole Hamiltonian involving mean field H_{AV} and residual interaction V_{res} is randomly generated using following expressions,

$$P_{ii}(H_{ii}) = \Big(\frac{C}{4\pi}\Big)^{1/2} e^{-\frac{C}{4}\,(H_{ii}-e_i)^2} \quad , \quad P_{ii}(H_{ij}) = \Big(\frac{C}{2\pi}\Big)^{1/2} e^{-\frac{C}{2}\,H_{ij}^2} \quad (12.138)$$

where opposite to (12.137) corrected energy exponent of the expression for the distribution $P_{ii}(H_{ii})$ is involved (taking into account the non-degeneracy of the mean field eigen-energies - compare (12.138) with (12.137));
- in such a way randomly created Hamiltonian matrix is finally diagonalized and corresponding spectrum of eigen-energies of the whole Hamiltonian matrix is found.
This procedure is repeated many times and obtained eigen spectra of Hamiltonian matrices form the RTBRE for each value J^{π} which can be further statistically analyzed.

Statistical working out of the TBRE or RTBRE spectra starts with "unfolding"of obtained spectra. The procedure of unfolding consists in the following steps. Each spectrum obtained by the diagonalization of each matrix from the ensemble is divided into small energy intervals (so called bins). In each interval the number of levels is determined and then these numbers for each bin with the given energy are summed from all spectra of the ensemble.

Numbers obtained in such a way for all bins are summed with increasing energy and obtained function $N(E)$ determines so called "staircase" function (that means $N(E)$ represents the number of levels from all spectra in the given ensemble with energies up to the energy E and the staircase character of the function $N(E)$ is connected with the creation of bins - see the Fig.12.6) Obtained staircase function is the fitted with a polynomial (in the

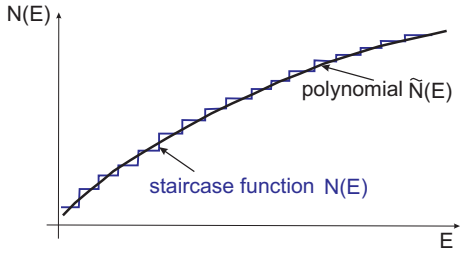


Figure 12.6: Staircase function (schematic figure)

paper [390] the polynomial of the degree 15 was used). This polynomial determines the smooth number of levels, $\tilde{N}(E)$, with the energy up to the value E. Its derivative, $\tilde{\rho}(E) \equiv \frac{d\tilde{N}(E)}{dE}$, gives the smooth value of the level density with the energy E in the ensemble. To perform unfolding in the given ensemble means to intoduce new variable $x_i \equiv \tilde{N}(E_i)$ and we get the function $N(x) = N(E(x))$. It is evident that the plot $N(x)$ fluctuates around the straight line $N(x) = x$ and that

$$\tilde{N}(x) = x \qquad \Rightarrow \qquad \tilde{\rho}(x) = \frac{d\tilde{N}(x)}{dx} = 1 \tag{12.139}$$

The transition from E_i to the new variables x_i is called as unfolding. All spectra of the whole ensemble are unfolded in this way. If we want to compare the unfolded TBRE or RTBRE spectra with experimental values we should unfold also experimental spectra. From (12.139) it is clear that after unfolding the mean field spacing in the unfolded spectrum is $\langle s \rangle = (\tilde{\rho}(x))^{-1} = 1$.

The unfolding discussed above can be done by two ways,

- All spectra belonging to given enesemble are combined into the one spectrum and the the "unfolding" of this spectra is done. As a result one "staircase" function is obtained for the whole ensemble. This global staircase function is then fitted with one polynomial and corresponding unfolded function $N(x)$ is gotten, which is then statistically worked out.

- In the alternative way the forming of bins and subsequent obtaing the staircase function is performed extra for each spectrum obtained by the

diagonalization of individual Hamiltonian matrix belonging to the ensemble. That means the unfolding is done separately for each spectrum and only then all obtained unfolded spectra (staircase functions) are summed into the one global spectrum of the whole ensemble. Then the statistical working out of the global spectra is performed.

Statistical analyses of unfolded spectrum usually involve comparisons of values of different quantities extracted from the TBRE or RTBRE spectrum with corresponding values extracted from experimental spectrum. For this aim following quantities are usually used.

$\mathbf{P(s)}$ - probability distribution of the neighboring level spacing in the unfolded spectrum (e.g. energy spacing of the ground state and the first excited state);

$\mathbf{N(L)}$ - number of levels with quantum numbers J^π (eventually also isospin T) lying in the energy interval L in the unfolded spectrum (usually interval $\langle 0, L\rangle$;

$\mathbf{\Sigma^i(L)} \equiv \langle|\big(\mathbf{N(L)} - \langle\mathbf{N(L)}\rangle\big)^{\mathbf{i}}|\rangle$ - $\frac{i}{2}$-th power of the mean square deviation of the quantity $N(L)$;

and (see [390])

$$\gamma_{\mathbf{1}}(\mathbf{L}) \equiv \frac{\mathbf{\Sigma^3(L)}}{(\mathbf{\Sigma^2(L)})^{\mathbf{2}}} \ ,$$

so called skewness, and

$$\gamma_{\mathbf{2}}(\mathbf{L}) \equiv \frac{\mathbf{\Sigma^4(L)}}{(\mathbf{\Sigma^2(L)})^{\mathbf{3/2}}} \ . \tag{12.140}$$

As an example of analyses of these quantities further some results taken from the paper [390] are shown. In this paper the TBRE statistical analyzes for following nuclear states are shown,

- states $J = 0$, $T = 0$ (basis dimension 325, number 500 of matrices involved in the TBRE);
- states $J = 0$, $T = 2$ (basis dimension 287, number 500 of matrices involved in the TBRE);
- states $J = 2$, $T = 0$ (basis dimension 1206, number 708 of matrices involved in the TBRE).

and RTBRE analyses for

- states $J = 0$, $T = 0$ (basis dimension 325, number 500 of matrices involved in the RTBRE).

From the point of view of statistical analyzes of the TBRE or RTBRE the spectra were divided into so called central part of spectra and edge part of spectra. For instance the statistical analyzes of the spacings between the ground state energy and the first excited level belongs to the spectral statistics of the edge region of the spectra.

i. Statistics in the center of the TBRE spectra

The results of the calculation of unfolded level spacing distribution $P(s)$ and of the number number variance $\Sigma^2(L)$ are shown in the Fig.12.6. The unfolding of the TBRE was performed once in the global spectrum obtained by the summation of all TBRE spectra in individual bins.

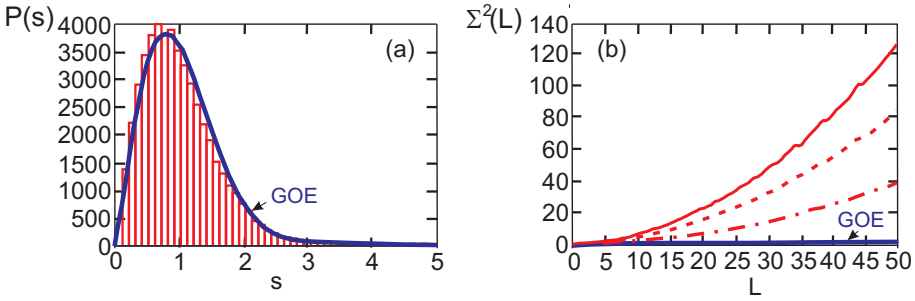


Figure 12.7: Left panel (a): Ensemble averaged nearest-neighbor spacing distribution of the TBRE ($J = 0$, $T = 0$) (red curves) at the center of the spectrum. The full solid blue curve corresponds to the GOE; the ordinate is normalized to show the number of spacings in each bin of the histogram, and the abscissa to the average spacing equal to 1. Right panel (b): Number variance $\Sigma^2(L)$ for the same case. The solid thin line corresponds to the ensemble average, the dashed line to the ensemble average after normalizing the spectrum widths, and the dashed-dotted line to the ensemble average after recentering the spectra. The GOE values are indicated by the thick solid line. The normalization of the average level spacing defined the scales. The figure is taken from [390], for details see therein.

In the Fig.12.7 the TBRE results (red curves) are compared with the GOE calculations (the full solid blue line). It can be seen in the panel (a) of the Fig.12.7, with the level spacing distribution $P(s)$, that in the region $s \to 0$ and $s > \langle s \rangle = 1$ the bin diagram with unfolded TBRE distribution differs a little bit from the full solid line with the GOE distribution. The panel (b) in the Fig.12.7 demonstrates the increasing differences between TBRE and GOE for the number of variance $\Sigma^2(L)$ with the increasing L. Generally it

w	σ_c	σ_v	σ_{tot}	σ_c/σ_{tot}	σ_c/σ_{tot}
TBRE $J=0,\ T=0$	20.1	4.5	39.7	0.51	0.11
TBRE $J=0,\ T=2$	22.1	4.3	37.1	0.59	0.12
TBRE $J=2,\ T=0$	20.3	4.2	38.2	0.53	0.11
RTBRE $J=0,\ T=0$	5.0	1.96	12.3	0.41	0.16
GOE	0.015	3.17×10^{-3}	1.0	1.5×10^{-2}	3.1×10^{-3}

Table 12.1: Standard deviation σ_c of the ensemble distribution of the average energies of each spectrum, standard deviation σ_v of the ensemble distribution of the average widths of each spectrum, standard deviation σ_{tot} of the width of energy levels in the global spectrum of the whole ensemble w. The index w enumerates individual ensembles. (Taken from [390].)

is possible to conclude that the fluctuation between individual spectra are much bigger for the TBRE bin the comparison with the GOE. This can be seen also from the Table 12.1 where we compare the following variances:
- variance $\sigma_c = \langle\mid \bar{E}^2 - \langle\bar{E}\rangle_w^2 \mid\rangle_w$ of ensemble distribution of average energies $\bar{E}$ of each individual spectrum in the given ensemble w;
- variance $\sigma_v = \langle\mid \bar{\Gamma}^2 - \langle\bar{\Gamma}\rangle_w^2 \mid\rangle_w$ of the average widths of energy levels of each individual spectrum in the given ensemble w;
- variance $\sigma_{tot} = \langle\mid \Gamma^2 - \langle\Gamma\rangle^2 \mid\rangle$ of the width of energy levels in the global spectrum of the whole ensemble w,
where w enumerates ensembles $(w = TBRE\ (J=0,T=0),\ TBRE\ (J=0,T=2),\ TBRE\ (J=2,T=0), RTBRE\ (J=0,T=0),\ GOE)$.

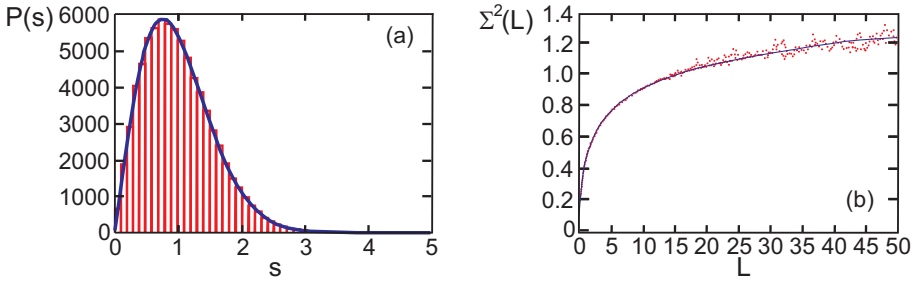


Figure 12.8: Left panel (a): Nearest-neighbor spacing distribution of the TBRE ($J=0$, $T=0$) after each spectrum is unfolded individually and then summed (red diagram). The solid blue line corresponds to the GOE. Right panel (b): Number variance $\Sigma^2(L)$ for the same case. Scales in as in the Fig.12.7. The red dots correspond to the value of the variance $\Sigma^2(L)$ obtained from individual unfolded TBRE spectra after their recentering and normalizing their widths. The full blue line is obtained for the GOE. The whole figure is taken from [390].

From the Table 12.1 follows that the GOE is ergodic ensemble because

its deviations σ_c, σ_v and σ_{tot} are very small [13]. The GOE distributions are extremely narrow. The TBRE calculations give much bigger variations σ_c, σ_v and σ_{tot}. The RTBRE fluctuations are less than those for TBRE but nevertheless bigger by two orders in the comparison with the GOE ones. Therefore it might seems the TBRE and RTBRE are not ergodic. However in the paper [390] it was shown that in fact the TBRE and RTBRE did not violate ergodicity. The problem consists in the unfolding performed for the whole ensemble. If authors of [390] performed the unfolding extra for each spectrum in the ensemble then they obtained distributions $P(s)$ and $\Sigma^2(L)$ shown in the Fig.12.8,

The GOE and the TBRE distributions in the Fig 12.8 are in good agreement and therefore we can expect that also the TBRE and RTBRE are ergodic. It is interesting, as it follows from the paper [390] and papers quoted there, that higher moments $\Sigma^3(L)$ and $\Sigma^4(L)$ involved in the expressions for $\gamma_1(L)$ and $\gamma_2(L)$ (see (12.140) did not demonstrate any difference between the TBRE (RTBRE) and the GOE regardless the unfolding is done for the whole ensemble spectrum or at first for individual spectra before their summation.

ii. Spectral characteristics for the edge spectra region

In the paper [393] so called Nuclear Table Ensemble (NTE) was introduced. This ensemble involves experimental data on the spacing between the lowest levels of big amount of nuclei. The comparison of statistical distributions of level spacings and other quantities from the NDE with those obtained by TBRE and/or RTBRE performed in [390] confirmed that both the TBRE and RTBRE are ergodic.

However the most interesting result concerning the statistics of the edge spectra region was published in [394, 395, 396]. It was found in these papers that the shell model calculations with different random ensembles of spherical nuclei two-body Hamiltonian matrices preferred the ground states with $J^\pi = 0^+$ separated from the first excited states by a large energy spacings (gaps). Particularly it was shown there that the $T = 0$ effective attractive pairing interaction (leading to the $J = 0$ for ground states of even-even nuclei - see the Chapter 6) is contained naturally in the randomly created residual interaction.

[13] In the section R7 of the Appendix R the ergodicity (its definition and its relation to the ensemble probability distribution and the probability distribution in the phase-space) is shortly discussed for classical systems. Possible indicia of the ergodicity in quantum system is also mentioned there (the ergodicity for a quantum system can be expected if the ensemble variations (fluctuations) of quantities connected directly with the system spectra are small.

nucleus	RQE	RQE-NP	TBRE	RQE-SPE	$J=0$ (total space)	$J=2$ (total space)
^{20}O	68%	50%	50%	49%	11.1%	14.8%
^{22}O	72%	68%	71%	77%	9.8%	13.4%
^{24}O	66%	51%	55%	78%	11.1%	14.8%
^{44}Ca	70%	46%	41%	70%	5.0%	9.6%
^{46}Ca	76%	59%	56%	74%	3.5%	8.1%
^{48}Ca	72%	53%	58%	71%	2.9%	7.6%
^{50}Ca	65%	45%	51%	61%	2.7%	7.1%
^{24}Mg	66%	-	44%	54%	4%	16%
^{26}Mg	62%	52%	48%	56%	4%	15%
^{28}Mg	59%	46%	44%	54%	4%	16%

Table 12.2: Percentage of ground states for selected random ensembles (2-d, 3-d,4-th, 5-th columns) that have $J=0$ for nucleus given in the first column, as compared to the percentage of all states in the model space that have these quantum numbers (6-th and 7-th columns) (table is taken from [395]).

As an example of this result the Table 12.2, taken from [395], is presented below. In the Table 12.2 the percentage of ground states for selected random ensemble that have many particle angular momentum $J=0$ and $J=2$ for selected nuclei given in the first column is shown. For the purpose of the comparison the fraction of the total many body states with the angular momenta $J=0$ and $J=2$ with any energy is presented in the table as well. Ensembles used in the shell model calculations involves Hamiltonian matrices with various randomly created two-body residual interactions and different single-particle mean fields. Various ensembles of two-body Hamiltonians been invariant with respect to the orthogonal rotational transformation of the two-particle basis states were used (that means additional rotational invariance of two-particle basis in which the matrices are constructed was supposed). This can be achieved by taking the two-body matrix elements to be Gaussian distributed around zero (GOE ensembles) with the widths possibly depending on the two-particle angular momenta $\mathcal{J}$ (we emphasize that $\mathcal{J}$ refer to quantum numbers of the angular momentum of two-body states, and not of the final many-body states (which are denoted by J). Concretely, randomly created two-body matrix elements have following form,

$$\begin{aligned} &\langle V^2_{\alpha,\alpha'}\rangle = c_{\mathcal{J}}\left(1+\delta_{\alpha\alpha'}\right)\bar{\nu}^{\,2} \\ &\langle V_{\alpha,\alpha'}\cdot V_{\beta,\beta'}\rangle = 0 \qquad \text{for } (\alpha,\alpha')\neq(\beta,\beta') \end{aligned} \tag{12.141}$$

Here $\bar{\nu}$ is an general scale factor, which in the most of ensembles is taken

as $\bar{\nu} = 1$ (with the exception of the RQE-SPE ensemble - see below). The coefficient $c_{\mathcal{J}}$ is defined by the concrete ensemble (see below). Then the diagonalization of randomly created matrices for Hamiltonian involving the single-particle mean field and random two-particle residual interactions within the many-particle wave functions with given J^{π} was performed. As a result the eigen many-body wave functions and correponding eigen-energies were obtained in the shell-model spaces for given many-body angular momentum J and parity π.

For the two-body matrix elements authors of [395] chose a basis of two-body states, labeled by α, which has sharp value of $\mathcal{J}$. These were 63 independent two-body matrix elements in the *sd* shell space and 195 in the *pf* shell space of nuclei in the Table 12.2, including neutrons and protons.

In the paper [395] following ensembles were taken into account:

1. **RQE (random quasiparticle interaction)**
   Here $c_{\mathcal{J}} = (2\mathcal{J}+1)^{-1}$ which is a result of the additional invariance impossed on the ensemble (two-body residual Hamiltonian is supposed to be invariant under orthogonal transformation in the basis of two-particle basis states). Single-particle energies of the nucleus mean field are supposed to be zero for this ensemble.

2. **TBRE (two-body random ensemble)**
   Here $c_{\mathcal{J}} = const$ (usually taken $c_{\mathcal{J}} = 1$). Historically this ensemble was the first two-particle random ensemble used for the analyzes of statistical properties of many particle spectra (see [389, 393] and citations therein) and it was already discussed in previous supsection. Single-particle energies of the nucleus mean field are supposed to be zero for this ensemble.

3. **RQE-NP (random quasiparticle - no pairing)**
   This is the same ensemble as the RQE, except all $\mathcal{J} = 0$ two-body matrix elements are set to zero. This ensemble shows whether the $\mathcal{J} = 0$ are necessary to produce the signatures of pairing. All single-particle energies of the nucleus mean field are supposed to be zero for this ensemble.

4. **RQE-SPE (random quasiparticle ensemble with nonzero single-particle energies)**
   All the previous ensembles had the single-particle energies set to zero. However, realistic interactions have nonzero single-particle energies and

these can affect pairing properties (at least they contribute to large shell gaps). For calculations in the *sd* shell the single-particle energies from the Wildenthal interaction [397] with the scaling $\bar{\nu} = 3.84$ MeV and for *pf* shell the single-particle energies from the modified KB3 interaction [398] and scaled by $\bar{\nu} = 4.43$ MeV. These scaling factors provide the best widths of two-particle matrix elements.

The Table 12.2 demonstrates that the most realistic ensemble RQE-SPE (see the 5-th column) gives the highest percentage of $J = 0$ ground states for the most of investigated nuclei from the 1-st column. Simultaneously the comparison of the 2-d column (ensemble RQE involving $\mathcal{J} = 0$ two-particle configurations) with the 3-d column (ensemble RQE-NP without $\mathcal{J} = 0$ two-particle configurations) show the importance of $\mathcal{J} = 0$ pairing configurations for forming of $J = 0$ ground state (the highest percentage for the RQE ensemble).

Statistical analyzes of properties of low-lying random matrices spectra (or edge part of spectra) and corresponding pair-transfer amplitudes performed in the pioneering papers [394, 395, 396], and in other papers with embedded random matrices topic which followed, confirmed the importance of the $\mathcal{J} = 0$ pairing leading to $J^\pi = 0^+$ ground states. That means $J = 0$ character of even-even spherical nuclei ground states and corresponding pairing properties of nuclear many-body Hamiltonian are not connected directly with the specific features of effective nucleon-nucleon interaction but rather are related to the Fock-space connectivity of the interacting shell model.

12.4 Strength function

Strength function of given quantity is usually defined as the probability distribution of this quantity in the dependence on the excitation energy of investigated system (nucleus). In this section two types of strength functions are discussed.

The first part of this section concerns the distribution of quantities which are proportional to the square of the amplitude of one components of the nucleus wave function. For instance this is the case of the distribution of the square of amplitude of the single-particle neutron state in the final nucleus after the neutron capture. As it was already discussed in the paragraph 12.3.3.1 the captured neutron has a tendency to occupy some single-particle state and this state can be supposed to form a one component of the collective

eigen-states of the compound nucleus nucleus Hamiltonian created after the neutron is captured.

The second part is devoted to so called photon strength functions, that means to the energy distribution of electromagnetic excitation of nuclei and its connection to the photo-absorption cross section.

12.4.1 Strength functions of the square of the amplitude of one basis vector in the excitation states of the system Hamiltonian

We start with the Hamiltonian (12.136) which is further rewritten in the following form,

$$\hat{H} = \hat{H}_0 + \hat{V} \tag{12.142}$$

where $\hat{H}_0$ is so called non-interaction (unperturbed) part of the system Hamiltonian (e.g. mean field Hamiltonian but not necessarily) and the symbol $\hat{V}$ stands for the two-particle interaction between eigen-states of the unperturbed Hamiltonian $\hat{H}_0$. We suppose that among the eigen-states of the Hamiltonian $\hat{H}_0$ there is one eigen-state $|a\rangle$, called further as the channel state, which we are interested in. As an example of such channel state we can referred to the single-particle neutron state occupied by the neutron after the neutron capture reaction [14]. Other eigen-states of the unperturbed Hamiltonian $\hat{H}_0$ are denoted by the index α (the index α enumerates all other eigen-states of $\hat{H}_0$, that means $\alpha \neq a$),

$$\begin{aligned} &\hat{H}_0\,|a\rangle = E_a^{(0)}|a\rangle \quad , \quad \langle a|a\rangle = 1 \\ &\hat{H}_0\,|\alpha\rangle = E_\alpha^{(0)}\,|\alpha\rangle \quad , \quad \langle \alpha|\alpha'\rangle = \delta_{\alpha\alpha'} \quad , \quad \langle a|\alpha\rangle = 0 \end{aligned} \tag{12.143}$$

Further we suppose that the unperturbed Hamiltonian $\hat{H}_0$ exhausts almost the whole Hamiltonian $\hat{H}$ and that the interaction $\hat{V}$ acts only between the channel state $|a\rangle$ and other eigen-states $|\alpha\rangle$,

$$\langle a|\hat{V}|a\rangle = \langle \alpha|\hat{V}|\alpha'\rangle = 0 \quad , \quad V_{a\alpha} \equiv \langle a|\hat{V}|\alpha\rangle = \langle \alpha|\hat{V}|a\rangle \neq 0 \tag{12.144}$$

Hamiltonians $\hat{H}$ and $\hat{H}_0$ are assumed to be time-reverse invariants and therefore the wave function phase convention can be always chosen in such a way that all matrix elements are real (see the text following the expression (1.44)). Expressions (12.143), (12.144) represent the definition of the channel state $|a\rangle$.

[14] Other examples of the channel state can be found in [6] (see the Appendix 2D therein).

Our aim is to describe how the amplitude for a particular channel $|a\rangle$ may be distributed over many stationary eigen-states $|i\rangle$ of the whole Hamitonian $\hat{H}$,

$$\hat{H}\,|i\rangle = E_i\,|i\rangle \tag{12.145}$$

Since we suppose that eigen-vectors of the unperturbed Hamiltonian $\hat{H}_0$, $|a\rangle$ and all $|\alpha\rangle$, form the complete basis we can look for the total Hamiltonian eigen-vectors in the following form,

$$|i\rangle = c_a^{(i)}|a\rangle + \sum_\alpha c_\alpha^{(i)}|\alpha\rangle \tag{12.146}$$

The substitution of (12.146) into (12.145) gives,

$$\begin{aligned} & c_a^{(i)}\,\hat{H}|a\rangle + \sum_\alpha c_\alpha^{(i)}\hat{H}|\alpha\rangle = E_i\,c_a^{(i)}|a\rangle + E_i\,\sum_\alpha c_\alpha^{(i)}|\alpha\rangle \\ \Rightarrow \quad & c_a^{(i)}\,(E_a^{(0)}+\hat{V})|a\rangle + \sum_\alpha c_\alpha^{(i)}\,(E_\alpha^{(0)}+\hat{V})|\alpha\rangle = \\ & \qquad = E_i\,c_a^{(i)}|a\rangle + E_i\,\sum_\alpha c_\alpha^{(i)}|\alpha\rangle \end{aligned} \tag{12.147}$$

The multiplying of (12.147) by $\langle a|$ yields (using (12.144)),

$$E_a^{(0)}c_a^{(i)} + \sum_\alpha c_\alpha^{(i)}\langle a|\hat{V}|\alpha\rangle = E_i\,c_a^{(i)} \tag{12.148}$$

and multiplying of (12.147) by $\langle\alpha|$ provides,

$$c_a^{(i)}\langle\alpha|\hat{V}|a\rangle + c_\alpha^{(i)}E_\alpha^{(0)} = E_i\,c_\alpha^{(i)} \tag{12.149}$$

Therefore,

$$c_a^{(i)} = -\frac{\sum_\alpha c_\alpha^{(i)}\,V_{a\alpha}}{E_a^{(0)}-E_i} \quad , \quad c_\alpha^{(i)} = -\frac{V_{a\alpha}\,c_a^{(i)}}{E_\alpha^{(0)}-E_i} \tag{12.150}$$

We substitute from the second equation in (12.150) into the first one ($V_{\alpha a} = V_{a\alpha}$),

$$(E_a^{(0)}-E_i)\,c_a^{(i)} = \sum_\alpha \frac{V_{\alpha a}V_{a\alpha}\,c_a^{(i)}}{E_\alpha^{(0)}-E_i} \quad \Rightarrow \quad E_a^{(i)}-E_i = \sum_\alpha \frac{V_{a\alpha}^{\,2}}{E_\alpha^{(0)}-E_i} \tag{12.151}$$

The equation (12.150) represents the equation for the eigen-energies E_i of the total Hamiltonian $\hat{H}$. For the eigen-vectors $|i\rangle$ the normalization to the unity 1 is supposed,

$$\langle i|i\rangle = c_a^{(i)\,2} + \sum_\alpha c_\alpha^{(i)\,2} = 1 \tag{12.152}$$

The substitution of the second equation in (12.150) into (12.152) gives the equation for amplitude $c_a^{(i)}$,

$$c_a^{(i)\,2}\big(1+\sum_\alpha \frac{V_{a\alpha}^2}{(E_\alpha^{(0)}-E_i)^2}\big)=1 \quad , \quad c_a^{(i)}=\big(1+\sum_\alpha \frac{V_{a\alpha}^2}{(E_\alpha^{(0)}-E_i)^2}\big)^{-1/2} \tag{12.153}$$

So for the searching for the total Hamiltonian eigen vectors $|i\rangle$ and corresponding eigen-energies E_i at first the equation (12.150) for E_i should be solved. Obtained E_i are substituted into (12.153) and we obtained amplitudes $c_a^{(i)}$ which are then substituted into the second equation in (12.150) which gives $c_\alpha^{(i)}$.

Amplitudes $c_a^{(i)}$ characterize the distribution of the channel state $|a\rangle$ over the spectrum of the total Hamiltonian eigen-energies E_i. This spectrum is often so dense that the smooth strength function can be introduced as follows, *The strength function $P_a(E)$ for the square $c_a^{(i)\,2}$ is defined as the mean value of the quantity $c_a^{(i)\,2}$ corresponding to the unit interval in the vicinity of the energy E.*
That means,

$$P_a(E)=\sum_i \rho(E_i-E)\,\langle c_a^{(i)\,2}\rangle \tag{12.154}$$

where $\rho(E_i-E)$ is the density of levels E_i (eigen-energies of the total Hamiltonian $\hat{H}$ and $\langle c_a^{(i)\,2}\rangle$ is the mean value of the quantity $c_a^{(i)\,2}$ obtained by its averaging in the narrow energy interval around the energy E.

In the case of energies E where the density of eigen-energies E_i is very high $\rho(x)$ in (12.153) is a function peaked around $x=0$ and quickly falling off for large $|x|$. Usually this function has following form (analogue of (7.373),

$$\rho(x)=\frac{1}{2\pi}\frac{\Delta}{x^2+(\Delta/2)^2} \stackrel{\Delta\to 0}{\longrightarrow} \delta(x) \tag{12.155}$$

with the normalization $\int_{-\infty}^{\infty}\rho(x)dx=1$. For discrete levels E_i (in the limit $\Delta\to 0$) the expression (12.154) can be rewritten as,

$$P_a(E)=\sum_i \delta(E_i-E)\,(c_a^{(i)})^2 \tag{12.156}$$

In the analogy with electromagnetic transition strength function (see the subsection 7.3.1.3.2.1, where the strength function (7.371) was discussed) the statistics of the distribution $P_a(E)$ can be analized using so called moments

of the strength function (see expressions (7.372),-,(7.382)),

$$
\begin{aligned}
m_0(a) &\equiv \int dE\ P_a(E) = \sum_i \int dE\ (c_a^{(i)})^2\ \delta(E - E_i) = \sum_i (c_a^{(i)})^2 \\
m_1(a) &\equiv \int dE\ P_a(E)\ E = \sum_i (c_a^{(i)})^2\ E_i \\
&\vdots \\
m_k(a) &\equiv \int dE\ P_a(E) E^k = \sum_i (c_a^{(i)})^2\ E_i^k
\end{aligned}
\tag{12.157}
$$

Knowing these moments we can immediately estimate the centroid $\bar{E}$ and the width of the distribution $P_a(E)$ (the direct analogue of (7.382)).

In the next paragraphs we will discuss in more details two cases: i) the strength finction $P_a(E)$ when the matrix elements $V_{a\alpha}$ are constant and the unperturbed basis vector energies E_α are equidistant, and ii) general case of the strength function $P_a(E)$ with the non-constant matrix elements $V_{a\alpha}$.

12.4.1.1 Strength function $P_a(E)$ (see (12.153), (12.156)) in the case of the constant matrix elements $V_{a\alpha}$

At first the simplest case is discussed when the matrix elements $V_{a\alpha}$ are supposed to be constant. Generally these matrix elements can fluctuate for different α but their mean values obtained by averaging over appropriate energy interval ΔE is assumed to be constant. Such assumption may be O.K. if the width of the whole strength function is small compared to the characteristic energies associated with systematic variations in $V_{a\alpha}$. Moreover further we will also suppose that the spectrum $E_\alpha^{(0)}$ of unperturbed states $|\alpha\rangle$ is equidistant. So overall assumption is,

$$
V_{a\alpha} = v = const \quad , \quad E_\alpha^{(0)} = \alpha D \quad , \quad \alpha = 0, \pm 1, \pm 2, \cdots \tag{12.158}
$$

where D is the spacing constant. Then the expressions (12.151) and (12.153) obtain following forms,

$$
\begin{aligned}
E_a - E_i = \frac{v^2}{D} \sum_{\alpha=0,\pm1,\cdots} \frac{1}{\alpha - \frac{E_i}{D}} &= \boxed{\begin{array}{c}\text{because - see [399]} \\ \pi\ cotg\frac{\pi E_i}{D} = \sum_{\alpha=0,\pm1,\cdots} \frac{1}{\frac{E_i}{D} - \alpha}\end{array}} = \\
&= -\frac{\pi v^2}{D}\ cotg\frac{\pi E_i}{D}
\end{aligned}
\tag{12.159}
$$

$$c_a^{(i)} = \Big(1 + \frac{v^2}{D^2} \sum_{\alpha=0,\pm1,\cdots} \frac{1}{(\alpha - \frac{E_i}{D})^{\,2}}\Big)^{-1/2} =$$

$$= \boxed{\begin{array}{c}\text{because}\\ \pi^2\, cosec^{\,2}\frac{\pi E_i}{D} = \sum_{\alpha=0,\pm1,\cdots} \frac{1}{(\alpha-\frac{E_i}{D})^{\,2}}\end{array}} =$$

$$= \Big(1 + \big(\frac{\pi v}{D}\big)^{\,2} cosec^{\,2}\frac{\pi E_i}{D}\Big)^{-1/2} = \boxed{\begin{array}{c}\text{see (2D-9) in [6]}\\ \text{and [399]}\end{array}} =$$

$$= \Big(1 + \big(\frac{\pi v}{D}\big)^{\,2} + \frac{(E_a^{(0)} - E_i)^{\,2}}{v^2}\Big)^{-1/2} \qquad (12.160)$$

where $cosec\Theta \equiv \frac{1}{sin\Theta}$. Further we will suppose that $v >> D$ and therefore it is possible to neglect unity 1 with respect to other terms in the bracket of (12.160). Then the strength function $P_a(E)$ (which, according to (12.154), gives probability of the state $|a\rangle$ per unit energy interval around E in the spectrum) has following form,

$$P_a(E) \approx \frac{1}{D}\left(c_a^{(i)}(E_i \approx E)\right)^{\,2} = \boxed{\begin{array}{c}\text{see}\\ (12.160)\end{array}} = \frac{1}{D}\frac{1}{\big(\frac{\pi v}{D}\big)^{\,2} + \frac{(E_a^{(0)}-E_i)^{\,2}}{v^2}} =$$

$$= \frac{1}{2\pi}\frac{\frac{2\pi\, v^2}{D}}{(E - E_a^{(0)})^{\,2} + \frac{1}{4}(\frac{2\pi v^2}{D})^{\,2}} = \frac{1}{2\pi}\frac{\Gamma}{(E_a^{(0)} - E)^{\,2} + (\frac{\Gamma}{2})^{\,2}} \qquad (12.161)$$

where the width $\Gamma \equiv 2\pi\frac{v^2}{D}$ was introduced. The assumption $v >> D$ in going from (12.160) to (12.161) is necessary in order to get component with $|a\rangle$ in more eigenstates $|i\rangle$ and to have a sense of the strength function.

From (12.160) we see that the Breight-Wigner resonance form (compare with (11.271)) is a direct consequence of the assumption about a constant coupling of the channel state $|a\rangle$ with other degrees of freedom (other unperturbed eigen-states $|\alpha\rangle$ of the Hamiltonian $\hat{H}_0$).

Further we will discuss the distribution of the channel $|a\rangle$ over the total Hamiltonian eigen-states in the dependence on time for the case of constant matrix elements $V_{a\alpha} = v$. So let us consider the probability amplitude $A_\alpha(t)$ of the situation that the system with the Hamiltonian $\hat{H}$ will be in the state $|a\rangle$ also in the time t when in the beginning (in the time $t = 0$) was in the state $|a\rangle$. From the quantum mechanics we know that such probability

amplitude $A_a(t)$ is given by,

$$A_a(t) = \langle a|e^{-\frac{i}{\hbar}\hat{H}t}|a\rangle = \boxed{\begin{array}{c}\text{using}\\ \sum_i |i\rangle\langle i| = 1\end{array}} = \sum_{ij}\langle a|i\rangle\langle i|e^{-\frac{i}{\hbar}\hat{H}t}|j\rangle\langle j|a\rangle =$$

$$= \sum_{ij} c_a^{(i)\,*}\,\langle i|e^{-\frac{i}{\hbar}\hat{H}t}|j\rangle\;\; c_a^{(j)} = \boxed{\begin{array}{c}\text{because}\\ \hat{H}|i\rangle = E_i|i\rangle\end{array}} = \sum_i |c_a^{(i)}|^{\,2}\, e^{-\frac{i}{\hbar}E_i t} \tag{12.162}$$

If we suppose validity of the conditions in (12.158) then we can substitute (12.160) for $c_a^{(i)}$ (with the neglecting of 1 in the comparison with other terms in the bracket which corresponds to $v >> D$) into (12.162),

$$A_a(t) = \sum_i \frac{1}{(\frac{\pi v}{D})^{\,2} + \frac{(E_a^{(0)} - E_i)^{\,2}}{v^2}}\, e^{-\frac{i}{\hbar}E_i t} \approx \int \frac{dE}{D}\frac{e^{-\frac{i}{\hbar}Et}}{(\frac{\pi v}{D})^2 + \frac{(E_a^{(0)} - E)^{\,2}}{v^2}} =$$

$$= \boxed{\begin{array}{c}\text{see expr. (2D-13)}\\ \text{in [6]}\end{array}} = e^{-\pi\frac{v^2}{D}|t| - \frac{i}{\hbar}E_a^{(0)}t} =$$

$$= \boxed{\begin{array}{c}\text{because } \Gamma = 2\pi\frac{v^2}{D}\\ \text{see the text under (12.161)}\end{array}} = e^{-\frac{\Gamma}{2}|t| - \frac{i}{\hbar}E_a^{(0)}t} \tag{12.163}$$

So we see that the assumption (12.158) corresponds to the exponentially degreesing of the amplitude $A_a(t)$ with the time (damping of the channel $|a\rangle$).

12.4.1.2 Strength function $P_a(E)$ (see (12.153), (12.156)) in the case when matrix elements $V_{a\alpha}$ are not constant

Let us consider the general case when $V_{a\alpha}$ in the expression (12.153) is not constant. The strength function $P_a(E)$ is given by (12.154). For a large density of levels E_i we can substitute $\rho(E_i - E) \approx \frac{1}{2\pi}\frac{\Delta}{(E-E_i)^{\,2}+\frac{\delta^2}{4}}$ (see (12.155) and for the $\langle (c_a^{(i)})^{\,2}\rangle$ we can use the expression (12.153). So the strength function $P_a(E)$ is,

$$P_a(E) = \sum_i \frac{1}{2\pi}\;\frac{\Delta}{(E - E_i)^{\,2} + \frac{\Delta^2}{4}}\;\frac{1}{1 + \sum_\alpha \frac{V_{a\alpha}^2}{(E_\alpha^{(0)} - E_i)^{\,2}}} \tag{12.164}$$

This expression can be understood as the result of the path integral in the complex plane $\lambda = Re\lambda + iIm\lambda$,

$$P_a(E) = \frac{i\Delta}{4\pi^2} \oint_{\mathscr{E}_1} \frac{d\lambda}{(E-\lambda)^2 + \frac{\Delta^2}{4}} \frac{1}{E_a^{(0)} - \lambda - \sum_\alpha \frac{V_{a\alpha}^2}{E_\alpha^{(0)} - \lambda}} \tag{12.165}$$

where $\mathscr{E}_1$ is the curve illustrated in the Fig.12.9. The equivalence of (12.164)

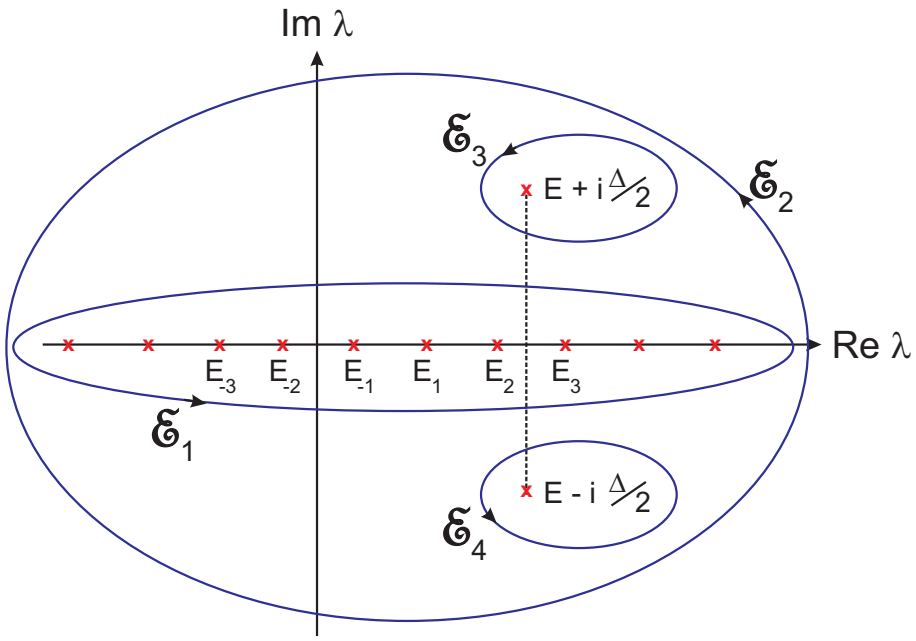


Figure 12.9: Schematic figure of the complex plane $\lambda \equiv Re\lambda + i\,Im\lambda$. Poles of the expression under the path integral in (12.165) are denoted by the red crosses and integral paths by blue curves.

and (12.165) can be proved using the residuum theorem as is shown below,

$$P_a(E) = \frac{i\Delta}{4\pi^2} \oint_{\mathscr{E}_1} d\lambda \frac{\varphi_1(\lambda)}{\psi_1(\lambda)} = \boxed{\begin{array}{c}\text{residuum}\\ \text{theorem}\end{array}} = \frac{i\Delta}{4\pi^2}\, 2\pi i \sum_i \frac{\varphi_1(\lambda = E_i)}{\psi_1'(\lambda = E_i)}$$

where from the point of view of the curve $\mathscr{E}_1$ we have only poles with real eigen-energies of the Hamiltonian $\hat{H}$ $(\lambda = E_i)$,

$$\varphi_1(\lambda) = \frac{1}{(E-\lambda)^2 + \frac{\Delta^2}{4}}$$

$$\psi_1(\lambda) = E_a^{(0)} - \lambda - \sum_\alpha \frac{V_{a\alpha}^2}{E_a^{(0)} - \lambda} \quad \Rightarrow \quad \psi_1'(\lambda) = -1 - \sum_\alpha \frac{V_{a\alpha}^2}{(E_a^{(0)} - \lambda)^2}$$

and we have,

$$\frac{i\Delta}{4\pi^2} \oint_{\mathscr{E}_1} d\lambda \frac{\varphi_1(\lambda)}{\psi_1(\lambda)} = \frac{\Delta}{2\pi} \sum_i \frac{1}{(E-E_i)^2 + \frac{\Delta^2}{4}} \frac{1}{1 + \sum_\alpha \frac{V_{a\alpha}^2}{(E_a^{(0)} - E_i)^2}} = (12.164)$$

So expressions (12.164) and (12.165) are really equivalent.

From the point of view of the whole complex plane (or curve $\mathscr{E}_2$) the expression under the integral in (12.165) has poles in the following points of the complex plane (index i enumerates eigen-energies of the Hamiltonian $\hat{H}$):

$$\lambda = E_i = \boxed{\begin{array}{c}\text{see}\\(12.151)\end{array}} = E_a^{(0)} - \sum_\alpha \frac{V_{a\alpha}^{\,2}}{E_\alpha^{(0)} - E_i}$$

and

$$\lambda = E \pm \frac{i\Delta}{2} \tag{12.166}$$

For a large values $|\lambda|$ the expression under the integral in (12.165) behaves like $1/\lambda^3$ and $\oint_{\mathscr{E}_2} \frac{1}{\lambda^3} d\lambda \to 0$ and therefore we can apply the Cauchy sentence from mathematics (the expression under the integral in (12.165) is denoted in (12.167) as Ξ)

$$\begin{aligned}
0 &= \oint_{\mathscr{E}_2} \Xi\, d\lambda = \oint_{\mathscr{E}_1} \Xi\, d\lambda + \oint_{\mathscr{E}_3} \Xi\, d\lambda + \oint_{\mathscr{E}_4} \Xi\, d\lambda \\
\Rightarrow \oint_{\mathscr{E}_1} \Xi\, d\lambda &= -\oint_{\mathscr{E}_3} \Xi\, d\lambda - \oint_{\mathscr{E}_4} \Xi\, d\lambda = \\
&= -\Big(\oint_{\mathscr{E}_3} + \oint_{\mathscr{E}_4} \Big) \frac{1}{(E-\lambda)^{\,2} + \frac{\Delta^2}{4}} \; \frac{1}{E_a^{(0)} - \lambda - \sum_\alpha \frac{V_{a\alpha}^2}{(E_a^{(0)} - \lambda)^{\,2}}}
\end{aligned} \tag{12.167}$$

Further the expression for $P_a(E)$ (see (12.165)) can be rewritten using (12.167) and residuum theorem,

$$\begin{aligned}
P_a(E) &= -\frac{i\Delta}{4\pi^2} \Big(\oint_{\mathscr{E}_3} + \oint_{\mathscr{E}_4} \Big) \frac{\varphi_{34}(\lambda)}{\psi_{34}(\lambda)} = \\
&= -\frac{i\Delta}{4\pi^2}\, 2\pi i \left[\frac{\varphi_{34}(\lambda = E + \frac{i\Delta}{2})}{\psi'_{34}(\lambda = E + \frac{i\Delta}{2})} + \frac{\varphi_{34}(\lambda = E - \frac{i\Delta}{2})}{\psi'_{34}(\lambda = E - \frac{i\Delta}{2})} \right]
\end{aligned} \tag{12.168}$$

where

$$\begin{aligned}
\varphi_{34}(\lambda) &= \frac{1}{E_a^{(0)} - \lambda - \sum_\alpha \frac{V_{a\alpha}^2}{E_\alpha^{(0)} - \lambda}} \\
\psi_{34}(\lambda) &= (E-\lambda)^{\,2} + \frac{\Delta^2}{4} \quad \Rightarrow \quad \psi'_{34}(\lambda) = -2\,(E-\lambda)
\end{aligned}$$

So the final expression for the distribution $P_a(E)$ is,

$$
\begin{aligned}
P_a(E) = \frac{\Delta}{2\pi} \Big\{ \Big(& \frac{1}{E_a^{(0)} - \lambda - \sum_\alpha \frac{V_{a\alpha}^2}{E_\alpha^{(0)} - \lambda}} \; \frac{1}{2(E-\lambda)} \Big)_{\lambda = E + \frac{i\Delta}{2}} \\
& + \Big(\frac{1}{E_a^{(0)} - \lambda - \sum_\alpha \frac{V_{a\alpha}^2}{E_\alpha^{(0)} - \lambda}} \; \frac{1}{2(E-\lambda)} \Big)_{\lambda = E - \frac{i\Delta}{2}} \Big\} = \\
= \frac{\Delta}{2\pi} \Big\{ & \frac{i}{\left[E_a^{(0)} - E - \frac{i\Delta}{2} - \sum_\alpha \frac{V_{a\alpha}^2}{E_\alpha^{(0)} - E - \frac{i\Delta}{2}} \right] \Delta} \\
& - \frac{i}{\left[E_a^{(0)} - E + \frac{i\Delta}{2} - \sum_\alpha \frac{V_{a\alpha}^2}{E_\alpha^{(0)} - E + \frac{i\Delta}{2}} \right] \Delta} \Big\} = \\
= \frac{1}{\pi} \, Im & \frac{1}{E_a^{(0)} - E - \frac{i\Delta}{2} - \sum_\alpha \frac{V_{a\alpha}^2}{E_\alpha^{(0)} - E - \frac{i\Delta}{2}}} = \\
= \frac{1}{2\pi} & \; \frac{\tilde{\Gamma} + \Delta}{(E_a^{(0)} + (\Delta E_a) - E)^{\,2} + \frac{1}{4}(\tilde{\Gamma} + \Delta)^{\,2}}
\end{aligned}
\tag{12.169}
$$

where

$$
\tilde{\Gamma} \equiv \sum_\alpha \frac{V_{a\alpha}^2 \, \Delta}{(E - E_a^{(0)})^{\,2} + \frac{\Delta^2}{4}} \quad , \quad (\Delta E_a) \equiv \sum_\alpha \frac{V_{a\alpha}^2 \, (E - E_\alpha^{(0)})}{(E - E_\alpha^{(0)})^{\,2} + \frac{\Delta^2}{4}} \tag{12.170}
$$

Expression (12.169) for the strength function $P_a(E)$ (the probability of the finding the channel $|a\rangle$ in the eigen-states of the Hamiltonian $\hat{H} = \hat{H}_0 + \hat{V}$ with the eigen-energies in the unity interval around the energy E) resembles the Breight-Wigner expression (11.271). However it is necessary to realize that quantities $\tilde{\Gamma}$ and (ΔE_a) are dependent on the energy E and therefore the expression (12.170) is not exact Breigth-Wigner type expression.

The expression (12.169) can be used e.g. for the description of the probability distribution of the capture of neutron through the channel $n + {}^{A}_{z}X$ (channel state $|a\rangle$ over the collective states of the resultant compound nucleus ${}^{A+1}_{Z}X$ with the energy in the unity energy interval around the energy E (see the subsection 12.3.3.1). However it should be pointed out that the expression (12.169) and (12.170) request the knowledge (or at least estimates) of matrix elements $V_{a\alpha}$ and energies E_α and this can be a problem in practice.

In the paper [400] the method for determination of the strength function described above was used to show that the damping of nuclear collective excitations (called in [400] as doorway channel states), connected with the

fragmentation of giant resonances of different types and multipolarities over the excitation spectrum, can be well described by the coupling of nuclear excitations to doorway states. Subsequent collision processes (reactions), which eventually lead the system into the compound nucleus eigen-states, do not increase the damping width. Particularly it was found that the damping of nuclear collective excitations J^π, caused by the decay fragmentation of the resonance doorway states J^π into many degrees of freedom associated with the compound nucleus formed in some collision reaction, is described by the strength function which is a hybrid of semicircle and Breight-Wigner shapes.

The idea of doorway states treated in the combination with the random matrices approach was used in the recent paper [401]. In this paper so called hybrid model was introduced where the coupling interaction between one-RPA phonon and two-RPA phonons states in spherical nuclei (see the assumed nucleus wave function (7.336)) was randomly created using the random matrices approach. As doorway states the one-RPA phonon states $|a\rangle$ (see (12.143)) were taken and the unperturbed states $|\alpha\rangle$ (called in [401] as background states)were formed by the two-RPA phonon states. The excitation $B(E1)$- strength function determined by the hybrid model was compared with the $B(E1)$- strength function calculated by the realistic Skyrme RPA model with the wave function (7.336). This comparison provided very good agreement of both approaches, with realistic Skyrme interaction and the interaction matrix elements generated randomly. This was an additional confirmation of the fact discussed already in the end of the subsection 12.3.4 that many of features of system properties can be described only by random statistics without knowledge of details of real interactions.

12.4.2 Photon strength function

Standard electromagnetic excitation strength function is usually understood as the distribution of the excitation electromagnetic probability over the excitation energy of the system (nucleus). It was introduced and discussed in details in the subsection 7.3.1.3.2, where $E0$, $E1$, $E2$, $M1$ giant resonances in spherical and deformed nuclei were discussed as the broad peaks observed in the corresponding strength function involving the square of the transition operator (see (7.371)).

However in many papers with the processing of experimental data (especially experimental data from neutron capture experiment) defines the photon strength function in the connection with photo-absorption cross section (see

e.g. [403] and citation therein). Certainly the photon strength function and the standard electromagnetic strength function describe the same physics and are mutually proportional. In this subsection the link between these strength functions is shown.

12.4.2.1 Partial radiation widths and their connection with photo-absorption cross-section

Let us consider electromagnetic deexcitation (see the Fig. 12.10)

$$|i\rangle \equiv |E_i J_i M_i \alpha_i\rangle \quad \rightarrow \quad |f\rangle \equiv |E_f J_f M_f \alpha_f\rangle$$

where E_i is the initial energy for the deexcitation, J_i - total angular momentum in the state $|i\rangle$, M_i - is the projection of the J_i, and $|\alpha_i\rangle$ characterizes other possible quantum numbers of the state $|i\rangle$; and similarly for the final state $|f\rangle$. We suppose that during the transition $|i\rangle \rightarrow |f\rangle$ the photon is emitted with the helicity (polarization) $\tau = \pm 1$ and with the energy $E_\gamma = \hbar\omega = \hbar kc = E_i - E_f > 0$ ($\hbar k$ is the absolute value of the linear momentum of the emitted photon).

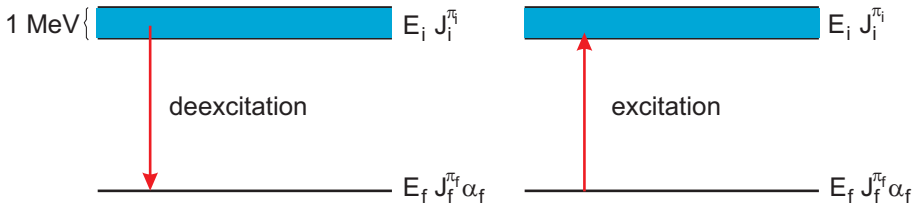


Figure 12.10: Schematic figure of the deexcitation transition (left figure) from the initial states, with fixed quantum numbers $J_i^{\pi_i}$ and energies in the unitary interval $I(E_i)$ around the value E_i, into the particular final state $|E_f J_f^{\pi_f} \alpha_f\rangle$. In the right figure the inverse excitation transition is depicted.

The probability $T_{\alpha_i J_i \rightarrow \alpha_f J_f}$ (see (2.114)) that during 1 second the nucleus passes from the non-oriented state $|i\rangle$ (arbitrary M_i) into the non-oriented state $|f\rangle$ (arbitrary M_f) with the simultaneous emission of the unpolarized photon (arbitrary τ) with the energy in the unitary energy interval around the energy $E_\gamma = E_i - E_f$ (we suppose the energy E_f is fixed while the E_i is not fixed and it falls into the unitary energy interval $I(E_i)$ around the value E_i - see the left panel in the Fig. 12.10) and flying to any direction,

determines so called radiation widths $\Gamma_{deex}(E_i J_i \to E_f J_f \alpha_f)$,

$$\Gamma_{deex}(E_i J_i \to E_f J_f \alpha_f) \equiv \hbar\, T_{J_i \to \alpha_f J_f}(E_\gamma = E_i - E_f) = \boxed{\begin{array}{c}\text{see}\\(2.114)\end{array}} =$$

$$= \frac{8\pi\alpha c}{e^2}\frac{1}{2J_i+1}\sum_J \frac{k^{2J+1}}{[(2J+1)!!\,]^2}\frac{J+1}{j}$$

$$\sum_{\alpha_i \in I(E_i)} \left[|\langle \alpha_f J_f || \hat{\mathscr{M}}^{(el)}_J || \alpha_i J_i \rangle|^2 + |\langle \alpha_f J_f || \hat{\mathscr{M}}^{(mg)}_J || \alpha_i J_i \rangle|^2 \right] =$$

$$= \sum_{|J_i - J_f| \le J \le J_i + J_f} \sum_{X = el,\, mg} \Gamma^{(XJ)}_{deex}(E_i J_i \to E_f J_f \alpha_f) \tag{12.171}$$

where the partial radiation width was introduced,

$$\Gamma^{(XJ)}_{deex}(E_i J_i^{\pi_i} \to E_f J_f^{\pi_f} \alpha_f) =$$

$$= \frac{8\pi\alpha_F}{e^2}\,\frac{E_\gamma^{2J+1}}{(\hbar c)^{2J}}\,\frac{J+1}{J\,[(2J+1)!!]^2}\,\frac{1}{2J_i+1}\sum_{\alpha_i \in I(E_i)} \left| \langle J_f \alpha_f || \hat{\mathscr{M}}^{(X)}_J || J_i \alpha_i \rangle \right|^2 =$$

$$= \boxed{\begin{array}{c}\text{see}\\(2.147)\end{array}} =$$

$$= \frac{8\pi\alpha_F}{e^2}\,\frac{E_\gamma^{2J+1}\,(J+1)}{(\hbar c)^{2J} J[(2J+1)!!]^2} \sum_{\alpha_i \in I(E_i)} B_{deex}(XJ;\; E_i J_i^{\pi_i} \alpha_i \to E_f J_f^{\pi_f} \alpha_f) \tag{12.172}$$

where the sum over α_i in (12.171) and (12.172) involves all states $|J_i^{\pi_i} M_i\, \alpha_i\rangle$ (with any $M_i = -J_i, \cdots, +J_i$, but fixed $J_i^{\pi_i}$) with energies falling to the unitary interval $I(E_i)$ of energies around $E_i = E_\gamma + E_f$ [15].

In (12.172) $B_{deex}(XJ;\; E_i J_i \alpha_i \to E_f J_f \alpha_f)$ stands for the deexcitation reduced probability defined by (2.147) and the symbol α_F represents the fine structure constant, $\alpha_F = \frac{e^2}{4\pi\epsilon_0 \hbar c} = \frac{1}{137}$, which is dimensionless. The long-wave

[15] Units necessary used in (12.172) are following:

$$[\langle J_f \alpha_f || \hat{\mathscr{M}}^{(X)}_J || J_i \alpha_i \rangle] = \begin{cases} e\, fm^J & \text{for } X = el \\ \mu_N fm^{J-1} & \text{for } X = mag \end{cases}$$

$$\Rightarrow \quad [B_{deex}(XJ)] = \begin{cases} e^2\, fm^{2J} & \text{for } X = el \\ \mu_N^2 fm^{2J-2} = (\frac{e\hbar}{2Mc})^2 fm^{2J-2} = 0.011\, e^2 fm^{2J} & \text{for } X = mag \end{cases}$$

$$\Rightarrow \quad [\Gamma^{(XJ)}_{deex}] = MeV$$

limit expressions for electromagnetic transition operators $\hat{\mathscr{M}}^{(X)}_{JM}$ are derived in the Chapter 2 (see the expr. (2.132) for electric $X = el$ case and the expr. (2.142) for magnetic one, $X = mg$),

$$\begin{aligned}
\hat{\mathscr{M}}^{(el)}_{J\,M} &\overset{long\,wave\,limit}{\longrightarrow} \sum_{i=1}^{A} e_i\, r_i^J\, Y_{JM}(\hat{r}_i) \\
\hat{\mathscr{M}}^{(mag)}_{JM} &\overset{long\,wave\,limit}{\longrightarrow} \mu_N\, \sqrt{J(2J+1)} \\
&\sum_{i=1}^{A} \Big(\frac{2g_i^{(l)}}{J+1} \big[\hat{l}_i \otimes Y_{J-1}(\hat{r})\big]_{JM} + g_i^{(s)} \big[\hat{s}_i \otimes Y_{J-1}(\hat{r})\big]_{JM} \Big)\, r^{J-1}
\end{aligned} \tag{12.173}$$

Electromagnetic transition operators $\hat{\mathscr{M}}^{(X)}_{JM}$ fulfill following symmetries with respect to the time-reverse and hermitian conjugation,

$$\begin{aligned}
&\hat{\mathscr{M}}^{(el)\,+}_{JM} = (-1)^M \hat{\mathscr{M}}^{(el)}_{J-M} \quad , \quad \hat{\mathscr{T}}^{-1} \hat{\mathscr{M}}^{(el)}_{JM} \hat{\mathscr{T}} = (-1)^M \hat{\mathscr{M}}^{(el)}_{J-M} \\
&\hat{\mathscr{M}}^{(mg)\,+}_{JM} = (-1)^M \hat{\mathscr{M}}^{(mg)}_{J-M} \quad , \quad \hat{\mathscr{T}}^{-1} \hat{\mathscr{M}}^{(mg)}_{JM} \hat{\mathscr{T}} = (-1)^{M+1} \hat{\mathscr{M}}^{(mg)}_{J-M} \\
&\Rightarrow \hat{\mathscr{T}}^{-1} \hat{\mathscr{M}}^{(X)}_{JM} \hat{\mathscr{T}} = \gamma_T^{(X)} \hat{\mathscr{M}}^{(X)\,+}_{JM}\,,\ \gamma_T^{(X)} = \begin{cases} +1 & \text{for } X = el \\ -1 & \text{for } X = mag \end{cases}
\end{aligned} \tag{12.174}$$

The phase of the laboratory wave function $|JM\alpha\rangle$ can be always chosen in such a way that (so called Bohr-Mottelson phase convention - see (1.48)),

$$\overline{|JM\alpha\rangle} = \mathscr{T}\,|JM\alpha\rangle = (-1)^{J+M}\,|J\,-M\,\alpha\rangle \tag{12.175}$$

Expressions (12.174) and (12.175) gives following symmetry relations for the matrix elements of electromagnetic transition operators,

$$\begin{aligned}
\langle f|\hat{\mathscr{M}}^{(X)}_{JM}|i\rangle &= \langle f|\hat{\mathscr{T}}^{-1}\hat{\mathscr{T}}\hat{\mathscr{M}}^{(X)}_{JM}\hat{\mathscr{T}}^{-1}\hat{\mathscr{T}}|i\rangle = \gamma_T^{(X)}\,\langle \bar{f}|\hat{\mathscr{M}}^{(X)\,+}_{JM}|\bar{i}\rangle^* = \\
&= \gamma_T^{(X)}\,\langle \bar{i}|\hat{\mathscr{M}}^{(X)}_{JM}|\bar{f}\rangle \\
\langle f|\hat{\mathscr{M}}^{(X)}_{JM}|\bar{i}\rangle &= \langle f|\hat{\mathscr{T}}^{-1}\hat{\mathscr{T}}\hat{\mathscr{M}}^{(X)}_{JM}\hat{\mathscr{T}}^{-1}\hat{\mathscr{T}}\hat{\mathscr{T}}|i\rangle = \boxed{\begin{matrix}\text{see}\\(1.50)\end{matrix}} = \\
&= \pm\,\gamma_T^{(X)}\,\langle \bar{f}|\hat{\mathscr{M}}^{(X)\,+}_{JM}|i\rangle^* = \pm\,\gamma_T^{(X)}\langle i|\hat{\mathscr{M}}^{(X)}_{JM}|\bar{f}\rangle = \\
&= \begin{cases} +\,\gamma_T^{(X)}\langle i|\hat{\mathscr{M}}^{(X)}_{JM}|\bar{f}\rangle & \text{for even A nuclei} \\ -\,\gamma_T^{(X)}\langle i|\hat{\mathscr{M}}^{(X)}_{JM}|\bar{f}\rangle & \text{for odd A nuclei} \end{cases}
\end{aligned} \tag{12.176}$$

These expressions together with the Wigner-Eckard theorem (see (A.12)),

$$\langle J_f M_f \alpha_f|\hat{\mathscr{M}}^{(X)}_{JM}|J_i M_i \alpha_i\rangle = \frac{1}{\sqrt{2J_f+1}}\, C^{J_f M_f}_{J_i M_i JM}\,\langle J_f\alpha_f||\hat{\mathscr{M}}^{(X)}_{J}||J_i\alpha_i\rangle \tag{12.177}$$

and using symmetries of Clebsch-Gordan coefficients (see(A.4)) provide,

$$\langle J_f\alpha_f||\hat{\mathscr{M}}_J^{(X)}||J_i\alpha_i\rangle = \gamma_T^{(X)}\,(-1)^{J_i+J_f+J+2M_F}\langle J_i\alpha_i||\hat{\mathscr{M}}_J^{(X)}||J_f\alpha_f\rangle$$
$$\Rightarrow \quad |\langle J_f\alpha_f||\hat{\mathscr{M}}_J^{(X)}||J_i\alpha_i\rangle|^2 = |\langle J_i\alpha_i||\hat{\mathscr{M}}_J^{(X)}||J_f\alpha_f\rangle|^2 \tag{12.178}$$

This implies following symmetry conditions between excitation and deexcitation reduced probabilities,

$$B_{deex}(XJ;\ E_iJ_i\alpha_i \to E_fJ_f\alpha_f) = \frac{1}{2J_i+1}\,|\langle J_f\alpha_f||\hat{\mathscr{M}}_J^{(X)}||J_i\alpha_i\rangle|^2 =$$
$$= \boxed{\begin{array}{c}\text{see}\\(12.178)\end{array}} = \frac{2J_f+1}{2J_i+1}\,\frac{1}{2J_f+1}\,|\langle J_i\alpha_i||\hat{\mathscr{M}}_J^{(X)}||J_f\alpha_f\rangle|^2 =$$
$$= \frac{2J_f+1}{2J_i+1}\,B_{ex}(XJ;\ E_fJ_f\alpha_f \to E_iJ_i\alpha_i) \tag{12.179}$$

and we obtain so called detailed equilibrium condition between excitation and deexcitation probabilities (see the Fig.12.10),

$$(2J_i+1)\,B_{deex}(XJ;\ E_iJ_i\alpha_i \to E_fJ_f\alpha_f) =$$
$$= (2J_f+1)\,B_{ex}(XJ;\ E_fJ_f\alpha_f \to E_iJ_i\alpha_i) \tag{12.180}$$

This condition valids also for partial radiation widths,

$$(2J_i+1)\,\Gamma_{deex}^{(XJ)}(E_iJ_i \to E_fJ_f\alpha_f) =$$
$$= (2J_f+1)\,\Gamma_{ex}^{(XJ)}(E_fJ_f\alpha_f \to E_iJ_i) \tag{12.181}$$

where total widths for the deexcitation and excitation transition $E_iJ_i \to E_fJ_f\alpha_f$ and $E_fJ_f\alpha_f \to E_jJ_i$ are (see (12.171), (12.172)),

$$\Gamma_{deex}(E_iJ_i \to E_fJ_f\alpha_f) = \sum_J \sum_{X=el,mg} \Gamma_{deex}^{(XJ)}(E_iJ_i \to E_fJ_f\alpha_f)$$
$$\Gamma_{ex}(E_fJ_f\alpha_f \to E_iJ_i) = \sum_J \sum_{X=el,mg} \Gamma_{ex}^{(XJ)}(E_fJ_fE_f \to E_iJ_i) \tag{12.182}$$

Further the connection between photoabsorption cross-section and corresponding inverse deexcitation reduced probability is discussed. Let us denote $\sigma(E_\gamma = \hbar\omega;\ E_fJ_f^{\pi_f}\alpha_f \to E_iJ_i^{\pi_i})$ as the photoabsorption cross-section when the nucleus absorbs the photon and simultaneously is excited from the state $|E_fJ_f\alpha_f\rangle$ into non-oriented states with $J_i^{\pi_i}$ and with energies in the unitary

interval $I(E_i)$ around the energy E_i. Then,

$$\sigma(E_\gamma = \hbar\omega;\ E_f J_f^{\pi_f} \alpha_f \to E_i J_i^{\pi_i}) = \boxed{\begin{array}{c}\text{see}\\(12.171)\end{array}} =$$

$$= \frac{8\pi^3 \hbar c^2 \alpha_F}{\omega\, e^2} \sum_J \sum_{X=el,mg} \frac{k^{2J}}{[(2J+1)!!]^2} \frac{J+1}{J}$$

$$\sum_{\alpha_i \in E(E_i)} B_{ex}(XJ;\ E_f J_f^{\pi_f} \to E_i J_i^{\pi_i} \alpha_i)\, \delta(E_\gamma - (E_i - E_f)) =$$

$$= \frac{8\pi^3 \alpha_F}{e^2} \sum_J \sum_{X=el,mg} \frac{E_\gamma^{2J-1}}{(\hbar c)^{2J-2}} \frac{J+1}{J\,[(2J+1)!!]^2}$$

$$\sum_{\alpha_i \in I(E_i)} B_{ex}(XJ;\ E_f J_f^{\pi_f} \to E_i J_i^{\pi_i} \alpha_i)\, \delta(E_\gamma - (E_i - E_f)) =$$

$$= \boxed{\begin{array}{c}\text{see}\\(12.179)\end{array}} =$$

$$= \frac{8\pi^3 \alpha_F}{e^2} \sum_J \sum_{X=el,mg} \frac{E_\gamma^{2J-1}}{(\hbar c)^{2J-2}} \frac{J+1}{J\,[(2J+1)!!]^2} \frac{2J_i+1}{2J_f+1}$$

$$\sum_{\alpha_i \in I(E_i)} B_{deex}(XJ;\ E_i J_i^{\pi_i} \alpha_i \to E_f J_f^{\pi_f} \alpha_f)\, \delta(E_\gamma - (E_i - E_f)) =$$

$$= \sum_{|J_i - J_f| \le J \le J_i + J_f} \sum_{\substack{X=el,mg \\ \pi_i \pi_f (-1)^J = 1 \text{ for } X=el \\ \pi_i \pi_f (-1)^J = -1 \text{ for } X=mg}} \sigma_{XJ}(E_\gamma;\ E_f J_f \alpha_f \to E_i J_i^{\pi_i}) \tag{12.183}$$

where we introduced partial cross-section,

$$\sigma_{XJ}(E_\gamma;\ E_f J_f^{\pi_f} \alpha_f \to J_i^{\pi_i} E_i) =$$

$$= \frac{8\pi^3 \alpha_F}{e^2} \frac{J+1}{J\,[(2J+1)!!]^2} \frac{E_\gamma^{2J-1}}{(\hbar c)^{2J-2}} \frac{2J_i+1}{2J_f+1}$$

$$\sum_{\alpha_i \in I(E_i)} B_{deex}(XJ;\ E_i J_i^{\pi_i} \alpha_i \to E_f J_f^{\pi_f} \alpha_f)\, \delta(E_\gamma - (E_i - E_f)) =$$

$$= \frac{8\pi^3 \alpha_F}{e^2} \frac{J+1}{J\,[(2J+1)!!]^2} \frac{E_\gamma^{2J-1}}{(\hbar c)^{2J-2}} S_{ex;\, E_f J_f^{\pi_f} \alpha_f \to J_i^{\pi_i}}(E_\gamma) \tag{12.184}$$

where the strength excitation function $S_{ex;\, E_f J_f^{\pi_f} \alpha_f \to J_i^{\pi_i}}(E_\gamma)$ of the excitation process $E_f J_f^{\pi_f} \alpha_f \;\to\; J_i^{\pi_i} E_i$ going into states $J_i^{\pi_i}$ by the absorption of the photon with the energy E_γ is (see (7.371)) [16]

$$
\begin{aligned}
& S_{ex;\, E_f J_f^{\pi_f} \alpha_f \to J_i^{\pi_i}}(E_\gamma) \\
& \equiv \sum_{\alpha_i \in I(E_i)} B_{ex}(XJ;\; E_f J_f^{\pi_f} \alpha_f \to E_i J_i^{\pi_i} \alpha_i)\;\; \delta(E_\gamma - E_i + E_f) = \\
& = \boxed{\begin{array}{c} \text{see} \\ (12.180) \end{array}} = \\
& = \frac{2J_i + 1}{2J_f + 1} \sum_{\alpha_i \in I(E_i)} B_{deex}(XJ;\; E_i J_i^{\pi_i} \alpha_i \to E_f J_f^{\pi_f} \alpha_i)\;\; \delta(E_\gamma - E_i + E_f)
\end{aligned}
\tag{12.185}
$$

where the sum over α_i involves all states $|J_i^{\pi_i} M_i \alpha_i\rangle$ (with any $M_i = -J_i, \cdots, +J_i$) with energies falling into the unitary interval $I(E_i)$ of energies around $E_i = E_\gamma + E_f$ (because of the presence of the Dirac δ- function $\delta(E_\gamma - E_i + E_f)$. Dimension of the strength function is: $[S_{ex;\, E_f J_f \alpha_f \to J_i}] = e^2\, fm^{2J}\, MeV^{-1}$. [17]

States $|E_i J_i^{\pi_i} \alpha_i\rangle$ and $|E_f J_f^{\pi_f} \alpha_f\rangle$ corresponds to the laboratory frame. However, in the case of deformed nuclei we should distinguish between laboratory frame and intrinsic frame which rotates together with the nucleus. For axially deformed nuclei the wave function of the nucleus in the laboratory frame has following form (see expressions (7.27), (7.29)),

$$
\begin{aligned}
& \Psi_{JMK\rho}(\xi, \theta) = \langle \xi, \theta | JMK\rho \rangle = \\
& = \sqrt{\frac{2J+1}{16\pi^2(1+\delta_{K0})}}\; \Big[\, D^J_{MK}(\theta)\, \psi_{K\rho}(\xi) + (-1)^J\, D^J_{M-K}(\theta)\, \hat{\mathscr{R}}_1(\pi) \psi_K(\xi) \Big]
\end{aligned}
\tag{12.186}
$$

where J is the total angular momentum in the laboratory frame, M is the total angular momentum projection on the z-axis of the laboratory frame, K

[16] The excitation strength function (12.185) is a generalization of the strength function (7.371) defined for pure electromagnetic excitation ($\Delta T = p$) from the ground state of even-even nucleus. The strength function (12.185) is general in the sense that it valids for any XJ- excitations from the fixed initial state $E_f J_f^{\pi_f} \alpha_f$ going to any states with given $J_i^{\pi_i}$ (see the Fig.12.10) in any nucleus (not only even-even nuclei).

[17] Dimension unit check of (12.184):
$[E_\gamma] = MeV$, $[B_{deex}(XJ)] = e^2\, fm^{2J}$, $\hbar c = 197\, MeV\, fm$, $[\delta(E)] = MeV^{-1}$
right side of (12.184): $MeV^{2J-1}\, MeV^{2J-2}\, fm^{-(2J-2)}\, fm^{2J}\, MeV^{-1} = fm^2$
left side of (12.184): fm^2
$[S_{ex}^{(XJ)}(E_\gamma)] = e^2\, fm^{2J}\, MeV^{-1}$

is the angular momentum projection on the 3-d intrinsic axis (symmetry axis) of the intrinsic rotating frame, $D^J_{MK}(\theta)$ are Wigner functions of Euler angles between intrinsic and laboratory frames, $\psi_{K\rho}(\xi)$ is the eigen-wave function of the intrinsic nucleus Hamiltonian $\hat{H}_{intr}$ ($\hat{H}_{intr}\psi_{K\rho}(\xi) = E_{K\rho}\psi_{K\rho}(\xi)$) where ξ represents all intrinsic variables and the index ρ enumerates all solutions of the stationary Schoedinger equation $\hat{H}_{intr}$ ($\hat{H}_{intr}\psi_{K\rho}(\xi) = E_{K\rho}\psi_{K\rho}(\xi)$). One should realize that the wave function (12.186) is the eigen-function of the total Hamiltonian $\hat{H} = \hat{H}_{intr} + \hat{H}_{rot}$ only in the case when the Coriolis and centrifugal terms in the total Hamiltonian are neglected (see (7.17). That means,

$$|E_i J_i^{\pi_i} \alpha_i\rangle \equiv |E_i J_i^{\pi_i} K_i \rho_i\rangle \quad , \quad |E_f J_f^{\pi_f} \alpha_f\rangle \equiv |E_f J_f^{\pi_f} K_f \rho_f\rangle$$

Then the reduced probability (12.177) has following form (see (7.42)),

$$\begin{aligned} &B_{deex}(XJ;\ E_i J_i^{\pi_i} K_i \rho_i \to E_f J_f^{\pi_f} K_f \rho_f) = \\ &= \Big| C^{J_f K_f}_{J_i K_i J K_f - K_i} \langle K_f \rho_f | \hat{\mathscr{M}}^{(X)\prime}_{JK_f - K_i} | K_i \rho_i \rangle \\ &\qquad + (-1)^{J_i} C^{J_f K_f}_{I_i - K_i J K_f + K_i} \langle K_f \rho_f | \hat{\mathscr{M}}^{(X)\prime}_{JK_f + K_i} \hat{\mathscr{R}}_1 | K_i \rho_i \rangle \Big|^2 \end{aligned} \tag{12.187}$$

and

$$\begin{aligned} &B_{ex}(XJ;\ E_f J_f^{\pi_f} K_f \rho_f \to E_i J_i^{\pi_i} K_i \rho_i) = \\ &= \frac{2J_i + 1}{2J_f + 1} B_{deex}(XJ;\ E_i J_i^{\pi_i} K_i \rho_i \to E_f J_f^{\pi_f} K_f \rho_f) = \\ &= \Big| C^{J_i K_i}_{J_f K_f J K_i - K_f} \langle K_i \rho_i | \hat{\mathscr{M}}^{(X)\prime}_{JK_i - K_f} | K_f \rho_f \rangle \\ &\qquad + (-1)^{J_f} C^{J_i K_i}_{I_f - K_f J K_i + K_f} \langle K_i \rho_i | \hat{\mathscr{M}}^{(X)\prime}_{JK_f + K_i} \hat{\mathscr{R}}_1 | K_f \rho_f \rangle \Big|^2 \end{aligned} \tag{12.188}$$

where $\hat{\mathscr{M}}^{(X)\prime}_{J\Delta K}$ means the transition operator in the intrinsic frame rotating with the nucleus. Keeping the assumption of the Coriolis and centrifugal terms in the Hamiltonian $\hat{H}$ neglected the reduced probability for so called intraband transition ($K_i\rho_i = K_f\rho_f = K\rho$) is given by (see (7.43)),

$$B_{ex}(XJ;\ E_f J_f^{\pi_f} K_f \rho_f \to E_i J_i^{\pi_i} K_i \rho_i) = \left(C^{J_i K}_{J_f K J\, 0} \right)^2 \left| \langle K\rho | \hat{\mathscr{M}}^{(X)\prime}_{J0} | K\rho \rangle \right|^2 \tag{12.189}$$

This expression excludes the intraband E1, E3, E5, ... and M2, M4, ... transitions (because of the parity selection rules). The intraband transitions are also drastically reduced for M1 (see the text below the expression (7.76)).

Further we will discuss the case of even-even nuclei with the photoabsorption starting with the ground state $|E_f = 0;\ J_f^{\pi_f} = 0^+; K_f = 0;\ \rho = gr\rangle$. In this case laboratory wave function (12.186) reads (ground state intrinsic wave function $\psi_{K_f=0\,\rho=gr}(\xi)$ corresponds to the signature $r = +1$ (see (7.34), $\hat{\mathscr{R}}_1(\pi)\,\phi_{K_f=0,gr}(\xi) = \phi_{K_f=0,gr}(\xi)$),

$$\Psi_{J_f=0\,M_f=0\,K_f=0\,\rho_f}(\xi,\theta) = \sqrt{\frac{1}{8\pi^2}}\ D^0_{00}(\theta)\,\psi_{K_f=0\rho_f=gr}(\xi) = \frac{\psi_{K_f=0\,\rho_f=gr}(\xi)}{\sqrt{8\pi^2}} \tag{12.190}$$

and corresponding reduced excitation probability (12.188) has following form,

$$\begin{aligned}
&B_{ex}(XJ; gr \to E_i - E_\gamma, J_i - J\ K_i\rho_i) = \\
&= \left(C^{00}_{00JK_i}\right)^2 |\langle K_i\rho_i|\hat{\mathscr{M}}^{(X)\,\prime}_{JK_i})|gr\ 0^+\rangle|^{\,2} = |\langle K_i\rho_i|\hat{\mathscr{M}}^{(X)\,\prime}_{JK_i})|gr\ 0^+\rangle|^{\,2} = \\
&= (2J_i+1)\,B_{deex}(XJ;\ J_i = J, K_i\rho_i \leftrightarrow gr\ 0^+) = \\
&= (2J_i+1)\left(C^{00}_{J_i-K_iJK}\right)^2 |\langle gr\ 0^+|\hat{\mathscr{M}}^{(X)\,\prime}_{J-K_i}|K_i\rho_i\rangle|^{\,2} = \\
&= |\langle K_i\rho_i|\hat{\mathscr{M}}^{(X)\,\prime}_{JK_i}|gr\ 0^+\rangle|^{\,2}
\end{aligned} \tag{12.191}$$

Corresponding excitation strength function is (see (12.185)),

$$\begin{aligned}
S_{ex;\,gr\,0^+\to E_iK_i^{\pi_i}\rho_i} &= \sum_{K_iE_i\rho_i} B_{ex}(XJ;\ gr\ 0^+ \to E_iK_i^{\pi_i}\rho_i)\ \delta_{J_iJ}\ \delta(E_\gamma - E_i) = \\
&= \sum_{K=-J}^{+J}\ \sum_{E_i\rho_i} B_{ex}(XJ;\ gr\ 0+ \to E_iK\rho_i)\,\delta_{J_iJ}\,\delta(E_\gamma - E_i) = \\
&= \sum_{K=-J}^{+J} S_{ex;\,gr\to K^{\pi_i}}(E_\gamma)
\end{aligned} \tag{12.192}$$

where we defined,

$$\begin{aligned}
S_{ex;\,gr\,0^+\to K^{\pi_i}}(E) &= \sum_{E_i\rho_i} B_{ex}(XJ;\ gr\ 0+ \to E_iK^{\pi_i}\rho_i)\,\delta(E_\gamma - E_i) = \\
&= (2J+1)\,S_{deex;\,K^{\pi_i}\to gr\,0^+}(E)
\end{aligned} \tag{12.193}$$

Corresponding total photoabsorption cross-section $\sigma_{phot}(E)$ when the nucleus is excited from its ground state $|E_\gamma = 0;\ gr\ 0^+\rangle$ into the final states with all

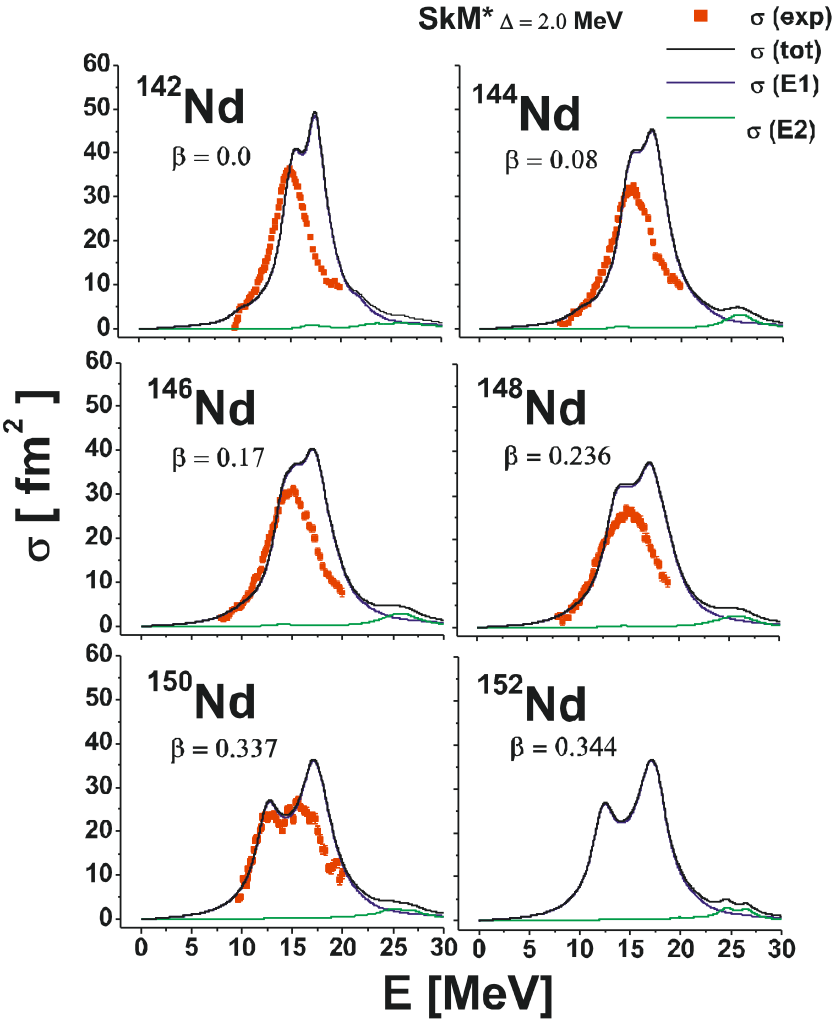


Figure 12.11: Photoasorption cross-section as a function of the excitation energy for the chain of the Nd isotopes (from the spherical ^{142}Nd up to the well- deformed ^{152}Nd). The axial deformation of each isotopes is characterized by the quadrupole deformation parameter β. The black curve is for the total cross-section $\sigma_{tot}(E)$, the blue one for the $\sigma_{E1}(E)$ and the green one for $\sigma_{E2}(E)$ (calculated using expressions (12.194), (12.195), (12.185), (7.371) and (7.374)). Experimental data (red squares) are taken from [199].

$J^{\pi=\pm 1}$ and with the excitation energy in the unitary energy interval around the energy E is following (see (12.183), (12.184),

$$\sigma_{phot}(E) = \sum_{\substack{J=1 \\ \pi_f=\pm 1}}^{\infty} \sum_{\substack{X=el,mg \\ \pi_i\pi_f(-1)^J=1 \text{ for } X=el \\ \pi_i\pi_f(-1)^J=-1 \text{ for } X=mg}} \sigma_{XJ}(E;\ gr\ 0^+ \to J^{\pi_f}\ E_f = E) =$$

$$= \sigma_{E1}(E) + \sigma_{E2}(E) + \cdots + \sigma_{M1}(E) + \sigma_{M2}(E) + \cdots \qquad (12.194)$$

where

$$\sigma_{E1}(E) = 0.402\ E\ S^{(E1)}_{ex;\,0^+\ gr\to J^\pi=1^-}$$
$$\sigma_{E2}(E) = 3.089\ 10^{-7}\ E^3\ S^{(E2)}_{ex;\,0^+\ gr\to J^\pi=2^+}$$
$$\sigma_{E3}(E) = 1.199\ 10^{-13}\ E^5\ S^{(E3)}_{ex;\,0^+\ gr\to J^\pi=3^-}$$
$$\sigma_{M1}(E) = 4.437\ 10^{-3}\ E\ S^{(M1)}_{ex;\,0^+\ gr\to J^\pi=1^+} \qquad (12.195)$$

where dimensions of individual quantities in (12.194) and (12.195) are following: $[S^{(EJ)}_{ex;\,0^+\ gr\to J^\pi}] = e^2\ fm^{2J}\ MeV^{-1}$, $[S^{MJ}_{ex;\,0^+\ gr\to J^\pi}] = \mu_N^2\ fm^{2J-2}\ MeV^{-1}$ and $[E] = MeV$.

From (12.195) follows that the dominant contribution into the photoabsorption cross-section (12.194) comes from $E1$ transitions. Contributions from higher transition multi-polarities J degrease quickly with the increasing J and it is possible to neglect them in the comparison with the $E1$ transition (see the text below the expression (7.386) in the Chapter 7).

As an example of the calculation of photoabsorption cross-section the Fig.12.11 is presented where the experimental values (taken from [199]) are compared with the calculated Skyrme-RPA calculations with the realistic SkM* Skyrme-RPA calculation (using expressions (12.195) for strength functions $S^{(XJ)}_{ex;\,0^+\ gr\to J^\pi}$ calculated in the framework of the RPA approach). From the Fig.12.11 it is clear that the $\sigma_{E1}(E)$ is dominant in (12.194) and the contributions from other (higher) multipolarities and types (different from E1 and E2) are not visible in the Fig.12.11.

12.4.2.2 Photon strength function and its connection with photoabsorption cross section

In many papers, especially those with the processing of experimental data, instead of excitation or deexcitation strength functions defined by (7.371) or (12.185) so called **photon strength functions** are introduced (see e.g. [403, 405] and citations therein). In this subsection the photon strength function and its connection with standard excitation or deexcitation strength function is discussed in details.

Expressions (12.183) and (12.184) give the cross section of the photoabsorption when the nucleus passes from its non-oriented initial state $|E_f J_f \alpha_f\rangle$ into non-oriented final states with $J_i^{\pi_i}$ and energies corresponding to the unitary energy interval $I(E_i)$ around the energy E_i (because of the presence of the Dirac δ- function $\delta(E_\gamma - (E_i - E_f))$ which has a dimension $1/MeV$) as is

schematically shown in the right panel of the Fig.12.10. One should realize that the number of such final states $|E_i J_i\rangle$ in this unitary energy interval is equal to the energy density $\rho(E_i, J_i^{\pi_i})$ of states with fixed $J_i^{\pi_i}$. So in order to obtain average photoabsorption cross section $\bar{\sigma}(E_\gamma;\ E_f J_f^{\pi_f} \alpha_f \to E_i J_i^{\pi_i})$ for particular states $|E_i J_i^{\pi_i} \alpha_i\rangle$ with energies $E_i \in I(E_i)$ it is necessary to divide the expression (12.183) by the energy density $\rho(E_i, J_I^{\pi_i})$,

$$\bar{\sigma}(E_\gamma;\ E_f J_f^{\pi_f} \alpha_f \to E_i J_i^{\pi_i}) \equiv \frac{\sigma(E_\gamma;\ E_f J_f^{\pi_f} \alpha_f \to E_i J_i^{\pi_i})}{\rho(E_i, J_i^{\pi_i})} =$$

$$= \boxed{\begin{array}{c}\text{see}\\ (12.183)\end{array}} = \sum_{|J_i - J_f| \le J \le J_i + J_f} \sum_{\substack{X=el,mg \\ \pi_i\pi_f(-1)^J=1 \text{ for } X=el \\ \pi_i\pi_f(-1)^J=-1 \text{ for } X=mg}} \bar{\sigma}_{XJ;\, J_f^{\pi_f} \alpha_f \to J_i^{\pi_i}}(E_\gamma) \tag{12.196}$$

where

$$\bar{\sigma}_{XJ;\, J_f^{\pi_f} \alpha_f \to J_i^{\pi_i}}(E_\gamma) \equiv$$

$$= \frac{8\pi^3 \alpha_F}{e^2} \frac{J+1}{J[(2J+1)!!]^2} \frac{E_\gamma^{2J-1}}{(\hbar c)^{2J-2}} \frac{S^{(XJ)}_{ex;\, E_f J_f^{\pi_f} \alpha_f \to J_i^{\pi_i} E_i}}{\rho(E_i, J_i^{\pi_i})} \tag{12.197}$$

Similarly for average radiation width, in order to obtain average radiation width corresponding to one particular state $|E_i J_i^{\pi_i} \alpha_i\rangle$ it is necessary to divide the expressions (12.171) and (12.172) by the energy density $\rho(E_i, J_i^{\pi_i})$,

$$\bar{\Gamma}_{deex}(E_\gamma;\ J_i^{\pi_i} \to E_f J_f^{\pi_f} \alpha_f) \equiv \frac{\Gamma_{deex}(E_\gamma;\ E_i J_i^{\pi_i} \to E_f J_f^{\pi_f} \alpha_f)}{\rho(E_i, J_i^{\pi_i})} =$$

$$= \boxed{\begin{array}{c}\text{see}\\ (12.171)\end{array}} =$$

$$= \sum_{|J_i - J_f| \le J \le J_i + J_f} \sum_{\substack{X=el,mg \\ \pi_i\pi_f(-1)^J=1 \text{ for } X=el \\ \pi_i\pi_f(-1)^J=-1 \text{ for } X=mg}} \bar{\Gamma}^{(XJ)}_{deex;\, J_i^{\pi_i} \to E_f J_f^{\pi_f} \alpha_f} \tag{12.198}$$

with the average partial deexcitation width $\bar{\Gamma}^{(XJ)}_{deex;\, J_i^{\pi_i} \to J_f^{\pi_f} \alpha_f}$ (for given XJ)

corresponding to one state to one state transition was introduced as,

$$\bar{\Gamma}^{(XJ)}_{deex;\, J_i^{\pi_i}\to J_f^{\pi_f}\alpha_f} = \frac{\bar{\Gamma}^{(XJ)}_{deex;\, J_i^{\pi_i}\to E_f J_f^{\pi_f}\alpha_f}}{\rho(E_i, J_i^{\pi_i})} = \boxed{\begin{array}{c}\text{see}\\ (12.172)\end{array}} =$$

$$= \frac{8\pi\alpha_F}{e^2}\,\frac{(J+1)\,E_\gamma^{2J+1}}{J[(2J+1)!!]^{\,2}\,(\hbar c)^{2J}}\,\frac{1}{\rho(E_i, J_i^{\pi_i})} \sum_{\alpha\in I(E_i)} B_{deex}(XJ;\; J_i^{\pi_i}\to E_f J_f^{\pi_f}\alpha_f)\,\delta(E_\gamma - E_i + E_f) =$$

$$= \frac{8\pi\alpha_F}{e^2}\,\frac{(J+1)\,E_\gamma^{2J+1}}{J[(2J+1)!!]^{\,2}\,(\hbar c)^{2J}}\,\frac{1}{\rho(E_i, J_i^{\pi_i})}\,S^{(XJ)}_{deex;\, J_I^{\pi_i}\to E_f J_f^{\pi_f}\alpha_f}(E_\gamma) \tag{12.199}$$

where (see (12.185)),

$$S^{(XJ)}_{deex;J_i^{\pi_i}\to E_f J_f^{\pi_f}\alpha_f}(E_\gamma) = \sum_{\alpha\in I(E_i)} B_{deex}(XJ;\; J_i^{\pi_i}\to E_f J_f^{\pi_f}\alpha_f)\,\delta(E_\gamma - E_i + E_f) = \frac{2J_f+1}{2J_i+1}\,S^{(XJ)}_{ex;\, E_f J_f^{\pi_f}\alpha_f\to J_i^{\pi_i}}(E_\gamma) \tag{12.200}$$

is the total partial (for given XJ) strength function for given one deexcitation final state $|E_f J_f^{\pi_f}\alpha_f\rangle$ and for deexcitation initial states with fixed $J_i^{\pi_i}$ and energies in the unitary interval $I(E_i)$.

The excitation partial radiation width can be expressed in terms of the partial photoabsorption cross section $\bar{\sigma}_{XJ;\, J_f^{\pi_f}\alpha_f\to J_i^{\pi_i}}$ (see (12.197), (12.199)),

$$\bar{\Gamma}^{(XJ)}_{ex;\, J_f^{\pi_f}\alpha_f\to J_i^{\pi_i}} = \frac{2J_i+1}{2J_f+1}\;\bar{\Gamma}^{(XJ)}_{deex;\, J_i^{\pi_i}\to J_f^{\pi_f}\alpha_f} = \frac{E_\gamma^2}{(\pi\hbar c)^2}\;\bar{\sigma}_{XJ;\, J_f^{\pi_f}\alpha_f\to J_i^{\pi_i}} \tag{12.201}$$

The **photon strength** function $f^{(XJ)}(E_\gamma)$, often used in the processing of

experimental data on γ- decays, was defined by Bartholomew [404],

$$f^{(XJ)}_{J_i^{\pi_i}\to E_f J_f^{\pi_f}\alpha_f}(E_\gamma) \equiv \frac{\rho(E_i,J_i^{\pi_i})}{E_\gamma^{2J+1}}\,\bar\Gamma^{(XJ)}_{deex;\,J_i^{\pi_i}\to J_f^{\pi_f}\alpha_f} = \boxed{\begin{array}{c}\text{see}\\ (12.199)\end{array}} =$$
$$= \frac{8\pi\alpha_F}{e^2}\,\frac{J+1}{J[(2J+1)!!]^2}\,\frac{1}{(\hbar c)^{2J}}\,S^{(XJ)}_{deex;\,J_i^{\pi_i}\to E_f J_f^{\pi_f}\alpha_f}(E_\gamma) =$$
$$= \frac{8\pi\alpha_F}{e^2}\,\frac{2J_f+1}{2J_i+1}\,\frac{J+1}{J[(2J+1)!!]^2}\,\frac{1}{(\hbar c)^{2J}}\,S^{(XJ)}_{ex;\,E_f J_f^{\pi_f}\alpha_f\to J_i^{\pi_i}}(E_\gamma) =$$
$$= \frac{1}{(\pi\hbar c)^2}\,\frac{2J_f+1}{2J_i+1}\,\frac{1}{E_\gamma^{2J-1}}\;\bar\sigma^{(XJ)}_{XJ;\,J_f^{\pi_f}\alpha_f\to J_i^{\pi_i}}(E_\gamma)\;\rho(E_i,J_i^{\pi_i}) \qquad (12.202)$$

and we have,

$$\rho(E_i,J_i^{\pi_i})\;\bar\sigma_{XJ;\,J_f^{\pi_f}\alpha_f\to J_i^{\pi_i}}(E_\gamma) = (\pi\hbar c)^2\,\frac{2J_i+1}{2J_f+1}\,E_\gamma^{2J-1}\;f^{(XJ)}_{J_i^{\pi_i}\to E_f J_f^{\pi_f}\alpha_f}(E_\gamma) \qquad (12.203)$$

In the processing of experimental data several approximations are used which are described further.

Experiments with the photoabsorption usually do not recognize individual components of the photoabsorption cross section $\bar\sigma_{XJ;\,J_f^{\pi_f}\alpha_f\to J_i^{\pi_i}}(E)$ with different final angular momenta $J_i^{\pi_i}$. From this point of view it is necessary to sum the expression (12.201) over all J_i (with fixed J and J_f) which are accessible from the given $J_f^{\pi_f}$ by the selection role for given XJ transition (that means $|J_f-J|\le J_i\le J_f+J$ and $\pi_i\pi_f=(-1)^J$ for $X=el$ or $\pi_i\pi_f=(-1)^{J+1}$ for $X=mag$). In this summation often the assumption is done that the deexcitation width $\Gamma^{(XJ)}_{deex;\,J_i^{\pi_i}\to E_f J_f^{\pi_f}\alpha_f}(E) = \rho(E_i,J_i^{\pi_i})\,\bar\Gamma^{(XJ)}_{deex;\,J_i^{\pi_i}\to J_f^{\pi_f}\alpha_f}(E)$ is not dependent on J_i and it can be substituted by some average value $(\overline{\rho\Gamma}(E))_{deex;\,J_f^{\pi_f}\alpha_f}$ defined as,

$$\bar\Gamma^{(XJ)}_{deex;\,J_i^{\pi_i}\to E_f J_f^{\pi_f}\alpha_f}(E) =$$
$$= \rho(E_i,J_i^{\pi_i})\;\bar\Gamma^{(XJ)}_{deex;\,J_i^{\pi_i}\to J_f^{\pi_f}\alpha_f}(E) \;\approx\; \big(\overline{\rho\Gamma}(E)\big)_{deex;\,J_f^{\pi_f}\alpha_f}$$

Provided this assumption is valid the total partial photoabsorption cross section $\sigma_{XJ;\,J_f^{\pi_f}\alpha_f\to tot}\equiv\rho(E_i,J_i^{\pi_i})\,\bar\sigma_{XJ;\,J_f^{\pi_f}\to tot}$ for transition XJ into all possible states reachable from the initial state $|E_f J_f^{\pi_f}\alpha_f\rangle$ by the selection rule of the

transition XJ reads,

$$\sigma_{XJ;\, J_f^{\pi_f}\alpha_f\to tot} \equiv \sum_{J_i=|J_f-J|}^{J_f+J} \bar{\sigma}_{XJ;\, J_f^{\pi_f}\alpha_f\to J_i^{\pi_i}}(E)\;\rho(E_i, J_i^{\pi_i}) =$$

$$= \boxed{\begin{array}{c}\text{see (12.201)}\\ \text{and the assumption above}\end{array}} =$$

$$\approx \frac{\pi^2\hbar^2c^2}{E^2}\left(\overline{\rho\Gamma}(E)\right)_{deex;\, J_f^{\pi_f}\alpha_f}(2J+1) = \boxed{\begin{array}{c}\text{see}\\ (12.202)\end{array}} =$$

$$= (\pi\hbar c)^2\, E^{2J-1}\,(2J+1)\, f^{(XJ)}_{tot\to E_f J_f^{\pi_f}\alpha_f}(E) \qquad (12.204)$$

where the photon strength function for all deexcitation transition XJ into the final state $|E_f J_f \alpha_f\rangle$ from all initial states $|E_i J_i \alpha_i\rangle$, accessible by selection rules of the transition XJ, is dependent only on $E = E_i - E_f$ and $J_f^{\pi_f}\alpha_f$ [18],

$$f^{(XJ)}_{tot\to E_f J_f^{\pi_f}\alpha_f}(E) = \frac{\sigma_{XJ;\, J_f^{\pi_f}\alpha_f\to tot}(E)}{E^{2J-1}\,\pi^2\hbar^2c^2\,(2J+1)} \qquad (12.205)$$

Further relatively rough approximation, usually used in the analyzes of partial radiative widths, is based on so called Brink- hypothesis that the photoabsorption cross-section does not depend on the quantum numbers $E_f J_f^{\pi_f}\alpha_f$. In such a case the expression (12.205) is dependent only on the energy $E = E_\gamma$ of the absorbed (in the photoabsorption) or emitted (in the γ- decay process) photon (that means $f_{tot\to E_f J_f^{\pi_f}\alpha_f}(E) \approx f^{(XJ)}(E) = \sigma_{XJ}(E)/[E^{(2J-1}\pi^2\hbar^2c^2(2J+1)]$ and the partial cross section $\sigma_{XJ}(E)$ is often estimated by some phenomenological function - see the next subsection). However, the more realistic models predict the dependence of the radiative widths on the quantum numbers $E_f J_f \alpha_f$ of the final states after the emission of the photon (this is true particularly for the low excitation energy E_f of the final states) as it is discussed in further subsections.

In numerical calculation the excitation strength function can be deter-

[18] Dimension units for the photon strength function are (see (12.202)),

$$[f^{(XJ)}] = \frac{1}{MeV^{2J}\,fm^{2J}}\,[S^{(XJ)}] = \begin{cases} e^2\,MeV^{-(2J+1)} & \text{for } X = el \\ \mu_N^2 MeV^{-(2J+1)} = 0.011\,e^2 MeV^{-(2J+1)} & \text{for } X = mag \end{cases}$$

mined as (see (12.185)),

$$
\begin{aligned}
&S^{(XJ)}_{ex;\, E_f J_f^{\pi_f} \alpha_f \to J_i^{\pi_i}}(E) = \\
&= \sum_{\alpha_i \in I(E_i)} B_{ex}(XJ;\; E_f J_f^{\pi_f} \alpha_f \to E_i J_i^{\pi_i} \alpha_i)\, \delta(E - E_i + E_f) \approx \\
&\approx S^{(XJ)}_{ex;\, E_f J_f^{\pi_f} \alpha_f \to J_i^{\pi_i}}(E, \Delta) \equiv \\
&\equiv \frac{1}{\Delta} \sum_{\alpha_i,\, E \in \Delta(E_i)} B_{ex}(XJ;\; E_f J_f^{\pi_f} \alpha_f \to E_i J_i^{\pi_i} \alpha_i) = \\
&= \frac{1}{\Delta}\, \frac{2J_i + 1}{2J_f + 1} \sum_{\alpha_i,\, E \in \Delta(E_i)} B_{deex}(XJ;\; E_i J_i^{\pi_i} \alpha_i \to E_f J_f^{\pi_f} \alpha_f)
\end{aligned}
\tag{12.206}
$$

where $\Delta(E_i)$ is arbitrary small energy interval in the vicinity of the energy E. Alternative possibility of the determination of the excitation strength function $S_{ex;\, E_f J_f^{\pi_f} \alpha_f \to J_i^{\pi_i}}(E)$ is to use Lorentzian averaging way (see (7.372)-(7.374)),

$$
\begin{aligned}
&S^{(XJ)}_{ex;\, E_f J_f^{\pi_f} \alpha_f \to J_i^{\pi_i}}(E, \Delta) = \\
&= \sum_{E_i, \alpha_i} B_{ex}(XJ;\; E_f J_f^{\pi_f} \alpha_f \to E_i J_i^{\pi_i} \alpha_i)\, \frac{1}{2\pi}\, \frac{\Delta}{[E - E_i + E_f]^{\,2} + \frac{\Delta^2}{4}} \\
&\stackrel{\Delta \to 0}{\longrightarrow} \sum_{E_i, \alpha_i} B_{ex}(E_f J_f^{\pi_f} \alpha_f \to E_i J_i^{\pi_i} \alpha_i)\, \delta(E - E_i + E_f)
\end{aligned}
\tag{12.207}
$$

And the connection between $S^{(XJ)}_{deex;\, J_i^{\pi_i} \to E_f J_f^{\pi_f} \alpha_f}(E)$ and $f^{(XJ)}_{J_i^{\pi_i} \to E_f J_f^{\pi_f} \alpha_f}(E)$ (see (12.202)) gives the corresponding value of the photon strength function,

$$
\begin{aligned}
&S^{(XJ)}_{deex;\, J_i^{\pi_i} \to E_f J_f^{\pi_f} \alpha_f}(E_\gamma; \Delta) = \\
&= \frac{1}{\Delta} \sum_{\alpha_i, E \in \Delta(E_i)} B_{deex}(XJ;\; E_i J_i^{\pi_i} \alpha_i \to E_f J_f^{\pi_f} \alpha_f) = \\
&= \Big\{ \frac{8\pi \alpha_F}{e^2}\, \frac{J+1}{J[(2J+1)!!]^{\,2}}\, \frac{1}{(\hbar c)^{2J}} \Big\}^{-1}\, f^{(XJ)}_{J_i^{\pi_i} \to E_f J_f^{\pi_f} \alpha_f}(E_\gamma)
\end{aligned}
\tag{12.208}
$$

More explicitly,

$$
\begin{aligned}
&\frac{1}{\Delta} \sum_{\alpha_i, E \in \Delta(E_i)} B_{deex}(el\; J;\; E_i J_i^{\pi_i} \alpha_i \to E_f J_f^{\pi_f} \alpha_f) = \\
&= \Big\{ \frac{8\pi \alpha_F}{e^2}\, \frac{J+1}{J[(2J+1)!!]^{\,2}}\, \frac{1}{(\hbar c)^{2J}} \Big\}^{-1}\, f^{(el\; J)}_{J_i^{\pi_i} \to E_f J_f^{\pi_f} \alpha_f}(E_\gamma)
\end{aligned}
$$

$$\frac{1}{\Delta}\sum_{\alpha_i, E\in\Delta(E_i)} B_{deex}(mag\ J;\ E_i J_i^{\pi_i}\alpha_i \to E_f J_f^{\pi_f}\alpha_f) =$$
$$= \{\frac{8\pi\alpha_F}{e^2}\ \frac{J+1}{J[(2J+1)!!]^2}\ \frac{0.011}{(\hbar c)^{2J}}\}^{-1}\ f^{(mag\ J)}_{J_i^{\pi_i}\to E_f J_f^{\pi_f}\alpha_f}(E_\gamma) \qquad (12.209)$$

where following units should be used in (12.209),
$[\Delta] = MeV$, $[B_{deex}(el\,J)] = e^2\,fm^{2J}$, $[f^{(el\,J)}] = e^2\,MeV^{-(2J+1)}$, $[B_{deex}(el\,J)] = \mu_N^2\,fm^{2J-2}$, $[f^{(el\,J)}] = e^2\,MeV^{-(2J+1)}$.

In the axially deformed nucleus the excitation transition $gr;\ 0^+ \to J_i^{\pi_i}$ (see (12.189) with $E_f = 0$) the excitation strength function reads,

$$S_{ex;\,gr0^+\to J_i^{\pi_i}}(E_\gamma) = \sum_{K_i E_i \rho_i} B_{ex}(XJ;\ gr0^+ \to E_i K_i \rho_i)\ \delta_{J_i J}\ \delta(E_\gamma - E_i) =$$
$$= \sum_{K_i=-J_i}^{+J_i}\ \sum_{E_i J_i} B_{ex}(XJ_i;\ gr0^+ \to E_i K_i \rho_i)\ \delta(E_\gamma - E_i) =$$
$$= \sum_{K_i=-J_i}^{+J_i} S^{(XJ)}_{ex;\,gr0^+\to K_i^{\pi_i}}(E_\gamma) \qquad (12.210)$$

where
$B_{ex}(XJ;\ gr0^+ \to E_i K^{\pi_i}\rho_i) = (\text{see (12.189)} = |\langle K^{\pi_i}\rho_i|\mathscr{M}^{(X)\prime}_{JK}|0^+\ gr\rangle|^2$.

12.4.3 Photon radiation widths for finite temperature

The usage of a temperature for nuclei was initiated by H.A.Bethe, V.F.Weiskopf and N.Bohr on the thirties [406, 407, 109] in the connection with the derivation of the expression for the energy level density (see the Section 12.2, expression (12.30) and the text in the end of the Subsection 12.2.2). The basic idea is that the complete information about the energy spectrum of the system (nucleus) is equivalent to the information involved in the canonical (or grandcanonical) partition function of the system. The expression for the level density (see (12.47), (12.60) or (12.61)) was derived using the inverse Laplace transformation of the Fermi gas partition function (see Subsections 12.2.1 - 12.2.4, and [6, 408]). However, it should be pointed out that all level density expressions mentioned above are only approximate from the point of view of the quantum mechanics when the nucleus is substituted by Fermi gas and the residual interaction in the Hamiltonian is neglected. Nevertheless the concept of the temperature is used up to now (see e.g. [409, 410, 402]) because the level density predictability of realistic microscopic models is still

very low. Further the using of the nuclear temperature for estimations of average transition probabilities between different points in the plane (energy, ang. momentum)$\equiv (E, J)$ are discussed.

Let us consider the ensemble of same nuclei (N, Z) in different state. Each state is characterized by the angular momentum J_n, parity π_n and energy E_n. The probability $p_T(n|J^{\pi_n})$ of the occupation of individual states for particular temperature T is given by the canonical partition function (see (12.1), (12.3) and (12.4)),

$$p_T(n|J^{\pi_n}) = \frac{e^{-E_n/T}}{Z(J^\pi, T)} \tag{12.211}$$

where $Z(n|J^\pi)$ is the parition function for the angular momentum$J$, parity π and nuclear temperature T. This partition function is given by (12.3),

$$Z(J^\pi, T) = \sum_{i \in I(J^\pi)} e^{-\frac{E_i}{T}} \approx \int dE\, \rho(J^\pi, E)\, e^{-\frac{E}{T}} \tag{12.212}$$

where $I(J^\pi)$ is the ensemble of nuclear states with the angular momentum J and parity π,

$$I(J^\pi) \equiv \left\{ i;\ J_i = J,\ \pi_i = \pi \right\} \tag{12.213}$$

The symbol $\rho(J^\pi, E)$ represents the energy density of states with the angular momentum J and the parity π in the vicinity of the energy E. Then the probability of finding the nucleus in the state with J^π and with the energy in the interval $(E, E + dE)$ with the temperature T can be obtained by the summation of (12.211) over all such states in the interval $I(J^\pi, E, \Delta E) \equiv \{i;\ J_i = J,\ \pi_i = \pi,\ E_i \in \langle E, E + dE \rangle\}$,

$$w_T(E|J^\pi)\, dE = \sum_{i \in I(J^\pi, E' dE)} p_T(i|J^\pi) \ \approx \frac{\rho(J^\pi, E)\, e^{-\frac{E}{T}} dE}{Z(J^\pi, T)} \tag{12.214}$$

The probability $w_T(E|J^\pi)$ for given J^π is given by the product of exponentially decreasing function of the energy E and the density $\rho(J^\pi, E)$ which, on the contrary, is increasing with the energy. If the density $\rho(J^\pi, E)$ does not behave as $e^{const\, E^k}$ with $k \geq 1$ then the distribution function $w_T(E|J^\pi)$ forms the peak with the maximum $E_T(J^\pi)$ and the width $D_T(J^\pi)$ dependent on the temperature T. Usually the energy maximum $E_T(J^\pi)$ corresponds to the expectation mean value $\int dE\, w_T(E|J^\pi)$ but it is not always the case.

The conclusion above is further demonstrated on the simple example. Let us consider the simplified version of the Fermi gas with the energy state

density (see (12.34)),

$$\rho(E) = \frac{e^{2\sqrt{aE}}}{D} \tag{12.215}$$

where a and D are the constants. According to (12.212) the corresponding partition function is,

$$\begin{aligned}
Z(T) &= \int_0^\infty dE\, \rho(E)\, e^{-\frac{E}{T}} = \frac{1}{D} \int_0^\infty dE\, e^{2\sqrt{aE}-\frac{E}{T}} = \\
&= \boxed{\begin{array}{c}\text{substitution} \\ x = \sqrt{E} \Rightarrow dE = 2\,x\,dx\end{array}} = \frac{1}{D} \int_0^\infty dx\, 2x\, e^{-\frac{1}{T}\,(x^2 - 2Tx\sqrt{a})} = \\
&= \frac{1}{D} \int_0^\infty dx\, 2x\, e^{-\frac{1}{T}\,(x^2 - 2Tx\sqrt{a} + aT^2) + aT} = \frac{2\,e^{aT}}{D} \int_0^\infty dx\, x\, e^{-\frac{1}{T}\,(x - T\sqrt{a})^2} = \\
&= \boxed{\begin{array}{c}\text{substitution } y = \frac{x - Ta}{\sqrt{T}} \\ \Rightarrow dy = \frac{dx}{\sqrt{T}};\; x = y\sqrt{T} + T\sqrt{a}\end{array}} = \\
&= \frac{2\,e^{aT}\sqrt{T}}{D} \int_{-\sqrt{aT}}^\infty dy\, e^{-y^2}\, (y\sqrt{T} + T\sqrt{a}) = \\
&= \frac{2\,e^{aT}T}{D} \int_{-\sqrt{aT}}^\infty dy\, e^{-y^2}\, y + \frac{2\,e^{aT}\sqrt{aT^3}}{D} \int_{-\sqrt{aT}}^\infty dy\, e^{-y^2} = \\
&= \boxed{\begin{array}{c}\text{substitution in the 1-st integral} \\ t = y^2 \Rightarrow dt = 2y\,dy\end{array}} = \\
&= \frac{e^{aT}}{D}\, T\, \left[e^{-t}\right]_{aT}^\infty + \frac{e^{aT}}{D}\, \sqrt{\pi\, a\, T^3}\; erfc(-\sqrt{aT}) = \\
&= \frac{1}{D} \left(T + \sqrt{\pi\, a\, T^3}\; e^{aT}\; erfc(-\sqrt{aT})\right)
\end{aligned} \tag{12.216}$$

where $erfc(x) \equiv \frac{2}{\sqrt{\pi}} \int_x^\infty e^{-t^2} dt$ is the Laplace-Gauss integral.
The substitution of (12.215), (12.216) into (12.214) gives,

$$w_T(E) = \frac{e^{2\sqrt{aE} - \frac{E}{T}}}{K} \tag{12.217}$$

where $K = T + \sqrt{\pi a T^3}\, e^{aT}\, erfc(-\sqrt{aT})$.m
The condition of the maximum of the function (12.217) is,

$$\begin{aligned}
&\frac{dw_T}{dE}|_{E=E_{max}} = \frac{e^{2\sqrt{aE} - \frac{E}{T}}}{K} \left(2\sqrt{a}\, \frac{1}{2\sqrt{E}} - \frac{1}{T}\right)|_{E=E_{max}} = 0 \\
&\Rightarrow \quad T\sqrt{a} = \sqrt{E_{max}} \quad \Rightarrow \quad E_{max} = aT^2
\end{aligned} \tag{12.218}$$

Further the width $D_T(f)$ of the energy interval in which the probability $w_T(E)$ is equal to the fraction $f\, w_T(E_{max})$ of its maximal value,

$$f\, w_T(E_{max}) \equiv \frac{f}{K}\, e^{2\sqrt{a^2T^2}-\frac{1T^2}{T}} = \frac{f}{K}\, e^{aT}$$

That means the value E_f is searched for when,

$$\begin{aligned} & w_T(E_f) = \frac{f}{K}\, e^{aT} \;\Rightarrow \\ & \Rightarrow e^{2\sqrt{aE_f}-\frac{E_f}{T}} = f\, e^{aT} \quad \Rightarrow \quad E_f - 2T\sqrt{aE_f} + aT^2 + T\, lnf = 0 \\ & \Rightarrow (E_f)_{1,2} = \frac{2T\sqrt{a} \pm \sqrt{4T\, ln\frac{1}{f}}}{2} = T\sqrt{a} \pm \sqrt{T\, ln\frac{1}{f}} \end{aligned}$$

So the width $D_T(f)$ of searched for interval is,

$$D_T(f) = (E_f)_1 - (E_f)_2 = 4\, T\sqrt{aT}\sqrt{ln\frac{1}{f}} = 4\sqrt{ln\frac{1}{f}}\sqrt{aT^3} \qquad (12.219)$$

the mean energy and the mean square deviation (or fluctuation) for given temperature can be determined from following expressions,

$$\begin{aligned} \langle E\rangle_T &= \int dE\; E w_T(E) = \frac{1}{K}\int_0^\infty dE\; E\, e^{2\sqrt{aE}-\frac{E}{T}} \\ \langle E^2\rangle_T &= \int dE\; E^2 w_T(E) = \frac{1}{K}\int_0^\infty dE\; E^2\, e^{2\sqrt{aE}-\frac{E}{T}} \end{aligned} \qquad (12.220)$$

and the r.m.s. fluctuation is $\sigma_T(E) = \sqrt{\langle E^2\rangle_T - \langle E\rangle_T^2}$.

The simple example above demonstrates the way of obtaing the temperature dependence of the probability $w_T(E)$ of finding the nucleus in the state with the excitation energy in the unitary energy in the vicinity of the given energy E starting with the known energy density of states $\rho(E)$ with the zero temperature. This way can be extended for more general state energy densities as $\rho(A, E_x, I^\pi)$ discussed in the Section 12.2 (see e.g. (12.61)).

Further we discuss the thermodynamic mean value of the general quantity A represented in the quantum mechanics by the operator $\hat{A}$ for the system (nucleus) with the temperature T and with the probability $w_T(E|J^\pi)$ (see (12.214)) of finding this system in the state J^π and with the energy in the unitary interval around the energy E. It is clear that this mean value is given by,

$$\langle A\rangle_{T,J^\pi} = \int dE\, \bar{A}(E, J^\pi)\, w_T(E|J^\pi) = \sum_{i\in I(J^\pi)} p_T(i|J^\pi)\, \langle i, J^\pi|\hat{A}|i, J^\pi\rangle \quad (12.221)$$

where $I(J^\pi)$ is the ensemble (12.213) of eigenstates of the nucleus Hamiltonian, $\bar{A}(E, J^\pi)$ is the averaged value of the quantity A for states with J^π in the unitary energy interval in the vicinity of the value E, $\langle i, J^\pi|\hat{A}|i, J^\pi\rangle$ is the quantum mechanics mean value of the quantity A in the concrete state $|iJ^\pi\rangle$, and the $p_T(i|J^\pi)$ is the probability (12.211) for the given temperature T.

In the end of this subsection it is necessary to point out again that the nuclear temperature T has nothing to do with the standard temperature. The nuclear temperature $T = \beta_0^{-1}$ represents only a parameter characterizing the mean value excitation energy E_{ex} ($\beta_0 = \frac{1}{T} \approx \sqrt{E_{ex}}$ - see e.g. (12.35)).

12.4.4 Simulation of γ- cascades in complex nuclei

As it was emphasized several times in many nuclear reactions high excited states in final nuclei are produced. In subsequent step these high energy states decay through radiative γ- transitions into ground state. These γ- cascades can generally proceed via many intermediate levels. For instance in the case of neutron capturing levels in heavier nuclei the overall number of the encountered intermediate levels is $10^5 - 10^7$ (see the Subsection 12.3.3.1). Such a huge number of intermediate states and corresponding radiation widths of electromagnetic transitions are not possible to be described by means of realistic microscopic or semi-microscopic nuclear models of shell model type (because of huge configuration spaces with huge dimensions of Hamiltonian matrices causing problems with the computer memory and with the real calculation time). Therefore it is necessary to use some statistical approaches for the description of γ- cascades which enable to avoid the determination of radiation width of each individual transition in each γ- cascade.

The decay of γ- cascades are products of a complex interplay between photon strength functions (PSF), $f^{(XJ)}_{J_i^{\pi_i}\to E_f J_f^{\pi_f}\alpha_f}(E)$, and the level density (LD), $\rho(E_i, J_i^{\pi_i})$, on one side and a complicated detector response on the other side. As a result strength functions and level densities cannot be directly extracted from experimental spectra. Therefore, usually simulation approaches are used for obtaining an information in strength functions and level density from experimental data on γ- cascade spectra. Each simulation method consists in the determination of simulated spectra applying some statistical method (recently the most used are Monte Carlo approaches) starting with various models for photons strength function and level densities. The comparison between simulated and experimental spectra allow to reject many models of

photon strength functions and level density models and choose most likely models to be valid.

As an example of simulation process further the analysis of γ- cascades following the neutron capture ^{161,163}Dy(n,γ)^{162,164}Dy performed in [405] is shortly described.

In [405] the thermal neutron capture (n,γ) experiment was done for target isotopes ^{161,163}Dy in the Los Alamos National Laboratory with the Detector for Advanced Neutron Capture Experiments (DANCE). It is known from the Subsection 12.3.3.1 that the resonance states $|c\rangle \equiv |E_c J_c^{\pi_c} \alpha_c\rangle$ of the final nucleus, in which the thermal neutron from the (n,γ) reaction is captured, are compound nucleus state with the angular momentum $J_c = J_0 \pm 1/2$ (see (12.122)) where J_0 is the angular momentum of the target nucleus state, usually its ground state. In [405] target nuclei are ^{161}Dy and ^{163}Dy with $J_0^{\pi_0} = \frac{5}{2}^+$ and $J_0^{\pi_0} = \frac{5}{2}^-$, respectively. Therefore angular momenta J_c of the capturing resonance states are $J_c = 2$ or $J_c = 3$ for corresponding final nuclei ^{262}Dy and ^{164}Dy. Capturing state energies are about ≈ 8 MeV for thermal neutron capture in final heavier nuclei. In total, 25 resonances with $J_c^{\pi_c} = 2^+$ and 22 resonances with $J_c^{\pi_c} = 3^+$ in ^{162}Dy and 14 resonances with $J_c^{\pi_c} = 2^-$ and 26 resonances with $J_c^{\pi_c} = 3^-$ in ^{164}Dy were found in [405] with corresponding decay γ- cascades. A lot of different γ- cascades can arise from one capturing resonance with different number M of γ- transitions (so called multiplicity M) and different intermediate states of the final nucleus. For each γ- cascade with the given multiplicity $M = 2, 3, 4$ so called multistep cascade (MCS) experimental spectrum was exctraced (see the Fig.4 in [405]) for both isotopes ^{162,164}Dy).

From theoretical point of view each MSC spectrum can be simulated starting with a priori supposed models of photon function and level density. In [405] the simulation process consists in two steps. In the first step the level scheme and decay branching intensities needed for the forming of each γ-cascade are randomly generated by means of the DICEBOX procedure (see [411]). In the second step for each γ- cascade generated by the DICEBOX code the response of the detector DANCE is mimic by the commonly used GEAN 4 detector response simulation code and corresponding simulated MSC spectrum is created. Farther the Monte Carlo DICEBOX code for a simulation of the γ- cascade following the thermal neutron capture is shortly described in order to obtain an idea about a simulation of the γ cascade.

At first in the DICEBOX algorithm some critical energy, E_{crit}, is chosen

below which the complete decay scheme of levels for final nucleus is known and is taken from existing data (^{162}Dy or ^{164}Dy in [411]) with the complete knowledge about the energies, angular momenta, parities and decay properties (deexcitation widths $\Gamma_{deex;\,|i\rangle\to|f\rangle}$ or photon strength functions $f^{(XJ)}_{|i\rangle\to|f\rangle}$ for all states $|i\rangle$ and $|f\rangle$ with energies E_i and E_f below the critical energy E_{crit}). The states above the critical energy E_{crit} up to the capturing state $|c\rangle$ are not known experimentally completely and they are generated using simulation codes starting with chosen models of level density $\rho(E_i, J_i^{\pi_i})$ and photon strength function $f^{(XJ)}_{|i\rangle\to|f\rangle}(E_\gamma)$ for all XJ taking into account ($XJ = E1$, $M1$ and $E2$ in [405], where contributions of higher transition multipolarities J were neglected). Concretely, averaged partial radiation widths $\bar{\Gamma}_{deex;\,|i\rangle\to|f\rangle}$ per one transition from the initial states $|i\rangle \equiv |E_i J_i^{\pi_i}\alpha_i\rangle$ into the final state $|f\rangle \equiv |E_f J_f^{\pi_f}\alpha_f\rangle$ with $E_i > E_{crit}$ were generated randomly using following expression originated from (12.198) and (12.202),

$$\bar{\Gamma}_{deex;\,|i\rangle\to|f\rangle} = \boxed{\begin{array}{c}\text{see}\\ 12.198\end{array}} =$$

$$= \sum_{|J_i-J_f|\le J\le J_i+J_f} \sum_{\substack{X=el,mg\\ \pi_i\pi_f(-1)^J=1 \text{ for } X=el\\ \pi_i\pi_f(-1)^J=-1 \text{ for } X=mg}} \xi^2_{XJ}\,\bar{\Gamma}^{(XJ)}_{|i\rangle\to|f\rangle} = \boxed{\begin{array}{c}\text{see}\\ 12.202\end{array}} =$$

$$= \sum_{|J_i-J_f|\le J\le J_i+J_f} \sum_{\substack{X=el,mg\\ \pi_i\pi_f(-1)^J=1 \text{ for } X=el\\ \pi_i\pi_f(-1)^J=-1 \text{ for } X=mg}} \frac{\xi^2_{XJ}\, f^{(XJ)}_{deex;\,E_iJ_i^{\pi_i}\alpha_i\to E_eJ_f^{\pi_f}\alpha_f}(E_\gamma, T)\;\; E_\gamma^{2J+1}}{\rho(E_i, J_i^{\pi_i})} \tag{12.222}$$

where ξ_{XJ} is the random number drawn from a normal (Gauss) distribution with the zero mean value and unit variance. This ensures that the individual widths $\bar{\Gamma}_{deex;\,|i\rangle\to|f\rangle}(E_\gamma)$ fluctuates according to the Porter-Thomas distribution (12.144) (see also [370]), T is the nuclear temperature corresponding to the energy E_f of the final states $|f\rangle = |E_f J_f^{\pi_f}\alpha_f\rangle$, which is a parameter of some models of the photon strength function (see the Section III B in [405] for details). The energy interval between E_{crit} and E_c is binned with the appropriately chosen energy width and the expression (12.222) is used for random generation of $\bar{\Gamma}_{deex;\,|i\rangle\to|f\rangle}$ for XJ- transitions between possible bines with energies E_i and E_f allowed by the XJ- selection rules ($E_i = E_f + E_\gamma$).

More precisely, through the random generation of so called seed number ξ_{XJ} by the random number generator and using a priori known $f^{(XJ)}_{deex}(E_\gamma, T)$ and $\rho(E_i, J_i^{\pi_i})$ from some chosen model the radiation widths are calculated by (12.222) and simultaneously starting with the initial capture resonance level energy E_c the decay level scheme of γ- cascades from the capturing state $|c\rangle$ down to the ground state $|gr\rangle$ can be determined many times.

Decay branching intensities $I_{i\to f} = \Gamma_{deex;\,|i\rangle\to|f\rangle}/\Gamma_{deex;\,tot\,|i\rangle}$ for transitions from any initial state $|i\rangle$ below the capture state $|c\rangle$ to various final levels $|f\rangle$ are determined from a full set of radiation widths $\Gamma_{deex;\,|i\rangle\to|f\rangle}$ of given initial state $|i\rangle$ simulated by (12.222) using the total radiation width corresponding to given $|i\rangle$ defined as $\Gamma_{deex;\,tot\,|i\rangle} \equiv \sum_f \Gamma_{deex;\,|i\rangle\to|f\rangle}$. In such a way the occupation of states with energies in all bins and corresponding deexcitation photon strength functions of all electromagnetic XJ transitions are determined for each simulated γ- cascade. Hereafter, the simulated system of levels E_i below the capturing state $|c\rangle$ grouped into bins with the width ≈ 100 keV and with corresponding averaged branching intensities $I_{i\to f}$ for transitions between bins is referred in [405] as a nuclear realization (NR) for a priori fixed models of photon strength function and level density.

In reality, decays of various neutron resonances (neutron capturing states $|c\rangle$) of the same angular momentum and parity, $J_c^{\pi_c}$, differs only in intensities of primary transitions, $|c\rangle \to |f_1\rangle$. In order to mimic this behavior the intensities of primary transitions were generated randomly within a given nuclear realization (NR).The set of primary decay branching intensities within a given NR was denoted as a nuclear subrealization.

In the way described above the huge number of γ- cascades are generated in terms of the DICEBOX algorithm (see [411]) and consequently for each simulated γ- cascade the multistep cascade (MSC) spectrun is obtained in terms of the detector response simulation GEANT 4 code. In [405] usually $\approx 10^5$ γ- cascades were randomly generated for each nuclear subrealization and for both investigated ^{161}Dy and ^{164}Dy nuclei authors of [405] produced 50 nuclear realizations with 50 nuclear subrealizations. However, it should be pointed out that all simulation process described above involves the assumption of of the validity of the Brink hypothesis that the photon strength function depends only on the photon energy E_γ (the dependence of $f^{(XJ)}_{deex;\,E_iJ_i^{\pi_i}\alpha_i\to E_fJ_f^{\pi_f}\alpha_f}(E_\gamma) = \frac{2J_f+1}{2J_i+1}\, f^{(XJ)}_{ex;\,E_fJ_f^{\pi_f}\alpha_f\to E_iJ_i^{\pi_i}\alpha_i}(E_\gamma)$ on the quantum numbers $E_f, J_f^{\pi_f}, \alpha_f$ is neglected) [19] .

[19]Original Brink hypothesis claims that the excitation photon strength function of the electromagnetic

So from the discussion above follows that inputs for the simulation of the multistep cascade (MSC) spectra are represented by the photon strength function (PSF) $f^{(XJ)}_{deex;\,|i\rangle\to|f\rangle} \approx \sigma_{XJ}(E_\gamma)\ /\ E^{2J-1}\pi^2\hbar^2c^2(2J+1)$ (see the text under (12.205) and using the Brink hypothesis) and the level density (LD) $\rho(E_i, J_i^{\pi_i})$ (see (12.222). In the paper [405] a lot of so called models of strength function and models of level density were involved into the MSC spectra analyzes. Some of PSF-s and LD-s are with and some without a temperature dependence.

All models of PSF used in [405] are not genuine models from the point of view of some true nuclear theory. All expressions used in [405] for $f^{(XJ)}_{deex;\,|i\rangle\to|f\rangle}(E_\gamma)$ (for $XJ = E1,\ M1,\ E2$) are mostly based on well-known experimental fact, known from photoabsorption and other experiments, that there exist giant dipole electric E1 resonance with one-peak character for spherical nuclei and two-peak character for axially deformed nuclei (see the expr. (7.391) and the text around it), and that for $M1$ transitions we have spin-flip two peak character part and the scissor (orbital) part of the magnetic dipole $M1$ transition (see Figs. 7.50 - 7.56). And that $E2$ transitions are formed by isoscalar and isovector parts of giant quadrupole resonance with its more complex (more peaks) character for deformed nuclei (see the Fig.7.48). Each of these parts of $E1$, $M1$ and $E2$ giant resonances manifests as a Lorentzian peak in the cross-section of photoabsorption or other processes from which partial excitation strength functions are extracted experimentally. The heights and widths of these Lorentzian peaks are usually fitted to experimental cross-sections of processes mentioned above. These Lorentzians describing all parts of $E1$, $M1$ and $E2$ PSF-s (with several their modifications connected with taking into account nuclear temperature, or nucleus deformation and other effects - see the section IIIB in [405]) are called as PSF models in [405], in spite of the fact that they have not been consequently derived from some theory of nuclear structure.

On the other side the using of not so precise word "model" for input phenomenological formula of PSF-s describing the experimental data on cross-sections of different processes for the simulation of the MSC spectra is only a formal drawback and it is necessary to admit that it is commonly used in many papers with this topic. For instance, in [405] for analyzes of MSC spectra the modified generalized Lorentzian (MGLO) "model" for $E1$ tran-

excitation $|f\rangle \to |i\rangle$ (or corresponding photoabsorption cross-section) does not depend on the quantum numbers $E_f, J_f^{\pi_f}, \alpha_f$ of the initial state $|f\rangle$ and is dependent only on the photon energy E_γ - see the text under the expr. (12.205) and [412].

sitions was used (see also [414]) and for $M1$ transitions so called composite $M1$ PSE "model" was applied. In the case of $E2$ transitions the simple giant resonance model was chosen, where the PSF $f^{(E2)}_{|i\rangle\rightarrow|f\rangle} = constant$ was adjusted to reproduce the ratio of partial radiation width $\Gamma(E1)/\Gamma E2 \geq 100$ at about $\approx 7MeV$ - see [413] (in [405] it is claimed that under this condition results do not depend in the choice of the $E2$ PSF model).

Similarly as for the photon strength function in [405] several models of level density were tested. The most of them is based on the Fermi-gas level density expression (12.60) with different parametrizations and slight modifications (see [416, 415]). Besides that the microscopic level density models as shell model Monte Carlo (SMMC) model [417] or Hartree-Fock-Bogoliubov models [418, 419] were also tested. The best description of the MSC spectra was obtained using back-shifted Fermi gas (BSF6) model with parameters from [415].

The main result of the paper [405] is the importance of the taking into account the scissor (orbital) part of the $M1$ resonance in the simulation of the MSC spectra. As it was mentioned above the composite $M1$ PSF model was used for $M1$ transitions when the both orbital and spin-flip parts of $M1$ transition operator were taken into account. In this model the partial $M1$ photon strength function was taken in the form of the sum of three terms,

$$f^{(M1)}_{|i\rangle\rightarrow|f\rangle}(E_\gamma) = f^{(M1)}_{SM;\,|i\rangle\rightarrow|f\rangle}(E_\gamma)(E_\gamma) + f^{(M1)}_{SF;\,|i\rangle\rightarrow|f\rangle} + f^{(M1)}_{SP;\,|i\rangle\rightarrow|f\rangle}(E_\gamma) \quad (12.223)$$

where $f^{(M1)}_{SP;\,|i\rangle\rightarrow|f\rangle}(E_\gamma)$ is in [405] called as a single-particle part of the $M1$ PSF with the value depending on used $E1$ PSF model (see [405] for details) which is a constant independent on E_γ with the value depending on used $E1$ PSF model. The $f^{(M1)}_{SF;\,|i\rangle\rightarrow|f\rangle}$ represents the spin-flip part of the $M1$ PSF and has the form of the double bump Lorentzian shape with a centroid 5 and 7 MeV (typical spin-flip resonance values - see the Figs 7.50 or 7.55 and 7.56 for ^{232}U and [420].

The $f^{(M1)}_{SM;\,|i\rangle\rightarrow|f\rangle}(E_\gamma)$ stands for the scissor $M1$ part (see the Fig. 7.51 and the text around) of the $M1$ PSF having the Lorentzian shape with the centroid in 2.8-3.0 MeV (almost independent on A) with the width $\approx$ 1-1.4 MeV (see the section VB in[405] for details). In [405] the importance of the taking into account the scissor part of the $M1$ giant resonance in the simulation process was tested by the switching on and off the term $f^{(M1)}_{SM;\,|i\rangle\rightarrow|f\rangle}(E_\gamma)$ in (12.223)) for both isotopes ^{162,164}Dy - see e.g. Figs. 7 and 9 for ^{162}Dy in [405] which are shown in one figure Fig.12.2 in this textbook. From the Fig.12.12 it

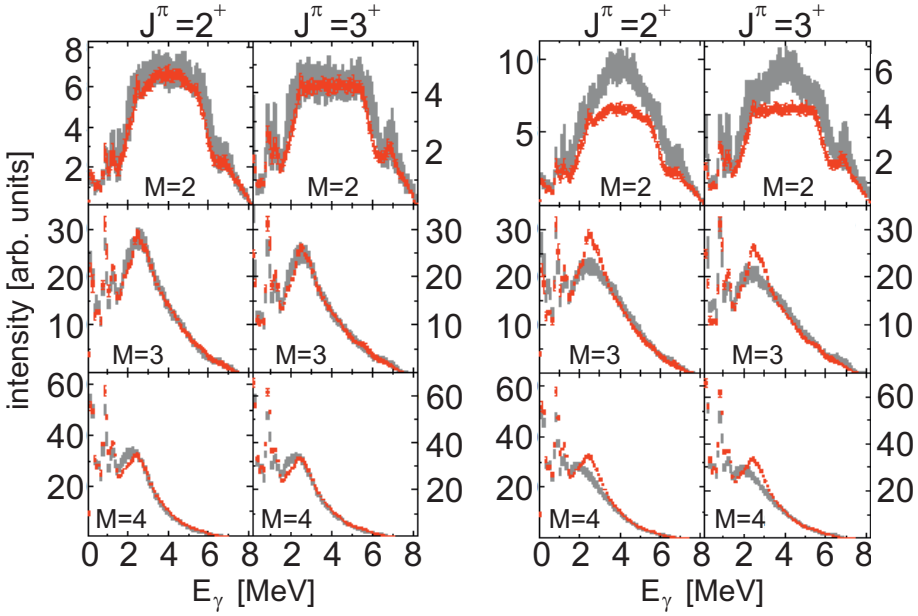


Figure 12.12: Comparison of ^{162}Dy mean experimental MSC spectra with simulations using the MGLO E1 PSF model and the composite M1 PSF model. The full red rectangles show the mean experimental MSC intensities I_{exp}. The gray band corresponds to the result of simulations drawn as two standard deviation corridors centered at average MSC intensities. The left panel corresponds to the simulations when the scissor term in (12.223) was taken into account and in the right panel there are mean MSC spectra simulated without involving the scissor M1 term in 12.223 (adapted from [405]).

can be clearly seen that the inclusion of the scissor mode term $f^{(M1)}_{SM;\,|i\rangle\to|f\rangle}(E_\gamma)$ improve the agreement of simulated MSC spectra with experimental ones for all multiplication M (number of γ- transitions in the given γ- cascade). By other words it means that the γ- cascades following the neutron capture feel the existence of the scissor $M1$ mode. However one should realize that analysis performed in [405] were performed assuming the validity of the Brink hypothesis.

The simulation approach used in [405] is presented here only as an example. In literature one can find several different simulation methods for theoretical investigation of γ- cascade specter following various nuclear reactions (not only neutron capture). For instance in [421, 422] so called Oslo method is applied for the extraction of "experimental" photon strength functions from ^{3}He- induced reactions.

A. Some expressions from the theory of angular moment

A.1 Coupling of two moments ($\vec{j} = \vec{j}_1 + \vec{j}_2$)

In the case of the coupling of two ang. moments two bases of eigen-states of the square of the ang. moment and its projection can be built in the Hilbert space:

$$\begin{array}{ll} \text{1-st basis:} & |j_1 m_1\rangle |j_2 m_2\rangle \\ \text{2-nd basis:} & |j_1 j_2\, jm\rangle \end{array} \tag{A.1}$$

These two bases are connected through the Clebsch-Gordan coefficients:

$$\begin{aligned} |j_1 j_2\, jm\rangle &= \sum_{m_1\, m_2} C^{jm}_{j_1 m_1 j_2\, m_2}\, |j_1 m_1\rangle |j_2 m_2\rangle \\ |j_1 m_1\rangle |j_2 m_2\rangle &= \sum_{j=|j_1 - j_2|}^{j_1+j_2} C^{jm}_{j_1 m_1 j_2 m_2}\, |j_1 j_2\, jm\rangle \end{aligned} \tag{A.2}$$

The orthogonality and the completeness of the both given above bases can be expressed as:

$$\begin{aligned} \sum_{m_1 m_2} C^{jm}_{j_1 m_1 j_2\, m_2} C^{j'm'}_{j_1 m_1 j_2\, m_2} &= \delta_{j\, j'} \delta_{m\, m'} \\ \sum_{j\, m} C^{jm}_{j_1 m_1 j_2\, m_2} C^{jm}_{j_1 m'_1 j_2\, m'_2} &= \delta_{m_1\, m'_1} \delta_{m_2\, m'_2} \end{aligned} \tag{A.3}$$

Clebsch-Gordan coefficients fulfil differents symmetries (see e.g. [2]) the most important of which are following:

$$\begin{aligned}
C^{jm}_{j_1 m_1 j_2\, m_2} &= (-1)^{j_1+j_2-j}\, C^{j-m}_{j_1 -m_1 j_2\, -m_2} \\
C^{jm}_{j_1 m_1 j_2\, m_2} &= (-1)^{j_1+j_2-j}\, C^{jm}_{j_2 m_2 j_1\, -m_1} \\
C^{jm}_{j_1 m_1 j_2\, m_2} &= (-1)^{j_1-m_1} \sqrt{\frac{2j+1}{2j_2+1}} C^{j_2 -m_2}_{j_1 m_1 j -m_1} \\
C^{jm}_{j_1 m_1 j_2\, m_2} &= (-1)^{j_2+m_2} \sqrt{\frac{2j+1}{2j_1+1}} C^{j_1 -m_1}_{j -m j_2 m_2}
\end{aligned} \tag{A.4}$$

Instead of Clebsch-Gordan coefficients sometimes so called 3j-symbols are used in the literature:

$$\begin{pmatrix} j_1 & j_2 & j_3 \\ m_1 & m_2 & m_3 \end{pmatrix} = (-1)^{j_3+m_3+2j_1}\, \frac{1}{2j_3+1}\, C^{j_3\, m_3}_{j_1\, -m_1\, j_2\, -m_2} \tag{A.5}$$

Symmetries of 3j-symbols:

- 3j-symbol is invariant with respect to the even permutations of columns;
- by each odd permutation of columns or by the change of signs of all projections 3j-symbol obtains the phase factor $(-1)^{j_1+j_2+j+3}$.

A.2 Coupling of three angular moments $(\vec{j} = \vec{j}_1 + \vec{j}_2 + \vec{j}_3)$

In this case we have three possibilities of the coupling with corresponding basis vactors in the Hilbert space of three ang. moments:

$$\begin{array}{lcl}
\vec{j}_1 + \vec{j}_2 = \vec{j}_{12}\ ,\ \vec{j}_{12} + \vec{j}_3 = \vec{j} & \leftrightarrow & \text{basis: } |j_1 j_2 (j_{12}),\ j_3;\ jm\rangle \\
\vec{j}_2 + \vec{j}_3 = \vec{j}_{23}\ ,\ \vec{j}_1 + \vec{j}_{23} = \vec{j} & \leftrightarrow & \text{basis: } |j_1, j_2 j_3 (j_{23});\ jm\rangle \\
\vec{j}_1 + \vec{j}_3 = \vec{j}_{13}\ ,\ \vec{j}_{13} + \vec{j}_2 = \vec{j} & \leftrightarrow & \text{basis: } |j_1 j_3 (j_{13}),\ j_2;\ jm\rangle
\end{array} \tag{A.6}$$

Each vector from one basis can be obtained as the linear combination of the other basis:

$$\begin{aligned}
|j_1 j_2 (j_{12}), j_3;\ jm\rangle \;=\; & \sum_{j_{23}} \langle j_1, j_2 j_3 (j_{23});\ j \mid j_1 j_2 (j_{21}, j_3;\ j\rangle \cdot \\
& \cdot |j_1, j_2 (j_{21}), j_3;\ jm\rangle
\end{aligned} \tag{A.7}$$

where amplitudes $\langle j_1, j_2 j_3(j_{23});\ j \mid j_1 j_2(j_{21}, j_3;\ j\rangle$ are determined by so called 6j-symbols $\begin{Bmatrix} j_1 & j_2 & j_{12} \\ j_3 & j & j_{23} \end{Bmatrix}$:

$$\begin{aligned} &\langle j_1, j_2 j_3(j_{23});\ j \mid j_1 j_2(j_{21}, j_3;\ j\rangle = \\ &= (-1)^{j_1+j_2+j_3+j}\ [(2j_{12}+1)(2j_{23}+1)]^{1/2} \begin{Bmatrix} j_1 & j_2 & j_{12} \\ j_3 & j & j_{23} \end{Bmatrix} \end{aligned} \tag{A.8}$$

A.3 Coupling of four angular moments $(\vec{j} = \vec{j}_1 + \vec{j}_2 + \vec{j}_3 + \vec{j}_4)$

We have again three possibilities of the coupling:

$$\begin{aligned} &\vec{j}_1 + \vec{j}_2 = \vec{j}_{12}\ ,\ \vec{j}_3 + \vec{j}_4 = \vec{j}_{34}\ ,\ \vec{j}_{12} + \vec{j}_{34} = \vec{j} \quad \leftrightarrow \\ &\qquad\qquad \text{basis: } |j_1 j_2(j_{12}),\ j_3 j_4(j_{34});\ jm> \\ &\vec{j}_1 + \vec{j}_3 = \vec{j}_{13}\ ,\ \vec{j}_2 + \vec{j}_4 = \vec{j}_{24}\ ;\ \vec{j}_{13} + \vec{j}_{24} = \vec{j} \quad \leftrightarrow \\ &\qquad\qquad \text{basis: } |j_1 j_3(j_{13}), j_2 j_4(j_{24});\ jm> \\ &\vec{j}_1 + \vec{j}_4 = \vec{j}_{14}\ ,\ \vec{j}_2 + \vec{j}_3 = \vec{j}_{23}\ ;\ \vec{j}_{14} + \vec{j}_{23} = \vec{j} \quad \leftrightarrow \\ &\qquad\qquad \text{basis: } |j_1 j_4(j_{13}),\ j_2 j_3(j_{23});\ jm> \end{aligned} \tag{A.9}$$

and similarly as in (A.8) the amplitudes of the linear combination transition from one basis to another one is given by so called 9j-symbols:

$$\begin{aligned} &\langle j_1 j_2(j_{12})\ ,\ j_3 j_4(j_{34})\ ;\ jm \mid j_1 j_3(j_{13})\ ,\ j_2 j_4(j_{24})\ ;\ jm\rangle = \\ &= [(2j_{12}+1)(2j_{34}+1)(2j_{13}+1)(2j_{24}+1)]^{1/2} \begin{Bmatrix} j_1 & j_2 & j_{12} \\ j_3 & j_4 & j_{34} \\ j_{13} & j_{24} & j \end{Bmatrix} \end{aligned} \tag{A.10}$$

where $\begin{Bmatrix} . & . & . \\ . & . & . \\ . & . & . \end{Bmatrix}$ are the 9j-symbols.

A.4 Tensor operators, reduced matrix elements

The ensamble of operators $\hat{T}_{\lambda\mu}$ ($\mu = -\lambda, -\lambda+1, \ldots, \lambda-1, \lambda$) are called tensor operators from the point of view of the group of rotations if the following relations are fulfilled [2]:

$$\begin{aligned} \left[\ \hat{I}_{\pm},\ \hat{T}_{\lambda\mu}\ \right] &= \sqrt{(\lambda \mp \mu)(\lambda \pm \mu + 1)}\ \hat{T}_{\lambda\,\mu\pm1} \\ \left[\ \hat{I}_{z},\ \hat{T}_{\lambda\mu}\ \right] &= \mu\, \hat{T}_{\lambda\,\mu} \end{aligned} \tag{A.11}$$

For the calculation of the matrix elements of tensor operators it is very usefull to apply Wigner-Eckart theorem (see e.g. [2]):

$$\langle \beta j_2 m_2 | \hat{T}_{\lambda\mu} | \alpha j_1 m_1 \rangle = \frac{1}{\sqrt{2j_2+1}} C^{j_2 m_2}_{j_1 m_1 \lambda \mu} \langle \beta j_2 || \hat{T}_\lambda || \alpha j_1 \rangle \tag{A.12}$$

where the reduced matrix element $\langle \beta j_2 \,||\hat{T}_\lambda||\, \alpha j_1 \rangle$ does not depend on projections m_1, μ and m_2.

If the investigated system is composed from two subsystems (e.g. two-particle system or a particle with the orbital moment and spin), that means if operators $\hat{T}_{\lambda\mu}$ depend on variables x_1 and x_2 related to single subsystems:

$$\begin{aligned} \hat{T}_{\lambda\mu}(x_1, x_2) \;&\equiv\; (F_{\lambda_1}(x_1) G_{\lambda_2}(x_2))_{(\lambda_1\lambda_2)\lambda\mu} = \\ &= \sum_{\mu_1\mu_2} C^{\lambda\mu}_{\lambda_1\mu_1\lambda_2\mu_2} \hat{F}_{\lambda_1\mu_1}(x_1)\, \hat{G}_{\lambda_2\mu_2}(x_2) \end{aligned} \tag{A.13}$$

then

$$\begin{aligned} &\langle (j_1' j_2') j' \,||\, \hat{T}_\lambda(x_1, x_2) \,||\, (j_1 j_2) j \rangle \;= \\ &= \qquad [(2\lambda+1)(2j+1)(2j_1'+1)(2j_2'+1)]^{1/2} \\ &\qquad \cdot \begin{Bmatrix} j_1 & j_2 & j \\ \lambda_1 & \lambda_2 & \lambda \\ j_1' & j_2' & j' \end{Bmatrix} \langle j_1' \,||\, \hat{F}_{\lambda_1} \,||\, j_1 \rangle \langle j_2' \,||\, \hat{G}_{\lambda_2} \,||\, j_2 \rangle \end{aligned} \tag{A.14}$$

Particularly,

$$\begin{aligned} &\langle (j_1' j_2') j' \,||\, (F_\lambda(x_1) G_\lambda(x_2))_{(\lambda\lambda)0} \,||\, (j_1 j_2) j \rangle \;= \\ &= (-1)^{\lambda+j+j_1+j_2'} \left[\frac{2j+1}{2\lambda+1}\right]^{1/2} [(2j_1'+1)(2j_2'+1)]^{1/2} \begin{Bmatrix} j_1 & j_2 & j \\ j_1' & j_2' & \lambda \end{Bmatrix} \\ &\qquad \cdot \langle j_1' \,||\hat{F}_{\lambda_1}||\, j_1 \rangle \langle j_2' | \hat{G}_{\lambda_2} ||\, j_2 \rangle \end{aligned} \tag{A.15}$$

A.5 Rotation, Wigner D-functions

Let us consider two coordinate systems $S(x, y, z)$ and $S'(x_1, x_2, x_3)$. Further the system S' is assumed to obtain from the system S by a rotation by angle φ round the axis directed along the unit vector $\vec{n}$. Let the $\psi(\vec{r'})$ is some wave function expressed in terms of x_1, x_2, x_3 (that means in the system S') and we want to express this wave function in terms of x, y, z (that means in the system S). This new expression of this function is denoted as $\psi^{(\varphi)}(\vec{r})$. We

will also assume that for $\varphi = 0$ both systems, S and S', coincides, that means $\psi^{(\varphi=0)}(\vec{r}) = \psi(\vec{r})$. Then we can write:

$$\psi^{(\varphi)}(\vec{r}) = \hat{R}(\vec{n},\varphi)\,\psi(\vec{r}) = \; e^{-i\vec{n}.\hat{\vec{J}}\varphi}\,\psi(\vec{r}) \tag{A.16}$$

$$\Rightarrow\; \psi^{(\varphi)}_{JM'}(\vec{r}) = \hat{R}(\vec{n},\varphi)\psi_{JM'}(\vec{r}) = \sum_{M} D^{J*}_{MM'}(\vec{n},\varphi),\varphi)\psi_{JM}(\vec{r}) \tag{A.17}$$

where Wigner function $D^{J}_{MM'}(\vec{n},\varphi)$ is defined as:

$$D^{J*}_{MM'}(\vec{n},\varphi) \;=\; \langle JM|e^{-i\vec{n}.\hat{\vec{J}}\varphi}\mid JM'\rangle \tag{A.18}$$

Up to now the rotation $S \;\rightarrow\; S'$ was specify by the angle φ and by the direction of the rotation axis given by the unit vector $\vec{n}$. In practice, more often the rotation specification is given by Euler angles α, β and γ. Let us denote $\hat{R}(\alpha,\beta,\gamma)$ as the transformation operator corresponding to the transformation $S \;\rightarrow\; S'$ consisting from the following sequence of rotations:

- 1-st rotation round the axis given by the unit vector $\vec{e}_z$ by angle $\alpha \in \langle 0, 2\pi\rangle$ (new axes $\vec{e''}_1,\ \vec{e''}_2,\ \vec{e''}_3 = \vec{e}_z$)
- 2-nd rotation round the axis given by the unit vector $\vec{e''}_2$ by angle $\beta \in \langle 0, \pi\rangle$ (new axes $\vec{e'''}_1,\ \vec{e'''}_2 = \vec{e''}_2,\ \vec{e'''}_3$)
- 3-th rotation round the axis given by the unit vector $\vec{e'''}_3$ by angle $\gamma \in \langle 0, 2\pi\rangle$ (new axes $\vec{e}_1,\ \vec{e}_2,\ \vec{e}_3 = \vec{e'''}_3$)

It can be shown that the definition of the Euler angles given above is fully equivalent to the following definition:

- 1-st rotation round the axis $\vec{e}_z$ by angle $\gamma \in \langle 0, 2\pi\rangle$
- 2-nd rotation round the old axis $\vec{e}_y$ by angle $\beta \in \langle 0, \pi\rangle$
- 3-th rotation round old axis $\vec{e}_z$ by angle $\alpha \in \langle 0, 2\pi\rangle$

So, according to the second definition of the Euler angles the operator of the transformation $S \;\rightarrow\; S'$ given by Euler angles can be writte as follows:

$$\hat{R}(\alpha,\beta,\gamma) \;=\; e^{-i\alpha\hat{J}_z}\,e^{-i\beta\hat{J}_y}\,e^{-i\gamma\hat{J}_z} \tag{A.19}$$

and in the analogy with (A.17) the wave function $\psi_{JM'}(\vec{r})$ in the system S transforned into the system S' is (three Euler angles α, β and γ are here denoted as one symbol θ :

$$\Rightarrow\; \psi^{(\theta)}_{JM'}(\vec{r}) = \hat{R}(\theta)\psi_{JM'}(\vec{r}) = \sum_{M} D^{J*}_{MM'}(\theta),\varphi)\psi_{JM}(\vec{r}) \tag{A.20}$$

where Wigner function $D^J_{MM'}(\theta)$ is now defined as:

$$D^{J*}_{MM'}(\theta) \;=\; \langle JM \mid e^{-i\alpha\hat{J}_z}\, e^{-i\beta\hat{J}_y}\, e^{-i\gamma\hat{J}_z} \mid JM' \rangle = \\ =\; e^{-iM\alpha}\, d^J_{MM'}(\beta)\, e^{-iM'\gamma} \tag{A.21}$$

with

$$d^J_{MM'}(\beta) = \langle JM \mid e^{-i\beta\hat{J}_y} \mid JM' \rangle \tag{A.22}$$

It is possible to show that $d^J_{MM'}(\beta)$ is the real matrix. Then (A.21) can be rewritten:

$$D^J_{MM'}(\alpha,\beta,\gamma) =\; e^{iM\alpha}\, d^J_{MM'}(\beta)\, e^{iM'\gamma} \tag{A.23}$$

The matrix $D^J_{MM'}(\alpha,\beta,\gamma)$ is in the literature usually called as Wigner D matrix [1] . Its matrix elements are called Wigner D functions.

Some properties of the Wigner D-functions [2]:

- symmetry:

$$D^{J*}_{MM'}(\alpha,\beta,\gamma) = D^J_{M'M}(-\alpha,-\beta,-\gamma) \tag{A.24}$$

- completeness:

$$\sum_M D^{J*}_{\mu M}(\theta)\, D^J_{\nu M}(\theta) = \delta_{\mu\nu} = \sum_M D^{J*}_{M\mu}(\theta)\, D^J_{M\nu}(\theta) \tag{A.25}$$

- combining:

$$D^{J_1}_{M_1M_1'}(\theta)\, D^{J_2}_{M_2M_2'}(\theta) = \sum_{J=|J_1-J_2|}^{J_1+J_2} C^{JM}_{J_1M_1J_2M_2}\, C^{JM}_{J_1M_1'J_2M_2'}\, D^J_{MM'}(\theta) \tag{A.26}$$

- orthogonality

$$\int D^J_{MM'}(\theta)\, d\theta = 8\pi^2\, \delta_{J0}\, \delta_{M0}\, \delta_{M'\,0}$$

$$\int D^{J_2\,*}_{M_2M_2'}(\theta)\, D^{J_1}_{M_1M_1'}(\theta)\, d\theta = \frac{8\pi^2}{2J_2+1}\, \delta_{J_1J_2}\, \delta_{M_1M_2}\, \delta_{M_1'M_2'}$$

$$\int D^{J_3\,*}_{M_3M_3'}(\theta)\, D^{J_2}_{M_2M_2'}(\theta)\, D^{J_1}_{M_1M_1'}(\theta)\, d\theta = \\ = \frac{8\pi^2}{2J_3+1}\, C^{J_3M_3}_{J_1M_1J_2M_2} C^{J_3M_3'}_{J_1M_1'J_2M_2'} \tag{A.27}$$

[1]The definition of the Wigner D matrix $D^J_{MM'}(\alpha,\beta,\gamma)$ is not unambiguous, e.g. in the books [2, 10] matrix elements of Wigner D matrix are defined as complex conjugated to those defined by (A.23) but the definition (A.23) is in the agreement with the definition of $D^J_{MM'}(\alpha,\beta,\gamma)$ used in [6, 11] and in order to obtain definition of D-functions given in [9] we should change $M \leftrightarrow M'$ in (A.23).

- other usefull expressions with D-matrices:

$$
\begin{aligned}
& d^J_{MK}(-\beta) = (-1)^{M-K}\, d^J_{MK}(\beta) \\
& d^J_{MK}(\pi) = (-1)^{J-K}\, \delta_{M\,-K} \\
& d^J_{MK}(-\pi) = (-1)^{J+K}\, \delta_{M\,-K} \\
& \Rightarrow\ D^J_{MK}(\alpha, \beta-\pi, -\gamma) = (-1)^{J+K}\, D^J_{M\,-K}(\alpha,\beta,\gamma)
\end{aligned}
\tag{A.28}
$$

Using the completeness of Wigner D-functions (A.25) the expression (A.20) can be inverted:

$$
\psi_{JM}(\vec{r}) = \sum_{M'} D^J_{MM'}(\theta)\, \psi^{(\theta)}_{JM}(\vec{r}) \tag{A.29}
$$

For many practical situations it is useful to consider the system S as the laboratory system and the system S' rotating with respect to S (for instance the system S' is tightly connected with the rotating nucleus). In such a case it is convenient to take the Euler angles $\theta(t)$ as dynamical quantities and to introduce the rotation angular moment $\vec{R}(t)$ as the conjugated quantity to the angles $\theta(t)$ (if the rotation is characterized by the direction $\vec{n}$ of the rotation axis and by the rotation angle $\varphi(t)$ then the dynamical rotational moment $\vec{R}(t)$ is directed along the unit vector $\vec{n}$). Then we can introduce the total angular moment $\vec{I}$ as a vector sum of the rotational moment $\vec{R}$ and the intrinsic angular moment $\vec{J}$:

$$
\hat{\vec{I}} = \hat{\vec{R}} + \hat{\vec{J}} \tag{A.30}
$$

where $\hat{\vec{I}}$ acts on the wave function $\psi^{(\theta)}(\vec{r})$ only by the action on $\vec{r}$ leaving θ unchanged (see (A.16) where the rotation is now given by Euler angles θ instead of φ). Oppositely, $\hat{\vec{R}}$ acts only on θ and does not act on $\vec{r}$. So we have (see footnote [2])

$$
\hat{\vec{I}}\, \psi^{(\theta)}(\vec{r}) = 0 \tag{A.31}
$$

Using (A.31) the application of the operator $\hat{\vec{I}}$ on the function $\psi_{JM}(\vec{r})$ (see(A.31))

[2]The expression (A.31) is evident if we assume one-dimensional rotation round the 3-d axis when the eigen function of the 3-d component $\hat{J}_3$ of the ang. moment is $\psi_m(\phi) = e^{im\varphi}$ ($\hat{J}_3\psi_m(\phi) = m\,\psi_m(\phi)$). Then, according to (A.16) this wave function, written in the rotating system S', is:

$$
\psi^{(\gamma)}_m(\phi) = \hat{R}(\hat{n}_3,\gamma)\, \psi_m(\phi) = e^{-i\hat{J}_3\gamma}\psi_m(\phi) = e^{im(\phi-\gamma)}
$$

and since rotational moment component $\hat{R}_3$ acts on γ ($\hat{R}_3 = -i\frac{\partial}{\partial\gamma}$) and $\hat{J}_3$ on ϕ ($\hat{J}_3 = -i\frac{\partial}{\partial\phi}$) we obtain (A.33):

$$
\hat{I}_3\, \psi^{(\gamma)}_m(\phi) = (\hat{R}_3 + \hat{J}_3) e^{im(\phi-\gamma)} = 0
$$

can be expressed as follows

$$\hat{\vec{I}}\,\psi_{JM}(\vec{r}) = \boxed{\begin{array}{c}\text{see}\\(A.29)\end{array}} = \hat{\vec{I}}\sum_K D^J_{MK}(\theta)\,\psi^{(\theta)}_{JK}(\vec{r}) = \boxed{\begin{array}{c}\text{see}\\(A.31)\end{array}} =$$
$$= \sum_K \left[\hat{\vec{I}}\,D^J_{MK}(\theta)\right]\,\psi^{(\theta)}_{JK}(\vec{r}) \qquad (A.32)$$

and also

$$\hat{\vec{I}}^{\,2}\,\psi_{JM}(\vec{r}) = J(J+1)\,\psi_{JM}(\vec{r}) = \boxed{\begin{array}{c}\text{see}\\(A.29)\end{array}} =$$
$$= J(J+1)\sum_K D^J_{MK}(\theta)\,\psi^{(\theta)}_{JK}(\vec{r}) =$$
$$= \boxed{\begin{array}{c}\text{on the other}\\\text{hand - }(A.32)\end{array}} = \sum_K \left[\hat{\vec{I}}^{\,2}\,D^J_{MK}(\theta)\right]\,\psi^{(\theta)}_{JK}(\vec{r})$$
$$\Longrightarrow \hat{\vec{I}}^{\,2}\,D^J_{MK}(\theta) = J(J+1)\,D^J_{MK}(\theta) \qquad (A.33)$$

At first we analyze the action of the total angular moment components in the lab. system S on Wigner D-functions.

$$\hat{I}_z\,\psi_{JM}(\vec{r}) = M\,\psi_{JM}(\vec{r}) = \boxed{\begin{array}{c}\text{see}\\(A.29)\end{array}} = M\sum_K D^J_{MK}(\theta)\,\psi^{(\theta)}_{JK}(\vec{r}) =$$
$$= \boxed{\begin{array}{c}\text{on the other}\\\text{hand - }(A.32)\end{array}} = \sum_K \left[\hat{I}_z\,D^J_{MK}(\theta)\right]\,\psi^{(\theta)}_{JK}(\vec{r})$$
$$\Longrightarrow \hat{I}_z\,D^J_{MK}(\theta) = M\,D^J_{MK}(\theta) \qquad (A.34)$$

and also

$$\tilde{\hat{I}}_\pm\,\psi_{JM}(\vec{r}) =$$
$$= (\hat{I}_x \pm i\,\hat{I}_y)\,\psi_{JM}(\vec{r}) = \sqrt{(J\mp M)(J\pm M+1}\,\psi_{J\,M\pm1}(\vec{r}) =$$
$$= \boxed{\begin{array}{c}\text{see}\\(A.29)\end{array}} = \sqrt{(J\mp M)(J\pm M+1}\sum_K D^J_{M\pm1\,K}(\theta)\,\psi^{(\theta)}_{JK}(\vec{r}) =$$
$$= \boxed{\begin{array}{c}\text{on the other}\\\text{hand - }(A.32)\end{array}} = \sum_K \left[\tilde{\hat{I}}_\pm\,D^J_{MK}(\theta)\right]\,\psi^{(\theta)}_{JK}(\vec{r})$$
$$\Longrightarrow \tilde{\hat{I}}_\pm\,D^J_{MK}(\theta) = \sqrt{(J\mp M)(J\pm M+1}\,D^J_{M\pm1\,K}(\theta) \qquad (A.35)$$

where $\hat{\tilde{I}}_{\pm} = \hat{I}_x \pm i\,\hat{I}_y$ are the step-up and step-down ang. moment operators acting in the lab. nonrotating system S.

The action of the total angular moment components in the rotationg S'-system on the Wigner D-functions can be also derived using (A.34) and using the fact that rotational moment $\hat{\vec{R}}$ acts only on θ:

$$\hat{\vec{R}}\,\psi_{JM}(\vec{r}) = 0 = \boxed{\begin{array}{c}\text{see}\\(A.29)\end{array}} = (\hat{\vec{I}} - \hat{\vec{J}})\sum_K D^J_{MK}(\theta)\,\psi^{(\theta)}_{JK}(\vec{r}) =$$

$$= \boxed{\begin{array}{c}\text{see}\\(A.32)\end{array}} = \sum_K \left[\left(\hat{\vec{I}}\,D^J_{MK}(\theta)\right)\psi^{(\theta)}_{JK}(\vec{r}) - D^J_{MK}(\theta)\,\left(\hat{\vec{J}}\psi^{(\theta)}_{JK}(\vec{r})\right)\right]$$

$$= 0 \tag{A.36}$$

From (A.36) it follows:

$$\sum_K \left[\hat{I}_3\,D^J_{MK}(\theta)\right]\psi^{(\theta)}_{JK}(\vec{r}) = \sum_K D^J_{MK}(\theta)\left[\hat{J}_3\,\psi^{(\theta)}_{JK}(\vec{r})\right] =$$

$$= \sum_K K\,D^J_{MK}(\theta)\,\psi^{(\theta)}_{JK}(\vec{r})$$

$$\Longrightarrow \qquad \hat{I}_3\,D^J_{MK}(\theta) = K D^J_{MK}(\theta) \tag{A.37}$$

and similarly

$$\sum_K \left[\hat{I}_{\pm}\,D^J_{MK}(\theta)\right]\psi^{(\theta)}_{JK}(\vec{r}) = \sum_K \left[(\hat{I}_1 \pm i\,\hat{I}_2)\,D^J_{MK}(\theta)\right]\psi^{(\theta)}_{JK}(\vec{r}) =$$

$$= \boxed{\begin{array}{c}\text{see}\\(A.36)\end{array}} = \sum_K D^J_{MK}(\theta)\left[(\hat{J}_1 \pm i\,\hat{J}_2)\,\psi^{(\theta)}_{JK}(\vec{r})\right] =$$

$$= \boxed{\begin{array}{c}\text{because}\\ \hat{J}_{\pm}\,\psi^{(\theta)}_{JK}(\vec{r}) = \sqrt{(J\mp K)(J\pm K+1)}\,\psi^{(\theta)}_{JK\pm1}(\vec{r})\end{array}} =$$

$$= \sum_K \sqrt{(J\mp K)(J\pm K+1)}\,D^J_{MK}(\theta)\,\psi^{(\theta)}_{J\,K\pm1}(\vec{r}) =$$

$$= \boxed{\begin{array}{c}\text{we change sumation}\\ \text{index: } K\pm1 \to\ K\end{array}} =$$

$$= \sum_K \sqrt{(J\pm K)(J\mp K+1)}\,D^J_{M\,K\mp1}(\theta)\,\psi^{(\theta)}_{JK}(\vec{r})$$

$$\Longrightarrow\ \hat{I}_{\pm}\,D^J_{MK}(\theta) = \sqrt{(J\pm K)(J\mp K+1)}\,D^J_{M\,K\mp1}(\theta) \tag{A.38}$$

where $\hat{I}_\pm \equiv \hat{I}_1 \pm i\,\hat{I}_2$ are step-up and step-down operators acting on the 3-d komponent of the total ang. moment in the rotating S'-system.

From the comparison of (A.38) and (A.35) one can see that the standard action of the step-up and step-down operators $\hat{\tilde{I}}_\pm$ in the nonrotationg lab. system S is opposite then the action of $\hat{I}_\pm$ in the rotation S' system in the sense that in the rotating S' system step-up operator $\hat{I}_+$ decreases unusually the the projection K by 1 and step-down operator $\hat{I}_-$ increases the projection K by 1.

Corresponding transformation of the rotation for tensor operators $\hat{T}_{\lambda\mu}$ (see (A.11)) is following:

$$\hat{T}_{\lambda\mu} = \sum_\nu D^\lambda_{\mu\nu}(\theta)\,\hat{T}^{(\theta)}_{\lambda\nu} \tag{A.39}$$

where $\hat{T}_{\lambda\mu}$ acts in the space of functions $\psi(\vec{r})$ (that means in the system S) while the operator $\hat{T}^{(\theta)}_{\lambda\nu}$ acts in the space of functions $\psi^{(\theta)}(\vec{r})$ (that means within the system S').

A.6 Spherical harmonics, vector spherical harmonics

Sperical harmonics $Y_{lm}(\vartheta,\varphi)$ are defined as the eigenfunctions of the operator of square of the orbital angular moment

$$\begin{aligned}\hat{\vec{L}}^{\,2} &= [\,-i\,(\vec{r}\times\vec{\nabla})\,]^{\,2} = \\ &= -\left[\frac{1}{sin\vartheta}\frac{\partial}{\partial\vartheta}\,(sin\vartheta) + \frac{\partial^{\,2}}{\partial\varphi^{\,2}}\frac{1}{sin^2\vartheta}\right]\end{aligned} \tag{A.40}$$

and its 3-d component

$$\hat{L}_3 = -\,i\,\frac{\partial}{\partial\varphi} \tag{A.41}$$

with corresponding eigenvalues $l\,(l+1)$ and m, respectively:

$$\begin{aligned}\hat{\vec{L}}^{\,2}\,Y_{lm}(\vartheta,\varphi) &= l\,(l+1)\,Y_{lm}(\vartheta,\varphi) \\ \hat{L}_3\,Y_{lm}(\vartheta,\varphi) &= m\,Y_{lm}(\vartheta,\varphi)\end{aligned} \tag{A.42}$$

where $l = 0,\ 1,\ \ldots,\ \infty$ and $m = -l,\ \ldots,\ +l$.

The most useful relations concerning spherical harmonics are following (see e.g [2])

$$\int_0^{2\pi} d\varphi \int_0^{\pi} d\vartheta\; sin\vartheta\; Y^*_{l_1m_1}(\vartheta,\varphi)\,Y_{l_2m_2}(\vartheta,\varphi) = \delta_{l_1\,l_2}\,\delta_{m_1\,m_2} \tag{A.43}$$

$$\sum_{l=0}^{\infty}\sum_{m=-1}^{+l} Y_{lm}(\vartheta_1,\varphi_1)\,Y^*_{lm}(\vartheta_2,\varphi_2) = \delta(\vartheta_1-\vartheta_2)\,\delta(\varphi_1-\varphi_2) \tag{A.44}$$

$$Y^*_{lm}(\vartheta,\varphi) = (-1)^{\,l}\,Y_{l\,-m}(\vartheta,\varphi) \tag{A.45}$$

$$\mathscr{P}\,Y_{lm}(\vartheta,\varphi) = Y_{lm}(\pi-\vartheta,\varphi+\pi) = (-1)^{\,l}\,Y_{lm}(\vartheta,\varphi) \tag{A.46}$$

$$R_1(\pi)\,Y_{lm}(\vartheta,\varphi) = Y_{lm}(\pi-\vartheta,2\pi-\varphi) = (-1)^{\,l}\,Y_{l-m}(\vartheta,\varphi) \tag{A.47}$$

$$R_2(\pi)\,Y_{lm}(\vartheta,\varphi) = Y_{lm}(\pi-\vartheta,\pi-\varphi) = (-1)^{\,l-m}\,Y_{l-m}(\vartheta,\varphi) \tag{A.48}$$

$$R_3(\pi)\,Y_{lm}(\vartheta,\varphi) = Y_{lm}(\vartheta,\pi-\varphi) = (-1)^{\,m}\,Y_{lm}(\vartheta,\varphi) \tag{A.49}$$

$$\int_0^{2\pi} d\varphi \int_0^{\pi} d\vartheta\; sin\vartheta\; Y_{lm}(\vartheta,\varphi) = \sqrt{4\pi}\;\delta_{l0}\;\delta_{m0} \tag{A.50}$$

$$\int_0^{2\pi} d\varphi \int_0^{\pi} d\vartheta\; sin\vartheta\; Y_{l_1m_1}(\vartheta,\varphi)\,Y_{l_2m_2}(\vartheta,\varphi)\,Y^*_{l_3m_3}(\vartheta,\varphi) = \\ = \frac{\sqrt{(2l_1+1)(2l_1+1)}}{4\pi\;(2l_3+1)} C^{\,l_3\,0}_{l_1 0\,l_2\,0}\,C^{\,l_3\,m_3}_{l_1m_1l_2m_2} \tag{A.51}$$

where $\mathscr{P}$ is the parity operator (invesrion of coordinate axes - see subsection 1.3.1), $R_i(\pi)$ is the operator of the rotation by angle π round the i-th coordinate axis and other notations are obvius.

Vector spherical harmonics $\vec{Y}_{LJM}(\hat{r})$ are defined as the eigenfunctions of the mutually commuting operators:

- $\hat{\vec{J}}^{\,2}$ - square of the total ang. moment ($\hat{\vec{J}} = \hat{\vec{L}} + \hat{\vec{S}}$, where spin operator $\hat{\vec{S}}$ corresponds to $S = 1$)
- $\hat{J}_3$ - the 3-d component of the total moment
- $\hat{\vec{L}}^{\,2}$ - square of the orbital ang. moment
- $\hat{\vec{S}}^{\,2}$ - quare of the spin-moment (where $S = 1$)

So,

$$\begin{aligned}
\hat{\vec{J}}^{\,2}\,\vec{Y}_{LJM}(\theta,\varphi) &= J\,(J+1)\,\hat{\vec{J}}^{\,2}\,\vec{Y}_{LJM}(\theta,\varphi) \\
\hat{J}_3\,\vec{Y}_{LJM}(\theta,\varphi) &= M\,\vec{Y}_{LJM}(\theta,\varphi) \\
\hat{\vec{L}}^{\,2}\,\vec{Y}_{LJM}(\theta,\varphi) &= L\,(L+1)\,\vec{Y}_{LJM}(\theta,\varphi) \\
\hat{\vec{S}}^{\,2}\,\vec{Y}_{LJM}(\theta,\varphi) &= S\,(S+1)\vec{Y}_{LJM}(\theta,\varphi) = 2\,\vec{Y}_{LJM}(\theta,\varphi)
\end{aligned} \tag{A.52}$$

where $J = L,\ L \pm 1$. The vector spherical harmonics may be constructed from the spherical harmonics $Y_{LM}(\theta,\varphi)$ ($\hat{\vec{L}}^{\,2} Y_{LM}(\theta,\varphi) = L\,(L+1)\; Y_{LM}(\theta,\varphi)$, $\hat{L}_3\; Y_{LM}(\theta,\varphi) = m\; Y_{LM}(\theta,\varphi)$) and from spin functions $\vec{\xi}_\mu$ (eigenfunctions of $\hat{\vec{S}}^{\,2}$ and $\hat{S}_3$ for $S = 1$, $\hat{\vec{S}}^{\,2}\vec{\xi}_\mu = S\,(S+1)\,\vec{\xi}_\mu = 2\,\vec{\xi}_\mu,\ \hat{\vec{S}}_3\vec{\xi}_\mu = \mu\,\vec{\xi}_\mu$) in accordance with the coupling scheme of two angular moments (see (A.2)):

$$\vec{Y}_{LJM}(\theta,\varphi) = \sum_{m\mu} C^{JM}_{Lm1\mu}\; Y_{Lm}(\theta,\varphi)\,\vec{\xi}_\mu \tag{A.53}$$

The spin functions $\vec{\xi}_\mu$ are constructed from the basis of the three unit vectors directed along the coordinate axes:

$$\vec{e}_1 = \begin{pmatrix} 1 \\ 0 \\ 0 \end{pmatrix} \qquad \vec{e}_2 = \begin{pmatrix} 0 \\ 1 \\ 0 \end{pmatrix} \qquad \vec{e}_3 = \begin{pmatrix} 0 \\ 0 \\ 1 \end{pmatrix} \tag{A.54}$$

by the following way.

From the quantum mechanics it is known that the operators of the spin components in the 3-dimensional Kartezian space (that means in the space of the basis vectors (A.54)) for the object with $S = 1$ (like photon) are given by

$$S_1 = \begin{pmatrix} o & 0 & 0 \\ 0 & 0 & -i \\ 0 & i & 0 \end{pmatrix},\ S_2 = \begin{pmatrix} o & 0 & i \\ 0 & 0 & 0 \\ -i & 0 & 0 \end{pmatrix},\ S_3 = \begin{pmatrix} o & -i & 0 \\ i & 0 & 0 \\ 0 & 0 & 0 \end{pmatrix} \tag{A.55}$$

Corresponding operator of the square of spin is:

$$\vec{S}^{\,2} = S_1^2 + S_2^2 + S_3^2 = \begin{pmatrix} 2 & 0 & 0 \\ 0 & 2 & 0 \\ 0 & 0 & 2 \end{pmatrix} \tag{A.56}$$

Since $[\vec{S}^{\,2},\ S_3] = 0$ we can search for the common system of eigenfunctions $\vec{\xi}_\mu$ of the operators $\vec{S}^{\,2}$ and S_3:

$$\begin{aligned} \vec{S}^{\,2}\,\vec{\xi}_\mu &= S\,(S+1)\,\vec{\xi}_\mu = 2\,\vec{\xi}_\mu \\ S_3\,\vec{\xi}_\mu &= \mu\,\vec{\xi}_\mu, \qquad \mu = 0,\ \pm 1 \end{aligned} \tag{A.57}$$

Spin functions $\vec{\xi}_\mu$ can be obtained from basis vectors $\vec{e}_1,\ \vec{e}_2,\ \vec{e}_3$ by the diago-

nalization of the matrix S_3:

$$S_3^{'} = U^{+}\, S_3\, U\,, \qquad\qquad U = \begin{pmatrix} -\frac{1}{\sqrt{2}} & 0 & \frac{1}{\sqrt{2}} \\ -\frac{i}{\sqrt{2}} & 0 & -\frac{i}{\sqrt{2}} \\ 0 & 1 & 0 \end{pmatrix}$$

$$\Longrightarrow S_3^{'} = \begin{pmatrix} 1 & 0 & 0 \\ 0 & 0 & 0 \\ 0 & 0 & -1 \end{pmatrix} \tag{A.58}$$

with the vectors $\vec{\xi}_\mu$ ($\mu = 0,\, \pm 1$) in the form $\vec{\xi}_\mu = \sum_i U_{i\mu}\, \vec{e}_i$:

$$\begin{aligned} \vec{\xi}_{+1} &= -\frac{1}{\sqrt{2}}\,(\vec{e}_1 + i\,\vec{e}_2) \\ \vec{\xi}_0 &= \vec{e}_3 \\ \vec{\xi}_{-1} &= \frac{1}{\sqrt{2}}\,(\vec{e}_1 - i\,\vec{e}_2) \end{aligned} \tag{A.59}$$

with the following symmetry

$$\vec{\xi}^{\,*}_\mu = (-1)^\mu\, \vec{\xi}_{-\mu} \tag{A.60}$$

The most important relations for vector spherical harmonics are following (see e.g. [2])

$$\begin{aligned} \vec{Y}^{\,*}_{LJM} &= \sum_{\mu=-1}^{1} C^{JM}_{L\,M-\mu\,1\,\mu}\, Y^{*}_{L\,M-\mu}\, \vec{\xi}^{\,*}_\mu = \boxed{\begin{array}{c}\text{see} \\ (A.60), (A.45), (A.4)\end{array}} = \\ &= (-1)^{J+L+1+M}\, \vec{Y}_{LJ\,-M}(\hat{r}) \end{aligned} \tag{A.61}$$

and (without a proof, see e.g. [2])

$$\begin{aligned} \vec{\nabla} f(r)\, Y_{JM}(\hat{r}) &= \sqrt{\frac{J}{2J+1}}\,\left(\frac{d}{dr} + \frac{J+1}{r}\right)\, f(r)\;\vec{Y}_{J-1\,J\,M}(\hat{r}) \\ &\quad -\sqrt{\frac{J+1}{2J+1}}\,\left(\frac{d}{dr} - \frac{J}{r}\right)\, f(r)\;\vec{Y}_{J+1\,J\,M}(\hat{r}) \end{aligned} \tag{A.62}$$

$$\begin{aligned} \vec{\nabla} \times f(r)\, \vec{Y}_{JJM}(\hat{r}) &= i\,\sqrt{\frac{J}{2J+1}}\,\left(\frac{d}{dr} - \frac{J}{r}\right)\, f(r)\;\vec{Y}_{J+1\,J\,M}(\hat{r}) \\ &\quad +i\,\sqrt{\frac{J+1}{2J+1}}\,\left(\frac{d}{dr} + \frac{J+1}{r}\right)\, f(r)\;\vec{Y}_{J-1\,J\,M}(\hat{r}) \end{aligned} \tag{A.63}$$

$$\hat{\vec{L}}\, Y_{JM}(\hat{r}) = -i\,(\vec{r}\times\vec{\nabla})\, Y_{JM}(\hat{r}) = \sqrt{J(J+1)}\,\vec{Y}_{JJM}(\hat{r}) \tag{A.64}$$

$$\int_0^{2\pi} d\varphi \int_0^{\pi} d\theta\; sin\theta\; \vec{Y}^{+}_{L_1\, J_1\, M_1}(\theta,\varphi)\cdot\vec{Y}_{L_2\, J_2\, M_2}(\theta,\varphi) = \\ = \delta_{L_1L_2}\,\delta_{J_1J_2}\,\delta_{M_1M_2} \tag{A.65}$$

where in (A.62), (A.63) $f(r)$ is arbitrary function of r.

B. Creation and annihilation operators of fermions

B.1 Introduction of creation and annihilation operators

Let us suppose a complete ensemble of orthonormal singleparticle wave functions $\varphi_\nu(\vec{r})$ (e.g the basis of eigenvectors of the 3-dimensional oscillator). Using this system we can construct the fully antisymmetrized A-particle wave function of the system of A-fermions (Slater determinant)

$$\Psi_{\alpha,\beta,\gamma,\ldots}(\vec{r}_1,\vec{r}_2,\vec{r}_3,\ldots,\vec{r}_A) \;=\; \langle \vec{r}_1\vec{r}_2\ldots\vec{r}_A \,|\, \alpha\beta\gamma\ldots\rangle \;= \\ = \frac{1}{\sqrt{A!}} \begin{vmatrix} \varphi_\alpha(\vec{r}_1) & \varphi_\beta(\vec{r}_1) & \varphi_\gamma(\vec{r}_1) & \ldots \\ \varphi_\alpha(\vec{r}_2) & \varphi_\beta(\vec{r}_2) & \varphi_\gamma(\vec{r}_2) & \ldots \\ \vdots & \vdots & \vdots & \\ \varphi_\alpha(\vec{r}_A) & \varphi_\beta(\vec{r}_A) & \varphi_\gamma(\vec{r}_A) & \ldots \end{vmatrix} \tag{B.1}$$

From the quantum mechanics it is known that in accordance with the Pauli principle for fermions this fully antisymmetrized wave function is the wave function of the ground state of the system (nucleus). From the quantum mechanics we also know that the ground state $|\,\alpha\beta\gamma\ldots\rangle$ of the system of fermions can be also written in terms of creation operators a^+_ν of the particle of the system in the singleparticle state $|\nu>$ as follows

$$|\,\alpha\beta\gamma\ldots\rangle \;=\; a^+_\alpha\, a^+_\beta\, a^+_\gamma \ldots |-\rangle \tag{B.2}$$

where $|->$ is the singleparticle vacuum:

$$a_\nu\,|-\rangle \;=\; 0 \qquad\qquad \text{for all } \nu \tag{B.3}$$

Creation a^+_ν and annihilation a_ν operators of the particle in the corresponding s.p. state $|\nu\rangle$ fulfil anti-commutator relations (following from the Pauli principle)

$$\{a_\beta, a^+_\alpha\} = \delta_{\alpha\,\beta}\,, \qquad \{a_\beta, a_\alpha\} = \{a^+_\beta, a^+_\alpha\} = 0 \tag{B.4}$$

Further we will use also creation and annihilation operators of particles (fermions) in the given point $\vec{r}$ of the space:

$$|\vec{r}\rangle \;=\; a^+_{\vec{r}}|-\rangle\,, \qquad \langle\vec{r}\,|\,\vec{r}\,'\rangle = \langle -|\,a_{\vec{r}}\,a^+_{\vec{r}\,'}\,|-\rangle = \delta(\vec{r}-\vec{r}\,') \\ \{a_{\vec{r}}, a^+_{\vec{r}\,'}\} = \delta(\vec{r}-\vec{r}\,') \tag{B.5}$$

Using the completeness relation, $\int d^3r|\vec{r}\rangle\langle\vec{r}| = 1$ the creation particle operator can be rewritten:

$$a^+_\nu\,|-\rangle = \int d^3r\,|\vec{r}\rangle\langle\vec{r}|\,a^+_\nu\,|-\rangle = \int d^3r\,\varphi_\nu(\vec{r})\,a^+_{\vec{r}}|-\rangle \\ \Rightarrow \quad a^+_\nu = \int d^3r\,\varphi_\nu(\vec{r})\,a^+_{\vec{r}} \tag{B.6}$$

where $\varphi_\nu(\vec{r}) = \langle\vec{r}|\nu\rangle = \langle\vec{r}|a^+_\nu|-\rangle$.

B.2 One-particle and two-particle operators expressed in terms of creation and annihilation operators

The operator of the number of particles in the given s.p. state is (see e.g. [14])

$$\hat{n}_\nu = a^+_\nu\,a_\nu \tag{B.7}$$

therefore, the operator of the total number of particles can be written as

$$\hat{n} = \sum_\nu a^+_\nu\,a_\nu$$

B.2.1 Single-particle operators

Let us assume some single-particle operator (e.g. the operator of the kinetic energy)

$$\hat{T} = \sum_{i=1}^{A} t_{(i)} \tag{B.8}$$

The expectation value of the operator $\hat{T}$ in the A-particle state $|\alpha\beta\gamma\ldots>$ is

$$\langle\alpha\beta\gamma\ldots|\hat{T}|\alpha\beta\gamma\ldots\rangle \;=\; T_{\alpha\alpha} + T_{\beta\beta} + T_{\gamma\gamma} + \ldots \tag{B.9}$$

where $T_{\alpha\beta} = \int d^3r\,\varphi^*_\alpha(\vec{r})\,T(\vec{r})\,\varphi_\beta(\vec{r})$ is the s.p. matrix element of the operator $\hat{T}$, which has the form $T(\vec{r})$ in the coordinate x-representation (e.g. in the case of the kinetic energy: $t(\vec{r}) = -\frac{\hbar^2\vec{\nabla}^2}{2M}$).

The matrix elements of the operator $\hat{T}$ between the A-particle wave functions differing only by the state of one particle are (generally nonzero):

$$\langle \alpha\beta\gamma \ldots |\hat{T}|\alpha\beta'\gamma \ldots\rangle \;=\; T_{\beta\beta'} \qquad \text{for } \; \beta \neq \beta' \tag{B.10}$$

and the matrix elements of the operator $\hat{T}$ between the A-particle wave functions differing only by two or more s.p. states of are zero

$$\langle \alpha\beta\gamma \ldots |\hat{T}|\alpha'\beta'\gamma \ldots\rangle \;=\; 0 \qquad \text{for } \; \alpha, \beta \neq \alpha', \beta' \tag{B.11}$$

It is known (see e.g. [14]) that such properties has the operator which can be written in terms of creation and annihilation operators as follows

$$\hat{T} = \sum_{\nu\nu'} T_{\nu\nu'}\, a^{+}_{\nu}\, a_{\nu'} \tag{B.12}$$

where

$$T_{\nu\nu'} = \langle \nu|\hat{T}|\nu'\rangle = \int d^3r \int d^3r' \langle \nu|\vec{r}\rangle\, \langle \vec{r}|\hat{T}|\vec{r}\,'\rangle\, \langle \vec{r}\,'|\nu'\rangle \tag{B.13}$$

If the assumed operator $\hat{T}$ is local then

$$\langle \vec{r}|\hat{T}|\vec{r}\,'\rangle = \delta(\vec{r} - \vec{r}\,')\, T(\vec{r}) \tag{B.14}$$

and the expression (B.13) is (because $\langle \vec{r}\,'|\nu'\rangle = \varphi_{\nu'}(\vec{r}\,')$, $\langle \nu|\vec{r}\rangle = \varphi^{*}_{\nu}(\vec{r})$)

$$T_{\nu\nu'} = \int d^3r\, \varphi^{*}_{\nu}(\vec{r})\, T(\vec{r})\, \varphi_{\nu'}(\vec{r}) \tag{B.15}$$

B.2.2 Two-particle operators

General two-particle operator $\hat{V}$ is usually written as follows

$$\hat{V} = \frac{1}{2} \sum_{ij=1}^{A} V_{ij} \tag{B.16}$$

Further we define two-particle antisymmetrized matrix elements of the operator $\hat{V}$

$$
\begin{aligned}
V_{\alpha\beta\,\alpha'\beta'} \equiv \langle\alpha\beta|\hat{V}|\widetilde{\alpha'\beta'}\rangle \equiv\ & \langle\alpha\beta|\hat{V}|\alpha'\beta'\rangle - \langle\alpha\beta|\hat{V}|\beta'\alpha'\rangle\ = \\
= \int d^3r_1 \int d^3r_2 \int d^3r_3 \int d^3r_4 & \langle\alpha|\vec{r}_1\rangle\langle\beta|\vec{r}_2\rangle\langle\vec{r}_1\vec{r}_2|\hat{V}|\vec{r}_3\vec{r}_4\rangle \\
& \langle\vec{r}_3|\alpha'\rangle\langle\vec{r}_4|\beta'\rangle \\
- \int d^3r_1 \int d^3r_2 \int d^3r_3 \int d^3r_4 & \langle\alpha|\vec{r}_1\rangle\langle\beta|\vec{r}_2\rangle\langle\vec{r}_1\vec{r}_2|\hat{V}|\vec{r}_3\vec{r}_4\rangle \\
& \langle\vec{r}_3|\beta'\rangle\langle\vec{r}_4|\alpha'\rangle\ = \\
= \int d^3r_1 \int d^3r_2 \int d^3r_3 \int d^3r_4 & \varphi^*_\alpha(\vec{r}_1)\,\varphi^*_\beta(\vec{r}_2)\,V(\vec{r}_1,\vec{r}_2;\vec{r}_3,\vec{r}_4) \\
& \varphi_{\alpha'}(\vec{r}_3)\,\varphi_{\beta'}(\vec{r}_4) \\
- \int d^3r_1 \int d^3r_2 \int d^3r_3 \int d^3r_4 & \varphi^*_\alpha(\vec{r}_1)\,\varphi^*_\beta(\vec{r}_2)\,V(\vec{r}_1,\vec{r}_2;\vec{r}_3,\vec{r}_4) \\
& \varphi_{\beta'}(\vec{r}_3)\,\varphi_{\alpha'}(\vec{r}_4)
\end{aligned}
\tag{B.17}
$$

Moreover, if the two-particle operator $\hat{V}$ has a local character then

$$
V(\vec{r}_1,\vec{r}_2;\vec{r}_3,\vec{r}_4) = \delta(\vec{r}_1-\vec{r}_3)\,\delta(\vec{r}_2-\vec{r}_4)\,V(\vec{r}_1,\vec{r}_2) \tag{B.18}
$$

and antisymmetrized two-particle matrix element (B.17) can be rewitten

$$
\begin{aligned}
V_{\alpha\beta\,\alpha'\beta'} = & \int d^3r_1 \int d^3r_2\ \varphi^*_\alpha(\vec{r}_1)\,\varphi^*_\beta(\vec{r}_2)\,V(\vec{r}_1,\vec{r}_2)\,\varphi_{\alpha'}(\vec{r}_1)\,\varphi_{\beta'}(\vec{r}_2) \\
& - \int d^3r_1 \int d^3r_2\ \varphi^*_\alpha(\vec{r}_1)\,\varphi^*_\beta(\vec{r}_2)\,V(\vec{r}_1,\vec{r}_2)\,\varphi_{\beta'}(\vec{r}_1)\,\varphi_{\alpha'}(\vec{r}_2)
\end{aligned}
\tag{B.19}
$$

From the definition (B.17) following symmetries of $V_{\alpha\beta\,\alpha'\beta'}$ can be deduced (the operator $\hat{V}$ is assumed to be hermitian)

$$
V_{\alpha\beta\,\alpha'\beta'} = -\,V_{\beta\alpha\,\alpha'\beta'} = -\,V_{\alpha\beta\,\beta'\alpha'} = V_{\beta\alpha\,\beta'\alpha'} \tag{B.20}
$$

Each two-particle operator $\hat{V}$ can be also expressed in terms of s.p. creation and annihilation operators [1]

$$
\hat{V} = \frac{1}{4} \sum_{\mu\nu\mu'\nu'} V_{\mu\nu\,\mu'\nu'}\, a^+_\mu\, a^+_\nu\, a_{\nu'}\, a_{\mu'} \tag{B.21}
$$

[1] In the expr. (B.21) for the two-particle operator antisymmetrized matrix elements $V_{\mu\nu\,\mu'\nu'}$ (see (B.17)) are involved. If we use standard nonantisymmetrized matrix elements $\langle\mu\nu|\hat{V}|\mu'\nu'\rangle$ then the expression (B.21) can be written as follows

$$
\hat{V} = \frac{1}{2} \sum_{\mu\nu\mu'\nu'} \langle\mu\nu|\hat{V}|\mu'\nu'\rangle\, a^+_\mu\, a^+_\nu\, a_{\nu'}\, a_{\mu'}
$$

We can check that the expression (B.21) gives the right two-particle matrix elements (B.17):

$$
\begin{aligned}
&\langle \alpha\beta\gamma\delta\ldots|\hat{V}|\alpha'\beta'\gamma\delta\ldots\rangle = \\
&= \frac{1}{4}\sum_{\mu\nu\mu'\nu'} V_{\mu\nu\,\mu'\nu'} \\
&\langle -|\ldots a_\delta a_\gamma a_\beta a_\alpha a^+_\mu a^+_\nu a_{\nu'} a_{\mu'} a^+_{\alpha'} a^+_{\beta'} a^+_\gamma a^+_\delta \ldots|-\rangle = \\
&= \frac{1}{4}\sum_{\mu\nu\mu'\nu'} V_{\mu\nu\,\mu'\nu'}\,\langle -|\ldots a_\delta a_\gamma a_\beta \\
&\qquad\qquad (\delta_{\alpha\,\mu} - a^+_\mu a_\alpha) a^+_\nu a_{\nu'} (\delta_{\mu'\,\alpha'} - a^+_{\alpha'} a_{\mu'}) a^+_{\beta'} a^+_\gamma a^+_\delta \ldots|-\rangle = \\
&= \boxed{\begin{array}{c}\text{successive application of (B.4) untill} \\ \text{we can use } \langle -|a^+_\mu = 0 \;\text{ or }\; a_{\mu'}|-\rangle = 0\end{array}} = \\
&= \frac{1}{4}\,(V_{\alpha\beta\,\alpha'\beta'} - V_{\beta\alpha\,\alpha'\beta'} - V_{\alpha\beta\,\beta'\alpha'} + V_{\beta\alpha\,\beta'\alpha'}) = \boxed{\begin{array}{c}\text{see} \\ (B.20)\end{array}} = \\
&= V_{\alpha\beta\,\alpha'\beta'}
\end{aligned}
\tag{B.22}
$$

B.3 Normal product of creation and annihilation operators

B.3.1 Normal product with respect to particle vacuum $|-\rangle$

Definition of the normal product:
in the expression involving product of creation and annihilation operators we rearrange operators in such a way that all creation operators stand right from annihilation operators. During the process of operator rearranging in each transposition of two operators we must change sign of the whole expression in the case when creation and annihilation operators concern fermions. Result of such rearranging is called normal product of creation and annihilation operators and resulting expression is written between two double dots, $: \ldots :$
Examples:

$$\begin{aligned} &: a_\alpha^+ \, a_\beta \; := a_\alpha^+ \, a_\beta \, , && : a_\alpha^+ \, a_\beta^+ \; := a_\alpha^+ \, a_\beta^+ = -a_\beta^+ \, a_\alpha^+ \\ &: a_\beta \, a_\alpha^+ \; := -a_\alpha^+ \, a_\beta \, , && : a_\alpha^+ \, a_\beta \, a_\gamma^+ \; := -a_\alpha^+ \, a_\gamma^+ \, a_\beta = a_\gamma^+ \, a_\alpha^+ \, a_\beta \end{aligned} \tag{B.23}$$

From the definition of the normal product and from (B.3) ($a_\nu|-\rangle = 0$, $\langle -| \, a_\nu^+ = 0$) it follows that the expectation value in the particle vacuum $|-\rangle$ of any normal product is zero:

$$\langle -| : \, A \, B \, C \ldots : |-\rangle = 0 \tag{B.24}$$

where A, B, C, D, $\ldots =$ a_α^+ or a_β for all α and β.

B.3.2 Normal product with respect to Hartree-Fock ground state $|HF\rangle$

The Hartre-Fock ground state $|HF\rangle$ of the system of fermions is the state when particles fill single-particle states one by one from the s.p. state with the lowest energy up to the s.p. state with the energy nearest below the Fermi level. All s.p. states with energies above Fermi level are not occupied (see the Chapter 4 and Fig. A1). Further we will denote always the particle states (above the Fermi level) by indexes with the subindex $>$ and hole states (below the Fermi level) by indexes wit the subindex $<$. Using such assignment the HF- ground state $|HF\rangle$ can be specified in the Fock space of the occupation

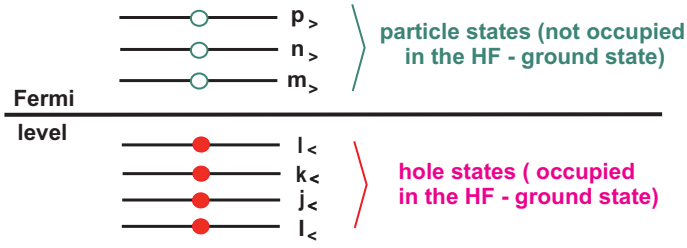


Figure B.1: Schematic figure of particle and hole states in the HF- ground state

numbers as folows.

$$|HF\rangle \quad = \quad | \quad \underbrace{i_< \, j_< \, k_< \, l_< \quad \ldots}_{\begin{array}{c}\text{list of indexes}\\ \text{of all s.p. states}\\ \text{below Fermi level}\end{array}} \quad >$$

In accordance with the Pauli principle (each s.p. state can be occupied only by one fermion) the following relations can be written

$$\begin{aligned} a^+_{i_<} \,|\, HF\rangle \;&=\; 0 \qquad \Leftrightarrow \qquad \langle HF \,|\, a_{i_<} = 0 \\ a_{m_>} \,|\, HF\rangle \;&=\; 0 \qquad \Leftrightarrow \qquad \langle HF \,|\, a^+_{m_>} = 0 \end{aligned} \tag{B.25}$$

On basis of (B.25) it is useful to introduce so called quasiparticle creation and annihilation operators (in this case quasiparticle operators are introduced in the framework of the model of independent particles, that means the pairing interaction is not taken into account) [2]

$$\begin{aligned} \alpha^+_{m_>} \;&\equiv\; a^+_{m_>} \qquad \text{(particle is created)} \\ \alpha^+_{i_<} \;&\equiv\; a_{i_<} \qquad \text{(hole is created)} \end{aligned} \tag{B.26}$$

Then the expression (B.25) can be rewritten in the more compact form

$$\alpha_\nu \,|HF\rangle = 0 \qquad \text{for all} \;\; \nu \tag{B.27}$$

So, the HF- ground state $|HF\rangle$ is the vacuum state for quasiparticle operators introduced by (B.26) (similarly as the state $|-\rangle$ in (B.3) was the vacuum for particle operators). This fact enables to introduce the normal products for quasiparticle operators where the role of the vacuum is played by the HF-

[2] The quasiparticle operators introduced by (B.26) should not be confused with the quasiparticle operators defined by the Bogoliubov transformation (6 ?).

ground state.
Examples:

$$
\begin{aligned}
&: \alpha_a^+ \, \alpha_b \, \alpha_c^+ \, \alpha_d \; := - \, \alpha_a^+ \, \alpha_c^+ \, \alpha_b \, \alpha_d \\
&: a_{m_>}^+ \, a_{i_<}^+ \, a_{j_<} \, a_{n_>} \; := : \; \alpha_{m_>}^+ \, \alpha_{i_<} \, \alpha_{j_<}^+ \, \alpha_{n_>} \; := \\
&\qquad = \; - \, \alpha_{m_>}^+ \, \alpha_{j_<}^+ \, \alpha_{i_<} \, \alpha_{n_>} \; = \; - \, a_{m_>}^+ \, a_{j_<}^+ \, a_{i_<}^+ \, a_{n_>}
\end{aligned}
\tag{B.28}
$$

Therefore the rule for normal products of quasiparticle operators (B.26) can be formulated as follows:
Particle operators in the product are arranged in such a way that any operator giving zero if acts on the HF- ground state $|HF\rangle$ stands always right to all operators which do not give zero if acts on the $|HF\rangle$.

Similarly as in (B.24) the expectation value of any normal product of quasiparticle operators in the HF- ground state is zero:

$$
\langle HF| : \, A \, B \; \ldots \; : \, |HF\rangle \; = \; 0 \tag{B.29}
$$

where A, B, C, $\ldots \; = \; \alpha_\nu^+ \; or \; \alpha_\nu$ for all ν.

B.4 Wick's theorem

For normal products of the creation and annihilation operators very important Wick's theorem is used (we present here Wick's theorem without a proof) [3]

$$
\begin{aligned}
&A \, B \, C \, D \; \ldots \; =: \; A \, B \, C \, D \; \ldots \; : \; + \\
&+ \; : \widehat{A \, B} \, C \, D \; \ldots \; : \; + \; : \widehat{A \, B \, C} \, D \; \ldots \; : \; + \; \ldots \\
&+ \; : \widehat{A \, B} \, \widehat{C \, D} \; \ldots \; : \; + \; : \widehat{A \, B} \, \widehat{C \, D \, E} \; \ldots \; : \; + \; \ldots \\
&+ \; \ldots
\end{aligned}
\tag{B.30}
$$

where A, B, C, D, $\ldots = a_\nu^+$ or a_ν (α_ν^+ or α_ν, respectively). In (B.30) the symbol $\widehat{A \, B}$ means the contraction of two operators A and B which is defined as the vacuum expectation value of these operators:

$$
\begin{aligned}
&: \widehat{A \, B} \, C \, D \; \ldots \; := \; \langle| \, A \, B \, |\rangle \; : C \, D \; \ldots \; : \\
&: \widehat{A \, B} \, \widehat{C \, D} \, E \; \ldots \; := \; \langle| \, A \, B \, |\rangle \, \langle| \, C \, D \, |\rangle \; : E \; \ldots \; : \\
&: \; \widehat{A \, B} \, \widehat{C \, D \, E} \; \ldots \; := \; - \; : \widehat{A \, B} \, \widehat{C \, E} \, D \; \ldots \; := \\
&\qquad\qquad = \; - \, \langle| \, A \, B \, |\rangle \, \langle| \, C \, E \, |\rangle \; : D \; \ldots \; :
\end{aligned}
\tag{B.31}
$$

[3] The Wick's theorem in the form of (B.30) valids for the case when operators A, B, C, ... do not depend on time. Original Wick's theorem [16] was formulated for time-dependent operators, where on the l.h.s. of (B.30) there is a time-ordered product, $T(ABCD \ldots)$, where operators A, B, C, , D ... are ordered according to the increasing time from the right to the left.

where we have to change the sign in the l.h.s. if the order of operators on the l.h.s. of (B.31) requires odd number of interchanges of two operators (so called odd- permutation) in order to be obtained from the order of operators on the r.h.s. of (B.31). The second row of (B.30) involves all possible terms with one contraction, in the third row there are all possible terms with two contractions, the fourth row all terms with three contractions, etc., up to the row where all operators are contracted.

For the product of two operators the proof of the Wick's theorem (B.30) is trivial. It is evident that

$$AB =: AB : + c_{(AB)} \tag{B.32}$$

where $c_{(AB)}$ is a constant depending on the fact if the product AB requires interchange in order to obtain the order given by the normal pruduct $: AB :$, or not:

$$c_{(AB)} = \begin{cases} 0 & \text{if the order } AB \text{ corresponds to the order of } : AB : \\ \{A, B\} & \text{if the interchange is necessary} \end{cases}$$

For instance: $a\, a^+ = \{a, a^+\} - a^+\, a = \{a, a^+\} + : a\, a^+ :$.

If we perform the vacuum expectation value of (B.32) we obtain the contraction of operators A and B:

$$\widehat{A\, B} \equiv \langle |A\, B| \rangle = \langle | : A\, B : | \rangle + c_{(AB)} = \boxed{\begin{array}{c}\text{see} \\ (B.29),\ (B.24)\end{array}} =$$

$$= c_{(AB)} \tag{B.33}$$

In exprs. (B.31), (B.32), (B.33) always proper vacuum $|\rangle$ participates, that means the vacuum with respect to which the annihilation operators involved in operators A, B, C, ... give the zero if they act on this vacuum ($|\rangle = |-\rangle$ if a_ν is involved in A, B, C, ... or $|\rangle = |HF\rangle$ if α_ν is involved in A, B, C, ...).

We will apply Wick's theorem especially in the case of the group of four

operators $a^+_\mu\, a^+_\nu\, a_{\nu'}\, a_{\mu'}$ involved in the two- particle operator (B.21):

$$\begin{aligned}
a^+_\mu\, a^+_\nu\, a_{\nu'}\, a_{\mu'} \;=\; & :a^+_\mu\, a^+_\nu\, a_{\nu'}\, a_{\mu'}: + :\widehat{a^+_\mu\, a^+_\nu}\, a_{\nu'}\, a_{\mu'}: \\
& - :\widehat{a^+_\mu\, a_{\nu'}}\, a^+_\nu\, a_{\mu'}: + :\widehat{a^+_\mu\, a_{\mu'}}\, a^+_\nu\, a_{\nu'}: + :\widehat{a^+_\nu\, a_{\nu'}}\, a^+_\mu\, a_{\mu'}: \\
& - :\widehat{a^+_\nu\, a_{\mu'}}\, a^+_\mu\, a_{\nu'}: + :\widehat{a_{\nu'}\, a_{\mu'}}\, a^+_\mu\, a^+_\nu: + :\widehat{a^+_\mu\, a^+_\nu}\, \widehat{a_{\nu'}\, a_{\mu'}}: \\
& - :\widehat{a^+_\mu\, a_{\nu'}}\, \widehat{a^+_\nu\, a_{\mu'}}: + :\widehat{a^+_\mu\, a_{\mu'}}\, \widehat{a^+_\nu\, a_{\nu'}}: \\
=: & a^+_\mu\, a^+_\nu\, a_{\nu'}\, a_{\mu'}: + \langle|a^+_\mu\, a^+_\nu|\rangle\; :a_{\nu'}\, a_{\mu'}: \\
& - \langle|a^+_\mu\, a_{\nu'}|\rangle\; :a^+_\nu\, a_{\mu'}: + \langle|a^+_\mu\, a_{\mu'}|\rangle\; :a^+_\nu\, a_{\nu'}: \\
& + \langle|a^+_\nu\, a_{\nu'}|\rangle\; :a^+_\mu\, a_{\mu'}: - \langle|a^+_\nu\, a_{\mu'}|\rangle\; :a^+_\mu\, a_{\nu'}: \\
& + \langle|a_{\nu'}\, a_{\mu'}|\rangle\; :a^+_\mu\, a^+_\nu: + \langle|a^+_\mu\, a^+_\nu|\rangle\, \langle|a_{\nu'}\, a_{\mu'}|\rangle: \\
& - \langle|a^+_\mu\, a_{\nu'}|\rangle\, \langle|a^+_\nu\, a_{\mu'}|\rangle: + \langle|a^+_\mu\, a_{\mu'}|\rangle\, \langle|a^+_\nu\, a_{\nu'}|\rangle
\end{aligned} \tag{B.34}$$

If $|\rangle = |HF\rangle$ (if $|\rangle$ is the HF- ground state with the sharp value of the number of particles) then $\langle HF|a^+_\mu\, a^+_\nu|HF\rangle = \langle HF|a_\nu\, a_\mu|HF\rangle = 0$ and the expr. (B.34) is simplified

$$\begin{aligned}
a^+_\mu\, a^+_\nu\, a_{\nu'}\, a_{\mu'} \;=\; & :a^+_\mu\, a^+_\nu\, a_{\nu'}\, a_{\mu'}: \\
& - \langle|a^+_\mu\, a_{\nu'}|\rangle\; :a^+_\nu\, a_{\mu'}: + \langle|a^+_\mu\, a_{\mu'}|\rangle\; :a^+_\nu\, a_{\nu'}: \\
& + \langle|a^+_\nu\, a_{\nu'}|\rangle\; :a^+_\mu\, a_{\mu'}: - \langle|a^+_\nu\, a_{\mu'}|\rangle\; :a^+_\mu\, a_{\nu'}: \\
& - \langle|a^+_\mu\, a_{\nu'}|\rangle\, \langle|a^+_\nu\, a_{\mu'}|\rangle: + \langle|a^+_\mu\, a_{\mu'}|\rangle\, \langle|a^+_\nu\, a_{\nu'}|\rangle
\end{aligned} \tag{B.35}$$

It is necessary to realize that $\langle|a^+_\mu\, a^+_\nu|\rangle$ or $\langle|a_\nu\, a_\mu|\rangle$ is equal to zero only in the case when the vacuum $|\rangle$ has a definite number of particles (and this is the case of the particle vacuum $|-\rangle$ (B.3) or the HF-ground state $|HF\rangle$ (B.25) which is the vacuum for quasiparticle annihilation operators α_ν (B.26), that means quasiparticles without the inclusion of the pairing interactions). In the case when the pairing interactions are taken into account (see the Chapter 6) the quasiparticle creation and annihilation operators are introduced by the Bogoliubov transformation (6.33)

$$\alpha^+_\nu = \mathscr{U}_\nu a^+_\nu - \mathscr{V}_\nu a_{\bar\nu}\;, \qquad \alpha^+_{\bar\nu} = \mathscr{U}_\nu a^+_{\bar\nu} + \mathscr{V}_\nu a_\nu \tag{B.36}$$

where $\alpha^+_{\bar\nu} = \alpha^+_{\nu,\sigma=-} = \mathscr{T}^{-1}\, a^+_\nu\, \mathscr{T}$. It is known that the Bogoliubov transformation does not preserve the number of particles in the system (nucleus) and as a consequence of it (see the Chapter 6 for details) the vacuum of the

quasiparticles (B.36), $|BCS\rangle$:

$$\alpha_\nu|BCS\rangle = 0\ , \qquad \alpha_{\bar{\nu}}|BCS\rangle = 0 \tag{B.37}$$

does not describe the state with definite number of particles. When we apply the Wick's theorem to the product $a^+_\mu\ a^+_\nu\ a_{\nu'}\ a_{\mu'}$ from the point of view of this $|BCS>$ vacuum then the expectation values $\langle BCS|\ a^+_\mu a^+_\nu\ |BCS\rangle$ do not vanish and we should take into account all terms in the r.h.s. of (B.34).

B.5 Thouless theorem

The Thouless theorem [17] gives the answer to the question what is the relation between two different vacua of given system (nucleus), for instance the relation between the particle vacuum $|-\rangle$ and quasiparticle vacuum $|BCS\rangle$.
Thouless theorem states:
Let $|\Phi\rangle$ is the vacuum for the system of fermion creation and annihilation operators $(\beta^+_k,\ \beta_k)$, $\beta_k|\Phi\rangle = 0$, and let $|\Psi\rangle$ is another vacuum for another system of fermion creation and annihilation operators $(\gamma^+_k,\ \gamma_k)$, $\gamma_k|\Psi\rangle = 0$. If the relation between both systems of operators $(\beta^+_k,\ \beta_k)$ and $(\gamma^+_k,\ \gamma_k)$ is supposed to be

$$\beta_k = \sum_l Q_{lk}\ \left(\gamma_l + \sum_{l'} Z_{l\,'l}\ \gamma^+_{l'}\right)$$

where $Z_{l\,'l} = Z_{l\,l'}$ and if vacua $|\Phi\rangle$ and $|\Psi\rangle$ are not orthogonal each other: $C_0 \equiv \langle\Phi|\Psi\rangle \neq 0$, then the relation between $|\Phi\rangle$ and $|\Psi\rangle$ is following

$$|\Phi\rangle = C_0\ e^{\frac{1}{2}\sum_{l\,l'} Z_{l\,l'}\ \gamma^+_l\ \gamma^+_{l'}}\ |\Psi\rangle \tag{B.38}$$

The proof of the Thouless theorem:
We have to prove that the state $|\Phi\rangle$ given by (B.38) is the vacuum of the system of operators $(\beta^+_k,\ \beta_k)$, that means

$$\beta_k\ |\Phi\rangle = \sum_l Q_{l\,k}\ \left(\gamma_l + \sum_{l'} Z_{l\,'l}\ \gamma^+_{l'}\right)\ C_0\ \ e^{\frac{1}{2}\sum_{l\,l'} Z_{l\,l'}\ \gamma^+_l\ \gamma^+_{l'}}\ |\Psi\rangle = 0 \tag{B.39}$$

Let us take

$$\begin{aligned}
&\left(\gamma_l + \sum_{l'} Z_{l\,'l}\,\gamma_{l'}^{+}\right)\;\; e^{\frac{1}{2}\sum_{l\,l'} Z_{l\,l'}\,\gamma_l^{+}\,\gamma_{l'}^{+}}\,|\Psi\rangle = \\
&= \left[\gamma_l\, e^{\frac{1}{2}\sum_{l\,l'} Z_{l\,l'}\,\gamma_l^{+}\,\gamma_{l'}^{+}} \;+\; (\sum_{l'} Z_{l\,'l}\,\gamma_{l'}^{+})\;\; e^{\frac{1}{2}\sum_{l\,l'} Z_{l\,l'}\,\gamma_l^{+}\,\gamma_{l'}^{+}}\right]|\Psi\rangle = \\
&= \boxed{\begin{array}{c}\text{because}\\ \{\gamma_l^{+},\gamma_k^{+}\}=0\end{array}} = \\
&= \left[\gamma_l\, e^{\frac{1}{2}\sum_{l\,l'} Z_{l\,l'}\,\gamma_l^{+}\,\gamma_{l'}^{+}} \;+\; e^{\frac{1}{2}\sum_{l\,l'} Z_{l\,l'}\,\gamma_l^{+}\,\gamma_{l'}^{+}}\,(\sum_{l'} Z_{l\,'l}\,\gamma_{l'}^{+})\right]|\Psi\rangle
\end{aligned} \tag{B.40}$$

Further the first term in (B.40) will be adapted

$$\begin{aligned}
&\gamma_l\, e^{\frac{1}{2}\sum_{l\,l'} Z_{l\,l'}\,\gamma_l^{+}\,\gamma_{l'}^{+}} = \gamma_l\;\left[1+\frac{1}{2}\sum_{k\,k'} Z_{k\,k'}\gamma_k^{+}\,\gamma_{k'}^{+},+\ldots\right] = \\
&= \gamma_l + \frac{1}{2}\sum k\,k'Z_{k\,k'}\gamma_l\,\gamma_k^{+}\,\gamma_{k'}^{+},+\ldots = \boxed{\begin{array}{c}\text{because}\\ \gamma_l\,\gamma_{k'}^{+}=\delta_{lk}-\gamma_k^{+}\,\gamma_l\end{array}} = \\
&= \gamma_l + \frac{1}{2}\;\sum_{k\,k'} Z_{k\,k'}\,(\delta_{lk}-\gamma_k^{+}\,\gamma_l)\,\gamma_{k'}^{+},+\ldots = \\
&= \gamma_l + \frac{1}{2}\;\sum_{k'} Z_{l\,k'}\gamma_{k'}^{+},-\frac{1}{2}\sum_{k\,k'} Z_{k\,k'}\gamma_k^{+}\,(\delta_{lk'}-\gamma_{k'}^{+},\gamma_l)+\ldots = \\
&= \gamma_l + \frac{1}{2}\;\sum_{k'} Z_{l\,k'}\gamma_{k'}^{+},-\frac{1}{2}\;\sum_{k} Z_{k\,l}\gamma_k^{+}+\frac{1}{2}\sum_{k\,k'} Z_{k\,k'}\gamma_k^{+}\gamma_{k'}^{+},\,\gamma_l+\ldots = \\
&= \boxed{\begin{array}{c}\text{because}\\ Z_{k\,l}=-Z_{k\,l}\end{array}} = \gamma_l - \sum_{k} Z_{k\,l}\gamma_k^{+}+\frac{1}{2}\sum_{k\,k'} Z_{k\,k'}\gamma_k^{+}\gamma_{k'}^{+}\gamma_l+\ldots = \\
&= \boxed{\begin{array}{c}\text{it can be shown that each term in the Taylor epansion}\\ \text{of } e^{1/2\sum_{kk'} Z_{kk'}}\gamma_k^{+}\gamma_{k'}^{+}\text{, during anticommutation with } \gamma_l\\ \text{gives itself times } (\gamma_l-\sum_k Z_{lk}\gamma_k^{+})\end{array}} =
\end{aligned}$$

$$= \left(1 + \frac{1}{2} \sum_{kk'} Z_{kk'} \gamma_k^+ \gamma_{k'}^+ + \ldots\right) \left(\gamma_l - \sum k Z_{kl} \gamma_k^+\right) =$$

$$= e^{\frac{1}{2}\sum_{kk'} Z_{kk'} \gamma_k^+ \gamma_{k'}^+} \left(\gamma_l - \sum_k Z_{kl}\, \gamma_k^+\right) \tag{B.41}$$

The substitution of (B.41) into (B.40) gives

$$\left(\gamma_l + \sum_{l'} Z_{l'l} \gamma_{l'}^+\right) e^{\frac{1}{2}\sum_{kk'} Z_{kk'} \gamma_k^+ \gamma_{k'}^+} |\Psi> =$$

$$= e^{\frac{1}{2}\sum_{kk'} Z_{kk'} \gamma_k^+ \gamma_{k'}^+} \left(\gamma_l - \sum_k Z_{kl} \gamma_{l'}^+\right) +$$

$$+ e^{\frac{1}{2}\sum_{kk'} Z_{kk'} \gamma_k^+ \gamma_{k'}^+} \left(\sum_{l'} Z_{l'l} \gamma_{l'}^+\right) = 0 \tag{B.42}$$

Therefore the relation (B.39) valids and the proof of the Thouless theorem is completed.

The constant C_0 in (B.38) is connected with the normalization of the wave functions $|\Phi>$ and $|\Psi>$ (if $<\Phi|\Psi>= 0$ then the normalization cannot be done - see [9] for details).

Further we will discuss a special case of the Thouless theorem. Let a_ν^+ are creation operators of some Hartree-Fock basis in the ground state of the nucleus

$$|HF\rangle = \prod_{i_<=1}^{A} a_{i_<}^+ |-\rangle \tag{B.43}$$

The Thouless theorem states that any other product $|HF\rangle'$ of other HF basis of given nucleus, which is not orthogonal to the original product $|HF\rangle$ ($\langle HF|HF\rangle' \neq 0$) should be expressed in the nonnormalized form by the following expression (using also Pauli principle)

$$|HF\rangle' = e^{\sum_{m_>} \sum_{i_<} C_{m_> i_<} a_{m_>}^+ a_{i_<}^+} |HF\rangle \tag{B.44}$$

where $C_{m_> i_<}$ determine the relation between the original HF basis with creaition aperators a_ν^+ and the new basis with the new creation operators b_ν^+ given by

$$b_{i_<}^+ = a_{i_<}^+ + \sum_{m_>} C_{m_> i_<}\, a_{m_>}^+$$

$$b_{m_>}^+ = a_{m_<}^+ + \sum_{i_<} C_{m_> i_<}\, a_{i_<}^+ \tag{B.45}$$

and (B.43) gives

$$|HF\rangle' = \prod_{i_<=1}^{A} b^+_{i_<} \, |-\rangle \tag{B.46}$$

C. Approximative solution of the nonstationary problems

C.1 Schroedinger and Dirac description of the time evolution

Let us suppose that some quantum system with the Hamiltonian $\hat{H}$ is in the state $|\varphi\rangle \equiv |\varphi(t_0)\rangle$ in some initial time t_0 and we are interested in the probability with which this system is found in some other state $|\psi\rangle$ in the time t ($t > t_0$). This question can be answered within so called Schroedinger or Dirac description of the time evolution of the system.

Schroedinger's description
The time evolution is given by the Schroedinger equation $i\hbar \frac{\partial|\varphi(t)\rangle}{\partial t} = \hat{H}\,|\varphi(t)\rangle$. If the system is in the state $|\varphi\rangle = |\varphi(t_0)\rangle$ in the time t_0 then its state $|\varphi(t)\rangle$ in the time t is

$$|\varphi(t)\rangle = \hat{U}(t,t_0)\,|\varphi\rangle = e^{-\frac{i}{\hbar}\hat{H}\,(t-t_0)}|\varphi\rangle\ , \quad (\hat{U}(t_0,t_0) = 1) \tag{C.1}$$

because in accordance with the Schroedinger equation we have

$$i\hbar\,\frac{\partial|\varphi(t)\rangle}{\partial t} = i\hbar\,(-\frac{i}{\hbar})\,e^{-\frac{i}{\hbar}\hat{H}\,(t-t_0)}\hat{H}\,|\varphi\rangle = \hat{H}\,|\varphi(t)\rangle$$

The probability that in the time t (when the system state is given by $|\varphi(t)\rangle$) the system is found in the concrete state $|\psi\rangle$ is (see e.g. [14])

$$w_{\varphi\to\psi}(t,t_0) = |\langle\psi\mid\varphi(t)\rangle|^2 = |\langle\psi\,|\hat{U}(t,t_0)|\,\varphi\rangle|^2 \tag{C.2}$$

The time dependence of the Schroedinger evolution operator $\hat{U}(t,t_0)$ is driven by the following equation (followd from (C.1))

$$i\hbar\,\frac{\partial\hat{U}(t,t_0)}{\partial t} = i\hbar(-\frac{i}{\hbar}\hat{H})e^{-\frac{i}{\hbar}\hat{H}\,(t-t_0)}i\hbar = \hat{H}\,\hat{U}(t,t_0) \tag{C.3}$$

$$\Longrightarrow$$

$$\hat{U}(t,t_0) =$$

$$= \frac{1}{i\hbar}\int_{t_0}^{t} dt'\, \hat{H}(t')\, \hat{U}(t',t_0) = \boxed{\begin{array}{c}\text{iterative}\\ \text{substitution of } \hat{U}(t,t_0)\end{array}} =$$

$$= 1 + \frac{1}{i\hbar}\int_{t_0}^{t} dt_1\, \hat{H}(t_1) + (\frac{1}{i\hbar})^2 \int_{t_0}^{t} dt_2 \hat{H}(t_2) \int_{t_0}^{t_2} dt_1 \hat{H}(t_1) \;+\; \ldots =$$

$$= \sum_{n=0}^{\infty} \hat{U}^{(n)}(t,t_0) \tag{C.4}$$

where

$$\hat{U}^{(n)}(t,t_0) =$$

$$= 1 + \frac{1}{(i\hbar)^n}\int_{t_0}^{t} \hat{H}(t_n)\, dt_n \int_{t_0}^{t_n} \hat{H}(t_{n-1})\, dt_{n-1} \ldots \int_{t_0}^{t_2} \hat{H}(t_1)\, dt_1 \tag{C.5}$$

for $n \geq 1$ and

$$\hat{U}^{(0)}(t,t_0) = 1$$

for $n = 0$.

Dirac's description

Dirac's description is suitable in the case when the Hamiltonian of the system is written in the form of the sum of unperturbed part $\hat{H}_0$ and the perturbation (interaction) part $\hat{H}_I$ ($[\, \hat{H}_0,\ \hat{H}_I \,] = 0$)

$$\hat{H} = \hat{H}_0 + \hat{H}_I \tag{C.6}$$

Instead of the standard Schroedinger wave function $|\varphi(t)\rangle$ we introduce so called Dirac's state $|\varphi_D(t)\rangle$ by the following definition

$$|\varphi_D(t) = \hat{S}_D(t,t_0)\, |\varphi(t)\rangle \tag{C.7}$$

where

$$\hat{S}_D(t,t_0) = e^{\frac{i}{\hbar}\,\hat{H}_0\,(t-t_0)} \tag{C.8}$$

The Dirac's wave function $|\varphi_D(t)\rangle$ is time-evoluted according to the following equation

$$\begin{aligned} & i\hbar\,\frac{\partial|\varphi_D(t)\rangle}{\partial t} = i\hbar\,\frac{\partial}{\partial t}\,\left(e^{\frac{i}{\hbar}\hat{H}_0\,(t-t_0)}|\varphi(t)\rangle\right) = \\ & = -\hat{H}_0\,\hat{S}_D(t,t_0)\,|\varphi(t)\rangle + \hat{S}_D(t,t_0)\,\hat{H}\,|\varphi(t)\rangle = \\ & = \boxed{\begin{array}{c}\text{because}\\ \left[\hat{H}_0,\hat{S}_D(t,t_0)\right]=0\end{array}} = \hat{S}_D(t,t_0)\,\hat{H}_I\,|\varphi(t)\rangle = \\ & = \left(\hat{H}_I\right)_D\,|\varphi_D(t)\rangle \end{aligned} \tag{C.9}$$

where

$$\left(\hat{H}_I\right)_D \equiv \hat{S}_D(t,t_0)\,\hat{H}_I\,\hat{S}_D^{-1}(t,t_0) \tag{C.10}$$

The differential equation (C.9) can be formally solved and we obtain

$$|\varphi_D(t)\rangle = e^{-\frac{i}{\hbar}\,(\hat{H}_I)_D\,(t-t_0)}\,|\varphi(t_0)\rangle \equiv \hat{S}(t,t_0)\,|\varphi\rangle \tag{C.11}$$

where $\hat{S}(t,t_0) = e^{-\frac{i}{\hbar}\,(\hat{H}_I)_D\,(t-t_0)}$ is the Dirac's evolution operator. Similarly as in (C.2) the probability of the finding of the system in the particular state $|\psi\rangle$ (with the Dirac's equivalent $|\psi\rangle_D = \hat{S}_D(t,t_0)\,|\psi\rangle$) at the time t ($t \geq t_0$) is given by

$$\begin{aligned} & w_{\varphi\to\psi}(t,t_0) = |\,\langle\psi_D\,|\,\varphi_D(t)\rangle|^2 = |\langle\psi|\hat{S}_D^{-1}(t,t_0)|\varphi_D(t)\rangle|^2 = \\ & = \left|\langle\psi\,|\hat{S}_D^{-1}(t,t_0)\,\hat{S}(t,t_0)|\,\varphi\rangle\right|^2 \end{aligned} \tag{C.12}$$

If, moreover, the states $|\varphi\rangle$ and $|\psi\rangle$ are eigenstates of the unperturbed Hamiltonian $\hat{H}_0$ ($\hat{H}_0|j\rangle = E_j^{(0)}|j\rangle,\ |\varphi\rangle = |j\rangle,\ \hat{H}_0|k\rangle = E_k^{(0)}|k\rangle,\ |\psi\rangle = |k\rangle$) then

$$\hat{S}_D(t,t_0)|\psi\rangle = e^{\frac{i}{\hbar}\,\hat{H}_0\,(t-t_0)}|k\rangle = e^{\frac{i}{\hbar}\,E_k^{(0)}\,(t-t_0)}|k\rangle$$

and therefore

$$\begin{aligned} & w_{j\to k}(t,t_0) = \left|e^{-\frac{i}{\hbar}\,E_k^{(0)}\,(t-t_0)}\right|^2\ \left|\langle k|\hat{S}(t,t_0)|j\rangle\right|^2 = \\ & = \left|\langle k|\hat{S}(t,t_0)|j\rangle\right|^2 \end{aligned} \tag{C.13}$$

From the definition of the Dirac's evolution operator (C.11), $\hat{S}(t,t_0) = e^{-\frac{i}{\hbar}(\hat{H}_I)_D\,(t-t_0)}$, it follows that it fulfils the following equation

$$i\hbar\,\frac{\partial\hat{S}(t,t_0)}{\partial t} = (\hat{H}_I)_D\,(t-t_0) \tag{C.14}$$

and this equation can be formally solved (in the analogy with (C.4)) [1]

$$\hat{S}(t,t_0) = \frac{1}{i\hbar}\int_{t_0}^{t} dt' \ \left(\hat{H}_I(t)\right)_D \ \hat{S}(t,t_0) =$$

$$= \boxed{\begin{array}{c}\text{in the analogy with}\\ (C.4)\end{array}} = \sum_{n=0}^{\infty} \hat{S}^{(n)}(t,t_0) \qquad \text{(C.15)}$$

where

$$\hat{S}^{(n)}(t,t_0) = \frac{1}{(i\hbar)^n}$$
$$\int_{t_0}^{t} \left(\hat{H}_I(t_n)\right)_D \ dt_n \int_{t_0}^{t_n} \left(\hat{H}_I(t_{n-1})\right)_D \ dt_{n-1} \ \ldots \int_{t_0}^{t_2} \left(\hat{H}_I(t_1)\right)_D \ dt_1 \qquad \text{(C.16)}$$

for $n \geq 1$ and

$$\hat{S}^{(n=0)}(t,t_0) = 1$$

for $n = 0$. From the comparison of exprs. (C.4), (C.5) with (C.15), (C.16) the advantage or the Dirac's description over the Schroedinger description can be seen. Since the Dirac's description is usually applied when the absolute values of the matrix elements of the perturbation, $|\langle k|(\hat{H}_I)_D|j\rangle|$, are less than the absolute values of the matrix elements of the total Hamiltonian, $|\langle k|\hat{H}|j\rangle|$, for all states $|k\rangle$ and $|j\rangle$, one can expect the faster convergence of the series (C.15) in the comparison with the series (C.4). Usually only the first $n = 1$ term of the series (C.15) is used in the expression (C.13) for the probability $w_{j\to k}(t,t_0)$ for the evolution of the nucleus from the initial state $|j\rangle$ to the final state $|k\rangle$ during the time interval $\langle t_0, t\rangle$. Then (C.13) is approximated by (the 1-st order of the perturbation theory)

$$w_{j\to k}(t,t_0) \approx |\langle k\,|\hat{S}^{(1)}(t,t_0)|j\rangle|^2 \qquad \text{(C.17)}$$

where

$$\langle k\,|\hat{S}^{(1)}(t,t_0)|\,j\rangle = \frac{1}{i\hbar}\int_{t_0}^{t} dt\,'\langle k\,|(\hat{H}_I(t\,'))_D|\,j\rangle =$$
$$= \frac{1}{i\hbar}\int_{t_0}^{t} dt\,'\langle k\,|\hat{S}_D(t\,',t_0)\,\hat{H}_I(t\,')\,\hat{S}_D^{-1}(t,t_0)|\,j\rangle =$$
$$= \frac{e^{-\frac{i}{\hbar}(E_k-E_j)\,t_0}}{i\hbar}\int_{t_0}^{t} dt\,'\,e^{\frac{i}{\hbar}\,(E_k-E_j)\,t\,'}\,\langle k\,|\hat{H}_I(t\,')|\,j\rangle \qquad \text{(C.18)}$$

[1] The series (C.15) is known in the literature as the Dyson series for the evolution operator in the Dirac's representation

D. Scattering of the spinless particle

D.1 Stationary states of the particle scattering on the spherically symmetric potential

If the spinless particle is scattered by the central potential $\hat{V}(r)$ depending only on the radial coordinate then the wave function of this particle can be written as follows ($\hat{r} \equiv \theta,\, \varphi$)

$$\Psi_{Elm}(\vec{r}) = R_{El}(r)\, Y_{lm}(\hat{r}) \tag{D.1}$$

where $Y_{lm}(\hat{r})$ is the spherical function depending on the angles of the spherical coordinate system and the radial function $R_{El}(r)$ is given by the stationary Schroedinger equation

$$\frac{d^2R_{EL}(r)}{dr^2} + \frac{2}{r}\frac{dR_{El}(r)}{dr} + \\ + \frac{2M}{\hbar^2}\left(E - \hat{V}(r) - \frac{\hbar^2}{2M}\,\frac{l(l+1)}{r^2}\right) R_{El}(r) = 0 \tag{D.2}$$

where E is the scattering energy. Energy scale is given by the asymptotic value of the potential $\hat{V}(r)$, $V_\infty = \lim_{r\to\infty} V(r)$:

for $E > V_\infty$ we have a smooth spectrum
for $E < V_\infty$ we have a discrete spectrum

Usually the energy scale is chosen so that

$$V_\infty = 0 \tag{D.3}$$

D.1.1 Scattering on a spherically symmetric finite-range potential ($\hat{V}(r) = 0$ for $r \geq a$)

For the region $r \geq a$ the Shroedinger equation (D.2) for the radial wave function $R_{El}(r)$ is (we suppose the scattering problem with $E > 0$)

$$\frac{d^2R_{EL}(r)}{dr^2} + \frac{2}{r}\frac{dR_{El}(r)}{dr} + \left(k^2 - \frac{l(l+1)}{r^2}\right) R_{El}(r) = 0 \tag{D.4}$$

with $k^2 = 2ME/\hbar^2$. This equation is the same as the differential equation determining the spherical Bessel function $j_l(kr)$ or spherical Neumann function $n_l(kr)$ (see e.g. [14]). Therefore the general solution of (D.4) can be written as the linear combination

$$R_{kl}(r) = A_l\, j_l(kr) + B_l\, n_l(kr) \tag{D.5}$$

with the well-known asymptotic behaviour of the spherical Bessel and Neumann functions

$$\begin{aligned} j_l(kr) &\stackrel{r\to\infty}{\longrightarrow} \frac{sin(kr - \frac{\pi l}{2})}{kr} \\ n_l(kr) &\stackrel{r\to\infty}{\longrightarrow} -\frac{cos(kr - \frac{\pi l}{2})}{kr} \end{aligned} \tag{D.6}$$

Instead of the amplitudes A_l and B_l we can introduce new ones, C and δ_l

$$A_l = C\, \cos\delta_l \qquad\qquad B_l = -\,C\, \sin\delta_l \tag{D.7}$$

and the radial wave function (D.5) can be rewritten as follows

$$\begin{aligned} R_{kl}(r) = C\, [\cos\delta_l\, j_l(kr) - \sin\delta_l\, n_l(kr)] &\stackrel{r\to\infty}{\longrightarrow} \\ \to \quad \frac{C}{kr}\, sin(kr - \frac{\pi l}{2} + \delta_l) & \end{aligned} \tag{D.8}$$

and the normalization condition $\int d^3r\, \Psi^*_{Elm}(\vec{r})\, \Psi_{E'l'm'}(\vec{r}) = \delta(E - E')\, \delta_{ll'}\, \delta_{mm'}$ gives $C = \sqrt{\frac{2}{\pi}}k$.

The radial wave function $R_{kl}(r)$ in the asymptotic region $r \to \infty$ feels the finite-range potential through the phase shift δ_l as it can be seen if we compare (D.8) with the asymptotic expression (D.6) for the spherical Bessel function. The value of the phase shift δ_l for given finite-range central potential $\hat{V}(r)$ can be obtained from the condition of the smoothness of the logaritmic derivative of $R_{El}(r)$ in the point $r = a$ (see e.g. [14])

$$\lim_{r\to a-} \frac{\frac{dR_{El}(r)}{dr}}{R_{El}(r)} = \lim_{r\to a+} \frac{\frac{dR_{kl}(r)}{dr}}{R_{kl}(r)} \tag{D.9}$$

where $R_{El}(r)$ is the solution of (D.2) for given potential $\hat{V}(r)$.

It can be shown that the asymptotic behaviour (D.8) is valid not only for the wave function $R_{El}(r)$ of the finite-range potential but also for all potentials which go to zero with $r \to \infty$ faster than $1/r$.

D.1.2 Scattering on the Coulomb potential $\hat{V}(r) = \frac{\gamma}{r}$

In this case we look for the solution of the equation

$$\frac{d^2 R_{EL}(r)}{dr^2} + \frac{2}{r}\frac{dR_{El}(r)}{dr} + \\ + \frac{2M}{\hbar^2}\left(E - \frac{\gamma}{r} - \frac{\hbar^2}{2M}\,\frac{l(l+1)}{r^2}\right) R_{El}(r) = 0 \tag{D.10}$$

This second order differential equation has always two linearly independent solutions for $E > 0$, $f_l(\gamma, kr)$ and $g_l(\gamma, kr)$, and these two solutions differ mutually (except other) by the asymptotic behaviour (similarly as the spherical Bessel function $j_l(kr$ differes from the spherical Neumann functions $n_l(kr)$ - see (D.6)):

$$R^{(1)}_{kl}(r) = \sqrt{\frac{2}{\pi}}\, k\, f_l(\gamma, kr) \qquad\qquad R^{(2)}_{kl}(r) = \sqrt{\frac{2}{\pi}}\, k\, g_l(\gamma, kr)$$

$$f_l(\gamma, kr) \quad \stackrel{r\to\infty}{\longrightarrow} \quad \frac{sin(kr - \eta\, ln2kr - \frac{\pi l}{2} + \sigma_l)}{kr}$$

$$g_l(\gamma, kr) \quad \stackrel{r\to\infty}{\longrightarrow} \quad -\frac{cos(kr - \eta\, ln2kr - \frac{\pi l}{2} + \sigma_l)}{kr} \tag{D.11}$$

where $\eta = \frac{\gamma}{\hbar}\sqrt{\frac{M}{2E}}$ and σ_l is so called Coulomb shift which is defined as (see e.g. [23])

$$\Gamma(l + 1 + i\,\eta) = |\Gamma(l + 1 + i\,\eta)|\; e^{i\sigma_l} \tag{D.12}$$

where $\Gamma(z)$ is the Γ- function known from the mathematics. If we switch off the Coulomb field the Coulomb functions $f_l(kr)$ and $g_l(kr)$ become spherical Bessel and spherical Neumann functions, respectively

$$\lim_{\gamma\to 0} f_l(\gamma, kr) = j_l(kr), \qquad \lim_{\gamma\to 0} g_l(\gamma, kr) = n_l(kr) \tag{D.13}$$

D.1.3 Scattering on a superposition of the finite-range central potential and the Coulomb potential

The radial wave function $R_{El}(r)$ in this case is the solution of the following equation

$$\frac{d^2 R_{EL}(r)}{dr^2} + \frac{2}{r}\frac{dR_{El}(r)}{dr} + \\ + \frac{2M}{\hbar^2}\left(E - \hat{V}(r) - \frac{\gamma}{r} - \frac{\hbar^2}{2M}\,\frac{l(l+1)}{r^2}\right) R_{El}(r) = 0 \tag{D.14}$$

where $\hat{V}(r) = 0$ for $r > a$. Therefore for $r > a$ the equation (D.14) takes the form (D.10) and the function $R_{El}(r)$ is a combination of the Coulomb functions $f_l(\gamma, kr)$ and $g_l(\gamma, kr)$ in the region $r > a$:

$$R_{kl}(r) = C\ [\cos\delta'_l\, f_l(kr) - \sin\delta'_l\, g_l(kr)] \quad \stackrel{r\to\infty}{\longrightarrow}$$

$$\boxed{\begin{array}{c}\text{see}\\(D.11)\end{array}} \to \quad \frac{C}{kr}\, sin(kr - \eta\, ln2kr - \frac{\pi l}{2} + \sigma_l + \delta'_l) \tag{D.15}$$

where $C = \sqrt{\frac{2}{\pi}}\, k$ and the phase shift δ'_l can be again determined from the condition of the smoothness of the logaritmic derivative of $R_{El}(r)$ in the point $r = a$ (see (D.9)) but now the function $R_{El}(r)$ in the region $r \leq a$ should be determined from (D.14). Again the presence of the phase shift δ'_l in the asymptotic radial wave function (D.15) reflects the presence of finite-range scattering central potential in the small region $r \leq a$ in the vicinity of the origin of coordinates.

D.2 Cross section of the spinless particle scattering

D.2.1 Elastic scattering of the spinless particle

Let us assume the spinless particle scattering on a fixed target in the laboratory system of coordinates [1] through central finite-range potential. The stationary wave function of the elastic scattered particles in the asymptotic region $r \to \infty$ can be searched for in the form of the sum of the plane wave (describing the incident beam of particles) and going out spherical wave (describing the scattered particles)

$$\Psi_{\vec{k},el}(\vec{r}) \quad \stackrel{r\to\infty}{\longrightarrow} \quad e^{i\,\vec{k}\cdot\vec{r}} + f_{el}(\vec{k}, \vec{k}\,')\, \frac{e^{ikr}}{r} \tag{D.16}$$

where $\hbar\vec{k}$ is the linear moment of the incident particle, $\vec{k}\,' = k\,\frac{\vec{r}}{r}$ (we suppose elastic scattering when $|\vec{k}\,'| = |\vec{k}| = k$ and the scattering center is placed into the origin of coordinates), $k^2 = 2ME/\hbar^2$ (M is the mass of the scattering particle and $E > 0$ is its energy). Further we introduce coordinate frame in such a way that the direction of the z-axis coincides with the direction of the

[1] The scattering of two particles in the center of mass frame is described by the same way as the scattering of one particle on a fixed target in the laboratory frame

vector $\vec{k}$. In such a case the scattering angle ϑ (the angle between vectors $\vec{k}$ and $\vec{k}\,'$) is simultaneously the angle between $\vec{k}$ and $\vec{r}$ (that means the ϑ angle from the spherical coordinate system - see fig D.1). The symbol $f_{el}(\vec{k},\vec{k}\,')$ in

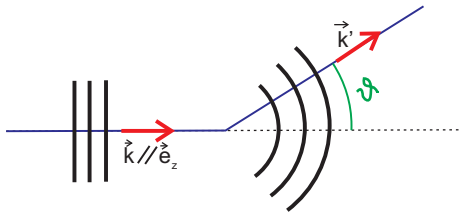


Figure D.1: Elastic scattering of the incident plane wave beam. Scattered particles are represented by outgoing spherical waves, ϑ is the scattering angle (schematic figure).

(D.16) stands for the scattering amplitude which determines the differential cross section $\frac{d\sigma_{el}}{d\Omega}$ of the eleastic scattering - see further (we suppose only eleastic scattering is present without any inelastic processes)

$$\frac{d\sigma_{el}}{d\Omega} = \frac{\left(\begin{array}{c}\text{the number of particles scattered on one target}\\ \text{particle into the unit space angle in the direction}\\ \text{of the vector } \vec{k}\,' \text{ in one second}\end{array}\right)}{\text{the intensity of the incident beam}} =$$

$$= \frac{\left|\vec{j}_R(\vec{r})\right|^2 r^2}{\left|\vec{j}_D(\vec{r})\right|^2} \qquad \text{(D.17)}$$

where $\vec{j}_D(\vec{r})$ is the probability current of the incident plane wave and $\vec{j}_R(\vec{r})$ is the radial probability current of the scattered out-going particles:

$$\vec{j}_D(\vec{r}) = \frac{\hbar}{2iM}\left[e^{-i\,\vec{k}\cdot\vec{r}}\vec{\nabla}e^{i\,\vec{k}\cdot\vec{r}} - e^{i\,\vec{k}\cdot\vec{r}}\vec{\nabla}e^{-i\,\vec{k}\cdot\vec{r}}\right] = \frac{\hbar\vec{k}}{M}$$

$$\vec{j}_R(\vec{r}) = \left(\begin{array}{c}\text{because } \vec{k}\,' = k\,\frac{\vec{r}}{r} = k\,\vec{e}_r\\ \vec{\nabla} = \vec{e}_r\,\frac{\partial}{\partial r} + \vec{e}_\vartheta\,\frac{1}{r}\frac{\partial}{\partial\vartheta} + \vec{e}_\varphi\,\frac{1}{r\sin\vartheta}\frac{\partial}{\partial\varphi}\end{array}\right) =$$

$$= \frac{\hbar\,\vec{e}_r}{2iM}\left|f_{el}(\vec{k},\vec{k}\,')\right|^2\left[\frac{e^{-ikr}}{r}\frac{\partial}{\partial r}\frac{e^{ikr}}{r} - \frac{e^{ikr}}{r}\frac{\partial}{\partial r}\frac{e^{-ikr}}{r}\right] =$$

$$= \frac{\left|f_{el}(\vec{k},\vec{k}\,')\right|^2}{r^2}\frac{\hbar\vec{k}\,'}{M} \qquad \text{(D.18)}$$

The substitution of (D.18) into (D.17) gives

$$\frac{d\sigma_{el}}{d\Omega} = \left| f_{el}(\vec{k}, \vec{k}\,') \right|^2 \tag{D.19}$$

In the case of the central scattering potential the wave function $\Psi_{\vec{k},el}(\vec{r})$ does not depend on the angle φ and the function $\Psi_{\vec{k},el}(\vec{r})$ can be decomposed into the Legendre polynomials $P_L(\cos\vartheta)$ as follows

$$\Psi_{\vec{k},el}(\vec{r}) = \Psi_{\vec{k},el}(r,\vec{\vartheta}) = \sum_{l=0}^{\infty} \frac{u_{lk}(r)}{r}\, P_l(\cos\vartheta) \tag{D.20}$$

where the function $u_{lk}(r)r$ fulfils the following equation

$$\left[\frac{d^2}{dr^2} + k^2 - \frac{2M}{\hbar^2}\, V(r) - \frac{l(l+1)}{r^2}\right]\, u_{lk}(r) = 0 \tag{D.21}$$

with the boundary condition $u_{lk}(r=0) = 0$ (we require the finite value of $u_{lk}(r)/r$ in the coordinate origing $r = 0$ fm because the particle wave function in the origin should be finite).

The plane wave function in the asymptotic expression for the function $\Psi_{\vec{r},\,el}(\vec{r})$ (see (D.16)) can be also decomposed into the Legendre polynomials $P_l(\cos\vartheta)$ (see e.g. [2])

$$\begin{aligned} e^{i\,\vec{k}\cdot\vec{r}} = e^{i\,kz} = e^{i\,kr\cos\vartheta} = \sum_{l=0}^{\infty}(2l+1)\, i^l\, j_l(kr)\, P_l(\cos\vartheta) \rightarrow \\ \overset{r\to\infty}{\longrightarrow} \quad \boxed{\begin{array}{c}\text{see}\\ (D.6)\end{array}} \rightarrow \sum_{l=0}^{\infty}(2l+1)\, i^l\, \frac{\sin\left(kr - \frac{\pi l}{2}\right)}{kr}\, P_l(\cos\vartheta) \end{aligned} \tag{D.22}$$

In the asymptotic region(where $V(r) = 0$) the presence of the nonzero $\hat{V}(r)$ in the vicinity of the coordinate origin comes out by the appearing of the phase shift δ_l in the asymptotic expression for $u_{lk}(r \to \infty)$ (compare with (D.8))

$$u_{lk}(r) \quad \overset{r\to\infty}{\longrightarrow} \quad (2l+1)\, i^{\,l}\, \frac{C_l}{k}\, \sin\left(kr - \frac{\pi l}{2} + \delta_l\right) \tag{D.23}$$

The function $u_{lk}(r)$ in (D.23) is not normalized as the function $r\, R_{kl}(r)$ in (D.8) and the parameter C_l is determined from the requirement that the function $\Psi_{\vec{k},\,el}(\vec{r}) - e^{i\,\vec{k}\cdot\vec{r}}$ should involve only spherical outgoing waves (in

accordance with (D.16))

$$\Psi_{\vec{k},\,el}(\vec{r}) - e^{i\,\vec{k}\cdot\vec{r}} \quad \stackrel{r\to\infty}{\longrightarrow} \quad \boxed{\begin{array}{c}\text{see}\\ (D.22)\text{ and }(D.23)\end{array}} \to$$

$$\to \sum_{l=0}^{\infty}(2l+1)\,i^{l}\,\frac{1}{kr}\,P_l(\cos\vartheta)$$

$$\cdot\left[C_l\,\sin\left(kr-\frac{\pi l}{2}+\delta_l\right)-\sin\left(kr-\frac{\pi l}{2}\right)\right]=$$

$$=\sum_{l=0}^{\infty}(2l+1)\,i^{\,l}\,\frac{1}{2ikr}\,P_l(\cos\vartheta)$$

$$\cdot\left[C_l\,\left(e^{i\,(kr-\frac{\pi l}{2}+\delta_l)}-e^{-i\,(kr-\frac{\pi l}{2}+\delta_l)}\right)-\left(e^{i\,(kr-\frac{\pi l}{2})}-e^{-i\,(kr-\frac{\pi l}{2})}\right)\right]=$$

$$=\sum_{l=0}^{\infty}(2l+1)\,i^{\,l}\,\frac{1}{2ikr}\,P_l(\cos\vartheta)$$

$$\cdot\left[e^{i\frac{\pi l}{2}}\left(1-C_l\,e^{-\delta_l}\right)\,e^{-ikr}+e^{-i\frac{\pi l}{2}}\left(C_l\,e^{\delta_l}-1\right)\,e^{ikr}\right]$$

In order this function is only outgoing spherical wave (containing only e^{ikr}/r) the following condition should be fulfiled

$$1-C_l\,e^{-i\delta_l}=0 \qquad \Rightarrow \qquad C_l=e^{i\,\delta_l}$$

and we have

$$\Psi_{\vec{r},\,el}(\vec{r}) - e^{i\,\vec{k}\cdot\vec{r}} \quad \stackrel{r\to\infty}{\longrightarrow}$$

$$\to \sum_{l=0}^{\infty}(2l+1)\,i^{\,l}\,P_l(\cos\vartheta)\frac{e^{ikr}}{2ikr}e^{-i\frac{\pi l}{2}}\,\left(e^{2i\delta_l}-1\right) \tag{D.24}$$

and corresponding scattering amplitude $f(\vec{k},\vec{k}\,')=f(\vartheta)$ is (using the comparison of (D.24) with (D.16) and $i^{\,l}=e^{i\frac{\pi l}{2}}$)

$$f_{el}(\vartheta)=\frac{1}{2ik}\,\sum_{l=0}^{\infty}(2l+1)\left[e^{2i\delta_l}-1\right]\,P_l(\cos\vartheta)=$$

$$=\frac{1}{k}\,\sum_{l=0}^{\infty}(2l+1)\,e^{i\delta_l}\,\sin\delta_l\,P_l(\cos\vartheta) \tag{D.25}$$

and the substitution of (D.25) into (D.19) gives the differential cross section of the elastic scattering

$$\frac{d\sigma_{el}}{d\Omega}(\vartheta) = \frac{1}{k^2} \left| \sum_{l=0}^{\infty} (2l+1)\, e^{i\,\delta_l}\, \sin\delta_l\, P_l(\cos\vartheta) \right|^2 \tag{D.26}$$

The integral cross section of the elastic scattering is then given by the integration of (D.26) over the whole space angle

$$\sigma_{el} = \int_0^{2\pi} d\varphi \int_{-1}^{+1} d(\cos\vartheta)\, \frac{d\sigma_{el}}{d\Omega} = \frac{\pi}{k^2} \sum_{l=0}^{\infty} (2l+1) \left| e^{2i\,\delta_l} - 1 \right|^2 \tag{D.27}$$

In the nuclear or particle physics literature so called scattering S-matrix is introduced for the case of the description of the nuclear or particle rections. In the case when only one outgoing final channel is opened for given initial channel (like in our case of the only elastic scattering on the central potential) the S-matrix is reduced to one element (see e.g. [23, 14])

$$S_{el}^{(l)} \equiv e^{2i\,\delta_l} \tag{D.28}$$

and the integral cross section (D.27) of the only elastic process is

$$\sigma_{el} = \frac{\pi}{k^2} \sum_{l=0}^{\infty} (2l+1) \left| S_{el}^{(l)} - 1 \right|^2 \tag{D.29}$$

In the case when several final channels f are opened for given initial channel i the S-matrix is more dimensional matrix and the integral cross-section of the process $i \to f$ is [14, 23]

$$\sigma_{i\to f} = \frac{\pi}{k_i^2} \sum_{l=0}^{\infty} (2l+1) \left| S_{fi}^{(l)} - \delta_{fi} \right|^2 \tag{D.30}$$

Going back to the pure elastic scattering the asymptotic expression for the wave function $\Psi_{\vec{k},el}(\vec{r})$ is following (using the substitution of (D.22) and (D.28) in (D.24)

$$\Psi_{\vec{k},el}(\vec{r}) \quad \stackrel{r\to\infty}{\longrightarrow} \quad \sum_{l=0}^{\infty} (2l+1)\, P_l(\cos\vartheta) \frac{1}{2ik} \cdot \left[S_{el}^{(l)}\, \frac{e^{ikr}}{r} - (-1)^l\, \frac{e^{-ikr}}{r} \right] \tag{D.31}$$

It is evident that if only elastic scattering is possible then the flux of the probability of the ingoing wave $\frac{e^{-ikr}}{r}$ should be the same as the probability flux of the outgoing wave $\frac{e^{ikr}}{r}$ and therefore [2]

$$\left|S_{el}^{(l)}\right|^2 = 1 \tag{D.32}$$

In the case when except the elastic channel also other inelastic final channels are opened the part of the probability, brought into the target by the ingoing spherical wave $\frac{e^{-ikr}}{r}$ of the elastic channel, is transformed to the outgoing spherical waves on other final channels. Therefore the outgoing spherical wave in the elastic channel has smaller flux than in the case of the only elastic channel opened (without other inelastic channels). So, if except the elastic channel also other inelastic channels are present, the equation (D.32) is changed into the following inequality

$$\left|S_{el}^{(l)}\right|^2 < 1 \tag{D.33}$$

This can be formally achieved if instead of the real phase shift δ_l in (D.28) the complex phase shift $\delta_l' = \delta_L^{(1)} + i\delta_l^{(2)}$ is used ($\delta_l^{(1)}$ and $\delta_l^{(2)}$ are real). Then

$$S_{el}^{(l)} = e^{2\,i\delta_l'} = e^{-2\delta_l^{(2)}}\; e^{2\,i\delta_l^{(1)}} \quad \Rightarrow \quad \begin{array}{l} ReS_{el}^{(l)} = e^{-2\delta_l^{(2)}}\cos 2\delta_l^{(1)} \\ ImS_{el}^{(l)} = e^{-2\delta_l^{(2)}}\sin 2\delta_l^{(1)} \end{array} \tag{D.34}$$

and $|S_{el}^{(l)}|^2 = e^{-4\delta_l^{(2)}} < 1$ for $4\delta_l^{(2)} > 0$.

The complex phase shift is connected with the fact that the presence of other inelastic channels can be simulated in the equation (D.2) for the radial wave function $R_{El}(r)$ of the elastic channel by the using of the complex potential $\hat{V}(r)$ (so called optical potential - see the Chapter 11 for details). The usage of the complex optical potential gives the complex phase shift δ_l' for the elastic scattering. It can be shown (see e.g. [14]) that the analysis of the only elastic channel in the presence of inelastic channels (knowledge of the elastic S-matrix $S_{el}^{(l)}$ (D.34)) gives not only elastic integral cross section

[2] The equation (D.32) is one-dimensional special case of the general unitary condition of the more-dimensional S-matrix for the many-channel formalism (see also Chapter 10)

$$\sum_c S_{bc}^{(l)}\, S_{ac}^{(l)\,*} = \delta_{ba}$$

or

$$S^{(l)}\, S^{(l)\,+} = S^{(l)\,+}\, S^{(l)} = I$$

σ_{el} but also the integral cross section of all inelastic channels σ_{inel} and, of course, the total integral cross section σ_{total} of all possible processes: [3]

$$\sigma_{el} = \sum_{l=0}^{\infty} \frac{\pi}{k^2} (2l+1) \left| S_{el}^{(l)} - 1 \right|^2 \tag{D.35}$$

$$\sigma_{inel} = \sum_{l=0}^{\infty} \frac{\pi}{k^2} (2l+1) \left(1 - |S_{el}^{(l)}|^2 \right) \tag{D.36}$$

$$\sigma_{total} = \sigma_{el} + \sigma_{inel} = \frac{2\pi}{k^2} \sum_{l=0}^{\infty} (2l+1) \left(1 - \Re e S_{el}^{(l)} \right) \tag{D.37}$$

The total integral cross section (D.37) can be compared with the elastic scattering amplitude for $\vartheta = 0$:

$$f_{el}(\vartheta = 0) = \boxed{\begin{array}{c}\text{see} \\ (D.25)\end{array}} =$$

$$= \frac{1}{2ik} \sum_{l=0}^{\infty} (2l+1) \left(S_{el}^{(l)} - 1 \right) P_l(1) = \boxed{\begin{array}{c}\text{because} \\ P_l(1) = 1\end{array}} =$$

$$= -\frac{i}{2k} \sum_{l=0}^{\infty} (2l+1) \left(\Re e\, S_{el}^{(l)} + i\, \Im m\, S_{el}^{(l)} - 1 \right) \tag{D.38}$$

and the comparison of (D.38) with (D.37) gives

$$\sigma_{total} = \frac{4\pi}{k} \Im m\, f_{el}(\vartheta = 0) \tag{D.39}$$

This relation is known in the literature as the optical theorem. It enables to obtain the total integral cross section involving both elastic and inelastic processes through the elastic scattering amplitude with $\vartheta = 0$.

[3] The elastic scattering amplitude, differential cross section $\frac{d\sigma_{el}}{d\Omega}$ and integral cross section σ_{el} in the case, when inelastic processes are also present, are again given by (D.25), (D.26) and (D.27), respectively, only δ_l should be substituted by $\delta\,'_l$. It gives the equation (D.35). Since in the case of presence of inelastic processes the S-matrix of the elastic scattering fulfils (D.33) the total flux to the whole space angle 4π of the elastic scattering wave function (D.31) is not equal to zero but it is negative. The absolute value of this flux determines the number of particles from the initial beam with the probability current $\vec{j}_D(\vec{r})$ which are absorbed from the elastic channel to all other inelastic channels in one second during the scattering on one targed particle. If we divide this flux by $|\vec{j}_D(\vec{r})|$ we obtain σ_{inel} (see (D.36)).

E. Lippman-Schwinger and Bethe-Goldstone equations, Born series for the scattering amplitude

E.1 Lippman-Schwinger equation

Let us consider the scattering of two particles with the same mass. The Hamiltonian of the problem is supposed to have the following form

$$\hat{H} = \hat{H}_0 + \hat{V} \tag{E.1}$$

where $\hat{H}_0$ is the single-particle (unperturbed) part of the Hamiltonian and the symbol $\hat{V}$ involves two-particle scattering potential. Further we suppose that $|\phi\rangle$ is the eigen vector of the unperturbed Hamiltonian $\hat{H}_0$ with the energy E and $|\psi\rangle$ is the eigen vector of the perturbed (total) Hamiltonian $\hat{H}$ with the same energy E

$$\hat{H}_0 |\phi\rangle = E |\phi\rangle \quad , \qquad \hat{H} |\psi\rangle = E |\psi\rangle \tag{E.2}$$

The combination of (E.1) and (E.2) gives

$$\left(\hat{H}_0 - E\right) |\phi\rangle = 0 \tag{E.3}$$

$$\left(\hat{H}_0 - E\right) |\psi\rangle = -\hat{V} |\psi\rangle \tag{E.4}$$

and we have

$$\left(\hat{H}_0 - E\right) (|\psi\rangle - |\phi\rangle) = -\hat{V} |\psi\rangle$$

$$\Rightarrow |\psi\rangle = |\phi\rangle - \frac{\hat{V}}{\hat{H}_0 - E} |\psi\rangle \tag{E.5}$$

The equation (E.5) represents the precise relation between perturbed function $|\psi\rangle$ and unperturbed function $|\phi\rangle$. Further we define the operator $\hat{G}$

$$\hat{G} |\phi\rangle = \hat{V} |\psi\rangle \tag{E.6}$$

The equation (E.6) means that the action of the potential $\hat{V}$ on the perturbed function $|\psi\rangle$ can be substituted by the action of the operator $\hat{G}$ on the unperturbed funtion $|\phi\rangle$. From (E.5) and (E.6) the following equation can be deduced

$$\hat{G}\,|\phi\rangle = \hat{V}\,|\psi\rangle = \hat{V}\,|\phi\rangle - \frac{\hat{V}^2}{\hat{H}_0 - E}\,|\psi\rangle = \boxed{\begin{array}{c}\text{see}\\ (E.6)\end{array}} =$$

$$= \hat{V}\,|\phi\rangle - \frac{\hat{V}}{\hat{H}_0 - E}\,\hat{G}\,|\phi\rangle$$

$$\Rightarrow \qquad \hat{G} = \hat{V} - \hat{V}\,\frac{1}{\hat{H}_0 - E}\,\hat{G} \tag{E.7}$$

The equation (E.7) in the connection with the definition (E.6) is known as the Lippman-Schwinger equation. This equation can be formally solved:

$$\hat{G} = \frac{\hat{V}}{1 + \frac{\hat{V}}{\hat{H}_0 - E}} \tag{E.8}$$

From this equation it can be seen that the action of the operator $\hat{G}$ is finite even in the case when the action of the potential $\hat{V}$ is divergent (as it is in the case of the nucleon-nucleon scattering due to the infinite repulsive core of the bare nucleon-nucleon potential).

Further we work in the linear momentum representation and we determine the matrix element of the equation (E.7) between the eigen states $|\vec{k}_1\,\vec{k}_2\rangle$ and $|\vec{k}'_1\,\vec{k}'_2\rangle$ of the unperturbed Hamiltonian $\hat{H}_0$ which is taken as the total kinetic energy of two scattering particles (we suppose the eleastic scattering when the total energy before and after the scattering is the same)

$$\begin{aligned}
\hat{H}_0\,|\vec{k}_1\,\vec{k}_2\rangle &= \left(\frac{\hbar^2 k_1^2}{2m} + \frac{\hbar^2 k_2^2}{2m}\right)\,|\vec{k}_1\,\vec{k}_2\rangle = E\,|\vec{k}_1\,\vec{k}_2\rangle \\
\hat{H}_0\,|\vec{k}\,'_1\,\vec{k}\,'_2\rangle &= \left(\frac{\hbar^2 k_1'^2}{2m} + \frac{\hbar^2 k_2'^2}{2m}\right)\,|\vec{k}\,'_1\,\vec{k}\,'_2\rangle = E\,|\vec{k}\,'_1\,\vec{k}\,'_2\rangle
\end{aligned} \tag{E.9}$$

and using the completeness of the basis $|\vec{t}_1\,\vec{t}_2\rangle$ and the Lipman-Schwinger equation (E.7) we have

$$\begin{aligned}
\langle\vec{k}_1\,\vec{k}_2\,|\hat{G}|\,\vec{k}\,'_1\,\vec{k}\,'_2\rangle = \langle\vec{k}_1\,\vec{k}_2\,|\hat{V}|\,\vec{k}\,'_1\,\vec{k}\,'_2\rangle + \\
\sum_{\vec{t}_1\,\vec{t}_2}\langle\vec{k}_1\,\vec{k}_2\,|\hat{V}|\,\vec{t}_1\,\vec{t}_2\rangle\,\frac{1}{E - \epsilon_{t_1} - \epsilon_{t_2}}\,\langle\vec{t}_1\,\vec{t}_2\,|\hat{G}|\,\vec{k}\,'_1\,\vec{k}\,'_2\rangle
\end{aligned} \tag{E.10}$$

where $\hat{H}_0 \mid \vec{t}_1\, \vec{t}_2\rangle = (\epsilon_{t_1} + \epsilon_{t_2}) \mid \vec{t}_1\, \vec{t}_2\rangle$, $\epsilon_{t_1} = \hbar^2\, t_1^2/2m$, $\epsilon_{t_2} = \hbar^2\, t_2^2/2m$.

If we substitute again and again for $\langle \vec{t}_1\, \vec{t}_2\, |\hat{G}|\, \vec{k}\,'_1\, \vec{k}\,'_2\rangle$ in the r.h.s. of (E.10) the equation (E.10) can be graphically interpreted as the sum over so called ladder diagrams - see Fig. E.1. In the Fig. E.1 the diagrams denoted by (a),

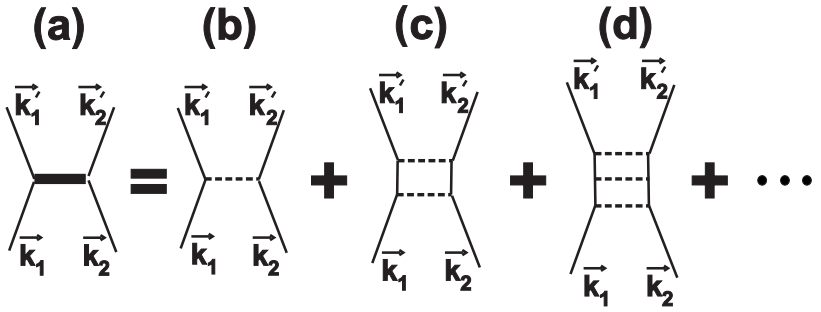


Figure E.1: Graphical demonstration of the equation (E.10) in terms of ladder diagrams.

(b), (c), ... represent the following expressions

$$\begin{aligned}
(a) \quad &\leftrightarrow \quad \langle \vec{k}_1\, \vec{k}_2\, |\hat{G}|\, \vec{k}\,'_1\, \vec{k}\,'_2\rangle \\
(b) \quad &\leftrightarrow \quad \langle \vec{k}_1\, \vec{k}_2\, |\hat{V}|\, \vec{k}\,'_1\, \vec{k}\,'_2\rangle \\
(c) \quad &\leftrightarrow \quad \sum_{\vec{t}_1 \vec{t}_2} \langle \vec{k}_1\, \vec{k}_2\, |\hat{V}|\, \vec{t}_1\, \vec{t}_2\rangle\, \frac{1}{E - \epsilon_{t_1} - \epsilon_{t_2}}\, \langle \vec{t}_1\, \vec{t}_2\, |\hat{V}|\, \vec{k}\,'_1\, \vec{k}\,'_2\rangle \\
\vdots \quad &\leftrightarrow \quad \vdots \qquad\qquad \vdots
\end{aligned}$$

The first term in the r.h.s. of (E.10) represents the 1-st order of the Born approximation (see further in this appendix) for the elastic scattering of two particles. The other terms correspond to the higher order terms in the perturbations series. The single diagrams in the Fig. E.1 can be divergent but it is possible to show that the whole sum in the r.h.s. of the Fig. E.1 is finite (see e.g. [19]).

If the linear momentum conservation is taken into account then the sum over linear momenta $\vec{t}_1, \vec{t}_2$ in (E.10) is reduced only over one linear momentum because the matrix element $< \vec{k}_1\, \vec{k}_2\, |\hat{G}|\, \vec{k}\,'_1\, \vec{k}\,'_2 >$ depends only on 3 linear momenta.

$$\vec{k}\,'_1 + \vec{k}\,'_2 = \vec{k}_1 + \vec{k}_2 \qquad\qquad \vec{q} = \vec{k}\,'_1 - \vec{k}_1 = \vec{k}_2 - \vec{k}\,'_2 \tag{E.11}$$

Therefore we have only 3 independent linear momenta, e.g. $\vec{k}_1$, $\vec{k}_2$, $\vec{q}$, because remain momenta $\vec{k}\,'_1$ and $\vec{k}\,'_2$ are given by

$$\vec{k}\,'_1 = \vec{k}_1 + \vec{q} \qquad , \qquad \vec{k}\,'_2 = \vec{k}_2 - \vec{q} \tag{E.12}$$

and we have

$$\begin{aligned}\langle \vec{k}_1\,\vec{k}_2\,|\hat{G}|\,\vec{k}\,'_1\,\vec{k}\,'_2\rangle &= G(\vec{k}_1,\,\vec{k}_2,\,\vec{q})\\ \langle \vec{k}_1\,\vec{k}_2\,|\hat{V}|\,\vec{k}\,'_1\,\vec{k}\,'_2\rangle &= \boxed{\begin{array}{c}\text{usually is}\\ \text{dependent only on } \vec{q}\end{array}} = V(\vec{q})\end{aligned} \tag{E.13}$$

and the Lippman-Schwinger equation (E.10) can be rewritten as follows ($\sum_{\vec{t}_1\,\vec{t}_2} \to \sum_{\vec{k}} \to \int \frac{d^3k}{(2\pi)^3}$)

$$\begin{aligned}&G(\vec{k}_1,\,\vec{k}_2,\,\vec{q}) = V(\vec{q}) +\\ &+\int \frac{d^3k}{(2\pi)^3} V(\vec{q}-\vec{k}) \frac{1}{\frac{\hbar^2 k_1^2}{2m} + \frac{\hbar^2 k_2^2}{2m} - \frac{\hbar^2(\vec{k}_1+\vec{k})^2}{2m} - \frac{\hbar^2(\vec{k}_2-\vec{k})^2}{2m}} G(\vec{k}_1,\,\vec{k}_2,\,\vec{k})\end{aligned} \tag{E.14}$$

This equation should be solved numerically for all values $\vec{q}$ when $\vec{k}_1$ and $\vec{k}_2$ are fixed.

E.2 Bethe-Goldstone equation

We consider again the elastic scattering of two nucleons (fermions) but now in the presence of other nucleons (other fermions). In such a case the Pauli principle should be taken into account. In the standard Lippman-Schwinger equation (concerning the scattering in the vacuum) there is no any restriction on intermediate states (all states $|\vec{t}_1\,\vec{t}_2\rangle$ are possible in the sum on the r.h.s. of (E.10)). For many fermion systems the Pauli principle claims that all states $|\vec{t}_1\,\vec{t}_2\rangle$ with the momenta $\vec{t}_1$ and $\vec{t}_2$ inside the Fermi sphere (k_F is the modulus of the Fermi linear momentum)

$$\frac{\hbar^2 t_1^2}{2m} \le \frac{\hbar^2 k_F^2}{2m} \qquad\qquad \frac{\hbar^2 t_2^2}{2m} \le \frac{\hbar^2 k_F^2}{2m} \tag{E.15}$$

are occupied by one nucleon and therefore such states cannot be occupied once more. Therefore all intermediate states $|\vec{t}_1\,\vec{t}_2\rangle$ fulfilling (E.15) should be excluded from the sum $\sum_{\vec{t}_1\vec{t}_2}$ in (E.10). For equation (E.14) it means the following modification

$$\begin{aligned}&G(\vec{k}_1,\,\vec{k}_2,\,\vec{q}) = V(\vec{q}) +\\ &+\int \frac{d^3k}{(2\pi)^3} V(\vec{q}-\vec{k}) \frac{(1-n_{\vec{k}_1+\vec{k}})\,(1-n_{\vec{k}_2-\vec{k}})}{\frac{\hbar^2 k_1^2}{2m} + \frac{\hbar^2 k_2^2}{2m} - \frac{\hbar^2(\vec{k}_1+\vec{k})^2}{2m} - \frac{\hbar^2(\vec{k}_2-\vec{k})^2}{2m}} G(\vec{k}_1,\,\vec{k}_2,\,\vec{k})\end{aligned} \tag{E.16}$$

where $n_{\vec{k}}$ is the usual Fermi distribution function (in the zero temperature - see Appendix H)

$$n_{\vec{k}} = \begin{cases} 1 & \text{if } k \leq k_F, \\ 0 & \text{if } k \geq k_F, \end{cases} \tag{E.17}$$

Equation (E.16) is called Bethe-Goldstone equation. The operator (or matrix) G is known in the literature as G-matrix. It is necessary to realize that the dependence of (E.16) on the Fermi linear momentum k_F in the fact means that the G-matrix depends on the medium (nuclear) density (because there is the relation between k_F and the density ρ - see e.g. (H.7)).

E.3 Born series for the scattering amplitude

The Lippman-Schwinger equation (E.5) has the following form in the coordinate representation

$$\psi_{\vec{k}}(\vec{r}) = \langle \vec{r} \,|\psi\rangle_{\vec{k}} = \langle \vec{r} \,|\phi\rangle_{\vec{k}} + \langle \vec{r} \,|\frac{\hat{V}}{E - \hat{H}_0}|\psi\rangle_{\vec{k}} \tag{E.18}$$

where $\vec{r}$ is the relative coordinate of two scattering particles (nucleons). In this case the Hamiltonian $\hat{H}_0$ is the kinetic energy of the relative motion of these particles,

$$\hat{H}_0 = \frac{\hat{\vec{p}}^{\,2}}{2m} \tag{E.19}$$

where $\vec{p}$ is the linear momentum of the relative motion. In such a case the unperturbed wave function $\langle \vec{r} \,|\phi\rangle$ is given by the plane wave

$$\langle \vec{r} \,|\phi\rangle_{\vec{k}} \approx e^{i\vec{k}\cdot\vec{r}} \tag{E.20}$$

and we have

$$\begin{aligned} \psi_{\vec{k}}(\vec{r}) = \langle \vec{r} \,|\psi\rangle_{\vec{k}} >= e^{i\vec{k}\cdot\vec{r}} + \langle \vec{r} \,|\frac{1}{E - \hat{H}_0}\,\hat{V}|\psi\rangle_{\vec{k}} = \\ = e^{i\vec{k}\cdot\vec{r}} + \int d^3r' \,\langle \vec{r} \,|\frac{1}{\frac{\hbar^2 k^2}{2m} - \frac{\hat{\vec{p}}^2}{2m}}|\vec{r}\,'\rangle \, V(\vec{r}\,') \, \psi_{\vec{k}}(\vec{r}\,') = \\ = e^{i\vec{k}\cdot\vec{r}} + \int d^3r' \,\langle \vec{r} \,|\frac{1}{k^2 - \frac{\hat{\vec{p}}^2}{\hbar^2}}|\vec{r}\,'\rangle \, \frac{2m}{\hbar^2} \, V(\vec{r}\,') \, \psi_{\vec{k}}(\vec{r}\,') = \\ = e^{i\vec{k}\cdot\vec{r}} + \int d^3r' \, G_k(\vec{r},\, \vec{r}\,') \, U(\vec{r}\,') \, \psi_{\vec{k}}(\vec{r}\,') \end{aligned} \tag{E.21}$$

where Green function $G_k(\vec{r},\, \vec{r}\,')$ was introduced

$$G_k(\vec{r},\, \vec{r}\,') = \langle \vec{r}\,| \frac{1}{k^2 - \frac{\hat{p}^2}{\hbar^2}} \,|\vec{r}\,'\rangle \tag{E.22}$$

and

$$U(\vec{r}) = \frac{2m}{\hbar^2}\, V(\vec{r}) \tag{E.23}$$

The expression (E.22) for the Green function can be modified as follows

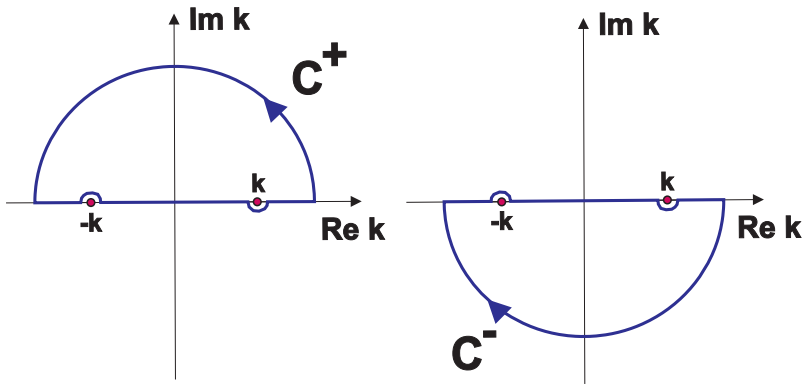


Figure E.2: Paths C^+ and C^- for the integration in the exp. (E.24).

$$\begin{aligned}
G_k(\vec{r},\, \vec{r}\,') &= \langle \vec{r}\,| \frac{1}{k^2 - \frac{\hat{p}^2}{\hbar^2}} |\vec{r}\,'\rangle = \\
&= \int d^3p\,' \,\langle \vec{r}\,| \frac{1}{k^2 - \frac{\hat{p}^2}{\hbar^2}} |\vec{p}\,'\rangle \,\langle \vec{p}\,' \,|\vec{r}\,'\rangle = \\
&= \hbar^3 \int d^3k\,' \,\frac{\langle \vec{r}\,|\,\vec{p}\,'\rangle \,\langle \vec{p}\,' \,|\,\vec{r}\,'\rangle}{k^2 - k\,'^2} = \\
&= \frac{\hbar^3}{(2\pi\hbar)^3} \int d^3k\,' \,\frac{e^{i\vec{k}\,'\cdot(\vec{r}-\vec{r}\,')}}{k^2 - k\,'^2} = \\
&= \frac{1}{(2\pi)^3} \int_0^\infty k\,'^2\, dk\,' \int_0^{2\pi} d\varphi \int_0^\pi \sin\vartheta\, d\vartheta \frac{e^{ik\,'|\vec{r}-\vec{r}\,'|\,\cos\vartheta}}{k^2 - k\,'^2} = \\
&= \frac{1}{(2\pi)^2\, i|\vec{r}-\vec{r}\,'|} \int_0^\infty k\,'\, dk\,' \,\frac{e^{-ik\,'|\vec{r}-\vec{r}\,'|} - e^{ik\,'|\vec{r}-\vec{r}\,'|}}{k^2 - k\,'^2} = \\
&= \frac{1}{2(2\pi)^2 iR} \int_0^\infty k\,'\, dk\,' \,\frac{e^{-ik\,'R} - e^{ik\,'R}}{k^2 - k\,'^2} = \\
&= \boxed{\begin{array}{c}\text{integration along the real axis is changed for} \\ \text{the integration along the curves } C^+ \text{ and } C^- \\ \text{- see Fig.E.2}\end{array}} =
\end{aligned}$$

$$= \frac{1}{2(2\pi)^2 iR}\left[\int_{C^-} \frac{e^{-ik'R}\,k'dk'}{(k'-k)(k'+k)} - \int_{C^+} \frac{e^{ik'R}\,k'dk'}{(k'-k)(k'+k)}\right] =$$

$$= \boxed{\begin{array}{c}\text{Cauchy's}\\ \text{integral formule}\end{array}} = -\frac{1}{4\pi}\frac{e^{ik|\vec{r}-\vec{r}\,'|}}{|\vec{r}-\vec{r}\,'|} \tag{E.24}$$

The substitution of (E.24) into (E.21) gives

$$\psi_{\vec{k}}(\vec{r}) = e^{i\vec{k}\cdot\vec{r}} - \frac{1}{4\pi}\int d^3r'\,\frac{e^{ik|\vec{r}-\vec{r}\,'|}}{|\vec{r}-\vec{r}\,'|}\,U(\vec{r}\,')\,\psi_{\vec{k}}(\vec{r}\,') \quad \stackrel{r\to\infty}{\longrightarrow}$$

$$= \boxed{\begin{array}{c}\text{in the asymptotic region } r >> r'\\ \frac{e^{ik|\vec{r}-\vec{r}\,'|}}{|\vec{r}-\vec{r}\,'|} \approx \frac{e^{ikr}}{r}e^{-i\vec{k}\,'\cdot\vec{r}\,'}\end{array}} =$$

$$= e^{i\vec{k}\cdot\vec{r}} - \frac{1}{4\pi}\frac{e^{ikr}}{r}\int d^3r'\,e^{-i\vec{r}\,'\cdot\vec{r}\,'}\,U(\vec{r}\,')\,\psi_{\vec{k}}(\vec{r}\,') \tag{E.25}$$

This expression can be compared with the following asymptotic expression (see (D.16) or (3.58))

$$\psi_{\vec{k}}(\vec{r}) \quad \stackrel{r\to\infty}{\longrightarrow} \quad e^{i\,\vec{k}\cdot\vec{r}} + f(\vec{k},\vec{k}\,')\,\frac{e^{ikr}}{r} \tag{E.26}$$

and for the scattering amplitude $f(\vec{k},\,\vec{k}\,')$ we have

$$f(\vec{k},\,\vec{k}\,') = -\frac{1}{4\pi}\int d^3r'\,e^{-i\vec{k}\,'\cdot\vec{r}\,'}\,U(\vec{r}\,')\,\psi_{\vec{k}}(\vec{r}\,') =$$

$$= -\frac{m}{2\pi\hbar^2}\int d^3r'\,e^{-i\vec{k}\,'\cdot\vec{r}\,'}\,V(\vec{r}\,')\,\psi_{\vec{k}}(\vec{r}\,') \tag{E.27}$$

By means of the successive substitution for $\psi_{\vec{k}}(\vec{r}\,')$ in the r.h.s. of (E.25) we obtain the following series

$$\psi_{\vec{k}}(\vec{r}) = \sum_{n=0}^{\infty}\psi_{\vec{k},n}(\vec{r}) \tag{E.28}$$

where

$$\begin{aligned}\psi_{\vec{k},0}(\vec{r}) &= e^{i\vec{k}\cdot\vec{r}}\\ \psi_{\vec{k},n}(\vec{r}) &= \int d^3r_1 \ldots \int d^3r_n\\ &\quad G_{\vec{k}}(\vec{r},\vec{r}_1)\,U(\vec{r}_1)\,G_{\vec{k}}(\vec{r}_1,\vec{r}_2)\ldots G_{\vec{k}}(\vec{r}_{n-1},\vec{r}_n)\,U(\vec{r}_n)\,e^{i\vec{k}\cdot\vec{r}_n}\end{aligned} \tag{E.29}$$

The substitution of (E.28) into (E.27) provides so called Born series for the scattering amplitude

$$f(\vec{k},\ \vec{k}\,') = \sum_{n=1}^{\infty} f^{(n)}(\vec{k},\ \vec{k}\,') \tag{E.30}$$

with

$$f^{(n)}(\vec{k},\ \vec{k}\,') = -\frac{m}{2\pi\hbar^2}\int d^3r\,'\, e^{-i\vec{k}\,'\cdot\vec{r}\,'}\, V(\vec{r}\,')\, \psi_{\vec{k},n-1}(\vec{r}\,') \tag{E.31}$$

Particularly, the first order approximation is

$$\begin{aligned} f^{(1)}(\vec{k},\ \vec{k}\,') &= -\frac{m}{2\pi\hbar^2}\int d^3r\, e^{-i\vec{k}\,'\cdot\vec{r}}\, V(\vec{r})\, e^{i\vec{k}\cdot\vec{r}} = \\ &= -\frac{m}{2\pi\hbar^2}\int d^3r\, e^{i\vec{q}\cdot\vec{r}}\, V(\hat{r}) \end{aligned} \tag{E.32}$$

where $\hat{q} = \hat{k} - \hat{k}\,'$ If the potential $V(\vec{r})$ is spherically symmeteric $V(\vec{r}) = V(r)$ then

$$\begin{aligned} f^{(1)}(\vec{k},\ \vec{k}\,') &= -\frac{m}{2\pi\hbar^2}\int_0^{\infty} r^2 dr \int_0^{2\pi} d\varphi \int_0^{\pi} \sin\vartheta\, d\vartheta\, e^{iqr\cos\vartheta} V(r) = \\ &= \frac{m}{\hbar^2}\int_0^{\infty} r^2 dr\, V(r)\, \left[\frac{e^{iqr\cos\vartheta}}{iqr}\right]_0^{\pi} = \\ &= -\frac{2m}{\hbar^2}\int_0^{\infty} r\, dr\, V(r)\, \sin qr \end{aligned} \tag{E.33}$$

where $\vec{q} = \vec{k} - \vec{k}\,'$.

F. Strutinski shell-model corrections

The liquid drop model Weiszacker formula (1.13) for the nuclear bind energy as a function of the mass number A gives the smooth dependence (see the solid line in the Fig. 1.1). The fluctuation (the difference between experimental values and the smooth solid line in the Fig. 1.1) were explained in the 60-ties by the introduction of Strutinski shell correction method. This method is based on the assumption that these fluctuations (oscillations) can be fully described in the framework of the shell model and therefore the total energy of the nucleus in the ground state can be written as follows (see (5.52)).

$$E = E_{LDM} + E_{OSC} = E_{LDM} + E_{SM} - \tilde{E}_{SM} \tag{F.1}$$

where E_{LDM} is the liquid drop model energy given by the Weiczacker expression (1.13) or (5.49), E_{OSC} is the oscillation part of the binding energy given by the difference between the shell model energy and the smooth part $\tilde{E}_{SM}$ energy.

The total shell model energy of the nucleus with the energy density $g(e)$ of nucleons is given by

$$E_{SM} = \int_{-\infty}^{\lambda} e\, g(e)\, de = \sum_i n_i\, e_i \tag{F.2}$$

with the nucleon density $g(e)$:

$$g(e) = \sum_i n_i\, \delta(e - e_i), \qquad A = \int_{-\infty}^{\lambda} g(e)\, de = \sum_i n_i \tag{F.3}$$

where e_i is the single-particle energy ($\hat{H}_{AV}\, |i\rangle = e_i\, |i\rangle$). The sumation in the (F.2) and (F.3) goes over all single-particle levels. The number n_i is the occupation number for given sinle-particle state $|i\rangle$ (in the ground state $n_i = 1$ for all single-particle states below the Fermi level and $n_i = 0$ for s.p. states above the Fermi level). The Fermi level λ is defined by the second equation in (F.3).

For the determination of the smooth part $\tilde{E}_{SM}$ of the total shell model energy it is suitable to introduce the smooth part $\tilde{g}(e)$ of the energy density of nucleons.

$$A = \int_{-\infty}^{\tilde{\lambda}} \tilde{g}(e)\, de = \sum_i \tilde{n}_i, \qquad \tilde{E}_{SM} = \int_{-\infty}^{\tilde{\lambda}} e\, \tilde{g}(e)\, de \tag{F.4}$$

where $\tilde{\lambda}$ is the "smooth" Fermi level and $\tilde{n}_i$ is the generalized (smooth) occupation number of the level e_i. The task is to determine the smooth part of the energy density $\tilde{g}(e)$ together with the corresponding Fermi level $\tilde{\lambda}$ (it should be pointed out that generally $\lambda \neq \tilde{\lambda}$). In the subsection 5.1.2.2 it was claimed that this smooth density is given by the averaging (convolution) (see (5.58)

$$\tilde{g}(e) = \frac{1}{\gamma} \int_{-\infty}^{\infty} g(e')\, f\left(\frac{e'-e}{\gamma}\right)\, de' \tag{F.5}$$

where the width of the averaging energy interval is $\gamma \approx \hbar\omega_0^{(0)}$. The averaging (convoluting) function $f\left(\frac{e'-e}{\gamma}\right)$ is given by the requirement that the convolution (F.5) when applied to $\tilde{g}(e)$ provides again the same function $\tilde{g}(e)$:

$$\tilde{g}(e) = \frac{1}{\gamma} \int_{-\infty}^{\infty} \tilde{g}(e')\, f\left(\frac{e'-e}{\gamma}\right)\, de' \tag{F.6}$$

Further the convoluting function $f\left(\frac{e'-e}{\gamma}\right)$ will be determined.

If the convoluting function f is the Dirac δ-function then

$$\begin{aligned} &\frac{1}{\gamma} \int_{-\infty}^{\infty} de'\, \tilde{g}(e')\, f\left(\frac{e'-e}{\gamma}\right) = \frac{1}{\gamma} \int_{-\infty}^{\infty} de'\, \tilde{g}(e')\, \delta\left(\frac{e'-e}{\gamma}\right) = \\ &= \boxed{\begin{array}{c}\text{because} \\ \delta(\alpha x) = \frac{1}{\alpha}\delta(x)\end{array}} = \frac{\gamma}{\gamma} \int_{-\infty}^{\infty} de'\, \tilde{g}(e')\, \delta(e'-e) = \tilde{g}(e) \end{aligned} \tag{F.7}$$

So we can see that in the case when the averaging function is the Dirac δ-function the condition (F.6) is fulfilled for arbitrary function $\tilde{g}(e)$. However, we want the condition (F.6) to be fulfilled only for the function $\tilde{g}(e)$ which does not contain any fluctuations. So we do not use in (F.6) the Dirac function as the averaging function but we can expect that the biggest contribution to the integral in the r.h.s. of (F.6) comes from the interval of e' in the vicinity of e. The Dirac δ-function can be decomposed into the complete set

of orthogonal polynomials of the second order (because δ-function is the even function), e.g. to the set of the Hermitian polynomials (see e.g. [58])

$$\delta(x) = \sum_{n=0}^{\infty} \frac{(-1)^n}{(2n)!!2^n} H_{2n}(x)\, e^{-x^2} \frac{1}{\sqrt{\pi}} \tag{F.8}$$

Suggestion of V.M. Strutinski [56] was to take as the averaging function $f\left(\frac{e'-e}{\gamma}\right)$ not the whole decomposition (F.8) but only several first terms of it.

Orthogonal polynomials are defined as the ensemble of polynomials $Q_m(x), m = 0, 1, \ldots, \infty$ which fulfil:

$$\int_{-\infty}^{\infty} Q_m(x)\, Q_{m'}(x)\, w(x)\, dx = \delta_{mm'} \tag{F.9}$$

where $w(x)$ is so called weight function [58]. For instance, if we choose $Q_m(x)$ to be Hernitian polynomials $H_m(x)$ then the weght function $w(x)$ is foolowing

$$w(x) = \frac{1}{\sqrt{\pi}}\, e^{-x^2} \tag{F.10}$$

So, according to V.V. Strutinski [56] we take orthogonal polynomial $Q_m(x)$ with the corresponding weight function $w(x)$ and the averaging function $f(x)$ is then defined as

$$f(x) = P(x)\, w(x) \tag{F.11}$$

where

$$P(x) = \sum_{n=0}^{M} Q_{2n}(x)\, Q_{2n}(e)$$

for arbitrary e.

We can easily prove that in this case the smooth energy density function $\tilde{g}(x)$ is

$$\tilde{g}(x) = \sum_{n} b_{2n}\, Q_{2n}(x) \tag{F.12}$$

Really we have

$$\int_{-\infty}^{\infty} \tilde{g}(x)\, f(x)\, dx = \int_{-\infty}^{\infty} \left(\sum_n b_{2n}\, Q_{2n}(x) \right)\, P(x)\, w(x)\, dx =$$
$$= \int_{-\infty}^{\infty} \left(\sum_n b_{2n}\, Q_{2n}(x) \right)\, \left(\sum_{n'=0}^{M} Q_{2n'}(x)\, Q_{2n'}(e) \right)\, w(x)\, dx =$$
$$= \sum_{n\,n'} b_{2n}\, Q_{2n'}(e)\, \int_{-\infty}^{\infty} dx\, Q_{2n}(x)\, Q_{2n'}(x)\, dx = \boxed{\begin{array}{c}\text{see}\\ (F.9)\end{array}} =$$
$$= \sum_{n\,n'} b_{2n}\, Q_{2n'}(e)\, \delta_{nn'} = \sum_n b_{2n}\, Q_{2n}(e) = \tilde{g}(e) \qquad \text{(F.13)}$$

So, if $\tilde{g}(x)$ is given by (F.12) and if $f(x)$ is equal to (F.11) then the condition (F.6) is fulfilled.

If we use in (F.11) and (F.12) Hermitian polynomials $H_{2n}(x)$ as the $Q_{2n}(x)$ then

$$w(x) = \frac{1}{\sqrt{\pi}}\, e^{-x^2}, \quad P(x) = \sum_{n=0}^{M} [2 \cdot (2n)!!]^{-1}\, H_{2n}(x)\, H_{2n}(0) = L_M^{1/2}(x) \quad \text{(F.14)}$$

where $L_M^{1/2}(x)$ are generalised Laquere polynomials.

So, conclusion is: using (F.11) we can construct the averaging function $f(x)$ and smooth density (F.12) which fulfil the following requirements.

- From the simple shell model spectra (which describe the experimental data on single-particle states) it is known that the fluctuation of the density $g(e)$ have frequency $\hbar\omega_0^{(0)} \approx 41\, A^{-1/3}\, MeV$. Therefore the width of the averaging interval is usually taken with values $\gamma \approx (1.0 - 1.5)\, \hbar\omega_0^{(0)}\, MeV$;

- The value of M is of the order of units (e.g. $M \approx 2$)

- The used values of γ and M should be taken in agreement with the requirement that the resultant smooth part $\tilde{E}_{SM}$ should not be dependent on the width γ of the averaging interval, that means

$$\frac{\partial \tilde{E}_{SM}}{\partial \gamma} = 0 \qquad \text{(F.15)}$$

The condition (F.15) is known as a plateau condition.

The smooth part $\tilde{g}(e)$ of the energy density is defined by (F.5). The substitution of (F.3) into (F.5) gives

$$\begin{aligned}\tilde{g}(e) &= \frac{1}{\gamma}\int_{-\infty}^{\infty} de\,'\, g(e\,')\, f\left(\frac{e\,'-e}{\gamma}\right) = \\ &= \frac{1}{\gamma}\int_{-\infty}^{\infty} de\,'\sum_i n_i\,\delta(e\,'-e_i)\, f\left(\frac{e\,'-e}{\gamma}\right) = \sum_i \frac{n_i}{\gamma}\, f\left(\frac{e-e_i}{\gamma}\right)\end{aligned} \tag{F.16}$$

and the "smooth" Fermi level $\tilde{\lambda}$ defined by the second equation in (F.4) can be determined from the following condition

$$\begin{aligned}A &= \int_{-\infty}^{\tilde{\lambda}} \tilde{g}(e)\, de = \sum_i \frac{n_i}{\gamma}\int_{-\infty}^{\tilde{\lambda}} f\left(\frac{e-e_i}{\gamma}\right)\, de = \\ &= \boxed{\begin{array}{c}\text{substitution}\\ x=\frac{e-e_i}{\gamma}\end{array}} = \sum_i \int_{-\infty}^{\tau_i} dx\, f(x) = \boxed{\begin{array}{c}\text{see}\\ (F.4)\end{array}} = \sum_i \tilde{n}_i\end{aligned} \tag{F.17}$$

where $\tau_i = \frac{\tilde{\lambda}-e_i}{\gamma}$ and the generalized "smooth" occupation numbers $\tilde{n}_i$ are

$$\tilde{n}_i = n_i \int_0^{\tau_i} f(x)\, dx \tag{F.18}$$

Then the smooth part (F.4) of the shell model energy can be written as

$$\begin{aligned}\tilde{E}_{SM} &= \int_{-\infty}^{\tilde{\lambda}} e\,\tilde{g}(e) = \boxed{\begin{array}{c}\text{see}\\ (F.16)\end{array}} = \sum_i \frac{n_i}{\gamma}\int_{-\infty}^{\tilde{\lambda}} f\left(\frac{e-e_i}{\gamma}\right)\, e\, de = \\ &= \sum_i \frac{n_i}{\gamma}\int_{-\infty}^{\tilde{\lambda}} f\left(\frac{e-e_i}{\gamma}\right)\, [e+e_i-e_i]\, de = \\ &= \sum_i \frac{n_i}{\gamma}\, e_i \int_{-\infty}^{\tilde{\lambda}} f\left(\frac{e-e_i}{\gamma}\right)\, de + \\ &\qquad + \sum_i \frac{n_i}{\gamma}\int_{-\infty}^{\tilde{\lambda}} [e-e_i]\, f\left(\frac{e-e_i}{\gamma}\right)\, de = \\ &= \boxed{\begin{array}{c}\text{see}\\ (F.17)\end{array}} = \sum_i e_i\,\tilde{n}_i + F\end{aligned} \tag{F.19}$$

where we define F:

$$F = \sum_i \frac{n_i}{\gamma} \int_{-\infty}^{\tilde{\lambda}} [e - e_i]\, f\left(\frac{e - e_i}{\gamma}\right) de = \boxed{\begin{array}{c}\text{substitution}\\ x = \frac{e-e_i}{\gamma}\end{array}} =$$
$$= \gamma \sum_i n_i \int_{-\infty}^{\tau_i} x\, f(x)\, dx \tag{F.20}$$

and the plateau condition gives

$$\frac{\partial \tilde{E}_{SM}}{\partial \gamma} = \frac{\partial}{\partial \gamma} \sum_i e_i\, \tilde{n}_i + \frac{\partial F}{\partial \gamma} =$$
$$= \frac{\partial}{\partial \gamma} \sum_i e_i\, \tilde{n}_i + \sum_i n_i \int_{-\infty}^{\tau_i} x\, f(x)\, dx + \gamma \sum_i n_i\, \tau_i\, f(\tau_i) \frac{\partial \tau_i}{\partial \gamma} =$$
$$= \frac{\partial}{\partial \gamma} \sum_i e_i\, \tilde{n}_i + \frac{F}{\gamma} + \gamma \sum_i n_i\, \tau_i\, f(\tau_i) \frac{\partial \tau_i}{\partial \gamma} =$$
$$= \frac{F}{\gamma} + \sum_i e_i \frac{\partial \tilde{n}_i}{\partial \gamma} + \gamma \sum_i n_i\, \tau_i\, f(\tau_i) \frac{\partial \tau_i}{\partial \gamma} = \boxed{\begin{array}{c}\text{see}\\ (F.18)\end{array}} =$$
$$= \frac{F}{\gamma} + \sum_i n_i\, e_i\, f(\tau_i) \frac{\partial \tau_i}{\partial \gamma} + \gamma \sum_i n_i\, \tau_i\, f(\tau_i) \frac{\partial \tau_i}{\partial \gamma} =$$
$$= \boxed{\begin{array}{c}\text{becaues}\\ \gamma\, \tau_i = \tilde{\lambda} - e_i\end{array}} =$$
$$= \frac{F}{\gamma} + \sum_i n_i\, e_i\, f(\tau_i) \frac{\partial \tau_i}{\partial \gamma} + \sum_i n_i\, [\tilde{\lambda} - e_i] f(\tau_i)\, \frac{\partial \tau_i}{\partial \gamma} =$$
$$= \frac{F}{\gamma} + \tilde{\lambda} \sum_i n_i\, f(\tau_i)\, \frac{\partial \tau_i}{\partial \gamma} = \boxed{\begin{array}{c}\text{because - see (F.18)}\\ \frac{\partial \tilde{n}_i}{\partial \gamma} = f(\tau_i)\, n_i\, \frac{\partial \tau_i}{\partial \gamma}\end{array}} =$$
$$= \frac{F}{\gamma} + \tilde{\lambda}\, \frac{\partial}{\partial \gamma} \sum_i \tilde{n}_i = \boxed{\begin{array}{c}\text{see}\\ (F.17)\end{array}} = \frac{F}{\gamma} + \tilde{\lambda}\, \frac{\partial A}{\partial \gamma} =$$
$$= \frac{F}{\gamma} = 0$$
$$\Rightarrow F = 0 \tag{F.21}$$

therefore (F.19) can be rewritten:

$$\tilde{E}_{SM} = \sum_i e_i\, \tilde{n}_i \tag{F.22}$$

and the oscillation (fluctuation) part of the total energy is (see (F.1))

$$E_{OSC} = E_{SM} - \tilde{E}_{SM} = \boxed{\begin{array}{c}\text{see}\\ (F.17), (F.2)\end{array}} = \sum_i e_i (n_i - \tilde{n}_i) \equiv \sum_i e_i \, \delta n_i \quad \text{(F.23)}$$

with

$$\delta n_i \equiv n_i - \tilde{n}_i = \boxed{\begin{array}{c}\text{see}\\ (F.18)\end{array}} = n_i - \int_{-\infty}^{\tau_i} f(x)\, dx \qquad \text{(F.24)}$$

Expressions (F.23) and (F.24) are final expressions for the fluctuation part

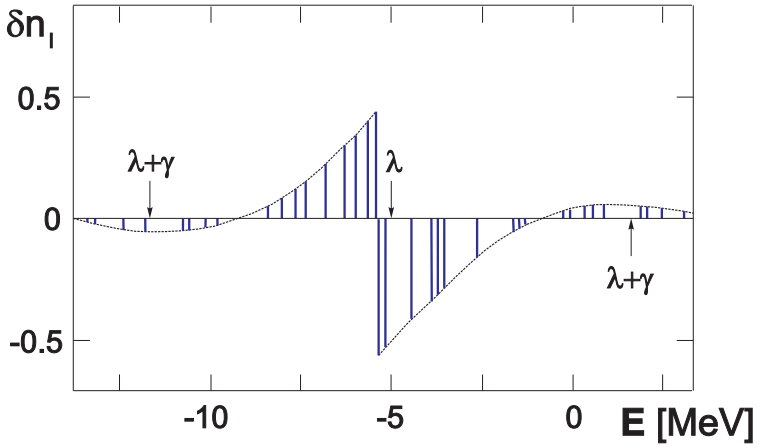


Figure F.1: Deviations δn_i as a function of the single-particle energy e in the energy interval in the vicinity of the Fermi level for the $Z = 94$ proton system. Calculation was done for the Wood-Saxon mean field potential (from [59])

E_{OSC} of the shell model energy ($\tau_i = \frac{\tilde{\lambda} - e_i}{\gamma}$, $f(x) = P(x)\, w(x)$, $P(x) = \sum_{n=0}^{M} Q_{2n}(x) Q_{2n}(0)$).

In the Fig. F.1 there is the demonstration of the deviations δn_i as a function of the single-particle energy e in the energy interval in the vicinity of the Fermi level λ. Calculation was done for the proton system $Z = 94$ using the mean field potential in the Wood-Saxon form (5.48) with the value $M = 2$ and the averaging width $\gamma = 6.6$ MeV.

One can see that the deviations δn_i are nonzero only in the vicinity of the Fermi level.

G. Penetration through the potential barrier

The probability or the coefficient of the penetration through the potential barrier can be obtained by means of the WKB (P.Wentzel, H.A.Kramers, L. Brilloin)(see [14, 70]). In this textbook the complete derivation of the quasi-classic WKB method is not given. We present here only a simple one-dimension example from which the reader can get a simple overall impression how the WKB method works.

Let us supose one-dimensional potential barrier (see Fig. G.1)

$$\begin{aligned} V(x) &= 0 \qquad \text{for } x < 0 \text{ and } x > d \\ V(x) &\neq 0 \qquad \text{for } 0 \leq x \leq d \end{aligned} \tag{G.1}$$

and the particles with the energy E ($E < V_{max}$) which hint at this barrier in

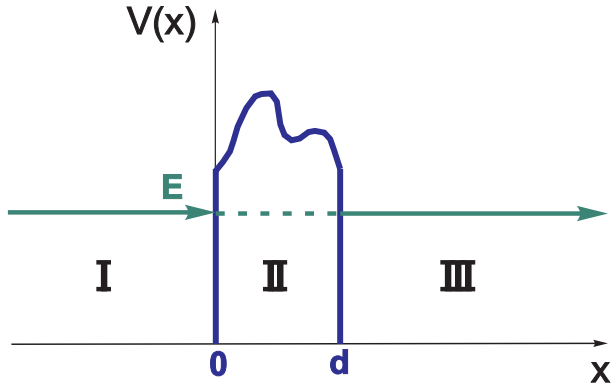


Figure G.1: Schematic figure - penetration through barrier (G.1).

the region I (see Fig. G1). That means the regions II and III are not accessible for particles from the point of view of the classical physics. However, from the point of view of the quantum mechanics there is some probabilty that particles penetrate through the barrier (region II) into the region III. Our aim is to determine this probability.

We will describe the particle beam which hint the barrier from the left (see Fig.G1) by means of the plane wave, $\psi_{im}(x) = A\, e^{ikx}$. Some particles are reflected by the barrier back to the region I and corresponding reflected beam

is again described by the plane wave, $\psi_{ref}(x) = B\, e^{-ikx}$. So, the complete wave function of parrticles in the region I is

$$\psi_I(x) = \psi_{im}(x) + \psi_{ref}(x) = A\, e^{ikx} + B\, e^{-ikx} \tag{G.2}$$

Particles penetrating to the region III go to the right direction and are described again by the plane wave:

$$\psi_{III}(x) = C\, e^{ikx} \tag{G.3}$$

In (G.2) and (G.2) $\hbar k$ stands for the linear momentum which is connected with the kinetic energy E of each particle by the following expression

$$E = \frac{\hbar^2 k^2}{2M} \tag{G.4}$$

where M is the particle mass.

The coefficients of the reflection, R, and of the penetration, D, are defined as follows

$$\begin{aligned} R &= \frac{|\text{ current of reflected particles }|}{|\text{ current of impacting particles }|} = \frac{j_{ref}}{j_{impact}} \\ D &= \frac{|\text{ current of penetrated particles }|}{|\text{ current of impacting particles }|} = \frac{j_{penetr}}{j_{impact}} \end{aligned} \tag{G.5}$$

The currents j_{impact}, j_{ref}, j_{penetr} are given by well-known expressions from the quantum mechanics

$$\begin{aligned} j_{impact}(x) &= -\frac{i\hbar}{2M}\left[\psi^*_{im}\frac{\partial\psi_{im}}{dx} - \psi_{im}\frac{\partial\psi^*_{im}}{dx}\right] = \frac{\hbar k}{M}\,|A|^2 \\ j_{ref}(x) &= -\frac{i\hbar}{2M}\left[\psi^*_{ref}\frac{\partial\psi_{ref}}{dx} - \psi_{ref}\frac{\partial\psi^*_{ref}}{dx}\right] = \frac{\hbar k}{M}\,|B|^2 \\ j_{penetr}(x) &= -\frac{i\hbar}{2M}\left[\psi^*_{III}\frac{\partial\psi_{III}}{dx} - \psi_{II}\frac{\partial\psi^*_{III}}{dx}\right] = \frac{\hbar k}{M}\,|C|^2 \\ &\Rightarrow \qquad R = \left|\frac{B}{A}\right|^2 \qquad D = \left|\frac{C}{A}\right|^2 \end{aligned} \tag{G.6}$$

The wave function $\psi_{II}(x)$ in the region II (classically not accessible region), where $0 \le x \le d$, is given by the WKB method, concretely by the following expression (see e.g. expression (7.256) in [14])

$$\psi_{II}(x) = \frac{1}{\sqrt{\kappa(x)}}\left\{\alpha\, e^{\int_0^x \kappa(y)\,dy} + \beta\, e^{-\int_0^x \kappa(y)\,dy}\right\} \tag{G.7}$$

where

$$\kappa(x) = \frac{1}{\hbar}\sqrt{2M\,(V(x) - E)}$$

with α and β normalization parameters.

Functions $\psi_I(x)$ (see (G.2)), $\psi_{II}(x)$ (see (G.8)), and $\psi_{III}(x)$ (see (G.3)) should be sewed together in the way that the final function is smooth and with smooth first derivative. The smmothness condition at the point $x = 0$ gives

$$A + B = \frac{1}{\sqrt{\kappa(0)}}\,(\alpha + \beta) \tag{G.8}$$

and the first derivative smoothness condition for $x = 0$ is

$$ik\,(A + B) = \sqrt{\kappa(0)}\,(\alpha - \beta) \tag{G.9}$$

The smoothness at the point $x = d$ is represented by

$$\frac{1}{\sqrt{\kappa(d)}}\,\alpha\,e^{\int_0^d \kappa(y)\,dy} + \frac{1}{\sqrt{\kappa(d)}}\,\beta\,e^{-\int_0^d \kappa(y)\,dy} = C\,e^{ikd} \tag{G.10}$$

and the first derivative smoothness condition for $x = d$ is

$$\sqrt{\kappa(d)}\,\alpha\,e^{\int_0^d \kappa(y)\,dy} - \sqrt{\kappa(d)}\,\beta\,e^{-\int_0^d \kappa(y)\,dy} = ik\,C\,e^{ikd} \tag{G.11}$$

Equations (G.8) - (G.11) form the system of 4 equations for 5 unknowns A, B, C, α, β (the fifth equation can be obtained from the normalization of the whole wave function):

$$\begin{aligned} \sqrt{a}\,(A + B) &= \alpha + \beta \\ ik\,(A - B) &= \sqrt{a}\,(\alpha - \beta) \end{aligned} \tag{G.12}$$

and

$$\begin{aligned} \alpha\,e^{\gamma} + \beta\,e^{-\gamma} &= c\,\sqrt{b}\,e^{ikd} \\ \sqrt{b}\,(\alpha\,e^{\gamma} - \beta\,e^{-\gamma}) &= ik\,e^{ikd} \end{aligned} \tag{G.13}$$

where

$$\begin{aligned} a &\equiv \kappa(0) = \frac{1}{\hbar}\sqrt{2M\,(V(0) - E)} \\ b &\equiv \kappa(d) = \frac{1}{\hbar}\sqrt{2M\,(V(d) - E)} \\ \gamma &\equiv \frac{1}{\hbar}\int_0^d dx\,\sqrt{2M\,(V(x) - E)} \end{aligned} \tag{G.14}$$

are known quantities.

From (G.12) the expressions for α and β can be obtained

$$\begin{aligned} \alpha &= \frac{1}{2}\left(\sqrt{b}+\frac{ik}{\sqrt{b}}\right) C\, e^{ikd-\gamma} \\ \beta &= \frac{1}{2}\left(\sqrt{b}-\frac{ik}{\sqrt{b}}\right) C\, e^{ikd+\gamma} \end{aligned} \tag{G.15}$$

The quasi-classical WKB solution for the wave function $\psi_{II}(x)$ in the classically not accessible region II (see (G.7) is applicable only for sufficiently broad barriers (see [14]). This means the high value for d and as a consequence of it $\gamma \approx d\bar{\kappa} >> 1$ and therefore $\beta >> \alpha$ (see (G.15)):

$$\begin{aligned} \sqrt{a}\,(A+B) &\approx \beta \\ ik\,(A-B) &\approx -\beta\sqrt{a} \end{aligned} \quad \Rightarrow \quad \begin{aligned} A+B &\approx \tfrac{\beta}{\sqrt{a}} \\ A-B &\approx -\tfrac{\beta\sqrt{a}}{ik} \end{aligned}$$

$$\Rightarrow A = \frac{1}{2}\left[\frac{\beta}{\sqrt{a}} - \frac{\beta\sqrt{a}}{ik}\right] \tag{G.16}$$

The coefficient C can be obtained e.g. from the second equation in (G.15)

$$\begin{aligned} C &= \frac{2\beta}{\sqrt{b}-\frac{ik}{b}}\, e^{-ikd-\gamma} \\ \Rightarrow \frac{C}{A} &= \boxed{\begin{array}{c}\text{see} \\ (G.16),\ (G.17)\end{array}} = \frac{4\, e^{-ikd-\gamma}}{\left(\frac{1}{\sqrt{a}}\right)\left(\sqrt{b}-\frac{ik}{\sqrt{b}}\right)} \end{aligned} \tag{G.17}$$

and the final expression for the penetration coefficient D is

$$D = \left|\frac{C}{A}\right|^2 = \frac{16\, e^{-2\gamma}}{\frac{b}{a}+\frac{ab}{k^2}+\frac{k^2}{ab}+\frac{a}{b}} \approx e^{-\frac{2}{\hbar}\int_0^d dx\,\sqrt{2M\,(V(x)-E)}} \tag{G.18}$$

The reflection coefficient R is then given by the condition:

$$R + D = 1 \tag{G.19}$$

The above obtained result (G.18) was derived for the barrier in the form of (G.1) ($V(x) = 0$ for $x < 0$ and $x > d$). It can be shown (see e.g. [14]) that the expression (G.18) is general (it valids for general barrier (see Fig 5.14)):

$$D \approx e^{-\frac{2}{\hbar}\int_a^b dx\,\sqrt{2M\,(V(x)-E)}} \tag{G.20}$$

where $V(a) = V(b) = E$ (see Fig. 5.14).

H. Density of Fermi gas and Fermi sphere

Fermi gas is defined as the system of mutually noninteracting fermions. That means the Hamiltonian of the system is given only by the kinetic energy operator with the corresponding single-particle eigen-wave function in the form of plane waves

$$\varphi_i(\vec{r}) = \frac{1}{V}\, e^{i\,\vec{k}\cdot\vec{r}}\,\chi_\mu\,, \qquad \hat{t}\,\varphi_i(\vec{r}) = -\frac{\hbar^2 k^2}{2m}\,\varphi_i(\vec{r}) \tag{H.1}$$

where χ_μ is the eigen-function of square of the spin and its z-projection ($\hat{s}^2\,\chi_\mu = 3/4\,\chi_\mu,\ \hat{s}_z\,\chi_\mu = \mu\,\chi_\mu$), $\mu = \pm 1/2$. The single-particle index i corresponds to given values of the linear momentum components $k_x,\ k_y,\ k_z$ (in the 3-dimesional space) and to the given value of the spin projection μ. Plane wave (H.1) is the periodical function in the spatial space with some periodic distance L. In the border of the cube with the side L the following condition should be fulfilled by the plane wave (we suppose 3-dimesional Fermi gas)

$$\begin{aligned} & e^{i\,k_x\,(x+L)} = e^{i\,k_x\,x}\,, \quad e^{i\,k_y\,(y+L)} = e^{i\,k_y\,y}\,, \quad e^{i\,k_z\,(z+L)} = e^{i\,k_z\,z}\,, \\ & \Rightarrow \quad e^{i\,k_j\,L} = e^{i\,2\pi\,n_j} \quad (j = x,\ y,\ z) \quad \Rightarrow \quad k_j = \frac{2\pi}{L}\,n_j \end{aligned} \tag{H.2}$$

where $j = x,\ y,\ z$ in the case of 3-dimensional Fermi gas (the nucleus case) and n_x, n_y, n_z are integer numbers. For general D-dimensional gas the volume of the cube with the side L is

$$V = L^D \tag{H.3}$$

and we have (see (H.2))

$$\begin{aligned} D=1 \quad & \to\ k = \frac{2\pi}{L}\,n, && n = 0,\ \pm 1,\ \pm 2, \ldots \\ D=2 \quad & \to\ \vec{k} = (\frac{2\pi}{L}\,n_x, \frac{2\pi}{L}\,n_y), && n_x,\ n_y = 0,\ \pm 1,\ \pm 2, \ldots \\ D=3 \quad & \to\ \vec{k} = (\frac{2\pi}{L}\,n_x, \frac{2\pi}{L}\,n_y, \frac{2\pi}{L}\,n_z), && n_x,\ n_y,\ n_z = 0,\ \pm 1,\ \pm 2, \ldots \end{aligned} \tag{H.4}$$

In the case of the Fermi gas the ground state is characterized by the occupation of all single-particle states with energies up to the Fermi energy $\hbar^2 k_F^2/2m$ (m is the nucleon mass). In the linear momentum space it means that in the ground state of the Fermi gas all single-particle states with $\vec{k}$ fulfilling

$$|\vec{k}| \leq k_F$$

and with given spin projection μ are occupied by one particle. So the number N of all fermions in the given Fermi gas is

$$\begin{aligned} N &= \sum_{\substack{n_x,n_y,n_z \\ \text{inside Fermi sphere}}} 1 = \sum_{\mu=\pm 1/2} \int d\vec{n} = \boxed{\begin{array}{c}\text{see} \\ (H.2)\end{array}} = \\ &= \left(\frac{L}{2\pi}\right)^D \sum_{\mu=\pm 1/2} \int n_k \, d\vec{k} \end{aligned} \tag{H.5}$$

where

$$n_k = \begin{cases} 1 & \text{for } |\vec{k}| \leq \vec{k}_F, \\ 0 & \text{for } |\vec{k}| > \vec{k}_F \end{cases} \tag{H.6}$$

Therefore the density of the Fermi gas depending on the dimension D of the space is

$$\begin{aligned} \rho^{(3D)} &= \frac{N}{L^3} = \frac{1}{(2\pi)^3}\, 2\, \frac{4}{3}\pi k_F^3 = \frac{k_F^3}{3\pi^2} \\ \rho^{(2D)} &= \frac{N}{L^2} = \frac{1}{(2\pi)^2}\, 2\, \pi\, k_F^2 = \frac{k_F^2}{\pi} \\ \rho^{(1D)} &= \frac{N}{L} = \frac{1}{(2\pi)}\, 2\, 2\, k_F = \frac{2k_F}{\pi} \end{aligned} \tag{H.7}$$

I. Collective Hamiltonian of the Liquid Drop Model (LDM)

In this appendix mass parameters B_λ and potential parameters C_λ involved in the LDM (or Bohr Geometrical Model - BGM) Hamiltonian H_C (see 7.31),

$$H_C = \frac{1}{2} \sum_{\lambda\mu} \left(B_\lambda \mid \dot{\alpha}_{\lambda\mu}|^2 + C_\lambda \mid \alpha_{\lambda\mu}|^2 \right) , \tag{I.1}$$

of arbitrary nuclear droplet are derived. Vibrations are described by collective coordinates $\alpha_{\lambda\mu}$ (see (7.30) ($\dot{\alpha}_{\lambda\mu} = \frac{d\alpha_{\lambda\mu}}{dt}$). Starting point of the derivation of parameters B_λ and C_λ is the assumption of the irrotationality and incompressibility of the nuclear liquid (matter) forming the droplet.

The assumption of the irrotationality of the nuclear liquid (that means the liquid without vortexes) can be expressed by the following condition

$$\vec{\nabla} \times \vec{v}(\vec{r}) = 0 \tag{I.2}$$

where $\vec{v}(\vec{r})$ stands for the velocity field of the liquid (velocity of the liquid in the given point $\vec{r}$). Since there is the mathematical identity

$$\vec{\nabla} \times \left(\vec{\nabla} \Psi(\vec{r}) \right) = 0 \, , \tag{I.3}$$

where $\Psi(\vec{r})$ is arbitrary scalar function of $\vec{r}$, the velocity field of the irrotational liquid can be written as the gradient of the scalar function $\Psi(\vec{r})$:

$$\vec{v}(\vec{r}) = -\vec{\nabla} \Psi(\vec{r}) \tag{I.4}$$

The requirement of the incompressibility of the nuclear liquid means that the nucleon density inside the whole volume of the nucleus is constant during the shape vibration, that means:

$$\dot{\rho} = 0 \tag{I.5}$$

This requirement can be rewritten using the continuity equation, $\vec{\nabla} \vec{j} + \frac{\partial \rho}{\partial t} = 0$ (where $\vec{j}(\vec{r}) = \rho(\vec{r}) \, \dot{\vec{r}}$ is the current density and the density ρ is supposed to

be constant inside the nucleus), as follows (we use also the approximation that $\vec{v}(\vec{r}) \approx \dot{\vec{r}}$) [1]

$$\vec{\nabla}\vec{v}(\vec{r}) = 0 \quad \Rightarrow \quad \Delta\Psi(\vec{r}) = 0 \tag{I.6}$$

From the mathematics it is known that the general solution of the equation (I.6) can be expressed as follows

$$\Psi(\vec{r}) = \sum_{\lambda\mu} d^*_{\lambda\mu}\, r^\lambda Y_{\lambda\mu}(\hat{r}) \tag{I.7}$$

where $Y_{\lambda\mu}(\hat{r})$ are spherical functions and amplitudes $d_{\lambda\mu}$ are determined below.

From the equation (I.4) it follows that the radial component of the velocity field $\vec{v}(\vec{r}\,)$ in the equilibrium shape on the nuclear surface, $r = R_0$, is

$$v_r(\vec{r}) = -\frac{\partial\Psi(\vec{r})}{\partial r}|_{r=R_0} = \boxed{\begin{array}{c}\text{see}\\ (I.7)\end{array}} = -\sum_{\lambda\mu} d^*_{\lambda\mu}\, \lambda\, R_0^{\lambda-1}\, Y_{\lambda\mu}(\hat{r}) \tag{I.8}$$

From the other side this radial component $v_r(\vec{r})$ can be determined from the exp. (7.45) (the distance from the center of the nucleus to its surface, where the nucleus center coincides with the origin of the coordinate frame):

$$v_r(\vec{r}) = \dot{R}(\vartheta,\varphi) = R_0 \sum_{\lambda\mu} \dot{\alpha}^*_{\lambda\mu}\, Y_{\lambda\mu}(\hat{r}) \tag{I.9}$$

and the comparison of (I.8) and (I.9) gives

$$d_{\lambda\mu} = -\frac{1}{\lambda}\, R_0^{2-\lambda}\, \dot{\alpha}_{\lambda\mu} \tag{I.10}$$

---

[1] From

$$\vec{\nabla}\vec{j} + \frac{\partial\rho}{\partial t} = 0\,, \qquad \vec{j}(\vec{r}) = \rho\,\vec{v}(\vec{r})$$

and

$$\dot{\rho} = \frac{d\rho}{dt} = \frac{\partial\rho}{\partial x_i}\frac{dx_i}{dt} + \frac{\partial\rho}{\partial t} = 0$$

it follows

$$\frac{\partial\rho}{\partial x_i}\frac{dx_i}{dt} - \vec{\nabla}\vec{j} = 0$$

and the substitution for $\vec{j}$ gives

$$\frac{\partial\rho}{\partial x_i}\frac{dx_i}{dt} - \vec{\nabla}\cdot\rho\vec{v} = \frac{\partial\rho}{\partial x_i}\frac{dx_i}{dt} - \frac{\partial\rho}{\partial x_i}v_i - \rho\frac{\partial}{\partial x_i}v_i \approx -\rho\frac{\partial}{\partial x_i}v_i = 0$$

So we have

$$\vec{\nabla}\vec{v}(\vec{r}) = 0$$

I.1 Derivation of B_λ

The kinetic energy of the nuclear drop is represented by the first term in (I.1). It is evident that it can be expressed also as follows (M is the nucleon mass and we suppose the constant density ρ_0 inside the nucleus)

$$T = \frac{1}{2}\, M \int_{(V)} d^3r\, \rho\, v^2 \approx \boxed{\begin{array}{c}\text{see}\\ (I.4)\end{array}} \approx \frac{M\,\rho_0}{2} \int_{(V)} d^3r \left|\vec{\nabla}\Psi\right|^2 =$$

$$= \boxed{\begin{array}{c}\text{because } (I.6) \text{ and}\\ \vec{\nabla}(\Psi^*\vec{\nabla}\Psi) = \left|\vec{\nabla}\Psi\right|^2 + \Psi^*\Delta\Psi\end{array}} = \frac{M\rho_0}{2} \int_{(V)} d^3r\, \vec{\nabla}(\Psi^*\vec{\nabla}\Psi) =$$

$$= \boxed{\begin{array}{c}\text{Gauss theorem}\\ \text{from mathematics}\end{array}} = \frac{M\rho_0}{2} \int_{(S)} \Psi^*(\vec{\nabla}\Psi)\cdot d\vec{S} =$$

$$= \boxed{\begin{array}{c}\text{see}\\ (I.7)\end{array}} = \frac{M\rho_0}{2} \int_{(S)} \sum_{\substack{\lambda\mu\\ \lambda'\mu'}} d^*_{\lambda\mu}\, d_{\lambda'\mu'}\, r^\lambda Y_{\lambda\mu}\, (\vec{\nabla} r^{\lambda'} Y^*_{\lambda'\mu'})\, d\vec{S} =$$

$$= \boxed{\begin{array}{c}\text{because - see (A.62):}\\ \vec{\nabla} r^{\lambda'} Y_{\lambda'\mu'} = \sqrt{\lambda'(2\lambda'+1)}\;\; r^{\lambda'-1}\, \vec{Y}_{\lambda'-1\;\lambda'\;\mu'}\end{array}} =$$

$$= \frac{M\rho_0}{2} \int_{(S)} \sum_{\substack{\lambda\mu\\ \lambda'\mu'}} d^*_{\lambda\mu}\, d_{\lambda'\mu'}\, r^\lambda Y_{\lambda\mu}\, r^{\lambda'-1}$$

$$\sqrt{\lambda'(2\lambda'+1)}\;\; r^{\lambda'-1}\, \vec{Y}^*_{\lambda'-1\;\lambda'\;\mu'} \cdot d\vec{S} =$$

$$= \boxed{\begin{array}{c}\text{because } d\vec{S} = \vec{n}\, dS \text{ and, see p. 219 in [2]}\\ \vec{n}\cdot\vec{Y}_{\lambda'-1\;\lambda'\;\mu'} = \sqrt{\frac{\lambda'}{2'\lambda'+1}}\, Y_{\lambda'\mu'}(\hat{r})\end{array}} =$$

$$= \frac{M\rho_0}{2} \int_{(S)} \sum_{\substack{\lambda\mu\\ \lambda'\mu'}} d^*_{\lambda\mu}\, d_{\lambda'\mu'}\, R_0^{\lambda+\lambda'-1}\, \lambda'\, Y_{\lambda\mu}\, Y^*_{\lambda'\mu'}\, dS =$$

$$= \boxed{\begin{array}{c}\text{because}\\ dS = R_0^2\, d\Omega\end{array}} =$$

$$= \frac{M\rho_0\, R_0^{\lambda+\lambda'+1}}{2} \sum_{\substack{\lambda\mu\\ \lambda'\mu'}} d^*_{\lambda\mu}\, d_{\lambda'\mu'}\, \lambda' \int d\Omega\, Y_{\lambda\mu}(\hat{r})\, Y^*_{\lambda'\mu'}(\hat{r}) =$$

$$= \boxed{\begin{array}{c}\text{because}\\ \int d\Omega\, Y_{\lambda\mu}(\hat{r})\, Y^*_{\lambda'\mu'}(\hat{r}) = \delta_{\lambda\lambda'}\, \delta_{\mu\mu'}\end{array}} = \frac{M\rho_0\, R_0^{2\lambda+1}}{2} \sum_{\lambda\mu} \lambda\, |d_{\lambda\mu}|^2 =$$

$$= \boxed{\begin{array}{c}\text{see}\\ (I.10)\end{array}} = \frac{M\rho_0\, R_0^5}{2} \sum_{\lambda\mu} \frac{1}{\lambda}\, |\dot{\alpha}_{\lambda\mu}|^2 \qquad \text{(I.11)}$$

The comparison of (I.11) with the first term in (I.1):

$$T = \frac{1}{2} \sum_{\lambda\mu} B_\lambda\, |\dot{\alpha}_{\lambda\mu}|^2 \qquad \text{(I.12)}$$

gives the expression for B_λ:

$$B_\lambda = \frac{M\rho_0\, R_0^5}{\lambda} = \boxed{\begin{array}{c}\text{because}\\ \rho_0 = \frac{A}{\frac{4}{3}\pi R_0^3}\end{array}} = \frac{3}{4\pi\lambda}\, A\, M\, R_0^2 \qquad \text{(I.13)}$$

I.2 Derivation of C_λ

The potential parameter C_λ in the collective oscillator potential in (I.1) can be determined in terms of the analysis of the dynamical change of the nucleus total energy during the shape vibrations. In the framework of the LDM the total nucleus energy is given by the Weizsacker formula (1.13):

$$B(Z,N) = b_V A + b_S A^{2/3} + b_C \frac{Z^2}{A^{1/3}} + b_{sym} \frac{(N-Z)^2}{A} + \delta(A) \qquad \text{(I.14)}$$

where parameters b_V, b_S, b_C, b_{sym} are described in (1.13). If we assume the incompressibility of the nuclear liquid then the first term (volume term) does not change during the nucleus vibrations. Similarly last two terms in (I.14) do not change as well. So the relevant terms in (I.14) for the nuclear shape vibrations are the second (surface) and third (Coulomb) ones. Only these two terms change during the surface vibrations. The potential energy

of these vibrations, given in the Hamiltonian (I.1) by the second term, is therefore given only by these surface and Coulomb terms in the Weizsacker formula

$$V = \frac{1}{2} \sum_{\lambda\mu} C_\lambda \mid \alpha_{\lambda\mu}|^2 = V_{surf} + V_{coul} \tag{I.15}$$

Further these two terms, V_{surf} and V_{coul}, are specified in the depedence on the collective variables $\alpha_{\lambda\mu}$.

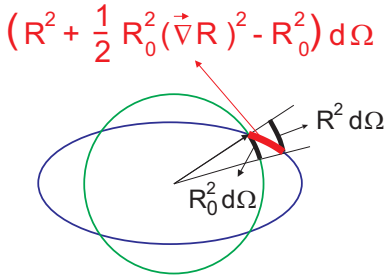


Figure I.1: Schematic figure of the change of the surface element under the space angle $d\Omega$ during the surface vibration.

At first the part V_{surf} will be determined. During surface vibrations the surface of the nucleus droplett changes (with the value ΔS). According to the classical physics this surface change corresponds to the potential energy V_{surf} given by the surface tension $\sigma = b_S/(4\pi r_0^2)$ (see the text below the exp. (1.14)):

$$V_{surf} = \sigma\, \Delta S =$$

$$= \boxed{\begin{array}{l}\text{from the geometrical analyses (see Fig. I.1 and [99])} \\ \text{it follows: } \Delta S = \int d\Omega \left(R^2(\vartheta,\varphi) + \frac{1}{2} R_0^2 \, (\vec{\nabla} R)^2 - R_0^2 \right)\end{array}} =$$

$$= \sigma \int d\Omega \left[R^2(\vartheta,\varphi) + \frac{1}{2} R_0^2 \, (\vec{\nabla} R)|^2_{r=R_0} - R_0^2 \right] =$$

$$= \sigma \int d\Omega \left[2\, R_0 \, (R - R_0) + (R - R_0)^2 + \frac{1}{2} R_0^2 \, (\vec{\nabla} R)|^2_{r=R_0} \right] =$$

$$= \boxed{\begin{array}{c}\text{because } \int d\Omega\, \vec{\nabla}\,(R\,\vec{\nabla} R) = 0 \\ \vec{\nabla}\,(R\,\vec{\nabla} R) = (\vec{\nabla} R)^2 + R\,\Delta R\end{array}} =$$

$$= \sigma \int d\Omega \left[2\,R_0\,(R - R_0) + (R - R_0)^2 - \frac{1}{2}\,R_0^2\,R\,(\Delta R)\big|_{\,r=R_0} \right] =$$

$$= \boxed{\begin{array}{c}\text{because } \Delta R\big|_{\,r=R_0} = \left(\frac{1}{r_2}\frac{\partial}{\partial r}(r^2 \frac{\partial}{\partial r}) - \frac{\vec{L}^2}{r^2} \right)\, R_0 \,\sum_{\lambda\mu} \alpha^*_{\lambda\mu}\, Y_{\lambda\mu} = \\ = -\frac{1}{R_0}\,\sum_{\lambda\mu} \alpha^*_{\lambda\mu}\,\lambda\,(\lambda+1)\,Y_{\lambda\mu}\end{array}} =$$

$$= \sigma \int d\Omega \left[2\,R_0^2 \sum_{\lambda\mu} \alpha^*_{\lambda\mu}\, Y_{\lambda\mu} + R_0^2 \sum_{\substack{\lambda\mu \\ \lambda'\mu'}} \alpha^*_{\lambda\mu}\,\alpha_{\lambda'\mu'}\, Y_{\lambda\mu}\, Y_{\lambda'\mu'} + \right.$$

$$\left. + \frac{1}{2}\,R_0^2 \sum_{\substack{\lambda\mu \\ \lambda'\mu'}} \lambda\,(\lambda+1)\,\alpha^*_{\lambda\mu}\,\alpha_{\lambda'\mu'}\, Y_{\lambda\mu}\, Y^*_{\lambda'\mu'} \right] =$$

$$= \boxed{\begin{array}{c}\text{because} \\ \int d\Omega\, Y_{\lambda\mu} = \delta_{\lambda 0}\,\delta_{\mu 0}\,\sqrt{4\pi}\,, \quad \int d\Omega\, Y^*_{\lambda\mu}\, Y_{\lambda'\mu'} = \delta_{\lambda\lambda'}\,\delta_{\mu\mu'}\end{array}} =$$

$$= \sigma\,R_0^2 \left[2\sqrt{4\pi}\,\alpha_{00} + \sum_{\lambda\mu} |\,\alpha_{\lambda\mu}|^{\,2} + \frac{1}{2} \sum_{\lambda\mu} \lambda\,(\lambda+1)\,|\,\alpha_{\lambda\mu}|^{\,2} \right] \qquad \text{(I.16)}$$

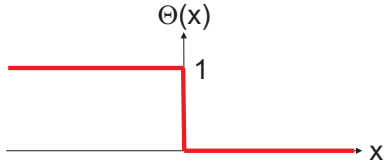


Figure I.2: The figure of the step function: $\Theta(x) = 1$ if $x < 0$, and $\Theta(x) = 0$ if $x > 0$. It is evident that the derivative of the step function is: $\frac{d\Theta}{dx} = -\,\delta(x)$.

Further the connection between α_{00} and $\sum_{\lambda\mu} |\alpha_{\lambda\mu}|^{\,2}$ is determined. If the incompressibility of the nuclear liquid is supposed with the constant value of the density inside the nucleus then the density of nucleons can be expressed by the step function $\Theta(x)$ (see Fig. I.2).

$$\rho(r, \vartheta, \varphi) = \rho_0\ \Theta(r - R(\vartheta, \varphi)) \qquad \text{(I.17)}$$

where the constant density ρ_0 is given by the following normalization condition

$$A = \int_0^\infty r^2\, dr \int d\Omega\, \rho(r, \vartheta, \varphi) \tag{I.18}$$

Since we suppose small vibrations with respect to deformation parameters $\alpha_{\lambda\mu}$ we can apply the Taylor expansion in (I.17) (it should be realized that the differentiation of the step function in the Taylor expansion is assumed to be performed in (I.17) with respect to $R(\vartheta, \varphi)$ in the vicinity of $R(\vartheta, \varphi) = R_0$)

$$\begin{aligned}
\rho(r, \vartheta, \varphi) &= \rho_0 \Big[\Theta(r - R_0) + \Theta'(r - R_0)\,(R - R_0) + \\
&\qquad + \frac{1}{2}\,\Theta''(r - R_0)\,(R - R_0)^2 + \ldots\Big] = \\
&= \boxed{\begin{array}{c}\text{see the capture of}\\ \text{the Fig. I.2}\end{array}} = \\
&= \rho_0 \Big[\Theta(r - R_0) + \delta(r - R_0)\,(R - R_0) \\
&\qquad - \frac{1}{2}\,\frac{d}{dr}\delta(r - R_0)\,(R - R_0)^2 + \ldots\Big]
\end{aligned} \tag{I.19}$$

where

$$\rho_0 = \frac{A}{\frac{4}{3}\,\pi\, R_0^3} \tag{I.20}$$

The substitution of (I.19) into (I.18) gives

$$\begin{aligned}
A &\approx \rho_0 \int d\Omega \int_0^\infty dr\, r^2 \Big[\Theta(r - R_0) + \delta(r - R_0)\,(R - R_0) \\
&\qquad - \frac{1}{2}\,(R - R_0)^2\,\frac{d}{dr}\delta(r - R_0) + \ldots\Big] = \\
&= \boxed{\begin{array}{c}\text{per partes integration}\\ \text{in the last term}\end{array}} = \\
&= \rho_0 \int d\Omega \int_0^\infty dr\, \Big[r^2\,\Theta(r - R_0) + r^2\,\delta(r - R_0)\,(R - R_0) \\
&\qquad + \frac{1}{2}\,(R - R_0)^2\,\delta(r - R_0)\,2r\Big] =
\end{aligned}$$

$$= \rho_0 \int d\Omega \left[\frac{R_0^3}{3} + R_0^3 \sum_{\lambda\mu} \alpha^*_{\lambda\mu}\, Y_{\lambda\mu} + \right.$$
$$\left. + R_0^3 \sum_{\lambda\mu} \sum_{\lambda'\mu'} Y_{\lambda\mu} Y^*_{\lambda'\mu'} \alpha^*_{\lambda\mu} \alpha_{\lambda'\mu'} \right] =$$

$$= \boxed{\begin{array}{c} \text{because of (I.20) and} \\ \int d\Omega\, Y_{\lambda\mu} = \delta_{\lambda 0}\delta_{\mu 0}\,\sqrt{4\pi}\,, \int d\Omega\, Y_{\lambda\mu} Y^*_{\lambda'\mu'} = \delta_{\lambda\lambda'}\delta_{\mu\mu'} \end{array}} =$$

$$= A + \alpha^*_{00}\,\rho_0\, R_0^3\,\sqrt{4\pi} + \rho_0\, R_0^3 \sum_{\lambda\mu} |\,\alpha_{\lambda\mu}|^{\,2} \qquad \text{(I.21)}$$

From (I.21) it follows

$$\alpha_{00}\,\sqrt{4\pi} = -\sum_{\lambda\mu} |\,\alpha_{\lambda\mu}|^{\,2} \qquad \text{(I.22)}$$

and the substitution of (I.22) for α_{00} into (I.16) gives

$$\begin{aligned} V_{surf} &= \sigma\, R_0^2 \left[-\sum_{\lambda\mu} |\,\alpha_{\lambda\mu}|^{\,2} + \frac{1}{2} \sum_{\lambda\mu} \lambda(\lambda+1)\,|\,\alpha_{\lambda\mu}|^{\,2} \right] \\ &= \frac{\sigma\, R_0^2}{2} \sum_{\lambda\mu} |\,\alpha_{\lambda\mu}|^{\,2}\,(\lambda-1)\,(\lambda+2) \end{aligned} \qquad \text{(I.23)}$$

Further the Coulomb contribution to the surface vibration potential energy (I.15) is derived. The change of the Coulomb energy during the spherical nucleus vibration is given by:

$$V_{coul} = \frac{1}{2} \int d^3r\, \rho^{(ch)}(\vec{r})\, \varphi^{(coul)}(\vec{r}) - \frac{1}{2} \int d^3r\, \rho_0^{(ch)}(\vec{r})\, \varphi_0^{(coul)}(\vec{r}) \qquad \text{(I.24)}$$

where $\rho_0^{(ch)}(\vec{r})$ and $\varphi_0^{(coul)}(\vec{r})$ are the charge density and the Coulomb potential of the spherical droplett in the equilibrium spherical shape, respectively. Symbols $\rho^{(ch)}(\vec{r})$ and $\varphi^{(coul)}(\vec{r})$ are also charge density and Coulomb potential but now in the general deformation shape during the vibration. The density vibration can be expressed in terms of the equilibrium $\rho_0^{(ch)}(\vec{r})$ and $\varphi_0^{(coul)}(\vec{r})$ as follows

$$\begin{aligned} \rho^{(ch)}(\vec{r}) &= \rho_0^{(ch)}(\vec{r}) + \delta\rho^{(ch)}(\vec{r}) \\ \varphi^{(coul)}(\vec{r}) &= \varphi_0^{(coul)}(\vec{r}) + \delta\varphi^{(coul)}(\vec{r}) \end{aligned} \qquad \text{(I.25)}$$

So the product $\rho^{(ch)}(\vec{r})\,\varphi^{(coul)}(\vec{r})$ involved in (I.24) is

$$\rho^{(ch)}(\vec{r})\,\varphi^{(coul)}(\vec{r}) = \rho_0^{(ch)}(\vec{r})\,\varphi_0^{(coul)}(\vec{r}) + \delta\rho^{(ch)}(\vec{r})\,\varphi_0^{(coul)}(\vec{r}) +$$
$$+ \rho_0^{(ch)}(\vec{r})\,\delta\varphi^{(coul)}(\vec{r}) + \delta\rho^{(ch)}(\vec{r})\,\delta\varphi^{(coul)}(\vec{r}) \qquad \text{(I.26)}$$

It can be shown that (see [99])

$$\int d^3r\, \delta\rho^{(ch)}(\vec{r})\, \varphi_0^{(coul)}(\vec{r}) = \int d^3r\, \rho_0^{(ch)}(\vec{r})\, \delta\varphi^{(coul)}(\vec{r})$$

Therefore the first term in (I.24) is following

$$\begin{aligned}
&\frac{1}{2} \int d^3r\, \rho^{(ch)}(\vec{r})\, \varphi^{(coul)}(\vec{r}) = \\
&= \frac{1}{2} \int d^3r \Big[\rho_0^{(ch)}(\vec{r})\, \varphi_0^{(coul)}(\vec{r}) + 2\, \delta\rho^{(ch)}(\vec{r})\, \varphi_0^{(coul)}(\vec{r}) + \\
&\qquad\qquad + \delta\rho^{(ch)}(\vec{r})\, \delta\varphi^{(coul)}(\vec{r}) \Big]
\end{aligned}$$

and (see (I.24))

$$V_{coul} = \int d^3r\, \delta\rho^{(ch)}(\vec{r})\, \varphi_0^{(coul)}(\vec{r}) + \frac{1}{2} \int d^3r\, \delta\rho(\vec{r})\, \delta\varphi^{(coul)}(\vec{r}) \tag{I.27}$$

In the framework of the approximation that the density is constant in the whole volume of the droplett and using expressions (I.19) and (I.20) we can write following expressions for $\rho_0^{(ch)}$ and $\delta\rho^{(ch)}$

$$\begin{aligned}
\rho_0^{(ch)}(\vec{r}) &= \frac{3Ze}{4\pi R_0^3}\, \Theta(r - R_0) \\
\delta\rho^{(ch)}(\vec{r}) &= \frac{3Ze}{4\pi R_0^3} \Big[(R(\vartheta,\varphi) - R_0)\, \delta(r - R_0) \\
&\qquad - \frac{1}{2}\, (R(\vartheta,\varphi) - R_0)^2\, \frac{d}{dr}\delta(r - R_0) \Big]
\end{aligned} \tag{I.28}$$

So

$$\int d^3r\ \delta\rho^{(ch)}(\vec{r})\ \varphi_0^{(coul)}(\vec{r}) =$$

$$= \frac{3Ze}{4\pi R_0^3}\left[(R(\vartheta,\varphi)-R_0)\,\delta(r-R_0)\right.$$

$$\left.-\frac{1}{2}\,(R(\vartheta,\varphi)-R_0)^2\,\frac{d}{dr}\delta(r-R_0)\right]\varphi_0^{(coul)}(\vec{r}) =$$

$$= \boxed{\begin{array}{c}\text{because}\\ R(\vartheta,\varphi)-R_0 = R_0\ \textstyle\sum_{\lambda\mu}\alpha^*_{\lambda\mu}\,Y_{\lambda\mu}(\vartheta,\varphi)\end{array}} =$$

$$= \frac{3Ze}{4\pi R_0^3}\int d\Omega\int dr\ r^2\left[\delta(r-R_0)\,R_0\sum_{\lambda\mu}\alpha^*_{\lambda\mu}\,Y_{\lambda\mu}(\vartheta,\varphi)\right.$$

$$\left.-\frac{R_0^2}{2}\sum_{\substack{\lambda\mu\\ \lambda'\mu'}}\alpha^*_{\lambda\mu}\,\alpha_{\lambda'\mu'}\,Y_{\lambda\mu}(\hat{r})\,Y^*_{\lambda'\mu'}(\hat{r})\,\frac{d}{dr}\delta(r-R_0)\right]\varphi_0^{(coul)}(\vec{r}) =$$

$$= \boxed{\begin{array}{c}\text{because }\ \textstyle\int d\Omega\,Y_{\lambda\mu}(\vartheta,\varphi)=\delta_{\lambda 0}\delta_{\mu 0}\sqrt{4\pi}\,;\\ \textstyle\int d\Omega\,Y_{\lambda\mu}(\hat{r})\,Y^*_{\lambda'\mu'}(\hat{r})=\delta_{\lambda\lambda'}\delta_{\mu\mu'}\text{ and per partes in the 2-d term}\end{array}} =$$

$$= \frac{3ZeR_0}{4\pi R_0^3}\,\alpha^*_{00}\,\sqrt{4\pi}\int_0^{R_0} dr\ r^2\,\delta(r-R_0)\,\varphi_0^{(coul)}(\vec{r}) +$$

$$+\frac{3ZeR_0^2}{8\pi R_0^3}\sum_{\lambda\mu}|\,\alpha_{\lambda\mu}|^2\int_0^{R_0} dr\,\delta(r-R_0)\,\frac{d(r^2\varphi_0^{(coul)}(\vec{r}))}{dr} =$$

$$= \frac{3Ze}{4\pi}\,\alpha^*_{00}\,\sqrt{4\pi}\,\varphi_0^{(coul)}(R_0)\ +$$

$$+\frac{3Ze}{8\pi R_0}\left[2\,R_0\,\varphi_0^{(coul)}(R_0)+R_0^2\,\frac{d\varphi_0^{(coul)}(R_0)}{dr}\right]\sum_{\lambda\mu}|\alpha_{\lambda\mu}|^2 =$$

$$= \boxed{\begin{array}{c}\text{see}\\ (I.22)\end{array}} =$$

$$= -\frac{3Ze}{4\pi}\,\varphi_0^{(coul)}(R_0)\sum_{\lambda\mu}|\,\alpha_{\lambda\mu}|^2+\frac{3Ze}{4\pi}\,\varphi_0^{(coul)}(R_0)\sum_{\lambda\mu}|\,\alpha_{\lambda\mu}|^2+$$

$$+\frac{3Ze}{8\pi}\,R_0\,\frac{d\varphi_0^{(coul)}(r)}{dr}\Big|_{r=R_0}\sum_{\lambda\mu}|\,\alpha_{\lambda\mu}|^2 =$$

$$= \boxed{\begin{array}{c}\text{because}\\ \varphi_0(r)\Big|_{r=R_0}=\frac{Ze}{4\pi\epsilon_0\,R_0}\,;\quad \frac{d\varphi_0(r)}{dr}\Big|_{r=R_0}=-\frac{Ze}{4\pi\epsilon_0 R_0^2}\end{array}} =$$

$$= -\frac{3}{8\pi}\,\frac{Z^2e^2}{4\pi\epsilon_0 R_0}\sum|\,\alpha_{\lambda\mu}|^2 \qquad \text{(I.29)}$$

The 2-d integral in (I.27) can be derived similarly using following expressions:

$$\varphi^{(coul)}(\vec{r}) = \int d^3r' \, \frac{\rho^{(ch)}(\vec{r}\,')}{4\pi\epsilon_0 \, |\vec{r} - \vec{r}'|}$$

$$\frac{1}{|\vec{r}_1 - \vec{r}_2|} = \boxed{\begin{array}{c}\text{see p. 165}\\ \text{in [2]}\end{array}} =$$

$$= \frac{4\pi}{r_2} \sum_{l=0}^{\infty} \left(\frac{r_1}{r_2}\right)^l \sum_{m=-l}^{+l} Y^*_{lm}(\hat{r}_1) \, Y_{lm}(\hat{r}_2) \; , \quad \text{for } r_1 < r_2 \tag{I.30}$$

and (see [99])

$$\varphi^{(coul)}(\vec{r}) = \varphi_0^{(coul)}(\vec{r}) + \delta\varphi^{(coul)}(\vec{r})$$

with

$$\delta\varphi^{(coul)}(\vec{r}) = \frac{Ze}{4\pi\epsilon_0 \, R_0} \sum_{\lambda\mu} \frac{3}{2\lambda+1} \, \alpha_{\lambda\mu} \, Y^*_{\lambda\mu}(\vartheta, \varphi) \begin{cases} \left(\frac{r}{R_0}\right)^{\lambda} & \text{if } r < R_0 \\ \left(\frac{R_0}{r}\right)^{\lambda+1} & \text{if } r > R_0 \end{cases}$$

The resulting expression for this 2-d integral in (I.27) is (see [99])

$$\frac{1}{2} \int d^3r \, \delta\rho^{(ch)}(\vec{r}) \, \delta\varphi^{(coul)}(\vec{r}) = \frac{9}{8\pi} \, \frac{Z^2e^2}{4\pi\epsilon_0 \, R_0} \sum_{\lambda\mu} \frac{|\, \alpha_{\lambda\mu}|^2}{2\lambda+1} \tag{I.31}$$

So, the substitution of (I.31) and (I.29) into (I.27) gives finally

$$V_{coul} = -\frac{3}{8\pi} \, \frac{Z^2e^2}{4\pi\epsilon_0 \, R_0} \sum_{\lambda\mu} |\, \alpha_{\lambda\mu}|^2 + \frac{9}{8\pi} \, \frac{Z^2e^2}{4\pi\epsilon_0 \, R_0} \sum_{\lambda\mu} \frac{|\, \alpha_{\lambda\mu}|^2}{2\lambda+1} =$$

$$= -\frac{3}{4\pi} \, \frac{Z^2e^2}{4\pi\epsilon_0 \, R_0} \sum_{\lambda\mu} \frac{\lambda-1}{2\lambda+1} \, |\, \alpha_{\lambda\mu}|^2 \tag{I.32}$$

The subsequent substitution of (I.32) and (I.23) into (I.15) provides the final expression for the droplet vibration potential energy:

$$V = \frac{\sigma R_0^2}{2} \sum_{\lambda\mu} |\, \alpha_{\lambda\mu}|^2 \, (\lambda-1) \, (\lambda+2)$$

$$- \frac{3}{4\pi} \, \frac{Z^2e^2}{4\pi\epsilon_0 \, R_0} \sum_{\lambda\mu} \frac{\lambda-1}{2\lambda+1} \, |\, \alpha_{\lambda\mu}|^2 \tag{I.33}$$

This expression should be compared with the second term in (I.1) and it gives us the expression for the potential parameter C_λ involved in (I.1) in the following form

$$C_\lambda = \sigma\, R_0^2\, (\lambda - 1)\, (\lambda + 1) - \frac{3}{2\pi}\, \frac{Z^2 e^2}{4\pi\epsilon_0\, R_0}\, \frac{\lambda - 1}{2\lambda + 1} \tag{I.34}$$

J. Some definitions and theorems from the group theory

In this appendix the basic elements of the group theory is presented. The only statements and theorems from the group theory are given which are necessary for the understanding of the algebraic models of nuclei. All theorems are shown without proofs. More details of the group theory for nuclear physics can be found e.g. in [112, 111].

J.1 Definition of the group

The ensamble G of elements $a, b, c, \ldots$ is called as **group** if their mutual multiplication is defined:

1. The product of arbitrary elements of the group G is also the element of this group
$$a, b \in G \qquad \Rightarrow \qquad ab \in G \tag{J.1}$$

2. The multiplication is associative, that means
$$a, b, c \in G \qquad (ab)\, c = a\, (bc) \tag{J.2}$$

3. There is only one unit element ($\equiv e$) fulfilling:
$$ea = ae = a \qquad \text{for all } a \in G \tag{J.3}$$

4. For each element $a \in G$ there exists one and only one inverse element $a^{-1} \in G$ fulfilling
$$a\, a^{-1} = a^{-1}\, a = e \tag{J.4}$$

If the group multiplication is commutative ($ab = ba$) then the group is called **abelian**.

The **order of the group** is defined as the number of its elements.

The element $b \in G$ of the group is **conjugated** to the element $a \in G$ of the group G if there exists element $c \in G$ such as

$$b = c\, a\, c^{-1} \tag{J.5}$$

According to (J.5) we can divide all elements of the group into **classes** of conjugated elements (all alements conjugated to the given element are also mutually conjugated).

Two groups G and $G^{'}$ are **isomorfic** ($G \cong G^{'}$) if there is one and only one mutual matching invariant with respect to the group multiplication. If this matching connects one element of the group $G^{'}$ with several elements of the group G then the group $G^{'}$ is **homomorfic** image of the group G.

If the group G contains subset $G^{'}$ which itself is the group (with the same definition of the group multiplication) then the $G^{'}$ is called as **subgroup** of the group G ($G \subset G$). The subgroup $G^{'}$ is **invariant subgroup** of the group G if for all $g \in G$ and $h \in G^{'}$ we have

$$g\, h\, g^{-1} \in G^{'} \tag{J.6}$$

The **direct product** of the group G and $G^{'}$ ($\equiv G \otimes G^{'}$) is the group with elements $(g, g^{'})$ where $g \in G$ and $g^{'} \in G^{'}$ with the following defintition of the group multiplication

$$(g_1, g_1^{'})(g_2, g_2^{'}) = (g_1 g_1^{'}, g_2 g_2^{'}) \tag{J.7}$$

The group G is the **simple group** if it does not contain any invariant subgroups. The group G is the **semisimple group** if it does not contain any abelian subgroups.

The important role in physics are played by groups, elements of which are operators and the group multiplication is identical with the multiplication of operators. The group of operators (acting in the Hilbert space $\mathscr{H}$) which represents the homomorfic image of the group G is called as the **representation** $D(G)$ of the group G. The dimension of the Hilbert space $\mathscr{H}$ defines the **dimension of given representation** $D(G)$. Further the different representation of given group G are distinguished by the upper index (e.g. $D(G)^{(1)}, D(G)^{(2)}, \ldots$). So in the representation $D(G)$ each element $g \in G$ is

connected with the operator $\hat{D}(g)$ by following way

$$\hat{D}(g_1) \neq \hat{D}(g_2) \qquad \Rightarrow \qquad g_1 \neq g_2 \tag{J.8}$$

$$\hat{D}(g_1) \cdot \hat{D}(g_2) = \hat{D}(g_1 g_2) \tag{J.9}$$

$$\hat{D}(e) = 1 \tag{J.10}$$

$$\hat{D}(g^{-1}) = \hat{D}^{-1}(g) \tag{J.11}$$

However, one operator can be affiliated with the more elements of the group G:

$$g_1 \neq g_2 \quad \text{does not mean that} \quad \hat{D}(g_1) \neq \hat{D}(g_2) \tag{J.12}$$

Relations (J.9) - (J.11) are invariant with respect to the similarity transformation, therefore operators

$$\hat{D}^{'}(g) \equiv \hat{S}^{-1} \hat{D}(g)\, \hat{S} \tag{J.13}$$

form also the representation of the group G (representations $D(G)$ and $D^{'}(G)$ are **equivalent**), Further we restrict ourselves to so called **linear representation**, that means the representation containing linear operators $\hat{D}(g)$.

If in the Hilbert space $\mathscr{H}$ of the n- dimensional representation $D(G)$ the basis of functions (kets) $|\psi)j\rangle$ $(j = 1, \ldots, n)$ is chosen then operators $\hat{D}(g)$ can be unambiguously represented by square matrices $\mathscr{D}(g)$ with matrix elements defined by the following relation

$$\hat{D}(g)\, |\psi_j\rangle) = \sum_{k=1}^{n} \mathscr{D}_{kj}(g)\, |\psi_k\rangle \tag{J.14}$$

Then the relations (J.9)-(J.11) can be rewritten in the matrix form

$$\mathscr{D}(g_1)\, \mathscr{D}(g_2) = \mathscr{D}(g_1 g_2) \tag{J.15}$$

$$\mathscr{D}(e) = 1 \tag{J.16}$$

$$\mathscr{D}(g^{-1}) = \mathscr{D}^{-1}(g) \tag{J.17}$$

and matrices $\mathscr{D}(g)$ form so called **matrix representation** of the group G.

the representation $D(G)$ is **irreducible** (irrep) if and only if in the representative Hilbert space $\mathscr{H}$ there is not possible to find any basis $|\psi_j\rangle$ $(j = 1, \ldots, n)$ in which all matrices $\mathscr{D}(g)$ have the following form

$$\mathscr{D}(g) = \begin{pmatrix} \mathscr{D}_1(g)) & \mathscr{C}(g) \\ 0 & \mathscr{D}_2(g) \end{pmatrix} \quad \text{for all } g \in G \tag{J.18}$$

(the first $n-m$ elements in the last m rows ($n > m > o$) are zero in all matrices $\mathscr{D}(g)$, $g \in G$). By other words, the given representation $D(G)$ is irrep if there is no any similarity transformation S which transforms all matrices $\mathscr{D}(g)$ into the form (J.18). If such similarity transformation is possible to find then the representation $D(g)$ is **reducible**.

Each reducible **unitary** representation is **fully reducible** if the unitary matrices $\mathscr{D}(g)$ for all $g \in G$ are possible to transform by a similarity transformation into the form (J.18) where the matrices $\mathscr{C}$ are zero. Then the matrices $\mathscr{D}_1(g)$ form unitary representation of the group G and the same valids for the matrices $\mathscr{D}_2(g)$. If some of these representations is still reducible it is again possible to transform corresponding matrices $\mathscr{D}_1(g)$ or $\mathscr{D}_2(g)$ for all $g \in G$ by other similarity transformation into the quasi-diagonal form. This procedure can be repeated untill we come into the irreducible representations. That means each unitary representation of the group G can be expressed as the direct sum of the irreps:

$$D(G) = \sum_{\sigma} \oplus D^{(\sigma)}(G) \tag{J.19}$$

or similarly for operators

$$\hat{D}(g) = \sum_{\sigma} \oplus \hat{D}^{(\sigma)}(g) \quad \text{for all } g,\ g \in G \tag{J.20}$$

where unitary operators $\hat{D}^{(\sigma)}(g)$ form the irreducible representation of the group G in the subspace $\mathscr{H}^{(\sigma)}$ and

$$\mathscr{H} = \sum_{\sigma} \oplus \mathscr{H}^{(\sigma)} \tag{J.21}$$

is the Hilbert space of the representation $D(G)$. This result for unitary representations is very important because it is possible to show that all representations of the finite groups (with the finite number of elements) are equivalent to unitary representations. The same equivalence valids for all infinite connected simple compact groups with the finite dimensions. Further we always assume that we discuss only unitary representations.

Let us suppose that matrices $\mathscr{D}^{(\mu)}(g)$ and $\mathscr{D}^{(\nu)}(g)$ for n_μ- and n_ν- dimensional irreducible representations of the finite group G, respectively. Then it is possible to prove the orthogonality relation for irreducible representations:

$$\sum_{g} \mathscr{D}^{(\mu)}_{jk}(g) \left(\mathscr{D}^{(\nu)}_{pq}(g)\right)^{*} = \frac{N}{n_\mu}\, \delta_{\mu\nu}\, \delta_{jp}\, \delta_{kq} \tag{J.22}$$

where the sum goes over all N elements of the group G and n_μ is the dimension of the representation $D^{(\mu)}(G)$ (for the case $\mu = \nu$ both matrices involved in the l.h.s. of (J.22) should be identical) [1]

Let us go back to exprs. (J.19) - (J.21). Among irreducible representations $D^{(\sigma)}(G)$ participating in (J.19) some of them can be equivalent. Therefore instead of (J.19) it is better to write

$$D(G) = \sum_{\mu\tau} \oplus D^{(\mu,\tau)}(G) \tag{J.23}$$

where the index μ enumerates labels of nonequivalent irreps and the index τ distinguishes among different mutually equivalent representations. Similarly instead of (J.20) and (J.21) we write

$$\hat{D}(g) = \sum_{\mu\tau} \oplus \hat{D}^{(\mu,\tau)}(g) \tag{J.24}$$

$$\mathscr{H} = \sum_{\mu\tau} \oplus \mathscr{H}^{(\mu,\tau)} \tag{J.25}$$

If $\{|\mu j;\ \tau\rangle,\ j = 1, \ldots, n\}$ is the orthonormal basis of the subspace $\mathscr{H}^{(\mu,\tau)}$ then matrices $\mathscr{D}^{\mu,\tau)}(g)$ with elements

$$\mathscr{D}^{(\mu,\tau)}_{jk} \equiv \langle \mu j;\ \tau|\hat{D}(g)|\mu k;\ \tau\rangle \tag{J.26}$$

form the irreducible representation of the group G. Since the matrices differing each other only by the index τ are connected by a similarity transformation (independent on g) we can always choose the basis $|\mu j;\ \tau\rangle$ in such a way that matrix are identical. Such a choice of the basis $|\mu j;\ \tau\rangle$ is further always supposed and therefore instead of (J.26) we write

$$\langle \mu j;\ \tau|\hat{D}(g)|\mu k;\tau\rangle = \mathscr{D}^{(\mu)}_{jk}(g) \tag{J.27}$$

$$\langle \nu j;\sigma|\hat{D}(g)|\mu k;\ \tau\rangle = \delta_{\nu\mu}\,\delta_{\sigma\tau}\,\mathscr{D}^{(\mu)}_{jk}(g) \tag{J.28}$$

[1] In the case of the infinite group G instead of the sum in (J.22) we have the integral and the factor $\frac{N}{n_\mu}$ is the concrete normalization factor, e.g. in the case of the group of rotations in the 3-dimensional space the expr. (J.22) reads as

$$\int d\Omega\ \mathscr{D}^{(j)}_{m_1 m_2}(\theta)\left(\mathscr{D}^{j'}_{m_1' m_2'}(\theta)\right)^* = \frac{8\pi}{2j+1}\,\delta_{jj'}\,\delta_{m_1 m_1'}\,\delta_{m_2 m_2'}$$

where $\mathscr{D}^{(j)}_{mm'}(\theta)$ are Wigner functions $D^j_{mm'}(\theta)$ discussed in the Appendix A (see (A.27)).

Let us choose another orthonormal basis of states in the space $\mathscr{H}^{(\mu)}$: $|\psi_m^{(\mu)}\rangle$ $(m = 1, \ldots, n_\mu)$. It can be shown that the action of any operator $\hat{D}(g)$ from the representation $D(G)$ on any function $|\psi_m^{(\mu)}\rangle$ is following (transformation according to irrep $D^{(\mu)}G$)

$$\hat{D}(g)\,|\psi_m^{(\mu)}\rangle = \sum_{m'=1}^{n_\mu} \mathscr{D}^{(\mu)}_{m'm}(g)\,|\psi_{m'}^{(\mu)}\rangle \tag{J.29}$$

Let the operators $\hat{D}^{(\mu)}(g)$ form the representation $D^{(\mu)}(G)$ in the space $\mathscr{H}^{(\mu)}$ and another representation $D^{(\nu)}(G)$ is formed by a set of operators $\hat{D}^{(\nu)}(g)$ in the space $\mathscr{H}^{(\nu)}$. Then it is possible to prove that the operators

$$\hat{D}(g) \equiv \hat{D}^{(\mu)}(g) \otimes \hat{D}^{(\nu)}(g) \tag{J.30}$$

form the representation

$$D(G) \equiv D^{(\mu)})(G) \otimes D^{(\nu)}(G)) \tag{J.31}$$

in the space

$$\mathscr{H} = \mathscr{H}^{(\mu)} \otimes \mathscr{H}^{(\nu)} \tag{J.32}$$

The representation (J.30) is called as the direct product of representations $D^{(\mu)}(G)$ and $D^{(\nu)}(G)$ of the group G. The direct product of two representations is usually reducible representation. Its decomposition into irreducible representations

$$D^{(\mu)}(G) \otimes D^{(\nu)}(G) = \sum_{\lambda\tau} \otimes D^{\lambda,\tau)}(G) \tag{J.33}$$

is known as the Clebsch-Gordan series. Two equivalent representations can be considered as two different realizations of one representation. In this sense the expression (J.33) can be rewritten as follows

$$D^{(\mu)}(G) \otimes D^{(\nu)}(G) = \sum_{\lambda} \oplus\, (\lambda\mu\nu)\, D^{(\lambda)}(G) \tag{J.34}$$

where the number $(\lambda\mu\nu)$ gives how many representations $D^{(\lambda,\tau)}$ with given λ participate in the r.h.s. of (J.33). That means the direct product of irreducible representations $D^{(\mu)}$ and $D^{(\nu)}$ contains given irreducible representation $D^{(\lambda)}$ $(\lambda\mu\nu)$- times. Let us suppose the vectors $|\mu m\rangle$, $m = 1, \cdots, n_\mu$ form the the orthonormal basis in the Hilbert space $\mathscr{H}^{(\mu)}$ and the vectors $|\nu k\rangle$ create the orthonormal basis in the space $\mathscr{H}^{(\nu)}$. So the vectors

$$|\mu m\rangle\,|\nu k\rangle\ ,\ m = 1, \ldots, n_\mu \text{ and } k = 1, \ldots, n_\nu \tag{J.35}$$

form the orthonormal basis in the space (J.32) ($\mathscr{H} = \mathscr{H}^{(\mu)} \otimes \mathscr{H}^{(\nu)}$) and the corresponding condition of the completeness of this basis is

$$\sum_{m=1}^{n_\mu} \sum_{k=1}^{n_\nu} |\mu m\rangle \, |\nu k\rangle \, \langle \nu k| \, \langle \mu m| = 1 \tag{J.36}$$

On the other side the expression (J.33) says that the Hilbert space (J.32) can be decomposed into the direct sum of invariant subspaces

$$\mathscr{H} = \sum_{\lambda\tau} \oplus \, \mathscr{H}^{\lambda,\tau)} \tag{J.37}$$

with the basis

$$|\lambda i; \, \mu\nu, \, \tau\rangle \qquad i = 1, \ldots, \, n_\lambda \tag{J.38}$$

with its completeness condition

$$\sum_{\lambda\tau} \sum_{i=1}^{n_\lambda} |\lambda i; \mu\nu; \, \tau\rangle\langle\lambda i; \, \mu\nu;\tau| = 1 \tag{J.39}$$

where the first sum goes over the same indexes $\lambda\tau$ as the sum in (J.37). Since the basis $|\lambda i; \, \mu\nu, \, \tau\rangle$ ($i = 1, \ldots, \, n_\lambda$) works in the same space as the basis $|\mu m\rangle|\nu k\rangle$ ($m = 1, \ldots, \, n_\mu$ and $k = 1, \ldots, \, n_\nu$) the vectors (J.38) can be expressed as the superposition of vectors (J.35)

$$|\lambda i; \, \mu\nu, \, \tau\rangle = \sum_{m=1}^{n_\mu} \sum_{k=1}^{n_\nu} C^{\lambda i,\tau}_{\mu m \nu k} \, |\, \mu m\rangle |\, \nu k\rangle \tag{J.40}$$

where

$$C^{\lambda i;\, \tau}_{\mu m \nu k} \equiv \langle \nu k| \, \langle \mu m| \, \lambda i; \, \mu\nu, \, \tau\rangle \tag{J.41}$$

are so called Clebsch-Gordan coefficients of the group G (for the Clebsch-Gordan coefficiets of the group of rotations see (A.2)). Using the completeness relations (J.40) we obtain the inverse relation:

$$|\mu m\rangle \, ||\nu k\rangle = \sum_{\lambda\tau} \sum_{i=1}^{n_\lambda} \left(C^{\lambda i, \, \tau}_{\mu m \nu k} \right)^* \, |\, \lambda i; \, \mu\nu; \, \tau\rangle \tag{J.42}$$

and the expression (J.39) together with (J.40) gives

$$\sum_{m=1}^{n_\mu} \sum_{k=1}^{n_\nu} C^{\lambda i, \, \tau}_{\mu m \nu k} \left(C^{\lambda' i', \, \tau'}_{\mu m \nu k} \right)^* = \delta_{ii'} \delta_{\lambda\lambda'} \delta_{\tau\tau'} \tag{J.43}$$

or

$$\sum_{\lambda\tau}\sum_{i=1}^{n_\lambda} C^{\lambda i,\,\tau}_{\mu m\nu k}\left(C^{\lambda i,\,\tau}_{\mu m'\nu k'}\right)^{*} = \delta_{mm'}\delta_{\lambda\lambda'} \tag{J.44}$$

Using these relations and (J.29) we can obtain the following equations

$$\sum_{mm'=1}^{n_\mu}\sum_{kk'=1}^{n_\nu}\left(C^{\lambda i,\,\tau}_{\mu m\nu k}\right)^{*}\mathscr{D}^{(\mu)}_{mm'}(g)\,\mathscr{D}^{(\nu)}_{kk'}(g)\,C^{\lambda' i',\,\tau'}_{\mu m'\nu k'} = \delta_{ii'}\delta_{\lambda\lambda'}\delta_{\tau\tau'}\,\mathscr{D}^{(\lambda)}_{ii'}(g)$$

and

$$\mathscr{D}^{(\mu)}_{mm'}(g)\,\mathscr{D}^{(\nu)}_{kk'}(g) = \sum_{\lambda\tau}\sum_{ii'} C^{\lambda i,\,\tau}_{\mu m\nu k}\,\mathscr{D}^{(\lambda)}_{ii'}(g)\left(C^{\lambda i',\,\tau}_{\mu m'\nu k'}\right)^{*} \tag{J.45}$$

Let the operators $\hat{D}(g)$ form the group G in the Hilbert space $\mathscr{H}$. The set of operators $\hat{A}(\rho s)$, $s = 1,\ldots,n_\rho$ is called as the set of the **tensor operators** of the group G if for all $g \in G$ the following expressions valid

$$\hat{D}(g)\,\hat{A}(\rho,s)\,\hat{D}^{-1}(g) = \sum_{s'=1}^{n_\rho}\mathscr{D}^{(\rho)}_{ss'}(g)\,\hat{A}(\rho,s')$$

The matrix element of the operator $\hat{A}(\rho,s)$ can be written in terms of the Wigner-Eckart theorem [2]

$$\langle\nu k|\hat{A}(\rho,s)|\mu m\rangle = \sum_{\tau}\left(C^{\nu k,\,\tau}_{\rho\mu sm}\right)\langle\nu||\hat{A}(\rho)||\mu\rangle \tag{J.46}$$

where $\langle\nu||\hat{A}(\rho)||\mu\rangle$ are so called reduced matrix elements which are not dependent on the basis indexes k and m and on the projection index s and depends only on the representation indexes ν, μ and on the tensor index ρ (for the Clebsch-Gordan coefficients of the group of rotations - see (A.2)).

Trace of the matrix $\mathscr{D}^{(\mu)}(g)$

$$\chi^{\mu}(\rho) = \sum_{m=1}^{n_\mu}\mathscr{D}^{(\mu)}_{mm}(g) \tag{J.47}$$

is called as the **character** of the element g in the representation $D^{(\mu)}(G)$. The trace of the matrix $\mathscr{D}^{(\mu)}(g)$ is invariant with respect to the similarity relation and therefore:

[2]The formulation (J.46) of the Wigner-Eckart theorem is general in contrast to the expr. (A.12) which is connected with the group of rotations in the 3D- space.

- characters of all elements belonging to the same class are equal each other;
- given element g has the same character in all equivalent representations.

The character of the direct sum of representations is equal to the sum of characters of the corresponding representations. The character of the direct product of representations is equal to the product of characters of corresponding representations:

$$\begin{aligned} \chi^{\mu \oplus \nu}(g) &= \chi^{\mu}(g) + \chi^{\nu}(g) \\ \chi^{\mu \otimes \nu}(g) &= \chi^{\mu}(g) \cdot \chi^{\nu}(g) \end{aligned} \tag{J.48}$$

Orthogonality relation (J.22) for irreducible representations implies the orthogonality relation for characters of irreducible representations:

$$\sum_{g \in G} \chi^{(\mu)}(g)\, \chi^{(\nu)\,*}(g) = N\, \delta_{\mu\nu} \tag{J.49}$$

where N is the number of elements of the given group G. This expression can be written also in the following form

$$\sum_{c} n_c\, \chi^{(\mu)}(c)\, \chi^{(\nu)\,*}(c) = N\, \delta_{\mu\nu} \tag{J.50}$$

where n_c is the number of elements of the class c and the summation over c goes over all classes. It can be proved that **the number of irreps of given group G is exactly equal to the number of its classes**. As a result of it the matrix constructed from the elements

$$\left(\frac{n_c}{N}\right)^{1/2} \chi^{\mu}(c)$$

where rows are enumerated by the index μ (irreducible representation) and the columns by the index c (classes) is the square matrix. However the unitary matrix has orthogonal not only rows vut also elements. Therefore

$$\sum_{\mu} \chi^{\mu}(c)\, (\chi^{\mu}(c^{'}))^{*} = \frac{N}{n_c}\, \delta_{cc'} \tag{J.51}$$

Another important statement is that the sum of squares of dimensions of all irreducible representations of the group G is equal to the number of elements (the order) of this group:

$$N = \sum_{\nu} n_{\nu}^2 \tag{J.52}$$

J.2 Lie groups and Lie algebras

Up to now we supposed that the group G is finite. From now on we shall consider the infinite order group G with elements which can be identified by means of the r real parameters $a_1,\ a_2,\ \ldots,\ a_r$ $(\equiv a)$:

$$g(a_1,\ \ldots,\ a_r) \equiv g(a) \tag{J.53}$$

The parametrization is usually chosen in such a way that the unit element e is characterized by zero values of all parameters

$$e \equiv g(0,\ \ldots,\ 0) \equiv g(0) \tag{J.54}$$

The symbol $\tilde{a}$ denotes the parameters corresponding to the inverse element with respect to the element $g(a)$

$$g(\tilde{a}) \equiv g^{-1}(a) \tag{J.55}$$

If the space (ensemble) $\mathscr{A}$ of parameters a corresponding to all elements of the group G is connected then we speak about the connected group G. If the space $\mathscr{A}$ is compact then the corresponding group G is compact [3].

Elements $g(a),\ g(b) \in G$ unamboguesly define the element

$$g(c) = g(b)\, g(a) \tag{J.56}$$

of the group G. The group multiplication is then given by r real functions φ:

$$c_k = \varphi_k(b_1,\ \ldots,\ b_r;\ a_1,\ \ldots,\ a_r), \quad k = 1,\ \ldots,\ r \quad \Leftrightarrow \quad c = \varphi(ba) \tag{J.57}$$

Because each element has one and only one inverse element there are r real functions f_k fulfilling

$$\tilde{a}_k = f_k(a_1, \ldots,\ a_r) \qquad k = 1, \ldots,\ r \qquad \Leftrightarrow \qquad \tilde{a} = f(a) \tag{J.58}$$

If all functions $f_k,\ \varphi_k$ $(k = 1, \ldots,\ r)$ have all derivatives than the group G is called as **the r- parameter Lie group**.

The group of operators $\hat{D}(a) \equiv \hat{D}(g(a))$ homorfic with the Lie group G is called as the representation of the group G in the Hilbert space $\mathscr{H}$ if and only if the elements $\langle\psi|\ \hat{D}(a)\ |\psi\rangle$ for all $|\psi\rangle \in \mathscr{H}$ are continuous function of

[3] The space (ensemble) M is called as connected if each of its 2 points can be connected by the polynomial chain (that means by the line formed by the finite number of streight line segmens). The space M is called as compact if each sequence of elements of this space converges to the element of this space

parameters a. So for operators forming the representation of the Lie group the following relations are valid

$$\hat{D}(a) \neq \hat{D}(b) \quad \Rightarrow \quad a \neq b \tag{J.59}$$
$$\hat{D}(b)\, \hat{D}(a) = D(\varphi(b,a)) \tag{J.60}$$
$$\hat{D}(0) = 1 \tag{J.61}$$
$$\hat{D}(\tilde{a}) = \hat{D}^{-1}(a) \tag{J.62}$$
$$\langle\psi|\, \hat{D}(a)\, |\psi\rangle \text{ is a continuous function of } a \tag{J.63}$$

In the physical applications it is usually sufficient to work not with the Lie groups but with only corresponding Lie algebras. Let us denote

$$|\psi,\, a\rangle = \hat{D}(a)\, |\psi\rangle \tag{J.64}$$

where $|\psi\rangle$ is the arbitrary vector from $\mathscr{H}$. It is evident that

$$\hat{D}(\varphi(b,a))\, |\psi,\, \tilde{a}\rangle = |\psi,\, b\rangle \tag{J.65}$$

The differentiation of this identity gives

$$\sum_{i=1}^{r} \frac{\partial \hat{D}(\varphi(b,a))}{\partial \varphi_i}\, \frac{\partial \varphi_i(b,a)}{\partial b_j}\, |\psi,\, \tilde{a}\rangle = \frac{\partial}{\partial b_j} |\psi,\, b\rangle \tag{J.66}$$

In the limit $a \to \tilde{b}$ the equation (J.66) gives

$$\sum_{i=1}^{r} S_{ij}(b)\, \hat{X}_i\, |\psi,\, b\rangle = \frac{\partial}{\partial b_j} |\psi,\, b\rangle \tag{J.67}$$

where

$$S_{ij}(b) \equiv \frac{\partial \varphi_i(b,a)}{\partial b_j}\Big|_{a=\tilde{b}} \tag{J.68}$$

and

$$\hat{X}_i \equiv \frac{\partial \hat{D}(a=0)}{\partial a_i} \qquad i = 1,\, \ldots,\, r \tag{J.69}$$

are so called **generators of the Lie group**.

On the other hand we know that

$$\varphi(b,0) = b \tag{J.70}$$

and therefore

$$S_{ij}(0) = \boxed{\begin{matrix}\text{see} \\ (J.68)\end{matrix}} = \delta_{ij} \tag{J.71}$$

So in the vicinity of the origin up to the linear terms in b we have (see (J.65), (J.69))

$$|\psi,\, b\rangle = \Big(1 + \sum_i b_i\, \hat{X}_i\Big)\, |\psi\rangle \tag{J.72}$$

Going to the higher orders of the accuracy we can write

$$|\psi,\, b\rangle = \Big(1 + \frac{1}{n} \sum_i b_i\, \hat{X}_i\Big)^n\, |\psi\rangle$$

and in the limit $n \to \infty$ this gives

$$|\psi,\, b\rangle = e^{\sum_i b_i \hat{X}_i} |\psi\rangle \tag{J.73}$$

and in terms of the comparison of (J.73) with (J.64) we obtain

$$\hat{D}(b) = e^{\sum_i b_i \hat{X}_i} \tag{J.74}$$

The further differentiation of (J.67) gives

$$\frac{\partial^2}{\partial b_k \partial b_j} |\psi;\, b\rangle = \sum_i \Big(\frac{\partial S_{ij}(b)}{\partial b_k} \hat{X}_i + S_{ij}(b) \hat{X}_i \frac{\partial}{\partial b_k} \Big)\, |\psi;\, b\rangle =$$

$$= \boxed{\begin{array}{c}\text{see} \\ (J.67)\end{array}} = \sum_i \Big(\frac{\partial S_{ij}(b)}{\partial b_k} \hat{X}_i + S_{ij}(b) \sum_l S_{lk}(b) \hat{X}_i \hat{X}_l \Big)\, |\psi;\, b\rangle \tag{J.75}$$

and if indexes k and j are exchanged

$$\frac{\partial^2}{\partial b_j \partial b_k} |\psi;\, b\rangle = \sum_i \Big(\frac{\partial S_{ik}(b)}{\partial b_j} \hat{X}_i + S_{ik}(b) \sum_l S_{lj}(b) \hat{X}_i \hat{X}_l \Big)\, |\psi;\, b\rangle \tag{J.76}$$

Since the l.h.s. of (J.75) is equal to the l.h.s. of (J.76) the right hand sides of (J.75) and (J.76) are also equal each other. The comparison of right hand sides of (J.75) and (J.76) for $b = 0$, with the use of (J.71) and of the fact that $|\psi\rangle$ is arbitrary, gives

$$[\hat{X}_j,\, \hat{X}_k] = \sum_{l=1}^{r} C_{jk}^l\, \hat{X}_l \qquad j, k = 1, \ldots,\, r \tag{J.77}$$

where

$$C_{jk}^l \equiv \Big(\frac{\partial S_{lk}(b)}{\partial b_j} - \frac{\partial S_{lj}(b)}{\partial b_k} \Big)_{b=0} \tag{J.78}$$

are so called **structural coefficients of the given group** G [4]. From the definition (J.78) the following symmetry follows

$$C^{l}_{jk} = - C^{l}_{kj} \tag{J.79}$$

For commutator we have Jacobi identity

$$\Big[\hat{A},\, [\hat{B},\, \hat{C}]\Big] + \Big[\hat{B},\, [\hat{C},\, \hat{A}]\Big] + \Big[\hat{C},\, [\hat{A},\, \hat{B}]\Big] = 0 \tag{J.80}$$

which implies the following expression for structural coefficients

$$\sum_{k} \Big(C^{k}_{ij}\, C^{l}_{ks} + C^{k}_{si}\, C^{l}_{kj} + C^{k}_{js}\, C^{l}_{ki} \Big) = 0 \tag{J.81}$$

The vector space $\mathscr{A}$ of parameters a is called as **the Lie algebra** if the "multiplication" $[a,\, b]$ of elements $a, b \in \mathscr{A}$ in this space is defined with the following properties

$$\begin{aligned} &1. \quad [(a+b),\, c] = [a,\, c] + [b,\, c] \\ &2. \quad [\alpha\, a,\, b] = \alpha\, [a,\, b] \\ &3. \quad [a,\, b] = - [b,\, a] \\ &4. \quad [a,\, [b,\, c]] + [b,\, [c,\, a]] + [c,\, [a,\, b]] = 0 \end{aligned} \tag{J.82}$$

where a, b, c are arbitrary elements from $\mathscr{A}$ and α is the arbitrary number. If the reality of the number α is required then we speak about the **real Lie algebra**.

The important role is played by algebras where elements are linear operators and corresponding multiplication is defined as commutators. The Lie algebra of operators homomorfic with the Lie algebra $\mathscr{A}$ is called as the representation of the lie algebra $\mathscr{A}$.

From the expression (J.77) one can see that to each Lie group G the Lie algebra $\mathscr{A}(G)$ can be assigned. The expression (J.77) says that the generators

[4] opposite to mathematical literature in physics the term "group generators" is used for the operators $\hat{Y}_j \equiv i\, \hat{X}_j$. Then the expression (J.74) reads as

$$\hat{D}(b) = e^{- \sum_i b_j \hat{Y}_j} \tag{J.74$'$}$$

with the commutator relations (J.77) in the form

$$[\hat{Y}_j,\, \hat{Y}_k] = i \sum_{l=1}^{r} C^{l}_{jk}\, \hat{Y}_l$$

The reason for this is the fact that the operators $\hat{Y}_l$ are Hermitian and in the quantum mechanics it is possible to identify them with physical observables.

of the group G form the basis of the corresponding algebra $\mathscr{A}(G)$. It can be proved that this statement can be reversed saying that we can find the corresponding Lie group to any Lie algebra. Therefore the problem of the classification of Lie groups can be transformed into the classification of Lie algebras which is simpler. The classification of the irreducible representations of the Lie groups is therefore based on the classification of corresponding algebras.

Let the operators $\hat{X}_j$ $(j = 1, \ldots, r)$ form the basis of the Lie algebra $\mathscr{A}(G)$. Using these basis operators $\hat{X}_j$ it is possible to construct n (but not more than n) independent operators $\hat{C}_1, \ldots, \hat{C}_n$ which fulfill the following relation

$$\left[\hat{C}_s,\, \hat{X}_j\right] = 0 \qquad \text{for } j = 1, \ldots, r \text{ and } s = 1, \ldots, n \tag{J.83}$$

than we say that the algebra $\mathscr{A}(G)$ is **of the order** n.

For given group G we can define so called **metric tensor** using the structural coefficients (J.78)

$$\eta_{jk} \equiv \sum_{lm} C^l_{jm}\, C^m_{kl} \tag{J.84}$$

It can be shown that the determinant of the metric tensor matrix η is nonzero only in the case when the group G is semi-simple. For semi-simple groups it is possible to define so callled (first) Casimir operator

$$\hat{C} \equiv \sum_{kl} \eta^{kl}\, \hat{X}_k\, \hat{X}_l \tag{J.85}$$

where η^{kl} are elements of the matrix η^{-1}. From the commutator relations (J.77) it is possible to derive the following identity

$$\left[\hat{C},\, \hat{X}_j\right] = 0 \qquad \text{for all } j = 1, \ldots, r \tag{J.86}$$

So, the first Casimir operator (J.85) is an example of the general Casimir operator C_s (see (J.83)).

J.3 Examples of Lie groups and Lie algebras

J.3.1 Orthogonal group (algebra) $O(n)$ and special orthogonal group (algebra) $SO(n)$

orthogonal group $O(n)$ = Lie group of $n \times n$ orthogonal matrices where group operation is the matric multiplication.

Determinants of orthogonal matrices are equal 1 or -1. If only othogonal matrices with the determinant equal to 1 are considered then we speak about a **special orthogonal group** $SO(n)$.

The most important in practice is the case of $n = 3$. The group $SO(3)$ is the group of rotations in 3- dimensional space. This group was already discussed in the Appendix A (see the section A.5), even though it was not mentioned explicitely there that the rotations in 3- dimensional space form the group $SO(3)$. Below the basic characteristics of the algebra $S0(3)$ are listed.

Rotations in the 3- dimensional space round the axis directed along the unit vector $\vec{n}$ can be always composed from rotations round the frame axes with unit vectors $\vec{e}_1$, $\vec{e}_2$, $\vec{e}_3$ and these rotations are represented by 3×3 orthogonal matrices:

$$R(\vec{e}_1,\, \varphi) = \begin{pmatrix} 1 & 0 & 0 \\ 0 & cos\,\varphi & -sin\,\varphi \\ 0 & sin\,\varphi & cos\,\varphi \end{pmatrix} = e^{-i\,\varphi\, M_1} \quad , \qquad \vec{e}_1 \equiv \begin{pmatrix} 1 \\ 0 \\ 0 \end{pmatrix}$$

$$R(\vec{e}_2,\, \varphi) = \begin{pmatrix} cos\,\varphi & 0 & sin\,\varphi \\ 0 & 1 & 0 \\ -sin\,\varphi & 0 & cos\,\varphi \end{pmatrix} = e^{-i\,\varphi\, M_2} \quad , \qquad \vec{e}_2 \equiv \begin{pmatrix} 0 \\ 1 \\ 0 \end{pmatrix}$$

$$R(\vec{e}_3,\, \varphi) = \begin{pmatrix} cos\,\varphi & -sin\,\varphi & 0 \\ sin\,\varphi & cos\,\varphi & 0 \\ 0 & 0 & 1 \end{pmatrix} = e^{-i\,\varphi\, M_3} \quad , \qquad \vec{e}_3 \equiv \begin{pmatrix} 0 \\ 1 \\ 0 \end{pmatrix} \tag{J.87}$$

where (see also (A.55))

$$M_1 = \begin{pmatrix} 0 & 0 & 0 \\ 0 & 0 & -i \\ 0 & i & 0 \end{pmatrix} \; M_2 = \begin{pmatrix} 0 & 0 & i \\ 0 & 0 & 0 \\ -i & 0 & 0 \end{pmatrix} \; M_3 = \begin{pmatrix} 0 & -i & 0 \\ i & 0 & 0 \\ 0 & 0 & 0 \end{pmatrix} \tag{J.88}$$

So each spatial vector $\vec{r} \equiv X$

$$X = \begin{pmatrix} x_1 \\ x_2 \\ x_3 \end{pmatrix} \tag{J.89}$$

is transformed by the rotation of the frame system round the exis directed along the unit vector $\vec{n}$ by angle φ, $S \equiv (x_1, x_2, x_3) \;\rightarrow\; S^{'} \equiv (x_1^{'}, x_2^{'}, x_3^{'})$, according to the following expression

$$X^{'} = R(\vec{n}, \varphi)\, X = e^{-i\,\varphi\, \vec{n}\cdot\vec{M}}\, X \tag{J.90}$$

where R is the orthogonal matrix ($R^T = R^{-1}$). All these matrix R form the representation of the group $SO(3)$. This representation is homomorfic with the representation od the $SO(3)$ group formed by the operators $\hat{D}(\vec{n}, \varphi)$ acting in the space of wave functions. These operators have the following form

$$\hat{D}(a) \equiv \hat{D}(\vec{n}, \varphi) = e^{-i\,\varphi\,\vec{n}\cdot\hat{\vec{J}}} \tag{J.91}$$

where $\hat{\vec{J}}$ is the operator of the vector of the angular momentum, $\hat{\vec{J}} \equiv (\hat{J}_1, \hat{J}_2, \hat{J}_3)$. The components of $\hat{\vec{J}}$ fulfil:

$$\left[\hat{J}_i,\ \hat{J}_j\right] = i\,\epsilon_{ijk}\,\hat{J}_k \tag{J.92}$$

The relations (J.92) can be compared with (J.77) and one can see that the components $\hat{J}_1,\ \hat{J}_2,\ \hat{J}_3$ can be identified with the generators of the algebra $SO(3)$ with the correspondent structural constants

$$C^l_{jk} = \epsilon_{jkl} \tag{J.93}$$

and the metric tensor

$$\eta_{jk} = -\,2\,\delta_{jk} \tag{J.94}$$

So, according to (J.84) the first Casimir operator of the group $SO(3)$ is given by the operator of the square of the angular moment, $\hat{J}^2 = \hat{J}_1^2 + \hat{J}_2^2 + \hat{J}_3^2$.

Operators $\hat{D}(\vec{n}, \varphi)$ (see (J.91)) give the unitary representation of the algebra $SO(3)$ spanned the Hilbert space with the basis $|jm\,a\rangle$

$$\begin{aligned}
&\hat{J}^2\,|jm\,a\rangle = j(j+1)\,|jm\,a\rangle && j = 0,\ 1/2,\ 1,\ 3/2, \ldots \\
&\hat{J}_3\,|jm\,a\rangle = m\,|jm\,a\rangle && m = -j,\ -j+1, \ldots, j-1,\ j \\
&\hat{A}\,|jm\,a\rangle = a\,|jm\,a\rangle &&
\end{aligned} \tag{J.95}$$

where the operator $\hat{A}$ (with the corresponding eigenvalue a) together with $\hat{J}^2$ and $\hat{J}_3$ form the total ensemble of commuting operators ($[\hat{J}^2,\ \hat{J}_3] = [\hat{J}^2,\ \hat{A}] = [\hat{A},\ \hat{J}_3] = 0$) and therefore have the common basis of eigenfunctions $|jm\,a\rangle$. Since all further given matrix elements are diagonal in a and not dependent on a further we omit the index a in all orthonormal basis vectors $|jm\,a\rangle$.

The matrix elements

$$\langle jm|\hat{D}(\vec{n}, \varphi)|j'm'\rangle = \delta_{jj'}\,D^j_{mm'}(\vec{n}, \varphi) = \delta_{jj'}\,e^{-i\,\varphi\,\vec{n}\cdot\vec{J}^{\,(j)}_{mm'}} \tag{J.96}$$

define the Wigner functions $D^j_{mm'}(\vec{n}, \varphi)$ (see (A.18)). In (J.96) the symbol $\vec{J}^{\,(j)}_{mm'}$ stands for the matrix elment

$$\vec{J}^{\,(j)}_{mm'} = \langle jm|\,\hat{\vec{J}}\,|jm'\rangle \tag{J.97}$$

If j goes over $j = 0,\ 1/2,\ 1,\ 3/2, \ldots$ then the matrices $D^j_{mm'}(\vec{n}, \varphi)$ represent all unitary representations of the group $SO(3)$.

It is evident that instead of the rotation around the axis in the direction of the unit vector $\vec{n}$ by an angle φ we can discuss the general rotation given by the Euler angles $\theta \equiv (\alpha, \beta, \gamma)$ - see (A.19). Then the expression (J.96) is modified (see(A.21))

$$\langle jm|\ \hat{D}(\theta)\ |j^{'}m^{'}\rangle = \delta_{jj'}\ D^j_{mm'}(\theta) \tag{J.98}$$

and Wigner functions $D^j_{mm'}(\theta)$ are now functions of the Euler angles θ (see(A.21)).

J.3.2 Unitary group (algebra) $U(n)$ and special unitary group (algebra) $SU(n)$

group $U(n)$ = Lie group of $n \times n$ unitary matrices where the group operation is the matrix multiplication. If determinants of these unitary matrices is 1 then we speak about the $SU(n)$ group.

The number of generators of the $U(n)$ algebra is n^2, the number of generators of the algebra $SU(n)$ is $n^2 - 1$.

The most important in the practise is the $SU(3)$ algebra and therefore the main properties of this algebra are discussed below. Practilally it is shown how to construct generators of the $SU(3)$ algebra from harmonic oscillator quanta.

The Hamiltonian of the harmonic oscillator in the 3- dimensional space is

$$\hat{H}_{osc} = \frac{\hat{\vec{p}}^{\,2}}{2M} + \frac{k^2 \hat{\vec{r}}^{\,2}}{2} = \left(\hat{p}^{\,2} + \hbar^2\alpha^2\hat{r}^2\right)\ 2M = \\ = \left(\alpha^{-2}\,\hat{p}^{\,2} + \hbar^2\alpha^2\hat{r}^{\,2}\right)\ \frac{\alpha^2}{2M} \tag{J.99}$$

where $\alpha = \sqrt{M\omega/\hbar}$, $\hbar\omega = \alpha^2/M = \hbar kc$. From the linear momentum $\hat{\vec{p}} \equiv (\hat{p}_1, \hat{p}_2, \hat{p}_3)$ and coordinate spatial $\hat{\vec{r}} \equiv (\hat{x}_1, \hat{x}_2, \hat{x}_3)$ vectors the creation and annihilation operators b^+_j and b_j $(j = 1, 2, 3)$ can be constructed:

$$b^+_j \equiv \frac{\alpha}{\sqrt{2}}\ \left(\hbar\hat{x}_j - i\,\alpha^{-2}\hat{p}_j\right)\ ,\ b_j \equiv \frac{\alpha}{\sqrt{2}}\ \left(\hbar\hat{x}_j + i\,\alpha^{-2}\,\hat{p}_j\right)\ ,\ j = 1, 2, 3 \tag{J.100}$$

which fulfil the boson commutator relations

$$[\, b_i^+,\, b_k^+\,] = [\, b_i,\, b_k\,] = 0 \quad , \qquad [\, b_j,\, b_k^+\,] = \delta_{jk} \tag{J.101}$$

Using these commutation relations it can be easily shown that the oscillator Hamiltonian (J.99) can be rewritten as follows

$$\hat{H}_{osc} = \sum_{j=1}^{3} \left(b_j^+ b_j + \frac{1}{2} \right) \hbar\omega \tag{J.102}$$

Further we introduce the following operators

$$\hat{X}_{ij} \equiv \left(b_i^+ b_j + b_j b_i^+ \right) = \left(2 b_i^+ b_j + \delta_{ij} \right) \frac{1}{2} =$$
$$= \left(b_i^+ b_j + \frac{\delta_{ij}}{2} \right) = \hat{X}_{ji}^+ \tag{J.103}$$

So the oscillator Hamiltonian $\hat{H}_{osc}$ can be expressed in terms of the operators $\hat{X}_{ii}$ $(i = 1, 2, 3)$ as follows

$$\hat{H}_{osc} = \left(\hat{X}_{11} + \hat{X}_{22} + \hat{X}_{33} \right) \hbar\omega \tag{J.104}$$

with

$$\left[\hat{H}_{osc}, \hat{X}_{ij} \right] = 0 \qquad \text{for all } ij = 1, 2, 3 \tag{J.105}$$

The operator $\hat{X}_{ij}$ (J.103) fulfill also the following commutation relations

$$\left[\hat{X}_{ij},\, \hat{X}_{kl} \right] = \boxed{\begin{array}{c}\text{using} \\ (J.101)\end{array}} = \delta_{ij}\, \hat{X}_{il} - \delta_{il}\, \hat{X}_{kj} \tag{J.106}$$

If we compare this commutator with (J.77) we can see that operators $\hat{X}_{ij}$ represent 9 generators of the Lie algebra $U(3)$. Elements of the corresponding Lie group $U(3)$ are formed by the operators $\hat{D}(a_{ij})$ defined as follows (see (J.74))

$$\hat{D}(a) \equiv e^{\sum_{jk} a_{jk}\, \hat{X}_{jk}} \quad , \qquad \hat{X}_{jk} = \frac{\partial \hat{D}(a)}{\partial a_{jk}}|_{a=0} \tag{J.107}$$

Because of (J.105) the oscillator Hamiltonian commutes with all operators $\hat{D}(a)$ to zero

$$\left[\hat{H}_{osc},\, \hat{D}(a) \right] = 0 \tag{J.108}$$

and we see that the $U(3)$ group of operators $\hat{D}(b)$ is the symmetry group of the oscillator Hamiltonian $\hat{H}_{osc}$

The $\hat{X}_{ij}$ $(i,j=1,2,3)$ (see(J.105)) form the tensor operator of the 2-d order in the cartesian indexes i, j. It is known from a mathematics (see e.g. [2]) that from 9 elements of any cartesian tensor of the 2-d order $(\hat{X}_{ij})$ we can construct 1 scalar $(\hat{\mathscr{E}})$, 1 irreducible tensor of the 1-st order $(\hat{\mathscr{L}}_\mu,\ \mu=0,\pm1)$ and 1 irreducible tensor of the 2-d order $(\hat{\mathscr{Q}}_\mu,\ \mu=0,\pm1,\pm2)$ from the point of view of the group $SO(3)$ of rotations:

$$\hat{\mathscr{E}} = \frac{1}{3}\sum_{i=1}^{3}\hat{X}_{ii} \tag{J.109}$$

$$\begin{aligned}
\hat{\mathscr{L}}_{+1} &= \frac{1}{2}\left(\hat{X}_{13}-\hat{X}_{31}\right)+\frac{i}{2}\left(\hat{X}_{23}-\hat{X}_{32}\right)\\
\hat{\mathscr{L}}_{-1} &= \frac{1}{2}\left(\hat{X}_{13}-\hat{X}_{31}\right)-\frac{i}{2}\left(\hat{X}_{23}-\hat{X}_{32}\right)\\
\hat{\mathscr{L}}_{0} &= i\left(\hat{X}_{21}-\hat{X}_{12}\right)
\end{aligned} \tag{J.110}$$

$$\begin{aligned}
\hat{\mathscr{Q}}_0 &= -\hat{X}_{11}-\hat{X}_{22}+2\,\hat{X}_{33}\\
\hat{\mathscr{Q}}_2+\hat{\mathscr{Q}}_{-2} &= \sqrt{6}\left(\hat{X}_{12}-\hat{X}_{21}\right)\\
\hat{\mathscr{Q}}_2-\hat{\mathscr{Q}}_{-2} &= i\sqrt{6}\left(\hat{X}_{12}+\hat{X}_{21}\right)\\
\hat{\mathscr{Q}}_1+\hat{\mathscr{Q}}_{-1} &= -i\sqrt{6}\left(\hat{X}_{32}-\hat{X}_{23}\right)\\
\hat{\mathscr{Q}}_1-\hat{\mathscr{Q}}_{-1} &= -\sqrt{6}\left(\hat{X}_{31}-\hat{X}_{13}\right)
\end{aligned} \tag{J.111}$$

If we substitute (J.103) into (J.110) and (J.111) and use the explicit expression of $rY_{1\mu}(\hat{r})$ and $r^2Y_{2\mu}(\hat{r})$ (see e.g. [2]) then the following expressions can be shown

$$\begin{aligned}
\hat{\mathscr{L}}_\mu &= \sum_{ij}\langle i|\ \left[\hat{\vec{r}}\times\hat{\vec{p}}\right]_\mu\ |j\rangle\ b_i^+b_j \quad , \qquad \mu=\pm1,0\\
\hat{\mathscr{Q}}_\mu &= \sum_{ij}\langle i|\ r^2\,Y_{2\mu}(\hat{r})\ |j\rangle\ b_i^+b_j \quad , \qquad \mu=\pm2,\pm1,0
\end{aligned} \tag{J.112}$$

Then, using (J.106) and (J.110) with (J.111), we obtain

$$\begin{aligned}
\left[\ \hat{\mathscr{L}}_\mu,\ \hat{\mathscr{L}}_{\mu'}\ \right] &= -\sqrt{2}\,C^{1\,\mu+\mu'}_{1\mu1\mu'}\ \hat{\mathscr{L}}_{\mu+\mu'}\\
\left[\ \hat{\mathscr{Q}}_\mu,\ \hat{\mathscr{L}}_{\mu'}\ \right] &= -\sqrt{6}\,C^{2\,\mu+\mu'}_{2\mu1\mu'}\ \hat{\mathscr{Q}}_{\mu+\mu'}\\
\left[\ \hat{\mathscr{Q}}_\mu,\ \hat{\mathscr{Q}}_{\mu'}\ \right] &= 3\sqrt{10}\,C^{1\,\mu+\mu'}_{2\mu2\mu'}\ \hat{\mathscr{L}}_{\mu+\mu'}
\end{aligned} \tag{J.113}$$

and we see that the commutator relations of operators $\hat{\mathscr{L}}_\mu$ $(\mu = 0, \pm 1)$ and $\mathscr{Q}_\mu$, $(\mu = 0, \pm 1, \pm 2)$ remain close in the space of these 8 operators. It can be shown (see e.g. [112]) that these operators $\hat{\mathscr{L}}_\mu$ $(\mu = 0, \pm 1)$ and $\mathscr{Q}_\mu$, $(\mu = 0, \pm 1, \pm 2)$ form generators of the algebra $SU(3)$. Then because of we know the structural coefficients of this $SU(3)$ algebra, using (J.83) and (J.85) the first Casimir operator (J.85) can be constructed for this representation of the $SU(3)$ algebra.

J.4 Symmetry groups, dynamical groups, dynamical subgroup chain

J.4.1 Symmetry groups (algebras)

Let us suppose that the investigated quantum system (nucleus—) has the Hamiltonian $\hat{H}$. The group G is called as the symmetry group for the Hamiltonian $\hat{H}$ if there is the operator representation $\hat{D}(G(a))$ of this group span the Hilbert space of the Hamiltonian $\hat{H}$ and the Hamiltonian is invariant with repect to all transformations (elements) $\hat{D}(g(a))$, where $g(a) \in G(a)$ for all a. That means

$$\hat{D}(g(a))\, \hat{H}\, \hat{D}^{-1}(g(a)) = \hat{H} \tag{J.114}$$

For instance, if the Hamiltonian $\hat{H}$ is invariant under $SO(3)$ rotations (in the case when the model Hamiltonian does not involve spin degrees of freedom) or $SU(2)$ rotations (when the Hamiltonian involves spin degrees of freedom) [5] then its eigenstates can be labelled by angular momentum numbers, $|\alpha JM\rangle$. Thus, if $\{|\alpha JM\rangle\}$ are orthonormal basis states for our system, where J and M are angular momentum quantum numbers and α distinquishes different $SO(3)$ (or $SU(2)$) irreps of the same J, then the Hamiltonian is bock- diagonal:

$$\langle \alpha JM \mid \hat{H} \mid \beta J^{'} M^{'} \rangle = \delta_{JJ'}\, \delta_{MM'}\, H^J_{\alpha\beta} \tag{J.115}$$

where $H^J_{\alpha\beta}$ is the M- independent matrix elements

$$H^J_{\alpha\beta} = \langle \alpha JM \mid \hat{H} \mid \beta JM \rangle \tag{J.116}$$

Thus, to determine a complete set of eigenstates of a Hamiltonian, it only remains to diagonalize the matrices H^J with respect to indices α, β which distinquish states with a common set of good, symmetry defined, quantum numbers, which in this example are J and M.

[5] If the rotation invariant Hamiltonian $\hat{H}$ does not involve spin degrees of freedom then the symmetry group is $SO(3)$; if $\hat{H}$ involves spin degrees of freedom then the symmetry group is $SU(2)$.

J.4.2 Dynamical groups (algebras)

Dynamical group is connected with the symmetry of the space of vectors which form the basis of wave functions for the description of given quantum system in the framework of given model. Usually the character of used model gives some concrete irreducible representation λ of the particular group $\hat{D}^{(\lambda)}(G)$ with respect to which the Hamiltonian $\hat{H}$ of the system is closed to be invariant. Naturally it is advantageous to choose the Hilbert subspace $\mathscr{H}^{(\lambda)}$ corresponding to $\hat{D}^{(\lambda)}(G)$ for the construction of the basis of vectors (kets) within which the eigenvectors of the Hamiltonian $\hat{H}$ are searched for. The group G corresponding to $\hat{D}^{(\lambda)}(G)$ is called dynamical group. So the definition of the dynamical group can be formulated as follows:

Dynamical group for the given model is a Lie group that has irreducible unitary representation as a group of transformations of the model Hilbert space which is close the symmetry group of the given model and which is convenient from the point of view of used model.

In order to be useful, the dynamical group should be such that its representation theory and that of its Lie algebra are of assistance in determining the spectral properties of the model.

For instance in the simple case when the Hamiltonian $\hat{H}$ is close to be rotational invariant with the particular angular momentum $\lambda = J$ it is favorable to choose the basis of kets $|JM\alpha\rangle$ with the angular momentum quantum numbers J and M ($M = -J, \ldots, +J$) and possible other quantum numbers α as the starting basis. That means the group $SU(2)$ is chosen to be a dynamical group. Then the eigenvectors and eigenvalues of the model Hamiltonian $\hat{H}$ can be obtained by the diagonalization of the matrix with elements $\langle JM\alpha|\hat{H}|JM'\beta\rangle$ and the eigenvectors are then linear combination of the basis vector $|JM\alpha\rangle$ with different α and M.

In the real physical problems the situation is usually complicated and the label λ of the irreducible representation of the dynamical group gives only the first fixed quantum number for basis vectors (like the quantum number J in the simple example given above). The other quantum numbers of the basis vectors can be determined using the different dynamical subgroup chains for the given representation $\hat{D}^{(\lambda)}(G)$ of the dynamical group G. This is discussed in the next subsection.

J.4.3 Dynamical subgroup chains [111]

Let us suppose that G is the dynamical group of the model Hamiltonian $\hat{H}$ of the investigated quantum system and λ is the label of the irreducible representation $\hat{D}^{(\lambda)}(G)$ of this group G corresponding to the assumed model Hilbert space. That means λ is the first quantum number of the basis states of the model. In order to determine other quantum numbers characterizing individual basis states we should choose a chain of subgroups of the dynamical group G. Particularly useful basis states for used model (without spin degrees of freedom [6]) are ones labelled by quantum numbers associated with the following chain of subgroups

$$\begin{array}{ccccccc} G & \supset & G_1 & \subset & SO(3) & \subset & SO(2) \\ & \rho & & \alpha & & & \\ \lambda & & \kappa & & L & & M \end{array} \qquad \text{(J.117)}$$

where λ, κ, L and M, respectively, label irreps of the groups G, G_1,$SO(3)$ and $SO(2)$ in the chain (the subgroups $SO(3)$ and $SO(2)$ are included in such subgroup chain when one wishes to define basis states with the good angular momentum numbers). Irrep labels provide quantum numbers for labelling basis states. However, there are generally missing labels in the sense that the set of quantum numbers given by the representative labels of the groups in the chain may be unsufficient to identify a state uniquely. Multiplicity labels must be then added to the set for a complete classification of basis states. For example, if multiple equivalent irreps of the group G_1, labelled by κ, occur within the space of a single irrep of G, labelled by λ, these irreps are distinquisged by a multiplicity index ρ.

Basis states $|\lambda\rho\kappa\alpha LM\rangle$, defined by the chain (J.117), are said to reduce the given subgroup chain. The representation theory for the groups in the chain then provides powerful tools for the deducing the energy spectrum and other properties of the system. A chain of subgroups of a dynamical group G for a model can imply also the existence of a corresponding chain of submodels each of which has a dynamical group given by an associated subgroup in the chain. For example, the Hilbert space spanned by all states $\{|\lambda\rho\kappa\alpha LM\rangle\}$ given by the chain (J.117) with fixed $(\lambda\rho\kappa)$ quantum numbers, carries an irrep κ of the subgroup $G_1 \subset G$ and is the Hilbert space for a submodel with G_1 as its dynamical group.

[6] If the model includes spin degrees of freedom the subgroup $SO(3)$ in the chain(J.117) should be replaced by $SU(2)$ and instead of indexes L (orbital angular momentum) we should use the index J (total angular momentum).

For given starting irrep λ of the dynamical group G there exist alternative chaines of subgroup chains that can be used for the construction of basis states for a model. As it is illustrated in the Appendix K and in the Subsection 7.2.2 for so called Interacting Boson Model (IBM) different subgroup chains of given irrep λ of the dynamical group G can be used for the analysis of symmetries and spectra of nuclear model Hamiltonian taken as the sums of the Casimir iperators (invariants) and other invariants of the groups in subgroup chains corresponding to different Hamiltonian parametrizations.

When a subgroup chain of a dynamical group contains a symmetry group of the Hamiltonian, then the corresponding irrep label is a good quantum number, i.e. a quantum number that is conserved by the Hamiltonian and can be used to label eigenstates of the Hamiltonian. For example, if a model Hamiltonian has a dynamical group G, with subgroups given by exp. (J.117) and it is rotationally invariant so that $SO(3)$ and $SO(2)$ are symmetry groups, then the labels L and M are good quantum numbers for the model. However, one should realize that a subgroup in a chain need not be a symmetry group of the Hamiltonian to provide good quantum numbers. In general, when a complete set of eigenstates of a model Hamiltonian $\hat{H}$ reduce some subgroup chain of a dynamical group, the Hamiltonian is said to have a dynamical symmetry defined by the subgroup chain.

J.4.4 Permutation symmetry, Young diagrams

Let $p_1, \cdots, p_n$ is the permutation of numbers $1, \ldots, n$. This is usually written as

$$P = \begin{pmatrix} 1 & 2 & \cdots & n \\ p_1 & p_2 & \cdots & p_n \end{pmatrix} \tag{J.118}$$

Let us consider other permutation

$$Q = \begin{pmatrix} 1 & 2 & \cdots & n \\ q_1 & q_2 & \cdots & q_n \end{pmatrix} \tag{J.119}$$

then the permutation product QP

$$\begin{aligned} QP &= \begin{pmatrix} p_1 & p_2 & \cdots & p_n \\ q_{p_1} & q_{p_{p_2}} & \cdots & q_{n_{p_n}} \end{pmatrix} \begin{pmatrix} 1 & 2 & \cdots & n \\ p_1 & p_2 & \cdots & p_n \end{pmatrix} = \\ &= \begin{pmatrix} 1 & 2 & \cdots & n \\ q_{p_1} & q_{p_2} & \cdots & q_{p_n} \end{pmatrix} \end{aligned} \tag{J.120}$$

is again the permutation, for instance

$$P = \begin{pmatrix} 1 & 2 & 3 & 4 & 5 & 6 \\ 2 & 3 & 1 & 4 & 6 & 5 \end{pmatrix} \quad , \quad Q = \begin{pmatrix} 1 & 2 & 3 & 4 & 5 & 6 \\ 2 & 1 & 4 & 5 & 6 & 3 \end{pmatrix}$$
$$\Rightarrow \qquad QP = \begin{pmatrix} 1 & 2 & 3 & 4 & 5 & 6 \\ 1 & 4 & 2 & 5 & 3 & 6 \end{pmatrix} \tag{J.121}$$

Identical permutation is defined as

$$E \equiv \begin{pmatrix} 1 & 2 & \cdots & n \\ 1 & 2 & \cdots & n \end{pmatrix} \tag{J.122}$$

and the inverse permutation with respect to P is

$$P^{-1} = \begin{pmatrix} p_1 & p_2 & \cdots & p_n \\ 1 & 2 & \cdots & n \end{pmatrix} \tag{J.123}$$

So, the ensemble of permutations of n elements forms the permutation group of the n-the order. This group is usually denoted as S_n.

In order to investigate properties of the permutation group S_n it is suitable to introduced the concept of a cycle. The cycle of the length k is defined as the following permutation of k elements

$$t_1 \to t_2 \to t_3 \to \ \cdots \ \to t_{k-1} \to t_k \to t_1 \tag{J.124}$$

and is usually labelled by the symbol

$$(t_1\, t_2\, t_3\, \cdots\, t_k) \tag{J.125}$$

Symbols of (J.125) type differing only by the permutation of arguments describe the same cycle, that means the symbol

$$(t_3\, \cdots\, t_k\, t_1\, t_2) \tag{J.126}$$

represents the same cycle as the symbol (J.124) or (J.125).

An arbitrary permutation is possible to decompose unambuguously to cycles not involving common elements (so called independent cycles). For instance for permutations P and Q in (J.121) these decompositions are following

$$P = (123)(56)(4) \qquad\qquad Q = (3456)(12) \tag{J.127}$$

The sequence, in which the independent cycles are written, is irrelevant. The cycles with one element are not usually presented, that means the permutation P in (J.127) can be also written as

$$P = (123)(56) \tag{J.128}$$

The cycles with the length 2 represent transpositions. Each permutation can be obtained as a product of several transpositions. For instance the permutation (J.128) can be also written as [7]

$$P = (13)(12)(56) \tag{J.129}$$

The permutation formed by the product of the even (odd) number of transpositions is called as the even (odd) permutation. The parity of given prmutation is defined as the number ϵ_P:

$$\epsilon_P = \begin{cases} +1 & \text{for even permutation } P, \\ -1 & \text{for odd permutation } P. \end{cases} \tag{J.130}$$

If the given permutation $P \in S_n$ is composed from ν_1 cycles of the length 1, ν_2 cycles of the length 2, $\cdots$, ν_n cycles of the length n then the cyclic structure of this permutation is defined as

$$(1^{\nu_1}, 2^{\nu_2}, \cdots, n^{\nu_n}) \tag{J.131}$$

Two permutations are conjugated (equivalent) if and only if they have the same cyclic structure. Therefore the cyclic structure determines the classes of S_n (by the class we understand the ensemble of permutations conjugated each other).

From the definition of numbers ν_j above the following relation arises

$$\sum_{j=1}^{n} j\, \nu_j = n \tag{J.132}$$

Every n positive numbers ν_j in (J.132) determine one class of the group S_n and simultaneously one irreducible representation of the group S_n.

Each cyclic structure (J.131) is unambiguously assiciated with n numbers λ_k $(k = 1, \cdots, n)$ defined as

$$\lambda_k = \sum_{j=k}^{n} \nu_j \qquad\qquad k = 1, \cdots, n \tag{J.133}$$

It is evident that

$$\lambda_1 \geq \lambda_2 \geq \cdots \geq \lambda_n \geq 0 \tag{J.134}$$

[7] Opposite to the decomposition (J.128) in (J.129) there is the same element 1 in the first two cycles. Therefore in this case (J.129) the sequence (order) of cycles is important.

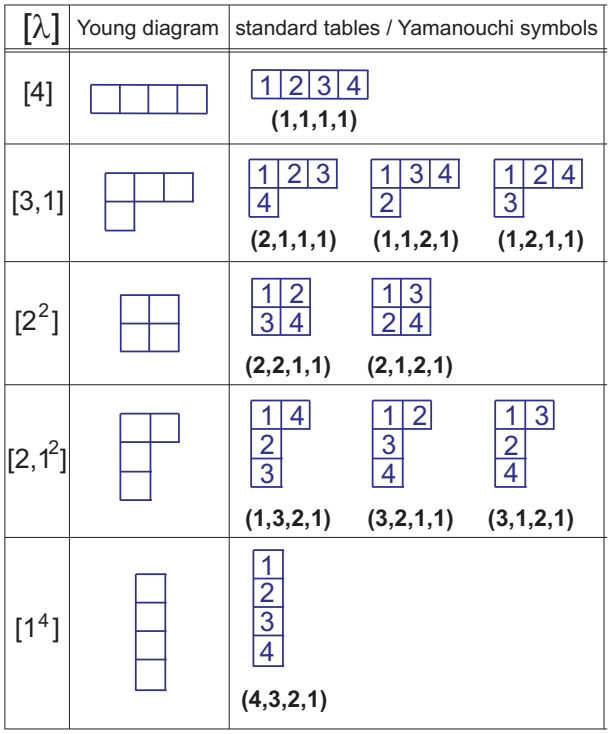


Figure J.1: Decompositions of the number $n = 4$ and corresponding Yung diagrans.

and from (J.132) it follows

$$\sum_{k=1}^{n} \lambda_k = \sum_{k=1}^{n} \sum_{j=k}^{n} \nu_j = \sum_{j=1}^{n} j\, \nu_j = n \tag{J.135}$$

Every n integer numbers $[\lambda] \equiv [\lambda_1, \cdots, \lambda_n]$ fulfilling (J.135), (J.134) are called as the decomposition of the number n. Since the numbers ν_j $(j = 1, \cdots, n)$ determine one irreducible representation of S_n and since the numbers λ_k $(k = 1, \cdots, n)$ are unambiguously given by the numbers ν_j according to (J.133) **each decomposition** $[\lambda]$ **of the number** n **corresponds to one and only one irreducible representation** $(\equiv D^{[\lambda]})$ **of the group** S_n.

Each decomposition $[\lambda]$ of the number n (and therefore each irreducible representation of the group S_n) is unambiguously connected with one Young diagram. The Young diagram is composed from n cells arranged to rows with lenths λ_1, λ_2, $\cdots$, in such a way that the cells of the k-th row lie under the first λ_k cells of the $(k-1)$-th row. As an example in the first two columns of the table shown in the Fig.J.1 there are all decompositions of the number $n = 4$ and corresponding Young diagrams. In the first column of this table there are so called standard tables which are the result from distribution of numbers (elements) 1,2,$\cdots$,n into the cells of each Young diagram presented

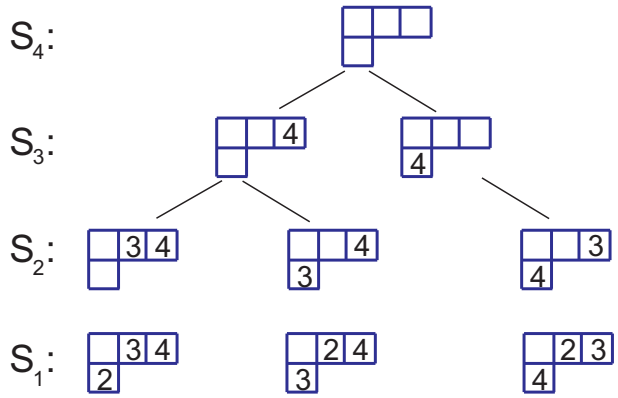


Figure J.2: Decomposition of the representation $D^{[3,1]}$ of the group S_4 into the direct sums of the representations of all subgroups of S_4.

in the 2-nd column in the increasing order in each row and column of the diagram.

If we restrict ourselves only to such permutations in S_n where the n-th element is untouched, that means to permutations of the following type

$$\begin{pmatrix} 1 & 2 & \cdots & n-1 & n \\ p_1 & p_2 & \cdots & p_{n-1} & n \end{pmatrix} \tag{J.136}$$

then we obtain the subgroup $S_{n-1} \in S_n$ and simultaneously the following statement valids:

Irreducible representation of the group S_n corresponding to the given Young diagram can be obtained as a direct sum of irreducible representations of the subgroup S_{n-1} corresponding to Young diagrams created from the original one by the cancellation of one cell by all possible ways.

By repeated application of this statement every irrediciuble representation of the group S_n can be decomposed into the direct sum of irreducible representations of the the arbitrary subgroup S_m with $m < n$. For instance, in the Fig.J.2 there is the decomposition of the representation $D^{(3,1)}$ of the group S_4 into the direct sum of representations of subgroups S_m with $m < 4$.

In the Fig.J.2 in each Young diagram the number denotes the cell abandoned in the transition from the Young diagram of the group S_n to the Young diagram of the group S_{n-1}. So the representation $D^{[3,1]}$ represents the direct sum of irreps of the subgroup S_m ($m \leq 4$) characterized by Yound diagrams as it is given in the Fig.J.3.

The group S_1 is trivial, it consists from one element and its only irrep is one-dimensional (with identical element). From the Fig.J.3 it follows that

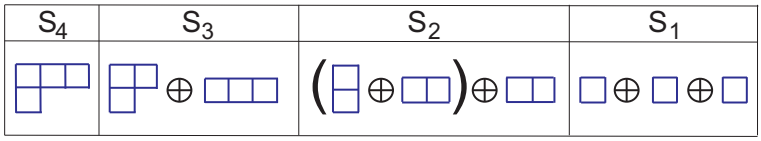


Figure J.3: Decomposition of the representation $D^{[3,1]}$ of the group S_4 into irreducible representations of subgroups S_m $(m < 4)$.

the irreducible representation $D^{[3,1]}$ of the group S_4 is 3- dimensional.

Each standard table is connected with the one vector of the basis of the representation $D^{[\lambda]}$ of the group S_n (which belongs simultaneously to the basis of the irreducible representation of the subgroup S_m $(m < n)$. The number of the standard tables corresponding to given representation $[\lambda]$ gives the dimension $(\equiv n_{[\lambda]})$ of this representation $D^{[\lambda]}$. The standard tables can be also characterized by the Yamanouchi symbols. Let r_j gives the number of rows in which the given element (number) j sits in the standard table. Then the Yamanouchi symbol

$$(r) \equiv (r_n, r_{n-1}, \cdots, r_2, r_1) \tag{J.137}$$

describes unambiguously the standard table. So, the Yamanouchi symbols are often used for labelling the vectors of the basis of given irreducible representation of the group S_n. This labelling is shown in the third column of the table in the Fig.7.1 for the case of the group S_4.

Two Young diagrams are conjugated each other if they differ only by exchange of rows or columns (Young diagram conjugated to the diagram $[\lambda]$ is usually denoted by $[\tilde{\lambda}]$). Corresponding representations are also conjugated. It is possible to prove easily that the mutual conjugated representations have the same dimensions. In the analogy the mutual conjugated standard tables and Yamanouchi symbols can be introduced.

Each group S_n $(n \geq 2)$ has two and only two one- dimensional (mutually conjugated) representations. The first one corresponds to the Young diagram with only one row and it it assigns the unity to each permutation:

$$D^{[n]}(P) = 1 \tag{J.138}$$

which means the totally symmetric representation.

The second one dimensional representation corresponds to the Young diagram with only one column and it assigns to each permutation its parity:

$$D^{[1^n]} = \epsilon_P \tag{J.139}$$

and this representation is totally antisymmetric.
All other representations are more dimensional than 1 and they correspond to the mixed-symmetry (for details of the mixed-symmetry more dimensional representations of the group S_n see e.g. Appendix O in the textbook [14]).

K. More details on the Interaction Boson Model

In this appendix the Interacting Boson Model (IBM) is discussed in a little bit more details than in the subsection 7.2.2.The IBM was established in the 70-ties with the aim to describe the low-lying collective states in even-even nuclei, particularly the change of the nuclear energy spectrum going from the spherical nuclei to deformed ones in the framework of one approach (see e.g.[113, 114, 115] and also [116, 117]). In this appendix we restrict ourselves to the IBM-1 version of the model where isospin degrees of freedom are not taken into account and neutrons and protons are considered as one type particles [103].

K.1 IBM Hamiltonian

The IBM-1 version of the model starts with the assumption that the lowest states of the even-even spherical as well as deformed nuclei has quadrupole collective character [1]. Therefore the assumed configuration space can be reduced to the multiboson space formed by quadrupole ($l = 2$) and monopole ($l = 0$) bosons with corresponding creation operators $d^+_\mu \equiv b^+_{l=2\,\mu}$ ($\mu = 0, \pm 1, \pm 2$) and $s^+ \equiv b^+_{l=0\,\mu=0}$, respectively. This simple model further supposes that these $l = 2$ and $l = 0$ bosons can fill only two levels: s- level ($L = 0$) with energy ϵ_s and d- level ($L = 2$) with energy ϵ_d (which is degenerated with respect to the angular momentum projection) and these quadrupole and monopole bosons interact mutually by the two- boson interaction $\mathscr{U}$. General multiboson Hamiltonian consists from one- boson and two- boson

[1] In the case of deformed nucleus the quadrupole character is supposed for the lowest intrinsic nonrotational states

parts as follows

$$\hat{H} = \sum_{\substack{l=0,2 \\ m}} \epsilon_l \, b^+_{lm} \, b_{lm} +$$

$$+ \frac{1}{2} \sum_{\substack{l_1,\, l_2=0,2 \\ m_1, m_2}} \sum_{\substack{l_1^{'},\, l_2^{'}=0,2 \\ m_1^{'}, m_2^{'}}} \langle \, l_1 m_1 l_2 m_2 | \hat{V} | \, l_1^{'} m_1^{'} l_2^{'} m_2^{'} \rangle \;\; b^+_{l_1 m_1} b^+_{l_2 m_2} b_{l_2^{'} m_2^{'}} b_{l_1^{'} m_1^{'}}$$

(K.1)

Using Clebsch-Gordan coefficients for the group $SO(3)$ of rotations (see(A.2)) the two- boson state $| \, l_1^{'} m_1^{'} l_2^{'} m_2^{'} \rangle$ reads [2]

$$| \, l_1^{'} m_1^{'} l_2^{'} m_2^{'} \rangle = \sum_{\substack{L^{'}=0,2,4 \\ M^{'} = m_1^{'} + m_2^{'}}} C^{L^{'} M^{'}}_{l_1^{'} m_1^{'} l_2^{'} m_2^{'}} \, | \, l_1^{'} l_2^{'};\; L^{'} m^{'} \rangle \qquad \text{(K.2)}$$

and similarly for the bra $\langle l_1 m_1 l_2 m_2 |$. So the expression (K.1) can be rewritten as follows

$$\hat{H} = \sum_{\substack{l=0,2 \\ m}} \epsilon_l \, b^+_{lm} \, b_{lm} +$$

$$+ \frac{1}{2} \sum_{\substack{l_1,\, l_2=0,2 \\ m_1, m_2}} \sum_{\substack{l_1^{'},\, l_2^{'}=0,2 \\ m_1^{'}, m_2^{'}}} \sum_{\substack{L=0,2,4 \\ M = m_1 + m_2}} \sum_{\substack{L^{'}=0,2,4 \\ M^{'} = m_1^{'} + m_2^{'}}} C^{L^{'} M^{'}}_{l_1^{'} m_1^{'} l_2^{'} m_2^{'}} \, C^{LM}_{l_1 m_1 l_2 m_2}$$

$$\langle \, l_1 l_2 L M | \hat{V} | \, l_1^{'} l_2^{'} L^{'} M^{'} \rangle \;\; b^+_{l_1 m_1} b^+_{l_2 m_2} b_{l_2^{'} m_2^{'}} b_{l_1^{'} m_1^{'}} =$$

$$= \boxed{\begin{array}{c} \text{because the matrix element } \langle \, l_1 l_2 L M | \hat{V} | \, l_1^{'} l_2^{'} L^{'} M^{'} \rangle \\ \text{does not depend on } M \text{ and } M^{'} \text{ and it involves } \delta_{LL^{'}} \\ \text{if } \hat{V} \text{ is scalar operator and because of} \\ C^{00}_{LML\,-M} = \frac{(-1)^{L+M}}{\sqrt{2L+1}} \end{array}} =$$

[2] For $l_1^{'} = l_2^{'} = 2$ the angular momentum $L^{'}$ can only be $L^{'} = 0, 2, 4$ because the wave function $|l_1^{'} l_1^{'} L^{'} M^{'}\rangle$ should be symmetric with respect to boson exchange. As a result the angular momentum $L^{'}$ can have only even values $L^{'} = 0, 2, 4$ (see (7.64)-(7.66) and the text around).

$$= \sum_{\substack{l=0,2\\ m}} \epsilon_l \, b^+_{lm} \, b_{lm} +$$

$$+ \frac{1}{2} \sum_{\substack{l_1,\, l_2=0,2\\ m_1,m_2}} \sum_{\substack{l_1^{'},\, l_2^{'}=0,2\\ m_1^{'},m_2^{'}}} \sum_{\substack{L,\, L^{'}=0,2,4\\ MM^{'}}} (2L+1)^{1/2} \langle \, l_1 l_2 L \mid \hat{V} \mid l_1^{'} l_2^{'} L^{'} \rangle$$

$$(-1)^{L+M} \, C^{00}_{LML\,-M} \, C^{L^{'}M^{'}}_{l_1^{'}m_1^{'}l_2^{'}m_2^{'}} \, C^{LM}_{l_1m_1l_2m_2} \, b^+_{l_1m_1} b^+_{l_2m_2} b_{l_2^{'}m_2^{'}} b_{l_1^{'}m_1^{'}} \tag{K.3}$$

Further we use the following coupling notation

$$\sum_{m_1} C^{LM}_{l_1m_1\, l_2\, M-m_1} \, b^+_{l_1m_1} \, b^+_{l_2m_2} \equiv \left(b^+_{l_1} \, b^+_{l_2}\right)_{(l_1l_2;\, LM)}$$

$$\sum_{m_1^{'}} C^{LM}_{l_1^{'}m_1^{'}\, l_2\, M-m_1^{'}} \, (-1)^{L+M} \, b_{l_2^{'}m_2^{'}} \, b_{l_1^{'}m_1^{'}} =$$

$$= \sum_{m_1^{'}} C^{L\,-M}_{l_1^{'}-m_1^{'}\, l_2\, -M+m_1^{'}} \, (-1)^{l_1^{'}+\, l_2^{'}-L+L+M} \, b_{l_2^{'}m_2^{'}} \, b_{l_1^{'}m_1^{'}} =$$

$$= \sum_{m_1^{'}m_2^{'}} C^{L\,-M}_{l_1^{'}m_1^{'}\, l_2m_2^{'}} \, (-1)^{l_1^{'}+m_1^{'}} \, b_{l_1^{'}-m_1^{'}} \, (-1)^{l_2^{'}+m_2^{'}} \, b_{l_2^{'}-m_2^{'}} =$$

$$\equiv \left(\tilde{b}_{l_1^{'}} \, \tilde{b}_{l_2^{'}}\right)_{(\, l_1^{'}l_2^{'};\, L\,-M)} \tag{K.4}$$

where we introduced

$$\tilde{b}_{l_1^{'}m_1^{'}} \equiv (-1)^{l_1^{'}+m_1^{'}} b_{l_1^{'}-m_1^{'}} \, , \qquad \tilde{b}_{l_2^{'}m_2^{'}} \equiv (-1)^{l_2^{'}+m_2^{'}} b_{l_2^{'}-m_2^{'}} \tag{K.5}$$

Then the expression (K.3) reads

$$\hat{H} = \sum_{\substack{l=0,2\\ m}} \epsilon_l \, b^+_{lm} \, b_{lm} +$$

$$+ \sum_{L=0,2,4} \frac{1}{2} \, (2L+1)^{1/2} \sum_{\substack{l_1=0,2\\ l_1^{'}=0,2}} \sum_{\substack{l_2=0,2\\ l_2^{'}=0,2}} \langle \, l_1 l_2 L \mid \hat{V} \mid l_1^{'} l_2^{'} L \rangle$$

$$\left[\left(b^+_{l_1} \, b^+_{l_2}\right)_{(\, l_1\, l_2;\, L)} \, \left(\tilde{b}_{l_1^{'}} \, \tilde{b}_{l_2^{'}}\right)_{(\, l_1^{'}l_2^{'};\, L)}\right]_{(LL;\, 00)} \tag{K.6}$$

and using the notation $d^+_\mu \equiv b^+_{l=2\,\mu}$ ($\mu = 0, \pm 1, \pm 2$) and $s^+ \equiv b^+_{l=0\,\mu=0}$ the final expression for the Hamiltonian (K.6) is:

$$\begin{aligned}
\hat{H} &= \epsilon_0\, s^+ s + \epsilon_2 \sum_{m=-2}^{2} d^+_m d_m + \\
&+ \sum_{L=0,\,2,\,4} \frac{\sqrt{2L+1}}{2}\, \langle\, d^{\,2} L|\, \hat{V}|\, d^2 L\rangle\, \Big[(d^+ d^+)_{(22;\,L)}\, (\tilde{d}\,\tilde{d})_{(22;\,L)}\Big]_{(LL;\,0)} \\
&+ \frac{\sqrt{5}}{2}\, \langle\, d^{\,2} L = 2|\, \hat{V}|\, dsL = 2\rangle \\
&\qquad \Big[(d^+ d^+)_{(22;\,2)}\, (\tilde{d}\,\tilde{s})_{(20;\,2)} + (d^+ s^+)_{(20;\,2)}\, (\tilde{d}\,\tilde{d})_{(22;\,2)}\Big]_{(22;\,0)} \\
&+ \frac{1}{2}\, \langle\, d^2 L = 0|\, \hat{V}|\, ssL = 0\rangle \\
&\qquad \Big[(d^+ d^+)_{(22;\,0)}\, (\tilde{s}\,\tilde{s})_{(00;\,0)} + (s^+ s^+)_{(00;\,0)}\, (\tilde{d}\,\tilde{d})_{(22;\,0)}\Big]_{(00;\,0)} \\
&+ \sqrt{5}\, \langle\, dsL = 2|\, \hat{V}|\, dsL = 2\rangle\, \Big[(d^+ s^+)_{(20;\,0)}\, (\tilde{d}\,\tilde{s})_{(20;\,2)}\Big]_{(22;\,0)} \\
&+ \frac{1}{2}\, \langle\, ssL = 0|\, \hat{V}|\, ssL = 0\rangle\, \Big[(s^+ s^+)_{(00;\,0)}\, (\tilde{s}\,\tilde{s})_{(00;\,00}\Big]_{(00;\,0)} = \\
&= \epsilon_0\, s^+ s + \epsilon_2 \sum_{m=-2}^{2} d^+_m d_m + \\
&\quad + \sum_{L=0,\,2,\,4} \frac{\sqrt{2L+1}}{2}\, c_L\, \Big[(d^+ d^+)_{(22;\,L)}\, (\tilde{d}\,\tilde{d})_{(22;\,L)}\Big]_{(LL;\,0)} \\
&\quad + \tilde{v}_2\, \Big[(d^+ d^+)_{(22;\,2)}\, (\tilde{d}\,\tilde{s})_{(20;\,2)} + (d^+ s^+)_{(20;\,2)}\, (\tilde{d}\,\tilde{d})_{(22;\,2)}\Big]_{(22;\,0)} \\
&\quad + \tilde{v}_0\, \Big[(d^+ d^+)_{(22;\,0)}\, (\tilde{s}\,\tilde{s})_{(00;\,0)} + (s^+ s^+)_{(00;\,0)}\, (\tilde{d}\,\tilde{d})_{(22;\,0)}\Big]_{(00;\,0)} \\
&\quad + \tilde{u}_2\, \Big[(d^+ s^+)_{(20;\,0)}\, (\tilde{d}\,\tilde{s})_{(20;\,2)}\Big]_{(22;\,0)} \\
&\quad + \tilde{u}_0\, \Big[(s^+ s^+)_{(00;\,0)}\, (\tilde{s}\,\tilde{s})_{(00;\,20}\Big]_{(00;\,0)}
\end{aligned} \tag{K.7}$$

where the single- boson energies ϵ_0, ϵ_2 and matrix elements of the two- boson interaction are taken as parameters:

$$c_L \equiv \langle\, d^{\,2} L|\, \hat{V}\,|\, d^{\,2} L\rangle \quad , \quad \tilde{v}_2 \equiv \frac{\sqrt{5}}{2} \langle\, d^{\,2} L = 2|\, \hat{V}\,|\, dsL = 2\rangle$$

$$\tilde{v}_0 \equiv \frac{1}{2}\langle\, d^{\,2}L=0|\,\hat{V}\,|\,s^{\,2}L=0\rangle \quad , \quad \tilde{u}_2 \equiv \sqrt{5}\,\langle dsL=2|\,\hat{V}\,|\,dsL=2\rangle$$
$$\tilde{u}_0 \equiv \frac{1}{2}\,\langle\, s^{\,2}L=0|\,\hat{V}\,|\,s^{\,2}L=0\rangle \tag{K.8}$$

One can see from (K.7) that the IBM-1 Hamiltonian involves generally 9 parameters ϵ_0, ϵ_2, $c_L\,(L=0,2,4)$, $\tilde{v}_2$, $\tilde{v}_0$, $\tilde{u}_2$, $\tilde{u}_0$. It is necessary also to realize that the operators $\hat{n}_s = s^+s$ and $\hat{n}_d = \sum_m d_m^+ d_m$ are the number of monopole and quadrupole bosons, respectively.

The other important aspect is the fact that the column vector

$$B^+ \equiv \begin{pmatrix} B_1^+ \\ B_2^+ \\ \vdots \\ B_6^+ \end{pmatrix} \equiv \begin{pmatrix} s^+ \\ d_2^+ \\ \vdots \\ d_{-2}^+ \end{pmatrix} \tag{K.9}$$

constructed from six boson creation operators, s^+, d_{+2}^+, d_{+1}^+, d_0^+, d_{-1}^+, d_{-2}^+, transforms according to the group $U(6)$ and the s and d multi- boson states

$$B_\mu^+ B_\nu^+ B_\kappa^+ \ldots |0\rangle \tag{K.10}$$

represent vectors in the Hilbert space for the totally symmetric representation of the group $U(6)$, which is characterized by the number of bosons N and which is further labeled by a single label $[N]$ (see [124]). The 36 bilinear combinations [3]

$$\hat{G}_{\mu\nu} \equiv B_\mu^+ B_\nu \qquad\qquad (\mu,\,\nu = 1,2,\ldots,6) \tag{K.11}$$

form the corresponding $U(6)$ algebra and are generators of this algebra that are closed under the commutation (J.77). From the point of view of the $U(6)$ algebra the Hamiltonian (K.7) can be written formally as follows

$$\hat{H} = \sum_\mu \epsilon_\mu \hat{G}_{\mu\mu} + \underbrace{\frac{1}{2}\sum_{\mu\nu\kappa\sigma} U_{\mu\nu,\,\kappa\sigma}\hat{G}_{\mu\nu}\hat{G}_{\kappa\sigma}}_{\hat{H}'} \tag{K.12}$$

where the first term in (K.12) should be identified with the first two terms in (K.7) and the rest of (K.7) is involved in $\hat{H}'$. This means that in the absence

[3] Explicitly these combinations forming generators of the $U(6)$ group are following:

$$G_{U(6)} \equiv \Big\{(s^+\tilde{s})_{(00;\,0)},\ (d^+\tilde{s})_{(20;\,2m)},\ (s^+\tilde{d})_{(02;\,2m)},\ (d^+\tilde{d})_{(22;\,0)},\ (d^+\tilde{d})_{(22;\,1m)},$$
$$(d^+\tilde{d})_{(22;\,2m)},\ (d^+\tilde{d})_{(22;\,3m)},\ (d^+\tilde{d})_{(22;\,4m)}\Big\}$$

of the interaction $\hat{H}'$ al possible states (K.10) for a given N are degenerated in the energy. The interaction $\hat{H}'$ thus split the different possible states for a given N and one needs to solve the eigenvalue equation to obtain energies and eigenvectors in the most general situation. However in some cases (with special sets of parameters mentioned above) the interaction part $\hat{H}'$ of the Hamiltonian (K.7) or (K.12) can be written as a sum of Casimir (invariant) operators of a complete chain of subgroups of the largest $U(6)$ group. In such cases the exact quantum numbers characterizing the eigenstates of the Hamiltonian $\hat{H}$ are given by labels of the irreducible representations of the subgroups in the chain and eigenvalues of the Hamiltonian are explicitely determined by these quantum numbers (see the subsection J.4.3 in the Appendix J). Such situations are discussed in details further (vibration and rotational limits of the IBM-1).

In the connection with the determination of electromagnetic transition probabilities within the IBM it is necessary to express the electric and/or magnetic transition operator in terms of the monopole and quadrupole boson creation and annihilation operators. Electromagnetic transition operators $\hat{\mathscr{M}}^{(el)}_{JM}$ and $\hat{\mathscr{M}}^{(mag)}_{JM}$ are tensor operators from the point of view of the $SO(3)$ group of rotations and they are single- boson operators. Therefore they can be expressed in terms of the boson creation and annihilation operators as follows ($X = el,\ mag$)

$$\hat{\mathscr{M}}^{(X)}_{JM} = \sum_{\substack{l_1=0,2\\ m_1}} \sum_{\substack{l_2=0,2\\ m_2}} \langle l_1 m_1 |\, \hat{\mathscr{M}}^{(X)}_{JM} \,|\, l_2 m_2 \rangle\, b^{+}_{l_1\, m_1} b_{l_2\, m_2} =$$

$$= \boxed{\begin{array}{c}\text{the Wigner-Eckart theorem}\\ \text{(A.12) is used}\end{array}} =$$

$$= \sum_{\substack{l_1=0,2\\ m_1}} \sum_{\substack{l_2=0,2\\ m_2}} \langle l_1 ||\, \hat{\mathscr{M}}^{(X)}_{J} \,||\, l_2 \rangle\, C^{l_1\, m_1}_{l_2 m_2 JM}\, \frac{1}{\sqrt{2l_1+1}}\, b^{+}_{l_1\, m_1} b_{l_2\, m_2} =$$

$$= \sum_{\substack{l_1=0,2\\ m_1}} \sum_{\substack{l_2=0,2\\ m_2}} \langle l_1 ||\, \hat{\mathscr{M}}^{(X)}_{J} \,||\, l_2 \rangle\, C^{J\, -M}_{l_2 m_2 l_1 -m_1}\, \frac{(-1)^{l_2-m_2}}{\sqrt{2J+1}}\, b^{+}_{l_1\, m_1} b_{l_2\, m_2} =$$

$$= \sum_{l_1=0,2} \sum_{l_2=0,2} \langle l_1 || \, \hat{\mathscr{M}}_J^{(X)} \, || \, l_2 \rangle \, C^{J\,-M}_{l_2 m_2 l_1 - m_1} \, \frac{1}{\sqrt{2J+1}} \, \left(b^+_{l_1} \tilde{b}_{l_2} \right)_{(l_1 l_2;\, JM)} =$$

$$= \tilde{\alpha}_J \, \delta_{J2} \, \left\{ (d^+ \tilde{s})_{(20;\, 2M)} + (s^+ \tilde{d})_{(02;\, 2M)} \right\} +$$

$$+ \beta_J \, (d^+ \tilde{d})_{(22;\, JM)} + \gamma_0 \, \delta_{J0} \delta_{M0} \, (s^+ \tilde{s})_{(00;\, 0)} \qquad \text{(K.13)}$$

where $J = 0, 1, 2, 3, 4$ and the folowing parameters $\tilde{\alpha}_J$, γ_0, β_J were introduced

$$\tilde{\alpha}_2 = \langle d || \, \hat{\mathscr{M}}^{(X)}_{J=2} \, || \, s \rangle \, \frac{1}{\sqrt{5}} \, , \qquad \beta_J = \langle d || \, \hat{\mathscr{M}}^{(X)}_J \, || \, d \rangle \, \frac{1}{\sqrt{2J+1}}$$

$$\gamma_0 = \langle s || \, \hat{\mathscr{M}}^{(X)}_J \, || \, s \rangle \qquad \text{(K.14)}$$

That means, for instance, the electric quadrupole transition operator is given by two parameters, $\tilde{\alpha}_2$ and β_2:

$$\hat{\mathscr{M}}^{(el)}_{2M} = \tilde{\alpha}_2 \, \left\{ (d^+ \tilde{s})_{(20;\, 2M)} + (s^+ \tilde{d})_{(20;\, 2M)} \right\} + \, \beta_2 \, (d^+ \tilde{d})_{(22;\, 2M)} \qquad \text{(K.15)}$$

and magnetic dipole transition operator by one parameter β_1:

$$\hat{\mathscr{M}}^{(mg)}_{1M} = \beta_1 \, (d^+ \tilde{d})_{(22;\, 1M)} \qquad \text{(K.16)}$$

Further the action of the Hamiltonian (K.7) within the basis of vectors $|[N]; s^{n_s = N - n_d} \, d^{\, n_d}; \Gamma L M \rangle$ is analysed. Here N is the total number of s- and d- bosons, n_d is the number of quadrupole phonons, $n_s = N - n_d$ is the number of monopole s- bosons, L is the angular momentum quantum number with the projection M of the whole system of N bosons and the symbol Γ represents all other possible quantum numbers. It is evident that

$$s^+ s \, |[N]; s^{n_s = N - n_d} \, d^{\, n_d}; \Gamma L M \rangle = (N - n_d) \, |[N] : s^{n_s = N - n_d} \, d^{\, n_d}; \Gamma L M \rangle \qquad \text{(K.17)}$$

$$\sum_{m=-2}^{2} d^+_m d_m \, |[N]; s^{n_s = N - n_d} \, d^{\, n_d}; \Gamma L M \rangle = n_d \, |[N] : s^{n_s = N - n_d} \, d^{\, n_d}; \Gamma L M \rangle \qquad \text{(K.18)}$$

$$\left[(d^+ s^+)_{(20;\, 2)} \, (\tilde{d} \tilde{s})_{20;2)} \right]_{(22;\, 0)} \, |[N]; s^{n_s = N - n_d} \, d^{\, n_d}; \Gamma L M \rangle =$$

$$= \sum_{m m'} C^{2m}_{2m00} \, C^{2m'}_{2m'00} \, C^{00}_{2m2-m'} \, (-1)^m \, d^+_{m'} s^+ d_m s$$

$$|[N] : s^{n_s = N - n_d} \, d^{\, n_d}; \Gamma L M \rangle =$$

$$= \boxed{\begin{array}{c} \text{because } \hat{n}_d = \sum_m d^+_m d_m \, , \; \hat{n}_d = \sum_m s^+ s \\ \text{and } C^{00}_{2m2-m'} \text{ contains } \delta_{m m'} \end{array}} =$$

$$= (N - n_d) \, n_d \, |[N]; s^{n_s = N - n_d} \, d^{\, n_d}; \Gamma L M \rangle \qquad \text{(K.19)}$$

and similarly

$$\left[(s^+s^+)_{(00;\,0)}\,(\tilde{s}\tilde{s}_{(00;\,0)}\right]_{(00;\,0)}\,|[N];s^{n_s=N-n_d}\,d^{\,n_d};\Gamma LM\rangle = \\ = (N-n_d)(N-n_d-1)\,|[N];s^{n_s=N-n_d}\,d^{\,n_d};\Gamma LM\rangle \tag{K.20}$$

$$\left[(d^+d^+)_{(22;\,2)}\,(\tilde{d}\tilde{s}_{(20;\,2)}\right]_{(22;\,0)}\,|[N];s^{n_s=N-n_d}\,d^{\,n_d};\Gamma LM\rangle = \\ = \sum_M C^{00}_{2M2-M}\,(d^+d^+)_{(22;\,2M)}\,(\tilde{d}\tilde{s})_{(20;\,2-M)} \\ |[N];s^{n_s=N-n_d}\,d^{\,n_d};\Gamma LM\rangle = \\ = \sum_M C^{00}_{2M2-M}\,(d^+d^+)_{(22;\,2M)}\,C^{2-M}_{2-M00}(-1)^M\,d_{-M}\,s \\ |[N];s^{n_s=N-n_d}\,d^{\,n_d};\Gamma LM\rangle = \\ = \left[(d^+d^+)_{(22;2)}\tilde{d}_2\right]_{(22;\,0)}\,s \\ |[N];s^{n_s=N-n_d}\,d^{\,n_d};\Gamma LM\rangle = \\ = \sqrt{N-n_d}\,\left[(d^+d^+)_{(22;2)}\tilde{d}_2\right]_{(22;\,0)} \\ |[N-1];s^{n_s=N-n_d-1}\,d^{\,n_d};\Gamma LM\rangle \tag{K.21}$$

$$\left[(d^+s^+)_{(20;\,2)}\,(\tilde{d}\tilde{d})_{(22;\,2)}\right]_{(22;\,0)}\,|[N];s^{n_s=N-n_d}\,d^{\,n_d};\Gamma LM\rangle = \\ = \boxed{\begin{array}{c}\text{similarly as in}\\ (K.21)\end{array}} = \\ = \left[d_2^+\,(\tilde{d}\tilde{d})_{(22;\,2)}\right]_{(22;\,0)}\,s^+\,|[N];s^{n_s=N-n_d}\,d^{\,n_d};\Gamma LM\rangle = \\ = \sqrt{N-n_d+1}\,\left[d_2^+\,(\tilde{d}\tilde{d})_{(22;\,2)}\right]_{(22;\,0)}|[N];s^{n_s=N-n_d}\,d^{\,n_d};\Gamma LM\rangle \tag{K.22}$$

$$\left[(d^+d^+)_{(22;\,0)}\,(\tilde{s}\tilde{s})_{(00;\,0)}\right]_{(00;\,0)}\,|[N];s^{N-n_d}\,d^{\,n_d};\Gamma LM\rangle = \\ = \sqrt{(N-n_d)(N-n_d+10)}\;(d^+d^+)_{(22;\,0)} \\ |[N-2];s^{N-n_d-2}\,d^{\,n_d};\Gamma LM\rangle \tag{K.23}$$

$$\left[(s^+s^+)_{(00;\,0)}\,(\tilde{d}\tilde{d})_{(22;\,0)}\right]_{(00;\,0)}\,|[N];s^{N-n_d}\,d^{\,n_d};\Gamma LM\rangle = \\ = \sqrt{(N-n_d+1)(N-n_d+2)}\;(\tilde{d}\tilde{d})_{(22;\,0)} \\ |[N+2];s^{N-n_d+2}\,d^{\,n_d};\Gamma LM\rangle \tag{K.24}$$

Therefore the action of the Hamiltonian (K.7) on the basis vector $|[N]; s^{N-n_d} d^{\,n_d}; \Gamma L M\rangle$ is following

$$\begin{aligned}
&\hat{H}\,|[N]; s^{N-n_d}\,d^{\,n_d}; \Gamma L M\rangle = \\
&= \Big\{\epsilon_s(N-n_d) + \epsilon_d n_d + \sum_{L=0,4} \frac{\sqrt{2L+1}}{2}\, c_L\, \left[(d^+d^+)_{(22;\,L)}\,(\tilde{d}\tilde{d})_{(22;\,L)}\right]_{(LL;\,0)} \\
&\quad + \tilde{u}_2(N-n_d)\,n_d + \tilde{u}_0(N-n_d)(N-n_d-1)\Big\}\,|[N]; s^{N-n_d}\,d^{\,n_d}; \Gamma L M\rangle \\
&\quad + \tilde{v}_2\,\Big\{\left[(d^+d^+)_{(22;\,2)}\,\tilde{d}_2\right]_{(22;\,0)}\sqrt{N-n_d}\;\,|[N-1]; s^{N-n_d-1}\,d^{\,n_d}; \Gamma L M\rangle \\
&\qquad + \left[d_2^+\,(\tilde{d}\tilde{d})_{(22;\,2)}\right]_{(22;\,0)}\sqrt{N-n_d+1}\;\,|[N+1]; s^{N-n_d+1}\,d^{\,n_d}; \Gamma L M\rangle\Big\} \\
&\quad + \tilde{v}_0\,\Big\{(d^+d^+)_{(22;\,0)}\,\sqrt{(N-n_d)(N-n_d-1)}\;\,|[N-2]; s^{N-n_d-2}\,d^{\,n_d}; \Gamma L M\rangle \\
&\qquad + (\tilde{d}\tilde{d})_{(22;\,0)}\sqrt{(N-n_d+1)(N-n_d+2)}\,|[N+2]; s^{N-n_d+2}\,d^{\,n_d}; \Gamma L M\rangle\Big\}
\end{aligned} \tag{K.25}$$

The number of s- bosons in the given state does not have a physical meaning. Therefore degrees of freedom connected with s- bosons are usually omitted in (K.25) and the action of the Hamiltonian can be rewritten as follows

$$\begin{aligned}
&\hat{H}\,|N; d^{\,n_d}; \Gamma L M\rangle = \\
&= \Big\{h_0 + \epsilon\,\hat{n}_d + \sum_{L=0,2,4} \frac{\sqrt{2L+1}}{2}\;c_L^{'}\;\left[(d^+d^+]_{(22;\,L)}\,(\tilde{d}\tilde{d})_{(22;\,L)}\right]_{(LL;\,0)} + \\
&\quad + \tilde{v}_2\,\Big(\left[(d^+d^+)_{(22;\,2)}\,\tilde{d}\right]_{(22;\,0)}\sqrt{N-n_d}\;\; + \\
&\qquad\qquad + \;\; \left[d^+\,(\tilde{d}\tilde{d})_{(22;\,2)}\right]_{(22;\,0)}\sqrt{N-n_d+1}\,\Big)\; + \\
&\quad + \tilde{v}_0\,\Big((d^+d^+)_{(22;\,0)}\,\sqrt{(N-n_d)(N-n_d-1)}\;\; + \\
&\qquad\qquad + \;\; (\tilde{d}\tilde{d})_{(22;\,0)}\,\sqrt{(N-n_d+1)(N-n_d+2)}\Big)\;\Big\} \\
&\quad |N; d^{\,n_d}; \Gamma L M\rangle
\end{aligned} \tag{K.26}$$

where

$$\begin{aligned}
&h_0 = \epsilon_s\,N \qquad , \qquad \epsilon = \epsilon_d + (\tilde{u}_2 - \tilde{u}_0)(N-n_d) \\
&c_L^{'} = c_L + \tilde{u}_0\,\delta_{L0}
\end{aligned} \tag{K.27}$$

Similarly we will analyze the action of the quadrupole transition operators

$\hat{\mathscr{M}}^{(el)}_{2M}$ (see (K.15)) on the general state $|[N];\ s^{N-n_d}d^{n_d};\ \Gamma LM\rangle$

$$(d^+s)_{(20;\,2M')}\,|[N];\ s^{N-n_d}d^{n_d};\ \Gamma LM\rangle =$$

$$= C^{2M'}_{2M'00}\,d^+_{M'}\,s\,|[N];\ s^{N-n_d}d^{n_d};\ \Gamma LM\rangle = \boxed{\begin{array}{c}\text{because}\\ s\,|s^n\rangle = \sqrt{n}\,|s^{n-1}\rangle\end{array}} =$$

$$= d^+_{M'}\ \sqrt{N-n_d}\ |[N-1];\ s^{N-n_d-1}d^{n_d};\ \Gamma LM\rangle \tag{K.28}$$

$$(s^+\tilde{d})_{(02;\,2M')}\,|[N];\ s^{N-n_d}d^{n_d};\ \Gamma LM\rangle = \boxed{\begin{array}{c}\text{because}\\ s^+\,|s^n\rangle = \sqrt{n+1}\,|s^{n+1}\rangle\end{array}} =$$

$$= \sqrt{N-n_d+1}\,(-1)^{M'}\ d_{-M'}\ |[N+1];\ s^{N-n_d+1}d^{n_d};\ \Gamma LM\rangle \tag{K.29}$$

So

$$\hat{\mathscr{M}}^{el}_{2M'}\,|[N];\ s^{N-n_d}d^{n_d};\ \Gamma LM\rangle = \boxed{\begin{array}{c}\text{see}\\ (K.15)\end{array}} =$$

$$= \tilde{\alpha}_2\left\{\sqrt{N-n_d}\,d^+_{M'}\,|[N-1];\ s^{N-n_d-1}d^{n_d};\ \Gamma LM\rangle + \right.$$

$$\left. + \sqrt{N-n_d+1}\ (-1)^{M'}\ d_{-M'}\,|[N+1];\ s^{N-n_d+1}d^{n_d};\ \Gamma LM\rangle\right\}$$

$$+ \quad \beta_2\,(d^+\tilde{d})_{(22;\,2M)}\,|[N];\ s^{N-n_d}d^{n_d};\ \Gamma LM\rangle \tag{K.30}$$

and if the degrees of freedom connected with s- bosons are omitted then

$$\hat{\mathscr{M}}^{el}_{2M'}\,|N;d^{n_d};\ \Gamma LM\rangle =$$

$$= \left\{\tilde{\alpha}_2\left[\sqrt{N-n_d}\,d^+_{M'} + \sqrt{N-n_d+1}\,(-1)^{M'}\,d_{-M'}\right] + \right.$$

$$\left. + \ \beta_2\,(d^+\tilde{d})_{(22;\,2M')}\right\}|N;d^{n_d};\ \Gamma LM\rangle \tag{K.31}$$

So, if in our configuration space only d- bosons are involved (basis vectors $|N;d^{n_d};\ \Gamma LM\rangle$ then from the expression (K.26) one can see that the IBM-1 Hamiltonian involves 7 parameters. The parameter h_0 determines only the absolute scale of the energy and therefore we can put e.g. $h_0 = 0$. Therefore in reality the IBM-1 Hamiltonian is determined by 6 parameters ϵ, c'_L $(L = 0, 2, 4)$, $\tilde{v}_2$ and $\tilde{v}_0$. From (K.30) it follows that the electric quadrupole transition operator $\hat{\mathscr{M}}^{(el)}_{2M'}$ is given by two parameters $\tilde{\alpha}$ and β_2.

Eigen-spectrum and eigen-vectors of the IBM-1 Hamiltonian $\hat{H}$ can be obtained by the diagonalization of the Hamiltonian matrix within the space of basis vectors $|N; d^{n_d}; \Gamma LM\rangle$ (after the specification of the additional quantum numbers Γ). However, for the special values of the parameters the IBM-1 Hamiltonian can be written as the combination of Casimir operators of chains of subgroups of the $U(6)$ algebra (it is necessary to remaind here that the IBM-1 Hamiltonian is constructed from generators of the $U(6)$ algebra - see (K.12)). In such cases the eigen-vectors of the IBM-1 Hamiltonian are characterized by the quantum numbers which label irreps of subgroups in the given chain and no diagonalization is needed. From the point of view of the IBM-1 Hamiltonian there are 3 possible subgroup chains of the group $U(6)$ (see subsection J.4.3 for more details of subgroup chain) (e.g. [118])

$$\begin{aligned} &U(6) \supset U(5) \supset SO(5) \supset SO(3) \supset SO(2) \; - \text{ vibrator limit} \\ &U(6) \supset SU(3) \supset SO(3) \supset SO(2) \quad - \quad \text{axial rotor limit} \\ &U(6) \supset SO(6) \supset SO(5) \supset SO(3) \supset SO(2) \; - \; \gamma\text{- unstable limit} \end{aligned} \tag{K.32}$$

which correspond to so called anharmonic vibrator limit, axial rotor limit and γ- unstable limit, respectively. As it will be shown in next subsections the anharmonic vibrator limit subgroup chain gives the low-lying spectrum which is similar to the spectrum of low-lying (vibrational) states in spherical nuclei while the axial-rotor limit subgroup chain corresponds to the low-lying rotational bands observed in well- deformed nuclei. If the dynamical symmetry of the IBM-1 Hamiltonian is given by the 3-d subgroup chain in (K.32) (the γ- unstable limit chain) then the corresponding low-lying spectrum resembles the low-lying spectrum of so called γ- unstable nuclei (the nuclei where the total energy as a function of the quadrupole deformation parameter γ (see (1.5)) does not provide any distinct minimum). In the next subsections all these limits are discussed in more details.

K.1.1 Anharmonic vibrator ($U(5)$) limit

In the case of this limit we restrict ourselves only to the configuration space of d- bosons (only basis states $|N; d^{n_d};\ \Gamma LM\rangle$) and the model Hamiltonian

$\hat{H}_{vib}$ involves only the second and third terms of (K.26) ($h_0 = \tilde{v}_2 = \tilde{v}_0 = 0$)

$$\hat{H}_{vib} = \epsilon \sum_{m=-2}^{2} d_m^+ d_m \; + \underbrace{\; + \sum_{L=0,2,4} \frac{2L+1}{2} \, c_L^{'} \left[(d^+ d^+)_{(22;\,L)} \, (\tilde{d}\tilde{d})_{(22;\,L)} \right]_{(LL;\,0)}}_{\hat{V}} \tag{K.33}$$

From (K.33) one can see that the Hamiltonian $\hat{H}_{vib}$ is constructed only from 25 bilinear quadrupole operator combinations $d_\mu^+ d_\nu$ ($\mu,\, \nu = -2, -1, 0, 1, 2$). These combinations represent generators of the $U(5)$ Lie algebra. The corresponding quadrupole transition operator $\hat{\mathscr{M}}_{2m}^{(el)}$ is taken in the following form (see (K.31))

$$\hat{\mathscr{M}}_{2M}^{(el)} = \tilde{\alpha}_2 \sqrt{N} \left[\sqrt{1 - \frac{n_d}{N}} \, d_M^+ \; + \; \sqrt{1 - \frac{n_d + 1}{N}} \, (-1)^M \, d_{-M} \right] \; + \; + \; \beta_2 \, (d^+ \tilde{d})_{(22;\,2M)} \; \rightarrow$$

$$= \boxed{\begin{array}{c} \text{for} \\ \text{higher N} \end{array}} \; \rightarrow \quad q_2 \left(d_M^+ + (-1)^M \, d_{-M} \right) + q_2^{'} \, (d^+ \tilde{d})_{(22;\,2M)} \tag{K.34}$$

with two parameters $q_2 = \tilde{\alpha}_2 \sqrt{N}$, $q_2^{'} = \beta_2$.

One should realize that the first term in the Hamiltonian $\hat{H}_{vib}$, $\epsilon \sum_{m=-2}^{2} d_m^+ d_m$, corresponds to the quadrupole $\lambda = 2$ part, $1/2 \, (B_2 \, |\hat{\dot{\alpha}}_{2M}|^2 + C_2 \, |\hat{\alpha}_{2M}|^2)$, of the quantum Bohr Hamiltonian $\hat{H}_C$ (see(7.54)) when the substitution (7.59) with $Q_{2M}^+ = d_M^+$ is done. Similarly the first term in (K.34) corresponds to the Bohr's expression (7.69) for the quadrupole electric transition operator $\hat{\mathscr{M}}_{2M}^{(el)}$ if the same substitution is done.

Further we will specify the basis vectors $|N; d^{n_d};\, \Gamma L M\rangle$, particularly the quantum numbers Γ. Instead $|N; d^{n_d}; \Gamma L M\rangle$ the new assignment $|n_d \nu n_\Delta L M\rangle$ is used further, where n_d is the number of quadrupole bosons, ν is so called seniority - the number of unpaired bosons when by the boson pair is always understood two bosons with the total angular momentum 0. So the seniority ν is connected with the number n_β of boson pairs with the zero angular momentum by the following relation

$$\nu = n_d - 2 n_\beta \tag{K.35}$$

The next quantum number n_Δ determines the number of the boson triplets with the zero angular momentum. Therefore its connection with the numbers n_d and n_β is following

$$n_d = 2n_\beta + 3n_\Delta + \lambda \tag{K.36}$$

where λ is the number of quadrupole bosons not involved in the pairs and triplets with the zero angular momentum. The quantum numbers L and M are the total angular momentum and its projection , respectively. It can be shown that in the case of λ quadrupole bosons not coupled to the zero ang. momentum pairs and triplets the total angular momentum L can have only following values

$$L = \lambda, \lambda+1, \lambda+2, \ \ldots \ , 2\lambda-2, 2\lambda \tag{K.37}$$

That means the value $L = 2\lambda - 1$ is always missing. Further it will be shown that the kets $|N; d^{n_d};\ \Gamma LM\rangle$ are eigen vectors of the Hamiltonian $\hat{H}_{vib}$:

$$\hat{H}_{vib}\,|N; d^{n_d};\ \Gamma LM\rangle = E_{n_d \nu L}\,|N; d^{n_d};\ \Gamma LM\rangle \tag{K.38}$$

with the eigen-energies $E_{n_d \nu L}$ degenerated with respect to n_Δ and M. Further the explicite expression for $E_{n_d \nu L}$ will be derived.

The two- boson interaction in the Hamiltonian $\hat{H}_{vib}$ (the second term in (K.33)) can be written in the following form (see e.g. [113, 114])

$$\begin{aligned} \hat{H}_{vib} &= \epsilon^{'}\,\hat{n}_d + \hat{V} \\ \hat{V} &\equiv \sum_{i<j} \hat{V}_{ij} = \sum_{i<j} \left(\alpha\,\hat{1}_{ij} + \beta\,\hat{\mathscr{P}}_{ij} + \gamma\,\hat{\mathscr{L}}_{ij} \right) \end{aligned} \tag{K.39}$$

where 1_{ij} are the matrix elements of the unity operator between i-th and j-th bosons, $\mathscr{P}_{ij}$ are matrix elements of so called boson pairing operator:

$$\begin{aligned} \hat{\mathscr{P}} \equiv 4\,\hat{S}_+\,\hat{S}_- \quad , \quad \hat{S}_+ &\equiv \frac{1}{2} \sum_{m=-2}^{2} (-1)^m d_m^+ d_{-m}^+ \\ \hat{S}_- &\equiv \frac{1}{2} \sum_{m=-2}^{2} (-1)^m d_m d_{-m} \end{aligned} \tag{K.40}$$

and $\mathscr{L}_{ij}$ in (K.39) is given by

$$\mathscr{L}_{ij} = 2\,\vec{l}_i \cdot \vec{l}_j \tag{K.41}$$

where $\vec{l}_i$, $\vec{l}_j$ are angular momenta of the i-th and j-th quarupole bosons, respectively. The connection of parameters α, β and γ with the parameters $c_L^{'}$ ($L = 0, 2, 4$) in (K.33) will be determined later (see).

In order to determine energies $E_{n_d\nu L}$ it is necessary to calculate expectation value $\langle n_d\nu n_\Delta LM|\,\hat{V}\,|n_d\nu n_\Delta LM\rangle$.

i. Expectation value of the operator $\hat{1} \equiv \sum_{ij} 1_{ij}$

$$\langle n_d\nu n_\Delta LM \mid \hat{1} \mid n_d\nu n_\Delta LM\rangle = \sum_{i<j}\langle n_d\nu n_\Delta LM|\,1_{ij}\,|n_d\nu n_\Delta LM\rangle =$$
$$= \langle n_d\nu n_\Delta LM \,\Big|\, \frac{1}{2}\big(\hat{n}_d^2 - \hat{n_d}\big)\,\Big| n_d\nu n_\Delta LM\rangle = \frac{1}{2}\,n_d(n_d-1) \qquad \text{(K.42)}$$

ii. Expectation value of the operator $\hat{\mathscr{L}} \equiv \sum_{i<j} \mathscr{L}_{ij}$

The connection of the operator $\hat{\mathscr{L}}$ with the total angular momentum operator $\hat{\vec{L}} = \sum_i \hat{\vec{l}}_i$ is following

$$\hat{\vec{L}}^2 = \sum_{ij} \hat{\vec{l}}_i \cdot \hat{\vec{l}}_j = \sum_i \hat{\vec{l}}_i^2 + 2\sum_{i<j} \hat{\vec{l}}_i \cdot \hat{\vec{l}}_j = \sum_i \hat{\vec{l}}_i^2 + \hat{\mathscr{L}}$$
$$\Rightarrow \langle n_d\nu n_\Delta LM \mid \hat{\mathscr{L}} \mid n_d\nu n_\Delta LM\rangle =$$
$$= L(L+1) - \langle n_d\nu n_\Delta LM \mid \sum_i \hat{\vec{l}}_i^2 \mid n_d\nu n_\Delta LM\rangle =$$
$$= L(L+1) - \sum_i 2.3 = L(L+1) - 6\,n_d \qquad \text{(K.43)}$$

ii. Expectation value of the boson pairing operator $\hat{\mathscr{P}} = 4\,\hat{S}_+\hat{S}_-$

Operators $\hat{S}_\pm$,from which the operators $\hat{\mathscr{P}}$ is built, can be added by the third operator:

$$\hat{S}_0 = \frac{1}{4}\sum_{m=-2}^{2}\big(d_m^+ d_m + d_m d_m^+\big) \qquad \text{(K.44)}$$

and as a result we obtain 3 operators $\hat{S}_+$, $\hat{S}_-$, $\hat{S}_0$ which create 3 generators of the $SU(2)$ algebra. Really, using the boson commutaton relations, $[d_\mu,\, d_{m'}^+] = \delta_{mm'}$, $[d_\mu,\, d_{m'}] = 0$, it is possible to obtain the following commutator relations

$$[\hat{S}_0,\ \hat{S}_\pm] = \pm\hat{S}_\pm \qquad\qquad [\hat{S}_+,\ \hat{S}_-] = -2\,\hat{S}_0 \qquad \text{(K.45)}$$

which are consistent with (J.77) and therefore they form generators of the algebra. Similarly as the components $\hat{L}_x$, $\hat{L}_y$, $\hat{L}_z$ of the angular momentum can

be obtained from the step-up and step-down operators $\hat{L}_\pm$ we can introduce the "components" $\hat{S}_x$, $\hat{S}_y$, $\hat{S}_z$ operators

$$\begin{aligned}\hat{S}_x &= \frac{1}{2}\left(\hat{S}_+ + \hat{S}_-\right)\\ \hat{S}_y &= \frac{1}{2i}\left(\hat{S}_+ - \hat{S}_-\right)\\ \hat{S}_z &= \hat{S}_0\end{aligned} \tag{K.46}$$

which filfil

$$[\hat{S}_i,\ \hat{S}_j] = i\,\epsilon_{ijk}\,\hat{S}_k \tag{K.47}$$

The first Casimir operator (see (J.85)) of the $SU(2)$ algebra of generators $\hat{S}_+$, $\hat{S}_-$, $\hat{S}_0$ (or $\hat{S}_x$, $\hat{S}_y$, $\hat{S}_z$) is given by

$$\hat{C} = \hat{S}_z^2 - \hat{S}_y^2 - \hat{S}_x^2 = \hat{S}_0^2 - \hat{S}_0 - \hat{S}^+\hat{S}_- \tag{K.48}$$

Again, using the boson commutation relations for d_μ, d_μ^+ operators, it can be proved that

$$[\hat{C},\ \hat{S}_i] = 0 \qquad\qquad i = x, y, z \tag{K.49}$$

Therefor we can search for the common eigen basis $|a, b\rangle$ of operators $\hat{C}$ and $\hat{S}_0$:

$$\begin{aligned}\hat{C}\mid a,b\rangle &= a\mid a,b\rangle\\ \hat{S}_0\mid a,b\rangle &= b\mid a,b\rangle\end{aligned} \tag{K.50}$$

Further we will find the quantum numbers a, b and their connection.

$$\begin{aligned}\hat{S}_0\,\hat{S}_+\mid ab\rangle &= (\hat{S}_+\,\hat{S}_0 + \hat{S}_+)\mid ab\rangle = (b+1)\,\hat{S}_+\mid ab\rangle\\ \hat{S}_0\,\hat{S}_-\mid ab\rangle &= (\hat{S}_-\,\hat{S}_0 - \hat{S}_-)\mid ab\rangle = (b-1)\,\hat{S}_+\mid ab\rangle\end{aligned} \tag{K.51}$$

Therefore

$$\begin{aligned}\hat{S}_+\mid ab\rangle &= \alpha^{(+)}(ab)\mid ab+1\rangle\\ \hat{S}_-\mid ab\rangle &= \alpha^{(-)}(ab)\mid ab-1\rangle\end{aligned} \tag{K.52}$$

where $\alpha^{(\pm)}(ab)$ are real numbers and because of $\hat{S}_+^+ = \hat{S}_-$ we have

$$\alpha^{(+)}(ab) = \langle ab+1|\hat{S}_+|\,ab\rangle = \langle ab|\hat{S}_-|\,ab+1\rangle = \alpha^{(-)}(ab+1) \tag{K.53}$$

Therefore

$$\begin{aligned}\hat{C}\mid ab\rangle = \boxed{\begin{array}{c}\text{see}\\ (K.48)\end{array}} &= \left(\hat{S}_0^2 - \hat{S}_0 - \hat{S}_+\,\hat{S}_-\right)\mid ab\rangle =\\ &= \left[b\,(b-1) - \alpha^{(-)}(ab)\,\alpha^{(+)}(a\,b-1)\right]\mid ab\rangle\end{aligned} \tag{K.54}$$

The using of (K.53) and comparing (K.54) with (K.48) give

$$a = b\,(b-1) - (\alpha^{(-)}(ab))^2$$
$$\Rightarrow \qquad \alpha^{(-)}(ab) = \alpha^{(+)}(a\,b-1) = \sqrt{b\,(b-1)-a} \tag{K.55}$$

It is also evident that using the operator $\hat{S}_-$ we can decrease the projection b down to some limit b_{min} for which

$$\hat{S}_- \mid a\,b_{min}\rangle = 0 \tag{K.56}$$

So

$$0 = \hat{S}_+\,\hat{S}_- \mid a\,b_{min}\rangle = \boxed{\begin{array}{c}\text{see}\\(K.45)\end{array}} = \big(\hat{S}_-\,\hat{S}_+ - 2\,\hat{S}_0\big) \mid a\,b_{min}\rangle =$$
$$= \big(-2\,b_{min} + b_{min}\,(b_{min}+1) - a\big) \mid a\,b_{min}\rangle$$
$$\Rightarrow \qquad a = b_{min}\,(b_{min}-1) \tag{K.57}$$

Further we introduce a new assignment $s \equiv b_{min}$, $s_0 = b$. Then we have

$$\hat{S}_+\,|s\,s_0\rangle = \boxed{\begin{array}{c}\text{see}\\(K.52),(K.55),(K.57)\end{array}} = \sqrt{s_0\,(s_0+1) - s\,(s+1)} =$$
$$= \sqrt{(s+s_0)\,(s_0-s+1)}\,|s\,s_0+1\rangle$$
$$\hat{S}_-\,|s\,s_0\rangle = \sqrt{(s-s_0)\,(s_0+s+1)}\,|s\,s_0-1\rangle \tag{K.58}$$

and the action of the pairing operator $\hat{\mathscr{P}} = 4\,\hat{S}_+\,\hat{S}_-$ on the basis vector $|s\,s_0\rangle$ is following

$$\hat{\mathscr{P}}\,|s\,s_0\rangle = 4\,\hat{S}_+\,\hat{S}_-\,|s\,s_0\rangle = 4\,\big[s_0\,(s_0-1) - s(s-1)\big]\,|s\,s_0\rangle \tag{K.59}$$

Now we can determine the connection between quantum numbers n_d, ν (see (K.35) - (K.37)) and s, s_0. On the base of (K.44) we can write

$$\hat{S}_0 = \frac{1}{4}\sum_{m=-2}^{+2}(d_m^+\,d_m + d_m\,d_m^+) = \frac{1}{2}\sum_{-2}^{+2} d_m^+ d_m + \frac{1}{4}\sum_{-2}^{+2} 1$$
$$\Rightarrow \qquad \hat{S}_0 \mid n_d\nu n_\Delta LM\rangle = (\frac{1}{2}\,n_d + \frac{5}{4})\,|n_d\nu n_\Delta LM\rangle \tag{K.60}$$

One should also realize that the operator $\hat{S}_+$ creates the boson pair with the zero angular momentum. It can be seen its action on the boson vacuum:

$$\hat{S}_+ \mid 0\rangle = \sum_{m=-2}^{+2}(-1)^m\,d_m^+ d_{-m}^+\,|0\rangle = \sqrt{5}\,\sum_{m=-2}^{+2} c^{00}_{2m2-m} \mid 2m,\,2-m\rangle =$$
$$= \sqrt{5}\;\mid 22;\,00\rangle \tag{K.61}$$

where $|\,22;\,00\rangle$ is the two- boson state with the zero angular momentum (see (K.2). From (K.60) it follows that for given value of the signature ν the state $|\,s = b_{min},\, s_0\rangle$ with minimal value of s_0 corresponds to the state $|\,n_d \nu n_\Delta LM\rangle$ with the minimal value of the n_d and according to (K.35) this is $(n_d)_{min} = \nu$ $(n_\beta = 0)$. So, according to (K.60) we have $(s = b_{min})$:

$$s = b_{min} = (s_0)_{min} = \frac{1}{2}\,\nu + \frac{5}{4} \tag{K.62}$$

with the general value of s_0 given by

$$s_0 = \frac{1}{2}\,n_d + \frac{5}{4} \tag{K.63}$$

The substitution of (K.62) and (K.63) into (K.59) gives

$$\begin{aligned}
&\langle n_d \nu n_\Delta LM|\hat{\mathscr{P}}|\,n_d \nu n_\Delta LM\rangle = \\
&\quad = 4\left[\big(\frac{1}{2}\,n_d + \frac{5}{4}\big)\big(\frac{1}{2} + \frac{1}{4}\big) - \big(\frac{1}{2} + \frac{5}{4}\big)\big(\frac{1}{2}\,\nu + \frac{1}{4}\big)\right] = \\
&\quad = n_d^4 + 3\,n_d - \nu^2 - 3\,\nu = \big(n_d - \nu\big)\big(n_d + \nu + 3\big)
\end{aligned} \tag{K.64}$$

Collecting the expressions (K.42), (K.43) and (K.64) the eigen-energy $E_{n_d \nu L}$ (see (K.38)) of the Hamiltonian (K.39) is

$$\begin{aligned}
&E_{n_d \nu l} = \langle n_d \nu n_\Delta LM|\hat{H}_{vib}|\,n_d \nu n_\Delta LM\rangle = \\
&\quad = \langle n_d \nu n_\Delta LM|\,\epsilon^{'} \sum_{m=-2}^{+2} d_m^+ d_m + \hat{V}|\,n_d \nu n_\Delta LM\rangle = \boxed{\begin{array}{c}\text{see}\\(K.39)\end{array}} = \\
&\quad = \epsilon^{'}\,n_d + \alpha\,\frac{1}{2}\,n_d\,(n_d - 1) + \beta\,(n_d - \nu)(n_d + \nu + 3) + \\
&\qquad\qquad + \gamma\,\big[L(L+1) - 6\,n_d\big]
\end{aligned} \tag{K.65}$$

and each level $E_{n_d \nu L}$ is degenerated according to the quantum numbers n_Δ and M.

So in the case of the anharmonic limit, where the Hamiltonian $\hat{H}_{vib}$ is given by (K.33) of $\hat{H}_{vib} = \epsilon \sum_{m=-2}^{+2} d_m^+ d_m + \hat{V}$ with $\hat{V}$ given by (K.39), the eigen system of the Hamiltonian is given by basis states $|\,n_d \nu n_\Delta LM\rangle$ with eigen energies $E_{n_d \nu L}$ in the explicite form (K.65).

It remains to determine the connection between parameters $\epsilon^{'}$, α, γ (see (K.39)) and ϵ, $c_L^{'}$ $(L = 0, 2, 4)$ (see (K.33)). This can be found by the comparison of the spectrum (K.65) with the expectation value of the (K.33) in

the state $|\, n_d \nu n_\Delta L M\rangle$ - see e.g. [118, 114] :

$$\begin{aligned} \epsilon &= \epsilon^{'} + \frac{10}{3}\,\beta \\ c_0 &= \alpha + \frac{10}{3}\,\beta - 12\,\gamma \\ c_2 &= \alpha + \frac{5}{3}\,\beta - 6\,\gamma \\ c_4 &= \alpha + \frac{5}{3}\,\beta + 8\,\gamma \end{aligned} \tag{K.66}$$

From the reason of the comparison of the calculated eigen energies $E_{n_d \nu L}$ with experimental energies the individual states $|\, n_d \nu n_\Delta L M\rangle$ are divided into the following "bands" [114]

$$\begin{aligned} \text{Y band} &: |\, n_d\,,\ \nu = n_d\,,\ n_\Delta = 0\,,\ L = 2\,n_d\,;\ M\rangle && n_d = 0, 1, 2, \ldots \\ \text{X band} &: |\, n_d\,,\ \nu = n_d\,,\ n_\Delta = 0\,,\ L = 2\,n_d - 2\,;\ M\rangle && n_d = 2, 3, 4 \ldots \\ \text{Z band} &: |\, n_d\,,\ \nu = n_d\,,\ n_\Delta = 0\,,\ L = 2\,n_d - 3\,;\ M\rangle && n_d = 3, 4, 5 \ldots \\ \text{X' band} &: |\, n_d\,,\ \nu = n_d\,,\ n_\Delta = 0\,,\ L = 2\,n_d - 4\,;\ M\rangle && n_d = 4, 5, 6 \ldots \\ \beta \text{ band} &: |\, n_d\,,\ \nu = n_d - 2\,,\ n_\Delta = 0\,,\ L = 2\,n_d - 4\,;\ M\rangle && n_d = 2, 3, 4 \ldots \\ & \qquad\qquad \vdots \end{aligned}$$

Corresponding level scheme is shown in the Fig. 7.13. If we compare the spectrum of levels $E_{n_d \nu L}$ given on the Fig. 7.13 with the experimental spectrum of the lowest states in the spherical nuclei (see e.g. the spectrum of ^{106}Pd in the Fig.7.6) one can see that the lowest levels of the spectrum of $E_{n_d \nu L}$ resembles the experimental spectrum, particularly the first 0_1^+, 2_1^+, 2_2^+, 0_2^+, 4_1^+ levels (see also fig. 7.12). It was the success of the simple IBM-1 model that the explicit expressions for $E_{n_d \nu L}$ describe the low-lying parts of the spectra of vibrational nuclei. The more detailed discussion concerning the comparison of the IBM-1 model results with experimental values can be found in the subsection 7.2.2.

In the end of this subsection some aspects of the electromagnetic transition probabilities are discussed. The electric $E2$ transition operator $\hat{\mathscr{M}}_{2M}^{(el)}$ in the vibrational limit is given by (K.34). The corresponding reduced probability $B(E2; L_i \to L_f)$ of the transition going from the state of the spherical nucleus with the angular momentum L_i to the state with L_f is determined by (see

(2.147))

$$B(E2;\ L_i \to L_f) = \frac{\left|\langle (n_d\nu n_{\Delta}L)_f\ ||\hat{\mathscr{M}}_2^{(el)}||\ (n_d\nu n_{\Delta}L)_i\rangle\right|^2}{2L_i+1} =$$

$$= \boxed{\begin{array}{c}\text{see}\\ (K.33)\end{array}} =$$

$$= \frac{\left|\langle (n_d\nu n_{\Delta}L)_f\ ||q_2\left(d^+ + \tilde{d}\right) + q_2^{'}\left(d^+\tilde{d}\right)_{(22;\,2)}||\ (n_d\nu n_{\Delta}L)_i\rangle\right|^2}{2L_i+1} \tag{K.67}$$

So it is given by the square of the reduced matrix elements of the operator $\hat{\mathscr{M}}_2^{(el)}$, which can be finally expressed by the reduced matrix elements $\langle (n_d\nu n_{\Delta}L)_f||\ d^+\ ||\ (n_d\nu n_{\Delta}L)_i\rangle$ which are determined by so called parentage (genealogic) coefficients [99]. For instance, for $n_d = 2$ we have (see [99], p.690)

$$\langle n_d = 2\ L_f||\ d^+\ ||\ n_d = 1\ L_i = 2\rangle = \left[2\ (2L_f+1)\right]^2 \tag{K.68}$$

For the case of the $M1$ transitions we start with the expression (K.13) for the general transition operator $\hat{\mathscr{M}}_{JM}^{(X)}$. For $M1$ only term $\beta_1\ (d^+\tilde{d})_{22;\,1M}$ can work in (K.13). So we have

$$\hat{\mathscr{M}}_{1M}^{(mag)} = m_1\ (d^+\tilde{d})_{22;\,1M} =$$

$$= m_1\ \sum_{m=-2}^{+2} C_{2m\,2\,M-m}^{1m}\ d_m^+\ \tilde{d}_{M-m} \tag{K.69}$$

and it can be easily shown that the reduced matrix of (K.69) is diagonal

$$\langle n_d\nu n_{\Delta}L||\hat{\mathscr{M}}_1^{(mag)}||\ n_d^{'}\nu^{'}n_{\Delta}^{'}L^{'}\rangle =$$

$$= m_1\ \sqrt{\frac{L(L+1)(2L+1)}{10}}\ \delta_{n_dn_d^{'}}\ \delta_{\nu\nu^{'}}\ \delta_{n_{\Delta}n_{\Delta}^{'}}\ \delta_{LL^{'}} \tag{K.70}$$

However it means that all $M1$ transitions with $L_i \to L_f$, $L_i \neq L_f$ are not possible if the corresponding $M1$ transition operator is given only by (K.69). Therefore in order to describe nonzero $M1$ transitions observed in experiments the additional second order term was introduced into $\hat{\mathscr{M}}_{1M}^{(mag)}$ (see [113, 114]):

$$\hat{\mathscr{M}}_{1M}^{(mag)} = m1\ (d^+\tilde{d})_{(22;\,1M)} +$$

$$+m_1^{'}\left\{\left[d^+\ (d^+\tilde{d})_{(22,\,1)}\right]_{(21;\,1M)} + \left[(d^+\tilde{d})_{(22;\,1)}\tilde{d}\right]_{(12,1M)}\right\} \tag{K.71}$$

where m_1 and $m_1^{'}$ are free parameters. In the analogy with (K.67)-(K.68) the $M1$ reduced probabilities can be also expressed in terms of the parentage genealogic coefficients (see [99]).

From the point of view of the group chain (particularly see the first group chain in (K.32)) the quantum numbers of the basis state $|N;\ n_d \nu n_\Delta L M\rangle$ of the vibrational limit Hamiltonian (K.33) label irreps of the subgroups of the chain as follows

$$\begin{array}{ccccccccc} U(6) & \supset & U(5) & \supset & SO(5) & \supset & SO(3) & \supset & SO(2) \\ \vdots & & \vdots & & \vdots & & \vdots & & \vdots \\ N & & n_d & & \nu & ..n_\Delta.. & L & & M \end{array} \tag{K.72}$$

The 25 generators of the $SU(5)$ group can be written as

$$G_{U(5)} \equiv \Big\{(d^+\tilde{d})_{(22;\,00)},\ (d^+\tilde{d})_{(22;\,1m)},\ (d^+\tilde{d})_{(22;\,2m)},\ (d^+\tilde{d})_{(22;\,3m)},\ (d^+\tilde{d})_{(22;\,4m)}\Big\} \tag{K.73}$$

The quantum numbers with the representation of this group is n_d. The set $G_{U(5)}$ contains a subset of 10 operators that are close under commutation, the generators of the group $SO(5)$

$$G_{SO(5)} \equiv \Big\{(d^+\tilde{d})_{(22;\,1m)},\ (d^+\tilde{d})_{(22;\,3m)}\Big\} \tag{K.74}$$

The representations of $SO(5)$ are labeled by ν, the boson seniority. The eigen values of the quadratic Casimir operator of $SO(5)$,

$$\hat{C}_2[SO(5)] = \frac{1}{3}\,(d^+\tilde{d})_{(22,\,1)} \cdot (d^+\tilde{d})_{(22,\,1)} + \frac{1}{3}\,(d^+\tilde{d})_{(22,\,3)} \cdot (d^+\tilde{d})_{(22,\,3)} \quad , \tag{K.75}$$

are given by $\frac{1}{6}\nu(\nu+3)$.

The $SO(5)$ group contains $SO(3)$, the angular momentum, as subgroup. The three generators are given by

$$G_{SO(3)} \equiv \Big\{(d^+\tilde{d})_{22;\,1m)}\Big\}$$

with the well-known Casimir operator

$$\hat{C}_2[SO(3)] \equiv \hat{L}^2 = 10\,(d^+\tilde{d})_{(22;\,1)} \cdot (d^+\tilde{d})_{(22;\,1)} \tag{K.76}$$

the eigen values of which are $L(L+1)$. In all $SO(3)$ multiplets the levels are distinquised by M, the projection of L on z-axis.

From the Casimir operators of $U(5)$ the most general two-body $U(5)$ Hamiltonian can be constructed (another form of the Hamiltonian (K.33) or (K.39))

$$\hat{H}_{vib} = \epsilon^{''}\,\hat{n}_d + \kappa_1\,\hat{n}_d(\hat{n}_d - 1) + \kappa_2\,\hat{C}_2[SO(5)] + \kappa_3\,\hat{L}^2 \tag{K.77}$$

where parameters $\epsilon^{''}$, κ_1, κ_2, κ_3 are connected with the parameters ϵ, c_0, c_2, c_4 involved in (K.33) by [118]

$$\begin{aligned}
\epsilon &= \epsilon^{''} + \frac{2}{3}\kappa_2 + 6\kappa_3 \\
c_0^{'} &= 2\kappa_1 - \frac{4}{3}\kappa_2 - 12\kappa_3 \\
c_2^{'} &= 2\kappa_1 + \frac{1}{3}\kappa_2 - 6\kappa_3 \\
c_4^{'} &= 2\kappa_1 + \frac{1}{3}\kappa_2 + 8\kappa_3
\end{aligned} \tag{K.78}$$

K.1.2 Axial rotor ($SU(3)$) limit

In the previous subsection the vibrator limit was discussed when the general IBM-1 Hamiltonian (K.7) is reduced to the $\hat{H}_{vib}$ given by (K.33) with corresponding eigen vectors $|N;\, n_d \nu n_\Delta\, LM\rangle$. In this case the Hamiltonian $\hat{H}_{vib}$ is written as the combination of Casimir operators of the subgroups in the group chain (K.72). Another simplification of the IBM-1 model occurs when the general Hamiltonian (K.7) is reduced to the Casimir operators of the subgroups in the group chain $U(6) \supset SU(3) \supset SO(3) \supset SO(2)$ (see (K.32)) which, as it is shown below, corresponds to so called axial rotor limit.

In the 50-ties J.P. Elliott (see [119]) showed that it is possible to find the analytical solution of the eigen state problem of the following Hamiltonian

$$\hat{H}^{'}_{rot} = -\kappa\,\hat{\vec{Q}}\cdot\hat{\vec{Q}} \tag{K.79}$$

where $\hat{\vec{Q}}\cdot\hat{\vec{Q}} \equiv \sum_{m=-2}^{+2}(-1)^m \hat{Q}^{(2)}_m \hat{Q}^{(2)}_m$, and $\hat{Q}^{(2)}_m = \sqrt{\frac{4\pi}{5}}\hat{Y}_{2m}$ are the quadrupole spherical function operators and κ is the corresponding strength constant. This Hamiltonian is written as the Casimir operator of the algebra $SU(3)$ and it is possible to find the basis where the Hamiltonian $\hat{H}^{'}_{rot}$ is diagonal. These eigen vectors are described by the quantum numbers labeling the irreps of the subbgroup chain $U(6) \supset SU(3) \supset SO(3) \supset SO(2)$, $|[N];\,(\lambda\mu)\,KLM\rangle$, where N characterizes the totally symmetric irreducible representation of the group $U(6)$, $(\lambda\mu)$ corresponds to the irrep of the subgroup $SU(3)$; L and M

label the angular momentum and its projection onto z- axis (the labels of $SO(3)$; and K is the additional quantum numbers which distinguishes the state with the same $\lambda\mu$ and L:

$$\begin{array}{ccccccc} U(6) & \supset & SU(3) & \supset & SO(3) & \supset & SO(2) \\ \vdots & & \vdots & & \vdots & & \vdots \\ N & & (\lambda\mu) & ..K.. & L & & M \end{array} \tag{K.80}$$

We will not go into details (see [119]) but quantum numbers λ, N, μ and M are tied by the following conditions

$$\begin{aligned} & 0 \leq \lambda \leq 2N - 2\mu - 6M \\ & M \geq 0 \quad \text{integer} \\ & \mu \geq 0 \quad \text{integer, even} \end{aligned} \tag{K.81}$$

In the original Elliott's paper [119] the physical meaning of the additional quantum number K in the basis state $|[N];\,(\lambda\mu)\,KLM\rangle$ was the projection of the angular momentum L onto the nucleus symmetry axis and the connection of K and L is

$$\begin{aligned} & L = K,\ K+1,\ K+2, \cdots,\ (K + max(\lambda,\mu)) \quad \text{for } K \neq 0 \\ & L = max(\lambda,\mu),\ max(\lambda,\mu) - 2, \cdots,\ 1 \text{ or } 0 \quad \text{for } K = 0 \end{aligned} \tag{K.82}$$

where

$$K = \text{ integer } = min(\lambda,\mu),\ \min(\lambda,\mu) - 2, \cdots,\ 1 \text{ or } 0 \tag{K.83}$$

It should be realized that opposite to the standard angular momentum case the new quantum number L can obtain only the finite number of values for given λ and μ. In [119] it was shown that the eigen energy corresponding to the eigen vector $|[N];\,(\lambda\mu)\,KLM\rangle$ is given by the following explicit expression

$$\begin{aligned} E^{'}([N](\lambda\mu)L) &= \langle [N];\,(\lambda\mu)\,KLM|\hat{H}^{'}|\,[N];\,(\lambda\mu)\,KLM\rangle = \\ &= \kappa\,\big[\frac{3}{4}\,L(L+1) - C(\lambda\mu)\big] \end{aligned} \tag{K.84}$$

with

$$C(\lambda\mu) = \lambda^2 + \mu^2 + \lambda\mu + 3\,(\lambda + \mu) \tag{K.85}$$

From (K.84) it follows that the eigen energies of the Hamiltonian $\hat{H}^{'}_{rot}$ do not depend on M. Later, after [119], it was shown (see e.g. [113, 114]) that the states $|[N];\,(\lambda\mu)\,KLM\rangle$ are eigen states of the more general Hamiltonian $\hat{H}_{rot}$

$$\hat{H}_{rot} = -\kappa\,\hat{\vec{Q}}\cdot\hat{\vec{Q}} - \kappa^{'}\,\hat{\vec{L}}\cdot\hat{\vec{L}} \tag{K.86}$$

with the eigen energy [4]

$$E([N](\lambda\mu)KL) = (\frac{3}{4}\kappa - \kappa^{'})\, L(L+1) - \kappa\, C(\lambda\mu) \tag{K.88}$$

where $\hat{\vec{Q}}\cdot\hat{\vec{Q}} = \sum_{m=-2}^{+2}(-1)^m\, \hat{Q}^{(2)}_m\, \hat{Q}^{(2)}_{-m}$ and $\hat{\vec{L}}\cdot\hat{\vec{L}} = \sum_{m=-1}^{+1}(-1)^m\, \hat{L}^{(1)}_m\, \hat{L}^{(1)}_{-m}$ are scalar products of the angular momentum and quadrupole operators, respectively. For $\hat{Q}^{(2)}_m$ and $\hat{L}^{(1)}_m$ we have (see also (K.13))

$$\begin{aligned}
\hat{Q}^{(2)}_m &= \sqrt{\frac{4\pi}{5}}\, \hat{Y}_{2m} = \boxed{\begin{array}{c}\text{see}\\ (K.13)\end{array}} = \\
&= \sqrt{\frac{4\pi}{5}} \sum_{l_1,l_2=0,2} \langle l_1||\hat{Y}_2||\, l_2\rangle \frac{1}{5}\, \left(b^{+}_{l_1}\tilde{b}_{l_2}\right)_{(\, l_1 l_2;\, 2m)} = \\
&= \sqrt{\frac{4\pi}{5}}\, \langle d||\hat{Y}_2||\, s\rangle\, \frac{1}{5}\, \left[(d^{+}\tilde{s})_{(\, 20;\, 2m)} + (s^{+}\tilde{d})_{(\, 02;\, 2m)}\right] + \\
&\quad + \sqrt{\frac{4\pi}{5}}\, \langle d||\hat{Y}_2||\, d\rangle\, \frac{1}{5}(d^{+}\tilde{d})_{(\, 22;\, 2m)} = \boxed{\begin{array}{c}\text{see}\\ [2]\end{array}} = \\
&= \left[(d^{+}\tilde{s})_{(\, 20;\, 2m)} + (s^{+}\tilde{d})_{(\, 02;\, 2m)}\right] - \frac{7^{1/2}}{2}\, (d^{+}\tilde{d})_{(\, 22;\, 2m)}
\end{aligned} \tag{K.89}$$

$$\begin{aligned}
\hat{L}^{(1)}_m &= \sum_{l_1,l_2=0,2} \langle l_1||\hat{L}^{(1)}||\, l_2\rangle\, \frac{1}{\sqrt{3}}\, (b^{+}_{l_1}\tilde{b}_{l_2})_{(\, l_1 l_2;\, 1m)} = \boxed{\begin{array}{c}\text{see}\\ [2]\end{array}} = \\
&= \sum_{l_1,l_2=0,2} \sqrt{l_1(l_1+1)(2l_2+1)}\, \frac{1}{\sqrt{3}}\, (b^{+}_{l_1}\tilde{b}_{l_2})_{(\, l_1 l_2;\, 1m)}\, \delta_{\, l_1 l_2} = \\
&= \boxed{\begin{array}{c}\text{only the case}\\ l = 2 \text{ can occur}\end{array}} = \sqrt{10}\, (d^{+}\tilde{d})_{(\, 22;\, 1m)}
\end{aligned} \tag{K.90}$$

[4] The Hamiltonian (K.80) is written in terms of generators of the $SU(3)$ group. The set of eight $SU(3)$ generators is given by 5 operators $\hat{Q}^{(2)}_m$ ($m = \pm 2, \pm 1, 0$) and 3 operators $\hat{L}^{(1)}_m$ ($m = \pm 1, 0$). The corresponding quadratic $SU(3)$ Casimir operator is

$$C_2[SU(3)] = 2\, \hat{Q}\cdot\hat{Q} + \frac{3}{4}\, \hat{L}\cdot\hat{L} \tag{K.87}$$

From the group theory it is known that if the Hamiltonian can be written in terms of the Casimir operators of the subgroups of the $SU(3)$ group then the Hamiltonian is diagonal in the basis of states with the quantum numbers which label the irreps of the corresponding $SU(3)$ subgroup chain (K.74)). Casimir operators of the given group is determined by its generators. In this sense the Hamiltonian (K.80) is the most general $SU(3)$ Hamiltonian ($C(\lambda,\mu)$ in (K.81) are the eigen values of the above quadratic Casimir operator of ($SU(3)$).

It should be noted that in later versions of the IBM-1 model instead of $\hat{Q}^{(2)}_m$ operator given in (K.89) a little bit modified and generalized operators was introduced

$$\hat{Q}^{(2)}_m(\chi) = \left[(d^+\tilde{s})_{(\,20;\,2m)} + (s^+\tilde{d})_{(\,02;\,2m)}\right] + \chi\,(d^+\tilde{d})_{(\,22;\,2m)} \tag{K.91}$$

where the additional parameter χ was introduced and the $SU(3)$ generator corresponds to $\chi = -\frac{\sqrt{7}}{2}$.

The substitution of (K.90) and (K.91) into (K.86) and subsequent comparison with (K.7) give the relation between parameters ϵ_s, ϵ_d, $c^{'}_L$ $(L = 0, 2, 4)$, $\tilde{v}_0$, $\tilde{v}_2$, $\tilde{u}_2$, $\tilde{u}_0$ and parameters κ, $\kappa^{'}$ which gives the reduction of the general IBM-1 Hamiltonian (K.7) into the rotor $SU(3)$ limit Hamiltonian (K.86) (se e.g. [118]):

$$\begin{aligned}
\epsilon_s &= -10\,\kappa & c_0 &= -7\,\kappa + 12\,\kappa^{'} \\
\epsilon_d &= -\frac{11}{2}\,\kappa - 6\,\kappa^{'} & c_2 &= \frac{3}{2}\,\kappa + 6\,\kappa^{'} \\
\tilde{v}_2 &= \sqrt{140}\,\kappa & c_4 &= -2\,\kappa - 8\,\kappa^{'} \\
\tilde{v}_0 &= -2\,\sqrt{5}\,\kappa & & \\
\tilde{u}_2 &= -4\,\sqrt{5}\,\kappa & & \\
\tilde{u}_0 &= -2\,\sqrt{5}\,\kappa & &
\end{aligned} \tag{K.92}$$

A typical $SU(3)$ limit spectrum (K.84) of the Hamiltonian (K.79) is shown in the fig.7.15. All levels are sorted according to the quantum numbers $(\lambda\mu)$ and K into bands. If we compare this spectrum with the spectrum of the lowest positive parity rotational band spectrum of the axially symmetric nuclei (see e.g. fig. 7.2 where the low-lying spectrum of well- deformed nucleus ^{154}Sm is shown) one can see that they are very similar. The main difference between $SU(3)$ limit spectrum (K.84) or (K.88) and axially symmetric rotor spectrum is that in the case of $SU(3)$ the bands are terminated at a certain angular momentum (see (K.82)) while in the axially symmetric rotor they continue up to infinity. The other difference is that in the case of axially symmetric rotor the rotational bands based on the β- and γ- vibrational states are not degenerate while in the $SU(3)$ scheme the levels with the same spin L and the same $(\lambda\mu)$ but with different K are degenerated in the energy. The comparison of the $SU(3)$ spectrum (K.88) with the experimental low-lying spectrum of ^{156}Gd is also shown in the fig. 7.16.

If the general E2 transition operator of eq. (K.34) or (K.91) is used, it is very hard to calculate the E2 transition probabilities analytically. As is the

case for the Hamiltonian simplification occur when the operator is written in terms of $SU(3)$ generators:

$$\hat{\mathscr{M}}^{(el)}_{2m} = e_2\,\hat{Q}^{(2)}_m = e_2\,\hat{Q}^{(2)}_m(\chi = -\frac{\sqrt{7}}{2}) \tag{K.93}$$

Using this E2 transition operator the $B(E2)$ values for transitions in the ground state band $(\lambda, \mu) = (2N, 0)$ are given by

$$B(E2;\ L+2 \to L) = e_2^2\,\frac{3}{4}\,\frac{(L+2)(L+1)}{(2L+3)(2L+5)}\,(2N-L)(2N+L+3) \tag{K.94}$$

where e_2 is the effective quadrupole charge. It should be noted that the factor $(2N - L)(2N + L + 3)$ gives rise to the phenomenon that beyond a critical value of the ang. momentum L the ground state band $B(E2)$ values actually decrease with increasing L. This causes some problems in the comparison of these $B(E2)$ values with the corresponding experimental values for axially deformed "γ soft" nuclei as it is discussed in the next subsection.

K.1.3 γ- unstable ($SO(6)$) limit

Finally we discuss the thirs limiting case corresponding to the third subgroup chain in (K.32), $U(6) \supset SO(6) \supset SO(5) \supset SO(3) \supset SO(2)$. This occurs if the Hamiltonian can be expressed in terms of the Caimir operators of $SO(6)$ and its subgroups.

The fifteen $SO(6)$ generators are

$$G_{SO(6)} \equiv \Big\{\big((s^+\tilde{d})_{(02;\,2m)} + (d^+\tilde{s})_{(20;\,2m)}\big),\ (d^+\tilde{d})_{(22;\,3m)},\ (d^+\tilde{d})_{(22;\,1m)}\Big\} \tag{K.95}$$

Ten operators

$$G_{SO(5)} \equiv \Big\{(d^+\tilde{d})_{(22;\,1m)},\ (d^+\tilde{d})_{(22;\,3m)}\Big\} \tag{K.96}$$

form the set of generators of the group $SO(5)$ and three operators

$$G_{SO(3)} \equiv \Big\{(d^+\tilde{d})_{(22;\,1m)}\Big\} \tag{K.97}$$

are generators of the group $SO(3)$. From (K.95) we see immediately that the generators of $SO(5)$ and $SO(3)$ are contained in the set of generators of $SO(6)$ and this gives rise to the group reduction $U(6) \supset SO(6) \supset SO(5) \supset$

$SO(3) \supset SO(2)$. The quadratic Casimir operator of $SO(6)$ is given by [115]

$$\begin{aligned}\hat{C}_2[SO(6)] = \hat{N}(\hat{N}+4) \\ -8\Big\{\frac{5}{4}\big[(d^+d^+)_{(22;\,0)}\,(\tilde{d}\tilde{d})_{(22;\,0)}\,\big]_{(00;\,0)} \\ -\frac{\sqrt{5}}{4}\,\big[(d^+d^+)_{(22;\,0)}\,(\tilde{s}\tilde{s})_{(00;\,0)} + h.c.\big]_{(00;\,0)} \\ +\frac{1}{4}\,\big[(s^+s^+)_{(00;\,0)}\,(\tilde{s}\tilde{s})_{(00;\,0)}\big]_{(00;\,0)}\Big\}\end{aligned} \tag{K.98}$$

This operator has eigen values $2\sigma(\sigma+4)$ where σ label the different $SO(6)$ multiplets [115].

According to the group reduction $U(6) \supset SO(6) \supset SO(5) \supset SO(3) \supset SO(2)$ the basis states are labeled as $|\,[N];\,\sigma\,\nu\,n_\Delta\,L\,M\rangle$:

$$\begin{array}{ccccccccc} U(6) & \supset & SO(6)) & \supset & SO(5) & \supset & SO(3) & \supset & SO(2) \\ \vdots & & \vdots & & \vdots & & \vdots & & \\ N & & \sigma & & \nu & ..n_\Delta.. & L & & M \end{array} \tag{K.99}$$

This resembles the labeling of irreps in the vibrator limit group chain (see (K.72)) but instead of the quantum number n_d now we have the quantum number σ. The numbers ν, n_d have the same meaning as in (K.72). The allowed values for the quantum numbers are [115, 118]

$$\begin{aligned}&\sigma = N,\ N-2,\ N-4, \cdots, 0 \text{ or } 1 \\ &0 \le \nu \le \sigma \\ &\lambda = \nu - 3n_\Delta \ge 0 \\ &L = \lambda,\ \lambda+1,\ \lambda+2, \cdots, 2\lambda-2,\ 2\lambda\end{aligned} \tag{K.100}$$

where the last two equalities are the same as in (K.35) - (K.37). The most general Hamiltonian with the $SO(6)$ symmetry can be then written as

$$\begin{aligned}\hat{H}_{\gamma-\,soft} = A\,\frac{1}{8}\,\big\{2\hat{N}(\hat{N}+4) - \hat{C}_2[SO(6)]\big\} + \\ +B\,\hat{C}_2[SO(5)] + C\,\hat{L}^2\end{aligned} \tag{K.101}$$

where $\hat{C}_2[SO(6)]$ is given by (K.98), $\hat{C}_2[SO(5)]$ by (K.75) and $\hat{L}^2$ by (K.76). The eigen values of (K.101) in the basis of states $|\,[N];\,\sigma\,\nu\,n_\Delta\,L\,M\rangle$ are

$$\begin{aligned}E(N,\sigma,\nu,n_\Delta,L) = A\,\frac{1}{4}(N-\sigma)(N+\sigma+4) + \\ +B\,\frac{1}{6}\nu(\nu+3) + C\,L(L+1)\end{aligned} \tag{K.102}$$

The $SO(6)$ limit Hamiltonian $\hat{H}_{\gamma-\,soft}$ (see (K.101)) corresponds to a particular choice of the coefficients of the general IBM-1 $U(6)$ Hamiltonian (K.7):

$$\begin{aligned}
&\epsilon_0 = 0 \quad , \qquad\qquad \epsilon_d = \frac{5}{2}\,A + \frac{2}{3}\,B + 6\,C\,, \\
&c_0 = -\frac{1}{3}\,B - 12\,C\,, \quad c_2 = \frac{1}{3} - 6\,C\,, \quad c_4 = \frac{1}{3}\,B + 8\,C \\
&\tilde{v}_2 = 0\,, \qquad \tilde{v}_0 = \frac{\sqrt{5}}{4}\,A\,, \qquad \tilde{u}_2 = 0\,, \qquad \tilde{u}_0 = \frac{1}{4}\,A
\end{aligned} \tag{K.103}$$

A typical spectrum is shown in the fig. 7.18. A characteristic property of this $SO(6)$ limit is the repeated occurrence of a sequence of states 0^+, 2^+ and a doublet $(4^+, 2^+)$, where the energy difference between the doublet and the ground 0^+ in each multiplet is about 2.5 times as large as the energy difference between the first 2^+ and ground 0^+ level of each (σ, n_Δ) multiplet. Although at the first glance the spectrum resembles that of the $U(5)$ limit (see Fig 7.13), there are an important difference. In the $U(5)$ limit there is a triplet of states $(0^+, 2^+, 0^+)$ at $E_x \approx 2\epsilon$ (see Fig. 7.13) while in $SO(6)$ there is only a doublet. Also marked differences occur in the $B(E2)$ transition probabilities as it will be discussed further.

The name "γ- soft" came from the paper of Meyer-ter-Vehn [120] where it was shown that the most resembles with $SO(6)$ limit is the γ- unstable model of Wilets and Jean [121]. This model corresponds to considering only $\sigma = N$ multiplets of $SO(6)$ in the limit of $N \to \infty$. As an example of the $SO(6)$ limit in the fig. 7.19 the spectrum of ^{196}Pt is shown. One can see very good agreement of the calculated energies with experimental ones in spite of the fact that we used a little number of parameters (A, B, C, N).

As was the case of the $SU(3)$ limit analytic formulas for $B(E2)$ values can be given if the $E2$ operator is written as a generator of the group (the group $SO(6)$ in our case now - see (K.95)), that means

$$\hat{\mathscr{M}}^{(el)}_{2m} = e_2 \left[(s^+ \tilde{d})_{(02;\,2m)} + (d^+ \tilde{s})_{(20;\,2m)} \right] \tag{K.104}$$

which corresponds to taking $\chi = 0$ in eqs. (K.93), (K.91). The selection rules for the E2 transitions are $\Delta\nu = \pm 1$. This selection rules give the $B(E2)$ strength for transitions within the ground band ($\sigma = N$, $n_\Delta = 0$, $L = 2\nu$) as follows

$$B(E2;\; L+2 \to L) = e_2\, \frac{(L+2)}{2(L+5)}\, (N - \frac{L}{2})(N + \frac{L}{2} + 4) \tag{K.105}$$

The $SO(6)$ nuclei are now well known in two regions: the Pt isotopes, especially ^{196}Pt and Xe-Ba nuclei near $A \approx 130$. A comparison of the ^{196}Pt level scheme with the $SO(6)$ limit is shown in the fig.7.19. Similar comparisons for other nuclei from regions mentioned above can be found e.g. in [118, 123]. Although the energy spectra obtained in the framework of the $U(5)$ and $SO(6)$ limits are quite similar the selection rule $\Delta\nu = \pm 1$ for E2 transitions in the $SO(6)$ limit gives much better results in the comparison with the experimental values of reduced probabilities than the $U(5)$ limit. This can be seen from the fig.7.20 where the experimental decay of the 1604.5 keV level in ^{196}Pt is compared with with the theoretical $SO(6)$ and $U(5)$ limit predictions.

In this appendix the IBM-1 model was discussed relatively in details. In the subsection 7.2.2. the brief summarization if the IBM-1 model is given together with the short description of its extension IBM-2 (neutron - proton interacting boson model) and also Fermion-Boson model for odd-A nuclei.

L. The quasiparticle representation of the general single-particle operator

In the appendix the general single-particle operator

$$\hat{G} = \sum_{ij} \langle i| \hat{G} |j\rangle \, a_i^+ a_j \tag{L.1}$$

is expressed in terms of the quasiparticle creation α_i^+ and annihilation α_i operators given by the Bogoliubov transormation (6.30), (6.33) from the single-particle ones (a_i^+, a_i)

$$\begin{aligned} a_i^+ &= \mathscr{U}_i \, \alpha_i^+ + \mathscr{V}_i \, \alpha_{\bar{i}} \\ a_{\bar{i}}^+ &= \mathscr{U}_i \, \alpha_{\bar{i}}^+ - \mathscr{V}_i \, \alpha_i \end{aligned} \tag{L.2}$$

where $\mathscr{U}_i$ and $\mathscr{V}_i$ are real pairing amplitudes.

Further we will suppose that the single-particle operator $\hat{G}$ is Hermitian, symmetric (positive) or antisymmetric (negative) with respect to the time-reverse transformation and that its single-particle matrix elements are real or purely imaginary:

$$\hat{G}^+ = \hat{G} \quad , \quad \hat{\mathscr{T}}^{-1} \hat{G} \, \hat{\mathscr{T}} = \gamma_T^{(G)} \, \hat{G} \quad , \quad \langle i| \hat{G} |j\rangle^* = \gamma_c^{(G)} \, \langle i| \hat{G} |j\rangle \tag{L.3}$$

where $\gamma_T^{(G)} = \pm 1$, $\gamma_c^{(G)} = \pm 1$. Then the single-particle matrix elements of such operator fulfill the following symmetry relations

$$\begin{aligned} \langle \bar{i}| \hat{G} |\bar{j}\rangle &= \langle i| \hat{\mathscr{T}}^{-1} \hat{G} \hat{\mathscr{T}} |j\rangle^* = \gamma_T^{(G)} \gamma_c^{(G)} \, \langle i| \hat{G} |j\rangle \\ \langle \bar{i}| \hat{G} |j\rangle &= \langle i| \hat{\mathscr{T}}^{-1} \hat{G} |j\rangle^* = - \gamma_T^{(G)} \gamma_c^{(G)} \, \langle i| \hat{G} |\bar{j}\rangle \end{aligned} \tag{L.4}$$

The substitution of (L.2) into (L.1) gives

$$\begin{aligned}
\hat{G} &= \sum_{ij} \langle i|\, \hat{G}\, |j\rangle\, a_i^+ a_j = \\
&= \sum_{ij\geq 0} \Big\{ \langle i|\, \hat{G}\, |j\rangle\, a_i^+ a_j + \langle i|\, \hat{G}\, |\bar{j}\rangle\, a_i^+ a_{\bar{j}} + \\
&\qquad + \langle \bar{i}|\, \hat{G}\, |j\rangle\, a_{\bar{i}}^+ a_j + \langle \bar{i}|\, \hat{G}\, |\bar{j}\rangle\, a_{\bar{i}}^+ a_{\bar{j}} \Big\} = \\
&= \boxed{\begin{array}{c}\text{see symmetries} \\ (L.3)\end{array}} = \\
&= \sum_{ij\geq 0} \Big\{ \langle i|\, \hat{G}\, |j\rangle\, \left(a_i^+ a_j + \gamma_T^{(G)}\gamma_c^{(G)}\, a_{\bar{i}}^+ a_{\bar{j}}\right) + \\
&\qquad + \langle i|\, \hat{G}\, |\bar{j}\rangle\, \left(a_i^+ a_{\bar{j}} - \gamma_T^{(G)}\gamma_c^{(G)}\, a_{\bar{i}}^+ a_j\right) \Big\} = \\
&= \boxed{\begin{array}{c}\text{the substitution} \\ \text{from } (L.2)\end{array}} = \\
&= \langle BCS|\, \hat{G}\, |BCS\rangle + \hat{G}^{(1)} + \hat{G}^{(2)}
\end{aligned} \tag{L.5}$$

where

$$\begin{aligned}
\langle BCS|\, \hat{G}\, |BCS\rangle &= \sum_{i\geq 0} \langle i|\, \hat{G}\, |i\rangle\, \mathscr{V}_i{}^2\, (1+\gamma_T^{(G)}) \\
\hat{G}^{(1)} &= \sum_{i,j\geq 0} \Big\{ \left(\mathscr{U}_i\mathscr{V}_i + \gamma_T^{(G)}\mathscr{U}_j\mathscr{V}_i\right) \langle i|\, \hat{G}\, |j\rangle\, \left(\alpha_i^+\alpha_{\bar{j}}^+ + \gamma_c^{(G)}\, \alpha_{\bar{j}}\alpha_i\right) \\
&\quad -\frac{1}{2}\left(\mathscr{U}_i\mathscr{V}_j + \gamma_T^{(G)}\mathscr{U}_j\mathscr{V}_i\right) \langle i|\, \hat{G}\, |\bar{j}\rangle\, \left(\alpha_i^+\alpha_j^+ + \gamma_c^{(G)}\, \alpha_j\alpha_i\right) \\
&\quad -\frac{1}{2}\,\gamma_c^{(G)}\gamma_T^{(G)}\left(\mathscr{U}_i\mathscr{V}_j + \gamma_T^{(G)}\mathscr{U}_j\mathscr{V}_i\right) \langle i|\, \hat{G}\, |\bar{j}\rangle\, \left(\alpha_{\bar{i}}^+\alpha_{\bar{j}}^+ + \gamma_c^{(G)}\, \alpha_{\bar{j}}\alpha_{\bar{i}}\right) \Big\} \\
\hat{G}^{(2)} &= \sum_{i,j\geq 0} \Big\{ \langle i|\, \hat{G}\, |j\rangle\, \Big[\mathscr{U}_i\mathscr{U}_j\, \left(\alpha_i^+\alpha_j + \gamma_c^{(G)}\gamma_T^{(G)}\, \alpha_{\bar{i}}^+\alpha_{\bar{j}}\right) \\
&\qquad\qquad -\mathscr{V}_i\mathscr{V}_j\, \left(\alpha_{\bar{j}}^+\alpha_{\bar{i}} + \gamma_c^{(G)}\gamma_T^{(G)}\, \alpha_j^+\alpha_i\right)\Big] + \\
&\qquad +\langle i|\, \hat{G}\, |\bar{j}\,\rangle\, \Big[\mathscr{U}_i\mathscr{U}_j\, \left(\alpha_i^+\alpha_{\bar{j}} - \gamma_c^{(G)}\gamma_T^{(G)}\alpha_{\bar{i}}^+\alpha_j\right) \\
&\qquad\qquad +\mathscr{V}_i\mathscr{V}_j\, \left(\alpha_j^+\alpha_{\bar{i}} - \gamma_c^{(G)}\gamma_T^{(G)}\, \alpha_i^+\alpha_{\bar{j}}\right)\Big]\, \Big\}
\end{aligned} \tag{L.6}$$

where in (L.5), (L.6) the symbol $ij \geq 0$ in sums over i, j means the summation goes over single-particle state i, j with the positive sign of the amg. momentum projection (time-noninverted s.p. states).

From (L.6) it follows, for instance, that the matrix elements between two-quasiparticle state $|ij\rangle = \alpha_i^+\alpha_j^+ \, |BCS\rangle$ and BCS ground state $|BCS\rangle$ are given by the $\hat{G}^{(1)}$ part:

$$\begin{aligned}
&\langle ij|\, \hat{G}\, |BCS\rangle = \langle BCS|\, \alpha_j\alpha_i\, \hat{G}^{(1)}\, |BCS\rangle = \\
&= -\frac{1}{2} \sum_{i'j'\geq 0} \langle i'|\, \hat{G}\, |\bar{j}'\rangle \left(\mathscr{U}_{i'}\mathscr{V}_{j'} + \gamma_T^{(G)}\, \mathscr{U}_{j'}\mathscr{V}_{i'}\right) \langle BCS|\, \alpha_j\alpha_i\alpha_{i'}^+\alpha_{j'}^+\, |BCS\rangle = \\
&= -\frac{1}{2} \sum_{i'j'\geq 0} \langle i'|\, \hat{G}\, |\bar{j}'\rangle \left(\mathscr{U}_{i'}\mathscr{V}_{j'} + \gamma_T^{(G)}\, \mathscr{U}_{j'}\mathscr{V}_{i'}\right) \left(\delta_{ii'}\delta_{jj'} - \delta_{ij'}\delta_{ji'}\right) = \\
&= \boxed{\begin{array}{c}\text{because of : } \langle i|\, \hat{G}\, |\bar{j}\rangle = -\langle i|\, \mathscr{T}^{-1}\mathscr{T}^{-1}\, \hat{G}\mathscr{T}|j\rangle = \\ = -\gamma_T^{(G)}\, \langle \bar{i}|\, \hat{G}\, |j\rangle^* = -\gamma_T^{(G)}\, \langle j|\, \hat{G}^+\, |\bar{i}\rangle = -\gamma_T^{(G)}\, \langle j|\, \hat{G}\, |\bar{i}\rangle\end{array}} = \\
&= -\langle i|\, \hat{G}\, |\bar{j}\rangle \left(\mathscr{U}_i\mathscr{V}_j + \gamma_T^{(G)}\, \mathscr{U}_j\mathscr{V}_i\right)
\end{aligned} \tag{L.7}$$

and similarly

$$\begin{aligned}
\langle \bar{i}\bar{j}|\, \hat{G}\, |BCS\rangle &= -\gamma_c^{(G)}\gamma_T^{(G)}\, \langle i|\, \hat{G}\, |\bar{j}\rangle \left(\mathscr{U}_i\mathscr{V}_j + \gamma_T^{(G)}\, \mathscr{U}_j\mathscr{V}_i\right) \\
\langle i\bar{j}|\, \hat{G}\, |BCS\rangle &= \langle i|\, \hat{G}\, |j\rangle \left(\mathscr{U}_i\mathscr{V}_j + \gamma_T^{(G)}\, \mathscr{U}_j\mathscr{V}_i\right)
\end{aligned} \tag{L.8}$$

For instance, in the case of the multipole and spin-multipole operators $\hat{M}_{\lambda\mu}$ and $\hat{S}_{l\lambda\mu}$ (see (1.56)) their symmetries with respect to the Hermitian conjugation, time reverse transformation $\hat{T}$, parity $\hat{\mathscr{P}}$ and the rotation $\hat{R}_1(\pi)$ by angle π round the 1-st frame axis are following (we use Condon-Shortley phase convention (see the subsection 1.3.2))

$$\begin{aligned}
&\hat{M}_{\lambda\mu}^+ = (-1)^\mu \hat{M}_{\lambda-\mu} \quad , \quad \hat{\mathscr{T}}^{-1}\hat{M}_{\lambda\mu}\hat{\mathscr{T}} = (-1)^\mu M_{\lambda-\mu} \\
&\hat{\mathscr{P}}^{-1}\hat{M}_{\lambda\mu}\hat{\mathscr{P}} = (-1)^\lambda M_{\lambda\mu} \quad , \quad \hat{R}_1^{-1}(\pi)\hat{M}_{\lambda\mu}\hat{R}_1(\pi) = (-1)^\lambda \hat{M}_{\lambda-\mu}
\end{aligned} \tag{L.9}$$

and

$$\begin{aligned}
&\hat{S}_{l\lambda\mu}^+ = (-1)^{\lambda+l+\mu+1}\hat{S}_{l\lambda-\mu} \quad , \quad \hat{T}^{-1}\hat{S}_{l\lambda\mu}\hat{T} = (-1)^{l+\lambda+\mu}\hat{S}_{l\lambda-\mu} \\
&\hat{\mathscr{P}}^{-1}\hat{S}_{l\lambda\mu}\hat{\mathscr{P}} = (-1)^l \hat{S}_{l\lambda\mu} \quad , \quad \hat{R}_1^{-1}(\pi)\hat{S}_{l\lambda\mu}\hat{R}_1(\pi) = (-1)^\lambda \hat{S}_{l\lambda-\mu}
\end{aligned} \tag{L.10}$$

Using the Condon-Shortley phase convention the imaginarity of the single-particle matrix elements of operators $\hat{M}_{\lambda\mu}$ and $\hat{S}_{l\lambda\mu}$ is:

$$\begin{aligned}
\langle i|\, \hat{M}_{\lambda\mu}\, |j\rangle^* = (-1)^\lambda\, \langle i|\, \hat{M}_{\lambda\mu}\, |j\rangle \quad &\Rightarrow \quad \gamma_c^{(M_{\lambda\mu})} = (-1)^\lambda \\
\langle i|\, \hat{S}_{l\lambda\mu}\, |j\rangle^* = (-1)^l\, \langle i|\, \hat{S}_{l\lambda\mu}\, |j\rangle \quad &\Rightarrow \quad \gamma_c^{(S_{l\lambda\mu})} = (-1)^l
\end{aligned} \tag{L.11}$$

Since the multipole operators $\hat{M}_{\lambda\mu}$ and $\hat{S}_{l\lambda\mu}$ (see the Chapter 2) are not Hermitian we cannot use expressions (L.5)-(L.8). In order to use them we should symmetrized them as follows (further $\mu \geq 0$)

$$\begin{aligned}
\hat{M}_{\lambda\mu}[r] &\equiv \frac{i^{\lambda+\mu+\frac{r+3}{2}}}{\sqrt{2(1+\delta_{\mu 0})}} \left(\hat{M}_{\lambda\mu} + (-1)^{\lambda+\frac{r+3}{2}} \hat{M}_{\lambda-\mu}\right) \quad , \quad r = \pm 1 \\
\hat{S}_{l\lambda\mu}[r] &\equiv \frac{i^{l+\mu+\frac{r+3}{2}+1}}{\sqrt{2(1+\delta_{\mu 0})}} \left(\hat{S}_{\lambda\mu} + (-1)^{\lambda+\frac{r+3}{2}} \hat{S}_{l\lambda-\mu}\right) \quad , \quad r = \pm 1
\end{aligned} \tag{L.12}$$

Then

$$\begin{aligned}
&\hat{M}^{+}_{\lambda\mu}[r] = \hat{M}_{\lambda\mu}[r] \quad , \quad \mathscr{T}^{-1}\hat{M}_{\lambda\mu}[r]\mathscr{T} = \hat{M}_{\lambda\mu}[r] \\
&\mathscr{P}^{-1}\hat{M}_{\lambda\mu}[r]\mathscr{P} = (-1)^{\lambda}\, \hat{M}_{\lambda\mu}[r] \;,\; \hat{R}_1^{-1}(\pi)\hat{M}_{\lambda\mu}[r]\hat{R}_1(\pi) = r\, \hat{M}_{\lambda\mu}[r] \\
&\langle i|\, \hat{M}_{\lambda\mu}[r]\, |j\rangle^{*} = (-1)^{\mu+\frac{r+3}{2}}\, \langle i|\, \hat{M}_{\lambda\mu}[r]\, |j\rangle
\end{aligned} \tag{L.13}$$

and

$$\begin{aligned}
&\hat{S}^{+}_{l\lambda\mu}[r] = \hat{S}_{l\lambda\mu}[r] \quad , \quad \mathscr{T}^{-1}\hat{S}_{l\lambda\mu}[r]\mathscr{T} = -\hat{S}_{l\lambda\mu}[r] \\
&\mathscr{P}^{-1}\hat{S}_{l\lambda\mu}[r]\mathscr{P} = (-1)^{l}\, \hat{S}_{\lambda\mu}[r] \;,\; \hat{R}_1^{-1}(\pi)\hat{S}_{l\lambda\mu}[r]\hat{R}_1(\pi) = r\, \hat{S}_{l\lambda\mu}[r] \\
&\langle i|\, \hat{S}_{l\lambda\mu}[r]\, |j\rangle^{*} = (-1)^{\mu+1+\frac{r+3}{2}}\, \langle i|\, \hat{S}_{\lambda\mu}[r]\, |j\rangle
\end{aligned} \tag{L.14}$$

So we have

$$\begin{aligned}
\gamma_T^{[M_{\lambda\mu}]} &= +1 \qquad , \qquad \gamma_c^{[M_{\lambda\mu}]} = (-1)^{\mu+\frac{r+3}{2}} \\
\gamma_T^{[S_{l\lambda\mu}]} &= -1 \qquad , \qquad \gamma_c^{[S_{\lambda\mu}]} = (-1)^{\mu+1+\frac{r+3}{2}}
\end{aligned} \tag{L.15}$$

with $r \pm 1$ (the number r is often called as signature of the given operator) and we can use expressions (L.5) - (L.7) for operators $\hat{M}_{\lambda\mu}[r]$ ($\mu \geq 0$) and $\hat{S}_{l\lambda\mu}[r]$ $(\mu \geq 0)$.

In the quantum mechanics we meet often the decomposition of local two-body potential into multipoles and spin-multipoles (see (1.55)). In such decompositions the sums $\sum_{\mu=-\lambda}^{+\lambda} \hat{M}^{+}_{\lambda\mu}\hat{M}_{\lambda\mu}$ and $\sum_{\mu=-\lambda}^{+\lambda} \hat{S}^{+}_{l\lambda\mu}\hat{S}_{l\lambda\mu}$ are present (see (1.55)). If the operators $\hat{M}_{\lambda\mu}$ and $\hat{S}_{l\lambda\mu}$ are symmetrized according to (L.12) than these sums can be rewritten as follows

$$\begin{aligned}
\sum_{\mu=-\lambda}^{+\lambda} \hat{M}^{+}_{\lambda\mu}\, \hat{M}_{\lambda\mu} &= \sum_{\mu=0}^{\lambda} \sum_{r=\pm 1} \hat{M}_{\lambda\mu}[r]\, \hat{M}_{\lambda\mu}[r] \\
\sum_{\mu=-\lambda}^{+\lambda} \hat{S}^{+}_{l\lambda\mu}\, \hat{S}_{l\lambda\mu} &= \sum_{\mu=0}^{\lambda} \sum_{r=\pm 1} \hat{S}_{l\lambda\mu}[r]\, \hat{M}_{l\lambda\mu}[r]
\end{aligned} \tag{L.16}$$

It should be also noted that the operator $\hat{M}_{\lambda\mu}$ can be (up to the charge factor) identified with electric type multipole operators (see (2.130) within the long wave approximation and similarly the spin-multipole operator is connected with the magnetic type multipole operator in the long wave approximation. So electric type transition operators are always connected with $\gamma_T^{(el)} = +1$ while magnetic type transition operators with $\gamma_T^{(mag)} = -1$.

M. Separable RPA

Let us suppose the model Hamiltonian in the form of (7.309), that means it has a form of a sum of the quasiparticle mean field $\hat{H}_{BCS}$ and the separable residual interaction (see (7.309))

$$\hat{H}'_{even-even} = \hat{H}_{BCS} - \frac{1}{2} \sum_{\tau\tau'} \sum_{kk'} \kappa_{k\tau\, k'\tau'}\, \hat{Z}^{(1)}_{k\tau} \hat{Z}^{(1)}_{k'\tau'} \tag{M.1}$$

where (see (6.50), (6.57) or (6.100))

$$\hat{H}_{BCS} = \sum_{\tau=neut,prot} \sum_{\substack{i>0 \\ i\in\tau}} E_i \left(\alpha^+_i \alpha_i + \alpha^+_{\bar{i}} \alpha_{\bar{i}}\right) \tag{M.2}$$

with single-quasiparticle creation and annihilation operators α^+_i and α_i and quasiparticle energies E_i. The residual interactions (the second term in (M.1)) contain products of two-quasiparticle parts of single-particle operators $\hat{Z}_k$. If these operators $\hat{Z}_k$ fulfill the symmetry conditions (7.301) then their two-quasiparticle parts $\hat{Z}^{(1)}_k$ are given by (L.6):

$$\begin{aligned} \hat{Z}_k &= \sum_{\tau=neut,prot} Z^{(1)}_{k\tau} = \\ &= 2 \sum_{\tau} \sum_{\substack{\varpi=ij,\, i\bar{j},\, \bar{i}j,\, \bar{i}\bar{j} \\ \varpi\in\tau,\, \varpi>0}} \xi_\varpi \langle\varpi|\, \hat{Z}_k\, |BCS\rangle \left(b^+_\varpi + \gamma_c^{(\hat{Z}_k)}\, b_\varpi\right) \end{aligned} \tag{M.3}$$

with (see (L.6))

$$\begin{aligned} &\langle\varpi|\, \hat{Z}_k\, |BCS\rangle = \\ &= \begin{cases} -\left(\mathscr{U}_i \mathscr{V}_j + \gamma_T^{(\hat{Z}_k)}\, \mathscr{V}_i \mathscr{U}_j\right) \langle i|\, \hat{Z}_k\, |\bar{j}\rangle & \text{if } \varpi = ij, \\ -\gamma_c^{(\hat{Z}_k)} \gamma_T^{(\hat{Z}_k)} \left(\mathscr{U}_i \mathscr{V}_j + \gamma_T^{(\hat{Z}_k)}\, \mathscr{V}_i \mathscr{U}_j\right) \langle i|\, \hat{Z}_k\, |\bar{j}\rangle & \text{if } \varpi = \bar{i}\bar{j}, \\ \left(\mathscr{U}_i \mathscr{V}_j + \gamma_T^{(\hat{Z}_k)}\, \mathscr{V}_i \mathscr{U}_j\right) \langle i|\, \hat{Z}_k\, |j\rangle & \text{if } \varpi = i\bar{j}. \end{cases} \end{aligned} \tag{M.4}$$

where b^+_ϖ and b_ϖ are two-quasiparticle creation and annihilation operators, respectively (see (L.6) and (7.306))

$$b^+_\varpi = \begin{cases} \alpha^+_i \alpha^+_j & \text{for } \varpi = ij, \\ \alpha^+_i \alpha^+_{\bar{j}} & \text{for } \varpi = i\bar{j}, \\ \alpha^+_{\bar{i}} \alpha^+_{\bar{j}} & \text{for } \varpi = \bar{i}\bar{j}. \end{cases} \tag{M.5}$$

and

$$\xi_\varpi = \begin{cases} 1/4 & \text{for } \varpi = ij \\ 1/2 & \text{for } \varpi = i\bar{j}, \\ 1/4 & \text{for } \varpi = \bar{i}\bar{j}. \end{cases} \tag{M.6}$$

and $\varpi > 0$ in the sum in (M.3) means that the summation goes over two-quasiparticle states ij, $i\bar{j}$, $\bar{i}\bar{j}$ with the positive sign of the angular momentum projection of the given two-quasiparticle states.

As it is discussed in the Chapter 7 (see (7.300) - (7.309)) Hamiltonian (M.1) (or (7.309)) is the simpliest Hamiltonian describing harmonic vibrations of even-even nuclei. Therefore it has an index $even - even$.

Further we suppose quasi-boson approximation for two-quasiparticle creation and annihilation operators b^+_ϖ and b_ϖ (see (7.220)):

$$\begin{aligned} &\left[b_{ij},\, b^+_{i'j'}\right] \approx \langle BCS| \left[b_{ij},\, b^+_{i'j'}\right] |BCS\rangle = \delta_{ii}\,\delta_{jj} - \delta_{ij}\,\delta_{ji} \\ &\left[b_{i\bar{j}},\, b^+_{i'\bar{j}'}\right] \approx \langle BCS| \left[b_{i\bar{j}},\, b^+_{i'\bar{j}'}\right] |BCS\rangle = \delta_{ii}\,\delta_{jj} \\ &\left[b_{ij},\, b^+_{i'j'}\right] \approx \delta_{ii}\,\delta_{jj} - \delta_{ij}\,\delta_{ji} \\ &\left[b_{ij},\, b_{i'j'}\right] \approx \left[b_{\bar{i}\bar{j}},\, b_{\bar{i}'\bar{j}'}\right] \approx \left[b_{ij},\, b^+_{i'\bar{j}'}\right] \approx \left[b_{ij},\, b^+_{\bar{i}'\bar{j}'}\right] \approx 0 \end{aligned} \tag{M.7}$$

In the framework of the RPA the lowest excited states of the intrinsic nuclear Hamiltonian of even-even nuclei have one-phonon character where the phonon (vibration harmonic vibration quantum) is created by the operator Q^+_νv (see (7.207)):

$$\begin{aligned} Q^+_\nu &= \frac{1}{2} \sum_{\tau=neut,prot} \sum_{\substack{\varpi=ij,\, i\bar{j},\, \bar{i}j,\, \bar{i}\bar{j} \\ \varpi\in\tau,\, \varpi>0}} \left(\tilde{X}^{(\nu)}_\varpi b^+_\varpi - \tilde{Y}^{(\nu)}_\varpi b_\varpi\right) = \\ &= \frac{1}{2} \sum_{\tau=neut,prot} \sum_{\substack{\varpi=ij,\, i\bar{j},\, \bar{i}\bar{j} \\ \varpi\in\tau,\, \varpi>0}} \left(X^{(\nu)}_\varpi b^+_\varpi - Y^{(\nu)}_\varpi b_\varpi\right) \end{aligned} \tag{M.8}$$

with the corresponding forward and backward two-quasiparticle amplitudes:

$$\begin{aligned} X^{(\nu)}_{ij} &= \tilde{X}^{(\nu)}_{ij} \qquad X^{(\nu)}_{\bar{i}\bar{j}} = \tilde{X}^{(\nu)}_{\bar{i}\bar{j}} \qquad X^{(\nu)}_{i\bar{j}} = \tilde{X}^{(\nu)}_{i\bar{j}} \\ Y^{(\nu)}_{ij} &= \tilde{Y}^{(\nu)}_{ij} \qquad Y^{(\nu)}_{\bar{i}\bar{j}} = \tilde{Y}^{(\nu)}_{\bar{i}\bar{j}} \qquad Y^{(\nu)}_{i\bar{j}} = \tilde{Y}^{(\nu)}_{i\bar{j}} \end{aligned} \tag{M.9}$$

In the quasi-boson approximation (M.7) phonon creation and annihilation operators behave like bosons:

$$\begin{aligned} &\left[Q_\nu,\, Q^+_{\nu'}\right] = \\ &= \frac{1}{2} \sum_{\tau=neut,\,prot} \sum_{\substack{ij>0 \\ ij\in\tau}} \left\{ X^{(\nu)\,*}_{ij} X^{(\nu')}_{ij} - Y^{(\nu)\,*}_{ij} Y^{(\nu')}_{ij} + \right. \\ &\qquad \left. + \; X^{(\nu)\,*}_{\bar{i}\bar{j}} X^{(\nu')}_{\bar{i}\bar{j}} - Y^{(\nu)\,*}_{\bar{i}\bar{j}} Y^{(\nu')}_{\bar{i}\bar{j}} \right\} + \\ &+ \frac{1}{4} \sum_{\tau=neut,prot} \sum_{\substack{i\bar{j}>0 \\ i\bar{j}\in\tau}} \left\{ X^{(\nu)\,*}_{i\bar{j}} X^{(\nu')}_{i\bar{j}} - Y^{(\nu)\,*}_{i\bar{j}} Y^{(\nu')}_{i\bar{j}} \right\} \;\approx\; 0 \end{aligned}$$

$$\left[Q_\nu,\, Q_{\nu'}\right] \approx 0 \tag{M.10}$$

The structure of phonons (amplitudes $X^{(\nu)}_{\varpi}$ and $Y^{(\nu)}_{\varpi}$) and corresponding phonon energies $\hbar\omega_\nu$ can be obtained from the solving of the oscillator RPA equations (7.212)

$$\left[\hat{H}'_{even-even}\,,\, Q^+_\nu\right] = \hbar\omega_\nu\, Q^+_\nu \qquad \left[\hat{H}'_{even-even}\,,\, Q_\nu\right] = -\,\hbar\omega_\nu\, Q_\nu \tag{M.11}$$

The substitution of (M.1) into (M.11) yields

$$\begin{aligned} &\left[\hat{H}'_{even-even}\,,\, Q^+_\nu\right] = \\ &\quad = \left[\hat{H}_{BCS}\,,\, Q^+_\nu\right] - \frac{1}{2} \sum_{\tau\tau'} \sum_{kk'} \kappa_{k\tau\,k'\tau'} \left[\hat{Z}^{(1)}_{k\tau}\, \hat{Z}^{(1)}_{k'\tau'}\,,\, Q^+_\nu\right] = \\ &\quad = \hbar\omega_\nu\, Q^+_\nu \end{aligned} \tag{M.12}$$

where

$$\left[\hat{H}_{BCS}\,,\, Q^+_\nu\right] = \boxed{\begin{array}{c}\text{see} \\ (M.2), (M.8)\end{array}} =$$

$$= \Big[\sum_{\tau} \sum_{\substack{i>0 \\ i\in\tau}} E_i \left(\alpha_i^+ \alpha_i + \alpha_{\bar{i}}^+ \alpha_{\bar{i}} \right),\ \frac{1}{2} \sum_{\tau'} \sum_{\substack{\varpi=ij,\, i\bar{j},\, \bar{i}\bar{j} \\ \varpi\in\tau,\, \varpi>0}} \left(X_{\varpi}^{(\nu)} b_{\varpi}^+ - Y_{\varpi}^{(\nu)} b_{\varpi} \right) \Big] =$$

$$= \boxed{\begin{array}{c} \text{using} \\ \left[\alpha_i^+ \alpha_i,\ \alpha_k^+ \alpha_{k'}^+ \right] = \delta_{ik}\, \alpha_i^+ \alpha_{k'}^+ - \delta_{ik'}\, \alpha_i^+ \alpha_k^+ \text{ and } E_i = E_{\bar{i}} \end{array}} =$$

$$= \frac{1}{2} \sum_{\tau\tau'} \sum_{ij\in\tau} \Big\{ \epsilon_{ij}\, X_{ij}^{(\nu)}\, \alpha_i^+ \alpha_j^+ + \epsilon_{ij}\, X_{\bar{i}\bar{j}}^{(\nu)}\, \alpha_{\bar{i}}^+ \alpha_{\bar{j}}^+ + \epsilon_{ij}\, X_{i\bar{j}}^{(\nu)}\, \alpha_i^+ \alpha_{\bar{j}}^+$$
$$+ \epsilon_{ij}\, Y_{ij}^{(\nu)}\, \alpha_i^+ \alpha_j^+ + \epsilon_{ij}\, Y_{\bar{i}\bar{j}}^{(\nu)}\, \alpha_{\bar{i}}^+ \alpha_{\bar{j}}^+ + \epsilon_{ij}\, Y_{i\bar{j}}^{(\nu)}\, \alpha_i^+ \alpha_{\bar{j}}^+ \Big\} \tag{M.13}$$

and

$$-\frac{1}{2} \sum_{\tau\tau'} \sum_{kk'} \kappa_{k\tau\, k'\tau'} \left[\hat{Z}_{k\tau}^{(1)} \hat{Z}_{k'\tau'}^{(1)}, Q_{\nu}^+ \right] =$$

$$= \boxed{\begin{array}{c} \text{using quasi-boson approximation (M.7) and} \\ \left[\hat{A}\hat{B},\, \hat{C} \right] = \hat{A} \left[\hat{B}, \hat{C} \right] + \left[\hat{A}, \hat{C} \right] \hat{B} \end{array}} =$$

$$- \sum_{\tau\tau'} \sum_{kk'} \kappa_{k\tau\, k'\tau'} \left\langle BCS \right| \left[\hat{Z}_{k\tau}^{(1)},\, Q_{\nu}^+ \right] \left| BCS \right\rangle Z_{k'\tau'}^{(1)} \tag{M.14}$$

where

$$\left\langle BCS \right| \left[\hat{Z}_{k\tau}^{(1)},\, Q_{\nu}^+ \right] \left| BCS \right\rangle = \boxed{\begin{array}{c} \text{see} \\ (M.7), (M.8) \end{array}} =$$

$$= \frac{1}{2} \sum_{\substack{\varpi=ij,\, i\bar{j},\, \bar{i}\bar{j} \\ \varpi\in\tau,\, \varpi>0}} \Big\{ X_{\varpi}^{(\nu)} \left\langle BCS \right| \left[\hat{Z}_{k\tau}^{(1)},\, b_{\varpi}^+ \right] \left| BCS \right\rangle$$
$$- Y_{\varpi}^{(\nu)} \left\langle BCS \right| \left[\hat{Z}_{k\tau}^{(1)},\, b_{\varpi} \right] \left| BCS \right\rangle \Big\} =$$

$$= \frac{1}{2} \sum_{\substack{\varpi=ij,\, i\bar{j},\, \bar{i}\bar{j} \\ \varpi\in\tau,\, \varpi>0}} \Big\{ X_{\varpi}^{(\nu)} \left\langle \varpi \right| \hat{Z}_{k\tau}^{(1)} \left| BCS \right\rangle^*$$
$$+ \quad Y_{\varpi}^{(\nu)} \left\langle \varpi \right| \hat{Z}_{k\tau}^{(1)} \left| BCS \right\rangle \Big\} \tag{M.15}$$

In (M.15) $\left| \varpi \right\rangle = b_{\varpi}^+ \left| BCS \right\rangle$ represent two- quasiparticle states of the BCS mean field and we suppose that two- quasiparticle matrix elements $\langle \varpi | \hat{Z}_{k\tau}^{(1)} | BCS \rangle$ are known.

After the substitution of (M.13), (M.14) and (M.15) into (M.12) and using (M.3), (M.8) the first equation in (M.12) reads

$$\begin{aligned}
&\left[\hat{H}^{'}_{even-even},\, Q^{+}_{\nu}\right] = \\
&= \frac{1}{2}\sum_{\tau} \sum_{\substack{\varpi=ij,\, i\bar{j},\, \bar{i}\bar{j} \\ \varpi\in\tau,\, \varpi>0}} \left\{\epsilon_{\varpi}\, X^{(\nu)}_{\varpi}\, b^{+}_{\varpi} + \epsilon_{\varpi}\, Y^{(\nu)}_{\varpi}\, b_{\varpi}\right\} \\
&- \sum_{\tau\tau^{'}} \sum_{kk^{'}} \kappa_{k\tau\, k^{'}\tau^{'}}\, \langle BCS|\, \left[\hat{Z}^{(1)}_{k\tau}, Q^{+}_{\nu}\right]\, |BCS\rangle \\
&\qquad \cdot \sum_{\substack{\varpi=ij,\, i\bar{j},\, \bar{i}\bar{j} \\ \varpi\in\tau^{'},\, \varpi>0}} 2\,\xi_{\varpi}\, \langle\varpi|\, \hat{Z}^{(1)}_{k^{'}\tau^{'}}\, |BCS\rangle\, \left(b^{+}_{\varpi} + \gamma_{c}^{(X_{k^{'}})}\, b_{\varpi}\right) = \\
&\qquad\qquad = \hbar\,\omega_{\varpi}\, \frac{1}{2} \sum_{\tau} \sum_{\substack{\varpi=ij,\, i\bar{j},\, \bar{i}\bar{j} \\ \varpi\in\tau,\, \varpi>0}} \left\{X^{(\nu)}_{\varpi} b^{+}_{\varpi} - Y^{(\nu)}_{\varpi} b_{\varpi}\right\}
\end{aligned} \tag{M.16}$$

The comparison of terms with given b^{+}_{ϖ} in the l.h.s. and r.h.s. of (M.16) yields ($\varpi \in \tau$)

$$\begin{aligned}
&\frac{1}{2}\,\epsilon_{\varpi}\, X^{(\nu)}_{\varpi} \\
&- \sum_{\tau^{'}} \sum_{kk^{'}} \kappa_{k\tau\, k^{'}\tau^{'}} \langle BCS|\, \left[\hat{Z}^{(1)}_{k^{'}\tau^{'}},\, Q^{+}_{\nu}\right]\, |BCS\rangle\, 2\,\xi_{\varpi}\, \langle\varpi|\, \hat{Z}^{(1)}_{k\tau}\, |BCS\rangle = \\
&\qquad = \frac{1}{2}\,\hbar\,\omega_{\nu}\, X^{(\nu)}_{\varpi}
\end{aligned} \tag{M.17}$$

The similar comparison in (M.16) of terms with the given b_{ϖ} provides the following equation ($\varpi \in \tau$)

$$\begin{aligned}
&\frac{1}{2}\,\epsilon_{\varpi}\, Y^{(\nu)}_{\varpi} \\
&- \sum_{\tau^{'}} \sum_{kk^{'}} \kappa_{k\tau\, k^{'}\tau^{'}} \langle BCS|\, \left[\hat{Z}^{(1)}_{k^{'}\tau^{'}},\, Q^{+}_{\nu}\right]\, |BCS\rangle\, 2\,\xi_{\varpi}\, \langle\varpi|\, \hat{Z}^{(1)}_{k\tau}\, |BCS\rangle^{*} = \\
&\qquad = -\frac{1}{2}\,\hbar\,\omega_{\nu}\, Y^{(\nu)}_{\varpi}
\end{aligned} \tag{M.18}$$

We would obtain the same equation as (M.17) and (M.18) if the expressions (M.13), (M.14) and (M.15) are substituted into the second equation in (M.11).

Equations (M.17) and (M.18) give ($\varpi \in \tau$)

$$
\begin{aligned}
& X^{(\nu)}_{\varpi} = 4\,\xi_{\varpi} \\
& \cdot \frac{\sum_{\tau'}\ \sum_{kk'}\kappa_{k\tau\,k'\tau'}\langle BCS|\left[\hat{Z}^{(1)}_{k'\tau'},\ Q^{+}_{\nu}\right]|BCS\rangle\ 2\,\xi_{\varpi}\ \langle\varpi|\ \hat{Z}^{(1)}_{k\tau}\ |BCS\rangle}{\epsilon_{\varpi} - \hbar\,\omega_{\nu}} \\
& Y^{(\nu)}_{\varpi} = 4\,\xi_{\varpi} \\
& \cdot \frac{\sum_{\tau'}\ \sum_{kk'}\kappa_{k\tau\,k'\tau'}\langle BCS|\left[\hat{Z}^{(1)}_{k'\tau'},\ Q^{+}_{\nu}\right]|BCS\rangle\ 2\,\xi_{\varpi}\ \langle\varpi|\ \hat{Z}^{(1)}_{k\tau}\ |BCS\rangle^{*}}{\epsilon_{\varpi} + \hbar\,\omega_{\nu}}
\end{aligned}
\tag{M.19}
$$

Further we introduce a new assignment for unknown quantities $\langle BCS|\left[\hat{Z}^{(1)}_{k\tau}, Q^{+}_{\nu}\right]|BCS\rangle$ ($k = 1, \cdots, N_{op}\,;\ \tau = neut, prot$)

$$
R^{(\nu)}_{k\tau} \equiv \langle BCS|\left[\hat{Z}^{(1)}_{k\tau},\ Q^{+}_{\nu}\right]|BCS\rangle \tag{M.20}
$$

After the substitution of (M.19) into (M.15) and using the new assignment (M.20) we obtain the following equation for unknowns $R^{(\nu)}_{k\tau}$ ($k = 1, \ldots, N_{op}; \tau = neut, prot$)

$$
\begin{aligned}
& R^{(\nu)}_{k\tau} = \\
& = \sum_{\substack{\tau'\varpi = ij,\, i\bar{j},\, \bar{i}\bar{j} \\ \varpi\in\tau'\,;\,\varpi>0}}\ \sum 2\,\xi_{\varpi}\ \frac{\sum_{\bar{k}\bar{k}'}\kappa_{\bar{k}\tau\,\bar{k}'\tau'}\ R^{(\nu)}_{\bar{k}\tau}\ \langle\varpi|\ \hat{Z}^{(1)}_{\bar{k}'\tau'}\ |BCS\rangle\ \langle\varpi|\ \hat{Z}^{(1)}_{k\tau}\ |BCS\rangle^{*}}{\epsilon_{\varpi} - \hbar\omega_{\nu}} \\
& + \sum_{\substack{\tau'\varpi = ij,\, i\bar{j},\, \bar{i}\bar{j} \\ \varpi\in\tau'\,;\,\varpi>0}}\ \sum 2\,\xi_{\varpi}\ \frac{\sum_{\bar{k}\bar{k}'}\kappa_{\bar{k}\tau\,\bar{k}'\tau'}\ R^{(\nu)}_{\bar{k}\tau}\ \langle\varpi|\ \hat{Z}^{(1)}_{\bar{k}'\tau'}\ |BCS\rangle^{*}\ \langle\varpi|\ \hat{Z}^{(1)}_{k\tau}\ |BCS\rangle^{*}}{\epsilon_{\varpi} + \hbar\omega_{\nu}} = \\
& = \sum_{\tau'}\sum_{\bar{k}\bar{k}'}\kappa_{\bar{k}\tau\,\bar{k}'\tau'}\ R^{(\nu)}_{\bar{k}\tau}\ \ F^{(\nu)}_{\bar{k}'\tau'\,k\tau}
\end{aligned}
\tag{M.21}
$$

where

$$
\begin{aligned}
& F^{(\nu)}_{\bar{k}'\tau'\,k\tau} \equiv \\
& \equiv 2\,\delta_{\tau\tau'}\sum_{\substack{\varpi = ij,\, i\bar{j} \\ \varpi\in\tau'\,;\,\varpi>0}}\ \frac{\epsilon_{\varpi}\ \langle\varpi|\ \hat{Z}^{(1)}_{\bar{k}'\tau'}\ |BCS\rangle\ \langle\varpi|\ \hat{Z}^{(1)}_{k\tau}\ |BCS\rangle^{*}}{\epsilon^{2}_{\varpi} - (\hbar\omega_{\nu})^{2}}
\end{aligned}
$$

for $\gamma_c^{(Z_{\bar{k}'})} = \gamma_c^{(Z_k)}$ and

$$F^{(\nu)}_{\bar{k}\tau' \, k\tau} \equiv$$
$$\equiv 2\,\delta_{\tau\tau'} \sum_{\substack{\varpi=ij,\, i\bar{j} \\ \varpi\in\tau' ;\, \varpi>0}} \frac{\hbar\omega_\nu \,\langle\varpi|\, \hat{Z}^{(1)}_{\bar{k}'\tau'} \,|BCS\rangle \,\langle\varpi|\, \hat{Z}^{(1)}_{k\tau} \,|BCS\rangle^*}{\epsilon^2_\varpi - (\hbar\omega_\nu)^2} \tag{M.22}$$

for $\gamma_c^{(Z_{\bar{k}'})} = -\,\gamma_c^{(Z_k)}$.

Equations (M.22) represent the equation system for unknowns $R^{(\nu)}_{k\tau}$:

$$\sum_{\bar{\tau}\tau'} \sum_{k'\bar{k}} \left\{ \kappa_{k\tau \; k'\tau'} \;\; F_{k'\tau' \, \bar{k}\bar{\tau}} - \delta_{k\bar{k}} \;\; \delta_{\tau\bar{\tau}}\, \delta_{kk'} \;\; \delta_{\tau\tau'} \right\} R^{(\nu)}_{\bar{k}\bar{\tau}} = 0 \tag{M.23}$$

for $\tau, \tau', \bar{\tau} = neut, prot$ and $k, k', \bar{k} = 1, \cdots, N_{op}$. The condition of solvability of this homogeneous equation system is

$$det\{\kappa\, F - 1\} = 0 \tag{M.24}$$

and it determines phonon energies $\hbar\omega_\nu$ where the index ν enumerates individual solutios of (M.24) and (M.23). One can see that the dimension of the algebraic homogeneous system of equations (M.23) is $2N_{op}$. The solving of (M.24) gives phonon energies $\hbar\omega_\nu$. Each such energy $\hbar\omega_\nu$ is then substituted into (M.22), (M.23) and the subsequent solving of (M.23) gives unknowns $R^{(\nu)} = \langle BCS|\, \left[Z^{(1)}_{k\tau}, Q^+_\nu\right] |BCS\rangle$ which determine phonon amplitudes $X^{(\nu)}_\varpi$ and $Y^{(\nu)}_\varpi$ of each one- phonon state $Q^+_\nu \,|RPA\rangle$ (see (M.19)). In such a way we obtain structures and energies of all phonons.

N. Projection method

N.1 Projection operator

Let us suppose that the Hamiltonian of our investigated system (nucleus), $\hat{H}$, commutes with some operators $\hat{R}(\Omega)$ ($[\hat{H},\ \hat{R}(\Omega)] = 0$) which form the group of the symmetry. Further it is also supposed that these operators depend on one or several continuous parameters Ω. As an example we can give the Hamiltonian symmetric with respect to the group of rotations, the each element of which depends on Euler angles $\Omega \equiv (a, b, c)$ (this case is discussed in details in the section N.3). Another examples are Hamiltonians symmetric with respect to the gauge group connected with the number of particle conservation discussed in the section N.2 where each alement is given by the angle φ_g of the rotation around the 3-d axis of the frame in the gauge coordinate space.

Further we assume that there exists some many-particle wave function $|\phi\rangle$ which violates the total Hamiltonian symmetry generated by the symmetry transformations $\hat{R}(\Omega)$ introduced above, that means $\hat{R}(\Omega)|\phi\rangle \neq |\phi\rangle$. Such situation occurs in the nuclear physics very often, for instance, when the total nuclear Hamiltonian in laboratory system is invariant with respect to rotations in the 3-dimensional space but the HF or HFB (BCS) deformed mean field together with its ground state $|\phi\rangle$ violates the rotational invariance. Another example is the BCS ground state (quasiparticle vacuum) violating the invariance with respect to the rotation around the 3-d axis of the gauge space (violation of the number of particle conservation).

Applying all elements $\hat{R}(\Omega)$ of the symmetry group on symmetry-violating wave function $|\phi\rangle$ we obtain a continous set of functions $|\phi(\Omega)\rangle$

$$|\phi(\Omega)\rangle = \hat{R}(\Omega)\,|\phi\rangle\,, \tag{N.1}$$

so called **generating functions** $\phi(\Omega)\rangle$, where Ω runs over the whole parameter space of the group. According to the assumtion of the symmetry

group

$$\left[\hat{H},\ \hat{R}(\Omega) \right] = 0 \quad \text{for all } \Omega \tag{N.2}$$

Therefore all generating functions $|\phi(\Omega)\rangle$ have the same energy. This fact lead Peierls and Yoccoz in 1957 (see [155]) to propose to use the generating functions (N.1) as the generator functions in the GCM technique (see $|\phi(\vec{q})\rangle$ in the subsection 7.3.3.2.1). Then we can make the following ansatz for the wave function $|\psi\rangle$ of the nucleus (for possible eigen-functions of the nucleus Hamiltonian $\hat{H}$)

$$|\psi\rangle = \int d\Omega\, f(\Omega)\, |\phi(\Omega)\rangle = \int d\Omega\, f(\Omega)\, \hat{R}(\Omega)\, |\phi\rangle \tag{N.3}$$

where the weight function $f(\Omega)$ can be obtained by the variational principle by zero variation of the energy (the expectation value $\langle\psi|\, \hat{H}\, |\psi\rangle$ with respect to $f(\Omega)$). It is equivalent to the diagonalization of the Hamiltonian $\hat{H}$ in the subspace spanned by the functions $|\phi(\Omega)\rangle$. This subspace is invariant under the elements $\hat{R}(\Omega)$ of the symmetry group [1]

$$\begin{aligned}
&\hat{R}(\Omega)\,|\,\psi\rangle = \int d\Omega^{'}\, \hat{R}(\Omega)\, f(\Omega^{'})\, \hat{R}(\Omega^{'})\,|\,\phi\rangle = \\
&= \int d\Omega^{'}\, \hat{R}(\Omega+\Omega^{'})\, f(\Omega^{'})\, |\phi\rangle = \boxed{\begin{array}{c}\text{substitution } \Omega^{''} = \Omega + \Omega^{'} \\ \text{for fixed } \Omega\end{array}} = \\
&= \int d\Omega^{''}\, f(-\Omega+\Omega^{''})\, \hat{R}(\Omega^{''})\,|\,\phi\rangle = \\
&= \int d\Omega^{''}\, f(-\Omega+\Omega^{''})\,|\,\phi(\Omega^{''})\rangle
\end{aligned} \tag{N.4}$$

That means the vector $\hat{R}(\Omega)\,|\,\psi\rangle$ belongs also to the subspace spanned by the functions $|\,\phi(\Omega)\rangle$ and we call this subspace as "collective" subspace and corresponding projector operator is denoted by $\hat{P}_{\phi}$. Since the "collective" subspace is closed to action of all symmetry operations $\hat{R}(\Omega)$ the projector $\hat{P}_{\phi}$ onto this subspace cummutes with the all symmetry operators $\hat{R}(\Omega)$. In other words, there exists a function $f(\Omega)$ which minimizes the energy and causes $|\psi\rangle$ (see (N.3)) to have the proper symmetry.

If the weight function $f(\Omega)$ in (N.3) is determined by the variation priciple discussed above the corresponding wave functions $|\,\psi\rangle$ from the "coollective"

[1] It is necessary to note that for the non Abelian groups the argument $(-\Omega+\Omega^{''})$ depends on the ordening and means the order of parameters $-\Omega$ and $\Omega^{''}$ correspondingly to the transformation $\hat{R}^{-1}(\Omega)\hat{R}(\Omega^{''})$.

subspace can be considered as the system wave functions for which the symmetry of the system Hamiltonian (given by the condition $\hat{R}^{-1}(\Omega)\hat{H}\hat{R}(\Omega) = \hat{H}$ for all Ω) violated by the function $|\phi\rangle$ is restored. So, in such a way obtained wave functions $|\,\psi\rangle$ span the physical Hilbert space of our system (nucleus).

N.2 Particle number projection (PNP)

The PNP is connected with the violation of the number of particle by the BCS function (6.28) which is the ground state of the quasiparticle mean field (see the subsection 6.2.2.). By other words, the particle number conservation, which is expressed as

$$\Big[\,\hat{H},\,\hat{N}\,\Big] = 0 \tag{N.5}$$

where $\hat{N}$ is the number of particle operator, is violated by the quasiparticle mean field which involves the pairing correlations. In the framework of the simple seniority model involving a single j- shell (see section 6.3) the pairing correlations are given by the effective pairing Hamiltonian (6.156), (6.169):

$$\hat{V}_{pair} = -G\,\hat{S}_{+}\hat{S}_{-} = -G\,\left(\hat{\vec{S}}\cdot\hat{\vec{S}} - \hat{S}_0^2 + \hat{S}_0\right) \tag{N.6}$$

where $\hat{\vec{S}} \equiv (\hat{S}_1, \hat{S}_2, \hat{S}_3)$ is the quasi-spin operators (see (6.167)) with corresponding quasi-spin step up and step down operators $\hat{S}_{\pm} = \hat{S}_1 \pm i\hat{S}_2$ and $\hat{S}_0 \equiv \hat{S}_3$ fulfilling the quasi-spin commutation relations (6.168). These commutation relations provide the eigen basis $|SS_0\rangle$ of eparators $\hat{S}^2$ amd $\hat{S}_3 = \hat{S}_0$ (see (6.171))

$$\begin{aligned}
&\hat{S}^2\,|SS_0\rangle = S(S+1)\,|SS_0\rangle \\
&\hat{S}_3\,|SS_0\rangle = S_0\,|SS_0\rangle \\
&\hat{S}_{\pm}\,|SS_0\rangle \equiv |SS_0 \pm 1\rangle
\end{aligned} \tag{N.7}$$

In the analogy with the standard orbital angular momentum projection operator $\hat{L}_3 = -i\frac{\partial}{\partial\varphi}$ (see (A.41)) the operator $\hat{S}_3 \equiv \hat{S}_0$ can be represented as

$$\hat{S}_3 = i\frac{\partial}{\partial\varphi_g} \tag{N.8}$$

where φ_g is the angle in the gauge space which is the analogue of the spherical coordinate angle φ in the standard space. So, the operator $\hat{S}_3$ represents the generator of rotations around the 3-d axis in the quasi-spin space (gauge

space). Such rotations are called gauge transormations and corresponding transformation operator is

$$\hat{R}(\varphi_g) = e^{i\varphi_g \hat{S}_3} \tag{N.9}$$

From the section 6.2 (expr. (6.170)) we know that the particle number operator $\hat{N}$ is related to $\hat{S}_3 = \hat{S}_0$:

$$\hat{N} = 2\,\hat{S}_3 + \Omega \tag{N.10}$$

where $\Omega = j + 1/2$ for the simple single j- shell seniority model. From the point of view of the gauge representation of operators $\hat{S}_3$ and $\hat{N}$ the Ω is a constant and the operation $\hat{N}$ is represented as (substitution from (N.8))

$$\hat{N} = 2i\frac{\partial}{\partial\varphi_g} + const \tag{N.11}$$

The eigen functions of the operator $\hat{S}_3 = i\frac{\partial}{\partial\varphi_g}$ are normalized exponents:

$$\phi_{S_0}(\varphi_g) = \frac{1}{2\pi} e^{-i\,S_0\,\varphi_g} \tag{N.12}$$

because

$$\hat{S}_3\,\phi_{S_0}(\varphi_g) = i\,\frac{\partial}{\partial\varphi_g}\,\phi_{S_0}(\varphi_g) = S_0\,\psi_{S_0}(\varphi_g) \tag{N.13}$$

and the same functions are eigenfunctions of the number of particle operator $\hat{N}$

$$\hat{N}\psi_n(\varphi_g) = 2\,i\,\frac{\partial}{\partial\varphi_g}\,\frac{1}{2\pi}\,e^{-i\,\frac{n}{2}\,\varphi_g} = n\,\phi_n(\varphi_g) \tag{N.14}$$

and a gauge rotation by angle φ_g round the third axis (see (N.9)) can be rewritten as

$$\hat{R}(\varphi_g) = e^{i\varphi_g \frac{\hat{N}}{2}} \tag{N.15}$$

These rotations for all possible gauge angles φ_g form the symmetry group connected with the symmetry (N.5) and we also have

$$\left[\hat{H},\ \hat{R}(\varphi_g)\right] = 0 \qquad\qquad \text{for all } \varphi_g \tag{N.16}$$

Comparing (N.16) with (N.2) we see that the role of Ω in (N.2) is now played by the gauge angle φ_g. Since the functions $\psi_n(\varphi_g) = \frac{1}{2\pi}e^{-i\varphi_g n/2}$ form the complete orthogonal basis in the space of functions of φ_g the weight function $f(\varphi_g)$ from (N.3) can be decomposed onto the basis of functions $\psi_n(\varphi_g)$:

$$f(\varphi_g) = \sum_n \psi_n(\varphi_g)\,g_n = \sum_n \frac{1}{2}\,e^{-i\varphi_g n/2}\,g_n \tag{N.17}$$

and the many body wave function $|\psi\rangle$ (see (N.3) reads

$$\begin{aligned}|\psi\rangle &= \int d\Omega\, f(\Omega)\, |\phi(\Omega)\rangle = \int d\Omega\, f(\Omega)\, \hat{R}(\Omega)\, |\phi\rangle = \\ &= \sum_n g_n \frac{1}{2} \int d\varphi_g\, e^{i\frac{\varphi_g}{2}(\hat{N}-n)}\, |\phi\rangle = \\ &= \sum_n g_n\, \hat{P}^{(n)}\, |\phi\rangle \end{aligned} \tag{N.18}$$

where

$$\hat{P}^{(n)} = \frac{1}{2\pi} \int_0^{2\pi} d\varphi_g\ e^{i\,\varphi_g\,(\hat{N}-n)} \tag{N.19}$$

is the projection operator onto the subspace of the total Hilbert space corresponding to the number of particle equal to n. The operator $\hat{P}^n$ is a projection operator in the mathematical sense ($(\hat{P}^{(n)})^2 = \hat{P}^{(n)},\ (\hat{P}^{(n)})^+ = \hat{P}$). To see this, we multiply $P^{(n)}$ from the left and from the right with the unity operator, expressed by a complete orthogonal set of wave functions $|N\alpha\rangle$ with the particle number N (α are other quantum numbers characterizing unambiguously given many-body state $|N\alpha\rangle$):

$$\begin{aligned}\hat{P}^{(n)} = &\sum_{\substack{N\alpha \\ N'\alpha'}} |N\alpha\rangle\langle N\alpha| \frac{1}{2\pi} \int_0^{2\pi} d\varphi\, e^{i\varphi(\hat{N}-n)}\, |N'\alpha'\rangle\langle N'\alpha'| = \\ = &\sum_{\substack{N\alpha \\ N'\alpha'}} |N\alpha\rangle\langle N\alpha| \frac{1}{2\pi} \int_0^{2\pi} d\varphi\, e^{i\varphi(N'-n)}\, |N'\alpha'\rangle\langle N'\alpha'| = \\ = &\sum_{\substack{N\alpha \\ N'\alpha'}} |N\alpha\rangle\langle N\alpha|N'\alpha'\rangle\langle N'\alpha'|\, \delta_{N'n} = \sum_\alpha |n\alpha\rangle\langle n\alpha| \end{aligned} \tag{N.20}$$

Since we are interested only in a wave function $|\psi\rangle$ with the proper nucleon number A, we find

$$g_n = 0 \qquad \text{for } n \neq A \tag{N.21}$$

with g_A normalization constant.

In the end of this section it is necessary to point out that in spite of the fact, that we introduced the number of particle operator as a derivative of the

gauge angle (see (N.11)) based on the simple quasi-spin model of the pairing correlations with the Hamiltonian (N.6), the final expressions (N.19), (N.21) valid for the general case when the used theory gives the many body wave function $|\phi\rangle$ violating the particle number conservation.

N.3 Angular momentum projection

As it was mentioned in the section N.1 we meet very often a situation when the HF or HFB mean field is deformed and therefore the mean field ground state $|\phi\rangle$ violates the rotational invariance of the total Hamiltonian (together with its many-particle eigenstates $|\psi\rangle$). Since the total Hamiltonian in the laboratory frame is invariant with respect to rotations the total angular momentum I is a good quantum number for its eigenstates $|\psi\rangle$. However, the angular momentum I cannot be a good quantum number for the deformed mean field gr. state $|\phi\rangle$. In order to obtain $|\psi\rangle$ from $|\phi\rangle$ we can use the projection method described in the section N.1 and project the state $|\phi\rangle$ onto the "collective" sub-space of the states $|\psi\rangle$ with good sharp value of the angular momentum. In this section we search for the corresponding projection operator.

In accordance with the recipe given in the section N.1 we start with the ansatz (N.3) where in the case of the group of rotations in the 3- dimensional space (symmetry group) the parameters Ω are represented by Euler angles, $\Omega \equiv (a, b, c)$ [2] and the group elements are rotation operators given by

$$\hat{R}(\Omega) = \boxed{\begin{array}{c}\text{see}\\(A.19)\end{array}} = e^{-ia\hat{J}_z} e^{-ib\hat{J}_y} e^{-ic\hat{J}_z} \tag{N.22}$$

Similarly as in (N.17) for the case of the projection onto the good number of particles also in the case of the ang. momentum projection the weight function $f(\Omega)$ in (N.3) can be expanded into a complete set of eigenfunctions of the corresponding symmetry operators $\hat{R}(\Omega)$ (see (N.22)) which are the Wigner functions $D^I_{MK}(\Omega)$ (see (A.21)). Taking into account the normalization of the Wigner D- functions (see (A.27)) the weight function $f(\Omega)$ reads:

$$f(\Omega) = f(a, b, c) = \frac{2I+1}{8\pi^2} \sum_{IMK} g_{IMK}\, D^I_{MK}(\Omega) \tag{N.23}$$

[2] Euler angles $a = \alpha$, $b = \beta$, $c = \gamma$ are defined in the appendix A (see the text below expr. (A.18)). In order to avoid a misunderstanding with other quantities denoted by Greek symbols α, β, γ in this section Euler angles are denoted by a, b, c.

and now expr. (N.3) has the following form (analogue of (N.18))

$$|\psi\rangle = \sum_{IMK} g_{IMK}\, \hat{P}^I_{MK}\, |\phi\rangle \tag{N.24}$$

with the projection operator (analogue of (N.19))

$$\hat{P}^I_{MK} = \frac{2I+1}{8\pi^2} \int d\Omega\, D^I_{MK}(\Omega)\, \hat{R}(\Omega) \tag{N.25}$$

and in the analogue with (N.20) we have

$$\begin{aligned}
\hat{P}^I_{MK} = & \sum_{\substack{M'\alpha' \\ M''\alpha''}} |IM'\alpha'\rangle\langle IM'\alpha'| \\
& \frac{2I+1}{8\pi^2} \int d\Omega\, D^I_{MK}(\Omega)\, \hat{R}(\Omega)\, |IM''\alpha''\rangle\langle IM''\alpha''| = \\
= & \boxed{\begin{array}{c}\text{see} \\ (A.21)\end{array}} = \\
= & \sum_{\substack{M'\alpha' \\ M''\alpha''}} |IM'\alpha'\rangle \int d\Omega\, D^I_{MK}(\Omega)\, D^{I*}_{M'M''}(\Omega)\, \langle IM''\alpha''| = \\
= & \boxed{\begin{array}{c}\text{see} \\ (A.27)\end{array}} = \sum_{\substack{M'\alpha' \\ M''\alpha''}} |IM'\alpha'\rangle \delta_{MM'}\delta_{KM''}\delta_{\alpha'\alpha''}\, \langle IM''\alpha''| = \\
= & \sum_{\alpha} |IM\alpha\rangle\langle IK\alpha|
\end{aligned} \tag{N.26}$$

where $|IM\alpha\rangle$ is a complete orthonormal set in the total Hilbert space and α characterize all quantum numbers besides the angular momentum quantum numbers I and M.

However, from (N.26) we see that $\hat{P}^I_{MK}$ are not projectors from the mathematical point of view (which is $\hat{P}^2 = \hat{P}$, $\hat{P}^+ = \hat{P}$). We only have the following

relations

$$\hat{P}^I_{MK}\,\hat{P}^{I'}_{M'K'} = \sum_{\alpha\alpha'} |IM\alpha\rangle\langle IK\alpha\,|\,I'M'\alpha'\rangle\langle I'K'\alpha'| =$$
$$= \sum_{\alpha} |IM\alpha\rangle\,\langle IK'\alpha|\,\delta_{II'}\,\delta_{KM'} = \delta_{II'}\,\delta_{KM'}\,\hat{P}^I_{MK'}$$
$$(\hat{P}^I_{MK})^+ = \sum_{\alpha} |IK\alpha\rangle\,\langle IM\alpha| = \hat{P}^I_{KM} \qquad \text{(N.27)}$$

We should also have in mind the assumption about the total Hamiltonian in lab. system to be rotational invariant. As a result of this assumption the total Hamiltonian eigenstates $|\psi^{IM}\rangle$ are simultaneously eigestates of the square of ang. momentum operator $\hat{I}^2$ and its projection $\hat{I}_z$ onto the z-axis of the lab. frame ($\hat{I}^2\,|\psi^{IM}\rangle = I(I+1)|\psi^{IM}\rangle$, $\hat{I}_z\,|\psi^{IM}\rangle = M\,|\psi^{IM}\rangle$). So, instead of the ansatz (N.24) we have to use the following general ansatz

$$|\psi^{IM}\rangle = \sum_K g^{(I)}_K\,\hat{P}^I_{MK}\,|\phi\rangle =$$
$$= \sum_K g^{(I)}_K\,\frac{2I+1}{8\pi^2}\int d\Omega\,D^I_{MK}(\Omega)\,\hat{R}(\Omega)\,|\phi\rangle \qquad \text{(N.28)}$$

In the special cases where the "internal" [3] wave function $|\phi\rangle$ has axial summetry, only the K- value K_0 contribute to the sum (N.28) and the coefficient $g^{(I)}_{K_0}$ is given by normalization. In general, however, we have to minimize the energy of the total Hamiltonian:

$$E^I_{proj} = \frac{\langle\psi^{IM}|\,\hat{H}\,|\psi^{IM}\rangle}{\langle\psi^{IM}\,|\,\psi^{IM}\rangle} = \frac{\sum_{kk'} g^{(I)*}_K\,g^{(I)}_{K'}\,h^I_{KK'}}{\sum_{KK'} g^{(I)*}_K\,g^{(I)}_{K'}\,n^I_{KK'}} \qquad \text{(N.29)}$$

with

$$h^I_{KK'} = \langle\phi|\,\hat{H}\,\hat{P}^I_{KK'}\,|\phi\rangle \quad , \qquad n^I_{KK'} = \langle\phi|\,\hat{P}^I_{KK'}\,|\phi\rangle \qquad \text{(N.30)}$$

which gives for $g^{(I)}_K$ the eigenvalue problem

$$\sum_{K'} h^I_{KK'}\,g^{(I)}_{K'} = E^I\,\sum_{K'} n^I_{KK'}\,g_{K'} \qquad \text{(N.31)}$$

It corresponds to a diagonalization of the Hamiltonian $\hat{H}$ in the space spanned by the nondiagonal system $\hat{P}^I_{MK}\,|\phi\rangle$.

[3] It should be pointed out the projection method discussed in this appendix as well as the Generalized Coordinate Method (GCM) discussed in the subsection 7.3.3.2.1 do not introduce any intrinsic non-rotating frame as in the appendix A. The connection between the "intrinsic" wave function $|\phi\rangle$ and the lab. wave function $|\psi\rangle$ is not given by a coordinate transformation, but by the GCM anstatz (N.3) or (N.24) or (N.28).

N.4 Projection before and after the variation

Up to now we have not specified the symmetry-violating internal wave function $|\phi\rangle$. Generally, there are two ways to determine this function.

(i) **Variation before the projection (VBP)**

In this case, at first, we minimize the energy $\langle\phi(\Omega)|\ \hat{H}\ |\phi(\Omega)\rangle$ using the variational principle (e.g. HF or HFB "intrinsic deformed" state for given Ω) :

$$\delta\frac{\langle\phi(\Omega)|\ \hat{H}\ |\phi(\Omega)\rangle}{\langle\phi(\Omega)\ |\ \phi(\Omega)\rangle} = 0 \tag{N.32}$$

and we obtain the solution $|\phi(\Omega)\rangle$ of this equation in the form of a superposition of eigenstates of the corresponding symmetry operator, for instance, of the angular momentum. Then we apply the projetor operator $\hat{P}^I$ onto the good value of the angular momentum I, and we get a wave function [4] (schematically)

$$|\psi^I\rangle = \hat{P}^I\ |\phi\rangle \tag{N.33}$$

which contains only components with the given ang. momentum I. The function $|\psi^I\rangle$ (e.g. (N.28)) is no longer a product wave function, but a complicated superposition of Slater determinants and it contains much more correlations than the function $|\phi\rangle$. Therefore, it has a lower energy expectation value and it is certainly a much better approximation of the exact wave function of the system (exact eigenfunction of the total Hamiltonian $\hat{H}$).

However, on the other hand side, the VBP is a relatively rough approximation. The variational equation (N.32) has to be solved only once (and from this point of view the VBP is simple) but this method does violates the total variational principle, because we do not vary the projected wave function $|\psi^I\rangle$ and it does not allow for changes of the self-consistent internal field within a rotational band.

(ii) **Variation after the projection (VAP)**

Here we use the proper variational principle

$$\delta\frac{\langle\psi^I|\ \hat{H}\ |\psi^I\rangle}{\langle\psi^I\ |\ \psi^I\rangle} = \delta\frac{\langle\phi(\Omega)|\ \hat{P}^I\ \hat{H}\ \hat{P}^I\ |\phi(\Omega)\rangle}{\langle\phi(\Omega)|\ \hat{P}^I\ \hat{P}^I\ |\phi(\Omega)\rangle} = 0 \tag{N.34}$$

[4] Here we give only a very qualitative discussion of the projection technique and the angular momentum I is used as an example, without going to the details of therotational group. The angular momentum can be replaced by any other symmetry operator.

which means the minimization is performed within projected wave functions and we have to minimize the expectation value of the projected Hamiltonian $\hat{P}^I \hat{H} \hat{P}^I$ within the set of symmetry violating functions $|\phi(\Omega)\rangle$.

In principle, this VAP method corresponds to a double variational GCM technique (see ??(4)) [5]

$$|\psi\rangle = \int d\vec{q}\, f(\vec{q})\, |\phi(\vec{q}\rangle \tag{N.35}$$

where the generalized coordinates $\vec{q}$ are identified with the parameters Ω of the symmetry group and the variation of the energy is performed with respect to both the weight function f and the generating function $|\phi\rangle$.

This method is certainly better in the comparison with the VBP, but it is also much more complicated. We must repeat the variation for each value of I again, and the operator $\hat{P}^I \hat{H} \hat{P}^I$ is a multi-body operator and $|\psi^I\rangle$ is multi-particle wave function (not only a product of the s.p. wave functions).

[5] To be more precise the VAP is equivalent to the VAMPIR method discussed in more details in the subsection .....

O. Sum rules of multipole strength functions

O.1 EWSR for isoscalar multipole operators

In this appendix at first we will discuss energy weighted sum rule (EWSR), $m_1(\hat{\mathscr{M}})$ (see (7.376)), for the isoscalar transition (excitation) single-particle operator $\hat{\mathscr{M}}$ (see (7.364))

$$\hat{\mathscr{M}}(\Delta T = 0) = \sum_{i=1}^{N} f(\vec{r}_i) + \sum_{i=1}^{Z} f(\vec{r}_i) \tag{O.1}$$

where in (7.364) $f(\vec{r}_i) = r_i^\lambda \, Y_{\lambda\mu}(\hat{r}_i)$. Further we suppose that this operator cummutes to zero with the interaction term $\hat{V}$ of the nuclear Hamiltonian $\hat{H}$, which is generally given by the sum of the kinetic energy term $\hat{T}$ and the interaction term $\hat{V}$ ($\hat{H} = \hat{T} + \hat{V}$), that means

$$\left[\hat{V},\, \hat{\mathscr{M}}\right] = 0 \tag{O.2}$$

This condition valids for a class of effective nucleon-nucleon interactions. This class of interaction, fulfilling (O.2), includes finite range interaction with exchange terms not depending on linear momentum (like Gogny interaction (3.148)) or the substantial part of the zero range current dependent Skyrme interaction (7.145). Even for effective nucleon-nucleon interactions for which equation (O.2) does not hold exactly the relative part of $\hat{V}$, which violates (O.2), gives the contribution to EWSR value $m_1(\hat{\mathscr{M}})$ which is usually negligible and can be ignored in the discussion of physical effects. Condition (O.2) is often called the local Galilean invariance.

The condition (O.2) implies the m_1 sum rule becomes

$$m_1(\hat{\mathscr{M}}(\Delta T=0)) = \boxed{\begin{array}{c}\text{see}\\(7.377)\end{array}} = \frac{1}{2}\,\langle 0|\,\big[\hat{\mathscr{M}}^+,\,[\hat{T},\,\hat{\mathscr{M}}\,]\,\big]\,|\,0\rangle =$$

$$= \frac{1}{2}\sum_{i=1}^{A}\langle 0|\,\hat{\mathscr{M}}^+\hat{T}\hat{\mathscr{M}} - \hat{T}\hat{\mathscr{M}}\hat{\mathscr{M}}^+ - \hat{\mathscr{M}}^+\hat{\mathscr{M}}\,\hat{T} + \hat{\mathscr{M}}\,\hat{T}\hat{\mathscr{M}}^+\,|\,0\rangle =$$

$$= -\frac{1}{2}\sum_i \frac{\hbar^2}{2m_i}\,\langle 0|\,\hat{\mathscr{M}}^+\vec{\nabla}_i^2\hat{\mathscr{M}} - \vec{\nabla}_i^2\hat{\mathscr{M}}^+\hat{\mathscr{M}} - \hat{\mathscr{M}}^+\hat{\mathscr{M}}\,\vec{\nabla}_i^2 +$$

$$+\,\hat{\mathscr{M}}\,\vec{\nabla}_i^2\hat{\mathscr{M}}^+\,|\,0\rangle =$$

$$= \sum_{i=1}^{A}\frac{\hbar^2}{2m_i}\langle 0|\,\big(\vec{\nabla}_i\hat{\mathscr{M}}^+\big)\,\big(\vec{\nabla}_i\hat{\mathscr{M}}\big)\,|\,0\rangle =$$

$$= \frac{\hbar^2}{2m}\sum_{i=1}^{A}\langle 0|\,\big(\vec{\nabla}_i f^+(\vec{r}_i)\big)\,\big(\vec{\nabla}_i f(\vec{r}_i)\big)\,|\,0\rangle \qquad (O.3)$$

For the electric type isoscalar multipole operator $\hat{\mathscr{M}}^{(el)}_{\lambda\mu}(\Delta T=0) = \sum_i f(\vec{r}_i) = \sum_i g(r_i)Y_{\lambda\mu}(\hat{r}_i)$ (see (7.364) we have $(f_{\lambda\mu}(\vec{r}_i) = g(r_i)Y_{\lambda\mu}(\hat{r}_i))$

$$\vec{\nabla} f_{\lambda\mu}(\vec{r}) = \vec{\nabla} g(r)Y_{\lambda\mu}(\hat{r}) = \boxed{\begin{array}{c}\text{see}\\(A.62)\end{array}} =$$

$$= \sqrt{\frac{\lambda}{2\lambda+1}}\big[\frac{dg}{dr} + \frac{\lambda+1}{r}g\big]\vec{Y}_{\lambda-1\,\lambda\,\mu}(\hat{r})$$

$$-\sqrt{\frac{\lambda+1}{2\lambda+1}}\big[\frac{dg}{dr} - \frac{\lambda}{r}g\big]\vec{Y}_{\lambda+1\,\lambda\,\mu}(\hat{r}) \qquad (O.4)$$

and

$$\sum_{\mu=-\lambda}^{+\lambda}\big(\vec{\nabla} f^+_{\lambda\mu}(\vec{r})\big)\,\big(\vec{\nabla} f_{\lambda\mu}(\vec{r})\big) = \boxed{\begin{array}{c}\text{because (see [2] p.221, rel.(81))}\\ \sum_\lambda \vec{Y}^+_{l\lambda\mu}(\hat{r})\cdot\vec{Y}_{l'\lambda\mu}(\hat{r}) = \frac{2\lambda+1}{4\pi}\,\delta_{ll'}\end{array}} =$$

$$= \frac{\lambda}{2\lambda+1}\big[\frac{dg}{dr} + \frac{\lambda+1}{r}g\big]^2\frac{2\lambda+1}{4\pi} +$$

$$+\frac{\lambda+1}{2\lambda+1}\big[\frac{dg}{dr} - \frac{\lambda}{r}g\big]^2\frac{2\lambda+1}{4\pi} =$$

$$= \frac{2\lambda+1}{4\pi}\big[\,\big(\frac{dg}{dr}\big)^2 + \lambda(\lambda+1)\frac{g^2}{r^2}\,\big] \qquad (O.5)$$

So we have for the EWSR

$$\sum_{\mu=-\lambda}^{+\lambda} m_1(\hat{\mathscr{M}}^{(el)}_{\lambda\mu}(\Delta T=0)) = \boxed{\begin{array}{c}\text{see}\\(O.3)\end{array}} =$$

$$= \frac{\hbar^2}{2m}\sum_{i=1}^{A}\langle 0|\sum_{\mu=-\lambda}^{+\lambda}\left(\vec{\nabla}_i f_{\lambda\mu}(\vec{r}_i)\right)\left(\vec{\nabla}_i f_{\lambda\mu}(\vec{r}_i)\right)|\,0\rangle = \boxed{\begin{array}{c}\text{see}\\(O.5)\end{array}} =$$

$$= \frac{\hbar^2}{2m}\,\frac{2\lambda+1}{4\pi}\int d^3r\,\rho(\vec{r})\,\Big[\,\Big(\frac{dg}{dr}\Big)^2+\lambda(\lambda+1)\,\frac{g^2}{r^2}\,\Big] \qquad (O.6)$$

where nucleon density $\rho(\vec{r})$ is normalized as:

$$\int d^3r\,\rho(\vec{r}) = \int d^3r\,\langle 0|\sum_i \delta(\vec{r}-\vec{r}_i)\,|\,0\rangle = A \qquad (O.7)$$

That means in the spherical case for one projection μ the corresponding EWSR is:

$$m_1(\hat{\mathscr{M}}^{(el)}_{\lambda\mu}(\Delta T=0)) = \frac{\hbar^2}{8\pi m}\int d^3r\,\rho(\vec{r})\,\Big[\,\Big(\frac{dg}{dr}\Big)^2+\lambda(\lambda+1)\,\frac{g^2}{r^2}\,\Big] \qquad (O.8)$$

Expressions (O.3) - (O.6) for EWSR valid for laboratory frame where the motion of the nucleus center of mass is not extracted (for the simplicity we suppose now that the nucleus is spherical without a rotation). The elimination of the spurious modes connected with the center of mass motion is discussed in the end of the Subsection 7.3.1.1.2. In the paper [53] (see the relation (6.11) therein) it is shown that the most of the effects due to the center of mass motion can be accounted by working with the kinetic energy operator in the following form [1]

$$\hat{T} = \frac{1}{2m}\sum_i \hat{\vec{p}}_i^{\,2} - \frac{1}{2mA}\Big(\sum_{i=1}^{A}\hat{\vec{p}}_i\Big)^2 \qquad (O.9)$$

and employing laboratory coordinates. So, the expression (O.3) should be modified by using of (O.9) instead of the standard kinetic energy operator

[1] Let us consider the system (nucleus) consisting from $i=1,\ldots,A$ identical particles, each with the mass m and with the coordinates $\vec{r}_i$ in the laboratory frame. The coordinates $\vec{R}$ and the linear momentum $\hat{\vec{P}}$ of the system center of mass in the laboratory frame are

$$\vec{R} = \frac{1}{A}\sum_{i=1}^{A}\vec{r}_i \qquad , \qquad \hat{\vec{P}} = -i\hbar\,\frac{\partial}{\partial\vec{R}}$$

$\frac{1}{2m}\sum_{i=1}^{A}\hat{\vec{p}}_i^{\,2}$. Then we have

$$
\begin{aligned}
\big[\hat{T},\,\hat{\mathscr{M}}\big] &= \boxed{\begin{array}{c}\text{see}\\ (O.9)\end{array}} = \\
&= \frac{1}{2m}\sum_{ik}\big[\hat{\vec{p}}_i^{\,2},\,f(\vec{r}_k)\,\big] - \frac{1}{2mA}\,\big[\big(\sum_i \hat{\vec{p}}_i\big)^2,\,\sum_k f(\vec{r}_k)\,\big] = \\
&= \frac{1}{2m}\sum_{ik}\Big\{\hat{\vec{p}}_i\,\big[\hat{\vec{p}}_i,\,f(\vec{r}_k)\,\big] + \big[\hat{\vec{p}}_i,\,f(\vec{r}_k)\,\big]\,\hat{\vec{p}}_i\,\Big\} \\
&\qquad -\frac{1}{2mA}\,\Big\{\big(\sum_i \hat{\vec{p}}_i\big)\,\big[\big(\sum_j \hat{\vec{p}}_j\big),\,\sum_k f(\vec{r}_k)\,\big] + \\
&\qquad\qquad + \big[\big(\sum_i \hat{\vec{p}}_i\big),\,\sum_k f(\vec{r}_k)\,\big]\,\big(\sum_j \hat{\vec{p}}_j\big)\,\Big\} = \\
&= \boxed{\begin{array}{c}\text{because}\\ \hat{\vec{p}}_i = -i\hbar\vec{\nabla}_i\,;\quad [\hat{\vec{p}}_i,\,f(\vec{r}_k)\,] = \delta_{ik}\,(\vec{\nabla} f(\vec{r}_i))\end{array}} =
\end{aligned}
$$

Coordinates of the i-th particle in the CoM frame are given as follows

$$
\begin{aligned}
&\vec{x}_i = \vec{r}_i - \frac{1}{A}\sum_{i=1}^{A}\vec{r}_i \qquad \text{or} \qquad \vec{r}_i = \vec{x}_i + \vec{R} \\
&\quad\Rightarrow \\
&-i\hbar\,\frac{\partial}{\partial\vec{r}} = -i\hbar\sum_{j=1}^{A}\big(\frac{\partial\vec{x}_j}{\partial\vec{r}_i}\big)\frac{\partial}{\partial\vec{x}_j} - i\hbar\,\big(\frac{\partial\vec{R}}{\partial\vec{r}_i}\big)\frac{\partial}{\partial\vec{R}} = -i\hbar\sum_{i=1}^{A}\big[\,\delta_{ij} - \frac{1}{A}\sum_{l=1}^{A}\big(\frac{\partial\vec{r}_l}{\partial\vec{r}_i}\big)\,\big]\frac{\partial}{\partial\vec{x}_j} - i\hbar\,\frac{1}{A}\frac{\partial}{\partial\vec{R}} = \\
&\quad = \hat{\vec{p}}_i - \frac{1}{A}\sum_{i=1}^{A}\hat{\vec{p}}_j + \frac{1}{A}\,\hat{\vec{P}}
\end{aligned}
$$

where $\hat{\vec{p}}_i = -i\hbar\,\frac{\partial}{\partial\vec{x}_i}$ is the linear momentum operator of the i-th particle in the CoM frame. Then the Hamiltonian in the laboratory frame is

$$
\begin{aligned}
\hat{H} &= -\frac{\hbar^2}{2m}\sum_{i=1}^{A}\big(\frac{\partial}{\partial\vec{r}}\big)^2 + V = \frac{1}{2m}\sum_{i=1}^{A}\big[\,\frac{1}{A}\,\hat{\vec{P}} + \hat{\vec{p}}_i - \frac{1}{A}\sum_{j=1}^{A}\hat{\vec{p}}_j\,\big]^2 + V = \\
&= \frac{\hat{\vec{P}}^2}{2Am} + \sum_{i=1}^{A}\frac{\hat{\vec{p}}_i^{\,2}}{2m} - \frac{1}{2Am}\,\big(\sum_{j=1}^{A}\hat{\vec{p}}_j\big)^2 + V = \frac{\hat{\vec{P}}^2}{2Am} + \hat{H}_{intr}
\end{aligned}
$$

where $\hat{H}_{intr} = \hat{T} + \hat{V}$ with $\hat{T} = \frac{1}{2m}\sum_{i=1}^{A}\hat{\vec{p}}_i^{\,2} - \frac{1}{2Am}\,\big(\sum_{i=1}^{A}\hat{\vec{p}}_i\big)^2$.

$$= -\frac{1}{2m}\Big\{\sum_i \hat{\vec{p}}_i \cdot \big(\vec{\nabla}_i f(\vec{r}_i)\big) + \sum_i \big(\vec{\nabla}_i f(\vec{r}_i)\big) \cdot \hat{\vec{p}}_i\Big\} +$$
$$+\frac{i\hbar}{2mA}\Big\{\big(\sum_i \hat{\vec{p}}_i\big) \cdot \big(\sum_j (\vec{\nabla}_j f(\vec{r}_j))\big) +$$
$$+\big(\sum_j (\vec{\nabla}_j f(\vec{r}_j))\big) \cdot \big(\sum_i \hat{\vec{p}}_i\big)\Big\} \qquad \text{(O.10)}$$

and finally

$$m_1(\hat{\mathscr{M}}(\Delta T = 0)) = \frac{1}{2}\,\langle 0|\,\big[\hat{\mathscr{M}}^+,\,[\hat{T},\,\hat{\mathscr{M}}\,]\,\big]\,|\,0\rangle =$$
$$= -\frac{ih}{4m}\,\langle 0|\,\big[\sum_k f^+(\vec{r}_k),\,\sum_i \hat{\vec{p}}_i \cdot \big(\vec{\nabla}_i f(\vec{r}_i)\big) + \sum_i \big(\vec{\nabla}_i f(\vec{r}_i)\big) \cdot \hat{\vec{p}}_i\,\big]\,|\,0\rangle$$
$$+\frac{ih}{4mA}\,\langle 0|\,\Big[\sum_k f^+(\vec{r}_k),\,\big(\sum_i \hat{\vec{p}}_i\big) \cdot \big(\sum_j (\vec{\nabla}_j f(\vec{r}_j))\big) +$$
$$+\big(\sum_j (\vec{\nabla}_j f(\vec{r}_j))\big) \cdot \big(\sum_i \hat{\vec{p}}_i\big)\,\Big]\,|\,0\rangle =$$

$$= \frac{\hbar^2}{2m}\,\langle 0|\,\sum_i \big(\vec{\nabla}_i\, f^+(\vec{r}_i)\big) \cdot \big(\vec{\nabla}_i\, f(\vec{r}_i)\big)\,|\,0\rangle$$
$$-\frac{\hbar^2}{2mA}\,\langle 0|\,\big(\sum_i (\vec{\nabla}_i\, f^+(\vec{r}_i))\big) \cdot \big(\sum_k (\vec{\nabla}_k\, f(\vec{r}_k))\big)\,|\,0\rangle \qquad \text{(O.11)}$$

Simpler result can be obtained neglecting the effects caused by the antisymmetrization and correlations in the calculation of the second term in (O.11). With such approximation the $m_1(\hat{\mathscr{M}})$ sum rule becomes (see [53])

$$m_1(\hat{\mathscr{M}}(\Delta T = 0)) = \frac{\hbar^2}{2m}\,\langle 0|\,\sum_i \big(\vec{\nabla}_i\, f^+(\vec{r}_i)\big) \cdot \big(\vec{\nabla}_i\, f(\vec{r}_i)\big)\,|\,0\rangle$$
$$-\frac{\hbar^2}{2mA}\,\langle 0|\,\sum_i \big(\vec{\nabla}_i\, f^+(\vec{r}_i)\big)\,|\,0\rangle \cdot \langle 0|\,\sum_k \big(\vec{\nabla}_k\, f^+(\vec{r}_k)\big)\,|\,0\rangle =$$
$$= \frac{\hbar^2}{2m}\,\Big\{\int d^3r\,\big|\vec{\nabla} f(\vec{r})\big|^2\,\rho(\vec{r}) - \frac{1}{A}\,\Big|\int d^3r\,\big(\vec{\nabla} f(\vec{r})\big)\,\rho(\vec{r})\,\Big|^2\,\Big\} \qquad \text{(O.12)}$$

Further the EWSR $m_1(\hat{\mathscr{M}})$ is specified for electric isoscalar multipole operators.

i) Operator $\hat{\mathscr{M}}^{(el)}_{1\mu}(\Delta T=0)=\sum_{k=1}^{A} r_k Y_{1\mu}(\hat{r}_k)$

In this case we have $f(\vec{r})=rY_{1\mu}(\hat{r})$ and $g(r)=r$. The first term in (O.12) for the operator $\sum_{\mu=-1}^{+1}\hat{\mathscr{M}}^{(el)}_{1\mu}(\Delta T=0)$ is given by:

$$\frac{\hbar^2}{2m}\sum_{\mu=-1}^{+1}\langle 0|\sum_{i=1}^{A}\left(\vec{\nabla}_i r_i Y_{1\mu}(\hat{r}_i)\right)^{+}\cdot\left(\vec{\nabla}_i r_i Y_{1\mu}(\hat{r}_i)\right)|\,0\rangle=\boxed{\begin{array}{c}\text{see}\\(O.6)\end{array}}=$$
$$=\frac{\hbar^2}{8\pi m}\,9\int d^3r\rho(\vec{r})=\frac{9\hbar^2}{8\pi m}\,A \tag{O.13}$$

For the determination of the second term in (O.12) at first the expression for $\vec{\nabla}rY_{1\mu}(\hat{r})$ should be specified

$$\vec{\nabla}rY_{1\mu}(\hat{r})=\boxed{\begin{array}{c}\text{see}\\(O.4)\end{array}}=\sqrt{\frac{1}{3}}\,3\,\vec{Y}_{01\mu}(\hat{r})-\sqrt{\frac{2}{3}}\,(1-1)\,\vec{Y}_{21\mu}(\hat{r})=$$
$$=\sqrt{3}\,\vec{Y}_{01\mu}(\hat{r})=\boxed{\begin{array}{c}\text{see}\\(A.53)\end{array}}=\sqrt{3}\,C^{1\,\mu}_{00\,1\mu}Y_{00}(\hat{r})\,\vec{\xi}_\mu=\sqrt{\frac{3}{4\pi}}\,\vec{\xi}_\mu \tag{O.14}$$

and the second term in (O.12) for $\sum_{\mu=-1}^{1}\hat{\mathscr{M}}^{(el)}_{1\mu}(\Delta T=0)$ is

$$-\frac{\hbar^2}{2mA}\sum_{\mu=-1}^{1}\langle 0|\sum_{i}\left(\vec{\nabla}_i r_i Y_{1\mu}(\hat{r})\right)^{+}|\,0\rangle\cdot\langle 0|\sum_{i}\left(\vec{\nabla}_i r_i Y_{1\mu}(\hat{r})\right)|\,0\rangle=$$
$$=-\frac{\hbar^2}{2mA}\sum_{\mu=-1}^{1}\Big|\int d^3r\,\rho(\vec{r})\sqrt{\frac{3}{4\pi}}\,\vec{\xi}_\mu\Big|^2=\boxed{\begin{array}{c}\text{because}\\\vec{\xi}^{+}_\mu\cdot\vec{\xi}_\mu=1\end{array}}=$$
$$=-\frac{\hbar^2}{2mA}\frac{9}{4\pi}A^2=-\frac{9\hbar^2}{8\pi m}A \tag{O.15}$$

So the EWSR value for the operator $\sum_{\mu=-1}^{1}\hat{\mathscr{M}}^{(el)}_{1\mu}(\Delta T=0)$ is zero

$$m_1\Big(\sum_{\mu=-1}^{1}\hat{\mathscr{M}}^{(el)}_{1\mu}(\Delta T=0)\Big)=0 \tag{O.16}$$

ii) Operator $\hat{\mathscr{M}}^{(el)}_{com\,1\mu}(\Delta T=0)=\sum_{k=1}^{A} r_k^3\,Y_{1\mu}(\hat{r}_k)$

This transition operator is incorrectly called in literature isoscalar dipole transition operator. More precise name is compression electric dipole transition operator. It is also known as squeezed dipole operator. For this operator we have $f(\vec{r}) = r^3\, Y_{1\mu}(\hat{r})$ and $g(r) = r^3$. The first term in (O.12) for the operator $\sum_{\mu=-1}^{1} \hat{\mathscr{M}}^{(el)}_{com\,1\mu}(\Delta T = 0)$ is

$$\frac{\hbar^3}{2m} \sum_{\mu=-1}^{+1} \langle 0| \sum_{i=1}^{A} \left(\vec{\nabla}_i\, r_i^3 Y_{1\mu}(\hat{r}_i)\right)^+ \cdot \left(\vec{\nabla}_i\, r_i^3 Y_{1\mu}(\hat{r}_i)\right) | \, 0\rangle = \boxed{\begin{array}{c}\text{see}\\ (O.5)\end{array}} =$$

$$= \frac{3\hbar^2}{8\pi m}\, 11 \int d^3r\, r^4\, \rho(\vec{r}) = \frac{3 \cdot 11\, \hbar^2}{8\pi m}\, A\, \langle r^4 \rangle_A \qquad \text{(O.17)}$$

where $\langle r^n \rangle_A$ is the single-particle expectation value:

$$\langle r^n \rangle_A \equiv \frac{1}{A} \int d^3r\, r^n\, \rho(\vec{r}) \qquad \text{(O.18)}$$

We also have

$$\vec{\nabla}\, r^3 Y_{1\mu}(\hat{r}) = \boxed{\begin{array}{c}\text{see}\\ (O.4)\end{array}} = \sqrt{\frac{1}{3}}\, 5\, r^2\, \vec{Y}_{01\mu}(\hat{r}) - \sqrt{\frac{2}{3}}\, 2\, r^2\, \vec{Y}_{21\mu}(\hat{r}) =$$

$$= \frac{5}{\sqrt{3}}\, r^2\, \frac{1}{\sqrt{4\pi}}\, \vec{\xi}_\mu - \frac{2\sqrt{2}}{\sqrt{3}}\, r^2\, \vec{Y}_{21\mu}(\hat{r})$$

$$\Rightarrow$$

$$\langle 0| \sum_{i=1}^{A} \vec{\nabla}\, r_i^3 Y_{1\mu}(\hat{r}_i) \, | \, 0\rangle =$$

$$= \int d^3r \left(\frac{5}{\sqrt{3}}\, r^2\, \frac{1}{\sqrt{4\pi}}\, \vec{\xi}_\mu - \frac{2\sqrt{2}}{\sqrt{3}}\, r^2\, \vec{Y}_{21\mu}(\hat{r})\right) \rho(\vec{r}) =$$

$$= \boxed{\begin{array}{c}\text{because - see [2], p.148, exp. (1)}\\ \int d\Omega\, Y_{lm}(\hat{r}) = \sqrt{4\pi}\, \delta_{l0}\, \delta_{m0}\end{array}} =$$

$$= \frac{5}{\sqrt{12\pi}}\, \vec{\xi}_\mu \int d^3r\, r^2\, \rho(\vec{r}) = \frac{5}{\sqrt{12\pi}}\, \vec{\xi}_\mu\, A\, \langle r^2 \rangle_A \qquad \text{(O.19)}$$

So the second term in (O.12) for the operator $\sum_{\mu=-1}^{+1} \hat{\mathscr{M}}^{(el)}_{com\,1\mu}(\Delta T=0)$ is

$$-\frac{\hbar^2}{2mA}\sum_{\mu=-1}^{1}\langle 0|\sum_i \left(\vec{\nabla}_i\, r_i^3 Y_{1\mu}(\hat{r})\right)^+ |\,0\rangle\cdot\langle 0|\sum_i \left(\vec{\nabla}_i\, r_i^3 Y_{1\mu}(\hat{r})\right)|\,0\rangle =$$

$$= \boxed{\begin{array}{c}\text{see (O.19) and because}\\ \vec{\xi}^{+}_{\mu}\cdot\vec{\xi}_{\mu}=1\end{array}} = -\frac{25\cdot 3}{3}\,\frac{\hbar^2}{8\pi mA}\,A^2\,\langle r^2\rangle_A^2 \tag{O.20}$$

and the EWSR value for the operator $\sum_{\mu=-1}^{+1}\hat{\mathscr{M}}^{(el)}_{com\,1\mu}(\Delta T=0)$ given by (O.12) is

$$m_1\Big(\sum_{\mu=-1}^{1}\hat{\mathscr{M}}^{(el)}_{com\,1\mu}(\Delta T=0)\Big) = \\ = \frac{3\hbar^2}{8\pi m}\,A\left\{\,11\,\langle r^4\rangle_A - \frac{25}{3}\,\langle r^2\rangle_A^2\,\right\} \tag{O.21}$$

iii) Operator $\hat{\mathscr{M}}^{(el)}_{\lambda\mu}(\Delta T=0)=\sum_{k=1}^{A} r_k^{\lambda}\,Y_{1\mu}(\hat{r}_k)$ for $\lambda>1$

In this case the second term in (O.12) is zero because $\vec{\nabla}\,r^{\lambda}\,Y_{\lambda\mu}(\hat{r})$ involves $\vec{Y}_{l\lambda\mu}(\hat{r})$ for $l=\lambda\pm 1$, $l>0$ and then for spherically symmetric case we always have $\int d^3r\;\rho(\vec{r})\;\vec{Y}_{l\lambda\mu}(\hat{r})=0$ and therefore $\langle 0|\sum_i r_i^{\lambda}\,Y_{\lambda\mu}(\hat{r}_i)\,|\,0\rangle=0$. So the EWSR value for the operator $\sum_{\mu=-1}^{+1}\hat{\mathscr{M}}^{(el)}_{\lambda\mu}(\Delta T=0)$ for $\lambda>1$ is given only by the first term in (O.12):

$$m_1\Big(\sum_{\mu=-\lambda}^{+\lambda}\hat{\mathscr{M}}^{(el)}_{\lambda\mu}(\Delta T=0)\Big) = \frac{\hbar^2}{2m}\sum_{\mu=-\lambda}^{+\lambda}\int d^3r\;\rho(\vec{r})\left|\vec{\nabla}\,r^{\lambda}\,Y_{\lambda\mu}(\hat{r})\right|^2 =$$

$$= \boxed{\begin{array}{c}\text{see}\\ \text{(O.5)}\end{array}} = \frac{\hbar^2}{2m}\int d^3r\;\rho(\vec{r})\,\frac{(2\lambda+1)^2\lambda}{4\pi}\,r^{2\lambda-2} =$$

$$= \frac{\hbar^2}{8\pi m}\,(2\lambda+1)^2\,\lambda\,A\,\langle r^{2\lambda-2}\rangle_A \tag{O.22}$$

Expressions (O.20). (O.21) and (O.22) concerned isoscalar multipole electric transition operators where the total isoscalar density $\rho(\vec{r})=\rho_n(\vec{r})+\rho_p(\vec{r})$ was used and corresponding $\langle r^n\rangle_A$ values were calculated with this total nucleon density (see (O.18)). However, these expressions (O.20). (O.21) and

(O.22) can be used also for the determination of the EWSR for true electromagnetic transitions connected with the transition operators $\hat{\mathscr{M}}^{(el)}_{\lambda\mu}(\delta T = p)$ - see (7.367), (7.368) where instead of the total nucleon density only proton density as charge density participates, only instead of the total density expectation values $\langle r^n \rangle_A$ (see (O.18) the proton density expectation values

$$\langle r^n \rangle_Z = \frac{1}{Z} \int d^3r \, \rho_p(\vec{r}) \, r^n \tag{O.23}$$

should be used in (O.20). (O.21) and (O.22).

In this subsection we do not discuss the EWSR values of magnetic type transitions. The derivation of the corresponding moments of strength functions of magnetic transitions can be found e.g. in [181, 53] and citations therein.

It should be reminded here that the EWSR expressions for electric isoscalar multipole operators (O.12) - (O.22) valid only in the case when the total Gallilean invariance condition (O.2) is fulfilled by the transition multipole operator. This is the case of the Gogny effective nucleon-nucleon interaction. In [53] it is shown that it is alo fulfilled with a good approximation for the Skyrme effective nucleon-nucleon interaction (in spite of the fact that the Skyrme interaction violates the condition (O.2)). In the next subsections the EWSR values for isovector electric transition multipole operators are discussed.

O.2 EWSR for isovector multipole operators

We consider one- body isovector excitation operator (for the simplicity no spin dependent). In the coordinate representation such transition isovector operator can be writte as (see the footnote under the (7.364))

$$\hat{\mathscr{M}}(\Delta T = 1) = \sum_{i=1}^{A} f(\vec{r}_i) \, (\hat{t}_z)_i = \boxed{\begin{array}{c}\text{because - see (1.15)} \\ (t_z)_n = 1/2, \quad (t_z)_p = -1/2\end{array}} =$$

$$= \frac{1}{2} \sum_{i=1}^{N} f(\vec{r}_i) - \frac{1}{2} \sum_{i=1}^{Z} f(\vec{r}_i) \equiv \hat{\mathscr{M}}_n - \hat{\mathscr{M}}_p \tag{O.24}$$

In this case the local Gallilean invariance condition (O.2) does not valid

$$\left[\hat{V}.\,\hat{\mathscr{M}}(\Delta T=1)\right]\neq 0 \tag{O.25}$$

even for the effective nucleon-nucleon interaction $\hat{V}$ not involving velocity dependent terms. So, opposite to the isoscalar case, now we should consider also the contribution to $m_1(\hat{\mathscr{M}}(\Delta T=1)$ going from the effective interaction $\hat{V}$. According to (7.376) we have

$$\begin{aligned} m_1\big(\hat{\mathscr{M}}(\Delta T=1)\big) &= \frac{1}{2}\,\langle 0|\,\big[\hat{\mathscr{M}}^{+}(\Delta T=1),\,[\,\hat{H},\,\hat{\mathscr{M}}(\Delta T=1)\,]\,\big]\,|\,0\rangle = \\ &= \frac{1}{2}\Big\{\langle 0|\,\big[\hat{\mathscr{M}}^{+}(\Delta T=1),\,[\,\hat{T},\,\hat{\mathscr{M}}(\Delta T=1)\,]\,\big]\,|\,0\rangle + \\ &\qquad +\langle 0|\,\big[\hat{\mathscr{M}}^{+}(\Delta T=1),\,[\,\hat{V},\,\hat{\mathscr{M}}(\Delta T=1)\,]\,\big]\,|\,0\rangle\Big\} = \\ &= \frac{1}{2}\,\langle 0|\,\big[\hat{\mathscr{M}}^{+}(\Delta T=1),\,[\,\hat{T},\,\hat{\mathscr{M}}(\Delta T=1)\,]\,\big]\,|\,0\rangle\,\Big(\,1+\mathscr{K}\,\Big) \end{aligned} \tag{O.26}$$

where we have introduced a factor $\mathscr{K}$ which characterizes the relative contribution of the nucleon-nucleon interaction to the energy weighted sum rule:

$$\mathscr{K}=\frac{\langle 0|\,\big[\hat{\mathscr{M}}^{+}(\Delta T=1),\,[\,\hat{V},\,\hat{\mathscr{M}}(\Delta T=1)\,]\,\big]\,|\,0\rangle}{\langle 0|\,\big[\hat{\mathscr{M}}^{+}(\Delta T=1),\,[\,\hat{T},\,\hat{\mathscr{M}}(\Delta T=1)\,]\,\big]\,|\,0\rangle} \tag{O.27}$$

and the EWSR value $m_1(\hat{\mathscr{M}}(\Delta T=1))$ is the sum of the kinetic energy and the interaction parts:

$$m_1\big(\hat{\mathscr{M}}(\Delta T=1)\big)=m_1^{(kin)}\big(\hat{\mathscr{M}}(\Delta T=1)\big)+m_1^{(\hat{V})}\big(\hat{\mathscr{M}}(\Delta T=1)\big) \tag{O.28}$$

Further the kinetic energy part of $m_1(\hat{\mathscr{M}}(\Delta T=1))$ will be determined:

$$m_1^{(kin)}\big(\hat{\mathscr{M}}(\Delta T=1)\big)=\frac{1}{2}\,\langle 0|\,\big[\hat{\mathscr{M}}^{+}(\Delta T=1),\,[\,\hat{T},\,\hat{\mathscr{M}}(\Delta T=1)\,]\,\big]\,|\,0\rangle \tag{O.29}$$

where, similarly as in the isoscalar case, the kinetic energy operator $\hat{T}$ is taken in the form (O.9) (that means assumed intrinsic kinetic energy). Similarly

as in (O.10) and (O.11) we obtain

$$\begin{aligned}\big[\hat{T},\, \hat{\mathscr{M}}(\Delta T=1)\,\big] &= \frac{1}{2m}\,\big[\,\sum_i \hat{\vec{p}}_i^{\,2},\, \sum_k f(\vec{r}_k)\,(\hat{t}_z)_k\,\big] = \\ &= -\frac{i\hbar}{2m}\,\Big\{\sum_{i=1}^{A}\hat{\vec{p}}_i\,\big(\vec{\nabla}_i\, f(\vec{r}_i)\,(\hat{t}_z)_i\big) + \sum_{i=1}^{A}\big(\vec{\nabla}_i\, f(\vec{r}_i)\,(t_z)_i\big)\,\hat{\vec{p}}_i\,\Big\} + \\ &\quad + \frac{i\hbar}{2mA}\,\Big\{\big(\sum_i \hat{\vec{p}}_i\big)\cdot\Big(\sum_j\big(\vec{\nabla}_j\, f(\vec{r}_j)\,(\hat{t}_z)_j\big)\Big) + \\ &\qquad + \Big(\sum_j\big(\vec{\nabla}_j\, f(\vec{r}_j)\big)\,(\hat{t}_z)_j\Big)\cdot\big(\sum_i \hat{\vec{p}}_i\big)\,\Big\}\end{aligned} \tag{O.30}$$

and (see also [53])

$$\begin{aligned} m_1^{(kin)}\big(\hat{\mathscr{M}}(\Delta T=1)\big) &= \frac{1}{2}\,\langle 0|\,\big[\hat{\mathscr{M}}^{+}(\Delta T=1),\,[\,\hat{T},\,\hat{\mathscr{M}}(\Delta T=1)\,]\,\big]\,|\,0\rangle = \\ &= \boxed{\begin{array}{c}\text{in analogy with}\\ \text{(O.11)}\end{array}} = \\ &= \frac{\hbar^2}{8m}\,\langle 0|\,\sum_{i=1}^{A}\big(\vec{\nabla}_i\, f^{+}(\vec{r}_i)\big)\cdot\big(\vec{\nabla}_i\, f(\vec{r}_i)\big)\,|\,0\rangle \\ &\quad - \frac{\hbar^2}{8mA}\,\langle 0|\,\Big(\sum_i\big(\vec{\nabla}_i\, f^{+}(\vec{r}_i)\big)\,(\hat{t}_z)_i\Big)\cdot\Big(\sum_k\big(\vec{\nabla}_k\, f^{+}(\vec{r}_k)\big)\,(\hat{t}_z)_k\Big)\,|\,0\rangle \end{aligned} \tag{O.31}$$

In heavy nuclei we can neglect effects of correlations and anti-symmetrization in the calculation of the center of mass correction in (O.31) (the second term) and we have (analogy with (O.12))

$$\begin{aligned} m_1^{(kin)}\big(\hat{\mathscr{M}}(\Delta T=1)\big) &= \\ &= \frac{\hbar^2}{8m}\,\Big\{\int d^3r\,\big|\vec{\nabla}\, f(\vec{r})\big|^2\,\rho(\vec{r}) - \frac{1}{A}\,\Big|\int d^3r\,\big(\vec{\nabla}\, f(\vec{r})\big)\,\rho_1(\vec{r})\Big|^2\,\Big\} \end{aligned} \tag{O.32}$$

where

$$\rho_1(\vec{r}) \equiv \rho_n(\vec{r}) - \rho_p(\vec{r}) \tag{O.33}$$

is the isovector nucleon density.

If we compare (O.32) with (O.12) and if we accept the approximation: $\rho_1(\vec{r}) \approx \frac{N-Z}{A}\,\rho(\vec{r})$ (which is often used - see e.g. [99]) then one can see that the second term in the r.h.s of (O.32) is quenched with respect to the comparing term in the isoscalar case (O.12) by a factor $(\frac{N-Z}{A})^2$. One can further see that the first term in (O.32) is a similar (up to a factor) as in the first term in (O.12) while the corresponding second terms are different.

For the case of isovector electric dipole mode ($\sum_{\mu=-1}^{+1} \hat{\mathscr{M}}^{(el)}_{1\mu}(\Delta T=1) = \sum_{\mu=-1}^{+1}\sum_{i=1}^{A} r\,Y_{1\mu}(\hat{r})\,2\,(\hat{t}_z)_i$) the first term in the expression (O.32) for the EWSR gives the same formula as the isoscalar electric dipole excitation, concretely

$$\sum_{\mu=-1}^{+1} \frac{\hbar^2}{8m} \int d^3r \left|\vec{\nabla}\, r\, Y_{1\mu}(\hat{r})\right|^2 \rho(\vec{r}) = \frac{9\hbar^2}{32\pi m}\, A \tag{O.34}$$

For the second term in (O.32) we have

$$\int d^3r\, \rho_1(\vec{r})\, \left(\vec{\nabla}\, r\, Y_{1\mu}(\hat{r})\right) = \boxed{\begin{array}{c}\text{see}\\ \text{(O.14)}\end{array}} = \sqrt{\frac{3}{4\pi}}\,\vec{\xi}_\mu \int d^3r\, \rho_1(\vec{r}) =$$

$$= \sqrt{\frac{3}{4\pi}}\,\vec{\xi}_\mu \left(\int d^3r\, \rho_n(\vec{r}) - \int d^3r\, \rho_p(\vec{r})\right) = \sqrt{\frac{3}{4\pi}}\,\vec{\xi}_\mu\,(N-Z) \tag{O.35}$$

$$\Longrightarrow -\frac{\hbar^2}{32mA} \sum_{\mu=-1}^{+1} \left| \int d^3r\, \rho_1(\vec{r})\, \left(\vec{\nabla}\, r\, Y_{1\mu}(\hat{r})\right) \right|^2 =$$

$$= -\frac{\hbar^2}{32mA} \sum_{\mu=-1}^{+1} \left| \sqrt{\frac{3}{4\pi}}\,\vec{\xi}_\mu\,(N-Z) \right|^2 = -\frac{9\,\hbar^2\,(N-Z)^2}{32\pi mA} \tag{O.36}$$

So the kinetic energy part of the EWSR for the isovector electric dipole transition operator is

$$m_1^{(kin)}\Big(\sum_{\mu=-1}^{+1} \hat{\mathscr{M}}^{(el)}_{1\mu}(\Delta T=1)\Big) = \frac{9\,\hbar^2}{32\pi m}\,A - \frac{9\,\hbar^2}{32\pi mA}\,(N-Z)^2 =$$

$$= \frac{9\,\hbar^2}{32\pi mA}\,\Big(\,(N+Z)^2 - (N-Z)^2\,\Big) = \frac{9\,NZ\,\hbar^2}{8\pi mA} \tag{O.37}$$

It should be noted that the same result (O.37) can be obtained of we work directly in the intrinsic c.o.m. frame with the standard kinetic energy operator $\frac{1}{2m}\sum_{i=1}^{A}\hat{\vec{p}}_i^{\,2}$, where the EWSR is given only by the first term in (O.32), but with the effective transition operator:

$$\hat{\mathscr{M}}^{(el)}_{1\mu}(eff) = \sum_{k=1}^{Z} e_k^{(eff)}\, r_k\, Y_{1\mu}(\hat{r}_k) + \sum_{k=1}^{N} e_k^{(eff)}\, r_k\, Y_{1\mu}(\hat{r}_k) = \\ = \frac{N}{A}\sum_{k=1}^{Z} r_k\, Y_{1\mu}(\hat{r}_k) - \frac{Z}{A}\sum_{k=1}^{N} r_k\, Y_{1\mu}(\hat{r}_k) \quad , \tag{O.38}$$

that means with the proton and neutron effective charges given by

$$e_p^{(eff)} = \frac{N}{A} \qquad\qquad e_n^{(eff)} = -\frac{Z}{A} \tag{O.39}$$

Then we really have (without the second term in (O.32)

$$m_1^{(kin)}\Big(\sum_{\mu=-1}^{+1}\hat{\mathscr{M}}^{(el)}_{1\mu}(eff)\Big) = \\ = \frac{\hbar^2}{2m}\sum_{\mu=-1}^{+1}\int d^3r\,\Big(\vec{\nabla}\, r\, Y_{1\mu}(\hat{r})\Big)^2\,\frac{Z^2}{A^2}\,\rho_n(\vec{r}) + \\ + \frac{\hbar^2}{2m}\sum_{\mu=-1}^{+1}\int d^3r\,\Big(\vec{\nabla}\, r\, Y_{1\mu}(\hat{r})\Big)^2\,\frac{N^2}{A^2}\,\rho_p(\vec{r}) = \\ = \boxed{\begin{array}{c}\text{see}\\ \text{(O.14)}\end{array}} = \frac{\hbar^2}{2m}\Big(\frac{9}{4\pi}\frac{Z^2}{A^2}N + \frac{9}{4\pi}\frac{N^2}{A^2}Z\Big) = \\ = \frac{9\,\hbar^2}{8\pi m}\frac{NZ}{A} \tag{O.40}$$

and this is the same as (O.37).

For the kinetic energy contribution to the $m_1(\hat{\mathscr{M}}(\Delta T = 1))$ for other isovector multipole operators $\hat{\mathscr{M}}^{(el)}_{\lambda\mu}(\Delta T = 1) = \sum_{i=1}^{A} r_i^{\lambda}\, Y_{\lambda\mu}(\hat{r}_i)\; 2\;(\hat{t}_z)_i$ for $\lambda > 1$ we can use the same expression as (O.22) (if we neglect the center of mass correction given by the second term in (O.31) or (O.32), which is good approximation for heavier nuclei):

$$m_1^{(kin)}\Big(\sum_{\mu=-1}^{+1}\hat{\mathscr{M}}^{(el)}_{\lambda\mu}(\Delta T = 1) = \sum_{i=1}^{A} r_i^{\lambda}\, Y_{\lambda\mu}(\hat{r}_i)\; 2\;(\hat{t}_z)_i\Big) \approx \\ \approx \frac{\hbar^2}{8\pi m}\,(2\lambda+1)^2\,\lambda\,A\langle r^{2\lambda-2}\rangle_A \tag{O.41}$$

for $\lambda > 1$ (the same expr. as (O.22)).

The value of the enhance factor $\mathscr{K}$ (see (O.26) and (O.27)), reflecting the violance of the local Gallilean invariance (see (O.25) by the velocity (or linear momentum) dependent terms in the effective nucleon-nucleon interaction, depends on the parametrization used for the particular effective nucleon-nucleon interaction. For some Skyrme interaction parametrizations this enhance factor $\mathscr{K}$ can reach the value up to 0.5 for isovector transitions (see [53]- table A1 and [181]). The analogous factor for isoscalar transitions is closed to zero, up to the value 0.1-0.2.

P. Selected expressions from quantum field theory

The probability of some process $|i\rangle \rightarrow |f\rangle$ is given by the square of the absolute value of the matrix element of the evolution operator $\hat{S}$ (here we use the Dirac description of the evolution - see the Appendix C),

$$\Gamma_{i\rightarrow f} \approx \left| \langle f| \hat{S} |i\rangle \right|^2 \tag{P.1}$$

where $|i\rangle$ is the initial state of the investigated quantum system (with N_i particles) and $|f\rangle$ is the final state (with N_f particles in the system). If the investigated process is described by the density $\hat{\mathcal{H}}_{intr}(x)$ of the interaction Hamiltonian (where $x \equiv (ct, \vec{r})$ is the coordinate in the 4D Minkowski space) then the evolution operator $\hat{S}$ is given by the Dyson perturbation decomposition (see (C.15) and C.16))

$$\hat{S} = \sum_{n=0}^{\infty} \frac{(-i)^n}{n!} \int d^4x_1 \int d^4x_2 \cdots \int d^4x_n \; T\{\hat{\mathcal{H}}_{int}(x_1)\, \hat{\mathcal{H}}_{int}(x_1) \cdots \hat{\mathcal{H}}_{int}(x_n)\} \tag{P.2}$$

where the symbol $T\{\ \}$ means the time ordering product of all operators involved in the complex parenthesis. For the matrix element $\langle f| \hat{S} |i\rangle$ it is possible to derive following expression (see any quantum field theory textbook - e.g. [13, 14])

$$\begin{aligned} &S_{fi} = \langle f| \hat{S} \,|\, i\rangle = \\ &= \delta_{ij} + (2\pi)^4\, \delta^{(4)}(\sum_f p_f^{'} - \sum_i p_i) \prod_i (\frac{1}{(2\pi)^3\, 2E_i}) \prod_f (\frac{1}{(2\pi)^3\, 2E_f^{'}})\, \mathcal{M}_{fi} \end{aligned} \tag{P.3}$$

where $p_f^{'} \equiv (E_f^{'}, \vec{p}_f^{\,'})$ $(f = 1, 2, \cdots, N_f)$ and $p_i \equiv (E_i, \vec{p}_i)$ $(f = 1, 2, \cdots, N_i)$ are 4D linear four- momenta of the f-th final particle and of i-th initial particle in the given process, respectively (with corresponding energies E_i and $E_f^{'}$ and corresponding linear momentum vectors $\vec{p}_f^{\,'}$ and $\vec{p}_i$). The symbol $\mathcal{M}_{fi}$ stands

for so called Feynman amplitude of given investigated process $|i\rangle \to |f\rangle$, and it is given by the following decomposition,

$$\mathcal{M}_{fi} = \sum_{n=1}^{\infty} \mathcal{M}_{if}^{(n)} \tag{P.4}$$

where $\mathcal{M}_{fi}^{(n)}$ is the Feynman amplitude of investigated process $|i\rangle \to |f\rangle$ for n-th order of the perturbation decomposition (P.3). The amplitude $\mathcal{M}_{fi}^{(n)}$ is directly connected with Feynman diagrams of the n-th order of given process according to Feynman rules (see e.g. [13]). In the case of the processes involving Dirac particles with the spin 1/2 and photons with the spin 0 this amplitude contains bispinor functions $u_r(\vec{p})$ (and/or $v_r(\vec{p})$) of Dirac particles (and/or Dirac antiparticles) and polarization vectors $\epsilon_r(\vec{k})$ of photons (in the linear momentum representation), and propagators of all intermediate interchanged particle created and then annihilated during given process (see [13, 256]).

For instance, in the quantum electrodynamic processes involving electromagnetic field with the four-potential $A_\mu(x)$ ($\mu = 0, 1, 2, 3$) and interacting with the quantum system consisted from Dirac particles with the charge q the density of the interaction Hamiltonian is [13],

$$\hat{\mathcal{H}}_{int}^{(elmag)}(x) = q\, \hat{\bar{\psi}}(x)\, \gamma^\mu\, \hat{\psi}(x)\, \hat{A}_\mu(x) \tag{P.5}$$

where

$$\begin{aligned}
\hat{\psi}(x) &= \sum_r \int \frac{d^3p}{(2\pi)^{3/2}\,(2p_0)^{1/2}} \left[b_r(\vec{p})\, u_r(\vec{p})\, e^{-ipx} + d_r^+(\vec{p})\, v_r(\vec{p})\, e^{ipx}\right] \\
\hat{\bar{\psi}}(x) &= \hat{\psi}^+(x)\, \gamma_0 = \\
&= \sum_r \int \frac{d^3p}{(2\pi)^{3/2}\,(2p_0)^{1/2}} \left[d_r(\vec{p})\, \bar{v}_r(\vec{p})\, e^{-ipx} + b_r^+(\vec{p})\, \bar{u}_r(\vec{p})\, e^{ipx}\right]
\end{aligned} \tag{P.6}$$

are Dirac bispinor functions in the coordinate representation. After the quantization of the Dirac field amplitudes $b_r(\vec{p})$ and $d_r(\vec{r})$ obtain the meaning of annihilation operators of corresponding Dirac particle (e.g. electron) and of antiparticle (positron), respectively (with corresponding creation operators $b_r^+(\vec{p})$ and $d_r^+(\vec{p})$. A similar plane-wave decomposition for the four- electromagnetic potential $A_\mu(x)$ is,

$$\hat{A}_\mu(x) = \sum_r \int \frac{d^3k}{(2\pi)^{3/2}(2k_0)^{1/2}} \left[\epsilon_r(\vec{k})\, a_r(\vec{k})\, e^{-ikx} + \epsilon_r^*(\vec{k})\, a_r^+(\vec{k})\, e^{ikx}\right] \tag{P.7}$$

where again $a_r(\vec{k})$ and $a_r^+(\vec{k})$ are the annihilation and creation operators of the photon with the helicity $r = \pm 1$ and linear momentum $\vec{k}$ and with the energy k_o, respectively. The bispinor functions $u_r(\vec{p})$ and $v_r(\vec{p})$ in the momentum representation can be expressed in terms of spinor functions χ_r as follows,

$$u_r(\vec{p}) = \sqrt{p_0 + m} \begin{pmatrix} \chi_r \\ \frac{\vec{\sigma}\cdot\vec{p}}{p_0+m}\,\chi_r \end{pmatrix} \quad , \quad v_r(\vec{p}) = \sqrt{p_0 + m} \begin{pmatrix} \frac{\vec{\sigma}\cdot\vec{p}}{p_0+m}\,\chi_r \\ \chi_r \end{pmatrix} \tag{P.8}$$

where $\chi_1 = \begin{pmatrix} 1 \\ 0 \end{pmatrix}$ and $\chi_2 = \begin{pmatrix} 0 \\ 1 \end{pmatrix}$ are spinors and $E \equiv p_0 = \sqrt{m^2 + |\vec{p}|^2}$ is the total energy of the Dirac particle in the given frame and with the rest energy (mass) m. The bispinor functions $u_r(\vec{p})$ and $v_r(\vec{p})$ are normalized as follows [13, 256] ($\bar{u}_r(\vec{p}) = u_r^+(\vec{p})\,\gamma_0$, $\bar{v}_r(\vec{p}) = v_r^+(\vec{p})\,\gamma_0$)

$$\begin{aligned} &\bar{u}_r(\vec{p})\, u_s(\vec{p}) = -\bar{v}_r(\vec{p})\, v_s(\vec{p}) = 2m\,\delta_{rs} \\ &\bar{u}_r(\vec{p})\, v_s(\vec{p}) = \bar{v}_r(\vec{p})\, u_s(\vec{p}) = 0 \end{aligned} \tag{P.9}$$

In the non-relativistic approximation (reduction), when $|\vec{p}| << m$, the bispinor functions reduce to

$$\begin{aligned} u_r(\vec{p} \to 0) &= \sqrt{2m} \begin{pmatrix} \chi_r \\ 0 \end{pmatrix} = \begin{pmatrix} U_r \\ 0 \end{pmatrix} \quad , \quad U_r \equiv \sqrt{2m}\,\chi_r \\ v_r(\vec{p} \to 0) &= \sqrt{2m} \begin{pmatrix} 0 \\ \chi_r \end{pmatrix} = \begin{pmatrix} 0 \\ U_r \end{pmatrix} \end{aligned} \tag{P.10}$$

Knowing the amplitude $\mathcal{M}_{fi}$ of the given process $|i\rangle \to |f\rangle$ ($1 + 2 \to 1^{'} + 2^{'} + \cdots$) where in the initial state $|i\rangle$ there are two particles with four- linear momenta $p_i \equiv (E_i, \vec{p}_i)$ ($i = 1, 2$) and with polarizations (helicities) r_i ($i = 1, 2$), and in the final state (in the end of the process) there are N_f particles with four- momenta $p_f^{'} \equiv (E_f^{'}, \vec{p}_f^{'})$ ($f = 1, \cdots, N_f$) and with polarizations $r_f^{'}$ ($f = 1, \cdots, N_f$), the corresponding differential cross section is,

$$\begin{aligned} d\sigma_{i\to f} \;=\; (2\pi)^4 \;\delta^{(4)}\Big(\sum_{f=1}^{N_f} p_f^{'} - \sum_{i=1,2} p_i\Big) \;\frac{1}{4E_1E_2\,v_{rel}} \\ \Big(\prod_{f=1}^{N_f} \frac{d^3p_f^{'}}{(2\pi)^3\,E_f^{'}}\Big)\,\Big|\mathcal{M}_{r_1p_1,\,r_2p_2\,;\;\,r_1^{'}p_1^{'},\cdots,\,r_{N_f}^{'}p_{N_f}^{'}}\Big|^2 \end{aligned} \tag{P.11}$$

where v_{rel} is the value of the relative velocity of initial particles 1 and 2.

If the investigated process is the decay of some mother particle with given four- linear momentum P and polarization r, and after the decay N_f particles are created with four- momenta $p_f^{'}$ and polarizations $r_f^{'}$ $(f = 1, \cdots, N_f)$, that means $(P, r) \to (p_f^{'}, r_f^{'})$ $(f = 1, \cdots, N_f)$, then the probability of the decay per 1 second is $(P \equiv (E, \vec{P}))$,

$$d\Gamma_{f\to i} = (2\pi)^4 \ \delta^{(4)}(\sum_{f=1}^{N_f} p_f^{'} - P) \ \frac{1}{2E} \ (\prod_{f=1}^{N_f} \frac{d^3 p_f^{'}}{(2\pi)^3 \ 2E_f^{'}}) \ \left|\mathcal{M}_{fi}\right|^2 \tag{P.12}$$

If in this decay only one final channel is open then exp. (P.12) determines whole differential probability of the decay. If more final channels are open during the decay,

$$A \to \begin{cases} a_1 + a_2 + \cdots \\ b_1 + b_2 + \cdots \\ c_1 + c_2 + \cdots \\ \vdots \end{cases} \tag{P.13}$$

then so called branching ration B_j for j-th channel is introduced

$$B_j = \frac{\Gamma_{i\to j}}{\sum_{k=a,b,c,\cdots} \Gamma_{i\to k}} \tag{P.14}$$

and the life time of the mother particle is

$$\tau = \frac{1}{\sum_{k=a,b,c,\cdots} \Gamma_{i\to k}} = \frac{B_j}{\Gamma_{i\to j}} \tag{P.15}$$

for any channel j.

Q. Selected expressions from scattering theory

In this appendix the basic expressions of the theory of the scattering (reaction) of particles and nuclei, relevant to energies of impacting particle (light nucleus) up to hundreds of MeV, are listed. The derivation of these expressions is not given in the appendix but it can be found for the most of the listed expressions in different sections of the Chapter 11.

Let $|\Psi\rangle$ is the channel $\alpha \equiv (a + A)$ wave function with the interaction $\hat{V}$ between the particle a and the nucleus A. Channel wave function fulfills stationary Schroedinger equation

$$(E - \hat{H})\,|\Psi_\alpha\rangle = 0 \tag{Q.1}$$

Total channel Hamiltonian $\hat{H}$ is supposed to be hermitian and consists from two terms,

$$\hat{H} = \hat{H}_0 + \hat{V} \tag{Q.2}$$

where $\hat{H}_0$ is the Hamiltonian of internal degrees of freedom of the particle a and the target nucleus A together with the kinetic energy Hamiltonian of the relative motion of the particle a with respect to the nucleus A. Let $|\Phi\rangle$ is the solution of the stationary Schroedinger equation with the Hamilonian $\hat{H}_0$ and with the same energy E as in (Q.1),

$$(E - \hat{H}_0)\,|\Phi_\alpha\rangle = 0 \tag{Q.3}$$

It is necessary to realize that $\hat{H}_0 = \lim_{\hat{V}\to 0} \hat{H}$ and $\hat{V} \to 0$ in the asymptotic region where the distance r between particle a and the nucleus A in the channel α is infinite. That means the wave function $|\Phi_\alpha\rangle$ represents the asymptotic form of the whole channel wave function $|\Psi_\alpha\rangle$ ($|\Phi_\alpha\rangle = \lim_{\hat{V}\to 0} |\Psi_\alpha\rangle = \lim_{r\to\infty} |\Psi_\alpha\rangle$).

Q.1 Lippman- Schwinger equation for the channel wave function, "in" and "out" waves

From (Q.1)-(Q.3) follows that wave funtions $|\Phi_\alpha\rangle$ and $|\Psi_\alpha\rangle$ fulfills conditions for Lippman-Schwinger equation (see the Appendix E, exprs. (E.6),(E.8)) and we can write (see also [23])

$$
\begin{aligned}
|\Psi_\alpha^{(+)}\rangle &= |\Phi_\alpha\rangle + \frac{1}{E^{(+)} - \hat{H}_0}\,\hat{V}\,|\Psi_\alpha^{(+)}\rangle = |\Phi_\alpha\rangle + \frac{1}{E^{(+)} - \hat{H}_0}\,\hat{V}\,|\Phi_\alpha\rangle + \cdots = \\
&= |\Phi_\alpha\rangle + \frac{1}{E^{(+)} - \hat{H}}\,\hat{V}\,|\Phi_\alpha\rangle \\
|\Psi_\alpha^{(-)}\rangle &= |\Phi_\alpha\rangle + \frac{1}{E^{(-)} - \hat{H}_0}\,\hat{V}\,|\Psi_\alpha^{(-)}\rangle = |\Phi_\alpha\rangle + \frac{1}{E^{(-)} - \hat{H}_0}\,\hat{V}\,|\Phi_\alpha\rangle + \cdots = \\
&= |\Phi_\alpha\rangle + \frac{1}{E^{(-)} - \hat{H}}\,\hat{V}\,|\Phi_\alpha\rangle
\end{aligned}
\tag{Q.4}
$$

with

$$
E^{(+)} \equiv E + i\eta \quad , \qquad E^{(-)} \equiv E - i\eta \quad , \qquad \eta \to 0+ \tag{Q.5}
$$

In the linear momentum representation channel kets $|\Psi_\alpha^{(+)}\rangle$ and $|\Psi_\alpha^{(-)}\rangle$ are represented by the following wave functions,

$$
\begin{aligned}
\Psi_\alpha^{(+)}(\vec{k}_\alpha, \xi_\alpha) &= \langle \vec{k}_\alpha, \xi_\alpha | \Psi_\alpha^{(+)} \rangle \\
\Psi_\alpha^{(-)}(\vec{k}_\alpha, \xi_\alpha) &= \langle \vec{k}_\alpha, \xi_\alpha | \Psi_\alpha^{(-)} \rangle
\end{aligned}
\tag{Q.6}
$$

where $\hbar\vec{k}_\alpha$ is the linear momentum of the particle a with respect to the nucleus A and ξ_α are internal coordinates of particle and the nucleus A.

Further the reaction $i \to f$ going from the initial channel $i \equiv (a + A)$ to the final channel $f \equiv (b + B)$ is discussed. Initial channel i is described by the initial channel wave function $|i; in\rangle = |\Psi_i^{(+)}\rangle$. In the time $t \to -\infty$ the whole system is in the channel i and the index i in the wave function $|\Psi_i^{(+)}\rangle$ characterizes the linear momentum of the impacting particle a with respect to the target nucleus A and the intrinsic structure of the particle a and the nucleus A. For $t \to -\infty$ the distance between the particle a and the nucleus A is infinite and in this asymptotic region the interaction $\hat{V}$ between a and A is zero, $\hat{V} \to 0$. That means for $t \to -\infty$ the wave function $|\Psi_i^{(+)}\rangle$ becomes the wave function $|\Phi_i\rangle$ describing free particle a and free nucleus A, $\lim_{t\to-\infty} |\Psi_i^{(+)}\rangle = |\Phi_i\rangle$. In the asymptotic wave function $|\Phi_i\rangle$ particle a and the nucleus A can be represented by the wave packets with so big sizes that the uncertainty in their linear momenta (energies) is very small. As a

result of this the relative linear momentum $\vec{k}_i$ and relative coordinate $\vec{r}$ of the particle a and the nucleus A can be used as simultaneous characteristics of state $|\Phi_i\rangle$. So in the coordinate (linear momentum) representation the asymptotic initial channel state $|\Phi_i\rangle$ with the energy E_i can be expressed in the following plane wave form [1]

$$\lim_{t\to-\infty}\langle\vec{k}_i \mid \Psi_i^{(+)}\rangle = \langle\vec{k}_i,\vec{r}\,|\,\Phi_i\rangle = e^{i\vec{k}_i\cdot\vec{r}}\,\sqrt{\rho_i} \tag{Q.7}$$

where ρ_i is the density of channel states at the energy E_i and with the relative coordinate $\vec{r}$ of the particle a and the target nucleus A (one should realize that the channel states involve also internal characteristics of the particle a and the nucleus A. The other things to be realized is the fact that $|\langle\vec{k}_i,\vec{r}\,|\,\Phi_i\rangle|^2 = \rho_i$).

Similarly the wave function $|f;out\rangle = |\Psi_f^{(-)}\rangle$ of the final channel f describing the final particle b and the final nucleus B becomes the wave function of free particle b and free nucleus B for time $t\to\infty$, $\lim_{t\to\infty}|\Psi_f^{(-)}\rangle = |\Phi_f\rangle$. And again in the coordinate representation the asymptotic final channel state $|\Phi_f\rangle$ with the energy E_f can be expressed in the following plane wave form

$$\lim_{t\to\infty}\langle\vec{k}_f \mid \Psi_i^{(-)}\rangle = \langle\vec{k}_f,\vec{r}\,|\,\Phi_f\rangle = e^{i\vec{k}_f\cdot\vec{r}}\,\sqrt{\rho_f} \tag{Q.8}$$

with ρ_f being the density of the final channel states at the energy E_f.

It is necessary to realize that if the initial and final channel states $|\Psi_i^+\rangle$, $|\Psi_f^-\rangle$, $|\Phi_i^+\rangle$ and $|\Phi_f^-\rangle$ are normalized as in (Q.7) and (Q.8), that mean using densities ρ_i and ρ_f then it is implicitly supposed that the internal coordinates of both the initial channel i and the final channel f are taken into account only by means of these densities and the only active coordinates in wave functions $\Psi_i^{(+)}(\vec{k}_i)$ and $\Psi_f^{(-)}(\vec{k}_i)$ are corresponding linear momenta $\vec{k}_i$ and $\vec{k}_f$. In such a case the Hamiltonian $\hat{H}_0$ in (Q.2), (Q.3) and (Q.4) is only the Hamiltonian of the kinetic energy of the particle-nucleus relative motion in the initial and/or final channel and energies E_i and E_f are only corresponding relative motion energies.

Q.2 S matrix

The amplitude of the process $i\to f$ is given by the matrix element S_{fi} of so called S-matrix defined as

$$S_{fi} \equiv \langle\Psi_f^{(-)} \mid \Psi_i^{+)}\rangle \tag{Q.9}$$

[1] Generally the wave packet describing the impacting particle a and the target nucleus A in the asymptotic region for $t\to-\infty$ can be expressed not only by plane wave form but also by another type of waves, e.g. by spherical waves.

If the Hamiltonian $\hat{H}$ if invariant with respect to the time-reverse ($\mathscr{T}\hat{H}\mathscr{T}^{-1} = \hat{H}$) then the time-reverse operator $\mathscr{T}$ transform the state $|\Psi_i^{(+)}\rangle$ into the state $|\Psi_{\bar{i}}^{(-)}\rangle$ (see e.g. [6, 23])

$$\begin{aligned}\mathscr{T}|i;in\rangle &= \mathscr{T}|\Psi_i^{(+)}\rangle = |\bar{i};out\rangle = |\Psi_{\bar{i}}^{(-)}\rangle \\ \mathscr{T}|i;out\rangle &= \mathscr{T}|\Psi_i^{(-)}\rangle = |\bar{i};in\rangle = |\Psi_{\bar{i}}^{(+)}\rangle \end{aligned} \qquad \text{(Q.10)}$$

where $|\bar{i};in\rangle = |\Psi_{\bar{i}}^{(+)}\rangle$ means the state which is obtained from $|i;in\rangle = |\Psi_i^{(+)}\rangle$ by the inversion of linear momenta and the transformation of the spin and angular momentum parts of the wave function in the correspondence with the action of the time-reverse operator (e.g. $|\overline{\vec{p},m_s}\rangle = (-1)^{s+m_s}|-\vec{p},-m_s\rangle$ and so on - see (1.42)), and similarly for the final channel. The expression (Q.10) gives the connection between S - matrix element of the process $i \to f$ and the time-reverse process $\bar{f} \to \bar{i}$,

$$\begin{aligned} S_{fi} &= \langle \Psi_f^{-)} \mid \Psi_i^{(+)}\rangle = \langle |\Psi_f^{(-)} \mid \mathscr{T}^{-1}\mathscr{T} \mid \Psi_i^{(+)}\rangle = \\ &= \boxed{\begin{array}{c}\text{see}\\ \text{(Q.10)}\end{array}} = \langle \Psi_{\bar{f}}^{(+)} \mid \Psi_{\bar{i}}^{(-)}\rangle^* = \langle \Psi_{\bar{i}}^{(-)} \mid \Psi_{\bar{f}}^{(+)}\rangle = S_{\bar{i}\bar{f}} \end{aligned} \qquad \text{(Q.11)}$$

It is possible to show (see e.g. [23]) that S_{fi} can be also expressed as

$$S_{fi} = \langle \Phi_f \mid \hat{S}(E^{(+)}) \mid \Phi_i\rangle \qquad \text{(Q.12)}$$

with the evolution operator $\hat{S}(E^{(+)})$ which evolved the state $|\Phi_i\rangle$ with the energy E_i to the state $|\Phi_f\rangle$ with the same energy $E = E_f = E_i$ within the time interval $(-\infty, \infty)$. This evolution operator (and therefore also S-matrix) is unitary.

$$\hat{S}\,\hat{S}^+ = \hat{S}^+\,\hat{S} = 1 \qquad \text{(Q.13)}$$

Q.3 Reaction matrix $\mathcal{T}$ and cross-section ($\hat{H}^+ = \hat{H}$)

Let us consider the reaction from the initial channel i to the final channel f. The reaction matrix element $\mathcal{T}_{fi}$ is given by

$$\mathcal{T}_{fi} = \langle \Psi_f^{(-)}|\hat{V}|\Phi_i^{(+)}\rangle = \langle \Phi_f^{(-)}|\hat{V}|\Psi_i^{(+)}\rangle = \langle \Phi_f^{(-)}|\hat{\mathcal{T}}(E^{(+)})|\Phi_i^{+)}\rangle \qquad \text{(Q.14)}$$

and using Lippman-Schwinger equation (Q.4) we obtain following expression for the reaction "evolution" operator (acting in the space of asymptotic

channel states) ,

$$\hat{\mathcal{T}}(E) = \hat{V} + \hat{V}\frac{1}{E - \hat{H}_0}\hat{\mathcal{T}}(E) = \hat{V} + \hat{V}\frac{1}{E - \hat{H}}\hat{V}(E) \tag{Q.15}$$

where $\Phi_i^{(+)}(\vec{r}, \vec{k}_i, \xi_i) = \lim_{\hat{V}\to 0} \Psi_i^{(+)}(\vec{k}_i, \xi_i)$ and $\Phi_f^{(-)}(\vec{r}, \vec{k}_f, \xi_f) = \lim_{\hat{V}\to 0} \Psi_f^{(-)}(\vec{k}_f, \xi_f)$ are asymptotic ingoing initial channel and asymptotic outgoing final channel wave functions, respectively.

Reaction probability w_{fi} (we suppose reaction goes to one final channel state with the energy E_f),

$$w_{fi} = \frac{2\pi}{\hbar} |\mathcal{T}_{fi}|^2 \, \delta(E_f - E_i) \tag{Q.16}$$

However, from the experimental point of view we are usually interested in the reaction going to final states with the unity energy interval around the energy E_f with the following probability

$$d\bar{w}_{fi} = \frac{2\pi}{\hbar} |\mathcal{T}_{fi}|^2 \, \rho_f \qquad \text{with } E_f = E_i \tag{Q.17}$$

where ρ_f is the density of final states with the energy E_f. For single final channel we have

$$\rho_f = \frac{1}{(2\pi)^3} \, k_f^2 \, \frac{dk_f}{dE} = \frac{1}{(2\pi)^3} \, \frac{\mu_f}{\hbar^2} \, k_f \tag{Q.18}$$

where μ_f is the reduced mass of particle and nucleus in the channel f.

Differential cross-section of the reaction $i \to f$ is directly proportional to the corresponding probability $d\bar{w}_{fi}$,

$$\frac{d\sigma_{fi}}{d\Omega_f} = \frac{d\bar{w}_{fi}}{j_i} \tag{Q.19}$$

where j_i is the value if the incident current,

$$j_i = \frac{\hbar k_i}{\mu_i} \tag{Q.20}$$

and the substitution of (Q.20),(Q.17) and (Q.18) into (Q.19) gives for the differential cross-section of the single final channel reaction,

$$\frac{d\sigma_{fi}}{d\Omega_f} = \frac{1}{(2\pi)^2} \frac{\mu_i \mu_f \, k_f}{\hbar^4 \, k_i} \, |\mathcal{T}_{fi}|^2 \tag{Q.21}$$

In the case when the interaction $\hat{V}$ in (Q.2) consists from two parts,

$$\hat{V} = \hat{V}_0 + \hat{V}_1 \tag{Q.22}$$

and at first the solution of the stationary Schroedinger equation with the Hamiltonian $\hat{H}_0 + \hat{V}_0$,

$$(\hat{H}_0 + \hat{V}_0)\,|\chi^{(\pm)}_{i(f)}\rangle = E^{(\pm)}\,|\chi^{(\pm)}_{i(f)}\rangle \tag{Q.23}$$

was found then the $\mathcal{T}$- matrix element $\mathcal{T}_{fi}$ can be expressed as

$$\mathcal{T}_{fi}(E^{(+)}) = \langle\Phi^{(-)}_f|\hat{V}_0|\chi^{(+)}_i\rangle + \langle\chi^{(-)}_f|\hat{V}_1|\Psi^{(+)}_i\rangle \tag{Q.24}$$

This is the scheme of the calculation when in the first step the distorted waves $|\chi_{i(f)}\rangle$ are found from (Q.23) with the optical potential $\hat{V}_0$ for the given ensemble of channels and in the second step the $\mathcal{T}$- matrix with matrix elements (Q.24) is constructed and diagonalized within the space of the finite ensemble of possible channels with the additional interaction $\hat{V}_1$ between channels. Then the diagonal matrix elements of diagonalized matrix $\mathcal{T}$ provide through the expr. (Q.21) corresponding differential cross-sections for all output channels reachable from the initial channel i by means of the interaction V_1.

There is the following connection between $\mathcal{T}$- and S- matrices (see e.g. [23])

$$S_{fi} = \delta_{if} - 2\pi\,\mathcal{T}_{fi}\,\delta(E_f - E_i) \tag{Q.25}$$

Q.4 Scattering amplitude

Scattering amplitude f_{fi} is defined through the corresponding asymptotic form of the final channel f ($f \neq i$) wave function (see (D.16) for the elastic scattering case)

$$\langle\vec{r}, \vec{k}_f, \xi_f|\Psi_f\rangle \quad \stackrel{r\to\infty}{\longrightarrow} \quad f_{fi}\;\frac{e^{ik_f r}}{r}\;\sqrt{\rho_f} \tag{Q.26}$$

It is connected with the corresponding $\mathcal{T}$- matrix element $\mathcal{T}_{fi}$ by (see (E.27) for elastic scattering)

$$f_{fi} = -\frac{\mu_f}{2\pi\hbar^2}\,\mathcal{T}_{fi} \tag{Q.27}$$

where $\mathcal{T}_{fi} = \langle\Phi^{(-)}_f|\hat{\mathcal{T}}(E^{(+)})|\Phi^{(+)}_i\rangle$ (see (Q.14)) with properly normalized asymptotic plane waves (or other types of asymptotic waves) $|\Phi_i\rangle$ and $|\Phi_f\rangle$,

$$\begin{aligned}\Phi_i(\vec{r}, \vec{k}_i) &= \langle\vec{r}, \vec{k}_i|\Phi_i\rangle = e^{i\vec{k}_i\cdot\vec{r}}\,\sqrt{\rho_i}\\ \Phi_f(\vec{r}, \vec{k}_f) &= \langle\vec{r}, \vec{k}_f|\Phi_f\rangle = e^{i\vec{k}_f\cdot\vec{r}}\,\sqrt{\rho_f}\end{aligned} \tag{Q.28}$$

Then the differential cross-section (Q.21) can be expressed in terms of f_{fi} as (the substitution of (Q.26) into (Q.21) - see also (D.19) for elastic scattering)

$$\frac{d\sigma_{fi}}{d\Omega_f} = \frac{\mu_i k_f}{\mu_f k_i} |f_{fi}|^2 \tag{Q.29}$$

It should be pointed out that all expressions $(Q.4)$-$(Q.29)$ should be modified if the Hamiltonian $\hat{H} = \hat{H}_0 + \hat{V}$ is not hermitian (see Appendix A in [23] and [348]).

R. Detailed derivations and discussions of selected expressions of the Chapter 12 (Statistical aspects of nuclear dynamics)

R.1 Derivation of the expression for energy density of quantum canonical system states (expressions (12.17) and (12.18))

We start with the expression (12.15) for the energy density of levels with the given energy E and given quantum numbers q,

$$\rho(E,q) = \frac{1}{(2\pi i)^2} \int_{-i\infty}^{\infty} d\beta \int_{-i\infty}^{\infty} d\alpha \, e^{lnZ(\beta,\alpha)+\beta E-\alpha q} =$$

$$= \boxed{\begin{array}{c}\text{Taylor expansion of the exponent around the stationary} \\ \text{point } (\beta_0,\alpha_0) \text{ and thanks to the condition (12.16) linear} \\ \text{terms in } \alpha-\alpha_0 \text{ and } \beta-\beta_0 \text{ are not present}\end{array}} =$$

$$= \frac{1}{(2\pi i)^2} \, e^{lnZ(\beta_0,\alpha_0)+\beta_0 E-\alpha_0 q} \int_{-i\infty}^{\infty} d\beta \int_{-i\infty}^{\infty} d\alpha \; e^{\frac{1}{2}\left\{A\,(\beta-\beta_0)^2+B\,(\alpha-\alpha_0)^2+2C\,(\alpha-\alpha_0)\,(\beta-\beta_0)\right\}} \tag{R.1}$$

where we introduced,

$$A \equiv \frac{\partial^2 \, lnZ(\beta,\alpha)}{\partial \, \beta^2}\Big|_{\alpha,\beta=\alpha_0,\beta_0} \quad , \quad B \equiv \frac{\partial^2 \, lnZ(\beta,\alpha)}{\partial \, \alpha^2}\Big|_{\alpha,\beta=\alpha_0,\beta_0}$$

$$C \equiv \frac{\partial^2 \, lnZ(\beta,\alpha)}{\partial \, \beta \, \partial\alpha}\Big|_{\alpha,\beta=\alpha_0,\beta_0} \tag{R.2}$$

Further the substitution $\beta - \beta_0 = ix$ $(d\beta = idx)$ and $\alpha - \alpha_0 = iy$ $(d\alpha = idy)$ is done:

$$\rho(E,q) = \frac{1}{(2\pi)^2}\, e^{lnZ(\beta_0,\alpha_0)+\beta_0 E-\alpha_0 q} \int_{-\infty}^{\infty} dx \int_{-\infty}^{\infty} dy\, e^{-\frac{1}{2}\left\{Ax^2+By^2+2Cxy\right\}} =$$
$$= \frac{1}{(2\pi)^2}\, e^{lnZ(\beta_0,\alpha_0)+\beta_0 E-\alpha_0 q} \int_{-\infty}^{\infty} dx \int_{-\infty}^{\infty} dy\, e^{-\frac{1}{2}\left\{(x\sqrt{A}+y\sqrt{B})^2+2xy(C-\sqrt{AB})\right\}}$$

Then we continue with substitutions,

$$\begin{array}{lll} u = x\sqrt{A} + y\sqrt{B} & & x = \frac{u+v}{2\sqrt{A}} \\ v = x\sqrt{A} - y\sqrt{B} & \Rightarrow & y = \frac{u-v}{2\sqrt{B}} \end{array} \quad \Rightarrow \quad xy = \frac{u^2-v^2}{4\sqrt{AB}}$$
$$\Rightarrow \quad dx\,dy = \begin{vmatrix} \frac{\partial x}{\partial u} & \frac{\partial x}{\partial v} \\ \frac{\partial y}{\partial u} & \frac{\partial y}{\partial v} \end{vmatrix} du\,dv = \frac{1}{2\sqrt{AB}}\, du\,dv \qquad \text{(R.3)}$$

and finally we have,

$$\rho(E,q) =$$
$$= \frac{e^{lnZ(\beta_0,\alpha_0)+\beta_0 E-\alpha_0 q}}{(2\pi)^2} \int_{-\infty}^{\infty} du \int_{-\infty}^{\infty} dv\, \frac{e^{-\frac{1}{2}\left\{u^2+\frac{2(u^2-v^2)\,(C-\sqrt{AB})}{4\sqrt{AB}}\right\}}}{2\sqrt{AB}} =$$
$$= \frac{e^{lnZ(\beta_0,\alpha_0)+\beta_0 E-\alpha_0 q}}{(2\pi)^2} \int_{-\infty}^{\infty} du \int_{-\infty}^{\infty} dv\, \frac{e^{-\frac{\sqrt{AB}+C}{4\sqrt{AB}}\,u^2}\, e^{-\frac{\sqrt{AB}-C}{4\sqrt{AB}}\,v^2}}{2\sqrt{AB}} =$$
$$= \boxed{\begin{array}{c}\text{Substitution} \\ t = \sqrt{\frac{\sqrt{AB}+C}{4\sqrt{AB}}}\, u \quad , \quad s = \sqrt{\frac{\sqrt{AB}-C}{4\sqrt{AB}}}\, v\end{array}} =$$
$$= \frac{e^{lnZ(\beta_0,\alpha_0)+\beta_0 E-\alpha_0 q}}{(2\pi)^2}\, \frac{1}{2\sqrt{AB}}\, \frac{4\sqrt{AB}}{\sqrt{AB-C^2}} \int_{-\infty}^{\infty} dt \int_{-\infty}^{\infty} ds\, e^{-t^2}\, e^{-s^2} =$$
$$= \frac{e^{lnZ(\beta_0,\alpha_0)+\beta_0 E-\alpha_0 q}}{(2\pi)^2}\, \frac{1}{2\sqrt{AB}}\, \frac{4\sqrt{AB}}{\sqrt{AB-C^2}}\, \sqrt{\pi}\,\sqrt{\pi} =$$
$$= \frac{1}{2\pi}\, \frac{e^{lnZ(\beta_0,\alpha_0)+\beta_0 E-\alpha_0 q}}{\sqrt{AB-C^2}} = \frac{1}{2\pi}\, \frac{e^{lnZ(\beta_0,\alpha_0)+\beta_0 E-\alpha_0 q}}{\sqrt{det\ R}} = (12.17) \qquad \text{(R.4)}$$

where

$$detR = \begin{vmatrix} \frac{\partial^2 lnZ(\beta_0,\alpha_0)}{\partial\beta^2} & \frac{\partial^2 lnZ(\beta_0,\alpha_0)}{\partial\beta\,\partial\alpha} \\ \frac{\partial^2 lnZ(\beta_0,\alpha_0)}{\partial\alpha\,\partial\beta} & \frac{\partial^2 lnZ(\beta_0,\alpha_0)}{\partial\alpha^2} \end{vmatrix} = \boxed{\begin{array}{c}\text{see} \\ \text{(R.2)}\end{array}} = AB - C^2 = (12.18) \qquad \text{(R.5)}$$

R.2 Derivation of the expression (12.23) for the logarithm of the partition function $lnZ(\beta,\alpha)$

We start with the partition function (12.21) expressed in terms of single-particle energies e_s of fermions forming the quantum system, $Z(\beta,\alpha) = \prod_s (1+e^{\alpha-\beta\, e_s})$ (here α,β are considered as real),

$$lnZ(\beta,\alpha) = \sum_s ln(1+e^{\alpha-\beta e_s}) = \boxed{\begin{array}{c}\text{see}\\ (12.22)\end{array}} = \int_0^\infty de\; g(e)\; ln(1+e^{\alpha-\beta e}) =$$

$$= \int_0^{\alpha/\beta} de\; g(e)\; ln(1+e^{\beta\,(\frac{\alpha}{\beta}-e)}) + \int_{\alpha/\beta}^\infty de\; g(e)\; ln(1+e^{\beta\,(\frac{\alpha}{\beta}-e)}) =$$

$$= \int_0^{\alpha/\beta} de\; g(e)\; (\alpha-\beta e) + \int_0^{\alpha/\beta} de\; g(e)\; \big[ln\big(1+e^{\beta(\frac{\alpha}{\beta}-e)}\big) - (\alpha-\beta e)\big]$$
$$+ \int_{\alpha/\beta}^\infty de\; g(e)\; ln(1+e^{\beta\,(\frac{\alpha}{\beta}-e)}) =$$

$$= \boxed{\begin{array}{c}\text{in the last two integrals}\\ \text{the substitution } e = \frac{\alpha}{\beta}+x\end{array}} =$$

$$= \int_0^{\alpha/\beta} de\; g(e)\; (\alpha-\beta e) + \int_{-\alpha/\beta}^0 dx\; g(\frac{\alpha}{\beta}+x)\; \big[ln\big(1+e^{-\beta x}\big) + \beta x\big] +$$
$$+ \int_0^\infty dx\; g(\frac{\alpha}{\beta}+x)\; ln\big(1+e^{-\beta x}\big) =$$

$$= \boxed{\begin{array}{c}\text{because}\quad ln\,(1+e^{\beta x}) =\\ = ln\, e^{\beta x}\,(1+e^{-\beta x}) = ln\, e^{\beta x} + ln(1+e^{-\beta x}) = \beta x + ln\,(1+e^{-\beta x})\end{array}} =$$

$$= \int_0^{\alpha/\beta} de\; g(e)\; (\alpha-\beta e) + \int_{-\alpha/\beta}^0 dx\; g(\frac{\alpha}{\beta}+x)\; ln\big(1+e^{\beta x}\big) +$$
$$+ \int_0^\infty dx\; g(\frac{\alpha}{\beta}+x)\; ln\big(1+e^{-\beta x}\big) =$$

$$= \boxed{\begin{array}{c}\text{because}\\ g(x) = 0 \text{ for } x<0\end{array}} =$$

$$= \int_0^{\alpha/\beta} de\, g(e)\,(\alpha - \beta e) + \int_{-\infty}^{0} dx\, g(\frac{\alpha}{\beta} + x)\, ln\big(1 + e^{\beta x}\big) +$$

$$+ \int_0^{\infty} dx\, g(\frac{\alpha}{\beta} + x)\, ln\big(1 + e^{-\beta x}\big) =$$

$$= \boxed{\begin{array}{l}\text{in the second integral}\\ \text{substitution } x \;\rightarrow\; -x\end{array}} =$$

$$= \int_0^{\alpha/\beta} de\, g(e)\,(\alpha - \beta e) + \int_0^{\infty} dx\, g(\frac{\alpha}{\beta} - x)\, ln\big(1 + e^{-\beta x}\big) +$$

$$+ \int_0^{\infty} dx\, g(\frac{\alpha}{\beta} + x)\, ln\big(1 + e^{-\beta x}\big) =$$

$$= \beta \int_0^{\alpha/\beta} de\, g(e)\,(\mu - e) + \int_0^{\infty} dx \left[g(\mu + x) + g(\mu - x)\right] ln\,(1 + e^{-\beta x}) \tag{R.6}$$

where $\mu = \alpha/\beta$ was introduced. The value of the logarithm $ln\,(1 + e^{-\beta x})$ is closed to zero for $x \to \infty$ (because $e^{-\beta x} \to 0$ and $ln1 = 0$). Since the stationary value of $\mu = \alpha_0/\beta_0$ is usually far from 0 (sufficiently big) we can consider the logarithm $ln\,(1 + e^{-\beta x})$ to be negligible in the vicinity of $\mu \approx \alpha_0/\beta_0$ where the discontinuities in $g(x)$ are the biggest. By other words we can assume that β and α are such that the arguments $\mu \pm x$ of the density g in (R.6) are far from the point (β_0, α_0) where the density is discontinuous and therefore we can use the Taylor expansion around the point μ:

$$\begin{aligned} g(\mu + x) &\approx g(\mu) + g'(\mu)\, x + \frac{1}{2} g''(\mu)\, x^2 \\ g(\mu - x) &\approx g(\mu) - g'(\mu)\, x + \frac{1}{2} g''(\mu)\, x^2 \\ \Rightarrow \quad & g(\mu + x) + g(\mu - x) \approx 2\, g(\mu) + g''(\mu)\, x^2 \end{aligned} \tag{R.7}$$

and the expression (R.6) can be rewritten as,

$$\begin{aligned} & ln\, Z(\beta, \alpha) \approx \\ & \approx \beta \int_0^{\mu} dx\, g(x)\,(\mu - x) + \int_0^{\infty} dx \left[2\, g(\mu) + g''(\mu)\, x^2\right] ln\,(1 + e^{-\beta x}) \end{aligned} \tag{R.8}$$

From (R.8) follows that it is necessary to determine integrals of the type:

$$I_n = \int_0^{\infty} dx\, x^n\, ln\,(1 + e^{-\beta x}) \tag{R.9}$$

where n is the integer number. We expand the logarithm $ln\,(1+e^{-\beta x})$ into the Taylor series and we have,

$$I_n = \int_0^\infty dx\, x^n \,(\sum_{m=1}^{\infty} \frac{(-1)^{m+1}}{m}\, e^{-m\beta x}) = \boxed{\begin{array}{c}\text{the substitution}\\ y=\beta x\end{array}} =$$

$$= \frac{1}{\beta^{n+1}} \int_0^\infty dy\, y^n \,(\sum_{m=1}^{\infty} \frac{(-1)^{m+1}}{m}\, e^{-my}) = \cdots =$$

$$= \frac{n!}{\beta^{n+1}} \,(1-\frac{1}{2^{n+1}}) \sum_{m=1}^{\infty} \frac{1}{m^{n+2}} = \frac{n!}{\beta^{n+1}} \,(1-\frac{1}{2^{n+1}})\, \zeta_{(n+2)}$$

where $\zeta_{(n)}$ is so called Riemann "zeta" function. For integer arguments n we obtain,

$$I_n = \frac{1}{\beta^{\,n+1}}\, \frac{2^{\,n+1}-1}{(n=1)(n+2)}\, \pi^{n+2}\, \left|B_{n=2}\right|$$

where $B_2 = \frac{1}{6},\ B_4 = -\frac{1}{30},\ B_6 = \frac{1}{42}$.
Concretly,

$$I_0 = \frac{1}{2}\,\frac{\pi^2}{6\beta} \qquad I_2 = \frac{7}{12}\,\frac{\pi^4}{30\beta^3}$$

The substitutions of these integrals into (12.8) gives finally the expression (7.23):

$$ln\, Z(\beta,\alpha) =$$
$$= \int_0^\mu de\, g(e)\,(\alpha-\beta e) + \frac{\pi^2}{6\beta}\, g(\mu) + \frac{7\pi^4}{360\beta^3}\, g''(\mu) + \cdots = (7.23) \qquad \text{(R.10)}$$

where $\mu = \alpha_0/\beta_0$ and g'' is the second derivative of g.

R.3 Classification of Gaussian ensembles of Hamiltonian matrices

In the Section (12.3) specific features of spectra of Hamiltonian matrices which are given by the random probability distributions of individual matrix elements are discussed. It is shown there, for instance, that the distribution $P(s)$ of the neighboring level spacing s has a Wigner distribution character, $P(s) \approx \frac{\pi}{2D^2}\, s\, e^{-\frac{\pi}{4}\frac{s^2}{D^2}}$, if the non-diagonal matrix elements of the Hamiltonian matrix constructed within some basis are big (strong interaction between unperturbed basis vectors). If non-diagonal matrix elements in the Hamiltonian

matrix are close to zero (basis vectors do not interact) then the distribution $P(s)$ corresponds to so called Poisson distribution, $P(s) \approx \frac{1}{D}\, e^{-\frac{1}{D}}$, which follows from the assumption that the eigen values of the Hamiltonian matrix are randomly distributed.

In the end of the Subsection 12.3.1.2 it is mentioned that depending in the symmetries of the Hamiltonian matrix (giving the number of independent matrix elements) and assuming the statistical independence of these matrix elements we obtain different character of distributions $P(s)$ (or $P(H)$). In the usual quantum systems (e.g. nuclei) the Hamiltonian is Hermitian and invariant with respect to the time-reverse transformation. In the Subsections 12.3.1.1 and 12.3.1.2 it is shown that these usual symmetries of the Hamiltonian give the distribution $P(H) = \prod_{i,j=1}^{N} P_{ij}(H_{ij})$ in the form of products of Gaussian distributions , $P_{ii} = (\frac{C}{4\pi})^{1/2}\, e^{-\frac{C}{4} H_{ii}^2}$ and $P_{ij} = (\frac{C}{2\pi})^{1/2}\, e^{-\frac{C}{2} H_{ij}^2}$ $(i \neq j)$ (see (12.73) and (12.20) with (12.74) or (12.94)).

This lead in the sixties, seventies and eighties to the investigation of so called Gaussian ensembles of matrices as the ensembles of Hermitian matrices with matrix elements distributed by Gauss distribution and with zero mean values , $\langle H_{ij} \rangle = 0$, for non-diagonal matrix elements $(i \neq j)$. Based on the symmetry of the Hamiltonian with respect to the time-reverse transformation, Hermitian matrices can be divided into three types:

1. real symmetric matrices (time-reverse invariant and invariant with respect to rotations);

2. complex Hamiltonian matrices (no time reverse invariant but invariant with respect to unitary transformations);

3. quaternian matrices (time reverse invariant and invariant with respect to so called "unitary symplectic"transformations.

These 3 possibilities are characterized by 3 values of so called Dyson parameter β. For instance, for the lowest dimensions of these matrices we have following examples of above possibilities:

- ad 1.

$$\beta = 1 \quad , \quad \begin{pmatrix} a & b \\ b & c \end{pmatrix}$$

  where a, b, c are real $\rightarrow$ Hamiltonian is time-reverse invariant and it is also invariant with respect to orthogonal transformations (rotations);

- ad 2.

$$\beta = 2 \quad , \quad \begin{pmatrix} a & x \\ x^* & b \end{pmatrix}$$

where a, b are real and x is complex $\rightarrow$ Hamiltonian is not time-reverse invariant and but is invariant with respect to unitary transformations;

- ad 3.

$$\beta = 4 \quad , \quad \begin{pmatrix} a & 0 & x & y \\ 0 & a & -y^* & x^* \\ x^* & -y & c & 0 \\ y^* & x & 0 & c \end{pmatrix}$$

where a, c are real and x, y are complex (non-diagonal matrix elements are complex) $\rightarrow$ Hamiltonian is time-reverse invariant and is also invariant with respect to so called "unitary symplectic" transformations (but not for rotations).

Corresponding ensembles formed by these matrices are called as
$\beta = 1 \rightarrow$ Gaussian orthogonal ensemble (GOE);
$\beta = 2 \rightarrow$ Gaussian unitary ensemble (GUE);
$\beta = 4 \rightarrow$ Gaussian symplectic ensemble (GSE).
In the Chapter 12 the GOE is only discussed.

R.4 Derivation of eigen values and eigen vectors of two- dimensional matrix H (derivation of exprs. (12.76)-(12.78))

The eigen vectors $|\alpha\rangle$ and $|\beta\rangle$ of two- dimensional matrix H ($H_{11} = \langle 1|\hat{H}|1\rangle$, $H_{12} = \langle 1|\hat{H}|2\rangle$, $H_{21} = \langle 2|\hat{H}|1\rangle$, $H_{22} = \langle 2|\hat{H}|2\rangle$) are supposed to be in the form of linear combinations,

$$|\alpha\rangle = a_\alpha|1\rangle + b_\alpha|2\rangle \quad , \quad |\beta\rangle = a_\beta|1\rangle + b_\beta|2\rangle \tag{R.11}$$

From (12.75) follows that the eigen values E and eigen vectors $a\,|1\rangle + b\,|2\rangle$ fulfil following equations,

$$\begin{aligned} (H_{11} - E)\, a + H_{12}\, b &= 0 \\ H_{21}\, a + (H_{22} - E)\, b &= 0 \end{aligned} \tag{R.12}$$

with the condition of solvability,

$$\begin{vmatrix} H_{11} - E & H_{12} \\ H_{21} & H_{22} - E \end{vmatrix} = 0 \quad \Rightarrow \quad (H_{11} - E)(H_{22} - E) - H_{12}H_{21} = 0 \tag{R.13}$$

and solutions of this quadratic equation is,

$$E_{\alpha,\beta} = \frac{H_{11}+H_{22}}{2} \pm \frac{1}{2}\sqrt{(H_{11}+H_{22})^2 - 4H_{12}H_{21}} \tag{R.14}$$

which gives (12.76) if $H_{21} = H_{12}$.
We substitute (R.14) into the first equation in (R.12),

$$\begin{aligned} & H_{21}\, a_\alpha + (H_{22} - E_\alpha)\, b_\alpha = 0 \\ \Rightarrow \quad & \frac{a_\alpha}{b_\alpha} = \frac{1}{2H_{21}}\left(H_{11} - H_{22} + \sqrt{(H_{11}-H_{22})^2 + 4H_{21}H_{12}}\right) \end{aligned} \tag{R.15}$$

or (R.14) into the second equation in (R.12),

$$\begin{aligned} & (H_{11} - E_\beta)\, a_\alpha + H_{12}\, b_\beta = 0 \\ \Rightarrow \quad & \frac{b_\beta}{a_\beta} = \frac{1}{2H_{12}}\left(H_{22} - H_{11} - \sqrt{(H_{11}-H_{22})^2 + 4H_{21}H_{12}}\right) \end{aligned} \tag{R.16}$$

Eigen vectors $|\alpha\rangle$ and $|\beta\rangle$ are orthonormal,

$$\begin{aligned} & \langle\alpha|\alpha\rangle = a_\alpha^* a_\alpha + b_\alpha^* b_\alpha = 1\ ,\ \langle\beta|\alpha\rangle = a_\beta^* a_\alpha + b_\beta^* b_\alpha = 0 \\ & \langle\beta|\beta\rangle = a_\beta^* a_\beta + b_\beta^* b_\beta = 1 \end{aligned} \tag{R.17}$$

and therefore we can introduce new parameter θ,

$$a_\alpha = \cos\theta \ \ , \ \ b_\alpha = \sin\theta \ \ , \ \ a_\beta = -\sin\theta \ \ , \ \ b_\beta = \cos\theta \tag{R.18}$$

Then equations (R.16), (R.17) give (12.78).

R.5 Poisson Distribution

The idea of the Poisson distribution appeared in nuclear physics for the first time in the connection with the detection of particles. Only in the sixties of the last century the Poisson distribution was used also for the case of the distribution of k levels in the given energy interval in the spectrum of randomly selected system from the ensemble of quantum systems described in the framework of the model of independent particles.

In this section the Poisson distribution is derived for the number of particles detected by a detector in some time interval and in the end it is shown that this distribution can be used also for the number of levels in the given

energy interval of the system when the corresponding particles sitting in eigen states of the mean field Hamiltonian do not interact mutually.

In the derivation of the distribution of particles registered by the detector in the given time interval we start with following assumptions.

- Let us denote $p_k(dt)$ the probability of the registration of k particles in the detector during the time dt if the detector is bombarded by the statistically independent particles;

- The probability $p_1(dt)$ of the registration of one particle in the time dt grows with the intensity n of the impacting beam of particles and with the time interval dt,
$$p_1(dt) = n\,dt \tag{R.19}$$
where n is the beam intensity (n can be dependent on t);

- The probability normalization gives,
$$p_0(dt) + p_1(dt) + p_2(dt) + \cdots = 1 \tag{R.20}$$
where we suppose that the time interval dt is so small that the probabilities $p_k(dt)$ of the registration of k particles for $k > 1$ are infinitezimally small in the comparison with $p_0(dt)$ and $p_1(dt)$. Therefore,
$$p_0(dt) \approx 1 - p_1(dt) = 1 - n\,dt \tag{R.21}$$

- We suppose that the registration of particles by the detector in different times are statistically independent $\Rightarrow$ the probability that particles are not detected in the time interval $t + dt$ is,
$$p_0(t + dt) = p_0(t) \cdot p_0(dt) = \boxed{\begin{array}{c}\text{see}\\ \text{(R.21)}\end{array}} = p_0(t) - n\,p_0(t)\,dt \tag{R.22}$$
From other side we have (from the definition of the derivative),
$$p_0(t + dt) \approx p_0(t) + \frac{dp_0(t)}{dt} \cdot dt \tag{R.23}$$
The comparison of (R.22) and (R.23) gives,
$$\frac{dp_0(t)}{dt} + n\,p_0(t) = 0 \quad \Rightarrow \quad p_0(t) = e^{-nt} \tag{R.24}$$

- Let us investigate the distribution of the registration of k particles ($k \neq 0$) in the time interval $t + dt$. We have following possibilities for their registration:
  $\rightarrow$ k particles are registered in the interval t and 0 particles in the interval dt;
  $\rightarrow$ $k - 1$ particles are registered in the interval t and 1 particle in the interval dt;
  $\rightarrow$ $k - 2$ particles are registered in the interval t and 2 particle in the interval dt;
  $\vdots$
  $\rightarrow$ 0 particles are registered in the interval t and k particles in the interval dt.

It is evident that if registrations in the interval t and dt are statistically independent then the whole probability that we detect k particles in the whole interval $t + dt$ is,

$$p_k(t + dt) = \\ = p_k(t) \cdot p_0(dt) + p_{k-1}(t) \cdot p_1(dt) + \cdots + p_1(t) \cdot p_{k-1}(dt) + p_0(t) \cdot p_k(dt) \tag{R.25}$$

Using the expression (R.21) and(R.19) the expression (R.25) can be rewritten as follows (up to the first power in dt),

$$\begin{aligned} p_k(t + dt) &= p_k(t)\,(1 - n\,dt) + p_{k-1}(t)\,n\,dt + \cdots = \\ &= p_k(t) + n\,(p_{k-1}(t) - p_k(t))\,dt + \cdots \end{aligned} \tag{R.26}$$

From other side $p_k(t + dt)$ can be expressed also as (using the definition of the derivative),

$$p_k(t + dt) = p_k(t) + \frac{dp_k(t)}{dt}\,dt \tag{R.27}$$

and the comparison of (R.26) with (R.27) gives the following equation,

$$\frac{dp_k}{dt} + n\,p_k = n\,p_{k-1} \tag{R.28}$$

The solution of this differential equation can be searched for in the form,

$$p_k(t) = C_k(t)\,e^{-n\,t} \tag{R.29}$$

The substitution of (R.29) into (R.28) enables to rewrite (R.28) as follows,

$$-n\,C_k\,e^{-nt} + \dot{C}_k\,e^{-nt} + n\,C_k\,e^{-nt} = n\,p_{k-1} \quad \Rightarrow \quad \dot{C}_k = n\,p_{k-1}\,e^{nt}$$

$$\Rightarrow \quad C_k(t) = \int_0^t dt'\, n\, p_{k-1}(t')\, e^{nt'} =$$

$$= \boxed{\begin{array}{c}\text{because}\\ p_{k-1}(t') = C_{k-1}(t')\, e^{-nt'} \int_0^{t''} dt''\, n\, p_{k-2}(t'')\, e^{nt''}\end{array}} =$$

$$= \int_0^t dt_1\, n\, e^{nt_1}\, e^{-nt_1} \int_0^{t_1} dt_2\, n\, p_{k-2}(t_2)\, e^{nt_2} = \cdots =$$

$$= \int_0^t dt_1\, n \int_0^{t_1} dt_2\, n \cdots \int_0^{t_{k-1}} dt_k\, n\, e^{nt_k}\, p_0(t_k) = \boxed{\begin{array}{c}\text{see}\\ (R.24)\end{array}} =$$

$$= n^k \int_0^t dt_1 \int_0^{t_1} dt_2 \cdots \int_0^{t_{k-1}} dt_k =$$

$$= \frac{n^k}{k!} \int_0^t dt_1 \int_0^t dt_2 \cdots \int_0^t dt_k = \frac{n^k\, t^k}{k!} \qquad \text{(R.30)}$$

And the substitution of (R.30) onto (R.29) provides,

$$p_k(t) = \frac{1}{k!}\, (nt)^k\, e^{-nt} \qquad \text{(R.31)}$$

If the beam intensity n is time dependent then instead of (R.31) we have,

$$p_k(t) = \frac{1}{k!} \Big(\int_0^t n(t')\, dt' \Big)^k\, e^{-\int_0^t dt'\, n(t')} \qquad \text{(R.32)}$$

Expression (R.31) or (R.32) is called as the Poisson distribution of number k of registered particles in the given time interval t. The distribution (R.31) (or (R.32)) can be also understood as the distribution of time intervals t needed for the registration of given number k of particles.

The same derivation as for (R.31), giving the distribution of the number k of particles registered by the detector during the time t, can be applied for the derivation of the distribution of the number k of levels of given quantum system with energies lying in the energy interval $\langle 0, E\rangle$, that means,

$$p_k(E) = a\, \frac{E^k}{k!}\, e^{-bE} \qquad\qquad a, b \text{ are parameters} \qquad \text{(R.33)}$$

is a probability that k levels are spread out the energy interval $\langle 0, E\rangle$. The crucial point of the derivation of (R.34) is mutual statistical independence of levels, that means

$$p_k(E + dE) = p_k(E) \cdot p_0(dE) + p_{k-1}(E) \cdot p_1(dE) + \\ \cdots + p_1(E) \cdot p_{k-1}(dE) + p_0(E) \cdot p_k(dE) \qquad \text{(R.34)}$$

with $p_0(E+dE) = p_0(E) \cdot p_0(dE)$. This corresponds to the fact that corresponding states are eigen states of the Hamiltonian matrices from the ensemble of statistically independent matrices. For $k = 0$ the probability $p_0(E)$ means that in the interval $\langle 0, E\rangle$ there is not any eigen energy (level). So the probability $p_0(E)$ can be interpreted as the distribution of level spacing s between neighboring levels, that means (see (12.88)),

$$P(s) = p_0(s) = \frac{1}{D}\, e^{-\frac{s}{D}} \tag{R.35}$$

R.6 Derivation of the expression for the distribution $P(C_1^{(\alpha)})$ (see (12.106)) of the amplitude $C_1^{(\alpha)}$ in the eigen vector of $N \times N$ matrices from GOE ensemble.

In this section the derivation of the distribution (12.106) for the amplitude $C_1^{(\alpha)}$ of the eigen vector $|\alpha\rangle = \sum_{j=1}^{N} C_j^{(\alpha)} |j\rangle$ (see (12.94)) of the GOE matrices is shorly described. The case of $N = 2$ was already discussed (see (12.90).

In the general case $N > 2$ we start with the distribution (12.104). For $N = 3$ we have,

$$P(C_1) = \int_0^\infty dC_2 \int_0^\infty dC_3\, P(C_1, C_2, C_3) =$$

$$= \frac{2}{\Omega_3} \int_{-\infty}^{\infty} dC_2 \int_{-\infty}^{\infty} dC_3\, \delta(1 - C_1^2 - C_2^2 - C_3^2) = \boxed{\begin{array}{c}\text{see}\\ (12.105)\end{array}} =$$

$$= \frac{1}{4\pi} \int_{-\infty}^{\infty} dC_2 \int_{-\infty}^{\infty} dC_3\, \delta(1 - C_1^2 - C_2^2 - C_3^2) =$$

$$= \boxed{\begin{array}{c}\text{polar coordinates for the space } (C_2, C_23)\\ C_2 = r\, \cos\varphi\ ,\ C_3 = r\, \sin\varphi\end{array}} =$$

$$= \frac{1}{2\pi} \int_0^\infty dr \int_0^{2\pi} dC_3\, r\, \delta(r^2 - (1 - C_1^2) = \int_0^\infty dr\, r\, \delta(r^2 - (1 - C_1^2) =$$

$$= \boxed{\begin{array}{c} r_1 = \sqrt{1 - C_1^2}\\ r_2 = -\sqrt{1 - C_1^2}\end{array}} = \int_0^\infty dr\, r \left(\frac{\delta(r - r_1)}{|\frac{d}{dr} r^2|_{r=r_1}} + \frac{\delta(r - r_2)}{|\frac{d}{dr} r^2|_{r=r_2}} \right) =$$

$$= \boxed{\begin{array}{c} r_2 \text{ does not}\\ \text{contribute}\end{array}} = \frac{1}{2} \tag{R.36}$$

which is in accordance with the general expression (12.106),

$$P(C_1) = \frac{\Omega_{N-1}}{\Omega_N} \left(1 - C_1^2\right)^{\frac{N-3}{2}} \tag{R.37}$$

if $N = 3$ (because $\frac{\Omega_2}{\Omega_3} = \frac{1}{2}$ - see (12.105)).

For general case N the polar coordinates are introduced for $(N-1)$-dimensional space,

$$dV_{N-1} = r^{N-2}\, d\Omega_{N-1}\, dr \qquad\qquad r^2 = \sum_{i=2}^{N} C_i^2 \tag{R.38}$$

where $d\Omega_{N-1}$ is the "space angle"element of the $(N-1)$- dimensional space. Then we can determine the integral,

$$\begin{aligned}
P(C_1) &= \boxed{\begin{array}{c}\text{see}\\ (12.104)\end{array}} = \\
&= \frac{2}{\Omega_N} \int_0^\infty dC_2 \int_0^\infty dC_3 \cdots \int_0^\infty dC_N\, \delta(1 - C_1^2 - \sum_{i=2}^{\infty} C_i^{(\alpha)\,2}) = \\
&= \frac{2}{\Omega_N} \int d\Omega_{N-1} \int_0^\infty dC_3 \cdots \int_0^\infty dC_N\, \delta\big(r^2 - (1 - C_1^2)\big) = \\
&= \frac{2\,\Omega_{N-1}}{\Omega_N} \int dr\, r^{N-2} \sum_{k=1,2} \frac{\delta(r - r_k)}{2r_k} = \\
&= \boxed{\begin{array}{c}\text{because } r_1 = \sqrt{1 - C_1^{(\alpha)\,2}} = -r_2\\ \text{and } r_2 \text{ does not contribute}\end{array}} = \frac{\Omega_{N-1}}{\Omega_N} \left(1 - C_1^{(\alpha)\,2}\right)^{\frac{N-3}{2}} = \\
&= (12.106) \text{ or } (R.37)
\end{aligned} \tag{R.39}$$

R.7 Ergodicity of canonical systems - canonical ensemble as the mean value of all possible distributions

In this section the ergodicity of canonical systems is discussed, particularly it is shown that the system state distribution in the canonical system is given by the most probable distribution in the phase space of this system.

We start with a classical microcanonical system. Let us denote $\rho(q, p)$ as the density of the probability (distribution function) that the investigated

microcanonical system of particles is found in the unity volume of the phase space in the vicinity of its point, $(p,q) \equiv (q_i, p_i)$ where $i = 1, \cdots, n_d$ enumerates degrees of freedom of the system (q_i are generalized coordinates and p_i are corresponding conjugated linear momenta). We suppose that the microcanonical system is in its thermodynamic equilibrium and therefore $\rho(q,p)$ does not depend on the time explicitly. It is also supposed that the density $\rho(p,q)$ is normalized to 1 ($\int dq\, dp\, \rho(q,p) = 1$). Then the mean (expectation) value of an arbitrary dynamical quantity $F(q,p)$ is

$$\langle F \rangle = \int dq\, dp\, \rho(q,p)\, F(q,p) \tag{R.40}$$

where $\rho(q,p) \neq 0$ for phase-space points on the given energy surface $E(q,p) = E$ for microcanonical systems. The quantity $F(t) = F(q(t), p(t))$ is dependent on the time t through the trajectory $(q(t), p(t))$ in the phase space (which is the solution of the equation of motion with the system Hamiltonian corresponding to the given system energy $E = H(q(t), p(t))$). Then there is a question if the expectation value $\langle F \rangle$ is or is not equal to the time mean field value,

$$\bar{F} = \lim_{\tau \to \infty} \int_{t_0}^{t_0+\tau} F(t) dt \tag{R.41}$$

where t_0 is arbitrary time. The answer for general (not microcanonical) system is that **generally $\langle F \rangle \neq \bar{F}$ and that $\langle F \rangle = \bar{F}$ only for so called ergodic systems**. The equivalence $\langle F \rangle = \bar{F}$ is understood as the definition for the ergodicity of the system. It is possible to show that this definition can be formulated also as is given below (see e.g. [131, 391]),
Given system is ergodic in some part of its phase-space if the the time average $\bar{F}$ and the phase space average $\langle F \rangle$ of any quantity F are equivalent, $\langle F \rangle = \bar{F}$. This is valid if during its time evolution the phase-space trajectory passed through each point of this part of the phase-space an equal number of times.

This condition, which was introduced by Boltzmann in 1871 as to be fulfilled in each microcanonical system located in the given energy surface $E = H(q,p)$, is known as the **ergodic hypothesis**.

For one dimensional case ($n_d = 1$) the statement that any microcanonical system is ergodic in the energy surface is clear from the discussion above. For higher dimensional systems, however, one can prove mathematically that the phase-space trajectory, in principle, can never pass through all points of the energy surface. The reason for this is that on the one hand Hamilton equations of motion always have a unique solution, so that the phase-space

trajectory can never cross itself, but on the other side it is problematic to map a one-dimensional time interval onto n_d- dimensional energy surface element. For the identity of time averages and phase-space (or ensemble - as will be discussed further) averages, it is not necessary that the phase-space trajectory really pass through every point of the energy surface. It is sufficient if the trajectory comes arbitrarily close to each point (this assumption is the so called quasi ergodic hypothesis - see e.g. [391] and strictly mathematically e.g. [392]).

Instead of one microcanonical system with the distribution function $\rho(q,p)$ we will consider now the ensemble of $\mathcal{N}$ identical microcanonical systems (all systems have the same number n_d of degrees of freedom, the same number of particles and the same energy surfaces). In general, these microsystems are different from each other, but they must lie in the same energy surface $\sigma(E)$ of their phase-spaces. Further we sub-divide the energy surface into equally large surface elements $\Delta\sigma_i$ ($\sigma(E) = \sum_i \Delta\sigma_i$). Each of these surface element contains a number n_i of systems. If we choose the surface elements to be sufficiently small, then each of these elements corresponds exactly to one micro-state (one state of the microcanonical system). Then we have,

$$\mathcal{N} = \sum_i n_i \tag{R.42}$$

Then the number $n_i/\mathcal{N}$ is the probability for the micro-state i to lie in the element Δ_i. The probability $p_i = n_i/\mathcal{N}$ therefore corresponds to $\rho(q,p)\,dq\,dp$ **(for $\mathcal{N} \to \infty$)**,

$$\frac{n_i}{\mathcal{N}} \quad \leftrightarrow \quad \rho(q,p)\,dq\,dp \tag{R.43}$$

One of the basic assumption of statistical physics is that all micro-states are, in principle, equally likely and thus have the same probability ω_i. This means that the probability p_i of finding a microcanonical system in the energy surface element $\Delta\sigma_i$ is proportional to its size (see [391]).

Now we will consider the ensemble of $\mathcal{N}$ identical **canonical systems** with corresponding phase-space Ω. In the canonical system the energy E_i of the system is not fixed. Therefore, all phase-space points $(q,p) \in \Omega$ with different energies can be occupied. We sub-divide the total phase-space Ω into equally sized enumerated cells $\Delta\Omega_i$. If these cells are sufficiently small, each of them corresponds to exactly one micro-state i and each of them is in one micro-state at fixed time. Let there be just n_i systems in each phase-space

cell $\Delta\Omega_i$. Then we have,

$$\mathcal{N} = \sum_i n_i \tag{R.44}$$

where the sum extends over all phase-space cells (not only over the energy surface as in (R.42) for microcanonical systems). However, just as in the microcanonical case, $p_i = n_i/\mathcal{N}$ is the probability that the micro-state i appears in the cell $\Delta\Omega_i$. We suppose that all systems are in the thermodynamical equilibrium and therefore a certain mean value of energy will be established in each system in the ensemble, which is further denoted as U. The quantity U must be given as a statistical mean value of all energies E_i which are actually assumed in the ensemble,

$$U = \langle E \rangle = \sum_i p_i \, E_i = \sum_i \frac{n_i}{\mathcal{N}} \, E_i \overset{\mathcal{N}\to\infty}{\longrightarrow} \int_{(q,p)\in\Omega} dq \, dp \, \rho(q,p) \, E(q,p) \tag{R.45}$$

That means for a large canonical ensemble ($\mathcal{N} \to \infty$) the ensemble mean energy is approximately equal to the system mean energy.

In the book [391] (see expressions (7.211), (7.212) therein) the following relation between the mean number $\langle n_i \rangle$ of the canonical systems in the micro-state i (or the cell with the index i which is equivalent for sufficiently big $\mathcal{N}$), corresponding standard deviation $\langle (\Delta n_i)^2 \rangle = \langle n_i^2 \rangle - \langle n_i \rangle^2$ and the number $\mathcal{N}$ of systems in the ensemble, was derived,

$$\frac{\langle (\Delta n_i)^2 \rangle}{\langle n_i \rangle^2} = \frac{1}{\langle n_i \rangle} - \frac{1}{N} \left[1 + \frac{(E_i - U)^2}{\langle (E_i - E)^2 \rangle} \right] \tag{R.46}$$

For $\mathcal{N} \to \infty$ all $\langle n_i \rangle \to \infty$, and therefore relative fluctuations in the micro-state i vanishes. In other words: **Not only is the mean energy in the canonical ensemble identical to the most probable energy (see (R.45)), but the phase-space distribution density is given also by the most probable ensemble distribution $p_i = \langle n_i \rangle / \mathcal{N}$ of all possible distributions (for $\mathcal{N} \to \infty$)**. The deviations (fluctuations) of this distribution vanishes for a large number of systems in the canonical ensemble ($\mathcal{N} \to \infty$). That means, for $\mathcal{N} \to \infty$ the ensemble system distribution of $\langle n_i \rangle / \mathcal{N}$ in the canonical ensemble corresponds exactly to the most probable density distribution $\rho(q,p)$ of the finding the canonical system in unit volume of the the phase-space in the vicinity of the point (q,p).

Since we speak about the most probable density distribution and/or mean ensemble distribution for canonical systems in the thermodynamical equilibrium it is possible to expect that this distribution is stable in time. Therefore,

in agreement with the definition of the ergodicity of the classical system (see the text below the expression (R.41)) it would seem that all canonical ensembles are ergodic in the full phase-space. However one should be careful. The problem with the canonical system consists in the fact that, opposite to microcanonical systems, all trajectories in the phase-space are not located at the same energy surfaces and the distribution of energy in the phase-space is not homogeneous. The inhomogeneity of the energy distribution is connected with the structure and symmetries of the system Hamiltonian with the increasing excitation energy of the system. Therefore, depending on the system Hamiltonian and its symmetries, the ergodicity of the canonical system is usually found only is some parts of the phase-space.

From the discussion below the expression (12.89) we know that if the mean distribution of the probability of finding the system in the point (q, p) of the phase-space is homogeneously spread and constant in some subspace of the phase-space the classical system behaves chaotically and if regular patterns can be recognized in the Poincare cuts of the phase-space then the system is regular with periodical trajectories in this subspace (see the footnote 6 in the Chapter 12). That means the statistical analyzes of the ensemble of canonical systems can give an information about the chaotic or regular character of the canonical system,

So far we have discussed classical systems. The situation with the quantum systems is more complicated because quantum systems have not clear trajectories in the phase-space, even the phase-space itself cannot be introduced in quantum mechanics. Nevertheless, in the case of the ensemble of quantum systems we can speak about chaotic or regular behavior. As it is discussed in the text below the expression (12.89) it is believed that quantum systems with the Wigner level spacing probability distribution $P(s)$ (see (12.88) tends to the regular behavior in classical physics while the Poisson distribution $P(s)$ (see (12.89)) corresponds rather to the chaotic character of the system if it is treated classically. As it concerns ergodicity in canonical quantum systems in the analogy with the classical expression (12.46) it is believed that the ergodicity can be expected for quantum ensembles if the ensemble variance (fluctuations)) of quantities connected directly with the system spectra are small (see e.g. [390]) and citations therein).

S. Importance sampling Monte Carlo integration

Monte Carlo integration (MCI) is the statistical method for the estimation of the integral using the random sampling. Further the idea of the MCI is shortly described.

We want to estimate an integral $I = \int_\Omega f(\vec{x})d\vec{x}$ on the area Ω with the volume $V = \int_\Omega d\vec{x}$. The naive Monte Carlo approach is to sample area points uniformly on the Ω by N samples $\vec{x}_1, \vec{x}_2, \cdots, \vec{x}_N$,

$$I \approx Q_N \equiv \sum_{i=1}^{N} \frac{V}{N} f(\vec{x}_i) \boxed{\begin{array}{c}\text{if sample points are}\\ \text{distributed uniformly}\end{array}} = \frac{V}{N}\sum_{i=1}^{N} f(\vec{x}_i) = V \cdot \langle f \rangle \tag{S.1}$$

Corresponding variances are:

$$\begin{aligned} Var(f) \equiv \sigma_N^2 &= \frac{1}{N}\sum_{i=1}^{N}\big(f(\vec{x}_i) - \langle f\rangle\big)^2 = \frac{1}{N}\sum_{i=1}^{N}(f(\vec{x}_i))^2 - \langle f\rangle^2 \\ Var(Q_N) &= \frac{V^2}{N^2}\sum_{i=1}^{N} Var(f) = V^2\frac{Var(f)}{N} = V^2\,\frac{\sigma_N^2}{N} \end{aligned} \tag{S.2}$$

So the mean square deviation of the uniformly sampled estimation Q_N is $\delta Q_N = \sqrt{Var(Q_N)} = V\frac{\sigma_N}{\sqrt{N}}$. That means the mean square deviation decreases with the increasing N as $\frac{1}{\sqrt{N}}$.

Let us suppose now that the sampling points are not distributed on the area Ω uniformly and that sampling points are distributed over Ω with some probability density $p(\vec{x})$. That means $p(\vec{x}_i)$ is the probability that in the unit volume around the point $\vec{x}_i \in \Omega$ there is a sampling point $\Rightarrow N \cdot p(\vec{x}_i)$ is the number of sampling points in the unit volume in the point $\vec{x}_i \in \Omega \Rightarrow$ i-th sampling point occupies the volume $1/(N \cdot p(\vec{x}_i))$ of the whole area Ω with the value $f(\vec{x}_i)$ of the integrand and therefore it contributes to the Q_N with the contribution $\frac{1}{N\cdot p(\vec{x}_i)} \equiv \frac{1}{G(\vec{x}_i)}$. Therefore the whole integral is approximated

by,

$$I \approx Q_N = \sum_{i=1}^{N} \frac{f(\vec{x}_i)}{N \cdot p(\vec{x}_i)} = \sum_{i=1}^{N} \frac{f(\vec{x}_i)}{G(\vec{x}_i)} \qquad \text{with} \qquad G(\vec{x}_i) \equiv N \cdot p(\vec{x}_i) \tag{S.3}$$

In our case (see (7.477) we take $G(\vec{\sigma}) = G(\sigma) = e^{-\beta|V|\sigma^2}$ (which is proportional to the Gauss probability distribution),

$$I = \int_{-\infty}^{\infty} d\sigma \, e^{-\beta|V|\sigma^2} e^{-\beta|V|\sigma\hat{Q}} = \sum_{i=1}^{N} \frac{e^{-\beta|V|\sigma_i^2} e^{-\beta|V|\sigma_i\hat{Q}}}{e^{-\beta|V|\sigma_i^2}} = \sum_{MC;\,\sigma} e^{\beta|V|\sigma\hat{Q}} \tag{S.4}$$

Bibliography

[1] Hofstadter R., Ann. Rev. Nuclear Sci. **7**, 231 (1957).

[2] Varshalovich D.A., Moskalev A.N., Khersonski V.K., Quantum Theory of Angular Momentum, (World Scientific, Singapore, 1976).

[3] von Weizsacker C.F., Z. Phys. **96**, 431 (1935).

[4] De Shalit A., Feshbach H., Theoretical Nuclear Physics, Vol.I, Nuclear Structure, Wiley N.Y., 1974.

[5] Hornyak W.F., Nuclear Structure, Academic N.Y., 1975.

[6] Bohr A., Mottelson B.R., Nuclear Structure I, Benjamin, N.Y., 1969.

[7] Soloviev V.G., Theory if Complex Nuclei, Nauka, Moscow, 1971 (in Russian) or Theory of Complex Nuclei, Pergamon Press, London, 1976 (in English)

[8] Soloviev V.G., Theory of Atomic Nuclei: Quasiparticles and Phonons, Institute of Physics, Bristol, 1993.

[9] Ring P., Schuck P., The Nuclear Many-Body Problem, Springer, New York, 1980.

[10] Rose M.E., Elementary Theory of Angular Momentum, J.Wiley and Sons, New York, 1957.

[11] Rowe D.J., Nuclear Collective Motion, Butler and Tanner Ltd., London, 1970.

[12] Sakurai J.J., Modern Quantum Mechanics - Revised Adition, Addison-Wesley Pub. Company Reading, N.Y. 1994.

[13] Mandl F., Shaw G., Quantum Field Theory, A.Wiley and sons Interscience Publication, N.Y. 1988.

[14] Formanek J., Introduction to Quantum Theory (in Czech), Academia, Praha 1983.

[15] Weisskopf V.F., Phys. Rev **83**, 1073 (1951).

[16] Wick G.C., Phys. Rev. **80**, 268 (1950).

[17] Thouless D.J., Nuclear Physics **21**, 225 (1960).

[18] Brueckner K.A., Phys. Rev. **97**, 1353 (1955).

[19] Day B.D., Rev. Mod. Phys. **39**, 719 (1967).

[20] Skyrme T.H.R., Phil. Mag. **1**, 1043 (1956).

[21] Gogny D., Nucl. Phys. **A237**, 399 (1975).

[22] Ring P., Prog. Part. Nucl. Phys. **37**, 193 (1996).

[23] Feshbach H., Theoretical Nuclear Physiscs Vol II, Nuclear reactions, John Wiley & Sons, N.Y. 1992.

[24] Bryan R.A., Proc. Int. Nuclear Physics Conf. Gattinburg, N.Y., p.603, (1967)

[25] Machleidt R., Entem D.R/, Chiral Effective Field Theory and Nuclear Forces, Physics Reports 503, 1 (2011)

[26] Papakonstantinen, Roth R., Paar N, Phys. Rev. **C75**, 014310 (2007).

[27] Sprung D.W., Banerjee P.K., Nuclear Physics **A168**, 273 (1971).

[28] Negele J., Phys. Rev. **C1**, 1260 (1970)

[29] Campi X., Sprung D.W.L., Nuclear Physics **A194**, 401 (1972)

[30] Song H.Q., Baldo M., Giansiracussa G., Lombardo U., Phys. Rev. Letters **81**, 1584 (1998)

[31] Lipparini E., Modern Many-Particle Physics - Atimic Gases, Quantum Dots and Quantum Fluids, World Scientific Pub. Co, Singapore, 2003

[32] Navratil P., Vary J.P., Barret B.R., Phys. Rev. **C62**, 054311 (2000)

[33] Skyrme T.H.R., Phil. Mag. 1, 1043 (1956); Nucl. Phys. 9, 615 (1959)

[34] Giambrone G., et al., Nucl. Phys. **A726**, 3 (2003)

[35] Vretenar D., Afanasjev A.V., Lalazissis G.A., Ring P., Physics Reports **409**, 101 (2005)

[36] Serot B.D., Walecka J.D., Adv. Nucl. Phys. **16**, 1 (1986)

[37] Sharma M.M., Nagarajan M.A., Ring P., Phys. Lett. **B312**, 377 (1993)

[38] Koopmans T., Physica 1, 104 (1934)

[39] Caurier E., Martinez-Pinedo G., Nowacki F., Poves A., Zucker A.P., Rev. Mod. Phys. **77**, 427 (2005)

[40] Haxton W.C., Johnson C.J., Phys. Rev. Letters **65**, 1325 (1990)

[41] Andreozzi F., Knapp F., Lo Iudice, Porino A., Kvasil J., Phys. Rev. **C78**, 054308 (2008)

[42] Dytrych T., Sviratcheva K.D., Bahri C., Draayer J.R., Vary J.P., Phys. Rev. Letters **98**, 1620503 (2007)

[43] Mulliken R.S., Phys. Rev. **41**, 49 (1937)

[44] Born M., Oppenheimer J.R., Annalen der Physik **389**, 457 (1927)

[45] Eckart C., Phys. Rev. **46**, 383 (1935)

[46] Seaborg G., Science **104**, 379 (1946)

[47] Myers W.D., Swiatecki J., Nucl. Phys. 81, 1 (1966)

[48] Goepert-Mayer M., Phys. Rev. **75**, 1969 (1949)

[49] Haxel O., Jensen J.H.D., Suess H.E., Phys. Rev. **75**, 1766 (1949)

[50] Nilsson S.G., Mat. Fys. Medd. Dan. Vid. Selsk **29**, No 16 (1955)

[51] Woods R.D., Saxon D.S., Phys. Rev. **95**, 577 (1954)

[52] Alarcon R., Laszewski R.M., Dale D.S., Phys. Rev **C40**, R1097 (1989)

[53] Lipparini E., Stringari S., Phys. Report **175** No 3+4, 103-261 (1989)

[54] Mayer M.G., Jensen J.H.D., Elementary Theory of Nuclear Shell Structure, Wiley, New York 1955

[55] Jain A.K., Sheline R.K., Sood P.C., Jain Kiran, Rev. Mod. Phys. **62**, No 2, 393 (1990)

[56] Strutinski V.M., Nucl. Phys. **A 95**, 420 (1967); Nucl. Phys. **A122**, 169 (1968)

[57] Soloviev V.G., Theory of Complex Nuclei, Pergamon, Oxford 1976

[58] Abramowitz M., Stegun A., Handbook of Mathematical Functions, Dover N.Y., 1965

[59] Brack M., Pauli H.C., Nucl. Phys. **A 207**, 401 (1973)

[60] Nilsson S.G., Tsang C.F., Sobiczewski A., Szymanski Z., Wycech C., Gustafson C., Lamm I.-L., Moeller P., Nilsson B., Nucl. Phys. **A131**, 1 1969

[61] Ragnarsson, Proc. 6th. Conf. on Atomic Masses, East Lansing, Michigan 1979 (Plenum Press New York 1890), p.87

[62] Meitner L., Hahn O., Strasman F., Z. Phys. **106**, 249 (1937)

[63] Meitner L., Frisch O.R., Nature **143**, 239 (1939)

[64] Frenkel J., Phys. Rev. **55**, 987 (1939)

[65] Bohr N., Wheeler J.A., Phys. Rev. **56**, 426 (1939)

[66] Vanderbosch R., Huizenga J.R., Nuclear Fission, Academic Press, N.Y. and London, 1973

[67] Nilsson S.G., Ragnarsson I., Shapes and Shells in Nuclear Structure, Cambridge Press, 2005

[68] Moeller P., Nix J.R., Proc. Third IAEA Symp. on Physics and Chemistry of Fission, Rochester, N.Y., IAEA Vienna, 1974

[69] Moeller P., Nilsson S.G., Phys. Lett. **B31**, 283 (1970)

[70] Landau L.D., Lifshitz E.M., Quantum Mechanics, Non-Relativistic Theory, London 1958

[71] Greiner W., Ivascu M., Poenaru D.N., Sandulescu A., in Treatise on Heavy-Ion Science, Vol 8: Nuclei Far From Stability, ed. D.A.Bromley, Plenum Press, N.Y. 1989

[72] Krappe H.J., Pomorski K., Theory of Nuclear Fission, Springer, Berlin 2013

[73] Baran A., Pomorski K., Lukasiak A., Sobiczewski A., Nucl. Phys. **A361**, 83 (1981)

[74] Dvorak J., et al., Phys. Rev. Letters **97**, 242501 (2006)

[75] Emsley J., Nature's Building Blocks, Oxford Univ. Press, 2001

[76] https://www-nds.iaea.org/relnsd/vcharthtml/VChartHTML.html

[77] Petermann I., Reinhard P.-G., Thielemann F.-K., Eur. Phys. J. **A48**, 122 (2012)

[78] Erler J., Langanke K., Loens H.P., Martinez-Pinedo G., Reinhard P.-G., Phys. Rev. **C85**, 025802 (2012)

[79] Kluepfel P., Reinhard P.-G., Buervenich T.J., Maruhn A.J., Phys. Rev. **C70**, 034310 (2009)

[80] Talmi I., Helv. Phys. Acta **25**, 185 (1952)

[81] Moshinsky M, Nucl. Phys. **13**, 104 (1959)

[82] Buck B., Merchant A.C., Nucl. Phys. **A600**, 387 1996

[83] Stone J.R., Reinhard P.-G., Progress in Particle and Nuclear Physics **58**, 587 (2007)

[84] Vautherin D., Brink D.M., Phys. Rev. **C5**, 626 (1972)

[85] Raimondi F., Carlsson B.G., Dobaczewski J., Phys. Rev. **C83**, 054311 (2011)

[86] Van Giai N., Sagawa H., Phys. Letters **B106**, 379 (1981)

[87] Reinhard P.-G., Flocard H., Nucl. Phys. **A584**, 467 (1995)

[88] Bartel J., Quentin P., Brack M., Guet C., Hakansson H.-B., Nucl. Phys. **A386**, 79 (1982)

[89] Reinhard P.-G., Dean D.J., Nazarewicz W., Dobaczewski J., Maruhn J.A., Strayer M.R. Phys. Rev. **C60**, 014316 (1999)

[90] Tondeur F., Brack M., Farine M., Pearson J.M., Nucl. Phys. **A420**, 297 (1984)

[91] Chabanat E., Bonche P., Hamsel P., Meyer J., Schaeffer R., Nucl. Phys. **A635**, 231 (1998)

[92] Kvasil J., Nesterenko V.O., Kleinig W., Bozik D., Reinhard P.-G., Lo Iudice N., Eur. Phys. J. **A49**, 119 (2013)

[93] Audi G., et al., Nucl Phys. **A729**, 337 (2013)

[94] Dobaczewski J., Bennaceur K., Raimondi F., Journal of Phys. **G39**, 125103 (3013)

[95] Mottelson B.R., Rendiconti della Scuola Internationale di Fisica, Corso XV, Varemma (Zanichelli, Bologna, 1962), p.44

[96] Bardeen J., Cooper L.N., Schrieffer J.R., Phys. Rev. **108**, 1975 (1957)

[97] Bogoliubov N.N., J. Phys. (USSR) **11**, 23 (1947)

[98] Bohr A., Mottelson B.R., Pines D., Phys. Rev **C110**, 936 (1958)

[99] Bohr A., Mottelson B.R., Nuclear Structure, Vol II, Benjamin N.Y., 1974

[100] Bloch C., Messiah A., Nuclear Physics **39**, 95 (1962)

[101] Kerman A.K., Ann. Phys. (N.Y.) 12, 300 (1961)

[102] Bohr A., Mat. Fys. Med. Dan. Vid. Selsk. **26**, No. 14 (1952)

[103] Iachello F., Talmi I., Rev. Mod. Phys. **58**, 339 (1982)

[104] Messiah A., Quantum Mechanics, North Holland, Amsterdam, 1961

[105] Nathan P., Nilsson S.G., Alpha-, Beta- and Gamma- Ray Spectroscopy, K. Siegbahn, Ed. North Holland, Amsterdam, 1965

[106] Suzuki T., Nuclear Physics **217**, 182 (1973)

[107] Eisenberg j.M., Greiner W., Microscopic Theory of the Nucleus, North Holland, Amsterdam 1987

[108] Bohr a., Mottelson B.R., Mat. Fys. Medd. Dan. Vid. Selsk **27**, No 16 (1953)

[109] Bohr N., Kalckar F., Mat. Fys. Medd. Dan. Vid. Selsk **14**, No10 (1937)

[110] Heyde K., Basic Ideas and Concepts in Nuclear Physics, Institute of Physics Publishing, Bristol, 1999

[111] Rowe D.J., Wood J.L., Fundamentals of Nuclear Models, World Scientific, Singapore, 2010

[112] Frank A., Van Isacker P., Symmetry Method in Molecules and Nuclei, S y G editors S.A. de C.V. Mexico D.F., 2005

[113] Arima A., Iachello F., Ann. Phys. (N.Y.) **99**, 253 (1976)

[114] Arima A., Iachello F., Ann. Phys. (N.Y.) **111**, 201 (1978)

[115] Arima A., Iachello F., Ann. Phys. (N.Y.) **123**, 201 (1979)

[116] Iachello F., Arima A., The Interacting Boson Model, Cambridge Univ. Press, Cambridge (1987)

[117] Janssen D., Jolos R.V., Doenau F., Nuclear Physics **A224**, 93 (1974); Jolos R.V., Doenau F., Janssen D., Sov. J. Nucl. Phys. **22**, 503 (1975)

[118] Scholten O., Prog. Part. Nucl. Phys. **14**, 189 (1985)

[119] Elliott J.P., Proc. Roy. Soc. Ser. **A245**, 562 (1958)

[120] Meyer-te-Vehn J., in "Interacting Bosons in Nuclear Physics", F. Iachello, ed., Plenum Press, New York, p.137 (1979)

[121] Wilets j., Jean M., Phys. Rev. **102**, 788 (1956)

[122] Cizewski J.A., Casten R.F., Smith G.J., Stelts M.L., Kan W.R., Boerner H.G., Davidson W.F., Phys. Rev. Lett. **40**, 167 (1978)

[123] Casten R.F., Nuclear Structure from a Simple Perspective, Oxford University Press, 1990

[124] Arima A., Iachello F., Phys. Rev. Lett. **35**, 1069 (1975)

[125] Schwinger J., in "Quantum Theory of Angula Momentum", L.Biedenharn and H.van Dam, ed., Academic Press, N.Y., p. 222 (1965)

[126] Iachello F., Van Isacker P., The Interacting-Fermion Model, Cambridge University Press, 1991

[127] Scholten O., Iachello F., Arima A., Ann. Phys. (N.Y.) **115**, 325 (1978)

[128] Iachello F., Zamfir N.V., Casten R.F., Phys. Rev. Lett. **81**, 1191 (1998)

[129] Cejnar P., Jolie J., Phys. Rev. **E58**, 387 (1998)

[130] Dipering A.E.L., Scholten O., Iachello F., Phys. Rev. Lett. **44**, 1747 (1980)

[131] Landau L.D., Lifshitz E.M¿, Statistical Physics, Course of Theoretical Physics, Butterworth -Heinsnann, Oxford, 2001, Part 1, Vol. V

[132] Schiffer J.P., True W.W., Rev. Mod. Phys. **48**, 191 (1976)

[133] Arima A., Otsuka T., Iachello F., Talmi I., Phys. Lett. **66B**, 205 (1977)

[134] Otsuka T., Arima A., Iachello F., Talmi I., Phys. Lett. **76B**, 139 (1978)

[135] Van Isacker P., Warner D.D., J. Phys. G: Nucl. Phys. **20**, 853 (1994)

[136] Kishimoto T., Tamura T., Nucl. Phys. **A 270**, 317 (1977)

[137] Holstein T., Promacoff H., Phys. Rev. **58**, 1098 (1940)

[138] Iachello F., Van Isacker P., The Interacting Boson-Fermion Model, Cambridge University Press, Cambridge, (1991)

[139] Rowe D.S., Wong S.S.M., Phys.Lett. **30B**, 147 (1969); Nucl. Phys. **A153**, 561 (1970)

[140] Iachello F., Phys. Rev. Lett. **85**, 3580 (2000)

[141] Iachello F., Phys. Rev. Lett. **87**, 052502 (2001)

[142] Iachello F., Phys. Rev. Lett. **91**, 132502 (2003)

[143] Bohm D., Pines D., Phys.Rev. **92**, 609 (1953)

[144] Gell-Mann M., Brueckner A., Phys.Rev. **106**, 364 (1957)

[145] Savada K, Phys.Rev. **106**, 372 (1957)

[146] Belyaev S.T., Zelevinskii V.G., Nucl. Phys. **39**, 582 (1962)

[147] Marshalek E.R., Nucl. Phys. **A224**, 221 (1974)

[148] Marumori T., Yamamura M., Tokunaga A., Progr. Theor. Phys. **31**, 1009 (1964)

[149] Marumori T., Yamamura M., Tokunaga A., Progr. Theor. Phys. **32**, 726 (1964)

[150] Ring P., Schuck P., Phys. Rev. **C16**, 801 (1977)

[151] Belyaev S.T., Mat.Fys.Medd.Dan.Vid.Selsk **31** (No11) (1959)

[152] Belyaev S.T., Nucl. Phys. **24**, 322 (1961)

[153] Sarriguren P., Moya de Guerra, Escudens A., Nuclear Physics **A691**, 631-648 (2001)

[154] Nesterenko V.O., Kvasil J., Reinhard P.-G., Phys. Rev. **C66**, 044307 (2002)

[155] Peierls R.E., Yoccoz J., Proc. Phys. Soc (London) **A70**, 381 (1957)

[156] Shirikova N.Yu., Suschkov A.V., Jolos R.V., Phys.Rev. **C88**, 064319 (2013)

[157] Suhonen J., Nucl. Phys. **A853**, 36 (2011)

[158] Suhonen J., From Nucleons to Nucleus, Springer-Verlag Berlin Heidelberg, 2007

[159] Kisslinger L.S., Sorensen R.A., Mat. Fys.. Dan. Vid. Selsk 32, No 9 (1960)

[160] Waroquier M., Heyde K., Wenes G., Nucl. Phys. **A404**, 269 (1983)

[161] Waroquier M., Wenes G., Heyde K., Nucl. Phys. **A404**, 298 (1983)

[162] Terasaki J., Engel J., Phys. Rev. **C84**, 014332 (2011)

[163] www.nndc.bnl.gov

[164] Soloviev V.G., Theory of Atom Nucleus, Energoatomizdat Moscow, 1989

[165] Bertsch G.F., Tsai S.F., Phys. Reports **18** (No.2), 125-158 (1975)

[166] Soloviev V.G., Sushkov A.V., Shirikova N.Yu., J. Phys. G: Nucl. Part. Phys. 20, 113-134 (1994)

[167] Soloviev V.G., Sushkov A.V., Shirikova N.Yu., Part. Nucl. **27**, No.6, 1643 (1996)

[168] Kim W., et al., Phys. Rev. **C45**, 229 (1992)

[169] Grigorev E.P., Soloviev V.G., Structure of even-even deformed nuclei, Nauka Moscow, 1974

[170] Fraile L.M., et al., Nucl. Phys. **A657**, 355 (1999)

[171] Aas A.J., et al., Nucl. Phys. **A657**, 281 (1996)

[172] Gaffney L.P., et al., Nature **497**, 199 (2013)

[173] Boisson J.P., Piepenbring R., Ogle W., Physics Report **26**, 99-147 (1976)

[174] de Shalit A., Phys. Rev. **91**, 1479 (1953)

[175] Nordheim L.W., Rev. Mod. Phys. **23**, 322 (1951)

[176] Paar V., Nucl. Phys. A331, 16 (1979)

[177] Maldeghem J., Heyde K., Phys. Rev. **C32**, 1067 (1985)

[178] Alexa P., Kvasil J., Nguyen Viet Minh, Sheline R.K., Phys. Rev. **C55**, 179 (1997)

[179] Prokofjevs P., et al., Phys. Rev. **C61**, 044305 (2000)

[180] Bohigas D., Lane A.M., Maitorell D., Phys. Report **51**, 267 (1979)

[181] Harakeh M.N., Van der Woude, "Giant Resonances", Clarendon Press Oxford, 2001

[182] Wentz C., Uberal H., Phys. Rev. **149**, 762 (1966)

[183] Harakeh M., et al., Phys. Rev. Letters **38**, 676 (1977)

[184] Youngblood D.H., Rozsa C.M., Moss J.M., Brown D.R., Bronson J.D., Phys. Rev. Letters **39**, 1188 (1977)

[185] Yongblood D.H., Clark H.L., Lui Y.-W., Proc. Selected Topics in Nuclear Excitations, eds. Dinh Dang N., Garg U. and Yamaji S., RIKEN Rev. **23**, 159 (1999)

[186] Shlomo S., Youngblood D.H., Phys. Rev. **C47**, 529 (1993)

[187] Blaizot J., Phys. Report **64**, 171 (1980)

[188] Vesely P., Toivanen J., Carlsson B.C., Dobaczewski J., Michel M., Pastore A., Phys. Rev. **C86**, 024303 (2012)

[189] Youngblood D.H., et al., Phys. Rev. **C69**, 034315 (2004); 054312 (2004); Phys. Rev. bf C88, 021301(R) (2004)

[190] Uchida M., et al., Phys. Rev. **C69**, 051301 (2004)

[191] Itoh M., et al., Phys. Rev. **C68**, 064602 (2003)

[192] Li T., et al., Phys. Rev. Lett. **99**, 162503 (2007)

[193] Youngblood D.H., et al., Phys. Rev. **C88**, 021301(R) (2013)

[194] Patel D., et al., Phys. lett. **B718**, 447 (2012)

[195] Yoshida K., Nakatsukasa T., Phys. Rev. **C88**, 034309 (2013)

[196] Kvasil J., Nesterenko V.O., Repko A., Bozik D., Kleinig W., reinhard P.-G., Jornal of Phys.: conf. ser. **580**, 012053 (2015)

[197] Li J., Colo G., Meng J., Phys. Rev. **C78**, 064304 (2008)

[198] Baldwin G.C., Klaiber G.S., Phys. Rev. **73**, 1156 (1948)

[199] Carlos P., Beil H., Bergere R., lepretre A., Veyssiere A., Nucl. Phys. **A172**, 437 (1971)

[200] Kvasil J., Nesterenko V.O., Kleinig W., Reinhard P.-G., vesely P., Phys. Rev. **C84**, 034303 (2011)

[201] Reinhard P.-G., Nesterenko V.O., Repko A., Kvasil J., Phys. Rev. **C89**, 024321 (2014)

[202] Stringari S., Physl. Letters **B108**, 232 (1982)

[203] Kneissl U., et al., J. Phys. **G32**, R217 (2006)

[204] Krasnahorkay A., et al., Phys. Rev. **C64**, 064302 (2001)

[205] Ryezava N., et al., Phys. Rev. Lett. **89**, 272502 (2002)

[206] Repko A., Reinhard P.-G., Nesterenko V.O., Kvasil J., Phys. Rev. **C87**, 024305 (2013)

[207] Paar N., Vretenar D., Khan E., Colo G., Rep. Prog. Phys. **70**, 691 (2007)

[208] Van Isacker P., Nagarjan M.A., Warner D.D., Phys. Rev. **C45**, R13 (1992)

[209] Vretenar D., Paar N., Ring P., Lalazisis P., Phys. Rev. **C63**, 047301 (2001)

[210] Kvasil J., Nesterenko V.O., Kleinig W., Reinhard P.-G., Physica Scripta **89**, 054023 (2014)

[211] Nesterenko V.O., Kvasil J., Repko A., Kleinig W., Reinhard P.-G., arXiv:1602.03326v1 [nucl-th] 10Feb2016, to be published in Phys.At.Nucl (Russian Journal)

[212] Repko A., "Theoretical description of nuclear collective excitations", Ph.D. Thesis, IPNP, Faculty of Maths. and Physics, Charles University, Prague (2015)

[213] Lo Iuduce N., Richter A., Phys. Letters **B304**, 193 (1993)

[214] Richter A., in Proc. Int. Symp. on New Fases of Spin Giant Resonance, Tokyo 1997, eds. Sakai H., Wakasa T., World Scientific, Singapure, p. 13

[215] Von Bretano R., et al., Prog. Part. Nucl. Phys. **46**, 197 (2001)

[216] Heyde K., Von Bretano P., Richter A., Rev. Mod. Phys. 82, 2365 (2010)

[217] Fearick R.W., et al., Nucl. Phys. **A727**, 41 (2003)

[218] Pai H., et al., Phys. Rev. **C93**, 014318 (2016)

[219] Vesely P., Kvasil J., Nesterenko V.O., Kleinig W., Reinhard P.-G., V.Yu. Ponomarev, Phys. Rev. **C80**, 031302(R) (2009)

[220] Woertche H.L., Ph.D. thesis, Technischen Hochschule Darmstadt, Germany, 1994

[221] Laszewski R.M., Alacron R., Dale D.S., Hoblit S.D., Phys. Rev. Lett. **61** , 1710 (1988)

[222] Shizuma T., at al., Phys. Rev. **C78**, 061303(R) (2008)

[223] Rodriguez T.R., Egido J.L., Phys. Rev. **C81**, 064323 (2010)

[224] Hofman D., Nucl. Phys. **A505**, 21c (1989)

[225] Godz A., Pomorski K., Brack M., Werner E., Nucl. Phys. **A442**, 16 (1985)

[226] Griffin J., Wheeler J.A., Phys. Rev. **108**, 311 (1957)

[227] Hill D.J., Wheeler J.A., Phys. Rev. **89**, 1102 (1953)

[228] De Toledo Piza A.F.R., De Passos E.J.V., Galetti D., Nemes M.C., Watanabe M., Phys. Rev. **C 15**, 1477 (1977)

[229] Bender M., Heenen P.-H., Reinhard P.-G., Rev. Mod. Phys. **75**, 121 (2013)

[230] Rodriguez T.R., Egido J.L., Phys. Rev. Letters **99**, 062501 (2007)

[231] Niksic T., Vretenar D., Ring P., Phys. Rev. **C74**, 064309 (2006)

[232] Rodrigues-Guzman R.R., Egido J.L., Robledo L.M., Nuclear Physics **A709**, 201 (2002)

[233] Rodriguez T.R., Egido J.L., Jungclaus A., Phys. Letters **B668**, 410 (2008)

[234] Bender M., Bonche P., Heenen P.-H., Phys. Rev. **C74**, 024312 (2008)

[235] Duguet T., Bender M., Bonche P., Heenen P.-H., Phys. Letters **B559**, 201 (2003)

[236] Rodriguez-Guzman R.R., Egido J.L., Robledo L.M., Phys. Rev. **C69**, 054319 (2004)

[237] Niksic T., Vretenar D., Lalazissis G.A., Ring P., Phys. Rev. Letters **99**, 092505 (2007)

[238] Rodriguez T.R., Egido J.L., Phys. Letters **B663**, 49 (2008)

[239] Yao J.M., Meng J., Ring P., Vretenar D., Phys. Rev. **C81**, 044311 (2010)

[240] Anguiano M., Egido J.L., Robledo L.M., Nucl. Physics **A696**, 467 (2001)

[241] Borrago M., Rodriguez T.R., Egido J.L., Phys. Letters **B746**, 341 (2015)

[242] Egido J.L., Borrago M., Rodriguez T.R., Phys. Rev. Letters **116**, 052502 (2016)

[243] Berger F., Girod M., Gogny D., Nucl. Physics **A428**, 23c (1984)

[244] Rodriguez T.R., Egido J.L., Robledo L.M., Rodriguez-Guzman R., Phys. Rev. **C71**, 044313 (2005)

[245] Schunck N., Egido J.L., Phys. Rev. **C78**, 064305 (2008)

[246] http://www.nndc.bnl.gov/ensdf/

[247] Caurier A.P., Martines-Pinedo G., Nowacki F., Poves A., Zuker A.P., Rev. Mod. Phys. **77** , 427 (2005)

[248] Tsunoda Y., Otsuka T., Shimizu N., Honna M., Utsuno Y., Phys. Rev. **C89**, 032301 (2014)

[249] Barrett B.R., Navratil P., Vary J.P., Prog. in Part. and Nucl. Physics **69**, 131 (2013)

[250] Suzuki K., Okamoto R., Profr. Theor. Phys. **68**, 1999 (1982)

[251] Machleidt R., Phys. Rev. **C63**, 024001 (2001)

[252] Wiringa R.B., Stoks V.G.J., Schiavilla R., Phys. Rec. **C51**, 38 (1995)

[253] Bogner S.K., Kuo T.T.S., Schwenk A., Phys. Rep. **361**, 1 (2003)

[254] Bogner S.K., Furnstahl R.J., Perry R.J., Phys. Rev. **C75**, 061001 (2007)

[255] Honma M., Otsuka T., Brown B.A., Misuzaki T., Phys. Rev. **C65**, 061301(R) (2002)

[256] Horejsi J.,"Fundamentals of Electroweak Theory", Charles University Prague, the Karolinum Press, 2002

[257] Hjorth-Jensen M. , Kuo T.T.S., Osnes E., Phys. Rep. **261** 125 (1995)

[258] Shimizu N., Abe T., Tsunoda Y., Utsuno Y., Yoshida T., Mizusaki T., Honma M., Otsuka T., Prog. Theor. Exp. Phys. 01A205 (2012)

[259] Otsuka T., Honma M., Mizusaki T., Shimizu N., Itsuno Y., Prog. Part. Nucl. Phys. **47**, 319 (2001)

[260] Shimizu N., Utsuno Y., Mizusaki T., Otsuka T., Abe T., Honma M., Phys. Rev. **C82**, 061305(R) (2010)

[261] De Gregorio G., Knapp F., Lo Iudice N., Vesely P., Phys. Rev. **C93**, 044314 (2016)

[262] Ekstrom A., et al., Phys. Rev. Lett. **110**, 192502 (2013)

[263] Bianco D., Knapp F., Lo Iudice N., Andreozzi F., Porrino A., Phys. Rev. **85**, 014313 (2012)

[264] Knapp F., "Multiphonon Equation of Motion Model, Doctoral Thesis, Faculty of Mathematics and Physics, Charles University, 2007

[265] Bianco D., Knapp F., Lo Iudice N., Andreozzi F., Porrino A., Phys. Rev. **C86**, 044327 (2012)

[266] Knapp F., Lo Iudice N., Vesely P., Andreozzi F., De Gregorio G., Porrino A., Phys. Rev. **C92**, 054315 (2015)

[267] Knapp F., Lo Iudice N., Vesely P., Andreozzi F., De Gregorion G., Porrino A., Phys. Rev. **C90**, 014310 (2014)

[268] De Gregorio G., Knapp F., Vesely P., Lo Iudice N., Phys. Rec. **C93**, 044314 (2016)

[269] Bianco D., Knapp F., Lo Iudice N., Vesely P., Andreozzi F., De Gregorio G., Porrino A., J. Phys. G: Nucl. Part. Phys. **41**, 025109 (2014)

[270] Litvinova E., Ring P., Tselyaev V., Langanke K., Phys. Rev. **C79**, 054312 (2009)

[271] Papakonstantinou P., Roth R., Phys. Rev. **C81**, 024317 (2010)

[272] Gambacurta D., Grasso M., Catara F., Phys. Rev. **C81**, 054312 (2010)

[273] Butler P.A., Nazarewicz W., Rev. Mod. Phys. **68**, 349 (1996)

[274] Jahn H.A., Teller E., Proc. Roy. Soc. **A161**, 220 (1937)

[275] Thouless D.J., Nucl.Phys. **22**, 78 (1961)

[276] Guest J.R., et al., Phys. Rev. Letter **98**, 093001 (2007)

[277] Cocks J., et al., Nucl. Phys. **A645**, 61 (1999)

[278] Dahlinger, M., et al., Nucl. Phys. **A484**, 337 (1988)

[279] Moller P., et al., At. Data Nucl. Data Tables **94**, 758 (2008)

[280] Bonche P., Heenen P.H., Flocard H., Vautherin D., Phys. Lett. **B175**, 387 (1986)

[281] Engel J., Bender M., Dobaczewski J., Jesus J.H., Olbratowski P., Phys. Rev. **C68**, 025501 (2003)

[282] Robledo L.M., Bertsch G.F., Phys. Rev. **C84**, 054302 (2011)

[283] Shneidman T.M., Adamian G.G., Antonenko N.V., Jolos R.V., Scheid W., Phys. Rev **C67** , 014313 (2013)

[284] Buck B., Merchant A.C., Perez S.M., J. Phys. **G35**, 085101 (2008)

[285] Zamfir N.V., Kusnecov D., Phys. Rev. **C63**, 054306 (2001)

[286] Nazarewicz W., Olander G.A., Ragnarsson I., Dudek J., Leander G.A., Moller P., Ruchowska E., Nucl. Phys. **429** (1984)

[287] Mach H., et al., Eur. Phys. J. **A52**, 172 (2016)

[288] Asarov F., Stephens F., Perlman I., Phys. Rev. **92**, 1495 (1953)

[289] Stephens F., Asarov F., Perlman I., Phys. Rev. **100**, 1543 (1955)

[290] Lee K., Inglis D.R., Phys. Rev. **108**, 774 (1957)

[291] Herzberg G., Molecular Spectra and Molecular Structure, Vol2: Infrared and Raman Spectra of Polyatomic Molecules, Van Nostrand, New York, 1945

[292] Neergard K., Vogel P., Nucl. Physics **A145**, 33 (1970)

[293] Neergard K., Vogel P., Nucl. Physics **A149**, 209 (1970)

[294] Jain A.K., Kvasil J., Sheline R.K, Hoff R.W., Phys. Rev. **C40**, 432 (1989)

[295] Wuerkner M, et al., Nucl. Phys. **A725**, 3 (2003)

[296] Levon A.I., et al., Nucl. Phys. **A598**, 11 (1996)

[297] Gulda K., et al., Nucl. Phys. **A703**, 45 (2002)

[298] Sheline R.K., Liang C.F., Paris P., Kvasil J., Nosek D., Phys. Rev/ **C51** , 1708 (1995)

[299] Liang C.F., Paris P., Sheline R.K., Nosek D., Kvasil J., Phys. Rev. **C51** , 1199 (1995)

[300] Nosek D., Sheline R.K., Sood P.C., Kvasil J., Zeit. f. Physik **A344**, 277 (1993)

[301] Stephens F.S., Rev. Mod. Phys. **47**, 57 (1975)

[302] Szymanski Z., Fast Nuclear Rotation, Clarendon Press, Oxford 1983

[303] Pal M.K., Theory of Nuclear Structure, Affiliation East-West Press, New Delhi 1981

[304] Faessler A., KFA (Julich) preprint, X-th International School on Nuclear Physics, Predeal, Romania 1976

[305] Nilsson S.G., Prior O., Mat. Fys. Medd. Dan. Vid. Selsk **32**, No 16 (1960)

[306] Kvasil J., Nazmitdinov R.G., Phys. Rev. **C73**, 014312 (2006)

[307] Johnson A., Ryde H., Sztarkier J., Phys. Lett. **B34**, 605 (1971)

[308] Johnson A., Ryde H., Hjorth S.A., Nucl. Phys. **A149**, 753 (1972)

[309] Cwiok S., Nazarewicz W., Dudek J., Szymanski Z., Phys. Rev. **C21**, 448 (1980)

[310] Kvasil J., Lo Iudice N., Andreozzi F., Knapp F., Porrino A., Phys. Rev. **C73**, 034302 (2006)

[311] Twin P.J., et al., Phys. Rev. Lett. **57**, 811 (1986)

[312] Nakatsukasa T., Matsuyanagi K., Mizutori S., Nazarewicz W., Physics Letter **B343**, 19 (1995)

[313] Lauritsen T., et al., Phys. Rev. lett. **89**, 282501 (2002)

[314] Dagnall P.J., et al., Phys. Lett. **B335**, 313 (1994)

[315] Hamamoto I., Nazarewicz W., Phys. Lett. **B297**, 25 (1992)

[316] Kvasil J., Lo Iudice N., Andreozzi F., Knapp F., Porrino A., Phys. Rev. **C75**, 034306 (2007)

[317] Purnima Singh, et al., Phys. Rev. **C86**, 067305 (2012)

[318] Petrache C.M., et al., Phys. Rev. **C92**, 064306 (2015)

[319] Frauendorf S., Rev. Mod. Phys. **73**, 463 (2001)

[320] Frauendorf S., Donau F., Phys. Rev. **C92**, 064306 (2015)

[321] Geiger H., Nuttall A., Philosophical Magazine, Series 6, Vol. 22, No130, 613-621 (1911)

[322] Gamow G., Zeit. fur Physik **51**, 204 - 212 (1928)

[323] Siegbahn K. (editor), "Alpha-, Beta- and Gamma- Ray Spectroscopy", North Holand Publ. Company, Amsterdam, 1965

[324] Mang H.J., Phys. Rev. **119**, 1069 (1960)

[325] Rasmussen J, Phys. Rev. **113**, 1593 (1959)

[326] Mang H.J., Rasmussen J., Mat. Fyz. Skr. Dan. Vid. Selsk. **2** (3) (1962)

[327] Fermi E., Zeit. Phys. **88**, 161 (1934)

[328] Wu C.S., et al., Phys. Rev. **105**, 1413 (1957)

[329] Aseev V.N. et al., Phys. Rev. **D84**, 112003 (2011)

[330] Eitel K., et al., Nucl. Physics (proc. Suppl.) **B143**, 197 (2005)

[331] Feynman R., Gell-Mann M., Phys. Rev. **109**, 183 (1958)

[332] Eisenberg J.M., Greiner W., "Excitation Mechanism of the Nucleus", North-Holland Pub. Company, Amsterdam 1976 (the 2-d edition)

[333] Primacoff H., Rosen S.P., Rep. Prog. Phys. **22**, 121 (1959)

[334] Wu C.S., Albert R.D., Phys. Rev. **75**, 315 (1949)

[335] Katrin collaboration, Status of the Karlsruhe Tritium Neutrino Mass Experiment KATRIN, Fusion Science and Technology **71(4)**, 485-490 (2017)

[336] Feenberg E., Trigg G., Rev. Mod. Phys. **22**, 399 (1950)

[337] Raman S., Walkiewicz T.A., Behrens H., Atomic Data and Nuclear Data Tables **16**, 451 (1975)

[338] Meyerhof W., "Elements of Nuclear Physics", N.Y., McGraw-Hill, 1967

[339] Niu Y.F., Colo G., Viggezzi E., Bai C.L., Sagawa H., Phys. Rev. **C94**, 064328 (2016)

[340] Niu Y.F., Colo G., Brenna M., Bortignon P.F., Meng J., Phys. Rev. **C85**, 034314 (2012)

[341] Pham K., et al., Phys. Rev. **C51**, 526 (1995)

[342] Sasano M., et al., Phys. Rev. **C79**, 024602 (2009)

[343] Taddeuci T.N., Carey C.A., Byrd R.C., Goodman C.D., Horen D.L., Rapaport J., Sugarbaker, Nucl. Phys. **A495**, 125 (1990)

[344] Bohr N., Nature **137**, 344 (1936)

[345] Hodgson P.E., Gadioli E., Gadioli Erba E., Introductory Nuclear Physics, Clarendon Press Oxford, 1997.

[346] Bertrand F.E., Peelle R.W., Phys. Rev. **C8**, 1045 (1973)

[347] Feshbach H., Poter C., Weiskopf, Phys. Rev. **96**, 448 (1954)

[348] Feshbach, Ann. Phys. (NY) **159**, 150 (1985)

[349] Block B., Feshbach H., Ann. Phys. (N.Y.) **23**, 47 (1963)

[350] Singh P.P., at al., Nucl. Phys. **65**, 577 (1965)

[351] Hodgson P.E., Nuclear Reactions and Nuclear Structure, Clarendon Press Oxford, 1971.

[352] Froebrich P. Lipperheide R., Theory of Nuclear Reactions, ClarendonPresss, Oxford, 1996.

[353] Morse P.M., Feshbach, Methods of theoretical physics, McGraw-Hill, 1953.

[354] Hodgson P.E., Phys. Rev. Letters **6**, 360 (1961)

[355] Beccetti F.D., Greenless G.W., Phys. Rev **182**, 1190 (1969)

[356] Satchler G.R., Nucl. Phys. **18**, 110 (1960)

[357] Buck B., Phys. Rev **127**, 940 (1962)

[358] Buck B., Stamp A.P., Hodgson P.E., Phil.Mag. **8**, 1805 (1963)

[359] Smith W.R., Nucl. Phys. **A130**, 657 (1969)

[360] Austern N., Direct nuclear reaction theories, Wiley N.Y., 1970

[361] Seth K.K., Picard J., Satchler G.R., Nucl. Phys. **A140**, 577 (1970)

[362] Lee L.L., et al., Phys. Rev. **136**, B971 (1964)

[363] Bechetti F.D., Greenless, Phys. Rev **182**, 1190 (1969)

[364] Macefield B.E.F., Middleton R., Pullen D.J., Nucl. Phys **44**, 309 (1963)

[365] Burjan V., et al., Eur. Phys. J. **A55**, 114 (2019)

[366] Hauser W., Feshbach H., Phys. Rev. **87**, 366 (1952)

[367] Blatt J.M., Biederham L.C., Rev.Mod.Phys. **24**, 258 (1952)

[368] Tucker A.B., Wells J.T., Meyerhof W.E., Phys. Rev. **B 137**, 1181 (1965)

[369] Moldauer P.A., Phys. Rev. **177**, 1841 (1969)

[370] Porter C.E., Thomas R.G., Phys. Rev. **104**, 483 (1956)

[371] Moldauer P.A., Rev. Mod. Phys. **36**, 1079 (1964)

[372] Dallimore P.J., Allardyce B.W., Nucl. Phys. **A 108**, 150 (1968)

[373] Felsteiner J., Serfaty R., Nucl. Phys. **A148**,428 (1970)

[374] Hausser D., von Bretano P., Mayer-Kuckuk T., Phys. Letters. **12**, 226 (1964)

[375] Gallmann A., Wagner P., Franck G., Wilmore D., Hodson P.E., Nucl. Phys. **88** , 654 (1966)

[376] Navratil P., Quaglioni S., Hupin G, at al., Physica Scripta **91**, 053002 (2016)

[377] Raimondi F., Hupin G., Navratil P., at al., Phys. Rev. **C 93**, 054606 (20161)

[378] Dohet-Eraly J., Navratil P., Quagliomi S., Horiuchi W., Raimondi F., Physics Letters **B757**, 430 (2016)

[379] Idini A., Barbieri C., Navratil P., Phys. Rev. Letters **122**, 092501 (2019)

[380] Gennari M., Vorabli M., Calci A., Navratil P., Phys. Rev. **C 97**, 034619 (2018)

[381] Landau L.D., Lifshitz, Statistical Physics, 3-d edition, Part 1, Butterwoth-Heinemann, Oxford, 1996

[382] Krticka M., Gorielly S., Hilaire S., Peru S., Valenta S., Phys. Rev. **C 99**, 044308 (2019)

[383] Garg J.B., Rainwater J., Petersen J.S., Havens W.W.,Jr., Phys. Rev. **134**, B985 (1964)

[384] Dyson F.J., Mehta M., Journal of Math.Phys. 4, 701 (1963)

[385] Haq R.U., Pandey A., Bohigas O, Phys. Rev. Letters **48**, 1086 (1982)

[386] Mehta M.L., Random Matrices, Elseviere, Amsterdam, 2004

[387] Bohigas O., Haq R.U., Pandey A., Nuclear Data for Science and technology, (ed. by K.H. Bockhoff), Reidel Publ. Comp., Dordrecht, p.809-813, 1983

[388] Phys. Lett. **B 33**, 449 (1970)

[389] Bohigas O., Flores J., Phys. Lett. **B 34**, 261 (1971)

[390] Flores J., Horoi M., Mueller M., Seligman T.M., Phys. Rev. **E 63**, 026204 (2001)

[391] Greiner W., Niese L., Stoecker H., Thermodynamics and Statistical Mechanics, Springer N.Y., 1995

[392] Farquhan I.E., Egodic Theory in Statistical Mechanics, Interscience Pu blisher, New York, 1964

[393] Brody T.A., Coha E., Flores J., Mello P.A., Nuclear Physics **A 259**, 87 (1976)

[394] Johnson C.W., Berch G.F., Dean D.J., Phys. Rev. Letters **80**, 2749 (1998)

[395] Johnson C.W., Berch G.F., Dean D.J., Talmi I., Phys. Rev. **C 61**, 014311 (1999)

[396] Bijker R., Frank A., Pittel S., Phys. Rev. **C 60**, 021302 (1999)

[397] Wildental B.H., Prog. Part. Nucl. Phys. **11**, 5 (1981)

[398] Poves A., Zuker A.P., Phys. Rep. **70**, 235 (1981)

[399] https://en.wikipedia.org/wiki/Trigonometric-functions

[400] Lauritzen B., Bortignon P.F., Broglia R.A., Zelevinsky V G, Phys. Rev. Letters **74**, 5190 (1995)

[401] Severyukhin A.P., Aberg S., Arsenyev N.N., Nazmitdinov R., Phys. Rev. **C 95**, 061305(R) (2017)

[402] Weidenmueller H.A., Mitchell G.E., Rev. Mod. Phys. **81**, 540 (2009)

[403] Kopecky J., Uhl M., Phys. Rev. **C 41**, 1941 (1990)

[404] Bartholomew G.A., Ann. Rev. Nucl. Sci. **11**, 259 (1961)

[405] Valenta S., et al., Phys. Rev **C 96**, 054315 (2017)

[406] Bethe H.A., Rev. Mod. Phys. **9**, 69 (1937)

[407] Weisskopf V.F., Phys. Rev. **52**, 295 (1937)

[408] Dilg W., Schantl W., Vonach H., Uhl M, Nucl. Phys. **A 217**, 269 (1973)

[409] Becvar F., Cejnar P., Chrien R.E., Kopecky J., Phys. Rev. **C 39** , 2398 (1992)

[410] Egido J.L., Weidenmueller H., Phys. Rev. **C 39**, 2398 (1989)

[411] Becvar F., Nucl.Inst.Methods **A417**, 434 (1998)

[412] Brink D.M., PhD Thesis, Oxford University, Oxford, UK, 1955

[413] Bollinger M., Thomas G.E.,Phys. Rev. **C 2** , 1951 (1970)

[414] Kroll J, at al., Phys. Rev. **C 88** , 034317 (2013)

[415] von Egidy T., Bucurescu D., Phys. Rev. **C 72**, 044311 (2005)

[416] von Egidy T., Bucurescu D., Phys. Rev. **C 80**, 054310 (2009)

[417] Alhassid Y., Fang L., Nakada H., Phys. Rev. Lett. **101**, 082501 (2008)

[418] Goriely S., Hilaire S., Konong A.J., Phys. Rev. **C 78**, 064307 (2008)

[419] Koning A.J., Hilaire S., Goriely S., Nucl. Phys. **A810**, 13 (2008)

[420] Capote R., et al., Nucl.Data Sheets **110**, 3107 (2009)

[421] Guttormsen M., Bagheri A., Chankova R., Rekstad J., Siem S., Schiller A., Voinov A., Phys. Rev. **C 68**, 064306 (2003)

[422] Nyhus H.T., Siem S., Guttormsen M., Larsen A.C., Buerger S., Syed N.U.H., Tveten G.M., Voinov A., Phys. Rev. **C 81**, 024325 (2010)